Food Chemistry 118 (2010) 1–10

Contents lists available at ScienceDirect

Food Chemistry

journal homepage: www.elsevier.com/locate/foodchem

Review

Pharmacological evidences for the extracts and secondary metabolites from plants of the genus *Hibiscus*

Elemar Gomes Maganha [a], Rafael da Costa Halmenschlager [b], Renato Moreira Rosa [a], João Antonio Pegas Henriques [a,b], Ana Lígia Lia de Paula Ramos [b], Jenifer Saffi [a,b,*]

[a] Laboratório de Genética Toxicológica e Programa de Pós-Graduação em Genética e Toxicologia Aplicada, Universidade Luterana do Brasil (ULBRA), Canoas, RS, Brazil
[b] Departamento de Biofísica, Instituto de Biociências, Universidade Federal do Rio Grande do Sul (UFRGS), Porto Alegre, RS, Brazil

ARTICLE INFO

Article history:
Received 13 January 2009
Received in revised form 24 February 2009
Accepted 1 April 2009

Keywords:
Hibiscus
Phytotherapics
Antioxidants
Medicinal plants

ABSTRACT

The scientific basis for the statement that plants and their active constituents play an important role in the prevention of chronic and degenerative diseases is continuously advancing. In fact, the origin of many therapeutic substances is due to secondary metabolism in the plant. The genus *Hibiscus* contains 220 species distributed around the world. It is an interesting source of potential bioactive molecules, as phenolic compounds, triterpene derivatives, phytosteroids, with antioxidant, cardioprotective, antihypertensive and antiproliferative activities. This work reviews the pharmacological evidence of extracts of plants from the genus *Hibiscus*, giving an overview of the most studied biological effects and the known phytochemical composition. Although more studies are necessary, *Hibiscus* spp. exhibits proven potential to become of important pharmacological interest.

Contents

1. Introduction

In recent times, focus on plant research has increased all over the world, and a large body of evidence has been collected to show the immense potential of medicinal plants used in traditional systems. Various medicinal plants have been identified and studied using modern scientific approaches. The results revealed the potential of medicinal plants in the field of pharmacology (Fiala, Reddy, & Weisburger, 1985; Tapsell et al., 2006; Triggiani et al., 2006).

Several human diseases, such as diabetes, neurodegenerative, cardiovascular diseases and specially carcinogenesis have been associated with oxidative stress. This condition occurs in a cell or in a tissue when the concentration of the reactive oxygen species (ROS) generated exceeds its antioxidant capability

* Corresponding author. Address: Laboratório de Genética Toxicológica, Avenida Farroupilha 8001, Bairro São José, CEP 92425-900, Canoas, RS, Brasil. Tel.: +55 51 34774000x2774; fax: +55 51 33167003.
E-mail address: jenifer.saffi@ulbra.br (J. Saffi).

0308-8146/$ - see front matter © 2009 Published by Elsevier Ltd.
doi:10.1016/j.foodchem.2009.04.005

(Nakabeppu et al., 2006; Valko, Izakovic, Mazur, Rhodes, & Telser, 2004, 2006). As a consequence, much attention has been directed to the research of naturally occurring protective antioxidants and their action mechanisms. In line with this, several plant extracts or their secondary metabolites have been found to show strong antioxidant activity and to protect against oxidant-induced damage (Collins, 2005; Hayatsu, Arimoto, & Negishi, 1988; Loo, 2003; Triggiani et al., 2006). Accordingly, many plant extracts have demonstrated potent cancer chemopreventive properties as observed in the last decade (Ames, 1998; Ames & Gold, 1998; Beckman & Ames, 1998; Borek, 2004; Cassady, Baird, & Chang, 1990). Most of these extracts are known to exert their effects by antioxidant mechanisms that either quench reactive oxygen species (ROS), inhibit lipid peroxidation or stimulate cellular antioxidant defenses (Valko et al., 2007; Yun et al., 1999).

Natural products extracted from plants which belong to the Malvaceae family are used in the treatment of many diseases worldwide. One important genus in this family is *Hibiscus* spp., with more than 220 species distributed in tropical and subtropical regions (Tseng & Lee, 2006). Species of the genus *Hibiscus* have been used in several applications in traditional medicine, as antidotes to poisoning with chemicals and venomous mushrooms and as a source of fibre in the pulp and paper industries. Members of the genus *Hibiscus* thrive in a variety of climates and produce a diversity of natural compounds with interesting bioactive properties (Holser, Bost, & Van Boven, 2004). Pharmacological investigations of the genus *Hibiscus* indicated the presence of some species with useful biological activities as antihypertensive, anti-inflammatory, antipyretic, hepatoprotective, anti-diarrhoeic, anti-spermatogenic, anti-tumour, antidiabetic, anticonvulsivant, antihelminthic immunomodulator, antioxidant and antimutagenic agents (Dafallah & Al-Mustafa, 1996; Sachdewa & Khemani, 2003). Amongst these species, less than 15 have had their biological effects studied. The majority of these studies mainly concentrated on *Hibiscus sabdariffa*. In this paper, we revised the phytochemical composition and the main pharmacological effects of the genus *Hibiscus*.

2. Materials and methods

2.1. Hibiscus syriacus

Hibiscus syriacus, the common garden *Hibiscus*, is called rose of Sharon in North America, a name given also to other plants. It is a flowering shrub native of Asia. The root bark of *H. syriacus* L. has been used as an antipyretic, antihelminthic, and antifungal agent in the east. From the stem and root bark of *H. syriacus*, saponarin, polyphenol compounds, betulin, canthin-6-one, carotenoids and anthocyanins have been previously isolated (Chen & Fang, 1993; Kwon, Hong, Kim, & Ahn, 2003). In this species, a lignan named hibiscuside ((+)-pinoresinol 4-*O*-[β-glucopyranosyl(1–2)-α-rhamnoside]) and a known lignan (syringaresinol) were present in the root bark of this plant, together with two feruloyltyramines and three known isoflavonoids: 6″-*O*-acetyldaidzin, 6″-*O*-acetylgenistin and 3-hydroxydaidzein. All compounds exhibited important antioxidant activity in vitro (Yoo et al., 1998). During screening for lipid peroxidation inhibitors, three naphthalene compounds: 2,7-dihydroxy-6-methyl-8-methoxy-1-naphthalenecarboxaldehyde, 2-hydroxy-6-hydroxymethyl-7,8-dimethoxy-1-naphthalene-carboxaldehyde and 1-carboxy-2,8-dihydroxy-6-methyl-7-methoxynaphthalenecarbolactone (1→8), designed as syriacusins A–C, were isolated from the chloroform extract of the root bark of this plant (Yoo et al., 1998). Recently, in investigations for biologically active substances, two pentacyclic triterpene caffeic acid esters were isolated (Fig. 1), increasing the number of molecules with potential pharmacodynamic interest in this species. These molecules inhibited lipid peroxidation in rat liver microsomes, indicating the existence of an antioxidant potential (Kwon et al., 2003; Yun et al., 1999; Yoo et al., 1998a). In the investigation of a methanolic extract of root bark, 8-hydroxy-5,6,7-trimethoxycoumarin, a derivative of coumarin, scopoletin and clemicosins A, C and D were identified (Fig. 1). The molecules with the coumarin core inhibited monoamine oxidase in vitro in a dose-dependent manner, while the coumarin derivative and clemicosin were potent antioxidative agents in vitro (Yun et al., 1999).

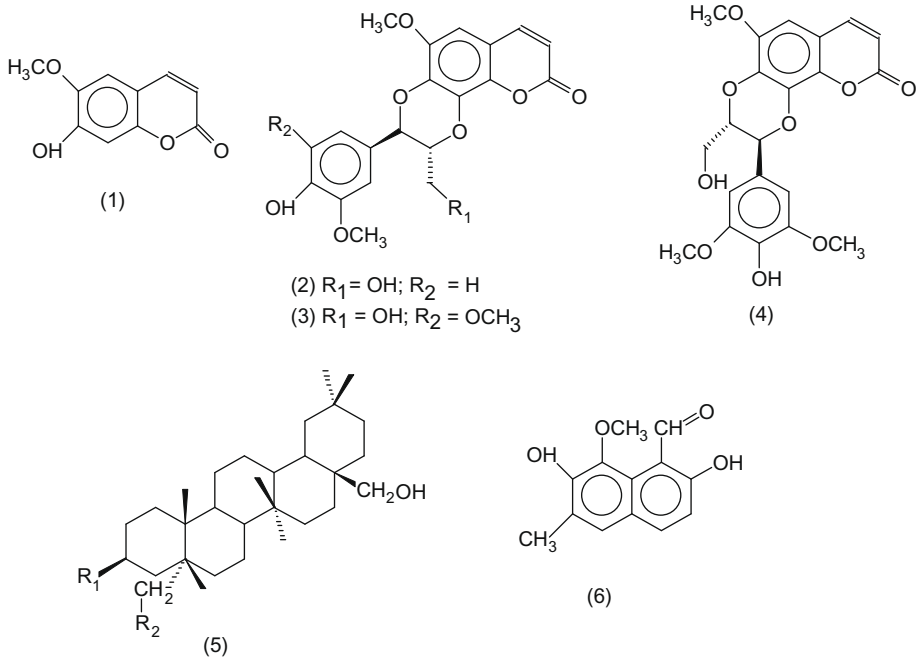

Fig. 1. Some biological compounds of *H. syriacus*: (1) scopoletin; (2) clemiscosin A; (3) clemiscosin C; (4) clemiscosin D; (5) structure of pentacyclic triterpenes; (6) syriacusin A.

More recently, the antiproliferative effect of an acetone extract of the root bark of *H. syriacus* was reported on human lung cancer cells in culture and using in vivo models, employing A549-xenograft. In this study, it was shown that this extract suppressed the expression of the proto-oncogene p53 and the apoptosis initiation factor (AIF), which can explain the cytotoxic effect of this extract, although the exact mechanisms and the molecules involved remain unclear (Cheng, Lee, Harn, Huang, & Chang, 2008).

2.2. Hibiscus cannabinus

Hibiscus cannabinus, known as kenaf, is an annual dicotyledonous herbaceous plant, well known in Asia and Africa, which has been cultivated in some Mediterranean areas. Kenaf has a long history of cultivation for its fibre by pulp and paper industries in India, Bangladesh, Thailand, parts of Africa and, to a small extent, in south eastern Europe (Moujir et al., 2007; Pappas, Tarantilis, & Polissiou, 2003).

In previous phytochemical investigations, the aliphatic composition of the bark and core were reported. In addition new lignans were identified and isolated from the core and new lignanamides were isolated, characterised and named grossamide K 1 and erythrocanabisine H 2. 2,5-Dimethyl-3-*O*-β-D-glucopyranosylnaphthol 3 was isolated and characterised as well as six other compounds from the acetone extract of the bark of kenaf (Seca et al., 2001a, 2001b). In contrast, the only previous report on the volatile leaf constituents of *H. cannabinus* concerns a biotype collected in Egypt. The authors mention the presence of 10 components, namely ethyl alcohol, isobutyl alcohol, limonene, phellandrene, R-terpenyl acetate, citral, and four unidentified components. In line with this, a group investigated the chemical composition of this essential oil: 58 components were characterised from *H. cannabinus* with (*E*)-phytol (28.2%), (*Z*)-phytol (8.02%), *n*-nonanal (5.70%), benzeneacetaldehyde (4.39%), (*E*)-2-hexenal (3.10%) and 5-methylfurfural (3.00%) as the major constituents and for which antibacterial activity was detected (Kobaisy et al., 2001). Recently, six lignans isolated from an acetone extract of the core and bark of this plant and two other compounds showed strong activity against three tumoural cell lines in several stages of cellular division (Moujir et al., 2007).

2.3. Hibiscus taiwanensis

Hibiscus taiwanensis Hu is a moderate shrub widely distributed throughout Taiwan (Wu, Wu, He, Su, & Lee, 2005). Three new phenylpropanoid esters: (7*S*,8*S*)-demethylcarolignan E, hibiscuwanin A, hibiscuwanin B and eight known phenylpropanoids: threo-carolignan E, erythro-carolignan E, cleomiscosin A, cleomiscosin C, 9,9′-*O*-feruloyl-(−)-secoisolariciresinol, dihydrodehydrodiconiferyl alcohol, boehmenan and (β)-syringaresinol have been isolated from this species (Wu et al., 2005). In the cytotoxicity evaluation of these phenyl propanoids, 9,9′-*O*-feruloyl-(β)-seco-isolariciresinol (Fig. 2) showed strong cytotoxic activity against human lung carcinoma and breast carcinoma cell lines in in vitro assays (Wu, Chuang, He, & Wu, 2004). Moreover, the crude methanolic extract has a promising cytotoxic activity against gastric and nasopharyngeal carcinoma cell lines. In addition, five new compounds, named as hibisculide A, hibisculide B, hibisculide C, hibiscutaiwanin, hibiscusin and 51 known compounds have been isolated from the stem of this species. Among them, mansonone H and uncarinic acid A inhibited HIV replication in H9 lymphocyte cells, and myriceric acid C and uncarinic acid A showed cytotoxic activity against human lung carcinoma and breast carcinoma (Wu et al., 2004).

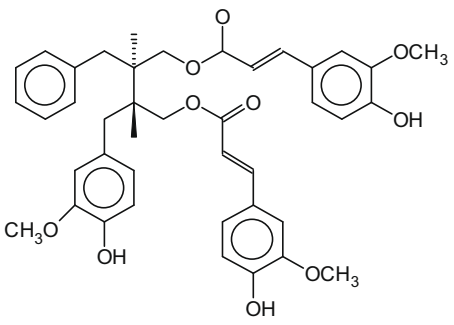

Fig. 2. The metabolite 9,9′-*O*-feruloyl-(-)secoisolariciresinol, a cytotoxic compound from *H. taiwanensis*.

2.4. Hibiscus macranthus

Hibiscus macranthus is a herbaceous plant widely distributed in tropical areas of Africa. In the western province of Cameroon, the aqueous extract from their leaf mixtures is used by tradipractioners to treat dysmenorrhoea, some cases of infertility in women and sexual weaknesses in men. Indeed, the aqueous extract from the fresh leaves was shown to increase testosteronemia in the adult male rat (Telefo, Moundipa, & Tchouanguep, 2002, 2004). Subsequently, a study evidenced the abundant presence of spermatozoa in the lumen of seminiferous tubules in rats, suggesting a useful potential of this plant in the treatment of cases of infertility due to oligospermia (Moundipa et al., 1999). Recently, Moundipa and co-workers showed that the dichloromethane and methanol extracts induced an increase in testosterone production by testes slices in vitro. However, further studies will be necessary for the isolation of androgenic bioactive components of this plant (Moundipa et al., 2005, 2006).

2.5. Hibiscus escullentus

Hibiscus escullentus L., known as lady's finger, is a very poorly studied species. The biological activity investigated in this species was the in vitro antioxidant potential. The major antioxidant molecules were identified to be quercetin derivatives and (−)-epigallocatechin (Shui & Peng, 2004).

2.6. Hibiscus vitifolius

Hibiscus vitifolius Linn is a well-adapted species in the United States of America. A new flavonol bioside from its flowers was found to exhibit significant hypoglycemic activity (Kunnumakkara et al., 2007).

2.7. Hibiscus abelmoschus

The aqueous extract of the roots of *Hibiscus abelmoschus* L. has larvicidal activity against the larvae of mosquitoes of the genera *Anopheles* and *Culex* (Dua, Pandey, Alam, & Dash, 2006). This is a useful approach to prophylaxis in countries with a high incidence of diseases transmitted by these vectors.

2.8. Hibiscus tiliaceus

Hibiscus tiliaceus L. is a common coastal plant native to Eastern and Northern Australia, Oceania and South-East Asia. The plant is also introduced as a feral species in several parts of the world including South-Western Australia and in Southern Africa. It is known by many names including hau (Hawaiian), purau (Tahitian) and "algodoeiro da praia" (Brazil) (Rosa et al., 2006). The flowers are widely used in birth control in Asian and African countries (Brondegaard, 1973). An infusion of the dried wood has been used

in folk medicine to expel the placenta and to combat postparturition disorders (Kobayashi, 1976). An aqueous extract of wood and fresh flowers has been reported to be useful to treat skin diseases (Singh, Ikahihifo, Panuve, & Slatter, 1884; Whistler, 1985). However, its chemical composition and biological and pharmacological effects are still poorly defined. Our research group has studied the biological activities of a methanolic extract of *H. tiliaceus* focusing on its antioxidant and antimutagenic effects. In preliminary work, a methanolic extract of *H. tiliaceus* flowers was studied to determine its in vivo antioxidant activity using *Saccharomyces cerevisiae* strains defective in antioxidant defense and exposed to oxidative stress induced by hydrogen peroxide and *tert*-butylhydroperoxide. The antioxidant effect verified was attributed to vitamin E and several derivatives of stigmasterol, which were identified in this extract (Rosa et al., 2006). Phytosterols present in this extract, such as stigmasterol, stigmastadienol and stigmastadienone are recognised as antioxidants and play a potential role in the chemoprevention of DNA damage in human cells induced by oxidative radicals (Wang et al., 2000).

Recently a new friedelane-type triterpene named 27-oic-3-oxo-28-friedelanoic acid and eight known triterpenoids involving five friedelane-type derivatives were isolated from the stem and bark of *H. tiliaceus* (Li et al., 2006). The knowledge of the phytochemical composition of the extracts has rapidly increased. Chen and coworkers found a new coumarin, hibiscusin and a new amide, hibiscusamide, together with 11 known compounds including vanillic acid, *p*-hydroxybenzoic acid, syringic acid, *p*-hydroxybenzaldehyde, scopoletin, *N-trans*-feruloyltyramine, *N-cis*-feruloyltyramine, a mixture of β-sitosterol and stigmasterol, a mixture of β-sitostenone and stigmasta-4,22-dien-3-one in the stem wood of this plant (Chen et al., 2006; Liu et al., 2006).

2.9. Hibiscus rosa-sinensis

Hibiscus rosa-sinensis is a glabrous shrub widely cultivated in the tropics as an ornamental plant, since it presents several forms with varying flower colours. In South Asian traditional medicine, various parts of the plant are used in the preparation of a variety of foods (Gilani, Bashir, Janbaz, & Shah, 2005). The leaves are used as a laxative, while the root is used in cough treatment. The flowers are considered to be aphrodisiac, emollient and emmenagogic and are used in bronchial catarrh, diarrhoea and fertility control (Gilani et al., 2005; Kasture, Chopde, & Deshmukh, 2000). Moreover, in India the herbal products in the market intended for hair growth include the extract of various parts of *H. rosa-sinensis* (Adhirajan, Ravi Kumar, Shanmugasundaram, & Babu, 2003).

The most ancient property studied in this species is the antifertility effect, since the benzene extract of the flowers was able to prevent pregnancy in rats (Kholkute, 1977b; Kholkute, Mudgal, & Udupa, 1977a). Other studies also show that this extract affects male fertility (Singh, Singh, & Udupa, 1882).

It is well accepted that the leaves and flowers of *H. rosa-sinensis* exhibit hair growth promoting properties in vitro and in vivo, as well as anti-greying properties, suggesting that the leaf extract could be included as a constituent in hair growth formulations (Adhirajan et al., 2003). Indeed, pharmaceutical interest in *H. rosa-sinensis* is focused on this property.

Investigations of the pharmacological properties have shown interesting effects. The ethanolic extract and acetone insoluble fractions exhibited anticonvulsant activity in pentylenetetrazol- and maximum electroshock-induced convulsion models, but failed to protect animals from strychnine-induced seizures. However, in lower doses these fractions produced signs of depression such as reduced locomotion and rearing, passivity, prostration, decreased muscle strength and diminished response to touch and noise (Kasture et al., 2000). This interesting finding suggests that the anticonvulsant action of the fractions is mediated by the chloride channel of GABA-benzodiazepine receptor complex, not by the chloride channel of glycine receptors.

The flowers of *H. rosa-sinensis*, have been reported in the ancient Indian medicinal literature to have beneficial effects in heart diseases, mainly in ischemic disease (Gauthaman et al., 2006). The mechanisms of the cardioprotective effect are controversial; in this respect, a study showed for the first time that the flower extract could enhance myocardial endogenous antioxidants by an adaptative response, without producing any cytotoxic effects. Therefore, the protection against myocardial ischemic reperfusion injury in the treated rats is attributed to enhanced endogenous antioxidant activity of this plant extract (Gauthaman et al., 2006).

In view of the traditional uses of *H. rosa-sinensis* in constipation and diarrhoea, the crude extract of aerial parts, and its subsequent fractions, were tested on isolated intestinal preparations to provide a pharmacological basis for their use in gut motility disorders. This study clearly shows the presence of two components (cholinomimetic and calcium antagonist) in the crude extract of aerial parts. The cholinomimetic activity is likely to play role as a mild laxative and provides a mechanistic basis for the possible use of the plant for constipation, while the calcium antagonistic activity provides pharmacological rationale for its use in diarrhoea (Gilani et al., 2005).

Studies have demonstrated the anti-diabetic activity of *H. rosa-sinensis* in rural populations and similar results were obtained with the leaf extract after repeated dosing in hyperglycemic rats (Sachdewa & Khemani, 1999; Sachdewa, Raina, Srivastava, & Khemani, 2001). In an elegant study using streptozotocin-induced diabetic rats, a comparable hypoglycemic effect was demonstrated after 7 and 21 days of oral administration of either the extract or glibenclamide. Besides, the extract lowered the total cholesterol and serum triglycerides and increased the HDL-cholesterol to a greater extent as compared to glibenclamide. In this manner, the hypoglycemic activity of this extract is comparable to that of glibenclamide, but is not mediated through insulin release, increasing the potential use of this species for human health purposes (Sachdewa & Khemani, 2003).

There is very important evidence of the anticancer action of this extract against the effect of benzoyl peroxide and ultraviolet radiation in mouse skin by means of antioxidant protection, decreasing the ornithine descarboxylase activity and thymidine incorporation in DNA. In this manner, *H. rosa-sinensis* extract exerts a protective effect against the tumour promotion stage of cancer development (Sharma, Khan, & Sultana, 2004b; Sharma & Sultana, 2004a).

Phytochemical studies revealed the presence of several chemicals, including flavonoids, flavonoid glycosides, hibiscetin, cyanidine, cyanidin glucosides, taraxeryl acetate, β-sitosterol, campesterol, stigmasterol, ergosterol, citric, tartaric and oxalic acids, cyclopropenoids and anthocyanin pigments (Ajay, Chai, Mustafa, Gilani, & Mustafa, 2007; Gauthaman et al., 2006; Gilani et al., 2005; Sachdewa & Khemani, 1999, 2003).

2.10. Hibiscus sabdariffa

H. sabdariffa L., an attractive plant, believed to be native to Africa, is cultivated in tropical areas as Sudan, Eastern Taiwan, and in Thailand (Chang, Huang, Hsu, Yang, & Wang, 2005; Hirunpanich et al., 2005; Lin, Chen, Kuo, & Wang, 2007). This is an annual herb that grows to 180 cm or more; stems are globular, while the lower leaves are ovate with the upper leaves being 3–5 palmately lobed. The flowers are auxiliary or in terminal racemes, the petals are white with a reddish centre at the base of the staminal column, the calyx enlarges at maturity and the fruit is fleshy and bright red. It is known as roselle (English), l'Oiselle (French), Spanish (Jamaica), karkade (Arabic), Krachiap daeng (in Thailand) and bissap

(Wolof). The calyces are used to make cold and hot beverages in many of the world's tropical and sub-tropical countries. The average consumption of these beverages in Nigeria is 150–180 mg/kg per day. Calyces are used in the West Indies to colour and flavour rum and the seeds have been used as an aphrodisiac coffee substitute. In addition, its fruits are edible too (Ali, Al Wabel, & Blunden, 2005).

The red persistent calyx of its flowers is the major component which has a sour taste and is commonly used in the preparation of cold and hot beverages and as a food colourant. Recently, it has gained an important position in the local soft drink market and commercial preparations of *H. sabdariffa* extract (HSE) are currently marketed as supplements due to their perceived potential health benefits (Ali et al., 2005). It is claimed to be a Thai traditional medicine for kidney and urinary bladder stones. It is also used as an antibacterial, antifungal, hypocholesterolemic, antispasmodic, diuretic, uricosuric, mild laxative, antihypertensive substance, against inflammation, mutagenicity and as an immune modulating compound (Ali, Salih, Mohamed, & Homeida, 1991; Chen et al., 2003; Dafallah & Al-Mustafa, 1996; Farombi & Fakoya, 2005).

The calyx and flowers of roselle have been known to contain many chemical constituents such as alkaloids, ascorbic acid, β-carotene, anisaldehyde, arachidic acid, citric acid, malic acid, tartaric acid, glycinebetaine, trigonelline, anthocyanins as cyanidin-3-rutinoside, delphinidin, delphinidin-3-glucoxyloside (also known as hibiscin, the major anthocyanin in *H. sabdariffa* flowers, Fig. 3), delphinidin-3-monoglucoside, cyanidin-3-monoglucoside, cyanidin-3-sambubioside, cyanidin-3,5-diglucoside; the flavonol glycosides hibiscetin-3-monoglucoside, gossypetin-3-glucoside, gossypetin-7-glucoside, gossypetin-8-glucoside and sabdaritrin; quercetin, protocatechuic acid, pectin, polysaccharides, mucopolysaccharides, stearic acid and wax (Hirunpanich et al., 2005). In the seed oil, the presence of campasterol, stigmasterol, ergosterol, β-sitosterol and α-spinasterol has been reported. The petals yielded 65% (dry weight) of mucilage, which on hydrolysis gave galactose, galacturonic acid and rhamnose. These molecules are bioactive in several biological models and responsible by the pharmacological effects presented by the extracts of this species. Various antioxidant constituents are found in the calyx and flower petals of roselle, such as *Hibiscus* anthocyanins, quercetin, ascorbic acid, steroid glycosides (such as β-sitosteroid glycoside) and protocatechuic acid (Tseng et al., 1997). Furthermore, HSE contained polyphenolic acids (1.7% dry weight), flavonoids (1.43% dry weight) and anthocyanins (2.5% dry weight) (Tsuda, Horio, & Osawa, 2000a; Tsuda, Shiga, Ohshima, Kawakishi, & Osawa, 1996).

Phenolic compounds are ubiquitous in vegetables, fruit and nuts, and several of them have been reported to be inhibitors of chemical carcinogenesis due to their antioxidant properties (Stich, 1991; Wattenberg, 1985). *Hibiscus* anthocyanins (HAs) (Kamei et al., 2003) are water-soluble and among the most important groups of plant pigments which significantly reduced oxidative stress induced by *tert*-butylhydroperoxide in rat hepatocytes, in vitro and in vivo. This is an important model for liver injury. They also significantly reduced the activities of the serum enzymes indicative of liver damage and ameliorated histological lesions (Chang, Huang, Huang, Ho, & Wang, 2006; Suboh, Bilto, & Aburjai, 2004; Wang et al., 2000). Similar dosages of HAs were effective in mitigating the toxicity induced by paracetamol in mice (Ali, Mousa, & El-Mougy, 2003).

Furthermore, anthocyanins not only possess antioxidant ability, but also mediate other physiological functions related to cancer suppression, which has roused increasing interest concerning the pharmaceutical function of these pigments (Kamei et al., 2003; Meiers et al., 2001; Pool-Zobel, Bub, Schroder, & Rechkemmer, 1999; Tsuda, Kato, & Osawa, 2000b). HAs have demonstrated an anti-tumour effect in HL-60 cells. The molecular mechanism underlying this effect could be described as the induction of apoptosis via activation of the p38 MAP kinase that subsequently phosphorylates the target protein c-jun and trigger the signal to further activate the apoptotic protein cascades that contain Fas-mediated signaling. As an outcome, cytochrome *c* is released from the mitochondria, leading to the cleavage of caspase-3 (Chang et al., 2005). In view of this, HAs were considered the major components of the antitumoural effect of HSE in human gastric adenocarcinoma and in promyelocytic cells in vitro, reflecting the chemopreventive potential of HSE (Lin, Chen, Kuo, & Wang, 2007).

Hibiscus protocatechuic acid (PCA) (Fig. 3) has been demonstrated to be an efficacious agent in inhibiting the carcinogenic action of various chemicals in different tissues, such as diethylnitrosamine in the liver, 4-nitroquinoline-1-oxide in the oral cavity, azoxymethane in the colon, *N*-methyl-*N*-nitrosourea in glandular stomach tissue and *N*-butyl-*N*-(4-hydroxybutyl)nitrosamine in the bladder, in murine models (Hirose et al., 1995; Tanaka, Kojima, Kawamori, & Mori, 1995; Tseng et al., 1998). PCA also shows mild cytotoxicity to PC14 and MKN45 human tumour cell lines and induces apoptosis in human leukaemia HL-60 cells by means of the reduction of retinoblastoma protein phosphorylation and Bcl-2 expression (Tseng et al., 2000). Thus, PCA possesses strong antioxidant and antitumour promotion effects and may play a role in dietary chemoprevention (Chewonarin et al., 1999; Hirose et al., 1995; Kawamori et al., 1994; Tseng et al., 1998). In addition, it has been reported that the topical application of PCA inhibited the 12-*O*-tetradecanoylphorbol-13-acetate-induced tumour promotion in the skin of mice initiated with benzo[*a*]pyrene. Moreover, it has strong potential in inhibiting LDL oxidation induced by copper or a nitric oxide donor, besides the protection against cytotoxicity and genotoxicity of *tert*-butylhydroperoxide in a primary culture of rat hepatocytes and in rat liver. This indicates that this antioxidative potential can be involved in the beneficial effects of HSE (Hirunpanich et al., 2005; Lee et al., 2002). Furthermore, PCA also inhibits lipopolysaccharide-induced rat hepatic damage (Lin et al., 2003).

Due to its chemical composition, HSE presents antioxidative potential and useful pharmacodynamic actions in diseases caused by oxidative stress, as cancer and cardiovascular pathologies. In vitro, the ethyl acetate fraction of the ethanol extract showed a strong ability to scavenge free radicals in the assay of quenching the 1,1-diphenyl-2-picrylhydrazyl radical, whereas the chloroform fraction showed the strongest inhibitory effect in the assay of xantine oxidase inhibition. Both fractions presented strong antioxidant potential in the model of *tert*-butylhydroperoxide-induced oxidative damage in the primary cultures of rat hepatocytes. In addition, HSE exerted its hepatoprotective activity against hepatic fibrosis induced by carbon tetrachloride exposure in rats with the participation, at least in part, of the antioxidant activity of protocatechuic

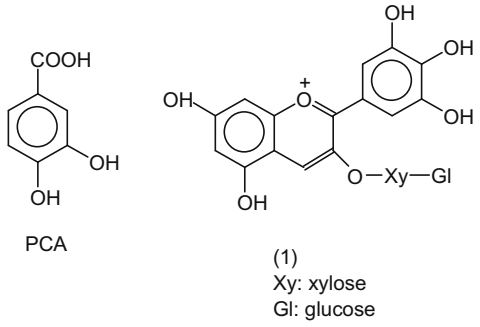

Fig. 3. Structure of delphinidin-3-glucoxyloside (1), the major anthocyanin from *H. sabdariffa* flowers, and protocatechuic acid (PCA).

Table 1
Some secondary metabolites found in the *Hibiscus* genus and its pharmacodinamic properties.

Species	Important compounds	Sources studied	Pharmacodynamic effects	References
H. syriacus	Hibiscuside Syringaresinol Feruloyltyramines Isoflavonoids Syriacusins A–C Pentacyclic triterpene caffeic acid esters Clemicosin A, C and D Scopoletin 8-Hydroxy-5,6,7-trimethoxycoumarin	Chloroform extract of root bark	Antioxidant in vitro Monoaminoxidase inhibitors	Yokota, Zenda, Kosuge, & Yamamoto, 1978; Kwon et al., 2003; Yoo et al., 1998; Yun et al., 1999
H. cannabinus	Grossamide K1 Erythrocanabisine H2 Phellandrene Phytol Nonanal 5-Methyl-furfural 2-Hexenal Benzene acetaldehyde	Leaf Acetone extract of root bark	Antibacterial	Pappas et al., 2003; Moujir et al., 2007; Seca et al., 2001a; Seca et al., 2001b
H. taiwanensis	(7*S*,8*S*)-Demethylcariolignan E Hibiscuwanin A Hibiscuwanin B Clemicosin A and C 9,9′-*O*-Feruloyl-(−)secoisolariciresinol Dehydroconifenyl alcohol β-Syringaresinol Erythro-cariolignan E Hibisculide A Hibisculide B Hibisculide C Hibiscutaiwanin Hibiscusin Mansonone H Uncarinic acid Myceric acid	Methanol extract of leaf	Cytotoxic against tumoral cells in vitro Inhibited HIV replication Cytotoxic against human lung carcinoma and breast carcinoma	Wu et al., 2004, 2005
H. macrantus		Aqueous extract of flowers	Androgenic effects	Moundipa et al., 1999, 2005, 2006; Telefo et al., 2004
H. esculentus	(−)-Epigallocatechin	Flowers	Antioxidant in vitro	Shui and Peng (2004)
H. vitifolius	Flavonol bioside	Flowers	Hypoglycemic activity	Kunnumakkara et al., 2007
H. abelmoschus		Aqueous extract of roots	Larvicidal activity	Dua et al., 2006
H. tilliaceus	Stigmasterol Stigmastadienol Stigmastadienone 27-Oic-3-oxo-28-friedelanoic acid Vanillic acid Syringic acid Scopoletin *N-trans*-Feruloyltiramine *N-cis*-Feruloyltyramine β-Sitostenone Stigmasta-4,22-dien-3-one	Methanol extract of flowers and leaves	Antioxidant activity in vitro	Kobayashi, 1976; Singh et al., 1884; Whistler, 1985

H. rosa sinensis	Hibiscetin	Aqueous extract of flowers and leaves	Anticonvulsivant action	Gilani et al., 2005; Adhirajan et al., 2003;
	Cyanidin			Kholkute, 1977b; Singh et al., 1882;
	Cyanidine glucosides		Cardioprotective effect	Gauthaman et al., 2006; Sachdewa & Khemani,
	Taraxeryl acetate			1999; Sachdewa et al., 2001; Sharma & Sultana,
	β-Sitosterol		Cholinomimetic activity	2004a; Sharma et al., 2004b; Ajay et al., 2007
	Campesterol		Hypoglycemic effects Antiproliferative effects in tumor xenografts vivo	
	Ergosterol			
	Cyclopropenoids			
H. sabdariffa	β-Carotene	Aqueous extract of flowers, leaves and bark	Aphrodisiac antibacterial, antifungal,	Dafallah & Al-Mustafa, 1996; Farombi &
	Anisaldehyde		hypocholesterolemic, antispasmodic a diuretic,	Fakoya, 2005; Chen & Fang, 1993; Ali et al.,
	Arachidic acid		uricosuric, mild laxative, antihypertensive substance,	1991, 2005; Osawa et al., 1996; Kamei et al.,
	Citric acid		against inflammation, mutagenicity and as immune	2003; Chang et al., 2006; Suboh et al., 2004;
	Malic acid		modulating	Pool-Zobel et al., 1999; Meiers et al., 2001
	Tartaric acid			
	Glycinebetaine			
	Trigonelline			
	Anthocyanins			
	Cyanidin-3-rutinoside			
	Delphinidin			
	Delphinidin-3-glucoxyloside			

acid and anthocyanins (Liu et al., 2006; Tseng, Wang, Kao, & Chu, 1996). Besides, some antioxidants such as L-ascorbic acid, vitamin E or garlic acid may play an important role in this effect (Sheweita, El-Gabar, & Bastawy, 2001). Recently, the pretreatment of rats with HSE reduced significantly the hepatotoxicity of cadmium. The extract also protected the rats against cadmium-induced liver, prostate, and testis lipoperoxidation. In this manner, the antioxidant ability of the aqueous extract can be used in cadmium poisoning (Asagba, Adaikpoh, Kadiri, & Obi, 2007). Interestingly, HSE reduced the extent of cisplatin-induced sperm abnormality and enhanced sperm motility through its antioxidant capacity, increasing the activities of testicular antioxidant enzymes, showing a possible employment of this plant in the treatment of fertility disorders (Amin & Hamza, 2006). In addition, the methanolic extracts of leaves of this species has radioprotective efficacy against gamma radiation-induced liver damage in rats, by stimulating the increase in hepatic superoxide dismutase production.

Two fractions of the ethanolic extract, the chloroform soluble fraction and ethyl acetate soluble fraction orally administered to mice simultaneously with intraperitoneal injection of ferrous chloride – ascorbic acid – ADP mixture reduced the formation of malondialdehyde content in rats and significantly inhibited the induction of micronucleated polychromatic erythrocytes by sodium arsenite showing that the antioxidant properties of this plant contribute to its antimutagenic potential (Adetutu et al., 2004; Farombi & Fakoya, 2005). The ethanolic extract of this species was also effective in decreasing the mutagenecity induced by heterocyclic amines in the *Salmonella* microsome assay and inhibits the formation of colon cancer at the initiation stage. Recently, the aqueous, ethyl acetate and chloroform extracts of the leaves of this species inhibited the mutagenicity induced by 1-nitropyrene in HeLa cells in a dose- response manner and showed an antiproliferative effect in these cells (Olvera et al., 2008).

The ancient use of *H. sabdariffa*, the best-studied species in this genus, is related to cardiovascular diseases (Ajay et al., 2007; Ali, Al Wabel, & Blunden, 2005). In this sense, several studies evaluated the anti-hypertensive effects of HSE in several biological models. The intravenous injection of HSE to anaesthetized cats and rats lowered the blood pressure in a dose-dependent manner, which was partially blocked by atropine and antihistamine H1 blockers, though the sectioning of the left and right vagi nerves did not have a significant effect on the fall in mean arterial blood pressure (Adegunloye et al., 1996; Ali et al., 1991). Recent pharmacological reports have shown that HSE significantly reduced blood pressure in humans and in experimental animals; in addition, the chronic administration of HSE decreased blood pressure and reduced cardiac hypertrophy in the 2-kidney-1-clip (2K-1C) rat model of hypertension and inhibited vascular tone in isolated vascular preparations including the rat thoracic aorta (Adegunloye et al., 1996; Ajay et al., 2007; Onyenekwe, Ajani, Ameh, & Gamaniel, 1999). However, the exact mechanisms responsible for these effects are not fully understood. In view of this, the possibility that HSE could produce a direct vasorelaxant effect was investigated: the methanolic extract of calyces induced a vasodilator effect in isolated aortas from spontaneously hypertensive rats via endothelium-dependent and -independent vasodilator pathways. The endothelium-dependent vasodilator component results from the activation of the endothelium-derived nitric oxide/cGMP-relaxant pathway, whereas the endothelium-independent component could be due to inhibition of calcium influx (Ajay et al., 2007). Thus, these findings provided rational evidence for the traditional use of the plant as an antihypertensive agent.

The first single trial involved 54 patients with moderate essential hypertension and it reported that the daily consumption of an aqueous extract resulted in a decrease of about 11% in blood pressure 12 days after the beginning of the treatment. In this study, 3

days after cessation of the treatment, the blood pressure rose again by about 6–8% (Haji-Faraji & Haji-Tarkhani, 1999). In 2004, a clinical trial involving 39 patients that were receiving HSE and 36 hypertensive patients that were treated with captopril shows that HSE was as effective and safe in the reduction of blood pressure as captopril was (Herrera-Arellano, Flores-Romero, Chavez-Soto, & Tortoriello, 2004). A recent study confirmed the anti-hypertensive effect using watery infusions, in which a natriuretic effect was also evidenced, in a randomized, controlled, and double-blind clinical trial. The results showed that the experimental treatment decreased blood pressure with therapeutic effectiveness of 65.1% as well as tolerability and safety of 100%. Under the experimental treatment, the serum chlorine level increased, the sodium level showed a tendency to decrease, while the potassium level was not modified. The possible mechanism underlying this effect could be the inhibition of angiotensin I converting enzyme, since its activity decreased in the plasma of treated patients.

Currently, the dried calyx extracts of this species are commercially prepared as health food products available in the form of granules and as tea, and are claimed to be diuretic, antihypertensive and mainly as hypolipidemic. However, the scientific data in respect of hypolipidemic efficacy of these extracts are relatively recent. In 1991, rats with hypercholesterolaemia were fed with HSE for 9 weeks and the treatment progressively lowered the different lipid fractions in plasma, heart, brain, kidney and liver. However, this treatment slightly raised the content of plasma phospholipids (El-Saadany, Sitohy, Labib, & El-Massry, 1991). In the study of Chen and co-workers, in 2003, the administration of HSE to rabbits which had been fed cholesterol for 10 weeks reduced the serum levels of triglycerides, total cholesterol and LDL, and mitigated atherosclerosis in the aorta. Moreover, it slightly decreased the susceptibility of LDL to oxidation induced by copper sulphate ex vivo and the rate of formation of conjugated dienes. Since phytoconstituents compounds such as β-sitosterol and pectin have been reported to possess a hypocholesterolemic effect in vivo, it may be speculated that the hypolipidemic effects are attributed to these compounds (Hirunpanich et al., 2006).

Many investigations highlight an additional role of polyphenolic acids, flavonoids, and anthocyanins, which may act as antioxidants or via other mechanisms, enhancing the cardioprotective actions (Hirunpanich et al., 2006; Rimm & Stampfer, 2000). This potent dose-dependent antioxidant effect in the protection of LDL oxidation induced by copper sulphate in vitro was demonstrated some years ago and stimulated the investigation of the antioxidant effect in vivo, as well as the determination of the active compounds and the correlation with the antiatherosclerotic effects (Hirunpanich et al., 2005). In some previous studies, HAs and PCA showed remarkable antioxidative activity and are able to inhibit LDL oxidation and lipid peroxidation in vitro (Wang et al., 2000). Therefore, dietary HSE may reduce the incidence of heart disease, such as atherosclerosis, through their antioxidant activity.

According to the oxidative hypothesis of atherosclerosis, LDL entrapped in the subendoethelial space of lesion-prone arterial sites is slowly oxidised through the action of resident vascular cells. In this manner, oxidation of LDL in the arterial wall is thought to be a very important step in atherogenesis. In this respect, HSE inhibits oxidation of LDL in the arterial wall, thereby exerting an antiatherosclerotic action, as observed in hystopatological and immunohistochemical analysis (Chen et al., 2003). It has been demonstrated that many antioxidants inhibit the development of atherosclerotic lesions in rabbits fed with high cholesterol diet through the prevention of LDL oxidation. In this manner, there is considerable interest in the cardioprotective potential of HSE in lowering the incidence of atherosclerosis and coronary heart disease.

Recently, new pharmacodynamic activities on this plant have been reported, as immunomodulatory effect of the ethanolic extracts of dried calyx in mouse (Falceve, Pal, Bawankule, & Khanuja, 2008) and anticandidal activity. Moreover, the extract of this plant inhibited the rat bladder and uterine contractility in a dose-dependent manner via a mechanism unrelated to local or remote autonomic receptors or calcium channels (Prasongwatana, Woottisin, Sriboonlue, & Kukorgvirivapan, 2008).

3. Concluding remarks

The main biological findings and the known phytochemical composition of the *Hibiscus* genus are summarised in Table 1. The studies conducted to date have demonstrated that the plants of the *Hibiscus* genus have the potential to provide biologically active compounds that act as antioxidants, as well as being cardioprotective, and that are able to deter the proliferation of malignant cells. Thus, the *Hibiscus* genus deserves additional evaluation as a provider of chemopreventive agents. Indeed, there is a current need for availability of new plant-derived bioactive molecules; thus *Hibiscus* sp. may be a great natural source for the development of new drugs and may provide a cost-effective mean of treating cancers and other diseases in the developing world.

References

Adegunloye, B. J., Omoniyi, J. O., Owolabi, O. A., Ajagbonna, O. P., Sofola, A. O., & Coker, H. A. (1996). Mechanisms of the blood pressure lowering effect of the calyx extract of *Hibiscus sabdariffa* in rats. *African Journal of Medicine and Medical Sciences, 25*, 227–235.

Adetutu, A., Odunola, A. O., Owoade, A. O., Adeleke, A. O., & Amuda, O. S. (2004). Anticlastogenic effects of *Hibiscus sabdariffa* fruits against sodium arsenite-induced micronuclei formation in erythrocytes in mouse bone marrow. *Phytotherapy Research: PTR, 18*, 862–866.

Adhirajan, N., Ravi Kumar, T., Shanmugasundaram, N., & Babu, M. (2003). *In vivo* and *in vitro* evaluation of hair growth potential of *Hibiscus rosa-sinensis* Linn. *Journal Ethnopharmacology, 88*, 226–235.

Ajay, M., Chai, H. J., Mustafa, A. M., Gilani, A. H., & Mustafa, M. R. (2007). Mechanisms of the anti-hypertensive effect of *Hibiscus sabdariffa* L. calyces. *Journal Ethnopharmacology, 109*, 15–388.

Ali, B. H., Al Wabel, N., & Blunden, G. (2005). Phytochemical, pharmacological and toxicological aspects of *Hibiscus sabdariffa* L.: A review. *Phytotherapy Research: PTRP*, 75–369.

Ali, B. H., Mousa, H. M., & El-Mougy, S. (2003). The effect of a water extract and anthocyanins of *Hibiscus sabdariffa* L. on paracetamol-induced hepatoxicity in rats. *Phytotherapy Research: PTR, 17*, 56–65.

Ali, M. B., Salih, W. M., Mohamed, A. H., & Homeida, A. M. (1991). Investigation of the antispasmodic potential of *Hibiscus sabdariffa* calyces. *Journal Ethnopharmacol, 31*, 57–249.

Ames, B. N. (1998). Micronutrients prevent cancer and delay aging. *Toxicology Letters, 102–103*, 5–18.

Ames, B. N., & Gold, L. S. (1998). The prevention of cancer. *Drug Metabolism Reviews, 30*, 201–224.

Amin, A., & Hamza, A. A. (2006). Effects of roselle and ginger on cisplatin-induced reproductive toxicity in rats. *Asian Journal of Andrology, 8*, 595–607.

Asagba, S. O., Adaikpoh, M. A., Kadiri, H., & Obi, F. O. (2007). Influence of aqueous extract of *Hibiscus sabdariffa* L. petal on cadmium toxicity in rats. *Biological Trace Element Research, 115*, 47–57.

Beckman, K. B., & Ames, B. N. (1998). The free radical theory of aging matures. *Physiological Reviews, 78*, 547–581.

Borek, C. (2004). Dietary antioxidants and human cancer. *Integraly Cancer, 3*, 333–374.

Brondegaard, V. J. (1973). Contraceptive plant drugs. *Planta Medica, 23*, 167–172.

Cassady, J. M., Baird, W. M., & Chang, C. J. (1990). Natural products as a source of potential cancer chemotherapeutic and chemopreventive agents. *Journal of Natural Products, 53*, 23–41.

Chang, Y. C., Huang, H. P., Hsu, J. D., Yang, S. F., & Wang, C. J. (2005). *Hibiscus anthocyanins* rich extract-induced apoptotic cell death in human promyelocytic leukemia cells. *Toxicology and Applied Pharmacology, 205*, 12–201.

Chang, Y. C., Huang, K., Huang, A. C., Ho, Y. C., & Wang, C. J. (2006). *Hibiscus anthocyanins*-rich extract inhibited LDL oxidation and oxLDL-mediated macrophages apoptosis. *Food and Chemical Toxicology, 44*, 73–1015.

Chen, R. T., & Fang, S. D. E. (1993). On the chemical constituents of cotton rose *Hibiscus*. *Traditional and Herbal, 24*, 227–229.

Chen, C. C., Hsu, J. D., Wang, S. F., Chiang, H. C., Yang, M. Y., Kao, E. S., Ho, Y. C., & Wang, C. J. (2003). *Hibiscus sabdariffa* extract inhibits the development of

atherosclerosis in cholesterol-fed rabbits. *Journal of Agricultural and Food Chemistry, 51*, 5465–5472.
Chen, J. J., Huang, S. Y., Duh, C. Y., Chen, I. S., Wang, T. C., & Fang, H. Y. (2006). A new cytotoxic amide from the stem wood of *Hibiscus tiliaceus*. *Planta Medica, 72*, 935–938.
Cheng, Y. L., Lee, S. C., Harn, H. J., Huang, H. C., & Chang, W. L. (2008). The extract of *Hibiscus syriacus* inducing apoptosis by activating p53 and AIF in human lung cancer cells. *American Journal of Chinese Medicine, 36*, 171–184.
Chewonarin, T., Kinouchi, T., Kataoka, K., Arimochi, H., Kuwahara, T., Vinitketkumnuen, U., & Ohnishi, Y. (1999). Effects of roselle (*Hibiscus sabdariffa* Linn.), a Thai medicinal plant, on the mutagenicity of various known mutagens in *Salmonella typhimurium* and on formation of aberrant crypt foci induced by the colon carcinogens azoxymethane and 2-amino-1-methyl-6-phenylimidazo(4,5-*b*) pyridine in F344 rats. *Food and Chemical Toxicology, 37*, 591–601.
Collins, A. R. (2005). Antioxidant intervention as a route to cancer prevention. *European Journal of Cancer, 41*, 1923–1953.
Dafallah, A. A., & Al-Mustafa, Z. (1996). Investigation of the antiinflamatory activity of Acacia nilotica and *Hibiscus sabdariffa*. *The American Journal of Chinese Medicine, 24*, 263–269.
Dua, V. K., Pandey, A. C., Alam, M. E., & Dash, A. P. (2006). Larvicidal activity of *Hibiscus abelmoschus* Linn. (Malvaceae) against mosquitoes. *Journal of the American Mosquito Control Association, 22*, 148–155.
El-Saadany, S. S., Sitohy, M. Z., Labib, S. M., & El-Massry, R. A. (1991). Biochemical dynamics and hypocholesterolemic action of *Hibiscus sabdariffa* (Karkade). *Nahrung, 35*, 490–567.
Falceve, T. O., Pal, A., Bawankule, D. U., & Khanuja, S. P. (2008). Immunomodulatory effect of extracts of *Hibiscus sabdariffa* L. (family Malvaceae) in a mouse model. *Phytotherapy, 22*, 664–672.
Farombi, E. O., & Fakoya, A. (2005). Free radical scavenging and antigenotoxic activities of natural phenolic compounds in dried flowers of *Hibiscus sabdariffa* L.. *Molecular Nutrition and Food Research, 49*, 1118–1120.
Fiala, E. S., Reddy, B. S., & Weisburger, J. H. (1985). Naturally occurring anticarcinogenic substances in foodstuffs. *Annual Review of Nutrition, 5*, 295–321.
Gauthaman, K. K., Saleem, M. T., Thanislas, P. T., Prabhu, V. V., Krishnamoorthy, K. K., Devaraj, N. S., & Somasundaram, J. S. (2006). Cardioprotective effect of the *Hibiscus rosa-sinensis* flowers in an oxidative stress model of myocardial ischemic reperfusion injury in rat. *BMC Complementary and Alternative Medicine, 6*, 32.
Gilani, A. H., Bashir, S., Janbaz, K. H., & Shah, A. J. (2005). Presence of cholinergic and calcium channel blocking activities explains the traditional use of *Hibiscus rosa-sinensis* in constipation and diarrhoea. *Journal Ethnopharmacology, 102*, 94–289.
Haji-Faraji, M., & Haji-Tarkhani, A. (1999). The effect of sour tea (*Hibiscus sabdariffa*) on essential hypertension. *Journal Ethnopharmacol, 65*, 225–231.
Hayatsu, H., Arimoto, S., & Negishi, T. (1988). Dietary inhibitors of mutagenesis and carcinogenesis. *Mutation Research, 202*, 46–429.
Herrera-Arellano, A., Flores-Romero, S., Chavez-Soto, M. A., & Tortoriello, J. (2004). Effectiveness and tolerability of a standardized extract from *Hibiscus sabdariffa* in patients with mild to moderate hypertension: A controlled and randomized clinical trial. *Phytomedicine, 11*, 82–375.
Hirose, Y., Tanaka, T., Kawamori, T., Ohnishi, M., Makita, H., Mori, H., Satoh, K., & Hara, A. (1995). Chemoprevention of urinary bladder carcinogenesis by the natural phenolic compound protocatechuic acid in rats. *Carcinogenesis, 16*, 2337–2376.
Hirunpanich, V., Utaipat, A., Morales, N., Bunyapraphatsara, N., Sato, H., Herumale, A., & Suthisisang, C. (2006a). Hypocholesterolemic and antioxidant effects of aquous extracts from the dried calyx of *Hibiscus sabdariffa* L. in hypercholesterolemic rats. *Journal of Ethnopharmacology, 103*, 252–260.
Hirunpanich, V., Utaipat, A., Morales, N. P., Bunyapraphatsara, N., Sato, H., Herunsale, A., & Suthisisang, C. (2006b). Hypocholesterolemic and antioxidant effects of aqueous extracts from the dried calyx of *Hibiscus sabdariffa* L. in hypercholesterolemic rats. *Journal of Ethnopharmacology, 103*, 60–252.
Hirunpanich, V., Utaipat, A., Morales, N. P., Bunyapraphatsara, N., Sato, H., Herunsalee, A., & Suthisisang, C. (2005). Antioxidant effects of aqueous extracts from dried calyx of *Hibiscus sabdariffa* L. (Roselle) *in vitro* using rat low-density lipoprotein (LDL). *Biological and Pharmaceutical Bulletin, 28*, 477–481.
Holser, R. A., Bost, G., & Van Boven, M. (2004). Phytosterol composition of hybrid *Hibiscus* seed oils. *Journal of Agricultural and Food Chemistry, 52*, 2546–2548.
Kamei, H., Kojima, T., Hasegawa, M., Koide, T., Umeda, T., Yukawa, T., & Terabe, K. (2003). Suppression of tumor cell growth by anthocyanins *in vitro*. *Cancer Investigation, 13*, 586–590.
Kasture, V. S., Chopde, C. T., & Deshmukh, V. K. (2000). Anticonvulsive activity of Albizzia lebbeck, *Hibiscus rosa-sinesis* and Butea monosperma in experimental animals. *Journal of Ethnopharmacology, 71*, 65–75.
Kawamori, T., Tanaka, T., Kojima, T., Suzui, M., Ohnishi, M., & Mori, H. (1994). Suppression of azoxymethane-induced rat colon aberrant crypt foci by dietary protocatechuic acid. *Japanese Journal of Cancer Research, 85*, 686–691.
Kholkute, S. D. (1977b). Effect of *Hibiscus rosa-sinensis* on spermatogenesis and accessory reproductive organs in rats. *Planta Medica, 31*, 92–127.
Kholkute, S. D., Mudgal, V., & Udupa, K. N. (1977a). Studies on the ant fertility potentiality of *Hibiscus*. *Planta Medica, 31*, 35–39.
Kobaisy, M., Tellez, M. R., Webber, C. L., Dayan, F. E., Schrader, K. K., & Wedge, D. E. (2001). Phytotoxic and fungitoxic activities of the essential oil of kenaf (*Hibiscus cannabinus* L.) leaves and its composition. *Journal of Agricultural and Food Chemistry, 49*, 3768–3771.
Kobayashi, J. (1976). Early Hawaiian uses of medicinal plants in pregnancy and childbirth. *The Journal of Tropical Pediatrics and Environmental Child Health, 22*, 260–262.
Kunnumakkara, A. B., Nair, A. S., Ahn, K. S., Pandey, M. K., Yi, Z., Liu, M., & Aggarwal, B. B. (2007). Gossypin, a pentahydroxy glucosyl flavone, inhibits the transforming growth factor β-activated kinase-1-mediated NF-kappaB activation pathway, leading to potentiation of apoptosis, suppression of invasion, and abrogation of osteoclastogenesis. *Blood, 12*, 5091–5112.
Kwon, S. W., Hong, S. S., Kim, J. I., & Ahn, I. H. (2003). Antioxidant properties of heat-treated *Hibiscus syriacus*. *Izvestiia Akademii nauk. Seriia biologicheskaia, 1*, 20–21.
Lee, M. J., Chou, F. P., Tseng, T. H., Hsieh, M. H., Lin, M. C., & Wang, C. J. (2002). *Hibiscus* protocatechuic acid or esculetin can inhibit oxidative LDL induced by either copper ion or nitric oxide donor. *Journal of Agricultural and Food Chemistry, 50*, 2124–2130.
Li, L., Huang, X., Sattler, I., Fu, H., Grabley, S., Lin, W., et al. (2006). Structure elucidation of a new friedelane triterpene from the mangrove plant *Hibiscus tiliaceus*. *Magnetic Resonance Chemistry, 44*, 624–628.
Lin, H. H., Chen, J. H., Kuo, W. H., & Wang, C. (2007). Chemopreventive properties of *Hibiscus sabdariffa* L. on human gastric carcinoma cell through apoptosis induction and JNK/p38 MAPK signaling activation. *Chemico-Biological Interactions, 165*, 59–75.
Lin, W. L., Hsieh, Y. J., Chou, F. P., Wang, C. J., Cheng, M. T., & Tseng, T. H. (2003). *Hibiscus protocatechuic* acid inhibits lipopolysaccharide-induced rat hepatic damage. *Archives of Toxicology, 77*, 35–42.
Liu, J. Y., Chen, C. C., Wang, W. H., Hsu, J. D., Yang, M. Y., & Wang, C. J. (2006). The protective effects of *Hibiscus sabdariffa* extract on CCl4-induced liver fibrosis in rats. *Food and Chemical Toxicology, 44*, 43–336.
Loo, G. (2003). Redox-sensitive mechanisms of phytochemical-mediated inhibition of cancer cell proliferation (review). *The Journal of Nutritional Biochemistry, 14*, 64–73.
Meiers, S., Kemeny, M., Weyand, U., Gastpar, R., von Angerer, E., & Marko, D. (2001). The anthocyanidins cyanidin and delphinidin are potent inhibitors of the epidermal growth-factor receptor. *Journal of Agricultural and Food Chemistry, 49*, 62–958.
Moujir, L., Seca, A. M., Silva, A. M., Lopez, M. R., Padilla, N., Cavaleiro, J. Á., & Neto, C. P. (2007). Cytotoxic activity of lignans from *Hibiscus cannabinus*. *Fitoterapia, 78*, 378–385.
Moundipa, P. F., Beboy, N. S., Zelefack, F., Ngouela, S., Tsamo, E., Schill, W. B., & Monsees, T. K. (2005). Effects of Basella alba and *Hibiscus macranthus* extracts on testosterone production of adult rat and bull Leydig cells. *Asian Journal of Andrology, 7*, 7–411.
Moundipa, F. P., Kamtchouing, P., Koueta, N., Tantchou, J., Foyang, N. P., & Mbiapo, F. T. (1999). Effects of aqueous extracts of *Hibiscus macranthus* and Basella alba in mature rat testis function. *Journal of Ethnopharmacology, 65*, 9–133.
Moundipa, P. F., Ngouela, S., Kamtchouing, P., Tsamo, E., Tchouanguep, F. M., & Carreau, S. (2006). Effects of extracts from *Hibiscus macranthus* and Basella alba mixture on testosterone production *in vitro* in adult rat testes slices. *Asian Journal of Andrology, 8*, 4–111.
Nakabeppu, Y., Sakumi, K., Sakamoto, K., Tsuchimoto, D., Tsuzuki, T., & Nakatsu, Y. (2006). Mutagenesi and carcinogenesis caused by the oxidation of nucleic acids. *Biological Chemistry, 387*, 9–373.
Olvera, G. V., Casta, T. E., Rezendiz, R. I., Reynoso, C. R., Gonzalez, E., Elizondo, G., et al. (2008). *Hibiscus sabdariffa* L. extracts inhibit the mutagenicity in microsuspension assay and the proliferation of HeLa cells. *Journal of Food Science, 73*, 75–81.
Onyenekwe, P. C., Ajani, E. O., Ameh, D. A., & Gamaniel, K. S. (1999). Antihypertensive effect of roselle (*Hibiscus sabdariffa*) calyx infusion in spontaneously hypertensive rats and a comparison of its toxicity with that in Wistar rats. *Cell Biochemistry and Function, 17*, 199–206.
Pappas, C. S., Tarantilis, P. A., & Polissiou, M. G. (2003). Isolation and spectroscopic study of pectic substances from kenaf (*Hibiscus cannabinus* L.). *Natural Product Research, 17*, 171–176.
Pool-Zobel, B. L., Bub, A., Schroder, N., & Rechkemmer, G. (1999). Anthocyanins are potent antioxidants in model systems but do not reduce endogenous oxidative DNA damage in human colon cells. *European Journal of Nutrition, 38*, 227–261.
Prasongwatana, V., Woottisin, S., Sriboonlue, P., & Kukorgvirivapan, V. (2008). Uricosuric effect of Roselle (*Hibiscus sabdariffa*) in normal and renal-stone former subjects. *Journal of Ethnopharmacology, 5*, 491–496.
Rimm, E. B., & Stampfer, M. J. (2000). Antioxidants for vascular disease. *The Medical Clinics of North America, 84*, 49–239.
Rosa, R. M., Melecchi, M. I., da Costa Halmenschlager, R., Abad, F. C., Simoni, C. R., Caramao, E. B., et al. (2006). Antioxidant and antimutagenic properties of *Hibiscus tiliaceus* L. methanolic extract. *Journal of Agricultural and Food Chemistry, 54*, 7324–7330.
Sachdewa, A., & Khemani, L. D. (1999). A preliminary investigation of the possible hypoglycemic activity of *Hibiscus rosa-sinensis*. *Biomedical and Environmental Sciences, 12*, 6–222.
Sachdewa, A., & Khemani, L. D. (2003). Effect of *Hibiscus rosa-sinensis* ethanol flower extract on blood glucose and lipid profile in streptozotocin induced diabetes in rats. *Journal of Ethnopharmacology, 89*, 61–66.
Sachdewa, A., Raina, D., Srivastava, A. K., & Khemani, L. D. (2001). Effect of Aegle marmelos and *Hibiscus rosa sinensis* leaf extract on glucose tolerance in glucose

induced hyperglycemic rats (Charles foster). *Journal of Environmental Biology, 22*, 7–53.

Seca, A. M., Silva, A. M., Silvestre, A. J., Cavaleiro, J. A., Domingues, F. M., & Pascoal-Neto, C. (2001a). Lignanamides and other phenolic constituents from the bark of kenaf *Hibiscus cannabinus*. *Phytochemistry, 58*, 23–1219.

Seca, A. M., Silva, A. M., Silvestre, A. J., Cavaleiro, J. A., Domingues, F. M., & Pascoal-Neto, C. (2001b). Phenolic constituents from the core of kenaf (*Hibiscus cannabinus*). *Phytochemistry, 56*, 67–759.

Sharma, S., Khan, N., & Sultana, S. (2004b). Effect of Onosma echioides on DMBA/croton oil mediated carcinogenic response, hyperproliferation and oxidative damage in murine skin. *European Journal of Cancer Prevention, 13*, 40–53.

Sharma, S., & Sultana, S. (2004a). Effect of *Hibiscus rosa-sinensis* extract on hyperproliferation and oxidative damage caused by benzoyl peroxide and ultraviolet radiations in mouse skin. *Basic and Clinical Pharmacology and Toxicology, 95*, 115–220.

Sheweita, S. A., El-Gabar, M. A., & Bastawy, M. (2001). Carbon tetrachloride changes the activity of cytochrome P450 system in the liver of male rats: Role of antioxidants. *Toxicology, 169*, 83–92.

Shui, G., & Peng, L. L. (2004). An improved method for the analysis of major antioxidants of *Hibiscus esculentus* Linn. *Journal of chromatography, 1048*, 17–24.

Singh, Y. N., Ikahihifo, T., Panuve, M., & Slatter, C. (1884). Folk medicine in Tonga. A study of the use of herbal medicines for obstetric and gynaecological conditions and disorders. *Journal of Ethnopharmacology, 12*, 301–305.

Singh, M. P., Singh, R. H., & Udupa, K. N. (1882). Anti-fertility activity of a benzene extract of *Hibiscus rosa-sinensis* flowers on female albino rats. *Planta Medica, 44*, 171–174.

Stich, H. F. (1991). The beneficial and hazardous effects of simple phenolic compounds. *Mutation Research, 259*, 307–331.

Suboh, S. M., Bilto, Y. Y., & Aburjai, T. A. (2004). Protective effects of selected medicinal plants against protein degradation, lipid peroxidation and deformability loss of oxidatively stressed human erythrocytes. *Phytotherapy Research: PTR, 18*, 276–280.

Tanaka, T., Kojima, T., Kawamori, T., & Mori, H. (1995). Chemoprevention of carcinogenesis in rats by flavonoids diosmin and hesperidin the combination. *Carcinogenesis, 75*, 1433–1475.

Tapsell, L. C., Hemphill, I., Cobiac, L., Patch, C. S., Sullivan, D. R., Fenech, M., Enrys, S., Keogh, J. B., Clifton, P. M., Williams, P. G., Fazio, V. A., & Inge, K. E. (2006). Health benefits of herbs and spices: The past, the present, the future. *The Medical Journal of Australia, 185*, S4–S24.

Telefo, P. B., Moundipa, P. F., & Tchouanguep, F. M. (2002). Oestrogenicity and effect on hepatic metabolism of the aqueous extract of the leaf mixture of Aloe buettneri, Dicliptera verticillata, *Hibiscus macranthus* and Justicia insularis. *Fitoterapia, 73*, 466–472.

Telefo, P. B., Moundipa, P. F., & Tchouanguep, F. M. (2004). Inductive effect of the leaf mixture extract of Aloe buettneri, Justicia insularis, Dicliptera verticillata and *Hibiscus macranthus* on *in vitro* production of estradiol. *Journal of Ethnopharmacology, 91*, 195–225.

Triggiani, V., Resta, F., Guastamacchia, E., Sabba, C., Licchelli, B., Ghiyasaldin, S., et al. (2006). Role of antioxidants, essential fatty acids, carnitine, vitamins, phytochemicals and trace elements in the treatment of diabetes mellitus and its chronic complications. *Endocrine, Metabolic and Immune Disorders Drug Targets, 6*, 77–93.

Tseng, T. H., Hsu, J. D., Lo, M. H., Chu, C. Y., Chou, F. P., Huang, C. L., & Wang, C. J. (1998). Inhibitory effect of *Hibiscus* protocatechuic acid on tumor promotion in mouse skin. *Cancer Letters, 126*, 199–207.

Tseng, T. H., Kao, T. W., Chu, C. Y., Chou, F. P., Lin, W. L., & Wang, C. J. (2000). Induction of apoptosis by *Hibiscus* protocatechuie acid in human leukemia cells via reduction of retinoblastoma (RB) phosphorylation and Bel-2 expression. *Biochemical Pharmacology, 60*, 307–315.

Tseng, T. H., Kao, E. S., Chu, C. Y., Chou, F. P., Lin Wu, W., & Wang, C. J. (1997). Protective effects of dried flower extract of *Hibiscus sabdariffa* L. against oxidative stress in rat primary hepatocytes. *Food and Chemical Toxicology, 35*, 1159–1164.

Tseng, T. H., & Lee, Y. J. (2006). Evaluation of natural and synthetic compounds from East Asiatic folk medicinal plants on the mediation of cancer. *Anti-cancer Agents in Medicinal Chemistry, 6*, 65–347.

Tseng, T. H., Wang, C. J., Kao, E. S., & Chu, H. Y. (1996). Hibiscus anthocyanin are potent antioxidants in human cells. *Chemico-Biological Interactions, 101*, 137–145.

Tsuda, T., Horio, F., & Osawa, T. (2000a). The role of anthocyanins as an antioxidant under oxidative stress in rats. *Biofactors, 13*, 122–133.

Tsuda, T., Kato, Y., & Osawa, T. (2000b). Mechanism for the peroxynitrite scavenging activity by anthocyanins. *FEBS Letters, 484*, 197–207.

Tsuda, T., Shiga, K., Ohshima, K., Kawakishi, S., & Osawa, T. (1996). Inhibition of lipid peroxidation and the active oxygen radical scavenging effect of anthocyanin pigments isolated from *Phaseolus vulgaris* L.. *Biochemical Pharmacology, 52*, 1022–1033.

Valko, M., Izakovic, M., Mazur, M., Rhodes, C. J., & Telser, J. (2004). Role of oxygen radicals in DNA damage and cancer incidence. *Molecular and Cellular Biochemistry, 266*, 37–56.

Valko, M., Leibfritz, D., Moncol, J., Cronin, M. T., Mazur, M., & Telser, J. (2007). Free radicals and antioxidants in normal physiological functions and human disease. *The International Journal of Biochemistry and cell Biology, 39*, 44–84.

Valko, M., Rhodes, C. J., Moncol, J., Izakovic, M., & Mazur, M. (2006). Free radicals, metals and antioxidants in oxidative stress-induced cancer. *Chemico-Biological Interactions, 160*, 1–40.

Wang, C. J., Wang, J. M., Lin, W. L., Chu, C. Y., Chou, F. P., & Tseng, T. H. (2000). Protective effect of *Hibiscus* anthocyanins against *tert*-butyl hydroperoxide-induced hepatic toxicity in rats. *Food and Chemical Toxicology, 38*, 6–411.

Wattenberg, L. W. (1985). Chemoprevention of cancer. *Cancer Research, 45*, 1–8.

Whistler, W. A. (1985). Traditional and herbal medicine in cook islands. *Journal of Ethnopharmacology, 13*, 239–280.

Wu, P. L., Chuang, T. H., He, C. X., & Wu, T. S. (2004). Cytotoxicity of phenylpropanoid esters from the stems of *Hibiscus taiwanensis*. *Bioorganic and Medicinal Chemistry, 12*, 2193–2200.

Wu, P. L., Wu, T. S., He, C. X., Su, C. H., & Lee, K. H. (2005). Constituents from the stems of *Hibiscus taiwanensis*. *Chemical and Pharmaceutical Bulletin, 53*, 47–56.

Yokota, M., Zenda, H., Kosuge, T., & Yamamoto, T. (1978). Studies on isolation of naturally occurring biologically active principles V. Antifungal constituents in Betulae cortex (author's transl). *Yakugaku Zasshi, 98*, 1508.

Yoo, I. D., Yun, B. S., Lee, I. K., Ryoo, I. J., Choung, D. H., & Han, K. H. (1998a). Three naphthalenes from root bark of *Hibiscus syriacus*. *Phytochemistry, 47*, 799–802.

Yoo, I. D., Yun, B. S., Lee, I. K., Ryoo, I. J., Choung, D. H., & Han, K. H. (1998b). Coumarins with monoamine oxidase inhibitory activity and antioxidative coumarins-lignans from *Hibiscus syriacus*. *Journal of Ethnopharmacology, 64*, 1238–1240.

Yun, B. S., Ryoo, I. J., Lee, I. K., Park, K. H., Choung, D. H., Han, K. H., et al. (1999). Two bioactive pentacyclic triterpene esters from the root bark of *Hibiscus syriacus*. *Journal of Natural Products, 62*, 764–770.

Food Chemistry 118 (2010) 11–16

Contents lists available at ScienceDirect

Food Chemistry

journal homepage: www.elsevier.com/locate/foodchem

Anthocyanins and polyphenol oxidase from dried arils of pomegranate (*Punica granatum* L.)

Vidhan Jaiswal [a], Ara DerMarderosian [a,b,*], John R. Porter [a,b]

[a] Program in Pharmacognosy, Department of Chemistry and Biochemistry, University of the Sciences in Philadelphia, Philadelphia, PA 19104, United States
[b] Department of Biological Sciences, University of the Sciences in Philadelphia, Philadelphia, PA 19104, United States

ARTICLE INFO

Article history:
Received 30 July 2008
Received in revised form 27 January 2009
Accepted 29 January 2009

Keywords:
Pomegranate
Punica granatum L.
Polyphenol oxidase
Anthocyanin

ABSTRACT

Anthocyanins are natural pigments responsible for red, purple, and blue colouration in plants. Human consumption of anthocyanins is increasing because of the rising awareness and interest in their potential health benefits. Pomegranate is one of the major sources of polyphenolic phytochemicals, such as anthocyanins. Dried pomegranate raisins (*anardana*) are consumed in large quantities in Asian countries, and contain substantial amounts of anthocyanins. Five anthocyanins were found to be present in pomegranate raisins. Drying adversely affected the amount of anthocyanins, with polyphenol oxidase (PPO) playing a possible role in oxidative degradation of anthocyanins. Anthocyanins are heat-stable compounds, and inactivation of PPO by processing at high temperature for short periods may prevent PPO-catalysed anthocyanin oxidation in pomegranate arils. Pomegranate PPO kinetics were partially characterised by investigating the effect of substrate (catechol) concentration; optimum pH for PPO activity was found to be 6.0.

1. Introduction

Anthocyanins are the largest and most important group of water-soluble pigments in nature. In plant tissues, they are responsible for producing red, purple, blue, and intermediate hues, depending upon the vacuolar pH and the presence of copigments (Brouillard, Figueiredo, Elhabiri, & Dangles, 1997; Clifford, 2000; Rapeanu, Loey, Smout, & Hendrickx, 2006). Anthocyanins are of considerable importance in the co-evolution of plant–animal interactions, as they contribute to the colourful appearance of flowers, fruits and vegetables, helping them to attract animals, leading to seed dispersal and pollination (Kong, Chia, Goh, Chia, & Brouillard, 2003). Anthocyanin stability is influenced by various factors such as temperature, pH, light, and oxygen. Anthocyanins also may be susceptible to degradation by oxidising enzymes.

Polyphenol oxidases (PPOs), or tyrosinases, are nuclear-coded enzymes with a dinuclear copper centre, which are able to insert oxygen in a position *ortho* to an existing hydroxyl group in an aromatic ring, followed by the oxidation of the diphenol to the corresponding quinone. These *o*-quinone intermediates are highly reactive and quickly polymerise to dark-coloured melanins (Rapeanu et al., 2006). PPO is widely distributed in animals, plants, fungi, and bacteria and plays an important role in various physiological and defence reactions (Mayer, 2006). PPO is inducible by both biotic and abiotic stresses, and is implicated in several physiological processes, including photoreduction of molecular oxygen by photosystem I (PSI), regulation of plastidic oxygen levels, aurone biosynthesis, and the phenylpropanoid pathway (Thipyapong, Stout, & Attajarusit, 2007).

The pomegranate (*Punica granatum* L.), from the Latin words *pomus* and *granatus*, meaning a seeded or granular apple, is native from Iran to the Himalayas in northern India, where it has been cultivated for thousands of years. There are over 1000 cultivars of *Punica granatum* (Levin, 1994) that are grown from Iran, eastward to China and India and westward through the Mediterranean region, on to the American Southwest, California and Mexico (Lansky & Newman, 2007). There has been a virtual explosion of interest in pomegranate as a medicinal and nutritional product because of its multifunctionality, and, as a result, the field of pomegranate research has experienced tremendous growth in the past decade. Polyphenols are the major class of pomegranate fruit phytochemicals, including flavonoids (anthocyanins), condensed tannins (proanthocyanidins) and hydrolysable tannins (ellagitannins and gallotannins) (Gil, Tomas-Barberan, Hess-Pierce, Holcroft, & Kader, 2000; Hernandez, Melgarejo, Tomas-Barberan, & Artes, 1999; Santagati, Duro, & Duro, 1984). Pomegranate juice may provide protection against cardiovascular diseases and stroke, by acting as a potent antioxidant against LDL oxidation and inhibition of atherosclerosis development (Aviram et al., 2002a, 2002b). Pomegranate

* Corresponding author. Address: Program in Pharmacognosy, Department of Chemistry and Biochemistry, University of the Sciences in Philadelphia, Philadelphia, PA 19104, United States. Tel.: +1 215 596 8915; fax: +1 215 596 8710.
E-mail address: a.dermar@usp.edu (A. DerMarderosian).

0308-8146/$ - see front matter © 2009 Elsevier Ltd. All rights reserved.
doi:10.1016/j.foodchem.2009.01.095

phytochemicals also show potential in chemoprevention of various types of cancers, by exerting antiproliferative effects on tumour cells (Kim et al., 2002; Shishodia, Adams, Bhatt, & Aggarwal, 2006).

Pomegranates are popularly consumed as fresh fruit, beverages (juice and wine) and other food products (jams and jellies). The presence of anthocyanins is responsible for the appealing bright red colour of juice and other products of pomegranate fruit. Pomegranate raisins (*anardana*) are dried arils of wild pomegranates that are manually separated from the rind and septa of the fruit and sun- or air-dried. Pomegranate raisins have a distinct sour or tart flavour, and are commercially available in many West and East Asian countries, where they are consumed in large quantities. The raisins are also used in the ayurvedic system of medicine, and are claimed to be digestive and stomachic (Pruthi & Saxena, 1984; Singh, Kingly, & Jain, 2007). Pomegranate juice, which is prepared by hydrostatic pressing of whole fruits, has been found to contain more than 26 different chemical compounds, whereas the seeds contain various fatty acids and steroidal compounds (Seeram, Zhang, Reed, Krueger, & Vaya, 2006). The aril (the seed and surrounding flesh) contains anthocyanins, which might be affected by the severity of the drying process employed for the raisin preparation.

Scarce information exists on the chemical constituents of *anardana*. This study was designed to evaluate the effect of drying on pomegranate aril anthocyanins and to investigate the role of PPO in aril anthocyanin oxidation.

2. Materials and methods

2.1. Plant material

Fresh pomegranates (*P. granatum* L. cv. Wonderful) were supplied by POM Wonderful company (Del Rey, CA). Arils were separated manually and kept in dark and cold (−80 °C) storage until analysed. Pomegranate raisins (*anardana*) were purchased from Deep Foods, Inc. (Union, NJ).

2.2. Chemicals

Cyanidin 3-glucoside (kuromanin chloride) standard for HPLC analysis, catechol, trifluoroacetic acid (TFA), acetone, acetonitrile, ethyl acetate, hexane, and methanol were purchased from Sigma–Aldrich (St. Louis, MO). Unless stated otherwise, all solvents were HPLC-grade. Diaion HP-20SS resin was purchased from Supelco (Bellefonte, PA). Triton X-100 was purchased from Bio-Rad (Richmond, CA).

2.3. Preparation of pomegranate raisins (anardana)

Commercially available *anardana* contains 2.7% moisture, whereas fresh pomegranate arils contain about 78.7% moisture. One batch of fresh pomegranate arils was dried in a cabinet dryer at 90 °C for 90 min, followed by 70 °C for 2 h, and finally 50 °C for an additional 9 h to remove the required 76% moisture. This drying regime was used following a variety of drying methods at various temperatures to achieve material that was similar to the commercial product. A second batch of fresh pomegranate arils was sun-dried in shallow trays in the summer months in the USP research greenhouse; the average temperature was 32–43 °C. The drying was continued until the arils lost the required 76% moisture.

2.4. Anthocyanin isolation and purification

Fresh and dried pomegranate arils were extracted exhaustively by maceration with acidic methanol (1:10, w/v) containing 1% 0.1 M HCl over 24 h at room temperature. The extract was filtered through a sintered glass funnel and concentrated *in vacuo* at 37 °C. The extract was partitioned sequentially with hexane and ethyl acetate, and the aqueous fraction containing the anthocyanins was lyophilised. Removal of other water-soluble constituents, such as sugars and ascorbic acid, was accomplished by chromatography over Diaion HP-20SS resin (Einbond, Reynertson, Luo, Basile, & Kennelly, 2004). The lyophilised, semi-purified anthocyanin extract was resuspended in 25 ml water, applied to the Diaion HP-20SS resin column (60 cm × 5 cm ID, 120 g) and allowed to adsorb for 20 min. The column was sequentially eluted with 500 ml water to remove sugars and then with 300 ml acidic methanol containing 0.1% 0.1 M HCl to elute all of the anthocyanins. Finally, the column was washed clean with 300 ml methanol:acetone (1:1) mixture. The methanol fraction containing anthocyanins was concentrated *in vacuo* at 37 °C and lyophilised.

2.5. Anthocyanin analysis by quantitative HPLC and LC–MS

Quantitative HPLC analysis was conducted on an Agilent 1100 HPLC system (Agilent Technologies, Santa Clara, CA) consisting of a low pressure quaternary pump, an autosampler and a photodiode array detector controlled by Agilent ChemStation [Rev. B. 01.03(204)] software. LC–MS analysis was conducted on a Shimadzu liquid chromatograph–mass spectrometer (Shimadzu, Columbia, MD), consisting of a dual-plunger parallel-flow solvent delivery module (LC-20AD), an autosampler (SIL-20AC), and a single-stage quadrupole mass analyser (LCMS-2010EV) monitored by LCMSsolution (ver.3.30) software (Shimadzu). The anthocyanin separation was done on a Zorbax SB-C8 column (4.6 mm ID × 75 mm, 3.5 μm) (Agilent). Anthocyanin samples were dissolved in HPLC-grade water containing 0.1% TFA and filtered through a 0.45 μm nylon filter (Fisher Scientific, Pittsburgh, PA) prior to the analysis. The binary mobile phase consisted of solvents **A**, 0.1% TFA in water, and **B**, acetonitrile acidified with 0.1% TFA. The gradient method was 0–10 min, 13–20% **B**; 10–18 min, 20–40% **B**; 18–21 min, 40% **B**; and post-run time of 5 min with 13% **B**. Solvent flow rate was 0.2 ml/min, and the sample injection volume was 10 μl. Detection was at 520 nm. The amounts of individual and total anthocyanins in samples extracted from fresh, oven-dried, and sun-dried pomegranate arils were quantified using a cyanidin 3-glucoside standard calibration curve ($r^2 \geqslant 0.99$).

2.6. Heat stability of anthocyanin

Cyanidin 3-glucoside was dissolved in distilled water at a concentration of 0.01 mg/ml. Two samples of 1 ml each were transferred into 5 ml glass vials. Air was replaced with nitrogen in one vial, and both vials were capped and sealed immediately. These samples were subjected to heat treatment as mentioned in the drying protocol for pomegranate raisins, i.e. heated in a cabinet dryer at 90 °C for 90 min, followed by 70 °C for 2 h, and finally at 50 °C for 9 h. The samples were cooled and analysed by HPLC to determine the amount of cyanidin 3-glucoside degraded by heat treatment. The results were compared to a freshly prepared 0.01 mg/ml standard sample.

2.7. Polyphenol oxidase enzyme extraction

Polyphenol oxidase enzyme extract was prepared following a modification of the procedure described by Coseteng and Lee (1987). Fresh and dried pomegranate arils (30 g each) were homogenised for 2 min in a prechilled blender with 50 ml ice-cold 0.1 M potassium phosphate buffer, pH 7.2, containing 1% Triton X-100. The homogenate was filtered through a sintered glass funnel and centrifuged (2 °C, 5000*g*) for 15 min in a Sorvall RC-5B+

centrifuge (Thermo Fisher Scientific, Inc. Waltham, MA). The supernatant was decanted and used as a crude enzyme preparation in the PPO activity assay.

2.8. PPO activity assay

The PPO activity was determined by measuring the initial rate of increase in absorbance at 420 nm as described by Gonzalez, de Ancos, and Cano (1999). The activity was assayed in 3 ml of reaction mixture consisting of 2.5 ml potassium phosphate buffer (pH 6.0), 0.3 ml substrate (0.5 M catechol) and 0.2 ml crude enzyme. The blank consisted of 3.0 ml potassium phosphate buffer (pH 6.0). The first control cuvette contained 2.7 ml buffer solution and 0.3 ml substrate, whereas the second control cuvette contained 2.8 ml buffer and 0.2 ml enzyme preparation. Absorbance values of these controls were subtracted from that of the sample. The enzyme activity was defined as the change in absorbance of 0.001 per min per ml enzyme.

2.9. Optimum pH for PPO activity

The effect of pH on pomegranate PPO activity was determined by catechol oxidation in 0.1 M sodium acetate buffer (pH 5.0 and 5.5) and 0.1 M potassium phosphate buffer (pH 6.0, 6.5, 7.0, 7.5, and 8.0). The sample cuvette contained 2.5 ml buffer solution (pH 5–8), 0.3 ml substrate and 0.2 ml enzyme.

2.10. Effect of boiling on PPO activity

PPO was extracted from fresh pomegranate arils and divided into two parts. The first sample was boiled for 2 min at 100 °C, and the PPO activity was determined using catechol as a substrate. The activity of boiled aril PPO was compared to that of untreated PPO from the second sample.

2.11. PPO kinetics: the Michaelis–Menten constant

Seven catechol solutions varying in concentration from 0.1 to 0.9 M were prepared, and the effect of substrate concentration on pomegranate PPO activity was investigated to partially characterise the enzyme kinetics. The sample cuvette contained 0.3 ml substrate (0.1–0.9 M catechol), 2.5 ml 0.1 M potassium phosphate buffer, pH 6.0, and 0.2 ml undiluted enzyme preparation. The Michaelis–Menten constant (K_m) and maximum velocity (V_{max}) were calculated from a double reciprocal plot of 1/velocity *vs.* 1/substrate concentration by the method of Lineweaver and Burk (1934). The reaction velocity was defined as change in optical density (ΔOD) of reaction mixture per min per ml of enzyme.

2.12. Effect of drying on anthocyanins and PPO activity

Anthocyanins were extracted from fresh, oven-dried and sun-dried pomegranate arils and quantified by HPLC using the cyanidin 3-glucoside standard calibration curve. The PPO was extracted from fresh, oven-dried and sun-dried pomegranate arils and activity determined by catechol oxidation assay.

2.13. Effect of boiling on anthocyanins and PPO activity

Two 25 g samples of fresh, frozen pomegranate arils were placed in glass bottles and immersed in an oil-bath at 100 °C. It took 14 min to bring the frozen arils (−80 °C) to 100 °C. The samples were maintained at 100 °C for 2 min (total 16 min). Anthocyanins were extracted from the first sample and quantified by HPLC using the cyanidin 3-glucoside standard calibration curve. PPO activity was determined in the second sample by the catechol oxidation assay. The results were compared to total anthocyanins and PPO activity of 25 g samples of fresh, untreated arils, extracted simultaneously.

2.14. Data analysis

Values are averages of three determinations. The results were analysed for variation (ANOVA) and statistical significance by *t*-test. Error bars shown in figures are standard deviations of the values.

3. Results and discussion

3.1. Anthocyanin analysis by quantitative HPLC and LC–MS

We determined the presence of anthocyanins delphinidin 3,5-diglucoside (*m/z* 627), cyanidin 3,5-diglucoside (*m/z* 611), delphinidin 3-glucoside (*m/z* 465), cyanidin 3-glucoside (*m/z* 449) and pelargonidin 3-glucoside (*m/z* 433) by LC–MS analysis (Fig. 1: peaks 1–5). These anthocyanins have been reported previously to be present in pomegranates (Hernandez et al., 1999; Santagati et al., 1984). The mass spectrum showed the presence of the molecular ion for the respective anthocyanin along with that of its aglycone. Depending on the variety of the pomegranates, the amount of total anthocyanins varies from 35 to 350 mg/kg fresh weight of arils (Hernandez et al., 1999). Quantitative HPLC analysis indicated that arils of the fresh pomegranates of Wonderful variety contained 250 mg/kg anthocyanins.

3.2. Heat stability of anthocyanin

The cyanidin 3-glucoside sample maintained under nitrogen showed only a small degradation that was not statistically different from the control of freshly prepared cyanidin 3-glucoside standard sample (Fig. 2). There was about 65% loss of cyanidin 3-glucoside in the sample maintained under air, signifying the role of oxygen in anthocyanin degradation. Pure anthocyanins were stable at high temperatures in the absence of oxygen, but they quickly degraded in the presence of oxygen.

3.3. Optimum pH for PPO activity

Depending upon the enzyme source and substrate, the optimum pH for browning reactions catalysed by PPO is between pH 4.0 and pH 7.0 (Severini, Baiano, De Pilli, Romaniello, & Derossi, 2003). The effect of pH on PPO activity was investigated using catechol as a substrate in the pH 5.0–8.0 range (Fig. 3). The optimum pH for pomegranate PPO activity was found to be about pH 6.0. The PPO activity decreased rapidly at pH below or above this optimum.

3.4. Effect of boiling on PPO activity

There was about a 73% decrease in activity when the PPO extract was boiled. PPO is relatively heat-labile, and temperatures above 50 °C for sufficient time result in a decrease of activity (Vámos-Vigyázó, 1981). In fact, the heat inactivation of PPO by blanching treatment is the most common method of preventing the browning reaction in fruits and vegetables (Chen, Collins, McCarty, & Johnston, 1971). However, PPO heat resistance depends on the species and cultivar of the plant from which it is extracted. The ability of the PPO assay to measure this decrease in activity indicates, to some degree, that the assay is capable of distinguishing the enzyme reaction from any chemical reactions that may be present.

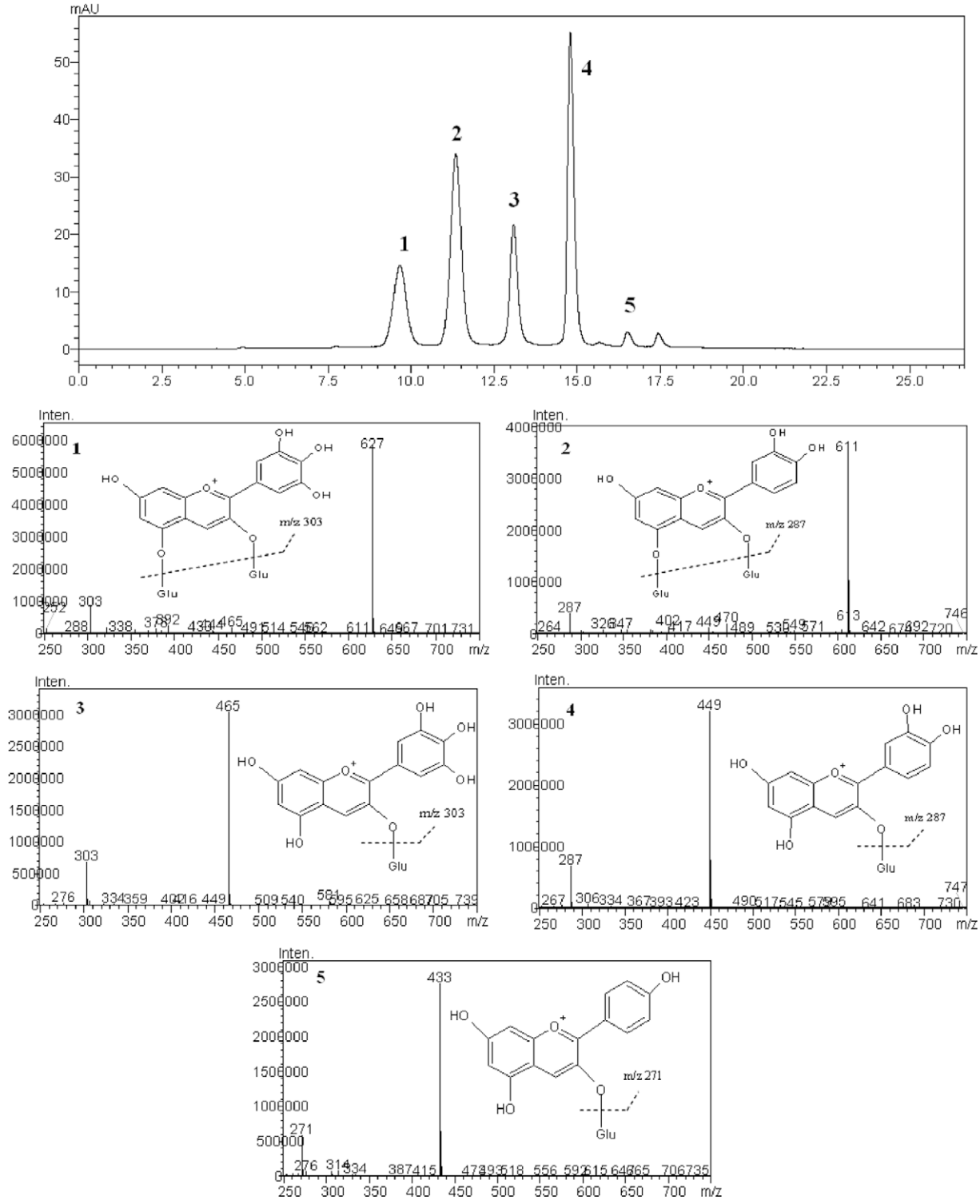

Fig. 1. Typical LC–MS chromatograms of anthocyanins from fresh, oven-dried and sun-dried pomegranate arils. Peak identities: 1 – delphinidin 3,5-diglucoside; 2 – cyanidin 3,5-diglucoside; 3 – delphinidin 3-glucoside; 4 – cyanidin 3-glucoside; 5 – pelargonidin 3-glucoside. Identity of the sixth peak is unknown.

3.5. PPO kinetics: the Michaelis–Menten constant

Pomegranate PPO kinetics were partially characterised by investigation of the effect of substrate concentration on PPO activity. The Michaelis–Menten constant (K_m) and V_{max} values were determined from a Lineweaver–Burk plot (Fig. 4). The K_m value was 635 mM, and the V_{max} value was 1.045 ΔOD/min/ml. Spinach PPO was considerably inhibited above its K_m value when dopamine was used as a substrate, whereas catechol is also shown to inhibit PPO activity at higher concentrations (Golbeck & Cammarata, 1981). Our results indicate a similar phenomenon; pomegranate PPO was inhibited above the catechol K_m value in a progressive manner proportional to the catechol concentration. Using catechol as a substrate in the PPO assay may be responsible for these non-classic enzyme kinetics. The high K_m value of 635 mM can be explained by the fact that catechol is a non-physiological substrate for pomegranate PPO.

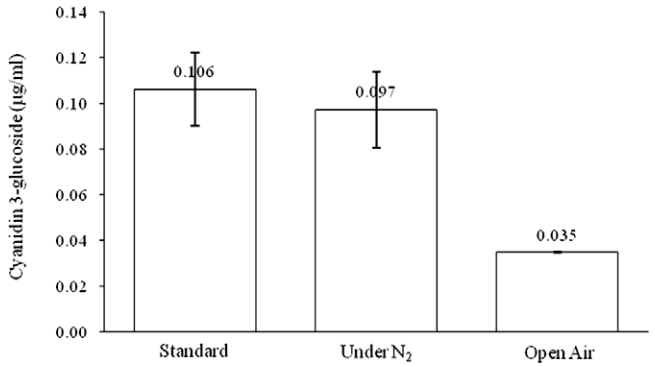

Fig. 2. Effect of temperature on anthocyanin stability. Values are averages of three determinations. Error bars are standard deviations of the values.

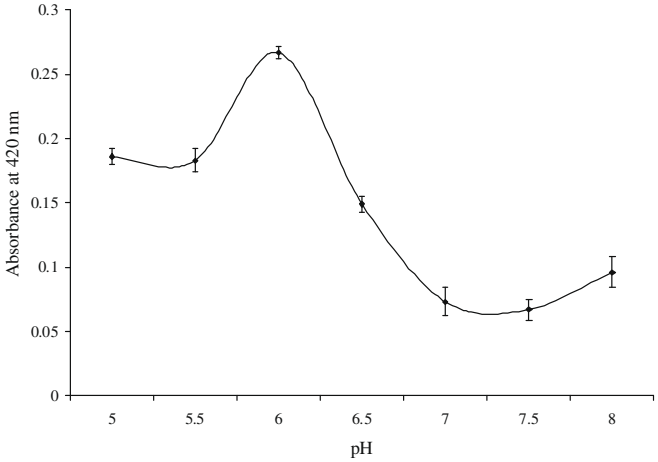

Fig. 3. Effect of pH on pomegranate PPO activity. Values are averages of three determinations. Error bars are standard deviations of the values.

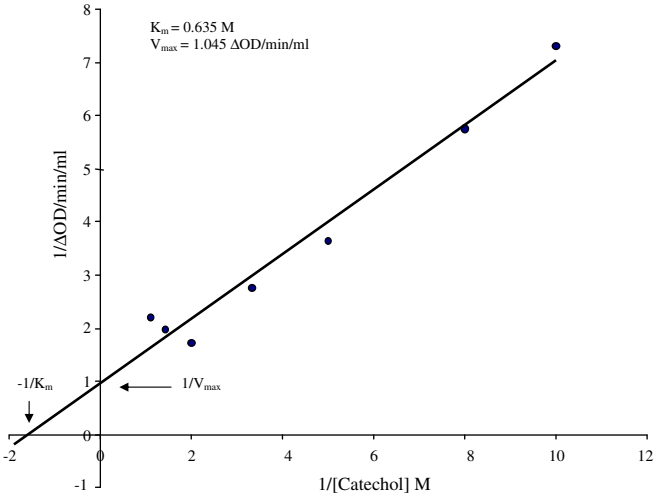

Fig. 4. Effect of substrate concentration on pomegranate PPO activity (Lineweaver–Burk plot of the reaction data). Average of three determinations.

3.6. Effect of drying on anthocyanins and PPO activity

Drying reduced the amount of anthocyanins and the PPO activity in fresh pomegranate arils (Table 1). Oven-drying resulted in 61% loss of anthocyanins and 68% loss of PPO activity. Sun-drying was more destructive to anthocyanins, resulting in about 83% loss, but only 45% loss was recorded in the PPO activity. Anthocyanins are stable at high temperatures, whereas PPO is heat-labile and is considerably inhibited above 80 °C (Severini et al., 2003). Inhibition of PPO by oven-drying at high temperature may be responsible for protecting the anthocyanins from oxidation by PPO. Sun-drying was apparently unable to inhibit PPO activity as much, resulting in enhanced anthocyanin oxidation.

Table 1
Anthocyanin amount and PPO activity in pomegranate arils. Values are averages of three determinations and the number in parentheses is the standard deviation of the corresponding value.

Characteristic	Fresh arils	Oven-dried arils	Sun-dried arils
Total anthocyanins (µg/g ± SD)	250.5 (±10.9)	97.4 (±1.8)	42.2 (±0.3)
PPO activity (units/ml ± SD)	647.7 (±9.9)	205.7 (±5.1)	356 (±23.6)

3.7. Effect of boiling on anthocyanins and PPO activity

To further investigate the role of PPO in anthocyanin degradation, the effect of boiling on anthocyanins and PPO activity in pomegranate arils was determined. PPO activity in boiled arils was reduced by 75% from that of fresh arils, whereas total anthocyanins were reduced by only 2.5% (Fig. 5). Anthocyanins were protected from oxidative degradation because of inactivation of PPO by boiling. The results of this experiment again indicate the possible involvement of PPO in anthocyanin degradation.

The role of PPO has always been speculated in anthocyanin degradation with mixed results. Although, our investigations were carried out on crude enzyme preparations, the results indicate a possible involvement of PPO in anthocyanin oxidation.

In the presence of very low levels of hydrogen peroxide, peroxidase (POD; EC 1.11.1.7) also catalyses the formation of quinones from phenolic compounds (Vaughn & Duke, 1984). To adequately understand the physiology of an enzyme, it is important that the assay used can distinguish that enzyme from all others. Unfortunately, however, the catechol oxidation assay is not sufficient to measure the true PPO activity and needs to be refined, in order to distinguish PPO activity from POD or other similar enzyme activities. Our results strongly indicate a likely involvement of PPO in anthocyanin oxidation in pomegranate arils, although further investigations are required. Instead of a non-physiological substrate, such as catechol, anthocyanin may be the most suitable substrate to evaluate the role of PPO in anthocyanin oxidative degradation.

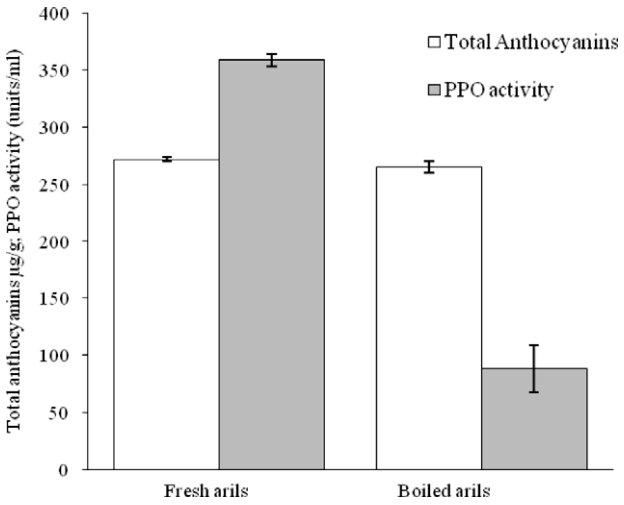

Fig. 5. Effect of boiling on total anthocyanins and PPO activity in pomegranate arils. Average of three determinations and error bars are standard deviations of the values.

References

Aviram, M., Dornfeld, L., Kaplan, M., Coleman, R., Gaitini, D., Nitecki, S., et al. (2002a). Pomegranate juice flavonoids inhibit low-density lipoprotein oxidation and cardiovascular diseases: Studies in atherosclerotic mice and in humans. *Drugs under Experimental and Clinical Research, 28*, 49–62.

Aviram, M., Fuhrman, B., Rosenblat, M., Volkova, N., Kaplan, M., Hayek, T., et al. (2002b). Pomegranate juice polyphenols decreases oxidative stress, low-density lipoprotein atherogenic modifications and atherosclerosis. *Free Radical Research, 36*(Suppl. 1), 72–73.

Brouillard, R., Figueiredo, P., Elhabiri, M., & Dangles, O. (1997). Molecular interactions of phenolic compounds in relation to the color of fruit and vegetables. *Proceedings of Phytochemical Society of Europe, 41*, 29–49.

Chen, S. C., Collins, J. L., McCarty, I. E., & Johnston, M. R. (1971). Blanching of white potatoes by microwave energy followed by boiling water. *Journal of Food Science, 36*, 742–743.

Clifford, M. N. (2000). Anthocyanins – Nature, occurrence and dietary burden. *Journal of the Science of Food and Agriculture, 80*, 1063–1072.

Coseteng, M. Y., & Lee, C. Y. (1987). Changes in apple polyphenoloxidase and polyphenol concentrations in relation to degree of browning. *Journal of Food Science, 52*, 985–989.

Einbond, L. S., Reynertson, K. A., Luo, X., Basile, M. J., & Kennelly, E. J. (2004). Anthocyanin antioxidants from edible fruits. *Food Chemistry, 84*, 23–28.

Gil, M. I., Tomas-Barberan, F. A., Hess-Pierce, B., Holcroft, D. M., & Kader, A. A. (2000). Antioxidant activity of pomegranate juice and its relationship with phenolic composition and processing. *Journal of Agricultural and Food Chemistry, 48*, 4581–4589.

Golbeck, J. H., & Cammarata, K. V. (1981). Spinach thylakoid polyphenol oxidase isolation, activation and properties of the native chloroplast enzyme. *Plant Physiology, 67*, 977–984.

Gonzalez, E. M., de Ancos, B., & Cano, M. P. (1999). Partial characterization of polyphenol oxidase activity in raspberry fruits. *Journal of Agricultural and Food Chemistry, 47*, 4068–4072.

Hernandez, F., Melgarejo, P., Tomas-Barberan, F. A., & Artes, F. (1999). Evolution of juice anthocyanins during ripening of new selected pomegranate (*Punica granatum*) clones. *European Food Research and Technology, 210*, 39–42.

Kim, N. D., Mehta, R., Yu, W., Neeman, I., Livney, T., Amichay, A., et al. (2002). Chemopreventive and adjuvant therapeutic potential of pomegranate (*Punica granatum*) for human breast cancer. *Breast Cancer Research and Treatment, 71*, 203–217.

Kong, J., Chia, L., Goh, N., Chia, T., & Brouillard, R. (2003). Analysis and biological activities of anthocyanins. *Phytochemistry, 64*, 923–933.

Lansky, E. P., & Newman, R. A. (2007). *Punica granatum* (pomegranate) and its potential for prevention and treatment of inflammation and cancer. *Journal of Ethnopharmacology, 109*, 177–206.

Levin, G. M. (1994). Pomegranate (*Punica granatum*) plant genetic resources in Turkmenistan. *Plant Genetic Resource. Newsletter, 97*, 31–37.

Lineweaver, H., & Burk, D. (1934). The determination of enzyme dissociation constant. *Journal of the American Chemical Society, 56*, 658–661.

Mayer, A. M. (2006). Polyphenol oxidases in plants and fungi: Going places? A review. *Phytochemistry, 67*, 2318–2331.

Pruthi, J. S., & Saxena, A. K. (1984). Studies on anardana (dried pomegranate seeds). *Journal of Food Science and Technology, 21*, 296–299.

Rapeanu, G., Loey, A. V., Smout, C., & Hendrickx, M. (2006). Thermal and high pressure inactivation kinetics of victoria grape polyphenol oxidase: From model systems to grape must. *Journal of Food Process Engineering, 29*, 269–286.

Santagati, N. A., Duro, R., & Duro, F. (1984). Study on pigments present in pomegranate seeds. *Journal of Commodity Science, 23*, 247–254.

Seeram, N. P., Zhang, Y., Reed, J. D., Krueger, C. G., & Vaya, J. (2006). Pomegranate phytochemicals. In N. P. Seeram, R. N. Schulman, & D. Heber (Eds.), *Pomegranates: Ancient roots to modern medicine* (pp. 3–29). Boca Raton, FL: Taylor and Francis.

Severini, C., Baiano, A., De Pilli, T., Romaniello, R., & Derossi, A. (2003). Prevention of enzymatic browning in sliced potatoes by blanching in boiling saline solutions. *Lebensmittel-Wissenschaft und - Technologie, 36*, 657–665.

Shishodia, S., Adams, L., Bhatt, I. D., & Aggarwal, B. B. (2006). Anticancer potential of pomegranate. In N. P. Seeram, R. N. Schulman, & D. Heber (Eds.), *Pomegranates: Ancient roots to modern medicine* (pp. 107–116). Boca Raton, FL: Taylor and Francis.

Singh, D. B., Kingly, A. R. P., & Jain, R. K. (2007). Studies on separation techniques of pomegranate arils and their effect on quality of anardana. *Journal of Food Engineering, 79*, 671–674.

Thipyapong, P., Stout, M. J., & Attajarusit, J. (2007). Functional analysis of polyphenol oxidases by antisense/sense technology. *Molecules, 12*, 1569–1595.

Vámos-Vigyázó, L. (1981). Polyphenol oxidase and peroxidase in fruits and vegetables. *Critical Reviews in Food Science and Nutrition, 15*, 49–127.

Vaughn, K. C., & Duke, S. O. (1984). Function of polyphenol oxidase in higher plants. *Physiologia Plantarum, 60*, 106–112.

Food Chemistry 118 (2010) 17–25

Contents lists available at ScienceDirect

Food Chemistry

journal homepage: www.elsevier.com/locate/foodchem

Chemical stability of açai fruit (*Euterpe oleracea* Mart.) anthocyanins as influenced by naturally occurring and externally added polyphenolic cofactors in model systems

Lisbeth A. Pacheco-Palencia, Stephen T. Talcott *

Department of Nutrition and Food Science, Texas A&M University, College Station, TX 77843, USA

ARTICLE INFO

Article history:
Received 2 December 2008
Received in revised form 7 January 2009
Accepted 16 February 2009

Keywords:
Euterpe oleracea
Açai
Anthocyanin
Cofactor
Colour
Copigmentation
Stability

ABSTRACT

The influence of different classes of naturally occurring and externally added polyphenolic cofactors on the phytochemical and colour stability of anthocyanins in açai fruit (*Euterpe oleracea*) was investigated. Model systems were based on anthocyanin isolates from açai fruit, rich in cyanidin-3-rutinoside (311 ± 27 mg/l) and cyanidin-3-glucoside (208 ± 18 mg/l), and isolated groups of naturally occurring polyphenolic cofactors in açai fruit (phenolic acids, procyanidins, and flavone-*C*-glycosides, each adjusted to ~50 mg/l). Anthocyanin degradation kinetics were assessed as a function of pH (3.0, 3.5, and 4.0) and storage temperature (5, 20 and 30 °C). During storage, anthocyanins experienced pH and temperature-dependent losses, and the half life cyanidin-3-rutinoside ($t_{1/2}$ = 2.67–210 days) was consistently longer than cyanidin-3-glucoside ($t_{1/2}$ = 1.13–144 days). The presence of flavone-*C*-glycosides induced significant hyperchromic shifts and enhanced anthocyanin stability at all pH and temperature combinations, while no significant effects were attributed to the presence of phenolic acids or procyanidins. Additional models using externally added cofactors from rooibos tea, also rich in flavone-*C*-glycosides, resulted in up to 45.5% higher anthocyanin colour and up to 40.7% increased anthocyanin stability compared to uncopigmented anthocyanin isolates and had similar copigmentation effects to a commercial rosemary-based colour enhancer. Results suggest flavone-*C*-glycosides offer potential for their use as colour enhancers and stabilizing agents in products rich in cyanidin glycosides, particularly açai fruit-containing foods, juice blends, and beverages.

1. Introduction

Anthocyanins have been categorized as the most important group of water-soluble pigments in plants, and are responsible for most blue, red, and related colours in flowers and fruits (Clifford, 2000). Anthocyanin colour is an important sensory characteristic and often a major quality parameter for a variety of fruit products. Açai (*Euterpe oleracea* Mart.), a palm fruit native to the Brazilian Amazon, has been the focus of increased international attention as a functional ingredient in fruit juices, beverage blends, dietary supplements, and dairy products (Del Pozo, Brenes, & Talcott, 2004; Schauss et al., 2006) and is a potential rich source of anthocyanins (Gallori, Bilia, Bergonzi, Barbosa, & Vincieri, 2004; Lichtenthaler et al., 2005; Pacheco-Palencia, Hawken, & Talcott, 2007a, 2007b). Two predominant anthocyanins, cyanidin-3-rutinoside and cyanidin-3-glucoside, are responsible for most of its characteristic dark purple colour, and are often a major source of colour in açai-containing juices and beverages (Lichtenthaler et al., 2005; Pacheco-Palencia et al., 2007a; Schauss et al., 2006). However, anthocyanins are highly reactive and generally experience extensive degradation during long-term storage, leading to dark, dull, brown hues (Jurd, 1972).

Anthocyanin colour changes are known to be influenced by several factors, including pH, temperature, light, and the presence of enzymes, sugars, metals, and phenolic cofactors (Markakis, 1982). Among these, the presence of non-anthocyanin polyphenolics may significantly affect anthocyanin colour, as they participate in copigmentation reactions in enhanced colour and increased stability during storage (Singleton, 1972). Intermolecular copigmentation reactions are common in nature and occur when colourless phenolic cofactors are attracted to anthocyanins via weak hydrophobic forces (Mazza & Brouillard, 1990). Anthocyanin copigmentation reactions are detected by both a hyperchromic shift, where absorbance at the λ_{max} of the absorption spectrum increases, and by a bathochromic shift, where a change toward higher wavelengths (nm) at the λ_{max} of the absorption spectrum occurs (Baranac, Petranovic, & Dimitric-Markovic, 1996; Malien-Aubert, Dangles, & Amiot, 2001).

* Corresponding author. Tel.: +1 979 862 4056; fax: +1 979 458 3704.
E-mail address: stalcott@tamu.edu (S.T. Talcott).

0308-8146/$ - see front matter © 2009 Elsevier Ltd. All rights reserved.
doi:10.1016/j.foodchem.2009.02.032

Previous studies have evaluated the use of externally added polyphenolic cofactors, particularly phenolic acids, to enhance and stabilize anthocyanin colour in berry juices (Eiro & Heinonen, 2002). External addition of commercial polyphenolic cofactors from rosemary (*Rosmarinus officinalis*) has also shown to result in enhanced anthocyanin colour and increased stability in grape juices (Brenes, Del Pozo-Insfran, & Talcott, 2005; Talcott, Brenes, Pires, & Del Pozo-Insfran, 2003). Thus, the natural occurrence and predominant presence of certain groups of polyphenolic cofactors in açai fruit, including phenolic acids, flavone-*C*-glycosides, and procyanidins (Gallori et al., 2004; Pacheco-Palencia et al., 2007b; Schauss et al., 2006), may play a significant role in the structural and pigment stability of anthocyanins in açai fruit juices. The role of flavone-*C*-glycosides is of particular interest, as their presence in other anthocyanin-rich fruits has not been previously reported. Moreover, the potential use of flavone-*C*-glycoside-rich extracts as anthocyanin colour enhancers and stabilizing agents has not been evaluated. Extracts rich in flavone-*C*-glycosides may be obtained from various botanical sources, among which, rooibos (*Aspalathus linearis)* tea, a leguminous shrub native to South Africa, is among the highest, most widely available, and easily extractable sources (Krafczyk & Glomb, 2008).

This study was conducted to evaluate the influence of different groups of naturally occurring polyphenolic cofactors on the stability of anthocyanins in açai models stored under different pH (3.0, 3.5, and 4.0) and temperature (5, 20, and 30 °C) conditions and assess the influence of externally added polyphenolic cofactors from rooibos tea, rich in flavone-*C*-glycosides, and from commercial rosemary extracts on the stability of açai anthocyanin models. Relations between anthocyanin degradation and sulfite bleaching resistance, reducing capacity, and antioxidant activity were additionally determined.

2. Materials and methods

2.1. Polyphenolic isolations

Phenolic acids and procyanidins were extracted from a previously characterized, polyphenolic-enriched açai oil (Pacheco-Palencia, Mertens-Talcott, & Talcott, 2008), which contained concentrated amounts of phenolic acids and procyanidins originally present in açai fruit pulp. Açai oil was extracted from a semi-solid filter cake obtained from the Bossa Nova Beverage Group (Los Angeles, CA), commercially used for açai pulp clarification, using a hydro-alcoholic solution, as described by Pacheco-Palencia et al. (2008). Açai oil was extensively extracted with an equal volume of a 1:1 (v/v) hexane:methanol solution until complete dissolution. A known volume of 0.1 M aqueous citric acid buffer at pH 3.0 was added to the mixture, to form a bi-layer, from which the hydrophilic phase was retained. Residual methanol in the hydrophilic phase was evaporated under reduced pressure (<40 °C) and the resulting aqueous solution recovered, adjusted to pH 7.0, and loaded onto C18 Sep-Pak Vac 20 cm^3 mini-columns (Waters Corporation, Milford, MA). Phenolic acids were eluted in the unbound fraction, while procyanidins were eluted with acidified methanol (0.01% HCl). The aqueous, phenolic acid-containing fraction was then acidified to pH 3.0, loaded onto a second Sep-Pak column, and eluted with acidified methanol (0.01% HCl). Methanol from each extraction was then evaporated under vacuum (<40 °C) and each fraction was re-dissolved in a known volume of the citric acid buffer.

In a second extraction, anthocyanins and naturally occurring flavone-*C*-glycosides in açai fruit were extracted from clarified açai pulp (Bossa Nova Beverage Group, Los Angeles, CA). Clarified açai pulp was likewise loaded onto Sep-Pak mini-columns (Waters Corporation, Milford, MA), and sequentially eluted with acidified water (0.01% HCl) to remove metals, sugars, and other water soluble components followed by ethyl acetate to remove phenolic acids. Flavone-*C*-glycosides and anthocyanins were finally eluted with acidified methanol. Following solvent evaporation and re-dissolution in the citric acid buffer, the methanolic fraction was loaded onto manually packed, lipophilic Sephadex LH-20 (Sigma–Aldrich, St. Louis, MO) 40 cm^3 mini-columns, previously equilibrated with water. Columns were washed with 30% aqueous methanol (v/v) to elute anthocyanins, followed by 60% aqueous methanol (v/v) to elute flavone-*C*-glycosides, and with 100% methanol to elute procyanidins. These procyanidins were combined with the procyanidin fraction previously obtained from açai oil. All solvents were finally evaporated under reduced pressure (<40 °C) and each resulting isolate was redissolved in the citric acid buffer (pH 3.0).

2.2. Anthocyanin models

Açai fruit models were created based on the predominant anthocyanins present in the fruit (cyanidin-3-rutinoside and cyanidin-3-glucoside), adjusted to a total concentration of approximately 500 mg/l in all models. Four different anthocyanin-based models were prepared by combining açai anthocyanins with a major group of naturally occurring polyphenolics present in the fruit. Models were created by combining phenolic acids, procyanidins, flavone-*C*-glycosides, and a non-copigmented anthocyanin control. Cofactor concentrations on each model were adjusted according to the original ratio of total phenolic cofactors to anthocyanins (1:10) naturally present in 100% clarified açai pulp. Models were adjusted to three different pH levels (3.0, 3.5, and 4.0), based on the pH range of commercial açai products, and equal amounts of each were loaded into screw-cap glass test tubes in triplicate. Treatments were stored in the dark at 5, 20, and 30 °C for up to 60 days. Sodium azide (50 mg/l) was added to prevent microbial growth during storage and individual tubes were removed from storage at predetermined time intervals and held at −20 °C until analysis.

Additional models with açai anthocyanins (~500 mg/l) were evaluated that contained externally added polyphenolic cofactors from a rooibos tea extract, rich in flavone-*C*-glycosides, as compared to a commercial rosemary extract (ColourEnhance, 3.5% rosmarinic acid, Naturex, South Hackensack, NJ) and a non-copigmented control. Rooibos tea extracts were obtained from rooibos tea, prepared by brewing 50 g of loose rooibos tea (Keekanne GmbH, Dusseldorf, Germany) in 50 ml boiling water for 30 min. Both rooibos tea and commercial rosemary extracts were subsequently diluted in citric acid buffer (0.1 M, pH 3.0) and further purified using Sep-Pak columns. Sugars, organic acids, and other water soluble components were removed with water, and polyphenolic components were recovered with ethyl acetate. Following solvent removal, compounds were redissolved in a known volume of citric acid buffer (0.1 M, pH 3.0), adjusted to equal soluble phenolic contents (10,000 mg gallic acid equivalents/l) and added to anthocyanin isolates to contain final concentrations of 0.2% v/v, based on previous reports using similar rosemary extracts (Brenes et al., 2005; Talcott et al., 2003). All models were finally adjusted to pH 3.0, 3.5, or 4.0, loaded into screw-cap glass tubes in triplicate, and stored at 30 °C for up to 30 days. Sodium azide (50 mg/l) was added to all treatments to retard microbial growth and pH was measured every other day to confirm its consistency during storage. Individual tubes were removed from storage every 3 days and held at −20 °C until analysis.

2.3. Chemical analyses

Polyphenolic compounds were analyzed by reversed phase HPLC with a Waters 2695 Alliance system (Waters Corporation, Milford, MA), using previously described chromatographic condi-

tions (Pacheco-Palencia et al., 2007a). Polyphenolic identification and quantification was based on spectral properties, retention time, and comparison to authentic standards. Phenolic acid, flavonol, and anthocyanin standards were obtained from Sigma Chemical Company (St. Louis, MO), and flavone-*C*-glycoside standards were obtained from Indofine Chemical Company (Hillsborough, NJ). Mass spectrometric analyses were additionally performed on a Thermo Finnigan LCQ Deca XP Max MS^n ion trap mass spectrometer equipped with an ESI ion source (ThermoFisher, San Jose, CA). Separations were conducted using a Dionex (Dionex Corporation, Sunnyvale, CA), Acclaim 120 column (4.6 × 250 mm; 5 μm) with a C18 guard column. Mobile phases consisted of 0.5% formic acid in water (phase A) and 0.5% formic acid in methanol (phase B) run at 0.30 ml/min. A gradient elution program in which phase B changed from 5% to 30% in 10 min, from 30% to 65% in 70 min, and from 65% to 95% in 30 min was used and held isocratic for 20 min prior each injection. Electrospray ionization in the negative ion mode was conducted under the following conditions: sheath gas (N_2), 60 units/min; auxiliary gas (N_2), 5 units/min; spray voltage, 3.5 kV; capillary temperature, 250 °C; capillary voltage, 1.5 V; tube lens offset, 0 V.

Total anthocyanin contents were determined spectrophotometrically at 520 nm, according to the pH differential method described by Wrolstad, Durst, and Lee (2005) and quantified using equivalents of cyanidin-3-glucoside (mg/l) with a molar extinction coefficient of 29,600 (Jurd & Asen, 1966). Anthocyanin sulfite bleaching resistance was also determined spectrophotometrically, based on colour retention in the presence of sodium sulfite (Rodriguez-Saona, Guisti, and Wrolstad, 1999). Total soluble phenolic contents were estimated from the total metal reducing capacity of each model in the Folin-Ciocalteu assay (Singleton & Rossi, 1965) and quantified in gallic acid equivalents (GAE). Antioxidant capacity was determined by the oxygen radical absorbance capacity assay (ORAC) (Talcott & Lee, 2002), using fluorescein as the fluorescent probe, and measured on a BMG Labtech FLUOstar fluorescent microplate reader (485 nm excitation and 538 nm emission). Results were quantified and expressed as μmole Trolox equivalents per milliliter.

2.4. Statistical analyses

A 4 × 3 × 3 factorial design that included four anthocyanin-based models, three pH levels, and three storage temperatures was employed. Data from each chemical analysis was analyzed by one-way analysis of variance (ANOVA) using SPSS version 15.0 (SPSS Inc., Chicago, IL) and mean separations were conducted using Tukey–Kramer HSD ($p < 0.05$) as a post-hoc analysis. Linear regression analyses and parametric correlations were conducted using a 0.05 significance level.

3. Results and discussion

3.1. Polyphenolic composition of anthocyanin models

Anthocyanins, phenolic acids, procyanidins, and flavone-*C*-glycosides present in açai anthocyanin models were characterized based on their spectral characteristics and mass spectrometric (MS) fragmentation patterns and quantified against authentic standards when available (Table 1). All models were adjusted to equal cyanidin-3-glucoside and cyanidin-3-rutinoside concentrations (519 ± 48 mg/l, Table 1). In addition, a group of naturally occurring phenolic cofactors in açai fruit (Pacheco-Palencia et al., 2007a, 2008), was present on each model and included phenolic acids (protocatechuic, *p*-hydroxybenzoic, vanillic, syringic, and ferulic acids), procyanidins (dimers and trimers), and flavone-*C*-glycosides (isoorientin, orientin, and isovitexin), and two additional flavone *C*-glycosides, tentatively identified as apigenin 6,8-di-*C*-glycosides. Phenolic cofactor concentrations were adjusted ranging from 48.9 to 56.1 mg/l (Table 1) to yield a phenolic cofactor-to-anthocyanin ratio of 1:10 that corresponded to the natural ratio of these cofactors originally present in clarified açai pulp (Pacheco-Palencia et al., 2007a, 2008).

Identification of flavone-*C*-glycosides was based on their characteristic MS patterns, as preferential fragmentation of the glycosidic moiety typically occurs to yield typical product ions at $[M-H-60]^-$, $[M-H-90]^-$, and $[M-H-120]^-$ (Ferreres, Silva, Andrade, Seabra, & Ferreira, 2003; Gattuso, Barreca, Gargiulli, Leuzzi, & Caristi, 2007; Pereira, Yariwake, & McCullagh, 2005). Tentative identification of apigenin-6-*C*-glucosyl-8-*C*-arabinoside was based on precursor ion signals at $m/z = 563.1$ ($[M-H]^-$), and respective product ions at $m/z = 503.1$ ($[M-H-60]^-$), $m/z = 473.2$ ($[M-H-90]^-$); and $m/z = 443.1$ ($[M-H-120]^-$) as indicated in Fig. 1. Fragmentation patterns corresponded to those previously reported for apigenin-6-*C*-glucosyl-8-*C*-arabinoside (shaftoside, $m/z = 563.1$, $[M-H]^-$) in quince seeds (Ferreres et al., 2003) and in *Scutellaria baicalensis* roots (Han et al., 2007). Likewise, tentative identifica-

Table 1
Polyphenolic composition of *Euterpe oleracea* anthocyanin models.

Anthocyanin model	Polyphenolic	$[M-H]^-$ (m/z)	Concentration (mg/l)
All anthocyanin models	Cyanidin-3-glucoside	447.0	208 ± 18
	Cyanidin-3-rutinoside	593.1	311 ± 27
	Total anthocyanins		*519 ± 48*
Anthocyanin-phenolic acid models	protocatechuic acid	153.1	6.15 ± 0.7
	p-Hydroxy benzoic acid	137.2	7.74 ± 0.6
	Vanillic acid	167.1	19.5 ± 1.3
	Syringic acid	197.0	13.8 ± 1.1
	Ferulic acid	193.1	1.67 ± 0.2
	Total phenolic acids		*48.9 ± 4.1*
Anthocyanin-flavone-*C*-glycoside models	Apigenin 6-*C*-glucosyl-8-*C*-Arabinoside (schaftoside)	563.1	5.14 ± 0.3[a]
	Apigenin 6,8-di-*C*-glucoside (vicenin-2)	593.5	5.07 ± 0.4[a]
	Luteolin 6-*C*-glucoside (isoorientin)	447.1	17.4 ± 1.5
	Luteolin 8-*C*-glucoside (orientin)	447.1	24.2 ± 2.2[a]
	Apigenin 6-*C*-glucoside (isovitexin)	431.0	4.19 ± 0.5[a]
	Total flavone-C-glycosides		*56.0 ± 4.9*[a]
Anthocyanin-procyanidin models	(+)-Catechin	289.0	2.33 ± 0.2
	Procyanidin dimers	577.2	18.8 ± 1.4[b]
	Procyanidin trimers	865.1	34.4 ± 3.5[b]
	Total procyanidins		*55.5 ± 5.6*[b]

[a] Isoorientin equivalents.
[b] (+)-Catechin equivalents.

tion of apigenin 6,8-di-*C*-glucoside was based on ion signals at *m/z* = 593.5, $[M-H]^-$, with a similar neutral loss to yield ions at *m/z* = 533.1 ($[M-H\text{-}60]^-$); *m/z* = 503.1 ($[M-H\text{-}90]^-$); and *m/z* = 473.1 ($[M-H\text{-}120]^-$). Mass fragmentation patterns were identical to those previously reported for apigenin 6,8-di-*C*-glucoside (vicenin-2, *m/z* = 593.5, $[M-H]^-$), in both wild basil leaves (Grayer, Kite, Abou-Zaid, & Archer, 2000) and quince seeds (Ferreres et al., 2003). These are the first tentative reports on the occurrence of apigenin-6-*C*-glucosyl-8-*C*-arabinoside and apigenin 6,8-di-*C*-glucoside in açai fruit.

3.2. Influence of natural phenolic cofactors on anthocyanin stability

The influence of naturally occurring polyphenolic cofactors on the stability of anthocyanins in açai fruit was evaluated by monitoring changes in anthocyanin concentrations of model juice systems adjusted to different conditions of temperature (5, 20, or 30 °C for up to 12 weeks) and pH (3.0, 3.5, and 4.0). Initial spectrophotometric determinations for total anthocyanin contents were consistent among anthocyanin controls and models combined with phenolic acids or procyanidins (522.9 ± 27.3 mg cyanidin-3-gluco-

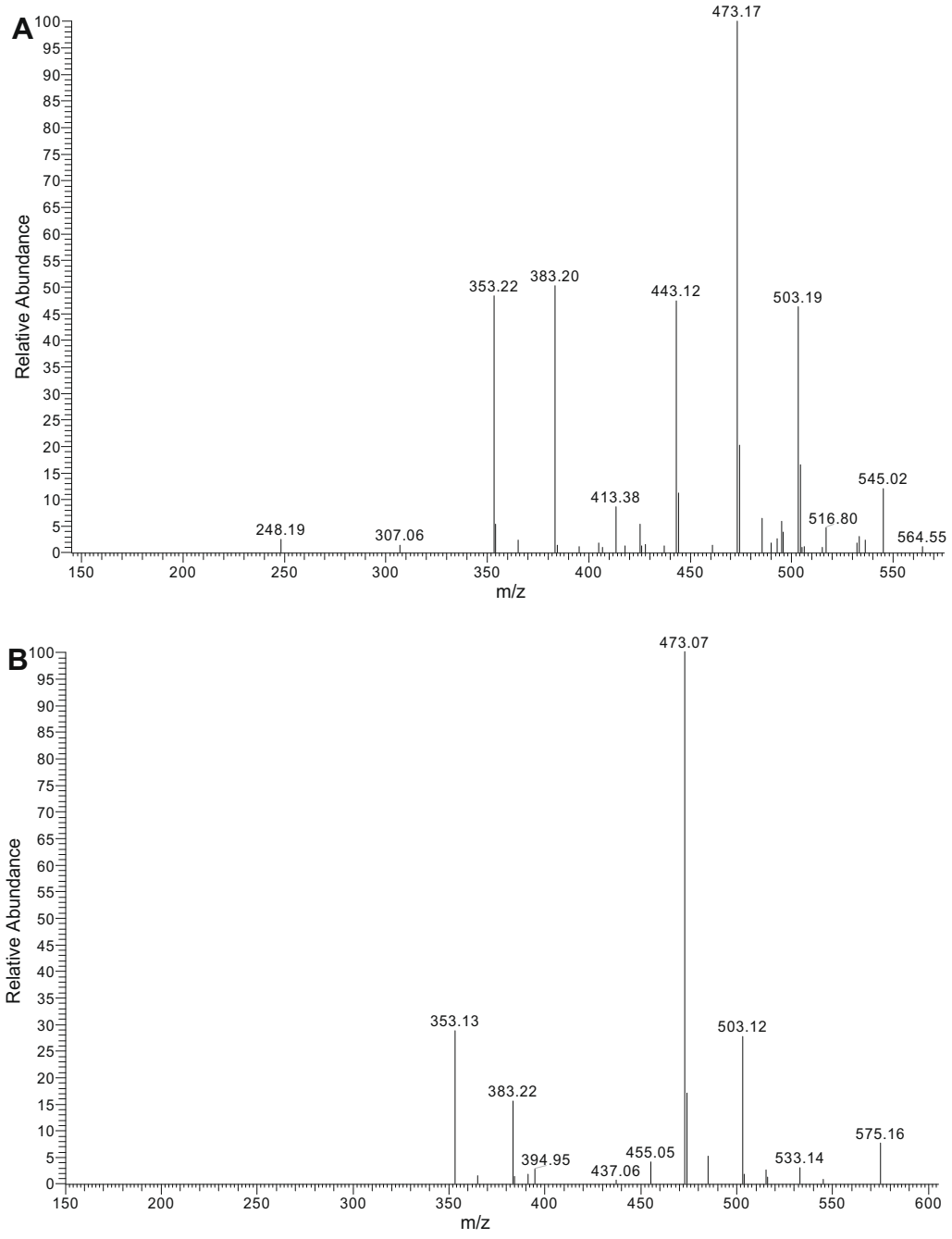

Fig. 1. ESI-MS negative product ion spectra of (A) apigenin-6-*C*-glucosyl-8-*C*-arabinoside (shaftoside, 563.1, $[M-H]^-$), and (B) apigenin 6,8-di-*C*-glucoside (vicenin-2, 593.5, $[M-H]^-$).

side equivalents/l). However, models containing flavone-*C*-glycosides were 18.0% higher in initial absorbance values (617.1 ± 30.1 mg/l), attributed to hyperchromic shifts that resulted from intermolecular copigmentation reactions with anthocyanins. These molecular associations between anthocyanins and other phenolics are commonly associated with enhanced anthocyanin colour, despite equivalent individual anthocyanin concentrations (Boulton, 2001). Copigmentation reactions are often accompanied by a bathochromic shift in the wavelength of maximum absorbance (Talcott et al., 2003); however, no change was observed in the presence of flavone-*C*-glycosides in these models.

Degradation rates for cyanidin-3-glucoside, cyanidin-3-rutinoside, and total anthocyanins followed first-order ($p < 0.01$) degradation kinetics. Rate constants (β_1, in days^{-1}), half-lives ($t_{1/2}$, time in days to achieve a 50% reduction in initial concentrations), and temperature quotients (Q_{10}, fold increase in degradation rate when temperature was increased from 20 to 30 °C) were calculated as previously described (Pacheco-Palencia et al., 2007b) and are shown in Tables 2–4. Anthocyanin models experienced significant pH- and temperature-dependent total anthocyanin losses, with half-lives ranging from 4.01 to 23.2 days for models stored at 30 °C, from 6.94 to 47.0 days when stored at 20 °C, and from 48.2 to 259 days for models kept at 5 °C (Table 2). Total anthocyanin losses were also influenced by acidity level, whereby a 45–60% increase in stability was observed when the pH was raised from 3.0 to 3.5, and by 90–100% when raised from 3.5 to 4.0, regardless of storage temperature or presence of cofactors. Similar pH and temperature-dependent degradation patterns were observed when individual cyanidin-3-glucoside and cyanidin-3-rutinoside concentrations were monitored (Tables 3 and 4) and both cyanidin-3-glucoside ($r = 0.94$) and cyanidin-3-rutinoside ($r = 0.93$) concentrations were highly correlated ($p < 0.001$) to total anthocyanin losses in all models throughout storage. However, temperature quotients (Tables 3 and 4) indicated cyanidin-3-glucoside was less stable to temperature changes ($Q_{10} = 2.9–3.2$) compared to cyanidin-3-rutinoside ($Q_{10} = 2.5–2.9$), and that individual anthocyanin concentrations were significantly less stable to temperature changes compared to total anthocyanin contents ($Q_{10} = 1.8–2.1$). Observed differences between total anthocyanin contents and changes in individual anthocyanin concentrations were likely due to the influence of other matrix components in the açai anthocyanin models (Wrolstad et al., 2005) as well as significant colour contributions from polymeric anthocyanins formed during storage.

Similar detrimental effects were observed at increasing pH values, and changes from pH 3.0 to 3.5 nearly doubled cyanidin-3-glucoside and cyanidin-3-rutinoside degradation rates (Tables 3 and 4) and increased total anthocyanin degradation rates by ~50% in all models. Detrimental effects of both high temperature and pH on anthocyanin stability and colour were attributed to shifts in the anthocyanin equilibrium toward the colourless pseudobase

Table 2
Kinetic parameters of total anthocyanin degradation during storage of açai models.

Anthocyanin model	pH	β_1[A]			$t_{1/2}$[B]			Q_{10}[C]
		5 °C	20 °C	30 °C	5 °C	20 °C	30 °C	20–30 °C
Anthocyanin control models	3.0	4.62	23.3	49.3	150 b[D]	29.7 b	14.1 b	2.10
	3.5	7.19	43.2	89.7	96.4 c	16.0 c	7.73 cd	2.07
	4.0	11.4	69.1	132	60.8 e	10.0 d	5.25 d	1.91
Anthocyanin-phenolic acid models	3.0	3.80	21.4	38.8	182 b	32.4 b	17.9 ab	1.81
	3.5	6.27	37.9	69.8	111 c	18.3 c	9.94 c	1.84
	4.0	11.8	68.9	136	58.9 e	10.1 d	5.11d	1.97
Anthocyanin-flavone-*C*-glycoside models	3.0	2.98	14.8	29.9	233 a	47.0 a	23.2 a	2.03
	3.5	4.61	25.2	50.8	150 b	27.5 b	13.6 b	2.02
	4.0	9.23	48.0	102	75.1 d	14.4 c	6.82 d	2.12
Anthocyanin-procyanidin models	3.0	2.68	20.8	40.2	259 a	33.3 b	17.2 b	1.93
	3.5	4.41	36.9	68.4	157 b	18.8 c	10.1 c	1.85
	4.0	8.29	67.0	133	83.6 d	10.3 d	5.22 d	1.98

[A] Reaction rate constant ($\beta_1 \times 10^3$ days^{-1}).
[B] Half-life (days) of initial absorbance for each anthocyanin model.
[C] Temperature coefficient of total anthocyanin degradation rate as influenced by a 10 °C increase in storage temperature.
[D] Values with different letters within columns are significantly different (student's t test, $p < 0.05$).

Table 3
Kinetic parameters of cyanidin-3-glucoside degradation during storage of açai models.

Anthocyanin model	pH	β_1[A]			$t_{1/2}$[B]			Q_{10}[C]
		5 °C	20 °C	30 °C	5 °C	20 °C	30 °C	20–30 °C
Anthocyanin control models	3.0	8.05	57.6	179	86.1 b[D]	12.0 b	3.87 b	3.11
	3.5	11.4	111	334	61.0 d	6.24 c	2.08 c	3.01
	4.0	20.4	189	612	33.9 f	3.67 d	1.13 d	3.24
Anthocyanin-phenolic acid models	3.0	5.42	42.8	128	128 a	16.2 a	5.42 a	2.98
	3.5	9.64	73.0	232	71.9 c	9.50 b	2.99 b	3.18
	4.0	17.3	136	411	40.0 e	5.10 c	1.68 c	3.03
Anthocyanin-flavone-*C*-glycoside models	3.0	4.82	41.8	124	144 a	16.6 a	5.57 a	2.98
	3.5	8.53	72.0	223	81.3 b	9.63 b	3.11 b	3.09
	4.0	15.4	128	394	45.1 e	5.40 c	1.76 c	3.07
Anthocyanin-procyanidin models	3.0	5.12	48.7	141	136 a	14.2 a	4.91 a	2.90
	3.5	9.01	84.5	259	77.0 bc	8.21 bc	2.68 b	3.06
	4.0	16.4	158	467	42.3 e	4.39 cd	1.48 cd	2.96

[A] Reaction rate constant ($\beta_1 \times 10^3$ days^{-1}).
[B] Half-life (days) of initial cyanidin-3-glucoside concentrations for each anthocyanin model.
[C] Temperature coefficient of cyanidin-3-glucoside degradation rate as influenced by a 10 °C increase in storage temperature.
[D] Values with different letters within columns are significantly different (student's t test, $p < 0.05$).

Table 4
Kinetic parameters of cyanidin-3-rutinoside degradation during storage of açai models.

Anthocyanin model	pH	β_1[A]			$t_{1/2}$[B]			Q_{10}[C]
		5 °C	20 °C	30 °C	5 °C	20 °C	30 °C	20–30 °C
Anthocyanin control models	3.0	4.06	24.4	66.3	171 a[D]	28.4 a	10.7 a	2.72
	3.5	7.80	42.1	119	88.9 b	16.4 b	5.81 b	2.83
	4.0	12.0	64.8	185	57.8 c	10.7 c	3.75 c	2.85
Anthocyanin-phenolic acid models	3.0	3.72	20.4	56.8	186 a	34.0 a	12.4 a	2.78
	3.5	6.62	34.3	101	105 b	20.2 b	6.87 b	2.95
	4.0	11.9	63.2	179	58.2 c	11.0 c	3.87 c	2.83
Anthocyanin-flavone-*C*-glycoside models	3.0	3.31	20.9	55.3	210 a	33.2 a	12.8 a	2.65
	3.5	5.85	33.8	96.8	118 b	20.5 b	7.16 b	2.86
	4.0	10.6	59.7	172	65.7 c	11.6 c	4.04 c	2.87
Anthocyanin-procyanidin models	3.0	3.51	23.2	58.8	197 a	29.9 a	12.0 a	2.53
	3.5	6.18	39.7	103	112 b	17.5 b	6.70 b	2.61
	4.0	11.2	73.5	187	61.7 c	9.43 c	3.71 c	2.54

[A] Reaction rate constant ($\beta_1 \times 10^3$ days^{-1}).
[B] Half-life (days) of initial cyanidin-3-rutinoside concentrations for each anthocyanin model.
[C] Temperature coefficient of cyanidin-3-rutinoside degradation rate as influenced by a 10 °C increase in storage temperature.
[D] Values with different letters within columns are significantly different (student's t test, $p < 0.05$).

and chalcone forms, expected to occur under these conditions (Clifford, 2000; Markakis, 1982). Structural differences also had a significant influence on anthocyanin stability whereas cyanidin-3-rutinoside was consistently more stable ($t_{1/2}$ = 2.67 to 210 days, Table 4) than cyanidin-3-glucoside ($t_{1/2}$ = 1.13 to 144 days, Table 3) in all models, regardless of variations in temperature, pH, or cofactor composition. These models were in agreement with our previous observations of anthocyanins stability in ascorbic acid-fortified açai juices (Pacheco-Palencia et al., 2007a). Moreover, in models that incorporated a cyanidin-3-rutinoside standard in aqueous buffer (pH 3.5) revealed a gradual conversion to cyanidin-3-glucoside over time that progressed at up to 12.5% after 20 days of storage at 30 °C, indicating hydrolysis of glycosidic bonds during storage. Applied to these fruit models, a gradual hydrolysis of glycosidic bonds would lead to increased cyanidin-3-glucoside and decreased cyanidin-3-rutinoside concentrations during storage of açai fruit anthocyanins and result in higher proportions of the more labile cyanidin-3-glucoside subsequently a more rapid rate of anthocyanin and colour degradation. Moreover, hydrolysis of the glycosidic bond has been proposed as one of the early steps in the degradation of anthocyanins, as the resulting aglycone is unstable and undergoes spontaneous ring fission and subsequent degradation (Adams, 1972, 1973; Clifford, 2000; Markakis, 1974).

The presence of phenolic cofactors had also a significant (p = 0.006) influence on the stability of açai fruit anthocyanins in all models. Overall, the presence of flavone-*C*-glycosides resulted in increased total anthocyanin stability at all temperature and pH combinations in relation to the anthocyanin control, while no significant effects were attributed to the presence of phenolic acids or procyanidins (Table 2). Protective effects were more pronounced for cyanidin-3-glucoside, where addition of flavone-*C*-glycosides resulted in higher anthocyanin stability in all models (Table 3). By contrast, cyanidin-3-rutinoside degradation rates were not significantly affected by the presence of flavone-*C*-glycosides (Table 4), likely due to its inherently higher stability in all models. Thus, the positive influence of flavone-*C*-glycosides on anthocyanin stability in açai fruit models was likely a result of their protective effect on cyanidin-3-glucoside and the colour contribution of cyanidin-3-glucoside to total anthocyanin measurements. Supporting models that used cyanidin-3-glucoside standards (205 ± 14 mg/l) adjusted to pH 3.5 and to which phenolic acid, flavone-*C*-glycoside, and procyanidin isolates from açai fruit were added confirmed the ability of flavone-*C*-glycosides to act as effective copigments and also resulted in increased ($p < 0.01$) anthocyanin stability during storage (Fig. 2). Stable anthocyanin copigment complexes with flavone-*C*-glycosides were reported to occur naturally in Iris flowers (Asen, Stewart, Norris, & Massie, 1970), yet this is the first report on the ability of flavone-*C*-glycosides to act as copigments in fruit juice anthocyanins.

Sulphite bleaching resistance of anthocyanins in açai models was also correlated ($p < 0.01$) to total anthocyanin contents (r = 0.77), and was indicative of hue changes in colour from dark red to brown. Temperature, pH, and phytochemical composition significantly ($p < 0.03$) influenced anthocyanin bleaching resistance, expressed as percent polymeric anthocyanin contents during storage. All phenolic cofactors decreased anthocyanin polymerization rates throughout storage with effects generally more pronounced in models adjusted to pH 3.0 or 3.5, regardless of storage temperature (Fig. 3).

Açai anthocyanin models were also evaluated for pH variations, soluble phenolic contents, as a measure of total reducing capacity, and for changes in antioxidant capacity throughout storage (Fig. 4). No significant pH variations were detected in any of the models following addition of phenolic cofactors or throughout storage. However, addition of phenolic copigments resulted in increased total soluble phenolic contents (23.1 ± 1.8% increase) and antioxidant capacity (30.2 ± 2.6% increase) in relation to uncopigmented anthocyanin controls that contained 974 ± 79 mg gallic acid equiv-

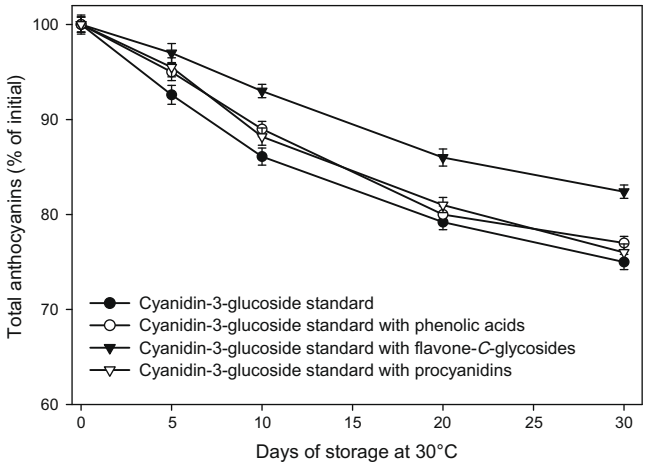

Fig. 2. Percent changes in total anthocyanin contents during storage (30 °C) of cyanidin-3-glucoside standard models adjusted to pH 3.0. Error bars represent the standard error of the mean (n = 3).

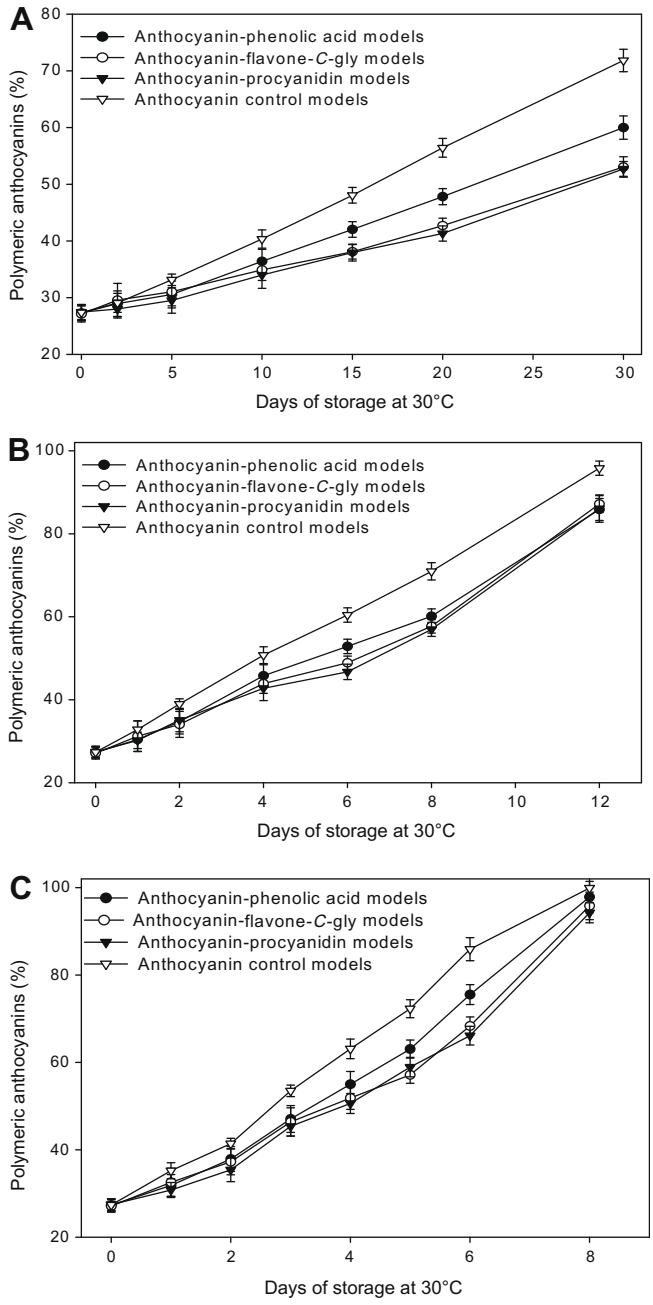

Fig. 3. Percent polymeric anthocyanins during storage (30 °C) of açai models adjusted to pH 3.0 (A), 3.5 (B), and 4.0 (C). Error bars represent the standard error of the mean ($n = 3$).

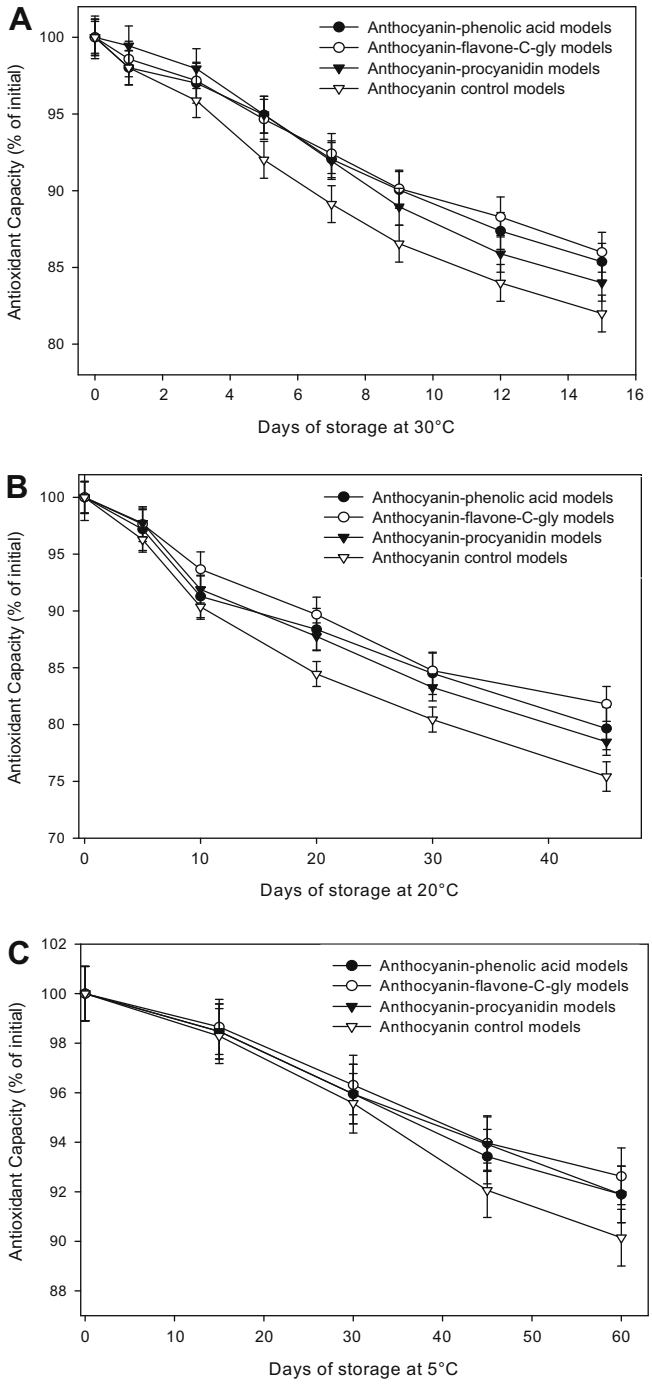

Fig. 4. Percent changes in antioxidant capacity of açai models adjusted to pH 3.0 during storage at 30 °C (A), 20 °C (B), and 5 °C (C). Error bars represent the standard error of the mean ($n = 3$).

alents/l and an antioxidant capacity of 23.8 ± 1.15 μM Trolox equivalents/ml. All phenolic cofactors resulted in higher soluble phenolic contents and antioxidant capacity throughout storage when compared to uncopigmented anthocyanins, at all temperature and pH conditions (Fig. 4). Moreover, changes in soluble phenolic contents and antioxidant capacity were correlated ($r = 0.47$ and 0.68, respectively) to variations in total cyanidin-3-glucoside and cyanidin-3-rutinoside concentrations during storage of açai anthocyanin models.

3.3. Stability of phenolic cofactors

The overall stability of naturally occurring polyphenolic cofactors during storage of açai anthocyanin models was additionally evaluated. Phenolic acid concentrations remained unchanged ($p < 0.05$) in models stored at up to 20 °C, yet losses were <10% at 30 °C. Similarly, flavonol derivatives were stable in models stored at 5 °C but experienced temperature-dependent losses following storage at both 20 and 30 °C, of up to 12.1 ± 1.3% after 30 days, regardless of pH differences. Specifically, the predominant flavone *C*-glycosides, orientin and isoorientin, experienced temperature-dependent losses of up to 11.1% during storage at 5 to 30 °C for up to 60 days, while no changes occurred for the flavone *C*-glycosides luteolin 6,8-di-*C*-glucoside, apigenin 6,8-di-*C*-glucoside, isovitexin, and scoparin.

Table 5
Kinetic parameters of total anthocyanin degradation during storage of açai models with externally added polyphenolic cofactors.

Anthocyanin model	β_1 [A]			$t_{1/2}$ [B]		
	pH 3.0	pH 3.5	pH 4.0	pH 3.0	pH 3.5	pH 4.0
Anthocyanin control models	64.5	120	294	10.7 c[C]	5.79 b	2.36 b
Anthocyanin-rooibos models	53.6	80.0	209	12.9 a	8.67 a	3.32 a
Anthocyanin-rosemary models	59.8	83.4	214	11.6 b	8.30 a	3.24 a

[A] Reaction rate constant ($\beta_1 \times 10^3$ days^{-1}).
[B] Half-life (days) of initial total anthocyanin content for each anthocyanin model.
[C] Values with different letters within columns are significantly different (student's t test, $p < 0.05$).

3.4. Influence of added phenolic cofactors on anthocyanin stability

The influence of externally added flavone-*C*-glycoside cofactors on the stability of anthocyanin isolates from açai fruit was additionally evaluated and compared to a commercially available anthocyanin colour enhancer isolated from rosemary. Extracts rich in flavone-*C*-glycosides were obtained from rooibos tea (*Aspalathus linearis*), which was previously identified to contain high amounts of flavone-*C*-glycosides (Bramati et al., 2002; Krafczyk & Glomb, 2008; Marnewick et al., 2005). Chemical analyses of rooibos extracts used in these trials revealed the presence of orientin (39.9 ± 2.8%), isoorientin (48.1 ± 3.1%), vitexin (19.9 ± 1.4%), and isovitexin (19.7 ± 1.3%), along with lower concentrations of *C*-linked dehydrochalcone glycosides (12.3 ± 1.1%), likely aspalathin and nothofagin (Krafczyk & Glomb, 2008; Marnewick et al., 2005). Copigmentation of anthocyanin isolates with rooibos extracts (0.2% v/v) resulted in immediate hyperchromic shifts of up to 45.5 ± 3.8% at pH 3.0, 30.2 ± 2.3% at pH 3.5, and 14.7 ± 1.3% at pH 4.0, that related to proportionally higher increases in visual red colour at all pH levels. A less pronounced hyperchromic shift was observed with the commercial rosemary extracts (0.2% v/v), which resulted in 27.5 ± 2.2%, 21.1 ± 1.3%, and 10.7 ± 0.9% higher absorbance at pH 3.0, 3.5, and pH 4.0, respectively. Moreover, kinetic parameters of total anthocyanin degradation, expressed as the sum of cyanidin-3-glucoside and cyanidin-3-rutinoside concentrations, revealed consistently higher ($p < 0.05$) anthocyanin half-lives for anthocyanin models containing rooibos ($t_{1/2}$ = 3.32–12.9 days) or rosemary extracts ($t_{1/2}$ = 3.24–11.6 days) as compared to an anthocyanin isolate control ($t_{1/2}$ = 2.36–10.7 days) (Table 5). Changes in total anthocyanin contents were inversely correlated ($p < 0.05$) to anthocyanin bleaching resistance (r = 0.72) and directly correlated to antioxidant capacity (r = 0.65). Thus, addition of rooibos extracts, rich in flavone-*C*-glycosides, not only resulted in higher colour intensities but also increased anthocyanin stability during long-term storage (30 °C) of açai anthocyanin models, in a comparable manner to a known copigment source such as rosemary extract. Results from model systems can be related to similar effects in natural açai juices, and are thus indicative of the potential of flavone-*C*-glycoside-rich extracts for anthocyanin stabilization in açai-containing foods, juice blends and beverages.

4. Conclusion

The influence of naturally occurring and externally added polyphenolic cofactors on the chemical and colour stability of predominant anthocyanins in açai fruit (*Euterpe oleracea*), cyanidin-3-glucoside and cyanidin-3-rutinoside, was investigated. Overall, the presence of flavone-*C*-glycosides induced an increase in anthocyanin colour and enhanced total anthocyanin stability, regardless of pH (3.0, 3.5, or 4.0) or storage temperature (5, 20, or 30 °C), while no significant effects were attributed to the presence of phenolic acids or procyanidins. External addition of flavone-*C*-glycoside-rich extracts from rooibos tea also resulted in up to ~45% higher anthocyanin colour and up to ~40% higher anthocyanin stability compared to uncopigmented anthocyanin isolates, and had similar copigmentation effects to a commercial anthocyanin colour enhancer extracted from rosemary. Results suggest flavone-*C*-glycosides are a potential alternative for the food and beverage industry for their use as colour enhancers and stabilizing agents in products containing non-acylated cyanidin glycosides, particularly açai fruit juice blends and beverages.

References

Adams, J. B. (1972). Changes in the polyphenols of red fruits during heat processing: the kinetics and mechanism of anthocyanin degradation. Campden Food Preservation Research Association Technology Bulletin No. 22.

Adams, J. B. (1973). Thermal degradation of anthocyanins with particular reference to the 3-glycosides of cyanidin. I. In acidified aqueous solution at 100 C. *Journal of the Science of Food and Agriculture, 24*, 747–762.

Asen, S., Stewart, R., Norris, K., & Massie, D. (1970). A stable blue non-metallic copigment complex of delphanin and C-glycosylflavones in Prof. *Blaauw Iris. Phytochemistry, 9*, 619–627.

Baranac, J., Petranovic, N., & Dimitric-Markovic, J. (1996). Spectrophotometric study of anthocyan copigmentation reactions. *Journal of Agricultural and Food Chemistry, 44*, 1333–1336.

Boulton, R. (2001). The copigmentation of anthocyanins and its role in the colour of red wine: a critical review. *American Journal of Enology and Viticulture, 52*, 67–87.

Bramati, L., Minoggio, M., Gardana, C., Simonetti, P., Mauri, P., & Pietta, P. (2002). Quantitative characterization of flavonoid compounds in Rooibos tea (*Aspalathus linearis*) by LC-UV/DAD. *Journal of Agricultural and Food Chemistry, 50*, 5513–5519.

Brenes, C., Del Pozo-Insfran, D., & Talcott, S. T. (2005). Stability of copigmented anthocyanins and ascorbic acid in a grape juice model system. *Journal of Agricultural and Food Chemistry, 53*, 49–56.

Clifford, M. (2000). Anthocyanins: Nature, occurrence and dietary burden. *Journal of the Science of Food and Agriculture, 80*, 1063–1072.

Del Pozo, D., Brenes, C., & Talcott, S. (2004). Phytochemical composition and pigment stability of açai (*Euterpe oleracea* Mart.). *Journal of Agricultural and Food Chemistry, 52*, 1539-1545.

Eiro, M., & Heinonen, M. (2002). Anthocyanin colour behavior and stability during storage: Effect of intermolecular copigmentation. *Journal of Agricultural and Food Chemistry, 50*, 7461–7466.

Ferreres, F., Silva, B., Andrade, P., Seabra, R., & Ferreira, M. (2003). Approach to the study of *C*-glycosyl flavones by ion trap HPLC-PAD-ESI/MS/MS: Application to seeds of quince (*Cydonia oblonga*). *Phytochemical Analysis, 14*, 352–359.

Gallori, S., Bilia, A., Bergonzi, M., Barbosa, L., & Vincieri, F. (2004). Polyphenolic constituents of fruit pulp of *Euterpe oleracea* Mart. (açai palm). *Chromatographia, 59*, 739-743.

Gattuso, G., Barreca, D., Gargiulli, C., Leuzzi, U., & Caristi, C. (2007). Flavonoid composition of citrus juices. *Molecules, 12*, 1641–1673.

Grayer, R., Kite, G., Abou-Zaid, M., & Archer, L. (2000). The application of atmospheric pressure chemical ionization liquid chromatography–mass spectrometry in the chemotaxonomic study of flavonoids: Characterisation of flavonoids from *Ocimum gratissimum* var. Gratissimum. *Phytochemical Analysis, 11*, 257–267.

Han, J., Ye, M., Xu, M., Sun, J., Wang, B., & Guo, D. (2007). Characterization of flavonoids in the traditional Chinese herbal medicine Huangqin by liquid chromatography coupled with electrospray ionization mass spectrometry. *Journal of Chromatography B, 848*, 355–362.

Jurd, L. (1972). Some advances in the chemistry of anthocyanin-type plant pigments. *Advances in Food Research Supplement, 3*, 123–142.

Jurd, L., & Asen, S. (1966). The formation of metal and co-pigment complexes of cyanidin 3-glucoside. *Phytochemistry, 5*, 1263–1271.

Krafczyk, N., & Glomb, M. (2008). Characterization of phenolic compounds in Rooibos tea. *Journal of Agricultural and Food Chemistry, 56*, 3368–3376.

Lichtenthaler, R., Belandrino, R., Maia, J., Papagiannopoulos, M., Fabricius, H., & Marx, F. (2005). Total antioxidant scavenging capacities of *Euterpe oleracea* Mart. (açai) fruits. *International Journal of Food Science and Nutrition*, *56*, 53-64.

Malien-Aubert, C., Dangles, O., & Amiot, M. (2001). Colour stability of commercial anthocyanin-based extracts in relation to the phenolic composition. *Protective effects by intra- and intermolecular copigmentation. Journal of Agricultural and Food Chemistry, 49*, 170–176.

Markakis, P. (1974). Anthocyanins and their stability in food. *Critical Reviews in Food Technology, 4*, 437–456.

Markakis, P. (1982). Stability of anthocyanins in foods. In P. Markakis (Ed.), *Anthocyanins as Food Colours* (pp. 163–180). London, UK: Academic Press Inc.

Marnewick, J., Joubert, E., Joseph, S., Swanevelder, S., Swart, P., & Gelderblom, W. (2005). Inhibition of tumor promotion in mouse skin by extracts of rooibos (*Aspalathus linearis*) and honeybush (*Cyclopia intermedia*), unique South African herbal teas. *Cancer Letters, 224*, 193–202.

Mazza, G., & Brouillard, R. (1990). The mechanism of co-pigmentation of anthocyanins in aqueous solutions. *Phytochemistry, 29*, 1097–1102.

Pacheco-Palencia, L., Hawken, P., & Talcott, S. (2007a). Juice matrix composition and ascorbic acid fortification effects on the phytochemical, antioxidant, and pigment stability of açai (*Euterpe oleracea* Mart.). *Food Chemistry*, *105*, 28–35.

Pacheco-Palencia, L., Hawken, P., & Talcott, S. (2007b). Phytochemical, antioxidant and pigment stability of açai (*Euterpe oleracea* Mart.) as affected by clarification, ascorbic acid fortification and storage. *Food Research International*, *40*, 620–628.

Pacheco-Palencia, L., Mertens-Talcott, S., & Talcott, S. T. (2008). Chemical composition, antioxidant properties, and thermal stability of a phytochemical enriched oil from açai (*Euterpe oleracea* Mart.). *Journal of Agricultural and Food Chemistry, 56*(12), 4631–4636.

Pereira, C., Yariwake, J., & McCullagh, M. (2005). Distinction of the *C*-glycosylflavone isomer pairs orientin/isoorientin and vitexin/isovitexin using HPLC-MS exact mass measurement and in-source CID. *Phytochemical Analysis*, 295-301.

Rodriguez-Saona, L., Guisti, M., & Wrolstad, R. (1999). Colour and pigment stability of red radish and red fleshed potato anthocyanins in juice model systems. *Journal of Food Science, 64*, 451–456.

Schauss, A., Wu, X., Prior, R., Ou, B., Patel, D., Huang, D., & Kababick, J. (2006). Phytochemical and nutrient composition of the freeze-dried amazonian palm berry, *Euterpe oleracea* Mart. (açai). *Journal of Agricultural and Food Chemistry*, *54*, 8598-8603.

Singleton, V. L. (1972). Common plant phenols other than anthocyanins, contributions to colouration and discolouration. *Advances in Food Research Supplement, 3*, 143–191.

Singleton, V., & Rossi, J. (1965). Colourimetry of total phenolics with phosphomolybdic-phosphotungstic acid reagents. *American Journal of Enology and Viticulture, 16*, 144–153.

Talcott, S., Brenes, C., Pires, D., & Del Pozo-Insfran, D. (2003). Phytochemical stability and colour retention of copigmented and processed muscadine grape juice. *Journal of Agricultural and Food Chemistry, 51*, 957–963.

Talcott, S., & Lee, J. (2002). Ellagic acid and flavonoid antioxidant content of muscadine wine and juice. *Journal of Agricultural and Food Chemistry, 50*, 3186–3192.

Wrolstad, R. E., Durst, R. W., & Lee, J. (2005). Tracking colour and pigment changes in anthocyanin products. *Trends in Food Science and Technology, 16*, 423–428.

Food Chemistry 118 (2010) 26–34

Contents lists available at ScienceDirect

Food Chemistry

journal homepage: www.elsevier.com/locate/foodchem

Proteins in white wines: Thermo-sensitivity and differential adsorbtion by bentonite

Francois-Xavier Sauvage *, Benoit Bach, Michel Moutounet, Aude Vernhet

UMR 1083 Sciences for Enology, INRA/Montpellier SupAgro, 2 Place Viala, 34 060 Montpellier Cedex 01, France

ARTICLE INFO

Article history:
Received 21 November 2008
Received in revised form 6 January 2009
Accepted 24 February 2009

Keywords:
White wine stability
Wine proteins
Thermo-sensitivity
Bentonite adsorption

ABSTRACT

Protein fractions in a Chardonnay wine (invertases, glucanases, chitinases and thaumatin-like proteins) were identified using 2D-electrophoresis and mass spectrometry. The sensitivity of these fractions to heat-induced denaturation and precipitation following heat-treatments at different temperatures was studied and compared to their affinity for bentonite, a clay used to adsorb proteins and stabilise wines with regards to protein hazes. The different proteins exhibited different sensitivity with regards to heat-induced precipitation, glucanases being the most sensitive and invertases the least. Thaumatines and chitinases were characterised by a wide range of behaviours attributed to structural micro-heterogeneities. Protein depletion upon the addition of increasing bentonite doses was also dependent on the considered fraction. A good correlation was shown between protein affinity for bentonite and their sensitivity to heat precipitation. Results were discussed considering the current winemaking practices used to assess white wine stability and define bentonite doses needed to achieve their stabilisation.

1. Introduction

Protein synthesis in grape berries quickly increases after veraison, along with sugar accumulation (Giribaldi, Perugini, Sauvage, & Schubert, 2007; Murphey, Spayd, & Powers, 1989; Pocock, Hayasaka, Mc Carthy, & Waters, 2000). Protein diversity in musts and wines is much lower than in grapes since only soluble proteins are extracted during the winemaking process (Ferreira, Piçarra-Pereira, Monteiro, Loureiro, & Teixeira, 2002; Murphey et al., 1989). Moreover, protein amounts in wines are always lower than in the corresponding musts. That decrease is attributed to proteolytic activity, to precipitation by polyphenols and to unfavourable conditions related to the low pHs and the increasing ethanol contents. Protein concentrations reported for white wines vary between 10 and about 500 mg l^{-1} (Santoro, 1995; Vincenzi, Polesani, & Curioni, 2005). Grape variety, maturity and winemaking process are some factors that strongly affect the final protein content. These proteins have molecular mass ranging from 9 to 66 kDa and isoelectric points ranging from 3 to 9 (Brissonnet & Maujean, 1993; Dawes, Boyes, Keene, & Heatherbell, 1994; Hsu & Heatherbell, 1987). Most of them, identified as being chitinases and thaumatin-like proteins, are found within the range 20–30 kDa and are acidic (Dawes et al., 1994; Hsu & Heatherbell, 1987; Mesquita et al., 2001; Murphey et al., 1989; Pocock et al., 2000; Pocock, Hayasaka, Peng, Williams, & Waters, 1998).

Though present in rather small amounts, proteins are of primary importance for the colloidal stability and clarity of white wines (Bayly & Berg, 1967; Hsu & Heatherbell, 1987; Waters, Wallace, & Williams, 1991). Haze or deposit formation in bottled wines, due to protein aggregation during storage, is a common defect of commercial wines making them unacceptable for consumers. Numerous works have been devoted to the identification of protein structures implied in colloidal instabilities, as well as to the elucidation of the factors that trigger or prevent haze formation (Dawes et al., 1994; Hsu & Heatherbell, 1987; Pocock, Alexander, Hayasaka, Jones, & Waters, 2007; Waters et al., 1991; Waters, Dupin, & Stockdale, 2000; Waters, Peng, Pocock, & Williams, 1995; Waters, Wallace, & Williams, 1992). Aggregation is usually attributed to slow protein unfolding during storage, induced by exposure to high temperatures. As a consequence, most studies to explore the development of these hazes have been conducted using heat-induced precipitation. Chitinases and thaumatin-like proteins, which constitute the major part of white wine proteins, are also important contributors to heat-induced protein instability (Dawes et al., 1994; Hsu & Heatherbell, 1987; Waters et al., 1992). Attempts to correlate the total wine protein contents to their sensitivity to protein haze failed (Bayly & Berg, 1967); this can be related to a different sensitivity of the various protein fractions to heat-denaturation (Hsu & Heatherbell, 1987; Waters et al., 1991, 1992), and/or to the influence of factors other than protein composition. Among others, haze formation was shown to be strongly affected by the presence of non-protein compounds such as polyphenols (Dawes et al., 1994; Waters et al., 1995), ions (Besse, Clarck, & Scollary; 2000; Pocock et al., 2007) and polysaccharides (Dupin et al., 2000; Mesquita et al., 2001).

Different tests have been proposed to assess wine stability/instability with regards to protein haze (Pocock & Waters, 2006). These tests are based upon different types of procedures, leading to protein aggregation and precipitation. Heat stability trials, based on heat-induced precipitation, are the most common. These tests

* Corresponding author. Fax: +33 (0) 4 99 61 28 57.
E-mail address: sauvage@supagro.inra.fr (F.-X. Sauvage).

0308-8146/$ - see front matter © 2009 Published by Elsevier Ltd.
doi:10.1016/j.foodchem.2009.02.080

are empirical and do not necessarily reflect changes and destabilisation phenomena liable to occur in real wine storage conditions. If needed, stability is usually obtained by bentonite fining, due to protein adsorption by the clay particles. The level of bentonite addition required for stabilisation is also determined by stability tests. These levels have increased during the last 20 years, so that doses in the order of 100–200 g hl^{-1} are often employed (Dubourdieu & Canal-Llaubère, 1989). Though effective, bentonite fining generates different problems, especially when such high doses are needed. First, this treatment is not selective enough and may adversely affect wine quality by inducing significant aroma losses and sometime colour alteration (Bayonove et al., 1995; Cabaroglu, Canbas, Lepoutre, & Gunata, 2002). Bentonite fining also causes substantial volume losses (between 3% and 10%) (Hoj et al., 2001) and the disposal of spent bentonites constitute a non negligible source of waste. Finally, bentonite handling is also of concern for occupational health and safety issues. For these reasons, increasing attention is given today to the development of alternative practices for protein stabilisation, that would maintain quality, reduce costs and be more sustainable (Waters et al., 2005).

Thorough knowledge of the structures and mechanisms involved is needed to be in position to control and prevent protein hazes while avoiding excessive and detrimental treatments. In addition to the identification of the role played by the other wine compounds, additional information regarding: (i) the sensitivity of the different wine proteins to heat-induced precipitation and (ii) their adsorption by bentonites is necessary. It is clear from previous works that the wine protein fractions exhibit different behaviours with regards to heat-induced precipitation and adsorption (Dawes et al., 1994; Hsu & Heatherbell, 1987; Murphey et al., 1989). In the present study the major proteins in a Chardonnay wine were identified using 2D-electrophoresis and mass spectrometry. This identification was used to study the sensitivity of each protein fraction to heat-treatment and to correlate this sensitivity to their adsorption by bentonite. To this end, a methodology to analyse and quantify wine proteins using 1D-electrophoresis coupled with image analysis was used, which is described first.

2. Materials and methods

2.1. Materials

2.1.1. Wine sample

The Chardonnay white wine used in this study was elaborated in 2005 at the Pech Rouge Experimental Unit (INRA Gruissan, France). Following to harvest, grapes were pressed without skin maceration and the must settled down (one night, 15 °C). Alcoholic fermentation was achieved at a temperature of 15 °C using the yeast Firmivin (DSM). After fermentation, the wine was racked and the SO_2 level was adjusted to prevent oxidation and malolactic fermentation. It was then stored during two months at 15 °C and bottled after a second racking and a membrane filtration.

2.1.2. Chemicals

The bentonite used was a commercial suspension of bentonite Electra® (Martin Vialatte). Thio-urea, urea, CHAPS, Triton X-100, Dithiothreitol, bromophenol blue, Tris buffer, glycine and Sodium Docedyl Sulfate were purchased from Sigma–Aldrich. Ampholines were from GE Healthcare.

2.2. Protein quantification in white wines using 1D-electrophoresis coupled with image analysis

Problems encountered to quantify proteins in wines using 1D electrophoresis and image analysis are related to their low concentrations and to the presence of non-protein compounds, especially polyphenols, that interfere with the analysis. To overcome these problems, a methodology was developed to obtain both protein concentration and separation. This was achieved by adsorption on bentonite of the proteins contained in a 1 ml wine aliquot, followed by their desorption using Laemmli buffer. Different bentonite doses, between 20 and 500 g hl^{-1}, were assayed. After bentonite addition and 30 min under soft shaking the mixture was centrifuged for 15 min at 20,000*g* and at 4 °C. The supernatant was removed and 100 μl of Laemmli buffer were added to the pellet to allow protein desorption. The suspension was shaken for 15 min and the bentonite separated by centrifugation, as described before. Several successive desorption steps were performed (up to 5 steps) and the supernatants analysed. With the experimental wines (protein concentrations below 150 mg l^{-1}) it was verified that no protein could be detected in the treated wines at a bentonite dose of 200 g hl^{-1} and higher. Up to 200 g hl^{-1} bentonite, the first washing step using 100 μl Laemmli buffer allowed the recovery of the whole protein fraction. Conditions for further experiments were then: wine sample, 1 ml; bentonite dose, 200 g hl^{-1} and Leammli buffer volume for desorption, 100 μl. Proteins in the buffer were concentrated 10 fold by comparison to the original wine. They were separated by 1D SDS–PAGE electrophoresis, performed in 14% acrylamide resolving gel (resolving gel length, 60 mm). As their initial concentration in wine was unknown, three different volumes (10, 20 and 40 μl) were deposited in the gel. Running was first conducted at 20 mA per gel all along the stacking gel and 30 mA per gel until the run end. Gels were then stained with colloidal CBB G-250 (Biorad) (Neuhoff, Arold, Taube, & Ehrhadt, 1988) and scanned at 300 dpi with an Image scanner (GE Biosciences). A low molecular weight calibration kit (Pharmacia, Biotech), ranging from 14 400 to 97,000 Da, was included in each electrophoretic run. Image elaboration and analysis were carried out with the Totallab software (Nonlinear Dynamics Ltd.). Image analysis was used to calculate the "volume" of each staining band from sample. This volume (product of the band area by the intensity of each pixel within this area) is proportional to the protein amount in each band provided saturation of the coloration has not been reached. It can be compared to the volume of the band obtained with a calibration protein. The volume of the Bovine Serum Albumin band of the low molecular weight calibration kit was used and results expressed in μg equivalent BSA. Quantification was performed for the three different deposited volumes (between 10 and 40 μl) and results represent the linear regression of the three measures.

2.3. Separation and identification of wine proteins by 2D-electrophoresis and mass spectrometry

2.3.1. Protein extract preparation for 2DE separation

To be in position to perform a 2D-electrophoresis separation of the wine proteins it was first required to purify (partial purification) and concentrate the whole wine protein content. Proteins were then dissolved under their native form by means of a suitable tensioactive mixture.

Polyphenols in the Chardonnay wine (750 ml aliquot) were first removed by adsorption using Fractogel (50 ml, Fractogel®TSK, Toyopearl HW50F, TosoHaas, Allemagne). Adsorption was realised in batches for 30 min, under gentle stirring. Adsorbent was removed by centrifugation (14,000*g*, 15 min, 4 °C) and the supernatant recovered. Protein concentration and purification from the dephenolysed wine was then achieved by successive ultrafiltration steps. The wine was first ultrafiltered using a 150 kDa plane membrane (50 cm^2, TAMI Industry, Nyons, France) using the spirelab device developed by TAMI (Nyons, France). This first step allowed the separation between wine polysaccharides, concentrated in the

retentate, and proteins (MW <150 kDa), recovered in the permeate. A second ultrafiltration step on a 5 kDa titanium/zirconium membrane (50 cm^2, TAMI Industry, Nyons, France), along with extensive diafiltration using deionised water (Milli-Q), allowed protein concentration and the removal of salts and small molecules. Diafiltration was monitored via conductivity measurements. The 5 kDa membrane was washed twice in 2 ml of an isoelectrofocusing (IEF) rehydration solution to recover adsorbed proteins. Washing solutions were added to the ultrafiltration retentate. The composition of the rehydratation solution was: 2 M thiourea, 7 M urea, 4% CHAPS, 0.5% Triton X-100, 65 mM DTT, traces of bromophenol blue, 5% ampholines mix. Protein concentration in the final extract (after 10 fold dilution) was assessed using CBB G-250 (Bio-Rad) with BSA as standard according to the Bradford's procedure (Bradford, 1976). It was adjusted to 1 μg μl^{-1} for next experiments.

2.3.2. 2DE Separation

Isoelectrofocusing (IEF) was carried out with 300 μg protein using 18 cm long Immobiline Dry-strips (pH interval 3–10, nonlinear, GE Healthcare). Sample loading was performed passively for 8 h at 20 °C in an IPGphor system (GE Healthcare). IEF migration program was as follows: active rehydration at 50 V during 9 h, ramping until 300 V in 1 min, start focusing at 300 V for 30 min, ramping again until 8000 V in 3 h, focusing for 11 h at 8000 V, decreasing until 300 V in 3 h. For a complete focusing the total power reached 105,000 Vh. Strips were then equilibrated twice upon gentle agitation for 15 min in a 50 mM Tris–HCl (pH 8.8) buffer containing 6 M urea, 10% glycerol and 2% SDS, added first with 1% DTT, and in a second time with 2.5% iodoacetamine (Görg, Weiss, & Dunn, 2004).

Second-dimension SDS–PAGE was performed on a 12% acrylamide gel using an ISODALT apparatus (GE Healthcare). Separation was achieved at 15 °C in a buffer (pH 8.3) containing 25 mM Tris, 0.192 M glycine, and 0.1% SDS. Running conditions were 1 h at 40 V and 30 mA per gel, 1 h at 70 V and 40 mA per gel, and then 11 h at 110 V per gel. Gels were stained and scanned as described before for 1D-electrophoresis. Image elaboration and 2D analysis were completed with the ImageMaster 2D-Platinium version 5 software (GE Healthcare). Molecular weights and isoelectric points of spots were determined according to migration of 2D standards (Bio-Rad).

2.3.3. In-gel digestion and mass spectrometry

Gels spots from 2D-electrophoresis were excised and washed twice with deionised water. Destaining was realised by at least three successive washes using a 50% acetonitrile aqueous solution (ACN) and 50 mM NH_4HCO_3, as described before (Görg et al., 2004). Gel fragments were successively dehydrated by ACN, re-hydrated and dehydrated again by NH_4HCO_3/ACN washes and finally dried under vacuum on a centrifugal evaporator. Final rehydration was achieved in a digestion solution composed of 0.1 M NH_4HCO_3, 5 mM $CaCl_2$ and 0.015 mg ml^{-1} trypsin (GOLD, Promega). Samples were first left on ice for 45 min to allow trypsin activation and then during one night at 37 °C to complete the in-gel protein digestion. To collect the digested peptides, gels spots were dehydrated/re-hydrated/dehydrated twice with ACN/NH_4HCO_3 (100 mM ACN), and washed twice in 5% formic acid and ACN. Washing solutions were pooled and dried in a vacuum centrifuge. The pellets (containing digested products) were re-suspended in 10 μl of 2% formic acid and desalted using C18 Zip Tips (Millipore Inc., France) according to manufacturer's instructions. The final peptide solution ACN/TFA/water (50%/0.1%/49.9%) was concentrated to a 2 μl volume by vacuum evaporation.

MS analyses were performed using an UltraFlex matrix-assisted laser desorption ionisation time-of-flight (MALDI-TOF) mass spectrometer (Bruker Daltonics, Bremen, Germany) in reflecton mode with an accelerating voltage of 19 kV. Different peptides ions generated by trypsin autolysis were used as internal standards for calibrating the mass spectra. Spots identified by MALDI-TOF were also analysed online using nanoflow HPLC nanospray ionisation on a quadrupole time-of-flight (Q-TOF) mass spectrometer. Spectra were recorded using Analyst QS 1.1 software (Applied Biosystems).

2.3.4. Identification by database search

The NCBI non-redundant database was explored with the MASCOT software (Matrix Science, London, UK). To confirm protein identities, the SWISS-PROT and Trembl databases were also explored with Peptident™ software. For identification by peptide mass fingerprinting (MALDI-TOF), the following parameters were used for database searches (Görg et al., 2004): (1) mass tolerance of 50 ppm, (2) a minimum of four peptide mass matching the protein, and (3) up to one missed cleavage was accepted only when two consecutive lysine or arginine residues were present or when residues were followed by a proline or acidic/basic residues. Sequence coverage was at least 15% for any identification. All MS/MS spectra were searched against the *Viridiplantae* entries of either the Swiss-Prot or Trembl database or ESTs in Genbank databases by using the Mascot v 2.1 algorithm, by sequence query analysis. All significant hits were manually inspected.

2.4. Thermo-sensibility of white wine proteins

Ten millilitre aliquots of the Chardonnay wine were heated to 30, 40, 50, 60, 70 or 80 °C in a waterbath during 30 min. Samples were cooled down and left at room temperature for at least one night. Then, they were centrifuged at 20,000*g* and at 4 °C during 20 min, to separate the precipitate. Proteins in the supernatants and in the pellets were identified and quantified by 1D-electrophoresis and image analysis, as described before. Experimental protocol for the supernatants was the same than that described for wine, except that in this case, a 12% acrylamide resolving gel was used. Precipitated proteins, recovered in the pellet, were solubilised in 1 ml Laemmli buffer before electrophoresis (Hsu & Heatherbell, 1987).

2.5. Protein adsorption on bentonite

Increasing volumes of a 10 g l^{-1} bentonite suspension were added to 1 ml Chardonnay wine aliquots to obtain final bentonite concentrations between 0 and 150 g hl^{-1}. Suspensions were shaken during 30 min at ambient temperature before being centrifuged (20,000*g*, 4 °C, 15 min). Proteins in the supernatants were analysed as described for wines. Adsorbed proteins on bentonites were recovered by washing the clay particles with 0.1 ml Laemmli buffer and directly analysed using electrophoresis (14% acrylamide resolving gel) and image analysis.

3. Results and discussion

3.1. Quantification of wine proteins by 1D-electrophoresis and image analysis

In the present work, the opportunity of improving protein patterns obtained from 1D-electrophoresis of white wines was experienced. The aim was to obtain profiles allowing protein quantification by image analysis. To this end, proteins have to be concentrated and separated first. This was achieved by an adsorption/desorption step on bentonite, clay being added in excess to ensure the adsorption of all proteins. Protein profiles obtained in this way for different white wines are shown in Fig. 1; pattern quality allowed the quantification of each protein band within

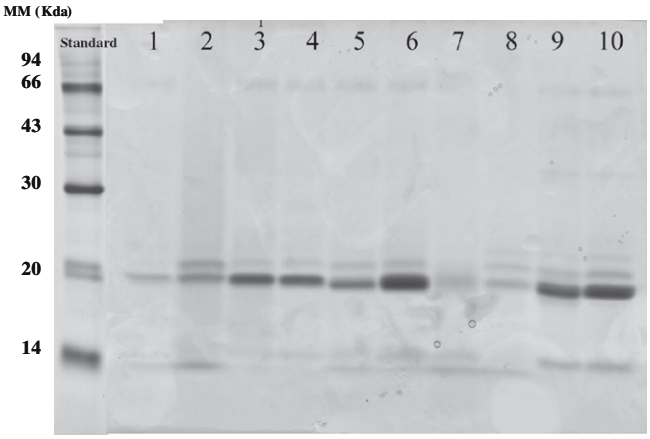

Fig. 1. Protein profiles obtained by 1D SDS–PAGE electrophoresis for white wines of different varieties and using the described extraction and concentration procedure. 1: Muscat, 2: Garganega, 3: Chasselas, 4: Moscatel, 5: Sauvignon, 6: Ugni Blanc, 7: Chardonnay I5, 8: Chardonnay I19, 9: Chardonnay I41, 10: Chardonnay I10.

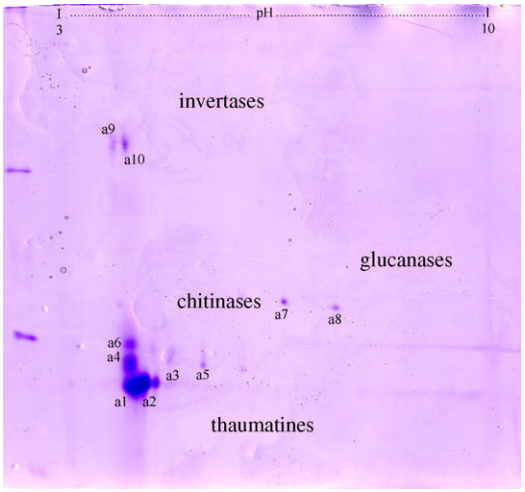

Fig. 3. Protein profile obtained by 2D-electrophoresis separation and staining using CBB-G-250. Proteins in the Chardonnay wine (I10) were identified by mass spectrometry and were: thaumatin-like proteins (spots a1, a2, a3, a5), chitinases (spots a4 and a6), glucanases (spots a7 and a8) and invertases (spots a9 and a10).

the whole pool. These patterns were typical of those reported in the literature for white wines (Dawes et al., 1994; Hsu & Heatherbell, 1987; Pocock et al., 2000), with protein fractions of molecular weight ranging from 14 to 66 kDa, the majority of them being comprised between 20 and 30 kDa.

The reproducibility of the quantification obtained via image analysis was assayed on the Chardonnay I10 wine (Fig. 2a), selected for further experiments due to its protein composition. The I10 protein pattern exhibited nine major bands so that this wine was characterised by the variety of its protein content. Results of protein quantification (Fig. 2b) represent a mean of six separate experiments, including the initial separation and concentration step. The I10 wine contained 142 mg l^{-1} protein in equivalent BSA, and the standard deviation between the six aliquots was 11%. It is important to note that when bands are quantified separately, the standard deviation may be different, depending on the concentration of each protein in the initial wine. For the I10 wine, these standard deviation fluctuated from 10% (band corresponding to the most concentrated protein fraction) to 25% (band corresponding to the less concentrated protein fraction).

3.2. Identification of white wine proteins

Proteins in the I10 wine were extracted and separated by 2D-electrophoresis for further identification by mass spectrometry. The protein profile evidenced ten major spots (Fig. 3), the number of spots detected onto 2DE gels being in agreement with the number of bands detected on 1D SDS–PAGE gels. MS analyses (Table 1) allowed identifying the different proteins in these spots: 4 thaumatin-like proteins (spots a1, a2, a3, a4), 2 chitinases (spots a5, a6), 2 glucanases (spots a7, a8) and 2 invertases (spots a9, a10). All these proteins, considered as pathogenesis-related proteins (PRPs) except for invertases, originated from grape and not from yeast. This specific grape origin of wine proteins is in accordance with previous data (Ferreira et al., 2000). However some proteins of fungal

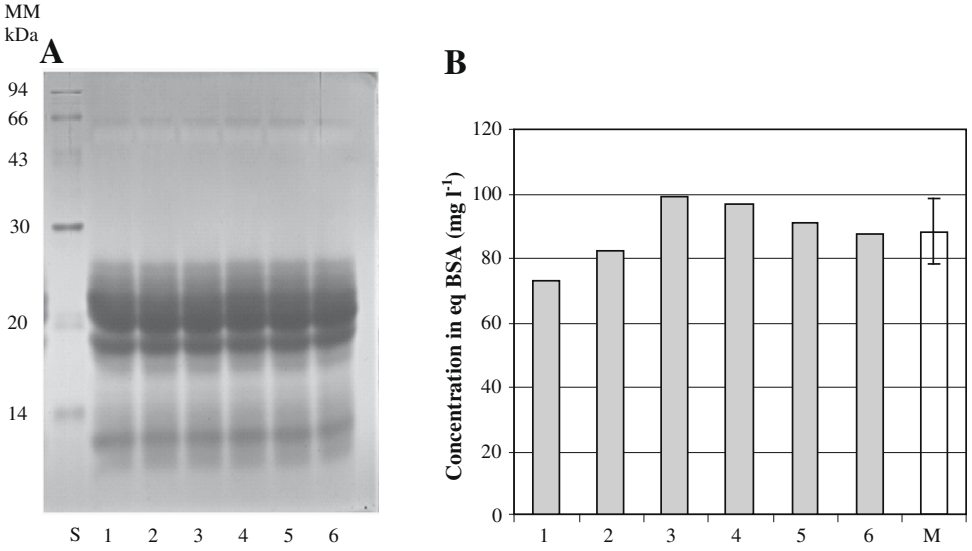

Fig. 2. (A) Protein profiles in the I10 Chardonnay wine obtained by 1D SDS–PAGE electrophoresis (14% acrylamide gel) for a deposited volume equivalent to 400 µl of wine. (B) Protein quantification on 6 aliquots, M being the average of the six quantifications. Under the experimental conditions this Chardonnay wine exhibited 9 different protein bands, corresponding to an average protein content of 142 mg l^{-1} equivalent BSA, with an 11% standard deviation.

Table 1
Protein identification by Maldi-TOF MS (results non shown) and peptide sequence determination using HPLC-ion trap MS/MS.

Spot number	Score* (peptide number)	Sequence	Access number** (SP Trembl)	Molecular mass (Da)	Name
a10	88(3)	SSLAVDDVDQR; VLVDHSIVEGFSQGGR; VYPTEAIYGAAR	Q9S944_VITVI	71,501	Vacuolar invertase 1
a9	144(5)	SSLAVDDVDQR; TFFCTDLSR; IYGSIVPVLDDEKPTMR; VLVDHSIVEGFSQGGR; VYPTEAIYGAAR	Q9S944_VITVI	71,501	Vacuolar invertase 1
a8, a7	75(2)	NIFNAISAAGLGNQIF; NLFDAILDAVYSALER	Q9M3U4_VITVI	37,489	β1-3 glucanase
a5, a6	45(4)	AAFLSALNSYSGFGNDGSTDANKR; AINGAVECNGGNTAAVNAR; AAFLSALNSYSGFGNDGSTDANK; DYCSQLGVSPGDNLTC	Q7XAU6_VITVI	28,366	Class IV chitinase
a4	122(1)	RTNCNFDASGNGK	Q7XAU7_VITVI	24,835	Thaumatin-like protein
	56(1)	RLDSGQSWTITVK	Q9LLB7_VITVI	25,269	Thaumatin-like protein
a3	167(4)	LDSGQSWTITVNPGTTNAR; TSLFTCTSGTNYK ; TSCTFDANGR; DRCPDAYSYPQDDK; rldsgqswtitvnpgttnar; GIQCSADINGQCPSELK	Q9M4G6_VITVI	24,947	Thaumatin-like protein
	52(2)	RTNCNFDASGNGK; GISCTADIVGECPAALK	Q7XAU7_VITVI	24,835	Thaumatin-like protein
a2	755(6)	LDSGQSWTITVNPGTTNAR; TSLFTCPSGTNYK; TSCTFDANGR ; DRCPDAYSYPQDDK; rldsgqswtitvnpgttnar; GIQCSVDINGQCPSELK	O04708_VITVI	24,866	Thaumatin-like protein (VVTL1)
	527(6)	LDSGQSWTITVNPGTTNAR; TSLFTCTSGTNYK; TSCTFDANGR; DRCPDAYSYPQDDK; rldsgqswtitvnpgttnar; GIQCSADINGQCPSELK	Q9M4G6_VITVI	24,947	Thaumatin-like protein
	56(1)	RTNCNFDASGNGK	Q7XAU7_VITVI	24,835	Thaumatin-like protein
a1	852(2)	RTNCNFDASGNGK; VLVDHSIVEGFSQGGR	Q7XAU7_VITVI	24,835	Thaumatin-like protein
	131(5)	LDSGQSWTITVNPGTTNAR; TSLFTTCSGTNYK ; TSCTFDANGR; DRCPDAYSYPQDDK; ldsgqswtitvnpgttnar	O04708_VITVI	24,866	Thaumatin-like protein (VVTL1)
	49(1)	SSLAVDDVDQR	Q9S944_VITVI	71,501	Vacuolar invertase 1

* Identification score along with the number of peptides (into brackets) that matched with peptides of the SP Trembl database.
** Identification number in the SP Trembl database.

or bacterial origin may also be present, though rarely evidenced (Monteiro et al., 2001). I10 wine proteins were mainly acidic, with isoelectric points (IEP) below 5, except for glucanases, the IEPs of which were found to be around 7. This also is in agreement with previous works (Cilindre, Castro, Clément, Jeandet, & Marchal, 2007; Dawes et al., 1994).

3.3. Heat-induced precipitation of white wine proteins

The conformational stability of proteins in a given solvent is weak and strongly affected by even small changes in the external variables (temperature, pH, salts, etc.). Changes from native to unfolded conformation, such as those induced by high temperature, are known to lead to protein aggregation (intermolecular interactions) and eventually precipitation (Chi, Krishnan, Randolph, & Carpenter, 2003; Murphy & Kendrick, 2007). However, complete unfolding is not required and also only partially unfolded structures may be prone to aggregate. In complex media such as wines, aggregation may involve proteins only, but can also result from attractive interactions between proteins and other non-protein compounds, as well-known for polyphenols. The presence of different protein structures, along with a large diversity in wine composition, makes the elucidation of mechanisms a very complex task and information is still required to rationalise both stability/instability trials and stabilization operations.

Thanks to the identification of the I10 wine protein composition it was possible to evaluate here the sensitivity of each protein family to heat-induced precipitation. Haze-forming precipitates were removed by centrifugation, and proteins in the pellets (results non shown) and non-precipitated proteins in the heat-treated wine (Fig. 4) were analysed and quantified by 1D-electrophoresis and image analysis. Results showed differences between the various protein families. The most heat-unstable were found to be glucanases (band 2); most of them were precipitated by a 30 min heat-treatment at a temperature as low as 40 °C. By contrast, temperatures higher than 60 °C were needed to significantly affect invertases (band 1). At 70 °C an important reduction of the invertase band was observed and most of them were removed when the temperature was raised to 80 °C. Chitinases (bands 3 and 4) and thaumatin-like proteins (bands 5, 6) exhibited different behaviours, depending on the considered structures. Increasing the temperature between 40 and 80 °C progressively induced an increasing precipitation of chitinases in band 4, most being eliminated after 30 min at 70 °C. Two different behaviours were observed for chitinases in band 3: most of them were highly sensitive to heat-induced precipitation (85% were precipitated at 40 °C, as glucanases) but others (15%) remained unaffected by temperatures below 80 °C. Thaumatin-like proteins were broadly more stable than chitinases, in accordance with previous results (Waters et al., 1992). The disparities observed here for chitinases and thaumatins could be related to the strong micro-heterogeneities evidenced between structurally similar wine proteins (Monteiro et al., 2001). Such micro-heterogeneities, which cannot be resolved by techniques based on separation according to the mass or the charge, were attributed to the limited proteolysis of common precursors during the wine-making process, generating a large number of structurally related but different polypeptides. Such a limited proteolysis is sufficient to induce subtle changes in the balance of intramolecular forces that affect protein conformational stability (Murphy & Kendrick, 2007). In the present conditions a large part of the proteins in the band 7 (40%) did not precipitate, even for temperatures as high as 80 °C. Proteins in band 7 were thaumatins (about 4 mg l^{-1}), along with low molecular weight (14 kDa) proteins (about 27 mg l^{-1}), not separated by the applied experimental conditions (12% acrylamide gel).

In most cases, heat-induced precipitation of wine proteins is studied using heat-tests performed at high temperature. The most widely used is that proposed by Pocock and Rankine (1973), which consists in a 6 h −80 °C treatment followed by cooling down during 12 h at 4 °C. Present results evidence that heat-induced aggregation is prone to occur for much less drastic conditions than those usually applied in these tests. They also emphasised the high heat-sensitivity of β-glucanases. This last protein class is not always found in white wines, where its presence was underlined only

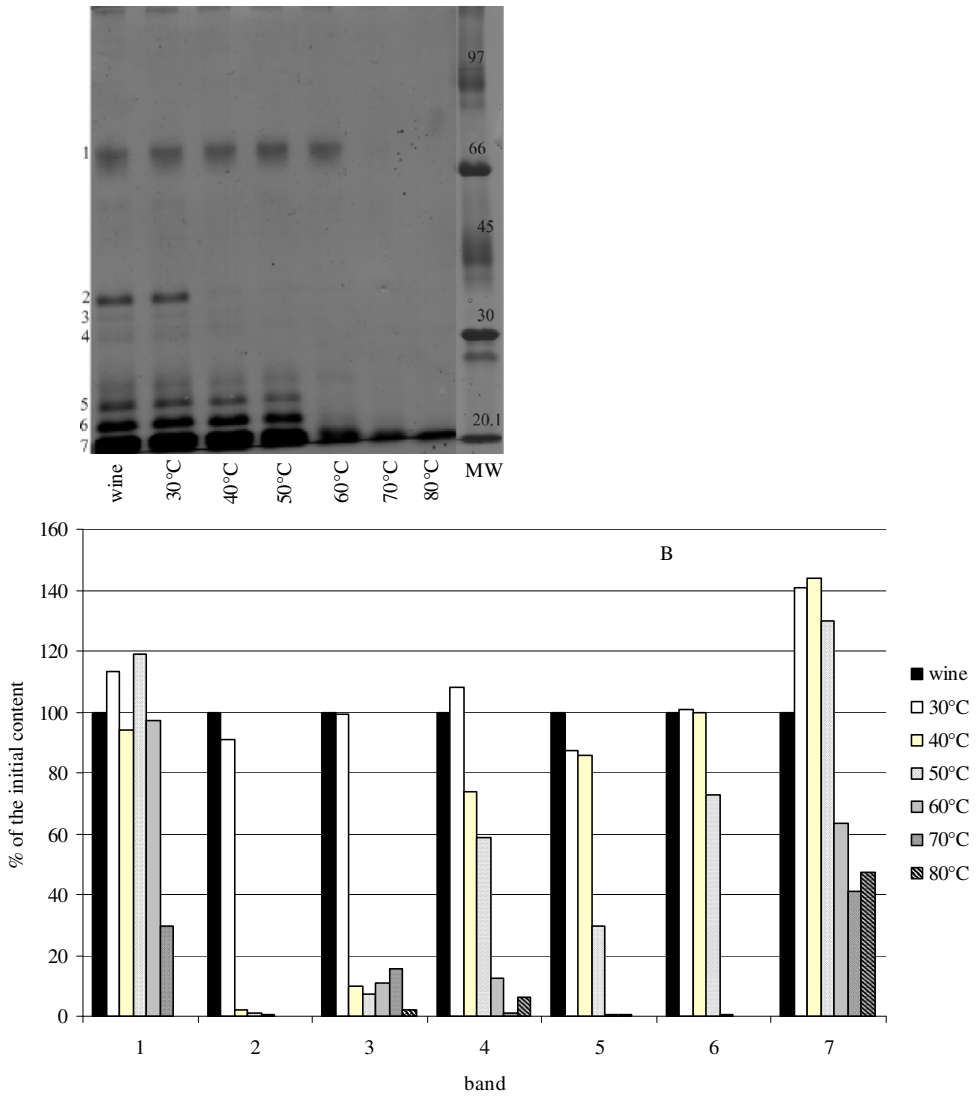

Fig. 4. Protein patterns in the I10 Chardonnay wine following to 30 min heat-treatments at different temperatures. (A) SDS–PAGE Electrophoresis (12% acrylamide resolving gel, Coomassie staining) performed on aliquots of heated-wine supernatants after cooling down and haze removal by centrifugation (molecular weight standard proteins on the right). (B) Protein contents in the supernatants as quantified by image analysis, in percentage of each protein band with regards to the initial wine. Band 1: invertases (initial content 12 mg l^{-1}); band 2: glucanases (initial content 9 mg l^{-1}); bands 3 and 4: chitinases (initial contents 8 and 11 mg l^{-1}, respectively); bands 5, 6: thaumatin-like proteins (initial contents 17 and 54 mg l^{-1}, respectively); band 7 (31 mg l^{-1}): low molecular weight unknown proteins (14 kDa, 87%) and thaumatins (13%), not separated here due to the experimental conditions (acrylamide percentage in gel of 12% and resolving gel length 60 mm).

three times (Cilindre et al., 2007; Esteruelas et al., 2009). It was recently found to be involved in naturally occurring hazes that had formed in a Sauvignon wine, along with VVTL1 thaumatin-like protein and ripening-related protein grip22 precursor (Esteruelas et al., 2009). Proteins in these spontaneous hazes were associated with phenolics and polysaccharides, present in quantitatively comparable levels. It is important to mention that β-glucanases in the I10 wine exhibited significantly higher isoelectric point (IEP) values than the other protein fractions (Fig. 3), and were then more distant from their IEP in the wine pH range. Heat-induced precipitation of proteins involves two distinct phenomena, protein unfolding and colloidal aggregation, which both are strongly influenced by protein charge (Chi et al., 2003). The influence of that charge on both intramolecular and intermolecular interactions is however complex and cannot be discussed on the only basis of protein isoelectric point; it also depends on the overall charge density and on the charged group distribution within the structure (random or anisotropic). Such structural information, along with information related to the other wine macromolecules (Vernhet, Pellerin, Prieur, Osmianski, & Moutounet, 1996), is needed to identify the exact physico-chemical mechanisms involved in protein instabilities in wines.

3.4. Protein adsorption on bentonite

Bentonite fining is the most common treatment applied to achieve white wine stabilization with regards to protein haze. One millilitre aliquots of the Chardonnay wine were treated with increasing bentonite doses, up to 150 g hl^{-1}. Adsorption was studied by the analysis of residual proteins in the fined wine along with that of the adsorbed proteins. More than 50% of the whole protein content was removed with 50 g hl^{-1} bentonite (Fig. 5). Increasing this dose up to 100 g hl^{-1} resulted in the removal of 85% of the protein content. About 15% of this protein content remained non-adsorbed even for a bentonite concentration as high as 150 g hl^{-1}, indicating that the concerned structures only have low affinity for the clay particles. Residual proteins all belonged to the thaumatin-like family. Protein patterns clearly showed selectivity in pro-

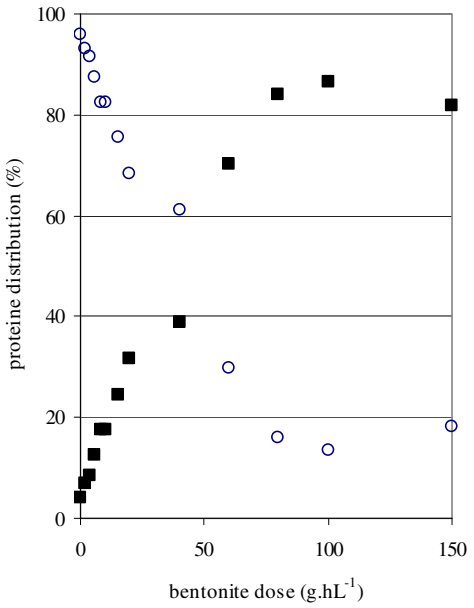

Fig. 5. Quantification of adsorbed (■) and non-adsorbed (○) proteins in the I10 wine after bentonite fining. Results are expressed in % of the whole protein content.

tein adsorption by bentonite (Fig. 6). Glucanases were adsorbed first, along with part of the thaumatin-like and low MW (14 kDa) proteins (in the order of 20%). Doses as low as 6 g hl^{-1} were enough to achieve glucanase depletion in the experimental wine. Chitinase adsorption started from 8 to 10 g hl^{-1} bentonite, progressively increased with increasing clay doses and was complete at 60 g hl^{-1}. The adsorption of thaumatin-like and 14 kDa proteins continued in parallel. A plateau value (70% adsorption) was reached for thaumatins at bentonite doses between 60 and 80 g hl^{-1}, while at 80 g hl^{-1} the depletion of 14 kDa proteins was achieved. Invertase adsorption only began at 20 g hl^{-1} and was total at 100 g hl^{-1}. Differences between wine proteins with regards to their removal by bentonite are in accordance with the earlier observations of Hsu and Heatherbell (1987). However in their work, the protein identities were still unknown.

Depletion of the protein fractions in the I10 wine as a function of bentonite concentration has to be compared to their sensitivity towards heat-induced precipitation. Glucanases, that exhibited the highest affinity for the clay, were the most heat-sensitive. Invertases, that needed the highest bentonite doses to be removed, were shown to be the most resistant to heat-induced precipitation. Chitinases, low molecular weight proteins and thaumatins exhibited intermediate behaviours, as observed with heat trials, and a specific part of the thaumatin (≈30%) remained unaffected for bentonite doses lower than 150 g hl^{-1} (it must be noted that this adsorption is achieved at a dose of 200 g hl^{-1}). Protein adsorption at interfaces often involves structural changes (partial or total unfolding) due to the formation of physico-chemical bonds between protein amino-acids and surface interaction sites (Haynes & Norde, 1995). Such structural changes have been evidenced for protein adsorption on negatively charged montmorillonites (main component of bentonites) when adsorption occur at pH values lower than the protein isoelectric point (Gougeon et al., 2003; Servageant-Noinville, Revault, Quiquampoix, & Baron, 2000). The relationship between protein adsorption on bentonite and their sensitivity to heat-induced precipitation could then be linked to their inherent conformational stability. As already discussed, the different behaviours observed in a given protein family, especially important for chitinases and thaumatins, could be related to micro-heterogeneities generated between structurally similar proteins by grape processing (Monteiro et al., 2001).

3.5. Consequences for stability tests and bentonite fining trials

Though the use of heat-stability tests to warrant white wine stability during transport and storage is a prevalent practice, the question of how they really predict situations that may occur during wine storage and transport is not yet solved. Indeed, only few works have been devoted to the study of the relationship between test procedures and long term stability of wines in real (long-time

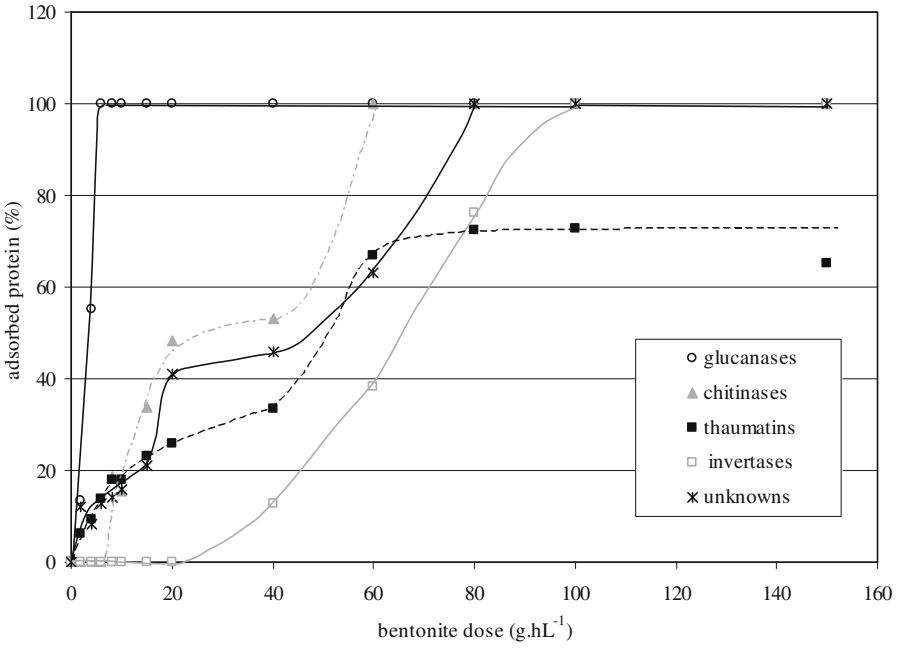

Fig. 6. Percentage of adsorbed proteins as a function of the bentonite dose, represented for each different protein family. Results showed selectivity in protein removal by the clay particles.

– low temperature) conditions (Pocock & Waters, 2006). The fact that the same tests, associated with bentonite fining trials, are used to determine the bentonite doses needed to stabilise wines raises the question of the relevance of these doses. Solving this question is a complex task due to wine variability and to incomplete knowledge concerning: (i) the precise structures and physico-chemical properties of wine proteins and, (ii) the mechanisms actually involved in their instability, including the influence of non-protein compounds. Results of the present work provide however some information to direct further studies devoted to the rationalisation of heat-test use.

With the experimental Chardonnay wine, a correlation was found between protein sensitivity to heat-induced precipitation and their removal by bentonite; the most heat-sensitive fractions were those that were also adsorbed first. These fractions are also those most likely to precipitate under excessive temperature exposure during practical storage and transport conditions. It could then be concluded that usual heat-tests, which induce the precipitation of almost all wine proteins including invertases, lead to an overestimation of the bentonite doses required for stabilization. These doses should be reasoned considering the different sensitivity of wine proteins and the conditions actually met in bottled wines. Additional information is needed to be in position to propose such less drastic heat-stability test conditions. First, heat-tests in the present study were performed at different temperatures but for a given incubation duration of 30 min. As temperature is known to affect protein unfolding rates, kinetics of heat-induced precipitation of the different protein classes have to be determined for different temperatures. Moreover, results must be validated using a large selection of wines because: (i) the wine composition is known to influence protein heat-stability and aggregation; (ii) if most wines were shown to contain the same set of structurally related proteins, the micro-heterogeneities evidenced within a same protein family (Monteiro et al., 2001) may be wine-dependent and induce conflicting results. Finally, all these results will have to be correlated with realistic storage conditions to validate the new test.

Acknowledgements

The authors thank VINIFLHOR for their financial support.

References

Bayly, F. C., & Berg, H. W. (1967). Grape and wine proteins of white wine varietals. *American Journal of Enology and Viticulture, 24*, 18–32.

Bayonove, C., Cabaroglu, T., Dufour, C., Razungles, A., Sapis, J.-C., Baumes, R., et al. (1995). *Influence du collage sur le potentiel aromatique variétal du vin*. Uruguay: XXIème Congrès de la Vigne et du Vin.

Besse, C., Clarck, A., & Scollary, G. (2000). Investigation of the role of total and free copper in protein haze formation. *The Australian Grapegrower and Winemaker, 437*, 19–20.

Bradford, M. (1976). A rapid and sensitive method for the quantification of microgram quantities of protein utilizing the principle of protein–dye binding. *Analytical Biochemistry, 72*, 248–254.

Brissonnet, F., & Maujean, A. (1993). Characterization of foaming proteins in a champagne base wine. *American Journal of Enology and Viticulture, 44*, 297–301.

Cabaroglu, T., Canbas, A., Lepoutre, J.-P., & Gunata, Z. (2002). Free and bound volatile composition of red wines of *Vitis vinifera L.* cv. Okuzgozu and Bogazkere grown in Turkey. *American Journal of Enology and Viticulture, 53*(1), 63–68.

Chi, E. Y., Krishnan, S., Randolph, T. W., & Carpenter, J. F. (2003). Physical stability of proteins in aqueous solutions: Mechanisms and driving forces in nonnative protein aggregation. *Pharmaceutical Research, 20*(9), 1325–1336.

Cilindre, C., Castro, A. J., Clément, C., Jeandet, P., & Marchal, R. (2007). Influence of Botritis cinerea infection on Champagne wine proteins (characterised by two-dimensional electrophoresis/immunodetection) and wine foaming properties. *Food Chemistry, 103*(1), 139–149.

Dawes, H., Boyes, S., Keene, J., & Heatherbell, D. A. (1994). Protein instability of wines: Influence of protein isoelectric point. *American Journal of Enology and Viticulture, 45*(3), 319–326.

Dubourdieu, D., & Canal-Llaubère, R. M. (1989). Influence of some colloids (polysaccharides and proteins) on the clarification and stabilization of wines. In *Proceedings of the seventh Australian wine industry technical conferences* (pp. 180–185) [13–17 August 1989].

Dupin, I. V. S., McKinnon, B. M., Ryan, C., Bouley, M., Markides, A. J., Jones, G. P., et al. (2000). *Saccharomyces cerevisiae* mannoproteins that protect wine from protein haze: Their release during fermentation and lees contact and a proposal for their mechanism of action. *Journal of Agricultural and Food Chemistry, 48*(8), 3098–3105.

Esteruelas, M., Poinsaut, P., Sieczkowski, N., Manteau, S., Fort, M. F., Canals, J. M., et al. (2009). Characterization of natural haze protein in sauvignon white wine. *Food Chemistry, 113*, 25–38.

Ferreira, R. B., Monteiro, S., Piçarra-Pereira, M. A., Tanganho, M. C., Loureiro, V. B., & Teixeira, A. R. (2000). Characterization of the proteins from grapes and wines by immunological methods. *American Journal of Enology and Viticulture, 51*(1), 22–28.

Ferreira, R. B., Piçarra-Pereira, M. A., Monteiro, S., Loureiro, V. B., & Teixeira, A. R. (2002). The wine proteins. *Trends in Food Science and Technology, 12*(6–7), 230–239.

Giribaldi, M., Perugini, I., Sauvage, F. X., & Schubert, A. (2007). Analysis of protein changes during grape berry ripening by 2-DE and MALDI-TOF. *Proteomics, 7*(17), 3154–3170.

Görg, A., Weiss, W., & Dunn, M. (2004). Current two-dimensional electrophoresis technology for proteomics. *Proteomics, 4*(12), 3665–3685.

Gougeon, R. D., Soulard, M., Miehé-Brendlé, J., Chézeau, J.-M., Le Dred, R., Jeandet, P., et al. (2003). Analysis of two bentonites of enological interest before and after commercial activation by solid Na_2CO_3. *Journal of Agricultural and Food Chemistry, 51*(14), 4096–4100.

Haynes, C. A., & Norde, W. (1995). Structures and stabilities of adsorbed proteins. *Journal of Colloid and Interface Science, 169*, 313–328.

Hoj, P. B., Tattersall, D. B., Adams, K., Pocock, K. F., Hayasaka, Y., van Heeswijck, R., & Waters, E. J. (2001). The ''haze proteins" of wine – A summary of properties, factors affecting their accumulationin grapes, and the amount of bentonite required for their removal from wines. In *Proceedings of the ASEV 50th anniversary meeting* (pp. 149–154). Seattle, Washington, USA.

Hsu, J.-C., & Heatherbell, D. A. (1987). Heat-unstable proteins in wine. I. Characterization and removal by bentonite fining and heat-treatment. *American Journal of Enology and Viticulture, 38*(1), 11–16.

Mesquita, P. R., Piçarra-Pereira, M. A., Monteiro, S., Loureiro, V. B., Teixeira, A. R., & Ferreira, R. B. (2001). Effect of wine composition on protein stability. *American Journal of Enology and Viticulture, 52*, 324–330.

Monteiro, S., Piçarra-Pereira, M. A., Mesquita, P. R., Loureiro, V. B., Teixeira, A. R., & Ferreira, R. B. (2001). The wide diversity of structurally similar wine proteins. *Journal of Agricultural and Food Chemistry, 49*(8), 3999–4010.

Murphey, J. M., Spayd, S. E., & Powers, J. R. (1989). Effect of grape maturation on soluble protein characteristics of gewürztraminer and white riesling juice and wine. *American Journal of Enology and Viticulture, 40*(3), 199–207.

Murphy, R. G., & Kendrick, B. S. (2007). Protein misfolding and aggregation. *Biotechnology Progress, 23*(3), 548–552.

Neuhoff, V., Arold, N., Taube, D., & Ehrhadt, W. (1988). Improved staining of proteins in polyacrylamide gels including isoelectric focusing gels with clear background at nanogram sensitivity using Coomassie Brilliant Blue G-250 and R-250. *Electrophoresis*(9), 255–262.

Pocock, K. F., Alexander, G. M., Hayasaka, Y., Jones, P. R., & Waters, E. J. (2007). Sulfate – A candidate for the missing essential factor that is riquired for the formation of protein haze in white wine. *Journal of Agricultural and Food Chemistry, 55*(5), 1799–1807.

Pocock, K. F., Hayasaka, Y., Mc Carthy, G., & Waters, E. J. (2000). Thaumatin-like proteins and Chitinases, the haze forming proteins of wine, accumulate during ripeninfg of grape (*Vitis vinifera*) berries and drought stress does not affect the final level per berry at maturity. *Journal of Agricultural and Food Chemistry, 48*(5), 1637–1643.

Pocock, K. F., Hayasaka, Y., Peng, Z., Williams, P. J., & Waters, E. J. (1998). The effect of mechanical harvesting and long-distance transport on the concentration of haze-forming proteins in grape juice. *Australian Journal of Grape and Wine Research, 4*, 23–29.

Pocock, K. F., & Rankine, B. C. (1973). Heat test for detecting protein instability in wine. *Australian Wine Brewing Spirit Revue, 91*, 42–43.

Pocock, K. F., & Waters, E. J. (2006). Protein hazes in bottled white wines: How well do stability tests and bentonite fining trials predict haze formation during storage and transport? *Australian Journal of Grape and Wine Research, 12*, 212–220.

Santoro, M. (1995). Fractionation and characterization of must and wine proteins. *American Journal of Viticulture and Enology, 46*(2), 250–254.

Servageant-Noinville, S., Revault, M., Quiquampoix, H., & Baron, M. H. (2000). Conformational changes of Bovine Serum Albumin induced by adsorption on different clay surfaces: FTIR analysis. *Journal of Colloid and Interface Science, 221*(2), 273–283.

Vernhet, A., Pellerin, P., Prieur, C., Osmianski, J., & Moutounet, M. (1996). Charge properties of some grape and wine polysaccharide and polyphenolic fractions. *American Journal of Enology and Viticulture, 47*(1), 25–30.

Vincenzi, S., Polesani, M., & Curioni, A. (2005). Removal of specific protein compounds by chitin enhanced protein stability in white wine. *American Journal of Viticulture and Enology, 56*(3), 246–254.

Waters, E. J., Alexander, G., Muhlack, R., Pocock, K. F., Colby, C., O'Neill, B. K., et al. (2005). Preventing protein haze in bottled white wine. *The Australian Journal of Grape and Wine Research, 11*, 215–225.

Waters, E. J., Dupin, I., & Stockdale, V. (2000). A review of current knowledge on polysaccharides which "protect" against protein haze in white wines. *The Australian Grapegrower and Winemaker, Annual Technical Issue* (pp. 14–16).

Waters, E. J., Peng, Z., Pocock, K. F., & Williams, P. J. (1995). Proteins in white wine, I: Procyanidin occurence in soluble proteins and insoluble protein hazes and its relationship to protein instability. *Australian Journal of Grape and Wine Research, 1*, 86–93.

Waters, E. J., Wallace, W., & Williams, P. J. (1991). Heat haze characteristics of fractionated wine proteins. *American Journal of Enology and Viticulture, 42*(2), 123–127.

Waters, E. J., Wallace, W., & Williams, P. J. (1992). Identification of heat-unstable proteins and their resistance to peptidases. *Journal of Agricultural and Food Chemistry, 40*(9), 1514–1519.

Food Chemistry 118 (2010) 35–41

Contents lists available at ScienceDirect

Food Chemistry

journal homepage: www.elsevier.com/locate/foodchem

Effects of Trolox and ascorbic acid on the riboflavin photosensitised oxidation of aromatic amino acids

Ramesh R. Yettella, David B. Min *

Department of Food Science and Technology, The Ohio State University, 2015 Fyffe Road, Columbus, OH 43210, United States

ARTICLE INFO

Article history:
Received 8 September 2008
Received in revised form 8 April 2009
Accepted 9 April 2009

Keywords:
Riboflavin
Aromatic amino acids
Singlet oxygen
Trolox
Ascorbic acid

ABSTRACT

The effects of 0, 100, 250, 500, 750 or 1000 ppm Trolox and ascorbic acid on the singlet oxygen oxidation of aromatic amino acids viz. phenylalanine, tryptophan, tyrosine in the presence of 25 ppm riboflavin were determined by measuring depleted headspace oxygen by gas chromatography and aromatic amino acid content by high performance liquid chromatography. The coefficients of variations (CVs) for headspace oxygen analysis and HPLC analysis of aromatic amino acids were 1.4% and 4.7%, respectively. Samples were stored under light (1000 lux) at 30 °C for 10 h. Both Trolox and ascorbic acid acted as antioxidants. As the concentration of Trolox and ascorbic increased from 0 to 1000 ppm, the head space oxygen depletion increased. This was due to the oxidation of Trolox and ascorbic acid along with amino acids in the presence of riboflavin. High performance liquid chromatography analysis of the samples clearly indicated that both Trolox and ascorbic acid minimised the degradation of phenylalanine, tryptophan, tyrosine significantly ($p < 0.05$), but did not prevent their oxidation completely. Trolox acted as a better antioxidant than ascorbic acid in protecting phenylalanine, tryptophan and tyrosine. Type-I mechanism was mainly responsible for riboflavin photosensitised degradation of aromatic amino acids.

1. Introduction

Riboflavin is naturally present in milk, eggs, meat products and vegetables. It is an active part of coenzymes such as flavin mononucleotide (FMN) and flavin adenine dinucleotide (FAD) that catalyse oxidation–reduction reactions (Choe, Huang, & Min, 2005). Riboflavin has complex photochemistry because of its ability to accept or lose a pair of hydrogen atoms (Crank & Pardijanto, 1995; Criado, Castillo, Yppolito, Bertolotti, & Garcia, 2003; Edwards et al., 1996; Kim, Kirschenbaum, Rosenthal, & Riesz, 1993; Li & Min, 1998; Viteri, Edwards, La Fuente, & Silva, 2003). Riboflavin under light can generate reactive oxygen species such as super oxide anions and singlet oxygen (Grzelak, Rycjlik, & Bartosz, 2001; Mahns, Melchheier, Suschek, Sies, & Klotz, 2003; Min & Boff, 2002). Formation of reactive oxygen species by riboflavin under light proceeds by both Type-I and Type-II mechanisms (Rochette, Birlouez-Aragon, Silva, & Morliere, 2003). After receiving light energy from light, riboflavin becomes excited triplet riboflavin. In the Type-I mechanism, the excited triplet riboflavin is reduced by abstraction of electrons or hydrogen ion from other food components to form riboflavin radical. In the Type-II mechanism, the excited triplet riboflavin reacts with atmosphere triplet oxygen to produce superoxide anion or singlet oxygen (Foote, 1985).

The interaction of singlet oxygen with biological molecules is of special interest both because of its effect on essential biological structures and also because in the treatment of malignancies by photodynamic therapy (Dougherty, 1992). Most of the research in the singlet oxygen oxidation of proteins has been done in the medical and pharmaceutical fields. Singlet oxygen reacts with proteins, peptides and amino acids in a variety of media (Kanofsky, 1990). The aromatic amino acids tyrosine and tryptophan as well as histidine and the sulphur containing methionine and cysteine are the major targets of attack by singlet oxygen, while aliphatic amino acids react with singlet oxygen at a significantly lower rate ($k \sim 10^4$–10^5 M^{-1} S^{-1}) (Lissi, Encinas, Lemp, & Rubio, 1993).

The indole ring of tryptophan, imidazole ring of histidine and phenol ring of tyrosine contain electron rich double bonds and can readily react with electrophilic singlet oxygen. Methionine and cysteine contain sulphur atoms with four non bonding electrons which readily react with electrophilic singlet oxygen. As amino acids become altered by singlet oxygen, the proteins and enzymes get denatured, lose functionality and can aggregate.

Song, An, and Jiang (1999) reported the use of histidine in several analytical techniques involving singlet oxygen. The reaction rate of singlet oxygen oxidation with amino acids and proteins depends on pH, temperature, the dielectric constant of the medium and the presence of singlet oxygen reactive amino acids as mentioned above. Bisby, Morgan, Hamblett, and Gorman (1999) reported that pH influences N-acetyl tyrosine ethyl ester and

* Corresponding author. Tel.: +1 614 292 7801; fax: +1 614 292 0218.
E-mail address: min.2@osu.edu (D.B. Min).

0308-8146/$ - see front matter © 2009 Elsevier Ltd. All rights reserved.
doi:10.1016/j.foodchem.2009.04.022

amino acids. Singlet oxygen rate constant (k_t) by histidine is greatest when the pH $\gg$ pK_a (5×10^7) compared to 10^6 when pH $\ll$ pK_a. Fully protonated histidine had a k_t of 10^4. Tryptophan does not have any ionisable protons in the ionisable groups in the tested pH range, so did not show any pH effect. Their research showed that deprotonation of phenols in tyrosine results in an increase in k_t.

Michaeli and Feitelson (1995) compared the singlet oxygen reaction rate of large peptides to a solution of a comparative concentration of amino acids to each respective peptide. The free amino acids had a higher oxidation rate than did the native peptide. The reaction between amino acids and singlet oxygen is solvent dependent (Miskoski & Garcia, 1993). Some amino acids act as both physical and chemical quenchers. The singlet oxygen reaction rate constant of proteins is dependent on the types of amino acids, their accessibility to singlet oxygen and the dielectric constant of the medium (Michaeli & Feitelson, 1994). Jung, Kim, and Kim (1995) reported that histidine and tyrosine accelerated the riboflavin sensitised destruction of ascorbic acid and suggested that intermediate products of amino acid and singlet oxygen accelerated the oxidation of ascorbic acid.

Trolox is a water soluble analogue of α-tocopherol. Trolox is similar in structure to tocopherol with chroman ring but lacks a hydrophobic tail (Priyadarshini, Kapoor, & Naik, 2001). The phytyl tail of α-tocopherol is substituted with a carboxylic group which makes Trolox soluble in polar media. Trolox has been proved to be a better antioxidant than α-tocopherol under a wide range of conditions and test systems (Cort et al., 1975). Ascorbic acid acts as a primary and secondary antioxidant. Ascorbic acid has strong quenching ability for reactive oxygen species such as singlet oxygen and superoxide anion radical by converting their hydroperoxides into stable products (Jung, Lee, & Kim, 2000).

Many studies have reported the riboflavin photosensitised oxidation of amino acids while none reported how to minimise the photosensitised oxidation of amino acids and the antioxidant properties of Trolox and ascorbic acid on the photosensitised oxidation of amino acids. The objectives of this study was to study the effects of Trolox and ascorbic acid on inhibiting the oxidation of phenylalanine, tryptophan and tyrosine in the presence of riboflavin in aqueous model system and to study the nature of reactions (i.e. Type-I or Type-II) during riboflavin photosensitised oxidation of phenylalanine, tryptophan and tyrosine.

2. Materials and methods

2.1. Materials

Trolox (>98.0%), ascorbic acid (>99.5%), riboflavin (>99.9%) phenylalanine (Phe), tryptophan (Trp), tyrosine (Tyr) and NaH_2PO_4 ($\geqslant$99.9%) were purchased from Sigma Chemical Co. (St. Louis, MO). HPLC grade acetonitrile ($\geqslant$99.9%) and methanol ($\geqslant$99.9%) were obtained from Sigma Chemical Co. (St. Louis, MO). Serum bottles, Teflon lined rubber septa and aluminium caps were purchased from Supelco Inc. (Beelfonte, PA). HPLC grade water (Sigma, St. Louis, MO) was used as solvent for sample preparation. The purity of all amino acids used in this study was $\geqslant$99.5%.

2.2. Effects of Trolox or ascorbic acid on the degradation of phenylalanine, tryptophan and tyrosine

Aqueous solutions of 0, 100, 250, 500, 750 or 1000 ppm Trolox or ascorbic acid with 25 ppm riboflavin and 1.25% of phenylalanine, tryptophan and tyrosine were prepared separately to study the effect of Trolox or ascorbic acid on the stability of Phe, Trp and Tyr. The bottles were stored in a light storage box of 1000 lux (Li, King, & Min, 2000) or in the dark at 30 °C. Phe, Trp and Tyr concentrations in the serum bottles were determined in duplicate after 2, 4, 6, 8, 10 h of storage in the light box.

Aqueous solutions of 0, 0.3, 0.6 and 0.9 mM Trolox or ascorbic acid with 100 μM riboflavin and 40 mM Phe, Trp and Tyr were prepared separately to study favourable pathway, i.e. Type-I or Type-II, in the riboflavin photosensitised oxidation of Phe, Trp and Tyr. The bottles were stored in a light storage box for 4 h as mentioned above.

2.3. Effect of Trolox or ascorbic acid on the head space oxygen depletion of samples containing phenylalanine, tryptophan and tyrosine

Aqueous solutions of 0, 100, 250, 500, 750 or 1000 ppm Trolox or ascorbic acid with 25 ppm riboflavin and 1.25% of Phe, Trp and Tyr were prepared separately to study the effect of Trolox or ascorbic acid on the head space oxygen depletion. The bottles were stored in a light storage box of 1000 lux (Li et al., 2000) or in the dark at 30 °C. The head space oxygen in the serum bottles was determined in duplicate after 2, 4, 6, 8, 10 h of storage in the light box.

2.4. Effects of riboflavin on the photosensitised oxidation of Trolox and ascorbic acid

Aqueous solutions of 500 ppm Trolox or ascorbic acid with 25 ppm riboflavin were prepared separately to study the effect of riboflavin on the photosensitised oxidation of Trolox or ascorbic acid. The bottles were stored in a light storage box of 1000 lux (Li et al., 2000) or in the dark at 30 °C. Trolox and ascorbic acid concentrations in the serum bottles were determined in duplicate after 2, 4, 6, 8, 10 h of storage in the light box.

2.5. Headspace oxygen determination

The head space oxygen of each sample was analysed every 0, 2, 4, 6, 8, 10 h for oxygen content after equilibration to 20 °C in a water bath (Precision® Model 260, Winchester, VA) for 15 min. Headspace oxygen in the sample bottles was analysed by injecting a 100 μL headspace sample into a HP 5890 gas chromatograph equipped with a stainless-steel molecular sieve column (13×, 80:100; Alltech, Deerfield, IL) and a thermal conductivity detector (GOW-MAC® Instrument Company, Bethlehem, PA) (King & Min, 1998). High-purity helium (99.99%) was used as carrier gas. The flow rate was 40 mL/min. The GC oven temperature was maintained at 40 °C. The temperature at the injector port and detector were maintained at 120 and 150 °C, respectively. Duplicated injections were performed for each sample bottle. Electronic counts were integrated on an HP 3396A integrator (King & Min, 1998; Yang, Lee, & Min, 2002).

2.6. Determination of phenylalanine, tryptophan and tyrosine content by HPLC

The concentrations of Phe, Trp and Tyr in the samples were determined by HPLC analysis (Agilent 1100, Santaclara, CA) equipped with C-18 Zorbax Eclipse AAA column (3.5 μm, 4.6 × 75 mm) (Agilent Technologies, Santaclara, CA), diode array detector (Agilent Technologies, Santaclara, CA), manual injector (Rheodyne Model 7725i, Oakharbor, WA) and Agilent HPLC software (Agilent Technologies, Santaclara, CA). Samples were filtered with a 0.2 μm membrane filter (Corning Inc., Corning, NY). The injection volume was 20 μL. The flow rate of the mobile phase was 1.0 mL/min. For the separation of amino acids the following gradient system was used; 100% A at 0 and 1 min; gradient to 43% A and 57% B at 9.8 min; 100% B at 10 and 12 min; 0% B at

12.5 and 14 min (Solvent A – NaH_2PO_4; Solvent B – acetonitrile (45):methanol (45):water (10)). Spectral data (210–350 nm) was collected during the whole run. Elution of compounds was monitored at wavelength 254 nm for phenylalanine and tyrosine and 257 nm for tryptophan. Phenylalanine, tryptophan and tyrosine concentrations were calculated using a standard curve.

2.7. Trolox and ascorbic acid analysis content by HPLC

Trolox and ascorbic acid concentration in the samples were determined by HPLC analysis (Agilent 1100, Santaclara, CA) equipped with an aqua C-18 column (5 μM, 150 mm × 4.60 mm) (Phenomenex, Torrance, CA), diode array detector (Agilent Technologies, Santaclara, CA), manual injector (Rheodyne Model 7725i, Oakharbor, WA) and Agilent HPLC software (Agilent Technologies, Santaclara, CA). Samples were filtered with 0.2 μM membrane filter (Corning Inc., Corning, NY) before injection. The injection volume was 20 μL. The flow rate of mobile phase (methanol:water = 3:7 (v/v)) was 1.0 mL/min. Spectral data (210–350 nm) was collected during the whole run. Elution of compounds was monitored at wavelength 254 nm for ascorbic acid and 294 nm for Trolox. The concentration of Trolox and ascorbic acid were calculated using a standard curve.

2.8. Light storage conditions for the oxidative study

The light storage box consisted of two rectangular chambers: a glass chamber (60 cm × 30 cm × 50 cm) for sample storage and the wooden box (70 cm × 50 cm × 60 cm) for light sources. The distance from the light sources to the glass chamber was 12 cm. Samples were placed on a wire netting which was 10 cm above the bottom of the glass chamber. The light sources, four Sylvania 15 W cool white fluorescent lamps (Danvers, MA), were placed on the bottom of the wooden box. The light intensity at the sample level was about 1000 lux.

2.9. Statistical analysis

All the experiments were done in duplicate. Analysis of variance (ANOVA) was used to determine if antioxidant levels, storage duration were significant factors in the photooxidation of amino acids. Means were compared using Tukey's studentised range using XLSTAT at $\alpha = 0.05$ (Microsoft 2007).

3. Results and discussion

3.1. Reproducibility of analysis

The coefficients of variation for headspace oxygen analysis and HPLC analysis of amino acids were 1.4% and 4.7%, respectively (data not shown). The low coefficients of variation were considered good and indicated that headspace oxygen and HPLC analyses were reproducible methods to study oxidation of amino acids in the presence of riboflavin.

3.2. Effects of Trolox and ascorbic acid on the headspace oxygen of aqueous solution containing 1.25% of phenylalanine, tryptophan and tyrosine

The effects of 0, 100, 250, 500, 750 and 1000 ppm of Trolox on the headspace oxygen of aqueous solution containing 1.25% of phenylalanine, tryptophan and tyrosine, with 25 ppm added riboflavin are shown in Figs. 1–3. As the concentration of Trolox increased from 0 to 1000 ppm, the depletion of headspace oxygen increased. After 10 h of storage under light, the headspace oxygen of samples with 0 ppm Trolox and 1.25% phenylalanine was 17.2%,

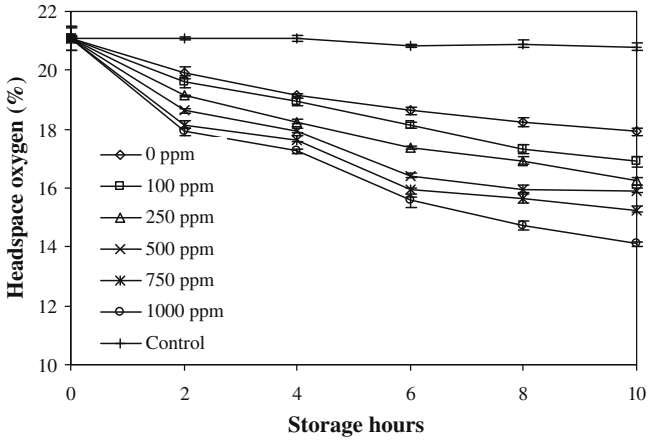

Fig. 1. Effects of Trolox on the headspace oxygen depletion of aqueous solution containing 1.25% phenylalanine and 25 ppm riboflavin under light. Data points represent means ($n = 3$) plus standard deviation.

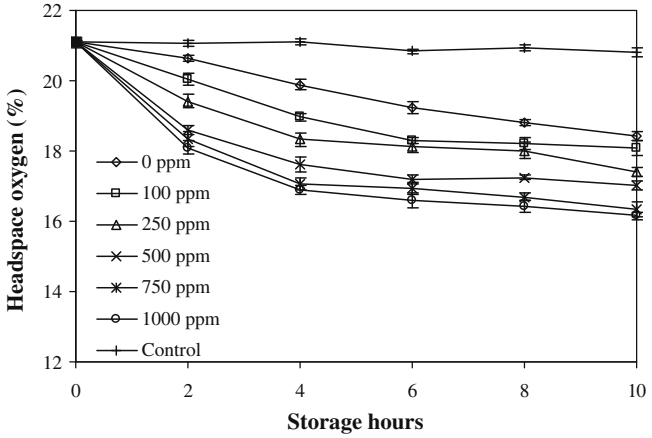

Fig. 2. Effects of Trolox on the headspace oxygen depletion of aqueous solution containing 1.25% tryptophan and 25 ppm riboflavin under light. Data points represent means ($n = 3$) plus standard deviation.

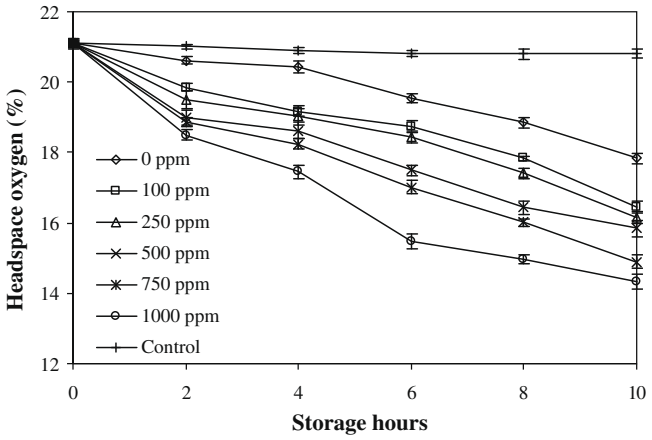

Fig. 3. Effects of Trolox on the headspace oxygen depletion of aqueous solution containing 1.25% tyrosine and 25 ppm riboflavin under light. Data points represent means ($n = 3$) plus standard deviation.

while the headspace oxygen of samples with 1000 ppm Trolox was 14.1% (Fig. 1). But under dark, after 10 h of storage the headspace oxygen remained almost the same at approximately 21% throughout the storage. Similarly, after 10 h of storage the head space

oxygen of the samples with tryptophan and tyrosine was 16.4% and 14.2%, respectively.

The effects of 0, 100, 250, 500, 750 and 1000 ppm of ascorbic acid on the headspace oxygen of aqueous containing 1.25% of phenylalanine, tryptophan, and tyrosine with 25 ppm added riboflavin are shown in Figs. 4–6. As the concentration of ascorbic acid increased from 0 to 1000 ppm, the depletion of headspace oxygen increased. After 10 h of storage under light, the headspace oxygen of samples with 0 ppm ascorbic acid and 1.25% phenylalanine was 16.8%, while the headspace oxygen of model system with 1000 ppm ascorbic acid was 12.6% (Fig. 4). But under dark, after 10 h of storage the headspace oxygen remained almost the same at approximately 21% throughout the storage. Similarly, after 10 h of storage the head space oxygen of the samples with tryptophan and tyrosine was 14.4% and 12.8%, respectively.

Riboflavin had a significant effect on the depletion of headspace oxygen in the samples stored under light but not in dark ($p < 0.05$). The disappearance of headspace oxygen in the airtight bottles was assumed to be a result of the reaction between oxygen, riboflavin and amino acids. Riboflavin in milk or soymilk increased the formation of volatiles and the depletion of headspace oxygen under light (Bradley, Kim, & Min, 2006; Huang, Choe, & Min, 2004c; King & Min, 1998). Jung, Lee, and Min (1998) removed riboflavin in milk by passing it though a Florisil column and the riboflavin-free milk did not produce volatiles during 8 h of storage under light. It suggested that the type of oxygen depleted from the headspace of sample bottles under light might not be the same as the type of oxygen depleted from the headspace of sample bottles in the dark. Ground state riboflavin having conjugated double bonds easily absorbs light and becomes excited singlet riboflavin. The excited singlet state riboflavin becomes excited triplet riboflavin through intersystem crossing mechanism. The diradical excited triplet riboflavin reacts with diradical triplet oxygen to produce singlet oxygen by triplet–triplet annihilation (Huang, Choe, & Min, 2004b; Min & Boff, 2002). Singlet oxygen is electrophilic, very reactive and a high-energy molecule. Singlet oxygen quickly reacts with food components containing double bonds such as riboflavin, polyunsaturated lipids and amino acids.

Singlet oxygen was detected in skim milk by electron spin resonance spectroscopy (Bradley et al., 2006), which showed singlet oxygen was formed in the presence of riboflavin and triplet oxygen. Singlet oxygen cannot be formed in dark, even in the presence of riboflavin. Therefore, the headspace oxygen in the airtight sample bottles stored under light probably decreased due to the formation of singlet oxygen. The type of oxygen lost from the headspace

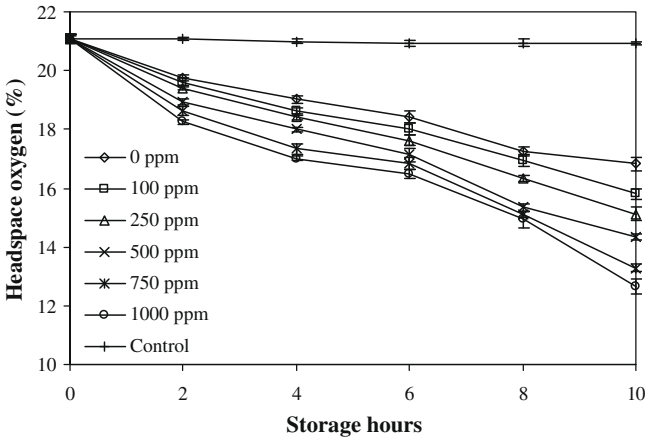

Fig. 4. Effects of ascorbic acid on the headspace oxygen depletion of aqueous solution containing 1.25% phenylalanine and 25 ppm riboflavin under light. Data points represent means ($n = 3$) plus standard deviation.

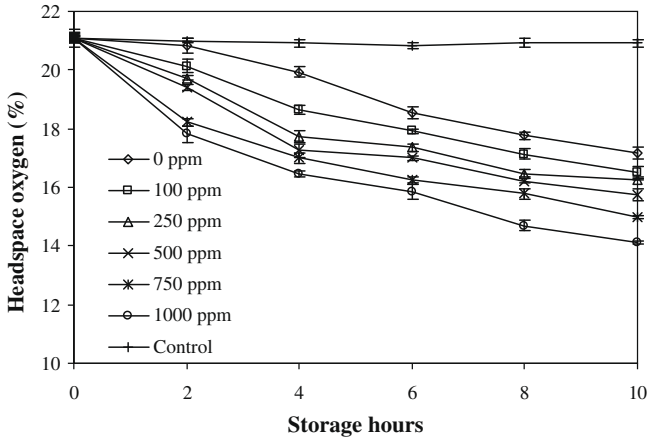

Fig. 5. Effects of ascorbic acid on the headspace oxygen depletion of aqueous solution containing 1.25% tryptophan and 25 ppm riboflavin under light. Data points represent means ($n = 3$) plus standard deviation.

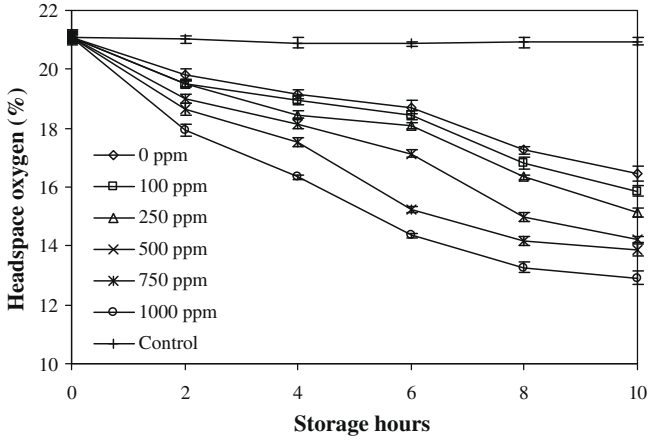

Fig. 6. Effects of ascorbic acid on the headspace oxygen depletion of aqueous solution containing 1.25% tyrosine and 25 ppm riboflavin under light. Data points represent means ($n = 3$) plus standard deviation.

of model system under light was presumably oxygen in its singlet state. The more singlet oxygen formed in model system, the more the headspace oxygen of samples decreased. The samples containing phenylalanine lost most head space oxygen (8.44%) followed by tyrosine (8.18%) and tryptophan (6.96%) at 10 h. But the samples stored in dark were relatively stable, remaining at approximately 21% of oxygen throughout storage.

3.3. Effects of Trolox and ascorbic acid on the retention (%) of phenylalanine, tryptophan and tyrosine (1.25%) under light

The effects of 0, 100, 250, 500, 750 and 1000 ppm of Trolox on the degradation of phenylalanine, tryptophan and tyrosine in the aqueous solution containing with 25 ppm added riboflavin are shown in Tables 1–3. As the concentration of Trolox increased from 0 to 1000 ppm, the degradation of amino acids decreased. After 10 h of storage under light, the samples with 0 ppm Trolox lost 23.6% phenylalanine while the samples with 1000 ppm Trolox lost 12.8% only. Trolox had a significant effect on the retention of phenylalanine, tryptophan and tyrosine at all levels of concentration.

The effects of 0, 100, 250, 500, 750 and 1000 ppm of ascorbic acid on the degradation of phenylalanine, tryptophan and tyrosine in the model system containing with 25 ppm added riboflavin are shown in Tables 4–6. As the concentration of ascorbic acid

Table 1
Effects of Trolox on the retention (%) of phenylalanine (1.25%) under light.[A]

Trolox (ppm)	Phenylalanine retention during storage (%) Storage hours					
	0	2	4	6	8	10
0	100[a]	92.4[a]	86.3[a]	81.4[a]	76.4[a]	73.6[a]
100	100[a]	95.1[b]	92.4[b]	87.0[b]	84.2[b]	79.4[b]
250	100[a]	96.4[c]	93.2[b]	89.2[c]	86.4[c]	81.0[c]
500	100[a]	97.4[c]	94.6[c]	89.6[c]	88.4[d]	84.6[d]
750	100[a]	98.1[d]	96.4[d]	91.1[d]	90.2[e]	86.4[e]
1000	100[a]	98.4[d]	97.1[e]	94.3[e]	92.1[f]	87.2[f]

[A] Numbers with different letters in the same column are significantly different at $\alpha = 0.05$.

Table 2
Effects of Trolox on the retention (%) of tryptophan (1.25%) under light.[A]

Trolox (ppm)	Tryptophan retention during storage (%) Storage hours					
	0	2	4	6	8	10
0	100[a]	94.4[a]	86.4[a]	82.8[a]	80.0[a]	76.3[a]
100	100[a]	96.6[b]	87.6[b]	85.4[b]	83.2[b]	80.4[b]
250	100[a]	96.8[b]	91.2[c]	87.2[c]	85.1[c]	82.1[c]
500	100[a]	97.0[b]	93.1[d]	89.0[d]	86.3[d]	84.5[d]
750	100[a]	98.6[c]	94.4[e]	91.4[e]	89.3[e]	87.3[e]
1000	100[a]	98.0[c]	96.3[f]	94.3[f]	92.4[f]	90.6[f]

[A] Numbers with different letters in the same column are significantly different at $\alpha = 0.05$.

Table 3
Effects of Trolox on the retention (%) of tyrosine (1.25%) under light.[A]

Trolox (ppm)	Tyrosine retention during storage (%) Storage hours					
	0	2	4	6	8	10
0	100[a]	92.1[a]	85.8[a]	82.4[a]	76.8[a]	71.4[a]
100	100[a]	94.4[b]	86.9[b]	84.8[b]	81.3[b]	78.8[b]
250	100[a]	95.6[c]	88.9[c]	86.6[c]	84.9[c]	81.1[c]
500	100[a]	96.4[d]	90.3[d]	88.9[d]	86.5[d]	84.3[d]
750	100[a]	98.0[e]	92.5[e]	90.1[e]	88.5[e]	85.4[e]
1000	100[a]	98.9[e]	94.3[f]	91.2[f]	89.4[e]	86.3[f]

[A] Numbers with different letters in the same column are significantly different at $\alpha = 0.05$.

increased from 0 to 1000 ppm, the degradation of amino acids decreased. After 10 h of storage under light, the samples with 0 ppm ascorbic acid lost 27.6% phenylalanine while the samples with 1000 ppm ascorbic acid lost 14.4% only. Ascorbic acid also had a significant effect on the retention of phenylalanine, tryptophan and tyrosine at all levels of concentration.

Trolox acted as a better antioxidant in preventing the degradation of aromatic amino acids than ascorbic acid. After 10 h of storage under light, 1000 ppm Trolox helped retain 87.2% of phenylalanine, 90.6% of tryptophan and 86.3% of tyrosine, while the samples containing ascorbic acid retained 85.6% of phenylalanine, 88.4% tryptophan and 83.2% of tyrosine. Cardoso, Olsen, and Skibsted (2007) reported that Trolox deactivates triplet-excited riboflavin in homogeneous aqueous solution (7:3 (v/v), *tert*-butanol/water).

Table 4
Effects of ascorbic acid on the retention (%) of phenylalanine (1.25%) under light.[A]

Ascorbic acid (ppm)	Phenylalanine retention during storage (%) Storage hours					
	0	2	4	6	8	10
0	100[a]	91.4[a]	84.3[a]	81.2[a]	75.8[a]	72.4[a]
100	100[a]	93.3[b]	86.4[b]	84.3[b]	80.4[b]	74.4[b]
250	100[a]	94.9[c]	89.1[c]	86.8[c]	83.4[c]	79.8[c]
500	100[a]	95.6[c]	90.2[d]	88.9[d]	86.4[d]	81.6[d]
750	100[a]	96.3[d]	91.4[d]	90.1[e]	87.8[e]	83.8[e]
1000	100[a]	97.8[e]	94.1[e]	90.6[e]	88.4[f]	85.6[f]

[A] Numbers with different letters in the same column are significantly different at $\alpha = 0.05$.

Table 5
Effects of ascorbic acid on the retention (%) of tryptophan (1.25%) under light.[A]

Ascorbic acid (ppm)	Tryptophan retention during storage (%) Storage hours					
	0	2	4	6	8	10
0	100[a]	91.2[a]	85.4[a]	82.4[a]	79.0[a]	78.4[a]
100	100[a]	92.4[b]	87.3[b]	84.0[b]	80.2[b]	80.4[b]
250	100[a]	92.1[b]	88.4[c]	85.2[c]	82.6[c]	81.3[c]
500	100[a]	94.3[c]	90.2[d]	86.0[d]	83.3[d]	82.5[d]
750	100[a]	95.3[d]	91.4[e]	88.9[e]	86.1[e]	85.3[e]
1000	100[a]	97.4[e]	92.8[f]	90.2[f]	89.4[f]	88.4[f]

[A] Numbers with different letters in the same column are significantly different at $\alpha = 0.05$.

Table 6
Effects of ascorbic acid on the retention (%) of tyrosine (1.25%) under light.[A]

Ascorbic acid (ppm)	Tyrosine retention during storage (%) Storage hours					
	0	2	4	6	8	10
0	100[a]	91.3[a]	83.2[a]	79.6[a]	74.5[a]	68.3[a]
100	100[a]	93.2[b]	84.9[b]	83.4[b]	80.2[b]	75.6[b]
250	100[a]	94.6[c]	87.1[c]	85.6[c]	84.4[c]	78.3[c]
500	100[a]	95.3[d]	89.3[d]	86.9[d]	85.6[d]	80.2[d]
750	100[a]	97.4[e]	91.3[e]	89.3[e]	86.5[e]	81.6[e]
1000	100[a]	98.0[e]	92.3[f]	90.2[e]	88.4[f]	83.2[f]

[A] Numbers with different letters in the same column are significantly different at $\alpha = 0.05$.

The reduction potentials of triplet riboflavin, tyrosine and tryptophan are 1.70, 0.93 and 1.01 V, respectively (Lu & Liu, 2002). Since, triplet riboflavin has a higher reduction potential than tryptophan and tyrosine, it can easily induce the photodegradation of amino acids by acting as strong oxidising species (Lu & Liu, 2002). Both Trolox and ascorbic acid quenches singlet oxygen (Huang, Choe, & Min, 2004a; Jung et al., 2000). So, the effect of Trolox and ascorbic acid can be used to estimate the relative contributions of Type-I or Type-II pathways on the degradation of phenylalanine, tryptophan and tyrosine under light. The degradation of Phe, Trp and Tyr without any singlet oxygen quencher under light is due to the sum of Type-I and Type-II pathways. The degradation observed under high concentrations of singlet oxygen of singlet oxygen quencher would be mainly contributed by the Type-I pathway (Huang et al., 2004a).

As shown in Fig. 7, the degradation rates of Phe, Trp and Tyr decreased as added Trolox increased. More than 15% of Phe, 48% of Trp and 45% of Tyr riboflavin photosensitised degradation can be prevented by 10 mM of Trolox. So, from this data, Type-I pathway was responsible for 85% degradation of Phe, 52% of Trp and 55% of Tyr. Similarly, as shown in Fig. 8, the degradation rates of Phe, Trp and Tyr decreased as added ascorbic acid increased. More than 17% of Phe, 48% of Trp and 43% of Tyr riboflavin photosensitised degradation can be prevented by 10 mM of Trolox. So, from this data, Type-I pathway was responsible for 83% degradation of Phe, 52% of Trp and 57% of Tyr. About 85% of Phe degraded through Type-I pathway in the presence of riboflavin indicating that Phe reacts with singlet oxygen at a significantly lower rate when compared to Trp and Tyr. Tryptophan and tyrosine have electron rich double

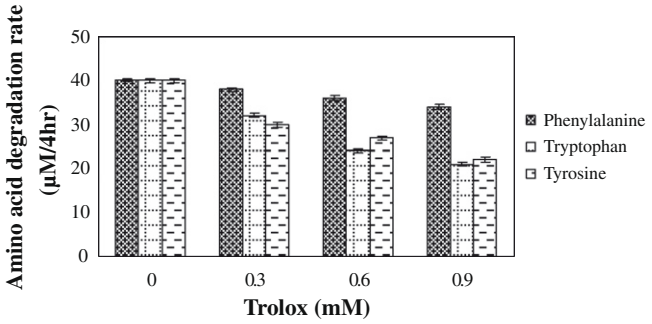

Fig. 7. Effects of 0, 0.3, 0.6 and 0.9 mM Trolox on degradation of phenylalanine, tryptophan and tyrosine. Data points represent means ($n = 3$) plus standard deviation.

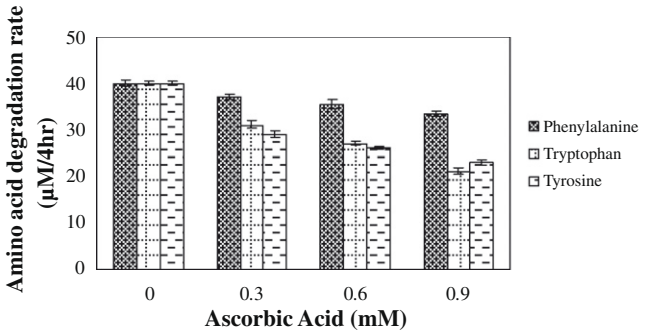

Fig. 8. Effects of 0, 0.3, 0.6 and 0.9 mM ascorbic acid on degradation of phenylalanine, tryptophan and tyrosine. Data points represent means ($n = 3$) plus standard deviation.

bonds and are excellent reactants for singlet oxygen oxidation. Photooxidation of tryptophan in the presence of riboflavin follows both Type-I and Type-II pathways (Rochette et al., 2000). Type-II pathway is favoured in riboflavin sensitised oxidation of tryptophan at high oxygen concentration under light (Rochette et al., 2000). However, in aqueous solutions the oxygen solubility is lower than other non-polar solvent systems. The lower availability of oxygen would favour the photosensitised reaction toward the Type-I pathway (Huang et al., 2004a). Cardoso, Franco, Olsen, Andersen, and Skibsted (2004) suggested that Type-I pathway may be major pathway for the light induced photooxidation of milk sensitised by riboflavin. The Type-I pathway proceeds via direct transfer of electrons from tryptophan and tyrosine side chains to triplet riboflavin yielding reduced riboflavin which subsequently generates reactive oxygen species (Cardoso et al., 2004).

The main photoproducts of tyrosine and tryptophan are bityrosine and a mixture of indole, flavin and indole flavin type aggregates, respectively (Rochette et al., 2000). Tryptophan degradation by riboflavin photosensitisation increased with oxygen concentration up to 40 μM oxygen and then decreased (Rochette et al., 2000). Ascorbic acid reduces the tryptophan photooxidation by interacting with excited triplet riboflavin (Garcia & Silva, 1997). Dalsgaard, Otzen, Nielsen, and Larsen (2007) studied riboflavin induced photooxidation of milk proteins and reported increase in carbonyl content during the oxidation of tryptophan as well as formation of dityrosine. Tyrosine and tryptophan in distilled water were oxidised in the presence of riboflavin at 7.5×10^{-6} M under light (Lu & Liu, 2002). At a low oxygen concentration of 5%, excited triplet riboflavin reacts with tyrosine (TyrOH) and produces riboflavin radicals ($RFH^{\cdot}_2$) and oxidised radicals of tyrosine ($TyrO^{\cdot}$) via electron transfer by Type-I pathway (Garcia & Silva, 1997; Viteri et al., 2003):

Table 7
Effects of light or dark on riboflavin (25 ppm) photosensitised oxidation of Trolox at 30 °C.

	Storage time (h)					
	0	2	4	6	8	10
Under light	100	95.0	88.3	83.7	80.0	75.1
In the dark	100	99.7	99.2	98.6	98.1	97.7

Table 8
Effects of light or dark on riboflavin (25 ppm) photosensitised oxidation of ascorbic acid at 30 °C.

	Storage time (h)					
	0	2	4	6	8	10
Under light	100	86.8	78.6	73.6	68.4	64.3
In the dark	100	98.8	98.2	97.6	97.1	96.4

$$3RFH^{*} + TyrOH \rightarrow RFH^{\cdot -} + TyrOH^{\cdot +}$$
$$RFH^{\cdot -} + TyrOH^{\cdot +} \rightarrow RFH^{\cdot}_2 + TyrO^{\cdot}$$

Peptides containing tryptophan were oxidised rapidly at pH 7.5 in the presence of 21 μM riboflavin and fluorescent light mostly by singlet oxygen. The oxidation rate was higher when tryptophan was bound on the carboxyl side in dipeptide than when it was bound to the amino side (Viteri et al., 2003). In tripeptide containing tryptophan, the oxidation rate was highest when tryptophan is in the carboxyl side and lowest when tryptophan is in the middle of a tripeptide (Kanner & Fennema, 1987). Tyrosine (TyrOH) reacts with hydrogen peroxide formed by riboflavin and produces phenoxyl radicals ($TyrO^{\cdot}$) and finally bityrosine by radical–radical coupling (Pichorner, Metodiewa, & Winterbourn, 1995):

$$2TyrOH + H_2O_2 \rightarrow 2TyrO^{\cdot} + 2H_2O$$
$$TyrO^{\cdot} + TyrO^{\cdot} \rightarrow TyrO{-}OTyr \ (\text{bityrosine})$$

3.4. Effects of riboflavin (25 ppm) on the photosensitised oxidation of Trolox and ascorbic acid

Generally, the addition of singlet oxygen quenchers like Trolox and ascorbic acid should decrease the loss of head space oxygen. But the higher rate of headspace oxygen depletion indicates that oxidation reactions are occurring. This may be because of simultaneous oxidation of Trolox and ascorbic acid along with amino acids. So, to confirm our hypothesis we studied the effect of riboflavin on the oxidation of Trolox and ascorbic acid. The effects of riboflavin (25 ppm) on the degradation of Trolox and ascorbic acid are presented in Tables 7 and 8. Riboflavin had a significant effect on the degradation of both Trolox and ascorbic acid. As the storage duration increased from 0 to 10 h, the degradation of both Trolox and ascorbic acid increased under light but not in dark. At the end of 10 h 24.9% of Trolox and 35.7% of ascorbic acid was degraded. So, the higher rates of headspace oxygen losses in the samples containing Trolox and ascorbic acid were mainly due to the oxidation of Trolox and ascorbic acid. Between Trolox and ascorbic acid, the degradation rate of ascorbic acid was higher.

4. Conclusions

In conclusion, riboflavin has contributed to the photosensitised oxidation of phenylalanine, tryptophan and tyrosine. Trolox and ascorbic acid increased the depletion of headspace oxygen in the samples. The loss of headspace oxygen in the samples could be attributed to the formation of singlet oxygen and the subsequent

oxidation riboflavin, Trolox, ascorbic acid and amino acids. Trolox and ascorbic acid quenched singlet oxygen and thus reduced reactions between riboflavin and singlet oxygen. Type-I mechanism was mainly responsible for riboflavin photosensitised degradation of aromatic amino acids. Trolox and ascorbic acid can be used to effectively protect Phe, Trp and Tyr from destruction under light in the presence of riboflavin.

References

Bisby, R. H., Morgan, C. G., Hamblett, I., & Gorman, A. A. (1999). Quenching of singlet oxygen by Trolox C, ascorbate and amino acids: Effects of pH and temperature. *The Journal of Physical Chemistry, 103*, 7454–7459.

Bradley, D. G., Kim, H. J., & Min, D. B. (2006). Effect, quenching mechanism, and kinetics of water soluble compounds in riboflavin photosensitized oxidation of milk. *Journal of Agricultural and Food Chemistry, 54*, 6016–6020.

Cardoso, D. R., Franco, D. W., Olsen, K., Andersen, M. L., & Skibsted, L. H. (2004). Reactivity of bovine whey proteins, peptides and amino acids towards triplet riboflavin. A laser flash photolysis study. *Journal of Agricultural and Food Chemistry, 52*, 6602–6606.

Cardoso, D. R., Olsen, K., & Skibsted, L. H. (2007). Mechanism of deactivation of triplet-excited riboflavin by ascorbate, carotenoids, and tocopherols in homogeneous and heterogeneous aqueous food model systems. *Journal of Agricultural and Food Chemistry, 55*, 6285–6291.

Choe, E., Huang, R., & Min, D. B. (2005). Chemical reactions and stability of riboflavin in foods. *Journal of Food Science, 70*, R28–R36.

Cort, W. M., Scott, J. W., Araujo, M., Mergens, W. J., Cannalonga, M. A., Osadca, M., et al. (1975). Antioxidant activity and stability of 6-hydroxy-2,5,7,8-tetramehtylchroman-2-carboxylic acid. *Journal of American Oil Chemists Society, 52*, 174–178.

Crank, G., & Pardijanto, M. S. (1995). Photooxidations and photosensitized oxidations of vitamin A and its palmitate ester. *Journal of Photochemistry and Photobiology A: Chemistry, 85*(1/2), 93–100.

Criado, S., Castillo, C., Yppolito, R., Bertolotti, S., & Garcia, N. A. (2003). The role of 4- and 5-aminosalicylic acids in a riboflavin-photosensitized process. *Journal of Photochemistry and Photobiology A: Chemistry, 155*(1–3), 115–118.

Dalsgaard, T. K., Otzen, D., Nielsen, J. H., & Larsen, L. B. (2007). Changes in structures of milk proteins upon photo-oxidation. *Journal of Agricultural and Food Chemistry, 55*, 10968–10976.

Dougherty, T. J. (1992). Photochemistry in the treatment of cancer. In D. Volman, G. Hammond, & D. Neckers (Eds.), *Advances in photochemistry* (pp. 275–311). New York: John Wiley and Sons.

Edwards, A. M., Bueno, C., Saldano, A., Silva, E., Kassab, K., Polo, L., et al. (1996). Photochemical and pharmacokinetic properties of selected flavins. *Journal of Photochemistry and Photobiology B: Biology, 48*(1), 36–41.

Foote, C. S. (1985). Chemistry of reactive oxygen species. In T. R. Richardson & J. W. Finley (Eds.), *Chemical changes in food processing* (pp. 17–31). Westport: AVI Publishing.

Garcia, J., & Silva, E. (1997). Flavin-sensitized photooxidation of amino acids present in a parenteral nutrition infuscate: protection by ascorbic acid. *The Journal of Nutrional Biochemistry, 8*, 341–345.

Grzelak, A., Rycjlik, B., & Bartosz, G. (2001). Light dependent generation of reactive oxygen species in cell culture media. *Free Radical Biology and Medicine, 30*(12), 1418–1425.

Huang, R., Choe, E., & Min, D. B. (2004a). Kinetics for singlet oxygen formation by riboflavin photosensitization and the reaction between riboflavin and singlet oxygen. *Journal of Food Science, 69*, C726–C732.

Huang, R., Choe, E., & Min, D. B. (2004b). Kinetics for singlet oxygen formation by riboflavin. *Journal of Agricultural and Food Chemistry, 35*, 71–76.

Huang, R., Choe, E., & Min, D. B. (2004c). Effects of riboflavin photosensitized oxidation on the volatile compounds of soymilk. *Journal of Food Science, 69*, C733–C738.

Jung, M. Y., Kim, S. K., & Kim, S. Y. (1995). Riboflavin-sensitized photooxidation of ascorbic acid: Kinetics and amino acid effects. *Food Chemistry, 53*, 397–403.

Jung, M. Y., Lee, K. H., & Kim, S. Y. (2000). Riboflavin sensitized photochemical changes in α-lactoglobulin in an aqueous buffer solution as affected by ascorbic acid. *Journal of Agricultural and Food Chemistry, 48*, 3847–3850.

Jung, M. Y., Lee, H. O., & Min, D. B. (1998). Singlet oxygen and ascorbic acid effects on dimethyl disulfide and off-flavor in skim milk exposed to light. *Journal of Food Science, 63*, 408–412.

Kanner, J. D., & Fennema, O. R. (1987). Photooxidation of tryptophan in the presence of riboflavin. *Journal of Food Science, 69*, C726–732.

Kanofsky, J. R. (1990). Quenching of singlet oxygen by human plasma. *Photochemistry and Photobiology, 57*, 299–303.

Kim, H., Kirschenbaum, L. J., Rosenthal, I., & Riesz, P. (1993). Photosensitized formation of ascorbate radicals by riboflavin: An ESR study. *Photochemistry and Photobiology, 57*(5), 777–784.

King, J. M., & Min, D. B. (1998). Riboflavin photosensitized singlet oxidation of vitamin D. *Journal of Food Science, 63*, 31–38.

Li, T. L., King, J. M., & Min, D. B. (2000). Quenching mechanisms and kinetics of carotenoids in riboflavin photosensitized singlet oxygen oxidation of vitamin D_2. *Journal of Food Biochemistry, 24*(6), 477–492.

Li, T. L., & Min, D. B. (1998). Stability and photochemistry of vitamin D_2 in model system. *Journal of Food Science, 63*, 413–417.

Lissi, E. A., Encinas, M. V., Lemp, E., & Rubio, M. A. (1993). Singlet oxygen O_2 ($^1\Delta_g$) bimolecular processes. Solvent effects. *Chemical Reviews, 93*, 699–723.

Lu, C. Y., & Liu, Y. Y. (2002). Electron transfer oxidation of tryptophan and tyrosine by triplet states and oxidized radicals of flavin sensitizers: A laser flash photolysis study. *Biochimica et Biophysica Acta, 1571*, 71–76.

Mahns, A., Melchheier, I., Suschek, C. V., Sies, H., & Klotz, L. O. (2003). Irradiation of cells with ultraviolet-A (320–400 nm) in the presence of cell culture medium elicits biological effects due to extracellular generation of hydrogen peroxide. *Free Radical Research, 37*, 391–397.

Michaeli, A., & Feitelson, J. (1994). Reactivity of singlet oxygen toward amino acids and peptides. *Photochemistry and Photobiology, 59*, 284–298.

Michaeli, A., & Feitelson, J. (1995). Reactivity of singlet oxygen towards large peptides. *Photochemistry and Photobiology, 61*, 255–260.

Min, D. B., & Boff, J. M. (2002). Chemistry and reaction of singlet oxygen in foods. *Comprehensive Reviews in Food Science and Food Safety, 1*(2), 58–72.

Miskoski, S., & Garcia, N. A. (1993). Influence of the peptide bond on the singlet molecular oxygen-initiated photooxidation of histidine and methionine dipeptides. A kinetic study. *Photochemistry and Photobiology, 57*, 447–452.

Pichorner, H., Metodiewa, D., & Winterbourn, C. (1995). Generation of superoxide and tyrosine peroxide as a result of tyrosyl radical scavenging by glutathione. *Archives of Biochemistry and Biophysics, 323*, 429–437.

Priyadarshini, K. I., Kapoor, S., & Naik, D. B. (2001). One and two electron oxidation reactions of Trolox by peroxynitrate. *Chemical Research in Toxicology, 14*, 567–571.

Rochette, A. D. L., Birlouez-Aragon, I., Silva, E., & Morliere, P. (2003). Advanced glycation end products as UVA photosensitizers of tryptophan and ascorbic acid: Consequences for the lens. *Biochimica et Biophysica Acta, 1621*, 235–241.

Rochette, A. D. L., Silva, E., Birlouez-Aragon, I., Mancini, M., Edwards, A. M., & Morliere, P. (2000). Riboflavin photodegradation and photosensitizing effects are highly dependent on oxygen and ascorbate concentrations. *Photochemistry and Photobiology, 72*, 815–820.

Song, Y. Z., An, J., & Jiang, L. (1999). ESR evidence of the photogeneration of free radicals ($GDHB^{\bullet}$, $O_2^{\bullet}$) and singlet oxygen ($^1O_2$) by 15-deacetyl-13-glycine-substituted hypocrellin B. *Biochimica et Biophysica Acta, 1472*, 307–313.

Viteri, G., Edwards, A. M., La Fuente, J. D., & Silva, E. (2003). Study of the interaction between triplet riboflavin and the α-, β_H- and β_L-crystallins of the eye lens. *Photochemistry and Photobiology, 77*, 535–540.

Yang, W. T., Lee, J. H., & Min, D. B. (2002). Quenching mechanisms and kinetics of α-tocopherol and b-carotene on the photosensitizing effect of synthetic food colorant FD&C Red No. 3. *Journal of Food Science, 67*, 507–510.

Food Chemistry 118 (2010) 42–47

Contents lists available at ScienceDirect

Food Chemistry

journal homepage: www.elsevier.com/locate/foodchem

ATP-regulation of antioxidant properties and phenolics in litchi fruit during browning and pathogen infection process

Chun Yi [a,b], Yueming Jiang [a], John Shi [b,*], Hongxia Qu [a,*], Sophia Xue [b], Xuewu Duan [a], Jingyu Shi [a], Nagendra K. Prasad [a]

[a] South China Botanical Garden, Chinese Academy of Sciences, Guangzhou 510650, PR China
[b] Food Research Center, Agriculture and Agri-Food Canada, Guelph, Ont., Canada N1G 5C9

ARTICLE INFO

Article history:
Received 14 January 2009
Received in revised form 7 April 2009
Accepted 20 April 2009

Keywords:
Litchi
ATP depletion
Energy
DNP
Antioxidant ability
Phenols
Pathogen infection

ABSTRACT

The impact of energy level on antioxidant properties in relation to pericarp browning and loss of disease resistance of litchi fruit was investigated. Litchi fruits were vacuum-infiltrated with distiled water (control), 1 mM adenosine triphosphate (ATP) and 0.5 mM 2,4-dinitrophenol (DNP) under 75 kPa for 3 min before being inoculated with *Peronophythora litchi* or not. ATP-treated fruits presented higher activities of antioxidant enzymes, including catalase (CAT), superoxide dismutase (SOD) and ascorbate peroxidase (APX). Higher activities of 1,1-diphenyl-2-picrylhydrazyl (DPPH) scavenging, reducing power and contents of phenolic compounds were also observed in ATP-treated fruit during storage. In contrast, DNP treatment lowered the enzymes activities, scavenging ability and the contents of phenolic compounds. Higher levels of antioxidant enzymatic system and non-enzymatic system were observed in *P. litchii*-inoculated fruits than those in non-inoculated fruits. Application of ATP and DNP exhibited a similar change patterns and effects in inoculated fruits. When related to previously reported ATP levels, the results suggested that ATP levels could regulate the antioxidant system. Sufficient available energy is crucial for inhibiting browning and preventing the loss of disease resistance in harvested litchi fruit.

1. Introduction

Adenosine triphosphate (ATP) serves as the 'energy currency of the cell' and is determinant of cell function and viability (Pradet & Raymond, 1983). Plant energy metabolism is considered as a mature field, but several important observations in plants initiated a research renaissance in ATP (both cellular and extracellular) in the last decade (Jiang, Jiang, Qu, Duan, & Jiang, 2007). This includes: (a) an ATP threshold existing for membrane lipid synthesis (Rawyler, Pavelic, Gianinazzi, Oberson, & Braendle, 1999); (b) effective preservative ways of horticultural crops closely associated with elevated ATP levels (Duan et al., 2004; Saquet, Streif, & Bangerth, 2001), energy deficiency, fruit browning and decay (Saquet, Streif, & Bangerth, 2000; Yi et al., 2008); and (c) extracellular nucleotides (eATP, eADP and hydrolyzable analogues of them) that function as regulatory agents in plant signal transduction (Roux, Song, & Jeter, 2006).

Mitochondrial oxidative phosphorylation is not only the main pathway of ATP production for eukaryotic cell, but also the major target of oxidative stress, mediated by reactive oxygen species (ROS), including superoxide anion ($O^{\cdot -}$), hydrogen peroxide (H_2O_2), hydroxyl ($HO^{\cdot}$), peroxyl ($ROO^{\cdot}$) and alkoxyl ($RO^{\cdot}$) (Bloknina, Virolainen, & Fagerstedt, 2003; Fleury, Mignotte, & Vayssiere, 2002). Such ROS, also termed active oxygen species, can disrupt cellular membranes, induce oxidative changes in DNA, and disturb cellular metabolism (Yu, 1994).

The accumulation of ROS could be prevented by two defence systems: non-enzymatic antioxidant system containing low molecular weight antioxidants (ascorbic acid, glutathione, tocopherols) and ROS-interacting enzymatic system comprising enzymes such as superoxide dismutases (SOD), peroxidase (POD), catalase (CAT), and ascorbate peroxidase (APX). Oxidative stress occurs due to the imbalance between ROS and ROS-scavenging compounds and enzymes. During senescence and stress conditions, plants cells could sense lethal dose of ROS and subsequently activate several defence enzymes and synthesise compounds as adaptional responses to scavenge ROS amount within a safe level. The processes for enzyme activation and synthesis of low molecular weight antioxidants require energy. Veltman, Lenthéric, Van der Plas, and Peppelenbos (2003) showed that energy production and ATP levels in tissues of pears play a role in regulating/inducing antioxidant enzymes, including SOD, CAT, and APX. Saquet et al. (2000) demonstrated that ATP played a vital role in the synthesis of ROS scavenging enzymes and non-enzyme scavengers in the ascorbate-gluthatione cycle. Energy depletion may result in a more dramatic oxidative stress, and consequently, damage the cell. Franck et al. (2007) suggested that membrane dysfunction, an early

* Corresponding authors. Tel.: +1 519 780 8035; fax: +1 519 829 2600 (J. Shi).
E-mail addresses: shij@agri.gc.ca (J. Shi), q-hxia@scib.ac.cn (H. Qu).

0308-8146/$ - see front matter Crown Copyright © 2009 Published by Elsevier Ltd. All rights reserved.
doi:10.1016/j.foodchem.2009.04.074

response to senescence and stresses, is characterised by shortage of ATP and an increase in ROS production.

Browning is a common symptom during senescence or injury in fruit, resulting from breakdown of cellular compartments and consequently reaction between polyphenol oxidase (PPO) and its substrates (phenolic compounds) (Jiang, 2000). During storage, excess ROS generation accelerates the oxidisation of phenolic compounds, resulting in decreased contents of phenolics and pericarp browning (Underhill & Critchley, 1994; Zhang, Quantick, & Grigor, 2000).

The infection by pathogens increases the amount of ROS produced during fruit storage, the so-called "oxidative burst" in response to pathogen attack (Bolwell & Wojtaszek, 1997). The oxidative burst is crucial for the disease resistance in higher plants, whilst it may result in peroxidative destruction of cellular constituents if they are not timely averted. Thus, the intracellular ROS level has to be kept under tight control to prevent cell damage (Bartoli, Simontacchi, Montaldi, & Puntarulo, 1996).

Litchi (*Litchi chinensis* Sonn.) is a subtropical/tropical fruit of high commercial value in the international trade. Harvested litchi fruits are highly perishable due to water loss, pericarp browning and disease development. The objectives of present work were to measure antioxidant enzymes activities, scavenging activities and phenolic compounds contents to test whether extrogenous ATP supply will regulate the balance between the ROS and its defence system in litchi fruit during browning and pathogen infection process.

2. Materials and methods

2.1. Sample preparation

Litchi fruits were harvested when commercially matured from a local orchard (Guangzhou, China). They were washed in water containing 0.1% thiabendazole, and then infiltrated under vacuum with sterile distilled water (SDW) as control, 1.0 mM ATP and 0.5 mM DNP solution under 75 kPa for 3 min, separatively. *Peronophythora litchii* was isolated from infected litchi fruits and cultured on potato dextrose agar medium at 28 °C for 4 days. Half of the litchi fruits treated above were inoculated as previously reported by Yi et al. (2008). The fruits were kept in covered plastic boxes ($5 \times 15 \times 4$ cm) and stored at 25 °C (85–90% RH). Twenty fruits from different treatments were randomly sampled every 2 days of storage until the end of storage time (0, 2, 4, 6 days for inoculated fruits; 0, 2, 4, 6, 7 days for non-inoculated fruits). Pericarp tissue were immediately frozen in liquid nitrogen and stored at −70 °C until analysis (less than 3 months).

2.2. Determination of SOD, CAT, APX activities

Litchi pericarp tissue (2 g) was homogenised in 10 mL 0.05 M potassium phosphate buffer (pH 7.8) for SOD activity, 0.1 M potassium phosphate buffer (pH 7.0) for CAT and APX activities. The homogenate was filtered through two layers of miracloth and centrifuged at 20,000*g* for 15 min at 4 °C. The resulting supernatants were collected for the enzyme assays described below. Protein content was determined according to the Bradford (1976) method with bovine serum albumin as standard.

SOD activity was assayed by measuring its ability to inhibit the photochemical reduction of nitroblue tetrazolium (NBT) using the method of Beyer and Fridovich (1987). One unit of SOD activity was defined as the amount of enzyme required to effect 50% inhibition of the reduction of NBT per mg protein as monitored at 560 nm.

CAT activity was assayed by measuring the disappearance of H_2O_2 according to Aebi (1984). The assay mixture (3 mL) contained 2.95 mL phosphate buffer (0.05 M, pH 7.0), 15 mM H_2O_2 and 50 μL of extract. CAT activity was usually calculated by a decrease in absorbance at 240 nm and was expressed as U per mg protein.

APX activity was measured following the oxidation of ascorbic acid at 290 nm (extinction coefficient 2.8 mM^{-1} cm^{-1}) according to Nakano and Asada (1981). The reaction mixture consisted of 50 mM potassium phosphate buffer (pH 7.0), 0.5 mM sodium ascorbate, 0.1 mM H_2O_2, 0.5 mM ethylene diamine tetraacetic acid and 1 mL of extract. APX activity was calculated by the change of absorbance per minute per mg protein.

2.3. Determination of Scavenging activities of DPPH radicals and reducing power

Litchi pericarp tissue (2 g) was ground in liquid nitrogen with a mortar and pestle and homogenised in 10 mL methanol by stirring for 30 min at room temperature. The homogenate was filtered through two layers of miracloth and extracted again. Combined extract were stored at −20 °C until analysis.

DPPH radical scavenging activity was measured according to Shimada, Fujikawa, Yahara, and Nakamura (1992) with slight modification. The reaction mixture contained 0.1 mL of sample extract and 2.9 mL of 0.1 mM DPPH methanol solution. The absorbance at 517 nm was measured after 30 min of incubation at 25 °C. The inhibition of DPPH radicals by samples was calculated according to the following equation: DPPH scavenging activity (%) = (1 − absorbance of sample/absorbance of control) × 100.

Reducing power was measured at 700 nm according to Duan, Jiang, Su, Zhang, and Shi (2007). A control, devoid of any hydrolysates and a blank, containing only hydrolysate samples, was used because proteins also absorb at the same wavelength. Increased absorbance of the reaction mixture indicated increased reducing power.

2.4. Determination of total phenolic compounds

Litchi pericarp tissue (5 g) from 12 fruits was extracted three times in 100 mL methanol containing 0.1 M HCl at 25 °C for 2 h. The extract solutions were filtered and combined for total phenolic determination. Phenolic content of the extract was determined by a modification of the Prussian blue assay of Price and Buttler (1977). The extracts (50 μL) was diluted with 3 mL distiled water, and then 100 μL of 50 mM $FeCl_3$ in 0.1 M HCl plus 100 μL of 8 mM $K_3Fe(CN)_6$ added to the solution, which was incubated for 20 min. Total phenolic compounds were determined by measuring the absorbance at 720 nm on a spectrophotometer with gallic acid as standard.

2.5. Statistical analysis

Significant differences were tested by one-way analysis of variance (ANOVA) (SPSS, version 10.0). Each experiment was repeated 2–4 times.

3. Results

3.1. Effects of ATP and DNP on SOD, CAT and APX in litchi fruits

As shown in Fig. 1A and B, both the activities of SOD and CAT in control fruits slightly fluctuated in the first 4 days of storage and then continuously decreased to lower values as compared that of 0 day. Significant enhancements of both SOD and CAT activities were observed after fruits were treated with ATP ($P < 0.05$). Different with those in control fruits, the activities of SOD and CAT in ATP-treated fruits increased 23% and 45% in the first 4 days of storage, respectively. DNP-treated fruits showed much lower SOD and CAT activities than both control and ATP-treated fruits. SOD activity started to decrease after 2 days of storage and CAT activity began to decline from the beginning of the storage. Moreover, no signifi-

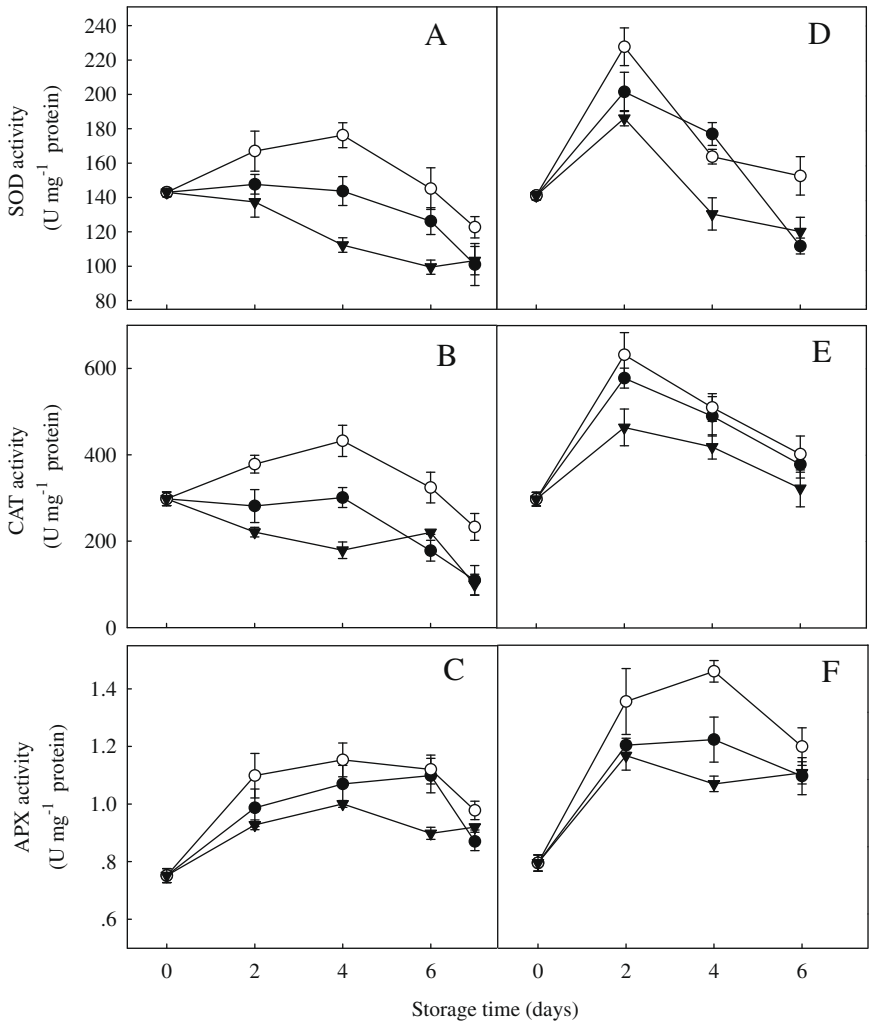

Fig. 1. Effects of ATP and DNP on SOD (A, D), CAT (B, E), APX (C, F) activities in non-inoculated (A, B, C) and *P. litchii*-inoculated (D, E, F) litchi fruits during storage. Each value is presented as mean ± standard error ($n = 3$). The vertical bars indicate standard errors where they exceeded the symbol size. (○, ATP; ●, Control; ▼, DNP).

cant difference of CAT activity between the control and DNP-treated fruits was observed in the last 3 days of storage. APX activity showed distinct change pattern with activities of other two enzymes. The activity increase from 0.75 to 1.09 U mg^{-1} protein as storage time proceeded and declined at the end of storage (Fig. 1C). ATP treatment markedly enhanced the APX activity, whilst DNP treatment lowered the activity.

The levels of SOD, CAT and APX activities in *P. litchi*-inoculated fruits were higher than those of non-inoculated fruits throughout the storage period (Fig. 1D, E, and F). Compared with non-inoculated fruits, inoculated fruits showed different trends in both SOD and CAT activities. SOD and CAT activities increased in the first 2 days of storage and then sharply decreased in the last 4 days of storage. The decrease in APX activity started from the 4 day of storage, which is 2 days earlier than that in the control and ATP-treated fruits. Likewise, higher activities of SOD, CAT and APX were found in ATP-treated fruit throughout the storage time, whilst lower activities were found in DNP-treated fruits than those in control and ATP-treated fruits.

3.2. Effect of ATP and DNP on DPPH scavenging ability and reducing power

Fig. 2 shows the effects of ATP and DNP treatment on DPPH radical scavenging ability and reducing power of litchi pericarp. In non-inoculated fruits, the scavenging activity of DPPH radicals gradually decreased as the storage time progressed. ATP treatment significantly reduced the activity of DPPH radicals (Fig. 2A). The DPPH scavenging ability decreased in DNP treated fruit. The change trends differed when the fruits were inoculated with *P. litchii*. DPPH radical scavenging ability in *P. litchii*-inoculated fruits was higher than those in inoculated fruits. It slightly increased from 100.1% to 105.2% in control fruits and significantly increased from 100.1% to 113.2% in the ATP-treated fruits in the first 2 days of storage, and then gradually declined (Fig. 2C). Also, remarkable enhancement of DPPH scavenging ability was observed in ATP-treated fruits and significantly lower scavenging ability was observed in DNP-treated fruits. The scavenging ability was in the order of ATP-treated *P. litchii*-inoculated fruit > *P. litchii*-inoculated fruit (control) > DNP-treated *P. litchii*-inoculated fruit > ATP-treated non-inoculated fruit > non-inoculated fruit (control) > DNP-treated non-inoculated fruit, throughout the storage period.

For both the non-inoculated and *P. litchii*-inoculated fruits, reducing powers of litchi pericarp extracts rapidly decreased from 1.6 to around 1.2 mg mL^{-1} (Fig. 2B and D). It was shown that the reducing power of ATP-treated fruits was higher than that in the control and DNP-treated fruits. After 2 day of storage, reducing powers in inoculated fruits were lower than those in non-inoculated fruits, suggesting stronger decline of antioxidant activity in infected tissues during storage.

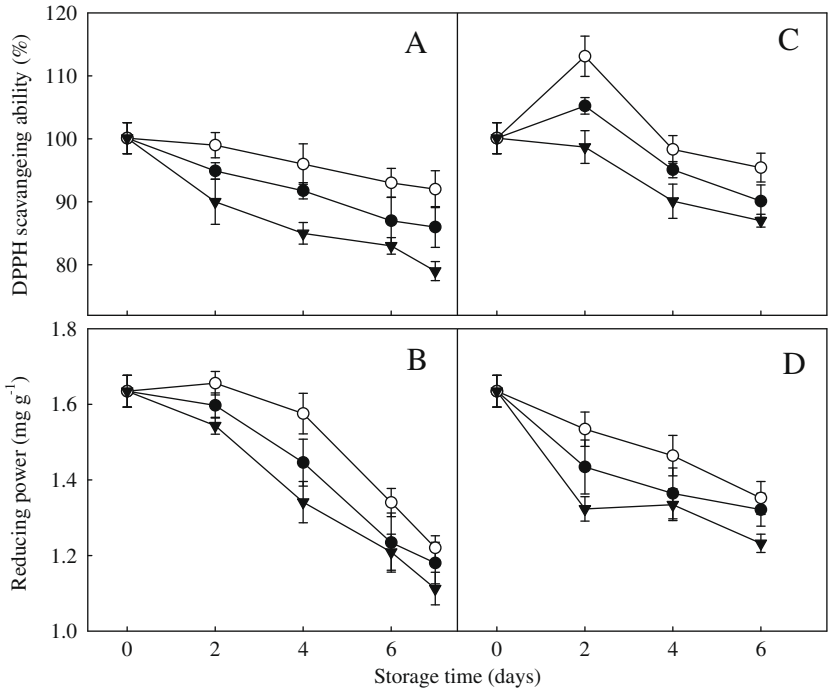

Fig. 2. Effects of ATP and DNP on DPPH scavenging activities (A, C) and reducing power (B, D) in non-inoculated (A) and *P. litchii*-inoculated (B) litchi fruits during storage. Each value is presented as mean ± standard error (n = 3). The vertical bars indicate standard errors where they exceeded the symbol size. (○, ATP; ●, Control; ▼, DNP).

3.3. Effect on the content of phenolic compounds

Contents of phenolic compounds of litchi fruit pericarp with different treatments are shown in Fig. 3. In the control fruits, the total phenolic contents decreased from 3.21 to 1.87 mg g^{-1} fresh weight (FW) in non-inoculated fruits and from 3.21 to 2.32 mg g^{-1} FW in *P. litchii*-inoculated fruits, respectively. Higher contents of total phenolic compounds in inoculated fruits were detected than non-inoculated fruits, even at the end of storage. There is a slight increase in all fruits after 2 days of inoculation. Treatment with ATP elevated the phenolic compounds contents of litchi fruit pericarp. At the second day of storage, the contents in ATP-treated fruits were 29% higher in non-inoculated fruits and 32% higher in *P. litchii*-inoculated fruits than those of DNP-treated fruits, respectively.

A correlation between the antioxidant activity in the DPPH assay and the contents of phenolic compounds were established (Fig. 4). As shown, there is a linear relationship between them with correlation coefficients of r^2 = 0.63. The increase of phenolic compounds contents will result an increase in DPPH scavenging ability.

4. Discussion

The data confirm that the ability of defence system of ROS gradually decrease during browning and pathogen infection process. According to previous results (Yi et al., 2008), ATP-treated fruits clearly exhibit less browning and disease symptom. This study shows the effects of ATP and DNP on the anti-oxidation system during browning or loss of disease resistance process.

Senescence and/or browning were caused by overproduction of ROS. The enzymes are involved in scavenging superoxide radicals, thus they could protects cells from oxidative stress (Buchanan-Wollaston et al., 2003). SOD converts two superoxide anions into a molecule of hydrogen peroxide and one of oxygen, and CAT could convert hydrogen peroxide to water and oxygen (Boonsiri, Ketsa, & van Doorn, 2007). APX prevents the accumulation of ROS by the ascorbate-gluthatione cycle (Asada, 1994). The results showed that all enzymes activities were higher in ATP-treated fruits and lower in DNP-treated fruits throughout the storage. The increased activities of SOD, CAT, and APX in ATP-treated fruits could contribute to

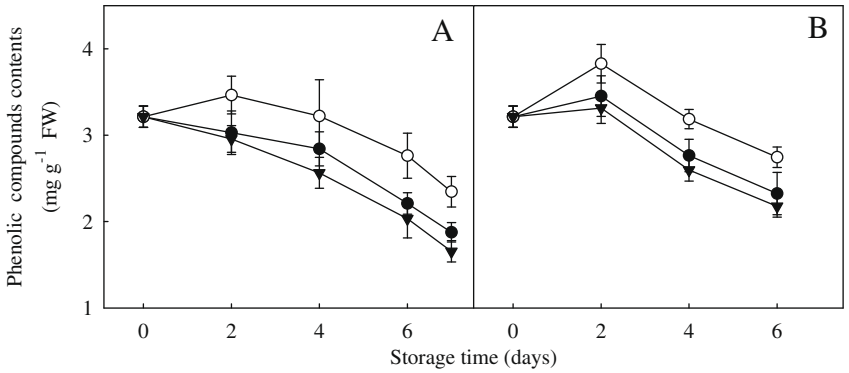

Fig. 3. Effects of ATP and DNP on contents of phenolic compounds in non-inoculated (A) and *P. litchii*-inoculated (B) litchi fruits during storage. Each value is presented as mean ± standard error (n = 3). The vertical bars indicate standard errors where they exceeded the symbol size. (○, ATP; ●, Control; ▼, DNP).

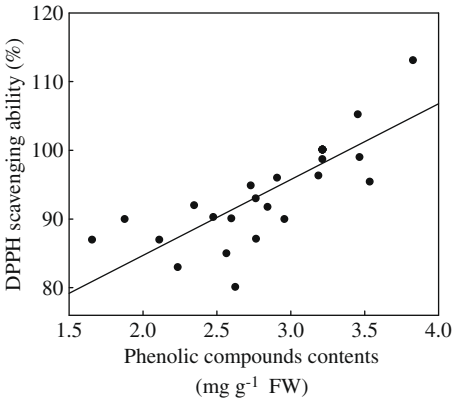

Fig. 4. Correlation between contents of phenolic compounds and DPPH scavenging ability in ATP-treated and DNP-treated litchi fruits.

avoiding or delaying the accumulation of ROS during ripening and then to prevent tissue damage.

Application of ATP to litchi fruits in the case of senescence and pathogen attack could protect the fruits against ROS generation via activating the enzymatic protecting system. Related to the ATP levels examined previously after ATP and DNP treatment, ATP treatment could elevate the ATP level and energy charge and then delay the browning process (Yi et al., 2008). By contrast, energy depletion in DNP-treated fruits fastened browning and decay process (Yi et al., 2008). Thus, the activities of SOD, CAT, and APX depended on the available energy in the cells. Therefore, energy level could regulate the balance between ROS generating and its enzymatic defence system, which could reduce the accumulation of ROS and prevent the abnormalities in cellular metabolism (Franck et al., 2007).

Free radical-scavenging is another known system for inhibiting lipid peroxidation by antioxidants. DPPH radical scavenging activity is one of the known methods used for evaluating antioxidant activity (Bloknina et al., 2003). The reducing power might also serve as a significant reflection of the antioxidant activity (Chang, Yen, Huang, & Duh, 2002). The noticeable elevated level of radical scavenging ability by ATP supply indicated that ATP might be involved in the synthesis of antioxidants, whilst decreased levels of radical scavenging ability in DNP-treated fruits corresponded to the accelerated browning process. Related to the energy levels previous examined, energy levels are positively correlated with the free radical scavenging ability. The energy level in litchi pericarp tissue could regulate the non-enzymatic ROS defence system.

Phenolic compounds are effective antioxidants in plants (Jiang, 2000), which are demonstrated by the correlation between the antioxidant activity in the DPPH assay and the contents of total phenolic compounds. The results suggested that sufficient ATP level was essential for the synthesis of phenolic compounds, and then consequently, enhance the antioxidant activity of litchi pericarp.

The results showed higher enzyme activities, higher free radical scavenging ability, and higher phenolic compounds after pathogen attack. The increased protection by enzyme activities could contribute to responses of ROS to the pathogen stress and defence pathways (Desikin, Mackerness, Hancock, & Neill, 2001). The induction of APX activity in response to stress has been reported by Garcia-Limones, Hervas, Navas-Cortes, Jimenez-Diaz, and Tena (2002). A previous study suggested two-stage behaviours with respect to pathogen invasion in litchi fruits (Yi et al., 2008). The first stage was characterised by increased ATP levels and better preserved membrane (0–4 days for non-inoculated fruits and 0–2 days for inoculated fruits), whilst the second stage was characterised by reductions in ATP contents and accumulation of lipid peroxide product (Yi et al., 2008). The present results are consistent with the two-stage behaviours as the enzyme activities remained constant or increased during the first stage and decreased during the second stage.

Moreover, phenolic compounds played vital roles in pathogen resistance (Nicholson & Hammerschmidt, 1992). Obviously, higher content and slower decrease trend of total phenolic in inoculated fruits suggested the induction of phenolic compounds synthesis under pathogen attack. A higher level of ATP may provide an advantage for phenolic compounds synthesis of rapid disease resistance in response to pathogen attack.

5. Conclusions

A fine balance between the maintenance of ATP levels and the confinement of ROS production within the amount of signal requirement is essential for inhibiting browning and loss of disease resistance. Exogenous ATP supply provides sufficient available energy to maintain or enhance the antioxidant systems and the synthesis ability of phenolic compounds, and consequently, to inhibit the accumulation of ROS and maintain the integrity of membrane. In other words, energy levels could regulate the balance between the ROS production and antioxidant system through enhancing both the enzymes activities and free radical scavenging ability.

Acknowledgements

This work was supported by National Natural Science Foundation of China (Grants 30400026, 30871740 & U0631004).

References

Aebi, H. (1984). Catalases. In H. U. Bergmeyer (Ed.). *Methods of enzymatic analysis* (Vol. 2, pp. 673–684). New York: Academic Press.

Asada, K. (1994). Production and action of active oxygen species in photosynthetic tissues. In C. H. Foyer & P. M. Mullineaux (Eds.), *Causes of photooxidative stress and amelioration of defense systems in plants* (pp. 77–104). Boca Raton: CRC Press.

Bartoli, C. G., Simontacchi, M., Montaldi, E., & Puntarulo, S. (1996). Oxidative stress, antioxidant capacity and ethylene production during aging of cut carnation (*Dianthus cariophyllus*) petals. *Journal of Experimental Botany, 47*, 595–601.

Beyer, W. F., & Fridovich, I. (1987). Assaying for superoxide dismutase activity: Some large consequences of minor changes in condition. *Analytic Biochemistry, 161*, 559–566.

Bloknina, O., Virolainen, E., & Fagerstedt, K. V. (2003). Antioxidants, oxidative damage and oxygen deprivation stress: A review. *Annals of Botany, 91*, 179–194.

Bolwell, G. P., & Wojtaszek, P. (1997). Mechanisms for the generation of reactive oxygen species in plant defense – A broad perspective. *Physiological and Molecular Plant Pathology, 51*, 347–366.

Boonsiri, K., Ketsa, S., & van Doorn, W. G. (2007). Seed browning of hot peppers during low temperature storage. *Postharvest Biology and Technology, 45*, 358–365.

Bradford, M. M. (1976). A rapid and sensitive method for the quantitation of microgram quantities of protein utilizing the principle of protein-dye binding. *Analytical Biochemistry, 72*, 248–254.

Buchanan-Wollaston, V., Earl, S., Harrison, E., Mathas, E., Navabpour, S., Page, T., et al. (2003). The molecular analysis of leaf senescence – A genomics approach. *Plant Biotechnology, 1*, 3–22.

Chang, L. W., Yen, W. J., Huang, S. C., & Duh, P. D. (2002). Antioxidant activity of sesame coat. *Food Chemistry, 78*, 347–354.

Desikin, R., Mackerness, S., Hancock, J., & Neill, S. J. (2001). Regulation of the Arabidopsis transcriptosome by oxidative stress. *Plant Physiology, 127*, 159–172.

Duan, X. W., Jiang, Y. M., Su, X. G., Liu, H., Li, Y. B., Zhang, Z. Q., et al. (2004). Role of pure oxygen treatment in browning of litchi fruit after harvest. *Plant Science, 167*, 665–668.

Duan, X. W., Jiang, Y. M., Su, X. G., Zhang, Z. Q., & Shi, J. (2007). Antioxidant property of anthocyanins extracted from litchi (*Litchi chinenesis* Sonn.) fruit pericarp tissues in relation to their role in the pericarp browning. *Food Chemistry, 101*, 1365–1371.

Fleury, C., Mignotte, B., & Vayssiere, J. L. (2002). Mitochondrial reactive oxygen species in cell death signaling. *Biochimie, 84*, 131–141.

Franck, C., Lammertyn, J., Ho, Q. T., Verboven, P., Verlinden, B., & Nicolai, B. M. (2007). Browning disorders in pear fruit. *Postharvest Biology and Technology, 43*, 1–13.

Garcia-Limones, C., Hervas, A., Navas-Cortes, J. A., Jimenez-Diaz, R. M., & Tena, M. (2002). Induction of an antioxidant enzyme system and other oxidative stress markers associated with compatible and incompatible interactions between chickpea (*Cicer arietinum* L.) and *Fusarium oxysporum* f. sp. ciceris. *Physiological and Molecular Plant Pathology, 61*, 325–337.

Jiang, Y. M. (2000). Role of anthocyanins, polyphenol oxidase and phenols in lychee pericarp browning. *Journal of the Science of Food and Agricultural, 80*, 305–310.

Jiang, Y. M., Jiang, Y. L., Qu, H. X., Duan, X. W., & Jiang, W. B. (2007). Energy aspects in ripening and senescence of harvested horticultural crops. *Stewart Postharvest Review, 3*, 1–5.

Nakano, Y., & Asada, K. (1981). Hydrogen peroxide is scavenged by ascorbate-specific peroxidase in spinach chloroplasts. *Plant Cell Physiology, 22*, 867–880.

Nicholson, R. L., & Hammerschmidt, R. (1992). Phenolic compounds and their role in disease resistance. *Annual Review of Phytopathology, 30*, 369–389.

Pradet, A., & Raymond, P. (1983). Adenine nucleotide ratios and adenylate energy charge in energy metabolism. *Annual Review of Plant Physiology, 34*, 199–224.

Price, M. L., & Buttler, L. G. (1977). Rapid visual estimation and spectrophotometric determination of tannin content of sorghum grain. *Journal of Agricultural and Food Chemistry, 25*, 1268–1273.

Rawyler, A., Pavelic, D., Gianinazzi, C., Oberson, J., & Braendle, R. (1999). Membrane integrity relies on a threshold of ATP production rate in potato cell cultures submitted to anoxia. *Plant Physiology, 120*, 293–300.

Roux, S. J., Song, C., & Jeter, C. (2006). Regulation of plant growth and development by extracellular nucleotides. In F. Baluska, S. Mancuso, & D. Volkmann (Eds.), *Communication in plants* (pp. 221–234). Berlin: Springer.

Saquet, A. A., Streif, J., & Bangerth, F. (2000). Changes in ATP, ADP and pyridine nucleotide levels related to the incidence of physiological disorders in 'Conference' pears and 'Jonagold' apples during controlled atmosphere storage. *The Journal of Horticultural Science and Biotechnology, 75*, 243–249.

Saquet, A. A., Streif, J., & Bangerth, F. (2001). On the involvement of adenine nucleotides in the development of brown heart in 'Conference' pears during delayed controlled atmosphere storage. *Gartenbauwissenschaft, 66*, 140–144.

Shimada, K., Fujikawa, K., Yahara, K., & Nakamura, T. (1992). Antioxidative properties of xanthan on the autoxidation of soybean oil in cyclodextrin emulsion. *Journal of Agricultural and Food Chemistry, 40*, 945–948.

Underhill, S., & Critchley, C. (1994). Anthocyanin decolorisation and its role in lychee pericarp browning. *Australian Journal of Experimental Agriculture, 34*, 115–122.

Veltman, R. H., Lenthéric, I., Van der Plas, L. H. W., & Peppelenbos, H. W. (2003). Internal browning in pear fruit (*Pyrus communis* L. cv Conference) may be a result of a limited availability of energy and antioxidants. *Postharvest Biology and Technology, 28*, 295–302.

Yi, C., Qu, H. X., Jiang, Y. M., Shi, J., Duan, X. W., Joyce, D. C., et al. (2008). ATP-induced disease resistance in postharvested litchi fruit. *Journal of Phytopathology, 156*, 365–371.

Yu, B. P. (1994). Cellular defenses against damage from reactive oxygen species. *Physiological Reviews, 74*, 139–162.

Zhang, D., Quantick, P. C., & Grigor, J. M. (2000). Changes in phenolic compounds in litchi (*Litchi chinensis* Sonn.) fruit during postharvest storage. *Postharvest Biology and Technology, 19*, 165–172.

Food Chemistry 118 (2010) 48–55

Contents lists available at ScienceDirect

Food Chemistry

journal homepage: www.elsevier.com/locate/foodchem

Impact of emulsifier microenvironments on acid–base equilibrium and activity of antioxidants

Kathleen Oehlke *, Anja Heins, Heiko Stöckmann, Karin Schwarz

Institute of Human Nutrition and Food Science, University of Kiel, 24118 Kiel, Germany

ARTICLE INFO

Article history:
Received 29 October 2008
Received in revised form 9 April 2009
Accepted 21 April 2009

Keywords:
Antioxidants
Emulsions
Acid–base equilibria
Emulsifier pseudophases
Microenvironment

ABSTRACT

Mechanisms by which emulsifiers influence the activity of antioxidants in emulsions were investigated. To evaluate the importance of the partitioning between the different phases, the proportions of ferulic acid (FA) and isoferulic acid (iFA) at the o/w interface, in the coexisting micellar phase and in the aqueous phase were experimentally determined. An increase of the total emulsifier concentration and hence the micellar concentration led to an increased solubilisation of FA and iFA by the emulsifier pseudophases. From the point of view that the solubilisation sites of the antioxidants have different properties and thereby affect their activity, the microenvironment of each antioxidant was characterised in terms of local pH values and electrostatic potential. The degree of dissociation of both FA and iFA decreased in the order CTAB > SDS ≈ Brij. Information about the relative locations of the antioxidants was deduced from the extents to which the dissociation equilibria were affected by their environment. It was concluded that (1) the proximity to the polar headgroup of SDS, (2) a high degree of dissociation in a CTAB environment and (3) a deeper intercalation into the headgroup region of Brij were favourable for the antioxidant activity.

1. Introduction

The activity of antioxidants in emulsions is a complex issue as a result of their partitioning into different phases, each being characterised by specific properties and possible interactions with other constituents. It was proposed that the antioxidant activity in emulsions was positively correlated to the proportion of the antioxidant at the o/w interface (Frankel, Huang, Kanner, & German, 1994). In addition, it has been hypothesised that the proportion of antioxidants which is solubilised by the micellar pseudophase is not antioxidatively active. Therefore, regarding the impact of the partitioning on the antioxidant activity, a distinction between the proportion at the interface and in the micelles is necessary (Stöckmann, Schwarz, & Huynh-Ba, 2000). The ultrafiltration (UF) technique allows a distinction between the bulk aqueous phase, the micellar pseudophase and the o/w interface and maintains the initial structure of the emulsions (Oehlke, Garamus, Heins, Stöckmann, & Schwarz, 2008). However, a separation of the o/w interface and the droplet interior is not possible. To overcome this uncertainty, Gunaseelan, Romsted, Gonzalez-Romero, and Bravo-Diaz (2004) have developed a kinetic method which is based on the reaction of the antioxidant with arenidazonium salts taking place exclusively at the interface (Gunaseelan et al., 2004). They have shown that antioxidants with high and moderate hydrophilicity are predominantly located at the o/w interface rather than in the oil droplet interior. The results were in good accordance with results from UF experiments published by Stöckmann et al. (2000) and Stöckmann and Schwarz (1999).

Depending on the emulsifier concentration, a considerable amount of micelles may be present. Therefore, mass transfer in emulsions by micelles, and thereby an exchange of solutes between micelles and the o/w interface, also has to be taken into consideration (Zana, 1996).

Whether and by which mechanisms the activity of phenolic antioxidants is influenced by the pH value of the system has been investigated (Amorati, Pedulli, Cabrini, Zambonin, & Landi, 2006). It has been observed that phenolic antioxidants possess a higher antioxidant activity at neutral pH values than in acidic media, which was explained by the positive effect of the dissociated carboxylic group (Amorati et al., 2006). Schreier, Frezzatti, Araujo, Chaimovich, and Cuccovia (1984) developed a model to describe the interaction between partitioning and pK_a values of drugs in model systems. Furthermore, it has been shown that the dissociation of phenolic acids can be affected by the presence of emulsifiers in solution (Drummond, Grieser, & Healy, 1989; Polewski, Kniat, & Slawinska, 2002). These changes were ascribed to differences between mean solvent properties of the bulk and the interfacial phase. Results were also explained in terms of interactions with the emulsifier micelles and probable partitioning effects. The main objective of the present study was to relate factors which are governed by the emulsifier to the activity of antioxidants in emulsions.

* Corresponding author.
E-mail address: koehlke@foodtech.uni-kiel.de (K. Oehlke).

0308-8146/$ - see front matter © 2009 Elsevier Ltd. All rights reserved.
doi:10.1016/j.foodchem.2009.04.078

The scope of this work embraced especially the acid base equilibria and the partitioning behaviour of antioxidants, utilising ferulic acid (FA) and isoferulic acid (iFA) as model compounds (Fig. 1).

2 Materials and methods

2.1. Chemicals

SDS (sodium dodecyl sulphate, ⩾99%), sodium acetate (⩾99%, anhydrous) and ferulic acid (>98%) were obtained from Carl Roth, Karlsruhe, Germany. CTAB (cetyl trimethyl ammonium bromide, ⩾99%), ABTS (2,2′-azino-bis(3-ethylbenzthiazoline-6-sulphonic acid), >99%) and potassiumperoxosulphoxide (⩾99%) were purchased from Fluka, Buchs, Switzerland. Brij 58 (polyoxy-ethylene-20-cetyl-ether) and isoferulic acid (97%) were obtained from Sigma–Aldrich, Seelze, Germany). All solvents were of analytical grade. The chemicals were used as received.

2.2. Emulsion preparation

Commercial corn oil was chromatographically purified on an aluminium oxide column and eluted with hexane according to the method of Lampi and Kamal-Eldin (1998). Hexane was evaporated under reduced pressure. The oil was stored under nitrogen at −20 °C until used.

The o/w emulsions consisted of 10 wt% purified corn oil triglycerides, 90 wt% acetic acid buffer solution (0.2 M, pH 5.0) and 10, 20 or 30 mM emulsifier, relative to the total emulsion. To prepare batches of 150 g, 15 g of oil were poured into plastic bottles, to which 60 ml of emulsifier solution were added. After shaking the solution to form pre-emulsions, sonication was applied for 30 s. During the next sonication step, the remaining 75 ml of buffer solution was added stepwise within one minute. The whole mixture was further sonicated for 120 s so that the total sonication time was 210 s (cycle 5, 40% power, Bandelin sonopuls, sonication probe VS 70, Berlin, Germany). Antioxidants were added via a concentrated ethanolic stock solution (50 μl) so that the antioxidant concentration in the emulsions was 50 μM, i.e., 500 μM relative to the oil phase. The ethanol volume was 0.2 vol% and was hence assumed to be negligible.

For the partitioning studies, emulsions were prepared with commercial corn oil, which was purchased in a local supermarket and used without any modification.

2.3. Determination of the partitioning behaviour

Ultrafiltration experiments were carried out using centrifugal devices as described earlier (Oehlke et al., 2008). Briefly, membranes with a low molecular weight cut-off (Vivaspin4 with reg. cellulose membrane, 3 kDa, Millipore, Schwalbach, Germany) were used to separate a small volume, usually not more than 10% of the initial sample volume, of the bulk aqueous phase containing emulsifier monomers and water-solubilised antioxidant molecules. To also separate a portion of the coexisting micellar phase, membranes with larger pores were utilised. Emulsions with SDS were filtered through regenerated cellulose membranes with an MWCO of 100 kDa (Centricon YM100, Millipore, Schwalbach, Germany), whereas emulsions with CTAB or Brij were filtered through inorganic membranes with a pore size of 20 nm (VectaSpin micro, Whatman, Dassel, Germany). Antioxidant concentrations in the filtrate were determined by HPLC analysis. All experiments were done in duplicate with three sampling steps each, so that the given results are means of six individual values. The experiments were carried out at room temperature.

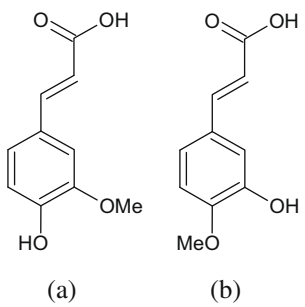

Fig. 1. Chemical structures of (a) ferulic acid (FA) and (b) isoferulic acid (iFA).

The total antioxidant concentration, $[A]_{tot}$, is the sum of the o/w interfacial concentration $[A]_{int}$, the micellar concentration $[A]_m$ and the free aqueous concentration $[A]_w$ (Eq. (1)), provided that all concentrations are given in mM (per total volume)

$$[A]_{tot} = [A]_{int} + [A]_m + [A]_w \quad (1)$$

By ultrafiltration, the different fractions are determined with

$$[A]_w = 0.903[A]_{low} \quad (2)$$

$$[A]_m = 0.903([A]_{high} - [A]_{low}) \quad (3)$$

$$[A]_{int} = [A]_{tot} - 0.903[A]_{high} \quad (4)$$

The subscripts "low" and "high" stand for the filtrate and permeate achieved with low and high MWCO membranes, respectively. The factor 0.903 accounts for the volume fraction of the oil phase, which does not directly solubilise the antioxidants (Gunaseelan et al., 2004).

2.4. Modified ABTS assay

The radical-scavenging activity was determined by a modified ABTS assay at different pH values (Ozgen, Reese, Tulio, Scheerens, & Miller, 2006). An ABTS solution was prepared (8 mM ABTS, 3 mM potassiumperoxosulphoxide in water) and left overnight in the dark. This solution was added to the different buffer solutions to yield an absorption of 1.4. From a 0.5 mM antioxidant stock solution, 50 μl were added to 2.95 ml of ABTS solution. A control sample was prepared by adding 50 μl of ethanol instead of antioxidant solution. Absorption of the samples was measured photometrically at 734 nm, before and 30 min after the addition of the antioxidant solution. The reduction of the absorption was calculated and corrected by values from the blank solutions. Between the measurements, the samples were kept at 25 °C in the dark. Measurements were done in duplicate with three independent antioxidant solutions, i.e., the given results are the means of six individual values.

2.5. Lipid oxidation experiments

The antioxidant activity was determined by a modified Schaaloven test. Samples were stored in gas-tight flasks at 40 °C in the dark and were analysed repeatedly over time. Hydroperoxide concentrations were determined by the ferric thiocyanate method modified by Stöckmann et al. (2000). The antioxidants were compared on the basis of the inhibition of hydroperoxide formation at the time when the control sample had reached a concentration of approximately 200 mmol hydroperoxides per kg of oil (Eq. (5)). This level corresponds to a peroxide value determined by iodometric titration of approximately 60 and was reached after 3–5 days, depending on the system.

$$\text{Inhibition} = 100\frac{C_{control} - C_{sample}}{C_{control}} \quad (5)$$

$C_{control}$ and C_{sample} are the hydroperoxide concentrations in the control and in the samples, respectively.

2.6. Spectrometric titration

The equilibria and species involved in the micellar solutions can be described by a thermodynamic cycle (Fig. 2) (Saikia, Bora, & Dutta, 2005; Schreier et al., 1984). It involves the dissociation of the antioxidant and the partitioning of the protonated and dissociated species between the aqueous phase and micelles.

For the determination of the pK_a values in buffer solution and buffered micellar solutions, pK_a^{obs}, solutions of 50 μM FA or iFA in acetic acid buffer solutions (0.2 M) in the pH range 3–6, with or without 30 mM of the respective emulsifiers, were prepared. Below pH 3.6 and above pH 5.6 the pH was adjusted with acetic acid to maintain a constant ionic strength in all samples. pH values were measured with a glass electrode (WTW, Weilheim, Germany). The calibration of the pH metre was carried out with a two point calibration curve. The pH value of each sample was measured until a stable value was obtained. UV absorption spectra were recorded with a spectrophotometre (Beckman Coulter, Krefeld, Germany) over the wavelength range from 200 to 400 nm. Samples were kept in a quartz cuvette with a path length of 1 cm (Hellma, Müllheim, Germany) and measurements were performed at 25 ± 0.2 °C.

For each wavelength, a curve of the absorbances vs. pH value was fitted according to a modified Boltzmann model with the software Origin 8. The pK_a^{obs} was given by the inflection point. Failed fits were discarded. The remaining 50–140 curves with the respective inflection points were used for further calculations.

2.7. Determination of acidity constants, local pH values and electric potentials

The total antioxidant concentrations and the pH value of the bulk were directly measured. The proportion of antioxidant in the bulk aqueous phase was analysed in the filtrate of UF tubes with a membrane cut-off of 3 kDa as described above. The difference of the total concentration was assigned to the micellar concentration. The resulting method to determine the acidity constants is similar to the procedure described by Schreier (1984) for drugs in a membrane model system. Abbreviations are given in Table 1.

The aqueous antioxidant concentration $[A]_w$ was determined in the ultrafiltrate of the tubes with 3 kDa membranes. The antioxidant in the aqueous phase is present in the dissociated and non-dissociated state:

$$[AH]_w + [A^-]_w = [A]_w \quad (6)$$

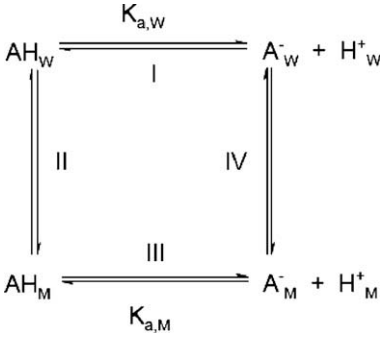

Fig. 2. Equilibria (roman numerals) and species involved in the partitioning of an antioxidant in a micellar solution (modified from Schreier et al. (1984) and Saikia et al. (2005)). *AH* and A^- represent the non-dissociated and dissociated forms of the antioxidant; for further abbreviations see Table 1.

Table 1
Abbreviations used in equations.

[]	Molar concentrations relative to the total solution
$[A]_w$	Total antioxidant in the aqueous phase: determined by UF
$[AH]_w$	Non-dissociated antioxidant in the aqueous phase[a]
$[A^-]_w$	Dissociated antioxidant in the aqueous phase[a]
$[H^+]_w$	Hydrogen ion concentration in the aqueous phase; measured with a pH electrode
$[A]_m$	Total antioxidant in micelles; determined by UF
$[AH]_m$	Non-dissociated antioxidant in micelles[b]
$[A^-]_m$	Dissociated antioxidant in micelles[b]
$[H^+]_m$	Hydrogen ion concentration in micelles
$K_{a,w}$	Acidity constant in water/the aqueous phase[b]
$K_{a,m}$	Acidity constant in micellar environment[b]
K_a^{obs}	Observed acidity constant in a micellar environment[b]
K_a^{app}	Apparent acidity constant in a micellar environment[b]

[a] Dissociation refers to the carboxylic group.
[b] For all acidity constants it is $pK_a = -\log K_a$.

The concentration of the dissociated species (Fig. 2, equilibrium II) was calculated by:

$$K_{a,w} = \frac{[A^-]_w[H^+]_w}{[AH]_w} \quad (7)$$

$K_{a,w}$ was determined in buffer solution by spectrometric titration experiments. The pH value, and hence $[H^+]_w$, was known, so that Eqs. (6) and (7) could be simultaneously solved to give $[A^-]_w$ and $[AH]_w$.

K_a^{obs} is the acidity constant which was directly observed in spectrometric titration experiments with micellar solutions. It includes dissociated and non-dissociated species in micelles and the bulk aqueous phase and can be described by:

$$K_a^{obs} = \frac{([A^-]_w + [A^-]_m)}{([AH]_w + [AH]_m)}[H^+]_w \quad (8)$$

The concentration of antioxidants solubilised by micelles $[A]_m$ was determined by UF. $[A^-]_w$ and $[AH]_w$ are known from Eq. (6) and (7). Further, the antioxidant molecules are known to be present in the micelles in both forms, dissociated and non-dissociated:

$$[AH]_m + [A^-]_m = [A]_m \quad (9)$$

Thus Eqs. (8) and (9) could be simultaneously solved, so that $[A^-]_m$, $[AH]_m$, $[A^-]_w$ and $[AH]_w$ are readily calculated.

K_a^{app} is the apparent dissociation constant in micelles and accounts for the partitioning of the solute (in contrast to K_a^{obs}). It is affected by the local pH value/electric potential and by polarity differences compared to the bulk aqueous phase.

2.8. Polarity effects in non-ionic micelles

Equilibrium III in Fig. 2 can be expressed as

$$K_{a,m} = \frac{[A^-]_m[H^+]_m}{[AH]_m} \quad (10)$$

The absence of an electric potential at the surface of non-ionic micelles makes it possible to determine the influence of a micellar environment on the acidic strength of a solute (Dupont-Leclerq, Giroux, Henry, & Rubini, 2007). Thus, if the concentrations of the acid and base forms of the compound in the micellar phase are known and the pH value is assumed to be equal to the pH value of the bulk, $K_{a,m}$ can be calculated (Eq. (10)). In the case of non-ionic micelles, $K_a^{app} = K_{a,m}$.

2.9. Potential and pH effects in ionic micelles

In ionic micelles, the electrostatic potential ψ at the micellar surface influences the local H^+ or OH^- concentration, and hence

the dissociation equilibrium of solubilised species. The influence of the electrostatic potential ψ at the micellar surface on the dissociation of acids was described by Fernandez and Fromherz (1977):

$$\Delta pK_a^{app} = pK_a^{app} - pK_{a,m} = -\frac{F}{2.3RT}\psi \quad (11)$$

with

$$pK_a^{app} = pH_w + \frac{[A^-]_m}{[AH]_m} \quad (12)$$

$pK_{a,m}$ accounts for the polarity of the local environment and therefore $pK_{a,m}^{SDS} = pK_{a,w}$ and $pK_{a,w}^{CTAB} = pK_{a,m}^{Brij}$.

The pH value at the solubilisation site (pH_{loc}) in SDS micelles was calculated according to the procedures previously described by Saikia et al. (2005) and Souza et al. (2006):

$$pH_{loc} = pK_{a,w} + \frac{[A^-]_m}{[AH]_m} \quad (13)$$

The pH_{loc} in CTAB micelles was calculated according to Pal and Jana (1996) and Dupont-Leclerq et al. (2007):

$$pH_{loc} = pK_{a,m} + \frac{[A^-]_m}{[AH]_m} \quad (14)$$

2.10. Calculation of the surface pH of ionic micelles according to the pseudophase ion exchange (PIE) model

The coverage of SDS micelles with H^+ ions is described by:

$$m_H^s = \frac{\beta[H^+]_w}{K_H^{Na}[Na]_w} \quad (15)$$

β is the micelle surface fraction covered with counter ions, K_H^{Na} is a constant which describes the exchange of protons and sodium ions between bulk and surface. $[Na]_w$ and $[H^+]_w$ are the sodium and hydrogen concentrations in the bulk.

m_H^s can be expressed as the proton concentration at the interface related to the volume of the Stern layer:

$$[H^+]_m = \frac{m_H^s[SDS]_m}{V_{Stern}} \quad (16)$$

From $[H^+]_m$, the pH value at the micellar surface can be calculated. With $K_H^{Na} = 1$, $\beta = 0.75$ and the molar volume of the Stern layer = 0.14 l, the surface pH was 3.3 in a 0.2 M sodium acetate buffer solution with pH 5.0 containing 0.03 M SDS. Values were taken from the literature (Romsted & Zanette, 1988).

A similar procedure was used for cationic micelles, but taking into account the exchange of OH^- and Br^- ions.

$$m_s^{OH} = \frac{\beta[OH]_w}{K_{OH}^{Br}[Br]_w} \quad (17)$$

$$[OH^-]_m = \frac{m_s^{OH}[CTAB]_m}{V_{Stern}} \quad (18)$$

Assuming the ion product of water to be 14 at the micellar surface, the pH can be calculated. With $K_{OH}^{Br} = 12$, $\beta = 0.8$ and the molar volume of the Stern layer = 0.14 l, the surface pH was 6.9 in a 0.2 M sodium acetate buffer solution with pH = 5.0 containing 0.03 M CTAB. Values were taken from the literature (Romsted, 1985).

3. Results

3.1. Partitioning of antioxidants

The partitioning of both antioxidants depended strongly on the type and concentration of the emulsifier (Table 2).

Table 2
Partitioning of FA and iFA in emulsions containing different emulsifiers and different emulsifier concentrations[a].

	P_w (%)	P_m (%)	P_i (%)
FA			
10 mM Brij	46.0 ± 0.4	1.0 ± 5.0	53.1 ± 5.0
20 mM Brij	34.2 ± 0.2	6.7 ± 3.3	59.1 ± 3.3
30 mM Brij	28.2 ± 0.6	13.7 ± 2.3	58.0 ± 2.5
10 mM SDS	78.0 ± 1.4	4.5 ± 1.4	17.5 ± 0.7
20 mM SDS	69.6 ± 0.4	7.5 ± 0.7	22.9 ± 0.5
30 mM SDS	64.1 ± 0.3	9.4 ± 0.5	26.5 ± 0.4
10 mM CTAB	15.3 ± 0.4	25.0 ± 1.8	59.7 ± 1.8
20 mM CTAB	10.5 ± 0.2	27.7 ± 1.7	61.8 ± 1.7
30 mM CTAB	8.9 ± 0.5	31.1 ± 2.9	60.0 ± 2.9
iFA			
10 mM Brij	50.9 ± 0.4	18.3 ± 3.2	30.9 ± 3.2
20 mM Brij	32.0 ± 2.2	35.3 ± 2.8	32.6 ± 1.8
30 mM Brij	26.7 ± 0.2	50.6 ± 1.8	22.7 ± 1.8
10 mM SDS	82.2 ± 0.3	5.5 ± 2.0	12.3 ± 2.0
20 mM SDS	72.6 ± 1.2	10.0 ± 0.8	17.4 ± 1.5
30 mM SDS	67.6 ± 3.9	11.0 ± 4.2	21.3 ± 1.5
10 mM CTAB	7.7 ± 0.1	32.4 ± 3.0	59.9 ± 2.9
20 mM CTAB	5.4 ± 0.1	31.9 ± 2.1	62.7 ± 2.1
30 mM CTAB	4.6 ± 0.1	30.5 ± 1.3	65.0 ± 1.3

[a] Errors correspond to the standard deviation according to Gauss error propagation, $n = 6$.

The proportions of FA in the aqueous phase decreased with increasing emulsifier concentration, regardless of the type of emulsifier. The highest concentrations in the aqueous phase were present in emulsions with SDS, followed by emulsions with Brij and CTAB. The micelle-bound FA concentrations increased with increasing total emulsifier concentrations. This effect was most pronounced in emulsions containing Brij 58, whereas SDS and CTAB concentrations had smaller effects. The proportion of FA at the o/w interface was not markedly affected by the total emulsifier concentration in the emulsions with CTAB and Brij, whereas an increased SDS concentration resulted in an enhanced interfacial FA concentration. The interfacial concentrations in the different emulsions decreased in the order CTAB > Brij > SDS.

The aqueous concentrations of iFA decreased in the order SDS > Brij > CTAB and were reduced with increasing emulsifier concentrations. Both micellar and interfacial concentrations decreased in the reversed order, i.e., CTAB > Brij > SDS compared to the aqueous phase in the same systems. The proportions solubilised by micelles increased with increasing Brij concentration and were less pronounced with increasing SDS concentrations. The total CTAB concentration did not influence the micellar concentration. The iFA concentrations at the o/w interface increased with increasing CTAB and SDS concentrations and decreased with increasing Brij concentration.

3.2. Apparent pK_a and local pH values

For the determination of local pH values and/or pK_a values in the respective micellar environment, the concentrations of the different species were calculated (Table 3). FA and iFA were incorporated to roughly the same extent in CTAB micelles. iFA was better solubilised by SDS micelles than FA, whereas FA was better solubilised by Brij than iFA.

The ratios of dissociated to non-dissociated acid were below 1.0 in Brij and SDS micelles, whereas they were 3.6 and 5.8 in CTAB micelles. In CTAB micelles, FA was less dissociated than was iFA. In contrast, FA was slightly more dissociated in SDS and Brij micelles. In buffer solution, the acidic strengths of both antioxidants were similar within errors. The observed pK_a values in micellar solutions

Table 3
Parametres to describe the acid base equilibria of FA and iFA in micellar solutions[a].

	% Mic.[b]	$\frac{[A^-]_m}{[AH]_m}$	$pK_{a,w}$[c]	pK_a^{obs}	pK_a^{app}	ΔpK_a[d]	pH_{loc}	ΔpH[e]	ψ_{loc}, mV
Brij									
FA	69.1 ± 0.5	0.17 ± 0.01	4.56 ± 0.01	5.31 ± 0.04	5.76 ± 0.06	1.20 ± 0.06	5.00 ± 0.01[f]	–	–
iFA	63.5 ± 0.4	0.12 ± 0.01	4.51 ± 0.01	5.27 ± 0.01	5.90 ± 0.06	1.39 ± 0.06	4.39 ± 0.01[f]	–	–
SDS									
FA	34.4 ± 0.7	0.26 ± 0.08	4.56 ± 0.01	4.93 ± 0.02	5.58 ± 0.09	–	3.95 ± 0.08	0.65 ± 0.3	−60 ± 6
iFA	40.1 ± 0.1	0.09 ± 0.02	4.51 ± 0.01	5.01 ± 0.01	6.03 ± 0.11	–	3.45 ± 0.12	0.15 ± 0.3	−90 ± 6
CTAB									
FA	82.7 ± 0.1	2.56 ± 0.08	4.56 ± 0.01	4.52 ± 0.01	4.51 ± 0.05	–	6.2 ± 0.1	0.7 ± 0.2	74 ± 4
iFA	94.8 ± 0.2	5.80 ± 0.2	4.51 ± 0.01	4.26 ± 0.01	4.16 ± 0.05	–	6.7 ± 0.1	0.2 ± 0.2	74 ± 4

[a] Mean ± standard deviation according to Gauss error propagation.
[b] Obtained in buffered micellar solutions with pH = 5.0.
[c] Obtained in buffer solution.
[d] Difference of pK_a between micelle and bulk.
[e] Difference of local pH and pH at the micellar surface according to the PIE model (pH_{SDS} = 3.3, pH_{CTAB} = 6.9).
[f] Local pH value was assumed to be equal to the pH value of the bulk Dupont-Leclerq et al. (2007).

increased for both antioxidants in the order CTAB < SDS < Brij. After the correction for the partitioning, this order was maintained with regard to FA, but slightly different for iFA. Furthermore, differences between the emulsifiers increased. Also, the differences of the pK_a values of FA and iFA increased. The difference of the pK_a value in a Brij micellar environment compared to water was larger for iFA than for FA. In ionic micelles, the local pH values and electric potentials were calculated. The solubilisation site of FA was characterised by a higher pH value and a less negative electric potential than the solubilisation site of iFA. In CTAB micelles, the difference between local pH and surface pH was slightly larger for FA and FA showed a lower electric potential than did iFA.

3.3. Radical-scavenging activity

The ability to scavenge radicals was determined by a modified ABTS assay in solutions with different pH values. The loss of absorption at 734 nm related to a 1 mM antioxidant solution was determined as a measure of the number of radicals scavenged. For all pH values tested, FA was a more efficient radical-scavenger than was iFA (Fig. 3). The radical-scavenging activity of FA and iFA increased with increasing pH. An increase of the pH value from 4.0 to 6.1 resulted in a 1.2-fold increase of the activity of FA. The activity of iFA increased 1.4-fold with the most pronounced step from pH 5 to 5.6.

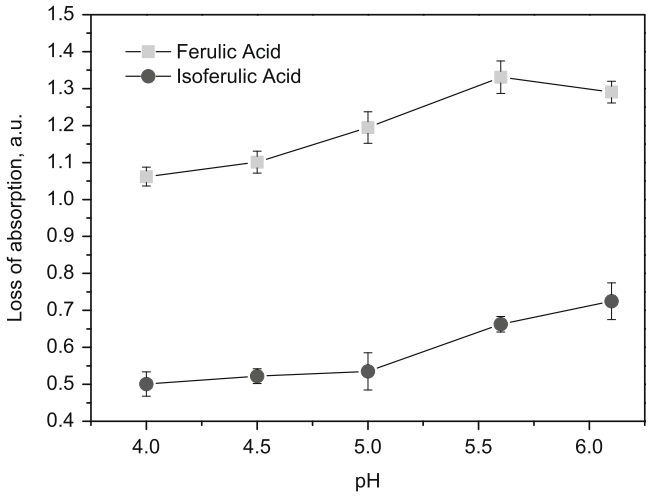

Fig. 3. ABTS radical scavenging activity of FA and iFA expressed as the reduction of absorption of the ABTS reaction solution at 734 nm after 30 min.

3.4. Inhibition of lipid oxidation

The ability of the antioxidants to inhibit the formation of hydroperoxides in emulsions during storage varied, depending on the type and concentration of the emulsifier used (Table 4). Both antioxidants showed the same trend, i.e. a decreasing activity in the order Brij > SDS > CTAB. In contrast to the ABTS assay, the inhibitory effect of iFA was stronger or comparable to that of FA. Hexanal concentrations were also measured to determine the inhibition of the formation of secondary oxidation products. The results showed the same trends (data not shown).

FA was not able to inhibit lipid oxidation in emulsions with CTAB. In emulsions with SDS, FA inhibited the formation of hydroperoxides only at the highest SDS concentration. In emulsions with Brij 58, FA had a moderate antioxidant activity, which increased with increasing Brij concentration.

In emulsions with 10 mM CTAB, hydroperoxide formation was inhibited by iFA to 16%, whereas no activity was observed when the CTAB concentration was increased. In emulsions with SDS, lipid oxidation was inhibited to 30–40% with a minimum at 20 mM SDS. In emulsions with Brij 58, iFA had moderate activity, which increased with the emulsifier concentration.

4. Discussion

4.1. Impact of the emulsifier on the partitioning

The partitioning of FA and iFA in emulsions was determined by ultrafiltration. The advantage of the technique, as applied in the present study, is the possibility to differentiate solute concentrations in the bulk aqueous phase, the micellar pseudophase and

Table 4
Inhibition of hydroperoxide formation by FA and iFA in emulsions stored at 40 °C in the dark.[a,b]

	FA	iFA
10 mM Brij	46 ± 2	56 ± 3
20 mM Brij	51 ± 2	52 ± 2
30 mM Brij	63 ± 1	60 ± 1
10 mM SDS	0 ± 2	40 ± 2
20 mM SDS	-3 ± 1	29 ± 1
30 mM SDS	13 ± 4	45 ± 1
10 mM CTAB	−7 ± 5	17 ± 2
20 mM CTAB	−127 ± 5	−11 ± 4
30 mM CTAB	−162 ± 13	−4 ± 4

[a]Errors correspond to the standard deviation according to Gauss error propagation, n = 9.
[b]The inhibition was calculated at a hydroperoxided level of 200 ± 40 mmol/kg oil in the control after three to 5 days of storage, depending on the samples.

the o/w interface without changing the physicochemical pattern of the emulsions. It was suggested earlier that the proportion of antioxidants in the micelles is antioxidatively inactive (Huang, Frankel, Aeschbach, & German, 1997; Huang, Hopia, Schwarz, Frankel, & German, 1996b). The distinction of antioxidant concentrations at the interface and in the coexisting micellar phase permits the testing of this hypothesis.

Generally, increased total emulsifier concentrations resulted in increased micellar and/or interfacial antioxidant concentrations to the expense of the proportions in the aqueous phase. Additionally, the increase of the micellar iFA concentration in emulsions with Brij was associated with decreased aqueous and interfacial concentrations.

This result reflects the partitioning of emulsifiers. When the interface is saturated with emulsifier molecules, a coexisting micellar pseudophase arises. Still, the interface had a higher solubilisation capacity than had the micellar pseudophase, which has been demonstrated by Stöckmann (1999). According to the LSER theory, hydrogen bonds in CTAB and Brij pseudophases can lead to an accumulation of antioxidants. The lower affinity of the antioxidants for the SDS pseudophases reflects the electrostatic repulsion on the one hand and the less favourable hydrogen bonding properties on the other hand (Stöckmann et al., 2000).

A direct exchange between ionic micelles and interfaces is unlikely, due to electrostatic repulsion, which would not allow a sufficient approximation of micelles and interface (Pena & Miller, 2006; Zana, 1996). In addition, the strong solubilisation of antioxidants by CTAB micelles results in an extended residence of solute molecules in the micelles (Zana, 1996). Therefore, an exchange with the aqueous phase is very slow, which results in restricted diffusion of the antioxidants to the interface. In contrast, interactions between the antioxidants and SDS molecules are very low and the exchange of antioxidants with the aqueous phase can be fast. The non-ionic Brij allows the direct exchange of solutes between the o/w interface and micelles. Therefore, it is concluded that antioxidants can freely diffuse between the phases and pseudophases, i.e., micelles could facilitate the transport of antioxidants to the o/w interface in emulsions stabilised by Brij 58 (Mukerjee & Ko, 1992; Pena & Miller, 2006).

4.2. Partitioning effects on the antioxidant activity

Regarding the activities of FA and iFA in the different emulsions, a similar trend was observed for both antioxidants, namely a decreasing activity in the systems in the order Brij > SDS > CTAB. According to the partitioning behaviour, an opposite trend would be expected, i.e., the highest activity in systems where the interfacial antioxidant concentrations are high, i.e., emulsions containing CTAB, followed by Brij and SDS.

In emulsions with the non-ionic Brij, partitioning seems to have a strong impact on the antioxidant activity. A higher proportion in micelles and interface roughly coincided with an increased activity of the antioxidants. This effect was less pronounced in emulsions containing SDS but not present in CTAB emulsions. It is suggested that Brij micelles contribute to an efficient inhibition of lipid oxidation by delivering antioxidant molecules, as discussed above. Due to the loose binding of FA and iFA by SDS, micelles may not negatively influence their activity. The presence of increasing micellar CTAB concentrations does not just inactivate the antioxidants, but promotes pro-oxidant behaviour. This is interpreted by molecular interactions or characteristic properties of the emulsifier pseudophases (Stöckmann et al., 2000).

4.3. Degree of dissociation and radical-scavenging activity

The radical-scavenging activity of FA and iFA increased with increasing pH value, the activity of iFA being slightly more sensitive to the pH value. Explanations for this may be obtained by taking mechanistic considerations into account.

The degree of dissociation changes electronic effects, which affect the mechanisms by which radicals are scavenged. Basically, many studies reveal that a dissociated carboxyl group is electron-donating and therefore activating other substituents in contrast to the non-dissociated electron-withdrawing COOH group. The positive effect on the activity may also be explained by the better stabilisation of the phenoxyl radical by the COO^- group. In addition, phenolic compounds with dissociated OH groups have been determined to be better radical-scavengers than are the parent compounds with non-dissociated phenolic OH groups. pK_a values of the phenolic OH of cinnamic acids are reported to be in the range of 8.5 (Silva et al., 2000). Amorati et al. (2006) reported that considerable dissociation of the phenolic OH started at pH 7–8. Hence, the concentration of this species is supposed to be very small under the conditions applied in this study.

The pH value can affect the activity of antioxidants in micellar solution and emulsions by two additional mechanisms. First, the partitioning and the location within micelles or the o/w interface depends on the degree of dissociation (Mei, McClements, & Decker, 1999). It was shown by Heins, McPhail, Sokolowski, Stöckmann, and Schwarz (2007) that the location in the interface has a strong impact, on the activity, which was explained by the importance of the spatial proximity of antioxidants and radicals. A high pH value may also be favourable, because metal ions, which act as pro-oxidants, can be better oxidised and thus mitigated in basic media, due to the more similar locations of metal ions and dissociated acids. In contrast, in acidic environments, phenolic acids, e.g., caffeic acids, were reported to reduce iron, thus acting as pro-oxidants themselves (Mei et al., 1999).

4.4. pH effects on antioxidant activity mediated by emulsifiers

4.4.1. pK_a values

pK_a values in buffer solution ($pK_{a,w}$) obtained by the spectroscopic method in the present study are in excellent accordance with values reported earlier (Erdemgil et al., 2007). The presence of micelles altered the dissociation equilibria of FA and iFA. The extent to which the micellar environment influences the dissociation equilibrium in micellar solutions (pK_a^{obs}) depends on the partitioning of the compound between the micellar phase and the bulk aqueous phase. Depending on the emulsifier, two effects may contribute to the influence of the micellar environment: solvation or polarity effects and the local pH (Losada Barreiro, Sánchez-Paz, Pastoriza Gallego, & Brávo-Díaz, 2008). In addition, there is a difference in the partitioning between ionised and non-ionised species, i.e., the non-dissociated forms of FA and iFA are subject to stronger hydrophobic attraction by micelles, which results in a higher incorporation (Saikia et al., 2005). On the other hand, electrostatic interactions may reduce the binding to anionic micelles and increase the binding to cationic micelles.

Drummond et al. (1989) described the impact of different emulsifiers on the pK_a value of phenolic compounds and found the same trends as reported in this work, namely an increase of the pK_a^{obs} value in the presence of SDS and Brij and a decrease in the presence of CTAB. They explained the results by the relatively low dielectric constant of the interfacial region and ascribed the effects to the difference between mean solvent properties of the interface and the bulk. The emulsifiers used in the present study have different properties and may thus provide different microenvironments as well as different solubilisation sites (Heins, Sokolowski, Stöckmann, & Schwarz, 2007). In the following sections, effects of each emulsifier will be described separately, because different mechanisms apply, depending on the charge of the emulsifier.

4.4.2. Effect of a Brij microenvironment on the acid base equilibrium and activity

The acidity constant in a homogeneous solvent mixture depends on the polarity of the mixture due to solvation effects, i.e. increasing organic solvent content increases the acidity constant (Beltrán et al., 2003). It has become common practice to evaluate the impact of a micellar environment on acid–base equilibria using non-ionic micelles, due to the altered polarity of the micellar environment compared to water (Fernandez & Fromherz, 1977; Pal & Jana, 1996; Whiddon, Bunton, & Söderman, 2003). On the other hand, it has been suggested that the acidity constant is an intrinsic property of a compound and is independent of the presence of micelles, as long as the environment is sufficiently hydrated. Hence, the acidity constants in water and in aqueous solution were set equal for further calculations in previous studies (Saikia et al., 2005; Souza et al., 2006). The dielectric constant of the headgroup region of non-ionic emulsifiers has been determined to be around 30–35 (Fernandez & Fromherz, 1977). In addition, non-ionic micelles have a higher solubilisation capacity for moderately polar compounds than has water and these compounds are located in the headgroup region of the micelles. As a conclusion, a polarity gradient is present between water and the headgroup region, which dominates over a possible pH gradient. These arguments are in line with the procedure described by Fernandez and Fromherz (1977), Pal and Jana (1996) and Whiddon et al. (2003) to evaluate the effect of the micellar environment. Thus, their method has been applied in the present study.

The pK_a^{app} values of both antioxidants were substantially higher in Brij micelles than were the $pK_{a,w}$ values obtained in buffer solution (Table 3). This is in accordance with results presented by other authors for a number of different compounds (Dupont-Leclerq et al., 2007; Pal & Jana, 1996; Whiddon et al., 2003). The difference between the pK_a values in buffer solution and in the micellar environment (ΔpK_a) was smaller for FA than for iFA. It is suggested that the larger the difference, the deeper is the probe buried in the headgroup region and thus the more non-polar is the solubilisation site. Therefore, it is concluded that FA is somewhat less deeply buried in the headgroup region of Brij micelles than is iFA.

Both FA and iFA exhibited a moderate antioxidant activity in emulsions, despite the lower radical-scavenging potential of iFA than for FA in the ABTS assay (Fig. 3, Table 4). The results show that the ratio of dissociated to non-dissociated acid ($[A^-]_m/[AH]_m$) is slightly higher for FA compared to iFA. This small difference may be superimposed by the effects of different locations. These are reflected by different pK_a^{app} values, so the proximity to radicals could be improved.

4.4.3. Effect of the SDS microenvironment on the acid–base equilibrium and activity

It has been demonstrated by NMR measurements that hydroxycinnamic acids are located in the Stern layer of SDS micelles (Heins, Sokolowski, et al., 2007). The Stern layer contains predominantly water and counter ions. The difference in the polarity between buffer solution and the outer Stern layer, where hydroxycinnamic acids are solubilised, therefore does not contribute to the pK_a^{app} value in the SDS micelle. Thus, $pK_{a,w}$ was used for calculating the pH value at the solubilisation site (pH_{loc}) according to Souza et al. (2006). In addition, it is possible to calculate the surface pH according to the PIE model. According to this model, at low pH, Na^+ of SDS is displaced from the micellar surface by H^+ (Romsted & Zanette, 1988). Increased pK_a^{app} values mean that the low pH in the Stern layer shifts the acid–base equilibria of solutes to the left (Fig. 2). For both FA and iFA, pH_{loc} was not equal to the surface pH calculated by the PIE model. The value of the pH-difference (ΔpH) could account for the distance of the molecule from the micelle surface. If a pH gradient is assumed from the micellar surface to the outer regions of the Stern layer, this would mean that iFA was closer to the surface than was FA. The electric potentials at the solubilisation sites of FA and iFA (ψ_{loc}) were in the range of values reported for SDS micelles at similar ionic strengths and led to the same conclusion (Fernandez & Fromherz, 1977).

$[A^-]_m/[AH]_m$ was higher for FA than for iFA. This result is in accordance to the local pH and electric potential, revealing a location closer to the micelle surface for iFA. The higher antioxidant activity of iFA compared to FA may thus be a result of a deeper intercalation at the o/w interface. A smaller distance to lipid radicals and a more efficient stabilisation of the antioxidant radical cation by the negatively charged headgroups may explain these results (Georges & Berthod, 1983; Murasecco-Suardi, Gassmann, Braun, & Oliveros, 1987). Thus, in an SDS microenvironment, a favourable location of an antioxidant may compensate a generally lower radical-scavenging ability.

4.4.4. Effect of the CTAB microenvironment on the acid–base equilibrium and activity

There is evidence from NMR measurements that hydroxycinnamic acids are located in the relatively hydrophobic palisade layer in CTAB micelles (Heins, Sokolowski, et al., 2007). CTAB micelles are generally drier due to a thinner Stern layer and lower water penetration than SDS or Brij micelles (Berr, 1987). The palisade layer of CTAB micelles still contains a considerable amount of water, but the polarity can be regarded to be below that of the bulk aqueous phase. Thus, a pK_a shift due to the low polarity of the micellar environment should be taken into account. The pK_a^{app} value obtained in Brij micelles, i.e., in a micellar environment without electrostatic effects, was used as $pK_{a,m}$ for the calculation of the pH_{loc} in CTAB micelles (Pal & Jana, 1996). The ionic nature of the micellar surface explains the demand for consideration of the surface pH. Any differences in the dissociation equilibrium between CTAB and Brij micelles were attributed to the electric potential of the cationic micelles and related effects. In addition, the surface pH was calculated according to the PIE model. The difference between the local pH at the solubilisation site of antioxidants and the surface pH may give information about the distance of FA and iFA from the surface plane.

According to the described procedure, FA and iFA experienced different pH values and electric potentials at their respective solubilisation sites (Table 3). The higher potential at the solubilisation site of iFA indicates that iFA is located at a smaller distance from the micellar surface plane than is FA. In addition, iFA was a stronger acid in CTAB micelles than was FA. The low or pro-oxidant activity of both antioxidants in CTAB emulsions is ascribed to the catalytic action of the cationic headgroup of CTAB which increases the homolytic decay of hydroperoxides similarly to catalytic metal ions (Pisarenko & Kasaikina, 2002). Antioxidant activity in metal ion-mediated oxidation processes, in turn, is low or even pro-oxidative (Frankel, 2005). The less pro-oxidant action of iFA compared to FA in CTAB emulsions may be related to the higher degree of dissociation, which is connected with a better stabilisation of the phenoxyl radical.

5. Conclusions

It was possible for the first time to determine the partitioning behaviour of antioxidants in emulsions by UF and to distinguish between the aqueous phase, the coexisting micellar phase and the o/w interface. It was shown that the partitioning of antioxidants in emulsions depends on the type and concentration of the emulsifier. The phenolic antioxidants used were of similar structure and polarity and are characterised by a roughly similar partitioning behaviour. From the oxidation experiments and

partitioning studies, it can be concluded that the partitioning alone cannot explain antioxidant activity in emulsions.

The comparison of the results obtained in the ABTS assay with the storage experiments reveals that the ABTS assay is not suitable for predicting the order of activity of two fairly similar antioxidants in emulsions. This is in agreement with earlier studies, which showed that the microenvironment or reaction field strongly influences the reaction of antioxidants and lipid radicals.

The microenvironment provided by the headgroup region of Brij micelles influenced the acidity of FA and iFA. The different degrees of dissociation and the location within the interface are closely related and affect the ability of the antioxidants to inhibit lipid oxidation. According to the comparison of FA and iFA, an orientation to the oil phase is favourable for increased activity. In addition, the direct exchange of micellar-bound antioxidants with the o/w interface may contribute to the high activities in emulsions with Brij 58.

The acid–base equilibria of FA and iFA in SDS micelles show that iFA was more closely located in the headgroups of SDS molecules than was FA. This decreases the dissociation rate of iFA, but could enhance the stabilisation of the iFA radical cation by the SDS headgroups, which in turn might reduce the tendency to participate in unfavourable side reactions.

In emulsions with CTAB a high degree of dissociation seems to be favourable for the antioxidant activity, as was demonstrated by the comparison of FA and iFA. However, both FA and iFA were weaker antioxidants than in the other emulsions, despite the favourable pH and degree of dissociation. It is suggested that the participation of phenolic antioxidants in side chain reactions is favoured in a CTAB environment, which may lead to the observed pro-antioxidant effects.

In conclusion, the relationships between the acid–base equilibrium of hydroxycinnamic acids, their location at the o/w interface and their ability to inhibit lipid oxidation have been investigated for the first time. Such relationships can only be detected and proven if the specific properties of emulsifiers are taken into account, so that each type of emulsifier has to be considered separately.

References

Amorati, R., Pedulli, G., Cabrini, L., Zambonin, L., & Landi, L. (2006). Solvent and pH effects on the antioxidant activity of caffeic and other phenolic acids. *Journal of Agricultural and Food Chemistry, 54*(8), 2932–2937.

Beltrán, J., Sanli, N., Fonrodona, G., Barrón, D., Özkanb, G., & Barbosa, J. (2003). Spectrophotometric, potentiometric and chromatographic pK_a values of polyphenolic acids in water and acetonitrile-water media. *Analytica Chimica Acta, 484*, 253–264.

Berr, S. (1987). Solvent isotope effects on alkyltrimethylammonium bromide micelles as a function of alkyl chain length. *Journal of Physical Chemistry, 91*, 4760–4765.

Drummond, C., Grieser, F., & Healy, T. (1989). Acid–base equilibria in aqueous micellar solutions. *Journal of the Chemical Society, Faraday Transactions, 85*, 521–535.

Dupont-Leclerq, L., Giroux, S., Henry, B., & Rubini, P. (2007). Solubilization of amphiphilic carboxylic acids in nonionic micelles: Determination of partition coefficients from measurements and NMR experiments. *Langmuir, 23*, 10463–10470.

Erdemgil, F., Sanli, S., Sanli, N., Özkan, G., Barbosa, J., Guiteras, J., et al. (2007). Determination of pK_a values of some hydroxylated benzoic acids in methanol–water binary mixtures by LC methodology and potentiometry. *Talanta, 72*, 489–496.

Fernandez, M. S., & Fromherz, P. (1977). Lipoid pH indicators as probes of electrical potential and polarity in micelles. *The Journal of Physical Chemistry, 81*, 1755–1761.

Frankel, E., Huang, S., Kanner, J., & German, J. (1994). Interfacial phenomena in the evaluation of antioxidants: Bulk oils vs. emulsions. *Journal of Agricultural and Food Chemistry, 42*, 1054–1059.

Frankel, E. N. (2005). *Lipid oxidation* (2nd ed.). The Oily Press.

Georges, J., & Berthod, A. (1983). Microenvironment influence on the electrochemical oxidation of n-methylphenothiazine in aqueous surfactant solutions and in a o/w microemulsion. *Electrochimica Acta, 28*, 735–741.

Gunaseelan, K., Romsted, L., Gonzalez-Romero, E., & Bravo-Diaz, C. (2004). Determining partition constants of polar organic molecules between the oil/interfacial and water/interfacial regions in emulsions: A combined electrochemical and spectrometric method. *Langmuir, 20*, 3047–3055.

Heins, A., McPhail, D., Sokolowski, T., Stöckmann, H., & Schwarz, K. (2007). The location of phenolic antioxidants and radicals at interfaces determines their activity. *Lipids, 42*(6), 573–582.

Heins, A., Sokolowski, T., Stöckmann, H., & Schwarz, K. (2007). Investigating the location of propyl gallate at surfaces and its chemical microenvironment by ^{1}H NMR. *Lipids, 42*, 561–572.

Huang, S.-W., Frankel, E., Aeschbach, R., & German, J. (1997). Partition of selected antioxidants in corn oil–water model systems. *Journal of Agricultural and Food Chemistry, 45*(6), 1991–1994.

Huang, S.-W., Hopia, A., Schwarz, K., Frankel, E., & German, J. (1996b). Antioxidant activity of a-tocopherol and trolox in different lipid substrates: Bulk oils vs oil-in-water emulsions. *Journal of Agricultural and Food Chemistry, 44*(2), 444–452.

Lampi, A., & Kamal-Eldin, A. (1998). Effect of α- and γ-tocopherols on thermal polymerization of purified high-oleic sunflower triacylglycerols. *Journal of the American Oil Chemists' Society, 75*, 1699–1703.

Losada Barreiro, S., Sánchez-Paz, V., Pastoriza Gallego, M. J., & Brávo-Díaz, C. (2008). Micellar effects on the reaction between an arenediazonium ion and the antioxidants gallic acid and octyl gallate. *Helvetica Chimica Acta, 91*, 21–34.

Mei, L., McClements, D. J., & Decker, E. A. (1999). Lipid oxidation in emulsions as affected by charge status of antioxidants and emulsion droplets. *Journal of Agricultural and Food Chemistry, 47*(6), 2267–2273.

Mukerjee, P., & Ko, J.-S. (1992). Solubilization of ethyl o-, m-, and p-aminobenzoates in micelles of different charge types: Interfacial adsorption and orientation effects. *Journal of Physical Chemistry, 96*(14), 6090–6094.

Murasecco-Suardi, P., Gassmann, E., Braun, A., & Oliveros, E. (1987). Determination of the quantum yield of intersystem crossing of rose bengal. *Helvetica Chimica Acta, 70*, 1760–1773.

Oehlke, K., Garamus, V., Heins, A., Stöckmann, H., & Schwarz, K. (2008). The partitioning of emulsifiers in o/w emulsions: A comparative study of SANS, ultrafiltration and dialysis. *Journal of Colloid and Interface Science, 322*, 294–303.

Ozgen, M., Reese, R., Tulio, A., Jr., Scheerens, J., & Miller, A. (2006). Modified 2,2-azino-bis-3-ethylbenzothiazoline-6-sulfonic acid (ABTS) method to measure antioxidant capacity of selected small fruits and comparison to ferric reducing antioxidant power (FRAP) and 2,2'-diphenyl-1-picrylhydrazyl (DPPH) methods. *Journal of Agricultural and Food Chemistry, 54*, 1151–1157.

Pal, T., & Jana, N. (1996). Polarity dependent positional shift of probe in micellar environment. *Langmuir, 12*, 3114–3121.

Pena, A., & Miller, C. (2006). Solubilization rates of oils in surfactant solutions and their relationship to mass transport in emulsions. *Advances in Colloid and Interface Science*, 241–257.

Pisarenko, L., & Kasaikina, O. (2002). Free radical formation during ethylbenzene oxidation catalyzed by cetyltrimethylammonium bromide. *Russian Chemical Bulletin, International Edition, 51*, 449–456.

Polewski, K., Kniat, S., & Slawinska, D. (2002). Gallic acid, a natural antioxidant, in aqueous and micellar environment: Spectroscopic studies. *Current Topics in Biophysics, 26*(2), 217–227.

Romsted, L. (1985). Quantitative treatment of benzimidazole deprotonation equilibria in aqueous micellar solutions of cetyltrimethylammonium ion (CTAX, X^- = Cl^-, Br^-, and NO^{3-}) surfactants. 1. Variable surfactant concentration. *Journal of Physical Chemistry, 89*, 5107–5113.

Romsted, L., & Zanette, D. (1988). Quantitative treatment of indicator equilibria in micellar solutions of sodium decyl phosphate and sodium lauryl sulfate. *Journal of Physical Chemistry, 92*, 4690–4698.

Saikia, P., Bora, M., & Dutta, R. (2005). Acid–base equilibrium of anionic dyes partially bound to micelles of nonionic surfactants. *Journal of Colloid and Interface Science, 285*, 382–387.

Schreier, S., Frezzatti, W., Araujo, P., Chaimovich, H., & Cuccovia, I. (1984). Effect of lipid membranes on the apparent pK of the local anesthetic tetracaine spin label and titration studies. *Biochimica et Biophysica Acta, 769*, 231–237.

Silva, F., Borges, F., Guimaraes, C., Lima, J., Matos, C., & Reis, S. (2000). Phenolic acids and derivatives: Studies on the relationship among structure, radical scavenging activity, and physicochemical parameters. *Journal of Agricultural and Food Chemistry, 48*, 2122–2126.

Souza, T., Zanette, D., Kawanami, A., de Rezende, L., Ishiki, H., do Amaral, A., et al. (2006). pH at the micellar interface: Synthesis of pH probes derived from salicylic acid, acid–base dissociation in sodium dodecyl sulfate micelles, and Poisson–Boltzmann simulation. *Journal of Colloid and Interface Science, 297*, 292–302.

Stöckmann, H. (1999). Untersuchungen zum Einfluss des Verteilungs- und Solubilisierungsverhaltens auf die Aktivität von Wirkstoffen in dispersen Systemen am Beispiel von Antioxidantien in O-W-Emulsionen. Diss., Univ. Hannover.

Stöckmann, H., & Schwarz, K. (1999). Partitioning of low molecular weight compounds in oil-in-water emulsions. *Langmuir, 15*(19), 6142–6149.

Stöckmann, H., Schwarz, K., & Huynh-Ba, T. (2000). The influence of various emulsifiers on the partitioning and antioxidant activity of hydroxybenzoic acids and their derivatives in oil-in-water emulsions. *JAOCS, 77*(5), 535–541.

Whiddon, C., Bunton, C., & Söderman, O. (2003). Titration of fatty acids in sugar-derived (APG) surfactants: A^{13} C NMR study of the effect of headgroup size, chain length, and concentration on fatty acid pK_a at a nonionic micellar interface. *Journal of Physical Chemistry B, 107*, 1001–1005.

Zana, R. (1996). Dynamics of organized assemblies of amphiphiles in solution. In V. Pillai & D. Shah (Eds.), *Dynamic properties of interfaces and association structures*. Champaign: AOCS Press.

Food Chemistry 118 (2010) 56–61

Contents lists available at ScienceDirect

Food Chemistry

journal homepage: www.elsevier.com/locate/foodchem

Thermal degradation of sucralose and its potential in generating chloropropanols in the presence of glycerol

Anja Rahn, Varoujan A. Yaylayan *

McGill University, Department of Food Science and Agricultural Chemistry, 21,111 Lakeshore, Ste. Anne de Bellevue, Quebec, Canada H9X 3V9

ARTICLE INFO

Article history:
Received 11 March 2009
Received in revised form 24 March 2009
Accepted 20 April 2009

Keywords:
Sucralose degradation products
Formation of chloropropanols
Levoglucosenone
Dehydrochlorination of sucralose

ABSTRACT

Sucralose, a polychlorinated synthetic high-intensity sweetener is being increasingly used in relatively large amounts in baked products under high temperature environments. This necessitates understanding its thermal decomposition and studying the consequences of hydrogen chloride release from sucralose and its ability to chlorinate various food related ingredients such as glycerol to generate chloropropanols a potentially toxic class of compounds. Studies conducted on the thermal degradation of sucralose under dry heating conditions have indicated that the glycosidic cleavage occurs through the formation of a galactopyranosyl cation contrary to sucrose where fructofuranosyl cation dictates the major breakdown products. Consequently the major product detected was levoglucosenone and its precursor. Subsequent degradation of the two monosaccharide derivatives causes dehydrochlorination and dehydration reactions to produce furan-related products. In addition, pyrolysis of sucralose in the presence of glycerol generated significant amounts of 3-monochloropropanediol and 1,2- and 1,3-dichloropropanols based on the relative intensities of their chromatographic peaks which amounted to 15% of the total chromatographic peak area.

1. Introduction

Sucralose, a non-nutritive, high–intensity sweetener that has replaced sucrose in a broad range of food products (Goldsmith & Merkel, 2001), due to the numerous toxicological studies confirming its safety (Goldsmith, 2000; Grice & Goldsmith, 2000; John, Wood, & Hawkins, 2000a, 2000b; Roberts, Renwick, Sims, & Snodin, 2000; Sims, Roberts, Daniel, & Renwick, 2000; Wood, John, & Hawkins, 2000). Although FDA allowed its use in food products however, it has yet to grant it GRAS status. The popularity of this food additive has lead to an average daily intake (ADI) of 1.1 mg/kg body weight (bw), while the ADI of the cumulative hydrolysis products; 1,6-dichloro-1,6-dideoxyfructose (1,6-DCF) and 4-chloro-4-deoxygalactose (4-CG), is estimated at 3.2 mg/kg bw (Grice & Goldsmith, 2000). Under alkaline conditions sucralose also generates 3′,6′-anhydro-4,1′-dichlorogalactosucrose (Barndt & Jackson, 1990). Although hydrolysis of the glycosidic bond, yielding 1,6-DCF and 4-CG, may occur in aqueous systems under acidic conditions as has been reported by Goldsmith and Merkel (2001), however, these results cannot be extrapolated to high temperature, low moisture environments such as baking. As has been suggested by many (Perez Locas & Yaylayan, 2008; Queneau, Jarosz, Lewandowski, & Fitremann, 2008) the hydrolysis of sucrose, into its corresponding monosaccharides, can be viewed as a secondary reaction in which the fructofuranosyl cation, initially formed, is then hydrolyzed in the presence of water. Sucralose, being sucrose analogue, one anticipates degrading in a similar fashion. In this paper we aim to investigate thermal degradation and dehydrohalogenation reactions of sucralose in high temperature and low moisture conditions as well as examine the capacity of glycerol in capturing any hydrogen chloride released and its conversion into chloropropanol derivatives. Barndt and Jackson (1990) attempted to demonstrate using radiolabeling techniques, that sucralose minimally degrades in baked goods (180–300 °C); however, these results lack credibility due to inefficient separation technique used in analysing the degradation products. As demonstrated later by Hutchinson (1996), sucralose completely degrades with the release of chloride ions at 180 °C in aqueous solutions at all pH levels (3, 7, and 11) studied. Analysis of the volatile compounds has also indicated that dehydrochlorination steps were important for their production (Hutchinson, Ho, & Ho, 1999).

2. Materials and methods

All reagents and chemicals were purchased from Aldrich Chemical Co. (Milwaukee, WI). Glycerol was purchased from Fluka (Steinheim, Germany). Sucralose was obtained from Tate & Lyle (Montreal, Canada).

* Corresponding author. Tel.: +1 514 398 7918; fax: +1 514 398 7977.
E-mail address: varoujan.yaylayan@mcgill.ca (V.A. Yaylayan).

0308-8146/$ - see front matter © 2009 Elsevier Ltd. All rights reserved.
doi:10.1016/j.foodchem.2009.04.133

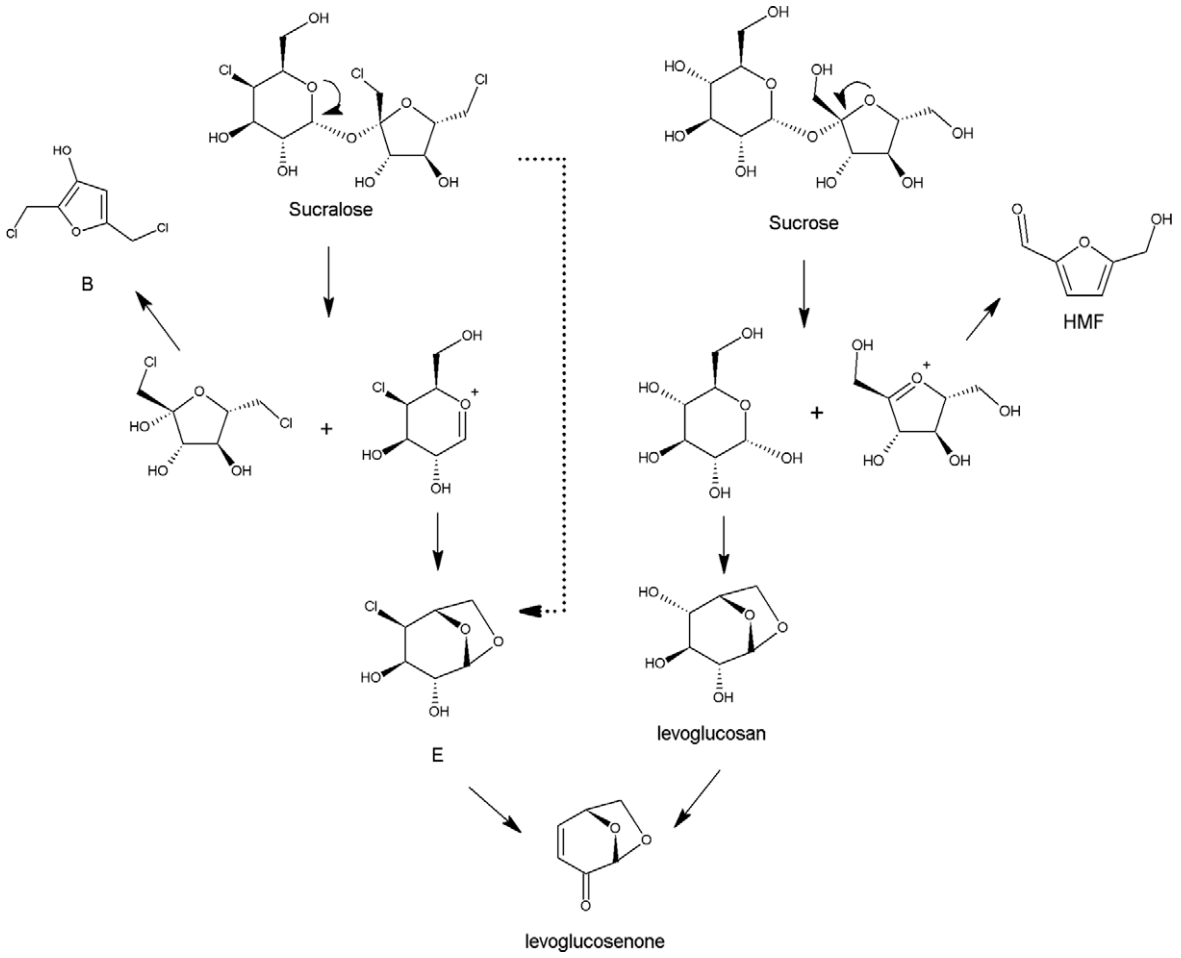

Fig. 1. Comparison of the degradation pathways of sucrose and sucralose.

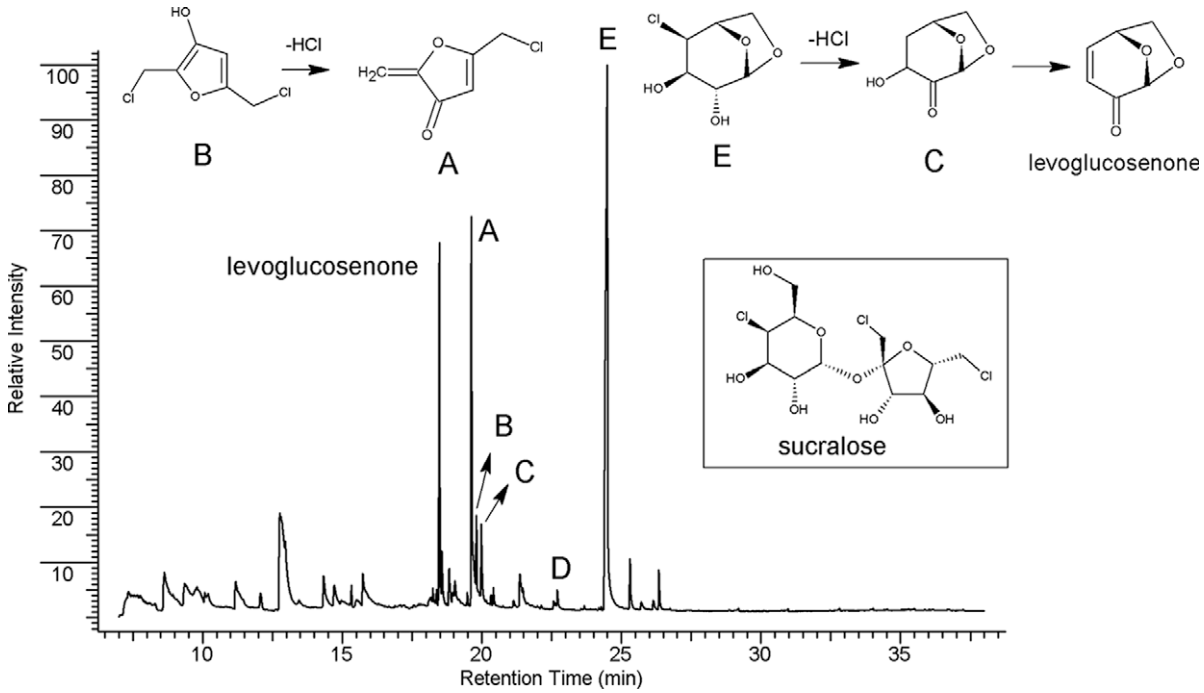

Fig. 2. Pyrogram of sucralose generated at 250 °C indicating proposed degradation products.

2.1. Pyrolysis-gas chromatography–mass spectrometry (Py-GC/MS) analysis

A Varian CP-3800 gas chromatograph coupled to a Saturn 2000 ion trap detector interfaced to a CDS Pyroprobe 2000 unit through a valved interface (CDS 1500) was used for Py-GC/MS analysis. In all experiments, the sucralose/glycerol model mixtures (1 mg, 1:2 M ratio) were introduced inside the quartz tube (0.3 mm thickness), which was plugged with quartz wool, and inserted into the coil probe. Prior to pyrolysis, argon gas was directed at the entrance of the pyroprobe interface to prevent the introduction of air into the pyroprobe interface. The temperature of the pyroprobe interface was set at 250 °C. Model systems were initially pyrolysed at 250 °C with a total heating time of 20 s. Samples were left in the interface for a total of 2 min, then removed. After 5 min, the sample was introduced into the interface under a steady stream of Helium. The initial temperature of the column was set at −5 °C for 5 min and then increased to 50 °C at a rate of 50 °C/min; immediately, the temperature was further increased to 280 °C at a rate of 8 °C/min and kept at 280 °C for 6 min. A constant flow of 1.5 mL/min was used during analysis. The capillary direct MS interface temperature was 250 °C; the ion source temperature was 175 °C. The ionisation voltage was 70 eV, and the electron multiplier was set at 1500 V. The mass range analysed was 20–650 amu. The column was a fused silica DB-5 MS column (50 m length, 0.2 mm i.d., and 0.33 μm film thickness; J&W Scientific). The identity and purity of the chromatographic peaks were determined by using NIST AMDIS version 2.1 software.

2.2. Pyrolysis in the presence of moisture and oxidative Py-GC/MS

Pyrolysis under air or in the presence of water was achieved through modification of the above-mentioned GC to allow gas stream switching and subsequent isolation of the pyrolysis chamber from the analytical stream. The pyrolysates generated under air or in the presence of moisture were initially collected onto the trap, which retained the organic volatiles and vented the carrier gas (air) and/or moisture. The trap was subsequently flushed with

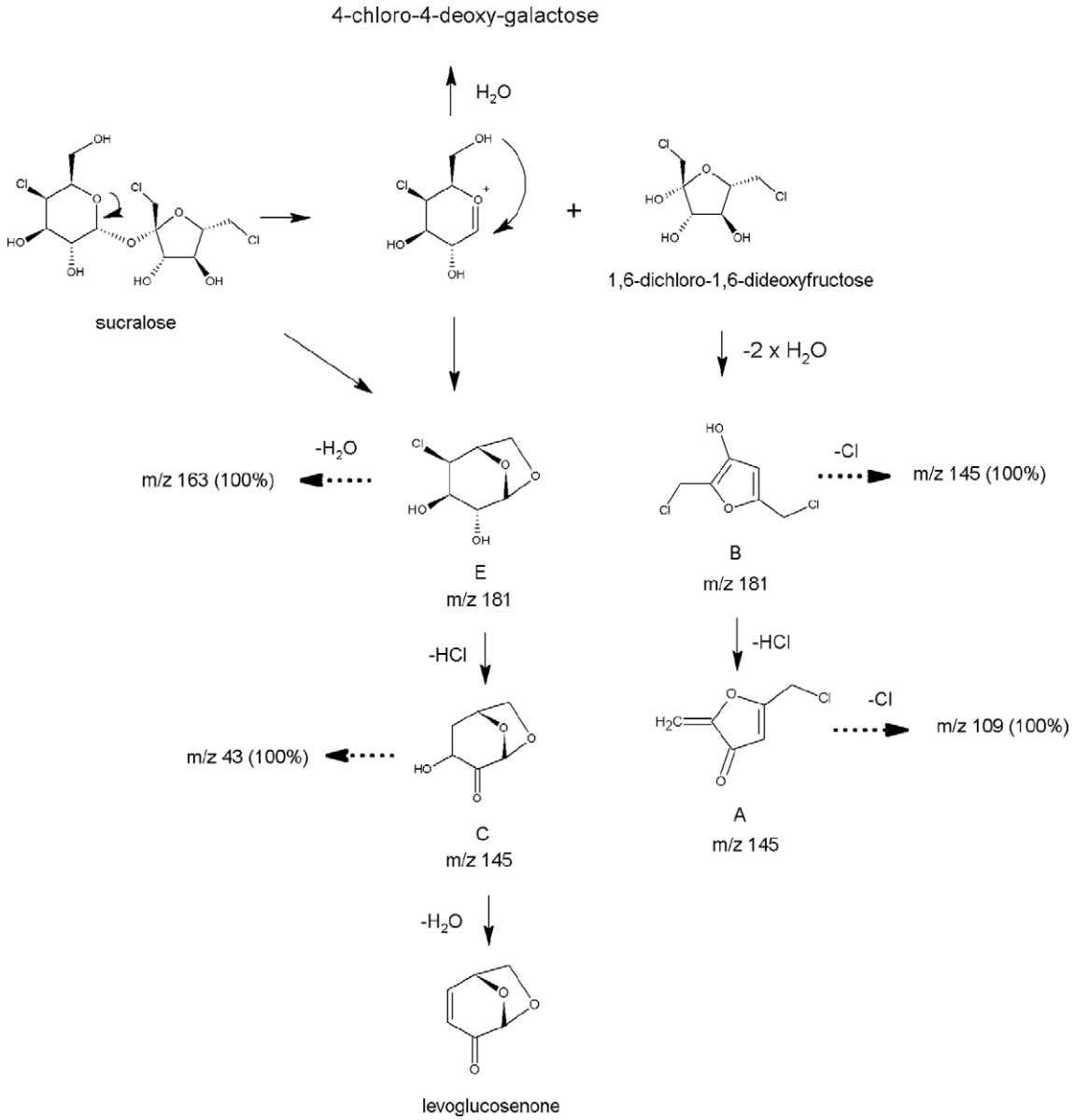

Fig. 3. Proposed mechanism of degradation of sucralose and formation of compounds A, B C, E, and levoglucosenone, showing their corresponding mass spectrometric base peaks.

helium and heated to desorb the collected volatiles. For detailed description see Yaylayan, Haffenden, Chu, and Wnorowski (2005).

2.3. Tentative characterisation of the thermal degradation products of sucralose

The mass spectra and chlorine content of the unknown peaks A to E shown in Figs. 1–3 are listed below. Chlorine content was estimated from the natural isotopic abundance of the ions in question.

- Unknown A. R_T = 19.631 min, MS 109(100), **145**(38), 144(23), 81(16), 53(13), 147(12), 146(10), 108(10), 52(9), 110(7). Number of chlorine atoms = 1, number of chlorine atoms in fragment at m/z 109 = 0.
- Unknown B. R_T = 19.810 min, MS 145(100), 39(54), 147(33), **181**(40), 40(19), 180(16), 183(25), 68(15), 43(14), 109(16). Number of chlorine atoms = 2, number of chlorine atoms in fragment m/z 145 = 1 and m/z 109 = 0.
- Unknown C. R_T = 19.986 min, MS 43(100), 29(93), 41(70), 39(66), **145**(62), 57(40), 27(39), 69(40), 70(35), 85(31). Number of chlorine atoms = 0.
- Unknown D. R_T = 22.703 min, MS 76(100), **180**(50), 39(45), 182(32), 41(35), 78(33), 48(17), 49(10), 27(10), 29(11). Number of chlorine atoms = 2, number of chlorine atoms in fragment at m/z 105 = 1 and m/z 76 = 1.
- Unknown E. R_T = 24.491 min, MS 163(100), **181**(47), 165(34), 39(21), 81(17), 162(24), 183(13), 103(14), 180(13), 97(13). Number of chlorine atoms = 1, number of chlorine atoms in fragment at m/z 163 = 1.

2.4. Statistical analysis

Statistical analysis was performed using SAS 9.1 TS level 1MS, (SAS Institute Inc., Cary, N.C., USA, 2002–2003). Two statistical tests were performed; analysis of variance (ANOVA) and least significant difference (LSD). A value of 0.05 for "alpha" was used throughout the statistical analysis. Shapiro–Wilk test was also used to establish the data collected came from a normally distributed population, while ANOVA was used to establish that the means for each compound significantly varied, depending on the reaction conditions listed in Tables 2 and 3. To distinguish the effect of each reaction on the production of each compound LSD was performed.

2.5. Identification of chloropropanols

All chloropropanols were identified by their retention times and through mass spectral library comparisons except 1,2-dichloropropanol which was confirmed only through NIST library match (see Table 1).

Table 2
Normalized relative formation efficiency[a] of levoglucosenone and chloropropanols in sucralose glycerol mixture heated at 250 °C for 20 s based on area/mole of sucralose ($\times 10^{10}$).

	Levoglucosenone	1,2-DCP	3-MCPD	1,3-DCP
He	1.1	3.4	105.2	19.4
Air	4.6	5.1	99.2	18.3
1 μL H_2O	2.4	1.3	55.2	16.5
2 μL H_2O	1.5	1.0	70.7	17.6

3-MCPD = 3-chloropropanediol; 1,3-DCP = 1,3-dichloropropanol; 1,2-DCP = 1,2-dichloropropanol.
[a] Based on three replicates with relative standard deviation of % 6.3.

Table 3
Relative and per cent chloropropanol distribution[a] in sucralose glycerol mixture heated at 250 °C for 20 s.

	1,2-DCP	3-MCPD	1,3-DCP
He	1 (2.6%)	31 (81.6%)	6 (15.7%)
Air	1 (4.1%)	19 (79.2%)	4 (16.6%)
1 μL H_2O	1 (1.7%)	43 (75.4%)	13 (22.8%)
2 μL H_2O	1 (1.1%)	71 (78.8%)	18 (20%)

3-MCPD = 3-chloropropanediol; 1,3-DCP = 1,3-dichloropropanol; 1,2-DCP = 1,2-dichloropropanol.
[a] Based on values reported in Table 2.

3. Results and discussion

3.1. Thermal degradation of sucralose

To gain insight into the thermal degradation pathways of sucralose, the degradation profile of sucrose generated by Pyrolysis-GC/MS was studied and compared due to their structural similarities and due to lack of available isotopically labelled sucralose. In a previous study, Perez Locas and Yaylayan (2008) using specifically ^{13}C-labelled sucrose at C-1 of the fructose moiety have identified the main event in the thermal degradation of sucrose under dry heating conditions to be the glycosidic bond cleavage initiated by the lone pair electrons of the ring oxygen of the fructofuranosyl moiety generating a free glucose and a fructofuranosyl cation (see Fig. 1). As a consequence of the formation of this reactive fructofuranosyl cation the efficiency of the conversion of sucrose into 5-(hydroxymethyl)-2-furaldehyde (HMF) was increased by 28-fold relative to glucose and that HMF generated from sucrose constituted one of the major peaks of the degradation product with 90% originating from the fructose moiety as indicated by the label incorporation into the HMF (Perez Locas & Yaylayan, 2008). The subsequent conversion of the glucose moiety into levoglucosan and levoglucosenone constituted only minor pathways of its degradation profile. Contrary to sucrose, the thermal degradation of sucralose under dry heat-

Table 1
Mass spectrometric data of glycerol/sucralose reaction products generated through pyrolysis at 250 °C for 20 s.

Compounds	m/z (% intensity)	Retention time
Levoglucosenone[a,b]	98(100), 96(34), 39(71), 53(41), 68(58), 97(56), 42(23), 41(17), 70(15), 29(54)	18.48
Levoglucosenone[b]	98(100), 96(81), 39(73), 53(69), 68(68), 97(50), 42(40), 41(36), 70(34), 29(32)	18.47
3-MCPD[b]	43(100), 44(63), 61(62), 79(35), 31(48), 79(35), 29(68), 27(18), 95(20), 57(20), 93(60)	15.75
3-MCPD[a,b]	43(100), 44(100), 61(98), 79(70), 31(42), 15(24), 81(23), 29(22), 27(16), 78(9)	15.30
1,3-DCP[b]	79(100), 43(55), 81(40), 49(20), 29(30), 39(13), 42(15), 51(6.5), 27(13), 75(35)	14.22
1,3-DCP[a,b]	79(100), 43(37), 81(36), 49(13), 29(6), 39(5), 42(5), 51(5), 27(4), 15(3)	14.31
1,2-DCP[b]	62(100), 64(32), 31(54), 27(30), 29(68), 63(9.2), 57(28), 66(1), 92(8), 61(13)	16.27
1,2-DCP[c]	62(100), 64(48), 31(32), 27(14), 29(9), 63(8), 57(8), 66(7), 92(6), 61(5)	–

3-MCPD = 3-chloropropanediol; 1,3-DCP = 1,3-dichloropropanol; 1,2-DCP = 1,2-dichloropropanol.
[a] Positive identification by NIST library.
[b] Standard.
[c] Library spectrum only (standard not available).

ing conditions generated levoglucosenone as one of the major peaks in the chromatogram (see Fig. 2) and this amounted to a 160-fold increase in intensity compared to sucrose under identical conditions. This dramatic increase in the intensity of the levoglucosenone may indicate a shift in the sucralose degradation pathway compared to sucrose. Due to the presence of two electron withdrawing chlorine atoms in the fructose moiety of sucralose, the electron flow during glycosidic bond cleavage may be directed towards fructose moiety away from galactose ring resulting in the formation of either a reactive galactopyranosyl cation or the direct formation of structure E; both can be considered as efficient precursors of levoglucosenone (Fig. 1). The galactopyranosyl cation can be easily converted into E through nucleophilic attack of the C-6 hydroxyl group or in the presence of water can be converted into 4-chloro-4-deoxygalactose (4-CG). The structure E which can be considered as equivalent to levoglucosan (see Fig. 1) through dehydration and dehydrochlorination reactions can be converted into levoglucosenone one of the major degradation products of sucralose. Further evidence was provided for the possible formation of the galactopyranosyl cation when sucralose was heated in refluxing methanol in the presence of *p*-toluenesulfonic acid and then analysed for the changes observed in the intensities of compound E and levoglucosenone. The results have indicated a significant reduction in the intensities of both compounds. As has been demonstrated in the case of sucrose (Perez Locas & Yaylayan, 2008), methanol is able to trap such cations as methyl glycosides and prevent their further degradation.

If the glycosidic cleavage of sucralose indeed proceeds as proposed in Fig. 1, then logical intermediates resulting from the degradation of E and 1,6-dichloro-1,6-dideoxyfructose should be formed and could tentatively be identified using the calculated molecular weights as shown in Fig. 3. The inspection of the pyrogram of sucralose has revealed that the major peak (24.49 min) in the pyrogram corresponded to the proposed structure E (see Fig. 2) having a molecular ion at *m*/*z* 181 and possessing only one chlorine atom based on natural isotope distribution pattern and generating a base peak at *m*/*z* 163 through a neutral loss of a water molecule. The base peak at *m*/*z* 163 retains the chlorine atom, consistent with the proposed structure. If intermediate E undergoes dehydrochlorination it should produce the structure C (see Figs. 2 and 3). A peak (19.98 min) in the chromatogram (Fig. 2) with a molecular ion at *m*/*z* 145 was identified and the natural isotope distribution pattern indicated that this compound does not contain a chlorine atom, consistent with proposed structure. On the other hand, 1,6-dichloro-1,6-dideoxyfructose can lose two molecules of water to generate structure B which in turn can undergo dehydrochlorination to generate structure A (see Figs. 2 and 3). Two peaks one eluting at 19.81 min (peak B) and other at 19.63 min (peak A) were identified in the pyrogram of sucralose (Fig. 2) that are consistent with the specifications of the two structures. Structure B contains two chlorine atoms and it generates a base peak at *m*/*z* 145 through loss of chlorine atom. The base peak at *m*/*z* 145 contains only one chlorine atom. Finally structure A with a molecular ion at *m*/*z* 145 containing a single chlorine atom was identified. The base peak generated through the loss of chlorine atom at *m*/*z* 109 that contains no other chlorine atoms supporting the proposed structure. Although all the intermediates A to E mentioned above are proposed logical structures, however, levoglucosenone was positively characterised using a mass spectral library and by the retention time of the suspected levoglucosenone peak with the known levoglucosenone peak resulting from pyrolysis of D-glucose and sucrose (Halpern, Riffer, & Broido, 1973; Riffer, 2000; Sharfizadeh, Furneaux, Stevenson, & Cochran, 1978) supporting the identity of the peak.

3.2. Sucralose as a chlorinating agent: formation of chloropropanols

As demonstrated above, degradation of sucralose through dehydrochlorination reactions is a viable pathway that can theoretically generate three moles of hydrochloric acid per mole of sucralose through such transformation as E–C and B–A. In addition, sucralose being utilised in baked goods at concentrations between 300–600 ppm (Chapello, 1998; Goldsmith & Merkel, 2001) can release hydrogen chloride in these products during baking that can react with glycerol generating various chloropropanols known for their toxicity. To evaluate the potential of sucralose to chlorinate glycerol, glycerol–sucralose mixtures were investigated using Py-GC/MS in the presence and absence of air and water to determine their effect on the efficiency of formation of chloropropanols. Analysis of the data (see Table 1) have indicated that indeed degradation of sucralose in the presence of glycerol generated the following three chloropropanols (amounting to 15% of the total area count of all the peaks); 3-monochloropropanediol (3-MCPD), 1,2-dichloropropanol (1,2-DCP) and 1,3-dichloropropanol (1,3-DCP) with relative amounts indicated in Table 2, however, 2-monochloropropanediol (2-MCPD) was not detected. Literature data (Collier, Cromie, & Davies, 1991) indicates that the initially formed 3-MCPD and 2-MCPD are further chlorinated to form 1,2- and 1,3-DCP with 3-MCPD and 1,3-DCP being always the major products consistent with our observation. Under pyrolytic conditions 2-MCPD formed may quickly be converted into 1,2-DCP and due to its lower yield may not be detected. When 3-MCPD was pyrolysed in the presence of sucralose the further chlorination resulted in the formation of 1,2- and 1,3-DCP in a ratio of 1:22 compared to 1:6 observed in sucralose glycerol model system (Table 3). This excess can be attributed to the formation of 1,2-DCP from the undetected 2-MCPD in sucralose glycerol model system. To evaluate the role of moisture and oxidative conditions on the production and the relative distribution of chloropropanols, statistical analysis was used to determine whether their generation was significantly affected by the experimental conditions. The results of such analysis have indicated that although oxidative pyrolysis or pyrolysis in the presence of moisture did not alter much relative distribution of chlorophenols in the reaction mixture, however, it did enhance slightly generation of 1,3-DCP on the expense of 3-MCPD.

4. Conclusion

Degradation of sucralose in the presence of glycerol may generate different chloropropanols in addition to levoglucosenone a well documented degradation product of sucrose and glucose. Caution should be exercised in the use of sucralose as a sweetening agent during baking of food products containing glycerol and or lipids due to the potential formation of toxic chloropropanols.

Acknowledgements

The authors acknowledge funding for this research by the Natural Sciences and Engineering Research Council of Canada (NSERC).

References

Barndt, R. L., & Jackson, G. (1990). Stability of sucralose in baked goods. *Food Technology, 44*(1), 62–66.

Chapello, W. J. (1998). The use of sucralose in baked goods and mixes. *Cereal Foods World, 43*(9), 716–717.

Collier, P. D., Cromie, D. D. O., & Davies, A. P. (1991). Mechanism of formation of chloropropanols present in protein hydrolysates. *JAOCS, 68*, 785–790.

Goldsmith, L. A. (2000). Acute and subchronic toxicity of sucralose. *Food and Chemical Toxicology, 38*, S53–S69.

Goldsmith, L. A., & Merkel, C. M. (2001). Sucralose. In L. O'Brien Nabors & R. C. Geladi (Eds.), *Alternative sweeteners* (pp. 185–207). New York: CRC Press.

Grice, H. C., & Goldsmith, L. A. (2000). Sucralose – An overview of the toxicity data. *Food and Chemical Toxicology, 38*, S1–S6.

Halpern, Y., Riffer, R., & Broido, A. (1973). Levoglucosenone (1,6-anhydro-3,4-dideoxy-δ-3-beta.-D-pyranosen-2-one). Major product of the acid catalyzed pyrolysis of cellulose and related carbohydrates. *The Journal of Organic Chemistry, 38*(20), 204–209.

Hutchinson, S. A. (1996). Ph.D. Dissertation. New Brunswick, New Jersey: Rutgers University.

Hutchinson, S. A., Ho, G. S., & Ho, Chi-Tang (1999). Stability and degradation of the high-intensity sweeteners: Aspartame, alitame, and sucralose. *Food Reviews International, 15*(2), 249–261.

John, B. A., Wood, S. G., & Hawkins, D. R. (2000a). The pharmacokinetics and metabolism of sucralose in the rabbit. *Food and Chemical Toxicology, 38*, S111–S113.

John, B. A., Wood, S. G., & Hawkins, D. R. (2000b). The pharmacokinetics and metabolism of sucralose in the mouse. *Food and Chemical Toxicology, 38*, S107–S110.

Perez Locas, C., & Yaylayan, V. (2008). Isotope labeling studies on the formation of 5-(hydroxymethyl)-2-furaldehyde (HMF) from sucrose by pyrolysis-GC/MS. *Journal of Agricultural and Food Chemistry, 56*, 6717–6723.

Queneau, Y., Jarosz, S., Lewandowski, B., & Fitremann, J. (2008). Sucrose chemistry and applications of sucrochemicals. *Advances in Carbohydrate Chemistry and Biochemistry, 61*, 218–271.

Riffer, Richard (2000). Nonsugars and sugar refining. In C. C. Chou (Ed.), *Handbook of sugar refining: A manual for design and operation of sugar refining facilities*. New York: John Wiley and Sons (p. 636).

Roberts, A., Renwick, A. G., Sims, J., & Snodin, D. J. (2000). Sucralose metabolism and pharmacokinetics in man. *Food and Chemical Toxicology, 38*, S31–S41.

Sharfizadeh, F., Furneaux, R. H., Stevenson, T. T., & Cochran, T. G. (1978). Acid-catalyzed pyrolytic synthesis and decomposition of 1,4:3,6-dianhydro-α-D-glucopyranose. *Carbohydrate Research, 61*, 519–528.

Sims, J., Roberts, A., Daniel, J. W., & Renwick, A. G. (2000). The metabolic fate of sucralose in rats. *Food and Chemical Toxicology, 38*, S115–S121.

Wood, S. G., John, B. A., & Hawkins, D. R. (2000). The pharmacokinetics and metabolism of sucralose in the dog. *Food and Chemical Toxicology, 38*, S99–S106.

Yaylayan, V. A., Haffenden, L., Chu, F. L., & Wnorowski, A. (2005). Oxidative pyrolysis and postpyrolytic derivatization techniques for the total analysis of Maillard model systems: Investigation of control parameters of Maillard reaction pathways. *The Maillard reaction: Chemistry at the interface of nutrition, aging and disease, 1043*, 41–54.

Food Chemistry 118 (2010) 62–66

Contents lists available at ScienceDirect

Food Chemistry

journal homepage: www.elsevier.com/locate/foodchem

Antioxidant and anticancer activities of 8-hydroxypsoralen isolated from wampee [*Clausena lansium* (Lour.) Skeels] peel

K. Nagendra Prasad [a], Haihui Xie [a], Jing Hao [a], Bao Yang [a], Shengxiang Qiu [a], Xiaoyi Wei [a], Fang Chen [b], Yueming Jiang [a,*]

[a] South China Botanical Garden, Chinese Academy of Sciences, Guangzhou 510650, People's Republic of China
[b] Department of Food Science and Human Nutrition, Clemson University, Clemson, SC 29634, USA

ARTICLE INFO

Article history:
Received 22 January 2009
Received in revised form 9 April 2009
Accepted 20 April 2009

Keywords:
8-Hydroxypsoralen
Antioxidant activity
Clausena lansium
Cytotoxicity

ABSTRACT

Fruits of wampee [*Clausena lansium* (Lour.) Skeels] contain a significant amount of coumarins with many health benefits. The activity-guided separation of an ethyl acetate-soluble fraction on a polyamide column followed by silica gel column and high performance liquid chromatography (HPLC) preparation afforded a pure compound, which was identified to be 8-hydroxypsoralen based on the ^{1}H, ^{13}C NMR (nuclear magnetic resonance), and ESI-MS (electrospray ionisation mass spectrometric) analysis. This isolate exhibited good scavenging activities against DPPH radical and superoxide anion as well as significant reducing power. It also showed potent proliferation inhibitory activity against human hepatocellular liver carcinoma cell line (HepG2), human lung adenocarcinoma epithelial cell line (A549) and human cervical carcinoma cell line (HELA). This is the first report on the antioxidant and cytotoxic properties of *C. lansium* fruit extract. The food and pharmaceutical industry could be benefited by the usage of this extract containing this constituent.

1. Introduction

Antioxidants possess the ability to protect the cellular organelles from damage caused by free radicals induced oxidative stress. Free radicals include hydroxyl radical, superoxide anion radical and hydrogen peroxide. Highly reactive free radicals which are formed by exogenous chemicals, stress or in the food system are capable of oxidising biomolecules, resulting in cancer, coronary heart disease and hypertension (Thomson, 1995). Generally, most of the free radicals generated from metabolism are scavenged by endogenous defence system such as catalase, superoxide dismutase and peroxidase–glutathione system (Hu, Louie, Cross, Motchink, & Halliwell, 1992). However, in many cases such as in unhealthy physical condition, ageing, or under stress environments, the exogenous antioxidants are either exhausted or insufficient to scavenge these radicals generated which resulted in diseases associated with oxidative stress and damage. Thus, the search for natural products represents an area of great interest in which the plant kingdom has been documented the most important source to provide many antioxidant and cancer chemopreventive agents with novel structures and unique mechanism of action (Kalt, 2001). Therefore, the phytochemicals from fruits and vegetables hold promising potential in the development of health foods, nutritional supplements and herbal medicines for the application as antioxidants and cancer chemopreventive agents.

Wampee [*Clausena lansium* (Lour.) Skeels] belongs to *Rutaceae* family which is distributed widely in India, southern China, Thailand and Vietnam. The fruit is about 2 cm in diameter, ripens from May to July and can be eaten with the peel at a full ripe stage. It contains 1–3 seeds and the pulp is highly acidic. The pulp can be added to fruit cups or made into pie, jam or jelly. Previous chemical studies on *C. lansium* included the characterisation of coumarin (Khan, Naqvi, & Ishratullah, 1983) from the bark, triterpene alcohol from aerial parts (Lakshmi, Raj, & Kapil, 1989), amide derivatives from the seeds (Lin, 1989), cyclic amides form the leaves (He, Yong, & Liang, 1988) and volatile compounds from leaf, fruit and seed (Chokeprasert, Charles, Sue, & Huang, 2007). The bioactivities from wampee are mainly focused on its leaf, stem and seed which include hepatoprotective activity (Liu, Li, Chen, & Wei, 1996), hypoglycemic (Ma, Wu, & Huang, 2008), antifungal and antiviral activities (Ng, Lam, & Fong, 2003), antiplatelet (Fan, Han, Kang, & Park, 2001), anti-inflammatory, antidiabetic and antioxidant activities (Adebajo et al., 2008). However, there is no study on the use of wampee peels even though it is applied as folk medicine in India and China for the treatment of stomachic and bronchitis as a vermifuge. Therefore, in the present study, the possibility of wampee

* Corresponding author. Address: South China Botanical Garden, Chinese Academy of Sciences, Plant Resource and Biotechnology, Guangzhou Reyiju, Guangdong, Guangzhou 510650, People's Republic of China. Tel.: + 86 20 37252525; fax: + 86 20 37253821.
E-mail address: ymjiang@scib.ac.cn (Y. Jiang).

0308-8146/$ - see front matter © 2009 Elsevier Ltd. All rights reserved.
doi:10.1016/j.foodchem.2009.04.073

peel used as natural antioxidant and anticancer agents was investigated for the first time, and the responsible compound for its activity was isolated and identified as well. This study can help the food industry use it as a natural compound for antioxidant and anticancer activities.

2. Materials and methods

2.1. Sample

Fresh fruits of wampee [*C. lansium* (Lour.) Skeels] at the mature stage were collected from an orchard in Guangzhou, China. Fruits with uniformity in shape and colour were chosen and washed carefully in potable water. The peels were manually separated, and then dried for 24 h using a hot air oven at 60 °C, and finally powdered using a blender. The moisture content of the dried peel was determined to be 85%.

2.2. Chemicals and reagents

1,1-Diphenyl-2-picrylhydrazyl (DPPH), nitro blue tetrazolium (NBT), methionine, riboflavin and 3-(4,5-dimethylthiazole-2yl)-2,5-diphenyl tetrazolium bromide (MTT) were purchased from Sigma Chemical Co. (St. Louis, Missouri, USA). Trypsin, RPMI-1640 medium (pH 7.4) was obtained from Gibco, Invitrogen, New York, USA while foetal bovine serum was supplied by Ebioway (Guangzhou, China). Butylated hydroxytoluene (BHT) was purchased from Sinopharm Chemical Reagent Co. (Shanghai, China). All other chemicals and solvents used in this study were of analytical grade and obtained from Tianjin Reagent Company (Tianjin, China).

2.3. Extraction and total phenolic content

The dried powder (50 g) of wampee peel was extracted for 24 h in a rotary shaker with 1000 ml of 50% ethanol in a conical flask at 30 °C. The extract was then filtered and concentrated using a rotary evaporator (RE-52A, Shanghai Woshi Co., Shanghai, China) and then partitioned sequentially with 100 ml of hexane, ethyl acetate and 1-butanol. The different fractions of hexane, ethyl acetate, butanol and water were separately collected. Total phenolic content of each fraction was determined by the method of Singleton and Rossi (1965) and then expressed as gallic acid equivalents.

2.4. Purification

Since the ethyl acetate-soluble fraction contained the highest phenolic content, it was selected for further purification. The ethyl acetate-soluble fraction (10 g) was subjected to a 450 × 25 mm column of polyamide (200 g, 20–40 mesh, Taizhou Luqiao Biochemical Corp. Taizhou, China), and eluted with a linear gradient of ethyl acetate/ethanol from 100:0 to 0:100 (v/v). About 40 fractions (50 ml per fraction) were collected and concentrated. After the analysis by TLC, these fractions were grouped into 21 major fractions (Fractions 1–21). Then, each fraction was reacted with 0.5% ferric chloride solution to detect the presence of polyphenol (Sun, Shi, Jiang, Xue, and Wei (2007). Among them, the major fraction (Fraction 5) containing the highest polyphenol content determined by the above method of Singleton and Rossi (1965) was concentrated under vacuum to obtain a brownish syrup (2 g). This syrup was re-chromatographed over a 400 × 25 mm silica gel (200 g, 60–100 mesh, Qiandao Marine Chemical Factory, Qingdao, China) column and eluted with the solvents of increasing polarity (hexane, hexane–ethyl acetate, ethyl acetate and ethyl acetate–methanol) to obtain 28 fractions which were pooled into 12 subfractions (Fractions 5.1–5.12) based on the TLC monitor. Each subfraction was allowed to react with 0.5% ferric chloride solution to identify the presence of polyphenol. Among them, the subfraction 5.5 (90 mg) containing the highest polyphenol content was finally purified by HPLC (LC-20 AT, Shimadzu Corporation, Tokyo, Japan) equipped with a Rheodyne injection valve and a 100-μl sample loop with a preparative column (Shim-Pack, PRC–ODS, 20 × 25 cm, Shimadzu, Kyoto, Japan) using a gradient system consisting of solvents A (2% acetic acid, v/v) and B (acetonitrile–methanol, 10:15, v/v) as mobile phase at a flow rate of 1.5 ml/min, and a diode array detector (Rheodyne, Waltham, Massachusetts, USA) with UV detection at 270 nm.

2.5. ^{1}H and ^{13}C NMR analyses

^{1}H NMR (400 MHz) and ^{13}C NMR (100 MHz) spectra of the purified compound were recorded on a Bruker DRX-400 NMR spectrometer (Bruker Co., Rheinstetten, Germany), using deuterated dimethylsulphoxide as the solvent residual peak as the reference standard. Chemical shifts (δ) were given in parts per million (ppm) relative to TMS.

2.6. ESI-MS analysis

Electrospray ionisation mass spectroscopic (ESI-MS) analysis was performed on an Applied Biosystems (API2000 LC/MS/MS System, ABI, Foster City, California, USA). Mass spectra were achieved by electrospray ionisation in both positive and negative modes. The capillary 4500 V (negative) and 5500 V (positive) were used in this study. The electrospray probe-flow was adjusted to 20 ml/min. Continuous mass spectra were obtained by scanning from 100 to 800 m/z.

2.7. Antioxidant activity determination

2.7.1. DPPH radical scavenging activity

The DPPH radical scavenging activities of the test samples were evaluated by the method of Blois (1958) with minor modifications. Initially, 0.1 ml of the samples at a concentration of 25, 50, 75 and 100 μg/ml was mixed with 1 ml of 0.2 mM DPPH (dissolved in methanol). The reaction mixture was incubated for 20 min at 28 °C under dark. The control contained all reagents without the sample while methanol was used as blank. The DPPH radical scavenging activity was determined by measuring the absorbance at 517 nm using a spectrophotometer. The scavenging DPPH radical activity (%) of the tested sample was calculated as (1 − absorbance of sample/absorbance of control) × 100. The DPPH radical scavenging activity of BHT was also assayed for comparison.

2.7.2. Superoxide anion radical scavenging activity

Superoxide anion radical scavenging activity was determined as described by Beauchamp and Fridovich (1971) with some modifications. All solutions were prepared in 0.2 M phosphate buffer (pH 7.4). The test samples at different concentrations (12.5, 25, 37.5 and 50 μg/ml) were mixed with 3 ml of reaction buffer solution (pH 7.4) containing 1.3 μM riboflavin, 0.02 M methionine and 5.1 μM nitro blue tetrazolium. The reaction solution was illuminated by exposing them to two 30 W fluorescent lamps for 20 min and the absorbance was measured at 560 nm. Butylated hydroxytoluene (BHT) was used as a comparison. The reaction mixture without any tested sample was used as control. The superoxide anion radical scavenging activity (%) was calculated as (1 − absorbance of sample/absorbance of control) × 100.

2.7.3. Determination of reducing power

The reducing power assay was determined according to the method of Oyaizu (1986) with little modification. The tested samples (0.1 ml) were mixed with phosphate buffer (2.5 ml, 0.2 M, pH

6.6) and potassium ferricyanide (2.5 ml, 1%). After the mixture was incubated at 50 °C for 20 min. Trichloroacetic acid (2.5 ml, 10%) was added to each sample and centrifuged at 650*g* for 10 min. A 5-ml aliquot of the upper layer was mixed with distilled water (5 ml) and ferric chloride (1 ml, 0.1%) was added and then the absorbance was measured at 700 nm against a blank which consists of all the reagents without the tested sample. The higher absorbance indicated higher reducing power. The reducing power of BHT was also determined for comparison.

2.8. Evaluation of cytotoxic activity

2.8.1. Cell line and culture

HepG2 (human hepatocellular liver carcinoma), A-549 (human lung adenocarcinoma epithelial cell line) and HELA (human cervical carcinoma) cell cultures were obtained from Biomedicine Research and Development Centre of Jinan University (Guangzhou, China). The cell lines were cultured in growth medium (RPMI-1640 medium, pH 7.4), supplemented with 10% foetal bovine serum (FBS) and antibiotics (penicillin, 100 U/ml) and streptomycin sulphate (100 μg/ml). The cell lines were grown in 50 cm^2 tissue culture flasks (Corning, New York, USA) and used for cytotoxicity assay.

2.8.2. Cytotoxicity assay

The cytotoxicity assay of the samples was determined according to the method of Zhao et al. (2007) by MTT (3-(4,5-dimethylthiazole-2yl)-2,5-diphenyl tetrazolium bromide) assay. In brief, human cancer cells were plated at 2×10^4 cells per well in 96-well microtitre plates (Costar 3599, Corning, New York, USA) with 100 μl RPMI-1640 growth medium and incubated for 24 h at 37 °C, with 5% CO_2 in a humidified atmosphere (Incu-Safe, Sanyo, Japan), during which period a partial monolayer was formed. Later, the medium was removed and fresh growth medium containing different concentrations (100, 50, 25, 12.5, 6.5 and 3.125 μg/ml) of the tested compound was added. After 2 days of incubation at 37 °C, with 5% CO_2, the growth medium was removed and MTT reagent (0.1 mg/ml) was added. After incubating at 37 °C for 4 h, the MTT reagent was removed and dimethylsulphoxide (100 μl) was added to each well and then shaken for another 15 min. The absorbance was then determined by an ELISA reader (Bio-Rad, Hercules, California, USA) at a wavelength of 492 nm. Control wells received only the media without the tested compound. The conventional anticancer drug, cisplatin, was used as a positive control in this study. The inhibition of cellular growth by the tested sample was calculated as the percent inhibitory activity and expressed as the IC_{50} value (concentration of the tested sample to inhibit 50% growth of the cells).

2.9. Statistical analysis

Data were expressed as means ± standard deviations (SD) of three replicate determinations and then analysed by SPSS V.13 (SPSS Inc., Chicago, Illinois, USA). One way analysis of variance (ANOVA) and the Duncan's New Multiple-range test were used to determine the differences among these means. p-Values < 0.05 were regarded to be significant.

3. Results and discussion

3.1. Total phenolic content

The ethyl acetate fraction exhibited the highest phenolic content (330 ± 9.9 μg/g dry weight, expressed as gallic acid equivalents), followed by water (54 ± 6 μg/g), butanol (30.3 ± 5.4 μg/g) and hexane fraction (7.9 ± 0.4 μg/g). Generally, hexane is used to extract nonpolar compounds and ethyl acetate is applied to extract medium polar compounds and glycosides while butanol and water are used for extracting polar compounds like aglycones, glucosides and sugars (Markham, 1982). Previously, the higher phenolic content was obtained in the ethyl acetate fraction of litchi fruit pericarp compared to butanol or water fraction (Prasad, Yang, Ruenroengklin, Zhao, & Jiang, 2009). Thus, the ethyl acetate fraction in this study was selected for further purification.

3.2. Purification of the ethyl acetate fraction

The ethyl acetate fraction obtained from wampee peel was first purified by polyamide column chromatography and then 40 fractions were collected and pooled into 21 major fractions as monitored by TLC (Fractions 1–21). Among them, Fraction 5 exhibited a highest polyphenol content. The fraction was then purified further by silica gel column chromatography. Twenty eight fractions were obtained and then grouped into 12 subfractions (Fractions 5.1–5.12) based on TLC analysis. Among them, the major subfraction (5.5, 90 mg) which exhibited a highest polyphenol content was further purified using the HPLC preparative column to get a pure compound (20 mg).

3.3. Structure elucidation of the purified compound

The purified compound isolated from wampee peels was identified as 8-hydroxypsoralen (xanthotoxol) (Fig. 1), on the bases of ESI-MS, ^1H and ^{13}C NMR analyses. The compound was obtained as white needle-like crystals with mp 247 °C. The ESI-MS in the positive and negative mode exhibited signals of quasi-molecular ions at m/z 203 $[M+H]^+$, 225 $[M+Na]^+$, and 201 $[M-H]^-$, respectively, which corresponded to a molecular formula of $C_{11}H_6O_4$ in combination of its 11 carbon signals in the ^{13}C NMR spectrum (DMSO-d_6, 100 MHz) at δ 160.54 (C-2), 114.26 (C-3), 146.01 (C-4), 116.70 (C-4a), 110.51 (C-5), 125.68 (C-6), 145.91 (C-7), 130.62 (C-8), 140.24 (C-8a), 147.87 (C-2′), and 107.50 (C-3′). The proton NMR spectrum (DMSO-d_6, 400 MHz) showed characteristic signals of a furanocoumarin at δ 6.40 (1H, d, J = 9.6 Hz, H-3), 8.11 (1H, d, J = 9.6 Hz, H-4), 7.45 (1H, s, H-5), 8.07 (1H, d, J = 2.0 Hz, H-2′), 7.04 (1H, d, J = 2.0 Hz, H-3′) and 3.36 (1H, br s, OH-8). The above NMR and ESI-MS data were in agreement with the reported values of 8-hydroxypsoralen in the literature (Harkar, Razdan, & Waight, 1984; Wei, Zhang, & Ito, 2004). Previously, 8-hydroxypsoralen was reported in the fruit of *Cnidium monnieri* (Ng, Liu, & Wang, 2000; Wei et al., 2004), roots of *Angelica officinalis* (Harkar et al., 1984) and the whole plant of *Saussurea involucrate* (Yang, Xie, Liu, & Wu, 2006).

3.4. Antioxidant activity

3.4.1. DPPH radical scavenging activity

The ethyl acetate-soluble fraction showed stronger DPPH free radical scavenging activity than 8-hydroxypsoralen and BHT at all the concentrations tested (Fig. 2). At 50 μg/ml, the highest percentage of DPPH radical scavenging activity of 95% was observed in

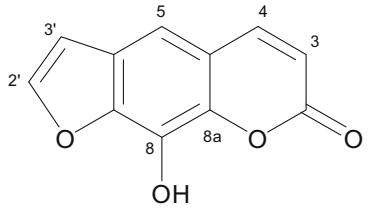

Fig. 1. The chemical structure of 8-hydroxylpsoralen.

the ethyl acetate-soluble fraction, significantly higher ($p < 0.05$) than that of BHT (73%) and 8-hydroxypsoralen (63.3%). From 0 to 50 μg/ml, the DPPH radical scavenging activity of 8-hydroxypsoralen increased but increased slowly when the concentration exceeded 50 μg/ml probably because the reaction of the scavenging radical activity gradually tended to stabilise at 50–100 μg/ml. A similar observation was noticed by Sun et al. (2007) in longan pericarp. Psoralen with free hydroxyl groups have a potent antioxidant activity while substitution of hydroxyl with methoxy or glucose can led to a dramatic drop in antioxidant activity (Ng et al., 2000). It is noteworthy that 8-hydroxypsoralen examined in the present investigation also possesses a hydroxyl group attached to an aromatic ring. It was found that the DPPH radical scavenging activity was reduced by the hydrogen donating ability (Prasad, Divakar, Shivamurthy, & Aradhya, 2005). The results revealed that the DPPH radical scavenging activity of ethyl acetate-soluble fraction and 8-hydroxypsoralen might be attributed to the electron donating ability.

3.4.2. Superoxide anion scavenging activity

In this study, the superoxide anion scavenging activities of ethyl acetate-soluble fraction, 8-hydroxypsoralen, and BHT were analysed, and were concentration dependent (Fig. 3). The ethyl acetate-soluble fraction exhibited an excellent superoxide anion scavenging activity, higher than 8-hydroxypsoralen and BHT in a dose-dependent manner. At 50 μg/ml, the superoxide anion scavenging activity of the ethyl acetate-soluble fraction, 8-hydroxypsoralen and BHT were 88 ± 2.2, 30 ± 1.4 and 25 ± 0.5%, respectively. Therefore, the superoxide anion scavenging activity was in increasing order, the ethyl acetate-soluble fraction > 8-hydroxypsoralen > BHT. It was reported that the superoxide anion scavenging activity could be due to the action of a free hydroxyl group (Siddhuraju, Mohan, & Becker, 2002). 8-Hydroxypsoralen has a free hydroxyl group at the 8th position and this might be responsible for its superoxide anion scavenging activity.

3.4.3. Reducing power

Reducing power is widely used to evaluate the antioxidant activity of polyphenols. The reducing power is generally associated with the presence of reductones, which exerts antioxidant action by breaking the free radical chain by donating a hydrogen atom (Duan, Wu, & Jiang, 2007). As shown in Fig. 4, the ethyl acetate-soluble fraction exhibited higher reducing power than BHT, suggesting that the fraction of wampee peels possessed a stronger electron donating capacity. Furthermore, a linear relationship existed between the concentration and reducing power of the ethyl

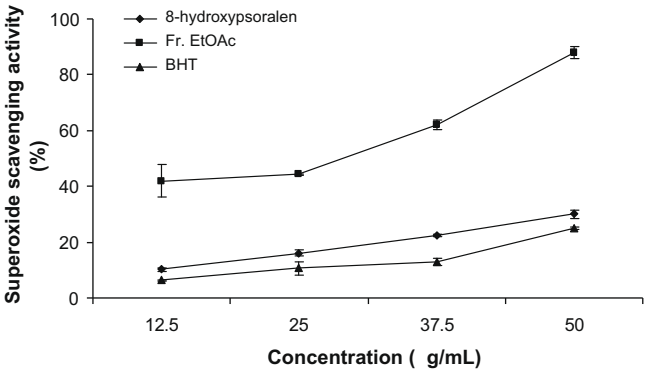

Fig. 3. Superoxide radical scavenging activity of the ethyl acetate fraction (Fr. EtOAc), 8-hydroxypsoralen and BHT.

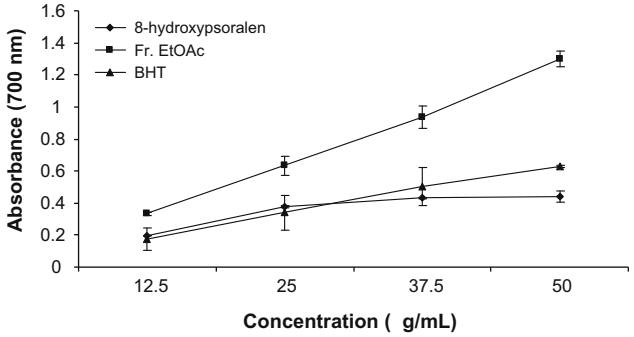

Fig. 4. Reducing power of the ethyl acetate fraction (Fr. EtOAc), 8-hydroxypsoralen and BHT. Higher absorbance values indicate higher reducing activity.

acetate-soluble fraction, 8-hydroxypsoralen and BHT, with their correlation coefficients of 0.9979 ($y = 0.0256x$), 0.9966 ($y = 0.527x + 3.2$) and 0.9968 ($y = 0.0122x + 0.0325$), respectively. Li, Wang, Li, Li, and Wang (2009) have reported the existence of linear relationships between antioxidant capacity (assessed as copper reducing power) and total phenol content in Chinese wine.

The antioxidant activity of 8-hydroxylpsoralen was previously reported by Ng et al. (2000) and the scavenging activity was due to the presence of hydroxyl group of 8-hydroxypsoralen. Usually, coumarins with free hydroxyl groups have a potent antioxidant activity while the substitution of the hydroxyl group with methoxy or sugar can lead to the decrease in the antioxidant activity. The

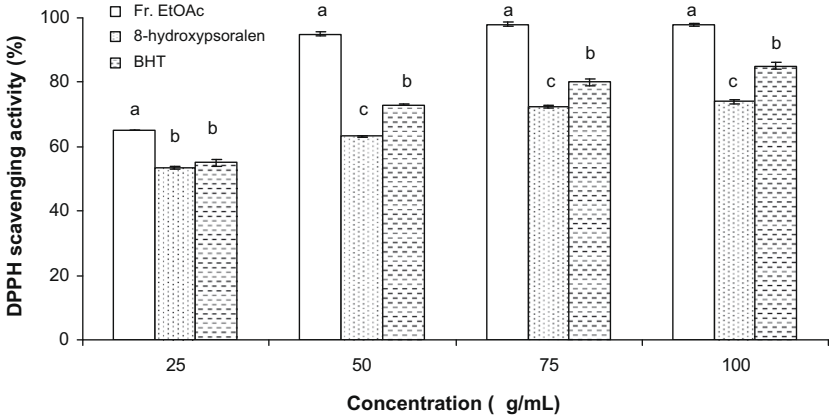

Fig. 2. DPPH radical scavenging activities of the ethyl acetate fraction (Fr. EtOAc), 8-hydroxypsoralen and BHT. For each treatment, the means within the same set followed by different letters were significantly different at $p < 0.05$.

Table 1
Anticancer activities of the ethyl acetate-soluble fraction (Fr. EtOAc) and 8-hydroxypsoralen isolated from wampee peels.

Sample	IC_{50} value (μg/ml)		
	Hep-G2	HELA	A-549
Fr. EtOAc	13.1 ± 0.9^{b}	ND	30.7 ± 2.4^{b}
8-Hydroxypsoralen	0.34 ± 0.02^{a}	0.013	28.2 ± 3.2^{a}
Cisplatin*	87.9 ± 2.3^{c}	349.9 ± 6.2	101.3 ± 1.2^{c}

IC_{50} value represents the concentration of the tested sample to kill 50% of the cancer cells. ND, Not determined; *, positive control; HepG-2, human hepatocellular liver carcinoma; HELA, human cervical carcinoma; and A-549, human lung adenocarcinoma epithelial cell line. For each treatment, the means within the column followed by different superscript letters were significantly different at $p < 0.05$.

antioxidant activity of the ethyl acetate-soluble fraction was more potent than 8-hydroxypsoralen, which might be due to the synergistic activity of other phenolics. Similar findings were reported by Prasad et al. (2005).

3.5. Anticancer activity

Anticancer activity of 8-hydroxypsorelen were reported by Gawron and Kruk (1987, 1992) and Madari and Jacobs (2004). In this study, the anticancer activities of the ethyl acetate-soluble fraction, 8-hydroxypsoralen and cisplatin were investigated using an 3-(4,5-dimethylthiazole-2yl)-2,5-diphenyl tetrazolium bromide assay on three human cancer cell lines, HELA, HepG2 and A-549. A mitochondrial enzyme in living cells, succinate-dehydrogenase, cleaves the tetrazolium ring and converts the MTT to an insoluble purple formazan and the amount of formazan produced is directly proportional to the number of viable cells (Lee, Hwang, & Lim, 2004). Table 1 shows that 8-hydroxypsoralen significantly inhibited ($p < 0.05$) the growth of cancer cells, HELA, A549 and HePG2 cell lines, compared to the ethyl acetate-soluble fraction and cisplatin. Our results are in agreement with the report of Gawron and Kruk (1987, 1992) and Madari and Jacobs (2004). The mechanism of action of anticancer activity of 8-hydroxypsoralen could be by disturbing the cellular division during mitosis at the telophase stage. It was also reported that 8-hydroxypsoralen decreased the amount of cellular protein and mitotic index, and the colony formation during cell proliferation (Gawron & Kruk, 1992).

4. Conclusions

In the present study, a compound was isolated and purified from wampee peels and then identified as 8-hydroxypsoralen, while its antioxidant and anticancer activities were evaluated. The study indicated that the 8-hydroxypsoralen exhibited high antioxidant and anticancer activities. Further work about the anticancer activity using *in vivo* models is worth investigation.

Acknowledgements

Research was supported by CAS/SAFEA international partnership program for creative research teams and the National Natural Science Foundation of China (Grant Nos. 30425040 and 30700557).

References

Adebajo, A. C., Iwalewa, E. O., Obuotor, E. M., Ibikunle, G.F., Omisore, N.O., Adewunmi, C. O., et al. (2008). Pharmacological properties of the extract and some isolated compounds of *Clausena lansium* stem bark: Anti-trichomonal, antidiabetic, antiinflammatory, hepatoprotective and antioxidant effects. *Journal of Ethnopharmacology*. doi:10.1016/j.jep.2008.11.015.

Beauchamp, C., & Fridovich, I. (1971). Superoxide dismutase: Improved assays and an assay applicable to acrylamide gels. *Analytical Biochemistry, 44*, 276–287.

Blois, M. S. (1958). Antioxidants determination by the use of a stable free radical. *Nature, 181*, 1199–1200.

Chokeprasert, P., Charles, A. L., Sue, K. H., & Huang, T. C. (2007). Volatile components of the leaves, fruits and seeds from wampee [*Clausena lansium* (Lour.) Skeels]. *Journal of Food Composition and Analysis, 20*(5), 2–56.

Duan, X., Wu, G., & Jiang, Y. (2007). Evaluation of antioxidant properties of phenolics from litchi fruit in relation to pericarp browning prevention. *Molecules, 12*, 759–771.

Fan, G. J., Han, B. H., Kang, Y. H., & Park, M. K. (2001). Evaluation of inhibitory potentials of Chinese medicinal plants on platelet-activating factor (PAF) receptor binding. *Natural Product Sciences, 7*, 33–37.

Gawron, A., & Kruk, G. (1987). Cytostatic activity of coumarins in vitro. *Planta Medica, 53*, 526–529.

Gawron, A., & Kruk, G. (1992). Cytotoxic effects of xanthotoxol (8-hydroxypsoralen) on TCTC cells in vitro. *Polish Journal of Pharmacology and Pharmacy, 44*, 51–57.

Harkar, S., Razdan, T. K., & Waight, E. S. (1984). Steroids, chromone and coumarins from *Angelica officinalis*. *Phytochemistry, 23*, 419–426.

He, Y. M., Yong, C. Y., & Liang, H. (1988). Three novel cyclic amides from *Clausena lansium*. *Phytochemistry, 27*, 445–450.

Hu, M. L., Louie, S., Cross, C. E., Motchink, P., & Halliwell, B. (1992). Antioxidant protection against hypochlorous acid in human plasma. *Journal of Laboratory and Clinical Medicine, 121*, 257–262.

Kalt, W. (2001). Healthy functional phytochemicals of fruits. *Horticultural Reviews, 27*, 269–314.

Khan, N. U., Naqvi, S. W. I., & Ishratullah, K. (1983). Wampetin, a furocoumarin from *Clausena wampi*. *Phytochemistry, 22*, 2624–2625.

Lakshmi, V., Raj, K., & Kapil, R. S. (1989). A triterpene alcohol, lansiol, from *Clausena lansium*. *Phytochemistry, 28*, 943–945.

Lee, J. Y., Hwang, W. I., & Lim, S. T. (2004). Antioxidant and anticancer activities of organic extracts from *Platycodon grandiflorum* A. De Candolla roots. *Journal of Ethanopharmacology, 93*(40), 9–415.

Li, H., Wang, X., Li, Y., Li, P., & Wang, H. (2009). Polyphenolic compounds and antioxidant properties of selected China wines. *Food Chemistry, 112*, 454–460.

Lin, J. H. (1989). Cinnamamide derivatives from *Clausena lansium*. *Phytochemistry, 28*, 621–622.

Liu, G. T., Li, W. X., Chen, Y. Y., & Wei, H. L. (1996). Hepatoprotective action of nine constituents isolated from the leaves of *Clausena lansium* in mice. *Drug Development Research, 39*, 174–178.

Ma, N., Wu, K., & Huang, L. (2008). An elegant synthesis of Zetaclausenamide. *European Journal of Medicinal Chemistry, 43*, 893–896.

Madari, H., & Jacobs, R. S. (2004). An analysis of cytotoxic botanical formulation used in the traditional medicine of ancient Persia as abortifacients. *Journal of Natural Product, 67*, 1204–1210.

Markham, K. R. (1982). *Techniques of flavonoid identification*. London: Academic Press.

Ng, T. B., Lam, S. K., & Fong, W. P. (2003). A homodimeric sporamin-type trypsin inhibitor with antiproliferative, HIV reverse transcriptaseinhibitory and antifungal activities from wampee (*Clausena lansium*) seeds. *Biological Chemistry, 384*, 289–293.

Ng, T. B., Liu, F., & Wang, Z. T. (2000). Antioxidative activity of natural products from plants. *Life Sciences, 66*, 709–723.

Oyaizu, M. (1986). Antioxidative activity of browning products of glucosamine fractionated by organic solvent and thin-layer chromatography. *Nippon Shokuhin Kogyo Gakkaishi, 35*, 771–775.

Prasad, N. K., Divakar, S., Shivamurthy, G. R., & Aradhya, S. M. (2005). Isolation of a free radical scavenging antioxidant from water spinach (*Ipomoea aquatica* Forsk). *Journal of the Science of Food and Agriculture, 85*, 1461–1468.

Prasad, N. K., Yang, B., Ruenroengklin, N., Zhao, M., & Jiang, Y. (2009). Application of ultrasonication or high pressure extraction of flavonoids from litchi fruit pericarp. *Journal of Food Process Engineering*. doi:10.1111/j.1745-4530.2008.00247.x.

Siddhuraju, P., Mohan, P. S., & Becker, K. (2002). Studies on the antioxidant activity of Indian Laburnum (*Cassia fistula* L.): A preliminary assessment of crude extracts from stem bark, leaves, flowers and fruit pulp. *Food Chemistry, 79*(6), 1–69.

Singleton, V. L., & Rossi, J. A. (1965). Colorimetry of total phenolics with phosphomolybdic–phosphotungstic acid reagents. *American Journal of Enology and Vitriculture, 16*, 144–158.

Sun, J., Shi, J., Jiang, Y., Xue, S. J., & Wei, X. (2007). Identification of two polyphenolic compounds with antioxidant activities in longan pericarp tissues. *Journal of Agriculture and Food Chemistry, 55*, 5864–5866.

Thomson, M. J. (1995). The role of free radicals and antioxidants: How do we know that they are working. *Critical Reviews in Food Science and Nutrition, 35*, 21–39.

Wei, Y., Zhang, T., & Ito, Y. (2004). Preparative isolation of osthol and xanthotoxol from common *Cnidium* Fruit (Chinese traditional herb) using stepwise elution by high-speed counter-current chromatography. *Journal of Chromatography A, 1033*, 373–377.

Yang, J. S., Xie, F. Z., Liu, Q. H., & Wu, X. (2006). Studies on coumarins from *Saussurea involucrate* Kar. et Kir. *Chinese Pharmaceutical Journal, 41*, 1774–1776.

Zhao, M., Yang, B., Wang, J., Liu, Y., Yu, L., & Jiang, Y. (2007). Immunomodulatory and anticancer activities of flavonoids extracted from litchi (*Litchi chinensis* Sonn.) pericarp. *International Immunopharmacology, 7*(16), 2–166.

Food Chemistry 118 (2010) 67–73

Contents lists available at ScienceDirect

Food Chemistry

journal homepage: www.elsevier.com/locate/foodchem

Heat-induced changes in dairy products containing sucrose

S.D. Rozycki [a,*], M.P. Buera [b], M.S. Pauletti [a]

[a] Instituto de Tecnología de Alimentos, Facultad de Ingeniería Química, Universidad Nacional del Litoral – Street: 1° de Mayo 3250, (3000) Santa Fe, Argentina
[b] Departamento de Industrias, Facultad de Ciencias Exactas y Naturales, 1428 Buenos Aires, Argentina

ARTICLE INFO

Article history:
Received 16 June 2008
Received in revised form 26 February 2009
Accepted 21 April 2009

Keywords:
Thermal gelation
Concentrated milk
Kinetics
Colour
Fluorescence

ABSTRACT

The aim of the present work was to analyse the influence of the variables reaction temperature, casein–sucrose ratio and pH, on the kinetic parameters of gelation reactions, the gelation time and the functionality of casein micelles in concentrated milk systems containing sucrose.

Global constant rate reaction order of gelation and were calculated, the first varying between four different orders of magnitude and the second between 1 and 7.

Mathematical models allowing the prediction of gelation time with a good fit ($r^2 > 0.94$) were obtained.

Activation energy (E_a) for gelation decreased as pH decreased. In presence of sucrose, E_a values showed a higher temperature dependence. Gel functionality showed to be pH independent. Although the kinetic aspects of the reactions were affected by pH, the thermodynamic ones remained almost unchanged. Aggregation and gelation were very fast at pH 6. When comparing gelation kinetics with those corresponding to fluorescence and colour development, gelation showed to be produced much earlier than the latter two phenomena.

1. Introduction

At temperatures above 100 °C, the thermal process of concentrated dairy systems containing sucrose induces thermal gelation of milk proteins (Pauletti, Castelao, & Seguro, 1996), which defines the texture of products such as milk jam (dulce de leche) and condensed milk, either during manufacture or sterilization (Moro & Hough, 1985).

Several authors have studied certain characteristics corresponding to this type of systems, such as density (Moro & Hough, 1985), rheological properties (Navarro, Ferrero, & Zaritzky, 1999) and colorimetric aspects (Rozycki, 1999, 2003). However, little research has been carried out on the influence of sucrose on gelation, fluorescence and colour development phenomena and on the comparison of the kinetics of these processes.

Comparatively, much more work has been performed on heat induced gelation of whey proteins, or on by acid and enzymatic induced gelation in milk, than on thermal gelation of milk proteins (Considine, Patel, Anema, Singh, & Creamer, 2007; Lucey, 2002). Moreover, various authors have studied heat-induced gelation of milk and dairy concentrates (Fox, 1981, 1982; McSweeney, Mulvihill, & O'Callaghan, 2004) but there has not been an in-depth investigation on sucrose effect yet. The knowledge of kinetic parameters corresponding to heat-induced gelation processes, such as the specific global constant of gelation reaction rate (k), its global pseudo-order of reaction (n) and its activation energy (E_a) are necessary to design continuous production equipments both for heat-gelified dairy products (milk jam – dulce de leche –, sterilized condensed milk) and those products in which this phenomenon is not desired (ice cream base, dairy desserts).

The most influential variables in the gelation processes of these systems are temperature (T), pH and protein concentration, which is determined by casein–sucrose ratio, here represented by R (the relative amounts whole milk powder (WMP)/sucrose (Rozycki, 1999).

Micellar hydration, related to zeta potential, is of great importance in gelation, its mechanism involving a kinetic scheme of controlled reaction where big particles react much faster than small ones. This leads to an "explosive" increase of aggregate size (Clark, 1992) where protein molecules, on hydration, increase their hydrodynamic volume and consequently the aggregation rate and gelation.

The main feature characterising the cascade mechanism applied to polymers is that each molecule or molecule aggregate has a number of reactive groups (f) which are able to join other molecules to form branched systems. As the process advances, cross-links between non-reacting branched groups take place, the relative average molecular mass tending faster and faster to infinity and reaching the gel point (Fox, 1982). The gel point was suggested to correspond to gelation time. For monodisperse systems, functionality f takes integer values: $f = 1$ for dimerization, $f = 2$ for linear polymerisation and $f = 3$ for branched polymerisation.

Under certain conditions, colour presents an induction period where colourless though fluorescent precursors occur, followed

* Corresponding author. Tel.: +54 342 4571150; fax: +54 342 4571164.
E-mail addresses: srozycki@fiq.unl.edu.ar, sdrozycki@hotmail.com (S.D. Rozycki).

0308-8146/$ - see front matter © 2009 Elsevier Ltd. All rights reserved.
doi:10.1016/j.foodchem.2009.04.096

by intermediate steps with brown, and also fluorescent compounds. In the final steps of heating, when the system achieves an intense brown colour (as in dulce de leche), colour formation rate begins to decrease, which is not the case for fluorescence. Hence, the fluorescent compounds would be considered the promoters of brown compounds (Petriella, Resnik, Lozano, & Chirife, 1985) in the initial steps, colour and fluorescence following parallel paths (Matiacevich & Buera, 2006).

As regards colour and fluorescence, numerous sugar–aminoacid model systems have been investigated, mainly under accelerated storing conditions (55 °C), but few have been carried out in "real" food systems, at low water activity a_w = 0.83–0.87 and temperatures above 100 °C, as in this study.

In the present work, the influence of the initial system pH, reaction temperature and casein concentration (R) on the heat-induced gelation process and its governing kinetic parameters was studied, comparing the kinetic aspects corresponding to colour development and fluorescence.

2. Material and methods

2.1. Sample preparation

Table 1 shows each sample formulation. Whole milk powder composition was: 25.05% protein (21.30% casein), 26.45% fat, 40.02% lactose, 6.05% minerals and 2.43% water. Total solids percentage (70%) was kept constant. Casein concentration of each sample, calculated from the whole milk powder (WMP) content was: 3.41%, 4.90%, 5.96%, 6.92% and 7.67%.

R value was defined as the ratio WMP/sucrose. The samples were obtained by mixing whole milk powder, sucrose and distilled water at 45 °C during 4 min, using a magnetic stirrer. The pH was adjusted with calcium hydroxide p.a. and/or lactic acid 1:10, as necessary.

2.2. Experimental design

To evaluate the influence of temperature, pH and R on gelation time, a factorial experimental design (Montgomery, 1991) involving two variables (T and R) in five levels and three pH values (6, 7 and 8) was selected. Table 2 shows coded and uncoded variable values.

After adjusting the pH to the desired value, about 2 g of each sample were put in Pyrex glass flame-sealed tubes (150 mm length, 8 mm inner diameter and 1 mm wall thickness). Three samples (replicates) of each formulation were taken and their individual gelation times were determined (gel point) at the five design temperatures. The same procedure was applied for pH 6, 7 and 8 and every experience was carried out in duplicate. Gelation time was obtained from the average of the times corresponding to replicates of at least two determinations (α = 0.05).

2.3. Determination of gelation time (t_g)

Each sample tube was put in an oscillating system of 5 cycle/minute, inside a thermostatic bath of silicon oil (Haake DC3, Karlsruhe, Germany) at controlled temperature (+0.1 °C). To determine t_g, the Subjective Test of Heat stability (Fox, 1982), proposed by Hyslop and Fox (1981), was used. Each tube was subjected to a complete oscillation every 12 s, the originally liquid mix flowing from one tube end to the other at 10 times per minute and twice per cycle. Gelation time, which is the time ranging from sample introduction into the bath and the occurrence of fluidity loss due to gelation, was visually determined.

Table 1
Composition of the formulations employed.

Content (g)	Samples				
	A	B	C	D	E
Sucrose (%)	54	49	44	39	34
WMP[a] (%)	16	21	26	31	36
Water (%)	30	30	30	30	30
R [b]	0.296	0.429	0.591	0.795	1.059

[a] WMP = whole milk powder.
[b] R = ratio WMP/sucrose [% w/w].

2.4. Colorimetric evaluation

Colorimetric measurements of each sample were made using non-standard white and black cylindrical plastic cells (28 mm diameter, 4 mm high). The reflectance values for 450, 560, and 685 nm were determined to obtain the Kubelka–Munk index (K/S) using the SBRT software (Shelf Backing Reflectance Transformation software) appropriate for small samples (Rozycki, 1999). Measurements were made using a Minolta CM 508d spectrophotometer with illuminant C, 2 degrees standard observer angle and specular component excluded.

2.5. Fluorescence and optical density measurements

Three gram of each sample were exactly weighed, mixed with about 15 ml of 80% ethanol (Park & Kim, 1983) and shacked at 150 agitation cycles per minute, during 30 min. The samples were filtered twice through filter paper in order to obtain a clear solution. Optical density (OD) at 420 nm was measured in an aliquot of this solution with a Génesis 5 UV–Visible spectrophotometer (Spectronic Instruments, Inc., Rochester, NY, USA). Another aliquot (1 ml) was diluted 10-fold with bi-distilled water and fluorescence was determined in a Biorad Versafluor fluorimeter TM, excitation maximum at 380 nm and emission maximum at 465 nm, employing a standard solution of quinine sulphate quinina, of 1 μg/ml de SO_4H_2 0.1 N (Park & Kim, 1983), which fluorescence value was 1435 UF (fluorescence units), as an average of triplicate measurements. The fluorescence of each sample was referred to as a percent of this reference.

2.6. Chemical determinations

Casein concentration was determined in a reconstituted sample of whole milk powder (13% total solids) and water, using a FIL-IDF standard method (International Dairy Federation, 1964). To determine pH, an E516 pHmeter (Metrom Herisau, Switzerland) was used.

2.7. Water activity determination

Water activity (a_w) was measured at 25 °C, in coded samples ($X_2 = X_3 = 0$), and for $R = -1$, 0 and +1 (Table 2). The equipment used was AQUA Lab – CX-2T (Washington, USA).

2.8. Functionality determination

Average functionality of casein monomers (f) was determined from the kinetic equations below, in accordance with Pauletti et al. (1996):

$$\ln t_g = [\ln(B/k)] - [(n-1)\ln C_o] \quad (1)$$

$$\ln k = \ln A - E_a/RT \quad (2)$$

$$\ln k/B = \ln A/B - E_a/RT \quad (3)$$

where t_g = gelation time [min]; C_o = casein concentration [% w/w]; k = specific global reaction rate coefficient [g casein^{-1} min^{-1}];

Table 2
Values of coded and uncoded variables.

WMP (%)	Sucrose (%)	X_1[a]	X_1 (coded)	X_2[b]	X_2 (coded)	X_3[c]	X_3 (coded)
16	54	0.296	−1	378	−1	6	−1
21	49	0.429	−0.5	388	−0.429		
26	44	0.591	0	395.5	0	7	0
31	39	0.795	+0.5	403	+0.429		
36	34	1.059	+1	413	+1	8	+1

[a] $X_1 = R$ = ratio WMP/sucrose.
[b] $X_2 = T$ = temperature (K).
[c] X_3 = pH.

n = global pseudo-order of reaction (adimensional); E_a = activation energy [kJ/mol].

B parameter is defined according to the following equation:

$$B = \frac{\left[\frac{f-1}{f-2}\right]^{n-1} - 1}{(n-1)\cdot f^{n-1}} \quad (4)$$

If B/k and n are known for every temperature, functionality can be obtained from an iterative process, since f value satisfies Eqs. (2)–(4).

2.9. Statistical analysis

Results were subjected to a multiple regression and variance analysis (Statgraphics Plus 3.0, 1994), t Student tests being used to determine the coefficient significance and standard error ($p > 0.95$). To determine multiple correlations between t_g and the design variables, Table Curve 3D (1993) program was used.

3. Results and discussion

For any R and pH studied, gelation times decreased as heating temperature increased, as shown in Fig. 1a–c for the samples with the different R (0.291, 0.678, and 1.059), and at initial pH values 6, 7 and 8. Temperature increase encourages several chemical changes in casein micelles, which result in their irreversible aggregation. These changes are probably related to whey protein denaturation, casein complex formation, Ca^{++} saturation in the soluble phase, and the resulting pH decrease (Fox, 1982).

Casein accounts for approximately 80% of bovine milk proteins and casein micelles constitute the basic blocks conforming the milk gel. The position of κ-casein on the micelle surface has a fundamental meaning in the gelation process (Horne, 1998). When milk is treated at temperatures above 70 °C, the different whey proteins inter-react in a very complex way, and soluble complexes are formed in the first stages, which act as intermediates in the association of β-lactoglobulin the casein micelles (Corredig & Dalgleish, 1999; Anema, Lowe, & Li, 2004) and with α-lactalbumin, which then precipitate on the surface of the casein micelles. Heat treatment markedly affects the interactions among whey denatured proteins, and among them and with the casein micelles. As shown in Fig. 1, gelation times were very high at 105 °C (278 K), and, in the case of samples with the lowest protein and the highest sucrose proportions (lowest R values) studied, gelation was still not complete after 3 h of heating.

As R increased, the gelation times decreased, regardless of the pH or temperature. This is due to the fact that at higher R values, the casein percentage in the medium is higher, which in turn increases, by cross-linking, the proportion of reactive sites involved in the gelation process (Donato, Guyomarch, Amiot, & Dagleish, 2007). Also, an increase of sucrose proportion (R decrease) resulted in an increase of the gelation time, which could be partly explained by the capacity of sugars to delay heat-induced protein denaturation (Carpenter, Chang, Garzón Rodríguez, & Randolph, 2002; Passot, Fonseca, Alarcon-Lorca, Rolland, & Marin, 2005), which, as discussed before, is fundamental for the gel development. Thus, as the relative amount of sugar decreases (R increases) it is expected that proteins are more subjected to denaturation and consequently to develop the different stages leading to gel formation.

As previously discussed, denaturation of whey proteins, and, particularly of β-lactoglobulin is the necessary initial step which allows the formation of a tri-dimensional network in milk (Donato et al., 2007). However, the modifications occurring on the surface of the casein micelles are also of fundamental importance (Anema & Li, 2003). These modifications are manifested by changes in the micelle volume, which are sensitive to even slight pH modifications (Anema & Li, 2003).

When comparing samples with the same composition and treatment temperatures, gelation times were very low (usually below 1 min) for samples with initial pH 6 (Fig. 1), and the highest gelation times were obtained for samples with an initial pH 7, since this pH is very close to that of maximum casein thermal stability (Walstra & Jenness, 1987a, chap. 17). Gelation times of samples with initial pH 8 were higher than those obtained for pH 6, though lower than those for pH 7.

Anema and Li (2003) showed that at pH 6.5, about 70% of denatured whey proteins are associated to the casein micelle, and the degree of association decreases as increasing pH. Thus, it could be expected that at pH 8 the gelation times would be the highest. However, the low gelation times observed at pH 8 (compared to those at pH 7) could be a consequence of the fact that alkaline conditions promote the kinetics of browning reactions, which contribute to a marked and faster pH decrease (Buera, Chirife, Resnik, & Wetzler, 1987) than those obtained with samples of initial pH 7, and, consequently, to a shorter gelation time. Sugar hydrocarbon chain fragmentation and heat-induced acid generation from lactose were reported to occur during heating, contributing to the acid formation and pH decrease (Fox, 1982; Rozycki, 1999). The faster pH decrease at pH 8 than that occurring at pH 7, would lead to gelation in a shorter time. There seems to be a kind of competition between the rate of pH decrease, caused by Maillard reaction, and the narrowness of conditions for the point of highest micelle stability.

pH has also opposite effects on sucrose hydrolysis (which is favoured at acid pHs (Flink, 1983)) and on Maillard reaction (which is favoured at neutral pHs) and a compromise between both types of reactions was reported (Buera et al., 1987). The values of (B/k) from the ordinate to the origin, and of $(n-1)$ from the slope, were obtained for all casein concentrations, with good correlation coefficients ($r^2 > 0.94$) for the different heating temperatures and pH values under study. Table 3 shows the kinetic parameter values (n, k and B).

As discussed before, at pH values 7 and 8, the kinetic parameters for gelation, B and n, were very similar, probably by a partial compensation of the above-mentioned effects.

The high values of n (Table 3) show the complexity of the reactions involved and the diversity of the changes produced (Walstra

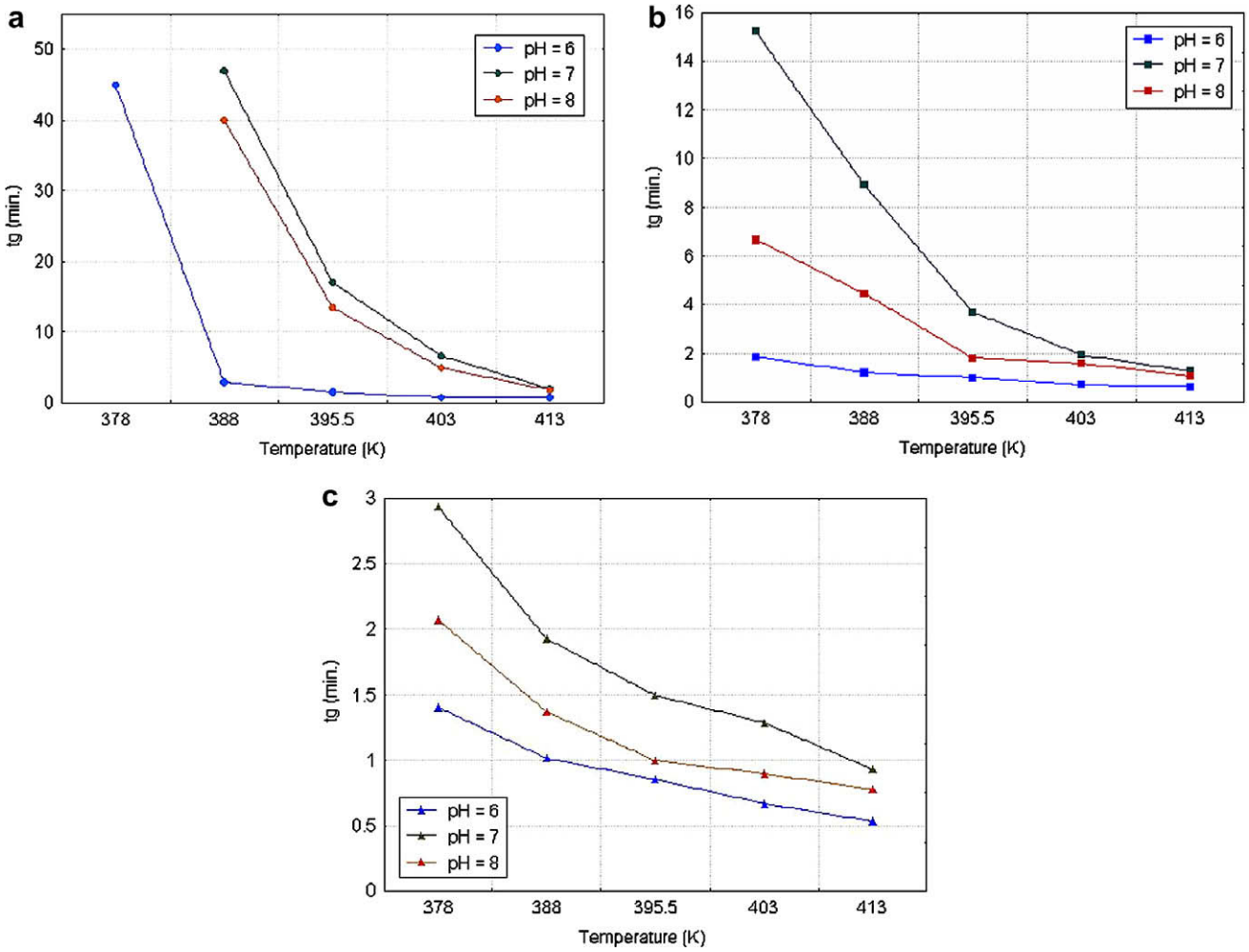

Fig. 1. Gelation time vs. temperature for samples with whole milk/sucrose ratios (R): $R = 0.291$ (a); $R = 0.678$ (b) and $R = 1.059$ (c), at different pH values.

Table 3
Kinetic parameters for the heat-induced gelation process, at different pH values.

pH	T (K)	n	B	k^a	P	s.e.	r^2
6.0	378	4.326	1.309	1.574E−03	0.014	1.099	0.947
	388	1.776	1.162	2.475E−01	0.019	0.282	0.948
	395.5	1.710	1.170	3.389E−01	0.001	0.103	0.979
	403	1.397	1.219	1.175	0.000	0.024	0.985
	413	1.241	1.250	1.235	0.007	0.060	0.949
7.0	378	6.214	0.983	8.529E−06	0.000	0.285	0.997
	388	5.180	0.882	8.792E−05	0.001	0.719	0.970
	395.5	4.092	0.833	1.212E−03	0.000	0.382	0.984
	403	3.089	0.847	1.115E−02	0.002	0.417	0.960
	413	1.981	0.960	1.444E−01	0.000	0.087	0.992
8.0	378	6.950	0.857	3.386E−06	0.002	0.935	0.975
	388	5.616	0.764	6.078E−06	0.002	0.703	0.976
	395.5	4.375	0.733	9.493E−04	0.003	0.631	0.965
	403	3.162	0.770	9.620E−03	0.000	0.210	0.989
	413	1.020	0.903	1.343E−01	0.001	0.149	0.978

s.e. = standard error.
[a] $(\text{g casein } 10^{-2}\ \text{g}^{-1})^{1-n}\ \text{min}^{-1}$.

& Jenness, 1987a, 1987b, chaps. 17, 10.2). Since thermal treatment at high temperatures can promote changes in the reaction mechanisms of the simultaneous reactions that take place, this could significantly influence n values (Villota & Hawkes, 1992, chap. 2).

The average casein micelle functionality (f), related to reactive sites in the casein micelles was calculated for all the samples by the method proposed by Pauletti et al. (1996). The f values obtained were the following: 2.37 (pH 6), 2.43 (pH 7) and 2.45 (pH 8), reflecting no significant changes on the average functionality of casein monomers when varying the mixture initial pH between 6 and 8. However, as shown in Table 3, k values at pH 6 were much higher than at pH 7 and 8. This could indicate that the pH 6 has a marked influence on the kinetic aspects of gelation reactions (k), but it does not significantly affect the thermodynamic aspects of gelation.

Consequently, the number of reactive (directly related to functionality f) sites per protein molecule is higher than 2 ($f > 2$) and it remains almost unchanged when varying pH between 6 and 8. It can be thus proposed that cross-linked branched polymers develop due to the thermal treatment, generating a three dimensional protein network involving the whole system, similar to other systems with whey and egg proteins (Rector, Matsudomi, & Kinsella, 1991).

The evolution of water activity (a_W) with reaction time was analysed in three samples, varying R between 0.296 and 1.059, keeping T (122.5°) and pH (7) constant and the results are shown in Table 4. At initial time (time = 0), as expected, a_W was lower as lower was the R value (higher the sucrose proportion). However, regardless of R, water activity decreased with increasing reaction time, which implies that as heating progresses, polymer–solvent interactions prevail over polymer–polymer one (Katsuta, Rector, & Kinsella, 1990). The solvation of the micelles, increases the hydrodynamic protein volume by increasing their "effective" radius which, according to the statistical gelation theory, would turn them more gelation reactive. Thus, the presence of sucrose limit

Table 4
a_W vs. reaction time, at $X_2 = X_3 = 0$.

t_g = 30–35 min[a]		t_g = 2.66 min		t_g = 1.3 min	
Time (min)	a_W ($R^b = -1$)	Time (min)	a_W ($R = 0$)	Time (min)	a_W ($R = +1$)
0	0.849	0	0.868	0	0.898
15	0.846	1.50	0.861	0.87	0.886
30	0.844	2.66	0.857	1.30	0.877
45	0.842	25	0.856	22	0.874
60	0.841	50	0.854	44	0.872

$X_2 = T$ (K).
X_3 = pH.
[a] Relatively noticeable gelation.
[b] R = LPE/sucrose (WMP = whole milk powder).

the water availability for micelle surface hydration, necessary for gelation to occur (Boye, Alli, Ramaswamy, & Raghavan, 1997). This would partly account for the fact that the higher the R (and the lower the S) values, the lower t_g and the more the amount of gelation reactive sites due to the increase in protein concentration.

By representing $\ln(k/B)$ for every pH as a function of $1/T$, straight lines were obtained (Fig. 2), and the obtained activation energy values resulting from their slopes are shown in Table 5.

The E_a values of the studied concentrated milk samples (Table 4) are more than twice higher than those corresponding to milk (100–120 kJ/mol), according to Pauletti et al. (1996). This effect can also be due to the sucrose–protein interaction, which increases micelle stability.

E_a values were significantly lower for the samples at pH 6 than for those at pH 7 and 8, which were similar. The little dependence on temperature for the samples at pH 6 may be associated to the fact that, at working temperature, there is a closer proximity in these samples to the optimum gelation pH for the concentrated milk. This could indicate that at pH 6 a different gelation mechanism could operate from that in the samples at PH 7 and 8.

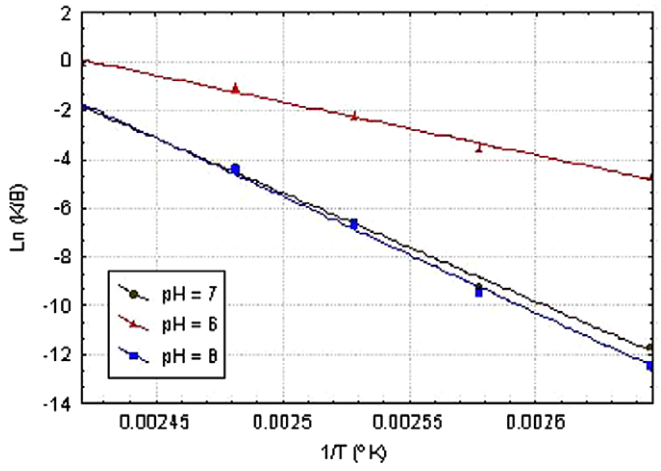

Fig. 2. Arrenhius plot for the gelation rate constants at different pH values.

Table 5
Activation energies and network formation energies values at different pH values.

pH	E_a[a] (kJ/mol)	r^{2b}	s.e.[c]	B^{*d}	r^{2b}	s.e.[c]
6.0	233.5	0.89	13.043	2,45,978	0.858	6953
7.0	371.3	0.996	4.274	3,69,285	0.995	1804
8.0	398.2	0.997	3.605	4,16,753	0.972	4883

[a] E_a = activation energy.
[b] r^2 = correlation coefficient.
[c] s.e = standard error.
[d] B^* = energy associated to network formation (kJ/mol).

Kim and Kinsella (1989) have defined the network formation energy, B^*, starting from a linear, Arrhenius-type, model

$$\ln k = \ln A - B^*(1/T) \quad (5)$$

where A = frequency factor; B^* = network formation energy.B^* is associated to the amount of consumed energy that is required for the network formation during gelation: as higher is B^* value, gelation is slower, thus favoring a wider micelle–micelle interaction and a denser network structure (Kim & Kinsella, 1989).

Using k values calculated above (Eqs. ((1)–(3)), and relating them with $(1/T)$ (Eq. (5)) by means of the linearisation method, B^* values are obtained from the slope of the straight lines, and are also shown in Table 5.

The analysis of these values shows that as the E_a values, the energy needed to form the network (B^*) increases with pH, being at pH 6 half the value of that at pH 8, and that energy is very similar for pHs 7 and 8.

By applying a multiple regression analysis (Statgraphics, 3.0) to the gel times and design variables (T, R and pH), the mathematical model represented by Eq. (6), which allows t_g value prediction, was obtained.

$$t_g = 4.681 - 11.255 \cdot X1 - 12.248 \cdot X2 + 3.510 \cdot X3 + 7.882 \cdot X12 + 9.755 \cdot X22 + 6.828 \cdot X32 + 17.481 \cdot X1 \cdot X2 - 4.870X1 \cdot X3 - 4.830 \cdot X2 \cdot X3 \quad (6)$$

($r^2 = 0.812$; standard error of estimation = 9.8515).

Linear regression coefficients show t_g to vary inversely with R and reaction temperature, gel time decreasing when casein proportion and temperature increase. Also, t_g is directly affected by initial pH, t_g decreasing when pH decreases.

When comparing linear and quadratic regression coefficients, it was observed that temperature was the most influential individual variable, though the influence of temperature–R interaction was also important.

In order to obtain simpler gel time prediction equations, and also a better fit, the regression analysis of experimental data (Table Curve 3D) as a function of two variables was carried out, at pH 6, 7 and 8, respectively. The following mathematical models were obtained ($r^2 > 0.94$):

$$\ln t_g = -3.661 + 1.356 \cdot e - X1 + 1.388 \cdot e - X2 \quad \text{pH6} \quad (7)$$

$$\ln t_g = 3.700 - 4.579 \cdot X1 - 1.936 \cdot e - X1 - 1.526 \cdot X2 \quad \text{pH7} \quad (8)$$

$$\ln t_g = 3.107 - 4.389 \cdot X1 - 1.705 \cdot e - X1 - 1.553 \cdot X2 \quad \text{pH8} \quad (9)$$

Heating affects the rate of two processes which mutually influence each other: gelation and non-enzymatic browning processes. The pH decrease promoted by non-enzymatic browning reactions affects system gelation. Gelation, in turn, causes variations in transport properties and sucrose hydrolysis kinetics, which influences directly and indirectly the kinetics of browning reactions.

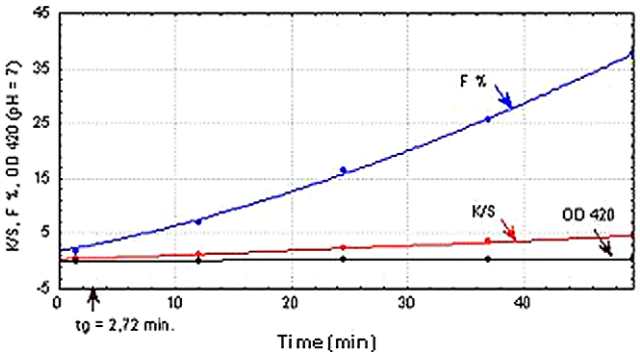

Fig. 3. Fluorescence, Kubelka–Munk index and optical density for the samples of $R = 0.591$, at pH 7, as a function of time. The arrow indicates the gelation time.

However, gelation and browning reactions have different kinetics, as activation energy and reaction pseudo-order values show (Rozycki, 1999).

In order to compare the kinetics of the gelation process in parallel to the non-enzymatic browning development, the browning indicators fluorescence (F), optical density at 420 nm (OD_{420}) and the Kubelka–Munk colour function K/S were measured and represented as a function of time. Fluorescence (F) presented higher sensitivity than the other colour functions or absorbance readings employed to follow browning development, as shown in Fig. 3, for the samples of $R = 0.591$, at pH 7. The corresponding gelation times (t_g), indicated as arrows noticeably show that the system gelation (at $T > 105$ °C) occurs much earlier than colour development can be appreciated, whereas fluorescence is clearly detected from the beginning of the reaction. It is concluded that both gelation and browning processes could be separated, as well as their individual design and control, which can be employed for the continuous production of concentrated and sucrose dairy products, whose organoleptic and texture characteristics would vary according to their future application.

4. Conclusions

The present work has shown temperature to be the most influential individual variable on the thermal-induced gelation of milk in the presence of sucrose. At temperatures close to the boiling point, at atmospheric pressure, both gelation and browning processes are slow and even below a certain proportion of milk solids there is no convenient system gelation. Also, the presence of sucrose increases gelation rate and its dependence on temperature.

At pHs 7 and 8, the system shows a similar behaviour, though sensibly different from that at pH 6, which shows the possibility of a change in the mechanism of the reactions involved in the gelation process.

The pH variation studied has no apparent influence on the thermodynamic aspects of gelation reactions and the average functionality of casein micelles, though it does influence the process kinetics, aggregation and gelation being fast at pH 6.

The mathematical models obtained were adequate to predict the system behaviour as far as its stability is concerned, combining technological variables commonly used in the industry.

pH was shown to noticeably affect the firmness and structural density of dairy gels obtained, these characteristics increasing at higher pHs (pH 8) since they produce a less fast (controlled) rate which allows a minimum heating time needed for establishing a higher number of bonds and the subsequent gel "reaffirmation".

System gelation occurs much earlier than the development of a noticeable brown colour.

These aspects are very useful for the development of continuous methods to obtain concentrated and sucrose products of different organoleptic and texture characteristics, for the optimisation of the designed processes, and the formulation of new products.

Acknowledgements

The authors acknowledge the financial support from Universidad Nacional de Litoral CAI + D 12/H624.

References

Anema, S. G., & Li, Y. (2003). Association of denatured whey proteins with the casein micelles in heated reconstituted skim milk and its effect on casein micelle size. *Journal of Dairy Research, 60*, 505–516.

Anema, S. G., Lowe, E. K., & Li, Y. (2004). Effect of pH on the viscosity of heated reconstituted skim milk. *International Dairy Journal, 14*, 541–548.

Boye, J. I., Alli, I., Ramaswamy, H., & Raghavan, V. G. (1997). Interactive effects of factors affecting gelation of whey proteins. *Journal of Food Science, 62*(1), 57–65.

Buera, M. P., Chirife, J., Resnik, S. L., & Wetzler, G. (1987). Nonenzymatic browning in liquid systems of high water activity: Kinetics of color changes due to Maillard's reaction between different single sugars and glycine and comparison with caramelization browning. *Journal of Food Science, 52*, 1063–1067.

Carpenter, J. F., Chang, B. S., Garzón Rodríguez, W., & Randolph, T. W. (2002). Rational design of stable lyophilised protein formulations: Theory and practice. *Pharmacology Biotechnology, 13*, 109–133.

Clark, A. H. (1992). Gels and gelling. In *Physical chemistry of foods*. M. Dekker.

Flink, M. J. (1983). Nonenzymatic browning of freeze-dried sucrose. *Journal of Food Science, 48*, 539–542.

Considine, T., Patel, H. A., Anema, S. G., Singh, H., & Creamer, L. K. (2007). Interactions of milk proteins during heat and high hydrostatic pressure treatments. *Innovative Food Science Engineering and Technology, 8*, 1–23.

Corredig, M., & Dalgleish, D. G. (1999). The mechanism of heat-induced interactions of whey proteins with casein micelles in milk. *International Dairy Journal, 9*, 233–236.

Donato, L., Guyomarch, F., Amiot, S., & Dagleish, D. G. (2007). Formation of whey protein/χ-casein complexes in heated milk: Preferential reaction of whey protein with χ-casein in the casein micelles. *International Dairy Journal, 17*, 1161–1167.

Fox, P. F. (1981). Heat-induced changes in milk preceding coagulation. *Journal of Dairy Science, 64*(11), 2127–2137.

Fox, P. F. (1982). Heat induced coagulation of milk. In P. F. Fox (Ed.), *Developments in dairy chemistry* (pp. 189–228). London: Elsevier Applied Science.

Horne, D. S. (1998). Casein interactions: Casting light on the black boxes, the structure in dairy products. *International Dairy Journal, 8*, 171–177.

Hyslop, D. B., & Fox, P. F. (1981). Heat stability of milk: Interrelationship between assay temperature, pH and agitation. *Journal of Dairy Research, 48*, 123–129.

International Dairy Federation – FIL-IDF (1964). Casein content of milk. IDF Standard 29. Int. Dairy Fed., Brussels, Belgium.

Katsuta, K., Rector, D., & Kinsella, J. E. (1990). Viscoelastic properties of whey protein gels: Mechanical model and effects of protein concentration on creep. *Journal of Food Science, 55*, 516–521.

Kim, B. Y., & Kinsella, J. E. (1989). Rheological changes during slow acid induced gelation of milk by D-glucono-(-lactone). *Journal of Food Science, 54*, 894–898.

Lucey, J. A. (2002). Formation and physical properties of milk protein gels. *Journal of Dairy Science, 85*, 291–294.

Matiacevich, S. B., & Buera, M. P. (2006). A critical evaluation of fluorescence as a potential marker for the Maillard reaction. *Food Chemistry, 95*, 423–430.

McSweeney, S. L., Mulvihill, D. M., & O'Callaghan, D. M. (2004). The influence of pH on the heat-induced aggregation of model milk protein ingredient systems and model infant formula emulsions stabilized by milk protein ingredients. *Food Hydrocolloids, 18*(1), 109–125.

Montgomery, D. C. (1991). *Diseño y Análisis de Experimentos* (Ed.) Grupo Editorial Iberoamericana S.A. de C.V., México.

Moro, O., & Hough, G. (1985). Total solids and density measurements in dulce de leche a typical argentine dairy product. *Journal of Dairy Science, 68*, 521–525.

Navarro, A. S., Ferrero, C., & Zaritzky, N. E. (1999). Rheological characterization of "Dulce de Lecheâ" by dynamic and steady shear measurements. *Journal of Texture Studies, 30*, 43–58.

Park, C. K., & Kim, D. H. (1983). Relationship between fluorescence and antioxidant activity of ethanol extracts of a Maillard browning mixture. *JAOCS, 60*(1), 22–26.

Passot, S., Fonseca, F., Alarcon-Lorca, M., Rolland, D., & Marin, M. (2005). Physical characterisation of formulations for the development of two stable freeze-dried proteins during both dried and liquid storage. *European Journal of Pharmaceutics and Biopharmaceutics, 60*, 335–348.

Pauletti, M., Castelao, E., & Seguro, E. (1996). Kinetics of heat coagulation of concentrated milk proteins at high sucrose contents. *Journal of Food Science, 61*(6), 1207–1210.

Petriella, S., Resnik, S., Lozano, R., & Chirife, J. (1985). Kinetics of deteriorative reactions in model food systems of high water activity: Color changes due to nonenzymatic browning. *Journal of Food Science, 50*, 622–626.

Rector, D. J., Matsudomi, N., & Kinsella, J. E. (1991). Changes in gelling behavior of whey protein isolate and (β-lactoglobulin during storage: Possible mechanism(s). *Journal of Food Science, 56*(3), 782–788.

Rozycki, S. D. (1999). Master Thesis in Food Science and Techonology. FIQ, UNL, Santa Fe, Argentina.

Rozycki, S. D. (2003). Cinética de Pardeamiento en Sistemas Lácteos Concentrados: Análisis Comparativos de Modelos. *Ciencia y Tecnología Alimentaria, 4*(2), 95–108.

Statgraphics Plus 3.0 (1994). Copyright 1994–1997. Statistical Graphics Corporation, USA.

Table Curve 3D (1993). Jandel Scientific Software, version 2 for Win 32. AISN Software Inc., USA.

Villota, R., & Hawkes, J. (1992). Reactions kinetics in food systems. In D. R. Heldman & Lund (Eds.), *Handbook of food engineering* (pp. 39–144). New York: Marcel Dekker.

Walstra, P. & Jenness, R. (1987a). Propiedades de los Concentrados Lácteos. In *Química y Física Lactológica* (p. 269–279). Acribia, Zaragoza, Spain.

Walstra, P., & Jenness, R. (1987b). Tratamientos Térmicos. In *Química y Física Lactológica* (p. 147–152). Acribia, Zaragoza Spain.

Food Chemistry 118 (2010) 74–77

Contents lists available at ScienceDirect

Food Chemistry

journal homepage: www.elsevier.com/locate/foodchem

Antimicrobial potential of *Coriandrum sativum* L. against different *Candida* species *in vitro*

A.F. Begnami [a], M.C.T. Duarte [b], V. Furletti [a], V.L.G. Rehder [b,*]

[a] *Piracicaba Dental School, University of Campinas, UNICAMP, Alexandre Cazellatto, Km 393, n. 999, 13140-000 Paulinia, Sao Paulo, Brazil*
[b] *Chemical, Biological and Agricultural Pluridisciplinary Research Center (CPQBA), University of Campinas, UNICAMP, Alexandre Cazellatto, Km 393, n. 999, 13140-000 Paulinia, Sao Paulo, Brazil*

ARTICLE INFO

Article history:
Received 17 December 2008
Received in revised form 8 April 2009
Accepted 21 April 2009

Keywords:
Essential oil
Antimicrobial activity
Coriandrum sativum

ABSTRACT

The aim of this study was to evaluate the chemical and antifungal activity of the essential oil from *Coriandrum sativum* L. (Apiaceae) against different *Candida* species. The essential oil (EO) was obtained by hydrodistillation and submitted to dry-column chromatography, resulting in six fractions, which were then submitted to TLC and GC–MS analysis. The main compounds identified were alcohols: 1-decanol (24.20%); 2E-decenol (18.00%); 2Z-dodecenol (17.60%); and aldehydes (89%). Antibacterial activity of the EO and its fractions was tested against five species of *Candida albicans*. The EO showed antimicrobial activity against all the species of *Candida* tested, except for *Candida tropicalis* CBS 94. Fractions 4 and 6 had a greater antibiotic spectrum, probably due to the presence of such alcohols as 3-hexenol, 1-decanol, 2E-decenol and 2Z-dodecenol. In conclusion, the EO and its fractions could be used as potential antimicrobial agents to treat or prevent *Candida* yeast infections.

1. Introduction

There has been a high incidence of nosocomial infections caused by opportunistic microorganisms, especially species of *Candida;* the therapeutic approach to such infections is a great challenge due to the resistance developed by pathogens towards a number of widely-used drugs (Chopra, 2007). *Candida* spp may cause several infections involving oral mucosal lesions (candidiasis or candidosis) and potential systemic dissemination, which might be due to antibiotics use, as they kill the competing bacterial flora, leading to an overgrowth of yeasts (Koneman, Allen, Janda, Schreckenberger, & Winn, 2001; Xu, Samaranayake, & Samaranayake, 1999).

A growing demand for natural antimicrobial agents has been observed in the past few years. Several studies have investigated the antimicrobial activity against *Candida albicans* of the essential oil and other substances extracted from medicinal plants; however, no phototherapeutic products with antimicrobial activity have been developed for human or animal use so far (Duarte, Figueira, Sartoratto, Rehder, & Delarmelina, 2005; Rosato, Vitalli, Gallo, Balenzano, & Mallamaci, 2008; Runyoro, Matee, Ngassapa, Joseph, & Mbwambo, 2006).

Coriandrum sativum L. (Umbelliferae/Apiaceae), popularly known as coriander, is commonly found in Brazilian cuisine and medicinally believed to have several therapeutic properties: hypoglycaemic (Otoom, Al-Safi, Kerem, & Alkofani, 2006; Waheed, Miana, Ahmad, & Khan, 2006), anti-inflammatory and hypolipidaemic (Chithra & Leelamma, 1997; Chithra & Leelamma, 2000; Lal, Tkumar, & Pillai, 2004), analgesic and sedative (Chaudhry & Tariq, 2006; Emamghoreishi & Heidari-Hamedani, 2006), anxiolytic (Emamghoreishi, Khasaki, & Aazam, 2005), antimutagenic (Cortes-Eslava, Gomez-Arroyo, Villalobos-Pietrini, & Espinosa-Aguirre, 2004), antihypertensive (Medhim, Hadharzy, Bakos, & Verzar-Petri,1986), diuretic (Benjumea, Abdala, Hernandez-Luiz, Pérez-Paz, & Martin-Herrera, 2005; Maghrani, Zwggwagh, Haloui, & Eddouks, 2005), antioxidant (Melo, Bion, Filho, & Guerra, 2003; Ramadan, Kroh, & Morsel, 2003), antimicrobial (Kubo, Fujita, Kubo, Hihei, & Ogura, 2004; Lo Cantore, Iacobelli, Marco, Capasso, & Senatore, 2004), and carminative, antispasmodic and relaxant (Vejdani et al., 2006).

Antimicrobial activity has been reported for the essential oil (EO) extracted from *C. sativum* seeds against different species of *Candida*, Gram-positive/negative bacteria, and fungi (Elgayyar, Draughon, Golden, & Mount, 2001; Hammer, Carson, & Riley, 1998; Lo Cantore et al., 2004).

Matasyoh, Maiyo, and Ngure (2008) reported antibacterial activity for the EO obtained from *C. sativum* leaves against Gram-positive (*Staphylococcus aureus, Bacillus* spp.) and Gram-negative bacteria (*Escherichia coli*, *Salmonella typhi*, *Klebsiella pneumoniae*, *Proteus mirabilis*, *Pseudomona aeruginosa*), as well as fungi (*C. albicans*). Duarte, Figueira, Delarmelina, and Sartoratto (2007) showed antimicrobial activity of *C. sativum* leaves against *Pityrosporum ovale*, while Wong and Kitts (2006) demonstrated antimicrobial activity for the ethanolic and aqueous extracts of *C. sativum* against *Bacillus subtilis* and *E. coli*.

* Corresponding author. Tel.: +55 19 2139 2869; fax: +55 19 2139 2850.
E-mail address: rehder@cpqba.unicamp.br (V.L.G. Rehder).

0308-8146/$ - see front matter © 2009 Published by Elsevier Ltd.
doi:10.1016/j.foodchem.2009.04.089

Therefore, the aim of the present study was to evaluate the antimicrobial activity of the EO extracted from *C. sativum* leaves and its fractions against different species of *Candida* (*C. albicans* CBS 562, *Candida tropicalis* CDS 94, *C. parapsilosis* CBS 604, *C. dubliniensis* CBS 7987, and *C. krusei* CBS 573), as well as to identify the chemical constituents responsible for such activity.

2. Materials and methods

2.1. Plant material

Leaves of *C. sativum* L. were obtained at CEASA (grocery wholesalers and retailers) in Campinas, January 2007.

2.2. Microorganisms

Microorganisms were obtained from the Department of Oral Diagnosis, Division of Microbiology and Immunology, at Piracicaba Dental School, University of Campinas (UNICAMP). Antibacterial assays involved such *Candida* species, as *C. albicans* CBS 562, *C. tropicalis* CDS 94, *C. parapsilosis* CBS 604, *C. dubliniensis* CBS 7987, and *C. krusei* CBS 573.

2.3. Distillation of essential oil and fractionation

The essential oil was obtained by the hydrodistillation of fresh leaves (7.5 kg) using a Clevenger-type apparatus for 4 h. The resulting oil/water mixture obtained was extracted using dichloromethane. The organic layer was then separated, dried over Na_2SO_4, filtered and the solvent removed by means of vacuum evaporation at room temperature, resulting in *C. sativum* essential oil (yield: 0.03% w/w).

The EO of the *C. sativum* (0.5 g) was further fractionated by dried column chromatography (cellulose 2 × 30 cm) using Si gel 60 (Merck; Darmstadt, Germany) and dichloromethane as the eluent. The columns were cut into six parts and extracted using dichloromethane, yielding the following fractions: **1** (84.3 mg), **2** (49.5 mg), **3** (21.6 mg), **4** (82.4 mg), **5** (164.8 mg), and **6** (50.9 mg). The fractions were analysed by thin layer chromatography and gas chromatography–mass spectrometry (GC–MS) and then submitted to antimicrobial assays.

2.4. Analysis

The EO and its fractions were analysed through thin layer chromatography (TLC) using silica gel 60 F_{254} layers (Merck) eluted with dichloromethane and visualised under UV 254 nm, following anisaldehyde solution application and drying at 105 °C for 5 min. The samples of the EO and its fractions were diluted in ethyl acetate (10 mg/ml). GC–MS analyses were carried out using gas chromatography (Agilent 6890), with mass selective detector (Agilent 5975; Agilent; Santa Clara, CA), using an HP-5 MS capillary column (25 m × 0.25 mm i.d. × 1.0 μm d.f.). Injection temperature was 220 °C, detector temperature was 250 °C, column temperature was increased from 60 °C to 240 °C at 3 °C per min. Carrier gas was He at 1.0 ml/min and split injection was used.

The programmed temperature retention index of each compound was determined in relation to *n*-alkanes. The MS was operated in the EI mode at 70 eV in the *m*/*z* range from 42 to 350. Compounds were identified by comparing the mass spectra with those in a mass spectral library database (NIST 05), co-injection of hydrocarbon standards to calculate the retention indices (RI's), and analysis of data described by Adams (2007). The relative proportions of the essential oil constituents were expressed as percentages obtained by peak area normalisation; all relative response factors were taken as one.

2.5. Anti-Candida assay – minimal inhibitory concentration (MIC) test

The yeast was grown overnight at 36 °C in Sabouraud dextrose agar (Merck) plates. Inocula for antimicrobial assays were prepared by diluting the scraped cell mass in 0.85% NaCl solution, adjusted to 0.5 McFarland scale and confirmed by spectrophotometric readings at 580 nm.

Cell suspensions were finally diluted to 10^4 CFU ml^{-1} (colony forming units) for use in the assays. Minimum inhibitory concentration (*MIC*) tests were carried out in RPMI-1640 medium according to NCCLS. (2002) using a tissue culture test plate (96 wells). The EO was diluted in 0.1% Tween 80 solution in sterile water and the stock solution transferred into the first well, and serial dilutions were performed, to obtain concentrations ranging between 0.003 and 2 mg/ml.

Nystatin (Merck) was used as the reference antimycotic control (5–60 μg/ml), the yeast inoculum was added to all wells and the plates were incubated at 36 °C for 24 h.

Table 1
Chemical composition of *Coriandrum sativum* leaves essential oil and fractions.

Compounds	Relative amount (%)						
	Oil	Fraction 1	Fraction 2	Fraction 3	Fraction 4	Fraction 5	Fraction 6
Alcohols							
3-Hexenol	10.30	–	–	–	0.70	10.50	16.30
2-Hexenol	3.80	–	–	–	0.40	4.40	6.20
2E-Hecenol	18.00	–	–	–	30.10	35.00	
1-Decanol	24.10	2.20	–	–	11.40	22.40	54.80
1-Undecanol	–	–	–	–	0.60	1.10	1.10
2Z-Dodecenol	17.60	–	–	–	39.90	20.70	6.20
2E-Tetradecenol	3.10	–	26.30	27.00	8.30	2.90	
	77.00	2.20	26.30	27.00	91.40	97.00	84.60
Aldehydes							
2-Hexenal	0.40			2.60	–	–	0.40
Decanal	4.80	24.80	24.90	4.40	–	–	–
2-Decenal	–	–	3.10	15.90	–	–	–
Dodecanal	–	2.90	1.90	–	–	–	–
Tridecanal	3.00	29.30	14.40	2.40	–	–	–
2-Dodecenal	2.90	0.60	14.90	30.40	–	–	–
Tetradecanal	0.90	13.00	3.30	0.50	–	–	–
	12.00	70.00	62.50	56.20	–	–	–
Total	89.00	72.20	88.80	83.20	91.40	97.00	85.00

Table 2
Antimicrobial activity of essential oil and its fractions from *Coriandrum sativum* against different species of *Candida*.

	MIC (μg/ml)								
Candida spp.	Oil	Fraction 1	Fraction 2	Fraction 3**	Fraction 4	Fraction 5	Fraction 6	Nistatin	Fluconazole
C. albicans CBS 562	500	*	1000	–	31	63	31	2	63
C. krusei CBS 573	250	*	125	–	63	250	63	0,5	15
C. parapsilosis CBS 604	125	31	1000	–	7	10	7	8	7
C. dubliniensis CBS 7987	250	*	500	–	7	31	15	1	7
C. tropicalis CBS 94	*	*	*	–	63	125	63	16	125

* MIC > 1000 μg/ml.
** The essential oil fraction three was not subjected to the tests of antimicrobial activity due the insufficient mass.

Minimal inhibitory concentration was determined as the lowest concentration of the EO to inhibit visible growth of yeast (RPMI medium is known to change colour, pink to yellow, as microbial growth occurs).

3. Results and discussion

The EO from the C. *sativum* obtained through hydrodistillation was submitted to GC–MS analysis. The main constituents identified were alcohols (78.13%) and aldehydes (11.96%), with linear chains ranging from 6 to 14 carbon atoms (Table 1). The major alcohols were 1-decanol (24.17%), 2E-decenol (18.05%), 2Z-dodecenol (17.55%) and 3-hexenol (10.34%), while the major aldehydes were decanal (4.76%), dodecanal (3.02%) and 2-dodecenal (2.88%).

These results were observed to be different from those concerning the EO of *C. sativum* leaves collected in Kenya (Matasyoh et al., 2008) and Tunisia (Msaada, Hosni, Ben Taarit, Chahed, & Marzouk, 2007), where the main compounds identified were the aldehydes (E)-2-decenal and (*E*)-2-dodecenal.

In the present study, the EO (*C. sativum*) showed antimicrobial activity, varying from 125 μg/ml (*C. parapsilosis* CBS 604) to 500 μg/ml (*C. albicans* CBS 562), against most of the Candida species tested, except for *C. tropicalis* CBS 94. These results showed a greater antimicrobial potential of the EO, when compared to those obtained by Matasyoh et al. (2008), reporting an *MIC* value of 163 mg/ml for *C. albicans*.

Fractionation of the EO through dry-column chromatography resulted in 6 fractions with different polarities and their main constituents were identified by GC–MS (Table 1).

Aldehydes were the main compounds observed in fractions **1**, **2** and **3** (56–71%) while alcohols were found in fractions **4**, **5** and **6** (85–97%). Results showed potential bacterial inhibition for fractions **4**, **5** and **6,** with *MIC* values varying from 7 to 250 μg/ml. The other fractions showed higher *MIC* values and lower antimicrobial activity, which might be explained by the greater concentration of aldehydes found.

Fractions **4**–**6** and the antibiotics tested showed similar antimicrobial activity against *C. albicans* CBS 562, *C. parapsilosis* CBS 604, *C. dubliniensis* CBS 7987, and *C. tropicalis* with *MIC* values ranging from 7 to 63 μg/ml. These values showed potential antimicrobial activity when compared to those obtained for the EO (125–500 μg/ml), which might be explained by the higher concentration of alcohols found (Table 2).

4. Conclusion

A high concentration of alcohols and aldehydes was observed for the EO of C. *sativum* fresh leaves, showing antimicrobial activity against different species of *Candida*, except for *C. tropicalis* CBS 94.

Chemical fractions of the EO possessed greater antimicrobial activity (*MIC*: 7–63 μg/ml), similar to that of standard antibiotics. The high concentration of alcohols found in these fractions might be responsible for such activity.

Acknowledgement

The authors thank CAPES (Brazilian Funding Agency) for the financial support.

References

Adams, R. P. (2007). *Identification of essential oil components by gas chromatography/ mass spectrometry* (4th ed., p. 804). Illinois: Allured Publishing Corporation.
Benjumea, D., Abdala, S., Hernandez-Luiz, F., Pérez-Paz, P., & Martin-Herrera, D. (2005). Diuretic activity of *Artemisia thuscula*, an endemic canary species. *Journal of Ethnopharmacology, 100*, 205–209.
Chaudhry, N. M. A., & Tariq, P. (2006). Bactericidal activity of black pepper, bay leaf, aniseed and coriander against oral isolates. *Pakistan Journal of Pharmacology and Science, 19*(3), 214–218.
Chithra, V., & Leelamma, S. (2000). *Coriandrum sativum*-effect on lipid metabolism in 1,2-dimethyl hydrazine induced colon cancer. *Journal of Ethnopharmacology, 71*, 457–463.
Chithra, V., & Leelamma, S. (1997). Hypolipidemic effect of coriander seed (*Coriandrum sativum*); mechanism of action. *Plant Foods and Human Nutrition, 51*(2), 167–172.
Chopra, I. (2007). The increasing use of silver-based products as antimicrobial agents: A useful development or a concern. *Journal of Antimicrobial Chemotherapy, 59*, 587–590.
Cortes-Eslava, J., Gomez-Arroyo, S., Villalobos-Pietrini, R., & Espinosa-Aguirre, J. J. (2004). Antimutagenicity of coriander (*Coriandrum sativum*) juice on the mutagenesis produced by plant metabolites of aromatic amines. *Toxicology Letters, 153*, 283–292.
Duarte, M. C. T., Figueira, G. M., Delarmelina, C., & Sartoratto, A. (2007). Investigação da atividade do oleo essencial de duas variedades de *Coriandrum sativum* contra microrganismos envolvidos com patologias dérmicas. *Horticultura Brasileira, 25*(1), s36.
Duarte, M. C. T., Figueira, G. M., Sartoratto, A., Rehder, V. L. G., & Delarmelina, C. (2005). Anti-Candida activity of Brazilian medicinal plants. *Journal of Ethnopharmacology, 97*(2), 305–311.
Elgayyar, M., Draughon, F. A., Golden, D. A., & Mount, J. R. (2001). Antimicrobial activity of essential oils from plants against selected pathogenic and saprophytic microorganisms. *Journal of Food Protection, 64*(7), 1019–1024.
Emamghoreishi, M., & Heidari-Hamedani, G. (2006). Sedative-hypnotic activity of extracts and essential oil of coriander seeds. *Iran Journal of Medicine and Science, 31*(1), 22–27.
Emamghoreishi, M., Khasaki, M., & Aazam, M. F. (2005). *Coriandrum sativum*: Evaluation of its anxiolytic effect in the elevated plus-maze. *Journal of Ethnopharmacology, 96*, 365–370.
Hammer, K. A., Carson, C. F., & Riley, T. V. (1998). In vitro activity of essential oils, in particular *Melaleuca alternifolia* (tea tree) oil and tea tree oil products, against *Candida* spp. *Journal of Antimicrobes and Chemotherapy, 42*, 591–595.
Koneman, E. W., Allen, S. D., Janda, W. M., Schreckenberger, P. C., & Winn, W. C. Jr., (2001). *Microbiological diagnosis: text and color atlas* (5th ed.). Rio de Janeiro: Medsi. 1465p.
Kubo, I., Fujita, K. I., Kubo, A., Hihei, K. I., & Ogura, T. (2004). Antibacterial activity of coriander volatile compounds against *Salmonella choleraesuis*. *Journal of Agriculture and Food Chemistry, 52*(11), 3329–3332.
Lal, A. A. S., Tkumar, P. B. M., & Pillai, K. S. (2004). Hypolipidemic effect of *Coriandrum sativum* L. Intriton-induced hyperlipidemic rats. *Indian Journal of Experimental Biology, 42*, 909–912.
Lo Cantore, P., Iacobelli, N. S., Marco, A., Capasso, F., & Senatore, F. (2004). Antibacterial activity of *Coriandrum sativum* L., and *Foeniculum vulgare* Miller Var Vulgare (Miller) essential oils. *Journal of Agriculture and Food Chemistry, 52*, 7862–7866.

Maghrani, M., Zwggwagh, N. A., Haloui, M., & Eddouks, M. (2005). Acute diuretic effect of aqueous extract of *Retama raetam* in normal rats. *Journal of Ethnopharmacology, 99*, 31–35.

Matasyoh, J. C., Maiyo, Z. C., & Ngure, R. M. (2008). Chemical composition and antimicrobial activity of the essential oil of *Coriandrum sativum*. *Food Chemistry, 113*(2), 526–529.

Medhim, D. G., Hadharzy, P., Bakos, P., & Verzar-Petri, G. (1986). Hypotensive effects of *Lupinus termis* and *Coriandrum sativum* in anesthetized rats. A preliminary study. *Acta Pharmaceutica Hungarica, 56*, 59–63.

Melo, E. A., Bion, F. M., Filho, J. M., & Guerra, N. B. (2003). In vivo antioxidant effect of aqueous and etheric coriander (*Coriandrum sativum*) extracts. *European Journal of Lipid Science and Technology, 105*, 483–487.

Msaada, K., Hosni, K., Ben Taarit, M., Chahed, T., & Marzouk, B. (2007). Variations in the essential oil composition from different parts of *Coriandrum sativum* L., Cultivated in Tunisia. *Italian Journal of Biochemistry, 56*, 47–52.

NCCLS. (2002). Reference method for testing the dilution in broth for determining the susceptibility of yeasts to antifungal therapy: Approved standard (2nd ed.). Pennsylvania: NCCLS document M27-A2, v.22, n.15, 51p.

Otoom, S. A., Al-Safi, S. A., Kerem, Z. K., & Alkofani, A. (2006). The use of medicinal herbs by diabetic Jordanian patients. *Journal of Herbal Pharmacotherapy, 6*(2), 31–41.

Ramadan, M. F., Kroh, L. W., & Morsel, J. T. (2003). Radical scavenging activity of black cumin (*Nigella sativa* L.), coriander (*Coriandrum sativum* L.) and niger (*Guizotia abyssinica* Cass.) crude seed oils and oil fractions. *Journal of Agricultural and Food Chemistry, 51*(696), 1–6969.

Rosato, A., Vitalli, C., Gallo, D., Balenzano, L., & Mallamaci, R. (2008). The inhibition of *Candida* species by selected essential oils and their synergism with amphotericin B. *Phytomedicinie, 15*, 635–638.

Runyoro, D. K. B., Matee, M. I., Ngassapa, O. D., Joseph, C. C., & Mbwambo, Z. H. (2006). Screening of Tanzanian medicinal plants for anti-Candida activity. *BMC Complementary and Alternative Medicine, 6*, 11. doi:10.1186/1472-6882-6-11.

Vejdani, R., Shalmani, H. R., Mir-Fattahi, M., Sajed-Nia, F., Abdollahi, M., & Zali, M. R. (2006). The efficacy of an herbal medicine, carmint, on the relief of abdominal pain and bloating in patients with irritable bowel syndrome: A pilot study. *Digestive Disease Science, 51*(8), 1501–1507.

Waheed, A., Miana, G. A., Ahmad, S. I., & Khan, M. A. (2006). Clinical investigation of hypoglycemic effect of *Coriandrum sativum* in type-2 (NIDDM) diabetic patients. *Pakistan Journal of Pharmacology, 23*(1), 7–11.

Wong, P. Y. Y., & Kitts, D. D. (2006). Studies on the dual antioxidant and antibacterial properties of parsley (*Petroselinum crispum*) and cilantro (*Coriandrum sativum*) extracts. *Journal of Agricultural and Food Chemistry, 97*, 505–515.

Xu, Y. Y., Samaranayake, Y. H., & Samaranayake, L. P. (1999). In vitro susceptibility of *Candida* species to lactoferrin. *Medical Mycology, 37*(1), 35–41.

Food Chemistry 118 (2010) 78–83

Contents lists available at ScienceDirect

Food Chemistry

journal homepage: www.elsevier.com/locate/foodchem

Authentication of extra virgin olive oils by Fourier-transform infrared spectroscopy

M.J. Lerma-García *, G. Ramis-Ramos, J.M. Herrero-Martínez, E.F. Simó-Alfonso

Department of Analytical Chemistry, Faculty of Chemistry, University of Valencia, 46100 Burjassot, Valencia, Spain

ARTICLE INFO

Article history:
Received 30 April 2008
Received in revised form 11 March 2009
Accepted 21 April 2009

Keywords:
Botanical origin
Extra virgin olive oil adulteration
Fourier-transform infrared spectroscopy
Linear discriminant analysis
Multiple linear regression

ABSTRACT

Fourier-transform infrared spectroscopy (FTIR), followed by multivariate treatment of the spectral data, was used to classify vegetable oils according to their botanical origin, and also to establish the composition of binary mixtures of extra virgin olive oil (EVOO) with other low cost edible oils. Oil samples corresponding to five different botanical origins (EVOO, sunflower, corn, soybean and hazelnut) were used. The wavelength scale of the FTIR spectra of the oils was divided in 26 regions. The normalized absorbance peak areas within these regions were used as predictors. Classification of the oil samples according to their botanical origin was achieved by linear discriminant analysis (LDA). An excellent resolution among all categories was achieved using an LDA model constructed with eight predictors. In addition, multiple linear regression models were used to predict the composition of binary mixtures of EVOO with sunflower, corn, soybean and hazelnut oils. For all the binary mixtures, models capable of detecting a low cost oil content in EVOO as low as 5% were obtained.

1. Introduction

Oil genuineness is a very important aspect of quality edible oils. Extra virgin olive oil (EVOO) has unique nutritional and sensory characteristics, being also a basic component of the Mediterranean diet. The importance of EVOO is mainly attributed to its high content of oleic acid and its richness in phenolic compounds, which act as natural antioxidants (Bendini et al., 2007). On the other hand, EVOO is expensive owing to the hard and time-consuming tasks involved in the cultivation of olive trees, the harvesting of the fruits, and the extraction of the oil. For these reasons, adulterations of EVOO with olive oils of lower quality, or with oils of a different botanical origin are occasionally detected (Catharino et al., 2005; Chiavaro, Vittadini, Rodriguez-Estrada, Cerretani, & Bendini, 2008; Marcos-Lorenzo, Pérez-Pavón, Fernández-Laespada, García-Pinto, & Moreno-Cordero, 2002; Mariani, Bellan, Lestini, & Aparicio, 2006; Poulli, Mousdis, & Georgiou, 2006; Tay, Singh, Krishnan, & Gore, 2002; Vlachos et al., 2006). For this reason, European Mediterranean countries, which are major suppliers of olive oil in the world market, have adopted common regulations to protect growers and consumers from fraud (European Union Commission, 1991).

To establish the authenticity of edible oils, a number of chromatographic (Brodnjak-Voncina, Kodba, & Novic, 2005; Marcos-Lorenzo et al., 2002; Mariani et al., 2006), thermal (Chiavaro et al., 2008) and spectroscopic methods, including fluorescence (Poulli et al., 2006; Sikorska, Górecki, Khmelinskii, Sikorski, & Kozioł, 2005), NIR (Christy, Kasemsumran, Du, & Ozaki, 2004; Downey, McIntyre, & Davies, 2002; Kasemsumran & Kang, 2005; Sato, 1994; Wesley, Pacheco, & McGill, 1996; Yang, Irudayaraj, & Paradkar, 2005), FTIR (Baeten et al., 2005; Dupuy, Duponchel, Huvenne, Sombret, & Legrand, 1995; Lai, Kemsley, & Wilson, 1999; Ozen & Mauer, 2002; Tay et al., 2002; Vlachos et al., 2006; Yang et al., 2005), FT-Raman (Baeten & Meurens, 1996; López-Díez, Bianchi, & Goodacre, 2003; Yang et al., 2005), NMR (Dais & Spyros, 2007; García-González, Mannina, D'Imperio, Segre, & Aparicio, 2004; Vigli, Philippidis, Spyros, & Dais, 2003) and MS (Catharino et al., 2005; Lay, Liyanage, Durham, & Brooks, 2006; Lerma-García, Ramis-Ramos, Herrero-Martínez, & Simó-Alfonso, 2007, 2008; Lerma-García, Simó-Alfonso, Ramis-Ramos, & Herrero-Martínez, 2007; Marcos-Lorenzo et al., 2002), followed by multivariate statistical analysis of the data, have been described. For this purpose, the contents of fatty acids (Brodnjak-Voncina et al., 2005), tocopherols (Lerma-García, Simó-Alfonso, et al., 2007; Sikorska et al., 2005), volatile compounds (Marcos-Lorenzo et al., 2002), amino acids (Lerma-García, Ramis-Ramos, et al., 2007) and sterols (Lerma-García et al., 2008; Mariani et al., 2006), have been used.

FTIR is a rapid and non-destructive powerful analytical tool for the study of edible oils and fats, requiring minimum sample preparation. FTIR is also an excellent tool for quantitative analysis, since the intensities of the spectral bands are proportional to concentration. For this reason, FTIR has been used to distinguish oils from different botanical origins using non-supervised classificatory techniques (Dupuy et al., 1995; Lai et al., 1999; Rusak, Brown, & Martin, 2003). FTIR has been also used to distinguish EVOOs from different geographical origins (Bendini, Cerretani, et al., 2007; Galtier et al., 2007; Tapp, Defernez, & Kemsley, 2003) and different genetic varieties (Gurdeniz, Tokatli, & Ozen, 2007). FTIR

* Corresponding author. Tel.: +34 96 354 43 34; fax: +34 96 354 44 36.
E-mail address: m.jesus.lerma@uv.es (M.J. Lerma-García).

0308-8146/$ - see front matter © 2009 Elsevier Ltd. All rights reserved.
doi:10.1016/j.foodchem.2009.04.092

applications addressed to detect olive oil adulteration with low cost edible oils (Baeten et al., 2005; Ozen and Mauer, 2002; Tay et al., 2002; Vlachos et al., 2006), to evaluate olive oil freshness (Sinelli, Cosio, Gigliotti, & Casiraghi, 2007), to study changes produced by frying (Valdes & Garcia, 2006) and to assess oil oxidation (Guillén & Cabo, 2002; Muik, Lendl, Molina-Diaz, Valcarcel, & Ayora-Canada, 2007; Vlachos et al., 2006) have been also described.

In this work, FTIR followed by linear discriminant analysis (LDA) of the spectral data was used to classify vegetable oils according to their botanical origin. Also, data treatment by multiple linear regression (MLR) was used to detect and quantify EVOO adulteration with other low cost edible oils, including sunflower, corn, soybean and hazelnut oils.

2. Experimental

2.1. Oil samples and mixtures

The vegetable oils employed in this study (Table 1) were either purchased at the local market or kindly donated by the manufacturers. The botanical origin and quality grade of all the samples were guaranteed by the suppliers. As indicated in Table 1, four samples of each botanical origin were used for training purposes in classification studies, being the other two samples of each category used to evaluate the prediction capability of the classification models. To estimate the adulteration of EVOO with low cost oils by using regression models, binary mixtures containing EVOO and increasing percentages of low cost oil (sunflower, corn, soybean or hazelnut) were prepared. To improve robustness of MLR models, the objects of the calibration matrix were prepared using EVOOs and low cost oils from different geographical origins. For instance, for the sunflower-EVOO pair, oils from different geographical origins were selected to prepare a total of seven mixtures containing 0%, 5%, 10%, 30%, 50%, 75% and 100% sunflower oil. Sets of mixtures containing the same percentages of low cost oil were also prepared for the corn-, soybean- and hazelnut-EVOO pairs. The resulting 28 mixtures were used as calibration set to construct regression models. Additional mixtures of the sunflower-, corn-, soybean- and hazelnut-EVOO pairs, also using oils from different geographical origins, and containing 5%, 50% and 80% low cost oil were prepared. These 12 additional binary mixtures were used to validate the prediction performance of the regression models.

Table 1
Botanical origin, number of samples, brand and use during LDA model construction of the oil samples.

Origin	No. of samples	Brand	LDA set
Hazelnut	2	Guinama	Training
	2	Percheron	Training
	2	Flumen	Evaluation
Sunflower	2	Koipesol	Training
	2	Hacendado	Training
	1	Capicua	Evaluation
	1	Coosol	Evaluation
Corn	1	Guinama	Training
	1	Asua	Training
	1	Artua	Evaluation
	1	Mazola	Evaluation
Corn germ	1	Guinama	Training
	1	Hacendado	Training
Extra virgin olive	1	Carbonell	Training
	1	Grupo Hojiblanca	Training
	1	Borges	Training
	1	Torrereal	Training
	1	Coosur	Evaluation
	1	Hacendado	Evaluation
Soybean	2	Guinama	Training
	2	Biolasi	Training
	2	Sojola	Evaluation

2.2. FTIR spectra

FTIR spectra were obtained using a Nicolet Nexus FTIR spectrophotometer (Thermo Electron Corporation, Waltham, MA, USA) with a resolution of 4 cm^{-1} at 32 scans. A small quantity of the oil samples (≈2 μL) was directly deposited between two well-polished KBr disks, creating a thin film. Duplicated spectra were recorded for all the oil samples and binary mixtures, except the 12 mixtures used as validation set in regression studies which were recorded three times each. Spectra were scanned in the absorbance mode from 4000 to 500 cm^{-1} and the data were handled with the EZ OMNIC 7.3 software (Thermo Electron Corporation).

2.3. Data treatment and construction of matrices

FTIR spectra were divided in the 26 wavelength regions described in Table 2. Each selected spectral region corresponds to a peak or a shoulder, representing structural or functional group information, either about the lipids or minor components of the oil samples (see Table 2). For each region, the peak/shoulder area was measured. In order to reduce the variability associated to the total amount of oil sample used, and to minimize other sources of variance also affecting the intensity of all the peaks, such as the thickness of the sample and radiation source intensity, normalized rather than absolute areas were used. Two normalization procedures were tried. In procedure A, for each spectrum, the area of each region was divided by the sum of the areas of the 26 regions. In procedure B, the area of each region was divided by each one of the areas of the other 25 regions; in this way, and since any pair of areas should be considered only once, $(26 \times 25)/2 = 325$ normalized variables were obtained.

For classification studies, two matrices containing 20 objects each, which corresponded to the averages of the duplicated spectra of the training samples of Table 1, were constructed. These matrices had either 26 or 325 predictors, according to normalization procedures A and B, respectively. A response column, containing the categories corresponding to the five botanical origins of the oils (corn and corn germ were considered as a single category), was added to the training matrices. In order to reduce the internal dispersion of the categories, which was important to reduce the number of variables selected during model construction, the means of the two spectra of each sample, instead of the individual spectra, were used. For evaluation purposes, two more matrices containing 10 objects each, which corresponded to the averages of the duplicated spectra of each evaluation sample of Table 1, were constructed. These matrices also had either 26 or 325 predictors, according to normalization procedures A and B, respectively.

Concerning to the regression studies, and for the sunflower-EVOO pair, two calibration matrices containing seven objects each, which corresponded to the averages of the duplicated spectra of the calibration mixtures, were constructed. According to normalization procedures A and B, the number of predictors was either 26 or 325, respectively. A response column, containing the low cost oil percentages of the mixtures, was added to these matrices. For validation of the prediction performance, two more matrices containing three objects each, which corresponded to the averages of triplicate spectra of validation mixtures, were constructed. The number of predictors was either 26 or 325 predictors, as indicated. Analogously, matrices for the corn-, soybean- and hazelnut-EVOO pairs were also constructed. Statistical treatment of the data was performed using SPSS (v. 12.0.1, Statistical Package for the Social Sciences, Chicago, IL, USA).

Table 2
FTIR spectral regions selected as predictor variables for statistical data treatment.

Identification no.	Range, cm^{-1}	Functional group	Nominal frequency	Mode of vibration
1	3029–2989	=C–H (trans)	3025[a]	Stretching
		=C–H (cis)	3006[a]	Stretching
2	2989–2946	–C–H (CH_3)	2953[a]	Stretching (asym)
3	2946–2881	–C–H (CH_2)	2924[a]	Stretching (asym)
4	2881–2782	–C–H (CH_2)	2853[a]	Stretching (sym)
5	1795–1677	–C=O (ester)	1746[a]	Stretching
		–C=O (acid)	1711[a]	Stretching
6	1486–1446	–C–H (CH_2)	1465[b]	Bending (scissoring)
7	1446–1425	–C–H (CH_3)	1450[b]	Bending (asym)
8	1425–1409	=C–H (cis)	1417[a]	Bending (rocking)
9	1409–1396	=C–H	1400[b]	Bending
10	1396–1382	=C–H	–[b]	Bending
11	1382–1371	–C–H (CH_3)	1377[a]	Bending (sym)
12	1371–1330	O–H	1359[b]	Bending (in plane)
13	1330–1290	Non-assigned	1319[a]	Bending
14	1290–1211	–C–O	1238[a]	Stretching
		$–CH_2–$		Bending
15	1211–1147	–C–O	1163[a]	Stretching
		$–CH_2–$		Bending
16	1147–1128	–C–O	1138[b]	Stretching
17	1128–1106	–C–O	1118[a]	Stretching
18	1106–1072	–C–O	1097[a]	Stretching
19	1072–1043	–C–O	–[b]	Stretching
20	1043–1006	–C–O	1033[a]	Stretching
21	1006–929	–HC=CH– (trans)	968[a]	Bending (out of plane)
22	929–885	–HC=CH– (cis)?	914[a]	Bending (out of plane)
23	885–802	$=CH_2$	850[b]	Wagging
24	802–754	–C–H	–[b]	Bending (out of plane)
25	754–701	$–(CH_2)_n–$	723[a]	Rocking
		–HC=CH– (cis)		Bending (out of plane)
26	701–640	C⋯C	685[b]	Bending (out of plane)
		O–H	650[b]	Bending (out of plane)

[a] According to Guillén and Cabo (1998).
[b] According to Silverstein, Bassler, and Morrill (1981).

3. Results and discussion

3.1. Classification of vegetable oils according to their botanical origin using LDA

FTIR spectra of the 30 oil samples of Table 1 were collected. Fig. 1 shows the spectra of five oils, one for each botanical origin, tailored at two absorbance units. As it can be observed, the differences between them were small. Interpretation of the absorption bands provides information about the molecular skeleton and functional groups (see Table 2); however, to obtain information about the botanical origin of the oils, band interpretation is not required. Information related to the origin was obtained by measuring the peak areas at the selected wavelength ranges. These data were conveniently handled by multivariate statistical techniques.

LDA, a supervised classificatory technique, is widely recognized as an excellent tool to obtain vectors showing the maximal resolution between sets of objects belonging to previously defined categories. In LDA, vectors minimizing the Wilks' lambda, λ_w, are obtained (Vandeginste et al., 1998). This parameter is calculated as the sum of squares of the distances between points belonging to the same category divided by the total sum of squares. Values of λ_w approaching zero are obtained with well resolved categories, whereas overlapped categories made λ_w to approach one. Up to $N-1$ discriminant vectors are constructed by LDA, being N the lowest value for either the number of predictors or the number of categories.

Using the normalized variables, LDA models capable of classifying the oil samples according to their botanical origin were constructed. To select the variables to be included in the model, the SPSS stepwise algorithm was used. According to this algorithm, a predictor is selected when the reduction of λ_w produced after its inclusion in the model exceeds F_{in}, the entrance threshold of a test of comparison of variances or F-test. However, the entrance of a new predictor modifies the significance of those predictors which are already present in the model. For this reason, after the inclusion of a new predictor, a rejection threshold, F_{out}, is used to decide if one of the other predictors should be removed from the model. The process terminates when there are no predictors entering or being eliminated from the model. The default probability values of F_{in} and F_{out}, 0.05 and 0.10, respectively, were adopted.

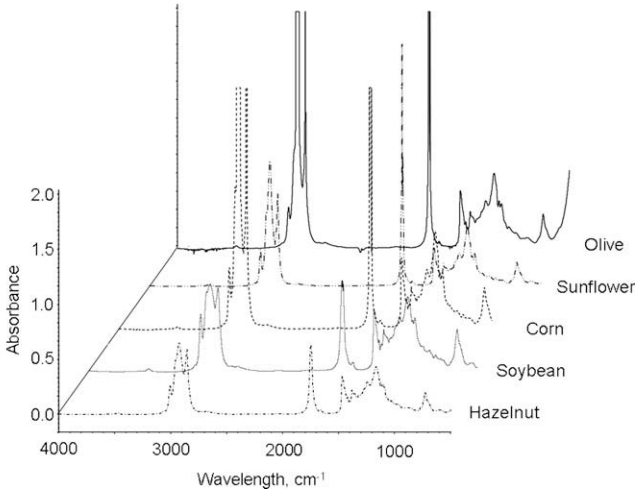

Fig. 1. FTIR spectra of representative samples of EVOO, sunflower, corn, soybean and hazelnut oils. Data were tailored at 2 absorbance units to better show the differences among small peaks.

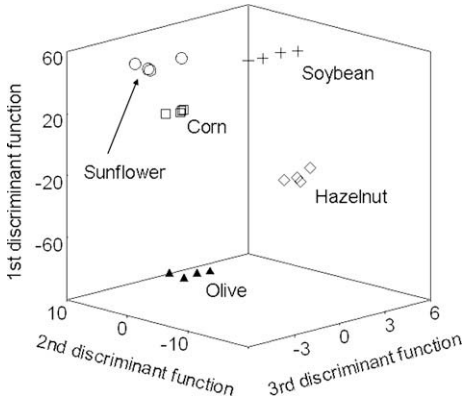

Fig. 2. Score plot on an oblique plane of the 3-D space defined by the three first discriminant functions of the LDA model constructed to classify vegetable oils according to their botanical origin.

Table 3
Predictors selected and corresponding standardized coefficients of the LDA model constructed to predict the botanical origin of vegetable oils.

Predictor[a]	f_1	f_2	f_3	f_4
8/9	19.00	8.20	5.14	3.63
10/12	0.75	9.37	4.03	0.92
11/13	−28.35	5.40	−3.19	−2.13
14/17	16.01	−3.49	−1.50	0.65
15/17	−6.81	5.74	−1.01	1.68
19/25	−13.73	4.33	1.25	0.91
21/26	12.51	−3.76	−0.64	−0.95
22/24	7.84	−5.13	2.26	−1.36

[a] Pairs of wavelength regions identified according to Table 2.

To classify oils according to the five botanical origins, two LDA models, one for each normalization procedure, were constructed. Normalization procedure B, which gave a model with a lower λ_w value and a smaller number of predictors than normalization procedure A, was selected for further studies. As shown in Fig. 2 for normalization procedure B, an excellent resolution between all category pairs was achieved ($\lambda_w = 0.362$). Taking into account that a large number of categories were simultaneously distinguished, this λ_w value was quite low. The predictors selected by the SPSS stepwise algorithm, and the corresponding standardized coefficients of the model, showing the predictors with large discriminant capabilities, are given in Table 3. According to Table 2, the main wavelength regions selected by the algorithm to construct the LDA model corresponded to =C–H (bending), O–H (bending in plane), –C–H (CH_3, bending sym), –C–O (stretching), –CH_2– (bending), –HC=CH– (trans, bending out of plane), O–H (bending out of plane) and C=C (bending out of plane). When leave-one-out validation was applied, all the objects of the training set were correctly classified. Concerning to the prediction capability of this model, and using a 95% probability, all the objects of the evaluation set were correctly assigned; thus, the prediction capability of the model was 100%. On the other hand, the variables obtained by measuring the peak areas along the 26 spectral regions of Table 2 were forced to be included in the model. An improvement of the LDA model was achieved but at the cost of introducing a large number of predictors with low significances. For this reason, variable selection by the stepwise algorithm was maintained.

Finally, an LDA model with all the available objects, including those used above for either training or evaluation, was constructed. The predictors selected by the SPSS stepwise algorithm were basically the same that those selected above, but the λ_w value was smaller (0.202), indicating a satisfactory stability of the model.

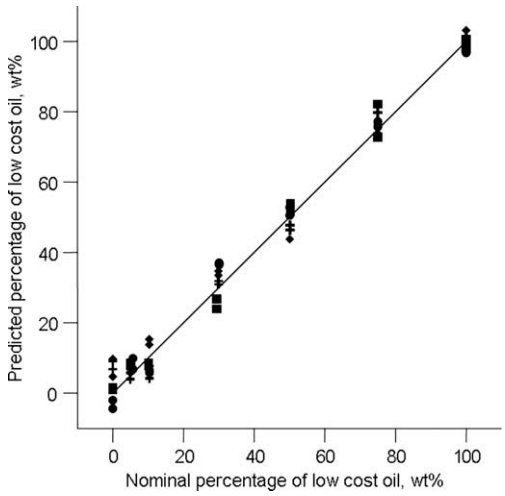

Fig. 3. Predicted (MLR) versus nominal oil percentages for binary mixtures of EVOO with sunflower (●), corn (■), soybean (+) and hazelnut (♦) oils. The straight-line is $y = x$.

3.2. Determination of EVOO adulteration by MLR

In order to quantify EVOO adulteration, the binary mixtures of EVOO with sunflower, corn, soybean and hazelnut oils (Section 2.1), were measured. To select the predictors used in the construction of MLR models, the SPSS stepwise algorithm, with the default probability values of F_{in} and F_{out}, 0.05 and 0.10, respectively, was adopted. MLR models, one for each binary combination of oils, and in each case according to normalization procedures A and B, were constructed. Normalization procedure B, which gave models with higher linear regression coefficients than normalization procedure A, was selected. A plot showing the predicted versus the nominal oil percentages for all the binary mixtures is shown in Fig. 3. The predictors selected and their corresponding non-standardized model coefficients are given in Table 4. It is interesting to observe that, except in the case of the corn-EVOO mixtures, a single predictor was selected to predict the composition of the other three binary mixtures. According to Table 2, the main wavelength transitions selected to construct the MLR model for the sunflower-EVOO pair were =CH_2 (wagging), O–H (bending out of plane) and C=C (bending out of plane). Analogously, for the hazelnut-EVOO pair, the selected transitions were =C–H (trans and cis, stretching), –C–O (stretching) and –CH_2– (bending). Those selected for the soybean-EVOO pair were –$(CH_2)_n$– (rocking) and –HC=CH– (cis, bending out of plane), and those selected for the corn-EVOO pair were –C–O (stretching) and =C–H (trans and cis,

Table 4
Predictors selected and their corresponding non-standardized model coefficients (coef.), linear regression coefficients (R^2), average prediction errors (av. pred. error) and limits of detection (LODs) obtained for the MLR models constructed to predict olive oil adulteration.

Binary mixture	Predictor	Coef.	R^2	Av. pred. error,%	LOD,%
Hazelnut-EVOO	1/15 Constant	−1080 348	0.912	2.0	4.8
Sunflower-EVOO	23/26 Constant	325 −270	0.989	1.7	4.0
Corn-EVOO	1/17 1/16 Constant	−353 221 309	0.994	1.5	1.3
Soybean-EVOO	13/25 Constant	324 −228	0.980	1.9	1.7

stretching). For all binary combinations of oils, a transition implying a double bond was selected, which suggest that unsaturated fatty acids were important in the quantification of the mixtures. The regression coefficients, average prediction errors (calculated as the sum of the absolute differences between expected and predicted oil percentages divided by the number of predictions) and the limits of detection (LODs, calculated as three times the standard deviation at 5% low cost oil level) are also given in Table 4. For all the MLR models and using leave-one-out validation, the average prediction errors were lower than 2%. The four sets of validation mixtures, one for each binary combination of oils ($4 \times 3 = 12$ mixtures), gave average prediction errors below 5%. LODs were in all cases below 5%, being lower than those previously reported in literature for binary mixtures of the same oils, namely 4% versus 6% (Vlachos et al., 2006) for sunflower-EVOO, 1.3% versus 9% (Vlachos et al., 2006) for corn-EVOO, 1.7% versus 6% (Vlachos et al., 2006) for soybean-EVOO and 4.8% versus 25% (Ozen and Mauer, 2002) and versus 8% (Baeten et al., 2005) for hazelnut-EVOO mixtures.

4. Conclusions

The possibility of classifying vegetable oils according to their botanical origin by using FTIR data has been demonstrated. Using eight wavelength regions, all the oil samples belonging to five different botanical origins were correctly classified with an excellent resolution among the categories. In addition, four MLR models constructed with one predictor for sunflower-, soybean- and hazelnut-EVOO mixtures, and with two predictors for corn-EVOO mixtures, were capable of detecting a low cost oil content in EVOO as low as 5%. Thus, the capability of the proposed method to identify the botanical origin of the oils, and to quantify low cost oils in EVOO has been demonstrated.

Acknowledgements

Project CTQ2007–61445 (MEC and FEDER funds). M.J.L.-G. also thanks the Generalitat Valenciana for an FPI grant for Ph.D. studies.

References

Baeten, V., Fernández Pierna, J. A., Dardenne, P., Meurens, M., García-González, D. L., & Aparicio-Ruiz, R. (2005). Detection of the presence of hazelnut oil in olive oil by FT-Raman and FT-MIR spectroscopy. *Journal of Agricultural and Food Chemistry, 53*, 6201–6206.

Baeten, V., & Meurens, M. (1996). Detection of virgin olive oil adulteration by Fourier transform Raman spectroscopy. *Journal of Agricultural and Food Chemistry, 44*, 2225–2230.

Bendini, A., Cerretani, L., Carrasco-Pancorbo, A., Gómez-Caravaca, A. M., Segura-Carretero, A., Fernández-Gutiérrez, A., et al. (2007). Phenolic molecules in virgin olive oils: a survey of their sensory properties, health effects, antioxidant activity and analytical methods. *An overview of the last decade. Molecules, 12*, 1679–1719.

Bendini, A., Cerretani, L., Di Virgilio, F., Belloni, P., Bonoli-Carbognin, M., & Lercker, G. (2007). Preliminary evaluation of the application of the FTIR spectroscopy to control the geographic origin and quality of virgin olive oils. *Journal of Food Quality, 30*, 424–437.

Brodnjak-Voncina, D., Kodba, Z. C., & Novic, M. (2005). Multivariate data analysis in classification of vegetable oils characterized by the content of fatty acids. *Chemometrics and Intelligent Laboratory Systems, 75*, 31–43.

Catharino, R. R., Haddad, R., Cabrini, L. G., Cunha, I. B. S., Sawaya, A. C. H. F., & Eberlin, M. N. (2005). Characterization of vegetable oils by electrospray ionization mass spectrometry fingerprinting: Classification, quality, adulteration, and aging. *Analytical Chemistry, 77*, 7429–7433.

Chiavaro, E., Vittadini, E., Rodriguez-Estrada, M. T., Cerretani, L., & Bendini, A. (2008). Differential scanning calorimeter application to the detection of refined hazelnut oil in extra virgin olive oil. *Food Chemistry, 110*, 248–256.

Christy, A. A., Kasemsumran, S., Du, Y., & Ozaki, Y. (2004). The detection and quantification of adulteration in olive oil by near-infrared spectroscopy and chemometrics. *Analytical Sciences, 20*, 935–940.

Dais, P., & Spyros, A. (2007). ^{31}P NMR spectroscopy in the quality control and authentication of extra-virgin olive oil: A review of recent progress. *Magnetic Resonance in Chemistry, 45*, 367–377.

Downey, G., McIntyre, P., & Davies, A. (2002). Detecting and quantifying sunflower oil adulteration in extra virgin olive oils from the Eastern Mediterranean by visible and near-infrared spectroscopy. *Journal of Agricultural and Food Chemistry, 50*, 5520–5525.

Dupuy, N., Duponchel, L., Huvenne, J. P., Sombret, B., & Legrand, P. (1995). Classification of edible fats and oils by principal component analysis of Fourier transform infrared spectra. *Food Chemistry, 57*, 245–251.

European Union Commission (1991). Regulation 2568/91, Official Journal of the European Communities.

Galtier, O., Dupuy, N., Le Dréau, Y., Ollivier, D., Pinatel, C., Kister, J., et al. (2007). Geographic origins and compositions of virgin olive oils determinated by chemometric analysis of NIR data. *Analytica Chimica Acta, 595*, 136–144.

García-González, D. L., Mannina, L., D'Imperio, M., Segre, A. L., & Aparicio, R. (2004). Using ^{1}H and ^{13}C NMR techniques and artificial neural networks to detect the adulteration of olive oil with hazelnut oil. *European Food Research and Technology, 219*, 545–548.

Guillén, M. D., & Cabo, N. (1998). Relationships between the composition of edible oils and lard and the ratio of the absorbance of specific bands of their Fourier transform infrared spectra. Role of some bands of the fingerprint region. *Journal of Agricultural and Food Chemistry, 46*, 1788–1793.

Guillén, M. D., & Cabo, N. (2002). Fourier transform infrared spectra data versus peroxide and anisidine values to determine oxidative stability of edible oils. *Food Chemistry, 77*, 503–510.

Gurdeniz, G., Tokatli, F., & Ozen, B. (2007). Differentiation of mixtures of monovarietal olive oils by mid-infrared spectroscopy and chemometrics. *European Journal of Lipid Science and Technology, 109*, 1194–1202.

Kasemsumran, S., & Kang, N. (2005). Partial least squares processing of near-infrared spectra for discrimination and quantification of adulterated olive oils. *Spectroscopy Letters, 38*, 839–851.

Lai, Y. W., Kemsley, E. K., & Wilson, R. H. (1999). Potential of Fourier transform infrared spectroscopy for the authentication of vegetable oils. *Journal of Agricultural and Food Chemistry, 42*, 1154–1159.

Lay, J. O., Liyanage, R., Durham, B., & Brooks, J. (2006). Rapid characterization of edible oils by direct matrix-assisted laser desorption/ionization time-of-flight mass spectrometry analysis using triacylglycerols. *Rapid Communications in Mass Spectrometry, 20*, 952–958.

Lerma-García, M. J., Ramis-Ramos, G., Herrero-Martínez, J. M., & Simó-Alfonso, E. F. (2007). Classification of vegetable oils according to their botanical origin using amino acid profiles established by direct infusion mass spectrometry. *Rapid Communications in Mass Spectrometry, 21*, 3751–3755.

Lerma-García, M. J., Ramis-Ramos, G., Herrero-Martínez, J. M., & Simó-Alfonso, E. F. (2008). Classification of vegetable oils according to their botanical origin using sterol profiles established by direct infusion mass spectrometry. *Rapid Communications in Mass Spectrometry, 22*, 973–978.

Lerma-García, M. J., Simó-Alfonso, E. F., Ramis-Ramos, G., & Herrero-Martínez, J. M. (2007). Determination of tocopherols in vegetable oils by CEC using methacrylate ester-based monolithic columns. *Electrophoresis, 28*, 4128–4135.

López-Díez, E. C., Bianchi, G., & Goodacre, R. (2003). Rapid quantitative assessment of the adulteration of virgin olive oils with hazelnut oils using Raman spectroscopy and chemometrics. *Journal of Agricultural and Food Chemistry, 51*, 6145–6150.

Marcos-Lorenzo, I., Pérez-Pavón, J. L., Fernández-Laespada, M. E., García-Pinto, C., & Moreno-Cordero, B. (2002). Detection of adulterants in olive oil by headspace-mass spectrometry. *Journal of Chromatography A, 945*, 221–230.

Mariani, C., Bellan, G., Lestini, E., & Aparicio, R. (2006). The detection of the presence of hazelnut oil in olive oil by free and esterified sterols. *European Food Research and Technology, 223*, 655–661.

Muik, B., Lendl, B., Molina-Diaz, A., Valcarcel, M., & Ayora-Canada, M. J. (2007). Two-dimensional correlation spectroscopy and multivariate curve resolution for the study of lipid oxidation in edible oils monitored by FTIR and FT-Raman. *Analytica Chimica Acta, 593*, 54–67.

Ozen, B. F., & Mauer, L. J. (2002). Detection of hazelnut oil adulteration using FT-IR spectroscopy. *Journal of Agricultural and Food Chemistry, 50*, 3898–3901.

Poulli, K. I., Mousdis, G. A., & Georgiou, C. A. (2006). Synchronous fluorescence spectroscopy for quantitative determination of virgin olive oil adulteration with sunflower oil. *Analytical and Bioanalytical Chemistry, 386*, 1571–1575.

Rusak, D. A., Brown, L. M., & Martin, S. D. (2003). Classification of vegetable oils by principal component analysis of FTIR spectra. *Journal of Chemical Education, 80*, 541–543.

Sato, T. (1994). Application of principal-component analysis of near-infrared spectroscopic data of vegetable oils for their classification. *Journal of the American Oil Chemists Society, 71*, 293–298.

Sikorska, E., Górecki, T., Khmelinskii, I. V., Sikorski, M., & Koziol, J. (2005). Classification of edible oils using synchronous scanning fluorescence spectroscopy. *Food Chemistry, 89*, 217–225.

Silverstein, R. M., Bassler, G. C., & Morrill, T. C. (1981). *Spectrometric identification of organic compounds*. Chichester: John Wiley & Sons.

Sinelli, N., Cosio, M. S., Gigliotti, C., & Casiraghi, E. (2007). Preliminary study on application of mid infrared spectroscopy for the evaluation of the virgin olive oil freshness. *Analytica Chimica Acta, 598*, 128–134.

Tapp, H. S., Defernez, M., & Kemsley, E. K. (2003). FTIR spectroscopy and multivariate analysis can distinguish the geographic origin of extra virgin olive oils. *Journal of Agricultural and Food Chemistry, 51*, 6110–6115.

Tay, A., Singh, R. K., Krishnan, S. S., & Gore, J. P. (2002). Authentication of olive oil adulterated with vegetable oils using Fourier transform infrared spectroscopy. *Lebensmittel-Wissenschaft und-Technologie, 35*, 99–103.

Valdes, A. F., & Garcia, A. B. (2006). A study of the evolution of the physicochemical and structural characteristics of olive and sunflower oils after heating at frying temperatures. *Food Chemistry, 98*, 214–219.

Vandeginste, B. G. M., Massart, D. L., Buydens, L. M. C., De Jong, S., Lewi, P. J., & Smeyers-Verbeke, J. (1998). *Data handling in science and technology part B* (p. 237). Amsterdam: Elsevier Science B.V.

Vigli, G., Philippidis, A., Spyros, A., & Dais, P. (2003). Classification of edible oils by employing ^{31}P and ^{1}H NMR spectroscopy in combination with multivariate statistical analysis. A proposal for the detection of seed oil adulteration in virgin olive oils. *Journal of Agricultural and Food Chemistry, 51*, 5715–5722.

Vlachos, N., Skopelitis, Y., Psaroudaki, M., Konstantinidou, V., Chatzilazarou, A., & Tegou, E. (2006). Applications of Fourier transform-infrared spectroscopy to edible oils. *Analytica Chimica Acta, 573–574*, 459–465.

Wesley, I. J., Pacheco, F., & McGill, A. E. J. (1996). Identification of adulterants in olive oils. *Journal of the American Oil Chemists Society, 73*, 515–518.

Yang, H., Irudayaraj, J., & Paradkar, M. M. (2005). Discriminant analysis of edible oils and fats by FTIR, FT-NIR and FT-Raman spectroscopy. *Food Chemistry, 93*, 25–32.

Food Chemistry 118 (2010) 84–89

Contents lists available at ScienceDirect

Food Chemistry

journal homepage: www.elsevier.com/locate/foodchem

Antioxidant activities of malt extract from barley (*Hordeum vulgare* L.) toward various oxidative stress *in vitro* and *in vivo*

Yang Qingming, Pan Xianhui, Kong Weibao, Yang Hong, Su Yidan, Zhang Li, Zhang Yanan, Yang Yuling, Ding Lan, Liu Guoan *

College of Life Science, Northwest Normal University, Lanzhou 730070, People's Republic of China

ARTICLE INFO

Article history:
Received 5 January 2009
Received in revised form 23 February 2009
Accepted 22 April 2009

Keywords:
Malt extract
Phenolic compounds
Antioxidant activity
Lipid peroxidation
Protein oxidation
DNA strand breakage
D-Galactose model

ABSTRACT

The antioxidant activities of malt extract from barley were evaluated by various methods *in vitro* and *in vivo*. Scavenging effects on the hydroxyl and superoxide radicals, and protection against reactive oxygen species induced lipid, protein and DNA damage were evaluated. The D-galactose induced mouse aging model was used to evaluate ability of malt extract to behave as an antioxidant *in vivo*. The extract exhibited high antioxidant activities both *in vitro* and *in vivo*, evidenced by its ability to scavenge hydroxyl- and superoxide-radicals, high reducing power, and protection against biological macromolecular oxidative damage. Furthermore, malt extract prevented the decrease of antioxidant enzyme activities, decreased liver and brain malondialodehyde levels and carbonyl content, and improved total antioxidant capability in D-galactose-treated mice. In conclusion, these results demonstrate potential antioxidant activities and antiaging effect of malt, providing scientific support for the empirical use of malt as an antioxidant for diseases caused by reactive oxygen species.

1. Introduction

It is commonly recognised that reactive oxygen species (ROS) are involved in a variety of physiological and pathological processes, including cellular signal transduction, cell proliferation, differentiation and apoptosis, as well as ischemia – reperfusion, inflammation, and many neurodegenerative disorders (Ames, Shigenaga, & Hagen, 1993; Bland, 1995). In healthy individuals, ROS production is continuously balanced by natural antioxidative defence systems. Oxidative stress is a process where the physiological balance between pro-oxidants and antioxidants is disrupted in favour of the former, ensuing in potential damage for the organism (Halliwell & Gutteridge, 1990). ROS production can induce DNA damage, protein carbonylation, and lipid peroxidation, leading to a variety of chromic health problems, such as cancer, aging, Parkinson's disease, Alzheimer's disease and amyotrophic lateral sclerosis (Collin, 1999; Floyd, 1999).

Dietary antioxidant intake may be an important strategy for inhibiting or delaying the oxidation of susceptible cellular substrates, and is thus relevant to disease prevention in many paradigms. Phenolic compounds such as flavonoids, phenolic acids, diterpenes and tannins have received attention for their high antioxidative activity (Rice-Evans, Miller, & Paganga, 1996). Converging evidence from both experimental and epidemiological studies have demonstrated that cereals, vegetables, and fruits contain a myriad of phenolic compounds.

Barley is a widely consumed cereal among the most ancient cereal crops, but mainly (80–90%) barley production is for animal feeds and malt (Liu & Yao, 2007). There are growing interests in barley products because of their high content of phenolic compounds such as phenolic acids (benzoic and cinnamic acid derivatives), proanthocyanidins, tannins, flavonols, chalcones, flavones, flavanones, and amino phenolic compounds (Goupy, Hugues, Boivin, & Amiot, 1999).

Malt, used for the manufacturing of beer, contains various compounds from barley (endogenous phenolic compounds) or from the malting process (Maillard reaction products) that can play a significant role in malting and brewing through their antioxidative properties (Maillard, Soum, Boivin, & Berset, 1996). Malting had significant influences on individual and total phenolic contents as well as antioxidant activities. The contents of some phenolic compounds and the antioxidant activities increased remarkably during the later stages of germination and subsequent kilning (Lu et al., 2007).

Barley and malt are now gaining renewed interests as ingredients for the production of functional foods due to their concentration of antioxidant compounds. Most previous studies reported the antioxidative properties of barley. Attention was paid above all to the identification of the individual components of the phenolic

* Corresponding author. Tel.: +86 931 7971414.
E-mail address: nwnuming@126.com (L. Guoan).

0308-8146/$ - see front matter © 2009 Elsevier Ltd. All rights reserved.
doi:10.1016/j.foodchem.2009.04.094

fraction and to their antioxidant effects (Bonoli, Verardo, Marconi, & Caboni, 2004; Zhao et al., 2006).

The objective of the present study was to evaluate the antioxidant activity of malt extract from barley *in vitro* and *in vivo*. While the antioxidant activity of barley or malt has been studied *in vitro*, there is no literature documenting an antioxidant role for barley or malt *in vivo*. In the present study we set out to determine the antioxidant properties of malt *in vitro*, by measuring scavenging effects on the hydroxyl radical and superoxide radical, reducing power, inhibition of lipid peroxidation, protein carbonlytaion and DNA damage. We then evaluated the potential antioxidant potential of malt *in vivo*, in the D-galactose induced mouse aging model.

2. Materials and methods

2.1. Chemicals and reagents

D-Galactose was purchased from Amresco. Commercial kits used for determination of T-AOC, MDA, SOD, GSH-Px and MAO were purchased from Jiancheng Institute of Biotechnology (Nanjing, China). 2,2′-azo (2-amidinopropane) dihydrochloride (AAPH), (Butylated hydroxytoluene) BHT, (bovine serum albumin) BSA, (sodium dodecyl sulphate) SDS, agarose, plasmid pBR322 DNA, ascorbic acid and 6-hydroxy-2,5,7,8-tetramethylchromancarboxylic acid (Trolox) were purchased from Sigma–Aldrich (St. Louis, MO, USA). Acrylamide, *N*,*N*′-methylene – bis–acrylamide and guanidine HCl were purchased from Fluka (Buchs, Switzerland). Dimethyl sulphoxide (DMSO) was purchased from the Sinopharm Chemical Reagent Co., Ltd. (Shanghai, China).

2.2. Preparation of malt samples

Malt was obtained from Lanzhou Huanghe Enterprise Co., Ltd. (Gansu, China). Two hundred grams of the defatted malt was separately extracted with 80% acetone (v/v) at room temperature for 24 h, following separation of the supernatant and the sediment by vacuum filtration. The residue was re-extracted with 80% acetone for another 24 h and supernatants obtained were pooled with those from the first extraction. The extraction solutions were concentrated by vacuum-evaporator at 50 °C. The resulting concentrated solutions were lyophilised for 72 h at −49 °C and 25×10^{-3} mbar. The dried extract was dissolved in DMSO to a concentration of 50 mg/ml and stored at 4 °C until analysis.

2.3. Animal treatment

Male Kunming mice weighing 20–24 g were purchased from the Experimental Animal Center of Lanzhou University. The mice were housed in the temperature and humidity controlled room with a 12 h light–dark cycle and free access to standard pellet diet and drinking water. After an adaptation period of 6 days, the mice were randomly divided into five groups and received intraperitoneal (i.p.) injections with 300 mg/kg D-galactose (0.9% saline solution) once a day for 60 days. The aging control group (group AC) mice were introgastric gavage (i.g.) administered with 0.2 ml of saline each; the malt extract treatment group (group MET) mice were i.g. administrated malt extract (100, 200 and 400 mg/kg, dispersed in 0.9% saline). The normal control group (group NC) mice were i.p. injected with 0.2 ml of saline for 60 days and i.g. administration 0.2 ml saline only (Song, Bao, Li, & Li, 1999).

2.4. Determination of total phenolic content

The Folin–Ciocalteu reagent assay was used to determine the total phenolic content in malt extract (Liu & Yao, 2007). About 1 ml of barley extract (0.25 mg/ml) was mixed with 2 ml of Folin–Ciocalteu reagent and 2 ml of 15% Na_2CO_3 were then added. After 1 h of reaction at room temperature, the absorbance was read at 760 nm. Total phenolics were expressed as milligrams of gallic acid equivalents (GAE) per gram of dry weight.

2.5. Hydroxyl radical scavenging assay

Hydroxyl radical ($OH^{\cdot}$) scavenging capacity was measured according to the method of Liu, Liu, Song, and Fang (2002). The reaction mixture contained 2.06×10^{-3} mM methyl violet, 0.2 mM Fe^{2+}, 0.35 M H_2O_2, and 0.1 M Tris–HCl (pH 4.7) and various concentrations of malt samples in a final volume of 5 ml. After incubation for 5 min at 20 °C, the absorbance of the methyl violet complex was measured at 582 nm. Trolox was used as control. The scavenging rate was obtained according to the formula: $OH^{\cdot}$ scavenging rate $(\%) = [1 - (A_0 - A_2)/(A_0 - A_1)] \times 100$. where A_0 was the absorbance of the negative control (without Fe^{2+} and H_2O_2), A_1 was the absorbance of the positive control (without extract), A_2 was the absorbance in the presence of the extract.

2.6. Superoxide radical scavenging assay

Superoxide radical ($O_2^{-\cdot}$) scavenging capacity of malt extract was examined by a pyrogallol autoxidation system with minor modifications (Xiang & Ning, 2008). The reaction mixture contained 70 μl 10 mM pyrogallol, 4.5 ml 50 mM Tris–HCl (pH 8.2) and 0.5 ml various concentrations of malt samples. The absorbance at 325 nm was recorded immediately at 30 s and then recorded once every minute. Trolox was used as control. The scavenging rate was obtained according to the formula: $O_2^{-\cdot}$ scavenging rate $(\%) = [1 - (A_1 - A_2)/A_0] \times 100$, where A_0 was the absorbance of the control (without extract), A_1 was the absorbance in the presence of the extract, A_2 was the absorbance of without pyrogallol.

2.7. Reducing power

The reducing power was determined by the method of Oyaizu (1986). About 1 ml of malt extract of varying concentrations was mixed with sodium phosphate buffer and potassium ferricyanide $[K_3Fe(CN)_6]$. The mixture was incubated at 50 °C for 20 min. followed by addition of trichloroacetic acid and then centrifugation at 3000 rpm for 10 min. The upper layer was mixed with deionized water and $FeCl_3$, then, the absorbance was measured at 700 nm. Increased absorbance of the reaction mixture indicated increased reducing power. Trolox was used for comparison.

2.8. Determination of lipid peroxidation

Peroxidation of liver microsomes was induced by Fe^{2+}/Vc. Liver microsomes were prepared and the lipid peroxidation assay was conducted according to Cai, Fang, Ma, Li, and Liu (2003). Briefly, 0.2–0.44 mg/ml microsomes were incubated with 1 mM Vc and 0.1 mM Fe^{2+} with various concentrations of malt samples. After incubation at 37 °C for 1 h, the formation of malondialdehyde (MDA) in the incubation mixture was measured at 532 nm. Trolox was used as control. The inhibitory rate was obtained according to the formula: inhibitory rate $(\%) = [1 - (A_1 - A_2)/A_0] \times 100$, where A_0 was the absorbance of the control (without extract), A_1 was the absorbance in the presence of the extract, A_2 was the absorbance of without liver microsomes.

2.9. Determination of protein oxidation

Protein oxidation was assayed as described previously (Kwon, Choi, Won, Kang, & Kang, 2000) with minor modifications. Oxida-

tion of BSA in PBS was initiated by AAPH and inhibited by various concentrations of test compounds. After incubation for 24 h at 37 °C, 0.02% BHT was added to the reaction mixture to prevent the formation of further peroxyl radical. The samples were then assayed with normal SDS–PAGE.

2.10. Determination of oxidative DNA strand breakage

Conversion of the supercoiled form of plasmid DNA to the open circular and further linear forms has been used as an index of DNA damage (Jung & Surh, 2001). To assay inhibition of DNA damage induced by peroxyl radical by the malt extract, 100 ng of pBR322 DNA was incubated with various concentrations of compounds and 10 mM AAPH in PBS for 1 h at 37 °C. Then the samples were electrophoresed in a horizontal slab gel apparatus in TAE buffer for 1 h. The agarose gel was stained with ethidium bromide and then photographed under a transilluminator.

2.11. Measurement of T-AOC in mouse blood

At the end of treatment, mice were decapitated and blood was collected. The total antioxidant capability (T-AOC) was examined by commercial kits (Nanjing Jiancheng Bioengineering Institute, Nanjing City, PR China). The spectrometric method was applied to evaluate T-AOC. In the reaction mixture ferric ion was reduced by antioxidant reducing agents and blue complex Fe^{2+}–TPTZ (2,4,6-tri(2-pyridyl)-*s*-triazine) is produced. The optical density was measured at 520 nm. One unit (U) of T-AOC was defined as the amount that increased the absorbance by 0.01 at 37 °C. Data were expressed as U/ml blood.

2.12. Measurement of SOD, GSH-Px and MAO activity in mouse brain and liver

After mice were sacrificed, their brain and liver were removed rapidly and homogenised in cold saline. The homogenate was centrifuged at 3000*g* at 4 °C for 20 min, and the supernatant was collected for analysis. The determination of the activity of superoxide dismutase (SOD), glutathione peroxide (GSH-Px) and (monoamine oxidase) MAO were performed using commercial kits (Nanjing Jiancheng Bioengineering Institute, Nanjing City, PR China).

The assay for total SOD was based on its ability to inhibit the oxidation of oxymine by the xanthine–xanthine oxidase system. One unit (U) of SOD activity was defined as the amount that reduced the absorbance at 550 nm by 50%, and data were expressed as U/mg protein. The activity of GSH-Px was determined by quantifying the catalysed reaction rate of GSH per minute on the base of its catalysis. The final result was expressed as a decrease of 1.0 μM GSH per 5 min at 37 °C after the nonenzymatic reaction is subtracted, and data were expressed as U/mg protein. Ultraviolet chromatometry was used for MAO activity determination. One unit (U) of MAO activity was defined as the amount that increased the absorbance by 0.01 at 37 °C, and the MAO activity was expressed as U/h/mg protein.

2.13. Measurement of MDA levels and carbonyl content in mouse brain and liver

The determination of the levels of MDA was performed using commercial kits (Nanjing Jiancheng Bioengineering Institute, Nanjing City, PR China). The level of lipid peroxidation was indicated by the content of MDA in tissue. Thiobarbituric acid reaction (TBAR) method was used to determine the MDA. MDA content was expressed as nmol per milligram of protein. Protein carbonyl contents was detected by the reaction with 2,4-dinitrophenylhydrazine (DNPH) method as reported by Levine et al. (1990). The results were expressed as μmol carbonyl groups per mg protein.

2.14. Protein assay

Protein concentration was measured by the Lowry method (Lowry, Rosebrough, Farr, & Randall, 1951). Bovine serum albumin was used as the standard.

2.15. Statistical analysis

The experimental results are expressed as means ± standard deviation (SD) of three measurements at least. Statistical Package for Social Science (SPSS 13) was used to analyse the variance (ANOVA). *P*-values < 0.05 were regarded as significant.

3. Results and discussion

3.1. Extract yields, total phenolic content

Previous studies reported that relatively higher phenolic compounds and antioxidant activities were observed from acetone extract in barley compared with the other solvents including water, ethanol and methanol (Liu & Yao, 2007; Zhao et al., 2006). We therefore used acetone as our extraction solvent and obtained a 7.425% yield of extracted materials from malt and 4.325% from barely, and the total phenolic content in malt was 3.19 mg GAE/g of d*w* and 3.11 mg GAE/g of d*w* in barley, indicating that both extract yields and total phenolic content are higher in malt than in barley. Those could partially be explained by the enzymatic release of bound phenolic compounds during malting or under the effect of temperature during kilning.

3.2. Antioxidative activities of malt extract

3.2.1. Hydroxyl radical scavenging assay

The hydroxyl radical is one of representative reactive oxygen species generated in the body. Fig. 1A depicts the scavenging capacity of malt extract. When the concentration is from 31.25 to 500 μg/ml, the percentage scavenging of malt extract ranged from 5.1% to 63.1%, and Trolox ranged from 23.3% to 72.9%, demonstrating enhanced hydroxyl radical scavenging ability relative to controls. That may be phenolic compounds in malt extract such as ferulic acid product in Maillard reaction contain phenolic hydroxyl group, with the ability to accept electrons, which can combine with free radical competitively to decrease hydroxyl radical (Thomas, Michaelh, & Jennifer, 2005).

3.2.2. Superoxide radical scavenging activity

The superoxide radical is the most common free radical generated *in vivo*. Pyrogallic acid can auto-oxidise in alkaline conditions to produce superoxide radical directly, and the constant rate of this auto-oxidation reaction is dependent on the pyrogallic acid concentration. In this study, as shown in Fig. 1B, malt extract and Trolox showed moderate superoxide radical scavenging activities. Even at 2000 μg/ml, malt extract and Trolox have only 47.1% and 42.1% scavenging effect, and malt extract is more efficient than Trolox.

3.2.3. Reducing power

The reducing power is associated with antioxidant activity and may serve as a significant reflection of the antioxidant activity (Meir, Kanner, Akiri, & Philosoph-Hadas, 1995). In this assay system, the presence of antioxidants causes the reduction of the Fe^{3+}/ferricyanide complex to the ferrous form (Fe^{2+}) monitored at 700 nm. As evidenced in Fig. 2, the malt extract presented a con-

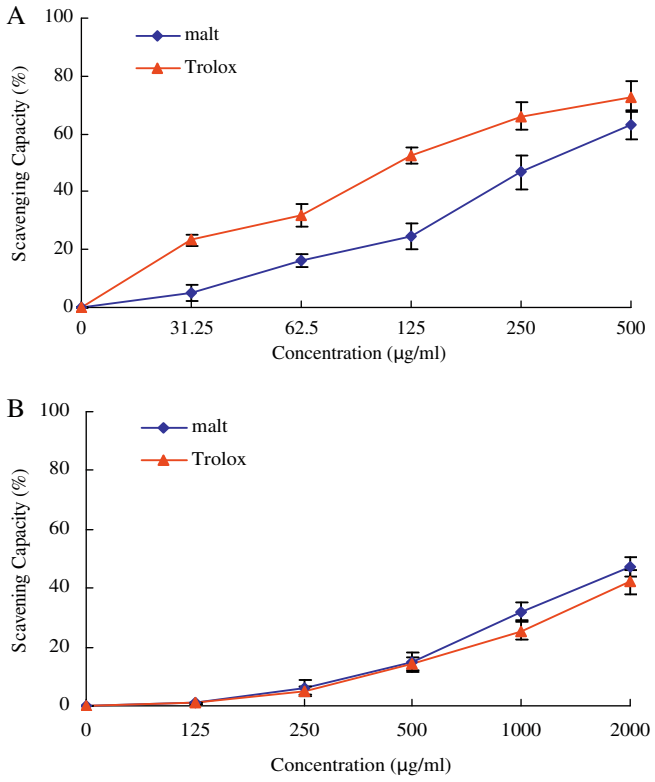

Fig. 1. (A) The hydroxyl radical scavenging capacity of malt extract and Trolox. (B) The superoxide radical scavenging capacity of malt extract and Trolox. Values are means ± SD of three parallel determinations.

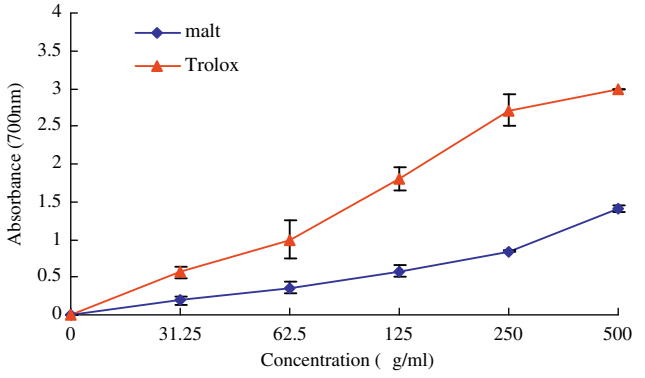

Fig. 2. Reducing power of malt extract and Trolox. Values are means ± SD of three parallel determinations.

centration-dependent activity increase. The malt extract absorbance varied from 0.19 (31.25 μg/ml) to 1.4 (500 μg/ml), while Trolox absorbance varied from 0.56 (31.25 μg/ml) to 3 (500 μg/ml). The reducing power of Trolox is stronger than malt extract in this system. Indeed, some phenolic compounds such as flavanoids and phenolic acids exhibited antioxidant activity through their reductive capacity in a Fe^{3+}–Fe^{2+} system (Zhao et al., 2006). The data presented here indicate that the marked reducing power of malt extracts seem to be attributed to their antioxidant activity.

3.2.4. Inhibition of lipid peroxidation

In biological systems, lipid peroxidation generates many aldehydes products, among which MDA is considered to be the most important derivative. Lipid peroxidation is a cause of cell membrane disruption and cell damage (Barrera, Pizzimenti, & Dianzani, 2008). This process is initiated by hydroxyl- and superoxide-radicals leading to the formation of peroxy radicals ($LOO^{\cdot}$) that ultimately propagates the chain reaction in lipids. Thus, antioxidants capable of scavenging peroxy radicals could prevent lipid peroxidation. In the present study, we measured the potential of malt extract to inhibit lipid peroxidation in rat liver microsomes, induced by the Fe^{2+}/ascorbate system. Trolox possesses increased inhibitory activity (IC_{50} = 22.74 μg/ml) relative to malt extract (IC_{50} = 231.49 μg/ml) (Fig. 3).

3.2.5. Inhibition of protein oxidation

A currently popular hypothesis postulates that a progressive accumulation of macromolecular oxidative damage is the fundamental underlying cause of senescence-associated deleterious alterations. Oxidation of cellular proteins has been described under many pathological conditions. The vulnerability of various amino acid residues of proteins to oxidation varies with reactive oxygen species. AAPH is a water–soluble initiator, which decomposes at physiological temperature producing alkyl radicals followed by fast reaction with oxygen to give alkyl peroxyl radicals (Cai et al., 2003) to initiate protein oxidation or DNA oxidative fragmentation.

The protection against protein oxidative damage was determined by the oxidation of BSA initiated by AAPH. After incubation for 24 h at 37 °C, the samples were assayed with normal SDS–PAGE. The results (Fig. 4) demonstrated that malt extract exhibited significant protective effect against oxidation of BSA (Fig. 4A lane 6), an effect that was augmented by increasing concentrations of extract. For example, at 2000 μg/ml (Fig. 4A lane 9), it completely inhibited the degradation of BSA. While Trolox at 1000 μg/ml (Fig. 4B lane 10), displayed a completely protective effect.

3.2.6. Inhibition of DNA damage

DNA damage alters replication and transcription, causes cell death or leads to mutations and neoplastic transformation in many organisms. Oxidative modifications of DNA have been suggested to contribute to aging and various diseases including cancer and chronic inflammation (Yang, Weissman, Bohr, & Mattson, 2008). To assay the potential of these compounds to prevent DNA damage, oxidative DNA strand breakage induced by peroxyl radical was measured with pBR322 DNA.

As showed in Fig. 5, the plasmid DNA was mainly of the supercoiled (bottom band) and open circular (top band) form in the absence of AAPH (Fig. 5 lane 1). With the addition of 10 mM AAPH the DNA supercoiled form decreased gradually and converted into the open circular and linear form (between the supercoiled and open circular, in Fig. 5 lane 2). Addition of malt extract or Trolox significantly inhibited the increasing of open circular and linear form of

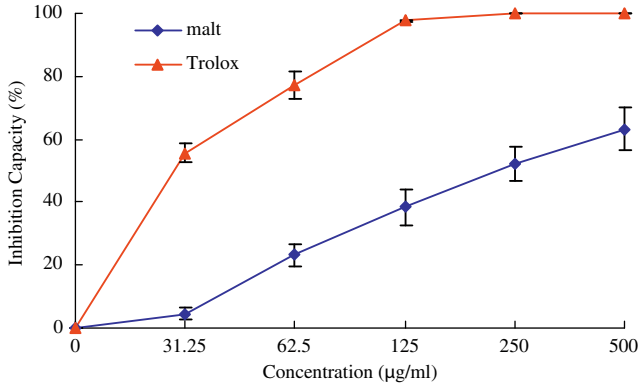

Fig. 3. Inhibition of lipid peroxidation by malt extract and Trolox in rat liver microsomes. Each value represents mean ± SD ($n \geqslant 3$).

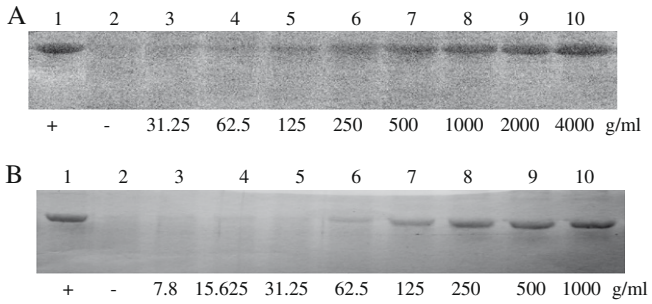

Fig. 4. The inhibitions of malt extract and Trolox to 20 mM AAPH induced BSA oxidative fragmentation. (A) BSA fragmentation was inhibited by malt extract in the presence of 20 mM AAPH. Lane 1, BSA; lane 2, BSA + 20 mM AAPH; lane 3–10, BSA + 20 mM AAPH + 31.25–4000 μg/ml malt extract. (B) BSA fragmentation was inhibited by Trolox in the presence of 20 mM AAPH. Lane 1, BSA; lane 2, BSA + 20 mM AAPH; lane 3–10, BSA + 20 mM AAPH + 7.8–1000 μg/ml Trolox.

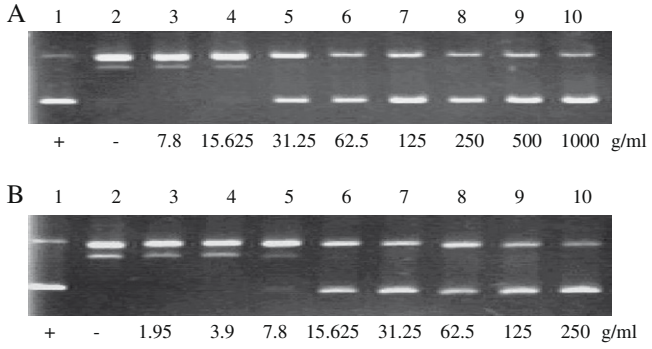

Fig. 5. The protections of malt extract and Trolox to 10 mM AAPH induced pBR322DNA strand breakage. (A) DNA damage was inhibited by malt extract in the presence of 10 mM AAPH. Lane 1, pBR322DNA; lane 2, pBR322DNA + 10 mM AAPH; lane 3–10, pBR322DNA + 10 mM AAPH + 7.8–1000 μg/ml malt extract. (B) DNA damage was inhibited by Trolox in the presence of 10 mM AAPH. Lane 1, pBR322DNA; lane 2, pBR322DNA + 10 mM AAPH; lane 3–10, pBR322DNA + 10 mM AAPH + 1.95–250 μg/ml Trolox.

pBR322 DNA, an effect dependent upon the concentration of compounds. Malt extract completely inhibited the DNA fragmentation at the concentration of 31.25 μg/ml (Fig. 5A lane 5), while Trolox (Fig. 5B lane 6) prevented DNA damage completely at 15.625 μg/ml.

3.3. Antioxidant effects of malt extract in D-galactose induced aging mice

The injection of D-galactose into mice induces a senescent phenotype (Song et al., 1999). The aging model shows neurological impairment, decreased activity of antioxidant enzymes, and compromised immune responses.

Long-term administration of D-galactose induced redox-related changes in these mice, including decrease in T-AOC, SOD, GSH-Px activities, as well as increase of the MAO activity, MDA level and carbonyl content. The activities of antioxidant enzymes SOD, GSH-Px in brain and liver were given in Table 1. A significant decrease in the activities of enzymates was observed in D-galactose treated mouse when compared with control ($P < 0.01$). In comparison to NC group mice, the SOD activity declined by 35.1% and 34.4% in brain and liver, the GSH-Px activity declined by 31.7% and 41.6% in brain and liver, respectively. Administration of malt extract to D-galactose treated mouse with 200 and 400 mg/kg increased the activities of these enzymatic antioxidants both in brain and liver ($P < 0.05$). Free-radical scavenging enzymes such as SOD and GSH-Px are the first line of defense against oxidative injury. SOD reduces superoxide radicals to form hydrogen peroxide, which in turn is decomposed to water and oxygen by GSH-Px and CAT, thereby preventing the formation of hydroxyl radicals (Yao et al., 2005). Therefore, malt extract may reduce oxidative stress and aging phenotypes by increasing SOD and GSH-Px activities, although these mechanisms remain to be elucidated.

Aging characteristics include an alteration of brain MAO metabolism. Studies involving MAO activity measurements in human and rodents brain or liver have shown a generalised age-related increase in MAO activity (Nicotra, Pierucci, Parvez, & Senatori, 2004). As shown in Table 1, MAO activity of brain and liver in D-galactose treated mice was significantly higher than NC group mice ($P < 0.01$). Malt extract, at doses of 200 and 400 mg/kg, inhibited brain and liver MAO activity significantly ($P < 0.01$).

Lipid peroxidation can reduce membrane fluidity, inactivate membrane-bound proteins, and decompose into cytotoxic aldehydes such as malondialdehyde or hydroxynonenal (Richter, 1987). The oxidative damage to proteins is reflected by increase in levels of protein carbonyls. Reaction of free radicals with the side chains of lysine, arginine, proline, threonine and glutamic acid residues of proteins leads to the formation of carbonyl derivatives (Stadtman & Berlett, 1997). Furthermore, aldehydes, such as 4-hydroxy-2-nonenal or malondialdehyde produced during lipid perox-

Table 1
Effect of malt extract on activities of SOD, GSH-Px, MAO, T-AOC, levels of MDA and content of protein carbonyl in tested organs in aged mice.

Parameters	NC	AC	MET (100 mg/kg)	MET (200 mg/kg)	MET (400 mg/kg)
Blood					
T-AOC (U/ml)	387.19 ± 38.58	247.69 ± 19.04[d]	271.50 ± 20.06	309.91 ± 23.93[a]	379.34 ± 33.14[b]
Brain					
SOD (U/mg protein)	140.00 ± 9.85	90.8 ± 7.22[d]	104.37 ± 7.16	118.92 ± 7.46[a]	129.21 ± 11.65[b]
GSH-Px (U/mg protein)	36.05 ± 5.06	24.63 ± 1.75[c]	25.19 ± 2.63	30.82 ± 2.61[a]	35.6 ± 2.69[b]
MAO (U/h/mg protein)	1.54 ± 0.05	2.08 ± 0.2[d]	2.06 ± 0.22	1.84 ± 0.15[a]	1.59 ± 0.15[b]
MDA (nmol/mg protein)	0.56 ± 0.04	1.18 ± 0.11[d]	1.00 ± 0.06	0.74 ± 0.05[b]	0.61 ± 0.05[b]
Protein carbonyl (μmol/mg protein)	4.52 ± 0.16	7.26 ± 0.32[d]	6.82 ± 0.37	5.92 ± 0.33[b]	5.19 ± 0.42[b]
Liver					
SOD (U/mg protein)	44.46 ± 2.56	29.18 ± 2.13[d]	32.20 ± 1.63	39.80 ± 3[a]	41.73 ± 3.6[b]
GSH-Px (U/mg protein)	17.73 ± 0.78	10.35 ± 0.71[d]	10.8 ± 0.57	14.16 ± 1.55[a]	16.47 ± 1.43[b]
MAO (U/h/mg protein)	0.59 ± 0.06	0.95 ± 0.09[d]	0.92 ± 0.1	0.81 ± 0.05[a]	0.69 ± 0.06[b]
MDA (nmol/mg protein)	0.51 ± 0.08	1.16 ± 0.08[d]	0.97 ± 0.07	0.72 ± 0.04[b]	0.60 ± 0.06[b]
Protein carbonyl (μmol/mg protein)	5.20 ± 0.43	9.43 ± 0.47[d]	8.83 ± 0.22	7.28 ± 0.22[a]	5.95 ± 0.29[b]

The data were expressed as means ± SD, ($n = 10$) and evaluated by one-way ANOVA. Differences were considered to be statistically significant if $P < 0.05$.
[a] $P < 0.05$, compared with AC group.
[b] $P < 0.01$, compared with AC group.
[c] $P < 0.05$, compared with NC group.
[d] $P < 0.01$ compared with NC group.

idation can be incorporated into proteins by reaction with either the ε-amino moiety of lysine or the sulfhydryl group of cysteine residues to form carbonyl derivatives (Uchida & Stadtman, 1993). Therefore, levels of MDA are a marker of lipid peroxidation and protein carbonyl content provide a reasonable marker for free radical induced protein oxidation.

In this study, the increase in the levels of MDA and protein carbonyl content in the D-galactose-treated mice was observed in Table 1. And both increased significantly compared with controls ($P < 0.01$). In the current study, malt extract treatment abrogated these effects in brain and liver ($P < 0.05$). Hence, lipid oxidation and protein oxidation is closely associated to aging caused by D-galactose, and malt extract effectively prevented the oxidation damage.

Age-induced oxidative injury was found to reduce the T-AOC, which reflects the non-enzymatic antioxidant defense system, as well as antioxidant enzyme levels (SOD, GSH-Px) in test organs of aged mice. Effect of the malt extract on T-AOC of the blood in aged mice was shown in Table 1. Significant differences in T-AOC were detected between normal control and aged control groups ($P < 0.01$). When treated with 200 and 400 mg/kg malt extract, the T-AOC increased significantly. This means the total antioxidant capability of the antioxidant systems in organism had been enhanced.

4. Conclusion

The results in the present work indicate the presence of phenolic compounds and antioxidant potential in malt extracts. We demonstrated that malt extract is able to scavenge the hydroxyl- and superoxide-radical, has high reducing power, conferred protection against biological macromolecular damage, significantly prevented the decrease of antioxidant enzyme activity in aging brain and liver, decreased brain and liver malondialodehyde level and carbonyl content, and improved total antioxidant capability in organism. The extract exhibited high antioxidant activities both *in vitro* and *in vivo*, and the phenolic compounds in extract were responsible for their effective antioxidant properties, this antioxidant property could be explained by a free-radical scavenging ability (such as scavenging hydroxyl-radical, superoxide-radical and carbon centred free radicals). It is proposed that hydroxyl was the most important factor in determining the antioxidant activities of the phenolic compounds.

The enhanced activity of SOD and GSH-Px and increased total antioxidant capacity in the aging animals can be very effective in scavenging the various types of oxygen free radicals and their products. So the inhibitory effect of malt extract on lipid peroxidation and protein oxidation might be, at least in part, attributed to its influence on the antioxidant enzymes and nonenzymatic system. In our previous study, malt extract showed significant scavenging activity on the superoxide anion and hydroxyl free radical. The direct oxygen free-radical scavenging activity of malt extract might also contribute to its *in vivo* antioxidant activity. In light of our observations that malt contains many phenolic compounds and significant antioxidant activities *in vitro* and *in vivo*, malt should be considered as a new source of natural antioxidant for pharmaceutical or dietary needs.

Acknowledgement

The authors gratefully acknowledge the cooperation of Mr. Hillel Zukor for his kind help and available discussion.

References

Ames, B. N., Shigenaga, M. K., & Hagen, T. M. (1993). Oxidants, antioxidants, and the degenerative diseases of aging. *Proceedings of the National Academy of Sciences of the United States of America, 90*, 7915–7937.

Barrera, G., Pizzimenti, S., & Dianzani, M. U. (2008). Lipid peroxidation: Control of cell proliferation, cell differentiation and cell death. *Molecular Aspects of Medicine, 29*, 1–8.

Bland, J. S. (1995). Oxidants and antioxidants in clinical medicine: Past, present and future potential. *Journal of Nutritional and Environment Medicine, 5*, 255–280.

Bonoli, M., Verardo, V., Marconi, E., & Caboni, M. F. (2004). Antioxidant phenols in barley (*Hordeum vulgare* L.) flour: Comparative spectrophotometric study among extraction methods of free and bound phenolic compounds. *Journal of Agriculture and Food Chemistry, 52*, 5195–5200.

Cai, Y. J., Fang, J. G., Ma, L. P., Li, Y., & Liu, Z. L. (2003). Inhibition of free radical-induced peroxidation of rat liver microsomes by resveratrol and its analogues. *Biochimica et Biophysica Acta, 1637*, 31–38.

Collin, A. R. (1999). Oxidative DNA damage, antioxidants, and cancer. *Bio-Essays, 21*, 238–246.

Floyd, R. A. (1999). Antioxidants, oxidative stress, and degenerative neurological disorders. *Proceedings of the Society for Experimental Biology and Medicine, 222*, 236–245.

Goupy, P., Hugues, M., Boivin, P., & Amiot, M. J. (1999). Antioxidant composition and activity of barley (*Hordeum vulgare*) and malt extracts and of isolated phenolic compounds. *Journal of Agriculture and Food Chemistry, 79*, 1625–1634.

Halliwell, B., & Gutteridge, J. M. C. (1990). Role of free radicals and catalytic metal ions in human disease: An overview. *Methods in Enzymology, 186*, 1–85.

Jung, Y. J., & Surh, Y. J. (2001). Oxidative DNA damage and cytotoxicity induced by copper-stimulated redox cycling of salsolinol, a neurotoxic tetrahydroisoquinoline alkaloid. *Free Radical Biology and Medicine, 30*, 1407–1417.

Kwon, H. Y., Choi, S. Y., Won, M. H., Kang, T. C., & Kang, J. H. (2000). Oxidative modification and inactivation of Cu, Zn-superoxide dismutase by 2,2′-azobis (2-amidinopropane) dihydrochloride. *Biochimica et Biophysica Acta, 1543*, 69–76.

Levine, R. L., Garland, D., Oliver, C. N., Amici, A., Climent, I., Lenz, A., et al. (1990). Determination of carbonyl content in oxidatively modified proteins. *Methods Enzymology, 186*, 464–478.

Liu, L. M., Liu, L. H., Song, G. W., & Fang, G. R. (2002). Determination of hydroxyl radical in Fenton reaction by spearophotometry. *Journal of Hubei University, 24*, 326–328. Natural Science Edition, China.

Liu, Q., & Yao, H. Y. (2007). Antioxidant activities of barley seeds extracts. *Food Chemistry, 102*, 732–737.

Lowry, O. H., Rosebrough, N. J., Farr, A. L., & Randall, R. J. (1951). Protein measurement with the Folin phenol reagent. *The Journal of Biological Chemistry, 193*, 265–275.

Lu, J., Zhao, H. F., Chen, J., Fan, W., Dong, J. J., Kong, W. B., et al. (2007). Evolution of phenolic compounds and antioxidant activity during malting. *Journal of Agricultural and Food Chemistry, 55*, 10994–11001.

Maillard, M. N., Soum, M. H., Boivin, P., & Berset, C. (1996). Antioxidant activity of barley and malt: Relationship with phenolic content. *Lebensmittel-Wissenschaft und-Technologie, 29*, 238–244.

Meir, S., Kanner, J., Akiri, B., & Philosoph-Hadas, S. (1995). Determination and involvement of aqueous reducing compounds in oxidative defense systems of various senescing leaves. *Journal of Agricultural and Food Chemistry, 43*, 1813–1819.

Nicotra, A., Pierucci, F., Parvez, H., & Senatori, O. (2004). Monoamine oxidase expression during development and aging. *NeuroToxicology, 25*, 155–165.

Oyaizu, M. (1986). Studies on products of browning reactions: Antioxidative activities of products of browning reaction prepared from glucosamine. *Japanese Journal of Nutrition, 44*, 307–315.

Rice-Evans, C. A., Miller, N. J., & Paganga, G. (1996). Structure-antioxidant activity relationships of flavonoids and phenolic acids. *Free Radical Biology and Medicine, 20*, 933–956.

Richter, C. (1987). Biophysical consequences of lipid peroxidation in membranes. *Chemistry and Physics of Lipids, 44*, 175–189.

Song, X., Bao, M. M., Li, D. D., & Li, Y. M. (1999). Advanced glycation in D-galactose induced mouse aging model. *Mechanisms of Aging and Development, 108*, 239–251.

Stadtman, ER., & Berlett, B. S. (1997). Reactive oxygen-mediated protein oxidation in aging and disease. *Chemical Research Toxicology, 10*, 485–494.

Thomas, S. S., Michaelh, H. G., & Jennifer, M. A. (2005). Antioxidant properties of malt model systems. *Journal of Agricultural and Food Chemistry, 53*, 4938–4945.

Uchida, K., & Stadtman, E. R. (1993). Covalent attachment of 4-hydroxy nonenal to glyceraldehyde-3-phosphate dehydrogenase a possible involvement of intra- and inter-molecular cross-linking reaction. *The Journal Biological Chemistry, 268*, 6388–6393.

Xiang, Z. N., & Ning, Z. X. (2008). Scavenging and antioxidant properties of compound derived from chlorogenic acid in South-China honeysuckle. *LWT – Food Science and Technology, 41*, 1189–1203.

Yang, J. L., Weissman, L., Bohr, V. A., & Mattson, M. P. (2008). Mitochondrial DNA damage and repair in neurodegenerative disorders. *DNA Repair, 7*, 1110–1120.

Yao, D. C., Shi, W. B., Gou, Y. L., Zhou, X. R., Tak, Y. A., & Zhou, Y. K. (2005). Fatty acid-mediated intracellular iron translocation: A synergistic mechanism of oxidative injury. *Free Radical Biology and Medicine, 39*, 1385–1398.

Zhao, H. F., Dong, J. J., Lu, J., Chen, J., Li, Y., Shan, L. J., et al. (2006). Effects of extraction solvent mixtures on antioxidant activity evaluation and their extraction capacity and selectivity for free phenolic compounds in barley (*Hordeum vulgare* L.). *Journal of Agriculture and Food Chemistry, 54*, 7277–7286.

Food Chemistry 118 (2010) 90–95

Contents lists available at ScienceDirect

Food Chemistry

journal homepage: www.elsevier.com/locate/foodchem

Effects of heat treatment and acid-induced gelation on aroma release from flavoured skim milk

V. Perreault [a,b,c], M. Britten [b,d,*], S.L. Turgeon [a,b], A.-M. Seuvre [e], P. Cayot [e], A. Voilley [e]

[a] Centre de recherche STELA, Faculté des sciences de l'agriculture et de l'alimentation, Pavillon Paul-Comtois, Université Laval, Québec, Canada G1K 7P4
[b] Institut des nutraceutiques et des aliments fonctionnels, Pavillon de l'INAF, Université Laval, 2440 rue Hochelaga, Québec, Canada G1K 7P4
[c] Institut de tourisme et d'hôtellerie du Québec, Centre d'expertise et de recherche, 3535 rue Saint-Denis, Montréal, Québec, Canada H2X 3P1
[d] Centre de recherche et de développement sur les aliments, Agriculture et Agroalimentaire Canada, 3600 Boul. Casavant, St-Hyacinthe, Québec, Canada J2S 8E3
[e] ENSBANA, Laboratoire d'ingénierie moléculaire et sensorielle des aliments et des produits de santé, Université de Bourgogne, 1 Esplanade Érasme, F21000 Dijon, France

ARTICLE INFO

Article history:
Received 18 December 2008
Received in revised form 20 April 2009
Accepted 21 April 2009

Keywords:
Aroma compound
Flavour
Release
Volatility
Kinetics
Headspace gas chromatography
Skim milk
Acid gel
Firmness

ABSTRACT

Time dependent aroma release was studied in skim milk, heated skim milk as well as in acid-induced gels derived from them using static headspace – gas chromatography analysis. A variable order kinetic model was fitted to experimental data and was used to determine headspace equilibrium concentration and initial rates of release. When compared to water, retention in milk based matrices was increased for hydrophobic aroma compounds, while it was decreased for more hydrophilic volatiles. Acid gelation reduced the initial rate of aroma release by a factor varying from 2.0 to 3.8, depending on the compound. Positive deviation from the first order kinetics was observed and suggests that a concentration gradient is established in the matrix during measurement. The interaction between milk based matrices and aroma compounds is discussed in relation to their chemical structure and the physico-chemical characteristics of the matrices.

1. Introduction

The growing demand for foods with improved nutritional qualities has prompted the food processing industry to cut down on ingredients such as fat, sugar and additives, thereby necessitating some important changes in sensory qualities that influence consumer acceptance of food products. Controlling food texture and aroma release represents a significant challenge for the industry. Both of these quality attributes are affected by changes in food composition, especially a reduction in fat. Furthermore, texture is thought to influence flavour perception.

From a physico-chemical standpoint, the release of aroma compounds depends not only on the properties of the compounds and their affinity for the product's components, but also on the structural complexity of the matrix. Interactions between macromolecules modify the nature and the number of binding sites available for aroma compounds. In general, these factors govern the equilibrium partitioning of aroma compounds between the different phases. The rate at which this equilibrium is achieved is driven by interfacial mass transport and diffusion phenomena (Taylor, 2002). Dairy proteins and lactose are the main components that affect aroma release from skim milk. In aqueous systems, increased volatility has been observed in the presence of lactose (van Willige, Linssen, & Voragen, 2000), suggesting that competition occurs between aroma compounds and lactose for interaction with water. In highly hydrated systems, however, proteins may bind aroma compounds via hydrophobic interactions (Fischer & Widder, 1997; Guichard & Langourieux, 2000; Landy, Druaux, & Voilley, 1995; O'Neill & Kinsella, 1987), although chemical bonds could be involved especially in the case of aldehydes (Fischer & Widder, 1997; Plug & Haring, 1993), which may react with amino groups of proteins to form imine bonds. Factors in food systems that influence protein conformation may have a considerable effect on the interaction between proteins and aroma compounds. The principal factors include ionic strength, concentration of other food components, temperature, pH and time (Fischer & Widder, 1997).

In yogurt production, milk is subjected to heat treatment, which is one of the most important processing parameters affecting the final product. The effects of milk heating on the

* Corresponding author. Address: Centre de recherche et de développement sur les aliments, Agriculture et Agroalimentaire Canada, 3600 Boul. Casavant, St-Hyacinthe, Québec, Canada J2S 8E3. Tel.: +1 450 773 1105; fax: +1 450 773 8461.
E-mail address: brittenm@agr.gc.ca (M. Britten).

0308-8146/$ - see front matter Crown Copyright © 2009 Published by Elsevier Ltd. All rights reserved.
doi:10.1016/j.foodchem.2009.04.095

rheological properties and microstructure of fat-free dairy gels have been studied fully (Harwalkar & Kalab, 1980; Lucey, Cheng, Munro, & Singh, 1999). Milk heating prior to acidification is known to increase yogurt firmness. Heating milk above 70 °C induces denaturation and aggregation of whey proteins and their association with casein micelles. The denatured whey proteins in the serum and those associated with casein micelles participate in the acid-induced gel structure. The highly branched structure of acid gels made from heated milks has been clearly shown using electron microscopy (EM) (Harwalkar & Kalab, 1980) or confocal scanning laser microscopy (CSLM) (Lucey et al., 1999). The increase in the number and strength of bonds linking protein particles helps to increase the firmness of acid gels made from heated milk.

The microstructure of the matrix itself may affect aroma release. Seuvre, Espinosa Diaz, Cayot, and Voilley (2004) compared the percentage of 2-nonanone release in set gels of β-lactoglobulin versus the same type of gel following destructuring; the release was slightly higher for the destructured gel. The gelled structure of polysaccharidic matrices has also been shown to cause increased retention of aroma compounds (Juteau, Doublier, & Guichard, 2004; Rega, Guichard, & Voilley, 2002) and slower transfer across the vapour/matrix interface (Juteau, Doublier, et al., 2004).

Milk heating is known to affect the microstructure and rheology of acid-induced dairy gels. However, little information is available about the associated impact on the release of aroma compounds. The objective of this project was to measure the influence of heat treatment (before aromatisation) and acid-induced gelation on the release of selected aroma compounds from flavoured skim milk matrices. Acid-induced gels were prepared from heated or unheated skim milk to study the relationship between gel firmness and aroma release from a complex dairy system. The thermodynamic and kinetic components of aroma release were both studied.

2. Material and methods

2.1. Materials

Spray dried low heat skim milk powder (32.9% protein) was obtained from Ingredia (Arras, France). Glucono-δ-lactone (GDL), ethyl acetate (EA), ethyl hexanoate (EH) and pentan-2-one (PO), hexanal (H) were obtained from Sigma–Aldrich (Steinheim, Germany). Ethyl butyrate (EB) was supplied by Aldrich (Milwaukee, USA). The purity of all the aroma products was higher than 97%.

2.2. Preparation of milk based matrices

Skim milk, heated skim milk, and gels from skim milk and heated skim milk were prepared from low heat skim milk powder rehydrated at ambient temperature in deionised water at 13.1% solids. From a previous study (Fairise, Cayot, & Lorient, 1999), reconstituted skim milk powder showed no sign of glycation or soluble protein denaturation and was considered similar to raw skim milk. Heat treatment was carried out at 90 °C for 5 min on 15 ml milk aliquots (Pyrex reaction tubes) according to the method of Cayot, Fairise, Colas, Lorient, and Brulé (2003). All of the aroma compounds (ethyl acetate, ethyl butyrate, ethyl hexanoate, pentan-2-one and hexanal) were added directly to skim milk and heated skim milk (500-g samples), each at 50 ppm concentration. The physico-chemical characteristics of the aroma compounds are presented in Table 1. Sodium azide (VWR, Prolabo, VWR International, Fontenay/Bois, France) was added at 0.02% to prevent microbial growth. Acid gels were produced by adding glucono-δ-lactone (GDL) to skim milk and heated skim milk. The GDL concentration was fixed to 1.7%, allowing the pH to drop to 4.5 after the incubation period. After the GDL was mixed with milk, liquid samples were quickly transferred to 21-ml vials for the gas chromatography measurements. Each vial was filled with 10 ml of the product and hermetically sealed with a Teflon-coated seal. In addition, beakers (80 ml) were filled with 65 g of the product for texture measurements and covered with two layers of parafilm. Samples were incubated at 30 °C for 10 h (Sanyo Incubator MIR 153, Sanyo Electric Co., Ltd., Japan) and then stored at 7 °C for 48 h before analysis.

2.3. Gel texture

The firmness of the gels was measured using a texture analyser (model 1122, Instron Ltd., Buckinghamshire, England) equipped with a stainless steel cylindrical sensor of 2.51×10^{-2} m^2 surface with constant compression speed (8.33×10^{-4} m s^{-1}). Penetration tests were performed at 20 ± 2 °C. Gel sample surface and thickness were 1.45×10^{-1} m^2 and 4.6×10^{-2} m, respectively. From the force-deformation data, the true stress–strain curve was derived, and Young's modulus of elasticity was obtained from the initial slope.

2.4. Static headspace analysis

Vials containing milk or acid gel samples were equilibrated at 20 °C in a water bath for at least 30 min before analysis. This temperature corresponds to the average temperature reached by a thick yogurt in the mouth during the first seconds of consumption (Paci Kora, 2003). Before the experiment started ($t = 0$), the vial headspace (11 ml) was flushed with nitrogen (150 ml min^{-1} for 25 s). The loss of each aroma compound during this operation was less than 1%. Samples were then sealed again and maintained at 20 °C for up to 300 min. At selected intervals, the headspace was analysed by gas chromatography, with a new sample being used for each analysis. Samplings and injections were carried out with a CombiPAL autosampler (CTC Analytics, Switzerland). The gas chromatograph (GC; CP3800; Varian Analytical Instruments, Walnut Creek, USA) was equipped with a 3-m stainless steel column (2.2 mm i.d.) packed with Chromosorb W-AW 80–100 mesh with a stationary phase of Carbowax 20 M-10%. The operating conditions were as follows: helium carrier flow rate 30 ml min^{-1}; hydrogen flow rate 30 ml min^{-1}; air flow rate 300 ml min^{-1}; injector (splitless) temperature 190 °C; flame ionisation detector (FID) temperature 200 °C. The oven temperature was maintained at 80 °C for 6 min and then increased to 140 °C at a rate of 5 °C min^{-1}, and finally to 180 °C at a rate of 10 °C min^{-1}. The chromatograms were recorded and analysed using the Star Chromatography Workstation software (v5.31, Varian Associates Inc.).

Six concentrations of the aroma compounds in pure water were analysed in quadruplicate for calibration, allowing quantification of the compounds in the gas phase. To verify that no aroma compounds were formed during the incubation, blank samples (non-aromatised) treated the same way as the experimental units were analysed after a 210-min equilibration.

2.5. Statistical analysis

The experiment was repeated four times according to a 2^2 factorial design, milk heat treatment and acid-gelation being the two variables under study. The analysis of variance (ANOVA) was used to determine whether the factors and their interactions had a significant effect on the measured parameters (SAS Institute Inc., Cary, NC).

Table 1
Physico-chemical characteristics of aroma compounds.

	Aroma compound				
	Ethyl acetate	Ethyl butyrate	Ethyl hexanoate	Hexanal	Pentan-2-one
Chemical class	Ester	Ester	Ester	Aldehyde	Ketone
Empirical formula	$C_4H_8O_2$	$C_6H_{12}O_2$	$C_8H_{16}O_2$	$C_6H_{12}O$	$C_5H_{10}O$
Molecular mass (g mol^{-1})	88.1	116.2	144.2	100.2	86.1
Molar volume (cm^3 mol^{-1})	107[a]	151[a]	196[a]	147[a]	121[a]
Boiling point at P_{atm} (°C)	75.0[b]	121.0[b]	168.0[b]	128.0[b]	102.0[b]
Log $P_{octanol/water}$	0.7 ± 0.2[c]	1.8 ± 0.2[c]	2.8 ± 0.2[c]	2.0 ± 0.2[c]	0.9 ± 0.2[c]
Water solubility at 25 °C (g L^{-1})	58.8 ± 4.3[e]	5.6[d] 4.4 ± 0.1[e]	0.5[d] 0.4 ± 0.0[e]	5.6 (30 °C)[f]	51.9 ± 2.2[e]
Saturated vapour pressure at 25 °C (Pa)	12 132[d] 12 510[h]	2306[d]	224[d] 215[h]	1517[h]	9464 (37 °C)[g]

[a] Reid, Prausnitz, and Poling (1987).
[b] Furia and Bellanca (1975).
[c] SciFinder Scholar (2005).
[d] Le Thanh (1992): experimental data.
[e] Philippe (2003): experimental data (mineral water).
[f] Paci Kora (2003): estimated with EPI software.
[g] Philippe et al. (2003): estimated with MPBP-Win software.
[h] Covarrubias Cervantes et al. (2004): experimental data.

3. Results and discussion

3.1. Time dependent release curves

Fig. 1a shows the time-dependent release curves for the different aroma compounds in flavoured raw skim milk. Aroma concentration in the gas phase increased until the thermodynamic equilibrium was reached. Final concentration in the gas phase increased in the following order: pentan-2-one (PO) < hexanal (H) < ethyl acetate (EA) ⩽ ethyl hexanoate (EH) < ethyl butyrate (EB). Partition between the aqueous and gas phases is driven by the physico-chemical characteristics of the flavour compounds and specific interactions with milk constituents (Nongonierma, Springett, Le Quéré, Cayot, & Voilley, 2006). The initial part of the release curves is presented in Fig. 1b. The concentration in the gas phase increased rapidly and half equilibrium concentration was reached between 0.8 and 3.0 min depending on aroma compound.

In order to describe the effect of heat treatment and acid-induced gelation on aroma release, and especially on its kinetic component, it is common practice to fit experimental data to an appropriate mathematical model. The variable order kinetic model (Eq. (1)) was compared to the Weibull function (Eq. (2)) as previously used by Juteau, Cayot, Chabanet, Doublier, and Guichard (2004).

$$C_t = C_\infty - (C_\infty^{1-n} + knt - kt)^{1/1-n} \quad (1)$$

$$C_t = a \times [1 - \exp(-b(t-d)^c)] \quad (2)$$

where C_t is the concentration in the headspace at time t; C_∞, the concentration in the headspace at equilibrium; n, the reaction order and k, the kinetic constant.

The two models showed good fit for t values larger than ~3 min. However, deviation from experimental data was observed with the Weibull function in the initial part of the curve. Fig. 2 shows the first 2 min of ethyl hexanoate release curve fitted with both models. The first derivative of the models, representing the rate of release, is also presented. The Weibull function is not defined for $t \lesssim d$ (when constant c is not a whole number), and cannot be used to estimate the initial rate of aroma release. The variable order kinetic model fitted the experimental data over the entire curve with a homogeneous distribution of residues and r^2 ranging from 0.988 to 0.999. The extrapolation of the first derivative (Eq. (3)) to $t = 0$ allows appropriate estimation of the initial rate of release.

$$dC/dt = k(C_\infty - C_t)^n \quad (3)$$

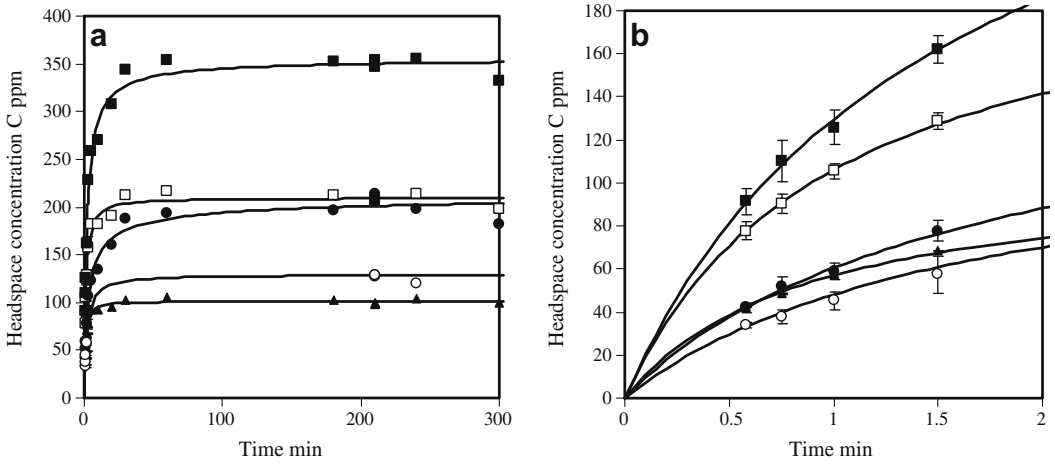

Fig. 1. Time-dependent aroma release from flavoured raw skim milk. (a) Entire experiment; (b) first 2 min. Aroma compounds were: ▲, pentan-2-one; ○, hexanal; ●, ethyl hexanoate; □, ethyl acetate and ■, ethyl butyrate. Experimental data were fitted to Eq. (1).

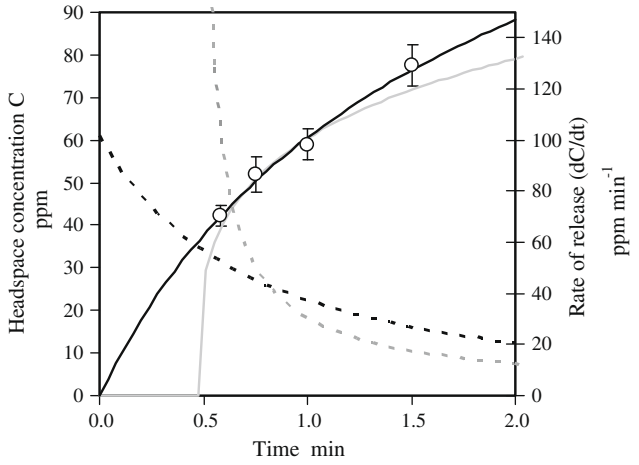

Fig. 2. Experimental data (○) from ethyl hexanoate release from raw skim milk (0–2 min) fitted to the variable order kinetic model (solid black line) and the Weibull function (solid grey line). First derivative (release rate) of these models is presented as dashed lines.

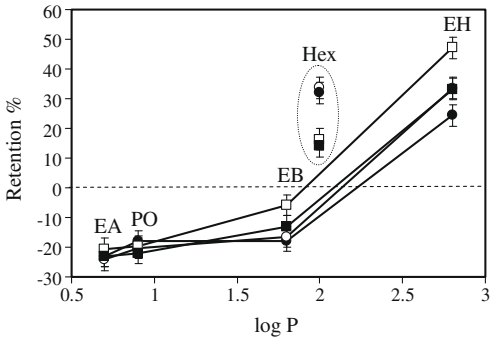

Fig. 3. Retention of aroma compounds (EA: ethyl acetate; PO: pentan-2-one; EB: ethyl butyrate; Hex: hexanal and EH: ethyl hexanoate) in: ○, raw skim milk; ●, heated skim milk; □, gel from raw milk and ■, gel from heated milk.

The variable kinetic order model was then used throughout the paper to characterise aroma release profiles.

3.2. Thermodynamic equilibrium

The equilibrium concentrations (C_∞) of aroma compounds in the headspace from milk based matrices and water are presented in Table 2. When dispersed in water, the homologous series of esters exhibited an increase in C_∞ with increasing carbon chain length and increasing hydrophobicity index (log *P*) (Table 1), which is in agreement with previous studies (Landy et al., 1995; Philippe, 2003). Among the compounds with the same number of carbons, the ester compound (ethyl butyrate) showed a higher C_∞ than the aldehyde (hexanal). The saturated vapour pressure of ethyl butyrate is higher than that of hexanal (Table 1), which could explain the difference (Covarrubias Cervantes, Mokbel, Champion, Jose, & Voilley, 2004).

Modification of flavour compound volatility in different matrices is attributed to physicochemical interaction with the matrices components (Landy et al., 1995). Percentages of retention, relative to water, were calculated according to Nongonierma et al. (2006) (Eq. (4)) and results are plotted as a function of hydrophobicity (log *P*) of each aroma compound (Fig. 3).

$$R\% = \left[1 - C_\infty^{\text{matrix}} / C_\infty^{\text{water}}\right] \times 100 \quad (4)$$

The four matrices under study showed negative retention (or rejection) for low hydrophobicity aroma compounds (log $P < 2$). Similar results were observed in non-fat stirred yogurts (Nongonierma et al., 2006) and suggest that competition for interaction with water occurred between aroma compounds and other milk solids. Lactose, which is highly hygroscopic, is present at a high concentration in milk based matrices (6.4%). Lactose has been shown to increase aroma compounds volatility in simple media (van Willige et al., 2000). In addition, it has been suggested that the high concentration of ions in milk could cause a salting-out effect, contributing to reduce aroma retention (Nongonierma et al., 2006). Ethyl hexanoate (log $P = 2.8$), was strongly retained in milk based matrices. Hydrophobic interactions with caseins (Fischer & Widder, 1997; Landy et al., 1995) and whey proteins, especially β-lactoglobulin (Guichard & Langourieux, 2000), could explain lower volatility of ethyl hexanoate in milk based matrices.

Heat treatment and acid gelation did not influence the retention for hydrophilic ethyl acetate and pentan-2-one (log $P < 1$). However, for more hydrophobic ethyl butyrate (log $P = 1.8$) and ethyl hexanoate (log $P = 2.8$), acid gelation increased retention. Heat treatment was shown to reduce retention only for ethyl hexanoate. Heat treatment induces unfolding and rearrangement of protein structures. Whey proteins are known to aggregate and associate with casein micelles in heated milk. These changes in protein structure affect its binding capacity for hydrophobic compounds. The affinity of thermally treated β-lactoglobulin for aroma compounds has been shown to be lower than that of native β-lactoglobulin (O'Neill & Kinsella, 1987). Well-defined hydrophobic cavities, known to be the binding sites for the majority of hydrophobic aroma compounds appear to be disrupted by heat treatments. Lowering of pH also causes changes in protein

Table 2
Headspace equilibrium concentration and initial rate of aroma release in milk based matrices.

	Raw milk	Heated milk	Raw milk gel	Heated milk gel	Water
Headspace equilibrium concentration C_∞ (ppm)					
Ethyl acetate	209	207	203	207	168
Ethyl butyrate	357	361	324	346	306
Ethyl hexanoate	217	247	172	218	326
Pentan-2-one	100	98	99	101	83
Hexanal	130	133	164	168	196
Initial rate of aroma release V_0 (ppm min^{-1})					
Ethyl acetate	196	215	57	60	416
Ethyl butyrate	211	226	57	57	335
Ethyl hexanoate	101	106	27	29	147
Pentan-2-one	111	120	37	49	237
Hexanal	77	84	40	41	163

Standard error for C_∞ and V_0 were, respectively, 10 ppm and 12 ppm min^{-1}.

conformation. With slow acidification of milk, colloidal calcium phosphate in the casein micelles gradually solubilises, casein micelles become unstable and aggregation occurs through hydrophobic interactions as pH approaches 4.6 (Cayot & Lorient, 1998). Acidification also induces dissociation of hydrophobic β-casein from the micelle. Retention of the more hydrophobic aroma compounds may be explained by increased accessibility of casein hydrophobic domains as a result of milk acidification.

The retention of hexanal by milk based matrices was higher than expected from its hydrophobicity index (Fig. 3). Furthermore, unlike ethyl hexanoate, retention of hexanal was not affected by milk heat treatment, but strongly decreased after acid gelation. Schiff's base formation resulting from the reaction of carbonyl with amino groups of proteins is likely to occur and explain high retention of hexanal in milk based matrices (Plug & Haring, 1993). The rate of Schiff's base formation is known to decrease with decreasing pH (Jirousova & Davidek, 1975) which explains the lower hexanal retention in acid gels (pH 4.5) than in non-acidified milks (pH 6.7). Mills and Solms (1984) reported similar finding for heptanal interaction with whey protein for pH ranging from 4.66 to 6.89.

3.3. Kinetics of flavour release

During the short time period of eating process, flavour behaviour will depend on the initial rate of release. The first derivative of the variable order kinetic model (Eq. (3)) was extrapolated to $t = 0$ to determine initial rate of flavour release (Table 2). Acid gelation was the most important factor controlling the initial rate of flavour release ($P < 0.0001$). Depending on aroma compound, acid gelation reduced the initial rate of release by a factor ranging from 2.0 (hexanal) to 3.8 (ethyl butyrate). Acid gelation eliminated convective transport of aroma compounds within the matrix which reduced the initial rate of release. Milk heat treatment had no significant effect on the initial rate of release ($P = 0.1626$).

The rate of aroma release is driven by interfacial mass transport and diffusion phenomena, but also depends on the volatility of aroma compounds. To better isolate the influence of the physical characteristics of milk based matrices on the rate of aroma release, kinetic data were normalised according to the equilibrium concentration. For that purpose the time required to reach 50% of the equilibrium concentration in the gas phase ($T_{1/2C_\infty}$) was calculated for each aroma compound. In agreement with the diffusion controlled transport to the interface (Seuvre, Philippe, Rochard, & Voilley, 2007), the $T_{1/2C_\infty}$ increased with increasing molar volume of aroma compound (Fig. 4a). Heat treatment had no significant effect on $T_{1/2C_\infty}$ ($P = 0.1373$) and half equilibrium concentration in the gas phases of skim milk and heated skim milk was reached within 0.8–3.3 min depending on aroma compound. Acid gelation significantly retarded aroma release from both raw and heated skim milks ($P < 0.0001$), and the $T_{1/2C_\infty}$ increased by an average factor of 3.2. However, no significant difference was observed between gels made from raw and heated skim milk ($P = 0.2418$). The firmness (Young's modulus) of acid gel made from heated milk (7116 ± 427 Pa) was higher than the firmness of gel made from raw milk (917 ± 62 Pa), suggesting that the structure of the matrix has little influence on the aroma release kinetics. Similar results were reported in the literature regarding the transport of aroma compounds in structured matrices (Juteau-Vigier et al., 2007). According to Juteau-Vigier et al. (2007), the presence of a macromolecular network would likely have little effect on diffusivity of small molecules. These authors have shown that the structural level of carrageenan matrices had negligible influence on diffusion properties of ethyl hexanoate and suggest that mobility through the open spaces is not disturbed. As predicted by the Stokes–Einstein equation, viscosity of the continuous phase would be the main factor driving the diffusion of aroma compounds. However, our results suggest that for matrices with low viscosity continuous phase, the formation of a gel eliminates convective transport and reduces aroma compounds mobility.

Fitting the kinetic model parameters (Eq. (1)) to the experimental data allows the determination of the kinetic order (n) for aroma release from the various matrices. In convective transfer conditions, with homogeneous aroma concentration in the matrix, a kinetic order of one is expected (Juteau, Cayot, et al., 2004). In the present study, aroma release experiments were performed in an unstirred closed system and kinetic orders larger than one were observed for milk based matrices (Fig. 4b). This deviation is attributed to the establishment of a concentration gradient between the surface layer and the bulk of the matrix (Juteau, Cayot, et al., 2004). The aroma concentration in the very first layers, located near the interface, is rapidly depleted and a gradient is established according to the mobility of aroma compounds in milk based matrices. The kinetic order increased with the molar volume of the aroma compound (Fig. 4b). According to the Wilke and Chang equation (1955), the diffusion coefficient is inversely related to the molar volume. Aroma compounds with high molar volume would be more prone to the establishment of a concentration gradient in milk based matrices. Milk heat treatment had no significant effect on the kinetic order, but an increase was observed in acid gels (Fig. 4b). As previously suggested, acid gelation eliminates convective transport in low viscosity media (milks), which further reduces macroscopic diffusion of aroma compounds. This, could be

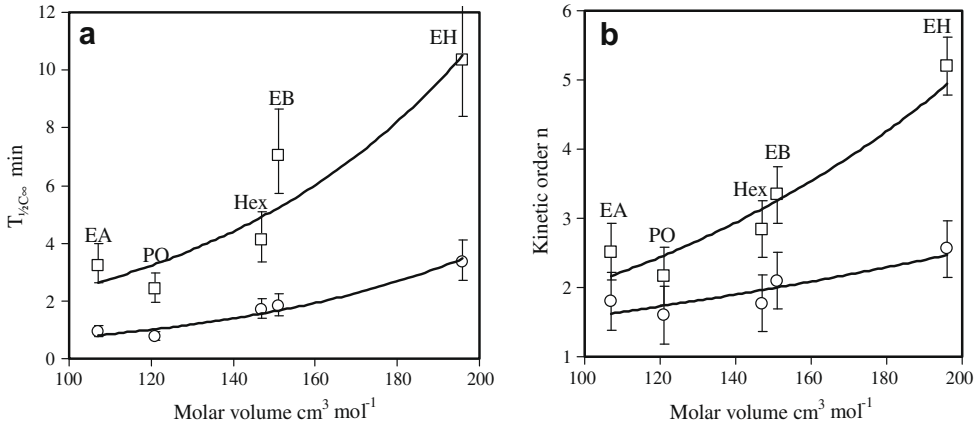

Fig. 4. Time required to reach 50% equilibrium concentration ($T_{1/2C_\infty}$) (a) and kinetic order of aroma release (b) in the headspace of ○, liquid skim milks and □, skim milk gels. EA: ethyl acetate; PO: pentan-2-one; EB: ethyl butyrate; Hex: hexanal and EH: ethyl hexanoate.

responsible for the establishment of a steeper concentration gradient in gels than in milks.

4. Conclusion

Milk heat treatment decreased retention of highly hydrophobic aroma compounds Ethyl hexanoate in milk based matrices, while acid-induced gelation retarded the release of all tested compounds. Gel formation reduced the rate of flavour release, but increasing gel firmness had no further effect. In an unstirred closed system, the formation of a concentration gradient between the surface layer and the bulk of the matrix controls the kinetics of aroma release in milk based matrices and this gradient depends on the characteristics of both, the aroma compound (molar volume) and the matrix. More targeted research is required to better understand the effect of matrix microstructure on the aroma release profile.

Acknowledgements

We wish to thank Valorisation-Recherche Québec for providing financial assistance for this collaborative project in which the IMS-APS Laboratory (ENSBANA, Université de Bourgogne) generously participated.

References

Cayot, P., Fairise, J.-F., Colas, B., Lorient, D., & Brulé, G. (2003). Improvement of rheological properties of firm acid gels by skim milk heating is conserved after stirring. *Journal of Dairy Research, 70*, 423–431.

Cayot, P., & Lorient, D. (1998). *Structures et technofonctions des protéines du lait*. Paris: Lavoisier Technique et Documentation. p. 363.

Covarrubias Cervantes, M., Mokbel, I., Champion, D., Jose, J., & Voilley, A. (2004). Saturated vapour pressure of aroma compounds at various temperatures. *Food Chemistry, 85*, 221–229.

Fairise, J.-F., Cayot, P., & Lorient, D. (1999). Characterization of the protein composition of casein micelles after heating. *International Dairy Journal, 9*, 249–254.

Fischer, N., & Widder, S. (1997). How proteins influence food flavour. *Food Technology, 51*, 68–70.

Furia, T. E., & Bellanca, N. (1975) (2nd ed.. In T. E. Furia & N. Bellanca (Eds.). *Fenaroli's Handbook of Flavor Ingredients* (Vol. 2, pp. 928). Cleveland, OH: CRC Press.

Guichard, E., & Langourieux, S. (2000). Interactions between β-lactoglobulin and flavour compounds. *Food Chemistry, 71*, 301–308.

Harwalkar, V. R., & Kalab, M. (1980). Milk gel structure. XI. Electron microscopy of glucono-δ-lactone-induced skim milk gels. *Journal of Texture Studies, 11*, 35–49.

Jirousova, J., & Davidek, J. (1975). Reactions of *n*-hexanal with glycine in model systems. *Zeitschrift-fuer-Lebensmittel-Untersuchung-und-Forschung, 157*, 269–276.

Juteau, A., Cayot, N., Chabanet, C., Doublier, J.-L., & Guichard, E. (2004). Flavour release from polysaccharide gels: Different approaches for the determination of kinetic parameters. *Trends in Food Science and Technology, 15*, 394–420.

Juteau, A., Doublier, J.-L., & Guichard, E. (2004). Flavor release from ι-carrageenan matrices: A kinetic approach. *Journal of Agricultural and Food Chemistry, 52*, 1621–1629.

Juteau-Vigier, A., Atlan, S., Deleris, I., Guichard, E., Souchon, I., & Trelea, I. C. (2007). Ethyl hexanoate transfer modeling in carrageenan matrices for determination of diffusion and partition properties. *Journal of Agricultural and Food Chemistry, 55*, 3577–3584.

Landy, P., Druaux, C., & Voilley, A. (1995). Retention of aroma compounds by proteins in aqueous solution. *Food Chemistry, 54*, 387–392.

Le Thanh, M. (1992). *Extraction de substances aromatisantes produites par voie microbiologique – Étude des interactions entre substances d'arôme et constituants d'un milieu de culture*. Ph.D. thesis. Dijon, France: University of Burgundy.

Lucey, J. A., Cheng, T. T., Munro, P. A., & Singh, H. (1999). Microstructure, permeability and appearance of acid gels made from heated skim milk. *Food Hydrocolloids, 12*, 159–165.

Mills, O. E., & Solms, J. (1984). Interaction of selected flavour compounds with whey proteins. *Lebensmittel Wissenschaft und Technologie, 17*, 331–335.

Nongonierma, A., Springett, M., Le Quéré, J.-L., Cayot, P., & Voilley, A. (2006). Flavour release at gas/matrix interfaces of stirred yoghurt models. *International Dairy Journal, 16*, 102–110.

O'Neill, T. E., & Kinsella, J. E. (1987). Binding of alkanone flavors to β-lactoglobulin: Effects of conformational and chemical modification. *Journal of Agricultural and Food Chemistry, 35*, 770–774.

Paci Kora, E. (2003). *Interactions physico-chimiques et sensorielles dans le yaourt brassé aromatisé: Quels impacts respectifs sur la perception de la texture et de la flaveur*? Ph.D. thesis. Paris, France: National Agronomic Institute Paris-Grignon.

Philippe, E. (2003). *Étude de différents paramètres physico-chimiques sur la rétention des composés d'arôme par des matrices possédant un comportement rhéologique similaire*. Ph.D. thesis. Dijon, France: University of Burgundy.

Philippe, E., Seuvre, A.-M., Colas, B., Langendorff, V., Schippa, C., & Voilley, A. (2003). Behaviour of flavour compounds in model food systems: A thermodynamic study. *Journal of Agricultural and Food Chemistry, 51*, 1393–1398.

Plug, H., & Haring, P. (1993). The role of ingredient–flavour interactions in the development of fat-free foods. *Trends in Food Science and Technology, 4*, 150–152.

Rega, B., Guichard, E., & Voilley, A. (2002). Flavour release from pectin gels: Effects of texture, molecular interactions and aroma compounds diffusion. *Sciences des Aliments, 22*, 235–248.

Reid, C., Prausnitz, J. M., & Poling, B. E. (1987). *Pressure–volume–temperature relation of pure gases and liquids* (4th ed.). *The properties of gases and liquids*. New York: McGraw-Hill Book Company.

SciFinder Scholar (2005). *Log P calculated using advanced chemistry development (ACD/labs) software Solaris v4.67 (1994–2005)*. American Chemical Society.

Seuvre, A.-M., Espinosa Diaz, M. A., Cayot, P., & Voilley, A. (2004). Influence of the composition and the structure of different media on the release of aroma compounds. *Le Lait, 84*, 305–316.

Seuvre, A.-M., Philippe, E., Rochard, S., & Voilley, A. (2007). Kinetic study of the release of aroma compounds in different model food systems. *Food Research International, 40*, 480–492.

Taylor, A. J. (2002). Release and transport of flavors in vivo: Physicochemical, physiological, and perceptual considerations. *Comprehensive Reviews in Food Science and Food Safety, 1*, 45–57.

van Willige, R. W. G., Linssen, J. P. H., & Voragen, A. G. J. (2000). Influence of food matrix on absorption of flavour compounds by linear low-density polyethylene: Proteins and carbohydrates. *Journal of Science of Food and Agriculture, 80*, 1779–1789.

Wilke, C. R., & Chang, P. C. (1955). Correlation of diffusion coefficients in dilute solutions. *AIChE Journal, 1*, 264–270.

Food Chemistry 118 (2010) 96–102

Contents lists available at ScienceDirect

Food Chemistry

journal homepage: www.elsevier.com/locate/foodchem

A novel angiotensin I converting enzyme inhibitory peptide from tuna frame protein hydrolysate and its antihypertensive effect in spontaneously hypertensive rats

Sang-Hoon Lee [a,1], Zhong-Ji Qian [b,1], Se-Kwon Kim [a,b,*]

[a] Department of Chemistry, Pukyong National University, Busan 608-737, Republic of Korea
[b] Marine Bioprocess Research Center, Pukyong National University, Busan 608-737, Republic of Korea

ARTICLE INFO

Article history:
Received 6 January 2009
Received in revised form 16 April 2009
Accepted 23 April 2009

Keywords:
ACE inhibitory peptide
Tuna frame protein
Enzymatic hydrolysate
Antihypertensive effect

ABSTRACT

Tuna frame protein was hydrolysed using Alcalase, Neutrase, pepsin, papain, α-chymotrypsin and trypsin. Peptic hydrolysate exhibited the highest ACE I inhibitory activity among them and was fractionated into three ranges of molecular weight (below 1, 1–5 and 5–10 kDa) using an ultrafiltration membrane bioreactor system. The 1–5 kDa fraction showed the highest ACE inhibitory activity and was used for subsequent purification steps. During consecutive purification, a potent ACE inhibitory peptide from tuna frame protein (PTFP), which was composed of 21 amino acids, Gly-Asp-Leu-Gly-Lys-Thr-Thr-Thr-Val-Ser-Asn-Trp-Ser-Pro-Pro-Lys-Try-Lys-Asp-Thr-Pro (MW: 2,482 Da, IC_{50}: 11.28 μm), was isolated. Lineweaver–Burk plots suggest that PTFP plays as a non-competitive inhibitor against ACE. Furthermore, antihypertensive effect in spontaneously hypertensive rats (SHR) also revealed that oral administration of PTFP can decrease systolic blood pressure significantly ($P < 0.01$). These results suggest that the PTFP would be a beneficial ingredient for nutraceuticals and pharmaceuticals against hypertension and its related diseases.

1. Introduction

Hypertension is one of the major risk factors for the development of cardiovascular diseases, stroke and the end stage of renal disease (Zhang et al., 2006). The renin–angiotensin system plays a key role in maintaining blood pressure homeostasis, as well as fluid and salt balance in mammals (Turner & Hooper, 2002; Weinberg, Weinberg, & Zappe, 2000). Angiotensin I converting enzyme (peptidyl carboxy peptidase, EC 3.4.15.1, ACE) belongs to the class of zinc proteases that needs zinc and chloride for activation. This enzyme plays an important physiological role in regulating blood pressure by virtue of the renin–angiotensin system (Fujita, Yokoyama, & Yoshikawa, 2000). ACE converts an inactive form of decapeptides, angiotensin I, to a potent vasopressor octapeptide, angiotensin II, and inactivates catalytic function of bradykinin. Therefore, inhibition of ACE is considered to be an important therapeutic approach for controlling hypertension. Since the discovery of ACE inhibitors in snake venom (Ferreira, Bartelt, & Greene, 1970), many studies have attempted to synthesise ACE inhibitors such as captopril, enalapril, alacepril and lisinopril which are currently used in the treatment of essential hypertension and heart failure in humans (Ondetti, 1977). However, these synthetic ACE inhibitors are believed to have certain side effects such as cough, taste disturbances and skin rashes (Atkinson & Robertson, 1979). Therefore, search for non-toxic ACE inhibitors as alternatives to synthetic drugs is of great interest among researchers and many natural ACE inhibitors have been isolated from functional food and natural bio-resources (Goretta, Ottaviani, & Fraga, 2006).

The peptides derived from food proteins are considered to be milder and safer compared with synthetic drugs. Furthermore, these peptides usually have multifunctional properties and are easily absorbed (Yike et al., 2006). Bioactive peptides usually contain 3–20 amino acid residues and their activity is based on their amino acid composition and sequence (Pihlanto, 2000). Bioactive peptides, which are inactive within the sequence of the parent protein, could be released by enzymatic hydrolysis and exhibit various regulatory effects such as antioxidant (Je, Qian, Byun, & Kim, 2007), immune defense (Tsuruki et al., 2003), opioid (Pihlanto, 2000) and antihypertensive activities (Yike et al., 2006). Many reports have demonstrated the antihypertensive effect of ACE inhibitory peptides or foods containing these bioactive peptides in hypertensive patients (FitzGerald & Meisel, 2000). Several studies on spontaneously hypertensive rats (SHR) suggested a significant

* Corresponding author. Address: Department of Chemistry, Pukyong National University 599-1, Daeyeon 3-Dong, Nam-gu, Busan 608-737, Republic of Korea. Tel.: +82 51 620 6753; fax: +82 51 621 0047.
E-mail address: sknkim@pknu.ac.kr (S.-K. Kim).
[1] Contributed equally to this work.

0308-8146/$ - see front matter Crown Copyright © 2009 Published by Elsevier Ltd. All rights reserved.
doi:10.1016/j.foodchem.2009.04.086

suppression of hypertension with a diet rich in ACE inhibitory peptides (Hong et al., 2008). Many ACE inhibitory peptides have been identified from the enzymatic hydrolysates of various natural sources such as cheese whey (Amhar, Saito, Aimar, & Itoh, 1996), casein (Yamamoto, Akino, & Takano, 1994), bovine skin gelatin (Kim, Byun, Park, & Shahidi, 2001), Alaska pollack skin gelatin (Byun & Kim, 2001), bigeye tuna dark muscle (Qian, Je, & Kim, 2007), oyster (Je, Park, Jung, & Kim, 2005) and yellowfin sole (Jung et al., 2006).

Tuna frame proteins are usually discarded as processing waste or used for animal feed because of its poor functional properties. However, frame proteins can be converted into value-added products by enzymatic hydrolysis, which may be widely applied to improve functional and nutritional properties of proteins. Previously, for the efficient recovery of fish frame proteins, we investigated the antioxidant properties of hoki and Alaska pollack frame protein hydrolysates using various enzymes. We also investigated the ACE inhibitory activity of yellowfin sole frame protein hydrolysate. In the present study, the objective was to isolate ACE inhibitory peptides from tuna frame protein hydrolysate (TFPH) and to characterise the isolated peptide with respect to ACE inhibitory activity. Furthermore, we have also investigated the inhibition pattern of the isolated peptide on ACE, toxicity on MRC-5 and its antihypertensive action by oral administration in SHR.

2. Materials and methods

2.1. Materials

Fresh tuna frame proteins were kindly donated by Dongwon fisheries Co. (Busan, Korea) and stored at −20 °C until use. Digestive proteases (pepsin, α-chymotrypsin, trypsin and papain), ACE (EC 3.4.15.1) from rabbit lung and hippuryl-histidyl-leucine (HHL) as a substrate peptide of ACE were products of Sigma Chemical Co. (St. Louis, MO). Other proteases (Alcalase and Neutrase) were purchased from Novozymes (Bagsvaerd, Denmark). Ultrafiltration membrane (UF) reactor system (Minitane) and membranes were purchased from Millipore Co. (Bedford, MA). MRC-5 (ATCC CCL-171) was obtained from American Type Culture Collection (Manassas, Va). Cell culture media and other materials required for culturing were obtained from Gibco (Grand Island, NY). All other reagents used in this study were reagent grade chemicals.

2.2. Preparation of tuna frame protein hydrolysate (TFPH)

To extract ACE inhibitory peptide from Tuna frame protein, enzymatic hydrolysis was performed using various commercial enzymes (Alcalase, α-chymotrypsin, papain, pepsin, Neutrase and trypsin) with each optimal condition. A 100 g substrate (on the basis of protein weight) and 1 g enzyme were mixed in a 10 L reactor with temperature and pH control devices. The mixture was incubated for 8 h at each optimal temperature with stirring and then heated in a boiling water bath for 10 min to inactivate the enzyme. Degree of hydrolysis was determined by measuring the nitrogen content soluble in 10% (v/v) trichloroacetic acid as discussed by Kim et al. (2001). The resultant TFPH were fractionated through UF membranes with a range of molecular weight cutoffs (M_{WCO}) of 1, 5 and 10 kDa, respectively. Fractionates were designed as follows: TFPH I with MW distribution of below 1 kDa, TFPH II with MW distribution of 1–5 kDa and TFPH III with MW distribution of 5–10 kDa. All recovered TFPH fractions were lyophilised and stored under −80 °C until used.

2.3. Measurement of ACE inhibitory activity

ACE inhibitory activity assay was performed using the method of Cushman and Cheung (1971) with slight modifications. The reaction mixture contained 5 mM HHL as a substrate, 0.3 M NaCl and 5 ml ACE in 50 mM sodium borate buffer (pH 8.3). A sample (50 μl) was added to the above reaction mixture (50 μl) and mixed with 8.3 mM HHL (150 μl) containing 0.5 M NaCl. After incubation at 37 °C for 30 min, the further reaction was stopped by the addition of 0.1 M HCl (250 μl). The resulting hippuric acid was extracted by the addition of 1.5 ml ethyl acetate. After centrifugation (800g, 15 min), 1 ml of the upper layer was transferred into a glass tube and evaporated at room temperature for 2 h in vacuum. The hippuric acid was redissolved in 3.0 ml of distilled water, and absorbance was measured at 228 nm using UV-spectrophotometer (Model U-3210, Hitachi Co., Tokyo, Japan). The IC_{50} value was defined as the concentration of inhibitor required to inhibit 50% of the ACE activity.

2.4. Purification of ACE inhibitory peptide

2.4.1. Ion exchange chromatography

The lyophilised TFPH (20 mg/ml) was loaded into a Hiprep 16/10 DEAE FF anion exchange column equilibrated with 20 mM sodium acetate buffer (pH 4.0, $CH_3COONa{\cdot}3H_2O$), and eluted with a linear gradient of NaCl (0–2 M) in the same buffer at a flow rate of 62 ml/h using fast protein liquid chromatography (FPLC, ÄKTA, Amersham Bioscience Co., Uppsala, Sweden). Each fraction was monitored at 280 nm, collected at a volume of 4 ml and concentrated using a rotary evaporator after removing salt. The lyophilised fraction having the highest ACE inhibitory activity was subjected to the next purification step.

2.4.2. High performance liquid chromatography (HPLC)

The fraction exhibiting the highest ACE inhibitory activity was further purified using reverse-phase HPLC on a Primesphere 10 C_{18} (20 × 250 mm, Phenomenex Co., Ltd., Torrance, CA, USA) column with a linear gradient of acetonitrile (0–50% for 20 min) containing 0.1% trifluoroacetic acid (TFA) at a flow rate of 2 ml/min. The absorbance of eluent was monitored at 215 nm. Active peak representing ACE inhibitory activity was pooled and lyophilised immediately. The active fraction from analytical column was further applied onto a Synchropak RPP-100 analytical column (4.6 × 250 mm, Eprogen, Inc., Chicago, IL, USA) with 15% acetonitrile containing 0.1% TFA at flow rate of 1.2 ml/min for 20 min. The finally purified peptide was analysed amino acid sequence.

2.5. Determination of amino acid sequence of the purified peptide

Molecular mass and amino acid sequence of purified peptide from tuna frame protein (PTFP) was determined by Q-TOF mass spectrometer (Micromass, Altrincham, UK) coupled with electrospray ionisation (ESI) source. The purified peptide dissolved in methanol/water (1:1, v/v) was infused into the ESI source and molecular mass was determined by doubly charged $(M + 2H)^{2+}$ state in the mass spectrum. Following molecular mass determination, peptide was automatically selected for fragmentation and sequence information was obtained by tandem MS analysis.

2.6. Determination of the inhibition pattern on ACE

To clarify the inhibitory mechanism of PTFP on ACE, Different concentrations of PTFP were added to each reaction mixture according to Bush, Herny, and Slusarchyk (1984) with slight modifications. The enzyme activities were measured with different concentrations of the substrate (HHL) following the above procedure.

The kinetics of ACE in the presence of the inhibitor was determined by the Lineweaver–Burk plots.

2.7. Cell culture and cytotoxic assessment using MTT assay

MRC-5, Human lung fibroblast cell line was cultured and maintained in Dulbecco's modification of eagle's medium (DMEM, GIBCO, New York, USA) containing 100 μg/ml penicillin–streptomycin, 10% fetal bovine serum (FBS) and maintained at 37 °C under a humidified atmosphere with 5% CO_2. Cytotoxicity levels of the purified peptide on MRC-5 were measured using MTT (3-(4,5-dimethyl-2-yl)-2,5-diphenyltetrazolium bromide) method as described by Hansen, Nielsen, and Berg (1989) with slight modifications. MRC-5 cells were cultured in 96-well plates at a density of 5×10^3 cells/well. After 24 h, cells were washed with fresh medium and were treated with different concentrations of PTFP. After 24 h of incubation, Cells were washed two times with PBS and 100 μl of MTT solution (1 mg/ml) was added to each well. After 4 h of incubation, 100 μl of dimethyl sulfoxide (DMSO) were added to solubilise the formazan salt. The optical density was measured at 540 nm by using UV microplate reader (Tecan Austria GmbH, Groedig, Austria). Relative cell viability was calculated compared to the non-treated blank group. The data were expressed as means of at least three independent experiments.

2.8. Animals and measurement of systolic blood pressure

Spontaneously hypertensive rats (SHR, 10-week-old, male, specific pathogen-free, 180–240 g body weight) with tail systolic blood pressure (SBP) over 180 mm Hg were obtained from Korea Research Institute of Bioscience and Biotechnology (Daejeon, Korea). SHRs were housed individually in steel cages in a room kept at 24 °C with a 12 h light–dark cycle, and fed a standard laboratory diet. Tap water was freely available. PTFP was dissolved in saline at a dose of 10 mg/kg body weight and injected orally using a metal gastric zoned in SHR. The lowering efficacy of PTFP on systolic blood pressure (SBP) was compared with that of captopril. Control rats were administrated with the same volume of saline solution. Following oral administration, SBP was measured by tail-cuff method with a Softron BP system (Softron BP-98A, Tokyo, Japan) after warming up SHR in a chamber maintained at 37 °C for 10 min.

2.9. Statistical analysis

All results were expressed as means ± S.E.M. (n = 3). The significance of the differences of SBPs between control group and administration group was analyzed using Student's t-test.

3. Results

3.1. Preparation of tuna frame protein hydrolysates (TFPH) and their ACE inhibitory activity properties

To produce ACE inhibitory peptides, tuna frame protein was separately hydrolysed using various commercial digestive enzymes. In this experiment, six proteolytic enzymes such as Alcalase, a-chymotrypsin, papain, pepsin, Neutrase and trypsin were selected to evaluate their effectiveness on degradation of tuna frame protein for ACE inhibitory activity. Degrees of hydrolysis

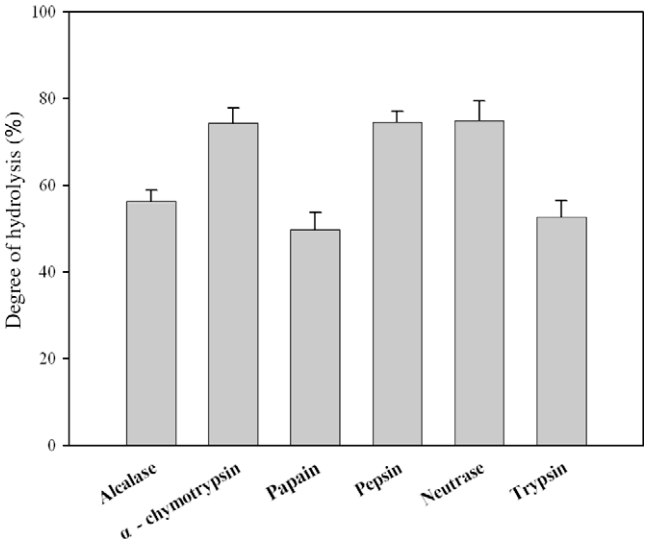

Fig. 1. Degrees of hydrolysis of tuna frame protein using various enzymes. Hundred gram substrate and 1 g enzyme were mixed in a 10 L reactor and the mixture was incubated for 8 h at optimal condition of each enzymes. Degrees of hydrolysis were determined by measuring the nitrogen contents soluble in 10% (v/v) trichloroacetic acid.

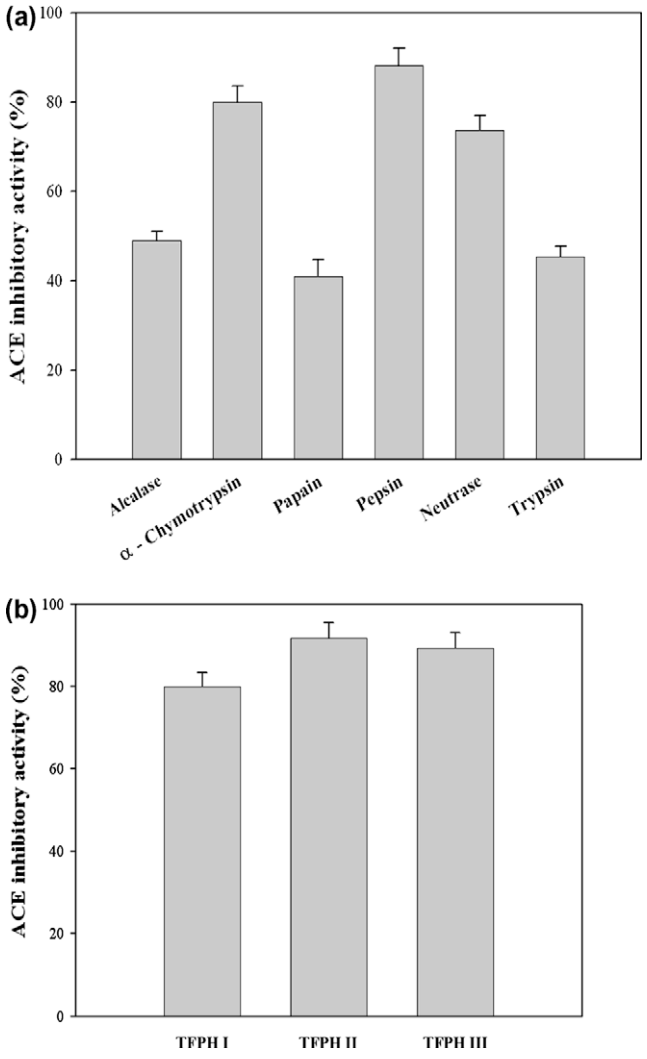

Fig. 2. (a) ACE inhibitory activities of enzymatic hydrolysates from tuna frame protein. Experiments were carried out in the presence or absence (control) of enzymatic hydrolysates as described in the text using HHL as the enzyme substrate for 30 min at 37 °C. (b) Comparison of ACE inhibitory activities of peptic hydrolysates of tuna frame protein with different molecular weight range. TFPH I (MW < 1 kDa), TFPH II (MW = 1–5 kDa) and TFPH III (MW = 5–10 kDa).

(DH) after proteolytic digestion were observed to be 74.3%, 74.5% and 74.8% for α-chymotrypsin, pepsin and Neutrase, respectively. However, the other proteolytic enzymes showed DH lower than 60% (Fig. 1). In ACE inhibitory activity assay (Fig. 2a), pepsin-proteolytic hydrolysate, which showed the highest ACE inhibitory activity (88.2%) among the tested hydrolysates at the concentration of 2 mg/ml, was selected for further study. Peptic hydrolysate was further separated into three MW groups, TFPH I (MW < 1 kDa), TFPH II (MW = 1–5 kDa) and TFPH III (MW = 5–10 kDa), using UF membrane (Mwco = 10, 5 and 1 kDa). The three MW groups were lyophilised and investigated by ACE inhibitory assay. As show in Fig. 2b, most of MW groups showed significant ACE inhibitory activity (over 80%) at the concentration of 1 mg/ml. Among the all MW groups, TFPH II exhibited highest ACE inhibitory activity (91.6%). However, TFPH III also exhibited similar activity (89.4%) compared to TFPH II. Bioactive peptides usually contain 3–20 amino acid residues and low MW peptides are more potent as bioactive peptides than high MW peptides (Pihlanto, 2000). Therefore, we selected TFPH II for the purification of the ACE inhibitory peptide.

3.2. Isolation of ACE inhibitory peptide

TFPH II was fractionated on a Hiprep 16/10 DEAE FF anion exchange column using FPLC. As shown in Fig. 3a, there were three major absorbance peaks at 280 nm and three fractions (F-1, F-2 and F-3) associated with the peaks were pooled and lyophilised for ACE inhibitory activity. F-3 which was eluted with 0.2–0.3 M NaCl exhibited a strong activity (76.4%) at the concentration of 0.2 mg/ml. The lyophilised active fraction, F-3 was further separated by reverse-phase HPLC on a Primesphere 10 C_{18} (20 mm × 250 mm) column with a linear gradient of acetonitrile (0–50% for 20 min) containing 0.1% TFA. The elution profiles of peptides are shown in Fig. 3b. Peptide peaks were separated into three fractions (F-3-1-1, F-3-2 and F-3-3) and each fraction was pooled and lyophilised for ACE inhibitory activity assay. F-3-3 showed the most potent ACE inhibitory activity (86.5%) at a concentration of 0.1 mg/ml. To obtain purified peptide, F-3-3 was further purified by reverse-phase HPLC on SynChropak RPP-100 analytical column (4.6 mm × 250 mm) with 15% acetonitrile containing 0.1% TFA (Fig. 3c). After two times of chromatography, finally we obtained the purified peptide from tuna frame protein (PTFP) and IC_{50} value of PTFP was 11.28 μM. In the N-terminal animo acid sequence analysis (Fig. 3d), it revealed that PTFP was composed of 21 amino acids, Gly-Asp-Leu-Gly-Lys-Thr-Thr-Thr-Val-Ser-Asn-Trp-Ser-Pro-Pro-Lys-Try-Lys-Asp-Thr-Pro (MW: 2,482 Da).

3.3. Determination of ACE inhibition pattern of PTFP

The ACE inhibition pattern of PTFP was investigated by Lineweaver–Burk plot and was found to be non-competitive (Fig. 4). This result means that the PTFP can combine with ACE molecule to pro-

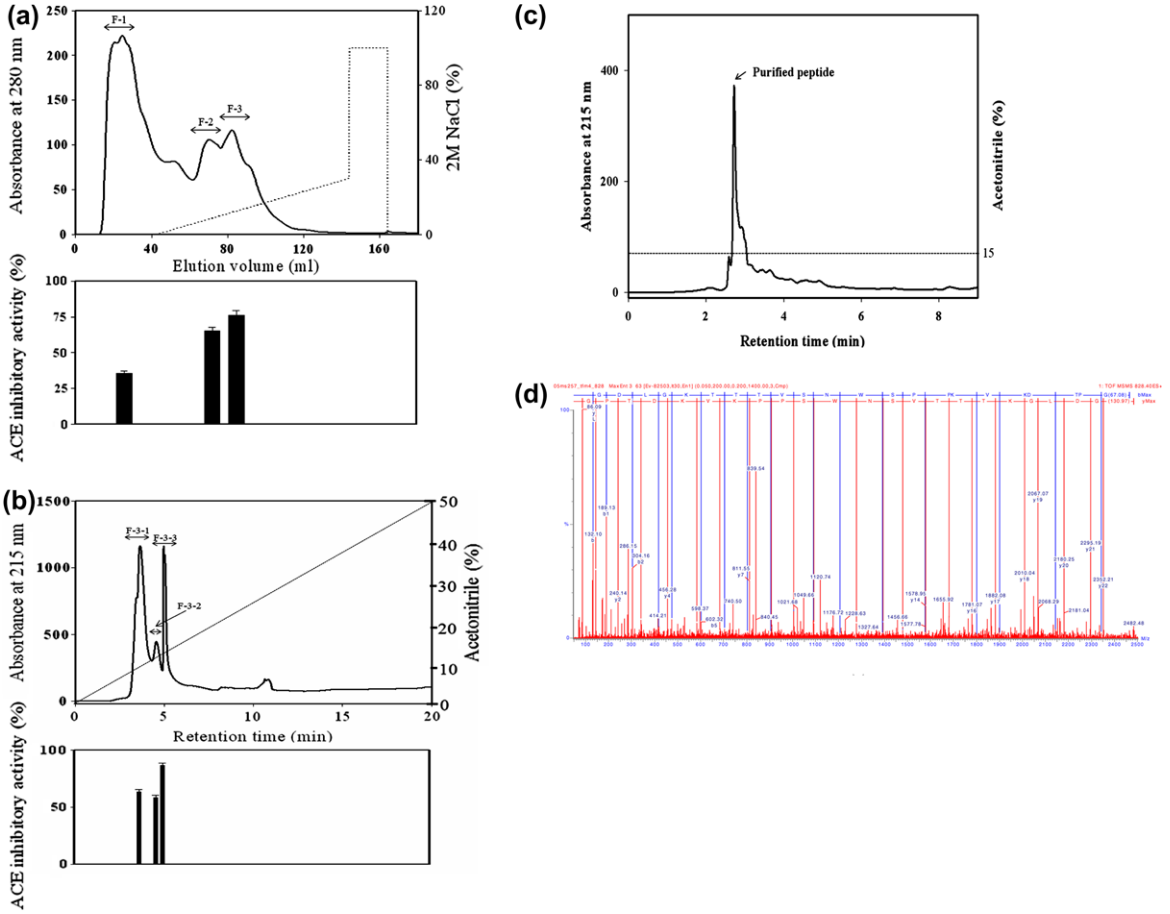

Fig. 3. (a) A FPLC chromatogram of TFPH II loaded on a Hiprep 16/10 DEAE FF ion-exchange column (upper panel) and the ACE inhibitory activity (lower panel). Active fractions were eluted with a NaCl linear gradient (0–2 M) at a flow rate of 62 ml/h. The sample concentration of each fraction was 0.2 mg/ml for measurement of ACE inhibitory activity. (b) A reverse-phase HPLC chromatogram of the active fraction (F-3) from FPLC loaded on Primesphere 10 C_{18} column (upper panel) and the ACE inhibitory activity (lower panel). Active fractions were eluted with an acetonitrile linear gradient (0–50% for 20 min) containing 0.1% TFA at a flow rate of 2 ml/min. The sample concentration of each fraction was 0.1 mg/ml for measurement of ACE inhibitory activity. (c) A reverse-phase HPLC chromatogram of the active fraction (F-3-3) on Synchoropak RPP-100 column using isocratic elution with 15% acetonitrile containing 0.1% TFA at a flow rate of 1.2 ml/min. (d) Identification of the molecular mass and amino acid sequence of the purified peptide (PTFP) using Q-TOF mass spectrometer.

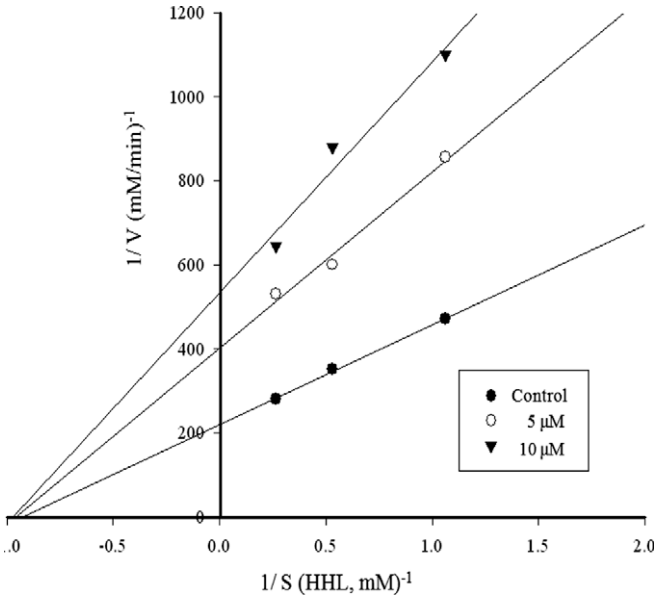

Fig. 4. Lineweaver–Burk plot for determination of inhibitory mode of PTFP on ACE. ACE inhibitory activity was determined in the presence or absence of PTFP (●; Control, ○; 5 μM, ▼; 10 μM) as described in the text using HHL as the enzyme substrate.

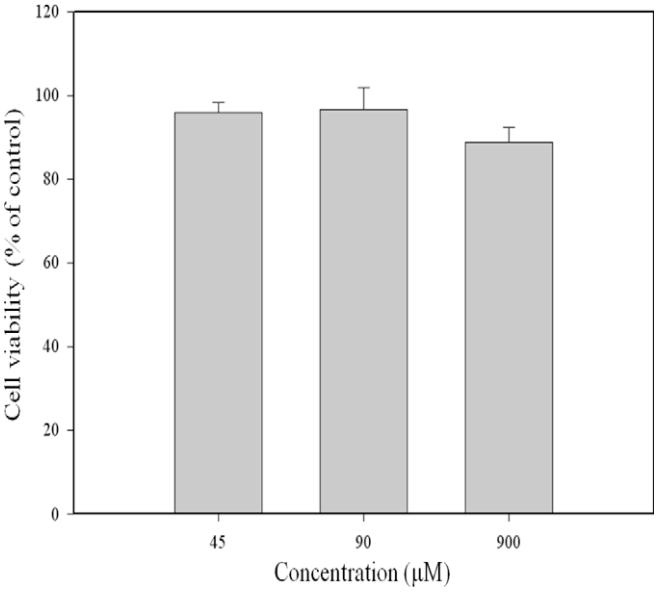

Fig. 5. Effect of PTFP on viability of MRC-5 cell lines using MTT assay. The cells were treated with various concentrations (45, 90 and 900 μM) of PTFP for 24 h. Values represent means ± S.E (n = 3).

duce a dead-end complex, regardless of whether a substrate molecule is bound or not.

3.4. Antihypertensive effect of PTFP on SHRs

For cytotoxic assessment of PTFP before oral administration in SHRs, cell viability of MRC-5 was tested using MTT assay after treatment of PTFP with various concentrations. PTFP showed no cytotoxicity up to 900 μM on MRC-5 (Fig. 5). Antihypertensive activity of PFTP was evaluated by measuring the change of systolic blood pressure (SBP) at 1, 2, 3, 6, and 9 h after oral administration of 10 mg/kg of body weight. Captopril was used as a positive control, and the control group was injected with the same volume of saline. As shown in Fig. 6, the SBP in quiescent state of SHR was 182 ± 2.0 mm Hg. After oral administration of PTFP and captopril, SBP was clearly decreased and the activities were maintained for 9 h. The maximal decrements in SBP of PTFP and captopril treatment groups were 21 and 26 mm Hg at 6 h, respectively.

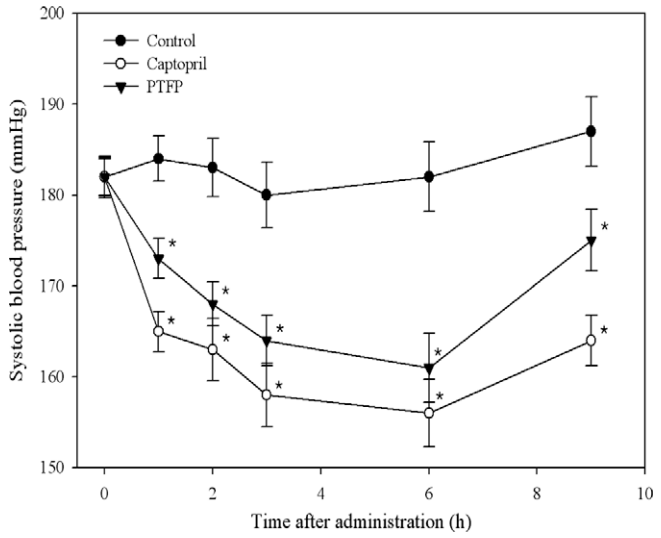

Fig. 6. Change of SBP after oral administration of PTFP in SHR. Captopril was used as a positive control. Single oral administration was performed with a dose of 10 mg/kg body weight, and SBP was measured 0, 1, 2, 3, 6 and 9 h after oral administration of PTFP. The significance of the difference from control at $^{*}P < 0.01$.

4. Discussion

To obtain the novel active ACE inhibitory peptide, six proteases were used under optimal conditions to hydrolyse tuna frame protein. Peptic hydrolysate showed the highest ACE inhibition and was fractionated in three portions (TFPH I = below 1 kDa, TFPH II = 1–5 kDa and TFPH III = 5–10 kDa) using UF membrane system. TFPH II showed highest ACE inhibitory activity and was selected for further isolation using FPLC and HPLC.

After three-step isolation, the novel ACE inhibitory PTFP which was composed of 21 amino acid was obtained. Several peptides derived from the enzymatic hydrolysates of various natural sources such as cheese whey (Amhar et al., 1996), casein (Yamamoto et al., 1994), bovine skin gelatin (Kim et al., 2001), Alaska pollack skin gelatin (Byun & Kim, 2001), sauce of fermented blue mussel (Je, Park, Byun, Jung, & Kim, 2005), bigeye tuna dark muscle (Qian et al., 2007) and porcine haemoglobin (Yike et al., 2006) are known to have ACE inhibitory activities and to exhibit antihypertensive activities in experimental animals. The identified ACE inhibitory peptides are Ile-Val-Tyr (IC_{50} = 0.48 μM) from wheat germ hydrolysate; Leu-Gln-Pro (IC_{50} = 9.6 μM) from zein; Glu-Val-Met-Ala-Gly-Asn-Leu-Try-Pro-Gly (IC_{50} = 2.98 μM) from sauce of fermented blue mussel; Leu-Gly-Phe-Pro-Thr-Thr-Lys-Thr-Tyr-Phe-Pro-His-Phe (IC_{50} = 4.92 μM) and Val-Val-Tyr-Pro-Trp (IC_{50} = 6.02 μM) from porcine hemoglobin; Trp-Pro-Glu-Ala-Ala-Glu-Leu-Met-Met-Glu-Val-Asp-Pro from bigeye tuna dark muscle (IC_{50} = 21.6 μM). In this study, the isolated ACE inhibitory PTFP was composed of Gly-Asp-Leu-Gly-Lys-Thr-Thr-Thr-Val-Ser-Asn-Trp-Ser-Pro-Pro-Lys-Try-Lys-Asp-Thr-Pro (MW: 2482 Da) and exhibited a higher or similar activity (IC_{50} = 11.28 μM) compared to other reports. The kinetic study revealed that ACE inhibitory PTFP acts as a non-competitive inhibitor, which means that it cannot bind at active site but at the other exclusive of the active site of ACE. Generally, ACE inhibitors contain one or more molecular functionalities such as a zinc

binding ligands (usually either a phosphate or carboxylate oxygen, or thiol sulphur), a hydrogen-bond donor and carboxyl-terminal group (Andrews, Carson, Caselli, Spark, & Woods, 1985). In case of ACE inhibitory peptides, the most potent and specific peptide inhibitors have similar structures and ACE activity is strongly influenced by the C-terminal tripeptide sequence of those. The tripeptides with Trp, Tyr, Phe, Pro and a hydrophobic amino acid at the C-terminal were effective for ACE inhibitory activity because of the interaction between three subsites at the active site of ACE (Pihlanto, 2000). In this study, a novel ACE inhibitory peptide from tuna frame protein hydrolysate (TFPH) contained hydrophobic amino acids and Pro at the C-terminal tripeptide sequence, which may contribute to ACE inhibitory activity.

A single oral administration (10 mg/kg) of PTFP showed a strong suppressive effect on SBP of SHRs and this antihypertensive activity was similar with captopril. Some antihypertensive drugs are known to cause side effects such as abnormal elevation of the blood pressure after administration. However, we could not observe any side effect after administration. Fujita and Yoshikawa (1999) classified the ACE inhibitory peptides into three groups based on the fates observed after preincubation with ACE. IC_{50} values of the inhibitor-type peptides (di- or tripeptides) are not affected by preincubation with ACE. Prodrug-type peptides were converted to their true inhibitors with smaller IC_{50} values by ACE, and substrate-type peptides exhibit an elevation of IC_{50} values after preincubation with ACE. According to this report, PTFP would be a prodrug-type inhibitor. It is well known that small peptides, such as di- or tripeptides are easily absorbed in their intact forms in the intestine. Even though PTFP has relatively high MW compared to other reports, the results clearly showed that PTFP exert a substantial effect on reduction of SBP in SHR. If this peptide was not effectively absorbed without digestion, it was difficult to observe this kind of antihypertensive effect on SHR. These results suggest that PTFP would be digested by gastric juice or protease in the small intestine, and then digested small peptide would be absorbed in the intestine. Matsui et al. (2004) reported an accumulation of ACE inhibitory dipeptide (Val-Tyr) in tissue of orally treated SHR. Val-Tyr accumulated in the kidney, lungs and abdominal aorta and caused decrease of ACE activity and angiotensin II levels. Matsui et al. (2003) demonstrated that Val-Tyr acts on the human rennin–angiotensin system through the retardation of angiotensin II formation-related enzyme activity. Therefore, further studies are needed to identify the mechanism of PTFP for the potent antihypertensive effect in SHR.

In conclusion, we isolated and characterised an ACE I inhibitory peptide (PTFP) to investigate beneficial effect against hypertension of tuna frame peptide hydrolysed using various digestive enzymes. PTFP exhibited potent inhibitory activity with 11.28 μM of IC_{50} value and was evaluated as a non-competitive inhibitor against ACE. Antihypertensive effect in SHR also revealed that oral administration of PTFP can decrease systolic blood pressure significantly. In addition, MTT assay showed no cytotoxicity on MRC-5. The result of this study suggests that the ACE inhibitory peptide from tuna frame protein hydrolysate could be potential candidates to develop nutraceuticals and pharmaceuticals against hypertension and its related disease. In addition, it is expected that this study will contribute to developing interest in basic research and potential application of bioactive peptides.

Acknowledgement

This research was supported by a grant from Marine Bioprocess Research Center of the Marine Biotechnology Program funded by the Ministry of Land, Transport and Maritime, Republic of Korea.

References

Amhar, A., Saito, T., Aimar, M. V., & Itoh, T. (1996). New derivation of the inhibitory activity against angiotensin converting enzyme (ACE) from sweet cheese whey. *Tohoku Journal of Agricultural Research, 47*, 1–8.

Andrews, P. R., Carson, J. M., Caselli, A., Spark, M. J., & Woods, R. (1985). Conformational analysis and active site modeling of angiotensin converting enzyme inhibitors. *Journal of Medicinal Chemistry, 28*, 393–399.

Atkinson, A. B., & Robertson, J. I. S. (1979). Captopril in the treatment of clinical hypertension and cardiac failure. *Lancet, 2*, 836–839.

Bush, K., Herny, P. R., & Slusarchyk, D. S. (1984). Muraceinsmuramyl peptides produced by *Norcardia orientalis* as angiotensin converting enzyme inhibitors. *Journal of Antibiotics, 37*, 330–335.

Byun, H. G., & Kim, S. K. (2001). Purification and characterization of angiotensin I converting enzyme inhibitory peptides from Alaska pollack (*Theragra chalcogramma*) skin. *Process Biochemistry, 36*, 1155–1162.

Cushman, D. W., & Cheung, H. S. (1971). Spectrophotometric assay and properties of the angiotensin-converting enzyme of rabbit lung. *Biochemistry and Pharmacology, 20*, 1637–1648.

Ferreira, S. H., Bartelt, D. C., & Greene, L. J. (1970). Isolation of bradykinin potentiating peptides from *Bothrops jararaca* venom. *Biochemistry, 9*, 2583–2593.

FitzGerald, R. J., & Meisel, H. (2000). Milk protein-derived peptide inhibitors of angiotensin-I-converting enzyme. *British Journal of Nutrition, 84*, 33–37.

Fujita, H., Yokoyama, K., & Yoshikawa, M. (2000). Classification and antihypertensive activity of angiotensin I-converting enzyme inhibitory peptides derived from food proteins. *Journal Food Science, 65*, 564–569.

Fujita, H., & Yoshikawa, M. (1999). LKPNM: A prodrug-type ACE inhibitory peptide derived from fish protein. *Immunopharmacology, 44*, 123–127.

Goretta, L. A., Ottaviani, J. I., & Fraga, C. G. (2006). Inhibition of angiotensin converting enzyme activity by flavanol-rich foods. *Journal of Agriculture and Food Chemistry, 54*, 229–234.

Hansen, M. B., Nielsen, S. E., & Berg, K. (1989). Re-examination and further development of a precise and rapid dye method for measuring cell growth/cell kill. *Journal of Immunological Methods, 119*, 203–210.

Hong, F., Ming, H., Yi, S., Zhanxia, L., Yongquan, W., & Chi, L. (2008). The antihypertensive effect of peptides: A novel alternative to drugs? *Peptides, 29*, 1062–1071.

Je, J. Y., Park, P. J., Byun, H. G., Jung, W. K., & Kim, S. K. (2005). Angiotensin I converting enzyme (ACE) inhibitory peptide derived from the sauce of fermented blue mussel, *Mytilus edulis*. *Bioresource Technology, 96*, 1624–1629.

Je, Y. J., Park, J. Y., Jung, W. K., & Kim, S. K. (2005). Isolation of angiotensin I converting enzyme (ACE) inhibitor from fermented oyster sauce, *Crassostrea gigas*. *Food Chemistry, 90*, 809–814.

Je, Y. J., Qian, Z. J., Byun, H. G., & Kim, S. K. (2007). Purification and characterization of an antioxidant peptide obtained from tuna backbone protein by enzymatic hydrolysis. *Process Biochemistry, 42*, 840–846.

Jung, W. K., Mendis, E., Je, J. Y., Park, P. J., Son, B. W., Kim, H. C., et al. (2006). Angiotensin I-converting enzyme inhibitory peptide from yellowfin sole (*Limanda aspera*) frame protein and its antihypertensive effect in spontaneously hypertensive rats. *Food Chemistry, 94*, 26–32.

Kim, S. K., Byun, H. G., Park, P. J., & Shahidi, F. (2001). Angiotensin I converting enzyme inhibitory peptides purified from bovine skin gelatin hydrolysate. *Journal of Agricultural and Food Chemistry, 49*, 2992–2997.

Matsui, T., Hayashi, A., Tamaya, K., Matsumoto, K., Kawasaki, T., Murakami, K., et al. (2003). Depressor effect induced by dipeptide, Val-Tyr, in hypertensive transgenic mice is due, in part, to the suppression of human circulating rennin–angiotensin system. *Clinical and Experimental Pharmacology and Physiology, 30*, 262–265.

Matsui, T., Imamura, M., Oka, H., Osajima, K., Kimoto, K., Kawasaki, T., et al. (2004). Tissue distribution of antihypertensive dipeptide, Val-Tyr, after its single oral administration to spontaneously hypertensive rats. *Journal of Peptide Science, 10*, 535–545.

Ondetti, M. A. (1977). Design of specific inhibitors of angiotensin-converting enzyme: New class of orally active antihypertensive agents. *Science, 196*, 441–444.

Pihlanto, L. (2000). Bioactive peptides derived from bovine whey proteins: Opioid and ace-inhibitory. *Trends in Food Science and Technology, 11*, 347–356.

Qian, Z. J., Je, J. Y., & Kim, S. K. (2007). Antihypertensive effect of angiotensin i converting enzyme-inhibitory peptide from hydrolysates of bigeye tuna dark muscle, *Thunnus obesus*. *Journal of Agricultural and Food Chemistry, 55*, 8398–8403.

Tsuruki, T., Kishi, K., Takahashi, M., Tanaka, M., Matsukawa, T., & Yoshikawa, M. (2003). Soymetide an immunostimulating peptide derived from soybean b-conglycinin, is an fMLP agonist. *FEBS Letter, 540*, 206–210.

Turner, A. J., & Hooper, N. M. (2002). The angiotensin-converting enzyme gene family: Genomics and pharmacology. *Trends in Pharmacological Sciences, 23*, 177–183.

Weinberg, M. S., Weinberg, A. J., & Zappe, D. H. (2000). Effectively targeting the renin–angiotensin–aldosterone system in cardiovascular and renal disease: Rationale for using angiotensin II receptor blockers in combination with angiotensin-converting enzyme inhibitors. *Journal of Renin–Angiotensin–Aldosterone System, 1*, 217–233.

Yamamoto, N., Akino, A., & Takano, T. (1994). Antihypertensive effect of the peptides derived from casein by an extracellular proteinase from *Lactobacillus helveticus* CP790. *Journal of Dairy Science, 77*, 917–922.

Yike, Y., Jianen, H., Yuji, M., Xuefang, B., Yuguang, D., & Bingcheng, L. (2006). Isolation and characterization of angiotensin I-converting enzyme inhibitory peptides derived from porcine hemoglobin. *Peptides, 27*, 2950–2956.

Zhang, Y., Lee, E. T., Devereux, R. B., Yeh, J., Best, L. G., Fabsitz, R. R., et al. (2006). Prehypertension, diabetes, and cardiovascular disease risk in a population based sample: The strong heart study. *Hypertension, 47*, 410–414.

Food Chemistry 118 (2010) 103–108

Contents lists available at ScienceDirect

Food Chemistry

journal homepage: www.elsevier.com/locate/foodchem

The effect of $MgCl_2$ on the kinetics of the Maillard reaction in both aqueous and dehydrated systems

Silvia B. Matiacevich [1], Patricio R. Santagapita [1], María del Pilar Buera [*,2]

Departamentos de Industrias y de Química Orgánica, Facultad de Ciencias Exactas y Naturales, Universidad de Buenos Aires, 1428, Buenos Aires, Argentina

ARTICLE INFO

Article history:
Received 10 February 2009
Received in revised form 12 March 2009
Accepted 23 April 2009

Keywords:
Maillard reaction
$MgCl_2$
Transversal relaxation time
Browning
Fluorescence
Browning inhibition

ABSTRACT

The modification of Maillard reaction kinetics induced by $MgCl_2$ was evaluated in both liquid and dehydrated model systems with special emphasis on the interactions of the salt with water and/or the sugars. In liquid trehalose systems, browning is accelerated by the presence of $MgCl_2$ due to the increased sugar hydrolysis and to the reduction of water mobility caused by the salt (shown by the decrease in ^1H NMR relaxation times T_2), counteracting the inhibitory effect of water on the reaction. In water restricted trehalose systems, $MgCl_2$ inhibited the Maillard reaction. The salt–sugar interactions, manifested by the delayed sugar crystallization, decreased the reaction rate by affecting the reactivity of reducing sugars. Molecular and supramolecular effects in the presence of $MgCl_2$ have been observed in the present work, and must be taken into account considering high technological interest in finding strategies to either inhibit or enhance the Maillard reaction depending on the application.

1. Introduction

The rate of the Maillard reaction and the nature of its products are governed by the immediate chemical environment of the reactants, defined by the chemical composition of the system (water content, pH, presence and type of buffer salts, temperature and exposure to light) (Baisier & Labuza, 1992; Bell, 1997; Cerruti, Resnik, Seldes, & Ferro Fontán, 1985; Petriella, Chirife, Resnik, & Lozano, 1988). The development of fluorescent products from the Maillard reaction (excitation 340–370 nm/emission 420–475 nm) was described during the storage of different types of food products and model systems. The application of fluorescence measurement is considered a potential tool for addressing key problems of food deterioration as it is an early marker or index of the biomolecular damage (Matiacevich, Santagapita, & Buera, 2005). The behaviour of model systems in the presence of divalent cations (Mg^{2+} or Ca^{2+}) was previously studied. Salts may affect important properties of sugar systems, including fluorescence and browning development from the Maillard reaction, the kinetics of sugar crystallization and sugar hydrolysis (Matiacevich & Buera, 2006; Santagapita & Buera, 2006; Santagapita & Buera, 2008; Schebor, Burin, Buera, & Chirife, 1999). Gökmen & Şenyuva (2007) showed that acrylamide formation is prevented by divalent cations during the Maillard reaction in fructose-asparagine model systems; however, ionic associations between the charged groups of asparagine and Ca^{2+} were not observed. Sugar–cation (Morel-Desrosier, Lhermet, & Morel, 1991) and brown pigment-cation complexes (O'Brien & Morrissey, 1997) have been shown to form in solution. The development of strategies for inhibiting the Maillard reaction employing additives other than sulphites (Lester, 1995) has a high technological interest. Alternatively, in other applications it may be beneficial to enhance the Maillard reaction. However, there has been little work carried out on the role of food-compatible salts in the kinetics of the Maillard reaction. The effect of cations can be analysed through their impact on the modification of solid–water interactions, and water availability, which govern and modulate the kinetics of the Maillard reaction (Acevedo, Schebor, & Buera, 2006).

Nuclear magnetic resonance (NMR) is a very useful technique for investigating the behaviour of water mobility in foods (Schmidt, 2007). The differences in relaxation times of protons from different environments have been exploited in NMR studies to measure the relative amounts of water with different degrees of interaction with solids and consequently, with different mobility (Acevedo et al., 2006; Farroni, Matiacevich, Guerrero, Alzamora, & Buera, 2008). The spin–spin or transversal relaxation time constants of protons (T_2) are related to the molecular mobility of protons in the system. The relaxation processes are affected by the chemical exchange taking place in sites of different mobility. Protons of water molecules which interact tightly with solids, and therefore have reduced mobility (although they are still exchangeable), show small T_2 values, whereas protons which are readily

* Corresponding author. Tel./fax: +54 11 4576 3366.
E-mail address: pilar@di.fcen.uba.ar (M. del P. Buera).
[1] Research fellow of Consejo Nacional de Investigaciones Científicas y Técnicas de la República Argentina (CONICET).
[2] Member of CONICET.

0308-8146/$ - see front matter © 2009 Elsevier Ltd. All rights reserved.
doi:10.1016/j.foodchem.2009.04.084

mobile have relatively long T_2 values (Kuo, Gunasekaran, Johnson, & Chen, 2001).

The purpose of the present work was to analyse the modification of Maillard reaction kinetics induced by the presence of $MgCl_2$ in both liquid and dehydrated model systems, with special emphasis on the interactions of the salt with water and/or the sugars.

2. Materials and methods

2.1. Preparation of model systems

2.1.1. Liquid systems

Liquid systems were prepared from 5% to 70% w/v of D(+)glucose (Merck, Darmstadt, Germany) or α-α-trehalose (Hayashibara Co, Ltd., Okayama, Japan) and 0.5% L-glycine (Merck) with and without $MgCl_2$ (Mallinckrodt Chemical Works, St. Louis, USA), in a 5:1 sugar:salt molar ratio; controls without $MgCl_2$ and glycine were also prepared. Aliquots (2.5 ml) of each model system were placed in 5 ml vials. The systems were prepared in 0.1 M phosphate buffer, pH 5 (Merck, Darmstadt, Germany). All reactants were analytical grade. The vials were hermetically sealed and stored at 70 ± 1 °C in a forced air convection oven.

2.1.2. Solid systems

Solid systems consisted of freeze-dried solutions containing 20% w/v trehalose and 1% w/v L-glycine. The systems were prepared in 0.1 M phosphate buffer at pH 5. The salt $MgCl_2$ was added in a 5:1 sugar:salt molar ratio; controls without $MgCl_2$ and without glycine were also prepared. Aliquots (2.5 ml) of each model were placed in 5 ml vials, frozen at −26 °C for 24 h and immersed in liquid nitrogen immediately before freeze-drying. Freeze-drying was performed in a Heto Holten A/S, cooling trap model CT 110 freeze-dryer (Heto Lab Equipment, Denmark) operating at a condenser plate temperature of −111 °C and a chamber pressure of 4×10^{-4} mbar. After freeze-drying, the systems were transferred to vacuum desiccators and exposed to different relative vapour pressure conditions (RVP): 22%, 43%, 52%, 84% and 97% (Greenspan, 1977) at 25 ± 1 °C for 2 weeks. After humidification, the vials were hermetically sealed and stored at 70 ± 1 °C in a forced air convection oven.

2.2. Determination of browning and fluorescence development

The progress of the Maillard reaction was followed by a browning index defined as absorbance units at 445 nm (UV–vis 1203 spectrophotometer, Shimadzu, Kyoto, Japan) multiplied by the dilution factor, and by fluorescence intensity with excitation at 340 nm/emission 492 nm (model USB 2000 spectrofluorometer, Ocean Optics Inc., FL, USA). The samples employed for the determination of fluorescence were diluted in order to avoid inner filter effect, with absorbance values lower than 0.1 at excitation wavelength (340 nm). Since trehalose is a non-reducing sugar, its participation in Maillard reaction can only occur after hydrolysis.

Browning and fluorescence development as a function of reaction time followed a quadratic dependence, which indicates a half order reaction, which results from the combination of two steps of zero and first order (Matiacevich & Buera, 2006).

The confidence intervals for browning and fluorescence values were 3% and 5% for 95% certainty, respectively.

2.3. Disaccharide hydrolysis

Sugar hydrolysis was analysed by measuring the amount of glucose released during the incubation time by means of an enzymatic method (Wiener Lab. S.A.I.C., Rosario, Argentina) described previously (Bergmeyer & Grassi, 1983).

2.4. Fluorescence quantum yield

Sugar systems solutions (70% w/v) were diluted in order to obtain absorbance below 0.05 to avoid inner filter effects (Lakowicz, 1999). Four dilutions (in duplicate) were prepared for each time of incubation. Fluorescence quantum yields (Φ_F) were determined using quinine sulphate in 0.1 N sulphuric acid as a reference fluorophore of known quantum yield ($\Phi_F = 0.546$) (Lakowicz, 1999), using the classical Eq. (2.1):

$$\Phi_F^S = \Phi_F^R \cdot \frac{I_\lambda^S}{I_\lambda^R} \cdot \frac{A_\lambda^R}{A_\lambda^S} \cdot \frac{n_S^2}{n_R^2} \tag{2.1}$$

where Φ_λ^S and Φ_λ^R are the fluorescence quantum yield of the sample (S) and the reference (R), respectively; I_λ^S and I_λ^R are the integrated areas of their fluorescence spectra; A_λ^S and A_λ^R are their absorbances at the excitation wavelength λ, and n_S and n_R are the refractive index of each solution. In Eq. (2.1), it is assumed that the sample and reference are excited at the same wavelength.

2.5. Nuclear magnetic resonance (NMR) measurements

Transversal or spin–spin relaxation times (T_2) were measured by time resolved proton nuclear magnetic resonance (^{1}H NMR) in a Bruker Minispec mq20 (Bruker Biospin Gmbh, Rheinstetten, Germany) with a 0.47 T magnetic field operating at a resonance frequency of 20 MHz. Proton populations of different mobility were measured using two spin-echo sequences: (a) Hahn (Hahn, 1950), for protons from solids or from water strongly interacting with the solid matrix, and (b) Carr–Purcell–Meiboom–Gill (CPMG) (Carr & Purcell, 1954; Meiboom & Gill, 1958), for more mobile protons. All samples were previously equilibrated at 25.00 ± 0.01 °C in a thermal bath (Haake, model Phoenix II C35P, Thermo Electron Corporation Gmbh, Karlsruhe, Germany).

2.5.1. Measurements using a Hahn sequence

Hahn spin-echo consists of a (90°–τ–180°) sequence. This method allows for analysis of the less mobile protons interacting with the solid matrix; the more mobile protons could not be analysed using this sequence due to diffusion problems during measurement at long times, caused by inhomogeneities in the magnetic field. Trehalose dehydrated systems humidified between 22% and 97% RVP were analysed using this sequence. The following settings were used: scans = 4, recycle delay = 1.5 s, gain = 75 dB, number of points = 20, time for decay curve display = 1 s and interpulse (τ) range of 0.001–0.5 ms. The interpulse range was selected in order to record the complete relaxation of the signal. No phase cycling was used. A polyvinylpyrrolidone (PVP of 58 000 Da) system equilibrated at 43% RVP was used for the automatic update of the equipment which tunes the pulse duration, detection angles, gain and magnetic field homogeneity.

2.5.2. Measurements using a CPMG sequence

Liquid systems were analysed using a CPMG sequence, which consists of $90^\circ_x - \tau - \left[180^\circ_y - \tau - \text{echo} - \tau\right]_n$ sequence, with the following setting: $\tau = 0.5$, scans = 4, number points = 256, dummy shots = 15, gain = 68 dB; phase cycling was used. The automatic update of the equipment was performed employing a 40% w/v trehalose system without thermal treatment.

For both sequence measurements, an exponential function (as stated below in Eq. (2.2)) was found to fit the experimental data adequately, from which transverse relaxation time constant (T_2) was obtained.

$$A = A^{(-t/T_2)} \quad (2.2)$$

where A is the signal amplitude that is proportional to the amount of protons in the sample relaxing after the pulse sequence. This mono-exponential model was used for the liquid samples and for most of the dehydrated systems, obtaining the contributions of protons in the most representative fraction. A bi-exponential model fitted some dehydrated systems with high water content (corresponding to samples at 97% and 84% RVP containing $MgCl_2$), but it is important to note that, for these samples, the signal amplitude of the detected second proton fraction represented a very small contribution to the total proton population, and the mono-exponential approach was selected as the best model for comparative purposes.

2.6. Determination of water content

The total water content of the trehalose solid rehumidified systems was determined gravimetrically by difference in weight before and after drying in a vacuum oven for 48 h at 96 ± 2 °C. These drying conditions were selected in previous studies with samples of similar composition (Mazzobre, Longinotti, Corti, & Buera, 2001) and they were adequate to determine water content in the studied systems with a confidence interval of 6% for a 95% certainty. Duplicate analyses were performed and the average of the results is reported on a dry basis (db).

2.7. Thermal transitions measurements

Melting events were determined by dynamic differential scanning calorimetry (DSC), in the temperature range from 20 to 120 °C, by means of a Mettler Toledo model 822 equipment (Mettler Toledo AG, Greifensee, Switzerland) at a heating rate of 10 °C/min. Melting temperature values were taken as peak temperatures. All measurements were made in duplicate with 10–25 mg sample mass using hermetically sealed aluminium pans of 40 μl inner volume (Mettler Toledo AG). An empty pan was used as a reference and average values are reported. The instrument was calibrated using standard compounds (indium and zinc) of defined melting point and heat of melting (ΔH_m). All thermograms were analysed using STAR^e Software v. 6.1 (Mettler Toledo AG). The samples were initially amorphous as determined by the absence of endothermal peaks in the DSC scans. The amount of trehalose dihydrate formed (degree of crystallization, ϕ) during the storage time was calculated from the ratio of the area of the endothermic melting peak of the sample and the calorimetric enthalpy of the melting of pure trehalose dihydrate measured under the same conditions in a dynamic DSC run, as Eq. (2.3).

$$\phi = \frac{\Delta H_m}{\Delta H_{mT}} * 100 \quad (2.3)$$

where ΔH_m is the heat of melting of trehalose in the sample and ΔH_{mT} is the heat of melting of pure trehalose (139 J/g) measured under the same conditions (Santagapita & Buera, 2006). The relative error for ϕ (calculated with a 95% confidence interval) was about 10% of the ϕ value.

3. Results and discussion

3.1. Maillard reaction development: fluorescence and absorbance data

3.1.1. Liquid systems

Browning and fluorescence development of the liquid systems increased with increasing storage time at 70 °C, for the whole composition range studied (5–70% w/v), as shown in Fig. 1 (a–d). The 70% w/v sugar systems, for example, showed corresponding visual colour changes: uncoloured → yellow → golden → cinnamon → reddish brown. The type and sugar concentration and the presence of $MgCl_2$ were critical for the rate of pigment and fluorescent compounds formation. In the model systems without amino acid (control samples), no increase in the absorbance or the fluorescence was detected, indicating that there was no contribution to colour or fluorescence due to caramelization in the experimental time frame. The decreasing order for browning development was found according to sugar reactivity/stability: glucose > trehalose (Burton, Mc Weeny, Pandhi, & Biltcliffe, 1962; O'Brien & Morrissey, 1997) in all analysed sugar concentrations, as shown in Fig. 1a and c for the 70% w/v samples. In liquid glucose systems, inhibitory effects of $MgCl_2$ on browning and development of fluorescent products, observed for the 70% w/v samples in Fig. 1a and b (respectively), were also noticed in the whole composition range studied (5–70% w/v), extending our previous results for 5% and 40% w/v samples (Matiacevich & Buera, 2006; Santagapita & Buera, 2006). However, as shown in Fig. 1c and d for the 70% w/v systems, an accelerating effect of $MgCl_2$ was observed for both browning and development of fluorescence in liquid systems containing trehalose, in the whole composition range studied. Fig. 2 shows the kinetic constants for browning development in trehalose systems, calculated through a quadratic model, plotted as a function of different water contents. Although trehalose is very stable to hydrolysis (Santagapita & Buera, 2006; Schebor et al., 1999), it was hydrolysed during heat treatment at 70 °C and the hydrolysis rate was accelerated by the presence of $MgCl_2$ (Santagapita & Buera, 2006), as confirmed by glucose analysis (data not shown). For example, for the range between 5% and 40% w/v trehalose system, the rate of trehalose hydrolysis was lower than 1% in systems without salt and increased to 2.3–2.5% in the presence of $MgCl_2$. Pigment development through the Maillard increased accordingly, as observed in Fig. 1c and d.

3.1.2. Solid systems

In the freeze-dried trehalose samples humidified at relative vapour pressures (RVPs) in the range 22–97%, the development of fluorescence was parallel to the development of browning, and the hydrolysis rate increased in the presence of salt as was seen in the analysed liquid systems (also in agreement with Santagapita & Buera, 2006). In the samples containing $MgCl_2$ at 10% (db) water content, only 1.1% trehalose was hydrolysed after 24 h at 70 °C. Under the same conditions, disaccharide hydrolysis was 0.13% for trehalose samples without salt. However, contrary to the results observed in trehalose liquid samples, in solid trehalose samples the presence of $MgCl_2$ delayed browning development, as shown in Fig. 2. It is clearly shown that $MgCl_2$ inhibited the Maillard reaction at low water contents in solid trehalose systems (Fig. 2, left side of the dotted line), but in liquid systems, the presence of the salt increased the reaction rate (Fig. 2, right side of the dotted line, and Fig. 1c). Thus, the effect of $MgCl_2$ on browning development in trehalose samples was dependent on the state of the systems.

3.2. Fluorescence characteristics and quantum yield study

In order to analyse the effects associated with sugar type and their interactions with $MgCl_2$ on the Maillard reaction kinetics in liquid systems shown in Fig. 1, fluorescence characteristics of the samples were studied. In agreement with previous studies (Matiacevich et al., 2005), the maximum wavelength for emission was 450 nm in all systems, and the fluorescence development at zero time of incubation was negligible. Fig. 3 shows the fluorescence emission spectra of trehalose or glucose systems with and without $MgCl_2$, after 0 and 120 h of storage at 70 °C. As seen in this figure, the spectral characteristics were independent of the studied

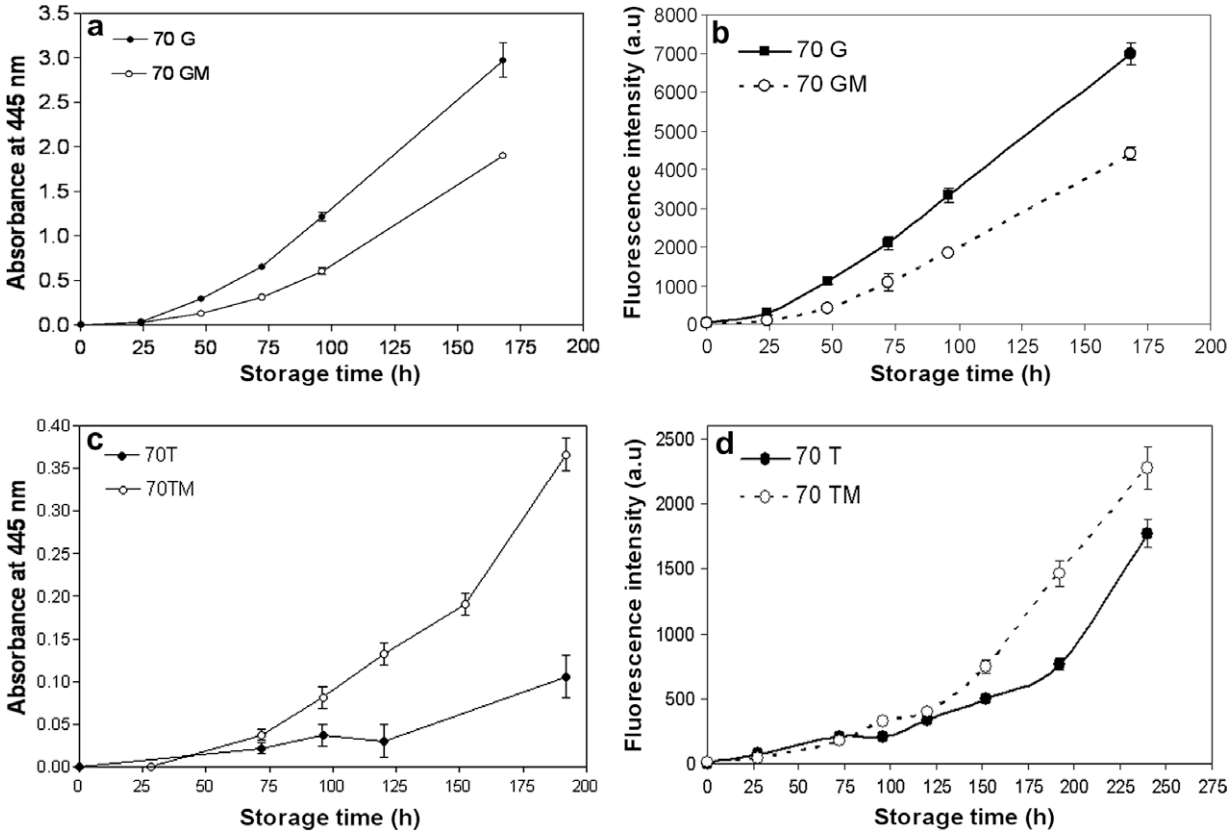

Fig. 1. Browning and fluorescence development for 70% w/v glucose (a, b), or trehalose (c, d) systems with $MgCl_2$ (open symbols) and without $MgCl_2$ (closed symbols) as a function of storage time at 70 °C. Excitation/emission 340/450 nm. T, trehalose; G, glucose; M, $MgCl_2$. Bars on symbols represent the 95% confidence interval.

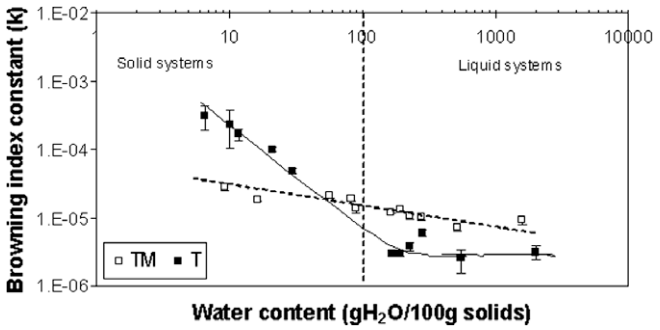

Fig. 2. Kinetic constants for the Maillard reaction (obtained by a quadratic model) as a function of water content for trehalose systems. Solid lines correspond to sugar systems without salt and dashed lines to $MgCl_2$ -containing systems. T, trehalose; M, $MgCl_2$. Bars on symbols represent the 95% confidence interval.

system, indicating that neither the type of sugar nor the presence of salt affected the type of fluorophore obtained in each system.

The fluorescence quantum yield, which is defined as the ratio between the number of photons involved in the emission and the total number of excited photons, may provide information on molecular structural properties of the fluorophores and their interactions. The fluorescence quantum yield was calculated for the samples as a function of heating time at 70 °C, in order to further analyse the effect of $MgCl_2$ on the Maillard reaction (shown in Figs. 1 and 2). As shown in Fig. 4, the fluorescence quantum yield was constant as a function of heating time in glucose systems after a slight initial increase. It is important to note that the presence of $MgCl_2$ did not affect the quantum yield. Thus, the increase of fluorescence observed in Fig. 1b is due to the increasing concentration of fluorophores with increased incubation time, and not to an increase of the fluorophores quantum yield. The same conclusion could be obtained for trehalose systems (Fig. 1d), considering that trehalose must be hydrolysed to two glucose units in order to participate of the Maillard reaction.

Therefore, in agreement with previous studies, the presence of $MgCl_2$ affected the kinetics of the reaction without affecting the chromatic and fluorescent spectral characteristics of samples (Matiacevich & Buera, 2006; Santagapita, Matiacevich, & Buera, in press) or the fluorescence quantum yield properties of the fluorophores.

3.3. Proton mobility studies by NMR

In order to evaluate the possible contribution of water–salt interactions in the results observed in Figs. 1 and 2, proton mobility in each liquid system was studied by ^1H NMR transversal relaxation times (T_2). In liquid systems, T_2 values were calculated after the spin-echo CPMG sequence by a mono-exponential decay model and the results are shown in Fig. 5. With increasing sugar concentration, T_2 values diminished for all sugar systems, indicating a reduced mobility of water protons. As also observed in Fig. 5, T_2 values were not affected by $MgCl_2$ in systems containing glucose (i.e., water–glucose interaction was unmodified by salt), whilst in trehalose systems they were between 6% and 14% lower in the presence of salt, reflecting a reduced mobility. The T_2 values obtained indicated that the $MgCl_2$ interaction affects water mobility in the trehalose samples, but not in glucose systems. Since an inhibitory effect of water has been observed on the Maillard reaction (Acevedo et al., 2006; Labuza, 1994), the accelerating effect of $MgCl_2$ on the reaction rate observed in the disaccharide samples in Figs. 1 and 2 can be associated with water–salt interactions. According to Miller and de Pablo (2000), the local environment

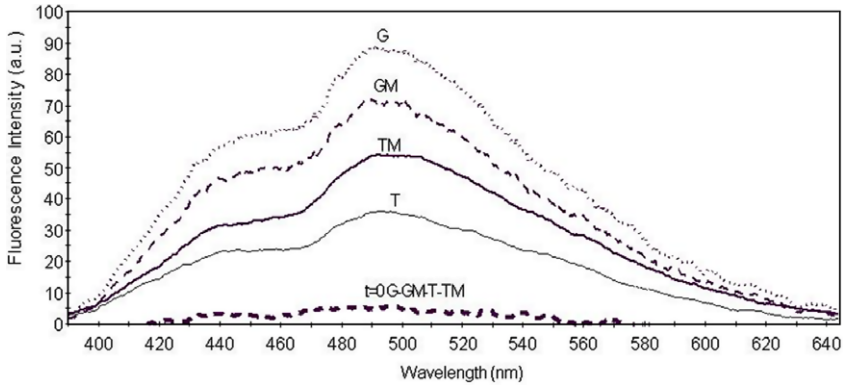

Fig. 3. Fluorescence emission spectra of 70% w/v sugar systems heated at 70 °C for 120 h (-.-.-.-.-. glucose, and —— trehalose systems; grey curves correspond to $MgCl_2$ containing systems). The curve labelled as $t = 0$ h, G or T corresponds to the fluorescence for zero time of incubation for all sugar systems. T, trehalose; G, glucose; M, $MgCl_2$.

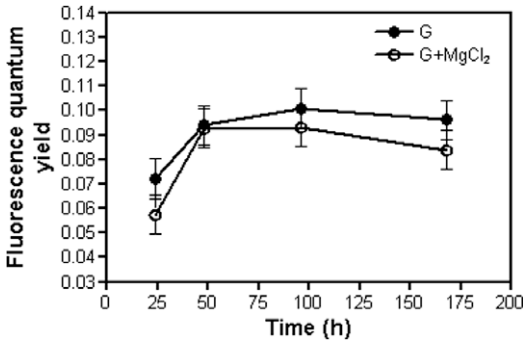

Fig. 4. Fluorescence quantum yield as a function of time of incubation for glucose systems with (open symbols) and without (closed symbols) $MgCl_2$. Excitation/emission 340/450 nm. G, glucose; M, $MgCl_2$. Bars on symbols represent the 95% confidence interval.

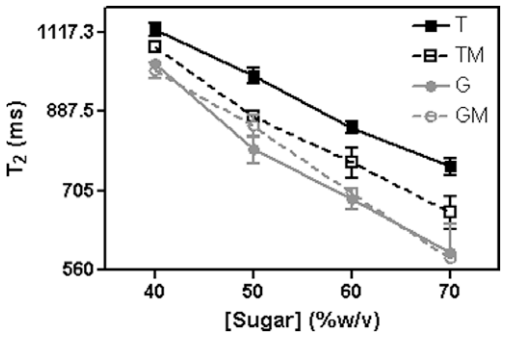

Fig. 5. ^1H NMR spin–spin relaxation times (T_2) obtained by a mono-exponential decay model, using a CPMG sequence as a function of sugar concentration for liquid systems. T, trehalose; G, glucose; M, $MgCl_2$. Bars on symbols represent the 95% confidence interval.

of the ions contained in a trehalose system has more water molecules compared to those uniformly distributed in water, which can explain the lower T_2 values obtained in the disaccharide-salt containing systems.

In the case of glucose liquid systems (Fig. 1a and b) the retarding effect of $MgCl_2$ can be attributed to sugar–salt interactions. The formation of sugar-cation complexes, which may affect the sugar availability for the reaction, has been previously reported and depends on the tautomeric forms and spatial position of the hydroxyl groups of the sugar (Angyal, 1973). It is to be noted that in trehalose systems, the reactant participating in the Maillard reaction is glucose, as in the pure glucose systems. However, in the trehalose

Table 1
Degree of trehalose crystallization (ϕ) obtained by differential scanning calorimetry for systems of different water contents (w.c., in % of dry basis) with or without $MgCl_2$.

W.C. ± 2 (% db)	ϕ (%)*	
	w.o. $MgCl_2$	with $MgCl_2$
11	38	6
24	86	61
27	88	54
32	80	35

* $\phi = \frac{\Delta H_m}{\Delta H_{mT}} * 100$; where ΔH_m is the melting enthalpy of trehalose at a given time and ΔH_{mT} is the melting enthalpy of pure trehalose (Santagapita & Buera, 2006). The relative error for ϕ (calculated for a 95% confidence interval) was about 10% of the ϕ value.

systems the reaction is accelerated by $MgCl_2$, whilst it is delayed in the glucose systems in the presence of salt. Thus, it is not an effect of the type of reactants involved in the reaction, but of the kind of water-matrix interactions: whilst in the glucose systems the water–glucose interactions were not affected by the presence of $MgCl_2$ (as shown by ^1H NMR relaxation times), in the trehalose systems a decreased relaxation time indicated lower water mobility in the presence of salt. A probable interaction between Mg^{2+} and phosphate buffer, which may cause the inhibition of Maillard reaction, has been reported (Akagawa, Miura, & Suyama, 2002) and must also be taken into account.

In other set of experiments, in the trehalose solid systems (with and without $MgCl_2$), the spin–spin ^1H NMR relaxation times were obtained by the spin-echo Hahn sequence (indicated as T_{2H}) in samples at different RVP. The T_{2H} values in samples of similar water content (between 10% and 20% db) were 25 ± 2 μs either in the presence of $MgCl_2$ or without the salt, showing no differences between them. The T_{2H} values obtained correspond to matrix and water protons displaying strong interactions with the matrix, and no changes in their mobility could be detected by the presence of $MgCl_2$. Therefore, the water–salt interactions manifested by the relaxation times from ^1H NMR in the trehalose solid systems could not explain the inhibitory effect of salts on the browning kinetics. Of the dehydrated systems, only the trehalose–$MgCl_2$ systems at RVP 84% and 97% and the trehalose systems at 97% showed a second set of T_{2H} with values higher than 1 ms, which correspond to water molecules of weak interactions with the solid matrix. It is to be noted that the effect of $MgCl_2$ in these solid systems (in which mobile water molecules were detected) was not as important on the browning kinetic constants of these systems as at lower water contents (Fig. 4).

Another effect of the salt interactions in restricted water environments could be manifested by the modification of the sugar

crystallization kinetics by $MgCl_2$. Table 1 shows that the degree of trehalose crystallization (ϕ) in solid trehalose systems containing $MgCl_2$ was lower than in samples without salt. The delay of sugar crystallization by the presence of salts in supercooled systems has been previously reported (Longinotti, Mazzobre, Buera, & Corti, 2002; Santagapita & Buera, 2008) and may be explained by dynamic water–salt–sugar interactions, which take place at a molecular level and are related to the charge/mass ratio of the cation present. An interaction/complexation between the magnesium cation and the Maillard reaction products has also been reported (O'Brien and Morrissey, 1997) and is not discarded as another factor influencing molecular mobility.

In conclusion, the Maillard reaction kinetics can be affected by the presence of salts to a different degree, depending on the type of sugar present (either acting as reactant or as part of the solid matrix) and the state of the system. Molecular and supramolecular effects of the presence of $MgCl_2$ have been observed in this work.

Due to the inhibitory effect of water on the Maillard reaction, modifications in water–solids interactions promoted by salts could be responsible for changes in the reaction rates. In liquid trehalose systems (or when mobile water protons were detected), the browning reaction is accelerated by the presence of $MgCl_2$ due to the increased sugar hydrolysis and the reduction of water mobility caused by the salt, counteracting the inhibitory effect of water on the Maillard reaction. On the other hand, in water restricted (freeze-dried) trehalose systems, $MgCl_2$ inhibited the Maillard reaction. In this case, the salt–sugar interactions, manifested by the delayed sugar crystallization, decreased the reaction rate by affecting the reactivity of reducing sugars.

Acknowledgements

This work was supported by Agencia Nacional de Promoción Científica y Tecnológica (PICT 20545), CONICET (PIP 5977) and Universidad de Buenos Aires (X024).

References

Acevedo, N., Schebor, C., & Buera, M. P. (2006). Water-solids interactions, matrix structural properties and the rate of non-enzymatic browning. *Journal of Food Engineering, 77*, 1108–1115.

Akagawa, M., Miura, T., & Suyama, K. (2002). Factors influencing the early stage of the Maillard reaction. *International Congress Series, 1245*, 196–203.

Angyal, S. J. (1973). Complex formation between sugars and metal ions. *Pure and Applied Chemistry, 35*, 131–146.

Baisier, W. M., & Labuza, T. P. (1992). Maillard browning kinetics in a liquid model system. *Journal of Agricultural and Food Chemistry, 40*, 707–713.

Bell, L. N. (1997). Maillard reaction as influenced by buffer type and concentration. *Food Chemistry, 1*, 143–147.

Bergmeyer, H. U., & Grassi, M. (1983). Reagents for enzymatic analysis: Enzyme α-glucosidase. In H. U. Bergmeyer (Ed.). *Methods of enzymatic analysis* (Vol. 2, pp. 205–206). Weinheim: Verlag Chemie Gmbh.

Burton, H. S., Mc Weeny, D. J., Pandhi, P. N., & Biltcliffe, D. O. (1962). Fluorescent compounds and non-enzymatic browning. *Nature, 98*, 948–950.

Carr, H. Y., & Purcell, E. M. (1954). Effects of diffusion on free precession in Nuclear Magnetic Resonance Experiments. *Physical Review, 94*, 630–638.

Cerruti, P., Resnik, S. L., Seldes, A., & Ferro Fontán, C. (1985). Kinetics of deteriorative reactions in food systems of high water activity: Glucose loss, 5-HMF accumulation and fluorescence development due to non-enzymatic browning. *Journal of Food Science, 50*, 627–636.

Farroni, A. E., Matiacevich, S. B., Guerrero, S., Alzamora, S. M., & Buera, M. P. (2008). A multi-level approach for the analysis of water effects in corn flakes. *Journal of Agricultural and Food Chemistry, 56*, 6447–6453.

Gökmen, V., & Şenyuva, H. Z. (2007). Acrylamide formation is prevented by divalent cations during the Maillard reaction. *Food Chemistry, 103*, 196–203.

Greenspan, L. (1977). Humidity fixed points of binary saturated aqueous solutions. *Journal of Research of the National Bureau of Standards-A. Physics and Chemistry, 81A*(1), 89–96.

Hahn, E. L. (1950). Spin echoes. *Physical Reviews, 80*, 580–594.

Kuo, M. I., Gunasekaran, S., Johnson, M., & Chen, C. (2001). Nuclear magnetic resonance study of water mobility in pasta filata and nonpasta filata mozzarella. *Journal Dairy Science, 84*, 1950–1958.

Labuza, T. P. (1994). Interpreting the complexity of the kinetics of the Maillard reaction. In T. P. Labuza, G. A. Reineccius, V. M. Monnier, J. ÓBrien & J. W. Baynes (Eds.), Maillard reactions in chemistry, food and health, The Royal Society of Chemistry (pp. 176–181). Cambridge.

Lakowicz, J. R. (1999). Instrumentation for fluorescence spectroscopy. In J. R. Lakowicz (Ed.), *Principles of fluorescence spectroscopy* (2nd ed., pp. 25–61). New York: Kluwer Academic/Plenum Publishers.

Lester, M. R. (1995). Sulfite sensitivity: Significance in human health. *Journal of the American College of Nutrition, 14*(3), 229–232.

Longinotti, M. P., Mazzobre, M. F., Buera, M. P., & Corti, H. R. (2002). Effect of salts on the properties of aqueous sugar systems, in relation to biomaterial stabilization. 2. Sugar crystallization rate and electrical conductivity behaviour. *Physical Chemistry-Chemical Physics., 4*, 533–540.

Matiacevich, S. B., Santagapita, P. R., & Buera, M. P. (2005). Fluorescence from the Maillard reaction and its potential application in food science. *Critical Reviews in Food Science & Nutrition, 45*, 483–495.

Matiacevich, S. B., & Buera, M. P. (2006). A critical evaluation of fluorescence as a potential marker for the Maillard reaction. *Food Chemistry, 95*, 423–430.

Mazzobre, M. F., Longinotti, M. P., Corti, H. R., & Buera, M. P. (2001). Effect of salt on the properties of aqueous sugar systems, in relation to biomaterial stabilization. 1. Water sorption behaviour and ice crystallization/melting. *Cryobiology, 43*(3), 199–210.

Meiboom, S., & Gill, D. (1958). Modified spin-echo method for measuring nuclear magnetic relaxation times. *The Review of Scientific Instruments, 29*, 688–691.

Miller, D. P., & de Pablo, J. J. (2000). Calorimetric solution properties of simple saccharides and their significance for the stabilization of biological structure and function. *Journal of Physical Chemistry B, 104*, 8876–8883.

Morel-Desrosier, N., Lhermet, C., & Morel, J. P. (1991). Interaction between cations and sugars. Part 6. Calorimetric method for simultaneous determination of the stability constant and enthalpy change for weak complexation. *Journal of the Chemical Society, Faraday Transactions, 87*, 2173–2177.

O'Brien, J., & Morrissey, P. A. (1997). Metal ion complexation by products of the Maillard reaction. *Food Chemistry, 58*, 17–27.

Petriella, C., Chirife, J., Resnik, S., & Lozano, R. (1988). A research note: Solute effects at high water activity on nonenzymatic browning of glucose–lysine solutions. *Journal of Food Science, 53*, 987–988.

Santagapita, P. R., & Buera, M. P. (2006). Chemical and physical stability of disaccharides as affected by the presence of $MgCl_2$. In M. P. Buera, J. Welti-Chanes, P. J. Lillford, & H. R. Corti (Eds.). *Water properties of food, pharmaceutical, and biological materials* (Vol. 9, pp. 663–669). CRC Press-Taylor and Francis.

Santagapita, P. R., & Buera, M. P. (2008). Electrolyte effects on amorphous and supercooled sugar systems. *Journal of Non-Crystalline Solids, 354*, 1760–1767.

Santagapita, P. R., Matiacevich, S. B., & Buera, M. P. (in press). Non-enzymatic browning may be inhibited or accelerated by $MgCl_2$ according to the level of water availability and saccharide specific interactions. In D. Reid & T. Sajjaanantakul (Eds.), Water properties in food, health, pharmaceutical and biological systems: ISOPOW 10 (Vol. 10). John Wiley & Sons Inc.

Schebor, C., Burin, L., Buera, M. P., & Chirife, J. (1999). Stability of hydrolysis and browning of trehalose, sucrose and raffinose in low-moisture systems in relation to their use as protectants of dried biomaterials. *Lebensmittel-Wissenschaft und-Technologie, 32*, 481–485.

Schmidt, S. J. (2007). Water mobility in foods. In G. V. Barbosa-Cánovas, A. J. Fontana, S. J. Schmidt, & T. P. Labuza (Eds.), *Water activity in foods: Fundamentals and applications* (pp. 47–108). Ames, IA: Blackwell Publishing.

Food Chemistry 118 (2010) 109–115

Contents lists available at ScienceDirect

Food Chemistry

journal homepage: www.elsevier.com/locate/foodchem

Effect of cultivar and environment on physicochemical and cooking characteristics of field pea (*Pisum sativum*) ☆

Ning Wang [a,*], David W. Hatcher [a], Thomas D. Warkentin [b], Ruth Toews [a]

[a] Canadian Grain Commission, Grain Research Laboratory, 1404-303 Main Street, Winnipeg, MB, Canada R3C 3G8
[b] Crop Development Centre, University of Saskatchewan, 51 Campus Drive, Saskatoon, SK, Canada S7N 5A8

ARTICLE INFO

Article history:
Received 29 October 2008
Accepted 23 April 2009

Keywords:
Field pea
Cooking time
Physico-chemical characteristics
Cultivar, growing location

ABSTRACT

The effects of cultivar, growing location and year on physicochemical and cooking characteristics of field pea (*Pisum sativum*) were investigated and the relationship between these characteristics was determined. Six diverse field pea cultivars were grown in five different growing locations for two subsequent years (2006 and 2007). Cultivar, location and year had a significant effect on the seed weight, seed size, water hydration capacity, cooking time and firmness of cooked peas. Significant cultivar and location differences in protein, starch, crude fibre, fat, ash and phytic acid contents of peas were observed. Most of the traits were significantly affected by the interactions: cultivar-by-location, cultivar-by-year and location-by-year. Both seed weight and seed size were negatively correlated with crude protein and crude fibre contents. Cooking time was negatively correlated with crude fibre, ash and phytic acid contents, but positively correlated with firmness and starch content. A significant positive correlation was observed between ash content and phytic acid level in peas.

1. Introduction

Pulses, including pea (*Pisum sativum*), play an important role in the diet of most of the people in the world because of their nutritive value. Pulses are consumed after cooking, both in the form of whole seed and decorticated splits in various types of food. Cooking time is one of the most important quality–determining processes for field peas for human consumption (Moscoso, Bourne, & Hood, 1984). One of the constraints in the utilisation of pulses is their long cooking time. Reduction in the nutritive value of the proteins, due to excessive cooking of pulses, has been reported (Walker & Kochhar, 1982). Apart from cooking time, cooked texture is also an important cooking quality characteristic for pulses. Cooking is required to render pulses edible and to ensure acceptable sensory quality (Bourne, 1982). Cooking causes some physicochemical changes in pulses, including gelatinization of starch, denaturation of proteins, solubilisation of some of the polysaccharides, and softening and breakdown of the middle lamella, a cementing material found in the cotyledon (Stanley & Aguilera, 1985; Vindiola, Seib, & Hoseney, 1986). Cooking also inactivates or reduces the levels of anti-nutrients such as trypsin inhibitors and flatulence-causing oligosaccharides, resulting in improved nutritional quality (Ayyagari, Rao, & Roy, 1989; Jood, Mehta, Singh, & Bhat, 1985; Wang, Hatcher, & Gawalko, 2008; Wang, Lewis, Brennan, & Westby, 1997).

Factors affecting cooking quality of pulses include cultivar, seed characteristics, composition of seeds, growing location and environment (Bishnoi & Khetarpaul, 1993; Gubbels & Ali-Khan, 1991; Gubbels, Chubey, Ali-Khan, & Stauvers, 1985; Stanley & Aguilera, 1985). Physical properties, such as size and weight, as well as seed coat and cotyledon characteristics, influence pulse cooking quality (Sefa-Dedeh & Stanley, 1979a). Pulses are generally soaked before cooking, to ensure uniform expansion of the seed coat and cotyledon for uniform cooking and to ensure their tenderness (Hoff & Nelson, 1965). The ability of seeds to hydrate has been linked to cooking quality. Bishnoi and Khetarpaul (1993) found that higher hydration capacity of peas was associated with shorter cooking time. The texture of cooked cowpeas (*Vigna unguiculata*) showed a negative correlation with the amount of water absorbed (Sefa-Dedeh, Stanley, & Voisey, 1978). Sefa-Dedeh and Stanley (1979b) reported that seed thickness and hilum size of cowpeas influenced water absorption during the initial stage of soaking whilst protein content became an important factor affecting water absorption in the later stages of soaking. Cooking brings about a number of changes in chemical composition of peas (Wang et al., 2008). However, little information is available on how cultivar and growing location affect the cooking quality attributes of field pea.

Variation in chemical composition in pulses might be due either to intrinsic factors (mainly genetic) or to extrinsic factors, such as storage, type of soil, agronomic practices (such as plant density, weeds, or soil fertility), climatic factors (such as rainfall, light

☆ Paper 1012 of the Grain Research Laboratory, Canadian Grain Commission, Winnipeg, MB, Canada R3C 3G8.

* Corresponding author. Tel.: +1 204 983 2154; fax: +1 204 983 0724.
E-mail address: ning.wang@grainscanada.gc.ca (N. Wang).

0308-8146/$ - see front matter Crown Copyright © 2009 Published by Elsevier Ltd. All rights reserved.
doi:10.1016/j.foodchem.2009.04.082

intensity, length of growing season, length of day or temperature (Eppendorfer & Bille, 1974; Holl & Vose, 1980; McLean, Sosulski, & Youngs, 1974; Nikolopoulou, Grigorakis, Stasini, Alexis, & Iliadis, 2006, 2007; Singh, Campbell, & Salunkhe, 1972) and technological treatments (Babiker, Elsheikh, Osman, & El Tinay, 1995; McLean et al., 1974). Data on the chemical composition and nutritive values of field pea have been reported (Davies, 1984; Petterson, Sipsas, & Mackintosh, 1997; Wang & Daun, 2004). However, information on the relationships amongst physical, cooking and chemical characteristics of peas is not readily available. This study aimed to investigate how cultivar, growing location and year affect the physicochemical and cooking characteristics of field peas, and to determine the relationships between these characteristics.

2. Materials and methods

2.1. Materials

Six registered field pea cultivars (CDC Striker, Cooper, Cutlass, Eclipse, SW Marquee and SW Sergeant) were grown over two seasons (2006 and 2007) at five locations (Indian Head, Melfort, Rosthern, Saskatoon and Swift Current) in Saskatchewan, Canada, in a randomized complete block design as part of the provincial regional variety trials. The cultivars chosen are commonly grown in western Canada (Saskatchewan Crop Insurance Corporation, personal communication). CDC Striker (Warkentin, Vandenberg, Banniza, & Slinkard, 2004) was developed by the Crop Development Centre (CDC), University of Saskatchewan; Cutlass (Blade, Warkentin, & Vandenberg, 2004) was jointly developed by the CDC and Alberta Agriculture; Cooper and Eclipse were developed by Cebeco Zaden, The Netherlands, and SW Marquee and SW Sergeant were developed by Svalof-Weibull, Sweden. Cutlass, Eclipse and SW Marquee have yellow cotyledons, whilst CDC Striker, Cooper and SW Sergeant have green cotyledons.

Growing season weather conditions at the five sites of the 2006 and 2007 Saskatchewan regional field pea variety trials are shown in Table 1. The Swift Current site was relatively warm and dry; the Indian Head site was relatively dry, whilst the Rosthern site was the wettest.

Broken and damaged seeds and foreign material were handpicked from the samples before testing commenced. Seed samples were ground into flour using an Udy grinder with a 0.5 mm sieve and stored at 4 °C in sealed plastic bags prior to further analysis.

2.2. Physical tests

Seed weight was determined according to the AACC method 56-35 (AACC, 2000) by counting one hundred seeds using a custom-made counting board and weighing. Results were expressed as means of duplicate determinations. Water hydration capacity was determined by soaking the 100-seed weight samples in deionized water at a ratio of 1:4 (sample weight:water weight) at room temperature for 16 h in accordance with the method AACC 56-35 (AACC, 2000). After the water was drained, the soaked seeds were blotted dry with a paper towel and weighed. Hydration capacity was expressed as the amount of water absorbed per kg of seeds (g H_2O/kg seeds) after soaking for 16 h. The mean diameter of pea seeds was determined using the image analysis technique of Shahin and Symons (2001).

2.3. Cooking quality

Cooking time of each pea sample was determined using an automated Mattson Cooker (Wang & Daun, 2005), which consists of 25 plungers, a cooking rack with 25 reservoir-like perforated saddles, a sensor assembly, which mounts on top of the cooking rack, an interface box, an input/output card and a computer. Each plunger was calibrated to a weight of 90 g by adjusting the lead buckshot inside each plunger. A pea sample (50 g) was soaked in distiled water at a ratio of 1:4 (seed:water, w/w) for 24 h at room temperature. Twenty-five soaked seeds were randomly selected and then positioned into each of the 25 saddles of the cooking rack so that the tip of each plunger rested on top of the soaked seed. The rack was then placed into a 2 l metal beaker containing 1.2 l of boiling water, which was placed on a hotplate. When a seed became sufficiently tender, the plunger penetrated the seed and dropped through the hole in the saddle. The time when each plunger dropped was recorded through a windows-based programme. The optimum cooking time was assigned when 80% of the seeds were cooked. The cooking time in minutes was determined as an average of triplicate determinations.

The firmness of cooked peas was measured with a TA-HDi texture analyzer (Texture Technologies Corp., Scarsdale, NY). A pea sample (50 g) was soaked in 300 ml of distiled water at room temperature for 24 h. After draining the water, the soaked sample was cooked in 1.0 l distiled water in a 2 l metal beaker placed on a hotplate for its predetermined cooking time, as described above. The cooked peas were drained for 15 s with a strainer and then the strainer was placed in a plastic container containing 700 ml of distiled water (20 ± 2 °C) for 30 s. The cooked seeds were drained and then transferred to another plastic container holding 700 ml of distiled water (20 ± 2 °C) for an additional 90 s to cool the cooked seeds to room temperature. The cooked seeds were then drained and transferred to a thermos flask, 250 ml capacity (Thermos L.L.C. Corp. Headquarters, Rolling Meadows, Illinois, USA), to keep the seeds at room temperature. Approximately 9.0 ± 0.5 g of cooked peas were loaded onto a TA-91 Kramer Shear Cell holder (Texture Technologies Corp., Scarsdale, NY). The TA-91 Kramer Shear Cell was attached to a load cell of 250 kg capacity. System parameters were: (a) arm speed prior to sample contact, 2.0 mm/s, (b) arm speed during compression of the sample, 1.5 mm/s, and (c) arm speed during

Table 1
Summary of growing season (May–August) mean temperature and total precipitation at five sites of the 2006 and 2007 Saskatchewan regional field pea variety trials[A].

Location	Soil zone	Year	Mean temperature (°C)	Total precipitation (mm)
Swift Current	Brown	2006	17.2	184
		2007	16.9	122
Saskatoon	Dark Brown	2006	16.5	210
		2007	16.6	274
Melfort	Black	2006	15.8	221
		2007	14.7	259
Rosthern	Black	2006	15.8	320
		2007	15.0	346
Indian Head	Black	2006	15.6	135
		2007	15.0	206

[A] Data source: based on the Environment Canada reporting site nearest to the field pea regional variety trial site.

retraction, 2.0 mm/s. The maximum shear force measured was recorded. The firmness of the cooked peas was defined as the maximum force required to shear the cooked peas and expressed as the maximum shear force per gram of cooked sample (N/g cooked sample). Values reported were averages of six determinations.

2.4. Chemical analysis

Nitrogen (N) was determined by the Dumas combustion method using a Leco FP-528 combustion nitrogen analyzer (Leco Corp. St. Joseph, MI, USA) calibrated with EDTA (AOAC, 2000). Crude protein content was calculated using N × 6.25. Moisture and ash contents were determined gravimetrically in accordance with AACC methods 44-17 and 08-16, respectively, (AACC, 2000). Starch content was determined colorimetrically as described by the method AACC 76-13 (AACC, 2000). Fat content was determined gravimetrically by hot extraction of the ground sample with petroleum ether for 2 h on a Soxtec extraction unit (Foss-Tecator, Höganäs, Sweden) (AOCS, 1998). Crude fibre (CF) was determined as described by the method of Ankom Technology (Ankom Technology, 1998) using the ANKOM^{2000} Fibre Analyzer (Ankom Technology, Macedon, NY).

Phytic acid was extracted and separated by ion-exchange chromatography, according to the method of AOAC (2000), before being quantified colorimetrically using an Ultrospec 3000 spectrophotometer (Biochrom Ltd., Cambridge, England) at 500 nm (Latta & Eskin, 1980). One gram of ground pea sample was extracted with 20 ml of 0.65 M HCl for 2 h at room temperature on a rotary shaker. The extract was centrifuged (3500 × *g*) at room temperature for 20 min and the supernatant was decanted. A 3 ml aliquot of the supernatant was diluted to 25 ml with deionized water. Diluted sample extract (10 ml) was passed through a column (7 × 150 mm) (Bio-Rad Laboratories, Inc., Hercules, CA) packed with 100–200 mesh AG1-X4 chloride anion-exchange resin (Bio-Rad Laboratories, Inc., Hercules, CA). Inorganic phosphorus was eluted with 15 ml 0.1 M NaCl, followed by elution of phytate with 0.7 M NaCl. The phytate content was measured colorimetrically at 500 nm, using the Wade reagent (0.03% $FeCl_3 \cdot 6H_2O$ and 0.3% sulfosalicylic acid in deionized water).

2.5. Statistical analysis

All statistical analyses were conducted using the SAS (v.9.1.3, SAS Institute, Cary, NC). The analysis of variance (ANOVA) for the main effects (cultivar, growing location and year) and interactions were determined using the GLM procedure. The Duncan multiple range test was used to separate means and significance was accepted at $p < 0.05$. The different parameters were correlated with each other by Pearson two-tailed significance correlation.

3. Results and discussion

3.1. Physical and cooking characteristics

A significant ($p < 0.001$) effect of cultivar, growing location and year on the physical characteristics of field peas was found (Table 2). Interaction of cultivar-by-location, cultivar-by-year and location-by-year also significantly affected 100-seed weight, seed size and water hydration capacity. Seed weights ranged from 16.6 to 31.7 g per 100 seeds whilst mean seed sizes varied from 6.1 to 7.5 mm (Table 3). Cultivar Cooper had the highest seed weight (26.8 g per 100 seeds) and the largest seed size (7.1 mm). The lowest seed weight and the smallest mean seed size were observed for cultivars SW Marquee and SW Sergeant. Pea samples from Indian Head, Melfort and Rosthern had significantly ($p < 0.05$) higher seed weight and larger seed size than had those from Saskatoon and Swift Current (Table 4). Results from the present study confirmed results of Singh, Erskine, Robertson, Nakkoul, and Williams (1988) who reported that seed size was a cultivar characteristic and was influenced by the environmental conditions. Water hydration capacity ranged from 936.0 to 1316.6 (g H_2O/kg seeds) (Table 3). Cultivar SW Marquee had the highest water hydration capacity whereas CDC Striker exhibited the lowest. Significantly ($p < 0.05$) higher water hydration capacity values were observed in peas from Swift Current than in those from other growing locations (Table 4). Peas grown in the 2006 season had significantly ($p < 0.05$) higher mean seed weights and larger mean seed sizes but had significantly ($p < 0.05$) lower mean water hydration capacities than in the 2007 season (Table 4).

Cultivar, growing location and year significantly affected cooking time and firmness of cooked pea samples (Table 2). Cultivar-by-location showed a significant effect on cooking time ($p < 0.001$) and firmness ($p < 0.01$) (Table 2). Cultivar-by-year had a significant effect on firmness ($p < 0.05$), but had no effect on cooking time. Location-by-year showed a significant effect on cooking time ($p < 0.001$), but no effect on firmness was observed. Cooking time and firmness varied from 6.2 to 33.5 min and 14.5 to 31.3 N/g seed, respectively, (Table 3). The cultivar Eclipse had the longest cooking time, whereas CDC Striker and SW Marquee exhibited the shortest (Table 3). Shorter cooking time is important from the point of view of convenience and nutritional value. Prolonged cooking of pulses has been reported to increase the percentage of leached solids, to destroy heat-labile vitamins and to decrease the protein quality of cooked product (Walker & Kochhar, 1982). Cultivars Eclipse and SW Sergeant had significantly ($p < 0.05$) higher firmness value than had the other cultivars (Table 3). Pea samples from Melfort and Swift Current had significantly ($p < 0.05$) longer cooking time and firmer texture than had those from Indian, Rosthern and Saskatoon (Table 3). Pea samples from 2006 exhibited significantly ($p < 0.05$) longer cooking time and firmer texture than did those from 2007 (Table 4).

3.2. Chemical composition

Analysis of variance showed a strong cultivar, growing location and year effect on crude protein, starch, crude fibre, fat, ash, and phytic acid contents (Table 2). Crude protein content (N × 6.25) varied from 213 to 284 g/kg dry matter with a mean of 248 g/kg dry matter (Table 3), in accordance with values previously reported (Black, Singh, & Meares, 1998; Owusuh-Ansah & McCurdy, 1991; Wang & Daun, 2004). The wide variations in protein content were due to a combination of genetic and environmental factors (growing location and year), confirming the findings reported previously (Nikolopoulou et al., 2007; Reichert & MacKenzie, 1982; Vidal-Valverde et al., 2003). Cultivar CDC Striker had the highest mean protein content whereas Cutlass had the lowest (Table 3). The highest protein level of the pea cultivars was observed at the location in Swift Current (Table 4). Starch content ranged from 433 to 496 g/kg dry matter, which was within the range reported by Borowska, Zadernowski, and Konopka (1996) and Wang and Daun (2004). Cooper and Cutlass had the highest starch contents, whilst CDC Striker had the lowest (Table 3). Pea samples from Melfort had the highest starch content, whereas pea samples from Indian Head and Swift Current had the lowest (Table 4). Peas grown in 2006 had significantly ($p < 0.05$) higher starch contents than those grown in 2007. Crude fibre content varied from 43.4 to 62.2 g/kg dry matter with a mean of 52.4 g/kg dry matter (Table 2). CDC Striker and SW Sergeant had the highest crude fibre contents, whereas Cooper had the lowest (Table 3). Pea samples from Rosthern and Saskatoon had significantly ($p < 0.05$) higher crude fibre content than had those from the other locations

Table 2
Analysis of variance of the effect of cultivar, location and year on physicochemical and cooking characteristics of field peas.

	Cultivar (C)	Location (L)	Year (Y)	C x L	C × Y	L × Y	G × L × Y
Physical characteristics							
100 seed weight (g)	***	***	***	**	***	***	***
Seed size (mm)	***	***	***	***	***	***	***
WHC[A] (g H_2O/kg seed)	***	***	***	***	**	***	**
Cooking time (min)	***	***	***	***	–	***	–
Firmness (N/g seed)	***	***	**	**	*	–	–
Composition (g/kg dry matter)							
Protein (N × 6.25)	**	***	*	***	***	***	**
Starch	***	***	**	*	*	***	–
Crude fibre	***	***	*	–	***	***	–
Fat	***	***	*	**	***	***	–
Ash	***	***	***	–	***	***	–
Phytic acid	**	***	***	–	**	***	*

***, **, * = significant at $p < 0.001$, $p < 0.01$, and $p < 0.05$, respectively.
– Blank spaces indicate no significance.
[A] WHC = water hydration capacity (g H_2O/kg seed).

Table 3
Mean values of physicochemical and cooking characteristics of six field pea cultivars grown in 2006 and 2007.

	Cultivar mean[C]							
	CDC Striker $n = 20$	Cooper $n = 20$	Cutlass $n = 20$	Eclipse $n = 20$	SW Marquee $n = 20$	SW Sergeant $n = 20$	Mean[D] $n = 120$	Range[D] $n = 120$
Physical characteristics								
100 seed weight (g)	22.6c[B]	26.8a	21.2d	23.2b	19.6e	19.8e	22.2	16.6–31.7
Seed size (mm)	6.7c	7.1a	6.5d	6.8b	6.4e	6.4e	6.7	6.1–7.5
WHC[A] (g H_2O/kg seed)	1040.5e	1139.2b	1063.7d	1066.4d	1183.6a	1088.3c	1096.9	936.0–1316.6
Cooking time (min)	11.0d	13.5c	15.9b	21.7a	9.6d	14.4c	14.3	6.2–33.5
Firmness (N/g seed)	18.4c	16.6e	19.1b	20.4a	17.4d	20.0a	18.6	14.5–31.3
Composition (g/kg dry matter)								
Protein (N × 6.25)	263a	242c	239d	249b	248b	245c	248	213–284
Starch	456c	476a	474a	472ab	472ab	470b	470	433– 496
Crude fibre	55.9a	48.5d	52.9b	49.7c	50.7c	56.7a	52.4	43.4–62.2
Fat	9.6b	8.5d	9.2c	8.1e	8.0e	10.1a	8.9	6.7–11.7
Ash	25.7d	27.4abc	27.9a	27.3bc	27.6ab	27.0c	27.2	23.0–31.3
Phytic acid	7.8 cd	8.8a	7.5d	8.2bc	8.4ab	7.8cd	8.1	4.2–11.9

[A] WHC = water hydration capacity (g H_2O/kg seed).
[B] Means within a row with the same letter are not significantly different ($p > 0.05$) as determined using Duncan's multiple range test.
[C] n = number of samples for each cultivar (5 sites × 2 years × 2 duplicates = 20).
[D] n = number of samples (6 cultivars × 5 sites × 2 years × 2 duplicates = 120).

Table 4
Physicochemical and cooking characteristics of field pea cultivars grown in different locations over two years.

	Location mean[C]					Year mean[D]	
	Indian Head $n = 24$	Melfort $n = 24$	Rosthern $n = 24$	Saskatoon $n = 24$	Swift Current $n = 24$	2006 $n = 60$	2007 $n = 60$
Physical characteristics							
100 seed weight (g)	22.8a[B]	23.1a	23.0a	21.4b	20.6c	22.5a	21.9b
Seed size (mm)	6.7b	6.7b	6.8a	6.6c	6.5d	6.7a	6.6b
WHC[A] (g H_2O/kg seed)	1072.0c	1103.5b	1079.3c	1095.1b	1134.5a	1087.9b	1106.0a
Cooking time (min)	11.6b	18.1a	12.6b	11.0b	18.4a	15.6a	13.1b
Firmness (N/g seed)	17.8b	19.8a	17.6b	18.4b	19.6a	19.2a	18.1b
Composition (g/kg dry matter)							
Protein (N × 6.25)	253b	240c	241c	242c	262a	247b	248a
Starch	467c	474a	472ab	470b	467c	471a	468b
Crude fibre	51.5b	51.3b	54.0a	53.9a	51.4b	52.7a	52.1b
Fat	8.6c	9.4a	9.1b	9.2b	8.4c	9.0a	8.8b
Ash	28.6a	25.9c	28.1b	28.2b	25.0d	26.5b	27.8a
Phytic acid	9.6a	6.7c	9.2b	8.9b	6.1d	7.4b	8.8a

[A] WHC = water hydration capacity (g H_2O/kg seed).
[B] Means within a row with the same letter are not significantly different ($p > 0.05$) as determined using Duncan's multiple range test.
[C] n = number of samples at each site (6 cultivars × 2 years × 2 duplicates = 24).
[D] n = number of samples for each year (6 cultivars × 5 sites × 2 duplicates = 60).

(Table 4). Crude fat content was in the range of 6.7–11.7 g/kg dry matter and ash content varied from 23.0 to 31.3 g/kg dry matter. SW Sergeant had the highest fat content (Table 3). Copper, Cutlass and SW Marquee had significantly ($p < 0.05$) higher ash content than had the other cultivars. Pea samples from Melfort had the highest mean fat content whilst samples from Indian Head had

the highest ash content (Table 4). Both fat and ash values in this study were in agreement with data reported (Nikolopoulou et al., 2007; Petterson et al., 1997; Wang & Daun, 2004). Phytic acid level ranged from 4.2 to 11.9 g/kg dry matter with a mean value of 8.1 g/kg dry matter (Table 3), which was comparable with that reported for peas, lentils and beans (Bhatty & Slinkard, 1989; Lolas & Markakis, 1975; Wang & Daun, 2004). Cooper showed the highest mean phytic acid level. Pea samples from Indian Head had the highest phytic acid content, whereas samples from Swift Current had the lowest. Higher phytic acid content could be attributed to higher soil phosphorus (P) content, since the major portion of total P in plant tissues is stored in the form of phytate (Ravindran, Ravindran, & Sivalogan, 1994). Higher phytic acid levels, due to higher P content in the soil of the cultivation area, have been observed for chickpeas (Nikolopoulou et al., 2006). Peas grown in 2006 had significantly ($p < 0.05$) higher crude fibre and fat contents but had significant ($p < 0.05$) lower ash and phytic acid contents than those grown in 2007 (Table 4).

3.3. Relationships between various characteristics

Seed weight had a significant positive correlation with seed size ($r = 0.95$, $p < 0.001$), which is expected (Table 5). Both seed weight and seed size were negatively correlated with protein ($p < 0.05$) and crude fibre contents ($p < 0.05$), indicating that smaller size seeds had higher protein and higher fibre contents than had larger size seeds. Seed size showed a significant negative correlation with fat content ($p < 0.05$). No correlations between seed weight/size and water hydration capacity were observed in this study. By contrast, Williams, Nakoul, and Singh (1983) and Singh, Williams, and Nakoul (1990) reported a positive correlation between seed size and water hydration capacity. Generally, the water absorption patterns of peas were characterised by rapid water uptake at initial soaking times (data not shown), after which the rate of water absorption slowed and reached a saturation level. In the present study, water hydration capacity was determined at 16 h of soaking when peas reached saturation level. Sefa-Dedeh and Stanley (1979b) reported that characteristics of seed coat and cotyledon structures for pulses were important factors affecting water absorption rate at initial stages of soaking. With increasing soaking time and consequent hydration of the seed coat, this structure no longer exerted an important influence on water absorption and other factors, such as intrinsic properties of the cotyledon components, the cotyledon structure and growing conditions, became important. It was observed that water hydration capacity was negatively correlated with crude fibre ($p < 0.001$) and fat contents ($p < 0.001$) (Table 5).

Cooking time was positively correlated with firmness of cooked peas ($p < 0.001$). A similar result for dry beans was reported by Deshpande and Cheryan (1986). Cooking time had no correlations with seed weight, seed size or water hydration capacity (Table 5). However, Black et al. (1998) reported that seed weight had a positive correlation with cooking time of peas. Cooking time was negatively correlated with crude fibre ($p < 0.05$) and ash ($p < 0.001$) but positively correlated with starch content ($p < 0.01$) (Table 5). Our results suggest that the composition of the cultivar and growing conditions play important roles in influencing cooking time. A significant negative correlation between cooking time and phytic acid content ($r = -0.61$, $p < 0.001$) was observed. This was in agreement with the results reported by other researchers (Stanley & Aguilera, 1985; Vindiola et al., 1986). It has been postulated that phytic acid chelates divalent cations (Ca^{2+}, Mg^{2+}) and prevents their binding to pectin in the cell wall for the formation of the insoluble calcium and magnesium pectates, thereby facilitating cell wall dissolution during the cooking process. In peas, grown under field conditions, the critical level of phytic acid sufficient to bind the divalent cations is not known. Nevertheless, reductions in phytic acid content of pea may increase its cooking time. Phytic acid has been implicated in reducing the availability of essential minerals, and possibly the utilisation of protein due to formation of phytate–mineral and phytate–protein complexes (Reddy, Sathe, & Pierson, 1988). However, phytic acid seems to have a beneficial role in reducing cooking time of pulses.

Firmness of cooked seeds was negatively correlated with seed weight ($p < 0.05$), seed size ($p < 0.05$) and water hydration capacity ($p < 0.05$), confirming the results reported by Wang, Daun, and Malcolmson (2003). However, Black et al. (1998) reported that firmness had a positive correlation with seed weight. Wang et al. (2003) reported that firmness is a function of both seed coat and cotyledon properties. They found that small size peas, having a greater surface to volume ratio than large size peas, had a greater proportion of seed coat to cotyledon, resulting in higher firmness value. Firmness also had a significant negative correlation with fat ($p < 0.05$), ash ($p < 0.001$) and phytic acid ($p < 0.001$) contents. It has been reported that softening of pulses during cooking was accompanied by structural changes in the seed, primarily breakdown of the middle lamella, leading to the easy separation of cells (Sefa-Dedeh et al., 1978; Vindiola et al., 1986). Other changes reported include the gelatinization of starch and the consequent deformation of the spherical granules. Differences in the gelatinization pattern of the starch and the susceptibility of the cell constituents (notably the protein matrix) to softening, may also contribute to the overall texture of the cooked seed.

Table 5
Correlation coefficients amongst physical characteristics and chemical composition of field peas ($n = 120$)[A].

Attribute	SW	SS	WHC	CT	FIRM	Protein	Starch	CF	Fat	Ash	PA
100 seed weight (SW)	1.00										
Seed size (SS)	0.95***	1.00									
WHC[B]	–	–	1.00								
Cooking time (CT)	–	–	–	1.00							
Firmness (FIRM)	−0.29**	−0.29**	−0.28**	0.48***	1.00						
Protein	−0.19*	−0.18*	–	–	–	1.00					
Starch	–	–	–	0.28**	–	−0.74***	1.00				
Crude fibre (CF)	−0.37***	−0.41***	−0.36***	−0.18*	–	–	−0.20*	1.00			
Fat	–	−0.18*	−0.41***	–	−0.23*	−0.34***	–	0.51***	1.00		
Ash	–	–	–	−0.49***	−0.39***	−0.32**	–	–	–	1.00	
Phytic acid (PA)	0.18*	0.20*	–	−0.61***	−0.48***	0.43***	–	–	–	0.88***	1.00

***, **, * = significant at $p < 0.001$, $p < 0.01$, and $p < 0.05$, respectively.
– Blank spaces indicate no significance.
[A] n = number of samples (6 cultivars × 5 sites × 2 years × 2 duplicates = 120).
[B] WHC = water hydration capacity (g H_2O/kg seed).

Protein content was negatively correlated with the starch content ($p < 0.001$) (Table 5), which is expected, since these two constituents form the bulk of the composition of pea seeds in reverse proportions. Similar significant correlations have been reported by others (Black et al., 1998; Wang & Daun, 2004). Protein content was also negatively correlated with fat ($p < 0.001$) and ash contents ($p < 0.01$) but positively correlated with phytic acid ($p < 0.001$). Crude fibre had a significant ($p < 0.001$) positive correlation with fat content. Ash content was positively correlated with phytic content ($r = 0.88$, $p < 0.001$), confirming the findings reported by Wang and Daun (2004).

4. Conclusions

Significant effects of cultivar, growing location and year were detected on the physical, chemical and cooking characteristics of diverse pea cultivars over two seasons at five locations in Saskatchewan, Canada. Significant cultivar-by-location interactions were noted for all quality parameters except crude fibre, ash and phytic acid contents. There were significant interactive effects of cultivar-by-year on all quality parameters except cooking time. Significant location-by-year interactions were also observed for all quality parameters, except firmness, of cooked peas. These findings indicated that selection of a field pea cultivar with required quality characteristics must take into consideration, not only the genetic factors, but also the environmental parameters, namely climate conditions and growing locations during the growing season.

Protein content was negatively correlated with starch, fat and ash contents but positively correlated with phytic acid. A significant positive correlation between ash and phytic acid contents was noted. Seed weight and seed size were negatively correlated with protein and crude fibre contents. There was a negative correlation between water hydration capacity and crude fibre contents. Cooking time was positively correlated with starch content, but negatively correlated with crude fibre, ash and phytic acid contents. Firmness of cooked seeds was positively correlated with cooking time, but negatively correlated with fat, ash, phytic acid content, seed weight, seed size and water hydration capacity. Our results suggest that the physical characteristics and chemical composition of peas played important roles in influencing cooking characteristics (cooking time and texture). Phytic acid content in peas had a beneficial role in reducing cooking time of peas. Knowledge of how cultivar and environment influence quality traits of field peas, and the variation in physicochemical and cooking characteristics of different cultivars will be useful for breeders in efforts to improve the quality of peas.

Acknowledgements

We gratefully acknowledge the technical assistance of L. Maximiuk and D. Shaluk of the Canadian Grain Commission, Grain Research Laboratory. We are also grateful to Pulse Canada for partially funding this project.

References

AACC (2000). *Approved methods of the AACC international. Methods 44-15A, 56-35, 76-13, and 08-16* (10th ed.). St. Paul, MN: The Association.

Ankom Technology, (1998). Method for determining crude fibre (CF).

AOAC (2000). *Official methods of analysis of AOAC international* (17th ed.). Washington, DC: Association of Official Analytical Chemists.

AOCS, (1998). Determination of oil content in oilseeds, AOCS Am 2-93.

Ayyagari, R., Rao, B. S., & Roy, D. N. (1989). Lectins, trypsin inhibitors, BOAA and tannins in legumes and cereals and the effects of processing. *Food Chemistry, 34*, 229–238.

Babiker, E. E., Elsheikh, E. A. E., Osman, A. G., & El Tinay, A. H. (1995). Effect of nitrogen fixation, N-fertilization and viral infection on yield, tannin and protein contents and in vitro protein digestibility of faba bean. *Plant Foods Human Nutrition, 47*, 257–263.

Bhatty, R. S., & Slinkard, A. E. (1989). Relationship between phytic acid and cooking quality in lentil. *Canadian Institute Food Science and Technology Journal, 22*, 137–142.

Bishnoi, S., & Khetarpaul, N. (1993). Variability in physicochemical properties and nutrient composition of different pea cultivars. *Food Chemistry, 47*, 371–373.

Black, R. G., Singh, U., & Meares, C. (1998). Effect of genootype and pretreatment of field peas (*Pisum sativum*) on their dehulling and cooking quality. *Journal of the Science of Food and Agriculture, 77*, 251–258.

Blade, S., Warkentin, T. D., & Vandenberg, A. (2004). Cutlass field pea. *Canadian Journal of Plant Science, 84*, 533–534.

Borowska, J., Zadernowski, R., & Konopka, I. (1996). Composition and some physical properties of different pea cultivars. *Nahrung, 40*(2), 74–78.

Bourne, M. C. (1982). *Food texture and viscosity: Concept and measurement*. New York: Academic Press Inc.

Davies, R. L. (1984). Field peas (*Pisum sativum*) as a feed for growing and finishing pigs 1. Nutrient levels in commercial crops. *Australian Journal of Experimental Agriculture and Animal Husbandry, 24*, 350–353.

Deshpande, S. S., & Cheryan, M. (1986). Water uptake during cooking of dry beans. *Quality Plant Foods Human Nutrition, 36*, 157–167.

Eppendorfer, W. H., & Bille, S. W. (1974). Amino acid composition as a function of total N (Nitrogen) in pea seeds grown on soils with P (phosphorous) and K (potassium) additions. *Plant soil, 41*, 33–39.

Gubbels, G. H., & Ali-Khan, S. T. (1991). Effect of seed quality on cooking quality and yield of a subsequent crop of field pea. *Canadian Journal of Plant Science, 71*, 857–859.

Gubbels, G. H., Chubey, B. B., Ali-Khan, S. T., & Stauvers, M. (1985). Cooking quality of field pea matured under various environmental conditions. *Canadian Journal of Plant Science, 65*, 55–61.

Hoff, J. E., & Nelson, P. E. (1965). An investigation of accelerated water-uptake in dry pea beans. *Indiana Agricultural Experiment Station Research progress Report, 221*.

Holl, F. B., & Vose, J. R. (1980). Carbohydrate and protein accumulation in the developing field pea seed. *Canadian Journal of Plant Science, 60*(4), 1109–1114.

Jood, S., Mehta, U., Singh, R., & Bhat, C. M. (1985). Effect of processing on flatus producing factors in legumes. *Journal of Agriculture and Food Chemistry, 33*, 268.

Latta, M., & Eskin, M. (1980). A simple and rapid colorimetric method for phytate determination. *Journal of Agricultural and Food Chemistry, 28*, 1313–1315.

Lolas, G. M., & Markakis, P. (1975). Phytic acid and other phosphorous compounds of (kidney) beans (*Phaseolus vulgaris L.*). *Journal of Agricultural and Food Chemistry, 23*(1), 13–15.

McLean, L. A., Sosulski, F. W., & Youngs, C. G. (1974). Effects of nitrogen and moisture on yield and protein in field peas. *Canadian Journal of Plant Science, 54*, 301–305.

Moscoso, W., Bourne, M. C., & Hood, L. F. (1984). Relationships between the hard-to-cook phenomenon in red kidney beans and water absorption, puncture force, pectin, phytic acid, and minerals. *Journal of Food Science, 49*, 1577.

Nikolopoulou, D., Grigorakis, K., Stasini, M., Alexis, M. N., & Iliadis, K. (2006). Effects of cultivation area and year on proximate composition and antinutrients in three different *Kabuli*-type chickpea (*Ciecer arientium*) varieties. *European Food Research and Technology, 223*(6), 737–741.

Nikolopoulou, D., Grigorakis, K., Stasini, M., Alexis, M. N., & Iliadis, K. (2007). Differences in chemical composition of field pea (*Pisum sativum*) cultivars: Effect of cultivation area and year. *Food Chemistry, 103*, 847–852.

Owusuh-Ansah, J., & McCurdy, S. M. (1991). Pea proteins: A review of chemistry, technology of production and utilization. *Food Reviews International, 7*(1), 103–134.

Petterson, D., Sipsas, S., & Mackintosh, J. B. (1997). *The chemical composition and nutritive value of Australian pulses*. Canberra, Australia: Grains Research and Development Corporation.

Ravindran, V., Ravindran, G., & Sivalogan, S. (1994). Total and phytate phosphorus contents of various foods and feedstuffs of plant origin. *Food Chemistry, 50*, 133–136.

Reddy, N. R., Sathe, S. K., & Pierson, M. D. (1988). Removal of phytate from great northern beans (*Phaseous vulgaris L.*) and its combined density fraction. *Journal of Food Science, 53*, 107.

Reichert, R. D., & MacKenzie, L. (1982). Composition of peas (*Pisum sativum*) varying widely in protein content. *Journal of Agricultural and Food Chemistry, 30*, 312–317.

Sefa-Dedeh, S., & Stanley, D. W. (1979a). Textural implications of the microstructure of legumes. *Food Technology, 33*, 77–83.

Sefa-Dedeh, S., & Stanley, D. W. (1979b). The relationship of microstructure of cowpeas to water absorption and dehulling properties. *Cereal Chemistry, 56*, 379–386.

Sefa-Dedeh, S., Stanley, D. W., & Voisey, P. W. (1978). Effect of storage time and cooking conditions on the hard-to-cook defect in cowpeas (*Vigna unguiculata*). *Journal of Food Science, 44*, 790.

Shahin, M. A., & Symons, S. J. (2001). *Lentil seed size distribution with machine vision*. *ASAE Paper No. 01-3058*, St. Joseph, Michigan.

Singh, B., Campbell, W. F., & Salunkhe, D. K. (1972). Effects of s-triazines on protein and fine structure of cotyledons of bush beans. *American Journal of Botany, 59*, 568–572.

Singh, K. B., Erskine, W., Robertson, L. D., Nakkoul, H., & Williams, P. C. (1988). Influence of pretreatment on cooking quality parameters of dry legumes. *Journal of the Science of Food and Agriculture, 44*, 135–142.

Singh, K. B., Williams, P. C., & Nakoul, H. (1990). Influence of growing season, location and planting time on some quality parameters of kabuli chickpea. *Journal of the Science of Food and Agriculture, 53*, 429–434.

Stanley, D. W., & Aguilera, J. M. (1985). A review of textural defects in cooked reconstituted legumes – The influence of structure and composition. *Journal of Food Biochemistry, 9*, 277–323.

Vidal-Valverde, C., Frias, J., Hernandez, A., Martin-Alvarez, P. J., Sierra, I., & Rodriguez, C. (2003). Assessment of nutritional compounds and antinutritional factors in pea (*Pisum sativum*) seeds. *Journal of the Science of Food and Agriculture, 83*, 298–306.

Vindiola, O. L., Seib, P. A., & Hoseney, R. C. (1986). Accelerated development of the hard-to-cook state in beans. *Cereal Foods World, 31*, 538–552.

Walker, A. F., & Kochhar, N. (1982). Effect of processing including domestic cooking on nutritional quality of legumes. *Proceedings of the Nutrition Society, 41*, 41–51.

Wang, N., & Daun, J. K. (2004). Effect of variety and crude protein content on nutrients and certain antinutrients in field peas (*Pisum sativum*). *Journal of the Science of Food and Agriculture, 84*, 1021–1029.

Wang, N., & Daun, J. K. (2005). Determination of cooking times of pulses using an automated Mattson cooker apparatus. *Journal of the Science of Food and Agriculture, 85*, 1631–1635.

Wang, N., Daun, J. K., & Malcolmson, L. J. (2003). Relationship between physico-chemical and cooking properties, and effects of cooking on anti-nutrients, of yellow field peas (*Pisum sativum*). *Journal of the Science of Food and Agriculture, 83*, 1228–1237.

Wang, N., Hatcher, D. W., & Gawalko, E. J. (2008). Effect of variety and processing on nutrients and certain anti-nutrients in field peas (*Pisum sativus*). *Food Chemistry, 111*, 132–138.

Wang, N., Lewis, M. J., Brennan, J. G., & Westby, A. (1997). Effect of processing methods on nutrients and anti-nutritional factors in cowpea. *Food Chemistry, 58*, 59–68.

Warkentin, T. D., Vandenberg, A., Banniza, S., & Slinkard, A. (2004). CDC Striker field pea. *Canadian Journal of Plant Science, 84*, 230–240.

Williams, P. C., Nakoul, H., & Singh, K. B. (1983). Relationship between cooking time and some physical characteristics in chickpea (*Cicer arietinum*). *Journal of the Science of Food and Agriculture, 34*, 492–496.

Food Chemistry 118 (2010) 116–119

Contents lists available at ScienceDirect

Food Chemistry

journal homepage: www.elsevier.com/locate/foodchem

Flavan-3-ol contents, anti-oxidative and α-glucosidase inhibitory activities of *Cynomorium songaricum*

Chao-Mei Ma [a,*], Naoto Sato [a], Xiao-Yu Li [b], Norio Nakamura [c], Masao Hattori [a,*]

[a] *Institute of Natural Medicine, University of Toyama, 2630 Sugitani, Toyama 930-0194, Japan*
[b] *Division of Immunology, Tokyo Women's Medical University, 8-1, Kawada-cho, Shinjuku-ku, Tokyo, Japan*
[c] *Faculty of Pharmaceutical Sciences, Doshisha Women's College of Liberal Arts, Kodo, Kyotanabe, Kyoto 610-0395, Japan*

ARTICLE INFO

Article history:
Received 16 February 2009
Received in revised form 15 April 2009
Accepted 23 April 2009

Keywords:
Cynomoriaceae
Tannin
Catechin
SOD
α-glucosidase

ABSTRACT

Flavan-3-ol oligomers from the stems of *Cynomorium songaricum* were found to show potent SOD-like activity with one of the dimers being most potent. The flavan-3-ols also showed inhibitory activity on α-glucosidase, implying the beneficial effects of this herb on diabetes patients. The total (extractable and non-extractable) tannin content of this herb was found to be as high as 18.3%. The contents of catechin, flavan-3-ol oligomers and extractable tannins using 70% acetone, methanol or water were analysed. It was found that 70% acetone was the most efficient extract solvent amongst these three solvents, especially for higher flavan-3-ol oligomers.

1. Introduction

The stems of *Cynomorium songaricum* Rupr (Cynomoriaceae) is a well known tonic in Traditional Chinese Medicine (State Administration of Traditional Chinese Medicine of People's Republic of China, 1999). This herb is also frequently added to teas and wines and consumed by the local people as vegetable or food. Previous studies have reported the occurrence of phenolic compounds, triterpenes and other compounds in this plant (Chu, Tian, Lin, & Ye, 2006; Jiang, Tanaka, Sakamoto, Jiang, & Kouno, 2001; Ma, Nakamura, Miyashiro, Hattori, & Shimotohno, 1999; Zhang, Xu, & Li, 1997; Zhang & Zhang, 1991). Phenolic compounds are known to have antioxidative activity and to have scavenging effects on reactive oxygen species (ROS) (Hatano et al., 1989; Shahidi, 1997a; Yokozawa, Dong, Liu, & Shimizu, 1997), whilst oxidative stress (free radicals) is believed to be a cause of ageing (Larsen, 1993). In addition to ageing process, it was suggested that increased ROS levels is an important trigger for insulin resistance in numerous settings and that antioxidant therapy might be a useful strategy in type 2 diabetes and other insulin-resistant states, such as cancer, obesity, and metabolic syndrome (Houstis, Rosen, & Lander, 2006). Glycosidases are hydrolytic enzymes that play a vital role in digestion of carbohydrates and biosynthesis of glycoproteins. Due to the ability to reduce blood glucose level, α-glucosidase inhibition, is one of the currently selected and preferred targets for development of anti-type II diabetes agents. Some inhibitors of this enzyme have been developed as clinical drugs, such as acarbose.

The present research was carried out to investigate the antioxidative (SOD-like) and α-glucosidase inhibitory activity of *C. songaricum* and to elucidate the active components of this herbal medicine. In addition, catechin and two flavan 3-ol dimers were quantified by HPLC–MS, the extractable and non-extractable tannin contents were determined, and the flavan 3-ol components in extracts using three different solvents were compared.

2. Materials and methods

2.1. Plant material

C. songaricum Rupr (Cynomoriaceae) stems were collected in Wulateqianqi, Innermongolia, China, in 1995 and kept in dark at 20–28 °C. Herbarium voucher specimens were deposited at Division of Metabolic Engineering, Institute of Natural Medicine, University of Toyama, Japan.

2.2. Extraction and purification of flavan 3-ols from the stems of *C. songaricum*

The ground powder (passed through a 20-mesh sieve, particle size < 0.853 mm, 200 g) of the stems of *C. songaricum* was extracted

* Corresponding authors. Tel.: +81 76 4347633; fax: +81 76 4345060.
E-mail addresses: mchaomei@hotmail.com (C.-M. Ma), saibo421@inm.u-toyama.ac.jp (M. Hattori).

0308-8146/$ - see front matter © 2009 Elsevier Ltd. All rights reserved.
doi:10.1016/j.foodchem.2009.04.083

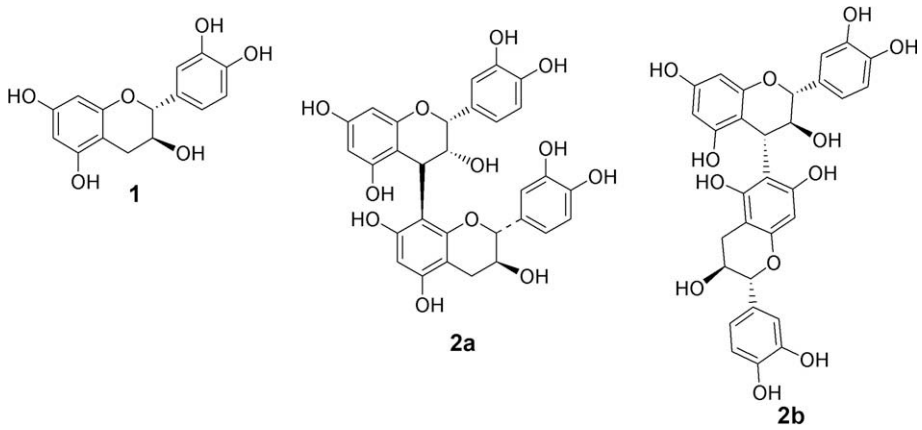

Fig. 1. Structures of catechin and the two flavan 3-ol dimers from the stems of *C. songaricum*.

twice, each with 2000 ml of 100% methanol by sonication at room temperature for 30 min. The combined solution was concentrated under vacuum to dryness to obtain 29 g of a methanol extract. The extract was chromatographed on a DIAION-HP20 (Mitsubishi Chemical Corporation, Tokyo, Japan) column (9 × 55 cm) eluted with water followed by methanol. The respective eluates were concentrated under vacuum to obtain 11 g of fraction I from the water eluate and 16 g of fraction II from the methanol eluate. Repeated column chromatograph of fraction II on Sephadex LH-20 (GE Healthcare Bio-Sciences AB, Uppsala, Sweden) and MCI gel CHP20P (Mitsubishi Chemical Corporation, Tokyo, Japan) furnished the flavan-3-ol monomer and oligomers. The flavan-3-ol monomer (**1**) and dimers (**2a** and **2b**) were isolated as pure compounds. The trimers (**3**), tetramers (**4**) and pentamers (**5**) were obtained as mixtures of isomers. The structures of these compounds were determined by comparing their NMR and MS spectral data with reported as described in the literature (Ma et al., 1999).

2.3. Quantification of total tannins in different extracts

The extraction was carried out in sealed centrifuge tubes under sonication for 30 min with an herb to solvent at ratio of 1:20 (w/v). Three solvents [acetone–H_2O (7:3, v/v) or MeOH or H_2O] were used for extraction to yield different extracts. For detection of total tannin contents, 10 mg of the herb powder were suspended in 0.2 ml of MeOH to determine the tannin content directly. Standard catechin was dissolved in MeOH at concentrations of 10, 5, 1 and 0.1 mg/ml.

The tannin contents were determined by *n*-BuOH–HCl–Fe^{III} method (Porter, Hrstich, & Chan, 1986). The reaction was carried out in 1.5 ml centrifuge tubes. To each tube was added 0.2 ml of an extract, 1.2 ml of a solution of *n*-BuOH-conc. HCl (95:5, v/v) and 40 μl of a ferric ammonium sulphate reagent. The reagent was a 2% (w/v) solution of ferric ammonium sulphate dodecahydrate ($NH_4Fe(SO_4)_2{\cdot}12H_2O$) in 2 M HCl. The tubes were capped and clamped with the top clips before the solutions were thoroughly mixed and heated at 95 °C for 40 min. The absorbance of released cyanidin at 560 nm was measured with a TECAN GENios plate reader (Wako, Osaka, Japan). The catechin equivalent was calculated by comparing the absorbance of samples with a concentration–absorbance curve of catechin.

2.4. HPLC–ESI/MS quantification of catechin and the two flavan 3-ol dimers

HPLC–PAD–MS was carried out on an Agilent 1100 system (Agilent Technologies, Waldbronn, Germany) equipped with degasser, binary pump, photodiode array detector and electrospray ionisation spectrometry (ESI, Esquire 3000^{plus}, Bruker Daltonik GmbH, Bremen, Germany). Data were acquired, integrated and analysed using a ChemStation with the software provided by the manufacturer. HPLC separation was performed on COSMOSIL 5C18-MS-II Waters columns (4.6 × 150 mm, Nacalai Tesque, Inc. Kyoto, Japan). The mobile phase containing solvents A and B, where A was water/formic acid (99.9:0.1, v/v) and B was acetonitrile/formic acid (99.9:0.1, v/v). The linear gradient profile was from 4% to 14% B in 10 min, 14–40% B in 6 min, 40–100% B in 1 min and kept at 100% B for 5 min. The flow rate was 1 ml/min for HPLC and 0.2 ml/min for MS detection with a splitter between PAD and MS detectors. ESI–MS was operated in negative mode with scanning range of *m/z* 200–1500 and trap drive of 47.6. High-purity nitrogen (99.99%) was used as dry gas at a flow rate of 9 l/min and temperature of 350 °C. Pure compounds **1**, **2a** and **2b**, in methanol at five concentrations (0.00167, 0.0333, 0.0667, 0.133 and 0.167 mg/ml) were used for the standard curves. Standard curves were plotted by using the areas of compound MS peaks in extract ion chromatograms as Y axis and the concentrations of compounds as X axis. Injection volumes were 10 μl for all compounds and extracts (see Fig. 1).

2.5. Assay for SOD-Like and α-glucosidase inhibitory activity

Superoxide dismutase (SOD)-like activity of the extract, fractions and compounds was evaluated on 96-well plates using a SOD Assay Kit-WST following the procedure provided by the supplier (Dojindo Chemical, Kumamoto, Japan). Briefly, 20 μl of sample solution and 200 μl of WST working solution were mixed in the well. The reaction was initiated by the addition of 20 μl of xanthine oxidase solution and the plates were incubated at 37 °C for 20 min. The absorbance at 450 nm was measured with an InterMed ImmunoReader (Nippon InterMed K.K. Tokyo, Japan) and the SOD-like activity (inhibition rate%) was calculated using the following equation. SOD-like activity (inhibition rate %) = $\{[(A_{\text{blank 1}} - A_{\text{blank 3}}) - (A_{\text{sample}} - A_{\text{blank 2}})]/(A_{\text{blank 1}} - A_{\text{blank 3}})\} \times 100$, where blank 1 contained water in place of sample solution; blank 2 contained buffer in place of enzyme; blank 3 contained water and buffer in place of sample solution and enzyme.

The α-glucosidase inhibitory activity was determined using 4-nitrophenyl α-D-glucopyranoside (purchased from TCI, Tokyo, Japan) in 100 mM potassium phosphate buffer (pH 7.0) as substrate and α-glucosidase from *B. stearothermophilus* as the enzyme. The assay was carried out on 96-well plates and the activities were calculated by the reported method (Ma, Hattori, Daneshtalab, & Wang, 2008).

Table 1
Contents of tannins in the stems of *C. songaricum*.

Sample	Catechin eq (mg)/g Herb	Tannin% of Herb	% of Total Tannin	RSD%
Total tannin	183.3	18.3		16.2
70% Acetone ext	65.0		35.4	3.1
Methanol ext	15.5		8.5	3.2
Water ext	9.6		5.2	8.3

The results are expressed as catechin equivalents.

3. Results and discussion

The *n*-BuOH–HCl–Fe^{III} method revealed that there were 18.3% of total flavan 3-ols (in catechin equivalent), in the stems of *C. songaricum*. Of these, 35.4%, 8.5% and 5.2% could be extracted with 70% acetone, 100% MeOH and 100% H_2O, respectively (Table 1). The contents of catechin and the small flavan-3-ol oligomers were investigated by HPLC–ESI/MS. The results indicated that in 1 g of the herb, there were 65 mg catechin equivalents of flavan 3-ols extractable by 70% acetone (Table 1), amongst which were 0.74 mg of catechin, 0.26 mg of the dimer **2a** and 0.62 mg of the dimer **2b** (Table 2). As there were no standard pure compounds available for the larger oligomers, their absolute contents were not determined, instead, the relative extraction efficiencies of the three solvents for the flavan-3-ols up to tetramers could be obtained by comparing the HPLC peak areas of the oligomers in different extracts. As shown in Fig. 2, extract ion chromatograms of these compounds displayed distinct peaks up to tetramers, and thus the relative contents of these compounds in methanol and water extracts compared to those in 70% acetone extract were summarised in Table 3. The 70% acetone is the best extract solvent for all these compounds. As the molecular weight increased, the extract efficiencies of methanol and water decreased, except for **2a** which was a little more exhaustively extracted with methanol or water than catechin was. For the tetramers, methanol and water could only extract 44.8% and 42.5% of that extracted by 70% acetone, respectively.

The antioxidative activities of the extract, fractions, isolated flavan-3-ol monomer and oligomers were evaluated as SOD-like activity using a SOD Assay Kit-WST. WST-1 produces a water-soluble formazan upon reduction with superoxide anion. The reduction rate is linearly related to the xanthine oxidase (XO) activity, and is inhibited by SOD or other antioxidative compounds. Therefore, the inhibition activity of the compounds can be determined by colorimetric measurement of the formazan dye. The activity was expressed as IC_{50} representing the concentration that inhibited the formation of WST-1 formazan by 50%. As shown in Table 4, the methanol extract of *C. songaricum* showed potent SOD-like activity (as methanol is a good solvent to extract not only tannins but also other constituents of plants, we used methanol for the activity guided fractionation). The methanol extract was fractionated to two fractions by DIAION-HP20 column chromatography. More potent activity was observed on Fraction II, from which flavan-3-ol monomer (**1**) and oligomers (**2a**, **2b** and **3**–**5**) were isolated. Flavan-3-ol monomer and oligomers noted showed significant SOD-like activity, with the IC_{50} of the oligomers being equal or lower than 0.01 μg/ml. Of the isolated compounds, the

Table 2
Contents of catechin and flavan-3-ol dimers in different extracts.

	r^2	t_R	HLQ (μg/ml)	LOQ (μg/ml)	mg/g herb ± RSD%		
					70% Acetone	MeOH	H_2O
1	0.9983	12.5	333	0.0033	0.74 ± 6.5	0.58 ± 9.4	0.56 ± 7.8
2a	0.9996	11.0	333	0.033	0.26 ± 4.0	0.22 ± 4.3	0.26 ± 7.5
2b	0.9998	11.8	333	0.033	0.62 ± 3.5	0.38 ± 6.7	0.44 ± 5.2

Results for the contents are the mean value of at least three experiments ± RSD.
r^2, regression value for the calibration curve; t_R, retention time; HLQ, high limit of quantification; LOQ, low limit of quantification (signal to noise ratio 10).

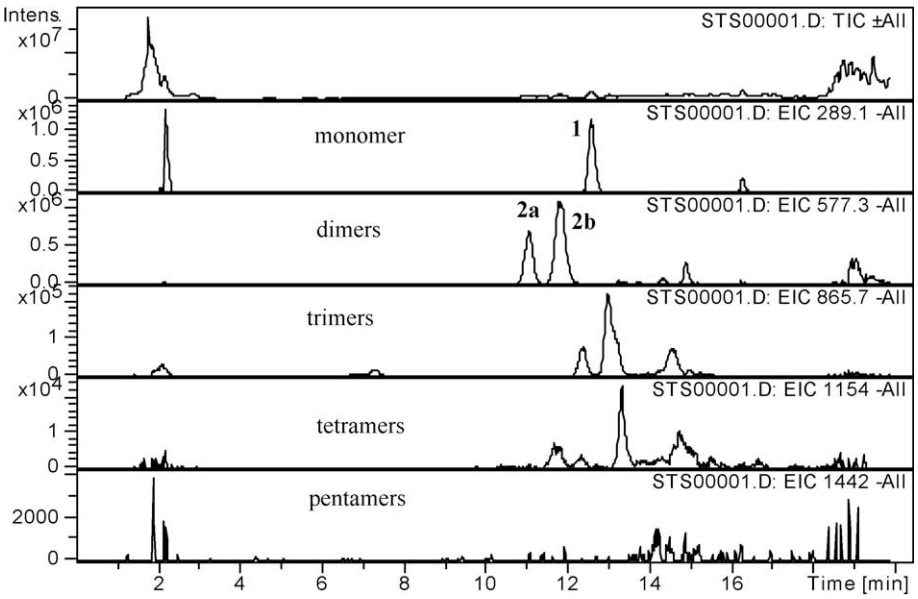

Fig. 2. Total ion chromatogram of a 70% acetone extract of *C. songaricum* and extracted ion chromatograms of catechin and flavan-3-ol oligomers.

Table 3
Contents of flavan-3-ols in methanol and water extracts compared to those in 70% acetone extract.

	% of Acetone extract				
	Catechin	**2a**	**2b**	Trimers	Tetramers
70% Acetone	100.0	100.0	100.0	100.0	100.0
MeOH	77.0	83.7	64.1	69.7	44.8
H_2O	73.8	97.0	73.0	52.8	42.5

Table 4
SOD-like and α-glucosidase inhibitory activity of *C. songaricum* extract, fractions and components.

Material	IC_{50} (μg/ml)	IC_{50g} (μg/ml)
Extract	0.300	180
Fraction I	7.000	>1000
Fraction II	0.200	120
Catechin (**1**)	0.030	970
Dimer (**2a**)	0.006	300
Dimer (**2b**)	0.010	430
Trimers (**3**)	0.009	90
Tetramers (**4**)	0.010	70
Pentamers (**5**)	0.007	30

IC_{50}: concentration that inhibited the formation of WST-1 formazan by 50% using a SOD Assay Kit-WST.
IC_{50g}: concentration that inhibited α-glucosidase activity by 50%.

most potent antioxidative activity belonged to one of the dimers, compound **2a**, with an IC_{50} of 0.006 μg/ml.

The α-glucosidase inhibitory activity was determined with 4-nitrophenyl α-D-glucopyranoside as substrate and the α-glucosidase from *B. stearothermophilus* as enzyme. The absorbance of released 4-nitrophenol at 405 nm was measured and the results were represented as IC_{50g}, the concentration at which 50% of α-glucosidase activity was inhibited. As shown in Table 4, the methanol extract of *C. songaricum* and the tannin-rich fraction (fraction II) showed moderate α-glucosidase inhibitory activity. Of the isolated flavan-3-ol monomer and oligomers, the α-glucosidase inhibitory activity increased as the molecular weight increased with a significant difference (32 times) in the potency between the strongest ones (pentamers) (Ma et al., 1999) and the weakest one (monomer). The strongest compounds (pentamers) showed an IC_{50} of 30 μg/ml.

Flavan-3-ol oligomers and polymers are known as condensed tannins and had been considered as antinutrients to herbivores and life stocks. However, in recent years, it has been proposed that some antinutrients, such as tannins may possess beneficial health effects and the mechanism by which the antinutritional and beneficial effects of food antinutrients operate are the same (Shahidi, 1997b). Tannins particularly those with smaller molecular weights (around 1000 or smaller) may show significant therapeutic and pharmaceutical potential for diseases in modern society that are associated with fundamental changes in nutrition and lifestyle (Ren & Chen, 2007). The present results that *C. songaricum* possessed potent SOD-like activity and moderate α-glucosidase inhibitory activity may suggest the use of this herbal medicine for the lifestyle-related diseases such as type II diabetes. The results also showed that *C. songaricum* is a rich source of condensed tannins and amongst the three solvents, 70% acetone is significantly better than MeOH and H_2O in extraction of these compounds, especially of relatively larger tannin oligomers. The result is consistent with the report in literature that 70–80% acetone is the best extract solvent for tannins (Naczk, Pegg, Zadernowski, & Shahidi, 2005).

References

Chu, Q. C., Tian, X. H., Lin, M., & Ye, J. N. (2006). Electromigration profiles of *Cynomorium songaricum* based on capillary electrophoresis with amperometric detection. *Journal of Agricultural and Food Chemistry, 54*, 7979–7983.

Hatano, T., Edamatsu, R., Hiramatsu, M., Mori, A., Fujita, Y., Yasuhara, T., et al. (1989). Effects of the interaction of tannins with co-existing substances. VI. Effects of tannins and related polyphenols and superoxide anion radical, and on 1,1-diphenyl-2-picrylhydrazyl radical. *Chemical and Pharmaceutical Bulletin, 37*, 2016–2021.

Houstis, N., Rosen, E. D., & Lander, E. S. (2006). Reactive oxygen species have a causal role in multiple forms of insulin resistance. *Nature, 440*, 944–948.

Jiang, Z. H., Tanaka, T., Sakamoto, M., Jiang, T., & Kouno, I. (2001). Studies on a medicinal parasitic plant: Lignans from the stems of *Cynomorium songaricum*. *Chemical and Pharmaceutical Bulletin, 49*, 1036–1038.

Larsen, P. L. (1993). Aging and resistance to oxidative damage in Caenorhabditis elegans. *Proceedings of the National Academy of Sciences of the United States of America, 90*, 8905–8909.

Ma, C. M., Hattori, M., Daneshtalab, M., & Wang, L. (2008). Chlorogenic acid derivatives with alkyl chains of different lengths and orientations: Potent α-glucosidase inhibitors. *Journal of Medicinal Chemistry, 51*, 6188–6194.

Ma, C. M., Nakamura, N., Miyashiro, H., Hattori, M., & Shimotohno, K. (1999). Inhibitory effects of constituents from *Cynomorium songaricum* and related triterpene derivatives on HIV-1 protease. *Chemical and Pharmaceutical Bulletin, 47*, 141–145.

Naczk, M., Pegg, R. B., Zadernowski, R., & Shahidi, F. (2005). Radical scavenging activity of canola hull phenolics. *Journal of the American Oil Chemists' Society, 82*, 255–260.

Porter, L. J., Hrstich, L. N., & Chan, B. G. (1986). The conversion of procyanidins and prodelphinidins to cyanidin and delphinidin. *Phytochemistry, 25*, 223–230.

Ren, Y., & Chen, X. (2007). Distribution, bioactivities and therapeutical potentials of pentagalloylglucopyranose. *Current Bioactive Compounds, 3*, 81–89.

Shahidi, F. (1997a). Natural antioxidants-and overview. In F. Shahidi (Ed.), *Natural antioxidants: Chemistry, health effects, and application* (pp. 1–10). Champaign, IL: The American Oil Chemists' Society.

Shahidi, F. (1997b). Beneficial health effects and drawbacks of antinutrients and phytochemicals in foods. In F. Shahidi (Ed.), *Antinutrients and phytochemicals in food (ACS symposium series 662)* (pp. 1–9). Washington, DC: American Chemical Society.

State Administration of Traditional Chinese Medicine of People's Republic of China, (1999). Zhong Hua Ben Cao (Vol. 5, pp. 722–724). Shang Hai: Shang Hai Science and Technology Press.

Yokozawa, T., Dong, E., Liu, Z. W., & Shimizu, M. (1997). Antioxidative activity of flavones and flavonols *in vitro*. *Phytotherapy Research, 11*, 446–449.

Zhang, C. Z., Xu, X. Z., & Li, C. (1997). Fructosides from *Cynomorium songaricum*. *Phytochemistry, 41*, 975–976.

Zhang, S. Z., & Zhang, S. Y. (1991). Chemical constituents of *Cynomorium songaricum*. *Zhongguo Yaoxue Zazhi, 26*, 649–651.

Food Chemistry 118 (2010) 120–127

Contents lists available at ScienceDirect

Food Chemistry

journal homepage: www.elsevier.com/locate/foodchem

Antioxidant activities of phenolic rich fractions (PRFs) obtained from black mahlab (*Monechma ciliatum*) and white mahlab (*Prunus mahaleb*) seedcakes

Abdalbasit Adam Mariod [a,c], Ramlah Mohamad Ibrahim [a,b], Maznah Ismail [a,b,*], Norsharina Ismail [a,b]

[a] Laboratory of Molecular Biomedicine, Institute of Bioscience, University Putra Malaysia, 43400 UPM Serdang, Selangor, Malaysia
[b] Department of Nutrition and Dietetic, University Putra Malaysia, 43400 UPM Serdang, Selangor, Malaysia
[c] Department of Food Science and Technology, Sudan University of Science and Technology, P.O. Box 71, Khartoum North, Sudan

ARTICLE INFO

Article history:
Received 6 March 2009
Received in revised form 16 April 2009
Accepted 23 April 2009

Keywords:
Antioxidant activity
β-Carotene–linoleic acid assay
1,1-Diphenyl-2-picrylhydrazyl (DPPH)
Phenolic rich fractions
Monechma ciliatum
Prunus mahaleb

ABSTRACT

The antioxidant activities of phenolic rich fractions (PRFs) from crude methanolic extract (CME), and its fractions using ethyl acetate (EAF), hexane (HF) and water (WF) of black mahlab (*Monechma ciliatum*) and white mahlab (*Prunus mahaleb*) seedcakes were investigated. The total phenolic compounds were found to be higher in white mahlab than black mahlab seedcakes. The antioxidant activity determined by the DPPH method revealed that black mahlab PRFs had the highest antioxidant activity, compared to white mahlab fractions. The presence of antioxidants in the two mahlab PRFs reduced the oxidation of β-carotene by hydroperoxides from these extracts/fractions. The effect of the two mahlab PRFs on the oxidative stability of corn oil at 70 °C was tested in the dark and compared with butylated hydroxyanisole (BHA). The CME performed better antioxidant activity in inhibiting the formation of both primary and secondary oxidation products. The qualitative and quantitative characterisation of phenolic compounds was carried out by HPLC/DAD.

1. Introduction

There is increasing evidence that consumption of a variety of phenolic compounds present in natural foods may lower the risk of serious health disorders because of the antioxidant activity of these compounds (Hertog, Feskens, Hollman, Katan, & Kromhout, 1993; Surh, 2002; Surh et al., 1999). When added to foods, antioxidants minimise rancidity, retard the formation of toxic oxidation products, maintain nutritional quality, and increase shelf life (Jadhav, Nimbalkar, Kulkarni, & Madhavi, 1996). The antioxidant activity of extracts of several plants, including their leaves, bark, roots (Mariod, Matthaus, & Hussein, 2008), fruits, seeds (Liyana-Pathirana & Shahidi, 2006; Malencic, Maksimovic, Popovic, & Miladinovic, 2008) and seedcake (Mariod, Matthaüs, Eichner, & Hussein, 2006; Matthaüs 2002) has been extensively studied. Tocopherol, tertiary-butylhydroquinone (TBHQ), butylated hydroxytoluene (BHT) and butylated hydroxyanisole (BHA) are the most commonly used primary antioxidant in oils. However, many researchers reported the adverse effects of synthetic antioxidants such as toxicity and carcinogenicity (Williams, Iatropoulos, & Whysner, 1999). Due to safety and limitation of synthetic antioxidant usage, natural antioxidants obtained from edible materials, edible by-products and residual sources have become alternately interesting (Moure et al., 2000).

Edible fats and oils, such as vegetable oils or lard, are usually used as substrates for evaluating the antioxidant activity from natural sources (Duh & Yen, 1997). Hydroperoxides are the primary products of lipid oxidation, and their content (i.e. peroxide value, PV) is often used as an indicator for the initial stages of oxidation. In the same time hydroperoxides decompose rapidly during storage. For these reasons, PV may not necessarily be indicative of the actual extent of lipid oxidation (Sherwin, 1978). The anisidine value is a more meaningful test for the assessment of the oils quality during heating than the peroxide value, because it measures aldehydes, which are formed as secondary products of oxidation reactions. These compounds are less easily destroyed under these conditions (Pantzaris, 1999).

Monechma ciliatum, family Acanthaceae is an annual glabrous herb, 30–65 cm high, known in Sudan as black mahlab, where the seeds are used as flavouring material in different food products e.g. Kisra (traditional fermented sorghum flour sheets) and bread. The seeds also used as an effective laxative, and contain a fixed oil which emits a sweet and pleasant odor. It's further used in traditional Sudanese fragrances, lotion and other cosmetics used for wedding preparation and childbirth (Sharief, 2002). *M. ciliatum* was used in remedy of general body pain, liver, cold, diarrhea and sterility in women and its leaves methanolic extract showed oxytocic property in vivo and in vitro (Ayoub & Babiker, 1981;

* Corresponding author. Address: Laboratory of Molecular Biomedicine, Institute of Bioscience, University Putra Malaysia, 43400 UPM Serdang, Selangor, Malaysia. Tel.: +60 3 8947 2115; fax: +60 3 8947 2116.
E-mail addresses: maznah@medic.upm.edu.my, myhome.e@gmail.com (M. Ismail).

0308-8146/$ - see front matter © 2009 Elsevier Ltd. All rights reserved.
doi:10.1016/j.foodchem.2009.04.085

Uguru, Okwuasaba, Ekwenchi, & Uguru, 1995). White mahlab (*Prunus mahaleb)* known as: English cherry, Rock cherry, St. Lucie cherry (in English) family Rosaceae is a deciduous tree, 1–2 m high. The kernels form an important source of protein (30.98%) and oil (40.40%). Its oil is valuable in the preparation of lacquers and varnishes; it contains little cyanogenic glycosides and coumarin derivatives (Aydin, Ogut, & Konak, 2002). In Sudan the kernels are used as a flavouring material in bread, as cosmetic in wedding preparation, and in remedy of diarrhoea in children.

High performance liquid chromatography (HPLC) with diode array detection (DAD) is an indispensable tool for the provisional identification of the main phenolic structures present in foods (Chirinos et al., 2009).

To the best of our knowledge this is the first report on polyphenol contents and antioxidant activity of the seedcakes of black and white mahlab. Hence, the aim of this study was to study and determine the total phenolic content (TPC) and antioxidant activities (AOA) of black and white mahlab seedcakes and their effect on the oxidation of corn oil. The different phenolic rich fractions (PRF) were applied to corn oil at levels of 0.25% and 0.5% to examine their antioxidative activity; the development of the peroxide conjugated diene, TBARS and anisidine values during oxidation of corn oil were evaluated at 70 °C for 72 h.

2. Materials and methods

2.1. Sample material, standards and reagents

All solvents used were of HPLC grade. Methanol, ethyl acetate, hexane, chloroform, butylated hydroxyanisole (BHA), β-carotene, linoleic acid and Folin–Ciocalteau reagent as well as polyoxyethylene sorbitan monopalmitate (Tween 40) were obtained from Merck (Merck, Darmstadt, Germany). Ferulic acid, chlorogenic acid *p*-coumaric acid, 3,4-dihydroxybenzoic acid, (−)-epicatechin and (+)-catechin, and syringic acid were obtained from Sigma–Aldrich (Hamburg, Germany), gallic acid and vanillin were obtained from Fluka Chemie AG (Buchs, Switzerland). The pure flavonoid compound quercetin was obtained from Extrasynthese (Genay Cedex, France).

Black and white mahlab seeds were obtained from a local store at Khartoum North, Sudan. The seeds were cleaned under running tap water for 10 min, rinsed twice with distilled water and air-dried in oven at 40 °C for overnight. The seeds were grinded to powder using an electric grinder (National, Model MX-915, Kadoma, Osaka, Japan) for 10 min and then passed through a 35 mm (42 mesh) sieve. The cakes were obtained after oils were extracted from the ground seeds by extraction with *n*-hexane (b.p. 50–60 °C) using Soxhlet apparatus for 6 h following the AOCS (1993) method Aa 4-38 and the obtained seedcakes were used to extract phenolic compounds.

2.2. Corn oil

The refined edible corn oil which was produced by Lam Soon edible oil Co. Ltd., Shah Alam, Selangor, Malaysia was obtained from local store Serdang Malaysia; the oil was free of any synthetic antioxidant.

2.3. Extraction of phenolic compounds

Twenty grams of the dried ground seedcakes from black and white mahlab were extracted with 80% methanol by sonication (Hwasin Technology, Seoul, Korea) to obtained crude methanolic extract (CME) with solid to solvent ratio of 1:10 (w/v) at room temperature for 1 h, the obtained CME was fractionated using the following solvent namely; hexane, ethyl acetate and water. Each extraction process involved homogenisation of CME and its fractions and solvent at 13000 rpm for 15 min followed by sonication (Hwasin Technology, Seoul, Korea) at constant temperature of 30 °C for 1 h. The CME and its fractions (hexane fraction, HF; ethyl acetate fraction, EAF; water fraction, WF) were filtered through filter paper Whatman no. 1. Then solvents were removed by using rotary evaporator (Buchi, Flawil, Switzerland). The yield of each extract and its fractions was measured before kept in −80 °C for further analysis.

2.4. Determination of total phenolic compounds (TPC) in black and white mahlab seedcakes

The total phenolic (TPC) contents of each extracts/fractions were determined using the Folin–Ciocalteu reagent (Zhou & Yu, 2006). The reaction mixture contained 1 ml of CME and each individual fraction, 0.5 ml of the Folin–Ciocalteu reagent, 3 ml of 20% sodium carbonate and 10 ml of distilled water. After 2 h of reaction at ambient temperature, the absorbance at 765 nm was measured using spectrophotometer (Shimazu Co. Ltd., Kyoto, Japan) and used to calculate the phenolic contents, using gallic acid as a standard. The total phenolic contents were then expressed as gallic acid equivalents (GAE), in mg/g dry sample.

2.5. Antioxidant activities (AOA) measurement

The antioxidant activities (AOA) of CME and its fractions of black and white mahlab seedcakes were addressed using the following methods.

2.5.1. 1,1-Diphenyl-2-picrylhydrazyl (DPPH) radical scavenging activity test

The hydrogen atom or electron-donation ability of the corresponding extracts/fractions was measured from the bleaching of a purple-coloured methanol solution of DPPH. The antioxidant activity of the extracts/fractions, on the basis of the scavenging activity of the stable 1,1-diphenyl-2-picrylhydrazyl (DPPH) radical, was determined by the method described by Gordon, Paiva-Martins, and Almeida (2001). A methanolic solution (100 μl) of the extracts/fractions was placed in a cuvette and 0.5 ml of a methanolic solution of DPPH (50 mg DPPH/100 ml MeOH) was added. After 30 min absorbance at 515 nm was determined using a spectrophotometer (Shimadzu Co. Ltd., Kyoto, Japan), and IC_{50}, was reported which is the concentration of antioxidant required for 50% scavenging of DPPH radicals in the specified time period. All determinations were performed in triplicate.

2.5.2. The β-carotene–linoleic acid assay

The antioxidant activity (AOA) of the different extracts/fractions was evaluated using the β-carotene–linoleic acid assay following the method of Amarowicz, Wanasundara, Wanasundara, and Shahidi (1993). In brief, a solution of β-carotene was prepared by dissolving 2 mg of β-carotene in 10 ml of chloroform. Two millilitres of this solution were pipetted into a 100 ml round-bottom flask. After chloroform was removed under vacuum, using a rotary evaporator at 40 °C, 40 mg of purified linoleic acid, 400 mg of Tween 40 as an emulsifier, and 100 ml of aerated distilled water were added to the flask with vigorous shaking. Aliquots (4.8 ml) of this emulsion were transferred into a series of tubes containing 200 μl of the extract (200 ppm in methanol). The total volume of the systems was adjusted to 5 ml with methanol. As soon as the emulsion was added to each tube, the zero time absorbance was measured at 470 nm with a Shimadzu spectrophotometer (Shimadzu Co. Ltd., Kyoto, Japan). Subsequent absorbance readings were recorded over a 2 h period at 20 min intervals by keeping the samples in a water

bath at 50 °C. Blank samples, devoid of β-carotene, were prepared for background subtraction.

2.5.3. Stability of corn oil as affected by the addition of different extracts/fractions from black and white mahlab seedcakes

Commercial edible corn oil was obtained from local market. It contained no added antioxidants originally. The dried extracts/fractions or BHA were mixed with a minimum amount of absolute methanol in an ultrasonic water bath (Hwasin Technology, Seoul, Korea) then applied directly to the oil samples at levels of 0.25% and 0.5% before the accelerated tests, and samples with no added antioxidants were kept as a control (Moure et al., 2000). The oxidative stability of storage oil (at 70 °C for 72 h) was evaluated by measuring the absorbance at 270 and 234 nm, and by determining the peroxide value (PV), conjugated diene (CD), thiobarbituric acid reactive substances (TBARS) and *p*-anisidine values (as indicators for the primary and secondary oxidation of the corn oil) following the method of AOCS (1993). The PVs, CD, TBARS and AVs were determined every 0, 6, 12, 24, 36, 48 and 72 h. All treatments were carried out three times. For the UV absorbance, 10 ml of each sample was mixed with 10 ml of isooctane, and the absorbance was followed at 234 and 270 nm using cells of 1 cm (Roussis, Tzimas, & Soulti, 2008). Pure isooctane was used as a reference. The conjugated diene values were calculated according to the equation below.

$$\text{CD value} = A/(C \times l)$$ (Shahidi, Desilva, & Amarowicz, 2003)

where CD = conjugated diene; A = absorbance at 234 nm; C = concentration (g/100 ml); and 1 = path length (cm).

TBARS test. Each sample (200 mg) was weighed into a 25-ml volumetric flask. It was then made up to the mark with 1-butanol (ACS grade) and mixed thoroughly. A 5-ml portion of this solution was transferred into a dry test tube, and a 5-ml quantity of fresh TBA reagent (200 mg TBA in 100 ml 1-butanol) was added to it. The tube was placed in a 95 °C water bath for 120 min. The tube was cooled, and the absorbance of the solution was read at 532 nm. The TBARS value was calculated as follows:

$$\text{TBARS value} = (A \times 0.415)/m$$ (Shahidi et al., 2003)

where A = absorbance at 532 nm and m = mass of the sample.

2.6. HPLC–DAD system for analysis of phenolic compounds

HPLC analysis was performed using Agilent G1310A pumps (Agilent, Stevens Creek Blvd. Santa Clara, CA, USA), with diode array detector and chromatographic separations were performed on a LUNA C-18 column (5 μm, 250 × 4.6 mm) (Phenomenex, Torrance, California, USA). The composition of solvents and used gradient elution conditions were described previously by Chirinos et al. (2009) with some modifications. The mobile phase was composed of solvent (A) water–acetic acid (94:6, v/v, pH 2.27) and solvent (B) acetonitrile. The solvent gradient was as follows: 0–15% B in 40 min, 15–45% B in 40 min, and 45–100% B in 10 min. A flow rate of 0.5 ml/min was used and 20 μl of sample were injected. Samples and mobile phases were filtered through a 0.22 μm Millipore filter, type GV (Millipore, Bedford, MA, USA) prior to HPLC injection. Each fraction was analysed in duplicate. Phenolic compounds were identified and quantified by comparing their retention time and UV–Vis spectral data to known previously injected standards (Chirinos et al., 2009).

2.7. Statistical analyses

Statistical analyses were conducted using SPSS (Statistical Program for Social Sciences, SPSS Corporation, Chicago, IL) version 12.0 for Windows. Analysis of variance (ANOVA) in a completely randomised design, Duncan's multiple range test and Pearson's correlation coefficients were performed to compare the data. All determinations were done at least in triplicate and all were averaged. The confidence limits used in this study were based on 95% ($P < 0.05$).

3. Results and discussion

3.1. Amount of extractable compounds vs extractable phenolic compounds

The results of using different solvents for the extraction/fractionation of phenolic compounds are given in Table 1. From this table it is clear that the different solvents had different abilities to extract substances from these seedcakes. In general, the amount of total extractable compounds decreased with decreasing polarity of the solvent in the order water, methanol, ethyl acetate and hexane. The extraction of phenolic compounds from mahlab seedcakes with water was found most effective. With this solvent, the highest amount of TEC was found to be 810.1 and 698.2 mg/g followed by CME 201.6, 185.8 mg/g, EA 107.6, 159.9 and hexane 85.9, 140.8 mg/g in black and white mahlab seedcake, respectively. The extraction with hexane showed the lowest TEC (85.9 and 140.8 mg/g, respectively) in comparison with that of the other solvents. The TEC were significantly different between the two mahlab seedcakes as well as between extracts/fractions ($P < 0.05$). These findings are in good agreement with that of Matthaüs (2002) who found that extraction with water gave the highest amounts of phenolic compounds from fat-free residues of different oilseeds.

Table 1
Total extractable compounds (TEC), total phenolic compounds (TPC), IC_{50} of different extracts/fractions obtained from seedcakes of black and white mahlab seeds.

Extraction	TEC (mg/g)	TPC (mg GAE/g extract/fraction)	TPC/TEC (%)	IC_{50} (μg/ml)
Black mahleb				
CME	201.6 ± 0.5	17.1 ± 0.04	8.5	0.460 ± 0.1
HF	85.9 ± 0.4	6.7 ± 0.02	7.8	0.648 ± 0.2
EAF	107.6 ± 0.2	26.3 ± 0.1	24.4	0.413 ± 0.1
WF	810.1 ± 0.6	9.9 ± 0.02	1.2	0.525 ± 0.3
Ascorbic acid				0.017 ± 0.01
White mahleb				
CME	185.8 ± 0.4	71.9 ± 0.31	38.7	2.942 ± 0.4
HF	140.8 ± 0.2	53.1 ± 0.41	37.7	5.563 ± 0.1
EAF	159.9 ± 0.3	72.9 ± 0.35	45.5	5.201 ± 0.2
WF	698.2 ± 0.6	65.7 ± 0.21	9.4	5.091 ± 0.2
Ascorbic acid				0.017 ± 0.01

3.2. Total phenolic compounds (TPC)

The content of the total phenolic compounds of CME and its different fractions (HF, EAF and WF) from black and white mahlab seedcakes determined using Folin–Ciocalteau method is shown in Table 1. Results in this table show that EAF in both black and white mahlab contained the highest amount of total phenolic compounds followed by CME, WF, and HF, respectively. Ethyl acetate is often used as an extraction solvent with a significant selectivity in the extraction of low-molecular-weight phenolic compounds and high-molecular-weight polyphenols (Scholz & Rimpler, 1989). The percentages of total phenolics that found in the TEC were significantly ($P < 0.05$) higher in all white mahlab fractions in comparison with that of black mahlab. The percentage of total phenolic compounds to the total extractable compounds ranged from 9.4% to 45.5% in white mahlab and from 1.2% to 24.4% in black mahlab (Table 1). From these results it can be understood that in white mahlab more than 50% of the extractable materials were compounds other than phenolic compounds. While in black mahlab more than 75% of the extractable materials were compounds other

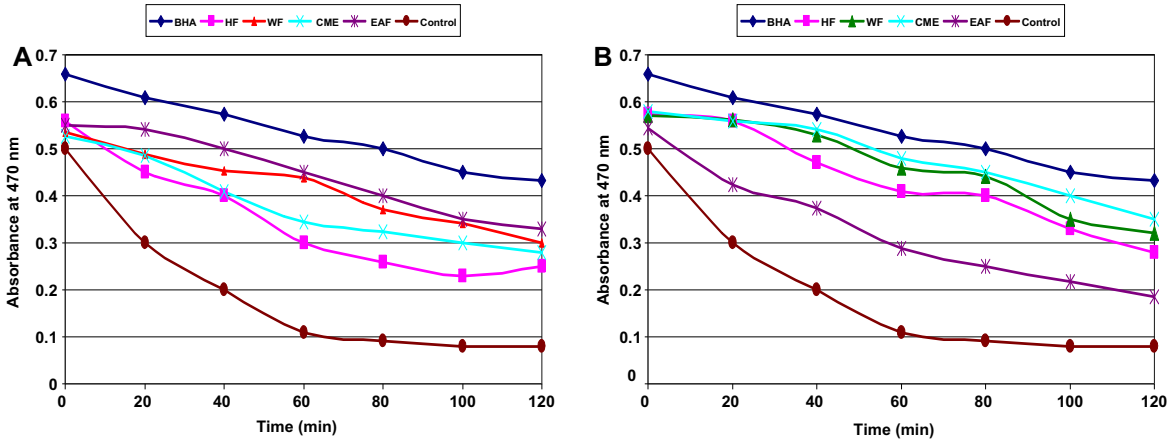

Fig. 1. Effect of black (A) and white (B) mahlab extract/fractions on oxidation of β-carotene/linoleic acid at 50 °C. BHA: butylated hydroxyanisole, HF: hexane fraction, WF: water fraction, CME: crude methanolic extract, EAF: ethyl acetate fraction.

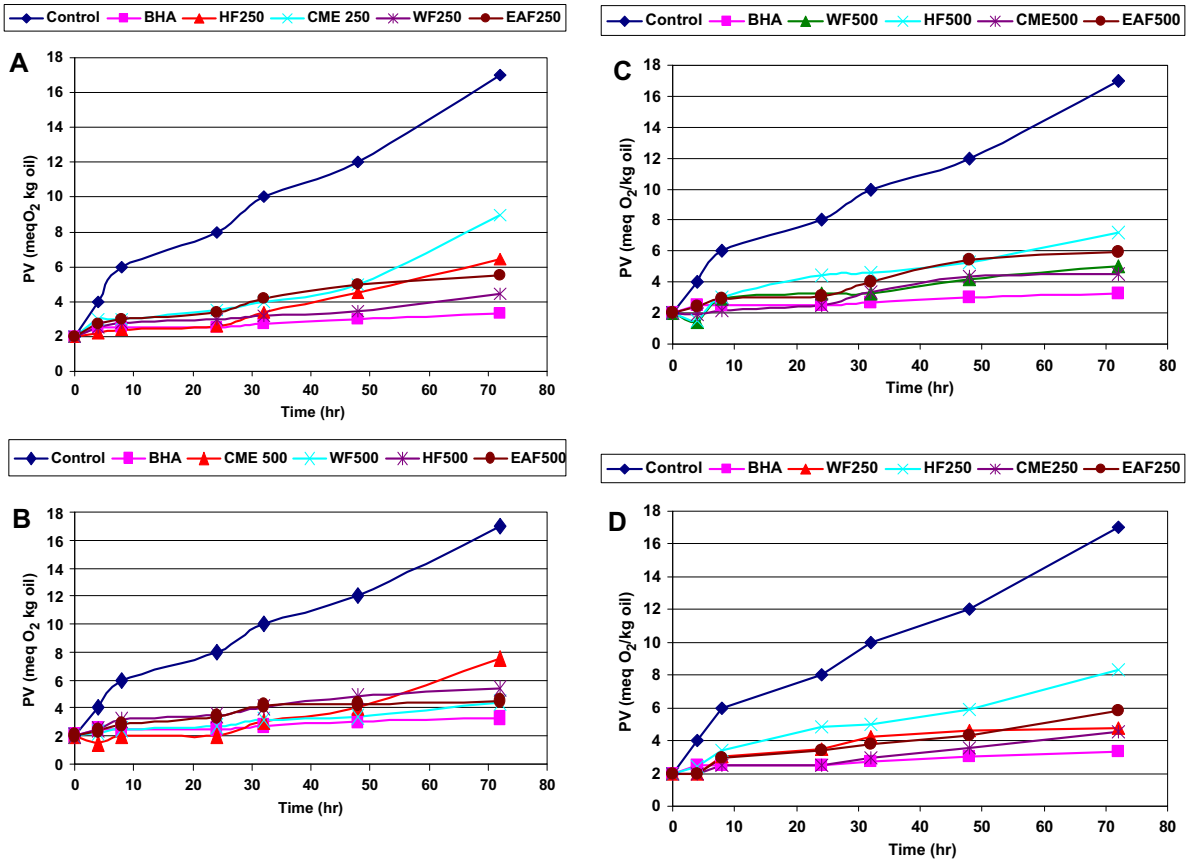

Fig. 2. Oxidation of corn oil treated with black mahlab (A, B) and white mahlab (C, D) CME and its fractions 250 and 500 mg /100 g oil during storage at 70 °C. BHA: butylated hydroxyanisole, HF: hexane fraction, WF: water fraction, CME: crude methanolic extract, EAF: ethyl acetate fraction.

than phenolic compounds. It becomes clear that the total phenolic compound was not related to the total extractable compounds. There was no significant correlation between the amount of total extractable compounds and the total phenolic compounds ($P < 0.05$). The extraction solvents influenced the amount of total phenolic compounds.

3.3. 1,1-Diphenyl-1-picrylhydrazyl (DPPH) radical scavenging activity test

The DPPH scavenging activities of different extracts/fractions of black and white mahlab seedcakes are shown in Table 1. The DPPH radical scavenging capacity assay was used to examine the antioxidant activity of black and white mahlab seedcakes extracts/fractions. The extracts/fractions were assayed over a range of dilutions to establish the concentration of each extract/fraction required to scavenge 50% of the DPPH radical present in the assay medium, referred to as the IC_{50} defined as the concentration of the antioxidant needed to scavenge 50% of DPPH present in the test solution. Lower IC_{50} value reflects better DPPH radical scavenging activity (Molyneux, 2004). Under the assay conditions employed here, the IC_{50} of ascorbic acid as standard was 0.017 μg/ml, between the extract/fractions of black mahlab seedcake EAF possessed greater DPPH radical scavenging activity with the lowest IC_{50} value of 0.413 μg/ml. DPPH scavenging activity of black mahlab seedcake extract/fractions increased in the order of ascorbic acid > EAF > CME > WF > HF. Among the extract/fractions of white mahlab seedcake, CME showed the greatest DPPH-scavenging activity with IC_{50} values of 2.94 μg/ml, followed by WF, EAF and HF, respectively, with IC_{50} of 5.091, 5.201 and 5.563 μg/ml, respectively (Table 1). In general, the black mahlab CME and its fractions showed higher DPPH radical scavenging activity ($P < 0.05$) than that of white mahlab, from Table 1 it can be said that, no significant correlation found between total phenolic content (TPC) and DPPH assay of black and white mahlab seedcake extract/fractions. Malencic et al. (2008) found that antioxidant activity of soya bean seed extracts increased proportionally to the polyphenol content with a linear relationship between DPPH values and total polyphenol. At the same time, they found that, there was no positive correlation between DPPH values and flavonoid content.

3.4. β-Carotene bleaching (BCB) assay

In the BCB assay, the oxidation of linoleic acid generates peroxyl free radicals due to the abstraction of hydrogen atom from diallylic methylene groups of linoleic acid (Kumaran & Karunakaran, 2006). The free radical then will oxidise the highly unsaturated β-carotene. The presence of antioxidants in the extract will minimise the oxidation of β-carotene by hydroperoxides. Hydroperoxides formed in this system will be decomposed by the antioxidants from the extracts. Thus, the degradation rate of β-carotene depends on the antioxidant activity of the extracts. Most studies showed there was no correlation between TPC and BCB (Amarowicz et al., 1993; Mariod et al., 2006; Matthaüs, 2002).

Effect of black mahlab extracts/fractions (CME, HF, WF and EAF) on oxidation of β-carotene/linoleic acid at 50 °C is shown in Fig. 1A. It was clear that the presence of antioxidants in the mahlab seedcakes extracts/fractions reduced the oxidation of β-carotene by hydroperoxides from these extracts/fractions. There were significant differences ($P < 0.05$) between the different extracts/fractions, control and BHA effect as shown in Fig. 1A. EAF, WF fractions were better in their effect on reducing the oxidation of β-carotene than

Table 2
Comparative inhibition of edible corn oil oxidation at 234 nm, 270 nm, *p*-anisidine and TBARS value by black mahlab seedcake phenolic rich fractions at 250 mg/100 g oil.

Time (h)	Control	BHA	HF	EAF	CME	WF
234 nm						
0	0.231 ± 0.01^{a,*}	0.115 ± 0.1b	0.231 ± 0.2^{a}	0.15 ± 0.06^{b}	0.112 ± 0.07^{b}	0.151 ± 0.05^{b}
6	0.568 ± 0.1^{a}	0.118 ± 0.05^{b}	0.254 ± 0.2^{c}	0.335 ± 0.1^{d}	0.123 ± 0.04^{b}	0.481 ± 0.01^{e}
12	0.685 ± 0.2	0.122 ± 0.01^{b}	0.447 ± 0.02^{c}	0.445 ± 0.01^{c}	0.125 ± 0.02^{b}	0.495 ± 0.01^{d}
24	0.899 ± 0.3^{a}	0.155 ± 0.02^{b}	0.589 ± 0.1^{c}	0.772 ± 0.2^{ac}	0.167 ± 0.01^{b}	0.564 ± 0.1^{c}
36	0.951 ± 0.4^{a}	0.198 ± 0.02^{b}	0.599 ± 0.1^{c}	0.789 ± 0.3^{d}	0.213 ± 0.1^{b}	0.689 ± 0.2^{d}
48	1.123 ± 0.5^{a}	0.255 ± 0.1^{b}	0.621 ± 0.2^{c}	0.876 ± 0.3^{d}	0.266 ± 0.1^{b}	0.694 ± 0.2^{cd}
72	1.543 ± 0.6^{a}	0.288 ± 0.1^{b}	0.65 ± 0.2^{c}	0.888 ± 0.3^{d}	0.289 ± 0.1^{b}	0.699 ± 0.2^{cd}
270 nm						
0	0.231 ± 0.1^{a}	0.112 ± 0.04^{b}	0.231 ± 0.1^{a}	0.254 ± 0.1^{c}	0.115 ± 0.03^{b}	0.251 ± 0.1^{c}
6	0.422 ± 0.1^{a}	0.123 ± 0.03^{b}	0.152 ± 0.01^{b}	0.253 ± 0.1^{c}	0.125 ± 0.04^{b}	0.212 ± 0.1^{d}
12	0.562 ± 0.2^{a}	0.182 ± 0.05^{b}	0.373 ± 0.1^{c}	0.415 ± 0.2^{d}	0.235 ± 0.1^{e}	0.381 ± 0.2^{c}
24	0.691 ± 0.3^{a}	0.185 ± 0.1^{b}	0.431 ± 0.2^{c}	0.521 ± 0.2^{d}	0.211 ± 0.1^{b}	0.451 ± 0.2^{c}
36	0.853 ± 0.6^{a}	0.221 ± 0.1^{b}	0.433 ± 0.2^{c}	0.621 ± 0.3^{d}	0.23 ± 0.1^{b}	0.462 ± 0.2^{c}
48	1.115 ± 0.6^{a}	0.232 ± 0.1^{b}	0.532 ± 0.2^{c}	0.771 ± 0.4^{d}	0.252 ± 0.1^{c}	0.571 ± 0.3^{c}
72	1.442 ± 0.6^{a}	0.255 ± 0.2^{b}	0.535 ± 0.3^{c}	0.864 ± 0.3^{d}	0.313 ± 0.1^{e}	0.541 ± 0.3^{c}
p-Anisidine value						
0	0.23 ± 0.1^{a}	0.11 ± 0.04^{b}	0.23 ± 0.1^{a}	0.35 ± 0.2^{c}	0.11 ± 0.04^{b}	0.25 ± 0.1^{a}
6	3.86 ± 0.5^{a}	1.86 ± 0.4^{b}	3.37 ± 0.6^{c}	3.55 ± 0.5^{d}	2.30 ± 0.5^{e}	3.49 ± 0.4^{c}
12	4.47 ± 0.6^{a}	2.71 ± 0.5^{b}	3.51 ± 0.6^{c}	3.93 ± 0.6^{d}	3.14 ± 0.5^{e}	3.54 ± 0.5^{c}
24	4.91 ± 0.6^{a}	3.14 ± 0.5^{b}	4.30 ± 0.5^{c}	4.46 ± 0.5^{c}	3.83 ± 0.4^{d}	4.35 ± 0.5^{c}
36	5.32 ± 0.4^{a}	3.52 ± 0.4^{b}	4.47 ± 0.4^{c}	4.69 ± 0.5^{c}	3.92 ± 0.4^{b}	4.51 ± 0.5^{c}
48	5.79 ± 0.4^{a}	3.87 ± 0.5^{b}	5.08 ± 0.5^{c}	5.31 ± 0.6^{d}	4.21 ± 0.5^{e}	5.37 ± 0.6^{d}
72	6.94 ± 0.4^{a}	4.21 ± 0.5^{b}	5.26 ± 0.6^{c}	5.72 ± 0.6^{d}	4.35 ± 0.5^{b}	5.52 ± 0.6^{d}
TBARS value						
0	0.231 ± 0.1^{a}	0.145 ± 0.1^{b}	0.242 ± 0.1^{c}	0.240 ± 0.1^{d}	0.130 ± 0.1^{b}	0.245 ± 0.1^{d}
6	0.562 ± 0.1^{a}	0.253 ± 0.1^{b}	0.354 ± 0.1^{c}	0.555 ± 0.2^{a}	0.252 ± 0.1^{b}	0.575 ± 0.2^{a}
12	0.666 ± 0.2^{a}	0.281 ± 0.1^{b}	0.422 ± 0.2^{c}	0.605 ± 0.4^{d}	0.261 ± 0.1^{b}	0.612 ± 0.2^{a}
24	0.784 ± 0.3^{a}	0.298 ± 0.1^{b}	0.541 ± 0.3^{c}	0.722 ± 0.5^{a}	0.305 ± 0.2^{b}	0.661 ± 0.3^{d}
36	0.863 ± 0.6^{a}	0.311 ± 0.2^{b}	0.569 ± 0.3^{c}	0.821 ± 0.5^{a}	0.355 ± 0.2^{b}	0.721 ± 0.5^{d}
48	1.215 ± 0.6^{a}	0.431 ± 0.2^{b}	0.635 ± 0.3^{c}	0.846 ± 0.^{d}	0.421 ± 0.3^{b}	0.794 ± 0.5^{e}
72	1.522 ± 0.6^{a}	0.489 ± 0.3^{b}	0.763 ± 0.4^{c}	0.932 ± 0.5^{d}	0.632 ± 0.4^{e}	0.832 ± 0.5^{f}

HF: hexane fraction, WF: water fraction, CME: crude methanolic extract, EAF: ethyl acetate fraction.
* Means in every row without a common superscript differ significantly at $P < 0.05$. BHA, butylated hydroxyanisol.

CME and HF fractions, and that their degradation rate of β-carotene clearly depends on their antioxidant activity. There was a correlation between the degradation rate and the bleaching of β-carotene; where the extract with the lowest β-carotene degradation rate exhibited the highest antioxidant activity. All extracts had a lower antioxidant activity than BHA (Fig. 1A).

Effect of white mahlab extracts/fractions (CME, HF, WF and EAF) on oxidation of β-carotene/linoleic acid at 50 °C is shown in Fig. 1B. The antioxidant activity of these extract/fractions was confirmed by this assay. β-Carotene molecules were protected by the extract/fraction to be bleached by linoleic acid. There is a significant difference ($P > 0.05$) between anti-bleaching effects of extract/fractions and positive control, BHA. From Fig. 1B the antioxidant activity of white mahlab extract/fractions reduces the oxidation of β-carotene in the order of CME, WF, HF and EAF, as CME exhibited the highest antioxidant activity.

3.5. Stability of corn oil as affected by the addition of different extracts/fractions from black and white mahlab seedcakes

Since the PRFs were effective as an antioxidant mixture in an emulsion (β-carotene–linoleate) and in DPPH, the next step was to test the activity of both the extracts/fractions in corn oil under accelerated conditions. Similar accelerated storage tests have been used by other authors to evaluate the efficacy of antioxidants (Shahidi et al., 2003; Mariod et al., 2006, 2008). Increasing primary and secondary lipid peroxidation products of corn oil during storage was measured by peroxide value and conjugated dienes (primary) and *p*-anisidine and TBARS values (secondary), during storage for the antioxidative effect of phenolic rich fractions from black and white mahlab seedcake. The effect of black and white mahlab extracts/fractions and BHA on oil oxidation measured by peroxide value is shown in Fig. 2A–D. From these figures the PV of corn oil (control) with and without black and white mahlab extracts/fractions (CME, HF, WF and EAF) added as 250, 500 mg/100 g oil or BHA (200 ppm), showed a gradual increase. As demonstrated in these figures a maximum PV of 17.5 meq O_2/kg was reached after 72 h of storage in the control without addition of extract or BHA. Significant differences ($P < 0.05$) were found between the control and CME, HF, WF and EAF or BHA, which decreased and slowed down the rate of peroxide formation, resulting in lower PVs after 72 h of storage at 70 °C. The PVs of corn oil containing WF, and EAF fractions from black mahlab were found to be less (more effective) than HF, and CME fractions (Fig. 2A and B) and all the fractions from black and white mahlab seedcakes were found to be less effective than the synthetic antioxidant. Using black and white mahlab seedcakes as natural antioxidants to prevent oxidation of corn oil in the rate of 250 mg/kg oil seem to be better and more effective and of course economically than using 500 mg (peroxide value data of black and white mahlab seedcakes extracts/fractions added as 500 mg/100 g was not shown).

Phenolic rich fractions from black and white mahlab seedcakes were tested as inhibitor of edible corn oil oxidation at 70 °C (Tables 2 and 3). The *A* 234 nm (conjugated dienes), *A* 270 nm, TBARS and *p*-anisidine values were monitored. All PRFs at 250 mg/100 g oil appeared to be strong inhibitors of corn oil oxidation. The most active fraction in both black and white mahlab was CME which exhibited an antioxidant activity seem to be similar to BHA at 200 mg/kg, the other three fractions (HF, EAF and WF) exhibited antioxidant activity lower than that of BHA. The antioxidant activity of black and white mahlab seedcakes PRFs was significantly different ($P < 0.05$). From the above studied results it was clear that

Table 3
Comparative inhibition of edible corn oil oxidation at 234 nm, 270 nm, *p*-anisidine value, and TBARS value by white mahlab seedcake phenolic rich fractions at 250 mg/100 g oil.

Time (h)	Control	BHA	HF	EAF	CME	WF
234 nm						
0	0.263 ± 0.1a	0.125 ± 0.1^{b}	0.221 ± 0.1^{c}	0.240 ± 0.1^{d}	0.165 ± 0.1^{b}	0.232 ± 0.1^{d}
6	0.561 ± 0.2^{a}	0.243 ± 0.1^{b}	0.354 ± 0.1^{c}	0.535 ± 0.2^{a}	0.255 ± 0.1^{b}	0.481 ± 0.2^{d}
12	0.782 ± 0.4^{a}	0.261 ± 0.1^{b}	0.447 ± 0.2^{c}	0.645 ± 0.4^{d}	0.265 ± 0.1^{b}	0.595 ± 0.2^{d}
24	0.893 ± 0.4^{a}	0.288 ± 0.1^{b}	0.589 ± 0.3^{c}	0.772 ± 0.5^{d}	0.325 ± 0.2^{e}	0.664 ± 0.3^{f}
36	0.984 ± 0.5^{a}	0.361 ± 0.2^{b}	0.599 ± 0.3^{c}	0.889 ± 0.5^{d}	0.375 ± 0.2^{b}	0.789 ± 0.5^{e}
48	1.344 ± 0.6^{a}	0.443 ± 0.2^{b}	0.662 ± 0.3^{c}	0.876 ± 0.^{d}	0.466 ± 0.3^{b}	0.794 ± 0.5^{e}
72	1.456 ± 0.5^{a}	0.555 ± 0.3^{b}	0.765 ± 0.4^{c}	0.912 ± 0.5^{d}	0.689 ± 0.4^{c}	0.899 ± 0.5^{d}
270 nm						
0	0.231 ± 0.1^{a}	0.112 ± 0.1^{b}	0.212 ± 0.1^{a}	0.260 ± 0.1^{c}	0.112 ± 0.06^{b}	0.251 ± 0.1^{c}
6	0.562 ± 0.3^{a}	0.153 ± 0.1^{b}	0.254 ± 0.2^{c}	0.272 ± 0.2^{d}	0.161 ± 0.07^{e}	0.262 ± 0.1^{c}
12	0.681 ± 0.4^{a}	0.125 ± 0.05^{b}	0.325 ± 0.2^{c}	0.424 ± 0.2^{d}	0.144 ± 0.1^{b}	0.354 ± 0.2^{c}
24	0.893 ± 0.4^{a}	0.126 ± 0.05^{b}	0.352 ± 0.2^{c}	0.511 ± 0.3^{d}	0.215 ± 0.2^{e}	0.455 ± 0.3^{f}
36	0.981 ± 0.6^{a}	0.154 ± 0.06^{b}	0.432 ± 0.2^{c}	0.632 ± 0.2^{d}	0.256 ± 0.2^{e}	0.552 ± 0.3^{f}
48	1.245 ± 0.6^{a}	0.156 ± 0.06^{b}	0.531 ± 0.3^{c}	0.771 ± 0.4^{d}	0.353 ± 0.2^{e}	0.643 ± 0.3^{f}
72	1.544 ± 0.7^{a}	0.252 ± 0.1^{b}	0.655 ± 0.3^{c}	0.863 ± 0.3^{d}	0.457 ± 0.2^{e}	0.674 ± 0.3^{c}
p-Anisidine value						
0	0.230 ± 0.1^{a}	0.11 ± 0.07^{b}	0.131 ± 0.1^{c}	0.152 ± 0.1^{d}	0.110 ± 0.06^{b}	0.150 ± 0.1^{d}
6	3.860 ± 0.2^{a}	1.84 ± 0.4^{b}	3.598 ± 0.6^{c}	3.654 ± 0.5^{c}	3.542 ± 0.4^{c}	3.640 ± 0.5^{c}
12	4.471 ± 0.4^{a}	2.71 ± 0.3^{b}	3.668 ± 0.4^{c}	3.715 ± 0.2^{c}	3.622 ± 0.5^{c}	3.697 ± 0.2^{c}
24	4.900 ± 0.5^{a}	3.14 ± 0.2^{b}	4.247 ± 0.4^{c}	4.403 ± 0.6^{c}	4.015 ± 0.6^{c}	4.354 ± 0.6^{c}
36	5.320 ± 0.3^{a}	3.52 ± 0.3^{b}	4.637 ± 0.4^{c}	4.903 ± 0.4^{d}	4.162 ± 0.6^{e}	4.722 ± 0.8^{f}
48	5.790 ± 0.4^{a}	3.87 ± 0.3^{b}	4.909 ± 0.7^{c}	5.457 ± 0.3^{d}	4.324 ± 0.3^{e}	4.976 ± 0.6^{c}
72	6.940 ± 0.6^{a}	4.11 ± 0.4^{b}	5.154 ± 0.5^{c}	5.780 ± 0.4^{d}	4.436 ± 0.5^{e}	5.766 ± 0.5^{d}
TBARS value						
0	0.231 ± 0.1^{a}	0.125 ± 0.1^{b}	0.241 ± 0.1^{c}	0.240 ± 0.1^{d}	0.135 ± 0.1^{b}	0.262 ± 0.1^{d}
6	0.462 ± 0.1^{a}	0.233 ± 0.1^{b}	0.364 ± 0.1^{c}	0.505 ± 0.2^{d}	0.255 ± 0.1^{b}	0.485 ± 0.2^{d}
12	0.566 ± 0.2^{a}	0.251 ± 0.1^{b}	0.421 ± 0.2^{c}	0.615 ± 0.4^{d}	0.265 ± 0.1^{b}	0.595 ± 0.2^{a}
24	0.734 ± 0.3^{a}	0.278 ± 0.1^{b}	0.511 ± 0.3^{c}	0.722 ± 0.5^{a}	0.300 ± 0.2^{b}	0.661 ± 0.3^{d}
36	0.853 ± 0.6^{a}	0.321 ± 0.2^{b}	0.599 ± 0.3^{c}	0.821 ± 0.5^{a}	0.345 ± 0.2^{b}	0.721 ± 0.5^{d}
48	1.215 ± 0.6^{a}	0.421 ± 0.2^{b}	0.665 ± 0.3^{c}	0.876 ± 0.^{d}	0.456 ± 0.3^{b}	0.794 ± 0.5^{e}
72	1.522 ± 0.6^{a}	0.487 ± 0.3^{b}	0.761 ± 0.4^{c}	0.912 ± 0.5^{d}	0.612 ± 0.4^{e}	0.832 ± 0.5^{f}

*Means in every row without a common superscript differ significantly at $P < 0.05$ BHA, butylated hydroxyanisol.
HF: hexane fraction, WF: water fraction, CME: crude methanolic extract, EAF: ethyl acetate fraction.

PRFs obtained from black and white mahlab seedcakes extracted by different solvents seem to be a good source of natural antioxidants that can be used to inhibit edible corn oil oxidation and these results were in agreement with different authors (Shahidi et al., 2003; Mariod et al., 2006, 2008; Roussis et al., 2008) who studied different extracts from different sources to be used as inhibitor of edible oil oxidation. Anisidine values of corn oil without black and white mahlab seedcakes extracts/fractions was rapidly increased ($P > 0.05$) to 6.94 after 72 h of storage and it was also significantly different to the other groups (BHA, HF, EAF, CME and WF) after the same period of storage, while corn oil containing 0.25% (w/w) of black and white mahlab seedcake extracts/fractions differed significantly from corn oil with 0.02% BHA after the 72 h storage at 70 °C (Tables 2 and 3). Addition of black and white mahlab extracts/fractions and BHA to corn oil had a significant ($P < 0.05$) effect on reducing TBARS formation as compared with the control sample in the following order: BHA > CME > HF > EAF > WF. CME was the strongest antioxidant among the PRFs tested.

3.6. Identification of phenolic compounds using HPLC–DAD

To know what is/are the responsible active ingredient(s) in black and white mahlab extracts/fractions, HPLC–DAD was used. Of the four solvent extracts, methanolic extracts exhibited high yield, and antioxidant activity (high in TPC and better AOA). Therefore, methanolic extract was used for further investigations towards identification by HPLC–DAD. The HPLC–DAD analysis of black and white mahlab seedcakes extracts revealed the presence of phenolic compounds. By this means, the crude methanolic extracts CME in the two samples were analysed. Fig. 3A and B shows a representative chromatogram of the CME of white and black mahlab seedcake PRFs, respectively, monitored at 280 nm. (+)-catechin, chlorogenic, hydroxybenzoic, *p*-cumeric and syringic acids were detected. These compounds have been identified according to their retention time and the spectral characteristics of their peaks compared to those of standards in Fig. 3C, as well as by spiking the sample with standards. Hydroxybenzoic acid was detected to be the major phenolic component in the two samples (white and black mahlab seedcake), contributing about 91.3% and 82.1% to the total amount, respectively, and showing the levels of 14.530 and 11.091 mg/100 g dry weight (DW) in CME of white and black mahlab, respectively. (+)-catechin, *p*-cumeric and syringic acid were also predominant in CME of white mahlab seedcake and showing the levels of 1.018, 0.234 and 0.125 mg/100 g DW, respectively. While in CME of black mahlab seedcake chlorogenic, (+)-catechin, and *p*-cumeric acid were the predominant phenolics showing the levels of 1.038, 0.885, and 0.404 mg/100 g DW, respectively. Results demonstrated that differences in CME of white and black

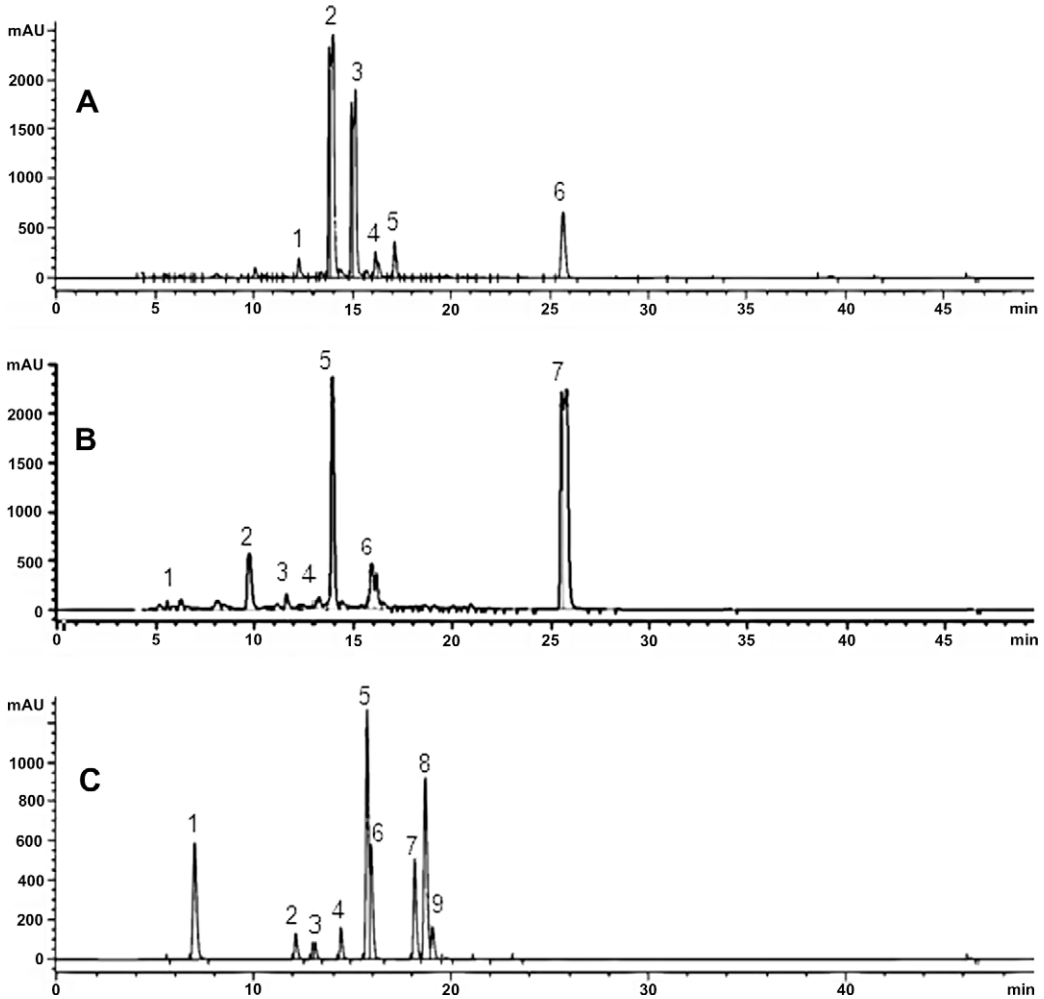

Fig. 3. (A) HPLC–DAD chromatogram of phenoilc compounds in white mahlab CME. Detection was at 280 nm. Peak: (1) (+)-catechin, (2) hydroxybenzoic acid (3) syringic acid, (4) *p*-cumeric (5) unknown, (6) unknown. (B) HPLC–DAD chromatogram of phenoilc compounds in black mahlab CME. Detection was at 280 nm. Peak: (1) gallic caid, (2) unknown, (3) (+)-catechin, (4) chlorogenic acid, (5) hydroxybenzoic acid, (6) *p*-cumeric, (7) unknown. (C) HPLC–DAD representative chromatogram of standards of phenolic acids recorded at 280 nm. Peak: (1) gallic caid, (2) (+)-catechin, (3) chlorogenic acid, (4) hydroxybenzoic acid, (5) syringic acid, (6) *p*-cumeric (7) vanillin, (8) ferulic (9) quercetin.

mahlab seedcake phenolic composition were significantly quantitative and qualitative, where white mahlab showed higher amounts in hydroxybenzoic and catechin than black mahlab. While, black mahlab seedcake contains chlorogenic acid which was not found in white mahlab seedcake. The levels of total phenolic compounds in CME of white and black mahlab determined by HPLC were 0.159 and 0.135 mg/g DW, respectively, and thus lesser than (71.9 and 17.1 mg/g) the ones obtained by the Folin–Ciocalteu method. This result is predictable due to the weak selectivity of the Folin–Ciocalteu reagent, as it reacts positively with different antioxidant compounds (phenolic and non-phenolic substances). The WF, EAF and HF fractions of black and white mahlab seedcake also presented some phenolic compounds with less area (data not shown). Previous studies reported that phenolic compounds such as hydroxybenzoic, syringic and *p*-cumeric containing significant antioxidant activities (Zhang, Liao, Moore, Wua, & Wang, 2009). The above mentioned HPLC–DAD results indicate that such phenolic rich fractions from black and white mahlab seedcake may inhibit the oxidation of corn oil. Isolation and characterisation of such PRFs may be useful in developing natural antioxidants.

4. Conclusions

This investigation shows that the peroxide, CD, TBARS and *p*-anisidine values were reliable methods that can be used to determine the lipid peroxidation in corn oil, containing various concentrations of black and white mahlab phenolic rich fractions (PRFs). Therefore, these PRFs can provide potential sources of natural antioxidants for inhibition of lipid oxidation. Six different individual phenolic compounds were identified in the studied samples by HPLC–DAD. All of the obtained results show that the black and white mahlab seedcakes extracts/fractions can be used as an easily accessible source of natural antioxidants and as a possible food supplement mainly in edible oils. Further studies in isolation of phenolic compounds using HPLC, GC/MS in mahlab seedcakes, and effects of these phenolics on antioxidant status in animal models are needed to evaluate their potential benefits.

Acknowledgements

The first author is grateful to IBS/UPM for the senior research fellowship granted during the period of this work. We thank Siti Muskinah, Laboratory of Molecular Biomedicine IBS/UPM for analysis in HPLC–DAD equipment and excellent technical expertise needed for this work. This study was funded by Intensifying Research Priority Areas (IRPA) grants provided by Government of Malaysia and Universiti Putra Malaysia.

References

Amarowicz, R., Wanasundara, U., Wanasundara, J., & Shahidi, F. (1993). Antioxidant activity of ethanolic extracts of flaxseed in a β-carotene–linoleate model system. *Journal of Food Lipids, 1*, 111–117.

AOCS (1993). In AOCS (Ed.), *Official methods and recommended practices of the American Oil Chemists' Society* (5th ed.) Champaign, IL official method Cc 13b-45 (reapproved (2000)).

Aydin, C., Ogut, H., & Konak, M. (2002). Some physical properties of Turkish mahaleb. *Biosystems Engineering, 82*(2), 231–234.

Ayoub, S. M., & Babiker, A. J. (1981). Component fatty acids from the oils of *Monechma ciliatum*. *Fitoterapia, 52*, 251–253.

Chirinos, R., Betalleluz, I., Humána, A., Arbizub, C., Pedreschi, R., & Campos, C. (2009). HPLC–DAD characterization of phenolic compounds from Andean oca (*Oxalis tuberose* Mol.) tubers and their contribution to the antioxidant capacity. *Food Chemistry, 113*, 1243–1251.

Duh, P. D., & Yen, Y. C. (1997). Antioxidant efficacy of methanolic extracts of peanut hulls in soybean and peanut oils. *Journal of the American Oil Chemists' Society, 74*, 745–748.

Gordon, M. H., Paiva-Martins, F., & Almeida, M. (2001). Antioxidant activity of hydroxytyrosol acetate compared with that of other olive oil polyphenols. *Journal of Agricultural and Food Chemistry, 49*, 2480–2485.

Hertog, M. L., Feskens, E. M., Hollman, P. H., Katan, M. B., & Kromhout, D. (1993). Dietary antioxidant flavonoids and risk of coronary heart-diseases the Zutphen elderly study. *Lancet, 342*, 1007–1011.

Jadhav, S. J., Nimbalkar, S. S., Kulkarni, A. D., & Madhavi, D. L. (1996). Lipid oxidation in biological and food systems. In D. L. Madhavi, S. S. Deshpande, & D. K. Salunkhe (Eds.), *Food antioxidants* (pp. 5–63). New York: Dekker Press.

Kumaran, A., & Karunakaran, J. R. (2006). Antioxidant and free radical scavenging activity of an aqueous extract of *Coleus aromaticus*. *Food Chemistry, 97*, 109–114.

Liyana-Pathirana, C. M., & Shahidi, F. (2006). Importance of insoluble bound phenolics to antioxidant properties of wheat. *Journal of Agricultural and Food Chemistry, 54*, 1256–1264.

Malencic, D., Maksimovic, Z., Popovic, M., & Miladinovic, J. (2008). Polyphenol contents and antioxidant activity of soybean seed extracts. *Bioresource Technology, 99*, 6688–6691.

Mariod, A. A., Matthaüs, B., Eichner, K., & Hussein, I. H. (2006). Antioxidant activity of extracts from *Sclerocarya birrea* kernel oil cake. *Grasas Y Aceites, 57*(4), 361–366.

Mariod, A. A., Matthaus, B., & Hussein, I. H. (2008). Antioxidant properties of methanolic extracts from different parts of *Sclerocarya birrea*. *International Journal of Food Science and Technology, 43*, 921–926.

Matthaüs, B. (2002). Antioxidant activity of extracts obtained from residues of different oilseeds. *Journal of Agricultural and Food Chemistry, 50*, 3444–3452.

Molyneux, P. (2004). The use of the stable free radical diphenylpicrylhydrazyl (DPPH) for estimating antioxidant activity. *Songklanakarin Journal of Science and Technology, 26*, 211–219.

Moure, A., Franco, D., Sineiro, J., Dominguez, H., Nunez, M. J., & Lema, J. M. (2000). Evaluation of extracts from Gevuina hulls as antioxidants. *Journal of Agricultural and Food Chemistry, 48*, 3890–3897.

Pantzaris, T. P. (1999). Palm oil in frying. In D. Boskou, & I. Elmadfa (Eds.), *Frying of food, oxidation, nutrient and non-nutrient antioxidants, biologically active compounds and high temperatures* (pp. 247–248). USA: CRC Press.

Roussis, I. G., Tzimas, P. C., & Soulti, K. (2008). Antioxidant activity of white wine extracts and phenolic acids toward corn oil oxidation. *Journal of Food Processing and Preservation, 32*, 535–545.

Scholz, E., & Rimpler, H. (1989). Proanthocyanidins from *Krameria triandra* root. *Planta Medica, 55*, 379.

Shahidi, F., Desilva, C., & Amarowicz, R. (2003). Antioxidant activity of extracts of defatted seeds of niger (*Guizotia abyssinica*). *Journal of the American Oil Chemists' Society, 80*, 443–450.

Sharief, M. T. (2002). *The Effect of sowing date and plant spacing on growth and yield of black mahlab (Monechma ciliatum)*. Khartoum, Sudan: M.Sc. thesis, University of Khartoum.

Sherwin, E. R. (1978). Oxidation and antioxidants in fat and oil processing. *Journal of the American Oil Chemists' Society, 55*, 809–814.

Surh, Y. J. (2002). Anti-tumor promoting potential of selected spice ingredients with antioxidative and anti-inflammatory activities: A short review. *Food and Chemical Toxicology, 40*, 1091–1097.

Surh, Y. J., Hurh, Y. J., Kang, J. Y., Lee, E., Kong, G., & Lee, S. J. (1999). Resveratrol, an antioxidant present in red wine, induces apoptosis in human promyelocytic leukemia (HL-60) cells. *Cancer Letters, 140*(1–2), 1–10.

Uguru, M. O., Okwuasaba, F. K., Ekwenchi, M. M., & Uguru, V. E. (1995). Oxytocic and oestrogenic effects of *Monechma ciliatum* methanol extract in vivo and in vitro in rodents. *Phytotherapy Research, 9*, 26–29.

Williams, G. M., Iatropoulos, M. J., & Whysner, J. (1999). Safety assessment to butylated hydroxyanisol and butylated hydroxytoluene as antioxidant food additives. *Food and Chemical Toxicology, 37*, 1027–1038.

Zhang, Z., Liao, L., Moore, J., Wua, T., & Wang, Z. (2009). Antioxidant phenolic compounds from walnut kernels (*Juglans regia* L.). *Food Chemistry, 113*, 160–165.

Zhou, K., & Yu, L. (2006). Total phenolic contents and antioxidant properties of commonly consumed vegetables grown in Colorado. *Lebensmittel-Wissenschaft und-Technologie, 39*, 1155–1162.

Food Chemistry 118 (2010) 128–132

Contents lists available at ScienceDirect

Food Chemistry

journal homepage: www.elsevier.com/locate/foodchem

Short communication

Determination of isoflavone content and antioxidant activity in *Psoralea corylifolia* L. callus cultures

Amit N. Shinde [a], Nutan Malpathak [a], Devanand P. Fulzele [b,*]

[a] Department of Botany, University of Pune, Pune 411 007, India
[b] Plant Biotechnology and Secondary Products Section, Nuclear Agriculture and Biotechnology Division, Bhabha Atomic Research Centre, Mumbai 400 085, India

ARTICLE INFO

Article history:
Received 19 December 2008
Received in revised form 8 April 2009
Accepted 22 April 2009

Keywords:
Psoralea corylifolia
Daidzein
Genistein
Antioxidant activity
Light intensity

ABSTRACT

Relation between isoflavones production and antioxidant activity in *Psoralea corylifolia* cell cultures was studied. High performance liquid chromatography analysis revealed that root-derived callus cultures produced maximum amount of daidzein whereas genistein by leaf-derived callus. Cell cultures grown under continuous illumination (40-μmol m^{-2} s^{-1}) produced several-fold more isoflavones daidzein (2.28% dry wt) and genistein (0.21% dry wt) than that of field grown plants. The antioxidant activity of extracts was determined using 1,1-diphenyl-2-picrylhydrazyl (DPPH) radical scavenging assay, phosphomolybdenum assay and correlated with the content of total phenolics in the extracts. Calli grown under continuous illumination exhibited strong antioxidant activities compared to dark grown callus cultures and explants materials.

1. Introduction

Psoralea corylifolia L. (Fabaceae) is a rich source of isoflavones daidzein (4′,7-dihydroxyisoflavone) and genistein (4′,5,7 trihydroxyisoflavone). In view of the action of natural dietary estrogens, they are recognised as potentially health-protective food compounds (neutraceuticals), which provide health benefits, including the prevention of sex hormone related ailments, cancer and cardiovascular diseases (Shinde, Malpathak, & Fulzele, 2009). Isoflavones also exert antioxidant properties thereby provide protective effect against oxidative damage (Akitha Devi et al., 2009; Slavin, Cheng, Luther, Kenworthy, & Yu, 2009).

Consumption of antioxidant constituents reported to have protection against oxidative damage induced degenerative and pathological processes including ageing and cancer (Tadhani, Patel, & Subhash, 2007). Antioxidant properties have been studied in several plant species for the development of natural antioxidant formulations in the areas of food, medicine and cosmetics (Miliauskas, Venskutonis, & Van Beek, 2004). However, chemical constituents of medicinal plants depending on several factors such as cultivation area, climatic conditions and genetic modification (Miliauskas et al., 2004; Santos-Gomes, Seabra, Andrade, & Fernandes-Ferreira, 2002).

Plant cell culture offers uniform secondary product synthesis by eliminating effect of unforeseen climatic conditions and diseases as observed in field grown plants. Plant tissue cultures have been used to derive isoflavones from various medicinal plants (Bouque, Bourgaud, Nguyen, & Guckert, 1998; Luczkiewicz & Glod, 2003; Matkowski, 2004). Light irradiation is one of the important factors that can act as a switch for controlling the expression of secondary metabolism to enhance the yield of useful bioactive compounds in plant cell cultures (Guo, Liu, Yan, & Liu, 2007; Park, Kim, Yang, Chung, & Choi, 2003).

No information is available about the influence of plant growth regulators and light regime on growth and isoflavones production in callus cultures of *P. corylifolia.* Further antioxidant potential of callus cultures was also not studied. This article deals with isoflavone production in callus cultures of *P. corylifolia* under influence of plant growth regulators and light intensity. Antioxidant potential of *in vitro* and *in vivo* cultures of *P. corylifolia* was also reported for the first time.

2. Material and methods

2.1. Plant material and tissue culture

Plants and seeds of *P. corylifolia* were collected from botanical garden, University of Pune, India. Plants were separated into different parts and analysed for daidzein and genistein content. *In vitro* seedlings were raised as described elsewhere (Shinde et al., 2009). Three-week-old *in vitro* germinated seedlings were used as a

* Corresponding author. Tel.: +91 22 25590230; fax: +91 22 25505326.
E-mail addresses: dfulzele@hotmail.com, dfulzele@barc.gov.in (D.P. Fulzele).

0308-8146/$ - see front matter © 2009 Elsevier Ltd. All rights reserved.
doi:10.1016/j.foodchem.2009.04.093

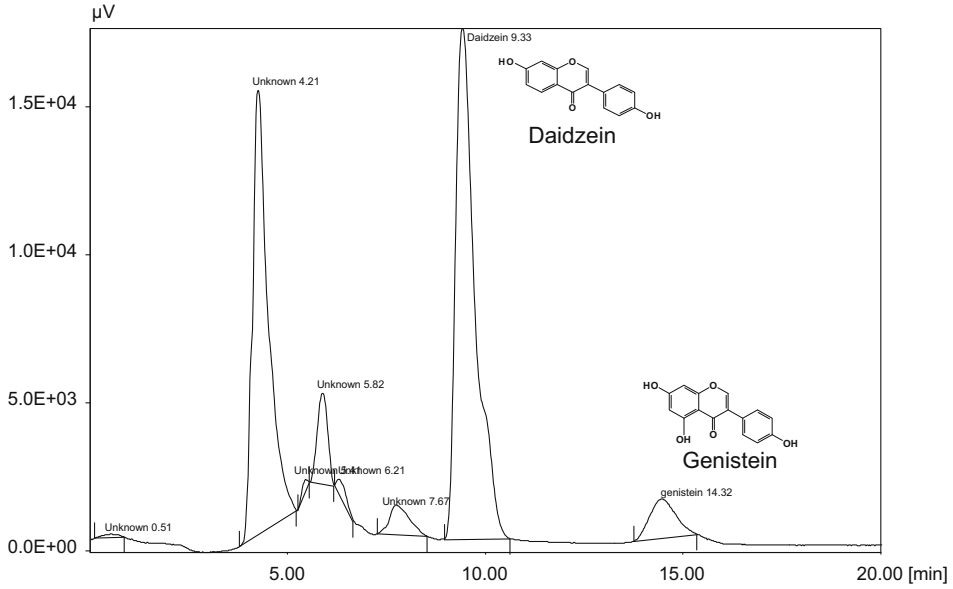

Fig. 1. HPLC analysis showing presence of daidzein and genistein in *P. corylifolia* extracts.

source of explants for initiation of callus cultures. Leaves and roots were incised into small pieces (9–10 mm) and cultured aseptically on MS medium (Murashige & Skoog, 1962) supplemented with different combinations and concentrations of 2,4-dichlorophenoxyacetic acid (2,4-D; 2.26–9.05 µM), α-naphthalene-acetic acid (NAA; 5.37–10.74 µM), Indole-3-acetic acid (IAA; 5.71–11.42 µM) and 6-bezylaminopurine (BAP; 4.40 µM) and denoted as (M1–M7) in Fig. 2. The cultures were maintained on similar media compositions and sub-cultured after every four weeks. After a period of 10-subculture, established callus cultures were taken up for growth study and quantification of isoflavones daidzein and genistein.

For light experiment, cultures were maintained under different light intensities ranges from 13 to 40 µmol m^{-2} s^{-1}. For studying the effect of photoperiod conditions, callus cultures were incubated under continuous light illumination, photoperiod (16 h light and 8 h dark) and in dark conditions.

2.2. Growth parameters

Callus cultures were gently pressed on filter papers (Whatman No. 1) to remove excess water for fresh weight (FW) determination. Cultures were dried in an oven at 55 °C for 16 h to get dry weight (DW). All experiments were replicated three times. Growth was determined as Growth index (GI) using formula:

$$\frac{\text{Final wt of Biomass} - \text{Initial wt of biomass}}{\text{Initial wt of biomass}}$$

2.3. Extraction of isoflavones and High Performance Liquid Chromatography analysis

Isoflavones were extracted from dried and powered plant material using method described elsewhere (Shinde et al., 2009). An isocratic analytical HPLC was performed on Jasco Liquid Chromatograph (Model 980, Japan) equipped with 25 µl loop and a variable wavelength detector (Model No. UV-975, Japan). Separations were performed on Inertsil C_{18} (250 mm × 4.6 I.D, Sigma, USA) column using acetonitrile:water (40:60 v/v) as a mobile phase. The flow rate was 0.6 ml/min and the elution was monitored at 250 nm (Shinde et al., 2009).

2.4. Preparation of extract for antioxidant activity

Callus cultures derived from roots and leaves grown under different conditions were used for antioxidant activities. Explant material was collected from greenhouse grown plants. Biomass was dried at 55 °C for 16 h and dried materials (1 g) mixed with 40 ml of methanol followed by sonication at 33 KH_z for 40 min. Thereafter, extracts were filtered by filter paper (Whatman No. 1) and filtrate evaporated under reduced pressure by BÜCHI Rotavapor (RI 111, Switzerland) at 45 °C. The residues were dissolved in an appropriate volume of methanol to obtained 100 mg/ml concentration and stored at −20 °C until used.

DPPH (2,2-diphenyl-1-pycrilhydrazil hydrate) and phosphomolybdenum reduction assay was carried out as described elsewhere (Ho, Tsai, Chen, Huang, & Lin, 2001; Prieto, Pineda, & Aguilar, 1999). The free radical (DPPH) scavenging activity was expressed as % inhibition whereas phosphomolybdenum reduction capacity of extract as equivalents of ascorbic acid (µmol/g of extract) at 50 µg/ml concentrations. Total phenolics content was estimated

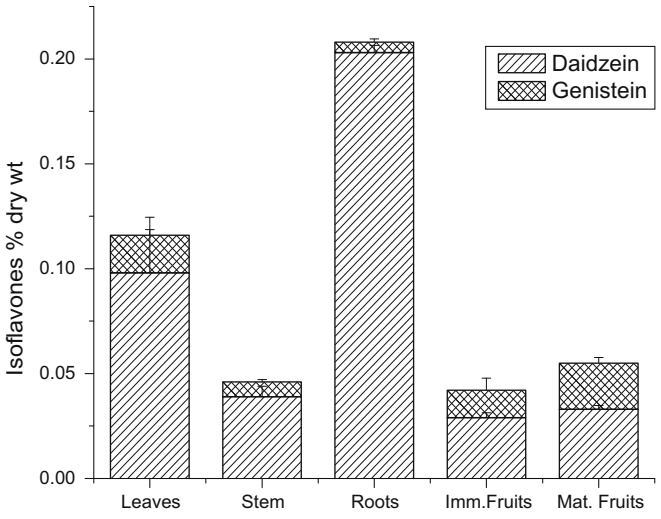

Fig. 2. Distribution of isoflavones daidzein and genistein in different organs of *P. corylifolia* plant. Results are the mean of five replicates ± SD.

as gallic acid equivalents (GAE) and expressed as mg gallic acid/g extract (Singleton, Orthofer, & Lamuela-Raventos, 1999).

2.5. Statistical analysis

The influence of various treatments on growth and isoflavones content was analysed by one-way analysis of variance (ANOVA). Values are mean of five replicates from two experiments. The data was analysed statistically by analysis of variance (ANOVA) and difference between means of the samples was analysed by the least significant difference (LSD) at a probability level of 0.05.

3. Results and discussion

3.1. Daidzein and genistein content in P. corylifolia plant material

Isoflavones content was determined in different parts of field grown plants (Fig. 1). The chromatographic analysis revealed that highest levels of daidzein was accumulated in roots (0.20% dry wt) whereas genistein (0.03% dry wt) by immature fruits (Fig. 2).

3.2. Callus growth and isoflavone production

Callus cultures were developed on MS medium supplemented with different combinations and concentrations of plant growth regulators (M1–M7). High growth index (8.4, 7.0 and 6.6) was achieved from root-derived callus on M6, M2 and M4 medium respectively. Leaf-derived callus exhibited slower growth (Growth index 6.1, 5.8, and 5.3) on similar media compositions (Fig. 3A and B). HPLC profiles revealed that highest daidzein (1.74% dry wt) was produced in callus derived from roots on M6 medium (Fig. 3A) whereas genistein (0.165% dry wt) by leaf-derived callus on similar medium (Fig. 3B). Medium containing 2,4-D was found to be optimum for isoflavone accumulation in callus cultures of *Pueraria lobata* and *Psoralea* sp. (Bouque et al., 1998; Matkowski, 2004). Similarly, present results indicated that the content of isoflavones

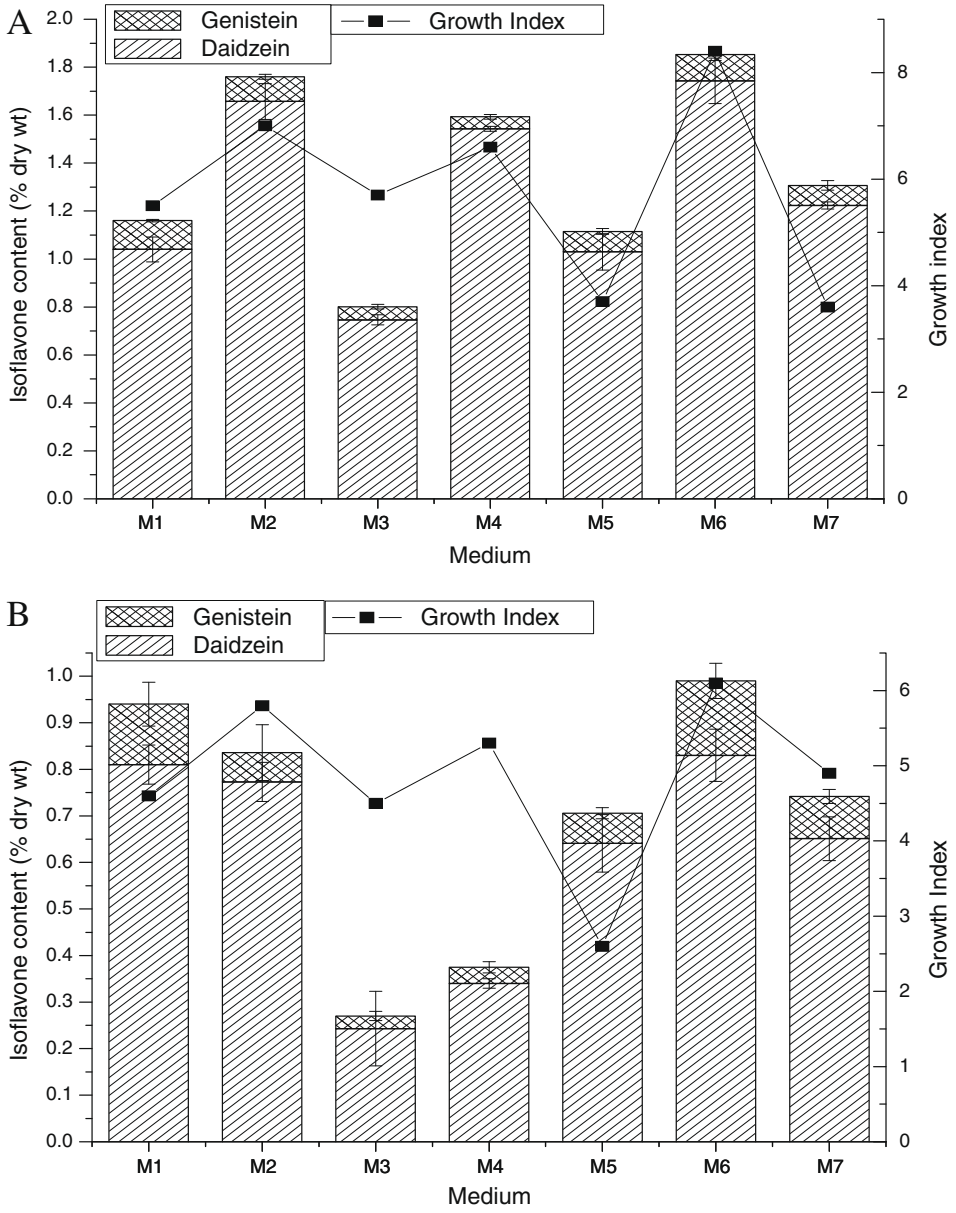

Fig. 3. Chromatographic analysis of daidzein and genistein in callus cultures obtained from roots (A) and leaf (B) explants on MS medium supplemented with different combinations and concentrations of plant growth regulators. Results are the mean of five replicates ± SD [M1: 2,4-D (4.52 μM) + BAP (4.40 μM); M2: 2,4-D (9.05 μM) + BAP (4.40 μM); M3: NAA (5.37 μM) + BAP (4.40 μM); M4: NAA (10.74 μM) + BAP (4.40 μM); M5: IAA (2.26 μM) + BAP (4.40 μM); M6: IAA (5.71 μM) + BAP (4.40 μM); M7: IAA (9.05 μM) + BAP (4.40 μM)].

Table 1
Effect of different light intensities and photoperiod conditions on growth and isoflavones production in callus cultures of *P. corylifolia* on 30th day.

Light intensity and photoperiod conditions	Dry wt (g)	Daidzein (% dry wt)	Genistein (% dry wt)
13.7 μmol $m^{-2}s^{-1}$, 16 h light + 8 h dark	0.20 ± 0.01^{b}	1.257 ± 0.13^{b}	0.09 ± 0.001^{ba}
27 μmol $m^{-2}s^{-1}$, 16 h light + 8 h dark	0.22 ± 0.03^{ab}	1.597 ± 0.12^{b}	0.11 ± 0.001^{b}
40 μmol $m^{-2}s^{-1}$, 16 h light + 8 h dark	0.25 ± 0.01^{a}	1.890 ± 0.20^{a}	0.15 ± 0.003^{ab}
40 μmol $m^{-2}s^{-1}$, continuous illumination	0.23 ± 0.01^{ab}	2.283 ± 0.11^{a}	0.21 ± 0.005^{a}
Dark condition	0.196 ± 0.01^{b}	0.623 ± 0.20^{c}	0.06 ± 0.002^{b}

Results are the mean of three replicates ± SD (Means with common letters (a–b) within column are not significantly different at $P \leqslant 0.05$ according to LSD test).

Table 2
Content of total phenolics and antioxidant activity of *in vitro* and *in vivo* cultures of *P. corylifolia*.

Plant material	DPPH assay EC_{50} value (μg/ml)	Phosphomolybdenum assay (50 μg/ml)	Total phenolic content (mg GAE/g dry wt)
Leaf	117.16 ± 2.48^{c}	84.5 ± 7.77^{b}	41 ± 1.41^{a}
Roots	273.27 ± 2.30^{a}	75.5 ± 5.16^{d}	28 ± 2.82^{e}
Leaf-derived callus	112.93 ± 2.80^{d}	53 ± 4.24^{e}	28.7 ± 1.76^{e}
Root-derived callus	104.89 ± 3.76^{e}	104 ± 8.48^{b}	39 ± 1.41^{c}
Dark grown callus	271.15 ± 5.99^{b}	78 ± 1.31^{c}	35.5 ± 0.70^{d}
Light grown callus	99.53 ± 2.95^{f}	169 ± 4.24^{a}	45 ± 0.10^{b}

Each value is expressed as the mean ± S.D. of three replicate determinations. (Means with common letters (a–f) within column are not significantly different at $P \leqslant 0.05$ according to LSD test).

in root and leaf-derived callus cultures was higher on 2,4-D and IAA containing medium. Matkowski (2004) reported that root-derived callus produced high concentrations of daidzin than leaf-derived callus of *P. lobata*. Similar to this, in case of *P. corylifolia*, root-derived callus cultures synthesized high amount of daidzein.

3.3. Effect of light intensity on growth and daidzein and genistein production

Root-derived callus cultures grown on M6 medium showed rapid growth and high accumulation of daidzein and genistein compared to other medium (M1–M7). Therefore, similar cultures were selected and consequently used for further experiments. The light intensities and different photoperiod conditions did not show significant effects on callus growth. Maximum light intensity (40 μmol m^{-2} s^{-1}) and continuous light illumination stimulated production of daidzein (2.28% dry wt) and genistein (0.21% dry wt) on day 30. It was observed that increased light intensity and illumination period enhanced isoflavones production level. On the contrary, absence of light inhibited the daidzein and genistein production (Table 1). Our findings strengthen the fact reported earlier that, presence of light enhanced isoflavone production in callus cultures of *Genista tinctoria* (Luczkiewicz & Glod, 2003). Similarly, edible legume seedlings showed enhanced levels of isoflavonoids production when grown in light compared to dark (Lal, Warber, Kirakosyan, Kaufman, & Duke, 2003). Light irradiation is one of the important factor that acts as a switch for controlling the expression of specific genes involved in growth and secondary metabolism of plants (Liu et al., 2006). Our findings are in agreement with the various results obtained for production of flavonoids by cell cultures exposed to light (Guo et al., 2007).

3.4. Antioxidant activities and total phenolics content

The most effective DPPH radical scavenging and phosphomolybdenum reducing property was shown by root-derived callus cultures grown under continuous illumination (at 40 μmol m^{-2} s^{-1} intensity) compared to dark grown cultures and explant material (Table 2). Similarly highest total phenol content was found in callus cultures grown under continuous illumination of light (45 mg GAE/g dry wt) compared to other callus cultures and explants used (Table 2). Correlation analysis indicated that content of phenolics is partially correlated with DPPH radical scavenging ($r = 0.4664$) and phosphomolybdenum reducing ($r = 0.7030$) activity. It is generally stated that only flavonoids of certain structure and with hydroxyl position in the molecule determine antioxidant properties. However antioxidant potential of the extracts does not solely depend on phenolics. Terpenes are another major group of chemicals showed antioxidant potential against lipid peroxidation and DPPH radical scavenging activity (Karagozler, Erdag, Emek, & Uygun, 2008) which could be an additional contributory factor for antioxidant activity of extracts.

In vitro cultures of *P. corylifolia* exhibited highest antioxidant activity compared to field grown plant parts. It was generally assumed that dedifferentiated cultures proved to be less active as antioxidants (Grzegorczyk, Matkowski, & Wysokinska, 2007). However, present results indicated that callus extracts showed significant antioxidant potential compared to *in vivo* materials, which could be explored further for source of natural antioxidants. Similar improved antioxidant activity was observed in *in vitro* cultures of *Salvia officinalis and Rosmarinus officinalis* compared to its field grown plant materials (Grzegorczyk et al., 2007; Yesil-Celiktas, Nartop, Gurel, Bedir, & Vardar-Sukan, 2007).

4. Conclusion

Levels of daidzein (2.28% dry wt) accumulated in callus cultures on day 30 was ~11-fold more than that of 60-day-old plants. These results exhibited that appropriate light intensities effectively enhanced accumulation of daidzein and genistein in callus cultures. In addition *in vitro* cultures of *P. corylifolia* exhibited highest antioxidant activity compared to field grown plant parts. Isoflavones production and antioxidant activities of *P. corylifolia* will help to select callus culture type as a source of natural antioxidants and nutraceuticals to enhance health benefits.

Acknowledgement

The SRF provided by Department of Atomic Energy, India, to Amit Shinde is gratefully acknowledged.

References

Akitha Devi, M. K., Gondi, M., Sakthivelu, G., Giridhar, P., Rajasekaran, T., & Ravishankar, G. A. (2009). Functional attributes of soybean seeds and products,

with reference to isoflavone content and antioxidant activity. *Food Chemistry, 114*, 771–776.
Bouque, V., Bourgaud, F., Nguyen, C., & Guckert, A. (1998). Production of daidzein by callus cultures of *Psoralea* species and comparison with the plants. *Plant Cell, Tissue and Organ Culture, 53*, 35–40.
Grzegorczyk, I., Matkowski, A., & Wysokinska, H. (2007). Antioxidant activity of extracts from *in vitro* cultures of *Salvia officinalis* L. *Food Chemistry, 104*, 536–541.
Guo, B., Liu, Y. G., Yan, Q., & Liu, C. Z. (2007). Spectral composition of irradiation regulates the cell growth and flavonoids biosynthesis of callus cultures of *Saussurea medusa* Maxim. *Plant Growth Regulation, 52*, 259–263.
Ho, K. Y., Tsai, C. C., Chen, C. P., Huang, J. S., & Lin, C. C. (2001). Screening of Brazilian plant extracts for antioxidant activity by the use of DPPH free radical method. *Phytotherapy Research, 15*, 127–130.
Karagozler, A. A., Erdag, B., Emek, Y. C., & Uygun, D. A. (2008). Antioxidant activity and proline content of leaf extracts from *Dorystoechas hastata*. *Food Chemistry, 111*, 400–407.
Lal, A., Warber, S., Kirakosyan, A., Kaufman, P. B., & Duke, J. A. (2003). Upregulation of isoflavonoids and soluble proteins in edible legumes by light and fungal elicitor treatments. *The Journal of Alternative and Complementary Medicine, 9*, 371–378.
Liu, Z., Qi, J., Chen, L., Ming, S., Wang, X., Pang, Y., et al. (2006). Effect of light on gene expression and shikonin formation in cultures *Onosma paniculatum* cells. *Plant Cell, Tissue and Organ Culture, 84*, 38–48.
Luczkiewicz, M., & Glod, D. (2003). Callus cultures of Genista plants – *In vitro* material producing high amounts of isoflavones of phytoestrogenic activity. *Plant Science, 165*, 1101–1108.
Matkowski, A. (2004). *In vitro* isoflavonoid production in callus from different organs of *Pueraria lobata* (Wild.) Ohwi. *Journal of Plant Physiology, 161*, 343–346.
Miliauskas, G., Venskutonis, P. R., & Van Beek, T. A. (2004). Screening of radical scavenging activity of some medicinal and aromatic plants. *Food Chemistry, 85*, 231–237.
Murashige, T., & Skoog, F. (1962). A revised medium for rapid growth and bioassay with tobacco tissue cultures. *Physiologia Plantarum, 15*, 475–479.
Park, Y. G., Kim, M. H., Yang, J. K., Chung, Y. G., & Choi, M. S. (2003). Light-susceptibility of camptothecin production from *in vitro* cultures of *Camptotheca acuminata* Decne. *Biotechnology & Bioprocess Engineering, 8*, 32–36.
Prieto, P., Pineda, M., & Aguilar, M. (1999). Spectrophotometric quantitation of antioxidant capacity through the formation of a phosphomolybdenum complex: Specific application to the determination of vitamin E. *Analytical Biochemistry, 269*, 337–341.
Santos-Gomes, P. C., Seabra, R. M., Andrade, P. B., & Fernandes-Ferreira, M. (2002). Phenolic antioxidant compounds produced by *in vitro* shoots of sage (*Salvia officinalis* L.). *Plant Science, 162*, 981–987.
Shinde, A. N., Malpathak, N., & Fulzele, D. P. (2009). Studied enhancement strategies for phytoestrogens production in shake flasks by suspension culture of *Psoralea corylifolia*. *Bioresource Technology, 100*, 1833–1839.
Singleton, V. L., Orthofer, R., & Lamuela-Raventos, R. M. (1999). Analysis of total phenols and other oxidation substrates and antioxidants by means of Folin–Ciocalteu reagent. In L. Packer (Ed.). *Methods in enzymology* (Vol. 299, pp. 152–315). San Diego, CA: Academic Press.
Slavin, M., Cheng, Z., Luther, M., Kenworthy, W., & Yu, L. (2009). Antioxidant properties and phenolic, isoflavone, tocopherol and carotenoid composition of Maryland-grown soybean lines with altered fatty acid profiles. *Food Chemistry, 11*, 420–427.
Tadhani, M. B., Patel, V. H., & Subhash, R. (2007). *In vitro* antioxidant activities of *Stevia rebaudiana* leaves and callus. *Journal of Food Composition and Analysis, 20*, 323–329.
Yesil-Celiktas, O., Nartop, P., Gurel, A., Bedir, E., & Vardar-Sukan, F. (2007). Determination of phenolic content and antioxidant activity of extracts obtained from *Rosmarinus officinalis*' calli. *Journal of Plant Physiology, 164*, 1536–1542.

Food Chemistry 118 (2010) 133–140

Contents lists available at ScienceDirect

Food Chemistry

journal homepage: www.elsevier.com/locate/foodchem

Analytical Methods

Separation and isolation of β-sitosterol oxides and their non-mutagenic potential in the Salmonella microsome assay

Karin Koschutnig [a], Suvi Kemmo [b], Anna-Maija Lampi [b], Vieno Piironen [b], Cornelia Fritz-Ton [a], Karl-Heinz Wagner [a,*]

[a] Department of Nutritional Sciences, University of Vienna, Althanstrasse 14, 1090 Vienna, Austria
[b] Department of Applied Chemistry and Microbiology, University of Helsinki, Latokartanonkaari 11, P.O. Box 27, FIN-00014 University of Helsinki, Finland

ARTICLE INFO

Article history:
Received 9 July 2008
Received in revised form 16 April 2009
Accepted 18 April 2009

Keywords:
Phytosterol oxidation products
HPLC
Salmonella microsome assay

ABSTRACT

The recent increase in phytosterol-enriched functional food provokes questions concerning the safety of their oxidation products. However, most of the existing toxicity studies have been performed with mixtures instead of single compounds, a consequence of the lack of pure phytosterol oxidation product (POP)-standards.

The objectives of this study were to take in use a method for the isolation of β-sitosterol oxidation products and to assess their mutagenic and pro-oxidative potential. Oxides were prepared by thermo-oxidation, purified by column chromatography and separated by a NP–HPLC–UV system. 7-ketositosterol, 7β-OH-sitosterol, 7α-OH-sitosterol, a mixture of 6β-OH-3-ketositosterol/6α-OH-3-ketositosterol (ratio 4:3) and a mixture of polar oxides were fractionated. Yields in the range of several milligrams per fraction were achieved within one HPLC-run. Identification and quantification was done by GC–MS and GC–FID, respectively. In the Ames test the collected fractions failed to show a mutagenic activity towards Salmonella typhimurium strains TA98, TA100 and TA102.

1. Introduction

Recently phytosterols (plant sterols) have become a focus of interest due to their serum cholesterol lowering effect and consequently their protection against cardiovascular diseases (Piironen, Lindsay, Miettinen, Toivo, & Lampi, 2000). According to the literature an uptake of 1.5–3 g phytosterols per day is recommended in order to achieve a reduction of 10–15% in serum LDL cholesterol (Katan et al., 2003). As the daily intake from natural sources is estimated to range from 150 to 440 mg a day, a wide variety of products fortified with phytosterols has been introduced to the market in order to reach the advised uptake levels. However, besides their positive aspects concerns in terms of health are emerging.

It is well known that during food preparation and storage cholesterol oxidation products (COPs) are formed from cholesterol through autoxidation, photoxidation and enzymatic oxidation (Boesinger, Luf, & Brandl, 1993). Mutagenic, carcinogenic, angiotoxic, cytotoxic and atherogenic properties of the thereby generated COPs are generally accepted and have already been extensively documented (for review see Osada, 2002).

Similar to cholesterol, phytosterols consist of a tetracyclic cyclopenta[α]phenanthrene ring, they mainly differ in their side chain (Piironen et al., 2000). Because of their structural similarities, phytosterols are expected to undergo analogous chemical reactions as cholesterol, including oxidation. But information on phytosterol oxidation products (POPs) is still rather limited.

Existing knowledge on POPs is mainly concentrated on their quantification in food. In first studies concerning their absorption in vivo a significant uptake of POPs was proven (Grandgirard et al., 2004).

Regarding their possible harmful effects only a few studies were conducted and most of them dealt with a potential cytotoxicity. Investigations with different cultured mammalian cells showed comparable damage to that caused by COPs, but higher concentrations of POPs were needed (Adcox, Boyd, Oehrl, Allen, & Fenner, 2001; Maguire, Konoplyannikov, Ford, Maguire, & O'Brien, 2003; Ryan, Chopra, McCarthy, Maguire, & O'Brien, 2005). So far only Lea, Hepburn, Wolfreys, and Baldrick (2004) investigated the mutagenic potential of POPs in the Ames test and reported no evidence of genotoxicity. However, in this investigation only a non-specified mixture with 30% of POPs was analysed. Due to the lack of commercial POP-standards in most cases a blend instead of single oxidation products has been used for toxicity studies. But evidence exists that compared to mixtures individual POPs behave in a different way (Maguire, Konoplyannikov, Ford, Maguire, & O'Brien, 2003). Therefore the biological and safety aspects of POPs remain rather unclear.

* Corresponding author. Tel.: +43 1 4277 54930; fax: +43 1 4277 9549.
E-mail address: karl-heinz.wagner@univie.ac.at (K.-H. Wagner).

0308-8146/$ - see front matter © 2009 Elsevier Ltd. All rights reserved.
doi:10.1016/j.foodchem.2009.04.062

Hence, the aim of the present study was to scale up a method for the isolation of single phytosterol oxidation products. ß-sitosterol served as the model compound as it is the most abundant plant sterol in nature. Gram scale amounts of toxicologically relevant oxidation products with sufficient purity were collected in order to undergo toxicity tests.

The second objective of this study was to investigate the collected oxides regarding their possible mutagenic and pro-oxidative properties in the Ames test. Since it is assumed that the toxicity of oxidation products varies depending on their chemical structure (Osada, 2002) a hierarchy of toxicity of the isolated compounds would be essential. In addition a mixture of all oxidation products was prepared and analysed in the same way, to further investigate whether or not single isolated products react differently from mixtures.

2. Materials and methods

2.1. Chemicals

24β-Ethylcholest-5-en-3β-ol (purity: β-sitosterol ~76%, sitostanol ~13%, campesterol ~9,5%, campestanol ~1,5%) was purchased from Fluka Chemie (Buchs, Switzerland). 5-Cholesten-3β-ol (cholesterol), Cholest-5-en-3β-ol-7-one (7-ketocholesterol) and Cholestan-5α,6α-epoxy-3β-ol (5α,6α-epoxycholesterol) were provided by Sigma Chemical Co. (St. Louis. MO, USA). Cholest-5-en-3β,7α-diol (7α-hydroxycholesterol), Cholest-5-en-3β,7β-diol (7β-hydroxycholesterol) and 5-Cholesten-3β,19-ol (19-hydroxycholesterol), the latter was used as an internal standard (ISTD) in GC-analysis, were obtained from Steraloids (Wilton, NH, USA). All the other cholesterol oxides were used as reference solutions in TLC and HPLC analysis, as standards of phytosterol oxides are not available.

Silica gel 60 (0.2–0.5 mm) for column chromatography and thin layer chromatography (TLC) plates (silica gel 60, 20 × 20 cm) were purchased from E. Merck (Darmstadt, Germany). Spots were visualized by staining with 10% sulphuric acid (H_2SO_4) (E. Merck) in methanol (Rathburn Chemicals Ltd., Walkerburn, Scotland). Bis(trimethylsilyl) trifluoroacetamide (BSTFA) and trimethylchlorosilane (TMCS) were obtained from E. Merck and Fluka Chemie, respectively, and were used as a 99:1 (v/v) mixture for silylation of the oxidation products. Analytical grade pyridine (>99%) from Sigma was also used. Ethyl acetate (E. Merck), diethyl ether (J.T. Baker, Deventer, The Netherlands), *n*-heptane and acetone (Rathburn Chemicals Ltd.), 99.5% ethanol (Primalco, Rajamäki, Finland) and water (purified by Milli-Q Plus, Millipore, Molsheim, France) all of analytical grade, were used.

All chemicals used for the Ames test were obtained from Sigma (Vienna, Austria), unless otherwise stated. The Salmonella typhimurium strains TA98, TA100 and TA102 were obtained from Discovery Partners International (San Diego, USA) and from Trinova Biochem GmbH (Giessen, Germany). The S9 liver homogenate (from Sprague–Dawley rats induced with Aroclor 1254 prepared as a KCL homogenate) was obtained from MP Biomedicals (Illkirch, France). Agar No. 1 and Nutrient Broth were obtained from Oxoid/Bertoni (Vienna, Austria), Dulbecco's PBS was from PAA (Pasching, Austria). All mutagens and other reagents were of analytical reagent grade or higher and stored at – 80 °C if necessary.

2.2. Production and isolation of phytosterol oxidation products

2.2.1. Preparation of oxides by thermo-oxidation

POPs were formed by thermo-oxidation. Commercial available β-sitosterol was heated in open glass vials (300 mg, 25 mm, I.D.) in a ventilated oven for 24 h at 130 °C. Optimal heating conditions were evaluated in pre-tests. Different temperatures and time periods (130 °C/24 h, 120 °C/48 h and 130 °C/48 h) were tested and resulting oxidation mixtures were analysed using GC–FID and GC–MS. After the heating period the samples were cooled down in a desiccator, dissolved in 15 mL of *n*-heptane/diethyl-ether (90:10, v/v), solubilised using a sonicator and finally stored in a freezer (−20 °C).

2.2.2. Purification and enrichment of phytosterol oxidation products by column chromatography (CC)

The purification method used was based on former investigations by Lampi, Juntunen, Toivo, and Piironen (2002) and Apprich and Ulberth (2004). Briefly, 72 g silica gel (loaded with 10% distilled water) was dry packed into a glass column and pre-wetted with 150 mL *n*-heptane. The whole sample (300 mg heated β-sitosterol/15 mL *n*-heptane/diethyl-ether (90:10, v/v)) was applied to the column and first nonoxidized sterols and apolar components were eluted with 150 mL *n*-heptane/diethyl-ether (90:10, v/v) followed by 450 mL *n*-heptane/diethyl-ether (50:50, v/v). Thereafter POPs were extracted with 150 mL acetone. The acetone fraction was evaporated to dryness. To get rid of the water ethanol was added during the evaporation step. The residue was dissolved in 550 μL *n*-heptane/2-propanol (93:7, v/v).

To confirm the performance of the CC TLC was conducted. 100 μL of the purified sample were applied to silica gel G 60 TLC plates (0.5 mm layer thickness). The identification of the single oxidation products was done using a standard solution, which contained 5α,6α-epoxy-, 7-hydroxy- and 7-ketocholesterol. As eluent *n*-heptane/ethyl-acetate (50:50, v/v) was used. Components were visualized by spraying with 10% sulphuric acid in methanol followed by heating for a few minutes at 100 °C.

2.2.3. Separation of single oxidation products by a NP–HPLC–UV system

For the collection of single oxidation products a preparative normal-phase HPLC-method was used. The method was based on papers published by Kemmo, Soupas, Lampi, and Piironen (2005) and Säynäjoki, Sundberg, Soupas, Lampi, and Piironen (2003) with some modifications. A preparative HPLC-instrument (Waters Delta Prep 3000, Milford, USA) equipped with a silica Supelcosil column (250 mm × 21.1 mm, 12 μm; Supelco, Bellefonte, PA, USA) and a UV detector at 206 nm (Waters 484 Milford, USA) was applied. Several mobile phase systems (90:10, 92:8, 93:7, 94:6, 95:5 and 97:3 *n*-heptane/2-propanol) and flow rates (5, 7, 9.9, 15 and 17 mL/min) were examined. Determination of purity levels and identification of the collected fractions was done by GC–MS. The best separation was achieved at room temperature under isocratic conditions using a mobile phase of *n*-heptane/2-propanol (93:7, v/v) with a flow rate of 17 mL/min. The injection volume was 1.8 mL. The performance of the separation was checked daily using a cholesterol oxides standard solution (7-ketocholesterol, 7β-hydroxycholesterol and 7α-hydroxycholesterol) by monitoring the retention times. For the generation of the mixture no HPLC separation was performed, therefore it includes all polar β-sitosterol oxidation products.

2.2.4. Identification and quantification

For identification and quantification of the collected fractions GC–mass spectrometry (GC–MS) and GC–flame ionization detection (GC–FID) were used, respectively. Both methods have been developed earlier by co-workers (Lampi et al., 2002; Soupas, Juntunen, Säynäjoki, Lampi, & Piironen, 2004) and are routinely used for analysing POPs.

Prior to the GC analysis the samples were converted to TMS-ether derivatives. Therefore 100 μL aliquots of each fraction and 1 mL of internal standard solution (19-OH-cholesterol, 18.55 μg/mL) were evaporated to dryness under nitrogen, dissolved in 100 μL of pyridine and subjected to silylation by 100 μL BSTFA/TMCS

(100 μL, 99:1, v/v) over night at room temperature. The reagent mixture was then evaporated and the residue was dissolved in 200 μL *n*-heptane before GC analysis.

2.2.5. GC–MS analysis

For identification of the collected oxidation products and verification of the purity of the fractions GC–MS was used as described in Soupas et al. (2004). The GC–MS equipment consisted of a Hewlett–Packard 6890 Series gas chromatograph (Wilmington, PA, USA) including a Rtx-5MS w/Integra fused-silica capillary column (60 m × 0.25 mm i.d., crossbond 5% diphenyl – 95% dimethyl polysiloxane, 0.1 μm film with 10 m Integra-Guard column; Restek, Bellefonte, PA, USA) and was coupled to an Agilent 5973 mass spectrometer (Palo Alto, CA, USA). Helium was used as carrier gas at 240 kPa. Initial oven temperature was 70 °C, after 1 min the temperature was raised to 280 °C at 40 °C/min and was then held at 280 °C for 35 min. Interface temperature and ion source were 280 °C and 230 °C, respectively. Spectra were scanned within the mass range of *m*/*z* 100–600 using the electron impact mode (70 eV).

2.2.6. GC–FID analysis

The quantification was done by GC–FID measurements using a Hewlett–Packard 6890 Series II gas chromatograph equipped with an HP-7673 autosampler (Hewlett–Packard, Karlsruhe, Germany), an automated on-column injection system, a flame ionization detector (FID), ChemStation 3.1 software and a RTX-5w/Integra fused-silica capillary column (60 m × 0.32 mm i.d., 5% diphenyl – 95% dimethyl polysiloxane, 0.1 μm film with 10 m Integra-Guard column; Restek, Bellefonte, PA, USA). Helium (99.996% AGA, Espoo, Finland) was used as the carrier gas at a constant flow (110 kPa at 200 °C). The initial temperature was 70 °C, which increased after 1 min to 245 °C by 60 °C/min. After 1 min at 245 °C it raised by 3 °C/min to 275 °C and remained at this temperature for 41 min. The detector temperature was 300 °C. The concentrations of the POPs were quantified by the added internal standard (19-OH-cholesterol).

2.3. Salmonella microsome assay

2.3.1. Preparation of reaction mixtures

Three individual oxidation products, 7-ketositosterol, 7β-OH-sitosterol, 7α-OH-sitosterol, a mixture of 6β-OH-3-ketositosterol/6α-OH-3-ketositosterol (ratio 4:3) and a mixture of the polar oxidation products of β-sitosterol were investigated. Considering the results of pre-tests, four concentrations (0.04, 0.2, 1.0 and 5.0 mg per plate (≈%)) of each compound were analysed. The concentration range used was a broad spectrum from very low physiological to nonphysiologically high concentrations, all below the solubility range, which is recommended for this test procedure.

Due to precipitation in the highest concentration of 7α-OH-sitosterol, only 3 doses of this compound could be used (0.04–1%). There were similar but minor solubility problems with the mixture of 6β-OH-3-ketositosterol/6-α-OH-3-ketositosterol, therefore as highest concentration 2.5 mg/plate was tested. On the other hand the mixture of all oxidation products showed very good solubility, so a 10 mg/plate dilution could also be included in the experiments (Table 1).

In order to obtain appropriate dilutions, each sample was predissolved in a mixture of acetone/tween80 (3:1, v/v). Afterwards two parts of sterile, distilled water was added to keep the concentration of acetone as low as possible and to avoid potential toxic effects on the bacterial strains. This procedure was tested to be safe for the strains in pre-experiments.

Table 1
Overview of the used concentrations of the sterol oxides in the study.

	10%	5%	2.5%	1%	0.2%	0.04%
7-ketositosterol		x		x	x	x
7β-OH-sitosterol		x		x	x	x
7α-OH-sitosterol				x	x	x
6α-OH-3-keto-/6β-OH-3-ketositosterol			x	x	x	x
Mixture	x	x		x	x	x

2.3.2. Metabolic activation

In order to simulate in vivo conditions the oxidation products were treated with a rat liver enzyme mixture (S9, which mainly consists of phase I enzymes) for metabolic activation. The S9 mix was prepared according to the recipes of Maron and Ames (1984) consisting of 19.75 mL distilled water, 25 mL of PBS buffer, 0.5 mL of $MgCl_2$ (0.85 M), 0.5 mL of KCl (1.65 M) and 2 mL of NaDP (90.8 mM), 250 μL of glucose-6-phosphate (1.08 M), and 2 mL of S9. The reagent was stored on ice throughout the whole experiment and discarded after 50 min.

2.3.3. Experimental design

The Ames Salmonella/microsome mutagenicity assay (Salmonella test, Ames test) was performed according to Maron and Ames (1984). The preincubation assay with an incubation period of 25 min (37 °C) was chosen, as reported earlier (Wagner, Reichhold, Koschutnig, Cheriot, & Billaud, 2007). Briefly, 500 μL of PBS or S9 mix, 200 μL of reaction mixture and 100 μL of overnight bacterial culture were added to test tubes. The tubes were shortly vortexed and then placed in an incubator on a rotary shaker and incubated for 25 min at 37 °C. After this period 2 mL of molten top agar were added to each tube. The mixture was vortexed and poured on glucose minimal agar plates. As soon as the agar had solidified the plates were inverted and stored in an incubator for 48 h at 37 °C. Thereafter his^+-revertants were counted manually.

In the present study three generally recommended tester strains (TA98, TA100 and TA102) were applied. TA98 gives information on frame-shift mutations, TA100 on base-pair substitutions and TA102 detects cross-linking agents, additionally it is specifically used to inform on oxidative stress. To further investigate the anti-/pro-oxidative effects the pro-oxidant tertiary-butyl hydroperoxide (*t*-BOOH, 0.7 mM) was used for a challenge test. The concentration of the oxidant was chosen in order to obtain suitable numbers of revertants on the plates. This test was performed with and without metabolic activation.

Each experiment included a positive control (2,4,7-Trinitro-9-fluorenone, Sodiumazide or 2-Aminofluorene), which confirmed the reversion capacity of the bacterial strains as well as a negative control, the sample solvent. All concentrations and the positive control were tested in triplicate. For the negative control even six plates were prepared. Each test was done at least twice ($n = 6$ in total).

2.3.4. Statistical analysis and evaluation of the mutagenic experiments

All data are expressed as mean ± SD (standard deviation). Obtained data ($n = 6$ for each concentration used) were analysed by one-way analysis of variance (ANOVA) and the Student's *t*-test since they were all normally distributed, using SPSS 15.0 for Windows. Statistical differences were considered significant at a value of $p < 0.05$.

In addition to the statistical, a nonstatistical evaluation was carried out. According to Mortelmans and Zeiger (2000) a compound is considered as "mutagenic" if the total number of his^+-revertants per plate was at least twice as high as the negative control (200%). Moreover a dose related increase of the number of his^+-revertants has to be shown.

3. Results and discussion

As already mentioned POPs are not commercially available, so they have to be laboratory-prepared. Applied methods are based on chemical synthesis (Bortolomeazzi, De Zan, Pizzale, & Conte, 1999; Zhang et al., 2005), thermo-oxidation in solid state (Lampi et al., 2002) or aqueous dispersion (Dutta & Appelqvist, 1997). Existing techniques are mostly very complex and time-consuming with the requirement of special equipment. Besides they are usually designed for the production of only small amounts of oxidation products. Therefore the initial target of this study was the development of a fast, simple and effective method for the isolation of common β-sitosterol oxides.

3.1. Performance of the method

3.1.1. Preparation of the test compounds by thermo-oxidation

In the present study thermo-oxidation in solid state was used for formation of oxides. Different temperatures and heating periods were tested and generated amounts of oxysterols were estimated by GC–FID (Fig. 1). Heat treatment for 24 h at 130 °C showed to be the best option, yielding to an oxidation rate of nearly 20%. The total amount of oxidation products decreased throughout longer heat exposure, even at a lower temperature (120 °C compared to 130 °C). This observation can be explained by conversion reactions to other secondary oxidation products as well as further reactions such as polymerisation, leading to non polar compounds, dimers and polymers. The latter occurs further particularly at higher heating conditions. The oxidation products observed in the heating experiments were analogous to those cited in the literature, mainly 7-ketositosterol followed by 7β-OH-sitosterol, 7α-OH-sitosterol, 5,6β-epoxy-sitosterol, 5,6α-epoxy-sitosterol, 6β-OH-3-ketositosterol, 6α-OH-3-ketositosterol, 6β-OH-sitosterol and 6-ketositosterol. Our findings supported those of Kemmo et al. (2005), who assessed that at different heating temperatures the same kind of oxidation products were formed, but the amount of the single products varied. Already Caboni, Costa, Rodriguez-Estrada, and Lercker (1997) noticed that the ratios of the formed products were influenced by the oxidation conditions.

The high amount of 7-ketositosterol and the generation of 7β-OH-sitosterol rather than 7α-OH-sitosterol was in accordance with previous studies (Chien, Wang, & Chen, 1998; Kemmo et al., 2005).

3.2. Purification and enrichment of the test compounds

When β-sitosterol is heated a mixture of oxidation products, non oxidized material and several unknown by-products is formed. Because of the complexity of the gained blend usually a combination of different separation techniques is applied to isolate single oxidation products. In this work CC was used for the first separation step. In contrast to the often employed solid-phase extraction (SPE) cartridges self prepared glass columns offer a higher loading capacity. Since our interest was focused on POPs with a higher polarity than non oxidized β-sitosterol a stepwise elution order to remove apolar components up to free sitosterol was applied.

Solvent mixtures of *n*-heptane/diethyl-ether in combination with silica gel and a final elution of the desired components with acetone were already successfully applied by others (Apprich & Ulberth, 2004; Lampi et al., 2002; Piironen, Toivo, & Lampi, 2002). TLC was used to confirm the separation process. No products with a lower polarity than β-sitosterol were detected. In addition a relevant reduction of non oxidized β-sitosterol could be noted. In other publications preparative TLC was also used to fractionate oxidation products. But this is only appropriate when small amounts of samples for analytical purpose are separated. In addition to its low loading capacity it also allows long exposure of the sample to air, which facilitates the possibility of artefact formation.

3.3. Separation, isolation and fractionating of the oxidation products by NP–HPLC–UV

The final separation of the oxidation products was achieved by a NP–HPLC–UV system. Due to its mild characteristics preparative HPLC is particularly suitable for the isolation of oxides. Both normal- and reverse phase chromatography has already been successfully used for the analyses of cholesterol (Caboni et al., 1997; Chien et al., 1998; Csallany, Kindom, Addis, & Lee, 1989; Mazalli, Sawaya, Eberlin, & Bragagnolo, 2006) and plant sterol (Kemmo, Ollilainen, Lampi, & Piironen, 2007; Kemmo et al., 2005) oxidation products. In general normal phase chromatography is considered to be the more effective option.

Table 2
Retention times and yield of single oxidation products (mg) within one HPLC-run (average values were obtained in over hundred HPLC-runs).

Compound	Retention time (min)	mg/injection
6β-OH-3-ketositosterol		5.7
6α-OH-3-ketositosterol	7.82	4.34
7-ketositosterol	11.09	16.9
7β-OH-sitosterol	13.36	11.03
7α-OH-sitosterol	14.82	6.12

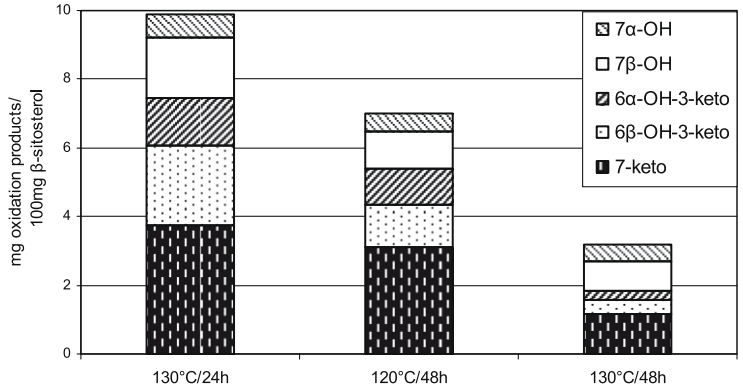

Fig. 1. Proportion of collected β-sitosterol secondary oxidation products (mg) after different oxidation conditions (130 °C/24 h, 120 °C/48 h and 130 °C/48 h) measured by a GC-FID system. Results are average values of at least two different heat treatments.

Different mobile phase systems with changing percentages of IPA were tested based on former investigations by Kemmo et al. (2007, 2005) and Säynäjoki et al. (2003). Best separation was achieved with a mobile phase of *n*-heptane/IPA (93:7, v/v). The same solvent system was already used earlier for the separation of COPs (Csallany et al., 1989). The elution order in this system was as follows: 6β-OH-3-ketositosterol/6α-OH-3-ketositosterol, 7-ketositosterol, 6β-OH-sitosterol, 7β-OH-sitosterol and 7α-OH-sitosterol. A rapid separation in one single HPLC-run was achieved within 20 min. The application of a big preparative silica column (25 cm × 21.2 mm, 12 μm) allowed an injection volume of 1.8 mL of the obtained oxidation mixture, containing the oxidation products derived from about 1000 mg unoxidized β-sitosterol (collected oxides of several purification steps by CC were combined). This led to yields in the range of several milligrams for the single fractions. Within one HPLC run, for example, 15–20 mg of 7-ketositosterol could be collected. For detailed information see Table 2.

Table 3
Purity of the obtained oxidation products as measured by GC–FID.

Fraction	Purity (%)	Campesterol counterpart (%)	Others (%)
6β-OH-3-ketositosterol/6α-OH-3-ketositosterol	88	12	
7-ketositosterol	82	10	8
7β-OH-sitosterol	90	10	
7α-OH-sitosterol	70	10	20

However, as already ascertained earlier no full resolution of the entire polarity range of the oxidation products is possible under isocratic conditions (Guardiola, Bou, Boatella, & Codony, 2004). 6β-OH-3-ketositosterol and 6α-OH-3-ketositosterol co-eluted, so they were collected in one fraction. When analysing the collected fractions with GC–FID high proportions of 7-ketositosterol were

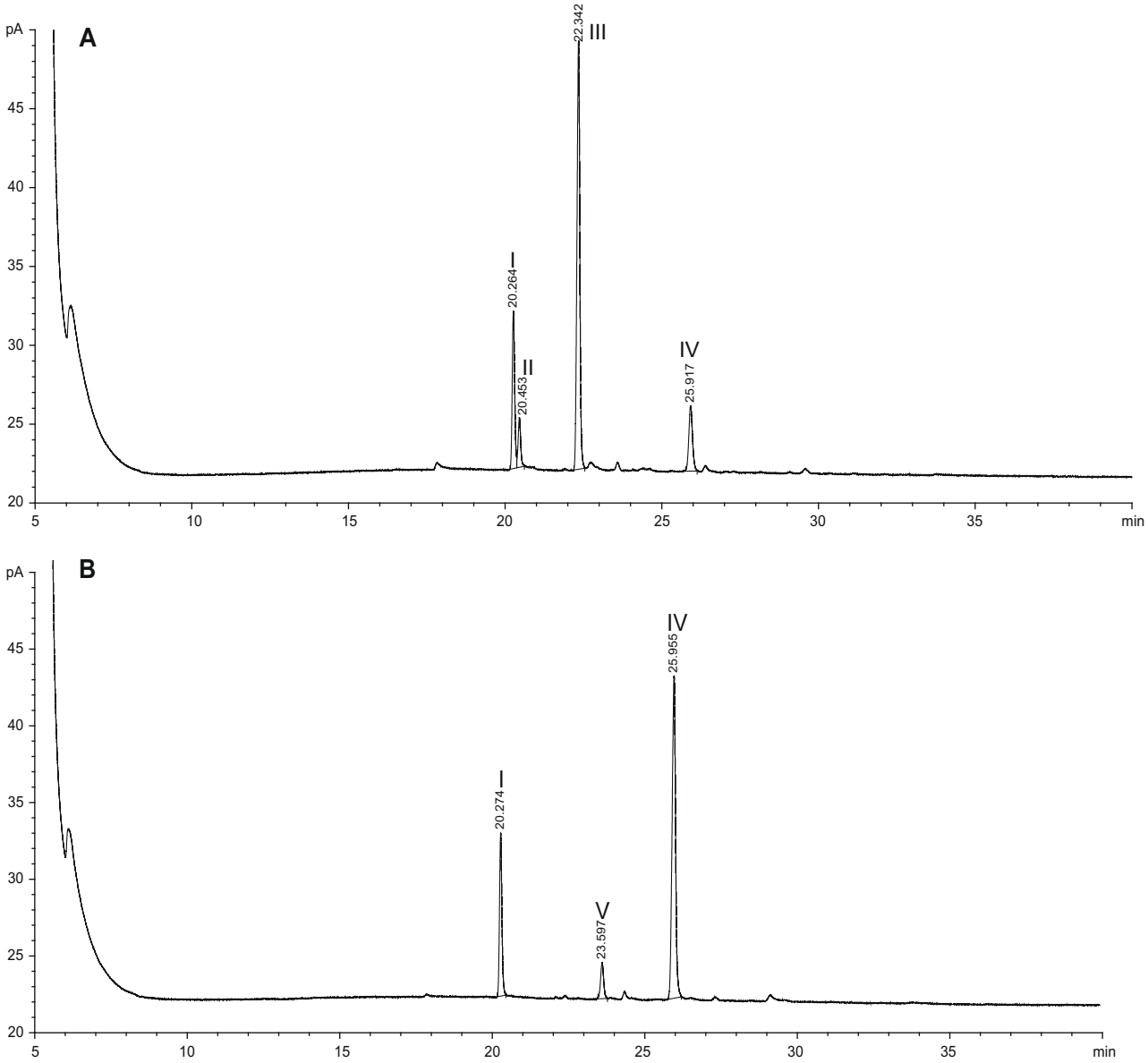

Fig. 2. GC–FID chromatograms of isolated β-sitosterol oxide fractions ((A) 7α-hydroxysitosterol; (B) 7β-hydroxysitosterol; (C) 7-ketositosterol; (D) 6α-OH-3-ketositosterol/6β-OH-3-ketositosterol) as TMS-ether derivatives on a RTX-5w/Integra fused silica capillary column (60 m × 0.25 mm i.d., 0.1 μm film). Analytical conditions are described in Section 2. Peaks are identified as: (I) 19-hydroxycholesterol (ISTD); (II) 7α-hydroxycampesterol; (III) 7α-hydroxysitosterol; (IV) 7β-hydroxysitosterol; (V) 7β-hydroxycampesterol; (VI) + (VII) unidentified compounds; (VIII) 7-ketocampesterol; (IX) 7-ketositosterol; (X) 6β-OH-3-ketocampesterol; (XI) 6β-OH-3-ketositosterol; (XII) 6α-OH-3-ketocampesterol; (XIII) 6α-OH-3-ketositosterol.

found in the 6β-OH-sitosterol-sample. Therefore 6β-OH-sitosterol was excluded from subsequent toxicology tests.

Moreover as already observed in earlier investigations (Dutta & Appelqvist, 1997) it was not possible to separate campesterol oxides from their sitosterol counterparts. Since the applied commercial β-sitosterol included some amount of campesterol (~10%) also a low amount of campesterol oxides (~10%) was present in the oxidation mixture. Average values of the purity of the collected compounds are listed in Table 3 and GC–FID chromatograms of each isolated oxide fraction are given in Fig. 2. However, bearing in mind the velocity of our method we put up with these minor impurities.

Among all detection systems available UV detection is still the most frequently applied for sterol analyses. Separation of the oxidation products was monitored using a wavelength of 206 nm. It is the common wavelength employed for oxysterols (Csallany et al., 1989). Since products without double bonds like epoxy-compounds and triols have poor UV absorption they were not included in collected oxides.

3.4. Bacterial tests

Although indications for adverse health effects exist, knowledge on biological properties of POPs is rather small. Further almost all of the so far conducted toxicology studies were done with cell lines, among others because of the small sample amounts needed for these assays. As data concerning the mutagenic potential of isolated POPs is lacking, the collected oxidation products were tested in Salmonella typhimurium strains TA98, TA100 and TA102 in the Ames test. To our knowledge it is the first time that single oxides of β-sitosterol are tested on their behaviour towards Salmonella typhimurium strains.

3.5. Mutagenicity testing

According to literature the here applied preincubation assay is the most sensitive form of the Ames test. It allows a closer contact of the test compounds and the indicator strain since the bacteria

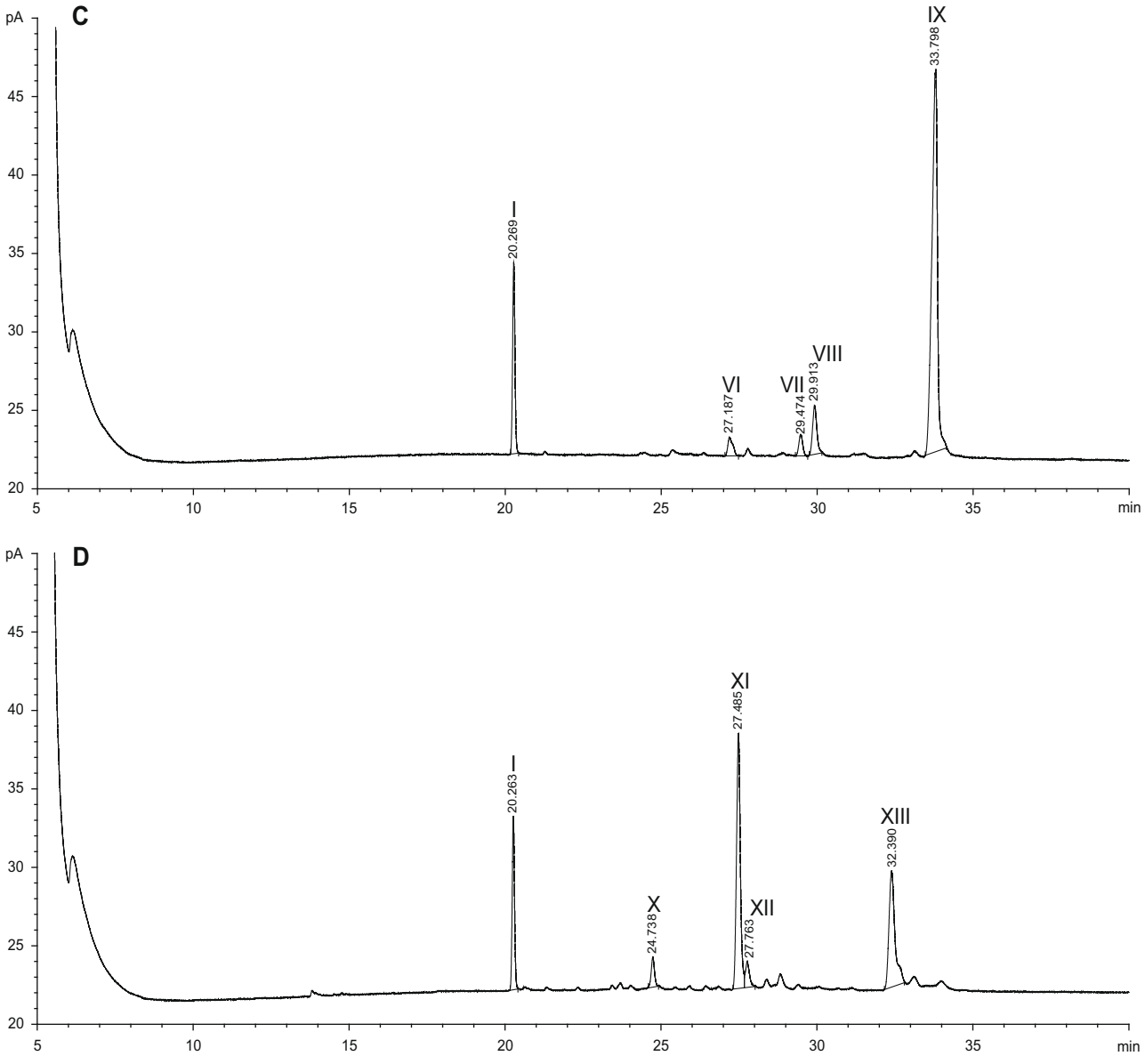

Fig. 2 (*continued*)

are able to react in a small volume, which is an advantage for detecting short-living mutagens (Mortelmans & Zeiger, 2000).

Throughout the whole test period the spontaneous mutation frequency of the strains was in accordance with the control levels published (Mortelmans & Zeiger, 2000) and each POP sample was significantly different to the positive control ($p < 0.05$).

In strain TA98 no mutagenic activity could be seen; neither with nor without metabolic activation. Also in TA100 the number of his$^+$-revertants remained in the range of the negative control and therefore were mutagenic not active (data not shown).

These results were in accordance with those published recently by Lea et al. (2004) who tested a mixture of oxidized and unoxidized products of β-sitosterol by using different Salmonella strains (TA98, TA100, TA102, TA1535 and TA1537). However, the amount of oxidation products in their tested samples was only 30%.

It is already well known that oxide mixtures react differently from individual oxidation products (Maguire, Konoplyannikov, Ford, Maguire, & O'Brien, 2003). Also additive, synergistic as well as inhibitory effects of single oxidation products in mixtures have been noted (O'Sullivan, O'Callaghan, & O'Brien, 2005). Therefore, in contrast to our study, the results of Lea et al. (2004) allow no sufficient information about the safety aspects of single oxidation products.

In the aforementioned publication also toxicity and precipitation problems during their work with TA102 were reported. Consequently in these experiments sample amounts had to be reduced. Throughout all of our research work no problems in this regard were observed.

Although in the present study none of the oxidation products were able to increase the number of revertants beyond the doubled negative control, yet for some oxides a certain response was observed in strain TA102 (Table 4). In the preincubation test without metabolic activation the highest concentrated fraction of 7-ketositosterol (5%) increased the number of his$^+$-revertants significantly, but not beyond twice of the negative control, which was set as threshold for mutagenic activity. Moreover a concentration-dependent tendency was seen for the lower concentrations but not for the 5%-fraction, mainly due to its higher standard deviation. With the addition of S9 the increase of 7-ketositosterol (5%) was even more pronounced ($p < 0.05$). On the other hand the highest concentrated fraction of 7β-OH-sitosterol (5%) reduced the number of his$^+$-revertants significantly compared to its lower concentrated fractions ($p < 0.05$).

The strain TA102 was chosen as besides its capability of detecting cross-linking agents it additionally informs on oxidative stress (Grey & Adlercreutz, 2003; Mortelmans & Zeiger, 2000). Based on that, the increase in revertants induced by 7-ketositosterol (5%) could be an indication of a pro-oxidant tendency. On the other hand the decline in revertant numbers of 7β-OH-sitosterol (5%) could be interpreted as a marginal sign of antioxidative effects. However, it could also be the result of increased cytotoxicity (Mortelmans & Zeiger, 2000).

To date no papers other than the one by Lea et al. (2004) had been published dealing with possible mutagenic actions of POPs. Hence, more information is available on mutagenic effects of COPs. Due to their structural similarity an analogous mode of action is expected. As early as in 1979 mixtures of COPs have been shown to possess mutagenic effects towards Salmonella typhimurium strains TA98, TA1535 and TA1537 (Smith, Smart, & Ansari, 1979). Several studies followed and in spite of contradictory results it seems that particularly epoxy and triol compounds of cholesterol possess mutagenic activity. Epoxy and triol compounds of β-sitosterol had never been tested before in regard of their mutagenicity and they were also not included in the present study. Oxysterols might in general possess rather cytotoxic properties whereas for epoxide epimeres and triols a mutagenic action could also be possible. For the mutagenic reactivity of COPs the authors also suggested ROS to be involved in the mutagenic action (Cheng, Kang, Shih, Lo, & Wang, 2005; Smith et al., 1979), as antioxidant enzymes diminished the mutagenic response.

Table 4
Overview of all obtained data in the preincubation assay with the strain TA102.

Compound	Concentration (mg/plate)	TA102 revertants/plate −S9	TA102 revertants/plate + S9	TA102 + tBOOH revertants/plate −S9	TA102 + tBOOH revertants/plate + S9
Negative control		571 ± 44[b]	847 ± 63[b]	747 ± 99[b]	1589 ± 349[b]
7-ketositosterol	5	701 ± 82[a,b]	1318 ± 41[a,b]	866 ± 24[a,b]	2038 ± 239[b]
	1	685 ± 16[a,b]	926 ± 28[b]	936 ± 66[a,b]	1714 ± 137[b]
	0.2	635 ± 36[a,b]	879 ± 108[b]	940 ± 75[a,b]	1891 ± 334[b]
	0.04	575 ± 45[b]	846 ± 81[b]	963 ± 52[a,b]	1974 ± 123[b]
7β-OH-sitosterol	5	607 ± 55[b]	675 ± 68[a,b]	525 ± 45[a,b]	1374 ± 60[b]
	1	589 ± 79[b]	853 ± 32[b]	776 ± 58[b]	1770 ± 146[b]
	0.2	582 ± 76[b]	840 ± 91[b]	840 ± 65[b]	1679 ± 146[b]
	0.04	606 ± 74[b]	793 ± 37[b]	804 ± 71[b]	1591 ± 103[b]
7α-OH-sitosterol	1	597 ± 101[b]	744 ± 97[b]	684 ± 56[b]	1222 ± 156[b]
	0.2	510 ± 27[a,b]	802 ± 16[b]	812 ± 36[b]	1252 ± 164[b]
	0.04	452 ± 103[a,b]	652 ± 34[a,b]	686 ± 111[b]	1317 ± 93[b]
6α-OH-3-keto/6β-OH-3-ketositosterol	2.5	684 ± 88[a,b]	1051 ± 28[a,b]	809 ± 51[b]	2119 ± 90[a,b]
	1	644 ± 51[a,b]	979 ± 12[a,b]	1031 ± 42[a,b]	2082 ± 32[a,b]
	0.2	609 ± 40[b]	990 ± 29[a,b]	801 ± 121[b]	2338 ± 29[a,b]
	0.04	644 ± 62[a,b]	953 ± 2[a,b]	814 ± 32[b]	2065 ± 70[b]
Mixture	10	713 ± 60[a,b]	1079 ± 107[a,b]	891 ± 14[a,b]	1501 ± 35[b]
	5	648 ± 94[a,b]	1008 ± 54[a,b]	797 ± 12[b]	1879 ± 158[b]
	1	598 ± 55[b]	967 ± 82[a,b]	842 ± 102[b]	1997 ± 5[a,b]
	0.2	556 ± 67[b]	829 ± 41[b]	902 ± 76[a,b]	2003 ± 19[b]
	0.04	625 ± 27[a,b]	731 ± 143[b]	851 ± 113[b]	2057 ± 175[b]
Positive control		2353 ± 422	3480 ± 165	2412 ± 71	3780 ± 271

Numbers of his$^+$-revertants are mean ± SD.
[a] $p < 0.05$ to negative control.
[b] $p < 0.05$ to positive control.

3.6. Antioxidant testing

To strengthen the information on oxidative stress challenge tests with the pro-oxidant *t*-BOOH were included in our experiments. *t*-BOOH is commonly used in in vitro assays, as it is known as an initiator of lipid peroxidation, where it leads to the formation of alkoxyl and alkyl radicals (Grey & Adlercreutz, 2003).

A prevention of the thereby caused mutagenicity would indicate possible antioxidant properties of the tested compounds. Per definition a reduction of the revertant colony number below 50% of the negative control level is necessary for an anti-mutagenic effect (Mortelmans & Zeiger, 2000). This was never seen in any of our conducted tests (Table 4). However, with the addition of *t*-BOOH 7β-OH-sitosterol (5%) caused a significant decrease in his^+-revertants ($p < 0.05$); even though not lower than the threshold level. With the addition of S9 the number of his^+-revertants was still lower compared with the less concentrated fractions, but here this tendency was not significant ($p = 0.196$).

4. Conclusion

The applied method was proven to be a powerful tool for the collection of oxidation products, as yields in the range of several milligrams per fractions were achieved within only one HPLC-run. Thus the collection of oxysterols for a later application in toxicity tests was possible.

The results of the Ames test demonstrated that the analysed common oxidation products of β-sitosterol were not mutagenic towards Salmonella typhimurium strains TA98, TA100 and TA102. Even though literature on the mutagenic response of COPs is conflicting, for some oxidation products a mutagenic action could be proved. In spite of their similar structure there could still be a difference in the mutagenic behaviour of cholesterol- and plant sterol oxidation products.

Acknowledgement

The work was supported by COST organization as a Cost 927 short term scientific mission, carried out at the University of Helsinki, by the Academy of Finland and by a research grant on behalf of the University of Vienna (F81-B Forschungsstipendium).

References

Adcox, C., Boyd, L., Oehrl, L., Allen, J., & Fenner, G. (2001). Comparative effects of phytosterol oxides and cholesterol oxides in cultured macrophage-derived cell lines. *Journal of Agricultural and Food Chemistry, 49*(4), 2090–2095.

Apprich, S., & Ulberth, F. (2004). Gas chromatographic properties of common cholesterol and phytosterol oxidation products. *Journal of Chromatography A, 1055*(1–2), 169–176.

Boesinger, S., Luf, W., & Brandl, E. (1993). 'Oxysterols': Their occurrence and biological effects. *International Dairy Journal, 3*, 1–33.

Bortolomeazzi, R., De Zan, M., Pizzale, L., & Conte, L. S. (1999). Mass spectrometry characterization of the 5alpha-, 7alpha-, and 7beta-hydroxy derivatives of beta-sitosterol, campesterol, stigmasterol, and brassicasterol. *Journal of Agricultural and Food Chemistry, 47*(8), 3069–3074.

Caboni, M. F., Costa, A., Rodriguez-Estrada, M. T., & Lercker, G. (1997). High-performance liquid chromatographic separation of cholesterol oxidation products. *Chromatographia, 46*(3/4), 151–155.

Cheng, Y. W., Kang, J. J., Shih, Y. L., Lo, Y. L., & Wang, C. F. (2005). Cholesterol-3-beta, 5-alpha, 6-beta-triol induced genotoxicity through reactive oxygen species formation. *Food and Chemical Toxicology, 43*(4), 617–622.

Chien, J. T., Wang, H. C., & Chen, B. H. (1998). Kinetic model of the cholesterol oxidation during heating. *Journal of Agricultural and Food Chemistry, 46*(7), 2572–2577.

Csallany, A. S., Kindom, S. E., Addis, P. B., & Lee, J. H. (1989). HPLC method for quantitation of cholesterol and four of its major oxidation products in muscle and liver tissues. *Lipids, 24*(7), 645–651.

Dutta, P. C., & Appelqvist, L. A. (1997). Studies on phytosterol oxides I: Effect of storage on the content in potato chips prepared in different vegetable oils. *Journal of the American Oil Chemists' Society, 74*(6), 647–657.

Grandgirard, A., Martine, L., Demaison, L., Cordelet, C., Joffre, C., Berdeaux, O., et al. (2004). Oxyphytosterols are present in plasma of healthy human subjects. *British Journal of Nutrition, 91*(1), 101–106.

Grey, C. E., & Adlercreutz, P. (2003). Ability of antioxidants to prevent oxidative mutations in Salmonella typhimurium TA102. *Mutation Research, 527*(1–2), 27–36.

Guardiola, F., Bou, R., Boatella, J., & Codony, R. (2004). Analysis of sterol oxidation products in foods. *Journal of AOAC International, 87*(2), 441–460.

Katan, M. B., Grundy, S. M., Jones, P., Law, M. F. R. C. P., Miettinen, T., & Paoletti, R. (2003). Efficacy and safety of plant stanols and sterols in the management of blood cholesterol levels. *Mayo Clinical Proceedings, 78*(8), 965–978.

Kemmo, S., Ollilainen, V., Lampi, A.-M., & Piironen, V. (2007). Determination of stigmasterol and cholesterol oxides using atmospheric pressure chemical ionization liquid chromatography/mass spectrometry. *Food Chemistry, 101*(4), 1438–1445.

Kemmo, S., Soupas, L., Lampi, A.-M., & Piironen, V. (2005). Formation and decomposition of stigmasterol hydroperoxides and secondary oxidation products during thermo-oxidation. *European Journal of Lipid Science and Technology, 107*(11), 805–814.

Lampi, A.-M., Juntunen, L., Toivo, J., & Piironen, V. (2002). Determination of thermo-oxidation products of plant sterols. *Journal of Chromatography B, 777*(1–2), 83–92.

Lea, L. J., Hepburn, P. A., Wolfreys, A. M., & Baldrick, P. (2004). Safety evaluation of phytosterol esters. Part 8. Lack of genotoxicity and subchronic toxicity with phytosterol oxides. *Food and Chemical Toxicology, 42*(5), 771–783.

Maguire, L., Konoplyannikov, M., Ford, A., Maguire, A. R., & O'Brien, N. M. (2003). Comparison of the cytotoxic effects of beta-sitosterol oxides and a cholesterol oxide, 7beta-hydroxycholesterol, in cultured mammalian cells. *British Journal of Nutrition, 90*(4), 1–10.

Maron, D. M., & Ames, B. N. (1984). Revised methods for the Salmonella mutagenicity test. In B. J. Kilbey, M. Legator, & C. Ramel (Eds.), *Handbook of mutagenicity test procedures* (pp. 93–140). Elsevier Science Publishers BV.

Mazalli, M. R., Sawaya, A. C. H. F., Eberlin, M. N., & Bragagnolo, N. (2006). HPLC method for quantification and characterization of cholesterol and its oxidation products in eggs. *Lipids, 41*(2), 615–622.

Mortelmans, K., & Zeiger, E. (2000). The Ames Salmonella/microsome mutagenicity assay. *Mutation Research, 455*(1–2), 29–60.

O'Sullivan, A. J., O'Callaghan, Y. C., & O'Brien, N. M. (2005). Differential effects of mixtures of cholesterol oxidation products on bovine aortic endothelial cells and human monocytic U937 cells. *International Journal of Toxicology, 24*(3), 173–179.

Osada, K. (2002). Cholesterol oxidation products: other biological effects. In P. C. Dutta, F. Guardiola, R. Codony, & G. P. Savage (Eds.), *Cholesterol and phytosterol oxidation products: Analysis, occurrence and biological effects* (pp. 278–318). Champaign, IL: AOCS Press.

Piironen, V., Lindsay, D. G., Miettinen, T. A., Toivo, J., & Lampi, A.-M. (2000). Plant sterols: biosynthesis, biological function and their importance to human nutrition. *Journal of the Science of Food and Agriculture, 80*(7), 939–966.

Piironen, V., Toivo, J., & Lampi, A. M. (2002). Plant sterols in cereals and cereal products. *Cereal Chemistry, 79*(1), 148–154.

Ryan, E., Chopra, J., McCarthy, F., Maguire, A. R., & O'Brien, N. M. (2005). Qualitative and quantitative comparison of the cytotoxic and apoptotic potential of phytosterol oxidation products with their corresponding cholesterol oxidation products. *British Journal of Nutrition, 94*(3), 443–451.

Säynäjoki, S., Sundberg, S., Soupas, L., Lampi, A. M., & Piironen, V. (2003). Determination of stigmasterol primary oxidation products by high-performance liquid chromatography. *Food Chemistry, 80*(3), 415–421.

Smith, L. L., Smart, V. B., & Ansari, G. A. (1979). Mutagenic cholesterol preparations. *Mutation Research, 68*(1), 23–30.

Soupas, L., Juntunen, L., Säynäjoki, S., Lampi, A. M., & Piironen, V. (2004). GC–MS method for characterization and quantification of sitostanol oxidation products. *Journal of the American Oil Chemists' Society, 81*(2), 135–141.

Wagner, K. H., Reichhold, S., Koschutnig, K., Cheriot, S., & Billaud, C. (2007). The potential antimutagenic and antioxidant effects of Maillard reaction products used as "natural antibrowning" agents. *Molecular Nutrition and Food Research, 51*(4), 496–504.

Zhang, X., Geoffroy, P., Miesch, M., Julien-David, D., Raul, F., Aoudé-Werner, D., et al. (2005). Gram-scale chromatographic purification of [beta]-sitosterol: Synthesis and characterization of [beta]-sitosterol oxides. *Steroids, 70*(13), 886–895.

Food Chemistry 118 (2010) 141–146

Contents lists available at ScienceDirect

Food Chemistry

journal homepage: www.elsevier.com/locate/foodchem

Analytical Methods

Application of artificial neural networks to the prediction of the antioxidant activity of essential oils in two experimental *in vitro* models

Alvaro Cortes Cabrera, Jose M. Prieto *

Center for Pharmacognosy and Phytotherapy, School of Pharmacy, University of London, 29-39 Brunswick Square, WC1N 1AX London, United Kingdom

ARTICLE INFO

Article history:
Received 13 March 2008
Received in revised form 15 April 2009
Accepted 18 April 2009

Keywords:
Artificial neural networks
Essential oils
Antioxidant activity
DPPH
Linoleic acid
Chemometrics

ABSTRACT

Introduction: The antioxidant properties of essential oils (EOs) have been on the centre of intensive research for their potential use as preservatives or nutraceuticals by the food industry. The enormous amount of information already generated on this subject provides a rich field for data-miners as it is conceivable, with suitable computational techniques, to predict the antioxidant capacity of any essential oil just by knowing its particular chemical composition. To accomplish this task we here report on the design, training and validation of an Artificial Neural Network (ANN) able to predict the antioxidant activity of EOs of known chemical composition.

Methods: A multilayer ANN with 30 input neurons, 42 in hidden layers (20 → 15 → 7) and one neuron in the output layer was developed and run using Fast Artificial Neural Network software. The chemical composition of 32 EOs and their antioxidant activity in the DPPH and linoleic acid models were extracted from the scientific literature and used as input values. From the initial set of around 80 compounds present in these EOs, only 30 compounds with relevant antioxidant capacity were selected to avoid excessive complexity of the neural network and minimise the associated structural problems.

Results and discussion: The ANN could predict the antioxidant capacities of essential oils of known chemical composition in both the DPPH and linoleic acid assays with an average error of only 3.16% and 1.46%, respectively. We also discuss on the contribution of different compounds to these chemical activities.

Conclusions: These results confirm that artificial neural networks are reliable, fast and cheap tools for predicting antioxidant activity of essential oils from some of its components and can be used to model biochemical properties of complex natural products including the prediction of parameters associated with nutraceutical properties of food ingredients.

1. Introduction

The antioxidant properties of essential oils (EOs) have been on the centre of intensive research for their potential use as preservatives, supplements, cosmeceuticals or nutraceuticals by the food and cosmetics industry. Literally 100s of works reporting both on the composition and antioxidant properties of EOs have been written during the last decade. However, this kind of work is under an increasing criticism as the inherent intra-specific variability of the essential oils composition – depending on the location, altitude, meteorology, type of soil and many other factors – make this kind of work virtually irreproducible.

To further complicate matters, the evaluation of the antioxidant capacity of different fractions or pure constituents of EOs often affords controversial results. For example, when Radonic and coworkers (Radonic & Milos, 2003) isolated the hydrocarbon fraction of *S. montana* EO, containing γ-terpinene, α-terpinene, *p*-cymene and terpinolene – which previously were identified as potential antioxidants – it showed the poorest effectiveness. On the other hand, thymol and carvacrol, the most active components of *Thymus pectinatus* EO were individually found to possess weaker antioxidant activity than the crude oil itself (Vardar-Ünlü et al., 2003). These data indicate that some of the constituents of the essential oils may act synergistically, and this interplay might be even more complex as antagonisms with other components cannot be discarded *a priori*.

Despite this controversy, the enormous amount of information produced on the antioxidant activity of EOs provides a rich field for data-miners, and it is conceivable to apply suitable computational techniques to predict the activity of any essential oil by just knowing its particular chemical composition. The challenge is the complexity of the countless chemical interactions between dozens of EOs components and the free radicals used as probes. It is virtually impossible to address all of them in the laboratory but it may be solved by the use of computational models such as artificial neural networks (ANNs). In fact, ANNs are algorithms which has the capacity of approximating an output value based on input data

* Corresponding author. Tel.: +44 2077535841; fax: +44 2077535909.
E-mail address: jose.prieto@pharmacy.ac.uk (J.M. Prieto).

0308-8146/$ - see front matter © 2009 Elsevier Ltd. All rights reserved.
doi:10.1016/j.foodchem.2009.04.070

without any previous knowledge of the model and regardless the complexity of its mechanisms, in this case the relationship between the antioxidant capacity of a given essential oil (input data) and its chemical composition (parameters affecting the assay).

An ANN is composed by a set of virtual/artificial neurons organised in interconnected layers. Each neuron has a specific weight in the processing of the information. The optimal weights are calculated with available pairs of input and output data constituting the training set. Using this pairs, the ANN is able to minimise output error modifying weights as required. While two of these layers are connected to the 'outside world' (input layer, where data is presented and output layer, where a prediction value is obtained), the rest of them (hidden layers) are defined by neurons connected to each other, avoiding connections between neurons of the same layer.

To our knowledge only one previous report (Buciński, Zieliński, & Kozłowska, 2004) show the possibility of applying ANNs to predict antioxidant capacity of food products. The authors chose to use the amount of total phenolics present in cruciferous sprouts as input data. Thus, no attempt has been made yet to use an ANN for the prediction of the antioxidant capacity of EOs, a popular subject in natural products chemistry. Moreover, all previous antecedents in the food field do not take into account more than 4–5 input variables whilst EOs would imply to use dozens of them. To accomplish this task we here report on the design, training and validation of an ANN in order to predict the antioxidant activity of EOs of known chemical composition in two widely used *in vitro* models of antiradical and antioxidant activity, namely DPPH and linoleic acid, respectively.

2. Materials and methods

2.1. Design of the ANN

An ANN was developed and run on a personal computer using Fast Artificial Neural Network software ver. 1.2.0-1 (Nissen, 2007). This package was downloaded from its original repository in http://leenissen.dk/fann/ and installed following the guidelines provided by the developers under Ubuntu 7.04 and Microsoft Windows XP Professional SP2.

FANN is a free, open source neural network library, which implements multilayer artificial neural networks in C language with support for both fully connected and sparsely connected networks. Cross-platform execution in both fixed and floating point is supported. We chose this software because it is versatile, well

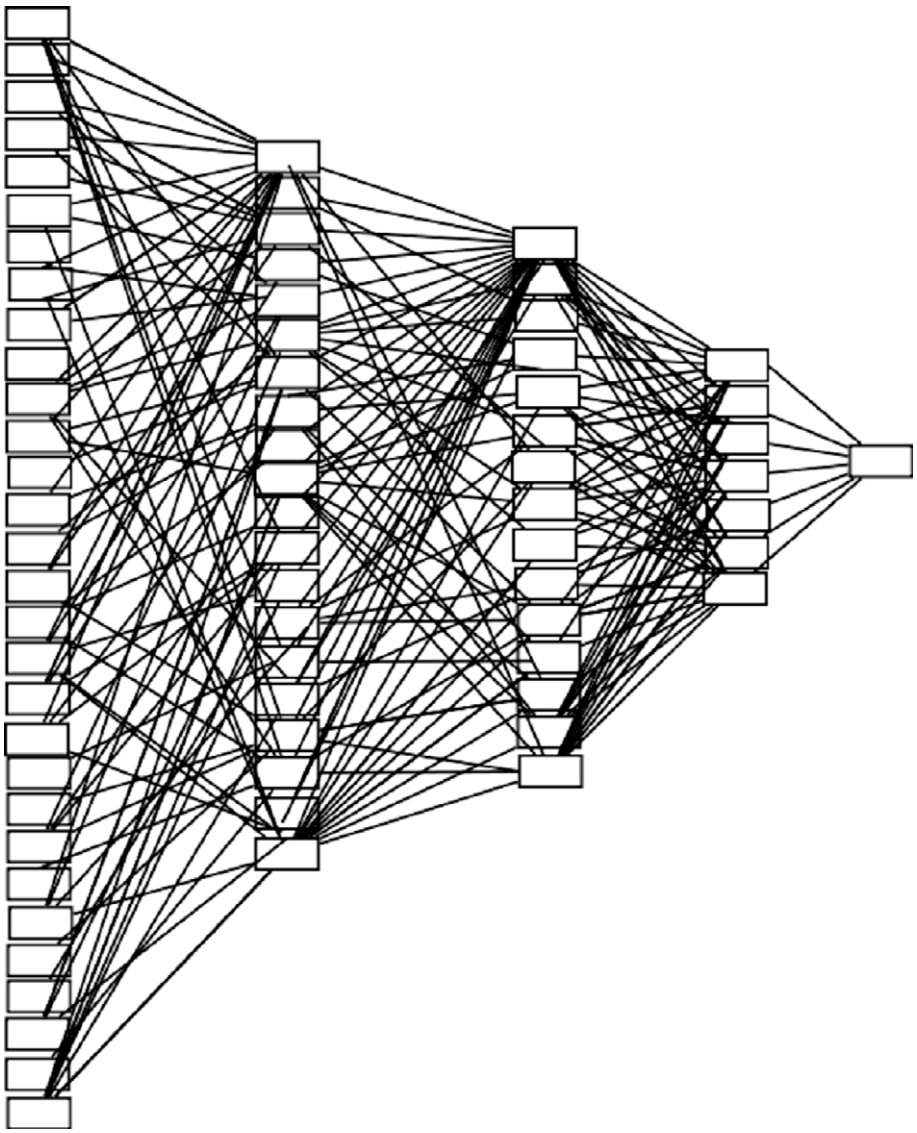

Fig. 1. Structure of the ANN (to reduce the complexity of the figure, not all the relationships between the neurons are displayed).

documented, and fast as well as including a framework for easy handling of training data sets (Nissen, 2007).

We design a multilayer ANN with 30 input neurones, 42 in hidden layers (20 → 15 → 7) and one neuron in the output layer. A general overview is shown in Fig. 1. Additionally, activation functions, both for hidden and output neurons, were set to FANN_SIGMOID_SYMETRIC. Training was based on a supervised method with back-propagation strategy and the parameters giving maximum accuracy were a learning rate equalled to 0.7, minimum error to 0.0001 and maximum epochs to 500,000.

The training-validating tests were run in automated manner by using an *ad hoc* program in C language developed by one of the authors (AC) running under Linux (Ubuntu 7.04). The most accurate networks were selected as potential candidates and further validated.

2.2. Data retrieval

All data selected were extracted from previous studies with similar results reported for the positive control butylhydroxytoluene (BHT) in order to reduce noise data as much as possible (Bozin, Mimica-Dukic, Samojlik, & Jovin, 2007; Burits & Bucar, 2000; Candan et al., 2003; Çetinus, Göze, Saraç, & Vural, 2007; Dermirci, Koşar, Dermirci, Dinç, & Başer, 2007; Eminagaoglu et al., 2007; Fraternale, Giamperi, Bucchini, & Ricci, 2007; Gülüce et al., 2007; 2003; Jirovetz et al., 2006; Kartal et al., 2007; Mimica-Dukic, Bozin, Sokovic, & Simin, 2004; Özer et al., 2007; Ricci et al., 2005; Sacchetti et al., 2004; Sharififar, Moshafi, Mansouri, Khodashenas, & Khoshnoodi, 2007; Sökmen et al., 2004a; Sökmen et al., 2004b; Tepe et al., 2006; Tepe, Daferera, Sihoglu-Tepe, Polissiou, & Sökmen, 2007; Tepe, Daferera, Sökmen, Polissiou, & Sökmen, 2004; Tepe et al., 2004; Tepe, Sihoglu-Tepe, Daferera, Polissiou, & Sökmen, 2007; Tepe et al., 2005; Tepe, Sökmen, Sökmen, Daferera, & Polissiou, 2005).

The chemical composition of the selected EOs consisted of up to 79 different compounds. To avoid excessive complexity of the neural network and minimise the associated structural problems, only 30 compounds with the higher antioxidant capacity according Ruberto and Baratta (2000) were selected as input values (Fig. 2). The resulting array of input sets is shown in Table 1 (Supplementary information), and the corresponding output values – i.e.

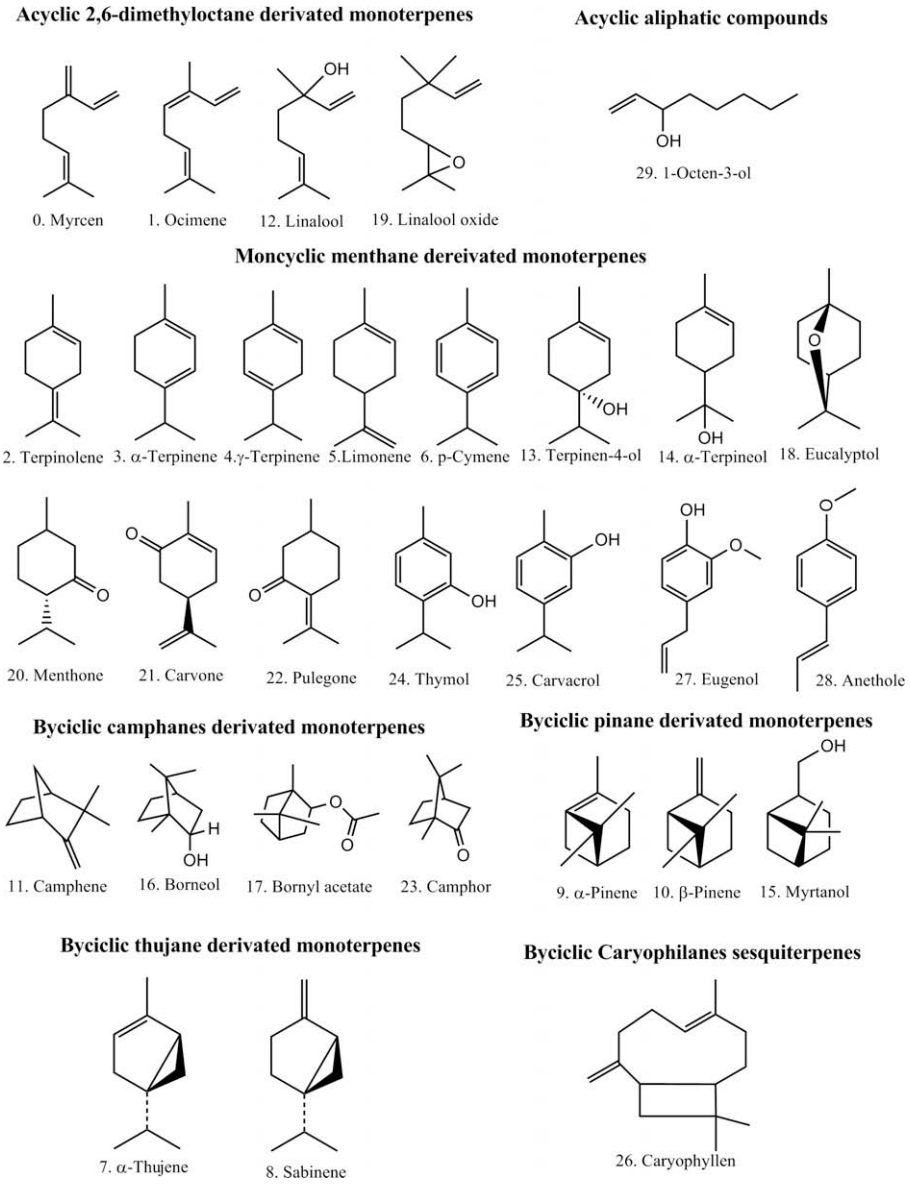

Fig. 2. Chemical structures of the 30 selected inputs.

antioxidant activity – are shown in Table 2 (Supplementary information).

2.3. Modelling the radical scavenging behaviour of essential oils in the DPPH assay

Chemical composition data – expressed in percentage of each compound – were retrieved from previous studies on the antioxidant activity of essential oils. Only studies reporting similar IC_{50} values for the reference compound BHT were selected to assure data uniformity among different articles/authors. The data were transformed into a suitable interval (0–1) for input neurons by dividing percentages by 100. The IC_{50} output values were reduced to an interval from 0 to 1 by applying Log in base 100,000. Then, all paired values were randomly divided in two sets: a learning set of 26 elements and a validating set of 4 elements.

2.4. Modelling the antioxidant behaviour of essential oils in the linoleic acid assay

In a second approach, the object of prediction was capacity of inhibition of the volatile organic compounds and the conjugated diene hydroperoxides arising from linoleic acid oxidation in a β-carotene–linoleic acid mixture.

Identical considerations for input data were taken in this estimation, using BHT positive controls to assure data uniformity and transforming values to 0–1 interval. In this case output values were transformed in a suitable set for output neurons dividing the reported percentages of inhibition (*%I*) by 100.

In this case, a training set of 27 elements and a validating set of 4 elements were used to predict percentage of inhibition of the linoleic acid oxidation.

2.5. Validation of the ANN

Statistical analyses were carried out to verify the accuracy of predictions in both cases. Output values of testing and validating sets were used in a linear regression test with ANOVA to determinate if they are statistically related with experimental values from the studies. All statistical analyses were performed using SPSS v. 15 (SPSS Inc. Chicago, USA).

3. Results and discussion

We could predict the antioxidant capacities of essential oils of known chemical composition in both the DPPH and linoleic acid assays using an artificial neuronal network (ANN) with an average error of only 3.16% and 1.46%, respectively.

A final set of the 30 compounds with the highest antioxidant activity according Ruberto and Baratta (2000) was used as inputs (Fig. 2). Fig. 3A shows the result of the ANN training with the reported values for the DPPH assay. As shown in Fig. 3B, all predicted values (Log in base 100,000 of IC_{50}) in the DPPH assay for the validating set could be correlated with the experimental values within an interval of confidence 95% with a relative error of 3.16% on average. Regression tests for the results in the linoleic acid assay are presented in Fig. 3C and D. They indicate that the prediction ability gained during the learning process was fully operational when using the validating set. The designed ANN proved to be able to produce values correlating well with experimental data (medium relative error of 1.46%). Furthermore, all statistical tests showed a significant relationship between experimental and predicted values ($p < 0.05$) in the validating set, the training set scoring even higher signification ($p < 0.0001$).

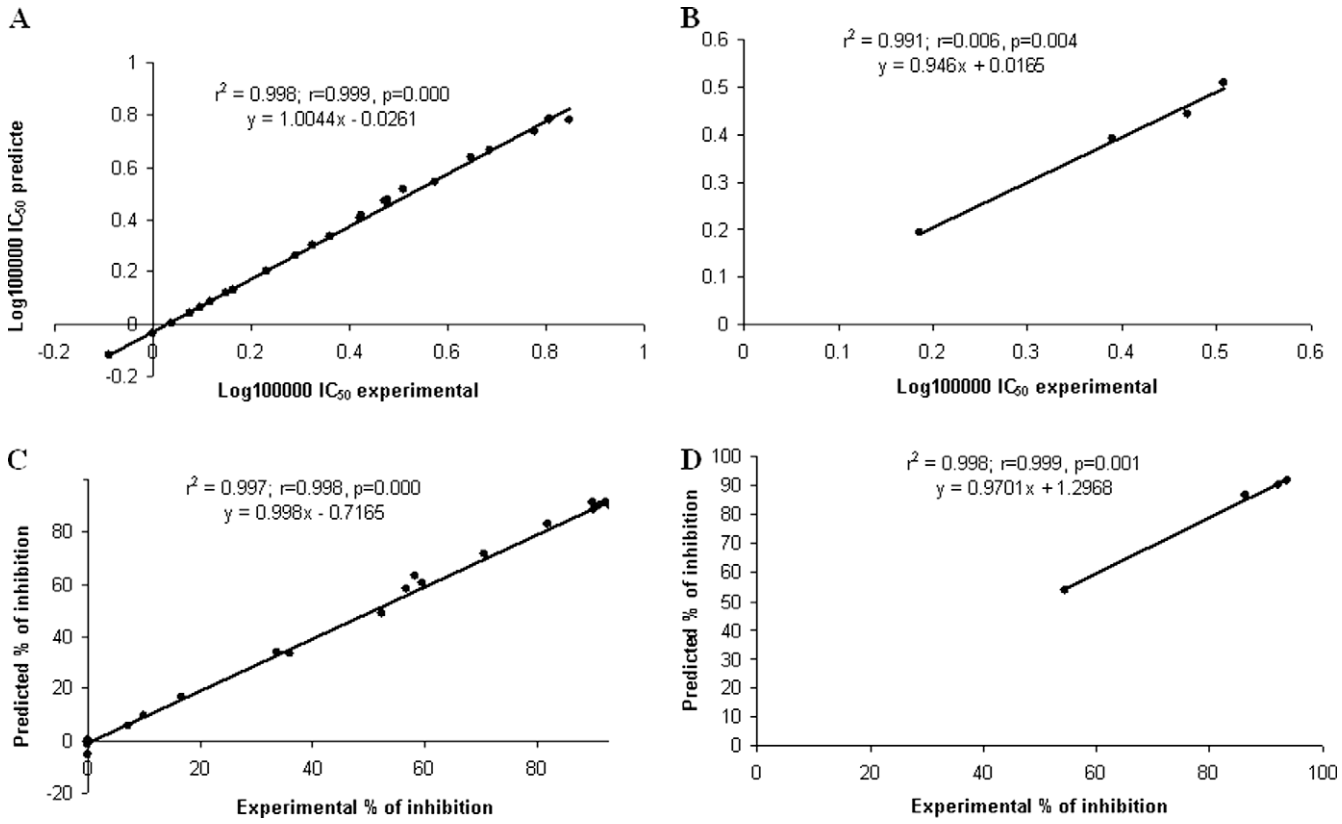

Fig. 3. Accuracy of the predictions. (A) Training set for the DPPH assay; (B) validating set for the DPPH assay; (C) training set for the linoleic acid assay; (D) validating set for the linoleic acid assay.

We could therefore successfully model the biochemical activity of essential oils in two standard, widely used and accepted *in vitro* chemical models whilst overcoming some of the limitations in the application of ANNs. Some of the reported problems in the application of ANNs are caused by their inherent structure and the most important are 'overtraining', 'peaking effect', and 'network paralysis'. Overtraining the ANN may lead to the noise of data used for training being fixed in the network weights. The peaking effect is experienced when an excessive number of hidden neurons minimise error in training but increase error in testing. Finally network paralysis appears when an excessive adjustment of neurons weight raise high negative or positive values leading to a near zero output with sigmoid activation functions (Kröse & van der Smagt, 1996). These limitations have to be taken into account and minimised with an adequate network topology and parameters. In our case noise reduction was achieved by selecting carefully the data sets by using only papers with similar values of BHT. By reducing the inputs to the most relevant compounds – i.e. keeping those with higher antioxidant activity as described in Section 2 – we could reduce the number of hidden neurons and all the problems associated with topology complexity. However, the number of inputs used in this work remains far higher than any of the previous attempts reported by the literature (Buciński et al., 2004; Torrecilla, Mena, Yáñez-Sedeño, & García, 2007) The reduced numbers of validating elements in both experiments are in line with previous studies confirming the possibility of using short sets for similar applications (Buciński et al., 2004).

Insights on the particular contribution of every single compound in the essential oil and their possible synergies/antagonism were not possible. Unfortunately our feed forward ANN did not allow us to determinate the final contribution of each input element – chemical compound – to the antioxidant activity of the EO due to the elevate number of hidden neurons. Therefore, relationships between all antioxidant compounds could not be established. According the literature phenolic compounds, eugenol, carvacrol and thymol, are known to be major players in the reduction of the DPPH radical (Brand-Williams, Cuvelier, & Berset, 1995). The linoleic acid oxidation assay occurs in a less polar environment than this of DPPH where phenols seem to be less soluble and therefore their antioxidant potential might be diminished. Interestingly, in our ANN model of the linoleic acid assay, the neurones weights for the first layer suggest significant initial contributions of non phenolic substances. In particular, *p*-ocimene seems to be an input as important as carvacrol or thymol, followed in less extend by eugenol and anethole, though this may not necessarily be important for the final output.

Antioxidant capacity is nowadays accepted as a criterion of food quality and to monitor the impact of food processing in the nutraceutical value of food products. As a consequence, developing ANNs able to predict antioxidant values of EOs could become an important tool for the food industry as they could predict their antioxidant capacity without implementing any experimental procedure within their premises.

Neural networks are fast-spreading in chemistry (Zupan & Gasteiger, 1991) but only a few applications to natural product's chemistry/food chemistry have been reported so far. Our results confirm that artificial neural networks are reliable, fast and cheap tools and open the way for predicting the antioxidant activity of essential oils. Therefore, can be used to model nutraceutical properties or predict the quality of food ingredients.

Acknowledgement

Alvaro Cortes Cabrera's participation in Erasmus Program is gratefully acknowledged.

Appendix A. Supplementary data

Supplementary data associated with this article can be found, in the online version, at doi:10.1016/j.foodchem.2009.04.070.

References

Bozin, B., Mimica-Dukic, N., Samojlik, I., & Jovin, E. (2007). Antimicrobial and antioxidant properties of rosemary and sage (*Rosmarinus officinalis* L. and *Salvia officinalis* L., Lamiaceae) essential oils. *Journal of Agricultural and Food Chemistry, 55*, 7879–7885.

Brand-Williams, W., Cuvelier, M. E., & Berset, C. (1995). Use of a free radical method to evaluate antioxidant activity. *Lebensmittel Wissenschaffen und Technologie, 28*, 25–30.

Buciński, A., Zieliński, H., & Kozłowska, H. (2004). Artificial neural networks for prediction of antioxidant capacity of cruciferous sprouts. *Trends in Food Science and Technology, 15*, 161–169.

Burits, M., & Bucar, F. (2000). Antioxidant activity of *Nigella sativa* essential oil. *Phytotherapy Research, 14*, 323–328.

Candan, F., Unlu, M., Tepe, B., Daferera, D., Polissiou, M., Sökmen, A., et al. (2003). Antioxidant and antimicrobial activity of the essential oil and methanol extracts of *Achillea millefolium* subsp. *millefolium* Afan. (Asteraceae). *Journal of Ethnopharmacology, 87*, 215–220.

Çetinus, A. Ş., Göze, İ., Saraç, B., & Vural, N. (2007). Scavenging effect and antispasmodic activity of the essential oil of *Cyclotrichium niveum*. *Fitoterapia, 78*, 129–133.

Dermirci, B., Koşar, M., Dermirci, F., Dinç, M., & Başer, K. H. C. (2007). Antimicrobial and antioxidant activities of the essential oil of *Chaerophyllum libanoticum* Boiss. et Kotschy. *Food Chemistry, 105*, 1512–1517.

Eminagaoglu, O., Tepe, B., Yumrutas, O., Akpulat, H. A., Daferera, D., Polissiou, M., et al. (2007). The in vitro antioxidative properties of the essential oils and methanol extracts of *Satureja spicigera* (K. Koch.) Boiss. and *Satureja cuneifolia* Ten. *Food Chemistry, 100*, 339–343.

Fraternale, D., Giamperi, L., Bucchini, A., & Ricci, D. (2007). Essential oil composition and antioxidant activity of aerial parts of *Grindelia robusta* from Central Italy. *Fitoterapia, 78*, 443–445.

Gülüce, M., Şahin, F., Sökmen, M., Ozer, H., Daferera, D., Sökmen, A., et al. (2007). Antimicrobial and antioxidant properties of the essential oils and methanol extract from *Mentha longifolia* L. ssp. *longifolia*. *Food Chemistry, 103*, 1449–1456.

Gülüce, M., Sökmen, M., Daferera, D., Ağar, G., Özcan, H., Kartal, N., et al. (2003). In vitro antibacterial, antifungal, and antioxidant activities of the essential oil and methanol extracts of herbal parts and Callus cultures of *Satureja hortensis* L.. *Journal of Agricultural and Food Chemistry, 51*, 3958–3965.

Jirovetz, L., Buchbauer, G., Stoilova, I., Stoyanova, A., Krastanov, A., & Schmidt, E. (2006). Chemical composition and antioxidant properties of clove leaf essential oil. *Journal of Agricultural and Food Chemistry, 54*, 6303–6307.

Kartal, N., Sökmen, M., Tepe, B., Daferera, D., Polissiou, M., & Sökmen, A. (2007). Investigation of the antioxidant properties of *Ferula orientalis* L. using a suitable extraction procedure. *Food Chemistry, 100*, 584–589.

Kröse, B. J. A., & van der Smagt, P. P. (1996). *An introduction to neural networks* (8th ed.). University of Amsterdam.

Mimica-Dukic, N., Bozin, B., Sokovic, M., & Simin, N. (2004). Antimicrobial and antioxidant activities of *Melissa officinalis* L. (*Lamiaceae*) essential oil. *Journal of Agricultural and Food Chemistry, 52*, 2485–2489.

Nissen, S. 2007. Fast artificial network library. <http://leenissen.dk/fann/> [last accessed 15.11.2007].

Özer, H., Sökmen, M., Gülüce, M., Adigüzel, A., Şahin, F., Sökmen, A., et al. (2007). Chemical composition and antimicrobial and antioxidant activities of the essential oil and methanol extract of *Hippomarathrum microcarpum* (Bieb) from Turkey. *Journal of Agricultural and Food Chemistry, 55*, 937–942.

Radonic, A., & Milos, M. (2003). Chemical composition and in vitro evaluation of antioxidant effect of free volatile compounds from *Satureja montana* L. *Free Radical Research, 37*, 673–679.

Ricci, D., Fraternale, D., Giamperi, L., Bucchini, A., Epifano, F., Burini, G., et al. (2005). Chemical composition, antimicrobial and antioxidant activity of the essential oil of *Teucrium marum* (*Lamiaceae*). *Journal of Ethnopharmacology, 98*, 195–200.

Ruberto, G., & Baratta, M. T. (2000). Antioxidant activity of selected essential oil components in two lipid model systems. *Food Chemistry, 69*, 167–174.

Sacchetti, G., Medici, A., Maietti, S., Radice, M., Muzzoli, M., Manfredini, S., et al. (2004). Composition and functional properties of the essential oil of Amazonian basil, *Ocimum micranthum* Willd., Labiatae in comparison with commercial essential oils. *Journal of Agricultural and Food Chemistry, 52*, 3486–3491.

Sharififar, F., Moshafi, M. H., Mansouri, S. H., Khodashenas, M., & Khoshnoodi, M. (2007). In vitro evaluation of antibacterial and antioxidant activities of the essential oil and methanol extract of endemic *Zataria multiflora* Boiss. *Food Control, 18*, 800–805.

Sökmen, A., Gülüce, M., Akpulat, A., Daferera, D., Tepe, B., Polissiou, M., et al. (2004a). The in vitro antimicrobial and antioxidant activities of the essential oils and methanol extracts of endemic *Thymus spathulifolius*. *Food Control, 15*, 627–634.

Sökmen, M., Serkedjieva, J., Daferera, D., Gülüce, M., Polissiou, M., Tepe, B., et al. (2004b). In vitro antioxidant, antimicrobial, and antiviral activities of the essential oil and various extracts from herbal parts and callus cultures of *Origanum acutidens*. *Journal of Agricultural and Food Chemistry, 52*, 3309–3312.

Tepe, B., Akpulat, A., Sökmen, M., Daferera, D., Yumrutas, O., Aydin, E., et al. (2006). Screening of the antioxidative and antimicrobial properties of the essential oils of *Pimpinella anisetum* and *Pimpinella flabellifolia* from Turkey. *Food Chemistry, 97*, 719–724.

Tepe, B., Daferera, D., Sihoglu-Tepe, A., Polissiou, M., & Sökmen, A. (2007). Antioxidant activity of the essential oil and various extracts of *Nepeta flavida* Hub.-Mor. from Turkey. *Food Chemistry, 103*(135), 8–1364.

Tepe, B., Daferera, D., Sökmen, M., Polissiou, M., & Sökmen, A. (2004). In Vitro Antimicrobial and antioxidant activities of the essential oils and various extracts of *Thymus eigii* M. Zohary et P.H. Davis. *Journal of Agricultural and Food Chemistry, 52*, 1132–1137.

Tepe, B., Donmez, E., Unlu, M., Candan, F., Daferera, D., Vardar-Ünlü, G., et al. (2004). Antimicrobial and antioxidative activities of the essential oils and methanol extracts of *Salvia cryptantha* (Montbret et Aucher ex Benth.) and *Salvia multicaulis* (Vahl). *Food Chemistry, 84*(51), 9–525.

Tepe, B., Sihoglu-Tepe, A., Daferera, D., Polissiou, M., & Sökmen, A. (2007). Chemical composition and antioxidant activity of the essential oil of *Clinopodium vulgare* L. *Food Chemistry, 103*, 766–770.

Tepe, B., Sökmen, M., Akpulat, A., Daferera, D., Polissiou, M., & Sökmen, A. (2005a). Antioxidative activity of the essential oils of *Thymus sipyleus* subsp. *sipyleus* var. *sipyleus* and *Thymus sipyleus* subsp. *sipyleus* var. *rosulans*. *Journal of Food Engineering, 66*, 447–454.

Tepe, B., Sökmen, M., Sökmen, A., Daferera, D., & Polissiou, M. (2005b). Antimicrobial and antioxidative activity of the essential oil and various extracts of *Cyclotrichium origanifolium* (Labill.) Manden. and Scheng. *Journal of Food Engineering, 69*(33), 5–342.

Torrecilla, J. S., Mena, M. L., Yáñez-Sedeño, P., & García, J. (2007). Application of artificial neural network to the determination of phenolic compounds in olive oil mill wastewater. *Journal of Food Engineering, 81*, 544–552.

Vardar-Ünlü, G., Candan, F., Sökmen, A., Daferera, D., Polissiou, M., Sökmen, M., et al. (2003). Antimicrobial and antioxidant activity of the essential oil and methanol extracts of *Thymus pectinatus* Fisch. et Mey. Var. *pectinatus* (*Lamiaceae*). *Journal of Agricultural and Food Chemistry, 51*, 63–67.

Zupan, J., & Gasteiger, J. (1991). Neural networks: a new method for solving chemical problems or just a passing phase? *Analytica Chimica Acta, 248*, 1–30.

Food Chemistry 118 (2010) 147–152

Contents lists available at ScienceDirect

Food Chemistry

journal homepage: www.elsevier.com/locate/foodchem

Analytical Methods

On-line HPLC–MS–DPPH assay for the analysis of phenolic antioxidant compounds in fruit wine: *Antidesma thwaitesianum* Muell.

Nitra Nuengchamnong [a], Kornkanok Ingkaninan [b,*]

[a] *Regional Medical Sciences Center Phitsanulok, Department of Medical Sciences, Ministry of Public Health, Phitsanulok 65000, Thailand*
[b] *Department of Pharmaceutical Chemistry and Pharmacognosy, Faculty of Pharmaceutical Sciences, Naresuan University, Phitsanulok 65000, Thailand*

ARTICLE INFO

Article history:
Received 30 July 2007
Received in revised form 15 April 2009
Accepted 18 April 2009

Keywords:
On-line HPLC–MS–antioxidant assay
Fruit wine
Characterisation
Antidesma thwaitesianum

ABSTRACT

A reversed phase high performance liquid chromatography (RP-HPLC) separation coupled with an electrospray ionisation mass spectrometry detection (ESI-MS) and the 2,2-diphenyl-1-picrylhydrazyl (DPPH) assay was used for the screening of multiple antioxidant compounds in *Antidesma thwaitesianum* Muell. fruit wine. The active compounds were identified by comparison with authentic standards and published mass spectra. With the help of the multidimensional information of LC–ESI-MS/MS and DPPH assay, the compounds with different chemical structures could be determined in one run successfully. The antioxidant compounds were separated and identified as gallic acid, cyanidin-3-sophoroside, monogalloyl glucoside, delphinidin-3-sambubioside, catechin, caffeic acid, and pelargonidin-3-malonyl glucoside. This result shows that an on-line HPLC–MS–DPPH assay can be a powerful technique for the rapid characterisation of antioxidant compounds in plant extracts.

1. Introduction

Over the last decade, the healthy effects of red wine have been studied in depth. Epidemiological studies have shown that moderate intake of red wine reduced the incidence of coronary heart disease (Criqui & Ringel, 1994; Serafini, Laranjinha, Almeida, & Mainai, 2000; Stanley & Mazier, 1999; Sun, Simonyi, & Sun, 2002). Fruit wines have also been claimed for health promoting effects which may be related to their antioxidant activity. The tropical climate and naturally fertile geography of Thailand is the home of some of the world's most exotic and delicious tropical fruits. Some of the fruits used for making particular wines are unique to this region. *Antidesma thwaitesianum* Muell. (Euphorbiaceae) is a wild plant found in the north-eastern area of Thailand. The fruits are round or ovoid, up to 1/3 in. (8 mm) in diameter, borne in grapelike, pendent clusters (often paired) which are extremely showy because the berries ripen unevenly. The pale yellowish-green, white, bright-red, and nearly black stages are all present at the same time. The trees flower in May–July and the fruits mature in August–October (Morton, 1987). The ripen fruits are consumed fresh or can be processed into juice or a type of wine. These fruits are believed to be a good source of natural antioxidants but it is still not clear which compounds are responsible for their antioxidant property. *A. thwaitesianum* red wine is another product that becomes more popular among Thai consumers as healthy nourishment.

HPLC methods coupled on-line with an antioxidants detection unit using post column reaction of the eluates with free radicals have been reported to be successfully applied to identify and quantify antioxidants in biological samples (Niederländer, van Beek, Bartasiute, & Koleva, 2008; Nuengchamnong & Ingkaninan, 2009). In several plant extracts, antioxidants are usually found as complex mixtures and the composition changes according to the plant examined. In such cases, hyphenated techniques are needed for the analysis of the extracts. In this study, we used a readily available on-line HPLC technique coupled to MS and an antioxidant activity detector using the DPPH method as a tool to directly screen and characterise the antioxidants in this fruit wine. The antioxidant compounds can be monitored spectrophotometrically by the decrease of the absorbance at 515 nm of the reduced form of the free radical, 2,2-diphenyl-1-picrylhydrazyl (DPPH). Combination of LC–MS techniques with on-line post-column detection of antioxidant compounds has an advantage of the simultaneous use of chromatography as a separation method, an ESI-MS/MS as an identification method, and a DPPH assay as an activity evaluation method.

In this paper, we report the evaluation of the antioxidant activity in Thai fruit wines using off-line DPPH assay and the use of an on-line HPLC–MS–DPPH assay for the analysis of phenolic antioxidant compounds in fruit wine, *A. thwaitesianum*. An LC–MS/MS in MRM mode was used to quantify the active compounds.

2. Materials and methods

2.1. Materials and reagents

Pure standards of gallic acid, caffeic acid, catechin, quercetin, were purchased from Sigma (St. Louis, MO, USA). DPPH was

* Corresponding author. Tel.: +66 55 261000x3618; fax: +66 55 261057.
E-mail address: k_ingkaninan@yahoo.com (K. Ingkaninan).

0308-8146/$ - see front matter © 2009 Elsevier Ltd. All rights reserved.
doi:10.1016/j.foodchem.2009.04.069

obtained from Sigma–Aldrich Chemie (Steinheim, Germany). Methanol (LC/MS reagent) was purchased from JT Baker (Mallinckrodt Baker, Inc. Phillipsburg, NJ, USA). Formic acid (analytical grade) was purchased for Merck (Darmstadt, Germany). Water was purified using Elga USF system (Bucks, England).

2.2. Wine samples

Thirty wine samples from 26 kinds of fruits were products from the "One Tambon One Product" (OTOP) project that supported by the Thai government. The name of the fruit wines and source of the product were listed in Table 1.

2.3. Sample preparation

The wine samples were tested for off-line antioxidant activity without any sample preparation. For the analyses using the on-line HPLC–MS–DPPH assay, *A. thwaitesianum* fruit wine from Mae Hong Sorn were filtered through a 0.2 μm Nylon syringe filter (Chrom Tech, Inc. MN, USA) and the filtrates were then injected into the on-line system.

2.4. Off-line DPPH assay for evaluation of antioxidant activity

The DPPH assay was slightly modified from the method of Brand-Williams, Cuvelier and Berset (1995). In the assay, 0.1 ml fruit wine was mixed with 2.9 ml of 0.1 mM DPPH in methanol and incubated in the dark at room temperature for 30 min. The absorbance (A) of the sample was measured on a Perkin Elmer Lambda II (Perkin Elmer, USA) spectrophotometer at 515 nm using methanol as a blank. All tests were performed in triplicate. The total antioxidant activity (TAA) was expressed in terms of percentage activity as calculated with the following equation: % TAA = $100 \times [(Ac - As/Ac)]$, where Ac is the absorbance of the control and As is the absorbance of the tested sample after 30 min.

2.5. On-line HPLC–MS–DPPH assay

An HPLC was on-line coupled to an MS (line A) and a continuous flow of DPPH assay (line B) as shown in Fig. 1. The details of the instrumental set up are as follows.

Line A represents the HPLC system. Agilent 1100 series HPLC system (Agilent Technologies, Palo Alto, CA, USA) is equipped with a binary pump, a degasser, an autosampler, a thermostated column compartment and a control module. The HPLC system was coupled to a PE SCIEX API 4000 triple quadrupole tandem mass spectrometer (Applied Biosystem, Foster City, CA) equipped with an electrospray ionisation interface. The Analyst 1.3.2 software was used for data acquisition and processing. The full scan mass spectra from m/z 100–1000 amu were acquired both in positive and negative ion modes. The optimum conditions of the interface were as follows: ESI-positive mode; ion spray voltage of 4500 V, curtain gas of 10 psi, ion source gas 1 of 65 psi, ion source gas 2 of 55 psi. The interface temperature was set at 400 °C. The entrance and declustering potential were 10 and 80 V, respectively. ESI-negative mode; ion spray voltage of −4500 V, curtain gas of 10 psi, ion source gas 1 of 65 psi, ion source gas 2 of 55 psi. The interface temperature was set at 400 °C. The entrance and declustering potential were −10 and −80 V, respectively.

The chromatographic separation was on a phenomenex Gemini column (5 μm, 250 × 4.6 mm i.d.) (Phenomenex, Torrace, CA) protected with an ODS C18 guard column, operated at 25 °C. The mobile phase consisted of 0.1% (v/v) formic acid in deionized water (solvent A) and methanol (solvent B), starting from 90% solvent A (4 min), from 90% to 80% solvent A (6 min), from 80% to 10% solvent A (30 min), constant at 10% solvent A (5 min), from 10% to 90% solvent A (5 min), and then constant at 90% solvent A for

Table 1
The percent total antioxidant activity (% TAA) of some fruit wines in Thailand evaluated by using DPPH assay. The activities shown are the means of three experiments ± standard deviations.

Common name	Scientific name	Source	% TAA
1. Java plum	*Syzygium cumini* (L.) Skeels	Kon kaen	95.9 ± 0.09
2. Emblica	*Phyllanthus emblica* L.	Chiang rai	94.3 ± 0.12
3. Roselle	*Hibicus sabdariffa* L.	Phayao	92.6 ± 0.10
4. Longan	*Dimocarpus longan* Lour.	Phayao	92.6 ± 0.10
5. Black ginger	*Kaempferia parviflora* Wall. ex Baker	Chiang mai	92.5 ± 0.10
6. Makiang	*Cleistocalyx nervosum* var. *paniala*	Chiang rai	91.2 ± 0.12
7. Santol	*Sandoricum Koetjape* (Burm.f) Merr.	Yala	91.2 ± 0.31
8. Mangosteen	*Garcinia mangostana* L.	Chumporn	89.9 ± 0.17
9. Strawberry	*Fragaria chiloensis* (L.) Duchense	Chiang mai	89.2 ± 0.14
10. Mao	*Antidesma thwaitesianum* Muell	Songkhla	88.8 ± 0.32
		Suratthani	87.7 ± 0.18
		Kon kaen	86.9 ± 0.21
		Mae Hong Sorn	81.3 ± 0.14
		Trang	74.9 ± 1.14
		Chiang rai	64.4 ± 0.36
11. Lychee	*Litchi chinensis* Sonn.	Chiang mai	86.7 ± 0.17
12. East Indian plum	*Flacourtia cataphracta* Roxb. ex willd.	Suratthani	86.2 ± 0.04
13. Plum	*Prunus domestica* L.	Mae Hong Sorn	86.2 ± 0.10
14. Peach	*Prunus persica* (L.) Batsch	Mae Hong Sorn	85.6 ± 0.11
15. Nutmeg	*Myristica fragrans* Houtt.	Chumporn	84.9 ± 0.72
16. Mullbery	*Morus alba* L.	Mae Hong Sorn	84.5 ± 0.20
17. Grape	*Vitis vinifera* L.	Nakornratchasima	83.7 ± 0.54
18. Apple	*Malus sp.*	Chiang rai	56.3 ± 0.67
19. Sala	*Salacca zalacca* (Gaertn.) Voss ex Vilm.	Suratthani	56.0 ± 0.98
20. Thao khan	*Cissus repens* Lam.	Suratthani	55.0 ± 0.33
21. Pineapple	*Ananas comosus* (L.) Merr.	Krabi	35.6 ± 0.45
22. Lime	*Citrus aurantifolia* (Christm.) Swingle	Chiang rai	20.1 ± 1.09
23. Tamarind	*Tamarindus indica* L.	Phitsanulok	15.7 ± 0.63
24. Garcinia	*Garcinia cambogia* Desr.	Songkhla	15.4 ± 0.21
25. Rambutan	*Nephelium lappaceum* L.	Suratthani	15.1 ± 0.26
26. Star gooseberry	*Phyllanthus acidus* (L.) Skeels	Kon kaen	14.8 ± 0.46

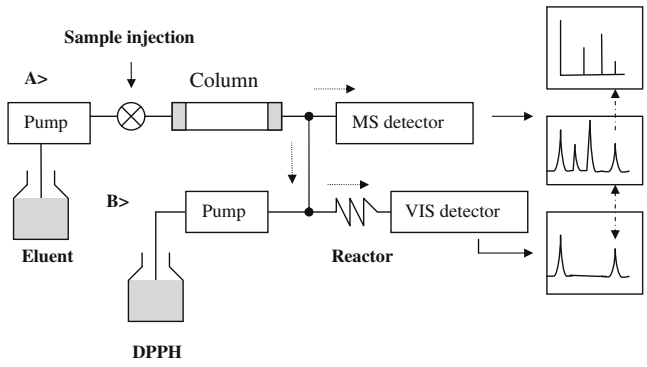

Fig. 1. Scheme of the on-line HPLC–MS–DPPH assay. The arrows indicate flow directions.

5 min for reconditioning of the column. A mass spectra was recorded within 55 min. The injection volume was 5 μl. The flow rate was set at 600 μl /min.

A polyetheretherketone (PEEK) tubing with the length of 10 cm and an i.d. of 0.25 mm was used as the post-column tubing. A 24 cm length of 0.17 mm (i.d.) PEEK tubing was coupled line A to line B by a Y-connector. A 30 cm 0.13 mm (i.d.) PEEK was connected to MS. The eluent flow was split in ratio of 8:2 between the MS ion source and DPPH line. Quercetin at concentration of 200 μg/ml was spiked into the wine sample and used as a standard to synchronise antioxidant activity in the DPPH trace with the mass trace.

Line B represents the continuous flow system for antioxidant activity detection. It consisted of an HPLC pump, LC20AD prominence (Shimadzu, Kyoto, Japan), home-made knitted reaction coil PEEK tubing with an inner diameter 180 μm and a total reaction coil volume of 100 μL. The flow of 0.1 mM DPPH was set to 0.2 ml/min and induced bleaching was detected as a negative peak at 515 nm using the UV–VIS detector (SPD 20AV, Shimadzu, Kyoto, Japan), and the LC solution software was used for data acquisition and processing. The polarity of the signal output was reversed in order to obtain positive signals. The system was operated at 25 °C.

To characterise the antioxidant peaks, the fragment ions from their corresponding parent ions in negative mode were induced with collision gas (CAD) of 6 psi, collision energy (CE) between −5 and −50 V and a collision cell exit potential (CXP) of −6 V, DP in the range of −20 to −110 V. In the positive mode, the ions were induced with CAD of 7 psi. CE, CXP, and DP were set in the range of 5–25, 3–13, and 20–100 V, respectively.

2.6. Peak identification

Peak identification was performed by comparison of the retention time and mass spectrum with reference compounds. Tentative identification of peaks of which standard compounds unavailable was obtained by comparing their elution order and their molecular ion with the data from the literature.

2.7. Quantitative analysis

For quantitative analysis of antioxidants, the same HPLC condition was used. The MS parameters were operated in negative multiple reactions monitoring (MRM) scan. The individual optimised parameters for each compound are provided in Table 2. Standard compounds, gallic acid, cathechin, and caffeic acid at the concentrations of 0.1–10 μg/ml were used for preparation of calibration curves. The curves were generated by linear regression based on peak area. Contents of antioxidant compounds in *A. thwaitesianum* fruit wine were determined in triplicate experiments.

3. Results and discussion

The antioxidant activities of 30 fruit wine samples were evaluated by DPPH assay. The method is based on the reduction of the stable radical, DPPH, to the formation a non radical form in the presence of hydrogen donating antioxidant. The fruit wines showed an antioxidant activity by reducing DPPH to the yellow coloured diphenylpicrylhydrazine derivatives. The results of the screening are shown in Table 1. Most of these fruit wines showed high antioxidant activity. *A. thwaitesianum* wine was selected for further study due to the fact that the chemical constituents of this plant had not been reported before. Investigation of its antioxidant components is, therefore, of interest.

3.1. Identification of phenolic antioxidants in A. thwaitesianum wine

An HPLC was linked to a triple quadrupole mass spectrometer and a DPPH assay for the rapid identification of antioxidant components of the fruit wine of *A. thwaitesianum* (Fig. 2). The DPPH assay monitors the activity of the antioxidant compounds that separated from the gradient reversed-phase HPLC system. The mass spectrometry was used to elucidate the structures based on their mass spectra and fragmentation patterns. Moreover tandem mass spectrometry (MS/MS), particularly product ion analysis and precursor ion analysis, was extensively used for the specific identification and characterisation of the antioxidants.

The separation of phenolic compounds in *A. thwaitesianum* wine was achieved using a reversed phase C_{18} column with gradient methanol under acidic condition as a mobile phase. The eluate was split to the activity monitor and to the mass spectrometer with an electrospray interface generated in full scan MS mode. The sample was analysed twice in positive ionisation and negative ionisation modes. The DPPH based antioxidant activity profile (Fig. 2a) showed that at least nine compounds had antioxidant activity. The deprotonated molecular ion $[M-H]^-$ peaks of a standard reference, quercetin, was found at 37.70 min. The delay time between the read out from the MS detector and the corresponding peak from the antioxidant activity assay (38.17 min) was calculated as ca. 0.47 min. The retention time (t_R) values of the DPPH-positive compound and MS data obtained with individual compounds are summarised in Table 3. Peaks 1, 3, 5, and 6 were analysed using negative ionisation mode, while better MS spectra of peaks 2, 4, 7, 8, and 9 were obtained with the positive ionisation mode (Fig. 2b and c).

In the negative ionisation mode, peak 1 with a $[M-H]^-$ at *m/z* 169.4 and a fragment ion at *m/z* 125.2 (170-H–CO_2) and peak 6 with a $[M-H]^-$ at *m/z* 179.1 and a fragment ion at *m/z* 135.2 were assigned as gallic acid and caffeic acid respectively by comparison of their retention times and their mass data with standard compounds.

Peak 3 showing a $[M-H]^-$ at *m/z* 331.3 was assigned as monogalloyl glucoside by comparison with published data (Nawwar, Marzouk, Nigge, & Linscheid, 1997; Zywicki, Reemtsma, & Jekel, 2002).

Peak 5 with an $[M-H]^-$ at *m/z* 289.2 and a fragment ion at *m/z* 245.2 was identified as catechin by comparison with published data (Rio et al., 2004) and a reference standard.

In positive ionisation, peak 2 showing a $[M+H]^+$ at *m/z* 611.5 and a fragment ion at *m/z* 287.6 (cyanidin; M-324, loss of the sophorosyl unit) was identified as cyanidin-3-sophoroside by comparison with published data (Mullen et al., 2002). In the same fashion, peak 4 with an $[M+H]^+$ at *m/z* 597.5 and a fragment ion at *m/z* 303.6 (M−293.9) and peak 7 showing an $[M+H]^+$ at *m/z* 519.7 and a fragment ion at *m/z* 271.7 (M−248) were identified as delphinidin-3-sambubioside (Giusti, Rodriguez-Saona, Griffin & Wrolstad, 1999), and pelargonidin-3-malonyl glucoside, respectively. The general structures and substitution patterns of compounds identified are shown in Fig. 3.

Table 2
Mass parameters in negative MRM scan mode for quantitative analysis.

Compound	Parent ion (*m/z*)	Product ion (*m/z*)	Declustering potential (V)	Collision energy (V)	Collision cell exit potential (V)
Gallic acid	169.0	125.1	−70	−20	−18
Catechin	288.9	245	−150	−22	−12
Caffeic acid	178.7	134.9	−70	−23	−20

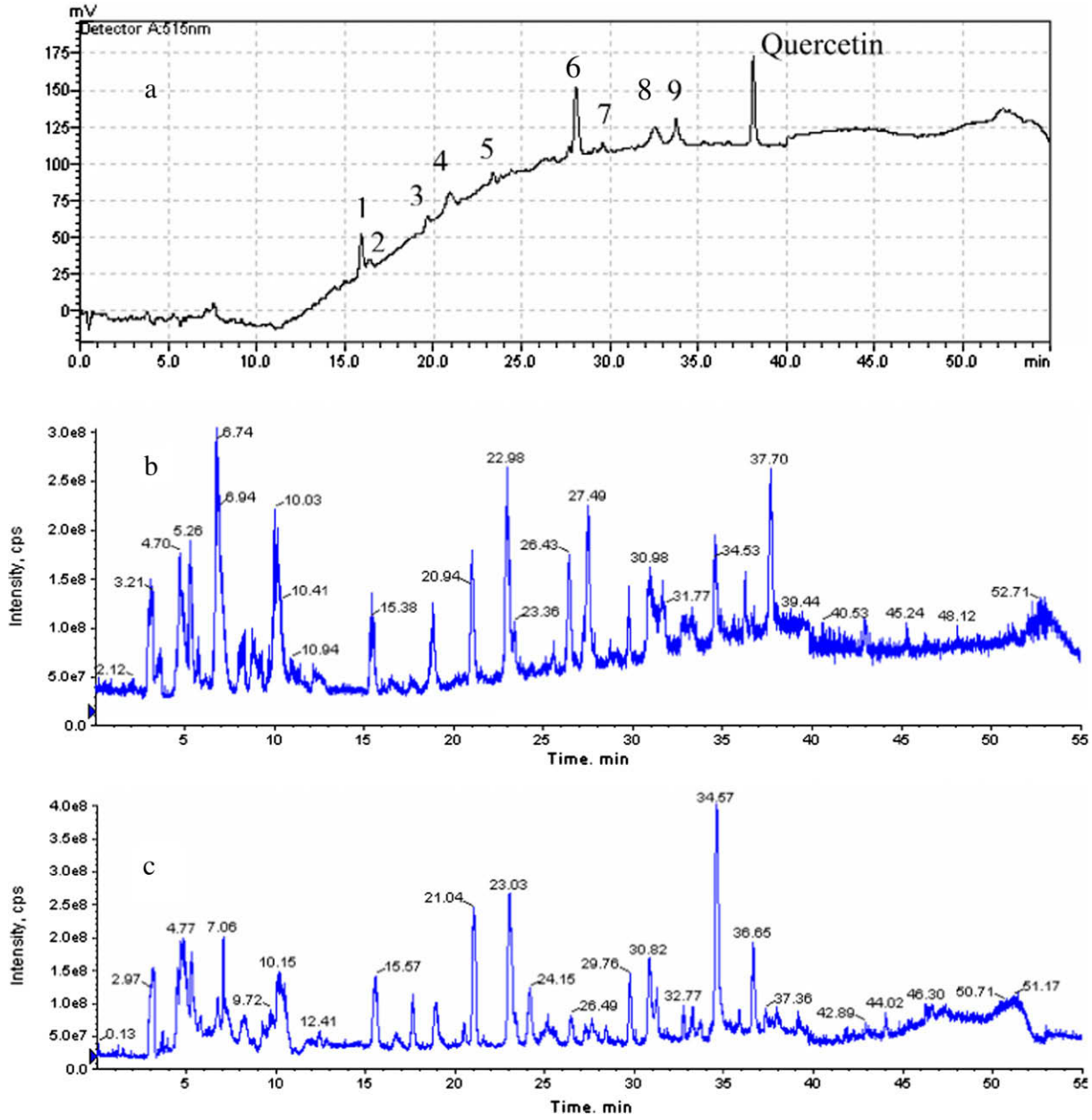

Fig. 2. The results from the analysis of *A. thwaitesianum* wine from Mae Hong Sorn using on-line HPLC–MS–DPPH assay. (a) The chromatogram from the antioxidant assay detection at 515 nm. (b) The total ion current (TIC) output from the ESI-MS in negative mode. (c) The total ion current (TIC) output from the ESI-MS in positive mode.

Peak 8 with fragment ions at *m/z* 401.3 and 385.5 and peak 9 with fragment ions at *m/z* 489.8 and 473.9 remained unidentified. Their structures still need to be elucidated by comparison of MS data with reference standards or using other spectroscopic techniques such as NMR.

Generally, an antioxidant activity depends on the number and positions of hydroxyl groups and other substituents and the glycosylation of the flavonoid molecules. Substitution pattern in the B ring and A ring as well as the 2,3-double bond and the 4-oxo group in the C ring also affect the antioxidant activity of flavonoids. Glycosylation of flavonoids reduces their activity (Rice-Evans, Miller, & Paganga, 1996). The aglycone of delphinidin, cyanidin, gallic acid, catechin pelargonidin, and caffeic acid showed high activity with the ABTS assay with TEAC value (mM) of 4.44, 4.40, 3.01, 2.40,

Table 3
Data from the on-line LC–MS–DPPH assay for characterisation of antioxidants in *A. thwaitesianum* wine.

Peak[a]	t_R[a] (min)	$[M-H]^-$ (*m/z*)	$[M+H]^+$ (*m/z*)	MS/MS (*m/z*)	Proposed compound
1	15.4	**169.4**[b], 125.2	–	125.2	Gallic acid[c]
2	15.6		611.5, 287.6	–	Cyanidin-3-sophoroside
3	19.2	**331.3**	–	169	Monogalloyl glucoside
4	20.5	–	597.5, 303.6	–	Delphinin-3-sambubioside
5	22.9	289.2, 245.2	–	–	Catechin[c]
6	27.5	**179.1**, 135.2	–	134.6	Caffeic acid[c]
7	29.7	–	519.7, 271.7	–	Pelargonidin-3-malonyl glucoside
8	32.2	–	**401.3**, 385.5	383.1	Unknown
9	33.3	–	489.8, 473.9	473.9	Unknown
10	37.7	**301.0**	–	179.1, 150.9	Quercetin (a reference standard)

[a] Peak numbers and retentions time refer to Fig. 2.
[b] *m/z* In bold was subjected to MS/MS analysis.
[c] Identified by comparison with reference standards.

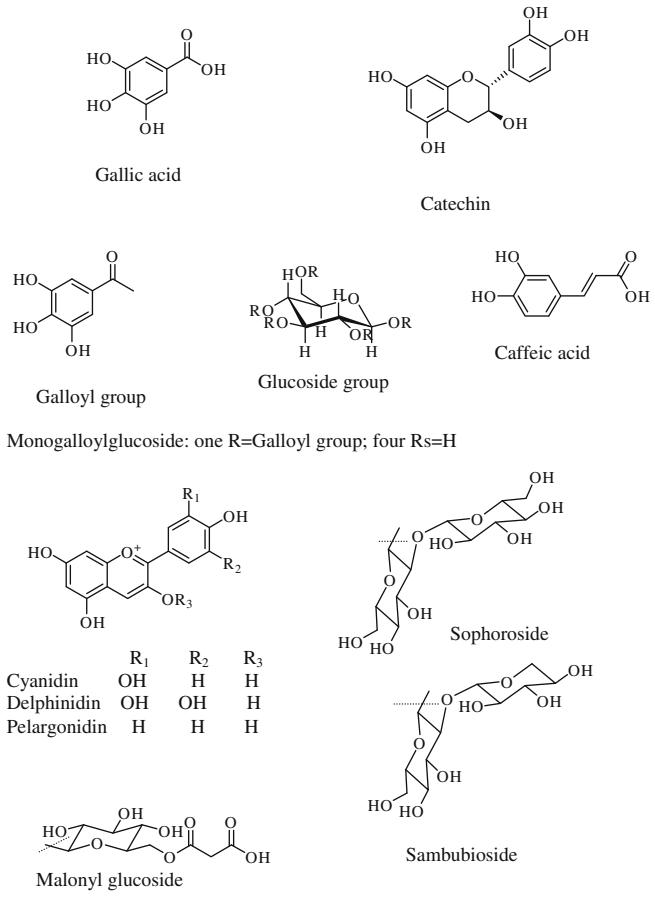

Fig. 3. Structure of phenolic compounds found in *A. thwaitesianum* wine: monogalloylglucoside; one R = galloyl group, four Rs = H; cyanidin: R_1 = OH,R_2,R_3 = H; delphinidin: R_1,R_2 = OH,R_3 = H; pelargonidin: R_1,R_2,R_3 = H; cyanidin-3-sophoroside: R_3 = sophoroside; Delphinidin-3-sambubioside: R_3 = sambubioside; Pelargonidin-3-malonyl glucoside: R_3 = malonyl glucoside.

1.30, 1.24, respectively (Cai, Sun, Xing, Luo, & Corke, 2006; Rice-Evans et al., 1996). In our previous study, it is proved that intensity of antioxidant peaks depend on both types and amounts of the antioxidant compounds present in the sample (Nuengchamnong et al., 2005).

Antioxidant compounds in *A. thwaitesianum* wine can be quantitatively analysed using LC–MS/MS in MRM mode if the standard compounds are available. In our studies, gallic acid, cathechin and caffeic acid at various concentrations were used for preparation of calibration curves. The satisfactory linearity was obtained. Regression equations ($1/x_2$ weighting) of gallic acid, cathechin, and caffeic acid were $Y = 8.49e + 005x + 5.49e + 003$, $Y = 1.47e + 004x - 6.62e + 004$, and $Y = 1.53e + 006x + 1.01e + 004$, with the *r* values of 0.9976, 0.9858, and 0.9995, respectively. The limits of detection (LOD) with signal to noise ratio of three were also determined. The LOD of gallic acid and caffeic acid were 0.05 ng while that of cathechin was 5.0 ng. The triplicate analyses of *A. thwaitesianum* fruit wine showed that caffeic acid was present in the highest amount (21.40 ± 0.26 μg/ml) comparing with gallic acid (16.9 ± 0.26 μg/ml) and catechin (4.91 ± 0.04 μg/ml). Unfortunately, not all antioxidant compounds in this wine were quantitatively determined due to lack of standard compounds.

4. Conclusions

The fruit wine of *A. thwaitesianum* was screened for antioxidant activity using an on-line HPLC–MS–DPPH assay. The active antioxidants were simultaneously monitored and identified. This is a clear example of how a hyphenated chromatographic technique can accelerate the procedure for identification of biologically active compounds in plants. The hyphenated technique used here successfully provided information of the antioxidant activity and the possible chemical structures of various phenolic antioxidant compounds in fruit wine of *A. thwaitesianum*.

Acknowledgements

We thank the staff from the Regional Medical Sciences Centers; Chiang Mai, Chiang Rai, Songkhla, Konkaen, Nakornratchasima and Chonburi for providing the samples and assisting in some of the preliminary analyses. Professor Dr. Hans Junginger is thanked for critically reviewing this manuscript. The Center of Excellence for Innovation in Chemistry (PERCH-CIC), Thailand is acknowledged for the support of the last author.

References

Brand-Williams, W., Cuvelier, M. E., & Berset, C. (1995). Use of a free radical method to evaluate antioxidant activity. *Lebensmittel-Wissenschaft Und Technologie, 28*, 25–30.
Cai, Y-Z., Sun, M., Xing, J., Luo, Q., & Corke, H. (2006). Structure–radical scavenging activity relationships of phenolic compounds from traditional Chinese medicinal plants. *Life Sciences, 78*, 2872–2888.
Criqui, M. H., & Ringel, B. L. (1994). Does diet or alcohol explain the French paradox? *Lancet, 344*, 1719–1723.
Giusti, M. M., Rodriguez-Saona, L. E., Griffin, D., & Wrolstad, R. E. (1999). Electrospray and tandem mass spectroscopy as tools for anthocyanin characterization. *Journal of Agricultural and Food Chemistry, 47*, 4657–4664.
Morton, J. (1987). Bignay. In Fruits of warm climates (pp. 210–212). Miami, FL.
Mullen, W., Mc Ginn, J., Lean, M. E. J., MacLean, M. R., Gardner, P., Duthie, G. G., et al. (2002). Ellagitannins, flavonoids, and other phenolics in red raspberries and

their contribution to antioxidant capacity and vasorelaxation properties. *Journal of Agricultural and Food Chemistry, 50*, 5191–5196.

Nawwar, W. A. M., Marzouk, M. S., Nigge, W., & Linscheid, M. (1997). High-performance liquid chromatography electrospray ionization mass spectrometric screening for polyphenolic compounds of *Epilobium hirsutum* – The structure of the unique Ellagictannin Epilobamide-A. *Journal of Mass Spectrometry, 32*, 645–654.

Niederländer, H. A. G., van Beek, T. A., Bartasiute, A., & Koleva, I. I. (2008). Antioxidant activity assays on-line with liquid chromatography. *Journal of Chromatography A, 1210*, 121–134.

Nuengchamnong, N., de Jong, C. F., Bruyneel, B., Niessen, W. M. A., Irth, H., & Ingkaninan, K. (2005). HPLC coupled on-line to ESI-MS and a DPPH-based assay for the rapid identification of anti-oxidants in *Butea superba*. *Phytochemical Analysis, 16*, 422–428.

Nuengchamnong, N., & Ingkaninan, K. (2009). On-line characterization of phenolic antioxidants in fruit wines from family Myrtaceae by liquid chromatography combined with electrospray ionization tandem mass spectrometry and radical scavenging detection. *LWT – Food Science and Technology, 42*, 297–302.

Rice-Evans, C., Miller, N. J., & Paganga, G. (1996). Structure–antioxidant activity relationships of flavonoids and phenolic acids. *Free Radical Biology and Medicine, 20*, 933–956.

Rio, D. D., Stewart, A. J., Mullen, W., Burno, J., Lean, M. E. J., Brighenti, F., et al. (2004). HPLC–MS^n analysis of phenolic compounds and purine alkaloids in green and black tea. *Journal of Agricultural and Food Chemistry, 52*, 2807–2815.

Serafini, M., Laranjinha, J. A. N., Almeida, L. M., & Mainai, G. (2000). Inhibition of human LDL lipid peroxidation by phenol rich beverages and their impact on plasma total antioxidant capacity in human. *Journal of Nutritional Biochemistry, 11*, 585–590.

Stanley, L. L., & Mazier, M. J. P. (1999). Potential explanations for the French paradox. *Nutrition Research, 19*, 3–15.

Sun, A. Y., Simonyi, A., & Sun, G. Y. (2002). The "French paradox" and beyond: neuroprotective effects of polyphenols. *Free Radical Biology and Medicine, 32*, 314–318.

Zywicki, B., Reemtsma, T., & Jekel, M. (2002). Analysis of commercial vegetable tanning agents by reversed-phase liquid chromatography–electrospray ionization-tandem mass spectrometry and its application to wastewater. *Journal of Chromatography A, 970*, 191–200.

Food Chemistry 118 (2010) 153–158

Contents lists available at ScienceDirect

Food Chemistry

journal homepage: www.elsevier.com/locate/foodchem

Analytical Methods

High-power gradient diffusion NMR spectroscopy for the rapid assessment of extra-virgin olive oil adulteration

Daniela Šmejkalová, Alessandro Piccolo *

Centro Interdipartimentale di Ricerca per la Spettroscopia di Risonanza Magnetica Nucleare (CERMANU), Via Università 100, 80055 Portici, Italy

ARTICLE INFO

Article history:
Received 10 October 2008
Received in revised form 21 January 2009
Accepted 21 April 2009

Keywords:
Olive oil
Adulteration
Diffusion NMR spectroscopy
Discriminant analysis

ABSTRACT

A high gradient diffusion NMR spectroscopy was applied to measure diffusion coefficients (*D*) of a number of extra-virgin olive, seed, and nut oils in order to ascertain the suitability of this rapid and direct method for discrimination of adulterated olive oils. Minimum adulteration levels that could be detected by changes in *D* were 10% for sunflower (SuO) and soybean oil (SoO), and 30% for hazelnut (HO) and peanut oil (PO). Qualitative and quantitative prediction of adulteration was achieved by discriminant analysis (DA). The highest prediction accuracy (98–100%) was observed only when two DA models were concomitantly used for sample classification. The first DA model provided recognition of high adulterated EVOO with more than 20% of SuO or SoO, and 30% with PO, whilst the second model could differentiate EVOO adulterated with 10% of SuO or SoO, and more than 30% of HO. The validation test performed with an independent set of randomly adulterated EVOO samples gave 100% classification success. The high accuracy levels together with minimal requirements of sample preparation, and short analyses time, prove the high-power gradient diffusion NMR spectroscopy as an ideal method for rapid screening of adulteration in valuable olive oils.

1. Introduction

High quality food products demanding higher market prices often become subjects of unscrupulous food mislabelling, or increased volume of good quality batches through adulteration with sub-standard procedure. With the increasing awareness of food safety and quality, consumers continuously demand reassurance of food origin and content (Schieber, 2008). Thus, there is a great effort, both from consumers and industrial site, to develop rapid, inexpensive, reliable and non-destructive screening techniques for the determination of food authenticity at any point of the distribution chain (Downey, Kelly, & Rodriguez, 2006; Schieber, 2008).

Recently, major concern was paid to frauds in olive oil industry. Production of olive oil represents about ~3% of the world oils and fat markets, with ~78% of global production taking place in Mediterranean countries (Aparicio & McIntyre, 1998; Rezzi et al., 2005), where oil industry is important in sustaining viability of agricultural economy (Vlachos et al., 2006). Virgin olive oils (VOO), and in particular, extra-virgin olive oils (EVOO), that are produced using solely cold pressing techniques, belong to the most sought after olive oil product on the account of their organoleptic (aroma and taste), antioxidant, and nutritional properties (Aparicio & McIntyre, 1998; Boscou, 1996; Harwood & Yaqoob, 2002). The cultivation of olive trees, harvesting of olive fruits, and extraction of olive oil are hard and time consuming tasks that add to its relatively high commercial price (Fragaki, Spyros, Siragakis, Salivaras, & Dais, 2005). Therefore, attempts to adulterate the high cost VOO with less expensive vegetable oils or low quality olive oils (López-Díez, Bianchi, & Goodacre, 2003) are by no means rare. Such fraud practise is not only unfair to consumers in terms of cost, but also comprises a threat for the economic development and prosperity of Mediterranean agricultural countryside communities, and, in addition, it may cause severe health and safety problems (López-Díez et al., 2003; Vlachos et al., 2006), such as the occurrence of food poisoning in Spain in 1981 (Wesley, Barnes, & McGill, 1995; World Health Organization, 1992).

Authentication and detection of VOO adulteration is based on the comparison of chemical compositions of suspected samples with identified characteristics of olive oils promulgated by the European Union (European Union, 1995, 1996). Despite the fact that composition of VOO differs with various factors such as geographical origin or weather conditions during growths and harvesting (Downey et al., 2006), good results were obtained applying classical analytical methods, such as gas chromatography (GC), high-performance liquid chromatography (HPLC), and pyrolysis mass spectrometry (Aparicio & Aparicio-Ruiz, 2000 and references therein). However, these methods are generally sample destructive and rather unsuitable for oil screening on a large scale,

* Corresponding author. Tel.: +39 081 253 91 60; fax: +39 081 253 91 86.
E-mail address: alessandro.piccolo@unina.it (A. Piccolo).

0308-8146/$ - see front matter © 2009 Elsevier Ltd. All rights reserved.
doi:10.1016/j.foodchem.2009.04.088

due to many necessary time-consuming steps required to achieve a complete quantification. Recent research, performed mainly in the last decade, is focused on the determination of adulterants using rapid spectroscopic techniques. Amongst these, Raman (López-Díez et al., 2003), ultraviolet (Aparicio & Aparicio-Ruiz, 2000), mid-infrared (Guillén & Cabo, 1997), near-infrared (Christy, Kasemsuran, Du, & Ozaki, 2004), fluorescence (Poulli, Mousdis, & Georgiou, 2007; Sayago, García-González, Morales, & Aparicio, 2007) and common solution-state NMR spectroscopy (Fauhl, Reniero, & Guillou, 2000; Mannina, Sobolev, & Segre, 2003; Sacchi et al., 1996; Vigli, Philippidis, Spyros, & Dais, 2003) were, with some limits, successfully proved as suitable tools for the detection of various adulterants.

This work discusses the potential of a high-power pulsed-field gradient NMR probe (Diff30) in enabling a direct observation of diffusion coefficient of viscous samples, and detecting adulterated EVOO oils. The suitability of this nondestructive, and rapid spectroscopic technique was evaluated on binary mixtures of olive oil adulterated with soybean, sunflower, peanut and hazelnut oil, all belonging to the most commonly found adulterants in VOO (Guimet, Ferré, & Boqué, 2005; Poulli et al., 2007). Discrimination of authentic and adulterated EVOO was assessed by chemometric approach, in particular, by discriminant analysis (DA).

2. Materials and methods

2.1. Materials

Twenty five extra-virgin olive oil (EVOO) samples of Leccino (L1–L6), Frantoio (F1–F6), Pendolino (P1–P7) and Coratina (C1–C6), obtained from the territory around Salerno, Italy, were kindly provided by the local producer "De Falco". Sunflower (SuO), soybean (SoO), hazelnut (HO), and peanut oil (PO) were purchased from local distributors. The authentic EVOO samples and the same ones but adulterated with 5%, 10%, 20%, 30% and 50% of SuO, SoO, PO and HO, reaching a total volume of 1 ml, were transferred into 5 mm NMR tubes, placed in the NMR probe, and left to equilibrate at 24.5 °C for 15 min prior to diffusion measurements.

2.2. Diffusion NMR measurements

Pulsed field gradient diffusion NMR measurement was carried out on a Bruker Wide-Bore Avance 300 MHz spectrometer, equipped with a 5 mm inverse Bruker high-power diffusion Diff30 probe yielding a maximum Z gradient strength of 350 G/cm. To avoid probe heating and control sample temperature, the probe was continuously cooled by flowing water at a constant temperature of 24.5 °C. Diffusion spectra (accumulation of four scans) were obtained using a spin-echo pulse sequence with a gradient pulse of 5 ms, diffusion time of 120 ms and gradient amplitude ranging from 11 to 140 G/cm in 128 increments. The total experimental time was 20 min per sample. Diffusion coefficients were calculated from the monoexponential decay dependence of attenuation of signal intensity on the gradient amplitude using Bruker Topspin 1.3 software. All measurements were performed in triplicate. A standard calibration sample (D_2O, $D = 1.872 \times 10^{-9}$ at 25 °C) was run prior to every set of experiments to ensure consistency between datasets.

2.3. Statistical analysis

All data were expressed as the means of at least three replications. Analysis of variance (ANOVA) was performed applying Duncan's multiple comparisons test to determine statistically significant differences at $P \leqslant 0.05$ confidence level. For discrimi-

Table 1
Mean values and standard deviations of diffusion coefficients ($D \times 10^{-12}$ m^2 s^{-1}) for different NMR peaks in spectra of extra-virgin olive (EVOO), hazelnut (HO), peanut (PO), sunflower (SuO), and soybean oil (SoO). Different letters indicate statistical differences (Duncan test) at $P \leqslant 0.05$ confidence level. Peak assignment is given in Table S1 in Supplementary data.

Oil sample	Peak					
	1	3	5	7[b]	8	9
EVOO[a]	8.98 ± 0.04*b*	8.15 ± 0.06*c*	9.01 ± 0.04*d*	14.35 ± 2.1*a*	9.27 ± 0.05*d*	9.31 ± 0.05*d*
HO	9.10 ± 0.06*a*	8.18 ± 0.02*c*	9.19 ± 0.02*c*	6.39 ± 0.91*c*	9.42 ± 0.05*c*	9.51 ± 0.06*c*
PO	8.41 ± 0.02*c*	7.56 ± 0.07*d*	8.50 ± 0.02*e*	6.21 ± 0.89*c*	8.66 ± 0.02*e*	8.79 ± 0.04*e*
SuO	ND	10.22 ± 0.05*b*	10.99 ± 0.04*b*	8.62 ± 0.64*b*	11.08 ± 0.03*b*	11.29 ± 0.04*b*
SoO	ND	10.41 ± 0.00*a*	11.25 ± 0.05*a*	8.08 ± 0.72*b*	11.33 ± 0.04*a*	11.46 ± 0.04*a*

[a] Means of 25 different EVOO.
[b] Diffusion coefficient was calculated within the range of amplitude gradient: 11–91 G/cm.

Table 2
Summary of classification results for independent test samples. EVOO, HO, PO, SuO and SoO refer to extra-virgin olive, hazelnut, peanut, sunflower, and soybean oil, respectively.

Sample	Adulteration	Observed classification model I	Correct assignment	Observed classification model II	Correct assignment
L1	10% SoO	EVOO	?	SuO, SoO 10%	Yes
P4	No	EVOO	?	EVOO	Yes
F2	20% SoO	SuO, SoO 20%	Yes	–	–
L6	No	EVOO	?	EVOO	Yes
C2	30% SuO	SuO, SoO 30%	Yes	–	–
P3	30% PO	PO 30–50%	Yes	–	–
P1	50% PO	PO 30–50%	Yes	–	–
C3	No	EVOO	?	EVOO	Yes
C3	50% SuO	SuO, SoO 50%	Yes	–	–
C5	50% SoO	SuO, SoO 50%	Yes	–	–
F1	No	EVOO	?	EVOO	Yes
P5	30% HO	EVOO	?	HO 30–50%	Yes
P7	50% HO	EVOO	?	HO 30–50%	Yes
F3	20% SuO	SuO, SoO 20%	Yes	–	–
F4	10% SuO	EVOO	?	SuO, SoO 10%	Yes

nant analysis (DA), all analysed samples were employed as training set in order to establish classification rules. The predictive ability of DA model was validated by a supplementary data set consisting of 15 randomly adulterated EVOO samples (Table 2). The statistical data processing was performed by XLSTAT 7.5.2 (Addinsoft SARL, Paris, France).

3. Results and discussion

3.1. ^{1}H NMR analysis

The main constituents of olive oil are variously substituted esters of glycerol and saturated (palmitic, stearic) or unsaturated (oleic, linoleic, linolenic) fatty acids (Sacchi, Addeo, & Paolillo, 1997). Due to the chemical similarity of these triglyceride esters, clusters of co-resonating signals are typically observed in ^{1}H NMR spectrum. This is reflected in Fig. 1 that shows ^{1}H NMR spectra of extra-virgin olive oil (EVOO) acquired with (a) Diff30 and (b) BBI (indirect) probe at 300 and 400 MHz, respectively. Although some resolution is lost when acquiring a spectrum with the Diff30 probe, the number of resonating clusters and their relative intensities are comparable to those observed by common ^{1}H NMR acquisition. The signal assignment of olive oil samples is well recognised and for the main signals is given in Table S1 in Supplementary data (Sacchi et al., 1996). Commonly reported resonance frequency of linolenyl chain, occurring at around 0.95 ppm, observable only upon enlargement of high resolution ^{1}H NMR spectra, was not detected with the Diff30 probe.

Inspection of ^{1}H NMR spectra, acquired with the Diff30 probe (Fig. 2) revealed that the composition of PO and HO did not significantly differ from that of EVOO. Conversely, significantly increased signal intensities can be noticed for peaks 1 and 4 in the spectrum of SoO and SuO. Peak 1 is attributed to the olefinic protons of all unsaturated fatty acids, whilst increased amount of peak 4 usually reflects larger amount of linoleic but at the same time smaller content of oleic acid (Vigli et al., 2003). The concentration of olefinic protons detected below peak 1 is one of the important input parameters for the estimation of the degree of oil unsaturation, known as iodine value (Sacchi et al., 1996). In fact, VOO having lower iodine value than SuO and SoO, are characterised by high amounts of monounsaturated fatty acid, such as oleic acid, and low content of polyunsaturated fatty acids, that include linoleic and linolenic acid (Vigli et al., 2003). The increased intensities of peak 1, and particularly of peak 4, were also noticeable for mixtures of EVOO containing more than 20% of SuO and SoO adulterants (data not shown).

3.2. Diffusion analysis

The mean values and standard deviations of diffusion coefficients (D) of all vegetable oils are summarised in Table 1. Diffusion values of signals 2, 4 and 6 are not reported since these peaks became undetectable under the optimised conditions for the applied NMR spin-echo sequence. This is noticeable in Fig. S1 in Supplementary data that reports 1D diffusion profiles of vegetable oils. With exception of peak 7, that was weighted by a maximum of

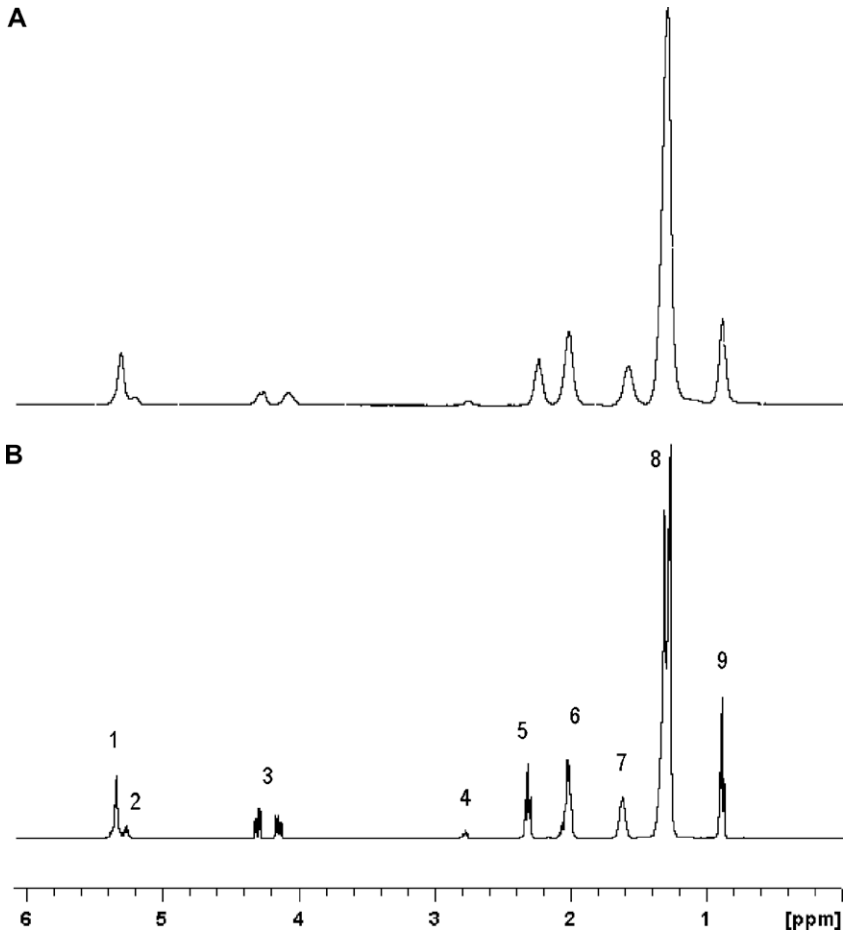

Fig. 1. ^{1}H NMR spectrum of olive oil obtained with: (A) diff30 probe (AV 300), and (B) BBI probe (AV 400, $CDCl_3$ solvent). Assignment of peaks is given in Table S1 in Supplementary data.

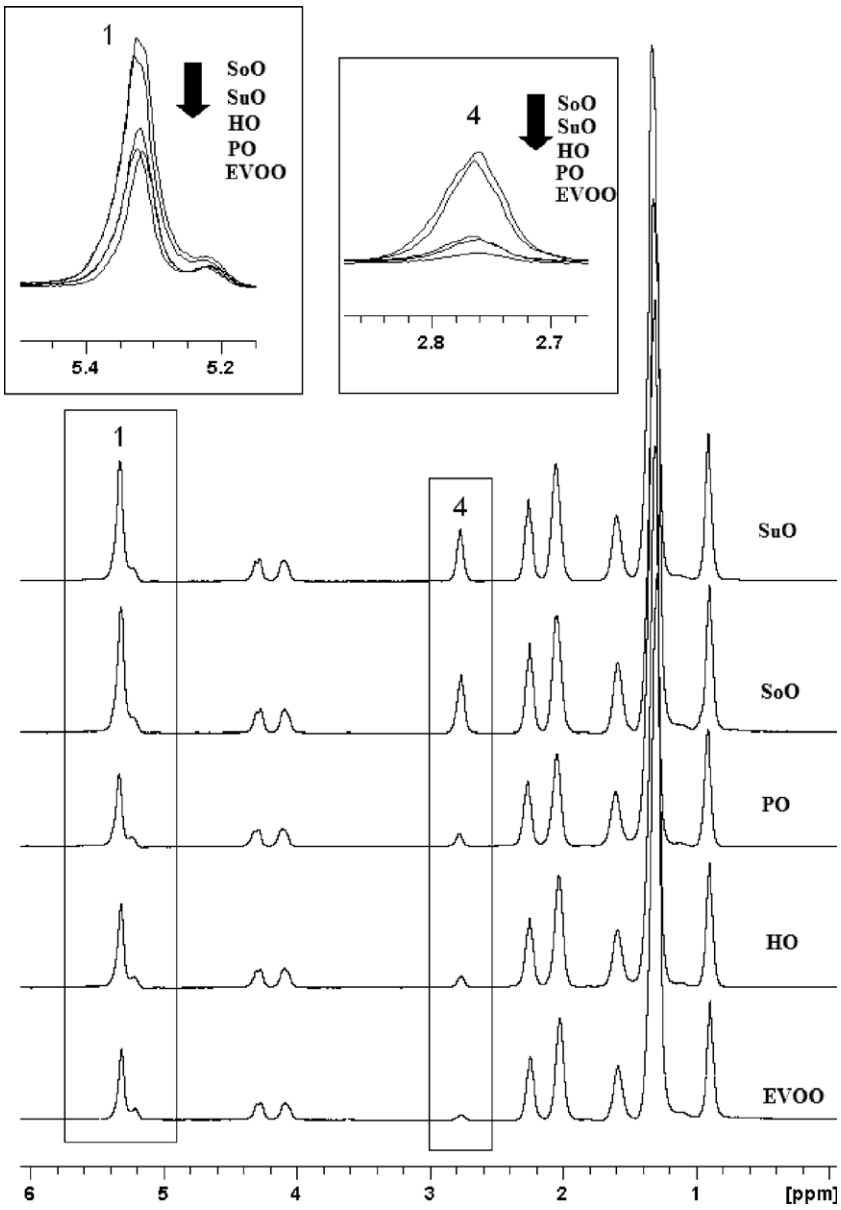

Fig. 2. ^{1}H NMR spectra of vegetable oils obtained with diff30 probe (AV 300). Assignment of peaks is given in Table S1 in Supplementary data. EVOO, HO, PO, SuO, and SoO refer to extra-virgin olive, hazelnut, peanut, sunflower, and soybean oil, respectively.

15% error (Table 1), standard deviations (SD) of less than 1% were observed for the triplicate diffusion measurements of SuO, SoO, PO and HO (Table 1), thereby indicating an excellent method reproducibility. Interestingly, low variability of diffusion coefficients for peaks 1, 3, 5, 8 and 9 was also noted for the 25 different EVOO samples (Table 1). The larger deviation observed for peak 7 was caused by the low signal/noise ratio of this resonance in the 1D diffusion spectra (Fig. S1 in Supplementary data).

The mean values for *D* (Table 1) further give information about dissimilarities in physical properties, namely viscosity, of seed and nut oils as compared to EVOO. The most similar diffusion behaviour to EVOO was noted for HO, whereby, except for signal 7, only a slight increase in *D* was observed for the remaining signals. The *D* value of signal 7 was also the only one greatly reduced in the case of PO, for which a small decrease in diffusion was otherwise noted. For these reasons, *D* calculated for signal 7 was later used as an input for statistical analysis, though it was weighted by a larger statistical error than similar coefficients observed for remaining signals. Unlike nut oils, a substantial difference in diffusion behaviour was noted for SuO and SoO. In comparison to EVOO, the SuO and SoO oils showed significantly larger diffusion for signals 3, 5, 8, and 9, and a smaller but still greatly varied diffusion coefficient for signal 7. In addition, signal 1 became undetectable in diffusion spectra of SuO and SoO under the experimental set-up conditions optimised for EVOO oils (Fig. S1 in Supplementary data).

3.3. Discriminant analysis

Dissimilarities of *D* reported in Table 1 suggested that high-power gradient diffusion NMR spectroscopy might be able to detect the presence of SuO, SoO, PO and HO in EVOO. To assess this possibility, diffusion spectra were collected for a set of 25 binary mixtures, each containing EVOO diluted with 5%, 10%, 20%, 30% and 50% of adulterant seed and nut oils. The obtained diffusion data were used as inputs for discriminant analysis (DA), a statistical technique applied for supervised pattern recognition. The main

DA task is to find the best linear discriminant functions of a set of variables, which reproduce, as far as it is possible, *a priori* grouping of the considered cases. The set of linear functions that are used to build a model for samples of known classes are then in turn used as predictors in order to determine group membership of anonymous samples (Brereton, 2003).

Preliminary DA analyses (DA plot not shown) performed on diffusion data of EVOO adulterated with HO indicated a strong overlay of authentic olive samples with samples adulterated up to 20%. Similar finding was observed for PO adulteration. In both cases, only the more largely adulterated samples were well separated from EVOO samples. The SuO- and SoO-diluted olive oil samples showed close grouping with EVOO for adulteration of 5%, acceptable separation for 10% adulteration, and well distinctive separation for adulteration larger than 20%. However, there was a strong overlay amongst groups adulterated with SuO and SoO. These findings indicate that the high-power gradient diffusion NMR technique was not sensitive enough to recognise adulterations lower than 20% in case of HO and PO, and 5% in case of SuO and SoO. Nor it was able to distinguish whether the adulteration was caused by SuO or SoO. To overcome this limitation in the development of a universal DA model, oil samples were divided into seven pre-defined groups. One group comprised all authentic EVOO; SuO and SoO adulterated EVOO samples were grouped together into four classes according to the adulteration percentage: 10%, 20%, 30% and 50%; and the last two predefined classes were formed by EVOO samples containing 30–50% of HO, and 30–50% of PO.

The best results were observed only when two DA models were used concomitantly. These models are shown in Figs. 3 and 4. The first DA model (Fig. 3) involved EVOO samples with an adulteration of 30–50% of PO, and 20%, 30% and 50% of SuO and SoO. The prediction ability of this training set was 98%. There was no prediction error in the classification of EVOO. A 2% error was observed due to the slight overlay between 20% and 30% adulterated samples with SuO and SoO. The second DA model (Fig. 4) is complementary to the first one and indicates the presence of SuO and SoO when as low as 10%, whereas that of HO was detected only when present from 30% to 50%. The prediction ability of the second DA model reached 100%. Therefore, due to the very good predictability of both model training sets, it is expected that the combined use of

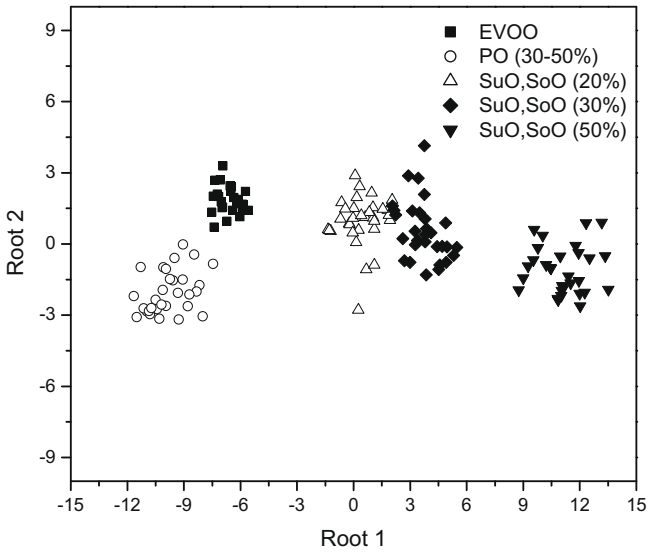

Fig. 3. Classification model I as calculated by discriminant analysis from diffusion data. EVOO, PO, SuO, and SoO refer to extra-virgin olive, peanut, sunflower, and soybean oil, respectively.

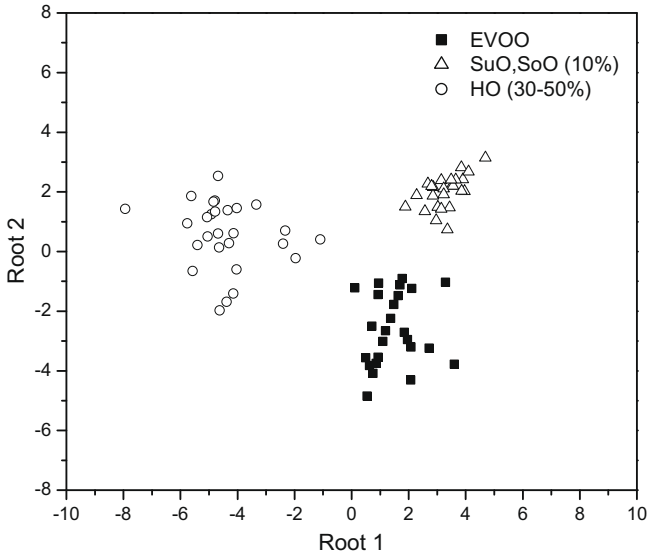

Fig. 4. Classification model II as calculated by discriminant analysis from diffusion data. EVOO, HO, SuO and SoO refer to extra-virgin olive, hazelnut, sunflower, and soybean oil, respectively.

the two DA models should ensure certain recognition of EVOO adulterated by more than 10% with SuO or SoO, and 30% with PO and HO. Concomitantly, olive oil samples classified by both models as EVOO are to be considered as unadulterated, or possessing smaller amounts of adulterants which are under the detection limits of the high-power gradient diffusion NMR technique, as indicated above.

In order to validate such approach, a set of randomly adulterated EVOO samples was prepared. The list of chosen EVOO and the amounts of added adulterants is shown in Table 2. The observed diffusion data were used as input variables in terms of supplementary observations, and the two DA models were applied to compute the probabilities by which such anonymous samples could be recognised in a specific group. The first DA model was initially employed to evaluate samples with high percentage adulteration (Fig. 3). As it is indicated in Table 2, samples F2, C2, P3, P1, C3, C5 and F3 were recognised as adulterated EVOO samples, whilst the remaining samples were temporarily labelled as belonging to unadulterated EVOO group. However, as discussed earlier, an authentic EVOO can be such only when both models classify it as unadulterated. Therefore, the second DA model (Fig. 4) was applied on the remaining dataset, and this time only four samples out of eight were further confirmed as unadulterated (Table 2). It can be noticed that these four samples (P4, L6, C3 and F1) were the only authentic EVOO amongst the independent test samples (Table 2). Moreover, a group membership was correctly recognised for all the 11 remaining adulterated test samples. Therefore, the validation gave 100% success.

Furthermore, it must be noted that the validation success can be expected to be somewhat reduced by interchanging class assignment of EVOO samples adulterated with 20% and 30% of both SuO and SoO. This may be due to the overlay between these two groups in the training set used to build the DA model (Fig. 3). Nevertheless, such reduction of validation does not have any effect on the recognition of an adulterated EVOO.

4. Conclusions

Using a limited number of authentic and adulterated oils, this work demonstrates that a combination of a high-power gradient

diffusion NMR technique with multivariate classification method can successfully discriminate between authentic and high adulterated EVOO with hazelnut (as low as 30%), peanut (as low as 30%), soybean (as low as 10%) and sunflower oil (as low as 10%). The main advantage of this approach is the rapid recognition (5–20 min of analysis) of such adulteration without employing any pre-extraction. The greatest classification success was observed by a combined use of two DA models, one of them involving high (more than 20%) adulteration with SuO, SoO and PO, whilst the other one was based on the diffusion data measured at low adulteration levels (10%) for SoO and SuO and high amount for HO (30–50%). The correct recognition of adulterated EVOO samples was as high as 98%, whilst, concomitantly, the detection accuracy of nonadulterated EVOO was 100%. Such high accuracy levels together with minimal requirements of sample preparation, call for the high-power gradient diffusion NMR spectroscopy as the ideal method for rapid screening of adulteration in olive oils. Only EVOO samples that pass such screening as authentic oils might undergo more costly and time consuming analyses in order to confirm their real authenticity. In addition, future diffusion NMR studies should indicate whether it is possible to apply this technique to detect adulteration of EVOO by an admixture of two and more vegetable oils.

Acknowledgement

This work was supported by the Regione Campania under programme "Legge 5" 2005.

Appendix A. Supplementary data

Supplementary data associated with this article can be found, in the online version, at doi:10.1016/j.foodchem.2009.04.088.

References

Aparicio, R., & Aparicio-Ruiz, R. (2000). Authentication of vegetable oils by chromatographic techniques. *Journal of Chromatography A, 881*(1–2), 93–104.

Aparicio, R., & McIntyre, P. (1998). Oils and fats. In M. Lees (Ed.), *Food authenticity: issues and methodologies* (pp. 231–269). France: Eurofins Scientific.

Boscou, D. (1996). Olive oil composition. In *Olive oil: Chemistry and technology* (pp. 52–83). Champaign: AOCS Press.

Brereton, R. G. (2003). *Chemometrics. Data analysis for the laboratory and chemical plant*. West Sussex, England: John Willey and Sons.

Christy, A. A., Kasemsuran, S., Du, Y., & Ozaki, Y. (2004). The detection and quantification of adulteration in olive oil by near-infrared spectroscopy and chemometrics. *Analytical Sciences, 20*(6), 935–940.

Downey, G., Kelly, J. D., & Rodriguez, C. P. (2006). Food authentication – Has near infrared spectroscopy a role? *Spectroscopy Europe, 18*, 10–14.

European Union (1995). *Official Journal of the Commission of the European Communities*. Regulation No. 656/95.

European Union (1996). *Official Journal of the Commission of the European Communities*. Regulation No. 2632/94, L280.

Fauhl, C., Reniero, F., & Guillou, C. (2000). ^{1}H NMR as a tool for the analysis of the mixtures of virgin olive oil with oils of different botanical origin. *Magnetic Resonance in Chemistry, 38*(6), 436–443.

Fragaki, G., Spyros, A., Siragakis, G., Salivaras, E., & Dais, P. (2005). Detection of extra virgin olive oil adulteration with lampante olive oil and refined olive oil using nuclear magnetic resonance spectroscopy and multivariate statistical analysis. *Journal of Agricultural and Food Chemistry, 53*(8), 2810–2816.

Guillén, M. D., & Cabo, N. (1997). Infrared spectroscopy in the study of edible oils and fats. *Journal of the Science of Food and Agriculture, 75*(1), 1–11.

Guimet, F., Ferré, J., & Boqué, R. (2005). Rapid detection of olive–pomace oil adulteration in extra virgin olive oils from the protected denomination of origin "Siurana" using excitation–emission fluorescence spectroscopy and three-way methods of analysis. *Analytica Chimica Acta, 544*(2), 143–152.

Harwood, J. L., & Yaqoob, P. (2002). Nutritional and health aspects of olive oil. *European Journal of Lipid Science Technology, 104*(9–10), 685–697.

López-Díez, E. C., Bianchi, G., & Goodacre, R. (2003). Rapid quantitative assessment of the adulteration of virgin olive oils with hazelnut oils using Raman spectroscopy and chemometrics. *Journal of Agricultural and Food Chemistry, 51*(21), 6145–6150.

Mannina, L., Sobolev, A. P., & Segre, A. L. (2003). Olive oil as seen by NMR and chemometrics. *Spectroscopy Europe, 15*(3), 6–14.

Poulli, K. I., Mousdis, G. A., & Georgiou, C. (2007). Rapid synchronous fluorescence method for virgin olive oil adulteration assessment. *Food Chemistry, 105*(2), 369–375.

Rezzi, S., Axelson, D. E., Héberger, K., Reniero, F., Mariani, C., & Guillou, C. (2005). Classification of olive oils using high throughput flow ^{1}H NMR fingerprinting with principal component analysis, linear discriminant analysis and probabilistic neural networks. *Analytica Chimica Acta, 552*(1–2), 13–24.

Sacchi, R., Addeo, F., & Paolillo, L. (1997). ^{1}H and ^{13}C NMR of virgin olive oil. An overview. *Magnetic Resonance in Chemistry, 35*(13), S133–S145.

Sacchi, R., Patumi, M., Fontanazza, G., Barone, P., Fiordiponti, P., Mannina, L., et al. (1996). A high field ^{1}H nuclear magnetic resonance study of the minor components in virgin olive oils. *Journal of the American Oil Chemist Society, 73*(6), 747–758.

Sayago, A., García-González, D. L., Morales, M. T., & Aparicio, R. (2007). Detection of the presence of refined hazelnut oil in refined olive oil by fluorescence spectroscopy. *Journal of Agricultural and Food Chemistry, 55*(6), 2068–2071.

Schieber, A. (2008). Introduction to food authentication. In D.-W. Sun (Ed.), *Modern Techniques for Food Authentication* (pp. 1–26). Elsevier: Amsterdam.

Vigli, G., Philippidis, A., Spyros, A., & Dais, P. (2003). Classification of edible oils by employing ^{31}P and ^{1}H NMR spectroscopy in combination with multivariate statistical analysis. A proposal for the detection of seed oil adulteration in virgin olive oils. *Journal of Agricultural and Food Chemistry, 51*(19), 5715–5722.

Vlachos, N., Skopelitis, Y., Psaroudaki, M., Konstantinidou, V., Chatzilazarou, A., & Tegou, E. (2006). Application of fourier transformed-infrared spectroscopy to edible oils. *Analytica Chimica Acta, 573–574*, 459–465.

Wesley, I. J., Barnes, R. J., & McGill, A. E. J. (1995). Measurement of adulteration of olive oils by near- infrared spectroscopy. *Journal of the American Oil Chemist Society, 72*(3), 289–292.

World Health Organization (1992). *Toxic oil syndrome, current knowledge and future perspectives*. Geneva, Switzerland: World Health Organization.

Food Chemistry 118 (2010) 159–162

Contents lists available at ScienceDirect

Food Chemistry

journal homepage: www.elsevier.com/locate/foodchem

Analytical Methods

Direct determination of free tryptophan contents in soy sauces and its application as an index of soy sauce adulteration

Yonghong Zhu *, Yan Yang, Zhaoxu Zhou, Genrong Li, Mei Jiang, Chun Zhang, Shiqi Chen

Quality Supervision and Inspection Center of Food, Chongqing Academy of Metrology and Quality Inspection, Chongqing 400020, China

ARTICLE INFO

Article history:
Received 12 May 2008
Received in revised form 12 March 2009
Accepted 21 April 2009

Keywords:
Tryptophan (Trp)
Fermented soy sauce (FSS)
Acid-hydrolysed vegetable protein (acid-HVP)
Blended soy sauce (BSS)
Adulteration
High performance liquid chromatography (HPLC)

ABSTRACT

A simple and rapid HPLC method using UV detector for determination of tryptophan (Trp) contents in pure fermented soy sauces, acid-HVP, and commercial soy sauces was developed. The method requires only simple sample pretreatment. The limit of detection (LOD) is estimated at 1 mg/L (signal-to-noise ratio of 3), and the recovery yields ranged from 92% to 108%. The analysis showed that Trp in all of the analysed acid-HVP samples was not detected and there was obvious detection of Trp (ranged from 136.4 to 261.8 mg/L) in all of the analysed fermented soy sauce samples. The observations suggest that Trp is a practical index of pure fermented soy sauce. The absence of Trp contents or lower level of Trp contents than that in pure fermented soy sauces suggests the soy sauces are not pure fermented soy sauces or presence of soy sauce adulteration. Simultaneous determination of levulinic acid (LV) in samples may be a good help in making assessment of soy sauce adulteration with acid-HVP.

1. Introduction

Soy sauce is a popular seasoning in many Asian countries. Two types of soy sauces are used for cooking and the preparation of diverse foods in China. One type is fermented soy sauce, which is manufactured by brewing of a mixture of cooked soybeans and wheat (National Standard of China, 2000). The second type is blended soy sauce, which is manufactured more economically by combining fermented soy sauce and acid-hydrolysed vegetable protein (acid-HVP) at an appropriate ratio (Food Industry Standard of China, 2000). Up to now, an ideal method for identification of soy sauce that is adulterated is still lacking. In fact, many commercial soy sauces labelled as "Pure fermented soy sauce" are blended soy sauce or produced solely with acid-HVP (Jiang, Ni, & Zhu, 2006; Peng, Yang, & Chen, 2007).

It was reported that levulinic acid (LV) was a proper index for determination of the acid-HVP content in blended soy sauce (Sano et al., 2007; Wang, Lin, Lee, & Choong, 1999). The analysis showed that there was no LV in naturally brewed soy sauce and there was apparent detection of LV in acid-HVP and blended soy sauces with acid-HVP (Sano et al., 2007). But it should be pointed out that levels of LV in some acid-HVP samples were very low. During our analysis, we also found that three commercial acid-HVP samples contained LV at levels (0.09–0.16 mg/mL) significantly lower than 1 mg/mL, which is the maxim allowed level of LV regulated by Soy sauce standard of Taiwan for fermented soy sauce (Taiwan CNS, 1993). Meanwhile, it was reported that LV can be detected in most of caramel colours, which was a common additive in soy sauce (Li & Geng, 2005). We also detected the presence of LV in caramel colour samples, although the detected level of LV (0.02–0.08 mg/mL) was not high. In view of the observations above, it is possible that sometimes LV can not be detected in soy sauce added with acid-HVP, but can be detected in the pure fermented soy sauce added with caramel colour.

Tryptophan (L-2-amino-3-(indol-3-yl)propionic acid, Trp) is a vital constituent of proteins and is indispensable in human nutrition for establishing and maintaining a positive nitrogen balance. As an essential amino acid, it is considered exceptional in its diversity of biological functions. In particular, it is the precursor of the neurotransmitter serotonin. Manufactures of nutritional products are often required to demonstrate an adequate Trp content in their products (Alwarthan, 1995; Delgado-Andrade, Rufián-Henares, Jiménez-Pérez, & Morales, 2006). As traditional seasonings, amino acids are the important constituents of soy sauces. For fermented soy sauces, the amino acids mainly come from the enzyme-catalysed protein hydrolysis under microbial fermentation. For the acid-HVP, the amino acids mainly come from the acid-induced protein hydrolysis. It is well known that, in the classical HCl hydrolysates, a considerable amount of Trp

* Corresponding author. Tel.: +86 23 6795 2759; fax: +86 23 6795 1136.
E-mail address: zyh218@yahoo.com.cn (Y. Zhu).

0308-8146/$ - see front matter © 2009 Published by Elsevier Ltd.
doi:10.1016/j.foodchem.2009.04.090

is destroyed (Molnár-Perl, 1997; Molnár-Perl, Pintér-Szakás, & Khalifa, 1993). So the contents of Trp might be a good index of soy sauce adulteration.

In the present work, we first developed a simple and rapid method for determination of Trp in soy sauce. Then we detected the content of Trp in acid-HVP, pure fermented soy sauces, commercial soy sauces and exploring the potential of Trp contents as an index of soy sauce adulteration.

2. Materials and methods

2.1. Soy sauce samples

Acid-HVP (11 samples, amino acid nitrogen contents $\geqslant$1.0 g/100 mL, formol nitrogen determination) were purchased from five manufactures in China. Pure fermented soy sauces (12 samples, amino acid nitrogen contents $\geqslant$0.4 g/100 mL, formol nitrogen determination) were obtained from six soy sauce companies in China. The authenticity of the 12 pure fermented soy sauces was guaranteed by sampling on the production spot. Commercial soy sauces (21 samples, amino acid nitrogen contents $\geqslant$0.4 g/100 mL, formol nitrogen determination) were purchased from local supermarkets in Chongqing.

2.2. Reagents

HPLC grade methanol was purchased from SK Chemicals (Korea). Trp standard was purchased from Beijing Dingguo Biological Technology Co., Ltd (China). Analytical grade ethanol was obtained from Chengdu Kelong Chemicals Factory (Sichuan province, China). All aqueous solutions were prepared with ultra-pure water purified with the Molecular® ΣH_2O system (Shanghai Molecular Biological Scientific & Technological Co., Ltd., China).

Standard stock solutions of Trp (1000 mg/L) were prepared in 10% ethanol and stored at 4 °C. Working solutions for Trp was prepared from the stock solution with 10% ethanol, and then five concentration levels (1.0, 2.0, 5.0, 10.0, and 20.0 μg/mL) were analysed. The stock solution was prepared every 2 weeks, and the working solutions were prepared the same day that they were used. For quantification, peak areas were correlated with the concentrations according to the calibration curve.

2.3. Instrumentation and chromatographic conditions

The HPLC system was a LC-20AB equipped with an autosampler SIL-20A, a system controller CBM-20A, a pump LC-20AB, a column oven CTO-20A, a UV–vis detector SPD-20AV (Shimadzu, Japan).

The chromatographic analysis was performed using an analytical scale (25 × 0.46 cm i.d.) venusil MP-C18 column with a particle size 5 μm (Agela Technologies, USA). The HPLC column temperature was set to 30 °C during all running procedures, and the injection volume was 10 μL. Absorbance was monitored at 280 nm. Two mobile phases were used to generate a gradient with 1 mL/min flow-rate. Mobile phase A is ultra-pure water, and mobile phase B was methanol. An isocratic elution gradient of 12% B was used.

2.4. Sample pretreatment

One volume of sample was placed in a centrifuge tube with cap. Three volumes of ethanol was then added. The mixture was mixed thoroughly and centrifuged at 4000 rpm for 5 min. The supernatant was diluted 4-fold with water. The diluted supernatant was then filtered through 0.45 μm membrane into HPLC vials for analysis and 10 μL of the final solution was injected into HPLC.

3. Results and discussion

Numerous methods for determination of Trp in complex samples have been proposed. Literature cited many efforts to apply a general method for Trp analysis in various samples (Molnár-Perl, 1997, 1999; Nielsen & Hurrell, 1985). Trp is degraded during classical aminogram analysis of proteins by acid hydrolysis. Several approaches have been proposed for direct Trp determination or after derivatisation, such as second-derivative spectroscopy, *p*-dimethylaminobenzaldehyde, *p*-phenylenediamine, *O*-phthaldehyde, and ninhydrin. Acidic (HCl, HCl with additives), alkaline (NaOH, LiOH) and enzymatic (pronase, pepsin, enzyme cocktail) hydrolysis of the protein has been carried out, followed by chromatographic (ion exchange or reversed-phase), colorimetric or fluorimetric determination of Trp (Aitken & Learmonth, 1996; Fabian, Pinter-Szakas, & Molnár-Perl, 1990; Fletouris, Botsoglou, Papageorgiou, & Mantis, 1993; Hugli & Moore, 1972; Ng, Pascaud, & Pascaud, 1987; Slump, Flissebaalje, & Haaksman, 1991; Yust, Pedroche, Girón-Calle, Vioque, & Millán et al., 2004). Direct spectrophotometric analysis is rapid and does not require hydrolysis of the protein. However, direct determination is subject to error due to interferences and can only be considered as an approximate procedure. Colorimetric methods can be tedious and suffer from problems such as colour stability and interferences (Yust et al., 2004). At present, HPLC is often used for the determination of Trp.

Up to now, the reports about HPLC method without derivatisation using UV detector for direct determination of free Trp in soy sauce samples were not seen. The reports about the application of the free Trp content in soy sauce adulteration were also not seen.

3.1. Sample pretreatment

A simple pretreatment method was developed in this work. The sample pretreatment steps only include precipitating sample with ethanol, dilution of supernatant fluid with water, and then directly analysed by HPLC-UV without further concentration and derivatisation. The simplified sample pretreatment procedures could shorten the analytical time and improve the repeatability of the method. It was found that ethanol could effectively precipitate solids of the samples, decolourise the sample and make the sample become more clarified. Because samples were pretreated directly without hydrolysis procedures, only free Trp in samples was determined.

3.2. HPLC separation and identification

To determine optimal chromatographic conditions for the determination of Trp, we performed preliminary tests with standard solution. When HPLC analysis for Trp standard solution was performed on different columns using different mobile phase, a good symmetrically shaped peak were easily obtained. But when the analysis for the soy sauce samples were performed, the interference peaks could be separated better from the target analyte by using hydrophilic HPLC columns (e.g. venusil MP-C18 columns) (Fig. 1).

The Trp was identified by comparison of retention times against those obtained from Trp standard solutions. The retention time of Trp in different samples was very stable, with the variability less than 0.2%.

3.3. Linearity, detection sensitivity, precision, and recovery yields

We found that there was a linear relationship between the concentrations and the peak area up to 104 mg/L (10 μL injected, $r^2 \geqslant 0.995$). The limit of detection (LOD) calculated from the

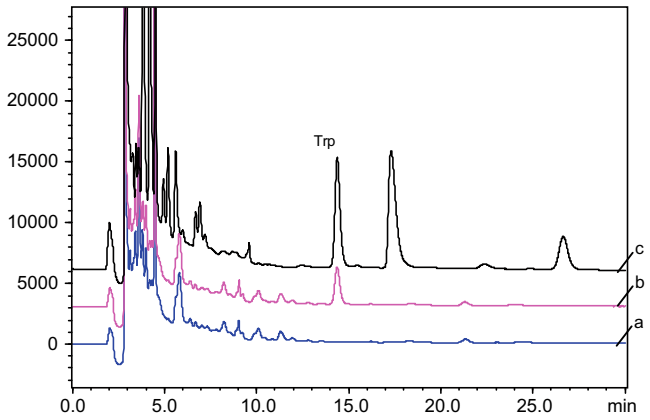

Fig. 1. HPLC–UV chromatograph at 280 nm of samples. (a) acid-HVP; (b) acid-HVP added with Trp (50 mg/L); (c) pure fermented soy sauce (170 mg/L). HPLC column: Venusil MP-C18 column.

measurement of standard solution is estimated at 1 mg/L (signal-to-noise ratio of 3), and the limit of quantitation (LOQ) at 3.3 mg/L (signal-to-noise ratio of 10).

The precision study was validated by replicate analysis of three different samples (including acid-HVP, pure fermented soy sauce, and commercial soy sauce added with large amount of caramel colour) under repeatability and intermediate reproducibility conditions. The samples were first analysed six times in parallel so as to get information about within-day variation. Good repeatability was obtained for three above-mentioned samples. The Trp content in the three samples ranged between 0 (not detected) and 170 mg/L, with repeatability relative standard deviations ranged between 2.1% and 4.7%. Additional precision data was obtained by duplicate analysis of the same products on three different days, which gave a low intermediate reproducibility relative standard deviations ranged between 3.2% and 4.9%.

The recovery of the method was determined in four tests employing the method of standard addition ranging from 50 to 150 mg/L. Three different samples (including acid-HVP, pure fermented soy sauce, and commercial soy sauce added with large amount of caramel colour) were selected. The recovery yields of Trp in acid-HVP, in which Trp was not detected, were estimated by adding 50 and 150 mg/L Trp. For the pure fermented soy sauce and commercial soy sauce, 150 mg/L Trp were added. Excellent percentage recovery yields (92–108%) were obtained according to the established method.

3.4. Determination of Trp in samples

3.4.1. Trp contents in acid-HVP

Totally 11 acid-HVP samples were analysed for determination of Trp contents. Results were listed in Table 1. It was found that Trp was not detected in all the acid-HVP samples. The results suggested that Trp in acid-HVP was destroyed nearly completely.

3.4.2. Trp contents in pure fermented soy sauce

Totally 12 pure fermented soy sauce samples were analysed for determination of Trp contents. Results were listed in Table 2. It was found that Trp was detected in all the pure fermented soy sauce samples. The contents of Trp in the samples were ranged from 136.4 to 261.8 mg/L. In view of that Trp was not detected in acid-HVP, it is possible to use Trp content as an index of soy sauce adulteration with acid-HVP. The absence or low level of Trp contents suggest the soy sauces are not pure fermented soy sauces or adulterated with Acid-HVP.

Table 1
Results of Trp levels in acid-HVP samples.

Sample no.	Content (mg/L)
HVP-1	n.d.[a]
HVP-2	n.d.
HVP-3	n.d.
HVP-4	n.d.
HVP-5	n.d.
HVP-6	n.d.
HVP-7	n.d.
HVP-8	n.d.
HVP-9	n.d.
HVP-10	n.d.
HVP-11	n.d.

[a] n.d.: not detected.

Table 2
Results of Trp levels in pure fermented soy sauces.

Sample no.	Content[a] (mg/L)
1	169.9
2	261.8
3	170.7
4	169.4
5	169.1
6	169.7
7	168.0
8	169.2
9	230.3
10	181.4
11	136.4
12	156.3

[a] Each point is the mean of three measurements.

3.4.3. Trp contents in commercial soy sauce

Totally 21 commercial soy sauce samples were analysed for the Trp contents. Of 21 samples, 3 samples were labelled as "blended soy sauce", 18 samples were labelled as "fermented soy sauces. The results were listed in Table 3. It was found that Trp was not detected in three blended soy sauces and five fermented soy sauces, which suggested that these soy sauces contained no fermented components and are faked fermented soy sauces and blended soy

Table 3
Results of Trp levels in commercial soy sauces.

Sample no.	Producer	Labels on the packages	Content[a] (mg/L)
1	China	FSS[b]	n.d.
2	China	BSS[c]	n.d.
3	China	FSS	n.d.
4	China	BSS	n.d.
5	China	BSS	n.d.
6	China	FSS	n.d.
7	China	FSS	n.d.
8	China	FSS	n.d.
9	China	FSS	29.93
10	China	FSS	37.14
11	China	FSS	46.28
12	China	FSS	62.06
13	China	FSS	83.99
14	China	FSS	157.46
15	China	FSS	168.36
16	China	FSS	186.29
17	China	FSS	248.15
18	Japan	FSS	172.57
19	Korea	FSS	23.86
20	Korea	FSS	14.23
21	Taiwan	FSS	78.73

[a] Each point is the mean of three measurements.
[b] FSS = fermented soy sauce.
[c] BSS = blended soy sauce.

sauces. According to (Food Industry Standard of China (2000), the blended soy sauce should contain an appropriate ratio of fermented components. It was also found that Trp contents (14.23–46.28 mg/L) in some samples (samples 9–11, 19 and 20) were significantly lower than that in pure fermented soy sauces, which strongly suggested that these samples contained some fermented components and were not "100% pure" fermented soy sauces. In view of the fact that acid-HVP adulteration was common in soy sauce adulteration, absence or low level of Trp in soy sauce could suggest the possibility of acid-HVP adulteration in soy sauce.

But for some samples whose Trp contents are not very low (62.06–83.99 mg/L) (e.g. samples 12, 13 and 21), it is relatively difficult to make a judgement about the presence of acid-HVP adulteration. In these instances, it is necessary to detect another useful indicator that could suggest the addition of acid-HVP. Although levulinic acid (LV) was not an ideal index for determination of acid-HVP as mentioned above, it is still useful as an indicator of acid-HVP at present. Simultaneous determination of LV in samples may be a good help in making assessment of sample authenticity. During this study, LV contents of the above tested commercial soy sauces were also determined. It was found that LV was detected in most of the samples not detected with Trp. Both Trp and LV were not detected only in one sample (sample 4). Of the samples detected with low levels of Trp (14.23–83.99 mg/L) (samples 9–13 and 19–21), 7 samples were detected with LV. Of the samples detected with relatively high levels of Trp (157.46–248.15 mg/L) (samples 14–18), none was detected with LV. But it should be pointed out that the presence of LV in samples sometimes cannot definitely indicate soy sauce adulteration with acid-HVP, especially when the detected LV contents were very low. Now we are screening other specific indicator that could identify acid-HVP adulteration or other adulteration.

Because Trp contents may be correlated with the contents of amino acid nitrogen or total nitrogen, the ratio of Trp and amino acid nitrogen (or total nitrogen contents) may be more meaningful for the authenticity measurement of soy sauce samples. For the soy sauces with a higher amino acid nitrogen contents, it should contain higher levels of Trp. For the soy sauces with a lower amino acid nitrogen contents, it should contain lower levels of Trp. Now we are exploring the experimental relationship between Trp and amino acid nitrogen content (or total nitrogen contents) in different soy sauce samples and the effects of different fermenting process and material components on the experimental relationship (ratio). If a relatively fixed ratio is existed, it is possible to add this ratio as a specification requirement for the fermented soy sauce products.

4. Conclusions

The HPLC method presented in this study is simple and reliable for determination of Trp contents in pure fermented soy sauces, acid-HVP, and commercial soy sauces. The method requires only a simple sample preparation. The analysis showed that Trp was not detected in all of the analysed acid-HVP samples and there was obvious detection of Trp (ranged from 136.4 to 261.8 mg/L) in all of the analysed fermented soy sauce samples. These results indicate that Trp is a practical index of pure fermented soy sauces. The absence or low level of Trp in soy sauces suggests that the soy sauces are not pure fermented soy sauces or may be adulterated with acid-HVP. In some instances, simultaneous determination of LV in samples may be a good help in making assessment of soy sauce adulteration with acid-HVP.

Acknowledgements

This research was financed by the Scientific & Research Project of Scientific Committee of Chongqing under Project No. CSTC, 2007AC1021 and National Commonweal Sci. & Tech. Project of China under Project No. 10–100.

References

Aitken, A., & Learmonth, M. (1996). Quantitation of tryptophan in proteins. In J. Walker (Ed.), *The protein protocols handbook* (pp. 29–31). Totowa, NJ: Humana Press.

Alwarthan, A. A. (1995). Chemiluminescent determination of tryptophan in a flow injection system. *Analytica Chimica Acta, 317*, 233–237.

Delgado-Andrade, C., Rufián-Henares, J. A., Jiménez-Pérez, S., & Morales, F. J. (2006). Tryptophan determination in milk-based ingredients and dried sport supplements by liquid chromatography with fluorescence detection. *Food Chemistry, 98*, 580–585.

Fabian, V., Pinter-Szakas, M., & Molnár-Perl, I. (1990). Gas chromatography of tryptophan together with other amino acids in hydrochloric acid hydrolysates. *Journal of Chromatography, 520*, 193–199.

Fletouris, D. J., Botsoglou, N. A., Papageorgiou, G. E., & Mantis, A. J. (1993). Rapid determination of tryptophan in intact proteins by derivative spectrophotometry. *Journal of the AOAC International, 76*, 1168–1173.

Food Industry Standard of China. (2000), SB 10336-2000. *Blended soy sauce.* PR China: National Bureau of Internal Trade.

Hugli, T. E., & Moore, S. (1972). Determination of the tryptophan content of proteins by ion exchange chromatography of alkaline hydrolysates. *Journal of Biological Chemistry, 247*, 2828–2834.

Jiang, Y., Ni, Y., & Zhu, H. (2006). Determination of levulinic acid in soy sauce by liquid chromatography. *Journal of Nanchang University (Natural Science), 30*, 40–42 (in Chinese).

Li, G., & Geng, Y. (2005). Determination of levulinic acid in soy sauce, hydrolyzed vegetable protein and caramel. *China Brewing, 150*, 51–52.

Molnár-Perl, I., Pintér-Szakás, M., & Khalifa, M. (1993). High-performance liquid chromatography of tryptophan and other amino acids in hydrochloric acid hydrolysates. *Journal of Chromatography, 632*, 57–61.

Molnár-Perl, I. (1997). Tryptophan analysis in peptides and proteins, mainly by liquid chromatography. *Journal of Chromatography A, 763*, 1–10.

Molnár-Perl, I. (1999). Advances in the analysis of tryptophan and its related compounds by chromatography. *Advances in Experimental Medicine and Biology, 467*, 801–806.

National Standard of China. (2000), GB 18186-2000. *Fermented soy sauce*. General Administration of Quality Supervision, Inspection and Quarantine of the People's Republic of China.

Nielsen, H. K., & Hurrell, R. F. (1985). Tryptophan determination of food proteins by HPLC after alkaline hydrolysis. *Journal of the Science of Food and Agriculture, 36*, 893–907.

Ng, L. T., Pascaud, A., & Pascaud, M. (1987). Hydrochloric acid hydrolysis of proteins and determination of tryptophan by reversed phase high-performance liquid chromatography. *Analytical Biochemistry, 167*, 47–52.

Peng, T., Yang, X., & Chen, S. (2007). Current situations and future applications of China soy sauce. *China Condiment, 9*, 26–29 (in Chinese).

Sano, A., Satoh, T., Oguma, T., Nakatoh, A., Satoh, J., & Ohgawara, T. (2007). Determination of levulinic acid in soy sauce by liquid chromatography with mass spectrometric detection. *Food Chemistry, 105*, 1242–1247.

Slump, P., Flissebaalje, T. D., & Haaksman, I. K. (1991). Tryptophan in food proteins: A comparison of two hydrolytic procedures. *Journal of the Science of Food and Agriculture, 55*, 493–496.

Taiwan CNS. (1993), 423-1993. *Soy sauce* (in Chinese).

Wang, M. L., Lin, H. J., Lee, M. H., & Choong, Y. M. (1999). A rapid method for direct determination of levulinic acid in soy sauce. *Journal of Food and Drug Analysis, 7*(2), 143–152.

Yust, M. M., Pedroche, J., Girón-Calle, J., Vioque, J., Millán, F., & Alaiz, M. (2004). Determination of tryptophan by high-performance liquid chromatography of alkaline hydrolysates with spectrophotometric detection. *Food Chemistry, 85*, 317–320.

Food Chemistry 118 (2010) 163–170

Contents lists available at ScienceDirect

Food Chemistry

journal homepage: www.elsevier.com/locate/foodchem

Analytical Methods

The potential of coupling information using three analytical techniques for identifying the geographical origin of Liguria extra virgin olive oil

Monica Casale *, Chiara Casolino, Paolo Oliveri, Michele Forina

Dipartimento di Chimica e Tecnologie Farmaceutiche ed Alimentari, Università di Genova, Via Brigata Salerno 13, I-16147 Genova, Italy

ARTICLE INFO

Article history:
Received 6 February 2008
Received in revised form 17 October 2008
Accepted 21 April 2009

Keywords:
Chemometrics
Fusion
Sampling design
Extra virgin olive oil
NIR
UV–visible
Head-space mass spectrometer

ABSTRACT

The combined use of data obtained from different analytical instruments is a complex problem.

In this paper the potential of coupling three analytical techniques for building a class model for extra virgin (e.v.) olive oil from Liguria, was investigated.

A sampling design for the Ligurian e.v. olive oil was developed by the selection of a representative subset from all possible e.v. olive oil samples of the Liguria region.

Thus, in order to choose this subset with uniform distribution on the production area and representative of the production density, two algorithms for sampling have been used: Kennard–Stone and Potential Function.

The samples were analysed by head-space mass spectrometry (electronic nose), UV–visible and NIR spectroscopy.

In particular, the exceptional possibility provided by Chemometrics to effectively extract and combine (fusion) the information from these multivariate and non-specific data and to build a class model for Liguria e.v. olive oil was studied.

1. Introduction

The development of new and increasingly sophisticated techniques for the authentication of food products continues with increasing consumer awareness of food safety and authenticity issues (Reid, O'Donnell, & Downey, 2006). Food authentication is also of concern to genuine food processors who do not wish to be subjected to unfair competition from unscrupulous processors who would gain an economic advantage from the misrepresentation of the food they are selling.

The rights of consumers and genuine food processors in terms of food adulteration and fraudulent or deceptive practices in food processing are set out in a European Union Regulation regarding food safety and traceability.

The European Council Regulation (EC) No. 2081/92 establishes that foodstuffs which are produced, processed and prepared in a given geographical area using recognised know-how, are indicated with the Protected Designation of Origin (PDO).

Among the numerous analytical methods applied to food authentication in the last decade, spectroscopy (UV, NIR, MIR, visible, Raman) and electronic nose have been frequently used.

IR spectroscopy is a rapid and non-destructive technique for the authentication of food samples. NIR spectroscopy utilises the spectral range from 14 000 to 4000 cm^{-1} and provides much more complex structural information relating to the vibrational behaviour of combinations of bonds. This technique is suited for use in an industrial setting due to its ease of use and the relatively low financial cost of obtaining and running the equipment. A lot of foods have recently been effectively tested for adulteration using NIR spectroscopy; with regards to olive oil, several studies are published (Christy, Du, & Ozaki, 2004; Galtier et al., 2007).

As far as the electronic nose is concerned, there has been some success using this technology for the differentiation of olive oils on the basis of geographical origin (Cerrato Oliveros, Boggia, Casale, Armanino, & Forina, 2005; Cosio, Ballabio, Benedetti, & Gigliotti, 2006). Electronic nose technology is based on the detection of the volatile compounds present in the headspace of a food sample and its advantages include the relatively small amount of sample preparation that is involved and the speed of analysis.

Regarding the UV–visible spectroscopy, the information of visible spectra has been evaluated for its ability to trace the geographical origin of e.v. olive oils coming from several Mediterranean regions (Forina, Boggia, & Casale, 2007) but in general the visible region has been rarely used in the characterisation of food origin.

All these analytical techniques provide multivariate and non-specific signals and for this reason Chemometrics is necessary to filter out the most relevant information from the data.

Chemometric methods for classification of olive oils have become of increasing importance (Aranda, Gómez-Alonso, Rivera

* Corresponding author. Tel.: +39 010 3532648; fax: +39 010 3532684.
E-mail address: monica@dictfa.unige.it (M. Casale).

0308-8146/$ - see front matter © 2009 Elsevier Ltd. All rights reserved.
doi:10.1016/j.foodchem.2009.04.091

del Álamo, Salvador, & Fregapane, 2004; Brescia, Alviti, Liuzzi, & Sacco, 2003; Casas, Bueno, Garcia, & Cano, 2003; Cichelli & Pertesana, 2004) and different Chemometric tools are applied in various laboratories.

Marini et al. (2004) authenticated e.v. olive oil varieties using linear discriminant analysis (LDA) and back propagation artificial neural networks (BP-ANN). Christy, Kasemsumran, Du, and Ozaki (2004) detected and quantified adulteration in olive oil by near-infrared spectroscopy and using Chemometric techniques: principal component analysis (PCA), partial least squares regression (PLS) and methods for data pretreatments such as multiplicative signal correction. Downey, McIntyre, and Davies (2003) studied the visible and NIR spectra of e.v. olive oils and correctly classified 94% of the samples according to the geographical origin, using PLS, LDA and *k*-nearest neighbour method (KNN).

In the literature, there are several examples that demonstrate the possibility of using "non conventional technologies", as spectroscopy and electronic nose, for the characterisation of e.v. olive oil, while papers about the coupling of information provided by different instruments are not frequent (Karoui et al., 2005; Mazerolles, Devaux, Dufour, Qannari, & Courcoux, 2002). On the contrary, the use of predictors from different instrumental sources, or with different treatments, should be one of the developmental directions in food chemistry in consequence of the fact that laboratories working on food problems have, in general, several instruments, many providing non specific information.

The objective of this study was to build a class model that would confirm the authenticity of e.v. olive oil from Liguria, an Italian region, using Chemometrics to extract and especially to combine the information from multivariate and non-specific data obtained by head-space mass spectrometry, UV–visible and NIR spectroscopy.

In order to reach this goal, two Chemometric strategies to manage all the information provided by three analytical techniques were developed.

Moreover, in order to select a representative subset of olive oil samples taken from the population of all possible samples in the Liguria region, a sampling strategy was developed. In classification and class-modelling problems, a sampling design should always be applied for the selection of samples to be used as a training set for building a class model, but, in reality, few sampling examples are present in the literature.

2. Materials and methods

2.1. Samples

One-hundred and eighty-nine extra virgin olive oils were analysed: 126 of these were authentic oils from Liguria and 63 were commercial samples.

The authentic samples were obtained from the 2005–2006 olive crop by collecting them directly and personally from farmers and oil mills in the Liguria region.

These samples comprehended both "fresh" and "bottled" oils, but they were defined "authentic" because their origin was guaranteed. Among these 126 samples, 65 representative samples were selected by means of a sampling strategy described below and used as training set to build a class model for Liguria olive oil.

The 63 commercial samples were bought in grocers and in supermarkets and comprehended 26 samples labelled as Ligurian e.v. olive oil (six of them labeled as PDO) and 37 samples of a different geographical origin (i.e. from Spain and other Italian regions).

The samples were stored in hermetically sealed topaz glass flask in a cold dark place until analysis in order to avoid losses or oxidations.

2.2. Sampling design

Sampling design in the context of this study refers to the selection of a statistical sample from the population of all (possible) samples.

A statistical sample should be representative of the population it is taken from, containing all variability of the relevant attributes describing its population.

The composition of olive oil is influenced by many factors, such as olive variety or cultivar, soil composition and climate, the procedure for collection of olives, pesticide treatments and phytosanitary conditions, month of collection, technology of production, manuring, transport and storage conditions before and after milling. Some of these factors are related to the specific production area while others cause a variation between oils of the same location as, for instance, month of collection, year of production, ripening or harvesting. In order to capture this variation, this study would need to be repeated over time.

In order to select Liguria e.v. olive oil samples with uniform distribution in the production area and representative of the production density, two algorithms for sampling have been sequentially used: Kennard–Stone design and Potential Function design.

2.2.1. Kennard and Stone algorithm

Kennard and Stone (1969) developed an algorithm for the selection of objects in multivariate space, such that the objects span the cloud of all objects as much as possible. This approach has been successfully applied in the field of Chemometrics, e.g. for the selection of a calibration set out of a population of samples. Here, this approach was applied to select a subset of samples with uniform distribution in the production area.

In this work, the Kennard and Stone algorithm was applied on the data matrix of 126 rows and 2 columns, containing the 126 Ligurian authentic samples described by the GPS coordinates of the oil mills in which they were collected.

The Kennard and Stone algorithm selects a predefined number of points (here the samples) in the space under the criterion that the sampled points are the best possible representation of the population of all points.

2.2.2. Potential Functions design

Many sampling designs are based on the statistical distribution of factor values, where a normal distribution is assumed to be the case. In many situations, however, a normal distribution is not appropriate, even after transformation of the data.

Complex distributions can be estimated by defining a Potential Function (Forina, Armanino, Leardi, & Drava, 1991). Potential Functions were introduced in Chemometrics several years ago for modelling groups (classes) of objects in multivariate space.

A sampling design based on the density functions was developed by Pizarro Millan, Forina, Casolino, and Leardi (1998) and in this study it was used to select samples representative of the production density of Liguria.

The probability density is determined as the sum of the individual contributions of each object. The individual contribution can have different shapes, however, one of the more common is the Gaussian-like shape (normal potential).

I is the number of training set objects. The selection of a subset of M objects from I ($I > M$) objects is performed as follows:

The object with the highest cumulative potential is selected.

Then, the potential in each point is recalculated after subtraction of the individual contribution of the selected object k multiplied by a selection factor r; r usually is $r = I/M$, i.e. the total number of objects I divided by the number of objects M to be selected.

In the new step, the object with the highest new potential is then selected as the second of the subset, and so on, till the predetermined number M of objects has been selected.

The density function computed with the selected objects must be very similar to the initial density function obtained from all the objects: this is a measure of the goodness of the representativity of the subset.

2.3. Apparatus and procedure

E.v. olive oil samples were measured with electronic nose, NIR and UV–visible spectrophotometers.

NIR measurements were performed with a FT near-infrared spectrometer based on a Polarization Interferometer (Buchi NIR-Flex N-500) in the 4000–10 000 cm^{-1} range at 4 cm^{-1} resolution. The samples were analysed in the transmittance mode using quartz cells with 5 mm path length. A total of 16 scans were averaged for every spectrum. Between samples, the cell components were washed with detergent in warm water, rinsed with acetone and then dried.

In order to eliminate the influence of the temperature in the variation between spectra, samples were measured in thermostatic conditions at 35 ± 0.5 °C.

Two replicates of each sample were taken and the average spectrum was calculated and used in subsequent analysis.

In order to remove the oil turbidity that could compromise the NIR spectra, in particular of the authentic samples, all the e.v. olive oils were centrifuged at 3000 rpm for 30 min before being analysed.

The electronic nose used in this study is not a traditional electronic nose based on sensors but it is a headspace mass spectrometer; it was assembled in our laboratory and is formed by an automatic sample introduction system, directly coupled to a mass detector without performing any chromatographic separation. A detailed description of this instrument and procedure of analysis can be found elsewhere (Cerrato Oliveros et al., 2005).

Absorption spectra in the ultraviolet and visible regions were obtained in the range 190–1100 nm using an Agilent 8453 spectrophotometer. The radiation source is a combination of a deuterium-discharge lamp for the ultraviolet wavelength range and a tungsten lamp for the visible wavelength range. The cells are rectangular cells in quartz glass with path length of 10 mm.

Isooctane (spectrophotometer grade) was used as a blank and it was purchased by Sigma–Aldrich (St. Louis, MO, USA). E.v. olive oils were directly analysed with no sample pre-treatment step other than filtration trough paper. Oil spectra were collected at room temperature, filling the quartz cell with samples (0.9 ml approximately).

2.4. Data analysis

The training set comprised two classes:

1. Authentic e.v. olive oils from Liguria, corresponding to the 65 samples selected using the sampling strategy.
2. Commercial e.v. olive oils from other regions corresponding to the 37 commercial samples of different geographical origin.

The 26 commercial samples labelled as Ligurian were joined to the 61 authentic Ligurian samples not selected by means of the sampling strategy and used only to test the class models.

Data analysis was performed using the Chemometric package V-PARVUS 2007 (Forina, Lanteri, Armanino, Casolino, & Casale, 2007).

As far as the NIR spectra is concerned, one segment of the signal without absorption was removed and only the range from 4380 to 10 000 cm^{-1} was considered. So, the data matrix had 189 rows (samples) and 1406 columns (variables, wavelengths).

Several mathematical transformations—standard normal variate (SNV) (Barnes, Dhanoa, & Lister, 1989), de-trending (DT) and derivatives—were tested to NIR transmittance spectra to eliminate the effect of particle size, scatter, and multi-collinearity and the use of first derivative only was effective in reducing the major factor inhibiting the interpretation of near-infrared spectra.

Therefore, the method of Savitzky and Golay (1964) with third-order smoothing polynomials through eleven points was used to compute the first derivatives of the NIR spectra that were used for all the subsequent analysis.

As far as the headspace mass spectrometry is concerned, the "spectral fingerprint" of each sample was obtained. The procedure is described in detail elsewhere (Cerrato Oliveros et al., 2005). The obtained data matrix for data analysis contained as many rows as samples (189) and as many columns as m/z recorded during the data acquisition time (151 m/z values, from 50 to 250). This data matrix was submitted to a row profile pre-treatment, a scaling that results in unit sum of the scaled elements:

$$y_{iv} = x_{iv} \Big/ \sum_{v=1}^{V} x_{iv}$$

As far as the UV–visible spectra is concerned, the parts of the signal saturated or without absorption were removed and only the range from 400 to 715 nm was considered. So, the data matrix had 189 rows (samples) and 316 columns (variables, wavelengths). Also in this case, first derivative spectra were calculated with a Savitzky–Golay filter using a third-order polynomial and an eleven point window.

The data from the three instruments were pre-treated separately and then, two strategies were considered:

1. The principal component analysis (PCA) was performed separately for each data set (HS-MS, UV–vis, NIR) and the first principal components of each data set were considered and joined. Then Unequal-Quadratic Discriminant Analysis (UNEQ-QDA) and Soft Independent Modelling of Class Analogy (SIMCA), as class-modelling techniques, were performed on these principal components.
2. The three data sets were joined and a procedure of variable selection was applied.

Then UNEQ-QDA and SIMCA were performed on the selected variables.

The two class-modelling techniques, SIMCA (Forina & Lanteri, 1984; Wold & Sjostrom, 1977) and UNEQ-QDA (Derde & Massart, 1986; Hotelling, 1947) were used to build a class model for Liguria e.v. olive oils.

SIMCA builds a class model based on the principal components of the category that are generally computed after individual category autoscaling.

K components are used to build the model. These K components define the inner space, the space of the structure.

The other dimensions are the outer space, the space of noise. The model of SIMCA is a hyper volume in the space of the first components, delimited by the range of the scores.

The Coomans plots (Coomans, 1982) were used to display the SIMCA results.

In these plots the coordinates of each object are the SIMCA distances from the models of two classes (in our case, distance from

class 1 on *X*-axis and distance from class 2 on *Y*-axis) or, better, their ratio to the critical distance corresponding to the boundary of the class space. The critical distances (95%) are drawn in the plot so that it is divided in four parts. The objects in the left bottom square are accepted by the models of the two classes because they have small distances from both models whereas the objects refused by both models are in the right upper square. The objects accepted by only one model fall in the other two parts (rectangles) of the Coomans plot.

UNEQ is the name currently used in Chemometrics for the class modelling technique developed by H. Hotelling and based on the Hotelling T^2 statistics. UNEQ is the class modelling version of quadratic discriminant analysis (QDA), where each category is described by the estimates of the means of the variables and the category variance-covariance matrix.

In this paper, classification and prediction abilities were computed as the average of the classification abilities for every class. The prediction ability was computed by the G-fold cross-validation method: the objects are divided into G cancellation groups. The objects are assigned to a cancellation group by their index *n* (row in the data matrix): the first object is assigned to the cancellation group 1, the second to group 2, the gth to the group G. Then the (g + 1)th is assigned again to group 1, and so on.

The model is computed G times. Each time, the objects in the corresponding cancellation group form the evaluation set. The objects in the other groups are the training set, used to compute the model parameters. At the end of the procedure, each object has been $(G - 1)$ times in the training set and once in the evaluation set. The final model is computed with all objects in the training set.

We used five cancellation groups for validation.

The *sensitivity* of a model (for a category) is the percentage of the objects of a class accepted by the class model. The specificity is the percentage of the objects of the categories different from the modelled one rejected by the class model.

The selection of discriminant variables was performed by means of a feature selection technique based on the stepwise decorrelation of the variables, SELECT (Forina, Lanteri, Casale, & Cerrato Oliveros, 2007; Kowalski & Bender, 1976), implemented in the V-PARVUS software.

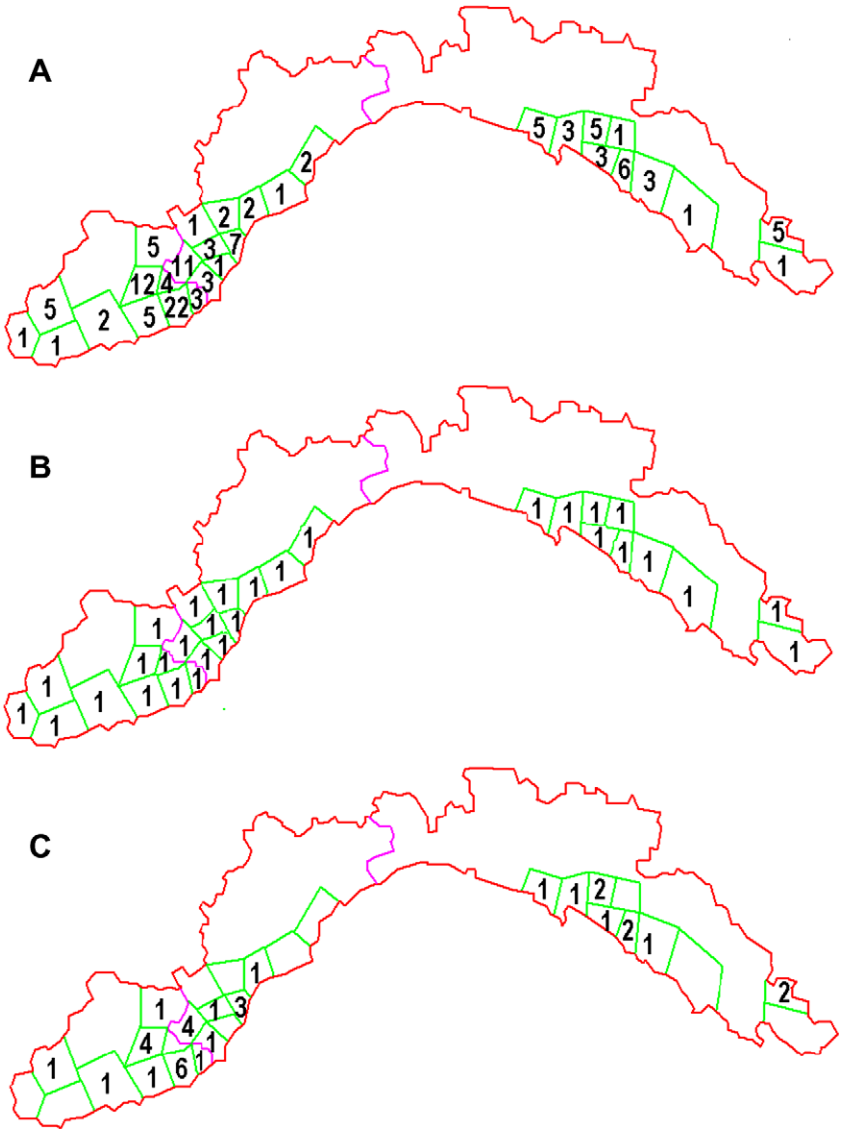

Fig. 1. (A) Repartition of oil-mills in the Liguria region; (B) distribution of the samples selected in the first step (Kennard Stone); (C) distribution of the samples selected in the second step (Potential Function). The three geographical denominations of the PDO "Riviera Ligure" are shown.

This technique generates a set of decorrelated variables ordered according to their Fisher weights. SELECT searches, at each step, for the variable with the largest classification weight. This variable is selected and decorrelated from the other variables; then the algorithm is repeated until a fixed number of variables is selected or the Fisher weight is lower than a specific cut-off value.

3. Results and discussion

3.1. Sampling design

The e.v. olive oil of Liguria is a PDO with name "Riviera Ligure", divided in three additional geographical denominations, namely "Riviera dei Fiori", "Riviera del Ponente Savonese" and "Riviera di Levante".

The sample distribution is analogous to the density of oliveyards, because an oil-mill receives olives from a relatively small neighbourhood. Fig. 1A, on the top, shows the repartition of oil-mills in the three geographical denominations of Liguria, that is the population of all (possible) samples.

For each of the three areas, the number of available samples was, respectively:

"Riviera dei Fiori"	60
"Riviera del Ponente Savonese"	33
"Riviera di Levante"	33

for a total of 126 samples.

The selection of a subset of samples was performed in two steps, using the sampling techniques described in Section 2.2.

1. Fist step – Kennard Stone algorithm was used to have a subset of 10 samples with uniform distribution on the production area of each geographical denomination; these 30 selected samples are shown in Fig. 1B.
2. Second step – The Potential Function design was used to select, among the samples not selected in the first step, a subset representative of the production density (and consequently of variability factors different from the geographical position). These selected samples are shown in Fig. 1C.

The number of samples selected in the second step was 15 for "Riviera dei Fiori", 10 for both "Riviera del Ponente Savonese" and for "Riviera di Levante". This difference can be justified by the fact that the "Riviera dei Fiori" has a larger production of olive oil.

The number of selected samples was:

"Riviera dei Fiori"	25
"Riviera del Ponente Savonese"	20
"Riviera di Levante"	20

for a total of 65 samples.

These 65 selected samples constituted the class 1 of the training set. The remainder 61 authentic samples were assigned to the test set.

Strategy 1: The PCA was performed separately for each of the three data set (HS-MS, UV–vis, NIR).

The first two principal components of each data set were considered and joined.

At first attempt, the PCA was applied as display method on these six principal components, after autoscaling.

Table 1
SIMCA and UNEQ-QDA results for Strategy 1 and Strategy 2, respectively.

SIMCA	(%)	UNEQ	(%)
Classification ability	96.1	Classification ability	99.0
Prediction ability (5CV)	92.2	Prediction ability (5CV)	97.1
Mean sensitivity	91.2	Mean sensitivity	90.7
Mean specificity	96.1	Mean specificity	100.0

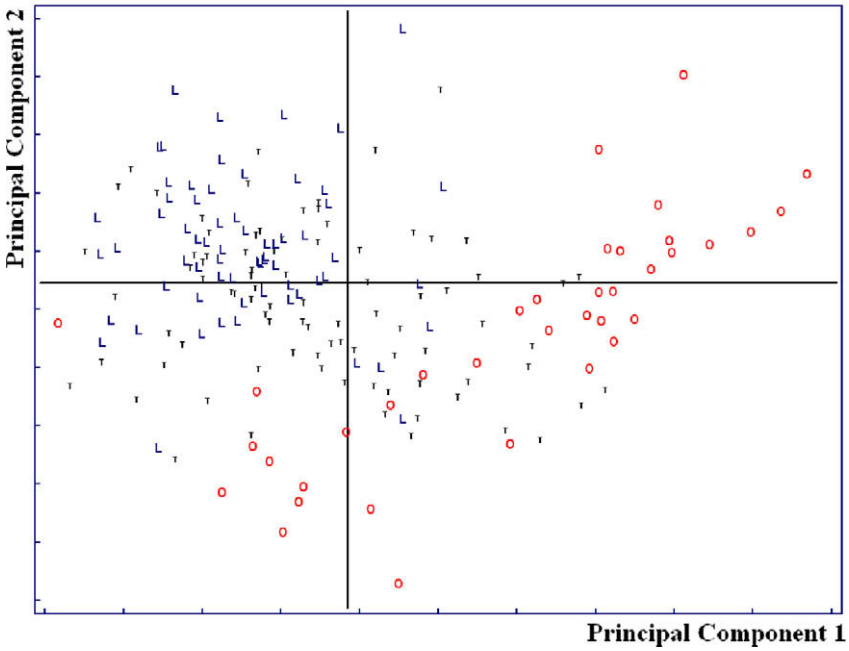

Fig. 2. Score plot on the first two principal components of the data fused according to Strategy 1. Samples are represented by a class symbol: L (Liguria), O (other regions), T (test set).

The first two PCs explained the 62.3% of total variance. In Fig. 2, score plot on the 1st–2nd components, a good discrimination between the two classes (authentic Ligurian oils and oils from other regions) is shown.

Then, in order to build class models in the multidimensional space, some class-modelling methods were applied using only the six principal components (the scores on the first two PCs for each of the three data sets).

Thus, UNEQ-QDA and SIMCA were performed as class-modelling tools; the results, shown in Table 1, were similar and both satisfactory. UNEQ-QDA allowed building Liguria class model with good predictive ability, high sensitivity and 100.0% specificity.

Fig. 3 shows the Coomans plot for the SIMCA models: the test set objects are not displayed, to make clearer the visualisation of the training set samples.

The samples having small distance from the model of class 1 fall in the vertical rectangle on the left, representing the model of authentic Ligurian e.v. olive oils. Four Ligurian samples are out of this model: the sensibility is not 100.0%. The horizontal rectangle on the right is the model of class 2 (oils from other regions). Four samples of class 2 are out of this model, its sensibility is 90.0% and the mean value between the sensitivities of the two classes 91.2%.

All samples of class 2 are rejected by the model of class 1: the specificity of this model is 100.0%. On the contrary, the model of class 2 accepts some Ligurian samples (those in the left bottom square), so that its specificity is lower. The value 96.1% reported in Table 1, is the mean value between the specificities of class 1 and 2.

Strategy 2: The three data sets were joined and SELECT, as feature selection technique, was applied to choose a subset of variables. In order to obtain a reliable model, there is a suggested number of samples to number of variables ratio, so 12 variables were retained.

Fig. 4 shows the score plot on the first two principal components of these 12 selected variables, after autoscaling. The use of autoscaling before computing principal components was necessary because the variables were of a different nature.

The first two PCs explained the 42.1% of total variance.

UNEQ-QDA and SIMCA were performed using these 12 variables; the results are shown in Table 1. Fig. 5 shows the Coomans plot for the SIMCA models: in this case, only three Ligurian samples are refused by the model of authentic Ligurian e.v. olive oils. Moreover, this model refuses all samples of class 2 and no Ligurian samples fall in the model of class 2: the mean specificity is 100.0% (no samples in the left bottom square).

The SIMCA and UNEQ-QDA results were improved by using the selected variables: as average values 100.0% of samples were correctly classified, 100.0% of total internal prediction (5 cross-validation groups) were achieved and both methods allowed building Liguria class models with good sensitivity and specificity.

Finally, the results (classification and prediction errors, sensitivity and specificity of the models) obtained by data fusion, were compared with the results obtained using the three data sets separately and this comparison showed that the results always improved through combining information from different sources. Using only the UV–visible variables, the prediction abilities were not so good (85.3% with SIMCA and 90.1% with UNEQ-QDA) and the specificities were lower (69.6% for SIMCA model and 55.5% for UNEQ-QDA model); also the results obtained using only the NIR spectra were worse: the prediction abilities were 91.2% for SIMCA and 84.3% for UNEQ-QDA but especially the specificities were not satisfactory (63.7% SIMCA and 46.0% UNEQ-QDA). Also using only the head-space mass spectrometry data, it was not possible to achieve the results

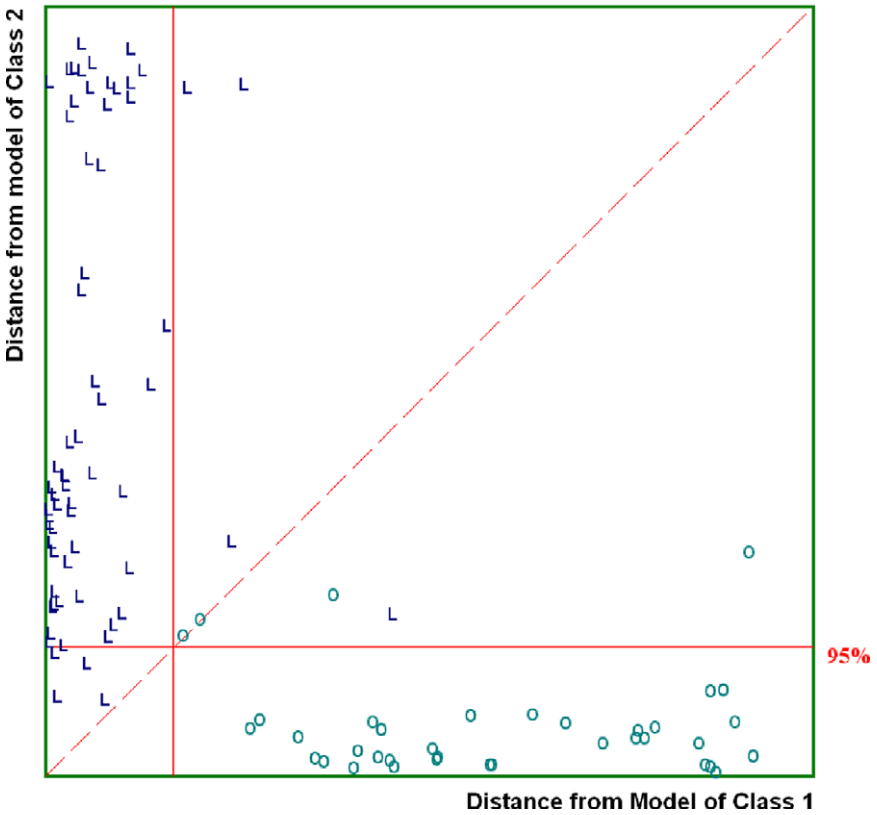

Fig. 3. Coomans plot for the SIMCA models computed according to Strategy 1. Samples are represented by a class symbol: L (Liguria), O (other regions).

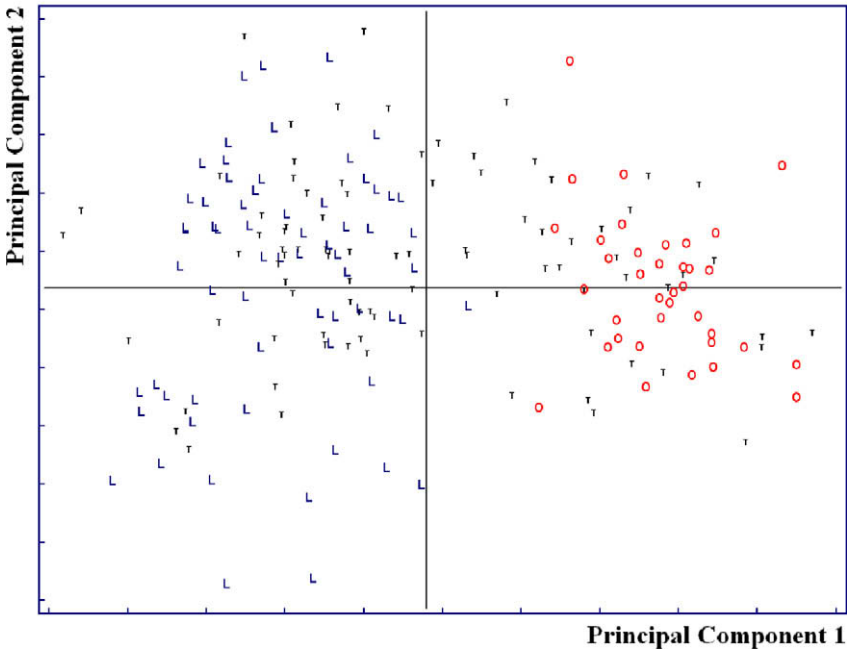

Fig. 4. Score plot on the first two principal components of the data fused according to Strategy 2. Samples are represented by a class symbol: L (Liguria), O (other regions), T (test set).

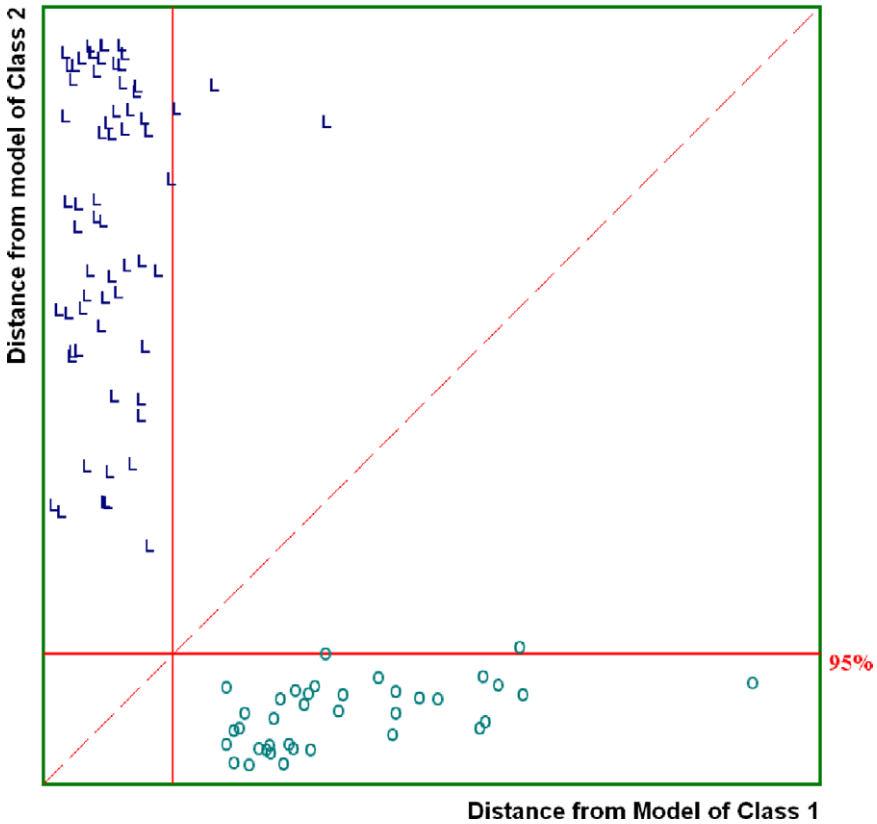

Fig. 5. Coomans plot for the SIMCA models previous feature selection by SELECT (Strategy 2). Samples are represented by a class symbol: L (Liguria), O (other regions).

obtained coupling the three analytical techniques: in this case the sensitivities of the models were worse (89.0% for SIMCA and 93.0% for UNEQ-QDA).

In addition, also as far as the test set is concerned, the results improved with the data fusion. In fact, with both strategies, the 61 authentic samples of the test set collected from oil mills in the Liguria region, were accepted by the class model of category

1: both SIMCA and UNEQ-QDA models had 100.0% of sensitivity considering the authentic samples. Otherwise, using the three data sets separately, some authentic samples were refused by the Liguria class model.

Among the 26 commercial samples of the test set labelled as Ligurian e.v. olive oils, some samples were accepted in the authentic Liguria e.v. olive oil model but other ones were refused by this model. It is interesting to note that the six PDO samples were always accepted from the model of authentic Liguria e.v. olive oils. In fact these commercial samples are of known and guaranteed origin. On the contrary, the remaining 20 samples were labelled as Ligurian samples, but their origin was dubious: these samples were produced in Liguria but not necessarily using Liguria olive cultivars.

4. Conclusion

In this paper, in order to build a class model for confirming the authenticity of Liguria e.v. olive oil, the fusion of data obtained by different instruments was tested.

In particular, non-specific data obtained by head-space mass spectrometry, UV–visible and NIR spectroscopy were considered and two Chemometric strategies to manage all the information provided by these three analytical techniques were developed.

In order to build a class model for a typical food as e.v. olive oil, that is a complex analytical matrix, it is necessary to extract an overall sample, constituted by a number of individual samples, representative of the food. For this reason a sampling strategy was developed and applied.

All the obtained results (classification and prediction errors, sensitivity and specificity of the models) were compared with the results obtained using the three data sets separately.

The results confirmed the potential of the fusion of data obtained by different analytical techniques (HS-MS, UV–Vis and NIR) using appropriate Chemometric methods for testing food authenticity.

Acknowledgement

This publication contains results from the EU project TRACE, No. 006942, funded under the Sixth Framework Program under the Food Quality and Safety Priority.

The authors are solely responsible for the content of the publication. It does not represent the opinion of the Community, nor is the Community responsible for any use that might be made of the data herein.

References

Aranda, F., Gómez-Alonso, S., Rivera del Álamo, R. M., Salvador, M. D., & Fregapane, G. (2004). Triglyceride, total and 2-position fatty acid composition of Cornicabra virgin olive oil: Comparison with other Spanish cultivars. *Food Chemistry, 86*(4), 485–492.

Barnes, R. J., Dhanoa, M. S., & Lister, S. J. (1989). Standard normal variate transformation and de-trending of near-infrared diffuse reflectance spectra. *Applied Spectroscopy, 43*(5), 772–777.

Brescia, M. A., Alviti, G., Liuzzi, V., & Sacco, A. (2003). Chemometric classification of olive cultivars based on compositional data of oils. *Journal of the American Oil Chemists' Society, 80*(10), 945–950.

Casas, J. J. S., Bueno, E. O., Garcia, A. M. M., & Cano, M. M. (2003). Study of fatty acid contents in monovariety oils elaborated from olives produced in Extremadura (Spain). *Grasas y Aceites, 54*(4), 371–377.

Cerrato Oliveros, M. C., Boggia, R., Casale, M., Armanino, C., & Forina, M. (2005). Optimisation of a new headspace mass spectrometry instrument. Discrimination of different geographical origin olive oils. *Journal of Chromatography A, 1076*(1–2), 7–15.

Christy, A. A., Du, Y. P., & Ozaki, Y. (2004). The detection and quantification of adulteration in olive oil by near-infrared spectroscopy and chemometrics. *Japanese Society of Analytical Chemistry, 20*, 935–940.

Christy, A. A., Kasemsumran, S., Du, Y. P., & Ozaki, Y. (2004). The detection and quantification of adulteration in olive oil by near-infrared spectroscopy and chemometrics. *Analytical Sciences, 20*(6), 935–940.

Cichelli, A., & Pertesana, G. P. (2004). High-performance liquid chromatographic analysis of chlorophylls, pheophytins and carotenoids in virgin olive oils: Chemometric approach to variety classification. *Journal of Chromatography A, 1046*(1–2), 141–146.

Coomans, D. (1982). PhD Thesis, Vrije Universiteit Brussel.

Cosio, M. S., Ballabio, D., Benedetti, S., & Gigliotti, C. (2006). Geographical origin and authentication of extra virgin olive oils by an electronic nose in combination with artificial neural networks. *Analytica Chimica Acta, 567*(2), 202–210. doi:10.1016/j.aca.2006.03.035.

Derde, M. P., & Massart, D. L. (1986). UNEQ: A disjoint modelling technique for pattern recognition based on normal distribution. *Analytica Chimica Acta, 184*, 33–51.

Downey, G., McIntyre, P., & Davies, A. N. (2003). Geographic classification of extra virgin olive oils from the eastern Mediterranean by chemometric analysis of visible and near-infrared spectroscopic data. *Applied Spectroscopy, 57*(2), 158–163.

Forina, M., & Lanteri, S. (1984). Data analysis in food chemistry. In B. R. Kowalski (Ed.), *Chemometrics: Mathematics and statistics in chemistry. NATO ASI series C* (Vol. 138, pp. 439). Dordrecht: Reidel Publ. Co..

Forina, M., Armanino, C., Leardi, R., & Drava, G. (1991). A class-modelling technique based on potential functions. *Journal of Chemometrics, 5*(5), 435–453.

Forina, M., Boggia, R., & Casale, M. (2007). The information content of visible spectra of extra virgin olive oil in the characterization of its origin. *Annali di Chimica, 97*(8), 615–693.

Forina, M., Lanteri, S., Armanino, C., Casolino, C., & Casale, M. 2007. V-PARVUS: An extendable package of programs for explorative data analysis, classification and regression analysis. Dip. Chimica e Tecnologie Farmaceutiche ed Alimentari, University of Genova. Free available at <http://www.parvus.unige.it>.

Forina, M., Lanteri, S., Casale, M., & Cerrato Oliveros, M. C. (2007). Stepwise orthogonalization of predictors in classification and regression techniques: An "old" technique revisited. *Chemometrics and Intelligent Laboratory Systems, 87*(2), 252–261. doi:10.1016/j.chemolab.2007.03.003.

Galtier, O., Dupuy, N., Le Dréau, Y., Ollivier, D., Pinatel, C., Kister, J., et al. (2007). Geographic origins and compositions of virgin olive oils determinated by chemometric analysis of NIR spectra. *Analytica Chimica Acta, 595*(1–2), 136–144. doi:10.1016/j.aca.2007.02.033.

Hotelling, H. H. (1947). Multivariate quality control. In C. Eisenhart, M. W. Hastay, & W. A. Wallis (Eds.), *Translator and editor techniques of statistical analysis* (pp. 111–115). New York: McGraw-Hill.

Karoui, R., Dufour, E., Pillonel, L., Schaller, E., Picque, D., Cattenoz, T., et al. (2005). The potential of combined infrared and fluorescence spectroscopies as a method of determination of the geographic origin of Emmental cheeses. *International Dairy Journal, 15*(3), 287–298.

Kennard, R. W., & Stone, L. A. (1969). Computer aided design of experiments. *Technometrics, 11*, 137–148.

Kowalski, B. R., & Bender, C. F. (1976). An orthogonal feature selection method. *Pattern Recognition, 8*(1), 1–4.

Marini, F., Balestrieri, F., Bucci, R., Magrý, A. D., Magrý, A. L., & Marini, D. (2004). Supervised pattern recognition to authenticate Italian extra virgin olive oil varieties. *Chemometric and Intelligent Laboratory System, 73*(1), 85–93.

Mazerolles, G., Devaux, M. F., Dufour, E., Qannari, E. M., & Courcoux, Ph. (2002). Chemometric methods for the coupling of spectroscopic techniques and for the extraction of the relevant information contained in the spectral data tables. *Chemometrics and Intelligent Laboratory Systems, 63*(1), 57–68.

Pizarro Millan, C., Forina, M., Casolino, C., & Leardi, R. (1998). Extraction of representative subsets by potential functions method and genetic algorithms. *Chemometrics and Intelligent Laboratory Systems, 40*(1), 33–52.

Reid, L. M., O'Donnell, C. P., & Downey, G. (2006). Recent technological advances for the determination of food authenticity. *Trends in Food Science and Technology, 17*(7), 344–353. doi:10.1016/j.tifs.2006.01.006.

Savitzky, A., & Golay, M. J. E. (1964). Smoothing and differentiation of data by simplified least squares procedures. *Analytical Chemistry, 36*(8), 1627–1639.

Wold, S., & Sjostrom, M. (1977). SIMCA: A method for analysing chemical data in terms of similarity and analogy. In B. R. Kowalski (Ed.), *Chemometrics, theory and application. ACS symposium series* (Vol. 52, pp. 243). Washington, DC: American Chemical Society.

Food Chemistry 118 (2010) 171–176

Contents lists available at ScienceDirect

Food Chemistry

journal homepage: www.elsevier.com/locate/foodchem

Analytical Methods

Tracing the geographical origin of honeys based on volatile compounds profiles assessment using pattern recognition techniques

I. Stanimirova [a], B. Üstün [b], T. Cajka [c], K. Riddelova [c], J. Hajslova [c], L.M.C. Buydens [b], B. Walczak [a,*]

[a] Institute of Chemistry, Department of Chemometrics, Silesian University, 9 Szkolna Street, Katowice 40-006, Poland
[b] Institute of Molecules and Materials, Department of Analytical Chemistry, Radboud University Nijmegen, Heyendaalseweg 135, 6525AJ Nijmegen, The Netherlands
[c] Institute of Chemical Technology, Prague, Faculty of Food and Biochemical Technology, Department of Food Chemistry and Analysis, Technicka 3, 166 28 Prague 6, Czech Republic

ARTICLE INFO

Article history:
Received 3 March 2008
Received in revised form 13 November 2008
Accepted 21 April 2009

Keywords:
Food analysis
Solid phase microextraction
Comprehensive two-dimensional gas chromatography
Time-of-flight mass spectrometry
Honey volatiles
Classification
LDA
DPLS
SIMCA
SVM

ABSTRACT

The goal of this study was to examine the possibility of verifying the geographical origin of honeys based on the profiles of volatile compounds. A head-space solid phase microextraction (SPME) combined with comprehensive two-dimensional gas chromatography–time-of-flight mass spectrometry (GC × GC–TOF-MS) was used to analyze the volatiles in honeys with various geographical and floral origins. Once the analytical data were collected, supervised pattern recognition techniques were applied to construct classification/discrimination rules to predict the origin of samples on the basis of their profiles of volatile compounds. Specifically, linear discriminant analysis (LDA), soft independent modeling of class analogies (SIMCA), discriminant partial least squares (DPLS) and support vector machines (SVM) with the recently proposed Pearson VII universal kernel (PUK) were used in our study to discriminate between Corsican and non-Corsican honeys. Although DPLS and LDA provided models with high sensitivities and specificities, the best performance was achieved by the SVM using PUK. The results of this study demonstrated that GC × GC–TOFMS combined with methods like LDA, DPLS and SVM can be successfully applied to detect mislabeling of Corsican honeys.

1. Introduction

Nowadays, the identification of the origin of food is one of the most important issues in food chemistry and in food quality control. Recently the European Commission has decided to introduce regulations for labeling food commodities. The origin of food, together with its main ingredients, should be available to the consumer. These regulations aim to guarantee product quality, safety, authenticity and to protect the rights of consumers. In light of the new regulations, there is an urgent demand to deliver cost-effective procedures for detecting fraudulent products and checking compliance with the quality specifications. This is essentially the goal of the EU-funded project "TRACE" (Tracing food commodities in Europe, www.trace.eu.org). This paper describes a part of the research done within the TRACE project on the commodity of honey.

Honey is a natural product, the consumption of which has increased in recent years. The traditional approach to recognizing the botanical origin of honey relies on a microscopic examination of its pollen (melissopalynology) (Anklam, 1998; Soria, González, de Lorenzo, Martínez-Castro, & Sanz, 2004). Melissopalynology can also be used to identify the geographical origin of honey if the pollen is specific enough in the area of interest. However, this method is expensive, time-consuming and strongly dependent on the qualifications and judgment of the analyst. Therefore, there is a tendency to replace pollen analysis by finding analytical and/or physicochemical markers for honey discrimination. Minerals and trace elements (Fernández-Torres et al., 2005; Hernández, Fraga, Jiménez, Jiménez, & Arias, 2005; Latorre et al., 1999), volatile compounds (Guyot, Scheirman, & Collin, 1999; Radovic et al., 2001; Soria et al., 2004), the protein pattern, flavonoids, physicochemical parameters like electrical conductivity, pH, total acidity and water activity (Acquarone, Buera, & Elizalde, 2007; Corbella & Cozzolino, 2006; Devillers, Morlot, Pham-Delegue, & Dore, 2004; Marini, Magrì, Balestieri, Fabretti, & Marini, 2004) are some of the parameters that have been extensively examined for the recognition of the floral and geographical origin of honeys.

Although the volatile composition has mainly been used for the characterization of the floral source of honey, the aim of this work was to evaluate whether the volatile profile also allowed for the identification of the geographical origin of honey. Specifically, its

* Corresponding author. Tel.: +48 32 359 2115; fax: +48 32 259 9978.
E-mail address: beata@us.edu.pl (B. Walczak).

0308-8146/$ - see front matter © 2009 Elsevier Ltd. All rights reserved.
doi:10.1016/j.foodchem.2009.04.079

use for discriminating between Corsican honeys and honeys from other geographical regions was studied. The reason for choosing Corsican honeys was to demonstrate the usefulness of the volatile profiles for tracing the origin of a PDO (protected designation of origin) commodity. The PDO label guarantees that the product consumers purchase is prepared, processed and produced in a specific region and consequently possesses unique properties. However, an emerging authenticity problem is the labeling of a non-PDO product as PDO. In other words, the aim of our study is to develop a reliable methodology to detect such a fraud in Corsican honey, i.e. a strategy for the successful differentiation of Corsican honeys from honeys originating from other regions (PDO or non-PDO) in Europe.

To meet the goal of the study, a large number of honey samples were collected in a two-year campaign (2006 and 2007) and their volatile constituents were analyzed using head-space solid phase microextraction (SPME) sampling followed by the separation/identification step employing comprehensive two-dimensional gas chromatography–time-of-flight mass spectrometry (GC × GC–TOFMS). This approach offers a quick (19 min GC run vs. 30–90 min using one-dimensional GC) and comprehensive analysis of honey volatiles, while minimizing the risk of their erroneous identification, which cannot be avoided in one-dimensional GC separation (Čajka, Hajšlová, Cochran, Holadová, & Klimánková, 2007).

A verification of the origin of food and/or checking the authenticity can be facilitated using chemometric approaches. The goal of supervised pattern recognition techniques is to create classification/discrimination rules using a set of training samples of a known origin and then using the created rules to predict the belongingness of new samples of an unknown origin to the available classes. Since the choice of a classification/discrimination method is strongly data dependent, performances of several pattern recognition methods (Berrueta, Alonso-Salces, & Héberger, 2007; González, 2007), which cover different aspects of data investigation, were evaluated for the two-class problem studied. These were linear discriminant analysis (LDA) (Fisher, 1936; Lebart, Morineau, & Warwick, 1984), discriminant partial least squares (DPLS) (Næs, Isaksson, Fearn, & Davies, 2002), soft independent modeling of class analogy (SIMCA) (Wold, 1976) and support vector machines (SVMs) (Vapnik, 1995) equipped with the recently proposed Pearson VII universal kernel (PUK) (Üstün, Melssen, & Buydens, 2006). The results of this study will help to confirm or reject the hypothesis that the volatile profiles of Corsican honeys can be used for tracing products that do not comply with the label information.

The following section describes the theoretical basis of LDA, DPLS, SIMCA and SVM. Next the experimental conditions and data are presented in Section 3. In Section 4, the results obtained from all the methods applied to the data collected in a two-year sampling campaign are discussed. Finally, the conclusions of the study are given in Section 5.

2. Theory

2.1. Linear discriminant analysis (LDA)

In LDA, it is assumed that the data of each class follow the normal distribution; the classes are linearly separable and the class variance–covariance matrices are equal. The objective of LDA is to find linear combinations of explanatory variables called discriminant functions that maximize the between-classes variance and at the same time minimize the within-classes variance. This is the well-known Fisher criterion (Fisher, 1936). The number of discriminant functions found is equal to the number of classes minus one, if the number of variables is larger than the number of classes. A disadvantage of LDA is that it is appropriate only for data in which the total number of objects is considerably larger than the number of variables. When this condition is not fulfilled, compression of data by means of PCA, regularized LDA, stepwise LDA or feature reduction methods (Wu et al., 1996) should be considered.

2.2. Discriminant partial least squares (DPLS)

The partial least squares model expresses a linear relationship between a response variable $\mathbf{y}$ ($n \times 1$) and a set of p explanatory variables $\mathbf{X}$ ($n \times p$). It can be seen as an extension of multiple linear regression that can deal with multicollinearity in the data by constructing new latent factors, $\mathbf{T}$ ($n \times f$), which maximize the covariance between $\mathbf{X}$ and $\mathbf{y}$. In discriminant PLS, the elements of $\mathbf{y}$ are usually coded as 0 and 1 (a binary variable) or as -1 and 1 (a bipolar variable) that provide information about the belongingness of n objects to two defined classes.

The optimal number of factors, f, is usually selected through the use of a cross-validation procedure and the model selected has a complexity for which the smallest root mean square error of cross-validation (RMSCV) is observed. The prediction power of a model is scored by a root mean square error (RMSEP) calculated for an external set of samples (test set) that is not used during the development of the model. Similar to LDA, an optimal DPLS model can be constructed when the training set is balanced i.e. it contains two classes with an equal number of samples and a comparable variance (Brereton, 2006).

2.3. Soft independent modeling of class analogy (SIMCA)

The main idea in SIMCA (Wold, 1976) is to build a confidence limit for each class with the help of principal component analysis (PCA) and then to project the unclassified samples into each principal components space and to assign them to the class in which they fit best.

Selection of the optimal number of PCs (f) is a key point in SIMCA and is usually determined using a leave-one object out cross-validation (Vandeginste et al., 1998). In our study, the classification of samples to a given category was done by means of the distance–distance plot (Daszykowski, Kaczmarek, Stanimirova, Vander Heyden, & Walczak, 2007). The Mahalanobis distance in the score space and the orthogonal distance from the PCA model constructed were calculated for each object. The default cut-off value for each of the absolute-centered distances (Mahalanobis or orthogonal) obtained using the cross-validated score values was determined at three times its standard deviation. By setting the cut-off value in this way, it was assumed that 99.90% of the centered distances for samples could be found within the interval of three times the standard deviation. One can make a distinction among regular samples and three categories of outlying observations. In general, each sample is fitted to each of the PCA models constructed and is assigned to the model for which its z-scores for the Mahalanobis and orthogonal distances are smaller than three.

2.4. Support vector machines (SVMs)

Support vector machine (SVM) is a binary classification tool that performs classification by constructing an optimal separating hyperplane (OSH) (Vapnik, 1995). The optimal separating hyperplane is defined as the one that maximizes the distance between the objects of the two classes (margin). Consider a data set $\{(x_1, y_1), \ldots, (x_n, y_n)\}$ with input data $\mathbf{x}_i \in \mathrm{R}^{\mathrm{d}}$ (d-dimensional input space) and output data y with binary class labeling $\mathbf{y} \in \{-1, +1\}$. SVM tries to separate the given set of binary-labeled data (two-class problem) with a hyperplane that is maximally distant from them. The objects lying on the margin are called support vectors

that control the discrimination power of the hyperplane. Moreover, SVM has a regularization constant *C* that controls the trade-off between errors of the SVM on the training data and the margin maximization. Using a non-linear kernel function, SVM can deal with complex, e.g. non-linear relationships in data. The kernel function transforms the original data into a high dimensional feature space, where non-linear relationships can be present in a linear form.

Some commonly used kernel functions in the literature are the inner-product based linear and polynomial kernels and the Euclidean distance-based Gaussian (Radial Basis Function (RBF)) kernel (Schölkopf & Smola, 2002). The particular choice of a kernel function greatly depends on the nature of the data, i.e. which kind of underlying relationship needs to be estimated to relate the input data to the desired output. The nature of the data is usually unknown, so the kernel function will be determined experimentally by applying and validating various kernel functions and selecting the one with the highest generalization performance. In this paper we used the recently proposed Pearson VII universal kernel (PUK) (Üstün et al., 2006). The PUK function has the flexibility to change easily from a Gaussian into a Lorentzian shape and into intermediate shapes as well. This flexibility results in a higher mapping power for PUK in comparison to the commonly used linear, polynomial and RBF kernel functions.

The PUK kernel contains two parameters, namely σ and ω. The parameters σ and ω control the width (also named Pearson width) and the actual shape (tailing behavior) of the Pearson VII function. In order to use SVM, both the kernel parameters and the SVM regularization constant, *C*, need to be defined by the user.

In this paper, those parameters were defined by means of a grid search optimisation. To decrease the number of parameter possibilities (time saving) an internal scaling factor β was introduced, according to (Melssen, Üstün, & Buydens, 2006).

3. Experimental

3.1. Honey samples

In total, 374 honey samples were collected within the framework of the EU TRACE project (www.trace.eu.org). The samples were obtained directly from the producers, which guarantees their authenticity. In 2006 (first harvest), 111 Corsican, 18 non-Corsican-French, 15 Italian, 18 Austrian, 2 Irish, and 18 German honey samples were collected. During 2007 (second harvest), 108 Corsican, 28 non-Corsican-French, 15 Italian, 23 Austrian, and 18 German samples were collected. Before distribution, each honey sample was incubated at 40 °C overnight in an air oven, then manually stirred, and adjusted with distilled water to a content of solids of 70° Brix. Prior to analysis, the honey sample (2 g) was placed into a 10 mL vial for SPME; after adding 2 mL of distilled water, the vial was sealed with a magnetic cap with PTFE/silicon septum and vortexed until complete homogenisation was achieved.

As regards the Corsican samples, products collected in spring and autumn, both with specified origin (maquis, bushes, sweet chesnut, strawberry-tree and Clémentinier – Citrus Reticulata) and non-specified were included in the experimental set.

3.2. Chemicals and materials

The SPME fibre 50/30 μm divinylbenzene/carboxen/polydimethylsiloxane, (DVB/CAR/PDMS) used for the sampling of honey volatiles was supplied by Supelco (Bellefonte, PA, USA). Prior to use, the fibre was conditioned following the manufacturer's recommendations.

The system used for GC × GC experiments comprised a DB-5 ms, 5% phenyl polysilphenylenesiloxane (J&W Scientific, Folsom, CA, USA) primary column; 30 m × 0.25 mm id, 0.25 μm film thickness, coupled via a column connector (Agilent, Palo Alto, CA, USA) to a SUPELCOWAX 10, polyethylene glycol (Supelco, Bellefonte, PA, USA) second column of dimension 1.25 m × 0.1 mm id, 0.1 μm film thickness.

The mixture of *n*-alkanes (C_8–C_{20}) dissolved in *n*-hexane employed for retention index determinations was supplied by Supelco (Bellefonte, PA, USA). The calculation was done for components eluting between *n*-octane and *n*-eicosane.

3.3. Instrumentation

A Pegasus 4D system consisting of an Agilent 6890 N gas chromatograph equipped with a split/splitless injector (Agilent Technologies, Palo Alto, CA, USA), an MPS2 autosampler for automated SPME (Gerstel, Mülheim an der Ruhr, Germany), and a Pegasus III high-speed time-of-flight mass spectrometer (Leco Corp., St. Joseph, MI, USA) was used. Inside the GC oven a cryogenic modulator (N_2 jets–hot air jets technology) and a secondary oven (Leco Corp., St. Joseph, MI, USA) were mounted. Resistively heated air was used as a medium for hot jets, while cold jets were supplied by gaseous nitrogen cooled by liquid nitrogen.

3.4. Operating conditions

The operating conditions of the optimised HS-SPME–GC × GC–TOFMS method were as follows (Čajka et al., 2007):

- HS-SPME: incubation time: 5 min; incubation temperature: 40 °C; agitator speed: 500 rpm; extraction time: 20 min; desorption temperature: 250 °C; desorption time: 45 s (splitless). After 6 min exposure in the injector the fibre is automatically withdrawn and incubation and extraction of the next sample ensues.
- GC × GC: primary oven temperature program: 45 °C (0.75 min), 10 °C/min to 200 °C, 30 °C/min to 245 °C (1.25 min); secondary oven temperature: +20 °C above the primary oven temperature;

Table 1
Honey volatiles (markers) used for chemometric analysis.

Number of compound	Marker
1	Hexanal
2	Furan-2-carbaldehyde (furfural)
3	Hexan-1-ol
4	Heptanal
5	Heptan-1-ol
6	Benzaldehyde
7	Methylsulfanyldisulfanylmethane (dimethyl trisulfide)
8	Octanal
9	1-Methyl-4-propan-2-yl-benzene (*p*-cymene)
10	2-Phenylacetaldehyde
11	Octan-1-ol
12	1-Phenylethanone
13	Ethyl heptanoate
14	Nonanal
15	2-Phenylethanol
16	3,5,5-Trimethylcyclohex-2-en-1-one (isophorone)
17	Lilac aldehyde I
18	2,6,6-Trimethylcyclohex-2-ene-1,4-dione (4-oxoisophorone)
19	Lilac aldehyde II
20	Lilac aldehyde III
21	Nonan-1-ol
22	Ethyl octanoate
23	Decanal
24	Decan-1-ol
25	Ethyl nonanoate
26	Ethyl decanoate

modulator offset: +35 °C above the primary oven temperature; modulation period: 3 s (hot pulse 0.6 s); carrier gas: helium (purity 99.9999%); column flow: 1.3 mL/min.
- TOFMS: electron ionisation mode (70 eV); ion source temperature: 220 °C; mass range: *m/z* 25–300; acquisition rate: 300 spectra/s; detector voltage: −1750 V (first harvest), −1500 V (second harvest).

ChromaTOF (LECO Corp.) software (v. 2.31) was used for instrument control, data acquisition, and data processing. Identification of compounds was based on a NIST 2005 mass spectra library search and was further confirmed by comparing the linear retention indexes available in the same library.

In total, 26 aroma compounds (markers) were selected on the basis of a careful examination of the GC × GC chromatograms of honey samples by identifying the peaks that significantly varied in their intensities or those that described the quality of the honeys. The list of the markers selected is given in Table 1.

For the markers selected, the repeatability of SPME–GC × GC–TOFMS measurements (expressed as relative standard deviation, RSD) ranged between 2.1% and 12% ($n = 10$). Also, the quality of mass spectra was checked during the data processing of real samples and only those target volatiles with a mass-spectral match (i.e. similarity) higher than 700 were considered for chemometric analysis.

3.5. Data preprocessing prior to chemometric analysis

Before the construction of any classification/discriminant model, the raw data (374 × 26) presented in the form of absolute peak intensities were preprocessed using the row-closure operation (Vandeginste et al., 1998). This procedure involves the division of each row element by the corresponding row-sum. Row-closure enables an easier comparison of the sample profiles.

4. Results and discussion

LDA, DPLS, SIMCA and SVM were used to construct models for the discrimination of Corsican from non-Corsican honeys for each year of sampling and for the data of both years. This was done in order to investigate whether the year of sampling might have an influence on the discrimination. To estimate properly the predictive abilities of the built models, the data were divided into training and external test sets, respectively. Since LDA and DPLS are sensitive to the number of samples in the training set, special attention was paid when selecting this number. Table 2 shows the number of samples included in the training and test sets for each set of data.

One can see that the training set is balanced, i.e. it contains an equal number of Corsican and non-Corsican samples. This number was chosen as 75% of the total non-Corsican samples of each year and of both years because, in general, a smaller number of non-Corsican samples are available in comparison with the Corsican samples. The subsets were selected randomly and the selection was applied to each class separately. A leave-one object out cross-validation procedure was adopted to optimise all the models constructed and two figures of merit such as sensitivity and specificity were used to characterize the quality of the models' predictions. For a two-class problem, sensitivity is defined as the percentage of samples from the first class that are correctly predicted by the model, while specificity is the percentage of samples that are correctly classified as belonging to the other class. The ideal model would have sensitivity and specificity of 100%. Together with the sensitivity and specificity, one can define the so-called efficiency, also known in the literature as the non-error rate, which is the total percentage of correctly classified test samples.

4.1. Classification/discrimination of the Corsican honeys using data from 2006

The efficiency, sensitivity and specificity obtained from all models are listed in Tables 3 and 4.

The LDA model has an efficiency of 89.5% (see Table 3), which is related to eight incorrectly classified samples in the test set. An analysis of these misclassified samples showed that 6 out of 58 Corsican samples were recognized as non-Corsican and two non-Corsican samples fell within the domain of the Corsican samples. This resulted in a high sensitivity of 89.7% and a specificity of 88.9% of the LDA model (see Table 4). A slightly worse efficiency of 85.5% was obtained from the DPLS model with complexity four. RMSCV was equal to 0.59 and RMSEP was 0.63. Similar to the LDA model, six Corsican samples were incorrectly classified as non-Corsican resulting in the same sensitivity of 89.7%. However, compared to the LDA model, the DPLS model showed a decrease of 16.7% in specificity because of five non-Corsican honeys that were identified as Corsican. In contrast to the quality of the predictions obtained from LDA and DPLS, the eight-component SIMCA model showed a relatively poorer efficiency of 77.5%. Even though the sensitivity of the SIMCA model is the highest observed (93.1%), the specificity is quite low (64.8%). A good performance was achieved using the SVM method combined with the Pearson VII universal kernel (PUK) function. The optimal values for σ, w and C are presented in Table 5.

A total of ten samples were misclassified, when the SVM model was tested, which resulted in an efficiency of 86.8%. Again six Corsican samples were incorrectly rejected and the sensitivity is the same as the one found for the LDA and DPLS models. Because of the four incorrectly identified non-Corsican honeys, the SMV model has a specificity of 77.8%.

Comparing the prediction abilities of the models built for data of year 2006, all the models, except SIMCA, showed the same sensitivity, but they present different specificities. This means that the probability of recognizing a Corsican honey as a non-Corsican is the same with all methods, while the probability of identifying a non-Corsican honey as a Corsican increases in the order LDA, SVM, DPLS and SIMCA (see Table 4).

4.2. Classification/discrimination of the Corsican honeys using data from 2007

Again four different models were built for a randomly chosen training set. The number of samples considered in the training

Table 2
Number of Corsican and non-Corsican samples in the training and test sets for 2006, 2007 and for the two-year sampling.

	Training set		Test set	
	Corsica	Non-Corsica	Corsica	Non-Corsica
2006	53	53	58	18
2007	63	63	45	21
Two-year sampling	116	116	103	39

Table 3
Efficiency (in percentage) of the models.

	LDA	DPLS	SIMCA	SVM
Corsica vs. non-Corsica				
2006	89.5	85.5	77.5	86.8
2007	89.4	83.3	60.0	95.5
Two-year sampling	85.2	86.6	64.3	91.5

Table 4
Sensitivity (in percent) and specificity (in percent) of the models.

	LDA		DPLS		SIMCA		SVM	
	Sensitivity	Specificity	Sensitivity	Specificity	Sensitivity	Specificity	Sensitivity	Specificity
Corsica vs. non-Corsica								
2006	89.7	88.9	89.7	72.2	93.1	64.8	89.7	77.8
2007	91.1	85.7	86.7	76.2	97.8	42.9	97.8	90.5
Two-year sampling	86.4	82.1	87.4	84.6	93.2	45.2	93.2	87.2

and test sets are presented in Table 2, while the efficiency, sensitivity and specificity of the models are shown in Tables 3 and 4. For honey data from 2007, all models, except SIMCA, presented comparable or improved efficiencies with respect to the corresponding models built for the data of the first year of sampling (see Table 3). The LDA model has an efficiency of 89.4%, when tested. After analyzing the misclassified test samples, it was found that four Corsican honeys were incorrectly recognized as non-Corsican and three non-Corsican honeys were found to have similar volatile compositions as the Corsican honeys. This analysis showed a fairly high sensitivity of 91.1% and a specificity of 85.7% for the LDA model.

The seven-component DPLS model with RMSCV equals 0.64 and a RMSEP of 0.72 lacks a correct assignment for six Corsican samples and therefore, a reduced sensitivity of 86.7% was observed in comparison with LDA. A decrease in specificity by 9.5% was also the result of the incorrect recognition of five non-Corsican honeys as Corsican. In contrast to both models built, the five-component SIMCA model had an efficiency of only 60.0% when tested. Although the model had a sensitivity of 97.8%, which is higher than the one found by LDA and DPLS, the majority of the non-Corsican honeys were assigned as Corsican and therefore, the specificity of the SIMCA model is considerably low (42.9%).

From the values presented in Table 3, it became clear that the SVM model has the best efficiency of 95.5% among the models built. Only three samples (one Corsican and two non-Corsican) were misclassified, when the SVM model was tested. Consequently, the SVM model offered the same fairly high sensitivity of 97.8% as the five-component SIMCA model and the best specificity (90.5%) among the all models constructed.

The difference in the classification results between the data of year 2006 and year 2007 might be explained by the possible differences in the volatile profiles of honeys from year to year.

4.3. Classification/discrimination of the Corsican honeys using the two-year data

One possibility is to construct a model for samples of one year and then to use this model to predict the belongingness of samples collected in the next year of sampling. However, due to the large variation in the sample profiles between the years possibly caused by different meteorological conditions, such a model would either be no longer valid or with poor predictive ability and therefore, a model updating would be required. A more reliable approach is to model the data of a two-year sampling together, i.e. for each class the training set contains representative samples of both years. Again, the training set was selected randomly and LDA, DPLS, SIMCA and SVM models were constructed.

Table 5
Optimal settings of σ, w and C of SVM models built using the PUK function.

	σ	w	C
Corsica vs. non-Corsica			
2006	2	10	10
2007	1	1	10^2
Two-year sampling	5	16	10^3

The efficiency of LDA (85.2%) is lower than that observed for the first and second year of sampling (see Table 3). There were 21 honey samples, which were incorrectly classified, when the model was tested. From the analysis of these samples, it followed that 14 Corsican and 7 non-Corsican honeys were predicted incorrectly, which led to a reduced sensitivity of 86.4% and a specificity of 82.1% in comparison with the predictions obtained from the LDA models constructed for the data from separate years of sampling (see Table 4).

DPLS showed an improved predictive ability compared to the LDA model. With DPLS, 13 out of 103 Corsican samples were identified as non-Corsican resulting in a sensitivity of 87.4%. Because 6 out of 39 non-Corsican honeys were recognized as Corsican, the specificity of the model was 84.6%. It should be noted that DPLS had a complexity of five factors, while RMSCV and RMSEP were both equal to 0.64.

Although, with the six-component SIMCA model 93.2% of the Corsican samples were predicted well, 54.8% of the non-Corsican samples were incorrectly recognized (see Table 4). Again, the worse predictive ability was observed for the SIMCA model.

The classification model constructed by SVM presented the best efficiency of 91.5% among all the methods. A total of 12 test samples (7 Corsican and 5 non-Corsican) were wrongly predicted and consequently the SVM model yielded a sensitivity of 93.2% and a specificity of 87.2%.

5. Conclusions

The main conclusion of this study is that the volatile profiles of Corsican honeys are specific enough and allow for their discrimination from honeys of different geographical origins. In general, all models, except SIMCA, showed good efficiencies, high sensitivities and specificities for data of separate sampling years and for data of both years. Moreover, all the models presented higher sensitivities than specificities. This demonstrates that the probability of recognizing Corsican honeys as non-Corsican on the basis of their volatile profiles is small. LDA, DPLS and especially SVM using the PUK function can be successfully used to detect the mislabeling of honeys.

Moreover, this study also demonstrated the flexibility of SVM using the PUK function in building models with better predictive abilities than those obtained from LDA and DPLS for the problem studied. The reason might be that the peak intensities of the 26 volatile compounds are not completely linearly related to the geographical origin of the honey samples.

It should be noted here that there is another important issue, namely which particular volatile compounds are the most descriptive in the classification/discrimination of the honey samples according to their origin. However, this matter will be the subject of a future study.

Disclaimer

Acknowledgements

The authors are grateful for the financial support concerning scientific activities within the Sixth Framework Programme of the European Union, project TRACE – "Tracing food commodities in Europe" (Project No. FOOD-CT-2005-006942). The implementation of TOFMS technology was funded by the project MSM 6046137305 supported by the Ministry of Education, Youth and Sports of the Czech Republic.

References

Acquarone, C., Buera, P., & Elizalde, B. (2007). Pattern of pH and electrical conductivity upon honey dilution as a complementary tool for discriminating geographical origin of honeys. *Food Chemistry, 101*, 695–703.

Anklam, E. (1998). A review of the analytical methods to determine the geographical and botanical origin of honey. *Food Chemistry, 63*(4), 549–562.

Berrueta, L. A., Alonso-Salces, R. M., & Héberger, K. (2007). Supervised pattern recognition in food analysis. *Journal of Chromatography A, 1158*, 196–214.

Brereton, R. (2006). Consequences of sample size, variable selection, and model validation and optimization, for predicting classification ability from analytical data. *TrAC – Trends in Analytical Chemistry, 25*, 1103–1111.

Čajka, T., Hajšlová, J., Cochran, J., Holadová, K., & Klimánková, E. (2007). Solid phase microexctraction–comprehensive two-dimensional gas chromatography–time-of-flight mass spectrometry for the analysis of honey volatiles. *Journal of Separation Science, 30*, 534–546.

Corbella, E., & Cozzolino, D. (2006). Classification of the floral origin of Uruguayan honeys by chemical and physical characteristics combined with chemometrics. *LWT – Food Science and Technology, 39*, 534–539.

Daszykowski, M., Kaczmarek, K., Stanimirova, I., Vander Heyden, Y., & Walczak, B. (2007). Robust SIMCA-bounding influence of outliers. *Chemometrics and Intelligent Laboratory Systems, 87*, 95–103.

Devillers, J., Morlot, M., Pham-Delegue, M. H., & Dore, J. C. (2004). Classification of monofloral honeys based on their quality control data. *Food Chemistry, 86*, 305–312.

Fernández-Torres, R., Pérez-Bernal, J., Bello-López, M., Callejón-Mochón, M., Jiménez-Sánchez, J., & Guiraúm-Pérez, A. (2005). Mineral content and botanical origin of Spanish honeys. *Talanta, 65*, 686–691.

Fisher, R. A. (1936). The use of multiple measurements in taxonomic problems. *Annals of Eugenics, 7*, 179–188.

González, A. G. (2007). Use and misuse of supervised pattern recognition methods for interpreting compositional data. *Journal of Chromatography A, 1158*, 215–225.

Guyot, C., Scheirman, V., & Collin, S. (1999). Floral origin markers of heather honeys: *Calluna vulgaris* and *Erica arborea*. *Food Chemistry, 64*, 3–11.

Hernández, O. M., Fraga, J. M. G., Jiménez, A. I., Jiménez, F., & Arias, J. J. (2005). Characterization of honey from the Canary Islands: Determination of the mineral content by atomic absorption spectrophotometry. *Food Chemistry, 93*, 449–458.

Latorre, M. J., Peña, R., Pita, C., Botana, A., Garcia, S., & Herrero, C. (1999). Chemometric classification of honeys according to their type. II. Metal content data. *Food Chemistry, 66*, 263–268.

Lebart, L., Morineau, A., & Warwick, K. M. (1984). *Multivariate descriptive analysis. Correspondence analysis and related techniques for large matrices*. USA: Wiley.

Marini, F., Magrì, A. L., Balestieri, F., Fabretti, F., & Marini, D. (2004). Supervised pattern recognition applied to the discrimination of the floral origin of six types of Italian honey samples. *Analytica Chimica Acta, 515*, 117–125.

Melssen, W. J., Üstün, B., & Buydens, L. M. C. (2006). SOMPLS: A supervised self-organising map partial least squares algorithm for multivariate regression problems. *Chemometrics and Intelligent Laboratory Systems, 86*, 299–309.

Næs, T., Isaksson, T., Fearn, T., & Davies, T. (2002). *A user-friendly guide to multivariate calibration and classification*. Chichester: NIR Publications.

Radovic, B. S., Careri, M., Mangia, A., Musci, M., Gerboles, M., & Anklam, E. (2001). Contribution of dynamic headspace GC–MS analysis of aroma compounds to authenticity testing of honey. *Food Chemistry, 72*, 511–520.

Schölkopf, B., & Smola, A. J. (2002). *Learning with kernels*. Cambridge: MIT press.

Soria, A. C., González, M., de Lorenzo, C., Martínez-Castro, I., & Sanz, J. (2004). Characterization of artisanal honeys from Madrid (Central Spain) on the basis of their melissopaynological, physicochemical and volatile data. *Food Chemistry, 85*, 121–130.

Üstün, B., Melssen, W. J., & Buydens, L. M. C. (2006). Facilitating the application of support vector regression by using a universal Pearson VII function based kernel. *Chemometrics and Intelligent Laboratory Systems, 81*, 29–40.

Vandeginste, B. M. G., Massart, D. L., Buydens, L. M. C., de Jong, S., Lewi, P. J., & Smeyers-Verbeke, J. (1998). *Handbook of chemometrics and qualimetrics*. Part B. Amsterdam: Elsevier.

Vapnik, V. (1995). *The nature of statistical learning theory*. New York: Springer.

Wold, S. (1976). Pattern recognition by means of disjoint principal components models. *Pattern Recognition, 8*, 127–139.

Wu, W., Mallet, Y., Walczak, B., Penninckx, W., Massart, D. L., Heuerding, S., et al. (1996). Comparison of regularized discriminant analysis, linear discriminant analysis and quadratic discriminant analysis applied to NIR data. *Analytica Chimica Acta, 329*, 257–265.

Food Chemistry 118 (2010) 177–181

Contents lists available at ScienceDirect

Food Chemistry

journal homepage: www.elsevier.com/locate/foodchem

Analytical Methods

A novel approach to authenticity control of whole grain durum wheat (*Triticum durum* Desf.) flour and pasta, based on analysis of alkylresorcinol composition

Matthias Knödler *, Maike Most, Andreas Schieber [1], Reinhold Carle

Institute of Food Science and Biotechnology, Chair Plant Foodstuff Technology, Garbenstrasse 25, Hohenheim University, Stuttgart, Germany

ARTICLE INFO

Article history:
Received 28 November 2008
Received in revised form 22 March 2009
Accepted 21 April 2009

Keywords:
Alkylresorcinols
Triticum durum Desf.
T. aestivum L.
Homologue composition
Whole grain pasta
Adulteration

ABSTRACT

Since durum wheat is ~20% more expensive than common wheat and considered of superior quality for the manufacture of pasta products, efficient methods for the detection of accidental or intentional admixtures of common wheat to durum wheat products are required. This paper describes a novel approach for the detection and quantification of whole grain common wheat adulteration in whole grain durum flour and dried pasta. We found that differences in the C17:0 to C21:0 alkylresorcinol homologue ratios between the two cereal species may serve as a suitable tool for whole grain durum product authentification. To detect and estimate adulteration, the C17:0/C21:0 ratios of flour and pasta admixtures with added whole grain flour of common wheat were analysed. A linear relationship between C17:0/C21:0 ratios and level of admixture in pasta samples showed that adulteration can be estimated within the range of 5–100% of admixture. Furthermore, di- and triunsaturated as well as oxygenated alk(en)ylresorcinols are reported to occur in *Triticum durum* Desf. for the first time.

1. Introduction

Traditionally, pasta is manufactured solely from durum wheat (*Triticum durum* Desf.), which results in a product considered to be of superior quality to pasta made from cheaper common wheat (*T. aestivum* L.) or a blend of the two species. Nevertheless, price differentials between both wheat species could provide some manufactures with the incentive to benefit economically by the undeclared addition of common wheat. The manufacture of pastas from mixtures of durum and common wheat without adequate labelling is usually considered as adulteration. National laws in Italy, France and Greece prohibit the inclusion of common wheat to pasta for sale in their countries, but not for subsequent export (Food Surveillance Paper No. 47, 1994). Durum wheat pasta for export outside the European Union may contain a maximum of 3% common wheat from unavoidable adventitious contamination during agricultural processing (EG Commission Regulation, Official Journal of the European Community, 1994; International Standard, ISO 11051: 1994 (E)).

Since pasta products purporting to be prepared solely from durum wheat are increasingly introduced in the market place, methods are consequently required that can be applied to these products to check the validity of such claims, if food legislation is to be enforced. The detection of the presence of *T. aestivum* in *T. durum* semolina and pasta can be addressed by a number of analytical methods, most of which rely upon detection of certain proteins expressed by the D-genome present in hexaploid wheat but absent from *T. durum* (Food Surveillance Paper No. 47, 1994). Electrophoretic methods are used, whereby D-genome encoded proteins like gliadins (Bonetti et al., 2004; Burgoon, Ikeda, & Tanner, 1985) or specific polyphenoloxidases (Feillet & Kobrehel, 1974) are separated and detected by gel electrophoresis. McCarthy, Scanlon, Lumley, and Griffin (1990) reported the use of RP-HPLC for the detection of common wheat flour in durum wheat flour/semolina, based on the separation and detection of specific gliadins, and the method has been extended for application to pasta products (Barnwell, McCarthy, Lumley, & Griffin, 1994). Specific D-genome encoded proteins have also been detected by free zone capillary electrophoresis (FZCE); however the method was only applied for blends of durum wheat and common wheat flour and has not been validated for quantitative analysis so far (Bonetti et al., 2004). Other techniques involve the separation and quantification of sterol palmitates by TLC (Gilles & Youngs, 1964) and HPLC (Sarwar & McDonald, 1993) or the detection of a specific DNA sequence amplified in the D-genome of common wheat by PCR (Bryan,

* Corresponding author. Present address: Wala Heilmittel GmbH, Bad Boll, Germany. Tel.: +49 711 45922995; fax: +49 711 45924110.
E-mail address: matthias-knoedler@gmx.de (M. Knödler).
[1] Present Address: Canada Research Chair in Functional Foods and Nutraceuticals, University of Alberta, Department of Agricultural, Food and Nutritional Science, Edmonton, Alberta, Canada.

0308-8146/$ - see front matter © 2009 Elsevier Ltd. All rights reserved.
doi:10.1016/j.foodchem.2009.04.080

Dixon, Gale, & Wiseman, 1998; Pasqualone, Montemurro, Griffin-Gofron, Sonnate, & Blanco, 2007).

However, environmental growing conditions and genetic variation between wheat cultivars may affect the expression of proteins used as markers of contamination (Food Surveillance Paper No. 47, 1994) or adversely influence sterol palmitates content used for verification of semolina and pasta authenticity (Sarwar & McDonald, 1993). The principal limitation of most of the methods involving protein extraction is the effect of denaturation, resulting from the widespread introduction of high-temperature drying processes (>70 °C), to accelerate drying of the product during pasta manufacture (Aktan & Khan, 1992).

In contrast, alkylresorcinols (Fig. 1) used as marker compounds in this study, have been shown to be thermostable during pasta manufacturing (Landberg, Kamal-Eldin, Andresson, & Åman, 2006) and even baking processes (Ross et al., 2003), thus meeting a fundamental criterion for authenticity control of dried pasta products. Alkylresorcinols (1,3-dihydroxy-5-alkylbenzene derivatives) are phenolic lipids present in a number of plants and bacteria. Of plants commonly used for food, apart from mango (Knödler, Kaiser, Carle, & Schieber, 2008), alkylresorcinols are present in high amounts in common wheat, durum wheat and rye kernels (~0.03–0.15% of dry kernel weight; Landberg et al., 2006; Ross et al., 2003). The odd-numbered alkyl side-chain of alkylresorcinols isolated from cereal grains varies from 13 to 27 carbon atoms (Knödler et al., 2008; Kozubek & Tyman, 1999). Recently, the ratio of the homologues C17:0 to C21:0 was found to be ~0.01 in whole grain durum wheat and products prepared thereof (Landberg et al., 2006), thus differing from that of common wheat which displays a C17:0/C21:0 ratio of ~0.1 (Andersson, Kamal-Eldin, Fras, Boros, & Åman, 2008; Chen, Ross, Åman, & Kamal-Eldin, 2004). Thus, the ratio of C17:0 to C21:0 can be used to distinguish between these cereals. Interestingly, 99% of alkylresorcinols are found in the hyaline layer, inner pericarp and testa of cereal grains (Landberg, Kamal-Eldin, Salmenkallio-Marttila, Rouau, & Åman, 2008), limiting the marker compounds for authentification of whole grain durum flour and pasta. However, with the whole grain trend in many countries, the consumption of pasta from whole grain durum wheat is rapidly increasing and, thus, demanding the development of methods valid for whole grain durum products. The following investigation reports the detection and estimation of whole grain common wheat flour adulteration in whole grain durum wheat flour and pasta, based on the analysis of the C17/C21 alkylresorcinols ratios.

2. Experimental

2.1. Cereals and pasta products

Ten samples of winter and spring durum wheat kernels (cv. Floradur, Prowidur, Durobonus, Topdur, Helidur, Ambrodur, Extradur and Rosadur) and ten samples of winter and spring soft wheat kernels (cv. Saturnus, Toronit, Capo, AC Vista and Cltr 17272) harvested in the years 2006 and 2007, respectively, were obtained from the Institute of Crop Cultivation and Plant Breeding at the University of Natural Resources and Applied Life Sciences in Vienna. Soft wheat kernels of the cultivars Tommi 220, Manhattan and Wasmo were cultivated at Ihinger Hof, Germany, an experimental station of Hohenheim University, in 2004.

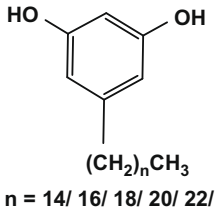

Fig. 1. Structures of 5-*n*-alkylresorcinols present in *Triticum durum* Desf. and *T. aestivum* L.

For the preparation of defined blends of whole grain flour and pasta, the durum wheat cultivar Rosadur and the common wheat cultivar Tommi 220 were used. Approximately 3 kg of durum and common wheat, respectively, were milled using an Ultra Centrifugal Mill ZM 200 (Retsch GmbH & Co. KG, Haan, Germany). Whole grain durum flours were blended with 0%, 20%, 40%, 60%, 80% and 100% common wheat flours).

Blended whole grain pasta samples with soft admixtures of 5%, 10%, 20%, 40%, 60%, 80% and 100%, respectively, were prepared with a Marcato pasta machine, (Marcato S.p.A., Padova, Italy). The pasta samples were dried at 90 °C to moisture content below 13%. Dry matter (DM) was determined using an infrared moisture-analyser (Sartorius AG, Göttingen, Germany).

2.2. Solvents and reagents

All reagents and solvents used were purchased from VWR (Darmstadt, Germany) and were of analytical or HPLC grade. Synthetic alkylresorcinols (5-pentadecylresorcinol, C15:0; 5-heptadecylresorcinol, C17:0; 5-nonadecylresorcinol, C19:0; 5-heneicosylresorcinol, C21:0; 5-tricosylresorcinol, C23:0; 5-pentacosylresorcinol, C25:0) were obtained from ReseaChem (Burgdorf, Switzerland).

2.3. Sample preparation

Cereal and pasta samples were ground using a water-cooled Yellow Line A10 laboratory mill (Ika-Werke, Staufen, Germany) and stored in vacuum-sealed polyethylene pouches at −20 °C until used for extraction. Ground samples (3 g) were extracted by continuous stirring with 50 ml ethyl acetate for 2 h under nitrogen atmosphere. Exhaustive extraction was ensured by extraction of the residue with 50 ml ethyl acetate for 1 h. After filtration through a paper filter, the extracts were evaporated to dryness *in vacuo* at 30 °C and the residue dissolved in 0.5 ml methanol. The solution was membrane filtered (0.45 μm, Whatman, Clifton, NJ) and used for HPLC–DAD and LC–MS/MS analysis.

2.4. HPLC and LC–MS/MS

Alkylresorcinol (AR) analyses were performed using an Agilent HPLC series 1100 (Agilent, Waldbronn, Germany) equipped with ChemStation software, a model G1322A degasser, a model G1312A binary pump, a model G1313A autosampler, a model G1316A column oven, and a model G1315A diode array detection system. The column used was a 150 × 3.0 mm i.d., 3 μm particle size, analytical scale Phenomenex C18 Aqua (Torrance, CA), with a C18 ODS guard column (4.0 × 2.0 mm, i.d.), operated at 25 °C. The mobile phase consisted of 100% methanol (eluent **A**) and 100% water (eluent **B**), and the following gradient programme was used: 11% **B**–0% **B** (38 min), 0% **B** isocratic (5.5 min), 0% **B**–11% **B** (3.5 min). Total run time was 50 min. The injection volume was 10 μl for cereal samples and 50 μl for blends of flour and pasta. All AR were monitored at 275 nm at a flow rate of 0.6 ml/min. Additionally, UV/Vis spectra were recorded in the range of 200–600 nm at a spectral acquisition rate of 1.25 scans/s (peak width 0.2 min).

LC–MS/MS analyses were performed with the HPLC system described above coupled to a model Esquire 3000+ ion trap mass spectrometer fitted with an APCI source (Bruker, Bremen, Germany). Data acquisition and processing were performed using

Esquire Control software. Positive ion mass spectra of the column eluate were recorded in the range of *m/z* 50–500 at a scan speed of 13,000 mass units/s (peak width 0.6 mass units, FWHM). Mass spectrometric conditions have been reported in detail in a recently published study (Knödler et al., 2008).

Individual compounds were identified by their retention times and UV and mass spectra (Knödler et al., 2008) and quantified using a calibration curve of the corresponding standard compound (Knödler, Reisenhauer, Schieber, & Carle, 2009).

3. Results and discussion

3.1. Differences in alkylresorcinols content and homologue composition of durum and soft wheat

In this novel approach to authenticity control of whole grain durum wheat flour and pasta prepared thereof, we have evaluated the detection and estimation of adulteration of whole grain durum wheat flour and pasta by flour of whole grain soft wheat using differences in the alkylresorcinol homologue composition between the two cereal species. While species-specific resorcinolic compounds could not be observed, we found that differences in the C17:0 to C21:0 homologue ratio between the hexaploid common wheat and durum wheat may serve as a suitable tool for the authentification of durum wheat products.

The HPLC pattern of alk(en)ylresorcinols with chain lengths varying from 15 to 25 carbons of durum and soft wheat extracts is illustrated in Fig. 2. Since their characterisation has recently reported in detail (Knödler et al., 2008), UV and mass spectrometric data are not given in the present communication. The use of tandem mass spectrometry in addition to diode array detection enabled the identification of up to 22 saturated, mono-, di- and triunsaturated and oxygenated alk(en)ylresorcinols, the latter three have so far not yet been reported in *T. durum* Desf.

While a number of qualitative and quantitative data on alkylresorcinols in common wheat are available (Andersson et al., 2008; Kozubek & Tyman, 1999; Kulawinek, Jaromin, Kozubek, & Zarnowski, 2008; Ross et al., 2003), only very few studies have reported on durum wheat (Andersson et al., 2008; Landberg et al., 2006; Sagi, Sagi, & Acs, 1983; Sagi-Lomnicizi & Sagi, 1982; Zarnowski, Suzuki, & Pietr, 2004). Total alkylresorcinol contents and homologue composition of saturated homologues of 10 durum wheat and 15 soft wheat samples are summarised in Table 1. Generally, soft wheat cultivars possessed higher total alkylresorcinol contents, ranging from 591 to 1077 mg/kg DM, compared to durum wheat cultivars, with contents of 430 to 797 mg/kg DM. Considerable differences in total alkylresorcinol contents were observed within some cultivars harvested within two consecutive vegetative years (e.g., cv. Prowidur and Saturnus harvested in 2006 and 2007), highlighting the advantage of using ratios of certain homologues, thus providing a tool for species authentification, irrespective of alkylresorcinol content, and hence, not being affected by varietal differences and environmental growing conditions. Total alkylresorcinol contents of soft and durum wheat varieties were exceptionally high, compared to those reported by other authors (Andersson et al., 2008; Landberg et al., 2006; Ross et al., 2003; Zarnowski et al., 2004), which may be explained by cultivar differences and by different methods of analysis. In accordance with previous findings (Landberg et al., 2006), the alkylresorcinol homologue composition in durum wheat was found to be completely different to that of common wheat, by having a higher proportion of the longer chained homologues, but was highly consistent within a given species (Table 1). The C17:0/C21:0 ratio, used as a marker to distinguish between durum and soft wheat in this study, was determined as ~0.01 for the durum wheats, which is different from that of common wheat cultivars displaying a C17:0/C21:0 ratio of ~0.1 (Table 1, Fig. 2, peaks highlighted in grey), which is consistent with previous investigations on durum (Andersson et al., 2008;

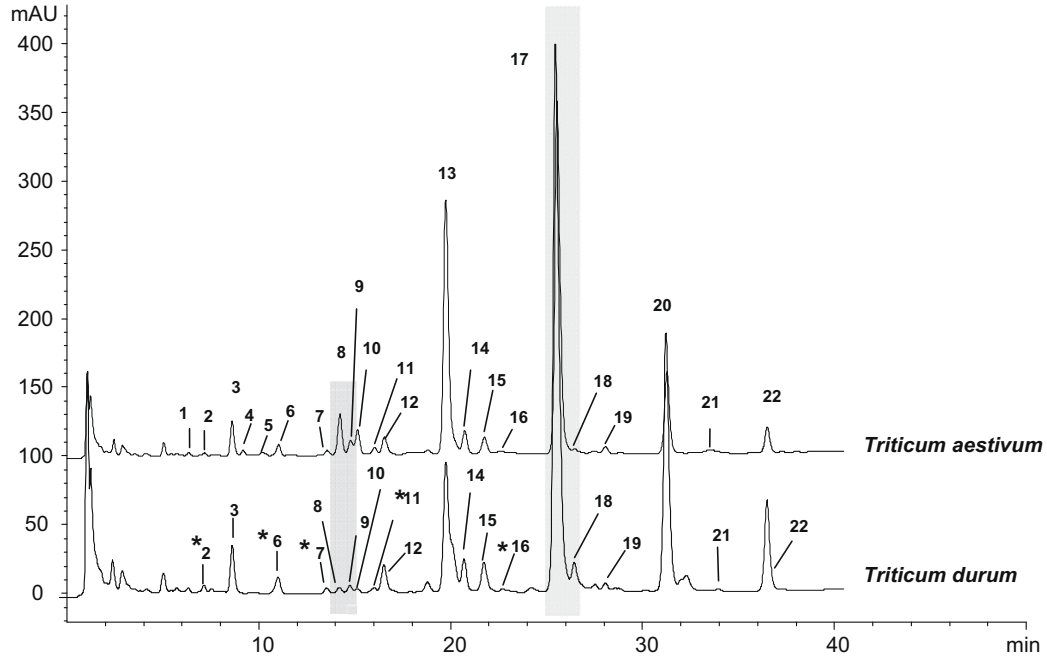

Fig. 2. HPLC separation (275 nm) of alk(en)ylresorcinols in common wheat (cv. Tommi 220) and durum wheat (cv. Rosadur) extracts. Peak assignments: **1**, heptadecadienylresorcinol (C17:2); **2**, nonadecatrienylresorcinol (C19:3); **3**, pentadecylresorcinol (C15:0); **4**, heptadecenylresorcinol (C17:1); **5**, hydroxynonadecenylresorcinol (C19:1-OH); **6**, nonadecadienylresorcinol (C19:2); **7**, heneicosatrienylresorcinol (C21:3); **8**, heptadecylresorcinol (C19:0); **9**, nonadecenylresorcinol (C19:1); **10**, nonadecenylresorcinol (C19:1); **11**, hydroxyheneicosenylresorcinol (C21:1-OH); **12**, heneicosadienylresorcinol (C21:2); **13**, nonadecylresorcinol (C19:0); **14**, heneicosenylresorcinol (C21:1); **15**, heneicosenylresorcinol (C21:1); **16**, hydroxytricosenylresorcinol (C23:1-OH); **17**, heneicosylresorcinol (C21:0); **18**, tricosenylresorcinol (C23:1); **19**, tricosenylresorcinol (C23:1); **20**, tricosylresorcinol (C23:0); **21**, pentacosenylresorcinol (C25:1); **22**, pentacosylresorcinol (C25:0). Novel compounds for durum wheat are marked with an asterisk (*).

Table 1
Total alkylresorcinol (AR) content, relative homologue composition and C17/C21 ratios in durum and common wheat cultivars.

	Cultivar	Total AR (mg/kg DM)	Homologue composition (%)						Ratio C17:0/C21:0
			C15:0	C17:0	C19:0	C21:0	C23:0	C25:0	
Triticum durum Desf.	Floradur^{S,07}	430 ± 6.6	tr.[a]	tr.	11.7	53.4	24.9	10.0	–
	Floradur^{S,06}	504 ± 18.9	tr.	0.5	10.9	54.3	24.5	9.8	0.01
	Prowidur^{W,07}	554 ± 29.4	tr.	0.8	14.2	58.4	20.3	6.3	0.01
	Prowidur^{W,06}	675 ± 20.6	tr.	0.7	13.9	60.2	19.3	5.9	0.01
	Durobonus^{S,07}	698 ± 5.4	tr.	0.6	15.1	51.0	23.2	10.1	0.01
	Topdur^{S,07}	673 ± 8.8	tr.	0.8	10.9	51.0	24.6	12.7	0.02
	Helidur^{S,07}	577 ± 20.3	tr.	0.9	10.2	52.0	25.1	11.8	0.02
	Ambrodur^{S,07}	696 ± 7.6	tr.	1.0	10.6	52.5	24.4	11.5	0.02
	Extradur^{S,07}	690 ± 8.2	tr.	1.0	11.9	51.6	24.1	11.4	0.02
	Rosadur^{S,06}	797 ± 70.3	tr.	0.5	14.6	50.3	23.8	10.8	0.01
T. aestivum L.	Saturnus^{W,07}	882 ± 51.6	tr.	4.5	31.2	49.4	10.6	4.3	0.09
	Saturnus^{W,06}	726 ± 16.8	tr.	4.7	32.5	48.0	10.6	4.2	0.1
	Toronit^{S,07}	862 ± 19.4	tr.	4.1	30.0	48.8	11.8	5.4	0.08
	Toronit^{S,06}	802 ± 8.6	tr.	5.0	34.7	47.9	9.3	3.1	0.1
	Capo^{W,07}	885 ± 18.0	tr.	4.7	31.4	49.8	10.3	3.8	0.1
	Capo^{W,06}	787 ± 13.5	tr.	4.8	32.3	48.6	10.6	3.7	0.1
	AC Vista^{S,06}	663 ± 38.1	tr.	3.9	27.1	50.6	12.3	6.1	0.08
	Cltr17272^{S,06}	809 ± 16.6	tr.	4.7	32.4	44.9	11.6	6.4	0.1
	Tommi 220^{W,04}	725 ± 35.6	0.7	5.2	30.3	51.1	9.6	3.1	0.1
	Wasmo^{W,04}	1077 ± 27.5	0.7	4.5	25.9	48.1	17.4	3.4	0.09
	Manhattan^{W,04}	591 ± 29.7	0.9	4.6	32.3	46.1	12.4	3.7	0.1

^{S}Spring wheat; ^{W}winter wheat; ^{07,06,04}harvested in 2007, 2006 and 2004, respectively.
[a] Trace.

Landberg et al., 2006) and soft wheat (Andersson et al., 2008; Chen et al., 2004), respectively. These authors analysed a number of cultivars grown in different countries and environmental growing conditions. Whereas the total content of alkylresorcinols varied between cultivars grown under different conditions, the profile and thus, the C17:0/C21:0 ratios, were found to be highly characteristic for durum and common wheat.

Striking differences with respect to species differentiation were also observed for the C19:0 and the C23:0 homologues, showing levels of 10–15% and 19–25%, respectively, in durum wheat and from 26% to 36% and 9% to 17%, respectively, in common wheat, which may serve as an additional tool for species authentification. However, compared to these homologue ratios, the C17:0/C21:0 ratios were found to be the most constant ones and, thus, most suitable for species differentiation.

3.2. Detection and quantification of whole grain soft wheat admixture to flour of whole grain durum wheat

Defined blends of whole grain durum wheat (cv. Rosadur) and whole grain soft wheat (cv. Tommi 220) flour, containing 0%, 20%, 40%, 60%, 80% and 100% durum and soft wheat, respectively, were analysed for their C17:0/C21:0 homologue ratios. Fig. 3 shows the plot of the calculated ratios, in relation to common wheat adulteration in the flour mixtures. It was found that the C17:0/C21:0 ratios increased linearly (R^2 = 0.986) with the level of common wheat admixture. The linear equation even permits quantitative estimation of common wheat proportions in the blended flours. Since this study mainly focused on the detection and quantification of common wheat adulteration in pasta samples, control samples containing <20% common wheat were not prepared for the flour mixtures. However, it was demonstrated that common wheat adulteration in whole grain durum flour can be detected easily by analysing the C17:0/C21:0 homologue ratios. For example, a C17:0/C21:0 ratio of >0.01 analysed for a suspect sample may generally indicate adulteration, if the durum wheat cultivars are known. For unknown durum wheat cultivars the significance may be of diminished value, considering varietal differences in the C17:0/C21:0 ratio within durum wheat (from 0.01 to 0.02) and soft wheat (from 0.08 to 0.1) cultivars. However, even when taking into account varietal differences within the species, a quantitative estimate of adulteration in a suspect sample is still feasible. Therefore, the proposed method for authentification may provide a powerful tool for inspection of incoming components at whole grain pasta manufacturers.

3.3. Detection and quantification of whole grain soft wheat admixture to whole grain durum wheat pasta

Alkylresorcinols are believed to form inclusion complexes with starch during thermal treatment, thus hindering quantitative recovery by conventional ethyl acetate extraction, while time-consuming extraction with hot water/1-propanol (1/3) was reported to allow their quantitative recovery (Ross et al., 2003). However,

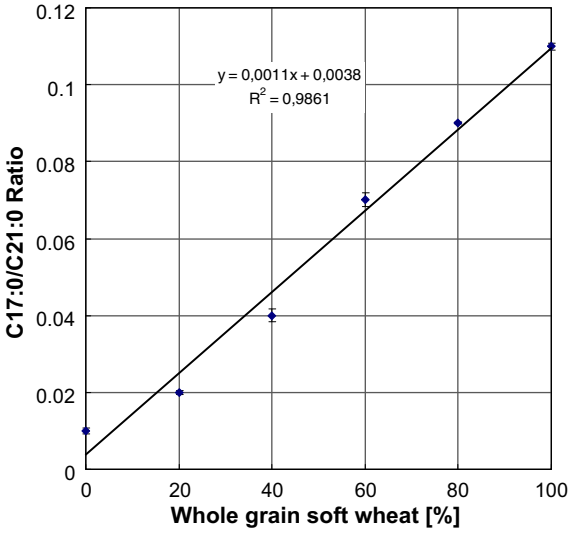

Fig. 3. Ratios of the homologues C17:0 to C21:0 determined in mixtures of whole grain durum wheat (cv. Rosadur) flour with 0%, 20%, 40%, 60%, 80% and 100% whole grain soft wheat (cv. Tommi 220) flour, respectively. In the graph, the linear equation and the coefficient of determination (R^2) of the standard curve is reported. Data points are means from two independent experiments, and bars represent SD where larger than symbol size.

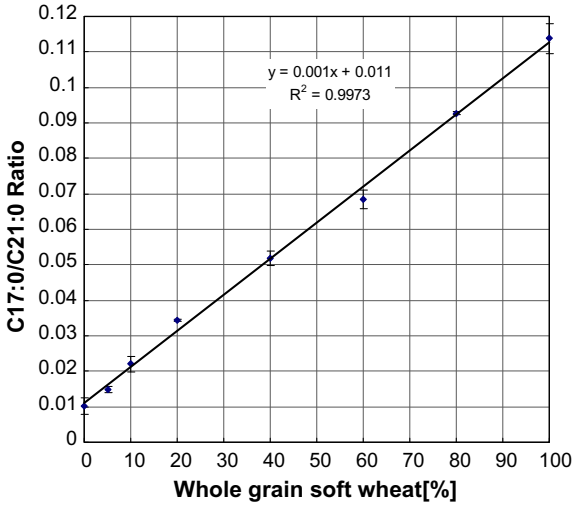

Fig. 4. Ratios of the homologues C17:0 to C21:0 determined in whole grain durum wheat (cv. Rosadur) pasta adulterated with 0%, 5%, 10%, 20%, 40%, 60%, 80% and 100% soft wheat (cv. Tommi 220), respectively. In the graph, the linear equation and the coefficient of determination (R^2) of the standard curve is reported. Data points are means from two independent experiments, and bars represent SD where larger than symbol size.

we observed that analysed homologue composition and hence C17:0/C21:0 ratio remained unchanged when comparing both extraction procedures (data not shown). Therefore, albeit not permitting quantitative recovery, pasta samples were extracted with ethyl acetate.

The effect of whole grain common wheat (cv. Tommi 220) adulteration of dried whole grain durum wheat (cv. Rosadur) pasta is illustrated in Fig. 4. The C17:0/C21:0 homologue ratios analysed for the control adulterated pasta samples containing 0%, 5%, 10%, 20%, 40%, 60%, 80% and 100% of soft wheat, respectively, increased with the level of admixture. A linear relationship between the C17:0/C21:0 ratios and adulteration level (R^2 = 0.997) provided a standard curve. As evident from Fig. 4, with the proposed method, adulteration may be estimated in the range of 5–100% by using linear regression analysis and thus approaching even small but economically most likely adulteration levels. Furthermore it could be shown that even high drying temperatures used in this study did not affect the applicability of alkylresorcinols as authentification markers, which was found to be the major disadvantage for methods involving proteinogenic markers (Surveillance Paper No. 47, 1994).

However, information on cultivar is often not obtained and commercial whole grain wheat flours often constitute blends of several cultivars and thus, the varietal differences in the ratios of the homologues C17:0/C21:0 within a species (Table 1) have to be considered when calculating adulteration levels using standard curves valid for a given cultivar.

With this study a novel approach to authenticity control of whole grain pasta, purporting to be made solely from durum wheat, was performed. It is expected that the present method can be further extended to the authentification of non-whole grain durum wheat products. Therefore, a method for the quantification of even very low alkylresorcinol contents in refined cereal products by MS/MS is currently being developed in our laboratory.

Acknowledgments

The authors express their gratitude to Mrs. Elke Rummel and Mr. Klaus Mix for their valuable technical assistance. Prof. Dr. Heinrich Grausgruber, University of Natural Resources and Applied Life Sciences, Vienna, Austria is gratefully acknowledged for providing the cereal samples.

References

Aktan, B., & Khan, K. (1992). Effect of high-temperature drying of pasta on quality parameters and on solubility, gel electrophoresis, and reversed phase high-performance liquid chromatography of protein components. *Cereal Chemistry, 69*, 288–295.

Andersson, A. A. M., Kamal-Eldin, A., Fras, A., Boros, D., & Åman, P. (2008). Alkylresorcinol in wheat varieties in the healthgrain diversity screen. *Journal of Agricultural and Food Chemistry, 56*, 9722–9725.

Barnwell, P., McCarthy, P. K., Lumley, I. D., & Griffin, M. (1994). The use of reversed-phase high-performance liquid chromatography to detect common wheat (*Triticum aestivum*) adulteration of durum wheat (*Triticum durum*) pasta products dried at low and high temperatures. *Journal of Cereal Science, 20*, 245–252.

Bonetti, A., Marotti, I., Catizone, P., Dinelli, G., Majetti, A., Tedeschi, P., et al. (2004). Compared use of HPLC and FZCE for cluster analysis of *Triticum* spp and for the identification of *T. durum* adulteration. *Journal of Agricultural and Food Chemistry, 52*, 4080–4089.

Bryan, G. J., Dixon, A., Gale, M. D., & Wiseman, G. (1998). A PCR-based method fort he detection of hexaploid bread wheat adulteration of durum wheat and pasta. *Journal of Cereal Science, 28*, 135–145.

Burgoon, A. C., Ikeda, H. S., & Tanner, S. N. (1985). A method for detecting adulteration in durum wheat pasta by polyacrylamide gel electrophoresis. *Cereal Chemistry, 62*, 72–74.

Chen, Y., Ross, A. B., Åman, P., & Kamal-Eldin, A. (2004). Alkylresorcinols as markers of whole grain wheat and rye in cereal products. *Journal of Agricultural and Food Chemistry, 52*, 8242–8246.

EG Commission Regulation (1994). *Official Journal of the European Community*, 1222/94 (Annex C) L136, p. 5.

Feillet, P., & Kobrehel, K. (1974). Determination of common wheat content in pasta. *Cereal Chemistry, 51*, 203–209.

Gilles, A., & Youngs, V. L. (1964). Evaluation of durum wheat and durum products. Separation and identification of the sitosterol esters of semolina. *Cereal Chemistry, 41*, 502–513.

International Standard (ISO 11051: 1994 (E)).

Knödler, M., Reisenhauer, K., Schieber, A., & Carle, R. (2009). Quantitative determination of allergenic 5-alk(en)ylresorcinols in mango (*Mangifera indica* L.) peels, pulp and fruit products by high-performance liquid chromatography. *Journal of Agricultural and Food Chemistry, 57*, 3639–3644.

Knödler, M., Kaiser, A., Carle, R., & Schieber, A. (2008). Profiling of alk(en)ylresorcinols in cereals by HPLC–DAD–APcI–MS^n. *Analytical Bioanalytical Chemistry, 391*, 221–228.

Kozubek, A., & Tyman, J. H. P. (1999). Resorcinolic lipids, the natural non-isoprenoid phenolic amphiphiles and their biological activity. *Chemical Reviews, 99*, 1–25.

Kulawinek, M., Jaromin, A., Kozubek, A., & Zarnowski, R. (2008). Alkylresorcinols in selected polish rye and wheat cereals and whole-grain cereal products. *Journal of Agricultural and Food Chemistry, 56*, 7236–7242.

Landberg, R., Kamal-Eldin, A., Andresson, R., & Åman, P. (2006). Alkylresorcinol content and homologue composition in durum wheat (*Triticum aestivum*) kernels and pasta products. *Journal of Agricultural and Food Chemistry, 54*, 3012–3014.

Landberg, R., Kamal-Eldin, A., Salmenkallio-Marttila, M., Rouau, X., & Åman, P. (2008). Localization of alkylresorcinols in wheat, rye and barley kernels. *Journal of Cereal Science, 48*, 401–406.

McCarthy, P. K., Scanlon, B. F., Lumley, I. D., & Griffin, M. (1990). Detection and quantification of adulteration of durum wheat flour by flour from common wheat using reverse phase HPLC. *Journal of the Science of Food and Agriculture, 50*, 211–226.

Pasqualone, A., Montemurro, C., Griffin-Gofron, A., Sonnate, G., & Blanco, A. (2007). Detection of soft wheat in semolina and durum wheat bread by analysis of DNA microsatellites. *Journal of Agricultural and Food Chemistry, 55*, 3312–3318.

Ross, A. B., Shepard, M. J., Schupphaus, M., Sinclair, V., Alfaro, B., Kamal-Eldin, A., et al. (2003). Alkylresorcinol in cereals and cereal products. *Journal of Agricultural and Food Chemistry, 51*, 4111–4118.

Sagi, F., Sagi, H., & Acs, E. (1983). Alkylresorcinols in durum wheat. Alkylresorcinol content of milling fractions and macaroni. *Acta Alimentaria Hungaria, 12*, 143–148.

Sagi-Lomnicizi, H., & Sagi, F. (1982). Alkylresorcinols in durum wheat. Varietal and kernel quality effects. *Acta Alimentaria Hungaria, 11*, 39–45.

Sarwar, M., & McDonald, C. E. (1993). Detection of bread wheat farina adulterant in durum wheat semolina and pasta dried at low, high, and ultra-high temperatures. *Cereal Chemistry, 70*, 405–411.

Surveillance Paper No. 47 (1995). *Dried durum wheat pasta*, HMSO.

Zarnowski, R., Suzuki, Y., & Pietr, S. J. (2004). Alkyl- and alkenylresorcinols of wheat grains and their chemotaxonomic significance. *Zeitschrift für Naturforschung, 59*, 190–196.

Food Chemistry 118 (2010) 182–189

Contents lists available at ScienceDirect

Food Chemistry

journal homepage: www.elsevier.com/locate/foodchem

Analytical Methods

Characterisation by SPME–GC–MS of the volatile profile of a Spanish soft cheese P.D.O. Torta del Casar during ripening

Francisco José Delgado [a], José González-Crespo [a], Ramón Cava [b], Jesús García-Parra [a], Rosario Ramírez [a,*]

[a] Instituto Tecnológico Agroalimentario de Extremadura (INTAEX) (Technological Institute of Food and Agriculture), Badajoz, Spain
[b] Departamento Tecnología de los Alimentos, Facultad Veterinaria, Universidad Extremadura, Cáceres, Spain

ARTICLE INFO

Article history:
Received 19 September 2008
Received in revised form 14 April 2009
Accepted 23 April 2009

Keywords:
Raw milk
Ripening
Vegetable rennet
Ewe
SPME
Volatile
Cheese

ABSTRACT

The volatile profile of the Spanish soft cheese of the Protected Designation of Origin (PDO) Torta del Casar, made from raw ewes' milk, was studied in four different stages of ripening (1, 30, 60 and 90 days) by the method of SPME–GC–MS. A total of 46 compounds were detected: 13 acids, 9 esters, 4 ketones, 7 alcohols, 3 aldehydes, 7 aromatic compounds and 3 compounds which could not be classified into those groups. Carboxylic acids were the most abundant group isolated; their levels significantly increased during ripening and comprised 61.5% of the total aroma extract at the end of ripening. At day 90, acids of microbial origin were the most abundant, followed by acids derived from amino acids while acids from lipolysis of triglycerides were the least abundant. Esters were the next most important group and their amount also increased significantly during maturation, as did ketones, while alcohols content slightly decreased at the end of the ripening. At day 90, the compounds at highest levels were acetic acid, 3-methylbutanoic acid, butanoic acid propyl ester and 2-butan-one; so these compounds, due to their high levels and their low threshold value could play an important role in the final aromatic profile of this cheese.

1. Introduction

Cheese flavour is one of the most important criteria determining consumer choice and acceptance. It is generally accepted that the volatile profile reflects the image of the odour and aroma of cheeses. So, the unique flavour of a cheese variety is the result of a complex balance among volatile and non-volatile chemical compounds, originating during the ripening process from milk fat, protein and carbohydrates (Fox & Wallace, 1997); as a consequence, each product has a characteristic and unique composition of volatile components (Plutowska & Wardencki, 2007). It is well-known that most cheese aroma volatile compounds are formed during ripening. The principal pathways for the formation of flavour compounds in cheese are metabolism of lactose and lactate, lipolysis and proteolysis. In the first pathway, depending on variety, microflora and ripening conditions, lactate may be metabolised by a number of pathways to various compounds which contribute to cheese flavour. The second pathway generates fat-derived compounds formed by lipolysis and lipid oxidation reactions, such as free fatty acids, esters, lactones and ketones, with low aroma thresholds (Kinsella, 1975; Siek, Albin, Sather, & Lindsay, 1971). Finally, proteolysis of caseins provides a range of small- and intermediate-sized peptides and free amino acids, which probably only contribute to the background flavour of most cheese varieties. However, free amino acids are important precursors for a range of poorly-understood catabolic reactions, which produce volatile compounds essential for flavour (McSweeney & Sousa, 2000).

Volatile compounds are generally analysed by gas chromatography (GC) coupled to mass spectrometry (MS), with a prior step involving the extraction and pre-concentration of the volatile fraction. The technique of solid phase microextraction (SPME) requires only a small amount of sample and permits the isolation of volatile analytes from matrices both in the solid and liquid states in a short time, in a simple way. For this reason, nowadays SPME is commonly used for the extraction of flavour compounds in cheese (Coda et al., 2006; Guillén, Ibargoitia, Sopelana, Palencia, & Fresno, 2004; Lecanu, Ducruet, Jouquand, Gratadoux, & Feigenbaum, 2002; Lee, Diono, Kim, & Min, 2003).

The volatile profile of some Spanish cheeses made from raw ewes' milk that belong to Protected Designation of Origins (PDO) have been previously studied, such as Manchego (Fernández-García, Carbonell, & Nuñez, 2002a, 2002b; Villaseñor, Valero, Sanz, & Martínez-Castro, 2000), La Serena (Carbonell, Núñez, & Fernández-García, 2002a, 2002b), Roncal (Izco & Torre, 2000), Zamorano (Fernández-García, Gaya, Medina, & Núñez, 2004b) and Idiazábal (Barron et al., 2007).

The soft cheese with the Protected Designation of Origin (PDO) Torta del Casar is produced in Extremadura region, in the southwest of Spain. It is a well-known cheese with an increasing production every year, since it is much appreciated by consumers for its

* Corresponding author. Tel.: +34 924 012690; fax: +34 924 012674.
E-mail addresses: mariarosario.ramirez@juntaextremadura.net, rramirez@unex.es (R. Ramírez).

0308-8146/$ - see front matter © 2009 Elsevier Ltd. All rights reserved.
doi:10.1016/j.foodchem.2009.04.081

high quality and unique flavour. This cheese has a light and thin semi-hard rind and a very soft texture. Raw milk, from Merino or Entrefina breed ewes reared outdoors, is used (DOE, 2001). In addition, no starter cultures are added, and vegetable rennet, previously obtained from maceration of thistle flowers (*Cynara cardunculus*) in water, is used to coagulate the milk. The most known cheeses made of raw ewes milk and vegetable coagulant are La Serena cheese (Spain) and Serra da Estrela cheese (Portugal). The use of Merino ewes' raw milk and plant coagulant provides characteristic slightly bitter taste and a spreadable texture.

Microbial characterisation of Torta del Casar cheese has been previously published (Cáceres, Castillo, & Pizarro, 1997; Poullet, Huertas, Sánchez, Cáceres, & Larriba, 1991; Poullet, Huertas, Sánchez, Cáceres, & Larriba, 1993). However, its volatile profile and changes during ripening have not been previously studied despite their importance. Therefore, the main objective of this paper are the characterisation of the volatile profile of the cheese Torta del Casar during the ripening process by SPME–GC–MS, in order to determine the compounds that provide its characteristic aroma.

2. Materials and methods

2.1. Cheese manufacture

Torta del Casar cheese was produced from Merino ewes' raw milk. No starter cultures were added and a plant coagulant obtained from the the flowers of the thistle *C. cardunculus* L. were used to coagulate the milk. The milk was heated to 28–32 °C, and coagulation took place after 50–80 min. The curd was cut to increase the surface area, which increases the movement of whey out of the curd. Then the curd was transferred into suitable moulds, where it was pressed for 3–4 h at pressures of 1–2.5 kg/cm^2. The cheeses were then salted with sodium chloride. Afterwards, they were ripened for 60–90 days at 4–12 °C and relative humidity of 75–90%. Legislation does not allow the consumption of these cheeses before 60 days of ripening since they are made with raw milk. According to the regulation of the PDO, the physicochemical properties must be a minimum of 50% of fat content in dry matter, a minimum of 50% of dry matter, a pH of 5.2–5.9 and a maximum of 3% NaCl (DOE, 2001).

Four cheeses from 3 different producers from the PDO were analysed at four different stages of ripening: 1, 30, 60 and 90 days. A total of 48 cheese were analysed, 12 at each stage of ripening. For each producer, four cheeses of the same batch were collected at each time of ripening. During the first 60 days of ripening, cheeses were matured in each dairy. The proximate composition of the cheeses after 60 days of ripening was 43.3% moisture, 32.5% fat and 16.9% protein and the pH was ~5.4, with a salt content of 1.29%. After 60 days of ripening, when cheeses can be sold, they were shrink-wrapped with a thin plastic film and put inside a thin wooden box (a decorative packaging) to simulate purchase conditions. For the last month, packed cheeses were stored at 5 °C. From each cheese, samples were taken from the inner part of the cheese and were stored at −20 °C until they were analysed (<2–3 weeks).

2.2. SPME–GC/MS

For the extraction of volatile compounds the method of Lee et al. (2003) was followed. Ten grams of cheese were placed in a 50-ml vial and then 10 ml NaH_2PO_4 (25%, w/v) were added. The sample was stirred for 30 min at 50 °C to accelerate equilibrium of headspace volatile compounds between the cheese matrix and the headspace. Then, volatile compounds extraction was carried out by injecting a 50/30 μm divinylbenzene/Carboxen/polydimethylsiloxane SPME fibre (Supelco, Bellefonte, PA) into the vial and exposing it to the headspace for 30 min at 50 °C. After extraction samples were directly desorbed into the injection port of the GC which was at 250 °C. The analyses of volatile compounds were performed on a Varian CP-3800 GC gas chromatograph coupled to a Varian Saturn 2200 MS (Varian Inc., Palo Alto, CA). Volatile compounds were separated using a capillary column (HP Innowax; 60 m × 0.25 mm ID × 0.50 μm film thickness; Agilent, Santa Clara, CA). The carrier gas was helium with a flow of 1 ml/min. The temperature programme was isothermal at 40 °C for 10 min, then raised at 5 °C/min to 240 °C and held for 11 min. The GC–MS transfer line temperature was at 280 °C. The MS operated in electron impact mode with electron impact energy of 70 eV; and collected data at a rate of 0.7 scans/s over a range of *m/z* 40–650. *n*-Alkanes (Sigma R-8769) were analysed under the same conditions to calculate retention indices (RI) for the volatile compounds. The compounds were identified by comparison with commercial reference compounds provided by Sigma–Aldrich (St. Louis, MO) by comparison of RI with those described in the literature and by comparison of their mass spectra with those contained in the NIST and Varian libraries.

2.3. Statistical analysis

The differences in the volatile profiles during ripening were analysed using the analysis of variance (ANOVA) procedure of SPSS, Version 14.0 (SPSS Inc., Chicago, IL). HSD Tukey's test was applied to compare the mean values of the volatile compounds of different days of ripening. Mean values with standard deviations are reported. The relationships between parameters were assessed by principal component analysis (PCA) using the Unscrambler 6.11 software (Camo Software AS, Oslo, Norway).

3. Results and discussion

3.1. General

Volatile compounds (area units, AU, $\times 10^5$) isolated from Spanish soft cheese Torta del Casar by SPME–GC–MS during 90 days of ripening are shown in Table 1. A total of 46 compounds were detected: 13 acids, 9 esters, 4 ketones, 7 alcohols, 3 aldehydes, 7 aromatic compounds and 3 compounds which could not be classified in these groups. Significant differences were found in the volatile compounds during ripening, as most of the volatile compounds detected tended to increase and new compounds were formed during maturation, while few tended to decrease. Compared to Day 1, an important increase of total area units (AU) was found in the first 60 days of ripening, while in the last 30 days, the amount of volatile compounds slightly increased (Day 1: 230×10^5 AU, Day 30: 808×10^5 AU, Day 60: 1426×10^5 AU, Day 90: 1530×10^5 AU). These results agree with the time when cheeses can be sold, after 60 days of maturation, so at purchase time they have developed most of the volatile compounds which form their characteristic profile.

Fig. 1 shows the evolution of volatile compounds grouped by their chemical nature. Total carboxylic acid content tended to increase during ripening, especially in the first 60 days. Lipolysis seems to be an important pathway of formation of linear carboxylic acids with more than 4 carbon atoms. However, the shorter carboxylic acids can also be derived from ketones, esters and aldehydes by oxidation (Molimard & Spinnler, 1996), as the metabolic products of lactose metabolism, deamination of amino acids and possibly lipid oxidation. Esters gradually increased during ripening, as very low levels of ester volatiles were detected at Day 1 and their levels were significantly increased after 90 days of ripening. Ketone volatiles followed a similar trend as described for

Table 1
Volatile compounds (AU × 10^5) isolated from Torta del Casar cheese at four different stages of ripening (mean ± standard deviation).

RI[w]	Id. Method[x]	Compounds	Day 1 (n = 12)	Day 30 (n = 12)	Day 60 (n = 12)	Day 90 (n = 12)	P[y]
Acids							
1460	RF, RI, TI	Acetic acid	7.37c ± 3.00	171.00b ± 26.00	312.00a ± 102.00	339.00a ± 86.50	**0.001**
1553	RF, RI, TI	Propanoic acid	0.00b ± 0.00	4.43b ± 3.65	21.10a ± 19.59	25.70a ± 11.20	**0.001**
1581	RI, TI	2-Methylpropanoic acid	0.00c ± 0.00	15.90bc ± 13.40	32.80ab ± 22.20	46.50a ± 27.70	**0.001**
1683	RF, TI	Butanoic acid	12.80 ± 2.85	56.10 ± 40.67	122.00 ± 284.00	16.60 ± 4.69	0.232
1678	RF, TI	3-Methylbutanoic acid	1.40c ± 1.41	78.30b ± 63.40	297.00a ± 532.00	265.00a ± 106.00	**0.029**
1736	RI, TI	Pentanoic acid	0.40b ± 0.40	0.61b ± 0.58	1.57a ± 0.87	0.49b ± 1.14	**0.003**
1817	RF, TI	Hexanoic acid	36.00b ± 4.25	87.20a ± 45.90	36.90b ± 29.70	28.00b ± 38.60	**0.001**
–	TI	(*E*)-3-hexenoic acid	30.9 ± 99.1	0.00 ± 0.00	23.10 ± 18.90	35.40 ± 30.50	0.372
1905	TI	Heptanoic acid	6.18 ± 14.5	1.22 ± 0.51	1.27 ± 0.40	0.55 ± 1.02	0.218
2064	RF, TI	Octanoic acid	34.50b ± 17.30	63.80a ± 11.60	62.80a ± 11.90	69.10a ± 15.90	**0.001**
–	TI	(*E,E*)-2,4-hexadienoic acid	0.00b ± 0.00	27.4ab ± 19.13	40.10a ± 26.50	53.70a ± 62.60	**0.004**
2113	RF, TI	Decanoic acid	51.40b ± 7.27	56.80b ± 21.3	71.50a ± 9.93	57.20b ± 10.30	**0.005**
2486	RF, TI	Dodecanoic acid	16.20ab ± 13.9	10.60ab ± 13.20	22.20a ± 19.00	3.73b ± 4.05	**0.013**
Percentage (%)[z]			***81.8***	***71.0***	***70.6***	***61.5***	
Esters							
892	RF, RI, TI	Acetic acid ethyl ester	0.00b ± 0.00	4.85a ± 2.53	4.04a ± 5.12	3.01a ± 1.16	**0.001**
1041	RF, RI, TI	Butanoic acid ethyl ester	0.12c ± 0.23	3.42b ± 1.29	6.03ab ± 4.34	7.50a ± 4.72	**0.001**
1070	TI	3-Methylbutanoic acid,ethyl ester	1.54ab ± 1.58	2.60a ± 1.38	1.50ab ± 0.77	1.23b ± 1.13	**0.049**
1121	TI	Acetic acid 3-methylbutyl ester	0.00c ± 0.00	1.36b ± 0.87	1.19b ± 1.07	2.70a ± 1.51	**0.001**
1232	RF, RI, TI	Hexanoic acid ethyl ester	0.33b ± 0.50	13.6a ± 9.01	8.21a ± 4.12	12.80a ± 6.01	**0.001**
1292	TI	Hex-4-enoic acid ethyl ester	0.00c ± 0.00	0.08c ± 0.13	1.46b ± 1.36	4.35a ± 2.43	**0.001**
1438	RF, RI, TI	Octanoic acid ethyl ester	0.23c ± 0.44	11.1a ± 5.41	6.77b ± 3.18	10.80a ± 4.36	**0.001**
–	TI	Butanoic acid propyl ester	1.48b ± 1.94	0.72b ± 0.41	173.00ab ± 242.00	230.00a ± 269.00	**0.004**
–	RF, TI	Dodecanoic acid ethyl ester	0.00b ± 0.00	0.85b ± 0.40	22.30b ± 32.40	57.30a ± 44.80	**0.001**
Percentage (%)			***0.0***	***10.9***	***19.0***	***24.5***	
Ketones							
818	RF, RI, TI	2-Propan-one	1.55a ± 0.59	0.51b ± 0.40	1.08ab ± 1.47	0.28b ± 0.36	**0.002**
906	RI, TI	2-Butan-one	0.29c ± 0.43	0.96c ± 0.83	41.70b ± 31.70	80.10a ± 52.10	**0.001**
1086	RF, RI, TI	2-Heptan-one	0.00b ± 0.00	0.00b ± 0.00	0.06b ± 0.22	24.60a ± 9.87	**0.001**
1309	RI, TI	3-Hydroxy-2-butan-one	0.17b ± 0.28	15.30a ± 21.04	4.34ab ± 1.71	6.06ab ± 1.53	**0.009**
Percentage (%)			***0.9***	***2.1***	***3.3***	***7.3***	
Alcohols							
940	TI	1-Methoxy 2-propan-ol	2.02d ± 0.66	47.70a ± 12.78	33.30b ± 11.90	22.40c ± 7.89	**0.001**
1026	RF, RI, TI	2-Butan-ol	0.26c ± 0.21	2.16c ± 1.74	12.50b ± 8.87	22.30a ± 15.70	**0.001**
1209	RF, RI, TI	3-Methyl-1-butan-ol	2.31c ± 1.65	49.39a ± 18.33	22.34b ± 13.13	0.00c ± 0.00	**0.001**
1219	RI, TI	2-Methyl-5-hex-en-3-ol	0.16b ± 0.37	0.00b ± 0.00	0.00b ± 0.00	5.17a ± 4.43	**0.001**
1499	TI	2,5-Dimethyl-3-hexan-ol	1.30ab ± 1.62	1.62a ± 1.44	0.90ab ± 0.90	0.25b ± 0.59	**0.049**
1598	TI	Hexa-2,4-dien-1-ol	0.00 ± 0.00	0.44 ± 0.39	0.47 ± 0.38	2.93 ± 7.43	0.220
–	TI	1-Dodecan-ol	15.70 ± 46.20	0.00 ± 0.00	3.03 ± 2.79	3.88 ± 3.47	0.378
Percentage (%)			***9.5***	***12.5***	***5.1***	***3.7***	
Aromatic compounds							
1049	RI, TI	Benzeneacetaldehyde	1.16a ± 1.01	0.19b ± 0.20	0.27b ± 0.62	0.00b ± 0.00	**0.001**
1085	RI,TI	Ethyldimethyl benzene	0.00b ± 0.00	0.19b ± 0.31	0.00b ± 0.00	1.97a ± 1.03	**0.001**
1265	RI, TI	Styrene	1.04 ± 0.80	0.62 ± 0.52	0.72 ± 0.73	1.20 ± 0.95	0.224
1531	RI, TI	Benzaldehyde	0.20b ± 0.37	0.44ab ± 0.21	0.36b ± 0.31	0.82a ± 0.62	**0.005**
–	RF, TI	Benzyl alcohol	2.13 ± 0.89	7.97 ± 12.21	4.90 ± 5.65	9.63 ± 4.79	0.065
1918	RF, RI, TI	2-Phenylethanol	0.00b ± 0.00	12.6a ± 3.58	12.4a ± 4.30	15.8a ± 5.14	**0.001**
–	TI	Phenol	0.57b ± 1.43	2.30b ± 3.21	4.24ab ± 6.56	9.60a ± 10.32	**0.007**
Percentage (%)			***2.2***	***3.0***	***1.6***	***2.5***	
Aldehydes							
923	RI, TI	3-Methylbutanal	0.56ab ± 0.29	1.07a ± 1.13	0.00b ± 0.00	0.00b ± 0.00	**0.001**
1422	TI	2,4-Hexa-dienal	0.49 ± 0.38	0.26 ± 0.25	0.10 ± 0.18	0.33 ± 0.64	0.131
–	RF, TI	Dodecanal	0.00b ± 0.00	0.00b ± 0.00	1.51ab ± 2.16	2.72a ± 2.37	**0.001**
Percentage (%)			***0.5***	***0.2***	***0.1***	***0.2***	
Others							
–	RF, TI	3-Methylpentane	0.97a ± 0.78	0.03b ± 0.10	0.14b ± 0.47	0.00b ± 0.00	**0.001**
–	RF, TI	3-(Methylthio)-1-propan-ol	1.71a ± 2.65	0.34ab ± 0.23	0.61ab ± 0.64	0.00b ± 0.00	**0.023**
2187	TI	δ-Decalactone	0.00b ± 0.00	1.81ab ± 0.76	3.17ab ± 1.68	5.20a ± 7.18	**0.011**
Percentage (%)			***2.2***	***3.0***	***1.6***	***2.5***	

a, b, c, d: Different letters in the same row indicate significant statistical differences (Tukey's Test, $p < 0.05$).
[w] RI: retention index.
[x] Method of identification: RF, mass spectrum and retention time identical with a reference compound; RI, mass spectrum and retention index from literature in agreement; TI, tentative identification by mass spectrum.
[y] P: Probability.
[z] Percentage (%): percentage of volatile compounds of each chemical group in each day of ripening of cheese.

esters. However, the levels of alcohols tended to increase in the first month of storage but tended to decrease after Day 30. This decrease could be probably due to the increase of esters, formed from the esterification of acids and alcohols. Finally, the level of aromatic compounds tended to increase at the beginning of the ripening but then remained constant.

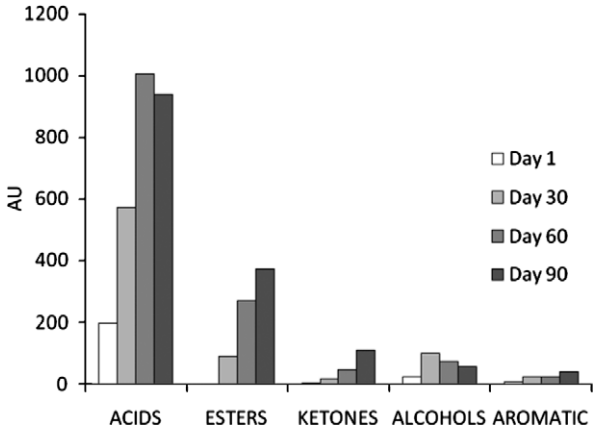

Fig. 1. Changes of the main chemical groups of volatile compounds (AU × 10^5) isolated in the soft cheese Torta del Casar during ripening.

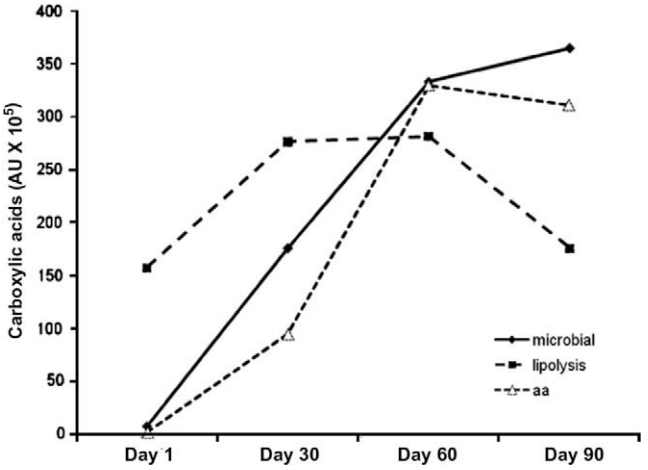

Fig. 2. Carboxylic acids with a microbial origin (acetic and propionic acids). Carboxylic acids with origin in lipolysis (butanoic, pentanoic, hexanoic, heptanoic, octanoic, decanoic and dodecanoic acids). Carboxylic acids with origin in amino acids (aa) (2-methylpropanoic and 3-methylbutanoic acids).

3.2. Carboxylic acids

Fig. 2 shows the evolution of carboxylic acids according to their most probable origin. During ripening of cheeses, carboxylic acids can originate from three main biochemical pathways: lipolysis, proteolysis and lactose fermentation (reviewed by Curioni & Bosset, 2002). Enzymes with lipolytic activity (esterases, lipases) may cause the release of linear-chain acids (butanoic, pentanoic, hexanoic, heptanoic, octanoic, decanoic and dodecanoic acids), whereas proteolytic enzymes are responsible for the formation of branched-chain acids (2-methylpropanoic and 3-methylbutanoic acids) by the deamination of amino acids, such as valine and leucine (Curioni & Bosset, 2002; Kuzdzal-Savoie, 1980). In this case, as these cheeses are made from raw milk, lipolysis could originate by the action of indigenous lipases from the milk, since no starter was added for the manufacture of the cheeses. Finally, acetic and propionic acids could have a microbial origin as a result of lactose fermentation, since the changes in those acids have been previously associated with the growth of lactic acid and propionic bacteria (Ziino, Condurso, Romeo, Giuffrida, & Verzera, 2005), respectively. The origin of (*E*)-3-hexenoic and (*E,E*)-2,4-hexadienoic acids is not clear in the literature, so they are not included in Fig. 2.

At Day 1, most acids detected came from lipolysis, while no acids had their origin in amino acid or microbial degradation. The amount of acids derived from lipolysis tended to increase in the first month of ripening, was constant until Day 60 and then decreased. However, carboxylic acids from amino acids increased during the first 60 days of ripening and then slightly decreased until Day 90. Acids with a microbial origin increased significantly during ripening, so at Day 90, they were the most abundant, followed by those acids derived from amino acids, while acids from lipolysis of triglycerides were the least abundant at the end of ripening. The high amount of acids derived from amino acids could be related to the high proteolysis of these cheeses during ripening, as a result of the addition of vegetable coagulant (Carbonell et al., 2002a; Fernández-Salguero & Sanjuan, 1999).

Carboxylic acids were the most abundant volatile compounds isolated in the headspace of Torta del Casar cheese on all days of ripening (Table 1) with a percentage of 61.5–81.8% of total compounds. They are not only aroma compounds by themselves but also they are precursors of other compounds, such as methyl ketones, alcohols, lactones, aldehydes and esters (Collins, McSweeney, & Wilkinson, 2003). Due to their low aroma thresholds, short and medium-chain carboxylic acids are considered to be important contributors to the flavour profile in a wide variety of cheeses (Kraggerud, Skeie, Høy, Røkke, & Abrahamsen, 2008; Moio & Addeo, 1998; Pinho, Ferreira, & Ferreira, 2003; Tavaria, Silva Ferreira, & Malcata, 2004; Woo & Lindsay, 1982; Zerfiridis, Vafopoulou-Mastrogiannaki, & Lipoulou-Tzanetaki, 1984).

At the beginning of maturation, the most abundant acids were hexanoic, (*E*)-3-hexenoic, octanoic and decanoic acids. However, at Day 90, high amounts of acetic acid and 3-methylbutanoic acid were isolated. Acetic acid content significantly increased after 90 days of ripening and it was the major compound isolated in the headspace of Torta del Casar soft cheese. The content of acetic acid, propanoic acid, 2-methylpropanoic acid, 3-methylbutanoic acid, octanoic acid and 2,4-hexanedienoic acid all significantly ($P < 0.05$) increased at the end of the ripening. However, the content of butanoic, pentanoic, decanoic and dodecanoic acids tended to decrease after 30 or 60 days of ripening, probably due to their transformation into other compounds, such as esters. High amounts of acetic and propanoic acids are related with vinegar odour, which could be associated with the slightly acid taste of these cheeses. Acetic acid originates from different reactions by the action of lactic acid bacteria (Ur-Rehman et al., 2000). The other major acid detected 3-methylbutanoic acid, has its origin in the breakdown of the aminoacid leucine (Kuzdzal-Savoie, 1980) and it provides a rancid, cheese and sweaty odour (Yvon & Rijnen, 2001). This compound could also originate from the oxidation of its Strecker aldehyde 3-methylbutanal. Of the other acids formed at high concentrations, propanoic acid has its origin in the metabolism of lactate by *Propionibacterium sp* (Steffen, Flueckiger, Bosset, & Ruegg, 1987) while 2-methylpropanoic acid is produced by the metabolism of the amino acid valine (Molimard & Spinnler, 1996; Urbach, 1997). Both propanoic and 2-methylpropanoic acids contribute with sour odour notes to cheese aroma (Avsar et al., 2004).

(*E*)-3-Hexenoic acid followed an opposite trend to hexanoic acid, since hexanoic acid tended to decrease after 30 days of ripening while the level of (*E*)-3-hexenoic acid tended to increase; we consider that probably there is a relationship between both compounds.

The volatile profile of La Serena cheese (Carbonell et al., 2002a, 2002b), with similar characteristics to Torta del Casar (made from raw ewes' milk, with vegetable coagulant), contained more alcohol compounds and less acids. These important differences could be explained by the different headspace extraction methods utilised, since they used purge-and-trap and we have used SPME. Mallia,

Fernández-García, and Bosset (2005) compared both methods and found that SPME fibres were more effective for extracting medium- and high-boiling compounds, especially volatile acids, while purge-and-trap was better for extracting highly volatile compounds and alcohols. However, these differences could also be evidence of the different volatile profiles of these cheeses.

3.3. Esters

Esters were the second most abundant compounds isolated in the headspace of Torta del Casar. The microorganisms involved in ester formation are mainly yeasts (Molimard & Spinnler, 1996); however, and also some lactic acid bacteria and *Micrococcaceae*, as well as chemical reactions, can also be responsible (Gripon, Monnet, Lamberet, & Desmazeaud, 1991). The action of the last two seems to be more probable in the Torta del Casar cheese (Cáceres et al., 1997; Poullet et al., 1991; Poullet et al., 1993).

Due to the microbial origin of esters, their levels were low at the beginning and then increased at the end of the ripening, especially butanoic acid propyl ester (propyl butyrate/butanoate).

Among the esters, 6 ethyl esters, 1 propyl ester and 1 3-methylbutyl ester were detected. Ethyl esters, due to their high amount, probably contribute to the overall flavour of Torta del Casar cheese as they have low detection thresholds. Some of the most important odorant compounds detected in other cheese varieties were ethyl esters such as butanoic acid ethyl ester (Cheddar, Emmental, creamy Gorganzola, Grana Padano, Pecorino, Ragusano), hexanoic acid ethyl ester (Cheddar, Emmental, natural Gorganzola, Grana Padano, Pecorino, Ragusano) and octanoic acid ethyl ester (Flor de Guia) (Curioni & Bosset, 2002). According to de Frutos, Sanz, and Martinez-Castro (1991), fruity notes provided by ethyl esters may minimise the sharpness of rancidity derived from excessive concentrations of carboxylic acids.

The increase of some esters, such as butanoic acid ethyl ester and butanoic acid propyl ester, could be associated with the decrease of butanoic acid at the end of ripening, although differences were not significant. Additionally, the reduction of some alcohols at the end of ripening, e.g., 3-methylbutan-1-ol, could also be related to the increase of esters, such as acetic acid 3-methylbutyl-1-ol ester. As far as we are concerned, these esters have not been previously isolated in other ewes' milk cheeses, so they could provide unique and characteristic aromatic notes to the Torta del Casar cheese. However, the increases during ripening of hexanoic acid ethyl ester and butanoic acid ethyl ester have been previously described in other ewes' milk cheeses (Barron et al., 2007; Carbonell et al., 2002a; Di Cagno et al., 2003; Mariaca, Fernández-García, Mohedano, & Nuñez, 2001).

3.4. Ketones

Ketones are abundant constituents of most dairy products, although in this case they were only 7.3% of the total compounds isolated at Day 90. They have typical odours and low perception thresholds. 2-Butan-one and 2-heptan-one were the most abundant ketones detected during ripening. They were not detected at trace levels at Day 1, but they greatly increased after 90 days of ripening, so they could play an important role in the final aroma of the Torta del Casar cheese. Similar results have been found in other cheeses made from raw ewes' milk such as Zamorano, Manchego and La Serena cheeses (Carbonell et al., 2002a, 2002b; Fernández-García et al., 2002a, 2002b). The opposite trend was found for 2-propan-one, which decreased during ripening, while, 3-hydroxy-2-butan-one (acetoin) increased at the beginning of ripening but then decreased slightly.

3.5. Alcohols

Alcohols were abundant at the beginning of the ripening, with a percentage of 10–12% of total volatiles detected at Day 30, while their level decreased to 3.7% at the end of ripening. These results contrast with those previously reported in other Spanish cheeses from ewes' raw milk, since alcohols were quantitatively the main chemical group found in the volatile fraction of Zamorano, Manchego, La Serena and Castellano cheeses (Carbonell et al., 2002a; Fernández-García, Gaya, Medina, & Núñez, 2004a; Fernández-García et al., 2004b). The levels of 1-dodecan-ol and 2,4-hexa-dien-1-ol did not change during ripening; however, the levels of 2-butanol and 2-methyl-5-hex-en-3-ol increased at the end of ripening, while the levels of 1-methoxy 2-propan-ol and 2,5-dimethyl-1-hexan-ol were the highest at Day 30 and then tended to decrease. These different patterns during ripening could be associated with the different metabolic pathways involved in the formation of alcohols in cheese, namely lactose metabolism, methyl ketone reduction, amino acid metabolism and degradation of linoleic and linolenic acids (Molimard & Spinnler, 1996).

3.6. Aromatic compounds

Most aromatic compounds tended to increase during ripening, except for benzeneacetaldehyde, which was not detected in Torta del Casar cheese samples after 90 days of ripening. So, the levels of ethyldimethylbenzene, benzaldehyde and phenol were significantly highest at Day 90, while the level of 2-phenylethanol was highest after 30 days of ripening and remained constant until Day 90. The amounts of styrene and benzyl alcohol did not change during ripening.

Some of the aromatic compounds detected originate from the Strecker reaction, e.g., benzaldehyde, which adds aromatic notes of bitter almond to cheese (Molimard & Spinnler, 1996), may be produced from the α-oxidation of phenyl acetaldehyde, as they followed an opposite trend; phenylacetaldehyde is derived from phenylalanine, *via* a Strecker reaction (Sieber, Buetikofer, & Bosset, 1995). On the other hand, Strecker degradation of phenylalanine is also responsible for 2-phenylethanol production and this reaction has been attributed to yeast metabolism (Correa Lelles Nogueira, Luachevsky, & Rankin, 2005).

3.7. Aldehydes

Aldehydes are not major compounds in cheese, as they are rapidly converted to alcohols or their corresponding acids (Lemieux & Simard, 1992), so their levels during ripening were 0.1–0.5% of total volatile compounds isolated. The low level of aldehydes indicated an optimal maturation because a high concentration of aldehydes may cause off-flavours (Moio & Addeo, 1998).

Three aldehydes were isolated which showed different patterns: 3-methylbutanal was detected at the beginning of maturation but not at Day 60 and 90, 2,4-hexa-dienal did not change during ripening, and dodecanal, which was only detected after 60 days of ripening reached its highest level at Day 90. The first is a Strecker aldehyde, while the other two could by formed by lipid oxidation of their respective alcohols. So the origin of dodecanal could be due to the oxidation of 1-dodecan-ol, as they followed an opposite pattern, and the same could happen with 2,4-hexa-dienal and 2,4-hexa-dien-1-ol.

3.8. Others

A branched alkane, 3-methylpentane, was isolated at the beginning of ripening, at Day 1, but its amount decreased during maturation and it was not detected at Day 90. The contribution of

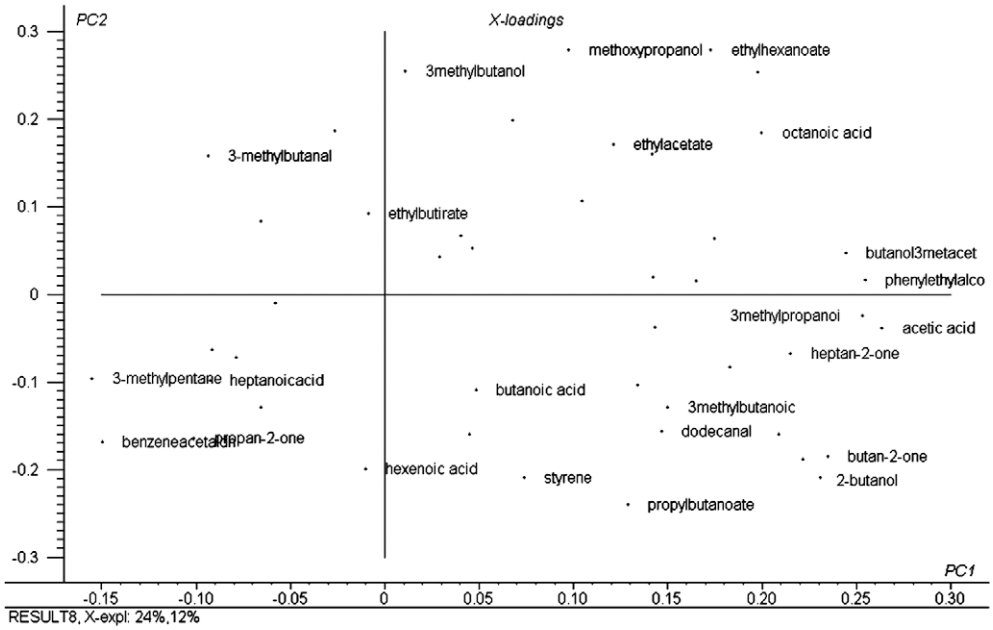

Fig. 3. Loading plots after principal components analysis of the variables in the plane defined by the two first principal components (PC #1 and PC #2).

aliphatic hydrocarbons to the global aroma of Torta del Casar cheese could be low as these compounds have high threshold values.

Only one sulphur compound, originating from methionine (Yvon & Rijnen, 2001) was found. 3-Methylthio-1-propan-ol or methionol probably has limited importance in the final aroma of Torta del Casar as it was not detected at the end of ripening.

Only one lactone was detected, δ-decalactone, which was not isolated at Day 1 but its level increased during ripening and the highest amount was found at Day 90. δ-Decalactone is one of the lactones most commonly detected in cheeses. Lactones have fruity and sweet, creamy, fermented notes (Dufosse, Latrasse, & Spinnler, 1994), so they could contribute pleasant odour notes to the aroma of Torta del Casar. δ-Lactones may be formed from δ-hydroxyacids following their release from triacylglycerides by lipolysis, so concentration of lactones usually correlate with lipolysis extent (Collins et al., 2003), which agrees with our results.

3.9. Multivariate analysis

A principal component analysis (PCA) was carried out to determine which were the most important volatile compounds on each day of maturation. PCA is a mathematical procedure for resolving sets of data into orthogonal components, whose linear combinations (principal components) approximate the original data to any desired degree of accuracy. In most cases, two principal components are sufficient to explain a great proportion of the variation in the original variables, thus resulting in a considerable

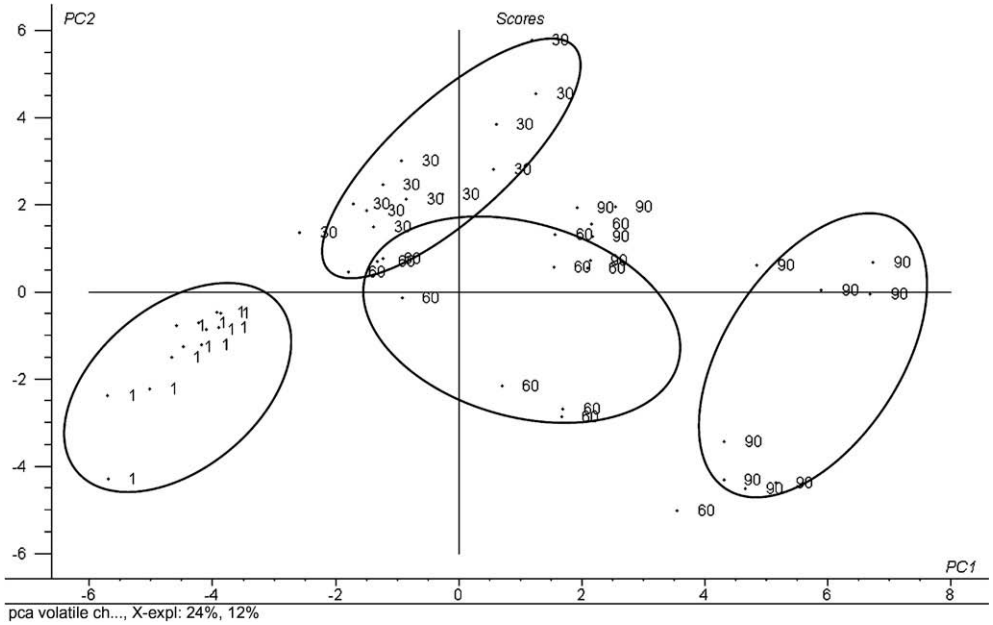

Fig. 4. Scores plot after principal component analysis of the individuals in the plane defined by the two first principal components (PC #1 and PC #2).

compression of the data. In this case, 24% and 12% of the variability was explained by principal components (PC) #1 and #2, respectively.

Fig. 3 shows the score plot of the different variables (coefficients of the eigenvectors) for the two first principal components (PC #1 and PC #2). Although all volatiles were included in the analysis, only volatile compounds which explained variation of the data have been identified in the figure. On the positive axis of PC #1, far from the origin and explaining an important part of the variation are located volatile compounds isolated to a higher extent in cheeses with 90 days of ripening, such as carboxylic acids (acetic acid, 3-methylbutanoic acid, 2-methylpropanoic acid), esters (acetic acid 3-methylbutyl-1-ol ester), ketones (2-heptan-one, 2-butan-one) and others (2-butan-ol, dodecanal). On the negative axis of PC #1 are compounds related to the flavour of cheese at the beginning of the ripening (3-methylpentane, heptanoic acid, benzeneacetaldehyde, 2-propan-one). Regarding PC #2, some volatile compounds were located in the positive axis of the plane (3-methyl-1-butanol, 1-methoxy-2-propanol, hexanoic acid ethyl ester) while others were located in the lower part of the plane in the negative axis (hexenoic acid, butanoic acid propyl ester).

The distribution of the scores on the first two PCs (Fig. 4) shows 4 separate groups of points, corresponding to the different days of ripening. Cheeses at Day 90 are located in the positive area of PC #1 while in the negative area are those with 1 day of ripening. In the middle of the plane are located cheeses with 30 and 60 days of ripening, so PC #1 cannot explain differences between these groups, however, PC #2 could explain differences between cheeses with 30 and 60 days of ripening as cheeses with one month of maturation are in the upper part of the plane and those with 2 months are in the low part of the plane. Volatile compounds located at the extremes of PC #2 are associated with the volatile profile of cheeses at 30 days and at 60 days of ripening.

4. Conclusions

The greater importance of carboxylic acids with origin in microbial activity (acetic and propionic acids) and amino acid degradation (2-methylpropanoic and 3-methylbutanoic acids) than those from lipolysis (butanoic, pentanoic, hexanoic, heptanoic, octanoic, decanoic and dodecanoic acids) is a unique characteristic, which could be associated with the typical aroma of Torta del Casar soft cheese, and which could differentiate its aroma from other cheeses on the market.

Acknowledgements

This work has been financed thanks to European Regional Development Fund (ERDF). Francisco José Delgado thanks Junta de Extremadura for the grant received for the development of this work (DOE 10.10.07). We thank the dairies "Quesos del Casar", "José Álvarez-Rocha" and "Jacinto M. Sánz Pérez/Tamussia" for providing the cheeses.

References

Avsar, Y. K., Karagul-Yuceer, Y., Drake, M. A., Singh, T. K., Yoon, Y., & Cadwallader, K. R. (2004). Characterization of nutty flavor in cheddar cheese. *Journal of Dairy Science, 87*, 1999–2010.

Barron, L. J. R., Redondo, Y., Aramburu, M., Gil, P., Pérez-Elortondo, F. J., Albisu, M., et al. (2007). Volatile composition and sensory properties of industrially produced Idiazabal cheese. *International Dairy Journal, 17*, 1401–1414.

Cáceres, P., Castillo, D., & Pizarro, M. (1997). Secondary flora of Casar de Cáceres cheese: Characterization of Micrococcaceae. *International Dairy Journal, 7*, 531–536.

Carbonell, M., Núñez, M., & Fernández-García, E. (2002a). Evolution of the volatile components of ewe raw milk La Serena cheese during ripening. Correlation with flavour characteristics. *Le Lait, 82*, 683–698.

Carbonell, M., Núñez, M., & Fernández-García, E. (2002b). Seasonal variation of volatile compounds in ewe raw milk La Serena cheese. *Le Lait, 82*, 699–711.

Coda, R., Brechany, E., De Angelis, M., De Candia, S., Di Cagno, R., & Gobbetti, M. (2006). Comparison of the compositional, microbiological, biochemical, and volatile profile characteristics of nine Italian ewes' milk cheeses. *Journal of Dairy Science, 89*, 4126–4143.

Collins, Y. F., McSweeney, P.-L. H., & Wilkinson, M. G. (2003). Review: Lipolysis and free fatty acid catabolism in cheese: a review of current knowledge. *International Dairy Journal, 13*, 841–866.

Correa Lelles Nogueira, M., Luachevsky, G., & Rankin, S. A. (2005). A study of volatile composition of Minas cheese. *Lebensmittel-Wissenschaft und-Technologie, 38*, 555–563.

Curioni, P. M. G., & Bosset, J. O. (2002). Key odorants in various cheese types as determined by gas chromatography–olfactometry. *International Dairy Journal, 12*, 959–984.

de Frutos, M., Sanz, J., & Martinez-Castro, J. (1991). Characterization of artisanal cheeses by GC/MS analysis of their medium volatile (SDE) fraction. *Journal of Agricultural and Food Chemistry, 39*, 524–530.

Di Cagno, R., Banks, J., Sheehan, L., Fox, P. F., Brechany, E. Y., Corsetti, A., et al. (2003). Comparison of the microbiological, compositional, biochemical, volatile profile and sensory characteristics of three Italian PDO ewes' milk cheeses. *International Dairy Journal, 13*, 961–972.

DOE (2001). *Diario Oficial de Extremadura (Regional Legislation of Extremadura)*, n° 119, 13th October 2001. Denominación de Origen. – Orden de 9 de octubre de 2001, por la que se aprueba el Reglamento de la Denominación de Origen (D.O.P.) Torta del Casar (pp. 10435–10448).

Dufosse, L., Latrasse, A., & Spinnler, H. E. (1994). Importance of lactones in food flavours: Structure, distribution, sensory properties and biosynthesis. *Sciences de Aliments, 14*, 17–50.

Fernández-García, E., Carbonell, M., & Nuñez, M. (2002a). Volatile fraction and sensory characteristics of Manchego cheese, 1. Comparison of raw and pasteurised milk cheese. *Journal of Dairy Research, 69*, 579–593.

Fernández-García, E., Carbonell, M., & Nuñez, M. (2002b). Volatile fraction and sensory characteristics of Manchego cheese 2. Seasonal variation. *Journal of Dairy Research, 69*, 595–604.

Fernández-García, E., Gaya, P., Medina, M., & Núñez, M. (2004a). Evolution of the volatile components of raw ewes' milk Castellano cheese: Seasonal variation. *International Dairy Journal, 14*, 39–46.

Fernández-García, E., Gaya, P., Medina, M., & Núñez, M. (2004b). Evolution of the volatile components of ewes' raw milk Zamorano cheese: Seasonal variation. *International Dairy Journal, 14*, 701–711.

Fernández-Salguero, J., & Sanjuan, E. (1999). Influence of vegetable and animal rennet on proteolysis during ripening in ewes' milk cheese. *Food Chemistry, 64*, 177–183.

Fox, P. F., & Wallace, J. M. (1997). Formation of flavour compounds in cheese. *Advances in Applied Microbiology, 45*, 17–85.

Gripon, J. C., Monnet, V., Lamberet, G., & Desmazeaud, M. J. (1991). Microbial enzymes in cheese ripening. In P. F. Fox (Ed.), *Food enzymes* (pp. 131–168). London: Elsevier Applied Science.

Guillén, M. D., Ibargoitia, M. L., Sopelana, P., Palencia, G., & Fresno, N. (2004). Components detected by means of solid-phase microextraction and gas chromatography/mass spectrometry in the headspace of artisan fresh goat cheese smoked by traditional methods. *Journal of Dairy Science, 87*, 284–299.

Izco, J. M., & Torre, P. (2000). Characterisation of volatile flavour compounds in Roncal cheese extracted by the purge and trap method and analysed by GC–MS. *Food Chemistry, 70*, 409–417.

Kinsella, J. E. (1975). Butter flavor. *Food Technology, 29*, 82–98.

Kraggerud, H., Skeie, S., Høy, M., Røkke, L., & Abrahamsen, R. K. (2008). Season and ripening temperature influence fatty acid composition and sensory properties of semi-hard cheese during maturation. *International Dairy Journal, 18*, 801–810.

Kuzdzal-Savoie, S.International Dairy Federation. (1980). Determination of free fatty acids in milk and milk products. *Annual Bulletin, 118*, 53–66.

Lecanu, L., Ducruet, V., Jouquand, C., Gratadoux, J. J., & Feigenbaum, A. (2002). Optimization of headspace solid-phase microextraction (SPME) for the odor analysis of surface-ripened cheese. *Journal of Agricultural and Food Chemistry, 50*, 3810–3817.

Lee, J. H., Diono, R., Kim, G. Y., & Min, D. (2003). Optimization of solid phase microextraction analysis for the headspace volatile compounds of Parmesan cheese. *Journal of Agricultural and Food Chemistry, 51*, 1136–1140.

Lemieux, L., & Simard, R. E. (1992). Bitter flavour in dairy products. A review of bitter peptides from caseins: their formation, isolation and identification, structure masking and inhibition. *Le Lait, 72*, 335–382.

Mallia, S., Fernández-García, E., & Bosset, J. O. (2005). Comparison of purge and trap and solid phase microextraction techniques for studying the volatile aroma compounds of three European PDO hard cheeses. *International Dairy Journal, 15*, 741–758.

Mariaca, R. G., Fernández-García, E., Mohedano, A. F., & Nuñez, M. (2001). Volatile fraction of ewe's milk semi-hard cheese manufactured with and without the addition of a cysteine proteinase. *Food Science and Technology, 212*, 239–246.

McSweeney, P. L. H., & Sousa, M. J. (2000). Biochemical pathways for the production of flavour compounds in cheeses during ripening: A review. *Le Lait, 80*, 293–324.

Moio, L., & Addeo, F. (1998). Grana Padano cheese aroma. *Journal of Dairy Research, 65*, 317–333.

Molimard, P., & Spinnler, H. (1996). Review: Compounds involved in the flavour of surface mold-ripened cheeses: origins and properties. *Journal of Dairy Science, 79*, 169–184.

Pinho, O., Ferreira, I. M. P. L. V. O., & Ferreira, M. A. (2003). Quantification of short-chain free fatty acids in "Terrincho" ewe cheese: intravarietal comparison. *Journal of Dairy Science, 86*, 3102–3109.

Plutowska, B., & Wardencki, W. (2007). Aromagrams – Aromatic profiles in the appreciation of food quality. *Food Chemistry, 101*, 845–872.

Poullet, B., Huertas, M., Sánchez, A., Cáceres, P., & Larriba, G. (1991). Microbial study of Casar de Cáceres cheese throughout ripening. *Journal of Dairy Research, 60*, 123–127.

Poullet, B., Huertas, M., Sánchez, A., Cáceres, P., & Larriba, G. (1993). Main lactic acid bacteria isolated during ripening of Casar de Cáceres cheese. *Journal of Dairy Research, 58*, 231–238.

Sieber, R., Buetikofer, U., & Bosset, J. O. (1995). Benzoic acid as a natural compound in cultured dairy products and cheese. *Journal of Reproductive Medicine, 40*, 227–246.

Siek, T. J., Albin, I. A., Sather, L. A., & Lindsay, R. C. (1971). Comparison of flavour thresholds of aliphatic lactones with those of fatty acids, esters, aldehydes, alcohols, and ketones. *Journal of Dairy Science, 54*, 1–4.

Steffen, C., Flueckiger, E., Bosset, J. O., & Ruegg, M. (1987). Swisstype varieties. In P. F. Fox (Ed.), *Cheese: Chemistry, physics and microbiology* (pp. 93–120). London: Elsevier Applied Science.

Tavaria, F. K., Silva Ferreira, A. C., & Malcata, F. X. (2004). Volatile free fatty acids as ripening indicators for Serra da Estrela cheese. *Journal of Dairy Science, 87*, 4064–4072.

Urbach, G. (1997). The chemical and biochemical basis of cheese and milk aroma. In B. A. Law (Ed.), *Microbiology and biochemistry of cheese and fermented milk* (pp. 253–298). London, UK: Blackie Academic and Professional.

Ur-Rehman, S., Banks, J. M., Bechany, E. Y., Muir, D. D., McSweeney, P. L. H., & Fox, P. F. (2000). Influence of ripening temperature on the volatiles profile and flavour of Cheddar cheese made from raw or pasteurised milk. *International Dairy Journal, 10*, 55–65.

Villaseñor, M. J., Valero, E., Sanz, J., & Martínez-Castro, I. (2000). Analysis of volatile compounds of Manchego cheese by dynamic headspace followed by automatic thermal desorption-GCMS. *Milchwissenschaft, 55*, 378–382.

Woo, A. H., & Lindsay, R. C. (1982). Rapid method for quantitative analysis of individual free fatty acids in Cheddar cheese. *Journal of Dairy Science, 65*, 1102–1109.

Yvon, M., & Rijnen, L. (2001). Cheese flavor formation by amino acids catabolism. *International Dairy Journal, 11*, 185–201.

Zerfiridis, G. K., Vafopoulou-Mastrogiannaki, A., & Lipoulou-Tzanetaki, E. (1984). Changes during ripening of commercial Gruyère cheese. *Journal of Dairy Science, 67*, 1397–1405.

Ziino, M., Condurso, C., Romeo, V., Giuffrida, D., & Verzera, A. (2005). Characterization of "Provola dei Nebrodi", a typical Sicilian cheese, by volatiles analysis using SPME–GC/MS. *International Dairy Journal, 15*, 585–593.

Food Chemistry 118 (2010) 191–198

Contents lists available at ScienceDirect

Food Chemistry

journal homepage: www.elsevier.com/locate/foodchem

Changes in durum wheat kernel and pasta proteins induced by toasting and drying processes

Carmela Lamacchia [a,b,*], Antonietta Baiano [a,b], Sara Lamparelli [a], Ennio La Notte [a,b], Aldo Di Luccia [c]

[a] Istituto per la Ricerca e le Applicazioni Biotecnologiche per la Sicurezza e la Valorizzazione dei Prodotti Tipici e di Qualità, Università degli Studi di Foggia, Via Napoli, 25-71100 Foggia, Italy
[b] Dipartimento di Scienze degli Alimenti, Università degli Studi di Foggia, Via Napoli, 25-71100 Foggia, Italy
[c] Dipartimento di Progettazione e Gestione dei Sistemi Agrozootecnici e Forestali, Università degli Studi di Bari, Via Amendola 165/A, 70126 Bari, Italy

ARTICLE INFO

Article history:
Received 2 February 2009
Received in revised form 22 April 2009
Accepted 24 April 2009

Keywords:
Protein size distribution
Intermediate aggregate proteins
Composite pasta
Toasted durum wheat seed
Toasted durum wheat flour

ABSTRACT

Durum wheat kernels were subjected to a toasting process and the proteins characterised by size exclusion-high performance liquid chromatography (SE-HPLC) and sodium dodecyl sulphate–polyacrylamide gel electrophoresis. With this physical process, albumins and globulins, as well as glutenins and gliadins, polymerised as seen by a shift of the SE-HPLC profile to lower elution times. The polymerisation seemed to happen mainly through disulphide bonds, even though the participation of ω-gliadins to the aggregation suggested the involvement of other kinds of interactions. It led to the revelation of a new peak originated by thermal aggregation of small polymeric proteins. The changes in the chromatographic profile were accompanied by increasing amounts of total unextractable polymeric proteins. The replacement of semolina with toasted durum wheat flour (5%, 10%, 15%, 20% and 30%) for the production of pasta in the shape of spaghetti significantly ($p < 0.001$) affected the molecular size distribution of the polymeric proteins, even though the replacement of semolina with 5% and 10% of toasted durum wheat flour (TDWF) did not significantly ($p > 0.05$) change the unextractable polymeric proteins (UPP) when compared with spaghetti made with 100% durum semolina. On the other hand, the replacements of semolina with 15–30% TDWF showed significant ($p < 0.001$) increase in UPP when compared with 100% durum semolina spaghetti.

1. Introduction

Wheat is currently the most important crop in the world, with total annual yields of almost 600 million tonnes. Much of the success of wheat stems from its processing properties and in particular its ability to form cohesive doughs which can be baked into bread or formed into pasta and noodles. These properties derive largely from the gluten proteins, which form a continuous viscoelastic network within the dough. Gluten contains hundreds of proteins components, which are present either as monomers or, linked by interchain disulphide bonds, as oligo- and polymers (Wrigley & Bietz, 1998). They are unique in terms of their amino acids composition, which are characterized by high contents of glutamine and proline and by low contents of amino acids with charged side groups. Traditionally gluten proteins have been divided into gliadins and glutenins, according to their polymerisation properties: gliadins are monomeric proteins that form only intra-molecular disulphide bonds, if present, whereas glutenins are polymeric proteins whose subunits are held together by inter-molecular disulphide bonds, although intra-chain bonds are also present. Among these storage proteins, glutenins (polymeric proteins) have been shown to be extremely important in determining rheological properties. Moreover, a certain amount of these polymers remains unextractable in various extracting systems (e.g. acetic acid solution or SDS–phosphate buffer) and the proportion of this fraction, known as unextractable polymeric proteins (UPP), is reported to be related to the technological response (Gupta, Khan, & MacRitchie, 1993; Jia, Fabre, & Aussenac, 1996).

Gluten proteins are susceptible to heat treatment and their behaviours subjected to relatively high temperatures have been studied by a numbers of workers. It was shown that molecular size of the glutenin aggregates increases and, hence, their extractability decreases (Booth et al., 1980; Schofield, Bottomley, Timms, & Booth, 1983; Weegels, de Groot, Verhoek, & Hamer, 1994b). At 100 °C, gliadins undergo similar changes. The extractability of gliadins from bread by 60% ethanol is much lower than that from flour, and α-and γ-giadins are more affected than ω-giadins (Wieser, 1998). The effects have been ascribed to sulphidryl

* Corresponding author. Address: Istituto per la Ricerca e le Applicazioni Biotecnologiche per la Sicurezza e la Valorizzazione dei Prodotti Tipici e di Qualità, Università degli Studi di Foggia, Via Napoli, 25-71100 Foggia, Italy. Tel.: +39 881 589 117; fax: +39 881 589 217.
E-mail address: c.lamacchia@unifg.it (C. Lamacchia).

0308-8146/$ - see front matter © 2009 Elsevier Ltd. All rights reserved.
doi:10.1016/j.foodchem.2009.04.100

(SH)-disulphide interchange reactions induced by heat, that affect all gluten proteins except the cysteine-free ω-giadins (Booth et al., 1980; Schofield et al., 1983). Morel, Redl, and Guilbert (2002) suggested that below 60 °C no changes in free sulphydryl groups occur. Heating to at least 90 °C leads to disulphide bond linked aggregates and conformational changes affecting mostly gliadins and low molecular weight albumins and globulins (Guerrieri, Alberti, Lavelli, & Cerletti, 1996). Although, Kokini, Cocero, Madeka, and de Graaf (1994) proposed that cross-links among gliadin molecules are formed above 70 °C in the absence of glutenins, others believed that gliadins cross-link only with glutenins (Redl, Morel, Bonicel, Vergnes, & Guilbert, 1999; Singh & MacRitchie, 2004). As a matter of fact, the incorporation of gliadin monomers in the glutenin network leads to a three-dimensional structure (Morel et al., 2002).

Apart from its fundamental interest, the effects of heating on gluten proteins are relevant to practical processes, such as drying of rain-damaged wheat, drying of gluten from starch/gluten manufacturing plants and, in relation to effects on gluten proteins during baking, pasta making and extrusion and the potential for producing modified glutens with unique technological properties. A traditional pasta used by poor Apulian people, which lived in Southern Italy, was home made brown pasta by durum semolina obtained from toasted kernel. The toasted kernel was the product of burning remained straw in the fields; in this way residual kernels were subjected to high temperature treatment. The poor people looked for toasted kernel in the straw ash and picked up it manually. Today pasta from toasted kernel, "Grano arso" called in Italy, is an actual commercial activity in Puglia.

To increase our insight into the behaviour of gluten proteins during heat treatment, the size exclusion-high performance liquid chromatography (SE-HPLC) was used to examine polymerisation of the different protein fractions of durum wheat kernels subjected to a toasting process and to evaluate their changes in molecular size distribution. In addition, the effect of the partial replacement of semolina with toasted durum wheat flour (5%, 10%, 15%, 20% and 30%) was studied to improve and optimize the process of traditional pasta production from "Grano arso". To reach this objective, SE-HPLC profiles and the UPP of the composite pasta were evaluated thus to gain a better understanding of size distribution and possible interactions at the molecular level.

2. Experimental

2.1. Raw materials

Semolina and toasted durum wheat flour (TDWF) derived from the same commercial blend of Italian durum wheats (Simeto, Ciccio, Arcangelo) were supplied by Molino Daddario Antonia (Cerignola, Foggia, Italy). The toasted meal was obtained by the milling of heat treated caryopses previously harvested and threshed. In particular, cleaned durum wheat grains were arranged on steel bearing placed into direct contact with a wood-fire for 120 s until kernels browned; then, grains were cleaned again and dampened; and after eight hours the grains were subjected to grinding using a roller mill. The particle size of the TDWF used was in the range of 200–355 μm.

2.2. Pasta production

Pasta was produced in a 2-kg pilot plant (NAMAD, Rome, Italy) consisting of a mixer, an extruder and a dryer. The flour was mixed with tap water (for 10 min) to obtain a dough water content of 44–45%. The extrusion conditions were as follows: temperature = 50 °C (the extrusion temperature varied between 45 °C and 55 °C); kneading time = 15 min, pressure = 60–125 atm as a function of the specific formulation and vacuum degree = 700 mm Hg. A Teflon die-plate of 1.70 mm diameter was used. Pasta in the shape of spaghetti was dried at 50 °C for 16 h. The diameter of the obtained spaghetti was about 1.70 ± 0.03 mm. Six kinds of spaghetti were produced: a control, made of 100% durum wheat semolina and pasta in which 5%, 10%, 15%, 20% and 30% of semolina was replaced with TDWF (named respectively as 5% TDWF-, 10% TDWF-, 15% TDWF-, 20% TDWF-, and 30% TDWF-wheat spaghetti).

2.3. Proteins extraction for SE-HPLC

Proteins from semolina, toasted durum wheat flour and milled spaghetti samples were extracted following the method of Gupta et al. (1993). Samples (10 mg) were suspended in 1 mL 0.5% sodium-dodecyl-sulphate (SDS)–phosphate buffer (pH 6.9) and mixed initially in a vortex-mixer and later kept at room temperature for 30 min. The suspensions were then centrifuged for 10 min at 17,000 g to obtain supernatant ("extractable" or "SDS-soluble" proteins).

The resulting residues were extracted with 0.9 ml 0.5% SDS–phosphate buffer (pH 6.9) by sonication for 15 s using a Microson Ultrasonic (Falc Instrument, Bergamo, Italy) cell distributor, ensuring that the samples were completely dispersed within the first 5 s and then heating to 35 °C for 30 min. The supernatants from centrifugation for 10 min at 17,000*g* were termed "unextractable" proteins. All extracts were filtered through a 0.45 μm PVDF filter prior to SE-HPLC analysis.

2.4. SE-HPLC analysis

Polymeric proteins from the semolina, toasted durum wheat flour and milled spaghetti samples were fractionated through size exclusion-high performance liquid chromatography (SE-HPLC) using a Phenomenex Biosep TM SEC 4000 column (Phenomenex) (Kuktaite, Johansson, & Juodeikiene, 2000; Kuktaite, Larsson, & Johansson, 2003). Proteins from semolina and milled spaghetti were extracted with a two step extraction procedure (Gupta et al., 1993). The first step in this method extracts the SDS-extractable proteins (soluble in diluted SDS), whilst the second extract contains the SDS-unextractable proteins (proteins soluble only after sonication). The extracted proteins were separated on SE-HPLC according to Tosi et al. (2005) by loading 20 μl of sample into an eluant of 50% (v/v) acetonitrile and water containing 0.05% (v/v) trifluoracetic acid (TFA) at a flow rate of 0.7 mL/min for 30 min. Proteins were detected at a wavelength of 214 nm. Three replicates of each samples were used for the investigation of protein composition. The percentage of unextractable polymeric protein (UPP) was calculated as described by Gupta et al. (1993). Briefly, the percentage of total UPP was calculated as [peak 1 + 2 area (unextractable)/peak 1 + 2 area (total)] × 100. Peak 1 + 2 (total) refers to the total of peak 1 + 2 (extractable) and peak 1 + 2 (unextractable) (Johansson, Prieto-Linde, & Jonsson, 2001; Kuktaite et al., 2000, 2003).

The SE-HPLC column was calibrated using protein standards with a range of molecular weights (KDa) as follows: ribonuclease A (13.7), chymotripsinogen (25.0), ovalbumin (43.0), bovine serum albumin (67.0), aldolase (158), catalase (232), ferritin (440) and thyroglobulin (669).

The molecular weights were calculated from the line of best fit through the calibration points, given by: log molecular weight = 8.1448–0.1995 × elution time (min).

2.5. SDS–PAGE (sodium dodecyl sulphate–polyacrilamide gel electrophoresis) analyses

One hundred gram were sequentially extracted by the Osborne procedure (Osborne, 1907) with modifications. Albumin and globulins

were extracted with 0.1 N NaCl for 30 min, vortexing for 1 min, every 10 min at 24 °C (room temperature). The mixture was centrifuged at 11,294*g* for 10 min at 24 °C using a Model IEC CL 31R Multispeed Centrifuge (Thermo Electron Corporation, 81 Wyman St. Waltham, MA 02454–9046 Stati Uniti). Four volumes of cold pure acetone were added to the supernatant (albumin/globulin extract) and stored at −20 °C overnight to precipitate the albumin/globulin. The solution was centrifugated at 4 °C for 10 min at 11,294*g* and the pellet was dissolved with buffer containing Tris–HCl 0.0625 M, SDS 2%, Glycerol 10% and Dithiotreitol (DTT) 1.5%.

The centrifuged albumin/globulin (pellet) was washed with deionized water for 30 min vortexing for 1 min, every 10 min at 24 °C. The mixture was centrifuged at 24 °C for 10 min at 11,294*g*. The washing was repeated four times with deionized water to reduce the effect of the salt in the centrifugate for the extraction of gliadins in the following steps. The gliadin fractions were extracted with 70% aqueous ethanol for 30 min, vortexing for 1 min, every 10 min at 24 °C. The mixture was centrifuged at 24 °C for 10 min at 11,294*g*. Four volumes of cold pure acetone were added to the supernatant (gliadins extract) and stored at −20 °C overnight to precipitate the gliadins. The solution was centrifuged at 4 °C for 10 min at 11,294*g* and the pellet was dissolved with buffer containing Tris–HCl 0.0625 M, SDS 2%, Glycerol 10% and 1.5% DTT. Glutenins were extracted by incubating the gliadins centrifuged (pellet) with 50% (v/v) 1-Propanol and 0.08 M Tris–HCl (pH 8.0) for 30 min, vortexed for 1 min every 10 min. The mixture was centrifuged at 24 °C for 10 min at 11,294*g*. Four volumes of cold pure acetone were added to the supernatant and stored at −20 °C overnight. The solution was centrifuged at 4 °C for 10 min at 11,294*g* and the pellet was dissolved with buffer containing Tris–HCl 0.0625 M, SDS 2%, Glycerol 10% and 1.5%. DTT. Each protein fraction (7.5 μl) was subjected to SDS–PAGE according to Laemmli (1970), at 25 mA for 3 h at 24 °C. The acrylamide content of a separation-slab-gel (13.5 × 11 cm) was 12.5%. The gels were stained with 0.25% w/v Coomassie Brilliant Blue (CBB) overnight.

2.6. Statistical analysis

The results were compared by one-way variance analysis (ANOVA). A Duncan's multiple range test, with the option of homogeneous groups ($p < 0.05$), was used to determine significant differences between samples. STATISTICA 7.1 for Windows (StatSoft, Inc, Tulsa, OK, USA) was used for this purpose.

3. Results and discussion

3.1. Effect of seed toasting on flour protein fractions

Proteins profile from semolina chromatogram is depicted in Fig. 1a. It shows a polymeric-protein peak of high molecular weight glutenin proteins at the extreme left of the profile and indicated as large polymeric protein (LPP), followed by a small peak of low molecular weight glutenin proteins, indicated as small polymeric proteins (SPP), and finally by a notable peak of large monomeric proteins (LMP) called gliadins and small peaks of albumins and globulins, indicated as small monomeric proteins (SMP) (Carceller & Aussenac, 2001; Larroque, Gianibelli, Batey, & MacRitchie, 1996, 1997; Tosi et al., 2005).

The SE-HPLC elution profile for TDWF (Fig. 1b) shows, respect to the semolina profile, a peak fusion, indicating a protein denaturation. Nevertheless, four main peaks are distinguishable: LPP, LMP, SMP and a new intermediate protein (IP) peak, with a molecular weight comprised between LMP and SMP. The TDWF profile shows a greatest proportion IP and a higher proportions of LPP than that of semolina. The chromatogram of TDWF did not show

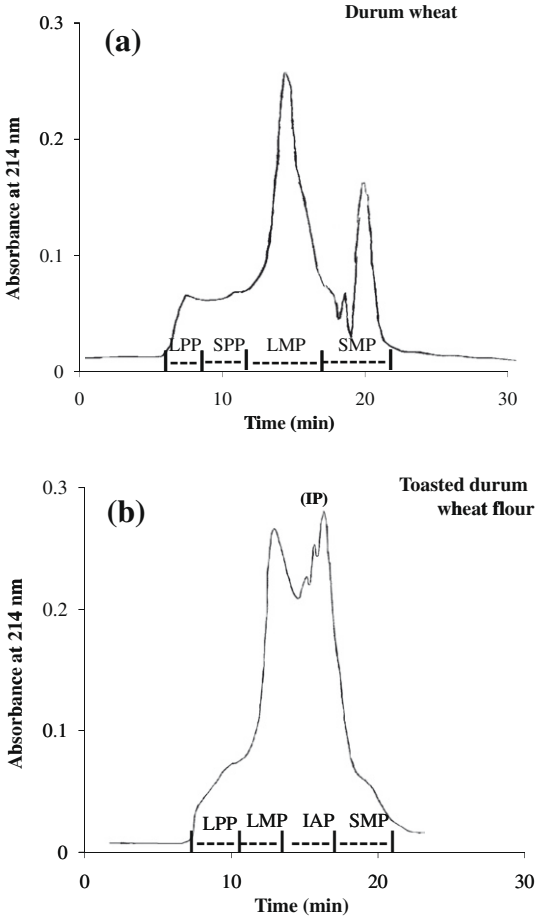

Fig. 1. SE-HPLC elution profile of durum wheat semolina (a) and TDWF (b). LPP: large polymeric proteins; LMP: large monomeric proteins; IAP: intermediate aggregates proteins; SMP: small polymeric proteins; IP: intermediate proteins.

the peak corresponding to the SPP in the semolina, that probably have been included in the LPP by polymerisation. This is consistent with results obtained by Singh and MacRitchie (2004) and Lamacchia et al. (2007), that observed the same changes in the polymerisation of gluten proteins when gluten was subjected to heating. The occurrence of the IP and the increase of the LPP are explainable with the concomitant decrease of the SMP and LMP peaks and the disappearance of the SPP. Considering that LPP, SMP and LMP are mainly represented by glutenin, albumin/globulin and gliadin proteins, respectively, (Carceller & Aussenac, 2001; Larroque et al., 1996), the high temperature applied may cause both the formation of intermolecular hydrogen bonding (Eckert, Amend, & Belitz, 1993) and disulphide cross-linking by the oxidation of glutenin free SH groups (Gobin, Ng, Buchanan, & Kobrehel, 1997; Weegels, Verhoek, de Groot, & Hamer, 1994a; Weegels et al., 1994b) among these proteins, leading to their aggregation into larger or new polymers (as evidenced from the SE-HPLC profile).

However the occurrence of the IP indicates that albumins and globulins have coagulated and reacted with gliadins forming protein aggregates. These data are not consistent with results obtained by Schofield et al. (1983), Lavelli, Guerrieri, and Cerletti (1996), Singh and MacRitchie (2004) and Lamacchia et al. (2007) that showed the incorporation, at high temperatures, of the albumins and globulins into high-molecular-weight polymers eluting in LPP peak.

A possible explanation for this phenomenon could be that the incorporation of albumins and globulins into the high-molecular-weight

polymers, during high temperature treatment, occur after gluten is already formed. In the case where the wheat proteins are subjected to high temperature treatment while present in the endosperm, polymerisation between the LPP and SMP protein classes cannot occur. This is probably due to the deposition of the two classes of proteins in different protein bodies. Indeed, it is well known that in the wheat endosperm two major transport routes run from the ER to the vacuole, one that by-passes the Golgi apparatus and another one that passes through it. Proteins travelling along either route converge as two types of protein bodies: the Endoplasmic Reticulum (ER)-derived protein bodies and the vacuolar protein bodies. Rubin, Levanony, and Galili (1992) reported that the glutenins (LPP and SPP) are retained predominantly within the ER, while the gliadins (LMP) are present in both ER-derived and vacuolar protein bodies. Furthermore, Krishnan, Franceschi, and Okita (1986) and Lending, Chesnut, Shaw, and Larkins (1989) found that cereal globulins (SMP) are deposited in vacuolar protein bodies via the Golgi apparatus.

The glutenin, gliadin and albumin/globulin fractions of semolina and TDWF were separated on SDS–PAGE under reducing (Fig. 2a) and non reducing conditions (Fig. 2b). As can be inferred by the gels, the toasting process caused both a decrease in the number of bands at higher molecular weight in the glutenins, gliadins and albumins/globulins lanes and a decrease in intensity of the bands at lower molecular weight, suggesting polymerisation of these proteins. The polymerisation seems to occur mainly through disulphide bonds, as evidenced by the non-reducing SDS–PAGE gel, although it is possible to notice some bands corresponding to ⟨omega⟩-gliadins disappear in the TDWF gliadins lane. Since ⟨omega⟩-gliadins do not contain cysteine residues, it can be suggested that the cross-linking is not occurring only through disulphide bonds.

3.2. Effect of substitution of semolina with increasing amount of toasted durum wheat flour on the pasta SE-HPLC profiles

Fig. 3 shows the SE-HPLC profiles for total proteins in spaghetti made of semolina and increasing amount (5%, 10%, 15%, 20% and 30%) of TDWF. The wheat spaghetti elution profile (Fig. 3a), used as a control, is essentially similar to that of semolina, showing a polymeric-protein peak of glutenins at the extreme left of the profile (LPP > 1,00,000 Da), followed by a large peak of monomeric gliadin proteins (LMP < 1,00,000 Da) and finally small peaks of albumins and globulins (SMP) (Larroque et al., 1996, 1997; Carceller & Aussenac, 2001). The SPP peak that contains low-molecular-weight glutenins (Larroque et al., 1996, 1997) is not present in the pasta elution profile, but present in the durum semolina profile. Lamacchia et al. (2007) demonstrated that SPP is included in the LPP, through polymerisation, during pasta drying cycles at ~60 °C. The temperatures used for pasta/spaghetti drying may promote the formation of both intermolecular hydrogen bonding between gluten protein subunits (Eckert et al., 1993) and protein disulphide cross-linking due to the oxidation of free SH groups of glutenin (Gobin et al., 1997; Weegels et al., 1994a,1994b), leading to aggregation of the pasta proteins into larger polymers. The elution profiles of 100% durum semolina spaghetti (Fig. 3a) and spaghetti with 5%, 10%, 15%, 20% and 30% semolina replaced with TDWF (Fig. 3b–f) were essentially similar. They all showed three main peaks (i.e., low-, medium- and high-molecular-weight), although their proportions varied on the basis of the percentage of TDWF added. In particular, it is possible to notice that the LPP peak of TDWF-wheat spaghetti increased significantly ($p < 0.001$) with respect to 100% durum semolina spaghetti. As the amount of TDWF increased to 15% there was an increase in the IP peak, while the LMP and SMP peaks decreased. On the contrary, in spaghetti made with 20% and 30% TDWF, the IP and SMP peaks decreased, while the

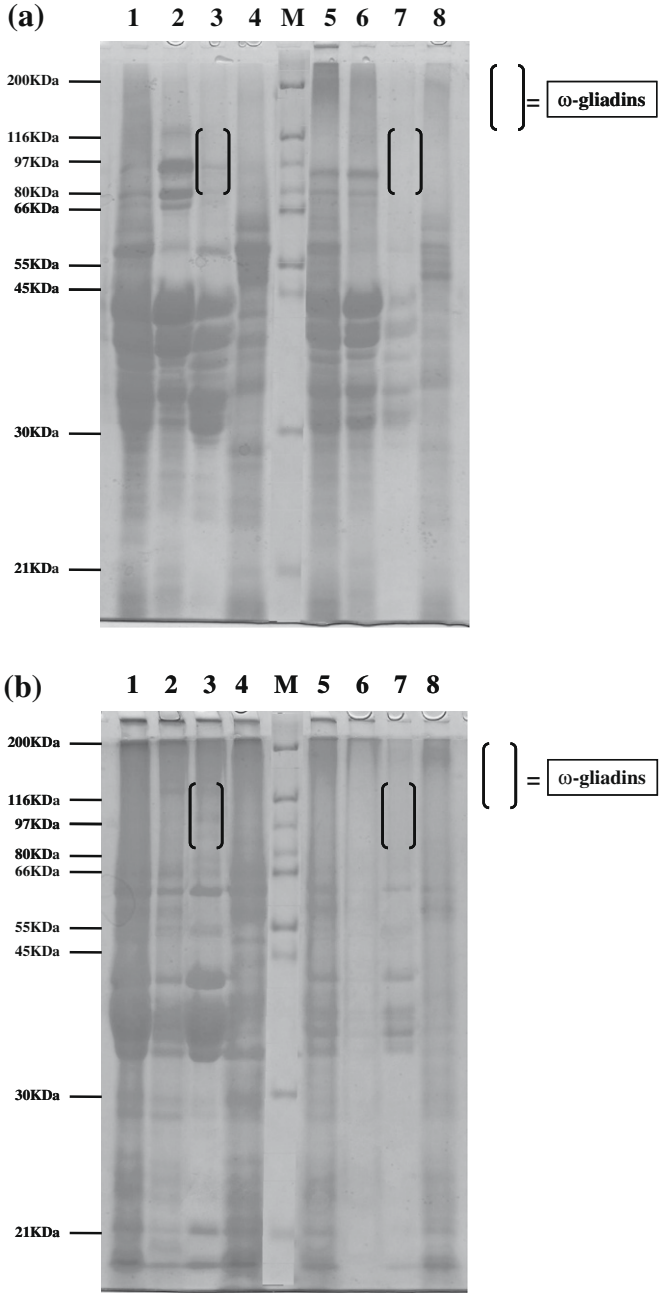

Fig. 2. SDS–PAGE separation of durum wheat semolina and TDWF protein fractions under reducing (a) and non reducing (b) conditions. Lane 1: durum wheat semolina total proteins; lane 2: durum wheat semolina glutenins; lane 3: durum wheat semolina gliadins; lane 4: durum wheat semolina albumins/globulins: M: marker; lane 5: TDWF total proteins; lane 6: TDWF glutenins; lane 7: TDWF gliadins; lane 8: TDWF albumins/globulins.

LMP peak increased. Therefore, it may be suggested that based on the amount of TDWF added for the preparation of spaghetti, two different aggregation arrangements occurred.

3.3. Changes in molecular weight distribution (MWD) and protein extractability

The changes in amount of protein measured by the chromatogram area, for the different protein fractions of TDWF and spaghetti samples, are shown in Table 1 and Table 2, respectively. The LPP peak increased significantly in TDWF when compared with semolina (Table 1), and a decrease of SPP, LMP and SMP peaks and

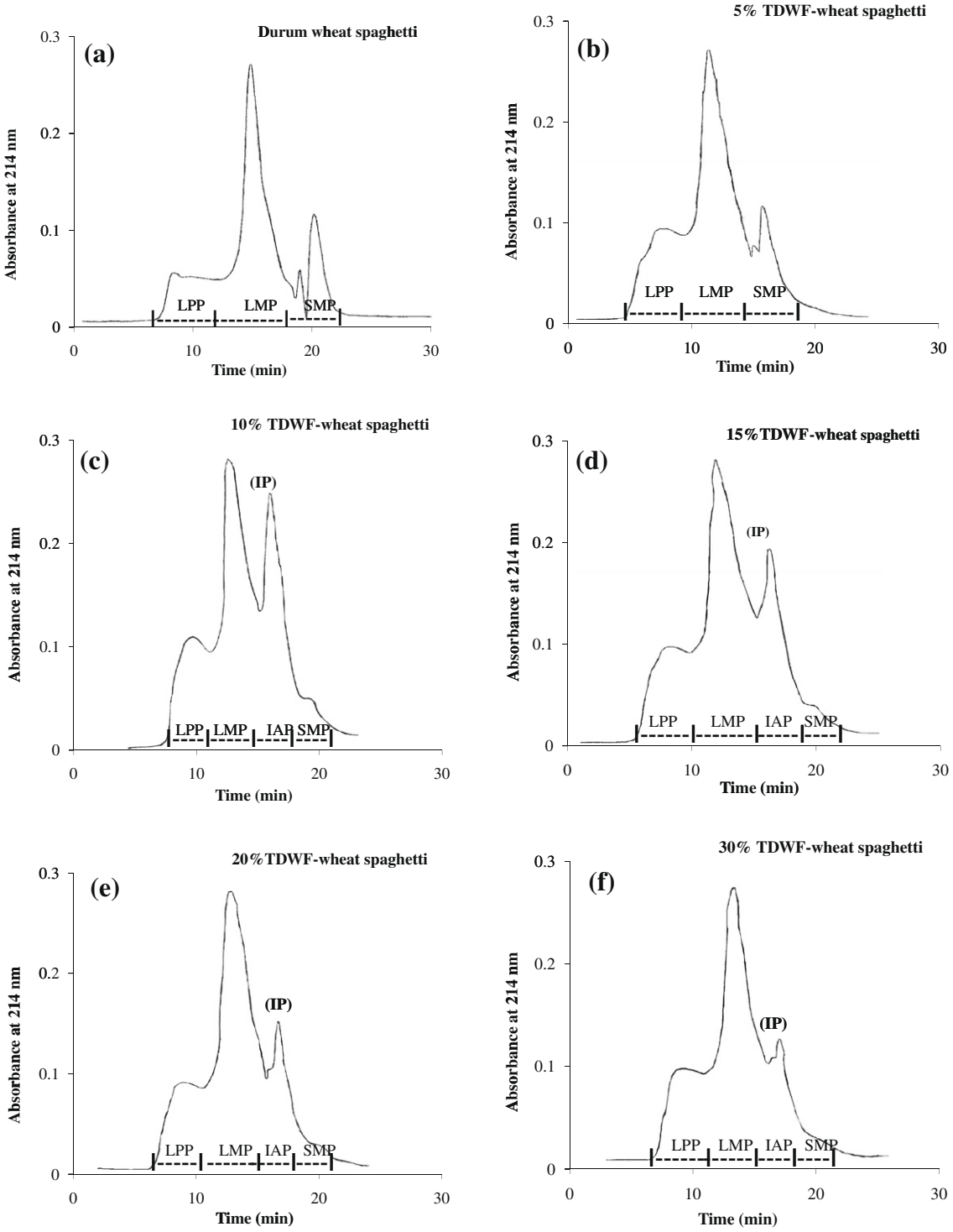

Fig. 3. SE-HPLC elution profile of spaghetti made of semolina (a) and semolina and increasing amount of TDWF: 5% TDWF-wheat spaghetti (b), 10% TDWF-wheat spaghetti (c), 15% TDWF-wheat spaghetti (d), 20% TDWF-wheat spaghetti (e) and 30% TDWF-wheat spaghetti (f).

the formation of an IP peak is detected (Table 1). It is evident that the toasting process caused a major upward shift in protein molecular weight distribution. Thus, the polymeric proteins with low-molecular weight (i.e., gliadins and albumins/globulins) were denatured and polymerised into high-molecular weight proteins eluting in the LPP and IP peaks. However, a decrease in the area of peaks SPP, LMP and SMP does not appear to be sufficient on its own to account for the increased area of the LPP peak and for the formation of the IP peak. In fact, Table 1 shows a significant decrease of total peak areas, indicating the possibility that part of the monomeric proteins and possibly SPP were denatured and made unextractable. These results are consistent with reports by Lagrain, Brijs, Veraverbeke, and Delcour (2005) and Lamacchia et al. (2007) who observed a similar phenomenon in both wheat proteins subjected to high temperature treatment and in wheat pasta proteins subjected to high temperature during the drying cycles. On the contrary, Table 2 shows a significant increase in the total peak area of the composite pasta (i.e., TDWF-wheat spaghetti) compared to

Table 1
Values of the SE-HPLC peaks area for the semolina and the TDWF.

	LPP peak area (%)	SPP peak area (%)	LMP peak area (%)	IAP peak area (%)	SMP peak area (%)	Total peaks area % (uV s)
Durum wheat	5.6 A	0.2 A	64.3 A	0 A	29.7 A	100 (5497292.6) A
Toasted durum wheat flour	11.6 B	0 B	39.5 B	48.3 B	0.5 B	100 (4842757.507) B

A, B = $P < 0.001$.
LPP: large polymeric proteins.
SPP: small polymeric proteins.
LMP: large monomeric proteins.
IAP: intermediate aggregated proteins.
SMP: small polymeric proteins.

Table 2
Values of the SE-HPLC peaks area for the investigated spaghetti samples.

Peaks	Durum wheat spaghetti	5% TDWF-wheat spaghetti	10% TDWF-wheat spaghetti	15% TDWF-wheatspaghetti	20% TDWF-wheat spaghetti	30% TDWF-wheat spaghetti
LPP peak area (%)	9.6 A	23 B	19.2 C	21.1 C	22.6B	23.7 B
LMP peak area (%)	66.6 A	63.7 B	48.9 C	54.2C	63.3 B	63 B
IAP peak area (%)	0 A	0 A	23.4 B	22 B	13.7 C	13.1 C
SMP peak area (%)	23.8 A	13.3B	8.5 B	2.7C	0.4 D	0.2D
Total peaks area % (μV s)	100(8 188 077.84) A	100(17509437.05) B	100 (20702 075.05) C	100(22477781.18) D	100 (23741970.6) E	100 (24572626.95) F

A, B, C, D, E ,F = $P < 0.001$.
LPP: large polymeric proteins.
LMP: large monomelic proteins.
IAP: intermediate aggregated proteins.
SMP: small polymeric proteins.

that of the traditional pasta (i.e., 100% durum semolina spaghetti). Even though only LPP and IP showed increased peak areas, the increase of these peaks was accompanied by a decrease in the SMP and LMP peak areas. In particular, in pasta containing 5% TDWF, the LMP and SMP were probably completely denatured at high temperature and incorporated into the high-molecular weight polymers eluting as LPP peak. In the spaghetti containing 10%, 15%, 20% and 30% TDWF, LMP and SMP were denatured and prob-

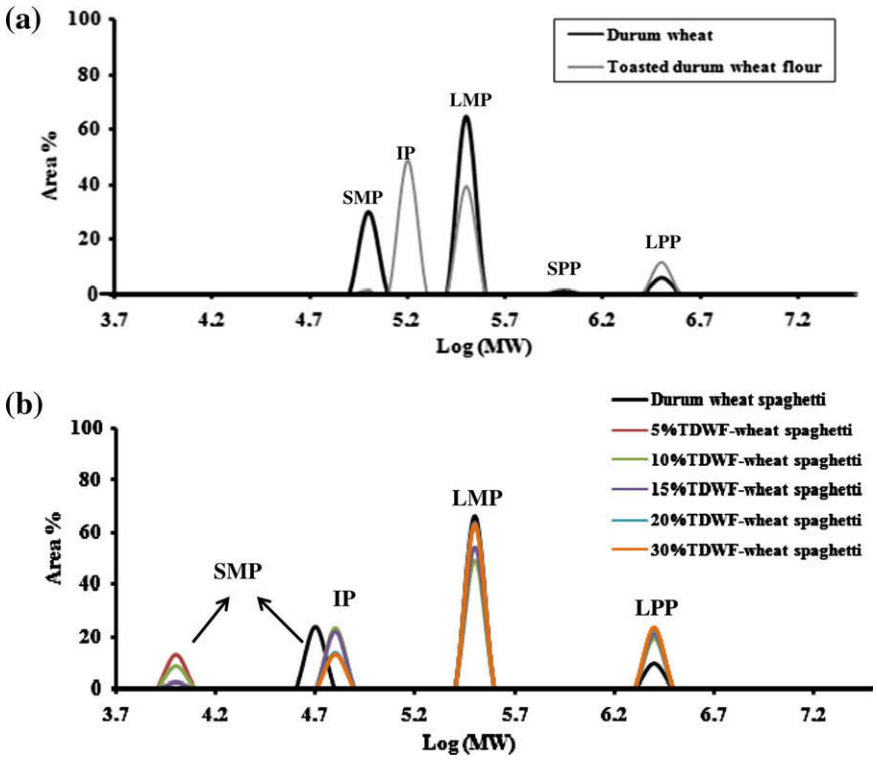

Fig. 4. Changes in molecular weight distribution induced by toasting process on durum semolina proteins (a): LPP: large polymeric proteins; SPP: small polymeric proteins; LMP: large monomeric proteins; IP: intermediate proteins; SMP: small monomeric proteins. Changes in molecular weight distribution (MWD) induced by replacement of durum wheat semolina with increasing amount of TDWF on spaghetti proteins (b): LPP: large polymeric proteins; LMP: large monomeric proteins; IP: intermediate proteins; SMP: small monomeric proteins.

ably incorporated into both LPP and IP peaks; and there seems to exist a sort of equilibrium between the LPP and IP polymers in the TDWF-wheat spaghetti. In fact, when the IP peak increased (i.e., in 10% TDWF-wheat spaghetti), a decrease in LMP, SMP and LPP peaks was detected, when compared with 5% TDWF-wheat spaghetti. On the other hand, when IP decreased (i.e., in 15%, 20% and 30% TDWF-wheat spaghetti), a decrease in SMP and an increase in LPP and LMP peak areas was detected, when compared with the 5% TDWF-wheat spaghetti. The increase in the LMP peak may suggest that the aggregates from IP and SMP assume a similar molecular weight to LMP, and that further aggregation among these produced other LPP. This indicated that SMP initially forms an intermediate aggregate, which we refer to as intermediate aggregated proteins (IAP) and corresponds to the IP peak. Therefore an aggregation sequence could occur according to the following schematic diagram.

- TDWF: LMP + SMP → IAP;
- 5% TDWF-wheat spaghetti: $\mathrm{LMP} + \mathrm{SMP} \xrightarrow{(\text{drying cycle } 60\ ^\circ\mathrm{C})} \mathrm{LPP}$;
- 10% TDWF-wheat spaghetti: (<LPP;>IP) $\mathrm{LMP} + \mathrm{SMP} + \mathrm{LPP} \xrightarrow{(\text{drying cycle } 60\ ^\circ\mathrm{C})} \mathrm{IAP}$;
- 15, 20, 30% TDWF-wheat spaghetti: (>LPP;<IP) $\mathrm{IAP} + \mathrm{SMP} \xrightarrow{(\text{drying cycle } 60\ ^\circ\mathrm{C})} \mathrm{LMP} + \mathrm{LPP}$;

An MWD curve (Fig. 4b) illustrates how this parameter changes with the replacement of durum wheat semolina with increasing amount of TDWF. On the contrary, Fig. 4a shows the changes in molecular weight distribution (MWD) induced by the toasting process on durum wheat proteins. These results also support our hypothesis of sequential aggregation, as shown in the schematic diagram above.

3.4. Effect of seed toasting on percentage of total UPP of durum wheat flour and composite pasta

The percentage of unextractable polymeric proteins in the total polymeric proteins in wheat flour and spaghetti samples were calculated from the chromatograms obtained by protein fractionation using SE-HPLC. The unextractable polymeric proteins of TDWF proteins (100% UPP) was significantly ($p < 0.001$) higher than that of semolina (20.33% UPP) (Fig. 5a). The higher proportion of UPP in TDWF may be explained by considering the fact that during the toasting process modification in sulphydryl (SH) and disulphide bonds occur and oxidation state generates dityrosyl bonds. This results in aggregation of monomeric and polymeric proteins to larger, insoluble protein aggregates. These results are consistent with the SE-HPLC profiles and the MWD curves, and are in agreement with reports by Ewart (1979), Graveland et al. (1985) and Gobin et al. (1997). Fig. 5b shows the percentage of total UPP in spaghetti samples; and surprisingly shows that the unextractable polymeric proteins in the 5% TDWF- and 10% TDWF-wheat spaghetti were not significantly ($p > 0.05$) different from spaghetti made with 100% durum semolina. On the contrary, the unextractable polymeric proteins in 15% TDWF-, 20% TDWF- and 30% TDWF-wheat spaghetti were significantly ($p < 0.001$) higher than 100%

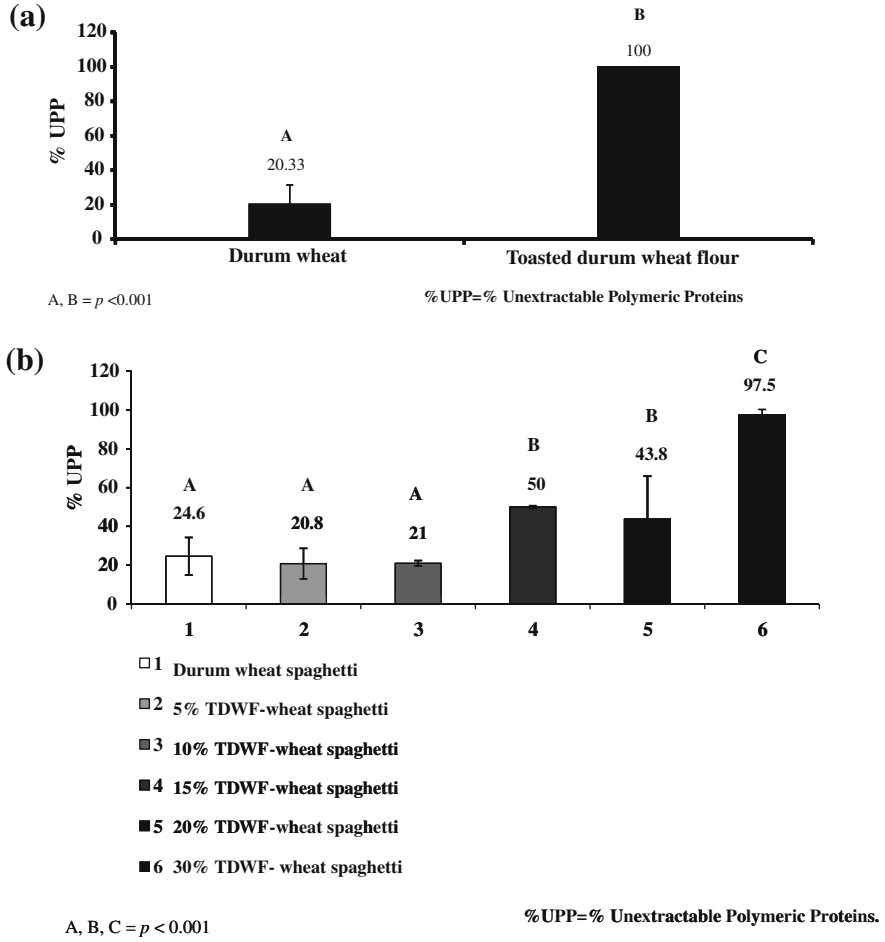

Fig. 5. Percentage of total UPP (unextractable polymeric proteins) of durum wheat semolina and TDWF (a) and in the investigated spaghetti samples (b).

durum semolina spaghetti. There was no significant difference ($p > 0.05$) between the 5% TDWF- and 10% TDWF-wheat spaghetti. Similarly there was no significant difference ($p > 0.05$) between the 15% TDWF- and 20% TDWF-wheat spaghetti. The fact that the UPP level is influenced by the different conformational structures derived from aggregate and polymer formation, may suggest that the large protein aggregates (formed by heat denaturation during the toasting of durum wheat kernels) further interacted with gluten proteins during the preparation of pasta. So, all aggregates derived from denatured proteins, since their hydrophobicity increased, interacted among them and this phenomenon is supported by covalent bonds induced by high temperature. Consequently, the formation of very large, insoluble and stable protein aggregates occurred.

4. Conclusions

The high temperature applied to durum wheat kernels induced significant changes in proteins. size exclusion-high performance liquid chromatography profile indicates that proteins were denatured and polymerised and that albumins and globulins tended to coagulate and interact with gliadins, to form protein aggregates of intermediate molecular weight revealed as a new Intermediate Protein (IP) peak, which corresponds to an Intermediate Aggregate Protein designated as IAP. The participation of the < omega > gliadins to the changes suggests that interactions other than disulphide bonds were involved. The physical modification process, to which the durum wheat kernels were subjected, altered also the size distribution of proteins that increased in size and insolubility. The replacement of durum wheat semolina with increasing percentage of Toasted durum wheat flour affects significantly the molecular weight distribution of derived pasta and induced variations in sodium-dodecyl sulphate-unextractable components, which become the major part of the proteins (97%) in the 30% of toasted durum wheat flour-wheat pasta.

Since an high content of sodium-dodecyl sulphate-unextractable polymeric proteins is known to be correlated with the good quality of the final wheat product, the best mixture to make pasta from ''Grano arso", on the basis of our results, was that containing higher percentage of toasted durum wheat flour.

References

Booth, M. R., Bottomley, R. C., Ellis, J. R. S., Malloch, G., Schofield, J. D., & Timms, M. F. (1980). The effect of heat on gluten-physico-chemical properties and baking quality. *Annales de Technologie Agricole, 1*, 399–408.

Carceller, J. L., & Aussenac, T. (2001). SDS–insoluble glutenin polymer formation in developing grains of hexaploid wheat: The role of the ratio of high to low molecular weight glutenin subunits and drying rate during ripening. *Australian Journal of Plant Physiology, 26*, 301–310.

Eckert, B., Amend, T., & Belitz, H.-D. (1993). The course of the SDS and Zeleny sedimentation tests for gluten quality and related phenomena studied using the light microscope. *Zeitschrift fur Lebensmittel-Untersuchung und-Forschung, 196*, 122–125.

Ewart, J. (1979). Glutenin structure. *Journal of the Science of Food and Agriculture, 30*, 482–492.

Gobin, P., Ng, P. K. W., Buchanan, B. B., & Kobrehel, K. (1997). Sulphydryl–disulfide changes in proteins of developing wheat grain. *Plant Physiology and Biochemistry, 35*, 777–783.

Graveland, A., Bosveld, P., Lichtendonk, W. J., Marseilled, J. P., Moonen, J. H. E., & Scheepstra, A. (1985). A model for the molecular structure of the glutenins from wheat flour. *Journal of Cereal Science, 3*, 1–16.

Guerrieri, N., Alberti, E., Lavelli, V., & Cerletti, P. (1996). Use of spectroscopic and fluorescence techniques to assess heat-induced molecular modifications of gluten. *Cereal Chemistry, 73*, 368–374.

Gupta, R. B., Khan, K., & MacRitchie, F. (1993). Biochemical basis of flour properties in bread wheats. I. Effects of variation in the quantity and size distribution of polymeric protein. *Journal of Cereal Science, 18*, 23–41.

Jia, Y. Q., Fabre, J.-L., & Aussenac, T. (1996). Effects of growing location on response of protein polymerization to increased nitrogen fertilization for the common wheat cultivar Soisson: Relationship with some aspects of the breadmaking quality. *Cereal Chemistry, 73*, 526–532.

Johansson, E., Prieto-Linde, M. L., & Jonsson, J. O. (2001). Effects of wheat cultivar and nitrogen application on storage protein composition and breadmaking quality. *Cereal Chemistry, 78*, 19–25.

Kokini, J. L., Cocero, A. M., Madeka, H., & de Graaf, E. (1994). The development of state of diagrams for cereal proteins. *Trends in Food Science and Technology, 5*, 281–288.

Krishnan, H. B., Franceschi, V. R., & Okita, T. W. (1986). Immunochemical studies on the role of the Golgi complex in protein-body formation in rice seeds. *Planta, 169*, 471–480.

Kuktaite, R., Johansson, E., & Juodeikiene, G. (2000). Composition and concentration of proteins in Lithuanian wheat cultivars: Relationships with bread-making quality. *Cereal Research Communications, 28*, 195–202.

Kuktaite, R., Larsson, H., & Johansson, E. (2003). Protein composition in different phases obtained by the ultracentrifugation of dough. *Acta Agronomica Hungarica, 51*, 163–172.

Lagrain, B., Brijs, K., Veraverbeke, W. S., & Delcour, J. A. (2005). The impact of heating and cooling on the physic-chemical properties of wheat gluten water suspensions. *Journal of Cereal Science, 42*(3), 327–333.

Lamacchia, C., Di Luccia, A., Baiano, A., Gambacorta, G., la Gatta, B., Pati, S., et al. (2007). Changes in pasta proteins induced by drying cycles and their relationship to cooking behaviour. *Journal of Cereal Science, 46*, 58–63.

Larroque, O. R., Gianibelli, M. C., Batey, I. L., & MacRitchie, F. (1996). Identification of elution subfractions from the first peak in SE-HPLC chromatograms of wheat storage proteins. In C. W. Wrigley (Ed.), *Proceedings of sixth international gluten workshop, cereal chemistry division* (pp. 228–293). North Melbourne, Australia: Royal Australian Chemical Institute.

Larroque, O. R., Gianibelli, M. C., Batey, I. L., & MacRitchie, F. (1997). Electrophoretic characterisation of fractions collected from gluten protein extracts subjected to size exclusion high-performance liquid chromatography. *Electrophoresis, 18*, 1064–1067.

Lavelli, V., Guerrieri, N., & Cerletti, P. (1996). Controlled reduction study of modifications induced by gradual heating in gluten proteins. *Journal of Agricultural and Food Chemistry, 44*, 2549–2555.

Lending, C. R., Chesnut, R. S., Shaw, K. L., & Larkins, B. A. (1989). Immunolocalization of avenin and globulin storage proteins in developing of *Avena sativa* L. *Planta, 178*, 315–324.

Morel, M.-H., Redl, A., & Guilbert, S. (2002). Mechanism of heat and shear mediated aggregation of wheat gluten upon mixing. *Biomacromolecules, 3*, 488–497.

Osborne, T. B. (1907). The proteins of the wheat kernel. *Publications of the Carnegie Institution Washington* No. 84, and for the Judd and Detweiler, Washington, USA

Redl, A., Morel, M. H., Bonicel, J., Vergnes, B., & Guilbert, S. (1999). Extrusion of wheat gluten plasticized with glycerol: Influence of process conditions on flow behaviour, rheological properties, and molecular size distribution. *Cereal Chemistry, 76*, 361–370.

Rubin, R., Levanony, H., & Galili, G. (1992). Evidence for the presence of two different types of protein bodies in wheat endosperm. *Plant Physiology, 98*, 718–724.

Schofield, J. D., Bottomley, R. C., Timms, M. F., & Booth, M. R. (1983). The effect of heat on wheat gluten and the involvement of sulphydryl–disulphide interchange reactions. *Journal of Cereal Science, 1*, 241–253.

Singh, H., & MacRitchie, F. (2004). Changes in proteins induced by heating gluten dispersions at high temperature. *Journal of Cereal Science, 39*, 297–301.

Tosi, P., Masci, S., Giovangrossi, A., D'Ovidio, R., Bekes, F., Larroque, O., et al. (2005). Modification of the low molecular weight (LMW) glutenin composition of transgenic durum wheat: Effects on glutenin polymer size and gluten functionality. *Molecular Breeding, 16*, 113–126.

Weegels, P. L., Verhoek, J. A., de Groot, A. M. G., & Hamer, R. J. (1994a). Effects on gluten of heating at different moisture contents. I. Changes in functional properties. *Journal of Cereal Science, 19*, 31–38.

Weegels, P. L., de Groot, A. M. G., Verhoek, J. A., & Hamer, R. J. (1994b). Effects on gluten of heating at different moisture contents. II. Changes in physico-chemical properties and secondary structure. *Journal of Cereal Science, 19*, 39–47.

Wieser, H. (1998). Investigation on the extractability of gluten proteins from wheat bread in comparison with flour. *Zeitschrift fur Lebensmittel-Untersuchung und-Forschung, 207*, 128–132.

Wrigley, C. W., & Bietz, J. A. (1998). Proteins and amino acids. In Y. Pomeranz (Ed.), *Wheat chemistry and technology* (3rd ed., pp. 159–275). St. Paul, MN, USA: AACC.

Food Chemistry 118 (2010) 199–207

Contents lists available at ScienceDirect

Food Chemistry

journal homepage: www.elsevier.com/locate/foodchem

Antioxidant and antiproliferative activities of phytochemicals from Quince (*Cydonia vulgaris*) peels

Daniela Alesiani [a], Antonella Canini [a], Brigida D'Abrosca [b], Marina DellaGreca [c], Antonio Fiorentino [b,*], Claudio Mastellone [b], Pietro Monaco [b], Severina Pacifico [b]

[a] *Dipartimento di Biologia, Università di Roma "Tor Vergata", Via della Ricerca Scientifica 1, I-00133 Rome, Italy*
[b] *Dipartimento di Scienze della Vita, Laboratorio di Fitochimica, Seconda Università degli Studi di Napoli, Via Vivaldi 43, I-81100 Caserta, Italy*
[c] *Dipartimento di Chimica Organica e Biochimica, Università Federico II, Via Cinthia 4, I-80126 Napoli, Italy*

ARTICLE INFO

Article history:
Received 29 July 2008
Received in revised form 20 March 2009
Accepted 24 April 2009

Keywords:
Quince
Cydonia vulgaris
Triterpenes
Carotenoids
Phenols
Antioxidant activity
Antiproliferative activity

ABSTRACT

Fifty-nine secondary metabolites have been isolated from *Cydonia vulgaris* peels and characterised on the basis of their spectroscopic features. Among them, five metabolites, 3β-(18-hydroxylinoleoyl)-28-hydroxyurs-12-ene (**12**), 3β-linoleoylurs-12-en-28-oic acid (**15**), 3β-oleoyl-24-hydroxy-24-ethylcholesta-5,28(29)-diene (**24**), tiglic acid 1-*O*-β-D-glucopyranoside (**35**), and 6,9-dihydroxymegastigmasta-5,7-dien-3-one 9-*O*-β-D-gentiobioside (**46**), have been isolated and elucidated for the first time. All of the compounds were tested for their radical-scavenging and antioxidant activities by measuring their capacity to scavenge the 2,2′-diphenyl-1-picrylhydrazyl (DPPH) radical, and anion superoxide radical and to induce the reduction of Mo(VI) to Mo(V). The antiproliferative activity of all the most abundant compounds by 3-(4,5-dimethylthiazol-2-yl)-2,5-diphenyl tetrazolium bromide (MTT) bioassay on murine B16-F1 melanoma cells has been also assessed.

1. Introduction

Plant-based foods provide, not only essential nutrients needed for life, but also other bioactive compounds for health promotion and disease prevention. In fact, fruit and vegetables contain significant amounts of phytochemicals that may afford desirable health benefits beyond basic nutrition and reduce the risk of chronic diseases (Liu, 2003). Numerous researches suggest that a wide variety of phytochemicals, such as phenolics and carotenoids, is able to prevent or slow down oxidative stress-induced damage leading to cancer. Kinghorn et al. (2004) reviewed the potential cancer chemopreventive effects of over 150 compounds in terms of the quinone reductase induction ability of flavonoids and withanolides and the cyclooxygenase-1 and -2 inhibitory activities of flavanones, flavones and stilbenoids. Epidemiological studies have shown that consumption of vegetables, mainly onion and garlic, reduces the risk of the intestinal stomach cancer (Gonzalez & Riboli, 2006).

In the investigation of health-protective compounds from edible plants, characteristic of the Campania Region (Italy), we identified several phytochemicals from local apple cultivars (Cefarelli et al., 2006; D'Abrosca, Fiorentino, Oriano, Monaco, & Pacifico, 2006; D'Abrosca, Pacifico, Cefarelli, Mastellone, & Fiorentino, 2007). Continuing this research we, recently, reported the isolation and antioxidant evaluation of carotenoid and phenol derivatives from *Cydonia vulgaris* fruits, also known as Quince (Fiorentino et al., 2006, 2007, 2008). *C. vulgaris* Pers. (sin. *C. oblonga* Mill.) is a small shrub belonging to the same family as apples and pears (Rosaceae). This species is the sole member of the genus. It is a small tree with bright golden yellow pome fruits, when mature. The fruit of *C. vulgaris*, known as Quince, resembles an apple, but differs in having many seeds in each carpel. Pomes of Quince, known in Italy as 'cotogna' apple, have hard flesh of high flavour, but very acid, and these are largely used for marmalade, liqueur, jelly and preserves. It has been reported that the leaves and fruits of Quince have some positive effects in the medical treatment of various conditions, including cardiovascular diseases, haemorroids, bronchial asthma, and cough (Yildirim, Oktay, & Bilaloğlu, 2001).

The present research reports the complete characterisation of the organic extracts of *C. vulgaris* peels. Among them, five metabolites, namely 3β-(18-hydroxylinoleoyl)-28-hydroxyurs-12-ene (**12**), 3β-linoleoylurs-12-en-28-oic acid (**15**), 3β-oleoyl-24-hydroxy-24-ethylcholesta-5,28(29)-diene (**24**), tiglic acid 1-*O*-β-D-glucopyranoside (**35**), and 6,9-dihydroxymegastigmasta-5,7-dien-3-one 9-*O*-β-D-gentiobioside (**46**), have been isolated and elucidated for the first time. All of the compounds were tested for their radical-scavenging and antioxidant activities by measuring their capacity to scavenge the 2,2′-diphenyl-1-picrylhydrazyl (DPPH)

* Corresponding author. Tel.: +39 0823274576; fax: +39 0823274571.
E-mail address: antonio.fiorentino@unina2.it (A. Fiorentino).

0308-8146/$ - see front matter © 2009 Elsevier Ltd. All rights reserved.
doi:10.1016/j.foodchem.2009.04.098

radical, and anion superoxide radical and to induce the reduction of Mo(VI) to Mo(V). The antiproliferative activities of terpenoid and isoprenoid constituents, as well as the most abundant polyphenol components, by 3-(4,5-dimethylthiazol-2-yl)-2,5-diphenyl tetrazolium bromide bioassay on murine B16-F1 melanoma cells have also been assessed.

2. Materials and methods

2.1. Fruit collection and extraction

C. vulgaris Pers. (syn. *Cydonia oblonga* Mill.) fruits were collected in Durazzano, near Caserta (Italy), in October, 2005, when the fruit had just been harvested. The fruits were sliced and the peels (3.1 kg) were infused in ethanol (5.0 l) for seven days in a refrigerated chamber at 4 °C in the dark. After removal of the ethanol, the peels were re-extracted first with Et_2O for seven days and then with petroleum ether (PE) for a further seven days. After distillation of the solvents in a vacuum, we obtained the EtOH crude extract (261.6 g), Et_2O crude extract (15.0 g) and a PE crude extract (13.0 g).

2.2. General experimental procedures

NMR spectra were recorded at 300 MHz for ^1H and 75 MHz for ^{13}C on a Varian Mercury 300 Fourier transform NMR or 500 MHz for ^1H and 125 MHz for ^{13}C on a Varian Inova Fourier transform NMR spectrometer in $CDCl_3$, DMSO d_6 or CD_3OD, at 25 °C. Proton-detected heteronuclear correlations were measured using HSQC (optimised for $^1J_{HC}$ = 140 Hz) and HMBC (optimised for $^nJ_{HC}$ = 8 Hz). UV spectra were recorded on a UV-1700 Shimadzu spectrophotometer in MeOH solution. Optical rotations were measured on a Perkin–Elmer (Perkin–Elmer Co., Norwalk, CT) 141 in MeOH solution. Electron ionisation mass spectra (EIMS) were obtained with a HP 6890 instrument equipped with a MS 5973 N detector. Electrospray mass spectra were recorded using a Waters ZQ mass spectrometer (Waters Co., Milford Massachusetts, USA) equipped with an electrospray ionisation (ESI) probe operating in positive or negative ion mode. The scan range was *m*/*z* 80–2000. The HPLC apparatus consisted of a pump (Shimadzu LC-10AD), a refractive index detector (Shimadzu RID-10A) and a Shimadzu Chromatopac C-R6A recorder. Preparative HPLC was performed using NH_2 (Luna 10 μm, 250 × 10 mm i.d., Phenomenex, Torrance, CA, USA) and SiO_2 (Kromasil 10 μm, 250 × 10 mm i.d., Phenomenex, Torrance, CA, USA) columns. Analytical HPLC was performed using RP-8 (Luna 5 μm, 250 × 4.6 mm i.d., Phenomenex, Torrance, CA, USA) or Polar-RP-80A (Synergi 4 μm, 250 × 4.6 mm i.d., Phenomenex, Torrance, CA, USA) columns. Analytical TLC was performed on Merck Kieselgel 60 F254 or RP-18 F254 plates with 0.2 mm layer thickness. Spots were visualised by UV light or by spraying with H_2SO_4/AcOH/H_2O (1:20:4). The plates were then heated for 5 min at 110 °C. Preparative TLC was performed on Merck Kieselgel 60 F254 plates, with 0.5 or 1.0 mm film thickness. Flash column chromatography (fcc) was performed on Merck Kieselgel 60 (230–400 mesh) at medium pressure. Column chromatography (CC) was performed on Merck Kieselgel 60 (70–240 mesh), Amberlite XAD-4 (Fluka, Buchs, Switzerland), Sephadex LH-20 (Pharmacia, Piscataway, U.S.A.), or on NH_2 silica (LiChroprep NH_2, 40–63 μm, Merck, Darmstadt, Germany).

2.3. Organic crude extracts fractionation and chemical characterisation

The EtOH extract (261.6 g) was dissolved in water and shaken with EtOAc to obtain an organic (8 g) and an aqueous fractions. The aqueous fraction (190.0 g) was chromatographed on Amberlite XAD-4, eluting with water first and then with MeOH. The methanolic fraction was chromatographed on Sephadex LH-20, eluting with water/methanol solutions to obtain fractions A–D. Fraction A, eluted with H_2O, was chromatographed on RP-8 CC, eluting with MeOH/MeCN/H_2O solutions to obtain six fractions. The first, purified by RP-8 HPLC, eluting with MeOH/MeCN/H_2O (1:1:8), furnished pure **25** (10.0 mg). The second fraction was purified by preparative TLC, eluting with the organic lower phase of $CHCl_3$/MeOH/H_2O (13:7:3) biphasic solution to give pure compound **37** (19.6 mg). The third fraction was purified by RP-8 HPLC using MeOH/MeCN/0.1% TFA (1:2:8) solution as mobile phase, to obtain metabolite **43** (3.0 mg); the fourth fraction was resolved by TLC, eluting with the organic lower phase of $CHCl_3$/MeOH/H_2O (13:7:2) biphasic solution to obtain pure **35** (3.0 mg), **36** (1.0 mg), **41** (3.5 mg) and **46** (2.0 mg). The fifth fraction was chromatographed by NH_2 HPLC, using (as mobile phase) a MeCN/H_2O solution (9:1), to obtain compounds **42** (2.3 mg), **44** (7.3 mg), and **45** (6.0 mg). Finally, the sixth fraction contained pure metabolite **40** (9.4 mg).

Fraction B, eluted with MeOH/H_2O (1:4), was chromatographed by RP-8 CC, eluting with MeOH/MeCN/H_2O solutions. The fraction eluted with MeOH/MeCN/H_2O (1:1:8) gave two fractions, identified respectively as the carotenoid glycoside **38** (15.3 mg) and its isomer **39** (8.0 mg). The fraction eluted with MeOH/MeCN/H_2O (5:1:1) afforded pure **47** (12.0 mg). The fraction eluted with MeOH/MeCN/H_2O (7:1:1) furnished pure **27** (12.0 mg) and a mixture which was resolved by TLC chromatography, eluting with the organic phase of $CHCl_3$/MeOH/EtOH/H_2O (10:7:5:5) to obtain the glucoside **26** (7.0 mg), and 4-hydroxybenzylamine **34** (5.0 mg). Fraction C, eluted with MeOH/H_2O (1:1), was purified by RP-8 HPLC-UV, using (as mobile phase) a MeOH/H_2O solution (1:149), to obtain metabolite **28** (11.0 mg). Fraction D, eluted with pure MeOH, was chromatographed by RP-8 HPLC-UV, eluting with MeOH/MeCN/H_2O (1:2:14), to obtain pure rutin **33** (23.1 mg).

The EtOAc organic fraction (7.4 g) of the ethanol extract was pooled with the Et_2O crude extract (15.0 g) and chromatographed by SiO_2 fcc to obtain two fractions E–F. Fraction E, eluted with CH_2Cl_2 and re-chromatographed by SiO_2 fcc, eluting with $CHCl_3$/MeOH (19:1), furnished three fractions: the first one was purified by SiO_2 CC, eluting with hexane/methylethylketone [MEK] (4:1), to give the pure ursane triterpenes **14** (312.1 mg), and **18** (66.1 mg); the second mixture was resolved by SiO_2 HPLC [hexane/MEK (41:9)] to obtain pure compounds **16** (43.2 mg), and **17** (4.5 mg), while the third fraction was purified by preparative TLC, eluting with hexane/MEK (3:2) to obtain the oleanane triterpene **9** (31.5 mg). Fraction F, eluted with CH_2Cl_2/MeOH (1:1), was re-chromatographed by SiO_2 fcc, eluting with the organic lower phase of $CHCl_3$/MeOH/H_2O (13:7:5) to give a fraction which, purified by RP-8 HPLC-UV [MeOH/H_2O (1:149)], yielding to chlorogenic acids **28** (62.0 mg), **29** (6.0 mg), **30** (35.2 mg), and **31** (10.1 mg).

The PE crude extract (13.0 g) was chromatographed on SiO_2 by aspiration under vacuum to obtain three fractions G–I.

Fraction G, eluted with pure CH_2Cl_2, was chromatographed on NH_2 silica, yielding three fractions. The first one, eluted with EtOAc/PE (1:19), furnished pure **4** (2.8 mg), **5** (31.0 mg) and **12** (30.7 mg) and a mixture which was chromatographed by RP-8 HPLC [MeOH/MeCN (4:1)], to give pure metabolite **24** (3.6 mg). The fraction eluted with EtOAc/PE (1:9), was purified by NH_2 CC, to give pure compound **15** (53.0 mg). The third fraction, eluted with EtOAc/PE (1:4), furnished a mixture which was chromatographed on SiO_2 by preparative TLC, eluting with PE/$CHCl_3$/EtOAc (6:3:1) to give two spots. The first contained the acyl benzoic acids **6a–c** (3.0 mg), which were separated by RP-18 HPLC, eluting with MeOH/MeCN (4:1), while the second consisted in the acyl benzaldehydes **7a–c** (4.0 mg).

Fraction H, eluted with CH_2Cl_2/acetone [Me_2CO] (1:1), chromatographed by SiO_2 fcc, eluting with hexane/$CHCl_3$/Me_2CO (13:6:1), furnished four fractions. The first one was purified by RP-18 HPLC, eluting with MeOH/MeCN (4:1) to give pure **1c** (2.5 mg), **1d** (2.1 mg), **1e** (2.2 mg), **1f** (1.8 mg), **2b** (2.9 mg) and **2c** (3.1 mg); the second fraction, purified under the same conditions, gave **1a** (2.6 mg), **1b** (2.3 mg), **2a** (3.2 mg), **3a** (1.0 mg) and **3b** (1.1 mg). The third fraction was purified by RP-8 CC to give pure **13** (30.1 mg), and mixtures A and B: mixture A was chromatographed by RP-8 CC [MeOH/MeCN (4:1)], to give pure metabolite **21** (61.7 mg); mixture B was purified by SiO_2 fcc [hexane/EtOAc (19:3)] to yield compound **20** (92.0 mg). The fourth fraction, chromatographed by RP-8 CC, furnished two fractions; the first was purified by RP-8 CC [MeOH/MeCN/H_2O (6:3:1)] to obtain pure **8** (119.8 mg), **11** (9.0 mg) and **32** (191.0 mg), while the second fraction was chromatographed by RP-8 HPLC, eluting with MeOH/MeCN/H_2O (7:2:1), to furnish metabolite **19** (4.9 mg).

Fraction I, eluted with CH_2Cl_2/MeOH (1:1), and chromatographed by SiO_2 fcc, furnished two fractions. The first, eluted with CH_2Cl_2/MeOH (19:1), was purified by preparative TLC [hexane/$CHCl_3$/MeOH (4:5:1)] to obtain compound **10** (7.8 mg), while the second fraction, eluted with CH_2Cl_2/MeOH (9:1), was chromatographed by preparative TLC [hexane/$CHCl_3$/MeOH (5:13:2)] to furnish metabolites **22** (21.0 mg) and **23** (26.0 mg).

2.4. Chemical characterisation

2.4.1. 3β-18-Hydroxylinoleoyl-uvaol (**12**)

$[\alpha]_D$ +23.9 (c = 0.82, $CHCl_3$); EIMS m/z 720 $[M]^+$; Anal. Calcd for $C_{48}H_{80}O_4$: C, 79.94; H, 11.18. Found: C, 80.01; H, 11.25. ^{1}H NMR (300 MHz, $CDCl_3$): see Table 1. ^{13}C NMR (75 MHz, $CDCl_3$): see Table 2.

2.4.2. 3β-Linoleoyl-ursolic acid (**15**)

$[\alpha]_D$ +30.6 (c = 0.15, $CHCl_3$); EIMS m/z 718 $[M]^+$; Anal. Calcd for $C_{48}H_{78}O_4$: C, 80.17; H, 10.93. Found: C, 80.22; H, 11.05; ^{1}H NMR (300 MHz, $CDCl_3$): see Table 1. ^{13}C NMR (75 MHz, $CDCl_3$): see Table 2.

Table 1
Selected ^{1}H NMR data of the new compounds **12**, **15** and **24** in $CDCl_3$ d = doublet, dd = doublet of doublet, m = multiplet, ov = overlapped, s = singlet, ob = obscured,; the J values are reported in the brackets.

Position	12	15	24
3	4.49 dd (8.1, 5.7)	4.49 dd (8.4, 5.5)	4.59 m
6	–		5.36 ov
12	5.12 t (3.6)	5.22 t (3.3)	
18		2.17 d (11.4)	0.68 s
19			1.01 s
21			0.95 d (6.6)
23	0.76 s	0.76 s	
24	0.98 s	0.85 s	
25	0.96 s	0.95 s	
26	0.84 s	0.84 s	0.88 ov
27	1.09 s	1.07 s	0.85 ob
28	3.52 d (10.8) 3.17 d (10.8)	–	5.74 d (18.0, 11.7)
29	0.83 d (6.7)	0.87 d (6.7)	5.27 dd (11.7, 1.5) 5.15 dd (18.0, 1.5)
30	0.90 d (6.6)	0.93 d (6.6)	
2′	2.29 t (7.5)	2.28 t (7.2)	2.35 t (7.2)
9′	5.34 ov	5.33 ov	5.36 ov
10′	5.34 ov	5.33 ov	5.36 ov
11′	2.76 t (5.7)	2.76 t (5.4)	2.00 m
12′	5.34 ov	5.33 ov	
13′	5.34 ov	5.33 ov	
18′	3.63 t (6.6)	0.88 ov	0.88 ov

2.4.3. 3β-Oleoyl-24-hydroxy-24-ethylcholesta-5,28(29)-diene (**24**)

$[\alpha]_D$ −25.9 (c = 0.19, $CHCl_3$); EIMS m/z 692 $[M]^+$; Anal. Calcd for $C_{47}H_{80}O_3$: C, 81.44; H, 11.63. Found: C, 81.52; H, 11.57. ^{1}H NMR (300 MHz, $CDCl_3$): see Table 1. ^{13}C NMR (75 MHz, $CDCl_3$): see Table 2.

2.4.4. Tiglic acid 1-O-β-D-glucopyranoside (**35**)

$[\alpha]_D$ +15.9 (c = 0.62, MeOH); ESIMS m/z 285 $[M+Na]^+$, 123 $[M-C_6H_5O_{10}+Na]^+$; Anal. Calcd for $C_{11}H_{18}O_7$: C, 50.38; H, 6.92. Found: C, 50.51; H, 6.77. ^{1}H NMR (300 MHz, CD_3OD): δ 7.00 (1H, dq, J = 6.9 and 1.5 Hz, H-3), 5.52 (1H, d, J = 7.2 Hz, H-1′), 3.83 (1H, dd, J = 12.0 and 1.8 Hz, H-6′a), 3.66 (1H, dd, J = 12.0 and 4.5 Hz, H-6′b), 3.50–3.33 (4H, ov, H-2′–H-5′), 1.84 (3H, d, J = 1.5 Hz, H-5), 1.82 (3H, d, J = 6.9 Hz, H-4). ^{13}C NMR (75 MHz, CD_3OD): δ 168.0 (C-1), 140.4 (C-3), 129.1 (C-2), 95.9 (C-1′), 78.8 (C-3′), 78.1 (C-5′), 74.0 (C-2′), 71.1 (C-4′), 62.3 (C-6′), 14.5 (C-4), 12.0 (C-5).

2.4.5. 6,9-Dihydroxymegastigmasta-5,7-dien-3-one 9-O-β-D-gentiobioside (**46**)

UV (EtOH) λ_{max} (log ε) 286.0 (2.66), $[\alpha]_D$ +10.5 (c = 0.15, MeOH); ESIMS: m/z 571 $[M+Na]^+$, 409 $[M-C_6H_5O_{10}+Na]^+$, 247 $[M-C_6H_5O_{10}-C_6H_5O_{10}+Na]^+$; Anal. Calcd for $C_{25}H_{40}O_{13}$: C, 54.74; H, 7.35. Found: C, 54.61; H, 7.47. ^{1}H NMR (300 MHz, CD_3OD): δ 5.84 (3H, ov, H-4, H-7, H-8), 4.24 (1H, d, J = 7.8. Hz, H-1′), 4.20 (1H, d, J = 7.6 Hz, H-1″), 4.13 dd (1H, dd, J = 11.9 and 2.1 Hz, H-6′), 3.81 (1H, dd, J = 11.9 and 5.3 Hz, H-6′), 2.52 (1H, d, J = 16.8 Hz, H-2), 2.17 (1H, d, J = 16.8 Hz, H-2), 1.92 (3H, d, J = 1.5 Hz, H-13), 1.30 and 1.29 (6H, s, H-11 and H-12), 1.03 (3H, d, J = 6.3 Hz, H-10). ^{13}C NMR (75 MHz, CD_3OD): δ 199.2 (C-3), 166.2 (C-5), 136.0 (C-8), 130.0 (C-4), 125.0 (C-7), 104.8 (C-1″), 102.2 (C-1′), 79.1 (C-9), 79.0 (C-6), 78.0 (C-3′, C-3″), 77.9 (C-5′, C-5″), 75.1 (C-2′, C-2″), 71.6 (C-4″), 71.4 (C-4′), 69.7 (C-6′), 62.7 (C-6″), 49.5 (C-2), 42.1 (C-1), 23.7 (C-12), 22.6 (C-13), 21.0 (C-10), 19.2 (C-11).

2.5. GC–MS analyses of fatty acid moieties

Pure ester (0.1 mg) was dissolved in 0.2 ml of 2 N KOH in methanol in a 1 ml vial. After stirring the solution for 30 min, heptane (0.8 ml) was added. The solution was mixed by a Vortex mixer and centrifuged, using a Beckman GS-15R centrifuge, for 10 min at 4000 rpm. Organic upper phase (1 μl) was analysed by GC–MS, fitted with 30 m × 0.25 mm i.d., 0.2 μm Zebron ZB5MS, fused silica capillary column (Phenomenex, Torrance, CA, USA). The column oven temperature was held at 80 °C for 1 min, then increased to 260 °C at 10 °C-min. Injector and detector temperatures were 250 and 150 °C, respectively; the carrier gas was He and the flow rate was 1.0 ml/min. The fatty acid methyl esters were identified on the basis of their EIMS spectra and by comparing their retention times with those of the standard fatty acid methyl esters (Supelco 37 Component FAME Mix).

2.6. DPPH radical-scavenging capacity

The DPPH radical-scavenging capacity of metabolites was measured according to the method of Brand-Williams, Cuvelier, and Berset (1995). DPPH· (2 mg) was dissolved in 54 ml of MeOH. The investigated metabolites were prepared by dissolving 0.4 μmol of each compound in 1 ml of MeOH. Then, 38 μl of each solution containing a compound were added to 1.46 ml of DPPH· solution at room temperature. The absorbance at 517 nm was measured in a cuvette at 30 min vs blank (38 μl MeOH in 1.46 ml of DPPH· solution), using a UV-1700 Shimadzu spectrophotometer. The analysis was carried out in triplicate and the results were expressed in terms of the percentage of radical-scavenging capacity (RCS).

Table 2
^{13}C NMR data of the new compounds **12**, **15** and **24** in $CDCl_3$.

Position	12	15	24	Position	12	15	24
1	38.6	38.5	37.2	25	16.0	15.7	39.9
2	28.2	27.4	32.1	26	17.6	17.0	16.8
3	80.8	80.8	73.9	27	23.5	23.8	17.9
4	38.2	39.7	42.5	28	70.1	184.3	149.2
5	55.4	55.5	139.9	29	16.9	17.2	116.6
6	18.4	18.4	122.8	30	21.6	21.4	-
7	32.9	35.0	29.9	1′	173.9	173.9	173.6
8	40.2	39.7	32.1	2′	35.1	33.9	32.1
9	47.8	48.2	50.2	3′	22.9	24.9	25.3
10	37.0	37.9	36.4	4′	29.3–29.9	30.4–29.5	29.7–29.1
11	23.6	24.3	21.2	5′	29.3–29.9	30.4–29.5	29.7–29.1
12	125.1	125.9	39.9	6′	29.3–29.9	30.4–29.5	29.7–29.1
13	139.0	138.2	42.6	7′	29.3–29.9	30.4–29.5	29.7–29.1
14	42.2	42.1	56.9	8′	28.2	27.7	27.4
15	26.0	29.3	24.5	9′	130.1	130.2	130.2
16	35.4	25.4	28.5	10′	128.1	128.1	130.0
17	37.9	47.7	56.1	11′	25.4	25.8	27.4
18	54.2	52.7	12.1	12′	128.3	128.3	29.7–29.1
19	39.5	39.2	19.6	13′	130.2	130.4	29.7–29.1
20	39.6	39.0	36.1	14′	28.2	27.7	29.7–29.1
21	30.0	31.7	19.1	15′	29.3–29.9	30.4–29.5	29.7–29.1
22	30.8	37.1	35.0	16′	25.4	30.4–29.5	32.1
23	28.3	28.3	36.8	17′	33.0	22.8	22.9
24	17.0	17.3	89.3	18′	63.3	14.3	14.4

2.7. Superoxide radical-scavenging activity

The assay of superoxide radical-scavenging capacity was based on the capacity of each isolated metabolite (0.4 mM) to inhibit the photochemical reduction of nitroblue tetrazolium (NBT) (Fluka, Buchs, Switzerland) in the riboflavin–light–NBT system (Dasgupta & De, 2004). Each 3 ml reaction mixture contained 50 mM sodium phosphate buffer (pH 7.8), 13 mM methionine (Fluka, Buchs, Switzerland), 2 μM riboflavin (Riedel-de Haën, Seelze, Germany), 100 μM EDTA (Carlo Erba Reagents, Rodano, Milano, Italy), 75 μM NBT and 100 μl of sample solution. The production was followed by monitoring the increase in absorbance at 560 nm after 10 min illumination from a fluorescent lamp. The analysis was carried out in triplicate and the results were expressed in terms of the percentage of radical-scavenging capacity (RCS).

2.8. Evaluation of total antioxidant capacity

Spectrophotometric evaluation of antioxidant capacity through the formation of a phosphomolybdenum complex was carried out according to Prieto, Pineda, and Aguilar (1999). Sample solutions (100 μl) containing reducing metabolites (0.4 μmol in 1 ml of dimethylsulphoxide) were combined in an Eppendorf tube with 1 ml of reagent solution (0.6 M sulphuric acid, 28 mM sodium phosphate and 4 mM ammonium molybdate). The tubes were capped and incubated in a thermal block at 95 °C for 90 min. After the samples were cooled to room temperature, the absorbance of aqueous solution of each was measured at 820 nm against a blank. The analysis was carried out in triplicate and the antioxidant activity was expressed as caffeic acid equivalents (CAE).

2.9. Cell line and culture conditions

Murine melanoma B16-F1 cells were purchased from the American Type Culture Collection (ATCC; Manassas, VA, USA). Freshly trypsinised cells were seeded and grown in RPMI-1640 medium supplemented with 10% (v/v) faetal bovine serum (FBS), 1% L-glutamine (v/v), 100 units/ml of penicillin and 100 μg/ml of streptomycin. The cells were grown at 37 °C in a humidified 5% CO_2 atmosphere.

2.10. MTT assay

To evaluate the effect of isolated metabolites on B16-F1 cells, the MTT colorimetric assay was performed as described by Mosmann (1983). The test is based upon the selective ability of living cells to reduce the yellow salt MTT [3-(4,5-dimethylthiazol-2-yl)-2,5-diphenyl tetrazolium bromide] to a purple-blue colour in soluble formazan precipitate. MTT was dissolved in phosphate buffer saline (PBS) at 5 mg/ml. Experiments were performed in 100 μl of media in sterile 96-well plates. After a 24 h incubation of B16-F1 cells at an initial density of 1×103 cells/well, medium was removed and replaced by 10% FCS medium containing test compounds (0–500 μM). After 24 h of incubation, stock MTT (Sigma–Aldrich) solution was added and plates were incubated at 37 °C in 5% CO_2 for 4 h. Blue crystals of MTT reduced by cells were dissolved with DMSO and cellular metabolism was determined by measuring the absorbance of samples at 570 nm in a microelisa reader.

3. Results and discussion

3.1. Chemical characterisation of phytochemicals

Structures of phytochemicals isolated from *C. vulgaris* extracts are shown in Figs. 1–4. The separation scheme of the secondary metabolites from the organic extracts of *C. vulgaris* is shown in Fig. 5. All of the structures were elucidated on the basis of 1D and 2D NMR experiments and by EI or ESI mass spectrometry. Compounds **1a–f** (Fig. 1) were identified as acyl derivatives of the *trans* isomer of the *p*-coumarylic alcohol. Compounds **2a–c** were identified as acyl derivatives of the *cis* isomer of the *p*-coumarylic alcohol. The structures of the fatty acid esters of *cis*-and *trans*-*p*-coumaryl alcohol were elucidated by GC–MS and ^{1}H and ^{13}C NMR spectroscopy after purification of the individual compounds by HPLC (Fiorentino et al., 2008). Compounds **3a**, **3b** and **4** were fatty acid esters characterised by the presence of a coniferyl alcohol moiety. In particular, metabolites **3a** and **b** were identified as acyl derivatives of the *E* isomer of the coniferyl alcohol, and compound **4** as the acyl derivative of its *Z* isomer. Compound **5**, identified for the first time in *C. vulgaris*, was characterised as *E*-

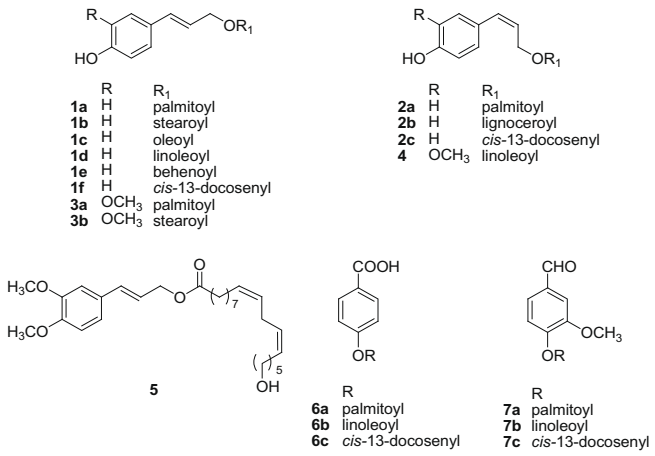

Fig. 1. Chemical structures of metabolites **1**–**7** from *C. vulgaris* peels.

3,4-dimethoxycinnamyl ω-hydroxylinoleate. Compounds **6a**–**c** were identified as 4-hydroxybenzoic acids, esterified through the 4-hydroxyl group to palmitic, linoleic and *cis*-13-docosenoic acids, respectively. Compounds **7a**–**c** were identified as 3-methoxy-4-hydroxy aldehydes, esterified by the hydroxyl group with the same fatty acid moiety as the previous compounds.

Compounds **8**–**10** (Fig. 2) were characterised as oleanane triterpenes: compound **8** was identified as oleananic acid (Kamiya, Yoshioka, Saiki, Ikuta, & Satake, 1997), while compounds **9** and **10** were identified as hederagenic acid (Bhandari & Rastogi, 1984) and its 2α-hydroxy derivative (Kojima & Ogura, 1988). The triterpenes **11**–**19** (Fig. 2) were characterised by the ursane skeleton. Compound **11** was identified as uvaol (Hota & Bapuji, 1994), and the new compound, **12**, as its acyl derivative. Its molecular formula was $C_{48}H_{80}O_4$, as suggested by the elemental analysis and the EIMS spectrum. The methyl signals in the ^{1}H and ^{13}C NMR spectra (Tables 1 and 2) were in good accordance with those of compound **11**, but some differences were evident. Besides, the H-12 proton at δ 5.12, in the ^{1}H NMR spectrum, further overlapped four olefinic protons, as a multiplet at δ 5.34, was present. In the same experiment, a methine at δ 4.49, and two methylenes as a triplet at δ 3.63 and as two doublets at δ 3.52 and 3.17 were also evident. In the upfield of the spectrum, seven methyls were detectable as five singlets at δ 1.09, 0.98, 0.96, 0.86 and two doublets at δ 0.90 and 0.83, besides signals due to doubly allylic protons at δ 2.76, a methylene at δ 2.29, methylene signals of the acyl chain in the range between 2.1 and 1.1 ppm, and a methylene triplet at δ 3.63. The downshifted H-3 proton at δ 4.49 indicated the linkage with an acyl group. The ^{13}C NMR and DEPT spectra were in good agreement with the presence of 48 carbons identified as 7 methyls, 23 methylenes, 11 methines and 7 tetrasubstituted carbons. These data led us to hypothesise the presence of the uvaol esterified with an unsaturated fatty acid. However, the absence of a methyl carbon, besides those of the triterpene, and the presence of the methylene at δ 63.3, suggested the presence of an ω-hydroxy fatty acid. The correlations in the HMBC experiment between the carbon at δ 173.9 (C-1′) with the protons at δ 4.49 (H-3), 2.29 (H-2′), and 1.62 (H-3′) confirmed this hypothesis. The acyl moiety was elucidated by GC–MS analysis of the methyl ester derivative of the fatty acid, obtained by reaction with KOH in MeOH, which showed a molecular peak at *m*/*z* 310. These data and the pattern of fragmentation, indicated the presence of the methyl ester of the ω-hydroxylinoleic acid, which was definitively confirmed by the 2D NMR data. Compounds **13** and **14** were identified as ursanaldehyde (Hota & Bapuji, 1994) and ursolic acid (Seo, Tomita, & Tori, 1975), respectively. The new compound **15** was identified as the 3-linoleoyl derivative of **14**. Its 1D NMR spectra (Tables 1 and 2) showed signals of the ursolic acid and signals attributable to a polyunsaturated fatty acid moiety. The downfield shift of the H-3 proton at δ 4.49 suggested the acylation point at the 3β-hydroxyl group of the triterpene. The acyl chain was confirmed by GC–MS analysis of the methyl derivatives obtained after methanolysis. Compounds **16**–**18** were characterised as 2α-hydroxy ursolic acid (Yamagishi et al., 1988), pomolic acid (Dong-Liang & Xiao-Ping, 1992) and

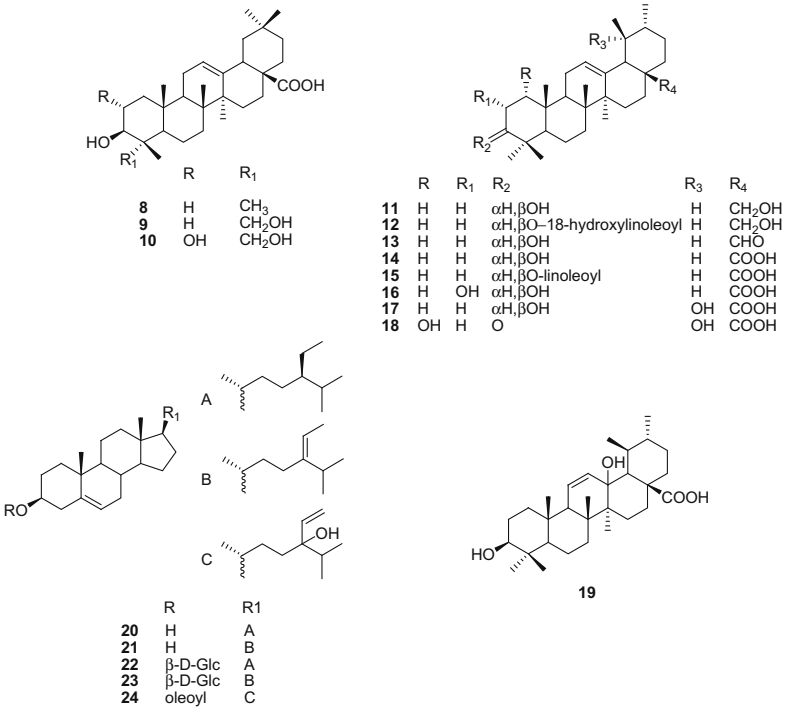

Fig. 2. Chemical structures of metabolites **8**–**24** from *C. vulgaris* peels.

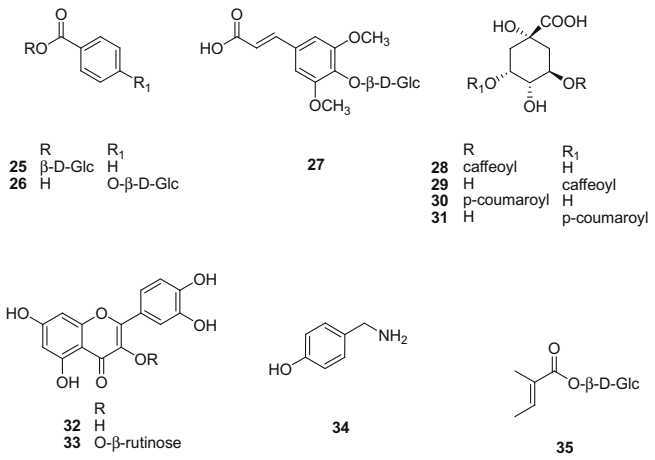

Fig. 3. Chemical structures of metabolites **25**–**35** from *C. vulgaris* peels.

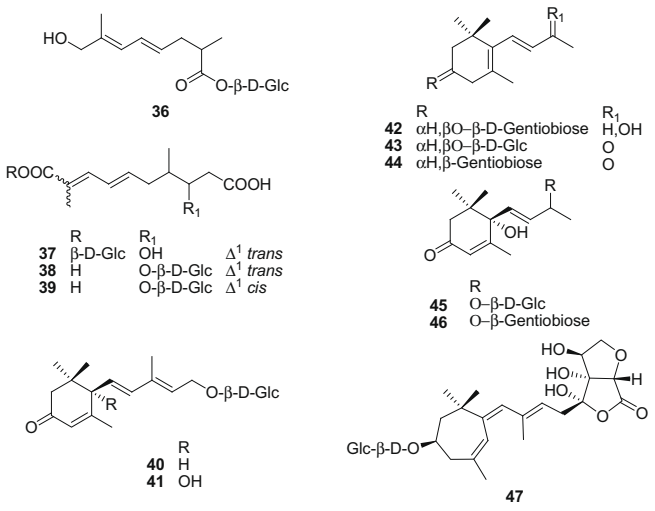

Fig. 4. Chemical structures of metabolites **36**–**47** from *C. vulgaris* peels.

annurcoic acid, respectively (D'Abrosca et al., 2006). Until now, this latter compound has been reported solely as a constituent of Annurca apple fruits. Finally, compound **19** was identified as 3β-13β-dihydroxyurs-11-en-28-oic acid (Huang, Sun, & Zhao, 1996).

All the steroids of *C. vulgaris* had a stigmastane skeleton (Fig. 2). Compounds **20** and **21** were identified as β-sitosterol (Wright et al., 1978) and fucosterol (Atta-ur-Rahman et al., 1999), while the glycosides **22** and **23** were characterised as 3-*O*-β-D-glucopyranoside derivatives (De Rosa, De Giulio, & Tommonaro, 1997; Tsai, Hsieh, Duh, & Chen, 1999). Compound **24** was characterised for the first time. It showed the molecular formula $C_{47}H_{80}O_3$ according to the elemental analysis and the EIMS spectrum showing the molecular peak at *m*/*z* 692. In the upfield region of the ^{1}H NMR spectrum (Table 1) methyl signals of a steroid were evident as two singlets at δ 0.68 and 1.01, and three methyl signals at δ 0.95, 0.87 and 0.85. In the downfield part of the spectrum, there were a multiplet at δ 4.59, and six olefin protons, three of which were present as an ABM spin system as three double doublets at δ 5.74, 5.27 and 5.15, suggesting the presence of a vinyl group, while the remaining protons were overlapped at δ 5.36. In the ^{13}C NMR (Table 2), there were a carboxyl carbon at δ 173.6, six olefinic carbons, confirming the presence of three double bonds, and two carbinol carbons at δ 73.9 and 89.3, besides other carbons ranging from 56.9 to 14.4 ppm. The DEPT experiment allowed us to identify all the carbons as 6 methyls, 25 methylenes, 11 methines and 5 quaternary carbons. The 2D NMR data allowed the complete assignment of all the protons and carbons in the molecule. In particular the tetrasubstituted carbinol at δ 89.3 correlated, in the HMBC experiment, with the vinyl protons, and with both the H-26 and H-27 methyls. These data suggested the presence of a hydroxyl group at the C-24 carbon and the double bond among the C-28 and C-29 carbons. ^{1}H and ^{13}C NMR values, relative to the steroidal skeleton, were in good accordance with the presence of a double bond at the C-5 carbon and an acyl group at the 3-hydroxyl, that was identified as oleic acid after reaction with KOH in MeOH and GC–MS analysis. The 2D NMR experiments confirmed our hypothesis.

Phenols **25**–**26** (Fig. 3) were identified as glucosides of benzoic acid, already identified from *Pinus contorta* needles (Higuchi & Donnelly, 1977) and from *Picea glauca* (Kraus & Spiteller, 1997); compound **27** was identified as synapyl acid 4-*O*-β-D-glucopyranoside (Beejmohun, Grand, Mesnard, Fliniaux, & Kovensky, 2004). Compounds **28**–**31** were characterised as chlorogenic acids, already reported as components of Hemerocallis (Clifford, Wu, & Kuhnert, 2006), while the flavones **32** and **33** were identified as quercetin and rutin, respectively (D'Abrosca et al., 2001). Compound **34** was identified as 4-hydroxybenzylamine (Lu, Rodriguez, Gu, & Silverman, 2003). Compound **35** was identified as the glucosyl derivative of tiglic acid. It showed a molecular formula $C_{11}H_{18}O_7$, as suggested by the ^{13}C NMR and ESIMS experiments. The ^{1}H NMR spectrum showed an olefinic quartet at δ 7.00, and two methyls as a singlet at δ 1.84 and a doublet at δ 1.82, a doublet of a sugar unity at δ 5.52, and a diastereotopic methylene as two double doublets at δ 3.83 and 3.66, besides four other protons geminal to oxygen in the range 3.50–3.33 ppm. The ^{13}C NMR spectrum revealed the presence of glucose, showing six carbinols at δ 95.9 (C-1′), 78.8, 78.1, 74.0, 71.1 and 62.3. The coupling constant of the anomeric proton was in good agreement with a β configuration for the C-1′ carbon. Furthermore, in the ^{13}C NMR spectrum, there were an ester carboxyl carbon at δ 168.0, two olefin signals as a methine at δ 140.4 and a tetrasubstituted carbon at δ 129.1 and two methyls at δ 14.5 and 12.0. The ^{13}C chemical shift values indicated the presence of a tiglic acid moiety in the molecule. Finally, the correlation between the carboxyl carbon and the anomeric proton confirmed the linkage of the glucose to the C-1 carbon of the aglycone trough an ester bond. Compounds **36**–**46** (Fig. 4) have been identified as carotenoid derivatives. Compound **36** was identified as (4*E*,6*E*)-8-hydroxy-2,7-dimethylocta-4,6-dienoic acid 1-*O*-β-D-glucopyranoside. This compound is reported as a precursor of isomeric marmelo lactones from Quince fruit (Winterhalter, Lutz, & Schreier, 1991). Carotenoids **37**–**40** (Fiorentino et al., 2006), **41** (Luts & Winterhalter, 1993), **42** (Winterhalter, Harmsen, & Trani, 1991) and **44** (Guldner & Winterhalter, 1991) were already reported as constituents of *C. vulgaris*, while compound **45** has been reported as a leaf constituent of *Alangium premnifolium* (Otsuka, Yao, Kamada, & Takeda, 1995). The new C_{13} norterpene glycoside, 46, had a molecular formula $C_{25}H_{40}O_{13}$ in accordance with ESIMS and ^{13}C NMR spectra. In the ^{1}H NMR, there were three overlapped protons at δ 5.84, two doublets at δ 4.20 and 4.24, two diastereotopic methylene protons at δ 2.52 and 2.17, three singlet methyls at δ 1.92, 1.29 and 1.30, and a doublet methyl at δ 1.03, besides other protons ranging from 4.18 to 3.10 ppm. In the ^{13}C NMR spectrum, 25 signals were evident, identified by a DEPT experiment, as four methyls, three methylenes, fourteen methines, and four tetrasubstituted carbons. The values of the carbinolic carbon were in good accordance with the presence of a gentiobiose moiety in the molecule. The remaining two carbinols were attributed to the C-6 and C-9 carbons on the basis of heterocorrelations shown in the HMBC experiment. In fact, the methyl at δ 1.92 correlated with the olefin carbons at δ 130.0 and 166.2, and with the tertiary carbinol at δ 79.0. The methyl doublet correlated with the carbons

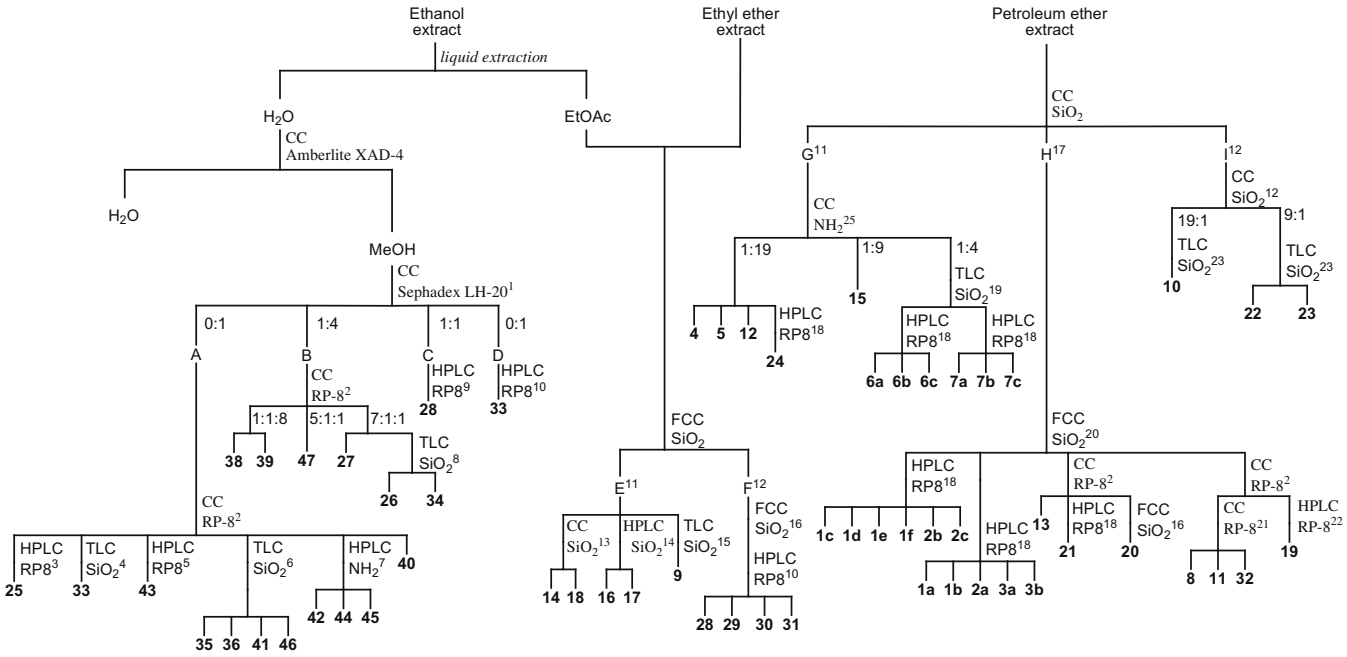

[1]MeOH-H_2O; [2]MeOH/MeCN/H_2O; [3]MeOH/MeCN/H_2O (1:1:8); [4]$CHCl_3$/MeOH/H_2O (13:7:3); [5]MeOH/MeCN/0.1% TFA (1:2:8); [6]$CHCl_3$/MeOH/H_2O (13:7:2); [7]MeCN/H_2O (9:1); [8]$CHCl_3$/MeOH/EtOH/H_2O (10:7:5:5); [9]MeOH/H_2O (1:149); [10]MeOH/MeCN/H_2O (1:2:14); [11]CH_2Cl_2; [12]CH_2Cl_2/MeOH (1:1); [13]hexane/MEK (4:1); [14]hexane/MEK (41:9); [15]hexane/MEK (41:9); [16]$CHCl_3$/MeOH/H_2O (13:7:3); [17]CH_2Cl_2/Me_2CO (1:1); [18]MeOH/MeCN (4:1); [19]PE/CH_2Cl_2/etOAc (6:3:1); [20]hexane/$CHCl_3$/Me_2CO (13:6:1); [21]MeOH/MeCN/H_2O (6:3:1); [22]MeOH/MeCN/H_2O (7:2:1); [23]hexane/$CHCl_3$/Me_2CO (4:5:1); [24]hexane/$CHCl_3$/Me_2CO (5:13:2); [25]EtOAc/PE;

Fig. 5. Isolation scheme of the secondary metabolites from *C. vulgaris* extracts.

at δ 136.0 and 79.1. This latter showed a cross peak with the anomeric proton of the gentiobiose at δ 4.24. Furthermore, the carbonil carbon at δ 199.2, attributed to the C-3 carbon, correlated with the methylenes at δ 2.52 and 2.17 and with the proton at δ 5.84. These data allowed us to assign the structure of 6,9-dihydroxy-megastigmast-4,7-dien-3-one 9-*O*-β-D-gentiobioside. Finally, compound **47** was identified as cydonioside A (Fiorentino et al., 2007).

3.2. Antioxidant and radical-scavenging capacities

All the isolated metabolites were tested for their antioxidant capacity, using three different methods. Two of these methods estimate the radical-scavenging activities of the investigated substances against the DPPH radical and the anion superoxide radical; the remaining test evaluates the capacity to induce the Mo(VI) reduction. The standards used in all the methods were α-tocopherol and ascorbic acid, known natural antioxidants, and the results are shown in Fig. 6.

When radical-scavenging capacities were tested, the strongest antioxidant capacity was observed for the flavonol quercetin (**32**) and its 3-*O*-rutinoside (**33**). In particular, quercetin reduced the DPPH radical by 56.7% and the anion superoxide radical by 80.4%. The quinic acid derivatives, chlorogenic acid (**28**) and neochlorogenic acid (**29**) determined an average DPPH radical reduction of 35.0% and were able to scavenge O_2^- by 52.8% and 51.8%, respectively. Among triterpenes, compounds **12** and **15** were the most active substances. In particular, uvaol ω-hydroxylinoleate (**12**) was able to reduce the DPPH radical absorbance by 15.7% and the anion superoxide radical by 22.5%. The uvaol acyl derivative showed a higher activity than did uvaol (**11**). Carotenoid derivative metabolites appeared to be strong radical-scavenger substances, exhibiting activities comparable to that of the positive standards. All the other compounds showed weak inhibiting capacities. Spectrophotometric quantisation of the antioxidant capacity of tested metabolites, through the formation of a phosphomolybdenum complex, showed that, in the complex, the substances were feebly able to induce the reduction of Mo(VI) to Mo(V). Quercetin and rutin exhibit a massive reducing capacity, greater than that exercised by α-tocopherol and ascorbic acid. Good antioxidant activity was observed for the phenylpropanoid esters **3a**, **3b** and **4**: they are able to induce the reduction of Mo(VI) to Mo(V), much more so than α-tocopherol.

3.3. Antiproliferative activity

The most abundant compounds present in the Quince peels, were subjected to the MTT bioassay on murine B16-F1 melanoma cells. Besides the isoprenoid and carotenoid metabolites, the main polyphenols isolated from *C. vulgaris* (Fiorentino et al., 2008) have also been tested. Besides the flavonoids quercetin (**32**) and rutin (**33**), four caffeoyl and *p*-coumaroyl derivatives of quinic acid (**28**–**31**), as well as the ester dimethoxycoumaryl alcohol (**5**) and the sinapic acid glucoside (**27**), were subjected to the bioassay. The results of the bioassays are listed in Table 3.

A significant antiproliferative activity was recorded for the triterpenoids. In particular, the most active metabolite was ursolic acid, **14**, with an IC_{50} of 10.2 μM. Compounds **8**, **9**, **11**, **13**, **18**, **19** and **21** showed very good activities toward B16-F1 cells in the range 32.7–80.5 μM. The presence of the acyl chain in the triterpenoid derivatives, **12** and **15**, determined a lower activity than those of the related **11** and **14**, respectively. Furthermore, the highest IC_{50}, recorded for the ursane triterpene, **16**, suggested that the introduction of a 2α-hydroxyl function was able to reduce the ursane skeleton antiproliferative ability. Interestingly, annurcoic acid showed an IC_{50} value of 77.6 μM. This compound has been reported in the cv Annurca apple alone, and the presence in the *C. vulgaris* peels led us to suppose its occurrence also in other apple cultivars (Rosaceae).

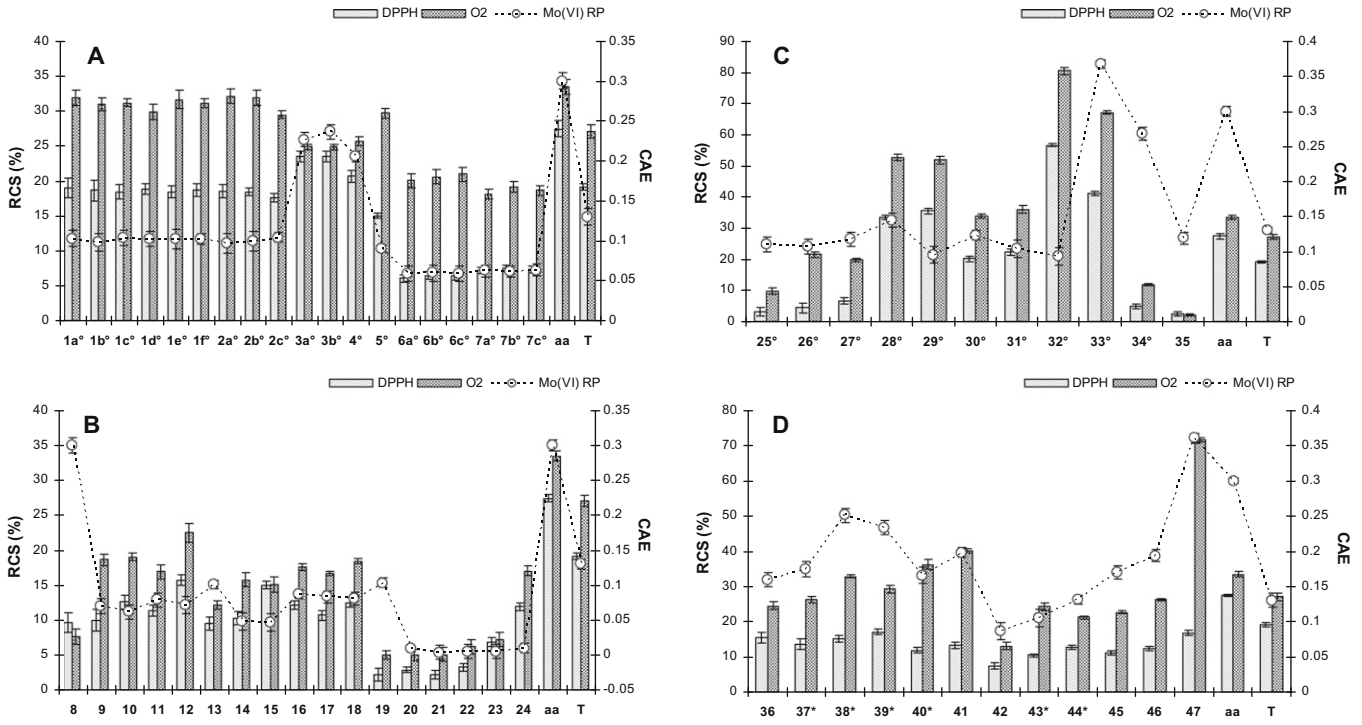

°Data according to Fiorentino *et al*., 2006; *Data according to Fiorentino *et al*., 2008.

Fig. 6. Radical-scavenging and antioxidant capacities of phenolic esters **1**–**7** (A), triterpenes **8**–**19** and steroids **20**–**24** (B), polyphenols **25**–**34** (C) and carotenoid derivatives **36**–**47** (D) isolated from *C. vulgaris*. (A) Values are presented as percentage differences from control ±SD. AA = ascorbic acid; T = α-tocopherol. CAE = caffeic acid equivalent.

Among polyphenolic compounds, quercetin (**32**) and rutin (**33**) were found to exhibit strong effects on B16-F1 cells with IC_{50} values of 85.1 and 92.5 μM, respectively.

Antiproliferative activity of the triterpenoids has been extensively reported in the literature. He and Liu (2007) demonstrated the high antiproliferative capacity of 13 triterpenoids isolated from apple peels against human HepG2 liver cancer cells, MCF-7 breast cancer cells, and Caco-2 colon cancer cells. They suggested that these phytochemicals, characterised by ursane or oleane skeletons, may be partially responsible for the anticancer activities of whole apples. Zuco et al. (2002) showed that betulinic acid exerted a selective cytotoxicity on nine neoplastic cell lines, including melanomas, small- and non-small cell lung carcinomas, ovarian and cervical carcinomas in a very narrow range of doses (1.5–4.5 μg/ml).

It has been suggested that phytosterols possess antitumour properties in both animals and humans. Rats (Raicht, Cohen, Fazzini, Sarwal, & Takahashi, 1980) administered methylnitrosourea, a direct acting carcinogen, produced a significantly higher incidence of tumours after 28 weeks compared to rats administered the same compound and fed a diet containing 0.2% β-sitosterol.

Carotenoids have been implicated as important dietary phytonutrients having cancer preventive activity (Van Poppel, 1993). Little is known about carotenoid derivatives' antiproliferative capacity. The metabolite **38**, a C-12 carotenoid saccharide derivative, with a diene α,ω-diacid skeleton, already isolated from the plant Oryctanthus, has been identified as an inhibitor of the vascular endothelial growth factor (VEGF) receptor (Hedge et al., 2005).

There is increasing interest in plant-derived dietary polyphenols, because several representatives of these compounds proved to be proliferation inhibitors and apoptosis inducers in tumour cells. Quercetin, has been shown to exhibit anti-carcinogenic properties by inducing cell cycle arrest and apoptosis, and inhibiting proliferation in diverse cancer cell lines as single compounds (Choi et al., 2001; Richter, Ebermann, & Marian, 1999; Yoshida, Yamamoto, & Nikaido, 1992).

Table 3
Growth inhibition (IC_{50}) of phytochemicals against murine B16-F1 melanoma cells.

Compounds	IC_{50} (μM)	Compounds	IC_{50} (μM)	Compounds	IC_{50} (μM)
5	NE	**20**	330	**37**	NE
8	61.6	**21**	45.3	**38**	NE
9	32.7	**27**	NE	**39**	233
11	80.5	**28**	404	**40**	NE
12	479	**29**	NE	**42**	NE
13	50.0	**30**	197	**43**	NE
14	10.2	**31**	470	**44**	NE
15	NE	**32**	85.1		
16	355	**33**	92.6		
18	75.0	**35**	484		
19	77.6	**36**	NE		

NE = no effect.

References

Atta-ur-Rahman, Choudhary, M. I., Hayat, S., Khan, A. M., Ahmad, A., & Malik, S. (1999). Spatozoate and varninasterol from the brown alga *Spatoglossum variabile*. *Phytochemistry, 52*, 495–499.

Beejmohun, V., Grand, E., Mesnard, F., Fliniaux, M.-A., & Kovensky, J. (2004). First synthesis of (1,2-$^{13}C_2$)-monolignol glucosides. *Tetrahedron Letters, 45*, 8745–8747.

Bhandari, P., & Rastogi, R. P. (1984). Triterpene constituents of *Caltha palustris*. *Phytochemistry, 23*, 2082–2085.

Brand-Williams, W., Cuvelier, M. E., & Berset, C. (1995). Use of a free radical method to evaluate antioxidant activity. *LWT – Food and Science Technology, 28*, 25–30.

Cefarelli, G., D'Abrosca, B., Fiorentino, A., Izzo, A., Mastellone, C., Pacifico, S., et al. (2006). Free radical scavenging and antioxidant activities of secondary metabolites from reddened cv. Annurca apple fruits. *Journal of Agricultural and Food Chemistry, 54*, 803–809.

Choi, J. A., Kim, J. Y., Lee, J. Y., Kang, C. M., Kwon, H. J., & Yoo, Y. D. (2001). Induction of cell cycle arrest and apoptosis in human breast cancer cells by quercetin. *International Journal of Oncology, 19*, 837–844.

Clifford, M. N., Wu, W., & Kuhnert, N. (2006). The chlorogenic acids of *Hemerocallis*. *Food Chemistry, 95*, 574–578.

D'Abrosca, B., DellaGreca, M., Fiorentino, A., Monaco, P., Previtera, L., Simonet, A. M., et al. (2001). Potential allelochemicals from *Sambucus nigra*. *Phytochemistry, 58*, 1073–1081.

D'Abrosca, B., Fiorentino, A., Oriano, P., Monaco, P., & Pacifico, S. (2006). Annurcoic acid: A new antioxidant ursane triterpene from fruits of cv. Annurca apple. *Food Chemistry, 98*, 285–290.

D'Abrosca, B., Pacifico, S., Cefarelli, G., Mastellone, C., & Fiorentino, A. (2007). 'Limoncella' apple fruit, an Italy apple cultivar: Phenol and flavonoid contents and antioxidant activity. *Food Chemistry, 104*, 1333–1337.

Dasgupta, N., & De, B. (2004). Antioxidant activity of *Piper betle* L. leaf extract *in vitro*. *Food Chemistry, 88*, 219–224.

De Rosa, S., De Giulio, A., & Tommonaro, G. (1997). Triterpenoids and sterol glucoside from cell cultuires of *Lycopersicon esculentum*. *Phytochemistry, 44*, 861–864.

Dong-Liang, C., & Xiao-Ping, C. (1992). Pomolic acid derivatives from the root of *Sanguisorba officinalis*. *Phytochemistry, 31*, 1317–1320.

Fiorentino, A., D'Abrosca, B., Pacifico, S., Mastellone, C., Piccolella, S., & Monaco, P. (2007). Isolation, structural elucidation, and antioxidant evaluation of cydonioside A, an unusual terpenoid from the fruits of *Cydonia vulgaris*. *Chemistry and Biodiversity, 4*, 973–979.

Fiorentino, A., D'Abrosca, B., Pacifico, S., Mastellone, C., Piscopo, V., Caputo, V., et al. (2008). Isolation and structure elucidation of antioxidant polyphenols from Quince (*Cydonia vulgaris*) peels. *Journal of Agricultural and Food Chemistry, 56*, 2660–2667.

Fiorentino, A., D'Abrosca, B., Pacifico, S., Mastellone, C., Piscopo, V., & Monaco, P. (2006). Spectroscopic identification and antioxidant activity of glucosilated carotenoid metabolites from *Cydonia vulgaris* fruits. *Journal of Agricultural and Food Chemistry, 54*, 9592–9597.

Gonzalez, C. A., & Riboli, E. (2006). Diet and cancer prevention: Where we are, where we are going. *Nutrition and Cancer, 56*, 225–231.

Guldner, A., & Winterhalter, P. (1991). Structures of two new ionone glycosides from Quince fruit (*Cydonia oblonga* Mill.). *Journal of Agricultural and Food Chemistry, 39*(214), 2–2146.

He, X., & Liu, R. H. (2007). Triterpenoids isolated from apple peels have potent antiproliferative activity and may be partially responsible for apple's anticancer activity. *Journal of Agricultural and Food Chemistry, 55*, 4366–4370.

Hedge, V. R., Pu, H., Patel, M., Jachens, A., Gullo, V. P., & Chan, T.-M. (2005). A new compound from the plant *Oryctanthus* sp. as a VEFG receptor binding inhibitor. *Bioorganic and Medicinal Chemistry Letters, 15*, 4907–4909.

Higuchi, R., & Donnelly, D. M. X. (1977). Pinus. Part 2. Glycosides from *Pinus contorta* needles. *Phytochemistry, 16*, 1587–1590.

Hota, R. K., & Bapuji, M. (1994). Triterpenoids from the resin of *Shorea robusta*. *Phytochemistry, 35*, 1073–1074.

Huang, H., Sun, H., & Zhao, S. (1996). Triterpenoids of *Isodon loxothyrsus*. *Phytochemistry, 42*, 1665–1666.

Kamiya, K., Yoshioka, K., Saiki, Y., Ikuta, A., & Satake, T. (1997). Triterpenoids and flavonoids from *Paeonia lactiflora*. *Phytochemistry, 44*, 141–144.

Kinghorn, A. D., Su, B.-N., Jang, D. S., Chang, L. C., Lee, D., Gu, J.-Q., et al. (2004). Natural inhibitors of carcinogenesis. *Planta Medica, 70*, 691–705.

Kojima, H., & Ogura, H. (1988). Configurational studies on hydroxyl groups at C2, 3 and 23 or 24 oleanene and ursine-type triterpenes by NMR spectroscopy. *Phytochemistry, 28*, 1703–1710.

Kraus, C., & Spiteller, G. (1997). Comparison of phenolic compounds from galls and shoots of *Picea glauca*. *Phytochemistry, 44*, 59–67.

Liu, R. H. (2003). Health benefits of fruit and vegetables are from additive and synergistic combinations of phytochemicals. *The American Journal of Clinical Nutrition, 78*, 517–520.

Lu, X., Rodriguez, M., Gu, W., & Silverman, R. B. (2003). Inactivation of mitochondrial monoamine oxidase B by methylthio-substituted benzylamines. *Bioorganic and Medicinal Chemistry, 11*, 4423–4430.

Luts, A., & Winterhalter, P. (1993). Abscisic alcohol glucoside in Quince. *Phytochemistry, 32*, 57–60.

Mosmann, T. (1983). Rapid colorimetric assay for cellular growth and survival: Application to proliferation and citotoxicity assays. *Journal of Immunological Methods, 65*, 55–63.

Otsuka, H., Yao, M., Kamada, K., & Takeda, Y. (1995). Alangionosides G–M: Glicosides of megastigmane derivatives from the leaves of *Alangium premnifolium*. *Chemical and Pharmaceutical. Bulletin, 43*, 754–759.

Prieto, P., Pineda, M., & Aguilar, M. (1999). Spectrophotometric quantitation of antioxidant capacity through the formation of a phosphomolybdenum complex: Specific application to the determination of vitamin E. *Analytical Biochemistry, 269*, 337–341.

Raicht, R. F., Cohen, B. I., Fazzini, E. P., Sarwal, A. N., & Takahashi, M. (1980). Protective effect of plant sterols against chemically induced colon tumors in rats. *Cancer Research, 40*, 403–405.

Richter, M., Ebermann, R., & Marian, B. (1999). Quercetin-induced apoptosis in colorectal tumor cells: Possible role of EGF receptor signaling. *Nutrition and Cancer, 34*, 88–99.

Seo, S., Tomita, Y., & Tori, K. (1975). Biosynthesis of arsene type triterpenes from sodium (1,2 ^{13}C] acetate in tissue cultures of *Isodon japonicus* Hara and reassignments of 13C-NMR signals in urs-12-ene. *JCS Chemical Communication, 270*, 954–955.

Tsai, I. L., Hsieh, C. F., Duh, C. Y., & Chen, I. S. (1999). Further study on the chemical constituents and their cytotoxicity from the leaves of *Persea obovatifolia*. *Chinese Pharmaceutical Journal, 51*, 335–345.

Van Poppel, G. (1993). Carotenoids and cancer: An update with emphasis on human intervention studies. *European Journal of Cancer, 29A*, 1335–1344.

Winterhalter, P., Harmsen, S., & Trani, F. (1991). A C13-norisoprenoid gentiobioside from Quince fruit. *Phytochemistry, 30*, 3021–3025.

Winterhalter, P., Lutz, A., & Schreier, P. (1991). Isolation of a glucosidic precursor of isomeric marmelo lactones from Quince fruit. *Tetrahedron Letters, 32*, 3669–3670.

Wright, J. L. C., Mcinnes, A. G., Shimizu, S., Smith, D. G., Walter, J. A., Idler, D., et al. (1978). Identification of C24 alkyl epimers of marin sterols by ^{13}C nuclear magnetic resonance spectroscopy. *Canadian Journal of Chemistry, 56*, 1898–1903.

Yamagishi, T., Zhang, D., Chang, J., McPhail, D. R., McPhail, A. T., & Lee, K. (1988). The cytotoxic principles of *Hyptis capitata* and the structures of the new triterpenes hyptatic acid-A and B. *Phytochemistry, 27*, 3213–3216.

Yildirim, A., Oktay, M., & Bilaloğlu, V. (2001). The antioxidant activity of the leaves of *Cydonia vulgaris*. *Turkish Journal of Medical Sciences, 31*, 23–27.

Yoshida, M., Yamamoto, M., & Nikaido, T. (1992). Quercetin arrests human leukemic T-cells in late G1 phase of the cell cycle. *Cancer Research, 52*, 6676–6681.

Zuco, V., Supino, R., Righetti, S. C., Cleris, L., Marchesi, E., Gambacorti-Passerini, C., et al. (2002). Selective cytotoxicity of betulinic acid on tumor cell lines, but not on normal cells. *Cancer Letters, 175*, 17–25.

Food Chemistry 118 (2010) 208–214

Contents lists available at ScienceDirect

Food Chemistry

journal homepage: www.elsevier.com/locate/foodchem

Antiproliferative and antioxidant properties of anthocyanin-rich extract from açai

Shelly Hogan [a], Hyun Chung [a], Lei Zhang [b], Jianrong Li [b], Yongwoo Lee [c], Yumin Dai [a], Kequan Zhou [a,*]

[a] Department of Food Science and Technology, Virginia Polytechnic Institute and State University, Blacksburg, VA 24061, USA
[b] College of Food Science, Biotechnology and Environmental Engineering, Zhejiang Gongshang University, Hangzhou 310035, PR China
[c] Department of Biomedical Engineering and Pathobiology, Virginia Tech, Blacksburg, VA 24061, USA

ARTICLE INFO

Article history:
Received 18 August 2008
Received in revised form 18 March 2009
Accepted 24 April 2009

Keywords:
Açai, Anthocyanins
Antiproliferative activity
C-6 glioma cells
Antioxidant properties

ABSTRACT

An anthocyanin-rich extract, generated from açai (AEA), was investigated for its antioxidant properties and antiproliferative activity against C-6 rat brain glioma cells and MDA-468 human breast cancer cells. AEA has an ORAC value of 2589 μmoles trolox equivalents (TE)/g dried powder and a DPPH radical-scavenging activity of 1208 μmoles TE/g, suggesting that AEA is an exceptional source of natural antioxidants. In addition, AEA remarkably suppresses proliferation of C-6 rat brain glioma cells, but has no effect on the growth of MDA-468 human breast cancer cells. Further experiments demonstrated that the AEA treatment dose-dependently inhibited the growth of C-6 rat glioma cells with an IC_{50} of 121 μg/ml. The DNA ladder fragmentation results indicated that AEA induced apoptosis of C-6 rat brain glioma cells. To compare açai with other anthocyanin-rich extracts, a number of berry extracts, including blueberry, strawberry, raspberry, blackberry and wolfberry, were assessed for potential antiproliferative activity against C-6 rat brain glioma cells. However, none of them showed suppressing effect. The results suggest that the active antiproliferative constituents in AEA are unlikely to be anthocyanins normally found in common berries.

1. Introduction

A growing body of epidemiological and clinical evidence suggests a beneficial role of foods rich in antioxidants in reducing incidences and mortality of certain cancers (Bandera, Kushi, Moore, Gifkins, & McCullough, 2007; Parsons et al., 2008). Fruits, especially berries, have been shown to contain high levels of antioxidant compounds, such as polyphenols, phenolic acids, flavonoids, and carotenoids (Wang & Lin, 2000). These antioxidants are thought to prevent chronic complications in part through their interactions with reactive oxygen species (ROS) and ability to scavenge free radicals (Seifried, Anderson, Fisher, & Milner, 2007). Mammalian cells are constantly exposed to ROS as a result of normal metabolic processes occurring during aerobic respiration (Wei & Lee, 2002). For instance, superoxide is a type of ROS that is generated within the mitochondria and can result in the induction of additional ROS, such as hydrogen peroxide and hydroxyl radicals (Grivennikova & Vinogradov, 2006). As a result, increased levels of these ROS create an environment referred to as oxidative stress, which has the potential to lead to DNA damage and subsequently promote the mutations that initiate tumour progression (Wiseman & Halliwell, 1996). Human tumour cell lines *in vitro* have been shown to produce ROS at a greater rate than non-transformed cell lines (Szatrowski & Nathan, 1991). ROS may cause damage to DNA, such as strand breaks, alterations in guanine and thymine bases, and sister chromatid exchanges (Wiseman & Halliwell, 1996).

Açai (*Euterpe oleracea* Mart.) is a native palm plant in northern South America which has recently emerged as a promising source of natural antioxidants. A recent study showed that the açai extract possessed noticeable activity against superoxide and the highest activity of any food reported to date, against the peroxyl radical when measured by the oxygen radical absorbance capacity assay ($ORAC_{FL}$) (Schauss et al., 2006a). The antioxidant activities of açai against the peroxynitrite and hydroxyl radicals were also noticeable (Schauss et al., 2006a). Similarly, other studies have reported significant antioxidant activities of açai berries and seeds by employing a variety of measurements (Hassimotto, Genovese, & Lajolo, 2005; Rodrigues et al., 2006). The potential beneficial effects attributed to açai-derived extracts are believed to be related to abundance of phenolic compounds found in this fruit. However, investigations of the medicinal role of the polyphenol-rich açai, in mediating cancer cells, are very limited, despite the recent increased interest in its antioxidant properties. The polyphenolic extract of açai has been shown, *in vitro,* to suppress proliferation of HL-60 leukaemia cells through caspase-3 activation in a dose- and time-dependent manner (Del Pozo-Insfran, Percival, & Talcott, 2006). Another study reported that a non-anthocyanin polyphenolic fraction from the açai pulp extract inhibited proliferation of HT-29 human colon adenocarcinoma cells (Pacheco-Palencia, Talcott,

* Corresponding author. Tel.: +1 540 231 9025; fax: +1 540 231 9293.
E-mail address: kzhou@vt.edu (K. Zhou).

0308-8146/$ - see front matter © 2009 Elsevier Ltd. All rights reserved.
doi:10.1016/j.foodchem.2009.04.099

Safe, & Mertens-Talcott, 2008). Açai fruit was reported to be rich in anthocyanins (Schauss et al., 2006b) and a number of anthocyanin-rich fruit extracts have exhibited the strong antiproliferative activities on different cancer cells (Balasundram, Bubb, Sundram, & Samman, 2003; Faria et al., 2005; Hosseinian et al., 2007b; Solomon et al., 2006; Vattem, Ghaedian, & Shetty, 2005). In this study, we have prepared an anthocyanin-rich extract from açai (AEA) and investigated its effect on proliferation of C-6 rat brain glioma cells and MDA-468 human breast cancer cells. The antioxidant properties of AEA were also assessed, as studies have shown that the anticancer effects of berry bioactives are partially mediated through their abilities to reduce and repair damage resulting from oxidative stress and inflammation (Seeram, 2008).

2. Materials and methods

2.1. Sample preparation

Lyophilised açai powder was obtained from the Van Drunen Farms (Momence, IL). The oil in the açai powder was removed with hexane by Soxhlet extraction at 45 °C for 3 h. The remaining residue was dried in a fume hood. Afterwards, 10 g of oil-free açai powder were extracted with 100 ml of 50% acetone at ambient temperature under stirring for 18 h. Extract was then filtered through a Whatman No. 4 filter paper. The residue was further extracted with 50 ml of 50% acetone. Following filtration, both filtrates were combined. The acetone in the extract was removed by a rotary evaporator (Thermo Scientific, Rockford, IL) at 45 °C. The remaining mixture was lyophilised. The anthocyanin-rich extract was obtained after purifying the lyophilised açai extract by solid phase extraction. Specifically, 100 mg of the açai crude extract were reconstituted in 10 ml of 15% methanol and then loaded onto a preconditioned Oasis HLB cartridge (Waters, Milford, MA). Water-soluble constituents, such as sugars, organic acids and minerals, were removed with distilled water. The anthocyanin fraction was eluted with 60% methanol in acidic water. The eluted material was collected and methanol was removed by a nitrogen evaporator (Organomation Associates, Berlin, MA). The collected residue was lyophilised (AEA) and stored at −20 °C for further investigation.

2.2. Total phenolic content (TPC)

TPC of AEA was determined using the Folin–Ciocalteu reagent with gallic acid as the phenolic standard (Zhou, Su, & Yu, 2004). In brief, appropriate dilutions of AEA were mixed with Folin–Ciocalteu reagent and 20% sodium carbonate (Na_2CO_3) at ambient temperature. After incubation for 2 h, the absorbance of blue colour developed in each assay mixture was recorded at 760 nm by a Genesys 10-UV scanning spectrophotometer (Thermo Electron Corporation, Madison, WI). The TPC of AEA was expressed in mg gallic acid equivalents (GAE) per gramme of dried AEA powder.

2.3. Total anthocyanin content

Total anthocyanin content of AEA was quantified using a pH differential method (Moyer, Hummer, Finn, Frei, & Wrolstad, 2002). In brief, 100 ml each of 0.025 M potassium chloride (pH 1.0) and 0.4 M sodium acetate (pH 4.5) buffer solutions were prepared. Each sample and standard (cyanidin 3-glucose) was diluted first with 0.025 M potassium chloride buffer (pH 1.0) and the absorbance was measured at 520 nm and 700 nm with a UV spectrophotometer (Genesys 10-UV scanning, Madison, WI) against a reagent blank (distilled water). A second aliquot of each sample was diluted to the same value with 0.4 M sodium acetate buffer (pH 4.5) and measured at 520 and 700 nm. The absorbance (A) was calculated using the following equation:

$$A = (A_{520\text{nm,pH 1.0}} - A_{700\text{nm,pH 1.0}}) - (A_{520\text{nm,pH 4.5}} - A_{700\text{nm,pH 4.5}}).$$

The total anthocyanin content was calculated and expressed as mg of cyanidin 3-glucoside equivalents (CGE) per gramme of AEA (mg/g).

2.4. Total flavonoid content

Total flavonoid content of AEA was analysed according to a reported colorimetric method (Veluri et al., 2006). In brief, 1 ml of AEA or standard (rutin) was mixed with 0.3 ml of 5% sodium nitrite, 0.3 ml of 10% aluminium chloride, and 2 ml of 1 M sodium hydroxide. All samples were run in duplicate and compared against a blank at an absorbance of 510 nm. Results were expressed as microgrammes rutin equivalents (RE) per gramme of AEA powder (mg/g).

2.5. Oxygen radical absorbance activity ($ORAC_{FL}$)

The $ORACFL_{FL}$ assay was conducted to measure the peroxyl radical-scavenging activity of AEA with trolox as the antioxidant standard (Zhou et al., 2007). A fluorescein stock solution (100 μM) in phosphate buffer (75 mM, pH 7.4) was prepared and kept at 4 °C in the dark. Fresh working fluorescein solution (100 nM) was prepared daily by diluting the stock solution in phosphate buffer. The fluorescein solution (200 μl) was added to each 40 μl of sample or trolox standard prepared in phosphate buffer (20, 40, 80, 100, and 200 μM) in a black 96-well plate and incubated for 20 min at 37 °C. The reaction was initiated by adding the peroxyl radical generator. Thirty-five microlitre of 0.36 M 2,2′-azobis-2-amidinopropane (AAPH), prepared in 75 mM phosphate buffer (pH 7.4), were added and the fluorescence was measured (λ_{ex} = 485 nm and λ_{em} = 535 nm) every minute using a Victor^3 multilabel plate reader (Perkin–Elmer, Turku, Finland) maintained at 37 °C until the reading had declined to less than 5% of the initial reading. Standards and samples were run in triplicate. Results for ORAC were determined by regression, relating trolox concentrations and the net area under the kinetic fluorescein decay curve. The $ORAC_{FL}$ value of each grape extract was expressed as micromoles of trolox equivalents per gramme of sample (μmoles/g).

2.6. DPPH·-scavenging activity

A high-throughput assay, based on the reduction of the free radical DPPH·, was carried out using a Victor^3 multilabel plate reader (Cheng, Moore, & Yu, 2006). The reaction mixture contained 100 μl of antioxidant açai extract and 100 μl of 0.208 mM DPPH$^•$ solution. The absorption at 515 nm was determined immediately after the reaction was initiated by gentle shaking. Each plate was read once every minute for 1.5 h. The relative DPPH$^•$-scavenging capacities (RDSC) were expressed as micromoles of trolox equivalents (TE) per gramme of sample (μmoles/g).

2.7. Cell culture

C-6 rat brain carcinoma cells and MDA-468 human breast cancer cells (American Type Culture Collection, Manassas, VA) were maintained at 37 °C in 5% CO_2 in a humidified incubator (Thermo Scientific, Rockford, IL) in Dulbecco's modified Eagle's medium (DMEM) containing 10% heat-inactivated foetal bovine serum and antibiotics (100 units/ml penicillin G, 100 μg/ml streptomycin) (Gibco BRL, Grand Island, NY). Cells (2.5×10^4 cells/ml) were plated in 48-well plates in complete media (FBS-containing media), and allowed to attach for 24 h.

2.8. Cell viability

C-6 brain carcinoma cells and MDA-468 breast cancer cells were treated for 24, 48, and 72 h in experimental media (without FBS in media) with sterile AEA dosed at 50, 100, and 200 μg/ml. The cell viability was assessed by the MTT assay according to the procedure previously described with slight modification (Chen, Jeng, Lin, Wu, & Chen, 2006). Cells were plated at a density of 2.5×10^4 cells/ml. After 24 h of incubation, the cells were washed with HBSS and then treated with AEA in the experimental medium or water alone, in a 48-well plate. Each treatment was repeated in 4 wells. The cells were further incubated for either 24, 48, or 72 h periods at 5% CO_2 37 °C in a humidified chamber. The treated media were removed at the end of each incubation period, washed with HBSS, and then cells were incubated for 4 h with 500 μl of MTT reagent solution (0.5 mg/ml in DMEM) added to each well; thus the tested AEA were present only during incubation treatments (24, 48, and 72 h). The MTT solution was aspirated and the formazan crystals were dissolved in dimethyl sulfoxide (DMSO) (500 μl) for 30 min on a plate rocker protected from UV light. Absorbance was recorded at 570 nm wavelength by a multilabel plate reader (Victor^3, Perkin–Elmer, Waltham, MA). Absorbance data acquired for cellular viability were expressed as percentages of the control (surviving control cells) in the experiment. After each treatment period, prior to MTT assays, cells were photographed with a Nikon microscope (Melville, NY) in order to observe gross cellular morphology of the cells after AEA treatments under 100× magnification.

2.9. DNA ladder fragmentation assay

Apoptosis or programmed cell death is a biological response of cells after exposure to DNA damage. DNA fragmentation in C-6 brain glioma cells was measured using a published method with the following modifications (Ray, Kamendulis, Gurule, Yorkin, & Corcoran, 1993). Briefly, C-6 glioma cells, treated with AEA (50–200 μg/ml) for 48 h, were washed with 1 × phosphate-buffered saline and harvested with plastic scrapers after trypsinization. Cells (15×10^4 cells per 100 mm culture dish) were lysed in 50 mM Tris–HCl, pH 7.5, 20 mM EDTA, and 1% Nonidet P-40 for approximately 10 s. This lysate was then centrifuged at 3000 rpm for 5 min at 4 °C to separate the fragmented DNA (supernatant) from the intact chromatin (pellet). A 10% SDS solution (10 μl) was added to the supernatant before it was treated with RNase A (final concentration of 5 μg/μl) and incubated for 2 h at 56 °C, followed by another incubation for 2 h at 37 °C with proteinase K (final concentration of 2.5 μg/μl). After extraction of the supernatant, fragmented DNA was precipitated with 100% cold ethanol and 0.5 M ammonium acetate for 1 h in −80 °C. Samples where then centrifuged at 12,000 rpm for 20 min, the supernatant was discarded and the white pellet was washed with 80% ice-cold ethanol and subsequently allowed to air-dry for 10 min at room temperature. The DNA sample was dissolved in 1× Tris–EDTA buffer, pH 8.0. DNA concentration was determined (Abs 260 nm) and 2% agarose gel electrophoreses of the same concentration of DNA was conducted (6 μg DNA per well). Electrophoresis was conducted in the TBE buffer for 120 min at 80 V. Gels were observed and photographed under UV light.

Table 1
Phenolic composition and antioxidant properties of AEA.

	AEA (lyophilized)
Total phenolic content	312 ± 5.6 mg GAE/g
Total flavonoids	124 ± 3.3 mg RE/g
Total anthocyanins	100 ± 2.4 mg CGE/g
ORAC	2589 ± 63.1 μmoles TE/g
DPPH scavenging activity	1208 ± 130 μmoles TE/g

GAE: gallic acid equivalents; RE: rutin equivalents; CGE: cyanidin 3-glycoside equivalents; TE: trolox equivalents.

2.10. HPLC–MS/MS detection of anthocyanins in AEA

Since anthocyanin compounds are the major components in AEA, its profile was analysed with HPLC–MS (high performance liquid chromatography–mass spectrometry). The chromatographic separation was performed with a Luna C18 column (150 × 2.1 mm, 4 μm dp; Phenomenex, Torrance, CA). AEA (20 μl) was injected onto the column with a Thermo Survey autosampler (San Jose, CA) maintained at 10 °C. Mobile phase A consisted of 1% aqueous formic acid, and mobile phase B consisted of 1% (*v*/*v*) formic acid in acetonitrile. The mobile phase was delivered to the HPLC column at a flow rate of 0.2 ml/min. The gradient elution programme was as follows: 0 min, 97/3 A/B; 40 min, 70/30 A/B; 45 min, 0/100 A/B; 50 min, 97/3 A/B). The HPLC column effluent was pumped directly without any split into a Finnigan LCQDUO mass spectrometer (Thermo Scientific, Waltham, MA) with electrospray ionisation. The MS/MS parameters were as follows: positive mode; nebulizer, 45 psi; dry gas, 11.0 psi, dry temperature, 340 °C; MS/MS, scan from *m*/*z* 350 to 1500; ion trap, scan from *m*/*z* 100 to 1500; maximum accrual time, 100.00 ms.

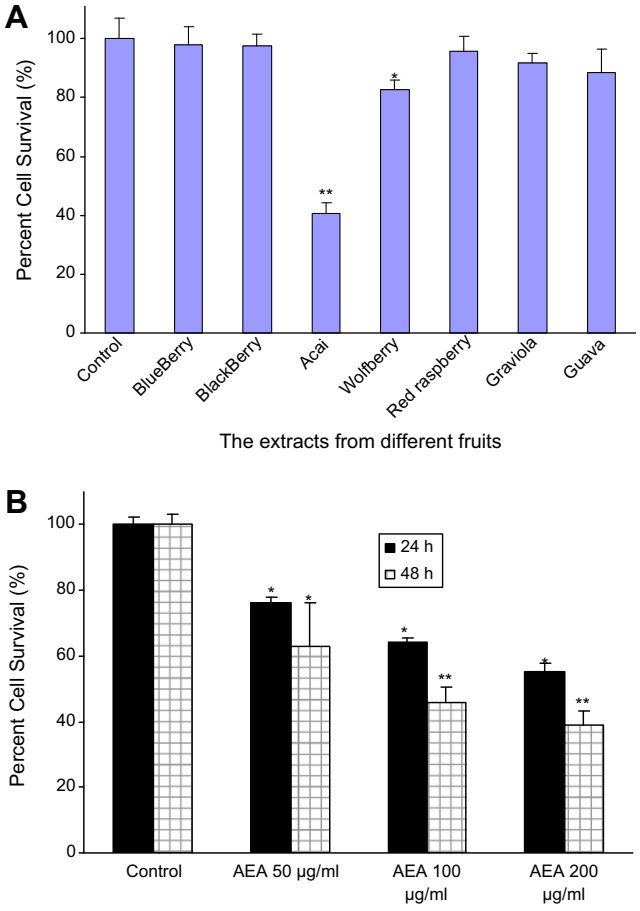

Fig. 1. Inhibitory effect of AEA on proliferation of C6 rat brain glioma cells. (A) AEA and other anthocyanin-rich fruit extracts on the cell growth. (B) Time and dose-dependent responses of AEA on the cell growth. C6 cells (2.5×104 cells/ml) followed 24 or 48 h exposure to AEA. The experiments were run in quadruplicate. * indicates significant difference compared to untreated control, ($P < 0.05$), ** indicates significant difference between 24 and 48 h of AEA treatments at the same dose.

2.11. Statistical analysis

Data were reported as means ± SD for triplicate determinations. Difference between two groups was analysed by two-tailed Student's *t* test and, between three or more groups, was analysed by one-way ANOVA multiple comparisons (SPSS 13.0, SPSS, Inc. Chicago, IL). Difference was considered statistically significant when the *P* value was <0.05.

3. Results and discussion

3.1. Total phenolic, flavonoid and anthocyanin contents

The total phenolic content of AEA was 312 mg gallic acid equivalents (GAE) per gramme (Table 1). This is considerably higher than in a previous report of 13.9 mg GAE per gramme of açai (Schauss et al., 2006a). The açai juice was reported to have TPC up to 2.1 mg GAE per ml of juice, predominantly consisting of anthocyanins and proanthocyanidins (Schauss et al., 2006b; Seeram et al., 2008). The result suggested that our AEA preparation method was able to efficiently extract and enrich phenolic compounds from açai powder. The flavonoid and anthocyanin contents in AEA were 124 mg rutin equivalents (RE) and 100 mg cyanidin 3-glycoside equivalents (CGE) per gramme, respectively, indicating that anthocyanins were the major flavonoids in AEA. Anthocyanins also were the major components in AEA and their concentration was well above those in certain other anthocyanin-rich fractions, such as grape skin (8.9 mg/g) (Munoz-Espada, Wood, Bordelon, & Watkins, 2004), Idared apple peels (0.3 mg/g) (Wolfe, Wu, & Liu, 2003), and a variety of berries (e.g. gooseberry, 0.8 and bilberry, 3.1 mg/g dry weight) (Kahkonen, Hopia, & Heinonen, 2001).

3.2. Oxygen radical absorbance capacity ($ORAC_{FL}$)

The hydrophilic $ORAC_{FL}$ value of AEA was 1800 μmol TE/g, which was more than twice higher than the 997 μmol TE/g of freeze-dried açai, as reported by Schauss et al. (2006a). AEA has considerably higher ORAC than have common phenolic-rich fruits or extracts, such as blueberry, strawberry, raspberry, chokecherry, and seabuckthorn, with ORAC values between 5.1 and 19.2 μmol TE/g fresh weight (Hosseinian et al., 2007a; Wang, Chen, Sciarappa, Wang, & Camp, 2008). This suggests that AEA is an exceptional source of natural antioxidants and consumption of AEA may provide potential antioxidant protection, thereby promoting human health.

3.3. $DPPH^{\bullet}$-scavenging activity

Traditional DPPH-scavenging assay measures the remaining radicals after reacting with antioxidants for a certain duration (30–90 min), which does not include an antioxidant standard. Thus, it is difficult to compare the data acquired from different laboratories because the experimental conditions, including temperature, reaction time, and sample/radical concentrations, can significantly affect the results. In this study, we used trolox as the antioxidant standard. The $DPPH^{\bullet}$-scavenging capacity of AEA was 839 μmol of TE/g. AEA, at 50 μg/ml, quenched 39.6% of DPPH radicals (1 mM) after 45 min of reaction. This result, along with the ORAC data, provided evidence that AEA is capable of interacting with different radicals, suggesting that AEA may have biomedical applications in reducing body oxidative stress, a deteriorating situation arising from elevation of various reactive oxygen species (ROS).

3.4. Cell viability

AEA treatments significantly suppressed proliferation of C-6 rat brain glioma cells (Fig. 1A and B). However, the growth of MDA-468 breast cancer cells was not affected by AEA treatments. For C-6 brain glioma cells, all three dosage treatments by AEA resulted in cell mortality. Specifically, 50, 100, and 200 μg/ml AEA treatments resulted in 62%, 45%, and 38% cell viability, respectively. The results revealed a distinct dose response and an IC_{50} value of 121 μg/ml after AEA treatments for 48 h. It appears that AEA inhibited the growth of C-6 glioma cells in a time-dependent manner as less pro-

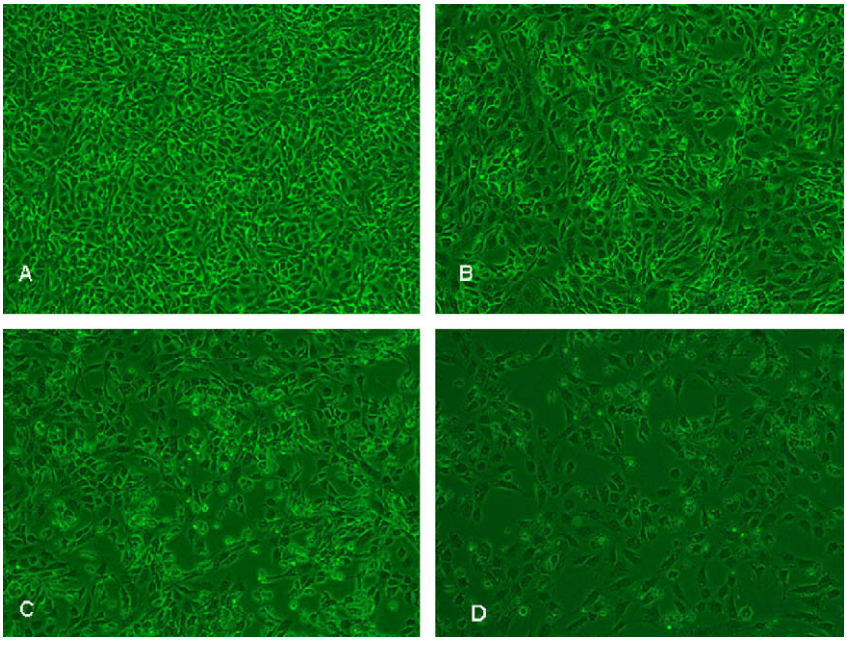

Fig. 2. Cell morphology of C-6 rat brain glioma cells after 48 h treatments by different doses of AEA. (A) The glioma cells grown in culture dishes were treated in experimental media only (control); (B) 50 μg/ml AEA treatment; (C) 100 μg/ml AEA treatment; (D) 200 μg /ml AEA treatment. Cell morphology was examined by microscopy under 100× magnification.

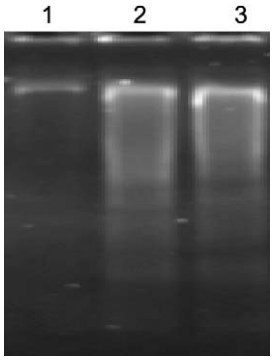

Fig. 3. DNA fragments of rat glioma C-6 cells treated with 100 and 200 μg/ml of açai for 48 h. Lane 1 represents control DNA from glioma cells in experimental media only, Lane 2 represents DNA fragments of glioma cells exposed to AEA at 200 μg/ml, Lane 3 represents DNA fragments after 100 μg/ml AEA treatments.

Table 2
Mass spectrometric data for identified phenolic compounds in AEA.

	Retention time (min)	Parent ion (*m*/*z*)	MS/MS fragments (*m*/*z*)
Cyanidin-3-glucoside	10.8	449	287
Cyanidin-3-rutinoside	11.34	595	449, 287
Peonidin-3-(6″-malonylglucoside)	13.20	549	463, 301
Delphinidin 3-(6″-acetoyl)glucoside	17.08	507	303
Peonidin-3-rutinoside	19.34	609	463, 301

nounced growth inhibitory effects were observed at 24 h treatments. The açai extract was recently reported to dose-dependently inhibit proliferation of HT-29 colon carcinoma cells (Pacheco-Palencia et al., 2008). The same research group also found that non-hydrolysed, anthocyanin-containing fractions of the açai extract strongly suppressed proliferation of HL-60 cells by inducing cell apoptosis (Del Pozo-Insfran et al., 2006). Anthocyanin-rich extracts, in particular berry extracts, have been widely investigated for their potential antiproliferative properties against a variety of cancer cells, and some have shown promising results. For instance, the strawberry and raspberry extracts strongly inhibited proliferation of CaCo-2 human colon cancer cells (McDougall, Ross, Ikeji, & Stewart, 2008); The bilberry extract was effective against HL-60 human leukaemia cells (Katsube, Iwashita, Tsushida, Yamaki, & Kobori, 2003); The blueberry and cranberry suppressed proliferation of MCF7 human breast cancer cells and HT-29 colon carcinoma cells (Seeram et al., 2006). In the cell experiments, we also evaluated other anthocyanin-rich extracts, including blueberry, strawberry, raspberry, blackberry, and wolfberry, against C-6 brain glioma cells as a comparison. However, none of the tested berry extracts inhibited proliferation of C-6 brain glioma cells (Fig. 1A). These observations indicate that the antiproliferative constituents, in AEA, on C-6 rat brain glioma cells, are unlikely to be the anthocyanins normally found in berries. Additional research is required to investigate the underlying mechanisms, and to characterise the chemical structures contributing to the antiproliferative capacity.

3.5. Cell morphology

To examine the effect of AEA on C-6 brain glioma cell proliferation, changes in cell morphology were also assessed at 48 h after AEA treatments with three different doses. Under experimental media-treated control conditions, C-6 cells appeared healthy and to be growing to 100% confluency (Fig. 2A). After exposure to 50 μg/ml of AEA for 48 h, C-6 cells numbers were noticeably reduced and appeared to be less dense (Fig. 2B). Further, at 100 μg/ml AEA concentration, cells exhibited the characteristic features of cell shrinkage, rounding, and partial detachment and demonstrated the lobulated appearance of apoptotic cells (Fig. 2C). When exposed to 200 μg/ml of AEA for 48 h, glioma cells had even more

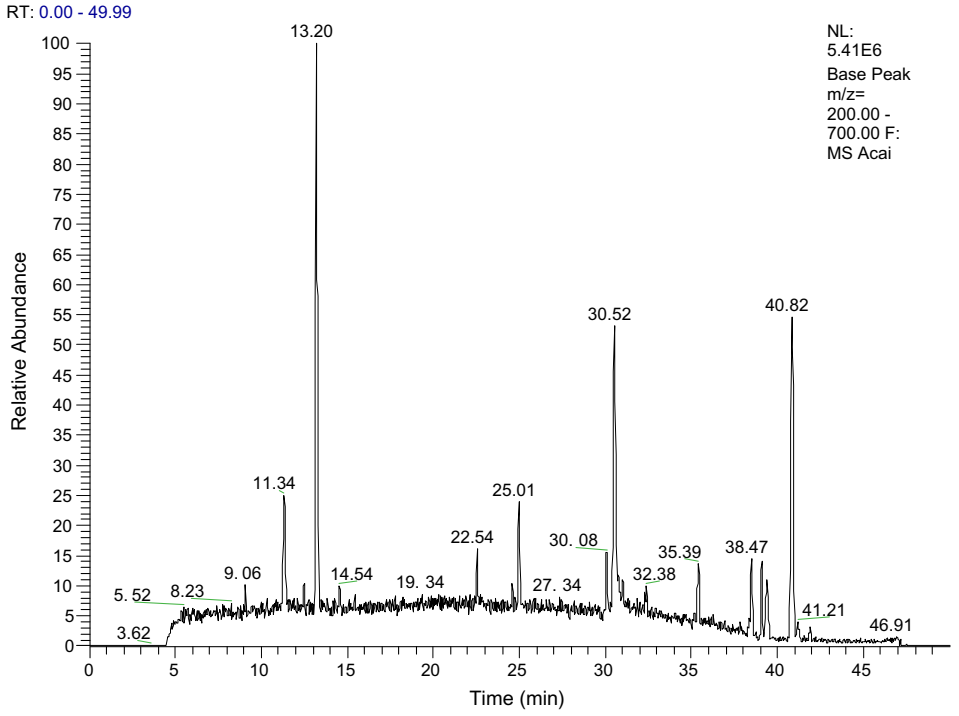

Fig. 4. HPLC–MS detection of anthocyanin compounds in AEA. The chromatograph was conditioned with the *m*/*z* range of 200–700. The peaks at the retention time of 10.80, 11.34, 13.20, 17.08, and 19.37 min represent cyanidin-3-glucoside, cyanidin-3-rutinoside, peonidin-3-(6″-malonylglucoside), delphinidin 3-(6″-acetoyl)glucoside, and peonidin-3-rutinoside, respectively.

profound features, characteristic of cell death (Fig. 2D). Similarly to the observations in the MTT experiments, the cell morphology results suggest that AEA reduced proliferation of C-6 brain glioma cells in a dose-dependent manner.

3.6. DNA ladder fragmentation

Fragmentation of DNA, observed from agarose gel results, is an indication of programmed cell death or apoptosis. No DNA fragmentation was detected in the control DNA from C-6 brain glioma cells in experimental media only (Fig. 3). However, fragmentation of DNA (laddering or banding observed in the image) was observed in C-6 glioma cells after 48 h treatments with either 100 or 200 μg/ml of AEA. The results suggest that the antiproliferative effect of AEA against C-6 glioma cells is caused by inducing cell apoptosis. The açai extract was previously reported to induce apoptosis in HL-60 human leukaemia cells by activating caspase-3 (Del Pozo-Insfran et al., 2006). In the future, it is necessary to examine whether the inhibition of AEA on C-6 glioma cells proliferation is through caspase-3 activation or other apoptotic pathways, to better understand antiproliferative mechanisms of AEA.

3.7. HPLC–MS/MS detection of anthocyanins in AEA

The chromatographic analysis identified three major anthocyanins in AEA with peonidin-3-(6″-malonylglucoside) being most abundant, followed by cyanidin-3-rutinoside, delphinidin 3-(6″-acetoyl)glucoside, and cyanidin-3-glucoside. In addition, one of the minor anthocyanins was identified as peonidin-3-rutinoside. The determination of anthocyanins was based on selective MS detection of the molecular ions and subsequent MS fragmentation experiments. Previous reports on the anthocyanin composition of açai fruit have been limited. A previous study determined cyanidin-3-glucoside and cyanidin-3-rutinoside as the major anthocyanins in açai (Lichtenthäler et al., 2005), while others found that cyanidin-3-arabinoside and cyanidin-3-arabinosylarabinoside were the most abundant (Bobbio, Bobbio, Oliveira, & Fadelli, 2002). However, both cyanidin-3-arabinoside and cyanidin-3-arabinosylarabinoside were not detectable in AEA under our experimental conditions. Moreover, AEA contained markedly more peonidin-3-(6″- malonylglucoside) than other anthocyanins. Table 2 presents the MS data for the identified compounds (see Fig. 4).

In summary, we have demonstrated that the anthocyanin-rich extract from açai possesses strong antioxidant activities and antiproliferative activity against C-6 brain glioma cells. The effect of AEA on C-6 glioma cells is unique as other selected anthocyanin-rich berry extracts do not have similar inhibitory activity. In addition, AEA has no effect on growth of MDA-468 human breast cancer cells, suggesting that it may specifically target C-6 glioma cells. The DNA ladder results indicated that AEA induces apoptosis in C-6 glioma cells. Further research is needed to identify active constituents in AEA and elucidate its inhibitory mechanisms on C-6 rat brain glioma cells.

References

Balasundram, N., Bubb, W., Sundram, K., & Samman, S. (2003). Antioxidants from palm (Elaeis guineensis) fruit extracts. *Asia Pacific Journal of Clinical Nutrition, 12*(Suppl.), S37.

Bandera, E. V., Kushi, L. H., Moore, D. F., Gifkins, D. M., & McCullough, M. L. (2007). Fruits and vegetables and endometrial cancer risk: A systematic literature review and meta-analysis. *Nutrition and Cancer, 58*(1), 6–21.

Bobbio, F. O., Bobbio, P. A., Oliveira, P. A., & Fadelli, S. (2002). Stability and stabilization of the anthocyanins from *Euterpe oleracea* Mart. *Acta Alimentaria, 31*, 371–377.

Chen, T. J., Jeng, J. Y., Lin, C. W., Wu, C. Y., & Chen, Y. C. (2006). Quercetin inhibition of ROS-dependent and- independent apoptosis in rat glioma C6 cells. *Toxicology, 223*(1–2), 113–126.

Cheng, Z., Moore, J., & Yu, L. (2006). High-throughput relative DPPH radical scavenging capacity assay. *Journal of Agricultural and Food Chemistry, 54*(20), 7429–7436.

Del Pozo-Insfran, D., Percival, S. S., & Talcott, S. T. (2006). Açai (Euterpe oleracea Mart.) polyphenolics in their glycoside and aglycone forms induce apoptosis of HL-60 leukemia cells. *Journal of Agricultural and Food Chemistry, 54*(4), 1222–1229.

Faria, A., Oliveira, J., Neves, P., Gameiro, P., Santos-Buelga, C., de Freitas, V., et al. (2005). Antioxidant properties of prepared blueberry (*Vaccinium myrtillus*) extracts. *Journal of Agricultural and Food Chemistry, 53*(17), 6896–6902.

Grivennikova, V. G., & Vinogradov, A. D. (2006). Generation of superoxide by the mitochondrial Complex I. *Biochimica et Biophysica Acta (BBA) – Bioenergetics, 1757*(5–6), 553–561.

Hassimotto, N. M., Genovese, M. I., & Lajolo, F. M. (2005). Antioxidant activity of dietary fruits, vegetables, and commercial frozen fruit pulps. *Journal of Agricultural and Food Chemistry, 53*(8), 2928–2935.

Hosseinian, F. S., Li, W., Hydamaka, A. W., Tsopmo, A., Lowry, L., Friel, J., et al. (2007a). Proanthocyanidin profile and ORAC values of manitoba berries, chokecherries, and Seabuckthorn. *Journal of Agricultural and Food Chemistry, 55*(17), 6970–6976.

Hosseinian, F. S., Li, W., Hydamaka, A. W., Tsopmo, A., Lowry, L., Friel, J., et al. (2007b). Proanthocyanidin profile and ORAC values of manitoba berries, chokecherries, and seabuckthorn. *Journal of Agricultural and Food Chemistry, 55*(17), 6970–6976.

Kahkonen, M. P., Hopia, A. I., & Heinonen, M. (2001). Berry phenolics and their antioxidant activity. *Journal of Agricultural and Food Chemistry, 49*(8), 4076–4082.

Katsube, N., Iwashita, K., Tsushida, T., Yamaki, K., & Kobori, M. (2003). Induction of apoptosis in cancer Cells by bilberry (*Vaccinium myrtillus*) and the anthocyanins. *Journal of Agricultural and Food Chemistry, 51*(1), 68–75.

Lichtenthäler, R., Rodrigues, R. B., Maia, J. G., Papagiannipoulos, M., Fabricius, H., & Marx, F. (2005). Total oxidant scavenging capacities of *Euterpe oleracea* Mart. (Açaí) fruit. *International Journal of Food Sciences and Nutrition, 56*(1), 53–64.

McDougall, G. J., Ross, H. A., Ikeji, M., & Stewart, D. (2008). Berry extracts exert different antiproliferative effects against cervical and colon cancer cells grown in vitro. *Journal of Agricultural and Food Chemistry, 56*(9), 3016–3023.

Moyer, R. A., Hummer, K. E., Finn, C. E., Frei, B., & Wrolstad, R. E. (2002). Anthocyanins, phenolics, and antioxidant capacity in diverse small fruits: Vaccinium, rubus, and ribes. *Journal of Agricultural and Food Chemistry, 50*(3), 519–525.

Munoz-Espada, A. C., Wood, K. V., Bordelon, B., & Watkins, B. A. (2004). Anthocyanin quantification and radical scavenging capacity of Concord, Norton, and Marechal Foch grapes and wines. *Journal of Agricultural and Food Chemistry, 52*(22), 6779–6786.

Pacheco-Palencia, L. A., Talcott, S. T., Safe, S., & Mertens-Talcott, S. (2008). Absorption and biological activity of phytochemical-rich extracts from Açai (*Euterpe oleracea* Mart.) pulp and oil in vitro. *Journal of Agricultural and Food Chemistry, 56*(10), 3593–3600.

Parsons, J. K., Newman, V. A., Mohler, J. L., Pierce, J. P., Flatt, S., & Marshall, J. (2008). Dietary modification in patients with prostate cancer on active surveillance. A randomized, multicentre feasibility study. *BJU International, 101*(10), 1227–1231.

Ray, S. D., Kamendulis, L. M., Gurule, M. W., Yorkin, R. D., & Corcoran, G. B. (1993). Ca2+ antagonists inhibit DNA fragmentation and toxic cell death induced by acetaminophen. *FASEB Journal, 7*(5), 453–463.

Rodrigues, R. B., Lichtenthaler, R., Zimmermann, B. F., Papagiannopoulos, M., Fabricius, H., Marx, F., et al. (2006). Total oxidant scavenging capacity of *Euterpe oleracea* Mart. (açai) seeds and identification of their polyphenolic compounds. *Journal of Agricultural and Food Chemistry, 54*(12), 4162–4167.

Schauss, A. G., Wu, X., Prior, R. L., Ou, B., Huang, D., Owens, J., et al. (2006a). Antioxidant capacity and other bioactivities of the freeze-dried Amazonian palm berry, *Euterpe oleraceae* mart. (açai). *Journal of Agricultural and Food Chemistry, 54*(22), 8604–8610.

Schauss, A. G., Wu, X., Prior, R. L., Ou, B., Patel, D., Huang, D., et al. (2006b). Phytochemical and nutrient composition of the freeze-dried Amazonian palm berry, *Euterpe oleraceae* mart. (açai). *Journal of Agricultural and Food Chemistry, 54*(22), 8598–8603.

Seeram, N. P. (2008). Berry Fruits for cancer prevention: Current status and future prospects. *Journal of Agricultural and Food Chemistry, 56*(3), 630–635.

Seeram, N. P., Adams, L. S., Zhang, Y., Lee, R., Sand, D., Scheuller, H. S., et al. (2006). Blackberry, black raspberry, blueberry, cranberry, red raspberry, and strawberry extracts inhibit growth and stimulate apoptosis of human cancer cells in vitro. *Journal of Agricultural and Food Chemistry, 54*(25), 9329–9339.

Seeram, N. P., Aviram, M., Zhang, Y., Henning, S. M., Feng, L., Dreher, M., et al. (2008). Comparison of antioxidant potency of commonly consumed polyphenol-rich beverages in the United States. *Journal of Agricultural and Food Chemistry, 56*(4), 1415–1422.

Seifried, H. E., Anderson, D. E., Fisher, E. I., & Milner, J. A. (2007). A review of the interaction among dietary antioxidants and reactive oxygen species. *The Journal of Nutritional Biochemistry, 18*(9), 567–579.

Solomon, A., Golubowicz, S., Yablowicz, Z., Grossman, S., Bergman, M., Gottlieb, H. E., et al. (2006). Antioxidant activities and anthocyanin content of fresh fruits of common Fig. (*Ficus carica* L.). *Journal of Agricultural and Food Chemistry, 54*(20), 7717–7723.

Szatrowski, T. P., & Nathan, C. F. (1991). Production of large amounts of hydrogen peroxide by human tumor cells. *Cancer Research, 51*(3), 794–798.

Vattem, D. A., Ghaedian, R., & Shetty, K. (2005). Enhancing health benefits of berries through phenolic antioxidant enrichment: Focus on cranberry. *Asia Pacific Journal of Clinical Nutrition, 14*(2), 120–130.

Veluri, R., Singh, R. P., Liu, Z., Thompson, J. A., Agarwal, R., & Agarwal, C. (2006). Fractionation of grape seed extract and identification of gallic acid as one of the major active constituents causing growth inhibition and apoptotic death of DU145 human prostate carcinoma cells. *Carcinogenesis, 27*(7), 1445–1453.

Wang, S. Y., Chen, C.-T., Sciarappa, W., Wang, C. Y., & Camp, M. J. (2008). Fruit quality, antioxidant capacity, and flavonoid content of organically and conventionally grown Blueberries. *Journal of Agricultural and Food Chemistry, 56*(14), 5788–5794.

Wang, S. Y., & Lin, H. S. (2000). Antioxidant activity in fruits and leaves of blackberry, raspberry, and strawberry varies with cultivar and developmental stage. *Journal of Agricultural and Food Chemistry, 48*(2), 140–146.

Wei, Y.-H., & Lee, H.-C. (2002). Oxidative Stress, mitochondrial DNA mutation, and impairment of antioxidant enzymes in aging. *Experimental Biology and Medicine, 227*(9), 671–682.

Wiseman, H., & Halliwell, B. (1996). Damage to DNA by reactive oxygen and nitrogen species: Role in inflammatory disease and progression to cancer. *Biochemical Journal, 313*(Pt 1), 17–29.

Wolfe, K., Wu, X., & Liu, R. H. (2003). Antioxidant activity of apple peels. *Journal of Agricultural and Food Chemistry, 51*(3), 609–614.

Zhou, K., Hao, J., Griffey, C., Chung, H., O'Keefe, S. F., Chen, J., et al. (2007). Antioxidant properties of fusarium head blight-resistant and- susceptible soft red winter wheat grains grown in Virginia. *Journal of Agricultural and Food Chemistry, 55*(9), 3729–3736.

Zhou, K., Su, L., & Yu, L. L. (2004). Phytochemicals and antioxidant properties in wheat bran. *Journal of Agricultural and Food Chemistry, 52*(20), 6108–6114.

Food Chemistry 118 (2010) 215–223

Contents lists available at ScienceDirect

Food Chemistry

journal homepage: www.elsevier.com/locate/foodchem

Structural characterisation and determination of prebiotic activity of purified xylo-oligosaccharides obtained from Bengal gram husk (*Cicer arietinum* L.) and wheat bran (*Triticum aestivum*)

M.S. Madhukumar, G. Muralikrishna *

Department of Biochemistry and Nutrition, Central Food Technological Research Institute, Mysore 570020, Karnataka, India

ARTICLE INFO

Article history:
Received 5 December 2008
Received in revised form 8 April 2009
Accepted 28 April 2009

Keywords:
Water extractable polysaccharides
Bengal gram husk
Wheat bran
Xylo-oligosaccharides
Prebiotic activity

ABSTRACT

Water extractable polysaccharides (WEPs) were isolated from Bengal gram husk and wheat bran. These WEP were subjected to driselase enzyme hydrolysis to obtain oligosaccharide mixtures, which were purified successively on Biogel P-2 and high performance liquid chromatographies. The molecular weight and structural features of the purified oligosaccharides were deduced using ESI-MS and ^{1}H NMR, respectively. The prebiotic properties of these purified oligosaccharides were studied by using *Bifidobacterium adolescentis* NDRI 236. Increase in dry cell mass (0.7–0.9 mg/ml) and decrease in pH (<5.8) due to production of short chain fatty acid (SCFA) indicated oligosaccharide fermentation. Acetate was the chief SCFA produced and its amount varied from 97.2% to 100%. The activities of xylanase (257–470 mU/ml), xylopyranosidase (53–60 mU/ml) and arabinofuranosidase (60–70 mU/ml) in the culture broth indicated the breakdown of xylo-oligosaccharides and their subsequent utilisation by the bacterium for its growth.

1. Introduction

Dietary fibres and their degradation products reaching the colon undergo different degrees of fermentation, out of which highly fermentable types include water-soluble hemicelluloses, pectins and gums and also include non-digestible oligosaccharides (NDOs) which resist digestion by endogenous enzymes within the human intestinal tract (Van Laere, Hartemink, Bosveld, Schols, & Voragen, 2000). Soluble dietary fibres, such as β-D-glucans and soluble arabinoxylans, are readily fermented by colonic microorganisms; where as insoluble dietary fibres are only degraded partially, resulting in an increase in the faecal bulk. Beneficial colonic bacteria such as lactic acid bacteria and bifidobacteria produce carbohydrate degrading enzymes which ferment the oligosaccharides and produce short chain fatty acids such as acetate, propionate and butyrate which provide metabolic energy for the host and help in the acidification of the bowel (Swennen, Courtin, & Delcour, 2006). Acidification can affect the balance of the bacterial species, bacterial metabolic activity and product formation as well as the epithelial proliferation. *Bifidobacterium* strains are largely described as capable of efficiently fermenting xylose-based oligo and polysaccharides (Crittenden et al., 2002).

Functional foods, which can enhance the health of the consumer, are having a large market in today's food industry. Of the currently known functional foods, non-digestible oligosaccharides hold an important position with respect to their prebiotic activity. A prebiotic is defined as "a non-digestible food ingredient that beneficially affects the host by selectively stimulating the growth and/or activity of one or a limited number of bacteria in the colon, and thus improves the host health" (Gibson & Roberfroid, 1995). Many studies have now confirmed that the prebiotics incorporated in the diet is a valid approach to the dietary manipulation of the colonic microflora (Gibson & Roberfroid, 1995). Health promoting bacteria also produce vitamins, SCFA and other nutrients for their host, providing up to 15% of the total caloric intake (Gibson, 1999). Prebiotic effect of fructo-oligosaccharides (FOS) and galacto-oligosaccharides (GOS) were reported (Delzenne & Kok, 2001). Studies on GOS and FOS have also shown that they are effective in increasing the mineral absorption (Chonan, Takahashi, & Watanuki, 2001). However, xylo-oligosaccharides as active prebiotic components have not yet been effectively exploited. Only few reports mention the fermentability of crude cereal non-starch polysaccharides/oligosaccharides (Cotta, 1993; Jaskari et al., 1998; Karppinen, Liukkonen, Aura, Forssell, & Poutanen, 2000).

Monitoring fermentation in vivo is very difficult. The fermentation of polysaccharides/oligosaccharides can be measured from faeces, but SCFA are readily absorbed in the colon and the amount found in faeces does not describe the true situation. Knowledge of the extent of fermentation of polysaccharides/oligosaccharides and of the SCFA production *in vitro* by beneficial bacteria are therefore of great importance. Bifidobacteria and lactic acid bacteria are

* Corresponding author. Tel.: +91 0821 2514876; fax: +91 0821 2517233.
E-mail address: krishnagm2002@yahoo.com (G. Muralikrishna).

0308-8146/$ - see front matter © 2009 Elsevier Ltd. All rights reserved.
doi:10.1016/j.foodchem.2009.04.108

shown to poorly utilise arabinoxylans, but readily utilised arabinoxylans hydrolysates (Jaskari et al., 1998). It was shown that arabinofuranosidase and xylopyranosidase cannot degrade long chain xylan and they act best on arabinoxylo-oligosaccharides (unpublished results). Acid hydrolysis of polysaccharides is nonspecific and restricts its wider application. Utilisation of enzymes might improve the technical and economic feasibility of biotechnological processes for arabinoxylan hydrolysis. Endoxylanase hydrolyses the arabinoxylans randomly producing xylo-oligosaccharides (Kormelink, Gruppen, Vietor, & Voragen, 1993) of varying degree of polymerisation (D.P. 2–10). Apart from their prebiotic effect, xylo-oligosaccharides are believed to alleviate disease symptoms such as diabetes, arteriosclerosis and colon cancer (Swennen et al., 2006).

Cereal brans and pulse husks (agricultural wastes) are available in plenty in India. They are used as feedstuffs for various non-ruminant farm animals. Arabinoxylans are rich in cereal bran and pulse husks. Development of an economically viable technology can therefore be explored in order to obtain high value added products such as bioactive oligosaccharides from agricultural wastes. Hence a study has been carried out by isolating xylo-oligosaccharides from the water extractable polysaccharides of agricultural wastes such as Bengal gram husk and wheat bran and the results pertaining to their purification, structural characterisation and determination of the prebiotic properties are reported here.

2. Materials and methods

2.1. Materials

Wheat bran (*Triticum aestivum*) was obtained from local market. Bengal gram (*Cicer arietinum*) was dehusked in the GST Department of C.F.T.R.I., Mysore, India. HPLC (μ-Bondapak-NH_2 carbohydrate) and GLC (OV-225 and PEG 20M) columns were obtained from Shimadzu Corporation, Kyoto, Japan. Sugars, enzymes (Driselase), substrates and other fine chemicals were purchased from Sigma Chemical Company, MO, USA. Microorganisms were obtained from National Dairy Research Institute (NDRI), Karnal, India. Microbiological culture media and media ingredients were obtained from HiMedia, Mumbai, India. All other chemicals and solvents were of analytical grade.

2.2. Isolation of water extractable polysaccharides (WEP)

Water extractable polysaccharides were isolated from wheat bran and Bengal gram husk as described earlier (Rao & Muralikrishna, 2004). In brief, bran/husk was powdered and extracted with water (200 ml × 4 at 25 °C), centrifuged (at 3000×*g* for 20 min) and the supernatant thus obtained was precipitated with three volumes of ethanol, which was separated out by centrifugation followed by dialysis (cut off range ≈8 Kda) and lyophilisation. These water-soluble fractions were further dissolved in water (10%) and insoluble portion was separated out by centrifugation (at 3000×*g* for 20 min). Soluble portion was heated at 95 °C for 10 min to denature associated enzymes and proteins. It was further centrifuged (at 7500×*g* for 10 min) and the supernatant thus obtained was dialysed and lyophilised to obtain water extractable polysaccharides.

2.3. Liberation of oligosaccharides from WEP

WEP of wheat bran and Bengal gram husk (500 mg each) were dissolved in acetate buffer (pH 4.8, 0.1 M, 10 ml) and incubated with driselase (0.28 U/mg protein) in a constant shaking water bath at 50 °C for 2 h. Subsequently the reaction was stopped by adding 3 volumes of ethanol and the precipitated material was removed by centrifugation (at 3000×*g* for 15 min). The resultant supernatant consisting of oligosaccharides was concentrated and used for further analysis.

2.4. Purification of oligosaccharides on Biogel P-2

The individual oligosaccharide mixtures obtained from WEP of wheat and Bengal gram by driselase action (10–15 mg) were separated on Biogel P-2 column (0.9 × 105 cm). Triple distilled, degassed water was used as the eluent at a flow rate of 6 ml/h and fractions (1 ml each) were collected (Guillon et al., 2004). The carbohydrate containing fractions were pooled and concentrated for further characterisation.

2.5. HPLC of oligosaccharides

Oligosaccharides obtained after purification on Biogel P-2 column chromatography were further purified by Shimadzu HPLC system using μ-Bondapak-NH_2 carbohydrate column (4.1 × 300 mm) using refractive index detector. The Biogel P-2 purified oligosaccharides (2 mg) were dissolved in water (0.2 ml) passed through a Millipore filter (0.2 micron), and an aliquot of 20 μl was injected to the column and eluted by using acetonitrile and water (70:30) at a flow rate of 1 ml/min (McGinnis & Fang, 1980).

2.6. Determination of neutral sugar composition of poly/oligosaccharides by GLC

The polysaccharides (10 mg) isolated from wheat bran and Bengal gram husk were suspended in water and were completely hydrolysed by prior solubilisation with 72% sulphuric acid at ice-cold temperature followed by diluting to 8% acid and heating at 100 °C for 10–12 h (Rao & Muralikrishna, 2004). The oligosaccharides (10 mg) were hydrolysed with sulphuric acid (2 N) for 8 h. The above mixtures were neutralised with barium carbonate (solid), filtered, deionized with Amberlite IR-120(H^+) resin and concentrated. Sodium borohydride (20 mg) was added to reduce the monosaccharides obtained from the polysaccharide/oligosaccharide hydrolysates and the tubes were kept at room temperature for 4–6 h. The excess borohydride was decomposed by adding acetic acid (2 N) drop wise till the effervescence of hydrogen stopped. The boric acid formed was removed by co-distillation with methanol (2 ml × 5). To the dry glycitols were added acetic anhydride and pyridine (1.0 ml each) and the mixture was kept at 100 °C for 2 h. After acetylation excess reagents were removed by co-distilling with water and toluene (2 ml × 3 each). The alditol acetates were extracted with chloroform, filtered through glass wool and dried by flushing nitrogen (Sawardekar, Slonekar, & Jeanes, 1965). The derivatives were taken in known amount of chloroform and analysed by GLC for qualitative and quantitative analysis.

2.7. Proton NMR spectra of oligosaccharides

Oligosaccharides samples (2–5 mg) were dissolved in D_2O (0.5 ml). The proton spectra collected with 7500 Hz spectral width with wet water suppression scheme. The proton spectra referenced with external TMS as standard (Hoffmann, Kamerling, & Vliegenthart, 1992). The experiments were done at 25 °C with 128 scans. The recycle delay kept at 3 s, with proton 90R above of 10.5 μs used.

2.8. ESI-MS of purified oligosaccharides

Mass spectra of the purified oligosaccharides were recorded by Alliance, Waters 2695 mass spectrometer instrument using

positive mode electrospray ionisation with the following operational conditions, i.e. capillary voltage 3.5 kV, core voltage 100 V, source temperature 80 °C, disolvation temperature 150 °C, core gas (Argon) 35 l/h and disolvation gas (nitrogen) 500 l/h (Fernandez, Obel, Scheller, & Roespstorff, 2004).

2.9. Uronic acid determination

To the test solutions (0.5 ml, kept in ice-cold temperature bath) was added conc. sulphuric acid (3 ml) and the solutions were mixed properly. The above mixture was kept in a boiling water bath for 20 min cooled and then carbazole solution (0.1 ml, 0.1% – prepared by dissolving recrystallized carbazole in alcohol) was added. The tubes were kept in dark for 2 h and the absorbance was read at 530 nm (Knutson & Jeanes, 1968). Uronic acid content was determined by referring to the standard graph prepared by using D-glucuronic acid (10–50 μg/0.5 ml). Averages of triplicate values were reported.

2.10. Protein determination

Protein concentration was determined according to the dye binding method of Bradford (1976) with bovine serum albumin (BSA) as standard. Averages of triplicate values were reported.

2.11. Microorganism and culture conditions

B. adolescentis NDRI 236 culture was used for the prebiotic activity determination studies. The culture was maintained at 6 °C in lactobacillus MRS broth medium supplemented with cysteine HCl (0.05%) and sub cultured at regular intervals of 30 days.

2.12. Inoculum

The culture was grown (24 h) in lactobacillus MRS broth medium supplemented with cysteine HCl (0.05%) and subjected to centrifugation (at 8000×*g* for 10 min at 4 °C) and the resultant cells were suspended in 0.85% normal saline. Serial dilutions were prepared to get the requisite cell population (10^{-6}). Lactobacillus MRS agar and broth medium and all the glassware, centrifuge tubes were sterilized (autoclaved at 121 °C for 15 min) and used for the microbiological experiments.

2.13. In vitro fermentation experiments

Membrane filter (0.22 mμ, Millipore) sterilized individual purified wheat bran oligosaccharides (WBO) and Bengal gram oligosaccharides (BGO) in 10× concentration were incorporated at 0.25% (w/v) level into 2 ml MRS broth medium (formulated without beef extract, yeast extract, sodium acetate and dextrose and replaced protease peptone to tryptone) and inoculated with 100 μl aliquots of culture suspension giving a cell number of 5×10^3 CFU/ml and incubated at 37 °C for up to 48 h. A change in the broth colour from colourless to deep yellow was considered as positive test. Growth of bacteria and utilisation of oligosaccharides by bacteria were monitored by measuring pH and absorbance of culture broth. Turbidity was monitored spectrophotometrically with an UV–Visible spectrophotometer at 600 nm. After 48 h of incubation, cultures were centrifuged (at 3000×*g* for 20 min) and cells were oven dried (for constant weight, at 80 °C) to determine the dry cell mass. Resultant supernatant was analysed for SCFA. Besides, viable cell population was enumerated by pour plating using lactobacillus MRS agar and incubating at 37 °C for 48 h. All the experimental values are averages of three independent experiments.

2.14. Enzyme assays

Culture broth (24 h old) was assayed for the presence of various enzyme activities. For determining the xylanase activity, larch wood xylan (1 ml, 0.5% in sodium acetate buffer, 0.1 M, pH 4.8) was incubated with sample (0.1 ml of culture broth) for 30 min at 50 °C. Reaction was stopped by adding 1 ml of DNS (dinitrosalicylic acid) reagent and the reducing sugar was quantified (Miller, 1959). One unit of activity was defined as the amount of enzyme required to liberate 1 μmol of xylose/min under assay conditions. β-D-xylopyranosidase (Beldman, Osuga, & Whitaker, 1996), α-L-arabinofuranosidase (Beldman et al., 1996), α-D-galactopyranosidase and β-D-galactopyranosidase activities were determined by monitoring the release of p-nitro phenol from respective substrates i.e. p-nitro phenol glycosides (0.5 ml of 2 mM substrate in sodium phosphate buffer, 0.1 M, pH 5.7) by incubating them with sample (0.1 ml of culture broth) for 1 h at 37 °C. For determining acetyl esterase activity, substrate (1 ml of saturated solution of p-nitro phenyl acetate in sodium potassium phosphate buffer, 0.2 M, pH 6.5) was incubated with sample (0.1 ml of culture broth) for 30 min at 25 °C. Reactions in the above enzyme assays were stopped by adding saturated solution of sodium tetra borate (0.5 ml). Absorbance was read at 400 nm. One unit of activity was defined as the amount of enzyme required to liberate 1 μmol of p-nitro phenol/min under assay conditions. Averages of triplicate values were reported.

2.15. SCFA analysis

The culture supernatant was acidified with sulphuric acid (50%) and extracted with diethyl ether (Karppinen et al., 2000) and analysed for SCFA by GLC on PEG-20 M by maintaining, column injector and detector temperatures at 120, 220 and 230 °C, respectively (Silvi, Rumney, Cresci, & Rowland, 1999), using nitrogen as the carrier gas (40 ml/min). Acetate, propionate and butyrate (10 μmol each/ml in diethyl ether) were used as standards. Quantity of individual SCFA in the sample was estimated by using peak area standard curve.

3. Results and discussion

3.1. Chemical composition of WEP extracted from Bengal gram husk and wheat bran

Water extractable polysaccharides (WEP) were isolated from Bengal gram husk and wheat bran (Rao & Muralikrishna, 2004) in yields of 2.78% and 4.8%, respectively. The protein content and uronic acid content of the polysaccharides were 2.5% and 24.6% (Bengal gram husk) and 6.4% and 11.3% (wheat bran). The neutral sugar composition of Bengal gram WEP showed rhamnose, arabinose, xylose, galactose and glucose in a ratio (mol%) of 12.5:17.8:16.7:30.9:22.6 whereas WEP of wheat bran consisted of rhamnose, arabinose, xylose, mannose, galactose and glucose in the ratio (mol%) of 1.3:21.2:38.5:1.6:26.4:11.3. The presence of high amount of uronic acid in these polysaccharides seems to be a characteristic of water-soluble arabinoxylans (Rao & Muralikrishna, 2004). However, presence of glucose and galactose in these polysaccharides may be due to the co-extraction of β-D-glucans and arabinogalacto-proteins present in the cell wall along with the enriched arabinoxylans (Loosveld et al., 1998).

3.2. Liberation of oligosaccharides from polysaccharides

The WEP from Bengal gram husk and wheat bran were subjected to commercial driselase (EC 3.2.1.8) hydrolysis in order to obtain oligosaccharides in the yields of 5.8% and 14.4% in Bengal

gram husk and wheat bran, respectively. Driselase from *Basidiomycetes* sp. is an endoxylanase, which cleaves arabinoxylans randomly (unbranched regions of both internal and external chains), resulting in the liberation of oligosaccharides with varying degree of polymerisation.

3.3. Purification of oligosaccharides

The oligosaccharides thus obtained from enzymatic hydrolysis of WEP of Bengal gram husk and wheat bran were separated by gel permeation chromatography (Biogel P-2 stationary media). Five major oligosaccharide fractions were obtained (elution volumes of oligosaccharides are given in parenthesis) in case of Bengal gram husk WEP and were designated as BGO-I (77 ml), BGO-II (83 ml), BGO-III (86 ml), BGO-IV (90 ml) and BGO-V (96 ml). Four fractions obtained in case of wheat bran WEP and were designated as WBO-I (72 ml), WBO-II (78 ml), WBO-III (86 ml) and WBO-IV (104 ml). BGO-V and WBO-IV exclusively consisted of monosaccharides, hence not taken for further studies.

Biogel P-2 purified oligosaccharides from Bengal gram husk (BGO-I and BGO-IV) and wheat bran (WBO-I and WBO-III), were further resolved into 1–3 sub fractions on HPLC (figures not shown). The major purified fractions were collected in each case and used for the structural characterisation and determination of their prebiotic activity.

3.4. ^{1}H NMR analysis of purified oligosaccharides

^{1}H NMR was used for elucidating the structures of the purified oligosaccharides. ^{1}H NMR analysis of purified oligosaccharides BGO-I, BGO-IV, WBO-I and WBO-III indicated chemical shifts in the region of δ 3.00 to δ 5.00 ppm characteristics of α-linked arabinofuranoside as well as β-linked xylopyranoside residues (Gruppen et al., 1992) (Table 1).

3.4.1. BGO-I fraction

The ^{1}H NMR spectrum of BGO-I (Fig. 1a) showed a peak at around δ 5.194 ppm representing the anomeric proton of xylopyranose at the reducing end, whereas δ 3.403 ppm represented that second β-xylopyranose (from reducing end) is linked to α-arabinofuranose residue at O-3 position (Gruppen et al., 1992). The signals at around δ 4.150 and δ 3.952 ppm represented the α-arabinofuranose linked to the O-2 position of third β-xylopyranose residue, which form the non-reducing end of the oligosaccharide. The signals at around δ 4.187 and δ 3.797 ppm represent that α-arabinofuranose linked to the O-3 position of second β-xylopyranose residue from reducing end. The ^{1}H NMR data is presented in Table 1 and the probable structure of BGO-I is as follows:

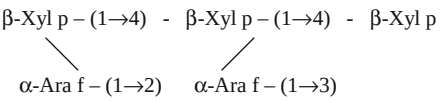

3.4.2. BGO-IV fraction

The ^{1}H NMR spectrum of BGO-IV fraction (Fig. 1b), gave a peak around δ 3.547 ppm representing the presence of β-xylopyranose residue at reducing end position. Signals at δ 3.292 and δ 3.765 ppm represents second β-xylopyranose residue from the reducing end, which is branched at O-3 position and forms the non-reducing end of the oligosaccharide (Gruppen et al., 1992). A signal at δ 3.914 and δ 3.800 ppm indicated that α-arabinofuranose might be linked to the O-3 position of the second β-xylopyranose residue. The ^{1}H NMR data is presented in Table 1 and the probable structure of BGO-IV is as follows:

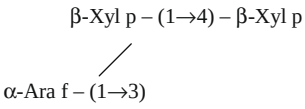

3.4.3. WBO-I fraction

The ^{1}H NMR spectrum of WBO-I (Fig. 2a) gave a peak at around δ 5.193 ppm representing the anomeric proton of xylopyranose at the reducing end. Signals at δ 3.546 and δ 3.730 ppm also indicated

Table 1
Chemical shifts[a] (δ) of proton resonances of purified oligosaccharides (^{1}H NMR data).

Oligosaccharide	Residue[b]	Chemical shifts (ppm)				
		H-1	H-2	H-3	H-4	H-5
BGO-I	Xyl *p*-1	5.194	3.547	3.730	–	3.820
	β-Xyl *p*-2^{II}	4.490	3.403	3.745	3.690	3.340
	β-Xyl *p*-3^{I}	4.475	3.400	3.579	3.663	3.340
	α-Ara *f*-A^{3X2}	5.427	4.159	3.902	4.187	3.797
	α-Ara *f*-A^{2X3}	5.221	4.150	3.952	3.829	3.817
BGO-IV	Xyl *p*-1	5.194	3.547	3.730	–	3.820
	β-Xyl *p*-2^{II}	4.421	3.292	3.765	3.795	4.004
	α-Ara *f*-A^{3X2}	5.443	4.162	3.914	4.308	3.800
WBO-I	Xyl *p*-1	5.193	3.546	3.730	–	3.820
	β-Xyl *p*-2	4.467	3.298	3.554	3.792	3.416
	β-Xyl *p*-3^{III}	4.639	3.572	3.670	3.724	3.431
	β-Xyl *p*-2	4.432	3.237	3.409	3.591	3.269
	α-Ara *f*-A^{2X3}	5.225	4.148	3.932	4.301	3.828
	α-Ara *f*-A^{3X3}	5.271	4.164	3.932	4.301	3.720
	β-Xyl *p*-4	4.432	3.237	3.409	3.591	3.269
WBO-III	Xyl *p*-1	5.194	3.547	3.73	3.820	–
	β-Xyl *p*-2^{III}	4.596	3.539	3.689	3.724	3.344
	α-Ara *f*-A^{2X2}	5.246	4.151	3.956	4.132	3.720
	α-Ara *f*-A^{3X2}	5.246	4.175	3.973	4.198	3.706

β-Xyl *p*-3^{I} means β-Xyl *p*-3 branched at O-2; β-Xyl *p*-3^{II} means β-Xyl *p*-3 branched at O-3; β-Xyl *p*-3^{III} means β-Xyl *p*-3 branched at both O-2, 3 and α-Ara *f*-A^{2X3} means α-arabinofuranose linked to O-2 of Xyl *p*-3, etc.

[a] Measured at 7500 Hz on solutions in D_2O at 25 °C.

[b] The Xyl *p*-1 means xylopyranose residue at reducing end position, etc.

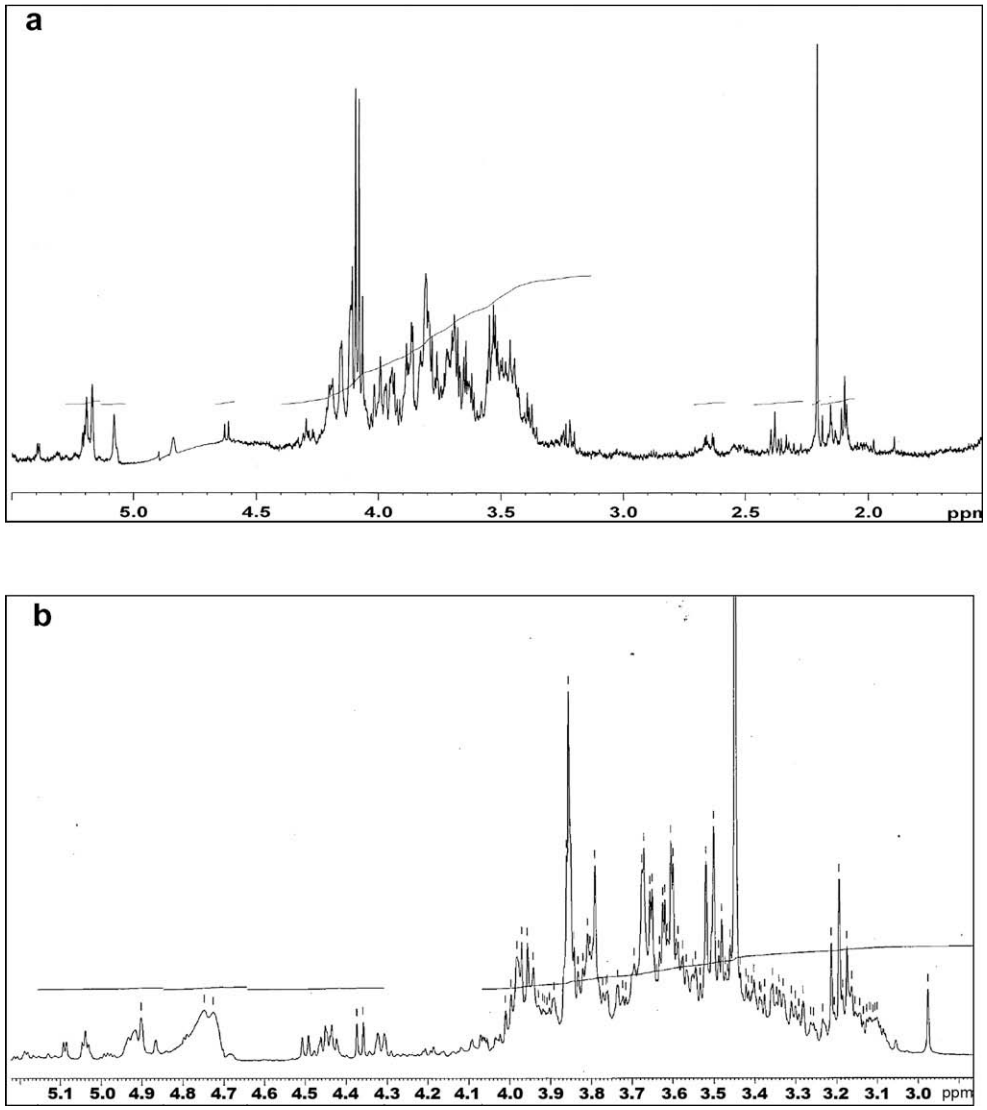

Fig. 1. ^{1}H NMR spectra of purified oligosaccharides: (a) BGO-I and (b) BGO-IV.

xylopyranose at the reducing end. Signals at δ 4.639 and δ 3.670 ppm represent the disubstituted β-xylopyranose residue which is present at position-3 from reducing end of the oligosaccharide. δ 5.271 ppm indicated that α-arabinose is linked to O-3 of xylopyranose-3 residue from the reducing end (Gruppen et al., 1992). δ 5.225 and δ 3.932 ppm represent α-arabinofuranose linked to O-2 position of 3rd β-xylopyranose residue from the reducing end. ^{1}H NMR signals at δ 4.432 and δ 3.237 ppm represent the fourth unbranched β-xylopyranose residue, which forms the non-reducing end (Harry Gruppen et al., 1992). The ^{1}H NMR data is recorded in Table 1 and the probable structure of WBO-I fraction is as follows:

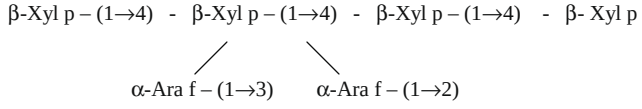

3.4.4. WBO-III fraction

The ^{1}H NMR spectrum of WBO-III fraction (Fig. 2b), gave a signal around δ 5.194 and δ 3.547 ppm which represents the presence of xylopyranose residue at reducing end. Signals at δ 4.596 and δ 3.689 ppm represent disubstituted xylopyranose-2 residue. Signals around δ 5.246 and δ 4.175 ppm represented that α-arabinofuranose is linked to O-3 position of xylopyranose-2 residue which forms the non-reducing end of the oligosaccharide (Harry Gruppen et al., 1992). The peaks around δ 5.238 and δ 4.151 ppm indicated that the α-arabinofuranose residue, which is linked to O-2 position of xylopyranose-2 residue. The ^{1}H NMR data is recorded in Table 1. Probable structure of WBO-III is given below:

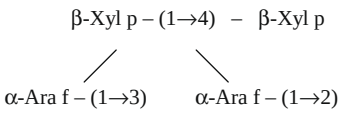

3.5. ESI-MS analysis of purified oligosaccharides

ESI-MS analysis of purified oligosaccharides of BGO-I, BGO-IV, WBO-I and WBO-III gave the molecular ion signals at *m*/*z* 701.3, 437.2, 833.3 and 569.2, respectively (Fig. 3A–D). The xylo-oligosaccharide ions present in the mass spectra were identified as sodium

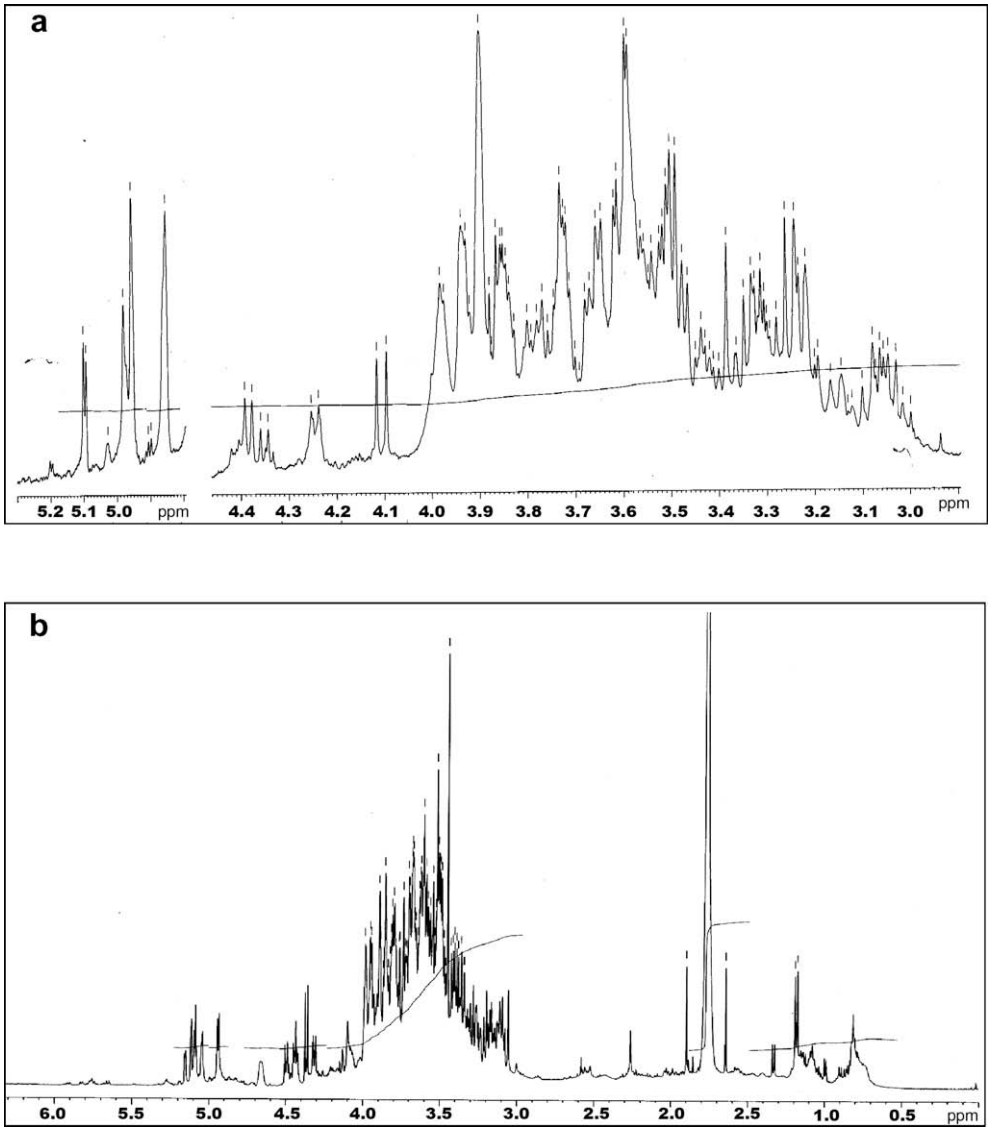

Fig. 2. ^{1}H NMR spectra of purified oligosaccharides: (a) WBO-I and (b) WBO-III.

adducts, $[M+Na]^{+}$ as described by Reis, Coimbra, Domingues, Ferrer-Correia, and Domingues (2002). ESI-MS analysis indicated BGO-I, BGO-IV, WBO-I and WBO-III as pentasaccharide (DP-5), trisaccharide (DP-3), hexasaccharide (DP-6) and tetrasaccharide (DP-4), respectively, varying in their arabinose and xylose ratio as determined by GLC analysis of the purified oligosaccharides (results not shown). These signals can be identified and assigned according to the nomenclature introduced by Domon and Castello (1998). From these spectra it was not possible to obtain information regarding the presence and branching pattern of arabinofuranosyl residues and their possible distribution along the xylopyranose backbone hence the oligosaccharides were taken for ^{1}H NMR analysis to elucidate the same.

3.6. In vitro fermentation of oligosaccharides

The strain of *Bifidobacterium* readily utilised both the WBO and BGO as indicated by increased biomass compared to control. There was a change in broth colour from colourless to deep yellow in all the culture tubes indicating oligosaccharides fermentation by the bacterium. There was an increase in the dry cell mass (0.7–0.9 mg/ml) compared to control value (0.04 mg/ml) (Table 2). Similar increase in the viable cell count was also observed (results not shown). *B. adolescentis* NDRI 236 growth is maximum in WBO-I (O.D. 0.518) followed by WBO-III, BGO-IV and BGO-I. A similar profile of decrease in pH, increase in dry cell mass and production of SCFA were observed (Table 2). There was a decrease in pH of the culture broth compared to control due to the production of SCFA by bifidobacteria. Decrease in pH can be used as an indication of the prebiotic effect of the oligosaccharides incorporated in the culture broth (Berggren, Bjorck, Nyman, & Eggum, 1993). The bacterium produced SCFA in different proportions in all the culture tubes inoculated with oligosaccharides as carbon source. The amount of total SCFA produced varied for individual oligosaccharides. Acetate was the chief SCFA produced and its amount varied from 97.2% to 100% (Table 2) similar results were reported for human faecal bacteria (Karppinen et al., 2000). Acetate, propionate and butyrate are the major SCFA produced during fermentation of carbohydrates in the large bowel. Acetate is mainly metabolized in human muscle, kidney, heart and brain, whereas propionate acts as a possible gluconeogenic precursor suppressing the cholesterol synthesis (Gibson, 1999). Butyrate is known to have pro-differentiation, anti-proliferation and anti-angiogenic effects on colonocytes (Mai & Morris, 2004).

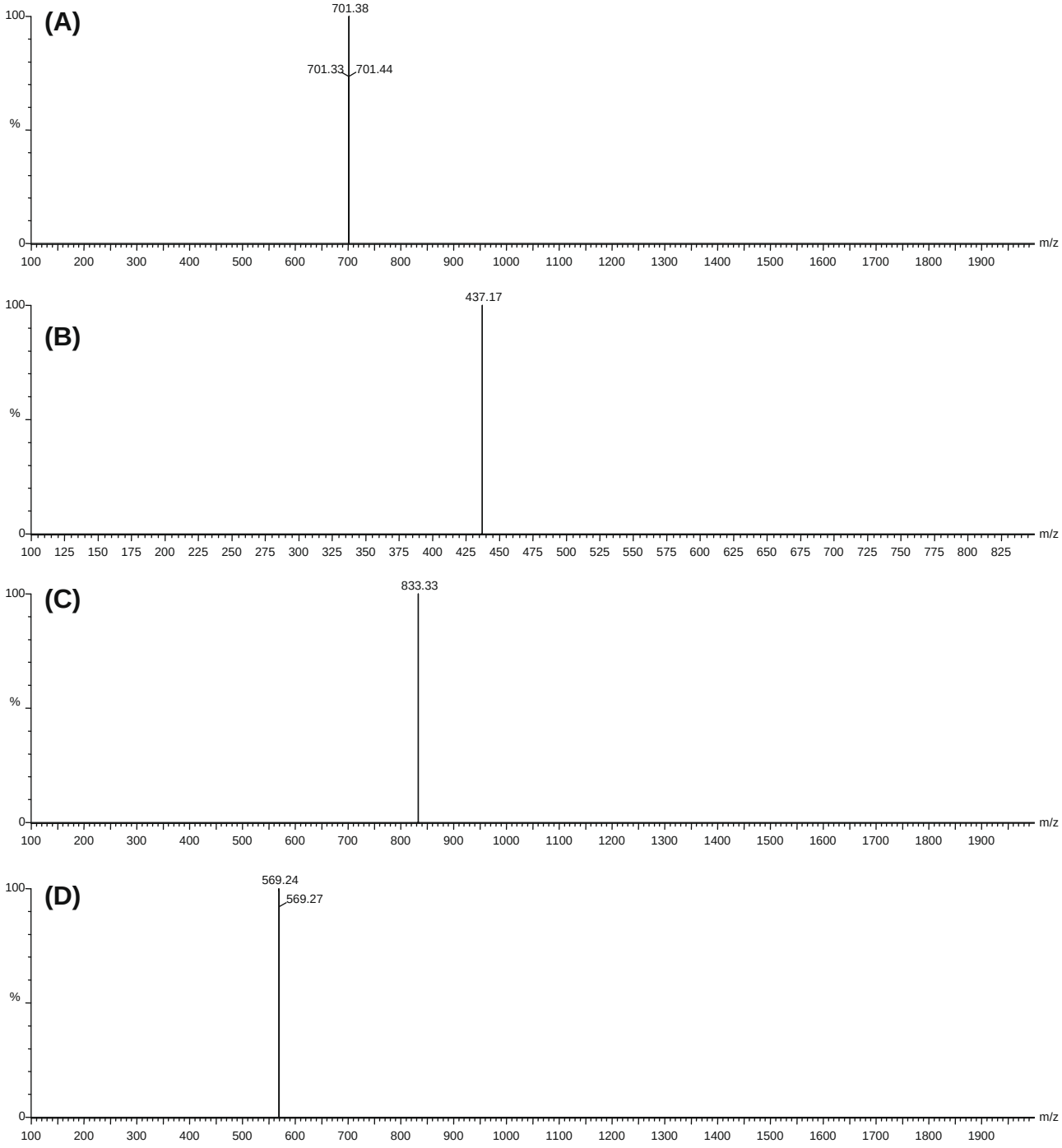

Fig. 3. ESI-MS of purified oligosaccharides: (A) BGO-I; (B) BGO-IV; (C) WBO-I and (D) WBO-III.

Table 2
Growth characteristics of *Bifidobacterium adolescentis* NDRI 236 on 0.25% (w/v) purified oligosaccharides.

Microorganism	Carbon source[a] (0.25%)	Absorbance at 600 nm	pH	Dry cell mass (mg/ml)	SCFA identified		
					Acetate	Propionate	Butyrate
Bifidobacterium adolescentis NDRI 236	Control[b]	0.031	6.65	0.04	–	–	–
	BGO-I	0.405	5.78	0.7	100	–	–
	BGO-IV	0.442	5.19	0.8	98.3	1.7	–
	WBO-I	0.518	5.03	0.9	97.2	1.8	1.0
	WBO-III	0.465	5.62	0.8	98.0	1.3	0.9

Reported values were corrected for the blank tube and baseline values.
[a] Carbon source is purified oligosaccharides incorporated to MRS broth.
[b] Control is culture broth without oligosaccharides and inoculated with microorganism.

Table 3
Enzyme activities (mU/min/ml) in *Bifidobacterium adolescentis* NDRI 236 culture filtrate grown on purified oligosaccharides as carbon source.

Microorganism	Carbon source (0.25%)	Xylanase	Xylosidase	Arabinosidase	α-Galactosidase	β-Galactosidase	Acetyl esterase
Bifidobacterium adolescentis NDRI 236	BGO-I	257.3	53.0	60.8	24.2	6.3	9.2
	BGO-II	268.6	57.5	62.9	27.5	9.6	9.9
	WBO-I	470.0	60.8	70.4	32.4	16.7	13.9
	WBO-III	445.3	59.0	64.8	28.8	13.4	12.2

Reported values were corrected with control values and blank tube values.

3.7. Determination of enzyme activities in the culture broth

The 24 h old cultures showed the presence of various enzyme activities such as xylanase, β-D-xylopyranosidase, α-L-arabinofuranosidase, α-D-galactopyranosidase, β-D-galactopyranosidase and acetyl esterase activities. All the cultures showed maximum xylanase activity. The activities of xylanase, xylopyranosidase and arabinofuranosidase were more compared to the α-D-galactopyranosidase, β-D-galactopyranosidase and acetyl esterase activities (Table 3). The relatively higher activities of xylanase, xylopyranosidase and arabinofuranosidase indicated the breakdown of arabinose and xylose, constituent sugars of xylo-oligosaccharides and subsequent utilisation of them by the bacteria for their growth. Bifidobacteria and lactic acid bacteria are shown to poorly utilise arabinoxylans, but readily utilise arabinoxylan hydrolysates (Jaskari et al., 1998). Arabinofuranosidase has been characterised and a large number of genes/proteins appeared to be specialised for catabolism of a variety of plant oligosaccharides were reported in bifidobacteria (Schley & Field, 2002; Shin, Park, Sung, & Kim, 2003). Xylanase activity is maximum in WBO-I (470 mU) followed by WBO-III (445 mU), BGO-IV (268.6 mU) and BGO-I (257.3 mU) (Table 3). The activity of enzyme xylopyranosidase is maximum in WBO-I (60.8 mU) followed by WBO-III (59.0 mU), BGO-IV (57.5 mU) and BGO-I (53.0 mU) (Table 3). The hydrolytic enzymes produced by the microorganisms help in the digestion of non-digestible oligosaccharides (NDOs) which escape digestion in the upper gastrointestinal tract and produce SCFA resulting in the reduction of pH of the culture broth. Decrease in pH in bowel creates acidic environment, which in turn reduces the number of pathogenic microorganisms (Morisse, Maurice, Boilletot, & Cotte, 1993).

4. Conclusions

In conclusion, the above study indicated that both Bengal gram husk and wheat bran are rich sources of arabinoxylans from which bioactive xylo-oligosaccharides can be obtained by driselase treatment. The purified xylo-oligosaccharides obtained from Bengal gram are penta and trisaccharides whereas from wheat bran they were found to be hexa and tetrasaccharides, respectively with varying ratios of arabinose and xylose. *B. adolescentis* NDRI 236 readily utilised purified oligosaccharides. Purified xylo-oligosaccharides from wheat bran are having much more potential than Bengal gram oligosaccharides as indicated by their prebiotic activity experiments.

Acknowledgements

We thank Dr. V. Prakash, F.R.Sc., Director, C.F.T.R.I., Mysore, for his keen interest in the work, and encouragement. The authors also thank Dr. M.C. Varadaraj, H.O.D, Human Resource Department, C.F.T.R.I., Dr. P. Srinivas, Head, PPSFT Department, C.F.T.R.I. and Mr. V.M. Pratape, G.S.T. Department, C.F.T.R.I., Mysore, for providing the facilities for prebiotic experiments, NMR experiments and for dehusking of Bengal gram, respectively. The investigators would like to thank sincerely the Department of Biotechnology (DBT), New Delhi, for the financial Grant. M.S.M. thanks the Council of Scientific and Industrial Research (C.S.I.R.), New Delhi, India for the Grant of senior research fellowship.

Appendix A. Supplementary data

Supplementary data associated with this article can be found, in the online version, at doi:10.1016/j.foodchem.2009.04.108.

References

Beldman, G., Osuga, D., & Whitaker, J. R. (1996). Some characteristics of β-D-xylopyranosidases, α-L-arabinofuranosidases and an arabinoxylan α-L-arabinofuranosidase from wheat bran and germinated wheat. *Journal of Cereal Science, 23*, 169–180.

Berggren, A. M., Bjorck, I. E. M., Nyman, E. M. G. L., & Eggum, B. O. (1993). Short-chain fatty acid content and pH in caecum of rats given various sources of carbohydrates. *Journal of the Science of Food and Agriculture, 63*, 397–406.

Bradford, M. M. (1976). A rapid and sensitive method for the quantitation of microgram quantities of protein utilizing the principle of protein-dye binding. *Analytical Biochemistry, 72*, 248–254.

Chonan, O., Takahashi, R., & Watanuki, M. (2001). Role of activity of gastrointestinal micro flora in absorption of calcium and magnesium in rats fed β-1, 4-linked galactooligosaccharides. *Bioscience, Biotechnology and Biochemistry, 65*, 1872–1875.

Cotta, M. A. (1993). Utilization of xylo-oligosaccharides by selected ruminal bacteria. *Applied and Environmental Microbiology, 59*, 3557–3563.

Crittenden, R., Karppinen, S., Ojanen, S., Tenkanen, M., Fagerstrom, R., & Matto, J. (2002). In vitro fermentation of cereal dietary fiber carbohydrates by probiotic and intestinal bacteria. *Journal of the Science of Food and Agriculture, 82*, 781–789.

Delzenne, N. M., & Kok, N. (2001). Effects of fructans-type prebiotics on lipid metabolism. *American Journal of Clinical Nutrition, 73*, 456S–458S.

Domon, B., & Castello, C. E. (1998). A systematic nomenclature for carbohydrate fragmentations in FAB–MS/MS spectra of glycoconjugates. *Glycoconjugate Journal, 5*, 397–409.

Fernandez, L. E. M., Obel, N., Scheller, V., & Roespstorff, P. (2004). Differentiation of isomeric oligosaccharide structure by ESI tandem MS and GC–MS. *Carbohydrate Research, 339*, 655–664.

Gibson, G. R. (1999). Dietary modulation of the human gut micro flora using the prebiotics oligofructose and inulin. *Journal of Nutrition, 129*, 1438S–1441S.

Gibson, G. R., & Roberfroid, B. (1995). Dietary modulation of the human colonic microflora: Introducing the concept of prebiotics. *Journal of Nutrition, 125*, 1401–1412.

Gruppen, H., Hoffmann, R. A., Kormelink, F. J. M., Voragen, A. G. L., Kamerling, J. P., & Vliegenthart, J. F. G. (1992). Characterization by ^{1}H-NMR spectroscopy of enzymatically derived oligosaccharides from alkali-extractable wheat-flour arabinoxylans. *Carbohydrate Research, 233*, 45–64.

Guillon, F., Tranquet, D., Quillien, L., Utille, J. P., Ortiz, J. J. O., & Saulnier, L. (2004). Generation of polyclonal & monoclonal antibodies against arabinoxylans and their use for immunocytochemical location of arabinoxylans in cell walls of endosperm of wheat. *Journal of Cereal Science, 40*, 167–182.

Hoffmann, R. A., Kamerling, J. P., & Vliegenthart, J. F. G. (1992). Structural features of a water-soluble arabinoxylan from the endosperm of wheat. *Carbohydrate Research, 226*, 303–311.

Jaskari, J., Kontula, P., Siitonen, A., Jousimies-Somer, H., Mattila-Sandholm, T., & Poutanen, K. (1998). Oat β-glucan and xylan hydrolysates as selective substrates for *Bifidobacterium* and *Lactobacillus* strains. *Applied Microbiology and Biotechnology, 49*, 175–181.

Karppinen, S., Liukkonen, K., Aura, A. M., Forssell, P., & Poutanen, K. (2000). In vitro fermentation of polysaccharides of rye, wheat and oat brans and inulin by human faecal bacteria. *Journal of the Science of Food and Agriculture, 80*, 1469–1476.

Knutson, C. A., & Jeanes, A. (1968). A new modification of the carbazole analysis: Application to heteropolysaccharides. *Analytical Biochemistry, 24*, 470–481.

Kormelink, F. J. M., Gruppen, H., Vietor, R. J., & Voragen, A. G. J. (1993). Mode of action of the xylan-degrading enzymes from *Aspergillus awamori* on alkali-extractable cereal arabinoxylans. *Carbohydrate Research, 249*, 355–367.

Loosveld, A., Maes, C., Vancasteren, W. H. M., Schols, H. A., Grobet, P. J., & Delcour, J. A. (1998). Structural variation and levels of water extractable arabingalactan-peptide in European wheat flours. *Cereal Chemistry, 75*, 815–819.

Mai, V., & Morris, J. G. Jr. (2004). Colonic bacterial flora: Changing understandings in the molecular age. *Journal of Nutrition, 134*, 459–464.

McGinnis, G. D., & Fang, P. (1980). High-performance liquid chromatography. *Methods in Carbohydrate Chemistry, 8*, 33–43.

Miller, G. L. (1959). Use of dinitrosalicylic acid reagent for determination of reducing sugar. *Analytical Chemistry, 31*, 426–428.

Morisse, J. P., Maurice, R., Boilletot, E., & Cotte, J. P. (1993). Assessment of the activity of a fructooligosaccharide on different caecal parameters in rabbits experimentally infected with *E. coli* 0.103. *Annals of Zootechnology, 42*(8), 1–87.

Rao, R. S. P., & Muralikrishna, G. (2004). Non-starch polysaccharide–phenolic acid complexes from native and germinated cereals and millet. *Food Chemistry, 84*, 527–531.

Reis, A., Coimbra, M. A., Domingues, P., Ferrer-Correia, A. J., & Domingues, M. R. M. (2002). Structural characterization of underivatized olive pulp xylo-oligosaccharides by mass spectroscopy using Matrix Assisted Laser Desorption/Ionization and Electrospray Ionization. *Rapid Communications in Mass Spectroscopy, 16*, 2124–2132.

Sawardekar, J. S., Slonekar, J. M., & Jeanes, A. (1965). Quantitative determination of monosaccharides as their alditol acetates by gas chromatography. *Analytical Chemistry, 37*, 1602–1604.

Schley, P. D., & Field, C. J. (2002). The immune-enhancing effects of dietary fibers and prebiotics. *British Journal of Nutrition, 87*, S221–S230.

Shin, H. Y., Park, S. Y., Sung, J. H., & Kim, D. H. (2003). Purification and characterization of α-L-arabinopyranosidase and α-L-arabinofuranosidase from *Bifidobacterium* breve K-110, a human intestinal anaerobic bacterium metabolizing ginsenoside Rb 2 and Rc. *Applied and Environmental Microbiology, 69*, 7116–7123.

Silvi, S., Rumney, C. J., Cresci, A., & Rowland, I. R. (1999). Resistant starch modifies gut micro flora and microbial metabolism in human flora associated rats inoculated with faeces from Italian and UK donors. *Journal of Applied Microbiology, 86*, 521–530.

Swennen, K., Courtin, C. M., & Delcour, J. A. (2006). Non-digestible oligosaccharides with prebiotic properties. *Critical Reviews in Food Science and Nutrition, 46*, 459–471.

Van Laere, K. M. J., Hartemink, R., Bosveld, M., Schols, H. A., & Voragen, A. G. J. (2000). Fermentation of plant cell wall derived polysaccharides and their corresponding oligosaccharides by intestinal bacteria. *Journal of Agricultural and Food Chemistry, 48*, 1644–1652.

Food Chemistry 118 (2010) 224–227

Contents lists available at ScienceDirect

Food Chemistry

journal homepage: www.elsevier.com/locate/foodchem

Amino acid and fatty acid compositions and nutritional quality of muscle in the pomfret, *Pampus punctatissimus*

Feng Zhao [a,b], Ping Zhuang [a,b,*], Chao Song [b], Zhao-hong Shi [a], Long-zhen Zhang [a]

[a] East China Sea Fisheries Research Institute, Chinese Academy of Fishery Sciences, Shanghai 200090, China
[b] College of Fisheries and Life Science, Shanghai Ocean University, Shanghai 201306, China

ARTICLE INFO

Article history:
Received 2 December 2008
Received in revised form 30 March 2009
Accepted 28 April 2009

Keywords:
Pampus punctatissimus
Nutrition
Amino acid
Fatty acid

ABSTRACT

The pomfret, *Pampus punctatissimus*, is an important fisheries resource in China, but little is known about its amino acid and fatty acid compositions. Pomfret muscle contained 18.6% crude protein and 4.95% crude fat. Pomfret protein has a well-balanced amino acid composition, with high amounts of glutamic acid (114 mg/g), lysine (82.8 mg/g), leucine (76.7 mg/g), and aspartic acid (76.0 mg/g). Twenty two fatty acids were found in pomfret oil and saturated fatty acids were the most abundant (48.3%). Palmitic acid (16:0) was the dominant fatty acid, followed by oleic acid (18:1), DHA (22:6n-3), myristic acid (14:0) and stearic acid (18:0), with percentages of 30.5, 26.3, 12.2, 7.37 and 6.86, respectively. The ratio of n-3/n-6 polyunsaturated fatty acids (PUFAs) was 8.04; thus, pomfret muscle is rich in n-3 PUFA.

1. Introduction

Muscle tissue of fish is an important source of protein for humans. The amino acid composition is one of the most important nutritional qualities of protein and the amino acid score (AAS; FAO/WHO, 1990) is used to evaluate protein quality world-wide (Iqbal, Khalil, Atgeeq, & Khan, 2006).

The nutritional quality of fish, is to a great extent, associated with its content of essential fatty acids (EFAs). Lipids of marine fish species are generally characterised by low levels of linoleic acid (18:2n6) and linolenic acid (18:3n3) and high levels of long-chain n3 polyunsaturated fatty acids (LC n-3 PUFA; Steffens, 1997). LC n-3 PUFA cannot be synthesised by humans and must be obtained from the diet (Alasalvar, Taylor, Zubcov, Shahidi, & Alexis, 2002). The n-3 fatty acids are essential for neural development in human infants *in utero* and during the first few years after birth (Montaño, Gavino, & Gavino, 2001). Also, n-3 PUFA have beneficial health effects in conditions of hypertension, inflammation, arrhythmias, psoriasis, aggression, depression, coronary heart disease, inflammatory and auto-immune disorders, and cancer (Candela, Astiasarán, & Bello, 1997; Pike, 1999).

The pomfret, *Pampus punctatissimus* (Temminck & Schlegel, 1845), is distributed in saline water along China's coast from the Yellow Sea to the South China Sea, and in Korean and Japanese coastal waters (Liu, Li, & Li, 2002). In 2006, Chinese fisheries of *Pampus spp.* captured almost 4,00,000 metric tons, and the pomfret was one of the main species in these fisheries.

Several papers have reported the compositions of pomfret fish; however, they are all about the silver pomfret *Pampus argenteus* (Chakraborty, Ghosh, & Bhattacharyya, 2005; Osman, Suriah, & Law, 2001). Determining the amino acid and fatty acid profiles of pomfret muscle will improve the nutritional information available to consumers. The objectives of this study were to analyse the amino acid and fatty acid composition of *P. punctatissimus* muscle and to determine its nutritional quality.

2. Materials and methods

2.1. Sample preparation

Fifteen adult pomfrets were caught from the wild in the waters of Zhoushan (30°39°N, 122°11 E), Zhejiang, China. Body length was 17.80–21.50 cm; wet body weight was 229.37–373.52 g. Sample fish were divided into three groups (five fish, each group). Boneless muscles, used for analysis, were collected from the back of the fish, and then mashed. Mashed muscle sample of each group (five fish) was mixed and stored in a plastic bag, and then kept in refrigerator at −20 °C.

2.2. Proximate composition analyses

Moisture content was determined by drying sample in an oven at 105 °C until a constant weight was obtained (AOAC, 1990).

* Corresponding author. Address: East China Sea Fisheries Research Institute, Chinese Academy of Fishery Sciences, 300 Jungong Road, Shanghai 200090, China. Fax: +86 021 65683926.
E-mail address: pzhuang@online.sh.cn (P. Zhuang).

0308-8146/$ - see front matter © 2009 Elsevier Ltd. All rights reserved.
doi:10.1016/j.foodchem.2009.04.110

Crude protein content was determined by the Kjeldahl method (AOAC, 1990), and a conversion factor of 6.25 was used to convert total nitrogen to crude protein. Fat was determined by using the Soxhlet extraction method (AOAC, 1990). Ash was determined by incineration in a muffle furnace at 550 °C for 24 h (AOAC, 1990).

2.3. Amino acid analyses

Amino acid content of samples was measured according to the GB/T14965-1994 in China: the sample was hydrolysed for 22 h at 110 °C with 6 M HCl in sealed glass tubes filled with nitrogen. The hydrolysed samples were taken, and the amino acid concentration was diluted to 50 nM with 0.2 N sodium citrate buffer, pH 2.2. The pH-adjusted samples were analysed by a Biochrom 20 Automatic Amino Acid Analyzer (GE, USA). The content of tryptophan was determined by the colorimetric method of Basha and Roberts (1977) after alkaline hydrolysis of each sample. All determinations were performed in triplicate.

2.4. Amino acid score

Essential amino acid score was calculated with respect to the FAO/WHO reference amino acid pattern of the pre-school child (age, 2–5 year; FAO/WHO/UNU, 1985).

$$\text{Amino acid score} = \text{Sample amino acid}/\text{Reference amino acid} \times 100$$

2.5. Fatty acid analyses

Fatty acids were extracted and fatty acid methyl esters (FAMEs) were prepared according to the ISO5509 method (ISO, 2000): first, Soxhlet extraction, and then, saponification, followed by esterification, and finally, extraction of FAMEs in hexane. FAMEs were subsequently analysed by capillary gas chromatography (column: 30 m × 0.25 mm I.D., 0.5 μm film thickness; Supelco. Flame ionisation detected temperature at 210 °C; carrier gas N_2 at 1.0 ml/min; injector temperature at 210 °C; oven temperature programmed from 180 to 250 °C) using an Agilent 6890 capillary gas chromatograph. Quantitative data were calculated using the peak area ratio (% total fatty acids).

3. Results and discussion

3.1. Proximate composition

The proximate composition of the pomfret is shown in Table 1. Crude protein, crude fat and crude ash contents of the pomfret muscle were 18.59%, 4.95% and 1.36%, respectively.

The crude fat content was higher than the amount found in silver pomfret, *P. argenteus* (Chakraborty et al., 2005; Osman et al., 2001). Based on the moisture and fat contents, the pomfret is a medium-fat fish, with a fat content of 5–10% by weight (Bennion, 1997). According to Feeley, Criner, and Watt (1972), low-fat fish have higher water contents, and as a result, their flesh is white in colour. Fatty fish store the fat in muscle tissue, and their flesh is yellow, grey, pink or another colour (Gurr, 1992). Fat content is influenced by species, season, geographical regions, age and maturity (Piggot & Tucker, 1990).

Table 1
Proximate composition of pomfret muscle.

	Moisture (%)[a]	Crude protein (%)[a]	Crude fat (%)[a]	Crude ash (%)[a]
Mean	75.35	18.6	4.95	1.36
SD	0.32	0.38	0.12	0.02

[a] Percentage of total wet weight.

3.2. Amino acid composition

The amino acid composition of pomfret muscle is shown in Table 2. Pomfret protein contained a high amount of glutamic acid (114 mg/g of crude protein), followed by lysine, leucine aspartic acid, arginine, valine, alanine in decreasing amounts.

Over the past 20 years, increasing evidence suggests the importance of glutamine in the function of many organ systems (Christina, Palmer, & Griffiths, 1999). Glutamine is the most abundant free amino acid in the body, comprising nearly 60% of the free intracellular amino acids in skeletal muscle. The efflux of glutamine from muscle in critical illness serves as an important carrier of ammonia (nitrogen) to the splanchnic area and the immune system (Deutz, Reijven, Athanasas, & Soeters, 1992). As a donor of nitrogen in the synthesis of purines and pyrimidines, glutamine is essential for the proliferation of cells.

Pomfret protein is also rich in lysine, which is the limiting amino acid in cereal-based diets of children in developing countries (Iqtidar & Khalil, 1995; Kim & Lall, 2000). Taurine, a sulfonated β-amino acid derived from methionine and cysteine metabolism, is not utilised in protein synthesis, but is found either as a free amino acid or in simple peptides (Jacobsen & Smith, 1968). Taurine plays a pivotal role in numerous physiological functions of human infants (Redmond, Stapleton, Neary, & Bouchier-Hayes, 1998; Stapleton, O'Flaherty, Redmond, & Bouchier-Hayes, 1998).

Table 2
Amino acid composition of pomfret muscle.

Amino acid	Content (% DW) Mean ± SD	Content (mg/g crude protein)
Taurine	0.11 ± 0.06	1.46
Serine	2.81 ± 0.06	37.2
Tyrosine	2.64 ± 0.29	35.0
Proline	1.92 ± 0.17	25.5
Aspartic acid	5.73 ± 0.07	76.0
Glutamic acid	8.61 ± 0.05	114
Glycine	3.03 ± 0.23	40.1
Alanine	3.72 ± 0.42	49.3
Histidine	1.51 ± 0.08	20.0
Arginine	4.20 ± 0.05	55.6
Methionine	1.76 ± 0.06	23.3
Phenylalanine	3.22 ± 0.04	42.6
Isoleucine	3.33 ± 0.00	44.2
Leucine	5.78 ± 0.19	76.6
Lysine	6.24 ± 0.16	82.7
Threonine	3.03 ± 0.13	40.2
Valine	3.89 ± 0.13	51.5
Tryptophan	1.25 ± 0.17	16.6

Table 3
Amino acid score of pomfret.

Amino acid	Content (mg/g crude protein)	Reference (mg/g protein)[a]	Score
Threonine	40.2	34	118
Tryptophan	16.6	11	151
Cysteine + Methionine	23.3	25	93
Valine	51.5	35	147
Phenylalanine + Tyrosine	77.6	63	123
Isoleucine	44.2	28	158
Leucine	76.6	66	116
Lysine	82.7	58	143

[a] Reference amino acid pattern of preschool children (2–5 years) (FAO/WHO/UNU, 1985).

Table 4
Fatty acid composition in pomfret muscle.

	Fatty acid	Mean ± SD	Fatty acid	Mean ± SD
Saturated fatty acid (SFA, %)[a]	C8:0	0.04 ± 0.00	C16:0	30.5 ± 0.26
	C12:0	0.09 ± 0.01	C17:0	2.07 ± 0.02
	C13:0	0.03 ± 0.00	C18:0	6.86 ± 0.19
	C14:0	7.37 ± 0.18	C22:0	0.07 ± 0.00
	C15:0	0.61 ± 0.00	C23:0	0.64 ± 0.04
	∑SFA	48.3 ± 0.26		
Monounsaturated fatty acid (MUFA, %)[a]	C14:1	0.10 ± 0.00	C18:1n-9	26.3 ± 0.02
	C16:1	5.22 ± 0.10	C24:1n-9	0.47 ± 0.01
	C17:1	0.66 ± 0.00	∑MUFA	32.5 ± 0.21
Polyunsaturated fatty acid (PUFA, %)[a]	C18:2n-6	0.85 ± 0.07	C20:4n-6	1.12 ± 0.03
	C18:3n-3	0.47 ± 0.01	C20:5n-3	4.47 ± 0.18
	C20:2n-6	0.33 ± 0.01	C22:6n-3	12.2 ± 0.42
	∑PUFA	19.3 ± 0.48		
Other fatty acid (%)[a]	∑PUFAn-3	17.1 ± 0.62	∑PUFAn-3/∑PUFAn-6	8.04
	∑PUFAn-6	2.13 ± 0.15	∑PUFAn-6/∑PUFAn-3	0.12

[a] Percentage of total fatty acids.

Amino acid scores are summarised in Table 3. When compared to the reference amino acid pattern of pre-school children (2–5 years old), all of the amino acid scores were >100, except for sulphur-containing amino acids (cysteine and methionine). According to the amino acid score, the amount of S-containing amino acids (cysteine and methionine) was the lowest amongst amino acids in pomfret. However, in this study, cysteine was totally lost when the muscle tissue was hydrolysed without performing acid oxidation; thus, the correct S-containing amino acid score would likely exceed 100. The protein in pomfret muscle was well-balanced in essential amino acid composition and is of high quality.

3.3. Fatty acid composition

Fatty acid composition is shown in Table 4. The fatty acid profile of the pomfret was dominated by saturated fatty acids (SFAs), which comprised about half (48.3%) of the total fatty acids. The SFA contents are similar to those published for silver pomfret (Chakraborty et al., 2005). Among the SFAs, palmitic acid (16:0) was the dominant saturated amino acid, accounting for 30.3% of the total fatty acids. Myristic acid (14:0) and stearic acid (18:0) were also abundant. Monounsaturated fatty acids (MUFAs) and polyunsaturated fatty acids (PUFAs) accounted for 32.5% of the total fatty acids and 19.3% of the total fatty acids, respectively. The main monounsaturated fatty acid was oleic acid (18:1), accounting for 26.3% of the total fatty acids, followed by palmitoleic acid (5.22%). The dominant PUFA was DHA (22:6n-3), accounting for 12.2% of the total fatty acids, followed by EPA (20:5n-3), AA (20:4n-6), LA (18:2n-6) and ALA (18:3n-3). However, except for EPA (4.47%), all of these three fatty acids were present in minor amounts (0.47–1.12%).

DHA and EPA prevent human coronary artery disease (Leaf & Webber, 1988). Bowman and Rand (1980) reported that AA is a precursor for prostaglandin and thromboxan, which influences clotting of blood and the healing process. Apart from this function, AA also plays a role in growth. Therefore, fish have been suggested as a key component for a healthy diet of humans (Abd Rahman, The, Osman, & Daud, 1995).

The n-3 and n-6 PUFAs of the pomfret accounted for 17.1% and 2.13% of the total fatty acids, respectively, and the ratio of n-3/n-6 was 8.04, which was greater than the values reported by Osman et al. (2001) for silver pomfret. As normal diets have lower amounts of n-3 fatty acids than n-6 fatty acids, a dietary intake of fish with a high ratio of n-3/n-6 would be beneficial. The n-3/n-6 ratio is a good index for comparing relative nutritional value of fish oils of different species, and a higher ratio of n-3/n-6 PUFAs has often been cited as an index of high nutritional value. The ratio of n-6/n-3 PUFAs found in this study was lower than the value (4.0 at maximum) recommended by the UK Department of Health (HMSO, 1994). Values higher than the maximum are harmful to health and may promote cardiovascular disease (Moreira, Visentainer, de Souza, & Matsushita, 2001).

Compared with the silver pomfret and other marine fish (Osman et al., 2001), the pomfret had higher amounts of SFAs and MUFAs, but lower amounts of PUFAs. Differences in fatty acids of fishes are based on their diet (Sargent, Bell, Bell, Henderson, & Tocher, 1995), and are also affected by size, age, reproductive conditions, and environmental conditions, especially water temperature, which can influence lipid content and fatty acid composition (Saito, Yamashiro, Alasalvar, & Konno, 1999).

In summary, pomfret muscle is a high quality protein source with a well-balanced composition of essential amino acids. With a n-3/n-6 PUFAs value of 8.04, it is also rich in n-3 PUFA.

Acknowledgements

We thank Prof. Boyd Kynard for his useful suggestions during the revision of the MS. This work was supported by the special research fund for national non-profit institutes (East China Sea Fisheries Research Institute, project No. 2007Z02).

References

Abd Rahman, S., The, S. H., Osman, H., & Daud, N. M. (1995). Fatty acid composition of some Malaysian fresh water fish. *Food Chemistry, 54*, 45–49.
Alasalvar, C., Taylor, K. D. A., Zubcov, E., Shahidi, F., & Alexis, M. (2002). Differentiation of cultured and wild sea bass (*Dicentrarchus labrax*): Total lipid content, fatty acid and trace mineral composition. *Food Chemistry, 79*, 145–150.
AOAC (1990). *Official methods of analyses of association of analytical chemist* (15th ed.). Washington, DC: AOAC.
Basha, S. M. M., & Roberts, R. M. (1977). A simple colorimetric method for the determination of tryptophan. *Analytical Biochemistry, 77*, 378–386.
Bennion, M. (1997). *Introductory foods* (7th ed.). New York, USA: Macmillan.
Bowman, W. C., & Rand, M. J. (1980). *Textbook of pharmacyology* (2nd ed.). Oxford: Blackwell.
Candela, M., Astiasarán, I., & Bello, J. (1997). Effects of frying and warmholding on fatty acid and cholesterol of sole (*Solea solea*), codfish (*Gadus morhua*) and hake (*Merluccius merluccius*). *Food Chemistry, 58*(3), 227–231.
Chakraborty, S., Ghosh, S., & Bhattacharyya, D. K. (2005). Lipid profiles of pomfret fish (*Pampus argenteus*) organs. *Journal of Oleo Science, 54*(2), 85–88.
Christina, J., Palmer, A., & Griffiths, R. D. (1999). Randomized clinical outcome study of critically ill patients given glutamine-supplemented enteral nutrition. *Nutrition, 15*, 108–115.
Deutz, N. E. P., Reijven, P. L. M., Athanasas, G., & Soeters, P. B. (1992). Post-operative changes in hepatic, intestinal, splenic and muscle fluxes of amino acids and ammonia in pigs. *Clinical Science, 83*, 607.

FAO/WHO (1990). *Report of the joint FAO/WHO Expert Consultation on Protein Quality Evaluation*. Bethesda, MD.

FAO/WHO/UNU (1985). *Energy and protein requirements. Report of a joint FAO/WHO/UNU Expert Consultation, World Health Organization technical report series 724*. Geneva: WHO. pp. 121–123.

Feeley, R. M., Criner, D. E. C., & Watt, B. K. (1972). Cholesterol content of foods. *Journal of the American Dietetic Association, 61*, 134–148.

Gurr, M. I. (1992). *Role of fats in food and nutrition* (2nd ed.). London, UK: Elsevier Applied Science.

HMSO, UK (1994). *Nutritional aspects of cardiovascular disease (report on health and sociall subjects No. 46)*. London: HMSO.

Iqbal, A., Khalil, I. A., Atgeeq, N., & Khan, M. S. (2006). Nutritional quality of important food legumes. *Food Chemistry, 97*, 331–335.

Iqtidar, A., & Khalil, S. K. (1995). Protein quality of Asian beans and their wild progenitor, *Vigna sublobata* (Roxb). *Food Chemistry, 52*, 327–339.

ISO (2000). ISO 5509: *Animal and vegetable fats and oils-preparation of methyl esters of fatty acids*. Geneva, Switzerland: International Organization for Standardization.

Jacobsen, J. G., & Smith, L. H. (1968). Biochemistry and physiology of taurine and taurine derivatives. *Physiological Review, 48*, 424–511.

Kim, J. D., & Lall, S. P. (2000). Amino acid composition of whole body tissue of Atlantic halibut (*Hippoglossus hippoglossus*), yellowtail flounder (*Pleuronectes ferruginea*) and Japanese flounder (*Paralichthys olivaceus*). *Aquaculture, 187*, 367–373.

Leaf, A., & Webber, P. C. (1988). Cardiovascular effects of n-3 fatty acids. *New England Journal of Medicine, 318*, 549–555.

Liu, J., Li, C., & Li, X. (2002). Phylogeny and biogeography of Chinese pomfret fishes (Pisces: Stromateidae). *Studia Marina Sinica, 44*, 235–239 (in Chinese).

Montaño, N., Gavino, G., & Gavino, V. C. (2001). Polyunsaturated fatty acid contents of some traditional fish and shrimp waste condiments of the Philippines. *Food Chemistry, 75*, 155–158.

Moreira, A. B., Visentainer, J. V., de Souza, N. E., & Matsushita, M. (2001). Fatty acids profile and cholesterol contents of three Brazilian Brycon Freshwater fishes. *Journal of Food Composition and Analysis, 14*, 565–574.

Osman, H., Suriah, A. R., & Law, E. C. (2001). Fatty acid composition and cholesterol content of selected marine fish in Malaysian waters. *Food Chemistry, 73*, 55–60.

Piggot, G. M., & Tucker, B. W. (1990). *Effects of technology on nutrition*. New York: Marcel Dekker.

Pike, H. I. (1999). *Health benefits from feeding fish oil and fish meal*. UK: International Fishmeal and Oil Manufactures Association.

Redmond, H. P., Stapleton, P. P., Neary, P., & Bouchier-Hayes, D. J. (1998). Immunonutrition: The role of taurine. *Nutrition, 14*, 599–604.

Saito, H., Yamashiro, R., Alasalvar, C., & Konno, T. (1999). Influence of diet on fatty acids of three subtropical fish, subfamily caseioninae (*Caesio diagrama* and *C. tile*) and family siganidae (*Siganus canaliculatus*). *Lipids, 34*, 1073–1082.

Sargent, J. R., Bell, J. G., Bell, M. V., Henderson, R. J., & Tocher, D. R. (1995). Requirements criteria for essential fatty acids. *Journal of Applied Ichthyology, 11*, 183–189.

Stapleton, P. P., O'Flaherty, L., Redmond, H. P., & Bouchier-Hayes, D. J. (1998). Host defense – A role of the amino acid taurine. *Journal of Parenteral and Enteral Nutrition, 22*, 42–48.

Steffens, W. (1997). Effects of variation in essential fatty acids in fish feeds on nutritive value of freshwater fish for humans. *Aquaculture, 151*, 97–119.

Temminck, C. J., & Schlegel, H. (1845). Pisces. In: Ph. Fr. von Siebold (Ed.), *Fauna Japonica. Lugdumi Batavorum*, Batavia. pp.121.

Food Chemistry 118 (2010) 228–238

Contents lists available at ScienceDirect

Food Chemistry

journal homepage: www.elsevier.com/locate/foodchem

Unusual sesquiterpene lactones with a new carbon skeleton and new acetylenes from *Ajania przewalskii*

Ying Zhu *, Li-Xia Zhang, Yan Zhao, Guo-Du Huang

State Key Laboratory of Applied Organic Chemistry, College of Chemistry and Chemical Engineering, Lanzhou University, Lanzhou 730000, PR China

ARTICLE INFO

Article history:
Received 26 November 2008
Received in revised form 25 March 2009
Accepted 28 April 2009

Keywords:
Asteraceae
Ajania prewalskii
Eudesmane
Guaianolide
Acetylenes
Cytotoxicity
Antioxidation

ABSTRACT

Four new compounds, a noreudesmanolide (**1**), a guaianolide (**4**), and acetylenes (**7**–**8**), together with 16 other known compounds, were isolated from *Ajania przewalskii*. The novel sesquiterpenolide (**1**) possesses a rare carbon skeleton. Acetylation of **1** gave **1a**. New compounds were elucidated as 1β-hydroxyl-2-noreudesm-4(15)-en-5α,6β,7α,11αH-12,6-olide (**1**), 1β-acetoxyoxyl-2-noreudesm-4(15)-en-5α,6β,7α,11αH-12,6-olide (**1a**), 8α-angeloyloxyl-3α,4α-dihydroxyguaia-1,9,11(13)-trien-6,12-olide (**4**), (E)-3β,4α-dihydroxyl-2-(2′,4′-hexadiynylidene)-1,6-dioxaspiro[4,5]decane (**7**) and 2-hydroxyl-2-[(E)-1α,2β,3-trihydroxyl-3-nonaene-5,7-diyne]-4H-pyran (**8**), by chemical and spectroscopic methods, including HRESIMS, 1D and 2D NMR. Cytotoxicity of nine compounds was assessed by their effects on selected cancer cell lines, K562, K562/ADM, BGC-823, and Hep-G2 cells. Phenolic acid **12** exhibited strong activity against K562 and K562/ADM cells and sesquiterpenolide **3** strong activity against K562/ADM cells. Radical-scavenging activities of 12 compounds, the mixed solvent extract (petrol ether–ether–methanol = 1:1:1), and the *n*-butanol extract were determined by ABTS and DPPH radical-scavenging assays. Phenols and coumarins (**11**–**16**), MSE, and *n*-BE displayed significant antioxidation (IC_{50} < 20 μg/ml).

1. Introduction

The genus *Ajania*, belonging to the family *Asteraceae*, includes around 28 species that are distributed over central and south Asia, China, and Japan. Most of them are widespread in the northwest of China. Some species of the genus have long been used as Chinese traditional folk medicines for treatments of intestinal ulcers, bronchitis, lung diseases, and rheumatism (Editorial Committee for Flora of the Chinese Academy of Science, 1983). So far, four species, *A. achilloides*, *A. fastigiata*, *A. fruticulosa*, and *A. przewalskii*, have been chemically investigated. Guaianolides, eudesmanolides, glaucolides, and phenolic constituents were isolated from *A. achilloides* (Belenovskaya & Markova, 1979; Zdero, Bohlmann, & Huneck, 1990). Guaianolides and flavonoids were isolated from *A. fastigiata* (Chumbalov, Glyzin, & Zhubaeva, 1974; Yusupov, Kasimov, & Abdullaev, 1982). Guaianolides, eudesmanolides, germacranolides, and flavonoids were isolated from *A. fruticulosa*. The guaianolides from this plant possess antifungal activity and have been used to inhibit the growth of *Candida albican*. Additionally, the flavonols have xanthine oxidase inhibitory activities (Adekenov et al., 1998; Li et al., 1999; Meng, Hu, Chen, & Tan, 2001). Lignans, flavonoids and phenolic compounds were isolated from *A. pzewalskii* Poljakov in our previous phytochemical investigation (Zhang, He, & Zhu, 2006).

In conjunction with our continuing interests in the chemical constituents of *A. przewalskii*, we further isolated four new compounds (**1**, **4**, **7**–**8**) and 16 known constituents: three eudesmane lactones (**1**–**3**), a highly oxygenated guaiane lactone (**4**), a bisabolene sesquiterpene (**5**), a monoterpene (**6**), five acetylenes (**7**–**10**), three phenylpropanoids (**11**–**13**), a phenolic glycoside (**14**), and six coumarins (**15**–**20**) by extraction with a mixed solvent (petrol ether–ether–methanol = 1:1:1) and by extraction with ethanol from *A. przewalskii* (Fig. 1). The structures of four new compounds were identified by chemical and spectroscopic methods, especially HRESIMS, ^1H–^1H COSY, HMQC, HMBC and 1D NOE experiments. The carbon skeleton of noreudesmanolide **1**, which was named Ajaniaolide A, was found to be rare and novel. Acetylation of **1** gave **1a**, further confirming the structure of **1**.

The cytotoxicity of compounds, **3**, **5**, **6**, **9**, **11**–**13**, **16**, and **18**, was evaluated by assessing their effects on the human erythroleukemia adriamycin-resistant subline (K562/ADM), compounds **9**, **11**–**13**, **16**, and **18** on the human erythroleukemia (K562), **3**, **5**, and **6** on the human stomach carcinoma (BGC-823), and **9**, **16**, and **18** on human hepatoma (Hep-G2) cell lines. Among them, sesquiterpene **3** exhibits strong activities against K562/ADM cell lines (IC_{50} 11.1 for 48 h and 13.1 μg/ml for 72 h) and phenolic acid **12** exhibits strong activities against K562 and K562/ADM cell lines (IC_{50} of 5.57 for 48 h and 0.78 μg/ml for 72 h on K562; 7.25 for 48 h and 3.29 μg/ml for 72 h on K562/ADM). Compounds **3**, **6**, **9**, and **11**–**19**, the mixed solvent extract (petrol ether–ether–methanol = 1:1:1, MSE), and the *n*-butanol extract (*n*-BE) were tested

* Corresponding author. Tel.: +86 931 3698769; fax: +86 931 8912582.
E-mail address: zhuy@lzu.edu.cn (Y. Zhu).

0308-8146/$ - see front matter © 2009 Elsevier Ltd. All rights reserved.
doi:10.1016/j.foodchem.2009.04.112

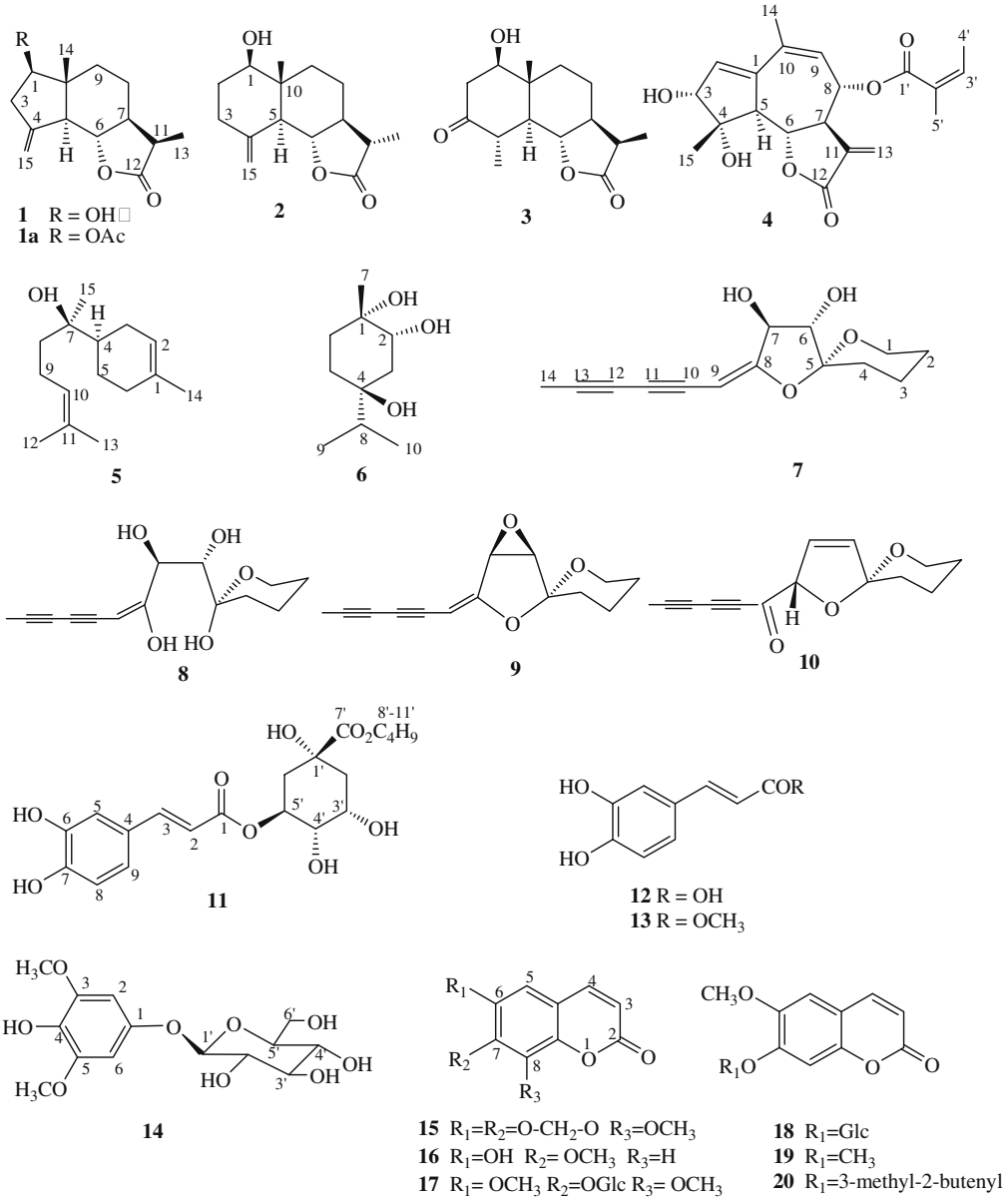

Fig. 1. The structures of compounds isolated from *A. przewalskii*.

by ABTS radical-scavenging assays, as well as six compounds, **3**, **11**, **13**–**15**, **17**, and **19** by DPPH radical-scavenging assays. The results indicated that phenols and coumarins (**11**–**16**), MSE, and *n*-BE display significant antioxidant activity (IC_{50}<20 μg/ml), especially, and phenolic compounds **12**, **13**, and coumarin **16** are strong antioxidants (IC_{50} of 2.83, 3.38 and 2.83 μg/ml by ABTS). Phenolic acid **12** shows, not only strong cytotoxic activity against K562 and K562/ADM cell lines, but also strong antioxidant activity.

2. Materials and methods

2.1. General methods

Melting points were measured on an uncorrected Koffler hot plate. Optical rotations were measured at 20 °C, in chloroform on a Perkin-Elmer Model 341 polarimeter. UV spectra were obtained on a Shimadzu UV-260 spectrophotometer. IR spectra were recorded on a Nicolet 170SX FT-IR instrument or Avatar 360 FT-IR over the range of 400–4000 cm^{-1}. EIMS data were obtained as measured on an HP5988 or a VG-ZAB-HS by a direct inlet at 70 ev and HRESIMS data were obtained on a Bruker Daltanics APEX II FT-ICR spectrometer. NMR spectra were recorded on a Varian MercuryPlus-300/400BB NMR spectrometer using TMS as an internal standard in chloroform-d_1, dimethyl sulfoxide-d_6 (DMSO-d_6), acetone-d_6 or deuterium oxide (D_2O). Column chromatography was carried out on Si gel (200–300 mesh and Type 60) and TLC on Si gel (GF_{254}, 10–40 μm), both supplied by Qingdao Marine Chemical Co.

2.2. Plant material

The whole plant of *A. przewalskii* was collected in Qinghai province, China in 2001, and identified by Professor Yao-Jia Zhang, the college of Life Science from Lanzhou University. A voucher specimen (Ap20010801) is preserved at the State Key Laboratory of Applied Organic Chemistry, Lanzhou University.

2.3. Extraction and isolation

The dried and powdered whole plants of *A. przewalskii* (6 kg) were extracted at room temperature by the mixed solvent of petrol ether (PE)–ether–methanol (1:1:1, v:v:v), three times, each using 20 l of the solvent for 4 days. The extracts were firstly concentrated under reduced pressure and then filtered. They afforded 220 g of the crude residue. The whole plants were again extracted by ethanol three times at room temperature (each 18 l, 3 days) to give 215 g of the residue. About 160 g of the mixed solvent crude residue were subjected to silica gel column chromatography (CC) using PE-acetone (1:0–0:1) to give 11 fractions, which were further isolated and purified. The ethanol extract was suspended in water (1.5 l) and then successively extracted with chloroform, ethyl acetate, and *n*-butanol. After concentration of the ethyl acetate-soluble fraction and *n*-butanol-soluble fraction, the ethyl acetate-soluble fraction (40 g) and the *n*-butanol-soluble fraction (42 g) were each subjected to silica gel CC. Isolation details are depicted in Fig. 2. In particular, the percentage values are the ratio of each compound's weight over the total weight of the air dried whole plant (6 kg).

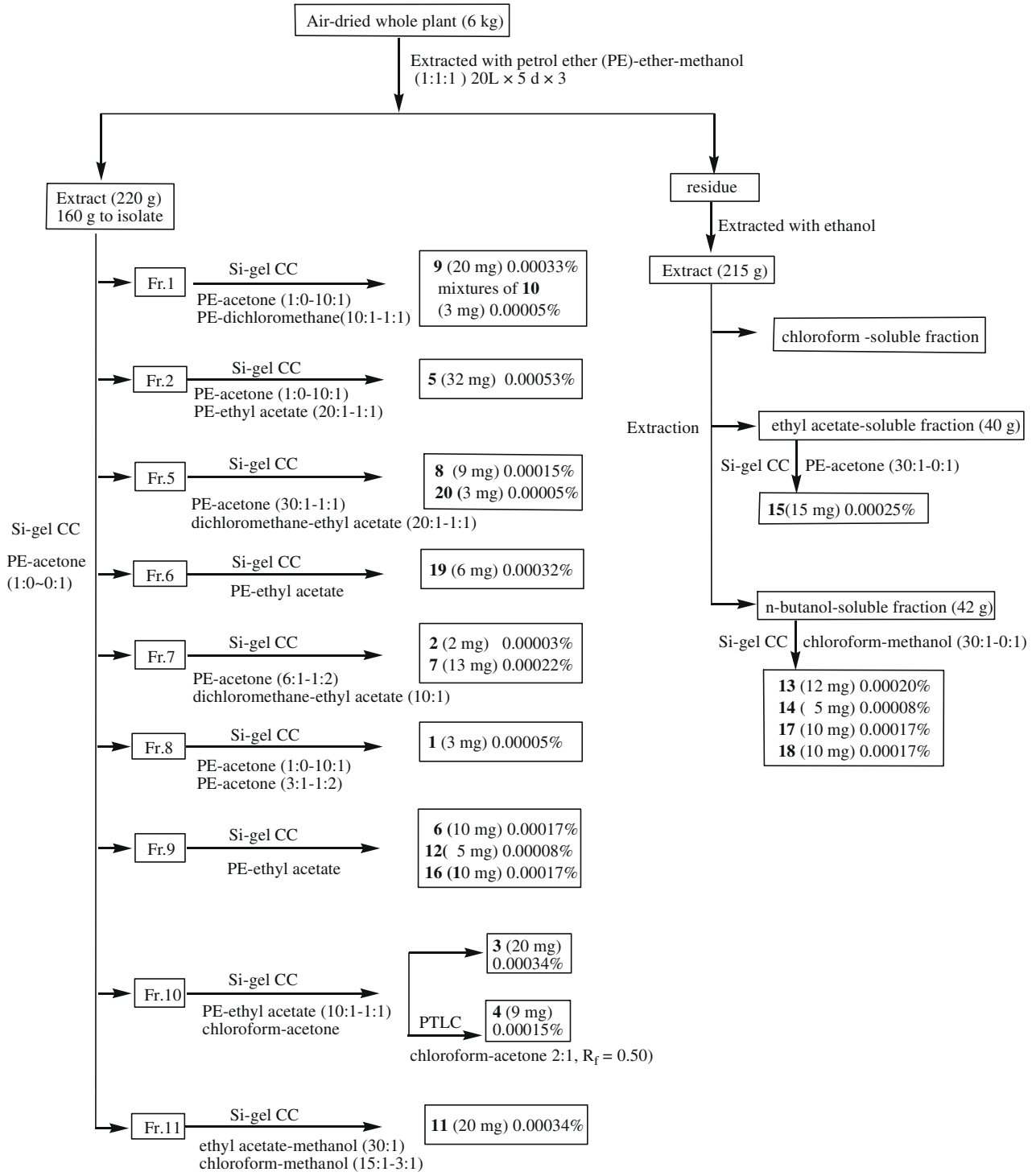

Fig. 2. Isolation scheme for *A. przewalskii*; the percentage values are the ratios of each compound's weight over the total weight of the whole plant (6 kg).

2.4. Acetylation of compound **1**

Four milligrammes of **1** were acetylated with a mixture (1:1) of Ac_2O in pyridine. The solution was allowed to stand overnight at room temperature. After the usual work-up, pure compound **1a** was obtained.

2.5. Cytotoxic assay

The cytotoxicity of the tested compounds was determined using the [3-(4,5-dimethylthiazol-2-yl)-2,5-diphenyltetrazolium bromide] (MTT) colorimetric assay, as previously reported (Hussain, Nouri, & Oliver, 1993). A stock solution of a compound under study was prepared by dissolving it in dimethyl sulfoxide. It was diluted to a working solution before usage and the final dimethyl sulfoxide concentration was 0.1% v/v. Logarithmically growing K562 cells, containing 2×10^8 cells/l, K562/ADM cells, containing 2×10^8 cells/l, BGC-823 cells, containing 1×10^8 cells/l, and Hep-G2 cells, containing 1×10^8 cells/l, were seeded in 96-well flat-microtitre plates (NUNC, Nunclon, Nagle, Denmark). After 24 h of incubation, the cells were treated with the tested samples at various concentrations (0, 10, 50, 100 and 200 μg/ml). Samples were grown in a humidified atmosphere at 37 °C in 5% CO_2 for 48 to 72 h. Parallel controls were performed in deionized water with the same dimethyl sulfoxide concentration. Three replicate wells were used for each point measurement. 10 μl of a MTT solution (5 mg/ml in PBS) were added to each well and then incubated for 4 h before the termination of culture. Then 100 μl of extraction buffer (10% SDS with 0.01 M HCl) were added to each well. After an overnight incubation at 37 °C, the absorbance was measured at a wavelength of 570 nm, using a microplate reader (Power Wave X200, Bio-TEK, USA) for calculating the inhibition rate (IR) of the cell proliferation. The IC_{50} value was defined as the concentration of sample which reduced absorbance by 50% relative to the vehicle-treated control. The cytotoxicity (IR) of a compound was calculated as

$$IR(\%) = [(A_{570} \text{ of untreated cells} - A_{570} \text{ of treated cells})/A_{570} \text{ of untreated cells}] \times 100\%.$$

By their structural features, the tested compounds **11–13** are strong antioxidants and can reduce MTT, whose cytotoxicity was not determined by MTT methods. Therefore the treated cells viability were observed by trypan blue dye exclusion, then counted by microscopy.

2.6. Antioxidant capacity assay

2.6.1. Chemicals

ABTS (2,2′-azino-bis(3-ethylbenzo-thiazoline-6-sulphonic acid) diammonium salt, 98%), BHA (butylated hydroxy anisole, 90%), DPPH· (2,2′-diphenyl-1-picrylhydrazyl, 90%), and trolox (6- hydroxy-2,5,7,8-tetramethylchroman-2-carboxylicacid, 97%) were purchased from Sigma Chemical Co. (St. Louis, MO, USA). All other chemicals and solvents were of analytical grade.

2.6.2. ABTS free radical-scavenging assay

The antioxidant capacity of the tested samples, to scavenge ABTS radical cation ($ABTS^{\cdot+}$), was measured by using a method previously reported (Re et al., 1999; Van den Berg, Haenen, Van den Berg, & Bast, 1999). $ABTS^{\cdot+}$ was generated by the reaction of a 7 mM aqueous solution of ABTS with a 2.45 mM aqueous solution of $K_2S_2O_8$ (final concentration), kept in the dark at room temperature for 16 h before use. The $ABTS^{\cdot+}$ solution was diluted with ethanol and phosphate buffered saline (PBS), pH 7.4, to an absorbance of 0.70 (±/0.02) at 734 nm and equilibrated at 30 °C. About 50 μl of an ethanolic solution of each sample were mixed with an ethanolic solution of $ABTS^{\cdot+}$ (2 ml). The vitamin E analogue, trolox, was used as a positive control. The optical density of the mixture was determined in comparison with $ABTS^{\cdot+}$ solution and pure ethanol. All testing samples were replicated at least three times. The scavenging ability of antioxidant was calculated, based on the following equation:

$$\text{Inhibition } (\%) = [A_0 - (A_t - B)]/A_0 \times 100\% \quad (t = 6 \text{ min})$$

where A_0 is the absorbance of the $ABTS^{\cdot+}$ solution without adding sample and A_t is the absorbance of sample after acting with $ABTS^{\cdot+}$ solution for 6 min, and B is the absorbance of the sample solution. IC_{50} values, which represented the concentration of samples that caused 50% neutralisation of $ABTS^{\cdot+}$ radicals, were calculated from the plot of inhibition percentage against concentration of the samples.

2.6.3. DPPH free radical-scavenging assay

The ability of the tested samples to scavenge DPPH stable radicals was measured by using the method previously reported (Von Gadow, Joubert, & Hansmann, 1997). Various concentrations of the samples were made, from 2.5 to 50.0 μg ml^{-1}. About 50 μl of an ethanol solution of each sample were mixed with 2 ml of 60 μM DPPH solution and made up with ethanol solution, to a final volume of 4 ml. The absorbances of the resulting solutions and the blank were recorded after 1 h at room temperature. The optical density of the mixture was determined in comparison with DPPH radical solution and pure ethanol. Ethanol was used to zero the spectrophotometer. Two reference antioxidants (BHA and trolox) were used as positive controls and standards for the evaluation of the antioxidant power of the tested samples. For each sample, three replicates were recorded. The disappearance of DPPH· was read spectrophotometrically at 515 nm using a spectrophotometer (Unico WFZ UV-2000, Tokyo, Japan). The inhibition percentage of the DPPH radical by the samples was calculated using the following equation:

$$\text{Inhibition } (\%) = [(A_0 - A_t)/A_0] \times 100\%$$

where A_0 is the absorbance of the DPPH radical solution without adding sample and A_t is the absorbance of sample after reacting with DPPH radical solution for 20 min. IC_{50} values, which represented the concentrations of samples that caused 50% neutralisation of DPPH radicals, were calculated from the plot of inhibition percentage against concentration of the samples.

2.7. Characteristic data of compounds

1β-Hydroxyl-2-noreudesm-4(15)-en-5α,6β,7α,11αH-12,6-olide (**1**). Colourless oil; $[\alpha]_D^{20} + 63$ (*c* 0.31, chloroform); HRESIMS *m/z*: 259.1306 (calcd. for $C_{14}H_{20}O_3 + Na^+$, 259.1305); IR (film) λ_{max}: 3390, 2929, 2859, 1773, 1652, 1121, 1065, 1038 and 1006 cm^{-1}; EIMS *m/z* (rel int): 236 (7) $[M]^+$, 218(9) $[M-18]^+$, 165 (44), 121 (18), 109 (31), 91 (47) and 55 (100); ^1H NMR see Table 1 and ^{13}C NMR (DEPT) see Table 2.

1β-Acetoxyoxyl-2-noreudesm-4(15)-en-5α,6β,7α,11αH-12,6-olide (**1a**). Colourless gum, $[\alpha]_D^{20} + 13$ (*c* 0.27, chloroform); UV (chloroform, log ε): λ_{max} 242 (0.37) nm; ^1H NMR see Table 1.

8α-Angeloyloxyl-3α,4α-dihydroxyguaia-1,9,11(13)-trien-6,12-olide (**4**). Colourless oil, $[\alpha]_D^{20} + 66$ (*c* 0.9, $CHCl_3$); HRESIMS: 378.1907 (calcd. for $C_{20}H_{24}O_6 + NH_4^+$, 378.1911); UV (chloroform, log ε): λ_{max} 244 (1.18) nm; IR (film) λ_{max}: 3422, 2926, 1770, 1712, 1647, 1455, 1379, 1361, 1228, 1146, 1038 and 961 cm^{-1}; EIMS *m/z* (rel int): 260 (4) $[M-AngOH]^+$, 99 (2), 100 (3), 83 (84), 55 (74) and 43 (100); ^1H NMR and ^{13}C NMR (DEPT) see Table 3.

1*S*,2*R*,4*S*-trihydroxyl-*p*-methane (**6**). NMR (acetone-d_6, 300 MHz): 3.5 (1H, brs, H-2), 3.0 (3H, brs, OH), 1.94 (dq, 14.2, 6.0, H-8), 1.85 (dd, 12.9, 3.6, H-3a), 1.58 (dd, 11.7, 5.7, H-3b),

Table 1
^{1}H NMR data for compounds **1a**, **1–3**.

No.	**1**[a]	**1a**[b]	**2**[b]	**3**[c]
1	3.95 (t, 8.4)	4.87 (dd, 8.4, 8.7)	3.51 (dd, 11.7, 4.8)	3.61 (dd, 11.7, 6.0)
2a	–	–	1.81–1.87 (m)	2.60–2.64 (m)
2b	–	–	1.61–1.66 (m)	2.55 (t, 6.5)
3a	2.82 (dd, 17.4, 8.4)	2.92 (dd, 17.4, 8.7)	2.30–2.33 (m)	
3b	2.16 (dd, 18.3, 8.1)	2.21 (dd, 17.1, 8.5)	2.11–2.17 (m)	
4				2.60 (br s)
5	2.23 (br d, 11.7)	2.31 (br d, 10.5)	2.05 (br d, 12.9)	1.46 (t, 11.1)
6	4.25 (t, 10.6)	4.23 (t, 10.5)	4.06 (t, 10.5)	4.35 (t, 10.5)
7	1.90–1.98 (m)	2.02–2.08 (m)	1.57–1.62 (m)	1.71–1.73 (m)
8a	1.72 (brd, 12.8)	1.72 (ddd, 12.9, 3.0, 3.9)	1.90–1.95 (m)	2.05–2.10 (m)
8b	1.61 (dddd, 12.7, 12.7, 12.6, 3.6)	1.56–1.59 (m)	1.54–1.57 (m)	1.67 (ddd, 12.6, 12.6, 3.9)
9a	1.94 (br d, 12.8)	1.84 (ddd, 12.3, 3.3, 2.8)	2.11–2.17 (m)	2.16–2.17 (m)
9b	1.29 (ddd, 12.8, 12.8, 3.9)	1.39 (ddd, 12.3, 12.3, 3.9)	1.27–1.31 (m)	1.33 (ddd, 12.9, 12.9, 4.7)
11	2.64 (dq, 7.5, 7.8)	2.64 (dq, 7.5, 7.8)	2.33–2.37 (m)	2.11-2.12 (m)
13	1.20 (d, 7.6)	1.19 (d, 7.8)	1.23 (d, 6.0)	1.12 (d, 6.9)
14	0.84 (s)	0.87 (s)	0.83 (s)	1.16 (s)
15a	5.17 (d, 2.8)	5.20 (d, 2.4)	4.97 (br s)	1.17 (d, 7.5)
15b	4.90 (d, 2.0)	4.91 (d, 2.4)	4.83 (br s)	
OAc	–	2.07 (s)		

The assignment of **1** was performed by ^{1}H–^{1}H COSY, HMBC and NOE experiments.
[a] 400 MHz, chloroform-d_1.
[b] 300 MHz, chloroform-d_1.
[c] 300 MHz acetone-d_6.

Table 2
^{13}C NMR (DEPT) data for compounds **1**–**3**.

NO.	**1**[a]	**2**[b]	**3**[c]
1	79.0 (C-1, d)	79.3 (d)	75.8 (d)
2		31.2 (t)	46.8 (t)
3	37.9 (C-2, t)	33.5 (t)	208.3 (s)
4	145.5 (C-3, s)	142.7 (s)	44.5 (d)
5	55.1 (C-4, d)	52.4 (d)	49.2 (d)
6	79.7 (C-5, d)	78.3 (d)	81.8 (d)
7	49.2 (C-6, d)	52.3 (d)	50.7 (d)
8	20.7 (C-7, t)	23.0 (t)	20.1 (t)
9	34.8 (C-8, t)	35.9 (t)	36.8 (t)
10	46.8 (C-9, s)	42.8 (s)	42.1 (s)
11	37.9 (C-10, d)	41.2 (d)	38.1 (d)
12	180.2 (C-11, s)	179.4 (s)	179.3 (s)
13	9.6 (C-12, q)	12.5 (q)	9.1 (q)
14	11.7 (C-13, q)	11.6 (q)	11.4 (q)
15	107.6 (C-14, t)	110.4 (t)	13.3 (q)

[a] 100 MHz, chloroform-d_1.
[b] 75 MHz, chloroform-d_1.
[c] 75 MHz, acetone-d_6.

1.51 (dd, 7.2, 6.9, H-6a), 1.37–1.45 (2H, m, H-5a, H-6b), 1.31 (brd, 10.5, H-5b), 1.25 (3H, s, H-7), 0.79 (6H, d, 6.6, H-9, H-10), 74.6(d, C-2), 73.9 (s, C-1), 70.4 (t, C-4), 33.8 (t, C-3), 29.3 (t, C-5, C-6), 27.1 (q, C-7), 38.4 (d, C-8), 16.6 (q, C-9), 16.6 (q, C-10).

(E)-3β,4α-Dihydroxyl-2-(2′,4′-hexadiynylidene)-1,6-dioxaspiro[4,5]decane (**7**). Colourless needles (from petrol ether-acetone); m.p. 220–222 °C; $[\alpha]_D^{20}$ − 50 (*c* 1.17, chloroform); HRESIMS *m/z*: 271.0944 (calcd. for $C_{14}H_{16}O_4 + Na^+$, 271.0941); UV (chloroform, log ε): λ_{max} 294 (1.12), 279 (1.32) and 266 (1.07) nm; IR (film) λ_{max}: 3367, 3033, 2948, 2882, 2139, 1651, 1449, 1425, 1360, 1283, 1226, 1182, 1160, 1073, 1024, 950, 899, 873 and 811 cm^{-1}; EIMS *m/z* (rel int): 249 (3) $[M+H]^+$, 248 (15) $[M]^+$, 230 (2) $[M-H_2O]^+$, 136 (33), 121 (26), 113 (83), 76 (66), 55 (88) and 43 (100); ^{1}H NMR and ^{13}C NMR (DEPT) see Tables 4 and 5.

2-Hydroxyl-2-[(E)-1α,2β,3-trihydroxyl-3-nonaene-5,7-diyne]-4H-pyran (**8**). Colourless crystals (from petrol ether-acetone); $C_{14}H_{18}O_5$; EIMS *m/z* (rel int): 266 (13) $[M]^+$, 230 (2) $[M-2H_2O]^+$, 154 (22) and 113 (100); ^{1}H NMR and ^{13}C NMR (DEPT) see Tables 4 and 5.

^{1}H NMR and ^{13}C NMR (DEPT) data for **9–10** see Tables 4 and 5; ^{1}H and ^{13}C NMR (DEPT) data for **11–13** see Table 6; ^{1}H data for **15–20** see Table 7.

4-Hydroxyl-3,5-dimethoxyl-6-*O*-β-D-glucosebenzene (**14**). ^{1}H NMR (chloroform-d_1, 300 MHz): δ 6.66(1H, brs, H-2), 6.60(1H, brs, H-6), 5.02(1H, brs, phenolic-OH), 4.89(1H, d, 5.1, H-1′), 4.64 (dd, 15.9, 3.6, H-6′a), 4.36 (1H, brs, OH), 4.16 (dd, 14.8, 7.2., 8.7, H-6′b), 4.64 (dd, 15.9, 3.6, H-6′a), 4.36 (1H, brs, OH), 4.16 (dd, 14.8, 7.2., 8.7, H-6′b), 3.81(dd, 5.4, 5.7, H-3′), 3.70–3.57 (m, H-2′), 3.76 (OCH_3), 3.75(OCH_3), 3.59(d, 11.7, H-3′), 3.18 (dd, 7.8, 5.1, H-4′), 3.00–3.07 (m, H-5′).

3. Results and discussion

3.1. Phytochemical investigation

Compound **1** was obtained as a colourless oil. The molecular formula was established as $C_{14}H_{20}O_3$ by HR ESI MS, which showed a quasimolecular ion peak $[M+Na]^+$ at *m/z* 259.1306 (calcd. 259.1305). The EIMS peaks at *m/z* 236 $[M]^+$ and 218 $[M-H_2O]^+$ suggested the presence of a hydroxyl group. IR spectrum showed the absorption bands for hydroxyl (3390 cm^{-1}), γ-lactone (1773 cm^{-1}), and terminal olefinic (1652, 917 and 891 cm^{-1}) groups. The ^{13}C NMR spectrum of **1** showed 14 carbon signals which are assigned to two methyls, four methylenes, five methines, and three quaternary carbons (Table 2). ^{1}H and ^{13}C NMR spectra showed the characteristic signals of Me-14 of an eudesmanolide at δ_H 0.84 (s) and δ_C 11.7, an α-methyl-γ-lactone moiety at δ_H 1.20 (d, *J* = 7.6 Hz, H-13), 4.25 (t, *J* = 10.6 Hz, H-6) and δ_C 79.7 (C-6), 49.2 (C-7), 180.2 (C-12) and 9.6 (C-13), one terminal double bond: at δ_H 5.17 (d, *J* = 2.8 Hz, H-15a) and 4.90 (d, *J* = 2.0 Hz, H-15b); δ_C 145.5 (C-4) and 107.6 (C-15), and a skeletal quaternary carbon signal at δ_C 46.8 (C-10). ^{1}H NMR data for **1** are similar to those of **2**, **3** and 1β-hydroxyeudesm-4(15)-en-5α,6β,7α,11αH-12,6-olide (Marco, 1989), except for the signals of H-2 and C-2 which are not present in **1**. All these data indicated that **1** is a 2-nor eudesmanolide. In Fig. 1, Tables 1 and 2, the atomic numbers of **1** are noted according to the normal eudesmanolide numbering convention, for the sake of comparing NMR data of **1** with those of eudesmanolides **2** and **3**.

Table 3
^{1}H and ^{13}C NMR (DEPT) data for compounds **4**–**5** (300 and 75 MHz, chloroform-d_1).

No.	**4**				**5**	
	^{1}H	^{13}C	^{1}H–^{1}HCOSY	HMBC	^{1}H	^{13}C
1	–	142.1 (s)		C-1/H-14, H-5, H-7, H-9		134.1 (s)
2	6.19 (br s)	132.4 (d)	H-2/H-3, H-5		5.36 (brs)	120.5 (d)
3	4.12 (br s)	78.6 (d)	H-3/H-2, H-15	C-3/H-15	1.89–2.09 (m) 1.78 (brdd, 15.9, 2.4)	26.9 (t)
4	–	79.2 (s)		C-4/H-15	1.50 (ddd, 11.1, 6.0, 1.8)	42.9 (d)
5	3.30 (br d, 9.9)	57.9 (d)	H-5/H-6, H-2, H-13	C-5/H-15, H-3	1.29 (ddd, 11.7, 6.0, 1.8) 1.24 (brs)	22.0 (t)
6	4.23 (t, 9.9)	77.0 (d)	H-6/H-7, H-5	C-6/H-5, H-7, H-15	1.89–1.99 (m) 2.09 (m)	31.0 (t)
7	3.28 (t, 9.9)	48.5 (d)	H-7/H-3′, H-6, H-8, H-13b	C-7/H-13a, H-8	–	74.3 (s)
8	5.69 (d, 3.0)	71.5 (d)	H-8/H-7	C-8/H-6	1.50 (ddd, 11.1, 6.0, 1.8)	40.1 (t)
9	5.50 (br s)	128.3(d)	H-9/H-14	C-9/H-14	1.89–1.99 (m) 2.09 (m)	23.2 (t)
10	–	130.6 (s)		C-10/-H-14	5.21 (t, 7.2)	124.5 (d)
11	–	135.9 (s)		C-11/-H-13a	–	131.7 (s)
12	–	169.1 (s)		C-12/H-4′	1.61 (s)	17.7 (q)
13a	6.25 (d, 3.6)	123.9 (t)	H-13b/H-7, H-5	H-13a/C-11, C-7, C-1′	1.67 (s)	25.7 (q)
13b	5.57 (d, 3)					
14	2.00 (s)	24.8 (q)	H-14/H-9	H-14/C-1, C- 9, C-10	1.64 (s)	23.1 (q)
15	1.38 (s)	20.6 (q)	H-15/H-3	H-15/C-3, C-4, C-5	1.10 (s)	23.3 (q)
OAng						
1′	–	166.7 (s)		C-1′/H-8, H-13a, H-3′		
2′	–	126.8 (s)		C-2′/H-4′, H-5′		
3′	6.29 (qq, 6, 1.2)	140.9 (d)	H-3′/H-4′, H-7	C-3′/H-4′, H-5′		
4′	1.94 (dq,7.2,1.8)	16.0 (q)	H-4′/H-3′	H-4′/C-2′, C-3′, C-12		
5′	2.04 (dq, 6, 1.8)	21.7 (q)		H-5′/C-2′, C-3′		

Table 4
^{1}H data for compounds **7–10** (300 MHz, chloroform-d_1).

No.	**7**	**8**	**9**	**10**
1a	3.87 (ddd,11.4, 11.1, 3.1)	3.87 (ddd, 11.3, 11.1, 3.4)	3.86 (ddd, 11.0, 11.0, 3.0)	4.11 (ddd, 11.0, 11.0, 4.0)
1e	3.74 (brd, 11.7)	3.76 (dd, 11.1, 4.2)	3.76 (dd, 11.0, 3.0)	3.82 (dd, 11.1, 2.4)
2	1.60–1.65 (m)	1.62 (dddd, 12.3, 10.5, 6.6, 4.8) 1.69 (brdd, 6.0, 3.6)	1.62–1.66 (m)	1.66–1.79 (m)
3	1.72–1.79 (m)	1.78 (brddd, 12.9, 8.9, 4.5)	1.75–1.78 (m)	1.75–1.84 (m)
4	1.92 (brs)	1.90 (ddd, 13.5, 4.2, 3.3)	1.92 (brd, 6.3)	2.01–2.08 (m)
6	3.95 (brs)	4.21 (brs)	3.80 (d, 3.0)	6.20 (d, 6.0)
7	4.59 (brs)	4.72 (brs)	4.29 (d, 2.4)	6.20 (d, 6.0)
8	–	–	–	4.60 (brs)
9	5.17 (brs)	5.18 (brs)	5.18 (brs)	–
14	1.96 (s)	1.98 (s)	2.00 (s)	2.00 (s)

The assignments of **7** and **8** were achieved by ^{1}H–^{1}H COSY, HMBC and NOE experiments.

Table 5
^{13}C NMR (DEPT) data for **7–10** (75 MHz, chloroform-d_1).

No.	**7**	**8**	**9**	**10**
1	62.7 (t)	57.9 (t)	63.2 (t)	64.5 (t)
2	24.5 (t)	24.7 (t)	24.8 (t)	24.7 (t)
3	18.5 (t)	19.1 (t)	18.6 (t)	19.3 (t)
4	27.3 (t)	28.1 (t)	28.8 (t)	32.8 (t)
5	110.5 (s)	111.4 (s)	105.9 (s)	113.1 (s)
6	79.0 (d)	81.7 (d)	51.9 (d)	138.2 (d)
7	76.3 (d)	63.0 (d)	60.0 (d)	126.9 (d)
8	171.1 (s)	168.6 (s)	164.9 (s)	168.2 (s)
9	83.7 (d)	84.8 (d)	85.8 (d)	78.9 (t)
10	79.8 (s)	79.5 (s)	79.6 (s)	80.6 (s)
11	70.0 (s)	69.9 (s)	69.8 (s)	71.0 (s)
12	83.7 (s)	81.0 (s)	76.6 (s)	79.0 (s)
13	64.7 (s)	65.0 (s)	64.7 (s)	64.5 (s)
14	4.6 (q)	4.9 (q)	4.6 (q)	5.0 (q)

^{1}H–^{1}H COSY correlations of H-1 to H-3, H-5 to H-6, H-8 to H-7 and H-9; H-11 to H-13 suggested that **1** possesses the structure shown in Fig. 1. The carbon skeleton was confirmed to be a noreudesmane sesquiterpene by HMBC correlations of C-1 at δ_C 79.0 to H-3b at δ_H 2.16, H-9b at δ_H 1.29, and H-14, C-3 to H-1, H-15a, and H-15b, C-4 to H-3a at δ_H 2.82 and H-3b, C-5 to H-14, H-15a, and H-15b, C-6 to H-7 and H-11, C-7 to H-8b at δ_H 1.61, C-8 to H-9b, C-9 to H-14 and H-1, C-11 to H-13, C-12 to H-11 and H-13, H-13 to C-7, C-11, and C-12, H-14 to C-1, C-5, C-9, and C-10. In order to confirm the position of the hydroxyl group, compound **1** was acetylated to **1a**. The ^{1}H NMR spectrum of **1a** showed the presence of an acetyl methyl signal. In addition, the downfield shift of signal of H-1 at δ_H 3.95 in **1** to δ_H 4.87 in **1a** indicated acetylation at C-1. This provided an evidence for the hydroxyl being located at C-1.

The stereochemistry of **1** was determined by the coupling constants and the NOE difference spectrum. The large coupling constants for H-6 (t, J = 10.6 Hz) suggested that H-6 should be in a β orientation, and H-5 and H-7 being α-oriented, which indicated the junction of *trans* A/B and *trans* B/C rings. The configuration of CH_3-13 was assigned as β by comparison between the chemical shift of C-13 of **2**, **3** and the reported value in the literature (Marco, 1989), about δ_C 9.5 for β-orientation and δ_C 12.5 for *a*-orientation. In the NOE difference spectrum experiments, irradiation of H-5 led to an enhancement of H-1 (+5.14%) and H-3a (+5.34%); irradiation of H-6 led to an enhancement of H-14 (+3.08%) and irradiation of H-13 led to an enhancement of H-6 (+4.46%). All of these observations suggested that H-1 has α-orientation, whereas both H-13 and H-14 have β-orientation. Therefore, the structure of **1** was assigned to a novel noreudesmanolide, 1β-hydroxyl-2-noreudesm-4(15)-en-5α,6β,7α,11αH-12,6-olide. A trivial name, Ajaniaolide A, was adopted for it.

Compound **4** was obtained as colourless oil. The molecular formula was established as $C_{20}H_{24}O_6$ by HRESIMS which gave the

Table 6
^{1}H- and ^{13}C NMR (DEPT) NMR data for compounds **11–13** (300 and 75 MHz).

No.	^{1}H			^{13}C		
	11[a]	**12**[b]	**13**[a]	**11**[a]	**12**[b]	**13**[a]
1	–	–	–	166.1 (s)	167.9 (s)	168.0 (s)
2	6.08 (d, 15.6)	6.28 (d, 15.9)	6.29 (d, 15.9)	114.5 (d)	115.0 (d)	115.1 (d)
3	7.35 (d, 15.9)	7.56 (d, 15.9)	7.54 (d, 15.6)	146.3 (d)	145.4 (d)	145.9 (d)
4	–	–	–	126.0 (s)	126.9 (s)	127.4 (s)
5	7.00 (brs)	7.18 (brs)	7.17 (d, 1.2)	115.2 (d)	114.3 (d)	114.9 (s)
6	–	–	–	149.2 (s)	145.7 (s)	146.3 (s)
7	–	–	–	145.9 (s)	148.1 (s)	148.9 (s)
8	6.74 (d, 6.9)	6.88 (d, 8.1)	6.87 (d, 8.4)	116.5 (d)	115.6 (d)	116.2 (d)
9	6.94 (d, 7.5)	7.04 (d, 8.4)	7.03 (d, 8.1)	122.0 (d)	121.9 (d)	122.6 (d)
OCH_3		–	3.72 (s)	–	–	51.6 (d)

11: 9.63(s, phenolic-OH), 9.21(s, phenolic-OH), 7.00 (s, OH_1), 5.65(s, OH_5), 5.01(2H, brs, OH_3+OH_4), 4.75 (brs, H-5′), 3.93 (m, H-4′), 3.86 (2H, m, H-8′), 3.55(brs, H-3′), 2.07–2.09(m, H-2′e), 2.07–2.09(m, H-6′e), 1.89 (brd, 13.2, H-6′a), 1.71–1.74(brt, 12, H-2′a), 1.46(2H, brs, H-9′), 1.20(2H, brd, 6.0, H-10′), 0.77–0.79(3H, m, H-11′), 173.9(s, C-7′), 73.7 (s, C-1′), 71.7 (d, C-4′), 69.9 (d, C-3′), 67.5(d, C-5′), 64.8(t, C-8′), 37.9(t, C-2′), 35.6 (t, C-6′), 30.7(t, C-9′), 19.2(t, C-10′), 14.2 (q, C-11′).
[a] Dimethyl sulfoxide-d_6.
[b] Acetone-d_6.

Table 7
^{1}H NMR data for compounds **15–20** (300 MHz).

No.	**15**[a]	**16**[a]	**17**[c]	**18**[b]	**19**[a]	**20**[a]
3	6.27 (d, 9.3)	6.27 (d, 9.3)	6.23 (d, 9.3)	6.32 (d, 9.6)	6.30(d, 9.3)	6.27 (d, 9.3)
4	7.57 (d, 9.9)	7.60 (d, 9.6)	7.72 (d, 9.9)	7.95 (d, 9.9)	7.63(d, 9.6)	7.61 (d, 9.6)
5	6.59 (s)	6.91(s)	6.87 (s)	7.29 (s)	6.86(s)	6.84 (s)
8	–	6.84 (s)	–	7.14 (s)	6.85(s)	6.84 (s)
OCH_3	3.93 (s)	3.95 (s)	3.82 (s) 3.70 (s)	3.80 (s)	3.93(s) 3.96(s)	3.90 (s)
OH		6.20 (brs)				
1′	6.17 (2H, s)	–	4.99 (d, 6.9)	5.07 (d, 5.4)	–	4.66 (d, 6.3)
2′	–	–	3.40 (dd, 6.9, 6.0)	3.74 (m)	–	5.49 (m)
3′	–	–	3.40 (dd, 9.6, 6.9)	3.70 (m)	–	1.77 (s)
4′	–	–	3.32 (t, 9.5)	3.27 (m)	–	1.79 (s)
5′	–	–	3.14–3.21 (m)	3.14 (d, 4.5)	–	–
6a′	–	–	3.61 (brd,12.3)	4.58 (m)	–	–
6b′			3.51 (dd,12.3, 5.4)	4.12 (dd, 12, 5.1)		

[a] Chloroform-d_1.
[b] Dimethyl sulfoxide-d_6.
[c] Deuterium oxide.

quasimolecular ion peak $[M+NH_4]^+$ at *m/z* 378.1907 (calcd. 378.1911). The EIMS peak at *m/z* 260 $[M-AngOH]^+$ suggested the presence of an angeloyloxy group. The presence of hydroxyl, γ-lactone, carbonyl, and a double band was characterised by IR bands at 3422, 1770, 1712, and 1647 cm^{-1}, respectively. ^{13}C NMR (DEPT) spectra (Table 3) showed 15 skeletal carbons which included one γ-lactone at δ_C 169.1, two methyls at δ_C 24.8 and 29.6, one exo-methylene at δ_C 123.9, seven methines containing three oxymethines at δ_C 78.6, 77.0, and 71.5, five quaternary carbons containing one oxyquaternary carbon at δ_C 79.2, and three vinylic quaternary carbons. ^{1}H and ^{13}C NMR were assigned to vinylic signals, δ_H 6.19 (1H, br s) and 5.50 (br s) and δ_C 142.1 s, 132.4 d, 128.3 d and 130.6 s, exhibiting the presence of a conjugated double bond system. This assignment was further confirmed by a UV (MeOH) absorption at λ_{max} (log ε) 244 nm. The characteristic NMR signals of an angeloyloxyl group are shown in Table 3. All these observations suggested that compound **4** was a highly oxygenated guaiane lactone (Meng et al., 2001). This assignment was confirmed by 2D NMR spectroscopic analyses (^{1}H–^{1}H COSY and HMBC). As a consequence, it allowed us to unambiguously assign all ^{1}H and ^{13}C NMR spectroscopic data in Table 3.

The conjugated double bond system was established to be located among C-1, C-2, C-9, and C-10, as deduced by correlation between H-2 and H-3 in the ^{1}H–^{1}H COSY, and the correlations between C-1 and H-5, H-9, H-14, and the correlations between H-14 and C-1, C-9, C-10 in HMBC experiments. The angeloyloxyl group was located at C-8 at δ_C 71.5, as deduced by HMBC correlations between the carbonyl carbon C-1′ at δ_C 166.7 and H-8 at δ_H 5.69. Two hydroxyl groups were located at C-3 and C-4, respectively, as deduced by HMBC correlations between the Me-15 at δ_H 1.38 and C-3 at δ_C 78.6, C-4 at δ_C 79.2, respectively.

The relative stereochemistry of **4** was determined by the coupling constants and NOE difference spectra. The large coupling constants, $J_{5,6} = J_{7,6} = J_{7,8} = 9.9$ Hz, suggested that H-6, H-7, and H-8 were all located at *trans* position. In the NOE difference spectrum, irradiation of H-6 led to an enhancement of H-15 (+3.70%), and irradiation of H-3 led to an enhancement of H-15 (+3.08%). These observations suggest that H-3, H-6, H-8, and H-15 were β-oriented, while H-5 and H-7 were α-oriented. Therefore, compound **4** was assigned as 8α-angeloyloxyl-3α,4α-dihydroxyguaia-1,9,11(13)-trien-6,12-olide, as shown in Fig. 1.

Compound **7** was isolated as colourless needles. Its molecular formula was established as $C_{14}H_{16}O_4$ from HRESIMS which gave the quasimolecular ion peak $[M+H]^+$ at *m/z* 249.1120 (calcd. 249.1123) and $[M+Na]^+$ at *m/z* 271.0944 (calcd. 271.0941). The IR spectrum showed absorbances for hydroxyl (3367 cm^{-1}) and conjugated acetylene-olefine (2139, 1651 cm^{-1}). The existence of the latter was also confirmed by the UV (MeOH) spectrum (λ_{max} 279 nm). ^{13}C NMR (DEPT) spectra showed peaks assigned to an acetylene skeleton: four acetylenic quaternary carbons at δ_C 79.8 (C-10), 70.0 (C-11), 83.7 (C-12), and 64.7 (C-13), an olefine conjugated with acetylene, signals at δ_C 83.7 (CH, C-9) and 171.1 (C, C-8). Two characteristic signals of the terminal methyl and the olefine proton were determined at δ_H 1.96 (H-14) and 5.17 (H-9), respectively. ^{1}H NMR data of **7** were similar

to those of a glycol reported by Matsuo, Uchio, Nakayama, and Hayashi (1974), whose structure is an acetylenic compound of dioxaspiro[4,5]decans. However, the relative stereochemistry of them is different because their optical rotation values are exactly opposite, i.e. $[\alpha]_D^{20} - 50$ (*c* 1.17, $CHCl_3$) for **7** and +112 (*c* 0.37%, $CHCl_3$) for the glycol. The structure of **7** and its ^1H and ^{13}C NMR assignment were confirmed by ^1H–^1H COSY and HMBC experiments.

A spirocyclic system was established by ^1H–^1H COSY correlations between H-2 and H-1, H-3, H-4, between H-3 and H-2, between H-6 and H-7, and between H-9 and H-14, H-7. A quaternary carbon, C-5 at δ_C 110.5, was also observed. The conjugated acetylene-olefine skeleton, connecting to a five-membered epoxide, was established by HMBC correlations between H-7 at δ_H 4.59 and C-5, C-6, between C-7 at δ_C 76.3 and H-6, H-9, between C-8 at δ_C 71.5 and H-6, H-9, and between the terminal methyl H-14 at δ_H 1.96 and C-10, C-11, C-12, C-13, C-8. These observations suggested two hydroxyl groups located at C-7 and C-8.

The relative stereochemistry of **7** was elucidated by coupling constants and NOE experiments. The chemical shift of a broad singlet H-9 at δ 5.17 indicated that the 8,9-double bond was in an *E* conformation (Matsuo et al., 1974). NOE experiments indicated that irradiation of H-7 did not lead to an enhancement of H-6, suggesting that an *anti* relationship between H-7 and H-6, exists, and irradiation of H-6 led to an enhancement of H-4 (6.51%), suggesting that H-7 was located at the α-orientation and both H-6 and H-4 at the β-orientation. Therefore, compound **7** was elucidated as 3β,4α-dihydroxy-2(*E*)-(2′,4′-hexadiynylidene)-1,6-dioxaspiro [4,5]decane.

Compound **8** was isolated as colourless needles. The molecular formula of **8** is found to be $C_{14}H_{18}O_5$ from the EIMS, which exhibits a molecular ion peak at *m/z* 266, and this is further confirmed by ^{13}C NMR (DEPT) spectra. The molecular weight of **8** was 18 amu more than that of **7** and its ^1H and ^{13}C NMR spectra are very similar to those of **7**. The ^{13}C NMR spectrum showed 14 carbons, assigned to one methyl, four methylenes, three methines, and six quaternary carbons. A ^1H–^1H COSY experiment showed couplings from H-9 to H-14, H-7, from H-7 to H-6, from H-3 to H-2 and H-4, from H-2 to H-1e, H-1a, H-3, and H-4. In comparison with **7**, chemical shifts of C-5, C-6 and C-9 moved downfield, whereas those of C-7 and C-8 moved upfield. These observations suggest that the five-membered ring was broken and two hydroxyl groups were located at C-5 and C-8 in **8**. Consequently, compound **8** was elucidated to be 2-hydroxyl-2-[(E)-1α,β,3-trihydroxyl-3-nonaene-5,7-diyne]-4H-pyran. Compound **8** was not stable. Even stored at 5 °C, it was completely decomposed within one week.

The known compounds were identified by comparing their physical and spectroscopic data with values reported in the literature. They are 1β-hydroxyeudesm-4(15)-en-5α,6β,7α, 11βH-12,6-olide (**2**) (Marco, 1989), 1β-hydroxyeudesm-3-oxo-4β, 5α,6β,7α,11αH-12,6-olide (**3**) (Ahmed et al., 2003; Marco, 1989), α-bisabol (**5**) (Jequier, Nicollier, Tabacchi, & Garnero, 1980), 1*S*,2*R*,4*S*-trihydroxyl-*p*-methane (**6**) (Gomes & Antunes, 2001), (*E*)-3β,4β-epoxy- 2-(2′,4′-hexadiynylidene)-1,6-dioxaspiro[4,5] decane (**9**) (Birnecker, Wallnöfer, Hofer, & Greger, 1988), 2β-(2′,4′-hexadiynoyl)-1,6-dioxaspiro[4,5]deca-3-ene (**10**) (Tan, Jia, Zhao, & Feng, 1992), chlorogenic acid butyl ester (**11**) (Rumbero-Sanchez & Vazquez, 1991), caffeic acid (**12**) and caffeic acid methyl ester (**13**) (Bolzani, Trevisan, & Young, 1991), 4-hydroxyl-3,5-dimethoxyl-6-*O*-β-D-glucosebenzene (14) (Cui et al., 1990), sabandinin (**15**) (Sarker, Gray, Waterman, & Armstrong, 1994), isoscopoletin (**16**) and scoparone (**19**) (Tsukamoto, Hisada, Nishibe, Roux, & Rourke, 1984), 6,8-dimethoxyl-7-*O*-β-D-glucosecoumarin (**17**) (Tsukamoto, Hisada, & Nishibe, 1985; De Rosa, Mitova, Handjieva, & Calis, 2002), scopolin (**18**) (Kuroyanagi et al., 1986), and 7-(3-methyl-2-butenyloxy)-6-methoxycoumarin (**20**) (Debenedetti, Nadinic, Coussio, De Kimpe, & Boeykens, 1998).

3.2. Anticancer activity

The cytotoxic activities of compounds **3**, **5**, **6**, **9**, **11–13**, **16**, and **18** were evaluated by assessing their effects on K562/ADM cell lines, **9**, **11–13**, **16**, and **18** on K562 cell lines, **3**, **5–6** on BGC-823 cell lines and **9**, **16**, and **18** on Hep-G2 cell lines using MTT colorimetric assay, as previously reported (Hussain et al., 1993). The results of the inhibition of compounds on the viabilities of cancer cells after 48 or 72 h of incubation are presented in Table 8, which does not include the compounds without inhibition toward selected cancer cell lines. IC_{50} values of all tested compounds are given in Table 9. Among them, sesquiterpene **3** and phenolic acid **12** exhibit strong activities against the K562/ADM lines: IC_{50} of 11.1 for 48 h and 13.1 μg/ml for 72 h for **3**, and 7.25 for 48 h and 3.29 μg/ml for 72 h for **12**. Compounds **5**, **11**, **13**, and **16** display weak activities (IC_{50} > 70 μg/ml), but **6**, **9**, and **18** display no activity toward K562/ADM cell lines. Compound **12** also exhibits strong activity against the K562 cell lines (IC_{50} of 5.57 for 48 h and 0.78 μg/ml for 72 h), while **11** and **13** display a moderate activity (IC_{50} of 82.3 μg/ml for 48 h and 45.4 μg/ml for 72 h for **11** and 65.0 μg/ml for 48 h and 22.5 μg/ml for 72 h for **11**), and **16** displays very weak activity (IC_{50} > 100 μg/ml), but **9** and **18** display no activity toward K562 cell lines. Compounds **3**, **5**, and **6** display very weak activity toward BGC-823 cell lines (IC_{50} > 100 μg/ml). Compound **16** displays very weak activity (IC_{50} > 100 μg/ml), but **9** and **18** show no activity toward Hep-G2 cell lines.

The data indicate that **3** is more sensitive to K562/ADM cancer cells than BGC-823 gastric cancer cells as measured by growth inhibition and apoptosis assays at the same drug concentration. This suggested that **3** might possess different anticancer activities toward solid tumours and hemocytein tumours. Experiment showed that **3** obviously inhibited the proliferation of K562/ADM cancer cells and induced apoptosis of tumour cells. Therefore, the interference mechanism of **3** on K562/ADM cancer cells was assumed to inhibit a variety of cellular functions which direct cells into apoptosis. From Fig. 3, compounds **3** and **12** possessed inhibitory effects upon K562/ADM cells growth at lower concentrations, suggesting that the observed growth inhibition was caused by a cytostatic effect, as also by **11–13** upon K562 cells (Fig. 4). However compounds **5**, **11**, **12**, **13**, and **16** possessed inhibitory effects upon K562/ADM cells growth at higher concentrations, suggesting that the observed growth inhibition was caused by a cytotoxic effect rather than a cytostatic effect (Fig. 3), as also for **16** upon K562 cells (Fig. 4). This showed a close agreement with previous work on potential mechanisms (Kampa et al., 2004).

Previous studies of natural sesquiterpenes and synthetic analogues show that the main determining factor responsible for the cytotoxicity and antitumor activity of compounds under study is the existence of an α,β-unsaturated system (Barla, Topçu, Öksüz, Tümen, & Kingston, 2007), which is likely to serve as an alkylating centre and can be a part of an ester, ketone, or lactone moiety. The activity of **3** may be relevant to the 6,12-lactonization in the molecule. The activity of **3** against K562/ADM cells might be due to the absence of an α-methylene bearing a γ-lactone moiety. We found that only **3** possessed an α-methyl-γ-lactone moiety among all tested compounds. Results for their bioassays indicate that bioactive molecules must possess an α-methyl-γ-lactone sesquiterpene skeletal type of structure. By means of its structural feature, caffeic acid, **12,** exhibits strong antioxidant and cytotoxic activity against K562 and K562/ADM cell lines, not only containing two hydroxyl groups and but also carboxyl groups (Gomes et al., 2003).

Table 8
Inhibition (ratios) of selected compounds in tested concentrations (0, 10, 50, 100, and 200 μg/ml), against K562, K562/ADM, BGC-823, and Hep-G2 cell lines (incubation time 48 and 72 h).

Compound No.	Time (h)	Concentration (μg/ml)				
		0	10	50	100	200
K562						
11	48	0.000 ± 0.045	0.096 ± 0.056	0.518 ± 0.031	0.524 ± 0.053	0.651 ± 0.085
12	48	0.000 ± 0.056	0.518 ± 0.021	0.657 ± 0.098	0.668 ± 0.033	0.681 ± 0.070
13	48	0.000 ± 0.033	0.091 ± 0.023	0.386 ± 0.037	0.734 ± 0.032	0.741 ± 0.022
16	48	0.000 ± 0.033	0.000 ± 0.027	0.000 ± 0.028	0.225 ± 0.029	0.447 ± 0.082
11	72	0.000 ± 0.015	0.182 ± 0.044	0.615 ± 0.073	0.663 ± 0.079	0.752 ± 0.038
12	72	0.000 ± 0.015	0.642 ± 0.039	0.773 ± 0.033	0.784 ± 0.033	0.791 ± 0.015
13	72	0.000 ± 0.023	0.303 ± 0.018	0.733 ± 0.013	0.779 ± 0.016	0.791 ± 0.028
16	72	0.000 ± 0.097	0.000 ± 0.045	0.000 ± 0.076	0.337 ± 0.025	0.493 ± 0.034
K562/ADM						
3	48	0.000 ± 0.053	0.555 ± 0.034	0.927 ± 0.011	0.979 ± 0.008	1.019 ± 0.005
5	48	0.000 ± 0.053	0.048 ± 0.012	0.122 ± 0.029	0.241 ± 0.018	0.523 ± 0.022
11	48	0.000 ± 0.039	0.000 ± 0.732	0.060 ± 0.138	0.433 ± 0.028	0.597 ± 0.065
12	48	0.000 ± 0.022	0.500 ± 0.028	0.693 ± 0.027	0.707 ± 0.091	0.714 ± 0.044
13	48	0.000 ± 0.055	0.002 ± 0.038	0.342 ± 0.083	0.550 ± 0.033	0.664 ± 0.038
16	48	0.000 ± 0.057	0.000 ± 0.027	0.000 ± 0.045	0.152 ± 0.027	0.327 ± 0.040
3	72	0.000 ± 0.037	0.348 ± 0.012	0.942 ± 0.013	1.011 ± 0.007	1.020 ± 0.008
5	72	0.000 ± 0.037	0.001 ± 0.064	0.347 ± 0.060	0.606 ± 0.041	0.767 ± 0.075
11	72	0.000 ± 0.012	0.000 ± 0.065	0.080 ± 0.021	0.446 ± 0.029	0.784 ± 0.076
12	72	0.000 ± 0.088	0.081 ± 0.026	0.995 ± 0.083	0.998 ± 0.022	0.998 ± 0.039
13	72	0.000 ± 0.011	0.083 ± 0.082	0.389 ± 0.035	0.579 ± 0.022	0.784 ± 0.028
16	72	0.000 ± 0.087	0.003 ± 0.031	0.000 ± 0.034	0.235 ± 0.028	0.485 ± 0.018
Hep-G2						
16	72	0.000 ± 0.263	0.000 ± 0.056	0.000 ± 0.022	0.176 ± 0.023	0.448 ± 0.018
BGC-823						
3	72	0.000 ± 0.011	0.096 ± 0.044	0.166 ± 0.066	0.235 ± 0.072	0.393 ± 0.012
5	72	0.000 ± 0.011	0.070 ± 0.044	0.147 ± 0.029	0.394 ± 0.065	0.964 ± 0.004
6	72	0.000 ± 0.011	0.088 ± 0.013	0.107 ± 0.033	0.129 ± 0.019	0.248 ± 0.059

Table 9
IC_{50} concentrations (μg/ml) of the tested compounds against K562, K562/ADM, BGC-823, and Hep-G2 cell lines (incubation time 48 and 72 h).

Compound No.	K562		K562/ADM		BGC-823		Hep-G2	
	48 h	72 h	48 h	72 h	48 h	72 h	48 h	72 h
3	ND	ND	11.1	13.1	>100	>100	ND	ND
5	ND	ND	>100	72.5	>100	69.63	ND	ND
6	ND	ND	NA	NA	>100	>100	ND	ND
9	NA	NA	NA	NA	ND	ND	NA	NA
11	82.25	45.41	>100	>100	ND	ND	ND	ND
12	5.57	0.78	7.25	3.29	ND	ND	ND	ND
13	65.02	22.52	>100	72.6	ND	ND	ND	ND
16	>100	>100	>100	>100	ND	ND	>100	>100
18	NA	NA	NA	NA	ND	ND	NA	NA

NA, no inhibitory activity; ND, not determined.

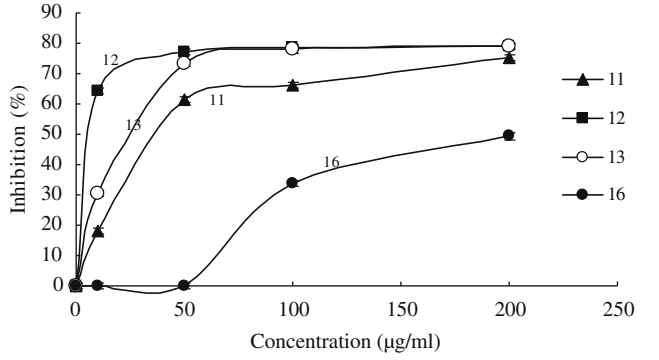

Fig. 4. Inhibition of compounds **11**–**13**, **16** against K562 cell lines (incubation time 72 h).

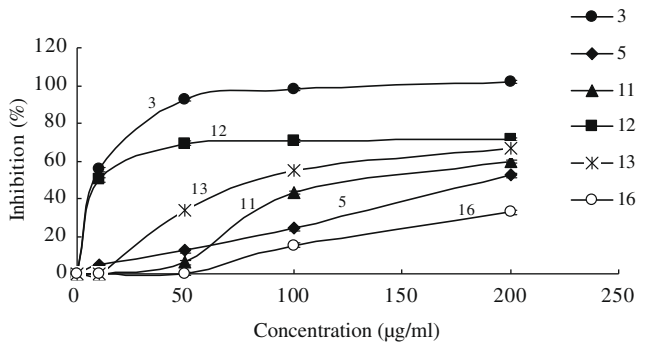

Fig. 3. Inhibition of compounds **3**, **5**, **11**–**13**, and **16** against K562/ADM cell lines (incubation time 48 h).

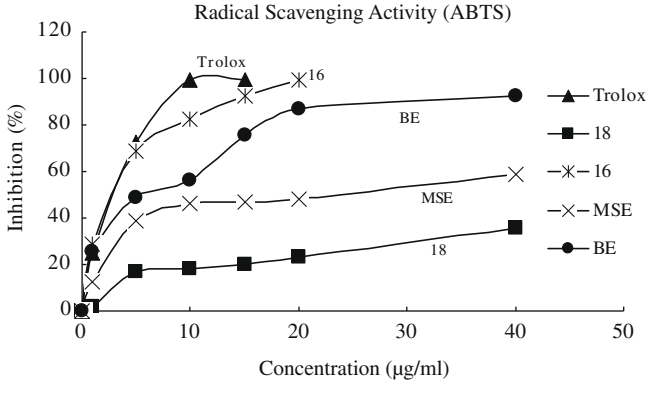

Fig. 5. ABTS· assay of compounds **16**, **18**, MSE, and BE in comparison to trolox.

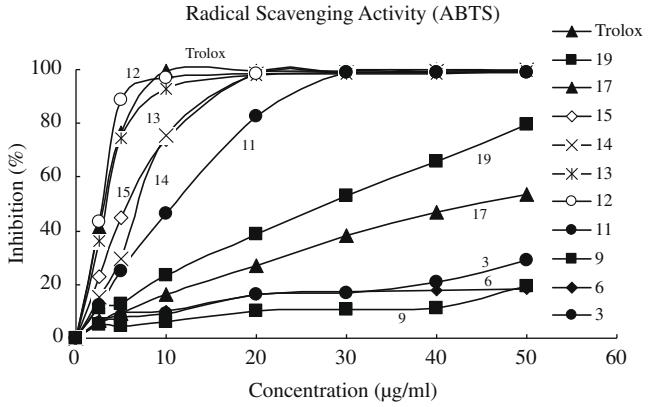

Fig. 6. ABTS· assay of compounds **3**, **6**, **9**, **11**–**15**, **17**, and **19** in comparison to trolox.

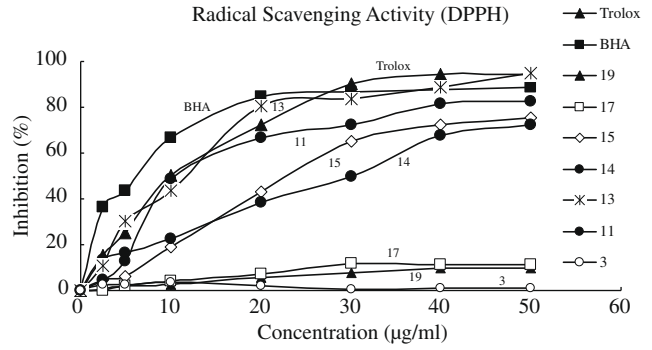

Fig. 7. DPPH· assay of compounds **3**, **11**, **13**–**15**, **17**, and **19** in comparison to BHA and trolox.

3.3. ABTS and DPPH free radical-scavenging activity

Free radical-scavenging activities of 12 compounds (**3**, **6**, **9**, **11**–**19**) as well as the mixed solvent extracts (MSE) and *n*-butanol extracts (*n*-BE) were evaluated in comparison with trolox, using ABTS·+ radical cation. Trolox was used as an antioxidant standard for ABTS·+. Free radical-scavenging activities of four compounds (**11** and **13**–**15**) were evaluated in comparison with trolox and BHA, using DPPH. Trolox and BHA were used as antioxidant standards for DPPH·. Free radical-scavenging capacities of the selected compounds, trolox and BHA measured by the ABTS· and the DPPH· assay are presented in Figs. 5–7 and their IC_{50} values are given in Table 10. Phenolic compounds and coumarins, **11**–**16**, MSE, and *n*-BE displayed significant scavenging capacities towards ABTS·+ and DPPH· (IC_{50} < 20 μg/ml). Coumarins **17**–**19** tested under the same conditions exhibited lower antioxidant activity, while non-phenolic compounds **3**, **6**, and **9** exhibited no antioxidant activity. Based on their IC_{50} values, the order of antioxidant activity of the compounds is as follows: **16** = **12** > trolox > **13** > **15** > **14** > **11** > **19** > **17** > **18** for ABTS· assay; BHT > trolox > **11** > **13** > **15** > **14** for DPPH· assay. In our study, an increase in the number of the OH ring substituents, and existence of the terminal carboxylate groups leads to higher antioxidant and cytotoxic activities. Therefore phenolic compounds **12**, **13**, and **16** are strong antioxidants.

Table 10
Scavenging IC_{50} values of ABTS and DPPH· radicals by the tested compounds, MSE and *n*-BE.

Compound No.	ABTS	DPPH
3	NA	NA
6	NA	ND
9	NA	ND
11	11.7	11.7
12	2.83	ND
13	3.38	11.90
14	6.98	28.7
15	5.56	23.4
16	2.83	ND
17	37.3	NA
18	65.9	ND
19	29.8	NA
MSE	18.8	ND
n-BE	6.01	ND
Trolox[a]	3.22	–
Trolox[b]	3.36	9.90
BHA	–	5.16

NA, no inhibitory activity at >60 μg/ml.
ND, not determined.
[a] ABTS· assay of compounds **16**, **18**, MSE and *n*-BE in comparison with trolox[a].
[b] ABTS· assay of compounds **3**, **6**, **9**, **11**–**15**, **17**, and DPPH· assay of **3**, **11**, **13**–**15**, **17**, **19** in comparison with trolox[b], respectively.

4. Conclusions

It is known that sesquiterpenes are characteristic constituents of the family Compositae (*Asteraceae*). Our results show that there are three different types of sesquiterpeneolides: eudesmane lactones, guaiane lactone, and bisabolene. Except for the typical eudesmane framework, a few other eudesmane types exist in nature. They are secoeudesmanes, lindelanes, cycloeudesmanes, isomeric eudesmanes, noreudesmanes, and dimers. Most of them contain two six-ring skeletons (Wu, Shi, & Jia, 2006). However, the rearranged eudesmanes, such as cyperane, iphionane, and oppositane skeleton, were few, and are not found in eudesmane sesquiterpene lactones. To our best knowledge, Ajaniaolide A (**1**) is a novel noreudesmane sesquiterpene lactone with a rare rearranged carbon skeleton.

According to the phytochemical studies on *A. przewalskii*, we isolated sesquiterpenolides, monoterpene, acetylenes, flavonoids, lignans, coumarins, phenylpropanoids, and aromatic compounds. The results showed that various natural products with diverse structures exist in *A. przewalskii*. Its compound types show a close relationship with the genus *Ajania* in which similar guaianolides, eudesmanolides, flavonoids, and aromatic compounds are present. Except for the above compounds, bisabolene-, acetylene-, monoterpene- and lignan-type compounds have been isolated from the genus *Ajania* for the first time.

We found that there are abundant phenolic compounds in *A. przewalskii*, including coumarins, flavonoids, lignans, phenylpropanoids, and aromatic compounds. Therefore, the potent antioxidant activity of *A. przewalskii* might be attributed to the presence of these important polyphenolics, flavonoids, and coumarin compounds, which are attractive additives for the food and drug industry and are of great interest for use in complementary medicine supplements.

Acknowledgments

This work was financially supported by the National Basic Research Program of China (973 Program, the Project No. 2007CB108903), the Natural Science Foundation of Gansu Province in China (No. ZS001-A25-002-Z) and University Key Teacher by the Ministry of Education. We are grateful to Prof. Hu-Lai Wei, School of Basic Medical Sciences, Lanzhou University, China, for his assistance in the bioassay.

References

Adekenov, S. M., Kulyjasov, A. T., Raldugin, V. A., Bagryanskaya, I. Y., Gatilov, Y. V., & Shakirov, M. M. (1998). Ajanolide A, a new germacranolide from *Ajania fruticulosa*. *Russian Chemical Bulletin, 47*(1), 169–172.

Ahmed, A. A., Gáti, T., Hussein, T. A., Ali, A. T., Tzakou, O. A., Couladis, M. A., et al. (2003). Ligustolide A and B, two novel sesquiterpenes with rare skeletons and three 1,10-seco-guaianolide derivatives from *Achillea ligustica*. *Tetrahedron, 59*(21), 3729–3735.

Barla, A., Topçu, G., Öksüz, S., Tümen, G., & Kingston, D. (2007). Identification of cytotoxic sesquiterpenes from *Laurus nobilis* L.. *Food Chemistry, 104*(4), 1478–1484.

Belenovskaya, L. M., & Markova, L. P. (1979). Phenol compounds of *Ajania achilleoids*. *Khiiya Prirodnykh Soedinenii*(2), 232–233.

Birnecker, W., Wallnöfer, B., Hofer, O., & Greger, H. (1988). Relative and absolute configurations of two naturally occurring acetylenic spiroketal enol ether epoxides. *Tetrahedron, 44*(1), 267–276.

Bolzani, V. da S., Trevisan, L. M. V., & Young, M. C M. (1991). Caffeic acid esters and triterpenes of *Alibertia macrophylla*. *Phytochemistry, 30*(6), 2089–2091.

Chumbalov, T. K., Glyzin, V. I., & Zhubaeva, R. A. (1974). Flavonoids of *Ajania fastigiata*. *Khimiya Prirodnykh Soedinenii*(6), 791–792.

Cui, C. B., Yezuka, Y., Kikuchi, K., Nakano, H., Tamaoki, T., & Park, J. H. (1990). Constituents of a fern, *Davallia mariesii* Moore. I. Isolation and structures of davallialactone and a new flavanone glucuronide. *Chemical and Pharmaceutical Bulletin, 38*(12), 3218–3225.

De Rosa, S., Mitova, M., Handjieva, N., & Calis, I. (2002). Coumarin glucosides from *Cruciata taurica*. *Phytochemistry, 59*(4), 447–450.

Debenedetti, S. L., Nadinic, E. L., Coussio, J. D., De Kimpe, N., & Boeykens, M. (1998). Two 6,7-dioxygenated coumarins from *Pterocaulon virgatum*. *Phytochemistry, 48*(4), 707–710.

Editorial Committee for Flora of the Chinese Academy of Science (1983). In Y. Ling, C. Shih (Eds.), *Flora of China*. Science Press, Beijing, 76(1), 105–125.

Gomes, C. A., da Cruz, T. G., Andrade, J. L., Milhazes, N., Borges, F., & Marques, M. P. M. (2003). Anticancer activity of phenolic acids of natural or synthetic origin: A structure-activity study. *Journal of Medicinal Chemistry, 46*(25), 5395–5401.

Gomes, M., Jr., & Antunes, O. A. C. (2001). Upjohn catalytic osmium tetroxide oxidation process: diastereoselective dihydroxylation of monoterpenes. *Catalysis Communications, 2*(6–7), 225–227.

Hussain, R. F., Nouri, A. M. E., & Oliver, R. T. D. (1993). A new approach for measurement of cytotoxicity using colorimetric assay. *Journal of Immunological Methods, 160*(1), 89–96.

Jequier, C., Nicollier, G., Tabacchi, R., & Garnero, J. (1980). Constituents of the essential oil of *Salvia stenophylla*. *Phytochemistry, 19*(3), 461–462.

Kuroyanagi, M., Shiotsu, M., Ebihara, T., Kawai, H., Ueno, A., & Fukushima, S. (1986). Chemical studies on *Viburnum awabuki* K. Koch. *Chemical and Pharmaceutical Bulletin, 34*(10), 4012–4017.

Kampa, M., Alexaki, V. I., Notes, G., Nifli, A. P., Nistikaki, A., Hatzoglou, A., et al. (2004). Antiproliferative and apoptotic effects of selective phenolic acids on T47D human breast cancer cells: Potential mechanism of action. *Breast Cancer Research, 6*, 63–74.

Li, H., Meng, J.-C., Cheng, C.-H.-K., Higa, T., Tanaka, J., & Tan, R.-X. (1999). New guaianolides and xanthine oxidase inhibitory flavonols from *Ajania fruticulosa*. *Journal of Natural Products, 62*(7), 1053–1055.

Marco, J. A. (1989). Sesquiterpene lactones from *Artemisia herba-alba* subsp. *Herba-alba*. *Phytochemistry, 28*(11), 3121–3126.

Matsuo, A., Uchio, Y., Nakayama, M., & Hayashi, S. (1974). Two new acetylenic compounds from *Chrysanthemum boreale*. *Tetrahedron Letters, 22*, 1885–1888.

Meng, J.-C., Hu, Y.-F., Chen, J.-H., & Tan, R.-X. (2001). Antifungal highly oxygenated guaianolides and other constituents from *Ajania fruticulosa*. *Phytochemistry, 58*(7), 1141–1145.

Re, R., Pellegrini, N., Proteggente, A., Pannala, A., Yang, M., & Rice-Evans, C. (1999). Antioxidant activity applying an improved ABTS radical cation decolorization assay. *Free Radical Biology and Medicine, 26*(9–10), 1231–1237.

Rumbero-Sanchez, A., & Vazquez, P. (1991). Quinic acid esters from *Isertia haenkana*. *Phytochemistry, 30*(1), 311–313.

Sarker, S. D., Gray, A. I., Waterman, P. G., & Armstrong, J. A. (1994). Coumarins from *Asterolasia trymalioides*. *Journal of Natural Products, 57*(11), 1549–1551.

Tan, R.-X., Jia, Z.-J., Zhao, Y., & Feng, S.-L. (1992). Sesquiterpenes and acetylenes from *Artemisia feddei*. *Phytochemistry, 31*(9), 3135–3138.

Tsukamoto, H., Hisada, S., Nishibe, S., Roux, D. G., & Rourke, J. P. (1984). Coumarins from *Olea africana* and *Olea capensis*. *Phytochemistry, 23*(3), 699–711.

Tsukamoto, H., Hisada, S., & Nishibe, S. (1985). Coumarins from bark of *Fraxinus japonica* and *F. mandshurica var. japonica*. *Chemical and Pharmaceutical Bulletin, 33*(9), 4069–4073.

Van den Berg, R., Haenen, G. R. M. M., Van den Berg, H., & Bast, A. (1999). Applicability of an improved Trolox equivalent antioxidant capacity (TEAC) assay for evaluation of antioxidant capacity measurements of mixtures. *Food Chemistry, 66*(4), 511–517.

Von Gadow, A., Joubert, E., & Hansmann, C. F. (1997). Comparison of the antioxidant activity of aspalathin with that of other plant phenols of rooibos tea (*Aspalathus linearis*), α-Tocopherol, BHT, and BHA. *Journal of Agricultural and Food Chemistry, 45*(3), 632–638.

Wu, Q.-X., Shi, Y-P., & Jia, Z.-J. (2006). Eudesmane sesquiterpenoids from the *Asteraceae* family. *Natural Product Reports, 23*(5), 699–734.

Yusupov, M. I., Kasimov, S. Z., & Abdullaev, N. D. (1982). Rupicolin B oxide and isochrysartemin B-new guaianolides from *Ajania fastigiata*. *Khimiya Prirodnykh Soedinenii*(2), 260–261.

Zdero, C., Bohlmann, F., & Huneck, S. (1990). Guaianolides and glaucolides from *Ajania achilleoides*. *Phytochemistry, 29*(2), 1585–1588.

Zhang, L.-X., He, Z.-W., & Zhu, Y. (2006). The lipophilic constituents from *Ajania prewalskii*. *Journal of Lanzhou University (Natural Sciences), 42*(6), 1–4.

Food Chemistry 118 (2010) 239–244

Contents lists available at ScienceDirect

Food Chemistry

journal homepage: www.elsevier.com/locate/foodchem

Suppressive effect of hot water extract of wasabi (*Wasabia japonica* Matsum.) leaves on the differentiation of 3T3-L1 preadipocytes

Tetsuro Ogawa [a,*], Hiromasa Tabata [a,b], Takuya Katsube [a], Yukari Ohta [a], Yukikazu Yamasaki [a], Masayuki Yamasaki [c], Kuninori Shiwaku [c]

[a] *Shimane Institute for Industrial Technology, 1 Hokuryo-cho, Matsue City, Shimane 690-0816, Japan*
[b] *Applied Molecular Bioscience, Graduate School of Medicine, Yamaguchi University, 1677-1, Yoshida, Yamaguchi City, Yamaguchi 753-8515, Japan*
[c] *Department of Environmental and Preventive Medicine, Shimane University School of Medicine, 89-1 Enya-cho, Izumo City, Shimane 693-8501, Japan*

ARTICLE INFO

Article history:
Received 19 November 2008
Received in revised form 30 March 2009
Accepted 28 April 2009

Keywords:
Wasabi
3T3-L1 cell
Adipocyte
Differentiation
PPARγ
C/EBPα

ABSTRACT

This study investigated the effect of hot water extract of wasabi (*Wasabia japonica* Matsum.) leaves (WLE), without its specific pungent constituents, such as allyl isothiocyanate, on the differentiation of 3T3-L1 preadipocytes. WLE suppressed the increase in glycerol-3-phosphate dehydrogenase (GPDH) activity and triglyceride (TG) accumulation, markers of adipogenesis, in a dose-dependent manner. Quantitative real time RT-PCR results showed that WLE significantly reduced the mRNA expression levels of peroxisome proliferator-activated receptor (PPAR) γ and CCAAT/enhancer-binding protein (C/EBP) α, both key adipogenic transcription factors, as subsequently were the mRNA expression levels of their target genes, such as adipocyte fatty acid binding protein 2 (aP2). Western blot analysis results showed that the protein expression levels of both PPARγ and C/EBPα were also inhibited by WLE. Thus, WLE suppressed the differentiation of 3T3-L1 preadipocytes, and the suppressive effect was mediated, in part, through the altered regulation of PPARγ, C/EBPα, and other specific genes, such as aP2. These results suggest that WLE may prevent obesity and insulin resistance by inhibiting the differentiation of preadipocytes.

1. Introduction

In humans, obesity has become a serious medical problem in developed countries as it is intimately implicated in metabolic syndrome and type 2 diabetes, which ultimately lead to atherosclerosis (Kopelman, 2000; Zimmet, Magliano, Matsuzawa, Alberti, & Shaw, 2005). Therefore, the prevention of obesity should naturally decrease the risk for developing these diseases. Obesity results from an imbalance between energy intake and expenditure, and is mainly characterized at the cell biological levels by an increase in the size of adipocytes differentiated from preadipocytes, through the conversion of extra energy to lipids and pooling in adipose tissues. In trials of obesity prevention, researchers have investigated whether some food components exhibit an ability to suppress intracellular lipid accumulation. For example, tea catechin has been reported to be effective in the inhibition of adipogenesis in 3T3-L1 cells (Furuyashiki et al., 2004), and *in vivo* studies have shown that oral administration of green tea decreases the weight of adipose tissue in rats and mice (Han, Takaku, Li, Kimura, & Okuda, 1999; Sayama, Lin, Zheng, & Oguni, 2000; Sayama, Ozeki, Taguchi, & Oguni, 1996). Also, the same suppressive effects have been demonstrated with mioga extract (*Zingiber mioga* Rosc.) (Iwashita, Yamaki & Tsushida, 2001), red yeast rice extract (Jeon et al., 2004), flavonoids (Harmon & Harp, 2001; Iwashita, Yamaki & Tsushida, 2001), and mushroom extracts (Ohtsuru, Horio, & Masui, 2000) on 3T3-L1 or C3H10T1/2 B_2C_1 adipocyte differentiation.

Wasabi (*Wasabia japonica* Matsum.) is a native Japanese plant and was used as a medicinal herb in ancient times. In most parts, wasabi is used as a spice or as pickles as it contains strong pungent constituents, including isothiocyanates such as allyl isothiocyanate. In previous studies, isothiocyanates have been reported to have various physiological properties, including antimicrobial activity (Isshiki, Tokuoka, Mori, & Chiba, 1992), antioxidative activity (Fukuchi et al., 2004), anti-platelet aggregative activity (Kumagai et al., 1994), and anti-carcinogenic activity (Fuke, Haga, Ono, Nomura, & Ryoyama, 1997). However, there have been few studies of the functional properties of other components, particularly in summer leaves, which are too late of stage, and have little pungency (Mochida & Ogawa, 2008).

To develop an effective use for summer leaves, which are discarded as an agricultural waste, we investigated the possible

* Corresponding author. Present address: Shimane Agricultural Technology Center, 388-3 Shimoko-cho, Hamada City, Shimane 697-0006, Japan. Tel.: +81 855 28 1881; fax: +81 855 28 1719.
E-mail address: ogawa-tetsuro@pref.shimane.lg.jp (T. Ogawa).

0308-8146/$ - see front matter © 2009 Elsevier Ltd. All rights reserved.
doi:10.1016/j.foodchem.2009.04.113

existence of any anti-obesity function of wasabi leaves, *i.e.* the effect of their hot water extract (WLE), without its specific pungent constituents, such as allyl isothiocyanate, on the differentiation of 3T3-L1 preadipocytes, measuring glycerol-3-phosphate dehydrogenase (GPDH) activity and triglyceride (TG) content in 3T3-L1 cells as markers of adipogenesis. To determine whether WLE affected the alteration in the differentiation programme, we also investigated the expression of PPARγ and C/EBPα, both of which act as central regulators of adipocyte differentiation, and their target genes, such as aP2.

2. Materials and methods

2.1. Reagents

Dulbecco's Modified Eagle's Medium (DMEM) was purchased from Invitrogen (Carlsbad, CA). Fetal bovine serum (FBS) was obtained from AGC Techno Grass Co. Ltd. (Chiba, Japan). Dexamethazone (DEX), gentamicin sulfate and insulin were purchased from Sigma–Aldrich Co. (St. Louis, MO). 3-Isobuthyl-1-methylxanthine (IBMX), (−)-epigallocatechin (EGC) and allyl isothiocyanate (AIT) were purchased from Wako Pure Chemical Industries, Ltd. (Osaka, Japan). ISOGEN, for total RNA isolation from cells, was purchased from Nippon Gene (Tokyo, Japan). ReverTra Ace -α-, for cDNA synthesis, was purchased from TOYOBO Co., Ltd. (Osaka, Japan). The PCR reagents and the oligonucleotide primers of mouse (Table 1) were obtained from Takara Bio Inc. (Shiga, Japan). Rabbit polyclonal antibodies against PPARγ and C/EBPα were purchased from Upstate (Lake Placid, NY) and Santa Cruz Biotechnology (Santa Cruz, CA), respectively. As secondary antibodies, horseradish peroxidase-conjugated goat anti-rabbit IgG, and chemiluminescent substrate (SuperSignal West Femto Maximum Sensitivity Substrate), to detect immunoreactive band, were obtained from Thermo Fisher Scientific Inc. (Rockford, IL). A polyvinylidene fluoride (PVDF) membrane (Immun-Blot PVDF Membrane) was purchased from Bio-Rad Laboratories (Hercules, CA). All other chemicals used were of analytical grade.

2.2. Preparations of wasabi extract

Wasabi (*W. japonica* Matsum.) leaves were harvested in Shimane Prefecture, Japan, in July, 2004, and pooled at −50 °C until used for experiments. After lyophilisation in a vacuum at room temperature for 3 days and milling with a vibrating sample mill TI-100 (Heiko Seisakusho Ltd., Tokyo, Japan), the samples were ready for experiment. One gramme of lyophilized sample of wasabi leaves in 10 ml of distilled water was boiled for 10 min in a hot water bath, and then centrifuged at 12,000*g* for 10 min at 4 °C; the supernatants were then filtered through a 0.45 μm membrane filter (Adovantec Toyo Kaisha Ltd., Tokyo, Japan). The solid contents of the extract were calculated by evaporating the sample in a vacuum and subsequently measuring the dry weight. Wasabi rhizomes and stalks were also used in this study. To examine the differences of suppressive effects of WLE, from samples of different harvesting periods, on adipocyte differentiation, wasabi leaves harvested from July, 2004, to June, 2005, were also used. The extract from these leaves, as well as from the rhizomes and stalks, was prepared as described above.

2.3. Cell culture and treatment

Murine 3T3-L1 cells (JCRB 9014) were obtained from the Health Science Research Resources Bank (Osaka, Japan). The cells were grown in maintenance medium (MM, DMEM supplemented with 10% FBS and 50 μg/ml of gentamicin) at 37 °C in 5% CO_2. The medium was changed every two or three days. For adipocyte differentiation, the cells were cultured in 6-well plates to full confluence for 2 days and were then treated with differentiation medium containing 0.25 μM DEX, 0.5 mM IBMX, and 1.5 μg/ml of insulin (DMI). After 2 days of induction (day 2), the medium was changed to MM containing 1.5 μg/ml of insulin, and WLE, at final concentrations of 333, 667 or 1333 μg/ml, was added every 2 days. In the case of examining the differences of suppressive effects on adipocyte differentiation of WLE from samples of the various harvesting periods, 15 μl of WLEs were added to 1.5 ml of MM containing 1.5 μg/ml of insulin. After 6 days of incubation from the initiation of differentiation, the cells were harvested. For quantitative real time RT-PCR and Western blot analysis, the cells were treated with WLE, or EGC as positive control, at the same time as DMI induction of differentiation (day 0), and then incubated in the same manner as described above. All samples were prepared in triple cell culture wells.

2.4. Measurement of GPDH activity and quantification of TG accumulation

The cells were washed twice with ice-cold 0.9% saline solution, collected in 1 ml of cold sonication buffer (25 mM Tris buffer

Table 1
PCR primers used in this study.

Gene name[a]	Sequences[b]	GenBank accession number
PPARγ	F: TGTCGGTTTCAGAAGTGCCTTG R: TTCAGCTGGTCGATATCACTGGAG	NM_011146
C/EBPα	F: TGCGCAAGAGCCGAGATAAAG R: TCACGGCTCAGCTGTTCCAC	NM_007678
aP2	F: TGGGAACCTGGAAGCTTGTCTC R: GCTGATGATCATGTTGGGCTTG	NM_024406
GLUT4	F: ACGACGGACACTCCATCTGTTG R: GGAGACATAGCTCATGGCTGGAA	NM_009204
LPL	F: TCCGAGTGAAAGCCGGAGA R: TGGCATTTCACAAACACTGCTG	NM_008509
SCD1	F: TCTTGTCCCTATAGCCCAATCCAG R: AGCTCAGAGCGCGTGTTCAA	NM_009127
CD36	F: GATGGCCTTACTTGGGATTGGA R: GGCTTTACCAAAGATGTAGCCAGTG	N M_007643
GAPDH	F: AAATGGTGAAGGTCGGTGTG R: TGAAGGGGTCGTTGATGG	NM_001001303

[a] PPARγ, peroxisome proliferator-activated receptorγ; C/EBPα, CCAAT/enhancer-binding proteinα; aP2, adipocyte fatty acid binding protein 2; GLUT4, glucose transporter 4; LPL, lipoprotein lipase; SCD1, stearoyl coenzyme A desaturase 1; GAPDH, glyceraldehyde-3-phosphate dehydrogenase.
[b] F: forward, R: reverse.

containing 1 mM EDTA, pH 7.5) using a cell scraper, and then sonicated. Twenty microlitres of suspension were used to measure TG concentrations, using a commercial kit (Triglyceride E-test Wako, Wako Pure Chemical Industries, Ltd., Osaka, Japan) according to manufacturer's instructions. The remaining portion of the suspension was centrifuged at 8000*g* for 10 min at 4 °C, and the supernatant was assayed for GPDH activity. This was done by measuring the decrease in the absorbance of NADH at 340 nm at 37 °C. Protein concentrations were determined using Protein Quantification Kit-Rapid (Dojindo Molecular technologies, Inc., Rockville, MD). The GPDH activity and the TG concentration per mg of protein in the cells were calculated and expressed as ratios (%) of the control value.

2.5. Analysis of allyl isothiocyanate (AIT) content in hot water extract of wasabi

The AIT contents of the test samples were measured by high-performance liquid chromatography (L-7100, Hitachi, Ltd., Tokyo, Japan), using the following analytical conditions: column, TSKGEL ODS-80TS (φ4.6 × 250 mm); mobile phase, acetonitrile–water = 50/50; flow rate, 1.0 ml/min; detection, UV 240 nm. On the HPLC analysis, limit of detection (LOD) and limit of quantification (LOQ) of AIT were 0.01 mM and 0.02 mM, respectively.

2.6. Quantitative real time RT-PCR

Total RNA was isolated from the cells using ISOGEN, according to the manufacturer's instructions. One microgramme of total RNA was used for the single strand cDNA synthesis with a cDNA synthesis kit, ReverTra Ace -α-. Gene expression levels were analyzed by quantitative real time RT-PCR, using the ABI PRISM 7000 Sequence Detection System (Applied Biosystems, Foster City, CA). The cDNA was denatured at 95 °C for 10 s, followed by 40 cycles of PCR (95 °C, 5 s; 60 °C, 31 s). Results were obtained from at least three independent experiments. The mRNA levels of all genes were normalized, using GAPDH as an internal control.

2.7. Western blot analysis

The cells were washed twice with ice-cold PBS, scraped with RIPA buffer, and allowed to stand on ice for 1 h to permit lysis. After centrifugation at 18,000*g* for 20 min at 4 °C, protein content in the supernatant was determined, using a DC-protein assay kit (Bio-Rad Laboratories, Hercules, CA), and aliquots (20 μg) of protein were separated by SDS-polyacrylamide gel electrophoresis and transferred onto a PVDF membrane. The membrane was blocked with 0.3% (w/v) non-fat dried milk in TBST (25 mM Tris–HCl, pH 7.4, 150 mM NaCl, and 0.1% (v/v) Tween 20) for 1 h, and then incubated for 1 h with primary antibody in TBST containing 0.3% (w/v) non-fat dried milk. The blots were treated with horseradish peroxidase-conjugated secondary antibody in TBST containing 0.3% (w/v) non-fat dried milk for 1 h, and then reacted with a chemiluminescent substrate. An immune complex was detected using a multiimager (Bio-Rad SU-115, Bio-Rad Laboratories, Hercules, CA).

2.8. Statistical analysis

Statistical analysis of the data was done with SPSS statistical analysis software (Version 17.0J, SPSS Inc., Tokyo, Japan). One-way ANOVA was used to assess the differences between the individual groups, and *post hoc* analyses were performed by the Bonferroni test for two independent variables. Differences were considered significant at $p < 0.025$. The significance of differences between two groups (samples and control) were analyzed by the Student's *t*-test, and were determined at $p < 0.05$.

3. Results

3.1. Suppressive effects of wasabi extract on GPDH activity and TG accumulation

The extracts from all parts of the wasabi plant suppressed the increase in GPDH activity and TG accumulation in a dose-dependent manner (Fig. 1). Particularly, the cells treated with 667 μg/ml of extract from leaves and stalks showed suppression of increase in GPDH activity up to 36% and 25%, respectively, in comparison with control cells. However, in the case of treatment with 1333 μg/ml of extract from them, the cells were damaged (#), so GPDH activity and TG accumulation could not be evaluated clearly. From the results obtained above, the adipocyte differentiation-inhibitory activities of the extracts of leaves and stalks were higher than those of rhizomes. Table 2 shows AIT content of the extracts. The extracts of all wasabi parts tested had little or no AIT, so we surmised that the results obtained here were not because of isothiocyanates, such as AIT. The differences in suppressive effects on adipocyte differentiation of WLE, from samples of the various harvesting periods were also examined (Fig. 2). The effects of WLE from samples harvested in winter were greater, on the whole, but the summer samples (July/2004) also showed significant effects. Hence we focused on WLE in this study, which also had inhibitory activity on adipogenesis.

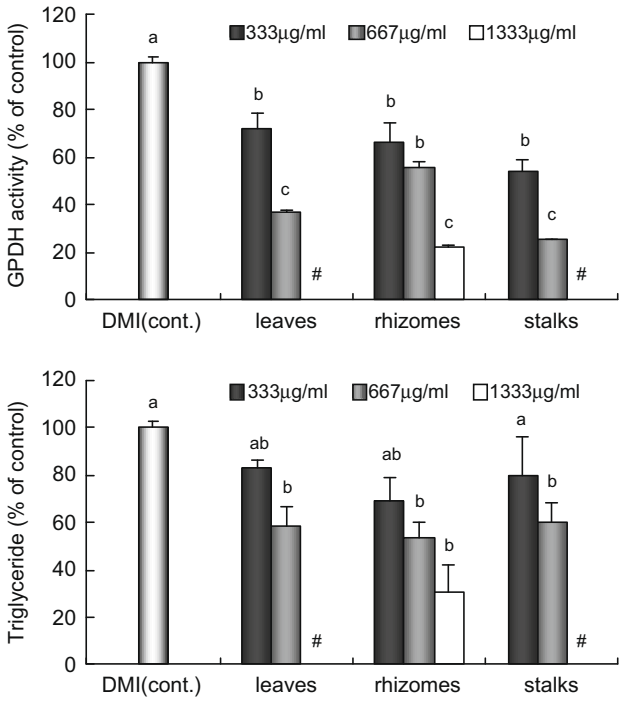

Fig. 1. Hot water extracts of wasabi leaves, rhizomes and stalks suppress glycerol-3-phosphate dehydrogenase (GPDH) activity and triglyceride accumulation in 3T3-L1 cells in a dose-dependent manner. Samples are used at indicated concentrations. Cells were treated with samples at 2 days after DMI induction of differentiation (day 2). All values are represented as a percentage of the results from control which is taken as 100%, and are expressed as means ± SE of triplicate experiments. Different letters between samples and control, or among samples in each part, indicate significant differences by the Student's *t*-test ($p < 0.05$) and the Bonferroni test ($p < 0.025$), respectively. #: GPDH activity and TG accumulation of the cells treated with 1333 μg/ml of extract from both leaves and stalks were not evaluated clearly because these treatments damaged the cells. DMI: a mixture of dexamethazone, 3-isobuthyl-1-methylxanthine and insulin.

Table 2
AIT content in hot water extract of the wasabi parts.

Parts	AIT contents (mM)
Leaves	ND[a]
Rhizomes	0.03
Stalks	0.04

The sample extracts were obtained as follows: 1 g of lyophilized samples in 10 ml of distilled water was boiled and centrifuged, and then the supernatants were filtered. AIT contents in the extracts were analyzed by HPLC. LOD: 0.01 mM, LOQ: 0.02 mM.
[a] Not detected.

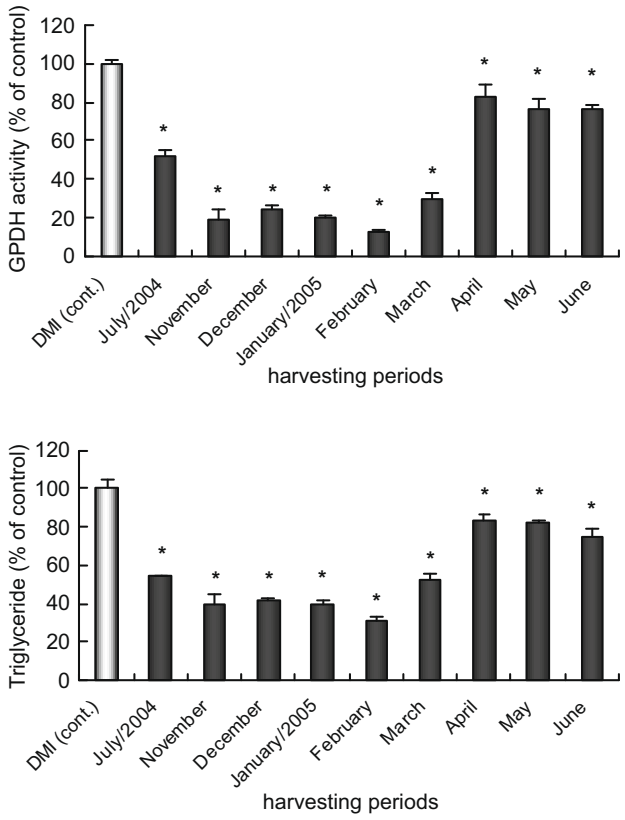

Fig. 2. Suppressive effects of WLE from samples harvested in different periods on GPDH activity and triglyceride accumulation in 3T3-L1 cells. Wasabi leaf samples were harvested at indicated periods and used. The sample extracts were obtained as follows: 1 g of lyophilized samples in 10 ml of distilled water was boiled and centrifuged, and then the supernatants were filtered. The cells were treated with 15 μl of sample extracts at 2 days after DMI induction of differentiation (day 2). All values are represented as a percentage of the results from control, which is taken as 100%, and are expressed as means ± SE of triplicate experiments. Asterisk indicates significant differences compared to the control ($*p < 0.05$). DMI: a mixture of dexamethazone, 3-isobuthyl-1-methylxanthine and insulin.

3.2. Suppressive effect of WLE on mRNA expression of adipogenic transcriptional factors

Adipocyte differentiation involves a series of programmed changes in gene expression. To determine whether the suppressed increase in GPDH activity and reduced TG accretion resulted from a WLE-mediated alteration in the differentiation programme, the expression of a number of adipogenic genes was investigated by quantitative real time RT-PCR. In the cells treated with WLE, as in those treated with EGC, we noted a significant decrease in the mRNA expression levels of PPARγ and C/EBPα, both key transcriptional factors, and followed by reduced mRNA expression levels of their target genes, such as aP2, in a dose-dependent manner (Fig. 3). For example, the mRNA expression level of PPARγ in cells treated with 333 or 667 μg/ml of WLE decreased to 76% and 40%, respectively, of that of the control cells.

3.3. Suppressive effect of WLE on protein expression of PPARγ and C/EBPα

During DMI induction of 3T3-L1 adipocyte differentiation, PPARγ and C/EBPs are activated by DMI (Rangwala & Lazar, 2000; Rosen & Spiegelman, 2000). To investigate the inhibitory mechanism of WLE, protein expression levels of PPARγ and C/EBPα were examined. We found that the WLE-associated attenuation of PPARγ and C/EBPα gene expressions was accompanied by a decrease in the corresponding proteins. For example, at 667 μg/ml of WLE, protein expression levels of PPARγ and C/EBPα decreased to 43% and 30%, respectively, of the control levels (Fig. 4).

4. Discussion

In the present study, we demonstrated that hot water extracts of several parts of the wasabi plant, suppressed the adipocyte differentiation in 3T3-L1 cells, while preventing increases in GPDH activity and TG accumulation, markers of adipogenesis, in a dose-dependent manner (Fig. 1). Iwashita et al. (2001) reported that only mioga (*Z. mioga* Rosc.) extract, among 15 edible-plant PBS-soluble extracts examined, proved effective in inhibiting 3T3-L1 adipocyte differentiation without cell damage, and that cells treated with 200 or 500 μg/ml of extract suppressed increases in GPDH activity to about 60% and 20%, respectively, of that of the control cells. Our results, where cells treated with 667 μg/ml of WLE suppressed increase in activity to about 40% compared to control cells, showed nearly the same as or slightly less than mioga extract.

At the molecular level, cells treated with WLE reduced mRNA and protein expression levels of PPARγ and C/EBPα, both of which act as key adipogenic transcription factors (Figs. 3 and 4). During subsequent terminal differentiations of preadipocytes into mature adipocytes with mitotic clonal expansion in adipose tissues, the adipocyte differentiation programme is regulated by transcriptional activators, such as C/EBPα, PPARγ2, fatty acid-activated receptor (FAAR), and transcriptional receptors, such as preadipocyte repressor element binding protein (PRE) and C/EBP undifferentiated protein (CUP) (MacDougald & Lane, 1995). For example, under induced preadipocyte differentiation into adipocyte in the presence of IBMX in 3T3-L1 cell cultures, C/EBPβ, belonging to a basic leucine zipper family of transcriptional factors, is induced temporarily at the early stage of differentiation (Ko et al., 2005), which, in turn, C/EBPβ induces downstream transcriptional factors, PPARγ and C/EBPα (Wu, Bucher, & Farmer, 1996), followed by the expression of genes, including ap2, GLUT4, LPL, SCD1 and CD36, which mediate fatty acid or glucose uptake into adipocyte, triglyceride hydrolysis and lipogenesis (Abumrad, El-Maghrabi, Amri, Lopez, & Grimaldi, 1993; Brun, Kim, Hu, Altiok, & Spiegelman, 1996; Long & Pekala, 1996; Miller & Ntambi, 1996; Tontonoz, Hu, Graves, Budavari, & Spiegelman, 1994). Thereafter, adipocytes incorporate glucose and free fatty acids to synthesize and accumulate lipids as energy, resulting in an increase in cell size. Huang et al. (2006) reported that berberine (BBR), a compound purified from *Cortidis rhizoma*, inhibited differentiation of 3T3-L1 adipocytes through PPAR pathways; not only were the mRNA and protein expression levels of PPARγ and C/EBPα directly affected, but levels of C/EBPβ were inhibited by BBR, resulting in the down-regulation of the target genes, such as CD36. In our study, in which the treatment with WLE suppressed adipocyte differentiation in 3T3-L1 cells, we supposed that PPARγ and C/EBPα gene expressions might be down-regulated directly, as with BBR, by reason that their expressions were also inhibited after treatment with WLE at 2 days after DMI induction of 3T3-L1 cells (day 2, data not shown). However, it re-

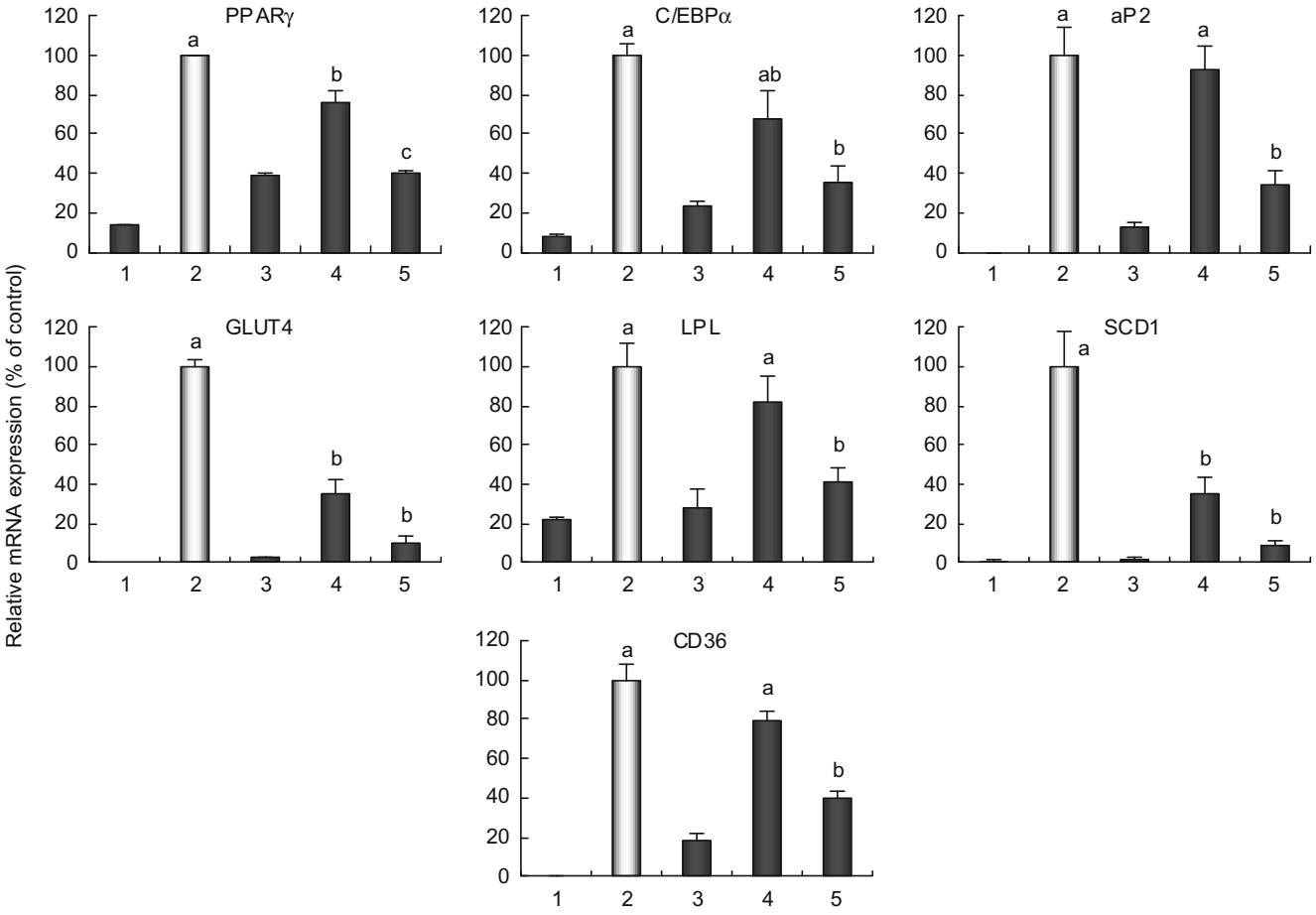

Fig. 3. WLE suppresses mRNA expressions of PPARγ, C/EBPα and their target genes in 3T3-L1 cells. The cells were treated with WLE at the same time as DMI induction of differentiation (day 0). Quantitative real time RT-PCR results are shown for (1) undifferentiated cells, (2) control cells differentiated by DMI, and cells treated with (3) 30 μM of EGC, (4) 333 μg/ml of WLE, and (5) 667 μg/ml of WLE, respectively. The mRNAs of GAPDH in the same samples were used as an internal control. All values are represented as a percentage of the results from control which is taken as 100%, and are expressed as means ± SE of triplicate experiments. Different letters among WLE samples and control indicate significant differences ($p < 0.025$). DMI: a mixture of dexamethazone, 3-isobuthyl-1-methylxanthine and insulin. EGC: (−)-epigallocatechin (positive control).

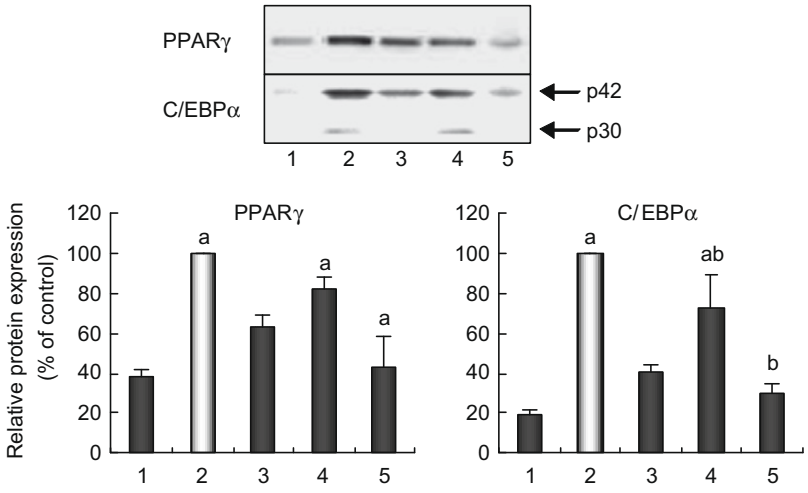

Fig. 4. WLE suppresses protein expressions of PPARγ and C/EBPα in 3T3-L1 cells. The cells were treated with WLE at the same time as DMI induction of differentiation (day 0). A set of representative Western blots for PPARγ and C/EBPα is shown in the upper panel. The quantitative changes of the target proteins are determined by densitometry, as shown in the lower panel. Lanes 1–5 are samples from (1) undifferentiated cells, (2) control cells differentiated by DMI, and cells treated with (3) 30 μM of EGC, (4) 333 μg/ml of WLE and (5) 667 μg/ml of WLE, respectively. All values are represented as percentages of the results from the control, which is taken as 100%, and are expressed as means ± SE of triplicate experiments. Different letters among WLE samples and control indicate significant differences ($p < 0.025$). DMI: a mixture of dexamethazone, 3-isobuthyl-1-methylxanthine and insulin. EGC: (−)-epigallocatechin (positive control).

mains unclear whether WLE affects upstream transcriptional factors, such as C/EBPβ.

In conclusion, we have demonstrated, in the present study, that WLE suppressed the differentiation of 3T3-L1 preadipocytes by

inhibiting increases in GPDH activity and TG accumulation, and that the suppressing effects were mediated, in part, through the altered regulation of adipogenic transcriptional factors, PPARγ and C/EBPα, and other specific genes, such as aP2. These results, combined with the findings that aP2 is central to the pathway that links obesity to insulin resistance (Hotamisligil et al., 1996), suggest that WLE may prevent obesity and insulin resistance by inhibiting the differentiation of preadipocytes.

References

Abumrad, N. A., El-Maghrabi, M. R., Amri, E.-Z., Lopez, E., & Grimaldi, P. A. (1993). Cloning of a rat adipocyte membrane protein implicated in binding or transport of long-chain fatty acids that is induced during preadipocyte differentiation. *Journal of Biological Chemistry, 268*, 17665–17668.

Brun, R. P., Kim, J. B., Hu, E., Altiok, S., & Spiegelman, B. M. (1996). Adipocyte differentiation: a transcriptional regulatory cascade. *Current Opinion in Cell Biology, 8*, 826–832.

Fuke, Y., Haga, Y., Ono, H., Nomura, T., & Ryoyama, K. (1997). Anti-carcinogenic activity of 6-methylsulfinylhexyl isothiocyanate, an active anti-proliferative principal of wasabi (*Eutrema wasabi* Maxim.). *Cytotechnology, 25*, 197–203.

Fukuchi, Y., Kato, Y., Okunishi, I., Matsutani, Y., Osawa, T., & Naito, M. (2004). 6-Methylsulfinylhexyl isothiocyanate, an antioxidant derived from *Wasabia japonica* Matum., ameliorates diabetic nephropathy in type 2 diabetic mice. *Food Science and Technology Research, 10*, 290–295.

Furuyashiki, T., Nagayasu, H., Aoki, Y., Bessho, H., Hashimoto, T., Kanazawa, K., et al. (2004). Tea catechin suppresses adipocyte differentiation accompanied by down-regulation of PPARγ2 and C/EBPα in 3T3-L1 cells. *Bioscience, Biotechnology, and Biochemistry, 68*, 2353–2359.

Han, L.-K., Takaku, T., Li, J., Kimura, Y., & Okuda, H. (1999). Anti-obesity action of oolong tea. *International Journal of Obesity and Related Metabolic Disorders, 23*, 98–105.

Harmon, A. W., & Harp, J. B. (2001). Differential effects of flavonoids on 3T3-L1 adipogenesis and lipolysis. *American Journal of Physiology, Cell Physiology, 280*, 807–813.

Hotamisligil, G. S., Johnson, R. S., Distel, R. J., Ellis, R., Papaioannou, V. E., & Spiegelman, B. M. (1996). Uncoupling of obesity from insulin resistance through a targeted mutation in aP2, the adipocyte fatty acid binding protein. *Science, 274*, 1377–1379.

Huang, C., Zhang, Y., Gong, Z., Sheng, X., Li, Z., Zhang, W., et al. (2006). Berberine inhibits 3T3-L1 adipocyte differentiation through the PPARγ pathway. *Biochemical and Biophysical Research Communications, 348*, 571–578.

Isshiki, K., Tokuoka, K., Mori, R., & Chiba, S. (1992). Preliminary examination of allyl isothiocyanate vapor for food preservation. *Bioscience, Biotechnology, and Biochemistry, 56*, 1476–1477.

Iwashita, K., Yamaki, K., & Tsushida, T. (2001a). Mioga (*Zingiber mioga* Rosc.) extract prevents 3T3-L1 differentiation into adipocytes and obesity in mice. *Food Science and Technology Research, 7*, 164–170.

Iwashita, K., Yamaki, K., & Tsushida, T. (2001b). Effect of flavonoids on the differentiation of 3T3-L1 adipocytes. *Food Science and Technology Research, 7*, 154–160.

Jeon, T., Hwang, S. G., Hirai, S., Matsui, T., Yano, H., Kawada, T., et al. (2004). Red yeast rice extracts suppress adipogenesis by down-regulating adipogenic transcription factors and gene expression in 3T3-L1 cells. *Life Sciences, 75*, 3195–3203.

Ko, B. S., Choi, S. B., Park, S. K., Jang, J. S., Kim, Y. E., & Park, S. (2005). Insulin sensitizing and insulinotropic action of berberine from *Cortidis rhizoma*. *Biological and Pharmaceutical Bulletin, 28*, 1431–1437.

Kopelman, P. G. (2000). Obesity as a medical problem. *Nature, 404*, 635–643.

Kumagai, H., Kashima, N., Seki, T., Sakurai, H., Ishii, K., & Ariga, T. (1994). Analysis of volatile components in essential oil of upland Wasabi and their inhibitory aggregation. *Bioscience, Biotechnology, and Biochemistry, 58*, 2131–2135.

Long, S. D., & Pekala, P. H. (1996). Regulation of GLUT4 gene expression by arachidonic acid. Evidence for multiple pathways, one of which requires oxidation to prostaglandin E_2. *Journal of Biological Chemistry, 271*, 1138–1144.

MacDougald, O. A., & Lane, M. D. (1995). Transcriptional regulation of gene expression during adipocyte differentiation. *Annual Review of Biochemistry, 64*, 345–373.

Miller, C. W., & Ntambi, J. M. (1996). Peroxisome proliferators induce mouse liver stearoyl-CoA desaturase 1 gene expression. *Proceedings of the National Academy of Sciences of the United States of America, 93*, 9443–9448.

Mochida, K., & Ogawa, T. (2008). Anti-influenza virus activity of extract of Japanese wasabi leaves discarded in summer. *Journal of the Science of Food and Agriculture, 88*, 1704–1708.

Ohtsuru, M., Horio, H., & Masui, H. (2000). Screening of various mushrooms with inhibitory activity of adipocyte conversion. *Nippon Shokuhin Kagaku Kogaku Kaishi, 47*, 394–396.

Rangwala, S. M., & Lazar, M. A. (2000). Transcriptional control of adipogenesis. *Annual Review of Nutrition, 20*, 535–559.

Rosen, E. D., & Spiegelman, B. M. (2000). Molecular regulation of adipogenesis. *Annual Review of Cell and Developmental Biology, 16*, 145–171.

Sayama, K., Lin, S., Zheng, G., & Oguni, I. (2000). Effects of green tea on growth, food utilization and lipid metabolism in mice. *In Vivo, 14*, 481–484.

Sayama, K., Ozeki, K., Taguchi, M., & Oguni, I. (1996). Effects of green tea and tea catechins on the development of mammary gland. *Bioscience, Biotechnology, and Biochemistry, 60*, 169–170.

Tontonoz, P., Hu, E., Graves, R. A., Budavari, A. I., & Spiegelman, B. M. (1994). mPPAR gamma 2: tissue-specific regulator of an adipocyte enhancer. *Genes and Development, 8*, 1224–1234.

Wu, Z., Bucher, N. L., & Farmer, S. R. (1996). Induction of peroxisome proliferators-activated receptor gamma during the conversion of 3T3 fibroblasts into adipocytes is mediated by C/EBPbeta, C/EBPdelta, and glucocorticoids. *Molecular and Cellular Biology, 16*, 4128–4136.

Zimmet, P., Magliano, D., Matsuzawa, Y., Alberti, G., & Shaw, J. (2005). The metabolic syndrome: a global public health problem and a new definition. *Journal of Atherosclerosis and Thrombosis., 12*, 295–300.

Food Chemistry 118 (2010) 245–250

Contents lists available at ScienceDirect

Food Chemistry

journal homepage: www.elsevier.com/locate/foodchem

Effects of addition of anka rice on the qualities of low-nitrite Chinese sausages

Deng-Cheng Liu, Shang-Wei Wu, Fa-Jui Tan *

Department of Animal Science, National Chung Hsing University, 250 Kuo Kuang Rd., Taichung 402, Taiwan

ARTICLE INFO

Article history:
Received 10 December 2008
Received in revised form 18 March 2009
Accepted 27 April 2009

Keywords:
Monascus
Anka rice
Low-nitrite
Chinese sausage

ABSTRACT

Anka rice (AR), previously inoculated with *Monascus purpureus*, was added during manufacturing of low-nitrite Chinese sausages. Chemical compositions and water activities of sausages were not affected. "*L*", "*a*", and "*b*" values of sausages with less nitrite (25 ppm) and 0.5% AR added were not significantly different from those with more nitrite (100 ppm) added. Colours of the sausages without AR were light red whereas those with AR added were darker red. Addition of AR did not inhibit lipid oxidation. Higher VBN (volatile basic nitrogen) values of the samples with AR added were observed. With addition of AR, the nitrite degrading rate was retarded. Microbial counts of the sausages with AR added were significantly higher than those of the controls (100 ppm nitrite). The low-nitrite Chinese sausage with addition up to 1.5% AR was acceptable when stored at 4 °C for 28 days.

1. Introduction

Monascus spp. which is a food fungus, has been widely applied for making wines and other fermented food products, especially in Taiwan, China, and many Asian areas for many years (Tseng, 1999). Many metabolic derivatives, such as ethanol, monascus pigments (red in colour), γ-aminobutyric, monacolins K, can be produced by *Monascus* spp. (Ma et al., 2000). In addition, it has also been reported in many ancient Chinese scripts to have some beneficial effects, such as improvement of food digestion and blood circulation (Ma et al., 2000). In Taiwan, as a natural food additive source, *Monascus* spp. has been granted edible natural colourant status and allowed in foods (DOH, 2008). Anka rice, also known as *Monascus*-fermented rice, monascal rice, and red koji, is a fermented food made by cultivating *Monascus* spp. on cooked rice, and has been widely used as a colouring and flavouring agent to make many Chinese roasted products (Tseng, Chen, & Lin, 2000).

Nitrite salts, mainly sodium nitrite and potassium nitrite, have been used in the preparation of cured meats for years and for many purposes. First, nitrite can be used as a potent anti-bacterial agent to provide protection against food microorganisms (Gill & Holley, 2003), as well as a potent antioxidant. In addition, nitrite is reduced to nitric oxide, which then interacts with myoglobin to produce nitric oxide myoglobin, which contributes to the characteristic pink cured meat colour (Honikel, 2008). Nitrite can also be applied to preserve desirable meaty flavour (Hedrick, Aberle, Forrest, Judge, & Merkel, 1994). Even though nitrite is known to participate in numerous reactions in cured meats, with many desirable functions, as mentioned previously, concern regarding the levels of nitrite used in meat curing has arisen because of the possibility of nitrosamine, which is a known carcinogen, being formed in cured meat (Osterlie & Lerfall, 2005). Therefore, many studies have been conducted to attempt to reduce the nitrite contents in cured meat products. Walsh et al. (1998) indicated that a combination of dietary vitamin E supplementation at a level of 500 mg α-tocopheryl kg feed^{-1} with nitrite at the level of 50 mg nitrite kg meat^{-1} could be used to produce cured pork products similar to those obtained from meat containing high nitrite levels (100 mg nitrite kg meat^{-1}). Osterlie and Lerfall (2005) recommended mixing minced meat with a lycopene-containing product that could be used to reduce nitrite levels. Jiménez-Colmenero, Carballo, and Cofrades (2001) pointed out that combining several compounds, which together have a cumulative effect on colour, flavour, antioxidant, and antimicrobial activity, could be considered when attempting to reduce the addition of nitrite in meat products. Functionality, such as colour enhancement and antioxidative properties, makes anka rice a potent candidate to be applied in low-nitrite products. Fink-Gremmels, Dresel, and Leistner (1992) indicated that *Monascus* extracts might be used as an alternative to nitrite in some meat products. Therefore, the purposes of this study were to compare the effects of anka rice on the qualities of low-nitrite Chinese sausages during refrigerated storage and to identify the volatile compounds from the anka rice and the sausages with anka rice added.

2. Materials and methods

2.1. Anka rice preparation

Monascus purpureus (CCRC No. 31499) was obtained from the Culture Collection and Research Center, Food Industry Research

* Corresponding author. Tel.: +886 4 22870613x246.
E-mail address: tanfj@dragon.nchu.edu.tw (F.-J. Tan).

0308-8146/$ - see front matter © 2009 Elsevier Ltd. All rights reserved.
doi:10.1016/j.foodchem.2009.04.114

and Development Institute, Hsinchu, Taiwan. The methods described by Tseng (1999) were utilised. *M. purpureus* was inoculated into a yeast glucose broth medium which contained 10% glucose and 0.8% yeast extract; the pH was adjusted to 5.5 and it was incubated at 35 °C with 120 rpm shaking (Yih Der LM-570R, shaker incubator, Taiwan) for 7 days. Then, the inocula were homogenised with a sterile blender (Waring Commercial, New Hartfor, Connecticut, USA) at high speed for 2 min. The microbial suspension was prepared accordingly. After being rinsed and soaked in water for 12 h, indica rice was shaken to remove excess water, autoclaved for 30 min, and then removed for cooling. The microbial suspension prepared previously [5% (w/w), with the yeast glucose broth as 100%], yeast glucose broth and pre-autoclaved rice (same weight as the yeast glucose broth) were mixed thoroughly, and then cultivated at 30 °C for 20 days. After drying in an oven (Model RHD, S-Tai Co., Kaohsiung, Taiwan) at 45 °C for 24 h, and cooling at room temperature, the mixture was ground with a grinder (Type 780A, Krups, Ireland), and then stored at −20 °C.

2.2. Sausage preparation

Frozen pork hams, frozen pork backfat, and salted natural pork casing were purchased from a local market in Nantou, Taiwan. Lean tissue and pork backfat were ground through a 10 mm plate. Ground pork was mixed thoroughly with non-meat ingredients, including 10% sugar, 2% rice wine, 1.6% salt, 0.5% monosodium glutamate, 0.2% polyphosphate, 0.08% onion powder, 0.05% white pepper powder, 0.05% five-spice powder, 0.02% clove powder, 0.02% sodium erythorbate, and sodium nitrite (25 ppm for treatments A, R1, R2, and R3 samples, and 100 ppm for treatment C samples), and then cured under refrigeration at 7 °C for 3 days. In addition, 0.5%, 1%, and 1.5% anka rice which were previously inoculated with *M. purpureus* were also added to the formula for the sample treatments R1, R2, and R3, respectively. Then, ground pork backfat (25%) was mixed with the meat mixture, and stuffed (Stuffer, Dick D-73779, Germany) into natural casings, which were previously soaked in water. Raw sausages were dried in a preheated oven (Model RHD, S-Tai Co., Kaohsiung, Taiwan) at 50 °C for 3 h. Following drying, sausages were cooled, vacuum-packaged (HAS02G, Europack, Holland) and stored at 4 °C.

2.3. Proximate composition, water activity and pH

Samples were first ground with a grinder (Type 780A, Krups, Ireland). Proximate compositions of samples, including moisture, crude fat, crude protein, and ash contents, were measured according to AOAC (1990) methods. Crude fat was measured using a fat extractor (Sotec System HT 1043 Extraction Unit, Tecator Co., Sweden) with ethyl ether as a solvent and extracted for 16 h. Crude protein was measured by the Kjeldahl method, using a digester (Model 2006, Foss tecator, Sweden) and a distillation unit (Model 2100, Foss tecator, Sweden). Approximately 2 g of ground samples were put into a holding cup, and measured with a water activity analyser (Aqualab-CX2, Decagon Devices Inc., USA). Eleven gramme samples were blended with 99 ml distilled water in a polyethylene bag for 1 min using a stomacher (Stomacher 400, Seward Ltd., England) at high speed, and then the pH of the mixture was measured using a pH meter (Micro-computer pH meter, Model 6210, Taiwan).

2.4. Instrumental colour measurement

Ground samples were placed in a measuring container, and then the "*L*" (lightness), "*a*" (redness), and "*b*" (yellowness) values of samples were measured with a colour meter (Spectrophotometer, Model TC1, Tokyo Co., Ltd. Japan). A standard plate with "*Y*" = 86.53, "*X*" = 82.45, and "*Z*" = 91.28 was used as a reference.

2.5. Thiobarbituric acid (TBARS) values and volatile basic nitrogen (VBN)

TBARS values of the samples were determined according the methods described by Faustman, Specht, Malkus, and Kinsman (1992). TBARS value was expressed as mg malonaldehyde/kg meat. Volatile basic nitrogen was determined according to CNS (1982) by the Conway micropipette diffusion method.

2.6. Nitrite residue

Nitrite residue was measured according to the methods of Lin (1984), briefly as follows: five grammes of ground sausage samples in a 250 ml flask were homogenised with 100 ml of 80 °C reverse osmosis water, using a homogenizer (Type PT 10/35, Brinkmann Instruments Inc., Westbury, NY, USA) for 60 s at 10,000 rpm. The homogenate was washed with reverse osmosis water to 150 ml totally, sealed with an aluminium foil cap, and heated for 30 min in an 80 °C shaking water bath (50 rpm). After adding 2 ml of saturated $HgCl_2$, cooling with ice water to room temperature, and filtering (Toyo No. 1) immediately, 10 ml of filtrate were transferred into a tube; 2 ml of Griess solution (a combination of sulfanilic acid solution and α-naphthlamine solution in a 1:1 ratio; 0.5 g sulfanilic acid was added to 150 ml of 15% acetic acid solution and 0.1 g α-naphthlamine was dissolved in 20 ml of boiled reverse osmosis water and 150 ml of 15% acetic acid solution) were placed in the tube, covered with aluminium foil, and kept for 30 min. OD values were measured, using a Spectrophotometer (U3210, Hitachi, Japan) at 540 nm wave-length. A nitrite standard curve was made by adding 0.2 g of $NaNO_2$ dissolved in 1000 ml DW and 10 ml of solution were withdrawn and diluted to 1000 ml. The concentration values were then determined according to the equation: $Y = 5.3527 \times X - 0.089$, with Y representing the concentration (ppm), and X representing OD values at 540 nm wave-length.

2.7. Microbial evaluation

Microbial qualities of samples were evaluated according to Bacteriological Analytical Manual for Foods (FDA, 1996), briefly follows: at specified sample times, sausages were aseptically removed from the bags. Eleven gramme samples were placed in a sterile bag containing 99 ml of sterile distilled water and homogenised with a stomacher (Stomacher blender, Model 400, Seward) for 1 min. Serial dilutions were then made. Plate count agar (PCA, Merck) and potato dextrose agar (PDA, Merck) were used for enumeration of total plate count, and mould count, respectively, using the pour plate method to enumerate bacteria. Total microflora and mould were incubated at 37 °C for 48 h and 37 °C for 96 h, respectively. For anaerobic plate counts, dilutions were poured into anaerobic agar (AA, Merck), placed in an anaerobic jar (BBL GasPak System, USA) and incubated at 37 °C for 48 h. Microbial counts in this study were expressed as $\log_{10}$ colony forming units (CFU) per gramme of sample.

2.8. Sensory evaluation

At days 0, 28 and 56, during storage, sausages were first cooked on a grill, until the internal temperature of the sausages reached and was held at 75 °C for 8 min, cooled to room temperature (approximately 25 °C), sliced (approximately 0.3 cm thickness), and then served to a sensory panel which consisted of 10 meat science-majored faculty and students. Sensory attributes, including colour, flavour, odour, and overall acceptance, was conducted using

a 1 to 7-point hedonic scale test, with 1, 4, and 7 representing extremely dislike, neither like nor dislike, and extremely like, respectively, for the attributes.

2.9. Statistical analyses

Data were analysed using the general linear model (GLM) of Statistical Analysis System's Procedures (SAS Institute Inc., Cary, NC) with a 5% level of significance. Means were separated using the Duncan's new multiple range test.

3. Results and discussion

3.1. Proximate composition, water activity and pH

The results showed that chemical compositions of low-nitrite Chinese sausages were not affected by the addition of different levels of anka rice (data not shown). The contents of moisture, crude protein, crude fat, and ash were 44.96–47.30%, 17.9–20.0%, 20.25–23.30%, and 2.78–3.07%, respectively, without significant ($P > 0.05$) differences between the samples. Also, the water activities of all treatments ranged from 0.92 to 0.93, and were not significantly different over storage time or between treatments ($P > 0.05$).

In this study, the sausage pH values significantly decreased from approximate pH 6.3 at day 0 to pH 4.7 at day 56. This pH reduction was probably due to the fact that lactic acid bacteria were the predominant microorganisms in vacuum-packaged meat products, which produced lactic acid, which then reduced pH values of products (Kuo & Chu, 2003). Banwart (1979) indicated that cured meat became sour, with lower pH values, because of the fermentation of carbohydrates by lactic acid bacteria. Similarly, Kuo and Chu (2003) reported that the pH values of Chinese sausages decreased during storage at 4 °C, when lactic acid bacterial counts increased over storage time. Typically, Chinese sausages had higher carbohydrate contents than had most sausages, for example, 10% sugar in this study, which probably could be utilised by lactic acid bacteria to produce more lactic acid, which could result in lower pH values during storage. In this study, the low-nitrite Chinese sausages with anka rice added, especially for the higher level of anka rice-added samples (R3), tended to have a slower pH decline during refrigerated storage. At days 0, 7 and 14, no significant differences of the pH values between the samples were observed. However, at day 28, the pH values of A (lower nitrite level added, i.e. 25 ppm sodium nitrite added) and C (higher level of nitrite added, i.e. 100 ppm sodium nitrite added) samples dropped rapidly to 4.68 and 4.92, respectively, while the pH values of the samples with anka rice added (R1, R2, and R3 treatments with lower level of nitrite added, i.e. 25 ppm sodium nitrite added) were 5.21, 5.17, and 5.38, respectively. In this study, a higher level of anka rice addition (R3, with 1.5% anka rice added) could retard the pH decrease rate for the low-nitrite Chinese sausage at day 28. After refrigeration for 56 days, all the pH values dropped to approximately 4.52–4.86, without significant differences between treatments.

3.2. Instrumental colour measurement

The data indicated that sausages with anka rice added (R1, R2, and R3) tended to have higher "*a*" values, indicating more red colour (Table 1). Especially, R2 (1% anka rice) and R3 (1.5% anka rice) samples had significantly higher "*a*" values than had those of A and C treatments (no anka rice added). In addition to monascin, ankaflavin and rubropunctatin, a red pigment, monascorubramine, was detected in *M. purpureus* extracts (Chen & Johns, 1993). These pigments, produced by *M. purpureus*, might contribute to the increase of redness of the samples observed in this study. In addition, there were no significant differences of the "*L*", "*a*" and "*b*" values between the C samples (with higher nitrite level, i.e. 100 ppm sodium nitrite added) and R1 samples (with lower level of nitrite, i.e. 25 ppm sodium nitrite and 0.5% anka rice added). Samples that had more anka rice added tended to have lower "*L*" values, indicating a darker colour. Especially, after storage for more than 7 days, R3 samples had significantly lower "*L*" values than had C and A samples. In this study, sausages without anka rice showed a lighter red colour whereas sausages with anka rice added had a darker red colour which could also be observed subjectively, through a sensory colour evaluation.

3.3. TBARS and VBN

TBARS values, which are indicators of lipid oxidation, are shown in Fig. 1a. The TBARS values of the sausage samples increased with

Table 1
Changes of colour values of Chinese sausages with addition of anka rice during storage at 4 °C.

Treatment[A]	Storage time (day)				
	0	7	14	28	56
L values					
C	$34.79 \pm 1.79a^{x}$	$36.75 \pm 2.91^{a,xy}$	$35.89 \pm 4.10^{a,x}$	$34.66 \pm 3.96^{a,xy}$	$42.48 \pm 3.30^{b,x}$
A	$33.91 \pm 2.88^{a,x}$	$38.55 \pm 3.42^{bc,x}$	$35.43 \pm 2.66^{ab,xy}$	$36.03 \pm 1.04^{ab,x}$	$41.00 \pm 3.28^{c,x}$
R1	$32.67 \pm 1.91^{a,x}$	$36.14 \pm 1.70^{a,xy}$	$34.28 \pm 3.07^{a,xyz}$	$31.34 \pm 2.13^{a,yz}$	$42.48 \pm 2.68^{b,x}$
R2	$31.26 \pm 1.80^{a,x}$	$34.03 \pm 1.55^{a,y}$	$31.61 \pm 2.58^{a,yz}$	$31.19 \pm 2.94^{a,yz}$	$39.98 \pm 4.88^{b,xy}$
R3	$30.66 \pm 3.18^{a,x}$	$26.63 \pm 3.51^{a,z}$	$30.23 \pm 1.44^{a,z}$	$27.75 \pm 2.93^{a,z}$	$38.20 \pm 2.79^{b,y}$
a values					
C	$12.08 \pm 2.38^{a,yz}$	$12.64 \pm 1.75^{a,yz}$	$13.46 \pm 2.11^{a,yz}$	$14.66 \pm 3.31^{a,z}$	$14.46 \pm 1.73^{a,yz}$
A	$11.51 \pm 1.48^{a,z}$	$11.56 \pm 2.21^{a,z}$	$10.79 \pm 1.24^{a,z}$	$11.42 \pm 2.58^{a,z}$	$12.34 \pm 0.87^{a,z}$
R1	$14.43 \pm 2.63^{a,xyz}$	$13.74 \pm 2.02^{a,xyz}$	$14.91 \pm 2.62^{a,y}$	$17.42 \pm 2.66^{a,yz}$	$17.43 \pm 2.47^{a,xy}$
R2	$16.54 \pm 2.61^{a,x}$	$17.05 \pm 2.39^{ab,wx}$	$18.30 \pm 2.12^{ab,x}$	$20.66 \pm 2.44^{b,xy}$	$19.61 \pm 2.67^{b,wx}$
R3	$20.05 \pm 2.77^{a,w}$	$21.13 \pm 2.27^{a,w}$	$19.96 \pm 2.72^{a,x}$	$22.07 \pm 2.06^{a,x}$	$21.32 \pm 1.79^{a,w}$
b values					
C	$7.28 \pm 1.54^{ab,x}$	$9.32 \pm 1.07^{c,xy}$	$7.04 \pm 1.53^{a,x}$	$7.60 \pm 1.36^{abc,x}$	$9.11 \pm 1.97^{bc,x}$
A	$6.89 \pm 1.14^{a,x}$	$8.33 \pm 2.52^{a,xy}$	$7.86 \pm 1.23^{a,x}$	$8.11 \pm 0.60^{a,x}$	$8.44 \pm 1.09^{a,x}$
R1	$7.75 \pm 1.35^{a,x}$	$10.12 \pm 0.95^{bc,y}$	$8.05 \pm 1.95^{a,x}$	$8.20 \pm 0.90^{ab,xy}$	$10.25 \pm 1.67^{c,x}$
R2	$8.04 \pm 2.72^{a,x}$	$10.13 \pm 1.36^{b,y}$	$8.66 \pm 2.05^{ab,x}$	$9.54 \pm 1.30^{ab,y}$	$9.65 \pm 1.06^{ab,x}$
R3	$8.16 \pm 1.62^{a,x}$	$7.77 \pm 1.09^{a,x}$	$6.74 \pm 0.87^{a,x}$	$8.54 \pm 1.46^{a,xy}$	$9.78 \pm 1.82^{a,x}$

[a–c]Means within the same row for the same test with different superscripts are significantly different ($P < 0.05$).
[w–z]Means within the same column for the same test with different superscripts are significantly different ($P < 0.05$).
[A] C: 100 ppm sodium nitrite; A: 25 ppm sodium nitrite; R1: 25 ppm sodium nitrite + 0.5% anka rice which was inoculated with *M. purpureus*; R2: 25 ppm sodium nitrite + 1.0% anka rice which was inoculated with *M. purpureus*; R3: 25 ppm sodium nitrite + 1.5% anka rice which was inoculated with *M. purpureus*.

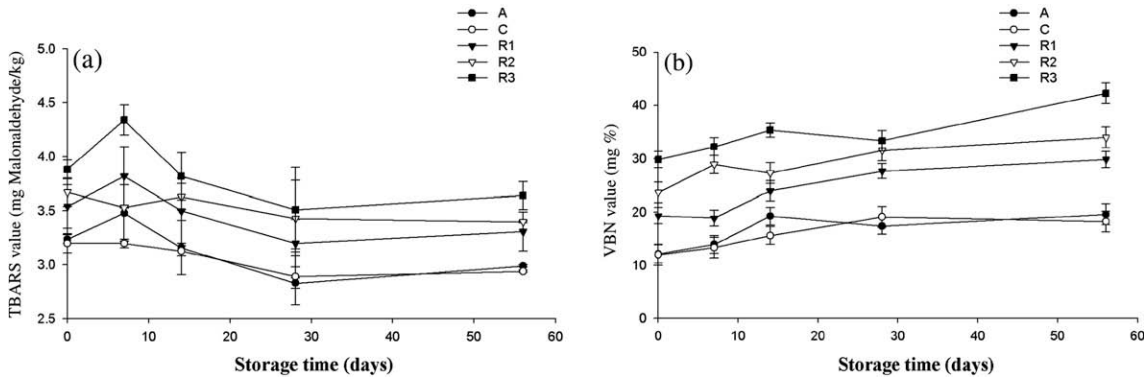

Fig. 1. Changes of (a) TBARS (thiobarbituric acid) and (b) VBN (volatile basic nitrogen) values of Chinese sausages with addition of anka rice during storage at 4 °C. A: 25 ppm sodium nitrite; C: 100 ppm sodium nitrite; R1: 25 ppm sodium nitrite + 0.5% anka rice which was inoculated with *M. purpureus*; R2: 25 ppm sodium nitrite + 1.0% anka rice which was inoculated with *M. purpureus*; R3: 25 ppm sodium nitrite + 1.5% anka rice which was inoculated with *M. purpureus*.

Table 2
Changes of nitrite residue (ppm) of Chinese sausages with addition of anka rice during storage at 4 °C.

Treatment[A]	Storage time (day)				
	0	7	14	28	56
C	$36.2 \pm 2.12^{a,x}$	$34.5 \pm 5.55^{a,y}$	$21.0 \pm 4.75^{b,y}$	$19.3 \pm 3.51^{b,y}$	$11.7 \pm 3.02^{c,y}$
A	$6.06 \pm 0.34^{a,z}$	$5.90 \pm 0.71^{a,z}$	$6.12 \pm 0.47^{a,z}$	$5.72 \pm 0.92^{a,z}$	$5.60 \pm 0.26^{a,z}$
R1	$8.27 \pm 0.86^{a,yz}$	$6.25 \pm 0.31^{a,z}$	$6.04 \pm 0.57^{a,z}$	$7.00 \pm 0.53^{a,z}$	$7.67 \pm 0.78^{a,yz}$
R2	$8.48 \pm 0.71^{a,y}$	$6.02 \pm 0.41^{a,z}$	$6.06 \pm 0.20^{a,z}$	$7.13 \pm 0.18^{a,z}$	$7.54 \pm 0.10^{a,yz}$
R3	$8.18 \pm 0.66^{a,yz}$	$6.08 \pm 0.31^{a,z}$	$6.28 \pm 0.82^{a,z}$	$7.00 \pm 0.29^{a,z}$	$7.63 \pm 0.04^{a,yz}$

[a–c]Means within the same row with different superscripts are significantly different ($P < 0.05$).
[x–z]Means within the same column with different superscripts are significantly different ($P < 0.05$).
[A] C: 100 ppm sodium nitrite; A: 25 ppm sodium nitrite; R1: 25 ppm sodium nitrite + 0.5% anka rice which was inoculated with *M. purpureus*; R2: 25 ppm sodium nitrite + 1.0% anka rice which was inoculated with *M. purpureus*; R3: 25 ppm sodium nitrite + 1.5% anka rice which was inoculated with *M. purpureus*.

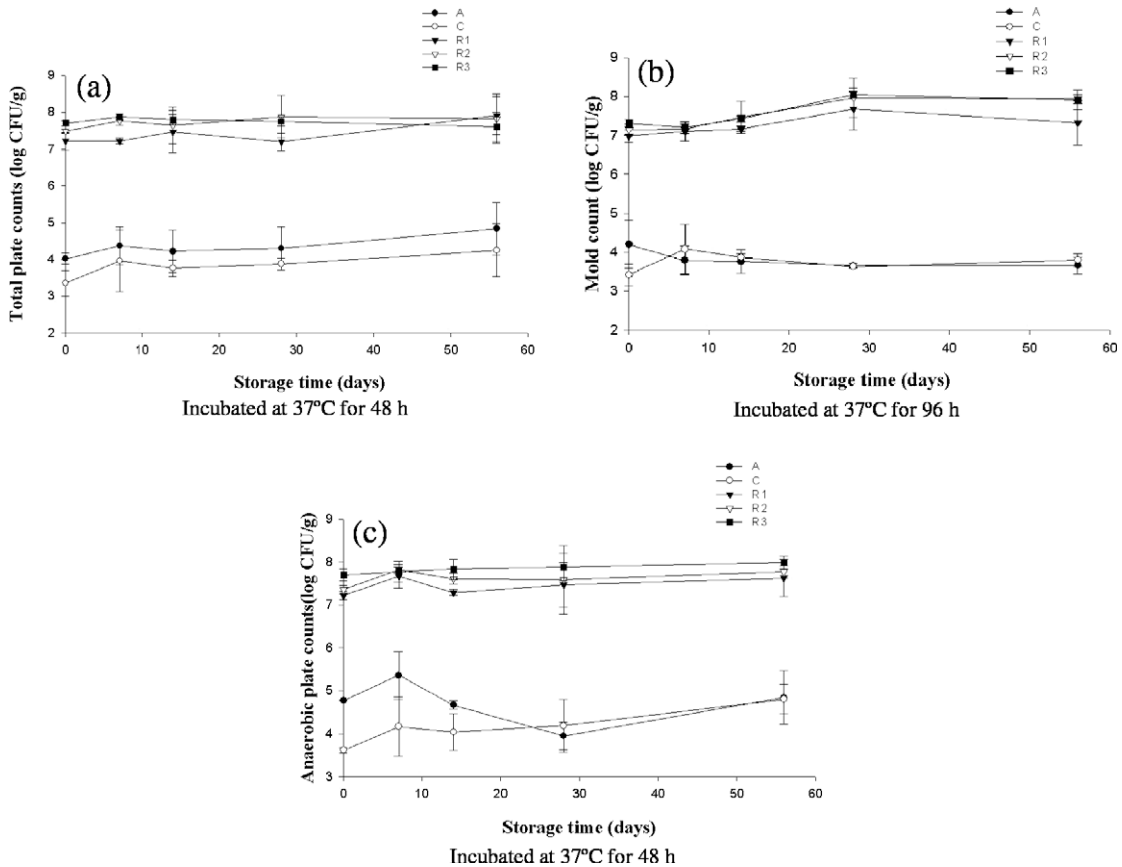

Fig. 2. Changes of (a) total plate counts (b) mould counts (c) anaerobic plate counts of Chinese sausages with addition of anka rice during storage at 4 °C. A: 25 ppm sodium nitrite; C: 100 ppm sodium nitrite; R1: 25 ppm sodium nitrite + 0.5% anka rice which was inoculated with *M. purpureus*; R2: 25 ppm sodium nitrite + 1.0% anka rice which was inoculated with *M. purpureus*; R3: 25 ppm sodium nitrite + 1.5% anka rice which was inoculated with *M. purpureus*.

refrigerated storage time during the first 7 days, indicating that lipid oxidation had occurred during this stage. This increase of TBARS values of Chinese sausages during storage has also been reported by other researchers (Kuo & Chu, 2003). In this study, TBARS values increased up to a maximum point at day 7, and then decreased gradually. Gokalp, Ockerman, Plimpoton, Parrett, and Cahill (1978) explained that, during storage, malonaldehyde, which is an intermediate by-product of lipid oxidation, is further oxidised to other organic acids and alcohols that can not react with TBA agent. This might be the reason why the TBARS values first increased and then decreased during storage. Also, a reduction in TBARS values of cooked meat during storage was probably due to interactions between malonaldehyde and proteins (Igene & Pearson, 1979). In this study, the TBARS values of the samples with anka rice added (R1, R2, and R3) were higher than those of the C and A samples. Higher TBARS values were observed when anka rice levels increased. This increase of TBARS values was probably due to the fact that *M. purpureus*, which was previously inoculated to the anka rice, might produce some lipases, and this then speeded up fat hydrolysis, and finally increased the TBARS values of samples (Tseng, 1999). The results of this study showed that the addition of anka rice did not inhibit the lipid oxidation of Chinese sausages, which agreed with other studies. When evaluating the TBARS values of samples, Cheng and Ockerman (1998) reported that addition of anka rice had little retarding effect on lipid oxidation in roast beef.

Increased amounts of volatile basic nitrogen (VBN), a result of decomposition of protein during storage by microorganisms, can be an index of loss of meat product freshness (Jay, 1992). Fig. 1b illustrates that VBN values of the sausage samples increased with storage time, as expected. This result agreed with other studies (Lin, Chen, & Yen, 1995). Also, samples with anka rice added (R1, R2, and R3) had significantly higher VBN values than had A and C samples. In addition, samples that had more anka rice added had significantly ($P < 0.05$) higher VBN values. This increase of VBN values was probably because anka rice itself had higher VBN values, which was also reported by Gui (1984). In this study, higher VBN values might suggest greater bacterial populations for the samples with more anka rice added, which were previously inoculated with *M. purpureus*, and this result was is in agreement with the microbial counts shown.

3.4. Nitrite residue

Table 2 illustrates the nitrite residue of sausages during storage. For the C samples, with high nitrite level (100 ppm), the nitrite contents dropped rapidly from 36.2 ppm at day 0 to 21.0 ppm at day 14, and 11.7 ppm at day 56. With addition of anka rice, the degrading rate of nitrite was reduced. Collins-Thomposon and Lopez (1981) reported that nitrite salts were converted to NO, NO_2, or N_2O by lactic acid bacteria isolated from vacuum-packed bologna, and depleted the nitrite contents in the samples. Similar nitrite depletion was also accomplished by lactic acid bacteria isolated from kimchi and other foods (Oh, Oh, & Kim, 2004). Faster nitrite depletion at lower pH values was also reported by Theiler, Sato, Aspelund, and Miller (1981). Therefore, a comparatively lower pH of the A samples (no anka rice added) in this study might be the reason why a lower residual nitrite content was observed after storage for more than 28 days.

3.5. Microbial qualities

In this study, the total plate counts of all samples remained stable during refrigerated storage (Fig. 2a). The total plate counts of Chinese sausage with different levels of anka rice added (R1, R2, and R3) were between 7.19 and 7.91 log CFU/g, which were significantly ($P < 0.05$) higher than those of the C and A groups (3.34–4.84 log CFU/g). The higher bacterial counts of the R1, R2, and R3 samples were probably due to the addition of *M. purpureus* to samples. Adding anka rice to the formula caused the samples (R1, R2, and R3) to have significantly higher mould counts (6.98–8.05 log CFU/g) during storage than those of the samples without anka rice added (3.14–4.19 log CFU/g). Samples with anka rice added (R1, R2, and R3) had anaerobic counts of 7.22–7.99 log CFU/g, which were significantly higher than those of the A and C samples during refrigerated storage. In addition, the C samples (without anka rice added, but with 100 ppm sodium nitrite added) had lower anaerobic counts than had the A samples (without anka rice, but with 25 ppm sodium nitrite added) during the first two weeks of storage. A higher nitrite level, which might inhibit some microbial growth, led to a lower count.

Table 3
Sensory evaluation[A] of Chinese sausages with addition of anka rice during storage at 4 °C.

Treatment[B]	Storage time (day)		
	0	28	56
Color			
C	4.1 ± 1.1^{ab}	3.5 ± 0.5^{cd}	4.0 ± 0.5^{ab}
A	3.8 ± 0.8^{b}	2.4 ± 0.7^{d}	3.8 ± 0.6^{b}
R1	4.3 ± 0.8^{ab}	4.9 ± 0.7^{abc}	5.0 ± 0.9^{ab}
R2	5.5 ± 0.5^{a}	5.1 ± 0.9^{ab}	5.4 ± 0.7^{a}
R3	5.0 ± 0.5^{a}	5.3 ± 0.7^{ab}	5.2 ± 1.2^{a}
Aroma			
C	$4.2 \pm 1.5^{a,x}$	$3.6 \pm 0.7^{a,xy}$	$3.1 \pm 1.0^{a,y}$
A	4.4 ± 1.3^{a}	3.1 ± 1.3^{a}	2.8 ± 1.1^{a}
R1	4.3 ± 1.3^{a}	4.1 ± 0.9^{a}	2.4 ± 1.0^{a}
R2	4.3 ± 1.2^{a}	4.5 ± 1.0^{a}	2.9 ± 1.3^{a}
R3	5.1 ± 1.1^{a}	3.8 ± 0.8^{a}	3.3 ± 1.2^{a}
Flavour			
C	$5.4 \pm 1.1^{a,x}$	$3.7 \pm 0.7^{ab,xy}$	$3.5 \pm 1.0^{a,y}$
A	4.4 ± 1.1^{a}	3.3 ± 0.9^{ab}	3.5 ± 1.3^{a}
R1	4.5 ± 1.3^{a}	4.5 ± 1.3^{ab}	3.0 ± 0.9^{a}
R2	4.2 ± 0.9^{a}	4.6 ± 0.7^{a}	3.2 ± 1.2^{a}
R3	5.2 ± 0.8^{a}	4.4 ± 1.0^{ab}	3.9 ± 1.1^{a}
Overall acceptance			
C	$5.6 \pm 1.3^{a,x}$	$3.4 \pm 0.8^{b,y}$	$3.1 \pm 1.0^{a,y}$
A	$5.0 \pm 1.1^{a,x}$	3.3 ± 1.2^{bx}	$3.1 \pm 1.4^{a,y}$
R1	$4.5 \pm 1.0^{a,x}$	$5.0 \pm 0.9^{ab,x}$	$2.3 \pm 1.1^{a,y}$
R2	$4.5 \pm 0.7^{a,x}$	$5.4 \pm 0.5^{a,x}$	$3.3 \pm 1.3^{a,y}$
R3	$5.8 \pm 0.8^{a,x}$	$4.2 \pm 0.9^{ab,xy}$	$3.6 \pm 1.2^{a,y}$

[a–d]Means within the same column for the same test with different superscripts are significantly different ($P < 0.05$).
[x–y]Means within the same row for the same test with different superscripts are significantly different ($P < 0.05$).
[A] A 7-point hedonic scale test was used in this study. 1 = extremely dislike, 4 = neither like nor dislike, 7 = extremely like.
[B] C: 100 ppm sodium nitrite; A: 25 ppm sodium nitrite; R1: 25 ppm sodium nitrite + 0.5% anka rice which was inoculated with *M. purpureus*; R2: 25 ppm sodium nitrite + 1.0% anka rice which was inoculated with *M. purpureus*; R3: 25 ppm sodium nitrite + 1.5% anka rice which was inoculated with *M. purpureus*.

3.6. Sensory evaluation

Table 3 illustrates the sensory evaluation results. A 7-point hedonic scale test was used in this study, where scores 1, 4, and 7 representing extremely dislike, neither like nor dislike, and extremely like, respectively. The sausages with anka rice added tended to have significantly higher colour scores than did the A and C samples. Also, all the colour scores of the anka rice-added sausages were higher than 4 over the entire storage time, whereas lower nitrite sausages (A) had the lowest colour scores. This result illustrates that addition of anka rice could improve colour acceptance of low-nitrite Chinese sausages. In this study, samples' aroma and flavour scores tended to decrease as storage time increased.

The aroma and flavour scores of the control samples with higher nitrite level (C) significantly decreased after 56 days of refrigerated storage. Overall, Chinese sausage with 0.5%, 1% and 1.5% anka rice (R1, R2, and R3) could be accepted when stored at 4 °C for 28 days, whereas the overall acceptance scores of the C and A samples were less than 4.

4. Conclusion

Addition of anka rice up to 1.5% (w/w), which was previously inoculated with *M. purpureus*, did not affect the chemical compositions and water activities of the Chinese sausages. Samples with anka rice added had darker red colours, higher TBARS values, higher microbial counts and less nitrite degradation. Based mainly on the results of overall acceptance, it could be concluded that anka rice, inoculated with *M. purpureus*, could be used in the production of low-nitrite Chinese sausages when stored at 4 °C for 28 days.

References

AOAC (1990). *Official methods for the analysis* (15th ed.). Arlington, Washington, DC: Association of Official Analytical Chemist.

Banwart, G. J. (1979). *Basic food microbiology*. Connecticut: AVI Publishing Company.

Chen, M. H., & Johns, M. R. (1993). Effect of pH and nitrogen source on pigment production by *Monascus purpureus*. *Applied Microbiology and Biotechnology, 40*, 132–138.

Cheng, J. H., & Ockerman, H. W. (1998). Effects of anka rice, nitrite, and phosphate on warmed-over flavor and palatability characteristics in roast beef. *Meat Science, 49*, 65–78.

CNS (Chinese National Standards). (1982). General No. 1451, Classified No. N6029. Bureau of Standards, Metrology and Inspection, M.O.E.A., R.O.C.

Collins-Thomposon, D. L., & Lopez, G. R. (1981). Depletion of sodium nitrite by lactic acid bacteria isolated from vacuum-packed bologna. *Journal of Food Science, 44*, 593–595.

DOH (Department of Health, Taiwan). (2008). *Sanitary standard for edible natural colorants (DOH Food No. 8246254)*. <http://food.doh.gov.tw/law/hygiene_standed_e_7.asp> Accessed 16.07.08.

Faustman, C., Specht, S. M., Malkus, L. A., & Kinsman, D. M. (1992). Pigment oxidation in ground veal: Influence of lipid oxidation, iron and zinc. *Meat Science, 31*, 351–362.

FDA (1996). *Bacteriological analytical manual for foods*. Washington, USA: US Government Printing Office.

Fink-Gremmels, J., Dresel, J., & Leistner, L. (1992). Use of *Monascus* extracts as an alternative to nitrite in meat products. *Fleischwirtschaft, 71*, 329–331.

Gill, A. O., & Holley, R. A. (2003). Interactive inhibition of meat spoilage and pathogenic bacteria by lysozyme, nisin and EDTA in the presence of nitrite and sodium chloride at 24 °C. *International Journal of Food Microbiology, 80*(3), 251–259.

Gokalp, H. Y., Ockerman, H. W., Plimpoton, R. F., Parrett, N. A., & Cahill, V. R. (1978). Effect of different packaging methods on objective quality characteristics of frozen and stored cow beef. *Journal of Food Science, 43*, 297–300.

Gui, C. H. (1984). *Effects of Monascus curing on the physic–chemical characteristics of porcine muscle*. National Chung-Hsing University, Master thesis, Taichung, Taiwan.

Hedrick, H. B., Aberle, E. D., Forrest, J. C., Judge, M. D., & Merkel, R. A. (1994). *Principles of Meat Science*. Dubuque, Iowa, USA: Kendall/Hunt Publishing Company.

Honikel, K. O. (2008). The use and control of nitrate and nitrite for the processing of meat products. *Meat Science, 78*(1–2), 68–76.

Igene, J. O., & Pearson, A. M. (1979). Role of phospholipids and triglycerides in warmed-over flavor development in meat model systems. *Journal Food Science, 44*, 1285–1290.

Jay, J. M. (1992). *Modern food microbiology*. New York: Chapman and Hall.

Jiménez-Colmenero, F., Carballo, J., & Cofrades, S. (2001). Healthier meat and meat products: Their role as functional foods. *Meat Science, 59*, 5–13.

Kuo, C. C., & Chu, C. Y. (2003). Quality characteristics of Chinese sausages made from PSE pork. *Meat Science, 64*, 441–449.

Lin, K. J. (1984). Studies on the relationship between curing time and nitrite residue in Chinese style semi-dry sausage. *Journal of the Chinese Society of Animal Science, 13*, 127–134.

Lin, L. C., Chen, C. M., & Yen, G. C. (1995). Relationship between biogenic amine contents and quality of lean meat of Chinese-style sausage prepared from pork ham stored at different temperature. *Food Science (Taiwan), 22*, 448–460.

Ma, J., Li, Y., Ye, Q., Li, J., Hua, Y., Ju, D., et al. (2000). Constituents of red yeast rice, a traditional Chinese food and medicine. *Journal of Agricultural and Food Chemistry, 48*, 5220–5225.

Oh, C. K., Oh, M. C., & Kim, S. H. (2004). The depletion of sodium nitrite by lactic acid bacteria isolated from kimchi. *Journal of Medicinal Food, 7*, 38–44.

Osterlie, M., & Lerfall, J. (2005). Lycopene from tomato products added minced meat: Effect on storage quality and colour. *Food Research International, 38*, 925–929.

Theiler, R. F., Sato, K., Aspelund, T. G., & Miller, A. F. (1981). Model system studies on N-nitrosamine formation in cured meat: The effect of curing solution ingredients. *Journal of Food Science, 46*, 996–999.

Tseng, Y. Y. (1999). *The utilization of Monascus purpureus as a curing agent in meat products*. National Chung-Hsing University, Ph.D. dissertation, Taichung, Taiwan.

Tseng, Y. Y., Chen, M. T., & Lin, C. F. (2000). Growth, pigments production and protease activity of *Monascus purpureus* as effect by salt, sodium nitrite, polyphosphate and various sugars. *Journal of Applied Microbiology, 88*, 31–37.

Walsh, M. M., Kerry, J. F., Buckley, D. J., Morrissey, P. A., Lynch, P. B., & Arendt, E. (1998). The effect of dietary supplementation with α-tocopheryl acetate on the stability of low nitrite cured pork products. *Food Research International, 31*, 59–63.

Food Chemistry 118 (2010) 251–255

Contents lists available at ScienceDirect

Food Chemistry

journal homepage: www.elsevier.com/locate/foodchem

Removal of oligosaccharides in soybean flour and nutritional effects in rats

Ana Paula Rodrigues Brasil [a], Sebastião Tavares de Rezende [a], Maria do Carmo Gouveia Pelúzio [b], Valéria Monteze Guimarães [a,*]

[a] BIOAGRO, Universidade Federal de Viçosa, Department of Biochemistry and Molecular Biology, Av. P. H. Rolfs, Campus UFV, Viçosa, MG 36570-000, Brazil
[b] Departamento de Nutrição e Saúde, Universidade Federal de Viçosa, Viçosa, MG 36570-000, Brazil

ARTICLE INFO

Article history:
Received 12 February 2009
Received in revised form 17 March 2009
Accepted 28 April 2009

Keywords:
Raffinose oligosaccharides
Debaryomyces hansenii
α-Galactosidase
Digestibility

ABSTRACT

The objectives of this work were to establish a safe and economically viable process for the removal of raffinose oligosaccharides (RO) from soy flour and compare the effects of RO elimination from diets with regard to nutritional parameters by testing in Wistar rats. *Debaryomyces hansenii* UFV-1 was cultivated in suspension of defatted soy flour (1:10 w/v). An increase in α-galactosidase activity was observed in the medium, with a consequent decrease in the RO concentration. A total reduction of RO was achieved at 36 h of incubation. The diet containing soy flour free of RO presented higher digestibility, 91.28%, in relation to the diet containing soy flour with RO, 87.14%. However, the removal of the oligosaccharides from the diet did not promote a significant improvement in the values of weight gain, and other nutritional parameters tested on rats, during the experimental period of 14 days.

1. Introduction

Soybeans and their derivatives possess excellent nutritional value, principally high protein levels. However, the consumption of this legume is limited due to the presence of raffinose oligosaccharides (RO), in particular raffinose and stachyose, which can cause abdominal discomfort in humans and monogastric animals, such as cramps, flatulency and diarrhoea. This occurs because the mucous in the small intestine does not possess the α-galactosidase (E.C. 3.2.1.22 α-galactoside galactohydrolase) enzyme necessary for the hydrolysis of the α-1,6 linkages present in RO, allowing these sugars to pass intact to the large intestine where they are fermented by anaerobic microorganisms creating excessive gas (Karr-Lilienthal, Kadzere, Grieshop, & Fahey, 2005). These compounds are also likely to be responsible for increasing viscosity of digesta, which interferes with digestion of nutrients by decreasing their interaction with digestive enzymes in the intestine (Smits & Annison, 1996).

As a result, there is a large demand for RO-free soybean products. Various processes for the reduction or elimination of RO have been proposed, such as the addition of α-galactosidases to the diet (Igbasan, Guenter, & Slominski, 1997; Smiricky et al., 2002) or the fermentation of soy products by microorganisms capable of producing this enzyme (Donkor, Henriksson, Vasiljevic, & Shah, 2007; Leblanc et al., 2004). The α-galactosidase is found in plants, microorganisms and animals (Kim et al., 2002). However, many α-galactosidase producing microorganisms do not present GRAS (generally recognised as safe) status for their use in foods. On the other hand, the use of isolated enzymes increases processing costs since the production and purification of enzymes are critical steps in order to make the enzymatic removal of RO economically viable. Isolated α-galactosidases from the *Debaryomyces hansenii* yeast have proven to be adequate for biotechnological applications, especially for RO hydrolysis in soy products (Viana et al., 2006, 2007). This is the most frequently used yeast in traditional cheese and sausages, contributing to the special flavours of these products (Saldanha-Da-Gama, Malfeito-Ferreira, & Loureiro, 1997) and there should be no restriction, regarding safety, for its use in food processing.

Despite various studies showing positive effects for the enzymatic removal of RO from soy based foods (Leblanc et al., 2004; Veldman, Veen, Barug, & Van Paridon, 1993), some authors have reported no improvements in protein digestibility when diets were supplemented with α-galactosidase (Irish, Barbour, Classen, Tyler, & Bedford, 1995; Smiricky et al., 2002).

The objectives of this work were to establish a safe and economically viable enzymatic process for the removal of RO from soy flour and compare the effects of RO elimination from diets with regard to nutritional parameters by testing in Wistar rats.

2. Materials and methods

2.1. Microorganisms and culture maintenance

The yeast strain used in this study was isolated from a dairy environment in Minas Gerais, Brazil, and maintained in the culture

* Corresponding author. Tel.: +55 31 3899 2374; fax: +55 31 3899 2373.
E-mail address: vmonteze@ufv.br (V.M. Guimarães).

0308-8146/$ - see front matter © 2009 Elsevier Ltd. All rights reserved.
doi:10.1016/j.foodchem.2009.04.124

collection of the Microorganism Physiology Laboratory, BIOAGRO, Federal University of Viçosa (UFV), Brazil. The yeast was identified by the Institute of Yeasts Identification, Centraalbureau voor Schimmelcultures, Utrecht, The Netherlands, as *D. hansenii* (Zopf) Lodder & Kreger-van Rij var *fabryi* Nakase & Suzuki. In this study, it is designated as *D. hansenii* UFV-1.

A stock culture of *D. hansenii* UFV-1 was maintained at −80 °C in glycerol and YPD medium (1% yeast extract, 2% peptone and 2% glucose). *D. hansenii* UFV-1 was streaked on a YPD agar surface (1.5% agar) and maintained in an incubation chamber at 30 °C for 36 h. The plates were maintained at 4 °C and this stock was restreaked monthly.

2.2. Treatment of soy flour with viable Debaryomyces hansenii cells

The yeast was activated in YPD liquid medium, incubated for 12–15 h, at 200 rpm and 30 °C and the culture was centrifuged (4000*g* for 5 min at 4 °C). Commercial fat-free soy flour was mixed with deionised water (1:10 w/v). The cells obtained after centrifugation were inoculated in the soy flour suspension and incubated at 200 rpm and 30 °C for 72 h. Samples of 2 ml were taken at 12 h intervals for the determination of α-galactosidase activity and percentage of RO hydrolysed. The reaction mixtures were dried, and the soluble sugars from 20 to 30 mg of lyophilised samples were extracted with 80% aqueous ethanol (v/v) according to Guimarães, de Rezende, Moreira, Barros, and Felix (2001). The solvent was evaporated at 50 °C, and the sugars were resuspended in 1 ml of 80% ethanol and analysed by high-performance liquid chromatography (HPLC). Hydrolysis efficiency was evaluated by the reduction of RO levels present in the soy flour suspension, as a function of incubation time with the yeast.

2.3. HPLC analysis of soluble sugars

Sugars were analysed by HPLC on a Shimadzu series 10A chromatograph equipped with an analytical column [aminopropyl ($-NH_2$)], eluted with an acetonitrile–water isocratic mixture (80:20 v/v) at 35 °C and a flow rate of 1 ml/min, according to Guimarães et al. (2001). The individual sugars were automatically identified and quantified by comparison with the retention times and standard sugar concentrations. Gentiobiose was used as an internal standard since it does not interfere with other sugars and is not found in soybean seeds.

2.4. Production of soybean flour free of raffinose oligosaccharides

Viable *D. hansenii* cells (equivalent to 0.533 mg/ml of dry cell mass) were mixed with an autoclaved suspension of defatted soy flour 1:10 (w/v) and the mixture was incubated at 200 rpm and 30 °C for 36 h. After this period, the suspension was lyophilised in order to obtain soy flour free of oligosaccharides. This flour was used as a protein source of the diet (D1). The soy flour containing oligosaccharides was prepared as described earlier, with the exception of the yeast cells being added to the soy flour suspension.

2.5. Enzyme assay

The enzyme was assayed using a reaction system (1 ml final volume) containing 650 μl of 0.1 M sodium acetate buffer, pH 5.0, 100 μl of enzyme preparation and 250 μl of 2 mM ρ-nitrophenyl α-D-galactopyranoside (ρNPGal) or, other synthetic substrates. The reaction was conducted for 15 min at 40 °C and stopped by the addition of 1 ml of 0.5 M sodium carbonate. The amount of ρ-nitrophenol (ρNP) released was determined at 410 nm. One unit of enzyme activity (U) was defined as the amount of protein required to produce 1 μmol of ρ-nitrophenol per minute.

2.6. Determination of the biochemical composition of the soy flours

Determination of the protein, lipid, ash and carbohydrate concentrations in the soy flours were performed according to the Association of Official Analytical Chemists (1997) method.

2.7. Biological assay

2.7.1. Diet preparation

The soy flours containing RO and no RO were used as protein sources in the experimental diets (Table 1). The diet composition was based on that of AIN-93G, according to Reeves, Nielsen, and Fahey (1993), with protein levels adjusted to 9–10%. The protein concentration of each diet was determined by the semimicro Kjeldahl method, using a conversion factor of 6.25 to obtain protein values.

2.7.2. Animals and experimental conditions

The male Wistar breed rats used were newly weaned, with an average age of 23 days and weight varying from 50 to 60 g. They were provided by the Biotery Center from the Center of Biological Sciences and Health (CCB) of the Federal University of Viçosa (UFV).

The rats were divided into four groups with each group containing six rats so that the difference in average weight between each group did not exceed 5 g. They were placed in individual cages where they received water and their *ad libitum* experimental diets for 14 days. The rats were maintained under controlled conditions of temperature (22 ± 3 °C) and luminosity (12 h photoperiod), with the weekly monitoring of feeding. Experimental procedures were approved by the Veterinary Commission Department of Ethics/UFV (protocol no. 57/2007).

2.7.3. Nutritional evaluation

In order to evaluate the effect of RO removal from the diets, the following were determined: animal weight gain, true digestibility, protein efficiency ratio (PER), and net protein ratio (NPR).

Animal weight gain: to compare weight gain, the animals were weighed before beginning the experiment and randomly distributed in the cages so that the difference between the average rat weight of each group did not exceed 5 g. At the end of each week the animals and diets were both weighed, discounting any remaining.

Table 1
Composition of experimental diets.[a]

Ingredient (%)	Diet			
	Aproteic	Casein	D1[a]	D2[b]
Casein	–	11.96	–	–
Soy flour	–	–	14.11	16.61
Dextrinized cornstarch	13.20	13.20	13.20	13.20
Sucrose	10.0	10.0	10.0	10.0
Soy oil	7.00	7.00	7.00	7.00
Fibre	5.00	5.00	2.80	2.80
Mineral mix (AIN-93G-MX)	3.50	3.50	3.50	3.50
Vitamin mix (AIN-93-VX)	1.00	1.00	1.00	1.00
Choline bitartrate	0.25	0.25	0.25	0.25
L-Cystine	0.30	0.30	0.30	0.30
Cornstarch	59.75	47.79	47.84	45.34

Font: Reeves et al. (1993).
[a] D1 – diet containing RO-free soy flour.
[b] D2 – diet containing soy flour with RO.

True digestibility: the diets were marked with 0.02% indigo carmin and the faeces were collected after 10 and 14 experimental days, packed in individual recipients and maintained under refrigeration. The faeces were dried at 105 °C for 24 h, cooled in a desiccator, weighed and ground. The nitrogen content in the faeces was determined using the semimicro Kjeldahl method, with tests being performed in triplicate. True digestibility was calculated by measuring the quantity of ingested nitrogen in the diet, quantity excreted in the faeces and the metabolic loss of nitrogen in the faeces, which corresponds to the faecal nitrogen from the aproteinic diet group. This was possible since one group of six rats was administered an aproteinic diet.

Protein efficiency ratio (PER): the PER was determined using the Osborne, Mendel and Ferry method, according to the Association of Official Analytical Chemists (AOAC) (1975).

Net protein ratio (NPR): the NPR was determined on the 14th experimental day, taking the weight gain of the test group plus the weigh loss from the group with the aproteinic diet, in relation to the protein consumption of the test group, according to the Bender and Doell (1957) method.

2.8. Extraction and concentration determination of short-chain fatty acids

The extraction and concentration determination of short-chain fatty acids (acetic, propionic and butyric) contained in the caecal was performed according to the techniques reported by Smiricky-Tjardes, Grieshop, Flickinger, Bauer, and Fahey (2003) with some modifications. Samples to be analysed for SCFA were mixed with 0.5 ml of 3.12 M metaphosphoric acid, precipitated at room temperature for 30 min, and then centrifuged at 16,100*g* for 30 min. The supernatant was decanted and again centrifuged at 16,000*g* for 20 min and frozen at −20 °C. After freezing, the supernatant was thawed and centrifuged at 13,000*g* for 10 min. Concentrations of SCFA were determined *via* gas–liquid chromatography. Concentrations of acetate, propionate, and butyrate were determined in the supernatant using a Shimadzu series 17A gas chromatograph and a 30 m × 0.25 mm Nukol column (Supelco Inc., Bellefonte, PA). Helium was the carrier gas with a flow rate of 1.90647 ml/min. The column temperature was maintained at 100 °C for 4 min and increased to 185 °C at a rate of 8.5 °C/min and maintained at this temperature for 15 min. The temperature of the detector (FID) and injector were 250 °C and 220 °C, respectively.

2.9. Statistical analysis

A statistical analysis (ANOVA) was used to determine the value of "*F*". For "*F*" significance, the Duncan test was used with a 5% significance level for comparison of the means. The dispersion of the means was expressed in the result tables with standard deviations from the average. Calculations were performed using SAEG version 9.1 (Federal University of Viçosa).

3. Results and discussion

During the cultivation of *D. hansenii* yeast in the soy flour suspension, an increase in α-galactosidase activity and a consequent decrease in the RO concentration present in soy flour was observed (Fig. 1). Various studies suggest the use of microorganisms, principally from the *Lactobacillus* and *Bifidobacterium* genus, for the removal of RO from soymilk and other products derived from soybeans (Scalabrini, Rossi, Spettoi, & Matteuzzi, 1998; Yoon & Hwang, 2008). However, there are no studies on the direct use of *D. hansenii* in soy products for the removal of RO. *D. hansenii* is

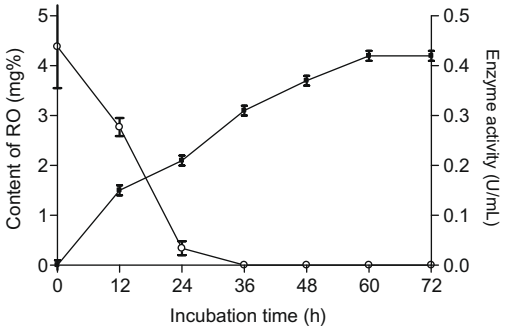

Fig. 1. α-Galactosidase activity (■) and raffinose oligosaccharides content (raffinose and stachyose) (○) in the suspension of defatted soy flour after inoculation of *Debaryomyces hansenii*.

the yeast most frequently found in several food products such as traditional cheese and sausages, and there should be no restriction regarding safety for its use in food processing.

Extracellular activity of α-galactosidase increased and stabilised after 60–72 h of *D. hansenii* cultivation in the soy flour suspension, and RO concentration reduced drastically during the first 24 h of cultivation (Fig. 1). Interestingly, the increase in the extracellular α-galactosidase activity, even after total reduction of RO, was observed (Fig. 1). Induction of α-galactosidase activity could be due to the higher concentration of galactose in the medium, which was released as a product of the RO hydrolysis. Galactose was considered to be the more efficient carbon source compared to raffinose and stachyose for the induction of α-galactosidase activity in microorganisms (Nobre, Lucas, & Leão, 1999; Yoshida, Tan, Shimokawa, Turakainen, & Kusakabe, 1997). Hydrolysis of RO may be achieved either by α-galactosidase, invertase or both. While α-galactosidase hydrolyses the α-1,6 linkage of raffinose producing galactose and sucrose, invertase hydrolyses α-1,2 linkage producing melibiose and fructose. During cultivation of *D. hansenii* in the soy flour suspension, no invertase activity was detected in the culture supernatant, indicating that RO hydrolysis was catalysed by α-galactosidase only. No hydrolysis was detected in the control samples, in which the soy flour suspension was not inoculated with any yeast.

The average raffinose and stachyose content in the defatted soy flour was 1.15% and 3.23%, respectively (Table 2). Oligosaccharides found in the majority of soybeans and its derivatives are stachyose followed by raffinose, making up approximately 4–6% of soybean flour's dry weight (Grieshop, Kadzere, Clapper, Frazier, & Fahey, 2003; Karr-Lilienthal et al., 2005). After 12 h of *D. hansenii* cultivation in the soy flour suspension, 96.2% of stachyose concentration was reduced and, the raffinose concentration increased by 132% in the culture medium (Table 2). This difference may be due to the accumulation of raffinose in the medium which is formed during hydrolysis of stachyose by cleaving of the α-1,6 bond and removal of the galactose residue. Kinetic studies of α-galactosidase

Table 2
Hydrolysis of oligosaccharides present in soybean flour by treatment with *Debaryomyces hansenii* UFV-1.

Incubation time (h)	Concentration (%) ± SD	
	Raffinose	Stachyose
0	1.15 ± 0.08	3.23 ± 0.75
12	2.67 ± 0.12	0.10 ± 0.06
24	0.34 ± 0.14	0
36	0	0
48	0	0
60	0	0
72	0	0

from *D. hansenii* confirm these results since the K_m value of the enzyme for the stachyose substrate was lower than the K_m value for raffinose, suggesting greater enzyme affinity for stachyose (Viana et al., 2006). Because stachyose is the most abundant nondigestible oligosaccharide found in soy flour, the high hydrolysis capacity of this sugar exhibited by α-galactosidase from *D. hansenii* makes its use extremely interesting as a biocatalyst for elimination of RO in soy products. Total reduction of RO was observed after 36 h of *D. hansenii* cultivation in the soy flour suspension. *Bifidobacterium breve*, *B. infantis* and *B. longum* incubated in soy milk for 48 h promoted the total reduction of raffinose and reduction of 68%, 73% and 35%, respectively in stachyose content (Scalabrini et al., 1998), while at the same time, *B. lactis* B94 promoted raffinose and stachyose content reductions of 77.4% and 63.5%, respectively (Donkor et al., 2007). The ability of *D. hansenii* to grow on the soy flour suspension, to produce α-galactosidases and to use the ROs, indicates the possibility of the direct utilisation of this yeast for RO reduction in soybean derivatives, what is advantageous in terms of facility and costs of the process.

The biochemical composition of soy flours free of RO (SF1) and containing RO (SF2) are presented in Table 3. Cultivation of yeast on soy flour promoted the increase in the protein content and decrease in the content of total carbohydrates in relation to the untreated soy flour. These data suggest that the treatment of soy flour with *D. hansenii* cells may be advantageous from a nutritional point of view since they eliminate RO, which are considered antinutritional factors, as well as increase the protein content of the flour.

For the evaluation of the nutritional effect of RO elimination from the soy flour, diets were prepared with soy flours SF1 and SF2, as well as the control diets (Table 1) and this was used to feed Wistar rats for a period of 14 days. The diet containing soy flour free of RO (D1) presented a digestibility of 91.28%, statistically significant ($p \leqslant 0.05$) and superior in relation to the diet containing soy flour with RO (D2), which presented a digestibility of 87.14% (Table 4). According to Graham, Kerley, Firman, and Allee (2002), the decrease in RO content may potentially reduce the viscosity of ingested food, increasing its retention time and promoting greater periods for enzyme digestion of substrates, consequently increasing the absorption of nutrients in the intestinal mucous. The presence of RO in swine diets containing concentrated soy proteins showed a significant reduction in the digestibility of proteins (Smiricky et al., 2002). Sakaguchi, Sakoda, and Toramaru (1998) confirmed a reduction in the true digestibility of proteins when RO was added to casein diets for rats. Veldman et al. (1993) also reported that the addition of soy molasses containing 18% RO to swine diets promoted a reduction of 25% in protein digestibility, but the addition of α-galactosidase improved the digestibility of these sugars and proteins. Therefore, RO reduction in diets can improve digestibility, both by reducing the viscosity of ingested food as well as promoting hydrolysis of these sugars into digestible monosaccharides. On the contrary, Gabert, Sauer, Mosenthin, Schimitz, and Abrens (1995) reported that swine diets produced from soy flour containing RO had no effect on the ileal digestibility of proteins and the majority of amino acids. Similarly, Irish et al. (1995) observed no effect on the ileal digestibility of proteins when α-galactosidase was added to chicken rations.

The values of weight gain, PER and NPR, did not differ statistically, with a 5% significance level, for the rats fed with the diet containing soy flour free of RO (D1) and containing RO (D2), during the experimental period (Table 4). Similarly, Graham et al. (2002) observed improvements in the digestibility of diets containing soy flour when supplemented with α-galactosidase, however, no variation in the weight gain of the broiler chickens was observed. Zdunczyk, Juskiewicz, Frejnagel, and Gulewicz (1998) reported that the presence of RO in rat diets decreased digestibility in relation to the same diet without these sugars, but the PER values for the two did not statistically differ.

The RO are considered indigestible carbohydrates due to their resistance to digestion in the small intestine, caused by the absence of the α-galactosidase in intestinal mucous in humans and monogastric animals (Sakaguchi et al., 1998). These sugars are kept intact until reaching the large intestine where they are fermented by anaerobic bacteria. The principal products of this fermentation are short-chain fatty acids (SCFA), which are absorbed and used as sources of energy by the epithelial cells in the large intestine (Roediger, 1980).

In this study, the production of SCFA does not statistically differ for animals fed with the diet containing soy flour free of RO (D1) and with RO (D2) during the experimental period (Table 5). Similarly, no difference in the production of SCFA was detected in the intestines of rats given a diet of bean flour with high and low RO contents during a period of 14 days (Henninsson, Margareta, Nyman, & Björck, 2001). Contrary to these results, Sakaguchi et al. (1998) found greater levels of propionic and butyric acid in rats when RO was added to a casein diet. Levrat, Behr, Rémésy, and

Table 3
Biochemical composition of treated (SF1)[a] and untreated (SF2)[b] soy flour.

Nutrient	Content (%) ± SD	
	SF1[a]	SF2[b]
Moisture	7.66 ± 0.11	7.17 ± 0.04
Ash	9.08 ± 0.01	7.64 ± 0.13
Fat	0.14 ± 0.07	0.11 ± 0.04
Protein	67.31 ± 0.69	57.19 ± 0.21
Carbohydrate	15.81 ± 0.05	27.89 ± 0.04

[a] SF1 – RO-free soy flour.
[b] SF2 – soy flour containing RO.

Table 5
Concentration[a] (μmol/g of sample) of short-chain fatty acids from rat caecum feed diets containing soybean flour.[b]

Dietary treatment	Acetic acid	Propionic acid	Butyric acid
D1	5.85[a] ± 0.63	1.97[a] ± 0.20	1.95[a] ± 0.21
D2	6.59[a] ± 0.70	1.86[a] ± 0.36	3.00[a] ± 1.19

[a] Mean ± standard deviation (sd) of triplicate determinations. Values with common superscript letter in each row are not significantly ($p > 0.05$) different by "*f*" test.
[b] D1 – diet containing RO-free soy flour; D2 – diet containing soy flour with RO.

Table 4
Protein digestibility *in vivo*, protein efficiency ratio (PER), net protein ratio (NPR), and animal weight gain[a] from diets containing casein or soybean flour (D1[b] and D2[c]).

Dietary treatment	Digestibility (% ± SD)	PER ± SD	NPR ± SD	Weight gain (g ± SD)
Casein	95.54[a] ± 2.56	3.76[a] ± 0.39	4.34[a] ± 0.46	66.00[a] ± 12.05
D1	91.28[b] ± 2.07	2.63[b] ± 0.14	3.56[b] ± 0.16	29.17[b] ± 4.26
D2	87.14[c] ± 2.98	2.71[b] ± 0.22	3.53[b] ± 0.22	33.83[b] ± 5.49

[a] Mean ± standard deviation of triplicate determinations. Values with common superscript letter in each row are not significantly ($p > 0.05$) different by Duncan test.
[b] D1 – diet containing RO-free soy flour.
[c] D2 – diet containing soy flour with RO.

Demigné (1991) observed that in rats given a soy based diet, the maximum production of SCFA occurred 16 days after beginning the experiment. However, the fermentation of RO and SCFA production was slower when RO was in the leguminous form, compared to when purified RO was added to the diet and production of gas and SCFA was greater when originating from the fermentation of raffinose compared to stachyose (Smiricky-Tjardes et al., 2003). In the present work, the low raffinose content in the diets and the short duration of the experiments probably explain why no significant differences were detected in SCFA production in the caecum of rats fed with a diet containing RO in relation to the diet free of RO.

4. Conclusions

The results presented in this study demonstrated that the removal of RO from soy flour using viable *D. hansenii* cells makes up a safe, simple and economical process. Rats administered a diet free of RO presented better protein digestibility compared to the rats given the diet containing RO, confirming preliminary results which indicated that RO may interfere in the absorption of nutrients in the diet, acting as an antinutritional factor. This suggests that the removal of RO can improve the nutritional values and the acceptance of products derived from soybeans for use in both human and animal nourishment.

References

Association of Official Analytical Chemists (AOAC) (1975). Official methods of analysis of the Association of Official Analytical Chemists (1.094 p). Washington.

Association of Official Analytical Chemists (1997). Official methods of analysis of AOAC international (16th ed.). v.2, Maryland.

Bender, A. E., & Doell, B. H. (1957). Note on the determination of net protein utilization by carcass analysis. *British Journal Nutrition, 11*, 138–143.

Donkor, O. N., Henriksson, A., Vasiljevic, T., & Shah, N. P. (2007). Galactosidase and proteolytic activities of selected probiotic and dairy cultures in fermented soymilk. *Food Chemistry, 104*, 10–20.

Gabert, V. M., Sauer, W. C., Mosenthin, R., Schimitz, M., & Abrens, R. (1995). The effect of oligosaccharides and lactitiol on the ileal digestibilities of amino acids, monosaccharides and bacterial populations and metabolites in the small intestine of weanling pigs. *Canadian Journal of Animal Science, 75*, 99–107.

Graham, K. K., Kerley, M. S., Firman, J. D., & Allee, G. L. (2002). The effect of enzyme treatment of soybean meal on oligosaccharide disappearance and chick growth performance. *Poultry Science, 81*, 1014–1019.

Grieshop, C. M., Kadzere, C. T., Clapper, G. M., Frazier, R. L., & Fahey, G. C. Jr., (2003). Chemical and nutritional characteristics of United States soybeans and soybean meals. *Journal of Agriculture and Food Chemistry, 51*, 7684–7691.

Guimarães, V. M., de Rezende, S. T., Moreira, M. A., Barros, E. G., & Felix, C. R. (2001). Characterization of α-galactosidases from germinating soybean seed and their use for hydrolysis of oligosaccharides. *Phytochemistry, 58*, 67–73.

Henninsson, A. M., Margareta, E., Nyman, G. L., & Björck, I. M. E. (2001). Content of short-chain fatty acids in the hindgut of rats fed processed bean (*Phaseolus vulgaris*) flours varying in distribution and content of indigestible carbohydrates. *British Journal of Nutrition, 86*, 379–389.

Igbasan, F. A., Guenter, W., & Slominski, B. A. (1997). The effect of pectinase and α-galactosidase supplementation on the nutritive value of peas for broiler chickens. *Canadian Journal of Animal Science, 77*, 537–539.

Irish, G. C., Barbour, G. W., Classen, H. L., Tyler, R. T., & Bedford, M. R. (1995). Removal of the alpha-galactosides of sucrose from soybean meal using either ethanol extraction or exogenous alpha-galactosidase and broiler performance. *Poultry Science, 74*, 1484–1494.

Karr-Lilienthal, L. K., Kadzere, C. T., Grieshop, C. M., & Fahey, G. C. Jr., (2005). Chemical and nutritional properties of soybean carbohydrates as related to nonruminants: A review. *Livestock Production Science, 97*, 1–12.

Kim, W. D., Kobayashi, O., Kaneco, S., Sakakibara, Y., Park, G. G., Kusakabe, I., et al. (2002). Galactosidase from cultured rice (*Oryza sativa* L. Var. Nipponbare) cells. *Phytochemistry, 61*, 621–630.

Leblanc, J. G., Garro, M. S., Silvestroni, A., Connes, C., Piard, J. C., Sesma, F., et al. (2004). Reduction of α-galactooligosaccharides in soyamilk by *Lactobacillus fermentum* CRL 722: *In vitro* and *in vivo* evaluation of fermented soyamilk. *Journal of Applied Microbiology, 97*, 876–881.

Levrat, M. A., Behr, S. R., Rémésy, C., & Demigné, C. (1991). Effects of soybean fiber on cecal digestion in rats previously adapted to a fiber-free diet. *Journal of Nutrition, 121*, 672–678.

Nobre, A., Lucas, C., & Leão, C. (1999). Transport and utilization of hexoses and pentoses in the halotolerant yeast *Debaryomyces hansenii*. *Applied and Environmental Microbiology, 65*, 3594–3598.

Reeves, P. G., Nielsen, F. H., & Fahey, G. C. Jr., (1993). AIN-93 purified diets for laboratory rodents: Final report of the American institute of nutrition ad hoc writing committee on the reformulation of the AIN-76. A rodent diet. *Journal of Nutrition, 123*, 1939–1955.

Roediger, W. E. W. (1980). Role of anaerobic bacteria in the metabolic welfare of the colonic mucosa in man. *Gut, 21*, 793–798.

Sakaguchi, E., Sakoda, C., & Toramaru, Y. (1998). Caecal fermentation and energy accumulation in the rat fed on indigestible oligosaccharides. *British Journal of Nutrition, 80*, 469–476.

Saldanha-Da-Gama, A., Malfeito-Ferreira, M., & Loureiro, V. (1997). Characterization of yeasts associated with Portuguese pork-based products. *International Journal Food Microbiology, 37*, 201–207.

Scalabrini, P., Rossi, M., Spettoi, P., & Matteuzzi, D. (1998). Characterization of *Bifidobacterium* strains for use in soymilk fermentation. *International Journal of Food Microbiology, 39*, 213–219.

Smiricky, M. R., Grieshop, C. M., Albin, D. M., Wubben, J. E., Gabert, V. M., & Fahey, G. C. J. (2002). The influence of soy oligosaccharides on apparent and true ileal amino acid digestibilities and fecal consistency in growing pigs. *Journal of Animal Science, 80*, 2433–2441.

Smiricky-Tjardes, M. R., Grieshop, C. M., Flickinger, E. A., Bauer, L. L., & Fahey, G. C. (2003). Dietary galactooligosaccharides affect ileal and total-tract nutrient digestibility, ileal and fecal bacterial concentrations, and ileal fermentative characteristics of growing pigs. *Journal Animal Science, 81*, 2535–2545.

Smits, C. H. M., & Annison, G. (1996). Non-starch plant polysaccharides in broiler nutrition- towards a physiologically valid approach to their determination. *World's Poultry Science Journal, 52*, 204–221.

Veldman, A., Veen, W. A. G., Barug, D., & Van Paridon, P. A. (1993). Effect of α-galactosides and α-galactosidase in feed on ileal piglet digestive physiology. *Journal of Animal Physiology and Animal Nutrition, 69*, 57–65.

Viana, P. A., De Rezende, S. T., Falkoski, D. L., Leite, T. A., José, I. C., Moreira, M. A., et al. (2007). Hidrolysis of oligosaccharides in soybean products by *Debaryomyces hansenii* UFV-1 α-galactosidases. *Food Chemistry, 103*, 331–337.

Viana, P. A., De Rezende, S. T., Marques, V. M., Trevizano, L. M., Passos, F. M. L., Oliveira, M. G. A., et al. (2006). Extracellular α-galactosidase from *Debaryomyces hansenii* UFV-1 and its use in the hydrolysis of raffinose oligosaccharides. *Journal of Agricultural and Food Chemistry, 54*, 2385–2391.

Yoon, M. Y., & Hwang, H. (2008). Reduction of soybean oligosaccharides and properties of α-D-galactosidase from *Lactobacillus curvatus* R08 and *Leuconostoc mesenteriodes* JK55. *Food Microbiology, 25*, 815–823.

Yoshida, S., Tan, C. H., Shimokawa, T., Turakainen, H., & Kusakabe, I. (1997). Substrate specificities of α-galactosidases from yeasts. *Bioscience, Biotechnology, Biochemistry, 61*, 359–361.

Zdunczyk, Z., Juskiewicz, J., Frejnagel, S., & Gulewicz, K. (1998). Influence of alkaloids and oligosaccharides from white lupin seeds on utilization of diets by rats and absorption of nutrients in the small intestine. *Animal Feed Science Technology, 72*, 143–154.

Food Chemistry 118 (2010) 256–265

Contents lists available at ScienceDirect

Food Chemistry

journal homepage: www.elsevier.com/locate/foodchem

Formation of dehydrodiisoeugenol and dehydrodieugenol from the reaction of isoeugenol and eugenol with DPPH radical and their role in the radical scavenging activity

Renzo Bortolomeazzi [a,*], Giancarlo Verardo [b], Anna Liessi [a], Alessandro Callea [b]

[a] Department of Food Science, University of Udine, via Sondrio 2ª, 33100 Udine, Italy
[b] Department of Chemical Sciences and Technologies, University of Udine, via Cotonificio 108, 33100 Udine, Italy

ARTICLE INFO

Article history:
Received 10 February 2009
Received in revised form 9 April 2009
Accepted 28 April 2009

Keywords:
Radical scavenging activity
DPPH radical
Isoeugenol
Eugenol
Dehydrodiisoeugenol
Dehydrodieugenol
Oxidative dimers
GC–MS
HPLC–MS

ABSTRACT

The aim of this work was to investigate the products of the reactions between isoeugenol and eugenol with the stable 2,2-diphenyl-1-picrylhydrazyl (DPPH) radical and their role in the radical scavenging mechanism. The reaction of isoeugenol and eugenol with the DPPH radical produced, as evidenced by GC–MS and HPLC–MS, a complex mixture of dimeric species in which dehydrodiisoeugenol and its adducts with methanol (reaction solvent) and dehydrodieugenol were the main reaction products, respectively. The antioxidant activity of dehydrodiisoeugenol, determined by the DPPH method, resulted lower than that of isoeugenol considering both the parameters Effective Concentration (EC_{50}) and Antiradical Efficiency (AE). In particular, due to its very slow kinetic behaviour ($T_{EC_{50}} = 201$ min), the possible contribution of dehydrodiisoeugenol to the DPPH radical scavenging activity of isoeugenol ($T_{EC_{50}} = 3.1$ min) was practically negligible. On the contrary, dehydrodieugenol had an antioxidant activity higher than that of eugenol and its lower $T_{EC_{50}}$ (85 min with respect to 126 min) made it possible to contribute to the DPPH radical scavenging activity of eugenol.

1. Introduction

Several analytical methods are routinely used to evaluate the antioxidant capacity of a large variety of compounds both in pure form and in complex mixture like herbs, spices, fruits and seeds extracts. Among them, the oxygen radical absorbance capacity (ORAC) assay, the 2,2-diphenyl-1-picrylhydrazyl (DPPH) radical assay, the trolox equivalent antioxidant capacity (TEAC) assay and the ferric reducing antioxidant power (FRAP) assay are probably the most widely used. The ORAC method is based on the scavenging of peroxyl radicals generated by an azo compound, and fluorescein is used as target molecule. The decrease in fluorescence in the absence and in the presence of an antioxidant is monitored. The assay is carried out in phosphate buffer at pH 7.4, and the results are expressed as trolox equivalents (Cao, Alessio, & Cutler, 1993; Ou, Hampsch-Woodill, & Prior, 2001). The DPPH method is based on the scavenging of the stable DPPH radical by the antioxidant. The decrease in absorbance of the radical is monitored at 515 nm, in methyl alcohol, until the reaction reaches a steady state. The results are expressed by the parameters Effective Concentration (EC_{50}) that represent the [antioxidant]/[DPPH] concentration ratio, which decreases the initial DPPH concentration by 50%, the stoichiometry value (n) defined as the DPPH moles scavenged by one mole of antioxidant and the Antiradical Efficiency defined as $AE = 1/(EC_{50} \times T_{EC_{50}})$, where $T_{EC_{50}}$ represents the time needed to reach the steady state for EC_{50} (Brand-Williams, Cuvelier, & Berset, 1995; Sanchez-Moreno, Larrauri, & Saura-Calixto, 1998). With a similar approach, the Trolox Equivalent Antioxidant Capacity (TEAC) method is based on the ability of a compound to scavenge the 2,2′-azinobis-(3-ethylbenzothiazoline-6-sulfonic acid) radical ($ABTS^{\bullet-}$) with respect to trolox C. The decrease in absorbance of the blue-green radical is monitored at 652 nm for 6–10 min. The assay is carried out in ethanol or in phosphate-buffered saline (PBS) at pH 7.4 and the results are expressed as trolox equivalents (Re et al., 1999). On the contrary, the FRAP method does not use free radical scavenging but is based on the reducing ability of the antioxidant versus the ferric-tripyridyltriazine complex. The increase in absorbance due to the formation of the coloured reduced ferrous complex is monitored and the results are expressed as trolox equivalents (Benzie & Strain, 1996). This brief description is enough to show the different approach and the different conditions of reaction time, reaction medium, temperature and treatment of the results used by these methods and the consequent difficulty to

* Corresponding author. Tel.: +39 0432558147; fax: +39 0432558130.
E-mail address: renzo.bortolomeazzi@uniud.it (R. Bortolomeazzi).

0308-8146/$ - see front matter © 2009 Elsevier Ltd. All rights reserved.
doi:10.1016/j.foodchem.2009.04.115

compare the results obtained for the same compounds. Foti and Ruberto (2001) observed a dependence of the antioxidant activity of some flavonoids and phenolic antioxidants on the hydrogen bond acceptor activity of the solvents. The effect of solvent and food components on the antioxidant activity obtained by applying the ORAC, DPPH, TEAC and FRAP methods to the mixture of catechin and gallic acid has been recently outlined by Perez-Jimenez and Saura-Calixto (2006). Also the oxidation processes involved are different: hydrogen atom transfer (HAT) in the case of the ORAC assay and single electron transfer (SET) in the other methods (Foti, Daquino, & Geraci, 2004; Huang, Ou, & Prior, 2005). These problems are even more enhanced by the possible occurrence of side reactions involving chemical species other than the antioxidant under testing. Studying the reaction mechanism of the DPPH radical with BHT, eugenol and isoeugenol, Brand-Williams et al. (1995) and Bondet, Brand-Williams, and Berset (1997) evidenced an inverse relationship between stoichiometry and reaction rates suggesting the intervention of a more complex reaction mechanism, eventually involving dimeric species, for the compounds with a slow kinetic behaviour such as eugenol. Recently, Ordoudi, Tsimidou, Vafiadis, and Bakalbassis (2006), studying the DPPH radical scavenging activity of guaiacol acid derivatives, reported the difficult to interpret the stoichiometry values of some compounds. Eklund et al. (2005) reported the formation of dimers in the reaction of lignans with DPPH radical. The EC_{50} of compounds with long reaction time can therefore reflect a radical scavenging capacity comprehensive not only of the contribution of the original antioxidant but also of other chemical species. Similar considerations were more recently outlined by Arts, Dallinga, Voss, Haenen, and Bast (2003) and Arts, Haenen, Voss, and Bast (2004) about the TEAC assay. In the reaction between $ABTS^{\cdot-}$ and the flavonoid chrysin, these authors reported the formation of a product with an antioxidant capacity higher than that of the parent compound. Hotta, Sakamoto, Nagano, Osakai, and Tsujino (2001) and Hotta, Nagano, Ueda, Tsujino, Koyama and Osakai (2002), studying the antioxidant capacity of natural compounds by column flow electrolysis, observed an increase of exchanged electrons by decreasing the flow and they attributed this effect to the oxidation of compounds formed by chemical reactions following the first oxidation process.

The aim of this work was to investigate the products formed by reaction of isoeugenol (**1**) and eugenol (**2**) with the DPPH radical under the same conditions used in the DPPH assay. The structural identification of these compounds, as well as the determination of their radical scavenging activity, may provide an insight into the antioxidant mechanism involved.

2. Materials and methods

2.1. Materials and reagents

All solvents were of analytical grade or LC–MS grade. 2,2-Diphenyl-1-picrylhydrazyl (DPPH) radical, eugenol (**1**), isoeugenol (**2**; mixture of *E* and *Z* isomers), N,O-bis(trimethylsilyl)trifluoroacetamide (BSTFA) and horseradish peroxidase (HRP, type II) were purchased from Sigma–Aldrich (Milan, Italy). Silica gel 60, 70–230 mesh ASTM and the thin-layer chromatography (TLC) silica gel plates, 0.25 mm thickness were provided by Merck (Darmstadt, Germany).

2.2. Melting point determination

Melting point determination was performed by differential scanning calorimetry (DSC) (Mettler TA 4000 system equipped with TC15 TA Controller, DSC 30 measuring cell and Star software version 8.10, Mettler, Greinfensee, Switzerland). Heat flow calibration was performed with indium, temperature calibration was done with *n*-hexane, distilled water and indium. Samples were placed into 40-μL aluminium pans that were hermetically sealed and scanned under 10 mL min^{-1} dry nitrogen flow to at least 10 °C above the endset of melting at a rate of 1 °C min^{-1}. The reported values were the average of two onset T_m.

2.3. ^1H and ^{13}C NMR spectra

^1H and ^{13}C NMR spectra were recorded on a Bruker AC-F 200 spectrometer at 200 and 50 MHz, respectively, using $CDCl_3$ as solvent at room temperature. NMR chemical shifts are reported as δ values from TMS.

2.4. Gas chromatography–mass spectrometry (GC–MS)

A Shimadzu gas chromatograph coupled to a quadrupole mass spectrometer QP-2010 (Shimadzu Corporation, Kyoto, Japan) was used. The column was a 30 m × 0.25 mm i.d., 0.25 μm film thickness, fused silica Equity 5 (Supelco, Sigma–Aldrich, Milan, Italy). The initial oven temperature was 60 °C for 2 min, then programmed to 280 °C at 15 °C min^{-1}. The injection was in splitless mode (2 min) with helium as carrier gas at a flow rate of 1 mL min^{-1}. The injector, transfer line and ion source temperatures were, respectively 280, 280 and 200 °C. The mass spectrometer operated in electron impact ionisation mode at 70 eV.

2.5. High performance liquid chromatography–mass spectrometry (HPLC–MS)

A Finnigan LXQ linear trap (Thermo Electron Corporation) was used for ESI-MS^n analysis in the positive and negative ion modes. The general conditions were capillary temperature 275 °C, sheath and auxiliary gas flows 25 and 5 (arbitrary units), respectively, source and capillary voltage in the positive polarity 4.0 kV and 2.0 V and 4.7 kV and −50.0 V in the negative polarity, respectively. Collision-induced dissociation (CID) multiple MS spectra (MS^n experiments) were acquired using helium as the collision damping gas in the ion trap at a pressure of 1 mTorr. Direct infusion of the standard solutions of pure dehydrodiisoeugenol (**3**) and dehydrodieugenol (**4**) and intact reaction mixtures diluted with MeOH or MeCN were performed with the aid of a syringe pump, using a flow rate of 5 μL min^{-1}. The LC-ESI-MS analyses were obtained with the same instrument coupled with a Finnigan Surveyor LC Pump Plus equipped with a Waters Spherisorb 5 μm ODS2 analytical column (4.6 × 250 mm) at 30 °C. Elution was carried out at a flow rate of 0.8 mL min^{-1} using an Accurate post-column flow splitter with a split ratio of 1:4 and MeCN/H_2O (65/35, v/v) as mobile phase.

2.6. DPPH radical scavenging method

The radical scavenging activity of the compounds was determined following the method used by Bortolomeazzi, Sebastianutto, Toniolo, and Pizzariello (2007). DPPH was dissolved in methanol at a final concentration of about 6×10^{-5} M. The exact concentration of DPPH was calculated from a calibration curve, ε = 11870 M^{-1} cm^{-1} at 515 nm. Different aliquots of a methanolic solution of the phenolic compounds were added to 2450 μL of DPPH solution and the volume was adjusted to a final value of 2500 μL with methanol. Five different concentrations were used for each assay. The decrease in the DPPH radical was followed at 515 nm until the reaction reached a steady state by using a Varian Cary 1E spectrophotometer equipped with a thermally controlled multicell block set at 25 °C. The concentrations of DPPH at the steady state, corrected for the natural disappearance of the DPPH radical, were plotted as a function of the molar concentration ratio

[AH]/[DPPH] to determine the Effective Concentration (EC_{50}). The time needed to reach the steady state for EC_{50} ($T_{EC_{50}}$) and the Antiradical Efficiency $AE = 1/(EC_{50} \times T_{EC_{50}})$ were also calculated.

2.7. Reaction of isoeugenol-DPPH radical

The conditions used to analyse the reaction products between isoeugenol (**1**) and DPPH were similar to those used in the DPPH assay. To 2450 μL of a methanolic DPPH solution were added 40 μL of methanol and 10 μL of an isoeugenol (**1**) methanolic solution. The final concentration was about 6×10^{-5} M and 4.4×10^{-5} M for DPPH and isoeugenol (**1**), respectively. After 5 min, the reaction mixture was reduced to dryness by a rotavapour at 40 °C, dissolved with 200 μL of acetonitrile and analysed by GC–MS. To the acetonitrile solution was then added 100 μL of BSTFA and was let to react for 1 h at room temperature before GC–MS analysis. The reaction was carried out also by using acetonitrile as solvent both for DPPH and isoeugenol (**1**) and analysed after 5 and 30 min.

2.8. Reaction of eugenol-DPPH radical

Similar conditions were used also for the analysis of the reaction products between DPPH radical and eugenol (**2**), final concentration was about 6×10^{-5} M and 4.7×10^{-5} M, respectively. The reaction was stopped after 10 min using methanol and after 30 min in the case of acetonitrile as solvents.

2.9. Synthesis of dehydrodiisoeugenol (*3*)

Dehydrodiisoeugenol (**3**) was prepared by oxidative coupling of isoeugenol (**1**) using the peroxidase-H_2O_2 system, following the method reported by Nascimento, Lopes, Davin and Lewis (2000) with minor modifications. To a solution of isoeugenol (**1**) (1.01 g, 6.2 mmol) in 30 mL of MeOH were added 275 mL of citrate–phosphate buffer (20 mM, pH 3) and horseradish peroxidase (8.5 mg, 1500 U) in 10 mL of buffer. 0.31 mL of H_2O_2 (3.05 mmol) was then added dropwise over 10 min and under magnetic stirring. The reaction mixture was stirred for an additional 10 min and then transferred in a separatory funnel and extracted with 100 mL of ethylacetate. The organic phase was washed with water, dried over anhydrous Na_2SO_4 and reduced to dryness. The crude product was loaded into a silica chromatography column (20 cm length × 2 cm i.d.) and eluted with *n*-hexane/ethylacetate mixture from an initial 8.5/1.5 (v/v) ratio. The chromatographic separation was monitored by TLC. The fractions containing the product (Rf 0.41, *n*-hexane/ethylacetate, 8/2, v/v) were combined, reduced to dryness (268 mg, 27%) and crystallised from MeOH/H_2O. m.p. 132.5 °C [lit. 128–130 °C (Shiba, Xiao, Miyakoshi, & Chen, 2000); 129–132 °C (Juhász, Kürti, & Antus, 2000)]; calcd. for $C_{20}H_{22}O_4$: C, 73.60; H, 6.79; found C, 73.56; H, 6.71. EIMS *m*/*z* (rel. int.): *m*/*z* 326 (M^+, 100), 311 (M^+-CH_3, 16), (1 × TMS) *m*/*z* 398 (M^+, 100), 383 (M^+-CH_3, 14), 368 ($M^+-2 \times CH_3$, 10). ESI (+)-MS (infusion, MeOH), *m*/*z*: 327 $[M + H]^+$ (MS^3 transitions 327 > 203 > 171), 349 $[M + Na]^+$, 675 $[2\,M + Na]^+$. ESI (−)-MS (infusion, MeOH), *m*/*z*: 325 $[M-H]^-$ (MS^5 transitions 325 > 310 > 295 > 277 > 249). ^1H NMR ($CDCl_3$/TMS): δ 1.37 (d, 3H, *J* = 6.8 Hz, ACH$_3$-9), 1.86 (dd, 3H, *J* = 6.4, 1.5 Hz, BCH$_3$-9), 3.37–3.52 (m, 1H, ACH-8), 3.86 (s, 3H, AMeO-3), 3.88 (s, 3H, BMeO-3), 5.09 (d, 1H, *J* = 9.5 Hz, ACH-7), 5.67 (br s, 1H, OH), 6.10 (dq, 1H, *J* = 15.6, 6.5 Hz, BCH-8), 6.36 (dd, 1H, *J* = 15.6, 1.5 Hz, BCH-7), 6.76 (br s, 1H, BCH-6), 6.78 (br s, 1H, BCH-2), 6.87–6.93 (m, 2H, ACH-5, ACH-6), 6.97 (br s, 1H, ACH-2). ^{13}C NMR ($CDCl_3$): δ 17.5 (AC-9), 18.3 (BC-9), 45.5 (AC-8), 55.8 (AMeO-3), 55.9 (BMeO-3), 93.7 (AC-7), 108.8 (AC-2), 109.1 (BC-2), 113.2 (BC-6), 114.0 (AC-5), 119.9 (AC-6), 123.4 (BC-8), 130.8 (BC-7), 132.0 (BC-1), 132.1 (AC-1), 133.2 (BC-5), 144.1 (BC-3), 145.7 (AC-4), 146.5 (BC-4), 146.6 (AC-3) (Scheme 1).

The GC–MS analysis of the crystallised product evidenced the presence of four compounds with practically the same mass spectra and M^+ at *m*/*z* 326. The relative retention times (RRTs) to the most abundant compound were 0.96, 0.97, 1, 1.01 and the corresponding percent chromatographic areas, calculated on the basis of the *m*/*z* 326 ion signal, were 2.1, 0.1, 95.7 and 2.1%, respectively. The HPLC–MS analysis of the same product evidenced the presence of three compounds with *m*/*z* 327 $[M + H]^+$ and the same fragmentation patterns till MS^3. Sarkanen and Wallis (1973) reported the formation of (*E*)-1-[(2*RS*,3*SR*)-2,3-dihydro-2-(4-hydroxy-3-methoxy phenyl)-7-methoxy-3-methyl-1-benzofuran-5-yl]-1-propene [(*E*)-(±)-*trans*-dehydrodiisoeugenol] (**3a**) and (*Z*)-1-[(2*RS*,3*SR*)-2,3-dihydro-2-(4-hydroxy-3-methoxyphenyl)-7-methoxy-3-methyl-1-ben zofuran-5-yl]-1-propene [(*Z*)-(±)-*trans*-dehydrodiisoeugenol] (**3b**) by peroxidase catalysed oxidation of (*E*)- and (*Z*)-isoeugenol, respectively. Due to the presence in isoeugenol (**1**) standard of both the (*E*)- and (*Z*)-isomers in the proportion of about 93% and 7%, respectively, the formation of both the dehydrodimers **3a** and **3b** would be expected. On this basis the structure of (*E*)-(±)-*trans*-dehydrodiisoeugenol (**3a**) has been assigned to the most abundant compound and the structure of (*Z*)-(±)-*trans*-dehydrodiisoeugenol (**3b**) to one of the other three compounds. Regarding the other two, the following structures (*E*)-1-[(2*RS*,3*RS*)-2,3-dihydro-2-(4-hydroxy-3-methoxyphenyl)-7-methoxy-3-methyl-1-ben zofuran-5-yl]-1-propene [(*E*)-(±)-*cis*-dehydrodiisoeugenol] (**3c**) and (*Z*)-1-[(2*RS*,3*RS*)-2,3-dihydro-2-(4-hydroxy-3-methoxyphenyl)-7-methoxy-3-methyl-1-benzofuran-5-yl]-1-propene [(*Z*)-(±)-*cis*-dehydrodiisoeugenol] (**3d**) have been hypothesised (Scheme 1). The ^1H and ^{13}C NMR spectra were in agreement with the structure of (*E*)-(±)-*trans*-dehydrodiisoeugenol (**3a**) (Barbosa-Filho, Leitão da-Cunha, & Sobral da Silva, 1998; Juhász et al., 2000; Shiba et al., 2000) which purity was about 95.7%. The structure-numbering system used in the ^1H and ^{13}C NMR data does not follow the actual compound names but is based on the numbering of the monomer so as to maintain consistency.

2.10. Synthesis of dehydrodieugenol (*4*)

Dehydrodieugenol (**4**) was prepared by oxidative coupling of eugenol (**2**) using potassium ferricyanide as oxidising agent following the method reported by De Farias Dias (1988). To a solution of eugenol (**2**) (1.0 g, 6.1 mmol) in an acetone/H_2O mixture (2:1, v/v, 30 mL) 18 mL of aqueous NH_4OH (28%) was added and the mixture was stirred for 10 min. To the mixture a saturated aqueous solution of $K_3Fe(CN)_6$ (2.0 g, 6.1 mmol) was then added dropwise over a period of about 5 h and then 18 mL of aqueous NH_4OH (28%) was added. The mixture was stirred for an additional 16 h at room temperature and then neutralised with HCl 10%. There was the formation of a solid precipitate which was filtered, washed with water and dried (720 mg, 72%). The crude product was crystallised from ethanol after decolourisation with activated charcoal. m.p. 105.8 °C, [lit. 105–106 °C, (De Farias Dias, 1988)]; calcd. for $C_{20}H_{22}O_4$: C, 73.60; H, 6.79; found C, 73.10; H, 6.84. EIMS *m*/*z* (rel. int.): *m*/*z* 326 (M^+, 100), 297 (M^+-HCO, 34), 285 ($M^+-CH_2CHCH_2$, 6), 284 [$M^+-(CH_2CHCH_2 + H)$, 7], 267 [$M^+-(CH_2CHCH_2 + H_2O)$, 6], 253 [$M^+-(CH_2CHCH_2 + H + CH_3O)$, 22], 244 ($M^+-2 \times CH_2CHCH_2$, 11), 221 [$M^+-(CH_2CHCH_2 + H + CH_3O + CH_3OH)$, 9]; (2 × TMS) *m*/*z* 470 (M^+, 100), 455 (M^+-CH_3, 46), 440 ($M^+-2 \times CH_3$, 36). ESI (+)-MS (infusion, MeOH), *m*/*z*: 327 $[M + H]^+$, 349 $[M + Na]^+$ (MS^3 transitions 349 > 308 > 277), 675 $[2\,M + Na]^+$. ESI (−)-MS (infusion, MeOH), *m*/*z*: 325 $[M-H]^-$ (MS^5 transitions 325 > 310 > 295 > 254 > 226). ^1H NMR ($CDCl_3$/TMS): δ 3.36 (d, 4H, *J* = 6.7 Hz, CH_2-7, CH_2-7′), 3.89 (s, 6H, 2 × OMe), 5.01–5.18 (m, 4H, CH_2-9, CH_2-9′), 5.87–6.09 (m, 2H, CH-8, CH-8′), 6.05 (br s, 2H, OH), 6.72 (d, 2H, *J* = 1.9, CH-2, CH-2'), 6.75 (d, 2H, J = 1.9, CH-6, CH-6′). ^{13}C NMR ($CDCl_3$): δ 39.9 (C-7, C-7′), 56.0

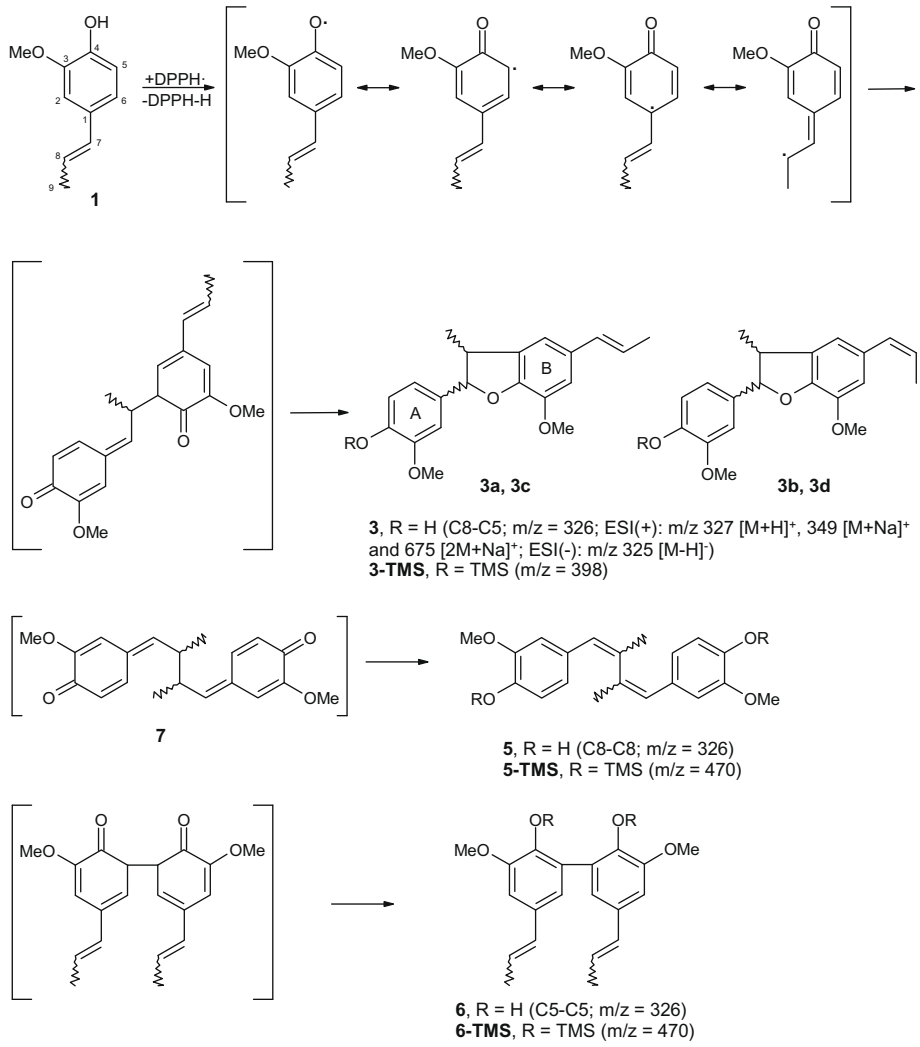

Scheme 1.

(2 × OMe), 110.6 (C-2, C-2′), 115.6 (C-9, C-9′), 123.0 (C-6, C-6′), 124.4 (C-5, C-5′), 131.8 (C-1, C-1′), 137.6 (C-8, C-8′), 140.8 (C-4, C-4′), 147.2 (C-3, C-3′). The ^{1}H and ^{13}C NMR spectra were in agreement with the data reported in literature (De Farias Dias, 1988).

3. Results and discussion

3.1. Reaction products of isoeugenol (*1*)

3.1.1. GC–MS analysis

The GC–MS chromatogram of the reaction mixture of isoeugenol (**1**) and DPPH radical in methanol evidenced the presence of two groups of compounds characterised by the M_r 326 and 358, respectively. The first group was composed of six compounds with M^+ at m/z 326 (Scheme 1), four of which had the same retention times of those present in the GC–MS chromatogram of the synthesised dehydrodiisoeugenol (**3**). In particular, the compound present in the highest amount (83.0%) had the same RT and mass spectrum of (*E*)-(±)-*trans*-dehydrodiisoeugenol (**3a**). The other two compounds with m/z 326 accounted for only 2.0% of the total chromatographic area.

The other group was composed of three compounds characterised by the same mass spectrum with M^+ at m/z 358. Compounds with M_r 358, which corresponded to an increase of 32 u with respect to the M_r 326, can be considered as the methanol adducts **9** arising from the addition of methanol to the C8–*O*–C4 quinone methide intermediate **8** (Scheme 2).

The formation of two diastereomeric forms of **9** was previously reported by Miller (1972) among the dimeric compounds obtained by 2,4,6-tri-*tert*-butylphenoxyl radical oxidation of (*E*)- or (*Z*)-isoeugenol in benzene/methanol solution. Also Chioccara et al. (1993) reported the formation of a mixture of *erythro* and *threo* diastereomers **9** by addition of methanol to a quinone methide intermediate formed by C8-*O*-C4 coupling of two phenoxyl radicals during the reaction of (*E*)-isoeugenol with hydrogen peroxide and HRP in aqueous buffer and methanol from 10% to 90%. The same authors observed an increase in the yields of these compounds with increasing methanol content. The addition of methanol to a quinone methide structure formed by reaction of lignans and DPPH radical was recently reported by Eklund et al. (2005). To confirm these structures, the reaction mixture was acetylated (Ac_2O, pyridine) and analysed by GC–MS. The analysis evidenced the presence of four compounds with m/z 400 (M^+) and fragment ions at m/z 237, 236, 209, 195, 194, 167 and 164. The M_r and the fragmentation patterns were in agreement with those reported by Chioccara et al. (1993) for the acetate derivatives of the methanol adducts of the C8–*O*–C4-coupled dimers **9**.

The GC–MS chromatogram of the TMS derivatives of the reaction products of isoeugenol (**1**) and DPPH radical in methanol is shown in Fig. 1A. Some compounds were detectable only after

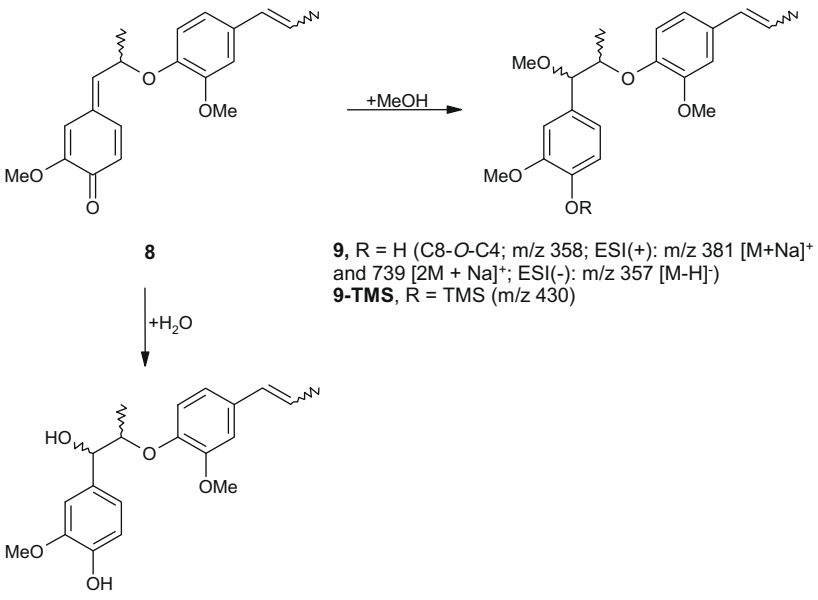

Scheme 2.

TMS derivatisation probably due to a better chromatographic behaviour of the TMS derivatives and, in particular, of the compounds present in very low amount. The GC–MS analysis evidenced the presence of four compounds with M^+ at m/z 398 corresponding to 326 + TMS, four compounds with M^+ at m/z 430 corresponding to m/z 358 + TMS, three compounds with M^+ at m/z 470 corresponding to 326 + 2 × TMS and three compounds with M^+ at m/z 502 corresponding to 358 + 2 × TMS. The mixture of products resulting from the reaction between DPPH radical and **1** was very complex, also due to the presence of (*E*)- and (*Z*)-isoeugenol, and can be rationalised by considering basically two groups of compounds characterised by M_r 326 and 358, respectively. The compounds with M_r 326 (Scheme 1) are dimeric form of **1** which, after silylation, produced two separate classes of isomers. The first class had originally one phenolic hydroxy group and the M_r of 398 corresponds to a mono-TMS derivative. Among the dimers with one phenolic hydroxy group, the most abundant was that corresponding to (*E*)-(±)-*trans*-dehydrodiisoeugenol (**3a**) arising from a C8–C5 coupling process (Scheme 1).

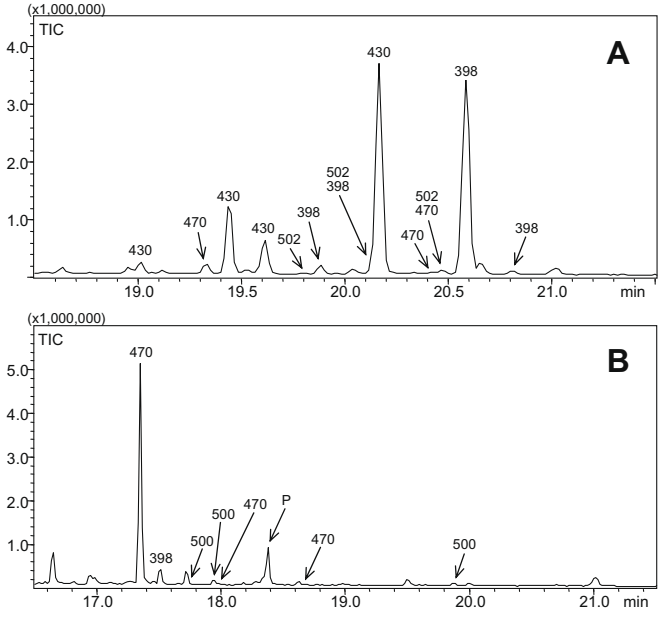

Fig. 1. GC–MS chromatograms of the dimer regions of the silylated reaction mixtures of isoeugenol (**1**) and eugenol (**2**) with DPPH radical in methanol. The number above the peaks represents the m/z ratio of the molecular ion of the corresponding compound. (**A**) isoeugenol – DPPH radical (for m/z 398 and 470 refer to Scheme 1, for m/z 430 refer to Scheme 2, for m/z 502 refer to Scheme 3); (**B**) eugenol – DPPH radical (for m/z 470 and 398 refer to Schemes 4 and 5, for m/z 500 refer to Scheme 6); P = phthalate contaminant.

The second class had two phenolic hydroxy groups and the M_r of 470 corresponded to a bis-TMS derivative. The dimers with two phenolic hydroxy groups **5** and **6** were present at a very low amount compared to **3a** and all the other compounds and can be originated from the C8–C8 and C5–C5 coupling processes, respectively, as hypothesised in Scheme 1. Sarkanen and Wallis (1973) reported the formation of compounds arising from the addition of water to a bisquinone methide system, such as **7** shown in Scheme 1, formed by a C8–C8 coupling process in the case of the enzyme-catalysed oxidation of both (*E*)- and (*Z*)-isoeugenol. Although the same authors did not report the formation of the C8–C8-coupled dimer **5** (Scheme 1), its formation in very low amount by aromatisation of bisquinone methide **7**, before the addition of water, cannot be excluded. Regarding the C5–C5-coupled dehydrodimer **6** (Scheme 1), Sarkanen and Wallis (1973) did not report its formation among the oxidation products of both (*E*)- and (*Z*)-isoeugenol. On the other hand, Ralph, Quideau, Grabber and Hatfield (1994) and Hatfield, Ralph and Grabber (1999) reported both the presence of C8–C8 and low amounts of the C5–C5 dehydrodimers of ferulic acid in plant cell wall extracts.

Like the compounds with M_r 326, also the compounds with M_r 358 produced, after silylation, two classes of isomers. The first class, which comprehended the methanol adducts of the C8–*O*–C4-coupled dimers **9**, had originally one phenolic hydroxy group and the M_r of 430 (326 + 32 + 72) corresponded to the mono-TMS derivatives **9-TMS** (Scheme 2).

The second class, present in very low amount, had two phenolic hydroxy groups and the M_r of 502 (326 + 32 + 2 × 72) corresponded to a bis-TMS derivative. The addition of methanol can take place only to the quinone methide intermediate **7** formed by the C8–C8 coupling process yielding **10** (Scheme 3). This consideration

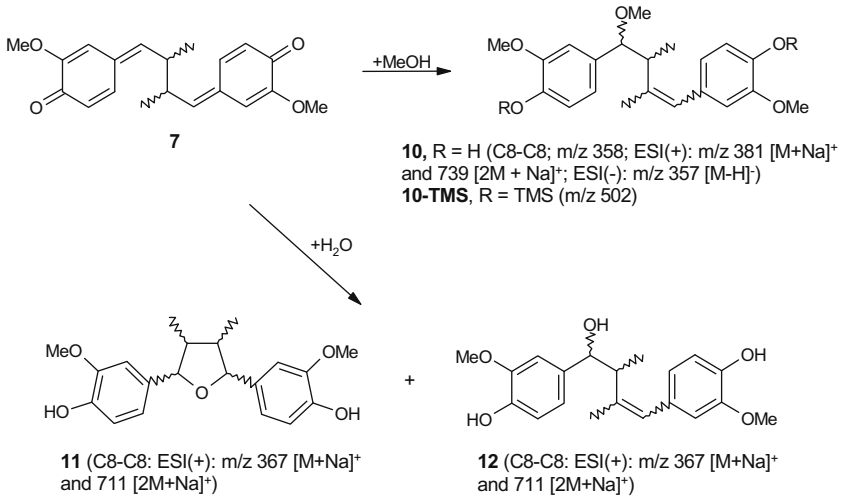

Scheme 3.

suggested that the dimers with two hydroxy groups were probably of the C8–C8 type (Scheme 1). The necessity of the presence of methanol to produce the adducts was demonstrated by carrying out the reaction in acetonitrile. In this case neither compounds with M_r 358, due to methanol addition, nor compounds with M_r 430 and 502 after silylation were observed.

Besides the dimers, other peaks corresponding to unreacted isoeugenol (**1**) and DPPH radical thermodegradation products were present in the GC–MS chromatogram, in particular diphenylamine and 2,4,6-trinitroaniline, which were the most abundant compounds in the reaction mixture as identified on the basis of the mass spectrum and comparison with the NIST library.

3.1.2. HPLC–MS analysis

Due to the possible risk of artifacts formation in the hot injection port of the gas chromatograph, the reaction mixture between isoeugenol (**1**) and DPPH radical was analysed also by HPLC–MS. The HPLC–MS analysis evidenced the presence of three compounds with ESI (+)-MS at m/z 327 $[M + H]^+$, 349 $[M + Na]^+$ and 675 $[2\,M + Na]^+$ and ESI (−)-MS at m/z 325 $[M - H]^-$ with the same retention times and fragmentation patterns of the synthesised dehydrodiisoeugenol (**3**). Moreover, three compounds with ESI (+)-MS at m/z 381 $[326 + 32 + Na]^+$ and 739 $[2 \times (356 + 32) + Na]^+$ and ESI (−)-MS at m/z 357 $[326 + 32 - H]^-$ which corresponded to the methanol adducts **9** and/or **10** were present (Schemes 2 and 3). These results confirmed the previous findings obtained by GC–MS apart from the number of isomers detected which can depend by the different resolving powers of the two chromatographic techniques. HPLC–MS analysis showed six other compounds with m/z at 367 $[326 + 18 + Na]^+$ and 711 $[2 \times (326 + 18) + Na]^+$ which probably corresponded to the addition of water to the quinone methides **7** and **8** with the formation of **11** and **12** (Scheme 3) and **13** (Scheme 2), respectively.

The formation of **11** (Sarkanen and Wallis, 1973) and **13** (Sarkanen and Wallis, 1973; Shiba et al., 2000) was previously reported in the case of the enzyme-catalysed oxidation of **1** moreover, like the addition of methanol leading to **10**, the addition of water to **7** could afford **12** (Scheme 3). The formation of water adducts could be due to the dilution of the methanolic reaction mixture with water to a final concentration of about 35% like the mobile phase prior to HPLC–MS analysis.

The HPLC–MS analysis of the reaction mixture carried out in acetonitrile and diluted with water, before analysis, evidenced the formation of the dimers of **1** and the water adducts, but not the formation of the methanol adducts, confirming the results obtained by GC–MS. The reactions carried out in acetonitrile were visibly slower than those carried out in methanol.

Neither termination products by coupling of **1** and DPPH radicals nor compounds arising by the abstraction of two hydrogen atoms from **1** were detected under our experimental conditions.

From the data obtained it can be concluded that the main products formed by reaction of isoeugenol (**1**) and DPPH radical in methanol were the (*E*)-(±)-*trans*-dehydrodiisoeugenol (**3a**) and the methanol adducts **9**.

*3.2. Reaction products of eugenol (**2**)*

3.2.1. GC–MS analysis

The GC–MS chromatogram of the TMS derivatives of the reaction products of eugenol (**2**) and DPPH radical in methanol is reported in Fig. 1B. The GC–MS analysis evidenced the presence of three peaks with M_r 470, one peak with M_r 398 and three peaks with M_r 500. The compounds with M_r 470 ($326 + 2 \times$ TMS) corresponded to the bis-TMS derivatives of eugenol dimers and the most abundant had the same retention time and mass spectrum of the TMS derivative of the dehydrodieugenol (**4**) synthesised, derived from a C5–C5 coupling process (Scheme 4). The other two compounds, which accounted for only 0.2% of the chromatographic area, could arise from the addition of eugenol-5-radical **14** at the 7 and 9 position of the quinone methide intermediate **15** affording **16** and **17**, respectively, as hypothesised in Scheme 5.

The compound with M_r 398 (326 + TMS) could be interpreted as mono-TMS derivative of eugenol dimer with only one hydroxy phenolic group, a C5–*O*–C4 coupling process could be the mechanism leading to compound **18** (Scheme 5). The formation of a compound formed by a C5–*O*–C4 coupling process was reported by Sy and Brown (1998) in the case of the oxidative coupling of 4-allylphenol.

The compounds with M_r 500 ($326 - 2 + 32 + 2 \times$ TMS), present in very low amount, could have structures **19** and **20**, corresponding to the bis-TMS derivatives of the addition products of methanol to the quinone methide **21**, as hypothesised in Scheme 6. As in the case of isoeugenol (**1**), the necessity of the presence of methanol to produce these adducts was demonstrated by carrying out the reaction in acetonitrile, in this case no compounds with M_r 500 were observed.

Unreacted eugenol (**2**) and DPPH radical thermodegradation products were also present in the GC–MS analysis of the reaction mixture.

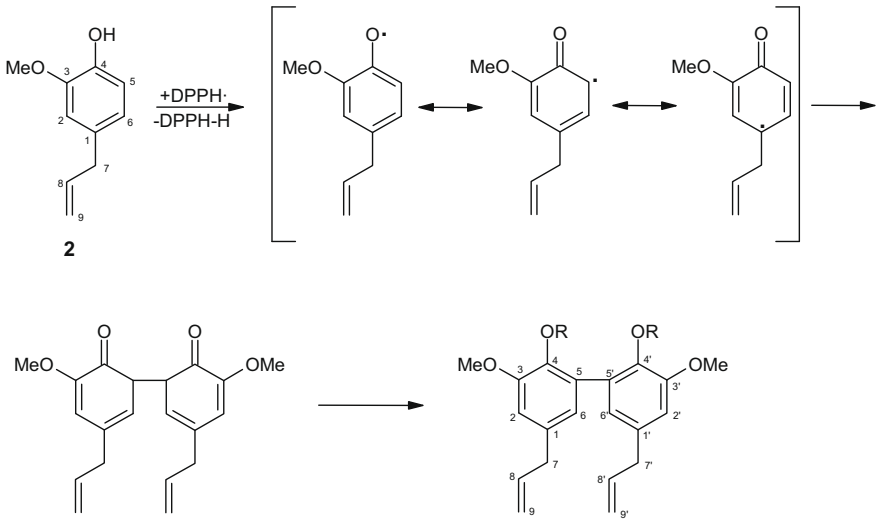

Scheme 4.

3.2.2. HPLC–MS analysis

The HPLC–MS analysis of the reaction mixture of eugenol (**2**) and DPPH radical evidenced the presence of a compound with ESI (+)-MS at *m/z* 327 $[M + H]^+$, 349 $[M + Na]^+$ and 675 $[2\,M + Na]^+$ and ESI (−)-MS at *m/z* 325 $[M - H]^-$ corresponding, as retention time and mass spectrum, to the synthesised dehydrodieugenol (**4**). Moreover, two compounds with *m/z* 379 $[326 - 2 + 32 + Na]^+$ and 355 $[326 - 2 + 32 - H]^-$ which could correspond to **19** and **20** (Scheme 6) were present. These results confirmed the previous findings obtained by GC–MS.

As in the case of isoeugenol (**1**), the reactions carried out in acetonitrile were visibly slower than those carried out in methanol, and neither termination products by coupling of **2** and DPPH radicals nor compounds arising by the abstraction of two hydrogen atoms from **2** were detected under our experimental conditions.

*3.3. DPPH radical scavenging activity of dehydrodiisoeugenol (**3**) and dehydrodieugenol (**4**)*

The DPPH radical scavenging activity of **3** and **4** was determined in order to evaluate their possible contribution to the activity of the corresponding parent compounds, isoeugenol (**1**) and eugenol (**2**), respectively. Only these two dimeric species have been considered from the point of view of the antioxidant activity being the most abundant among the products originated from the reactions of **1** and **2** with the DPPH radical. The results expressed as EC_{50}, stoichiometry (*n*), $T_{EC_{50}}$ and AE are reported in Table 1 together with the radical scavenging activity of **1** and **2** previously determined by Bortolomeazzi et al. (2007) under similar conditions of analysis.

The EC_{50} of dehydrodiisoeugenol (**3**) was slightly higher than that of isoeugenol (**1**) and one mole of both compounds roughly scavenged one mole of DPPH, with a stoichiometry value of 0.7 and 0.9, respectively, corresponding to the number of phenolic OH present in the molecular structure. On the contrary, their kinetic behaviour was completely different with **3** acting much more slowly ($T_{EC_{50}} = 201$ min) than **1** ($T_{EC_{50}} = 3.1$ min). The very rapid kinetic of **1** has been explained by the presence, at the para position relative to phenol, of a propenyl group with the double bond conjugated to the benzene ring. This allows a better stabilisation of the phenoxyl radical by extending the delocalisation and lowers the Bond Dissociation Enthalpy (BDE) of the phenolic O–H bond (Barclay, Xi, & Norris, 1997; Wrigth, 2002; Wrigth, Johnson, & Di Labio, 2001). This structure was lost in the formation of **3** and the eventually stabilising electron-donating (+I) effect of the aliphatic part of new heterocyclic moiety was moreover impaired by the −I effect of the oxygen linked to the ᴀC7 in **3** (Scheme 1).

The radical scavenging activity of the methanol adducts **9** was not determined, due to the lack of the pure compounds; however, on the basis of their structure it was sensible to hypothesise an antioxidant activity similar to that of **3**.

Sanchez-Moreno et al. (1998) outlined the presence of compounds with comparable EC_{50} but with very different kinetic behaviour. These authors introduced the parameter AE that takes into account both the radical scavenging activity (EC_{50}) and the kinetic behaviour ($T_{EC_{50}}$). On the basis of the AE values, isoeugenol (**1**) resulted about 90 times more active than its corresponding dimer dehydrodiisoeugenol (**3**) (Table 1).

Dehydrodieugenol (**4**) had an EC_{50} value lower than that of eugenol (**2**) and one mole can scavenge about 2.7 mol of DPPH, whereas **2** scavenged 2 mol of DPPH radical. Also the $T_{EC_{50}}$ value was lower and, on the basis of the AE parameter, the antioxidant activity of **4** resulted about twice that of **2** (Table 1). The higher activity of **4** with respect to **2** can be explained by the presence of two phenolic OH groups and an ortho benzene ring which allowed an extensive conjugation stabilising the phenoxyl radical of **4**.

The $T_{EC_{50}}$ values of the compounds analysed deserve some more comments. The $T_{EC_{50}}$ of isoeugenol (**1**) was very low in comparison to those of dehydrodiisoeugenol (**3**) and eugenol (**2**) attributing this effect to the lower BDE of the phenolic OH bond in **1** as a consequence of the extended conjugation. A similar consideration has been applied also to **4** although, in this case, the substituent is attached to the ortho position, relative to the two phenolic OH. Wrigth et al. (2001) reported that a vinyl group in the ortho position relative to phenol showed a stabilising electronic effect only slightly lower than in the para position. On this basis, the kinetic behaviour of dehydrodieugenol (**4**) could be expected to be more rapid with a $T_{EC_{50}}$ more similar to that of isoeugenol (**1**). The slow reaction between **4** and DPPH radical can, however, be explained

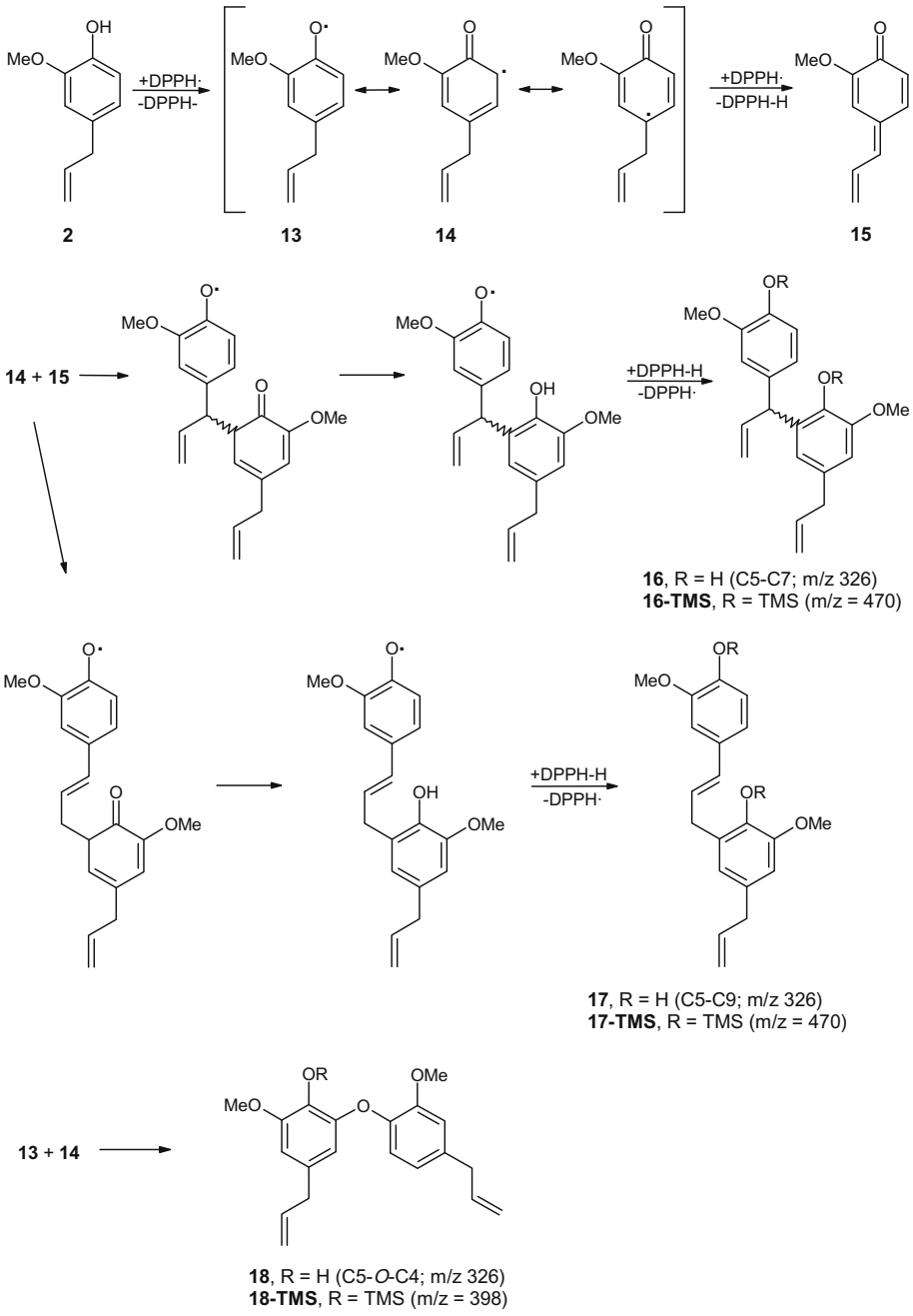

Scheme 5.

by the intervention of steric hindrance which can interfere with the planar conformation of **4** necessary to achieve optimal stabilisation of the phenoxyl radical by resonance as hypothesised by Barclay et al. (1997) in the case of 2,2′-dihydroxy-3,3′-dimethoxy-5,5′-dimethoxymethylbiphenyl.

Brand-Williams et al. (1995) and Bondet et al. (1997) reported that in the case of compounds reacting very quickly, the number of DPPH molecules reduced equals the number of hydroxyl groups present in the antioxidant molecule ($n = 1$). On the contrary, in the case of slow reacting compounds the stoichiometric value is, in general, larger than one ($n > 1$). This aspect was evidenced by the behaviour of isoeugenol (**1**) and eugenol (**2**) which had a kinetic fast (0.5 min) and slow (120 min) and $n = 1.1$ and 1.9, respectively. These authors explained the finding of stoichiometric values larger than one by hypothesising three reaction pathways after the initial formation of the antioxidant radical, such as donation of a second hydrogen atom to DPPH radical, dimerisation by coupling of two antioxidant radicals and coupling of antioxidant and DPPH radicals. In particular, for **2**, these authors suggested a dimerisation mechanism, while in the case of **1** none of these reactions would take place.

The results obtained in our work evidenced that, contrary to the hypothesis of Brand-Williams et al. (1995) and Bondet et al. (1997), the phenoxyl radical of isoeugenol (**1**) underwent extensive dimerisation and, moreover, the solvent methanol was involved in the reaction mechanism. The 0.9 stoichiometric value of **1** (Table 1) can, however, be explained by the very low kinetic behaviour of dehydrodiisoeugenol (**3**) with respect to **1**. When the DPPH method was applied to **1**, the time of the analysis was too short for the formed **3**, and eventually the methanol adducts **9**, to reveal their contribution to the total radical scavenging activity of **1**.

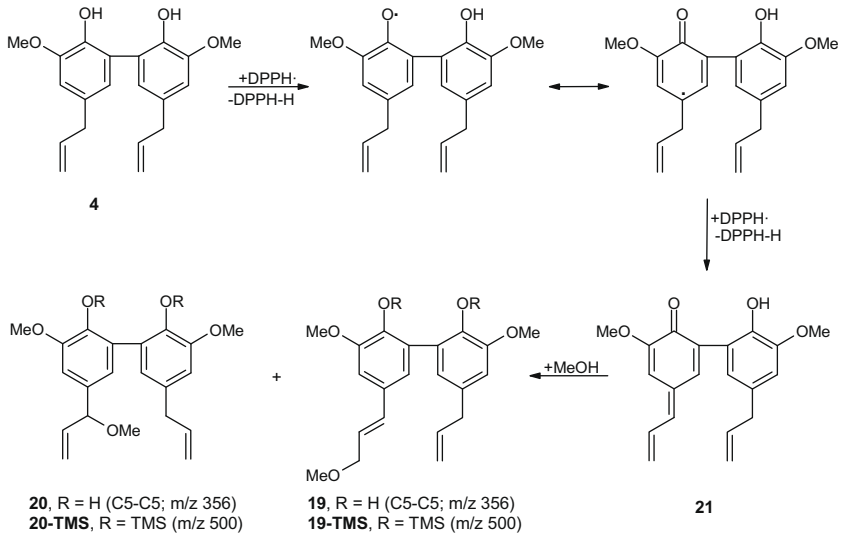

Scheme 6.

Table 1
Effective Concentration (EC_{50}), stoichiometry (n), $T_{EC_{50}}$ and antiradical efficiency (AE) obtained with the DPPH assay. (The values are the mean of three determinations ± standard deviation).

Compound	EC_{50}[a]	n[b]	$T_{EC_{50}}$[c]	AE × 10^3[d]
Isoeugenol (**1**)	0.54[e] ± 0.04	0.93 ± 0.07	3.12 ± 0.06	592 ± 45[e]
Dehydrodiisoeugenol (**3**)	0.74 ± 0.02	0.67 ± 0.02	201 ± 3	6.7 ± 0.3
Eugenol (**2**)	0.26[e] ± 0.01	1.94 ± 0.07	126 ± 8	31 ± 2[e]
Dehydrodieugenol (**4**)	0.184 ± 0.002	2.72 ± 0.03	85 ± 1	64 ± 1

[a] Mol AH/mol DPPH.
[b] Mol DPPH/mol AH.
[c] Min.
[d] Mol DPPH/(mol AH × t); AH, phenolic antioxidant.
[e] Bortolomeazzi et al. (2007).

In the case of eugenol (**2**), the formation of dehydrodieugenol (**4**), as the main reaction product, confirmed the hypothesis of Brand-Williams et al. (1995) and Bondet et al. (1997) regarding the dimerisation of **2**. The 1.9 stoichiometry value of **2** (Table 1) can then be explained by the formation of the dimer and its reaction with DPPH radical. In fact, considering the $T_{EC_{50}}$ of **2** and **4**, the time window of the reaction between DPPH radical and **2** can overlap with that of the reaction between DPPH radical and **4** which can then contribute to the radical scavenging activity of eugenol (**2**).

The formation of a complex mixture of dimeric compounds originated by different coupling processes and finding that also the solvent, methanol, and eventually water can be involved, evidenced that the reaction mechanism can be more complex than previously hypothesised. The possible contribution of the reaction products to the radical scavenging activity of a compound limits the use of the DPPH method to evaluate structure–activity relationship and the possibility to correlate the results with the antioxidant activity obtained by other methods.

References

Arts, M. J. T. J., Dallinga, J. S., Voss, H.-P., Haenen, G. R. M. M., & Bast, A. (2003). A critical appraisal of the use of the antioxidant capacity (TEAC) assay in defining optimal antioxidant structures. *Food Chemistry, 80*, 409–414.

Arts, M. J. T. J., Haenen, G. R. M. M., Voss, H.-P., & Bast, A. (2004). Antioxidant capacity of reaction products limits the applicability of the trolox equivalent antioxidant capacity (TEAC) assay. *Food and Chemical Toxicology, 42*, 45–49.

Barbosa-Filho, J. M., Leitão da-Cunha, E. V., & Sobral da Silva, M. (1998). Complete assignment of the ^1H and ^{13}C NMR spectra of some lignoids from lauraceae. *Magnetic Resonance in Chemistry, 36*, 929–935.

Barclay, L. R. C., Xi, F., & Norris, J. Q. (1997). Antioxidant properties of phenolic lignin model compounds. *Journal of Wood Chemistry and Technology, 17*, 73–90.

Benzie, I. F. F., & Strain, J. J. (1996). The Ferric reducing ability of plasma (FRAP) as a measure of "antioxidant power": The FRAP assay. *Analytical Biochemistry, 239*, 70–76.

Bondet, V., Brand-Williams, W., & Berset, C. (1997). Kinetics and mechanisms of antioxidant activity using the DPPH free radical method. *Lebensmittel-Wissenschaft und-Technologie, 30*, 609–615.

Bortolomeazzi, R., Sebastianutto, N., Toniolo, R., & Pizzariello, A. (2007). Comparative evaluation of the antioxidant capacity of smoke flavouring phenols by crocin bleaching inhibition, DPPH radical scavenging and oxidation potential. *Food Chemistry, 100*, 1481–1489.

Brand-Williams, W., Cuvelier, M. E., & Berset, C. (1995). Use of a free radical method to evaluate antioxidant activity. *Lebensmittel-Wissenschaft und-Technologie, 28*, 25–30.

Cao, G., Alessio, H. M., & Cutler, R. G. (1993). Oxygen-radical absorbance capacity assay for antioxidants. *Free Radical Biology & Medicine, 14*, 303–311.

Chioccara, F., Poli, S., Rindone, B., Pilati, T., Brunow, G., Pietikäinen, P., et al. (1993). Regio- and diastereo-selective synthesis of dimeric lignans using oxidative coupling. *Acta Chemica Scandinavica, 47*, 610–616.

De Farias Dias, A. (1988). An improved high yield synthesis of dehydrodieugenol. *Phytochemistry, 27*, 3008–3009.

Eklund, P. C., Långvik, O. K., Wärnå, J. P., Salmi, T. O., Willför, S. M., & Sjöholm, R. E. (2005). Chemical studies on antioxidant mechanisms and free radical scavenging properties of lignans. *Organic and Biomolecular Chemistry, 3*, 3336–3347.

Foti, M., Daquino, C., & Geraci, C. (2004). Electron-transfer reaction of cinnamic acids and their methyl esters with DPPH radical in alcoholic solution. *Journal of Organic Chemistry, 69*, 2309–2314.

Foti, M., & Ruberto, G. (2001). Kinetic solvent effects on phenolic antioxidants determined by spectrophotometric measurements. *Journal of Agricultural and Food Chemistry, 49*, 342–348.

Hatfield, R. D., Ralph, J., & Grabber, J. H. (1999). Cell wall cross-linking by ferulates and diferulates in grasses. *Journal of the Science of Food and Agriculture, 79*, 403–407.

Hotta, H., Nagano, S., Ueda, M., Tsujino, Y., Koyama, J., & Osakai, T. (2002). Higher radical scavenging activities of polyphenolic antioxidants can be ascribed to chemical reactions following their oxidation. *Biochimica et Biophysica Acta, 1572*, 123–132.

Hotta, H., Sakamoto, H., Nagano, S., Osakai, T., & Tsujino, Y. (2001). Unusually large numbers of electrons for the oxidation of polyphenolic antioxidants. *Biochimica et Biophysica Acta, 1526*, 159–167.

Huang, D., Ou, B., & Prior, R. L. (2005). The chemistry behind antioxidant capacity assay. *Journal of Agricultural and Food Chemistry, 53*, 1841–1856.

Juhász, L., Kürti, L., & Antus, S. (2000). Simple synthesis of benzofuranoid neolignans from *Myristica fragrans*. *Journal of Natural Products, 63*, 866–870.

Miller, I. J. (1972). The dimerization of isoeugenol by free radicals. *Tetrahedron Letters, 49*, 4955–4958.

Nascimento, I. R., Lopes, L. M. X., Davin, L. B., & Lewis, N. G. (2000). Stereoselective synthesis of 8,9-licarinediols. *Tetrahedron, 56*, 9181–9193.

Ordoudi, S. A., Tsimidou, M. Z., Vafiadis, A. P., & Bakalbassis, E. G. (2006). Structure-DPPH· scavenging activity relationships: Parallel study of catechol and guaiacol acid derivatives. *Journal of Agricultural and Food Chemistry, 54*, 5763–5768.

Ou, B., Hampsch-Woodill, M., & Prior, R. L. (2001). Development and validation of an improved oxygen radical absorbance capacity assay using fluorescein as the fluorescent probe. *Journal of Agricultural and Food Chemistry, 49*, 4619–4626.

Perez-Jimenez, J., & Saura-Calixto, F. (2006). Effect of solvent and certain food constituents on different antioxidant capacity assays. *Food Research International, 39*, 791–800.

Ralph, J., Quideau, S., Grabber, J. H., & Hatfield, R. D. (1994). Identification and synthesis of new ferulic acid dehydrodimers present in grass cell walls. *Journal of the Chemical Society. Perkin Transactions, 1*, 3485–3498.

Re, R., Pellegrini, N., Proteggente, A., Pannala, A., Yang, M., & Rice-Evans, C. (1999). Antioxidant activity applying an improved ABTS radical cation decolorization assay. *Free Radical Biology & Medicine, 26*, 1231–1237.

Sanchez-Moreno, C., Larrauri, J. A., & Saura-Calixto, F. (1998). A procedure to measure the antiradical efficiency of polyphenols. *Journal of the Science of Food and Agriculture, 76*, 270–276.

Sarkanen, K. V., & Wallis, A. F. A. (1973). Oxidative dimerizations of (E)- and (Z)-isoeugenol (2-methoxy-4-propenylphenol) and (E)- and (Z)-2,6-dimethoxy-4-propenylphenol. *Journal of the Chemical Society. Perkin Transactions, 1*, 1869–1878.

Shiba, T., Xiao, L., Miyakoshi, T., & Chen, C.-L. (2000). Oxidation of isoeugenol and coniferyl alcohol catalyzed by laccases isolated from *Rhus vernicifera* Stokes and *Pycnoporus coccineus*. *Journal of Molecular Catalysis. B, Enzymatic, 10*, 605–615.

Sy, L.-K., & Brown, G. D. (1998). Biomimetic synthesis of *Illicium* oligomeric neolignans. *Journal of Chemical Research (S)*, 476–477.

Wrigth, J. S. (2002). Predicting the antioxidant activity of curcumin and curcuminoids. *Journal of Molecular Structure, 591*, 207–217.

Wrigth, J. S., Johnson, E. R., & Di Labio, G. A. (2001). Predicting the activity of phenolic antioxidants: Theoretical method, analysis of substituent effects, and application to major families of antioxidants. *Journal of the American Chemical Society, 123*, 1173–1183.

Food Chemistry 118 (2010) 266–271

Contents lists available at ScienceDirect

Food Chemistry

journal homepage: www.elsevier.com/locate/foodchem

Berry juices, teas, antioxidants and the prevention of atherosclerosis in hamsters

Jean-Max Rouanet [a,*], Kelly Décordé [a], Daniele Del Rio [b], Cyril Auger [c], Gina Borges [c], Jean-Paul Cristol [a], Michael E.J. Lean [d], Alan Crozier [c]

[a] Unité Mixte de Recherche 204-Prévention des Malnutritions et des Pathologies Associées, CC 023, Université Montpellier, 2, Place Eugène Bataillon, 34095 Montpellier, France
[b] Department of Public Health, University of Parma, Via Volturno 39, 43100 Parma and National Institute of Biostructures and Biosystems (INBB), Italy
[c] Division of Environmental and Evolutionary Biology, Faculty of Biomedical and Life Sciences, University of Glasgow, Glasgow G12 8QQ, United Kingdom
[d] Human Nutrition Section, University of Glasgow Division of Developmental Medicine, Queen Elizabeth Building, Royal Infirmary, Glasgow G31 2ER, United Kingdom

ARTICLE INFO

Article history:
Received 20 February 2009
Received in revised form 17 March 2009
Accepted 28 April 2009

Keywords:
Atherosclerosis
Nutrition
Phenolic compounds
Antioxidants
Berry juices
Teas

ABSTRACT

The effects of raspberry, strawberry and bilberry juices and green and black tea on early atherosclerosis in hamsters were investigated. They received an atherogenic diet and at the same time either a juice or a tea at a daily dose corresponding to the consumption of 275 ml by a 70 kg human. After 12 weeks berry juices and teas inhibited aortic lipid deposition by 79–96% and triggered reduced activity of hepatic antioxidant enzymes, not accompanied by lowered plasma cholesterol. These findings suggest that moderate consumption of berry juices and teas can help prevent the development of early atherosclerosis. There were substantial differences between the five beverages in terms of composition and concentration of individual phenolic compounds that were present. This indicates that anti-atherosclerotic effects can be induced by a diversity of phenolic compounds rather than a few specific components. The possible mechanisms by which this is brought about are discussed.

1. Introduction

The postulated involvement of lipid peroxidation in atherogenesis invoked intensive research on antioxidants. Consumption of fruits and vegetables has been linked with lower prevalence of coronary heart disease (Bazzano, 2006; Dauchet, Amouyel, Hercberg, & Dallongeville, 2006; Feldman, 2001; Liu et al., 2000). Drinking tea has also been linked with reduced mortality arising from cardiovascular disease (Kuriyama et al., 2006), although some epidemiological data are inconclusive (Yang & Landau, 2000). Fruits, vegetables and teas contain a wide range of antioxidant compounds, including phenolic compounds and vitamins. Phenolic compounds, such as anthocyanins, flavan-3-ols, flavonols, hydroxycinnamates and tannins, are widespread in fruits and vegetables, with especially high quantities being found in berries and teas. Berries are rich in anthocyanins and can also contain substantial quantities of ellagitannins, while flavan-3-ols and their related derivatives predominate in teas (Crozier, Jaganath, Marks, Saltmarsh, & Clifford, 2006).

Golden Syrian hamsters represent an useful test system because when fed a fat-rich diet they develop dyslipidemia and atherosclerotic plaques, similar in many respects to human atheroma (Auger et al., 2002).

A relatively straight-forward way to evaluate influences on atherosclerosis progression in animal models is to measure the extent of fatty streak development, the continuous accumulation of lipids (due mainly to large accumulations of macrophages) in the subendothelial space. Using this approach, we have evaluated the effects of raspberry, strawberry and bilberry juices and green and black tea, sources of potentially anti-atherogenic phenolic compounds, by feeding the beverages to golden Syrian hamsters on a high fat diet for a 12-week period.

2. Materials and methods

2.1. Chemicals

5-*O*-Caffeoylquinic acid, procyanidin B2, (−)-epicatechin (+)-catechin, (−)-gallocatechin, (−)-epicatechin, (−)-epicatechin gallate, (−)-epigallocatechin, (−)-epigallocatechin gallate, gallic acid, caffeine, theobromine, theaflavins and ellagic acid were purchased from Sigma–Aldrich (Poole, UK). Quercetin, myricetin, quercetin-3-*O*-rutinoside, quercetin-3-*O*-glucoside, quercetin-3-*O*-arabinoside, quercetin-3-*O*-galactoside, kaemperol-3-*O*-rutinoside, kaemperol-3-*O*-glucoside, caffeic acid and *p*-coumaric acid were obtained from AASC Ltd. (Southampton, UK). Cyanidin-3-*O*-glucoside was purchased from Extrasynthese (Genay, France). Methanol and acetonitrile were obtained from Rathburn Chemicals (Walkerburn, Peebleshire, UK). Formic acid was obtained from Fisher Scientific (Loughborough, UK).

* Corresponding author. Fax: +33 0467143521.
E-mail address: jm.rouanet@univ-montp2.fr (J.-M. Rouanet).

0308-8146/$ - see front matter © 2009 Elsevier Ltd. All rights reserved.
doi:10.1016/j.foodchem.2009.04.116

2.2. Berries juices and teas

Bouvrage raspberry (*Rubus idaeus* L.;1 ml = 0.6 g berries), bilberry (*Vaccinium myrtillus*; 1 ml = 0.32 g berries) and strawberry juices (*Fragaria ananassa*; 1 ml = 0.22 g berries) drinks were obtained from Ella Drinks Ltd. (Alloa, Clackmannanshire, UK). The green and black teas (The Tetley Group, Greenford, Middlesex, UK) were prepared by adding 300 ml of boiling water to 3 g of leaves. After brewing for 3 min with continuous stirring, tea solids were removed by filtration through a sieve and the resulting tea was allow to cool before preparation of aliquots which were stored at −20 °C prior to use.

2.3. HPLC–PDA–MS^2 analysis of berry juices and teas

Berry juices and teas were analysed on a Surveyor HPLC system comprising of a HPLC pump, photodiode array detector (PDA) scanning from 250 to 700 nm, and an autosampler set at 4 °C (Thermo Finnigan, San Jose, USA) with the separation carried out using a 250 × 4.6 mm i.d. 4 μm Synergi RP-Max column (Phenomenex, Macclesfield, UK) eluted at a flow rate of 1 ml/min. A mobile phase consisting of a 5–40% gradient over 60 min of acetonitrile in 0.1% formic acid was used for the analysis of all samples. After passing through the flow cell of the diode array detector the column eluate was split and 0.3 ml was directed to a LCQ Deca XP ion trap mass spectrometer fitted with an electrospray interface (Thermo Finnigan, San Jose, USA). Analysis was carried out using full scan mode from 100 to 2000 amu, with data dependent tandem MS (MS^2) scanning, in both negative and positive ion mode.

A combination of co-chromatography with authentic standards, where available, absorbance spectra and mass spectra, using MS^2, were used to confirm the identity of compounds previously reported in the literature (Stewart, Mullen, & Crozier, 2005). Quantitative estimates are based on calibrations generated by the PDA detector using the compound under study when a standard was available – see Chemicals. When this was not possible, a closely related derivative was used instead. For instance, all anthocyanins, were quantified by reference to cyanidin-3-*O*-glucoside, while chlorogenic acids, such as 3-*O*-*p*-coumarylquinic acid were quantified by reference to the appropriate aglycone. In all instances the standard curve of reference compounds ranged from 2 to 500 ng.

The thearubigin content of the black tea was estimated as described by Stewart et al. (2005).

2.4. Animals, diets and experimental design

Sixty weanling male Syrian golden hamsters (Elevage Janvier, Le Genest-St-Isle, France) weighing ca.100 g were maintained in plastic cages in a temperature controlled environment (23 ± 1 °C) subjected to a 12-h light/dark cycle and allowed free access to both food and water. Hamsters were handled according to the guidelines of the Committee on Animal Care at the University of Montpellier and NIH guidelines (National Research Council, 1985).

They were randomly assigned to six groups of 10 not statistically different for weight. For 12 weeks all the hamsters were fed a semi-purified atherogenic diet (Scientific Animal Food and Engineering, Augy, France) consisting of casein (200 g/kg), L-methionine (3 g/kg), corn starch (393 g/kg), sucrose (154 g/kg), cellulose (50 g/kg), lard (150 g/kg), and cholesterol (5 g/kg) (Auger et al., 2002). The diet also contained vitamin (10 g/kg) and mineral mixes (35 g/kg). It was formulated according to AIN-93 guidelines (Reeves, Nielsen, & Fahey, 1993) and was devoid of selenium, vitamin C and vitamin E. During the 12-week period, the hamsters received either water (control), raspberry juice, strawberry juice, bilberry juice, green tea or black tea daily by gavage. The volume of solutions fed was adjusted daily to the weight of hamsters. The calculation is based on a consumption of 275 ml/day for a 70 kg human as based on the US Food and Drug Administration Center for Drug Evaluation and Research dose calculator (http://www.fda.gov/cder/cancer/animalframe.htm).

2.5. Analytical procedures

At the end of the 12-week experimental period the hamsters were fasted overnight and blood was drawn by cardiac puncture under anesthesia. Plasma was prepared by centrifugation at 2000*g* for 10 min at 4 °C, and then stored at −80 °C before analysis. The liver was perfused with saline to remove residual blood, rapidly excised, rinsed in ice cold saline, blotted dry, weighted, sectioned for analyses and stored in liquid nitrogen. The aortic tissues were then processed as described below.

Following blood collection and liver removal, the intact aorta was first perfused with phosphate buffered saline containing 1 mmol/l $CaCl_2$ and 15 mmol/l glucose for 5 min, then with 0.1 mmol/l sodium cacodylate buffer pH 7.4 containing 2.5 mmol/l $CaCl_2$, 2.5% paraformaldehyde and 1.5% glutaraldehyde for the fixation of the vasculature. The aorta was carefully dissected and processed as previously described (Auger et al., 2002), lipids being stained in Oil red O. An image acquisition and analysis system (ImageJ, Scion Corporation, Frederick, MD) incorporated in an Olympus microscope was used to capture and analyse the total Oil Red O stained area of each aortic arch. The area covered by foam cells (aortic fatty streak area or AFSA) was expressed as a percentage of the total area.

Plasma total cholesterol (TC) and HDL cholesterol (HDL-C) were determined by commercially available enzymatic methods (respectively Nos. CH 200 and CH 203, Randox Laboratories Ltd., Crumlin, UK) on a Pentra 400 automated analyser (HORIBA ABX, Montpellier, France). Plasma very low- + low-density lipoprotein cholesterol (referred to as « non-HDL-C in the data tables) was precipitated with phosphotungstate reagent and HDL-C was measured in the supernatant.

The liver was homogenised in 5 vol of 0.15 M KCl buffer (pH 7.4) and the homogenate was spun at 13,000*g* for 15 min at 4 °C. The supernatant was stored at −80 °C prior to the assay of glutathione peroxidase (GSHPx) and superoxide dismutase (SOD) activity on a Pentra 400 analyser. GSHPx activity was measured by the method of Randox (Randox Laboratories Ltd., Crumlin, UK) using a commercial kit (Ransel, No. RS505). Superoxide dismutase (SOD) activity was determined using a Randox kit (Ransod, No. SD 125).

To extract and analyse livers by HPLC–PDA–MS^2, the livers from two hamsters from each feeding group were combined and homogenised in 2 ml of methanol/water (v/v) containing 5% formic acid and 20 mM sodium diethyldithiocarbamate using an Ultraturrax homogeniser. The resultant homogenate was shaken continuously for 30 min before being centrifuged at 2000*g* for 20 min. The supernatant was decanted and the pellet re-extracted twice. The three supernatants were combined and reduced to dryness *in vacuo*. The extract was dissolved in 25 μl methanol in 475 μl aqueous 1% formic acid and loaded onto an activated 2 g Sep–Pak C_{18} cartridge (Waters, Milford, MA, USA) which was washed with 4 ml acidified water (pH 3.0) before elution with 4 ml methanol containing 1% formic acid. The methanolic eluates were reduced to dryness and resuspended in 50 μl methanol in 950 μl aqueous 1% formic acid before analysis for anthocyanin and flavan-3-ol metabolites by HPLC–PDA–MS^2 using single and selected ion monitoring.

2.6. Statistical analyses

Data are shown as the means ± SEM, $n = 10$ measurements/group. Tea and berry juices samples were analysed in triplicate.

Statistical analysis of the data was carried out using the Stat View IV software (Abacus Concepts, Berkeley, CA, USA) by one-way ANOVA followed by Fisher's Protected Least Significant Difference test. Differences were considered significant at $p < 0.05$.

3. Results

3.1. Phenolic compounds in berry juices and teas

Twenty seven phenolic compounds were detected in the bilberry juice (Table 1) with the 13 anthocyanins comprising 599 nmoles/ml of a total flavonoid and phenolic content of 744 nmoles/ml. The juice also contained 76 nmoles/ml of gallic acid and smaller quantities of flavan-3-ols and a number of flavonols in low concentrations. The major components in the raspberry juice were anthocyanins (164 nmoles/ml), principally cyanidin-3-sophoroside and cyanidin-3–2^G-glucosylrutinoside, and the ellagitannins, lambertianin C and sanguiin H-6 (Table 2). The strawberry juice contained much lower overall levels of flavonoids and phenolics, 181 nmoles/ml (Table 3), than the bilberry and raspberry juices. The main constituents were pelargonidin-3-glucoside (91 nmoles/l) and a *p*-coumaric acid hexose conjugate (46 nmoles/l) (Table 3).

The compositions of the two teas are summarised in Table 4. Both green and black tea contained higher amounts of phenolic compounds than the juices, with 2894 and 2285 nmoles/ml, respectively for green and black tea. The main green tea constituents were catechins which comprised a group of eight flavan-3-ols, accounting for 2414 nmoles/ml with the major component being (−)-epigallocatechin (921 nmoles/ml). Black tea contained much lower concentrations of catechins (52 nmoles/ml) than green tea, but a large amount of theaflavins and thearubigins (1839 nmoles/ml) that were not present in green tea. Both teas also contained broadly similar levels of chlorogenic acids and a diverse array of flavonols.

Table 1
Concentration of phenolic compounds in bilberry juice. Data expressed as nmoles/ml ± SEM ($n = 3$).

Compound	Concentration
Gallic acid	76 ± 1
5-Caffeoylquinic acid	22 ± 1
Caffeic acid hexoside	12 ± 0
Total gallic and caffeic acid derivatives	*110*
Delphinidin-3-galactoside	38 ± 2
Delphinidin-3-glucoside	75 ± 2
Delphinidin-3-arabinoside	45 ± 0
Cyanidin-3-galactoside	32 ± 1
Cyanidin-3-glucoside	120 ± 1
Cyanidin-3-arabinoside	46 ± 1
Petunidin-3-glucoside	64 ± 1
Petunidin-3-arabinoside	12 ± 0
Peonidin-3-galactoside	4.8 ± 0.1
Peonidin-3-glucoside	45 ± 1
Malvidin-3-galactoside	31 ± 1
Malvidin-3-glucoside	74 ± 1
Malvidin-3-arabinoside	12 ± 1
Total anthocyanins	*599*
(−)-Epicatechin	8.1 ± 0.2
Procyanidin dimer	7.4 ± 0.5
Procyanidin trimer	3.2 ± 0.1
Total flavan-3-ols	*19*
Myricetin-3-galactoside	1.6 ± 0.0
Myricetin-3-glucoside	2.6 ± 0.1
Myricetin-3-glucuronide	1.1 ± 0.0
Quercetin-3-galactoside	2.9 ± 0.0
Quercetin-3-glucoside	1.5 ± 0.0
Quercetin-3-glucuronide	3.6 ± 0.1
Myricetin	1.2 ± 0.0
Quercetin	1.2 ± 0.0
Total flavonols	*16*
Total phenolics and flavonoids	*744*

3.2. Effects of berry juices and teas on fatty steak deposits

Fig. 1A shows the effects of bilberry, raspberry and strawberry juice consumption on aortic fatty streak deposits in hamsters fed a high-fat diet for 12 weeks. In the control animals, which ingested water rather than juice, fatty streaks covered 21.2 ± 2.7% of the aortic wall. The extent of these deposits when juices or teas were administered to hamsters, were dramatically and significantly lower with respect to controls (all $p < 0.001$ when compared to water control). The aortic fatty streak area was 4.5 ± 0.5% for the group fed with bilberry juice, 2.4 ± 0.5% with strawberry juice, 1.1 ± 0.2% with raspberry juice and finally 0.75 ± 0.13% and 1.40 ± 0.31% for green and black tea, respectively. Representative pictures of fatty streak deposits are presented in Fig. 2.

Table 2
Concentration of phenolic compounds in raspberry juice. Data expressed as nmoles/ml ± SEM ($n = 3$).

Compound	Concentration
Cyanidin-3-sophoroside	108 ± 1
Cyanidin-3-(2^G-glucosylrutinoside)	32 ± 1
Cyanidin-3-glucoside	12 ± 0
Pelargonidin-3-sophoroside	4.1 ± 0.1
Cyanidin-3-rutinoside	5.6 ± 0.1
Pelargonidin-3-(2^G-glucosylrutinoside)	2.0 ± 0.1
Total anthocyanins	*164*
Procyanidin dimer B4	1.5 ± 0.1
Total flavan-3-ols	*1.5*
Sanguiin H-10	46 ± 1
Lambertianin C	59 ± 2
Sanguiin H-6	235 ± 6
Ellagic acid	16 ± 0.1
Ellagic acid-4-acetylpentose	0.9 ± 0.0
Total hydrolysable tannins and ellagic acid derivatives	*357*
Quercetin-3-hexosyl-rhamnoside	0.2 ± 0.1
Quercetin-3-galactosylrhamnoside	0.6 ± 0.0
Quercetin-3-rutinoside	0.2 ± 0.0
Quercetin-3-galactoside	2.2 ± 0.1
Quercetin-3-glucoside	0.7 ± 0.0
Quercetin-3-glucuronide	2.4 ± 0.1
Quercetin	0.5 ± 0.0
Total flavonols	*7.7*
Total phenolics and flavonoids	*530*

Table 3
Concentration of phenolic compounds in strawberry juice. Data expressed as nmoles/ml ± SEM ($n = 3$).

Compound	Concentration
p-Coumaric acid-hexose	46 ± 1
Total hydroxycinnamates	*46*
Pelargonidin-3-glucoside	91 ± 1
Pelargonidin-3-(6-malonylglucoside)	22 ± 0
Total anthocyanins	*113*
Procyanidin dimer B1	0.9 ± 0.0
Procyanidin dimer B3	4.9 ± 0.1
Procyanidin trimer	2.8 ± 0.0
Total flavan-3-ols	*8.6*
Sanguiin	9.9 ± 0.2
Ellagic acid rhamnoside	2.0 ± 0.0
Total hydrolysable tannins and ellagic acid derivatives	*12*
Quercetin-3-glucuronide	0.9 ± 0.1
Kaempferol-3-glucoside	0.3 ± 0.0
Kaempferol-malonyl-hexoside	0.7 ± 0.0
Total flavonols	*1.9*
Total phenolics and flavonoids	*181*

Table 4
Concentration of phenolic compounds, and purine alkaloids in green and black tea infusions. Data expressed as nmoles/ml ± SEM (n = 3).

Compound	Green tea	Black tea
Gallic acid	6.3 ± 0.2	132 ± 7
5-Galloylquinic acid	64 ± 1	77 ± 1
Total gallic acid derivatives	*70*	*209*
(−)-Gallocatechin	225 ± 2	n.d.
(−)-Epigallocatechin	921 ± 11	19 ± 1
(+)-Catechin	168 ± 6	7.4 ± 0.2
(−)-Epicatechin	459 ± 10	6.8 ± 0.1
(−)-Epigallocatechin-3-gallate	494 ± 25	7.4 ± 0
(−)-Epicatechin-3-gallate	147 ± 5	11 ± 0
Total flavan-3-ols	*2,414*	*52*
3-Caffeoylquinic acid	30 ± 1	5.0 ± 0.2
5-Caffeoylquinic acid	118 ± 1	32 ± 0.1
4-*p*-Coumaroylquinic acid	85 ± 2	76 ± 1
Total caffeic and coumaric acid derivatives	*233*	*113*
Quercetin-rhamnosylgalactoside	4.5 ± 0.2	3.6 ± 0.1
Quercetin-3-rutinoside	39 ± 1	29 ± 1
Quercetin-3-galactoside	46 ± 1	29 ± 1
Quercetin-rhamnose-hexose-rhamnose	7.2 ± 0.2	5.9 ± 0
Quercetin-3-glucoside	72 ± 1	46 ± 1
Kaempferol-rhamnose-hexose-rhamnose	7.7 ± 0	7.4 ± 0.2
Kaempferol-3-galactoside	17 ± 1	12 ± 1
Kaempferol-3-rutinoside	21 ± 1	18 ± 1
Kaempferol-3-glucoside	41 ± 0	28 ± 2
Kaempferol-3-arabinoside	2.0 ± 0.1	n.d.
Unknown quercetin conjugate	0.8 ± 0.1	0.9 ± 0.1
Unknown quercetin conjugate	6.7 ± 0.2	4.9 ± 0.2
Unknown kaempferol conjugate	2.0 ± 0	n.d
Unknown kaempferol conjugate	0.4 ± 0.0	10 ± 0.0
Total flavonols	*267*	*185*
Theaflavin	n.d.	20 ± 1
Theaflavin-3-gallate	n.d.	16 ± 1
Theaflavin-3′-gallate	n.d.	8.8 ± 0.1
Theaflavin-3,3′-digallate	n.d.	13 ± 0
Thearubigins	n.d.	1781
Total theaflavins and thearubigins	*n.d.*	*1839*
Total phenolics and flavonoids	*2984*	*2285*
Theobromine	57 ± 1	25 ± 1
Caffeine	804 ± 15	503 ± 3
Total purine alkaloids	*861*	*528*

n.d. – not detected.

3.3. Effects of berry juices and teas on circulating cholesterol and hepatic antioxidant enzymes

The lower fatty streak deposition in juice and tea hamster groups was not accompanied by lower circulating cholesterol levels (total cholesterol, HDL-cholesterol and non-HDL-cholesterol were not significantly different between all groups; not shown here) but was associated to a reduced activity of liver antioxidant defense system in hamsters fed antioxidant rich beverages in comparison to controls (Fig. 1B and C). Teas induced a greater inhibition in the antioxidant enzymes compared to berry juices. Analysis of liver extracts by HPLC-mass spectrometry operating in selected ion and selected reaction monitoring mode did not detect the presence of any flavonoids or phenolic compounds derived from the teas or berry juices despite the hamsters being fed the supplements for a period of 12 weeks.

4. Discussion

Daily consumption of each of the test beverages for a 12-week period resulted in a substantially lower fatty streak deposition in the arteries of the hamsters compared to water-treated controls, with stronger effects for green tea and raspberry juice (Figs. 1A and 2). This marked limitation of the onset of atherosclerosis was not associated with any significant change in plasma cholesterol profile.

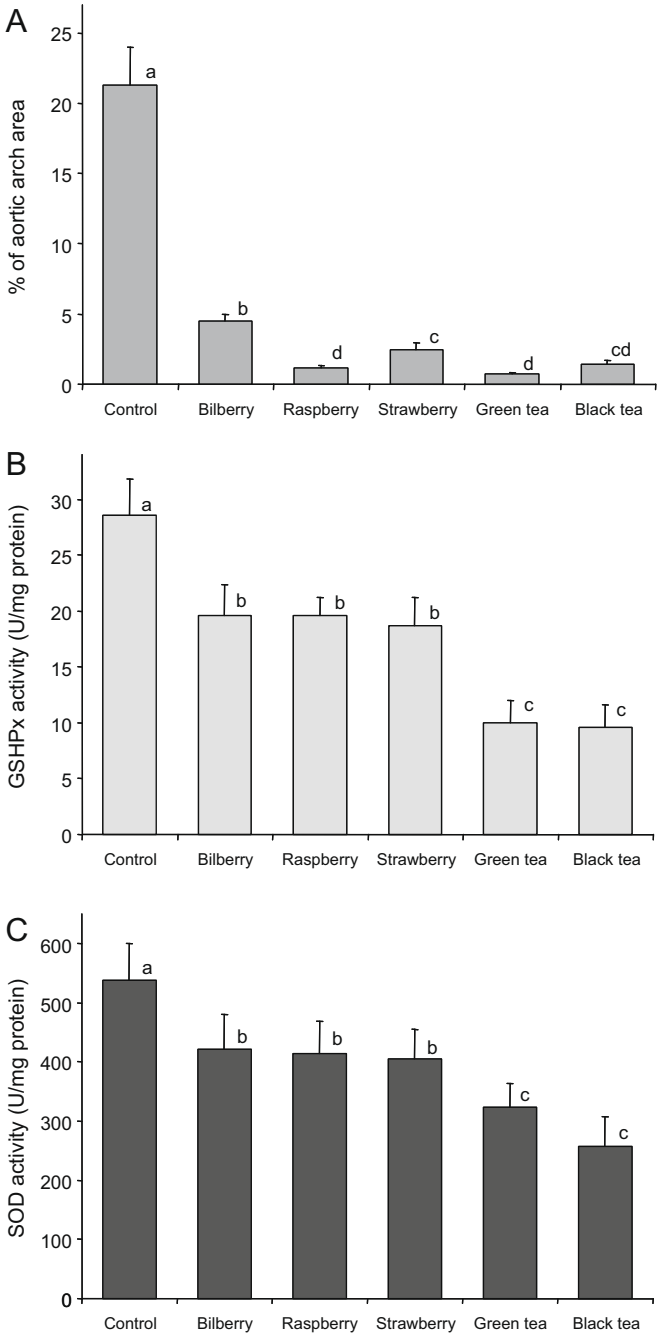

Fig. 1. Effects of dietary treatments on aortic fatty streak area and hepatic antioxidant enzymes activities. Mean values expressed as (A) a percent of aortic area ± SEM (n = 10) for aortic arch area, and as units per mg of hepatic proteins ± SEM (n = 10) for (B) SOD and (C) GSHPx activity. Bars with different letters are significantly different (p < 0.05).

The observation that the plasma cholesterol profile did not change among groups of hamsters (Table 5) is in keeping with the work of Andrews et al. (1995) that demonstrates that absolute cholesterolaemia is not pivotal in determining the aortic fatty streak deposition. These results thus strengthen the hypothesis that oxidation of LDL, more than their plasma level, must be implicated in the pathogenesis of atherosclerosis (Breinholt, Lauridsen, & Dragsted, 1999). This can explain, at least in part, the effects observed on aortic atherosclerosis after antioxidant juices and tea consumption.

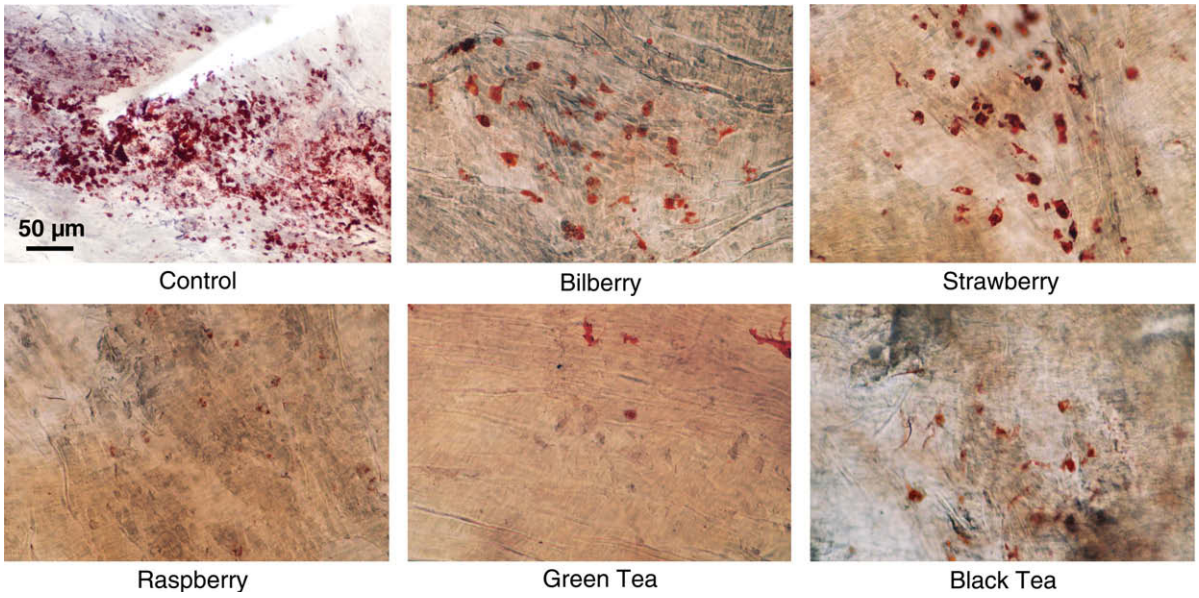

Fig. 2. Photomicrographs of hamster aortic arches after 12 weeks on an atherogenic diet (control) and 12 weeks on an atherogenic diet supplemented with either strawberry juice, bilberry juice, raspberry juice, green tea or black tea. The micrographs are examples of the aortic arch surface covered by lipid inclusion in the intima with lipids coloured red using Oil Red O stain. Quantifications of fatty streaks are summarised in and Fig. 1A. All micrographs have the same scale.

There are reports that consumption of fruit juice and green tea both increase the activity of hepatic antioxidant enzymes (Lin et al., 1998; Young et al., 1999). This contrasts with the findings of the present study where berry juice and tea consumption lowered hepatic GSHPx and SOD activities (Fig. 1B and C), and agree with previous results in hamsters receiving either pure catechin, quercetin or resveratrol (Auger et al., 2005) or phenolics from purple grape, apple, purple grape juice and apple juice (Décordé, Teissèdre, Auger, Cristol, & Rouanet, 2008). One explanation for this down regulation is that it is a consequence of dietary antioxidants being able to scavenge oxygen radicals and thus reduce the need for enzymatic endogenous antioxidants.

The prevention of fatty streak deposition by berry juice and tea consumption does seemingly involve mechanisms allowing the possibility of phenolic compounds to induce local antioxidant effects which cannot be ruled out. Recent data suggests that dietary phenolics can modulate inflammatory pathways, hence reducing the severity of local inflammation (Rahman, Biswas, & Kirkham, 2006). The pathogenesis of atherosclerosis has been linked to the occurrence of inflammatory processes inside the arterial wall during the initiation of lesions (Call, Deliargyris, & Newby, 2004). Compounds derived from the ingested phenolics could, therefore, delay the progression of atherosclerosis by inhibition of arterial wall inflammation.

Endothelial dysfunction is also associated with the increased production of the vasoconstrictive peptide endothelin-1, which has been linked with chronic inflammation of the arterial wall (Feletou & Vanhoutte, 2006; Schiffrin, 2005). Endothelin is also related with the onset and development of atherosclerosis, with atherosclerotic plaques containing an increased endothelin concentration (Bacon, Cary, & Davenport, 1996). Moreover, endothelin-1 production is induced by oxidised LDL, which in turn can recruit macrophages and monocytes in the arterial wall (Schiffrin, 2001). Endothelin, thus, plays a pivotal role in development of diseases related to vascular function. As demonstrated by Corder et al. (2006), phenolic compounds, principally procyanidins, are able to reduce the production of endothelin-1 by endothelial cells. The green tea polyphenol (−)-epigallocatechin gallate is also reported to reduce endothelin expression (Spinella et al., 2006). Inhibition of endothelin-1 over-expression is, therefore, a further potential mechanism for the observed protective effects of juice and tea consumption.

Tea antioxidants, in particular catechins, act either as activators or inhibitors of signal transduction kinases interfering with multiple pathways of signal transduction in cardiovascular relevant cells (Stangl, Dreger, Stangl, & Lorenz, 2007). Arguably, this could explain the strong effect of green tea with respect to the other beverages in this study.

The fact that the five beverages, which reduced the onset of atherosclerosis, contained a very different spectrum of phenolics implies that a wide variety of compounds may be bioactive and that the observed preventive effects may be due to the influence of several constituents working either independently or in tandem. What compounds enter the circulatory system, reduce the arterial fatty streaks deposition and the activity of hepatic SOD and GSHPx remains to be determined. Analysis of the livers of hamsters after 12 weeks plus an overnight treatment between last feed and sacrifice showed no trace of either the parent compounds from the beverages or their glucuronyl-, methyl- or sulfo-metabolites, indicating that they do not accumulate in these tissues, at least in detectable quantities.

In conclusion, we have demonstrated that berry juices and teas fed to hamsters under atherogenic diet are able to facilitate a very strong inhibition of aortic fatty streaks deposition. These effects are physiologically relevant as they were induced by a daily supplement equivalent to 275 ml of beverage consumed on a daily base by a 70 kg human. The features and progression of the lesions observed in the hamster model of atherosclerosis are morphologically similar to atheromatous lesions observed in humans. The hamster is therefore considered to be a good animal model to study the formation of atheromas in humans (Yamanouchi et al., 2000). It is also of interest to note while both bilberry and strawberry juices prevent aortic lipid deposition in hamsters, blueberry, a close relative of bilberry, and strawberry extracts both bring about improvements in neuronal function and behaviour in a rodent model of accelerated aging (Shukitt-Hale, Carey, Jenkins, Rabin, & Joseph, 2007).

Carotid atherosclerosis is associated with aortic atherosclerosis (Shimizu et al., 2003) and the intima-media thickness of the common carotid artery has been shown to predict coronary events and

is, therefore, a non-invasive predictor of future ischemic stroke incidence (Chambless, Folsom, Clegg, Sharrett, & Shahar, 2000). Thus, polyphenol-rich berry juices and green and black tea intake may be of significant relevance to clinical and public health.

Conflict of interest statement

The authors declare that there are no conflicts of interest.

References

Andrews, B., Burnand, K., Paganga, G., Browse, N., Rice-Evans, C., Sommerville, K., et al. (1995). Oxidisability of low density lipoproteins in patients with carotid or femoral artery atherosclerosis. *Atherosclerosis, 112*(1), 77–84.

Auger, C., Caporiccio, B., Landrault, N., Teissèdre, P. L., Laurent, C., Cros, G., et al. (2002). Red wine phenolic compounds reduce plasma lipids and apolipoprotein B and prevent early aortic atherosclerosis in hypercholesterolemic golden Syrian hamsters (Mesocricetus auratus). *Journal of Nutrition, 132*(6), 1207–1213.

Auger, C., Teissèdre, P. L., Gérain, P., Lequeux, N., Bornet, A., Serisier, S., et al. (2005). Dietary wine phenolics catechin, quercetin, and resveratrol efficiently protect hypercholesterolemic hamsters against aortic fatty streak accumulation. *Journal of Agricultural and Food Chemistry, 53*(6), 2015–2021.

Bacon, C. R., Cary, N. R., & Davenport, A. P. (1996). Endothelin peptide and receptors in human atherosclerotic coronary artery and aorta. *Circulation Research, 79*(4), 794–801.

Bazzano, L. A. (2006). The high cost of not consuming fruits and vegetables. *Journal of the American Dietetic Association, 106*(9), 1364–1368.

Breinholt, V., Lauridsen, S. T., & Dragsted, L. O. (1999). Differential effects of dietary flavonoids on drug metabolizing and antioxidant enzymes in female rat. *Xenobiotica, 29*(12), 1227–1240.

Call, J. T., Deliargyris, E. N., & Newby, L. K. (2004). Focusing on inflammation in the treatment of atherosclerosis. *Cardiology Review, 12*(4), 194–200.

Chambless, L. E., Folsom, A. R., Clegg, L. X., Sharrett, A. R., & Shahar, E. (2000). Carotid wall thickness is predictive of incident clinical stroke: The Atherosclerosis Risk in Communities (ARIC) study. *American Journal of Epidemiology, 151*(5), 478–487.

Corder, R., Mullen, W., Khan, N. Q., Marks, S. C., Wood, E. G., Carrier, M. J., et al. (2006). Red wine procyanidins and vascular health. *Nature, 444*(7119), 566.

Crozier, A., Jaganath, I. B., Marks, S., Saltmarsh, M., & Clifford, M. N. (2006). Secondary metabolites as dietary components in plant-based foods and beverages. In A. Crozier, M. N. Clifford, & H. Ashihara (Eds.), *Plant secondary metabolites: Occurrence, structure and role in the human diet* (pp. 208–230). Oxford: Blackwell Publishing.

Dauchet, L., Amouyel, P., Hercberg, S., & Dallongeville, J. (2006). Fruit and vegetable consumption and risk of coronary heart disease: A meta-analysis of cohort studies. *Journal of Nutrition, 136*(10), 2588–2593.

Décordé, K., Teissèdre, P. L., Auger, C., Cristol, J. P., & Rouanet, J. M. (2008). Phenolics from purple grape, apple, purple grape juice and apple juice prevent early atherosclerosis induced by an atherogenic diet in hamsters. *Molecular Nutrition and Food Research, 52*(4), 400–407.

Feldman, E. B. (2001). Fruits and vegetables and the risk of stroke. *Nutrition Reviews, 59*(1), 24–27.

Feletou, M., & Vanhoutte, P. M. (2006). Endothelial dysfunction: A multifaceted disorder. *American Journal of Physiology – Heart and Circulatory Physiology, 291*(3), H985–H1002.

Kuriyama, S., Shimazu, T., Ohmori, K., Kikuchi, N., Nakaya, N., Nishino, Y., et al. (2006). Green tea consumption and mortality due to cardiovascular disease, cancer, and all causes in Japan: The Ohsaki study. *Journal of the American Medical Association, 296*(10), 1255–1265.

Lin, Y. L., Cheng, C. Y., Lin, Y. P., Lau, Y. W., Juan, I. M., & Lin, J. K. (1998). Hypolipidemic effect of green tea leaves through induction of antioxidant and Phase II enzymes including superoxide dismutase, catalase, and glutathione *S*-transferase in rats. *Journal of Agricultural and Food Chemistry, 46*(5), 1893–1899.

Liu, S., Manson, J. E., Lee, I. M., Cole, S. R., Hennekens, C. H., Willett, W. C., et al. (2000). Fruit and vegetable intake and risk of cardiovascular disease: the Women's Health Study. *American Journal of Clinical Nutrition, 72*(4), 922–928.

National Research Council. Guide for the Care and the Use of Laboratory Animals. (1985). Publication Nos. 85-23(rev.). National Institutes of Health, Bethesda, MD.

Rahman, I., Biswas, S. K., & Kirkham, P. A. (2006). Regulation of inflammation and redox signaling by dietary polyphenols. *Biochemical Pharmacology, 72*(11), 1439–1452.

Reeves, P. G., Nielsen, F. H., & Fahey, G. C. Jr., (1993). AIN-93 purified diets for laboratory rodents: final report of the American Institute of Nutrition ad hoc writing committee on the reformulation of the AIN-76A rodent diet. *Journal of Nutrition, 123*(11), 1939–1951.

Schiffrin, E. L. (2001). Role of endothelin-1 in hypertension and vascular disease. *American Journal of Hypertension, 14*(6), 83S–89S.

Schiffrin, E. L. (2005). Vascular endothelin in hypertension. *Vascular Pharmacology, 43*(1), 19–29.

Shimizu, Y., Kitagawa, K., Nagai, Y., Narita, M., Hougaku, H., Masuyama, T., et al. (2003). Carotid atherosclerosis as a risk factor for complex aortic lesions in patients with ischemic cerebrovascular disease. *Circulation Journal, 67*(7), 597–600.

Shukitt-Hale, B., Carey, A. N., Jenkins, D., Rabin, B. M., & Joseph, J. A. (2007). Beneficial effects of fruit extracts on neuronal function and behavior in a rodent model of accelerated aging. *Neurobiology of Aging, 28*(8), 1187–1194.

Spinella, F., Rosano, L., Di, C. V., Decandia, S., Albini, A., Nicotra, M. R., et al. (2006). Green tea polyphenol epigallocatechin-3-gallate inhibits the endothelin axis and downstream signaling pathways in ovarian carcinoma. *Molecular Cancer Therapeutics, 5*(6), 1483–1492.

Stangl, V., Dreger, H., Stangl, K., & Lorenz, M. (2007). Molecular targets of tea polyphenols in the cardiovascular system. *Cardiovascular Research, 73*(2), 348–358.

Stewart, A. J., Mullen, W., & Crozier, A. (2005). On-line high-performance liquid chromatography analysis of the antioxidant activity of phenolic compounds in green and black tea. *Molecular Nutrition and Food Research, 49*(1), 52–60.

Yamanouchi, J., Nishida, E., Itagaki, S., Kawamura, S., Doi, K., & Yoshikawa, Y. (2000). Aortic atheromatous lesions developed in APA hamsters with streptozotocin induced diabetes: a new animal model for diabetic atherosclerosis. 1 Histopathological studies. *Experimental Animals, 49*(4), 259–266.

Yang, C. S., & Landau, J. M. (2000). Effects of tea consumption on nutrition and health. *Journal of Nutrition, 130*(10), 2409–2412.

Young, J. F., Nielsen, S. E., Haraldsdottir, J., Daneshvar, B., Lauridsen, S. T., Knuthsen, P., et al. (1999). Effect of fruit juice intake on urinary quercetin excretion and biomarkers of antioxidative status. *American Journal of Clinical Nutrition, 69*(1), 87–94.

Food Chemistry 118 (2010) 272–277

Contents lists available at ScienceDirect

Food Chemistry

journal homepage: www.elsevier.com/locate/foodchem

Emitted and endogenous volatiles in 'Tsugaru' apple: The mechanism of ester and (*E*,*E*)-α-farnesene accumulation

Yusuke Ban [a,b], Naomi Oyama-Okubo [c], Chikako Honda [d], Masayoshi Nakayama [a,c], Takaya Moriguchi [a,b,*]

[a] *Graduate School of Life and Environmental Sciences, University of Tsukuba, Tsukuba, Ibaraki 305-8572, Japan*
[b] *National Institute of Fruit Tree Science, 2-1 Fujimoto, Tsukuba, Ibaraki 305-8605, Japan*
[c] *National Institute of Floricultural Science, Tsukuba, Ibaraki 305-8519, Japan*
[d] *National Institute of Fruit Tree Science, Morioka, Iwate 020-0123, Japan*

ARTICLE INFO

Article history:
Received 10 February 2009
Received in revised form 8 April 2009
Accepted 27 April 2009

Keywords:
Alcohol acyltransferase (MdAAT)
Apple (*Malus* × *domestica*)
Ethylene
(*E*,*E*)-α-farnesene synthase (MdAFS1)
Volatile compounds

ABSTRACT

Volatile compound production was studied in terms of biosynthetic gene expression in apple ('Tsugaru'). To this end, we first analysed the endogenous and emitted volatiles in the skin of ripened apple fruit. GC–MS and GC analyses suggested that the boiling point of the endogenous compounds in apple skin is an important determinant of the composition and amount of emitted volatiles. Since esters and (*E*,*E*)-α-farnesene are the major endogenous volatiles in apple, key biosynthetic genes were isolated from apple skin and their expression patterns were analysed with ethylene biosynthetic genes. During fruit development, the onset of alcohol acyltransferase (*pMdAAT*) expression in the skin, which is responsible for ester biosynthesis, coincided with the accumulation of *1-aminocyclopropane-1-carboxylate synthase* (*MdACSs*, *MdACS5B*) mRNA. Thereafter, *pMdAAT* expression remained at a high level, even when no *MdACS* transcripts were observed. On the other hand, the accumulation of (*E*,*E*)-α-*farnesene synthase* (*pMdAFS1*) transcripts in the skin was associated with the expression of *MdACSs* and *1-aminocyclopropane-1-carboxylate oxidase* (*MdACO1*). After harvest, the inhibition of *pMdAAT* expression in 1-methylcyclopropene (1-MCP)-treated apple skin was incomplete. In contrast, the expression of *pMdAFS1* was repressed by 1-MCP treatment concomitant with considerable inhibition of ethylene production. These results suggest that *pMdAFS1* expression is controlled by ethylene, whereas *pMdAAT* expression is developmentally regulated in the skin of 'Tsugaru'.

1. Introduction

Volatile compounds are one of the factors that determine apple (*Malus* × *domestica*) fruit quality (Kondo, Setha, Rudell, Buchanan, & Mattheis, 2005). Apples emit a complex mixture of volatile compounds including alcohols, esters, aldehydes, ketones, and sesquiterpenes (Dimick & Hoskin, 1983). The major aromatic compounds in apples are volatile esters (Brackmann, Streif, & Bangerth, 1993; Olías, Sanz, Rios, & Perez, 1992). Esters are, associated with the 'fruity' attributes of a fruit's flavour and, are important aromatic components in many ripened fruits (Aharoni et al., 2000). Esters are derived from amino acids and fatty acids (Dixon & Hewett, 2000). Alcohol acyltransferase (AAT), a BAHD enzyme superfamily, is a key enzyme in ester biosynthesis, catalysing the final step in ester formation by linkage of an acyl moiety from acyl-CoA to the appropriate alcohol (Fellman, Miller, Mattison, & Mattheis, 2000). Studies have reported that apple *AAT* (*MdAAT*) is expressed at a later stage during fruit ripening (Defilippi, Kader, & Dandekar, 2005; Souleyre, Greenwood, Friel, Karunairetnam, & Newcomb, 2005), and studies based on *in situ* hybridization suggested that *MdAAT2* is primarily located in the fruit skin (Li et al., 2006). MdAAT is able to use a range of alcohols and CoA acids to produce the range of esters found in apple fruit (Souleyre et al., 2005). Apart from esters, apples also produce a large amount of (*E*,*E*)-α-farnesene (Girard & Lau, 1995), a sesquiterpene that is biosynthesized via the mevalonate pathway (Pechous & Whitaker, 2004). The products of (*E*,*E*)-α-farnesene oxidation can induce superficial scald disorder, an important disease in the apple industry; several studies have conducted comparative analyses of (*E*,*E*)-α-farnesene biosynthesis in resistant and susceptible cultivars (Lurie et al., 2005; Pechous, Watkins, & Whitaker, 2005; Tsantili, Gapper, Arquiza, Whitaker, & Watkins, 2007). (*E*,*E*)-α-farnesene synthase (AFS), encoded by *MdAFS1* in apple, is a key enzyme in (*E*,*E*)-α-farnesene biosynthesis, catalysing the conversion of farnesyl diphosphate to (*E*,*E*)-α-farnesene in the final steps of sesquiterpene biosynthesis (Pechous & Whitaker, 2004).

Ethylene is a key regulatory molecule for ripening and senescence and it is thought to regulate fruit ripening by coordinating

* Corresponding author. Address: National Institute of Fruit Tree Science, 2-1 Fujimoto, Tsukuba, Ibaraki 305-8605, Japan. Tel.: +81 29 838 6500; fax: +81 29 838 6437.
E-mail address: takaya@affrc.go.jp (T. Moriguchi).

0308-8146/$ - see front matter © 2009 Elsevier Ltd. All rights reserved.
doi:10.1016/j.foodchem.2009.04.109

the expression of many genes, which are responsible for chlorophyll degradation, carotenoid synthesis, conversion of starch to sugars, cell-wall modulation, and so on (Theologis, 1992). It is well-known that volatile biosynthesis is also regulated by ethylene. Kondo et al. (2005) showed that chemical inhibition of ethylene action suppresses volatile production. Moreover, several studies show that the genes responsible for volatile biosynthesis are regulated by ethylene. For example, an antisense experiment with *MdACO1* shows that *MpAAT1* and *MdAFS1* were expressed only after exogenous ethylene application in *MdACO1*-antisense apple transformants (Schaffer et al., 2007).

To date, research aimed at identifying the volatiles and their biosynthetic regulation in apple (e.g. Young, Chu, Lu, & Zhu, 2004) has focused on the relationship between the emitted volatile compounds and their related gene expression, despite the fact that the quality and quantity of endogenous volatiles may influence the emitted volatiles such as in petunia (Oyama-Okubo et al., 2005) and that gene expression should be directly related to endogenous, rather than emitted, volatiles in apple, because the genes function in the tissues in which endogenous volatiles biosynthesis took place. In addition, information regarding the volatile biosynthesis in 'Tsugaru' apple is not available, despite being a major cultivar in Japan. Therefore, in this study, we investigated the emitted and endogenous volatiles and the expression of *pMdAAT*, *pMdAFS1* and ethylene biosynthetic genes in 'Tsugaru' apple skin to gain insight into the regulatory mechanism underlying volatile compound production via ethylene action in this cultivar. To this end, we analysed the emitted and endogenous volatiles using capillary gas chromatography–mass spectrometry (GC–MS) and GC. Furthermore, we analysed the expressions of *pMdAAT*, *pMdAFS1*, apple *1-aminocyclopropane-1-carboxylate synthase* (*MdACSs*), and apple *1-aminocyclopropane-1-carboxylate oxidase* (*MdACO1*) in 1-methylcyclopropene (1-MCP)-treated skins as well as during fruit development. On the basis of the results, we discuss the possible regulation of volatile compound production via ethylene action in 'Tsugaru' apple skin.

2. Materials and methods

2.1. Plant materials

Fruit of 'Tsugaru' apple (pale red cultivar) was obtained from an orchard at the National Institute of Fruit Tree Science in Morioka, Japan. In this area, the commercial harvest time is mid-September for 'Tsugaru'. The mature fruit of 'Tsugaru' apple was harvested about one week after the commercial harvest. Fruits were also periodically harvested from young fruitlet to mature stages, which corresponded to 16, 37, 60, 79, 102 and 116 days after full bloom (DAFB). The last harvesting date of 116 DAFB corresponds to about one week after commercial harvest. The mature fruits were used for the GC–MS and GC analyses. The entire skin, including 1 mm of the cortical tissue, was collected. The collected skin was immediately frozen in liquid nitrogen, and stored at −80 °C until used for RNA isolation. In a preliminary experiment, the specificity of skin preparation was confirmed by the specific expression pattern of a MYB transcription factor gene (*MdMYBA*), which is responsible for anthocyanin accumulation in apple skin (Ban et al., 2007).

For 1-MCP treatment, 'Tsugaru' fruits were harvested at the preclimacteric stage (3 days before commercial harvest). Fruits without injury were selected and temporarily stored at 4 °C for 16 h before being transferred to 24 °C. 1-MCP treatment was carried out essentially as described by Tatsuki and Endo (2006). Fruits were placed in 117 l plastic containers and treated with 1.0 μl l^{-1} 1-MCP (SmartFresh™, AgroFresh, Inc., Spring House, PA, USA) for 24 h at 25 °C. As a control, fruits were left in the air for 24 h at 25 °C. All fruits were then stored for 5 days at 25 °C. Following ethylene measurement, the skins were collected and stored at −80 °C for RNA isolation.

2.2. Determination of ethylene concentration

Ethylene was measured by placing each fruit in a sealed desiccator (about 1,500 ml) for 1 h at 25 °C. A 1.0 ml sample of the gas was then withdrawn with a syringe and injected into a gas chromatograph (GC-14B, Shimadzu, Kyoto, Japan) equipped with a flame ionisation detector. Activated alumina (60–80 mesh) in a glass column (2.0 mm i.d. × 2 m) was used with helium as the carrier gas at 100 kPa pressure. The column, injector, and detector temperatures were 60, 80 and 200 °C, respectively.

2.3. Extraction of the emitted and endogenous volatiles

We used three fruits for extraction of the emitted and endogenous volatiles. The weights of fruits were 410.56, 369.37 and 441.11 g, respectively. The extraction of the emitted and endogenous volatiles was conducted with three biological replicates from three fruits. The emitted volatile compounds were collected by the headspace method (Oyama-Okubo et al., 2005). Mature apple fruits were separately placed in Tedlar Bags (5000 ml volume, GL Science, Tokyo, Japan). A constant stream of air (approx. 500 ml min^{-1}) was filtered through activated charcoal and then piped through the bag, and the volatiles were collected for a 1 h period using Tenax-TA (150 mg, GL science) traps. The relative humidity in the bags was approximately 50%. The emitted volatile compounds were extracted four times from the Tenax-TA traps using pentane and diethyl ether (5 ml each) alternately (Oyama-Okubo et al., 2005). After the addition of ethyl decanoate (20 μg) as an internal standard, the extract was dehydrated with anhydrous sodium sulphate and concentrated to about 15 μl at 40 °C in a water bath.

For analysis of the endogenous volatiles, the fruit skins from the three fruits were separately harvested after collecting the emitted volatile compounds. Extraction of the endogenous volatiles from the skins was carried out essentially as described by Kondo, Oyama-Okubo, Ando, Marchesi, and Nakayama (2006). The skin (5 g) from each sample was ground with a mortar and pestle in liquid nitrogen until a fine powder was obtained. The samples were then extracted twice with pentane (10 ml each) in a microwave oven (700 W) for 20 s. Ethyl decanoate (20 μg) was added as an internal standard. Each extract was then dehydrated with anhydrous sodium sulphate and concentrated to about 15 μl at 40 °C in a water bath.

2.4. GC–MS and GC analyses

The compounds were identified and quantified by GC–MS and GC analyses, respectively. GC–MS analysis was performed using an Agilent 6890N gas chromatograph coupled to an Agilent 5973N Mass Selective Detector (Agilent Technologies, Wilmington, DE, USA) (Kondo et al., 2006; Oyama-Okubo et al., 2005). The GC was equipped with a splitless injector and a DB-WAX capillary column (0.25 mm i.d. × 30 m, 0.25 μm film thickness). The column oven temperature was kept at 45 °C for the first 2 min, then increased by 3 °C min^{-1} to 220 °C and maintained at 220 °C for 10 min. The injection, interface, and MS source temperatures were 250, 280, and 250 °C, respectively. Helium was used as the carrier gas at 50 ml min^{-1}. GC analysis was performed using an Agilent 6850 gas chromatograph (Agilent Technologies) monitored by a flame ionisation detector. The analytical conditions were the same as those described above for GC–MS. Identification of compounds was confirmed by comparison of collected mass spectra with those

in the NIST02 library provided with the GC–MS software. The amount of each compound was calculated by comparison with the peak area of the internal standard. Only reproducible peaks within three biological replicates were extracted as data for analysis.

2.5. Isolation of the partial AAT and AFS genes from 'Tsugaru'

To isolate the partial fragment of *MdAAT* (*pMdAAT*), total RNA was extracted from mature fruit skin using the hot borate method (Wan & Wilkins, 1994). First-strand cDNA was synthesized using a SMART RACE cDNA Amplification Kit (Clontech, Palo Alto, CA, USA) and was then used as the template for amplification of the fragments. Reverse transcription-PCR (RT-PCR) was carried out with forward (5′-CGCATCCAGTAACCAGTCAA-3′) and reverse (5′-TGAGGTCGCCCTCTTAGTACC-3′) primers designed based on the sequences of *MpAAT1* (Souleyre et al., 2005) and *MdAAT2* (Li et al., 2006). Each reaction was performed in a total volume of 10 μl containing 20 ng of cDNA, 200 μM dNTPs, 1 mM $MgCl_2$, 3 pmol of each primer, 2 U of KOD plus (TOYOBO, Osaka, Japan), and 1× PCR buffer (TOYOBO). After pre-heating at 94 °C for 2 min, the tubes were subjected to 35 cycles of 94 °C for 15 s, 57.5 °C for 30 s, and 68 °C for 1.5 min. The products were then cloned into pCR-Blunt using a Zero Blunt PCR Cloning Kit (Invitrogen, San Diego, CA, USA) and sequenced. In contrast, the partial cDNA of *MdAFS1* (*pMdAFS1*) was identified from a subtracted cDNA library constructed using 'Tsugaru' fruit skin (Ban et al. unpublished data); consequently, we were able to use the clone directly. The sequences of *pMdAAT* (411 bp) and *pMdAFS1* (486 bp) have been deposited in the DNA Data Bank of Japan (DDBJ) under accession numbers AB370229 and AB370228, respectively.

2.6. RNA gel blot analysis

Total RNA was isolated from the skins of 1-MCP-treated fruit and during fruit development using the methods described above. Total RNA (5 μg) was electrophoresed on a 1.2% agarose/formaldehyde gel then blotted onto a nylon membrane (Hybond-N, Amersham Biosciences, Piscataway, NJ, USA) by capillary transfer. The insert DNAs in the identified cDNA clones (*pMdAAT* and *pMdAFS1*), the full-length *MdACS* cDNAs; *MdACS1* (accession number U89156), *MdACS3* (U73816), *MdACS4* (Kim, Silverstone, Yip, Dong, & Yang, 1992), *MdACS5A* (AB034992) and *MdACS5B* (AB034993), and apple *ACO* (*MdACO1*, X61390) were labelled with digoxigenin-dUTP (Roche Diagnostics, Mannheim, Germany) using M13 forward and reverse primers by PCR. Prehybridization, hybridization, washing, and detection were carried out according to the methods of Ban et al. (2007). Notably, our probe for *pMdAAT* contained the conserved region in *MpAAT1* (Souleyre et al., 2005), *MdAAT2* (Li et al., 2006) and *MdAAT3* (Zhu, Rudell, & Mattheis, 2008). Therefore, at least these signals could be detected under our conditions.

3. Results

3.1. Components of the emitted and endogenous volatiles in the skin of mature apple fruit

Emitted volatile compounds were first analysed using intact fruits. Twelve emitted volatiles were detected in mature 'Tsugaru' apple (Table 1). The total amount of emitted volatiles was 8.23 ng g^{-1} fresh weight (FW) of fruit. Esters were the predominant compound, accounting for 84.83% of the total emitted volatiles. Among the esters, hexyl 2-methylbutanoate and 2-methylbutyl acetate were predominantly detected. (*E*,*E*)-α-farnesene was also detected, but its content was 12-times lower than the ester content. Next, since volatile compounds are primarily synthesized in the skin (Knee & Hatfield, 1981), the endogenous volatiles in the skin were analysed. Fourteen endogenous volatiles were detected in the mature 'Tsugaru' apple skins (Table 1). The total amount of endogenous volatiles was 15,455.08 ng g^{-1} FW of skin. (*E*,*E*)-α-farnesene was the predominant compound, accounting for 65.1% of the total endogenous volatiles. Esters were also detected as endogenous volatiles; however, their content was about two times lower than the (*E*,*E*)-α-farnesene content. Among the esters, hexyl 2-methylbutanoate was predominantly detected. Nine compounds were detected in both the emitted and endogenous samples, including hexyl 2-methylbutanoate, 2-methylbutyl acetate, and (*E*,*E*)-α-farnesene. Conversely, a number of compounds were detected only in either the emitted or the endogenous samples.

3.2. Relationship between the boiling points and emission ratios

For the nine compounds that were detected in both the emitted and endogenous samples, the logarithm of the ratio of emitted to endogenous amounts was plotted against the boiling point (Fig. 1). The compounds included in the analysis were 2-methylbutyl acetate, butyl butanoate, hexyl acetate, butyl 2-methylbutanoate, hexyl propanoate, hexyl 2-methylbutanoate, hexyl butanoate, butyl hexanoate, and (*E*,*E*)-α-farnesene. Our results show a nearly linear negative correlation between the emission ratio and boiling point of each compound.

3.3. Expression of pMdAAT, pMdAFS1 and ethylene biosynthetic genes

Since esters and (*E*,*E*)-α-farnesene were the major endogenous volatiles in 'Tsugaru' apple skin, expression analysis of their biosynthetic genes and ethylene biosynthetic genes was conducted

Table 1
Composition of the emitted and endogenous volatiles in mature 'Tsugaru' apple.

Compounds[a] (boiling point)	Emitted		Endogenous	
	(ng g^{-1} FW fruit)	(%)	(ng g^{-1} FW skin)	(%)
Ester	6.98 ± 0.45[b]	(84.83)	4573.65 ± 951.24	(29.59)
2-Methylbutyl acetate (140 °C)	2.06 ± 0.12	(24.99)	268.03 ± 63.30	(1.73)
Butyl butanoate (164 °C)	0.31 ± 0.03	(3.82)	115.71 ± 17.43	(0.75)
Hexyl acetate (168 °C)	0.42 ± 0.03	(5.11)	189.34 ± 50.79	(1.23)
Butyl 2-methylbutanoate (174 °C)	0.52 ± 0.02	(6.36)	209.16 ± 48.23	(1.35)
Hexyl propanoate (180 °C)	0.07 ± 0.01	(0.88)	83.54 ± 21.53	(0.54)
Hexyl 2-methylbutanoate (203 °C)	2.96 ± 0.45	(35.98)	2772.26 ± 661.96	(17.94)
Hexyl butanoate (204 °C)	0.24 ± 0.01	(2.97)	191.30 ± 28.00	(1.24)
Butyl hexanoate (207 °C)	0.39 ± 0.05	(4.73)	174.19 ± 38.90	(1.13)
Butyl octanoate (240 °C)	n.d.[c]	–	72.77 ± 3.61	(0.47)
Hexyl hexanoate (245 °C)	n.d.	–	497.34 ± 82.20	(3.22)
Carboxylic acid	0.57 ± 0.09	(6.91)	337.33 ± 58.26	(2.18)
Acetic acid (117 °C)	0.28 ± 0.03	(3.39)	n.d.	–
2-Methylbutanoic acid (176 °C)	n.d.	–	337.33 ± 58.26	(2.18)
Hexanoic acid (202 °C)	0.29 ± 0.08	(3.52)	n.d.	–
Aldehyde	–	–	678.86 ± 270.43	(4.39)
(E)-2-hexenal (146 °C)	n.d.	–	570.32 ± 243.29	(3.69)
1-Nonanal (200 °C)	n.d.	–	108.55 ± 30.10	(0.70)
Other	0.68 ± 0.05	(8.26)	9865.24 ± 1154.89	(63.83)
Acetophenone (202 °C)	0.09 ± 0.02	(1.08)	n.d.	–
(*E*,*E*)-α-farnesene (260 °C)	0.59 ± 0.06	(7.18)	9865.24 ± 1154.89	(63.83)
Total	8.23 ± 0.38	(100)	15455.08 ± 1205.48	(100)

[a] Compounds were identified and quantified by GC–MS and GC analyses.
[b] Values are mean ± standard error ($n = 3$).
[c] n.d.: not detected.

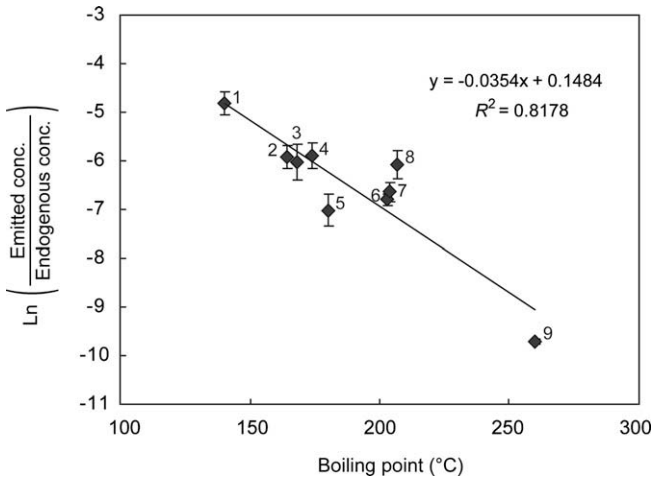

Fig. 1. Relationship between the boiling point and the natural logarithms of the ratios of emitted to endogenous concentrations of volatile compounds in mature 'Tsugaru' apple. 1,2-Methylbutyl acetate (boiling point, 140 °C); 2, Butyl butanoate (164 °C); 3, Hexyl acetate (168 °C); 4, Butyl 2-methylbutanoate (174 °C); 5, Hexyl propanoate (180 °C); 6, Hexyl 2-methylbutanoate (203 °C); 7, Hexyl butanoate (204 °C); 8, Butyl hexanoate (207 °C); and 9, (*E*,*E*)-α-farnesene (260 °C). Bars indicate the SE.

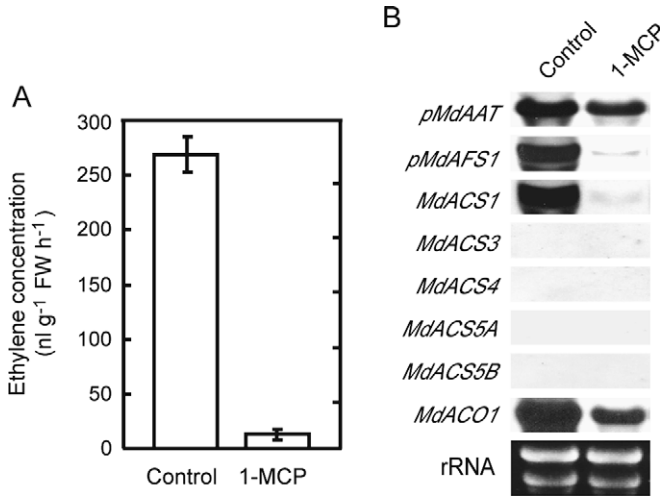

Fig. 3. Effect of 1-MCP on ethylene production (A) and the expression of *pMdAAT*, *pMdAFS1*, *MdACSs*, and *MdACO1* (B) in 'Tsugaru' at 5 days after treatment. 1-MCP was applied to fruits at the pre-climacteric stage (3 days before commercial harvest). The ethylene concentration is shown as the mean ± SE (n = 5). Ethidium bromide staining shows equal loading of rRNA.

using RNA isolated from fruit skins at different developmental stages. The transcript of *pMdAAT* was first detected at 16 DAFB, and its level increased continuously during fruit ripening, peaking at 116 DAFB (Fig. 2). *pMdAFS1* mRNA was abundant at 116 DAFB but rare at 16 DAFB. Ethylene production during fruit development was not monitored in this study. Instead, expressions of *MdACS*s and *MdACO1* were investigated using the same fruit skins because it is generally accepted that the expression level of *ACS* completely corresponds to ethylene production during fruit ripening (Dal Cin et al., 2007; Itai et al., 1999). *MdACS3*, *MdACS4*, and *MdACS5A* were not expressed at any stage in 'Tsugaru' (Fig. 2). However, *MdACS1* mRNA was detected at 116 DAFB. Furthermore, *MdACS5B* transcripts were observed at 16 and 37 DAFB. On the other hand, *MdACO1* mRNA was detected in young fruitlet (16 DAFB) and ripe fruit stages (102 and 116 DAFB). *MdACS5B* and *MdACO1* expression in young fruitlet (16 DAFB) might contribute to a system I ethylene (McMurchie, McGlasson, & Eaks, 1972), although this hypothesis is not yet confirmed.

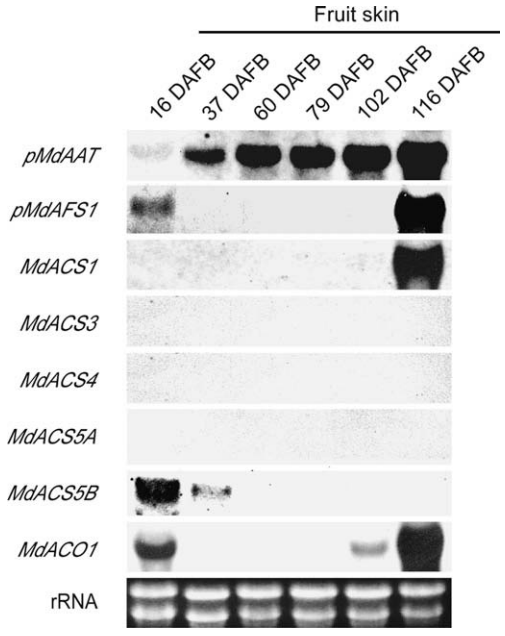

Fig. 2. RNA gel blot analysis of *pMdAAT*, *pMdAFS1*, *MdACSs*, and *MdACO1* in 'Tsugaru' fruit skin during fruit development. Ethidium bromide staining shows equal loading of rRNA.

To further investigate the regulation of *pMdAAT* and *pMdAFS1* by ethylene after harvest, ethylene action was inhibited by 1-MCP in the fruit after harvest. Treatment with 1-MCP effectively inhibited ethylene action at 5 days after treatment (DAT) (Fig. 3A). When the expression of *pMdAAT* and *pMdAFS1* was analysed, *pMdAAT* underwent only a minor change at 5 DAT; its expression was only slightly affected by ethylene signalling inhibitor (Fig. 3B). In contrast, *pMdAFS1* expression was notably inhibited by 1-MCP at 5 DAT. When expression analysis of the genes in the ethylene biosynthetic pathway was conducted, *MdACS1* expression clearly corresponded to ethylene production, whereas *MdACO1* did not tightly correspond to the amount of ethylene in 1-MCP-treated apple skin. Except for *MdACS1*, expression of *MdASC3*, *MdACS4*, *MdACS5A* and *MdACS5B*, was not detected in the skins from harvested apple.

4. Discussion

In this study, we intended to clarify the physiological regulation of volatile compound production in terms of biosynthetic gene expression and ethylene production in 'Tsugaru' apple skin. To this end, we first analysed the endogenous and emitted volatiles in the skin of ripened apple fruit, because it is generally believed that volatile production consists of two steps, endogenous production and evaporation of the endogenous volatile compounds (Oyama-Okubo et al., 2005). We, therefore, measured the composition and amount of both emitted and endogenous volatiles. As for emitted volatiles, 'Tsugaru' displayed esters and (*E*,*E*)-α-farnesene as major volatiles, which is comparable to other cultivars (e.g. Fellman et al., 2000) (Table 1), but the composition and concentration of emitted volatiles other than these major compounds in 'Tsugaru' were not identical to other cultivars. Interestingly, the composition and amount of emitted volatiles was distinct from that of the endogenous volatiles (Table 1). For example, (*E*,*E*)-α-farnesene was a major component of the endogenous samples, but its composition was largely reduced in the emitted samples. Evaporative properties such as the boiling point of volatile compounds may contribute

to floral scent in *Petunia axillaries*, and a negative correlation between the emitted/endogenous ratio and boiling point has been suggested (Kondo et al., 2006; Oyama-Okubo et al., 2005). Accordingly, we also considered the boiling points of the identified compounds. In general, those compounds with a lower boiling point tended to be emitted at higher levels (Table 1), indicating that the differences in composition and amount between the endogenous and emitted volatiles in apple skin might be partly ascribed to the different boiling points of the substances. In addition, the linear negative correlation between the emission ratio and boiling point also suggests the importance of the boiling point in determining emitted volatiles (Fig. 1). On the other hand, a number of compounds were detected either as emitted or endogenous volatiles only; i.e., acetic acid, hexanoic acid, and acetophenone were detected only as emitted volatiles but undetected as endogenous volatiles. Since the endogenous volatiles present in other tissues were not measured in this study, the possibility that these compounds were derived from the flesh and core tissues cannot be ruled out. Conversely, hexyl hexanoate, 2-methylbutanoic acid, and (*E*)-2-hexenal were not detected as emitted volatiles despite their high concentrations endogenously. It is worth noting that (*E*)-2-hexenal has a relatively low boiling point (146 °C); however, it was not detected as emitted volatile, indicating that unknown factor(s) other than boiling point may be involved in this process. Similar results were observed in *P. axillaries* (Kondo et al., 2006). Thus, it is difficult to show a clear-cut reason(s) for the relationships between emitted and endogenous volatiles possibly due to the involvement of many factors, such as enzyme and temperature in this process. It could, however, be suggested that the composition and amount of the emitted volatiles largely depend on the endogenous volatile compounds and their boiling points in apple.

Since GC–MS and GC analyses showed that the production of endogenous compounds is important for volatile production, we analysed the expression of volatile biosynthetic genes and ethylene biosynthetic genes to elucidate the regulatory process of endogenous volatile biosynthesis via ethylene action. Esters and (*E*,*E*)-α-farnesene were the major endogenous volatiles in apple skin. Therefore, we isolated their key biosynthetic genes, *pMdAAT* and *pMdAFS1*. During fruit development, *pMdAAT* expression was first detected at 16 DAFB, concomitant with abundant *MdACS5B* mRNA. After that, *pMdAAT* transcript levels were increasing towards 102 DAFB, even when no *MdACS* transcripts were observed. On the other hand, *pMdAFS1* expression paralleled that of *pMdACS*s; high or low expression at the fruitlet or ripe stage coincided with the expression of *MdACS5B* and *MdACS1*, respectively. Although we did not measure ethylene production during fruit development, a positive correlation has been shown between ethylene biosynthesis and *ACS* expression as suggested by Dal Cin et al. (2007) and Itai et al. (1999). Accordingly, one might suppose that *pMdAFS1* expression should have been detected at 37 DAFB because of the apparent existence of *MdACS5B* mRNA. However, *MdACO1* expression could not be detected at 37 DAFB. Therefore, we assume that ethylene cannot be synthesized at this stage, possibly due to the lack of an *MdACO1* signal (i.e., the final step in ethylene biosynthesis). Thus, onset of *pMdAAT* expression may be triggered by ethylene because of the concomitant expression of *pMdAA*T and *MdACS5B*. This hypothesis is not yet clarified. However, *pMdAAT* expression after 16 DAFB could be developmentally regulated in this cultivar. In contrast, ethylene may regulate *pMdAFS1* expression at the transcriptional level, as previously reported (Pechous & Whitaker, 2004; Schaffer et al., 2007). 1-MCP treatment also showed the incomplete inhibition pattern of *pMdAAT* and concomitant repression pattern of *MdAFS1* with ethylene production (Fig. 3), which supports our aforementioned assumption.

Recently, Zhu et al. (2008) suggested that *MdACS3* was responsible for the expression of *MdAAT1* and *MdAAT2* during ripening processes, since *MdACS3* was always detected throughout ripening processes in 'Golden Delicious'. In our study, only the signal for *MdACS5B* was apparent at 16 and 37 DAFB. No other *MdACSs* transcripts were detected during ripening processes until mature stage at 116 DAFB in which only *MdACS1* transcript was detected. Meantime, *pMdAAT* expressed stably throughout the ripening processes (Fig. 2). Moreover, Zhu et al. (2008) also suggested that *MdACS3* elicited the *MdAAT1* expression when ethylene action was inhibited by 1-MCP, since both *MdACS3* and *MdAAT1* expression were not repressed by 1-MCP treatment. However, in our study, only *MdACS1* transcript was detected at 5 DAT of 1-MCP treatment, and its expression was largely inhibited by 1-MCP concomitant with the large reduction of ethylene production, whereas *pMdAAT* expression underwent only a minor change (Fig. 3). Furthermore, if *pMdAAT* is truly ethylene-regulated gene in 'Tsugaru', similar expression pattern as those for *MdAFS1* should be expected both before and after harvest (Figs. 2 and 3). On the other hand, Defilippi et al. (2005) found small increment of *MdAAT* transcript level during fruit development in transgenic apple trees with suppressed ACC or ACO activity. This indicated that *MdAAT* expression can be induced even under negligible ethylene level conditions. Based on this observation, Defilippi et al. (2005) hypothesized that regulatory mechanisms other than ethylene action may be involved in the regulation of *MdAAT* during fruit development. Similar observation was reported in melon; in the transgenic melon with antisense-*ACO*, whose ethylene production was highly reduced, *CM-AAT1* transcription was not completely suppressed during fruits development (Yahyaoui et al., 2002). Therefore, based on our results and the previous observation of the transgenic plants (Defilippi et al., 2005; Yahyaoui et al., 2002), the expression of *pMdAAT* is regulated by developmental factors rather than ethylene in 'Tsugaru', although ethylene may trigger the onset of *pMdAAT* expression possibly due to the coexistence of *MdACS5B*, *MdACO1* and *pMdAAT* transcripts at 16 DAFB (Fig. 2). Since the cultivar used in this study ('Tsugaru') is different from those examined by Defilippi et al. (2005, 'Greensleeves') and by Zhu et al. (2008, 'Golden Delicious'), the possibility of the different regulatory mechanism of *MdAAT* in the different apple cultivars, needs to be further elucidated in the future.

Taken together, our results indicate that: (i) the boiling point of endogenous compounds is an important determinant of the composition and amount of emitted volatiles and (ii) *pMdAFS1* expression is controlled by ethylene, whereas *pMdAAT* expression is developmentally regulated in the skin of 'Tsugaru'. Our data could provide further insight on the mechanisms of volatile production in apple skin.

Acknowledgements

We thank Dr. Masatoshi Kondo (University of Tsukuba, Japan) and Dr. Miho Tatsuki (National Institute of Fruit Tree Science, Japan) for their valuable suggestions regarding our experiments. We are also grateful to Dr. Benjamin Ewa Ubi (Ebonyi State University, Nigeria) for his critical reading of our manuscript.

References

Aharoni, A., Keizer, L. C. P., Bouwmeester, H. J., Sun, Z. K., Alvarez-Huerta, M., Verhoeven, H. A., et al. (2000). Identification of the SAAT gene involved in strawberry flavor biogenesis by use of DNA microarrays. *Plant Cell, 12*(5), 647–661.

Ban, Y., Honda, C., Hatsuyama, Y., Igarashi, M., Bessho, H., & Moriguchi, T. (2007). Isolation and functional analysis of a MYB transcription factor gene that is a key regulator for the development of red coloration in apple skin. *Plant Cell and Physiology, 48*(7), 958–970.

Brackmann, A., Streif, J., & Bangerth, F. (1993). Relationship between reduced aroma production and lipid-metabolism of apples after long-term controlled-

atmosphere storage. *Journal of the American Society for Horticultural Science, 118*(2), 243–247.

Dal Cin, V., Danesin, M., Botton, A., Boschetti, A., Dorigoni, A., & Ramina, A. (2007). Fruit load and elevation affect ethylene biosynthesis and action in apple fruit (*Malus domestica* L. Borkh) during development, maturation and ripening. *Plant Cell and Environment, 30*(11), 1480–1485.

Defilippi, B. G., Kader, A. A., & Dandekar, A. M. (2005). Apple aroma: alcohol acyltransferase, a rate limiting step for ester biosynthesis, is regulated by ethylene. *Plant Science, 168*(5), 1199–1210.

Dimick, P. S., & Hoskin, J. C. (1983). Review of apple flavor – State of the art. *CRC Critical Reviews in Food Science and Nutrition, 18*(4), 387–409.

Dixon, J., & Hewett, E. W. (2000). Factors affecting apple aroma/flavour volatile concentration: A review. *New Zealand Journal of Crop and Horticultural Science, 28*(3), 155–173.

Fellman, J. K., Miller, T. W., Mattison, D. S., & Mattheis, J. P. (2000). Factors that influence biosynthesis of volatile flavor compounds in apple fruits. *HortScience, 35*(6), 1026–1033.

Girard, B., & Lau, O. L. (1995). Effect of maturity and storage on quality and volatile production of 'Jonagold' apples. *Food Research International, 28*(5), 465–471.

Itai, A., Kawata, T., Tanabe, K., Tamura, F., Uchiyama, M., Tomomitsu, M., et al. (1999). Identification of 1-aminocyclopropane-1-carboxylic acid synthase genes controlling the ethylene level of ripening fruit in Japanese pear (*Pyrus pyrifolia* Nakai). *Molecular and General Genetics, 261*(1), 42–49.

Kim, W. T., Silverstone, A., Yip, W. K., Dong, J. G., & Yang, S. F. (1992). Induction of 1-aminocyclopropane-1-carboxylate synthase mRNA by auxin in mung bean hypocotyls and cultured apple shoots. *Plant Physiology, 98*(2), 465–471.

Knee, M., & Hatfield, S. G. S. (1981). The metabolism of alcohols by apple fruit tissue. *Journal of the Science of Food and Agriculture, 32*(6), 593–600.

Kondo, M., Oyama-Okubo, N., Ando, T., Marchesi, E., & Nakayama, M. (2006). Floral scent diversity is differently expressed in emitted and endogenous compounds in *Petunia axillaris* lines. *Annals of Botany, 98*(6), 1253–1259.

Kondo, S., Setha, S., Rudell, D. R., Buchanan, D. A., & Mattheis, J. P. (2005). Aroma volatile biosynthesis in apples affected by 1-MCP and methyl jasmonate. *Postharvest Biology and Technology, 36*(1), 61–68.

Li, D., Xu, Y., Xu, G., Gu, L., Li, D., & Shu, H. (2006). Molecular cloning and expression of a gene encoding alcohol acyltransferase (*MdAAT2*) from apple (cv. golden delicious). *Phytochemistry, 67*(7), 658–667.

Lurie, S., Lers, A., Shacham, Z., Sonego, L., Burd, S., & Whitaker, B. (2005). Expression of α-farnesene synthase *AFS1* and 3-hydroxy-3-methylglutaryl-coenzyme A reductase *HMG2* and *HMG3* in relation to α-farnesene and conjugated trienols in 'Granny Smith' apples heat or 1-MCP treated to prevent superficial scald. *Journal of the American Society for Horticultural Science, 130*(2), 232–236.

McMurchie, E. J., McGlasson, W. B., & Eaks, I. L. (1972). Treatment of fruit with propylene gives information about the biosynthesis of ethylene. *Nature, 237*(5352), 235–236.

Olías, J. M., Sanz, L. C., Rios, J. J., & Perez, A. G. (1992). Inhibitory effect of methyl jasmonate on the volatile ester-forming enzyme-system in golden delicious apples. *Journal of Agricultural and Food Chemistry, 40*(2), 266–270.

Oyama-Okubo, N., Ando, T., Watanabe, N., Marchesi, E., Uchida, K., & Nakayama, M. (2005). Emission mechanism of floral scent in *Petunia axillaris*. *Bioscience, Biotechnology and Biochemistry, 69*(4), 773–777.

Pechous, S. W., Watkins, C. B., & Whitaker, B. D. (2005). Expression of α-farnesene synthase gene *AFS1* in relation to levels of α-farnesene and conjugated trienols in peel tissue of scald-susceptible 'Law Rome' and scald-resistant 'Idared' apple fruit. *Postharvest Biology and Technology, 35*(2), 125–132.

Pechous, S. W., & Whitaker, B. D. (2004). Cloning and functional expression of an (E,E)-α-farnesene synthase cDNA from peel tissue of apple fruit. *Planta, 219*(1), 84–94.

Schaffer, R. J., Friel, E. N., Souleyre, E. J. F., Bolitho, K., Thodey, K., Ledger, S., et al. (2007). A genomics approach reveals that aroma production in apple is controlled by ethylene predominantly at the final step in each biosynthetic pathway. *Plant Physiology, 144*(4), 1899–1912.

Souleyre, E. J. F., Greenwood, D. R., Friel, E. N., Karunairetnam, S., & Newcomb, R. D. (2005). An alcohol acyltransferase from apple (cv. Royal Gala), MpAAT1, produces esters involved in apple fruit flavor. *FEBS Journal, 272*(12), 3132–3144.

Tatsuki, M., & Endo, A. (2006). Analyses of expression patterns of ethylene receptor genes in apple (*Malus domestica* Borkh.) fruits treated with or without 1-methylcyclopropene (1-MCP). *Journal of the Japanese Society for Horticultural Science, 75*(6), 481–487.

Theologis, A. (1992). One rotten apple spoils the whole bushel: the role of ethylene in fruit ripening. *Cell, 70*(2), 181–184.

Tsantili, E., Gapper, N. E., Arquiza, J. M. R. A., Whitaker, B. D., & Watkins, C. B. (2007). Ethylene and α-farnesene metabolism in green and red skin of three apple cultivars in response to 1-methylcyclopropene (1-MCP) treatment. *Journal of Agricultural and Food Chemistry, 55*(13), 5267–5276.

Wan, C-Y., & Wilkins, T. A. (1994). A modified hot borate method significantly enhances the yield of high-quality RNA from cotton (*Gossypium hirsutum* L.). *Analytical Biochemistry, 223*(1), 7–12.

Yahyaoui, F. E. L., Wongs-Aree, C., Latché, A., Hackett, R., Grierson, D., & Pech, J.-C. (2002). Molecular and biochemical characteristics of agene encoding an alcohol acyl-transferase involved in the generation of roma volatile esters during melon ripening. *European Journal of Biochemistry, 26*(9), 2359–2366.

Young, J. C., Chu, C. L. G., Lu, X., & Zhu, H. (2004). Ester variability in apple varieties as determined by solid-phase microextraction and gas chromatography–mass spectrometry. *Journal of Agricultural and Food Chemistry, 52*(26), 8086–8093.

Zhu, Y., Rudell, D. R., & Mattheis, J. P. (2008). Characterization of cultivar differences in alcohol acyltransferase and 1-aminocyclopropane-1-carboxylate synthase gene expression and volatile ester emission during apple fruit maturation and ripening. *Postharvest Biology and Technology, 49*(3), 330–339.

Food Chemistry 118 (2010) 278–282

Contents lists available at ScienceDirect

Food Chemistry

journal homepage: www.elsevier.com/locate/foodchem

Antioxidant activities from the aerial parts of *Platycodon grandiflorum*

Chang-Ho Jeong [a], Gwi Nam Choi [a], Ji Hye Kim [a], Ji Hyun Kwak [a], Dae Ok Kim [b], Young Jun Kim [c], Ho Jin Heo [a,*]

[a] Division of Applied Life Sciences, Institute of Agriculture and Life Science, Gyeongsang National University, Jinju 660-701, Republic of Korea
[b] Department of Food Science and Technology, Institute of Life Science and Resources, Kyung Hee University, Yongin 446-701, Republic of Korea
[c] Department of Food and Biotechnology, Korea University, Yeongi 339-700, Republic of Korea

ARTICLE INFO

Article history:
Received 29 January 2009
Received in revised form 10 March 2009
Accepted 28 April 2009

Keywords:
Platycodon grandiflorum
Antioxidant activities
Luteolin-7-O-glucoside

ABSTRACT

In order to obtain basic data necessary for the utilisation of aerial parts from *Platycodon grandiflorum* as a functional substance in Korea, the antioxidant activities of solvent fractions from the ethanol extract of *P. grandiflorum* aerial parts were examined. The butanol fraction from *P. grandiflorum* showed the most potent antioxidant activities in each assay, showing 91.31% in the DPPH radical scavenging method, 99.62% in the ABTS radical scavenging method, 7.84% in the reducing power method, and 1.29% in the FRAP method at a concentration of 10 mg/ml. The DPPH, ABTS, reducing power, and FRAP assay indicated that the butanol fraction of aerial parts of *P. grandiflorum* was the most potent radical-scavengers and reducing agents compared to the other two extracts. Therefore, our study verified that the butanol fraction has strong antioxidant activities which are correlated with its high level of phenolics, particularly luteolin-7-O-glucoside and apigenin-7-O-glucoside. This extract of *P. grandiflorum* aerial parts can be utilised as an effective and safe source of functional food materials such as natural antioxidants.

1. Introduction

Platycodon grandiflorum is a perennial grass that grows autogenously in Korea, and the northeastern region of China and Japan. The roots of *P. grandiflorum* (Korean name, 'Doraji', Japanese name, 'Kikyo', and Chinese name, 'Jiegeng'), which belongs to the Campanulaceae family, have been used as either a food material or a traditional oriental medicine in Korea (Lee, Hwang, & Lim, 2004). It has been used more often for food than for medicinal purposes since old times. In the Korean traditional medicine, it has been shown that *P. grandiflorum* is good for cough, phlegm, sore throat having a close relation to a pulmonary disorder, amusia, dysuria, diarrhoea, tenesmus and the like (Lee et al., 2004). The roots of *P. grandiflorum* are used as a traditional material of kimchi, and pickled fresh roots are consumed to prevent obesity in Korea and China. Moreover, the roots of *P. grandiflorum*, as one of the most important traditional herbal medicines are used for functional resources on hyperlipidemia, hypertension, and diabetes in Korea (Xu, Zheng, & Sung, 2004). In some studies, its immunopharmacological effects have been studied (Nagao, Matsuda, Namba, & Kubo, 1986), and some active compounds, such as the triterpenoid saponin (Fu et al., 2007) have been identified. Several researches even extended the cultivation period of *P. grandiflorum* to 22 years using a patented method (Lee, 1991), and reported that its aqueous extracts were effective in preventing hypercholesteroleamia, hyperlipidemia, and CCl_4-induced hepatotoxicity (Lee & Jeong, 2002). Recently, it was reported that *P. gradiflorum* had effects on the protection of the liver against acetaminophen in mice (Lee et al., 2001), anti-inflammatory (Kim et al., 2001), anti-lipidemic (Zheng, He, Ji, Le, & Zhang, 2007), anti-hypercholesteroleamic (Zhao et al., 2006), and antiobesity properties (Zhao, Harding, Marinangeli, Kim, & Jones, 2008). However, antioxidative activities from aerial parts of *P. grandiflorum* have not previously been reported.

Reactive oxygen species (ROS) such as hydrogen peroxide (H_2O_2), singlet oxygen ($^1O_2$), superoxide anion radical ($\cdot O_2^-$), hydroxyl radical ($\cdot OH$) are generated from the auto-oxidation of lipids, as well as reactive nitrogen species (RNS) (Aruoma, 1996; Singh, 1989). Formations of these excess ROS and RNS by UV irradiation, smoking and drug metabolism are likely to damage several cellular components such as lipids, proteins, nucleic acid, and DNAs through oxidation or nitration processes (Sawa, Akaike, & Maeda, 2000). In addition, these reactive oxygen species cause inflammation or lesions on various organs and are associated with various degenerative diseases, including cancer, ageing, arteriosclerosis, and rheumatism (Choi, Choi, Han, Bae, & Chung, 2002; Squadrito & Pryor, 1998).

Edible plants contain a wide variety of chemicals that have potential antioxidant activity. The best known phytochemical antioxidants are traditional nutrients, such as β-carotene, ascorbic acid, and α-tocopherol. However, there is growing evidence that a significant portion of the antioxidant capacity of many edible plants is due to the phytochemicals other than the traditional vitamins (Cao, Sofic, & Prior, 1996). Recently, researchers have sought to isolate powerful and non-toxic natural antioxidants from edible plants not only to prevent autoxidation and lipid peroxidation,

* Corresponding author. Tel.: +82 55 751 5476; fax: +82 55 753 4630.
E-mail address: hjher@gnu.ac.kr (H.J. Heo).

0308-8146/$ - see front matter © 2009 Elsevier Ltd. All rights reserved.
doi:10.1016/j.foodchem.2009.04.134

but also to replace synthetic antioxidants. In this respect, the research into the determination of the natural antioxidant source is very important to promote public health. Since the antioxidant activities of extract of *P. grandiflorum* aerial parts have not previously been reported, the objectives of the present study were to assess various antioxidative activities and identify the antioxidant active compounds of *P. grandiflorum* aerial parts which are normally wasted during frequent pruning in order to obtain the possibilities for functional foods. In line with the efforts to balance the conservation of biodiversity and encouraging controlled exploitation of plant resources for economic gains, especially in biopharming, wastage of valuable resources should be minimised.

2. Materials and methods

2.1. Chemicals

Folin–Ciocalteu's reagent, 1,1-diphenyl-2-picrylhydrazyl (DPPH), 2,2′-azino-bis(3-ethylbenzothiazoline-6-sulphonic acid (ABTS), potassium persulfate, potassium ferricyanide, trichloroacetic acid, ferric chloride, sodium acetate, 2,4,6-tripyridyl-S-triazine, α-tocopherol, ascorbic acid, and all solvents used were of analytical grade and purchased from Sigma Chemical Co. (St. Louis, MO, USA). The aerial parts of *P. grandiflorum* were collected from Jinju, Korea in September, 2007, and were authenticated by Institute of Agriculture and Life Sciences, Gyeongsang National University where voucher specimens were maintained. The plant samples, including stem, flower and leaves, were washed and oven-dried at 45 °C.

2.2. Extraction from the aerial parts of P. grandiflorum

Each solvent fraction of freeze-dried *P. grandiflorum* aerial parts (60 mesh particle size) was obtained as follows. Powdered *P. grandiflorum* aerial parts (100 g) were suspended and extracted with 400 ml of ethanol at 80 °C for 2 h. The extracts were filtered through Whatman No. 2 filter paper (Whatman International Limited, Kent, England) and evaporated to dryness. The dry materials were re-dissolved in 200 ml of distilled water. The solution was consecutively portioned in a separatory funnel with the equivalent amount of chloroform, butanol and water. Each fraction was concentrated in a vacuum evaporator (Eeyla NE, Tokyo Rikakikai Co., Ltd., Tokyo, Japan) at 40 °C. The water filtrate was frozen and lyophilised. The fractions were place in a glass bottle and stored at −20 °C until used. The lyophilised fractions were re-dissolved in ethanol to a concentration of 10 mg/ml.

2.3. DPPH free radical-scavenging activity

This was carried out according to Blois method with a slight modification (Blois, 1958). Briefly, a 1 mM solution of DPPH (Sigma Chemical Co., St. Louis, MO, USA) radical solution in ethanol was prepared, and then 4 ml of this solution was mixed with 1 ml of extract solution in ethanol containing 0.075–10 mg/ml of dried extract; finally, after 30 min, the absorbance was measured at 517 nm (UV-1201, Shimadzu, Tokyo, Japan). This activity was given as percentage DPPH scavenging that is calculated as

$$\%\text{DPPH scavenging} = [(\text{control absorbance} - \text{extract absorbance})/(\text{control absorbance})] \times 100$$

2.4. $ABTS^{\cdot+}$ radical-scavenging activity

$ABTS^{\cdot+}$ was dissolved in water to make a concentration of 7 mmol/l. $ABTS^{\cdot+}$ was produced by reacting the ABTS stock solution with 2.45 mmol/l potassium persulfate (final concentration) and allowing the mixture to stand in the dark at room temperature for 12–16 h before use. For the test of samples, the $ABTS^{\cdot+}$ stock solution was diluted with phosphate-buffered saline 5 mmol/l (pH 7.4) to an absorbance of 0.70 at 734 nm. After the addition of 1.0 ml of diluted $ABTS^{\cdot+}$ to 10 μl of sample, the absorbance reading was taken 5 min after the initial mixing (Fellegrin, Ke, Yang, & Rice-Evans, 1999). This activity is given as percentage $ABTS^{\cdot+}$ scavenging that is calculated as.

$$\%\ ABTS^{\cdot+}\text{scavenging activity} = [(\text{control absorbance} - \text{extract absorbance})/(\text{control absorbance})] \times 100$$

2.5. Reducing power

This was carried out as Oyaizu's study (Oyaizu, 1986). Briefly, extracts in 1 ml of appropriate solvents were mixed with 2.5 ml of phosphate buffer (0.2 M, pH 6.6) and 2.5 ml of potassium ferricyanide $[K_3Fe(CN)_6]$ (1%), and then the mixture was incubated at 50 °C for 30 min. Afterwards, 2.5 ml of trichloroacetic acid (10%) was added to the mixture, which was then centrifuged at 3000 rpm for 10 min. Finally, 2.5 ml of the upper layer solution was mixed with 2.5 ml distilled water and 0.5 ml $FeCl_3$ (0.1%), and the absorbance was measured at 700 nm (UV-1201, Shimadzu, Tokyo, Japan).

2.6. The ferric reducing ability of plasma (FRAP) assay

The FRAP assay developed by Benzie and Strain (Benzie & Strain, 1996). In short, 1.5 ml of working, pre-warmed 37 °C FRAP reagent (10 vol of 300 mmol/l acetate buffer, pH 3.6 + 1 vol of 10 mmol/l 2,4,6-tripyridyl-S-triazine in 40 mmol/l HCl + 1 vol of 20 mmol/l $FeCl_3$) was mixed with 50 μl of test samples and standards. This was vortex mixed and the absorbance at 593 nm was read against a reagent blank at a pre-determined time after sample-reagent mixing. The test was performed at 37 °C and a 0–4 min reaction time window was used.

2.7. Determination of total phenolics

The total phenolics were determined by the spectrophotometric method (Kim, Jeong, & Lee, 2003). In brief, a 1 ml portion of appropriately diluted extracts was added to a 25 ml volumetric flask containing 9 ml of deionised distilled water. Reagent blank using deionised distilled water was prepared. One ml of Folin–Ciocalteu's phenol reagent was added to the mixture and then shaken. After 5 min, 10 ml of a 7% Na_2CO_3 solution was added with mixing. The mixed solution was then immediately diluted to volume (25 ml) with deionised distilled water and mixed thoroughly. After 90 min at 23 °C, the absorbance was read at 750 nm. The standard curve for total phenolics was made using gallic acid standard solution (0–100 mg/l) under the same procedure as above. The total phenolics in aerial parts of *P. grandiflorum* were expressed as milligrams of gallic acid equivalents (GAE) per 100 g of dried sample.

2.8. Quantification by HPLC

Phenolic compounds were measured at 280 nm using an Agilent HPLC (1100 series, Agilent Co., USA). Separation was achieved with a TSK gel column ODS-80Tm (4.6 mmΦ × 15 mm). The mobile phase consisted of water with 0.1% acetic acid (A) and methanol with 0.1% acetic acid (B). The linear gradient was 0–100% (B) in 60 min, at a flow rate of 1.0 ml/min and the injection volume was 20 μl. Compounds were detected by monitoring the elution

at 280 nm. Identification of the phenolic compounds was carried out by comparing their retention times to those of standards. Content of phenolic compounds was expressed in mg/g extract.

2.9. Statistical analysis

All data were expressed as mean ± SD. Analysis of variance was performed by the ANOVA procedures. Duncan's new multiple-range test was used to determine the difference of means, and $P < 0.05$ was considered to be statistically significant.

3. Results and discussion

3.1. Scavenging effect on DPPH radical

The radical-scavenging activities of the fractions from aerial parts of *P. grandiflorum* were estimated by comparing the percentage inhibition of formation of DPPH radicals by the extracts and those of α-tocopherol and ascorbic acid. It was found that the radical-scavenging activities of the positive control and various solvent extract increased with increasing concentration (Fig. 1). The ability to scavenge DPPH radicals of various solvent extracts from *P. grandiflorum* was in the order of butanol fraction (90.63%) > chloroform fraction (58.68%) > water fraction (28.49%) at the concentration of 5 mg/ml. An almost linear correlation between DPPH radical-scavenging activity and concentrations of polyphenolic compounds in various vegetable and fruits have been reported (Pyo, Lee, Logendra, & Rosen, 2004). This indicates that DPPH radical-scavenging activities of all extracts from aerial parts of *P. grandiflorum* were related to the amount of antioxidant extracted from aerial parts of *P. grandiflorum* by various solvents. These results revealed that the butanol fraction from aerial parts of *P. grandiflorum* has free radical scavengers, acting possibly as primary antioxidants.

3.2. Scavenging effect on $ABTS^{\cdot+}$ radical

All fractions from aerial parts of *P. grandiflorum* exhibited $ABTS^{\cdot+}$ radical-scavenging activities to different extents in a concentration-dependent manner; although the activity levels of all of the tested samples were lower than that of α-tocopherol and ascorbic acid.

The butanol fractions from aerial parts of *P. grandiflorum* exhibited the highest radical-scavenging activities when reacted with the $ABTS^{\cdot+}$ radicals (Fig. 2). In contrast, the chloroform and water extracts only showed low activities; approximately 4–7 times lower than the butanol fraction. Fig. 2 presented a steady increase in the percentage inhibition of the $ABTS^{\cdot+}$ radicals by the butanol fraction from aerial parts of *P. grandiflorum* and maximum inhibition was achieved above 10 mg/ml. The water extract showed a percentage inhibition of less than 50% at the highest concentration studied (10 mg/ml). In addition, the chloroform fraction from aerial parts of *P. grandiflorum* did not show a leveling off at the highest concentration; however, its radical scavenging effects were much less than the butanol fraction.

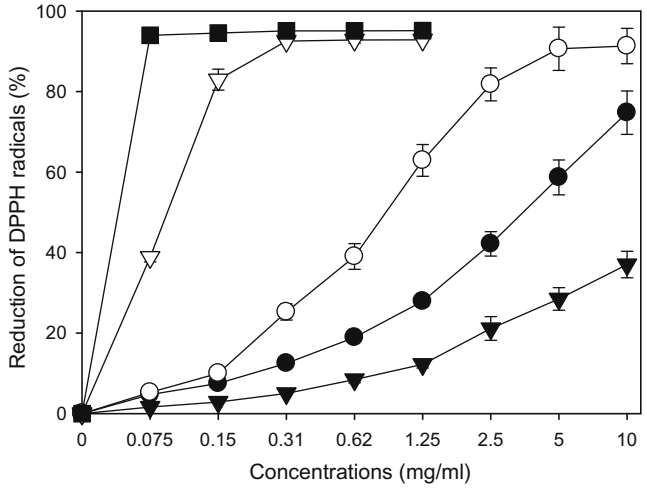

Fig. 1. DPPH radical-scavenging activities of different extracts from the ethanol crude extract of *P. grandiflorum* aerial parts by different solvents at different concentrations. Each value represents a mean ± SD ($n = 3$). (●) chloroform fraction; (○) butanol fraction; (▼) water fraction; (▽) α-tocopherol; (■) ascorbic acid.

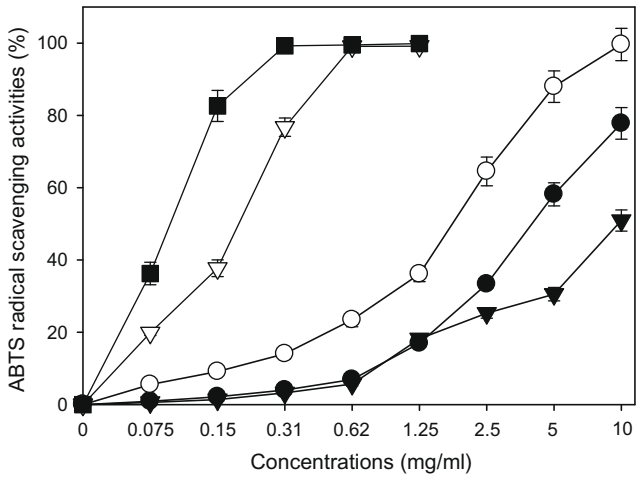

Fig. 2. ABTS radical-scavenging activities of different extracts from the ethanol crude extract of *P. grandiflorum* aerial parts by different solvents at different concentrations. Each value represents a mean ± SD ($n = 3$). (●) chloroform fraction; (○) Butanol fraction; (▼) water fraction; (▽) α-tocopherol; (■) ascorbic acid.

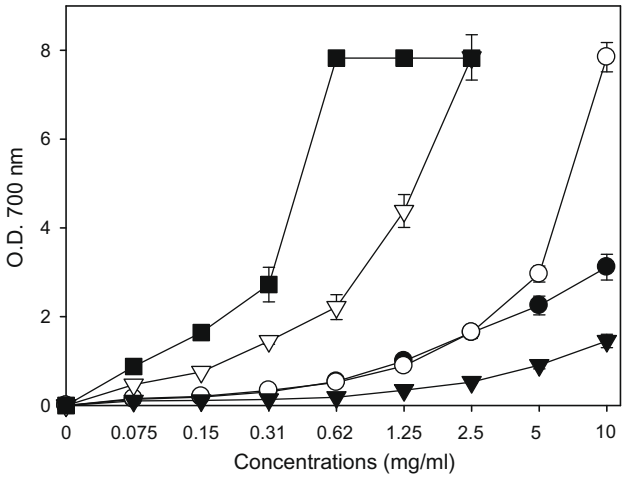

Fig. 3. Reducing power of different extracts from the ethanol crude extract of *P. grandiflorum* aerial parts by different solvents at different concentrations. Each value represents a mean ± SD ($n = 3$). (●) chloroform fraction; (○) butanol fraction; (▼) water fraction; (▽) α-tocopherol; (■) ascorbic acid.

3.3. Reducing power

In the reducing power assay, the presence of reductants (antioxidants) in the samples would result in the reducing of Fe^{3+} to Fe^{2+} by donating an electron. The amount of Fe^{2+} complex can be monitored by measuring the formation of Perl's Prussian blue at 700 nm. Increasing absorbance at 700 nm indicates an increase in reductive ability. Fig. 3 shows the dose–response curves for the

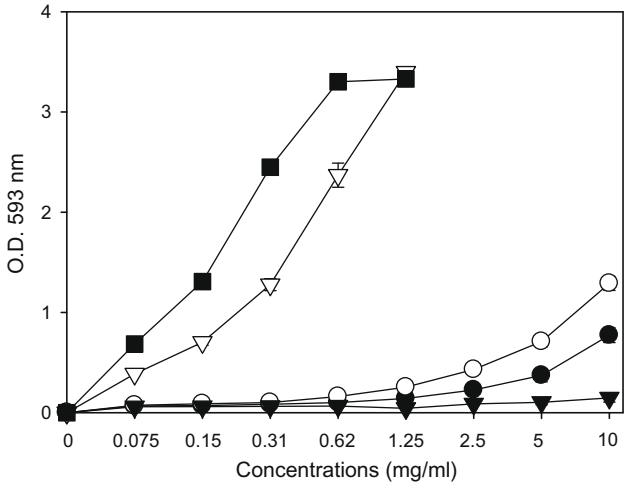

Fig. 4. Ferric reducing activities of different extracts from the ethanol crude extract of *P. grandiflorum* aerial parts by different solvents at different concentrations. Each value represents a mean ± SD ($n = 3$). (●) chloroform fraction; (○) butanol fraction; (▼) water fraction; (▽) α-tocopherol; (■) ascorbic acid.

Table 1
Total phenolics content of various solvent extracts and phenolic compounds content of butanol extract from the crude ethanol extract of *P. grandiflorum* aerial parts.

Samples	Content (mg/100 g fraction)
Fractions	
Chloroform	615 ± 32[a]
Butanol	9482 ± 325
Water	494 ± 18
Butanol fraction	
Chlorogenic acid	1214 ± 93
Luteolin-7-O-glucoside	2304 ± 219
Apigenin-7-O-glucoside	1994 ± 72
Luteolin	687 ± 53
Apigenin	151 ± 12

[a] Data are means ± SD of triplicates.

reducing powers of all extracts from aerial parts of *P. grandiflorum*. It was found that the reducing powers of all the extracts also increased with the increase of their concentrations. The various solvent fractions from aerial parts of *P. grandiflorum* exhibited a good reducing power of 3.11, 7.84 and 1.45 at 10 mg/ml, respectively. This data suggested that butanol fraction has a remarkable ability to react with free radicals to convert them into more stable non-reactive species and to terminate radical chain reaction.

3.4. Determination by FRAP assay

In this assay, extracts were used in a redox-linked reaction whereby the antioxidants present in the sample act as the oxidants. Reduction of the ferric-tripyridyltriazine to the ferrous complex forms an intense blue colour which can be measured at a wavelength of 593 nm. The intensity of the colour is related to the amount of antioxidant reductants in the extracts. The trend for ferric ion-reducing activities of different fractions from aerial parts of *P. grandiflorum* in the present study is shown in Fig. 4. For chloroform, butanol, and water fractions, the absorbance clearly increased due to the formation of the Fe^{2+}-TPTZ complex with increasing concentration. The highest reducing activity was for the butanol fraction, compared to those of the other fractions (Fig. 4). Similar to the results obtained from the DPPH to ABTS assay, the butanol fraction showed relatively strong ferric ion-reducing activity. Chloroform and water fractions showed lower ferric ion-reducing activities.

Some authors have reported similar correlations between polyphenols and antioxidant activity measured by various methods (Awika, Rooney, Wu, Prior, & Cisneros-Zevallos, 2003). A strong correlation between the mean values of the total polyphenol content and FRAP deserves detailed attention, because it implies that polyphenols in aerial parts of *P. grandiflorum* are capable of reducing ferric ions.

3.5. Total phenolics

The Folin–Ciocalteu's assay is a fast and simple method to rapidly determine the content of phenolics in samples. Phenolics or polyphenols are secondary plant metabolites that are present in every plant and plant product. Many of the phenolics have been shown to contain high levels of antioxidant activities. The total phenolic content of the three fractions from the ethanol extract of *P. grandiflorum* aerial parts are presented in Table 1. The butanol fraction exhibited the highest total phenolics content (9482 mg GAE/100 g fraction). It is approximately 15-fold more than the chloroform fraction (615 mg GAE/100 g fraction) and 19-fold more than the water fraction (494 mg GAE/100 g fraction).

3.6. Analysis of butanol fraction by HPLC

Since the butanol fraction exhibited the strongest antioxidant activity, it was subjected to further analysis by HPLC. The butanol fraction contained a variety of phenolic compounds (Fig. 5). By comparing the retention time of these compounds with those of standards, five phenolic compounds were identified (Table 1).

Furthermore, the HPLC results (Fig. 5, Table 1) indicated that luteolin-7-O-glucoside (2304 mg/100 g fraction) was the predominant compound in this extract, followed by apigenin-7-O-glucoside (1994 mg/100 g fraction). Flavonoids, and phenolic acids are important contributing factors to the antioxidant activity of the human diet. Based on the results for the phenolic composition of the butanol fraction from aerial parts of *P. grandiflorum*, we can conclude that these compounds (particularly luteoline-7-O-glucoside and apigenin-7-O-glucoside) may contribute to the antioxidant activities of the butanol extract. The activity of the butanol

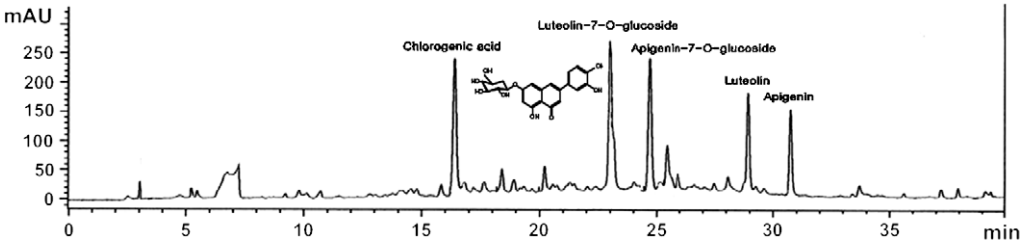

Fig. 5. HPLC chromatograms of the butanol fraction from the ethanol extract of *P. grandiflorum* aerial parts.

fraction is attributed to these phenolic compounds and in particular to luteolin-7-O-glucoside and apigenin-7-O-glucoside.

4. Conclusions

The results obtained in this work are noteworthy, not only with respect to the antioxidant activities of the butanol fraction of *P. grandiflorum* aerial parts, but also with respect to its content of a variety of phenolic compounds. The activity of this extract is attributed to these phenolic compounds and in particular to luteolin-7-O-glucoside and apigenin-7-O-glucoside. Since luteolin-7-O-glucoside is the predominant phenolic compound detected in the butanol extract, the safety of luteolin-7-O-glucoside for use as an antioxidant agent is very important. Consequently, our results presented that the butanol fraction of *P. grandiflorum* aerial parts which are normally wasted during frequent pruning has very strong antioxidant activities, and suggested that the extract can be utilised as an effective and safe antioxidant source, although the antioxidant activities of butanol fraction were lower than that of α-tocopherol and ascorbic acid.

Acknowledgments

This work was supported by the Korea Research Foundation Grant funded by the Korean Government (No. KRF-2008-521-F00074), and supported by Technology Development Program for Agriculture and Forestry, Ministry of Agriculture and Forestry, Korea.

References

Aruoma, O. I. (1996). Assessment of potential prooxidant and antioxidant actions. *Journal of American Oil Chemists Society, 73*, 1617–1625.

Awika, J. M., Rooney, L. W., Wu, X., Prior, R. L., & Cisneros-Zevallos, L. (2003). Screening methods to measure antioxidant activity of Sorghum (*Sorghum bicolor*) and Sorghum products. *Journal of Agriculture and Food Chemistry, 51*, 6657–6662.

Benzie, I. F. F., & Strain, J. J. (1996). The ferric reducing ability of plasma (FRAP) as a measure of "antioxidant power": The FRAP assay. *Analytical Biochemistry, 239*, 70–76.

Blois, M. A. (1958). Antioxidant determination by the use of a stable free radical. *Nature, 181*, 1199–1200.

Cao, G., Sofic, E., & Prior, R. (1996). Antioxidant capacity of tea and common vegetables. *Journal of Agriculture and Food Chemistry, 44*, 3426–3431.

Choi, H. R., Choi, J. S., Han, Y. N., Bae, S. J., & Chung, H. Y. (2002). Peroxynitrite scavenging activity scavenging activity of herb extracts. *Phytotherapy Research, 16*, 364–367.

Fellegrin, N., Ke, R., Yang, M., & Rice-Evans, C. (1999). Screening of dietary carotenoids and carotenoid-rich fruit extracts for antioxidant activities applying 2,2'-azinobis(3-ethylbenzothiazoline-6-sulfonic acid) radical cation decolorization assay. *Methods in Enzymology, 299*, 379–389.

Fu, W. F., Dou, D. Q., Zhao, C. J., Shimizu, N., Pei, Y. P., Pei, Y. H., et al. (2007). Triterpenoid saponins from *Platycodon grandiflorum*. *Journal of Asian Natural Products Research, 9*, 35–40.

Kim, D. O., Jeong, S. W., & Lee, C. Y. (2003). Antioxidant capacity of phenolic phytochemicals from various cultivars of plums. *Food Chemistry, 81*, 321–326.

Kim, Y. P., Lee, E. B., Kim, S. Y., Li, D., Ban, H. S., Lim, S. S., et al. (2001). Inhibition of prostaglandin E2 production by platycodin D isolated from the root of *Platycodon grandiflorum*. *Planta Medica, 67*, 362–364.

Lee, S. H. (1991). *Patent on the method of cultivating the perennial balloonflower*. Patent No. 045971, Korea.

Lee, K. J., Choi, C. Y., Chung, Y. C., Kim, Y. S., Ryun, S. Y., Rohm, S. H., et al. (2004). Protective effect of saponins derived from roots of *Platycodon grandiflorum* on tert-butyl hydroperoxide-induced oxidative hepatotoxicity. *Toxicology Letters, 147*, 271–282.

Lee, J. Y., Hwang, W. I., & Lim, S. T. (2004). Antioxidant and anticancer activities of organic extracts from *Platycodon grandiflorum* A. De Candolle roots. *Journal of Ethnopharmacology, 93*, 409–415.

Lee, K. J., & Jeong, H. G. (2002). Protective effect of *Platycodi radix* on carbon tetrachloride-induced hepatotoxicity. *Food and Chemical Toxicology, 40*, 517–525.

Lee, K. J., You, H. J., Park, S. J., Kim, Y. S., Chung, Y. C., Jeong, T. C., et al. (2001). Hepatoprotective effects of *Platycodon grandiflorum* on acetaminophen-induced liver damage in mice. *Cancer Letters, 174*, 73–81.

Nagao, T., Matsuda, H., Namba, K., & Kubo, M. (1986). Immune pharmacological studies on *Platycodi radix*. II. Antitumor activity of inulin from *Platycodi radix*. *Shōyakugaku Zasshi, 40*, 375–380.

Oyaizu, M. (1986). Studies on products of browning reaction: Antioxidative activities of products of browning reaction prepared from glucosamine. *Japanese Journal of Nutrition, 44*, 307–315.

Pyo, Y. H., Lee, T. C., Logendra, L., & Rosen, R. T. (2004). Antioxidant activity and phenolic compounds of Swiss chard (*Beta vulgaris* subspecies cycla) extracts. *Food Chemistry, 85*, 19–26.

Sawa, T., Akaike, T., & Maeda, H. (2000). Tyrosine nitration by peroxynitrite formed from nitric oxide and superoxide generated by xanthine oxidase. *Journal of Biological Chemistry, 275*, 32467–32474.

Singh, A. (Ed.). (1989). *Chemical and biochemical aspects of activated oxygen. Singlet oxygen, superoxide anion, and related species* Mequel, J., Quintanilha, A. T., & Weber, H. (Eds.). *CRC handbook of free radical and antioxidant in biomedicine* (vol. 1, pp. 17–28). Boca Raton, FL, USA: CRC Press, Inc..

Squadrito, G. L., & Pryor, W. A. (1998). Oxidative chemistry of nitric oxide: The role of superoxide, peroxynitrite, and carbon dioxide. *Free Radical Biology & Medicine, 25*, 392–403.

Xu, B. J., Zheng, Y. N., & Sung, C. K. (2004). Quality control and evaluation of *Platycodon grandiflorum* implications for future management. *Natural Product Sciences, 10*, 141–151.

Zhao, H. L., Cho, K. H., Ha, Y. W., Jeong, T. S., Lee, W. S., & Kim, Y. S. (2006). Cholesterol-lowering effect of platycodon D in hypercholesterolemic ICR mice. *European Journal of Pharmacology, 53*, 166–173.

Zhao, H. L., Harding, S. V., Marinangeli, C. P. E., Kim, Y. S., & Jones, P. J. H. (2008). Hypocholesterolemic and anti-obesity effects of saponine from *Platycodon grandiflorum* in hamsters fed atherogenic diets. *Journal of Food Science, 73*, H195–H200.

Zheng, J., He, J., Ji, B., Le, Y., & Zhang, X. (2007). Antihyperglycemic effects of *Platycodon grandiflorum* (Jacq.) A. DC. Extract on streptozotocin-induced diabetic mice. *Plant Foods for Human Nutrition, 62*, 7–11.

Food Chemistry 118 (2010) 283–290

Contents lists available at ScienceDirect

Food Chemistry

journal homepage: www.elsevier.com/locate/foodchem

Investigation of off-odour and off-flavour development in boiled potatoes

Giampaolo Blanda *, Lorenzo Cerretani *, Patrizia Comandini, Tullia Gallina Toschi, Giovanni Lercker

Dipartimento di Scienze degli Alimenti, Università di Bologna, P.zza Goidanich, 60, 47023 Cesena (FC), Italy

ARTICLE INFO

Article history:
Received 17 February 2009
Received in revised form 9 April 2009
Accepted 27 April 2009

Keywords:
Potato
Off-flavours
HS-SPME
Sensory analysis
Volatile compounds

ABSTRACT

The present study focused on the development of a sensory evaluation system, using a quantitative descriptive analysis (QDA) scheme, to define the sensory attributes of boiled potato slices. A HS-SPME–GC–MS technique for a rapid determination of volatile components in boiled potatoes was also investigated. In addition to the mechanism of generation of off-odours and off-flavours in boiled potatoes (POF), the effects of the use of food additives after cooking were examined. POF formation, analysed by both sensory evaluation and HS-SPME, demonstrated an oscillating mechanism of formation of volatile compounds, probably related to enzymatic lipid oxidation and hydroperoxide generation. In particular, POF were strongly correlated with the presence of 2-pentenal, 2-hexenal, 2-heptenal, 2-pentylfuran and 2-decenal. In all, about 50 compounds were detected by HS-SPME technique. Treatment with ascorbate or citrate, after cooking and before storage, did not prevent the formation of off-flavours, in contrast to sodium pyrophosphate. Potassium meta-bisulphite prevented POF formation, but caused the creation of other off-flavours detected by a trained panel.

1. Introduction

Potatoes (*Solanum tuberosum*), originating from the Andes Mountains about 8000 years ago, have widely spread to the rest of the world as a result of their nutritional properties and their adaptability to different climate conditions. The year 2008 was declared the "International Year of the Potato" to highlight the importance of potatoes as a fundamental food resource and to promote the development of sustainable potato-based systems; such actions aim to ensure food security for the increasing world population and also contribute in protecting natural resources (http://www.potato2008.org/en/index.html).

Potatoes may be served in a variety of ways: fried, steam cooked, baked or boiled, with inter-changeable preferences in different regions. Boiled potatoes have a flavour that is rather weak, but which is typical and clearly distinguishable from that of raw or cooked potatoes, and is one of the most important qualitative criteria in assigning different potato varieties to a fresh or processed food market. Volatile compounds responsible for the flavour of boiled potatoes are created by typical chemical precursors of raw tubers, which are characterised by different flavours (Petersen, Poll, & Larsen, 1998).

More than 140 volatile compounds have been identified in boiled potatoes (Ulrich, Hoberg, Neugebauer, Tiemann, & Darsow, 2000), whereas over 250 have been found in baked potatoes (Whitfield & Last, 1991) due to the high temperature and long cooking time that cause the degradation of the large compounds. Different potato varieties, cultivation techniques, storage and cooking methods, in addition to the extraction and the analytical techniques employed, have identified a broad set of aromatic compounds in boiled potatoes, which are quite variable and not always in agreement in different publications (Petersen, Poll, & Larsen, 1999, 2003; Petersen et al., 1998; Ulrich et al., 2000).

The typical aroma of boiled potatoes is mainly due to the presence of essential compounds such as methional and various pyrazines (Ulrich et al., 2000) produced by the Maillard reaction and Strecker degradation. Moreover, lipoxidase (lipoxygenase and lipoperoxidase) enzymes oxidise the fatty acids in boiled potatoes. Palmitic, linoleic and linolenic acids represent more than 90% of the total fatty acids in potatoes (Galliard, 1973), thus creating numerous aldehydes (Josephson & Lindsay, 1987; Petersen et al., 1998).

As reported by Petersen et al. (1999), during storage of boiled potatoes there is production of cardboard-like off-flavours within a few hours from preparation, that is due to lipid oxidation; such compounds, in fact, are strictly related to the presence of oxygen. This problem is particularly significant for the production of potato-based foodstuffs that are stored in modified atmosphere. Under these conditions, the creation of off-flavours slows but does not stop completely. Moreover, the production of volatile components also varies as a function of the amount of oxygen inside the packaging and the permeability of the latter to atmospheric gases. Such reactions may reduce the shelf life of ready-to-eat or ready-to-cook products that contain boiled potatoes.

* Corresponding authors. Tel.: +39 0547 338121; fax: +39 0547 382348.
E-mail addresses: giampaolo.blanda2@unibo.it (G. Blanda), lorenzo.cerretani@unibo.it (L. Cerretani).

0308-8146/$ - see front matter © 2009 Elsevier Ltd. All rights reserved.
doi:10.1016/j.foodchem.2009.04.135

To the best of our knowledge, the extraction techniques widely employed for the separation of aromatic compounds from boiled potatoes are the Lickens-Nickerson method, Dynamic Headspace (DH) and solid–liquid extraction. Over the years, the Lickens-Nickerson method has been performed with numerous variations from the original version (Buttery, Seifert, & Ling, 1970; Mutti & Grosch, 1999; Nursten & Sheen, 1974; Ulrich et al., 2000), but it is essentially based on steam distillation of volatile compounds at high temperatures for extended times. Due to the analytical conditions required, this process may lead to the creation of new aromatic substances, especially during extended treatments. The extraction is performed with dedicated equipment and assures good detection limits.

The DH technique is based on stripping of volatile components with a flow of inert gas (e.g. N_2, He) and their subsequent adsorption by polymers. Quantitative extraction is granted by high temperatures, such as those employed by Salinas, Hartman, Karmas, Lech, and Rosen (1994), which extracted the aromatic compounds from cooked and reconstituted dehydrated potatoes at 100 °C for 1 h, or by extended treatments such as those of Josephson and Lindsay (1987) who performed an extraction for 15 h at 21 °C. Under these conditions, enzymatic reactions may take place and synthesise ex novo aromatic components that were not present before the extraction.

The extraction procedure has been employed in several works by Petersen et al. (1998, 1999, 2003) to investigate the volatile fraction of potatoes. However, if the aromatic compounds in boiled potatoes are extracted with an organic solvent, a large quantity of sample has to be analysed due to the small concentration of aromas in the food matrix. Moreover, the extraction technique frequently leads to the separation of non-volatile chemical compounds that interfere with the analysis and increase the detection limits.

In 1990, headspace solid-phase microextraction (HS-SPME) has been introduced by Arthur and Pawliszyn as an alternative to the DH technique as a sample preconcentration method prior to chromatographic analysis. In addiction to the analysis of pollutants in water, this method has been applied to various food flavour analyses, and its suitability in qualitative and quantitative analysis of the volatile fraction of virgin olive oil has been frequently reported (Baccouri et al., 2008; Vichi, Pizzale, Conte, Buxaderas, & Pez-Tamames, 2003). It has moreover been used in the analysis of oxidation products of refined vegetable oils (Jelen, Obuchowska, Zavirska-Wojtasiak, & Wasowicz, 2000) and milk, where it demonstrated better precision, accuracy, repeatability and linearity of response than DH (Marsili, 1999).

The objectives of the present research were to perform a sensory evaluation system, using a quantitative descriptive analysis (QDA) scheme, to define the odour, flavour and texture features of boiled potato slices, and to develop a HS-SPME–GC–MS method for a rapid determination of volatile components in boiled potatoes. We also investigated the mechanism of generation of off-odours and off-flavours in boiled potatoes, with particular attention to the effects of treatment with food additives after cooking.

2. Experimental

2.1. Samples

Potatoes (*Solanum tuberosum*) of the Marabel variety were harvested in July and stored for three months at controlled temperature and relative humidity. Potato dry matter was 19.94% at the moment of analysis. From the initial stock of potatoes, only average size tubers (150–180 g) were selected.

All tubers were washed with tap water to remove soil residue before manual peeling. The central portion of each tuber was divided into 5–6 slices (5 mm thickness), and the rest of the tuber was rejected in order to obtain slices with a similar size. About 6.5 kg of potatoes slices were boiled in 24 L of tap water for 12 min. After boiling, slices were split in groups (W, AA, CA, PP, MB) and subjected to various treatments (immersion in hot water or in food additive solutions), as shown in Table 1. Slices were then cooled for 10 min at room temperature (22 °C), put in open PET containers, stored in refrigeration conditions (at a temperature of 5 °C and air exposed) until obtaining thermal equilibrium with

Table 1
Schematic representation of the boiled potato samples analysed.

Samples ID	Post-cooking treatment	Cooling conditions	Storing conditions	SPME extraction temperature (°C)	SPME enzymatic inhibition	QDA analysis	QDA of sample purees before SPME adsorption
WA0i	Water immersion for 1 min at 80 °C	10 min at 22 °C	30 min at 5 °C	70	NaCl	No	Yes
WA0j	Water immersion for 1 min at 80 °C	10 min at 22 °C	30 min at 5 °C	70	–	No	Yes
WA0	Water immersion for 1 min at 80 °C	10 min at 22 °C	30 min at 5 °C	37	NaCl	Yes	Yes
WA2	Water immersion for 1 min at 80 °C	10 min at 22 °C	2 h at 5 °C	37	NaCl	Yes	Yes
WA4	Water immersion for 1 min at 80 °C	10 min at 22 °C	4 h at 5 °C	37	NaCl	Yes	Yes
WA6	Water immersion for 1 min at 80 °C	10 min at 22 °C	6 h at 5 °C	37	NaCl	Yes	Yes
WA8	Water immersion for 1 min at 80 °C	10 min at 22 °C	8 h at 5 °C	37	NaCl	Yes	Yes
WA10	Water immersion for 1 min at 80 °C	10 min at 22 °C	10 h at 5 °C	37	NaCl	Yes	Yes
WA24	Water immersion for 1 min at 80 °C	10 min at 22 °C	24 h at 5 °C	37	NaCl	Yes	Yes
AA24	Ascorbic acid solution immersion(3 g/L) for 1 min at 80 °C	10 min at 22 °C	24 h at 5 °C	37	NaCl	Yes	Yes
CA24	Citric acid solution immersion (3 g/L)for 1 min at 80 °C	10 min at 22 °C	24 h at 5 °C	37	NaCl	Yes	Yes
PP24	Sodium acid pyrophosphate solution immersion (3 g/L) for 1 min at 80 °C	10 min at 22 °C	24 h at 5 °C	37	NaCl	Yes	Yes
MB24	Potassium meta-bisulphite solution immersion (3 g/L) for 1 min at 80 °C	10 min at 22 °C	24 h at 5 °C	37	NaCl	Yes	Yes

the temperature refrigeration (30 min at 5 °C) or for different times (2, 4, 6, 8, 10, 24 h at 5 °C), before extraction and analysis of the volatile fraction.

W samples, after boiling, were immediately immerged in hot water (80 °C) for 1 min (water/potatoes, 3:1).

WA0j: HS-SPME–GC–MS analysis of volatile compounds was carried out at 70 °C, without the addition of an enzymatic inhibitor to the extraction solution.

WA0i: during volatile compound extraction, carried out at 70 °C, NaCl was added to the extraction solution to inhibit enzymatic reactions.

WA0: volatile components extraction was performed at 37 °C with the addition of NaCl to the extraction solution.

WA2, 4, 6, 8, 10, 24 samples were obtained using the same extraction conditions of WA0 (temperature: 37 °C, inhibitor: NaCl), but were stored, respectively, for 2, 4, 6, 8, 10 and 24 h at 5 °C, before analysis.

After boiling, samples AA24, CA24, PP24, MB24 were immediately immerged, respectively, in ascorbic acid, citric acid, sodium acid pyrophosphate and meta-bisulphite solutions (3 g/L) for 1 min at 80 °C (solution/potatoes, 3:1). Each of these food additives was of commercial grade (CHIMAB S.p.A., Padova, Italy). After immersion, all further steps were the same as for sample W24 (storage: 24 h at 5 °C, HS-SPME extraction temperature: 37 °C, enzyme inhibitor: NaCl).

2.2. Sensory analysis

Quantitative Descriptive Analysis (QDA, Stone & Sidel, 1992; Stone, Sidel, Oliver, Woolsey, & Singleton, 1974) was carried out in the laboratory of sensory analysis at the "Campus of Food Science" at the University of Bologna. A panel of 12 judges, with experience in sensory evaluation of different foods, were trained to carry out QDA of boiled potatoes.

The best features for sensory description of boiled potatoes (attributes) were developed during a focus session. Then, additional six training sessions were held to enhance the ability of each panel member to recognise and quantify the descriptors previously stated.

Standard solutions of some descriptors were used to calibrate the panelists, when reference compounds were not available the descriptors learning and alignment procedure was realised without reference standards, as described by Sulmont, Lesschaeve, Sauvageo, and Issanchou (1999).

Based on repeatability and reproducibility of panel results only some attributes were judged during evaluation of potato samples. The descriptors "Other off-odours" and "Other off-flavours" were defined as defected odours and flavours different from the cardboard-like ones. Judges could identify the qualitative nature of the defects perceived and quantify them, using their personal lexicon developed in previous sensory evaluation experiences. The descriptors were evaluated on a continuous scale from 1 to 9 points. A score of 1 indicated no detectable perception, whilst 9 indicated maximum perception. The repeatability of each descriptor was also determined. Only the eight judges with the best analytical capacity (and best repeatability) were selected to perform the sensory evaluation described in Table 1.

A specific and standardised test was performed for sensory evaluation of boiled potatoes: the slices of boiled potato were cut into quarters, and each piece was served to the assessors in plastic dishes. Sensory analysis was made in individual booths equipped with red light to avoid any influence of potato colour on sample judgment; older samples, in fact, could have been identified from fresh samples as they had a paler pulp. After tasting each sample, the judges rinsed their mouth with water. Each sample cited in Table 1, except for WA0j and WA0i, was analysed four times.

A cardboard-like off-odour descriptor was also analysed on all sample purees immediately after HS-SPME extraction of volatile compounds, as described in paragraph 2.3.

Values of the median of sensory data and the robust standard deviation were calculated (Giomo, 2000).

2.3. HS-SPME–GC–MSD analysis

Potatoes slices (about 200 g for each sample) were put in a 1000 mL bottle and homogenised with 500 mL of NaCl 0.30 M using an Ultraturrax. The extraction solution was at a temperature suitable to bring the homogenate to 37 °C.

The bottle was closed with a silicon cap and then introduced in a heating bath at 37 °C for 10 min. After this step, the silicon cap was perforated with the divinylbenzene/carboxen/polydimethylsiloxane (DVB/CAR/PDMS, 50/30 μm, coating 2 cm) fibre holder (Supelco Ltd., Bellefonte, PA, USA) and equilibrated for 10 min, with the heating bath kept at 37 °C. Finally, the fibre was exposed for 30 min and immediately desorbed for 3 min at 250 °C in the gas chromatograph.

After removing the fibre from the bottle, each sample puree (2 repetitions) was immediately smelled by the panel judges directly from the bottle of extraction, and the cardboard-like off-odour perception was evaluated using the same scale of the other descriptors analysed during QDA.

Volatile compounds were identified and peak area was integrated by gas chromatography coupled to quadrupolar mass-selective spectrometry using an Agilent 6890 N Network gas chromatograph and an Agilent 5973 Network detector (Agilent Technologies, Palo Alto, CA, USA). Analytes were separated on a ZB-WAX Phenomenex column 30 m × 0.25 mm ID, 1.00 μm film thickness. Column temperature was held at 40 °C for 10 min and increased to 200 °C at 3 °C min^{-1}. The ion source and the transfer line were set to 175 °C and 280 °C, respectively. Electron impact mass spectra were recorded at 70 eV ionisation energy in the 20–250 amu mass range (2 scan/sec). Volatile compounds present in boiled potatoes were tentatively identified basing on computer matching against commercial libraries (NIST/EPA/NIH Mass Spectral Library 2005) as well as our laboratory-made spectral library of pure substances, Kovats retention indices (KI) and literature data. Retention indices were calculated for each compound using homologous series of C9–C19 n-alkanes (Van Den Dool & Kratz, 1963).

As the aim of the present work was to compare the use of the different additives and storage times, and thus absolute quantification was not necessary, data are reported as peak areas.

2.4. Statistical analysis

Data were analysed using Statistica 7.0 (Statsoft Inc., Tulsa, OK, USA) statistical software. The significance of differences at 5% level amongst means was determined by one-way ANOVA using Tukey's test. The data were also analysed by principal component and classification analysis to determine the correlation between the analyses and demonstrate differences between samples.

3. Results and discussion

Developing a QDA test is particularly complex, owing to intense training of assessors and the availability of artificial standards to calibrate the attributes. In this investigation, thanks to a high number of panel trainings, it was possible to get optimal repeatability of the attributes used, as shown in Table 2. As previously defined, the 10 attributes evaluated were the most repeatable between those developed during the focus session; particular attention was given to off-flavour and off-odour attributes generated during

Table 2
Description of the attributes evaluated during quantitative descriptive analysis of boiled potato slices.

Attribute	Definition	Standard employed to train the panel	Mean CVr% of attribute
Typical odour	Typical fragrance or aroma of boiled potatoes as perceived by the nose from sniffing through the external nares (Lawless and Heymann, 1998)	Solutions of Quest Aroma of boiled potatoes	10.5
Cardboard-like off-odour	Defected odour, characteristic of oxidised milk, perceived by sniffing boiled potatoes slices (Amerine, Pangborn, & Roessler, 1965)	Potatoes at different ageing degree	9.0
Other off-odours	Other defected odours perceived by sniffing boiled potatoes samples.	Not employed	3.7
Hardness	Force required dividing the potato in two parts by the front teeth (Thygesen, Thybo, & Engelsen, 2001)	Potatoes (variety Marabel) at different cooking degree	6.7
Mealiness	How mealy/crumbly the potato is felt in the mouth after chewing (Thygesen et al., 2001)	Potatoes (variety Innovator) at different cooking degree	13.9
Adhesiveness	Force required removing the potato sticking to teeth and palate after chewing (Thygesen et al., 2001)	Not employed	12.7
Sweetness	Sweet taste perceived during chewing of boiled potatoes slices	Sucrose aqueous solutions. Potato samples cooked in solutions at different sucrose concentration	8.7
Typical flavour	Typical boiled potato retronasal smell originated in the mouth via transportation of the stimulus molecules up to the back of the nasopharynx and into the region of the olfactory receptors (Lawless and Heymann, 1998)	Potato samples cooked in solutions at different Quest aroma concentrations.	9.4
Cardboard-like off-flavour	Defected retronasal smell, similar to the characteristic defected odour of oxidised milk, perceived after deglutition of boiled potato slices (Amerine et al., 1965)	Not employed	3.2
Other off-flavours	Other defected retronasal smell perceived after deglutition of boiled potatoes slices	Not employed	2.6

sample ageing, as also described by Petersen et al. (1999). The results of sensory analysis of boiled potato samples is reported on Table 3; PCA of the same data is shown in Fig. 1. For all sensory analyses, the CVr% were less than 20%, and were thus considered acceptable for sensory data (data not shown).

In the present work, the Marabel variety was used due to its marked tendency to develop off-flavours and rancidity (Thybo, Christiansen, Kaak, & Petersen, 2006).

As seen in Table 3, boiled potatoes analysed only a few minutes after cooking (WA0) presented a typical odour that was very high and no cardboard-like off-odour was detected. Hardness, mealiness and adhesiveness were 5.6, 5.5 and 5.1, respectively. Sweetness was 3.3, and typical flavour and off-flavours had a trend similar to the correspondent values of odour attributes.

WA0 and WA2 were very similar (Fig. 1), whilst at increasing storage times (4, 6, 8, 10 and 24 h) typical odour, typical flavour, off-odours and off-flavours changed, whereas the other characteristics evaluated did not vary considerably. Off-odours and off-flavour did not increase linearly during storage: they reached a maximum value after 6 h of storage (WA6), further decreased after 8 and 10 h (WA8 and WA10) and finally increased again after 24 h of storage (WA24). Typical odour and typical flavour have a complementary tendency.

The off-odour and off-flavour concentration of samples WA2,4,6,8,10,24 might be explained by a kinetic mechanism involving the formation of hydroperoxides during the first hours of storage, their increase with time and finally their transformation to yield aldehydes that are responsible for potato off-flavour (POF). Due to air exposure during refrigeration, some volatile components evaporate, and a decrease in POF in samples WA8 and WA10 was observed. The increase of off-odours and off-flavours after 10 h storage, in our view, may be due to further oxidation of the remaining lipid portion.

Volatile compounds are generated by enzymatic and chemical oxidation of the lipid fraction of boiled potatoes, which takes place on the surface of the food in contact with oxygen. Autooxidation reactions of linoleic and linolenic acids create hydroperoxides which are then broken with the formation of volatile compounds responsible for off-flavours. As reported on literature, the generation of hydroperoxides from food fatty acids is not linear during the time, because when a limit concentration is reached, the bimolecular interaction of hydroperoxides and the decomposition of secondary oxidation products leads to the increase of compounds with a great impact on flavour, like aldehydes, esters and other degradation products (Frankel, 1982, 1985).

Hydroperoxides may be cleaved also by enzymatic reactions catalysed by lipoperoxidase creating further off-flavours. Owing to the reproductive functions of the potato tubers, enzymatic activity is very high; its inhibition at elevated temperatures is not immediate, and it proceeds step-by-step and at lower temperatures during the initial stages of cooking. As a result, enzymatic reactions are accelerated. The consequences of these mechanisms

Table 3
Quantitative descriptive analysis results of boiled potato slices. Data presented is the median of 16 values (8 judges and 2 replicates); in brackets CVr% are reported.

Attributes	WA0	WA2	WA4	WA6	WA8	WA10	WA24	AA24	PP24	CA24	MB24
Typical odour	5.0 (7.3)	6.1 (4.5)	3.5 (13.2)	2.2 (12.6)	3.6 (12.7)	4.0 (10.3)	3.5 (7.9)	3.2 (15.3)	5.5 (3.6)	2.0 (13.3)	3.0 (14.9)
Cardboard-like off-odour	1.0 (11.2)	1.0 (9.0)	4.0 (8.3)	4.8 (12.0)	2.5 (11.4)	1.9 (7.5)	4.0 (8.8)	5.0 (12.3)	1.0 (7.3)	4.0 (6.3)	1.0 (5.3)
Other off-odours	1.0 (0.0)	1.0 (8.3)	1.0 (4.7)	1.0 (0.0)	1.0 (2.6)	1.0 (5.7)	1.0 (4.0)	1.0 (7.0)	1.0 (3.3)	1.0 (2.3)	5.0 (2.6)
Hardness	5.6 (11.0)	5.3 (8.0)	6.4 (4.5)	5.6 (5.9)	5.4 (10.5)	4.6 (8.8)	4.5 (7.7)	6.0 (4.8)	8.0 (3.8)	4.0 (2.3)	4.5 (6.7)
Mealiness	5.5 (13.1)	4.8 (9.9)	4.7 (10.9)	4.6 (6.8)	4.6 (15.7)	4.0 (18.7)	6.5 (19.4)	4.5 (6.7)	2.0 (19.9)	6.0 (16.6)	6.5 (14.7)
Sweetness	3.3 (8.1)	3.3 (13.5)	3.3 (17.0)	2.4 (13.5)	3.1 (18.3)	3.4 (12.1)	4.0 (12.1)	2.8 (11.7)	3.0 (8.1)	3.0 (12.7)	3.2 (12.7)
Adhesiveness	5.1 (9.0)	5.1 (6.7)	5.3 (12.4)	5.0 (12.3)	4.4 (5.8)	4.0 (3.9)	5.0 (13.0)	4.2 (11.5)	2.0 (8.5)	6.0 (5.7)	6.0 (7.2)
Typical flavour	5.5 (3.4)	5.9 (16.4)	3.0 (12.7)	1.6 (9.7)	3.6 (4.7)	3.3 (9.4)	5.0 (12.4)	1.8 (7.8)	5.0 (8.9)	2.0 (12.5)	2.0 (5.8)
Cardboard-like off-flavour	1.0 (0.0)	1.0 (2.5)	4.3 (6.5)	5.1 (2.6)	3.4 (7.7)	2.1 (3.9)	2.5 (2.0)	6.2 (0.0)	1.0 (2.3)	4.0 (3.2)	1.0 (4.5)
Others off-flavours	1.0 (2.4)	1.0 (0.0)	1.0 (4.5)	1.0 (0.0)	1.0 (0.0)	1.0 (8.7)	1.0 (0.0)	1.0 (5.6)	1.0 (0.0)	4.0 (2.2)	6.0 (5.6)

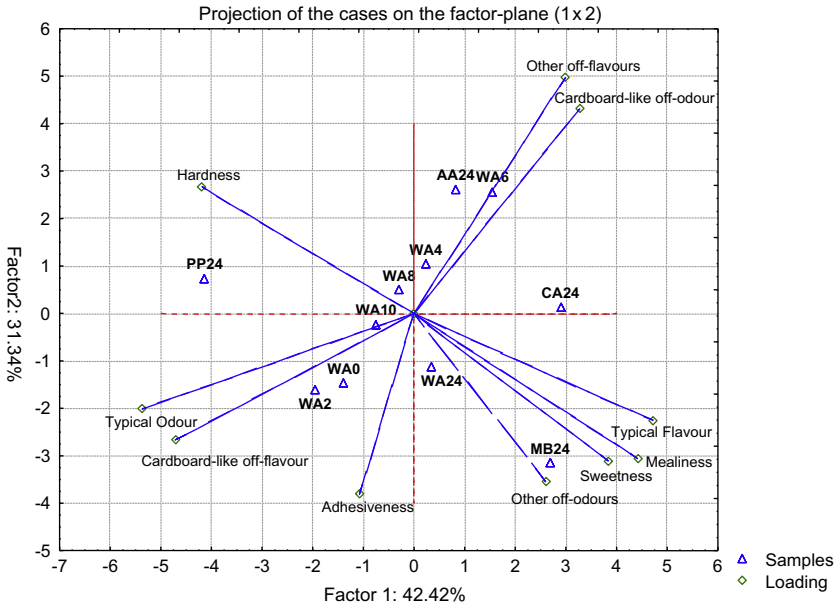

Fig. 1. Principal component analysis of sensory analysis results of boiled potato slices.

are the slow release of volatile components from the food matrix during the successive analytical phases. Another enzymatic mechanism that may be involved is the partial inactivation of potato enzymes, which continue to undergo oxidation even after boiling from atmospheric oxygen (Grosch, 1987; Lercker, Bortolomeazzi, & Pizzale, 1998; Lercker, Capella, & Conte, 1984; Selke, Frankel, & Neff, 1978).

Samples treated with different food additives and stored for 24 h (AA24, CA24, MB24 and PP24) are distant from either WA0 (analysed immediately after cooking) or WA24 (analysed after 24 h of storage without addition of food additives), as shown in the factorial plane of Fig. 1. These results indicate that the additives used do not allow the characteristics of boiled potato slices to remain unchanged, and determine a different evolution of sensorial attributes, with respect to those promoted by different storage times.

AA24 sample has a cardboard-like off-flavour and off-odour that was more intense than the control sample WA24. CA24 sample also differed substantially from WA24, mainly for the presence of other off-flavours defined by the panel judges as "dry", "hay", "biting", which were likely generated by the pH change induced by employing the food additive. These results demonstrate that neither ascorbic acid nor citric acid had any antioxidant effects on the lipid fraction of boiled potatoes, a finding that may be related to their hydrophilic nature, which does not allow them to protect the lipid portion. Moreover, it seems that these acids do not inhibit the activity of oxidative enzymes, which appears higher owing to a pH shift towards more favourable values.

The addition of potassium meta-bisulphite seems to prevent the creation of cardboard-like off-flavour and off-odour. In fact, whilst sample MB24 did not present such attributes, but had other negative characteristics described by the panel members as "beast" and "putrid". These features may be correlated with the capacity of meta-bisulphite to increase the reduction potential and create reduced molecules, with sulphhydryl functional groups.

Sample PP24 was interesting as it had no defects in flavour, odour or taste, but compared to the other samples it was harder and had a lower mealiness. The absence of off-flavours is probably due to the increase of the reduction potential of the system, and it is still unknown if these effects are due to direct inhibition of enzymatic processes. Textural changes in boiled potatoes, in our opinion, are probably due to the creation of a large number of interactions between calcium ions and wall cell pectins, with an increase in calcium pectate and subsequent hardness of boiled potato slices.

These results highlight that further research is needed to explain the reaction mechanisms of additives in boiled potatoes.

During preliminary tests (data not shown), the solid–liquid extraction technique described by Petersen et al. (1999) was applied, but the GC–MS chromatographic traces obtained did not present any significant peaks that were distinguishable from the limits of detection. Differences between our application of the solid–liquid extraction and those reported in literature include the variety of potatoes used (Marabel *vs*. Bintje) and the analysis of slices and not whole tubers. The apparently discrepant results we obtained might be due to the high surface/volume ratio of boiled potatoes, which enable a greater dispersion of volatile compounds, either during the cooking phase or during storage before analysis. However, in our opinion, the solid/liquid extraction technique has the disadvantage of extracting too many interferents that increase the limit of detection. For these reasons, potato slices evaluated by QDA were also analysed by HS-SPME–GC–MS to determine volatile compounds.

HS-SPME extraction was chosen since it is very fast and utilises small amounts of sample. Moreover, it does not extract interferent compounds. Volatile compound analysis by HS-SPME was able to characterise different potatoes samples very well, and in particular those treated with different food additives. Fig. 2 shows the PCA biplot of potato samples and the most representative volatile compounds identified by HS-SPME. Factor analysis was used to determine which variables had greater factor loadings or weights, with those having a value greater than 0.70 being considered significant. Principal components analysis identified two factors that explain 90.69% of the variance: factor 1 explains 63.33% of the variance, whilst factor 2 represents 27.36%. The variables most closely associated with factor 2 were *n*-hexyl acetate, hexyl butanoate and hexyl hexanoate. 2-Pentenal, 2-hexenal, 2,4-heptadienal, 2-heptenal, 2-pentyl furan, 2-nonenal, 2,4 decadienal, and 2-decenal were significantly associated with factor 1.

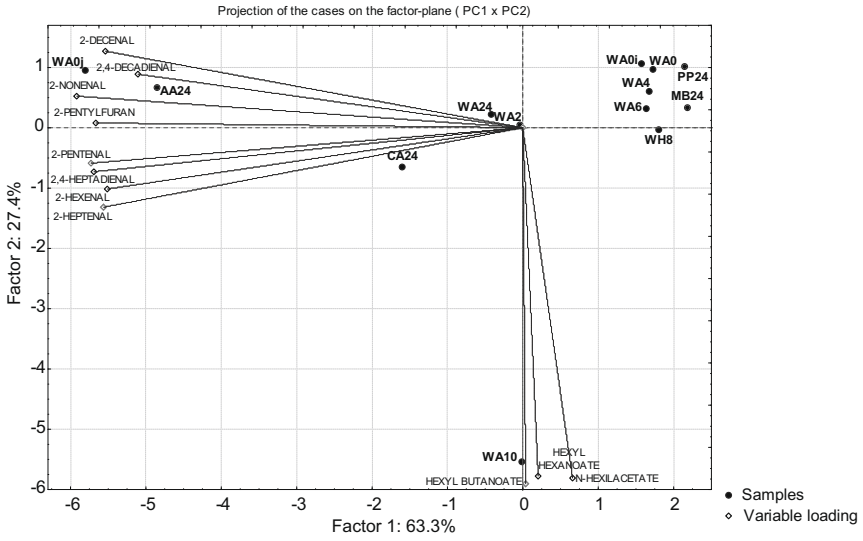

Fig. 2. Principal component analysis of solid-phase microextraction gas chromatography–mass spectrometry analysis results of boiled potato slices.

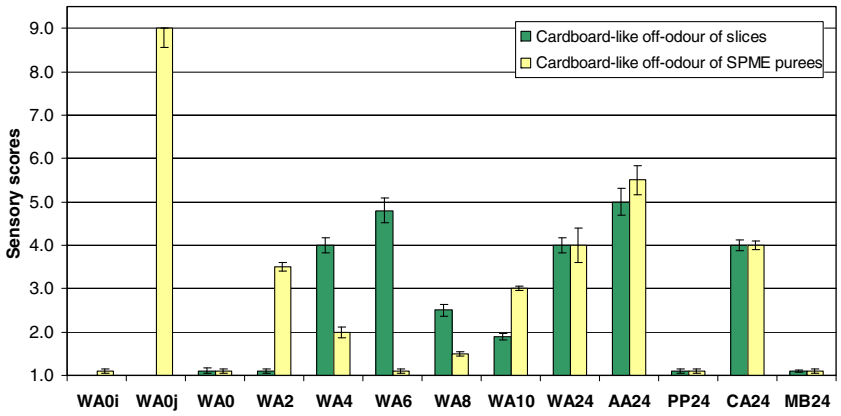

Fig. 3. Quantitative descriptive analysis of cardboard-like off-odour on boiled potato slices and potatoes pureed immediately before solid-phase microextraction analysis.

Samples WA0j and WA0i were analysed to verify the enzymatic production of volatile compounds during the analysis. WA0j, which was extracted with an aqueous solution without enzymatic inhibitor, had an elevated content of aldehydes, probably created by enzymatic processes before and during the adsorption on the fibre. WA0i sample, in contrast, which was extracted with NaCl 0.25 M at the same temperature as WA0j (70 °C), was not substantially different from WA0, which was extracted at 37 °C. In our opinion, this result highlights that temperature does not significantly influence the analysis, and that the oxidation reactions which take place during extraction are exclusively enzymatic. For these reasons, before analysing the volatile fraction in boiled potatoes, it is fundamental to inactivate the enzymatic fraction during the extraction.

In other experiments (data not published), the use of different adsorption temperatures (35, 37, 45, 55 and 70 °C) resulted in aromatic profiles that were very similar, with the same differences in absolute contents of volatile components, but not in the relative ones. In the present work, the temperature selected for absorption of the fibre was 37 °C, which simulated as much as possible that of the human mouth.

In addition, the cardboard-like off-odour attribute was evaluated directly from sample purees after fibre exposure, as described in paragraph 2.2, and the results were compared to those of the same attribute (cardboard-like off-odour) of boiled potatoes slices (Fig. 3). Several differences between slices and purees of the same samples may be noted. WA2 sample slices, which did not have either off-odour or off-flavour, when mashed, showed an increase in these attributes. On the other hand, WA6 had higher POF in slices, which was not detected in the puree. It is likely that this phenomenon was due to the preparation of the puree, which included shredding and homogenising boiled potatoes with NaCl 0.25 M in an aqueous solution at a suitable temperature to bring the system to 37 °C. It is evident that the analyses employed influences the volatile compounds profile.

The presence of cardboard-like off-odour in slices and purees was not seen for all samples, but for slices a trend of this attribute was observed. It did not show linear variations during storage from 2 to 24 h, but there was a maximum of perception at different times for slices and purees that demonstrated peroxide kinetics, as previously assumed.

Good agreement between the sensory evaluation of puree and HS-SPME–GC–MS analysis of volatile compounds was found, as reported below.

As stated by Petersen et al. (1999), the off-flavour of boiled potatoes is mainly due to 8 characteristic aldehydes (reported in thick type in Table 4). In this investigation, we confirmed previously reported results and found a greater number of oxidation products correlated with cardboard-like off-odours and off-flavours. These samples were characterised by the presence of 2-pentenal, 2-hexenal, 2-heptenal, 2-pentylfuran and 2-decenal.

Table 4
Headspace-solid-phase microextraction gas chromatography–mass spectrometry analysis of volatile compounds of potato slices. Different letters in the same row indicate statistically significantly differences (Honestly Significant Differences or HSD by Tukey $p < 0.05$). Values are expressed as peak area integration value (ion abundance x time). Compounds in bold are those identified by Petersen et al. (1999) as responsible for POF generation. Compounds in italics are employed to describe samples in PCA.

Rt (min)	Lib. Acc.	KI	Volatiles	Potato samples																									
				WA0i		WA0j		WA0		WA2		WA4		WA6		WA8		WA10		WA24		AA24		PP24		CA24		MB24	
8.9	91	940.06	2-Ethylfuran	0.0	c	6.2	a	1.1	b	1.9	b	0.0	c	0.6	b	1.0	b	1.6	b	0.0	c	4.9	a	0.0	c	3.5	a	0.0	c
10.5	**90**	**968.64**	**Pentanal**	**0.0**	**c**	**11.5**	**b**	**48.3**	**a**	**39.6**	**a**	**21.2**	**b**	**20.1**	**b**	**14.7**	**b**	**37.5**	**ab**	**37.0**	**ab**	**25.2**	**ab**	**56.6**	**a**	**34.1**	**ab**	**65.7**	**a**
13.3	88	1029.71	1-Penten-3-one	0.0	b	0.0	b	0.0	b	1.7	a	0.8	a	0.0	b	0.0	b	0.0	b	0.0	b	4.2	a	0.0	b	0.0	b	0.0	b
14.7	90	1060.75	2-Butenal	0.0	b	7.0	a	0.0	b	2.2	a	0.0	b	0.0	b	0.0	b	1.3	ab	0.0	b	5.6	a	0.0	b	0.0	b	0.0	b
17.2	**90**	**1116.19**	**Hexanal**	**0.0**	**a**	**19.2**	**a**	**41.3**	**a**	**25.1**	**a**	**25.5**	**a**	**34.9**	**a**	**23.4**	**a**	**26.7**	**ab**	**50.6**	**ab**	**32.3**	**a**	**0.0**	**b**	**33.0**	**a**	**0.0**	**b**
19.6	61	1169.40	Ethylbenzene	0.0	b	0.0	b	0.0	b	0.0	b	0.0	b	0.0	b	0.0	b	0.0	b	0.0	b	0.0	b	0.0	b	0.0	b	13.4	a
20.3	94	1184.92	*2-Pentenal*	0.0	c	10.6	a	0.0	c	3.9	b	0.0	c	0.0	c	0.0	c	4.2	b	0.0	c	11.2	a	0.0	c	4.4	b	0.0	c
20.5	36	1189.36	p-Xylene	0.0	b	0.0	b	0.0	b	0.0	b	0.0	b	0.0	b	0.0	b	0.0	b	0.0	b	0.0	b	0.0	b	0.0	b	14.6	a
23.4	90	1240.98	Heptanal	0.0	c	3.2	b	1.1	b	3.3	b	0.9	b	1.1	b	0.0	c	2.2	b	3.1	b	8.8	a	0.0	c	3.5	b	0.0	c
23.9	96	1249.45	d-Limonene	4.7	b	2.7	b	0.0	c	9.0	b	0.0	c	0.0	c	4.8	b	19.2	b	0.0	c	0.9	c	2.0	c	210	a	10.3	b
24.6	74	1261.30	Methylbutyl butanoate*	0.0	b	0.0	b	0.0	b	0.0	b	0.0	b	0.0	b	0.0	b	6.4	ab	0.0	b	0.0	b	0.0	b	0.0	b	0.0	b
24.9	85	1266.38	Butyl butanoate*	0.0	c	0.0	c	0.0	c	0.0	c	1.8	b	2.9	b	3.4	b	13.9	ab	2.9	b	0.0	c	0.0	c	0.0	c	0.0	c
25.1	78	1269.77	Methyl butanoate*	0.0	b	0.0	b	0.0	b	2.9	a	0.0	b	0.0	b	0.0	b	0.0	b	0.0	b	0.0	b	0.0	b	0.0	b	6.7	a
25.4	98	1274.85	*2-Hexenal*	0.0	b	7.1	a	0.0	b	3.5	a	0.0	b	0.0	b	0.0	b	3.7	ab	5.8	ab	7.7	a	0.0	b	5.8	a	0.0	b
26.0	90	1285.01	*2-Pentylfuran*	40.6	ab	115	a	18.3	b	30.1	b	7.2	b	8.9	b	11.0	b	33.8	b	33.1	b	90.5	a	3.4	b	85.9	a	6.6	b
27.0	86	1301.95	1-Pentanol	0.0	b	3.2	a	0.0	b	1.2	a	0.0	b	0.0	b	0.0	b	0.9	ab	0.0	b	1.4	a	0.0	b	0.0	b	0.0	b
27.2	–	1305.33	Unknown	0.0	b	0.0	b	0.0	b	0.0	b	0.0	b	0.0	b	0.0	b	0.0	b	0.0	b	0.9	a	0.0	b	0.0	b	0.0	b
28.2	92	1322.27	*n-Hexyl acetate*	0.0	c	0.0	c	0.0	c	13.2	b	7.6	b	12.6	b	15.6	b	75.0	ab	12.1	b	1.7	b	0.8	b	21.9	b	25.8	b
29.1	91	1337.51	Octanal	3.4	b	6.6	b	3.8	b	11.2	ab	2.2	b	1.9	b	0.0	c	0.0	c	5.0	b	20.0	a	1.1	b	14.2	a	0.0	c
29.8	57	1349.36	1-Octen-3-one	0.0	c	0.0	c	2.7	b	6.9	ab	1.4	b	1.2	b	0.0	c	6.0	ab	4.1	ab	14.4	a	0.0	c	9.3	ab	0.0	c
30.9	94	1367.99	*2-Heptenal*	7.5	ab	92.4	a	18.0	ab	58.6	a	18.7	ab	18.1	ab	14.1	ab	58.3	ab	62.4	ab	91.4	a	1.6	b	60.8	a	0.0	c
31.4	43	1376.46	Hexyl propanoate	0.0	c	0.0	c	0.0	c	0.0	c	0.0	c	0.0	c	0.0	c	7.0	ab	0.0	c	0.0	c	0.0	c	0.0	c	1.1	b
34.2	**98**	**1430.65**	**Nonanal**	**23.4**	**b**	**26.4**	**b**	**10.3**	**b**	**22.0**	**b**	**3.2**	**b**	**3.0**	**b**	**3.7**	**b**	**26.1**	**b**	**20.0**	**b**	**80.8**	**a**	**4.6**	**b**	**28.0**	**b**	**2.3**	**b**
34.9	80	1445.87	Butyl hexanoate*	0.0	c	0.0	c	0.0	c	10.7	b	4.0	b	5.9	b	9.6	b	83.4	ab	9.4	b	0.0	c	0.0	c	30.6	ab	10.5	b
35.0	70	1448.04	3-Octen-2-one	0.0	b	8.5	a	0.0	b	0.0	b	0.0	b	0.0	b	0.0	b	0.0	b	8.7	ab	0.0	b	0.0	b	0.0	b	0.0	b
35.1	83	1450.22	*Hexyl butanoate*	0.0	c	0.0	c	0.0	c	3.9	b	2.1	b	3.1	b	5.2	b	30.9	ab	0.0	c	0.0	c	0.0	c	9.5	ab	0.0	c
35.5	90	1458.91	3-Ethyl-2-methyl-1,3-hexadiene*	0.0	b	14.6	a	0.0	b	0.0	b	0.0	b	0.0	b	0.0	b	0.0	b	13.8	ab	26.7	a	0.0	b	0.0	b	0.0	b
35.9	35	1467.61	Ethyl octanoate	0.0	b	0.0	b	0.0	b	0.0	b	0.0	b	0.0	b	0.0	b	0.0	b	0.0	b	0.0	b	0.0	b	0.0	b	1.2	a
36.0	**90**	**1469.78**	**2-Octenal**	**8.3**	**b**	**109**	**ab**	**10.0**	**b**	**43.6**	**b**	**13.9**	**b**	**10.8**	**b**	**11.2**	**b**	**56.3**	**b**	**69.3**	**b**	**181**	**a**	**1.5**	**b**	**103**	**ab**	**0.0**	**c**
36.7	90	1485.00	1-Octen-3-ol	1.7	b	27.5	a	4.3	b	14.2	ab	4.7	b	5.4	b	3.4	b	13.9	ab	16.2	ab	20.7	ab	0.9	b	15.3	ab	0.0	c
37.7	**95**	**1506.74**	***2,4-Heptadienal***	**0.0**	**c**	**15.8**	**a**	**1.3**	**b**	**5.4**	**b**	**3.1**	**b**	**2.5**	**b**	**2.1**	**b**	**7.4**	**ab**	**11.3**	**ab**	**16.5**	**a**	**0.0**	**c**	**11.2**	**ab**	**0.0**	**c**
38.4	–	1521.96	Unknown	0.0	b	0.0	b	1.6	a	0.0	b	0.0	b	0.0	b	0.0	b	0.0	b	0.0	b	0.0	b	0.0	b	0.0	b	3.7	a
38.9	90	1532.83	Decanal	13.2	b	0.0	c	5.8	b	32.4	b	4.4	b	3.0	b	3.4	b	41.5	b	27.9	b	161	a	2.6	b	54.7	b	0.0	c
40.0	71	1556.74	3,5-Octadien-2-one	0.0	b	0.0	b	0.0	b	3.9	a	1.1	a	1.0	a	0.9	a	3.7	ab	7.0	ab	0.0	b	0.0	b	8.8	a	0.0	b
40.1	93	1558.91	6-Undecanone*	0.0	b	19.4	a	0.0	b	0.0	b	0.0	b	0.0	b	0.0	b	0.0	b	0.0	b	18.2	a	0.0	b	0.0	b	0.0	b
40.4	97	1565.43	Benzaldehyde	1.9	b	6.9	a	0.0	c	1.8	b	0.7	b	0.6	b	0.7	b	2.1	b	0.0	c	6.0	a	0.0	c	3.4	ab	0.0	c
40.6	**97**	**1569.78**	***2-Nonenal***	**1.6**	**b**	**25.8**	**a**	**0.5**	**b**	**3.3**	**b**	**1.0**	**b**	**0.8**	**b**	**0.7**	**b**	**4.1**	**ab**	**6.1**	**ab**	**22.0**	**a**	**0.0**	**c**	**8.8**	**ab**	**0.0**	**c**
41.3	90	1585.00	n-Octanol	1.3	b	5.3	ab	0.6	b	2.0	b	0.0	c	0.6	b	0.0	c	2.0	b	0.0	c	7.3	a	0.0	c	4.0	ab	0.0	c
42.4	98	1600.00	Hexadecane	2.4	ab	0.0	a	0.0	b	0.0	b	0.0	b	0.0	b	0.0	b	0.0	b	0.0	b	0.0	b	0.0	b	0.0	b	0.0	b
43.3	87	1633.21	*Hexyl hexanoate*	0.0	c	0.0	c	0.0	c	0.0	c	0.0	c	0.6	b	1.1	b	9.2	ab	0.0	c	0.0	c	0.0	c	0.0	c	0.0	c
43.4	91	1635.74	Undecanal*	0.0	b	8.5	a	0.0	b	0.0	b	0.0	b	0.0	b	0.0	b	0.0	b	0.0	b	7.7	a	0.0	b	0.0	b	0.0	b
44.3	94	1658.56	6-Dodecanone*	0.0	b	12.9	a	0.0	b	0.0	b	0.0	b	0.0	b	0.0	b	0.0	b	0.0	b	4.8	a	0.0	b	0.0	b	0.0	b
45.1	92	1678.83	2-Decenal	1.2	b	15.4	a	0.0	c	1.6	b	0.5	b	0.4	b	0.0	c	0.0	c	0.0	c	16.6	a	0.0	c	2.6	ab	0.0	c
47.5	**91**	**1739.67**	**2,4-Nonadienal**	**0.0**	**c**	**105**	**a**	**0.0**	**c**	**6.2**	**b**	**0.0**	**c**	**0.0**	**c**	**3.1**	**b**	**12.1**	**b**	**24.3**	**ab**	**61.6**	**ab**	**0.0**	**c**	**27.0**	**ab**	**0.0**	**c**
48.0	93	1752.34	4-Ethylbenzaldehyde	0.0	c	24.3	a	0.0	c	0.0	c	0.0	c	0.0	c	0.0	c	1.4	b	3.0	b	8.7	ab	0.0	c	2.8	b	0.0	c
49.3	90	1785.30	2-Undecenal	0.0	c	115	a	0.0	c	4.3	b	1.8	b	1.1	b	1.3	b	6.2	b	7.1	b	54.9	a	0.0	c	9.1	b	0.0	c
49.9	**90**	**1800.56**	**2,4-Decadienal**	**0.0**	**c**	**83.9**	**a**	**0.0**	**c**	**3.0**	**b**	**0.0**	**c**	**7.1**	**b**	**1.2**	**b**	**4.7**	**b**	**4.4**	**b**	**28.7**	**ab**	**0.0**	**c**	**7.4**	**b**	**0.0**	**c**
51.9	–	1857.06	Unknown	5.9	ab	0.0	c	0.0	c	0.0	c	0.0	c	0.0	c	0.0	c	0.0	c	1.1	b	0.0	c	0.0	c	9.2	a	0.0	c
52.7	83	1879.66	1-Dodecen-3-ol*	19.1	a	0.0	b	0.0	b	0.0	b	0.0	b	0.0	b	0.0	b	0.0	b	3.1	a	0.0	b	0.0	b	0.0	b	0.0	b
53.3	90	1896.61	2-Dodecenal	59.3	a	0.0	b	0.0	b	0.0	b	0.0	b	0.0	b	0.0	b	0.0	b	14.5	a	0.0	b	0.0	b	0.0	b	0.0	b

Lib.Acc.: Library accordance, KI: Kovats Indices.
* Volatile compounds tentatively identified only with mass spectra libraries search.

Whilst other compounds like *n*-hexyl acetate, hexyl butanoate, hexyl hexanoate were formed during storage, they were not however correlated with the perception of oxidised flavour. Their appearance was slow in samples stored for 2, 4, 6 and 8 h, was rapid after 10 h and finally reduced in samples stored for 24 h, even in presence of food additives.

POF in sample WA10 were higher than those in WA2, probably as result of the different volatility of the compounds present. For example, esters are created slowly at low temperatures by condensation of an alcohol with an acid, but since their volatility is very high, their decrease over time is reasonable.

HS-SPME–GC–MS analysis confirmed the efficiency of some food additives in preventing the formation of POF. As an example, sample PP24 did not show significant differences with respect to WA0, whilst CA24 and AA24 samples had a high content of aldehydes that could be responsible for POF. AA24, in particular, had a content of aldehydes that was similar to those of the sample extracted at 70 °C without food additives (WA0j). These results confirm a promoting effect on the formation of aldehydes, in agreement with data obtained by sensory evaluation of boiled potato slices.

Sample MB24, however, did not have cardboard-like off-flavour and, as illustrated on Fig. 2, was not well represented by factor 1. Therefore, it did not contain significant quantities of the aldehydes responsible for cardboard-like off-flavour. By GC analysis, it was shown that this sample did not have a volatile profile that differentiated it from the samples without defects. These results are in contrast with those of sensory evaluation, which identified off-odour and "beast-like" off-flavour. The reason for this discrepancy may be related to the characteristics of HS-SPME analysis as it does not detect these chemical compounds.

Finally, in the samples analysed in the present study, about 50 different compounds were identified, although no pyrazines were detected, in disagreement with previous reports. This is probably due to the low limits of detection of the method used.

4. Conclusions

In this study, it was found that the POF formation could be due to lipoxidase activity and was strongly correlated with a high content of 2-pentenal, 2-hexenal, 2-heptenal, 2-pentylfuran and 2-decenal. During storage of boiled potato slices many other volatiles were produced, and about 50 compounds were detected by the HS-SPME technique in samples treated under different conditions. In particular, the use of some commonly used food additives led to some interesting effects on potato slices: ascorbic acid and citric acid did not prevent the formation of POF, but actually enhanced it. Potassium meta-bisulphite prevented POF formation and caused the formation of other off-flavours. The best additive was sodium pyrophosphate, and potato slice flavour was almost unchanged during storage.

Acknowledgements

The authors would like to thank all the panel members, L. Alessandrini, C. Antico, S. Barbieri, M. Bonoli, A.U. Mattioli, F. Pasini, B. Rossetti and V. Verardo for their valued help in sensory evaluation. We are also grateful to A. Cardinali for technical assistance.

References

Amerine, M. A., Pangborn, R. M., & Roessler, E. B. (1965). *Principles of sensory evaluation of food*. London: Academic Press. pp. 540–564.

Arthur, C. L., & Pawliszyn, J. (1990). Solid phase microextraction with thermal desorption using fused silica optical fibres. *Analytical Chemistry, 62*, 2145–2148.

Baccouri, O., Bendini, A., Cerretani, L., Guerfel, M., Baccouri, B., Lercker, G., et al. (2008). Comparative study on volatile compounds from Tunisian and Sicilian monovarietal virgin olive oils. *Food Chemistry, 111*, 322–328.

Buttery, R. G., Seifert, R. M., & Ling, L. C. (1970). Characterization of some volatile potato components. *Journal of Agricultural and Food Chemistry, 18*(3), 538–539.

Frankel, E. N. (1982). Volatile lipid oxidation products. *Progress in Lipid Research, 22*, 1–33.

Frankel, E. N. (1985). Chemistry of free radical and singlet oxidation of lipids. *Progress in Lipid Research, 23*, 197–221.

Galliard, T. (1973). Lipids of potato tubers. 1. Lipid and fatty acid composition of tubers from different varieties of potato. *Journal of the Science of Food and Agriculture, 24*, 617–622.

Giomo, A. (2000). Organoleptic assessment of virgin olive oil. COI/T.20/Doc. N.15/Rev.1: a new robust statistical approach to classify the oils. *European Conference "Food Industry and Statistics"*, 19–21 January 2000.

Grosch, W. (1987). Reactions of hydroperoxides-products of low molecular weight. In H. W. S. Chan (Ed.), *Autoxidation of unsaturated lipids* (pp. 95–139). London: Academic Press.

Jelen, H. H., Obuchowska, M., Zavirska-Wojtasiak, R., & Wasowicz, W. (2000). Headspace solid-phase microextraction use for the characterization of volatile compounds in vegetable oils of different sensory quality. *Journal Agricultural and Food Chemistry, 48*, 2360–2367.

Josephson, D. B., & Lindsay, R. C. (1987). C4-Heptenal: An influential volatile compound in boiled potato flavour. *Journal of Food Science, 52*(2), 328–331.

Lawless, H. T., & Heymann, H. (1998). *Sensory evaluation of food: Principles and practices*. New York: Chapman & Hall. pp. 28–82.

Lercker, G., Capella, P., & Conte, L. S. (1984). Thermo-oxidative degradation products of methyl oleate. *La Rivista Italiana delle Sostanze Grasse, 61*, 337–344.

Lercker, G., Bortolomeazzi, R., & Pizzale, L. (1998). Thermal degradation of single methyl oleate hydroperoxides obtained from photosensitized oxidation. *Journal of the American Oil Chemists' Society, 75*, 1115–1120.

Marsili, R. T. (1999). Comparison of solid-phase microextraction and dynamic headspace methods for the gas chromatographic–mass spectrometric analysis of light induced lipid oxidation products in milk. *Journal of Chromatographic Science, 37*(1), 17–23.

Mutti, B., & Grosch, W. (1999). Potent odorants of boiled potatoes. *Nahrung, 43*(5), 302–306.

Nursten, H. E., & Sheen, M. R. (1974). Volatile flavour components of cooked potato. *Journal of the Science of Food and Agriculture, 25*, 643–663.

Petersen, M. A., Poll, L., & Larsen, M. L. (1998). Comparison of volatiles in raw and boiled potatoes using a mild extraction technique combined with GC odour profiling and GC–MS. *Food Chemistry, 61*(4), 461–466.

Petersen, M. A., Poll, L., & Larsen, M. L. (1999). Identification of compounds contributing to boiled potato off-flavour ('POF'). *Lebensmittel-Wissenschaft Und-Technologie-Food Science and Technology, 32*, 32–40.

Petersen, M. A., Poll, L., & Larsen, M. L. (2003). Changes in flavor-affecting aroma compounds during potato storage are not associated with lipoxygenase activity. *American Journal of Potato Research, 80*(6), 397–402.

Salinas, J. P., Hartman, T. G., Karmas, K., Lech, J., & Rosen, R. T. (1994). Lipid-derived aroma compounds in cooked potatoes and reconstituted dehydrated potato granules. In C. T. Ho & T. G. Hartmann (Eds.), *Lipids in food flavours* (pp. 108–129). Washington, DC: American Chemical Society.

Selke, E., Frankel, E. N., & Neff, W. E. (1978). Thermal decomposition of methyl oleate hydroperoxides and identification of volatile components by gas chromatography–mass spectrometry. *Lipids, 13*, 511–513.

Stone, H., Sidel, J. L., Oliver, J., Woolsey, A., & Singleton, R. C. (1974). Sensory evaluation by quantitative descriptive analysis. *Food Technology, 28*(11), 24–34.

Stone, H., & Sidel, J. L. (1992). *Sensory evaluation practices*. Orlando, FL: Academic Press, Inc.. pp. 206–240.

Sulmont, C., Lesschaeve, I., Sauvageo, F., & Issanchou, S. (1999). Comparative training procedures to learn odor descriptors: Effects on profiling performance. *Journal of Sensory Studies, 14*(4), 467–490.

Thybo, A. K., Christiansen, J., Kaak, K., & Petersen, M. A. (2006). Effect of cultivars, wound healing and storage on sensory quality and chemical components in prepeeled potatoes. *LWT, 39*, 166–176.

Thygesen, L. G., Thybo, A. K., & Engelsen, S. B. (2001). Prediction of sensory texture quality of boiled potatoes from low-field ^{1}H NMR of raw potatoes. The role of chemical constituents. *Lebensmittel-Wissenschaft Und-Technologie-Food Science and Technology, 34*, 469–477.

Ulrich, D., Hoberg, E., Neugebauer, W., Tiemann, H., & Darsow, U. (2000). Investigation of the boiled potato flavour by human sensory and instrumental methods. *American Journal of Potato Research, 77*, 111–117.

Van Den Dool, H., & Kratz, P. D. (1963). A generalization of the retention index system including linear temperature programmed gas–liquid partition chromatography. *Journal of Chromatography, 11*, 463–471.

Vichi, S., Pizzale, L., Conte, L. S., Buxaderas, S., & Pez-Tamames, E. L. (2003). Solid-phase microextraction in the analysis of virgin olive oil volatile fraction: Modifications induced by oxidation and suitable markers of oxidative status. *Journal of Agricultural and Food Chemistry, 51*, 6564–6571.

Whitfield, F. B., & Last, J. H. (1991). Vegetables. In H. Maarse (Ed.), *Volatile compounds in foods and beverages* (pp. 203–281). New York: Marcel Dekker Inc.

Food Chemistry 118 (2010) 291–299

Contents lists available at ScienceDirect

Food Chemistry

journal homepage: www.elsevier.com/locate/foodchem

Effect of thermal treatment and storage on the stability of organic acids and the functional value of grapefruit juice

M. Igual, E. García-Martínez, M.M. Camacho, N. Martínez-Navarrete *

Universidad Politécnica de Valencia, Food Technology Department, Food Investigation and Innovation Group, Camino de Vera s/n, 46022 Valencia, Spain

ARTICLE INFO

Article history:
Received 10 February 2009
Received in revised form 16 March 2009
Accepted 29 April 2009

Keywords:
Grapefruit juice
Pasteurisation
Microwaves
Organic acids
Ascorbic acid
Vitamin C
Total phenols
Antioxidant capacity
Chilling and frozen storage

ABSTRACT

The effect of conventional and microwave pasteurisation on the main bioactive compounds of grapefruit juice and their stability during 2 months' refrigerated and frozen storage was evaluated. Ascorbic acid (AA), vitamin C and organic acids were analysed by HPLC, whereas total phenols and antioxidant capacity (%DPPH) were measured by spectrophotometry. The results showed that conventional treatment led to a significant decrease in citric acid (from 1538 to 1478 mg/100 g) and AA (from 36 to 34.3 mg/100 g), whilst microwave pasteurisation preserved these compounds. Frozen storage maintained AA and vitamin C, especially in treated samples. Frozen non-treated samples and conventional pasteurised ones preserved about a 75% and 20% of the total phenols and antioxidant capacity, respectively, whilst in frozen microwave pasteurised juices this preservation was of 82% and 33%. From these results, the use of microwave energy may be proposed as an alternative to traditional heat pasteurisation in order to preserve the natural organoleptic characteristics and essential thermolabile nutrients of grapefruit juice.

1. Introduction

Evidence from a large number of epidemiological, *in vitro* and *in vivo* studies has shown that the consumption of citrus fruit is generally good for the health and contributes to the prevention of degenerative processes, particularly lowering the incidence and mortality rate of cancer and cardio and cerebro-vascular diseases (Poulose, Harris, & Patil, 2005). Citrus juice is an important dietary source of bioactive compounds, whose beneficial health effects are ascribed, in part, to its high content of ascorbic acid. Vitamin C is a natural antioxidant that may inhibit the development of major oxidative human reactions. In addition to the well-known vitamin C, citrus juice also contains phenolic compounds which contribute to their antioxidant capacity and that may produce beneficial effects by scavenging free radicals (Xu et al., 2008). Vinson and Bose (1988) emphasised the importance of ascorbic acid as a natural component in citrus juice where other natural compounds present in the juice, such as flavonoids, increase the bioavailability of this acid. On the other hand, organic acids, including citric, tartaric and malic acids in citrus juice are important components which contribute to flavour attributes and are usually used as "fingerprints" to detect the quality of the juice and accomplish its authentication (Cen, Bao, He, & Sun, 2007). High concentrations of organic acids and low pH in most fruits are critical for the preservation of derivative products. They also help to stabilise ascorbic acid and anthocyanins (Wang, Chuang, & Ku, 2007).

Nowadays, consumers demand the maximum preservation of the endogenous sensory, nutritional and health related qualities of fruit products. Traditional heat pasteurisation of citrus juices is necessary in order not only to destroy microorganisms and reduce pectin methylesterase (PME) enzymatic activity, but it also leads to detrimental changes in the quality (Elez-Martínez, Aguiló-Aguayo, & Martín-Belloso, 2006). The colour and flavour are different from those of freshly squeezed juice and there is also a decrease in the number of biochemical compounds. PME inactivation is important because this enzyme catalyses pectin degradation and alters the colloid stabilizing power of the pectin, which imparts the favourable appearance and mouth feel to orange juice. As PME is more resistant to heat than microorganisms, thermal treatments are focussed on the inactivation of this enzyme. The search for new technologies that cause minimum damage to the organoleptic and nutritional characteristics may be considered as an alternative to conventional thermal juice pasteurisation. In this sense, the use of microwave energy seems to cause smaller changes in the fruit quality attributes (Nikdel, Chen, Parish, MacKellar, & Friedrich, 1993). Several studies have successfully been carried out into the microwave pasteurisation of fruit juices, as it preserves the natural organoleptic characteristics of the juice and reduces the time of exposure to energy, with the subsequently lower risk of losing

* Corresponding author.
E-mail address: nmartin@tal.upv.es (N. Martínez-Navarrete).

0308-8146/$ - see front matter © 2009 Elsevier Ltd. All rights reserved.
doi:10.1016/j.foodchem.2009.04.118

essential thermolabile nutrients (Cañumir, Celis, Brujin, & Vidal, 2002).

The aim of this work was to characterise the main bioactive compounds (vitamin C, total phenol, organic acids) and their relative contribution to the antioxidant capacity of freshly squeezed grapefruit juice and assess the effect of conventional and microwave pasteurisation on these compounds and their antioxidant capacity. Their stability during 2 months' refrigerated and frozen storage was also evaluated.

2. Materials and methods

2.1. Raw material

For this work, grapefruits (*Citrus paradise* var. Star Ruby) from the city of Murcia were purchased from a local supermarket. Grapefruits were selected on the basis of a similar degree of ripeness (ratio °Brix/acidity ≈ 4) and apparent fruit quality (firmness, size, colour and absence of physical damages). Fruit was processed in the laboratory immediately after being purchased.

2.2. Treatments

Freshly squeezed (FS) grapefruit juice was extracted through a domestic squeezer (Braun Citromatic Pulp Control MPZ6), filtered using a sieve (light of mesh diameter 1 mm, Cisa 029077, 1 series) and immediately processed. To obtain conventional pasteurised juice (CP) samples of 40 ml were heated in glass tubes in a thermostatic water bath (Precisterm, Selecta, Spain) operating at 95 °C. In this way, the juice took 80 s to reach 80 ± 2.5 °C and it remained at this temperature for 11 s. In the case of microwave pasteurised juice (MP), samples of 20 ml were heated in 25 ml glass tubes at 900 W for 30 s using a microwave (Moulinex 5141 AFW2, Spain). Treated samples were immediately cooled in ice-water till juice reached 30 °C. Both processes were previously optimised to reach ≈10% of fresh juice pectimethylesterase (PME) residual activity.

2.3. Enzymatic determinations

2.3.1. Pectin methylesterase (PME) activity measurement

PME activity in grapefruit juice was measured using the Kimball (1999) method. Briefly 10 ml of grapefruit juice and 40 ml of 1% peel citrus pectin dissolution (60% degree of esterification, Fluka Biochemika, Switzerland) containing 0.02 M NaCl, previously tempered to 30 °C in a thermostat bath, were mixed and kept in continuous agitation. NaOH was used to adjust the resulting solution to pH 7.7 (Consort C830 pH meter, Belgium) and then 100 µl of 0.05 N NaOH were immediately added. The exact time needed to lower the pH back to 7.7 by enzyme's action was then measured. As it is a first order reaction, the enzyme activity (A) can be calculated according to the concentration of acid produced using Eq. (1).

$$A = \frac{(V_{NaOH}) \times (N_{NaOH})}{(t_R) \times (W_{sample})} \quad (1)$$

where V_{NaOH} is the NaOH volume used in the titration (ml), N_{NaOH} is the normality of the NaOH solution used (mEq ml^{-1}), t_R is the reaction time (min) and W_{sample} is the weight of the sample (g).

The percentage of residual enzyme activity (RA) was defined as indicated by Eq. (2):

$$RA = 100 \times \frac{A_t}{A_0} \quad (2)$$

where A_t and A_0 were the enzyme activities of treated and untreated samples, respectively. A_t and A_0 were determined immediately after processing to avoid the effects of storage time.

2.3.2. Polyphenoloxidase (PPO) activity measurement

PPO activity was measured by spectrophotometry. The enzyme was extracted from grapefruit juice using the method of Valero, Varón, and García-Carmona (1988) modified by Rapeanu, Van Loey, Smout, and Hendrickx (2006). Briefly 100 µl of clarified juice were added to 1 ml substrate (0.1 M cathecol in McIlvaine buffer, pH 5) and the increase in absorbance at 400 nm at 25 °C was recorded automatically for 30 min (Thermo Electron Corporation, USA). One unit of PPO activity was defined as a change in absorbance at 400 nm min^{-1} ml^{-1} of enzymatic extract. Enzyme activity was calculated from the linear part of the curve. The percentage of residual enzyme activity was calculated using Eq. (2).

2.3.3. Peroxidase (POD) activity measurement

POD activity in grapefruit juice was measured using the method described by Cano, Hernández, and De Ancos (1997) with some modifications made by Elez-Martínez et al. (2006). Briefly 10 ml of sample were homogenised with 20 ml 0.2 M sodium phosphate buffer (pH 6.5) and centrifuged (15,000 rpm, 20 min) at 4 °C (P-Selecta Medifrigar BL-S, Spain) to obtain the enzymatic extract. POD activity was assayed spectrophotometrically by placing 2.7 ml 0.2 M sodium phosphate buffer (pH 6.5), 0.2 ml *p*-phenylenediamine (10 g kg^{-1}), 0.1 ml hydrogen peroxide (15 g kg^{-1}) and 0.1 ml of enzymatic extract in a 1 cm oath cuvette. The oxidation of *p*-phenylenediamine was measured at 485 nm and 25 °C using a Thermo Electron Corporation spectrophotometer (USA). POD activity was determined by measuring the initial rate of the reaction, which was computed from the linear portion of the plotted curve. One unit of POD activity was defined as a change in absorbance at 485 nm min^{-1} ml^{-1} of enzymatic extract. The percentage of residual enzyme activity was calculated using Eq. (2).

2.4. Analytical determinations

2.4.1. Soluble solids

Total soluble solids were estimated as °Brix with a refractometer (Abbe Atago 89553 by Zeiss, Japan) at 20 °C.

2.4.2. pH

To determine the pH, a Consort C830 pH meter (Belgium) with a penetration electrode was used.

2.4.3. Organic acids

HPLC (Jasco, Italy) was applied to the quantitative determination of citric (CA), malic (MA) and tartaric acid (TA) according to Cen et al. (2007). Samples were centrifuged at 10,000 rpm for 15 min and filtered by 0.22 µm membrane. HPLC method and instrumentation was: Ultrabase-C18, 5 µm (4.6 × 250 mm) column (Spain); mobile phase 0.01 mol/l potassium dihydrogen phosphate solution, volume injection 20 µl, flow rate 1 ml/min, detection at 215 nm at 25 °C. Standard curves of each reference acid (Panreac, Spain) were used to quantify the acids.

2.4.4. Ascorbic acid and total vitamin C

Ascorbic acid (AA) and total vitamin C (ascorbic acid + dehydroascorbic acid) were determined by HPLC (Jasco, Italy). To determine the ascorbic acid (Xu et al., 2008), 1 ml sample was extracted with 9 ml 0.1% oxalic acid for 3 min and immediately filtered before injection. The procedure employed to determine total vitamin C was the reduction of dehydroascorbic acid to ascorbic acid, using DL-dithiothreitol as the reductant reagent (Sanchez-Mata, Cámara-Hurtado, Diez-Marques, & Torija-Isasa, 2000; Sánchez-Moreno, Plaza, De Ancos, & Cano, 2006). A 0.5 ml aliquot sample was taken to react with 2 ml of a 20 g/l dithiothreitol solution for 2 h at room temperature and in darkness. Afterwards, the same procedure as that used for the ascorbic acid method was performed. The HPLC

method and instrumentation was: Ultrabase-C18, 5 μm (4.6 × 250 mm) column (Spain); mobile phase 0.1% oxalic acid, volume injection 20 μl, flow rate 1 ml/min, detection at 243 nm and at 25 °C. AA standard solution (Panreac, Spain) was prepared.

2.4.5. Total phenols

The extraction of total phenols (Tomás-Barberán et al., 2001) consisted of homogenising 35 g of the sample (T25 Janke and Kunkel turrax) for 5 min with 40 ml of methanol, 10 ml of HCl and NaF to inactivate polyphenol oxidases and prevent phenolic degradation. The homogenate was centrifuged (10,000 rpm, 10 min, 4 °C) to obtain the supernatant. Total phenols (TF) were quantified by using the method reported by Selvendran and Ryden (1990) and Benzie and Strain (1999) based on the Folin–Ciocalteu method. Absorbance was measured at 765 nm in a UV–visible spectrophotometer (Thermo Electron Corporation, USA). The total phenolic content was expressed as mg of gallic acid equivalents (GAE) (Sigma–Aldrich, Germany) per gram of sample, using a standard curve range of 0–800 mg of gallic acid/ml.

2.4.6. Antioxidant capacity

Antioxidant Capacity was assessed using the free radical scavenging activity of the samples evaluated with the stable radical DPPH·, as described by Sánchez-Moreno, Plaza, and De Ancos, Cano (2003). Briefly, 0.1 ml of grapefruit juice sample was added to 3.9 ml of DPPH· (0.030 g/l, Sigma–Aldrich, Germany) in methanol. A Thermo Electron Corporation spectrophotometer (USA) was used to measure the absorbance at 515 nm at 0.25 min intervals until the reaction reached a plateau (time at the steady state). The changes in absorbance were measured at 25 °C. Appropriately diluted juice samples were used on the day of preparation. The percentage of DPPH· (%DPPH·) was calculated as Eq. (3):

$$\%\mathrm{DPPH}^{\cdot} = \frac{(A_{\mathrm{control}} - A_{\mathrm{sample}})}{A_{\mathrm{control}}} \quad (3)$$

where A_{control} is the absorbance of the control and A_{sample} the absorbance of the sample.

2.5. Storage conditions

Samples (FS, CP and MP) were stored immediately after treatment in sterile polypropylene packages and kept in darkness at 4 and −18 °C during a period of 60 days.

2.6. Statistical analysis

Significant differences between treatments and storage time were calculated by means of the analysis of variance (ANOVA). Differences of $p < 0.05$ were considered to be significant. Furthermore, a correlation analysis between antioxidant activity and all the studied components with a 95% significance level was carried out. All statistical analyses were performed using Statgraphics Plus 5.1.

3. Results and discussion

Pectimethylesterase (PME) residual activity detected in samples after thermal treatments was 12.04% ± 3.86% and 10.07% ± 0.63% in CP and MP, respectively. These are intermediate values in the 0–18% range found by Snir, Koehler, Sims, and Wicker (1996), who carried out the heat treatment at 70 °C for 5 min. Nevertheless, they are high enough to obtain good quality products with a convenient cloud stabilisation, which will be kept under refrigeration conditions with low level bacteria growth. According to studies performed by Sentandreu, Carbonell, Rodrigo, and Carbonell (2006), PME had a greater heat resistance than microorganisms.

As in some studies of fresh orange juice carried out by other authors (Cano et al., 1997), analyses of freshly squeezed and pasteurised grapefruit juice did not show PPO activity. According to Dziezak (1993), citric acid, which is an important component of grapefruit juice, provokes the copper quelation present in this enzyme, disabling the activity of the PPO.

With regard to the POD activity of fresh grapefruit juice, the obtained result (5.2 ± 0.2) was similar to values found in the bibliography for citric juices (Cano et al., 1997). In CP, an inactivation of 94.3% ± 0.7% was reached, which in the case of MP was 88.1% ± 0.3%, showing the significant differences that exist between them.

Table 1 shows the physicochemical and compositional parameters of freshly squeezed grapefruit juice, conventional pasteurised juice and that which has been microwave treated. In general, FS obtained for this work presented the characteristic physicochemical parameters shown in the bibliography for grapefruit juice (Moraga, Moraga, Fito, & Martínez-Navarrete, 2009). As was observed, neither pasteurisation process affected °Brix, at a range between 9.9–10.1, or pH (2.92–3). Similar results were found by Kim and Tadini (1999), who showed that temperature and holding time had no effect on pH and °Brix of conventional pasteurised juice. These quality parameters are important as they are closely related with the stability of the bioactive compounds in fruit products (Sánchez-Moreno et al., 2006). A significant ($p < 0.05$) decrease in CA and TA content was observed in the pasteurisation treatments of the juice; the citric acid content was less affected when microwaves were applied to pasteurised juice. In no case did the pasteurisation treatment influence the malic acid content. Cañumir et al. (2002) studied the effect of microwaves comparing them with conventional pasteurisation in apple juice and they observed that total acidity tended to increase when microwave pasteurisation was used, whereas the pH tended to be lower.

Vitamin C is used as reference in different industrial processes since its presence ensures a high nutritional quality of the final product due to its easy degradation (Klimczak, Malecka, Szlachta, & Gliszczynska, 2007). The initial values of ascorbic acid and vitamin C in the fresh juice were similar, 36.0 ± 0.1 mg/100 ml and 34.0 ± 1 mg/100 ml, respectively. This is the AA grapefruit value obtained by Leong and Shui (2002). No significant differences between AA and vitamin C content were observed, as reported by other authors (Plaza et al., 2006). Vitamin C shows great thermal stability at the low pH of citrus fruits (Sánchez-Moreno et al., 2003) and in fact it was not affected by the treatments applied in this case. The conventionally pasteurised juice presented the lowest, statistically significant ($p < 0.05$) ascorbic acid content. In this

Table 1
Mean values (with standard deviation) of °Brix, pH, CA, MA, TA, AA, vitamin C, TP and %DPPH in freshly squeezed (FS), conventional pasteurised (CP) and microwave pasteurised (MP) juice.

	FS	CP	MP
°Brix	9.9 (0.1)^{a}	10.1 (0.1)^{a}	10.1 (0.1)^{a}
pH	3.00 (0.01)^{a}	2.98 (0.01)^{a}	2.92 (0.01)^{b}
CA	1538 (3)^{a}	1478 (30)^{b}	1518 (11)^{ab}
MA	574 (8)^{a}	562 (1)^{a}	570 (5)^{a}
TA	272 (16)^{a}	236 (1)^{b}	237 (1)^{b}
AA	36.0 (0.1)^{a}	34.3 (0.1)^{b}	36 (0.3)^{a}
Vitamin C	34 (1)^{a}	33 (1)^{a}	35 (1)^{a}
TP	82 (3)^{a}	69 (1)^{b}	70 (2)^{b}
%DPPH	44.4 (0.3)^{a}	26.7 (0.1)^{b}	26.1 (0.1)^{b}

The same letter in superscript indicates homogeneous groups established by the ANOVA ($p < 0.05$).
In columns: FS, freshly squeezed juice; CP, conventional pasteurised juice; MP, microwave pasteurised juice.
In rows: CA, citric acid; MA, malic acid; TA, tartaric acid; AA, ascorbic acid; TP, total phenols.

Table 2
Mean values (with standard deviation) of °Brix and pH evolution of grapefruit juices stored at 4 °C (A) and −18 °C (B) for 2 months.

Storage		° Brix			pH		
T (°C)	*t* (d)	FS	CP	MP	FS	CP	MP
4	1	9.9 (0.1)^{ab}	10.0 (0.1)^{a}	10.0 (0.1)^{a}	3.09 (0.01)^{a}	3.12 (0.01)^{a}	3.08 (0.01)^{a}
	4	9.9 (0.1)^{ab}	10.1(0.1)^{ab}	10.0 (0.1)^{a}	3.15 (0.01)^{b}	3.12 (0.01)^{a}	3.13 (0.01)^{b}
	12	9.7 (0.1)^{a}	9.6 (0.1)^{c}	9.6 (0.1)^{b}	2.92 (0.01)^{cd}	2.89 (0.01)^{b}	2.91 (0.01)^{c}
	25	10.0 (0.1)^{ab}	10.1 (0.1)^{ab}	9.6 (0.1)^{b}	2.95 (0.01)^{de}	2.90 (0.01)^{b}	2.86 (0.01)^{d}
	35	10.0 (0.1)^{ab}	10.0 (0.1)^{a}	10.1 (0.1)^{a}	2.95 (0.01)^{de}	2.95 (0.01)^{c}	2.93 (0.01)^{cef}
	45	10.1 (0.1)^{b}	10.1 (0.1)^{ab}	10.1 (0.1)^{a}	3.00 (0.01)^{f}	3.00 (0.01)^{d}	3.00 (0.01)^{h}
	60	10.1 (0.1)^{b}	10.2 (0.1)^{ab}	10.1 (0.1)^{a}	3.01 (0.01)^{f}	2.99 (0.01)^{d}	2.99 (0.01)^{h}
−18	1	10.0 (0.1)^{ab}	10.4 (0.1)^{b}	10.3 (0.1)^{a}	3.20 (0.01)^{g}	3.12 (0.01)^{a}	3.15 (0.01)^{b}
	4	9.9 (0.1)^{ab}	10.1 (0.1)^{ab}	10.1 (0.1)^{a}	3.11 (0.01)^{a}	3.16 (0.01)^{f}	3.15 (0.01)^{b}
	12	9.7 (0.1)^{a}	9.5 (0.1)^{c}	9.6 (0.1)^{b}	2.92 (0.01)^{cd}	3.00 (0.01)^{d}	2.92 (0.01)^{ce}
	25	10.1 (0.1)^{b}	10.2 (0.1)^{ab}	9.6 (0.1)^{b}	2.90 (0.01)^{c}	2.85 (0.01)^{e}	2.87 (0.01)^{d}
	35	10.1 (0.1)^{b}	10.2 (0.1)^{ab}	10.2 (0.1)^{a}	2.93 (0.01)^{cd}	2.95 (0.01)^{c}	2.95 (0.01)^{efg}
	45	10.1 (0.1)^{b}	10.1 (0.1)^{ab}	10.1 (0.1)^{a}	2.98 (0.01)^{ef}	2.95 (0.01)^{c}	2.98 (0.01)^{gh}
	60	10.1 (0.1)^{b}	10.2 (0.1)^{ab}	10.2 (0.1)^{a}	3.00 (0.01)^{f}	3.01 (0.01)^{d}	2.96 (0.01)^{fgh}

The same letter in superscript indicates homogeneous groups in the same physico-chemical property and treatment during storage (temperature, *T* and time, *t*) established by the ANOVA ($p < 0.05$).
In columns: FS, freshly squeezed juice; CP, conventional pasteurised juice; MP, microwave pasteurised juice.

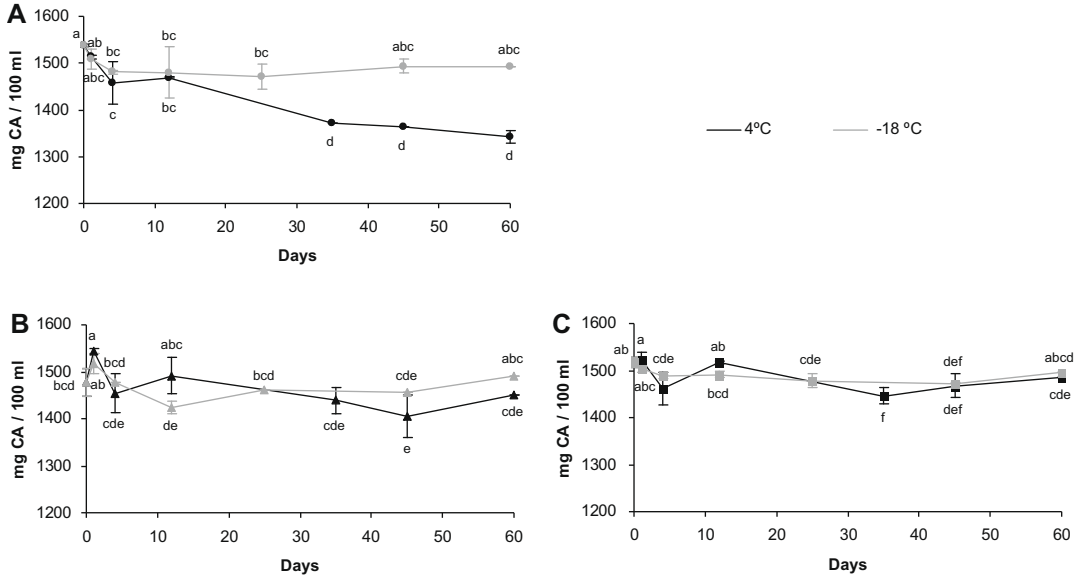

Fig. 1. Evolution of citric acid (CA) of FS (A), CP (B) and MP (C) grapefruit juices stored at 4 and −18 °C for 2 months. Letters indicate homogeneous groups established by the ANOVA ($p < 0.05$).

sense, the obtained results were the expected ones, since according to Vadivambal and Jayas (2007), ascorbic acid retention is superior in the microwave treatment than in the traditional one. In this respect, in order to diminish the impact on quality provoked by processing the juice, it would be preferable to apply microwave pasteurisation since a greater proportion of this compound is preserved.

Total phenols and %DPPH of FS were similar to the values found for orange juice by other authors (Klimczak et al., 2007). Pasteurisation provoked a significant ($p < 0.05$) decrease of the total phenol content and %DPPH. This decrease was similar in both treatments, producing a total phenol and %DPPH loss of 14.64% and 40%, respectively. Studies performed on other fruits, for example strawberry (Klopotek, Otto, & Bohm, 2005), demonstrate that there is a relationship between the decrease of antioxidant capacity, ascorbic acid, phenol content and anthocyanins and the processing necessary to obtain pasteurised juice. In general, the obtained results are comparable to those observed for citrus juices by other authors (Klimczak et al., 2007; Xu et al., 2008). In this case, antioxidant activity seems to be more related to total phenols than to ascorbic acid.

Table 2 shows the °Brix and pH obtained for fresh and pasteurised samples stored in refrigeration and freezing conditions for 2 months. From the statistical analysis and the evolution of the values, it can be stated that °Brix remained stable for all the samples, affected neither by storage conditions nor by storage time. Nevertheless, there is a general increase in pH, with no observed differences between the samples stored at 4 °C and those kept at −18 °C.

Fig. 1 shows that, in refrigeration conditions, the citric acid content of all the samples remained stable for the first 24 h, but sharply and significantly ($p < 0.05$) decreased during the next 3 days. After 12 days, the CA continued to decrease significantly in FS but remained constant in MP and CP. No significant decrease in CA was observed throughout storage at −18 °C.

As Fig. 2 shows, the storage conditions (refrigeration and freezing) affected the malic acid content of all the samples in the same way: the MA content remained constant for the first 25 storage days. Then, there was a significant ($p < 0.05$) drop in the content

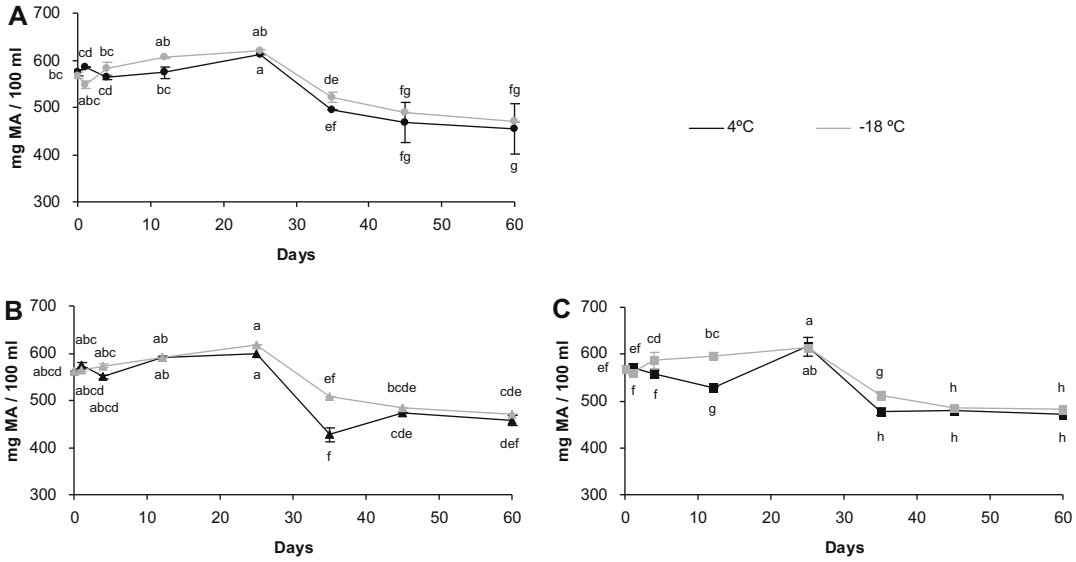

Fig. 2. Evolution of malic acid (MA) of FS (A), CP (B) and MP (C) grapefruit juices stored at 4 and −18 °C for 2 months. Letters indicate homogeneous groups established by the ANOVA ($p < 0.05$).

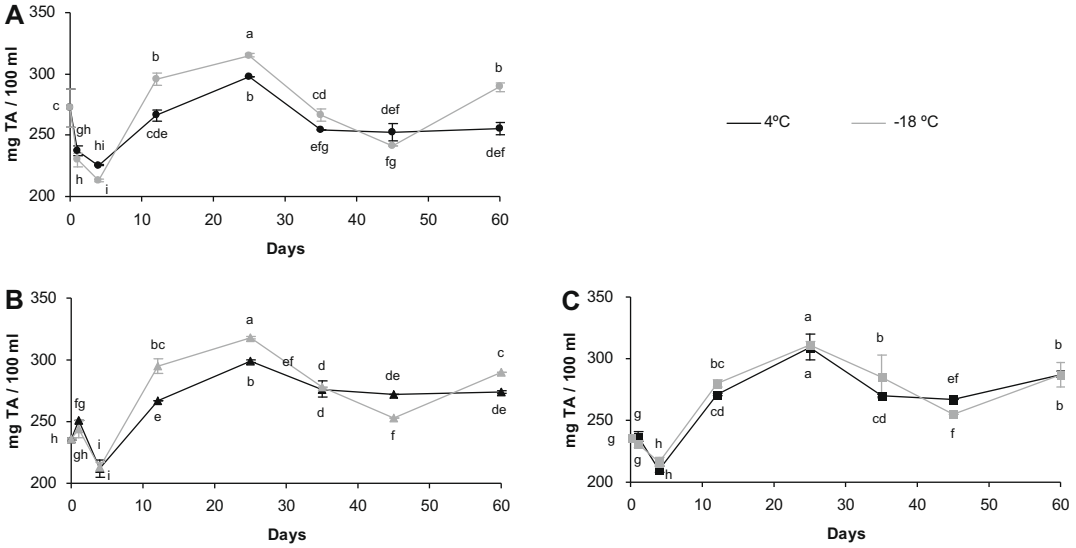

Fig. 3. Evolution of tartaric acid (TA) of FS (A), CP (B) and MP (C) grapefruit juices stored at 4 and −18 °C for 2 months. Letters indicate homogeneous groups established by the ANOVA ($p < 0.05$).

which, once again, stabilised till the end of the storage. With regards to the TA content (Fig. 3), a significant ($p < 0.05$) decrease took place during the first 4 days, with a subsequent recovery. There were no clear differences observed between the TA stability of the different samples and under differing storage conditions.

The evolution of the ascorbic acid content of grapefruit juices stored at 4 and −18 °C for 2 months is presented in Fig. 4. In general, the AA content of all juice samples studied behaved in a similar way whether under refrigeration or freezing conditions and no significant ($p < 0.05$) changes were observed till 12 days of storage. From this moment on, the samples stored under frozen conditions seem to maintain the AA content till the end of storage, whilst in the refrigerated juice the proportion of this component decreased significantly ($p < 0.05$). In this respect, from an industrial point of view, it would be advisable to freeze the pasteurised juice, for example, in the case of overproduction (Gil-Izquierdo, Gil, & Ferreres, 2002). According to the published data, the content of AA in different juices decreases during storage, depending on temperature, oxygen and light access (Klimczak et al., 2007). The degradation of AA follows both aerobic and anaerobic pathways. The oxidation of ascorbic acid occurs mainly during the processing of citrus juices, whereas anaerobic degradation, which is particularly observed in thermally preserved citrus juices, mainly appears during storage (Burdulu, Koca, & Karadeniz, 2006). For instance, Polydera, Galanou, Stoforos, and Taoukis (2004) reported that thermally pasteurised juice (80 °C, 60 s) showed 72% AA retention after 1 month at 5 °C. With regards to our CP and MP samples, 75% and 78% AA retention was reached after 25 days refrigeration, respectively, whereas in freezing conditions the retention was 84% in CP and 85% in MP. The loss of ascorbic acid during storage might be a quality indicator and a critical factor for the shelf life of some products, such as citrus juices (Plaza et al., 2006).

Fig. 5 shows the vitamin C evolution of grapefruit juices stored for 2 months at 4 °C and −18 °C. In the CP and MP juice samples,

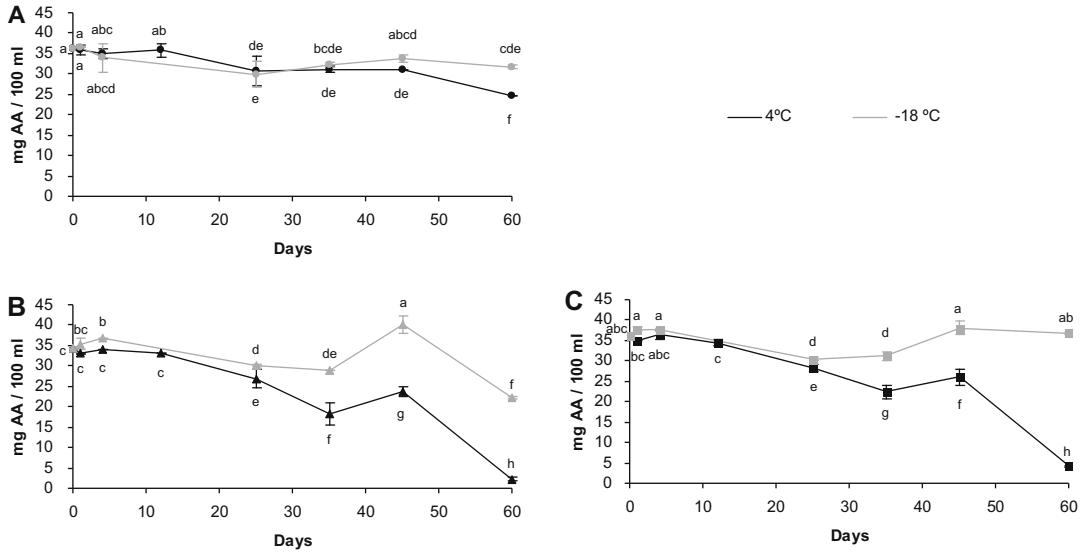

Fig. 4. Evolution of ascorbic acid (AA) of FS (A), CP (B) and MP (C) grapefruit juices stored at 4 and −18 °C for 2 months. Letters indicate homogeneous groups established by the ANOVA ($p < 0.05$).

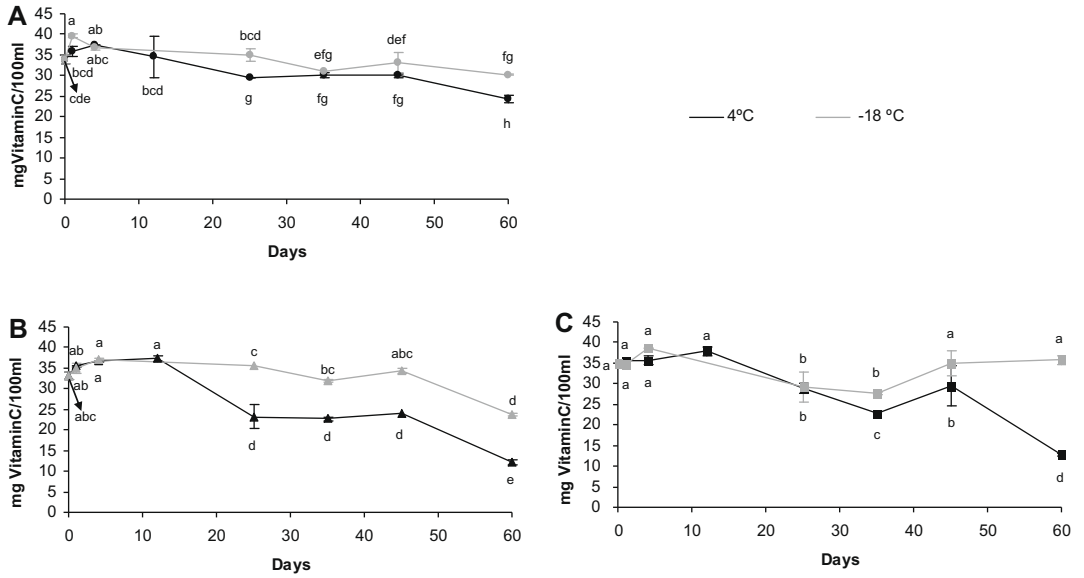

Fig. 5. Evolution of vitamin C of FS (A), CP (B) and MP (C) grapefruit juices stored at 4 and −18 °C for 2 months. Letters indicate homogeneous groups established by the ANOVA ($p < 0.05$).

the vitamin C content behaved in a similar way whether under refrigeration or freezing conditions and no significant ($p < 0.05$) changes occurred till 12 days in the case of CP samples and 25 days in the case of MP samples. From this moment on, under frozen conditions, the vitamin C content of CP samples suffered a significantly ($p < 0.05$) smaller decrease than that of refrigerated juice. In the case of frozen MP samples, this component remained stable whereas it dropped under refrigerated conditions.

At the end of the refrigerated storage, there were some significant ($p < 0.05$) differences observed between the AA and vitamin C content in pasteurised samples. As other authors suggest, the changes observed in the ascorbic acid concentration of the samples stored under refrigeration, suggest the continuation of the oxidative degradation reactions of ascorbic acid to other oxidised forms such as dehydroascorbic acid, which also presents biological activity as vitamin C (Rusell, 2004). The mechanism for enzyme degradation could be direct, by ascorbic acid oxidase, or indirect through polyphenoloxidase, cytochrome oxidase or peroxidase (Belizt & Grosch, 1997). This could be the reason why the values of vitamin C were higher than those of AA at the end of storage of treated samples.

During the storage time studied (Fig. 6), storage temperature seems not to affect FS phenol content since it evolved in a similar way whether stored under refrigeration or frozen, whereas PT significantly ($p < 0.05$) diminished till 25 days, after which it remained constant. In this way, Tavirini, D'Innocenti, Remorini, Massai, and Guidi (2008) reported that phenols did not change in kiwifruits stored for 2 months at 0 °C, but they observed a significant rise after a long storage (6 months at 0 °C) which further increased after a week at ambient temperature. In CP and MP refrigerated samples, the phenol content significantly ($p < 0.05$) diminished after day four, whilst under freezing conditions, the evolution of TP was constant.

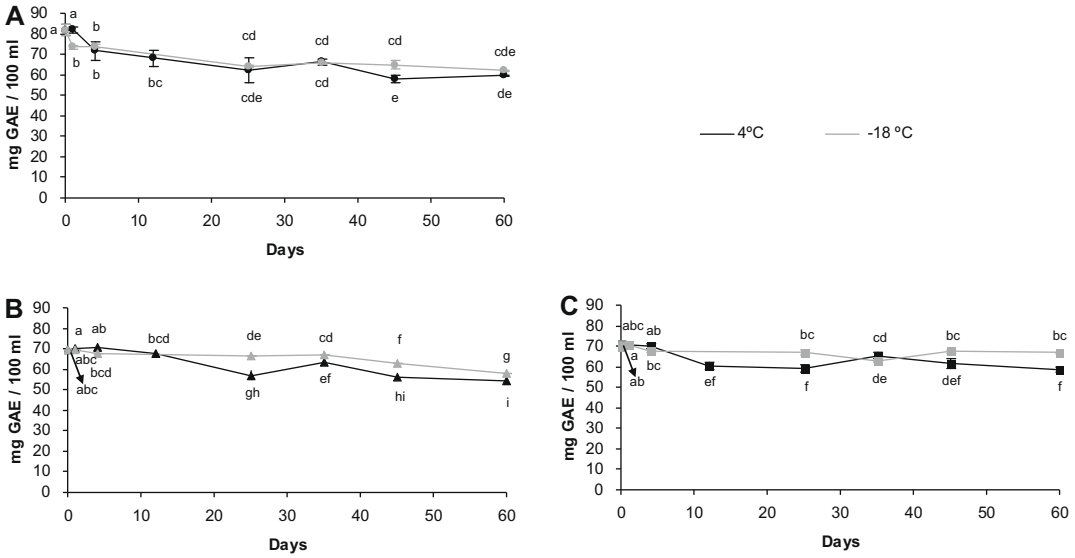

Fig. 6. Evolution of total phenols (mg GAE / 100 ml) of FS (A), CP (B) and MP (C) grapefruit juices stored at 4 and −18 °C for 2 months. Letters indicate homogeneous groups established by the ANOVA ($p < 0.05$).

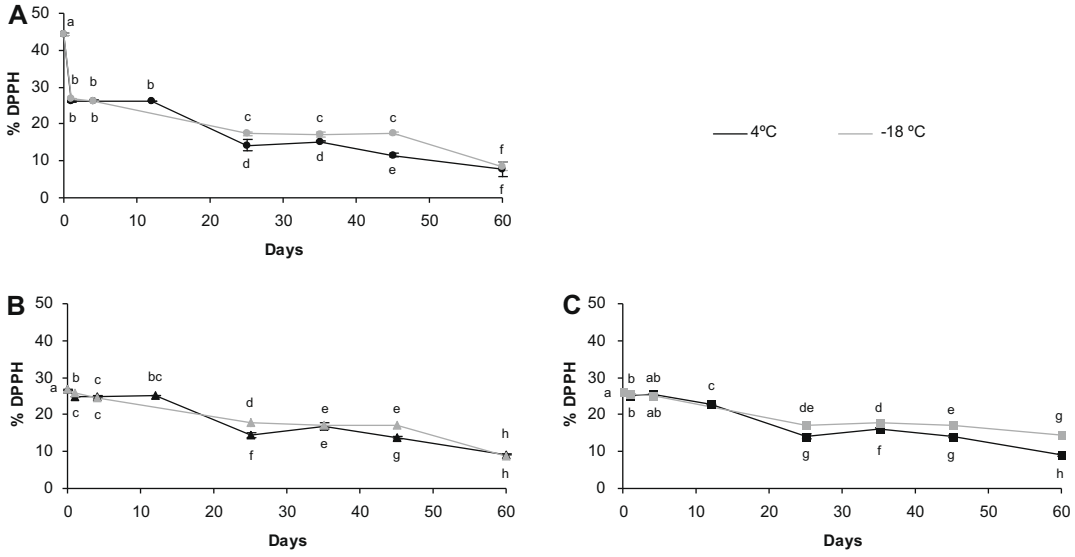

Fig. 7. Evolution of antioxidant activity (%DPPH) of FS (A), CP (B) and MP (C) grapefruit juices stored at 4 and −18 °C for 2 months.

Table 3
Mean values (with standard deviation) of variation of components (%) due to treatment and after 60 days of storage.

	Refrigeration			Frozen		
	FS	CP	MP	FS	CP	MP
°Brix	1.21 (0.01)^{a}	2.21 (0.01)^{b}	1.31 (0.14)^{a}	1.21 (0.01)^{a}	2.37 (0.22)^{b}	2.32 (0.14)^{b}
pH	0.33 (0.01)^{c}	−0.33 (0.01)^{b}	−0.33 (0.01)^{b}	−0.33 (0.47)^{b}	0.50 (0.23)^{c}	−1.33 (0.01)^{a}
CA	−12.64 (2.87)^{a}	−5.59 (2.68)^{b}	− 3.38 (0.27)^{b}	−3.02 (0.14)^{b}	−2.83 (0.24)^{b}	−3.09 (0.13)^{b}
MA	−20.63 (8.17)^{a}	−20.29 (2.81)^{a}	−17.51 (2.11)^{a}	− 18.21 (1.36)^{a}	−16.83 (0.10)^{a}	−15.60 (0.90)^{a}
TA	−5.96 (3.56)^{a}	0.89 (5.25)^{ab}	5.85 (5.27)^{ab}	6.57 (4.80)^{ab}	7.56 (7.19)^{b}	3.46 (5.40)^{ab}
AA	− 31.80 (0.13)^{d}	−93.85 (1.26)^{a}	−88.53 (0.43)^{b}	−11.89 (2.77)^{e}	−38.45 (1.02)^{c}	−0.85 (0.39)^{f}
Vitamin C	−28.41 (5.03)^{b}	−63.75 (2.82)^{a}	−62.27 (0.18)^{a}	−10.72 (3.18)^{c}	−29.84 (1.72)^{b}	6.05 (6.63)^{d}
TP	−27.37 (1.03)^{a}	−33.62 (2.44)^{a}	−28.23 (0.40)^{a}	−24.61 (0.77)^{a}	−28.11 (3.15)^{a}	−18.35 (0.89)^{b}
%DPPH	−82.67 (4.86)^{a}	−79.24 (0.51)^{a}	−79.67 (0.70)^{a}	− 80.73 (2.69)^{a}	−80.45 (0.91)^{a}	−67.10 (1.26)^{b}

The same letter in superscript indicates homogeneous groups established by the ANOVA ($p < 0.05$).
In columns: FS, freshly squeezed juice; CP, conventional pasteurised juice and MP, microwave pasteurised juice.
In rows: CA, citric acid; MA, malic acid; TA, tartaric acid; AA, ascorbic acid; TP, total phenols.

As can be observed in Fig. 7, the antioxidant capacity of both thermally treated grapefruit juices was affected by the storage conditions in a similar way. On the other hand, the antioxidant capacity of both the chilled and frozen fresh juice decreased during the first 24 h of storage. From 24 h of storage on, the FS sample evolved in a similar way to pasteurised juices, regardless of storage conditions and till the end of the study. In general, the %DPPH of all the samples decreased throughout the storage. Frozen stored MP samples had a significantly ($p < 0.05$) greater antioxidant capacity at the end of the period.

In Table 3, the variation of components due to treatment and 60 days of storage can be observed. These values were calculated as the difference of each compound in fresh or treated juice at the end of storage related to fresh juice and referred to 100 g of fresh juice. In general, frozen juices showed the smallest losses. The greatest losses were produced in FS refrigerated samples, except in the cases of AA and vitamin C, which were in greater proportions in CP refrigerated samples. When frozen, the vitamin C and AA content of the pasteurised samples remained the highest. Nevertheless, the studied bioactive compounds in the frozen MP juices maintained a greater stability and the smaller observed losses in antioxidant capacity point to this fact.

As regards to organic acids, refrigerated FS samples showed the greatest significant ($p < 0.05$) loss in CA (−12.64%). No significant ($p < 0.05$) differences were observed for the other acids in the rest of the samples and storage conditions (mean value of the loss is 3.58%, 18.18% and 3.06% for CA, MA and TA, respectively). AA and vitamin C were more stable when the samples were frozen, especially in the case of microwave-treated samples. Nevertheless, in refrigerated samples, FS juice contained the greatest amount of these compounds. In both cases, the greatest loss was observed in CP samples. Neither treatment nor storage temperature affected total phenols and antioxidant activity significantly ($p < 0.05$), except in the case of frozen MP samples which showed the lowest significant ($p < 0.05$) loss of TP (−18.35%) and %DPPH (−67.1%).

In order to explain the influence of the different compounds quantified in this study on the antioxidant capacity of the samples, correlation statistical analyses were performed. Only TA showed a negative Pearson's correlation coefficient with %DPPH (−0.5258, $p < 0.05$). Total phenols played a mayor role in the antioxidant capacity of grapefruit juices (0.8389, $p < 0.05$), followed by the vitamin C (0.7216, $p < 0.05$), ascorbic acid (0.5563, $p < 0.05$), malic acid (0.5548, $p < 0.05$), citric acid (0.4785, $p < 0.05$). Other studies (Bahorun, Luximon-Ramma, Crozier, & Aruoma, 2004) confirm the existence of a positive relationship between the phenolic content of a fruit and its antioxidant capacity. Fruits with high antioxidant activity generally contain a great quantity of antioxidant substances, especially phenolic compounds and specifically flavonoids (Tavirini et al., 2008).

4. Conclusion

Contrary to conventional treatment which leads to a significant decrease in CA and AA in grapefruit juice, microwave treatment preserved these compounds. Moreover, frozen microwave pasteurised juices better preserved total phenols and antioxidant capacity when compared with fresh or conventional pasteurised ones and maintained the amount of AA and vitamin C, especially in pasteurised samples. Therefore, the use of microwave energy offers a good alternative to conventional pasteurisation.

Acknowledgement

The authors thank the Ministerio de Educación y Ciencia for the financial support given throughout the Project AGL 2005–05994.

References

Bahorun, T., Luximon-Ramma, A., Crozier, A., & Aruoma, O. (2004). Total phenol, flavonoid, proanthocyanidin and vitamin C levels and antioxidant activities of Mauritian vegetables. *Journal of Science of Food and Agriculture, 84*, 1553–1561.

Belizt, H. D., & Grosch, W. (1997). *Química de los Alimentos*. Zaragoza: Acribia.

Benzie, I. F. F., & Strain, J. J. (1999). Ferric reducing/antioxidant power assay: Direct measure of total antioxidant activity of biological fluids and modified version for simultaneous measurement of total antioxidant power and ascorbic acid concentration. *Methods in Enzymology, 299*, 15–27.

Burdulu, H. S., Koca, N., & Karadeniz, F. (2006). Degradation of vitamin C in citrus juice concentrates during storage. *Journal of Food Engineering, 74*, 211–216.

Cano, M. P., Hernández, A., & De Ancos, B. (1997). High pressure and temperatures effects on enzyme inactivation in strawberry and orange products. *Journal of Food Science, 62*, 85–88.

Cañumir, J. A., Celis, J. E., Brujin, J., & Vidal, L. (2002). Pasteurisation of apple juice by using microwaves. *Lebensmittel-Wissenschaft und Technologie, 35*, 389–392.

Cen, H., Bao, Y., He, Y., & Sun, D. W. (2007). Visible and near infrared spectroscopy for rapid detection of citric and tartaric acids in orange juice. *Journal of Food Engineering, 82*, 253–260.

Dziezak, J. D. (1993). Natural acid and acidulants. In R. Macrac, R. K. Robinson, & M. J. Sadler (Eds.). *Encyclopedia of food science, food technology and nutrition* (Vol. 1, pp. 10–16). San Diego: Academic Press.

Elez-Martínez, P., Aguiló-Aguayo, I., & Martín-Belloso, O. (2006). Inactivation of orange juice peroxidase by high-intensity pulsed electric fields as influenced by process parameters. *Journal of the Science of Food and Agriculture, 86*, 71–81.

Gil-Izquierdo, A., Gil, M., & Ferreres, F. (2002). Effect of processing techniques at industrial scale on orange juice antioxidant and beneficial health compounds. *Journal of Agricultural and Food Chemistry, 50*, 5107–5117.

Kim, H. B., & Tadini, C. C. (1999). Effect of different pasteurisation conditions on enzyme inactivation of orange juice in pilot-scale experiments. *Journal of Food Process Engineering, 22*, 395–403.

Kimball, D. A. (1999). *Procesado de cítricos*. Zaragoza: Acribia.

Klimczak, I., Malecka, M., Szlachta, M., & Gliszczynska, A. (2007). Effect of storage on the content of polyphenols, vitamin C and the antioxidant activity of orange juices. *Journal of Food Composition and Analysis, 20*, 313–322.

Klopotek, Y., Otto, K., & Bohm, V. (2005). Processing strawberries to different products alters the vitamin C, total phenolics, total anthocyanins and antioxidant capacity. *Journal of Agricultural and Food Chemistry, 53*, 5640–5646.

Leong, L. P., & Shui, G. (2002). An investigation of antioxidant capacity of fruits in Singapore markets. *Food Chemistry, 76*, 69–75.

Moraga, M. J., Moraga, G., Fito, P. J., & Martínez-Navarrete, N. (2009). Effect of vacuum impregnation with calcium lactate on the osmotic dehydration kinetics and quality of osmodehydrated grapefruit. *Journal of Food Engineering, 90*(3), 372–379.

Nikdel, S., Chen, C., Parish, M., MacKellar, D., & Friedrich, L. (1993). Pasteurization of citrus juice with microwaves energy in a continuous-flow unit. *Journal of Agricultural and Food Chemistry, 41*, 2116–2119.

Plaza, L., Sánchez-Moreno, C., Elez-Martínez, P., Ancos, B., Martín-Belloso, O., & Cano, M. P. (2006). Effect of refrigerated storage on vitamin C and antioxidant activity of orange juice processed by high-pressure or pulsed electric fields with regard to low pasteurization. *European Food Research Technology, 223*, 487–493.

Polydera, A. C., Galanou, E., Stoforos, N. G., & Taoukis, P. S. (2004). Inactivation kinetics of pectin methyl esterase of greek Navel orange juice as function of high hydrostatic pressure and temperature process conditions. *Journal of Food Engineering, 62*, 291–298.

Poulose, S. M., Harris, E. D., & Patil, B. S. (2005). Citrus limonoids induce apoptosis in human neuroblastoma cells and have radical scavenging activity. *Journal of Nutrition, 135*, 870–877.

Rapeanu, G., Van Loey, A., Smout, C., & Hendrickx, M. (2006). Biochemical characterization and process stability of polyphenoloxidase extracted from Victoria grape (*Vitis vinifera* sp. *Sativa*). *Food Chemistry, 94*, 253–261.

Rusell, L. F. (2004). *Handbook of food analysis. Physical characterisation and nutrient analysis* Vol. 1, pp. 487–571. New York: Marcel Dekker.

Sanchez-Mata, M. C., Cámara-Hurtado, M., Diez-Marques, C., & Torija-Isasa, M. E. (2000). Comparison of HPLC and spectrofluorimetry for vitamin C analysis of green beans. *European Food Research International, 210*, 220–225.

Sánchez-Moreno, C., Plaza, L., De Ancos, B., & Cano, M. P. (2006). Nutritional characterisation of commercial traditional pasteurised tomato juices: Carotenoids, vitamin C and radical-scavenging capacity. *Food Chemistry, 98*, 749–756.

Sánchez-Moreno, C., Plaza, L., De Ancos, B., & Cano, M. P. (2003). Quantitative bioactive compounds assessment and their relative contribution to the antioxidant capacity of commercial orange juices. *Journal of the Science of Food and Agriculture, 83*, 430–439.

Selvendran, R. R., & Ryden, P. (1990). *Methods in plant biochemistry* Vol. 2, p. 549. London: Academic Press.

Sentandreu, E., Carbonell, L., Rodrigo, D., & Carbonell, J. V. (2006). Pulsed electric fields versus thermal treatment: Equivalent processes to obtain equally acceptable citrus juices. *Journal of Food Protection, 69*(8), 2016–2018.

Snir, R., Koehler, P. E., Sims, K. A., & Wicker, L. (1996). Total and thermostable pectinesterases in citrus juices. *Journal of Food Science, 61*(2), 379–382.

Tavirini, S., D'Innocenti, E., Remorini, D., Massai, R., & Guidi, L. (2008). Antioxidant capacity, ascorbic acid, total phenols and carotenoids changes during harvest and after storage of Hayward kiwifruit. *Food Chemistry, 107*, 282–288.

Tomás-Barberán, F. A., Gil, M. I., Cremin, P., Waterhouse, A. L., Hess-Pierce, B., & Kader, A. A. (2001). HPLC–DAD–ESIMS analysis of phenolic compounds in nectarines, peaches, and plums. *Journal of Agricultural and Food Chemistry, 49*, 4748–4760.

Vadivambal, R., & Jayas, D. S. (2007). Changes in quality of microwave-treated agricultural products – A review. *Biosystems Engineering, 98*, 1–16.

Valero, E., Varón, R., & García-Carmona, F. (1988). Characterization of polyphenol oxidase from Airen grapes. *Journal of Food Science, 53*, 1482–1485.

Vinson, J. A., & Bose, P. (1988). Comparative bioavailability to humans of ascorbic acid alone or in a citrus extract. *American Journal of Clinical Nutrition, 48*, 601–604.

Wang, Y., Chuang, Y., & Ku, Y. (2007). Quantitation of bioactive compounds in citrus fruits cultivated in Taiwan. *Food Chemistry, 102*, 1163–1171.

Xu, G., Liu, D., Chen, J., Ye, X., Ma, Y., & Shi, J. (2008). Juice components and antioxidant capacity of citrus varieties cultivated in China. *Food Chemistry, 106*, 545–551.

Food Chemistry 118 (2010) 300–306

Contents lists available at ScienceDirect

Food Chemistry

journal homepage: www.elsevier.com/locate/foodchem

In vitro evaluation of red and green lettuce (*Lactuca sativa*) for functional food properties

Vanisree Mulabagal [a], Mathieu Ngouajio [b], Ajay Nair [b], Yanjun Zhang [c], Aditya L. Gottumukkala [a], Muraleedharan G. Nair [a,*]

[a] Bioactive Natural Products and Phytoceuticals, Department of Horticulture, 173 National Food Safety and Toxicology Center, Michigan State University, East Lansing, MI 48824, USA
[b] Department of Horticulture, Michigan State University, East Lansing, MI, USA
[c] UCLA Center for Human Nutrition, David Geffen School of Medicine, 900 Veteran Avenue, Los Angeles, CA 90095, USA

ARTICLE INFO

Article history:
Received 25 August 2008
Received in revised form 31 March 2009
Accepted 29 April 2009

Keywords:
Phenolics
Lactuca sativa
Anthocyanins
Antioxidant
Cyclooxygenase enzyme

ABSTRACT

Lettuce (*Lactuca sativa*) is an important leafy vegetable consumed fresh or in salad mixes. We have compared the functional food properties of selected commercial red and green lettuce varieties grown under field conditions. Both lettuce cultivars were extracted with water at biological (38 °C) and room temperatures (22 °C) at pH 2. The residues from each extraction were further extracted, sequentially with methanol and ethyl acetate. The extracts were evaluated for their *in vitro* lipid peroxidation (LPO) and cyclooxygenase enzyme (COX) inhibitory activities. Amongst the extracts tested, all three extracts of red lettuce showed higher LPO and COX-1 and -2 enzyme inhibitory activities than did the green lettuce extracts. Red lettuce contained a single anthocyanin, cyanidin-3-*O*-(6″-malonyl-β-glucopyranoside) (**1**), which immediately converted to cyanidin-3-*O*-(6″-malonyl-β-glucopyranoside methyl ester) (**2**) and cyanidin-3-*O*-β-glucopyranoside (**3**) under laboratory conditions. Anthocyanins **1** and **2** inhibited LPO by 88% and 91.5%, respectively, at 0.25 μM concentration. Also, they inhibited COX-2 enzyme by 78.9% and 84.3% and COX-1 by 64% and 65.8%, respectively, at 5 μM. The chicoric acid (**4**), amongst other phenolics, such as quercetin glucoside, ferulic and caffeic acids, isolated from both green and red lettuce, showed 85.6%, 45.6% and 94% of LPO, COX-1 and -2 enzyme inhibitions at 50 μM, respectively. This is the first report of the LPO, COX-1 and -2 enzyme inhibitory activities of compounds **1**, **2** and **4**. The variation of phenolics in the red and green lettuces, and specifically the lack of anthocyanins in green lettuce, might account for the higher biological activity obtained with the red variety in our study.

1. Introduction

Numerous studies have shown a correlation between the consumption of fresh fruits and vegetables and their health benefits. Epidemiological studies have further demonstrated the relationship between dietary habits and disease risk and established that food has a direct impact on health. Lettuce, *Lactuca sativa*, is an important dietary leafy vegetable that is primarily consumed fresh or in salad mixes due to its perception as being amongst healthier foods (Dupont, Mondi, Willamson, & Price, 2000). A number of lettuce varieties have been investigated recently and reported to contain phenolic compounds with antioxidant activities (Llorach, Martinez-Sanchez, Tomas-Barberan, Gil, & Ferrers, 2008; Rice-Evans, Miller, Bolwell, Bramley, & Pridham, 1995). The health benefits of lettuce have also been attributed to the presence of Vitamin C, phenolic compounds and fibre content (Nicolle & Cardinault et al., 2004; Nicolle & Carnat et al., 2004. In folk medicine, lettuce seeds are used in the treatment of asthma, cough and as an analgesic.

In 2006, over 4,338,000 metric tons of lettuce plants were harvested from over 306,600 acres with a total value of over $2 billion. Iceberg, romaine and leaf lettuces represented 61%, 18% and 21% of the total national production (by weight), respectively. Despite a relatively small proportion of the total production (21%), leaf lettuce, including red and green types, continues to have the highest value. In 2006, leaf lettuce was valued at $8,451/acre compared to $5,596/acre and $7,016/acre for iceberg and romaine types, respectively. Iceberg lettuce is so far the most common lettuce used (especially in fast food restaurants). The antioxidant phenolics in lettuce vary amongst varieties due to growing practices, processing and storage conditions (Baur, Klaiber, Koblo, & Carle, 2004). Currently, red lettuce is popular in salad mixes due to its anthocyanin content that contributes to the higher value it fetches compared to the green lettuce (Gazula, Kleinhenz, Scheerens, & Ling, 2007). The increased demand of fresh vegetables associated with health benefits has led to an increase in the quality, quantity and variety of produce available to the consumer. Various approaches, involving

* Corresponding author. Fax: +1 (517) 432 2310.
E-mail address: nairm@msu.edu (M.G. Nair).

0308-8146/$ - see front matter © 2009 Elsevier Ltd. All rights reserved.
doi:10.1016/j.foodchem.2009.04.119

environmental, cultural and management practices, have been used to enhance the quality of lettuce, specifically in the areas of phytochemical contents and health-promoting attributes (Kleinhenz, French, Gazula, & Scheerens, 2003).

Anthocyanins are water-soluble phenolic glycosides that colour fruits, flowers, vegetables and cereals. Apart from imparting colour to plants, anthocyanins exhibit an array of health-promoting benefits. We have reported that anthocyanins isolated from various plants inhibited lipid peroxidation (LPO) and cyclooxygenase (COX) enzymes (Mulabagal, Van Nocker, DeWitt, & Nair, 2007; Seeram, Cichewez, Chandra, & Nair, 2003; Tall, Seeram, Zhao, Nair, & Meyer, 2004; Wang, Nair, & Strasburg, 1999). The ability of anthocyanidins to inhibit LPO and COX enzymes has also been reported (Seeram & Nair, 2002). Both anthocyanins and anthocyanidins stimulated insulin release by rodent pancreatic β-cells (INS-1 832/13) *in vitro* (Jayaprakasam, Vareed, Olson, & Nair, 2005). Also, a purified anthocyanin mixture from *Cornus mas* fruits has demonstrated an ability to ameliorate obesity and insulin resistance in C57BL/6 mice fed a high-fat diet (Jayaprakasam, Olson, Schutzki, Tai, & Nair, 2006). In another *in vivo* study, anthocyanins up-regulated the adipocyte-specific gene and genes involved in lipid metabolism (Tsuda, Ueno, Kojo, Yoshikawa, & Osawa, 2005; Tsuda et al., 2004).

Although red lettuce costs more than green lettuce, it is becoming very popular amongst consumers. This is probably due to its red colour and its association with better health as in the case of red fruits and berries. Therefore, in this study, we have compared both green and red lettuce, using *in vitro* bioassays and chemical composition studies and evaluated their functional food advantages.

2. Materials and methods

2.1. Materials

Seeds of green (Var. North Star) and red lettuce (Var. Cherokee) were purchased from Siegers Seeds Company (Holland, MI). The COX-1 enzyme was prepared from ram seminal vesicles purchased from Oxford Biomedical research, Inc. (Oxford, MI). The COX-2 enzyme was prepared from prostaglandin endoperoxide-H synthase-2 (PGHS-2)-cloned insect cell lysate. Solvents used for isolation and purification were of ACS grade and purchased from Sigma–Aldrich Chemical Co., Inc. (St. Luis, MO). Positive controls, t-butyl hydroquinone (TBHQ), butylated hydroxyanisole (BHA) and butylated hydroxytoluene (BHT), used in the anti-oxidant assay, were purchased from Sigma Chemical Company.

2.2. Equipment

Samples were homogenised using a Kinematica CH-6010 (Roxdale, ON, Canada) homogenizer and centrifuged (model RC5C, Sorvall Instruments, Hoffman Estates, IL) at 10,000*g* for 20 min at 4 °C. The NMR (^{1}H & ^{13}C) experiments were recorded on Varian INOVA (300 MHz) and VRX (500 MHz) instruments. The chemical shifts were measured in DMSO-*d6* and CD_3OD/DCl solutions and are expressed in δ (ppm). Fractionation of anthocyanin was carried out on a XAD-2 column (500 g, Amberlite resin, mesh size 20–50; Sigma Chemical Co., St. Louis, MO) and purified on a C-18 MPLC column (350 × 40 mm). Anthocyanin detection was carried out with a Waters 2010 HPLC system (Waters Corp.) equipped with Empower Software, Shodex Degasser, Auto sampler (Waters 717) and a Photodiode Array Detector (Waters 996). HPLC analysis was carried out by using a Capcell Pak column (DyChrom, Santa Clara, CA) C-18 column (150 × 4.6 mm i.d.; 5 μm particle size). Preparative HPLC purification of anthocyanin was carried out by using a Capcell Pak (DyChrom, Santa Clara, CA) C-18 column (250 × 4.6 mm i.d.; 5 μm particle size).

2.3. Plant material

Lettuce transplants were produced in the greenhouse using 72-cell flats filled with commercial greenhouse potting mix. At the two-leaf stage, the seedlings were transplanted to the field. Field experiments were conducted at Michigan State University Horticulture Teaching and Research Center. The lettuce seedlings were transplanted on raised beds covered with black plastic mulch and drip-irrigated using two staggered rows per bed. Spacing was 30 cm between the rows and 30 cm between plants inside each row. The plants were grown in the absence of any pesticide.

2.4. LC/MS analysis

Samples were analysed on a Surveyor HPLC system equipped with a diode array absorbance detector (DAD), measuring at 520 nm, and an autosampler cooled to 4 °C (Thermo Finnigan, San Jose, USA). An Agilent Zorbax SB C-18 column, 150 × 2.1 mm, i.d.; 5 μm particle size (Agilent, USA), was used and solvent elution consisted of a gradient system over 50 min of methanol (1% acetic acid) and H_2O (1% acetic acid) at a flow rate of 0.19 ml/min. The linear gradient system started from 5% methanol (1% acetic acid) and 95% of H_2O (1% acetic acid) to 95% methanol (1% acetic acid) and 5% of H_2O (1%) at 50 min. The column was maintained at 25 °C. After passing through the flow cell of the DAD, eluate was directed to a LCQ Advantage ion trap mass spectrometer fitted with an Eelectrospray Interface (ESI). Analyses utilised the positive ion mode (*m/z* $M + H^+$) for detection of anthocyanins. Preliminary analyses were carried out using full scan, data-dependent MS/MS scanning from *m/z* 250 to 1000. The capillary temperature was set at 275 °C and the sheath and auxiliary gas at 45 and 0 units/min, respectively. The source voltage was 4 kV. MS/MS and fragmentation were carried out with 50% energy.

2.5. Extraction of lettuce

Fresh leaves of red lettuce (1.2 kg) were blended and extracted at 22 °C with acidic water (0.1% HCl, 1 l 3×) and centrifuged. Supernatants were lyophilised to get water extract (19.1 g). The residue was further extracted with methanol (500 ml 3×), followed by ethyl acetate (500 ml 3×) and the organic extracts evaporated to dryness under reduced pressure. The yields of methanol and ethyl acetate extracts were 7 and 0.2 g, respectively. Similarly, green lettuce (300 g) leaves were blended and extracted with acidic water (200 ml 3×) and the water-soluble portions were centrifuged and lyophilised (3.4 g). Residue was extracted further with methanol (100 ml 3×), followed by ethyl acetate (100 ml 3×) and the resulting extracts evaporated under vacuum to afford 0.3 and 0.4 g of dried extracts, respectively.

To mimic *in vivo* conditions, another extraction was carried out at 38 °C and pH = 2. Red lettuce leaves (350 g) were blended with acid water (0.1% HCl, 300 ml 3×) and allowed to stand at 38 °C and pH = 2 for 4 h. The mixture was then centrifuged and the supernatant lyophilised to yield a powder (14.7 g). The residue was then extracted sequentially with methanol (200 ml 3×) and ethyl acetate (200 ml 3×). The yields of methanol and ethyl acetate extracts from this procedure were 4.9 and 0.8 g, respectively. The green lettuce leaves (200 g) were also extracted in a similar manner (75 ml 3×), followed by methanol (75 ml 3×) and ethyl acetate (75 ml 3×) to afford 3.4, 0.3 and 0.4 g of dried extracts, respectively.

2.6. Purification of anthocyanin from red lettuce

The crude extract (14 g) from red lettuce was dissolved in 200 ml of water and fractionated by an XAD-2 column (35 × 6 cm) according to the published procedure (Nair, 2002). The resin with adsorbed anthocyanins was then washed with water (2 × 1 l). The water fraction was lyophilised (4.9 g). The adsorbed anthocyanin was eluted with acidic methanol (1% HCl, 2 × 1 l), concentrated at reduced pressure (35 °C) and lyophilised to yield a dark red residue (8.5 g). An aliquot of this residue (3 g) was purified further by a C-18 MPLC column (350 × 40 mm) using water:methanol (1% HCl) as the mobile phase under gradient conditions, starting with 80% H_2O. Five fractions, I (H_2O:MeOH, 80:20, 250 ml); II (H_2O:MeOH, 70:30, 200 ml); III (H_2O:MeOH, 60:40, 200 ml); IV (H_2O:MeOH, 60:40, 200 ml) and V (H_2O:MeOH, 50:50, 500 ml) were obtained. All fractions were evaporated under vacuum and analysed by HPLC for purity and anthocyanin content. Based on HPLC, Fraction II contained pure cyanidin-3-*O*-β-glucopyranoside (**3**, 12 mg) as confirmed by NMR studies (Vareed, Reddy, Schutzki, & Nair, 2006).

Fraction IV (75 mg) showed two peaks by HPLC and was further purified by preparative HPLC using Capcell Pak (4.6 × 250 mm, 5 μm). The solvent system consisted of solvent A (water-trifluoroacetic acid (TFA) 99.99:0.1 v/v) and B (water–acetonitrile–acetic acid–TFA, 50.4%, 48.5%, 1%, 0.1%, v/v/v). The linear gradient began at 80% A and 20% B, was allowed to reach 40% A and 60% B in 26 min, and then reverted back to the initial condition of 80% A and 20% B in 30 min, where it remained for 20 min. The flow rate was 1 ml/min. The peaks detected at 520 nm (Fig. 3b) were collected, evaporated to dryness and characterised by NMR spectral methods as cyanidin-3-*O*-β-glucopyranoside (**3**, 6 mg), cyanidin-3-*O*-(6″-malonyl-β-glucopyranoside (**1**, 28 mg) and the methyl ester of cyanidin-3-*O*-(6″-malonyl-β-glucopyranoside (**2**, 15 mg). It is important to note that anthocyanins **2** and **3** are conversion products of anthocyanin **1** (Fig. 3a) produced during purification in the presence of acidic methanol. The structures of anthocyanins **1, 2** and **3** were further confirmed by comparison of NMR and mass spectral data with those of published data (Andersen & Fossen, 1995; Vareed et al., 2006).

2.7. Isolation of bioactive compounds from red and green lettuce

The MeOH extract (3.6 g) of red lettuce prepared at 38 °C was subjected to a silica gel MPLC column (350 × 40 mm) and eluted with $CHCl_3$ and mixtures of $CHCl_3$ and MeOH with increasing polarity. The fractions were analysed by TLC and similar fractions were combined to give fractions A (0.28 g, $CHCl_3$:MeOH; 9:1), B (0.75 g, $CHCl_3$:MeOH; 8:2), C (1.3 g, $CHCl_3$:MeOH; 7:3) and D (0.9 g, $CHCl_3$:MeOH; 1:1). Fraction A showed a single spot on TLC, using hexane and EtOAc (8:2) as mobile phase, and was characterised as linoleic acid (15 mg). Purification of Fraction B by silica gel TLC using hexane and EtOAc mixtures as the mobile phase gave a yellow solid, quercetin (22 mg). The compounds yielded from Fraction C by silica gel MPLC purification, followed by crystallization, were ferulic (7 mg) and caffeic acids (11 mg). The purification of fraction D by silica gel TLC gave a yellow solid, chicoric acid (**4**, 6 mg). The structures of all compounds were confirmed by comparison of NMR spectral data with those of published data (Bilia, Ciampi, Mendez, & Morelli, 1996; Dutta, Mazumdar, Mishra, Dastidar, & Park, 2007; Maeda et al., 2006; Zhang, Mills, & Nair, 2003).

Methanol extract of green lettuce (300 mg), prepared at 38 °C, was also purified by silica gel MPLC, as in the case of red lettuce extract. Fractions were collected in 5 ml aliquots and analysed by TLC. Fractions that showed identical TLC profiles were combined to obtain fractions I (78 mg, chloroform:methanol, 9:1), II (40 mg, chloroform:methanol, 8:2), III (80 mg, chloroform:methanol, 6:4) and IV, (90 mg, chloroform:methanol, 1:1). Fraction I contained primarily chlorophylls and was kept aside. Further purification of fractions II–IV by silica gel MPLC and preparative TLC resulted in the isolation of linoleic acid (12 mg), quercetin glucoside (20 mg), and chicoric acid (**4**, 15 mg), respectively. Structures of the isolates were confirmed by comparison of NMR and mass spectral data with those of published data (Bilia et al., 1996; Dutta et al., 2007; Maeda et al., 2006; Zhang et al., 2003).

2.8. Lipid peroxidation inhibitory assay

Lettuce extracts, pure anthocyanins and compounds were tested *in vitro* for their abilities to inhibit the oxidation of large unilamellar vesicles (LUV's), according to published procedure (Arora & Strasburg, 1997). Peroxidation was initiated by addition of 20 μl of $FeCl_2$–$4H_2O$ (0.5 mM) for positive controls and test samples. Fluorescence was measured at 384 nm and the decrease of relative fluorescence intensity with time indicated the rate of peroxidation. Extracts were assayed at 100 ppm, anthocyanins at 0.25 μM and compound **4** at 25 μM concentrations. Positive controls t-butyl hydroquinone (TBHQ), butylated hydroxyanisole (BHA) and butylated hydroxytoluene (BHT), used in the anti-oxidant assay, were tested at 10 μM. Water extracts and pure anthocyanins were assayed as solutions prepared in water. Compound **4** and methanolic extracts were assayed as solutions prepared in DMSO.

2.9. Cyclooxygenase enzyme inhibitory assay

All the lettuce extracts, anthocyanins and other phenolics were tested for their COX-1, and COX-2 enzyme inhibitory assay accord-

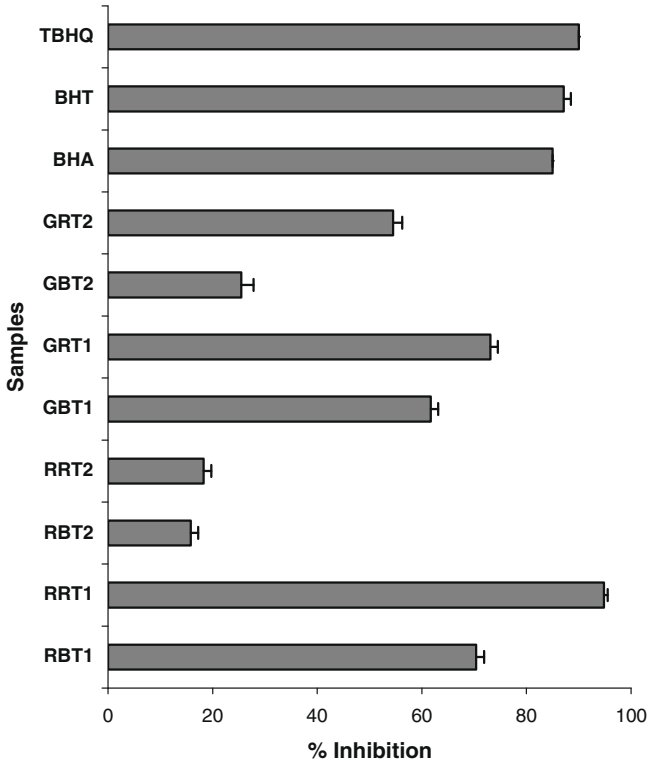

Fig. 1. Lipid peroxidation inhibitory activities of green and red lettuce extracts tested at 100 ppm (RBT1, RRT1: red lettuce water-extracts at 38 °C and 22 °C; RBT2, RRT2: red lettuce methanolic extracts of the residue from water extraction at 38 °C and 22 °C; GBT1, GRT1: green lettuce water-extracts at 38 °C and 22 °C; GBT2, GRT2: green lettuce methanolic extracts of the residue from water extraction at 38 °C and 22 °C). Positive controls BHA (butylated hydroxyanisole), BHT (butylated hydroxytoluene) and TBHQ (t-butyl hydroquinone) were tested at 10 μM in DMSO. Vertical bars represent the averages of two experiments ± SD.

ing to the previously published procedure from our laboratory (Vareed et al., 2006). COX-1 enzyme was prepared from ram seminal vesicles whereas; COX-2 enzyme was prepared from insect cell lysate. The rate of oxygen consumption during the initial phase of the enzyme-mediated reaction, with arachidonic acid as substrate, was measured using a Model 5300 biological oxygen monitor (Yellow Spring Instruments Inc., Yellow Spring, OH). Aspirin (60 μM), Celebrex (26 nM), Vioxx (32 nM) and Arcoxia (120 nM) were used as positive controls. Extracts were assayed at 100 ppm, anthocyanins at 5 μM and compound **4** at 50 μM concentrations. Water extracts and pure anthocyanins were assayed as solutions prepared in water. Compound **4** and methanolic extracts were assayed as solutions prepared in DMSO.

3. Results and discussion

Although the production of red lettuce is increasing, consumers still pay a higher price for red lettuce than for green lettuce. This is probably due to the health benefits attributed to the red colour, such as by anthocyanins, in red lettuce. This assumption and price difference prompted us to compare the functional food qualities, using *in vitro* bioassays, of commercial red and green lettuce grown under field conditions.

For comparison, green and red lettuces were extracted sequentially with water and methanol under laboratory conditions (22 °C). The resulting extracts were then assayed for lipid peroxidation (LPO) and cyclooxygenase enzyme (COX) inhibitory activities at 100 ppm. Amongst the extracts tested, the water extract of red lettuce prepared at 22 and 38 °C inhibited LPO by 94.8% and 70.4%, respectively, (Fig. 1). Similarly, water extracts of green lettuce prepared at 22 and 38 °C gave 73.1% and 61.7% of LPO inhibition, respectively, at 100 ppm (Fig. 1). The COX enzyme inhibitory assays for red and green lettuce extracts were performed by using COX-1, and -2 isozymes. The water and methanol extracts of red lettuce, prepared at 22 and 38 °C, inhibited COX-2 enzyme by 89.7%, 84.9% and 87.8%, 72.2%, respectively, (Fig. 2). The water

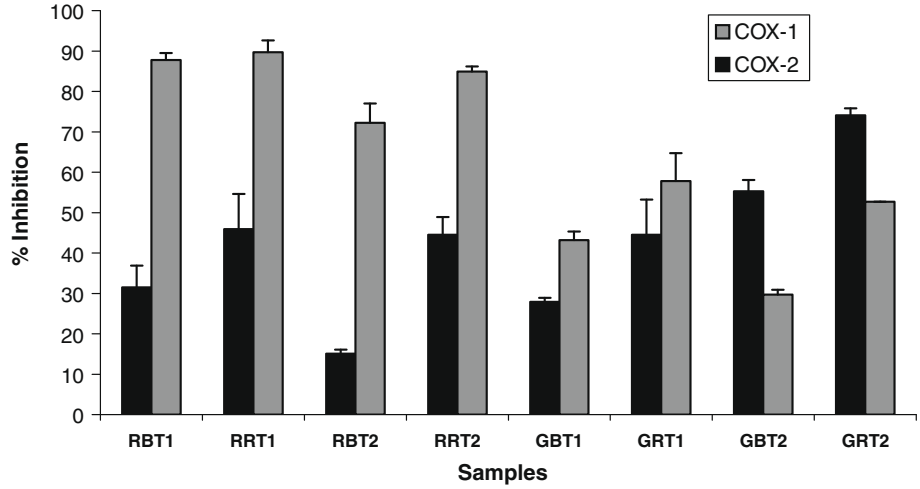

Fig. 2. *In vitro* COX-1 and COX-2 enzyme inhibitory activities of red and green lettuce extracts at 38 °C and 22 °C (RBT1, RRT1: red lettuce water-extracts at 38 °C and 22 °C; RBT2, RRT2: red lettuce methanolic extracts of the residue from water extraction at 38 °C and 22 °C; GBT1, GRT1: green lettuce water-extracts at 38 °C and 22 °C; GBT2, GRT2: green lettuce methanolic extracts of the residue after water extraction at 38 °C and 22 °C). The extracts were tested at 100 ppm. Vertical bars represent the averages of two experiments ± SD.

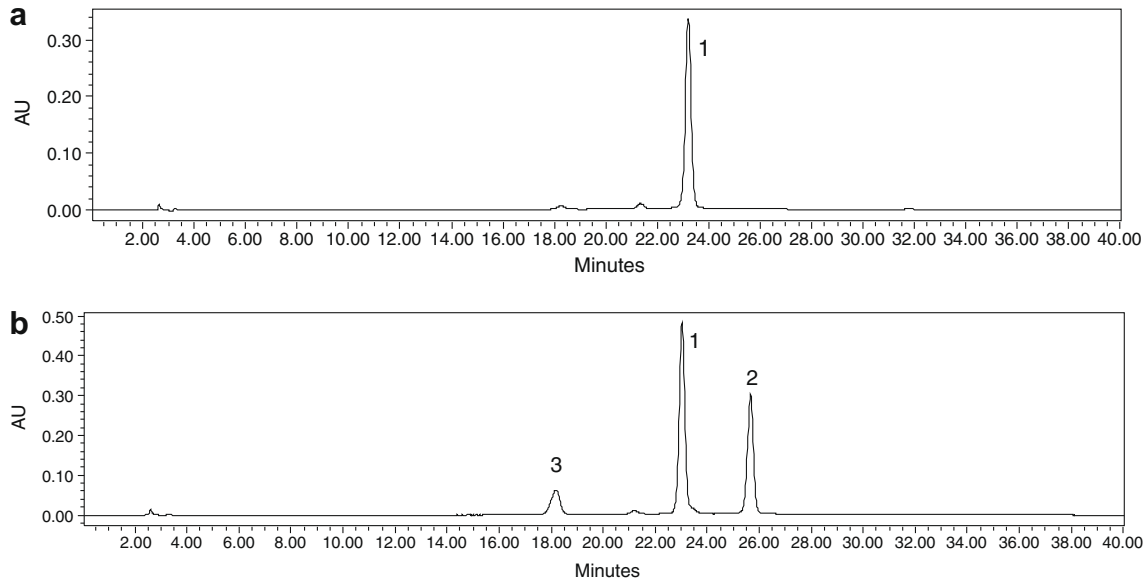

Fig. 3. (a) HPLC profile of anthocyanin in red lettuce, variety "Cherokee". Peak 1. (cyanidin 3-*O*-(6″-malonyl-β-glucopyranoside) and (b) HPLC profile of anthocyanins in the extract of red lettuce stored at room temperature for 1 h. Peak 1. (cyanidin 3-*O*-(6″-malonyl-β-D-glucopyranoside); Peak 2. (methyl ester of cyanidin-3-*O*-(6″-malonyl-β-D-glucopyranoside) and Peak 3. (cyanidin-3-*O*-β-D-glucopyranoside).

extracts of red lettuce, yielded at 22 and 38 °C, were similar in their COX-2 enzyme inhibition at 100 ppm test concentration. Water and methanol extracts of green lettuce prepared at 22 °C inhibited COX-2 enzyme by 57.8% and 52.7%, respectively, at 100 ppm (Fig. 2). Interestingly, the methanol extract of green lettuce showed 74.1% of inhibition against COX-1 enzyme (Fig. 2). Although the activity seems to be higher at 100 ppm for extracts prepared at 22 °C, the percentage weight of extracts obtained at 38 °C treatment was 3-fold higher than that of extracts at 22 °C. Therefore, the overall biological activity of fresh lettuce on a per gramme basis is higher at *in vivo* temperature than under laboratory conditions.

The primary difference between red and green lettuce is in their anthocyanin contents. Since the water extract of the red lettuce showed higher biological activity and contained anthocyanin, we have characterised the anthocyanin in the red lettuce variety studied. The HPLC profile of the extract showed only one anthocyanin, when analysed immediately after extraction, and it was characterised as cyanidin-3-*O*-(6″-malonyl-β-glucopyranoside (**1**) (Fig. 3a). However, purification or storage of the extract results in the methylation or loss of the malonic acid moiety to yield anthocyanins **2** and **3** (Figs. 3b and 4). Anthocyanins were purified using XAD-2 resin, C-18 MPLC followed by HPLC. During this process, anthocyanin **1** was converted to anthocyanin **2** (cyanidin-3-*O*-(6″-malonyl-β-glucopyranoside methyl ester) and then finally to **3** (cyanidin-3-*O*-β-glucopyranoside) (Figs. 3b and 4). The structures of anthocyanin **1** and its conversion products were elucidated by NMR and mass spectral analysis. The data were in agreement with the published spectral data of anthocyanins **1** and **2** (Andersen & Fossen, 1995). The isolation and characterisation of the acylated anthocyanins **1** and **2** from commercial red lettuce variety "Cherokee" are here reported for the first time.

The reported isolation of several anthocyanins from fruits with LPO and COX enzyme inhibitory activities (Mulabagal et al., 2007; Seeram et al., 2003; Tall et al., 2004; Wang et al., 1999), prompted us to evaluate similar biological activities of anthocyanins **1** and **2** isolated from red lettuce. Based on our experience with cyanidin-3-*O*-glucoside (**3**) and related anthocyanins, we tested **1** and **2** for LPO and COX enzyme inhibitory activities. The biological activities observed were similar to all three anthocyanins (Figs. 5 and 6). The positive controls used in the LPO assay were BHA, BHQ and TBHQ and were tested at 10 μM concentration. Similarly, anti-inflammatory drugs, Arcoxia (128 nM), Aspirin (60 μM), Celebrex (26 nM) and Vioxx (32 nM) were used as positive controls in the COX assay. Anthocyanins **1** and **2** inhibited COX-2 enzyme by 78.9% and 84.3%, respectively, when tested at 5 μM (Fig. 6). Both anthocyanins inhibited COX-1 enzyme by 64% and 65.8%, respectively, when tested at the same concentration (Fig. 6). Excellent LPO and COX inhibitory activities of anthocyanin **3** have recently been reported from our laboratory and hence were not repeated in this study (Mulabagal et al., 2007). This is the first report of the LPO, COX-1 and -2 enzyme inhibitory activities of anthocyanins **1** and **2**. Also, the activity of anthocyanins in red lettuce accounts for the higher activity observed for red lettuce than for green lettuce.

We have also analysed the methanolic extracts of red and green lettuce for bioactive principles. The red lettuce extract was fractionated by a silica gel MPLC column, using chloroform and mixtures of chloroform and methanol with increasing polarities. Low polar fractions yielded a fatty acid, linoleic acid, and a flavanone, quercetin. Medium and high polar fractions were purified to yield phenolic acids, caffeic, ferulic and chicoric (**4**) acids. The structures of these compounds were determined by comparison of NMR and mass spectral data with those of the published spectral data (Bilia et al., 1996; Dutta et al., 2007; Maeda et al., 2006; Zhang et al., 2003). This is the first report on the isolation of phenolic acids from red lettuce variety 'Cherokee'.

The purification of the methanolic extract of green lettuce resulted in the isolation of linoleic acid, quercitin glucoside, and chicoric acid (**4**). The majority of the extract contained chlorophyll, along with these compounds in minor quantities. Also, linoleic acid is considered as an essential dietary ingredient, with antioxidant

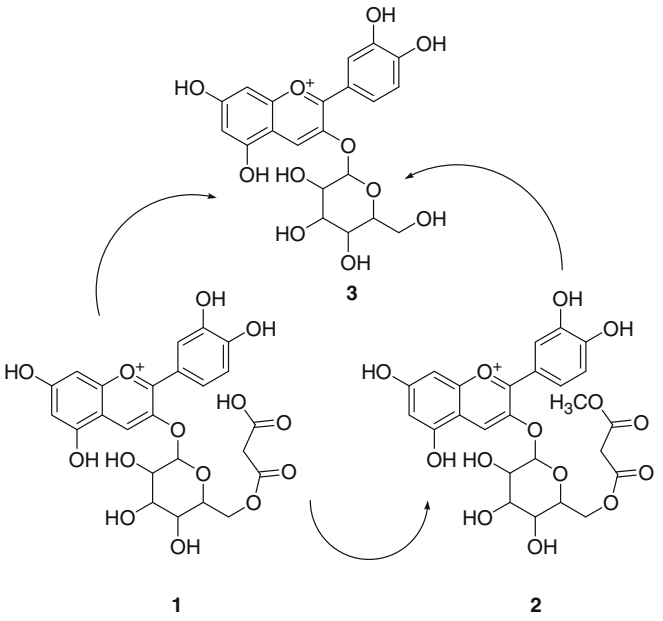

Fig. 4. Structure of anthocyanin **1** (cyanidin-3-*O*-(6″-malonyl-β-D-glucopyranoside), **2** (cyanidin-3-*O*-(6″-malonyl-β-D-glucopyranoside methyl ester) and **3** (cyanidin-3-*O*-β-D-glucopyranoside).

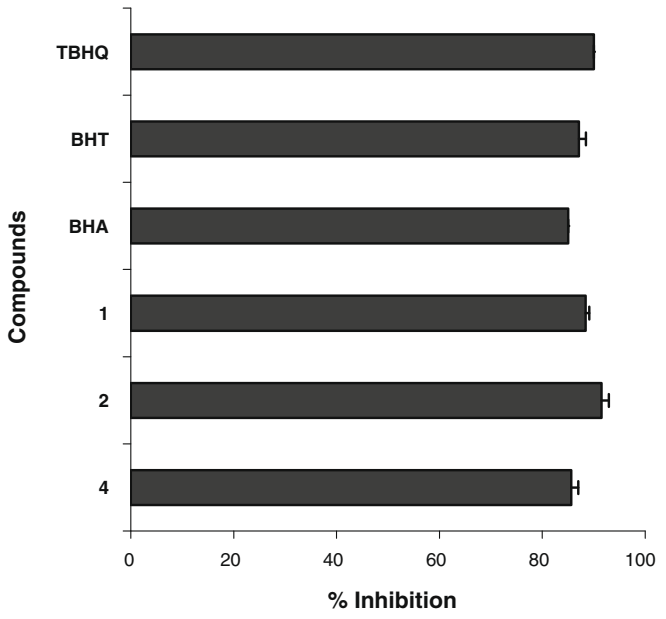

Fig. 5. Lipid peroxidation inhibitory activity of compounds **1** (cyanidin-3-*O*-(6″-malonyl-β-D-glucopyranoside), **2** (cyanidin-3-*O*-(6″-malonyl-β-D-glucopyranoside methyl ester) and **4** (chicoric acid). Compounds **1** and **2** were tested at 0.25 μg/ml. Compound **4** was tested at 50 μM. Positive controls BHA (butylated hydroxyanisole), BHT (butylated hydroxytoluene) and TBHQ (t-butyl hydroquinone) were tested at 10 μM concentration. The percent inhibition was calculated with respect to solvent control (DMSO) and values represent means ± SD ($n = 2$). Activity of anthocyanin **3** (cyanidin-3-*O*-β-D-glucopyranoside) was reported earlier from our laboratory (Mulabagal et al., 2007).

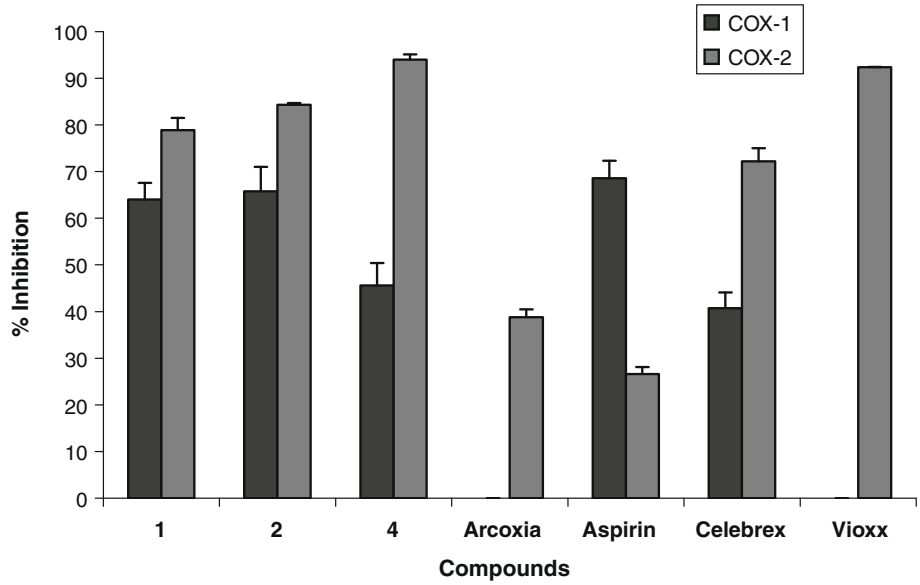

Fig. 6. *In vitro* COX-1 and COX-2 enzyme inhibitory activities of compounds **1** (cyanidin-3-*O*-(6″-malonyl-β-D-glucopyranoside at 0.25 μM), **2** (cyanidin-3-*O*-(6″-malonyl-β-D-glucopyranoside methyl ester at 0.25 μM) and **4** (chicoric acid at 50 μM) and positive controls, Arcoxia (128 nM), Aspirin (60 μM), Celebrex (26 nM) and Vioxx (32 nM). Vertical bars represent the averages of two experiments ± SD. Activity of anthocyanin **3** (cyanidin-3-*O*-β-D-glucopyranoside) was reported earlier from our laboratory (Mulabagal et al., 2007).

and anti-inflammatory properties (Henry, Momin, Nair, & Dewitt, 2002). Isolation of quercetin, caffeic acid, chicoric acid and anthocyanins was reported from other varieties of lettuce (Nicolle & Cardinault et al., 2004; Nicolle & Carnat et al., 2004; Romani et al., 2002). The chicoric acid (**4**), isolated from both green and red lettuce, showed 85.6%, 45.6% and 94% of LPO, COX-1 and -2 enzyme inhibitions at 50 μM, respectively. Other phenolic compounds, monocaffeoyltartaric acid, dicaffeoyltartaric acid, 5-caffeoylquinic acid, caffeoylmalic acid and 3,5-di-*O*-caffeoylquinic acid, have also been reported from lettuce and their contents may vary according to harvesting period (Sobolev, Brosio, Gianferri, & Segre, 2005). This is the first report of the LPO, COX-1 and -2 enzyme inhibitory activities of chicoric acid (**4**) (Figs. 5 and 6).

Most green vegetables contain large quantities of the green pigment chlorophyll. Previous studies from our laboratory have demonstrated that chlorophyll, quercetin and quercetin glucoside inhibited COX-1 and COX-2 enzymes (Reddy, Alexander-Lindo, & Nair, 2005; Vanisree, Alexander-Lindo, DeWitt, & Nair, 2008) *in vitro*. Studies have shown that chicoric acid had antioxidant activity (Thygesen, Thulin, Mortensen, Skibsted, & Molgaard, 2007) and inhibited the replication of HIV virus in tissue culture (Lee, Shin, Lee, & Lee, 2007). From the present study, it is clear that the biological activities observed for the methanolic extracts of red and green lettuce are due to the presence of phenolic compounds.

4. Conclusions

Our results have shown that both red and green lettuce had strong antioxidant and anti-inflammatory activities. However, the anthocyanin in red lettuce may be considered as an additional source of biological activity, based on a number of *in vitro* and *in vivo* experiments suggesting its health-beneficial activities. Our results also demonstrated the difference in biological activities between green and red lettuce due to the variation in phenolic composition. Higher amounts of phenolics, including the anthocyanin, present in red lettuce, may indicate that consumption of red lettuce may provide better health-benefits than green lettuce.

References

Andersen, O. M., & Fossen, T. (1995). Anthocyanins with unusual acylation pattern from stem of *Allium victorialis*. *Phytochemistry, 40*, 1809–1812.
Arora, A., & Strasburg, G. M. (1997). Development and validation of fluorescence spectroscopic assays to evaluate antioxidant efficacy. Application to metal chelator. *Journal of the American Oil Chemists Society, 74*, 1031–1040.
Baur, S., Klaiber, R. G., Koblo, A., & Carle, R. (2004). Effect of different washing procedures on phenolic metabolism of shredded, packaged iceberg lettuce during storage. *Journal of Agricultural and Food Chemistry, 52*, 7017–7025.
Bilia, A. R., Ciampi, L., Mendez, J., & Morelli, I. (1996). Phytochemical investigation of *Licania* genus. Flavanoids from *Licania pyrifolia*. *Pharmceutica Acta Helvictica, 71*, 199–204.
Dupont, S., Mondi, Z., Willamson, G., & Price, K. (2000). Effect of variety, processing, and storage on the flavonoid glycoside and composition of lettuce and chicory. *Journal of Agricultural and Food Chemistry, 48*, 3957–3964.
Dutta, N. K., Mazumdar, K., Mishra, U. S., Dastidar, S. G., & Park, J.-H. (2007). Isolation and identification of flavone (quercetin) from *Butea frondosa* bark. *Pharmaceutical Chemistry Journal, 41*, 269–271.
Gazula, A., Kleinhenz, M. D., Scheerens, J. C., & Ling, P. P. (2007). Anthocyanin levels in nine lettuce (*Lactuca sativa*) cultivars: Influence of planting date and relations among analytic, instrumented, and visual assessments of color. *Hortscience, 42*, 232–238.
Henry, G. E., Momin, R. A., Nair, M. G., & Dewitt, D. L. (2002). Antioxidant and cyclooxygenase activities of fatty acids found in food. *Journal of Agricultural and Food Chemistry, 50*, 2231–2234.
Jayaprakasam, B., Olson, L. K., Schutzki, R. E., Tai, M.-H., & Nair, M. G. (2006). Amelioration of obesity and glucose intolerance in high-fat-fed C57BL/6 mice by anthocyanins and ursolic acid in Cornelian Cherry (*Cornus mas*). *Journal of Agricultural and Food Chemistry, 54*, 243–248.
Jayaprakasam, B., Vareed, S. K., Olson, L. K., & Nair, M. G. (2005). Insulin secretion by bioactive anthocyanins and anthocyanidins present in fruits. *Journal of Agricultural and Food Chemistry, 53*, 28–31.
Kleinhenz, M. D., French, D. G., Gazula, A., & Scheerens, J. C. (2003). Variety, shading, and growth stage effects on pigment concentrations in lettuce grown under contrasting temperature regimens. *Hort Technology, 13*, 677–683.
Lee, S. U., Shin, C. G., Lee, C. K., & Lee, Y. S. (2007). Caffeoylglycolic and caffeoylamino acid derivatives, halfmers of L-chicoric acid, as new HIV-1 integrase inhibitors. *European Journal of Medicinal Chemistry, 42*, 1309–1315.
Llorach, R., Martinez-Sanchez, A., Tomas-Barberan, F. A., Gil, M. I., & Ferrers, F. (2008). Characterization of polyphenols and antioxidant properties of five lettuce varieties and escarole. *Food Chemistry, 108*, 1028–1038.
Maeda, G., Takara, K., Wada, K., Oki, T., Masuda, M., Ichiba, T., et al. (2006). Evaluation of antioxidant activity of vegetables from Okinawa prefecture and determination of some antioxidative compounds. *Food Science and Technology Research, 12*, 8–14.
Mulabagal, V., Van Nocker, S., DeWitt, D. L., & Nair, M. G. (2007). Cultivars of apple fruits that are not marketed with potential for anthocyanin production. *Journal of Agricultural and Food Chemistry, 55*, 8165–8169.

Nair, M. G. (2002). *Method and compositions for producing cherry derived products*. US Patent No. 6, 423-365.

Nicolle, C., Cardinault, N., Gueux, E., Jaffrelo, L., Rock, E., & Mazur, A. (2004). Health effect of vegetable-based diet: Lettuce consumption improves cholesterol metabolism and antioxidant status in the rat. *Clinical Nutrition, 23*, 605–614.

Nicolle, C., Carnat, A., Fraisse, D., Lamaison, J.-L., Rock, E., Michel, H., et al. (2004). Characterization and variation of antioxidant micronutrients in lettuce (*Lactuca sativa*). *Journal of the Science of Food and Agriculture, 84*, 2061–2069.

Reddy, M. K., Alexander-Lindo, R. L., & Nair, M. G. (2005). Relative inhibition of lipid peroxidation, cyclooxygenase enzymes, and human tumor cell proliferation by natural food colors. *Journal of Agricultural and Food Chemistry, 52*, 9268–9273.

Rice-Evans, C. A., Miller, N. J., Bolwell, P. G., Bramley, P. M., & Pridham, J. B. (1995). The relative antioxidant activity of plant derived polyphenolic flavonoids. *Free Radical Research, 22*, 375–383.

Romani, A., Pinelli, P., Galardi, C., Sani, G., Cimato, A., & Heimler, D. (2002). Polyphenols in greenhouse and open-air-grown lettuce. *Food Chemistry, 79*, 337–342.

Seeram, N. P., Cichewez, R. H., Chandra, A., & Nair, M. G. (2003). Cyclooxygenase inhibitory and antioxidant compounds from crab apple fruits. *Journal of Agricultural and Food Chemistry, 51*, 1948–1951.

Seeram, N. P., & Nair, M. G. (2002). Inhibition of lipid peroxidation and structure–activity-related studies of the dietary constituents anthocyanins, anthocyanidins, and catechins. *Journal of Agricultural and Food Chemistry, 50*, 5308–5312.

Sobolev, A. P., Brosio, E., Gianferri, R., & Segre, A. L. (2005). Metabolic profiles of lettuce leaves by high field NMR spectra. *Magnetic Resonance Chemistry, 43*, 625–638.

Tall, J. M., Seeram, N. P., Zhao, C. S., Nair, M. G., & Meyer, R. A. (2004). Tart cherry anthocyanins suppress inflammation-induced pain behavior in rat. *Behavioral Brain Research, 153*, 181–192.

Thygesen, L., Thulin, J., Mortensen, A., Skibsted, L. H., & Molgaard, P. (2007). Antioxidant activity of chicoric acid and alkamides from *Echinacea purpurea*, alone and its combination. *Food Chemistry, 101*, 74–81.

Tsuda, T., Ueno, Y., Aoki, H., Koda, T., Horio, F., Takahashi, N., et al. (2004). Anthocyanin enhances adipocytokine secretion and adipocyte-specific gene expression in isolated rat adipocytes. *Biochemistry and Biophysical Research Communications, 316*, 149–157.

Tsuda, T., Ueno, Y., Kojo, H., Yoshikawa, T., & Osawa, T. (2005). Gene expression profile of isolated rat adipocytes treated with anthocyanins. *Biochimica et Biophysica Acta, 1733*, 137–147.

Vanisree, M., Alexander-Lindo, R. L., DeWitt, D. L., & Nair, M. G. (2008). Functional food components of *Antigonon leptopus* tea. *Food Chemistry, 106*, 487–492.

Vareed, S. K., Reddy, M. K., Schutzki, R. E., & Nair, M. G. (2006). Anthocyanins in *Cornus alternifolia*, *Cornus controversa*, *Cornus kousa* and *Cornus florida* fruits with health benefits. *Life Sciences, 78*, 777–784.

Wang, H., Nair, M. G., & Strasburg, G. M. (1999). Antioxidant and anti-inflammatory activities of anthocyanins and their aglycon from tart cherries. *Journal of Natural Products, 62*, 294–296.

Zhang, Y., Mills, G. L., & Nair, M. G. (2003). Cyclooxygenase inhibitory and antioxidant compounds from the fruiting body of an edible mushroom, *Agrocybe aegerita*. *Phytomedicine, 10*, 386–390.

Food Chemistry 118 (2010) 307–314

Contents lists available at ScienceDirect

Food Chemistry

journal homepage: www.elsevier.com/locate/foodchem

Effects of steaming the root of *Panax notoginseng* on chemical composition and anticancer activities

Shi Sun [a,b], Chong-Zhi Wang [a,b], Robin Tong [a,b], Xiao-Li Li [a,b], Anna Fishbein [a,b], Qi Wang [c], Tong-Chuan He [d], Wei Du [e], Chun-Su Yuan [a,b,*]

[a] Tang Center for Herbal Medicine Research, The Pritzker School of Medicine, University of Chicago, 5841 South Maryland Avenue, MC 4028, Chicago, IL 60637, USA
[b] Department of Anesthesia and Critical Care, The Pritzker School of Medicine, University of Chicago, Chicago, IL, USA
[c] Center for Studies in Constitution Research of Traditional Chinese Medicine, School of Basic Medicine, Beijing University of Chinese Medicine, Beijing, China
[d] Department of Surgery, The Pritzker School of Medicine, University of Chicago, Chicago, IL, USA
[e] Ben May Department for Cancer Research, The Pritzker School of Medicine, University of Chicago, Chicago, IL, USA

ARTICLE INFO

Article history:
Received 25 September 2008
Received in revised form 17 April 2009
Accepted 29 April 2009

Keywords:
Panax notoginseng
Steaming
Saponin
Ginsenoside
High performance liquid chromatography (HPLC)
SW-480 human colorectal cancer cells
Antiproliferation
Apoptosis

ABSTRACT

The root of *Panax notoginseng* has been shown to change its saponin composition upon steaming. This study examines the effects of different steaming times and temperature on notoginseng root for saponin composition and anticancer activities. Steaming decreased the content of notoginsenoside R1, ginsenosides Rg1, Re, Rb1, Rc, R2, Rb3 and Rd, but increased the content of Rh1, Rg2, 20*R*-Rg2, Rg3 and Rh2. Steaming significantly influenced the transformation of Rg3. The amount of ginsenoside Rg3, an anticancer compound, was 5.23-fold greater in root steamed for 2 h at 120 °C than at 100 °C, and 3.22-fold greater when steamed for 4 h than for 1 h at 120 °C. For anticancer effects, the extract of steamed root significantly inhibited proliferation of SW-480 human colorectal cancer cells. The IC_{50} of the steamed extract for 1, 2, 4 and 6 h at 120 °C was 259.2, 131.4, 123.7 and 127.1 μg/mL, respectively; the effect of unsteamed extract was low. Flow cytometric analysis demonstrated that the apoptotic cell induction rates of SW-480 cells were 56.3% and 64.4% with 150.0 and 200.0 μg/mL extract steamed for 6 h. Compared with Rg1 and Rb1, only Rg3 had a significant antiproliferative effect.

1. Introduction

Panax notoginseng belongs to the family of flowering plants known as the Araliaceae. Notoginseng root is used in traditional Chinese medicine to remove blood stasis, stop bleeding, relieve swelling and alleviate pain. The root is the principal component in Yun-Nan-Bai-Yao, a formula used to stop bleeding, decrease inflammation, and relieve pain, and it is the main component of other traditional formulas for coronary heart disease such as Fu-Fang-Dan-Shen-Pian (Compound Salvia Tablet) and Guan-Xin-Dan-Shen-Pian (Guanxin Danshen Tablet) (Commission, 2005). Notoginseng root is also used to treat hyperlipemia and chronic infectious hepatitis (Wang, McEntee, Wicks, Wu, & Yuan, 2006). Based on the US Dietary Supplement Health and Education Act (DSHEA) of 1994 (103rd Congress, 1994), herbal medicines and food supplements, including notoginseng, were classified as dietary supplements. Thus, in the US health food market, notoginseng tea or capsules are being sold as over-the-counter dietary supplements.

Saponins are the main active constituents in notoginseng root (Wang, McEntee et al., 2006). The alcohol extract of the root, which contains 12.4% of saponins, shortened bleeding time and had better haemostatic effects than no treatment or treatment with lipophilic extract or placebo (White, Fan, Song, Tsikouris, & Chow, 2001). The saponin extract of notoginseng also had haemostatic effects when applied externally (White, Fan, & Chow, 2000). Saponins from notoginseng increased the blood flow of the coronary arteries (Huang et al., 1999) and decreased the consumption of oxygen by heart muscles (Chen et al., 1983). So far 59 saponins have been identified in notoginseng root (Wang, McEntee et al., 2006). These saponins have a dammarane structure: 35 belong to the protopanaxadiols (PPD) group, and 24 belong to the protopanaxatriols (PPT) group, and include ginsenosides, notoginsenosides, and gypenosides. Ginsenosides Rg1, Rb1, Rd, and notoginsenoside R1 are considered the major saponins in the root. These saponins, with the exception of R1, are also found in Asian ginseng (*P. ginseng*) and American ginseng (*P. quinguefolius*) (Wang, Mehendale, & Yuan, 2007). Oleanane-type

* Corresponding author. Address: Tang Center for Herbal Medicine Research, The Pritzker School of Medicine, University of Chicago, 5841 South Maryland Avenue, MC 4028, Chicago, IL 60637, USA. Tel.: +1 773 702 1916; fax: +1 773 834 0601.
E-mail address: cyuan@uchicago.edu (C.-S. Yuan).

0308-8146/$ - see front matter © 2009 Published by Elsevier Ltd.
doi:10.1016/j.foodchem.2009.04.122

saponins in Asian and American ginseng, however, have not been found in notoginseng.

In Korea, processed Asian ginseng is called red ginseng. Red ginseng's ability to inhibit lung tumour induced by urethane and/or 9,10-dimethyl-1,2-benzanthracene (DMBA) has been reported (Yun, Yun, & Han, 1983). Subsequently, other reports of ginseng's anticancer activity after different processing methods were published (Keum et al., 2000; Kim et al., 2000; Kitts, Popovich, & Hu, 2007; Popovich & Kitts, 2004). Pharmacological tests attributed the anticancer activity to the derivatives of the primary ginsenosides naturally generated by intestinal bacteria or by acid hydrolysis (Bae, Han, Kim, & Kim, 2004), not by the primary ginsenosides themselves. Some experiments (Wang, Zhao et al., 2007) suggested that the number of sugar moieties, and the differences in the substituent groups affect anticancer activity. This information may be useful for evaluating the structure–function relationship of other ginsenosides and their aglycones and for development of novel anticancer agents. For example, 20(*R*)-dammarane-3β,12β,20,25-tetrol and 20(*S*)-protopanaxadiol had significant dose-dependent effects on apoptosis, proliferation, and cell cycle progression (Wang, Zhao et al., 2007). Steaming Asian or American ginseng transformed original ginsenosides into anticancer compounds (Nam, 2005; Wang, Zhang et al., 2006; Wang, Aung et al., 2007).

Notoginseng root, too, has been shown to have anticancer activity (Konoshima, Takasaki, & Tokuda, 1999; Wang, Xie et al., 2007), and steaming it can increase its anticancer activity (Wang, Xie, 2007). However, the steaming parameters that affect saponin content and anticancer activities in notoginseng have not been systematically evaluated. The aim of this study was to analyse the influence of different steaming temperatures and duration on changes in saponin content of notoginseng root and to correlate the observed changes to antiproliferative activities in SW-480 human colorectal cancer cells.

2. Materials and methods

2.1. Cell lines, chemicals and biochemicals

SW-480 human colorectal cancer cells were purchased from American Type Culture Collection (Manassas, VA). All solvents were of high-performance liquid chromatography (HPLC) grade (Fisher Scientific, Norcross, GA). Milli Q water was supplied by a water purification system (US Filter, Palm Desert, CA). Standards for ginsenosides Rb1, Rb2, Rc, Rd, Re and Rg1 were obtained from the Indofine Chemical Company (Somerville, NJ); for ginsenosides Rb3, Rg2, Rg3, Rh1, Rh2 and 20(*R*)-ginsenoside Rg2 (20*R*-Rg2), from the Delta Information Center for Natural Organic Compounds (Xuancheng, Anhui, China). All standards were of biochemical-reagent grade and at least 95% pure as confirmed by HPLC. Plastic materials were purchased from Falcon Labware (Franklin Lakes, NJ). Trypsin, Leibovitz's L-15 medium, foetal bovine serum (FBS), and penicillin/streptomycin solution were obtained from Mediatech Inc. (Herndon, VA). A CellTiter 96 Aqueous One Solution Cell Proliferation Assay kit was obtained from Promega (Madison, WI). An Annexin V-FITC Apoptosis Detection kit was obtained from BD Biosciences (San Diego, CA).

2.2. Plant material and preparation of the extract

The roots of *P. notoginseng* were obtained from Wenshan, Yunnan, China. The voucher samples were deposited at the Tang Center for Herbal Medicine Research at University of Chicago.

Notoginseng root was pulverised, passed through a 40 mesh screen and was steamed at 100 °C for 2 h, or at 120 °C for 1, 2, 4 and 6 h. The steamed samples were frozen for 2 h before being lyophilised.

For the HPLC analysis, dried steamed notoginseng samples were pulverised, and 0.5 g of the ground unsteamed or steamed samples was extracted with 100% methanol in a Soxhlet extractor for 8 h while the water bath was maintained at 85 °C. The extracts were concentrated *in vacuo*, transferred into a 25 mL volumetric flask, and diluted to the desired volume with methanol; the solutions were stored at −20 °C until HPLC analysis.

For the *in vitro* anticancer studies, 10 g of dried powders of unsteamed or steamed notoginseng were extracted with 200 mL of 70% ethanol for 4 h; the water bath was maintained at 90 °C. When cooled, the solution was filtered with P8 filter paper (Fisher Scientific, Pittsburgh, PA) and the filtrate was collected. The residue was extracted with 100 mL of 70% ethanol once more and then filtered while the solution was cooled. The filtrates were combined, and the solvent was evaporated *in vacuo*. The dried extract was dissolved in 100 mL of water and then extracted with water-saturated *n*-butanol. The *n*-butanol phase was evaporated under vacuum and then frozen for 2 h and lyophilised.

2.3. HPLC analysis

The HPLC system included a Waters 2965 instrument (Milford, MA) with a quaternary pump, an automatic injector, a photodiode array detector (Model 996), and Waters Millennium 32 software for peak identification and integration.

HPLC conditions: Prodigy ODS (2) column, (5 μ, 3.2 × 250 mm; Phenomenex), with a guard column, (5 μ, 3.2 × 7.5 mm; Phenomenex). Solvent system: A – MeCN, B – H_2O; Gradient 17.5–21% over 20 min, 21–26% over 3 min, 26% A for 19 min, 26–36% A over 13 min, 36–50% A over 9 min, 50–68% A over 9 min, 68–80% A over 2 min, 80% A for 3 min, 80–17.5% A over 5 min, 17.5% A for 6 min. Flow rate: 1 mL/min; Injection volume: 20 μL; DAD conditions: 202 nm. The linearity of this method was assayed by analysing standard solutions in the range of 2–400 μg/mL for notoginsenoside R1 and 12 other ginsenosides. Calibration curves were constructed from the measured peak areas and the related amount of ginsenosides.

Notoginsenoside R1, ginsenosides Rb1, Rb2, Rb3, Rc, Rd, Re, Rg1, Rg2, 20*R*-Rg2, Rg3, Rh1, and Rh2 identified in extract samples were identified by comparison of their retention times with those obtained from the chromatograms of mixed ginsenoside standards. The content of saponins in each sample was calculated using standard curves of notoginsenoside and ginsenosides.

2.4. Cell culture

SW-480 human colorectal cancer cells were grown in the Leibovitz's L-15 medium supplemented with 10% FBS and 50 IU penicillin/streptomycin in a humidified atmosphere at 37 °C. When the cells were in the late log/early plateau phase (with about 90% of the surface area covered) and healthy and free of contamination, the cell culture medium was removed. After the cells were washed with PBS to remove any trace of serum that would inactivate trypsin, the PBS was discarded. One millilitre of trypsin was added to a 25 mL flask to break the cell–cell and cell–substrate links. Fresh culture medium containing serum (5 mL) was then added to inactivate the trypsin in the cell suspension. After pipetting this suspension, a single-cell suspension was prepared. The cell suspension was then counted for accurate cell density. An aliquot of the cell suspension was placed into a new 25 mL flask with the full amount of cell culture medium (10 mL) required for the flask size. The medium was then changed if necessary until the next subculture.

2.5. Cell proliferation analysis

Unsteamed or steamed notoginseng root extracts, and ginsenosides, were dissolved in 50% ethanol and then stored at −20 °C before use. Cells were seeded in a flat-bottomed 96-well plate with a multichannel pipet (1×10^4 cells/well). After 24 h, the medium was removed and 200 μL of fresh culture medium was added to each well. Various concentrations of extracts were added to the wells. The final concentration of ethanol in tested groups was 0.5%. Controls were exposed to culture medium containing the same quantity of ethanol without drugs. All experiments were performed at least in triplicate.

At the end of the drug exposure period (48 h), the medium was removed from all wells and 100 μL of fresh medium and 20 μL of CellTiter 96 aqueous solution was added to each well. CellTiter 96 aqueous solution is composed of a tetrazolium compound, 3-(4,5-dimethylthiazol-2-yl)-5-(3-carboxymethoxyphenyl)-2-(4-sulphophenyl)-2*H*-tetrazolium, an electron-coupling reagent (phenazine methosulphate), and buffer. When the solution contacts viable cells, it is bioreduced by dehydrogenase enzymes in metabolically active cells into a formazan product. The quantity of formazan product, measured by the amount of absorbance at 490 nm, is directly proportional to the number of living cells in culture. The plate was then incubated for 1 h in a humidified atmosphere at 37 °C; 60 μL of medium from each well were transferred to an ELISA 96-well plate, and the absorbance of the formazan product at 490 nm was measured. The blank was recorded by measuring the absorbance at 490 nm with wells containing medium but no cells. Results were expressed as per cent of control (ethanol vehicle set at 100%).

2.6. Apoptosis assay using flow cytometry

Annexin V is a Ca^{2+}-dependent phospholipid-binding protein that binds strongly to phosphatidylserine residues on the cell membrane. In a normal cell, these residues are on the inner surface of the membrane and therefore inaccessible to annexin V. In the early stage of apoptosis, the phosphatidylserine residues are translocated to the outside of the cell at which point the cells die. Cell apoptosis can be assayed by flow cytometry after staining with annexin V (Vermes, Haanen, Steffens-Nakken, & Reutelingsperger, 1995). Cells were seeded in 24-well tissue culture plates. After culture for 2 days, the medium was changed and notoginseng extracts were added. After treatment for 48 h, cells floating in the medium were collected. The adherent cells were detached with trypsin. Then culture medium containing 10% FBS (and floating cells) was added to inactivate trypsin. After being pipetted gently, the cells were centrifuged for 5 min at 600*g*. The supernatant was removed, and cells were stained with annexin V-FITC. Untreated cells were used as control. Cells were analysed immediately after staining using a FACScan flow cytometer (Becton Dickinson, Mountain View, CA) and FlowJo software (Tree Star, Ashland, OR). For each measurement, at least 20,000 cells were counted.

2.7. Statistical analysis

Data are presented as mean ± standard deviation (SD). A one-way ANOVA was employed to determine whether the results had statistical significance. In some cases, Student's *t*-test was used

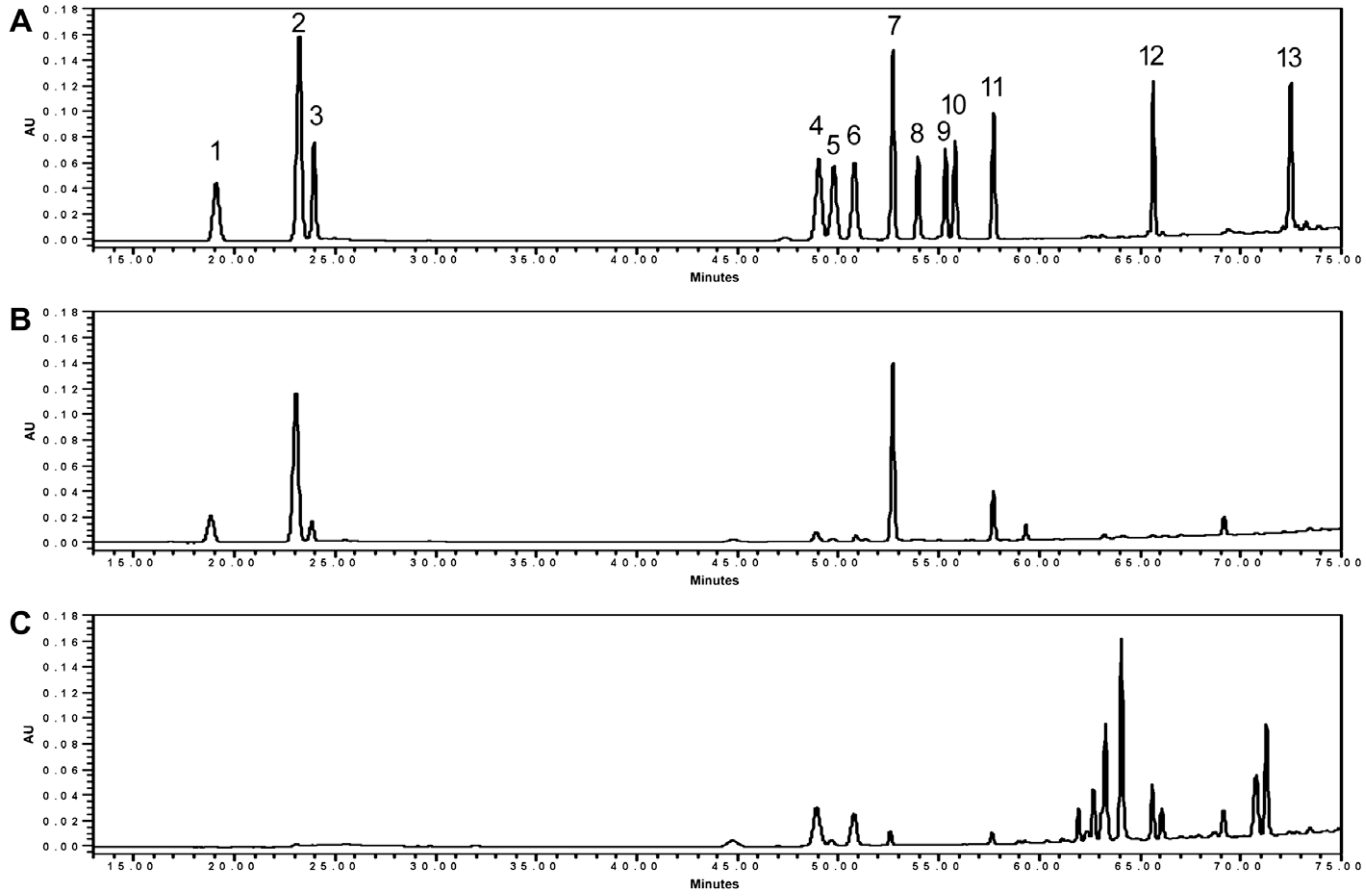

Fig. 1. Typical chromatograms of standard (A), unsteamed (B), and steamed (C) at 120 °C for 4 h notoginseng recorded at 202 nm. Peaks: notoginsenoside R1 (**1**), ginsenosides Rg1 (**2**), Re (**3**), Rh1 (**4**), Rg2 (**5**), 20*R*-Rg2 (**6**), Rb1 (**7**), Rc (**8**), Rb2 (**9**), Rb3 (**10**), Rd (**11**), Rg3 (**12**) and Rh2 (**13**).

Table 1
Saponin content in notoginseng root steamed at 100 °C or 120 °C (mean ± SD).

Notoginsenoside/Ginsenosides	Unsteamed	Steamed				
		100 °C 2 h	120 °C 1 h	120 °C 2 h	120 °C 4 h	120 °C 6 h
R1	6.78 ± 0.05	5.48 ± 0.09	2.71 ± 0.09	1.01 ± 0.04	N.D.	N.D.
Rg1	23.17 ± 0.15	19.90 ± 0.42	9.82 ± 0.18	4.16 ± 0.07	0.42 ± 0.02	0.24 ± 0.02
Re	3.29 ± 0.01	2.64 ± 0.10	1.26 ± 0.01	0.52 ± 0.05	N.D.	N.D.
Rh1	1.49 ± 0.02	2.39 ± 0.06	5.19 ± 0.15	7.23 ± 0.29	9.48 ± 0.06	9.99 ± 0.16
Rg2	0.48 ± 0.05	0.58 ± 0.05	0.80 ± 0.05	0.94 ± 0.10	1.12 ± 0.03	0.95 ± 0.10
20*R*-Rg2	N.D.	0.85 ± 0.02	3.48 ± 0.07	5.54 ± 0.19	8.17 ± 0.15	8.43 ± 0.47
Rb1	26.91 ± 0.12	21.28 ± 0.57	13.75 ± 0.11	8.46 ± 0.09	2.46 ± 0.03	2.02 ± 0.10
Rc	0.23 ± 0.06	0.10 ± 0.01	0.09 ± 0.02	N.D.	N.D.	N.D.
Rb2	0.22 ± 0.08	0.11 ± 0.01	0.06 ± 0.01	N.D.	N.D.	N.D.
Rb3	0.08 ± 0.01	0.37 ± 0.52	0.08 ± 0.01	N.D.	N.D.	N.D.
Rd	5.71 ± 0.19	4.91 ± 0.09	3.61 ± 0.02	2.80 ± 0.07	1.54 ± 0.03	1.51 ± 0.02
Rg3	0.33 ± 0.01	0.90 ± 0.01	2.77 ± 0.09	4.70 ± 0.45	8.50 ± 0.08	9.19 ± 0.06
Rh2	N.D.	N.D.	0.11 ± 0.02	0.20 ± 0.01	0.39 ± 0.02	0.44 ± 0.01

$n = 3$; N.D., not detected; values are expressed as mg/g of dry weight.

for comparing two groups. The level of statistical significance was set at $p < 0.05$.

3. Results and discussion

3.1. Effects of temperature on notoginseng constituents

Typical HPLC chromatograms of saponin standards, and unsteamed and steamed notoginseng root are shown in Fig. 1. The content of 13 ginsenosides in steamed notoginseng is shown in Table 1. Compared to unsteamed notoginseng, in root steamed at 100 °C for 2 h, the total content of confirmed saponins decreased slightly from 68.70 to 59.50 mg/g. Among the main saponins, ginsenoside Rg1 decreased from 23.17 to 19.90 mg/g, and Rb1 decreased from 26.90 to 21.28 mg/g; notoginsenoside R1 decreased from 6.78 to 5.48 mg/g; ginsenoside Rg3 increased from 0.33 to 0.90 mg/g. At 120 °C for 2 h, total ginsenoside content decreased to 35.56 mg/g. Rg1 was 4.16 mg/g; Rb1, 8.46 mg/g; notoginsenoside R1, 1.01 mg/g; Rg3, 4.70 mg/g. The changes in saponin content in notoginseng (Fig. 2) were the same as those in American ginseng berry (Wang, Zhang et al., 2006); total saponin content was reduced significantly, while Rg3 increased significantly.

Processing red ginseng with heat inactivates catabolic enzymes that deteriorate antioxidant-like substances, which inhibit formation of lipid peroxide (Nam, 2005). Steaming ginseng at temperatures higher than 100 °C enhanced biological activity (Kim et al., 2000). In our study total saponin content decreased at 120 °C, but ginsenoside Rg3, a recognised active anticancer reagent (Mochizuki et al., 1995), was increased by more than three-fold at 2 h compared to notoginseng root steamed at 100 °C for 2 h. This change shows that the chemical properties of steamed notoginseng root can markedly influence its pharmacological properties.

3.2. Effects of steaming duration on notoginseng root constituents

Typical HPLC chromatograms of notoginseng root steamed at 120 °C for 4 h are shown in Fig. 1C. The content of 13 ginsenosides in steamed notoginseng root is shown in Table 1. Compared to unsteamed notoginseng, in root steamed at 120 °C for 1, 2, 4 and 6 h, the total content of confirmed saponins significantly decreased from 68.70 to 43.74, 35.56, 32.07 and 32.78 mg/g, respectively. After steaming for 4 h, total saponin content was not shown to be significantly different, but notoginseng R1 and ginsenosides Rg1, Re, Rb1, R3, Rb2, Rb3 and Rd decreased during the steaming process. After 4 h of steaming, R1, Re, Rc, Rb2, Rb3 and Rd, were difficult to detect in the chromatogram (Table 1). On the other hand, ginsenoside Rg3, which is a trace saponin in unsteamed notoginseng root, significantly increased during the steaming process (Fig. 1C). The peak areas of four ginsenosides, Rh1, Rg2, 20*R*-Rg2, and Rh2, and two other peaks that could not be identified for lack

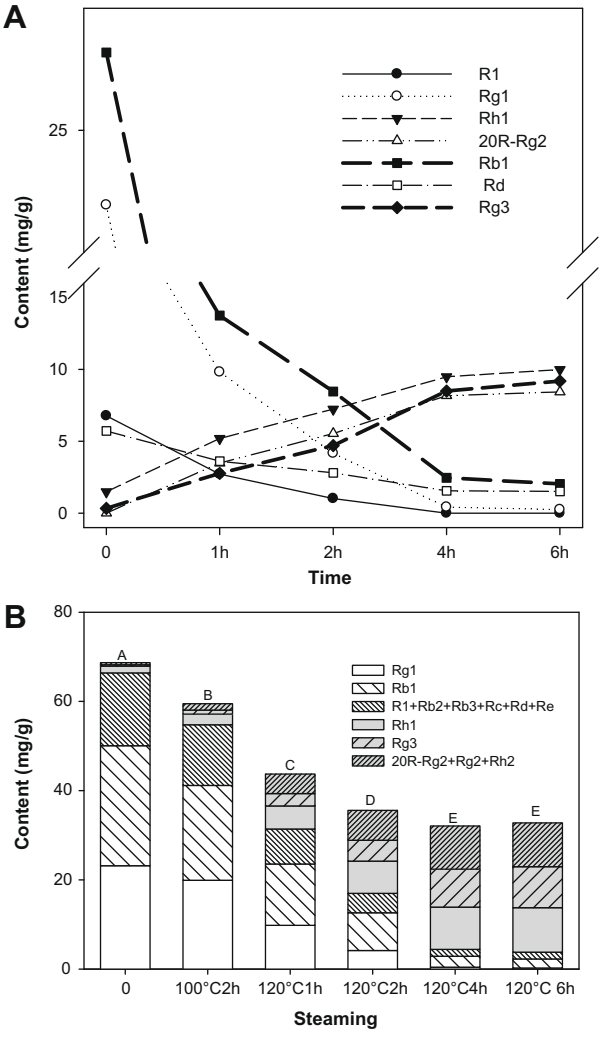

Fig. 2. Saponin content in steaming notoginseng root. The content of (A) typical ginsenosides was changed during the steaming at 120 °C: notoginsenoside R1, ginsenoside Re, Rc, Rb2 and Rb3 disappear as steaming time increases, ginsenosides 20*R*-Rg2, Rh1, and Rg3 significantly increase; and (B) the total ginsenoside content also was changed and with a significant difference between unsteaming and steaming at 100 °C for 2 h, at 120 °C for 1, 2, 4 and 6 h (not between steaming at 120 °C for 4 and 6 h) by multiple comparison [using analysis of least significant difference (LSD) and shortest significant ranges (SSR)].

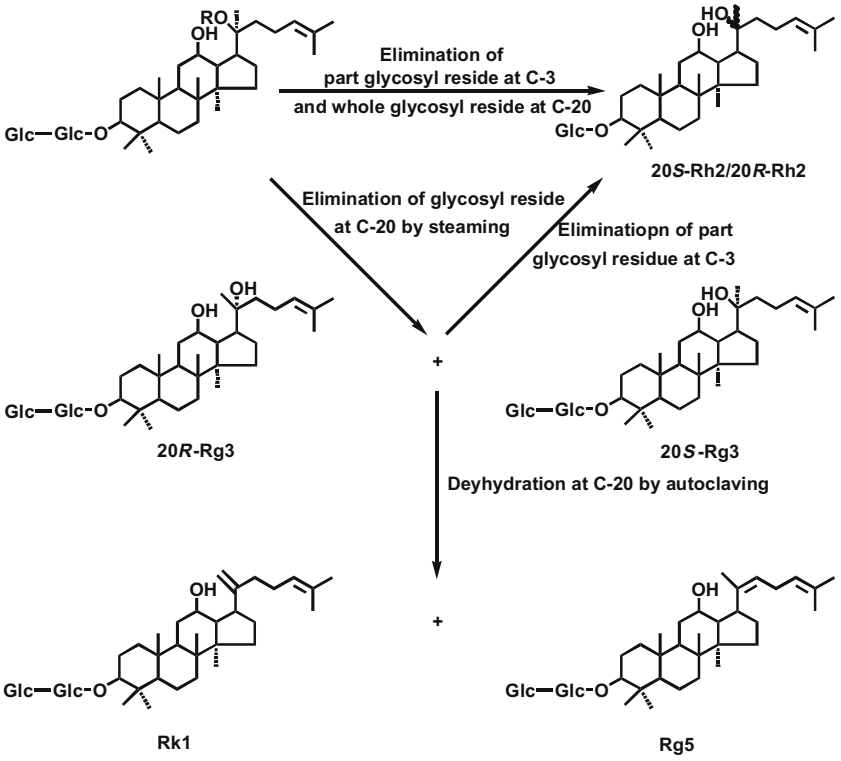

Fig. 3. Proposed saponin transformation in notoginseng root after steaming.

of standards were significantly increased. These two unidentified peaks may be derivates of ginsenoside Rg3, and based on their chromatographic pattern and previous isolation from steamed notoginseng, could be ginsenosides Rk1 and Rg5 (Fig. 3) (Lau, Seo, Woo, & Koh, 2004; Liao, Wang, Zhang, & Yang, 2008).

In some experiments Rk1 (Park et al., 2002) and Rg5 (Park et al., 2002; Yun, 2003) had more anticancer activity than did Rg3. Yun (2003) indicated that Asian ginseng may be a non-organ-specific cancer-preventive agent and the effect of *P. ginseng* could be attributed to ginsenosides Rg3, Rg5 and Rh2. In an MTT assay using SK-Hep-1 hepatoma cancer cells, the GI_{50} (the concentration that inhibits growth by 50%) of Rk1 and Rg5 was 11 and 13 μg/mL, respectively, lower than that of 41 μg/mL for Rg3.

The identity of the confirmed saponins following heating is shown in Fig. 2A. Ginsenoside Rb1 (26.91 mg/g) and Rg1 (23.17 mg/g), the main constituents in notoginseng root, were influenced significantly by steaming temperature and duration. After steaming at 120 °C for 1 h, Rb1 and Rg1 decreased 51.1% and 41.4%, respectively; after 6 h they decreased from 13.75 and 9.8 mg/g to 2.02 and 0.24 mg/g, respectively. Notoginsenoside R1, ginsenoside Rd and Re also decreased with time during steaming (Fig. 2A). Compared to the unsteamed root containing 6.78 mg/g of R1, steaming from 1 to 4 h decreased its content from 2.71 mg/g to undetectable; Rd was decreased from 5.71 mg/g in unsteamed root to 3.6 mg/g after steaming for 1 h and to 1.5 mg/g after 6 h; Re changed from 3.29 mg/g in the unsteamed root to 1.26 mg/g after steaming for 1 h and to undetectable after 4 h (Table 1 and Fig. 2A).

The levels of ginsenosides Rh1, 20*R*-Rg2, and Rg3, on the other hand, significantly increased during the steaming process (Fig. 2A). Rh1 increased from 1.49 mg/g in unsteamed notoginseng root to 5.19 mg/g after steaming for 1 h and to 9.99 mg/g after 6 h; 20*R*-Rg2 was undetectable in unsteamed root and after 1 h steaming was increased to 3.48 mg/g, and after 6 h to 8.43 mg/g; Rg3 increased from 0.33 mg/g to 2.77 and 9.19 mg/g, respectively. Steaming duration changed total saponin content from 49.1% in

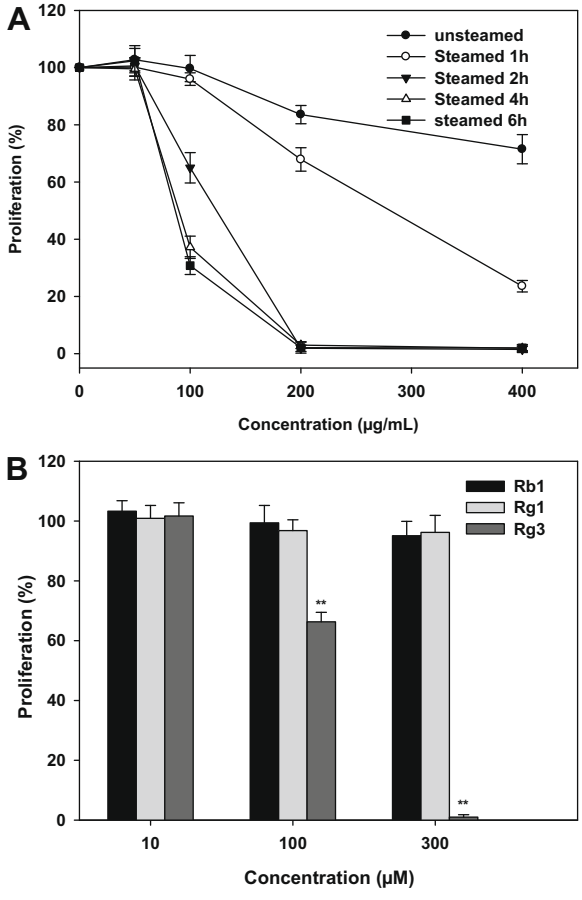

Fig. 4. Percentage of proliferation of SW-480 human colorectal cells treated for 48 h with (A) extract of unsteamed notoginseng or notoginseng steamed for 1–6 h, and (B) three ginsenosides. Statistical significance (**) was set at $p < 0.01$.

notoginseng root after steaming for 2 h, to 81.5% after 4 h, and to 84.2% after 6 h. The differences were not significant when steaming duration was longer than 4 h.

Ginsenoside Rg3 has been found to inhibit the growth of tumour cells (Mochizuki et al., 1995). Rg3 can be obtained via biological transformation or chemical synthesis (Bae et al., 2004), but the process is complicated and the yield is limited. The chemical structure of ginsenoside Rg3 is (3β,12β)-12,20-dihydroxydammar-24-en-3-yl 2-*O*-β-D-glucopyranosyl-β-D-glucopyranoside, and it may be naturally derived from other ginsenosides that are glycosylated at C-20 (S) as shown in Fig. 3. Shibata, Ando, and Tanaka (1966) obtained Rg3 following mild acidic hydrolysis of ginsenosides Rb1, Rb2 and Rc, and it can be isolated from white ginseng (Kaku & Kawashima, 1974) and red ginseng (Kitagawa, Yoshikawa, Yoshihara, Hayashi, & Taniyama, 1983). Rg3 content is lower in white ginseng than in red ginseng, which is produced by steaming at a temperature of 100 °C. When steaming temperature was increased to 120 °C, ginsenoside Rg3 was increased significantly compared to steaming at 100 °C. The result was similar to steaming American ginseng at 120 °C (Wang, Zhang et al., 2006; Wang, Aung et al., 2007), except that the main substrate was slightly different. Ginsenoside Rb1 may be the parent moiety of Rg3 as it is one of the main constituents in notoginseng root with structural similarity.

3.3. Effects of steamed notoginseng root extract on human colorectal cancer cells

The active principal constituents of notoginseng include saponins, polysaccharides, flavonoids, and volatile oils (Wang, McEntee et al., 2006). Investigations of the anticancer activity of notoginseng have focused on the same saponins from red ginseng: ginsenoside Rg3 and Rh2. Extracts from notoginseng root unsteamed or steamed at 100 °C for 2 h or at 120 °C for 1, 2, 4 or 6 h were tested for their effects on SW-480 human colorectal cancer cells (Fig. 4).

SW-480 cells treated for 48 h with an unsteamed, alcohol extract of notoginseng root at concentrations of 50–400 μg/mL showed no significant antiproliferative effects. In notoginseng root steamed for 1, 2, 4 or 6 h, IC_{50} was 259.2, 131.4, 123.7 and 127.1 μg/mL, respectively. Steaming significantly increased the anticancer effect of notoginseng root. At the lower concentration, cell growth was significantly inhibited when steaming lasted for more than 2 h (Fig. 4A).

To confirm the exact constituent responsible for antiproliferation, Rb1 and Rg1, major constituents in unsteamed notoginseng root, and Rg3, a major constituent in steamed notoginseng root, were tested for antiproliferative effects on human colon cancer cells. At concentration of 300 μM, Rb1 and Rg1 inhibited proliferation by <5%, whereas the same concentration of Rg3 inhibited proliferation by approximately 99% antiproliferative effect on SW-480 cells.

Whereas unsteamed root contained approximately 0.33 mg/g ginsenoside Rg3, when steamed for 6 h, the Rg3 content was 9.19 mg/g and produced maximum inhibitory effects on cell proliferation. Steamed notoginseng root may possess other active components besides Rg3 to inhibit the proliferation of SW-480 cells. For example, at a concentration of 100 μM (78.5 μg/mL), ginsenoside Rg3 itself inhibited cell proliferation by 33.7%; however, the extract inhibited cell proliferation by 69.2% at 100 μg/mL (Fig. 4). Further study should examine the potential role of ginsenosides Rk1 and Rg5 in the ability of extract to inhibit cancer cell proliferation.

3.4. Effects of steamed notoginseng root extract on cancer cell apoptosis

Apoptosis is essential in the homeostasis of normal tissues of the body. Apoptosis is a process of programmed cell death

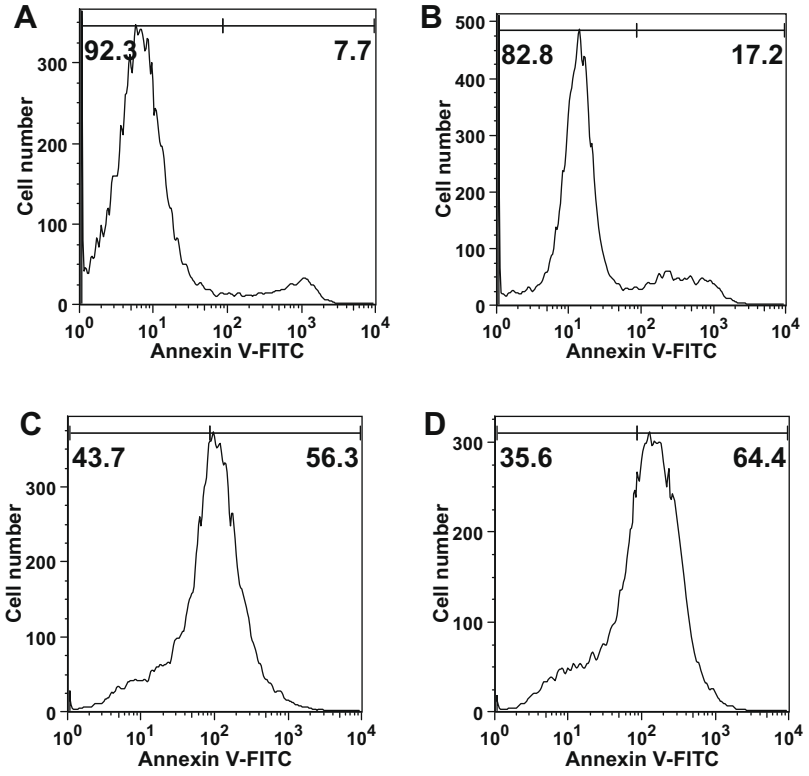

Fig. 5. Apoptotic induction activities of extract from notoginseng root steamed at 120 °C for 6 h on SW-480 human colorectal cells (treated for 48 h). A: unsteamed (control); B: 0.1 mg/mL; C: 0.15 mg/mL; D: 0.2 mg/mL.

through the activation of an intracellular pathway. The pathway produces pathogenomic cellular changes distinct from cellular necrosis. The processes of neoplastic transformation, progression and metastasis alter normal apoptotic pathways. Chemotherapeutic agents exert their cytotoxic activity by indirectly engaging apoptosis. Most chemotherapeutic agents, radiation, immunotherapy, and cytokines induce cancer cell death via the apoptotic pathway (Lowe & Lin, 2000). Compounds found in botanical products such as ginsenosides have been suggested as cancer-preventive agents because of their apoptotic effects (Yun et al., 1983).

In SW-480 cells treated for 48 h with either 0.2 mg/mL of extract from notoginseng root unsteamed and or with 0.10, 0.15 and 0.20 mg/mL of extract from the root steamed for 6 h, cell apoptosis rate was 7.7, 17.2, 56.3 and 64.4%, respectively (Fig. 5). Cells stained with annexin V-FITC dye showed apoptosis mainly in the earlier stage, confirming that decreased cell number may be due to apoptosis and increasing cell death. The exact mechanism still awaits elucidation. The most compelling links between apoptosis and treatment sensitivity in human cancer cells take place with adjuvant chemotherapy. Botanical products boost the immune system to decrease chemotherapy-induced side effects (Wong et al., 2005). American ginseng berry extract has been tested for reduction of gastric side effects induced by cisplatin (Wang, Luo et al., 2007). Anticancer agents induce apoptosis, and disruption of apoptotic programs can reduce treatment sensitivity; anticancer agents with distinct primary targets that induce apoptosis through similar mechanisms and mutations produce multi-drug resistance (Lowe, Ruley, Jacks, & Housman, 1993). Steamed notoginseng extract may become a new adjuvant chemotherapeutic reagent in case of drug resistance.

Induction of apoptosis in SW-480 cells by treatment extract from steamed notoginseng root is similar to results of experiments with steamed American ginseng root or berry (Wang, Zhang et al., 2006; Wang, Aung et al., 2007), but steamed notoginseng root has a higher dose-dependent potency. This difference may be the result of the higher accumulations of various compounds or of different ratios of ginsenoside derivatives with higher bioactivities from processing. Derivates of ginsenoside Rg3 have shown potential for inhibition of cancer cells (Bae, Han, Choo, Park, & Kim, 2002) or for hydroxyl radical scavenging activity (Kang et al., 2007). The relationship between transformation and activities of saponins needs further investigation.

In this study, the equivalent concentration of ginsenoside Rg3 presented lower inhibition *in vitro* than notoginseng root extract at lower dosage. In our previous reports, notoginseng root extract enhanced the actions of two chemotherapeutic agents, 5-fluorouracil and irinotecan on HCT-116 human colorectal cancer cells and may decrease the dosage of 5-FU needed for colorectal cancer treatment (Wang, Luo et al., 2007). Whether the saponins themselves in steamed notoginseng root convey a mutual additive or synergistic effect is not known.

4. Conclusions

There was a significant difference in ginsenoside content after steaming notoginseng root. No differences were observed in total ginsenoside content and antiproliferative effect between steaming treatment for 4 h and 6 h. After steaming, ginsenoside Rg3 content increased significantly, an increase that was partially responsible for the increase in anticancer activity. On the other hand, ginsenoside Rh2 content was increased only slightly by steaming. Thus, some other active anticancer components, in addition to Rg3 and Rh2, may form in notoginseng root extract after the steaming process.

Acknowledgements

This work was supported in part by Grants from the NIH/NCCAM AT003255 and AT004418 (to C.S.Y.), from the NIH/NCI CA106569 and American Cancer Society RSG-05-254-01DDC (to T.C.H.), and from the NIH GM074197 and the American Cancer Society RSG-05-230-01DDC (to W.D.).

References

103rd Congress. (1994). Dietary supplement health and education act of 1994. *Pub Law* 103–417. 108 Stat 4325.

Bae, E. A., Han, M. J., Choo, M. K., Park, S. Y., & Kim, D. H. (2002). Metabolism of 20(S)- and 20(R)-ginsenoside Rg3 by human intestinal bacteria and its relation to in vitro biological activities. *Biological and Pharmaceutical Bulletin, 25*(1), 58–63.

Bae, E. A., Han, M. J., Kim, E. J., & Kim, D. H. (2004). Transformation of ginseng saponins to ginsenoside Rh2 by acids and human intestinal bacteria and biological activities of their transformants. *Archives of Pharmacal Research, 27*(1), 61–67.

Chen, Z. H., Wang, D. C., Li, H. L., Wei, J. X., Wang, J. F., & Du, Y. C. (1983). Hemodynamic effects of san chi (*Panax notoginseng*) root, leaf, flower and saponins on anesthetized dogs. *Yao Xue Xue Bao, 18*(11), 818–822.

China Pharmacopoeia Commission (Ed.). (2005). *China Pharmacopoeia 2005*. Beijing: Chemical Industry Press.

Huang, Y. S., Yang, Z. C., Yan, B. G., Hu, X. C., Li, A. N., & Crowther, R. S. (1999). Improvement of early postburn cardiac function by use of *Panax notoginseng* and immediate total eschar excision in one operation. *Burns, 25*(1), 35–41.

Kaku, T., & Kawashima, Y. (1974). Studies on Panax ginseng C. A. Meyer. Part 3. Use of fractional precipitation in the column and isolation of Rg2 and Rg3. *Yamanouchi Seiyaku Kenkyu Hokoku, 3*, 45–49.

Kang, K. S., Kim, H. Y., Baek, S. H., Yoo, H. H., Park, J. H., & Yokozawa, T. (2007). Study on the hydroxyl radical scavenging activity changes of ginseng and ginsenoside-Rb2 by heat processing. *Biological and Pharmaceutical Bulletin, 30*(4), 724–728.

Keum, Y. S., Park, K. K., Lee, J. M., Chun, K. S., Park, J. H., Lee, S. K., et al. (2000). Antioxidant and anti-tumor promoting activities of the methanol extract of heat-processed ginseng. *Cancer Letters, 150*(1), 41–48.

Kim, W. Y., Kim, J. M., Han, S. B., Lee, S. K., Kim, N. D., Park, M. K., et al. (2000). Steaming of ginseng at high temperature enhances biological activity. *Journal of Natural Products, 63*(12), 1702–1704.

Kitagawa, I., Yoshikawa, M., Yoshihara, M., Hayashi, T., & Taniyama, T. (1983). Chemical studies of crude drugs (1). Constituents of Ginseng radix rubra. *Yakugaku Zasshi, 103*(6), 612–622.

Kitts, D. D., Popovich, D. G., & Hu, C. (2007). Characterizing the mechanism for ginsenoside-induced cytotoxicity in cultured leukemia (THP-1) cells. *Canadian Journal of Physiology and Pharmacology, 85*(11), 1173–1183.

Konoshima, T., Takasaki, M., & Tokuda, H. (1999). Anti-carcinogenic activity of the roots of *Panax notoginseng*. II. *Biological and Pharmaceutical Bulletin, 22*(10), 1150–1152.

Lau, A. J., Seo, B. H., Woo, S. O., & Koh, H. L. (2004). High-performance liquid chromatographic method with quantitative comparisons of whole chromatograms of raw and steamed *Panax notoginseng*. *Journal of Chromatography A, 1057*(1–2), 141–149.

Liao, P. Y., Wang, D., Zhang, Y. J., & Yang, C. R. (2008). Dammarane-type glycosides from steamed notoginseng. *Journal of Agricultural and Food Chemistry, 56*(5), 1751–1756.

Lowe, S. W., & Lin, A. W. (2000). Apoptosis in cancer. *Carcinogenesis, 21*(3), 485–495.

Lowe, S. W., Ruley, H. E., Jacks, T., & Housman, D. E. (1993). P53-dependent apoptosis modulates the cytotoxicity of anticancer agents. *Cell, 74*(6), 957–967.

Mochizuki, M., Yoo, Y. C., Matsuzawa, K., Sato, K., Saiki, I., Tono-oka, S., et al. (1995). Inhibitory effect of tumor metastasis in mice by saponins, ginsenoside-Rb2, 20(R)- and 20(S)-ginsenoside-Rg3, of red ginseng. *Biological and Pharmaceutical Bulletin, 18*(9), 1197–1202.

Nam, K. Y. (2005). The comparative understanding between red ginseng and white ginsengs, processed ginsengs (*Panax ginseng* C. A. Meyer). *Journal of Ginseng Research, 29*(1), 1–18.

Park, I. H., Piao, L. Z., Kwon, S. W., Lee, Y. J., Cho, S. Y., Park, M. K., et al. (2002). Cytotoxic dammarane glycosides from processed ginseng. *Chemical and Pharmaceutical Bulletin, 50*(4), 538–540.

Popovich, D. G., & Kitts, D. D. (2004). Ginsenosides 20(S)-protopanaxadiol and Rh2 reduce cell proliferation and increase sub-G1 cells in two cultured intestinal cell lines, Int-407 and Caco-2. *Canadian Journal of Physiology and Pharmacology, 82*(3), 183–190.

Shibata, S., Ando, T., & Tanaka, O. (1966). Chemical studies on the oriental plant drugs. XVII. The prosapogenin of the ginseng saponins (ginsenosides-Rb1, -Rb2, and -Rc). *Chemical and Pharmaceutical Bulletin, 14*(10), 1157–1161.

Vermes, I., Haanen, C., Steffens-Nakken, H., & Reutelingsperger, C. (1995). A novel assay for apoptosis. Flow cytometric detection of phosphatidylserine expression on early apoptotic cells using fluorescein labelled Annexin V. *Journal of Immunological Methods, 184*(1), 39–51.

Wang, C. Z., Aung, H. H., Ni, M., Wu, J. A., Tong, R., Wicks, S., et al. (2007). Red American ginseng: Ginsenoside constituents and antiproliferative activities of heat-processed *Panax quinquefolius* roots. *Planta Medica, 73*(7), 669–674.

Wang, C. Z., Luo, X., Zhang, B., Song, W. X., Ni, M., Mehendale, S., et al. (2007). Notoginseng enhances anti-cancer effect of 5-fluorouracil on human colorectal cancer cells. *Cancer Chemotherapy and Pharmacology, 60*(1), 69–79.

Wang, C. Z., McEntee, E., Wicks, S., Wu, J. A., & Yuan, C. S. (2006). Phytochemical and analytical studies of *Panax notoginseng* (Burk.) F.H. Chen. *Journal of Natural Medicines, 62*(2), 97–106.

Wang, C. Z., Mehendale, S. R., & Yuan, C. S. (2007). Commonly used antioxidant botanicals: Active constituents and their potential role in cardiovascular illness. *American Journal of Chinese Medicine, 35*(4), 543–558.

Wang, C. Z., Xie, J. T., Zhang, B., Ni, M., Fishbein, A., Aung, H. H., et al. (2007). Chemopreventive effects of *Panax notoginseng* and its major constituents on SW-480 human colorectal cancer cells. *International Journal of Oncology, 31*(5), 1149–1156.

Wang, C. Z., Zhang, B., Song, W. X., Wang, A., Ni, M., Luo, X., et al. (2006). Steamed American ginseng berry: Ginsenoside analyses and anticancer activities. *Journal of Agricultural and Food Chemistry, 54*(26), 9936–9942.

Wang, W., Zhao, Y., Rayburn, E. R., Hill, D. L., Wang, H., & Zhang, R. (2007). In vitro anti-cancer activity and structure–activity relationships of natural products isolated from fruits of *Panax ginseng*. *Cancer Chemotherapy Pharmacology, 59*(5), 589–601.

White, C. M., Fan, C., & Chow, M. (2000). An evaluation of the hemostatic effect of externally applied notoginseng and notoginseng total saponins. *The Journal of Clinical Pharmacology, 40*(10), 1150–1153.

White, C. M., Fan, C., Song, J., Tsikouris, J. P., & Chow, M. (2001). An evaluation of the hemostatic effects of hydrophilic, alcohol, and lipophilic extracts of notoginseng. *Pharmacotherapy, 21*(7), 773–777.

Wong, C. K., Bao, Y. X., Wong, E. L., Leung, P. C., Fung, K. P., & Lam, C. W. (2005). Immunomodulatory activities of Yunzhi and Danshen in post-treatment breast cancer patients. *American Journal of Chinese Medicine, 33*(3), 381–395.

Yun, T. K. (2003). Experimental and epidemiological evidence on non-organ specific cancer preventive effect of Korean ginseng and identification of active compounds. *Mutation Research, 523–524*, 63–74 (Special Issue).

Yun, T. K., Yun, Y. S., & Han, I. W. (1983). Anticarcinogenic effect of long-term oral administration of red ginseng on newborn mice exposed to various chemical carcinogens. *Cancer Detection and Prevention, 6*(6), 515–525.

Food Chemistry 118 (2010) 315–322

Contents lists available at ScienceDirect

Food Chemistry

journal homepage: www.elsevier.com/locate/foodchem

Anti-inflammatory effects of *Punica granatum* Linne *in vitro* and *in vivo*

Chia-Jung Lee [a], Lih-Geeng Chen [b], Wen-Li Liang [a], Ching-Chiung Wang [a,*]

[a] School of Pharmacy, College of Pharmacy, Taipei Medical University, 250 Wu-Hsing Street, Taipei 110, Taiwan
[b] Graduate Institute of Biomedical and Biopharmaceutical Sciences, College of Life Sciences, National Chiayi University, 300 University Road, Chiayi 600, Taiwan

ARTICLE INFO

Article history:
Received 1 July 2008
Received in revised form 22 April 2009
Accepted 29 April 2009

Keywords:
Punica granatum L.
Granatin B
Ellagictannin
Anti-inflammation
Nitric oxide
Inducible nitric oxide synthase
Cyclooxygenase-2

ABSTRACT

Inflammation can cause various physical dysfunctions. *Punica granatum* Linne (pomegranate), a high phenolic content fruit, is widely used as an antipyretic analgesic in Chinese culture. Pomegranate has shown potential nitric oxide (NO) inhibition in LPS-induced RAW 264.7 macrophage cells. Moreover, pomegranate (100 mg/kg) significantly decreased carrageenan-induced mice paw edema for 1, 3, 4, and 5 h. Therefore, column chromatography combined with *in vitro* bioassay-guided fractionation was used to isolate the active anti-inflammatory components from the pomegranate. Punicalagin (**1**), punicalin (**2**), strictinin A (**3**), and granatin B (**4**) were obtained with yields of 0.093%, 0.015%, 0.003%, and 0.013%, respectively. All these hydrolysable tannins inhibited NO production and iNOS expression in RAW 264.7 cells. Among them, **4** showed the strongest iNOS and COX-2 inhibitory effects, and exhibited these effects in the inhibition of paw swelling and the PGE_2 level in carrageenan-induced mice. Taken together, we suggest that **4** could be used as a standard marker for the anti-inflammatory effect of pomegranate.

1. Introduction

Punica granatum Linne, pomegranate (Punicaceae), a common fruit in the Mediterranean and Iran, is widely used for therapeutic formulae, cosmetics, and food seasoning. Pomegranate, also easily acquired from traditional medicine markets, was usually used as an astringent agent (Alper & Acar, 2004), for eliminating parasites (Mudzhiri, 1954; Raj, 1975) and as an antipyretic. The pharmacological functions of pomegranate include antioxidation (Lansky & Newman, 2007), anti-tumour (Khan, Afaq, Kweon, Kim, & Mukhtar, 2007; Lansky & Newman, 2007), anti-hepatotoxicity (Kaur, Jabbar, Athar, & Alam, 2006), anti-lipoperoxidation (Reddy, Gupta, Jacob, Khan, & Ferreira, 2007) and anti-bacteria properties (Menezes, Cordeiro, & Viana, 2006). In hematology, pomegranate could reduce the common carotid intima-medium thickness, thus lowering blood pressure and decreasing low-density lipoprotein (LDL) oxidation and the incidence of heart disease (Aviram et al., 2002, 2004). In our previous studies, we found that extract from the dried peel of the pomegranate could significantly inhibit NO production. Hence, we suggested pomegranate contains the anti-inflammatory activity components.

In the last few years, many important functions of fresh fruits and vegetables have been reported, and they are now recognised as being good sources of natural antioxidants (Joseph, Shukitt-Hale, & Lau, 2007), such as grapes, apples, and guavas. The antioxidants can prevent lipid peroxidation, and DNA and protein damage. Polyphenols have been acknowledged to have health-beneficial effects, owing to derived products such as flavonoids, tannins, coumarins, and lignans. According to recent reports, the pomegranate is rich in polyphenols, including mainly ellagitannins, gallotannins (punicalin, punicalagin, pedunculagin, punigluconin, granatin B, and tellimagrandin I) (Satomi et al., 1993) and anthocyanins (delphinidin, cyanidine and pelargonidin) (Noda, Kaneyuki, Mori, & Packer, 2002). However, the correlation between the phytochemicals and the anti-inflammatory properties of the dried peel of the pomegranate has not been investigated. Therefore, this study aimed to clarify the anti-inflammatory activities of pomegranate and its active components.

Inflammation, the first physiological defense system in the human body, can protect against injuries caused by physical wounds, poisons, etc. This defense system, also called short-term inflammation, can destroy infectious microorganisms, eliminate irritants, and maintain normal physiological functions. However, long-term over-inflammation might cause dysfunctions of the regular physiology, i.e., asthma and rheumatic arthritis.

We used *in vitro* and *in vivo* models to confirm the anti-inflammatory activity of pomegranate. Lipopolysaccharide (LPS)-induced RAW 264.7 murine macrophages were used in the *in vitro* study, and carrageenan-induced paw edema in mice served as the *in vivo* study. LPS can induce several cytokines, such as prostaglandins and nitric oxide (NO), which are involved in pro-inflammatory processes. NO can kill bacteria and viruses and is also an important

* Corresponding author. Tel.: +886 2 27361661x6161; fax: +886 2 27329368.
E-mail addresses: m303092003@tmu.edu.tw (C.-J. Lee), lgchen@mail.ncyu.edu.tw (L.-G. Chen), wenlee@tmu.edu.tw (W.-L. Liang), crystal@tmu.edu.tw (C.-C. Wang).

0308-8146/$ - see front matter © 2009 Elsevier Ltd. All rights reserved.
doi:10.1016/j.foodchem.2009.04.123

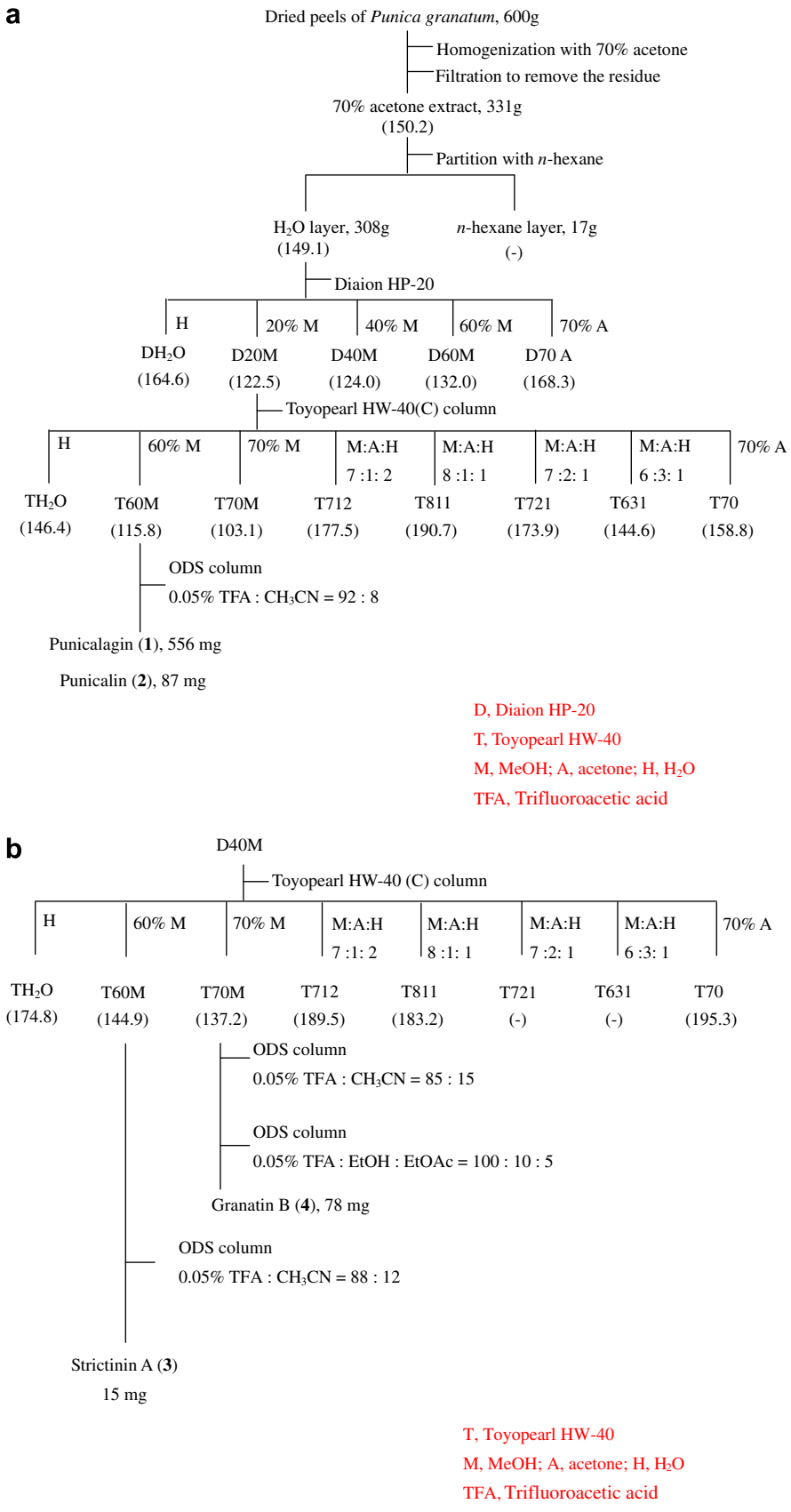

Fig. 1. Isolation flowchart of *Punica granatum* L. using anti-inflammation bioassay-guided fractionation. Numbers in the parentheses were the IC_{50} values (μg/ml) of NO inhibition. All test fractions displayed less than 10% cytotoxicity at 200 μg/ml, except D20M, D40M, D20M –TH_2O, and D20M – T60M. The IC_{50} values of the test sample exceeded 200 μg/ml.

mediator of vasodilatation; but too much NO might cause hypotension or septicemia (Moncada & Higgs, 2006). Prostaglandins have many physiological activities, such as inducing inflammation. Many tissues acutely or chronically generate excess NO and prostaglandin E_2 (PGE_2) by the overexpression of inducible nitric oxide synthase (iNOS) and cyclooxygenase-2 (COX-2) in the presence of various inflammatory stimulators. RAW 264.7 cells induced by LPS can produce the overexpression of NO and PGE_2, and their regulatory proteins, iNOS and COX-2. Therefore, we used this strategy, combined with chromatography, to isolate the active components, and we used carrageenan-induced paw edema in mice to confirm the *in vivo* anti-inflammatory effects of pomegranate.

2. Materials and methods

2.1. Chemicals

Dimethyl sulphoxide (DMSO), lipopolysaccharide (LPS), 3-(4.5-dimethylthiazol -2-yl) 2.5-diphenyltetrazolium bromide (MTT), indomethacin, *N*-nitro-L-arginine methyl ester (L-NAME), and the other chemicals were purchased from Sigma Industries (St. Louis, MO, USA). Dubecco's modified Eagle medium (DMEM), fetal bovine serum (FBS), antibiotics, and glutamine were purchased from GIBCO BRL (Grand Island, NY, USA). Diaion HP-20 gels were bought from Mitsubishi Chemical Industry (Tokyo, Japan). Western blotting was performed using an antibody specific to mouse. iNOS (sc-650), anti-COX-2 (sc-1745), and anti-GAPDH (sc-32233) were purchased from Santa Cruz Biotechnology (Santa Cruz, CA, USA).

2.2. Sample preparation

Test solutions of pomegranate were prepared by dissolving pomegranate in 10% DMSO, which was then stored at 4 °C and used within 1 month. Serial dilutions of test solutions with culture medium were prepared before the *in vitro* assays.

2.3. Determination of total phenols

The total phenol content was determined by the Folin-Ciocalteu method. Pomegranate extract was dissolved in distilled water and mixed with the Folin-Ciocalteu reagent and 7.5% aqueous Na_2CO_3 solution. After standing for 5 min at 50 °C, the absorbance was measured at 600 nm in an ELISA reader. The amount of total phenol was expressed as gallic acid equivalents (GAE, μg gallic acid/mg sample) through the calibration curve of gallic acid. The calibration curve ranged from 7.8 to 250 μg/ml (R^2 = 1) (Dudonné, Vitrac, Coutière, Woillez, & Mérillon, 2009).

2.4. Determination of the total flavones content

The total flavanol content was determined by the vanillin assay. Vanillin was dissolved in 80% H_2SO_4 to prepare the vanillin reagent. Pomegranate extract was dissolved in the distilled water and mixed with the vanillin reagent. After standing for 15 min at room temperature, the absorbance was measured at 530 nm in an ELISA reader. The amount of total flavanol was expressed as catechin equivalents (CE, μg catechin/mg sample) through the calibration curve of catechin. The calibration curve ranged from 7.8 to 250 μg/ml (R^2 = 1) (He, Liu, & Liu, 2008).

2.5. Determination of NO produced from LPS-induced RAW 264.7 cells

RAW 264.7 cells, a murine macrophage cell line, was obtained from American Type Cell Culture (ATCC no. TIB-71; Rockville, MD, USA). Cells were cultured in DMEM supplemented with 10% FBS, 1% L-glutamine, and 1% penicillin-streptomycin, and maintained at 37 °C and 5% CO_2. RAW 264.7 cells (4.0×10^5 cells/ml) were seeded in 96-well plates and then co-treated with LPS (500 ng/ml) and the test samples. After 18 h, the NO production was determined by mixing the culture supernatant with Griess reagent, and the absorption was detected in an ELISA reader at 530 nm. Anti-inflammatory activity was presented in terms of the NO production inhibition percentage. The viability of RAW 264.7 cells was detected by the MTT assay (Tseng, Lee, Chen, Wu, & Wang, 2006).

2.6. Isolation of polyphenols from P. granatum

Dried pomegranate peels (600 g) were purchased from a traditional Chinese medicine store in Taipei, pulverised and filtered through a 20# mesh. Pulverised peels were then homogenised with 70% aqueous acetone (3 L × 4) and the homogenate was then filtered. The filtrate was concentrated by evaporation under reduced pressure (*ca.* 40 °C) and further freeze-dried to yield the 70% acetone extract (330 g, yield 55%). The 70% acetone extract was dissolved in water and then partitioned with *n*-hexane to remove the non-polar compounds. The aqueous layer was chromatographed over a Diaion HP-20 gel column (9.5 × 40 cm) with stepwise aqueous MeOH ($H_2O \rightarrow 20\%$ MeOH → 40% MeOH → 60% MeOH → 70% acetone). Column chromatography was combined with an NO inhibition assay to clarify the bioactive fractions. We found that the 20% MeOH (D20M) and 40% MeOH (D40M) fractions of the Diaion column exhibited greater NO inhibition. Furthermore, the D20M fraction was chromatographed on a Toyopearl HW-40 (C) (Tosoh Bioscience, Montgomeryville, PA, USA) gel column (2.5 × 40 cm) and eluted stepwise with $H_2O \rightarrow 70\%$ MeOH → MeOH–acetone–H_2O (8:1:1, v/v/v) → MeOH–acetone–H_2O (7:2:1, v/v/v) → MeOH–acetone–H_2O (6:3:1, v/v/v) → 70% acetone. The 70% MeOH (D20M –T70M) eluate was applied to an ODS column (0.05% trifluoroacetic acid:CH_3CN, 92:8) and HLB® extraction cartridges (Waters, Milford, MA, USA) to yield punicalagin (556 mg, **1**) and punicalin (87 mg, **2**). The D40M fraction was chromatographed on a Toyopearl HW-40 (C) gel column (2.5 × 40 cm) and eluted stepwise with $H_2O \rightarrow 70\%$ MeOH → MeOH–acetone–H_2O (8:1:1, v/v/v) → MeOH–acetone–H_2O (7:2:1, v/v/v) → MeOH–acetone–H_2O (6:3:1, v/v/v) → 70% acetone. The 60% MeOH eluate (D40M –T60M) was purified on an ODS column with 0.05% trifluoroacetic acid–CH_3CN (88:12) to obtained 15 mg of strictinin A (**3**). The

Table 1
NO inhibitory effects of four hydrolysable tannins.

Compound	LPS-induced RAW 264.7 macrophage cells			Free radical-scavenging activity
	NO inhibition[a]	iNOS activity[b,c]		$ONOO^-$ scavenging[c]
	IC_{50} values (mM)	NO inhibition (%)	Cytotoxicity (%)	SNP clearance (%)
1	69.8	15.7 ± 0.4	35.5 ± 0.7	24.7 ± 6.4
2	78.6	46.7 ± 7.0	67.6 ± 1.4	30.7 ± 1.0
3	63.1	25.4 ± 2.4	45.8 ± 1.1	32.3 ± 0.0
4	33.6	14.8 ± 1.0	41.7 ± 0.7	29.5 ± 0.7
L-NAME[d]	–	46.4 ± 2.9	7.5 ± 1.6	–

Results are expressed as the mean ± SD of three experiments.
[a] Co-treatment of LPS and each test compound for 18 h and no cytotoxicites were found in these IC_{50} values.
[b] RAW 264.7 cells were stimulated with 1 μg/ml LPS and incubated overnight.
[c] Each test compound was 100 μM.
[d] L-NAME was used as positive control and its concentration was 400 μM.

70% MeOH eluate (D40M – T70M) was purified on an ODS column with 0.05% trifluoroacetic acid–CH_3CN (85:15) and 0.05% trifluoroacetic acid–EtOH–EtOAc (100:10:5, v/v/v) to obtain 78 mg of granatin B (**4**) (Fig. 1). The structures of these four compounds were identified by nuclear magnetic resonance and the purity of each compound (>99.0%) was confirmed by high-performance liquid chromatography. The formulae and molecular weights of punicalagin (**1**), punicalin (**2**), strictinin A (**3**), and granatin B (**4**) are $C_{43}H_{28}O_{30}$ (MW 1048.7), $C_{34}H_{22}O_{22}$ (MW 782.53), $C_{43}H_{28}O_{30}$ (MW 634.46), and $C_{41}H_{28}O_{27}$ (MW 952.66), respectively.

2.7. Determination of NO radical-scavenging activity

Sodium nitroprusside (SNP) is a stable NO donor. We used SNP as an NO donor to evaluate the direct NO radical clearance of samples. The SNP solution was prepared with H_2O. Test solution was added to the sample volume of SNP solution (50 mM). The mixture was incubated at 37 °C, for 5 h. Then, we took the supernatant (1, mixed it with the Griess reagent, and read the absorption on an ELISA reader at 530 nm (Bor, Chen, & Yen, 2006).

2.8. iNOS activity assay in LPS-induced RAW 264.7 cells

Initially, RAW 264.7 cells were pre-stimulated by 1 μg/ml LPS for 24 h to activate the iNOS. Then, cells were collected and washed twice with PBS to remove the excessive LPS, and the activated RAW 264.7 cells (4.0×10^5 cell/ml) were seeded in 96-well plates. Crude extract and active components were immediately added to the cells. The 96-well plate was incubated at 37 °C overnight. The NO detecting method was the same as previously described. We used *N*-nitrol-arginine methyl ester (L-NAME, 400 μM), a specific inhibitor of NO synthase enzyme, and as the positive control.

2.9. iNOS and COX-2 expression assay in LPS-induced RAW 264.7 cells

Total cellular protein was extracted with a RIPA solution (radioimmuno-precipitation assay buffer) at −20 °C overnight. We used BSA (bovine serum albumin) as a protein standard to calculate equal total cellular protein amounts. Protein samples (15 μg) were resolved by denaturing sodium dodecyl sulfate–polyacrylamide gel electrophoresis (SDS–PAGE) using standard methods, and then were transferred to nitrocellulose (Hybond-PVDF) membranes by electroblotting and blocking with 1% BSA. The membranes were probed with the primary antibodies (iNOS, COX-2 and GAPDH) at 4 °C overnight, washed three times with PBST, and incubated for 1 h at 37 °C with alkaline phosphatase-conjugated secondary antibodies. Then, we used an NBT/BCIP commercial kit (Gibco) as the visualising agent. The intensity of the bands was quantified by computer-assisted image analysis using AlphaInnotech Digital Imaging Systems. Western blotting results are representative of three independent experiments for every data point.

2.10. Model of 1% carrageenan-induced paw edema in ICR mice

Male ICR mice weighing 25 ± 2 g were bought from the National Science Council, Taipei, Taiwan, and maintained at 21 ± 2 °C with food and water *ad libitum*. They were kept on a 12-h light/12-h dark cycle. All mice used in this experiment were cared for according to

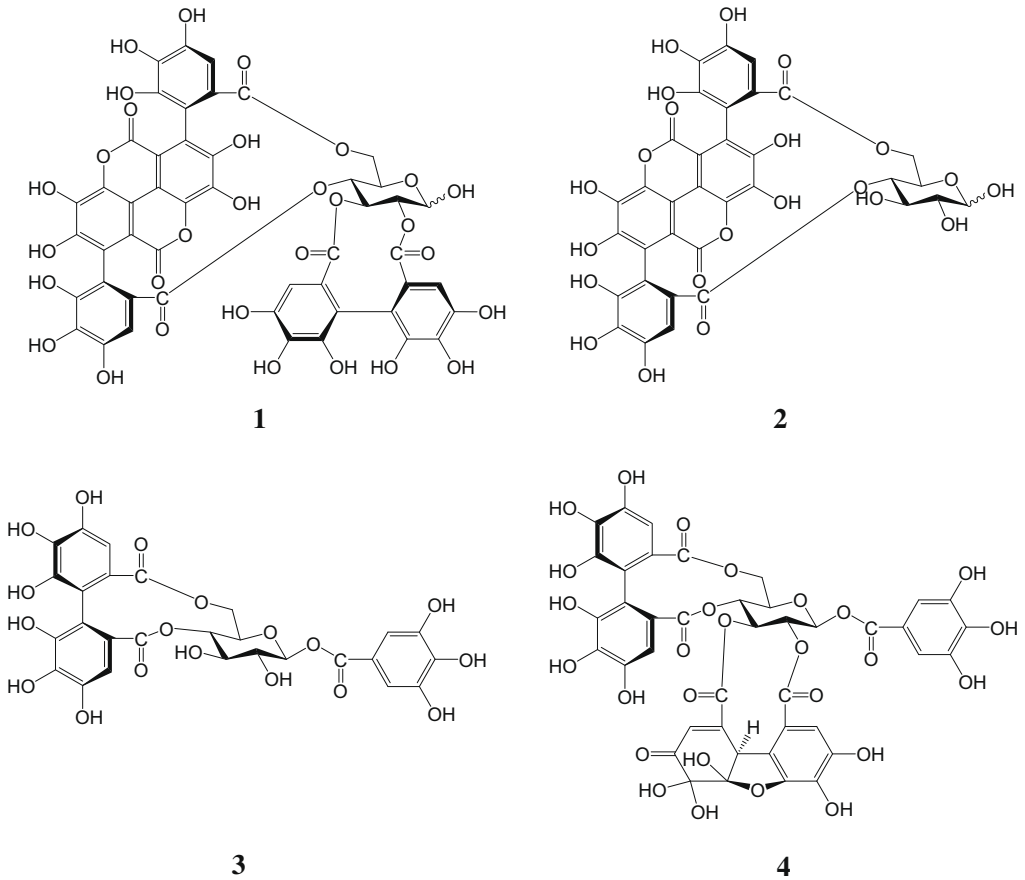

Fig. 2. Structures of the four hydrolysable tannins, punicalagin (**1**), punicalin (**2**), strictinin A (**3**), and granatin B (**4**), isolated from *Punica granatum* L.

the Ethical Regulations on Animal Research of our university. Edema in the left hind paw of the mice was induced by injecting 50 μl of 1% (w/v) carrageenan into the subplantar region. The perimeter of the paw was measured 1 h before the carrageenan injection and after 1–6 h, using calipers. One hour before the injection, the pomegranate (100 mg/kg), the active component (2.5 and 10 mg/kg), and indomethacin (10 mg/kg, as a positive control) were given orally, while the control group was given distilled water. The blank group was injected with normal saline and given distilled water. Each group consisted of five animals. After 6 h, mice were sacrificed and the serum collected for the PGE_2 measurement (Tseng et al., 2006).

2.11. Measurement of PGE_2 production

Serum and cell culture mediums were determined the PGE_2 concentrations by the PGE_2 ELISA kit (Amersham Pharmacia Biotech, Buckinghamshire, UK).

2.12. Statistical analysis

The data are presented as mean and standard deviation (SD). Significance was calculated using the Student's *t*-test. Differences were considered significant for $p < 0.05$.

3. Results

3.1. Polyphenols isolation from P. granatum L.

The phytochemical components of the 70% acetone extract of pomegranate peels were screened using the Folin-Ciocalteu method and vanillin assay. The screening found that pomegranate was rich in total phenol and flavanol (471.0 ± 32.0 μg gallic acid equivalent/mg in total phenol and 257.0 ± 19.6 μg catechin equivalent/mg in total flavanol).

The NO inhibition bioassay-guided fractionation flowchart of pomegranate is shown in Fig. 1. These four hydrolysable tannins, punicalagin (**1**), punicalin (**2**), strictinin A (**3**), and granatin B (**4**), were isolated from D20M and D40M of the pomegranate fractions, with stronger inhibition of NO production; the yields were 0.093%, 0.015%, 0.003% and 0.01%, respectively.

3.2. NO inhibitory effects of four hydrolysable tannins

The NO inhibitory effects of **1**–**4** were measured in LPS-induced RAW 264.7 cells for 18 h. We collected the culture medium to detect the NO levels using the Griess reaction. Compounds **1**–**4** showed less than 10% cytotoxicities in LPS-induced RAW 264.7 cells for 18 h. Compound **4** displayed a more potent NO inhibition

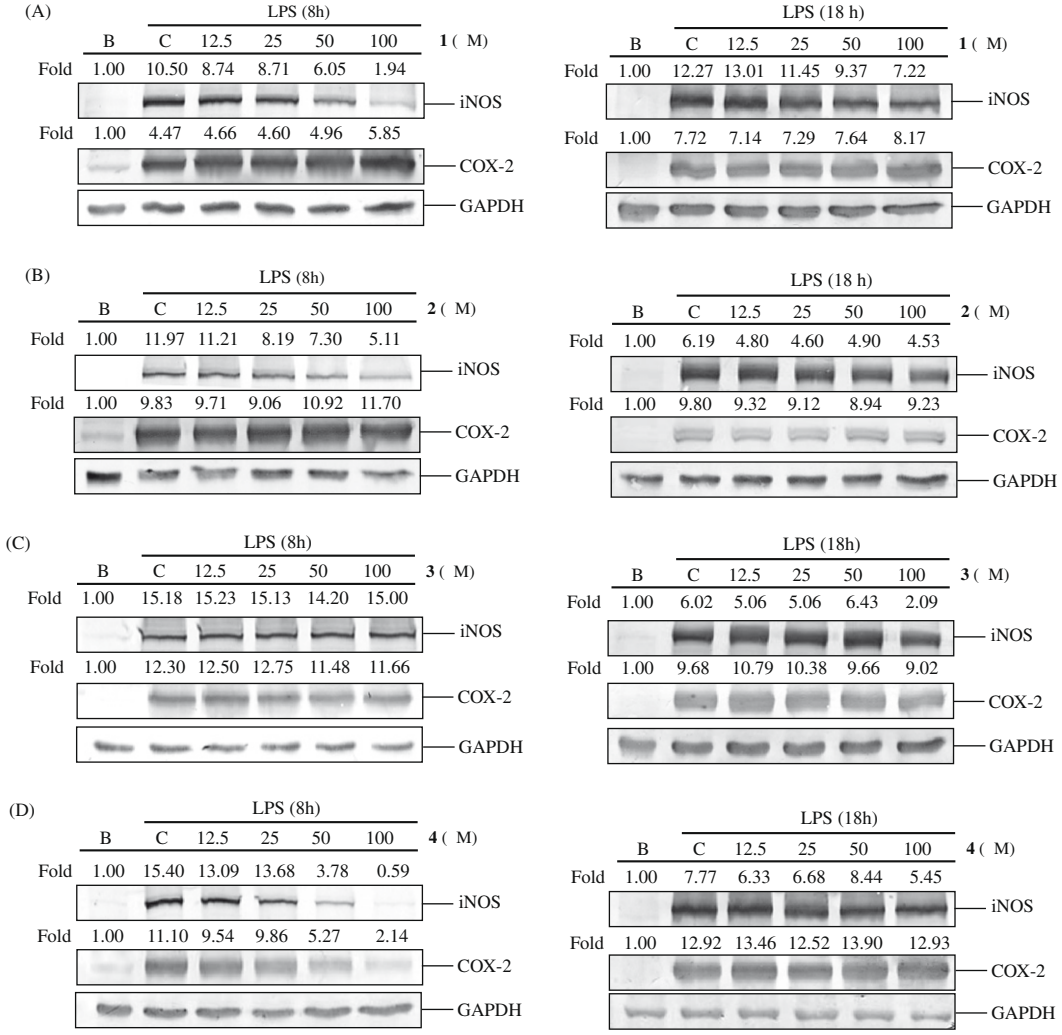

Fig. 3. Inducible NOS and COX-2 expression of punicalagin (A), punicalin (B), strictinin A (C) and granatin B (D) induced by LPS (500 ng/ml) in RAW 264.7 cells for 8 and 18 h. (B) Non-LPS-induced group. (C) Solvent control group (H_2O). GAPDH was used as an internal control to identify equal amounts of protein loading in each lane. The intensity of the iNOS and COX-2 protein was examined by densitometrus analysis, and expressed as the ratio of iNOS/GAPDH and COX-2/GAPDH. Data from three separate experiments were used, and the picture for one of which is shown.

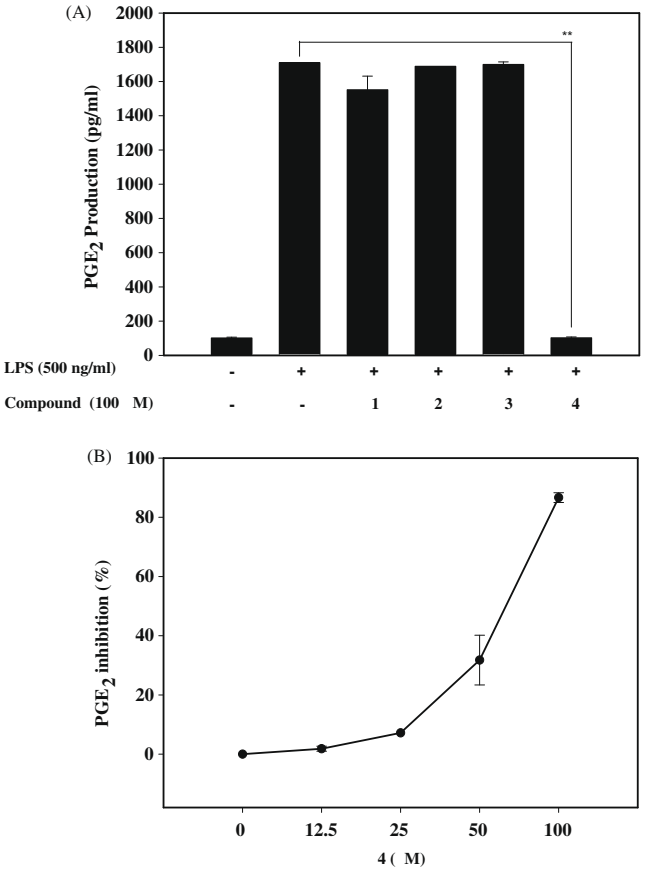

Fig. 4. Prostaglandin E_2 production of **1**–**4** (A) and a series dose–response curve of **4** (B) induced by LPS-induced RAW 264.7 cells for 8 h. $^{**}p < 0.001$. $n = 3$ All data were expressed as the mean ± SD.

in LPS-induced RAW 264.7 cells for 18 h than did the others, and its IC_{50} value was 33.6 μM (Table 1).

Nevertheless, we would like to clarify whether these hydrolysable tannins had NO radical-scavenging activity or not. SNP was used as an NO radical donor to evaluate the NO-scavenging activity of these four hydrolysable tannins. As shown in Table 1, the four hydrolysable tannins did not significantly exhibit SNP clearance at 100 μM.

3.3. iNOS expression and activities of four hydrolysable tannins in LPS-induced RAW 264.7 cells

Based on the above data, we suggest that the NO inhibition effects of the four hydrolysable tannins could be brought about through the influence of iNOS protein expression or activity. The iNOS protein expression in LPS-induced RAW 264.7 cells for 8 and 18 h were observed by Western blot assay. As shown in Fig. 3, the four hydrolysable tannins displayed dose-dependently inhibitory effects on the iNOS expression at 12.5–100 μM. In addition, the 8 h group expressed more significantly iNOS inhibitory effects than the 18 h group. Therefore, these four hydrolysable tannins could decrease the iNOS protein expressions from the early stage (8 h) to the late stage (18 h). Taken together, **1**–**4** significantly decreased the iNOS expressions in LPS-induced RAW 264.7 cells, and **4** was the strongest among them.

On the other hand, RAW 264.7 cells were pretreated with LPS for 24 h to observe the iNOS activity inhibition of these four hydrolysable tannins. As seen in Table 1, L-NAME acted as a positive control and displayed significant iNOS activity inhibition at 400 μM. However, these four hydrolysable tannins had no iNOS activity inhibitory effects and even exhibited cytotoxicity at 100 μM. Hence, these four hydrolysable tannins inhibited NO production through directly decreasing the iNOS protein expressions.

3.4. COX_2 and PGE_2 inhibitory effects of four hydrolysable tannins

The COX-2 and PGE_2 inhibitory effects of these four hydrolysable tannins were evaluated in LPS-induced RAW 264.7 cells for 8 and 18 h. As shown in Fig. 3, Compound **4** inhibited COX-2 protein expression in dose-dependent (Fig. 3) and PGE_2 productions (Fig. 4A) more significantly than the others after treatment with LPS for 8 h. Moreover, **4** inhibited PGE_2 productions in a dose-dependent manner, and the IC_{50} value was 66.22 ± 9.4 μM (Fig. 4D). However, COX-2 protein expression of LPS-induced RAW 264.7 cells was not inhibited after treatment with the four hydrolysable tannins for 18 h (Fig. 3). Hence, we suggested that **4** could inhibit COX-2 and PGE_2 production in the early stage (8 h) because there was less COX-2 expression at that stage, but in the late stage (18 h), COX-2 expression reached a stable state, so **4** had difficulty inhibiting its expression.

3.5. Inhibitory effect of pomegranate and 4 on carrageenan-induced paw edema in ICR mice

Carrageenan-induced paw edema in ICR mice was used to evaluate the *in vivo* anti-inflammatory model. We used indomethacin, a common non-steroidal anti-inflammatory drug (NSAID) as a positive control. Mice were treated with pomegranate (100 mg/kg) or indomethacin (10 mg/kg) 1 h before carrageenan induction, and had detected paw edema for 6 h. Results showed that carrageenan significantly induced paw edema during the entire experiment in the control group (Table 2). Pomegranate significantly reduced paw edema by more than 50% at 1–5 h after the carrageenan injection, and had even greater potential paw edema inhibitory effects than indomethacin.

Table 2
Effects of pomegranate and granatin B on the paw perimeter of carrageenan-induced mice paw edema.

Group	Time after injection of carrageenan (h)					
	1	2	3	4	5	6
Control	1.74 ± 0.30	1.41 ± 0.17	1.41 ± 0.23	1.21 ± 0.13	0.92 ± 0.16	0.88 ± 0.08
Indomethacin (10 mg/kg)	0.70 ± 0.35*	0.90 ± 0.34*	0.79 ± 0.33*	0.72 ± 0.15*	0.75 ± 0.09*	0.62 ± 0.19*
Pomegranate (100 mg/kg)	0.86 ± 0.10*	0.60 ± 0.07**	0.59 ± 0.28*	0.42 ± 0.30*	0.4 ± 0.36*	0.34 ± 0.50
*Granatin B (**4**)*						
2.5 mg/kg	1.08 ± 0.13*	0.84 ± 0.20*	0.77 ± 0.07**	0.75 ± 0.17*	0.63 ± 0.03*	0.59 ± 0.15*
10.0 mg/kg	0.98 ± 0.40*	0.89 ± 0.19*	0.68 ± 0.29*	0.50 ± 0.41*	0.23 ± 0.52*	0.48 ± 0.26*

Values were presented as the mean ± SD of the increasing mice paw edema (mm) of four animals for each group.
* $p < 0.05$.
** $p < 0.001$ were presented as significantly different from the control.

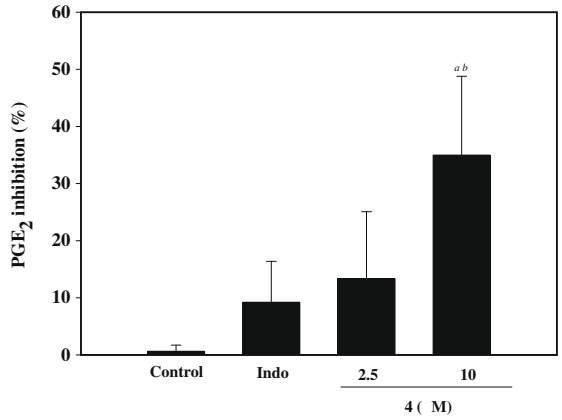

Fig. 5. Prostaglandin E_2 concentrations of **4** on carrageenan-induced mice paw edema for 6 h. Indomethacin served as a positive control and 10 mg/kg dosage used. [a]$p < 0.01$. The p value was calculated by comparison with the control group. [b]$p < 0.05$. The p value was calculated by comparison with the indomethacin group ($n = 3$). All data were expressed as mean ± SD.

Since **4** showed the strongest COX-2 and iNOS inhibitory effects in the *in vitro* study, we examined the *in vivo* anti-inflammatory effect of **4**. We found that **4** (2.5 and 10 mg/kg) could significantly and dose-dependently reduce paw edema, and the inhibitory abilities of the higher dose (10 mg/kg) were the same as that of the indomethacin (Table 2). In addition, **4** had more significant PGE_2 inhibitory effects than the indomethacin at 6 h (Fig. 5).

4. Discussion

Pomegranate has been used for centuries as a therapeutic agent for the treatment of inflammatory diseases. According to current reports, pomegranate is a polyphenol-rich fruit, and showed potential as an anti-inflammatory, anti-oxidative and anti-cancer agent in several experimental models (Shukla, Gupta, Rasheed, Khan, & Haqqi, 2008). Chemical analyses have also shown that the phenol compounds of pomegranate contain significantly high levels of hydrolysable tannins, such as punicalin, punicalagin, pedunculagin, punigluconin (Dudonné et al., 2009). Therefore, we used an NO inhibition assay combined with column chromatography to determine which components in pomegranate would have effective anti-inflammatory activity. In this paper, four hydrolysable tannins, punicalagin (**1**), punicalin (**2**), strictinin A (**3**), and granatin B (**4**), were isolated from pomegranate by bioassay-guided fractionation. Each of them displayed a dose-dependently and significantly inhibitory effect on NO production in LPS-induced RAW 264.7 cells (Table 1). Furthermore, granatin B (**4**) more strongly inhibited PGE_2 production and COX-2 expression in LPS-induced RAW 264.7 cells than the others.

Structure–activity relationships (SAR) of natural products have been found to influence the various pharmacological functions, such as antioxidant and anti-inflammation activities. Up to the present, over 3000 kinds of tannins have been identified, chiefly as secondary metabolites in green plants. Tannin is involved in a large proportion of phenolic derivatives in plants and is divided into two types: hydrolysable and condensed tannins. Many possible permutations are offered by substitution and conjugation, and this could explain why so many tannin derivatives occur naturally (Fylaktakidou, Hadjipavlou-Litina, Litinas, & Nicolaides, 2004). Based on the structural similarities of these four hydrolysable tannins, we divided them into two groups. One was punicalagin (**1**) and punicalin (**2**) and the other was strictinin A (**3**) and granatin B (**4**) (Fig. 2). Among them, **1** and **2** were previously recognised as inhibitors of the pro-inflammatory for anti-edematogenic activity on carrageenan-induced paw edema in rats (10 mg/kg) (Lin, Hsu, & Lin, 1999). However, there is no scientific evidence that **3** and **4** have anti-inflammatory activities. In this study, we first found that both **3** and **4** had potential NO inhibitory effects in LPS-induced RAW264.7, and that **4** was the better one (Table 1). Moreover, **4** showed the strongest COX-2 and iNOS inhibitory effects in an *in vitro* assay, and significantly reduced paw edema and PGE_2 inhibitory effects in an *in vivo* assay.

Dehydrohexahydroxydiphenoyl (DHHDP), a substitution in C-2 and C-3 of **4**, was the difference between **4** and **3**, and probably played an important role in anti-inflammation. In related investigations, tannins with DHHDP units invariably had strong anti-inflammatory and anti-oxidant activity. (Feldman, 2005) Geraniin, a well-documented hydrolysable tannin, has been reported to have excellent NO radical-scavenging and iNOS inhibitory activities (Kumaran & Karunakaran, 2006). Mallotusinic acid and euphorbin E also had potent scavenging effects on DPPH free radicals. (Okuda, 2005) Hence, we concluded once the hydrolysable tannins had the DHHDP group, they would appear to have better anti-inflammatory activities.

Many studies have demonstrated that the massive production of NO and PGE_2 *via* the pro-inflammatory proteins iNOS and COX-2 played an important physiological role in inflammation. Evidence has shown that NO production was initiated by treating LPS for 8 h and reached a stable state for 18 h, and that COX-2 expression began at 6–8 h and reached the maximal level at 16–24 h. (Caughey, Cleland, Penglis, Gamble, & James, 2001; Reher, Harris, Whiteman, Haiand, & Meghji, 2002). Therefore, we used two treatment times (8 and 18 h) to measure the anti-inflammatory effects of these hydrolysable tannins, because of the different mechanism and production time of these inflammation mediators (COX-2, iNOS, etc.). On the basis of the above results, we found that **4** could significantly decrease NO and PGE_2 production through inhibiting iNOS and COX-2 expression. Little NO production was found in LPS-induced RAW 264.7 for 8 h. NO was released from the process of converting L-arginine to L-citruline by iNOS, while NO was initially produced at 8 h and reached the maximum level at 18 h; therefore, NO production from LPS-induced RAW 264.7 was not detected at 8 h. Unlike NO production, activated COX-2 could convert arachidonic acid to PGE_2 in only 30 min. Hence, the COX-2 and PGE_2 inhibitory effects of **4** from LPS-induced RAW 264.7 at 8 h were stronger than those at 18 h. In summary, we suggest that **4** is an effective anti-inflammatory compound and has dual roles in anti-inflammation, by decreasing PGE_2 production in the early stage and decreasing NO production in the late stage.

In conclusion, **4** not only displayed the best NO inhibitory abilities in LPS-induced RAW 264.7, but also had the strongest PGE_2 inhibitory effects in the *in vitro* and *in vivo* assays. Taken together, **4** could be used as a standard marker compound to determine the potential anti-inflammatory effect of pomegranate.

References

Alper, N., & Acar, J. (2004). Removal of phenolic compounds in pomegranate juices using ultrafiltration and laccase-ultrafiltration combinations. *Die Nahrung, 48*(3), 184–187.

Aviram, M., Dornfeld, L., Kaplan, M., Coleman, R., Gaitini, D., Nitecki, S., et al. (2002). Pomegranate juice flavonoids inhibit low-density lipoprotein oxidation and cardiovascular diseases: Studies in atherosclerotic mice and in humans. *Drugs under Experimental and Clinical Research, 28*(2–3), 49–62.

Aviram, M., Rosenblat, M., Gaitini, D., Nitecki, S., Hoffman, A., Dornfeld, L., et al. (2004). Pomegranate juice consumption for 3 years by patients with carotid artery stenosis reduces common carotid intima-media thickness, blood pressure and LDL oxidation. *Clinical Nutrition, 23*(3), 423–433.

Bor, J. Y., Chen, H. Y., & Yen, G. C. (2006). Evaluation of antioxidant activity and inhibitory effect on nitric oxide production of some common vegetables. *Journal of Agricultural and Food Chemistry, 54*(5), 1680–1686.

Caughey, G. E., Cleland, L. G., Penglis, P. S., Gamble, J. R., & James, M. J. (2001). Roles of cyclooxygenase (COX)-1 and COX-2 in prostanoid production by human

endothelial cells: Selective up-regulation of prostacyclin synthesis by COX-2. *Journal of Immunology, 167*(5), 2831–2838.

Dudonné, S., Vitrac, X., Coutière, P., Woillez, M., & Mérillon, J. M. (2009). Comparative study of antioxidant properties and total phenolic content of 30 plant extracts of industrial interest using DPPH, ABTS, FRAP, SOD, and ORAC Assays. *Journal of Agricultural and Food Chemistry*.

Feldman, K. S. (2005). Recent progress in ellagitannin chemistry. *Phytochemistry, 66*, 1984–2000.

Fylaktakidou, K. C., Hadjipavlou-Litina, D. J., Litinas, K. E., & Nicolaides, D. N. (2004). Natural and synthetic coumarin derivatives with anti-inflammatory/ antioxidant activities. *Current Pharmaceutical Design, 10*(30), 3813–3833.

He, X., Liu, D., & Liu, R. H. (2008). Sodium borohydride/chloranil-based assay for quantifying total flavonoids. *Journal of Agricultural and Food Chemistry, 56*(20), 9337–9344.

Joseph, J. A., Shukitt-Hale, B., & Lau, F. C. (2007). Fruit polyphenols and their effects on neuronal signaling and behavior in senescence. *Annals of the New York Academy of Sciences, 1100*, 470–485.

Kaur, G., Jabbar, Z., Athar, M., & Alam, M. S. (2006). *Punica granatum* (pomegranate) flower extract possesses potent antioxidant activity and abrogates Fe-NTA induced hepatotoxicity in mice. *Food and Chemical Toxicology, 44*(7), 984–993.

Khan, N., Afaq, F., Kweon, M. H., Kim, K., & Mukhtar, H. (2007). Oral consumption of pomegranate fruit extract inhibits growth and progression of primary lung tumors in mice. *Cancer Research, 67*(7), 3475–3482.

Kumaran, A., & Karunakaran, R. J. (2006). Nitric oxide radical scavenging active components from *Phyllanthus emblica* L.. *Plant Foods for Human Nutrition, 61*(1), 1–5.

Lansky, E. P., & Newman, R. A. (2007). *Punica granatum* (pomegranate) and its potential for prevention and treatment of inflammation and cancer. *Journal of Ethnopharmacology, 109*(2), 177–206.

Lin, C. C., Hsu, Y. F., & Lin, T. C. (1999). Effects of punicalagin and punicalin on carrageenan-induced inflammation in rats. *The American Journal of Chinese Medicine, 27*(3–4), 371–376.

Menezes, S. M., Cordeiro, L. N., & Viana, G. S. (2006). *Punica granatum* (pomegranate) extract is active against dental plaque. *Journal of Herbal Pharmacotherapy, 6*(2), 79–92.

Moncada, S., & Higgs, E. A. (2006). The discovery of nitric oxide and its role in vascular biology. *British Journal of Pharmacology, 147*(Suppl. 1), S193–S201.

Mudzhiri, M. S. (1954). *Punica granatum* bark extract as a therapeutic agent in tapeworm infection. *Meditsinskaia Parazitologiia i Parazitarnye Bolezni, 4*, 311–313.

Noda, Y., Kaneyuki, T., Mori, A., & Packer, L. (2002). Antioxidant activities of pomegranate fruit extract and its anthocyanidins: Delphinidin, cyanidin, and pelargonidin. *Journal of Agricultural and Food Chemistry, 50*(1), 166–171.

Okuda, T. (2005). Systematics and health effects of chemically distinct tannins in medicinal plants. *Phytochemistry, 66*, 2012–2031.

Raj, R. K. (1975). Screening of indigenous plants for anthelmintic action against human *Ascaris lumbricoides*: Part-II. *Indian Journal of Physiology and Pharmacology, 19*(1), 47–49.

Reddy, M. K., Gupta, S. K., Jacob, M. R., Khan, S. I., & Ferreira, D. (2007). Antioxidant, antimalarial and antimicrobial activities of tannin-rich fractions, ellagitannins and phenolic acids from *Punica granatum* L. *Planta Medica, 73*(5), 461–467.

Reher, P., Harris, M., Whiteman, M., Haiand, H. K., & Meghji, S. (2002). Ultrasound stimulates nitric oxide and prostaglandin e2 production by human osteoblasts. *Bone, 31*(1), 236–241.

Satomi, H., Umemura, K., Ueno, A., Hatano, T., Okuda, T., & Noro, T. (1993). Carbonic anhydrase inhibitors from the pericarps of *Punica granatum* L.. *Biological and Pharmaceutical Bulletin, 16*(8), 787–790.

Shukla, M., Gupta, K., Rasheed, Z., Khan, K. A., & Haqqi, T. M. (2008). Consumption of hydrolyzable tannins-rich pomegranate extract suppresses inflammation and joint damage in rheumatoid arthritis. *Nutrition, 24*(7–8), 733–743.

Tseng, S. H., Lee, H. H., Chen, L. G., Wu, C. H., & Wang, C. C. (2006). Effects of three purgative decoctions on inflammatory mediators. *Journal of Ethnopharmacology, 105*(1–2), 118–124.

Food Chemistry 118 (2010) 323–327

Contents lists available at ScienceDirect

Food Chemistry

journal homepage: www.elsevier.com/locate/foodchem

Effects of alkaline treatment on the structure of phosphorylated wheat starch and its digestibility

Yijun Sang [a], Paul A. Seib [a], Alvaro I. Herrera [b], Om Prakash [b], Yong-Cheng Shi [a,*]

[a] Department of Grain Science and Industry, Kansas State University, Manhattan, KS 66506, USA
[b] Department of Biochemistry, Kansas State University, Manhattan, KS 66506, USA

ARTICLE INFO

Article history:
Received 9 December 2008
Received in revised form 21 April 2009
Accepted 29 April 2009

Keywords:
Phosphorylated starch
Digestibility
Resistant starch
Dietary fibre

ABSTRACT

Phosphorylated wheat starch (PWS) was prepared with sodium trimetaphosphate and sodium tripolyphosphate (99/1, w/w), and the modified starch gave 88.8% total dietary fibre by the Prosky method and 68.7% resistant starch (RS) by the Englyst method. The stability of the phosphate esters in aqueous sodium hydroxide was investigated and related to total dietary fibre and RS contents. The phosphorylated starch was slurried (40%, w/w) at 40 °C for 4 h at pH 9.0, 10.0, 11.0, and 12.0. The phosphorus content of the PWS decreased from 0.37% to 0.29% after treatment at pH 12.0, whereas only a slight decrease in phosphorus content occurred after treatments at pH 9.0–11.0. Despite the 22% decrease in total phosphorus content, total dietary fibre content and RS content of the alkali-treated PWS changed only slightly. ^{31}P nuclear magnetic resonance spectroscopy showed that after the alkali treatment at pH 12.0, cyclic monostarch monophosphate and monostarch diphosphate were not detectable and that the level of total monostarch monophosphate decreased from 0.077% to 0.067%. Conversely, distarch monophosphate increased from 0.17% to 0.20%, of ≈18%. The increase in distarch monophosphate (cross-linking) content after alkali treatment at pH 12.0 probably explained the retention of total dietary fibre and RS contents in the alkali-treated PWS.

1. Introduction

Nutritionally, starches are classified into rapidly digestible starch (RDS), slowly digestible starch (SDS), and resistant starch (RS) on the basis of their digestion rate in humans (Englyst, Kingman, & Cummings, 1992). A low ratio of RDS to the sum of SDS and RS in a starchy food indicates a low glycemic index (Englyst, Englyst, Hudson, Cole, & Cummings, 1999). Foods with a low glycemic index improve satiety (Warren, Henry, & Simonite, 2003) and may help prevent obesity and Type II diabetes (Bjorck, Liljeberg, & Ostman, 2000; Jenkins, Jerkins, Kendall, Augustine, & Vuksan, 2001; Roberts, 2000). RS is desirable for its additional prebiotic effect and can be fermented in the colon to produce short-chain fatty acids, which inhibit the development of colon cancer cells (Brown, McNaught, Andrew, & Morita, 2001; Topping & Clifton, 2001).

Chemical modifications, such as phosphorylation, may be used to change starch functionality and digestibility. Different levels and chemical forms of phosphate esters may give different functionalities to phosphorylated starch. Monostarch phosphate, whose structure is a single phosphate group esterified to a starch hydroxyl, imparts improved appearance, hygroscopicity, solution transparency, swelling, and viscosity at 0.1–0.4% P (Rutenberg & Solarek, 1984; Tomasik & Schilling, 2004). In contrast, distarch phosphate, whose structure is a single phosphate group esterified (cross-linked) to two starch hydroxyls, gives improved thickening properties even at very low levels of phosphorus (<0.04%). Distarch phosphate linkages (cross-links) import paste stability to heat, acid, and shearing (Rutenberg & Solarek, 1984; Tomasik & Schilling, 2004).

Monosubstitution of starch with phosphate groups has been shown to decrease starch digestibility with α-amylase (Janzen, 1969). However, it is the phosphate cross-link that can dramatically decrease starch digestion by α-amylase. A distarch phosphate with a high level of phosphorus content (≈0.4%) is high in RS and total dietary fibre (TDF) content (Woo & Seib, 2002). Distarch monophosphate (DSMP), monostarch monophosphate (MSMP), monostarch diphosphate (MSDP), and cyclic monostarch monophosphate (cyclic-MSMP) have been found in the phosphorylated cross-linked RS (Sang, Prakash, & Seib, 2007). The cross-linking of starch with sodium trimetaphosphate (STMP) and phosphoryl chloride are conducted at alkaline pH, and a reaction mechanism for cross-linking of polysaccharides with STMP has been proposed recently (Lack, Dulong, Picton, Cerf, & Condamine, 2007). Lack and coworkers reacted STMP with methyl α-D-glucopyranoside as a model substance for polysaccharides that are soluble at alkaline pH, and they followed the reaction by high-resolution NMR spectroscopy (^{31}P, ^{1}H and ^{13}C). However, the reaction of starch granules

* Corresponding author. Tel.: +1 785 532 6771; fax: +1 785 532 7010.
E-mail address: ycshi@ksu.edu (Y.-C. Shi).

0308-8146/$ - see front matter © 2009 Elsevier Ltd. All rights reserved.
doi:10.1016/j.foodchem.2009.04.121

with STMP is a two-phase, heterogeneous reaction conducted on starch slurries at concentrations of ~30%. The novelty of our work on the reaction of starch granules with STMP is to determine how slurry pH affects the ratio of mono-substituted (MSMP and MSDP) phosphate esters to cross-linked (DSMP) phosphate esters. In addition, we examine the stability of various starch phosphate esters in aqueous sodium hydroxide at different pH levels, and the effects of the various esters on starch digestibility.

2. Materials and methods

2.1. Materials

Wheat starch (Midsol 50) was obtained from MGP Ingredients Inc. (Atchison, KS). Potato starch was obtained from Avebe America Inc (Princeton, NJ). Sodium trimetaphosphate (STMP), sodium tripolyphosphate (STTP), phosphoric acid (85%), phosphocreatin, tetra sodium ethylenediaminetetraacetate (Na_4EDTA), and deuterium oxide were purchased from Sigma Chemical Company (St. Louis, MO). Thermally stable α-amylase (E-BLAAM; 3,000 Ceralpha Units/mL) and glucoamylase (E-AMGDF; 200 *p*-NP β-Maltoside Units/mL) were purchased from Megazyme International Ireland Ltd (Bray, Ireland). All chemicals were reagent grade.

2.2. General methods

Moisture content was determined by drying at 130 °C for 1 h (AACC, 2000) and phosphorus content was determined by the procedure of Smith and Caruso (1964). Total dietary fibre was determined by the Prosky method (AOAC, 2000) using a TDF assay kit from Megazyme (Megazyme International Ireland Ltd, Bray, Ireland). Starch samples were subjected to sequential enzymatic digestion by heat-stable α-amylase, protease and amyloglucosidase, and the enzyme resistant fraction was counted as TDF.

2.3. Preparation of cross-linked phosphorylated wheat starch (PWS)

Phosphorylated wheat starch was prepared according to the method described by Woo and Seib (2002). Wheat starch (50.0 g, db) was added into water (70.0 g) containing STMP (5.94 g), STPP (0.06 g), sodium sulphate (5.0 g), and sodium hydroxide to pH 11.5. The reaction mixture was stirred at 45 °C for 3 h, after which time reaction pH decreased to 10.8. The reaction mixture was adjusted to pH 6.5 by adding 1 M hydrochloric acid, and the slurry was centrifuged. The sedimented starch was collected and washed with distilled water seven times. The purified product was dried at 40 °C overnight and ground to give ≈50 g of PWS.

2.4. Treatment of PWS with aqueous sodium hydroxide

Phosphorylated wheat starch (50.0 g, db) was slurried in water (70.0 g), and the pH was adjusted to 9.0, 10.0, 11.0, and 12.0 by adding 1 M sodium hydroxide. The slurry was stirred at 40 °C for 4 h, cooled to 25 °C, and adjusted to pH 6.5. The starch was isolated and purified as described previously.

2.5. Conversion of PWS to phosphodextrins for ^{31}P nuclear magnetic resonance (^{31}P NMR) spectroscopy

Phosphorylated wheat starch (1.0 g, db) was added to a 50-ml centrifuge tube containing 2.0 mM calcium chloride (50 mL) at pH 8.2. Heat-stable α-amylase (100 μL) was added, and the tube was heated in a boiling-water bath for 30 min. The α-amylase digestion was repeated after adding another 100 μL of heat-stable α-amylase. The mixture was cooled and adjusted to pH 4.5 then incubated with amyloglucosidase (200 μL) for 1 h at 60 °C. The mixture was adjusted to pH 7.0, centrifuged, and the supernatant was freeze-dried. Recovery of phosphodextrins from the phosphorylated starch was estimated to be greater than 95% by mass balance.

2.6. ^{31}P NMR spectra of the phosphodextrins

The freeze-dried starch digest (≈1.0 g) was dissolved in deuterium oxide (1.0 ml) containing 20 mM EDTA and 0.002% sodium azide, and the pH was adjusted to 8.0 by adding 0.1 M sodium hydroxide. The proton-decoupled ^{31}P NMR data were acquired on a 11.75 Tesla Varian NMR System (Varian Inc., Palo Alto, CA,) operating at 499.84 MHz for ^{1}H and 202.34 MHz for ^{31}P, respectively (Sang et al., 2007). The ^{31}P NMR experiments were performed at 25 °C using a delay of 6 s between pulses with pulse width at 15.0 μs and sweep width at 12,730 Hz. The spectra were processed and analysed with Varian software VNMRJ Version 2.2C. Chemical shifts were reported in δ (ppm) from the reference signal of external 85% phosphoric acid (0.0 ppm).

2.7. In vitro digestion profiles of starch and calibration samples

In vitro digestion of starch and calibration samples were done by a modified Englyst procedure (Sang & Seib, 2006). In the modified method, the digestion with pancreatin was done in the presence of 30 glass beads of 6 mm diameter instead of 5 glass balls of 15 mm diameter, and the shake conditions were 90 strokes/min at a displacement of 25 mm instead of 160 strokes/min at 35 mm displacement. In addition, five times more IU (1112 vs.106–208 IU) of glucoamylase was used than in the original Englyst method. Control samples of potato starch and a 70% extraction hard white wheat flour ('Betty') were used to calibrate the degree of shaking so that the RS in potato starch and wheat flour matched their vivo levels determined in ileostomy patients (Englyst et al., 1999). Percentage of RS was calculated by total starch −% RDS −% SDS.

2.8. Differential scanning calorimetry (DSC)

Starch (≈10.0 mg) and deionized water (≈20 mg) were weighed into a stainless steel pan, and after sealing, the mixture was equilibrated overnight.

Differential scanning calorimeter (Q100, TA Instruments) was used to determine starch gelatinisation parameters with an empty stainless steel pan used as a reference. Starch samples were heated at 10 °C/min from 5 °C to 130 °C, and onset temperature (T_o), peak temperature (T_p), completion temperature (T_c), and enthalpy (ΔH) were calculated from the thermograms.

2.9. X-ray diffraction

X-ray diffraction patterns of the starch samples were recorded on a Philips APD 3520 X-ray diffractometer with Philps XRG 3100 X-ray generator. CuKα radiation at 35 kV and 20 mA, a curved crystal graphite monochromator, and a scanning rate of 2° 2θ/min were used. The degree of crystallinity was estimated from the ratio of the area of peaks to the total area of a diffractogram (Komiya & Nara, 1986).

3. Results and discussion

3.1. Effect of alkaline treatment on total phosphorus content of the PWS

The PWS was produced at 45 °C in a slurry (~35% starch) reaction starting at pH 11.5 and ending at pH 10.8. The purified PWS had a

total phosphorus content of 0.37% (dry basis). Exposure of the purified PWS to sodium hydroxide at pH 9.0 and 40 °C for 4 h caused no significant change of total phosphorus content (Table 1). At pH 10 and 11, only a slight decrease of phosphorus content was noted. However, the phosphorus content was reduced to 0.29% P when the PWS was held at pH 12, indicating that more than 22% of covalently bound phosphate was removed from the starch. Similar results were found when PWS with initial phosphorus of 0.029% P was treated at alkaline pH.

3.2. ^{31}P NMR spectra – effects of alkaline treatment on the chemical forms of the phosphate esters on starch

Repeated digestion of PWS with heat-stable α-amylase gave highly water-soluble phosphodextrins in ~95% yield, and a 50% concentration of those dextrins in D_2O were analysed by proton-decoupled ^{31}P NMR (Sang et al., 2007). Fig. 1A shows that PWS had four types of phosphate esters: cyclic-MSMP, MSMP, DSMP, and MSDP, which had a signal centred at δ 15.9 ppm, δ 3–5 ppm, δ −1 to 1 ppm, and δ −5 and −10 ppm, respectively. No cyclic phosphate or grafted pyrophosphate groups were detected on methyl α-D-glucopyranoside when it reacted with STMP at pH 13.5 → 10 (Lack et al., 2007). The broadening of the ^{31}P signals in Fig. 1A was a reflection of mixed molecules. The amylolytic enzymes do not hydrolyse the glucosidic bonds near phosphate groups (Kasemsuwan & Jane, 1996). Therefore, the various phosphate esters occur on phosphodextrins of different chain lengths, and the ^{31}P-signals of each type ester do not coincide.

The major type of phosphate ester in this sample of PWS was DSMP which showed a broad multiplet of ^{31}P peaks centred at ~0 ppm (Fig. 1). The integrated intensity of the multiplet indicated the modified starch contained 0.17% P as DSMP, or 46% of total phosphate content (Table 1 and 2). The prominence of the DSMP signal in Fig. 1 shows that cross-linking is a major pathway when starch is reacted with STMP in alkali. The second most abundant ester form was MSMP which showed two ^{31}P-signals between δ 3 and 5 and corresponded to 0.077% P (dry starch basis), or 21% of total phosphorus in the modified starch. The peak centred at δ 3.717 ppm, which was 1.04 ppm downfield from the inorganic phosphate peak in the sample, was from the monophosphate ester substituted at C-6 of the D-glucose unit (Lim and Seib, 1994), and the peak at δ 4.584 ppm was from C-3 bound monophosphate. The C-3 and 6 monophosphate peak assignments were confirmed by the spectrum of potato phosphodextrin (Fig. 2), which is known to contain monophosphate esters at C-3 and C-6 on its D-glucose repeat units (Blennow, Bay-Schmidt, Olsen, & Moller, 1998; Haebel, Hejazi, Frohberg, Heydenreich, & Ritte, 2008). The proportions of phosphate bound to the C-6 and C-3 positions of the D-glucose residues in potato starch is approximately 70–80% and 20–30%, respectively, which agrees with the intensities of the peaks in Fig. 2. The peak at 2.677 ppm in Fig. 1was confirmed to be inorganic phosphate (Pi) by spiking the PWS sample with phosphate salt.

It is interesting to note that starch phosphorylation is a key part of starch biosynthesis in potato. Glucan water dikinase catalyses phosphorylation at the C-6 position from ATP, and subsequently, C-3 can be phosphorylated by phosphoglucan water dikinase

Table 1
Total phosphorus contents of phosphorylated wheat starch (PWS) and of PWS after stirring for 4 h at 40 °C in aqueous sodium hydroxide at pH 9.0, 10.0, 11.0, and 12.0.

Samples	*P* (% dry basis)	Change (%)
PWS	0.37 ± 0.002	–
PWS treated at pH 9.0	0.37 ± 0.01	0
PWS treated at pH 10.0	0.36 ± 0.004	3
PWS treated at pH 11.0	0.35 ± 0.009	5
PWS treated at pH 12.0	0.29 ± 0.006	22

Table 2
Levels of different phosphate esters (%, dry basis) in phosphorylated wheat starch (PWS) and in PWS treated at pH 9.0, 10.0, 11.0, and 12.0 at 40 °C.

Samples	P content (%, dry basis) in the form of				
	Cyclic-MSMP	MSMP		MSDP	DSMP
		C-3	C-6		
PWS	0.010	0.034	0.043	0.042	0.17
PWS treated at pH 9.0	0.009	0.035	0.041	0.046	0.17
PWS treated at pH 10.0	0.006	0.036	0.040	0.043	0.16
PWS treated at pH 11.0	0.008	0.025	0.033	0.045	0.17
PWS treated at pH 12.0	0	0.040	0.027	0	0.20
Pooled standard deviation	0.006	0.007	0.005	0.009	0.005

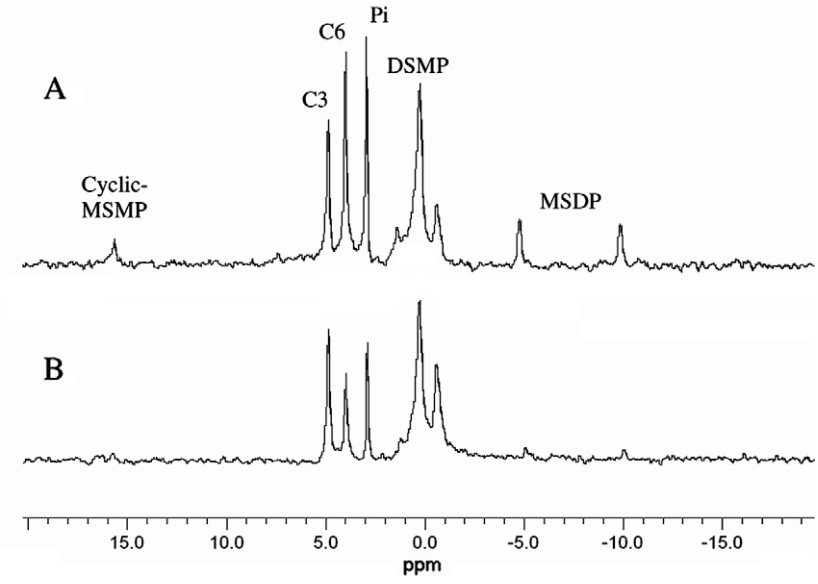

Fig. 1. ^{31}P nuclear magnetic resonance spectra of dextrin prepared from phosphorylated wheat starches (PWS) (A) and the PWS treated at pH 12.0 (B).

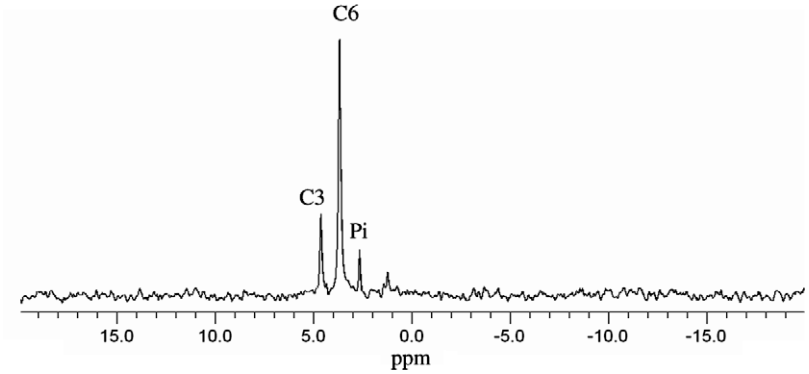

Fig. 2. ^{31}P nuclear magnetic resonance spectra of dextrin prepared from potato starch.

Table 3
Starch *in vitro* digestion by a modified Englyst's method and total dietary fibre content of phosphorylated wheat starch (PWS) and the PWS treated at pH 9.0, 10.0, 11.0, and 12.0.

Samples	*In vitro* digestion (%, db)			TDF (%, db)
	RDS	SDS	RS	
Controls				
Potato starch (Englyst et al., 1999)	4.5	25.5	70	
Potato starch (this work)	4.9	28.1	77	
Wheat flour (Englyst et al., 1999)	48	49.2	2.8	
Wheat flour (this work)	38	59	3.0	
Test samples				
PWS	7.3 ± 0.3	24.4 ± 0.3	68.7 ± 0.1	88.8 ± 0.8
PWS treated at pH 9.0	8.1 ± 0.2	25.5 ± 1.1	66.3 ± 0.9	85.6 ± 0.2
PWS treated at pH 10.0	7.5 ± 0.3	24.4 ± 0.3	68.0 ± 0.6	87.4 ± 0.2
PWS treated at pH 11.0	7.6 ± 0.2	24.9 ± 1.3	67.4 ± 1.2	86.8 ± 1.3
PWS treated at pH 12.0	9.0 ± 0.1	28.3 ± 0.4	62.7 ± 0.4	86.5 ± 0.9

(Haebel et al., 2008). C-6 bound phosphate was found to have a smaller effect on helix packing than C-3 bound phosphate. The C-6 phosphate group aligns well in one of the double-helix surface grooves (Blennow, Engelsen, Nielsen, Baunsgaard, & Mikkelsen, 2002).

The phosphate ester pattern did not significantly change when the PWS was treated at pH 9–11 and 40 °C, but did show changes when the starch was treated at pH 12.0 (Table 2). Phosphorus signals from cyclic-MSMP and MSDP were not detected in the phosphodextrin after PWS was treated at pH 12.0, suggesting that cyclic-MSMP and MSDP are unstable at pH 12. In addition, at pH 12, C-6 bound monophosphate decreased 38% from 0.043% to 0.027%, while C-3 bound monophosphate increased from 18% 0.034–0.040% (dry matter basis). Apparently at pH 12 some of the C6- phosphate groups are lost by alkaline hydrolysis. The increase of C-3 bound monophosphate may result from the alkaline hydrolysis of cyclic-MSMP or MSDP. Moreover, even though total bound phosphorus content decreased, *DSMP (cross-linked esters) increased* ~18% after the PWS was held at pH 12.0 for 4 h. New DSMP may result from the reaction at pH 12 of MSDP or cyclic MSMP with a hydroxyl on another starch chain. Overall, the stability of phosphate esters at pH 12.0 was in the order: cyclic-MSMP ≈ MSDP < MSMP < DSMP.

3.3. Starch enzyme digestion property

The PWS prepared in this study (12% STMP, initial pH 11.5, 45 °C for 3 h) had a high level of the sum of RS (68.7%) and SDS (24.4%). The digestion profile did not change after the starch phosphate was treated at pH 9.0, 10.0, and 11.0 (Table 3). Treating the PWS at pH 12.0 slightly increased enzyme digestion of the starch. The RS content decreased from 68.7% to 62.7%, but TDF content was little changed (88.8% vs. 86.5%) even though the total phosphorus decreased by 22%. It seems that DSMP is more important at inhibiting enzyme digestion than the total phosphorus substitution. After the starch phosphate was treated at pH 12.0, the amount of cross-linking phosphate esters (DSMP) increased ≈18%, which compensated the 22% loss of total phosphorus.

Total phosphorus content in STMP/STPP modified starch for food applications can not exceed the regulatory level of 0.4% P, dry basis in the USA (CFR, 2001). This study suggests that incubating phosphorus cross-linked starch at pH 12.0 can reduce total phosphorus content without significantly changing its digestion property.

3.4. Thermal properties

Gelatinisation of PWS and the PWS treated at pH 9.0, 10.0, 11.0, and 12.0 were investigated by using DSC. The PWS and the PWS after treatment at pH 9.0 to 12.0 showed an endothermic peak due to starch gelatinisation. No melting of an amylose-lipid peak was observed apparently because the alkaline pH saponifies the lipid and somewhere disrupts that complex (Matsunaga & Seib, 1997). Gelatinisation of the PWS started at 66.0 °C (T_o), peaked at 71.3 °C (T_p), and completed at 81.8 °C (T_c) with an enthalpy of 11.3 J/g (Table 4). No significant differences of gelatinisation properties were found after the phosphorylated starch was treated at pH 9.0 to 12.0. Native starch granules do not start gelatinisation until pH 13.0 in sodium hydroxide (Polzinger, 2003). It appears that the alkaline condition used in this study did not change the crystalline phase of the granular structure.

3.5. X-ray diffraction

The PWS and the PWS treated at pH 9.0 to 12.0 had a typical A-type pattern with strong peaks at 2θ values of 13°, 17°, and 23°. The degree of crystallinity of the PWS and the PWS treated

Table 4
Thermal properties of phosphorylated wheat starches (PWS) and the PWS treated at pH 9.0, 10.0, 11.0, and 12.0, respectively.

Starches	Temperature (°C)			ΔH (J/g)
	T_o	T_p	T_c	
PWS	66.0 ± 0.2	71.3 ± 0.3	81.8 ± 0.4	11.3 ± 0.3
PWS treated at pH 9.0	65.8 ± 0.1	71.1 ± 0.2	81.7 ± 0.2	11.3 ± 0.2
PWS treated at pH 10.0	66.0 ± 0.1	71.3 ± 0.1	82.4 ± 0.2	11.5 ± 0.1
PWS treated at pH 11.0	66.1 ± 0.3	71.3 ± 0.1	82.2 ± 0.1	11.6 ± 0.3
PWS treated at pH 12.0	66.4 ± 0.1	72.0 ± 0.1	81.8 ± 0	11.5 ± 0.3

at pH 9.0, 10.0, 11.0, and 12.0 was 24%, 25%, 24%, 23%, and 23%, respectively, confirming that no change in degree of crystallinity occurred after the PWS was treated at pH 9.0–12.0.

4. Conclusions

Four chemically unique phosphate ester forms were detected by ^{31}P NMR when wheat starch was reacted with STMP and STPP in sodium hydroxide starting at pH 11.5. Approximately half of the total phosphate ester was in the form of cross-linked starch diester. The levels of phosphate esters of starch were stable at pH 9.0, but they began to change at pH 10 and 11. At pH 12, the level of substituted phosphate esters decreased ≈22% but distarch monophosphate esters (cross-linked bonds) increased ≈18%. Even though the total amount of phosphate esters significantly decreased after the starch was treated at pH 12.0, the TDF of the starch barely changed, suggesting that the level of the cross-linked phosphate diesters play a key role in making the phosphorylated starch resistant to α-amylase and amyloglucosidase digestion. More work should be conducted to create reaction conditions that can form more cross-linking bonds so that smaller amounts of chemical reagents are used.

Acknowledgement

This work was supported in part by funds provided NIH-NCRR-S10RR22392 and NSF EPS-0236913 to OP. We also thank KSU COBRE and Targeted Excellence Programs support for NMR studies. Contribution No. 09-150-J from the Kansas Agricultural Experiment Station.

References

AACC. (2000). *Approved methods of the AACC* (10th ed.). St. Paul, MN: AACC.
AOAC. (2000). *Approved methods of the AOAC* (17th ed.). Gaithersburg, MD: AOAC (Method 991.43. Total dietary fiber enzymatic gravimetric method. First action. 1992).
Blennow, A., Bay-Schmidt, A. M., Olsen, C. E., & Moller, B. L. (1998). Analysis of starch-bound glucose 3-phosphate and glucose 6-phosphate using controlled acid treatment combined with high-performance anion-exchange chromatography. *Journal of Chromatography A, 829*, 385–391.
Blennow, A., Engelsen, S. B., Nielsen, T. H., Baunsgaard, L., & Mikkelsen, R. (2002). Starch phosphorylation: A new front line in starch research. *Trends in Plant Science, 7*, 445–450.
Bjorck, I., Liljeberg, H., & Ostman, E. (2000). Low glycaemic index foods. *British Journal Nutrition, 83*(Suppl. 1), S149–S155.
Brown, I. J., McNaught, K. J., Andrew, D., & Morita, T. (2001). Resistant starch: Plant breeding, application, development, and commercial use. In B. V. McCleary & L. Prosky (Eds.), *Advanced dietary fiber technology* (pp. 401–412). London, UK: Blackwell Science.
CFR. (2001). Code of federal regulations. Food starch modified. In *Food additives permitted in food for human consumption*. Washington, DC: U.S. Government Printing Office (Title 21. Chapter 1, Part 172. Sect 172.892).
Englyst, H. N., Kingman, S. M., & Cummings, J. H. (1992). Classification and measurements of nutritionally important starch fractions. *European Journal of Clinical Nutrition, 46* (Supp. I), S33–S50.
Englyst, K. N., Englyst, H. N., Hudson, G. J., Cole, T. J., & Cummings, J. H. (1999). Rapidly available glucose in food: An invitro measurement that reflects the glycemic response. *American Journal Clinical Nutrition, 69*, 448–454.
Haebel, S., Hejazi, M., Frohberg, C., Heydenreich, M., & Ritte, G. (2008). Mass spectrometric quantification of the relative amounts of C6 and C3 position phosphorylated glucosylresidues in starch. *Analytical Biochemistry, 379*, 73–79.
Janzen, J. G. (1969). Digestibility of starch and phosphated starches by pancreatin. *Starke, 21*, 231–235.
Jenkins, D. J. A., Jerkins, A. L., Kendall, C. W. C., Augustine, L., & Vuksan, V. (2001). Dietary fiber, carbohydrate metabolism, and chronic disease. In B. V. McCleary & L. Prosky (Eds.), *Advanced dietary fiber technology* (pp. 162–167). Ames, IA: Iowa State University Press.
Kasemsuwan, T., & Jane, J. J. (1996). Quantitative method for the survey of starch phosphate derivatives and starch phospholipids by ^{31}P nuclear magnetic resonance spectroscopy. *Cereal Chemistry, 73*, 702–707.
Komiya, T., & Nara, S. (1986). Changes in crystallinity and gelatinization phenomena of potato starch by acid treatment. *Starch, 38*, 9–13.
Lack, S., Dulong, V., Picton, L., Cerf, D. L., & Condamine, E. (2007). High-resolution nuclear magnetic resonance spectroscopy studies of polysaccharides crosslinked by sodium trimetaphosphate: A proposal for the reaction mechanism. *Carbohydrate Research, 342*, 943–953.
Lim, S., & Seib, P. A. (1994). Location of phosphate esters in a wheat starch phosphate by ^{31}P-nuclear magnetic resonance spectroscopy. *Cereal Chemistry, 70*, 145–152.
Matsunaga, N., & Seib, P. A. (1997). Extraction of wheat starch with aqueous sodium hydroxide. *Cereal Chemistry, 74*, 851–857.
Polzinger, R. (2003). US Patent 6669772. Method for preparing an adhesive for corrugated paperboard.
Roberts, S. B. (2000). High-glycemic index foods, hunger and obesity: Is there a connection? *Nutrition Review, 58*, 163–169.
Rutenberg, M. W., & Solarek, D. (1984). Starch derivatives: Production and uses. In R. L. Whistler, J. N. BeMiller, & E. F. Paschall (Eds.), *Starch chemistry and technology* (pp. 312–388). Orlando, FL: Academic Press.
Sang, Y., & Seib, P. A. (2006). Resistant starches from amylose mutants of corn by simultaneous heat-moisture treatment and phosphorylation. *Carbohydrate Polymers, 63*, 167–175.
Sang, Y., Prakash, O., & Seib, P. A. (2007). Characterization of phosphorylated cross-linked resistant starch by ^{31}P nuclear magnetic resonance (^{31}P NMR) spectroscopy. *Carbohydrate Polymers, 67*, 201–212.
Smith, R. J., & Caruso, J. (1964). Determination of phosphorus. *Methods in Carbohydrate Chemistry, 4*, 42–46.
Tomasik, P., & Schilling C. H. (2004). Chemical modification of starch. In: *Advances in carbohydrate chemistry and biochemistry* (Vol. 59, pp. 175–403).
Topping, D. L., & Clifton, P. M. (2001). Short chain fatty acids and human colonic function: Roles of resistant starch and nonstarch polysaccharides. *Physiology Review, 81*, 1031–1064.
Warren, J. M., Henry, C. J. K., & Simonite, V. (2003). Low glycemic index breakfast and reduced food intake in preadolescent child. *Pediatrics, 112*, E414–E419.
Woo, K., & Seib, P. A. (2002). Cross-linked resistant starch: Preparation and properties. *Cereal Chemistry, 79*, 819–825.

Food Chemistry 118 (2010) 328–332

Contents lists available at ScienceDirect

Food Chemistry

journal homepage: www.elsevier.com/locate/foodchem

Isoflavone during protease hydrolysis of defatted soybean meal

Jianping Wu *, Alister D. Muir

Agriculture and Agri-Food Canada, Saskatoon Research Station, 107 Science Place, Saskatoon, SK, Canada S7N 0X2

ARTICLE INFO

Article history:
Received 31 December 2008
Received in revised form 20 April 2009
Accepted 29 April 2009

Keywords:
Protease
Soybean flour
pH
Isoflavones
Aglycone
β-Glucosidase

ABSTRACT

The study examined the effects of proteases on the isoflavones during enzymatic hydrolysis of soybean flour. Protease itself did not affect the isoflavones during hydrolysis, whereas the applied conditions and contaminated β-glucosidase in the enzyme could greatly affect the content and composition of isoflavones. Soybean flour hydrolysis by ENZECO Alkaline Protease L-FG at high pH (10) resulted in complete loss of malonylglucosidic and acetylglucosidic conjugates in the hydrolysate. However, these conjugates such as 6″-*O*-malonylgenistin and 6″-*O*-malonyldaidzin remained as the principal compounds accounting for 66.2, 58.3 and 70.5% of the total isoflavones in the Protease M "Amano", Alcalase 2.4L, and neutral enzyme ENZECO Neutral Protease-NBP-L hydrolysates, respectively, compared to that of 57.8% in the original soybean flour. The residue prepared by Protease M contained 10 times higher aglycones than that of soy flour, which was due to the contaminated β-glucosidase activity in the enzyme preparation. Our result showed that β-glucosidase contaminated in Protease M has a unique selectivity compared to that of the purified almond β-glucosidase. Results from the study indicated that hydrolysis of soybean flour may provide another alternative approach to enrich aglycone isoflavones in soybean-containing products.

1. Introduction

Soybeans have been used for centuries as an important part of diet in many Asian countries. Consumption of soybean products has been seen an explosive growth worldwide, driven primarily by the US Food and Drug Administration (FDA) health claim concerning the role of soy protein in reducing the risk of heart disease (FDA, 1999). In addition to protein, isoflavones are also touted as one of the most important components responsible for preventing and attenuating cardiovascular diseases, certain cancers and osteoporosis (Brouns, 2002; Messina 1999; Setchell 1998; Setchell & Cassidy, 1999). The content and composition of aglycones in soy foods are largely decided by the genotype, environment, storage and processing conditions (Coward, Smith, Kirk, & Barnes, 1998; Eldridge & Kwolekm, 1983; Hoeck, Fehr, Murphy, & Welke, 2000; Hou & Chang, 2002; Nurmi, Mazur, Heinonen, Kokkonen, & Adlercreutz, 2002). It is believed that isoflavone aglycones, the predominant form in fermented soyfoods (Coward et al., 1998), display greater bioavailability than their corresponding glycosides (Izumi et al., 2000; Watanabe et al., 1998). Setchell et al. (2002) concluded that isoflavone β-glycosides do not cross the intestine of healthy humans, and their bioavailability requires initial hydrolysis of the sugar moiety by intestinal β-glucosidase for uptake to the peripheral circulation. Attempts have been made to increase purposely the aglycone forms mediated by β-glucosidase or microbial fermentation (Obata et al., 2002; Tsangalis, Ashton, Mcgill, & Shah, 2003; Xie, Hettiarachchy, Cai, Tsuruhami, & Koikeda, 2003).

Enzymatic modifications of soybean proteins are extensively explored to improve protein functionalities, nutritional quality, or produce specific population diets/clinical supplements, or as a flavour enhancer (Aaslyng et al., 1998; Clemente, 2000; Lahl & Braun, 1994; Were, Hettiarachchy & Kalapathy, 1997; Wu & Cadwallader, 2002). Recent studies have shown that soybean-derived peptides may have antihypertension (Wu & Ding, 2001), anti-cancer (Galvez, Chen, Macasieb, & de Lumen, 2001; Hellerstein, 1999), lowering cholesterol (Chen, Chiou, Shieh, & Yang, 2002) and immunostimulation activities (Chen, Suetsuna, & Yamauchi, 1995). Compared with many reports on the effect of enzymes on the functional and biological properties of soybean proteins, there is limited information on the effect of proteases on isoflavones that are associated with many soybean products and ingredients. The objectives of this study were to study the effect of proteases on the content and composition of isoflavones.

2. Materials and methods

2.1. Materials

Nutrisoy 7B flour (Lot# 991201C) was obtained from Archer Daniels Midland Co. (Decatur, IL, USA). Protease M (*Aspergillus oryzae,* Amano Enzyme USA Co., Ltd. Elgin, IL, USA), ENZECO

* Corresponding author. Present address: Department of Agricultural, Food and Nutritional Science, University of Alberta, Edmonton, AB, Canada T6H 2V8. Tel.: +1 780 492 6885; fax: +1 780 492 4346.
E-mail address: jwu3@ualberta.ca (J. Wu).

0308-8146/$ - see front matter © 2009 Elsevier Ltd. All rights reserved.
doi:10.1016/j.foodchem.2009.04.129

Neutral Protease-NBP-L (*Bacillus subtilis,* Enzyme Development Co., New York, NY, USA), ENZECO Alkaline Protease L-FG (*B. subtilis,* Enzyme Development Co., New York, NY, USA) and Alcalase 2.4L (*Bacillus licheniformis,* Novozymes North America, Inc., Franklinton, NC, USA) were gifts upon request. Almond-derived β-glucosidase was purchased from Sigma Chemical Co. (St. Louis, MO, USA). Isoflavone standards (daidzin, 6″-*O*-acetyldaidzin, daidzein, genistein, 6″-*O*-acetylgenistin, 6″-*O*-malonylgenistin, genistin, glycitin, 6″-*O*-acetylglycitin and glycitein,) were purchased from LC Labs (Woburn, MA, USA). HPLC-grade acetonitrile, acetic acid and spectranalyzed-grade dimethyl sulphoxide (DMSO) were obtained from Fisher Scientific (Pittsburgh, PA, USA). HPLC-grade water generated by Milli-Q system (Millipore, Bedford, MA, USA) was used for the preparation of the mobile phase.

2.2. Enzymatic hydrolysis of soybean flour

Enzymatic hydrolysis of soybean flour was performed in a temperature- and pH-controlled reaction vessel equipped with a stirrer. Nutrisoy 7B flour was mixed thoroughly using a magnetic stirrer with distilled water into a 5% (w/w, protein/water) slurry. The pH and temperature of the slurry was adjusted to the conditions of individual enzyme, such as 4.5 and 50 °C for Protease M (PM), or 7 and 40 °C for ENZECO Neutral Protease-NBP-L (EN), or 10 and 50 °C for ENZECO Alkaline Protease L-FG (EA), or 8 and 50 °C for Alcalase 2.4L; enzyme was then added at the level of 4% (w/w, on the basis of protein content of the slurry) to initiate the digestion. Temperature was kept stable using a circulating water bath and pH was kept constant during protein digestion with continuous addition of 0.5 M NaOH or 0.5 M HCl if necessary. After 3 h incubation, residue was separated from the slurry after centrifugation at 6,000*g* for 25 min; the residue was re-suspended in 100 mL water and centrifuged under the same condition above. The hydrolysates combined as the resulting clear supernatants and the residues were freeze dried and kept −20 °C till further use.

2.3. Isoflavones extraction

Approximately 0.5 g of soy flour was accurately weighted into a screw cap test tube (125 mm × 20 mm) and was extracted at room temperature for 2 h on a rotary mixer with 10 mL of methanol/acetonitrile/water (4:3:2, v/v/v). After a brief centrifugation (2000*g* for 10 min), a portion of the supernatant was removed with a syringe, filtered through a 0.45-μm filter into a sample vial, and analysed by HPLC.

2.4. Isoflavones analysis

Separation and quantification of isoflavones were performed on a symmetry® C_{18} reverse-phase column (4.6 × 250 mm, 5 μm particle size, Waters, Milford, MA, USA) according to Griffith and Collison (2001) with slight modifications as reported (Wu & Muir, 2008). All samples were run automatically via sample management system at a fixed injection volume of 10 μL on an HPLC Waters™ 2690 Separation Module System (Waters Inc.; Milford, MA, USA). UV absorbance was scanned from 200 to 350 nm using a Model Waters 996 Photodiode Array Detector, and peak area was integrated automatically with the supplied software at 254 nm. The sample compartment temperature and column temperature were kept at 15 and 34 °C, respectively. Column was eluted by a two-solvent system: (A) 0.1% acetic acid in water and (B) 0.1% acetic acid in acetonitrile. The column was held constantly at 15% B for the first 10 min, increased to 35% B over 45 min, then to 55% B over 10 min. The concentration of B was brought back to 15% over 5 min and held for another 5 min before the next run.

Individual isoflavone standards were used for peak identification according to elution time, UV spectra and spiking tests. Isoflavone quantification was based on calibration curves for each of the 10 isoflavone standards; quantification of 6″-*O*-malonyldaidzin and 6″-*O*-malonylglycitin, however, was based on their corresponding glucosides adjusted for the molecular weight difference (Kudou et al., 1991). Each sample was analysed in duplicate and mean values were reported.

2.5. β-Glucosidase activity analysis

β-Glucosidase activity in four proteases was determined according to the method of Grover (1977) by measuring the rate of hydrolysis of *p*-nitrophenyl-β-D-glucopyranoside (pNPG). One unit of the enzyme activity was defined as the amount of β-glucosidase that release 1 μmol of *p*-nitrophenol from the substrate pNPG per milliliter per minute.

2.6. Standard isoflavone incubation

Isoflavone standards (a mixture of 0.2 mg of daidzin, acetyldaidzin, malonyldaidzin, genistin, acetylgenistin and malonylgenistin) were dissolved by 1.0 mL of DMSO and extracted solvent mixture (1:1, v/v), diluted 10 times with 0.2 M acetic acid buffer (pH 4.5). Equal volume isoflavone standard solution was incubated with Protease M "Amano" or with β-glucosidase (15 U) at the same condition used for protein hydrolysis as stated above. Samples (0.6 mL) were taken at various incubation intervals at 0, 0.25, 1, 3, 6 and 24 h and the enzyme was inactivated by adding 0.9 mL of acetonitrile whilst stirring under room temperature. After mixed with 1.5 mL HPLC-grade water, the samples were filtered through a 0.45 μm filter prior to HPLC analysis.

3. Result and analysis

3.1. Isoflavones during protease hydrolysis

Four proteases with different pH optimums were used to study their effects on the isoflavones during hydrolysis. Compared to the soybean flour, the content and composition of isoflavones in both the hydrolysate and resultant residues were significantly affected by the proteases and their associated conditions (Table 1). The resultant residues tended to contain higher amount of isoflavones than those of the hydrolysates; the amount of isoflavones in the Protease M residue was more than three times higher than that of the hydrolysate. With the exception of EA hydrolysis, whose recovery of total isoflavones was only 71.6%, the average recovery of isoflavones after hydrolysis was 91.3%; the lower recovery percentage in EA hydrolysis was probably due to the high pH value (10) applied. Hydrolysis under high pH conditions such as in ENZECO Alkaline Protease L-FG resulted in complete loss of malonylglucosidic and acetylglucosidic conjugates both in the hydrolysate and residue (Table 1). However, these conjugates, such as 6″-*O*-malonylgenistin and 6″-*O*-malonyldaidzin remained as the principal compounds accounting for 66.2% in Protease M hydrolysate, 58.3% in Alcalase 2.4L hydrolysate, 70.5% in ENZECO Neutral Protease-NBP-L (EN) hydrolysate, respectively, compared with 57.8% in soybean flour and 0% in EA hydrolysate (Table 1). It is well known that malonylglucosidic and acetylglucosidic conjugates are the most fragile compounds among these isoflavone chemicals and their stability were vulnerable to environmental factors and processing conditions (Coward et al., 1998; Griffith & Collison, 2001; Kudou et al., 1991). With the exception of EA hydrolysis, there were relative high total amount of malonylglucosidic and acetylglucosidic conjugates left in hydrolysates and residues compared

Table 1
Effect of proteases on the isoflavones (values are the mean of duplicate determinations, expressed in the form of μg aglycone/g of dry weight) distribution in the hydrolysates and their residues.

Enzyme	Alcalase 2.4L		Protease M "Amano"		ENZECO Neutral Protease		ENZECO Alkaline Protease		Flour
Isoflavone	Hydrolysate	Residue	Hydrolysate	Residue	Hydrolysate	Residue	Hydrolysate	Residue	
Daidzein	67.7	344.0	67.2	604.1	79.2	317.7	42.9	240.4	37.5
Daidzin	180.4	112.1	51.2	48.3	66.5	44.5	334.1	156.6	252.4
6″-*O*-Acetyldaidzin	412.8	210.0	329.8	310.6	537.6	305.0	–	–	482.5
6″-*O*-Malonyldaidzin	–[a]	0.9	5.4	7.6	35.6	–	–	–	12.5
Genistein	49.4	590.4	52.9	1012.5	60.9	547.4	27.2	365.6	47.5
Genistin	186.7	227.4	43.1	90.9	63.9	82.5	576.8	624.4	288.4
6″-*O*-Acetylgenistin	395.5	420.4	250.2	515.5	408.8	520.9	0.0	0.0	557.1
6″-*O*-Malonygenistin	5.1	16.6	3.6	27.6	0.0	17.2	0.0	0.0	11.4
Glycitein	17.8	57.6	11.9	95.5	15.9	57.8	9.2	40.3	–
Glycitin	31.7	22.1	21.8	14.1	17.9	8.4	63.3	36.6	36.7
6″-*O*-Acetylglycitin	40.1	19.2	29.7	34.4	53.3	29.0	–	–	48.6
6″-*O*-Malonylglycitin	12.4	3.9	9.3	–	2.7	5.9	–	–	23.3
Total	1399.6	2024.5	876.3	2761.0	1342.3	1936.3	1053.6	1463.9	1797.9

[a] Not detected.

with their original values in soybean flour (Table 1). In contrast with the total loss of malonylglucosidic and acetylglucosidic conjugates under extreme pH (10.0) hydrolysis conditions, hydrolysis under mild enzymatic conditions had relatively small influence on the stability of these isoflavones (Table 1). The reaction temperature is 50 °C for both alkaline enzymes, but the pH was 8 in Alcalase 2.4L hydrolysis whereas 10 in ENZECO Alkaline Protease L-FG hydrolysis; these results indicated that the difference in pH played an important role in deciding the stability of the conjugated isoflavones. We previously explained that the high water content and the buffering environment formed during enzymatic hydrolysis might be the reasons for the enhanced stability of conjugated chemicals (Wu & Muir, 2008).

Interestingly, 6″-*O*-malonyldaidzin and 6″-*O*-malonygenistin were no longer the predominant chemicals in the PM residue. There was a large increase in aglycone content in the residue, e.g. the contents of daidzein, genistein and glycitein in PM residue were 604.1, 1012.5 and 95.5 μg aglycone/g compared to those of 37.5, 47.5 and 0 μg aglycone/g in the soybean flour; these three aglycones accounted for 62% of the total isoflavones in PM residue compared to that of 4.7% in soy flour. Similar trend existed in other enzymatic residues where the aglycone fraction accounted for 49.0% in Alcalase 2.4L residue, 44.1% in EA residue and 44.7% in EN residue of the total isoflavone content. The increase in aglycone content in our residues compared favourably with lactic acid fermented soymilk, showing a 63–67% increase in aglycone (Otieno & Shah, 2007). Using β-glycosidase from *Penicillium multicolour*, Xie et al. (2003) reported that the amount of genistein, daidzein, and glycitein in β-glycosidase treated soymeal were increased from 1.23, 1.25, and 1.51 mmol/g to 3.21, 2.02, and 2.12 mmol/g, respectively. Our results suggested that the major portion of aglycones formed during hydrolysis was remained in their residues after centrifugal separation; the residues accounted for 84.1, 90.9 and 73.3% of the total aglycones produced during the hydrolysis of soybean meal by EN, PM and Alcalase 2.4L, respectively.

The increase in aglycone content in EA treated sample could be attributed to the high pH applied in enzymatic hydrolysis; however, the remarkable increase in their aglycones under mild conditions could be attributed to the contaminated β-glucosidase present in these protease preparations rather than the temperature and pH applied during incubation. It was reported that β-glucosidase has superior activity for conversion of isoflavones glycosides to aglycones (Matsuura & Obata, 1993; Xie et al., 2003). β-Glucosidase from microorganisms such as *bifidobacteria* and *lactic acid* bacteria have also been studied in hydrolysing isoflavone glycosides into aglycones (Matsuyama, Setoguchi, Arai, & Kiyosawa, 1990; Tsangalis et al., 2003). Microbially derived protease preparations tend to contaminate more or less amount of β-glucosidase; the activity of β-glucosidase in PM, EN, Alcalase 2.4L and EA were determined to be 18.5, 0.09, 0.03, 0 U/g, respectively. The contaminated β-glucosidase in these bacterial proteases contributed greatly to the isoflavones conversion observed during hydrolysis with the exception of EA. Since the optimal pH for β-glucosidase is acidic pH, it is in a good alignment with the result that PM shows the highest β-glucosidase activity among the enzymes tested. However, the increase in aglycones could not be attributed totally to the conversion of their manyolglucosidic and acetylglucosidic conjugates, since the increase magnitude in daidzein (from 546 μg total aglycones in soy flour to 4207.1 μg total aglycones in hydrolysate and residue) was far greater than the total manyolglucosidic (from 7030.0 in soybean flour to 4483.4 μg total aglycones in hydrolysate and residue) and acetylglucosidic conjugates (from 182.1 to 88.5 μg total aglycones) in PM treated samples; furthermore, a significant higher conversion percentage was observed from glucosidic isoflavones to aglycones than malonylglucosidic and acetylglucosidic conjugates to aglycones. It was calculated that 81.1% of daidzin was converted into daidzein, 78.8% of genistin into genistein, compared with 36.2% of 6″-*O*-malonygenistin into daidzein, 51.4% of 6″-*O*-acetyldaidzin into daidzein, and 37.1% of 6″-*O*-malonygenistin into genistein. These results suggested that the activity of β-glucosidase in PM might have a different enzyme selectivity from the reported β-glucosidase (*P. multicolour*) (Xie et al., 2003).

3.2. Standard isoflavone incubation

In order to address the unique enzyme specificity of β-glucosidase in the Protease M, we tested its activity on authenticated isoflavone standards; purified β-glucosidase from almond was also used for comparison. Fig. 1 shows the chromatograms of these standard isoflavones under different incubation intervals using Protease M or purified almond β-glucosidase. Daidzin was completely converted into aglycone in the first 15 min in both enzymes; genistin was not detected in PM treated samples whereas there was trace amount of genistin left in the β-glucosidase treated samples. Matsuura and Obata (1993) reported that β-glucosidase from soybean had a conversion percentage of 16.9% from genistin to genistein and 14.3% for daidzin to daidzein in soymilk, which was much less than the results we reported. The content of malonyldaidzin decreased gradually with the incubation time; percentage conversion reached 74.5 and 61.1% for PM and β-glucosidase treated samples at 24 h, respectively (Fig. 2). It appeared that

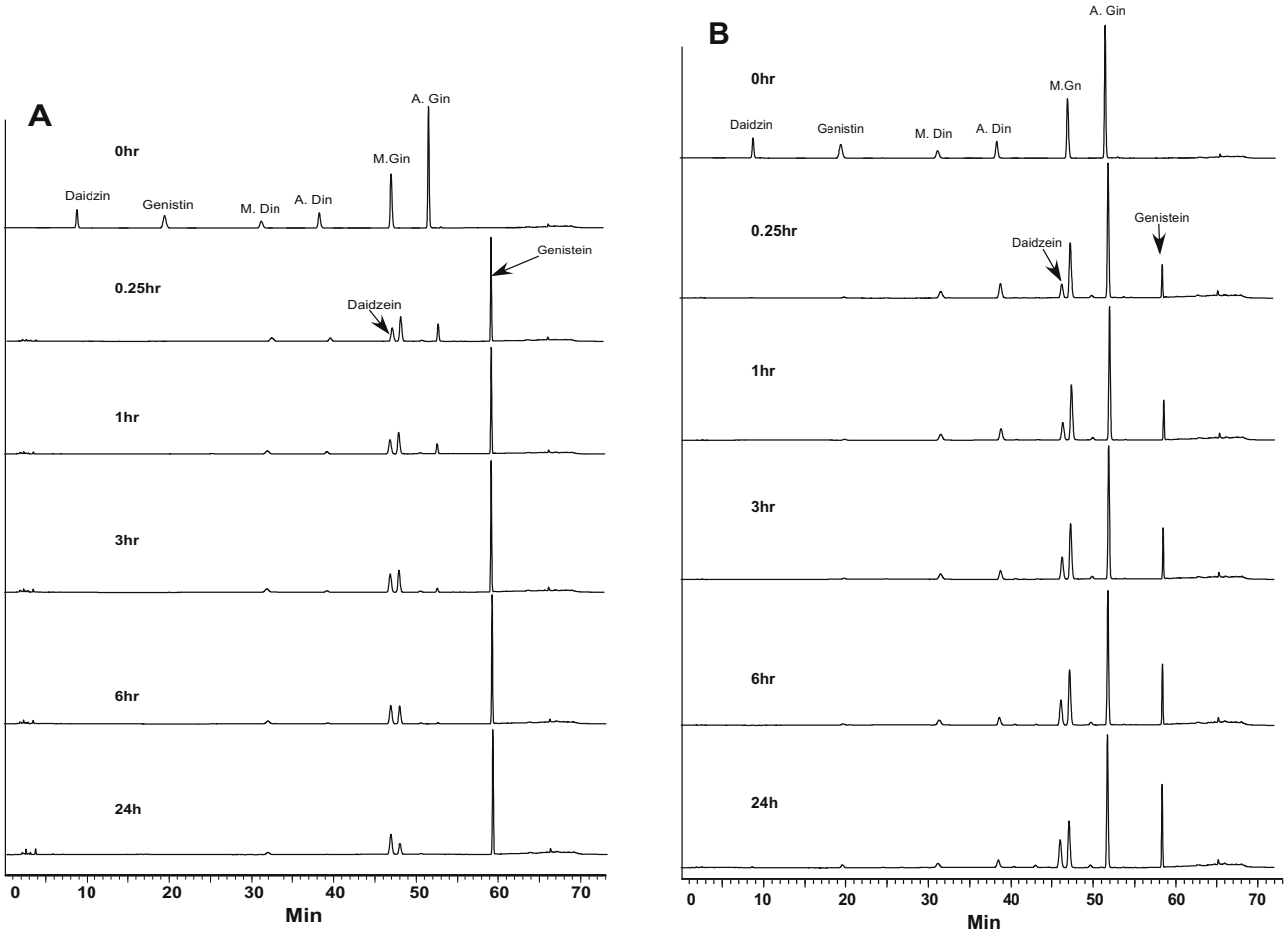

Fig. 1. Chromatograms of standard isoflavones under different incubation intervals with Protease M "Amano" (A) and purified β-glucosidase (B).

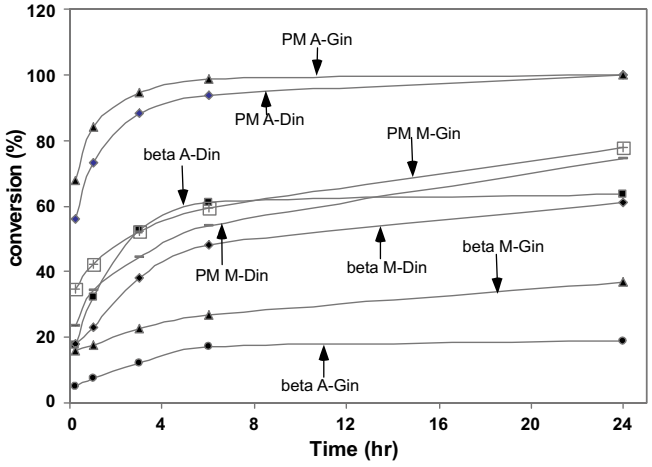

Fig. 2. The conversion percentage of standard isoflavone under various incubation intervals with PM and almond β-glucosidase at the same activity of β-glucosidase. Abbreviations: PM, Protease M "Amano"; β, almond purified β-glucosidase; A-Gin, acetylgenistin; A-Din, acetyldaidzin; M-Din, malonyldaidzin; M-Gin, malonylgenistin.

β-glucosidase from both PM and almond could not convert all malonyldaidzin into daidzein under the condition tested. Generally speaking, acetyldaidzin showed a higher conversion percentage than that of malonyldaidzin (Fig. 2). At 24 h, there was no acetyldaidzin left in PM treated sample whereas there was 36% of acetyldaidzin left in β-glucosidase treated sample. It seemed that β-glucosidase in PM had a higher efficiency than that of almond-derived β-glucosidase and therefore, the conversion percentage from acetylgenistin and malonylgenistin into genistein with PM was higher than that of almond-derived β-glucosidase. The difference between their specificity and efficiency for the conversion of glucosides to aglycones had a great impact on the content of aglycones. Consequently, the contents of daidzein and genistein in PM treated samples were significantly higher than those of almond β-glucosidase treated samples (Fig. 1). The content of daidzein in PM treated sample was 237.1 μg daidzein/mL compared with 156.2 μg daidzein/mL in almond β-glucosidase treated sample at 0.25 h and this difference remained significant within 6 h but not at 24 h incubation. It appeared that the conversion from glucosides to aglycones with PM was higher and faster than that of the almond β-glucosidase (Fig. 2); the greatest conversion happened within 3 h, reached a plateau after 6 h incubation. The content of genistein in PM treated sample increased rapidly to 659.6 μg aglycone/mL at 15 min, compared with 161.4 μg aglycone/mL at 15 min and 356.8 μg glycone/mL at 24 h incubation in almond β-glucosidase.

4. Conclusions

This study showed that protease hydrolysed soybean products contained significant amount of isoflavones, and the content and composition of isoflavones were greatly affected by the applied reaction conditions and presence of β-glucosidase activity in the

commercial protease enzyme. The microbial conversion of isoflavone forms has been reported in soybean products during fermentation efforts to convert conjugated isoflavones into their aglycone forms using bacterial β-glucosidase to develop aglycone-enriched products have been reported (Otieno & Shah, 2007, 2008; Xie et al. 2003). Our results indicated that the β-glucosidase present in commercial protease enzyme preparations has a unique specificity for the conversion of isoflavone chemicals, which was different from almond-derived β-glucosidase. Previous studies also showed that strain-dependent β-glucosidase activity in soymilk (Otieno & Shah 2007, 2008). In addition to β-glucosidase activity, enzyme specificity should be taken into consideration in bioconversion of isoflavones. PM hydrolysis of soybean flours not only resulted in potent bioactive peptides, but also produced a residue with an exceptional high content of aglycones. Our results indicated that protease hydrolysed residues contained more than 10 times higher concentration of aglycones than that of soy flour, thus provided another alternative approach to enrich aglycone isoflavones in soy-containing products. Our further study aims to develop an integrated technology to produce bioactive peptides and enriched aglycone isoflavones from soybean meal. Further research on the purification of the β-glucosidase from the PM preparation is needed to characterise its properties and compare with other sources of β-glucosidase.

References

Aaslyng, M. D., Martens, M., Poll, L., Nielsen, P. M., Flyge, H., & Larsen, L. M. (1998). Chemical and sensory characterization of hydrolyzed vegetable protein, a savory flavoring. *Journal of Agricultural and Food Chemistry, 46*, 481–489.

Brouns, F. (2002). Soya isoflavones: A new and promising ingredient for the health foods sector. *Food Research International, 35*, 187–193.

Chen, J. R., Chiou, S. F., Shieh, M. M., & Yang, S. C. (2002). The effects of soybean protein-derived hydrolysate on lipid metabolism in rats fed a high cholesterol diet. *Journal of Food Biochemistry, 26*, 431–442.

Chen, J. R., Suetsuna, K., & Yamauchi, F. (1995). Isolation and characterization of imunostimulative peptides from soybean. *Nutritional Biochemistry, 6*, 310–313.

Clemente, A. (2000). Enzymatic protein hydrolysates in human nutrition. *Trends in Food Science & Technology, 11*, 254–262.

Coward, L., Smith, M., Kirk, M., & Barnes, S. (1998). Chemical modification of isoflavones in soyfoods during cooking and processing. *American Journal of Clinical Nutrition, 68*, 1486S–1491S.

Eldridge, A. C., & Kwolekm, W. F. (1983). Soybean isoflavones: Effect of environment and variety on composition. *Journal of Agricultural and Food Chemistry, 31*, 394–396.

FDA. (1999). Food labeling health claims, soy protein and coronary heart disease. Food and Drug Administration, 21 Code of Federal Regulations, Part 101.

Galvez, A. F., Chen, N., Macasieb, J., & de Lumen, B. O. (2001). Chemopreventive property of a soybean peptide (Lunasin) that binds to deacetylated histones and inhibits acetylation. *Cancer Research, 61*, 7473–7478.

Griffith, A. P., & Collison, M. W. (2001). Improved methods for the extraction and analysis of isoflavones from soy-containing foods and nutritional supplements by reverse-phase high-performance liquid chromatography and liquid chromatography-mass spectrometry. *Journal of Chromatography (A), 913*, 397–413.

Grover, A. K. (1977). Studies on almond emulsin β-D-glucosidase. *Biochimica et Biophysica Acta, 482*, 98–108.

Hellerstein, M. (1999). Antimitotic peptide characterized from soybean: Role in protection from cancer? *Nutrition Review, 57*, 359–361.

Hoeck, J. A., Fehr, W. R., Murphy, P. A., & Welke, G. A. (2000). Influence of genotype and environment on isoflavone contents of soybean. *Crop Science, 40*, 48–51.

Hou, H. J., & Chang, K. C. (2002). Interconversions of isoflavones in soybeans as affected by storage. *Journal of Food Science, 67*, 2083–2089.

Izumi, T., Piskula, M. K., Osawa, S., Obata, A., Tobe, K., Saito, M., et al. (2000). Soy isoflavone aglycones are absorbed faster and in higher amounts than their glucosides in humans. *Journal of Nutrition, 130*, 1695–1699.

Kudou, S., Fleury, Y., Welti, D., Magnolato, D., Uchida, T., Kitamura, K., et al. (1991). Malonyl isoflavone glucosides in soybean seeds (*Glycine max* Merrill). *Agricultural and Biological Chemistry Journal, 55*, 2227–2233.

Lahl, W. J., & Braun, S. D. (1994). Enzymatic production of protein hydrolysates for food use in overview: Outstanding symposia in food science and technology. *Food Technology, 48*, 68–71.

Matsuura, M., & Obata, A. (1993). The β-glucosidases from soybeans hydrolyze daidzin and genistin. *Journal of Food Science, 58*, 144–147.

Matsuyama, J., Setoguchi, T., Arai, C., & Kiyosawa, I. (1990). Hydrolytic profiles of soybean isoflavone glycosides with β-glycosidases in the cultures of bifidobacteria and lactic acid bacteria. *Bulletin of the Faculty of Agriculture Tamagawa University (Japan), 30*, 33–42.

Messina, M. J. (1999). Legumes and soybeans: Overview of their nutritional profiles and health effects. *American Journal of Clinical Nutrition, 70*, 439S–450S.

Nurmi, T., Mazur, W., Heinonen, S., Kokkonen, J., & Adlercreutz, H. (2002). Isoflavone content of the soy base supplements. *Journal of Pharmaceutical and Biomedical Analysis, 28*, 1–11.

Obata, A., Manaka, T., Tobe, K., Izumi, T., Saito, M., & Kikuchi, M. (2002). Process for producing isoflavone aglycone-containing composition. US Patent, 6,444, 239

Otieno, D. O., & Shah, N. P. (2007). Comparison of changes in the transformation of isoflavones in soymilk using varying concentrations of exogenous and probiotic-derived endogenous β-glucosidases. *Journal of Applied Microbiology, 103*, 601–612.

Otieno, D. O., & Shah, N. P. (2008). Production of β-glucosidase and hydrolysis of isoflavone phytoestrogens by *Lactobacillus acidophilus*, *Bifidobacterium lactis*, and *Lactobacillus casei* in soymilk. *Journal of Food Science, 73*, M15–M20.

Setchell, K. D. R. (1998). Phytoestrogens: The biochemistry, physiology, and implications for human health of soy isoflavones. *American Journal of Clinical Nutrition, 68*, 1333S–1346S.

Setchell, K. D. R., Brown, N. M., Zimmer-Nechemias, L., Brashear, W. T., Wolfe, B. E., Kirschner, A. S., et al. (2002). Evidence for lack of absorption of soy isoflavone glycosides in humans, supporting the crucial role of intestinal metabolism for bioavailability. *American Journal of Clinical Nutrition, 76*, 447–453.

Setchell, K. D. R., & Cassidy, A. (1999). Dietary isoflavones: Biological effects and relevance to human health. *Journal of Nutrition, 129*, 758S.

Tsangalis, D., Ashton, J. F., Mcgill, A. E. J., & Shah, N. P. (2003). Biotransformation of isoflavones by bifidobacteria in fermented soymilk supplemented with D-glucose and L-cysteine. *Journal of Food Science, 68*, 623–631.

Watanabe, S., Yamaguchi, M., Sobue, T., Takahashi, T., Miura, T., Arai, Y., et al. (1998). Pharmacokinetics of soybean isoflavones in plasma, urine and feces of men after ingestion of 60 g baked soybean powder (Kinako). *Journal of Nutrition, 128*, 1710–1715.

Were, L., Hettiarachchy, N. S., & Kalapathy, U. (1997). Modified soy proteins with improved foaming and water hydration properties. *Journal of Food Science, 62*, 821–823. 850.

Wu, J., & Ding, X. (2001). Hypotensive effect of angiotensin converting enzyme inhibitory peptides derived from defatted soybean meal on spontaneously hypertensive rats (SHR). *Journal of Agricultural and Food Chemistry, 49*, 501–506.

Wu, Y. F. G., & Cadwallader, K. R. (2002). Characterization of the aroma of a meatlike process flavoring from soybean-based enzyme-hydrolyzed vegetable protein. *Journal of Agricultural and Food Chemistry, 50*, 2900–2907.

Wu, J., & Muir, A. D. (2008). Isoflavone content and its potential contribution to the antihypertensive activity in soybean angiotensin I converting enzyme inhibitory peptides. *Journal of Agricultural and Food Chemistry, 56*, 9899–9904.

Xie, L., Hettiarachchy, N. S., Cai, R., Tsuruhami, K., & Koikeda, S. (2003). Conversion of isoflavone glycosides to aglycones in soyLife and soymeal using β-glycosidase. *Journal of Food Science, 68*, 427–430.

Food Chemistry 118 (2010) 333–340

Contents lists available at ScienceDirect

Food Chemistry

journal homepage: www.elsevier.com/locate/foodchem

Marine collagen peptide isolated from Chum Salmon (*Oncorhynchus keta*) skin facilitates learning and memory in aged C57BL/6J mice

Xinrong Pei [a], Ruiyue Yang [a], Zhaofeng Zhang [a], Lifang Gao [b], Junbo Wang [a], Yajun Xu [a], Ming Zhao [a], Xiaolong Han [a], Zhigang Liu [a], Yong Li [a,*]

[a] Department of Nutrition and Food Hygiene, School of Public Health, Peking University, Beijing 100191, China
[b] Center for Food and Drug Safety Evaluation, Capital Medical University, Beijing, China

ARTICLE INFO

Article history:
Received 3 November 2008
Received in revised form 21 April 2009
Accepted 29 April 2009

Keywords:
Bioactive peptides
Learning and memory
Aging
Brain-derived neurotrophic factor
Postsynaptic density protein 95

ABSTRACT

To observe the neuroprotective effects of marine collagen peptide (MCP) isolated from Chum Salmon (*Oncorhynchus keta*) skin by enzymatic hydrolysis, 20-month-old female C57BL/6J mice were fed with chow diet, 0.22%, 0.44% or 1.32% (wt/wt) MCP diet for 3 months. Comparing with aged control group, the abilities of passive avoidance and spatial memory and learning were significantly enhanced evaluated by step-down test and Morris water maze respectively. Furthermore, the abilities of learning and memory had no significant difference between 0.44% and 1.32% MCP treated groups and young control group. The alleviated oxidative stress, reduced apoptotic neurons, up-regulated expression of brain-derived neurotrophic factor (BDNF) and postsynaptic density protein 95 (PSD95) were observed in MCP treated groups compared with aged control group. Our research revealed that there were no significant difference between 0.44% and 1.32% MCP treated groups and young control group. These findings suggest that MCP could be a candidate for functional food to relieve memory deficits associated with aging.

1. Introduction

Cognitive deficits including learning impairment and delayed amnesia may be caused by age-related deterioration in brain function (Erickson & Barnes, 2003). While the world's population is aging in the 21st century (Kalache, Aboderin, & Hoskins, 2002), a fast growing number of aged people suffer from neurodegenerative diseases, such as Alzheimer's disease (AD) and Parkinson's disease (PD), two of the most common diseases among the elderly that impairs the cognitive ability (Morrison & Hof, 1997).

Mounting evidence suggests that lifestyle factors, especially the diet, may account for the development of chronic diseases, such as cardiovascular disease, diabetes and neurodegenerative disease (Ferrari, 2007). Nowadays, while major dietary intervention has been applied to prevent such diseases as diabetes and heart disease, the potential impact of diet on aging process-associated neurodegeneration has been neglected. Apparently, the potential effect of nutrition on slowing down the neuropathies deserves increasing public concern (Paliyath, 2006). And it is well known that in protein, it is bioactive peptides that act out the biological activity.

Since the first bioactive peptide was revealed by Mellander (1950), the potential physiological functions of bioactive peptides derived from dietary protein have aroused a lot of scientific interest and attention (Korhonen & Pihlanto, 2003; Mellander, 1950). As specific protein fragments, a wide range of activities of bioactive peptides have been described, including antimicrobial, blood pressure-lowering, cholesterol-lowering, antioxidative and immunomodulatory effects, etc. (Hartmann & Meisel, 2007; Miraliakbari & Shahidi, 2008). Moreover, some peptides can influence higher brain functions, such as learning and memory, in humans and animals (McLay, Pan, & Kastin, 2001).

Theoretically, bioactive peptides can be released from dietary proteins through digestion in the gut; the amount of peptides, however, is too small to induce any significant effects. In contrast, enzymatic hydrolysis of dietary proteins offers a rapid and reproducible method for the production of considerable bioactive peptide fractions, and they are likely to become potential health-beneficial-food ingredients or nutraceutical preparations (Hartmann & Meisel, 2007).

During the past five decades, fish proteins were widely studied and their various multifunctional properties were well described (Aneiros & Garateix, 2004; Chavan, McKenzie, & Shahidi, 2001). We still do not know, however, whether bioactive peptides from fish proteins have preventive effect against age-related cognitive decline. It is certain now that oxidative stress can lead to cell and tissue damage, thus resulting in age-related cognitive decline and our previous research demonstrated that bioactive peptides derived from fish skin has antioxidant function in D-galactose induced Sprague-Dawley rats. Hence, it is reasonable to hypothesise that

* Corresponding author. Tel./fax: +86 10 82801177.
E-mail addresses: liyongbmu@163.com, liyong@bjmu.edu.cn (Y. Li).

0308-8146/$ - see front matter © 2009 Elsevier Ltd. All rights reserved.
doi:10.1016/j.foodchem.2009.04.120

fish protein may be a valuable source of neuroprotective peptides. The purpose of the present study was to investigate the promnestic effects of Marine Collagen Peptide (MCP), compounds of low molecular weight peptides derived from Chum Salmon (*Oncorhynchus keta*) skin by enzymatic hydrolysis, on the cognition of aged C57BL/6J mice. Despite broadly comparable patterns of cognitive decline with normal aging for males and females, some groups of females may be more vulnerable than males to cognitive dysfunction as they age. Most remarkable is the observation that Alzheimer's disease is two to threefold higher in women than in men after the age of 65 years (Andersen, Launer, & Dewey, 1999; Hebda-Bauer, Luo, Watson, & Akil, 2007). This gender difference persists even after correcting for differences in life expectancy. So, we used female mice in this study. In addition, we intended to explore cellular and molecular mechanisms and how MCP regulates the plasticity of the brain to repair itself in response to the effect of aging. Furthermore, we also wanted to determine whether MCP might become a candidate for functional food or pharmaceutical applications to relieve memory deficits associated with aging.

2. Materials and methods

2.1. Chemicals

Commercial kits used for determination of T-SOD, GSH-Px and TBARS were purchased from Jiancheng Institute of Biotechnology (Nanjing, China). Mouse monoclonal anti-BDNF was purchased from Santa Cruz Biotechnology (Santa Cruz, CA, USA). Rabbit monoclonal anti-PSD95 was purchased from Chimicon (Temecula, CA). ECL plus western blotting detection system was obtained from Amerscham Pharmacia Biotech (Buckinghamshire, England). All other chemicals were reagent grade or the highest quality available from Sigma–Aldrich Co. (St. Louis, MO, USA). MCP was purified by reversed phase chromatography using a 250 × 10 mm C18 column (Phenomenex Inc., Torrace, CA, USA).

2.2. Preparation and identification of MCP

Marine Collagen Peptide (MCP) was derived from the skin of wild-caught Chum Salmon (*O. keta*) (average body weight, 1.47 kg) and donated by CF Haishi Biotechnology Ltd. Co. (Beijing, China). In brief, skin of Chum Salmon was cleaned and the adherent tissue was scraped manually by a scalpel. Then the skin was minced and defatted by vigorous stirring in chill water. The materials were homogenised and emulsified in distilled water, and added into complex protease (3000 U/g protein), which including 7% of trypsin, 65% of papain and 28% of alkaline proteinase, with the constant temperature at 40 °C and pH value of 8, for 3 h. The resultant hydrolysate was centrifuged at 10,000*g* by decanter centrifuge at first, and then it was centrifuged at 15,000*g* by tube centrifuge to get rid of the impurity. After centrifuge, the liquid was subsequently separated through ceramic membrane (200 μm) to purify it. The mineral salt was removed from the liquid through a procedure of nanofiltration at pH 6.5–7.5 with a concentration of solid material between 2.2–2.6 g/100 ml. Then the purified liquid was condensed by cryoconcentration under vacuum at 70 °C with an evaporation rate of 500 kg/h. When the concentration of the condensed liquid was almost 30 Baume degrees, it was decoloured with 12% of active carbon at 75 °C for 1 h, and then got rid of the carbon by filtration. When all the process above was finished, removed most of the water by spray drying with the pressure of 20 MPa at an evaporation rate of 200 kg/h, MCP powder used in the following investigation was obtained.

High-performance liquid chromatography (HPLC, Waters Corp., Milford, MA, USA) of peptide sample was performed using a Phenomenex C_{18} column (10 × 250 mm), which used acetonitrile-0.05 mol/L phosphate buffer (PH 3.2) (10:90) as the mobile phase with a flow rate of 2.0 mL/min and monitored at 208 nm using a Water 486 tunable UV detector. Then the molecular weight distribution of the sample was ascertained by LDI-1700 matrix-assisted laser desorption ionisation time-of-flight mass spectrometry (MALDI-TOF-MS) (Liner Scientific Inc., Reno, NV, USA). In addition, the amino acid composition was further analysed by an H835–50 automatic amino acid analyzer (Hitachi, Tokyo, Japan). The result indicated that the molecular weight distribution of MCP was 100–860 Da. Furthermore, 85.86% of the molecular weight distributed between 300 and 860 Da. So, the main composition of MCP was oligopeptides. The amino acid composition of MCP was shown in Table 1.

2.3. Animals and diet

C57BL/6 J female mice were obtained from the Animal Service of Health Science Center, Peking University. Control animals were fed AIN93M Diet from Vital River Limited Company (Beijing, China). The mice in the experimental groups were fed with 0.22%, 0.44% or 1.32% (wt/wt) MCP in AIN93M diet, respectively. The composition of the AIN93M diet include 20.26% of protein, 4.24% of fat, 25.19% of carbohydrate, 3.60 mg/100 g vitminA, 0.25 mg/100 g vitminD, 44.00 mg/100 g vitminE, 5.00 mg/100 g vitminK, 1.10 g/kg choline chloride and 25.90 g/kg mineral mix. The weight and food consumption were measured every week. No significant differences in diet or weight gain had been found between the un-supplemented aged mice and the old supplemented mice (data were not shown). The young mice were 3 month-old, while aged mice 20 monthly at the start of the experiment. All animals were acclimatised at animal colony facilities in laboratory of animal service of Peking University for at least 1 week before treatment. Mice were housed four to five per cage and provided with MCP-supplemented diet or standard diet for 3 months. All animals were maintained at a constant temperature (23 ± 1 °C) and humidity (60 ± 10%) environment under a 12-h light/dark cycle (light on 07:30–19:30 h) with free access to food and water. Animal treatment and maintenance were carried out in accordance with the Principle of Laboratory Animal Care (NIH publication No. 85–23, revised 1985) and the guidelines of the Peking University Animal Research Committee.

2.4. Behavioral test

2.4.1. Passive avoidance task (step-down test)

A step-down passive avoidance was examined by using apparatus consisted of a box (25 × 25 × 40 cm), a floor with stainless-

Table 1
Amino acid composition of MCP from salmon skin.

Amino acid	No. residues/100 residues
Glycine	23.77
Alanine	6.59
Serine	4.23
Proline	9.79
Valine	2.94
Threonine	2.53
Leucine	4.64
Isoleucine	2.57
Aspartic acid	7.29
Lysine	5.66
Arginine	6.08
Glutamic acid	12.22
Methionine	0.03
Histidine	1.61
Phenylalanine	2.51
Tyrosine	0.03
Hydroxy proline	7.51

steel grids 2 mm in diameter at 8 mm intervals, and a rubber platform (4 cm diameter, 4 cm height) set on the grid in one corner. Electric stimulation was given through the grid connected with a scrambled shock generator. After 3 months of treatment, an acquisition trial was performed. In this trial, each mouse was placed gently on the platform and allowed to habituate freely for 3 min, and then electric shocks (0.4 mA) were delivered to the grid. If the mouse stepped down from the platform, the electric shock was delivered to the mouse on the grid floor. The cutoff time was 5 min. A retention trial was performed 24 h after the acquisition trial. Each mouse was again placed on the platform. The time (step-down latency) that elapsed until the mouse stepped down from the platform was recorded. If the mouse did not step down from the platform within 300 s, the retention trial was terminated and the maximal step down latency of 300 s was recorded. Each error was counted whenever the mouse stepped down from the platform and the number of errors made within 5 min was recorded.

2.4.2. Morris water maze

The experimental apparatus which used in the Morris water maze test consisted of a circular water tank (120 cm in diameter, 35 cm in height), containing water (24 ± 1 °C) to a depth of 20 cm, which was rendered opaque by adding milk. A platform (4.5 cm in diameter, 19 cm in height) was submerged 1 cm below the water surface and placed at the midpoint of one quadrant. The pool was located in a test room, which contained various prominent visual cues. Each mouse received four training periods per day for seven consecutive days. Before the first trail, each mouse was put on the platform for 10 s, and then it was given 30 s free swim and then was assisted to the platform where it was remained for another 10 s rest. For each trial, mouse was placed in the water facing the wall at one of four starting positions, and the time required for the released mouse to find the hidden platform was recorded. Mouse that found the platform was allowed to remain on the platform for 10 s and then returned to its cage for the inter-trial interval. A mouse failed to find the platform within 90 s was placed on the platform for 10 s at the end of the trial. Latency to escape from the water maze (finding the submerged escape platform), swimming distance and average speed to reach the platform were recorded for each trial.

To measure the strength of the spatial memory, on day 7, a "probe test" was performed, during which, mice were swimming freely for 60 s in the pool without platform. In the "probe test" calculated were: (1) the time (in seconds) spent by mice in the target quadrant in which the platform was hidden during acquisition trails, and (2) the number of times exactly crossing over the previous position of the platform.

Swimming behavior during the test was video-recorded using a commercial VCR and analysed by a PC computer.

2.5. Detection of SOD, GSH-Px and TBARS in serum

Superoxide dismutase (SOD), glutathione peroxidase (GSH-Px) and thiobarbituric acid-reactive substances (TBARS) in serum were examined by reagent kit (Jiancheng Institute of Biotechnology, Nanjing, China). The principles of these kits are as follows. The method which was used to measure SOD employs xanthine and xanthine oxidase to generate superoxide radicals. Activity of GSH-Px was reflected by the speed of enzymatic reaction, in which GSH-Px promote glutathione hormone (GSH) to generate oxidised form glutathione (GSSG). Lipid peroxidation is known to result in formation of malonaldehyde (MDA) and other structurally similar compounds, which react with triobarbitrric acid (TBA) to form TBARS that absorbs at 532 nm. The TBARS levels in serum were expressed as malondialdehyde (MDA) equivalents (Shahidi & Ho, 2007).

2.6. Morphological analysis

After behavioral analyses, five mice in each group were deeply anesthetised with pentobarbital and perfused intracardially with normal saline followed by 4% paraformaldehyde in phosphatebuffered saline (PBS). The brains were removed, post-fixed with the same fixative and cryoprotected with 30% sucrose containing PBS. Sections (10 μm) containing hippocampus were obtained using a rotary microtome (HM505E; MICROM International GmbH, Walldorf, Germany), mounted on slides, and stored at −20 °C until use.

Morphology of the hippocampal was monitored using nissl staining. The slide-mounted brain sections were soaked in cresyl violet solution for 10 min, dehydrated through a graded series of ethanol–water solutions, coverslipped, and analysed under a bright field microscope. Nissl-positive neuronal cell numbers were manually and rigidly counted within the hippocampal pyramidal cell layer (CA1 and CA3 regions and the dentate gyrus). The total cell counts were averaged from at least three sections per animal.

2.7. Western blot analysis

Mice were deeply anesthetised and their hippocampuses were rapidly removed and stored at −80 °C until use. The tissue samples were pooled and lysed in a buffer containing 50 mM Tris–HCl, pH 6.8, 10% glycerol, 2% sodium dodecyl sulfate, and 5% β-mercaptoethanol. 50 μg protein lysate were separated by 8% SDS–PAGE and transferred onto polyvinylidene difluoride (PVDF) membrane. After blocking in a 5% non-fat dry milk solution in washing buffer containing 10 mM Tris (pH7.5), 150 mM NaCl, and 0.05% Tween-20, membranes were incubated overnight at 4 °C with primary antibody (monoclonal anti-BDNF, 1:1000, Santa Cruz Biotechnology, USA; monoclonal anti-PSD95, 1:250, Chemicon, Temecula, CA). After washing three times with TBS, membranes were incubated for 1.5 h with horseradish peroxidase-coupled secondary antibody at room temperature. Following the post-secondary washes, the resulting antigen–antibody-peroxidase complex was detected using the ECL kit (Amersham Pharmacia Biotech) and visualised by exposures of various lengths to Kodak film.

2.8. Statistical analyses

All statistical analyses were performed with the Statistical Package for social sciences for Windows version 11.0 (SPSS Inc. Chicago, IL. USA). Data were expressed as mean ± SEM. Effects on escape latencies and swimming distance in Morris water maze between groups were evaluated using Repeated-measures two-way ANOVA followed by a least significant difference test as a post hoc test. To evaluate other effects of MCP, difference between all groups were compared using one-way ANOVA followed by a least significant difference test as a post hoc test or Dunnett's test. For all statistical tests $p < 0.05$ was considered significant.

3. Results

3.1. Effect of MCP on latency and number of errors in step-down test

One-way ANOVA revealed that the latency and number of errors in step-down test had significant difference among all five groups ($p < 0.01$, $p < 0.05$ respectively). As shown in Fig. 1, aged control showed significantly memory loss with respect to young mice. The error-number increased while latency reduced significantly in aged control with respect to young mice ($p < 0.01$). Treatment with 0.44% and 1.32% MCP prolonged the latency in the testing day compared with aged control ($p < 0.05$). Further-

more, there was no significant latency difference between young mice and 0.44% or 1.32% MCP treated mice. Regarding to mice treated with 0.22% MCP, a reduction in the latency was showed with respect to young control ($p < 0.05$) (Fig. 1A). As shown in Fig. 1B, treatment with 0.44% MCP showed a significant difference in the error-number compared to aged control ($p < 0.05$). No difference was observed between 0.22% or 1.32% MCP supplementation groups and aged control group. Compared with young mice, the error-number in all MCP treated mice had no significant difference.

3.2. MCP improves spatial learning and memory in Morris water maze

Morris water maze is a sensitive method for revealing the impairment of spatial learning and memory. Once animals learn where the hidden platform is located, they can remember the location and swim rapidly to it from any starting point. Both the time taken to reach the platform and the swimming distance traveled were measured. As shown in Fig. 2A and B, the mean latency to find the platform and swimming distance declined progressively during the training days in all animals. However, the aged control demonstrated markedly longer escape latencies and swim-traveling distance than young control group. MCP treatment to aged mice resulted in a significant decrease in escape latency and swim-traveling distance. The main effects for day on escape latency and swim-traveling distance were statistically significantly [$F(5, 370) = 210.32$, $p < 0.01$; $F(5, 370) = 292.22$, $p < 0.01$ respectively]. The main effects for group on escape latency and swim-traveling distance were also statistically significant [$F(4, 74) = 9.71$, $p < 0.01$; $F(4, 74) = 21.38$, $p < 0.01$ respectively]. The day × group interaction was not significant [$F(20, 370) = 0.73$, $p > 0.05$; $F(20, 370) = 1.20$, $p > 0.05$ respectively]. Post hoc test revealed a significant increase in escape latency and swim-traveling distance in aged control mice compared with young control mice and MCP-treated mice ($p < 0.05$). There were no differences between MCP treated and control mice in the swimming speed (data not shown).

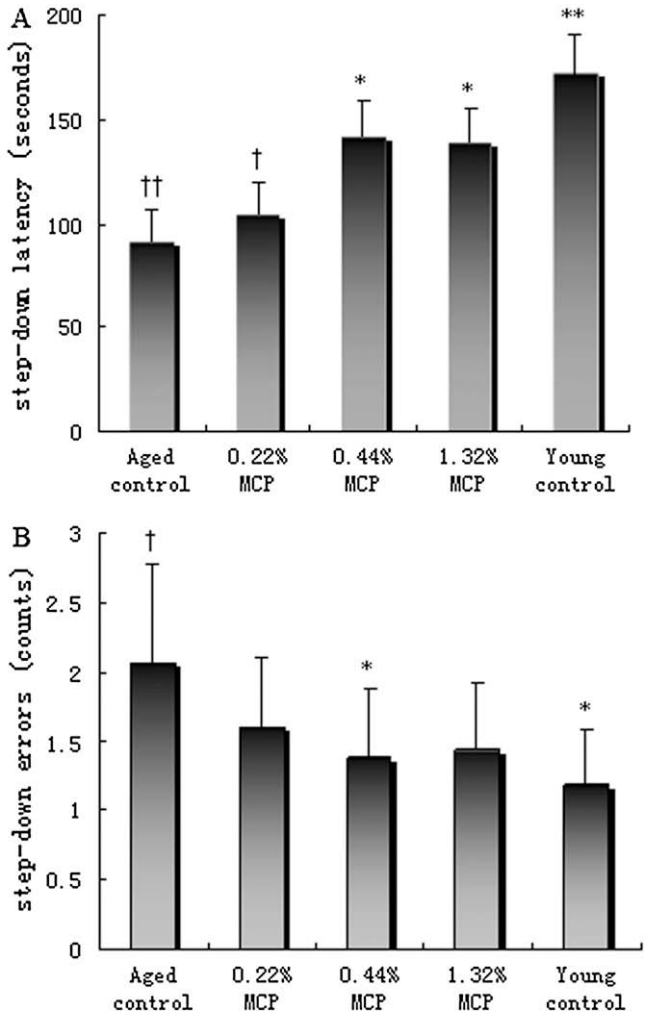

Fig. 1. Effects of MCP on latency (A) and number of errors (B) in step-down passive avoidance test. After daily oral treatment with MCP supplemented diet or standard diet for 3 months, animals were tested in step-down avoidance task. Values were presented as means ± SEMs of 15–16 mice. $^{*}p < 0.05$ compared to aged control mice; $^{**}p < 0.01$ compared to aged control mice; $^{\dagger}p < 0.05$ compared to young control mice; $^{\dagger\dagger}p < 0.01$ compared to young control mice (By Xinrong Pei, Ruiyue Yang, Zhaofeng Zhang, Lifang Gao, Junbo Wang, Yajun Xu, Ming Zhao, Xiaolong Han, Zhigang Liu, Yong Li*).

During the probe test, mice were swimming in the vicinity of the place that contained escape platform during the acquisition trial. There were significant differences on the time spent at target quadrant and number of times crossing over the platform among five groups ($p < 0.01$, $p < 0.05$ respectively). Young mice showed higher precision of the search for the platform as revealed by more time spent at the former platform position and higher number of crossing than aged control mice did (Fig. 2C and D). MCP seemed to restore the lost procedural subcomponent of spatial memory in aged mice, but only the 0.44% MCP had significantly effect on the time spent at target quadrant. On the other hand, 1.32% MCP could increase the number of times crossing over the platform site compared with aged control.

3.3. Effects of MCP on SOD, GSH-Px activities and TBARS level in serum

As regard to activity of SOD, all five groups of animals had significant difference ($p < 0.01$). Compared with young mice, the activity of SOD in serum significantly declined by 33.6% in aged control mice and MCP (0.22%, 0.44% or 1.32%) increased the activities of SOD nearly to 70.9%, 85.7% and 77.3% of the young mice, respectively (Table 2). The dose group of 0.44% MCP reached significant levels ($p < 0.05$) versus aged control.

Analysis on activity of GSH-Px also revealed a significant difference in five groups ($p < 0.01$). The activity of GSH-Px in serum of aged control group mice was significantly lower compared with young control group (Table 2, $p < 0.01$). MCP treatment resulted in an elevation in the activity of this enzyme. The dose group of 1.32% MCP ($p < 0.05$ versus aged control group) had more significant effect than other groups.

Aged control mice showed significant increase in TBARS level compared with the young mice ($p < 0.01$). This increase in TBARS was also attenuated in MCP treated mice.

3.4. Effect of MCP on morphological change in aged mice hippocampus

In order to discuss the neuroprotective effect of MCP, morphological change in hippocampus was observed using nissl staining method. In the young control group, multiple layers of pyramidal neurons with a dense and orderly arrangement were defined easily. However, in the aged control group, pyramidal neurons were less compact than those of young control group. Table 3 numerically expresses nissl positive cells in the CA1, CA3 regions and dentate gyrus (DG) of hippocampus. Measurement of total number in hippocampal CA1, CA3 and DG did not reveal any significant age-related change, although a slight age-related decline was observed. Similarly, no difference was seen in hippocampus between aged control and MCP treated groups.

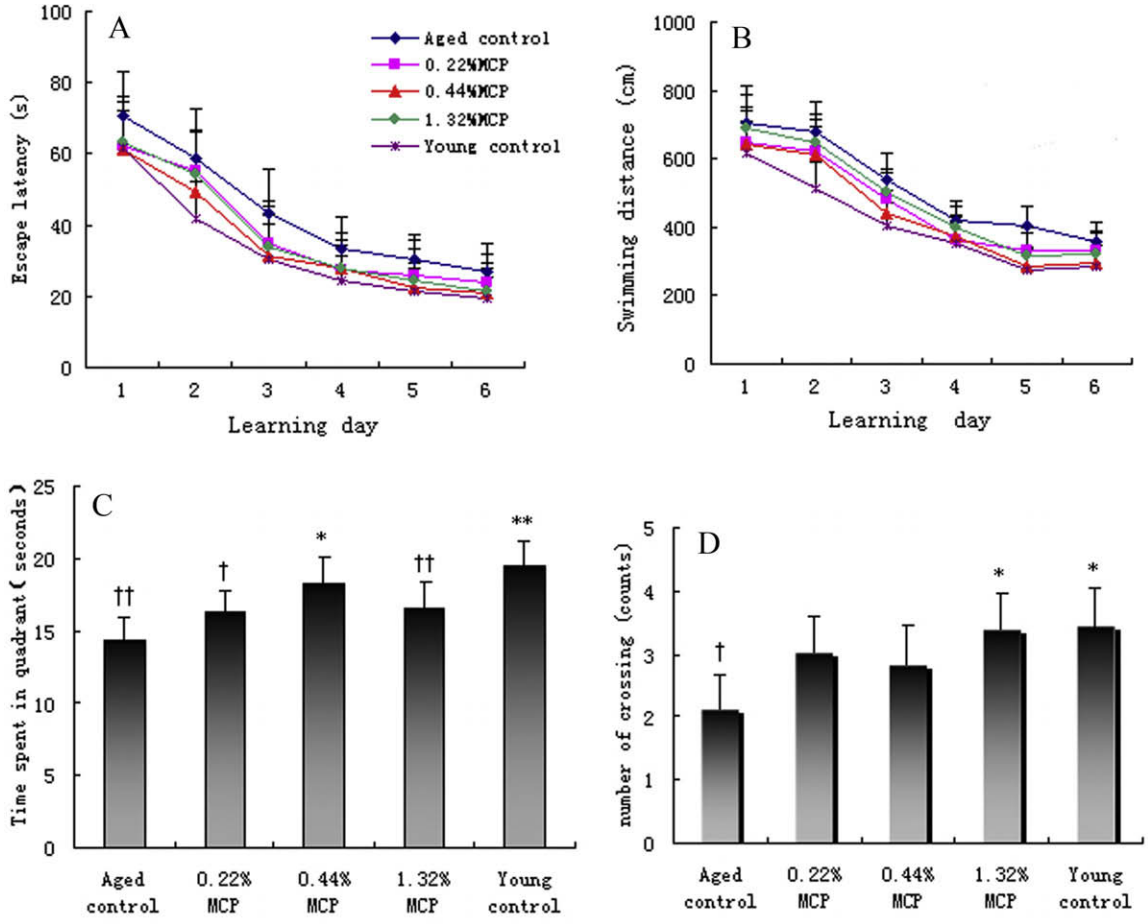

Fig. 2. Effects of MCP on spatial learning and memory of mice in Morris water maze test. The number for aged control group was 15, and 16 for other groups. (A) Escape latency to find the hidden platform. Two-way repeated measures ANOVA revealed statistically significant difference [group, $F(4, 74) = 9.71$, $p < 0.01$, day, $F(5, 370) = 210.32$, $p < 0.01$]. This difference was attributed to the longer latencies of aged control mice (post hoc LSD test $p < 0.01$ vs. all other groups) and shorter latencies of young control mice (post hoc LSD test $p < 0.01$vs. aged control group, $p < 0.05$ vs. 0.22% and 1.32% MCP treated groups). (B) Swimming distance travel to the goal platform. Two-way repeated measures ANOVA revealed statistically significant difference [group, $F(4, 74) = 21.38$, $p < 0.01$, day, $F(5, 370) = 292.22$, $p < 0.01$]. This difference was attributed to the longer distance of aged control (post hoc LSD test $p < 0.01$ vs. all other groups) and shorter distance of young control mice (post hoc LSD test $p < 0.01$vs. all other groups). (C) Presented were means ± SEMs time spent in target quadrant [one way ANOVA using LSD test, $^{*}p < 0.05$ compare with aged control mice, $^{**}p < 0.01$ compare with aged control; $^{\dagger}p < 0.05$ comparing with young control mice, $^{\dagger\dagger}p < 0.01$ comparing with young control mice]. (D) Presented were means ± SEMs numbers of crossing during the "probe test" [one way ANOVA using LSD test, $^{*}p < 0.05$ when compared with aged control mice; $^{\dagger}p < 0.05$ as compare with young control mice] (By Xinrong Pei, Ruiyue Yang, Zhaofeng Zhang, Lifang Gao, Junbo Wang, Yajun Xu, Ming Zhao, Xiaolong Han, Zhigang Liu, Yong Li*).

Table 2
Effects of MCP on superoxide dismutase (SOD), glutathione peroxidase (GSH-Px) and thiobarbituric acid-reactive substances (TBARS) in serum.

Group	*n*	SOD (U/mg protein)	GSH-Px (U/mg protein)	TBARS (MDA nmol/mg protein)
Aged control	8	81.56 ± 23.18††	818.63 ± 116.73††	2.67 ± 0.27††
0.22% MCP	8	87.13 ± 25.02†	874.02 ± 99.31†	2.18 ± 0.24*,†
0.44% MCP	8	105.37 ± 18.22*	886.54 ± 101.01†	1.78 ± 0.33*
1.32% MCP	8	95.00 ± 21.39†	945.14 ± 109.74*	2.31 ± 0.63†
Young control	8	122.87 ± 13.08**	1028.86 ± 161.80**	1.67 ± 0.52**

* $p < 0.05$ compared to aged control.
** $p < 0.01$ compared to aged control.
† $p < 0.05$ compared to young control.
†† $p < 0.01$ compared to young control.

3.5. Effect of MCP on expression of BDNF and PSD95 in hippocampus

As shown in Fig. 3, compared the aged control mice with the young mice, hippocampal BDNF and PSD95 decreased by 30% ($p < 0.01$) and 34% ($p < 0.01$) respectively.

The expression of hippocampal BDNF was significant up-regulated (29%, 26%) in aged mice treated with 0.44% and 1.32% MCP for 3 months ($p < 0.01$, $p < 0.05$ respectively) (Fig. 3). However the difference of hippocampal BDNF expression between aged control mice and 0.22% treated mice had no significant ($p > 0.05$).

The results also indicated that the level of PSD95 was significantly higher (38%) in 0.44% MCP treated mice than that of the aged control mice ($p < 0.01$) (Fig. 3). There was no significant difference of hippocampal PSD95 expression between aged control mice and 0.22%, 1.32% MCP treated mice ($p > 0.05$).

Table 3
Effect of MCP on nissl-positive cell numbers in hippocampal CA1, CA3 regions and DG.

Group	Nissl-positive cells (numbers/mm^2)		
	CA1	CA3	DG
Aged control	7591 ± 1392	5164 ± 665	17822 ± 996
0.22% MCP	7811 ± 1217	5314 ± 857	18302 ± 1292
0.44% MCP	7915 ± 1050	5639 ± 591	18115 ± 1026
1.32% MCP	7050 ± 1149	5505 ± 586	17989 ± 1134
Young control	7972 ± 759	6213 ± 1128	18044 ± 1058

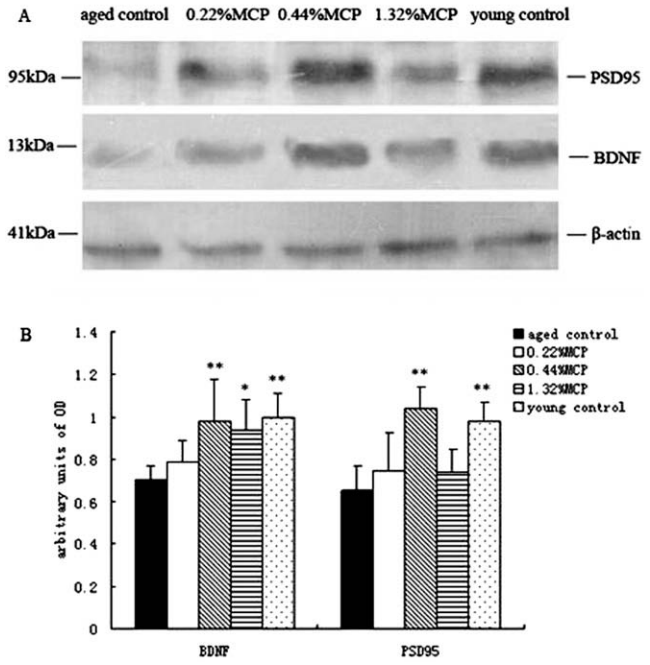

Fig. 3. Immunoblot analysis of BDNF and PSD95 in the hippocampus of the young, aged and MCP-treated mice. (A) Western blot from the aged group showed weak hippocampal BDNF and PSD95 compared with the young mice. Reinforced BDNF and PSD95 expression was observed in the MCP-treated groups, especially the 0.44% MCP treated group. Molecular weight markers (kDa) were shown on the left. (B) Quantitative analysis showed that hippocampal levels of BDNF and PSD95 protein of the young control mice and 0.44% MCP-treated mice were obviously higher than that of the aged mice. $^{*}p < 0.05$, $^{**}p < 0.01$ vs. the aged control group (By Xinrong Pei, Ruiyue Yang, Zhaofeng Zhang, Lifang Gao, Junbo Wang, Yajun Xu, Ming Zhao, Xiaolong Han, Zhigang Liu, Yong Li*).

4. Discussion

Unlike other dietary proteins, fish protein is likely to contain a lot of specific and potent bioactive sub-sequences in nutritional perspective for their competitive and aggressive living conditions (Aneiros & Garateix, 2004). Thus if the potent bioactive compounds were extracted and the functions were revealed, it would open a new perspective for pharmaceutical and functional food development.

MCP, compounds of proline and hydroxyl proline-rich oligopeptides, was derived from Chum Salmon (*O. keta*) skin which usually causes wastage and pollution in fish-processing industry (Kim et al., 2001). The low molecular weight distribution (100–860 Da) and small amounts of free amino acids, fat and carbohydrate, confirmed that the main composition of MCP was oligopeptides. The present study demonstrated that dietary administration of MCP could facilitate acquisition of spatial learning and increase the passive avoidance ability, bringing these to the level observed in young subjects. Furthermore, we found that these results were probably due to the antioxidative activity and protective effect on BDNF and PSD95 expression. To our knowledge, the present study is the first to reveal the neuro-protective effect of MCP on age-related deficit in rodents.

While the exact molecular basis of aging remains uncertain, the increasing accumulated related knowledge suggests that it may be related with the increase of free radical and neuroplasticity loss (Burke & Barnes, 2006). According to Free Radical Theory of Aging, the increase of lipid peroxides and the decrease activities of antioxidant enzymes, such as SOD and GSH-Px, are involved in the course of aging (Ceballos-Picot, Nicole, Clement, Bourre, & Sinet, 1992). The alterations are considered to play important roles in learning and memory deficits. In the present study, the activities of SOD and GSH-Px in serum showed a significant decline in aged control mice compared with young control; moreover, the activities of anti-oxidative enzymes such as SOD and GSH-Px were significantly increased in MCP treated group. As lipid peroxidation may also contribute to the neurotoxicity in mice, the peroxides could be indirectly estimated by measuring TBARS, a measure of lipid peroxidation and widely used as a biomarker of oxidative stress (Shahidi & Ho, 2007; Wanasundara & Shahidi, 1998). An obvious enhancement of the level of TBARS was shown in the aged control mice in this study, and it could be significantly reduced after MCP administration. The results indicate that MCP, to some extent, attenuates the oxidative injury in aging. In other words, the protection of MCP against oxidative stress to brain may be involved in the mechanism of its action to ameliorate the impairments of learning and memory.

Although neuronal cell loss was considered the main cause of learning and memory impairments during normal aging historically, more recent studies of rodents and humans demonstrated that the number of neurons in the hippocampal formation remained stable in aged subjects, irrespective of cognitive status (Calhoun et al., 1998; Rasmussen, Schliemann, Sorensen, Zimmer, & West, 1996). These data indicate that cognitive impairment may occur in aging, independent of neurodegeneration. Our analysis of the morphology of the hippocampal using nissl staining revealed that there was no evidence of aged-induced alterations in aged subjects compared to young control. In line with our observations, Nyffeler also reported that there was no difference in mean total volume of the hippocampus between performance groups as well (Nyffeler, Zhang, Feldon, & Knuesel, 2007). Nyffeler's and our findings support the assumption that aged-related cognitive impairments are not induced by gross morphological changes but rather associated with subtle connectional and synaptic reorganisation within the hippocampal formation (Nyffeler et al., 2007). There is now considerable evidence supporting the view that normal age-related memory deficits can be caused by functional changes, without the occurrence of major neuronal cell loss (Rapp, Deroche, Mao, & Burwell, 2002).

It is well established that brain-derived neurotrophic factor (BDNF), a crucial mediator of neuronal vitality and function, regulates the morphology through acting on both presynaptic and postsynaptic (Suzuki et al., 2004). It is emerging as a major player in neuronal events underlying learning and memory (Castren, Berninger, Leingartner, & Lindholm, 1998). The present study reported that BDNF in hippocampus of aged control group was lower than that of the young group, in agreement with previous data on age-related BDNF expression (Hwang et al., 2006). Furthermore, the results showed that when aged control group compared with 0.44% or 1.32% MCP-treated group, hippocampal BDNF increased by 29% and 26%, respectively. Although no information about how MCP regulates BDNF expression is provided in the present study, the authors think that there are several possible interpretations for MCP increasing BDNF expression: (1) It is well known that the generation of free radicals can lead to cell and tissue damage

paralleled by alterations in the function of the genetic apparatus, resulting in aging and untimely cell death (Droge & Schipper, 2007). MCP is confirmed to have antioxidant function, which can protect cerebral cells and reduce neuron cell apoptosis, therefore enhance the BDNF secretion indirectly or may probably protect the secreted BDNF directly from the oxidant damage. (2) The loss of elasticity and increasing rigidity of the aging vascular are considered as one of the factors leading progressively to severe arteriosclerosis and vascular dementia (Stewart, 2007). Collagen is well proved to improve vascular elasticity and reduce vascular rigidity, consequently increase the blood supply of brain (Bailey, Paul, & Knott, 1998; Silver, Horvath, & Foran, 2001), therefore protect the neuron cells and promote the expression of BDNF. Such effect may be another mechanism of how MCP increases BDNF expression. Despite lacking of direct evidence, the present results suggest that chronic MCP supplementation may prevent age-related learning and memory decline through increasing the expression of BDNF in hippocampus. However, further examinations are needed to elucidate the detail mechanisms on how MCP affects BDNF expression in brain.

BDNF does not only promote neuronal survival and differentiation, but also regulates synaptic transmission and plasticity in the central nervous system (CNS). There is now some considerable evidence indicating that brain has a decreased capacity for plastic response in aging process. Particularly, the hippocampus shows a reduction of synapticplasticity during aging (Teter & Ashford, 2002; Uylings & de Brabander, 2002). Consistent with these data, this study provided evidence for a concomitant decrease in PSD95 protein expression in the hippocampus of the aged mice. Nakata and Nakamura previously demonstrated that the expression of PSD95, a membrane-associated guanylate kinase protein enriched in the postsynaptic density (PSD), was increased upon BDNF addition (Nakata & Nakamura, 2007). Therefore, the PSD95 level in hippocampus was tested using immunoblot analysis in our research. A remarkable decrease in hippocampal PSD95 expression in the aged mice was found in the study, which supported previous reports of reduced PSD expression in aging brain (Head et al., 2007). At the same time, we presented reliable evidence of increasing hippocampal PSD95 of the aged mice receiving MCP administration. Furthermore, our results showed that PSD95 expression changed in an age-dependent manner, and BDNF revealed a similar expression pattern as compared with PSD95 in the hippocampus; also in MCP-treated groups, BDNF level increased in hippocampus accompanied with enhanced PSD95. PSD95 is thought to serve various functions at the synapse, implicate in the regulation of ion-channel function, synaptic activity, and intracellular signaling (Craven, El-Husseini, & Bredt, 1999). Therefore, the increased PSD95 expression induced by BDNF addition may represent a potential molecular substrate by which MCP increases hippocampal synaptic plasticity.

As mentioned above, MCP produced a biphasic effect, of which 0.44% MCP is an optical dose for memory, on the learning and memory in aged mice. This finding is not surprising, because numerous findings indicate that the U-shaped nature of the dose–response curve for the effects of promnestic agents on learning and memory is typical in that low doses have opposite effects from high dose, such as leptin, neuropeptide Y, colostrinin, et al. (Farr, Banks, & Morley, 2006; Flood, Hernandez, & Morley, 1987; Popik, Bobula, Janusz, Lisowski, & Vetulani, 1999).

In conclusion, the present study demonstrates that MCP can facilitate learning and memory in aged mice through reducing oxidative damage in the brain and increasing BDNF and PSD95 expression level. The increase in life expectancy in the 21st century has resulted in an increase in the prevalence of age-dependent diseases such as depression, Alzheimer's disease (AD) and other dementias. It is, therefore, crucial to develop appropriate health care means to deal with age-related neurodegenerative disorders, including cognitive deficits. Considering both the lack and the need of functional food or drugs proven to be effective in improving memory retrieval, the neuroprotective effect of MCP reported here is of vital importance and practical value. Undoubtedly it could be a candidate for functional food or drugs to manage/reduce memory deficits associated with aging.

Acknowledgements

The authors of the paper are grateful to the company CF Haishi Biotechnology Ltd. for providing the samples used in this study. This research was supported by the foundation (No. 2006BAD27B08) from the Ministry of Science and Technology of the People's Republic of China.

References

Andersen, K., Launer, L. J., & Dewey, M. E. (1999). Gender differences in the incidence of AD and vascular dementia: The EURODEM Studies.EURODEM Incidence Research Group. *Neurology, 53*(9), 1992–1997.

Aneiros, A., & Garateix, A. (2004). Bioactive peptides from marine sources: Pharmacological properties and isolation procedures. *Journal of Chromatography B, 803*(1), 41–53.

Bailey, A. J., Paul, R. G., & Knott, L. (1998). Mechanisms of maturation and ageing of collagen. *Mechanisms of Ageing and Development, 106*, 1–56.

Burke, S. N., & Barnes, C. A. (2006). Neural plasticity in the ageing brain. *Nature Reviews Neuroscience, 7*(1), 30–40.

Calhoun, M. E., Kurth, D., Phinney, A. L., Long, J. M., Hengemihle, J., Mouton, P. R., et al. (1998). Hippocampal neuron and synaptophysin-positive bouton number in aging C57BL/6 mice. *Neurobiology of Aging, 19*(6), 599–606.

Castren, E., Berninger, B., Leingartner, A., & Lindholm, D. (1998). Regulation of brain-derived neurotrophic factor mRNA levels in hippocampus by neuronal activity. *Progress in Brain Research, 117*, 57–64.

Ceballos-Picot, I., Nicole, A., Clement, M., Bourre, J. M., & Sinet, P. M. (1992). Age-related changes in antioxidant enzymes and lipid peroxidation in brains of control and transgenic mice overexpressing copper–zinc superoxide dismutase. *Mutation Research, 275*(3–6), 281–293.

Chavan, U. D., McKenzie, D. B., & Shahidi, F. (2001). Functional properties of protein isolates from beach pea (*Lathyrus maritimus* L.). *Food Chemistry, 74*(2), 177–187.

Craven, S. E., El-Husseini, A. E., & Bredt, D. S. (1999). Synaptic targeting of the postsynaptic density protein PSD-95 mediated by lipid and protein motifs. *Neuron, 22*(3), 497–509.

Droge, W., & Schipper, H. M. (2007). Oxidative stress and aberrant signaling in aging and cognitive decline. *Aging Cell, 6*(3), 361–370.

Erickson, C. A., & Barnes, C. A. (2003). The neurobiology of memory changes in normal aging. *Experimental Gerontology, 38*(1–2), 61–69.

Farr, S. A., Banks, W. A., & Morley, J. E. (2006). Effects of leptin on memory processing. *Peptides, 27*(6), 1420–1425.

Ferrari, C. K. B. (2007). Functional foods and physical activities in health promotion of aging people. *Maturitas, 58*(4), 327–339.

Flood, J. F., Hernandez, E. N., & Morley, J. E. (1987). Modulation of memory processing by neuropeptide Y. *Brain Research, 421*(1–2), 280–290.

Hartmann, R., & Meisel, H. (2007). Food-derived peptides with biological activity: From research to food applications. *Current Opinion in Biotechnology, 18*(2), 163–169.

Head, E., Corrada, M. M., Kahle-Wrobleski, K., Kim, R. C., Sarsoza, F., Goodus, M. & Kawas, C. H. (2007). Synaptic proteins, neuropathology and cognitive status in the oldest-old. *Neurobiology of Aging*. 10.1016/j.neurobiolaging.2007.10.001.

Hebda-Bauer, E. K., Luo, J., Watson, S. J., & Akil, H. (2007). Female CREB$^{\alpha\ \delta-}$ deficient mice show earlier age-related cognitive deficits than males. *Neuroscience, 150*(2), 260–272.

Hwang, I. K., Yoo, K. Y., Jung, B. K., Cho, J. H., Kim, D. H., Kang, T. C., et al. (2006). Correlations between neuronal loss, decrease of memory, and decrease expression of brain-derived neurotrophic factor in the gerbil hippocampus during normal aging. *Experimental Neurology, 201*(1), 75–83.

Kalache, A., Aboderin, I., & Hoskins, I. (2002). Compression of morbidity and active ageing: Key priorities for public health policy in the 21st century. *Bulletin of the World Health Organization, 80*(3), 243–244.

Kim, S. K., Kim, Y. T., Byun, H. G., Nam, K. S., Joo, D. S., & Shahidi, F. (2001). Isolation and characterization of antioxidative peptides from gelatin hydrolysate of Alaska pollack skin. *Journal of agricultural and food chemistry, 49*(4), 1984–1989.

Korhonen, H., & Pihlanto, A. (2003). Food-derived bioactive peptides – opportunities for designing future foods. *Current Pharmaceutical Design, 9*(16), 1297–1308.

McLay, R. N., Pan, W., & Kastin, A. J. (2001). Effects of peptides on animal and human behavior: A review of studies published in the first twenty years of the journal Peptides. *Peptides, 22*(12), 2181–2255.

Mellander, O. (1950). The physiological importance of the casein phosphopeptide calcium salts. II. Peroral calcium dosage of infants. *Acta Societatis Medicorum Upsaliensis, 55*(5–6), 247–255.

Miraliakbari, H., & Shahidi, F. (2008). Antioxidant activity of minor components of tree nut oils. *Food Chemistry, 111*(2), 421–427.

Morrison, J. H., & Hof, P. R. (1997). Life and death of neurons in the aging brain. *Science, 278*(5337), 412–419.
Nakata, H., & Nakamura, S. (2007). Brain-derived neurotrophic factor regulates AMPA receptor trafficking to post-synaptic densities via IP3R and TRPC calcium signaling. *FEBS Letters, 581*(10), 2047–2054.
Nyffeler, M., Zhang, W. N., Feldon, J., & Knuesel, I. (2007). Differential expression of PSD proteins in age-related spatial learning impairments. *Neurobiology of Aging, 28*(1), 143–155.
Paliyath, G. (2006). Functional foods, ageing and degenerative disease. *Trends in Food Science & Technology, 17*(8), 466–467.
Popik, P., Bobula, B., Janusz, M., Lisowski, J., & Vetulani, J. (1999). Colostrinin, a polypeptide isolated from early milk, facilitates learning and memory in rats. *Pharmacoogyl Biochemistry and Behavior, 64*(1), 183–189.
Rapp, P. R., Deroche, P. S., Mao, Y., & Burwell, R. D. (2002). Neuron number in the parahippocampal region is preserved in aged rats with spatial learning deficits. *Cerebral Cortex, 12*(11), 1171–1179.
Rasmussen, T., Schliemann, T., Sorensen, J. C., Zimmer, J., & West, M. J. (1996). Memory impaired aged rats: No loss of principal hippocampal and subicular neurons. *Neurobiology of Aging, 17*(1), 143–147.
Shahidi, F., & Ho, C. -T. (2007). Antioxidant Measurement and Applications. *ACS Symposium Series* (p. 956). Washington, DC: American Chemical Society.
Silver, F. H., Horvath, I., & Foran, D. J. (2001). Viscoelasticity of the vessel wall: The role of collagen and elastic fibers. *Critical Reviews in Biomedical Engineering, 29*(3), 279–301.
Stewart, J. T. (2007). Psychiatric and behavioral manifestations of vascular dementia. *The American Journal of Geriatric Cardiology, 16*(3), 165–170.
Suzuki, S., Numakawa, T., Shimazu, K., Koshimizu, H., Hara, T., Hatanaka, H., et al. (2004). BDNF-induced recruitment of TrkB receptor into neuronal lipid rafts: Roles in synaptic modulation. *The Journal of Cell Biology, 167*(6), 1205–1215.
Teter, B., & Ashford, J. W. (2002). Neuroplasticity in Alzheimer's disease. *Journal of Neuroscience Research, 70*(3), 402–437.
Uylings, H. B., & de Brabander, J. M. (2002). Neuronal changes in normal human aging and Alzheimer's disease. *Brain and Cognition, 49*(3), 268–276.
Wanasundara, U. N., & Shahidi, F. (1998). Antioxidant and pro-oxidant activity of green tea extracts in marine oils. *Food Chemistry, 63*(3), 335–342.

Food Chemistry 118 (2010) 341–348

Contents lists available at ScienceDirect

Food Chemistry

journal homepage: www.elsevier.com/locate/foodchem

Influence of the in vivo addition of alpha-tocopheryl acetate with three lipid sources on the lipid oxidation and fatty acid composition of Beluga sturgeon, *Huso huso*, during frozen storage

Seyed Vali Hosseini [a], Abdolmohammad Abedian-Kenari [a,*], Masoud Rezaei [a], Rajab Mohammad Nazari [b], Xesús Feás [c], Mohammad Rabbani [d]

[a] Department of Fisheries, Tarbiat Modares University, P.O. Box 46414-356, Noor, Mazandaran, Iran
[b] Rajaee Sturgeon Hatchery Center, P.O. Box 833, Sari, Mazandaran, Iran
[c] Departamento de Química Analítica, Nutrición y Bromatoloxía, Universidade de Santiago de Compostela, E-27002 Lugo, Galiza, Spain
[d] Department of Fisheries, Islamic Azad University–Tehran Shomal Branch, P.O. Box 1973733583, Tehran, Iran

ARTICLE INFO

Article history:
Received 31 December 2008
Received in revised form 10 March 2009
Accepted 30 April 2009

Keywords:
Beluga sturgeon
Vitamin E
Frozen storage
Lipid oxidation
Fish oil
Soybean oil
Canola oil

ABSTRACT

This study was conducted to investigate the effect of dietary alpha-tocopheryl acetate (vitamin E) and oil sources on fish flesh quality characteristics of *Huso huso* during frozen storage. Practical-type diets containing 0 or 250 mg vitamin E kg^{-1} with three lipid sources, fish oil (FO), soybean oil (SO) and canola oil (CO), were fed to *H. huso* for 120 days. Fillet samples were analysed fresh or after storage at −18 ± 1 °C for 12 months. Replacement of FO by SO and CO in diets for *H. huso* significantly altered the fatty acid (FA) profile, which also influenced the FA composition during frozen storage. Dietary vitamin E had a significant effect on muscle vitamin E content and lipid oxidation during storage ($P > 0.05$). Oxidation was reduced for fish fed vitamin E and results showed that dietary vitamin E supplementation can slow down the level of lipid oxidation in *H. huso* muscles during frozen storage.

1. Introduction

The importance of fish oil for human cardiovascular health is well known. The *n*3-polyunsaturated fatty acids (PUFA) are particularly beneficial and fish continue to be their main source in the human diet. Numerous studies over the years have suggested that the dietary consumption of fish/fish oils containing *n*−3 fatty acids may favourably influence a number of biological factors associated with cardiovascular disease (independent of blood-cholesterol lowering) (Abedian-Kenari et al., 2009). However, the *n*−3 fatty acids are highly unsaturated, and therefore, susceptible to oxidation in fish fillets during storage.

It is well established that during freezing and frozen storage, lipid hydrolysis and oxidation leads to a PUFA decrease with an increase of peroxides, which are two of the most important factors contributing to post mortem deterioration of fish meat quality (Pirini, Gatta, Testi, Trigari, & Monetti, 2000). This process is promoted by the abundance of PUFA and high lipid content. Oxidation of lipids initiates other changes that affect the nutritional quality, wholesomeness, safety, colour, flavour, and texture of foods (Shahidi & Wanasundara, 1992).

The use of antioxidants can be an effective way to minimise or delay the oxidation process, retarding the formation of toxic oxidation products, maintaining nutritional quality and prolonging the shelf life of foods (Sau, Paul, Mohanta, & Mohanty, 2004). One way to improve product stability is through dietary supplementation with antioxidants such as vitamin E (DL-α-tocopheryl acetate), which has been reported to improve the stability of fish tissue lipids (Chaiyapechara, Casten, Hardy, & Dong, 2003; Pirini et al., 2000; Ruff, Fitzgerald, Cross, Hamre, & Kerry, 2003; Sant'Ana and Mancini-Filho, 2000; Sau et al., 2004; Yildiz, Şener, & Gün, 2006).

DL-α-tocopheryl acetate, the form of synthetic vitamin E commonly added to fish feed, functions as a lipid soluble antioxidant that protects biological membranes, lipoproteins and lipid stores. Its main function is to protect unsaturated fatty acids against free radical-mediated oxidation (Sau et al., 2004). It is fairly stable during feed storage and only becomes active as an antioxidant after the hydrolysis of the acetate group in the fish's body, and therefore, it is not an antioxidant in the feed (Chaiyapechara et al., 2003).

* Corresponding author. Tel.: +98 122 6253101; fax: +98 122 6253499.
E-mail address: aabedian@modares.ac.ir (A. Abedian-Kenari).

0308-8146/$ - see front matter © 2009 Published by Elsevier Ltd.
doi:10.1016/j.foodchem.2009.04.131

In the aquaculture industry, marine fish oil (MFO) is the main oil supplement in fish diets to increase their energy content and provide essential fatty acids. A major challenge for future aquaculture production is a stable, predictable and high quality feed supply (Şener, Yildiz, & Savaş, 2005). Due to the decreased availability and increased cost of MFO, there needs to be consideration of the possible replacement with vegetable oils (e.g., soybean and canola oil). At present, partial or total replacement of MFO by vegetable oils in diets for farmed fish such as sturgeon species (i.e., white sturgeon, Xu, Hung, & German, 1993; adriatic sturgeon, McKenzie et al., 1999; and Russian sturgeon, Şener et al., 2005), are practiced without compromising growth, feed efficiency, reproduction or the health of fish. However, it is well known that the dietary fatty acid (FA) profile strongly affects the nutritional quality of the fish (Abedian-Kenari et al., 2009; Sargent, Bell, Bell, Henderson, & Tocher, 1995). Thus, it is important to understand the impact of vegetable oils on quality related characteristics in farmed Beluga sturgeon after ice- or frozen storage.

In recent years the intensive culture of certain sturgeon species has been developed as an alternative to other more traditional fish species such as salmonids and cyprinids. The Beluga sturgeon (*Huso huso*) is an increasingly important aquaculture species in Russia, Eastern Europe, Turkey, Japan and Iran because of the dwindling natural sources for its caviare and meat. This fish is a commercially important fish and is commonly processed into frozen fillets. Although microbial deterioration of fish muscle can be inhibited by frozen storage, as mentioned previously, fish lipids undergo a number of changes that affect the flavour and texture of the flesh (Dragoev, Kiosev, Danchev, Ioncheva, & Genov, 1998). These changes are important since they determine the storage life of the frozen product and are a major consideration in grading the quality of frozen fish. However, to our knowledge, no study has been performed on the effects of vitamin E and frozen storage on the quality of Beluga sturgeon grown using vegetable oils as the principle lipid in their diet.

Therefore, the purpose of the present study was to investigate the effects of vitamin E supplementation, and dietary oil sources on muscle fatty acid composition and flesh quality parameters (mainly lipid oxidation) of Beluga sturgeon during frozen storage (−18 °C). Flesh quality parameters were analysed on day 0 (post-rigor) and during frozen storage (1, 2, 3, 4, 5 and 6 months). Fish were also analysed after long-term frozen storage (12 months) to show whether an altered fatty acid profile due to inclusion of dietary vitamin E and vegetable oils influenced lipid deterioration (peroxide value, PV; free fatty acid, FFA; thiobarbituric acid, TBA; heme iron, HI) and consumer quality indexes [fatty acid (FA) profile; atherogenic index, AI; thrombogenic index, TI; water holding capacity, WHC].

2. Materials and methods

2.1. Feeding trial and fish diets

During 120 days between May and October, the experiments were carried out at the Iranian government's sturgeon hatchery, Shahid Rajaei (Sari, Mazandaran, Iran. Latitude 36° 37′N, Longitude 53° 05′E). The fish were from a genetically homogenous stock obtained from a mesocosm hatchery (land-based pond), weaned and adapted to a compound diet. During the acclimatisation period, fish were fed (five times and 5% of body weight) daily with a semi-moist pellet diet that was provided by a local manufacturer of livestock and aquatic feeds in Mazandaran-Sari (Iran).

Two hundred and seventy Beluga sturgeon juveniles, with near uniform biomass, were selected and distributed randomly into three replicated groups for each treatment in 2000 l fibreglass tanks (18 tanks and 15 fish per tank) for the feeding trials. The initial weight and length of the experimental fish was 209 ± 12 g and 348 ± 11 mm. Fish were reared with an earth bottom and supplied with flowing water constantly overflowing (with a flow rate of around 15 l min^{-1}). The water quality parameters observed during the experimental period were temperature (19–23 °C), oxygen saturation (73–88%), total alkalinity (136 ± 2.11 mg l^{-1} as $CaCO_3$), pH (6.95–7.75) and salinity ⩽ 1 ppt. Tanks were indoors and the light cycle was 16 h light and 8 h darkness.

In the present study, kilka fish oil (FO) rich in eicosapentaenoic acid (EPA, 20:5*n*3) and docosahexaenoic acid (DHA, 22:6*n*3) was chosen as the fish oil, soybean (SO), rich in linoleic acid (LN, 18:2*n*−6) and canola oil (CO) rich in oleic acid (OA, 18:1*n*−9) and α-linolenic acid (ALA, 18:3*n*−3) were chosen as the vegetable oil sources, and DL-α-tocopheryl acetate (Sigma Chemical Co., St. Louis, MO, USA) was used as the antioxidant. FO was provided by a local manufacturer of livestock and aquatic feeds in Mazandaran-Sari and SO and CO were provided by a local manufacturer of vegetable oil extraction (Khazar Yeganeh Oil Seed Co, Agh ghala, Iran). Six experimental fish meal-based diets (practical-type) were formulated by LINDO software-linear programming (LINDO

Table 1
Major ingredients and nutrient content of the experimental diets.[a]

Ingredient (%)	Experimental diet		
	FO	SO	CO
Fish meal	50.5	50.5	50.5
Soybean meal (defatted)	15	15	15
Fish oil	5.4	0	0
Soybean oil	0	5.4	0
Canola oil	0	0	5.4
Wheat flour	5	5	5
Molasses	3	3	3
Wheat bran	3	3	3
Filler (cellulose)	12	12	12
Binder (sodium alginate)	0.6	0.6	0.6
Vitamin mix (vitamin E free)[b]	1.5	1.5	1.5
Mineral mix[c]	2.5	2.5	2.5
Attractant[d]	1.5	1.5	1.5
DL-α-tocopheryl acetate	0.05	0.05	0.05
Nutrient content (% dry base)			
Moisture	10.4	11.7	11.3
Crude protein	42.5	42.1	41.7
Crude fat	12.4	11.8	12.1
Ash	7.02	7.09	7.13
Crude fibre	15.6	15.9	15.9
NFE[e]	12.1	11.4	11.9
Carbohydrate[f]	27.7	27.3	27.8
Gross energy (kJ g^{-1} diet)[g]	19.7	19.3	19.4
Gross energy/protein (kJ g^{-1} protein)	46.3	45.8	46.5
Vitamin E (mg kg^{-1} diet) added[h]	246	264	259

[a] FO, fish oil (kilka fish oil); SO, soybean oil; CO, canola oil. Proximate composition and gross energy of the diets were not significantly different ($P > 0.05$).

[b] Vitamin mixture: The mixture was diluted in cellulose and provides the following vitamin activities in mg or IU kg^{-1} of diet. Vitamin A (as acetate) 3000 IU; vitamin D3, 1500 IU; menadione sodium bisulphite, 10; choline chloride, 2000; niacin, 50; riboflavin, 20; pyridoxine, 10; thiamin mononitrate, 10; pantothenic acid, 40; folic acid, 5; vitamin B12, 0.02; biotin, 1; inositol, 400; vitamin C, 200.

[c] Mineral mixture (g/100 g): NaCl, 1.0; $MgSO_4{\cdot}7H_2O$, 15.0; $NaH_2PO_4{\cdot}2H_2O$, 25.0; KH_2PO_4, 32.0; $Ca(H_2PO_4)2{\cdot}H_2O$, 20; Fe-Citrate, 2.5; Ca-Lactate, 3.5; Trace element mixture*, 1.0 (*Trace element mixture (g/100 g): $ZnSO_4{\cdot}7H_2O$, 35.3; $MnSO_4{\cdot}4H_2O$, 16.2; $CuSO_4{\cdot}5H_2O$, 3.1; $CoCl_2{\cdot}6H_2O$, 0.1; Cellulose, 45.0).

[d] A mixture of amino acids including lysine, methionine, and betaine (Merck Chemical Co.).

[e] Nitrogen Free Extract.

[f] NFE + crude fibre.

[g] Calculated on the basis of 23.6, 39.5 and 17.2 kJ g^{-1} of protein, fat and carbohydrate, respectively (NRC, 1993).

[h] Vitamin E is supplemented as DL-α-tocopheryl acetate at 250 mg kg^{-1} diet. Analysed vitamin E contents in control diets of FO, SO and CO were found to be 18.2, 41.7 and 28.3 mg kg^{-1} diet, respectively.

Systems Inc., Chicago, IL, USA) to have similar protein and lipid by adding of FO, SO or CO. DL-α-tocopheryl acetate was added to the basal diet (dietary oil treatment) at the expense of small amounts of cellulose to provide the desired quantity of 250 mg kg^{-1}. The basal diet without the addition of DL-α-tocopheryl acetate is referred to as the control diet.

The dietary treatments were randomly assigned to the experimental tanks. All diets were prepared in the aquatic nutrition laboratory of Tarbiat Modares University, Noor (Iran). The experimental diets' ingredient composition is presented in Table 1 and the fatty acid profile of the initial fish, oil used and the diets is presented in Table 2. The diets were stored in airtight freezer bags at −18 ± 1 °C until used. All groups of fish were fed their respective diet by hand to visual satiety (visual observation of first feed refusal). The fish were fed the experimental diets five times a day at 8, 12 16, 20 and 24 h for 120 days.

At the end of the feeding trials, all fish in each tank were collected and immediately killed in a tank containing fresh water and ice (hypothermia), and transferred to the laboratory within ~2 h in foamed polystyrene, self-draining boxes with a suitable quantity of flaked ice (the ice/fish ratio was 3:1, w/w). After passing into rigor, fish were washed with potable water, and then eviscerated manually (head and skin were not removed). During preparation, fish were kept in ice and the process was carried out at room temperature (~14 °C). The samples from each trial group were separately packed into a black nylon bag (un-vacuumed) then transferred to an air-blast freezer and kept at −18 °C for different times (0 or fresh, 1, 2, 3, 4, 5, 6 and 12 months). At the time designated, samples were randomly chosen from every group and were subjected to chemical analysis. Before analysis, samples were thawed (in the original bag) in a refrigerator (Yakhsaran, Tehran, Iran) at 3 ± 1 °C for approximately 10 h.

Table 2
Fatty acid profile of the initial fish (*Huso huso*), oils (fish, soybean and canola oil) and of the experimental diets.[a]

Fatty acid	Initial fish[b]	Oils			Experimental diets		
		FO	SO	CO	FO	SO	CO
C14:0 (Myristic acid)	3.24	4.57	0.75	0.30	5.30	1.91	1.09
C15:0 (Pentadecanoeic acid)	0.94	0.83	0.28	–	0.694	0.407	0.261
C16:0 (Palmitic acid)	20.1	15.2	7.81	4.31	18.0	10.4	7.21
C18:0 (Stearic acid)	9.48	6.11	2.68	1.17	6.01	3.65	4.02
C16:1*n*7 (Palmitoleic acid)	4.37	4.18	3.76	1.83	8.49	2.88	6.39
C18:1*n*9 (Oleic acid)	18.6	19.5	22.4	54.1	19.6	20.8	43.2
C18:2*n*6 (Linoleic acid)	9.89	8.91	51.1	24.7	5.72	37.9	17.6
C18:3*n*3 (Linolenic acid)	4.69	1.28	4.56	5.11	3.90	7.13	7.54
C20:4*n*6 (Arachidonic acid)	0.49	0.43	–	–	0.585	0.224	0.206
C20:5*n*3 (Eicosapentanoic acid, EPA)	4.42	9.57	–	–	7.64	1.89	1.90
C22:1*n*11(Cetolic acid)	7.53	6.11	1.17	1.74	7.06	4.77	3.72
C22:6*n*3 (Decosahexanoic acid, DHA)	9.71	15.3	–	–	12.0	2.10	1.89
Total (Calculated value)	93.4	92.0	94.9	93.5	95.0	94.0	95.0
Other	6.56	8.02	5.10	6.50	5.01	5.97	5.03
∑SFA[c]	33.8	26.7	11.5	5.78	30.0	16.4	12.6
∑MUFA[d]	30.5	29.8	27.3	57.7	35.1	28.5	53.3
∑PUFA[e]	29.2	35.5	5.58	29.8	29.9	49.2	29.1
∑PUFA-*n*3	18.8	26.2	4.65	5.11	23.6	11.1	11.3
∑PUFA-*n*6	10.4	9.34	51.1	24.7	6.31	38.1	17.8
∑TUFA[f]	59.7	65.3	83.2	87.5	65.0	77.7	82.4
PUFA/SFA	0.86	1.33	4.85	5.16	0.99	3.01	2.31
n−3/*n*−6	1.81	2.80	0.093	0.207	3.74	0.292	0.637
n−6/*n*−3	0.55	0.357	10.7	4.83	0.268	3.42	1.57
SFA/TUFA	0.57	0.409	0.138	0.066	0.462	0.211	0.153
DHA/EPA	2.20	1.60	0.00	0.00	1.57	1.11	0.992

[a] Values are % of the total fatty acid expressed as the mean. See Table 1 for diet abbreviations.
[b] Mean proximate composition of initial fish on % of dry weight basis except for moisture: Moisture, 74.7 ± 1.10; Protein, 70.4 ± 2.56; Lipid, 20.3 ± 1.74 and Ash, 4.37 ± 0.85. Vitamin E content in initial fish was 6.02 mg kg^{-1} weight.
[c] Saturated fatty acids: C14:0 + C15:0 + C16:0 + C18:0.
[d] Monounsaturated fatty acids: C16:1*n*7 + C18:1*n*9.
[e] Polyunsaturated fatty acids: C18:2*n*6 + C18:3*n*3 + C20:4*n*6 + C20:4*n*6 + C20:5*n*3 + C22:6*n*3.
[f] Total unsaturated fatty acids: ∑MUFA + ∑PUFA.

2.2. Chemical analysis

2.2.1. Sampling procedure

For the chemical analyses, a slice sample (about 15 g in front of the dorsal fin) was taken for water holding capacity (WHC, %) analysis as described by Pastoriza, Sampedro, Herrera, and Cabo (1998) and the rest was homogenised (without skin and backbone), twice, in a meat blender (SAYA, Model: Promeat W-1800, Tehran, Iran) for around 2 min and sieved through a 4 mm mesh. In the present study, PV, FFA, TBA, HI and WHC were analysed for all sampling occasion, but the FA profile, lipid quality index and vitamin E content were only analysed on 0 (fresh), and at 6 and 12 months.

An initial sample of 12 fish was taken at the start of the experiment to determine baseline levels for proximate compositions, FA profile and vitamin E in muscle (without separation of white and dark muscle). After passing into rigor, fish were washed with potable water, and then headed, gutted, skinned, deboned and filleted manually, using a new sterile scalpel for each fish within 30–45 min, on both sides. The right side was used for the proximate composition assays and the other side was used for determination of FA profile and vitamin E content. The same day, the fillets were homogenised, twice, in a meat blender and immediately analysed for proximate compounds, FA profile and vitamin E content. The preparation process was carried out at room temperature (19 ± 3 °C).

2.2.2. Proximate analysis

The proximate composition at the start and also at the end of the feeding trials were done according to the procedures of the Association of Official Analytical Chemists (AOAC, 2005). Moisture, ash, crude fibre, protein and fat contents were assayed by methods 934.01, 920.153, 973.18, 954.01 and 991.36, respectively. Moisture was determined by drying the samples in an oven (Heraeus, D-63450, Hanau, Germany) at 105 °C to constant weight; ash was determined by incineration in a muffle furnace (Isuzu, Tokyo, Japan) at 600 °C for 3 h; crude fibre was determined by the acid detergent fibre (ADF) method (Fibertec System1010 Heat Extractor, Höganäs, Sweden); crude protein was determined by the Kjeldahl method (N × 6.25) using an automatic Kjeldahl system (230-Hjeltec Analyzer, Foss Tecator, Höganäs, Sweden); crude fat content was measured by gravimetry after extraction with petroleum ether using an automatic Soxtec device (FOSS, Soxtec™ 2050, Höganäs, Sweden); Nitrogen Free Extracts (NFE) was calculated following the formula below and NFE plus fibre was expressed as carbohydrate:

$$\text{Nitrogen Free Extract (NFE)} = 100 - (\text{Crude Protein} + \text{Crude Lipid} + \text{Fibre} + \text{Ash} + \text{Moisture})$$

$$\text{Carbohydrate} = \text{NFE} + \text{Fibre}$$

2.2.3. Analysis of vitamin E, heme iron and lipid (lipid extraction, PV, FFA, TBA, FA profile, AI and TI)

Vitamin E content of fish muscle and feed samples was determined by high-performance liquid chromatography (HPLC)

according to the extraction procedure of Liu, Scheller, and Schaefer (1996), and Vitamin E content was reported as mg kg^{-1} of muscle or feed. Total heme iron (ppm) was determined using the method of Clark, Mahoney, and Carpenter (1997). PV, expressed as meq of peroxide oxygen kg fat^{-1}, and FFA, expressed as % of oleic acid, were determined according to Egan, Kirk, and Sawyer (1981) on the extracted lipids obtained from homogenised fish by the Bligh and Dyer (1959) procedure. The TBA was determined according to Kirk and Sawyer (1991) method. The colour development was measured at 532 nm by using a UV–vis spectrophotometer (JENWAY 6305, Germany). The TBA value was expressed as mg malonaldehyde (MA) kg^{-1} of fish flesh. Total lipids in the diets and the fillets were extracted from a homogenised sample using the methodology described by Folch, Lees, and Sloan-Stanley (1957) and the extracted lipids were used for the FA profile analysis in diets and fish sample, and was done on the extracted lipids as previously described (Abedian-Kenari et al., 2009). Briefly, FA methyl esters were obtained by transmethylation using 20% BF_3 in methanol (Merck, Darmstadt, Germany). They were analysed by gas liquid chromatography (GLC) on a Phillips GLC-PU4400 (Phillips Scientific, Cambridge, United Kingdom), equipped with a fused silica capillary polar column (BPX70, 60 m × 0.32 mm ID, 0.25 μm film thickness, SGM, Victoria, Australia), and a flame ionisation detector (FID). The carrier gas was helium and the split ratio was 1:20. A thermal gradient from 160 to 230 °C at 45 °C min^{-1} was used with the injector and FID temperatures at 240 and 280 °C, respectively. The relative quantity of each FA was determined by measuring the area under the peak corresponding to a particular FA (% of total FA). The total quantity of identified FA was similar between sampling times (90–94%).

The lipid quality indices, i.e., the atherogenic index (AI) and the thrombogenic index (TI), were calculated according to Ulbricht and Southgate (1991) on the basis of fatty acid percentages including the saturated, monounsaturated fatty acids (MUFA) and PUFA:

$$AI = [12:0 + 4(14:0) + 16:0]/[MUFA + n-3PUFA + n-6PUFA]$$

$$TI = [14:0 + 16:0 + 18:0]/[0.5MUFA + 0.5(n-6PUFA) + 3(n-3PUFA) + (n-3PUFA/n-6PUFA)]$$

2.3. Statistical analysis

Descriptive statistics of the analysis results were calculated for each treatment. All data were subjected to one-way analysis of variance (ANOVA) to test the effects of experimental diets. The data were tested for homogeneity of variances at a significant level of $P < 0.05$ by the One-Sample Kolmogorov–Smirnov Test and probability values less than 0.05 were considered as statistically significant. Paired sample *t*-test was used for mean comparison of dietary vitamin E within dietary oil sources. Excel and SPSS version 13.5 (SPSS Inc., Chicago, IL, USA) computer programs were used for data manipulations and statistical analysis.

3. Results and discussion

The proximate compositions of the measured edible portions (muscle) of *H. huso* fed experimental diets are shown in Table 3. Slight changes were observed for some measured components ($P < 0.05$). Muscle lipid content in fish fed the SO diet (with or without vitamin E) was greater than other dietary groups. Conversely, the muscle protein content was lower in fish fed the SO diet compared with all other treatments, but statistical analysis did not show significant differences ($P < 0.05$). This relationship between muscle protein and lipid content has been observed in previous study with Russian sturgeon (Şener et al., 2005) and salmonids (Bell et al., 2001). On the other hand, dietary lipids and the retention of lipids, particularly in fillets, are parameters often discussed in connection with quality. In farmed fish the fatty acids as well as other fillet lipids may be altered by feeding (Bell et al., 2001), so controlled diets can be used to manipulate the FA profile of tissue lipids.

Vitamin E content in fillets from the fish fed the experimental diets is shown in Fig. 1. Dietary vitamin E had a significant effect on the α-tocopherol content of fish muscle ($P < 0.05$). At the end of the feeding trial, the supplemented fillets were 17.7, 19.4 and 17.9 mg kg^{-1} muscle, respectively, for FO, SO, and CO. Results from the present study are consistent with previous studies where the dietary supplementation of vitamin E increased the concentration of tocopherol in the edible tissues of fish (Chaiyapechara et al., 2003; Jitinandana, Kenney, Slider, Kamireddy, & Hankins, 2006; Pirini et al., 2000; Sau et al., 2004; Yildiz et al., 2006). During frozen storage, muscle α-tocopherol content decreased in all feeding groups ($P < 0.05$) and the highest reduction was observed for the FO + E diet (about 60% reduction). Decreased α-tocopherol content during frozen storage has been reported in rainbow trout (Jitinandana et al., 2006).

DL-α-tocopheryl acetate did not affect the FA composition of the feed ($P > 0.05$). For this reason, the data presented in Table 2 are the mean values of each dietary group with and without supplementation. In addition, DL-α-tocopheryl acetate did not affect the FA composition of the fresh muscle ($P > 0.05$, Table 4). This observation is supported by Jitinandana et al. (2006) and Yildiz et al. (2006) who also found that dietary vitamin E did not affect fish muscle FA composition. The FA profile also confirms that the

Table 3
Mean concentrations (% dry weight basis except for % moisture) of proximate constituents in the Beluga sturgeon, *Huso huso*, reared on different diets.[A]

Proximate constituent	Initial fish	Dietary treatment					
		FO	SO	CO	FO + E	SO + E	CO + E
Muscle							
Moisture	74.7 ± 1.10a	72.5 ± 1.37	72.1 ± 2.31	73.1 ± 1.85	72.9 ± 1.50	71.5 ± 1.78^{b}	72.4 ± 0.76
Crude lipid	20.3 ± 1.74	24.9 ± 1.05	27.1 ± 2.15	24.8 ± 1.27	24.5 ± 1.69	26.9 ± 1.72	25.1 ± 0.50
Crude protein	70.4 ± 2.56	70.6 ± 0.96	69.3 ± 1.88	70.4 ± 1.01	70.1 ± 0.96	68.9 ± 1.86	70.6 ± 0.52
Ash	4.37 ± 0.85	4.07 ± 0.16	4.19 ± 0.21$_{x}$	4.50 ± 0.17$^{ab}{}_{x}$	4.31 ± 0.17	5.07 ± 0.24$^{a}{}_{y}$	3.97 ± 0.22$_{y}$

Different superscripts a, b & c indicate significant ($P < 0.05$) differences between all dietary treatments (irrespective of dietary vitamin E and oil source) and different subscript x & y indicate significant ($P < 0.05$) difference between the diet with vitamin E within a single dietary oil source.
[A] See Table 1 for diet abbreviations.

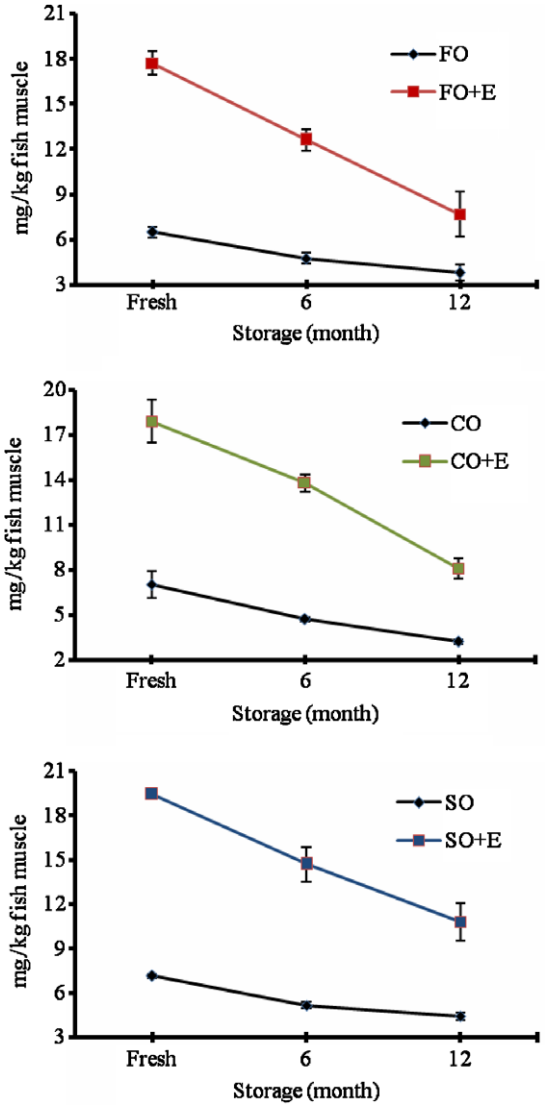

Fig. 1. Muscle vitamin E content (mg kg^{-1} muscle) of Beluga sturgeon, *Huso huso*, fed the experimental diets at 0 (fresh), 6 and 12th months frozen storage. See Table 1 for diet abbreviations.

assimilation patterns of dietary fatty acids in fish muscle reflect the content of the dietary lipid sources. This correspondence with diet content is not only related to the high presence of C16:0, C18:1*n*−9 and C_{18} PUFAs, but also to the high percentage of *n*−3 HUFA (EPA and DHA), which are definitely of exogenous origin. As shown in Tables 2 and 4, feeding sturgeon with diets rich in C_{18} PUFA (SO, CO diets) resulted in relatively good levels of EPA and DHA in the fish muscle. These results showed that *H. huso* have the ability to de-saturate and elongate C_{18} PUFA to EPA and DHA. This is in agreement with the obtained results on other sturgeon fish (Deng, Hung, & Conklin, 1998; Şener et al., 2005; Xu et al., 1993;). Furthermore, with the exception of the SO group, the *n*3/*n*6 ratio obtained from the present study was within the recommended ratio (1:1–1:5) for a healthy human diet (Osman, Suriah, & Law, 2001), but it was lower than that of the other cultured sturgeons [(4.26 for *Acipencer* spp.; 6.74 for *A. naccarii* × *A. baerii* (hybrid); and 4.94 for *H. huso* (reported by Abedian-Kenari et al., 2009)]. In the present study, the major fatty acids found in *H. huso* were palmitic (16:0), oleic acid (OA, 18:1*n*−9), linoleic acid (LN, 18:2*n*−6) and DHA, which is in agreement with the results of Abedian-Kenari et al. (2009) on *H. huso* at different ages.

In this trial fish fed supplemented diets with vitamin E had less significant variation in FA composition in comparison to the control diets during frozen storage at 18 ± 1 °C (Table 4). The FA composition of the muscle underwent slow changes during frozen storage. Fish muscles had higher concentrations of total SFA at 12 months compared to day 0 (fresh) for all dietary treatments ($P < 0.05$). The MUFA levels of the fillet were similar during the 12 months of storage ($P > 0.05$). The *n*−3/*n*−6 ratio of the fillet was the highest on day 0 and the lowest on month 12 ($P < 0.05$). The EPA and DHA levels decreased significantly from day 0 to month 12 ($P < 0.05$), but this reduction was less with the vitamin E treatments. The same trends during storage were observed by Jitinandana et al. (2006) and Yildiz et al. (2006) for rainbow trout fed different levels of dietary vitamin E, but similar results were not observed by Pirini et al. (2000), who found dietary vitamin E supplementation had no affect on general fatty acid composition, MUFA and PUFA content of experimental fish during storage.

Lipid nutritional quality and the AI or TI values are inversely related (Ulbricht & Southgate, 1991). In the present study the lipid quality indices (AI and TI) showed significant variation during frozen storage, but were lower in fish fed diets containing vegetable oils ($P < 0.05$, Table 4). These results showed that the use of vege-

Table 4
Main muscle fatty acid composition (% of total fatty acid expressed as mean) of Beluga sturgeon, *Huso huso*, fed the experimental diets (with and without vitamin E) at 0, 6 and 12th months frozen storage.[A]

Fatty acid	Fish oil diet						Soybean oil diet						Canola oil diet					
	0	0 + E	6	6 + E	12	12 + E	0	0 + E	6	6 + E	12	12 + E	0	0 + E	6	6 + E	12	12 + E
C16:0	16.9^{ab}	16.5^{b}	17.7^{ab}	16.8^{b}	18.3^{a}	17.4^{ab}	13.8	13.9	14.7	14.3	15.1	14.8	12.8^{b}	12.4^{b}	14.0^{a}	12.8^{b}	13.9^{a}	12.5^{b}
∑SFA	27.9^{cA}	27.3^{A}	29.7^{b}	27.8^{cA}	32.4^{a}	29.2^{bc}	19.5	19.4	20.8^{abc}	20.1^{bc}	22.3^{a}	21.4^{ab}	18.6^{b}	18.3^{b}	20.3^{a}	18.7^{b}	20.9^{a}	18.4^{b}
C18:1*n*9	21.4^{a}	21.3^{a}	20.6^{ab}	20.9^{ab}	19.2^{b}	20.3^{ab}	20.7	20.5	21.0	20.0	20.4	20.1	34.6^{a}	34.4^{a}	34.4^{a}	34.3^{a}	33.9^{a}	34.1^{a}
∑MUFA	34.2^{a}	34.1^{a}	34.4^{a}	33.7^{a}	33.2^{a}	33.9^{a}	30.6	30.2	30.7	30.2	31.2	29.7	41.8^{a}	41.7^{a}	41.9^{a}	41.5^{a}	41.3^{a}	41.4^{a}
C18:2*n*6	5.94^{a}	5.98^{a}	5.77^{ab}	5.98^{a}	5.58^{b}	5.71^{ab}	26.8	26.9	26.6	26.8	26.9	27.1	12.3^{a}	12.2^{a}	12.8^{a}	12.1^{a}	12.7^{a}	12.4^{a}
∑PUFA-*n*6	6.55^{a}	6.59^{a}	6.38^{ab}	6.59^{a}	6.19^{b}	6.32^{ab}	27.2	27.4	27.0	27.2	27.3	27.6	12.6^{a}	12.5^{a}	13.1^{a}	12.4^{a}	13.0^{a}	12.7^{a}
C18:3*n*3	4.91^{a}	4.89^{a}	4.68^{a}	4.70^{a}	4.46^{a}	4.57^{a}	6.72	6.78	6.43	6.76	6.22	6.47	7.91^{a}	7.97^{a}	7.78^{a}	8.04^{a}	7.59^{a}	7.91^{a}
C20:5*n*3	7.05^{a}	7.08^{a}	5.82^{b}	7.01^{a}	4.67^{c}	6.88^{a}	4.83^{a}	4.79^{a}	3.35^{c}	4.15^{b}	2.89^{c}	4.08^{b}	3.85^{a}	3.92^{a}	3.08^{ab}	3.72^{a}	2.55^{b}	3.45^{ab}
C22:6*n*3	11.5^{a}	11.8^{a}	10.2^{b}	11.5^{a}	9.25^{c}	11.3^{a}	5.43	5.49	3.98^{bc}	5.34^{a}	3.03^{c}	4.95^{ab}	7.64^{a}	7.73^{a}	6.70^{bc}	7.45^{ab}	5.87^{A}	6.62^{cA}
∑PUFA-*n*3	23.4^{a}	23.8^{a}	20.7^{b}	23.2^{a}	18.4^{c}	22.7^{ab}	17.0	17.1	13.8^{b}	16.3^{a}	12.1^{b}	15.5	19.4^{ab}	19.6^{a}	17.6^{bc}	19.2^{ab}	16.0^{c}	18.0^{ab}
PUFA/SFA	1.08^{a}	1.11^{a}	0.91^{b}	1.07^{a}	0.758^{c}	0.99^{ab}	2.27	2.29	1.96^{c}	2.16^{ab}	1.77^{A}	2.01^{bc}	1.72^{ab}	1.76^{a}	1.51^{c}	1.69^{b}	1.39^{A}	1.67^{ab}
n−3/*n*−6	3.58^{a}	3.61^{a}	3.25^{ab}	3.52^{a}	2.97^{b}	3.59^{a}	0.624^{a}	0.624^{a}	0.510^{bc}	0.597^{ab}	0.444^{c}	0.562^{ab}	1.54^{a}	1.57^{a}	1.34^{bc}	1.55^{a}	1.23^{c}	1.41^{ab}
DHA/EPA	1.63^{c}	1.67^{bc}	1.76^{b}	1.65^{bc}	1.98^{a}	1.64^{c}	1.12	1.15	1.19	1.29	1.05	1.21	1.99^{a}	1.97^{a}	2.18^{a}	2.00^{a}	2.30^{a}	1.92^{a}
AI[B]	0.536^{b}	0.518^{b}	0.607^{b}	0.537^{b}	0.695^{a}	0.561^{b}	0.299^{c}	0.295^{c}	0.352^{b}	0.308^{c}	0.394^{a}	0.348^{b}	0.291^{a}	0.287^{a}	0.328^{b}	0.295^{b}	0.362^{a}	0.292^{a}
TI[C]	0.288^{c}	0.279^{c}	0.337^{b}	0.290^{c}	0.407^{a}	0.310^{bc}	0.235^{c}	0.234^{c}	0.286^{b}	0.251^{c}	0.328^{a}	0.275^{b}	0.209^{ab}	0.204^{b}	0.243^{b}	0.212^{c}	0.267^{a}	0.218^{c}

[A] Different superscripts a, b & c indicate significant ($P < 0.05$) differences between each dietary treatments (irrespective of dietary vitamin E). See Table 2 for fatty acid abbreviation and equations.
[B] Atherogenic index.
[C] Thrombogenic index.

table oils in *H. huso* diet is effective in reducing the SFA, AI and TI, with consequent benefits on the nutritional quality for human consumption. In this regard, Abedian-Kenari et al. (2009), reported AI and TI values of 0.465–0.698 and 0.441–0.486 for *H. huso* at different ages, respectively.

Lipid deterioration is the main cause of shortened shelf life of fish (mainly in fatty fish) due to progressive oxidation (PV and TBA) and enzymatic hydrolysis (FFA) of unsaturated fatty acids and as mentioned previously, the use of antioxidants is an effective way to minimise or delay these reactions. The activity of an antioxidant can be estimated by quantitatively determining primary (PV) or secondary (TBA) products from the autoxidation of lipids or by monitoring other variables, such as accelerated oxidation studies and model systems tests (Shahidi & Wanasundara, 1992).

In the present trial, though the fat content in Beluga sturgeon was similar (Table 3) in all the dietary groups, the degree of lipid oxidation was different (Fig. 2, $P < 0.05$). The differences in lipid oxidation possibly resulted from the different FA compositions. The inclusion of vegetable oils in fish diet reduces lipid peroxidation in fish muscle (e.g., Atlantic salmon, Regost, Jakobsen, & Rørå, 2004; and red hybrid tilapia, Ng & Bahurmiz, 2009), and thereby might enhance the sensorial attributes of the flesh for human consumption. In the present work, replacement of FO by SO and CO decreased lipid oxidation irrespective of vitamin E supplemen-

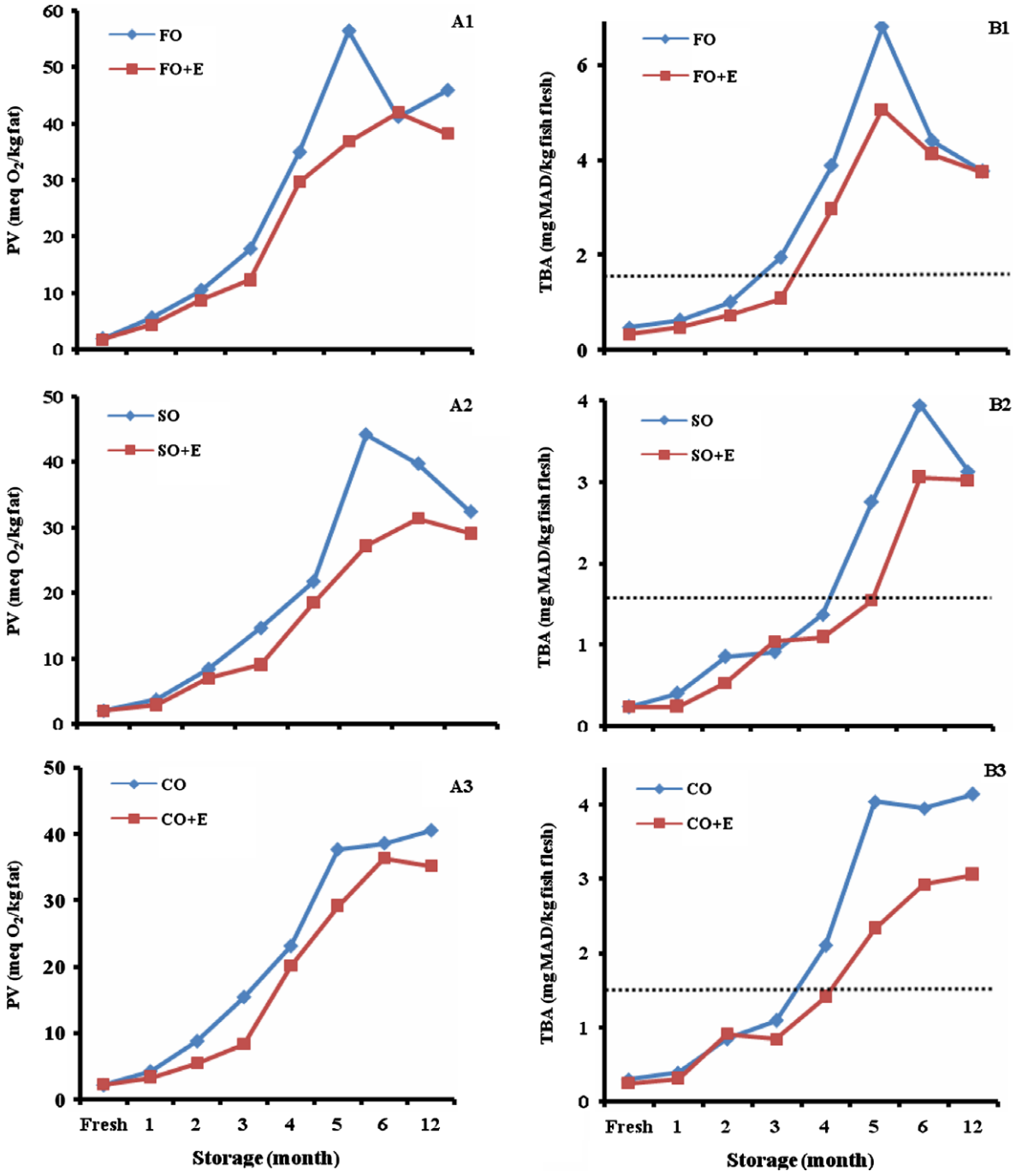

Fig. 2. Muscle peroxide value (PV. A1–3) and thiobarbituric acid (TBA, B1–3) levels of Beluga sturgeon, *Huso huso*, fed the experimental diet for 120 days during frozen storage at −18 °C. See Table 1 for diet abbreviations. (The dotted line represent limit acceptance. Error bar not shown.)

tation (Fig. 2). In addition, the deposition of tocopherols and tocotrienols in diets containing vegetable oil enhanced oxidative stability.

As shown in Fig. 2, the PV and TBA levels were found to be low in all vitamin E groups ($P < 0.05$) throughout the storage period, but as frozen storage time lengthened, PV and TBA levels gradually increased. This may be related to the loss of vitamin E (Fig. 1) that was caused by lipid peroxidation (Yildiz et al., 2006). In addition, it is significant that the Beluga sturgeon used in this study were stored at −18 °C and protected from light, capable of starting lipid oxidation, by a dark sheet of plastic. These conditions most likely contributed to the inhibition of lipid degradation even at low vitamin E concentrations. Frigg, Probucki, and Ruhdel (1990) indicated that when the α-tocopherol concentration in rainbow trout fillet increased to approximately 20 μg g^{-1} then fillet oxidation in fish tissue was effectively prevented. A similar effect of dietary vitamin E concentration in reducing fillet lipid oxidation was observed in rainbow trout (Chaiyapechara et al., 2003; Jitinandana et al., 2006; Yildiz et al. 2006), pacu (Sant'Ana and Mancini-Filho, 2000) and sea bass (Pirini et al., 2000). Since vitamin E prevents the development of rancidity, vitamin E levels and TBA values could be used as indices for fish quality evaluation. However, Auburg (1993) reported that TBA values may not give the actual rates of lipid oxidation since malondialdehyde can interact with other components of fish such as nucleosides, nucleic acids, proteins, amino acids, phospholipids and other aldehydes that are end-products of lipid oxidation. According to a sensory study of various fresh and frozen fish by Ke, Cervantes, and Robles-Martinez (1984), fish flesh with TBA greater than 21 μmol MDA kg^{-1} (1.51 mg MDA kg^{-1}) should be considered rancid and unacceptable. It is important to note that the TBA level for the SO group observed in this study reached this level later than the FO and CO groups (with or without dietary vitamin E).

DL-α-tocopheryl acetate did not affect lipid hydrolysis (FFA), WHC and HI (Fig. 3, $P > 0.05$). For this reason, the data presented in Fig. 3 are the mean values of each dietary oil group. As shown in Fig. 3, progressive development of lipid hydrolysis was observed ($P < 0.05$) during frozen storage but there was no significant differences among experimental diets. These results showed that even the low temperature (−18 °C) could not stop lipid hydrolysis. As a result of the hydrolysis, the original fish lipid structure is destroyed. In the process, significant amounts of FFA are released. They can then be included in the lipid oxidative processes started by free radicals, metal ion initiators, different enzymes or light. This finding is in agreement with that of Dragoev et al. (1998) who found progressive lipid hydrolysis ($P < 0.05$) in carp and mackerel during frozen storage.

The WHC of the muscle is an important flesh quality property of fish, since water is essential for maintaining good texture properties (Ng & Bahurmiz, 2009). Protein denaturation during frozen storage can cause loss of WHC in thawed fish. In the present study muscle WHC in the experimental fish was fairly stable and gradually decreased ($P > 0.05$) as the frozen storage time increased. Although no significant variation was found between the dietary groups ($P > 0.05$), there was a tendency for *H. huso* fed the SO diet to have a higher WHC during the frozen storage. The observed difference in WHC between *H. huso* fed the FO diet and *H. huso* fed vegetable oil diets seemed to be related to the unsaturated FA (Regost et al., 2004), but this aspect needs further investigation. Published reports on the effects of dietary oil on the WHC of fish are limited, and the results are often contradictory. Regost et al. (2004) reported significant differences in WHC in fillets of Atlantic salmon fed different dietary oils. Contradictory results were reported on the red hybrid tilapia by Ng and Bahurmiz (2009), who reported that WHC was not influenced by the dietary oil source, which is in agreement with the results of the present study.

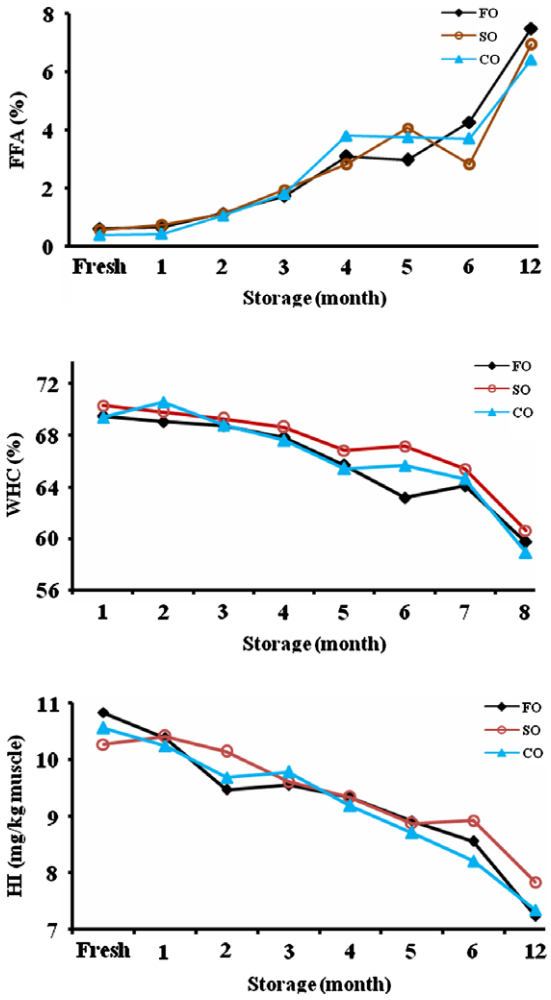

Fig. 3. Muscle free fatty acid (FFA), water holding capacity (WHC) and heme iron (HI) during frozen storage (−18 °C) of Beluga sturgeon, *Huso huso*, fed experimental diets (error bar not shown). See Table 1 for diet treatment.

In the present study, the HI decreased with increasing storage time ($P < 0.05$). Transition metal ions, notably iron, are important in the generation of free radicals that can initiate lipid peroxidation. During storage and processing of fish, heme complexes may have been destroyed and "free" iron released, the latter being considered as the main catalyst of the lipid peroxidation processes in muscle (Dragoev et al. 1998). In the present study, significant correlations were observed between HI values and lipid oxidation for all samples. The results corroborates the experimental findings of Dragoev et al. (1998).

4. Conclusion

This study showed that although proximate composition of Beluga sturgeon, *H. huso*, is not influenced by dietary oil sources. The muscle FA profiles reflected dietary FA profile. Also, there were no significant effects of dietary DL-α-tocopheryl acetate on proximate composition and FA composition of fish muscles. Muscle α-tocopherol content of fish fed diets supplemented with DL-α-tocopheryl acetate increased. The increased muscle α-tocopherol concentration allowed this antioxidant to perform its antioxidant role during storage. Reduced muscle α-tocopherol content was observed during frozen storage fillets compared with fresh fillets. Feeding DL-α-tocopheryl acetate at 250 mg kg^{-1} to *H. huso* for 120 days before slaughter improved the quality of frozen fillets by slowing down

the level of lipid oxidation and would justify the cost of supplementing with vitamin E. It is important that cultured *H. huso* maintain its level of $n-3$ HUFA in the edible flesh and preserve other aspects important to human acceptability i.e., colour, taste, texture during frozen storage. Therefore, further studies are necessary using other levels of vitamin E supplementation in fish dietary to further reduce lipid oxidation during long-term frozen storage. In addition, future study about the effect of such supplementation and also vegetable oil inclusion in *H. huso* diet on FA composition in the liver, histological aspects on intestine and muscle, different size and age fish, and enzymatic activities should be conducted to confirm the results found in this study.

Acknowledgements

This study has been financed jointly by *Tarbiat Modares University*, Tehran, Iran and *Mazandaran Livestock and Aquatic's Feed Co*., Sari, Iran. The authors thank the "University Research Deputy" and the general manager of the company for their support. We sincerely thank Prof. Joe M. Regenstein, from the Department of Food Sciences, Cornell University, USA, and Prof. Barbara Rasco, from the Department of Food Science, Washington State University, USA, for their critically reading of the manuscript and for making a number of helpful suggestions. We are also grateful to Seyedeh Hakimeh Hosseini, Reza Tahergorabi, Hoshang Fayazi and Ali Bagheri for their assistance with the chemical measurements.

References

Abedian-Kenari, A., Regenstein, J. M., Hosseini, S. V., Rezaei, M., Tahergorabi, R., Nazari, R. M., et al. (2009). Amino acid and fatty acid composition of Cultured Beluga (*Huso huso*) of different ages. *Journal of Aquatic Food Product Technology*. doi:10.1080/10498850902758586.

AOAC (2005). *Official methods of analysis* (18th ed.). Gaithersburg, MD, USA: Association of Official Analytical Chemists.

Auburg, S. P. (1993). Review: Interaction of malondialdehyde with biological molecules – new trends about reactivity and significance. *International Journal of Food Science and Technology, 28*, 323–335.

Bell, J. G., McEvoy, J., Tocher, D. R., McGhee, F., Campbell, P. J., & Sargent, J. R. (2001). Replacement of fish oil with rapeseed oil in diets of Atlantic salmon (*Salmo salar)* affects tissue lipid compositions and hepatocyte fatty acid metabolism. *Journal of Nutrition, 131*, 1535–1543.

Bligh, E. G., & Dyer, W. J. (1959). A rapid method of total lipid extraction and purification. *Journal of Biochemistry and Physiology, 37*, 911–917.

Chaiyapechara, S., Casten, M. T., Hardy, R. W., & Dong, F. M. (2003). Fish performance, fillet characteristics, and health assessment index of rainbow trout (*Oncorhynchus mykiss*) fed diets containing adequate and high concentration of lipid and vitamin E. *Aquaculture, 219*, 715–738.

Clark, E. M., Mahoney, A. W., & Carpenter, C. E. (1997). Heme and total iron in ready -to- eat chicken. *Journal of Agriculture and Food Chemistry, 45*, 124–126.

Deng, D. F., Hung, S. S. O., & Conklin, D. E. (1998). White sturgeon (*Acipencer transmontanus*) require both $n-3$ and $n-6$ fatty acids. *Aquaculture (Abstracts Lipids and Fatty Acids), 161*, 333–335.

Dragoev, S. G., Kiosev, D. D., Danchev, S. A., Ioncheva, N. I., & Genov, N. S. (1998). Study on the oxidative processes in frozen fish. *Bulgarian Journal of Agricultural Science, 4*, 55–65.

Egan, H., Kirk, R. S., & Sawyer, R. (1981). *Pearson's chemical analysis of foods*. Churchill Livingstone: UK, Edinburgh (pp. 535–536).

Folch, J., Lees, M., & Sloan-Stanley, G. H. (1957). A simple method for the isolation and purification of total lipids from animal tissues. *Journal of Biological Chemistry, 226*, 497–509.

Frigg, M., Probucki, M. L., & Ruhdel, E. U. (1990). Effect of dietary vitamin E levels on oxidative stability of trout fillets. *Aquaculture, 84*, 145–158.

Jitinandana, S., Kenney, P. B., Slider, S. D., Kamireddy, N., & Hankins, J. S. (2006). High dietary vitamin E affects storage stability of frozen-refrigerated trout fillets. *Journal of Food Science, 71*, 91–96.

Ke, P. J., Cervantes, E., & Robles-Martinez, C. (1984). Determination of thiobarbituric acid reactive substances (TBARS) in fish tissue by an improved distillation spectrophotometric method. *Journal of Food Sciences and Agriculture, 35*, 1248–1254.

Kirk, R. S., & Sawyer, R. (1991). *Pearson's composition and analysis of foods* (9th ed.). London: Longman Scientific and Technical.

Liu, Q., Scheller, K. K., & Schaefer, D. M. (1996). Technical note: A simplified procedure for vitamin E determination in beef muscle. *Journal of Animal Science, 74*, 2406–2410.

McKenzie, D. J., Piraccini, G., Agnisola, C., Steffensen, J. F., Bronzi, P., Bolis, C. L., et al. (1999). The influence of dietary fatty acid composition on the respiratory and cardiovascular physiology of Adriatic sturgeon (*Acipenser naccarii*): A review. *Journal of Applied Ichthyology, 15*, 265–269.

Ng, W.-K., & Bahurmiz, O. M. (2009). The impact of dietary oil source and frozen storage on the physical, chemical and sensorial quality of fillets from market-size red hybrid tilapia, *Oreochromis* sp. *Food Chemistry, 113*, 1041–1048.

NRC, National Research Council (1993). *Nutrient requirements of fish*. USA, Washington DC: National Academy Press.

Osman, H., Suriah, A. R., & Law, E. C. (2001). Fatty acid composition and cholesterol content of selected marine fish in Malaysian waters. *Food Chemistry, 73*, 55–60.

Pastoriza, L., Sampedro, G., Herrera, J. J., & Cabo, M. L. (1998). Influence of sodium chloride and modified atmosphere packaging on microbiological, chemical and sensorial properties in ice storage of slices of hake (*Merluccius merluccius*). *Food Chemistry, 61*, 23–28.

Pirini, M., Gatta, P. P., Testi, S., Trigari, G., & Monetti, P. G. (2000). Effect of refrigerated storage on muscle lipid quality of sea bass (*Dicentrarchus labrax*) fed on diets containing different levels of vitamin E. *Food Chemistry*, 289–293.

Regost, C., Jakobsen, J. V., & Rørå, A. M. B. (2004). Flesh quality of raw and smoked fillets of Atlantic salmon as influenced by dietary oil sources and frozen storage. *Food Research International, 37*, 259–271.

Ruff, N., Fitzgerald, R. D., Cross, T. F., Hamre, K., & Kerry, J. P. (2003). The effect of dietary vitamin E and C level on market-size turbot (*Scophthalmus maximus*) fillet quality. *Aquaculture Nutrition, 9*, 91–103.

Sant'Ana, L. S., & Mancini-Filho, J. (2000). Influence of the addition of antioxidants in vivo on the fatty acid composition of fish fillets. *Food Chemistry, 68*, 175–178.

Sargent, J. R., Bell, J. G., Bell, M. V., Henderson, R. J., & Tocher, D. R. (1995). Requirement criteria for essential fatty acids. *Journal of Applied Ichthyology, 11*, 183–198.

Sau, S. K., Paul, B. N., Mohanta, K. N., & Mohanty, S. N. (2004). Dietary vitamin E requirement, fish performance and carcass composition of rohu (*Labeo rohita*) fry. *Aquaculture, 240*, 359–368.

Şener, E., Yildiz, M., & Savaş, E. (2005). Effects of dietary lipids on growth and fatty acid composition in Russian sturgeon (*Acipenser gueldenstaedtii*) juveniles. *Turkish Journal of Veterinary and Animal Sciences, 29*, 1101–1107.

Shahidi, F., & Wanasundara, P. D. (1992). Phenolic antioxidants. *Critical Review for Food Science and Nutrition, 32*, 67–103.

Ulbricht, T. L. V., & Southgate, D. A. T. (1991). Coronary heart disease: Seven dietary factors. *The Lancet, 338*, 985–994.

Xu, R., Hung, S. S. O., & German, J. B. (1993). White sturgeon tissue fatty acid compositions are affected by dietary lipids. *Journal of Nutrition, 123*, 1685–1692.

Yildiz, M., Şener, E., & Gün, H. (2006). Effect of refrigerated storage on fillet lipid quality of rainbow trout (*Oncorhynchus mykiss* W.) Fed a diet containing different levels of DL-α-tocopherol acetate. *Turkish Journal of Veterinary and Animal Sciences, 30*, 143–150.

Food Chemistry 118 (2010) 349–356

Contents lists available at ScienceDirect

Food Chemistry

journal homepage: www.elsevier.com/locate/foodchem

Purification, structural elucidation, and anti-inflammatory effect of a water-soluble 1,6-branched 1,3-α-D-galactan from cultured mycelia of *Poria cocos*

Mei-Kuang Lu [1], Jing-Jy Cheng [1], Cha-Yui Lin, Chia-Chuan Chang *

National Research Institute of Chinese Medicine, 155-1 Li-Nung St., Sec. 2, Shipai, Peitou, Taipei 112, Taiwan, ROC

ARTICLE INFO

Article history:
Received 13 October 2008
Received in revised form 31 March 2009
Accepted 30 April 2009

Keywords:
Poria cocos
Polysaccharides
Galactan
Endothelial cell
Inflammation

ABSTRACT

Poria cocos has recently been commercially used to formulate nutraceuticals and functional foods in Taiwan. In this study, *P. cocos*, was cultured and polysaccharides were extracted, followed by fractionation with size-exclusion column chromatography to give a water-soluble 1,6-branched 1,3-α-D-galactan (PC-II). The predominant monosaccharide was galactose after complete hydrolysis of the polysaccharide. The chemical structure was characterised by a monosugar analysis, along with ^{1}H, ^{13}C, and 2D nuclear magnetic resonance spectroscopy, including NOESY and HMBC experiments for linkage and sequence analysis. This polysaccharide is composed of a high-galactose-type undecasaccharide repeating unit with the following structure:

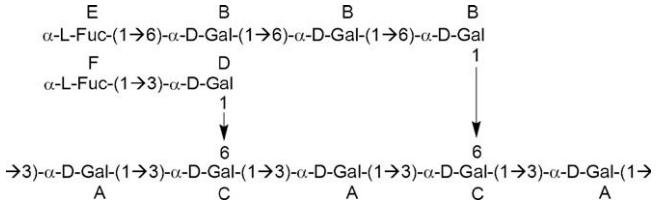

PC-II showed no toxicity to endothelial cells (ECs) and dose-dependently suppressed production of the interferon (IFN)-γ-induced inflammation marker, IP-10. However, PC-II showed no effect on cancer cell cytotoxicity or antiangiogenic activity. These results suggest that PC-II may play roles in regulating the anti-inflammatory process.

1. Introduction

Mushrooms constitute a flavourful and nutritious food group. They contain all of the essential amino acids. Mushrooms have long been used in oriental herbal traditions, and also as dietary supplements and natural cosmetics (Kaneno et al., 2004). *Poria cocos* (called *fu ling* in Chinese) is a medicinal fungus of the family *Polyporaceae* that grows on the roots of old, dead pine trees. It has been used in traditional Chinese medicine for many centuries. *P. cocos* has not only long been utilised to treat a wide variety of diseases, but also has recently attracted the attention of the pharmaceutical industry. Traditionally, it has been used to treat diabetes, dysentery, chronic fatigue syndrome, diarrhea, dizziness, edema, insomnia, kidney problems, nervousness, urination problems, and weakness. *P. cocos* is commercially available and is popularly used in the formulation of nutraceuticals, tea supplements, cosmetics, and functional foods in Asia. Chemical compounds found in *P. cocos* include triterpenes (Tai, Akira, Tetsuro, Tohru, & Yasuhiro, 1995; Yasukawa et al., 1998) and β-pachyman, a polysaccharide composed of β-pachymarose, pachymic acid, and poricoic acid. Recently, a growing body of evidence has indicated that *P. cocos* exhibits anticancer (Chen & Chang, 2004; Huang, Yong, Zhang, Cheung, & Kennedy, 2007; Jin et al., 2003), anti-inflammatory (Ukiya et al., 2002), and immunomodulating (Lee & Jeon, 2003) effects. The bioactivities of polysaccharides are related to their physical and chemical properties, such as the monosaccharide composition,

* Corresponding author. Tel.: +886 2 28201999x6641; fax: +886 2 28264266.
E-mail address: changch@nricm.edu.tw (C.-C. Chang).
[1] These two authors contributed equally to this work.

0308-8146/$ - see front matter © 2009 Elsevier Ltd. All rights reserved.
doi:10.1016/j.foodchem.2009.04.126

molecular weight, degree of branching, glycosidic linkages and substituents. For example, a linear 1,6-α-D-glucan from *P. lobata* shows antioxidant activity when the 2-*O*, 3-*O* and 4-*O* positions are sulfated (Cui et al., 2008); a mucilage, 1,4-β-D-glucomannan, from *Dendrobium huoshanense*, which exhibits cytokine-secretion activity, is 2-*O* and 3-*O* acetylated (Hsieh et al., 2008). In addition, a number of physicochemical properties, such as solubility, primary structure, molecular weight, extent of branching by side-chain substituents (Bohn & BeMiller, 1995), and the charge on the polymer, may influence the biological activities (Vetvicka & Yvin, 2004).

Since *P. cocos* is commercially available and is popularly used in Asia, it is worthwhile to fully characterise its activities. Use of cultured mycelia as metabolic factories, instead of whole fruiting bodies, can circumvent problems associated with inappropriate targeting and provide the opportunity to fine-tune the biosynthetic pathway. Polysaccharides isolated from different sources (fruiting bodies, mycelia, and biomass-free broth) differ somewhat in structure, composition, and physiological activities. It is also worthwhile to elevate the total polysaccharide production from the culturing system with a scalable method for pharmaceutical applications. Thus, cultured mycelia of *P. cocos* were used in this study. In nature, polysaccharides occur as mixtures of heterogeneous cellular components (Kim et al., 2003), and it is first necessary to isolate, purify, and structurally characterise these polysaccharides. In this study, the purification and partial characterisation of polysaccharides from an *in vitro* culture system of *P. cocos* were performed. A novel polysaccharide structure of a 1,3-α-galactan (denoted PC-II) from fractionated polysaccharides of cultured mycelia of *P. cocos* is reported. The overall objective of this study was to examine the structure and functions of PC-II from *P. cocos*. The results indicated that the biological properties of PC-II may play roles in regulating the anti-inflammatory process.

2. Material and methods

2.1. Poria cocos

Poria cocos (BCRC 36022) was purchased from the Bioresource Collection and Research Center, Hsinchu, Taiwan.

2.2. Isolation of polysaccharides

Polysaccharides were isolated from a 49 day-old culture of *P. cocos* (Cheng, Lin, Lur, Chen, & Lu, 2008).

2.3. Fractionation of polysaccharides by gel filtration column chromatography

Forty milligrammes of the lyophilised polysaccharide-containing preparation were dissolved in 3 ml of a buffer, containing 150 mM NaCl and 10 mM NaH_2PO_4, at pH 6.8, and analysed on a column of Fractogel BioSec 80 × 1.5 cm (Merck, Darmstadt, Germany) which had been equilibrated with the buffer mentioned above. The eluted fractions (2.8 ml/tube) were assayed for hexose by the phenol-sulphuric acid method (Zevenhuizen, Scholten-Koerselman, & Posthumus, 1980), and the absorbance at 488 nm was recorded.

2.4. Molecular weight and homogeneity determination

Molecular weight determination of the polysaccharide PC-II was determined by the same system as described in Section 2.3. A calibration curve was constructed using a dextran series (Sigma, Saint Louis, MO, USA) containing average molecular weights of 5 mg each of 69.8, 40.0, and 10.5 kDa (kilo-Daltons) in 3 ml of the buffer stated above. The regression equation was made between the log [Mw] (Y) and the fraction number (X) as $Y = 10.55–0.17X$; $R^2 = 0.9860$. Homogeneity of PC-II was confirmed by high performance size exclusion chromatography with an evaporative light scattering detector (HPSEC–ELSD) (Shimadzu, Kyoto, Japan) equipped with a TSK-GEL G-3000PW_{XL} 7.8 × 300 mm column (Tosoh, Tokyo, Japan) eluted with isocratic 100% de-ionised H_2O at a flow rate of 1 ml/min.

2.5. Compositional analysis of PC-II

Acid hydrolysis of PC-II and determination of monosaccharides composition were carried out according to Cheng et al. (2008). Monosaccharides were identified by comparing retention times of sample peaks with those of standards. Quantification of each monosaccharide was carried out by integration of the chromatographic peak on a PeakNet system (Dionex, Sunnyvale, CA, USA). Standards of monosaccharide were dissolved in Q-water. Myo-inositol, sorbitol, fucose, galactosamine, glucosamine, galactose, glucose, and mannose were obtained from Sigma. Sodium hydroxide solution was obtained from Fisher Scientific (Pittsburg, PA, USA).

2.6. One-(1D) and two-dimensional (2D) nuclear magnetic resonance (NMR)

Six milligrammes of PC-II sample was deuterium-exchanged in D_2O, lyophilised, and redissolved in 0.5 ml of D_2O. 1D ^1H (500 MHz), ^{13}C (125 MHz), and 2D NMR spectra of PC-II were recorded on a Varian Unity 500 MHz NMR spectrometer in D_2O (99.9%, Cambridge Isotope Laboratories, Andover, MA, USA) at 25 °C with a Varian 5 mm ^1H–$^{19}F/^{15}N$–^{31}P PFG switchable broadband probe. Chemical shifts were referenced to the HDO (δ_H 4.78) and acetone-d_6 (δ_C 30.89) resonances at 25 °C as the internal standards. 2D DQF-COSY (double-quantum filter correlation spectroscopy), HSQC (heteronuclear single quantum coherence), and HMBC (heteronuclear multiple-bond correlation) spectra were obtained using the standard pulse sequence. TOCSY (total correlation spectroscopy) spectra were recorded with a mixing time of 100 ms and relaxation delay of 2 s. The NOE (nuclear Overhauser enhancement) spectrum was obtained from the standard 2D ^1H–^1H ROESY spectra.

2.7. Endothelial cells culture

Human vascular endothelial cells (ECs) were maintained in Dulbecco's modified Eagle's medium (DMEM, Invitrogen, Carlsbad, CA, USA) supplemented with 2 mM L-glutamine and 10% heat-inactivated fetal bovine serum (FBS) (Life Technologies, Kibbutz, Israel). The cells' viability and the number of cells were determined by the trypan blue dye-exclusion method (Raimondi et al., 2006).

2.8. Determination of cells viability

To assess cell viability, the alamar blue (AB) assay (dye purchased from Biosource International, Nivelles, Belgium) was used as previously described (Fatokun, Stone, & Smith, 2008). At the end of each treatment period, a final concentration of 10% v/v AB was added to each well. Plates were incubated at 37 °C for 6 h prior to measuring the absorbance at 540 and 595 nm wavelengths using a spectrophotometric plate reader (DYNEX Technologies, Chantilly, VA, USA). The ratio of surviving cells is shown as the percentage of untreated control cells.

2.9. Matrigel EC tube formation assays

Matrigel (12.5 mg/ml) was thawed at 4 °C, and 50 μl were quickly added to each well of a 96-well plate and allowed to solidify for 10 min at 37 °C. Once solidified, wells were incubated for 30 min with ECs (25,000 cells/well). After adhesion of the cells, the medium was removed and replaced with fresh medium supplemented (or not) with PC-II and then incubated at 37 °C for 18 h. The growth tubes were visualised with an inverted microscope at a magnification of 10×.

2.10. Transient transfection and promoter activity assay

To evaluate the gene expression alternation of IP-10, a full-length IP-10 promoter construct with a reporter gene (luciferase) conjugation was purified using an EndoFree Plasmid Maxi Kit DNA Purification System (Qiagen, Valencia, CA, USA). Transfection to introduce these constructs into cells was performed by the LipofecTAMINE method (Invitrogen, CA, USA), and a pSV-β-galactosidase plasmid was co-transfected to normalise the transfection efficiency. When promoter activity is turned-on, luciferase will be translated in the cells and the activity of luciferase detected by its substrate equals the promoter activity of the target gene. Besides, β-galactosidase can be detected by its substrate and represents the same amount of cells in each test. In brief, ECs were plated onto 6-well plates at a density 1×10^5 cells/well and grown overnight. Cells were co-transfected with 2 μg of each promoter construct and 1 μg of the pSV-β-galactosidase plasmid for 5 h by the LipofecTAMINE method. After transfection, cells were recovered with 10% FBS medium with vehicle (DMSO) or drugs for 24 h. Luciferase and β-galactosidase activities were assayed using the assay systems according to the procedures of the manufacturer (Promega, Madison, WI, USA). Luciferase activity was normalised to β-galactosidase activity in cell lysates and was expressed as the average of three independent experiments.

2.11. Detection of IP-10 protein release

Levels of IP-10 secreted into the culture supernatant collected from ECs after interferon (IFN)-γ stimulation, with or without pretreatment with PC-II, were determined using a sandwich enzyme-linked immunosorbent assay (ELISA) kit (R&D Systems, Minneapolis, MN, USA) according to the manufacturer's instructions. Supernatants, as pools of triplicates, were collected and stored at −20 °C prior to use in the ELISA. Concentrations of secreted IP-10 were determined using ELISA readers from BioSource (Camarillo, CA, USA).

2.12. Statistical analysis

The data are presented as means ± standard error (SE), and n represents the number of experiments. In bar graphs, SE values are indicated by error bars. Statistical analyses were carried out with Student's unpaired t-tests when applicable; p values of <0.05 were considered significant.

3. Results

3.1. Characterisation of polysaccharides from cultured mycelia of P. cocos

Polysaccharides were isolated according to the methodology previously described and their profiles were evaluated into I (26–34), II (35–38), III (39–41), IV (41–47) and V (48–54), and the estimated Mn values (average molecular weight) of the five

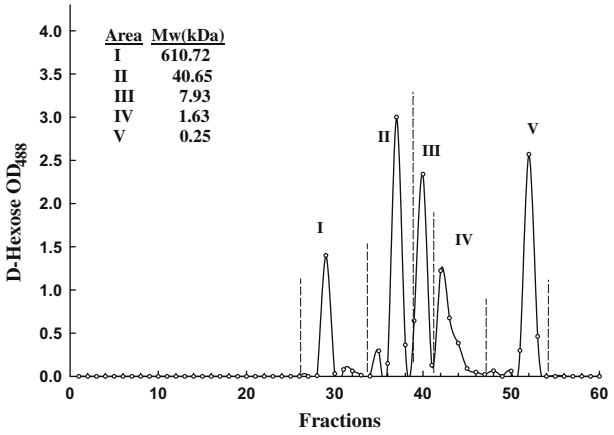

Fig. 1. Gel filtration profile of polysaccharides of *P. cocos*.

polysaccharide populations were determined to be 610.7, 40.7, 7.9, 1.6, and 0.3 kDa for fractions I–V, respectively, using a dextran series (Sigma) containing average molecular weights of 69.8, 40.0, and 10.5 kDa as standards (Fig. 1). In addition, HPSEC on a TSK-GEL G3000PW$_{XL}$ coupled with an ELSD was utilised as an alternative approach to evaluate the homogeneity of PC-II. The consistent retention time (18.3 min) and the peak symmetry double-confirmed that only one sample existed in PC-II (data not shown).

Compositional analysis showed that myo-inositol, sorbitol, fucose, galactosamine, glucosamine, galactose, glucose and mannose were the neutral sugars in the polysaccharide of *P. cocos* (Table 1). Galactose was the predominant species in fractions I, II, and IV.

3.2. 1D and 2D NMR

3.2.1. General

To enhance the quality of spectra and avoid the undesired line broadening effect arising from the high viscosity of the polysaccharide, the PC-II sample was diluted in D_2O to a concentration of 1.2×10^{-2} g cm^{-3} to diminish the intermolecular interaction. The ^{1}H and ^{13}C NMR spectra of PC-II are shown in Fig. 2. The completely assigned spectrum of the polysaccharide, given in Table 2, was derived from 2D DQF-COSY, TOCSY, NOESY, HSQC, and HMBC NMR spectra.

The ^{1}H NMR spectrum (Fig. 2A) of PC-II contained four signals of six embedded anomeric protons at δ 5.02, 4.95, 4.92 and 4.90. The sugar residues were designated as follows: δ 5.02 for residues A and D, δ 4.95 for residues E and F, δ 4.92 for residue B, and δ 4.90 for residue C (Table 2), according to the decreasing chemical shifts of the anomeric protons. The four low-field signals with the *galacto* configuration all appeared as singlets ($^3J_{1,2}$ < 3 Hz) and represent sugars with the α-anomeric configuration. The ^{13}C NMR spectrum (Fig. 2B) contained signals for three anomeric carbons at δ 98.0–102.5, one CH_3–C group (C-6 of Fuc) at δ 15.8,

Table 1
Sugar composition of the fractionated polysaccharide (PS) of *Poria cocos*.

PS (μmole/g)	I	II	IV	V
Myo-inositol	13.8 ± 1.15	6.26 ± 0.23	9.98 ± 0.12	18.5 ± 0.58
Sorbitol	6.29 ± 0.11	3.14 ± 0.07	–	0.67 ± 0.02
Fucose	35.6 ± 2.32	44.4 ± 1.44	33.1 ± 0.36	17.8 ± 0.38
Galactosamine	55.9 ± 0.36	3.94 ± 0.03	–	8.22 ± 0.29
Glucosamine	67.9 ± 0.32	–	–	6.31 ± 0.65
Galactose	104 ± 6.99	159 ± 0.05	35.1 ± 1.99	11.0 ± 0.05
Glucose	47.2 ± 1.57	0.94 ± 0.08	3.69 ± 0.12	2.25 ± 0.18
Mannose	77.4 ± 0.08	16.5 ± 0.13	6.80 ± 0.03	5.36 ± 0.48

one signal for the unsubstituted hydroxymethylene carbon at δ 61.3 (C-6 free), and one substituted hydroxymethylene carbon at δ 66.7 (C-6 glycosylated). As judged by the absence from the ^{13}C NMR spectrum of signals within δ 82–88, all sugar residues were in the pyranose form.

The ^{1}H and ^{13}C chemical shifts of the PC-II sample were fully assigned (Table 2), based on 1D ^{1}H, ^{13}C (Fig. 2), ^{13}C, DEPT-135, ROESY, 2D COSY, TOCSY (data not shown), HSQC (Fig. 3A), and HMBC (Fig. 3B) NMR experiments. The HSQC spectrum showed correlations between four α-^{1}H signals and three ^{13}C signals in the anomeric region, representative of five anomeric protons in the repeating unit. Integration of the H-1 signals and those in the HSQC spectra for residues A–F gave a ratio of around 3:3:2:1:1:1 (residues A–F, respectively), suggesting that the PC-II repeating unit is a high-galactose-type undecasaccharide.

3.2.2. Assignment of residue A

The COSY spectrum showed stepwise connectivities from the H-1 signal at δ 5.02 to H-2 at δ 3.98, H-3 at δ 3.67, H-4 at δ 3.58, H-5 at δ 3.81, and H-6a at δ 3.66, indicative of an α-pyranosyl moiety. The HMBC spectrum (Fig. 3B) demonstrated correlations between H-4 at δ 3.58 and C-3, C-5, and C-6 signals at δ 73.6, 70.5, and 61.3, respectively. In addition, the C-3 and C-5 signals demonstrated $^{3}J_{C,H}$ correlations with H-1 at δ 5.02, and the C-4 signal at δ 67.0 showed correlations with δ 3.98 (H-2), 3.81 (H-6b), and 3.67 (H-3). After the protons had been identified, the chemical shifts of their corresponding carbons were readily determined (Table 2) from the HSQC spectrum (Fig. 3A) between the carbon and proton in C–H pairs. The carbon and proton chemical shifts with a downfield-shifted carbon signal at δ 73.6 (C-3) indicated a 3-substituted α-pyranoside. Since galactose was the predominant monosaccharide identified by the monosaccharide analysis, and the absolute configuration of D for galactose was assumed as the natural occurring polysaccharide, residue A was a 3-substituted α-D-Gal residue, specifically α-D-galactopyranoside.

3.2.3. Assignment of residue B

Using similar approaches, the complete proton and carbon chemical shifts of the spin system beginning from the H-1 signal at δ 4.92 (residue B) was obtained (Table 2). The TOCSY spectrum

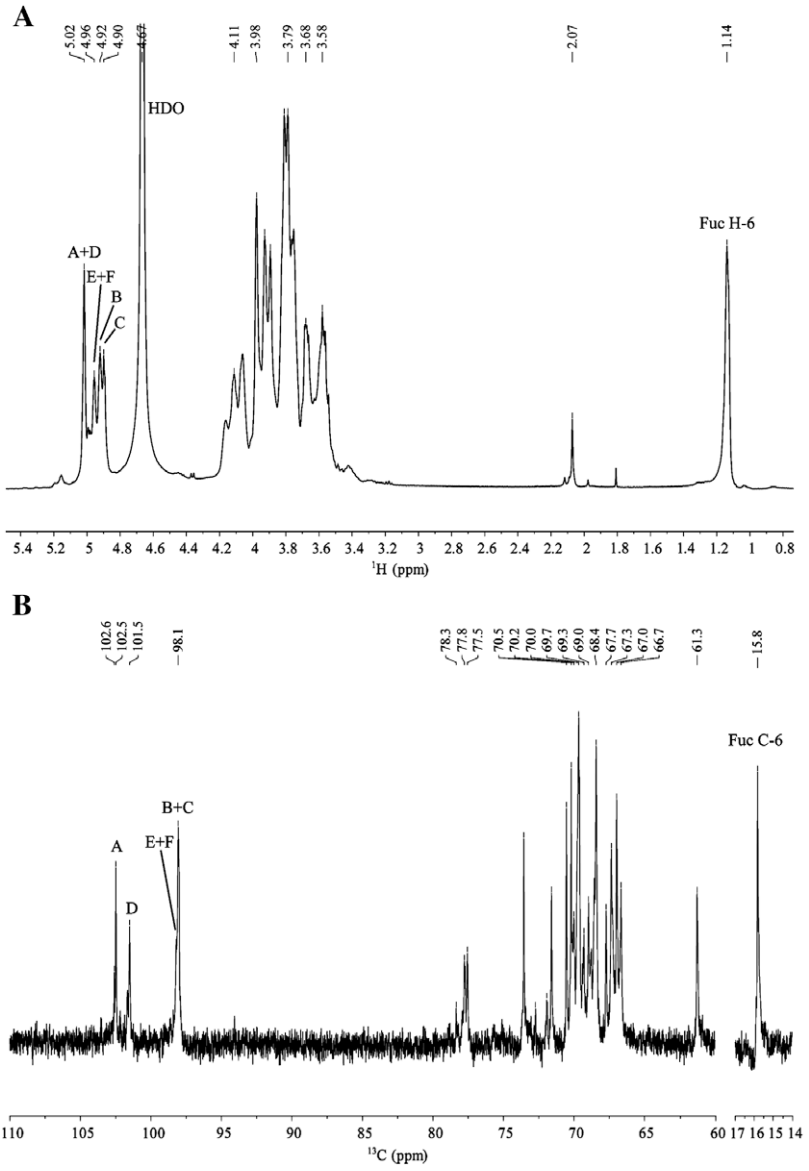

Fig. 2. ^{1}H and ^{13}C nuclear magnetic resonance spectra of 1,6-branched 1,3-α-D-galactan PC-II from *Poria cocos* in D_2O at 25 °C. Anomeric protons and carbons are labelled A–F. The chemical shifts are shown in δ ppm.

Table 2
^{1}H and ^{13}C chemical shift data of the monosaccharides constituting (1,3)-α-D-galactan PC-II from *Poria cocos*.

Residue	$^{1}H/^{13}C$					
	1	2	3	4	5	6
A	5.02	3.98	3.67	3.58	3.81	3.66 (a), 3.81 (b)
α-D-$Gal_{5,02}$	102.5	70.2[a]	73.6	67.0	70.5	61.3
B	4.92	3.93	3.75	3.8	3.81	3.88 (a), 3.59 (b)
α-D-$Gal_{4,92}$	98.1	69.9	68.4	67.0	70.2	67.0
C	4.90	4.06	3.91	4.11	3.79	3.82 (a), 3.59 (b)
α-D-$Gal_{4,92}$	98	69.5	77.5	69.0	70.2	66.7
D	5.02	3.88	3.75	3.58	3.98	3.66 (a), 3.81 (b)
α-D-$Gal_{5,02}$	101.5	67.0	77.8	67.0	70.2	61.3
E	4.95	3.59	3.98	3.89	4.08	1.14
α-L-$Fuc_{4,95}$	98.2	67.7	70.5	71.6	67.3	15.8
F	4.95	3.88	3.75	3.89	4.08	1.14
α-L-$Fuc_{4,95}$	98.2	67.0	69.7	71.6	67.3	15.8

showed connectivities from the H-1 signal at δ 4.92 to H-2 at δ 3.93 and H-3 at δ 3.75, from H-3 to H-4 at δ 3.80 and H-5 at δ 3.81, and from H-5 to H-6b at δ 3.59, one of the 6-substituted pyranosyl proton signals. Their corresponding ^{13}C chemical shifts were readily assigned from the HSQC spectrum (Fig. 3A) between the carbon and proton of C–H pairs (Table 2). The HMBC spectrum showed correlations of δ 98.1 (C-1) with δ 3.75 (H-3), and of δ 68.4 (C-3) with δ 3.93 (H-2) and 3.81 (H-5). The DEPT-135 spectrum showed a substituted hydroxymethylene carbon at δ 67.0, indicative of a glycosidic linkage on C-6. Accordingly, residue B was identified as a 6-substituted α-D-galactopyranoside.

3.2.4. Assignment of residue C

The complete proton and carbon chemical shifts of residue C, beginning from the peak at δ 4.90 (H-1), were obtained using the aforementioned approaches (Table 2). Signals for H-2, H-3, H-4, and H-5 were determined by cross peaks in the HMBC spectrum, including C-2 to H-1, C3 to H-4 and H-5, and C4 to H-5. The COSY spectrum demonstrated a correlation between δ 4.11 (H-4) and 3.82 (H-6a). Their corresponding ^{13}C chemical shifts were assigned, based on C–H pairs in the HSQC spectrum. From the downfield-shifted ^{13}C signals at δ 77.5 (C-3) and the substituted hydroxymethylene carbon at δ 67.0 (C-6), as confirmed by the DEPT-135 spectrum, residue C was assigned as 3,6-disubstituted α-D-galactopyranoside.

3.2.5. Assignment of residue D

The complete proton and carbon chemical shifts (Table 2) of the spin system beginning from the peak at δ 5.02 (residue D) was obtained from 2D TOCSY, ROESY, and HMBC. The TOCSY spectrum demonstrated correlations of H-1 at δ 5.02 with H-2 at δ 3.88, H-5 at δ 3.98, and H-6a at δ 3.81. The ROESY spectrum showed the correlations between the peaks at δ 5.02 (D H-1) and 3.88 (D H-2), indicative of the α-configuration. The HMBC spectrum revealed correlations between C-2 and H-4, and between C-3 and H-5, and the assignments of H-2 and H-3 were therefore confirmed. From the downfield-shifted ^{13}C signal at δ 77.8 (C-3), residue D was a 3-substituted α-D-galactopyranoside.

3.2.6. Assignment of residues E and F

The TOCSY spectrum showed stepwise connectivities from the H-1 (E and F) signal at δ 4.95 to F H-3 at δ 3.75, H-5 at δ 4.08, and H-6 at δ 1.14 (*d*, *J* = 1.35 Hz), indicative of a 6-deoxy-sugar. The HMBC spectrum showed correlations between H-6 at δ 1.14 and the peaks at δ 71.6 and 67.3, indicative of C-4 and C-5 peaks, respectively. In addition, correlations between the peaks at δ 98.2 (C-1) and 3.59, 3.75, and 3.88, and between the carbon signal at δ 67.7 (E C-2) and 3.89 (H-4), and between δ 70.5 (E C-3, $^{1}J_{C,H}$ to E H-3 at δ 3.98) and 3.59 (E H-2) resulted in the assignment of H-2 (E: δ 3.59; F: δ 3.88) and H-3 (E: δ 3.98; F: δ 3.75) signals. The ROESY spectra demonstrated correlations between the signals at δ 4.95 (E H-1) and 3.75 (F H-3), and between δ 3.75 and 4.08 (E and F H-5), indicative of H-3 (δ 3.75) and H-5 (δ 4.08) signals. Furthermore, the COSY, TOCSY, ROESY, and HMBC spectra showed correlations between the signal at δ 1.14 (H-6) and the peak at δ 4.08, which also confirmed the assignment of H-5. Both the carbon and proton chemical shifts (Table 2) are typical of a 6-deoxyhexopyranose. Since L-Fuc was the only sugar identified by the monosaccharide analysis (Table 1), residues E and F were assigned as the fucose residue, specifically as α-L-fucopyranoside. Minor differences were observed in the H-2 and H-3 signals, while their carbon signals were almost identical.

3.2.7. Assignment of remaining residues

After the ^{1}H and ^{13}C spectra for residues A–F had been virtually completely assigned, the sequence of the glycosyl residues in the undecasaccharide was determined by the observed inter-residue connectivities shown in the ROESY and HMBC spectra. ROESY connectivities were observed between A H-1 (and the overlapping D H-1 signal) and the three signals of A H-2, C H-3, and C H-6, indicative of A(1 → 3)C and D(1 → 6)C linkages. Moreover, the ROESY spectrum demonstrated inter-residue correlations between C C-1 and A H-3, and between B C-1 and B H-6, indicative of C(1 → 3)A and B(1 → 6)B linkages. These linkages were further supported by the inter-residue $^{3}J_{C,H}$-connectivities observed in the HMBC spectrum. In the anomeric carbon atom resonance region of the HMBC spectrum, correlations were seen between F C-1 and D H-3, between E C-1 and B H-6, and between F C-1 and D H-6, respectively indicative of F(1 → 3)D, E(1 → 6)B, and F(1 → 6)D linkages.

In the ^{13}C NMR spectra, C-3 signals of residues A, C, and D ranged from δ 73.6 to 77.8, indicative of 1,3-α-D-galactan (Moule, Galbraith, Cox, & Wilkinson, 2004; Vinogradov, Korenevsky, & Beveridge, 2003; Stroop, Xu, Retzlaff, Abeygunawardana, & Bush, 2002) and dissimilar to that of 1,3-β-galactan, 1,3-β-glucan and 1,3-α-glucan at δ 83.0 (Leon de Pinto, Martinez, Ludovic de Corredor, Rivas, & Ocando, 1994), 86.0 (Wang et al., 2004), and 82.0 (Huang & Zhang, 2005; Huang et al., 2007), respectively.

After a comprehensive analysis of the aforementioned 1D and 2D NMR spectral studies of PC-II summarised in Table 2, a putative undecasaccharide repeating unit for the neutral 1,6-branched 1,3-α-D-galactan was depicted as the following structure:

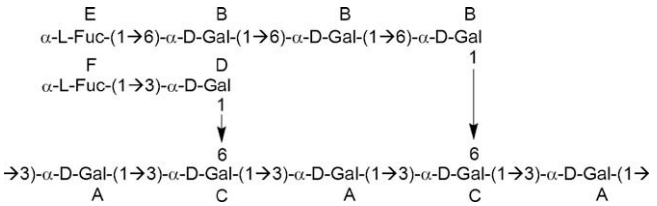

The main skeleton of the repeating unit is composed of three A residues and two C residues, and the two branches F–D and E–B–B–B are both connected to the C residues.

3.3. Toxicity of PC-II

To evaluate the toxicity of PC-II toward EC viability, an alamar blue (AB) assay was performed. The sensitivity and evaluation protocol of AB assay is now well recognised as better than the MTT assay used in our previous study. After ECs had reached confluence, the medium was changed to serum-free medium. Serial dilutions of PC-II were used to assay the toxicity toward ECs for 24 h. PC-II showed no toxicity toward ECs up to a concentration of 250 μg/ml (see Supplementary Table 1).

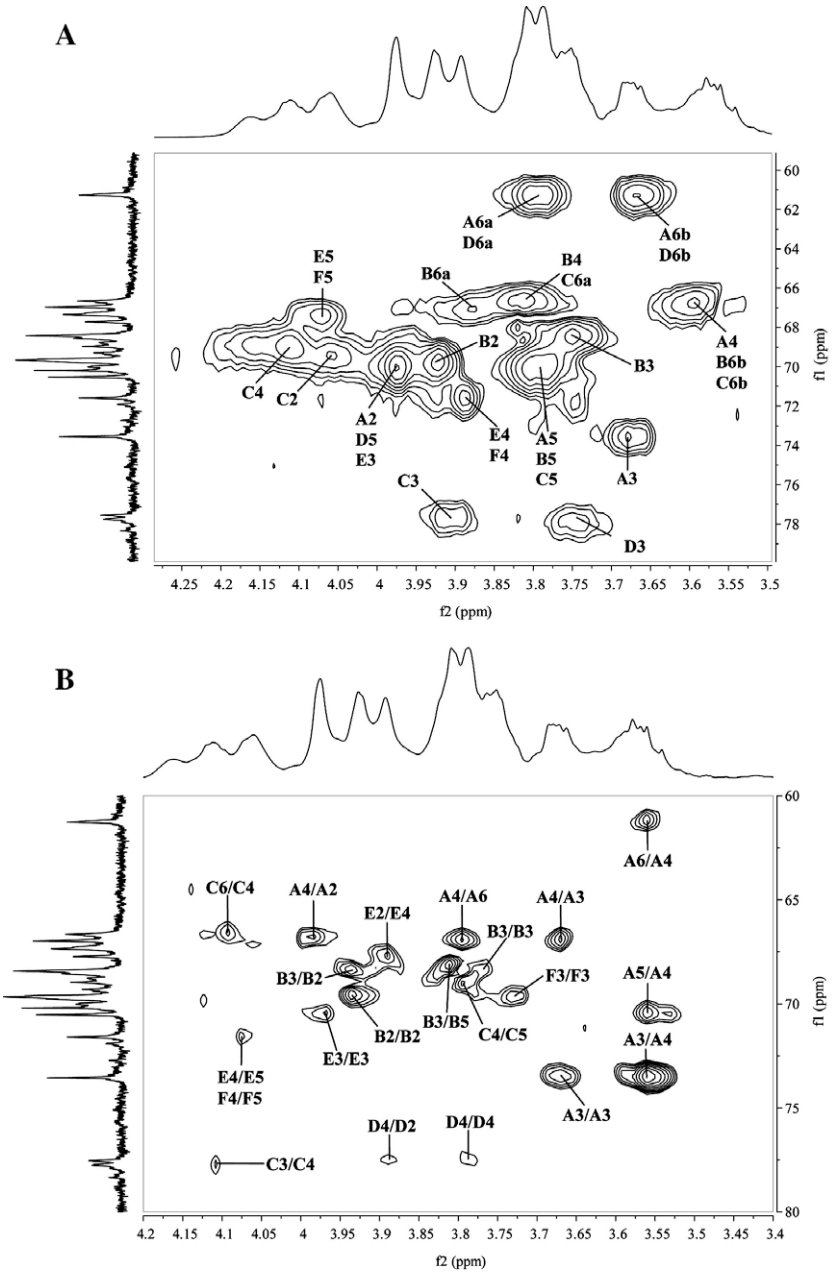

Fig. 3. 2D HSQC (A) and HMBC (B) nuclear magnetic resonance spectrum of 1,6-branched 1,3-α-D-galactan PC-II from *Poria cocos* in D_2O at 25 °C. (A) Cross-peaks marked by capital letters indicate $^1J_{CH}$ correlations. (B) Cross-peaks marked by capital letters indicate $^1J_{CH}$, $^2J_{CH}$, and $^3J_{CH}$ correlations from C to H atoms in selected ranges (^{1}H: 3.4–4.2 ppm; ^{13}C: 60–80 ppm).

3.4. Influences of PC-II on IFN-γ-induced IP-10 secretion

The inhibitory effects on IP-10 protein release and promoter activity induced by IFN-γ, stimulated by PC-II, were evaluated. As shown in Fig. 4A, IFN-γ treatment of ECs increased IP-10 protein release. PC-II pretreatment of ECs suppressed IFN-γ-induced IP-10 protein release in a dose-dependent manner. However, in the IP-10 promoter activity assay, PC-II pretreatment showed no influence on IFN-γ-induced IP-10 promoter activities (Fig. 4B). This result indicates that PC-II might play a role in regulating inflammation.

3.5. Influences of PC-II on cancer cell cytotoxicity

To study the effects of PC-II on cancer cell cytotoxicity, four cancer cell lines were used, including MCF-7 (breast cancer), H460 (lung cancer), HT29 (colon cancer), and CEM (leukemia cancer). Serial dilutions were evaluated for their cytotoxic effects on these four cancer cell lines in the same way as described in the viability assay (see Supplementary Table 2). PC-II exhibited no cytotoxic effect on cancer cells.

3.6. Influences of PC-II on EC tube formation

To study the effects of PC-II on angiogenesis, an *in vitro* Matrigel tube formation model was used. Serial dilutions were evaluated for their effects on VEGF-induced angiogenesis, as revealed by tube formation on Matrigel (see Supplementary Fig. 1). PC-II exhibited no inhibitory effect on EC tube formation compared to VEGF-treated control cells.

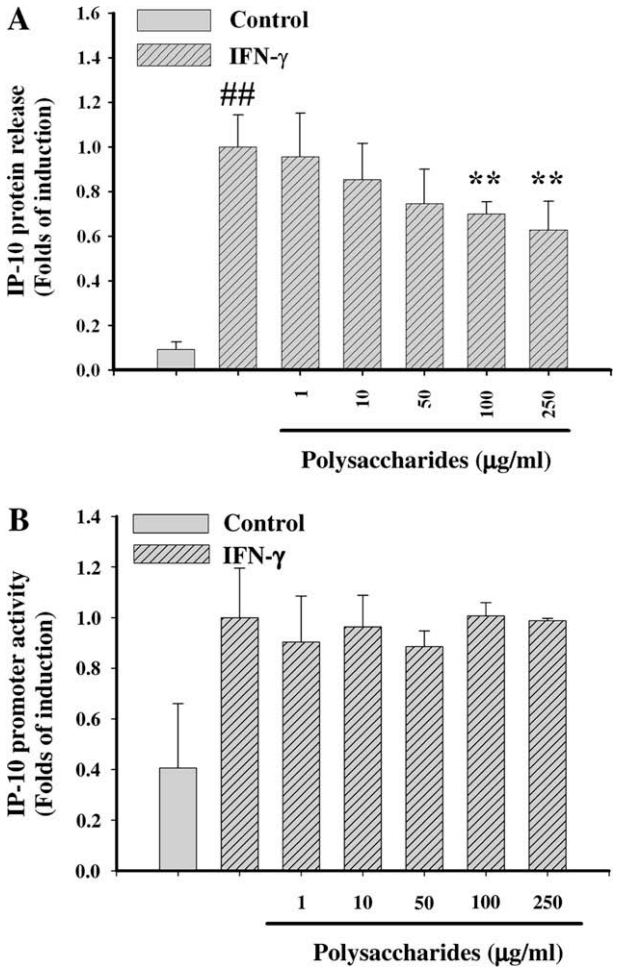

Fig. 4. Influences of PC-II on interferon (IFN)-γ-induced IP-10 secretion. (A) Effects of PC-II on IFN-γ-induced IP-10 protein release from ECs after being pretreated with PC-II at the indicated concentrations for 3 h, followed by IFN-γ (10 ng/ml) stimulation for 24 h. IP-10 protein release into medium is expressed as pg/mg of total protein and is presented as the mean ± SE from three independent experiments. $^{\#\#}p < 0.01$ vs. the control; $^{**}p < 0.01$ vs. IFN-γ treatment. (B) Effect of PC-II on IP-10 promoter activity in ECs. Luciferase activity (represents promoter activity) was normalised to β-galactosidase activity in cell lysates and was expressed as an average of three independent experiments.

4. Discussion

For the species studied in this report, *P. cocos*, a number of polysaccharides have been identified, including a 1,3-β-glucan (Chen, Xu, Zhang, & Kennedy, 2009), 1,3-α-glucan (Lin et al., 2004; Huang & Zhang, 2005), 1,3-α-glucan with 1,6-branches (Kanayama, Adachi, & Togami, 1983), and 1,6-α-glucan (Zjawiony, 2004). In this article, we report the isolation and identification of a 1,3-α-D-galactan with 1,6-branches and an α-L-fucosyl terminal from cultured mycelia of *P. cocos*, and this is the first report of an 1,3-α-galactan from *P. cocos*. The skeleton of 1,3-α-galactosyl moieties has also been found in a number of bacteria, such as *Shewanella* spp. MR-4 (Vinogradov, Kubler-Kielb, & Korenevsky, 2008) and *Streptococcus pneumoniae* type 1 (Stroop et al., 2002). In addition, a fucogalactan with 1,6- and 1,4,6-α-D-galactosyl skeleton and 2-β-galactosyl and 2-α-fucosyl side chains, which elicited the release of TNF-a and NO from murine macrophages, has also been isolated from a mushroom *Sarcodon aspratus* (Mizuno et al., 2000).

In addition to the structure of PC-II, composed of a 1,3-α-D-Gal main skeleton and 1,6-α-D-Gal side chains, at a ratio of 1:1, another possible structure composed of α-1,6- and α-1,3 interlaced D-Gal main skeleton with 1,3-α-D-Gal side chains was also proposed and analysed. However, the strong correlation between C C-1 and A H-3 and the weak correlation between B C-1 and C H-6 in HMBC spectra eliminated the possibility. Besides, for the minor mannose composition of PC-II (at a ratio of 1:10 to galactose) in Table 1, five signals of the 1,4-β-mannosyl moiety (Hsieh et al., 2008) were observed in the 2D HSQC (Fig. 3A) and HMBC (Fig. 3B) NMR spectra, including δ 4.99/101.6 (H-1/C-1) 3.64/71.0 (H-3/C-3), 3.82/77.9 (H-4/C-4) and 3.54/72.4 (H-5/C-5). However, weak 1D NMR signals and insufficient HMBC evidence of the 1,4-β-Man impeded further assignment of this moiety to the putative structure.

Inflammation is a general phenomenon in many diseases. IFN-γ is one of the major mediators which predisposes ECs toward inflammatory/immunological responses. In this study, pretreatment with the PC-II dose-dependently inhibited IFN-γ-induced inflammatory gene IP-10 protein release (Fig. 4A). However, PC-II showed no inhibitory effect on IP-10 promoter activity (Fig. 4B). Furthermore, the profiles and toxicity of PC-II were first evaluated. PC-II showed no toxicity to ECs, indicating the safety of the use of this fungus (see Supplementary Table 1). This result indicated that the effect of PC-II on IP-10 expression was regulated at the translational and not at the transcriptional level and thus it may participate in regulating inflammatory-related diseases.

Polysaccharides are known to have anticancer and antiangiogenic activities (Cheng, Huang, Chang, Wang, & Lu, 2005), and this formed the rationale for investigating the effects of polysaccharides from *P. cocos* on these two processes. Because VEGF is an angiogenic inducer which induces proliferation, migration, and differentiation of ECs, we investigated the effects of PC-II on VEGF-induced EC tube formation on Matrigel. As a result, PC-II did not inhibit VEGF-induced EC tube formation (see Supplementary Fig. 1). In addition, PC-II exhibited no cytotoxic activities on cancer cells (see Supplementary Table 2). Therefore, related diseases due to the anti-inflammatory property of PC-II remain for further elucidation. Furthermore, in comparison with our previous study that extracts from *Fomitopsis pinicola* (Cheng et al., 2008), PC-II from *P. cocos* in this study showed less potency than did *F. pinicola* both in Matrigel tube formation and IP-10 release inhibition. Nevertheless, the purpose of this study is to demonstrate the novel structure we discovered in *P. cocos* and its biological functions. Besides the functions we tested in this study, there may exist other biological functions, and this requires further investigation.

In conclusion, we report a novel polysaccharide of cultured *P. cocos* with 1,6-branched 1,3-α-D-galactan structure and an anti-inflammation function of the fractionated polysaccharide (PC-II). Further investigations on optimisation of the submerged culture to achieve the demands of commercial-scale mycelial and polysaccharide production are required.

Acknowledgements

We thank Mr. D.P. Chamberlin for critically reading the manuscript. This work was supported in part by grants (NRICM-97-DHM-05) to MKL, (NRICM97-DBCM-10) to JJC, and (NRICM-97-DMC-04) to CCC from the National Research Institute of Chinese Medicine, Taipei, Taiwan.

Appendix A. Supplementary data

Supplementary data associated with this article can be found, in the online version, at doi:10.1016/j.foodchem.2009.04.126.

References

Bohn, J., & BeMiller, J. (1995). (1 → 3)-ß-D-glucan as biological response modifiers: A review of a structure-functional activity relationships. *Carbohydrate Polymers, 28*, 3–14.

Chen, X., Xu, X., Zhang, L., & Kennedy, J. F. (2009). Flexible chain conformation of (1 → 3)-ß-D-glucan from *Poria cocos* sclerotium in NaOH/urea aqueous solution. *Carbohydrate Polymers, 75*, 586–591.

Chen, Y., & Chang, H. (2004). Antiproliferative and differentiating effects of polysaccharide fraction from fu-ling (*Poria cocos*) on human leukemic U937 and HL-60 cells. *Food and Chemical Toxicology, 42*, 759–769.

Cheng, J., Huang, N., Chang, T., Wang, L., & Lu, M. (2005). Study for anti-angiogenic activities of polysaccharides isolated from *Antrodia cinnamomea* in endothelial cells. *Life Sciences, 76*, 3029–3042.

Cheng, J., Lin, C., Lur, H., Chen, H., & Lu, M. (2008). Properties and biological functions of polysaccharides and ethanolic extracts isolated from medicinal fungus, *Fomitopsis pinicola*. *Process Biochemistry, 43*, 829–834.

Cui, H., Liu, Q., Tao, Y., Zhang, H., Zhang, L., & Ding, K. (2008). Structure and chain conformation of a (1 → 6)-α-D-glucan from the root of *Pueraria lobata* (Willd). Ohwi and the antioxidant activity of its sulfated derivative. *Carbohydrate Polymers, 74*, 771–778.

Fatokun, A., Stone, T., & Smith, R. (2008). Prolonged exposures of cerebellar granule neurons to S-nitroso-N-acetylpenicillamine (SNAP) induce neuronal damage independently of peroxynitrite. *Brain Research, 1230*, 265–272.

Hsieh, Y. S. Y., Chien, C., Liao, S. K. S., Liao, S. F., Hung, W. T., Yang, W. B., et al. (2008). Structure and bioactivity of the polysaccharides in medicinal plant *Dendrobium huoshanense*. *Bioorganic and Medicinal Chemistry, 16*, 6054–6068.

Huang, Q., Yong, J., Zhang, L., Cheung, P., & Kennedy, J. (2007). Structure, molecular size and antitumor activities of polysaccharides from *Poria cocos* mycelia produced in a fermenter. *Carbohydrate Polymers, 70*, 324–333.

Huang, Q., & Zhang, L. (2005). Solution properties of (1 → 3)-α-D-glucan and its sulfated derivative from *Poria cocos* mycelia via fermentation tank. *Biopolymers, 79*, 28–38.

Jin, Y., Zhang, L., Zhang, M., Chen, L., Cheung, P. C., Oi, V. E., et al. (2003). Antitumor activities of heteropolysaccharides of *Poria cocos* mycelia from different strains and culture media. *Carbohydrate Research, 338*, 1517–1521.

Kanayama, H., Adachi, N., & Togami, M. (1983). A new antitumor polysaccharide from the mycelia of *Poria cocos* Wolf. *Chemical and Pharmaceutical Bulletin, 31*, 1115–1118.

Kaneno, R., Fontanari, L., Santos, S., Di Stasi, L., Rodrigues, F., & Eira, A. (2004). Effects of extracts from Brazilian sun-mushroom (*Agaricus blazei*) on the NK activity and lymphoproliferative responsiveness of Ehrlich tumor-bearing mice. *Food and Chemical Toxicology, 42*, 909–916.

Kim, S., Xu, C., Hwang, H., Choi, J., Kim, C., & Yun, J. (2003). Production and characterisation of exopolysaccharides from an entomopathogenic fungus *Cordyceps militaris* NG3. *Biotechnology Progress, 19*, 428–435.

Lee, K., & Jeon, Y. (2003). Polysaccharide isolated from *Poria cocos* sclerotium induces NF-(B/Rel activation and iNOS expression in murine macrophages. *International Immunopharmacology, 3*, 1353–1362.

Leon de Pinto, G., Martinez, M., Ludovic de Corredor, A., Rivas, C., & Ocando, E. (1994). Chemical and ^{13}C NMR studies of *Enterolobium cyclocarpum* gum and its degradation products. *Phytochemistry, 37*, 1311–1315.

Lin, Y., Zhang, L., Chen, L., Jin, Y., Zeng, F., Jin, J., et al. (2004). Molecular mass and antitumor activities of sulfated derivatives of α-glucan from *Poria cocos* mycelia. *International Journal of Biological Macromolecules, 34*, 231–236.

Mizuno, M., Shiomi, Y., Minato, K., Kawakami, S., Ashida, H., & Tsuchida, H. (2000). Fucogalactan isolated from *Sarcodon aspratus* elicits release of tumor necrosis factor-alpha and nitric oxide from murine macrophages. *Immunopharmacology, 46*, 113–121.

Moule, A. L., Galbraith, L., Cox, A. D., & Wilkinson, S. G. (2004). Characterisation of a tetrasaccharide released on mild acid hydrolysis of LPS from two rough strains of *Shewanella* species representing different DNA homology groups. *Carbohydrate Research, 339*, 1185–1188.

Raimondi, F., Crivaro, V., Capasso, L., Maiuri, L., Santoro, P., Tucci, M., et al. (2006). Unconjugated bilirubin modulates the intestinal epithelial barrier function in a human-derived *in vitro* model. *Pediatric Research, 60*, 30–33.

Stroop, C. J., Xu, Q., Retzlaff, M., Abeygunawardana, C., & Bush, C. A. (2002). Structural analysis and chemical depolymerization of the capsular polysaccharide of *Streptococcus pneumoniae* type 1. *Carbohydrate Research, 337*, 335–344.

Tai, T., Akira, A., Tetsuro, S., Tohru, K., & Yasuhiro, T. (1995). Triterpene from the surface layer of *Poria cocos*. *Phytochemistry, 39*, 1165–1169.

Ukiya, M., Akihisa, T., Tokuda, H., Hirano, M., Oshikubo, M., Nobukuni, Y., et al. (2002). Inhibition of tumor-promoting effects by poricoic acid G and H and other lanostane-type triterpenes and cytotoxic activity of poricoic acid A and G from *Poria cocos*. *Journal of Natural Products, 65*, 462–465.

Vetvicka, V., & Yvin, J. (2004). Effects of marine β-1,3-glucan on immune reactions. *International Journal of Immunopharmacology, 4*, 721–730.

Vinogradov, E., Korenevsky, A., & Beveridge, T. J. (2003). The structure of the rough-type lipopolysaccharide from *Shewanella oneidensis* MR-1, containing 8-amino-8-deoxy-Kdo and an open-chain form of 2-acetamido-2-deoxy-D-galactose. *Carbohydrate Research, 338*, 1991–1997.

Vinogradov, E., Kubler-Kielb, J., & Korenevsky, A. (2008). The structure of the carbohydrate backbone of the LPS from *Shewanella* spp. MR-4. *Carbohydrate Research, 343*, 2701–2705.

Wang, Y., Zhang, M., Ruan, D., Shashkov, A. S., Kilcoyne, M., Savage, A. V., et al. (2004). Chemical components and molecular mass of six polysaccharides isolated from the sclerotium of *Poria cocos*. *Carbohydrate Research, 339*, 327–334.

Yasukawa, K., Kaminaga, T., Kitanaka, S., Tai, T., Nunoura, Y., Natori, S., et al. (1998). 3-Beta-p-hydroxybenzoyldehydrotumulosic acid from *Poria cocos*, and its anti-inflammatory effect. *Phytochemistry, 48*, 1357–1360.

Zevenhuizen, L., Scholten-Koerselman, I., & Posthumus, M. (1980). Lipopolysaccharides of *Rhizobium*. *Archives of Microbiology, 125*, 1–8.

Zjawiony, J. K. (2004). Biologically active compounds from *Aphyllophorales* (polypore) fungi. *Journal of Natural Products, 67*, 300–310.

Food Chemistry 118 (2010) 357–363

Contents lists available at ScienceDirect

Food Chemistry

journal homepage: www.elsevier.com/locate/foodchem

Effect of farm and industrial processing on the amino acid profile of cocoa beans

E.I. Adeyeye *, R.O. Akinyeye, I. Ogunlade, O. Olaofe, J.O. Boluwade

Department of Chemistry, University of Ado Ekiti, P.M.B. 5363, Ado Ekiti, Nigeria

ARTICLE INFO

Article history:
Received 19 July 2008
Received in revised form 26 March 2009
Accepted 30 April 2009

Keywords:
Cocoa beans
Farm fermentation
Industrial processing
Amino acids

ABSTRACT

An investigation into the amino acid profiles of unfermented and fermented cocoa nibs, as well as process-line cocoa nibs (P-LCN) and processed cocoa cake samples (PCCS) was carried out. In the unfermented cocoa nibs, Glu (128 mg/g crude protein i.e. 128 mg/gcp) was the most abundant amino acid whilst the most concentrated essential amino acid in the same sample was Leu (72.2 mg/g crude protein); in the fermented cocoa nibs, a similar trend was observed, with respective values of Glu (153 mg/gcp) and Leu (62.4 mg/gcp). Lys (181 mg/gcp) was most abundant amino acid in P-LCN and Ile (63.3 mg/gcp) was the second most abundant; also, in PCCS, Lys (52.7 mg/gcp) was the most abundant amino acid but Asp (43.7 mg/gcp) was the second most abundant. The total amino acid content was (mg/gcp), 641 (unfermented nibs), 708 (fermented nibs), 635 (P-LCN) and 368 (PCCS), with corresponding essential amino acids of 300, 287, 478 and 185 (all with His), respectively. Based on whole hen's egg, the limiting amino acids for the samples were: Ser (unfermented nibs), Met (fermented nibs), Ala (P-LCN) and Val (PCCS), whereas under provisional amino acid scoring pattern, they were: Met + Cys (unfermented nibs), Met + Cys (fermented nibs), Thr (P-LCN) and Val (PCCS). Prolonged and high heat treatments appeared to have reduced the essential amino acids of the PCCS as compared to the P-LCN. Significant differences existed between contents of essential amino acids and non-essential amino acids at $p < 0.05$ in unfermented cocoa nibs, fermented cocoa nibs and P-LCN.

1. Introduction

Cocoa bean was the foremost Nigerian foreign exchange earner before the advent of crude oil and it is currently in the second position after petroleum. The annual production in Nigeria is about 165,000 metric tonnes (MT) (Akinyeye, 1999). A small percentage of the annual production is processed, locally, to cocoa butter and cocoa cake, whilst the bulk is exported. The cocoa beans of commerce are the seeds of the tree –*Theobroma cacao* (Linnaeus), properly harvested, fermented and dried. It originated from Latin America about 500 years ago and thence to Europe, from where it was introduced to other parts of the world (International Cocoa and Commodities Organisation, 2000). Cocoa bean is an oil seed, just like palm kernel, groundnut, sesame seed or any of the other oilseeds. However, it is rarely processed in the same way as the other oil seeds in order to get the oil. The reason for this is probably due to the unique physicochemical characteristics of the beans and its constituents, especially the fat. The Aztecs (of Mexico) prepared the first cocoa drink called "Chocolatl" about 500 years ago (Minife, 1989). This chocolate drink was prepared from a mixture of ground, roasted whole beans or "nibs" and sugar. The drink was extremely rich because of the high fat content. The richness of the beverage made the Aztecs believe that the cocoa tree was of divine origin, hence the name – "Theobroma" meaning, *food for the gods.* The drink has aphrodisiac properties and was held in high esteem as a nuptial aid.

To obtain cocoa, the harvested pods are fermented, by naturally occurring bacteria and yeasts to eliminate their natural, bitter, astringent quality, during which the seeds are cured and roasted. The clean kernels obtained after the removal of the shell, called cocoa nibs, are manufactured into various products. The larger percentage of the nibs is fat, removed by pressure, and is called cocoa butter which is used in fine soaps and cosmetics and in medicine for emollients and suppositories. The residue is ground to a powder (cocoa) and used for beverages and flavouring. Chocolate is a product in which the cocoa butter has been retained. Cocoa products have a high food value because of the large proportion of fat, carbohydrates, and protein. Cacao is classified in the division Magnoliophyta, class Magnoliopsida, order Malvales and family Sterculiaceae.

Cocoa products are eaten mainly because they are liked, by young and old, owing to their attractive flavours and appearance which give pleasure in eating (Minife, 1989). The nutritional parameters of cocoa are determined largely by the chemical composition of the material. The energy contribution to daily diets is dependent on the quantum of proteins, carbohydrates and fats in the cocoa product and its corresponding digestibility coefficient (Minife, 1989). Cocoa powder is mainly used for low calorie food products. The minerals present in cocoa powder are important

* Corresponding author. Tel.: +234 8035782925.
E-mail address: eiadeyeye@yahoo.com (E.I. Adeyeye).

0308-8146/$ - see front matter © 2009 Elsevier Ltd. All rights reserved.
doi:10.1016/j.foodchem.2009.04.127

for their nutritional value. Olaofe, Oladeji, and Ayodeji (1987) and Olaofe and Onajeta (1986) reported on the quality parameters of cocoa beans from Nigeria, as well as on cocoa-based beverages of different brands consumed in the Nigerian market. The level of fermentation, degree of alkalisation, roasting and fat content determine the colour and flavour of cocoa products. Fermentation helps to generate proper aroma and reduce the level of acetic acid, which causes off-flavour in chocolate. The pH of cocoa liquors prepared from well fermented and dried West African beans is around 5.5 whilst those of unfermented or poorly fermented beans are 5.0 or less (The Biscuit, Cake, Chocolate, and Confectionary Alliance (BCCCCA), 1996). Cocoa is added to cigarettes for flavour enhancement. It also contains various psychoactive compounds, such as theobromine, caffeine, serotonin, histamine, tryptophan, trytamine, tyramine, phenylethylamine, octopamine and anandamide (Rambali et al., 2002). The levels of these compounds in added cocoa in cigarettes are thus critical to curtail possible addiction to cigarette smoking. Theobromine and theophylline, as well as caffeine, all found in this plant, are used as a diuretic, stimulant and also, in modern medicine, as an antiasthmatic (Morgan, 1994).

There is, at present, scanty information on the amino acid profile of cocoa beans and the effect of farm and industrial processing on their relative concentrations. This study attempts to evaluate the amino acid composition of dried unfermented and fermented cocoa beans from a major cocoa-producing town in south-west Nigeria vis-à-vis that of the in-process cocoa nibs and processed cocoa cake from a major cocoa processing industry in Nigeria. The effects of fermentation and heat treatment during the course of milling are to be evaluated. Direct processing of the same batch of beans collected from the selected farm location could not be conducted because of the enormous quantity required for batch processing. Consequently, heterogeneous samples of beans supplied, from different locations (thoroughly mixed together to a representative sample), were used for evaluating the effect of heat treatment during milling. This means the analyses were on four samples in two major groups; they are fermented and unfermented samples from the same farm in Aisegba Ekiti and this is the Forastero Amazonian Group (Opeke, 1992); the second group is the factory sample group consisting of the process-line cocoa nibs (P-LCN) and the processed cocoa cake samples (PCCS). The factory samples (P-LCN and PCCS) came from a blend of cocoa beans from different sources of the same species, which is the Forastero Amazonian Group.

2. Materials and methods

2.1. Materials

Cocoa bean seeds were collected from fully ripe pods harvested from some cocoa trees in a farm plantation located at Aisegba Ekiti in Ekiti State of Nigeria in December 2007, during the main crop season. The harvested beans were divided into two portions immediately after they were taken out of the pods. Whilst the first portion was directly sun-dried in open air, the second portion was fermented by a heaping method, using plantain leaves to cover the beans for 6 days before sun-drying. The dried beans were deshelled, dry-milled and labelled as unfermented and fermented nibs, respectively. These formed the group one samples. Similarly, in-process cocoa beans (heterogeneous) of indefinite source, and kibbled cake were collected from the production floor of Co-operative Cocoa Products Limited, Akure, Ondo State, Nigeria in December 2007, for comparative analysis.

The process-line cocoa nibs (P-LCN) were prepared from blended, cleaned and destoned dried cocoa beans from the factory's cleaner/destoner machine. The processed cocoa cake sample (PCCS) was a product that resulted from further processing of the P-LCN. The processes involve microwave heating of the beans at a temperature range of 90–100 °C for a period of about 15 min on a vibratory bed (this makes the cocoa bean shell puff for easy winnowing), automated roasting (at temperature range of 90–100 °C for about 20 min in a rotary evaporator), refining to over 98% fineness to obtain cocoa liquor (masse) which is further heat-treated at 80–90 °C for about 12 h in storage tanks. The liquor is later fed in batches of about 200 kg sizes into a steam-jacketed vacuum mixer, where liquor homogenisation and further heating takes place for about 10 min before final pressing to obtain cocoa butter and cocoa cake. The final heating and homogenisation are used to take the liquor from about 80 °C to about 105 °C and to ensure maturation of the liquor. This also further ensures a final rapid evaporation of residual moisture to <1% in the cocoa liquor and guarantees acceptable sterilisation of the liquor. The pressed cake is kibbled mechanically to obtain smaller sizes of the cocoa cake solid, otherwise called processed cocoa cake samples (PCCS). The factory samples were labelled process-line cocoa nibs (P-LCN) and processed cocoa cake samples (PCCS), respectively. These formed the group two samples.

2.2. Sample treatment

The samples were homogenised and ground to fine powder, using a Mouliness blender. The ground portions were kept in plastic rubbers in the freezer (−4 °C) pending analysis. The values reported for each test were averages of two or more determinations.

2.3. Determination of crude protein

Nitrogen was determined by the micro-Kjeldahl method, as described by Pearson (1976) and the percentage nitrogen was converted to crude protein by multiplying by 6.25.

2.4. Determination of amino acids

The amino acids profile in the cocoa samples was determined using methods described by Adeyeye and Afolabi (2004). The cocoa samples were dried to constant weight. The mass was subsequently defatted, hydrolysed, filtered to remove the humins and evaporated to dryness at 40 °C under vacuum in a rotary evaporator. Each residue was dissolved with 5 ml of acetate buffer (pH 2.0) and stored in a plastic specimen bottle and kept inside the deep freezer pending subsequent analysis. The Technicon Sequential Multisample Amino Acid Analyser (TSM), Technicon Instruments Corporation, New York was used for the analysis. The principle is based on ion-exchange chromatography (IEC) (FAO/WHO, 1991). The equipment is designed to separate free acidic, neutral and basic acids of the hydrolysate. The amount loaded for each sample was 5–10 μl and about 76 min elapsed for each analysis. The column flow rate was 0.50 ml/min at 60 °C with reproducibility consistent within ±3%. The net height of each peak produced by the chart record of the TSM was measured and calculated for the amino acid it was representing. The averages of two determinations were reported. All chemicals used were of analytical grade.

2.5. Estimation of quality of dietary protein

The essential amino acid score was calculated using the following formula (FAO/WHO, 1973): amino acid score = amount of amino acid per test protein (mg/g)/amount of amino acid per protein in reference pattern (mg/g).

Amino acid score (for both essential and non-essential amino acids) was also calculated based on whole hen's egg (Paul, Southgate, & Russel, 1976).

The ratio of total essential amino acid (TEAA) to the total amino acid (TAA), i.e. (TEAA/TAA), total sulphur amino acid (TSAA), percentage cystine in TSAA (%Cys/TSAA), total aromatic amino acid (TArAA), and the Leu/Ile ratios were calculated whilst the predicted protein efficiency ratio (P-PER) was determined using one of the equations developed by Alsmeyer, Cunningham, and Happich (1974), i.e. P-PER = −0.468 + 0.454 (Leu) − 0.105 (Tyr).

Calculations completed were the grand mean, standard deviation, coefficients of variation in percentage, correlation coefficient, regression and F-test, setting the confidence level at 95% (Christian, 1980).

3. Results and discussion

The crude protein levels of the unfermented and fermented samples are shown in Table 1. Also, the crude protein levels in the process-line cocoa nibs (P-LCN) and processed cocoa cake samples (PCCS) are shown in Table 2. The level of crude protein in fermented cocoa bean was 15.2 g/100 g which was better than the value in unfermented cocoa bean (13.6 g/100 g) by 1.58 g/100 g or 10.4%. This meant that the fermentation process had improved the level of the crude protein in the fermented sample compared to the unfermented sample. In the case of the group two samples, P-LCN had a crude protein level of 23.2 g/100 g which was better than the PCCS sample (18.4 g/100 g) by 4.8 g/100 g or 20.7%. This meant that the heat involved in the processing reduced the level of protein. This reduction could have been due to the Maillard reactions which are an interaction between the carbonyl group of a reducing sugar and the free amino acid group from an amino acid or protein. The resulting condensation product is converted by the Amadori rearrangement to the 1-deoxy-2-ketosyl compound. Browning then proceeds along complex pathways, the exact sequence being dependent on pH, temperature, concentration and the identity of the reactants (Muller & Tobin, 1980). However, Ala increased in the PCCS.

The amino acids composition of the unfermented and fermented cocoa nibs is presented in Table 1. The amino acid concentrations were variously distributed amongst the two samples, and this could easily be seen both in the various samples and in the coefficient of variation percentage (CV%). Glutamic acid (Glu) was the most concentrated amino acid amongst the samples: 128 mg/g crude protein (cp) (in unfermented cocoa nibs) and 153 mg/gcp (fermented cocoa nibs). Another acidic amino acid, aspartic acid (Asp), occupied the second position in both samples with values of 100 mg/gcp (unfermented sample) and 82.5 mg/gcp (fermented sample). Cystine (Cys) was the least concentrated, in both samples, with values of 7.8 mg/gcp (unfermented cocoa nibs) and 6.9 mg/gcp (fermented nibs). The fermented cocoa nibs were richer than were unfermented cocoa nibs in the following amino acids: Lys, His, Arg, Ser, Glu, Gly, Ala, Val, Ile, Tyr and Phe, whereas Pro (or one amino acid, 5.88%) was of equivalent level (12.5 mg/gcp in both samples). This meant that the fermented cocoa nibs were 64.7% richer in the amino acids than were the unfermented nibs; whereas the unfermented sample was only better in five (or 29.4%) of the amino acids. Therefore, fermentation improved the amino acid profile of the cocoa nibs. This is particularly true for most of the essential amino acids: Lys, His, Arg, Thr, Val, Ile and Phe. The improvement of amino acid concentration by fermentation followed the trend observed in guinea corn, where steeping of the grains improved the amino acid profile over the raw and germinated samples in Arg, His, Met, Phe, Thr, Val, Ala, Cys, Gly, Pro, Ser, and Tyr (Adeyeye, 2008).

Table 1
Amino acid profiles (mg/g crude protein) of unfermented and fermented cocoa nibs from a farm location.

Amino acid	Unfermented nibs	Fermented nibs	Mean	SD	CV%
Lys*	42.0 ± 0.02	52.6 ± 0.02	47.3	7.50	15.9
His*	20.0 ± 0.00	23.3 ± 0.02	21.7	2.33	10.7
Arg*	43.6 ± 0.01	51.4 ± 0.20	47.5	5.52	11.6
Asp	100 ± 0.10	82.5 ± 0.11	91.3	12.4	13.6
Thr*	29.9 ± 0.03	23.3 ± 0.10	26.6	4.67	17.6
Ser	23.7 ± 0.01	32.6 ± 0.03	28.2	6.29	22.3
Glu	128 ± 0.20	153 ± 0.40	141	17.7	12.6
Pro	12.5 ± 0.02	12.5 ± 0.03	12.5	0.00	–
Gly	20.5 ± 0.01	32.0 ± 0.02	26.3	8.13	30.9
Ala	29.8 ± 0.20	40.1 ± 0.03	35.0	7.28	20.8
Cys	7.8 ± 0.01	6.9 ± 0.02	7.35	0.64	8.71
Val*	32.1 ± 0.10	35.1 ± 0.02	33.6	2.12	6.31
Met*	9.9 ± 0.01	8.0 ± 0.00	8.95	1.34	15.0
Ile*	21.4 ± 0.02	29.3 ± 0.20	25.4	5.59	22.0
Leu*	72.2 ± 0.30	62.4 ± 0.20	67.3	6.93	10.3
Tyr	18.6 ± 0.02	27.0 ± 0.01	22.8	5.94	26.1
Phe*	28.6 ± 0.01	36.3 ± 0.02	32.5	5.44	16.7
Try*	–[a]	–	–	–	–
Crude protein (g/100 g)	13.6 ± 0.30	15.2 ± 0.21			

* Essential amino acids.
[a] Not determined.

Table 2
Amino acid profiles (mg/g crude protein) of process-line cocoa nibs and processed cocoa cake samples from a processing industry.

Amino acid	P-LCN[a]	PCCS[b]	Mean	SD	CV%
Lys	181 ± 0.05	52.7 ± 0.03	117	90.7	77.5
His	11.7 ± 0.01	4.4 ± 0.01	8.05	5.16	64.1
Arg	46.3 ± 0.02	29.4 ± 0.20	37.9	12.0	31.7
Asp	37.4 ± 0.03	43.7 ± 0.20	40.6	4.45	11.0
Thr	15.9 ± 0.02	8.7 ± 0.01	12.3	5.09	41.4
Ser	21.4 ± 0.00	23.1 ± 0.02	22.3	1.20	5.38
Glu	37.4 ± 0.10	43.5 ± 0.02	40.5	4.31	10.6
Pro	28.1 ± 0.02	25.1 ± 0.01	26.6	2.12	7.97
Gly	2.9 ± 0.01	5.0 ± 0.01	3.95	1.48	37.5
Ala	1.5 ± 0.01	20.1 ± 0.02	10.8	13.2	122
Cys	15.3 ± 0.02	10.8 ± 0.01	13.1	3.18	24.3
Val	39.2 ± 0.03	2.4 ± 0.01	20.8	26.0	125
Met	4.3 ± 0.01	3.7 ± 0.02	4.0	0.42	10.5
Ile	63.3 ± 0.30	31.9 ± 0.05	47.6	22.2	46.6
Leu	47.2 ± 0.02	37.0 ± 0.20	42.1	7.21	17.1
Tyr	13.6 ± 0.02	12.1 ± 0.11	12.9	1.06	8.22
Phe	21.8 ± 0.02	14.8 ± 0.01	18.3	4.95	27.0
Try	–	–	–	–	–
Crude protein (g/100 g)	23.2 ± 0.20	18.4 ± 0.03			

[a] Process-line cocoa nibs.
[b] Processed cocoa cake samples.

Our results, in both the unfermented and fermented cocoa nibs, followed the trends in *Cola acuminata, Garcinia kola* and *Anacardium occidentale*, where Glu was the most concentrated amino acid and Asp was the second most concentrated in *C. acuminata* and *G. kola* (Adeyeye, Asaolu, & Aluko, 2007). Our trend in Glu and Asp agreed with the results of Olaofe, Adeyemi, and Adediran (1994) who found that Glu and Asp, respectively, were the first and second most concentrated amino acids in some oilseeds. The differences in the levels of the amino acids in the two samples were shown by the various levels of the CV%; when subjected to the F-test the differences were not significant at $p < 0.05$ since F_c (1.11) < F_t (2.35). Also, the correlation coefficient was high at $r_{0.96}$ and regression (R_c) was 3.51.

Table 2 contains the amino acid profiles for the process-line cocoa nibs (P-LCN) and processed cocoa cake samples (PCCS). In both samples, Lys was the most concentrated amino acid with values of 181 mg/gcp in P-LCN and 52.7 mg/gcp in PCCS; whilst Ile (63.3 mg/gcp) was the second most concentrated in P-LCN, it was Asp (43.7 mg/gcp) in PCCS. The following amino acids were more concentrated in P-LCN than in PCCS (mg/gcp): Lys, His, Arg, Thr, Pro, Cys, Val, Met, Ile, Leu, Tyr and Phe, or 70.6% better in amino acid

concentration. This meant that P-LCN would be a better protein food ingredient than would PCCS. Here some of CV% levels were well above 50.0 and the data, when subjected to F-test analysis, showed that significant differences existed at $p < 0.05$ between the P-LCN and PCCS amino acid profiles, since F_c (6.86) > F_t (2.35). The $r_{0.70}$ was less than the value obtained in Table 1 but the R_c was 12.4 which was much higher than the value in Table 1.

It is interesting to note the high differences in the amino acids, Lys, His, Arg, and Cys between P-LCN and PCCS samples. The availability of some amino acids, for example, Lys, Met, Arg, Try, Cys and His, is often severely impaired when the protein in the food is heated, e.g. in processing, or where it is improperly stored. This impairment occurs when the Amadori rearrangement goes beyond the deoxy-ketosyl stage due to heat treatment. This is particularly serious when intravenous drip fluids containing sugars and proteins undergo Maillard reactions during sterilisation (Muller & Tobin, 1980). Carpenter has used the susceptibility of Lys to heat damage in the presence of moisture as a basis for estimating the extent of the damage (Muller & Tobin, 1980). Although Val may be thermally stable, it may also be possible that it takes part in this type of browning reaction which will definitely reduce its concentration during heat processing.

The processed cocoa cake samples (PCCS) underwent various heat processing unit operations which lasted for 13 h or more. This would have led to a very serious heat effect on the amino acids. Looking critically at Table 2, where the values of P-LCN and PCCS are compared, wide variation existed between the essential amino acids of the two samples. For example, loss of amino acid concentration from P-LCN to PCCS goes thus (mg/g crude protein) Lys, 128 (78.7%); His, 7.3 (62.4%); Arg, 16.9 (36.6%); Thr, 7.2 (45.3%); Cys, 4.5 (29.4%); Val, 36.8 (90.9%); Met, 0.6 (1.40%); Ile, 31.4 (49.6%); Tyr, 1.5 (11.0%) and Phe, 7.0 (32.1%). These values show serious reductions in the available essential amino acids, unlike the non-essential amino acids of the PCCS. Usually, the method used for the amino acid analysis will only detect L-amino acids from animal and plant proteins that do not produce racemisation (White et al., 1973). The reasons for these serious reductions of the amino acids from P-LCN to PCCS would likely be due to Amadori rearrangement that goes beyond the deoxy-ketosyl stage and the formation of D-amino acids which are both due to high and prolonged heat treatment (Fennema, 1985; Muller & Tobin, 1980).

Various parameters are presented in Tables 3 and 4. The total amino acids (TAA) in unfermented cocoa nibs was 641 mg/gcp and it was 708 mg/gcp in fermented cocoa nibs (Table 4) whilst it was 635 mg/gcp in P-LCN and 368 mg/gcp in PCCS (Table 3). The TAA in unfermented cocoa nibs was close to the value of 659 mg/gcp in *A. occidentale* and also the value of TAA in PCCS was close to the value of 356 mg/gcp in *C. acuminaa* (Adeyeye et al., 2007). The level of TAA in fermented cocoa nibs was close to the values of 703–917 mg/gcp of dehulled samples of African yam bean (Adeyeye, 1997). The total non-essential amino acids (TNEAA) for the samples were (mg/gcp): 341 (unfermented nibs), 421 (fermented nibs) – see Table 3, 158 (P-LCN) and 183 (PCCS) – see Table 4. The TNEAA of 341–421 mg/gcp was close to the value of 327–454 mg/gcp in African yam bean (Adeyeye, 1997) and also to 323 mg/gcp in *A. occidentale* (Adeyeye et al., 2007). However, in the composition of the total essential amino acids (TEAA), there was a reversal of concentration which followed this pattern (mg/gcp, with His): 478 (P-LCN) > 300 (unfermented nibs) > 287 (fermented nibs) > 185(PCCS). On a percentage basis, this trend was not consistent amongst the samples. The percent TNEAA ranged between 53.3% (unfermented nibs) and 59.5% (fermented nibs) with a low value of CV% (7.77) (Table 3); from Table 4 it ranged from 24.8% (P-LCN) to 49.8% (PCCS) with a high value of CV% (64.8). The % TEAA (with His) ranged between 75.2% (P-LCN) and 50.2% (PCCS) with CV% of 28.2 (Table 4). These results showed that the industrial processed cake was again lower in the TEAA than in the process on line by a wide margin. The total neutral amino acids (TNAA) levels were close in (mg/gcp); 228 (unfermented nibs), 235 (fermented nibs) but low in P-LCN (74.8) and PCCS (87.2).

The TEAA in melon and gourd oilseeds with respective values of 534 mg/g and 536 mg/gcp (Olaofe et al., 1994) were reportedly higher than all of our values, that ranged between 185 mg/gcp and 478 mg/gcp; with the exception of 478 mg/gcp (P-LCN), all of our EAA values were lower than those in soybean (444 mg/gcp) (Kuri, Sundar, Kahuwi, Jones, & Rivett, 1991). Our present samples were either close to or lower than the following TEAA levels (mg/gcp): pigeon pea (452) (Nwokolo, 1987), pumpkin seed (396)

Table 3
Concentrations of essential, non-essential, acidic, neutral, sulphur, aromatic (mg/g crude protein) of unfermented and fermented cocoa nibs.

Amino acid	Unfermented Nibs	Fermented nibs	Mean	SD	CV%
Total amino acid (TAA)	641	708	675	43.4	6.43
Total non-essential amino acid (TNEAA)	341	421	381	56.6	14.9
Total essential amino acid (TEAA)					
–With His	300	287	294	9.19	3.13
–No His	280	263	272	12.0	4.41
% TNEAA	53.3	59.5	56.4	4.38	7.77
% TEAA					
–With His	46.8	40.5	43.7	4.5	10.2
–No His	43.6	37.2	40.4	4.53	11.2
Total neutral amino acid (TNAA)	307	346	327	27.6	8.44
% TNAA	47.9	48.8	48.4	0.64	1.32
Total acidic amino acid (TAAA)	228	235	232	4.95	2.13
% TAAA	35.6	33.2	34.4	1.7	4.94
Total basic amino acid (TBAA)	106	127	117	14.8	12.6
% TBAA	16.5	18.0	17.3	1.06	6.13
Total sulphur amino acid (TSAA)	17.7	14.9	16.3	1.98	12.1
% TSAA	2.76	2.11	2.44	0.46	18.9
% Cys in TSAA	44.1	46.3	45.2	1.56	3.45
Total aromatic amino acid (TArAA)	47.2	63.3	55.3	11.4	20.6
% TArAA	7.36	8.94	8.15	1.12	13.7
P-PER*	3.55	2.55	3.05	0.71	23.3
Leu/Ile ratio	3.37	2.13	2.75	0.88	32.0
Leu-Ile (difference)	50.8	33.1	42.0	12.5	29.8
% Leu-Ile	70.4	53.0	61.7	12.3	19.9

* Predicted protein efficiency ratio.

Table 4
Concentrations of essential, non-essential, acidic, neutral, sulphur, aromatic amino acids (mg/g crude protein) of P-LCN and PCCS.

Amino acid	P-LCN*	PCCS*	Mean	SD	CV%
Total amino acid (TAA)	635	368	502	189	37.6
Total non-essential amino acid (TNEAA)	158	183	171	17.7	10.4
Total essential amino acid (TEAA)					
–With His	478	185	332	207	62.3
–No His	466	181	324	202	62.3
% TNEAA	24.8	49.8	27.3	17.7	64.8
% TEAA					
–with His	75.2	50.2	62.7	17.7	28.2
–no His	73.3	49.0	61.2	17.2	28.1
Total neutral amino acid (TNAA)	322	195	259	89.8	34.7
% TNAA	50.7	52.9	51.8	1.56	3.01
Total acidic amino acid (TAAA)	74.8	87.2	81.0	8.77	10.8
% TAAA	11.8	23.7	17.8	8.4	47.2
Total basic amino acid (TBAA)	239	86.5	163	108	66.3
% TBAA	37.6	23.5	30.6	9.97	32.6
Total sulphur amino acid (TSAA)	19.6	14.5	17.1	3.61	21.1
% TSAA	3.09	3.94	3.52	0.60	17.0
% Cys in TSAA	78.1	74.5	76.3	2.55	3.34
Total aromatic amino acid (TArAA)	35.4	26.9	31.2	6.01	19.3
% TArAA	5.57	7.31	6.44	1.23	19.1
P-PER*	2.47	2.02	2.25	0.32	14.2
Leu/Ile ratio	0.75	1.16	0.96	0.29	30.2
Leu-Ile (difference)	−16.1	5.1	10.6	7.78	73.4
% Leu-Ile	−34.1	13.8	24.0	14.4	60.0

* See Table 2.

(Aisegbu, 1987), cowpea (426) (Olaofe, Umar, & Adediran, 1993) and *Cajanus cajan* (436) (Oshodi, Olaofe, & Hall, 1992). This meant that unfermented nibs, fermented nibs and PCCS protein in the samples were of lower quality than those in cowpea, soybean and pigeon pea. However, whilst Cys was 0.0 mg/gcp in melon, pumpkin seed and gourd seed (Olaofe et al., 1994) and 11.3 mg/gcp in *A. occidentale*, 2.5 mg/gcp in *G. kola* and 4.5 mg/gcp in *C. acuminata* (Adeyeye et al., 2007), it was (mg/gcp): in unfermented nibs (17.7), fermented nibs (14.9), P-LCN (19.6) and PCCS (14.5). Generally, most of our results were better in many of the amino acids (essential and non-essential) than was pumpkin seed (Olaofe et al., 1994).

Whilst it is known that cystine can spare part of the requirement for methionine, FAO/WHO/UNICEF (1985) does not give any indication of the proportion of total sulphur amino acids that can be met by Cys. For the rat, chick and pig, the proportion is about 50% (FAO/WHO, 1991). Most animal proteins are low in cystine; in contrast, many vegetable proteins, especially the legumes, contain substantially more Cys than methionine. Thus, for animal protein, Cys is unlikely to contribute more than 50% of the total sulphur amino acids (FAO/WHO, 1991). For our samples, the percentages of Cys in total sulphur amino acids were: 44.1% (unfermented nibs), 46.3% (fermented nibs) – see Table 3; 78.1 (P-LCN) and 74.5 (PCCS) – see Table 4. Whilst the Cys/TSAA% in unfermented and fermented nibs followed the trend in *G. kola* (37.8%) and *C. acuminata* (44.3%) (Adeyeye et al., 2007), as well as in animals: 36.3% (*Macrotermes bellicosus*) (Adeyeye, 2005a), 25.6% (*Zonocerus variegatus*) (Adeyeye, 2005b), 35.5% (*Archachatina marginata*), 38.8% (*Archatina archatina*) and 21.0% (*Limicolaria* sp.) (Adeyeye & Afolabi, 2004), the Cys/TSAA% in P-LCN and PCCS followed the trend in *A. occidentale* (50.5%) (Adeyeye et al., 2007), coconut endosperm (62.9%) (Adeyeye, 2004), raw guinea corn (58.9%), steeped guinea corn (72.0%) and germinated guinea corn (71.1%) (Adeyeye, 2008). This meant that, whilst both unfermented and fermented cocoa nibs behaved like animal proteins under these conditions, the P-LCN and PCCS behaved like plant proteins. FAO/WHO (1973), states that Cys may supply up to one-third of the need for total sulphur amino acids whilst tyrosine may also supply up to one-third of the need for total aromatic amino acids.

The predicted protein efficiency ratios (P-PER) were better in the unfermented (3.55) and fermented (2.55) cocoa nibs than in the P-LCN (2.47) and PCCS (2.02) samples. The experimentally determined PER usually ranged from 0.0 for a very poor protein to a maximum possible of just over 4 (Muller & Tobin, 1980). These results showed that P-LCN and PCCS would likely be less utilised in the body than would the other two samples.

The Leu/Ile ratio values ranged as follows: 3.37 (unfermented nibs), 2.13 (fermented nibs), 0.75 (P-LCN) and 1.16 (PCCS). From Table 1, the level of Leu was more than twice that of Ile in unfermented and fermented nibs whilst, in Table 2, the level of Leu was just above one half that of Ile in P-LCN and slightly above Ile in PCCS. It has been suggested that an amino acid imbalance from excess leucine might be a factor in the development of pellagra in sorghum consumption (FAO, 1995).

High Leu in the diet impairs tryptophan and niacin metabolism and is responsible for niacin deficiency in sorghum eaters (Belavady, Srikantia, & Gopalan, 1963) . This leads to the hypothesis that excess Leu in sorghum is aetiologically related to pellagra in sorghum-eating populations (FAO, 1995). The study of Krishnaswamy and Gopalan (1971) suggested that Leu/Ile balance is more important than dietary excess of Leu alone in regulating the metabolism of Try and niacin and hence the disease process. Experiments in dogs have shown that animals fed sorghum proteins (with less than 110 mg/gcp of Leu) did not suffer from nicotinic acid deficiency (Belavady & Udayasekhara Rao, 1979). None of our samples had levels of Leu up to 110 mg/gcp.

Table 5 contains the amino acid scores, based on the provisional amino acids, for the unfermented and fermented cocoa nibs whilst Table 6 contains the scores of P-LCN and PCCS, based on the same formula. In Table 5, the limiting amino acids for both unfermented and fermented cocoa nibs were Met + Cys with respective values of 0.51 (unfermented nibs) and 0.43 for fermented nibs. The entire CV% was low and no significant differences existed between the two samples at $p < 0.05$ (F-test). Therefore, in order to fulfil the day's needs for the EAA in unfermented cocoa nibs, 100/51 or 1.96 times as much unfermented nibs would have to be eaten when it is the sole protein in the diet; in fermented nibs, it would be 100/43 or 2.33 times the protein level. In Table 6, Thr was the limiting

Table 5
Essential amino acid scores of the unfermented and fermented cocoa nibs based on provisional amino acid scores.

Amino acid	Unfermented nibs	Fermented nibs	Mean	SD	CV%
Ile	0.54	0.73	0.64	0.13	20.3
Leu	1.07	0.89	0.98	0.13	13.3
Lys	0.76	0.96	0.86	0.14	16.3
Met + Cys	0.51	0.43	0.47	0.06	12.8
Phe + Tyr	0.79	1.06	0.93	0.19	20.4
Thr	0.76	0.58	0.67	0.13	19.4
Try	–	–	–	–	–
Val	0.64	0.7	0.67	0.04	5.97

Table 6
Essential amino acid scores of the P-LCN and PCCS based on provisional amino acid scores.

Amino acid	P-LCN*	PCCS*	Mean	SD	CV%
Ile	1.58	0.80	1.19	0.55	46.2
Leu	0.67	0.53	0.60	0.10	16.7
Lys	3.28	0.96	2.12	1.64	77.4
Met + Cys	0.56	0.41	0.49	0.11	22.4
Phe + Tyr	0.59	0.45	0.52	0.11	19.2
Thr	0.40	0.22	0.31	0.13	41.9
Try	–	–	–	–	–
Val	0.78	0.05	0.42	0.52	124

Table 7
Amino acid scores of the four samples based whole hen's egg.

Amino acid	Unfermented nibs	Fermented nibs	P-LCN	PCCS
Lys	0.68	0.85	2.92	0.85
His	0.83	0.97	0.49	0.18
Arg	0.71	0.84	0.76	0.48
Asp	0.93	0.77	0.35	0.41
Thr	0.59	0.46	0.31	0.17
Ser	0.3	0.41	0.27	0.29
Glu	1.07	1.28	0.31	0.36
Pro	0.33	0.33	0.74	0.66
Gly	0.68	1.07	0.1	0.17
Ala	0.55	0.74	0.028	0.37
Cys	0.43	0.38	0.85	0.6
Val	0.43	0.47	0.52	0.032
Met	0.31	0.25	0.13	0.12
Ile	0.38	0.52	1.13	0.57
Leu	0.87	0.75	0.57	0.45
Tyr	0.47	0.68	0.34	0.3
Phe	0.56	0.71	0.43	0.29
Try	–	–	–	–

amino acid in P-LCN (0.40) and Val in PCCS (0.05); their correction values would be 2.50 times the protein in P-LCN and 20 times in PCCS. There were CV% levels of 124 (Val), 77.4 (Lys) and 46.2 (Ile) and significant differences existed between the P-LCN and PCCS samples at $p < 0.05$ when subjected to F-test analysis.

Table 7 contains the amino acid scores of the four samples based on whole hen's egg amino acid profile. Serine was the limiting amino acid in unfermented nibs (0.30), Met in fermented nibs (0.25), Ala in P-LCN (0.028) and Val in PCCS (0.032). The respective corrections would then be 100/30 or 3.3 (unfermented nibs), 100/25 or 4.0 (fermented nibs), 100/2.8 or 35.7 (P-LCN) and 100/3.2 or 31.3 (PCCS) times the protein of each sample where they serve as the sole protein sources.

The data obtained for TNEAA, TEAA and EAA scores were all subjected to the F-test as follows: TNEAA/TNEAA, TEAA/TNEAA and EAA score/EAA score for the pairs of unfermented/fermented nibs and P-LCN/PCCS setting the $p < 0.05$ (Christian, 1980). The following results were obtained. In unfermented/fermented cocoa nibs, TNEAA/TNEAA $F_c < F_t$ and in P-LCN/PCCS result was $F_c < F_t$, results not significantly different; in TEAA/TNEAA in unfermented nibs, $F_c > F_t$; in fermented nibs, $F_c > F_t$, in P-LCN, $F_c > F_t$ meaning all the values were significantly different but, in PCCS, $F_c < F_t$; hence results were not significantly different. For the EAA score/EAA score, in unfermented/fermented nibs, $F_c < F_t$, but not significant; for P-LCN/PCCS, $F_c > F_t$, and results were significantly different at $p < 0.05$.

In conclusion, the findings of this study showed that there was a more positive build up of AA in fermented nibs than in unfermented nibs. In the processing, about 40% of the AA was destroyed; this might have resulted from the series of reactions involving amino acids, nitrates and antioxidants during the heat processing of cocoa. Finally, more cake (PCCS) would be required for complementation/fortification than would have been used if the unprocessed nibs were to be used. Also the differences observed in the fermented and unfermented samples (group one) and P-LCN and PCCS (group two) could be due to planting material, climate, varieties, application of fertiliser, heat treatments and storage between the group one and two samples.

Acknowledgement

The authors are grateful to Dr. Segun Awolumate, the Managing Director of Co-operative Cocoa Products Limited, Akure, Nigeria for his collaborative support.

References

Adeyeye, E. I. (1997). Amino acid composition of six varieties of dehulled African yam bean (*Sphenostylis stenocarpa*) flour. *International Journal of Food Sciences and Nutrition, 48*, 345–351.
Adeyeye, E. I. (2004). The chemical composition of liquid and solid endosperm of ripe coconut. *Oriental Journal of Chemistry, 20*(3), 471–476.
Adeyeye, E. I. (2005a). The composition of the winged termites, *Macrotermes bellicosus*. *Journal of Chemical Society of Nigeria, 30*(2), 145–149.
Adeyeye, E. I. (2005b). Amino acid composition of variegated grasshopper, *Zonocerus variegatus*. *Tropical Science, 45*(4), 141–143.
Adeyeye, E. I. (2008). The intercorrelation of the amino acid quality between raw, steeped and germinated guinea corn (*Sorghum bicolor*) grains. *Bulletin of the Chemical Society of Ethiopia, 22*(1), 11–17.
Adeyeye, E. I., & Afolabi, E. O. (2004). Amino acid composition of three types of land snails consumed in Nigeria. *Food Chemistry, 85*, 535–539.
Adeyeye, E. I., Asaolu, S. S., & Aluko, A. O. (2007). Amino acid composition of two masticatory nuts (*Cola acuminata* and *Garcinia kola*) and a snack nut (*Anacardium occidentale*). *International Journal of Food Sciences and Nutrition, 58*(4), 241–249.
Aisegbu, J. E. (1987). Some biochemical evaluation of fluted pumpkin seed. *Journal of the Science of Food and Agriculture, 40*, 151–155.
Akinyeye, R. O. (1999). *Causes of capacity under-utilization in cocoa processing industries in Nigeria*. Akure, Nigeria: MBA Thesis, Federal University of Technology.
Alsmeyer, R. H., Cunningham, A. E., & Happich, M. L. (1974). Equations to predict PER from amino acid analysis. *Food Technology, 28*, 34–38.
Belavady, B., & Udayasekhara Rao, P. (1979). Leucine and isoleucine content of jowar and its pellagragenicity. *Indian Journal of Experimental Biology, 17*, 659–661.
Belavady, B., Srikantia, S. G., & Gopalan, C. (1963). The effect of oral administration of leucine on the metabolism of tryptophan. *Biochemical Journal, 87*, 652–655.
Christian, G. D. (1980). *Analytical chemistry* (3rd ed.). New York, USA: John Wiley and Sons Inc.
FAO (1995). *Sorghum and millets in human nutrition.*. Rome, Italy: FAO Food Nutrition Series, No. 27, Food and Agriculture Organisation of the United Nations.
FAO/WHO (1973). *Energy and protein requirements*. Geneva, Switzerland: Technical Report Series No. 522, WHO.
FAO/WHO (1991). *Protein quality evaluation*. Rome, Italy: Report of Joint FAO/WHO Expert Consultation, FAO Food and Nutrition Paper 51.
FAO/WHO/UNICEF (1985). *Energy and protein requirement*. Geneva, Switzerland: WHO Technical Report Series No. 724, WHO.
Fennema, O. R. (1985). *Principles of food science* (2nd ed.). New York: Marcel Dekker, Inc..
International Cocoa and Commodities Organisation (2000). *ICCO celebration of cocoa 2000*. London: K.P. Partners in Publishing.
Kuri, Y. E., Sundar, R. K., Kahuwi, C., Jones, G. P., & Rivett, D. E. (1991). Chemical composition of *Monerdica charantis* L. fruits. *Journal of Agricultural and Food Chemistry, 39*, 1702–1703.
Minife, B. W. (1989). *Chocolate, cocoa and confectionary* (3rd ed.). London: Chapman and Hall.

Morgan, J. (1994). Chocolate: A flavour and texture unlike any other. *American Journal of Clinical Nutrition, 60*(6), 1065–10675.
Muller, H. E., & Tobin, G. (1980). *Nutrition and food processing*. London: Crown Helm.
Nwokolo, E. (1987). Nutritional Evaluation of Pigeon Pea meal. *Plant Foods for Human Nutrition, 37*, 283–290.
Olaofe, O., Adeyemi, F. O., & Adediran, G. O. (1994). Amino acid and mineral compositions and functional properties of some oil seeds. *Journal of Agricultural and Food Chemistry, 42*, 878–881.
Olaofe, O., Oladeji, E. O., & Ayodeji, O. E. (1987). Metal contents of some cocoa beans produced in Ondo State, Nigeria. *Journal of the Science of Food and Agriculture, 41*, 241–244.
Olaofe, O., & Onajeta, C. C. (1986). Quality assessment of some cocoa-based beverages in the Nigerian market. *Nigerian Journal of Nutrition Science, 7*(2), 81–85.
Olaofe, O., Umar, Y. O., & Adediran, G. O. (1993). The effect of nematicides on the nutritive value and functional properties of cowpea seeds (*Vigna unguicalata* L. walp). *Food Chemistry, 46*(4), 337–342.
Opeke, L. K. (1992). *Tropical tree crops*. Ibadan: Spectrum Books Limited.
Oshodi, A. A., Olaofe, O., & Hall, G. M. (1992). Amino acid, fatty acid and mineral composition of pigeon pea (cajanus cajan). *International Journal of Food Sciences and Nutrition, 42*, 187–191.
Paul, A. A., Southgate, D. A. T., & Russel, J. (1976). *First supplement to Mclance and Widdowson's the composition of Foods*. London, UK: HMSO.
Pearson, D. (1976). *Chemical analysis of foods* (7th ed.). London: J.A. Churchhill.
Rambali, B., Van Andel, I., Schenk E., Wolterink, G., Van de Werken, G., Stevenson, H., & Vleenming, W. (2002). The contribution of cocoa additive to cigarette smoking addiction. *RIVM report* 650270002/2002.
The Biscuit, Cake, Chocolate, Confectionary Alliance (BCCCCA) (1996). *Cocoa beans, chocolate manufacturers' quality requirements* (4th ed.). London: BCCCCA.
White, A., Handler, P., & Smith, E. L. (1973). *Principles of biochemistry* (5th ed.). New York: McGraw-Hill, Inc.

Food Chemistry 118 (2010) 364–368

Contents lists available at ScienceDirect

Food Chemistry

journal homepage: www.elsevier.com/locate/foodchem

Effect of methylation on the structure and radical scavenging activity of polysaccharides from longan (*Dimocarpus longan* Lour.) fruit pericarp

Bao Yang [a], Mouming Zhao [b], K. Nagendra Prasad [a], Guoxiang Jiang [a], Yueming Jiang [a,*]

[a] South China Botanical Garden, Chinese Academy of Sciences, Guangzhou 510650, PR China
[b] College of Light Industry and Food Sciences, South China University of Technology, Guangzhou 510640, PR China

ARTICLE INFO

Article history:
Received 19 January 2009
Received in revised form 10 March 2009
Accepted 30 April 2009

Keywords:
Longan
Polysaccharide
Methylation
Structure
Radical scavenging activity

ABSTRACT

Polysaccharides of longan fruit pericarp (PLFP) were purified by gel filtration chromatography and methylated by methyl iodide. The structure of methylated PLFP was identified by gas chromatography/mass spectrometry. The results indicated that the percentages of methylated Ara, Glc and Gal increased gradually to a maximal value with increasing volume of methyl iodide. Methylation resulted in a decrease in the DPPH radical scavenging activity of PLFP, while the superoxide anion radical scavenging activity of PLFP decreased with increasing the degree of methylation. When the degree of methylation reached up to 47.4% or a higher value, a promoted effect on the generation of superoxide anion was observed. Furthermore, a high correlation coefficient between degree of methylation and superoxide anion radical scavenging activity of PLFP was determined, which indicated the important role of hydroxyl groups of monosaccharide units in the radical scavenging activity of PLFP.

1. Introduction

Longan (*Dimocarpus longan* Lour.) is an exotic subtropical fruit mainly planted in Southeast Asia, especially in China (Yang, Jiang, Wang, Zhao, & Sun, 2009). It is a desirable fruit gradually accepted by consumers over the world due to its sweet juicy mouthfeel and health benefits (Rangkadilok et al., 2007). In addition, the flesh, seed and pericarp of the fruit have been used as bioactive ingredients in traditional Chinese medicines for different treatments, such as improving women's health after childbirth and increasing the immunomodulatory capacity. Our previous work suggested that longan fruit pericarp tissue contained a large quantity of polysaccharides (Yang, Zhao et al., 2008). Thus, it is worthwhile to purify the polysaccharides from longan fruit pericarp and then evaluate their contribution to the pharmaceutical properties of the fruit.

In recent decades, plant polysaccharides have attracted a great deal of attention in the biomedical field due to their broad spectra of therapeutic properties and relatively low toxicity (Schepetkin & Quinn, 2006). A variety of bioactivities, such as antioxidation, immunomodulation, anti-tumour and hypoglycemic activity, have been confirmed for polysaccharides (Kardošová & Machová, 2006; Luk, Lai, Tam, & Koo, 2000). Plant polysaccharides have showed a strong antioxidant activity and can be explored as novel potential antioxidants (Tseng, Yang, & Mau, 2008). Some plant polysaccharides have been commercially developed into the important components of therapeutic drugs and skin care products (Deters, Dauer, Schnetz, Fartasch, & Hensel, 2001; Wang & Fang, 2002). It is well known that methylation of polysaccharides is a commonly used derivatization technique for the identification of polysaccharide structure (Kim, Reuhs, Michon, Kaiser, & Arumugham, 2006). It is also an effective method to modify the bioactivities and functions of natural products through partial derivatization of functional groups such as hydroxyl groups (Ouk, Thiebaud, Borredon, Legars, & Lecomte, 2002).

The antioxidant activity of polysaccharides of longan fruit pericarp (PLFP) and its structure has been investigated in a previous work (Yang et al., 2009). However, the relationship between PLFP structure and antioxidant activity is still unclear. In this study, PLFP was partially methylated to various extents. The DPPH and superoxide anion radical scavenging activities of the methylated PLFP were evaluated. The effect of methylation on the structure and radical scavenging activity of PLFP was also analysed.

2. Materials and methods

2.1. Plant materials

Fresh longan (*D.* longan Lour. cv. Shixia) fruit at the commercially mature stage were purchased from a local commercial market in Guangzhou, China. Fruit were selected for uniformity of shape and colour. The fruit pericarp was manually separated and collected.

* Corresponding author. Tel.: +86 20 37252525; fax: +86 20 37252831.
E-mail address: ymjiang@scib.ac.cn (Y. Jiang).

0308-8146/$ - see front matter © 2009 Elsevier Ltd. All rights reserved.
doi:10.1016/j.foodchem.2009.04.128

2.2. Chemicals

Galactose, phenol and sulphuric acid were obtained from Guangzhou Reagent Co. (Guangzhou, China), while methyl iodide was purchased from Mingfeng Chemical Co. (Juzhou, China). 1,1′-Diphenyl-2-picrylhydrazyl (DPPH), nitroblue tetrazolium, riboflavin and methionine were purchased from Sigma Chemical Co. (St. Louis, MO, USA). All the other chemicals were of analytical grade.

2.3. Extraction and purification of PLFP

PLFP was extracted by hot-water following the method of Yang, Jiang, Zhao, Shi, and Wang (2008). Briefly, the lyophilised longan fruit pericarp tissues were pulverised. After passing through a 60-mesh stainless steel sieve, an aliquot (5 g) of the pericarp powder was extracted for 120 min with 100 ml of distilled water at 55 °C in a 150 ml conical flask. The extract was then filtered through a Whatman No. 1 paper (Whatman plc., Shanghai, China), and then concentrated to 25 ml at 65 °C using a vacuum rotary evaporator (BC-R203, Shanghai Biochemical Equipment Co., Shanghai, China). The proteins in the PLFP extract were removed by the Sevag reagent (Navarini et al., 1999), while protein content was estimated by Folin–Ciocalteu reagent using bovine serum albumin as standard (Lowry, Rosebrough, Farr, & Randall, 1951). After removal of the proteins from the PLFP extract, anhydrate ethanol (100 ml) was added and then maintained overnight at 4 °C to precipitate polysaccharides, which were finally obtained after centrifugation at 3860*g* for 15 min. The precipitated polysaccharides were collected and then dissolved in distilled water to a concentration of 2 mg/ml. The amount of polysaccharides was determined by the phenol-sulphuric acid method (Dubois, Gilles, Hamilton, Rebers, & Smith, 1956), by which the recovery of PLFP was expressed as mg galactose equivalents/g dry pericarp, while galactose was prepared in a serial of concentrations to make a standard curve for the PLFP calculation. Three milliliters of 2 mg/ml PLFP was loaded onto a Sephadex G-100 gel column (10 × 500 mm), and then eluted with 100 ml of distilled water at a flow rate of 0.5 ml/min. All the fractions were quantified for polysaccharide content and an elution profile was then drawn. The highest peak was collected and then lyophilised. It was subjected to methylation and radical scavenging activity analyses.

2.4. Methylation of PLFP

Methylation of PLFP was carried out by the method of Needs and Sevendran (1993) with minor modifications. The dried PLFP powder (10 mg) was dissolved in 5.0 ml of dimethyl sulfoxide at 60 °C before 200 mg of NaOH was added. The mixture was treated for 10 min using ultrasonic wave with an ultrasonic cleaner (KQ-300DE, Kunshan Ultrasonic Equipment Co., Kunshan, China, 40 kHz). After incubation for 1 h at 25 °C, methyl iodide at different volumes (0.1, 0.2, 0.4, 0.6 and 0.8 ml) were added to prepare partially methylated PLFP. The sample was kept for 1 h in the dark before 5.0 ml of distilled water was used to decompose the methyl iodide remained. The mixture was transferred into a dialysis bag with a molecular weight cut-off of 8000 Da, which was kept in distilled water. The water was changed every 6 h for four times. The methylated PLFP was concentrated at low pressure by a rotary evaporator (RE52AA, Yarong Instrument Co., Shanghai, China) and then freeze-dried.

2.5. Identification of PLFP structure

After hydrolysis of methylated PLFP (10 mg) with 10 ml of 2 M trifluoracetic acid, the methylated PLFP hydrolysate was dissolved in 5 ml of 0.2% (w/w) NaOH. Twenty milligrams of $NaBH_4$ was added to reduce the uronic acid. After 30 min of incubation at 40 °C, glacial acetic acid (100 μl) was added to terminate the reduction. The sample was dried at low pressure and then acetylated with 2 ml of acetic anhydride and 2 ml of pyridine. The reaction was maintained for 1 h at 100 °C. Two milliliters of distilled water was used to decompose the acetic anhydride remained. The acetylated derivatives were extracted with 4 ml of methylene chloride. A gas chromatography/mass spectrometer (GCMS-QP 2010, Shimadzu, Kyoto, Japan) was used to analyse the glycosidic linkage. The acetylated derivatives (1 μl) were loaded into a HP-1 capillary column. The split ratio was 50:1. The initial temperature of the column was 150 °C, which increased to 180 °C at 10 °C/min, then to 260 °C at 15 °C/min and finally held for 5 min at 260 °C. The injection temperature was 220 °C. The ion source of mass spectrometer was set at 200 °C. Helium was used as the carrier gas. Identification of monosaccharide derivatives was based on comparisons of their mass spectra with those recorded in the National Institute of Standards and Technology database. The contents of monosaccharide derivatives were quantified by the peak area normalisation method. The degree of methylation was calculated as the percentage sum of the methylated monosaccharides.

2.6. Assay of DPPH radical scavenging activity

The DPPH radical scavenging activity was measured by the method of Yang, Zhao, Shi, Yang, and Jiang (2008). The methylated PLFP was precisely weighted and dissolved in distilled water to obtain a final concentration of 100 μg/ml. Two milliliters of 0.2 mM DPPH in ethanol was added to 1 ml of the PLFP solution. The absorbance was measured at 517 nm after 20 min of incubation at 25 °C. Ethanol instead of DPPH was used for the control while distilled water instead of sample was used for the blank. The DPPH radical scavenging activity of the sample was calculated by the following equation:

$$\text{DPPH radical scavenging activity } (\%) = [1 - (A_{\text{sample}} - A_{\text{control}})/A_{\text{blank}}] \times 100$$

where A_{sample}, A_{control} and A_{blank} are the absorbances of sample, control and blank, respectively.

2.7. Assay of superoxide anion radical scavenging activity

Superoxide anion radical scavenging activity was determined by the method of Prasad et al. (2009) with some modifications. The methylated PLFP was dissolved in distilled water to obtain a final concentration of 100 μg/ml. One milliliter of 100 μg/ml methylated PLFP was mixed with 0.3 ml of 50 μM riboflavin, 0.3 ml of 0.13 M methionine and 0.3 ml of 510 μM nitroblue tetrazolium, and then 0.2 M phosphate buffer (pH 7.8) was added to obtain a final volume of 5 ml. The reaction solution was exposed to a fluorescent lamp with a power of 40 W for 20 min and the absorbance was then measured at 560 nm. The reaction mixture without sample was used as control. The superoxide anion radical scavenging activity (%) was calculated as (1 − absorbance of sample/absorbance of control) × 100.

2.8. Statistical analysis

Data were expressed as means ± standard deviations of three replicated determinations. One way of variance analysis was applied for determining significant difference at $P < 0.05$ between the results.

3. Results and discussion

3.1. Extraction and purification of PLFP

Hot water was used to extract the crude water-soluble polysaccharides from longan fruit pericarp. The crude water-soluble polysaccharide was determined to be 10.6 ± 0.7 mg galactose equivalents/g dry pericarp, which accounted for 93.3 ± 2.7% of the dry extract. In contrast, the protein content in the aqueous extract only accounted for 1.1 ± 0.1%, which was due to the removal by the Sevag reagent at the first step of purification. After the isolation and purification by the gel filtration chromatography, the major polysaccharide fraction was collected, which accounted for 65.4% (w/w) of the total PLFP (Yang et al., 2009).

3.2. Methylation of PLFP

Methyl iodide was used to form methoxyl group with glycoside units of PLFP molecular chain in this work. Table 1 shows the percentages of the methylated and unmethylated monosaccharide units. The structural analysis indicated that the purified PLFP without methylation contained 32.8% Ara, 17.6% Glc and 49.6% Gal. Due to the reduction by $NaBH_4$, the GalA residue was reduced to Gal and, thus, the percentage of Gal in this study represented the sum of Gal and GalA. The addition of 0.1 ml of methyl iodide led to the formation of methylated Ara (7.7%) and Gal (9%), but Glc did not change. Furthermore, the methylated Glc (3.8%) was formed when the volume of methyl iodide was up to 0.2 ml. By increasing the methyl iodide volume, the percentages of methylated Ara, Glc and Gal increased gradually. As shown in Table 1, when 0.6 ml of methyl iodide was used, the percentages of unaffected Ara, Glc and Gal were 5.3, 6.0 and 30.7%, respectively. However, a similar degree of methylation was observed when a larger amount of 0.8 ml of methyl iodide was used, with the percentage sum of unaffected Ara, Glc and Gal being 41.1%. This indicated that the degree of methylation had reached a maximum.

Hot water extraction is a commonly used method for polysaccharide extraction. The pectins and water-soluble hemicelluloses are easily prepared by this technique. In this work, the PLFP comprised of Ara, Glc, Gal and GalA, which belongs to the hemicellulose family. Natural polysaccharides have complex structures due to their heterogeneity comprising of different kinds of monosaccharide units and, thus, it is difficult to elucidate the relationship between structure and bioactivity (Yoshida, 2001). Methylation is an important sample preparation step for structural identification of complex polysaccharides (Jay, 1996). The general mechanism of polysaccharide methylation is based on the substitution of the proton from polysaccharide hydroxyl group with a methyl group. Two steps are involved: deprotonation of hydroxyl groups by NaOH and nucleophilic attachment of the alkoxyl ion to the methylation reagent. In complex polysaccharides, the reactivity of hydroxyl group relies on the intramolecular hydrogen bond interactions and steric effects (Ciucanu, 2006). This might explain the low methylation rate of Glc when 0.1 ml of methyl iodide was used in this work. From the methylation percentages obtained, Ara was more easily accessible to the methylation reagent, compared with Glc and Gal. The steric position of Ara in the PLFP chain might be responsible for this result.

3.3. DPPH radical scavenging activity

The DPPH radical scavenging activity of methylated PLFP and purified PLFP were determined to evaluate their antioxidant activities. As shown in Fig. 1, the DPPH radical scavenging activity of the purified PLFP was 22.1%, significantly ($P < 0.05$) higher than all the methylated PLFP samples. From the results obtained in this study, a high volume of methyl iodide represented a high degree of methylation for PLFP. By increasing the degree of methylation, the DPPH radical scavenging activity decreased. However, no further decrease was observed when the volume of methyl iodide increased in the range of 0.2–0.8 ml. The correlation coefficient between degree of methylation and DPPH radical scavenging activity was determined to be 0.72.

The DPPH radical scavenging activity is widely used to evaluate antioxidant ability in a relatively short time (Yuan et al., 2005). This method is based on the reduction of ethanolic $DPPH^-$ solution in the presence of a hydrogen donating antioxidant, leading to the formation of non-radical form DPPH–H. The polysaccharides have been proved to be able to reduce the stable DPPH radical to yellow diphenylpicrylhydrazine (Tsai, Song, Shih, & Yen, 2007), and the antioxidant activity of polysaccharides is highly related to their chemical structure (Rao & Muralikrishna, 2006). In this study, a good DPPH radical scavenging activity of purified PLFP was observed. As the hydroxyl group of the monosaccharide unit can donate proton to reduce the DPPH radical, the formation of a methoxyl group eliminates the hydrogen donating property of the monosaccharide unit. Therefore, the DPPH radical scavenging activity of PLFP decreased with enhanced methylation. Ara and Gal played important roles in the DPPH radical scavenging activity of PLFP. When 7.7% Ara and 9.0% Gal were methylated, a significant ($P < 0.05$) decrease in the DPPH radical scavenging activity was observed. With the further increase of the methylation degree, the DPPH radical scavenging activity of PLFP had no significant ($P > 0.05$) change. The highly reactive hydroxyl groups in the PLFP molecule are methylated more easily during the methylation reaction, compared with the other hydroxyl groups. When the volume of methyl iodide was 0.2 ml, it was hypothesised that most of the highly reactive hydroxyl groups were methylated. Therefore, further increase of the volume of methyl iodide could not decrease the DPPH radical scavenging activity of PLFP.

Table 1
Structural analyses of partially methylated PLFP and control*.

Monosaccharide units	Molar percentage					
	Control	Volume of methyl iodide				
		0.1 ml	0.2 ml	0.4 ml	0.6 ml	0.8 ml
Ara	32.8%	25.1%	18.4%	10.2%	5.3%	5.1%
Glc	17.6%	17.6%	13.8%	8.5%	6.0%	6.0%
Gal	49.6%	40.6%	37.5%	33.9%	30.7%	30.0%
Methylated Ara	0%	7.7%	14.4%	22.6%	27.5%	27.7%
Methylated Glc	0%	0%	3.8%	9.1%	11.6%	11.6%
Methylated Gal	0%	9%	12.1%	15.7%	18.9%	19.6%
Degree of methylation	0%	16.7%	30.3%	47.4%	58.0%	58.9%

* Control was the purified PLFP without methylation.

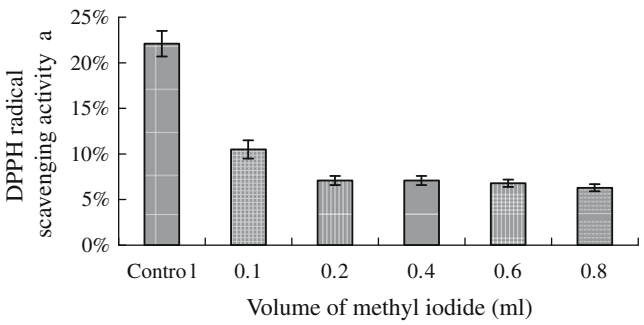

Fig. 1. DPPH radical scavenging activities of the methylated and purified PLFPs at 100 μg/ml.

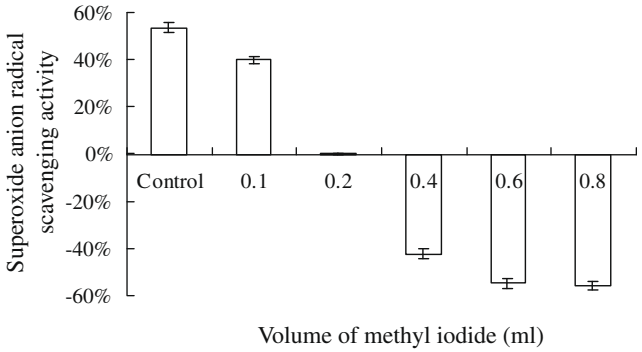

Fig. 2. Superoxide anion radical scavenging activities of the methylated and purified PLFPs at 100 μg/ml.

3.4. Superoxide anion radical scavenging activity

In this study, superoxide anion radical scavenging activity of the methylated PLFP and purified PLFP were measured to understand the effect of methylation (Fig. 2). The purified PLFP exhibited a superoxide anion radical scavenging activity of 53.6% and the activity decreased to 40% and 0.1% when 0.1 and 0.2 ml of methyl iodide were applied, respectively. The correlation coefficient between degree of methylation and superoxide anion scavenging activity was determined to be 0.98. Therefore, enhanced methylation led to a decrease in the superoxide anion scavenging activity of PLFP.

Superoxide anion radical ($O_2^{\cdot-}$) is one of reactive oxygen species (ROS) which are physiological metabolites (Jun et al., 2001). Many reports have indicated that exposure to ROS leads to damage to normal cell functions, such as enzyme inactivation, oxidative DNA damage (Halliwell, 1999) and induction of the aging process (Beckman & Ames, 1998). Polysaccharides can exert their capacities by scavenging ROS or preventing the generation of ROS. A nitroblue tetrazolium reduction system was used to determine the generation of superoxide anion radicals in this work. The general mechanism is the mixture of riboflavin and methionine can produce superoxide anion radicals, which reduce nitroblue tetrazolium from yellow to blue colour (Kang, 2008). From the results obtained in this work, an increase of degree of methylation would lead to a decrease of superoxide anion radical scavenging activity of PLFP, even promoting the generation of superoxide anion radicals when the volume of methyl iodide was in the range of 0.4–0.8 ml. It confirmed the importance of free hydroxyl groups of PLFP for its radical scavenging activity.

4. Conclusions

PLFP was purified by gel filtration chromatography and then methylated by different amounts of methyl iodide. In this study, no Glc unit was methylated while the percentage of methylated Ara and Gal were 7.7% and 9.0%, respectively, as 0.1 ml of methyl iodide was applied, and the percentages of methylated Ara, Glc and Gal increased gradually to the maximal point with increasing the methyl iodide amount, thereafter there was no further increase. The enhanced methylation resulted in the decreases in the scavenging activities of DPPH and superoxide anion radicals. As the effect of methylation on radical scavenging activity of PLFP was relatively complicated, further elucidation of the mechanism related to the group linkages of the PLFP should be conducted.

Acknowledgements

The financial support from National Natural Science Foundation of China (Nos. 30425040 and 30700557), International Foundation of Science (No. F/4451-1), the Chinese Academy of Sciences Fund for the Innovative Team of International Partnership Plan on Preservation and Sustainable Utilization of Plant Resources, and Scientific Research Foundation of South China Botanical Garden (No. 200807) was appreciated.

References

Beckman, K. B., & Ames, B. N. (1998). The free radical theory of aging matures. *Physiological Reviews, 71*, 547–581.

Ciucanu, I. (2006). Per-O-methylation reaction for structural analysis of carbohydrates by mass spectrometry. *Analytica Chimica Acta, 576*, 147–155.

Deters, A., Dauer, A., Schnetz, E., Fartasch, M., & Hensel, A. (2001). High molecular compounds (polysaccharides and proanthocyanidins) from *Hamamelis virginiana* bark: Influence on human skin keratinocyte proliferation and differentiation and influence on irritated skin. *Phytochemistry, 58*, 949–958.

Dubois, M., Gilles, K. A., Hamilton, J. K., Rebers, P. A., & Smith, F. (1956). Colorimetric method for determination of sugars and related substances. *Analytical Chemistry, 28*, 350–356.

Halliwell, B. (1999). Oxygen and nitrogen are pro-carcinogens. Damages to DNA by reactive oxygen, chlorine and nitrogen species: Measurement, mechanism and the effects of nutrition. *Mutation Research/Genetic Toxicology and Environmental Mutagenesis, 443*, 37–52.

Jay, A. (1996). The methylation reaction in carbohydrate analysis. *Journal of Carbohydrate Chemistry, 15*, 897–923.

Jun, W. J., Han, B. K., Yu, K. W., Kim, M. S., Chang, I. S., Kim, H. Y., et al. (2001). Antioxidant effects of *Origanum majorana* L. on superoxide anion radicals. *Food Chemistry, 75*, 439–444.

Kang, N. J. (2008). Inhibition of powdery mildew development and activation of antioxidant enzymes by induction of oxidative stress with foliar application of a mixture of riboflavin and methionine in cucumber. *Scientia Horticulturae, 118*, 181–188.

Kardošová, A., & Machová, E. (2006). Antioxidant activity of medicinal plant polysaccharides. *Fitoterapia, 77*, 367–373.

Kim, J. S., Reuhs, B. L., Michon, F., Kaiser, R. E., & Arumugham, R. G. (2006). Addition of glycerol for improved methylation linkage analysis of polysaccharides. *Carbohydrate Research, 341*, 1061–1064.

Lowry, O. H., Rosebrough, N. J., Farr, A. L., & Randall, R. J. (1951). Protein measurement with the folin phenol reagent. *The Journal of Biological Chemistry, 193*, 265–275.

Luk, J. M., Lai, W., Tam, P., & Koo, M. W. (2000). Suppression of cytokine production and cell adhesion molecule expression in human monocytic cell line THP-1 by *Tripterygium wilfordii* polysaccharide moiety. *Life Sciences, 67*, 155–163.

Navarini, L., Gilli, R., Gombac, V., Abatangelo, A., Bosco, M., & Toffanin, R. (1999). Polysaccharides from hot water extracts of roasted *Coffea arabica* beans: Isolation and characterization. *Carbohydrate Polymers, 40*, 71–81.

Needs, P. W., & Sevendran, R. R. (1993). Avoiding oxidative degradation during sodium hydroxide methyl iodide-mediated carbohydrate methylation in dimethyl sulfoxide. *Carbohydrate Research, 245*, 1–10.

Ouk, S., Thiebaud, S., Borredon, E., Legars, P., & Lecomte, L. (2002). O-Methylation of phenolic compounds with dimethyl carbonate under solid/liquid phase transfer system. *Tetrahedron Letters, 43*, 2661–2663.

Prasad, N. K., Yang, B., Zhao, M. M., Wang, B. S., Chen, F., & Jiang, Y. M. (2009). Effects of high-pressure treatment on the extraction yield, phenolic content and antioxidant activity of litchi (*Litchi chinensis* Sonn.) fruit pericarp. *International Journal of Food Science and Technology*. doi:10.1111/j.1745-4530.2008.00247.x.

Rangkadilok, N., Sitthimonchai, S., Worasuttayangkurn, L., Mahidol, C., Ruchirawat, M., & Satayavivad, J. (2007). Evaluation of free radical scavenging and antityrosinase activities of standardized longan fruit extract. *Food and Chemical Toxicology, 45*, 328–336.

Rao, R. S. P., & Muralikrishna, G. (2006). Water soluble feruloyl arabinoxylans from rice and ragi: Changes upon malting and their consequence on antioxidant activity. *Phytochemistry, 67*, 91–99.

Schepetkin, I. A., & Quinn, M. T. (2006). Botanical polysaccharides: Macrophage immunomodulation and therapeutic potential. *International Immunopharmacology, 6*, 317–333.

Tsai, M. C., Song, T. Y., Shih, P. H., & Yen, G. C. (2007). Antioxidant properties of water-soluble polysaccharides from *Antrodia cinnamomea* in submerged culture. *Food Chemistry, 104*, 1115–1122.

Tseng, Y. H., Yang, J. H., & Mau, J. L. (2008). Antioxidant properties of polysaccharides from *Ganoderma tsugae*. *Food Chemistry, 107*, 732–738.

Wang, Q., & Fang, Y. (2002). Analysis of sugars in traditional Chinese drugs. *Journal of Chromatography B, 812*, 219–231.

Yang, B., Jiang, Y. M., Wang, R., Zhao, M. M., & Sun, J. (2009). Ultra-high pressure treatment effects on polysaccharides and lignins of longan fruit pericarp. *Food Chemistry, 112*, 428–431.

Yang, B., Jiang, Y. M., Zhao, M. M., Chen, F., Wang, R., Chen, Y. L., et al. (2009). Structural characterisation of polysaccharides purified from longan (*Dimocarpus longan* Lour.) fruit pericarp. *Food Chemistry, 115*(60), 9–614.

Yang, B., Jiang, Y. M., Zhao, M. M., Shi, J., & Wang, L. Z. (2008). Effects of ultrasonic extraction on the physical and chemical properties of polysaccharides from longan fruit pericarp. *Polymer Degradation and Stability, 93*, 268–272.

Yang, B., Zhao, M. M., Shi, J., Cheng, G. P., Ruenroengklin, N., & Jiang, Y. M. (2008). Variations in water-soluble saccharides and phenols in longan fruit pericarp after drying. *Journal of Food Process Engineering, 31*, 66–77.

Yang, B., Zhao, M. M., Shi, J., Yang, N., & Jiang, Y. M. (2008). Effect of ultrasonic treatment on the recovery and DPPH radical scavenging activity of polysaccharides from longan fruit pericarp. *Food Chemistry, 106*, 685–690.

Yoshida, T. (2001). Synthesis of polysaccharides having specific biological activities. *Progress in Polymer Science, 26*, 379–441.

Yuan, H., Zhang, W., Li, X., Lu, X., Li, N., Gao, X., et al. (2005). Preparation and in vitro antioxidant activity of k-carrageenan oligosaccharides and their oversulfated, acetylated, and phosphorylated derivatives. *Carbohydrate Research, 340*, 685–692.

Food Chemistry 118 (2010) 369–376

Contents lists available at ScienceDirect

Food Chemistry

journal homepage: www.elsevier.com/locate/foodchem

Effect of macerating enzyme treatment on the polyphenol and polysaccharide composition of red wines

Marie-Agnès Ducasse [a,b,c], Rose-Marie Canal-Llauberes [b], Marie de Lumley [c], Pascale Williams [a], Jean-Marc Souquet [a], Hélène Fulcrand [a], Thierry Doco [a], Véronique Cheynier [a,*]

[a] INRA, Joint Research Unit 1083 Sciences for Oenology, 2 Place Viala, F-34060 Montpellier, France
[b] NOVOZYMES France, La cité Mondiale, 23 Parvis des Chartrons, 33074 Bordeaux Cedex, France
[c] Laffort Oenologie, 126 quai Souys, 33100 Bordeaux, France

ARTICLE INFO

Article history:
Received 14 January 2009
Received in revised form 11 March 2009
Accepted 30 April 2009

Keywords:
Wine
Enzymes
Polyphenols
Tannins
Anthocyanins
Colour
Pectic polysaccharides
RG-II

ABSTRACT

Effect of macerating enzymes on the polyphenol and polysaccharide composition of Merlot wines after 20 months of ageing was studied over three vintages (2004, 2005, 2006). Pectinase rich enzyme preparations, by degrading grape berry cell walls, led to a modification of the molecular weight distribution of polysaccharides released into the wines. Enzyme-treated wines contained more Rhamnogalacturonan II (RG-II) and less polysaccharides rich in arabinose and galactose (PRAGs) over the three vintages. The enzyme treatment also modified wine polyphenol composition. An increase of colour intensity, of derived pigments resistant to sulphite bleaching and of proanthocyanidins (condensed tannins) was observed, modulated by vintage effect. Principal Component Analysis of all the data indicated both vintage and enzyme effects. Beside the vintage effect separating the wine samples, the impact of enzyme treatment on wines was established for each year.

1. Introduction

Pectinase rich enzyme preparations obtained from *Aspergillus* sp. are commonly used in red wine-making to maximise the extraction of free-run juice during maceration, to aid in clarification and filtration, and to facilitate the processes (Canal-Llaubères, 1993). Pectinases act on the pectic substances which occur as the structural polysaccharides in the middle lamella and primary grape cell wall (Pinelo, Arnous, & Meyer, 2006). The polysaccharidic fraction of wines includes polysaccharides rich in arabinose and galactose (PRAGs) such as type II arabinogalactan-proteins (AGPs) and arabinans, Rhamnogalacturonans (RG-I and RG-II) coming from the pecto-cellulosic cell walls of grape berries (Doco & Brillouet, 1993; Pellerin et al., 1996; Pellerin, Vidal, Williams, & Brillouet, 1995; Vidal, Williams, Doco, Moutounet, & Pellerin, 2003), and mannoproteins (MPs) released by the yeasts during fermentation (Llaubères, Dubourdieu, & Villettaz, 1987; Waters, Wallace, Tate, & Williams, 1993). The structure and amounts of polysaccharides released in wines depend on the wine-making process and can be modified by enzyme treatment (Ayestaran, Guadalupe, & Leon, 2004; Doco, Williams, & Cheynier, 2007; Guadalupe, Palacios, & Ayestaran, 2007). Polysaccharides are one of the main groups of macromolecules of wine. They have been thoroughly studied because of their technological and sensory properties in wines. They play a role in the colloidal stability of wines through their ability to interact and aggregate with tannins. Polysaccharides do not prevent initial tannin aggregation but they influence particle size evolution (Riou, Vernhet, Doco, & Moutounet, 2002). RGII enhances tannin particle size, suggesting co-aggregation between RGII and tannins. It has been shown to decrease astringency in wine-like model solutions (Vidal et al., 2004) and is also known to inhibit hydrogen tartrate crystallisation (Gerbaud et al., 1996). The effect of enzymes on wine polysaccharide composition has been already studied (Doco et al., 2007): an increase of RG-II and a decrease of PRAGs were observed, along with a particular modification of AGPs, with loss of their terminal arabinose residues. Addition of macerating enzymes to the mash is also commonly performed to increase the extraction of phenolic compounds, and especially anthocyanins which are the red pigments of grapes, and thus to enhance wine colour intensity. However, studies on the effect of enzymes on wine colour and anthocyanin content have led to conflicting results (Sacchi, Bisson, & Adams, 2005): some publications have shown an increase of anthocyanins (Kelebek, Canbas,

* Corresponding author. Tel.: +33 4 99 61 22 98; fax: +33 4 99 61 28 57.
E-mail address: cheynier@supagro.inra.fr (V. Cheynier).

0308-8146/$ - see front matter © 2009 Elsevier Ltd. All rights reserved.
doi:10.1016/j.foodchem.2009.04.130

Cabaroglu, & Selli, 2007; Revilla & Gonzalez-SanJose, 2003) or an increase of colour (Bakker, Bellworthy, Reader, & Watkins, 1999; Ducruet, An, Canal-Llauberes, & Glories, 1997), while others have reported a decrease of anthocyanins (Wightman, Price, Watson, & Wrolstad, 1997) or of colour (Bautista-Ortin, Martinez-Cutillas, Ros-Garcia, Lopez-Roca, & Gomez-Plaza, 2005). These discrepancies may be due to differences in grape polyphenol compositions, in their extraction rates into the wines, and in their reactions in wine, depending on many parameters, such as the cultivar, the maturity of grape berries, and the wine-making techniques. Indeed, the colour of red wine is not only due to anthocyanins extracted from the grape skins but also to various products formed during wine-making and ageing. In particular, tannins (i.e. proanthocyanidins, which are oligomers and polymers of flavan-3-ols such as catechins) that play a significant role in the taste of wines (Cheynier et al., 2006) and contribute to the colour stability of red wines as they react with anthocyanins to form derived pigments such as tannin–anthocyanin and anthocyanin–tannin adducts (Fulcrand, Atanasova, Salas, & Cheynier, 2004; Salas, Fulcrand, Meudec, & Cheynier, 2003). Tannin extraction is modulated by their interactions between them and with polysaccharides. In particular, it can be impeded by their adsorption on polysaccharides of the cell and vacuole walls (Renard, Baron, Guyot, & Drilleau, 2001). The effect of macerating enzymes on tannin concentration has been evaluated using a precipitation method (Romero-Cascales, Fernandez-Fernandez, Ros-Garcia, Lopez-Roca, & Gomez-Plaza, 2008), and from absorbance measurements at 280 nm performed directly on wines (Kelebek et al., 2007) or after fractionation of wine proanthocyanidins (Bautista-Ortin et al., 2005): an increased extraction of tannins was commonly observed. However, to our knowledge, no information is available on the effect of enzyme treatments on wine proanthocyanidin composition. Methods based on acid-catalysed cleavage in the presence of a nucleophilic agent (thiolysis, phloroglucinolysis), followed by HPLC analysis of the resulting depolymerisation products, have been developed to determine the quantitative and qualitative composition of wine proanthocyanidins. Their application has enabled the characterisation of seed (Prieur, Rigaud, Cheynier, & Moutounet, 1994), skin (Souquet, Cheynier, Brossaud, & Moutounet, 1996) and pulp (Mane et al., 2007) proanthocyanidins, thus making it possible to monitor their extraction into the wine (Morel-Salmi, Souquet, Bes, & Cheynier, 2006) and to establish relationships between tannin composition and astringency (Vidal, Francis et al., 2003). In this study, the effect of macerating enzymes on the polysaccharide and polyphenol composition and the colour of Merlot wines was determined over three vintages. Due to their importance in red wine quality, proanthocyanidin quantitative and qualitative compositions were determined by phloroglucinolysis.

2. Materials and methods

2.1. Grape materials

Raw materials for this study were grapes from *Vitis Vinifera* var. Merlot grown in an experimental parcel located near Bordeaux in Southern France and harvested at maturity (Table 1) over three vintages (2004, 2005 and 2006). Analyses at harvest [reducing sugars (RS) measured by a colorimetric method (OIV, 2005), total acidity (TA), weight of grape berries (W), pH, anthocyanins at pH 3.2 determined by Glories's method (Ribéreau-Gayon, Glories, Maujean, & Dubourdieu, 2004) (ApH3.2), absorbance at 280 nm (DO280)] were performed by SARCO (Laffort laboratory, France).

2.2. Preparation of trials

One hundred and seventy kilograms of grapes, representive sampling of the parcel, were destemmed and crushed, and distributed into 200 l stainless steel tanks. Bisulphite (6 g/hl) was first added. After homogenisation, different enzymatic preparations were added: enzyme A (Vinozym Vintage FCE, Novozymes, Denmark, a preparation of pectinases, mainly containing polygalacturonase purified from cinnamoyl esterase activity for red wine-making) was applied at 3.5 g/100 kg either alone or together with enzyme B (Vinoflow FCE, Novozymes, Denmark, a purified preparation of pectinases and beta-glucananses for red wine maturation) at 5 g/hl. Abbreviations used for trials are the following: control wine (control); enzyme A (A); enzymes A and B (AB), vintages: 2004 coded 04, 2005 coded 05, 2006 coded 06.

2.3. Wine-making

After 12 h of maceration at 12 °C, all fermentations were started by implanting Excellence SP (commercial yeast, Lamothe-Abiet, Bordeaux, France) at 20 g/hl and were carried out in 200 l stainless steel tanks equipped with temperature control enabling to regulate fermentation kinetics. Alcoholic fermentation started at 15 °C; the temperature was allowed to rise during fermentation and was then maintained at around 24–25 °C. When alcoholic fermentation was finished (11 days), the free-run juice of each trial was transferred to one 200 l tank. After devatting, the young wines were kept at 20–21 °C to favour malolactic fermentation using thermoregulation. Freeze dried bacteria culture was inoculated at 1 g/hl to induce malolactic fermentation. Wines were filtered after 6 months of ageing on clarifying 20×20 cm cellulose-Kieselguhr Seitz K200 plates prior to bottling. Wine samples were stored in the wine experimental cellar until analysis. All wines were analysed after the same period of ageing, i.e. 20 months after the end of alcoholic fermentation.

2.4. Preparation of total soluble polysaccharides of wines

The wine polysaccharides were isolated as previously described (Vidal, Williams et al., 2003). Wine (2.5 ml) was evaporated in centrifugal evaporator (EZ-2, Genevac®, Ipswich, UK). The residue was dissolved in 0.5 ml of water to obtain wine concentrated five times. Ethanol (2.66 ml, 95%) containing 0.5% HCl was added to obtain a final concentration of 80% ethanol. After one night at 4 °C, wine polysaccharides were precipitated and the supernatant was eliminated after centrifugation (10 min, 15,000 rpm). The pellet that corresponds to total wine colloids was dissolved in 1 ml of H_2O (Millipore). The oligosaccharides and salts contained in the total colloids were eliminated by retention on a column (4 ml) of an

Table 1
Enological data at harvest of the three vintages.

Vintage	Date of harvest	RS[1] (g/l)	TA[2] (H_2SO_4 g/l)	W[3] (200 grape berries) (g)	pH	A[4] pH = 3.2 (mg/l)	DO280[5]
2004	09/29/2004	215	2.8	379	3.5	852	57
2005	09/19/2005	222	3.64	312	3.34	1017	65
2006	09/21/2006	232	3.54	350	3.47	963	62

1: Reducing sugars, 2: total acidity, 3: weight of 200 grape berries, 4: anthocyanins at pH = 3.2 determined by Glories method, 5: absorbance at 280 nm.

ion exchange mixed resin (Mix Bed Resin AG 501-X8, Bio Rad); wine polysaccharides, not retained, were eluted by 2.5 bed volumes of H_2O. Total soluble polysaccharides were obtained after the freeze drying of water eluted materials.

2.5. Analysis of polysaccharides

The molecular weight distribution of the wine polysaccharides was determined by high-performance size-exclusion chromatography (HPSEC) using a system equipped with a 234-Gilson sampling injector (Roissy, France), a LC-10 AS Shimadzu pump (Kyoto, Japan). HPSEC elution was performed on two serial Shodex Ohpak KB-803 and KB-805 columns (0.8 × 30 cm; Showa Denkko, Japan) connected to a ERC-7512 refractometer (Erma, Japan) at 1 ml/min flow rate in 0.1 M $LiNO_3$. The apparent molecular weights were deduced from the calibration curve established with a pullulan calibration kit (P-400, M_W = 380,000 P-200, M_W = 186,000; P-100, M_W = 100,000; P-50, M_W = 48,000; P-20, M_W = 23,700; P-10, M_W = 12,200; P-5, M_W = 5800; Showa Denko K.K., Japan). The calibration equation was log $M_W = 28.321 - 1.04 \times tR$ (tR = column retention-time at peak maximum, and $r^2 = 0.997$). Neutral monosaccharides were released after hydrolysis of wine polysaccharides with 2 M trifluoroacetic acid (75 min at 120 °C) (Albersheim, Nevins, English, & Karr, 1967). They were then converted to the corresponding alditol acetate derivatives by reduction and acetylation and quantified by GC analysis (Harris, Henry, Blakeney, & Stone, 1984) using a fused silica DB-225 (210 °C) capillary column (30 m × 0.32 mm i.d., 0.25 μm film) with H_2 as the carrier gas on a Hewlett–Packard Model 5890 gas chromatograph. The different alditol acetates were identified on the basis of their retention time by comparison with standard monosaccharides. Neutral sugar amounts were calculated relative to the internal standard (myo-inositol). Polysaccharide composition of each wine was estimated from the concentration of individual glycosyl residues, determined by GC after hydrolysis, reduction, and acetylation, that are characteristic of the known wine polysaccharides as previously described (Vidal, Williams, O'Neill & Pellerin, 2001). The calculation of the wine polysaccharide concentrations takes account of the composition of characteristic monosaccharides as well as hydrolysis yield (Doco, Quellec, Moutounet, & Pellerin, 1999).

2.6. Sample preparation and analysis of wine polyphenols

2.6.1. Analysis of anthocyanins and tannin–anthocyanin dimer adducts

Anthocyanins and tannin–anthocyanin dimer adducts were analysed by direct injection of wines into the HPLC system. HPLC–DAD analyses were performed using a Waters 2690 system equipped with an autosampler system, a Waters 996 photodiode array detector, and a Millenium 32 chromatography manager software (Waters, Milford, MA). Separation was achieved on a reversed-phase Atlantis dC18 column (250 × 2.1 mm i.d., 5 μm packing) protected with a guard column of the same material (20 × 2.1 mm i.d., 3 μm packing) (Waters, Milford, MA). The elution conditions were as follows: 0.250 ml/min flow rate; oven temperature 30 °C; solvent A, water/formic acid (95/5 v/v); solvent B, acetonitrile/water/formic acid (80/15/5 v/v/v); elution began isocratically with 0% B during 5 min, then continued with linear gradients from 0% to 10% B in 20 min, from 10% to 20% B in 15 min, from 20% to 45% B in 15 min, from 45% to 60% B in 15 min, from 60% to 80% B in 5 min, followed by washing and re-equilibration of the column. The injection volume for all samples was 5 μl. A calibration curve was established using malvidin 3-*O*-glucoside from Extrasynthese (Genay, France) to quantify red pigments at 520 nm as equivalent malvidin 3-*O*-glucoside.

2.6.2. Analysis of tannins

Tannins were analysed by HPLC after acid-catalysed cleavage in the presence of excess phloroglucinol as previously described (Kennedy & Jones, 2001). The protocol was adapted for analysis of wine tannins as follows. Wine (4 ml) was evaporated in centrifugal evaporator (EZ-2, Genevac®, Ipswich, UK). The residue was dissolved in 4 ml of water/acetic acid (98/2 v/v) and 1 ml was applied on a C-18 solid phase extraction cartridge (Waters, Vac tC18 3cc) using the RapidTrace®SPE workstation (Caliper Life Sciences, Hopkinton, MA). Sugars and organic acids were eluted with 5 ml of water/acetic acid (98/2 v/v) and phenolic compounds recovered with 8 ml of methanol. Methyl paraben (2 g/l) was added as an internal standard. An eluent volume of 8 ml was evaporated to dryness under vacuum, redissolved in 200 μl of MeOH containing 0.2 N HCl, 50 g/l phloroglucinol, and 10 g/l ascorbic acid and heated for 20 min at 50 °C. Then, an equivalent volume of aqueous 200 mM sodium acetate was added to stop the reaction. Released terminal subunits and extension subunit-phloroglucinol adducts were analysed by HPLC using a Waters 2690 system with a reversed-phase Atlantis dC18 column (Waters, Milford, MA; 5 μm packing, 250 × 4.6 mm i.d.) protected by a guard column of the same material (20 × 4.6 mm i.d.; Waters, Milford, MA) and with a Securityguard™ cartridge C18 (Phenomenex, Torrance, CA; 4.0 × 3.0 mm i.d.). The mobile phase was a gradient of water/acetonitrile/formic acid (80/18/2 v/v/v; solvent B) in water/formic acid (98/2 v/v; solvent A), at a flow rate of 1 ml/min at 30 °C. Proportions of solvent B were as follows: 0–5 min with 0% B; 5–35 min, 0–10%; 35–70 min, 10–20%; 70–75 min, 20–100%; and 75–80 min, 100–0%. The injection volume for all samples was 10 μl. The proanthocyanidin units were detected by a Waters 996 photodiode array detector and quantified from peak areas at 280 nm using external calibration with known concentrations of flavan-3-ol monomers from Sigma (Saint Louis, MO) and flavan-3-ol-phloroglucinol adducts, purified in the laboratory. Each analysis was performed in triplicate. These analyses gave access to total proanthocyanidin content, their mean degree of polymerisation (mDP), and the percentage of each constitutive unit (i.e. catechin, epicatechin, epicatechin gallate (%gal), epigallocatechin (%egc). The mDP was calculated as the ratio between the summed molar concentrations of all released constitutive units and the summed molar concentrations of terminal constitutive units.

2.7. Spectrophotometric measurements

Absorbance measurements were made with a SAFAS® UV mc2 spectrophotometer (Monaco) and colour indices were deduced from these absorbance measurements as previously described (Atanasova, Fulcrand, Cheynier, & Moutounet, 2002; Glories, 1984; Somers & Evans, 1977). All the absorbance measurements were converted to a 10-mm light path cell and a dilution of 1 before calculating indices. Absorbance values at 420, 520, and 620 nm were measured, 30 min after addition of acetaldehyde, in a 1-mm light path cell. Hue (H) was calculated as A420/A520 and colour intensity corrected of bisulphite (CIcorr) as A420 + A52O + A620. Wine pigments corrected of bisulphite at wine pH (WPcorr) was defined as the absorbance at 520 nm, 30 min after addition of acetaldehyde. Colour due to derivatives resistant to sulphite bleaching was determined at 520 nm in a 1-mm light path cell, 30 min after addition of a metabisulphite solution, and sulphite bleaching resistant pigments (PR_{SO2}) was calculated. Total pigments at acidic pH ($P_{pH<1}$) was determined from absorbance at 520 nm with a 10-mm light path, 4 h after a 100-fold dilution in HCl 1 M. Total polyphenol index (TPI) was determined from absorbance at 280 nm with a 10-mm light path after a 100-fold dilution.

2.8. Statistical analysis

Data are expressed as the average of three measurements. ANalysis Of VAriance (ANOVA) and Principal Component Analysis (PCA) were carried out with the software XLSTAT (Addinsoft, Paris, France). The analytical data were centred and normalised before being treated by PCA.

3. Results and discussion

3.1. Effect of enzymes on wine polysaccharide profile

The polysaccharides isolated from Merlot wines have the same molecular weight distribution as previously described in Carignan (Doco et al., 1999) and Tempranillo (Guadalupe & Ayestaran, 2007) wines (Fig. 1). A first peak eluting between 14 and 16.5 min corresponds to mannoproteins (MPs) released from yeast during fermentation; a second peak eluting between 16.5 and 18 min corresponds mainly to a mixture of arabinogalactan-proteins (AGPs), arabinans, and few MPs; and a third peak eluting between 18 and 19.2 min corresponds mainly to Rhamnogalacturonan II (RG-II) with AGPs and MPs of lower molecular weight. Pectinase addition leads to a modification of the molecular weight distribution of wine polysaccharides (Fig. 1). A shift from higher to lower molecular weight polysaccharides is observed in enzyme-treated wines; the decrease in the second peak indicates that AGPs and arabinans have been partly degraded to lower molecular weight polysaccharides, while the increase of the third peak may reflect a release of both lower molecular weight polysaccharides and of RGII due to an extended cell wall degradation, as shown earlier (Doco et al., 2007). The enzyme effect on the AGP peak seems to be dependent of vintage. The decrease of the AGP peak in enzyme-treated wines was more pronounced in 2004 and 2006 (Fig. 1A and C, respectively) than in 2005 (Fig. 1B). This phenomenon may be due to a difference of maturity (Table 1) of grape berries between the three vintages.

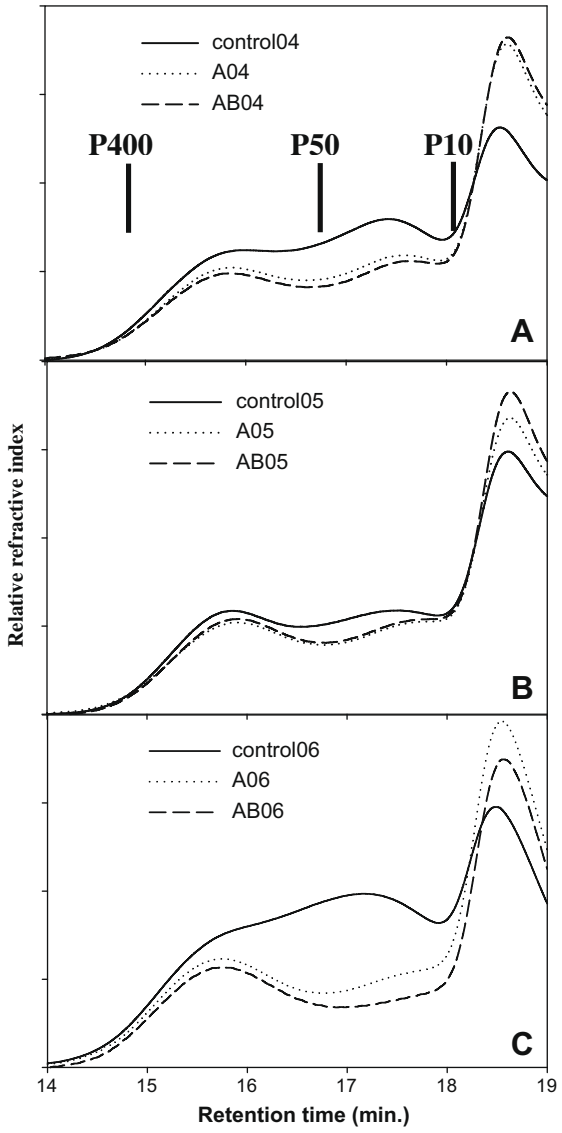

Fig. 1. Molecular weight distribution of polysaccharides isolated from 2004 wines (A), 2005 wines (B), 2006 wines (C).

3.2. Effect of enzymes on polysaccharide composition

Concentrations in MPs, PRAGs and RG-II were estimated from the concentration of individual glycosyl residues (mannose, arabinose, galactose, rhamnose, fucose, xylose, apiose, 2-*O*-methyl-fucose and 2-*O*-methyl-xylose) determined by GC after hydrolysis, reduction and acetylation. All the mannose is attributed to yeast MPs. PRAGs, representing mainly arabinogalactan–proteins and arabinans in wines, are estimated from the sum of galactose and arabinose residues. RG-II is calculated from the concentration of apiose, 2-*O*-methyl-fucose and 2-*O*-methyl-xylose. Fig. 2 presents the concentrations of MPs, PRAGs and RG-II in mg/l in wines. The data confirms the interpretation of molecular weight distribution profiles. The use of pectolytic enzymes modified the composition of the polysaccharides released from cell walls in wines as shown by a decrease of PRAG concentration and an increase of RG-II concentration. The loss of PRAGs was more pronounced in 2006 than in 2004 (Fig. 2A and C, respectively) and was not observed in 2005 (Fig. 2B). Again, this may be related to differences in grape maturity between the three vintages, as suggested above. As expected, no significant effect of pectolytic enzymes on MPs was observed.

3.3. Effect of enzymes on wine colour

Total polyphenol and wine colour indices (Table 2) were deduced from the absorbance measurements (Glories, 1984; Somers & Evans, 1977). Colour intensity was measured after addition of acetaldehyde to release anthocyanins eventually involved in bisulphite adducts (Atanasova et al., 2002). Large vintage differences were observed in the absorbance values. Thus, the total polyphenol and colour intensity values were higher in 2005 than in 2004 and 2006 at 20 months of ageing, suggesting that higher maturity was reached in this vintage. Indeed, monitoring of colour intensity and total polyphenol index during alcoholic fermentation (Fig. 3) shows a faster increase of these indices during the first days of fermentation in 2005 (Fig. 3B) than in 2004 and 2006 (Fig. 3A and C, respectively). In 2005, the extraction kinetics were identical in enzyme-treated wines and in the control wine. In contrast, in 2004 and 2006, TPI values were significantly higher in the treated wines than in the controls throughout fermentation. The total polyphenol index values after 20 months of ageing were also significantly higher in the enzyme-treated wines than in the control except for enzyme A in 2006. This suggests that the plant cell wall degradation induced by the enzyme treatment resulted in increased phenolic extraction from grapes and/or that changes in the wine polysaccharide composition enhanced the solubility and stability of phenolic compounds during wine ageing. The absorbance at 520 nm (WPcorr) and colour intensity (CIcorr) values were also higher in the enzyme-treated wines, after 20 months of ageing,

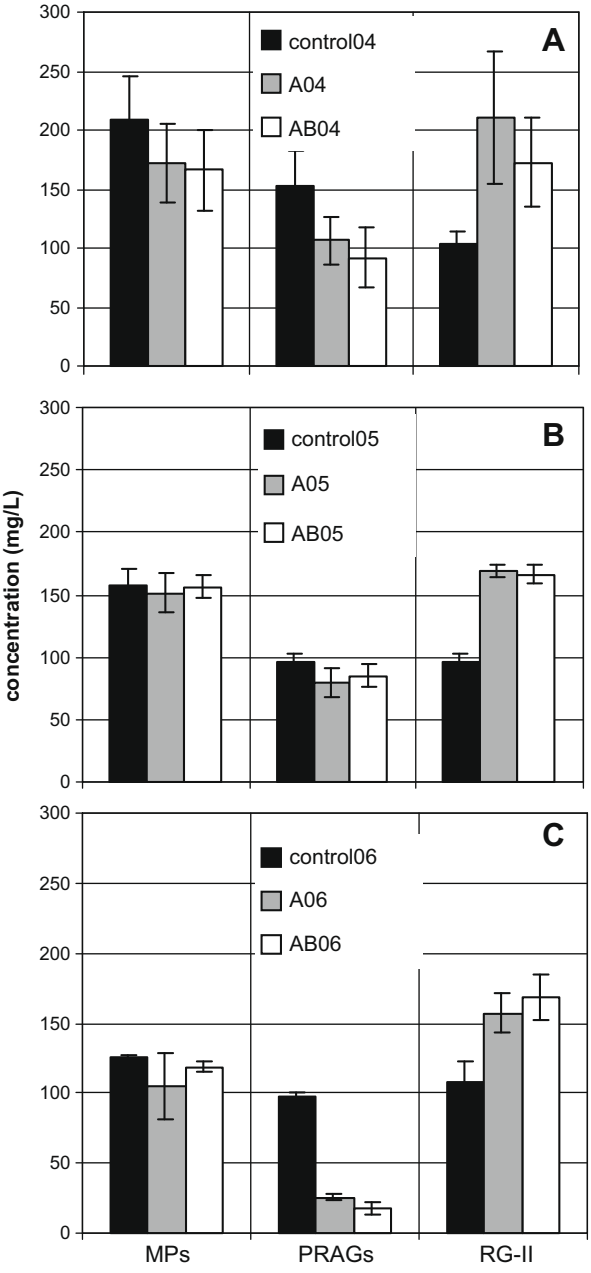

Fig. 2. Concentration (mg/l) of mannoproteins (MPs), polysaccharides rich in arabinose and galactose (PRAGs), and RhamnoGalacturonan II (RG-II) in 2004 wines (A), 2005 wines (B), 2006 wines (B).

for vintages 2004 and 2006, suggesting higher extraction of pigments from the grape berries and/or higher conversion of anthocyanins to derived pigments in wines obtained with enzymatic treatments. The latter hypothesis is confirmed by a higher level of sulphite bleaching resistant pigments (PR_{SO2}) in the treated wines than in the control wines, as genuine grape anthocyanins are bleached by sulphites while some derived pigments are not. This was not observed for the 2005 wines which showed higher values compared to the others. It seems that enzyme addition has no effect on Total Polyphenol Index (TPI) and Colour Intensity (CI) when using grapes with high initial values of these parameters, as above mentioned and shown by their monitoring of during alcoholic fermentation (Fig. 3B). Finally, the total pigment values measured in acidic conditions (ensuring conversion of all anthocyanins and derivatives to their flavylium pigment forms) were constant over the three vintages and little affected by the enzyme treatments. This indicates that the higher colour intensities measured in the 2005 wines are due to enhanced stabilisation of the pigments in the wines through formation of derived pigments or copigmentation rather than to a higher concentration of grape anthocyanins. Indeed, the sulphite bleaching resistant pigments contributed about 50% of the red colour in the 2005 wines and only 40% in the other two vintages, confirming that conversion of anthocyanin pigments occurred faster in the 2005 wines. The hue values were higher in the 2006 wines than in the other two series but were not modified by enzyme treatment.

3.4. Effect of enzymes on polyphenol composition

Tannin concentration (*T*) their qualitative composition (mDP, %gal, %egc), anthocyanin (ACN) concentration and tannin–anthocyanin adduct (TA) concentration are presented in Table 3. The enzyme-treated wines contained larger amounts of tannins than the control wines over the three vintages. Tannin composition was also qualitatively different in the treated wines. Their mDP were slightly higher than in the control wines. This may be due to easier extraction of higher molecular weight tannins as a results of the increased degradation of grape cell walls induced by enzyme addition. In all cases, tannins released into the wines are mainly tannins from skins as evidenced by the %egc. A slight but significant effect of enzymes on %gal was observed in 2004 and 2006. Inconsistent effects of enzyme treatments on the concentrations of anthocyanins and tannin–anthocyanin adducts measured by HPLC were observed (Table 3 ACN, TA). It should be emphasised that the concentration of native anthocyanins reflects both their extraction from the grape and their subsequent reactions in wine. The colour properties are not related to anthocyanin concentrations but depend, on one hand, on the nature and proportions of genuine anthocyanins and derivatives formed from them during wine-making, on the other hand on copigmentation phenomenon. Anthocyanin derivatives include TA adducts which are mostly colourless at wine pH but also other types of pigments that contribute colour in wine. The relative amounts of these various compounds depend on the concentrations of tannins and anthocyanins and on their molar ratio which are modified by enzyme treatment. The increase of colour intensity of enzyme-treated wines was not

Table 2
Wine colour indices over the three vintages.

Trials	CIcorr[1,2]	H[1,3]	TPI[1,4]	WPcorr[1,5]	PR_{SO2}[1,6]	$P_{pH<1}$[1,7]
2004 vintage						
Control04	10.07 a	0.574 b	36.9 a	5.78 a	2.31 a	12.4 ab
A04	10.86 b	0.567 a	44.7 c	6.27 b	2.58 b	13.0 b
AB04	11.40 c	0.572 b	40.3 b	6.49 c	2.70 c	11.7 a
p-Value	*p < 0.0001*	*p < 0.01*	*p < 0.01*	*p < 0.0001*	*p < 0.0001*	*p < 0.05*
2005 vintage						
Control05	14.79 c	0.581 a	40.5 a	8.09 c	4.41 b	12.5 a
A05	13.51 a	0.579 a	44.3 c	7.64 a	3.75 a	13.6 b
AB05	14.26 b	0.588 b	41.8 b	8.01 b	3.80 a	13.5 b
p-Value	*p < 0.0001*	*p < 0.05*	*p < 0.001*	*p < 0.0001*	*p < 0.001*	*p < 0.05*
2006 vintage						
Control06	9.62 a	0.636 b	36.7 a	5.49 a	2.02 a	12.8 b
A06	10.80 c	0.613 a	36.6 a	5.97 c	2.41 c	12.1 a
AB05	10.32 b	0.647 c	39.1 b	5.86 b	2.28 b	13.1 b
p-Value	*p < 0.0001*	*p < 0.001*	*p < 0.05*	*p < 0.0001*	*p < 0.0001*	*p < 0.05*

1: Average of three measurements, one-factor ANOVA a same letter means no significant difference within each vintage, 2: colour intensity corrected (Abs 420 nm + Abs 520 nm + Abs 620 nm with acetaldehyde), 3: hue (Abs 420 nm/Abs 520 nm without acetaldehyde), 4: Total Polyphenols Index: absorbance at 280 nm, 5: wine pigments corrected (Abs 520 nm with acetaldehyde), 6: pigments resisting to sulphite bleaching (Abs 520 nm with SO_2), 7: pigments at acidic pH < 1(Abs 520 nm in HCl).

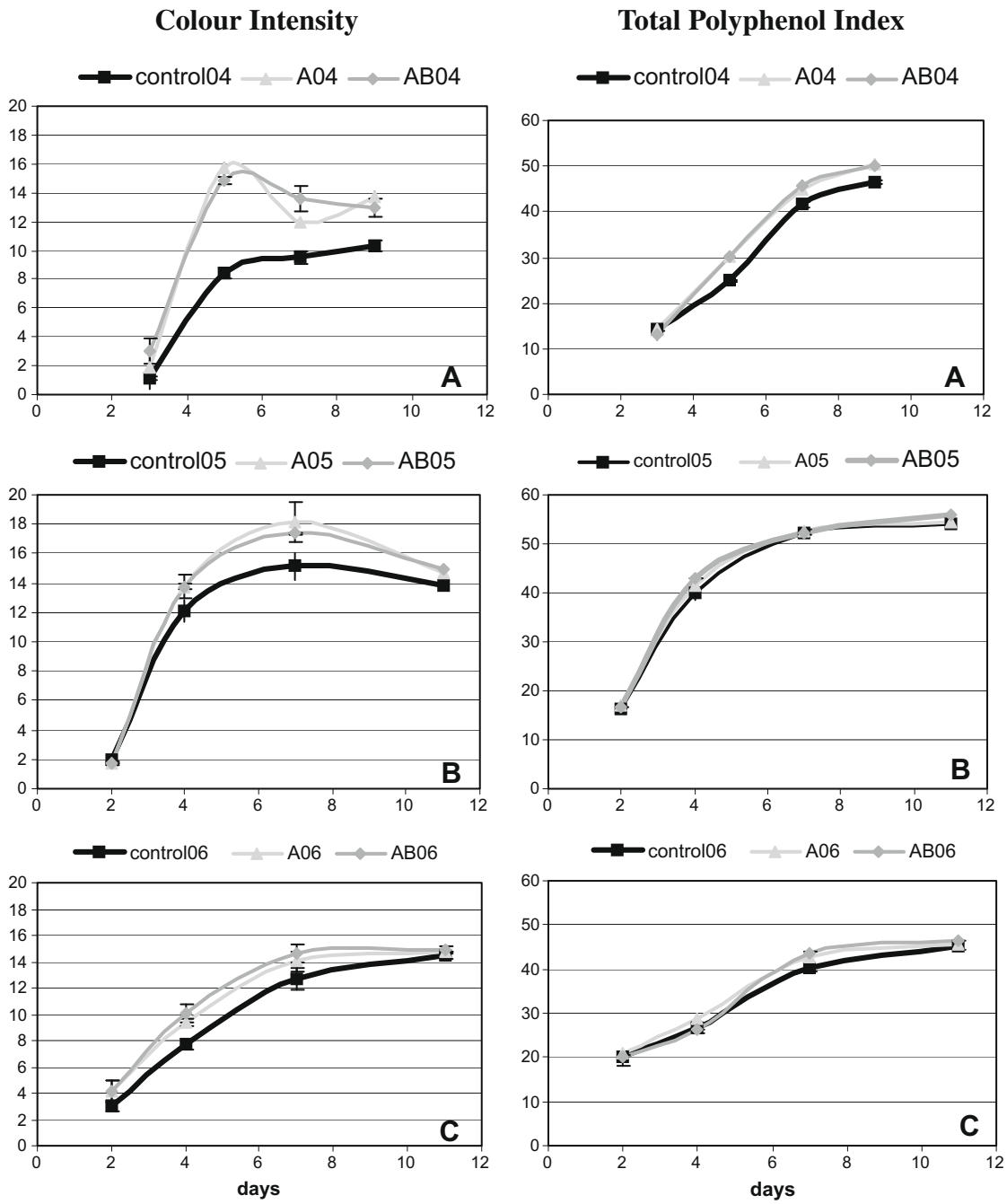

Fig. 3. Evolution of colour intensity (to the left) and total polyphenol index (to the right) during alcoholic fermentation of 2004 wines (A), 2005 wines (B) and 2006 wines (C).

related to a higher concentration of residual native anthocyanins in these wines. Thus, it is presumably due to other phenomena such as increased formation of derived pigments and enhanced copigmentation as a result of increased extraction of tannins (Fulcrand et al., 2004; Salas et al., 2003). It has been shown that the colour stability of malvidin 3-glucoside solutions was decreased in the presence of flavan-3-ol monomers but enhanced in the presence of procyanidin oligomers, especially as their the degree of polymerisation increased (Malien-Aubert, Dangles, & Amiot, 2002).

3.5. Vintage effect versus enzyme effect

Principal Component Analysis was performed on all the data generated from polysaccharide and polyphenol analysis and spectrophotometric measurements of the nine wines. The first and second Principal Components explained together 65.71% (PC1 36.43% and PC2 29.28%) of the total variance (Fig. 4). Projection of the wines on the first two PCs (Fig. 4A) shows a separation of the three vintages along the first two axes while control wines and enzyme-treated wines are separated along the second axis. PC1 is mainly associated positively with anthocyanins (ACN), hue (H), and tannins, and negatively with MPs, PRAGs, CIcorr, WPcorr, TPI, and PR_{SO2} (Fig. 4B). It contrasts 2006 wines, which show higher levels of free anthocyanins, H, and tannins, lower values of polysaccharides, and lower total polyphenol index, with the 2005 and, to a lesser extent, 2004 wines that exhibit higher values for total polyphenol and colour indices. Anthocyanin concentration is anti-correlated with CIcorr ($R = -0.76$), absorbance at 520 nm at wine pH

Table 3
Polyphenol composition of Merlot wines over the three vintages.

Trials	T[1,2] (mg/l)	mDP[1,3]	%gal[1,4]	%egc[1,5]	ACN[1,6] (mg/l)	TA[1,7] (mg/l)
2004 vintage						
Control04	425 a	4.65 a	2.38 a	17.90 a	63.3 b	1.35 a
A04	518 b	4.98 b	3.29 b	18.42 a	55.5 a	1.33 a
AB04	524 b	5.12 b	3.33 b	18.78 a	55.4 a	1.42 a
p-Value	*p < 0.01*	*p < 0.01*	*p < 0.001*	*n.s.*	*p < 0.05*	*n.s.*
2005 vintage						
Control05	447 a	4.84 a	2.42 b	22.53 a	25.1 a	1.18 a
A05	558 b	5.32 b	3.16 c	22.31 a	52.9 b	2.25 b
AB05	520 ab	6.11 c	1.35 a	23.43 a	58.4 c	1.89 b
p-Value	*p < 0.05*	*p < 0.01*	*p < 0.001*	*n.s.*	*p < 0.0001*	*p < 0.05*
2006 vintage						
Control06	572 a	4.96 a	1.68 a	24.35 c	85.2 b	1.62 c
A06	583 a	5.18 b	2.10 b	24.02 b	57.6 a	1.31 a
AB06	648 b	5.11 b	2.18 c	23.39 a	83.3 b	1.46 b
p-Value	*p < 0.0001*	*p < 0.01*	*p < 0.0001*	*p < 0.0001*	*p < 0.0001*	*p < 0.01*

1: Average of three measurements, one-factor ANOVA a same letter means no significant difference within each vintage, *n.s.* indicate no significant, 2: tannin concentration, 3: mean degree of depolymerization, 4:% of epicatechin gallate subunits, 5: % of epigallocatechin subunits, 6: anthocyanin concentration, 7: flavanol anthocyanin dimer concentration.

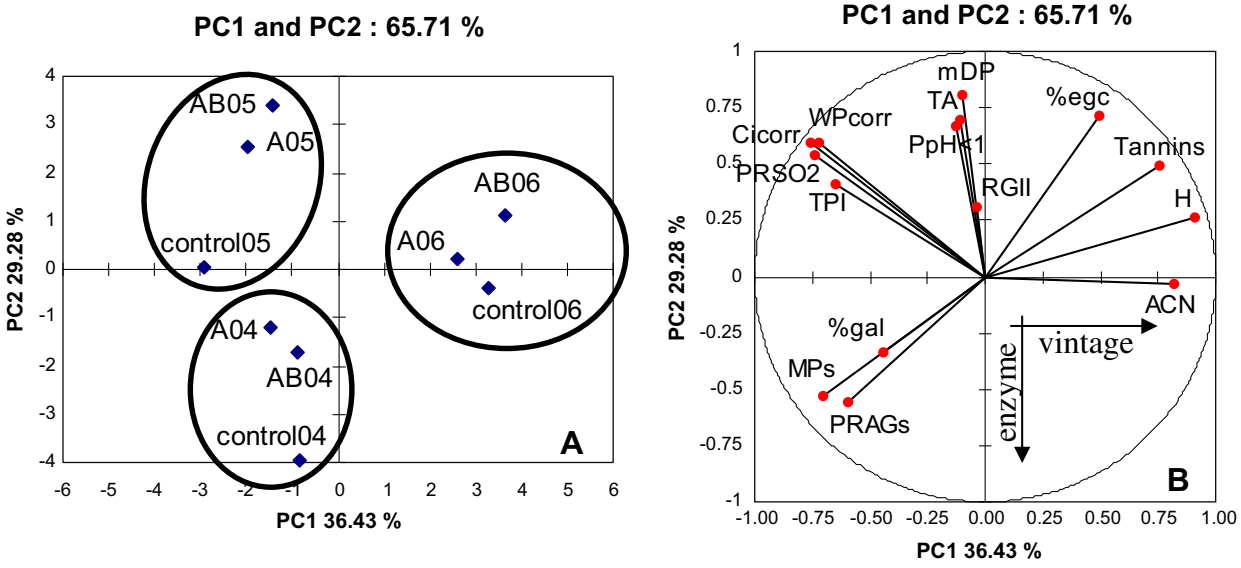

Fig. 4. Principal Component Analysis of the polysaccharide, polyphenol and spectrophotometric data of 2004, 2005, 2006 wines: projection of the wines on principal component 1 (PC1) and principal component 2 (PC2), control wine coded control; enzyme A coded A; enzymes A and B coded AB over three vintages: 2004 coded 04, 2005 coded 05, 2006 coded 06, (B) Correlation scatterplot of the chemical and spectrophotometric variables with PC1 and PC2.

(WPcorr; $R = -0.74$) and PR_{SO2} ($R = -0.78$), these three values being highly correlated, again meaning that wine colour after 20 months of ageing is mostly due to derived pigments (Fulcrand et al., 2004; Salas et al., 2004). Total polyphenol index appears correlated with colour indices but not with anthocyanins or tannins and thus is mostly contributed by derived pigments. PC2 is associated positively with mDP, $P_{pH<1}$, T–A, %egc, and, to a lesser extent, to tannins and colour indices and negatively with PRAGs and MPs concentrations (Fig. 4B). TA and $P_{pH<1}$ are positively correlated ($R = +0.72$), suggesting that the T–A dimers can serve as markers of a large class of T–A adducts which represent the majority of pigments in wine acidified to pH < 1. These adducts, like anthocyanins, are coloured at acidic pH but do not contribute much to red colour at the wine pH. Within each vintage, the enzyme-treated wines are distinguished from the control wines along the second axis, on one hand, by their higher contents of RGII and lower levels of PRAGs, related to enzymatic degradation of plant cell walls, on the other hand, by their higher tannin content, higher values of mDP, indicating an increased extraction of tannins as a result of increased cell wall degradation. The 2004 wines are also distinguished from the other two vintages by their higher amounts of PRAGs and MPs.

In conclusion, the effect of enzyme treatment has been demonstrated for each vintage, especially with regards to RG-II and tannin concentrations. This effect is more or less marked depending on the vintage. In particular, the increase in colour and degradation of PRAGs was not observed in 2005, possibly due to differences in grape maturity. This should be investigated further. No effect on wine anthocyanin concentration was observed. However, in 2004 and 2006, higher colour indices in the enzyme-treated wines indicate that the enzyme treatment either resulted in higher anthocyanin extraction followed by their conversion to other pigments or favoured reaction mechanisms yielding derivatives that are pigmented in wine. Indeed, the enzyme treatment leads to an increase of pigments resistant to sulphite bleaching which contribute to wine colour. No effect was observed on the concentration of TA adducts which are mostly colourless at wine pH but appeared

correlated to the red colour measured under acidic conditions (pH < 1). Finally, changes in polysaccharide composition induced by enzyme treatments may impact the colloidal structure and the mouth-feel properties of phenolic compounds in wines, as shown earlier in model solutions.

Acknowledgments

We thank Frederic Veran (UMR SPO) for technical assistance and all the staff of the wine experimental cellar for assistance with the wine-making experiments.

References

Albersheim, P., Nevins, D. J., English, P. D., & Karr, A. (1967). A method for the analysis of sugars in plant cell wall polysaccharides by gas–liquid-chromatography. *Carbohydrate Research, 5*, 340–345.

Atanasova, V., Fulcrand, H., Cheynier, V., & Moutounet, M. (2002). Effect of oxygenation on polyphenol changes occurring in the course of wine making. *Analytica Chimica Acta, 458*, 15–27.

Ayestaran, B., Guadalupe, Z., & Leon, D. (2004). Quantification of major grape polysaccharides (Tempranillo v.) released by maceration enzymes during the fermentation process. *Analytica Chimica Acta, 513*(1), 29–39.

Bakker, J., Bellworthy, S. J., Reader, H. P., & Watkins, S. J. (1999). Effect of enzymes during vinification on color and sensory properties of port wines. *American Journal of Enology and Viticulture, 50*(3), 271–276.

Bautista-Ortin, A. B., Martinez-Cutillas, A., Ros-Garcia, J. M., Lopez-Roca, J. M., & Gomez-Plaza, E. (2005). Improving colour extraction and stability in red wines: the use of maceration enzymes and enological tannins. *International Journal of Food Science and Technology, 40*(8), 867–878.

Canal-Llaubères, R. M. (1993). Enzymes in winemaking. In F. GH (Ed.), wine microbiology and biotechnology (Vol. 886, pp. 477–506). Washington, DC: Hardwood Academic Publishers.

Cheynier, V., Dueñas-Paton, M., Salas, E., Maury, C., Souquet, J.-M., Sarni-Manchado, P., et al. (2006). Structure and properties of wine pigments and tannins. *American Journal of Enology and Viticulture, 57*(3), 298–305.

Doco, T., & Brillouet, J.-M. (1993). Isolation and characterisation of a RhamnoGalacturonan II from red wine. *Carbohydrate Research, 243*(2), 333–343.

Doco, T., Quellec, N., Moutounet, M., & Pellerin, P. (1999). Polysaccharide patterns during the aging of Carignan noir red wines. *American Journal of Enology and Viticulture, 50*(1), 28–32.

Doco, T., Williams, P., & Cheynier, V. (2007). Effect of flash release and pectinolytic enzyme treatments on wine polysaccharide composition. *Journal of Agricultural and Food Chemistry, 55*(16), 6643–6649.

Ducruet, J., An, D., Canal-Llauberes, R. M., & Glories, Y. (1997). Influence des enzymes pectolytiques sélectionnées pour l'oenologie sur la qualité et la composition des vins rouges. *Revue Française d'Oenologie, 166*, 16–19.

Fulcrand, H., Atanasova, V., Salas, E., & Cheynier, V. (2004). The fate of anthocyanins in wine: Are there determining factors? In A. L. Waterhouse, & J. Kennedy (Eds.), Red wine color: Revealing the mysteries (Vol. 886, pp. 68-85). Washington, DC: American Chemical Society.

Gerbaud, V., Gabas, N., Laguerie, C., Blouin, J., Vidal, S., Moutounet, M., et al. (1996). Effect of wine polysaccharides on the nucleation of potassium hydrogen tartrate in model solutions. *Chemical Engineering Research and Design, 74*(A7), 782–790.

Glories, Y. (1984). La couleur des vins rouges. 2eme partie. Origine et interprétation. *Connaissance de la vigne et du vin, 18*(25), 3–271.

Guadalupe, Z., & Ayestaran, B. (2007). Polysaccharide profile and content during the vinification and aging of Tempranillo red wines. *Journal of Agricultural and Food Chemistry, 55*(26), 10720–10728.

Guadalupe, Z., Palacios, A., & Ayestaran, B. (2007). Maceration enzymes and mannoproteins: A possible strategy to increase colloidal stability and color extraction in red wines. *Journal of Agricultural and Food Chemistry, 55*(12), 4854–4862.

Harris, P. J., Henry, R. J., Blakeney, A. B., & Stone, B. A. (1984). An improved procedure for the methylation analysis of oligosaccharides and polysaccharides. *Carbohydrate Research, 127*(1), 59–73.

Kelebek, H., Canbas, A., Cabaroglu, T., & Selli, S. (2007). Improvement of anthocyanin content in the cv. Okuzgozu wines by using pectolytic enzymes. *Food Chemistry, 105*(1), 334–339.

Kennedy, J., & Jones, G. P. (2001). Analysis of proanthocyanidin cleavage products following acid-catalysis in the presence of excess phloroglucinol. *Journal of Agricultural and Food Chemistry, 49*(4), 1740–1746.

Llaubères, R. M., Dubourdieu, D., & Villettaz, J. C. (1987). Exocellular polysaccharides from Saccharomyces in wine. *Journal of the Science of Food and Agriculture, 41*, 277–286.

Malien-Aubert, C., Dangles, O., & Amiot, M. J. (2002). Influence of procyanidins on the color stability of oenin solutions. *Journal of Agricultural and Food Chemistry, 50*(11), 3299–3305.

Mane, C., Souquet, J. M., Olle, D., Verries, C., Veran, F., Mazerolles, G., et al. (2007). Optimization of simultaneous flavanol, phenolic acid, and anthocyanin extraction from grapes using an experimental design: application to the characterization of champagne grape varieties. *Journal of Agricultural and Food Chemistry, 55*(18), 7224–7233.

Morel-Salmi, C., Souquet, J. M., Bes, M., & Cheynier, V. (2006). The effect of flash release treatment on phenolic extraction and wine composition. *Journal of Agricultural and Food Chemistry, 54*, 4270–4276.

OIV. (2005). *Recueil des méthodes internationales d'analyse des vins et des moûts* (Vol. 1). MA-F-AS311-301-SUCRED.

Pellerin, P., Doco, T., Vidal, S., Williams, P., Brillouet, J. M., & Oneill, M. A. (1996). Structural characterization of red wine RhamnoGalacturonan II. *Carbohydrate Research, 290*(2), 183–197.

Pellerin, P., Vidal, S., Williams, P., & Brillouet, J.-M. (1995). Characterization of five type II arabinogalactan-protein fractions from red-wine of increasing uronic acid content. *Carbohydrate Research, 277*, 135–143.

Pinelo, M., Arnous, A., & Meyer, A. S. (2006). Upgrading of grape skins: Significance of plant cell-wall structural components and extraction techniques for phenol release. *Trends in Food Science and Technology, 17*(11), 579–590.

Prieur, C., Rigaud, J., Cheynier, V., & Moutounet, M. (1994). Oligomeric and polymeric procyanidins from grape seeds. *Phytochemistry, 36*, 781–784.

Renard, C., Baron, A., Guyot, S., & Drilleau, J.-F. (2001). Interactions between apple cell walls and native apple polyphenols: Quantification and some consequences. *International Journal of Biological Macromolecules, 29*, 115–125.

Revilla, I., & Gonzalez-SanJose, M. L. (2003). Compositional changes during the storage of red, wines treated with pectolytic enzymes: Low molecular-weight phenols and flavan-3-ol derivative levels. *Food Chemistry, 80*(2), 205–214.

Ribéreau-Gayon, P., Glories, Y., Maujean, A., & Dubourdieu, D. (2004). Chimie du vin, stabilisation et traitements. In Dunod (Ed.), *Traité d'OEnologie* (Vol. 2, pp. 240–242). France.

Riou, V., Vernhet, A., Doco, T., & Moutounet, M. (2002). Aggregation of grape seed tannins in model – Effect of wine polysaccharides. *Food Hydrocolloids, 16*, 17–23.

Romero-Cascales, I., Fernandez-Fernandez, J. I., Ros-Garcia, J. M., Lopez-Roca, J. M., & Gomez-Plaza, E. (2008). Characterisation of the main enzymatic activities present in six commercial macerating enzymes and their effects on extracting colour during winemaking of Monastrell grapes. *International Journal of Food Science and Technology, 43*(7), 1295–1305.

Sacchi, K. L., Bisson, L. F., & Adams, D. O. (2005). A review of the effect of winemaking techniques on phenolic extraction in red wines. *American Journal of Enology and Viticulture, 56*(3), 197–206.

Salas, E., Atanasova, V., Poncet-Legrand, C., Meudec, E., Mazauric, J., & Cheynier, V. (2004). Demonstration of the occurrence of flavanol–anthocyanin adducts in wine and in model solutions. *Analytica Chimica Acta, 513*, 325–332.

Salas, E., Fulcrand, H., Meudec, E., & Cheynier, V. (2003). Reactions of anthocyanins and tannins in model solutions. *Journal of Agricultural and Food Chemistry, 51*(27), 7951–7961.

Somers, T. C., & Evans, M. E. (1977). Spectral evaluation of young red wines: Anthocyanin equilibria, total phenolics, free and molecular SO_2. *Journal of the Science of Food and Agriculture, 28*, 279–287.

Souquet, J.-M., Cheynier, V., Brossaud, F., & Moutounet, M. (1996). Polymeric proanthocyanidins from grape skins. *Phytochemistry, 43*(2), 509–512.

Vidal, S., Courcoux, P., Francis, L., Kwiatkowski, M., Gawel, R., Williams, P., et al. (2004). Use of an experimental design approach for evaluation of key wine components on mouth-feel perception. *Food Quality and Preference, 15*(3), 209–217.

Vidal, S., Francis, L., Guyot, S., Marnet, N., Kwiatkowski, M., Gawel, R., et al. (2003). The mouth-feel properties of grape and apple proanthocyanidins in a wine-like medium. *Journal of the Science of Food and Agriculture, 83*(6), 564–573.

Vidal, S., Williams, P., Doco, T., Moutounet, M., & Pellerin, P. (2003). The polysaccharides of red wine: total fractionation and characterization. *Carbohydrate Polymers, 54*(4), 439–447.

Vidal, S., Williams, P., O'Neill, M. A., & Pellerin, P. (2001). Polysaccharides from grape berry cell walls. Part I: Tissue distribution and structural characterization of the pectic polysaccharides. *Carbohydrate Polymers, 45*, 315–323.

Waters, E. J., Wallace, W., Tate, M. E., & Williams, P. J. (1993). Isolation and partial characterization of a natural haze protective factor from wine. *Journal of Agricultural and Food Chemistry, 41*(5), 724–730.

Wightman, J. D., Price, S. F., Watson, B. T., & Wrolstad, R. E. (1997). Some effects of processing enzymes on anthocynains and phenolics in Pinot noir and Cabernet sauvignon wines. *American Journal of Enology and Viticulture, 48*(1), 39–48.

Food Chemistry 118 (2010) 377–383

Contents lists available at ScienceDirect

Food Chemistry

journal homepage: www.elsevier.com/locate/foodchem

Influence of the refrigeration technique on the colour and phenolic composition of syrah red wines obtained by pre-fermentative cold maceration

F.J. Heredia [a,*], M.L. Escudero-Gilete [a], D. Hernanz [b], B. Gordillo [a], A.J. Meléndez-Martínez [a], I.M. Vicario [a], M.L. González-Miret [a]

[a] Lab. Food Colour and Quality, Dept. Nutrition and Food Science, Faculty of Pharmacy, Universidad de Sevilla, 41012 Sevilla, Spain
[b] Department of Analytical Chemistry, Faculty of Experimental Sciences, Universidad de Huelva, Spain

ARTICLE INFO

Article history:
Received 22 January 2009
Received in revised form 13 March 2009
Accepted 30 April 2009

Keywords:
Colour
Tristimulus colorimetry
Red wine
Syrah
Pre-fermentative cold maceration
Refrigeration techniques

ABSTRACT

The vinification technique called pre-fermentative cold maceration is used to enhance the anthocyans diffusion from the skins to the must, increasing the pigments extraction. For using this technique the application of low temperatures is needed. In this study, two different refrigerating methods (dry ice and cooling of grapes) have been assessed regarding the colour and the phenolic composition of the Syrah wines elaborated by applying pre-fermentative cold maceration. Results showed more intense and stable colours when grapes were previously refrigerated in cold-storage rooms, which showed higher values of chroma and more red-bluish hues. As regards phenolic composition, the cold maceration technique used yields to significant differences among the levels of phenolics, having higher levels of anthocyanins and some non-coloured phenols as flavonols in PR wines. Regarding the colour-composition relationships, it has been highlighted the importance of the co-pigments such as flavonols and cinnamic acids for classify the two groups of samples.

1. Introduction

Colour is one of the main characteristic defining the quality of wines. During the storage the red-bluish colour of young wines changes to red–orange hues and their astringency diminishes. These sensory changes are induced by the transformation of phenolic compounds along the vinification. At the first steps of the winemaking process the wine shows bluish hues and high colour intensity since monomeric anthocyanins are implicated in co-pigmentation reactions. Nevertheless, the co-pigmentation complexes trend to disappear in the next few months of ageing due to the transformation of monomeric anthocyanins into polymeric pigments. This conversion yields to the colour stabilization of wine which shows brownish hues and less intensity colour (Boulton, 2001; Hermosín, Sánchez-Palomo, & Vicario, 2005). Anthocyans are the pigments accounting for the colour of red wines, which are transferred to the wine during the maceration stage. The final colour of the wine depends on the extraction of phenolics from the must, which is determined by factors like the grape variety, as well as length and temperature of skin-contact, among others (Gómez & Heredia, 2004; Gómez-Plaza, Gil-Muñoz, López-Andreu, Martínez, & Fernández-Fernández, 2001).

Syrah has been described as an excellent and robust grape, easy to cultivate and little vulnerable to diseases. It is recommended to monitor the harvests, perform a long fermentation, watch carefully the temperature, and carry out the ageing in oak barrels in order to produce quality wines from this grape (Robinson, 1996). Syrah wines exhibit high acidity, high levels of tannins and colourants, and floral and fruity aroma, with characteristic scent of violet and cassis and smoked touches.

In the last years, a new trend aimed at implementing the production of high quality red wines has been observed, which is being possible thanks to important investments in technology and the application of novel procedures intended to enhance the extraction of grape components responsible for the colour of wine. In this sense, the pre-fermentative cold maceration, also known as cold soaking or cryomaceration, is being increasingly used by enologists worldwide in order to improve some important quality characteristics of wines such as colour and aroma. This technique consists in maintaining the crushed grapes at low temperatures (5–10 °C) for a variable period (from one to several weeks), and thus the beginning of the fermentation process is delayed. During this period the extraction of polyphenols from the skins to the must takes place in the absence of ethanol. Later on, the temperature is raised to 20–25 °C and the fermentation starts in contact with the skins. The removal of the skins is performed a few days later, when the alcoholic fermentation is practically finished.

The cold needed to achieve the required low temperature can be obtained in diverse manners. Some studies have revealed that the effects of the cold maceration over the final quality of the wine are different depending on the cryogenic and the temperature

* Corresponding author. Tel.: +34 954556495; fax: +34 954557017.
E-mail address: heredia@us.es (F.J. Heredia).

0308-8146/$ - see front matter © 2009 Elsevier Ltd. All rights reserved.
doi:10.1016/j.foodchem.2009.04.132

used. In this sense, it is necessary to study comparatively refrigeration techniques employed to achieve the temperatures required for the pre-fermentative cold maceration. The most widely used technique is probably the addition of dry ice (solid carbon dioxide) which induces a thermal shock that cools down the must rapidly and inhibits the polyphenoloxidases enzymes. On the other hand, the saturation caused by the carbon dioxide produced by the sublimation of the dry ice displaces completely the oxygen present in the medium. Therefore, both the aroma compounds and the anthocyanic pigments become protected from oxidative reactions. Likewise, due to the freezing of the grape skins there are cellular breakdowns that favour the release and solubilisation of the pigments (Zamora, 2003, 2004). Other refrigeration method is cooling down (chilling) the grapes which will be used to produce the wine. This method consists in maintaining the grapes in a cold-storage room (below 4 °C) for 24 h prior crushing. In this case, the winery needs special equipments (cold-storage room) which are not habitual, and hence, this is not a usual process for vinification.

To gain insight into the etiology of colour it is necessary to relate the chromatic variables with the chemical compounds that account for it. Thus, there were initiatives where the anthocyanic pigments in solution (Gonnet, 1998, 1999, 2001; Heredia, Francia-Aricha, Rivas-Gonzalo, Vicario, & Santos-Buelga, 1998; Iñarrea, Negueruela, & Echavarri, 1992; Torskangerpoll & Andersen, 2005) or in the wine (Fernández de Simón, Hernández, Cadahía, Dueñas, & Estrella, 2003; Gómez-Cordovés & González-SanJosé, 1995; Gómez-Miguez, González-Manzano, Escribano-Bailon, Heredia, & Santos-Buelga, 2006) were studied.

The knowledge of the effects of the pre-fermentative cold maceration technique on the final quality of the wine is rather empirical; hence it is difficult to find related bibliography, and the scarce reports available are somewhat confusing. For instance, there are reports on the improvement of the colour and the phenolic content of wines through macerations with skins at around 15 °C (Gómez-Plaza, Gil-Muñoz, López-Andreu, & Martínez, 2000). Similarly, there are studies where the cold maceration is followed up with a raise in the temperature of fermentation to produce Syrah wines with higher colour intensity and varietal aromas (Reynolds, Cliff, Girard, & Kopp, 2001) in which authors recommend for this variety the use of temperatures of fermentation close to 30 °C along with a pre-fermentative cold maceration and a prolonged post-fermentative maceration.

The repercussion of the pre-fermentative cold maceration on the final colour and flavour of Syrah wines produced in Andalusia (southwest of Spain) have been already studied (Gómez & Heredia, 2004; Gómez-Míguez, González-Miret, & Heredia, 2007). The results revealed that the extraction of anthocyanins and other phenolic compounds was higher, and darker and less brown wines were obtained when the cold skin-contact process was applied.

Thus, the main objective of this study is to assess the influence of the application of two different refrigeration procedures for developing the pre-fermentative cold maceration on the colour and phenolic composition of Syrah wines. In this sense, the definition of chemical and colorimetric characteristics of the wines produced by pre-fermentative cold maceration, as well as the possible relationships between colour and chemical composition as a function of the technique of production have been assessed.

2. Materials and methods

2.1. Wine samples and vinification process

Six hundred and forty-four samples of musts and wines, corresponding to six different vinifications, were analysed. The wines were elaborated under different cold-maceration conditions, by using two different cooling techniques to achieve low temperatures: direct refrigeration (DR) of the crushed grapes (must and solid parts) by adding carbonic ice (three assays average: 10 days CM at 5–10 °C), and previous refrigeration (PR), that is the refrigeration of the grapes in a cold-storage room at 0° for 24 h prior crushing (three assays average: 10 days CM at 3–8 °C).

All wines were elaborated in triplicate. In order to avoid effects due to other factors different from the refrigeration technique, all the processes involving the winemaking were carried out under the same conditions for all the six assays, as detailed below.

Healthy grapes of *Vitis vinifera* cv. Syrah, grown in southwest Spain, were harvested at optimum maturity (average 13.3° Baumé). Grapes were manually harvested, placed in 20 kg plastic boxes and transported to an experimental wine-production centre. About 1500 kg of grapes per assay were processed. The grapes were destemmed and crushed and then transferred into 1000 l stainless steel tanks. The cold-maceration was carried out controlling the skin contact time (10 days) and temperature (below 10 °C) by using an industrial refrigeration system, consisted of a refrigeration unit (HITSA-TOPAIR, mod RAE-101, Madrid, Spain) for the recirculation of refrigerant liquid (water:glycerol at 2–7 °C) through cooling water jackets to keep low temperatures. The cold-maceration conditions for each assay were those indicated above. After the cold-maceration period was completed, the temperature of the tanks was left to rise up to 20 °C to allow starting the alcoholic fermentation, which was conducted at controlled temperature (21–23 °C). The fermentation caps were punched down once a day for 4 days during this phase. After this, the mash was drawn off to remove the skins and other solid parts, and the free-run musts were left to finish the fermentation under the same conditions. At the end of fermentation, which occurred after 25 days, the wine was racked and stored in 500 l stainless steel tanks.

The treatments were adjusted at the same levels for all the assays: 50 mg/l total sulphur dioxide, 7 g/l total acidity expressed as tartaric acid.

2.2. HPLC–DAD phenols analysis

High performance liquid chromatography was applied for the phenolic content determination by direct injection of the samples, previously filtered through a 0.45 μm Nylon filter, in an Agilent 1100 (Palo Alto, CA), equipped with a quaternary pump, an UV–Vis diode-array detector, an automatic injector, and the ChemStation software. All analyses were made in triplicate.

The *anthocyans* identification was performed following a modification of the method described in Gómez and Heredia (2004). Anthocyanins were separated on a Zorbax C18 column (250 × 4.6 mm, 5 μm particle size) maintained at 38 °C. Water–acetonitrile–formic acid (3:10:87) as solvent A, and water–acetonitrile–formic acid (50:10:40) as solvent B were used. The elution profile was as follows: 0–10 min 94% A–6% B; 10–15 min 70% A–30% B; 15–25 min 60% A–40% B; 25–35 min 55% A–45% B; 35–40 min 50% A–50% B; 40–42 min 40% A–60% B; 42–43 min 94% A–6% B. The flow-rate was 0.8 ml/min and the injection volume was 50 μl. UV–Vis spectra were recorded from 200 to 800 nm with a bandwidth of 2.0 nm. The quantification was made at 525 nm by comparing the areas and the retention times with malvidin 3-glucoside standard. The HPLC determination of the non-coloured phenolics was carried out as described in Hernanz et al. (2007). The wavelengths of detection were 280 nm (benzoic acids and tyrosol), 320 nm (cinnamic acids and their tartaric esters) and 360 nm (flavonols). The external calibration method was used for quantification, by comparing the areas with patrons of gallic, caffeic, *p*-coumaric, *m*-coumaric, protocatechuic, *p*-hydroxybenzoic and ferulic acids, catechin, epicatechin, tyrosol,

Table 1
Mean values and standard deviations of the CIELAB colorimetric parameters, for direct refrigeration (DR) and previous refrigeration (PR) assays. *p*-Values of the ANOVA analysis.

Colorimetric parameter (CIELAB units)	DR (n = 402)	PR (n = 242)	*p*-Values (ANOVA)
Lightness L^*	82.49 ± 4.99	73.50 ± 9.47	0.00
Coordinate a^*	22.21 ± 6.33	28.40 ± 14.36	0.00
Coordinate b^*	−3.66 ± 2.57	−3.59 ± 3.55	0.00
Chroma C^*_{ab}	23.14 ± 7.38	31.96 ± 11.67	0.00
Hue h_{ab}	−7.98 ± 4.74	−9.74 ± 4.85	0.00

Table 2
Mean values and standard deviations of the anthocyanic composition, for direct refrigeration (DR) and previous refrigeration (PR) assays. *p*-Values of the ANOVA analysis.

Anthocyanin *(mg/l)*	DR (n = 402)	PR (n = 242)	*p*-Values (ANOVA)
Delphinidin-3-glucoside	4.30 ± 3.10	8.37 ± 4.04	0.00
Cyanidin-3-glucoside	0.35 ± 1.05	1.45 ± 1.99	0.00
Petunidin-3-glucoside	9.57 ± 3.19	14.86 ± 4.69	0.00
Peonidin-3-glucoside	5.69 ± 6.16	15.20 ± 8.76	0.00
Malvidin-3-glucoside	110.89 ± 19.75	116.28 ± 28.88	0.01
Petunidin-acetate	4.96 ± 1.13	5.06 ± 1.38	0.35
Peonidin-acetate	7.48 ± 2.05	9.03 ± 2.12	0.00
Malvidin-acetate	59.44 ± 15.29	56.37 ± 14.21	0.01
Petunidin-coumarate	2.84 ± 0.83	4.40 ± 1.54	0.00
Peonidin-coumarate	5.46 ± 2.45	8.27 ± 3.00	0.00
Malvidin-coumarate	20.46 ± 12.22	31.83 ± 10.58	0.00
Total anthocyans	231.44 ± 48.29	271.11 ± 65.93	0.00

Table 3
Mean values and standard deviations of the phenolic composition, for direct refrigeration (DR) and previous refrigeration (PR) assays. *p*-Values of the ANOVA analysis.

Phenolic compound (mg/l)	DR (n = 402)	PR (n = 242)	*p*-Values (ANOVA)
Gallic acid	12.65 ± 6.69	9.89 ± 7.54	0.01
Protocatechuic acid	4.05 ± 1.25	3.61 ± 1.03	0.01
p-Hydrobenzoic acid	6.33 ± 5.46	7.63 ± 7.52	0.17
Caffeic acid	2.46 ± 0.83	2.34 ± 0.60	0.23
Caftaric acid	32.21 ± 3.73	28.48 ± 5.32	0.00
Ferulic acid	1.35 ± 0.43	2.90 ± 0.83	0.00
Fertaric acid	1.50 ± 0.13	1.53 ± 0.36	0.40
p-Coutaric acid	6.39 ± 1.25	5.82 ± 1.42	0.00
p-Coumaric 1 derivatives	2.07 ± 0.62	3.12 ± 0.92	0.00
p-Coumaric 2 derivatives	1.45 ± 0.37	1.86 ± 0.46	0.00
p-Coumaric 3 derivatives	0.98 ± 0.34	0.74 ± 0.19	0.00
p-Coumaric 4 derivatives	0.89 ± 0.16	1.46 ± 0.37	0.00
Ethyl *p*-coumarate	0.78 ± 0.23	0.87 ± 0.26	0.01
m-Coutaric acid	3.04 ± 0.58	6.02 ± 1.07	0.00
Catechin	65.91 ± 18.89	55.03 ± 19.67	0.00
Epicatechin	106.15 ± 26.08	76.14 ± 24.36	0.00
Quercetin 1 derivatives	11.76 ± 4.04	16.27 ± 4.60	0.00
Quercetin 2 derivatives	7.17 ± 1.83	12.70 ± 3.45	0.00
Quercetin-3-rutinoside	13.10 ± 4.19	23.40 ± 13.96	0.00
Quercetin-3-D-galactoside	3.57 ± 1.04	7.31 ± 2.19	0.00
Quercetin 3 derivatives	6.06 ± 1.54	12.87 ± 2.85	0.00
Quercetin 4 derivatives	4.50 ± 1.49	9.16 ± 2.46	0.00
Kaempherol	3.04 ± 4.64	27.56 ± 22.69	0.00
Tyrosol	16.36 ± 15.90	39.06 ± 37.89	0.00
Total benzoic derivatives	23.04 ± 3.92	21.13 ± 4.78	0.00
Total *p*-coumaric derivatives	12.48 ± 2.19	13.87 ± 2.15	0.00
Total hydroxycinnamic derivatives	53.04 ± 4.91	55.14 ± 7.08	0.02
Total phenolic acids	76.08 ± 6.95	76.28 ± 8.82	0.86
Total flavonols	221.28 ± 51.25	240.44 ± 67.39	0.02
Total non-coloured phenolics	297.36 ± 55.71	316.71 ± 69.51	0.03
Total phenolics (Folin Ciocalteau)	1288.33 ± 421.53	2841.57 ± 1012.74	0.00

rutin, quercetin, kaempherol and quercetin-3-D-galactoside. For the identification of quercetin derivatives and the tartaric esters of the cinnamic acids their spectra were comparing to those from quercetin and the corresponding free acids, respectively.

2.3. Spectrophotometric colour measurement

Spectrophotometric measurement of the visible absorption spectrum (380–770 nm) at constant intervals ($\Delta\lambda$ = 2 nm) was made, using distiled water as reference. The spectra were integrated by the CromaLab® software (Heredia, Álvarez, González-Miret, & Ramírez, 2004), which takes into consideration the Commission Internationale de l'Éclairage (CIE) recommendations

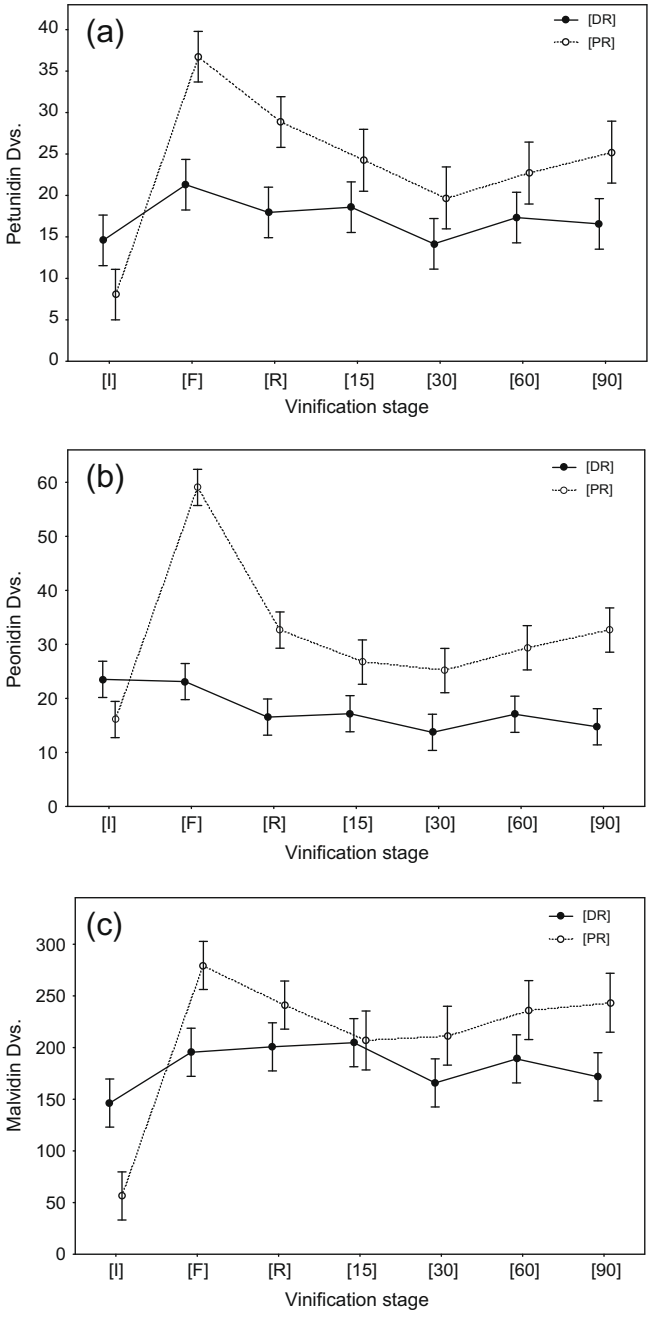

Fig. 1. Evolution of the major anthocyanidins occurring in the wine. (a) Petunidin derivatives, (b) peonidin derivatives, (c) malvidin derivatives.

(CIE, 2004). The colour coordinates of the uniform space CIE 1976-($L^*a^*b^*$) (CIELAB) were obtained considering the 10° Standard Observer and the Standard Illuminant D65 (Wyszecki & Stiles, 1982).

2.4. Statistical analysis

Analysis of variance (ANOVA/MANOVA), Principal Components Analysis (PA), and Stepwise Discriminant Analysis were applied in order to evaluate whether significant differences among the samples exist as well as to select the variable that most influence the differences between them. For the statistical treatment of the data the Statistica v.6.0 software (StatSoft Inc., 2001) was used.

3. Results and discussion

The colour of Syrah wines obtained by the application of different procedures of pre-fermentative cold maceration was objectively evaluated by tristimulus colorimetry. An exhaustive follow-up of the winemaking process allows us to acquire valuable information on the changes in pigments and colour of the wines.

The assessment of the changes in the levels of the pigments occurring along different stages is decisive to establish the points at which the different techniques have a greater impact in the quality of the wines. In this sense, the following stages were considered in the study: the initial point or grape crushing [I], the beginning of the fermentation [F], the skin removal [R], and 15, 30, 60 and 90 days after the removal of the skins. The mean values and the standard deviations of the colorimetric parameters, as well as the anthocyanic and phenolic composition for each type of chilling process are shown in Tables 1–3, respectively.

Regarding the colour, it can be observed that the chroma C^*_{ab} was higher in the wines obtained with previous refrigeration of the grapes and their lightness L^* was lower (darker wines). According to these results, higher anthocyanic and other phenolics contents were found in PR wines than in DR ones. Moreover, the analysis of variance (ANOVA) revealed significant differences among the levels of all the 3-glucoside anthocyanins as a function of the cold-maceration technique used, with high levels of significance in most of cases: $p < 0.001$ for delphinidin (Dp3g), cyanidin (Cy3g), petunidin (Pt3g) and peonidin (Pn3g); $p < 0.05$ for malvidin (Mv3g).

The evolutions of the compounds grouped by the anthocyanidin and the substituent were studied. When the major anthocyans

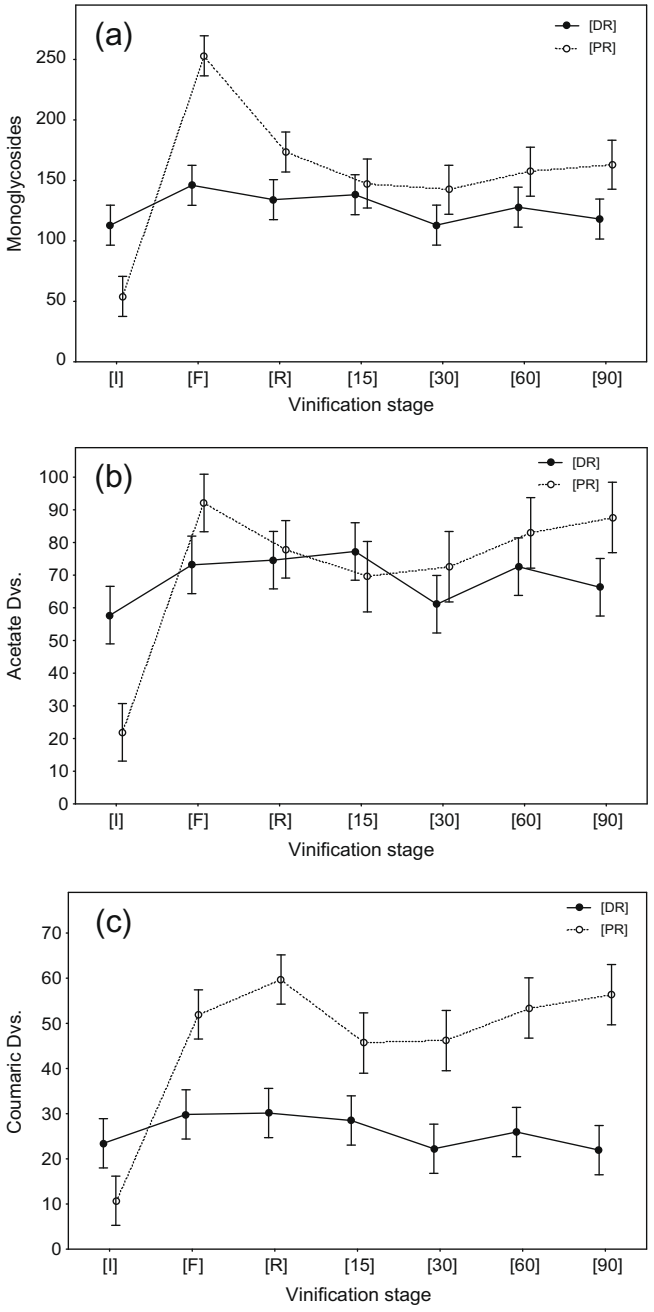

Fig. 2. Changes in the main anthocyanin groups. (a) Monoglycosides, (b) acetate derivatives, (c) coumaric derivatives.

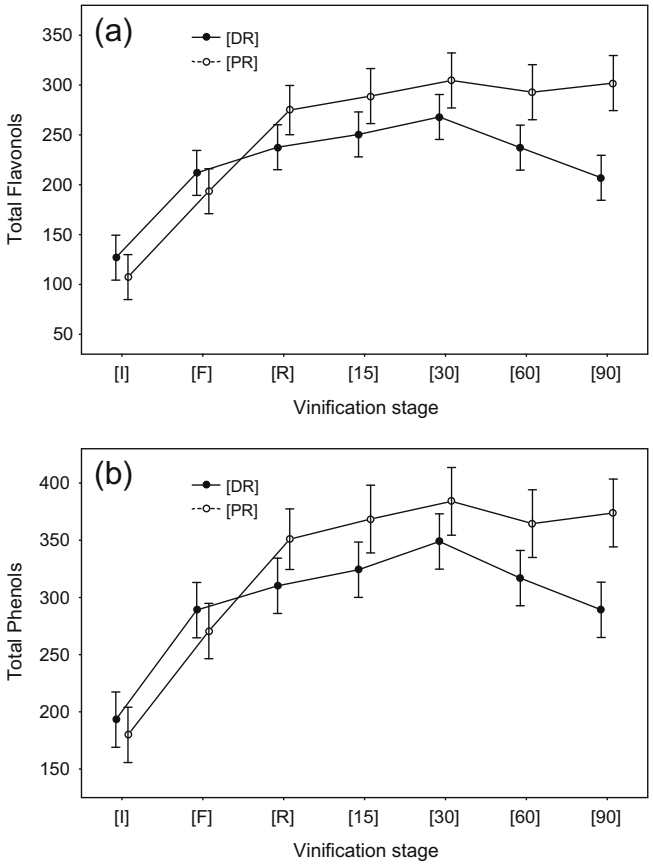

Fig. 3. Changes in phenolic composition along the vinification process, for each assay. (a) Total flavonols, (b) total phenols.

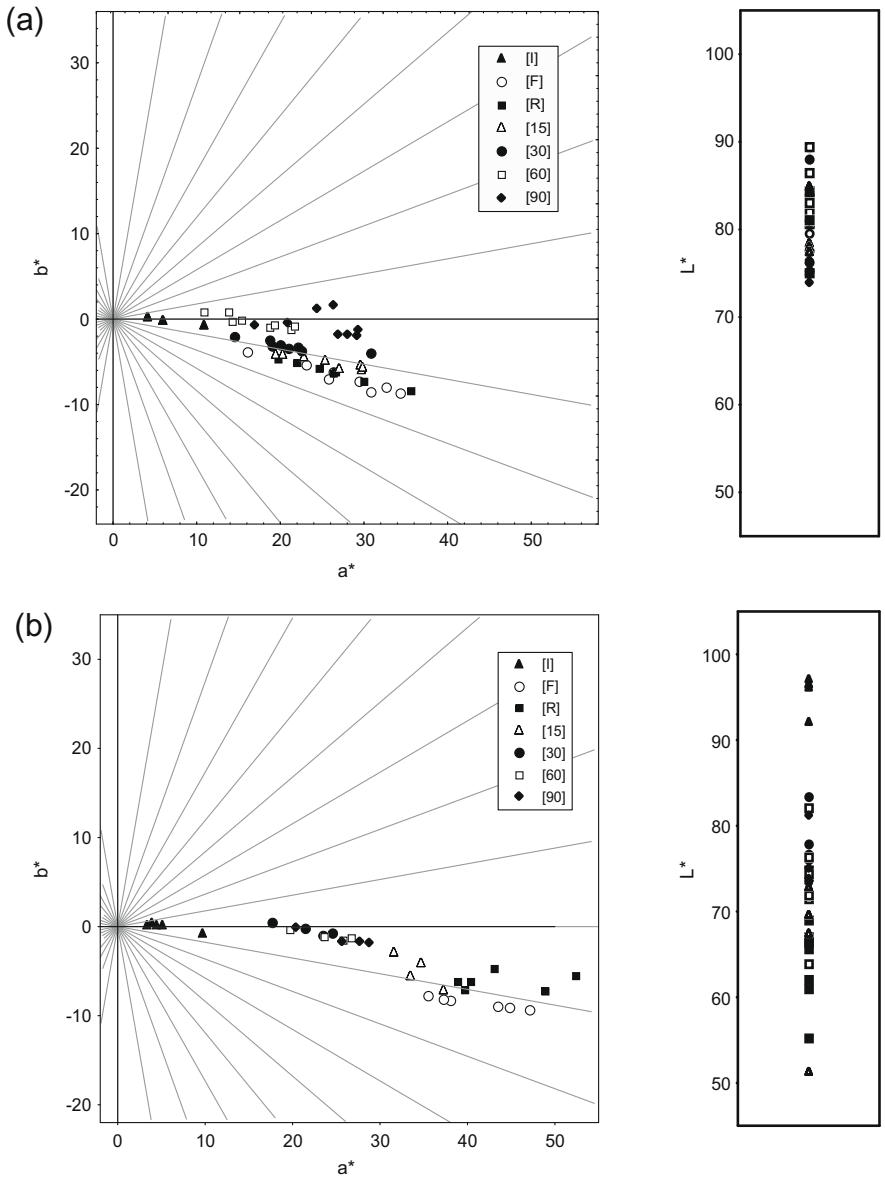

Fig. 4. CIELAB colour space (a^*b^*)-plane and lightness (L^*) for (a) direct refrigeration and (b) previous refrigeration assays.

were grouped by the anthocyanidin (Fig. 1) a very higher increase of the concentration along the cold-skin maceration was observed in all cases for the wines produced with previous refrigeration (PR). During the fermentation stage, these levels diminished, although they were always above those corresponding to the wines obtained by direct refrigeration (DR), especially for peonidin derivatives. DR wines showed a certain trend to diminish the levels of the anthocyanins and its derivatives, whilst the PR wines showed a slight ascending trend.

In general, the assays corresponding to the PR technique led to higher levels of each individual monoglycoside. It is worth stressing the changes in Mv3g, the major monoglycoside by far. Thus, it was noticed that the levels reached in both cases were similar, although in the case of the direct application of cold (DR) the appearance of the maximum levels holds back up to the removal of the skins, which denotes a slower extraction when dry ice is employed.

Considering the evolution of the groups of anthocyans, regarding the substituent (Fig. 2), it is observed that the changes in the levels of monoglycosides (Fig. 2a) were much similar (except for the cryomaceration stage, where higher levels were obtained for PR wines), although some differences and maybe a higher stability was perceived in the PR wines. The changes in the levels of acetate derivatives of the anthocyans (Fig. 2b) were different and were clearer in the case of the coumarates (Fig. 2c), being their levels always higher when the previous refrigeration is used.

It could be expected that the use of carbonic ice (DR) affects the extraction of chemical components due to the breakage of the grape skins occurring during the freezing. Nevertheless, the PR wines showed higher levels (Tables 2 and 3) of anthocyanins and most of non-coloured phenols than the DR wines. It could be due to the local effect of the ice just in the mass being directly in contact with the carbonic ice, and so the increase of the extraction due to the effect of freezing is not in the whole mass. Moreover, this effect leads to more unspecific extractions which can induce reactions involving anthocyanins, yielding to less colour wines.

Considering the non-coloured phenolics, the flavonoids encompass different compounds such as the flavonols, which exhibit a great capacity to stabilize the colour of anthocyans by co-pigmentation phenomena (Gómez-Miguez et al., 2006). Differences

between the two methodologies were observed, having higher levels in the samples from previously refrigerated grapes (PR), as observed in Fig. 3a (total flavonols), and b (total phenols).

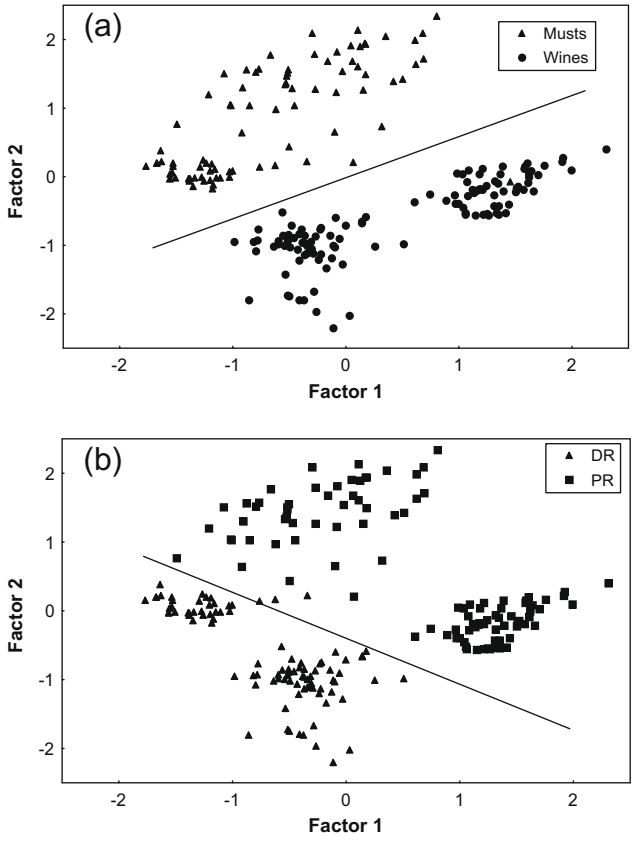

Fig. 5. Principal Components Analysis results based on the phenolic composition, regarding (a) the vinification stage, (b) the chilling process.

Table 4
Principal Components Analysis results.

	Factor 1	Factor 2
Gallic acid	0.554	−0.664
Protocatechuic acid	−0.124	−0.350
p-Hydroxybenzoic acid	−0.526	**0.722**
Caffeic acid	0.255	−0.412
Caftaric acid	−0.390	0.031
Ferulic acid	0.786	0.327
Fertaric acid	−0.435	0.460
p-coutaric acid	0.133	−0.362
p-coumaric 1 drv.	**0.937**	−0.150
p-coumaric 2 drv.	**0.860**	−0.234
p-coumaric 3 drv.	0.057	−0.679
p-coumaric 4 drv.	0.608	0.484
Ethyl *p*-coumarate	0.325	−0.048
m-coutaric acid	**0.786**	0.480
Catechin	0.448	−0.618
Epicatechin	0.219	−0.690
Quercetin-3-rutinoside	0.339	0.477
Quercetin-3-galactoside	0.545	0.108
Quercetin 1 drv.	**0.822**	0.096
Quercetin 2 drv.	0.648	0.585
Quercetin 3 drv.	**0.781**	0.470
Quercetin 4 drv.	**0.923**	0.202
Kaempherol	**0.827**	0.035
Tyrosol	**0.782**	−0.377
Variance	8.868	4.565
Total	0.370	0.190

Bold letter means significant value ($p < 0.05$).

The definition of the colour by tristimulus colorimetry enables to establish objectively the chromatic characteristics of the wines and, above all, their variability. The colour points represented in the (a^*b^*)-colour diagram as well as their lightness are shown in Fig. 4a (DR wines) and b (PR wines). It can be noticed that practically all of samples are located in the fourth quadrant (positive a^*, negative b^*) of the (a^*b^*)-plane, corresponding to the purple or red-bluish colours region. The (a^*b^*)-colour diagram allows one to observe a clear trend in the evolution of colour. In general for both chilling techniques, during the pre-fermentative cold maceration a net rise in the chroma C^*_{ab} together to a decrease in the lightness L^* is observed, whilst the hue h_{ab} remains virtually constant. Along the active maceration (simultaneous to the alcoholic fermentation) and during the first stage after the removal of the skins slight changes in hue are noticed, although the values of chroma lie high. As the vinification proceeds, a reduction in the levels of chroma is observed, along with increase of hue towards 0°, i.e., towards the net red. Considering separately both techniques, after the pre-fermentative cold maceration the PR wines reached higher levels of chroma C^*_{ab} than the DR wines (48.1 and 35.4 CIELAB units, respectively), and lower lightness L^* values (63% and 76%, respectively). Comparing the final wines (after 90 days of stabilization) the PR wines kept the purple hues (nega-

Table 5
Coefficients of the classification functions obtained by SDA, considering the anthocyanic composition of the wines.

Anthocyans	DR	PR
Pt-3 g	−0.16	0.18
Mv_ac	−0.17	−0.42
Pt_cm	−2.77	−0.11
Pn-3 g	0.20	0.35
Pn_cm	0.05	0.27
Pn_ac	1.76	2.38
Dp-3 g	−0.67	−1.06
Pt_ac	1.03	0.18
Cy-3 g	0.38	0.89
Mv-3 g	0.29	0.31
Constant	−15.08	−19.49
	Correct classification (%)	
Direct refrigeration (DR)	94.94	
Previous refrigeration (PR)	89.78	
Total	93.08	

Table 6
Coefficients of the classification functions obtained by SDA, considering the non-coloured phenolic composition of the wines.

	DR	PR
m-Coutaric acid	−2.46	3.90
Epicatechin	0.20	0.06
Quercetin 4 derivatives	−1.44	3.47
Caffeic acid	8.49	3.57
Ferulic acid	−3.96	3.11
Caftaric acid	2.05	0.52
Quercetin-3-galactoside	3.53	0.83
Quercetin 3 derivatives	−0.99	0.58
Quercetin 1 derivatives	−0.02	−0.66
Catechin	0.07	−0.18
p-Coumaric 4 derivatives	1.24	12.04
p-Coutaric acid	0.25	2.55
Quercetin 2 derivatives	−0.16	−1.12
p-Hydroxybenzoic acid	0.53	0.98
Constant	−53.10	−56.04
	Correct classification (%)	
Direct refrigeration (DR)	100	
Previous refrigeration (PR)	100	
Total	100	

tive h_{ab} values) while some DR wines changed towards higher hue values.

The capability of different groups of variables for discriminating between types of wines (regarding the refrigeration technique) has been studied, highlighting the repercussion on the most relevant chemical components over the colour that is pigments and co-pigments.

The inclusion of the chemical information yielded by the non-coloured phenols on the PCA model allows us to reach very good discriminations, both between musts and wines, as expected (Fig. 5a), as well as between chilling technique (Fig. 5b), which makes possible to state conclusions about the colour stabilization by co-pigmentation reactions. In the second case (regarding the technology), the differentiations is mainly due to the Factor 1, which includes different phenolics considered good co-pigments as cinnamic acids and specially several flavonols (Table 4). Since the PCA is a non-conditioned technique, the results are of great enological value because they demonstrate the advantages of the pre-refrigeration of the grapes over the direct refrigeration for achieving a better colour stabilization in red wines by means of co-pigmentation.

On the other hand, Stepwise Discriminant Analysis (SDA) is a conditioned technique, so the groups of samples are previously defined. Its objective is to find a model which better classify the samples into their corresponding group based on the information given by the variables included in the study or to find the variables which better classify the samples. In this study, these variables are those phenolics presenting the major influence on the differences marked by the refrigeration technique used for the pre-fermentative cold maceration. The classification functions obtained showed that it is necessary to include almost all the anthocyans for reaching a good discrimination (up to 95%, Table 5). Nevertheless, 100% of cases correctly classified is achieved by including only fourteen phenolics (Table 6), most of them flavonols and cinamic acids, which are considered as good co-pigments.

4. Conclusions

It can be concluded that regarding the cooling technique used for reaching the low temperatures needed for the pre-fermentative cold maceration process the refrigeration of the grapes before crushing leads to wines with higher concentrations of anthocyanins as well as other phenolics than those wines obtained by using dry ice. Furthermore, higher values of chroma and red-bluish hues are shown in these wines. Thus, the technique used for obtaining the low temperature influences the final chemical composition of the wine, especially regarding the phenolic compounds having high co-pigmentation power, which are of great interest on the stability of the colour of wines submitted to aging process.

Acknowledgments

Authors are indebted to Ministerio de Ciencia y Tecnología (Government of Spain) for the financial support (AGL2003-02972 Research Project) as well as to Vinícola del Condado Winery (Huelva, Spain) for supplying grapes and wine samples.

References

Boulton, R. (2001). *American Journal of Enology Viticulture, 52*(2), 67–87.
CIE (2004). *Colorimetry*. Viena, Austria: Technical Report CIE 15.2, 3 ed.
Fernández de Simón, B., Hernández, T., Cadahía, E., Dueñas, M., & Estrella, I. (2003). *European Food Research and Technology, 216*, 150–156.
Gómez, M., & Heredia, F. J. (2004). *Journal of Agricultural and Food Chemistry, 52*, 5117–5123.
Gómez-Cordovés, C., & González-SanJosé, M. L. (1995). *Journal of Agricultural and Food Chemistry, 43*, 557–561.
Gómez-Miguez, M., González-Manzano, S., Escribano-Bailon, M. T., Heredia, F. J., & Santos-Buelga, C. (2006). *Journal of Agricultural and Food Chemistry, 54*, 5422–5429.
Gómez-Míguez, M., González-Miret, M. L., & Heredia, F. J. (2007). *Journal of Agricultural and Food Chemistry, 79*, 271–278.
Gómez-Plaza, E., Gil-Muñoz, R., López-Andreu, F. J., Martínez, A., & Fernández-Fernández, J. I. (2001). *American Journal of Enology Viticulture, 52*, 266–270.
Gómez-Plaza, E., Gil-Muñoz, R., López-Andreu, F. J., & Martínez, A. (2000). *Journal of Agricultural and Food Chemistry, 48*, 736–741.
Gonnet, J. F. (1998). *Food Chemistry, 63*, 409–415.
Gonnet, J. F. (1999). *Food Chemistry, 66*, 387–394.
Gonnet, J. F. (2001). *Food Chemistry, 75*, 473–485.
Heredia, F. J., Álvarez, C, González-Miret, M. L., & Ramírez, A. (2004). *CromaLab®*. Sevilla, España: Registro General de la Propiedad Intelectual SE-1052-04.
Heredia, F. J., Francia-Aricha, E. M., Rivas-Gonzalo, J. C., Vicario, I. M., & Santos-Buelga, C. (1998). *Food Chemistry, 63*, 491–498.
Hermosín, I., Sánchez-Palomo, E., & Vicario, A. (2005). *Food Chemistry, 92*, 269–283.
Hernanz, D., Recamales, A. F., González-Miret, M. L., Gómez-Míguez, J., Vicario, I. M., & Heredia, F. J. (2007). *Journal of Food Engineering, 80*, 327–335.
Iñarrea, M., Negueruela, A. I., & Echavarri, J. F. (1992). *Óptica Pura y Aplicada, 25*, 93–107.
Reynolds, A., Cliff, M., Girard, B., & Kopp, T. G. (2001). *American Journal of Enology Viticulture, 52*, 235–240.
Robinson, J. (1996). *Guide to wine grapes*. Oxford: Oxford University Press.
StatSoft Inc. (2001). *STATISTICA (data analysis software system)*. version 6. <www.statsoft.com>.
Torskangerpoll, K., & Andersen, O. M. (2005). *Food Chemistry, 89*, 427–440.
Wyszecki, G., & Stiles, W. S. (1982). *Color science. Concepts and methods. Quantitative data and formulae* (2nd ed.). New York: John Wiley and Sons, Inc.
Zamora, F. (2003). *Elaboración y crianza del vino tinto. Aspectos científicos y prácticos*, AMV ed. Madrid: Editorial Mundi-Prensa.
Zamora, F. (2004). *Enólogos, 32*, 36–39.

Food Chemistry 118 (2010) 384–390

Contents lists available at ScienceDirect

Food Chemistry

journal homepage: www.elsevier.com/locate/foodchem

Rapid Communication

Effect of photoperiod on flavonoid pathway activity in sweet potato (*Ipomoea batatas* (L.) Lam.) leaves

Isabel S. Carvalho [a,*], Teresa Cavaco [a], Lara M. Carvalho [b], Paula Duque [b]

[a] IBB-Institute for Biotechnology and Bioengineering, FCT-Faculdade de Ciências e Tecnologia, University of Algarve, Campus de Gambelas, 8005-139 Faro, Portugal
[b] Instituto Gulbenkian de Ciência, Rua da Quinta Grande, 6, 2780-156 Oeiras, Portugal

ARTICLE INFO

Article history:
Received 14 November 2008
Received in revised form 31 March 2009
Accepted 5 May 2009

Keywords:
Anthocyanins
Catechins
Flavonoid pathway
Flavonols
HPLC
Hydroxycinnamic acids
Hydroxybenzoic acids
Photoperiod
RT-PCR, sweet potato
Gene expression

ABSTRACT

Compared with those of major commercial leafy vegetables, leaves of sweet potato have higher contents of flavonoids and phenolic acids, which provide significant health benefits and may be used as natural colourants. We have analysed the expression of key flavonoid biosynthesis genes using RT-PCR and the accumulation of polyphenolic compounds using high-performance liquid chromatography coupled to a photodiode-array detector, during the development of leaves of sweet potato plants growing under either long day or short day photoperiods. A massive induction of flavonoid pathway gene expression, correlating with a dramatic increase in the content of an anthocyanin, catechins, flavonols, hydroxycinnamic acids and hydroxybenzoic acids, was observed during sweet potato leaf exposure to a long day photoperiod. These results provide further support for the protective role of flavonoids and phenolic acids against enhanced light exposure in plants.

1. Introduction

In recent years, there has been a global trend toward the use of natural phytochemicals present in natural resources—such as vegetables, fruits, oilseeds and herbs—as antioxidants and functional ingredients (Elliott, 1999; Kaur & Kapoor, 2001; Larson, 1988; Namiki, 1990). Sweet potato (*Ipomoea batatas* (L.) Lam.) ranks as the world's seventh most important crop. It is more tolerant to diseases, pests and high moisture than are many other leafy vegetables grown in the tropics or the Mediterranean region. As a crop, sweet potato is used both for food and as an industrial source of starch (Mano, Ogasawara, Sato, Higo, & Minobe, 2007), but its leaves have been largely neglected, except for occasional use as livestock feed.

Polyphenolic compounds are a large group of secondary metabolites widely distributed in plants, which can be divided into two major subgroups: flavonoids and phenolic acids. Flavonoids, perhaps the most important single group of phenolics in foods, comprise a group of over 4000 aromatic plant compounds, which include anthocyanins, proanthocyanidins, flavonols and catechins. Phenolic acids, on the other hand, include hydroxycinnamic acids (*e.g.* caffeic or ferulic acid conjugates, sinapic acid) and hydroxybenzoic acids (*e.g.* benzoic, gentisic or *p*-anisic acids) (Li et al., 2007).

Recent experimental work has revealed that, compared with major commercial leafy vegetables, such as brassicas and lettuce, sweet potato leaves have higher contents of flavonoids, mainly anthocyanins, and phenolic acids (Kaur & Kapoor, 2001), which have significant medicinal value for certain human diseases and may also be used as natural food colourants. These polyphenolics show various kinds of physiological functions—such as radical-scavenging, anti-mutagenic, anti-diabetes and anti-bacterial activities *in vitro* or *in vivo*—which may be important in maintaining and promoting human health (Mazza, Pomponi, Janiri, Bria, & Mazza, 2007).

Flavonoids fulfill many plant functions, including the production of yellow, red or blue pigmentation. Different flavonoid subclasses have been found to play protective roles in plant tissues and the biosynthesis of flavonoids often increases in response to external stress factors, such as drought, cold temperatures, wounding or excess UV light (Chalker-Scott, 1999; Winkel-Shirley, 2002). Indeed, in addition to coloured anthocyanin pigments, other

* Corresponding author. Tel.: +351 289800040; fax: +351 289811419.
E-mail address: icarva@ualg.pt (I.S. Carvalho).

0308-8146/$ - see front matter © 2009 Elsevier Ltd. All rights reserved.
doi:10.1016/j.foodchem.2009.05.005

flavonoids and phenolic acids, especially sinapate esters and other hydroxylated or methoxylated cinnamic acid derivatives, have been found to play a role in photoprotection. These compounds accumulate mainly in the epidermal cells of plant tissues after light stress induction (Landry, Chapple, & Last, 1995; Winkel-Shirley, 2001). Flavonoids are synthesized via the general phenylpropanoid pathway, with the key steps of the main flavonoid pathway being well known (for review, see Holton & Cornish, 1995; Weisshaar & Jenkins, 1998; Winkel-Shirley, 2001).

The aim of the present study was to analyse the expression of key flavonoid pathway genes—chalcone synthase (*CHS*), chalcone flavanone isomerase (*CHI*), flavanone 3-hydroxylase (*F3H*), dihydroflavonol 4-reductase (*DFR*) and UDP-glucose flavonoid 3-O-glucosyl transferase (*UFGT*)—and the qualitative and quantitative composition of polyphenolic compounds in leaves of sweet potato plants exposed to long day (16 h light) or short day (8 h light) photoperiods. Flavonoids (anthocyanins, catechins and flavonols), as well as hydroxycinnamic and hydroxybenzoic acids, were identified and quantified in sweet potato leaves by high-performance liquid chromatography (HPLC), coupled to a photodiode-array detector. Results show induction of gene expression, indicating activation of the flavonoid pathway, and higher content of flavonoids and phenolic acids in leaves exposed to a long day photoperiod, suggesting a role for these compounds in the protection against enhanced light exposure in sweet potato plants. The study of plant polyphenolic compounds is an important scientific agenda for food and nutritional sciences, which may contribute to the improvement of conventional foods with added health benefits.

2. Materials and methods

2.1. Plant material

Sweet potato (*I. batatas* (L.) Lam.) was planted in sandy soil in 1 l pots with a layer of gravel at the bottom. Six replicate pots per cultivar were used, with one plant per pot. Plants were grown for 30 days under photosynthetic active radiation (PAR 400–700 nm) at 150 μmol m^{-2} s^{-1} and 22 °C, under either long day (16 h photoperiod) or short day (8 h photoperiod) conditions. Leaves of sweet potato plants were harvested at day 10 and day 30 from the two different photoperiod conditions, immediately frozen in liquid nitrogen and stored at −80 °C until used.

2.2. RT-PCR analysis of flavonoid pathway genes

Total plant RNA was extracted from plant material stored at −80 °C using the Tri-Reagent (Sigma–Aldrich) according to the manufacturer's instructions. The integrity of the isolated RNA was verified in a 1% (w/v) ethidium bromide-stained agarose gel, being judged by the sharpness of ribosomal RNA bands. No degradation was detected in any of the samples tested. Total RNA concentration and quality were determined spectrophotometrically by absorbance at 280 nm (A_{280}), 260 nm (A_{260}) and 230 nm (A_{230}) with a NanoDrop (UV-160A, Shimadzu, Kyoto, Japan). In all tested samples, the A_{260}/A_{230} ratios were greater than 1.8, indicating that only weak contamination by polysaccharide or polyphenol occurred. The A_{260}/A_{280} ratios ranged between 1.6 and 2, indicating little or no protein contamination.

cDNA was synthesized using the Superscript III First-Strand Synthesis System (Invitrogen). Transcriptional analysis of five key genes from the flavonoid pathway, encoding chalcone synthase (*CHS*), chalcone flavanone isomerase (*CHI*), flavanone 3-hydroxylase (*F3H*), dihydroflavonol 4-reductase (*DFR*) and UDP-glucose flavonoid 3-O-glucosyl transferase (*UFGT*), as well as of the housekeeping 18*S* ribosomal RNA gene, used as a loading control, was performed by semi-quantitative PCR using *Taq* DNA Polymerase with ThermoPol Buffer (Biolabs, New England) and the following gene-specific primer sets: 5′-TTCCGTGAAGCGCCTCATGATGTA-3′ and 5′-ACTTGTCCTCCACTTGGTCCAGAA-3′ (*CHS*), 5′-TCCCTT-TG AGAAGCTGACACGGAT-3′ and 5′-0TCCGACAGCGGCTTGTTCTCTAT T-3′ (*CHI*), 5′-ACGGCCACTTTCTGAGTAATGGGA-3′ and 5′-TACGATT TGCTGCTGCTCCTTTGC-3′ (*F3H*), 5′-AGCTTTGATGAAGCCAT-TGCA GGG-3′ and 5′-TCGCAGAGATCATCCAGATGCACA-3′ (*DFR*), 5′-ACCC ACGAGGAGTTCATCATG-3′ and 5′-AAGCAGGTGCACTAATT-CTTGG AA-3′ (*UFGT*), and 5′-CTGCCAGTAGTCATATGCTTGTC-3′ and 5′-GT GTAGCGCGCTGCGGCCC-3′ (18*S* ribosomal RNA gene). The correct PCR products were obtained with all primer sets when amplifying genomic DNA.

For all genes, the following PCR conditions were used: initial denaturation was performed at 94 °C for 2 min, followed by 25 cycles at 94 °C for 30 s, 55 °C for 45 s and 72 °C for 1 min. The final extension was performed at 72 °C for 10 min. PCR products were resolved by electrophoresis in 1% (w/v) ethidium bromide-stained agarose gels.

2.3. Preparation of sweet potato extracts

Leaves of sweet potato (0.3 g) were homogenised at room temperature with 3 ml of methanol (Merck) in a rotary mixer (Edmund Buhler Gmg H-Ks 15, Germany) at 45 °C angle and 220 rpm for 24 h and the mixture was then centrifuged at 1600*g* for 10 min. The supernatant was filtered though Whatman no. 4 filter paper and kept at 4 °C before analysis. The resulting extracts were used for different experimental analyses.

2.4. Colour analyses

A direct measurement of absorbance at 420, 520, and 620 nm in methanolic extracts was carried out using an Ultrospec 1100 pro-UV/visible spectrophotometer (GE Healthcare Life Sciences, England). The following variables were calculated: colour intensity (CI) as the sum of 420, 520, and 620 nm absorbances; proportions of yellow (Ye%), red (Rd%) and blue colour (Bl%) were calculated by dividing the absorbances at 420, 520 and 620 nm by the colour intensity (CI), respectively (Kelebek, Canbas, & Selli, 2008).

2.5. Determination of chlorophylls a and b

A direct measurement of absorbance at 652, 665, and 750 nm in methanolic extracts was carried out using an Ultrospec 1100 pro-UV/visible spectrophotometer (GE Healthcare Life Sciences, England). The following variables were calculated (in mg l^{-1}): Chl a = $(16.29 \times OD_{665}) - (8.54 \times OD_{652})$ and Chl b = $(30.66 \times OD_{652}) - (13.58 \times OD_{665})$. Each OD value was corrected for the absorbance at 750 nm (*e.g.* $OD_{665} = A_{665} - A_{750}$) (Porra, Thompson, & Kriedemann, 1989).

2.6. Determination of total phenolic compounds

Each methanol extract (0.2 ml) was mixed with 1.0 ml of Folin–Ciocalteau's reagent and 0.8 ml of saturated sodium carbonate solution (7.5%). After a 30 min incubation at room temperature, the absorbance was read at 765 nm against a blank in an Ultrospec 1100 pro-UV/visible spectrophotometer (GE Healthcare Life Sciences, England). A linear calibration curve of gallic acid, in the range 20–500 μg ml^{-1} with an r^2 value of 0.999, was constructed (data not shown), and the total phenolic content was expressed as gallic acid equivalents (GAE) in g/100 g of fresh material (Huang, Chang, & Shao, 2006).

2.7. Quantification of flavonoids and phenolic acids

Methanol extracts were filtered through a 0.45 μm filter. HPLC analyses of flavonoids and phenolic acids were conducted with a Dionex liquid chromatograph (USA) equipped with a model P580 solvent pump (USA), a ASI-100 autosampler (USA), a PDA-100 photodiode-array detector (USA) and Dionex Software. A Lochrospher 100 RP-18, with a reversed-phase column (25 cm × 4 mm, 5 μm; Merck, Darmstadt, Germany), was used throughout this study. Phenolic acids and flavonoids were detected at 280 and 360 nm, with the exception of anthocyanins, which were detected at 510 nm. The mobile phase was 5% formic acid and methanol in a linear gradient starting at 15% and reaching 35% in 15 min (then isocratic until 20 min), at a flow rate of 1 ml/min and an injection volume of 20 μl. Phenolic compounds were identified by comparison of their retention times with those of pure standards and quantified individually, based on standard curves of each flavonoid or phenolic acid type. Quantitation was performed with the linear calibration curves of standard compounds according to Jaakola, Määttä, Pirttilä, Törrönen, and Kärenlampi (2002) and Jaakola, Määttä-Riihinen, Kärenlampi, and Hohtola (2004).

2.8. Expression of data and statistical analysis

All data presented are means ± standard deviations. Significant differences between means ($p < 0.05$) were estimated by Student's *t*-tests using SPSS 16.0.

3. Results

3.1. Colour parameters and chlorophyll and total phenolic contents

While growing sweet potato plants in either short day or long day photoperiods, striking differences were observed between leaves of plants grown for 30 days under these two light conditions (Fig. 1). Leaves of plants growing under a long day photoperiod (16 h light/8 h dark) were slightly larger, with both the blade and the petiole displaying a reddish colour not evident in leaves growing under a short day photoperiod (8 h light/16 h dark). This prompted us to examine colour parameters, as well as the total phenolic and chlorophyll contents of sweet potato leaves exposed to the two light regimes.

Colour parameters were analysed by direct measurement of absorbance at 420, 520 and 620 nm in methanolic extracts. Results presented in Table 1 indicate higher colour intensity (CI) in leaves growing under a long day photoperiod when compared with leaves growing under a short day photoperiod. In particular, enhanced red colour in leaves that were exposed to long day, when compared with leaves exposed to short day conditions was observed. By contrast, yellow colour was reduced in leaves exposed to a long day photoperiod when compared with leaves exposed to a short day photoperiod. No differences in blue colour were observed between leaves exposed to the two different photoperiods, indicating a preponderant role for red and yellow colours in leaves under long and short day conditions, respectively (Table 1). Leaf colour was therefore clearly affected by the photoperiod regime in sweet potato.

Chlorophyll a and b contents were determined by direct measurements of absorbance at 652, 665 and 750 nm in methanolic extracts. Experimental results obtained show that the photoperiod had no effect on leaf chlorophyll content, but an overall reduction of approximately 63% (averages of 0.24–0.09 mg/100 g fw) in chlorophyll a and 61% (averages of 0.23–0.09 mg/100 g fw) in chlorophyll b contents was observed between days 10 and 30 of light exposure (Table 1). The reduction in chlorophyll content has a negative effect on plant photosynthetic efficiency, as the latter is dependent on the light harvesting properties of the chlorophylls (Demmig-Adams & Adams, 1992). Our results show that both chlorophylls decrease with time under both light treatments (Table 1).

Total phenolic content was estimated by the Folin–Ciocalteau colourimetric method, based on the procedure of Taga, Miller, and Pratt (1984), using gallic acid as a standard phenolic compound. As shown in Table 1, there is a large variation in the total phenolic content of the plant material analysed, ranging from 4.94 to 25.0 g GAE/100 g fresh weight for leaves exposed for 10 days to short day and 30 days to long day conditions, respectively. Higher amounts of total phenolic compounds were obtained in extracts of leaves exposed to a long day (8.63–25.0 GAE g/100 g), whereas leaves exposed to a short day photoperiod had a lower phenolic content (4.94–5.76 GAE g/100 g).

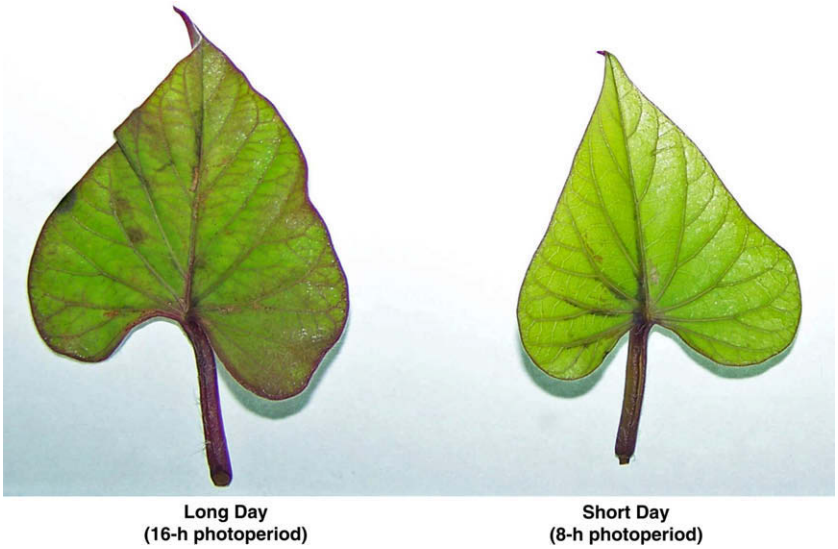

Fig. 1. Detached leaves from sweet potato plants 30 days after light exposure. Plants were grown in chambers with photosynthetic active radiation (PAR 400–700 nm) at 150 μmol m^{-2} s^{-1} and 22 °C under long day (16 h photoperiod) or short day (8 h photoperiod) conditions.

Table 1
Colour parameters (CI, Ye, Rd and Bl) and concentrations of chlorophylls a and b (mg/100 g fresh sample) and total phenolic compounds (g GAE/100 g fresh sample) in sweet potato leaves collected at days 10 and 30 of exposure to long day (16 h photoperiod) or short day (8 h photoperiod) conditions. Values are means ± SD of duplicate assays.

	Short day 10 days	Long day 10 days	Short day 30 days	Long day 30 days
Colour intensity (CI)	3.11 ± 0.005[a]	4.51 ± 0.006[b]	2.89 ± 0.032[a]	3.96 ± 0.045[b]
Yellow colour (Ye%)	62.1 ± 1.023[a]	53.7 ± 0.876[b]	70.2 ± 0.567[a]	60.8 ± 1.005[b]
Red colour (Rd%)	16.7 ± 0.123[a]	23.6 ± 0.233[b]	16.2 ± 0.087[a]	22.2 ± 0.457[b]
Blue colour (Bl%)	21.2 ± 1.789[a]	22.7 ± 1.675[a]	13.6 ± 3.089[a]	17.1 ± 2.478[a]
Chlorophyll a (mg/100 g)	0.20 ± 0.002[a]	0.27 ± 0.015[a]	0.07 ± 0.004[b]	0.10 ± 0.005[b]
Chlorophyll b (mg/100 g)	0.19 ± 0.001[a]	0.26 ± 0.001[a]	0.08 ± 0.005[b]	0.10 ± 0.003[b]
Total phenolic compounds (g GAE/100 g)	4.94 ± 0.126[a]	8.63 ± 0.234[b]	5.76 ± 0.562[a]	25.0 ± 1.002[c]

Means ± SD ($n = 2$). Different letters in the same rows are significantly different at $p < 0.05$.

3.2. Expression of flavonoid pathway genes

RT-PCR analysis was performed to analyse the expression of five key genes of the flavonoid pathway (Fig. 2A). Expression of one of these genes, *CHS*, coding for chalcone synthase, was undetectable in the plant material analysed (Fig. 2B). Regarding each of the other four flavonoid pathway genes, chalcone flavanone isomerase (*CHI*), flavanone 3-hydroxylase (*F3H*), dihydroflavonol 4-reductase (*DFR*) and UDP-glucose flavonoid 3-O-glucosyl transferase (*UFGT*), higher transcript levels were always detected in leaves of plants grown under a long day photoperiod, except for the *UFGT* gene after 10 days (Fig. 2B). In leaves of plants growing under short day conditions, it was not possible to detect expression of *CHI* and *DFR*, and only low levels of transcript were observed for the *F3H* and *UFGT* genes. With the exception of the *UFGT* gene, which was expressed at a low level at day 10 and undetectable at day 30 under a short day photoperiod, the number of days of light exposure did not apparently affect the expression of any of the flavonoid pathway genes studied (Fig. 2B). In summary, expression of the examined flavonoid pathway genes was largely higher in leaves of sweet po-

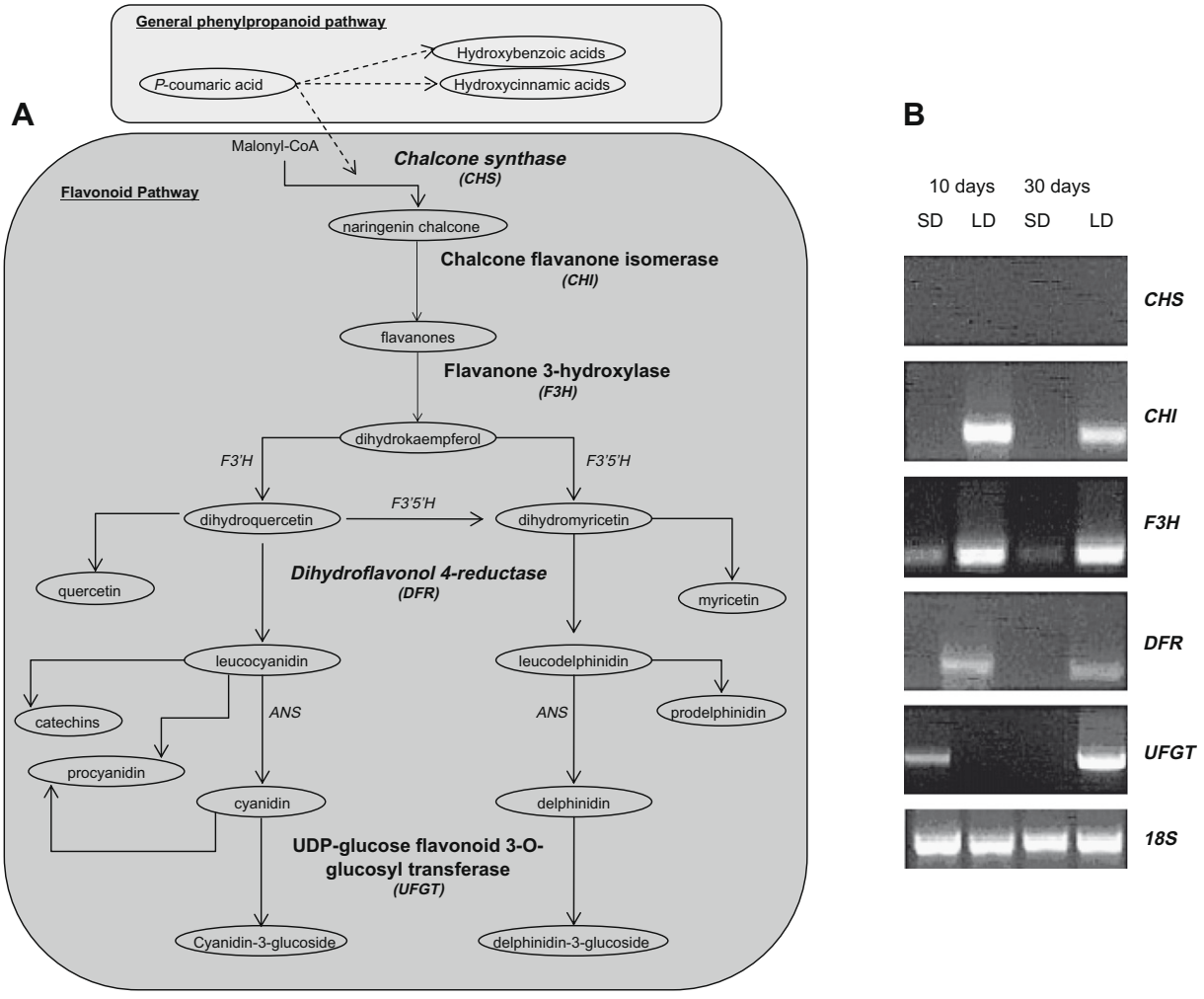

Fig. 2. (A) Schematic representation of the flavonoid pathway. Genes whose expression was determined are shown in bold. (B) RT-PCR analysis of the expression of five flavonoid pathway genes in sweet potato leaves collected at days 10 and 30 of exposure to long day (16 h photoperiod) or short day (8 h photoperiod) conditions. Amplification of 18*S* ribosomal RNA was used as a loading control. Results are representative of three independent experiments.

tato plants growing under long day than in leaves of plants growing under short day conditions, independently of the time of light exposure (10 or 30 days).

3.3. Flavonoid and phenolic acid composition

Anthocyanins, catechins, proanthocyanidins, flavonols, hydroxycinnamic acids and hydroxybenzoic acids from the sweet potato leaves under study were identified and quantified using high-performance liquid chromatography combined with a photodiode-array detector (HPLC–PDA). HPLC–PDA analyses, showing the separation of 13 flavonoids and phenolic acids from leaves of sweet potato plants after 10 and 30 days of growth under short day or long day photoperiods, are illustrated in Fig. 3. A good separation could be achieved in a short separation time of 30 min. The concentration of the identified components was calculated using the obtained calibration curves (data not shown).

Although typical anthocyanins are not abundant in green leaves, it was possible to detect delphinidin-3-glucoside (960 g g^{-1} fw) in leaf extracts of sweet potato plants grown for 30 days under a long day photoperiod (Table 2). High levels of delphinidin-3-glucoside detected under these growth conditions correlate with a higher expression of the *UFGT* gene (see Fig. 2B), which catalyses the conversion of delphinidin to delphinidin-3-glucoside (see Fig. 2A). These results are consistent with a redder colour of leaves under a long day photoperiod when compared with leaves of plants growing under short day conditions, which were mainly green (see Fig. 1). Higher transcript levels of the *CHI* and *F3H* flavonoid pathway genes were also observed in leaves of plants growing under a long day (see Fig. 2B), correlating with higher concentrations of the flavonol kaempferol in leaves under a long day as compared with leaves growing under a short day photoperiod (Table 2). These results provide further support to the protective role of flavonoids in plants growing under high photoperiod (Tawaha, Alali, Gharaibeh, Mohammad, & El-Elimat, 2007).

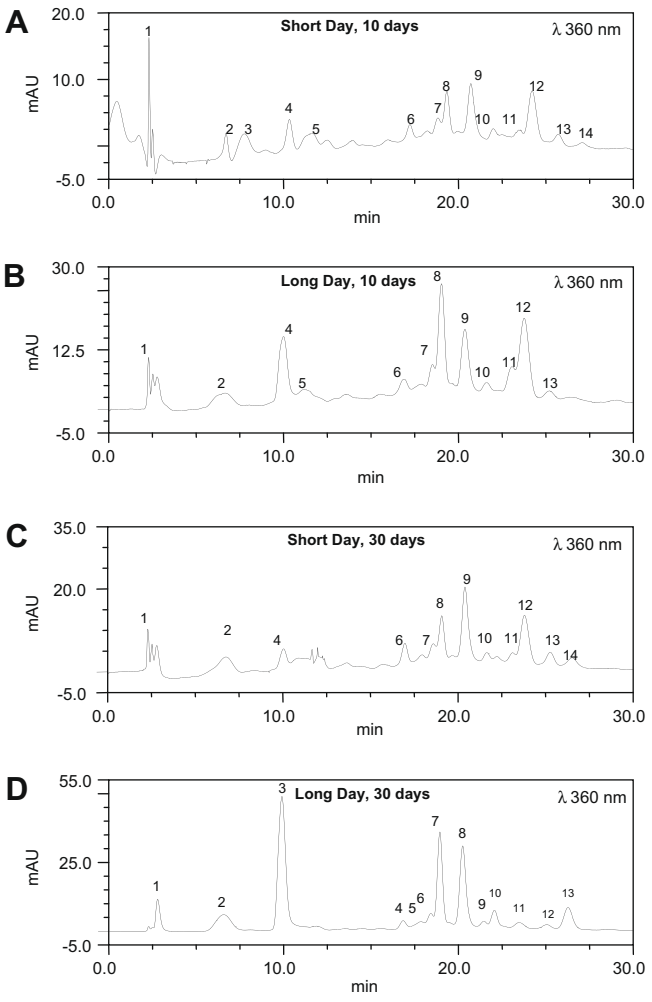

Fig. 3. HPLC chromatogram at 360 nm of different flavonoids and phenolic acids in sweet potato leaves collected at days 10 (A and B) and 30 (C and D) of exposure to long day (B and D) or short day (A and C) conditions. Peaks: 1 – gallic acid; 2 – gentisic acid; 3 – catechin; 4 – chlorogenic acid; 5 – caffeic acid; 6 – epicatechin; 7 – *p*-coumaric acid; 8 – sinapic acid; 9 – benzoic acid; 10 – anisic acid; 11 – kaempferol; 12 – myricetin; 13 – cinnamic acid; 14 – quercetin.

The flavonols (+)-catechin and (−)-epicatechin were also identified and quantified (Table 2). Again, the results obtained indicate higher amounts of total catechins (65.0 g g^{-1}) in leaves of sweet potato plants growing under a long day photoperiod for 30 days. The quantitative compositions of flavonols (quercetin, myricetin and kaempferol), hydroxycinnamic acids (*p*-coumaric, caffeic or ferulic acid conjugates and chlorogenic, sinapic and cinnamic acids) and hydroxybenzoic acids (benzoic, gentisic and *p*-anisic acids) were also consistently higher in leaves of plants growing under a long day photoperiod, with the exception of quercetin and myricetin that were not detected under this light regime.

Hydroxycinnamic acids, namely *p*-coumaric acid conjugates (415 g g^{-1}) and sinapic acid (480 g g^{-1}), were the major phenolic acids detected in sweet potato leaves exposed to a long day photoperiod for 30 days, as compared with those of plants growing under short day conditions for the same period of time (12.2 and 31.4 g g^{-1}, respectively). Similar results were obtained for hydroxybenzoic acids, namely benzoic (106 g g^{-1}), and *p*-anisic acids (48.0 g g^{-1}), which were present in higher amounts in leaves under a long day for 30 days than in leaves of plants exposed to a short day photoperiod for the same length of time (3.53 and 2.98 g g^{-1}, respectively). The levels of gentisic acid were also significantly higher (approximately fourfold) under long day than under short day conditions, but in this case no effect of exposure time was detected.

4. Discussion

Flavonoid compounds of fruits and vegetables have been considered as therapeutic agents due to their beneficial health effects, such as their supposed protection against certain cancers, cardiovascular diseases and aging (Ross & Kasum, 2002). Moreover, they have also been deemed a source of colours for food products, mainly anthocyanins (Espìn, Soler-Rivas, Wichers, & Garcìa-Viguera, 2000), alternative to synthetic dyes whose harmful effects upon human health have often been assumed and, in some cases, demonstrated. According to Mano et al. (2007), sweet potato accumulates flavonoid compounds in various tissues, such as flowers, leaves, stems and non-tuberous, as well as tuberous, roots. In the present study, attention was focused on sweet potato edible leaves and on the effects of different light treatments on their compositions in polyphenolic compounds.

Previous work has established that the antioxidant properties of some vegetables and fruits are partly due to low molecular weight phenolic compounds, particularly flavonoids, which are known to be potent antioxidants (Wang, Nair, Strasburg, Booren, & Gray, 1999). The total concentration of phenolic acid compounds in leaves of sweet potato reported in the present study is lower than that reported by Huang et al. (2006) for sweet potato tubers, but comparable to that reported for other edible plant leaves (Gins, Kolesnikov, Kononkov, Trishin, & Gins, 2000; Takenaka, Nagata, & Yoshida, 2000). These were found to be rich in chlorogenic acid,

Table 2
Concentrations ($\mu g\ g^{-1}$ fresh sample) of anthocyanins, catechins, flavonols, and hydroxycinnamic and hydrobenzoic acids in sweet potato leaves collected at days 10 and 30 of exposure to long day (16 h photoperiod) or short day (8 h photoperiod) conditions. Values are means ± SD of duplicate assays.

	Short day 10 days	Long day 10 days	Short day 30 days	Long day 30 days
Anthocyanins				
Cyanidin-3-glucoside	*ND*	*ND*	*ND*	*ND*
Cyanidin-3-galactoside	*ND*	*ND*	*ND*	*ND*
Cyanidin-3-arabinoside	*ND*	*ND*	*ND*	*ND*
Cyanidin aglycon	*ND*	*ND*	*ND*	*ND*
Delphinidin-3-glucoside	*ND*	*ND*	*ND*	960.10 ± 3.902
Delphinidin-3-galactoside	*ND*	*ND*	*ND*	*ND*
Delphinidin-3-arabinoside	*ND*	*ND*	*ND*	*ND*
Malvidin-3-glucoside	*ND*	*ND*	*ND*	*ND*
Malvidin-3-galactoside	*ND*	*ND*	*ND*	*ND*
Malvidin-3-arabinoside	*ND*	*ND*	*ND*	*ND*
Peonidin-3-glucoside	*ND*	*ND*	*ND*	*ND*
Peonidin-3-galactoside	*ND*	*ND*	*ND*	*ND*
Peonidin-3-arabinoside	*ND*	*ND*	*ND*	*ND*
Petudinin-3-glucoside	*ND*	*ND*	*ND*	*ND*
Petudinin-3-galactoside	*ND*	*ND*	*ND*	*ND*
Petudinin-3-arabinoside	*ND*	*ND*	*ND*	*ND*
Hydroxycinnamoyl conjugates	*ND*	*ND*	*ND*	*ND*
Catechins				
(+)-Catechin	6.52 ± 0.505[a]	3.94 ± 0.435[b]	2.65 ± 0.124[b]	22.4 ± 0.367[c]
(−)-Epicatechin	5.05 ± 0.005[a]	6.54 ± 0.789[b]	6.10 ± 0.004[b]	42.7 ± 0.005[c]
Flavonols				
Quercetin	4.58 ± 0.301[a]	*ND*	5.49 ± 0.345[a]	*ND*
Myricetin	32.9 ± 1.089[a]	*ND*	56.3 ± 0.905[b]	*ND*
Kaempferol	32.1 ± 0.980[a]	65.6 ± 3.566[b]	54.25 ± 2.879[b]	93.0 ± 1.23[c]
Hydroxycinnamic acids				
p-Coumaric acid conjugates	11.3 ± 0.122[a]	30.1 ± 0.145[b]	12.2 ± 0.089[a]	415 ± 4.034[c]
Caffeic or ferulic acid conjugates	4.31 ± 0.100[a]	2.83 ± 0.056[a]	3.71 ± 0.023[a]	18.0 ± 0.665[b]
Chlorogenic acid	3.66 ± 0.111[a]	5.30 ± 0.030[a]	5.11 ± 0.344[a]	15.0 ± 0.677[b]
Sinapic acid	17.1 ± 0.005[a]	25.7 ± 1.355[b]	31.4 ± 0.780[b]	480 ± 5.678[c]
Cinnamic acid	*ND*	5.44 ± 0.566[a]	7.98 ± 0.789[a]	32.2 ± 1.044[b]
Hydroxybenzoic acids				
Benzoic acid	4.56 ± 0.444[a]	5.89 ± 0.022[a]	3.53 ± 0.345[a]	106 ± 1.003[b]
Gentisic acid	11.5 ± 0.389[a]	45.4 ± 2.001[b]	10.1 ± 0.039[a]	45.0 ± 1.02[b]
p-Anisic acid	3.77 ± 0.038[a]	4.84 ± 0.267[a]	2.98 ± 0.067[a]	48.0 ± 1.011[b]

Means ± SD ($n = 2$). Different letters in the same rows are significantly different at $p < 0.05$. *ND*, not detected.

caffeic or ferulic acid conjugates and quercetin. This is in agreement with our results, in which increases in hydroxycinnamic acids, such as chlorogenic acid and caffeic or ferulic acid conjugates, under a long day photoperiod correlated with an increase in total phenolic compounds.

The biosynthesis of flavonoid compounds is catalysed by several enzymes, namely *CHS*, *CHI*, *F3H*, *DFR* and *UFGT*. *CHS* is the first committed enzyme of flavonoid biosynthesis, while *DFR* is the first committed enzyme of anthocyanin biosynthesis (see Fig. 2A). Expression of the genes coding for these enzymes is regulated by environmental cues, particularly light and temperature (Owens et al., 2008). In the present study, expression of the *CHS* gene was undetectable, whereas *DFR* was expressed only in leaves of sweet potato plants exposed to a long day photoperiod. This may explain why chalcones and anthocyanins were not detected in methanolic extracts, except for leaves growing for 30 days under a long day photoperiod, where a large amount of delphinidin-3-glucoside was detected in parallel with high levels of expression of the *UFGT* gene. After 10 days, under a short day photoperiod, significant levels of the *UFGT* transcript were detected, but this did not correlate with detectable amounts of the anthocyanin. High amounts of delphinidin-3-glucoside could result in a non-proportional increase in flavonoid compounds, such as hydroxycinnamic and hydroxybenzoic acids, or even catechins and kaempferol. In fact, the major flavonoid compounds found in sweet potato leaves were hydroxycinnamic acids, mainly *p*-coumaric acid conjugates and sinapic acid, present in almost equal proportions and representing about 85% of the total pigment content.

Hydroxycinnamic acids are thought to have the ability to shield the underlying tissues from harmful UV radiation. Indeed, Burchard, Bilger, and Weissenböck (2000) detected an increase in hydroxycinnamic acid concentrations in grape (*Vitis vinifera*) leaves as a consequence of strong visible radiation whereas, in the same study, the flavonoid production was specifically enhanced by UV radiation. In the present work, the high levels of *p*-coumaric acid, a precursor of both the flavonoid pathway and the biosynthesis of other hydroxycinnamic acid conjugates, detected after 30 days of exposure of sweet potato leaves to a long day photoperiod, may explain the overall activation of flavonoid production, as well as the sharp increase in hydroxycinnamic acid contents.

The qualitative and quantitative compositions of flavonols and phenolic acids also differed within leaves of plants growing under different photoperiod regimes. Kaempferol, the major flavonol in the sweet potato leaves studied, was detected in higher amounts under long day exposure, whereas quercetin and myricetin were detected only under a short day photoperiod, probably because high levels of kaempferol, produced upstream in the metabolic pathway, prevent accumulation of these compounds.

Strikingly, sweet potato leaf colour was affected by the photoperiod. Leaves exposed to long day conditions displayed enhanced red colour compared with yellow/green leaves from plants under a short day light photoperiod. The detected higher expression of all examined flavonoid pathway genes, as well as larger amounts of catechins, flavonols, and particularly the anthocyanin delphinidin-3-glucoside, under a long day photoperiod, explains the redder colour of leaves growing under these light conditions.

In summary, the results obtained in the present study show that photoperiod regimes influence the accumulation of phenolic acids, anthocyanins and other flavonoids in sweet potato leaves by increasing the total contents of these compounds under long day conditions, and that this accumulation is correlated with up-regulation of key flavonoid pathway gene expression. The results suggest that flavonols and the anthocyanin delphinidin-3-glucoside, together with hydroxycinnamic and hydroxybenzoic acids, play a predominant role in the defence against increased light exposure in sweet potato leaves. A dramatic induction of the synthesis and accumulation of flavonoids has previously been observed in response to high (sun)light. Although flavonoids are increasingly recognised as playing important roles as antioxidants, further work is necessary to uncover the full potential of these compounds in the improvement of human health, as well as to identify their presence in various foods and elucidate environmental effects on their contents in plants.

5. Conclusion

To our knowledge, this is the first work reporting the quantification of individual polyphenolic compounds in leaves exposed to different light regimes of sweet potato. Results show that the increased light exposure imposed by a long day photoperiod induces the expression of at least four key flavonoid pathway genes (*CHI*, *F3H*, *DFR* and *UFGT*), which positively correlates with the accumulation of an anthocyanin, catechins and the flavonol kaempferol, as well as hydroxycinnamic and hydroxybenzoic acids, in sweet potato leaves, suggesting a protective role for these compounds in plant tissues under increased light exposure.

References

Burchard, P., Bilger, W., & Weissenböck, G. (2000). Contribution of hydroxycinnamates and flavonoids to epidermal shielding of UV-A and UV-B radiation in developing rye primary leaves as assessed by ultraviolet-induced chlorophyll fluorescence measurements. *Plant Cell and Environment, 23*, 1373–1380.

Chalker-Scott, L. (1999). Environmental significance of anthocyanins in plant stress responses. *Photochemistry and Photobiology, 70*, 1–9.

Demmig-Adams, B., & Adams, W. W. (1992). Photoprotection and other responses of plants to high light stress. *Annual Review of Plant Physiology and Plant Molecular Biology, 43*, 599–626.

Elliott, J. G. (1999). Application of antioxidant vitamins in foods and beverages. *Food Technology, 53*, 46–48.

Espìn, J. C., Soler-Rivas, C., Wichers, H. J., & Garcìa-Viguera, C. (2000). Anthocyanin based natural colorants: A new source of antiradical activity for foodstuff. *Journal of Agriculture and Food Chemistry, 48*, 1588–1592.

Gins, V. K., Kolesnikov, M. P., Kononkov, P. F., Trishin, M. E., & Gins, M. S. (2000). Oxyanthraquinones and flavonoids from garland chrysanthemum. *Prikladnaia Biokhimiia Mikrobiologiya, 36*, 344–353.

Holton, T. A., & Cornish, E. C. (1995). Genetics and biochemistry of anthocyanin biosynthesis. *Plant Cell, 7*, 1071–1083.

Huang, Y. C., Chang, Y. H., & Shao, Y. Y. (2006). Effects of genotype and treatment on the antioxidant activity of sweet potato in Taiwan. *Food Chemistry, 98*, 259–538.

Jaakola, L., Määttä, K., Pirttilä, A. M., Törrönen, R., & Kärenlampi, S. (2002). Expression of genes involved in anthocyanin biosynthesis in relation to anthocyanin, proanthocyanidin, and flavonol levels during bilberry fruit development. *Plant Physiology, 130*, 729–739.

Jaakola, L., Määttä-Riihinen, K., Kärenlampi, S., & Hohtola, A. (2004). Activation of flavonoid biosynthesis by solar radiation in bilberry (*Vaccinium myrtillus* L.) leaves. *Planta, 218*(72), 1–728.

Kaur, C., & Kapoor, H. C. (2001). Antioxidants in fruits and vegetables – The millennium's health. *International Journal of Food Science and Technology, 36*, 703–725.

Kelebek, H., Canbas, A., & Selli, S. (2008). Determination of phenolic composition and antioxidant capacity of blood orange juices obtained from cvs. Moro Sanguinello (*Citrus sinensis* (L.) Osbeck) grown in Turkey. *Food Chemistry, 107*, 1710–1716.

Landry, L. G., Chapple, C. C. S., & Last, R. L. (1995). *Arabidopsis* mutants lacking phenolic sunscreens exhibit enhanced ultraviolet-B injury and oxidative damage. *Plant Physiology, 109*, 1159–1166.

Larson, R. A. (1988). The antioxidants of higher plants. *Phytochemistry, 27*, 969–978.

Li, H., Cheng, K., Wong, C., Fan, K., Chen, F., & Jiang, Y. (2007). Evaluation of antioxidant capacity and total phenolic content of different fractions of selected microalgae. *Food Chemistry, 102*, 771–776.

Mano, H., Ogasawara, F., Sato, K., Higo, H., & Minobe, Y. (2007). Isolation of a regulatory gene of anthocyanin biosynthesis in tuberous roots of purple-fleshed sweet potato. *Plant Physiology, 143*, 1252–1268.

Mazza, M., Pomponi, M., Janiri, L., Bria, P., & Mazza, S. (2007). Omega-3 fatty acids and antioxidants in neurological and psychiatric diseases: An overview. *Progress in Neuro-psychopharmacology and Biological Psychiatry, 31*, 12–26.

Namiki, M. (1990). Antioxidants/antimutagens in food. *Food Science and Nutrition, 29*, 273–300.

Owens, D. K., Alerding, A. B., Crosby, K. C., Bandara, A. B., Westwood, J. H., & Winkel, B. S. J. (2008). Functional analysis of a predicted flavonol synthase gene family in *Arabidopsis*. *Plant Physiology, 147*, 1046–1061.

Porra, R. J., Thompson, W. A., & Kriedemann, P. E. (1989). Determination of accurate extinction coefficients and simultaneous equations for assaying chlorophylls a and b extracted with four different solvents: Verification of the concentration of chlorophyll standards by atomic absorption spectroscopy. *Biochimica et Biophysica Acta, 975*, 384–394.

Ross, J. A., & Kasum, C. M. (2002). Dietary flavonoids: Bioavailability, metabolic effects, and safety. *Annual Review of Nutrition, 22*, 19–34.

Taga, M. S., Miller, E. E., & Pratt, D. E. (1984). Chia seeds as a source of natural lipid antioxidants. *Journal of American Oil Chemists' Society, 61*, 928–931.

Takenaka, M., Nagata, T., & Yoshida, M. (2000). Stability and bioavailability of antioxidants in garland (*Chrysanthemum coronarium* L.). *Bioscience, Biotechnology and Biochemistry, 64*, 2689–2691.

Tawaha, K., Alali, F. Q., Gharaibeh, M., Mohammad, M., & El-Elimat, T. (2007). Antioxidant activity and total phenolic content of selected Jordanian plant species. *Food Chemistry, 104*(4), 1372–1378.

Wang, H., Nair, M. G., Strasburg, G. M., Booren, A. M., & Gray, J. I. (1999). Antioxidant polyphenols from tart cherries (*Prunus cerasus*). *Journal of Agricultural and Food Chemistry, 47*, 840–844.

Weisshaar, B., & Jenkins, G. I. (1998). Phenylpropanoid biosynthesis and its regulation. *Current Opinion in Plant Biology, 1*, 251–257.

Winkel-Shirley, B. (2001). Flavonoid biosynthesis. A colorful model for genetics, biochemistry, cell biology and biotechnology. *Plant Physiology, 126*, 485–493.

Winkel-Shirley, B. (2002). Biosynthesis of flavonoids and effects of stress. *Current Opinion in Plant Biology, 5*, 218–223.

Food Chemistry 118 (2010) 391–397

Contents lists available at ScienceDirect

Food Chemistry

journal homepage: www.elsevier.com/locate/foodchem

Physical, biochemical and antioxidant properties of some Indian honeys

Sudhanshu Saxena, Satyendra Gautam, Arun Sharma *

Food Technology Division, Bhabha Atomic Research Centre, FIPLY, Trombay, Mumbai 400085, Maharashtra, India

ARTICLE INFO

Article history:
Received 23 February 2009
Received in revised form 24 March 2009
Accepted 5 May 2009

Keywords:
Indian honeys
Phenolics content
Antioxidant
Radical scavenging activity
DPPH
Proline

ABSTRACT

The study was intended to characterise the physicochemical and antioxidant properties of some commercial brands of Indian honeys. All the samples showed considerable variations with reference to their level of total phenolics, protein, radical scavenging activity, ascorbic acid equivalent antioxidant content (AEAC) and ferric reducing antioxidant potential (FRAP). Comparative studies of Indian honeys indicated the strong correlation between proline content and AEAC as well as 2,2-diphenyl-1-picryl-hydrazyl (DPPH) scavenging activity whereas phenol content was strongly correlated with FRAP values. Thus, overall antioxidant activity seems to be contributed by proline and phenol contents. Besides these major factors, colour pigments (ABS_{460}) were also found to contribute significantly to the overall observed antioxidant activity.

1. Introduction

Honey, produced by the honeybee, is a natural supersaturated sugar solution, which is mainly composed of a complex mixture of carbohydrates. Besides this, it also contains certain minor constituents viz., proteins, enzymes (invertase, glucose oxidase, catalase, phosphatases), amino and organic acids (gluconic acid, acetic acid, etc.), lipids, vitamins (ascorbic acid, niacin, pyridoxine etc.), volatile chemicals, phenolic acids, flavonoids, and carotenoid like substances and minerals (Blasa et al., 2006). The composition of honey depends on the plant species visited by the honeybees and the environmental, processing and storage conditions (Bertoncelj, Dobersek, Jamnik, & Golob, 2007; Guler, Bakan, Nisbet, & Yavuz, 2007). Blossom or nectar honey is derived from the nectaries of flowers and honeydew honey comes from the sugary excretion of some hemipterous insects on the host plant or from the exudates of the plants.

Honey has been traditionally used for different purposes and has a great potential to serve as a natural food antioxidant. In recent years much attention has been focused on the use of natural dietary antioxidants as an effective protection against oxidative damage. Enzymes in honey serve as antioxidants by promoting the removal of oxygen (Oszmianski & Lee, 1990). Honey consumption has been reported to be effective in increasing the total plasma antioxidant and reducing capacity in humans (Gheldof, Wang, & Engeseth, 2003).

The comparative physicochemical characterisation of different honeys from other regions of the world has been carried out extensively (Azeredo, Azeredo, De Souza, & Dutra, 2003; Finola, Lasagno, & Marioli, 2007; Guler et al., 2007; Ouchemoukh, Louaileche, & Schweizer, 2007). Although in India honey is produced and consumed on a large scale, there is a lack of information on the comparative biochemical properties of Indian honeys. Therefore, the objective of the current study was to investigate the physical, biochemical and antioxidant properties of Indian honeys and also to study their possible interdependence.

2. Materials and methods

2.1. Chemicals

Ascorbic acid, Folin–Ciocalteu's phenol reagent, gallic acid and L-proline were procured from Sigma Chemical Co. Ltd. (St. Louis, Mo., USA). Bovine serum albumin (10 mg/ml) was obtained from Bangalore Genei, Bangalore, India. Sodium chloride (NaCl) and trichloroacetic acid (TCA) were purchased from S.D. Fine-Chem. Ltd., Mumbai, India.

2.2. Honey samples

The present study was carried out using seven reputed commercial Indian honey brands. Fresh honey samples weighing 250 g, packed and sealed in glass bottles, were purchased from a

* Corresponding author. Tel.: +91 22 25595742/25592539; fax: +91 22 25505151/25519613.
E-mail address: ksarun@barc.gov.in (A. Sharma).

0308-8146/$ - see front matter © 2009 Published by Elsevier Ltd.
doi:10.1016/j.foodchem.2009.05.001

local market, and stored at 4 °C. The samples were analysed at the earliest in such a way that none of the samples exceeded the storage period beyond six months. The honey samples were kept at ambient temperature (26 ± 2 °C) overnight before the analyses were performed.

2.3. Physical analysis

2.3.1. Viscosity

Viscosity is the measure of the internal friction of a fluid. The viscosity measurements were performed at ambient temperature, using a Brookfield disc-type viscometer (model RVDVI+, Brookfield Engineering Labs, INC. Stoughton, MA 02072, USA). All the commercial honey samples were non-crystalline liquid honeys and any air bubbles which could interfere in the viscosity analysis were removed. The spindle type and spindle speed (shear rate in rpm) were S-6 and 50 rpm, respectively. A 35 ml aliquot of honey sample was withdrawn in a Falcon tube and used to measure the viscosity. The measurement was repeated thrice for each sample and the mean viscosity (cP) was calculated.

2.3.2. Water activity

A small aliquot of honey sample weighing approximately 1 g was used for determining water activity (a_w) using a water activity meter. This measures the water activity of the sample based on its equilibrium relative humidity (ERH). The relationship between a_w and ERH is a_w = ERH (in percentage)/100 (AqualabCX2T, Decagon Devices, USA) (Chirife, Zamora, & Motto, 2006). The measurements were performed in triplicates for each sample and the mean was determined.

2.3.3. Moisture content

The moisture content was determined based on the refractometric method. In general, the refractive index increases with the increase in the solid content. The refractive indices of honey samples were measured at ambient temperature using an Atago hand refractometer and the readings were further corrected for a standard temperature of 20 °C by adding the correction factor of 0.00023/°C. Moisture content was determined in triplicate and the% moisture content values corresponding to the corrected refractive index values were calculated using Wedmore's table (AOAC, 1990).

2.3.4. pH

The pH was measured using a pH meter (Elico ph analyser, Elico Pvt Ltd., Mumbai) for a 10% (w/v) solution of honey prepared in milli Q water.

2.3.5. Ash content

The ash content was determined by placing 2–3 g of honey samples in a crucible in a muffle furnace and heating at 640 °C for 6 h. Measurements of ash were done in triplicate and the mean was expressed in g% (AOAC, 1990).

2.3.6. Electrical conductivity

The measurement of electrical conductivity is based on the determination of the electrical resistance. The electrical conductivity was measured using a conductivity bridge (type CLOI/02A) for a 20% (w/v) solution of honey suspended in milli Q water (Bogdanov et al., 1997). The electrical conductivity of the milli Q water was < 10 μS/cm. Each sample was analysed in triplicate and the mean was expressed in mS/cm.

2.3.7. Total soluble solids (TSS) and total solids (TS)

The total soluble solids of the honey samples were measured by refractometry using a Atago hand held refractometer and the results were expressed in °Brix. All the measurements were done at ambient temperature and the readings were corrected for a standard temperature of 20 °C by adding the correction factor of 0.00023/°C (AOAC, 1990). The total solid content (%) in the honey samples was calculated by using the formula: TS (%) = 100 - moisture content (Amin, Safwat, & El-Iraki, 1999).

2.3.8. Colour measurement

For colour analyses a 30 ml aliquot of honey sample was packed and sealed in high-density polyethylene packets. The colour of the honey samples was measured based on reflectance measurement using a Minolta CM-3600D Spectrophotometer (Konica Minolta Sensing, Inc., Osaka, Japan). The reflectance of the whole visible spectrum (360–780 nm) was recorded at a wavelength interval of 10 nm. An illuminant C and 2° viewing angle were used as the standard light source and observer, respectively. The instrument was first calibrated with a black and white standard and then the reflectance was measured. The CIE colour parameters used were L^*(Lightness: L^* = 100 for white and 0 for black), a^*(redness/greenness axis: positive a^* is red and negative a^* is green), b^*(yellowness/blueness axis: positive b^* is yellow and negative b^* is blue), C^*(chroma or saturation index), and H^*(Hue). These parameters were analysed using JAYPAK 4808 software (Quality Control System, Version 1.2).

2.3.9. Colour intensity: ABS_{450}

The net absorbance of the honey samples was determined by the method of Beretta, Granata, Ferrero, Orioli, and Facino (2005). The honey samples were diluted to 50% (w/v) with warm (45–50 °C) milli Q water and the solution was filtered through a 0.45 μm filter. There was a complete absence of coarse particles in the honey solutions as all the commercial samples were non-crystalline liquid honeys. The absorbance was measured using a spectrophotometer at 450 and 720 nm and the difference in absorbance was expressed as mAU (Beretta et al., 2005).

2.4. Biochemical analysis

2.4.1. Reducing sugar and total sugar

The total reducing sugar was determined using 3,5-dinitrosalicylic acid (DNSA). In principle the reducing sugar reduces DNSA to 3- amino- 5-nitrosalicylic acid resulting in the formation of reddish–orangeish colouration which is measured spectrophotometrically at 540 nm (Khalil et al., 2001). The honey solution (0.1 g/ml) was diluted 100 fold with milli Q water. A 1 ml aliquot of this diluted solution was mixed with equal amounts of the DNSA solution and incubated in a boiling water bath for 10 min. The mixture was allowed to cool to ambient temperature, mixed with 7.5 ml of milli Q water and the absorbance was measured at 540 nm using a spectrophotometer. A glucose solution of known concentration was used as a standard. The estimation of total sugar content was performed following the inversion of sucrose (a non-reducing sugar) to a reducing sugar and subsequently measuring its concentration as discussed before (Sawhney & Singh, 2000). Briefly, the honey solution (0.1 g/ml) was diluted 33 fold with milli Q water and to 1 ml of the diluted solution, concentrated hydrochloric acid was added to obtain a final concentration of 2 N. The mixture was incubated at 68 °C for 8 min for the complete inversion of sucrose to a reducing sugar. The acid hydrolysed solution was cooled to ambient temperature and neutralised by the addition of sodium hydroxide. The total volume was adjusted to 2 ml with milli Q water. From this, a 500 μl aliquot was withdrawn for quantifying the total sugar content in terms of reducing sugar as per the method described above. Measurements were performed in triplicate. The sucrose concentration (%) in honey samples was calculated using the equation: sucrose (%) = (total sugar−total reducing sugar) × 0.95 (Amin et al., 1999).

2.4.2. Total protein content

The total protein content was determined by Lowry's method of protein estimation which is based on the formation of a copper–protein complex and the reduction of phosphomolybdate and phosphotungstate present in Folin–Ciocalteau reagent to hetero polymolybdenum blue and tungsten blue, respectively. Bovine serum albumin (0–100 μg/ml) was used as a standard for preparing the calibration curve.

2.4.3. Total phenolic content

The total phenolic content was determined by the Folin–Ciocalteu method (Singleton, Orthofer, & Lamuela-Raventos, 1999). Thirty microlitre of honey solution (0.1 g/ml) was mixed with 2.37 ml of milli Q water and 150 μl of 0.2 N Folin–Ciocalteu reagent. The solution was thoroughly mixed by vortexing and incubated for 2 min at ambient temperature. Four hundred and fifty microlitre of sodium carbonate solution (0.2 g/ml) was added to the reaction mixture and further incubated for 2 h at ambient temperature. The absorbance was measured at 765 nm using a spectrophotometer. The total phenolic content was determined by comparing with a standard curve prepared using gallic acid (0–200 mg/l). The mean of at least three readings was calculated and expressed as mg of gallic acid equivalents (mg GAE)/100 g of honey.

2.5. Analysis of antioxidant activities

2.5.1. Antioxidant content

The antioxidant content in terms of ascorbic acid equivalent antioxidant content (AEAC) was determined using the method of Meda, Lamien, Romito, Millogo, and Nacoulma (2005). The honey sample was dissolved in methanol to a final concentration of 0.03 g/ml. A 0.75 ml aliquot of the methanolic honey solution was mixed with 1.5 ml of 0.02 mg/ml of DPPH solution prepared in methanol. The mixture was incubated at room temperature for 15 min and the absorbance was measured at 517 nm using a spectrophotometer. The blank used was 0.75 ml of methanolic honey solution mixed with 1.5 ml of methanol. Ascorbic acid standard solutions (0–10 μg/ml) prepared in milli Q water were used to plot the calibration curve. Measurements were performed in triplicate and the mean value was expressed as mg of ascorbic acid equivalent antioxidant content (AEAC) per 100 g of honey.

2.5.2. DPPH radical scavenging activity

The DPPH (2,2-diphenyl-1-picryl-hydrazyl) radical scavenging effect (H/e^- transferring ability) of honey samples was measured as per the method described by Chen, Lin, and Hsieh (2007). The DPPH was dissolved in absolute ethanol to a 0.2 mM concentration. A 100 μl aliquot of honey solution (0.1 g/ml) was diluted to 500 μl with 70% ethanol, and vigorously mixed with 400 μl of DPPH solution by vortexing. The mixture was incubated at room temperature for 15 min and the absorbance of the solution (T_1) was measured at 517 nm. Sample blank (B_1) consisted of 600 μl of 70% ethanol and 400 μl of DPPH whereas DPPH blank (B_2) contained 100 μl of honey sample, 500 μl of 70% ethanol and 400 μl of absolute ethanol. The DPPH scavenging activity was calculated using the following formula:

$$\text{DPPH scavenging activity } (\%) = [1 - \{(T_1 - B_2)/B_1\}] \times 100$$

Where T_1, B_1, and B_2 are the absorbencies of the sample, sample blank and DPPH blank, respectively.

2.5.3. Ferric reducing/antioxidant power (FRAP) assay

The reducing power of the ethanolic extracts of honey was determined according to the method of Oyaizu (1986). A 1 ml aliquot of ethanolic honey extract (10% v/v) was mixed with 2.5 ml of phosphate buffer (0.2 M, pH 6.6) and 2.5 ml of potassium ferri-cyanide (1%). The mixture was incubated at 50 °C for 20 min. After this, 2.5 ml of 10% trichloroacetic acid was mixed by vortexing. The mixture was centrifuged at 3000 rpm for 10 min. A 2.5 ml aliquot of the supernatant was mixed with an equal amount of milli Q water and 0.5 ml of 0.1% $FeCl_3$. The absorbance was measured at 700 nm using a spectrophotometer. Precipitation or flocculation was never observed. Assays were performed in triplicate. Ascorbic acid (1.0 mg/ml) was used as a reference standard. The increase in absorbance provided an indication of higher reducing power of the samples being analysed.

3. Results and discussion

3.1. Physical analysis

3.1.1. Ash content and electrical conductivity

The percentage ash content is an indicator of the mineral content. It is considered as a quality criterion indicating the possible botanical origin of honey. Its value in the analysed samples ranged from 0.03 to 0.43 g% (Table 1). For most of the honeydew honeys from Romania, ash values ranged from 1.17 to 1.23, whereas, for floral honeys (acacia, sun-flower and lime), it ranged from 0.03 to 0.40 (Al et al., 2009). Generally, the ash content of blossom honey is $\leqslant$0.6% as compared to honeydew honey or blends of honeydew and blossom honeys where this value is $\geqslant$1.2% (Ouchemoukh et al., 2007). Thus based on this criterion, the analysed Indian honeys could be similar to the blossom honeys and the ash content values are comparable to the blossom honeys of Romania as mentioned above and also with Algerian honeys, for which the reported values are in the range of 0.06–0.54% (Ouchemoukh et al., 2007). The variability in the ash content of honeys could be due to harvesting processes, beekeeping techniques and the material collected by the bees during the foraging on the flora

Table 1
Comparative physical parameters of analysed honeys.

Honey	a_w[a]	Moisture (%)	Viscosity (cP)	TS[b] (%)	TSS[c] (°Brix)	RI[d]	Ash (%)	EC[e] (mS/cm)	pH
I	0.58 ± 0.002	18.2	5018 ± 11	81.8	79.6	1.4912	0.23 ± 0.02	0.64 ± 0.01	4.0 ± 0.003
II	0.57 ± 0.004	17.8	7150 ± 79	82.2	79.8	1.4918	0.23 ± 0.06	0.57 ± 0.01	4.4 ± 0.01
III	0.61 ± 0.003	20.0	2580 ± 29	80.0	77.8	1.4866	0.15 ± 0.05	0.50 ± 0.01	3.7 ± 0.00
IV	0.70 ± 0.004	17.2	8500 ± 43	82.8	80.4	1.4933	0.24 ± 0.09	0.68 ± 0.01	3.8 ± 0.001
V	0.65 ± 0.005	21.6	1140 ± 29	78.4	76.2	1.4825	0.03 ± 0.01	0.36 ± 0.01	3.9 ± 0.002
VI	0.58 ± 0.001	18.8	6383 ± 89	81.2	79.4	1.4894	0.43 ± 0.04	0.94 ± 0.01	4.2 ± 0.001
VII	0.64 ± 0.001	19.6	2765 ± 27	80.4	78.2	1.4876	0.07 ± 0.01	0.33 ± 0.01	3.7 ± 0.001

[a] Water activity.
[b] Total solids.
[c] Total soluble solids.
[d] Refractive index.
[e] Electrical conductivity.

(Finola et al., 2007). The electrical conductivity (mS/cm) in honey samples varied in the range of 0.33–0.94. A linear relationship is known to exist between the ash content and the electrical conductivity which is expressed as $C = 0.14 + 1.74\,A$, where C is the electrical conductivity and A is the ash content (Bogdanov et al., 2000). The coefficient of correlation between electrical conductivity and ash was found to be 0.98, which indicated a strong positive correlation between the two parameters. Similarly, a correlation value of 0.92 has been found to exist between the electrical conductivity and ash content for some Algerian honeys (Ouchemoukh et al., 2007).

3.1.2. pH

All the Indian honeys analysed were found to be acidic in character. Their pH values ranged from 3.7 to 4.4 (Table 1). In general, honey is acidic in nature irrespective of its variable geographical origin. The pH values of Algerian, Brazilian, Spanish and Turkish honeys have been found to vary between 3.49 to 4.53, 3.10 to 4.05, 3.63 to 5.01 and 3.67 to 4.57, respectively (Azeredo et al., 2003; Kayacier & Karaman, 2008; Ouchemoukh et al., 2007).

3.1.3. Moisture content

The moisture content (%) in the investigated samples ranged from 17.2 to 21.6. Except for sample V, all other tested Indian honeys had moisture contents below 20%, which is the maximum prescribed limit for the moisture content as per the Codex standard for honey (Codex Alimentarius, 2001). The moisture level of the analysed samples was consistent with the previous reported values for some Indian honeys for which the corresponding values ranged from 18.7% to 21.8% (Singh & Bath, 1997). The moisture content of honeys of different origins show varietal differences and it may range from 13% to 29% (Kayacier & Karaman, 2008). A higher moisture content could lead to undesirable honey fermentation during storage caused by the action of osmotolerant yeasts resulting in the formation of ethyl alcohol and carbon dioxide. The alcohol can be further oxidised to acetic acid and water resulting in a sour taste (Chirife et al., 2006). The moisture content of honey depends on various factors such as harvesting season, degree of maturity reached in the hive and climatic factors (Finola et al., 2007).

3.1.4. Water activity and viscosity

The water activity of the honey samples varied from 0.57 to 0.70 (Table 1). Our results are quite similar to those of Greek honeys for which the a_w values ranged from 0.53 to 0.67 (Lazaridou, Biliaderis, Bacandritsos, & Sabatini, 2004). The water activity is an important factor, which governs the food stability by preventing or limiting microbial growth. The osmotolerant yeasts are able to grow at a minimal water activity of 0.6 (Chirife et al., 2006). The honey sample IV, which had the lowest moisture content was found to have the highest water activity. Such observations are occasionally observed in certain honey samples probably due to the variation in the constituents and/or levels of individual sugar components (Abramovič, Jamnik, Burkan, & Kač, 2008). Viscosity is known to be affected by the water content and in our study an inverse correlation was found between the water activity and viscosity, with a correlation value of −0.9308. The viscosity of the samples ranged from 1140 to 8500 cP. All the analysed Indian honey samples were Newtonian with reference to their rheological behaviour and satisfactorily followed an Arrhenius model within a temperature range from 5 to 40 °C (Saxena et al., 2009, unpublished data).

3.1.5. Colour characteristics

The colour characteristics are presented in Table 2. Honey samples having an L value >50 are lighter honeys, whereas, samples having an L value ⩽50 are dark honeys. Therefore, based on this classification, the studied Indian honeys can be regarded as dark honeys because the L values of the samples ranged from 26.3 to 36.8. The 'a' values varied from 0.12 to 4.9; 'b' values ranged from 0.7 to 14.4; 'C' values ranged from 3.1 to 14.7 and 'H' value ranged from 44.7 to 89.4. Thus it is apparent that all the samples being darker had red and yellow components. The colour intensity (ABS_{450}) is supposed to be related to pigments (carotenoids, flavonoids etc.), which are also known to have antioxidant properties (Frankel, Robinson, & Berenbaum, 1998). The ABS_{450} values for the samples ranged from 524 to 1678 mAU (Table 2). The reported ABS_{450} values for some Italian and Slovenian honeys are in the range of 25 to 3413 mAU and 70 to 495 mAU, respectively (Beretta et al., 2005; Bertoncelj et al., 2007).

3.2. Biochemical analysis

3.2.1. Sugar

The total sugar and the total reducing sugar content in the honey samples ranged from 45.3% to 66.7% and 43.3% to 65%, respectively (Table 3). The data indicated that the majority of soluble sugars in honey samples are reducing sugars. The sucrose content (%) in the samples ranged from 0.4 to 8.8. Except for sample number VII, all other samples had sucrose levels below 5% which is the maximum prescribed limit as per the Codex standard (Codex Alimentarius, 2001). A higher sucrose content observed in one sample could be attributed to reasons such as overfeeding of honeybees with sucrose syrup, adulteration, or an early harvest of honey, wherein sucrose has not been fully transformed into glucose and fructose (Anklam, 1998; Azeredo et al., 2003; Guler et al., 2007). Some unifloral honeys like Banskia, Citrus, Hedysarum,

Table 3
Analysis of sugars in honeys.

Honey	Total sugar (%)	Total reducing sugar (%)	Sucrose (%)
I	61.3 ± 0.7	60.8 ± 0.3	0.4 ± 0.1
II	50.0 ± 0.6	49.0 ± 0.3	1.0 ± 0.4
III	62.6 ± 1.5	58.1 ± 0.5	4.3 ± 0.4
IV	45.3 ± 1.2	43.3 ± 0.5	2.0 ± 0.5
V	66.7 ± 2.1	65.5 ± 0.7	1.1 ± 0.7
VI	59.0 ± 1.5	57.0 ± 0.3	2.0 ± 0.6
VII	57.0 ± 0.9	47.8 ± 0.4	8.8 ± 0.7

Table 2
Colour characteristics of honeys.

Honey	L^*	a^*	b^*	C^*	H^*	ABS_{450} (mAU)
I	36.3 ± 1.7	1.2 ± 1.2	14.2 ± 0.5	14.3 ± 0.4	85.3 ± 5.1	1202 ± 0.7
II	34.6 ± 0.5	2.9 ± 0.03	12.7 ± 1.0	13.0 ± 1.0	76.8 ± 1.2	524 ± 3.5
III	33.5 ± 0.2	4.9 ± 0.3	11.4 ± 0.6	12.4 ± 0.7	66.4 ± 0.1	1008 ± 2.8
IV	26.3 ± 0.1	3.0 ± 0.01	0.7 ± 0.07	3.07 ± 0.04	44.7 ± 12.0	1678 ± 1.4
V	35.8 ± 0.1	1.3 ± 0.03	13.0 ± 0.1	13.1 ± 0.14	84.3 ± 0.1	1460 ± 2.1
VI	36.8 ± 0.3	0.1 ± 0.08	13.2 ± 0.1	13.3 ± 0.12	89.5 ± 0.4	1338 ± 0.7
VII	36.3 ± 0.3	2.7 ± 1.9	14.4 ± 0.7	14.7 ± 1.01	79.6 ± 7.1	796 ± 3.5

Medicago and Robinia contain up to 10% sucrose, whereas, up to 15% sucrose has been reported for Lavandula honeys (Bogdanov et al., 2000). Reducing sugars, which include mainly glucose and fructose, are the major constituents of honey (Küçük et al., 2007). A lime honey from Romania had 42.49% of combined glucose and fructose content (Al et al., 2009). Overheating of honey samples during processing or storage for very long periods could lead to the conversion of sugars to hydroxy methyl furfural (HMF). A low level of HMF is an indicator of the freshness of honey. In a parallel study, the HMF content of honey samples has been determined. In many of the samples the HMF content was found to be more than internationally recommended limit of 80 mg/kg (Saxena et al., 2009, unpublished data).

3.2.2. The protein content

In the current study the protein content (μg/g of honey) in the Indian honeys ranged from 480 to 2293, which was determined using the bovine serum albumin (BSA) as standard (R^2 = 0.9931). The protein content in Indian honeys was comparable to that found in Brazilian honeys where it varied from 199 to 2236 μg/g (Azeredo et al., 2003). Relatively higher protein levels ranging from 3700 to 9400 μg/g have been reported in Algerian honeys (Ouchemoukh et al., 2007). The protein content in honeys can be attributed to the presence of enzymes, some of which are introduced by bees themselves, and others are thought to be derived from the nectar. The protein content of honey is normally less than 5 mg/g (Anklam, 1998). The level of protein is dependent on the type of flora and thus it is variable. Proline is the predominant amino acid found in honey. The proline content in the honey samples was found to vary from 133 to 674 mg/kg (Saxena et al., 2009, unpublished data).

3.2.3. The total phenolic content

The total phenolic content (mg GAE/100 g of honey) of Indian honeys was found in the range of 47 to 98, which was determined using gallic acid as standard (R^2 = 0.9988). A similar level of phenolic content was also observed for Romanian honeydew honeys for which the phenolic content varied from 23.0 to 125.0 mg GAE/100 g (Al et al., 2009). For Algerian and Slovenian honeys, the phenolic content ranged from 64 to 1304 and 448 to 2414 mg GAE/100 g, respectively (Bertoncelj et al., 2007; Ouchemoukh et al., 2007). The concentration and type of polyphenolic substances in honey is variable and depends on the floral origin of honey (Küçük et al., 2007).

3.2.4. Antioxidant activity

Due to the lack of a specific official analytical approach for determination of antioxidant property of honey, different antioxidant assays have been used to evaluate the antioxidant properties of Indian honeys (Bertoncelj et al., 2007). Commonly used antioxidant assays are the FRAP (Ferric reducing antioxidant power) assay, percentage DPPH (1,1-diphenyl-2-picrylhydrazyl) scavenging activity, and ascorbic acid equivalent antioxidant content (AEAC). These methods are in wide use for assessing the antioxidant activity of different plant extracts (Chen et al., 2007).

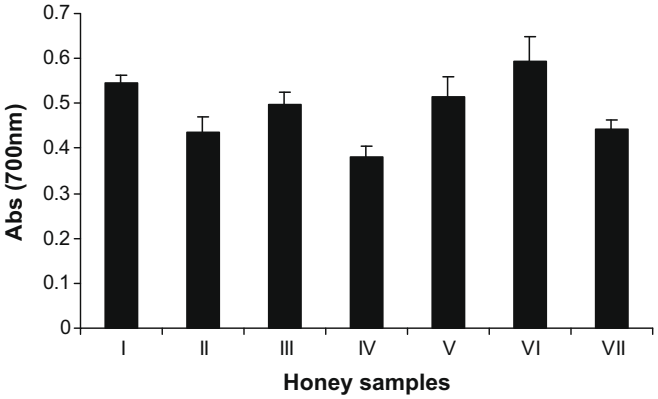

Fig. 1. Ferric reducing antioxidant power (FRAP) of the honey samples. The absorbance value at 700 nm for 1 mg/ml conc. of ascorbic acid (used as standard) was 1.543.

3.2.5. DPPH scavenging activity

DPPH is a stable nitrogen centred radical and has been widely used to test the free radical scavenging ability of various samples. The higher the DPPH scavenging activity, the higher the antioxidant activity of the sample. The presence of an odd electron is responsible for the strong absorption maxima at 517 nm for DPPH, which results in a purple colour. The decolourisation of DPPH occurs from purple to yellow when the unpaired electron of DPPH forms a pair with a hydrogen donated by a free radical scavenging antioxidant, thus converting DPPH into its reduced form. The DPPH radical scavenging effect of Indian honeys is presented in Table 4. The percentage DPPH scavenging activity ranged from 44 to 71. Five Indian honeys showed scavenging activity greater than 50% except for two samples whose scavenging activities were below 50%.

3.2.6. Ascorbic acid equivalent antioxidant content (AEAC)

Using the standard curve of ascorbic acid (R^2 = 0.9826), it was found that the ascorbic acid equivalent antioxidant content (mg AEAC/100 g of honey) of the analysed Indian honeys ranged from 15 to 30. The AEAC values for the multifloral Burkina Fasan honeys ranged from 10.20 to 37.87 mg AEAC/100 g (Meda et al., 2005). Thus our AEAC results are similar to those reported for multifloral Burkina Fasan honeys.

3.2.7. FRAP assay

The FRAP assay of all the Indian honeys tested are displayed in Fig. 1. The absorbance values in FRAP assay varied from 0.38 to 0.59. A relatively higher absorbance value indicated more reduction of ferric ions to ferrous ions. Samples having a higher reducing

Table 4
DPPH scavenging activity, ascorbic acid equivalent antioxidant content (AEAC), phenol content, and protein content of tested honeys.

Honey	DPPH scavenging activity (% ± SD)[a]	AEAC[b] (mg/100 g ± SD)	Phenol content (mg GAE/100 g ± SD)	Protein content (μg/g ± SD)
I	64 ± 0.7	24.4 ± 0.8	98 ± 1.2	1789 ± 5.5
II	59 ± 0.5	21.2 ± 0.9	47 ± 0.2	1567 ± 29.4
III	61 ± 0.9	26.0 ± 1.2	83 ± 1.1	2162 ± 37.8
IV	44 ± 0.6	15.1 ± 0.7	67 ± 0.8	480 ± 10.7
V	67 ± 1.1	27.1 ± 1.6	91 ± 1.4	2293 ± 22.5
VI	71 ± 1.3	29.5 ± 1.8	94 ± 0.8	2090 ± 27.0
VII	48 ± 0.8	15.3 ± 0.5	49 ± 1.3	821 ± 19.3

[a] Standard deviation.
[b] Ascorbic acid equivalent antioxidant content.

Table 5
Correlation matrix showing the interrelation amongst ascorbic acid equivalent antioxidant content, DPPH scavenging, FRAP, proline, phenol, and ABS_{450}.

	AEAC	DPPH scavenging	FRAP	Proline	Protein	Phenol	ABS_{450}
AEAC	1	0.97	0.82	0.94	0.95	0.84	0.74
DPPH scavenging	0.97	1	0.84	0.96	0.88	0.80	0.72
FRAP	0.82	0.84	1	0.73	0.64	0.90	0.83
Proline	0.94	0.96	0.73	1	0.92	0.78	0.77
Protein	0.95	0.88	0.64	0.92	1	0.77	0.67
Phenol	0.83	0.80	0.9	0.78	0.77	1	0.90
ABS_{450}	0.74	0.72	0.83	0.77	0.67	0.90	1

power had a higher absorbance value at 700 nm. Similar observations have also been observed for Turkish honeys (Küçük et al., 2007).

3.3. Correlation amongst the biochemical parameters and antioxidant properties

The correlation matrix (Table 5) showed a significant correlation between the biochemical and antioxidant parameters. The correlation values between ABS_{450} and FRAP, ABS_{450} and AEAC and ABS_{450} and percentage DPPH scavenging were 0.83, 0.74 and 0.72, respectively. Thus the colour pigments may have a role in the observed antioxidant activities of the honey samples. A strong correlation value of 0.90 was obtained between the ABS_{450} and phenolic content and 0.83 between the ABS_{450} and FRAP values. Almost similar values were obtained between ABS_{450} and phenolic content (=0.90) and between ABS_{450} and FRAP values (=0.85) for Slovenian honeys (Bertoncelj et al., 2007). A good correlation was observed between the ABS_{450} and percentage DPPH scavenging activity, FRAP and AEAC values indicating probable involvement of pigments conferring antioxidant property to honey.

There are reports indicating the role of amino acids in exhibiting antioxidant properties. In our study, the best interrelation was observed between the proline content and the DPPH scavenging activity for which the correlation value was 0.96 followed by a correlation value of 0.94 between proline content and AEAC. Previous work by Meda et al. (2005) has shown that the level of proline is a major factor responsible for radical scavenging activity as evident from their higher correlation values ($R = 0.75$) compared to that between radical scavenging activity and total phenolics ($R = 0.5$). Thus the percentage of total proline content in honey samples might be a critical factor responsible for their observed antioxidant activity. Protein can also work as an effective antioxidant as reported by Sivapriya and Srinivas (2007). The seminal work of Rice-Evans, Miller, and Paganga (1996), has very clearly indicated that not all plant products bear the same phenolic composition and not all phenolics posses the same antioxidant capacity. Therefore, it is not the quantity but the quality of polyphenols, which serves as the major determinant of the antioxidant capacity of food. This may explain the possible moderate correlation observed between the total phenol content and the antioxidant capacity of the analysed Indian honeys ($R = 0.80$ between phenol and DPPH scavenging activity; $R = 0.83$ between phenol and AEAC). The FRAP values correlated well with the phenolic content with a correlation value of 0.9. Previous studies on honey indicate that the presence of compounds such as polyphenols and flavonoids may function as potential natural antioxidants (Beretta et al., 2005; Blasa et al., 2006). The antioxidant activity of phenolics is mainly due to their redox properties. It can be summarised that the overall antioxidant property in the studied Indian honeys can be attributed to various contributing factors such as proline, phenolics, colour pigments and proteins though the relevance of proline appears prominent as shown by the correlation value.

4. Conclusion

All the seven commercial Indian honeys demonstrated antioxidant activities, which may have therapeutic potential. Though honey has a significant amount of phenols it is felt that the antioxidant property of honey is mainly due to its proline content as evidenced by the significant correlation observed between the antioxidant activity and proline content.

Acknowledgement

Authors thank Mr. Sanjeev Kumar, Mr. Sadanand Mayekar and Mr. Arvind Chaubey for their technical assistance during the course of this study.

References

Abramovič, H., Jamnik, M., Burkan, L., & Kač, M. (2008). Water activity and water content in Slovenian honeys. *Food Control, 19*, 1086–1090.
Al, M. L., Daniel, D., Moise, A., Bobis, O., Laslo, L., & Bogdanov, S. (2009). Physico-chemical and bioactive properties of different floral origin honeys from Romania. *Food Chemistry, 112*(4), 863–867.
Amin, W. A., Safwat, M., & EI-Iraki, S. M. (1999). Quality criteria of treacle (black honey). *Food Chemistry, 67*, 17–20.
Anklam, E. (1998). A review of the analytical methods to determine the geographical and botanical origin of honey. *Food Chemistry, 63*, 549–562.
AOAC (1990). Official methods of analysis. In K. Helrich (Ed.) (15th ed.). Arlington, VA, USA: Association of official Analytical Chemists, Inc.
Azeredo, L. D. C., Azeredo, M. A. A., De Souza, S. R., & Dutra, V. M. L. (2003). Protein content and physicochemical properties in honey samples of *Apis Mellifera* of different floral origins. *Food Chemistry, 80*, 249–254.
Beretta, G., Granata, P., Ferrero, M., Orioli, M., & Facino, R. M. (2005). Standardization of antioxidant properties of honey by a combination of spectrophotometric/fluorimetric assays and chemometrics. *Analytica Chimica Acta, 533*, 185–191.
Bertoncelj, J., Dobersek, U., Jamnik, M., & Golob, T. (2007). Evaluation of the phenolic content, antioxidant activity and colour of Slovenian honey. *Food Chemistry, 105*, 822–828.
Blasa, M., Candiracci, M., Accorsi, A., Piacentini, M. P., Albertini, M. C., & Piatti, E. (2006). Raw Millefiori honey is packed full of antioxidants. *Food Chemistry, 97*, 217–222.
Bogdanov, S., Lüllman, C., Martin, P., Ohe, W. V. D., Russmann, H., Vorwohl, G., et al. (2000). *Honey quality methods of analysis and international regulatory standards: Review of the work of the international honey commission*. Swiss Bee Research Centre.
Bogdanov, S., Martin, P., Lüllman, C., Borneck, R., Morlot, M., Heritier, J., et al. (1997). Harmonised methods of the European honey commission. *Apidologie, 1*(extra issue), 59.
Chen, H. Y., Lin, Y. C., & Hsieh, C. L. (2007). Evaluation of antioxidant activity of aqueous extract of some selected nutraceutical herbs. *Food Chemistry, 104*(4), 1418–1424.
Chirife, J., Zamora, M. C., & Motto, A. (2006). The correlation between water activity and % moisture in honey: Fundamental aspects and application to Argentine honeys. *Journal of Food Engineering, 72*, 287–292.
Codex Alimentarius Commission Standards (2001). CODEX STAN 12-1981, Rev.1 (1987), Rev.2.
Finola, M. S., Lasagno, M. C., & Marioli, J. M. (2007). Microbiological and chemical characterisation of honeys from central Argentina. *Food Chemistry, 100*, 1649–1653.
Frankel, S., Robinson, G. E., & Berenbaum, M. R. (1998). Antioxidant capacity and correlation characteristics of 14 unifloral honeys. *Journal of Apiculture Research, 37*, 27–31.
Gheldof, N., Wang, X. H., & Engeseth, N. J. (2003). Buckwheat honey increases serum antioxidant capacity in humans. *Journal of Agricultural and Food Chemistry, 51*, 1500–1505.

Guler, A., Bakan, A., Nisbet, C., & Yavuz, O. (2007). Determination of important biochemical properties of honey to discriminate pure and adulterated honey with sucrose (*Saccharum officinarum* L.) syrup. *Food Chemistry, 105*(111), 9–1125.

Kayacier, A., & Karaman, S. (2008). Rheological and some physicochemical characteristics of selected Turkish honeys. *Journal of Texture Studies, 39*(1), 17–27.

Khalil, M. I., Motallib, M. A., Anisuzzaman, A. S. M., Sathi, Z. S., Hye, M. A., & Shahjahan, M. (2001). Biochemical analysis of different brands of unifloral honey available at the northern region of Bangladesh. *The Sciences, 1*(6), 385–388.

Küçük, M., Kolaylı, S., Karaoğlu, S., Ulusoy, E., Baltacı, C., & Candan, F. (2007). Biological activities and chemical composition of three honeys of different types from Anatolia. *Food Chemistry, 100*, 526–534.

Lazaridou, A., Biliaderis, C. G., Bacandritsos, N., & Sabatini, A. G. (2004). Composition, thermal and rheological behaviour of selected Greek honeys. *Journal of Food Engineering, 64*, 9–21.

Meda, A., Lamien, C. E., Romito, M., Millogo, J., & Nacoulma, O. G. (2005). Determination of total phenolic, flavonoid and proline contents in Burkina Fasan honey, as well as their radical scavenging activity. *Food Chemistry, 91*, 571–577.

Oszmianski, J., & Lee, C. Y. (1990). Inhibition of polyphenol oxidase activity and browning by honey. *Journal of Agricultural Food Science, 38*, 1892–1895.

Ouchemoukh, S., Louaileche, H., & Schweizer, P. (2007). Physicochemical characteristics and pollen spectrum of some Algerian honey. *Food Control, 18*, 52–58.

Oyaizu, M. (1986). Antioxidative activity of browning products of glucosamine fractionated by organic solvent and thin-layer chromatography. *Nippon Shokuhin Kogyo Gakkaishi, 35*, 771–775.

Rice-Evans, C., Miller, N. J., & Paganga, G. (1996). Structure-antioxidant activity relationships of flavonoids and phenolic acids. *Free Radical Biology and Medicine, 20*, 933–956.

Sawhney, S. K., & Singh, R. (2000). *Carbohydrate. Introductory practical biochemistry*. New Delhi: Narosa Publising House.

Singh, N., & Bath, P. K. (1997). Quality evaluation of different types of Indian honey. *Food Chemistry, 58*(1–2), 129–153.

Singleton, V. L., Orthofer, R., & Lamuela-Raventos, R. M. (1999). Analysis of total phenols and other oxidation substrates and antioxidants by means of Folin–Ciocalteu reagent. *Methods in Enzymology, 299*, 265–275.

Sivapriya, M., & Srinivas, L. (2007). Isolation and purification of a novel antioxidant protein from the water extract of Sundakai (*Solanum torvum*) seed. *Food Chemistry, 104*, 510–517.

Food Chemistry 118 (2010) 398–402

Contents lists available at ScienceDirect

Food Chemistry

journal homepage: www.elsevier.com/locate/foodchem

Correlation of fatty acid composition of vegetable oils with rheological behaviour and oil uptake

Juyoung Kim [a], Deok Nyun Kim [a], Sung Ho Lee [b], Sang-Ho Yoo [a], Suyong Lee [a,*]

[a] Department of Food Science and Technology and Carbohydrate Bioproduct Research Center, Sejong University, 98 Gunja-dong Gwangjin-gu, Seoul 143-747, Republic of Korea
[b] Genencor, A Danisco Division, 2600 Kennedy Dr. Beloit, WI 53511, USA

ARTICLE INFO

Article history:
Received 9 February 2009
Received in revised form 6 April 2009
Accepted 5 May 2009

Keywords:
Vegetable oils
Viscosity
Fatty acid
Oil uptake

ABSTRACT

The fatty acid compositions of seven edible vegetable oils were investigated and correlated with their rheological behaviours and the amount of absorbed oils to fried products. All oil samples showed constant viscosity as a function of shear rate, exhibiting Newtonian behaviours. The highest viscosity was observed in hazelnut oil, followed by olive, canola, corn, soybean, sunflower, and grapeseed oils. In addition, a high correlation (R^2 = 0.94) demonstrated that the flow behaviours of vegetable oils were positively governed by their major components (18:1 and 18:2 fatty acids). It was also shown that a more rapid change in viscosity with temperature was observed in the oils containing more double bonds (R^2 = 0.71). Furthermore, even though the overall tendency was that the potato strips fried in the oils with high viscosity appeared to cause more oil uptake, a significant effect of oil types on oil uptake was not observed.

1. Introduction

Frying has been widely used for food industrial and household purposes as a typical way to prepare for foods. Frying is a very complex process where a variety of chemical and physical phenomena take place such as starch retrogradation, Maillard reactions, surface porosity, oil degradation, and etc. (Mellema, 2003). Specially, in terms of heat and mass transfer, heat is transferred from hot oils to foods and water is evaporated from the surface of the foods. Consequently, the pores caused by water evaporation are occupied by oils, thus causing a significant increase in the oil content of the product. Therefore, it seems that frying belongs to a dehydration process (Budzaki & Seruga, 2005).

Frying provides good sensory properties such as crisp texture, brownish colour, and juicy taste. Nonetheless, a negative aspect of fried foods has recently come to the attention of consumers since such products may contain undesirable components such as acrylamide, trans/saturated fatty acids, and a high amount of oil, even up to 50% of the total weight (Funami, Funami, Tawada, & Nakao, 1999). Specifically, since trans fatty acids are widely reported to be a causative factor in health problems such as coronary heart disease (Van de Vijver et al., 2000; Willett & Ascherio, 1994), non-hydrogenated vegetable oils have been receiving great attractions, consequently causing a dramatic increase in its use as an edible frying medium. This comprehensive trend is also supported by the new food guide pyramid of the United States Department of Agriculture (Goldie, 2005), which recommends to consume vegetable oils high in mono- or polyunsaturated fats and low in saturated fats. Therefore, a variety of natural oils from vegetable sources have been used, which include soybean, corn, palm, sunflower, canola, olive oils, and etc.

Basically, frying is the immersion and cooking of foods in hot oils. Therefore, the first step to understand the frying process would be to characterise the quality of the frying oils being used. Thus, a number of previous studies on vegetable oils have been found where a focus was mainly placed on their chemical (Abdulkarim, Long, Lai, Muhammad, & Ghazali, 2007; Dobarganes, Márquez-Ruiz, & Velasco, 2000) and rheological (Erhan, Asadauskas, & Adhvaryu, 2002; Wan Nik, Ani, Masjuki, & Eng Giap, 2005) properties. However, detailed correlations between such properties have not yet been analysed and only limited sources of vegetable oils have been utilised in preceding studies.

In addition, few reports are available on the amount of absorbed oils to foods depending on the type of vegetable oils, even though the oil uptake is a critical issue in a frying process. A couple of studies demonstrated that oil uptake was related to the oxidative degradation of vegetable oils (Dobarganes et al., 2000; Tseng, Moreira, & Sun, 1996). However, to our knowledge, there was only a report in 2007 (Kita, Lisinska, & Golubowska, 2007) in which the oil uptake and texture of foods fried in sunflower, soybean, peanut, rapeseed, olive, palm, and modified oils were compared as a function of frying temperature. Unfortunately, this study did not provide detailed information on the effect of the oil type on the oil uptake.

* Corresponding author. Tel.: +82 2 3408 3227; fax: +82 2 3408 4319.
E-mail address: suyonglee@sejong.ac.kr (S. Lee).

0308-8146/$ - see front matter © 2009 Elsevier Ltd. All rights reserved.
doi:10.1016/j.foodchem.2009.05.011

Therefore, in this study, the flow behaviours of seven vegetable oils were investigated and then correlated with their fatty acid composition. Also, the effect of the type of vegetable oils on the oil uptake of fried potato strips was investigated.

2. Materials and methods

2.1. Experimental materials

Seven edible vegetable oils (canola, corn, grapeseed, hazelnut, olive, soybean, and sunflower oils) were purchased from a commercial source. All chemicals used in this study were of analytical grade.

2.2. Measurement of fatty acid composition

Fatty acid composition of fresh vegetable oils was investigated by using GC–MS (6890N, Agilent Technologies, DE, USA). After each oil sample was methylated with boron trifluoride (Seiichi, Akiko, Yasue, & Chiemi, 2007), the fatty acid methyl esters were injected into a capillary DB-23 column (0.25 mm ID × 60 m × 0.25 μm film thickness, J & W Scientific, CA, USA). Oven temperature was programmed to be 100 °C for 1 min and then raised to 195 °C (15 °C/min), to 210 °C (1 °C/min), and to 240 °C (10 °C/min), which was held for 10 min. Helium was used as carrier gas. Fatty acid composition was expressed as percentage of the total peak area of all the fatty acids in the oil sample.

2.3. Rheological measurement

The flow behaviours of vegetable oils were measured by using a controlled-stress rheometer (Rheostress RS1, Thermo Hakke, Germany) with parallel plates (35 mm diameter). Shear rates in the range of 10–1000 s^{-1} under steady shear conditions were applied to oil samples of which resulting shear stress was measured at 25 °C. Also, in order to investigate the effect of temperature on oil viscosity, the oils were sheared at a constant shear rate of 100 s^{-1} over temperatures ranging from 20 to 70 °C and their viscosity was then measured.

2.4. Frying experiments

Potatoes were hand-peeled and cut into strips (0.9 × 0.9 × 5 cm) using a rectangular-shaped mould and knife. The potato strips were fried at 170 °C for 1 min in each oil by using a deep fryer (T-Fal, Serie F18-R, France). They were then placed in a strainer, allowing for the excessive oil to drain off and air-cooled at ambient conditions. Frying experiments were run in triplicate and fresh oil was used for each batch.

2.5. Oil content analysis

Total oil content in fried potato strips was determined using the soxhlet extraction method (AOAC, 2000).

2.6. Statistical analysis

All experiments were carried out in triplicate and a randomized complete block design was applied to statistically analyse the experimental results using the SAS system (SAS Institute Inc., Cary, NC, USA), followed by Duncan's multiple range test. The rheological curves reported were the mean values of three measurements.

3. Results and discussion

The fatty acid compositions of seven different vegetable oils were analysed as shown in Table 1. For all of the oils tested in this study, the percent amount of total saturated and unsaturated fatty acids ranged from 12% to 22% and from 78% to 88%, respectively. Specially, canola and hazelnut oils contained a great amount of unsaturated fatty acids, relatively compared to the other oil samples. The predominant component of olive, canola, and hazelnut oils was oleic acid (18:1) whilst the others were rich in linoleic acid (18:2). The presence of linolenic acid was found in soybean (7.8%) and canola (13.0%) oils which were relatively higher than other vegetable oils. These results are in great agreement with a previous study (Shahidi, 2004).

The flow behaviours of vegetable oils were characterised by steady shear measurements at 25 °C. All of the oil samples showed the similar flow pattern which could be characterised by straight lines as shown in Fig. 1, indicating that the shear stress is directly proportional to the shear rate. Therefore, the characteristics of this type of flow were adequately described by the equation given below

$$\sigma = \eta \cdot \dot{\gamma}$$

where σ is shear stress, $\dot{\gamma}$ is shear rate, and η is viscosity. Since viscosity is given by the slope of the shear stress vs. shear rate curve, the viscosity of all oil samples appeared to remain constant regardless of the shear rates tested. It was previously recognised that fresh vegetable oils showed Newtonian flow behaviours because of their long chain molecules (Maskan, 2003; Santos et al., 2004). However, the values of viscosity (that is, the slope of each curve) varied distinctly depending on the type of oil samples. The highest viscosity was observed in hazelnut oil, followed by olive, canola, corn, soybean, sunflower, and grapeseed oils (Table 2).

The dependence of viscosity on the type of vegetable oils was investigated by correlating the oil viscosity with fatty acid composition. First, an effort was made to investigate how the degree of

Table 1
Fatty acid composition (%) of edible vegetable oils.

Fatty acid	Grapeseed	Sunflower	Soybean	Corn	Canola	Olive	Hazelnut
C14:0	0.1	0.1	0.1	–	0.1	–	–
C16:0	9.9	9.1	14.6	16.1	6.9	15.9	9.5
C16:1	0.1	0.1	0.1	0.1	0.1	1.2	0.2
C18:0	5.0	4.6	4.9	2.6	2.9	5.4	4.1
C18:1	17.2	26.4	20.6	28.3	54.4	68.4	75.5
C18:2	66.9	57.8	50.5	50.6	19.0	7.2	10.0
C18:3	0.4	0.1	7.8	1.2	13.0	1.0	0.2
C20:0	0.2	0.3	0.5	0.6	0.9	0.6	0.2
C20:1	0.2	0.2	0.3	0.3	2.0	0.3	0.3
C22:0	–	1.0	0.6	0.2	0.5	–	–
C24:0	–	0.3	–	–	0.2	–	–
Saturated	15.2	15.4	20.7	19.5	11.5	21.9	13.8
Unsaturated	84.8	84.6	79.3	80.5	88.5	78.1	86.2

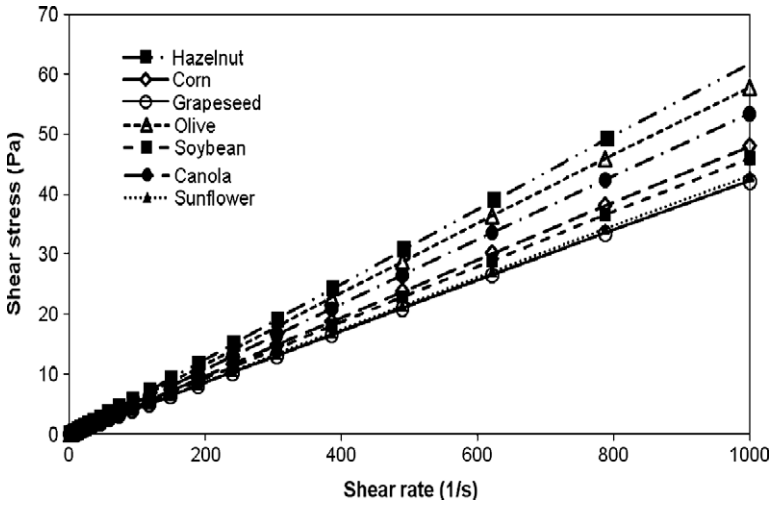

Fig. 1. Curves of shear stress vs. shear rate of edible vegetable oils at 25 °C.

unsaturation affected oil viscosity. Unfortunately, any positive correlation was not observed between viscosity and total saturated (or unsaturated) fatty acids (R^2 = 0.01). However, when the viscosities of the vegetable oils were plotted against either 18:1 or 18:2 fatty acids, it was interesting to note that there were highly positive correlations between them (R^2 = 0.94) as shown in Fig. 2. This relatively good fit demonstrated that the major components of the vegetable oils (18:1 and 18:2 fatty acids) appeared to make a great contribution to their flow behaviours. Especially, a decrease in the oil viscosity was distinctly observed with increasing portion of 18:2 fatty acids and a decreasing portion of 18:1 fatty acids, which indicated more double bonds in the chain, as shown in Table 1. Since each double bond with a *cis* configuration form causes a kink in the straight chain (Abramovic & Klofutar, 1998), the presence of double bond does not allow fatty acid molecules to stack closely together, consequently interfering with packing in the crystalline state. Thus, fatty acids with more double bonds do not have a rigid and fixed structure, being loosely packed and more fluid-like.

Furthermore, the flow behaviours of vegetable oils were investigated as a function of the temperature ranging from 20 to 70 °C. As can be seen in Fig. 3, all of the oil samples exhibited the same viscosity pattern over temperature, which was a non-linear decrease in viscosity with increasing temperature. This temperature effect on oil viscosity has been attributed to decreased intermolecular interactions by great thermal molecular movement (Santos, Santos, & Souza, 2005a). A favourably good agreement was found when the results were compared with other studies (Caristi, Bellocco, Gargiulli, Toscano, & Leuzzi, 2006; Maskan, 2003; Santos, Santos, & Souza, 2005b). In addition, the effect of temperature on the oil viscosity was evaluated by means of the Arrhenius temperature model, which describes the exponential decrease of the viscosity over temperature

$$\eta = A \cdot \mathrm{EXP}(E_a/RT)$$

where η is the oil viscosity, A is the pre-exponential factor, E_a is the activation energy, R is the gas constant, and T is the absolute temperature.

As also presented in Table 2, the calculated values of the activation energy and constant of the vegetable oils were ranged from 24.6 to 26.9 kJ/mol and from 1.18×10^{-6} to 2.23×10^{-6} Pa·s, respectively. The highest value of the activation energy was observed in olive oil, followed by hazelnut, corn, canola, soybean,

Table 2
Viscosity of edible vegetable oils at 25 °C and their Arrhenius model parameters (means with different letters in the same column are significantly different at the 5% level).

Vegetable oils	Viscosity (Pa·s)	Ea (J/mol)	A (Pa·s)
Grapeseed	0.043d	2.49E+04c	1.95E−06ab
Sunflower	0.044d	2.46E+04c	2.23E−06a
Soybean	0.047cd	2.51E+04bc	1.88E−06abc
Corn	0.049c	2.60E+04abc	1.46E−06bc
Canola	0.054b	2.55E+04abc	1.80E−06abc
Olive	0.059a	2.69E+04a	1.18E−06c
Hazelnut	0.063a	2.65E+04ab	1.38E−06bc

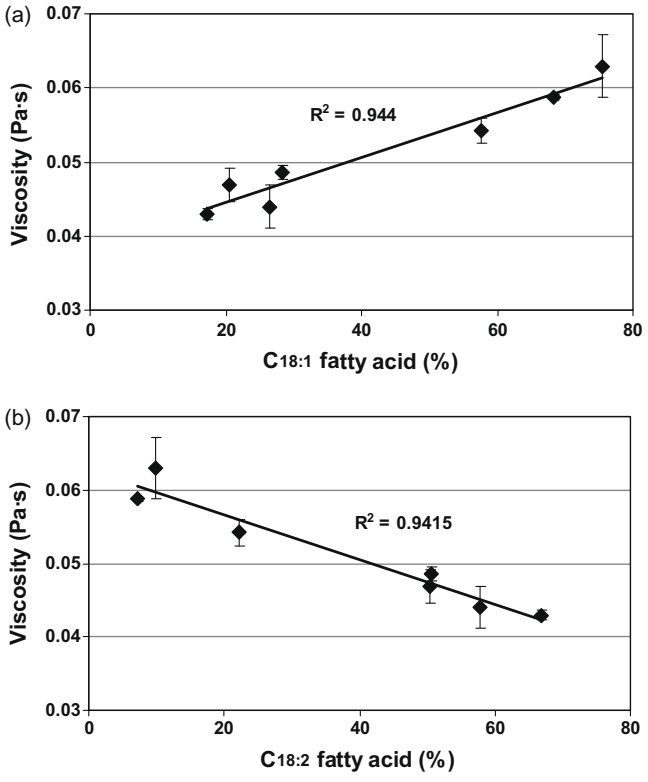

Fig. 2. Correlation of fatty acid composition of vegetable oils with their flow behaviours ((a) 18:1 fatty acid and (b) 18:2 fatty acid).

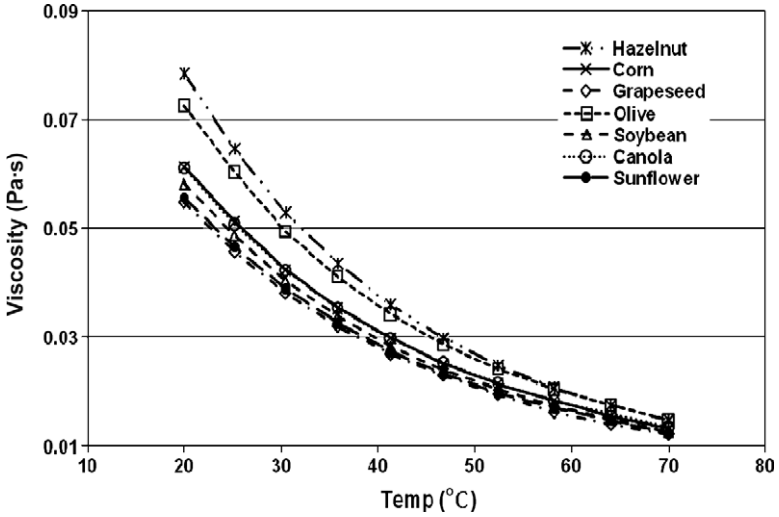

Fig. 3. Effect of temperature on the flow behaviours of vegetable oils.

grapeseed, and sunflower oils. Since the activation energy indicates the sensitivity of a material to temperature changes (Steffe, 1996), the statistical results demonstrated that the flow behaviours of corn, canola, olive, and hazelnut oils were highly dependent on temperature change, compared to the other oil samples. Also, when the activation energy value of each oil sample was plotted against the content of 18:2 fatty acid (data not shown), there was a reasonable correlation ($R^2 = 0.71$) suggesting that the oils containing more double bonds exhibited less activation energy.

In addition, another effort was made to investigate whether there is any correlation between the viscosity of vegetable oils and the oil uptake of fried foods that are cooked in the oils. For doing so, potato strips were fried in five different vegetable oils (olive, canola, soybean, corn, grape oils) and the amount of absorbed oil to the potato samples were analysed. It is generally recognised that the higher viscosity of frying oils, the greater oil content of fried foods (Dana & Saguy, 2006). This would be explained by the fact that high viscosity can allow the oils to be accumulated more easily on the surface of fried foods and enter inside during the cooling period (Maskan, 2003). Therefore, before this frying experiment started, the potato samples fried in olive or canola oils would be expected to have greater oil uptake due to their high viscosity. However, significant differences amongst the samples could not be detected as presented in Table 3. It indicates that viscosity might not be the only factor to affect the oil content. Another possible explanation would be that a more substantial difference in the viscosity amongst the oils might be needed to cause a significant change in the oil uptake. Nonetheless, an overall increase in the oil content by high viscosity could be observed from the mean values of the oil content. Table 3 showed that the highest mean value was observed in the samples fried in olive oil, followed by canola, corn, soybean, and grapeseed oils. Kita et al. (2007) reported the oil pickup of potato crisps, depending on the type of oils that were sunflower, soybean, peanut, rapeseed, olive, palm, and modified oils. Even though this study did not clearly explain the oil uptake difference amongst the used oils, it demonstrated that the samples fried in olive oil contained the highest oil content, which could be favourably compared to our results.

Table 3
Oil uptake of the potato strips fried in different vegetable oils (means with different letters in the same column are significantly different at the 5% level).

Vegetable oils	Oil content (%)
Grapeseed	5.21a
Soybean	5.30a
Corn	5.30a
Canola	5.39a
Olive	5.57a

4. Conclusions

As a principal and essential frying component, edible vegetable oils were characterised in terms of their fatty acid composition, flow behaviours, and oil uptake. The results demonstrated that there was a high correlation between oil viscosity and fatty acid composition, suggesting that the oils with more double bonds appeared to have lower viscosity due to their loosely-packed structure. Also, their flow behaviours over temperature could be well characterised by the Arrhenius model. Unexpectedly, the contribution of oil type to oil uptake of fried foods was not statistically effective. Thus, as long as fresh vegetable oils are used for frying applications, it seems that the effect of the oil type on the oil uptake of fried foods can be disregarded. However, since the quality stability of oils over time could vary depending on the oil type, further research would be necessary to investigate how pertinent quality parameters of the oils and their consequent oil uptake patterns are changed by frying conditions (time and temperature) and repeated use.

Acknowledgements

Thanks go to Mr. Hong Gyoon Oh for his great support during frying experiments. This work was supported by the Korea Research Foundation Grant funded by the Korean Government (MOEHRD, Basic Research Promotion Fund) (KRF-2007-331-F00046).

References

Abdulkarim, S. M., Long, K., Lai, O. M., Muhammad, S. K. S., & Ghazali, H. M. (2007). Frying quality and stability of high-oleic *Moringa oleifera* seed oil in comparison with other vegetable oils. *Food Chemistry, 105*(4), 1382–1389.

Abramovic, H., & Klofutar, C. (1998). The temperature dependence of dynamic viscosity for some vegetable oils. *Acta Chimica Slovenica, 45*(1), 69–77.

AOAC (2000). *Official methods of analysis of AOAC INTERNATIONAL*. Gaithersburg, Maryland, USA: AOAC INTERNATIONAL.

Budzaki, S., & Seruga, B. (2005). Determination of convective heat transfer coefficient during frying of potato dough. *Journal of Food Engineering, 66*(3), 307–314.

Caristi, C., Bellocco, E., Gargiulli, C., Toscano, G., & Leuzzi, U. (2006). Flavone-di-C-glycosides in citrus juices from Southern Italy. *Food Chemistry, 95*(3), 431–437.

Dana, D., & Saguy, I. S. (2006). Review: Mechanism of oil uptake during deep-fat frying and the surfactant effect-theory and myth. *Advances in Colloid and Interface Science, 128–130*, 267–272.

Dobarganes, C., Márquez-Ruiz, G., & Velasco, J. (2000). Interactions between fat and food during deep-frying. *European Journal of Lipid Science and Technology, 102*, 521–528.

Erhan, S. Z., Asadauskas, S., & Adhvaryu, A. (2002). Correlation of viscosities of vegetable oil blends with selected esters and hydrocarbons. *Journal of the American Oil Chemists' Society, 79*, 1157–1161.

Funami, T., Funami, M., Tawada, T., & Nakao, Y. (1999). Decreasing oil uptake of doughnuts during deep-fat frying using curdlan. *Journal of Food Science, 64*(5), 883–888.

Goldie, M. P. (2005). The new food pyramid. *International Journal of Dental Hygiene, 3*(3), 155–158.

Kita, A., Lisinska, G., & Golubowska, G. (2007). The effects of oils and frying temperatures on the texture and fat content of potato crisps. *Food Chemistry, 102*(1), 1–5.

Maskan, M. (2003). Change in colour and rheological behaviour of sunflower seed oil during frying and after adsorbent treatment of used oil. *European Food Research and Technology, 218*, 20–25.

Mellema, M. (2003). Mechanism and reduction of fat uptake in deep-fat fried foods. *Trends in Food Science and Technology, 14*(9), 364–373.

Santos, J. C. O., Santos, I. M. G., Conceição, M. M., Porto, S. L., Trindade, M. F. S., Souza, A. G., et al. (2004). Thermoanalytical, kinetic and rheological parameters of commercial edible vegetable oils. *Journal of Thermal Analysis and Calorimetry, 75*, 419–428.

Santos, J. C. O., Santos, I. M. G., & Souza, A. G. (2005a). Effect of heating and cooling on rheological parameters of edible vegetable oils. *Journal of Food Engineering, 67*(4), 401–405.

Santos, J. C. O., Santos, I. M. G., & Souza, A. G. (2005b). Effect of heating and cooling on rheological parameters of edible vegetable oils. *Journal of Food Engineering, 67*(4), 401–405.

Seiichi, S., Akiko, S., Yasue, S., & Chiemi, S. (2007). A rapid method for trans-fatty acid determination using a single capillary GC. *Journal of Oleo Science, 56*, 53–58.

Shahidi, F. (2004). *Bailey's industrial oil & fat products*. Hoboken, NJ: John Wiley & Sons.

Steffe, J. F. (1996). *Rheological methods in food process engineering*. East Lansing, MI: Freeman Press.

Tseng, Y. C., Moreira, R., & Sun, X. (1996). Total frying-use time effects on soybean-oil deterioration and on tortilla chip quality. *International Journal of Food Science and Technology, 31*(3), 287–294.

Van de Vijver, L. P. L., Kardinaal, A. F. M., Couet, C., Aro, A., Kafatos, A., Steingrimsdottir, L., et al. (2000). Association between trans fatty acid intake and cardiovascular risk factors in Europe: The TRANSFAIR study. *European Journal of Clinical Nutrition, 54*, 126–135.

Wan Nik, W. B., Ani, F. N., Masjuki, H. H., & Eng Giap, S. G. (2005). Rheology of bio-edible oils according to several rheological models and its potential as hydraulic fluid. *Industrial Crops and Products, 22*(3), 249–255.

Willett, W. C., & Ascherio, A. (1994). Trans fatty acids: Are the effects only marginal? *American Journal of Public Health, 84*(5), 722–724.

Food Chemistry 118 (2010) 403–410

Contents lists available at ScienceDirect

Food Chemistry

journal homepage: www.elsevier.com/locate/foodchem

Antioxidant activity and functional properties of porcine plasma protein hydrolysate as influenced by the degree of hydrolysis

Qian Liu [a], Baohua Kong [a,*], Youling L. Xiong [b], Xiufang Xia [a]

[a] College of Food Science, Northeast Agricultural University, Harbin, Heilongjiang 150030, China
[b] Department of Animal and Food Sciences, University of Kentucky, Lexington, KY 40546, USA

ARTICLE INFO

Article history:
Received 22 November 2008
Received in revised form 18 April 2009
Accepted 5 May 2009

Keywords:
Functional properties
Purification
Antioxidant peptide
Porcine plasma protein hydrolysate

ABSTRACT

Antioxidant activity and functional properties of porcine blood plasma protein hydrolysates (PPH) prepared with Alcalase at 6.2%, 12.7% and 17.6% of degree of hydrolysis (DH) were investigated. The PPH showed stronger radical-scavenging ability and possessed stronger Cu^{2+}-chelation ability and a reducing power compared to non-hydrolysed plasma protein ($P < 0.05$). The antioxidant activity of PPH, indicated by thiobarbituric acid-reactive substance (TBARS) values in a liposome-oxidising system, increased with increasing DH ($P < 0.05$). The Alcalase hydrolysis increased protein solubility from its original 68.46–81.79% (non-hydrolysed) to 82.95–94.94% (hydrolysed) over a broad pH range (3.0–8.0). However, hydrolysis decreased surface hydrophobicity and suppressed emulsifying and foaming capacity of the plasma protein. To identify antioxidant peptide, PPH was subjected to ultrafiltration, ion-exchange chromatography and reverse-phase high performance liquid chromatography (RP-HPLC), and the amino acid sequences of isolated peptides were determined by liquid chromatography/tendem mass spectrometry (LC–MS/MS). The peptide with the strongest antioxidant activity had the amino acid sequence of His-Asn-Gly-Asn. The results indicated that PPH could be used as a novel antioxidant but may be of limited utility as an emulsifying or foaming agent.

1. Introduction

Functional properties of proteins can be modified by physical, chemical and enzymatic treatments through changing the protein structure. Enzymatic treatment is a particularly attractive technique to modify proteins due to the milder process conditions required, the relative ease to control the reaction, and minimal formation of by-products (Mannheim & Cheryan, 1992). Selective enzymatic hydrolysis under controlled conditions has been used to improve the solubility and enhance the emulsifying and foaming properties of wheat gluten (Agyare, Xiong, & Addo, 2008) and fish protein (Shahidi, Han, & Synowiecki, 1995).

The cleavage of peptide bonds leads to an increase in the concentration of free amino and carboxyl groups, which increases solubility. Hydrolysis also disrupts the protein tertiary structure and reduces the molecular weight of the protein and, consequently, alters the functional properties of proteins (Adler-Nissen, 1986; Kristinsson & Rasco, 2000). However, extensive hydrolysis could have a negative impact on the functional properties (Kristinsson & Rasco, 2000).

In addition to their functionalities, protein hydrolysates, such as hydrolysed wheat protein (Liyana-Pathiranaa & Shahidi, 2007), zein protein (Kong & Xiong, 2006), and porcine haemoglobin (Chang, Wu, & Chiang, 2007), have been shown to possess antioxidant activity. A typical enzymatic protein hydrolysate is a mixture of proteoses, peptones, peptides, and free amino acids (Chang et al., 2007). The levels and compositions of free amino acids and peptides were reported to determine the antioxidant activities of protein hydrolysates (Wu, Chen, & Shiau, 2003). The type of proteases used and the degree of hydrolysis also affect the antioxidant activity (Kong & Xiong, 2006).

Many antioxidative peptides also have been identified from a variety of food proteins, such as royal jelly protein (Guo, Kouzuma, & Yonekura, 2009) and egg yolk (Park, Jung, Nam, Shahidi, & Kim, 2001). Marcuse (1962) reported that several amino acids, such as Tyr, Met, His, Lys, Gly and Trp, are generally accepted as antioxidants despite their prooxidative effects in some cases. Kawashima, Itoh, Miyoshi, and Chibata (1979) noted that some di- and tri-peptides containing aromatic amino acid residues, as well as peptides containing Tyr, Pro and His, showed strong antioxidant activity.

Animal blood, collected from packing plants, is a valuable protein source from which bioactive peptides can be produced. Presently, the utilisation of porcine serum protein is limited. The production of protein hydrolysates with antioxidant activity and improved functional properties would be of economical interest as well as processing significance. Unlike bovine plasma protein and its hydrolysates, which are restricted or banned from food uses due to the concern with potential transfer of animal diseases,

* Corresponding author. Tel.: +86 451 55191794; fax: +86 451 55190577.
E-mail address: Kongbh63@hotmail.com (B. Kong).

0308-8146/$ - see front matter © 2009 Elsevier Ltd. All rights reserved.
doi:10.1016/j.foodchem.2009.05.013

plasma protein from wholesome swine is considered safe for human consumption.

In this study, the antioxidant activity of porcine plasma protein hydrolysates (PPH) prepared by Alcalase-hydrolysis was evaluated. The surface hydrophobicity, solubility, and emulsifying and foaming properties in relation to the degree of hydrolysis were examined. Meanwhile, the antioxidative peptides were isolated from the hydrolysate, and their amino acid sequences were determined.

2. Materials and methods

2.1. Materials and chemicals

Porcine plasma protein was obtained from Beidahuang Meat Corporation (Harbin, Heilongjiang, China). The dry porcine plasma protein powder contained 70% protein as determined by the Kjeldahl method of determination (AOAC, 2000). Alcalase 2.4 L (6×10^4 u/g) was obtained from Novozymes (Bagsvaerd, Denmark). Testing chemicals, including 3-(2-pyridyl)-5,6-bis(4-phenyl-sulphonic acid)-1,2,4-triazine (ferrozine), 2,4,6-tris(2-pyridyl)-S-triazine (TPTZ), 1,1-diphenyl-2-picrylhydrazyl (DPPH), Soybean L-α-phosphatidylcholine, and 1-anilino-8-naphthalene-sulphonate (ANS) were purchased from Sigma Chemical Co. (St. Louis, MO, USA). All other chemicals and reagents used were of analytical grade.

2.2. Preparation of porcine plasma protein hydrolysates (PPH)

Porcine plasma protein solution (40 mg protein/mL) was heat pretreated (90 °C, 5 min) and then hydrolysed with Alcalase at 55 °C. The enzyme to substrate ratio (E/S) was 2:100 (g/g). The pH of the porcine plasma protein solution was adjusted to the optimal values for Alcalase (pH 8.0) before hydrolysis was initiated, and it was readjusted to the optimal value every 15 min during hydrolysis with 1 M NaOH. The hydrolysates were produced by varying the hydrolysed time to 0.5, 2 and 5 h, which yielded 6.2%, 12.7%, and 17.6% of degrees of hydrolysis (DH), respectively.

After hydrolysis, the pH of the solution was brought to 7.0, and the solution was then heated at 95 °C for 5 min to inactivate the enzyme. The hydrolysates were freeze-dried (LGJ-1 Freeze-Dryer, Shanghai, China), pulverised, placed in sealed bags, and stored at 4 °C until use. DH of hydrolysed protein was determined using a pH-stat method (Adler-Nissen, 1986).

2.3. Determination of antioxidant activities

2.3.1. Thiobarbituric acid-reactive substances (TBARS)

The antioxidant activity of PPH was initially assessed by means of TBARS analysis in an oxidising liposome system. Liposomes were prepared from soybean phosphatidylcholine according to the method of Decker and Hultin (1990). A series of mixed solutions of 5 mL of liposome with 1 mL of PPH (40 mg protein/mL) at 6.2%, 12.7%, and 17.6% of DH were prepared. The control solution was prepared by mixing 1 mL of water instead of 1 mL of protein solution (40 mg protein/mL) with 5 mL of liposome. Oxidation was initiated by adding 0.1 mL of 50 mM $FeCl_3$ and 0.1 mL of 10 mM sodium ascorbate into the liposome/protein solution and continued for 60 min in a 37 °C water bath. The concentrations of TBARS (secondary products from lipid oxidation), with or without the presence of PPH, were determined according to the method which outlined by Kong and Xiong (2006).

2.3.2. 2,2-Diphenyl-1-picryhydrazyl (DPPH) radical scavenging activity

The DPPH radical scavenging activity was determined according to the method of Yen and Hsieh (1995) with slight modification. Aliquots (4.0 mL) of the DPPH radical solution (1×10^{-4} M, in methanol) were each incubated with 1.0 mL of PPH (40 mg protein/mL in distilled water) at room temperature for 30 min in the dark. The absorbance of reacted solutions was measured at 517 nm.

2.3.3. Reducing power

The reducing power of PPH was measured using the ferric reducing/antioxidant power (FRAP) assay (Benzie & Strain, 1996). Absorbance (593 nm) of samples was taken at 30 s intervals for up to 8 min. Sample FRAP values were calculated based on a $FeSO_4$ standard curve (prepared with 100–1000 μM $FeSO_4{\cdot}7H_2O$), and were expressed as $FeSO_4$ equivalent (μM).

2.3.4. Metal chelating activity

The metal chelating effect was determined as previously described (Kong & Xiong, 2006).

2.4. Surface hydrophobicity

The determination of superficial hydrophobicity followed the method described by Akita and Nakai (1990) using 1-anilino-8-naphthalene-sulphonate (ANS) as the fluorescence probe. Fluorescence intensity (FI) was measured with a fluorometer (F-4500 model, Hicathi, Tokyo, Japan) at an excitation wavelength of 374 nm and an emission wavelength of 485 nm. After drawing a graph of the fluorescence as a function of protein concentration, the inclination was calculated and considered as the hydrophobicity.

2.5. Determination of functional properties

2.5.1. Solubility

To determine protein solubility, 200 mg of PPH samples were dispersed in a buffer solution (0.02 M sodium phosphate and 0.01 M citric acid), in pH 3.0–8.0. The mixtures were stirred at room temperature for 30 min and centrifuged at 7500g for 15 min. Protein contents in the supernatants were determined using the Biuret method (Gornall, Bardawill, & David, 1949). Total protein content in PPH samples was determined after solubilisation of the samples in 0.5 M NaOH. Protein solubility was calculated as follows:

$$\text{Solubility } (\%) = (A/B) \times 100$$

where A is protein content in supernatant and B is total protein content in sample.

2.5.2. Emulsifying properties

The emulsifying properties were determined according to the method of Pearce and Kinsella (1978) with a slight modification. Vegetable oil (10 mL) and 30 mL of 0.2% PPH solution were mixed in a buffer solution (0.02 M sodium phosphate and 0.01 M citric acid, pH 3.0–8.0) and homogenised at 20,000 rpm for 1 min using a homogenizer (IKA T18 basic, IKA-Werke GmbH & Co., Staufen, Germany). An aliquot of the emulsion (50 μL) was pipetted from the bottom of the container at 0 and 10 min after homogenisation and mixed with 5 mL of 0.1% sodium dodecyl sulphate (SDS) solution. Absorbance at 500 nm was measured using a spectrophotometer (UT-1800, Pgeneral, Beijing, China), using 0.1% SDS solution as the blank. The emulsifying activity index (EAI) and the emulsion stability index (ESI) was calculated as follows:

$$\text{EAI}(\text{m}^2/\text{g}) = (2 \times 2.303 \times A_{500})/[0.25 \times \text{Protein weight}(\text{g})]$$

where A_{500} represents the absorbance at 500 nm.

$$\mathrm{ESI(min)} = A_0 \times \Delta t / \Delta A$$

where $\Delta A = A_0 - A_{10}$ and $\Delta t = 10$ min, A_{10} and A_0 represent the absorbance after 10 min and time zero, respectively, at 500 nm.

2.5.3. Foaming properties

Foaming capacity and foaming stability of PPH were determined according to the method of Sathe and Salunkhe (1981) with a slight modification. Protein solutions (20 mL of 0.5%), prepared in a buffer (0.02 M sodium phosphate and 0.01 M citric acid, pH 3.0–8.0), were homogenised at 16000 rpm for 2 min using a homogenizer (IKA T18 basic, IKA-Werke GmbH & Co., Staufen, Germany). The whipped sample was immediately transferred into a 25 mL cylinder and the total volume was read after 30 s. The foaming capacity (FC) was calculated according to the following equation:

Foaming capacity (%) = $[(A - B)/B] \times 100$where A is the volume after whipping (mL); B is the volume before whipping (mL).

The whipped sample was allowed to stand at 20 °C for 3 min and the volume of whipped sample was then recorded. Foam stability (FS) was calculated as follows:

Foam stability (%) = $[(A - B)/B] \times 100$where A is the volume after standing (mL); B is the volume before whipping (mL).

2.6. Isolation of antioxidant peptides

PPH with DH of 17.6%, which exhibited the strong antioxidant activity, was fractionated by ultrafiltration (Amicon Stirred Cell 8400, Millipore, USA) with membranes having three different molecular weight cut-offs (3*k*, 6*k* and 10*k*). Four fractions (<3*k*, 3–6*k*, 6–10*k*, and > 10*k*) were separated, lyophilised and then stored at −20 °C until use. The antioxidant activity of these four fractions was determined by reducing power and DPPH radical scavenging activity.

The <3*k* fraction that exhibited high antioxidant activity was dissolved in 20 mM sodium acetate buffer (pH 4.0) and fractionated by ion-exchange chromatography on a SP Sepharose Fast Flow column (2 × 25 cm; GE Healthcare Bio-Sciences AB, Sweden) equilibrated and eluted with a linear gradient of NaCl concentrations from 0 to 1 M. Fractions of 3 mL were collected at a flow rate of 1 mL/min, and the eluted peaks were detected by ultraviolet (UV) absorbance at 280 nm. The fractions showing the highest antioxidant activity were pooled and lyophilised. The antioxidant fraction was dissolved in distilled water and separated by reversed-phase high performance liquid chromatography (RP-HPLC) on an octadecylsilyl ODS column (5 μm, 4.6 × 250 mm; Phenomenex, Macelesfield, United Kingdom) using a linear gradient of acetonitrile containing 0.05% trifluoroacetic acid (TFA) at a flow rate of 0.5 mL/min. The eluted peaks were detected by UV absorbance at 215 nm. Fraction which showed the highest antioxidative activity was further purified by RP-HPLC on an ODS column using a linear gradient of acetonitrile containing 0.05% TFA at a flow rate of 0.75 mL/min. The eluted peaks were detected by UV absorbance at 215 nm.

2.7. Peptide sequence analysis

Molecular mass and peptide sequence of purified fraction was determined using an ultra performance LC–MS/MS (ACQUITY TQD, Waters, New Castle, Delaware, USA). The amino acid sequence of antioxidant activity peptide was obtained over the m/z range 50–1500 and was identified using the SEQUEST sequencing algorithm.

2.8. Statistical analysis

All the experiments were carried out in triplicate. Data were analyzed using the General Linear Models procedure of Statistix 8.1 software package (Analytical Software, St. Paul, MN) for microcomputer. Analysis of variance (ANOVA) was done to determine the significance of the main effects. Significant differences ($P < 0.05$) between means were identified using Tukey procedures.

3. Result and discussion

3.1. Effect of DH on antioxidant activity of PPH

3.1.1. TBARS, DPPH radical scavenging activity and reducing power

The PPH prepared by Alcalase exhibited significant inhibition of TBARS formation, and the inhibition was more pronounced at increasing DH (Table 1). TBARS were lowered by 25.4%, 28.8% and 38.6% at 6.2, 12.7 and 17.6 of DH, respectively, compared to the non-hydrolysed plasma protein. The effect of PPH to inhibit TBARS formation in the liposome system suggested that lipid peroxides generated in the oxidising liposome system were readily decomposed into malondialdehyde or other secondary, TBA-reactive compounds. DPPH radical scavenging activity and reducing power of PPH with different DHs are also depicted in Table 1. As the DHs increased DPPH radical scavenging activity significantly increased ($P < 0.05$), which presented 21.72%, 31.3%, 45.4% and 76.8% scavenging activity corresponding to 0%, 6.2%, 12.7% and 17.6% of DH, respectively. The reducing power (4 min FRAP value) of PPH correlated well with DPPH radical scavenging activity, and it presented 3.0-fold increase for 17.6% of DH sample compared to non-hydrolysed plasma protein.

The ability of PPH to chemically inhibit lipid oxidation as demonstrated in the present study may be attributed, in part, to protein structural changes. Non-hydrolysed plasma protein, because of its compact structure, had a minimal antioxidant activity. Disruption of the native protein structure by enzyme hydrolysis resulted in the opening and exposure of active amino acid residues and patches capable of reacting with oxidants (Kong & Xiong, 2006). Fragmentation of plasma proteins would contribute to the antioxidant activity as well. Hirose and Miyashita (1999) postulated that besides acting as a free radical scavenger, a protein hydrolysate

Table 1
TBARS value, DPPH radical scavenging activity, reducing power (4 min FRAP value) and metal chelating activity of porcine PPH solution (40 mg/mL) produced using Alcalase with different degree of hydrolysis.

Sample	TBARS value (mg/L)	Reducing power (μM)	DPPH radical scavenging activity (%)	Metal chelating activity (%)	
				Cu^{2+}	Fe^{2+}
DH: 0%	2.05 ± 0.01[a]	456.4 ± 1.4d	21.43 ± 0.09[d]	15.82 ± 0.58[d]	5.62 ± 0.30[c]
DH: 6.2%	1.53 ± 0.01[b]	713.1 ± 8.8[c]	31.16 ± 0.93[c]	23.23 ± 0.99[c]	6.80 ± 0.62[c]
DH: 12.7%	1.48 ± 0.01[c]	1303.4 ± 8.2[b]	45.14 ± 1.51[b]	31.98 ± 1.53[b]	9.67 ± 0.30[b]
DH: 17.6%	1.37 ± 0.01[d]	1407.9 ± 9.9[a]	76.53 ± 1.51[a]	44.45 ± 2.01[a]	12.03 ± 0.52[a]

[a–d] Means in the same row with different superscript letters differ significantly ($P < 0.05$).

could serve as a protecting membrane surrounding lipid droplets against oxidation initiators. Presumably, by converting to more amphoteric and structurally flexible short peptides, hydrolysate fragments could readily diffuse to the water–oil interface, where they would adsorb or loosely bind to the phospholipids membrane in the liposome where oxidation occurs.

DPPH is a stable free radical that shows maximal absorbance at 517 nm in ethanol. When DPPH encounters a proton-donating substance (H^+), the radical is scavenged by changing colour from purple to yellow and the absorbance is reduced. In our DPPH test, the protein hydrolysates reduced the DPPH radical to a yellow-coloured compound, apparently due to the DPPH radical accepting an electron or hydrogen to become a stable diamagnetic molecule. Wu et al. (2003) reported that for mackerel protein hydrolysate, its DPPH scavenging activity was improved gradually with increasing hydrolysis time. Qian, Jung, and Kim (2008) noted that antioxidant peptide from bullfrog skin protein inhibited lipid peroxidation more efficiently than α-tocopherol.

The strong reducing power of PPH may be attributed to the increased availability of hydrogen ions (protons and electrons) due to peptide cleavages. Cumby, Zhong, Naczk, and Shahidi (2008) reported that for canola protein hydrolysate, the reducing power increased with increasing DH. It is known that Alcalase acts as an endo peptidase, thus cleaving peptide bonds at the interior of the polypeptide chain. Therefore, Alcalase mainly produces small- and medium-sized oligopeptides or polypeptides, some of which were antioxidative.

3.1.2. Metal chelating activity

Metal chelating activity of PPH with different DHs is shown in Table 1. The Cu^{2+} chelating activity increased markedly with increasing DH ($P < 0.05$), which presented 24.23%, 31.98% and 44.45% chelating activity for 6.2%, 12.7% and 17.6% of DH, respectively. In contrast, the Fe^{2+} chelating activity of hydrolysates, which was relatively low (5.62% at 0 DH), increased slightly with DH.

Transition metals may act as catalysts that promote the generation of the first few radicals, which initiate the oxidative chain reactions. Chelating agents may reduce the availability of transition metals and inhibit the radical-mediated oxidative chain reactions in biological or food systems, and consequently improve human health, and food quality, stability, and safety. Transition metal ions react very quickly with peroxides by acting as one-electron donors to form alkoxyl radical (Gordon, 2001). The chelating activity of peptides in PPH suppressed lipid oxidation. Presumably, peptide cleavages led to an enhanced metal ion binding due to an increased concentration of carboxylic groups and amino groups in branches of the acidic and basic amino acids, thus removing prooxidative free metal ions from the hydroxyl radical system. The direct relationship between soluble protein/peptide concentration and the increase in the chelating capability supported this premise. Kong and Xiong (2006) reported that hydrolysed zein possessed far stronger Cu^{2+} binding activity than Fe^{2+} binding. Haga, Fujinaga, and Kuboi (2005) also noted a far weaker Fe^{2+} binding than Cu^{2+} binding (875 fold difference) by dehydrin, a protein found in higher plants and yeast.

3.2. Surface hydrophobicity

Changes in surface hydrophobicity as a result of proteolysis influence the functional properties, especially the interfacial properties, of the hydrolysates. As is shown in Fig. 1a, the surface hydrophobicity of PPH with different DHs was significantly affected by pH; the highest value was reached at pH 3.0, and higher DH had lower surface hydrophobicity ($P < 0.05$). At pH 7.0, the hydrophobicity of 0%, 6.2%, 12.7% and 17.6% of DH were 64.83%, 26.34%, 6.38% and 4.53% (photons), respectively. Due to shortening of peptide chains, proteolysis is accompanied by gain or loss in hydrophobicity, depending mainly on the nature of the hydrolysed protein and molecular weight size of the formed peptides (Calderon de la Barca, Ruiz-Salazar, & Jara-Marini, 2000). In our present work, enzymatic hydrolysis by Alcalase was accompanied by a decrease of surface hydrophobicity. The possible reason is that peptides released from the native structure of porcine plasma protein reveal great flexibility, which helped them to adopt a conformation with hydrophilic groups more exposed outward.

3.3. Effect of DH on functional properties of PPH

3.3.1. Solubility

The solubility of PPH in the pH range of 3.0–8.0 is shown in Fig. 1b. All hydrolysates were soluble over a wide pH range with more than 78% solubility, significantly higher than that of non-hydrolysed plasma protein ($P < 0.05$). At pH 7.0, the solubility of PPH of 0%, 6.2%, 12.7% and 17.6% DH were 77.5%, 89.2%, 90.3% and 91.7%, respectively. Because smaller peptides resulting from

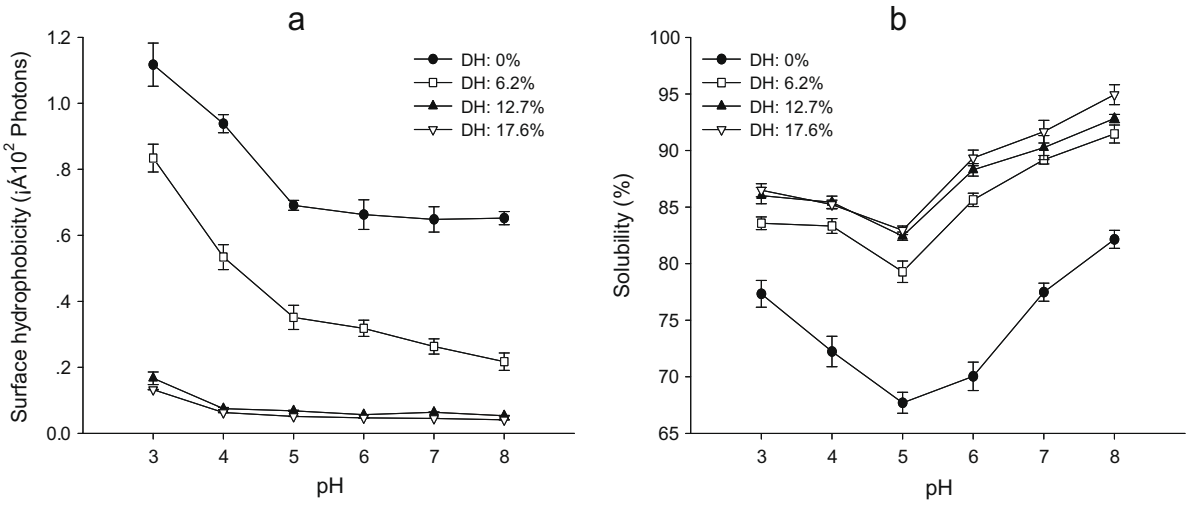

Fig. 1. Surface hydrophobicity (a) and solubility (b) of porcine PPH prepared using Alcalase with different degree of hydrolysis as influenced by pHs. Results are the means from three replicates.

hydrolysis are more polar than polypeptides in non-hydrolysed proteins, they can form stronger hydrogen bonds with water and thereby being more soluble in aqueous solutions.

3.3.2. Emulsifying and foaming properties

The EAI and ESI of hydrolysates are shown in Fig. 2a and b. Both EAI and ESI decreased ($P < 0.05$) with increasing DH. The peptides with low molecular weights probably had a reduced amphiphilicity required for producing a good emulsion. Turgeon, Gauthier, and Paquin (1991) also showed that hydrolysis resulted in a drastic loss of emulsifying properties. Although small peptides diffuse rapidly toward the interface, they are less efficient in stabilizing emulsions because they may not readily agglomerate to produce a fat globule membrane due to charge repulsions.

Foams are biphasic colloidal systems with a continuous liquid or aqueous phase and a dispersed gas or air phase. A degradation of FC and FS ($P < 0.05$) with increasing DH was observed in the present study (Fig. 2c and d), which corresponded to the decrease of emulsifying properties. Klompong, Benjukal, Kantachote, and Shahidi (2007) reported reduced foaming properties for capelin protein hydrolysates at high DHs. A foam stability reduction occurs since more microscopic peptides do not have the strength needed to maintain the stable foam (Shahidi et al., 1995). The molecular properties that are relevant for foaming are similar to those required for emulsification.

When determining the effect of pH on emulsifying and foaming properties, the lowest EAI, ESI, FC and FS were found at pH 5.0, with coincided with the minimal protein solubility. Since the lowest solubility occurred at pH 5.0 (the PI of porcine plasma protein), peptides could not move rapidly to the interface. Protein solubility makes an important contribution to the emulsifying and foaming behaviour of protein. The pH of the dispersing medium dramatically influences foaming properties, especially foam stability.

3.4. Isolation of antioxidant peptides and determination of amino acid sequences

The antioxidant activity of four ultrafiltration fractions with different molecular weights (<3*k*, 3–6*k*, 6–10*k*, and >10*k*) was shown in Table 2. The <3*k* fraction exhibited the highest reducing power and DPPH radical scavenging activity ($P < 0.05$). Guo et al. (2009) reported that the low molecular weight fraction

Table 2
Antioxidant activity of peptide fractions (40 mg/mL) of hydrolysate (DH of 17.6%) with different molecule weight.

Fraction (*k*)	Reducing power (μM)	DPPH radical scavenging activity (%)
>10	557.3 ± 16.3[d]	31.11 ± 1.07[d]
6–10	664.9 ± 22.4[c]	41.30 ± 1.23[c]
3–6	866.6 ± 12.5[b]	50.38 ± 2.06[b]
<3	1206.4 ± 31.5[a]	70.07 ± 1.86[a]

[a–d] Means in the same row with different superscript letters differ significantly ($P < 0.05$).

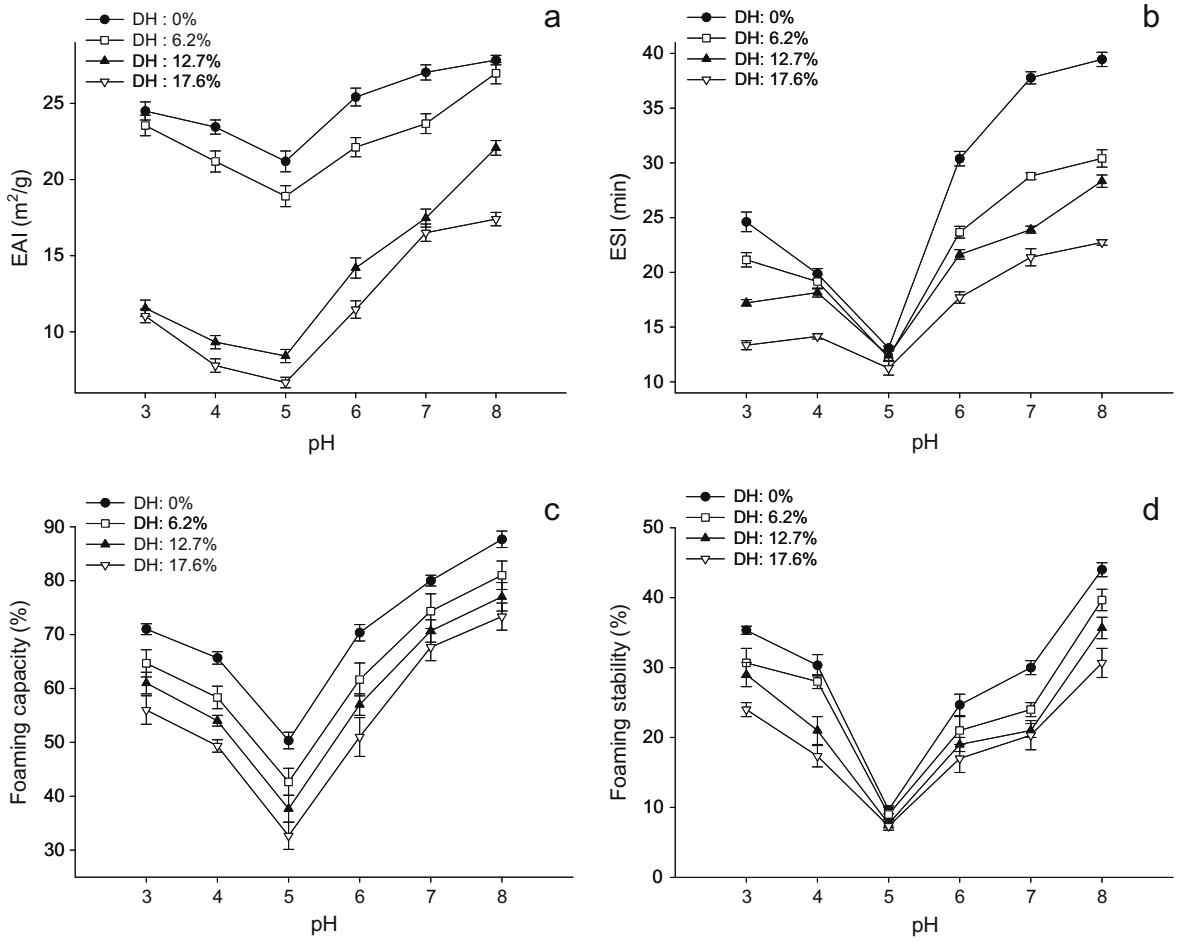

Fig. 2. Emulsifying activity index (a), emulsion stability index (b), foaming capacity (c) and foam stability (d) of porcine PPH prepared using Alcalase with different degree of hydrolysis as influenced by pHs. Results are the means from three replicates.

(<1*k*) from the protease N hydrolysate of royal jelly proteins had the greatest antioxidant activity. Park et al. (2001) also noted that <5*k* hydrolysate from egg yolk protein had the highest antioxidant activity.

To identify the antioxidant peptides derived from PPH, the <3*k* antioxidant hydrolysate, which had the highest antioxidant activity, was separated by ion-exchange chromatography into six fractions (A, B, C, D, E, and F) (Fig. 3). Fraction *E* was found to

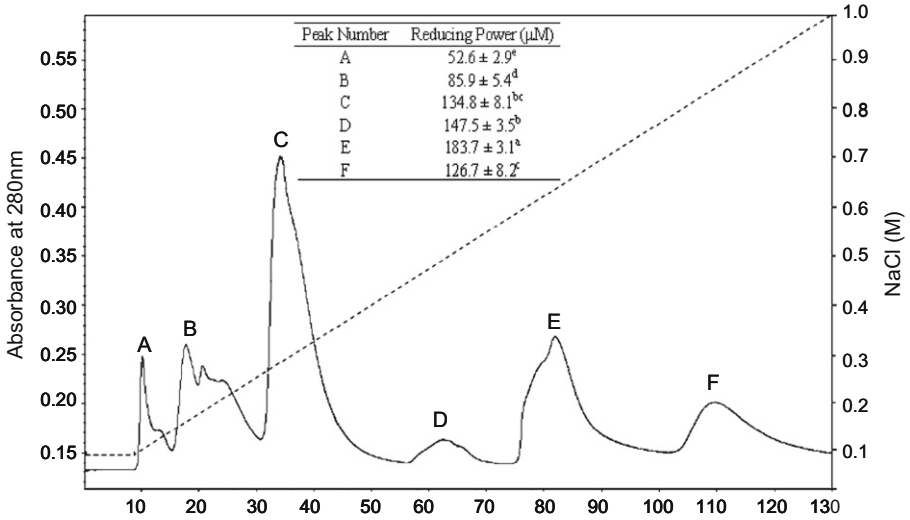

Fig. 3. Elution profile of the fraction (MW < 3*k*) from the hydrolysate (DH of 17.6%) was separated by ion-exchange chromatography. Antioxidative activity was determined by the method of reducing power. Protein concentration is 1 mg/mL.

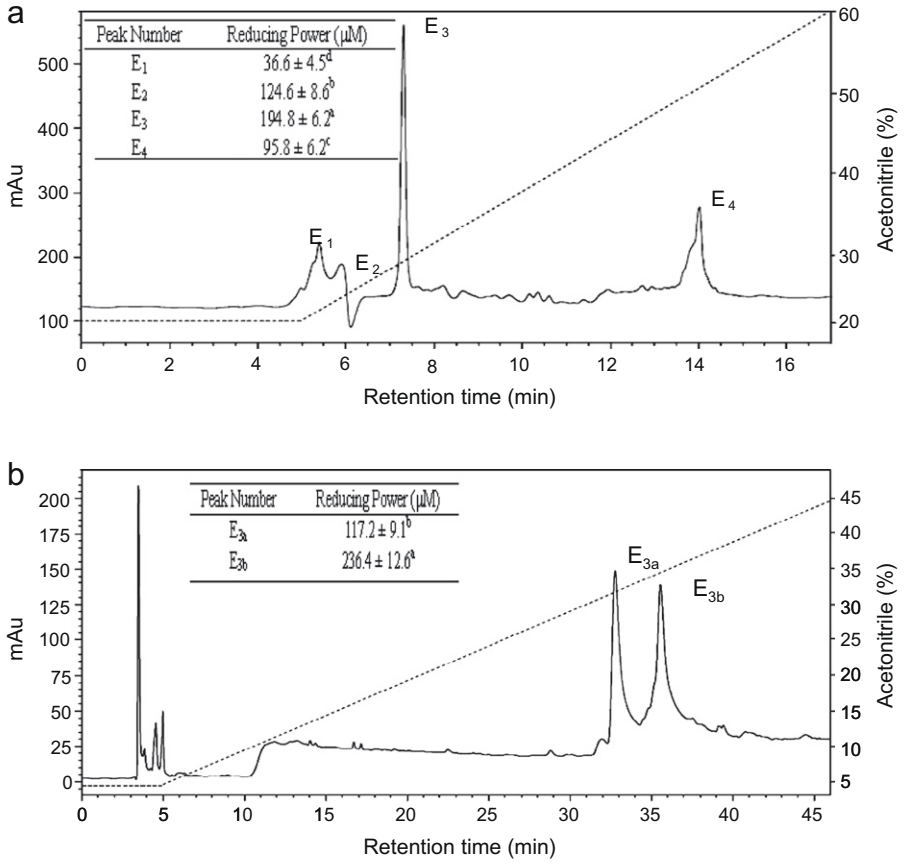

Fig. 4. Isolation of antioxidant peptides. (a) Reversed-phase HPLC pattern on a C_{18}-HPLC column of fraction *E* from Fig. 3 eluted on the ion-exchange chromatography and antioxidant activities of the fractions measured by the method of reducing power. HPLC operation was equilibrated with 0.05% TFA in H_2O and eluted with a linear gradient of 0.05% TFA in acetonitrile at a flow rate of 0.5 mL/min, using an UV detector at 215 nm. (b) Further separation of subfraction E_3 reversed-phase HPLC. HPLC operation was equilibrated with 0.05% TFA in H_2O and eluted with a linear gradient of 0.05% TFA in acetonitrile at a flow rate of 0.75 mL/min, using an UV detector at 215 nm. Protein concentration is 1 mg/mL.

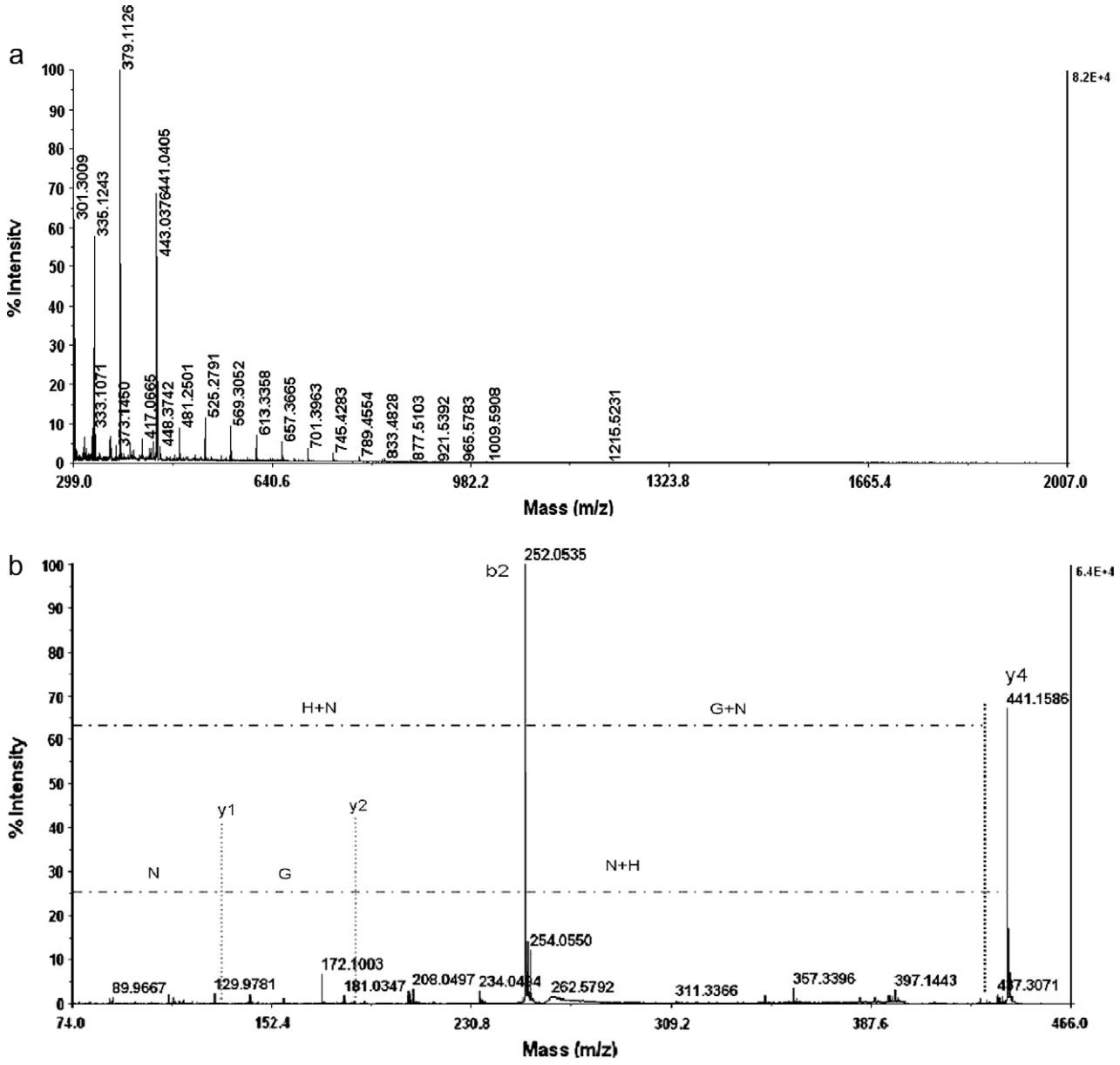

Fig. 5. Identification of amino acid sequence of the antioxidative peptide using UPLC/MS/MS tandem mass spectrometer. (a) The mass spectrum of active fraction E_{3b} separated from ultra performance liquid chromatography. (b) The MS/MS spectrum of active fraction E_{3b} separated from ultra performance liquid chromatography.

possess strong antioxidant activity. This fraction was further separated by RP-HPLC using 0.05% TFA-acetonitrile system and fractionated to four fractions (E_1, E_2, E_3, and E_4) (Fig. 4a). Subfraction E_3 possessed the highest antioxidant activity. Subfraction E_3 was further separated by RP-HPLC using the same solvent system. Two fractions (E_{3a} and E_{3b}) were obtained, and E_{3b} had the higher antioxidant activity (Fig. 4b). The reducing power of fraction E_{3b}, E_3 and E were 236.4, 194.8 and 183.7 μM, respectively, at protein concentration of 1 mg/mL.

Consequently, the E_{3b} fraction was analyzed for amino acid sequencing and the result is shown in Fig. 5. This antioxidative peptide had an amino acid sequence of His-Asn-Gly-Asn, and the molecular weight was 441 (Fig. 5a and b). Rajapakse, Mendis, Jung, Je, and Kim (2005) noted that the peptide isolated from fermented mussel sauce contained Gly, Phe and His, and it exhibited the highest radical scavenging activity and metal chelating activity. In the free radical-mediated lipid peroxidation system, antioxidant activity of peptide or protein is dependent on molecular size and chemical properties such as hydrophobicity and electron transferring ability of amino acid residues in the sequence. Guo et al. (2009) also reported 29 antioxidative peptides that were isolated from royal jelly proteins hydrolysate, and found that some small peptides with 2–4 amino acid residues (Phe-Lys, Ala-Leu, Arg-Tyr, Tyr-Tyr, and Lys-Asn-Tyr-Pro) had strong antioxidant activity. Our result indicated that the antioxidant activity of the peptides isolated from PPH depends on their special amino acid sequences.

4. Conclusions

The hydrolysis by Alcalase enhanced the antioxidant activity of hydrolysates from porcine plasma protein in a liposome model system. The antioxidant activity increased with increasing DH. Further analyses suggested the possible involvement of multiple reactions and processes leading to the inhibition of lipid oxidation, i.e., the

ability to donate hydrogen, to stabilize or terminate radicals, and to sequester prooxidative metal ions. The antioxidant activity of the peptides isolated from PPH depends on their special amino acid sequences. However, hydrolysis had enormously negative effects on the functional properties, notably emulsifying and foaming capacity of the plasma protein. Therefore, PPH could be used as a potential antioxidant but may not be suitable as a functional food ingredient.

Acknowledgement

This study was supported by foundation of Science and Technology of 11th Five-year Plan of Heilongjiang (Grant No. GB06B403).

References

AOAC (2000). *Official methods of analysis* (17th ed.). Gaithersberg, MD: Association of Official Analytical Chemists.

Adler-Nissen, J. (1986). *Enzymic hydrolysis of food proteins. Barking* (Vols. 9–56). UK: Elsevier. pp. 110–169.

Agyare, K. K., Xiong, Y. L., & Addo, K. (2008). Influence of salt and pH on the solubility and structural characteristics of transglutaminase-treated wheat gluten hydrolysate. *Food Chemistry, 107*(3), 1131–1137.

Akita, E. M., & Nakai, S. (1990). Liophilization of β-lactoglobulin: Effect no hydrophobicity, conformation and surface functional properties. *Journal of Food Science, 55*, 711–717.

Benzie, I. F. F., & Strain, J. J. (1996). The ferric reducing ability of plasma (FRAP) as a measure of "antioxidant power": The FRAP assay. *Analytical Biochemistry, 239*, 70–76.

Calderon de la Barca, A. M., Ruiz-Salazar, R. A., & Jara-Marini, M. E. (2000). Enzymatic hydrolysis and synthesis of soy protein to improve its amino acid composition and functional properties. *Journal of Food Science, 65*, 246–253.

Chang, C. Y., Wu, K. C., & Chiang, S. H. (2007). Antioxidant properties and protein compositions of porcine haemoglobin hydrolysates. *Food Chemistry, 100*, 1537–1543.

Cumby, N., Zhong, Y., Naczk, M., & Shahidi, F. (2008). Antioxidant activity and water-holding capacity of canola protein hydrolysates. *Food Chemistry, 109*, 144–148.

Decker, E. A., & Hultin, H. O. (1990). Factors influencing catalysis of lipid oxidation by the soluble fraction of mackerel muscle. *Journal of Food Science, 55*, 947–950, 953.

Gordon, M. (2001). Antioxidants and food stability. In J. Pokorny, N. Yanishlieva, & M. Gordon (Eds.), *Antioxidant in Food* (pp. 7–21). New York, USA: CRC Press.

Gornall, A. G., Bardawill, C. J., & David, M. M. (1949). Determination of serum proteins by means of the biuret reaction. *Journal of Biological Chemistry, 177*, 751–766.

Guo, H., Kouzuma, Y., & Yonekura, M. (2009). Structures and properties of antioxidative peptides derived from royal jelly protein. *Food Chemistry, 113*, 238–245.

Haga, M., Fujinaga, M., & Kuboi, T. (2005). Metal binding by citrus dehydrin with histidine-rich domains. *The Journal of Experimental Botany, 56*, 2695–2703.

Hirose, A., & Miyashita, K. (1999). Inhibitory effect of proteins and their hydrolysates on the oxidation of triacylglycerols containing docosahexaenoic acids in emulsion. *Journal of the Japanese Society for Food Science and Technology, 46*, 799–805.

Kawashima, K., Itoh, H., Miyoshi, M., & Chibata, I. (1979). Antioxidant properties of branched-chain amino acid derivatives. *Chemical Pharmacological Bulletin, 27*, 1912–1916.

Klompong, V., Benjukal, S., Kantachote, D., & Shahidi, F. (2007). Antioxidative activity and functional properties of protein hydrolysate of yellow stripe trevally (*Selaroides leptolepis*) as influenced by the degree of hydrolysis and enzyme type. *Food Chemistry, 102*, 1317–1327.

Kong, B. H., & Xiong, Y. L. (2006). Antioxidant activity of zein hydrolysates in a liposome system and the possible mode of action. *Journal of Agricultural and Food Chemistry, 54*, 6059–6068.

Kristinsson, H. G., & Rasco, B. A. (2000). Biochemical and functional properties of Atlantic salmon (*Salmo salar*) muscle hydrolyzed with various alkaline proteases. *Journal of Agriculture and Food Chemistry, 48*, 657–666.

Liyana-Pathiranaa, C. M., & Shahidi, F. (2007). Antioxidant and free radical scavenging activities of whole wheat and milling fractions. *Food Chemistry, 101*, 1151–1157.

Mannheim, A., & Cheryan, M. (1992). Enzyme-modified proteins from corn gluten meal: Preparation and functional properties. *Journal of the American Oil Chemist's Society, 69*, 1163–1169.

Marcuse, R. (1962). The effect of some amino acids on the oxidation of linoleic acid and its methyl ester. *Journal of the American Oil Chemist's Society, 39*, 97–103.

Park, P. J., Jung, W. K., Nam, K. S., Shahidi, F., & Kim, S. K. (2001). Purification and characterization of antioxidative peptides from protein hydrolysate of lecithin-free egg yolk. *Journal of the American Oil Chemist's Society, 78*, 651–656.

Pearce, K. N., & Kinsella, J. E. (1978). Emulsifying properties of proteins: Evaluation of a turbidimetric technique. *Journal of Agricultural and Food Chemistry, 26*, 716–723.

Qian, Z. J., Jung, Q. K., & Kim, S. K. (2008). Free radical scavenging activity of a novel antioxidative peptide purified from hydrolysate of bullfrog skin, Rana catesbeiana Shaw. *Bioresource Technology, 99*, 1690–1698.

Rajapakse, N., Mendis, E., Jung, W. K., Je, J. Y., & Kim, S. K. (2005). Purification of a radical scavenging peptide from fermented mussel sauce and its antioxidant properties. *Food Research International, 38*, 175–182.

Sathe, S. K., & Salunkhe, D. K. (1981). Functional properties of the Great Northern Bean (*Phaseolus vulgaris* L.) proteins: Emulsion, foaming, viscosity and gelation properties. *Journal of Food Science, 46*(7), 1–74.

Shahidi, F., Han, X. Q., & Synowiecki, J. (1995). Production and characteristics of protein hydrolysates from capelin (*Mallotus villosus*). *Food Chemistry, 53*, 285–293.

Turgeon, S. L., Gauthier, S. F., & Paquin, P. (1991). Interfacial and emulsifying properties of whey peptides fraction obtained with a two step ultrafiltration process. *Journal of Agricultural and Food Chemistry, 39*(4), 637–676.

Wu, H. C., Chen, H. M., & Shiau, C. Y. (2003). Free amino acids and peptides as related to antioxidant properties in protein hydrolysates of mackerel (*Scomber austriasicus*). *Food Research International, 36*, 949–957.

Yen, G., & Hsieh, P. (1995). Antioxidant activity and scavenging effects on active oxygen of xylose-lysine Maillard reaction products. *Journal of the Science of Food and Agriculture, 67*, 415–420.

Food Chemistry 118 (2010) 411–417

Contents lists available at ScienceDirect

Food Chemistry

journal homepage: www.elsevier.com/locate/foodchem

Hepatoprotective effect of the root extract of *Decalepis hamiltonii* against carbon tetrachloride-induced oxidative stress in rats

Anup Srivastava [a,*], T. Shivanandappa [b]

[a] Department of Pathology, Center for Free Radical Biology, University of Alabama at Birmingham, 901, 19th St. S., Rm #347, Birmingham, AL 35294, USA
[b] Department of Food Protectants and Infestation Control, Central Food Technological Research Institute, Mysore-570020, Karnataka, India

ARTICLE INFO

Article history:
Received 4 February 2009
Received in revised form 27 April 2009
Accepted 5 May 2009

Keywords:
Decalepis hamiltonii
Hepatoprotective
Antioxidant enzymes
Lipid peroxidation, protein carbonyls

ABSTRACT

Decalepis hamiltonii, a climbing shrub, grows in the forests of peninsular India and is consumed for its health promoting properties. The hepatoprotective activity of the aqueous extract of the roots of *D. hamiltonii* with known antioxidant constituents was studied against carbon tetrachloride (CCl_4)-induced oxidative stress and liver injury in rats. Pretreatment of rats with aqueous extract of the roots of *D. hamiltonii*, single (50, 100 and 200 mg/kg b.w.) and multiple doses (50 and 100 mg/kg b.w. for 7 days) significantly prevented the CCl_4 (1 ml/kg b.w.) induced hepatic damage as indicated by the serum marker enzymes (AST, ALT, ALP, and LDH). Parallel to these changes, the root extract also prevented CCl_4-induced oxidative stress in the rat liver by inhibiting lipid peroxidation and protein carbonylation, and restoring the levels of antioxidant enzymes (SOD, CAT, GPx, GR, and GST) and glutathione. The biochemical changes were consistent with histopathological observations suggesting marked hepatoprotective effect of the root extract in a dose dependent manner. Protective effect of the aqueous extract of the roots of *D. hamiltonii* against CCl_4-induced acute hepatotoxicity could be attributed to the antioxidant constituents.

1. Introduction

Liver damage is a widespread pathology which in most cases involves oxidative stress and is characterised by a progressive evolution from steatosis to chronic hepatitis, fibrosis, cirrhosis, and hepatocellular carcinoma. Various xenobiotics are known to cause hepatotoxicity one among them is carbon tetrachloride (CCl_4) (Kodavanti, Joshi, Young, Meydrech, & Mehendale, 1989). Reductive dehalogenation of CCl_4 by the P450 enzyme system to the highly reactive trichloromethyl radical initiates the process of lipid peroxidation which is considered to be the most important mechanism in the pathogenesis of liver damage induced by CCl_4 (Demirdag et al., 2004). Trichloromethyl radical can even react with sulfhydryl groups of glutathione (GSH) and protein thiols. In addition, CCl_4 also alters the antioxidant profile of the liver including the antioxidant enzymes like superoxide dismutase (SOD), catalase (CAT), glutathione peroxidase (GPx), glutathione reductase (GR), and glutathione transferase (GST) (Sheweita, El-Gabar, & Bastawy, 2001).

Steroids, vaccines, and antiviral drugs, have been used as therapies for liver pathologies, have potential adverse side-effects, especially if administered chronically or sub-chronically. Therefore, herbal products and traditional medicines with better effectiveness and safe profiles are needed as a substitute for chemical therapeutics. As oxidative stress plays a central role in liver pathologies and their progression, the use of antioxidants have been proposed as therapeutic agents, as well as drug co-adjuvants, to counteract liver damage. A number of studies have shown that the plant extracts having antioxidant activity protect against CCl_4 hepatotoxicity by inhibiting lipid peroxidation and enhancing antioxidant enzyme activity (Shahjahan, Sabitha, Jainu, & Devi, 2004; Sheweita et al., 2001).

Decalepis hamiltonii (Wight and Arn.) (family: Asclepiadaceae), a climbing shrub, grows in the forests of peninsular India. Its tuberous roots are consumed as pickles and juice for its health promoting properties in southern India. The roots are also used in folk medicine and ayurvedic (the ancient Indian traditional system of medicine) preparations as general vitaliser and blood purifier (Nayar, Shetty, Mary, & Yoganarshimhan, 1978). We have earlier shown that the roots of *D. hamiltonii* possess potent antioxidant properties, which could be associated with their health benefits (Srivastava, Shereen, Harish, & Shivanandappa, 2006). Our recent work has shown that the aqueous extract of the roots of *D. hamiltonii* is a cocktail of antioxidants (activity guided purification) namely, 4-hydroxyisophthalic acid, ellagic acid, 14-aminotetradecanoic acid, 4-(1-hydroxy-1-methylethyl)-1-methyl-1, 2-cyclohexane diol, 2-hydroxymethyl-3-methoxybenzaldehyde, 2,4,8 trihydroxybicyclo [3.2.1]octan-3-one; out of these five are novel antioxidants (Srivastava, Harish, & Shivanandappa, 2006;

* Corresponding author. Tel.: +1 205 975 9576; fax: +1 205 975 7447.
E-mail address: anup@uab.edu (A. Srivastava).

0308-8146/$ - see front matter © 2009 Elsevier Ltd. All rights reserved.
doi:10.1016/j.foodchem.2009.05.014

Srivastava, Rao, & Shivanandappa, 2007). We have also reported that the methanolic extract contains several antioxidant compounds (Harish, Divakar, Srivastava, & Shivanandappa, 2005). The present study investigates the hepatoprotective potential of *D. hamiltonii* aqueous extract pretreatment against CCl_4-induced liver toxicity in rats.

2. Materials and methods

2.1. Chemicals

Nicotinamide adenine dinucleotide phosphate reduced (NADPH), 1-chloro-2,4-dinitrobenzene (CDNB), thiobarbituric acid (TBA), glutathione (GSH), oxidised glutathione (GSSG), glutathione reductase (GR), cumene hydroperoxide (CHP), pryogallol, bovine serum albumin (BSA), 2,4-dinitrophenyl hydrazine (DNPH), tetraethoxypropane were purchased from Sigma Chemical Co. (St. Louis, MO, USA). Trichloroacetic acid (TCA), hydrogen peroxide (H_2O_2), 5,5′dithiobis(2-nitrobenzoic acid) (DTNB) and other chemicals were purchased from Sisco Research Laboratories, Mumbai, India. All the chemicals used were of highest purity grade available.

2.2. Preparation of the root powder and extraction

Roots of *D. hamiltonii* were washed with water, followed by crushing with a roller to separate the inner woody core from the outer fleshy layer. The fleshy portions were pooled, dried at 40 °C in a hot air oven and fine powdered. The powder was used for extraction.

The aqueous extract was prepared by homogenising the root powder in warm water (50 °C) and allowed to stand for 24 h, filtered with Whatman paper No. 1 and the filtrate was lyophilised and weighed (17% of root powder). To quantify/characterise the extract composition total polyphenolic content was measured. The aqueous extract had a total polyphenolic content of 13.8 mg/g extract. Aqueous extract of *D. hamiltonii* (DHA) was chosen for this study as it shows highest antioxidant activity among the different solvent extracts (Srivastava et al., 2006).

2.3. Animals and treatments

Sixty day old adult male Wistar rats (180–200 g) were divided into groups of eight each. Appropriate guidelines of the local animal ethics committee were followed for the animal experiments. In a 90 days dietary study on rats it was established that the root extract of *D. hamiltonii* is safe to the mammalian system at the highest dose used in this study. Based on the preliminary experiments the hepatoprotective dose of the aqueous extract of *D. hamiltonii* was decided. In single dose pretreatment (oral) experiment, administration of aqueous extract of the roots of *D. hamiltonii* at 50, 100 and 200 mg/kg b.w. was followed, after 1 h, by oral administration of CCl_4 (1/2 LD_{50}-1 ml/kg b.w.). In multiple dose pretreatment experiment, aqueous extract of the roots of *D. hamiltonii* was administered for seven consecutive days at 50 and 100 mg/kg b.w. followed by a single oral dose of CCl_4 (1 ml/kg b.w.) on the 7th day. Animals were sacrificed by anesthesia 16 h after CCl_4 administration, the liver perfused with saline were dissected out and processed immediately for biochemical assays.

2.4. Experimental groupings

Single dose: Group I – control; Group II – CCl_4 (sunflower oil was used as the vehicle); Group III – *D. hamiltonii* aqueous extract (DHA) 50 mg/kg b.w. + CCl_4; Group IV – DHA 100 mg/kg b.w. + CCl_4; Group V – DHA 200 mg/kg b.w. + CCl_4; Group VI – DHA 200 mg/kg b.w.

Multiple dose: Group I – Control; Group II – CCl_4; Group III – DHA 50 mg/kg b.w. + CCl_4; Group IV – DHA 100 mg/kg b.w. + CCl_4; Group V – DHA 100 mg/kg b.w.

2.5. Serum enzymes

Blood samples were collected in tubes, allowed to clot and the serum was collected by centrifugation at 2000*g* for 10 min and stored at 4 °C for biochemical analysis. Serum transaminases (alanine transaminase (ALT) and aspartate transaminase (AST)) were determined by the method of Reitman and Frankel (Reitman & Frankel, 1957). The reaction mixture containing the substrates (L-alanine (200 mM) or L-aspartate (200 mM) with α-ketoglutarate) and enzyme in phosphate buffer (0.1 M, pH 7.4) was incubated for 30 min and 60 min for ALT and AST, respectively. After incubation, DNPH (1 mM) was added and kept for another 30 min at room temperature. The colour was developed by the addition of NaOH (0.4 M) and read at 505 nm in a spectrophotometer. Lactate dehydrogenase (LDH) activity was assayed by the method of Kornberg (1955). The reaction mixture consisted of NADH (0.02 M), sodium pyruvate (0.01 M) in sodium phosphate buffer (0.1 M, pH 7.4). The change in the absorbance was recorded at 340 nm at 30 s interval for 3 min. Alkaline phosphatase (ALP) activity was assayed by the method of Walter and Schutt (1974) with *p*-nitrophenyl phosphate (1.25 mM) as the substrate. The enzyme activity was calculated using the extinction coefficient, $1.85 \times 10^{-3}\ M^{-1}\ cm^{-1}$ for *p*-nitrophenol.

2.6. Lipid peroxidation

Lipid peroxidation (LPO) in the tissue homogenate was measured by estimating the formation of thiobarbituric acid reactive substances (TBARS) (Ohkawa, Ohishi, & Yagi, 1979). Tissue homogenate (10% w/v in 50 mM phosphate buffer, pH 7.4) was boiled in TCA (10%) and TBA (0.34%) for 15 min, cooled and centrifuged. Absorbance of the supernatant was read at 535 nm. TBARS was calculated using tetraethoxypropane as the standard.

2.7. Antioxidant enzymes

Liver tissue was homogenised (10% w/v) in ice-cold 50 mM phosphate buffer (pH 7.4), centrifuged at 10,000*g* for 20 min at 4 °C and the supernatant was used to assay the enzyme activities. Superoxide dismutase (SOD) activity was measured using pyrogallol (2 mM) autoxidation in Tris buffer (Marklund & Marklund, 1974). Catalase (CAT) activity was measured using H_2O_2 (3%) as the substrate in phosphate buffer (Aebi, 1974). Glutathione peroxidase (GPx) activity was measured by the indirect assay method using glutathione reductase. Cumene hydroperoxide (1 mM) and glutathione (0.25 mM) were used as substrates and oxidation of NADPH by glutathione reductase (0.25 U) in tris buffer (0.05 M, pH 7.4) was monitored at 340 nm (Mannervik, 1985). Glutathione reductase (GR) activity was estimated using oxidised glutathione (0.5 mM) and NADPH (2 mM) in potassium phosphate buffer (0.1 M, pH 7.4) (Calberg & Mannervik, 1985). Glutathione-S-transferase (GST) activity was assayed by the method of Warholm, Guthenberg, Bahr, and Mannervik (1985) in phosphate buffer (0.1 M, pH 7.6) containing glutathione (0.5 mM) and CDNB (0.5 mM) and change in the absorbance at 344 nm was monitored in a UV–visible spectrophotometer.

2.8. Glutathione

A 10% (w/v) liver homogenate was prepared in 5% (w/v) trichloroacetic acid, centrifuged at 2000*g* for 10 min and the

glutathione (GSH) content in the deproteinised supernatant was estimated by Ellman's reagent with a standard curve (Ellman, 1959).

2.9. Protein carbonyls

Liver homogenate (10% w/v) was prepared in 20 mM Tris–HCl buffer, pH 7.4 with 0.14 M NaCl, centrifuged at 10,000*g* for 10 min at 4 °C. Supernatant (1.0 ml) was precipitated with an equal volume of 20% TCA and centrifuged. The pellet was resuspended in 1.0 ml of DNPH (10 mM in 2 M HCl) and allowed to stand at room temperature for 60 min with occasional vortexing. 0.5 ml of 20% TCA was added to the reaction mixture and centrifuged, the pellet obtained was washed three times with acetone and 1.0 ml of 2% of SDS (in 20 mM Tris–HCl, 0.1 M NaCl, pH 7.4) was added to solublise the pellet. The absorbance of the solution was read at 360 nm and the carbonyl content was calculated using a molar extinction coefficient of 22,000 M^{-1} cm^{-1} (Levine et al., 1990).

Protein content was estimated by the method of Lowry, Rosenbrough, Farr, and Randall (1951) with bovine serum albumin as the standard.

2.10. Histopathological examination

Pieces of liver from the left lobe were fixed in Bouin's fluid for 24 h and processed for paraffin embedding. Sections (6 μm thick) were stained with hematoxylin and eosin and imaged with Olympus photomicroscope.

2.11. Statistics

Data were expressed as mean ± SE ($n = 8$) and significant difference between the groups was statistically analysed by Duncan's multiple range test (Statistica Software, 1999). A difference was considered significant at $p < 0.05$.

3. Results

The food consumption and body weights of the DHA treated rats were comparable to the control group.

3.1. Serum enzymes

Levels of the serum marker enzymes of hepatic damage, AST, ALT, LDH, and ALP increased significantly in CCl_4 treated rats compared to the control group. In single dose experiment, DHA at 100 and 200 mg/kg b.w. prevented the liver damage as judged by the restored enzyme levels (Fig. 1). Multiple pretreatment of DHA at a lower dose (50 mg/kg b.w.) was more effective than that of single administration (Fig. 2).

3.2. Lipid peroxidation

The effect of DHA on CCl_4-induced lipid peroxidation in the liver is shown in Tables 1 and 2. CCl_4 increased the hepatic TBARS concentration significantly which was inhibited by DHA pretreatment. Single dose pretreatment with the highest dose of DHA (200 mg/kg b.w.) was most effective in inhibiting the hepatic lipid peroxidation.

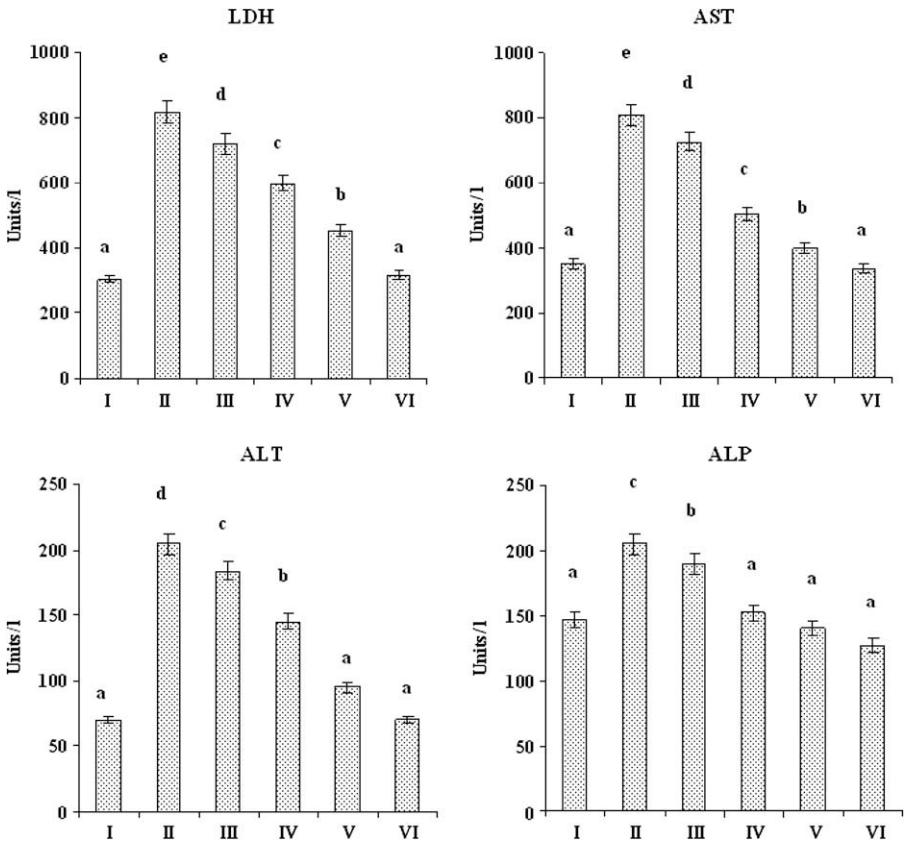

Fig. 1. Protective effect of the aqueous extract of the roots of *D. hamiltonii* (pretreatment-single dose) on CCl_4 hepatotoxicity: serum enzymes. Group I – control; Group II – CCl_4; Group III – DHA 50 mg/kg b.w. + CCl_4; Group IV – DHA 100 mg/kg b.w. + CCl_4; Group V – DHA 200 mg/kg b.w. + CCl_4; Group VI – DHA 200 mg/kg b.w. LDH, lactate dehydrogenase; ALT, alanine aminotransferase; AST, aspartate aminotransferase; ALP, alkaline phosphatase. Each bar represents the mean ± SE, $n = 8$; bars with different alphabets differ significantly at $p < 0.05$ level (DMRT).

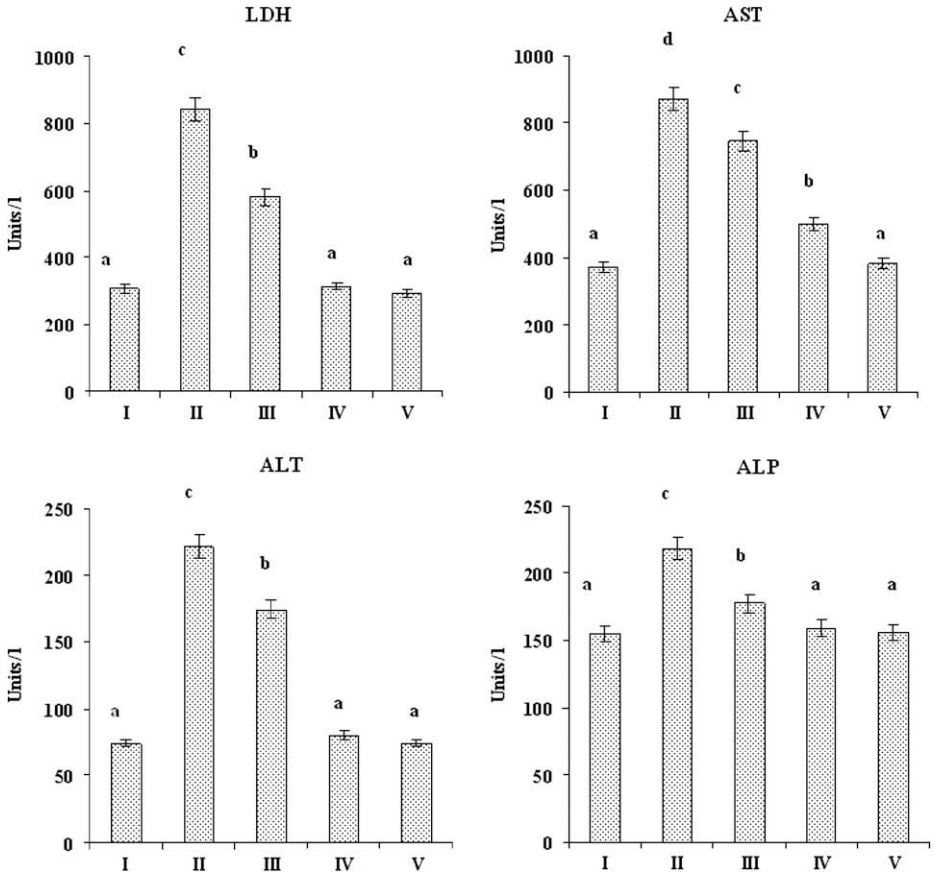

Fig. 2. Protective effect of the aqueous extract of the roots of *D. hamiltonii* (pretreatment-multiple dose) on CCl_4 hepatotoxicity: serum enzymes. Group I – control; Group II – CCl_4; Group III – DHA 50 mg/kg b.w. + CCl_4; Group IV – DHA 100 mg/kg b.w. + CCl_4; Group V – DHA 100 mg/kg b.w. LDH, lactate dehydrogenase; ALT, alanine aminotransferase; AST, aspartate aminotransferase; ALP, alkaline phosphatase. Each bar represents the mean ± SE, $n = 8$; bars with different alphabets differ significantly at $p < 0.05$ level (DMRT).

3.3. Antioxidant enzymes

The hepatic antioxidant enzyme activities were decreased in the liver of rats administered with CCl_4. Activities of SOD, CAT, GPx, GR and GST were restored by DHA pretreatment. Multiple dose pretreatment of the root extract was more effective in the restoration of biochemical changes than a single dose at a given DHA dose. Further, DHA multiple dose pretreatment, by itself, significantly boosted the antioxidant enzyme activities (except SOD) in the liver (Tables 1 and 2).

3.4. Glutathione

Administration of CCl_4 decreased the hepatic GSH level which was restored to normal level by DHA at higher doses in both single and multiple pretreatments (Tables 1 and 2). Pretreatment of DHA

Table 1
Effect of *D. hamiltonii* aqueous root extract (pretreatment-single dose) on hepatic lipid peroxidation, antioxidant profile and protein carbonylation of rats intoxicated with CCl_4.

Group	LPO[A]	SOD[B]	CAT[C]	GPx.[D]	GR[D]	GST[E]	GSH[F]	PC[G]
I	$3.79^{a} \pm 0.28$	$2.48^{a} \pm 0.21$	$5.08^{c} \pm 0.46$	$107.87^{b} \pm 9.95$	$234.47^{d} \pm 21.23$	$134.82^{b} \pm 12.44$	$17.82^{c} \pm 1.61$	$30.73^{a} \pm 2.62$
II	$3.51^{a} \pm 0.31$	$2.58^{a} \pm 0.19$	$5.39^{c} \pm 0.52$	$109.66^{b} \pm 9.92$	$246.75^{d} \pm 22.78$	$159.01^{c} \pm 13.49$	$18.50^{c} \pm 1.73$	$30.93^{a} \pm 2.46$
III	$5.21^{c} \pm 0.046$	$0.48^{c} \pm 0.03$	$3.35^{a} \pm 0.31$	$83.76^{a} \pm 7.82$	$167.48^{b} \pm 15.49$	$135.28^{b} \pm 12.38$	$15.43^{b} \pm 1.32$	$50.42^{b} \pm 4.51$
IV	$4.43^{b} \pm 0.39$	$1.28^{b} \pm 0.11$	$4.17^{b} \pm 0.38$	$79.83^{a} \pm 7.33$	$208.79^{c} \pm 18.37$	$143.27^{bc} \pm 13.28$	$17.32^{bc} \pm 1.64$	$33.68^{a} \pm 3.24$
V	$3.68^{a} \pm 0.27$	$2.15^{a} \pm 0.19$	$4.90^{c} \pm 0.35$	$105.91^{b} \pm 9.56$	$230.00^{d} \pm 21.26$	$152.18^{bc} \pm 11.56$	$18.06^{c} \pm 1.75$	$32.32^{a} \pm 3.11$
VI	$5.45^{c} \pm 0.44$	$0.28^{c} \pm 0.02$	$3.00^{a} \pm 0.27$	$80.73^{a} \pm 7.87$	$128.40^{a} \pm 11.24$	$97.09^{a} \pm 8.41$	$13.09^{a} \pm 1.21$	$49.16^{b} \pm 3.56$

Treatments – I: control; II: DHA (200 mg/kg); III: DHA (50 mg/kg) + CCl_4 (1 ml/kg); IV: DHA (100 mg/kg) + CCl_4 (1 ml/kg); V: DHA (200 mg/kg) + CCl_4 (1 ml/kg); VI: CCl_4 (1 ml/kg).
Means with different suffix letters differ significantly ($p < 0.05$).
[A] nmoles MDA/mg protein.
[B] Units/mg proteins.
[C] μmole H_2O_2/min/mg protein.
[D] nmoles NADPH/min/mg protein.
[E] μmole CDNB conjugate/min/mg protein.
[F] μg/mg protein.
[G] μmole/mg protein.

Table 2
Effect of *D. hamiltonii* aqueous root extract (pretreatment-multiple dose) on hepatic lipid peroxidation, antioxidant profile and protein carbonylation of rats intoxicated with CCl_4.

Group	LPO[A]	SOD[B]	CAT[C]	GPx.[D]	GR[D]	GST[E]	GSH[F]	PC[G]
I	$3.92^{b} \pm 0.21$	$2.35^{a} \pm 0.22$	$4.34^{d} \pm 0.39$	$105.55^{d} \pm 10.17$	$227.77^{c} \pm 21.36$	$170.93^{c} \pm 16.20$	$16.17^{c} \pm 1.38$	$33.20^{a} \pm 2.91$
II	$3.47^{a} \pm 0.29$	$2.69^{a} \pm 0.21$	$4.65^{e} \pm 0.42$	$117.70^{e} \pm 10.26$	$278.01^{d} \pm 22.19$	$189.34^{d} \pm 17.55$	$17.41^{d} \pm 1.59$	$33.38^{a} \pm 3.27$
III	$4.99^{c} \pm 0.36$	$0.76^{c} \pm 0.052$	$3.49^{b} \pm 0.31$	$89.12^{b} \pm 7.99$	$196.50^{b} \pm 17.48$	$120.35^{a} \pm 11.45$	$14.36^{b} \pm 1.24$	$38.45^{b} \pm 3.43$
IV	$4.08^{b} \pm 0.37$	$1.69^{b} \pm 0.13$	$3.92^{c} \pm 0.33$	$99.84^{c} \pm 8.46$	$226.65^{c} \pm 20.34$	$150.21^{b} \pm 12.38$	$14.50^{c} \pm 1.32$	$33.68^{a} \pm 3.24$
V	$5.80^{d} \pm 0.49$	$0.30^{d} \pm 0.02$	$2.67^{a} \pm 0.24$	$78.76^{a} \pm 7.21$	$118.35^{a} \pm 10.18$	$115.96^{a} \pm 10.38$	$11.72^{a} \pm 1.07$	$50.42^{c} \pm 4.12$

Treatments – I: control; II: DHA (100 mg/kg); III: DHA (50 mg/kg) + CCl_4 (1 ml/kg); IV: DHA (100 mg/kg) + CCl_4 (1 ml/kg); V: CCl_4 (1 ml/kg).
Means with different suffix letters differ significantly ($p < 0.05$).
[A] nmoles MDA/mg protein.
[B] Units/mg proteins.
[C] μmole H_2O_2/min/mg protein.
[D] nmoles NADPH/min/mg protein.
[E] μmole CDNB conjugate/min/mg protein.
[F] μg/mg protein.
[G] μmole/mg protein.

alone raised the hepatic GSH levels which was significant with multiple dose pretreatment.

3.5. Protein carbonyls

CCl_4 treatment increased the protein carbonyl content in the rat liver. DHA pretreatment prevented CCl_4-induced protein carbonyl formation in dose dependent manner except for the lowest dose in single dose experiment (Tables 1 and 2).

3.6. Histopathology

Histopathological examination of the liver of CCl_4 administered rats revealed degenerative changes such as vacuolisation and pyc-

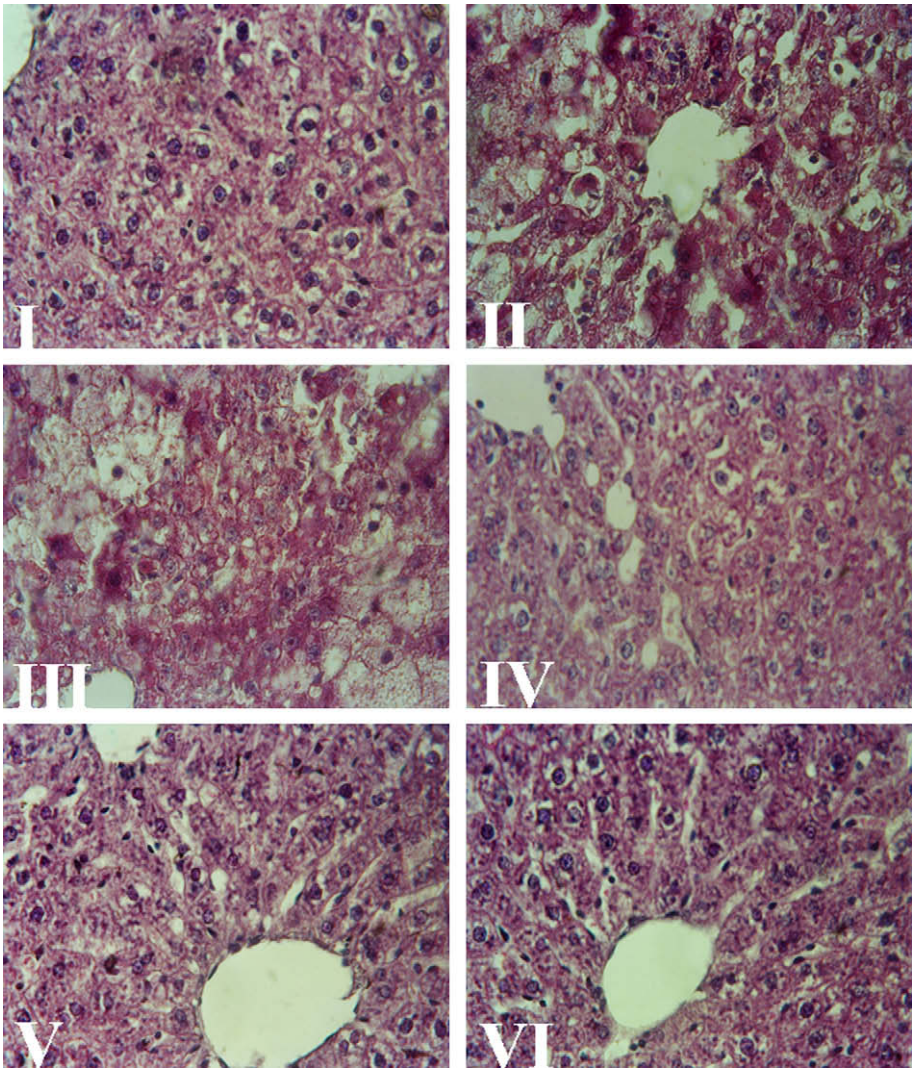

Plate 1. Hepatoprotective effect of *D. hamiltonii* aqueous extract pretreatment (single dose) on CCl_4-induced liver damage. H and E staining, magnification,×400. Group I – control; Group II – CCl_4; Group III – DHA 50 mg/kg b.w. + CCl_4; Group IV – DHA 100 mg/kg b.w. + CCl_4; Group V – DHA 200 mg/kg b.w. + CCl_4; Group VI – DHA 200 mg/kg b.w.

notic nuclei in the parenchymal cells in the centrilobular areas which were significantly reduced with DHA pretreatment at higher doses. Histological picture of the liver of rats pretreated with DHA did not reveal degenerative signs and was comparable to that of control (Plates 1 and 2).

4. Discussion

Hepatotoxicity induced by CCl_4 is the most commonly used model system for the screening of hepatoprotective activity of plant extracts/ drugs. Administering CCl_4 to rats markedly increases serum AST, ALT, ALP, and LDH levels which reflects the severity of liver injury (Lin, Yao, Lin, & Lin, 1996). In this study, significant increase in AST, ALT, ALP, and LDH in the serum were observed after administration of CCl_4, as reported earlier. The leakage of large quantities of enzymes into the blood stream was associated with centrilobular necrosis and ballooning degeneration of the liver. However, the increased levels of these enzymes were significantly decreased by pretreatment with *D. hamiltonii* aqueous extract, implying that the extract prevented the liver damage which was further confirmed by the reduced amount of histopathological injuries.

Lipid peroxidation has been implicated in the pathogenesis of hepatic injury by the free radical derivatives of CCl_4 and is responsible for cell membrane damage and consequent release of marker enzymes of heptotoxicity (Danni et al., 1991). In the present study, significantly elevated levels of TBARS, products of membrane lipid peroxidation, observed in CCl_4 administered rats indicated hepatic damage. Pretreatment of *D. hamiltonii* extract prevented lipid peroxidation which could be attributed to the radical scavenging antioxidant constituents (Srivastava et al., 2006).

GSH is the major non-enzymatic antioxidant and regulator of intracellular redox homeostasis, ubiquitously present in all cell types (Meister & Anderson, 1983). Mechanistic studies on CCl_4-induced studies reveal that GSH conjugation plays a critical role in eliminating the toxic metabolites, which are the major cause of liver pathology (Lee, Shimoji, Hossain, Sunakawa, & Aniya, 2008). CCl_4 administration leads to a significant decrease in the glutathione level which can be an important factor in the CCl_4 toxicity. The mechanism of hepatoprotection by *D. hamiltonii* extract against CCl_4 toxicity might be due to restoration of the GSH level. Multiple dose pretreatments of *D. hamiltonii, per se*, increased the levels of GSH which may possibly be due to enhancing of GSH synthesising enzyme activities such as γ-glutamylcysteine synthetase (γ-GCS) and GSH synthetase; this needs further investigation.

One of the major consequences of oxidative stress is irreversible protein modification, such as generation of carbonyls or loss of thiol residues (Berlett & Stadman, 2001). As CCl_4 toxicity is mediated by free radical metabolites, in CCl_4 intoxicated rats a significant increase in the protein carbonyl content was observed

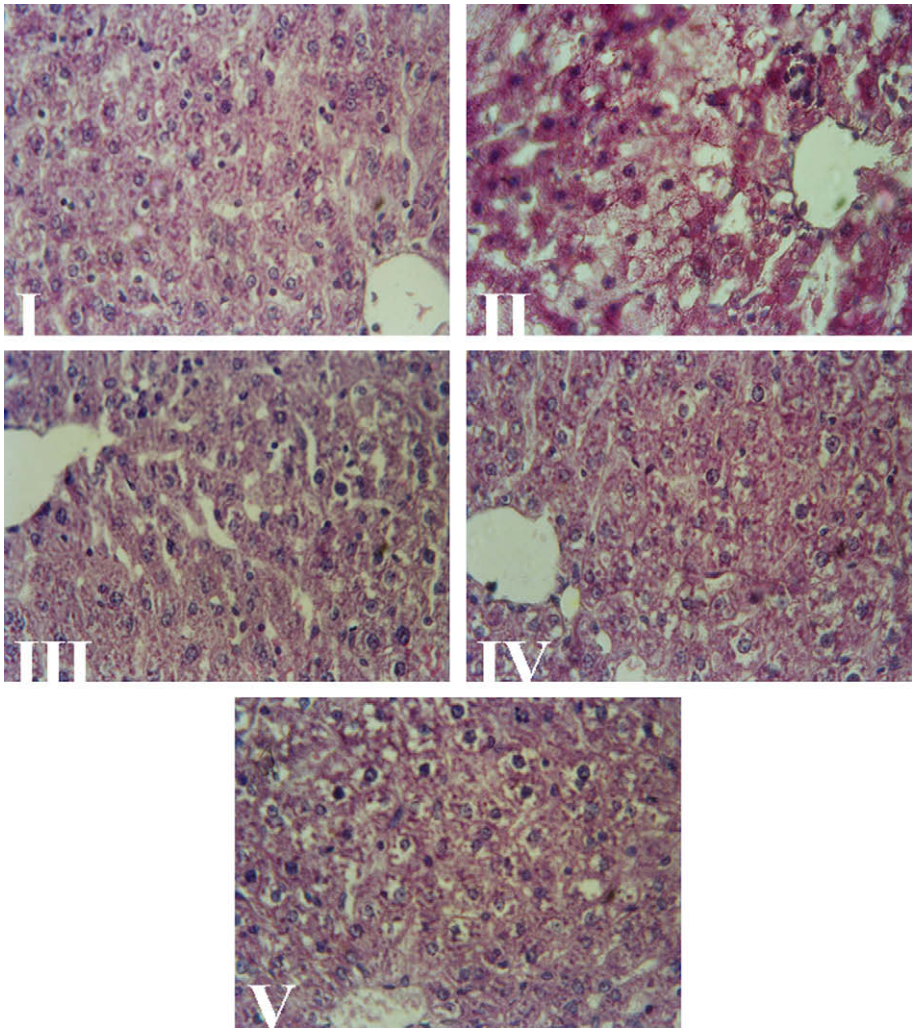

Plate 2. Hepatoprotective effect of *D. hamiltonii* aqueous extract pretreatment (multiple dose) on CCl_4-induced liver damage. H and E staining, magnification, ×400. Group I – Control; Group II – CCl_4; Group III – DHA 50 mg/kg b.w. + CCl_4; Group IV – DHA 100 mg/kg b.w. + CCl_4; Group V – DHA 100 mg/kg b.w.

which was restored to normalcy by *D. hamiltonii* extract pretreatment. The antioxidant activity of *D. hamiltonii* extract and its GSH status elevating effect could be responsible for this observation.

Among the cellular antioxidants, SOD, CAT, GST, GPx, and GR have received extensive studies. SOD catalyses the dismutation of superoxide anion to H_2O_2 and O_2. Because H_2O_2 is still harmful to cells, catalase and GPx further catalyse the decomposition of H_2O_2 to water. In the reaction catalysed by GPx, GSH is oxidised to GSSG, which can then be reduced back to GSH by GR. GSH is also a cofactor for GST, a phase II enzyme, primarily involved in the detoxification of electrophilic xenobiotics via catalysing the formation of GSH-electrophile conjugate (Hayes, Flanagan, & Jowsey, 2005). Thus, the coordinate actions of various cellular antioxidants in mammalian cells are critical for effectively detoxifying free radicals. CCl_4 administration to rats declined antioxidant capacity of the rat liver as evinced in decreased activity of the antioxidant enzymes, which is in agreement with earlier reports (Shahjahan et al., 2004). *D. hamiltonii* extract pretreatment prevented the reduction in the antioxidant enzyme activities and consequent oxidative damage to the liver. In fact, the multiple dose pretreatment of *D. hamiltonii* extract alone significantly boosted the antioxidant enzyme activities. Similar studies have shown a positive effect of different classes of polyphenols on antioxidant enzyme activities *in vivo* (Molina, Sanchez-Reus, Iglesias, & Benedi, 2003; Scharf, Prustomersky, Knasmuller, Schulte-Hermann, & Huber, 2003).

In conclusion, the *D. hamiltonii* aqueous extract effectively prevented CCl_4-induced hepatotoxicity which explains its health promoting property. Our previous study with ethanol, an inducer of oxidative stress, also shows hepatoprotective effect of *D. hamiltonii* extract (Srivastava & Shivanandappa, 2006). Even though ethanol and CCl_4 have different mechanisms of toxicity *D. hamiltonii* aqueous extract could protect the rat liver. The hepatoprotective activity of *D. hamiltonii* extract could be a result of free radical scavenging activity or boosting the antioxidant capacity of the liver. The bioactive antioxidant principles of the aqueous extract that have been identified (Srivastava et al., 2006) could be responsible for the observed hepatoprotective effect. Further studies with the individual antioxidant compounds isolated from *D. hamiltonii* root extract on hepatocytes are underway which will enable us to understand the exact mechanism of hepatoprotective action by *D. hamiltonii*.

Acknowledgements

This work was done at Central Food Technological Research Institute, Mysore, India. The authors wish to thank the Director of the institute for his keen interest in this study. The first author acknowledges Council for Scientific and Industrial Research, New Delhi for awarding the research fellowship.

References

Aebi, H. (1974). Catalase. In H. U. Bergmeyer (Ed.), *Methods of enzymatic analysis*. *Vol. 2* (pp. 674–678). Weinheim: Verlag Chenie.

Berlett, B. S., & Stadman, E. R. (2001). Protein oxidation in aging, disease and oxidative stress. *Journal of Biological Chemistry, 272*, 20313–20316.

Calberg, I., & Mannervik, B. (1985). Glutathione reductase. In A. Meister (Ed.). *Methods in enzymology* (Vol. 113, pp. 484–490). FL: Academic Press.

Danni, O., Chiarpotto, E., Aragno, M., Biasi, F., Comoglio, A., Belliardo, F., et al. (1991). Lipid peroxidation and irreversible cell damage: Synergism between carbon tetrachloride and 1,2-dibromoethane in isolated rat hepatocytes. *Toxicology and Applied Pharmacology, 110*, 216–222.

Demirdag, K., Bakcecioglu, I. H., Ozercan, I. H., Ozden, M., Yilmaz, S., & Kalkan, A. (2004). Role of L-carnitine in the prevention of acute liver damage induced by carbon tetrachloride in rats. *Journal of Gastroenterology and Hepatology, 19*, 333–338.

Ellman, G. L. (1959). Tissue sulfhydryl groups. *Archives of Biochemistry and Biophysics, 82*, 70–77.

Harish, R., Divakar, S., Srivastava, A., & Shivanandappa, T. (2005). Isolation of antioxidant compounds from the methanolic extract of the roots of *Decalepis hamiltonii* (Wight and Arn.). *Journal of Agricultural and Food Chemistry, 53*, 7709–7714.

Hayes, J. D., Flanagan, J. U., & Jowsey, I. R. (2005). Glutathione transferases. *Annual Reviews in Pharmacology and Toxicology, 45*, 51–88.

Kodavanti, P. R., Joshi, U. M., Young, Y. A., Meydrech, E. F., & Mehendale, H. M. (1989). Protection of hepatotoxic and lethal effects of CCl_4 by partial hepatectomy. *Toxicology and Pathology, 17*, 494–505.

Kornberg, A. (1955). Lactic dehydrogenase of muscle. *Methods in Enzymology, 1*, 441–443.

Lee, K. K., Shimoji, M., Hossain, Q. S., Sunakawa, H., & Aniya, Y. (2008). Novel function of glutathione transferase in rat liver mitochondrial membrane: Role for cytochrome *c* release from mitochondria. *Toxicology and Applied Pharmacology, 232*, 109–118.

Levine, R. L., Garland, D., Oliver, C. N., Amici, A., Climent, I., Lenz, A., et al. (1990). Determination of carbonyl content of oxidatively modified proteins. *Methods in Enzymology, 186*, 464–478.

Lin, S. C., Yao, C. J., Lin, C. C., & Lin, Y. H. (1996). Hepatoprotective activity of Taiwan folk medicine: *Eclipta prostrate* Linn. against various hapatotoxins induced acute hapatotoxicity. *Phototherapy Research, 10*, 483–490.

Lowry, O. H., Rosenbrough, N. J., Farr, A. L., & Randall, R. J. (1951). Protein measurement with Folin-Phenol reagent. *Journal of Biological Chemistry, 193*, 265–275.

Mannervik, B. (1985). Glutathione peroxidase. In A. Miester (Ed.). *Methods in enzymology* (Vol. 113, pp. 490–495). FL: Academic Press.

Marklund, S., & Marklund, G. (1974). Involvement of the superoxide anion in the autoxidation of pyrogallol and a convenient assay for superoxide dismutase. *European Journal of Biochemistry, 47*, 469–474.

Meister, A., & Anderson, M. E. (1983). Glutathione. *Annual Reviews in Biochemistry, 52*, 711–760.

Molina, M. F., Sanchez-Reus, I., Iglesias, I., & Benedi, J. (2003). Quercetin, a flavonoid antioxidant, prevents and protects against ethanol-induced oxidative stress in mouse liver. *Biological and Pharmaceutical Bulletin, 26*, 1398–1402.

Nayar, R. C., Shetty, J. K. P., Mary, Z., & Yoganarshimhan, S. N. (1978). Pharmacognostical studies on the root of *Decalepis hamiltonii* Wt. and Arn. and comparison with *Hemidesmus indicus* (L.) R. Br. *Proceedings of Indian Academy of Sciences, 87*, 37–48.

Ohkawa, H., Ohishi, N., & Yagi, K. (1979). Assay for lipid peroxides in animal tissues by thiobarbituric acid reaction. *Analytical Biochemistry, 95*, 351–358.

Reitman, S., & Frankel, S. (1957). A colorimetric method for the determination of serum oxaloacetic and glutamic pyruvic transaminases. *American Journal of Clinical Pathology, 28*, 56–63.

Scharf, G., Prustomersky, S., Knasmuller, S., Schulte-Hermann, R., & Huber, W. W. (2003). Enhancement of glutathione and g-glutamylcystein synthetase, the rate limiting enzyme of glutathione synthesis, by chemoprotective plant-derived food and beverage components in the human hepatoma cell line Hep G2. *Nutrition and Cancer, 45*, 74–83.

Shahjahan, M., Sabitha, K. E., Jainu, M., & Devi, C. S. S. (2004). Effect of *Solanum trilobatum* against carbon tetrachloride induced hapatic damage in albino rats. *Indian Journal of Medical Research, 120*, 194–198.

Sheweita, S. A., El-Gabar, M. A., & Bastawy, M. (2001). Carbon tetrachloride-induced changes in the activity of phase II drug-metabolizing enzyme in the liver of male rats: Role of antioxidants. *Toxicology, 165*, 217–224.

Srivastava, A., Harish, R., & Shivanandappa, T. (2006). Novel antioxidant compounds from the aqueous extract of the roots of *Decalepis hamiltonii* (Wight and Arn.) and their inhibitory effect on low-density lipoprotein oxidation. *Journal of Agricultural and Food Chemistry, 54*, 790–795.

Srivastava, A., Rao, L. J. M., & Shivanandappa, T. (2007). Isolation of ellagic acid from the aqueous extract of the roots of *Decalepis hamiltonii*: Antioxidant activity and cytoprotective effect. *Food Chemistry, 103*, 224–233.

Srivastava, A., Shereen, Harish, R., & Shivanandappa, T. (2006). Antioxidant activity of the roots of Decalepis hamiltonii (Wight and Arn.). *LWT-Food Science and Technology, 39*, 1059–1065.

Srivastava, A., & Shivanandappa, T. (2006). Hepatoprotective effect of the aqueous extract of the roots of *Decalepis hamiltonii* against ethanol-induced oxidative stress in rats. *Hepatology Research, 35*, 267–275.

Walter, K., & Schutt, C. (1974). Acid and alkaline phosphatase in serum (Two point method). In H. U. Bergmeyer (Ed.). *Methods of enzymatic analysis* (Vol. 2, pp. 856–860). Deerfield Beach, FL: Verlag Chemie.

Warholm, M., Guthenberg, C., Bahr, C. V., & Mannervik, B. (1985). Glutahtione transferase from human liver. *Methods in enzymology* (Vol. 113, pp. 499–504). Deerfield Beach, FL: Academic Press.

Food Chemistry 118 (2010) 418–425

Contents lists available at ScienceDirect

Food Chemistry

journal homepage: www.elsevier.com/locate/foodchem

Persistence of pasture feeding volatile biomarkers in lamb fats

Guilhem Sivadier, Jérémy Ratel, Erwan Engel *

INRA UR370 Qualité des Produits Animaux, 63122 Saint-Genès-Champanelle, France

ARTICLE INFO

Article history:
Received 8 August 2008
Received in revised form 26 January 2009
Accepted 22 February 2009

Keywords:
Authentication
Meat product
GC–MS
Volatile compounds
Adipose tissues
Ruminant
Persistence
Drift correction

ABSTRACT

Recent studies have evidenced volatile biomarkers in ruminant tissues that distinguish between exclusive pasture and exclusive concentrate diets. As ruminants usually alternate these diets, we set out to monitor the persistence of volatile tracers of pasture diet in perirenal fat and caudal subcutaneous fat in lambs ($n = 28$) fed on pasture and then fattened at increasing levels with concentrate: Four groups of lambs ($n = 7$) were stall-finished to achieve a final weight gain of 0, 4, 8, and 12 kg, respectively. Thirty nine pasture diet tracers including terpenes, 2,3-octanedione and toluene were found that distinguish between the four different diets in both tissues. According to their clearance rates monitored in the adipose tissues of lambs fattened with different amounts of concentrate, different types of persistence were evidenced. Most of the compounds exhibited a "short" persistence, e.g. 2,3-octanedione and terpenes, while some displayed a "medium" or "long" persistence. Finally, performing discriminant analysis on ratios of tracers from the two adipose tissues enabled the correct differentiation of the four different diets.

1. Introduction

There is an increasing demand from consumers, commercial entities and bodies operating product certification systems for the development of robust analytical tools to authenticate ruminant feeding based on meat products. Numerous studies have found the analysis of the volatile fraction of dairy (Engel et al., 2007) and meat products (Engel & Ratel, 2007; Sebastian, Viallon-Fernandez, Berge, & Berdague, 2003; Vasta & Priolo, 2006) to allow the construction of robust models for animal diet authentication. These studies were conducted on samples from animals fed exclusively either pasture or concentrate. However, ruminants are usually fed diets in which pasture and concentrate periods alternate. Some authors (Aurousseau, Bauchart, Faure, et al., 2007; Aurousseau, Bauchart, Galot, et al., 2007; Larick & Turner, 1990; Larick et al., 1987; Noziere et al., 2006) have studied the variations in levels of diet biomarkers in meat or milk samples from animals fed with alternating diets consisting of an exclusive pasture feeding period followed by a concentrate-finishing period of variable duration. Monitoring the level of carotenoids (Noziere et al., 2006) or fatty acids (Aurousseau, Bauchart, Faure, et al., 2007; Aurousseau, Bauchart, Galot, et al., 2007) allowed only the differentiation of diets exhibiting marked differences in the concentrate-finishing levels. By analysing the volatile fraction of beef samples, Larick et al. (1987) showed that volatile compounds could segregate diets into graduated concentrate-finishing durations. However, the list of the feeding tracers identified differs from other literature reports and may not be reliable, given the harsh operating conditions used by these authors. Recent developments in volatile compound analysis such as instrumental drift correction (Arvanitoyannis & Van Houwelingen-Koukaliaroglou, 2003; Deport, Ratel, Berdague, & Engel, 2006) and gentle operating conditions limiting the occurrence of artefacts caused by heat (Vasta, Ratel, & Engel, 2007) identified dozens of relevant discriminant compounds with identifiable metabolic origins.

The objective of this three-step study was to determine the persistence of volatile tracers of pasture diet in adipose tissues of lambs initially fed on pasture and stall-fattened to achieve a final weight gain of 0 kg (P), 4 kg (PC4), 8 kg (PC8), or 12 kg (PC12). Two adipose tissues, the perirenal fat (PRF) and the caudal subcutaneous fat (CSCF), were analysed in each animal, as we had previously found in preliminary study that the parallel analysis of volatile diet tracers from the two tissues improved the power of differentiation between exclusive pasture and exclusive concentrate diets (Sivadier, Ratel, Bouvier, & Engel, 2008). The aim of the first step was to identify the volatile pasture diet tracers by comparing the volatile compound composition in the two tissues of lambs fed on pasture and then fattened for either 0 or 12 kg with concentrate. The second step aimed at characterising the persistence rates of these tracers by determining their relative abundances in adipose tissues of lambs stall-finished for a final weight gain of 0, 4, 8, or 12 kg. The third step

* Corresponding author. Tel.: +33 (0)473624589; fax: +33 (0)473624731.
E-mail address: erwan.engel@clermont.inra.fr (E. Engel).

0308-8146/$ - see front matter © 2009 Elsevier Ltd. All rights reserved.
doi:10.1016/j.foodchem.2009.02.088

aimed at assessing the relevance of these findings concerning the persistence of the pasture diet tracers for distinguishing between different concentrate fattening degrees in grazing lambs on the basis of conventional GC–MS analysis of their adipose tissues.

2. Materials and methods

2.1. Animal products

A herd of 28 male INRA401 lambs born at the INRA research centre (Theix, France) during a 6-week period were divided, after a 45-day weaning period, into four groups of seven lambs each. The first group (P) was fed exclusively at pasture (consisting predominantly of Graminaceae) with no other additional feed. The animals were slaughtered according to the conventional EU procedures at the targeted weight of 40 kg, corresponding to a mean age of 186 days. The other three groups were initially fed at pasture until they reached the target weights of 28 kg (PC12), 32 kg (PC8), and 36 kg (PC4). Each of these three groups was installed in a large stall where they were offered a pelleted concentrate diet consisted of (w/w) 30% hay and 70% commercial concentrate containing barley (20%), wheat bran (15%), wheat (15%) and sugar beet (15%) as main constituents (THIVAT Nutrition Animale, Saint-germain-de-salles, France). The animals were all slaughtered at the target weight of 40 kg weight, corresponding to a mean age of 163 days.

Perirenal and subcutaneous fats were chosen for the study according to a preliminary work (Sivadier et al., 2008), in which it was established that the simultaneous data treatment of the volatile fraction of these two adipose tissues improved diet authentication. In addition, Vezinhet, Prud'hon, and Benevent (1974) reported different growth rates: perirenal fat is developed early in the lamb's life, while subcutaneous fat starts growing in the post-natal period. Diet information may thus have different implications in both tissues.

2.2. Preparation of samples

At 1 h *postmortem* a sample of each adipose tissue was excised from the lamb carcass: perirenal fat (PRF) was adipose tissue directly covering the left kidney, and caudal subcutaneous fat (CSCF) was tissue 10 cm from the tail. The adipose samples were trimmed free of all traces of muscle and immediately immersed in liquid nitrogen, wrapped in aluminium foil, vacuum packed and stored at −80 °C until the next preparation step.

Two days before the analysis each adipose tissue was immersed in liquid nitrogen, cut into small cubes (less than 0.1 g) and ground in liquid nitrogen with a crushing machine (Dangoumeau, Prolabo, Nogent-sur-Marne, France) to a fine homogeneous powder. Three grams of powder were then placed in glass vials (Wheaton Science Products) under a nitrogen flow and heated for 15 min at 70 °C in a 100–800 oven (Memmert, Schwabach, Germany). A mean of 1.2 g of liquid lipid phase was obtained, placed in glass vials sealed under nitrogen flow, and stored at −20 °C until analysis. Just before analysis, the frozen extracts were thawed for 7.5 min at 70 °C.

2.3. Addition of the standards

The comprehensive combinatory standard correction (CCSC) was used to correct instrument drifts, according to Deport et al. (2006). As previously stated by Engel and Ratel (2007), six standards were chosen according to various criteria including: (i) boiling point compatibility with the experimental conditions, (ii) stability, (iii) absence in samples before analysis, (iv) purity of commercially available solutions, (v) relative specificity of mass spectrometry fragmentation and (vi) safeness. The standards used were 2-methyl-pentane (S1; purity 99.5%), fluoro-benzene (S2; purity 99.7%), 1-bromo-butane (S3; purity 99.7%), bromo-benzene (S4; purity 99.5%), 1-fluoro-naphthalene (S5; purity 99.0%) and 1-phenyl-nonane (S6; purity 99.8%) (Sigma–Aldrich Chimie, Saint-Quentin-Fallavier, France). A mixture of the six standards was made and co-analysed with the lipid liquid extract at a final concentration of approx. 50 ppm for each standard (w/w).

2.4. Dynamic headspace–gas chromatography–mass spectrometry (DH–GC–MS) analysis

A plug of glass wool (0.2 g) (VWR International, Fontenay-sous-Bois, France) was introduced into a glass extraction cartridge (diameter 28 mm, length 100 mm, Ets. Maillière, Aubière, France). A 1 g aliquot of sample was placed on the glass wool and 10 µl of the mixture of standards was added on a second plug of 0.1 g of glass wool placed on the sample. The volatile fraction was extracted by dynamic headspace using a purge-and-trap device (3100 Sample Concentrator, Tekmar, Cincinnati, OH, USA). After a pre-purge of 5 min and a preheat of 15 min, the headspace of the sample was purged for 30 min under a 65 ml min^{-1} helium flow (He U quality, purity 99.995%, Messer, St.-Georges-d'Espéranche, France). The temperature of the sample during the DH extraction step was set at 70 °C. The volatiles were trapped by adsorption on a porous-polymer adsorbent Tenax trap column (Tenax TA, straight, 12″ × 30.5 cm, 24 cm of adsorbent, Supelco, Bellefonte, PA, USA) maintained at 36 °C. After a dry purge at 36 °C for 5 min, the volatile compounds were desorbed for 10 min at 230 °C under a helium flow (He N55, purity 99.9995%, Messer). Extracted compounds were then transferred to the head of a capillary column after cryoconcentration at −150 °C. After desorption, the Tenax trap was further heated for 30 min at 230 °C.

The compounds condensed at the head of the column were analysed by GC (model 6890, Hewlett–Packard, PA, USA); the interface was heated at 225 °C for 2 min followed by injection of the compounds in splitless mode into the non-polar phase of the capillary column (SPB5, 60 m × 0.32 mm × 1 µm, Sigma–Aldrich, St. Louis, MO, USA). The oven temperature was held at 40 °C for 5 min, and then increased to 230 °C with a gradient of 3 °C.min^{-1}, and maintained at this temperature for 10 min. The GC column was connected to a mass spectrometer (model 5973A, Hewlett–Packard). The temperature of the transfer line was set at 230 °C. The temperature was fixed at 180 °C in the MS source and at 150 °C in the MS quadrupole. The electron impact energy was set at 70 eV and data were collected in the range of *m/z* 33 to 230 at a scan range of 6.85 scans per second. Tentative identification of volatiles was based on: (i) mass spectra by comparison with MS spectra database including NBS 75 K, Wiley 275L or Masslib (MSP Kofel, Zollikofen, Switzerland) and (ii) comparison of retention indices (RI) with published RI values (Kondjoyan & Berdague, 1996) or with those of our internal data bank. The peak area of the tentatively identified compounds was integrated from the specific ion for each of the molecules to avoid co-elution problems. The integrations were performed with the Enhanced ChemStation software (version D.01.02.16, Hewlett–Packard).

2.5. Data treatment

Data were processed using the Statistica Software release 8.0 package (Statsoft, Maisons-Alfort, France) and the R software version 2.1.4. R development Core Team (2006). R: A language and environment for statistical computing. R Foundation for Statistical Computing, Vienna, Austria. ISBN 3-900051-07-0, URL http://www.R-project.org.

DH–GC–MS raw data were processed with CCSC according to Engel and Ratel (2007). The mixture of the six selected standards was analysed together with the sample, and the abundance of each compound specific ion was normalised by the sum of the abundances of the specific ion of standards, selected among the $\sum_{p=1}^{6} C_6^p$ possible sums where p represents the number of standards in a given sum, enabling the best product discrimination.

To determine which compounds distinguished between the exclusive pasture diet (P) and the alternate pasture then 12 kg concentrate-finishing diet (PC12), a one-way analysis of variance (ANOVA) was performed according to the model: CCSC pre-treated abundance of compound specific ion: type of feeding, $p < 0.05$. Principal component analyses (PCA) were performed on the CCSC pre-treated abundances of the discriminant compound specific ions to visualise the structure of the data.

To monitor the persistence of specific tracers of the four types of diet in PRF and CSCF, the compounds that discriminated between P and PC12 were filtered by one-way ANOVA (model: CCSC pre-treated abundance of compound specific ion: type of feeding, $p < 0.05$) according to the four modalities: P, PC4, PC8, and PC12. A Newman–Keuls mean comparison test was then performed on the resulting dataset to determine which compound distinguished between the four diets with increasing concentrate quantities.

To establish the possibility of distinguishing between the four types of diet on the basis of the volatile compounds from the lipid liquid extracts of the two adipose tissues, the most robust volatile tracers were obtained by filtering previous datasets of PRF and CSCF with a one-way ANOVA (with same factor) followed by a leave-one-out cross validation procedure ($p < 0.05$). A PCA was then performed on the filtered tracers from each adipose tissue and from the two pooled together in the same dataset ($n = 35$), to visualise the structure of the data. A Newman–Keuls mean comparison test was performed on the coordinates of the observations on the first principal component to assess its significance in the differentiation of the four diets. The gain in discriminative power obtained by processing the two adipose tissue volatile tracers in parallel was assessed by performing a discriminant analysis (DA) carried out on the previous datasets. The Wilk's λ values, which give the quality of differentiation of the four diets, were determined for the combinations of three tracers (triplets) from one or the two adipose tissues, built up according to the "best subset" algorithm. The optimisation of the differentiation of the four diets was obtained via ratios of tracer abundances. On the basis of the tracers from the two tissues previously selected ($n = 35$), the A_{35}^2 possible ratios were calculated and filtered by a one-way ANOVA (model: ratio of CCSC pre-treated abundances of compound specific ions: type of feeding, $p < 0.05$) followed by a leave-one-out cross validation procedure. Among the selected ratios, when several involved the same compound in the same tissue, only the one with the best Fisher F was selected. After processing the data with a PCA a Newman–Keuls mean comparison test was performed on the coordinates of the observations on the two principal components of the first map to assess their significance in the differentiation of the four diets.

3. Results and discussion

3.1. Identification of pasture diet tracers in the adipose tissues

A list of 125 volatile compounds known as potential tracers of pasture or concentrate feeding diets (Engel & Ratel, 2007; Maruri & Larick, 1992; Sebastian et al., 2003; Sivadier et al., 2008; Vasta & Priolo, 2006) were semi-quantified in perirenal fat (PRF) and caudal subcutaneous fat (CSCF) of P- and PC12-lambs. The compounds distinguishing between P and PC12 diets were selected by one-way

Table 1
Compounds identified as lamb pasture feeding tracers in PRF and CSCF tissues.

LRI[a]	Compounds[b] ($n = 54$)	PRF[c] ($n = 41$)	CSCF[c] ($n = 36$)	Ref.[d]
Alkanes				
857	Heptane, 2,3-dimethyl-	X		
900	Nonane	X		
972	Nonane, 3-methyl-	X		[2]
1200	Dodecane	X	X	
1264	Undecane, 2,10-dimethyl-	X		
1300	Tridecane	X		
1364	Tridecane, 2-methyl-	X		
1378	Dodecane, 2,6,10-trimethyl-	X		
1400	Tetradecane	X	X	[1]
1463	Decane, 2,3,7-trimethyl-	X	X	[1]
1472	Tetradecane, 3-methyl-	X		
1488	Cyclododecane, 1-ethyl-2-methyl-	X	X	
1500	Pentadecane	X	X	[1]
1600	Hexadecane	X	X	[1]
1700	Heptadecane		X	[1]
Alkenes				
488	1-Pentene	X		
796	(Z)-4-Octene	X	X	[2]
806	(E)-4-Octene	X	X	[2]
815	(E)-2-Octene	X	X	[2]; [4]
1495	1-Pentadecene	X	X	
Alcohols				
684	1-Penten-3-ol	X	X	
767	1-Pentanol		X	
Aldehydes				
593	Butanal	X		
648	2-Butenal		X	[2]
696	Pentanal		X	[2]
755	(E)-2-Pentenal		X	[2]
854	(E)-2-Hexenal		X	
900	(Z)-4-Heptenal	X	X	[2]; [1]
1014	2,4-Heptadienal	X	X	[2]; [1]
Benzene compounds				
663	Benzene	X		
771	Toluene	X	X	[2]
898	Styrene	X	X	
901	o-Xylene		X	
970	Benzaldehyde	X		[2]; [4]
1036	Benzene, 1,3,5-trimethyl-	X	X	[2]
Ketones				
591	2,3-Butanedione		X	
889	Ethanone, 1-(1-cyclohexen-1-yl)-	X		
979	1-Octen-3-one		X	[2]
982	2,3-Octanedione	X		[2]; [1]; [3]
1074	(E,E)-3,5-Octadien-2-one	X	X	[2]
1079	Acetophenone	X	X	[2]
1297	2-Undecanone	X		
1500	2-Tridecanone	X		
Chlorine compounds				
962	Heptane, 1-chloro-	X	X	
Nitrogen compounds				
748	Pyridine	X		
Oxygen compounds				
605	Furan, 2-methyl-	X		[2]
702	Furan, 2-ethyl-		X	
Sulfur compounds				
908	Methional		X	[3]
916	Sulfone, dimethyl-	X	X	[2]; [3]
Terpenes				
944	α-Pinene		X	
1034	p-Cymen		X	[2]; [3]
1407	α-Copaene	X	X	[2]
1461	β-Caryophyllene	X	X	[2]; [3]
1554	*trans*-Cadina-1(6),4-diene	X	X	[2]; [3]

[a] Linear retention index on a SPB5 capillary column.
[b] Compounds ($n = 54$) tentatively identified on the basis of both mass spectra by comparison with MS databases and linear retention indices of data banks.
[c] Adipose tissues: PRF = perirenal fat, and CSCF = caudal subcutaneous fat.
[d] Literature references where compounds stated as pasture diet tracers. [1]: Sebastian et al. (2003); [2] Engel and Ratel (2007); [3]: Vasta and Priolo (2006); [4]: Maruri and Larick (1992).

ANOVA ($p < 0.05$). Forty-one and 36 compounds were selected in the PRF and CSCF, respectively. Twenty-three were common to the two tissues studied (Table 1). The fact that some compounds were found to be discriminant in one tissue but not in the other (18 in PRF, and 14 in CSCF) supports the informative complementarity of the two tissues and the usefulness of studying them in parallel. The first map of the PCA performed on discriminant compounds of the two tissues is shown in Fig. 1. It reveals a clear differentiation between the two diets, confirming that the volatile fraction of these two tissues allows the authentication of the lamb diets.

Among the compounds distinguishing between P and PC12 diets in the two tissues ($n = 54$), 28 compounds had been determined as pasture diet tracers by several previous studies (Engel & Ratel, 2007; Sebastian et al., 2003; Sivadier et al., 2008; Vasta & Priolo, 2006). The common determination of these 28 pasture diet tracers in fat tissues of lambs raised with different husbandry practises (e.g. animal breed, type of pasture & concentrate, lamb growth rate...) validate the relevance of these compounds for a robust authentication of fats of pasture fed lambs (Table 1).

3.1.1. 2,3-Octanedione

This compound is the most widely recognised pasture diet tracer in the literature (Sivadier et al., 2008; Vasta & Priolo, 2006). According to Young, Berdague, Viallon, Rousset-Akrim, and Theriez (1997), it originates from the oxidation of linoleic acid by the action of the enzyme lipoxygenase, which is present in leafy plants but absent in seeds, except for soybeans. Three other ketones (1-octen-3-one, (E,E)-3,5-octadien-2-one, and acetophenone) were identified as tracers in several previous studies (Sivadier et al., 2008; Vasta & Priolo, 2006).

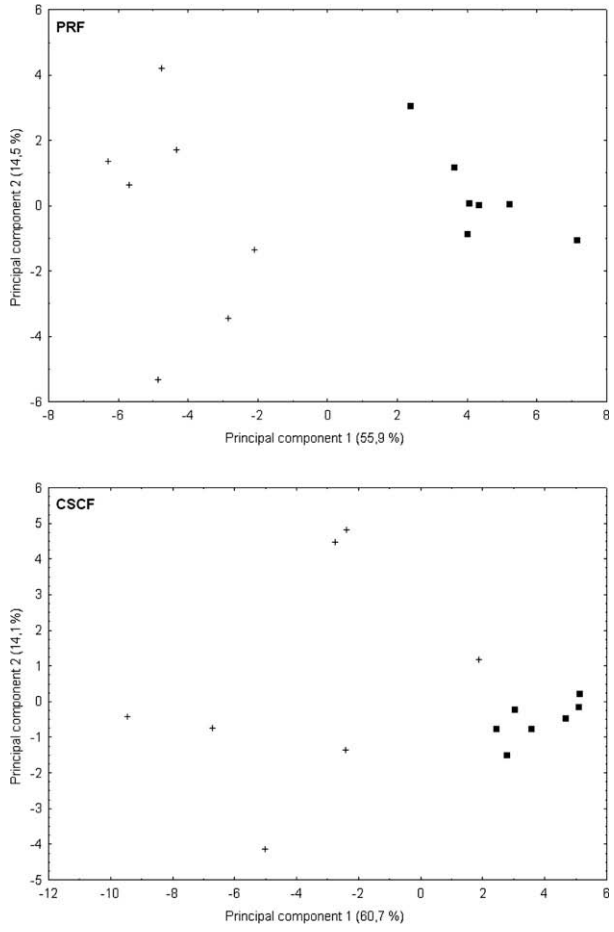

Fig. 1. Differentiation of concentrate- and pasture fed lambs based on GC–MS analysis of their adipose tissues: exclusive pasture (+/cross) and alternating pasture and fattening for 12 kg with concentrate (■/solid square). First map of normed PCAs carried out from the CCSC pre-treated abundances of the volatile compounds determined affected by the two types of diet by one-way ANOVA ($p < 0.05$). Forty-one compounds were selected in perirenal fat (PRF), and 36 in caudal subcutaneous fat (CSCF).

3.1.2. Alkanes

Similarly, six alkanes (3-methyl-nonane, 2,3,7-trimethyl-decane, tetradecane, pentadecane, hexadecane, and heptadecane) were identified as reliable pasture diet tracers (Engel & Ratel, 2007; Larick et al., 1987; Sebastian et al., 2003; Sivadier et al., 2008). As regards the four non-branched alkanes (C_{14}—C_{17}), their relation with the pasture diet could be explained by the higher amounts of long chain polyunsaturated fatty acids in the tissues of pasture fed lambs in comparison with concentrate fed lamb tissues (Aurousseau, Bauchart, Faure, et al., 2007; Aurousseau, Bauchart, Galot, et al., 2007). According to Watanabe and Sato (1971), these saturated alkanes may derive from decarboxylation and splitting of carbon–carbon chains.

3.1.3. Benzene compounds

Benzaldehyde, 1,3,5-trimethyl-benzene, and toluene were detected in higher amounts in adipose tissues of pasture fed lambs than in tissues of lambs fed with any of the three concentrate-finishing diets. According to Rios, Fernandez-Garcia, Minguez-Mosquera, and Oerez-Galvez (2008), the toluene may arise from the degradation of carotenoids supplied by pasture. These three compounds are also atmosphere pollutants which are known to be retained by green plants (Binnie, Cape, Mackie, & Leith, 2002).

3.1.4. Terpens

Mainly originating from green herbages (Body, 1977), terpenes are commonly detected in adipose tissues of pasture fed lambs (Priolo et al., 2004; Sivadier et al., 2008). They are generally too specific to some plant species to be used as generic tracers of a pasture diet (Engel & Ratel, 2007). However, p-cymen, α-copaene, β-caryophyllene, and trans-cadina-1(6),4-diene are identified as recurrent pasture diet tracers in the literature (Engel & Ratel, 2007; Sivadier et al., 2008; Vasta & Priolo, 2006) and can be considered as generic pasture diet tracers.

3.1.5. Aldehydes

2-Butenal, pentanal, (E)-2-pentenal, (Z)-4-heptenal, and 2,4-heptadienal were found to be characteristic of the pasture diet by some previous studies (Engel & Ratel, 2007; Sebastian et al., 2003; Sivadier et al., 2008). In contrast with Brown, Melton, Riemann, and Backus (1979), who proposed that some aliphatic aldehydes (e.g. pentanal) were related to the pasture feeding, Vasta and Priolo (2006) showed there was no consensus for relating these compounds to a given diet. Because they originate from lipid oxidation, their occurrence may be favoured by many factors other than the type of feeding, such as the temperature used for volatile compound extraction.

3.1.6. (E)-2-Octene

This compound, derived from α-linolenic acid according to Elmore et al. (2004), was determined as a pasture diet tracer in both this study and the literature (Engel & Ratel, 2007; Maruri & Larick, 1992; Sivadier et al., 2008).

To our knowledge, there is no evidence indicating the metabolic origin of methional, dimethyl-sulfone, 2-methyl-furane, and (E)- and (Z)-4-octene. Nevertheless, these compounds were also identified as pasture diet tracers in previous data (Engel & Ratel, 2007; Sivadier et al., 2008; Vasta & Priolo, 2006).

Among the compounds that were not found to distinguish between diets P and PC12, some were recurrently identified as pasture diet tracers in the literature (Engel & Ratel, 2007; Maruri & Larick, 1992; Sebastian et al., 2003). These compounds are: 1-methyl-cyclohexane, hexane, (Z)-2-octene, heptanal, m-cymen, and 3 alkyl-benzenes (2-ethyl-1,3-dimethyl-benzene, 1,2,3,4- and 1,2,4,5-tetramethyl-benzene). These discrepancies with the literature may be explained by differences between the rearing protocol used by the previous and the present studies. The PC12 diet consisted in pasture feeding for approximately 80 days after weaning, followed by concentrate feeding for about the same duration, while the exclusive concentrate feeding periods in the previous studies (Engel & Ratel, 2007; Maruri & Larick, 1992; Sebastian et al., 2003) were 101, 113, and 175 days after weaning. Hence we can assume that using the PC12 diet, the duration of the period where concentrate is given may be too short to significantly decrease the level of these compounds. Accordingly, we can assume that these compounds are particularly persistent pasture diet tracers. Concerning the other compounds found discriminant in previous studies but not in the present work, these may

Table 2
Persistence of pasture feeding tracers in perirenal and caudal subcutaneous lamb fat tissues.

Compounds[a] (n = 39)	PRF[b] (n = 32)						CSCF[b] (n = 22)					
	P[c]	PC4[c]	PC8[c]	PC12[c]		Persistence degree[d]	P[c]	PC4[c]	PC8[c]	PC12[c]		Persistence degree[d]
Alkanes												
Nonane	100%^{A}	74%^{A}	50%^{B}	48%^{B}	–	Medium						
Decane							100%^{AB}	188%^{A}	59%^{B}	61%^{B}	–	Other
Undecane							100%^{AB}	218%^{A}	56%^{B}	58%^{B}	–	Other
Dodecane	100%^{AB}	126%^{A}	70%^{B}	62%^{B}	–	Other						
Tridecane	100%^{AB}	132%^{A}	84%^{B}	73%^{B}	–	Other						
Dodecane, 2,6,10-trimethyl-	100%^{A}	31%^{B}	35%^{B}	31%^{B}	–	Short						
Tetradecane	100%^{A}	64%^{B}	48%^{B}	42%^{B}	–	Short						
Decane, 2,3,7-trimethyl-	100%^{A}	48%^{B}	33%^{B}	22%^{B}	–	Short	100%^{A}	45%^{B}	30%^{B}	26%^{B}	–	Short
Cyclododecane, 1-ethyl-2-methyl-	100%^{A}	27%^{B}	17% ^{B}	11%^{B}	–	Short	100%^{A}	42%^{B}	17%^{B}	14%^{B}	–	Short
Pentadecane	100%^{A}	51%^{B}	43%^{B}	37%^{B}	–	Short						
Hexadecane	100%^{A}	70%^{B}	50%^{B}	41%^{B}	–	Short	100%^{A}	82%^{A}	48%^{B}	44%^{B}	–	Medium
Alkenes												
1-Pentene	100%^{A}	79%^{A}	57%^{B}	58%^{B}	–	Medium						
(Z)-4-Octene	100%^{A}	33%^{B}	25%^{B}	33%^{B}	–	Short	100%^{A}	52%^{B}	39%^{B}	30%^{B}	–	Short
(E)-4-Octene	100%^{A}	30%^{B}	28%^{B}	36%^{B}	–	Short	100%^{A}	40%^{B}	33%^{B}	25%^{B}	–	Short
(E)-2-Octene	100%^{A}	28%^{B}	28%^{B}	35%^{B}	–	Short	100%^{A}	35%^{B}	35%^{B}	26%^{B}	–	Short
1-Pentadecene	100%^{A}	30%^{B}	18%^{B}	11%^{B}	–	Short	100%^{A}	40%^{B}	16%^{B}	15%^{B}	–	Short
Alcohols												
1-Penten-3-ol	100%^{A}	53%^{B}	37%^{B}	48%^{B}	–	Short	100%^{A}	55%^{A}	27%^{B}	22%^{B}	–	Medium
Aldehydes												
Butanal	100%^{A}	56%^{B}	40%^{B}	55%^{B}	–	Short						
(Z)-4-Heptenal	100%^{A}	39%^{B}	26%^{B}	24%^{B}	–	Short	100%^{A}	72%^{A}	34%^{B}	28%^{B}	–	Medium
2,4-Heptadienal	100%^{A}	56%^{B}	38%^{B}	37%^{B}	–	Short						
Benzene compounds												
Benzene	100%^{A}	78%^{A}	57%^{B}	7%^{B}	–	Medium						
Toluene	100%^{A}	2%^{B}	2%^{B}	2%^{B}	–	Short	100%^{A}	7%^{B}	4%^{B}	4%^{B}	–	Short
Styrene	100%^{A}	75%^{A}	49%^{B}	59%^{B}	–	Medium	100%^{A}	97%^{A}	40%^{B}	33%^{B}	–	Medium
Ketones												
2,3-Butanedione							100%^{A}	76%^{A}	53%^{A}	34%^{B}	–	Long
2,3-Octanedione	100%^{A}	50%^{B}	30%^{B}	25%^{B}	–	Short						
(E,E)-3,5-Octadien-2-one	100%^{A}	53%^{B}	56%^{B}	26%^{B}	–	Short						
Acetophenone	100%^{A}	102%^{A}	63%^{A}	59%^{A}	–	Persistant						
2-Undecanone	100%^{A}	62%^{A}	74%^{A}	44%^{B}	–	Long						
2-Tridecanone	100%^{A}	54%^{B}	52%^{B}	43%^{B}	–	Short						
Chlorine compounds												
Heptane, 1-chloro-							100%^{B}	276%^{A}	84%^{B}	70%^{B}	–	Other
Nitrogen compounds												
Pyridine	100%^{A}	53%^{B}	34%^{B}	54%^{B}	–	Short						
Oxygen compounds												
Furane, 2-methyl-	100%^{A}	69%^{B}	44%^{B}	62% ^{B}	–	Short						
Sulfur compounds												
Methional							100%^{AB}	188%^{A}	64%^{B}	32%^{B}	–	Other
Sulfone, dimethyl-	100%^{A}	5%^{B}	2%^{B}	2%^{B}	–	Short	100%^{A}	11%^{B}	5%^{B}	7%^{B}	–	Short
Terpenes												
α-Pinene							100%^{A}	39%^{B}	45%^{B}	30%^{B}	–	Short
p-Cymen							100%^{A}	27%^{B}	24%^{B}	21%^{B}	–	Short
α-Copaene	100%^{A}	11%^{B}	14%^{B}	4%^{B}	–	Short	100%^{A}	43%^{B}	37%^{B}	11%^{B}	–	Short
ß-Caryophyllene	100%^{A}	32%^{B}	28%^{B}	29%^{B}	–	Short	100%^{A}	61%^{A}	44%^{B}	34%^{B}	–	Medium
trans-Cadina-1(6),4-diene	100%^{A}	16%^{B}	11%^{B}	10%^{B}	–	Short	100%^{A}	23%^{B}	22%^{B}	13%^{B}	–	Short

[a] Compounds found to distinguish between the four types of diet. The amounts of the compounds in the volatile fraction of the tissues are expressed in percentages of their amount in the exclusive pasture diet (P).

[b] Adipose tissues: PRF = perirenal fat, and CSCF = caudal subcutaneous fat.

[c] Diets: P = exclusive pasture; PC4, PC8, PC12 = alternating pasture and fattening for 4 kg, 8 kg, and 12 kg, respectively with concentrate. For each tissue and each compound, values with different letters (A and B) within a same row were found significantly different ($p < 0.05$) according to a Newman–Keuls mean comparison test.

[d] Persistence degree resulting from the Newman–Keuls mean comparison test.

be too specific to experimental features to be considered as generic.

3.2. Persistence of pasture diet tracers in adipose tissues

The 54 compounds found to distinguish between the P and PC12 diets were semi-quantified in the adipose tissues of the lambs fed with the PC4 and PC8 diets. The compounds distinguishing between the four diets were determined by ANOVA ($p < 0.05$). Thirty-two and 22 compounds were selected as feeding tracers in the PRF and CSCF, respectively, with 15 in common (Table 2). Thirty-three of these 39 pasture feeding tracers decreased significantly when animals are finished with concentrate. This decrement confirms first that these compounds are pasture diet tracers, and second that the switch to concentrate diet results in a more or less fast decrease in the abundance of these tracers in lamb adipose tissues. These data are in agreement with the study performed by Larick et al. (1987) which showed a decrease of pasture diet tracers in fat tissue of beef finished with concentrate.

Twenty-four compounds in PRF and 13 in CSCF were shown to distinguish between P and each of the other alternating diets and can so be considered as pasture diet tracers with "short" persistence (see Table 2). Similarly, most of the volatile pasture diet tracers evidenced in beef fat by Larick et al. (1987) were shown to decrease significantly whatever the duration of the concentrate-finishing diet. The short persistence pointed out for 2,3-octanedione in both studies suggests an interspecific genericity. Four compounds in PRF and 5 in CSCF distinguished between P diet and pasture diets followed by a concentrate fattening for a final weight gain greater than or equal to 8 kg (PC8 and PC12). The latter compounds were considered as tracers with "medium" persistence. Similarly, 2-undecanone in PRF and 2,3-butanedione in CSCF that distinguish between the P and PC12 diets were considered as exhibiting a "long" persistence. Most of the pasture tracers which were commonly identified in PRF and CSCF exhibited the same persistence degree in the two tissues suggesting that the mechanisms responsible for the decrement of these compounds are common to PRF and CSCF. Finally, the results presented in Table 2 also confirm the different content in pasture diet tracers of both tissues which was previously evidenced by Sivadier et al. (2008).

All tracers that were alkenes or terpenes exhibited the same persistence, suggesting similar clearance mechanisms within the same chemical family. Considering the terpenes, the prompt variations in amounts of these compounds in response to a pasture-concentrate switch is consistent with previous work on ground beef (Larick et al., 1987). In contrast, other compounds exhibited different persistence within a given chemical family, suggesting that chemical family is not, in most cases, the only factor explaining the persistence of these tracers. The between-diet variation exhibited for linear *n*-alkanes suggest that the chain length of the compounds could be one of the other factors to consider. A systematic short persistence was found for tetra-, penta- and hexadecane in agreement with the result found by Larick et al. (1987) for hexa-, hepta- and octadecane. In contrast, a systematic higher amount in the 4 kg fattening (PC4) has been pointed out for decane, undecane, dodecane and tridecane. These C10—C13 linear alkanes may be suitable for segregating the four feeding situations together with pasture diet tracers with short, medium and long persistence.

3.3. Differentiation of four lamb diets varying in concentrate finishing duration

To determine the relevance of analysing the volatile fraction of the two adipose tissues to distinguish between the four types of diet, the most discriminative tracers listed in Table 2 were selected by a leave-one-out procedure ($p < 0.05$). A PCA was performed on

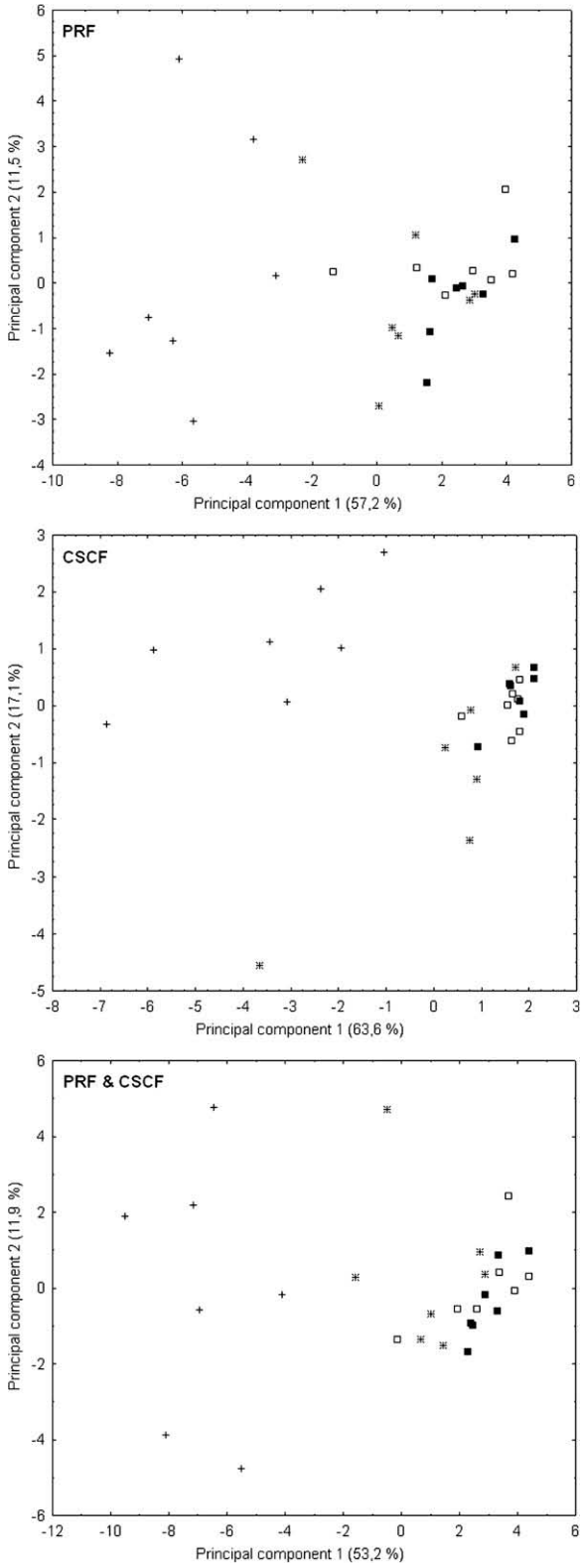

Fig. 2. Differentiation of pasture fed lambs fattened for various weight gain with concentrate based on GC–MS analysis of their adipose tissues: exclusive pasture (+/cross) and alternating pasture and fattening with concentrate for a final gain of weight of 4 kg (⁎/star), 8 kg (□/open square), or 12 kg (■/solid square). First map of normed PCAs carried out from the CCSC pre-treated abundances of the volatile compounds determined distinguishing between the four types of diet by one-way ANOVA followed by a leave-one-out cross validation procedure ($p < 0.05$). Twenty-five compounds were selected in perirenal fat (PRF) and 10 in caudal subcutaneous fat (CSCF). The pooled datasets thus comprised 35 compounds.

the resulting compounds selected in PRF ($n = 25$) and CSCF ($n = 10$) tissues, respectively. Whatever the tissue, the first maps (Fig. 2) show a clear segregation between the pasture and the three other diets. The Newman–Keuls mean comparison test performed on the coordinates of the observations on the first principal component confirmed that only the exclusive pasture diet was significantly differentiated from the three other concentrate-finishing diets in the two adipose tissues (data not shown). This may be explained in part by the fact that most of the tracers involved in the PCA had a "short" persistence.

To assess the usefulness of the combined analysis of PRF and CSCF, the tracers from the two tissues were pooled together in the same dataset ($n = 35$), and a PCA was run on these data (Fig. 2). The Newman–Keuls mean comparison test on the coordinates of the observations on the first principal component revealed a clear segregation of P, PC4, and the two other diets (data not shown). This improvement of the segregation compared with single tissue data confirms previous report showing that the parallel treatment of the data from different adipose tissues improves diet authentication (Sivadier et al., 2008).

The complementarity of PRF and CSCF tissues for differentiating the four diets was assessed by carrying out discriminant analyses (DA) on tracers either from one, or from the two adipose tissues. The tracers ($n = 35$) were combined into all possible triplets, and their Wilk's λ values, which indicate the quality of the distinction between the four diets, were calculated. The 120 most discriminative combinations (i.e. showing the lowest Wilk's λ values) formed by triplets involving tracers from PRF, CSCF and the two adipose tissues were considered. Fig. 3 shows that CSCF exhibits tracers which were less discriminant than PRF, and that the combination of the two datasets resulted in an improvement in the animal diet discrimination. However, this improvement was not sufficient to distinguish between PC8 and PC12 even in the most highly discriminant models (data not shown).

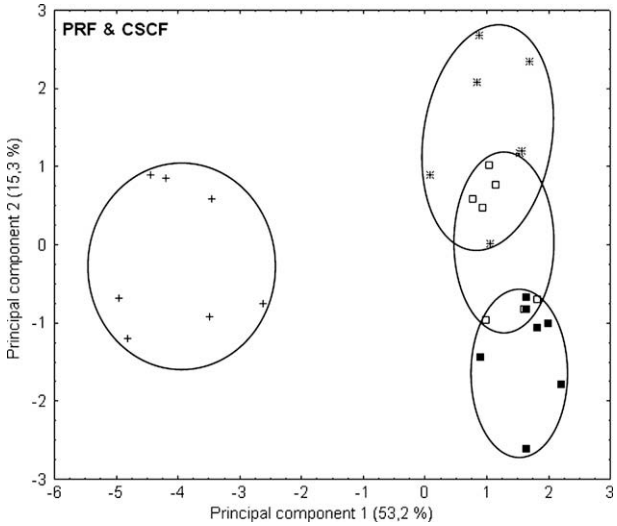

Fig. 4. Differentiation of pasture fed lambs fattened for various weight gain with concentrate based on GC–MS analysis of their adipose tissues: exclusive pasture (+/cross) and alternating pasture and fattening for 4 kg (✳/star), 8 kg (□/open square), or 12 kg (■/solid square) with concentrate. First map of normed PCA carried out from 11 selected ratios. To illustrate the differences in diets, the projection of lambs were clustered into ellipses.

To maximise the discrimination, the abundances of the 35 discriminative compounds from the two adipose tissues were built up into ratios according to Engel et al. (2007). All possible ratios ($n = 1225$) were then filtered by ANOVA ($p < 0.05$) followed by

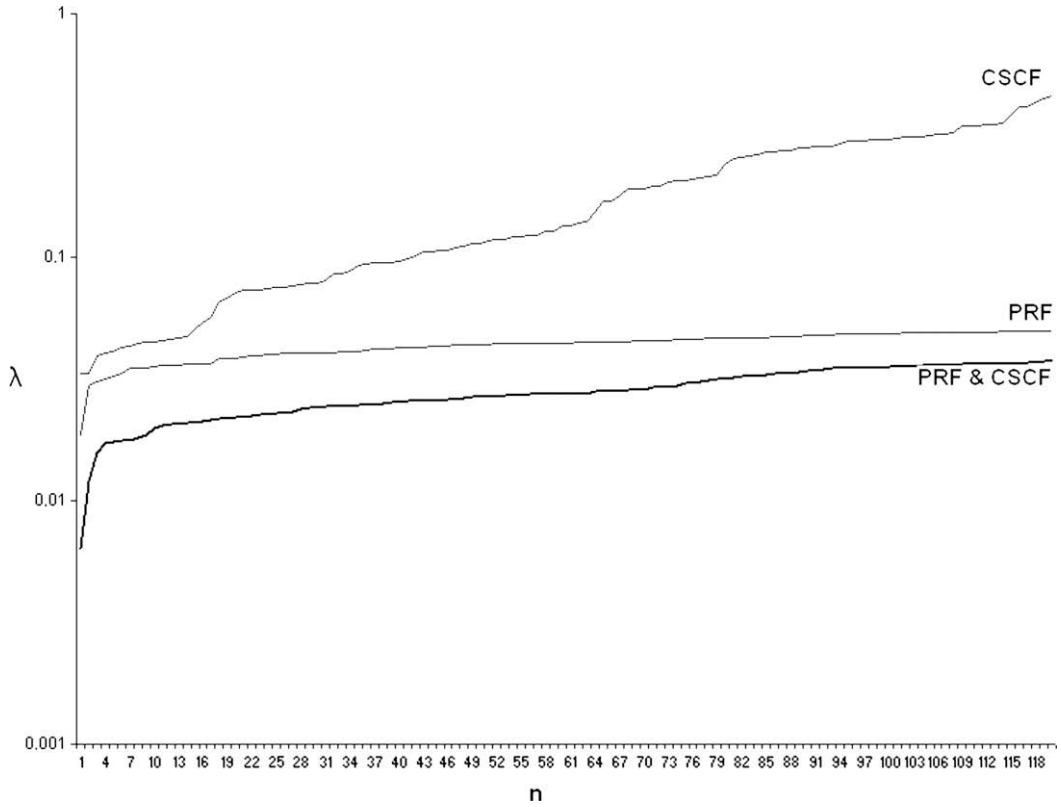

Fig. 3. Comparison of the quality of the diet differentiation by parallel analysis of the adipose tissues. Diagram of Wilk's λ values (λ) calculated for each triplet ($n = 120$) composed by diet tracers from one or the two adipose tissues (PRF = perirenal fat, and CSCF = caudal subcutaneous fat), after a discriminant analysis (DA).

leave-one-out cross validation procedure. 271 discriminant ratios were finally selected. Among the ratios involving the same compound from the same tissue (numerator or denominator), the ratio that exhibited the best Fisher *F* was selected. A PCA (Fig. 4) was carried out on the dataset formed by the 11 selected ratios. The first plane of the PCA revealed a strong segregation of the pasture diet and the three other diets displayed by the first principal component, while the second one segregated the three diets. Newman–Keuls test performed on the coordinates of the observations on both axes of the PCA confirmed that by considering the first and second principal components of the PCA, the four diets were significantly differentiated.

4. Conclusions

In the present study, DH–GC–MS technique and instrumental drift correction were used to extract the relevant information contained in the volatile fraction of the perirenal fat (PRF) and the caudal subcutaneous fat (CSCF) of lambs fed four different diets. The compounds distinguishing between the diets exhibited all the possible degrees of persistence, with most tracers exhibiting a "short" persistence. Only the combined treatment of the diet tracers from the two adipose tissues allowed efficient segregation of the four types of diet. To authenticate the feeding history of grazing ruminants, it is essential to determine the persistence of pasture diet tracers in their tissues, but it is also important to assess the latency rates of these tracers. This will be the subject of a further study.

Acknowledgement

The lambs used in this experiment were produced at the Herbivore Research Unit (INRA, UR1213, Theix, France) facilities; the authors acknowledge the active contribution of M. Bernard, J.C. Bonnefoy, C. Coustet, R. Jailler and S. Prache to the raising and the slaughtering of the animals.

References

Arvanitoyannis, I. S., & Van Houwelingen-Koukaliaroglou, M. (2003). Implementation of chemometrics for quality control and authentication of meat and meat products. *Critical Reviews in Food Science and Nutrition, 43*(2), 173–218.

Aurousseau, B., Bauchart, D., Faure, X., Galot, A. L., Prache, S., Micol, D., et al. (2007). Indoor fattening of lambs raised on pasture: (1) Influence of stall finishing duration on lipid classes and fatty acids in the longissimus thoracis muscle. *Meat Science, 76*, 241–252.

Aurousseau, B., Bauchart, D., Galot, A. L., Prache, S., Micol, D., & Priolo, A. (2007). Indoor fattening of lambs raised on pasture: (2) Influence of stall finishing duration on triglyceride and phospholipid fatty acids in the longissimus thoracis muscle. *Meat Science, 76*, 417–427.

Binnie, J., Cape, J. N., Mackie, N., & Leith, I. D. (2002). Exchange of organic solvents between the atmosphere and grass – The use of open top chambers. *The Science of the Total Environment, 285*, 53–67.

Body, D. R. (1977). Characterization of bovine rumen liquor isoprenoid hydrocarbons with reference to dietary phytol. *Lipids, 12*, 204–207.

Brown, H. G., Melton, S. L., Riemann, M. J., & Backus, W. R. (1979). Effects of energy intake and feed source on chemical changes and flavor of ground beef during frozen storage. *Journal of Animal Science, 48*, 338–347.

Deport, C., Ratel, J., Berdague, J. L., & Engel, E. (2006). Comprehensive combinatory standard correction: A calibration method for handling instrumental drifts if gas chromatography–mass spectrometry systems. *Journal of Chromatography A, 1116*(2), 248–258.

Elmore, J. S., Warren, H. E., Mottram, D. S., Scollan, N. D., Enser, M., Richardson, R. I., et al. (2004). A comparison of the aroma volatiles and fatty acids compositions of grilled beef muscle from Aberdeen Angus and Holstein-Fresian steers fed diets based on silage or concentrates. *Meat Science, 68*(1), 27–33.

Engel, E., Ferlay, A., Cornu, A., Chilliard, Y., Agabriel, C., Bielicki, G., et al. (2007). Relevance of isotopic and molecular biomarkers for the authentication of milk according to production zone and type of feeding of the cow. *Journal of Agricultural and Food Chemistry, 55*, 9099–9108.

Engel, E., & Ratel, J. (2007). Correction of the data generated by mass spectrometry analyses of biological tissues: Application to food authentication. *Journal of Chromatography A, 1154*, 331–341.

Kondjoyan, N., & Berdague, J. L. (1996). *A compilation of relative retention indices for the analysis of aromatic compounds*. Clermont-Ferrand, France: Laboratoire Flaveur.

Larick, D. K., Hedrick, H. B., Bailey, M. E., Williams, J. E., Hancock, D. L., Garner, G. B., et al. (1987). Flavor constituents of beef as influenced by forage- and grain-feeding. *Journal of Food Science, 52*(2), 245–251.

Larick, D. K., & Turner, B. E. (1990). Headspace volatiles and sensory characteristics of ground beef from forage- and grain-fed heifers. *Journal of Food Science, 54*(3), 649–654.

Maruri, J. L., & Larick, D. K. (1992). Volatile concentration and flavor of beef as influenced by diet. *Journal of Food Science, 57*(6), 1275–1281.

Noziere, P., Grolier, P., Durand, D., Ferlay, A., Pradel, P., & Martin, B. (2006). Variations in carotenoids, fat-soluble micronutrients, and color in cows' plasma and milk following changes in forage and feeding level. *Journal of Dairy Science, 89*, 2634–2648.

Priolo, A., Cornu, A., Prache, S., Krogmann, M., Kondjoyan, N., Micol, D., et al. (2004). Fat volatile tracers of grass feeding in sheep. *Meat Science, 66*, 475–481.

Rios, J. J., Fernandez-Garcia, E., Minguez-Mosquera, M. I, & Oerez-Galvez, A. (2008). Description of volatile compounds generated by the degradation of carotenoids in paprika, tomato and marigold oleoresins. *Food Chemistry, 106*, 1145–1153.

Sebastian, I., Viallon-Fernandez, C., Berge, P., & Berdague, J. L. (2003). Analysis of the volatile fraction of lamb fat tissue: Influence of the type of feeding. *Sciences des Aliments, 23*, 497–511.

Sivadier, G., Ratel, J., Bouvier, F., & Engel, E. (2008). Authentication of meat products: Determination of animal feeding by parallel GC-MS analysis of three adipose tissues. *Journal of Agricultural and Food Chemistry, 56*(21), 9803–9812.

Vasta, V., & Priolo, A. (2006). Ruminant fat volatiles as affected by diet: A review. *Meat Science, 73*(2), 218–228.

Vasta, V., Ratel, J., & Engel, E. (2007). Mass spectrometry analysis of volatile compounds in raw meat for the authentication of the feeding background of farm animals. *Journal of Agricultural and Food Chemistry, 55*(12), 4630–4639.

Vezinhet, A., Prud'hon, M., & Benevent, M. (1974). Evolution des différents types de dépôts adipeux après la naissance chez des agneaux *Mérinos d'Arles* normaux ou hypophysectomisés. *Annales de Biologie Animale, Biochimie et Biophysique, 14*, 117–129.

Watanabe, K., & Sato, Y. (1971). Gas chromatographic and mass spectral analysis of heated flavour compounds of beef fats. *Agricultural and Biological Chemistry, 35*(5), 756–763.

Young, O. A., Berdague, J. L., Viallon, C., Rousset-Akrim, S., & Theriez, M. (1997). Fat-borne volatiles and sheepmeat odour. *Meat Science, 45*(2), 183–200.

Food Chemistry 118 (2010) 426–429

Contents lists available at ScienceDirect

Food Chemistry

journal homepage: www.elsevier.com/locate/foodchem

Rapid Communication

Protective effects of quercetin-3-rhamnoglucoside (rutin) on ischemia-reperfusion injury in rat small intestine

Shirou Itagaki, Setsu Oikawa, Jiro Ogura, Masaki Kobayashi, Takeshi Hirano [1], Ken Iseki *

Laboratory of Clinical Pharmaceutics and Therapeutics, Department of Biopharmaceutical Sciences and Pharmacy, Division of Biopharmaceutical Sciences and Pharmacy, Faculty of Pharmaceutical Sciences, Kita 12-jo NIshi 6-chome, Kita-ku, Hokkaido University, Sapporo 060-0812, Japan

ARTICLE INFO

Article history:
Received 24 October 2008
Received in revised form 23 March 2009
Accepted 27 April 2009

Keywords:
Reactive oxygen substances
Rutin
Ischemia-reperfusion
EGCG

ABSTRACT

Quercetin-3-rhamnoglucoside (rutin) has a wide spectrum of biochemical and pharmacological activities. Orally administered compounds are absorbed in the intestine. Although absorption of rutin from the jejunum of the rat was good, binding of rutin to the intestinal wall components may limit its absorption from the small intestine. The physiological importance of an orally administered compound depends on its interaction with target tissues. Since there is limited information on the importance of rutin *in vivo*, we focused on the protective effect of rutin on intestinal injury. The intestinal mucosa is extremely sensitive to reactive oxygen species. We used a rat mesenteric ischemia-reperfusion (I/R) injury model as a model of oxidative injury and investigated the antioxidant activities of rutin *in vivo*. We found that rutin, which has combined antioxidant activity from radical-scavenging, xanthine oxidase inhibition and chain-breaking effects, exhibits a protective effect on I/R injury in the rat small intestine.

1. Introduction

Common buckwheat is recognised as a healthy food in many countries, such as China, Nepal and Japan, because it is rich in flavonoids, vitamins, amino acids and other substances. One of the most important components of buckwheat is quercetin-3-rhamnoglucoside (rutin), a flavonol glycoside compound. This natural substance has a wide spectrum of biochemical activities, including antioxidant, antiviral, antitumor, antiinflammatory and antiallergic activities, and is a stimulant of the immune system (Watanabe, 1998). Moreover, rutin is commercially prepared and used as dietary supplements. Orally administered compounds are absorbed in the intestine. It has been reported that absorption of rutin from the jejunum of the rat was good and that rutin is mainly absorbed in its unmetabolized form (Spencer, Chowrimootoo, Choudhury, Debnam, & Srai et al., 1999). However, it has also been reported that binding of rutin to the intestinal wall components may greatly limit its absorption from the small intestine (Carbonaro & Grant, 2005). The physiological importance of an orally administered compound depends on its interaction with target tissues. Thus, we focused on the effect of rutin on the jejunum.

The interest in using rutin in cosmetic and pharmaceutical formulations is to enhance their antioxidant and vasoprotective properties for promoting relief of symptoms of lymphatic and venous insufficiency and for reducing capillary fragility (Calabrò, Tommasini, Donato, Stancanelli, & Raneri et al., 2005). Production of reactive oxygen species (ROS) in tissue contributes to the development of various chronic diseases, such as cancer, neurodegenerative diseases and cardiovascular diseases (Benzie, 2000). Administration of antioxidants to patients may therefore help in removing ROS and thus improving their clinical outcome. Dietary antioxidants can improve the activities of cellular antioxidant defence systems including enzymes, such as superoxide dismutase and glutathione peroxidase, and help to prevent oxidation damage to cellular components. There has been considerable public and scientific interest in therapeutic use of natural antioxidants. In addition to buckwheat, rutin is found in fruits and vegetables, such as kale, apple and orange juice (Careri, Elviri, Mangia, & Musci, 2000; Paganga, Miller, & Rice-Evans, 1999). In order to evaluate *in vitro* antioxidant activities of various compounds, a screening procedure such as *in vitro* radical-scavenging assay is widely used. However, there is little information on the importance of dietary flavonoids, including rutin, as antioxidants *in vivo*, or evidence for such activity *in vivo*.

The intestinal mucosa is extremely sensitive to ROS (Kong, Blennerhassett, Heel, McCauley, & Hall, 1998). Since there is limited information on the importance of rutin as an antioxidant *in vivo*, we focused on the protective effect of rutin on intestinal oxidative injury. It is well known that ROS are responsible for intestinal isachemia-reperfusion (I/R) injury (Adam, Crespy, Levrat-Verny, Leenhardt, & Leuillet et al., 2002). Intestinal I/R is a common clinical problem in the settings of severe burns, circulatory shock and strangulation ileus. Furthermore, intestinal I/R injury is a serious medical problem often necessitating surgical intervention. In this study, we used a rat mesenteric I/R injury model as a model of oxi-

* Corresponding author. Tel./fax: +81 11 706 3770.
E-mail address: ken-i@pharm.hokudai.ac.jp (K. Iseki).
[1] Present address: Department of Pharmacy, Kobe University Hospital, Kobe, Japan.

0308-8146/$ - see front matter © 2009 Elsevier Ltd. All rights reserved.
doi:10.1016/j.foodchem.2009.04.103

dative injury and investigated the antioxidant activities of rutin *in vivo*.

2. Materials and methods

2.1. Chemicals

Rutin, (−)-epigallocatechin gallate (EGCG), thiobarbituric acid (TBA), 2,2′-azobis(4-methoxy-2,4-dimethylvaleronitrile) (MeO-AMVN), luminol, hydrogen peroxide, diethylenetriamine-N,N,N′,N″,N″-pentaacetic acid (DTPA) and iron (II) sulphate heptahydrate were purchased from Wako (Osaka, Japan). Xanthine oxidase was purchased from Nacalai Tesque (Kyoto, Japan). Hypoxanthine was purchased from Sigma (St. Louis, MO). 4,4-Difluoro-5-(4-phenyl-1,3-butadienyl)-4-bora-3a,4a,-diaza-s-indacene-3-propionic acid saccinimidyl ester (BODIPY) was purchased from Invitrogen (Carlsbad, CA). All other reagents were of the highest grade available and used without further purification.

2.2. Animals

Male Wistar rats, aged 6 weeks (180–200 g in weight), were obtained from Japan Laboratory Animals (Tokyo, Japan). The housing conditions were the same as those described previously (Itagaki, Kurokawa, Nakata, Saito, & Oikawa et al., 2009). The rats were housed for at least 1 week at 23 ± 3 °C and 50 ± 10% relative humidity and were maintained on a 12-h light/dark cycle. During the acclimatisation, the rats were allowed free access to food and water. The experimental protocols were reviewed and approved by the Hokkaido University Animal Care Committee in accordance with the "Guide for the Care and Use of Laboratory Animals".

2.3. Measurement of superoxide anion-scavenging activity

Superoxide anion-scavenging activity was measured by the chemiluminescent superoxide anion probe method, using a superoxide anion-2-methyl-6-methoxyphenylethynylimidazopyrazynone (MPEC) reaction kit (ATTO Corp., Osaka, Japan) according to the manufacturer's instructions (Itagaki et al., 2009).

2.4. Measurement of hydroxyl radical-scavenging activity

The method is based on the generation of HO· by Fenton reaction and the determination of HO· by chemiluminescence (Hirayama & Yida, 1997). For the Fenton reaction, H_2O_2 solution (1 mM) was prepared by diluting hydrogen peroxide solution with 25 mM imidazole-nitrite solution (pH 7.0); ferrous sulphate solution (1 mM) was prepared by dissolving $FeSO_4 \cdot 7H_2O$ in distilled water and DTPA solution (1 mM) was prepared in distilled water. As a chemiluminescent reagent, luminol solution (1 mM) was prepared by dissolving luminol in 200 mM borate buffer (pH 9.5). The reaction solution was composed of 0.16 mM ferrous sulphate, 0.16 mM DTPA, 0.25 mM hydrogen peroxide, and 0.16 mM luminal, with or without tested compounds (final concentrations of 0.001, 0.01, 0.1, 1 and 10 mM, respectively). The ferrous iron (Fe^{II})–H_2O_2–luminol chemiluminescence signal profile was obtained by the multilabel counter, Wallac 1420 ARVOse. The results are expressed as inhibition, representing the percentage of inhibition of luminol chemiluminescence with respect to that occurring in a control:

$$\text{Inhibition rate} = [(AUC_{control} - AUC_{sample})/AUC_{control}] \times 100$$

where $AUC_{control}$ and AUC_{sample} represent the area under the curve (AUC) of luminol chemiluminescence kinetics in the control and samples, respectively.

2.5. Measurement of radical chain-breaking activity

The assay was carried out as described in a previous report (Itagaki et al., 2009).

2.6. Intestinal I/R model

Surgical procedures and tissue sampling were carried out as described in a previous report (Itagaki et al., 2009).

2.7. TBA analysis

The amount of lipid peroxide in the intestine was determined as that of malondialdehyde (MDA) (Itagaki et al., 2009).

2.8. Evaluation of changes in vascular permeability

Extravasation of Evans blue dye into tissue was used as an index of increased vascular permeability. Evans blue dye (20 mg/kg) was injected (1 ml/kg) through the jugular vein 5 min prior to reperfusion. Sixty min after reperfusion, fragments of the loop were cut and Evans blue dye was extracted using 4 ml of formamide (24 h at 37 °C).

2.9. Data analysis

Nonlinear regression analysis was performed by using Origin® (version 6.1J). Student's *t*-test was used to determine the significance of differences between two group means. Statistical significance among means of more than two groups was determined by one-way analysis of variance (ANOVA). A value of $p < 0.05$ was considered significant.

3. Results and discussion

ROS are continuously generated by metabolism in the body and exert physiological actions (Gate, Paul, Ba, Tew, & Tapiero, 1999). Although the action of ROS is normally limited by the antioxidant defence system of the body, an excess of ROS induces oxidative damage in vulnerable targets, such as membrane unsaturated fatty acids, protein thiols, and DNA bases (Ceconi, Boraso, Cargnoni, & Ferrari, 2003). Since oxidative stress is an imbalance between ROS production and antioxidant defence, the antioxidant capacity in patients is likely to be compromised. Much interest has been shown in the discovery of new antioxidants in recent years, due to their potential applications in the treatment of ROS-induced diseases. For the prevention of these diseases, an approach focusing on the health aspects of natural antioxidants should be beneficial. However, there is not much available experimental evidence of their physiological functions, in comparison with experimental evidence of the physiological functions of pharmaceutical drugs.

In this study, we compared the antioxidative activities of rutin with those of EGCG, a well-known antioxidative flavonoid. In the first part of this study, the antioxidant activities of rutin were evaluated using an *in vitro* system. The superoxide radical anion appears to play a central role, since other ROS are formed in reaction sequences starting with the superoxide radical anion. Xanthine/xanthine oxidase is also a main source of ROS (Chambers, Parks, Patterson, Roy, & McCord et al., 1985). Moreover, the intestinal mucosa is one of the richest sources of xanthine oxidase. In this study, we therefore used a xanthine/xanthine oxidase system to generate superoxide anions. EGCG and rutin inhibited the light emission induced by xanthine oxidase in a concentration-dependent manner. IC_{50} values of EGCG and rutin for light emission induced by xanthine oxidase are listed in Table 1. EGCG and rutin

prevented the light emission induced by xanthine oxidase. Highly reactive free radicals, such as peroxyl radicals involved in auto-oxidation of lipoproteins and of biological membranes, are responsible for microvascular damage. Since hydroxyl radical production plays a significant role in the initiation of lipid peroxidation, we investigated the hydroxyl radical-scavenging activities of EGCG and rutin. The results showed that EGCG and rutin both exhibit hydroxyl radical-scavenging activities (Table 1). Since the influence of free radical-mediated oxidation is amplified, because it is proceeded by a chain mechanism, the role of chain-breaking activity is important as well as radical-scavenger activity (Riley, 1994). Recently, Beretta, Aldini, Facino, Russell, & Krinsky et al., (2006) reported a method that enables specific measurements of chain-breaking activities of tested compounds, using BODIPY, and showed that EGCG acts as a chain-breaking antioxidant, as well as a radical-scavenger. We therefore investigated the chain-breaking activity of rutin using BODIPY. EGCG and rutin inhibited BODIPY oxidation, and the TAP values of these compounds increased in a concentration-dependent manner (Table 2).

Evidence supporting an antioxidant function for flavonoids is usually derived from *in vitro* assays. However, evidence that flavonoids, including rutin, act directly or indirectly as antioxidants *in vivo* is limited. Antioxidant studies using laboratory animals should be carried out to obtain a mechanistic basis and safety profiles before they can be applied to humans for intervention trials. As a model of ROS-induced diseases, we selected intestinal I/R injury (Adam et al., 2002; Kong et al., 1998). We confirmed *in vivo* antioxidant activities of EGCG and rutin, using a rat I/R injury model. Lipid peroxidation is an integral process in the oxidation of unsaturated fatty acids via a radical chain reaction, and overproduction of lipid peroxide contributes to small intestinal injury. The increase in the amount of lipid peroxide after I/R was significantly inhibited by treatment with EGCG and rutin (Fig. 1). Since vascular permeability has been shown to be significantly higher in rats with I/R than in sham-operated rats, elevated vascular permeability is also one of the indicators of I/R injury (Pompermayer, Amaral, Fagundes, Vieira, & Cunha et al., 2007). We therefore investigated the effects of these compounds on increased vascular permeability, as assessed by reduction in the level of Evans blue dye. Elevation of vascular permeability by intestinal I/R was attenuated by treatment with EGCG and rutin (Fig. 2). I/R injury occurs clinically during abdominal aortic aneurysm surgery, small bowel transplantation, cardiopulmonary bypass, strangulated hernias and neonatal necrotizing enterocolitis. Moreover, reperfusion of ischemic vascular beds may lead to recruitment and activation of leukocytes, release of mediators of the inflammatory process and further injury to the affected vascular bed and remote sites (Lefer & Lefer, 1996). Thus, strategies that limit the damage induced by the reperfusion process may be useful in the treatment of ischemic disorders in various organs (Willerson, 1997). The protective effect of rutin on intestinal I/R injury may be relevant to human health.

As stated above, I/R injury is considered to be a major clinical problem and occurs in many kinds of tissues, including the stomach, pancreas, and cardiac and skeletal muscle (Harris, Leiderer, Peer, & Messmer, 1996; Reiter & Tan, 2003). In addition to I/R injury, ROS are thought to play an important role in many diseases (Benzie, 2000; Gate et al., 1999). The doses of rutin, with clinically

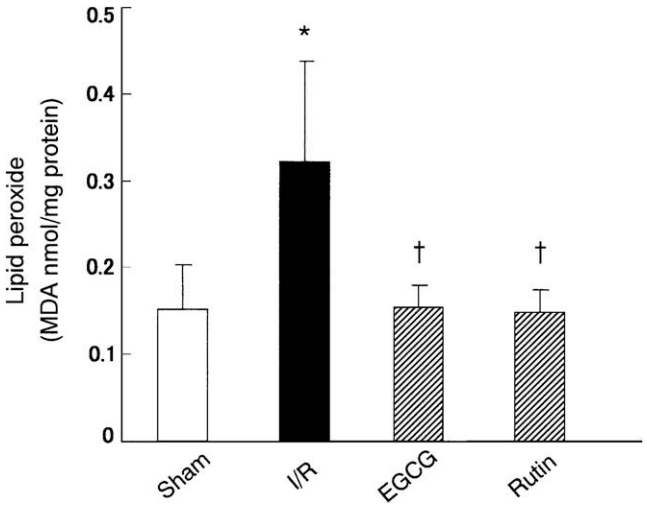

Fig. 1. Effects of EGCG and rutin (1 mM) on the amount of lipid peroxide in the small intestine after I/R. Each value is the mean with S.D. of 3 rats (I/R + rutin), 4 rats (I/R + EGCG) or 11 rats (sham, I/R). $^{*}P < 0.05$, significantly different from nonischemia control animals. $^{\dagger}P < 0.05$, significantly different from animals not treated with compounds (I/R animals). *Abbreviations:* MDA, malondialdehyde; I/R, ischemia-reperfusion; EGCG, (−)-epigallocatechin gallate.

Table 1
IC_{50} values of EGCG and rutin on xanthine oxidase-induced light emission and superoxide anion-scavenging activity

	Xanthine oxidase-induced light emission	Superoxide anion-scavenging activity
	IC_{50} (M)	
EGCG	9.13 ± 0.70	0.80 ± 0.02
Rutin	71.7 ± 11.1	10.6 ± 1.59

Each value represents the mean with S.D. of three independent experiments.
Abbreviation: EGCG, (−)-epigallocatechin gallate.

Table 2
Antioxidant activities of EGCG and rutin determined by the TAP assay.

Concentration (mM)	EGCG	Rutin
	TAP value (%)	
0.0001	0.95 ± 6.82	15.6 ± 16.1
0.001	35.9 ± 8.90	35.1 ± 5.01
0.01	78.9 ± 3.68	62.0 ± 3.42
0.1	85.8 ± 3.68	81.7 ± 2.01
1	78.6 ± 4.18	84.5 ± 0.31

Each value represents the mean with S.D. of three independent experiments.
Abbreviations: EGCG, (−)-epigallocatechin gallate; TAP, total antioxidant performance.

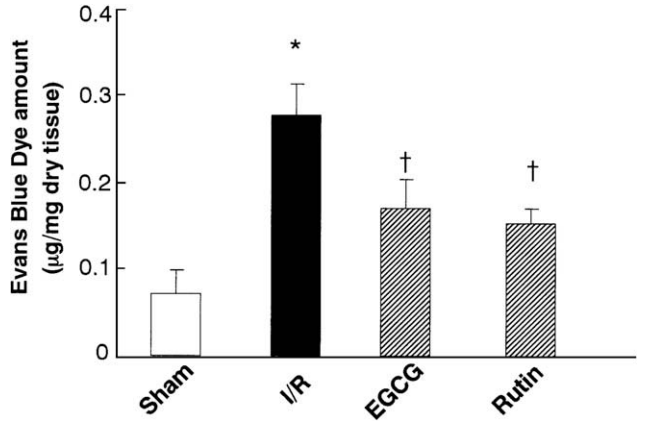

Fig. 2. Effects of EGCG and rutin (1 mM) on changes in vascular permeability in the small intestine. Each value is the mean with S.D. of 4 rats (I/R + rutin), 5 rats (sham) or 6 rats (I/R, I/R + EGCG). $^{*}P < 0.05$, significantly different from nonischemia control animals. $^{\dagger}P < 0.05$, significantly different from animals not treated with compounds (I/R animals). *Abbreviations:* I/R, ischemia-reperfusion; EGCG, (−)-epigallocatechin gallate.

clearly demonstrated effects, have been reported to be between 180 and 350 mg (Schilcher, Patz, & Schimmel, 1990). Thus, the intake of 100 g of buckwheat flour or bran in food would cover ~10% of the therapeutic doses. These are well below the therapeutic doses but could meet the demands of preventive nutrition and post-therapeutic nutritional treatment, especially with the consideration that, besides buckwheat, other foods and/or beverages could also be consumed as natural nutritional sources of rutin. A recommended daily intake of rutin has not been established. Further studies are needed to establish the recommended daily doses of rutin and food sources of dietary rutin.

For the prevention of ROS-induced diseases, an approach focusing on the health aspects of functional foods should be beneficial (Swinbanks & O'Brien, 1993). In order to develop new functional foods, it is important to select a suitable ingredient that has a scientific background. The results of this study should provide a scientific background of the usefulness of rutin as a functional food ingredient.

In summary, we have found that rutin, which has combined antioxidant activity from radical-scavenging, xanthine oxidase inhibition and chain-breaking effects, exhibits a protective effect on I/R injury in the rat small intestine. Rutin might be useful for prevention of oxidative injury in humans and for *in vivo* studies.

Acknowledgements

This work was supported in part by the Towa Food Research Foundation.

References

Adam, A., Crespy, V., Levrat-Verny, M. A., Leenhardt, F., Leuillet, M., Demigné, C., et al. (2002). The bioavailability of ferulic acid is governed primarily by the food matrix rather than its metabolism in intestine and liver in rats. *Journal of Nutrition, 132*, 1962–1968.

Benzie, I. F. (2000). Evolution of antioxidant defense mechanisms. *European Journal of Nutrition, 39*, 53–61.

Beretta, G., Aldini, G., Facino, R. M., Russell, R. M., Krinsky, N. I., & Yeum, K. J. (2006). Total antioxidant performance. A validated fluorescence assay for the measurement of plasma oxidizability. *Analytical Biochemistry, 354*, 290–298.

Careri, M., Elviri, L., Mangia, A., & Musci, M. (2000). Spectrophotometric and coulometric detection in the high-performance liquid chromatography of flavonoids and optimization of sample treatment for the determination of quercetin in orange juice. *Journal of Chromatography A, 881*, 449–460.

Calabrò, M. L., Tommasini, S., Donato, P., Stancanelli, R., Raneri, D., Catania, S., et al. (2005). The rutin/beta-cyclodextrin interactions in fully aqueous solution: Spectroscopic studies and biological assays. *Journal of Pharmaceutical and Biomedical Analysis, 36*, 1019–1027.

Carbonaro, M., & Grant, G. (2005). Absorption of quercetin and rutin in rat small intestine. *Annals of Nutrition and Metabolism, 49*, 178–182.

Ceconi, C., Boraso, A., Cargnoni, A., & Ferrari, R. (2003). Oxidative stress in cardiovascular disease: Myth or fact? *Archives of Biochemistry and Biophysics, 420*, 217–221.

Chambers, D. E., Parks, D. A., Patterson, G., Roy, R., McCord, J. M., Yoshida, S., et al. (1985). Xanthine oxidase as a source of free radical damage in myocardial ischemia. *Journal of Molecular and Cellular Cardiology, 17*, 145–152.

Gate, L., Paul, J., Ba, G. N., Tew, K. D., & Tapiero, H. (1999). Oxidative stress induced in pathologies: The role of antioxidants. *Biomedicine and Pharmacotherapy, 53*, 169–180.

Harris, A. G., Leiderer, R., Peer, F., & Messmer, K. (1996). Skeletal muscle microvascular and tissue injury after varying durations of ischemia. *American Journal of Physiology, 271*, H2388–H2398.

Hirayama, O., & Yida, M. (1997). Evaluation of hydroxyl radical-scavenging ability by chemiluminescence. *Analytical Biochemistry, 251*, 297–299.

Itagaki, S., Kurokawa, T., Nakata, C., Saito, Y., Oikawa, S., Kobayashi, M., et al. (2009). In vitro and in vivo antioxidant properties of ferulic acid: A comparative study with other natural oxidation inhibitors. *Food Chemistry, 114*, 466–471.

Kong, S. E., Blennerhassett, L. R., Heel, K. A., McCauley, R. D., & Hall, J. C. (1998). Ischaemia-reperfusion injury to the intestine. *Australian and New Zealand Journal of Surgery, 68*, 554–561.

Lefer, A. M., & Lefer, D. J. (1996). The role of nitric oxide and cell adhesion molecules on the microcirculation in ischaemia-reperfusion. *Cardiovascular Research, 32*, 743–751.

Paganga, G., Miller, N., & Rice-Evans, C. A. (1999). The polyphenolic content of fruit and vegetables and their antioxidant activities. What does a serving constitute? *Free Radical Research, 30*(15), 3–162.

Pompermayer, K., Amaral, F. A., Fagundes, C. T., Vieira, A. T., Cunha, F. Q., Teixeira, M. M., et al. (2007). Effects of the treatment with glibenclamide, an ATP-sensitive potassium channel blocker, on intestinal ischemia and reperfusion injury. *European Journal of Pharmacology, 556*, 215–222.

Reiter, R. J., & Tan, D. X. (2003). Melatonin: A novel protective agent against oxidative injury of the ischemic/reperfused heart. *Cardiovascular Research, 58*, 10–19.

Riley, P. A. (1994). Free radicals in biology: Oxidative stress and the effects of ionizing radiation. *International Journal of Radiation Biology, 65*, 27–33.

Schilcher, H., Patz, B., & Schimmel, K. (1990). Ch; Klinische Studie mit einem Phytopharmakon zur Behandlung von Mikrozirkulationsstorungen. *Ärztezeitschrift fur Naturheilverfahren, 31*, 819–826.

Spencer, J. P., Chowrimootoo, G., Choudhury, R., Debnam, E. S., Srai, S. K., & Rice-Evans, C. (1999). The small intestine can both absorb and glucuronidate luminal flavonoids. *FEBS Letters, 458*, 224–230.

Swinbanks, D., & O'Brien, J. (1993). Japan explores the boundary between food and medicine. *Nature, 364*, 180.

Watanabe, M. (1998). Catechins as antioxidants from buckwheat (*Fagopyrum esculentum* Moench) groats. *Journal of Agricultural and Food Chemistry, 46*, 839–845.

Willerson, J. T. (1997). Pharmacologic approaches to reperfusion injury. *Advances in Pharmacology, 39*, 291–312.

Food Chemistry 118 (2010) 430–435

Contents lists available at ScienceDirect

Food Chemistry

journal homepage: www.elsevier.com/locate/foodchem

Short communication

Oxygen species scavenger activities and phenolic contents of four West African plants

G. Kouakou-Siransy [a,b], S. Sahpaz [d], G. Irié-Nguessan [b], Y.J. Datte [c], J. Kablan [b], B. Gressier [a], F. Bailleul [d,*]

[a] Laboratoire de Pharmacologie, Pharmacocinétique et Pharmacie Clinique, Faculté des Sciences Pharmaceutiques et Biologiques, Université Lille Nord de France, 3 rue du Professeur Laguesse, B.P. 83, 59006 Lille Cedex, France
[b] Laboratoire de Pharmacologie, Pharmacocinétique et Pharmacie Clinique, UFR des Sciences Pharmaceutiques et Biologiques, Université de Cocody, Abidjan, Côte d'Ivoire
[c] Laboratoire de Nutrition et Pharmacologie, UFR des Biosciences, Université de Cocody, Abidjan, Côte d'Ivoire
[d] Laboratoire de Pharmacognosie, E.A. 1043, Faculté des Sciences Pharmaceutiques et Biologiques, Université Lille Nord de France, 3 rue du Professeur Laguesse, B.P. 83, 59006 Lille Cedex, France

ARTICLE INFO

Article history:
Received 9 December 2008
Received in revised form 1 April 2009
Accepted 29 April 2009

Keywords:
Antioxidant
Phenolics
Flavonoids
ROS
Alchornea cordifolia
Baphia nitida
Cassia occidentalis
Boerhavia diffusa

ABSTRACT

In West Africa, *Alchornea cordifolia*, *Baphia nitida*, *Cassia occidentalis* and *Boerhavia diffusa* leaves are used in food and drinks, as well as in traditional medicine, to treat rheumatic ailments which incur oxidative stress. First, these plants were evaluated for their antioxidant properties through a scavenger effect on reactive oxygen species (ROS), such as hydrogen peroxide and hypochlorous acid. All of them showed dose-dependent antioxidant activity. The values obtained were comparable to those of antioxidant pharmacological substances: N-acetylcysteine and Mesna. Second, rates of total phenolic, flavonoid and proanthocyanidin contents were evaluated. The highest rates were to be found in the most active extracts, indicating that antioxidant activity could be influenced by these phytochemical groups.

The results of our study confirm the traditional use of these plants in inflammatory diseases, and demonstrate that they could contribute, through their phenolic contents, to attenuating tissue damage due to ROS. These plants can also be beneficial for health as a source of antioxidants when they are included in food and drinks.

1. Introduction

In West Africa, numerous plants are included in food or drinks and are also successfully used in traditional medicine, e.g. *Alchornea cordifolia* (Schumach. & Thonn.) Müll. Arg. (Euphorbiaceae), *Baphia nitida* Lodd. (Fabaceae), *Cassia occidentalis* L. (Fabaceae) and *Boerhavia diffusa* L. (Nyctaginaceae) leaves. On the one hand, *A. cordifolia* and *C. occidentalis* leaves are used as decoctions in water instead of coffee and as a drink mixed with pineapple fruit juice (Motte, 1980). *B. diffusa* leaves, mixed with *Afromomum melegueta* fruits and *Zingiber officinale* rhizomes, are included in foodstuffs, as well as *B. nitida* leaves, which are used alone (Chastanet, Fauvelle-Aymar, & Juhé-Beaulaton, 2002). On the other hand, all these plants prevent or cure several illnesses, including those with severe inflammatory components, such as bronchial asthma and rheumatic ailments (Adjanohoun & Ake Assi, 1979). On the pharmacological level, they share anti-inflammatory properties (Mavar-Manga, Brkic, Marie, & Quetin-Leclercq, 2004). In addition, many scientific works report evidence of their effectiveness in antimicrobial (Agrawal, Srivastava, Srivastava, & Srivastava, 2004), antispasmodic (Borrelli et al., 2005), diuretic (Mishra & Singh, 1980), and immuno-modulating (Pandey, Maurya, Singh, Sathiamoorthy, & Naik, 2005) treatments. Our study, which is the first of its kind, aims at investigating the capacity of all four plants to scavenge reactive oxygen species (ROS) and at determining the compounds responsible for this effect.

Activation of neutrophils or macrophages, through inflammatory substances is known to generate ROS (Roos, 1991), such as hydrogen peroxide (H_2O_2), and hypochlorous acid (HOCl). At low rates, ROS act as signalling molecules in various intracellular processes and are produced continuously in most tissues. Antioxidants within the human body tend to limit oxidant rate. Any excessive increase in their production in the course of oxidant stress is particularly preponderant, on the one hand, in illnesses such as chronic inflammatory diseases (Sahinoglu, Stevens, Bhatt, & Blake, 1996), rheumatoid arthritis (Afonso, Campy, Mitrovic, & Collin, 2007) or pulmonary diseases (Chabot, Mitchell, Guteridge, & Evans, 1998) and, on the other hand, in others such as atherosclerosis, brain and heart ischemia, cancer, neurodegenerative diseases and acute kidney failure (Yoshioka & Ichikawa, 1989). ROS are associated with cell damage as they react with different macromolecules, such as membrane proteins, lipids and DNA. Therapeutic action aimed at correcting oxidant–antioxidant imbalance is a clinical challenge,

* Corresponding author. Tel./fax: +33 320 964039.
E-mail address: francois.bailleul@univ-lille2.fr (F. Bailleul).

0308-8146/$ - see front matter © 2009 Elsevier Ltd. All rights reserved.
doi:10.1016/j.foodchem.2009.04.117

and has increasingly been the object of research work. Several articles have reported that polyphenols, such as flavonoids and proanthocyanidins, which are widely distributed in the vegetable kingdom, show antioxidant properties (Hatano et al., 1989). Previous phytochemical works have indicated the presence of flavonoids and phenolic acids, such as ellagic acid and two glycosides of quercetol, in *A. cordifolia* leaves (Ogungbamila & Samuelsson, 1990) and the presence of cinnamoyl derivatives, quercetin, kaempferol and their glycosides, in *B. diffusa* leaves (Ferreres et al., 2005). No polyphenolic compounds had previously been isolated and identified in *B. nitida* and *C. occidentalis* leaves.

The aim of this study was therefore to determine the antioxidant activity of the four studied plant leaves versus ROS and to correlate this activity with the total phenolic, flavonoid and proanthocyanidin contents of each plant. This could explain, at least partly, their traditional anti-inflammatory uses.

2. Materials and methods

2.1. Chemicals and instruments

All chemicals were purchased from Sigma Chemical Co. (USA) and from Merck (France). Thin-layer chromatography (TLC) was performed on Merck silica gel F_{254} plates. Natural standard products (gallic acid, cyanidin and hyperoside, ellagic acid, quercetin, kaempferol and hyperin) were obtained from Extrasynthèse (France). All absorbances were measured with a Kontron Uvikon 869 spectrophotometer.

2.2. Plant material

Fresh leaves of *A. cordifolia*, *B. nitida*, *C. occidentalis* and *B. diffusa* were harvested at the Floristic National Center of Abidjan and verified by an expert botanist (Prof. Aké Assi, Department of Botany, University of Abidjan) to be identical to samples from the Herbarium at the centre (Table 1). Voucher specimens were deposited in the Botanical Department of the Centre National de Floristique at the Cocody University of Abidjan (Côte d'Ivoire). The leaves were collected and dried in darkness in a 25 °C air-conditioned room. These conditions were the most appropriate in order to protect the polyphenolic content of each plant.

2.3. Preparation of ethyl acetate and aqueous extracts

2.3.1. Ethyl acetate extract

The dried leaves were powdered (50 g) and macerated for 24 h at room temperature in 500 ml of methanol/acetone/water (70:70:30 v/v/v); then the filtrates were low pressure-concentrated at 30 °C to remove the methanol and acetone phases. The remaining water was extracted three times with ethyl acetate. The ethyl acetate phases obtained were evaporated to dryness and conserved at 4 °C (Table 2). This powder was dissolved in the appropriate solvents for further studies.

2.3.2. Aqueous extract

The fine powder (50 g) of dried leaves were macerated for 48 h at room temperature in 500 ml of distilled water. The aqueous extracts obtained were lyophilised and conserved at 4 °C, and aliquots of lyophilised powder were dissolved in the appropriate solvents for chemical and pharmacological studies (Table 2).

Table 2
Yields in percent of dry matter after extraction.

Plant	Aqueous extract	Ethyl acetate extract
Alchornea cordifolia	7.0	8.3
Baphia nitida	8.4	11.5
Cassia occidentalis	12.0	40.3
Boerhavia diffusa	6.6	6.3

2.4. Phenolic content

2.4.1. General

The extracts were tested by thin-layer chromatography (TLC) and colorimetric methods to determine the presence of flavonoids, proanthocyanidins and total phenolics. All measurements were made three times. The results were expressed in mg/mg of dry extract and compared with standards treated under the same conditions.

2.4.2. Thin-layer chromatography (TLC) analysis

TLC of phenolic extracts was performed on Merck 5554 Silicagel F_{254} aluminium sheets. Proanthocyanidins were analysed with toluene/acetone/formic acid, 3:3:1 (v/v). Detection: visible, UV alone (550 nm), anisaldehyde/H_2SO_4 (anisaldehyde, 0.2 ml/MeOH, 85 ml/AcOH, 10 ml/H_2SO_4, 5 ml) then 3–4 min at 105 °C. Flavonoids were analysed with ethyl acetate/formic acid/water, 8:1:1 (v/v). Detection: visible, UV alone (365), aminoethyl-diphenyl borinate in MeOH with 3% PEG 300 (visible and UV).

2.4.3. Determination of total phenolic content

Total phenolics were quantified by the colorimetric method adapted from Singleton, Joseph, and Rossi (1965), using Folin–Ciocalteu reagent (7 ml distilled H_2O, 0.5 ml Folin–Ciocalteu reagent); 0.5 ml of each aqueous extract solution was added. After 3 min, 2 ml of 20% Na_2CO_3 were added and the whole heated to 100 °C for 1 min in a water bath. Absorbance was measured at a wavelength of 680 nm and compared with a standard of gallic acid.

2.4.4. Determination of proanthocyanidin content

The method used in experimentation was similar to that of Porter, Hrtich, and Chan (1986). The results were compared with those obtained with a standard of cyanidin.

2.4.5. Determination of flavonoid content

Total flavonoid contents were determined with the aluminium chloride ($AlCl_3$, $6H_2O$) method used by Lamaison and Carnat (1991). A volume of 1 ml of methanolic extract solution was added to 1 ml of 2% methanolic aluminium chloride. Absorbance was measured 10 min later at a wavelength of 394 nm and compared with a standard of hyperoside.

2.5. Pharmacological activities

2.5.1. General

The aqueous and ethyl acetate extracts were both dissolved in phosphate buffered saline (PBS) 0.5 M, pH 7.4. The concentrations

Table 1
Plants and parts used for analysis.

Family	Plant	Aspect (m)	Part used	Herbarium no.
Euphorbiaceae	*Alchornea cordifolia*	Shrub (5–12)	Leaf	183
Fabaceae	*Baphia nitida*	Three (3–8)	Leaf	257
	Cassia occidentalis	Herb (1)	Leaf	317
Nyctaginaceae	*Boerhavia diffusa*	Herb (1)	Leaf	386

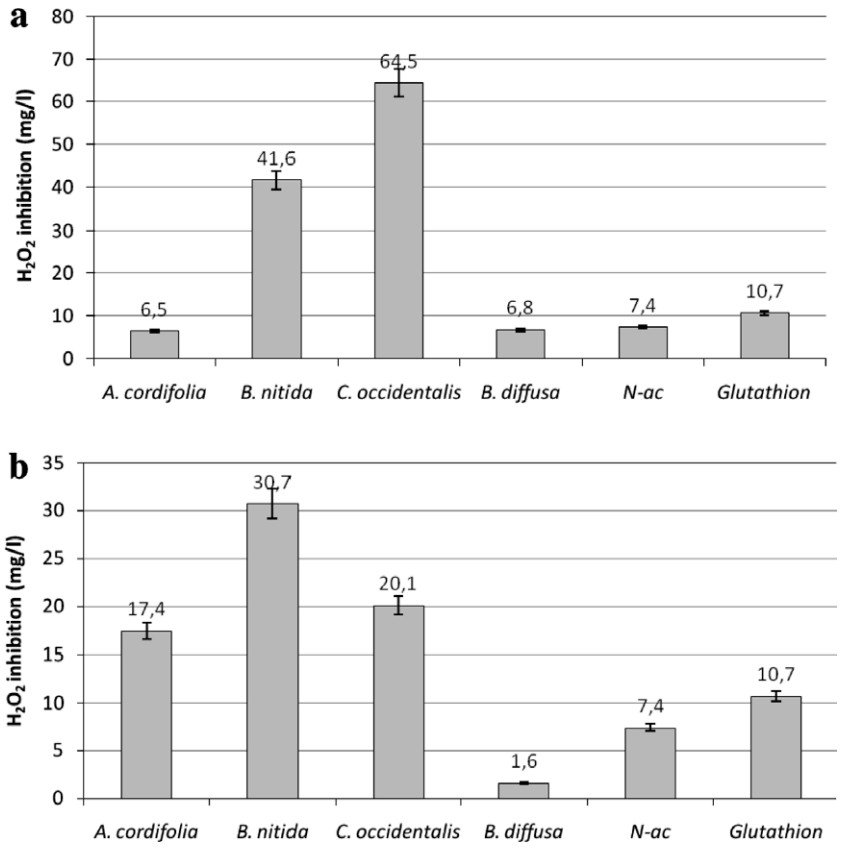

Fig. 1. Scavenger activities of plant extracts. Inhibitory concentrations (IC_{50}) of aqueous (a) and ethyl acetate (b) extracts towards H_2O_2. Histograms represent 3–4 experiments. Values are means ± S.E.M. ($p < 0.5$).

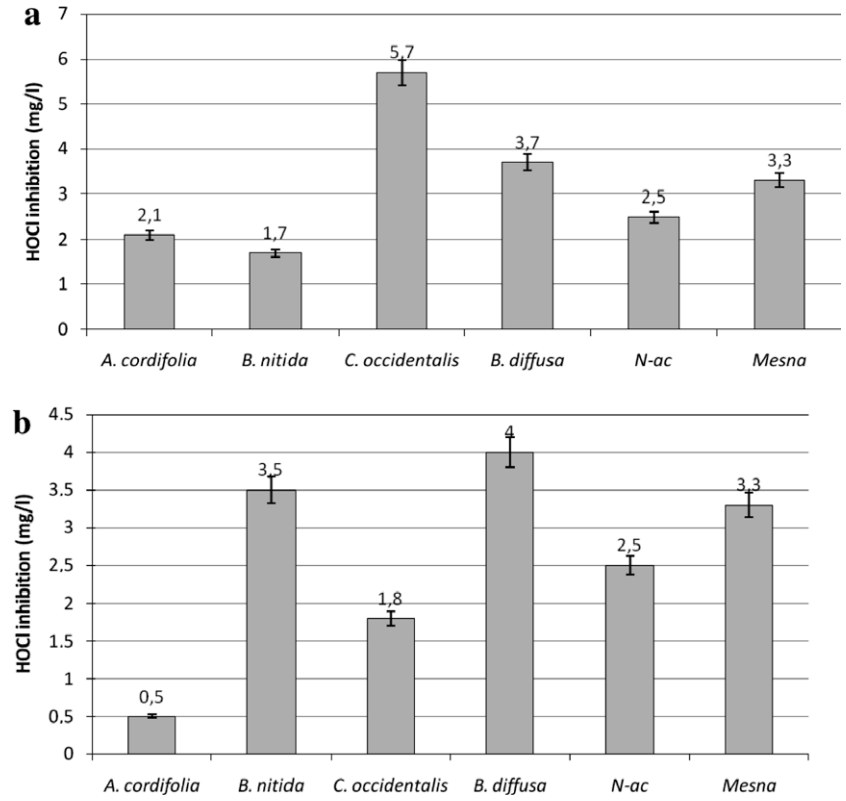

Fig. 2. Scavenger activities of plant extracts. Inhibitory concentrations (IC_{50}) of aqueous (a) and ethyl acetate (b) extracts towards HOCl. Histograms represent 3–4 experiments. Values are means ± S.E.M. ($p < 0.5$).

inhibiting 50% activity (IC_{50}) of extracts were obtained with a computer programme graphpad (prism 4, Mo, USA). They were uniformly expressed as the corresponding dry matter weight. All experiments were carried out three times.

2.5.2. Scavenging of hypochlorous acid (HOCl)

The amount of HOCl was measured by taurine chlorination (Weiss, Klein, Slivka, & Wei, 1982). Sample aliquots contained 100 µl of sodium hypochlorite (600 mM), 100 µl taurine (150 mM) and 100 µl of each extract solution from each plant in a final volume of 1 ml PBS pH 7.4. Absorbance was measured at a wavelength of 350 nm against a reference aliquot after adding 10 µl of potassium iodide (2 M).

The percentage of HOCl production inhibited by each plant extract was then calculated and results expressed in IC_{50} values.

2.5.3. Scavenging of hydrogen peroxide (H_2O_2)

H_2O_2 was measured according to Pick and Keisari (1980). Sample aliquots contained 100 µl of H_2O_2 (120 mM), 100 µl of each plant extract (in ranging concentrations) and the total volume of each vial was completed to 1 ml by adding phosphate buffered saline (PBS), pH 7.4. After 15 min at 37 °C, 1 ml of phenol red (0.2 mg/ml) containing horseradish peroxidase (17 U/ml), was added to induce the oxidation of phenol red by H_2O_2. After 15 min at 37 °C, 50 µl of NaOH (1 N) were added and the amount of H_2O_2 was determined by measuring absorbance at a wavelength of 610 nm against a reference aliquot. H_2O_2 concentrations were derived from a standard curve, using reagent grade H_2O_2. The percentage of H_2O_2 production inhibited by each plant extract was then calculated and results expressed in IC_{50} values.

2.6. Statistical analysis

Results were expressed as means ± S.E.M. and values were compared using the Wilcoxon test. Differences were considered to be statistically significant when $p < 0.05$.

3. Results

Assessment was made of the antioxidant activities of two extracts from each plant: an aqueous extract and an ethyl acetate extract. *In vitro* assays were performed in the two scavenging systems of H_2O_2 and HOCl (Figs. 1 and 2). Activity evaluation of plant

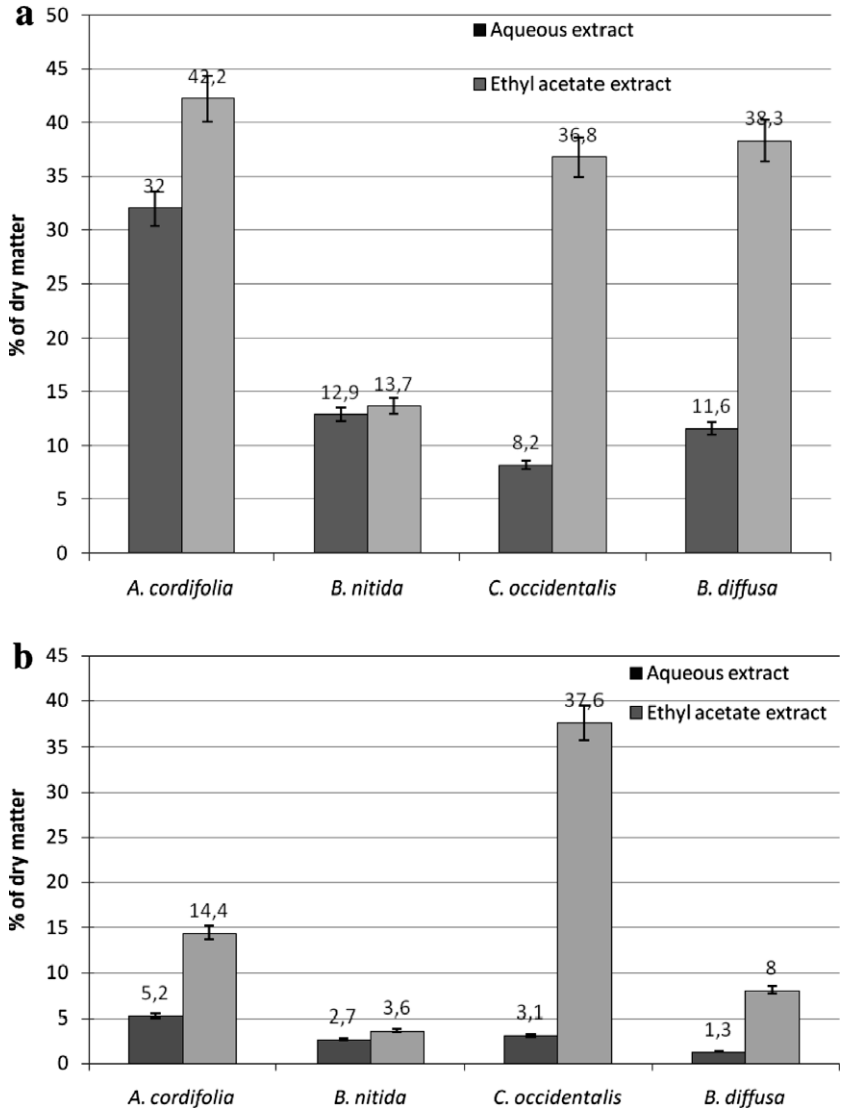

Fig. 3. Phenolic contents of aqueous and ethyl acetate extracts: total phenols (a) and flavonoids (b). Histograms represent 3–4 experiments. Values are means ± S.E.M. ($p < 0.5$).

extracts towards H_2O_2 and HOCl showed the capacity of the four plants to scavenge these ROS in a dose-dependent manner.

Activities towards H_2O_2, (Fig. 1) indicate that the ethyl acetate and aqueous extracts of *B. diffusa* (IC_{50} values of 1.6 and 6.8 mg/l, respectively), as well as the aqueous extract of *A. cordifolia* (IC_{50} values of 6.5 mg/l), had the best antioxidant activities of the tested extracts and were superior to N-acetylcysteine and Mesna reference substances (IC_{50} values of 7.4 and 10.7 mg/ml, respectively).

Activities towards HOCl (Fig. 2) reveal that aqueous extracts of *A. cordifolia* and *B. nitida* (IC_{50} values of 2.1 and 1.7 mg/l, respectively) and ethyl acetate extracts of *A. cordifolia* and *C. occidentalis* (IC_{50} values of 0.5 and 1.8 mg/l, respectively) had strong antioxidant activities, superior to those of N-acetylcysteine and Mesna reference substances (IC_{50} values of 2.5 and 3.3 mg/l, respectively).

Chromatographic analysis on thin-layer silica gel revealed the presence of flavonoids and the absence of proanthocyanidins in the four plants. As previously indicated, ellagic acid, quercetin and hyperin were identified in *A. cordifolia*, and quercetin and kaempferol in *B. diffusa*, when compared with authentic samples. Numerous other flavonoids were present in all four plant extracts. Proportions of total phenolics and flavonoids were measured for each plant according to the methods of Singleton et al. (1965) and Lamaison and Carnat (1991), respectively. Fig. 3a and b shows the concentrations of total phenolics and flavonoids: the former vary from 8.2% to 42.2% of dry extracts and the latter from 1.3% to 37.6%. For all four plants, concentrations are higher in the ethyl acetate extracts than in the aqueous ones.

4. Discussion

The IC_{50} values versus ROS (H_2O_2 and HOCl) observed in extracts from all four plants are comparable with those of pharmacological substances such as N-acetylcysteine and Mesna (Gressier, Cabanis, & Lebègue, 1994) which were previously reported to be effective ROS scavengers in therapeutics (Göksel, Levent, Özer, Feriha, & Nursal, 2006). The most efficient species are *A. cordifolia* and *B. diffusa* as they present the lowest IC_{50} values, between three and ten times lower than those of the other two plants. These data are very interesting as this is the first time they have been obtained for these plants whose strong antioxidant properties are therefore confirmed through a different experimental protocol.

Comparison of total phenolic and flavonoid contents with antioxidant activities shows a good correlation in the case of *A. cordifolia*, *B. nitida* and *B. diffusa* ethyl acetate and aqueous extracts. The antioxidant activity of *C. occidentalis* seems to be due to the high flavonoid content of the ethyl acetate extract (Figs. 2 and 3).

These scavenger activities of the studied plants could, at least partly, justify their traditional anti-inflammatory use, as phenolics, including flavonoids, are known for their antioxidant properties, which could be partially involved in anti-inflammatory mechanisms (Sala et al., 2003). First they act as antioxidants against free radicals which can attract various inflammatory mediators contributing to a general inflammatory response and tissue damage (Nijveldt et al., 2001). Second, the anti-inflammatory activity of flavonoids may be due to a decrease in the activation of the Nuclear Factor κB by ROS, such as HOCl and H_2O_2, which induce the transcription of inflammatory cytokines and cyclo-oxygenase-2 implicated in inflammatory mechanisms *in vivo* (Schinella, Tournier, Prieto, Mordujovich de Buschiazzo, & Ríos, 2002).

These results confirm those obtained by other authors, following different experimental protocols. The work undertaken on *A. cordifolia* (Mavar-Manga et al., 2004) and *B. nitida* (Onwukaeme, 1995) showed that flavonoid concentration was correlated to anti-inflammatory activity. Antioxidant activity, following yet another protocol, was assessed in *B. diffusa* (Devaki, Shivashangari, Ravikumar, & Govindaraju, 2005) through its protective effect against the intoxication of hepatocytes *via* carbon tetrachloride and ethanol in rats and mice. Oxygen species have been reported to have an important role in inflammatory processes after intoxication by ethanol, carrageenan and carbon tetrachloride (Yoshikawa, Tanaka, & Kondo, 1983). *B. diffusa* reduced oedema on mouse paw induced by carrageenan (Mugdal, 1975) confirming its antioxidant action. Jafri, Jalis Subhani, Javed, and Singh (1999) reported that *C. occidentalis* leaves could protect rat liver against intoxication induced by ethanol. This protective action could be due to an antioxidant effect of *C. occidentalis* revealed in our tests.

In conclusion, our study assesses, for the first time, the antioxidant activity of *A. cordifolia*, *B. nitida*, *C. occidentalis* and *B. diffusa* against ROS and its correlation with their phenolic and flavonoid contents. According to these results it is probable that the anti-inflammatory effects of the four plants, which have been confirmed in certain experimental models, could be at least partly related to their antioxidant activities. All of these results confirm the beneficial effects of these plants in traditional medicine, and as sources of antioxidants in food and drinks.

Acknowledgements

The authors wish to thank Professor Aké-Assi Laurent for identifying the plant species.

References

Adjanohoun, E. J., & Ake Assi, L. (1979). *Contribution au recensement des plantes médicinales en Côte d'Ivoire*. Abidjan: Edition CRESS. pp. 41, 66, 56, 118, 205, 218.

Afonso, V., Champy, R., Mitrovic, D., & Collin, P. (2007). Radicaux libres dérivés de l'oxygène et superoxydes dismutases: Rôle dans les maladies rhumatismales. *Revue du Rhumatisme et des Maladies Osteo-Articulaires, 74*, 636–643.

Agrawal, A., Srivastava, S., Srivastava, J. N., & Srivastava, M. M. (2004). Inhibitory effect of the plant *Boerhavia diffusa* L. against the dermatophytic fungus "*Microsporum fulvum*". *Journal of Environmental Biology, 25*, 307–311.

Borrelli, F., Milic, N., Ascione, V., Capasso, R., Izzo, A., Capasso, F., et al. (2005). Isolation of new rotenoids from *Boerhavia diffusa* and evaluation of their effect on intestinal motility. *Planta Medica, 71*, 928–932.

Chabot, F., Mitchell, J. A., Guteridge, C. M. M., & Evans, T. W. (1998). Reactive oxygen species in acute lung injury. *European Respiratory Journal, 11*, 745–757.

Chastanet, M., Fauvelle-Aymar, F. X., & Juhe-Beaulaton, D. (2002). *Cuisine et Société en Afrique: Histoire, Saveurs, Savoir-faire*. Paris: Edition Karthala. pp. 1–300.

Devaki, T., Shivashangari, K. S., Ravikumar, V., & Govindaraju, P. (2005). Effect of *Boerhavia diffusa* on tissue anti-oxidant defense system during ethanol-induced hepatotoxicity in rats. *Journal of Natural Remedies, 5*, 102–107.

Ferreres, F., Sousa, C., Justin, M., Valentão, P., Andrade, P. B., Llorach, R., et al. (2005). Characterisation of the phenolic profile of *Boerhavia diffusa* L. by HPLC–PAD–MS/MS as a tool for quality control. *Phytochemical Analysis, 16*, 451–458.

Göksel, Ş., Levent, K., Özer, Ş., Feriha, E., & Nursal, G. (2006). Mercaptoethane sulfonate (MESNA) protects against biliary obstruction-induced oxidative damage in rats. *Hepatology Research, 35*, 140–146.

Gressier, B., Cabanis, A., & Lebegue, S. (1994). Decrease of hypochlorous acid and hydroxyl radical generated by stimulated human neutrophils: Comparison *in vitro* of some thiol-containing drugs. *Methods and Findings in Experimental and Clinical Pharmacology, 16*, 9–13.

Hatano, T., Edmatsu, R., Hiramatsu, M., Moti, A., Fujita, Y., Yasuhara, T., et al. (1989). Effects of the interaction of tannins and related polyphenols on superoxide anion radical, and on 1,1-diphenyl-2-picrylhydrazyl radical. *Chemical and Pharmaceutical Bulletin, 37*, 2016–2021.

Jafri, M. A., Jalis Subhani, M., Javed, K., & Singh, S. (1999). Hepatoprotective activity of leaves of *Cassia occidentalis* against paracetamol and ethyl alcohol intoxication in rats. *Journal of Ethnopharmacology, 66*, 355–361.

Lamaison, J. L., & Carnat, A. (1991). Teneur en principaux flavonoïdes des fleurs et des feuilles de *Crataegus monogyna* Jacq. et de *Crataegus laevigita* (Poiret) DC. (Rosaceae). *Pharmaceutica Acta Helvetiae, 65*, 315–320.

Mavar-Manga, M. H., Brkic, D., Marie, D. E. P., & Quetin-Leclercq, J. (2004). *In vivo* anti-inflammatory activity of *Alchornea cordifolia* (Schumach. &Thonn.) Müll. Arg. (Euphorbiaceae). *Journal of Ethnopharmacology, 92*, 209–214.

Mishra, J. P., & Singh, R. H. (1980). Studies on the effect of indigenous drug *Boerhaavia diffusa* Rom. on kidney regeneration. *Indian Journal of Pharmacy, 12*, 59–64.

Motte, E. (1980). *Les plantes chez les Pygmées Aka et les Mozombo de La Lobaye (Centreafrique)*. Paris: Edition Société d'Etudes Linguistiques et Anthropologiques. p. 271.

Mugdal, V. (1975). Studies on medicinal properties of *Convolvulus plurucaulis* and *Boerhaavia diffusa*. *Planta Medica, 28*, 62–68.

Nijveldt, R. J., Van Nood, E., Van Hoorn, D. E. C., Boelens, P. G., Van Norren, K., & Van Leeuwen, P. A. M. (2001). Flavonoids: A review of probable mechanisms of action and potential applications. *American Journal of Clinical Nutrition, 74*, 418–425.

Ogungbamila, F. O., & Samuelsson, G. (1990). Smooth muscle relaxing flavonoids from *Alchornea cordifolia*. *Acta Pharmaceutica Nordica, 2*, 421–422.

Onwukaeme, N. D. (1995). Anti-inflammatory activities of flavonoids of *Baphia nitida* Lodd. (Leguminosae) on mice and rats. *Journal of Ethnopharmacology, 46*, 121–124.

Pandey, R., Maurya, R., Singh, G., Sathiamoorthy, B., & Naik, S. (2005). Immunosuppressive properties of flavonoids isolated from *Boerhaavia diffusa* Linn. *International Immunopharmacology, 5*, 541–553.

Pick, E., & Keisari, Y. (1980). A simple colorimetric method for measurement of hydrogen peroxide produced by cells in culture. *Journal of Immunological Methods, 38*, 161–170.

Porter, L. J., Hrtich, L. N., & Chan, B. G. (1986). The conversion of procyanidins and prodelphinidins to cyanidin and delphinidin. *Phytochemistry, 25*, 223–230.

Roos, D. (1991). The respiratory burst of phagocytic leukocytes. *Clinical Drug Investigations, 3*, 48–58.

Sahinoglu, T., Stevens, C. R., Bhatt, B., & Blake, D. R. (1996). The role of reactive oxygen species in inflammatory disease: Evaluation of methodology. *Methods, 9*, 628–634.

Sala, A., Recio, M. C., Schinella, G. R., Máñez, S., Giner, R. M., Cerdá-Nicolás, M., et al. (2003). Assessment of the anti-inflammatory activity and free radical scavenger activity of tiliroside. *European Journal of Pharmacology, 461*, 53–61.

Schinella, G. R., Tournier, H. A., Prieto, J. M., Mordujovich de Buschiazzo, P., & Ríos, J. L. (2002). Antioxidant activity of anti-inflammatory plant extracts. *Life Sciences, 70*, 1023–1033.

Singleton, V. L., Joseph, A., & Rossi, J. R. (1965). Colorimetry of total phenolics with phosphomolybdic–phosphotungstic acid reagents. *American Journal of Enology and Viticulture, 16*, 144–153.

Weiss, S. J., Klein, R., Slivka, A., & Wei, M. (1982). Chlorination of taurine by human neutrophils. *Journal of Clinical Investigation, 70*, 598–607.

Yoshioka, T., & Ichikawa, I. (1989). Glomerular dysfunction induced by polymorphonuclear leukocyte-derived oxygen species. *American Journal of Physiology, 257*, F53–59.

Yoshikawa, T., Tanaka, H., & Kondo, M. (1983). Effect of vitamin E on adjuvant arthritis in rats. *Biochemical Medicine, 29*, 227–234.

Food Chemistry 118 (2010) 436

Contents lists available at ScienceDirect

Food Chemistry

journal homepage: www.elsevier.com/locate/foodchem

Corrigendum

Corrigendum to "Influence of malt browning degree on lipoxygenase activity" [Food Chemistry 99 (2006) 711–717]

Silvia Sovrano *, Stefano Buiatti, Stefano Cossi, Monica Anese

Dipartimento di Scienze degli Alimenti, University of Udine, via Marangoni 97, 33100 Udine, Italy

The authors of the above paper regret that an author was missed from the author listing. The correct author listing is updated.

DOI of original article: 10.1016/j.foodchem.2005.08.048
* Corresponding author. Tel.: +39 432 590732; fax: +39 432 590719.
E-mail address: silvia.sovrano@radicifilm.com (S. Sovrano).

0308-8146/$ - see front matter
doi:10.1016/j.foodchem.2009.06.027

Food Chemistry 118 (2010) 437–444

Contents lists available at ScienceDirect

Food Chemistry

journal homepage: www.elsevier.com/locate/foodchem

Analytical Methods

Laccase-generated tetramethoxy azobismethylene quinone (TMAMQ) as a tool for antioxidant activity measurement

Endry Nugroho Prasetyo [a], Tukayi Kudanga [a], Walter Steiner [b], Michael Murkovic [c], Gibson S. Nyanhongo [a,*], Georg M. Guebitz [a]

[a] Institute of Environmental Biotechnology, Graz University of Technology, Petersgasse 12/1, A-8010 Graz, Austria
[b] Institute of Biotechnology and Bioprocess Engineering, Graz University of Technology, Petersgasse 12/1, A-8010 Graz, Austria
[c] Institute of Food Chemistry and Technology, Graz University of Technology, Petersgasse 12/1, A-8010 Graz, Austria

ARTICLE INFO

Article history:
Received 5 February 2009
Received in revised form 20 April 2009
Accepted 26 April 2009

Keywords:
Antioxidant activity assay
Antioxidants
Tetramethoxy azobismethylene quinone
Laccase

ABSTRACT

The potential of laccase-generated tetramethoxy azobismethylene quinone (TMAMQ) for measuring antioxidant activity of a wide range of structurally diverse molecules present in food and humans was investigated for the first time. All the tested antioxidants including simple phenolics, polyphenols and vitamins quenched TMAMQ. The antioxidant activity of phenolics and polyphenolics depended on the position and number of hydroxyl groups on the benzene ring. Equally interesting was the ability of amino acids like cysteine, tryptophan and methionine as well as peptides (glutathione) and proteins (albumin) to quench TMAMQ, demonstrating the great potential of TMAMQ for analysis of antioxidant activity of serum samples. Further, TMAMQ is promising is a more reliable tool for measuring antioxidant activity of amino acids when considering conflicting reports on antioxidant activity of some of the amino acids. The extracts from various food samples showed varying antioxidant activity with highest for spinach (4.36 mg methanol extract/mmol TMAMQ) followed by kiwi (13.95 mg methanol extract/mmol TMAMQ) and lettuce (40 mg methanol extract/mmol TMAMQ). The use of the laccase generated TMAMQ can be exploited for the development of laccase based biosensors for complex and coloured samples thereby facilitating online monitoring of antioxidants in food, cosmetic and health industries.

1. Introduction

The human body is exposed to a large variety of reactive species (free radicals) from both endogenous and exogenous sources. Endogenous free radical species (superoxide, nitric oxide and hydrogen peroxide) are products of normal cellular function. These cellular functions include mitochondrial respiration (Serrano, Goni, & Saura-Calixto, 2007), activated phagocytes, arachidonic acid metabolism, ovulation and fertilization (Magalhaes, Segundo, Reis, & Lima, 2008; Singh, Sharad, & Kapur, 2004). Exogenous sources of free radicals include pollutants such as car exhaust, industrial contaminants encompassing many types of nitrogen reactive species, drugs and xenobiotics (toxins, pesticides, herbicides etc.) (Kohen & Nyska, 2002; Valko et al., 2007). Cell damage caused by free radicals has been implicated in the pathogenesis of at least 50 diseases conditions (Dalle-Donne, Rossi, Colombo, Giustarini, & Milzani, 2006; Halliwell, 1994). Similarly, in food, for example the oxidation of lipids by free radicals has historically been a major problem for food processing industries responsible for the formation of off-flavours and undesirable chemical compounds which may be detrimental to health (Jadhav, Nimbalkar, Kulkarni, & Madhavi, 1996).

To protect the cells and organs against free radicals, biological systems have evolved a highly sophisticated and complex antioxidant protection system. These antioxidants therefore constitute the body's first line of defence against free radical damage. The antioxidants include biologically built-in mechanism of neutralizing free radicals for example glutathione peroxidase, catalase, and superoxide dismutases, glutathione and albumin (Singh et al., 2004; Valko, Rhodes, Moncol, Izakovic, & Mazur, 2006). The exogenous sources of antioxidants are mainly of dietary origin including vitamin C, tocopherols, carotenoids, flavonoids (Singh et al., 2004; Valko et al., 2006). Endogenous and exogenous antioxidants function interactively and synergistically to neutralize free radicals. When the availability of antioxidants is limited, cell damage and food oxidation occurs. Strangely, despite the well recognised importance of antioxidants for human health and food preservation, currently there is no nutritional standard index available related to antioxidants for food labelling because of the lack of standardised methods (Ou, Huang, Hampsch-Woodill, Flanagan, & Deemer, 2002). However, recently determining antioxidant capacity has become a very active research topic as recently demonstrated by international efforts to standardise assay methods (Prior, Wu, & Schaich, 2005).

* Corresponding author. Tel.: +43 316 873 8312; fax: +43 316 873 8819.
E-mail addresses: gnyanhongo@yahoo.com, g.nyanhongo@tugraz.at (G.S. Nyanhongo).

0308-8146/$ - see front matter © 2009 Elsevier Ltd. All rights reserved.
doi:10.1016/j.foodchem.2009.04.102

Recently, we have discovered that laccase oxidised syringaldazine was a reliable tool for measuring antioxidant activity of vitamin C and vitamin E (Nugroho Prasetyo et al., 2009). The performance of laccase oxidised syringaldazine was comparable to the commercially available 2,2-diphenyl-l-picrylhydrazyl (DPPH) radical.

Syringaldazine is a yellowish compound which is converted to tetramethoxy azobismethylene quinone (TMAMQ) with maximum absorbance at 530 nm (deep purple colour) upon oxidation by laccases (Harkin, Larsen, & Obstharkin, 1974; Holm, Nielsen, & Eriksen, 1998). It is a well known laccase substrate which is also used to detect peroxidase activities. The reaction of laccase with syringaldazine first generates a free radical and loss of the second electron can either proceed enzymatically or by disproportionation forming a deep purple coloured quinone (TMAMQ – Fig. 1) which is not prone to polymerisation under appropriate conditions (Kuznetsova & Romakh, 1996; Thurston, 1994). Further, electrochemical and pulse radiolysis studies of the oxidation of syringaldazine confirmed a reversible two-electron-two-proton transfer leading to the formation of a deep purple compound (Hapiot, Pinson, Neta, & Rolando, 1993).

Syringaldazine can also be oxidised by chlorine and is currently used for the colorimetric determination of chlorine in water (Bauer & Rupe, 1971; Cooper, Roscher, & Slifker, 1982). This work, is the first to explore the ability of laccase generated TMAMQ to measure the antioxidant activity of a wide variety of structurally different antioxidants relevant to both the food industry and human health. The study is also extended to investigate the ability of laccase generated TMAMQ to measure antioxidant activity of crude extracts of known important dietary sources. This knowledge will allow the development of laccase based biosensors for complex thereby facilitating online monitoring of antioxidants in food, cosmetic and health industries.

2. Materials and methods

2.1. Chemicals and enzyme

All the used antioxidants molecules were of analytical grade. The phenolics were purchased from Sigma–Aldrich, Steinheim, Germany while the flavonoids were purchased from Carl Roth GmbH, Karlsruhe Germany. All the other chemicals were purchased from Merck, Darmstadt, Germany. The *Trametes hirsuta* laccase was produced and purified as previously described by Almansa, Kandelbauer, Pereira, Cavaco, and Guebitz (2004). Food samples of onion (*Allium cepa*), green and fermented tea (*Camellia sinensis*), *kiwi* (*Actinidia arguta*), apple (*Malus domestica*), carrot (*Daucus carota subsp. sativus*), roasted coffee (*Coffea robusta*), lettuce (*Lactuca sativa*), spinach (*Spinacea oleracea*), pumpkin seed (*Curcubita maxima*), tomato (*Solanum lycopersicum*) and garlic (*Allium sativum*) were purchased from local markets in Graz, Austria.

2.2. Laccase activity assay

The activity of laccase was determined spectrophotometrically by monitoring the oxidation of 2,2′-Azino-bis(3-ethylbenzothiazoline-6-sulfonic acid) diammonium salt (ABTS) (ε_{436} = 29,300 M^{-1} cm^{-1}) as a substrate at 436 nm in 50 mM sodium succinate buffer at pH 4.5 and 30 °C (Nugroho Prasetyo et al., 2009). The spectrophotometric measurements were done by recording the absorbance in the time scan mode for 2 min using a Hitachi U-2001 UV–vis spectrophotometer.

2.3. Generation of TMAMQ

TMAMQ stock solutions were prepared by incubating syringaldazine (0.17 mM) with 50 μl of laccase (20 nkat ml^{-1}) in 50 mM sodium succinate buffer at pH 4.5. The reaction mixture (1 ml) was incubated at 30 °C for 10 min while shaking at 140 rpm in a thermomixer (Eppendorf AG, Germany). The oxidation process was monitored at 530 nm using a Hitachi U-2001 UV–vis spectrophotometer in disposable cuvettes of 1 cm pathway. To this stock solution of laccase generated TMAMQ, methanol was added to a final concentration of 80% (v/v) to stop laccase activity and to stabilize the TMAMQ (Nugroho Prasetyo et al., 2009).

2.4. Determination of antioxidant activity of pure molecules

Different concentrations of pure antioxidant molecules dissolved in methanol (0–20 μM) were added to 800 μl of TMAMQ dissolved in 80% methanol (final absorbance of 0.8) in order to obtain a dose response curve. The mixture was thoroughly mixed and incubated at 30 °C while shaking in a thermomixer (Eppendorf AG, Germany) at 140 rpm until full completion of the reaction as evidenced by no further decrease in absorbance. The degree of decoloration of the solution indicates the scavenging efficiency of the added antioxidant sample. The stoichiometrical reduction of TMAMQ (μM of TMAMQ reduced by 1 μM antioxidant) was then calculated from a dose response curve of added antioxidant.

2.5. Preparation of food samples and extraction of antioxidants

2.5.1. Recovery of simple phenolic compounds

Food samples were purchased fresh from local markets, and the edible parts blended using a blender GT800 (Uetendorf, Switzerland) and then freeze-dried. The procedure followed for extraction of antioxidants was as previously described by Saura-Calixto, Serrano, and Goni (2007) with slight modifications. The first extraction procedure involved suspending 0.5 g of freeze dried food sample in 20 ml of 98% methanol/water (50:50 v/v) in a 250 ml Erlenmeyer flask and incubating at 25 °C while mixing at 150 rpm for 1 h. The mixture was then centrifuged at 2500 g for 20 min and the supernatant recovered. The residue was then washed with 20 ml of 98% acetone/water (70:30 v/v) and centrifugation repeated as described above to maximally recover remaining antioxidants as recommended by previous researchers (Perez-Jimenez et al., 2008). The antioxidant activity of the different extracts was determined separately after adjusting pH to 7 using NaOH to stabilize the extracts (Perez-Jimenez et al., 2008).

2.5.2. Recovery of hydrolysed tannins

The residues arising from methanol extracts were mixed with 20 ml of methanol and 2 ml of concentrated sulphuric acid. Sam-

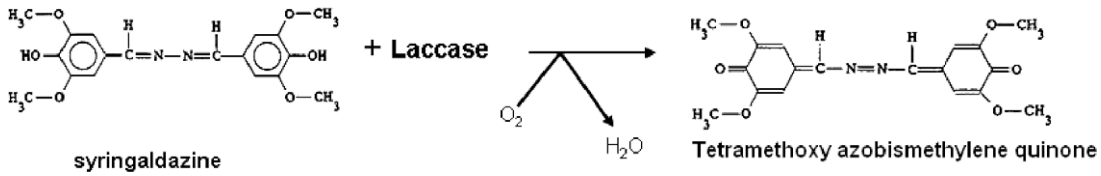

Fig. 1. Laccase oxidation of syringaldazine results in the formation of a water molecule and tetramethoxy azobismethylene quinone (TMAMQ).

ples were then incubated at 85 °C for 20 h in a shaking water bath. The samples were then centrifuged at 2500*g* for 20 min and supernatants recovered; subsequently the pH of supernatant was adjusted to 7 using NaOH. This fraction contained hydrolysable tannins and other phenolics linked to carbohydrates and proteins (Hartzfeld, Forkner, Hunter, & Hagerman, 2002).

2.5.3. Recovery of condensed tannins

The remaining residues from the two extraction processes were further treated with 37% HCl/98% butanol/$FeCl_3$ (5:95, v/v) at 100 °C for 3 h. Samples were centrifuged as described above and the supernatants recovered. The precipitates were further washed twice with 37% HCl/98% butanol (5:95 v/v) (Porter, 1989). The samples were then centrifuged at 2500*g* for 20 min and supernatants recovered. The pH of the antioxidant fractions from this extraction step corresponding to condensed tannins were adjusted to 7 as described above.

2.5.4. Determination of antioxidant capacity of food samples

The different extracts obtained above were incubated separately with the TMAMQ as described above for pure antioxidants. The extracts were mixed in varying amounts to obtain a dose response curve. The mixture was thoroughly mixed and incubated at 30 °C while shaking at 140 rpm until full completion of the reaction as evidenced by no further decrease in absorbance. The stochiometrical reduction of TMAMQ was then calculated from the decrease in absorbance as described above.

2.5.5. Antioxidant activity of oils

Extra-virgin olive oil and maize oil produced by Warenhandels-AG, Salzburg, Austria and Unilever, Wien, Austria respectively were used directly without any modification. Total antioxidant capacity was determined directly after diluting aliquots in ethyl acetate (Espin, Soler-Rivas, & Wichers, 2000). The mixture was thoroughly mixed and incubated at 30 °C while shaking at 140 rpm until full completion of the reaction as evidenced by no further decrease in absorbance. The stoichiometrical reduction of TMAMQ was then calculated from the dose response curve as described above.

2.5.6. Measurement of total phenols

The phenol content of the extracts was determined according to the Folin–Ciocalteu procedure (Singleton & Rossi, 1965). Briefly, test sample (100 μl) was mixed with 100 μl of Folin–Ciocalteau reagent and swirled. Subsequently, 500 μl of nanopure water, 50–100 μl of sample, and 100 μl of Folin–Ciocalteu reagent were added to a 2 ml eppendorf reaction tube. The contents were mixed and allowed to stand for 5–8 min at 25 °C. Thereafter, 1 ml of a 7% sodium carbonate solution was added, followed by the addition of nanopure water. Solutions were mixed and allowed to stand at 30 °C again for 2 h. Total phenolic content was determined using TECAN Infinite M200 plate reader (Tecan Austria GmbH, Grödig, Austria) at 650 nm wavelength. Total phenolic content was determined as gallic acid equivalents (GAE) expressed as milligrams per litre of gallic acid per milligram of extract (Peschel et al., 2006).

3. Results and discussion

In a first stage, the antioxidant scavenging activity of different pure molecules (phenolics, amino acids, peptides, proteins and vitamins) was investigated followed by the antioxidant activity of food extracts.

3.1. Antioxidant activity of phenolics

Among phenolic compounds, phenolic acids, flavonoids and tannins are regarded as the main dietary antioxidants (Pellegrini et al., 2007; Sikora, Cieslik, & Topolska, 2008) and were therefore selected. The antioxidant activity of simple phenolics increased with increasing number of hydroxyl groups in the order (guaiacol [0.01 μM] < pyrogallol [5.79 μM]) (Table 1). A similar trend was also observed with hydroxybenzoic acids in the order 4-hydroxybenzoic acid [no activity] < 2,5-hydroxybenzoic [0.63 μM] < gallic acid [3.91 μM] (Table 1). Substitution of the 3- and 5-hydroxyl group in gallic acid with methoxy groups as in syringic acid reduced the antioxidant activity from 3.91 μM to 1.03 μM, respectively. However the presence of the two methoxy groups in syringic acid adjacent to the OH group enhanced antioxidant activity as compared with vanillic acid (Table 1).

The antioxidant activity of hydroxycinnamic acids also increased with increasing number of hydroxyl groups (Table 1). Like the monohydroxy benzoic acid (4-hydroxybenzoic acid), p-coumaric acid showed no antioxidant activity in terms of hydrogen donating capacity towards TMAMQ. However, the presence of another hydroxyl group for example in caffeic acid as compared with p-coumaric showed an antioxidant activity of 2.47 μM (Table 1). The antioxidant behaviour of hydroxybenzoic acids and hydroxycinnamic acids in the presence of TMAMQ is consistent with previous observation (Rice-Evans, Miller, & Paganga, 1996; Villano, Fernandez-Pachon, Moya, Troncoso, & Garcia-Parrilla, 2007) when these respective antioxidants were incubated with ABTS and *N,N-*

Table 1
Amount of TMAMQ quenched by 1 μM of the phenolics tested.

Phenolics	Number of OH	Amount of TMAMQ (μM) reduced by 1 μM of phenolics
Simple phenolics		
Guaiacol	1	0.01 ± 0.004
Catechol	2	2.57 ± 0.30
Pyrogallol	3	5.78 ± 0.14
Hydroxybenzoic acids		
4-hydroxybenzoic acid	1	–
2,5-hydroxybenzoic acid	2	0.63 ± 0.02
Gallic acid	3	3.91 ± 0.02
Vannilic acid	1	0.67 ± 0.03
Syringic acid	1	1.03 ± 0.04
Hydroxycinnamic acids		
ρ-coumaric	1	–
Cafeic acid	2	2.47 ± 0.31
Eugenol	1	0.2 4 ± 0.15
Ferulic acid	1	1.23 ± 0.12
Sinapic acid	1	3.58 ± 0.22

(–) no antioxidant activity detected.

diphenyl-picryl hydrazyl (DPPH) radicals. The introduction of methoxyl groups at *meta* and *para* positions in hydroxybenzoic acids increased the antioxidant activity when comparing vannilic acid (0.67 μM) and syringic acid (1.03 μM). A similar trend was also observed for hydroxycinnamates when comparing caffeic acid (2.47 μM) to sinapic acid (3.58 μM). However, substitution of the 3-hydroxyl group only of caffeic acid by a methoxy group (ferulic acid) considerably decreased the antioxidant activity of hydroxycinnamates (Table 1). The antioxidant activity of the tested hydroxycinnamic acids was in the order sinapic acid > cafeic acid > ferulic acid > p-coumaric acid (Table 1).

In agreement with previous studies using other assay procedures, the antioxidant activity of phenolic antioxidants depended on the number and positions of the hydroxyl groups in relation to the carboxyl functional group and presence of methoxyl groups (Balasundram, Sundram, & Samman, 2006; Monach, Williamson, Morand, Scalbert, & Rémésy, 2005; Robards, Prenzler, Tucker, Swatsitang, & Glover, 1999) For example, the increase in antioxidant activity of phenolics with increasing degree of hydroxylation and the decrease in antioxidant activity with substitution of the hydroxyl groups at the 3- and 5-position with methoxyl groups as in syringic acid has also been reported by Rice-Evans and her co-workers (Rice-Evans et al., 1996). Further, in this study just as in previous studies (Andreasen, Landbo, Christensen, Hansen, & Meyer, 2001), generally the hydroxycinnamic acids exhibited higher antioxidant activity compared to the corresponding hydroxybenzoic acids. The high antioxidant activity of hydroxycinnamic acids has been attributed to the presence of CH=CH–COOH group, which ensures greater H-donating ability and radical stabilisation than the –COOH group in the hydroxybenzoic acids (Rice-Evans, Miller, & Paganga, 1997). However, comparing ferulic acid and eugenol which basically share similar functional groups, the presence of $CH_2CH{=}CH_2$ negatively influenced the antioxidant activity of the later (Table 1).

3.2. Antioxidant activity of polyphenols

The antioxidant activity of anthocyanins, flavonols, flavones and flavan-3-ols was investigated (Table 2). Among the anthocyanins tested, delphinidin chloride reduced 5.40 μM TMAMQ, pelargonidin chloride reduced 3.68 μM TMAMQ and paeonidin chloride reduced 2.89 μM of TMAMQ. Cyanin chloride and oenin chloride each reduced 0.88 μM and 0.94, respectively. malvidin chloride (1 μM) showed the highest antioxidant activity reducing 13.01 μM of TMAMQ although in previous studies its antioxidant activity was similar to that of peonidin. This result is consistent with results obtained with hydroxbenzoic and hydroxycinnamic acids when comparing antioxidants with one methoxyl group and two methoxyl groups demonstrating the advantage of this method over the DPPH and ABTS methods. Increase in methoxyl groups enhances the electron donating ability of the antioxidant. The B-ring hydroxyl configuration has been reported to be the most significant determinant for radical scavenging ability of flavonoids (Balasundram et al., 2006; Burda & Oleszek, 2001; Cao, Sofic, & Prior, 1996). The antioxidant activity of quercetin (4.80 μM), a flanovol was more than twice that of rutin hydrate (2.01 μM) a flavone, similar to that reported by (Lien, Ren, Bui, & Wang, 1999; Silva et al., 2002). This also adds evidence to the premise that flavonols are more effective free radical scavengers than flavones (Lien et al., 1999; Rice-Evans et al., 1996) and that glycosylation of flavonoids reduces their antioxidant activity when compared to the corresponding aglycones. Although quercetin has an identical number of hydroxyl groups in the same positions as catechin, the 2,3-double bond in the C ring and the 4-oxo group maybe responsible for enhancing the antioxidant activity of the later. Epigallocatechin gallate had an antioxidant activity three times that of catechin (Table 2) which shows the contribution of gallic units on the former.

Generally the antioxidant activity responses of polyphenols and phenolics were in good agreement with the proposed structure-activity relationship as summarised by previous reports (Balasundram et al., 2006; Heim, Tagliaferro, & Bobilya, 2002; Rice-Evans et al., 1997).

3.3. Antioxidant activity of endogenous antioxidants and free amino acids

Of the 21 free amino acids tested, only cysteine, tryptophan, serine, arginine, methionine and glycine quenched TMAMQ as shown in Table 3. A higher antioxidant activity (0.47) was obtained with cysteine (containing a free –SH group) followed by tryptophan (0.16), an aromatic containing amino acid. Many contradictory results are found in the literature when comparing the antioxidant activity of amino acids. For example, Trianitis and co-workers (Triantis, Yannakopoulou, Nikokavoura, Dimotikali, & Papadopoulos, 2007) using the luminal-sodium hypochlorite chemiluminescence observed antioxidant activity with 13 of the amino acids listed in Table 3 while another previous report (Perez-Jimenez & Saura-Calixto, 2006) using ORAC and ABTS recorded antioxidant activity for tyrosine, trypotophan and arginine. Interestingly, Meucci and Mele (1997) using ABTS and Triantis et al. (2007) using DPPH reported antioxidant activity only for a few amino acids. In another report,

Table 2
Amount of TMAMQ quenched by 1 μM of the polyphenolics tested.

Antioxidants	Position and number of free –OH substituents	Amount of TMAMQ (μM) reduced by 1 μmol antioxidant
Anthocyanidins		
Malvin chloride	7, 4′	0.17 ± 0.03
Oenin chloride	5, 7, 4′	0.94 ± 0.20
Malvidin chloride	3, 5, 7, 4′	13.01 ± 0.51
Pelargonidin chloride	3, 5, 7, 4′	3.68 ± 0.32
Paeonidin chloride	3, 5, 7, 4′	2.89 ± 0.44
Cyanin chloride	3, 5, 7, 3′, 4′	0.88 ± 0.21
Delphinidin chloride	3, 5, 7, 3′, 4′, 5′	5.40 ± 0.52
Flavan-3-ols		
Epigallocatechin gallate	3, 5, 7, 3′, 4′, 3″, 4″, 5″	14.33 ± 2.00
Catechin	3, 5, 7, 3′, 4′	5.98 ± 0.41
Flavonols		
Quercetin	3, 5, 7, 3′, 4′	4.80 ± 0.31
Flavones		
Rutin hydrate	5, 7, 3′, 4′	2.01 ± 0.21

Table 3
Antioxidant activity of free amino acids, other serum antioxidants and vitamins as measured with laccase generated TMAMQ.

Antioxidant	μmol TMAMQ reduced per 1 μmol antioxidant
Amino acids	
Cysteine	4.7×10^{-1}
Tryptophan	1.6×10^{-1}
Serine	4.0×10^{-4}
Arginine	4.7×10^{-3}
Methionine	9.0×10^{-4}
Aspartic acid	–
Lysine	–
Proline	–
Histidine	–
Alanine	–
Tyrosine	–
Valine	–
Isoleucine	–
Threonine	–
Phenylalanine	–
Glutamic acid	–
Asparagine	–
Leucine	–
Glycine	3.0×10^{-5}
Other serum antioxidants	
Uric acid	6.6×10^{-1}
Glutathione	3.0×10^{-1}
Albumin	1.8×10^{-1}
Vitamins	
L-ascorbic acid 6-palmitate	8.6×10^{-1}
Vitamin E	13×10^{-1}
β-carotene	5×10^{-2}

Ahmad, Al-Hakim, Adel, and Shehata (1983) found that lysine, arginine, glutamic acid, methionine, and hydroxyproline had high antioxidant activity. From structural point of view lysine and glutamic acid may not be antioxidants and this was confirmed by TMAMQ. This may indicate the superiority of TMAMQ as a more reliable tool to measure antioxidant activity of serum amino acids and proteins. Nevertheless, despite this controversy, the antioxidant activities of cysteine, tryptophan, methionine just as observed with TMAMQ are well established (Hernandez-Ledesma, Davalos, Bartolome, & Amigo, 2005; Levine, Mosoni, Berlett, & Satdtman, 1996; Masella, Di Benedetto, Vari, Filesi, & Giovannini, 2005; Pastore, Federici, Bertini, & Piemonte, 2003).

The antioxidant activities of cysteine, methionine and glycine when discussed in connection with the observed antioxidant activity of glutathione and serum albumin justify its already known role as a major antioxidant source in humans. Further, the observed antioxidant activity of cysteine, glutathione and albumin strengthens the crucial role of sulphydryl groups as source of antioxidants in proteins or peptides. For example glutathione is a tripeptide composed of cysteine, glutamic acid and glycine which is viewed as the principal non-protein thiol involved in the antioxidant cellular defence (Masella et al., 2005; Pastore et al., 2003). Albumin which also showed antioxidant activity with TMAMQ is believed to contribute 70% of the free radical-trapping activity of serum (Bourdon & Blache, 2001) and its antioxidant activity is attributed to cysteine residues (Oettl & Stauber, 2007).

Another widely reported human endogenous antioxidant is uric acid which also quenched TMAMQ (Table 3). Uric acid is reported as a selective antioxidant responsible for quenching hydroxyl radicals and hypochlorous acid (Genestra, 2007; Kohen & Nyska, 2002).

3.4. Antioxidant activity of vitamins and other compounds

The antioxidant activity of vitamin E was almost similar to that of ascorbic acid (Table 3) as determined in a previous study (Nugroho Prasetyo et al., 2009). The antioxidant activity of β-carotene was weak compared to Vitamin C and E (Table 3). Similarly low antioxidant activity of β-carotene was also reported using DPPH radical (Jimenez-Escrig, Jimenez-Jimenez, Sanchez-Moreno, & Saura-Calixto, 2000; Lee, Ozcelik, & Min, 2006). This may be attributed to antioxidant mechanisms of carotenoids which have been known to quench singlet oxygen radicals primarily by physical mechanism in which the excess energy of the singlet oxygen is transferred to the carotenoid's electron rich structure. The excited carotenoid then enters into its ground state by losing the extra energy as heat (Sies & Wilhelm, 2004). This means that the electron/hydrogen transfer mechanism is not the major route justifying the low antioxidant values. Equally interestingly was oleuropein which gives extra-virgin olive oil its bitter, pungent taste, which was also able to quench 0.82 μM TMAMQ confirming earlier reports that it is a powerful antioxidant (Tripoli et al., 2005).

3.5. Total phenolic content and antioxidant activity of extracts of food samples

The antioxidant activity of common fruits and vegetables found in Austrian food markets (Graz) was investigated. The different antioxidants in the food samples were extracted sequentially using different solvents (methanol, acetone, acidified methanol and butanol). The antioxidant activity as well as the total phenols of each solvent extract was analysed separately as summarised in Table 4 and Fig. 2, respectively. The different solvents extracted different antioxidants as reflected by the different antioxidants activities obtained with the different fractions (Table 4). The antioxidant activity of the methanol extract of spinach was the highest (4.36 mg extract/mmol TMAMQ) followed by kiwi (13.95 mg extract/mmol TMAMQ) and lettuce (40 mg extract/mmol TMAMQ), respectively. The rank order of the antioxidant activity of the methanol extracts of spinach, kiwi and lettuce reflected the total phenols content of the respective fractions in that order (Fig. 2). This antioxidant activity rank order agrees well with the Oxygen Radical Absorbance Capacity (ORAC) method which ranked spinach > white onion > tomato > carrot (Ou et al., 2002). Other previous reports (Cao et al., 1996; Kaur & Kapoor, 2001; Prior & Cao, 2000) also consistently reported high antioxidant activity of the same food samples using the ORAC assay. In other similar studies, (Perez-Jimenez et al., 2008) also observed that efficient extraction of antioxidants required the use solvents with different polarities. The different solvents extracted different antioxidants as reflected by the different antioxidants activities obtained with the different fractions. The antioxidant capacities of kiwi have been previously attributed to high levels of vitamin C present in the fruit (Chun et al., 2005; Halvorsen et al., 2002; Wang, Cao, & Prior, 1996) and could explain the antioxidant activity of the methanol extract. Although methanol extracts exhibited the highest concentration of phenolics in the other samples (Fig. 2), in pumpkin seeds the total phenolics were highest in hydrolysed tannins fractions. Surprisingly the acetone fraction of the pumpkin seeds showed the highest antioxidant activity of 13.44 mg extract per 1 mmol TMAMQ (Table 4). The data also show that different solvents are required for the extraction of different antioxidants contained in various food samples (Table 4).

The hydrolysed tannins and condensed tannins fractions of garlic acid also showed a high antioxidant activity when compared to the antioxidant activity of other fractions (Table 4). The antioxidant activity of tomato fractions and kiwi were generally high for all the fractions (Table 4). High levels of carotenoids especially lycopene in tomato and tocopherols in all chlorophyll containing tissues for example lettuce and spinach have been shown to contribute significantly to their antioxidant activity (Piironen, Syvaeoja, Salminen, & Koivistoinen, 1986). The antioxidant activity of all extracts from ap-

Table 4
Antioxidant activity of different foods samples as measured with laccase generated TMAMQ.

Food sample	mg dry weight of the extract required to reduce 1 mmol TMAMQ			
	Methanol/water (50:50 v/v)	Acetone/water 70:30 v/v	Acidified methanol	Acidified butanol/$FeCl_3$
Fruits and vegetables				
Apple	556 ± 1	149 ± 3	555 ± 2	189 ± 2
Carrots	98 ± 2	270 ± 1	476 ± 4	185 ± 4
Garlic	588 ± 2	135 ± 3	53 ± 3	37 ± 3
Kiwi	14 ± 1	44 ± 1	68 ± 3	141 ± 2
Lettuce	41 ± 3	182 ± 3	270 ± 1	263 ± 2
Onion	345 ± 2	39 ± 4	370 ± 3	46 ± 3
Pumpkin seed	159 ± 3	13 ± 2	154 ± 3	79 ± 3
Spinach	4 ± 0.5	30 ± 2	100 ± 2	476 ± 1
Tomato	62 ± 3	38 ± 3	50 ± 4	82 ± 2
Beverages	*Water extract*			
Green tea	1.2 ± 0.01			
Fermented tea	0.6 ± 0.01			
Coffee	0.7 ± 0.03			
Oils	*Oil extract*			
Maize corn oil	26 ± 1			
Extra-virgin olive oil	20 ± 3			

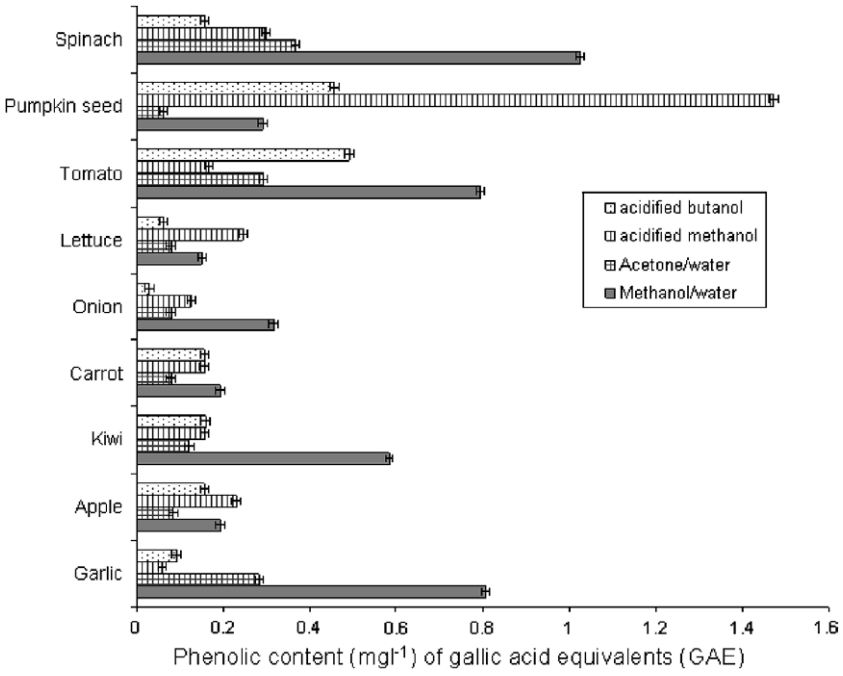

Fig. 2. Total phenol content in the different food extracts.

ples was generally low (Table 4) which probably can be justified by earlier reports that the major source of antioxidants in apples are found in the peel which is believed to contain about 7-times higher antioxidants than the pulp (Sikora et al., 2008).

3.6. Antioxidant activity of beverages and oils

The water extracts obtained from green, fermented teas and coffee were very active in quenching TMAMQ (Table 4) as compared to food samples in Table 4. The antioxidant activity of teas is mainly attributed to catechins namely; epigallocatechin gallate, epigallocatechin, gallic acid, epicatechin and catechin (Balasundram et al., 2006; Sikora et al., 2008). The antioxidant activity of green tea (0.59 g/mmol) was twice as effective as that of fermented tea (1.15 mg/mmol (Table 4). The decrease in antioxidant activity in fermented tea is attributed to changes occurring during the fermentation process where the flavanols in green tea leaves (mainly catechins and their gallic esters) undergo an oxidative polymerization by polyphenol oxidases, turning the leaves black (Daglia, Papetti, Gregotti, Berte, & Gazzani, 2000; Richelle, Tavazzi, & Offord, 2001; Wei, Zhou, Cai, Yang, & Liu, 2006). The antioxidant activity of coffee was lower as compared to that of green tea (Table 4). Coffee processing like in teas leads to the modification and loss of some polyphenolic antioxidants during roasting (Daglia et al., 2000; Tubaro, Micossi, & Ursini, 1996). Extra virgin olive oil quenched TMAMQ and its activity of 20.32 ml may partly be attributed to the presence oleuropein already shown above to quench TMAMQ as well as other phenolics described by earlier researchers as a powerful antioxidants both *in vivo* and *in vitro* (Tripoli et al., 2005). Maize oil also showed antioxidant activity (Table 4). Different oils have different antioxidants-contributing compounds as described by Pennington (2002).

Although generally the rank order of antioxidant activity of most of the known pure antioxidants and food samples investigated in

this work agree with previous studies using different approaches (ORAC, DPPH, ABTS), the actual values obtained vary. There may be several underlying factors among which are effects of solvents. Solvents have been shown to influence the reaction of antioxidants (Dangles, Dufoura, & Fargeixa, 2000) as well as the reaction mechanism favouring hydrogen atom transfer in apolar solvents and electron transfer mechanisms in polar solvents (Perez-Jimenez & Saura-Calixto, 2006; Saito & Kawabata, 2004). There is therefore a need to investigate the effects of solvents as well as other reaction conditions which might influence accurate measurement of antioxidant activity of given samples using TMAMQ.

4. Conclusions

All known different classes of antioxidants molecules tested (dietary and endogenous) were able to quench TMAMQ. This observation demonstrates the great potential application of TMAMQ for antioxidant activity measurement in both food, cosmetic and health industries. The TMAMQ seem to be more reliable than both DPPH and ABTS method when considering antioxidant activity of amino acids and this may well extend to antioxidant activity of serum proteins. Adding to this interesting observation, the extensive information accrued in the development of laccase based biosensors for phenolics detection in wine, beer, tea and vegetable extracts (Franzoi, Dupont, Spinelli, & Vieira, 2009; Gamella, Campuzano, Reviejo, & Pingarron, 2008; Jarosz-Wilkolazka, Ruzgas, & Gorton, 2004, 2005; Merle et al., 2008; Portaccio et al., 2006; Roy, Abraham, Abhijith, Kumar, & Thakur, 2005; Shleev et al., 2006) makes the development of an automated method for antioxidant activity determination feasible. In this case the immobilized laccase on the biosensor can be designed in such a way that laccase oxidises immobilized syringaldazine to TMAMQ which is further reduced to syringaldazine upon addition of a sample containing antioxidants molecules. The resulting oxygen consumption can be easily monitored (Nugroho Prasetyo et al., 2009) and converted into electrochemical signals.

Acknowledgements

This work was made possible by the support offered by the Austrian Academic Exchange Service (ÖAD) and European Union Biorenew Project [Sixth Framework Programme (FP6-2004-NMP-NI-4)].

References

Ahmad, M. M., Al-Hakim, S., Adel, A., & Shehata, Y. (1983). The antioxidant activity of amino acids in two vegetable oils. *Journal of the American Oil Chemists' Society, 60*, 837–840.

Almansa, E., Kandelbauer, A., Pereira, L., Cavaco, P., & Guebitz, G. M. (2004). Influence of structure on dyedegradation with laccase mediator systems. *Biocatalysis and Biotransformation, 22*, 315–324.

Andreasen, M. F., Landbo, A. K., Christensen, L. P., Hansen, A., & Meyer, A. S. (2001). Antioxidant effects of phenolic rye (*Secale cereale* L.) extracts, monomeric hydroxycinnamates, and ferulic acid dehydrodimers on human low-density lipoproteins. *Journal of Agricultural and Food Chemistry, 49*, 4090–4096.

Balasundram, N., Sundram, K., & Samman, S. (2006). Phenolic compounds in plants and agri-industrial by-products: Antioxidant activity, occurrence, and potential uses. *Food Chemistry, 99*, 191–203.

Bauer, R., & Rupe, C. O. (1971). Use of syringaldazine in a photometric method for estimating "free" chlorine in water. *Analytical Chemistry, 43*, 421–425.

Bourdon, E., & Blache, D. (2001). The importance of proteins in defense against oxidation. *Antioxidants & Redox Signaling, 3*, 293–311.

Burda, S., & Oleszek, W. (2001). Antioxidant and antiradical activities of flavonoids. *Journal of Agricultural and Food Chemistry, 49*, 2774–2779.

Cao, G., Sofic, E., & Prior, R. L. (1996). Antioxidant capacity of tea and common vegetables. *Journal of Agricultural and Food Chemistry, 44*, 3426–3431.

Chun, O. K., Kim, D. O., Smith, N., Schroeder, D., Han, J. T., & Lee, C. Y. (2005). Daily consumption of phenolics and total antioxidant capacity from fruit and vegetables in the American diet. *Journal of the Science of Food and Agriculture, 85*, 1715–1724.

Cooper, W. J., Roscher, N. M., & Slifker, R. A. (1982). Determining free available chlorine by DPD-colorimetric, DPD-Steadifac (colorimetric), and FACTS procedures. *Journal American Water Works Association, 74*, 362–368.

Daglia, M., Papetti, A., Gregotti, C., Berte, F., & Gazzani, G. (2000). In vitro antioxidant and ex vivo protective activities of green and roasted coffee. *Journal of Agricultural and Food Chemistry, 48*, 1449–1454.

Dalle-Donne, I., Rossi, R., Colombo, R., Giustarini, D., & Milzani, A. (2006). Biomarkers of oxidative damage in human disease. *Clinical Chemistry, 52*, 601–623.

Dangles, O., Dufoura, C., & Fargeixa, G. (2000). Inhibition of lipid peroxidation by quercetin and quercetin derivatives: antioxidant and prooxidant effects. *Journal of the Chemical Society, Perkin Transactions, 2*, 1215–1222.

Espin, J. C., Soler-Rivas, C., & Wichers, H. J. (2000). Characterization of the total free radical scavenger capacity of vegetable oils and oil fractions using 2,2-diphenyl-1-picrylhydrazyl radical. *Journal of Agricultural and Food Chemistry, 48*, 648–656.

Franzoi, A. C., Dupont, J., Spinelli, A., & Vieira, I. C. (2009). Biosensor based on laccase and an ionic liquid for determination of rosmarinic acid in plant extracts. *Talanta, 77*, 1322–1327.

Gamella, M., Campuzano, S., Reviejo, A. J., & Pingarron, J. M. (2008). Integrated multienzyme electrochemical biosensors for the determination of glycerol in wines. *Analytica Chimica Acta, 609*, 201–209.

Genestra, M. (2007). Oxyl radicals, redox-sensitive signalling cascades and antioxidants. *Cellular Signalling, 19*, 1807–1819.

Halliwell, B. (1994). Free radicals, antioxidants, and human disease: Curiosity, cause, or consequence? *The Lancet, 344*, 721–724.

Halvorsen, B. L., Holte, K., Myhrstad, M. C. W., Barikmo, I., Hvattum, E., Remberg, S. F., et al. (2002). A systematic screening of total antioxidants in dietary plants. *Journal of Nutrition, 132*, 461–471.

Hapiot, P., Pinson, J., Neta, P., & Rolando, C. (1993). Electrochemical behaviour of syringaldazine, a colorimetric redox reagent. *Journal of Electroanalytical Chemistry, 353*, 225–235.

Harkin, J. M., Larsen, M. J., & Obstharkin, J. R. (1974). Use of syringaldazine for detection of laccase in sporophores of wood rotting fungi. *Mycologia, 66*, 469–476.

Hartzfeld, P. W., Forkner, R., Hunter, M. D., & Hagerman, A. E. (2002). Determination of hydrolyzable tannins (gallotannins and ellagitannins) after reaction with potassium iodate. *Journal of Agricultural and Food Chemistry, 50*, 1785–1790.

Heim, K. E., Tagliaferro, A. R., & Bobilya, D. J. (2002). Flavonoid antioxidants: Chemistry, metabolism and structure–activity relationships. *The Journal of Nutritional Biochemistry, 13*, 572–584.

Hernandez-Ledesma, B., Davalos, A., Bartolome, B., & Amigo, L. (2005). Preparation of antioxidant enzymatic hydrolysates from a-lactalbumin and ß-lactoglobulin. Identification of active peptides by HPLC-MS/MS. *Journal of Agricultural and Food Chemistry, 53*, 588–593.

Holm, K. A., Nielsen, D. M., & Eriksen, J. (1998). Automated colorimetric determination of recombinant fungal laccase activity in fermentation sarples using syringaldazine as chromogenic substrate. *Journal of Automatic Chemistry, 20*, 199–203.

Jadhav, S. J., Nimbalkar, S. S., Kulkarni, A. D., & Madhavi, D. L. (1996). Lipid oxidation in biological and food system. In D. L. Madhavi, S. S. Deshpande, & D. K. Salunkhe (Eds.), *Food antioxidant* (pp. 5–63). New York: Dekker.

Jarosz-Wilkolazka, A., Ruzgas, T., & Gorton, L. (2004). Use of laccase-modified electrode for amperometric detection of plant flavonoids. *Enzyme and Microbial Technology, 35*, 238–241.

Jarosz-Wilkolazka, A., Ruzgas, T., & Gorton, L. (2005). Amperometric detection of mono- and diphenols at Cerrena unicolor laccase-modified graphite electrode: Correlation between sensitivity and substrate structure. *Talanta, 66*, 1219–1224.

Jimenez-Escrig, A., Jimenez-Jimenez, I., Sanchez-Moreno, C., & Saura-Calixto, F. (2000). Evaluation of free radical scavenging of dietary carotenoids by the stable radical 2,2-diphenyl-1-picrylhydrazyl. *Journal of the Science of Food and Agriculture, 80*, 1686–1690.

Kaur, C., & Kapoor, H. C. (2001). Antioxidants in fruits and vegetables – The millennium's health. *International Journal of Food Science & Technology, 36*, 703–725.

Kohen, R., & Nyska, A. (2002). Oxidation of biological systems: Oxidative stress phenomena. *Toxicology Pathology, 30*, 620–650.

Kuznetsova, Y. A., & Romakh, V. B. (1996). Syringaldazine new attractive electron donor of prostaglandin H synthase. *Applied Biochemistry and Biotechnology, 61*, 205–209.

Lee, J. H., Ozcelik, B., & Min, D. B. (2006). Electron donation mechanisms of ß-carotene as a free radical scavenger. *Journal of Food Science, 68*, 861–865.

Levine, R. L., Mosoni, L., Berlett, B. S., & Satdtman, E. R. (1996). Methionine residues as endogenous antioxidants in proteins. *Proceedings of the National Academy of Sciences of the United States of America, 93*, 15036–15040.

Lien, E. J., Ren, S., Bui, H. H., & Wang, R. (1999). Quantitative structure–activity relationship analysis of phenolic antioxidants. *Free Radical Biology and Medicine, 26*, 285–294.

Magalhaes, L. M., Segundo, M. A., Reis, S., & Lima, J. L. F. C. (2008). Methodological aspects about in vitro evaluation of antioxidant properties. *Analytica Chimica Acta, 613*, 1–19.

Masella, R., Di Benedetto, R., Vari, R., Filesi, C., & Giovannini, C. (2005). Novel mechanisms of natural antioxidant compounds in biological systems: Involvement of glutathione and glutathione-related enzymes. *The Journal of Nutritional Biochemistry, 16*, 577–586.

Merle, G., Brunel, L., Tingry, S., Cretin, M., Rolland, M., Servat, K., et al. (2008). Electrode biomaterials based on immobilized laccase. Application for enzymatic reduction of dioxygen. *Materials Science and Engineering: C, 28*, 932–938.

Meucci, E., & Mele, M. C. (1997). Amino acids and plasma antioxidant capacity. *Amino acids, 12*, 373–377.

Monach, C., Williamson, G., Morand, C., Scalbert, A., & Rémésy, C. (2005). Bioavailability and bioefficacy of polyphenols in humans. I. Review of 97 bioavailability studies. *The American Journal of Clinical Nutrition, 81*, 230–242.

Nugroho Prasetyo, E., Kudanga, T., Steiner, W., Murkovic, M., Nyanhongo, G., & Guebitz, G. (2009). Antioxidant activity assay based on laccase-generated radicals. *Analytical and Bioanalytical Chemistry, 393*, 679–687.

Oettl, K., & Stauber, R. E. (2007). Physiological and pathological changes in the redox state of human serum albumin critically influence its binding properties. *British Journal of Pharmacology, 151*, 580–590.

Ou, B., Huang, D., Hampsch-Woodill, M., Flanagan, J. A., & Deemer, E. K. (2002). Analysis of antioxidant activities of common vegetables employing oxygen radical absorbance capacity (ORAC) and ferric reducing antioxidant power (FRAP) assays: A comparative study. *Journal of Agricultural and Food Chemistry, 50*, 3122–3128.

Pastore, A., Federici, G., Bertini, E., & Piemonte, F. (2003). Analysis of glutathione: Implication in redox and detoxification. *Clinica Chimica Acta, 333*, 19–39.

Pellegrini, N., Colombi, B., Salvatore, S., Brenna, O. V., Galaverna, G., Del Rio, D., et al. (2007). Evaluation of antioxidant capacity of some fruit and vegetable foods: Efficiency of extraction of a sequence of solvents. *Journal of the Science of Food and Agriculture, 87*, 103–111.

Pennington, J. A. T. (2002). Food composition databases for bioactive food components. *Journal of Food Composition and Analysis, 15*, 419–434.

Perez-Jimenez, J., Arranz, S., Tabernero, M., Rubio, M. E., Serrano, J., Goni, I., et al. (2008). Updated methodology to determine antioxidant capacity in plant foods, oils and beverages: Extraction, measurement and expression of results. *Food Research International, 41*, 274–285.

Perez-Jimenez, J., & Saura-Calixto, F. (2006). Effect of solvent and certain food constituents on different antioxidant capacity assays. *Food Research International, 39*, 791–800.

Peschel, W., Sanchez-Rabaneda, F., Diekmann, W., Plescher, A., Gartzia, I., Jimenez, D., et al. (2006). An industrial approach in the search of natural antioxidants from vegetable and fruit wastes. *Food Chemistry, 97*, 137–150.

Piironen, V., Syvaeoja, E.-L., Salminen, K., & Koivistoinen, P. (1986). Tocopherols and tocotrienols in cereal products from Finland. *Cereal Chemistry, 63*, 78–81.

Portaccio, M., Di Martino, S., Maiuri, P., Durante, D., De Luca, P., Lepore, M., et al. (2006). Biosensors for phenolic compounds: The catechol as a substrate model. *Journal of Molecular Catalysis B: Enzymatic, 41*, 97–102.

Porter, L. J. (1989) Tannins. In P. M. Dey & J.B Harbomi (Eds.), *Method in Plant Biochemistry*, *Vol. 1. Plant Phenolics* (pp. 389–417).

Prior, R. L., & Cao, G. (2000). Analysis of botanicals and dietary supplements for antioxidant capacity: A review. *Journal of AOAC International, 83*, 950–956.

Prior, R. L., Wu, X., & Schaich, K. (2005). Standardized methods for the determination of antioxidant capacity and phenolics in foods and dietary supplements. *Journal of Agricultural and Food Chemistry, 53*, 4290–4302.

Rice-Evans, C. A., Miller, N. J., & Paganga, G. (1996). Structure–antioxidant activity relationships of flavonoids and phenolic acids. *Free Radical Biology and Medicine, 20*, 933–956.

Rice-Evans, C., Miller, N., & Paganga, G. (1997). Antioxidant properties of phenolic compounds. *Trends in plant science, 2*, 152–159.

Richelle, M., Tavazzi, I., & Offord, E. (2001). Comparison of the antioxidant activity of commonly consumed polyphenolic beverages (coffee, cocoa, and tea) prepared per cup serving. *Journal of Agricultural and Food Chemistry, 49*, 3438–3442.

Robards, K., Prenzler, P. D., Tucker, G., Swatsitang, P., & Glover, W. (1999). Phenolic compounds and their role in oxidative processes in fruits. *Food Chemistry, 66*, 401–436.

Roy, J. J., Abraham, T. E., Abhijith, K. S., Kumar, P. V. S., & Thakur, M. S. (2005). Biosensor for the determination of phenols based on Cross-Linked Enzyme Crystals (CLEC) of laccase. *Biosensors and Bioelectronics, 21*, 206–211.

Saito, S., & Kawabata, J. (2004). Synergistic effects of thiols and amines on antiradical efficiency of protocatechuic acid. *Journal of Agricultural and Food Chemistry, 52*, 8163–8168.

Saura-Calixto, F., Serrano, J., & Goni, I. (2007). Intake and bioaccessibility of total polyphenols in a whole diet. *Food Chemistry, 101*, 492–501.

Serrano, J., Goni, I., & Saura-Calixto, F. (2007). Food antioxidant capacity determined by chemical methods may underestimate the physiological antioxidant capacity. *Food Research International, 40*, 15–21.

Shleev, S., Persson, P., Shumakovich, G., Mazhugo, Y., Yaropolov, A., Ruzgas, T., et al. (2006). Laccase-based biosensors for monitoring lignin. *Enzyme and Microbial Technology, 39*, 835–840.

Sies, H., & Wilhelm, S. (2004). Carotenoids and UV protection. *Photochemical and Photobiological Sciences, 3*, 749–752.

Sikora, E., Cieslik, E., & Topolska, K. (2008). The sources of natural antioxidants. *Acta Scientiarum Polonorum, 7*, 5–17.

Silva, M. M., Santos, M. R., Caroco, G., Rocha, R., Justino, G., & Mira, L. (2002). Structure–antioxidant activity relationships of flavonoids: A re-examination. *Free Radical Research, 36*, 1219–1227.

Singh, R. P., Sharad, S., & Kapur, S. (2004). Free radicals and oxidative stress in neurodegenerative diseases: Relevance of dietary antioxidants. *Journal, Indian Academy of Clinical Medicine, 5*, 218–225.

Singleton, V. L., & Rossi, J. A. Jr., (1965). Colorimetry of total phenolics with phosphomolybdic–phosphotungstic acid reagents. *American Journal of Enology and Viticulture, 16*, 144–158.

Thurston, C. F. (1994). The structure and function of fungal laccases. *Microbiology, 140*, 19–26.

Triantis, T. M., Yannakopoulou, E., Nikokavoura, A., Dimotikali, D., & Papadopoulos, K. (2007). Chemiluminescent studies on the antioxidant activity of amino acids. *Analytica Chimica Acta, 591*, 106–111.

Tripoli, E., Giammanco, M., Tabacchi, G., Di Majo, D., Giammanco, S., & La Guardia, M. (2005). The phenolic compounds of olive oil: Structure, biological activity and beneficial effects on human health. *Nutrition Research Reviews, 18*, 98–112.

Tubaro, F., Micossi, E., & Ursini, F. (1996). The antioxidant capacity of complex mixtures by kinetic analysis of crocin bleaching inhibition. *Journal of the American Oil Chemists' Society, 73*, 173–179.

Valko, M., Leibfritz, D., Moncol, J., Cronin, M. T. D., Mazur, M., & Telser, J. (2007). Free radicals and antioxidants in normal physiological functions and human disease. *The International Journal of Biochemistry & Cell Biology, 39*, 44–84.

Valko, M., Rhodes, C. J., Moncol, J., Izakovic, M., & Mazur, M. (2006). Free radicals, metals and antioxidants in oxidative stress-induced cancer. *Chemico-Biological Interactions, 160*, 1–40.

Villano, D., Fernandez-Pachon, M. S., Moya, M. L., Troncoso, A. M., & Garcia-Parrilla, M. C. (2007). Radical scavenging ability of polyphenolic compounds towards DPPH free radical. *Talanta, 71*, 230–235.

Wang, H., Cao, G., & Prior, R. L. (1996). Total antioxidant capacity of fruits. *Journal of Agricultural and Food Chemistry, 44*, 701–705.

Wei, Q. Y., Zhou, B., Cai, Y. J., Yang, L., & Liu, Z. L. (2006). Synergistic effect of green tea polyphenols with trolox on free radical-induced oxidative DNA damage. *Food Chemistry, 96*, 90–95.

Food Chemistry 118 (2010) 445–448

Contents lists available at ScienceDirect

Food Chemistry

journal homepage: www.elsevier.com/locate/foodchem

Analytical Methods

A novel size-exclusion high performance liquid chromatography (SE-HPLC) method for measuring degree of amylose retrogradation in rice starch

Yaoqi Tian [a,b], Yin Li [c], Xueming Xu [a,b], Zhengyu Jin [a,b,*], Aiquan Jiao [a,b], Jinpeng Wang [a,b], Bo Yu [a,b]

[a] The State Key Lab of Food Science and Technology, Jiangnan University, 1800 Lihu Road, Wuxi 214122, China
[b] School of Food Science and Technology, Jiangnan University, 1800 Lihu Road, Wuxi 214122, China
[c] Department of Plant Science, North Dakota State University, Fargo 58105, ND, USA

ARTICLE INFO

Article history:
Received 11 November 2008
Received in revised form 31 March 2009
Accepted 26 April 2009

Keywords:
SE-HPLC
Amylose retrogradation
Rice starch
Molecular simulation

ABSTRACT

The objective of this study was to develop a new method to measure the degree of amylose retrogradation in rice starch using size-exclusion high performance liquid chromatography (SE-HPLC). This developed method is based on the change in molecule size related to the retention time of amylose. Results showed that SE-HPLC was able to provide accurate data to evaluate the amylose retrogradation by comparing with other well-established methods. The principle of the measurement was further studied in molecular level by molecular dynamic (MD) simulation. It indicated that amylose molecules were transformed from disordering configuration to ordering one due to the increase in Van der Waals (Vdw) and hydrogen forces, and decrease in bonded interaction during the short-term storage.

1. Introduction

Amylopectin and amylose, as major rice starch components, have different roles in starch retrogradation. Much evidence suggests that the changes in amylopectin properties are responsible for all long-term rheological and structural deteriorations (Miles, Morris, Orford, & Ring, 1985). Amylose, however, is related to the short-term change completing in a few hours (Khanna & Tester, 2006; Ring et al., 1987). Amylose crystallite is especially considered as a nucleus for amylopectin recrystallization, resulting in acceleration of the whole retrogradation process (Gudmundsson & Eliasson, 1990). It is therefore of importance to determine amylose retrogradation during the short-term storage of rice starch.

It is known that many methods have been applied in the measurement of starch retrogradation (Karim, Norziah, & Seow, 2000). Bao, Shen, and Jin (2007) evaluated the short-term retrogradation of rice starch by using near-infrared spectroscopy; whereas the direct determination was not reported in their work. X-ray diffraction studies clearly showed that the development of crystallinity occurred in an aging starch gel (Miles, Morris, & Ring, 1985; Miles et al., 1985). Nevertheless, the sensitivity of this method was too low to detect the minor extent of recrystallization during a rapid storage (Smits, Ruhnau, Vliegenthart, & van Soest, 1998). Differential scanning calorimetry (DSC) was apparently used for measuring retrogradation of starch and proved to be a valuable tool to quantify the crystallinity of amylopectin rather than amylose recrystallite since this recrystallite was transformed at much higher temperature (120–160 °C), at which the pans would be leaked before the transition occurred (Eerlingen, Jacobs, & Delcour, 1994; Russell, 1987). Enzymatic method (EN), based on measuring the resistance of starch to enzymatic hydrolysis, was performed to determine retrogradation degree; but this retrogradation is related to the amylose recrystallite as well as the retrograded amylopectin (Eerlingen, Crombez, & Delcour, 1993; Tsuge, Hishida, Iwasaki, Watanabe, & Goshima, 1990). Size-exclusion high performance liquid chromatography (SE-HPLC) has been used in the estimation of molecular weight (M_w) of starch components, according to the different retention time (T_R) for its components (Dias, Fernandes, Mota, Teixeira, & Yelshin, 2008). However, to the best of our knowledge, no other literatures related to this topic were found to exam amylose retrogradation by analysing the change in T_R.

The research presented here had two objectives. The first objective was to evaluate the possibility of measuring amylose retrogradation in rice starch using SE-HPLC method. The second objective was to clarify the principle of this method in molecular level by molecular dynamic (MD) simulation.

* Corresponding author. Address: School of Food Science and Technology, Jiangnan University, 1800 Lihu Road, Wuxi 214122, China. Tel./fax: +86 510 85913299.
E-mail addresses: zjin@jiangnan.edu.cn, jinlab2008@yahoo.com (Z. Jin).

0308-8146/$ - see front matter © 2009 Elsevier Ltd. All rights reserved.
doi:10.1016/j.foodchem.2009.04.107

2. Materials and methods

2.1. Materials

Rice starch (amylose content 29.7%, proteins content $\leqslant$ 0.2%, lipids content $\leqslant$ 0.1%) was isolated and purified from various milled fresh grains (Shandong Province, China) according to previously described protocols (Takeda, Hizukuri, & Juliano, 1986). α-Amylase from *Bacillus subtilis* was kindly provided from Genencor Biotechnology Inc. (Wuxi, China). All other chemicals and reagents were of analytical grade unless otherwise stated.

2.2. Preparation of the different aging samples

Rice starch (1.0 g) was dispersed in water (2 mL) and shook by a blender. The blend was heated at 100 °C for 20 min in a vacuum oven before the mixture was stored at 4 °C for the required time (0, 1, 3, 5, 7, 14, and 24 h) to accelerate the aging process. The resulting gelatinized and retrograded samples were dried at 40 °C in a vacuum oven until the water was evaporated to get dry powders.

2.3. SE-HPLC

A serial of dried powders (0.1 g) was dispersed in NaOH (0.5 mol/L, 2 mL) and mildly shook. The volume of this suspension was later diluted to 100 mL before incubation at 45 °C for 2 h. The resultant solution (about 2 mL) was centrifuged at 10,000*g* for 15 min and filtered with a 0.2 μm filter. From each supernatant, a volume of 10 μL (w/w, 0.1%) was injected for HPLC analysis. The HPLC system comprised a Waters 2410 pump equipped with auto-sampler and differential refractive index detector (Waters, Model 410, Milford, MA). An ultrahydrogel linear column (7.8 mm × 300 mm, Waters Corporation) and detector were maintained at 37 °C. The mobile phase was sodium acetate-acetic acid buffer (0.05 mol/L, pH 5.0) containing sodium nitrate (w/w, 0.02%) at a flow rate of 0.9 mL/min. The final retention time (T_R) of samples was collected and analysed by the following described Eq. (1) to perform a calculation of retrogradation degree

$$R(t) = \frac{A \cdot (T_t - T_0)}{(T_\infty - T_0)} \cdot 100\% \quad (1)$$

where $R(t)$ represents the recrystalline fraction of amylose (%) developed at time t, T_t is retention time of the sample stored for t hours, T_0 is the retention time of the gelatinized sample, T_∞ is limiting retention time of 24 h storage sample, and A is the amylose area (%) occupied of the peaks.

2.4. Differential scanning calorimetry

Thermal analysis was performed by using a Pris 1 DSC (Pekin-Elmer Inc., USA) under ultrahigh-purity nitrogen atmosphere. The equipment was calibrated with indium and tin standards. The prepared sample of 3.0 mg and distilled water (6 μL) were together added into an aluminum pan. The sealed sample were equilibrated at 25 °C for 8 h and then heated from 25 to 100 °C at a constant rate of 8 °C/min to analyse the enthalpy change (ΔH) in phase transition. An aluminum pan containing 6 μL of distilled water was meantime used as a reference. The final retrogradation degree of samples was calculated as following Eq. (2) (Baik, Kim, Cheon, Ha, & Kim, 1997)

$$X(t) = \frac{\Delta H_t - \Delta H_0}{\Delta H_\infty - \Delta H_0} \quad (2)$$

where $X(t)$ represents the crystalline fraction (%) developed at time t, ΔH_0 is enthalpy change (J/g) at time zero (the gelatinized sample), ΔH_t is enthalpy change at time t, and ΔH_∞ is limiting enthalpy change (4 weeks for all samples).

2.5. Enzymatic measurement

The degree of starch retrogradation was measured with the method previously described by Tsuge et al. (1990) with minor modifcation. Basically, 20 mg of starch was dispersed by water (3 mL), acetate buffer (0.1 mol/L, 2 mL), and α-amylase solution (8 unit, 2 mL). This suspension was incubated at 37 °C for 20 min before terminated this enzymatic reaction by NaOH (4 mol/L, 5 mL). The pH of the resultant solution was adjusted to neutrality with HCl (4 mol/L). The total volume was made up to 100 mL with water. From each sample, 10 mL of the digested solution was collected and mixed with I_2-KI solution (w/w, 0.2:2%, 5 mL) in a volumetric flask. The resulting solution was again made up to 100 mL with water and kept at 25 °C for 20 min. The absorbance of each samples was measured at 625 nm in calculation of degree of retrogradation (DR, %)

$$DR\ (\%) = \frac{100 \cdot (b - c)}{(a - c)} \quad (3)$$

where a represents the absorbance of total starch fraction, b is the absorbance of starch fraction to be tested, and c is the absorbance of the complete digestion of starch.

2.6. Molecular dynamic (MD) simulation

Amylose fraction and waters' interactions were simulated in a required periodic box (56 × 38 × 38 Å) by using MD module of HYPERCHEM 8.0 software (Hypercube Inc., Waterloo, Canada). In brief, the proposed model of amylose fraction was comprised eighteen polymeric glucose units in a rather stiff left-handed helix and dissolved in the water (60%, w/w) (Fig. 1). By imposing a restraint on a gradient of 0.01 × 4.186 8 kJ/(mol Å), this model of the interaction was energetically optimised using the AMBER force field. The resulting configuration was directly performed at a step size of 0.001 ps under 100 °C (373 K) for 2 ps. This optimised model was further simulated for 2 ps at a lower temperature of 4 °C (277 K) to analyse the changes of the structures and energies during the process of temperature decreasing. Some important parameters including molecular volume, solvent-accessible surface (grid), bonded interaction, and non-bonded interaction were collected and analysed.

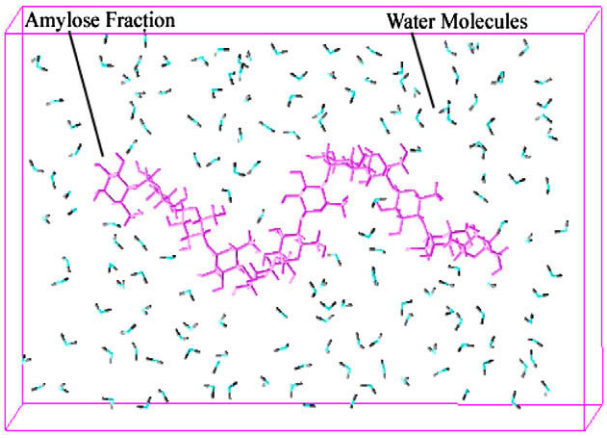

Fig. 1. The interaction model of amylose fraction and water (60%, w/w).

2.7. Statistic analysis

Statistical analysis was performed by using ORIGIN 7.5 (OriginLab. Inc., USA). Data were expressed as means of triplicate and analysed by a one-way analysis of variance (ANOVA). Treatment means were considered significantly different at $P \leqslant 0.05$.

3. Results and discussion

3.1. SE-HPLC analysis

Data obtained from SE-HPLC for rice starch samples with different storage time are summarised in Table 1. Rice starch displayed two elution profiles: the former one corresponding to the amylopectin (T_R around 13 min) and the second assigned to amylose fractions (T_R around 16 min). These profiles correspond to the results of previous studies (Suortti, Gorenstein, & Roger, 1998). Retention time (T_R) of amylopectin was not obviously affected by the storage time increasing from 0 h to 24 h. This can be attributed to the larger molecular size of amylopectin as retention time will not be affected by the molecular size that exceeds the separation range of ultrahydrogel (1×10^4–1×10^6 Da). Nevertheless, the aging treatment did significantly increase T_R of amylose but not affect area of amylose fraction compared to that of gelatinized starch ($P \leqslant 0.05$). This increase in T_R was corresponding to the structure change of amylose molecules during the short-term storage. It has been proposed that gelatinized amylose was transformed from disordering to an ordering one by hydrogen bond increasing (Miles et al., 1985; Tang & Copeland, 2007). The ordering amylose molecules, therefore, could be probable easily incorporated into the core of hydrogel, resulting in the increase of retention time. Upon this potential principle, we proposed the SE-HPLC method that can be used to evaluate the degree of amylose retrogradation in rice starch.

3.2. Comparison of different methods for determination of amylose retrogradation degree of rice starch

As shown in Table 2, there is significant difference in the degree of retrogradation of rice starch between SE-HPLC and DSC ($P \leqslant 0.05$). This significance is mainly ascribed to the different principles of both methods. DSC has been reported to be sensitive to the amylopectin fraction of the gels but not to the major proportion of amylose crystallite (Russell, 1987); whereas SE-HPLC is directly related to conformational changes of amylose molecules in a molecular level. The degree of retrogradation determined by SE-HPLC, however, showed a good accordance with that by enzymatic measurement. The similar accordance was shown between SE-HPLC and EN–DSC (the value determined by EN minus the value from DSC), which is suitable for the evaluation of the degree of amylose retrogradation. The relative coefficient ($R = 0.98$) between the two methods further showed a good linearity. These results strongly indicate that the SE-HPLC is able to be used to measure the amylose retrogradation in rice starch. Nevertheless, a major disadvantage of enzymatic measurement is associated with other food constituents (Tsuge et al., 1990). This disadvantage is not for the SE-HPLC determination in this work since we have removed the protein contained in starch and dispersed rice starch by NaOH solution. The dispersion presented could disrupt amylose–lipid complex formation and exclude the potential effect of this complex on the determination before the injection of samples.

3.3. Volume and surface values analysis

An optimised model of the amylose fraction/waters' interaction was achieved in the MD runs and a stable configuration in the equilibrium state was yielded at different temperature (100 or 4 °C). As can be seen in Table 3, the volume of amylose fraction as well as the solvent-accessible surface obviously decreases during the aging process of decreasing the simulation temperature ($P \leqslant 0.05$). This decrease in molecule size was related to the ordering of amylose fraction, which was often achieved at a lower energy (Ogura & Yamamoto, 1995). This ordering conformation indicates that the more retention time taken for the retrograded rice amylose is required to get through hydrogel column in SE-HPLC system. In addition, some main forces that may cause the change of molecular size were analysed by the final single point energies. Van der Waals (Vdw) and hydrogen bond energies ("-" in Table 3 means the force orientation) increased significantly ($P \leqslant 0.05$), but not for electro-

Table 1
Main parameters of SE-HPLC for rice starch samples in the treatment of different storage time.

Storage time (h)	Peak 1		Peak 2	
	Area (%)	Retention time (min)	Area (%)	Retention time (min)
0	72.42 ± 0.44^{A}[a]	13.22 ± 0.04$^{A, b}$	27.58 ± 0.37^{A}	15.98 ± 0.03^{A}
1	72.27 ± 0.67^{A}	13.21 ± 0.03^{A}	27.73 ± 0.54^{A}	16.08 ± 0.04^{B}
3	71.89 ± 0.53^{A}	13.24 ± 0.02^{A}	28.11 ± 0.52^{A}	16.15 ± 0.04^{BCD}
5	71.95 ± 0.41^{A}	13.25 ± 0.04^{A}	28.05 ± 0.57^{A}	16.21 ± 0.03^{CDE}
7	71.78 ± 0.84^{A}	13.24 ± 0.03^{A}	28.22 ± 0.82^{A}	16.25 ± 0.02^{EF}
14	72.17 ± 0.73^{A}	13.26 ± 0.05^{A}	27.83 ± 0.32^{A}	16.30 ± 0.03^{FG}
24	72.10 ± 0.67^{A}	13.23 ± 0.03^{A}	27.90 ± 0.25^{A}	16.34 ± 0.02^{G}

[a] Values are means ± standard deviations of three determination.
[b] Sample values with different superscript capital letters in the same column are significantly different at $P \leqslant 0.05$.

Table 2
Comparison of determination of retrogradation degree of rice starch by SE-HPLC, DSC, enzymatic measurement (EN), and EN-DSC.

Methods	Retrogradation degree (%)					Relative coefficient (R)			
	1 h	3 h	5 h	7 h	14 h	SE-HPLC	DSC	EN	EN–DSC
SE-HPLC	7.20 ± 0.13[a]	13.27 ± 0.10	17.92 ± 0.14	21.17 ± 0.12	24.73 ± 0.14	1.0000	0.8559	0.9855*	0.9893*
DSC	–	–	0.38 ± 0.05	0.92 ± 0.03	2.27 ± 0.08	0.8559	1.0000	0.8779	0.8768
EN	7.39 ± 0.15	13.17 ± 0.14	16.93 ± 0.11	23.73 ± 0.12	28.44 ± 0.16	0.9855*	0.8779	1.0000	0.9986*
EN–DSC[b]	7.39 ± 0.15	13.17 ± 0.14	16.55 ± 0.08	22.81 ± 0.11	26.17 ± 0.13	0.9893*	0.8768	0.9986*	1.0000

* $P \leqslant 0.05$ at $R \geqslant r_{0.05}(3) = 0.8780$.
[a] Values are means ± standard deviations from three determination.
[b] EN–DSC represents the value determined by EN minus the value from DSC.

Table 3
Structure properties and single point energy[a] of starch fraction with water molecules (60%, w/w) at different simulation temperatures.

Temperature (°C)	QSAR properties		Single point energies (kJ mol^{-1})			
	Volume (Å^3)	Surface (grid) (Å^2)	Bonded interaction	Vdw	Hydrogen bond	Electrostatic
100	4331.15 ± 10.52^{Ab}	2191.45 ± 7.54^{A}	75.41 ± 0.87^{A}	−20.32 ± 0.32^{A}	−33.59 ± 0.24^{A}	−62.47 ± 1.33^{A}
4	4273.73 ± 8.73^{B}	2147.03 ± 9.27^{B}	73.42 ± 1.10^{A}	−28.14 ± 0.19^{B}	−41.44 ± 0.52^{B}	−64.53 ± 1.54^{A}
100 → 4[c]	57.42 ± 0.85	44.42 ± 0.74	1.99 ± 0.14	7.82 ± 0.08	7.85 ± 0.17	2.06 ± 0.13

[a] Values are means standard deviations of three determination.
[b] Sample values with different superscript capital letters in the same column are significantly different at $P \leqslant 0.05$.
[c] "100 → 4" represents the difference from 4 to 100 °C.

static energy during the aging process. It suggests that the ordering structure formation at lower temperature was mainly ascribed to the change of Vdw attraction and hydrogen bond force. This finding was partially in agreement with the results of that Vdw attraction was the dominant driving force in the formation of ordering polymer (Xie & Soh, 2005). In general, the more negative the force energy was, the more thermodynamically favourable was the formation of the ordering structure (Yousef, Zughul, & Badwan, 2007). Especially, the change in bonded interaction was exothermal judged from the negative enthalpy change (−1.99 ± 0.14 kJ mol^{-1}), although the change was found less significant in comparison to the non-bonded interaction energy including Vdw attraction, hydrogen bond, and electrostatic force. This result indicates that the bonded interaction also accelerates the deformation of amylose molecules during the aging process.

4. Conclusions

This work clarified that the degree of amylose retrogradation is abele to be measured by a SE-HPLC method. Compared to other well-known methods, SE-HPLC method was proved to be an effective measurement of amylose retrogradation during the short-term storage of rice starch. The principle of this method could be studied in molecular level by MD simulation. It indicates that amylose recrystallization was induced by Vdw attraction, hydrogen bond force, and bonded interaction, resulting in the transformation of amylose molecule to the final ordering configuration. This study as well suggested the theoretical calculation provided a good reference for practical guidance.

Acknowledgements

This study was financially supported by Key Program of Ministry Education (No. 109080), and Programs of State Key Laboratory of Food Science and Technology, Jiangnan University (SKLF-TS-200810 and SKLF-MB-200804), Nature Science Foundation of Jiangsu Province (BK2008003) and International Science and Technology Cooperation Program (No. 2007DFA31120).

References

Baik, M. Y., Kim, K. J., Cheon, K. C., Ha, Y. C., & Kim, W. S. (1997). Recrystallization kinetics and glass transition of rice starch gel system. *Journal of Agricultural and Food Chemistry, 45*, 4242–4248.

Bao, J., Shen, Y., & Jin, L. (2007). Determination of thermal and retrogradation properties of rice starch using near-infrared spectroscopy. *Journal of Cereal Science, 46*, 75–81.

Dias, R. P., Fernandes, C. S., Mota, M., Teixeira, J., & Yelshin, A. (2008). Starch analysis using hydrodynamic chromatography with a mixed-bed particle column. *Carbohydrate Polymers, 74*, 852–857.

Eerlingen, R. C., Crombez, M., & Delcour, J. A. (1993). Enzyme-resistant starch. I. Quantitative and qualitative influence of incubation time and temperature of autoclaved starch on resistant starch formation. *Cereal Chemistry, 70*, 339–344.

Eerlingen, R. C., Jacobs, H., & Delcour, J. A. (1994). Enzyme-resistant starch. V. Effect of retrogradation of waxy maize starch on enzyme susceptibility. *Cereal Chemistry, 71*, 351–355.

Gudmundsson, M., & Eliasson, A. C. (1990). Retrogradation of amylopectin and the effects of amylose and added surfactants/emulsifiers. *Carbohydrate Polymers, 13*, 295–315.

Karim, A. A., Norziah, M. H., & Seow, C. C. (2000). Methods for the study of starch retrogradation. *Food Chemistry, 71*, 9–36.

Khanna, S., & Tester, R. F. (2006). Influence of purified konjac glucomannan on the gelatinization and retrogradation properties of maize and potato starches. *Food Hydrocolloids, 20*, 567–576.

Miles, M. J., Morris, V. J., Orford, P. D., & Ring, S. G. (1985). The roles of amylose and amylopectin in the gelation and retrogradation of starch. *Carbohydrate Research, 135*, 271–281.

Miles, M. J., Morris, V. J., & Ring, S. G. (1985). Gelation of amylose. *Carbohydrate Research, 135*, 257–269.

Ogura, I., & Yamamoto, T. (1995). Molecular dynamics simulation of large deformation in an amorphous polymer. *Polymer, 36*, 1375–1381.

Ring, S. R., Colonna, P., l'Anson, K. J., Kalichevsky, M. T., Miles, M. J., Morris, V. J., et al. (1987). The gelation and crystallization of amylopectin. *Carbohydrate Research, 162*, 277–293.

Russell, P. L. (1987). The ageing of gels from starches of different amylose/amylopectin content studied by differential scanning calorimetry. *Journal of Cereal Science, 6*, 147–158.

Smits, A. L. M., Ruhnau, F. C., Vliegenthart, J. F. G., & van Soest, J. J. G. (1998). Ageing of starch based systems as observed with FT–IR and solid state NMR spectroscopy. *Starch/Stärke, 50*, 478–483.

Suortti, T., Gorenstein, M. V., & Roger, P. (1998). Determination of the molecular mass of amylose. *Journal of Chromatography A, 828*, 515–521.

Takeda, Y., Hizukuri, S., & Juliano, B. O. (1986). Purification and structure of amylose from rice starch. *Carbohydrate Research, 148*, 299–308.

Tang, M. C., & Copeland, L. (2007). Investigation of starch retrogradation using atomic force microscopy. *Carbohydrate Polymers, 70*, 1–7.

Tsuge, H., Hishida, M., Iwasaki, H., Watanabe, S., & Goshima, G. (1990). Enzymatic evaluation for the degree of starch retrogradation in foods and foodstuffs. *Starch/Stärke, 42*(6), 213–216.

Xie, Y. H., & Soh, A. K. (2005). Investigation of non-covalent association of single-walled carbon nanotube with amylose by molecular dynamics simulation. *Materials Letters, 59*, 971–975.

Yousef, F. O., Zughul, M. B., & Badwan, A. A. (2007). The modes of complexation of benzimidazole with aqueous β-cyclodextrin explored by phase solubility, potentiometric titration, 1H-NMR and molecular modeling studies. *Journal of Inclusion Phenomena and Macrocyclic Chemistry, 57*, 519–523.

Food Chemistry 118 (2010) 449–455

Contents lists available at ScienceDirect

Food Chemistry

journal homepage: www.elsevier.com/locate/foodchem

Analytical Methods

Flow injection analysis of BHA by NiHCF modified electrode

S.J. Richard Prabakar, S. Sriman Narayanan *

Department of Analytical Chemistry, School of Chemical Sciences, University of Madras, Guindy Campus, Chennai, TN 600 025, India

ARTICLE INFO

Article history:
Received 20 October 2008
Received in revised form 21 April 2009
Accepted 26 April 2009

Keywords:
Nickel hexacyanoferrate
Butylated hydroxy anisole
Electrocatalytic oxidation
Amperometric determination
Flow injection analysis

ABSTRACT

Flow injection method is described for the determination of the antioxidant *tert*-butylhydroxy anisole (BHA) based on its catalytic oxidation at a nickel hexacyanoferrate (NiHCF) surface modified graphite wax composite electrode fabricated using a new approach. The electrochemical characteristics of the modified electrode were studied using cyclic voltammetry. The voltammetric response of BHA at the modified electrode showed current densities remarkably higher than the bare graphite electrode and occurred at a reduced over voltage of 200 mV. Linear calibration graphs were obtained in the range of 1.2×10^{-6}–1.07×10^{-3} M. A detection limit of 6×10^{-7} M was obtained with a correlation coefficient of 0.9983 based on S/N = 3. Reliable results were obtained by applying the proposed flow injection method to determine BHA spiked in dehydrated potato flakes. Results suggest that the developed method can be effectively employed for the determination of BHA from food samples.

1. Introduction

Antioxidants have extensive use in the food industry, being added to a wide variety of foods in order to improve their stability and especially to prevent rancidity in products containing lipids or fats. They also find their use in food packaging, animal feed, cosmetics, pharmaceutical preparation, in rubber and petroleum products. Lipid oxidation can be retarded by oxygen removal or by using antioxidants. The latter are mostly phenolic compounds, such as *tert*-butylhydroxyanisole (BHA), propyl gallate (PG) and BHT (Hudson, 1990) that provide the best results in combination with a chelating agent. Recently, people have found that these artificial antioxidants may cause loss of nourishment and even produce toxic substances to harm human health. The concentration of these additives present in a particular food is limited by legislation in many countries (Furia, 1980). The most widespread trend is to reduce the use of these compounds. As the potential harmful effects of these compounds on health have been extensively discussed (Grice, 1988; Witschi, 1986). It has become important to determine their contents in those materials that are used by people. It is reported that it is more effective to use a mixture of two or more antioxidants rather than a single compound in practical use (Robards & Dilli, 1987).

Several methods, usually involving separation steps, have been proposed for the determination of phenolic antioxidants. In the past few years, few electroanalytical methods have been described. Generally, chromatographic methods are often used for the analysis of these compounds (Delgado-Zamarren, Gonzalez-Maza, Sanchez-Perez, & Carabias Martınez, 2007; Lee, Lin, Li, & Tsai, 2006). Determination of BHA by preconcentration on a carbon paste electrode has been reported (Wang & Freiha, 1983). HPLC methods with an electrochemical detector have been reported for the determination of BHA (Andrikopoulos, Brueschweiler, Feber, & Taeschleer, 1991). Even though they appear to be sensitive tool for the determination of phenolic antioxidants, these methods are time consuming. Chemically modified electrodes pave way for the reliable and time effective determination of these compounds with greater sensitivity.

The use of conventional electrodes for electrochemical detection has a number of limitations. The limitations are low sensitivity and reproducibility, slow electron transfer reaction, low stability over a wide range of solution composition, surface fouling and high overpotential. The use of mediators showing electrocatalytic activity to modify electrode surfaces constitutes an interesting approach to fabricate sensing surfaces for analytical purposes. In operation, the redox active sites shuttle electrons between the analyte and the electrodes with significant reduction in activation overpotential. A further advantage of the chemically modified electrodes is that they are less prone to surface fouling and oxide formation compared to inert substrate electrodes. A wide variety of compounds have been used as electron transfer mediators for modification of electrode surfaces with various procedures. Metal hexacyanoferrates show interesting redox chemistry that is accompanied by changes in their electrochromic behaviour and have been potentially applied in solid-state batteries, electrode materials, electroanalytical, ion exchange and electrocatalytic purposes (Chen, 1996a, 1996b; Honda & Hayashi, 1987; Kubota & Tamamushi, 1995; Lin & Bocarsly, 1991).

* Corresponding author. Tel.: +91 44 22202717; fax: +91 44 22352494.
E-mail addresses: sriman55@yahoo.com, sriman55@gmail.com (S. Sriman Narayanan).

0308-8146/$ - see front matter © 2009 Published by Elsevier Ltd.
doi:10.1016/j.foodchem.2009.04.104

The modification of electrode surfaces with metal hexacyanoferrate is possible in different ways such as electrodeposition, adsorption, entrapping into a polymer matrice, electroless deposition, mechanically attaching the insoluble metal-hexacyanoferrate or by the reaction between metal hexacyanoferrate with self-assembled monolayer of an organosulfur compound on a gold electrode (Cai, Ju, & Chen, 1995; Gao, Wang, Li, & Zhao, 1991; Golabi & Noor Mohammadi, 1998; Mortimer, 1997; Pournaghi-Azar & Razmi-Nerbin, 1998; Reddy, Dostal, & Scholz, 1996; Xu, Wang, & Chen, 2000). The electrochemical deposition process that leads to the formation of the metal hexacyanoferrate (MHCF) on the electrode surface needs to be carefully controlled and hence it is pertinent to develop a simple and reliable method to fabricate stable MHCFs in short time. Most of the research activities use Au (Cox, Jaworski, & Kulesza, 1991), Pt, or Glassy Carbon (Lin & Bocarsly, 1991) as matrices for the preparation of modified electrodes in electroanalytical studies. These matrices may be replaced by a low cost and better anchoring functionalized surfaces because in this case the attachment of some transition metals, on these surfaces may be performed using a simple chemical method.

Very few reports are available for the determination of BHA using modified electrodes. A nickel pthalocyanin modified carbon paste electrode and a polymer coated glassy carbon electrode for the amperometric determination of BHA were reported (Ruiz, Blazquez, & Pingarron, 1995; Ruiz, Calvo, & Pingarron, 1994;). The simultaneous determination of BHA and TBHQ (tert-butylhydroquinone) at a polypyrrole electrode modified with a nickel pthalocyanin complex is also reported (De La Fuente, Acuna, Vazquez, Tascon, & Batenero, 1999). Our previous works include the use of Silver Hexacyanoferrate, Manganese Hexacyanoferrate modified graphite electrode used for the amperometric determination of BHA (Jayasri & Sriman Narayanan, 2006, 2007). Another new technique was adopted for the fabrication of cobalt hexacyanoferrate electrode using an amine adsorbed graphite powder as the substrate, which was used for the amperometric determination of BHA (Richard Prabakar & Sriman Narayanan, 2006). A similar modification procedure is adopted in the present work for the fabrication of a Nickel Hexacyanoferrate surface modified graphite wax composite electrode (GWCE). The modified electrode was found to have excellent mediation properties and was able to catalyze BHA oxidation effectively.

The present paper describes a method involving the coordination of nickel on a amine adsorbed graphite surface as an electrode matrix and the chemical derivatization of nickel anchored on the electrode to nickel hexacyanoferrate (NiHCF) film. The modification was achieved by adsorbing p-phenylenediamine onto graphite, which was used for making a graphite wax composite electrode. The electrode served as the base over which Ni^{2+} ions were coordinated to the adsorbed amine. It was followed by derivatization of the metal to its stable hexacyanoferrate thin film on the electrode surface. The NiHCF film was effectively used for the amperometric determination of BHA as it was found to have excellent catalytic activity over the oxidation of BHA. Differential pulse voltammetry (DPV) and flow injection technique were effectively used for the determination of the analyte from commercially available potato chips samples spiked with BHA. An amperometric method for the determination of Hydrazine from industrial wastewater samples using the electrode has been reported by us (Richard Prabakar & Sriman Narayanan, 2008).

2. Experimental

2.1. Chemicals and reagents

Graphite powder (1–2 μm) was purchased from Aldrich chemicals, Germany. All other reagents were of analytical grade. All aqueous solutions were prepared using doubly distilled water. Studies on effect of pH were carried out by adjusting the pH using 0.1 M HCl and 0.1 M NaOH solutions. *p*-Phenylenediamine solution (PPD) (10 mM) and $NiCl_2$ solution (0.01 M) were prepared by dissolving appropriate quantity in dry DMF and dry ethanol, respectively. All measurements were done after carefully degassing the solutions with pure nitrogen.

2.2. Flow injection procedure

A custom-built single channel flow cell was used in this work. A solution of 0.1 M $NaNO_3$ in phosphate buffer (pH 7.0) was used as the carrier (C) at a flow rate of 4.0 mL min^{-1}. The solution contained in the sample loop was injected and transported by the carrier stream after the baseline had reached a steady state value.

2.3. Treatment of commercial food sample

BHA spiked in commercially available potato chips (containing no BHA as the preservative) was analysed. The commercial sample was powdered in a mortar and pestle. 1 g of the powdered sample was weighed and spiked with a calculated amount of BHA. About 1 g of the spiked sample was placed in a centrifuge tube. To this 5 mL of 10% methanol solution was added and mechanically shaken for 20 min. The supernatant was collected after centrifuging. This extraction was repeated three times with 5 mL aliquots of 10% methanol solution and the supernatants were added together and concentrated to one third of its volume. The resulting extract was then diluted to the required concentration using the carrier solution (C). The same extract solution was used for differential pulse voltammetric determination and flow injection technique. Similar procedure was extended for other potato chips samples.

2.4. Apparatus

Electrochemical measurements were done using an Electrochemical workstation [CH Instruments (660B)] interfaced to an IBM personal computer with standard three-electrode configuration. The surface modified NiHCF graphite wax composite electrode was used as the working electrode. A platinum wire served as the counter with standard calomel electrode as the reference. Solutions were deoxygenated by bubbling high-purity nitrogen for 5 min prior to electrochemical experiments and all experiments were carried out at 25 °C.

FIA was done using a high pressure Michlins peristaltic pump PP10 (India) and a Rheodyne (Cotati, CA) model 7725 injection valve equipped with a 20 μL loop, coupled to a custom built radial flow cell with a platinum wire counter electrode and a Ag/AgCl ($E_{Ag/AgCl}$ = 0.1939 V vs. SHE) reference electrode connected to Electrochemical workstation CH Instruments (660B) controlled by an IBM personal computer for data acquisition. The reference electrode was filled with 3 M KCl solution. Working electrode was a 3 mm diameter NiHCF graphite paraffin wax composite electrode. The measurements made were converted to the standard calomel electrode values.

2.5. Electrode preparation

The fabrication of the surface modified NiHCF electrode involves four main steps as reported in our previous work (Richard Prabakar & Sriman Narayanan, 2008). In short, a graphite wax composite electrode was prepared using the p-phenylenediamine adsorbed graphite powder. An optimised composition was followed for the preparation of the electrode. The electrode was polished and surface was dipped in $NiCl_2$/EtOH to coordinate the metal cation (Ni^{2+}) to the adsorbed amine. The irreversibly bound metal

cation was then derivatized to its stable insoluble hexacyanoferrate form by cycling in potassium ferrocyanide solution. A stable thin layer was formed on the electrode surface.

3. Results and discussion

3.1. Electrochemical response of the modified electrode

The ions have a considerable role in the electrochemical behaviour of the modified electrode. In order to maintain the electro neutrality of the modified film during the electrochemical process, ions usually enter or leave the immobilized film. So ions have a considerable effect on the electrochemical behaviour of the modified electrode may be indicative of some characteristics of the film, depending on the nature or size of the alkali metal cations in the solution. The effect of different electrolytes on the electrochemical behaviour of the film was investigated by changing the cation and anion in the electrolyte solution. From our previous investigation it was found that 0.1 M $NaNO_3$ produced well defined and resolved peaks. Hence 0.1 M $NaNO_3$ was chosen as the background electrolyte for further electrochemical studies (Richard Prabakar & Sriman Narayanan, 2008).

The cyclic voltammogram obtained for NiHCF film in 0.1 M $NaNO_3$ (pH 7.0) displayed a single and well-defined redox couple (with peak potentials: E_{pa} – 0.330 V, E_{pc} – 0.286 V) in this electrolyte solution. The ratio of I_{pa}/I_{pc} remains almost equal to unity, as expected for a surface-type behaviour. The peak potentials are almost unchanged, and the peak potential separation is at least 25 mV at scan rate of 25 mV s^{-1}. The formal potential for the redox peak appeared at a potential of 0.312 V, at a scan rate of 50 mV s^{-1}. Generally, in this potential range only hexacyanoferrate is electroactive and not the metal cation as the latter requires a less positive potential for electrochemical transformation. Hence the redox peak is attributed to the hexacyanoferrate (II/III) system. It is interesting to note that the value obtained is appreciably lower when compared to previous reports (Pournaghi-Azar & Razmi-Nerbin, 1998).

3.2. Electrocatalytic behaviour of the NiHCF modified electrode

Fig. 1 shows the cyclic voltammograms of the bare and NiHCF modified electrodes in the absence and presence of BHA. As seen in Fig. 1. BHA at the bare graphite electrode is electroactive in this electrolytic solution at a higher overpotential (curve d). The NiHCF modified wax composite electrode in the blank solution (pH 7.0, 0.1 M $NaNO_3$) exhibits a well-behaved redox reaction at 330 mV (curve a). Upon the addition of 1×10^{-4} M BHA, an enhancement in the anodic peak current was observed (curve b). The anodic peak current observed increases with increasing BHA concentration in the solution. The increase in current on the addition of BHA is mainly due to the $Fe(CN)_6^{4-}/Fe(CN)_6^{3-}$ system. The iron in the NiHCF system gets electrochemically oxidised from Fe^{2+} to Fe^{3+}. The oxidised iron centre catalytically oxidises BHA to Tertiary butyl quinone thereby getting converted to the ferro form. This process repeat in a cyclic fashion producing the large anodic current increase.

As seen in Fig. 2a the cyclic voltammogram of the NiHCF modified electrode at various scan rates in the presence of 2.5×10^{-5} M BHA reveal that the catalytic effect of the NiHCF film appeared even at high scan rates of up to 100mV s^{-1} due to a considerable catalytic reaction rate. It can also be noted from Fig. 2a that with increasing scan rate, the peak potential for the catalytic oxidation of BHA shifts to more positive potentials, suggesting a kinetic limitation in the reaction between the redox sites of the NiHCF film and BHA. However, the oxidation current for BHA increased linearly with the square root of the scan rate (inset b), suggesting that

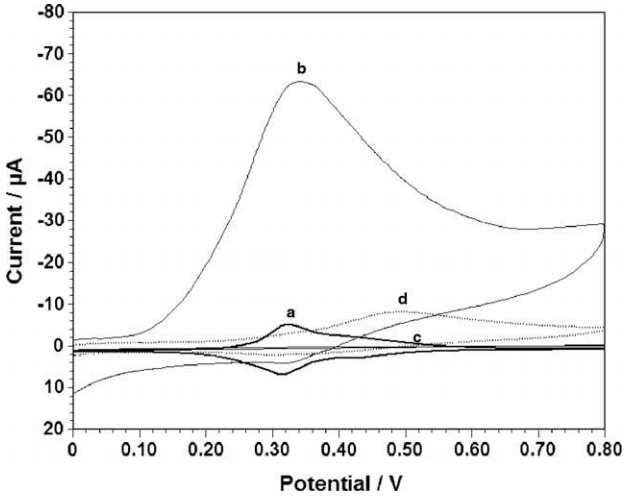

Fig. 1. Cyclic voltammogram in 0.1 M $NaNO_3$ for (a) NiHCF surface modified GWCE, (b) with 2.5×10^{-4} M of BHA at the modified electrode, (c) unmodified GWCE electrode and (d) with 2.5×10^{-4} M of BHA; scan rate 50 mV s^{-1}.

the reaction is mass transfer controlled. Also, a plot of the scan rate–normalised current ($I/v^{1/2}$) versus scan rate (inset c), exhibits linearity typical of an EC_{cat} process.

The influence of pH on the NiHCF modified electrode in the presence of analyte was studied in the pH range of 2–9. As observed in Fig. 2d, a maximum current response was observed at pH 7.0; the reason could be that at low pH, oxidation of BHA could be hindered by the production of H^+ ions. Since H^+ ions are one of the products formed during oxidation of BHA leading to a common ion effect. At pH greater than 7.0, a decrease in catalytic effect was observed. This decrease in alkaline range is also observed for other Prussian blue analogues (Pournaghi-Azar & Datangoo, 2002). The possible reason could be due to the hydrolysis of Fe^{2+} of $[Fe(CN)_6]^{4-}$ to $Fe(OH)_2$. Therefore pH 7.0 was selected as the optimum pH value for this work.

The cyclic voltammetric results lead to the conclusion that the oxidation of BHA at the NiHCF modified electrode could be due to diffusion of BHA to the electrode surface in the solution.

3.3. Hydrodynamic study

Hydrodynamic voltammetry was performed with the NiHCF modified electrode to study the response in dynamic conditions and also to optimise its operational potential for amperometric studies. The resulting steady state current was measured by increasing the potential of the working electrode in steps under stirred condition. The plot of current versus applied potential of the (a) bare electrode and (b) modified electrode in the presence of 1.5×10^{-5} M of BHA is shown in Fig. 3. The current starts to increase from 0.26 V and attains a maximum at 0.37 V. So an operational potential for amperometric studies could be chosen from a range starting from 0.37 V. A potential of 0.4 V was chosen as the operational potential for flow injection analysis studies.

3.4. Flow injection analysis

The NiHCF electrode showed excellent and strong mediation properties that enabled the determination of BHA at low potential. Fig. 4a shows the flow injection response of the NiHCF electrode to BHA at three different concentrations. As shown in the figure three successive additions of 2.98×10^{-5}, 3.96×10^{-5} and 4.95×10^{-5} M of BHA showed a well defined and near constant response. The modified electrode offered a sharp rise in current with every

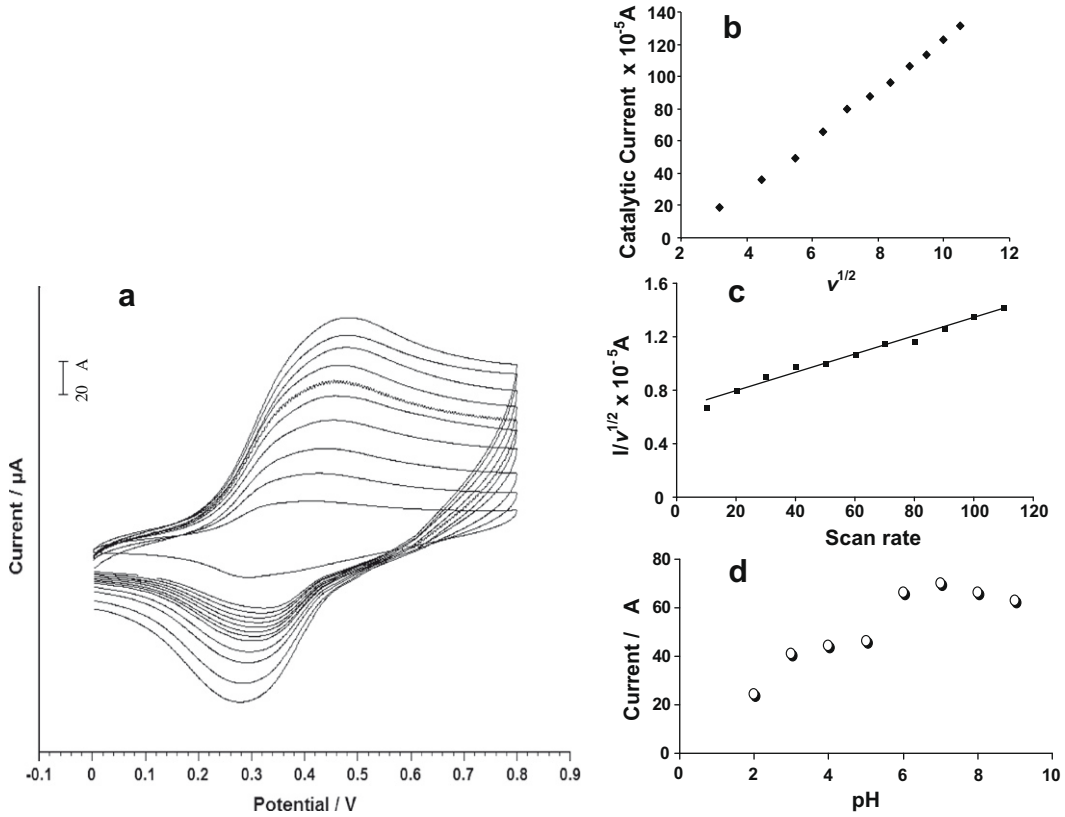

Fig. 2. (a) Dependence of the cyclic voltammetric response at a NiHCF surface modified graphite wax composite electrode on scan rate in 0.1 M $NaNO_3$ (pH 7.0, phosphate buffer solution) solution containing 2.5×10^{-5} M BHA. Scan rate: 10–150 mV s^{-1} with increments of 10 mV s^{-1}, respectively. (b) Variation of the catalytic current with the square root of scan rate. (c) Plot of normalised current vs. scan rate, (d) effect of pH on catalytic current of the NiHCF surface modified GWCE with 4.95×10^{-5} M of BHA; in 0.1 M $NaNO_3$.

addition of BHA. The signal appeared in a response time of less than 4 s. Fig. 4b shows the amperometric response of the modified electrode to equivalent concentrations of BHA recovered from potato chips spiked with BHA. Comparing the results, both appear synonymous with respect to sensitivity and results also confirmed that the detection limits were appreciably low. The NiHCF electrode also offered a highly invariable response over a long period of time. At a fixed potential of 0.4 V the catalytic current observed was also linearly dependent on the BHA concentration in the range 1.2×10^{-6}–1.07×10^{-3} M. Fig. 4c shows that the anodic peak current was linearly dependent on the BHA concentration, with a correlation coefficient better than 0.996 and the detection limit was 6×10^{-7} M.

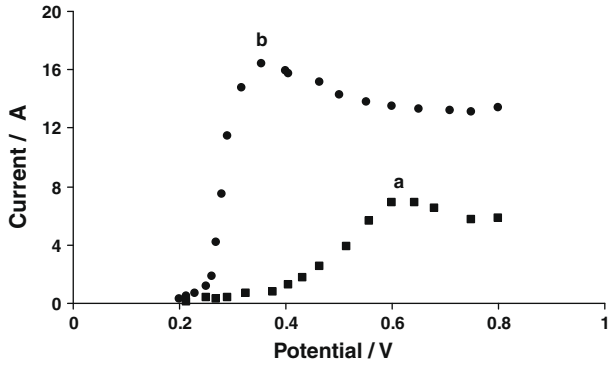

Fig. 3. Hydrodynamic voltammograms of: (a) unmodified GWCE and (b) NiHCF surface modified GWCE for 2×10^{-5} M BHA in 0.1 M $NaNO_3$; pH 7.0 (PBS); stirring rate 300 rpm.

The influence of flow rate of carrier solution was studied. On increasing the flow rate, the response of the sensor decreases and at flow rates higher than 4.0 mL min^{-1}, the response of the modified electrode to 2.48×10^{-5} M of BHA concentration is almost constant (figure not included). Therefore, a flow rate of 4.0 mL min^{-1} was used in all subsequent experiments.

3.5. Precision, linearity and detection limit

Under the selected conditions given above, the response of the NiHCF modified electrode to BHA concentration was linear over the range 1.2×10^{-6}–1.07×10^{-3} M, with a detection limit of 6×10^{-7} M (S/N = 3). The regression equation was I/mV = 1.6913 + 4.972 [BHA/10^{-6} M]. The correlation coefficient was 0.9965. These results further show that the NiHCF modified electrode, compared with the bare graphite electrode, offered a better sensitivity for BHA. It was also found that the NiHCF modified electrode showed good long-term stability in a flow stream. For evaluating the reproducibility of the NiHCF electrode a series of replicate additions of BHA of the same concentration was done and its chrono amperometric response was analysed. A relative standard deviation (RSD) of 2.4% was observed for 30 repetitive injections of 4×10^{-6} M BHA.

To determine the intra- and inter-day precision of this method, a series of seven repetitive injections of BHA containing 4×10^{-6} M were analysed on different days. For repeatability, the relative standard derivations (RSDs) of the peak current were 2.5%. Such good precision reflects the excellent antifouling surface of NiHCF surface modified GWCE. For reproducibility, the RSDs for the peak current (2.8%) show that the proposed method was both stable and reproducible.

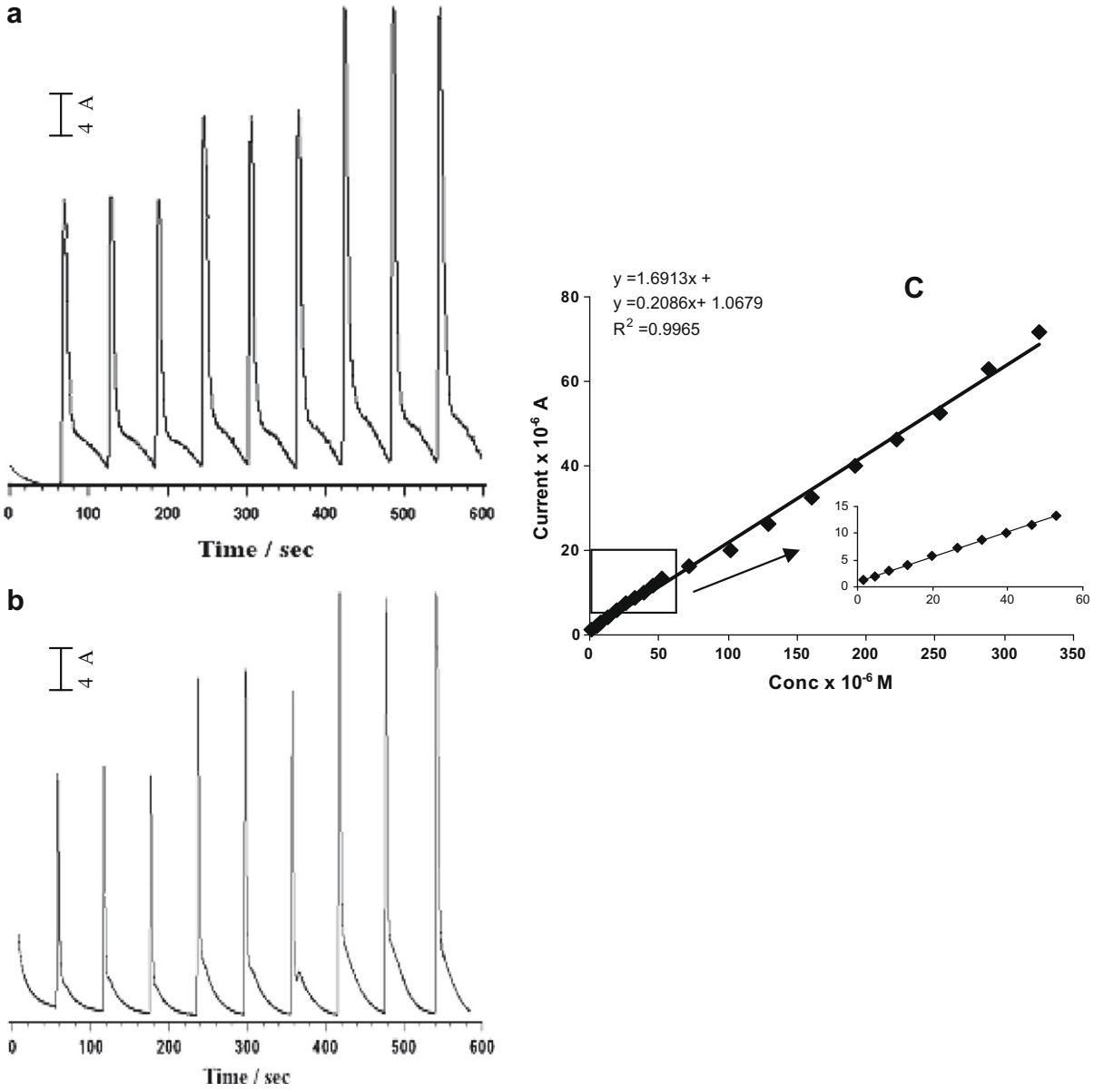

Fig. 4. (a) Flow injection response of the NiHCF modified GWCE at 0.4 V in 0.1 M $NaNO_3$ (pH, 7.0 phosphate buffer) for three replicate additions of 2.98×10^{-5} M, 3.96×10^{-5} M and 4.95×10^{-5} M of BHA from standard sample. (b) Flow injection response of the NiHCF modified GWCE at 0.4 V in 0.1 M $NaNO_3$ (pH, 7.0 phosphate buffer) for three replicate additions of 2.98×10^{-5} M, 3.96×10^{-5} M and 4.95×10^{-5} M of BHA recovered from spiked potato chips sample flow rate 4.0 mL min^{-1}. (c) Calibration plot for variation of catalytic current vs. BHA concentration.

3.6. Interferences

Different substances commonly present in commercial antioxidant mixtures (Citric acid, Propyl gallate (PG), BHT, ascorbic acid and propylene glycol) were tested during the chrono amperometric measurements at the modified electrode (at 0.4 V) in order to check their interference with the BHA signals. A concentration of 200:1 (interferent:BHA) was the maximum ratio tested. Under the experimental conditions described for the determination of BHA at a concentration of 5 μM, citric acid, BHT and propylene glycol showed no significant effect on response even at a interferents to analyte ratio of 1:200, 1:100 and 1:160, respectively.

It was found that ascorbic acid and propyl gallate interfered with BHA determination even with interferents to analyte ratio 0.7:1 and 1:1, respectively. However, in practise, ascorbic acid will be easily cleaned up by the extraction procedure described in the experimental section, because it is water-soluble (hence, its general use in beverages and solid food products). However the interference from propyl gallate could not be eliminated. Further research on improving the selectivity of the modified electrode is in progress.

3.7. Model sample analysis

Model sample analysis was done to evaluate the applicability of the NiHCF modified electrodes utility .The studies were carried out by spiking a known amount of BHA in commercially available potato chips. BHA was extracted as discussed in Section 2.3. Differential pulse voltammetry (DPV) was employed for the determination. Fig. 5 shows the differential pulse voltammetric response of the modified electrode response to increasing additions of BHA. Table. 1 shows the results obtained and the values obtained are an average of five replicate measurements. The

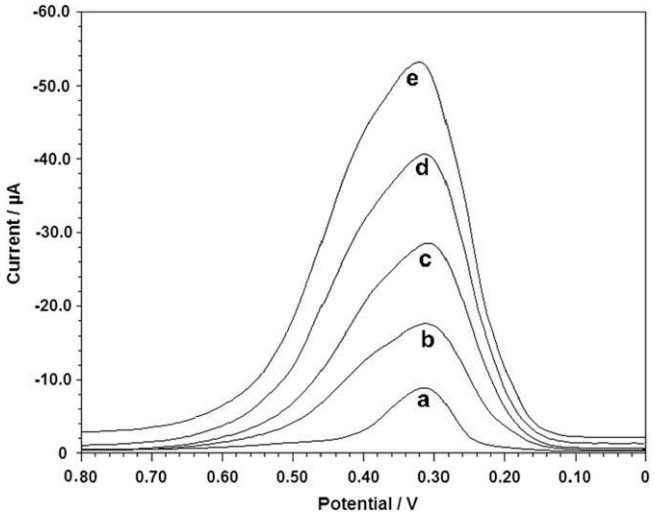

Fig. 5. Differential pulse voltammetric response of the (a) NiHCF surface modified GWCE in 0.1 M $NaNO_3$ (pH 7.0, PBS) for BHA in commercial potato chips sample (Sample a) with successive addition of (b–e) 20 μM of BHA successively in 0.1 M $NaNO_3$, pH 7.0 (phosphate buffer solution).

Table 1
Determination of BHA in spiked potato chips.

Potato chips sample[a]	Concentration of BHA (μM)		Recovery (%)
	Added	Found*	
Sample A	25	24.7 ± 0.7	98.8
	50	49.4 ± 0.6	98.8
	75	75.1 ± 0.7	100
Sample B	25	24.2 ± 0.9	96.8
	50	50.2 ± 0.6	100
	75	74.7 ± 0.8	99.6
Sample C	25	24.9 ± 0.5	99.6
	50	49.9 ± 0.6	99.8
	75	74.8 ± 0.5	99.7

* Average of five replicate measurements ± r.s.d.
[a] Samples A, B and C are potato chips supplied by three different companies.

samples analysed were potato chips obtained from local market containing no added BHA.

4. Conclusion

The results above demonstrated that the NiHCF film was firmly immobilized to the electrode surface and the new approach for fabrication of NiHCF electrode onto an amine adsorbed graphite composite electrode appeared to be stable. The NiHCF electrode effectively catalyzes the oxidation of BHA via a surface layer mediated transfer. The NiHCF modified electrode is stable for long periods that enable it as an effective and rapid sensor for the determination of BHA. Low detection limit and high catalytic effect with lack of electrode surface fouling by the oxidised products of BHA. Hydrodynamic and flow injection analysis show that the NiHCF modified electrode as a definite candidate for the determination of BHA in flow systems and also as a promising tool that can be employed for the routine analysis of BHA from food samples.

Acknowledgment

The authors acknowledge the financial assistance from Centre for Scientific and Industrial Research – Senior Research Fellowship (CSIR-SRF), New Delhi, for the support of this work.

References

Andrikopoulos, N. K., Brueschweiler, H., Feber, H., & Taeschleer, C. (1991). HPLC analysis of phenolic antioxidants, tocopherols and triglycerides. *Journal of American oil Chemists Society, 68*(6), 359–364.
Cai, C. X., Ju, H. Y., & Chen, H. Y. (1995). Cobalt hexacyanoferrate modified microband gold electrode and its electrocatalytic activity of NADH. *Journal of Electroanalytical Chemistry, 397*(2), 185–190.
Chen, S. M. (1996a). Electro polymerization of iron phenanthrolines and voltammetric response for pH and applications on electrocatalytic sulfite oxidation. *Journal of Electroanalytical Chemistry, 401*(1–2), 147–156.
Chen, S. M. (1996b). Electrocatalytic oxidation of thiosulphate by metal hexacyanoferrate film modified electrodes. *Journal of Electroanalytical Chemistry, 417*(1–2), 145–153.
Cox, J. A., Jaworski, R. K., & Kulesza, P. J. (1991). Electroanalysis with electrodes modified by inorganic films. *Electroanalysis, 3*(9), 869–877.
De La Fuente, C., Acuna, J. A., Vazquez, M. D., Tascon, M. L., & Batenero, P. S. (1999). Voltammetric determination of phenolic antioxidant 3-*tert*-butyl-4-hydroxyanisole and *tert*-butlyhydroquinone at a polypyrrole electrode modified with nickel pthalocyanin complex. *Talanta, 49*(2), 441–452.
Delgado-Zamarren, M. M., Gonzalez-Maza, I., Sanchez-Perez, A., & Carabias Martınez, R. (2007). Analysis of synthetic phenolic antioxidants in edible oils by micellar electrokinetic capillary chromatography. *Food Chemistry, 100*(4), 1722–1727.
Furia, T. E. (Ed.). (1980) (2nd ed.). *CRC handbook of food additives* (Vol. II). FL, USA: CRC Press.
Gao, Z., Wang, G., Li, P., & Zhao, Z. (1991). Electrochemical and spectroscopic studies of cobalt hexacyanoferrate film modified electrodes. *Electrochimica Acta, 36*(1), 147–152.
Golabi, S. M., & Noor Mohammadi, F. J. (1998). Electrocatalytic oxidation of Hydrazine at cobalt hexacyanoferrate-modified glassy carbon, Pt and Au electrodes. *Journal of Solid State Electrochemistry, 1*, 30–37.
Grice, H. C. (1988). Safety evaluation of butylated hydroxyanisole (BHA) from the perspective of effect on fore stomach and oesophageal squamous epithelium. *Food and Chemical Toxicology, 26*(8), 717–723.
Honda, K., & Hayashi, H. (1987). Prussian Blue containing Nafion composite films as rechargeable battery. *Journal of Electrochemical Society, 134*(6), 1330–1334.
Hudson, B. J. F. (1990). *Food antioxidants*. London: Elsevier. pp. 5–7.
Jayasri, D., & Sriman Narayanan, S. (2006). Electrocatalytic oxidation and amperometric determination of BHA at graphite–wax composite electrode with silver hexacyanoferrate as electrocatalyst. *Sensors and Actuators B, 119*(1), 135–142.
Jayasri, D., & Sriman Narayanan, S. (2007). Manganese (II) hexacyanoferrate based renewable amperometric sensor for the determination of butylated hydroxyanisole in food products. *Food Chemistry, 101*(2), 607–614.
Kubota, L. T., & Tamamushi, R. (1995). Voltammetry in low temperature liquid solutions and frozen media hexacyanoferrate (II/III) redox systems in aqueous LiCl solution at temperatures between 170 K and 300 K. *Journal of Electroanalytical Chemistry, 380*(1–2), 279–282.
Lee, M. R., Lin, C. Y., Li, Z. G., & Tsai, T. F. (2006). Simultaneous analysis of antioxidants and preservatives in cosmetics by supercritical fluid extraction combined with liquid chromatography–mass spectrometry. *Journal of Chromatography A, 1120*(1–2), 244–251.
Lin, C., & Bocarsly, A. (1991). Catalytic electro oxidation of hydrazine at the nickel hexacyanoferrate modified electrode: Can an array of surface bound one-electron redox centers act in concert? *Journal of Electroanalytical Chemistry, 300*(1–2), 325–345.
Mortimer, R. J. (1997). Electrochromic materials. *Chemical Society Reviews, 26*(3), 147–156.
Pournaghi-Azar, M. H., & Datangoo, H. (2002). Electrochemical characteristics of an aluminum electrode modified by a palladium hexacyanoferrate film, synthesized by a simple electroless procedure. *Journal of Electroanalytical Chemistry, 523*(1–2), 23–26.
Pournaghi-Azar, M. H., & Razmi-Nerbin, H. (1998). Voltammetric behavior and electrocatalytic activity of aluminum electrode modified with nickel and nickel hexacyanoferrate films, prepared by electroless deposition. *Journal of Electroanalytical Chemistry, 456*(1–2), 83–90.
Reddy, S. J., Dostal, A., & Scholz, F. (1996). Solid state electrochemical studies of mixed nickel–iron hexacyanoferrates with the help of abrasive stripping voltammetry. *Journal of Electroanalytical Chemistry, 403*(2), 209–212.
Richard Prabakar, S. J., & Sriman Narayanan, S. (2006). Surface modification of amine-functionalized graphite for preparation of cobalt hexacyanoferrate (CoHCF)-modified electrode: An amperometric sensor for determination of butylated hydroxyanisole (BHA). *Analytical and BioAnalytical Chemistry, 386*(7–8), 2107–2115.
Richard Prabakar, S. J., & Sriman Narayanan, S. (2008). Amperometric determination of hydrazine using a surface modified nickel hexacyanoferrate graphite electrode fabricated following a new approach. *Journal of Electroanalytical Chemistry, 617*(2), 111–120.
Robards, K., & Dilli, S. (1987). Analytical chemistry of synthetic food antioxidants. A review. *Analyst, 112*(7), 933–943.
Ruiz, M. A., Blazquez, M. G., & Pingarron, J. M. (1995). Electrocatalytic and flow injection of the antioxidant *tert*-butlyhydroxyanisole at a nickel pthalocyanin polymer modified electrode. *Analytica Chimica Acta, 305*(1–3), 49–56.

Ruiz, M. A., Calvo, M., & Pingarron, J. M. (1994). Catalytic voltammetric determination of the antioxidant *tert*-butylhydroxyanisole (BHA) at a nickel pthalocyanin modified carbon paste electrode. *Talanta, 41*(2), 289–294.

Wang, J., & Freiha, B. H. (1983). Preconcentration and differential pulse voltammetry of butylated hydroxy anisole at a carbon paste electrode. *Analytica Chimica Acta, 154*, 87–94.

Witschi, H. C. (1986). Enhanced tumor development by butylated hydrotoluene (BHT) in the liver, lung and gastrointestinal tract. *Food and Chemical Toxicology, 24*(10–11), 1127–1130.

Xu, J. J., Wang, C., & Chen, H. Y. (2000). Electrochemical characteristics of nickel hexacyanoferrate monolayer anchoring to bi-(2-aminoethyl)-aminodithio carboxyl acid self assembled film-modified electrodes. *Analytical Science, 16*(2), 231–235.

Food Chemistry 118 (2010) 456–461

Contents lists available at ScienceDirect

Food Chemistry

journal homepage: www.elsevier.com/locate/foodchem

Analytical Methods

Solid-phase microextraction gas chromatography–mass spectrometry (HS-SPME-GC–MS) determination of volatile compounds in *orujo* spirits: Multivariate chemometric characterisation

S. García-Martín *, C. Herrero, R.M. Peña, J. Barciela

Departamento de Química Analítica, Nutrición y Bromatología, Facultad de Ciencias, Universidad de Santiago de Compostela, Av. Alfonso X El Sabio s/n, 27002 Lugo, Spain

ARTICLE INFO

Article history:
Received 4 September 2008
Received in revised form 14 April 2009
Accepted 26 April 2009

Keywords:
Volatile compounds
Orujo spirits
Headspace solid-phase microextraction
Gas chromatography–mass spectrometry
Chemometrics

ABSTRACT

A headspace solid-phase microextraction gas chromatography mass spectrometric procedure (HS-SPME-GC–MS) was developed and applied in order to determine 22 volatile compounds (including alcohols, esters, aldehydes and terpenes) in different *orujo* spirit samples from the Geographic Denomination "*Orujo de Galicia/Augardente de Galicia*". The *orujo* samples considered in this study were elaborated from *Albariño* variety grapes grown in the *Rías Baixas* restricted geographical area, and *Albariño* variety grapes grown in other geographical areas of Galicia (NW Spain) using two of the traditional distillation techniques: alembic and steam distillation. HS-SPME adequate results were obtained using a 65 μm carbowax-divinylbencene fibre during a headspace extraction at 40 °C with constant magnetic stirring for 15 min, and after a 5 min period of pre-equilibrium time. Desorption was performed directly in the gas chromatograph injector port for 5 min at 250 °C using the splitless mode. The applied method was demonstrated to be sensible, accurate, precise, and linear over more than one order of magnitude. Multivariate chemometric techniques (such as cluster analysis, principal component analysis and linear discriminant analysis) were used to characterise the *orujo* samples according to the geographical origin of the grapes and the distillation system employed in their elaboration on the basis of the chemical information provided for their volatile composition data.

1. Introduction

The alcoholic beverage *orujo* is produced in Galicia (NW Spain) by distillation of fermented grape pomace. Galicia is the only region in Spain which could obtain a geographic denomination for *orujo* alcoholic distillates, in the same category as French *marcs*, Italian *grappas*, Portuguese *bagaceiras* and Greek *tsipouros* (European Regulation, EEC, 1989). This beverage has come to be a product of an important economic interest for producers and not merely as a complementary activity to wine elaboration.

The resulting *orujo* distillates undergo strict quality controls established by the Directive Council of the Geographic Denomination "*Orujo de Galicia/Augardente de Galicia*" (DOG, 1993). This Council defined the origin of the raw material, the authorised grape varieties, the geographical production areas, and several other characteristics which are necessary in order to be classified as a quality product under the brand "*Orujo de Galicia*". Among these, the concentration limits of different volatile compounds in the distilled spirit (ethanol, methanol, the total content of higher alcohols, ethyl acetate, and acetaldehyde) must be determined to ensure the product meets these standards.

More than 300 different compounds are present in *orujo* distillates, mainly alcohols, esters, carboxylic acids, aldehydes and acetals. These compounds produce key notes which characterise the flavour and aroma of these beverages. There are many factors in the production of distillates which influence the sensorial characteristics appreciated in the final commercial products: the raw material, the different distillation systems and the distillate maturation in wood (when this takes place) (Silva, Macedo, & Malcata, 2000). In the case of an unaged distillate, this set of compounds is composed of the volatile substances present in the grapes and of the ones formed either during fermentation or generated during distillation (Silva & Malcata, 1999; Silva, Malcata, & De Revel, 1996). Some of these compounds are present in relatively large amounts and can be determined by direct gas chromatography. Other compounds are present at much lower concentrations. Therefore, the determination of these constituents often requires the use of sophisticated preconcentration procedures before gas chromatography.

Chemometric pattern recognition techniques have been widely applied in food chemistry (Brown, Bear, & Blank, 1992; Forina & Lanteri, 1984) to elucidate the chemical information provided for

* Corresponding author. Tel.: +34 982 285900; fax: +34 982 285872.
E-mail address: sagrario.garcia.martin@usc.es (S. García-Martín).

0308-8146/$ - see front matter © 2009 Elsevier Ltd. All rights reserved.
doi:10.1016/j.foodchem.2009.04.105

the different multicomponent analytical techniques. Since the pioneering works done by Kwan, Kowalski, and Skogerboe (1979) and Kwan and Kowalski (1980) on the classification of wines of *Vitis vinifera* cv. Pinot Noir from France and the United States, a number of examples reported in previous studies demonstrate the useful combination of chemical analysis and chemometrics to solve different problems in a variety of food products. These include the characterisation of the geographic classification of olives (Pinheiro & Esteves da Silva, 2005), ciders (Alonso-Salces, Guyot, et al., 2004; Alonso-Salces, Herrero, et al., 2004), coffees (Rocha, Maeztu, Barros, Cid, & Coimbra, 2003; Zambonin, Balest, De Benedetto, & Palmisano, 2005) and wines (Jurado et al., 2008; Martí, Busto, & Guasch, 2004), etc.

In this work, a headspace solid-phase microextraction (HS-SPME) and gas chromatography-selective ion monitoring/mass spectrometry (GC-SIM/MS) procedure was applied in order to determine 22 volatile compounds (alcohols, esters, aldehydes and terpenes) in *orujo* spirit samples from the Geographic Denomination "*Orujo de Galicia/Augardente de Galicia*". Using the chemical information obtained and applying multivariate chemometrical tools–such as cluster analysis, principal component analysis and linear discriminant analysis–the *orujo* samples were characterised according to their geographical and botanical origins, and also to the distillation system employed in their elaboration.

2. Experimental

2.1. Orujo samples

Thirty commercial *orujo* spirit samples that were provided by the Directive Council of the Geographic Denomination "*Orujo de Galicia/Augardente de Galicia*" in order to guarantee their geographical origin and authenticity were used in this study. All samples were *orujo* monovarietal spirits (2004 vintage) obtained from the distillation of *Albariño* variety grapes. Nine of the samples were obtained from the alembic distillation of grapes grown in the *Rías Baixas* restricted geographical area (for identification purposes, these were coded as class 1). The remaining twenty one samples were obtained using steam distillation: 11 of them (coded as class 2) from grapes grown in the *Rías Baixas* restricted geographical area and the other 10 (coded as class 3) from grapes grown any place in Galicia other than the *Rías Baixas* area. All samples were collected in 400 mL glass bottles and stored at 4 °C before analysis.

2.2. Reagents

All volatile compound standards such as alcohols: 1-propanol, 2-methyl-1-propanol, 3-methyl-1-butanol, 2-phenylethanol, 3-octanol (used as an internal standard); esters: ethyl hexanoate, ethyl lactate, ethyl octanoate, ethyl decanoate, diethyl succinate, 2-phenyl ethyl acetate, ethyl dodecanoate, ethyl tetradecanoate; acids: acetic, hexanoic, octanoic, decanoic; aldehydes: benzaldehyde; and terpenes: linalool, α-terpineol, citronellol, nerol, geraniol, were supplied by Aldrich Flavor and Fragrances (Alcobendas, Madrid, Spain). The sodium chloride, used to control the ionic strength, was supplied by Panreac (Barcelona, Spain). Absolute ethanol (Panreac, Barcelona, Spain) and ultra-pure Milli-Q water (Millipore Co., Bedford, USA) were used as solvents. All solvents and reagents used were analytical grade.

Stock standard solutions of 10^3 or 10^4 mg $L^{-1}$of each component were prepared by dissolving the pure standards in 40% (v/v) ethanol. Then they were stored at 4 °C. Working standard solutions of each compound were prepared daily by mixing an aliquot of each individual solution and diluting them with ultrapure water to obtain a final ethanol content of 10% (v/v).

2.3. Apparatus and methods

2.3.1. Analytical determinations

Twenty two volatile compounds such as alcohols: 1-propanol, 2-methyl-1-propanol, 3-methyl-1-butanol, 2-phenylethanol, 3-octanol (used as an internal standard); esters: ethyl hexanoate, ethyl lactate, ethyl octanoate, ethyl decanoate, diethyl succinate, 2-phenyl ethyl acetate, ethyl dodecanoate, ethyl tetradecanoate; acids: acetic, hexanoic, octanoic, decanoic; aldehydes: benzaldehyde; and terpenes: linalool, α-terpineol, citronellol, nerol, geraniol were analysed using HS-SPME-GC–MS All determinations were carried out in triplicate and the average values were calculated.

2.3.2. HS-SPME

A manual fibre-holder and two types of fibres–100 μm polydimethylsiloxane (PDMS) and 65 μm carbowax-divinylbenzene (CW-DVB)–were obtained from Supelco (Bellefonte, PA, USA). In all cases, the fibres were conditioned before use by inserting them into the GC injector port for 1 h at 250 °C (PDMS) and for 30 min at 220 °C (CW-DVB). Between injections, the fibres were desorbed for 10 min at 250 °C in split mode in order to prevent any contamination. Due the high ethanol content of the *orujo* spirits (40% v/v) a dilution to 10% ethanol before solid-phase microextraction was necessary. The SPME process was carried out by introducing 6 mL of diluted *orujo* spirit into a 12 mL PTFE coated septum-closed vial; 1.5 g of sodium chloride and 20 mg L^{-1} of the internal standard (3-octanol) were added. SPME extractions were performed by inserting the fibre in the headspace for 15 min at 40 °C using continuous magnetic stirring of the liquid phase at 1100 rpm. Before the extraction, the sample with 25% (w/v) of NaCl was maintained at 40 °C for 5 min in order to establish equilibrium between headspace and sample. After each extraction, the fibre was inserted into the GC injector port using a 0.75 mm i.d. liner (in order to improve the GC resolution). Desorption time and temperature were 5 min and 250 °C, respectively. All experiments and sample measurements were carried out in triplicate and the average values were calculated.

2.3.3. GC–MS

Chromatographic analysis were performed using an Agilent 6890 gas chromatograph equipped with a mass spectrometric detector (MSD) model 5973 N (Agilent Technologies Deutschland Gmbh, Waldbronn, Germany). The capillary column used was a HP-Innowax (30 m × 0.25 mm i.d., film thickness 0.25 μm) from Agilent Technologies. The gas chromatographic operation conditions were as follows. The injector temperature was 250 °C; the carrier gas employed was Helium (purity 99.9995%) at a constant flow rate of 1 mL min^{-1}. The oven temperature program was 5 min at 40 °C, then 1.5 °C min^{-1} up to 80 °C, and finally 5 °C min^{-1} up to 200 °C. This final temperature was maintained for 0.5 min. The injection was made in splitless mode for 2 min at a temperature of 250 °C and using a SPME inlet guide and pre-drilled Thermogreen LB-2 septa from Supelco (Bellefonte, PA, USA).

The mass spectrometer was operated in electron impact mode with the following conditions. The source temperature was 230 °C; the quadrupole temperature selected was 150 °C and the relative electron multiplier voltage (EM) applied was 400 V with a resulting voltage of 1553 V. In order to improve the detection limits, the selected ion monitoring (SIM) mode was used. The data acquisition was carried out with the HP-Chemstation software version D.00.00.38 (Agilent Technologies). The compounds were identified using the NIST98 version 2.0 mass spectra library. Each compound was further confirmed by comparing its mass spectra,

linear retention index (LRI), and retention times with those obtained for the standards.

2.3.4. Data analysis and chemometrical procedures

A matrix ($X_{30\times22}$) with the chemical data was constructed. The rows of this matrix were the different *orujo* samples (objects) and the columns were the 22 variables (features) measured for each object. Therefore, each *orujo* sample could be represented in the 22-multidimensional space by a data vector (an assembly of 22 features). Data vectors belonging to the different categories were analysed using chemometrical procedures (Latorre, Peña, Garcia, & Herrero, 2000; Padin et al., 2001; Rodriguez et al., 2006). Cluster analysis (CA) and principal component analysis (PCA) were applied to obtain visualisation in a reduced dimension of the structure of the data. The linear discriminant analysis (LDA) was focused in order to develop a classification model to differentiate samples in function of classes 1, 2 or 3. The statistical and chemometrical analysis were performed by means of the following statistical software packages: Statgraphics (Statgraphics plus 5.1, 2000), Parvus (Forina, Lanteri, Armanino, Casolino, & Casale, 2007) and SPSS (SPSS for windows v. 15.0, 2006).

3. Results and discussion

3.1. HS-SPME extraction

Two fibre coatings, PDMS and CW-DVB, were used in order to determine which coating was more appropriate for the determination of flavor volatiles present in *orujo* spirits. Considering the peak areas, CW-DVB fibre provided the best results except for terpenes where the performance of both fibres was similar.

In order to optimise the SPME method, some parameters controlling the performance of the extraction were taken into account. The variables studied and the ranges considered were sample volume (6–10 mL), extraction temperature (30–50 °C), amount of NaCl to control the ionic strength (25–30% w/v), extraction time (5–25 min), pre-equilibrium time (0–10 min), desorption temperature (150–250 °C) and desorption time (1–5 min). The best conditions were as follows: 6 mL of the *orujo* sample diluted to 10% ethanol and 25% of NaCl were placed into a 12 mL PTFE coated septum-closed vial. SPME extractions were performed by inserting the fibre in the headspace for 15 min at 40 °C using continuous magnetic stirring of the liquid phase at 1100 rpm. Before the extraction, the sample with 25% (w/v) of NaCl was maintained at 40 °C for 5 min in order to establish equilibrium between headspace and sample. Desorption time and temperature were 5 min and 250 °C, respectively. The optimisation of the extraction procedure has been described in detail in previous work (Peña, Barciela, Herrero, & Garcia-Martín, 2008).

3.2. Performance of the method

The performance characteristic of the method such as linearity, precision, recovery and limit of detection and quantification, were tested. The results demonstrated that the proposed method is sensible (with detection limits between 0.0045 and 0.2399 mg L^{-1}), precise (with coefficients of variation in the range 0.99–8.18%) and linear over more than one order of magnitude. The developed method presented recoveries comprised between 76.0% and 112.4%.

3.3. Volatile profiles of orujo samples

The results of the HS-SPME-GC–MS determination for the 22 volatile compounds in *orujo* samples are summarised in Table 1. Mean, standard deviation, maximum and minimum values for each feature are presented. Alcohols constitute the group of compounds with the highest concentration in distilled beverages and they are responsible for their flavouring aromas. The level of these compounds depends on the grape variety, fermentation conditions and distillation technique. The predominant alcohol in *orujo* spirits was 3-methyl-1-butanol (isoamyl alcohol) with a mean value of 448.8 mg L^{-1}. This alcohol together with 2-methyl-1-butanol quantitatively accounts for the most of the higher alcohols and they may be considered predictors of sensory character in distilled products. Other alcohols like 2-methyl-1-propanol and 1-propanol are present in *orujo* spirits at high mean concentrations (170.5 and 146.7 mg L^{-1}, respectively). Another alcohol studied: 2-phenyl ethanol (mean value found in *orujo* samples 5.019 mg L^{-1}) is an aromatic alcohol that introduces a pleasant rose like aroma to

Table 1
Results of volatile compounds determined. All results are in mg L^{-1}.

	Rías Baixas, alembic				*Rías Baixas*, steam distillation				Non-*Rías Baixas*, steam distillation			
n	9				11				10			
Compound	Mean	SD	Max	Min	Mean	SD	Max	Min	Mean	SD	Max	Min
1-Propanol	161.6	37.6	225.2	124.5	158.2	63.2	304.3	92.40	120.1	24.1	154.8	93.36
2-Methyl-1-propanol	169.7	33.9	223.0	105.0	196.6	57.4	336.1	135.7	145.3	34.0	211.3	102.3
3-Methyl butanol	415.9	43.6	478.8	362.3	449.2	96.4	599.1	310.1	481.3	138.9	771.9	294.5
Ethyl hexanoate	4.118	1.677	6.844	1.155	2.488	1.137	5.036	1.112	3.243	0.654	4.646	2.307
Ethyl lactate	68.06	22.18	107.0	40.47	98.96	58.05	212.2	39.83	141.9	38.2	206.1	86.88
Ethyl octanoate	13.67	11.75	29.08	1.401	3.121	1.555	5.660	0.635	5.873	2.345	9.099	1.986
Acetic acid	134.7	46.4	198.6	61.06	71.61	55.48	186.9	19.51	177.6	187.6	661.4	23.69
Benzaldehyde	0.847	0.279	1.240	0.479	2.220	1.297	4.456	0.871	2.130	1.016	4.401	0.844
Linalool	2.041	0.530	2.936	1.331	1.692	0.721	2.860	0.658	1.133	0.239	1.431	0.550
Ethyl decanoate	56.84	60.26	178.8	1.604	8.581	13.460	48.46	0.647	13.66	7.68	26.76	1.329
Diethyl succinate	2.034	0.709	2.675	0.920	6.470	5.335	16.70	0.763	12.08	3.41	18.94	6.690
α-Terpineol	0.580	0.181	0.856	0.347	0.535	0.177	0.811	0.276	0.477	0.135	0.724	0.284
Citronellol	0.120	0.057	0.205	0.024	0.354	0.153	0.645	0.147	0.275	0.087	0.431	0.163
Nerol	0.069	0.053	0.180	ND	0.107	0.089	0.266	0.023	0.050	0.038	0.098	0.008
2-Phenyl ethyl acetate	0.273	0.138	0.606	0.125	0.286	0.095	0.470	0.139	0.421	0.426	1.588	0.170
Ethyl dodecanoate	96.62	69.00	211.2	6.582	2.616	5.396	18.75	0.330	7.897	13.430	41.88	0.945
Geraniol	0.576	0.436	1.388	0.268	0.436	0.250	0.976	0.136	0.372	0.152	0.629	0.216
Hexanoic acid	3.505	1.445	6.613	1.968	2.792	2.048	7.354	1.250	4.498	2.054	7.735	1.242
2-Phenyl ethanol	3.217	1.626	7.032	1.234	4.040	2.650	8.325	1.115	7.800	3.585	16.53	3.001
Ethyl tetradecanoate	9.401	6.066	20.86	4.469	2.242	2.538	8.685	0.432	1.551	1.248	4.595	0.535
Octanoic acid	5.088	1.697	7.898	3.194	7.234	8.208	28.64	1.930	11.40	8.19	28.45	1.861
Decanoic acid	5.221	1.999	8.630	3.377	7.033	7.192	24.52	1.910	12.71	10.18	31.94	2.276

distillates. The distillation technique plays an important role in the content of this alcohol.

Fatty acid esters are probably the group of compounds that contribute the most to the distillates aroma and quality. Ethyl esters are produced during the fermentation. They gain access to the spirits and increase during ageing. Grape variety is an important factor in determining the concentration of ethyl esters in these beverages (Milicevic, Banovic, Kovacevic-Ganic, & Gracin, 2002). The results obtained for these compounds in the analysed samples showed values in the range from 3.283 mg L^{-1} for ethyl hexanoate to 35.71 mg L^{-1} for ethyl dodecanoate.

Acetic acid esters, like 2-phenyl ethyl acetate, isoamyl acetate and hexyl acetate, are responsible for the flowery and fruity aroma of distillates while ethyl acetate, ethyl lactate and diethyl succinate derive mainly from bacterial spoilage of the distillate marc. The concentration obtained for 2-phenyl ethyl acetate, ethyl lactate and diethyl succinate was 0.327, 103.0 and 6.862 mg L^{-1}, respectively. The low value of ethyl lactate means that the maintenance of the pomace was satisfactory and no undesirable lactic and acetic fermentations took place.

Long chain fatty acids (such as hexanoic, octanoic and decanoic acids) are a group of compounds that affect the flavor to a lesser extent than the ones previous described. The concentration obtained for these acids was 3.598 mg L^{-1}, 7.906 and 8.321 mg L^{-1} for hexanoic, octanoic and decanoic acids, respectively. Other volatile carboxylic acids, such as acetic, showed a mean concentration of 128.0 mg L^{-1}. Benzaldehyde was also analysed because the formation of this compound is associated with microbial development during the ensilage of grape pomace. The mean concentration obtained for the samples measured was 1.732 mg L^{-1}.

Terpenes are another very important chemical group which has an important effect on flavor and aroma. These compounds are present in the grapes and can be used for varietal differentiation of wines and other related products. Five terpenic alcohols were identified in *orujo* samples: linalool, α-terpineol, citronellol, nerol and geraniol. The mean concentrations were 1.622 mg L^{-1} and 0.075 mg L^{-1} for linalool and nerol, respectively. There was only one sample in which nerol was not detected; thus, it is obvious that the spirits produced from *Albariño* grape pomace are characterised for their intense aromas.

In spite of certain differences in the mean values, there are no significant differences in the volatile levels of the *orujo* samples according to the distillation technique employed or to the geographical origin of the grapes. The examination of the box-whisker plots constructed for each individual variable showed an overlap between ranges of concentration. When measured alone, none of the variables, were able to discriminate between different classes of *orujo*. Therefore, a multivariate approach must be evaluated.

3.4. Data reduction and visualisation

When a multivariate data set is analysed, the first approach is the search for natural groupings in the samples. For this goal two unsupervised chemometric procedures were applied: principal component analysis (PCA) and cluster analysis (CA).

3.4.1. Principal component analysis

Principal component analysis was used to provide a partial visualisation of data in a reduced-dimension plot. The principal components or eigenvectors are orthogonal and they are a linear combination of the original variables (Jolliffe, 2002). PCA was performed on the autoscaled data to avoid the effect of different size variables. The study of loadings for the variables in the first two principal components (Fig. 1) shows that fatty acids, ethyl lactate and diethyl succinate, were the dominant features in the first principal component which represented 29.10% of the total variability.

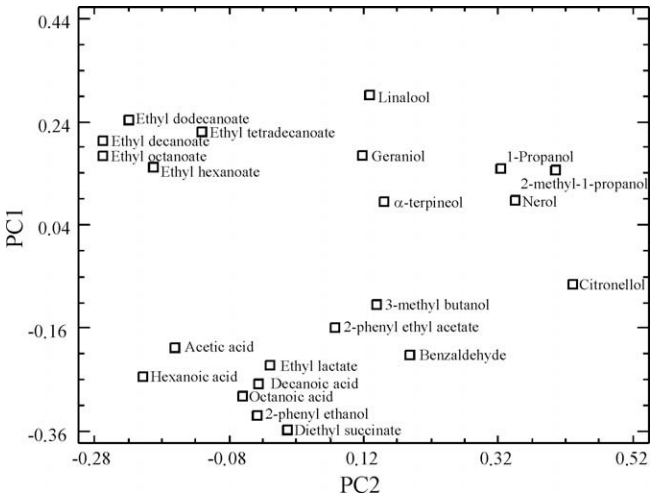

Fig. 1. Loadings of the variables in the first two principal components.

1-propanol, 2-methyl-1-propanol, citronellol and nerol (positive part of PC2) and fatty acid ethyl esters (negative part) dominate the second principal component which accounted for 17.41% of the total data variance. Chemically, the first principal component or eigenvector can be interpreted in relation to compounds that do not have a significant influence in the flavor of *orujo* samples (fatty acids); some of them are related to the bacterial spoilage of these beverages (ethyl lactate and diethyl succinate). Major contributions to the second principal component are from analytes related to the grape variety, fermentation conditions and distillation procedure such as alcohols, terpenes and fatty acids ethyl esters. When the score analysis of *orujo* samples on the space formed by the first three principal components (62.1% of total variability accounted) was carried out, a natural separation between the three classes of *orujo* samples considered was detected. As can be seen in Fig. 2, *orujo* samples of class 1 formed a separated group in the positive part of PC1. Samples of class 3 formed another group in the negative part of the first principal component. Samples from class 2 are located in a point between the two previous classes. Since the score plot of Fig. 2 provides a reduced vision in three dimensions of the sample 22-dimensional space, it can be concluded that the three classes of *orujo* are distributed in different areas in the high dimensional space considered.

3.4.2. Cluster analysis

Cluster analysis (CA) is an unsupervised chemometric technique that reveals the natural groupings existing between samples char-

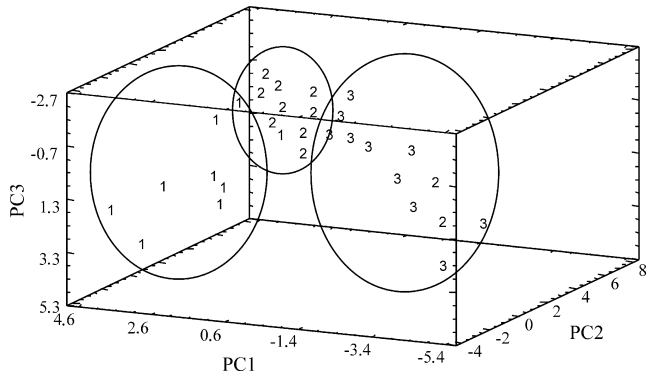

Fig. 2. PCA score plot of the *orujo* samples. 1: *Albariño-Rías Baixas*-alembic; 2: *Albariño-Rías Baixas*-steam distillation; 3: *Albariño*-Galicia-steam distillation.

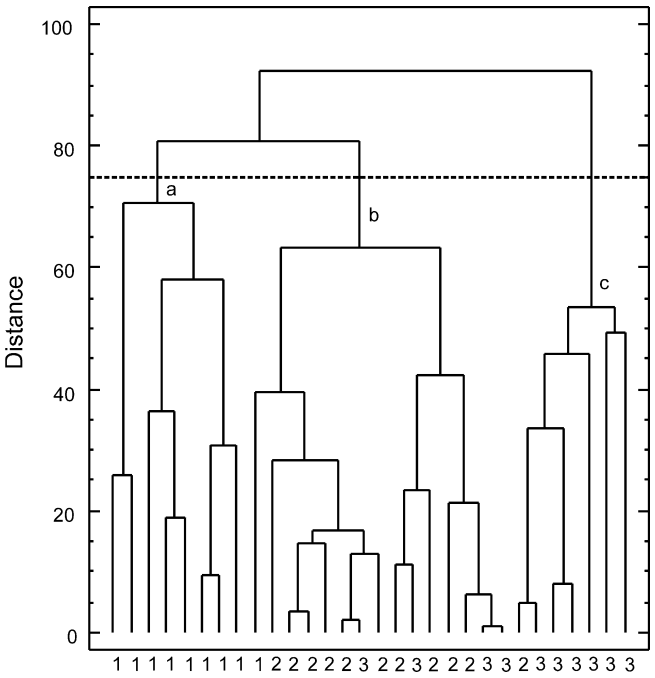

Fig. 3. Dendogram obtained for cluster analysis (Ward's method) of the *orujo* samples. 1: *Albariño-Rías Baixas*-alembic; 2: *Albariño-Rías Baixas*-steam distillation; 3: *Albariño*-Galicia-steam distillation.

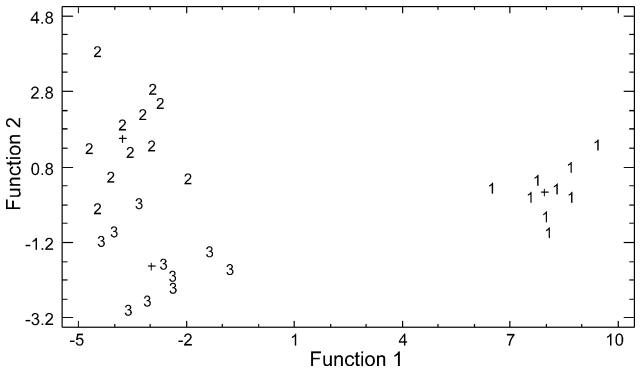

Fig. 4. Linear discriminant plot of the *orujo* samples. 1: *Albariño-Rías Baixas*-alembic; 2: *Albariño-Rías Baixas*-steam distillation; 3: *Albariño*-Galicia-steam distillation.

Table 2
Classification of *orujo* samples using LDA in validation set.

Category	1	2	3	% Correct classification
1	9	0	0	100
2	0	10	1	90.9
3	0	1	9	90.0

acterised by the values of a set of measured variables. CA is commonly applied together with PCA to study the structure of a data set before applying other multivariate pattern recognition procedures with classification purposes. In the present work, CA was applied to the autoscaled data to avoid the variable size; the similarities between samples were calculated on the basis of the Euclidean distance, whereas Ward's method was used as a linkage procedure to establish the clusters (Massart & Kaufman, 1993). The results achieved are presented in a graphic mode as a dendrogram (see Fig. 3). At a distance level of 75, three clusters (coded a-c) can be identified. From the left, the first cluster (cluster a) is a group made of class 1 samples. The second cluster (b) is mainly formed by samples from class 2, even though four class 3 samples were also present. The last cluster (c) includes the other remaining samples of class 3 plus one sample coded as 2. This chemometric technique demonstrated (as well as PCA) that there exists a certain overlap between categories 2 and 3. The two unsupervised displaying procedures used, PCA and CA, produced consistent results for the study of latent structures in the *orujo* samples data set. It can be concluded that the volatile compounds data may provide enough information to develop classification systems to differentiate different kinds of *orujo* samples of class 1, 2, and 3.

3.5. Pattern recognition analysis: linear discriminate analysis

In this section, volatile data of the *orujo* samples were processed by a chemometrical pattern recognition procedure in order to develop a classification rule to relate the volatile compounds content of the analysed *orujo* samples with the geographical origin of the grapes and the distillation procedure employed in their elaboration. Linear discriminant analysis (LDA) was applied to search for optimal linear boundaries between categories in the 22-dimensional space. The discriminant functions are established to achieve the highest discrimination among the given categories, maximising the ratio between-class variance to within-class variance in any particular data set to guarantee the maximal class separability (Vandeginste et al., 1998). LDA was operated over the autoscaled data matrix $X_{30\times22}$ to characterise *orujo* samples in the established categories 1, 2 and 3. In order to validate the classification rule developed for this study, a test set was constructed on the basis of the leave-one-out algorithm (Miller & Miller, 1988).

In Fig. 4, a plot of the samples in the space defined by the two discriminant functions was shown. There is a clear trend for the samples to cluster among themselves. As can be seen in Table 2, all samples in the validation set for class 1 were correctly classified in the appropriate group. The successful classification for classes 2 and 3 were lower but acceptable (one sample misclassified in each class). The average percentage of correct classification was 93.33%. These results are concordant with those provide by visualisation techniques in which a certain overlap between class 2 and 3 was pointed out.

4. Conclusions

An HS-SPME-GC–MS method has been used to determine the concentration of 22 volatile compounds of *orujo* spirits from the Geographic Denomination "*Orujo de Galicia/Augardente de Galicia*". Samples were obtained from the alembic or steam distillation of grape pomace from *Albariño* variety grapes grown in the *Rías Baixas* restricted geographical area or in other zones of Galicia. In spite of certain differences in the mean values, there are no significant differences in the volatile levels of the *orujo* samples according to the distillation technique employed or to the geographical origin of the grapes. Therefore a multivariate approach has been evaluated. PCA and CA show that the three classes of *orujo* considered naturally appear separated; thus, the available volatile compounds data may provide enough information to develop classification systems to differentiate different kinds of *orujo* samples. A lineal model (LDA) was constructed and recognition abilities in the range 90–100% were obtained.

In conclusion, this study shows that the combination of chemical information obtained in a single analysis and chemometrical analysis was able to differentiate *orujo* spirits elaborated with different distillation procedures and with grapes produced in different geographical areas.

Acknowledgments

We express our gratitude to *orujo*-producers and to the *Consello Regulador das Denominacións Xeográficas dos Augardentes e Licores Tradicionais de Galicia* (Certification Council of CBO) for providing *orujo* samples with guaranteed origin.

References

Alonso Salces, R. M., Guyot, S., Berrueta Herrero, L. A., Drilleau, J. F., Gallo, B., & Vicente, F. (2004). Chemometric characterization of Basque and French ciders according to their polyphenolic profiles. *Analytical and Bioanalytical Chemistry, 379*, 464–475.

Alonso Salces, R. M., Herrero, C., Barranco, A., Berrueta, L. A., Gallo, B., & Vicente, F. (2004). Technological classification of Basque cider Apple cultivars according to their polyphenolic profiles by pattern recognition analysis. *Journal of Agricultural and Food Chemistry, 52*, 8006–8016.

Brown, S. D., Bear, R. S., & Blank, T. B. (1992). Chemometrics. *Analytical Chemistry, 64*, 22–49.

DOG (1993). Orde de 16 de setembro de 1993. *Diario Oficial de Galicia, 193*, 1699–1723.

Commission of the European Communities (EEC) (1989). Council regulation No. 1576/89. *Official Journal of the European Community, L 160*, 1–17.

Forina, M., & Lanteri, S. (1984). Data analysis in food chemistry. In B. R. Kowalski (Ed.), *Chemometrics, mathematics and statistics in chemistry* (pp. 305–351). Dordrecht: Riedel Publishing.

Forina, M., Lanteri, S., Armanino, C., Casolino, C., & Casale, M., V-Parvus (2007). Dipartimento Chimica e Tecnologie Farmaceutiche ed Alimentari, University of Genova, Genova, Italy.

Jolliffe, I. T. (2002). *Principal component analysis*. New York: Springer.

Jurado, J. M., Ballesteros, O., Alcázar, A., Pablos, F., Martín, M. J., Vílchez, J. L, et al. (2008). Differentiation of certified brands of origins of Spanish White wines by HS-SPME-GC and chemometrics. *Analytical and Bioanalytical Chemistry, 390*, 961–970.

Kwan, W. O., & Kowalski, B. R. (1980). Pattern recognition analysis of gas chromatographic data. Geographic classification of wines of *Vitis vinifera* cv. pinot noir from France and the United States. *Journal of Agricultural and Food Chemistry, 28*, 356–359.

Kwan, W. O., Kowalski, B. R., & Skogerboe, R. K. (1979). Pattern recognition analysis of elemental data. Wines of *Vitis vinifera* cv. pinot noir from France and the United States. *Journal of Agricultural and Food Chemistry, 27*, 1321–1326.

Latorre, M. J., Peña, R. M., Garcia, S., & Herrero, C. (2000). Authentification of Galician (NW Spain) honeys by multivariate techniques base don metal content data. *The Analyst, 125*, 307–312.

Martí, M. P., Busto, O., & Guasch, J. (2004). Application of a headspace mass spectrometry system to the differentiation and classification of wines according to their origin, variety and ageing. *Journal of Chromatography A, 1057*, 211–217.

Massart, D. L., & Kaufman, L. (1993). *The interpretation of analytical chemical data by the use of cluster analysis*. New York: Wiley.

Milicevic, B., Banovic, M., Kovacevic-Ganic, K., & Gracin, L. (2002). Impact of grape varieties on wine distillates flavor. *Food Technology and Biotechnology, 40*, 227–232.

Miller, J. N., & Miller, J. C. (1988). *Statistics and chemometrics for analytical chemistry* (2nd ed.). Chichester, England: Ellis Horwood Ltd..

Padin, P. M., Peña, R. M., García, S., Iglesias, R., Barro, S., & Herrero, C. (2001). Characterization of Galician (NW Spain) quality brand potatoes: A comparison study of several pattern recognition techniques. *The Analyst, 126*, 97–103.

Peña, R. M., Barciela, J., Herrero, C., & Garcia-Martín, S. (2008). Headspace solid-phase microextraction gas chromatography–mass spectrometry analysis of volatiles in *orujo* spirits from a defined geographical origin. *Journal of Agricultural and Food Chemistry, 56*, 2788–2794.

Pinheiro, P. B. M., & Esteves da Silva, J. C. G. (2005). Chemometric classification of olives from three Portuguese cultivars of *Olea europaea* L. *Analytica Chimica Acta, 544*, 229–235.

Rocha, S., Maeztu, L., Barros, A., Cid, C., & Coimbra, M. A. (2003). Screening and distinction of coffee brews base don headspace solid phase microextraction/gas chromatography/principal component analysis. *Journal of the Science of Food and Agriculture, 84*, 43–51.

Rodriguez, J. C., Iglesias, R., Peña, R. M., Barciela, J., Garcia, S., & Herrero, C. (2006). Preliminary chemometric study on the use of honey as an environmental marker in Galicia (Northwestern Spain). *Journal of Agricultural and Food Chemistry, 54*, 7206–7212.

SPSS for Windows, version 15.0. SPSS Inc., © 1989–2006.

Silva, M. L., Macedo, A. C., & Malcata, F. X. (2000). Review: Steam distilled spirits from fermented grape pomace. *Food Science and Technology International, 6*(4), 285–300.

Silva, M. L., Malcata, F. X., & De Revel, G. (1996). Volatile contents of grape marcs in Portugal. *Journal of Food Composition and Analysis, 9*, 72–80.

Silva, M. L., & Malcata, F. X. (1999). Effects of time of grape pomace fermentation and distillation cuts on the chemical composition of grape marcs. *Zeitschrift fur Lebensmittel-Untersuchung und-Forschungz A, 208*, 134–143.

Statgraphics plus 5.1. Statistical Graphics Corporation, © 1994–2000.

Vandeginste, B. G., Massart, L., Buydens, L. M., De Jong, S., Lewi, P. J., & Smeyers-Verbeke, J. (1998). *Handbook of chemometrics and qualimetrics*. Amsterdam, The Netherlands: Elsevier.

Zambonin, C. G., Balest, L., De Benedetto, G. E., & Palmisano, F. (2005). Solid-phase microextraction-gas chromatography mass spectrometry and multivariate analysis for the characterization of roasted coffees. *Talanta, 66*, 261–265.

Food Chemistry 118 (2010) 462–466

Contents lists available at ScienceDirect

Food Chemistry

journal homepage: www.elsevier.com/locate/foodchem

Analytical Methods

Gold nanoparticle-based lateral flow assay for detection of staphylococcal enterotoxin B

Shyu Rong-Hwa *, Tang Shiao-Shek, Chiao Der-Jiang, Hung Yao-Wen

Institute of Preventive Medicine, National Defense Medical Center, P.O. Box 90048-700, Taipei, Taiwan, ROC

ARTICLE INFO

Article history:
Received 27 November 2007
Received in revised form 27 April 2009
Accepted 27 April 2009

Keywords:
Lateral flow assay
Staphylococcal enterotoxin B
Colloidal gold

ABSTRACT

The lateral flow assay (LFA), a rapid, sensitive, and reproducible technique, was successfully applied to detect staphylococcal enterotoxin B (SEB). The assay was based on a double-antibody sandwich format on a porous nitrocellulose membrane. When SEB-containing samples were applied to the LFA-device, the toxin initially reacted with polyclonal antibody (Pab)-coated colloidal gold particles and then reacted with the fixed Pab on the membrane. These reactions resulted in a red line at the detection zone, with intensity proportional to the SEB concentration (under 100 ng/ml). With this method, 1 ng/ml of SEB can be detected in less than 5 min and was highly reproducible. Signal can be amplified to 10 pg/ml by silver enhancement. This assay also showed no cross-reaction with other SEs, such as SEA, SEC, SED and SEE. The assay was significantly faster than the ELISA or real-time PCR assay and should facilitate early and rapid SEB detection in clinical and food samples.

1. Introduction

Staphylococci are gram-positive bacteria with the appearance of immobile, grape-like clusters. Recently, *Staphylococci* are becoming increasingly resistant to antibiotics and cause a wide range of diseases. They can cause illness directly by infection, or indirectly through their products, such as the toxins that are responsible for food poisoning and toxic shock syndrome (TSS) (Balaban & Rasooly, 2000). The low molecular weight staphylococcal enterotoxins (SEs, 27–30 kDa) produced by different strains of *Staphylococcus aureus* are the main cause of gastroenteritis resulting from the ingestion of contaminated foods. In addition, hospital-acquired infection causes thousands of deaths every year (Altekruse, Cohen, & Swerdlow, 1997). Many *S. aureus* strains produce one or more serotypes of specific exotoxins, including SEs A to E (SEA to SEE), SE-like toxins (SEls); and TSS toxin-1 (Bohach, Dinges, Mitchell, Ohlendorf, & Schlievert, 1997; Bohach, Fast, Nelson, & Schlievert, 1990; Dinges, Orwin, & Schlievert, 2000; Marrack & Kappler, 1990; McCormick, Yarwood, & Schlievert, 2001). These toxins are responsible for specific acute clinical syndromes such as TSS (due to both TSS toxin-1 SEs and SEls), food poisoning (due to SEs), and staphylococcal scarlet fever (a mild form of TSS) (Holtfreter & Broker, 2005; Muller-Alouf, Carnoy, Simonet, & Alouf, 2001; Proft & Fraser, 2003). According to previous studies, little as 100 ng of SEB may make a person ill with symptoms of classic food poisoning (nausea, vomiting and/or diarrhoea) (Evenson, Hinds, Berstein, & Bergdoll, 1988), and the inhalation exposure of SEB could cause a clinically ill in only a few hours (Franz et al., 1997).

It is also well-known that several countries considered SEB as an attractive choice for a biological aerosol weapon to contaminate food or water supplies due to its inherent stability, high morbidity rate, high intoxication effect, and ease of dissemination (Poli, Rivera, & Neal, 2002; Ulrich, Sidell, Taylor, Wilhlmsen, & Franz, 1997). It is currently listed as a restricted (B-list) agent by the Center for Disease Control and Prevention (CDC) (Ferguson, 1997) and is considered by NATO to be a significant threat as a potential biological aerosol weapon. Therefore, the development of a highly sensitive and specific detection method to monitor the toxin in the nares, blood, serum, urine or tissues of individuals would be desirable. Many investigators have reported highly sensitive SEB immunoassay methods, such as enzymatic bionanotransduction and enzyme-linked immunosorbent assays (ELISA). The detection limit of SEB of the former was 10 ng/ml in 4 h assay time (Branen, Hass, Maki, & Branen, 2007), and the latter were 2.8 ng/ml (Chan et al., 2003) and 3.9 ng/ml (Sapsford, Francis, Sun, Kostov, & Rasooly, 2009) respectively. However, these assays are either time consuming (including overnight incubations and complex assay procedures), require special equipment (ELISA reader), or are labor-intensive (require training to perform the analysis).

The lateral flow assay (LFA), also called the immunochromatographic assay or the strip assay, has been under development for several years, such as for antibodies (Peng et al., 2007; Smits, Abdoel, Solera, Clavijo, & Diaz, 2003), allergens (Schubert-Ullrich et al., 2009; Tsay, Williams, Mitchell, & Chapman, 2002) and for antigens (Chiao, Shyu, Hu, Chiang, & Tang, 2004; Diederen & Peeters, 2006; Shyu, Shyu, Liu, & Tang, 2002). This technique is based on an

* Corresponding author. Tel.: +886 2 8177 7038x19887; fax: +886 2 673 6954.
E-mail address: shyu11@yahoo.com.tw (S. Rong-Hwa).

0308-8146/$ - see front matter © 2009 Elsevier Ltd. All rights reserved.
doi:10.1016/j.foodchem.2009.04.106

immunochromatographic procedure that utilises antigen–antibody properties and enables rapid detection of the analyte. It includes several benefits, such as a user-friendly format, rapid results, long-term stability over a wide range of weather conditions, and relatively low manufacturing costs. These characteristics render it ideally suited for on site testing by untrained personnel.

Recent studies have used monoclonal antibodies based on this assay to detect ricin (Shyu et al., 2002) and sulfonamides (Wang et al., 2007) and a polyclonal antibody (Pab) to detect botulinum neurotoxin (Chiao, Wey, Shyu, & Tang, 2008; Chiao et al., 2004). In this research, we used a Pab to develop a rapid and sensitive sandwich immunochromatographic assay that can detect SEB contamination in food or clinical samples.

2. Materials and methods

2.1. Materials

Purified SEB toxin (Sigma–Aldrich, St. Louis, MO, USA) was stored at −20 °C until use. The thawed toxin was diluted in phosphate-buffered saline (PBS) and stored at 4 °C. Other SE toxins (A–E) were purchased from Denka Seiken Co., Ltd. (reversed passive latex agglutination (RPLA) kit; Tokyo, Japan) and stored at 4 °C according to the manufacturer's recommendations.

Anti-SEB IgG was purified from anti-SEB sera with a thiophilic gel (T-gel), which is an IgG specific immunosorbent (Pierce, Rockford, IL, USA). The anti-SEB sera were obtained from SEB immunized rabbits (New Zealand), and the sera titers were determined by ELISA. High-flow nitrocellulose (NC) membranes (AE 98), glass fiber conjugated pad (AccuFlow™ G), sample application pad (#12-S) and reagent adsorption pad (470 Zuschnitte/Cuts) were all purchased from Schleicher & Schuell GmbH (Dassel, Germany). Goat anti-rabbit IgG and silver enhancer reagent were obtained from Sigma.

2.2. Preparation of colloidal gold probes

Colloidal gold probes, measuring 25 nm (Fig. 1), were prepared with sodium citrate by using a modified citrate reduction method (Grabar, Freeman, Hommer, & Natan, 1995). Briefly, an aqueous chloroauric acid solution (200 ml of 0.01% $HAuCl_4$, Sigma) was boiled with vigorous stirring, followed by the rapid addition of 2 ml of 1% sodium citrate to the solution. Boiling was continued for 10 min; the heat source was then removed and stirring was continued for an additional 15 min. After the solution reached room temperature (RT), the probes were filtered through a 0.8 μm Gelman membrane (Voigt Global Distribution Inc., Lawrence, Kansas, USA). The size of the colloidal gold particles was analysed by transmission electron microscopy (TEM) (H-600; Hitachi Instrument Co., Tokyo, Japan); the particles can be stored at 4 °C for several weeks in a dark glass bottle.

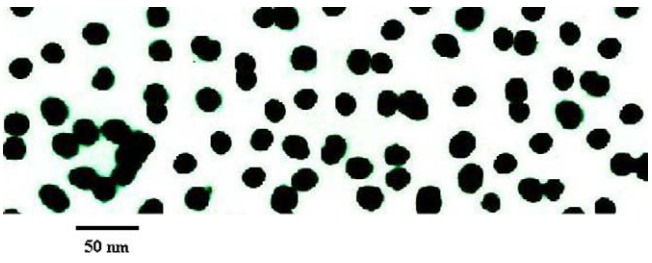

Fig. 1. TEM image of colloidal gold particles. Colloidal gold particle are examined by TEM imaging. The probe size is approximately 25 nm (100,000×), suggesting that the generated gold probes are suitable for conjugation of antibodies.

2.3. Conjugation of antibody to colloidal gold nanoparticles

The pH value of the colloidal gold solution (1%, w/v) was adjusted to 8.5 with NaOH. T-gel purified anti-SEB IgG (0.2 ml; 2 mg/ml; in 5 mM potassium carbonate buffer; pH 8.5) was added to 40 ml pH-adjusted colloid gold solution. The mixture was gently mixed for 30 min and then centrifuged for 30 min (4 °C, 1550*g*; 8178 swing-out rotor, Labofuge 400R; Heraeus Instruments). After centrifugation, the colloid gold pellets were suspended in 20 mM Tris/HCl, pH 8.2 containing 1% BSA and adjusted the optical density to 5.0 at O.D.520. The anti-SEB IgG-coated colloidal gold nanoparticles were ready for use without further preparation.

2.4. Preparation of immunochromatographic test strips

The schematic description and composition of the immunochromatographic test device has been described previously (Biagini et al., 2006; Chiao et al., 2008; Fong et al., 2000; Shyu et al., 2002). Briefly, goat anti-rabbit IgG and rabbit anti-SEB IgG were separately sprayed onto a NC membrane AE 98, using a Biodot dispensing apparatus (Biodot XYZ 3000 1414) to form a control region (C) and a test region (T). The membrane was then mounted in a plastic cassette with an additional reagent adsorbent filter, colloidal gold conjugate pad, and a sample application pad (Fig. 2). This test device was prepared as follows: 2 μl of goat anti-rabbit IgG (0.5 mg/ml, Sigma) and 2 μl of rabbit anti-SEB IgG (1 μg/ml in K_2CO_3, pH 8.5) were separately applied near one end (top) of the strip membrane; the membrane was then dried for 1 h at RT to fix the antibodies. Any remaining active sites on the membrane were blocked by incubation with 1% (w/v) low-melting-point polyvinyl alcohol (in 20 mM Tris/HCl, pH 7.4) for 30 min at RT. The membrane was washed once with water, dried, and immersed in a 5% sucrose solution to assist free mobility of the labeled reagent and dried again. Sucrose can protect the colloidal gold probe from irreversibly adsorbing to the membrane surface when dried. The membrane was then adhered to an adhesive paper plate (2.44 × 11.81 in., Adhesives Research Inc., Taiwan).

On the other hand, the SEB IgG-coated colloidal gold nanoparticles were sprayed onto the sliced conjugated pad (1 × 10 cm, 50 μl/cm) by Biodot AirJet dispensing apparatus (Biodot XYZ 3000 1414). The pad was then kept in a 37 °C incubator for 2 h until fully dried. After that the pad was adhered to the adhesive plate at the bottom end of the sucrose-coated membrane. Finally, a sample application pad (2 × 10 cm) and a reagent adsorption pad

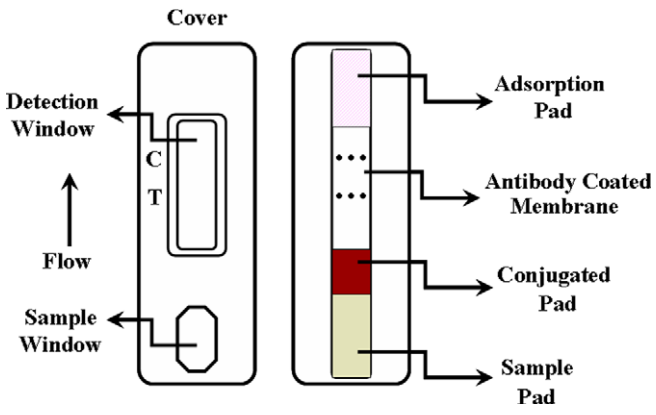

Fig. 2. The schematic description of immunochromatographic test device in a plastic cassette. The device is assembled with a nitrocellulose membrane, a sample pad, a conjugate pad and an adsorption pad. Sample and conjugate pad provide equivalent mixture of the liquid sample and serve as a reservoir for the assay reagents. The adsorption pad adsorbs extra liquid and ensures sufficient flow-through.

(1.2 × 10 cm) were adhered onto the plate to complete the fabrication of the device. The plate was then cut into 5-mm wide strips (by Biodot CM4000) and then mounted in a plastic cassette.

2.5. ELISA for determination of anti-SEB titer

Three rabbits were immunized with the SEB toxin (150 μg toxin/rabbit/boost) to induce anti-SEB Pab. Vaccination was carried out by intramuscular injection every 2 weeks. Whole blood was collected from each rabbit after three boosts, stored overnight at 4 °C, and then purified by further centrifugation (4 °C, 500*g*; 8178 swing-out rotor, Labofuge 400R; Heraeus Instruments, Hanau, Germany) to remove blood cells. Purified sera were stored at 4 °C. For ELISA analysis, all the sera were serially diluted 40,000- to 160,000-fold, with PBS.

2.6. Sensitivity and specificity test

Toxin samples (volume, 80 μl) containing an appropriate amount of SEB (1000–0.1 ng/ml) were applied onto the strip at sample window for the sensitivity assay. To help the sample to migrate, a half volume (40 μl) of tracing buffer (PBS) was applied. With the aim of detecting the very low levels of toxin content, a silver enhancement process was applied to intensify the binding signal of the colloidal gold: following the strip assay, the tested strips were washed once with PBS containing 0.1% (w/v) tween 20 and twice with distilled water, the washed strips were then soaked in a silver enhancer reagent (Sigma) for 5 min and fixed with sodium thiosulfate at room temperature.

For the specificity test, samples containing different enterotoxins (SEA, SEB, SEC, SED, and SEE) were assayed using the SEB test strip by the methods described above.

2.7. Practicability of the SEB test strip with simulated samples

For the purpose of evaluating the practicability of the SEB test strip in natural conditions, three different matrices were used as toxin diluents to mimic actual samples. The samples were prepared by diluting SEB (1 μg/ml) in a stock solution with the appropriate volume of human serum (1:5 in PBS), urine (1:1 in PBS), and cow milk powder (2% w/v in PBS). The serum required dilution because it was too viscous to flow through the membrane, while the urine required dilution because it was a weak acid and would interfere with the antigen–antibody reaction, and the milk need to be diluted because the milk particles and lipid would have blocked the pores of the membrane. Control samples were prepared by directly diluting the various matrices with PBS. All mimic samples were assayed on SEB test strips.

3. Results

3.1. Sensitivity of SEB test strip

Different concentrations of SEB toxin were assayed by the SEB test strip. Results were determined by the appearance of (positive result) or absence of (negative result) a red line in the test area, respectively, under the condition that a red line could be visualised at the control zone. Analyses were completed in less than 5 min, and the detection limit of SEB was 1 ng/ml (Fig. 3). All the results were highly reproducible throughout the assay. The intensity of the red color is proportional to the SEB concentration (under 100 ng/ml). However, in the absence of SEB (buffer only), no immunogold was bound to the solid-phase test antibody; hence no red signal can be visualised in this region. In the case of silver enhancement, the strong binding between silver molecules and colloidal gold particles developed a dark line at the place of the colloidal gold particles. By using silver enhancement, 10 pg/ml of the SEB toxin could be detected (Fig. 4). False positive results were not obtained in any of the assays performed.

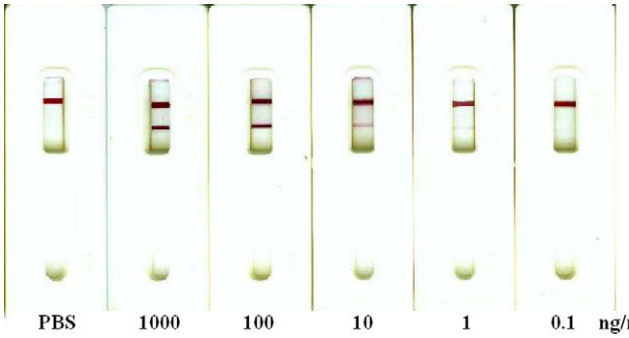

Fig. 3. Immunochromatographic assay of SEB. A series of dilutions (1000–0.1 ng/ml) of SEB was prepared in PBS. The detection limit of SEB toxin was 1 ng/ml. False positive was not detected in the absence of SEB.

3.2. Cross-reactivity of SEB test strip

The cross-reactivity of SEA, SEC, SED, and SEE on the SEB strip was examined. Samples of five different SEs (A through E) were each diluted in PBS buffer. When 100 ng/ml of each toxin was tested, only SEB produced a red band in the test region (Fig. 5), which suggests a clear specificity of the strips.

3.3. Detection of SEB in various matrices

Simulated samples (SEB toxin diluted in human urine, serum and cow milk powder) were also assayed by the SEB test strips. The results showed that SEB diluted in urine (Fig. 6a) or milk powder (Fig. 6b) provides better detection sensitivity than SEB diluted in serum (Fig. 6c). The detection limit of SEB in the simulated urine and milk samples was 10 ng/ml, which was 1-fold less sensitive than the detection limit of SEB in PBS; however, it was more sensitive than that of SEB in serum (100 ng/ml).

4. Discussion

The *Staphylococcus* toxin SEB poses a serious threat to the food industry and human health. Unfortunately, there is no effective

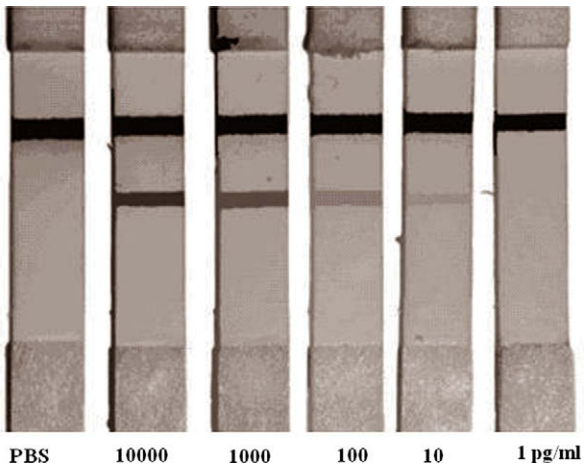

Fig. 4. Silver enhancement of immunochromatographic detection of SEB. The tested membranes were immersed in silver enhancer solution to amplify detection limitation. Sensitivity of the SEB strip can be intensified to 10 pg/ml after the silver enhancement.

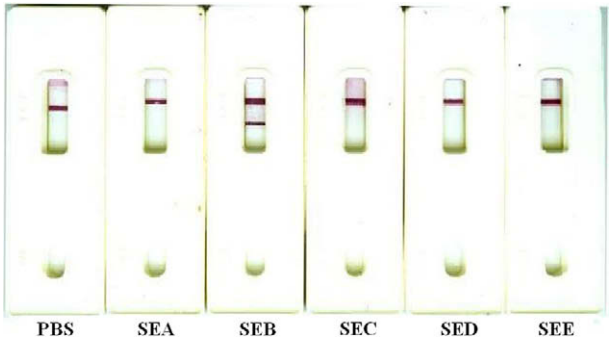

Fig. 5. Cross-reactivity assay of SEB test strip. Samples containing SE toxins (SEA–SEE, 100 ng/ml each) were applied to SEB test strip, while only SEB produced a red band in the test region. Non-specific binding was not visualised in the absence of SEB.

vaccine or specific anti-toxin to treat SEB poisoning. Therefore, a simple and rapid method to screen for SEB toxin would provide an important tool to protect the food supply.

In this paper, a SEB immunochromatographic assay was developed that utilises colored colloidal gold nanoparticles as a tracer which provides clear evidence of SEB identification. The criterion for reactivity was judged by the formation of red lines at both the test and control areas within 5 min but no longer than 10 min after sample addition. Formation of a red line at the control position other than the test position was classified as a negative result, while the absence of a red line at the control position was treated as an invalid result, and thus need to be reanalysed. The detection limit of the SEB toxin in the SEB strips was 1 ng/ml, and it could be enhanced to 10 pg/ml with the silver enhancer reagent. In contrast, since the Pab-based SEB test strips had no cross-reaction with other SEs (SEA, SEC, SED, and SEE) even when 1 μg/ml of the toxins was tested, suggesting that these SEB strips have high specificity for SEB.

In Fig. 3, there seems no difference in staining intensity observed between 1000 and 100 ng, previous studies explained this phenomenon: Chan et al. (2003) found that when using LFA to detect heart-type fatty acid-binding protein, the linear range of the detection was laid between 2.8–125 ng/ml, which suggested the staining intensity may reach an equilibrium value in LFA if the antibody exceeds a certain amount. Qian and Bau (2003) also established a mathematical model explained when the target analyte concentration is low, the signal level increases nearly linearly as the target analyte concentration increases; however, once the target analyte concentration exceeds a certain value, the signal reaches a plateau.

In strip analyses, the purified IgGs from the immunized rabbits were applied onto the devices. We could not measure the amount of specific anti-SEB IgG contained in the T-gel-purified IgG because the purified IgG was total IgG rather than specific IgG. Nevertheless, we obtained good detection specificity and sensitivity in the SEB strip test by using this total IgG as a reagent. On the other hand, previous studies (Chiao et al., 2004; Sharma, Eblen, Bull, Burr, & Whiting, 2005) discovered that in LFA, some components in urine, serum or milk may interfere the antigen–antibody reaction and result in a weak signal. In our study of SEB, although the signal intensity in simulated tests was not as sensitive as that in PBS only, the strips are still with sufficient sensitivity to detect SEB in food.

There are several steps in the immunochromatographic assay procedure. First, two antibodies are immobilized on the membrane: a suitable concentration of antibody (e.g., 1 μg/ml) against the test antigen, and an antibody against the IgG of the animal spe-

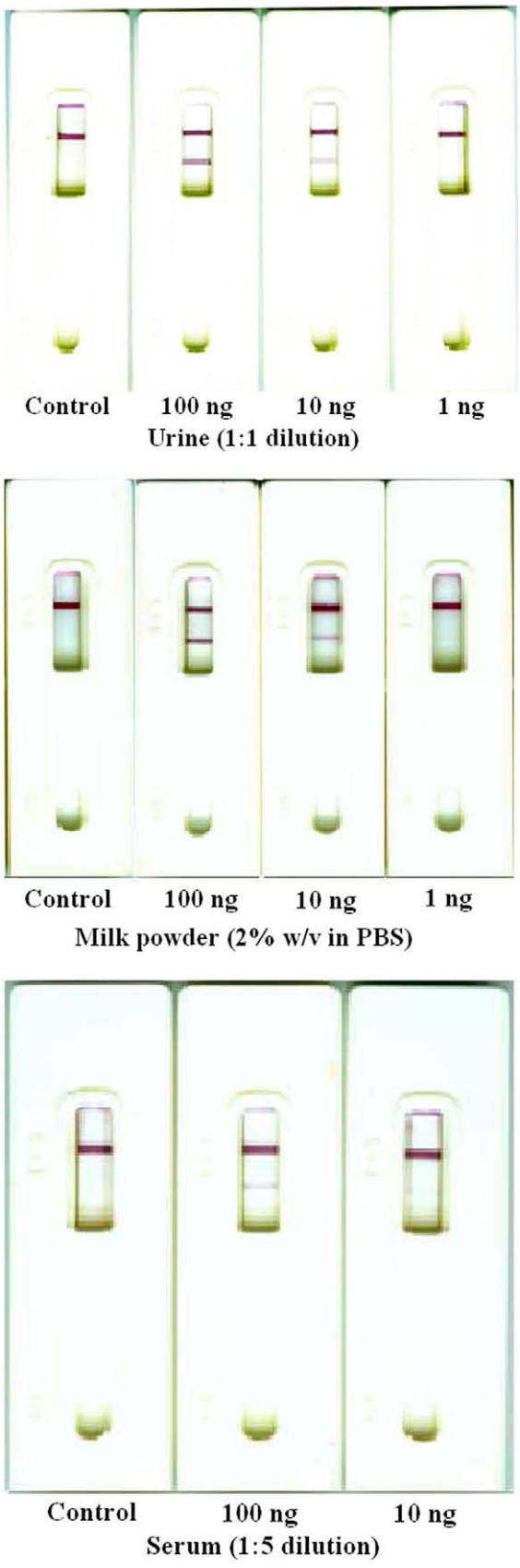

Fig. 6. Detection of SEB in various matrices. Simulated samples were assayed by SEB test strip. All the SEB samples were diluted in the control reagents that diluted in PBS (urine, 1:1 dilution (a); milk powder, 2% w/v (b); serum, 1:5 dilutions (c)). Simulated samples in urine and milk powder have same detection limit (10 ng/ml), while in serum, detection sensitivity has ten times less (100 ng/ml).

cies from which the pathogen antibody is derived. The antibodies are strongly adsorbed by the membrane and remain attached to the surface throughout the procedure. Second, any remaining sites on the membrane still capable of binding protein are blocked by other chemicals, such as polyvinyl alcohol, to reduce the nonspecific binding of antibody or antigen to the membrane. Third, when samples containing the toxin antigen are added to the device, the liquid mixture migrates along the NC membrane. As a result, the sample reacts with the two antibodies bound on the membrane and forms a visible line(s). The color intensity is proportional to the concentration of the pathogen. To avoid nonspecific binding and to prevent undesired cross-reactivity of the antibodies with the test line, all the procedures require conscientious development and optimisation of various capture lines.

The strip assay described above exhibits potential as a general assay method for the detection of the SEB toxin in biological fluids. The detection of the SEB toxin by the device requires approximately 5 min; this is much quicker than the time required for ELISA or radioimmunoassay; further, the results also can be read directly by the naked eye. Therefore, the strip assay is a highly specific, easy to operate, low cost, and sensitive assay for the rapid and reproducible detection of the SEB toxin.

In summary, we have successfully developed a polyclonal-based strip test kit that can rapidly detect SEB without cross-reaction with antibodies against other SEs. The results imply that the strip assay is sufficiently sensitive to support the detection of SEB contamination in clinical or food samples.

Acknowledgements

This work was supported by Institute of Preventive Medicine, National Defense Medical Center (IPMC I9601).

References

Altekruse, S. F., Cohen, M. L., & Swerdlow, D. L. (1997). Emerging foodborne diseases. *Emerging Infectious Diseases, 3*, 285–293.

Balaban, N., & Rasooly, A. (2000). Staphylococcal enterotoxins. *International Journal of Food Microbiology, 61*, 1–10.

Biagini, R. E., Sammons, D. L., Smith, J. P., MacKenzie, B. A., Striley, C. A., Snawder, J. E., et al. (2006). Rapid, sensitive, and specific lateral-flow immunochromatographic device to measure anti-anthrax protective antigen immunoglobulin G in serum and whole blood. *Clinical and Vaccine Immunology, 13*(5), 541–546.

Bohach, G. A., Dinges, M. M., Mitchell, D. T., Ohlendorf, D. H., & Schlievert, P. M. (1997). Exotoxins. In K. B. Crossley & G. L. Archer (Eds.), *The staphylococci in human disease* (pp. 83–111). New York: Churchill Livingstone.

Bohach, G. A., Fast, D. J., Nelson, R. D., & Schlievert, P. M. (1990). Staphylococcal and streptococcal pyrogenic toxins involved in toxic shock syndrome and related illnesses. *Critical Reviews in Microbiology, 17*, 251–272.

Branen, J. R., Hass, M. J., Maki, W. C., & Branen, A. L. (2007). An enzymatic bionanotransduction system for multianalyte biological detection. *Journal of Applied Microbiology, 102*, 892–908.

Chan, C. P. Y., Sum, K. W., Cheung, K. Y., Glatz, J. F. C., Sanderson, J. E., Hempel, A., et al. (2003). Development of a quantitative lateral-flow assay for rapid detection of fatty acid-binding protein. *Journal of Immunological Methods, 279*, 91–100.

Chiao, D. J., Shyu, R. H., Hu, C. S., Chiang, H. Y., & Tang, S. S. (2004). Colloidal gold-based immunochromatographic assay for detection of botulinum neurotoxin type B. *Journal of Chromatography B, 809*, 37–41.

Chiao, D. J., Wey, J. J., Shyu, R. H., & Tang, S. S. (2008). Monoclonal antibody-based lateral flow assay for detection of botulinum neurotoxin type A. *Hybridoma, 27*(1), 31–35.

Diederen, B. M. W., & Peeters, M. F. (2006). Evaluation of rapid U Legionella plus test, a new immunochromatographic assay for detection of *Legionella pneumophila* serogroup 1 antigen in urine. *European Journal of Clinical Microbiology & Infectious Diseases, 25*, 733–735.

Dinges, M. M., Orwin, P. M., & Schlievert, P. M. (2000). Exotoxins of *Staphylococcus aureus*. *Clinical Microbiology Reviews, 13*, 16–34.

Evenson, M. L., Hinds, W. M., Berstein, R. S., & Bergdoll, M. S. (1988). Estimation of human dose of staphylococcal enterotoxin A from a large outbreak of staphylococcal food poisoning involving chocolate milk. *International Journal of Food Microbiology, 7*(4), 311–316.

Ferguson, J. R. (1997). Biological weapons and US law. *The Journal of the American Medical Association, 278*, 357–360.

Fong, W. K., Modrusan, Z. J., McNevin, P., Marostenmaki, J., Zin, B., & Bekkaoui, F. (2000). Rapid solid-phase immunoassay for detection of methicillin-resistant *Staphylococcus aureus* using cycling probe technology. *Journal of Clinical Microbiology, 38*(7), 2525–2529.

Franz, D. R., Jahrling, P. B., Friedlander, A. M., McClain, D. J., Hoover, D. L., Bryne, W. R., et al. (1997). Clinical recognition and management of patients exposed to biological warfare agents. *The Journal of the American Medical Association, 278*(5), 399–411.

Grabar, K. C., Freeman, R. G., Hommer, M. B., & Natan, M. J. (1995). Preparation and characterization of Au colloid monolayers. *Clinical Chemistry, 67*, 735–743.

Holtfreter, S., & Broker, B. M. (2005). Staphylococcal superantigens: Do they play a role in sepsis? *Archivum immunologiae et therapiae experimentalis, 53*, 13–27.

Marrack, P., & Kappler, J. (1990). The staphylococcal enterotoxins and their relatives. *Science, 248*, 705–711.

McCormick, J. K., Yarwood, J. M., & Schlievert, P. M. (2001). Toxic shock syndrome and bacterial superantigens: An update. *Annual Review of Microbiology, 55*, 77–104.

Muller-Alouf, H., Carnoy, C., Simonet, M., & Alouf, J. E. (2001). Superantigen bacterial toxins: State of the art. *Toxicon, 39*, 1691–1701.

Peng, D. P., Hu, S. S., Hua, Y., Xiao, Y. C., Li, Z. L., Wang, X. L., et al. (2007). Comparison of a new gold-immunochromatographic assay for the detection of antibodies against avian influenza virus with hemagglutination inhibition and agar gel immunodiffusion assays. *Veterinary Immunology and Immunopathology, 117*, 17–25.

Poli, M. A., Rivera, V. R., & Neal, D. (2002). Sensitive and specific colorimetric ELISAs for *Staphylococcus aureus* enterotoxins A and B in urine and buffer. *Toxicon, 40*, 723–1726.

Proft, T., & Fraser, J. D. (2003). Bacterial superantigens. *Clinical and Experimental Immunology, 133*, 99–306.

Qian, S., & Bau, H. H. (2003). A mathematical model of lateral flow bioreactions applied to sandwich assays. *Analytical Biochemistry, 322*, 89–98.

Sapsford, K. E., Francis, J., Sun, S., Kostov, Y. & Rasooly, A. (2009). Miniaturized 96-well ELISA chips for staphylococcal enterotoxin B detection using portable colorimetric detector. *Analytical and Bioanalytical Chemistry Mar 17* (Published online).

Schubert-Ullrich, P., Rudolf, J., Ansari, P., Galler, B., Führer, M., Molinelli, A., et al. (2009). Commercialized rapid immunoanalytical tests for determination of allergenic food proteins: An overview. *Analytical and Bioanalytical Chemistry Mar 24*. (Published online).

Sharma, S. K., Eblen, B. S., Bull, R. L., Burr, D. H., & Whiting, R. C. (2005). Evaluation of lateral-flow *Clostridium botulinum* neurotoxin detection kit for food analysis. *Applied Environmental Microbiology, 71*(7), 3935–3941.

Shyu, R. H., Shyu, H. F., Liu, H. W., & Tang, S. S. (2002). Colloidal gold-based immunochromatographic assay for detection of ricin. *Toxicon, 40*, 255–258.

Smits, H. L., Abdoel, T. H., Solera, J., Clavijo, E., & Diaz, R. (2003). Immunochromatographic Brucella-specific immunoglobulin M and G lateral flow assays for rapid serodiagnosis of human brucellosis. *Clinical and Diagnostic Laboratory Immunology, 10*(6), 1141–1146.

Tsay, A., Williams, L., Mitchell, E. B., & Chapman, M. D. (2002). Multi-Centre Study group. A rapid test for detection of mite allergens in homes. *Clinical & Experimental Allergy, 32*(11), 1596–1601.

Ulrich, R. G., Sidell, S., Taylor, T. J., Wilhlmsen, C. L., & Franz, D. R. (1997). Staphylococcal enterotoxin B and related pyrogenic toxins. In R. Zatjchuk (Ed.), *Textbook of military medicine: Medical aspects of chemical and biological warfare* (pp. 621–630). Washington, DC: Office of the Surgeon General, Department of Army.

Wang, X., Li, K., Shi, D., Xiong, N., Jin, X., Yi, J., et al. (2007). Development of an immunochromatographic lateral-flow test strip for rapid detection of sulfonamides in eggs and chicken muscles. *Journal of Agricultural and Food Chemistry, 55*(6), 2072–2078.

Food Chemistry 118 (2010) 467–471

Contents lists available at ScienceDirect

Food Chemistry

journal homepage: www.elsevier.com/locate/foodchem

Analytical Methods

Development of a new monoclonal antibody based direct competitive enzyme-linked immunosorbent assay for detection of brevetoxins in food samples

Yu Zhou *, Yan-Song Li, Feng-Guang Pan, Yuan-Yuan Zhang, Shi-Ying Lu, Hong-Lin Ren, Zhao-Hui Li, Zeng-Shan Liu, Jun-Hui Zhang

Key Laboratory of Zoonosis Research, Ministry of Education, Institute of Zoonosis, Jilin University, Changchun 130062, PR China

ARTICLE INFO

Article history:
Received 18 November 2008
Received in revised form 13 April 2009
Accepted 2 May 2009

Keywords:
Hybridoma cell line
Monoclonal antibody
Enzyme-linked immunosorbent assay
Brevetoxin
Cross-reactivity
Recovery

ABSTRACT

Brevetoxin B (PbTx-2) was covalently linked to carrier protein bovine serum albumin and human gamma globulin. A monoclonal antibody against PbTx-2, which showed high cross-reactivity values with PbTx-1, PbTx-3 and PbTx-9 (more than 89%) was obtained from ascites and some characteristics of monoclonal antibody were studied. An direct competitive enzyme-linked immunosorbent assay (ELISA) for detection of PbTxs was developed, which showed an IC50 value of 5.3 ng mL^{-1} with a detection limit of 0.6 ng $well^{-1}$. The recoveries of PbTxs from cockle (88.4%–102.3%) and oyster (89.4%–104.3%) demonstrated that the matrices of cockle and oyster where PbTxs are found do not interfere with the assay. The newly developed competitive ELISA appears to be a reliable and useful method for mass monitoring of PbTxs in mollusk.

1. Introduction

Brevetoxins (PbTxs) are potent marine neurotoxins produced by the planktonic red tide dinoflagellate *Karenia brevis* and are accumulated in filter-feeding molluscan shellfish by dietary transfer. They are lipid-soluble polycyclic polyether compounds and are the only molecules known to activate voltage sensitive sodium channels in mammals through a specific interaction with site 5 of the alpha subunit of the sodium channel (Dechraoui, Naar, Pauillac, & Legrand, 1999). Human ingestion of toxic shellfish causes neurotoxic shellfish poisoning (NSP). Although PbTxs can be used as powerful tools in neuroscience research (Naar, Branaaa, Bottein-Dechraoui, Chinain, & Pauillac, 2001), their detrimental effects on human health and negative impact on seafood industries have mainly raised global awareness. Therefore it is very important to develop a precise, sensitive, reproducible and specific detection method as an alternative to the conventional mouse intraperitoneal (i.p.) bioassay (Lewis, 1995), solid-phase extraction (SPE) assay, receptor binding assay (RBA), radioimmuno-assay (RIA), and liquid chromatography–mass spectrometry (LC–MS) (Twiner et al., 2007), competitive electro-chemiluminescence-based immunoassay (Poli et al., 2007), cell based assay (Fairey, Bottein Dechraoui, Sheets, & Ramsdell, 2001) and in vitro assays (Plakas et al., 2008).

Immunological methods based on antibodies are simple, sensitive, economical and high throughput procedure for quantifying biologically relevant compounds, but require a continuous supply of well-defined specific antibodies. To date, Polyclonal and monoclonal antibodies to PbTx-2-type brevetoxins (Naar et al., 2001) and polyclonal antisera to PbTxs have been raised in animals such as mice (Trainer & Baden, 1990), goats (Melinek, Rein, Schultz, & Baden, 1994; Poli, Rein, & Baden, 1995; Trainer & Baden, 1991), and rabbits (Levine & Shimizu, 1992). Although they exhibit high affinity, but usually available in only limited supply and require batch standardisation and continual supply of antigen for booster injections. On the other hand, the antigens (PbTxs) are very expensive, so it is restricted to detect this kind of compounds by polyclonal antisera.

It is one of the key steps to generate a hybridoma cell line, which permanent secreting high affinity monoclonal antibody (mAb) against PbTxs, for the establishment of a precise, sensitive, and specific immunoenzymatic assay for PbTxs. Since PbTxs are small molecules, haptens must be synthesised and coupled to carrier proteins to induce antibody production. In this study, we aimed at obtaining mAbs against PbTxs and developing mAb-based enzyme-linked immunosorbent assay (ELISA) with better performance using a larger number of haptens as competitors.

* Corresponding author. Tel.: +86 0431 87836718.
E-mail address: zhouyu69@sina.com (Y. Zhou).

0308-8146/$ - see front matter © 2009 Elsevier Ltd. All rights reserved.
doi:10.1016/j.foodchem.2009.05.015

2. Materials and methods

2.1. Materials

PbTx-1, PbTx-2, PbTx-3, PbTx-9, ciguatoxin-1 (the purity ⩾ 98% by HPLC), okadaic acid, microcystin LR and dinophysistoxin (the purity ⩾ 95% by HPLC) were obtained from Sigma Chemicals Co. (St. Louis, MO, USA). Agarose, complete and incomplete Freund/s adjuvant, polythylene glycol-4000 (PEG), RPMI 1640, foetal bovine serum (FBS), horseradish peroxidase-conjugated goat anti-mice IgG (HRP–IgG), bovine serum albumin (BSA), human gamma globulin (HGG), HT and HAT were purchased from Express China. All other reagents were of analytical grade. The ELISA was carried out in 96-well polystyrene microtiter plates (Stripwell plate 2592, Costar, Changchun, China). Well absorbencies were read with a MK3 microplate reader (Thermo, Shanghai, China).

2.2. Animals

Female Balb/C mice, 6- to 7-week old and 9- to 10-week old, being immunized and using to produce ascites, respectively, were obtained from Changchun Institute of Biological Products, Jilin province China.

2.3. Buffers and solutions

The buffers used regularly were coating buffer, 50 mmol L^{-1} carbonate buffer (pH 9.5); phosphate buffered saline (PBS), 10 mmol L^{-1} sodium phosphate buffer (pH 7.4) containing 140 mmol L^{-1} NaCl; dilution buffer, PBS containing 0.1% (w/v) gelatin; washing buffer (PBST), 10 mmol L^{-1} sodium phosphate buffer (pH 7.4) containing 140 mmol L^{-1} NaCl and 0.05% (v/v) Tween 20; and TMB solution, 70 μL of 0.65% H_2O_2, 250 μL of 10 mg mL^{-1} 3,3/5,5/-tetramethylbenzidine (TMB) in dimethylsulfoxide (DMSO) per 25 mL of phosphate citrate buffer, pH 5.4.

2.4. Preparation of PbTx–protein conjugates

Conjugates were prepared according to a modified method of Naar et al. (2001). Briefly, A 10-fold molar excess of succinic anhydride solubilised in 10 mL of anhydrous pyridine was added to 8 mg of crystalline PbTx-2. After incubation (6 h at 65 °C) the solvent was evaporated under a stream of nitrogen and the residue was reacted with a 10-fold molar excess of tributylamine and isobutyl chlorocarbonate as 1/10th dilutions in dry peroxide-free dioxan for 30 min at room temperature. Then the carrier protein HGG and BSA (the same hapten/carrier molar ratio) were added at room temperature and incubated for more than 30 min, that were used for immunisation (PbTx–HGG) and antibody screening (PbTx–BSA) respectively. Conjugates were recovered by acetone precipitation, resuspended in 1 mL distilled water, filter sterilised (0.22 μm), dispensed into sterile tubes then freeze-dried overnight and stored at −20 °C until use.

2.5. Conjugate analysis

The conjugates were analysed using a modification of the methods of Kamps, Carlin, and Shefield (1993). Briefly, TAE was employed for electrophoresis buffer and the mixture solution of 0.04% bromophenoland blue and 6.67% sucrose was used as loading buffer. Each sample (5 μg $μL^{-1}$) 1 μL mixed with an equal volume of loading buffer was applied to the gel and samples were separated at 230 V for 30–40 min. The gel was fixed with 20% trichloroacetic acid for 30 min, stained with Coomassie blue R-250 for more than 2 h and destained with ethanol–acetic acid (250 mL 95% ethanol + 80 mL acetic acid, distilled water to 1000 mL) with several changes until be satisfied. The pictures of the gels were taken by ultraviolet irradiation (UVI) gel auto imaging system.

2.6. Immunization

Immunogen (PbTx–HGG 100 μg, in 0.1 mL PBS, pH 7.4) and freunds complete adjuvant (0.1 mL) was injected (female Balb/C mice, 6- to 7-week old) at multiple subcutaneously (s.c.) sites as the first immunization. The subsequent injections were intraperitoneally (i.p.) with 50 μg of immunogen (0.1 mL) and the same volume Freunds incomplete adjuvant at the 3rd, 5th, 7th, and 9th week, respectively. After the third immunization, at the 10th day of each injection, the animals were bled by tail–tip cut method, and the serum was tested for its ability to bind to PbTx–BSA or the carrier protein HGG and BSA. The animals, whose serum titres (serum antibody titres) bind to PbTx–BSA were 4 × 103 or higher were selected to be spleen donors for hybridoma production, and received intravenous injection (i.v.) boosts of 20 μg immunogen conjugate in PBS (pH 7.0). Four days after the final boost, spleens were removed from immunized mice.

2.7. Hybridoma screening and generation

The immunized mice spleen cells were mixed with myeloma cells (SP2/0) at a 5–10:1 (spleen: myeloma) ratio in the presence of polyethylene glycol (PEG), mol. wt 4000, and plated into 96-well tissue culture plates filled with RPMI + 20% FBS/HAT medium at 37 °C in an atmosphere of 5% CO_2. Specific antibody-secreting hybridoma were screened by ELISA employing PbTx–BSA as target antigen, BSA and HGG as non-relevant control antigens. Hybridoma showing significant PbTx-specific inhibition were cloned three times by limiting dilution. One clone was chosen for further study.

2.8. Ascites produce and mAb affinity determination

Hybridoma (2×10^6 cells for each mice) were injected into abdomens of the 9- to 10-week old Balb/C mice for seven days after liquid olefin was injected. The ascites were obtained through the needle of a 20 mL injector about seven days later. The mAb was purified from ascites using the method of Zhou et al. (2006). MAb subtyping was performed by an ELISA commercial kit "mouse monoclonal antibody isotyping reagents" (Sigma), and the operational procedure based on its manufacturer's instructions. The affinity of mAb for PbTxs was measured by a competitive enzyme immunoassay according to the method of Dong and Wang (2002).

2.9. Protocol of direct competitive ELISA

A direct competition ELISA format was utilised to measure PbTx-2 binding and cross-reactivity (CR) to related compounds PbTx-1, PbTx-3, PbTx-9, ciguatoxin-1, okadaic acid, microcystin LR and dinophysistoxin. Indirect ELISA was carried out as follows: (1) 200 μL of coating antigen PbTx–BSA diluted with the coating buffer at 0.5 μg mL^{-1} was added into a microtiter plate and incubated overnight at 4 °C. (2) Plates were washed three times using 300 μL $well^{-1}$ of PBST (10 mM PBS containing 0.05% Tween 20, pH 7.4) and then followed by incubation with 50 μL $well^{-1}$ of standard analyte (for inhibition assay) in 0.01 M PBS at different dilutions or sample solution or blank together with the mAb (1:8000 with the dilution buffer solution, 50 μL $well^{-1}$) for 30 min at 37 °C. (3) After washing three times, 100 μL of HRP–IgG (working concentration recommend 1:4000) was then added to each well and incubated for 30 min at 37 °C. (4) The plates were washed

again, and 100 μL well^{-1} of TMB solution was added. (5) After incubation for 15 min at 37 °C, the reaction was stopped by adding 50 μL of 2 M H_2SO_4 well^{-1}. (6) The absorbance was measured at 450 nm and recorded. Standard curves were obtained by plotting absorbance against the logarithm of analyte concentration.

2.10. Spiking of mollusk extracts

Non-toxic cockle *Austrovenus stuchibuli* and oyster *Crassostrea virginica* were purchased from a local supermarket. The tissue was thoroughly disrupted in dimethyl sulfoxide (50% w/v) and then centrifuged at 1500 g for 15 min. The supernatant was passed sequentially through a 100 mm nylon mesh, Whatman No. 1 filter and then finally through a Whatman GF/B filter yielding a slightly opalescent yellowcolored extract. Standard analyte of PbTx-2, PbTx-1, PbTx-3 and PbTx-9 was incorporated respectively at the required concentrations using vortexing. Recoveries were determined at concentrations of 4, 40 and 400 ng/g of whole shellfish meat ($n = 5$) by the use of non-toxic cockle or oyster homogenates spiked with standard analytes.

In order to see if the under- or overestimation in recoveries can be rationalised by the matrix effect of the extract of the mollusks, unspiked cockles or oysters were extracted with 10 mL of dimethyl sulfoxide as described above and standard analyte of PbTx-2, PbTx-1, PbTx-3 and PbTx-9 was spiked respectively into the extract to obtain standard curves. The standard curve in the buffer was also obtained.

3. Results and discussion

3.1. Analysis of the conjugates

Conjugates were prepared according to the procedure described in Section 2. In nondenaturing agarose gel electrophoresis, the more negative charged protein migrates further in the gel towards the anode (+) than the more positive charged protein. The coupling of protein with protein modifier and haptens will induce the changes of the protein charge, therefore the migration of carrier protein, treated protein and hapten-carrier protein will be different. Fig. 1 illustrates the results of nondenaturing agarose gel electrophoresis for conjugates. The net charge of PbTx–HGG (lane 3) becomes more negative than that of treated HGG (lane 2) and untreated HGG (line 1), so it migrates to a greater extent towards the anode (+), and the migration of PbTx–HGG and treated HGG became decentralized. The conjugate band migrations were different from those of treated proteins and carrier proteins alone. The net charge of PbTx–BSA (lane 6) becomes more negative, so PbTx–BSA migrates to a greater extent towards the anode (+) than that of treated BSA and untreated BSA, and the migration of PbTx–BSA and treated BSA became decentralized. The results indicated that PbTx was coupled with BSA and HGG successfully.

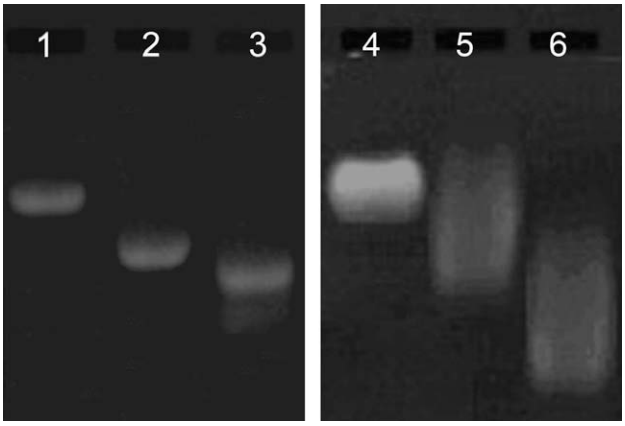

Fig. 1. Analysis of PbTx–HGG and PbTx–BSA conjugations by non-denaturing agarose gel electrophoresis. Lane 1. HGG, lane 2: treated HGG (the procedure was performed according to Section 2, only PbTxs was not added), lane 3: PbTx–HGG conjugates, lane 4: BSA, lane 5: treated BSA (the procedure was performed according to Section 2, only PbTxs was not added), lane 6. PbTx–BSA conjugates.

3.2. Antisera titres of immunized mice and screening of hybridoma

Like most other marine toxins, PbTx, as hapten, has no immunogenicity and must be conjugated to a protein carrier to add immunogenicity. A previous study indicated that the titres of produced antibody for the hapten changed according to the carrier protein used in the conjugation and different mice (Kentaro, Yonekazu, & Tamao, 1999). In the present study, six mice were immunized by PbTx–HGG. Table 1 shows the results of serum titres of immunized mice. There are four mice whose serum titres were 4×10^3 higher. No. 6 mouse was selected to be spleen donors for hybridoma production. Hybridoma supernatants were screened by ELISA for binding to target and control antigens in parallel, then positive clones were checked for PbTx-2 reactivity by competitive inhibition ELISA. A screened hybridoma cell line designated 2C4, was established after being subcloned for 3 cycles by "limiting dilution".

3.3. The characteristics of mAb

The hybridoma cells were expanded and injected into Balb/C mouse abdomen. The mAb was obtained from ascites and purified by the caprylic/ammonium sulphate precipitation (CA–AS) method. The protein concentration of ascites was 24.5 mg mL^{-1}, calculated as following equation (Liu, Cai, Wang, & Li, 1999): Concentration (mg mL^{-1}) = $1.45 \times OD_{280} - 0.74 \times OD_{260}$. Here OD_{280} is the absorption value of ascites at 280 nm, OD_{260} is the absorption value of ascites at 260 nm. The ELISA titres of ascites and purified mAb were 3.2×10^5 and 6.4×10^5, respectively. The mAb secreted by 2C4 belongs to the IgG1 class.

The average affinity of mAb was 0.82×10^9 M^{-1} calculated as following equation (Dong & Wang, 2002):

$$Ka = \frac{n-1}{2(n[Ab'] - [Ab])} \quad (1)$$

Here n is the concentration time of two different concentration plate coating antigens in one group, [Ab'] and [Ab] are the mAb concentrations (ng L^{-1}) correspond to 50% of maximum absorption values of two different concentration plate coating antigens.

The CR was calculated according to the following equation:

$$CR\% = \frac{\text{standard}IC_{50}}{\text{cross-reactant}IC_{50}} \quad (2)$$

Table 1
Titres of antisera from the immunized mice by indirect ELISA[a].

Mouse no.	Titers of antiserum		
PbTx–HGG[b]	PbTx–BSA[c]	BSA[c]	HGG[c]
1	1:8000	Negative	1:16000
2	1:400	1:200	1:8000
3	1:16000	Negative	1:64000
4	1:8000	Negative	1:32000
5	1:4000	1:400	1:1600
6	1:32000	Negative	1:64000

[a] The titrations by indirect ELISA were performed for the serum of mice after the fourth booster.
[b] As immunogen.
[c] As plate-coating antigen.

IC50 is PbTx concentration reducing the ELISA maximum response to 50%. CR (%) of PbTx-2 was defined as 100%. The CR of the mAb with some other marine toxins is shown in Table 2. The mAb showed high CR values with PbTx-1, PbTx-3 and PbTx-9, low CR values with ciguatoxin-1 and okadaic acid, and no significant CR values with microcystin LR and dinophysistoxin in the direct competitive ELISA. Therefore the mAb secreted by 2C4 is class-selective and has potential to be used for broad spectrum assay of PbTx-1, PbTx-2, PbTx-3 and PbTx-9. It is expensive and time consuming to produce the brevetoxin antiserum, which depends on the continual supply of animals and brevetoxins, and it is difficult to get the uniform antiserum due to the individual difference of animals. The uniform mAb can be readily obtained which dose not need brevetoxins.

Table 2
Specificity of the mAb to different marine toxins in the competitive ELISA[a] using PbTx–BSA as coating antigen.

Compound	IC_{50} (ng mL^{-1})[b]	CR (%)
PbTx-2	6.4	100.00
PbTx-1	6.57	97.45
PbTx-3	5.31	120.63
PbTx-9	7.15	89.56
Ciguatoxin-1	175.82	3.64
Okadaic acid	216.22	2.96
Microcystin LR	#[c]	<0.1
Dinophysistoxin	#[c]	<0.1

[a] Antigen coating solution was made in PBS at 500 ng mL^{-1} and final ascites dilution was 1:64,000 in PBS-T.
[b] Data represent the means of five experiments.
[c] The IC_{50} cannot be evaluated.

3.4. Extraction recovery

In order to understand the under- and overestimation in recovery values, unspiked cockles or oysters were extracted with 10 mL of dimethyl sulfoxide and standard analyte of PbTx-2, PbTx-1, PbTx-3 and PbTx-9 was spiked respectively into the extract to obtain standard curves. The standard curves obtained in the matrix extract are presented in Fig. 2. No remarkable matrix extract intersecting appears in standard curves of buffer, cockle and oyster matrix extract.

Recoveries of PbTx-2, PbTx-1, PbTx-3 and PbTx-9 extracted from tissue homogenates spiked at three dose levels are shown in Table 3. Recoveries of PbTx-2, PbTx-1, PbTx-3 and PbTx-9 were 98.7%–104.3%, 92.9%–101.2%, 95.4%–103.2% and 88.4%–99.3%, respectively and the recoveries of analytes from cockle (88.4%–102.3%) and oyster (89.4%–104.3%) were very similar, which is consistent with the corresponding standard curves in the matrix extract intersecting the standard curve in the buffer (Fig. 2). The results demonstrated that the matrices of cockle and oyster where PbTxs are found do not interfere remarkably with the assay. The optimised ELISA detection limit was calculated by taking the mean absorbance value of 10 blank wells plus 2 times standard deviations of the mean. The detection limit was found to be

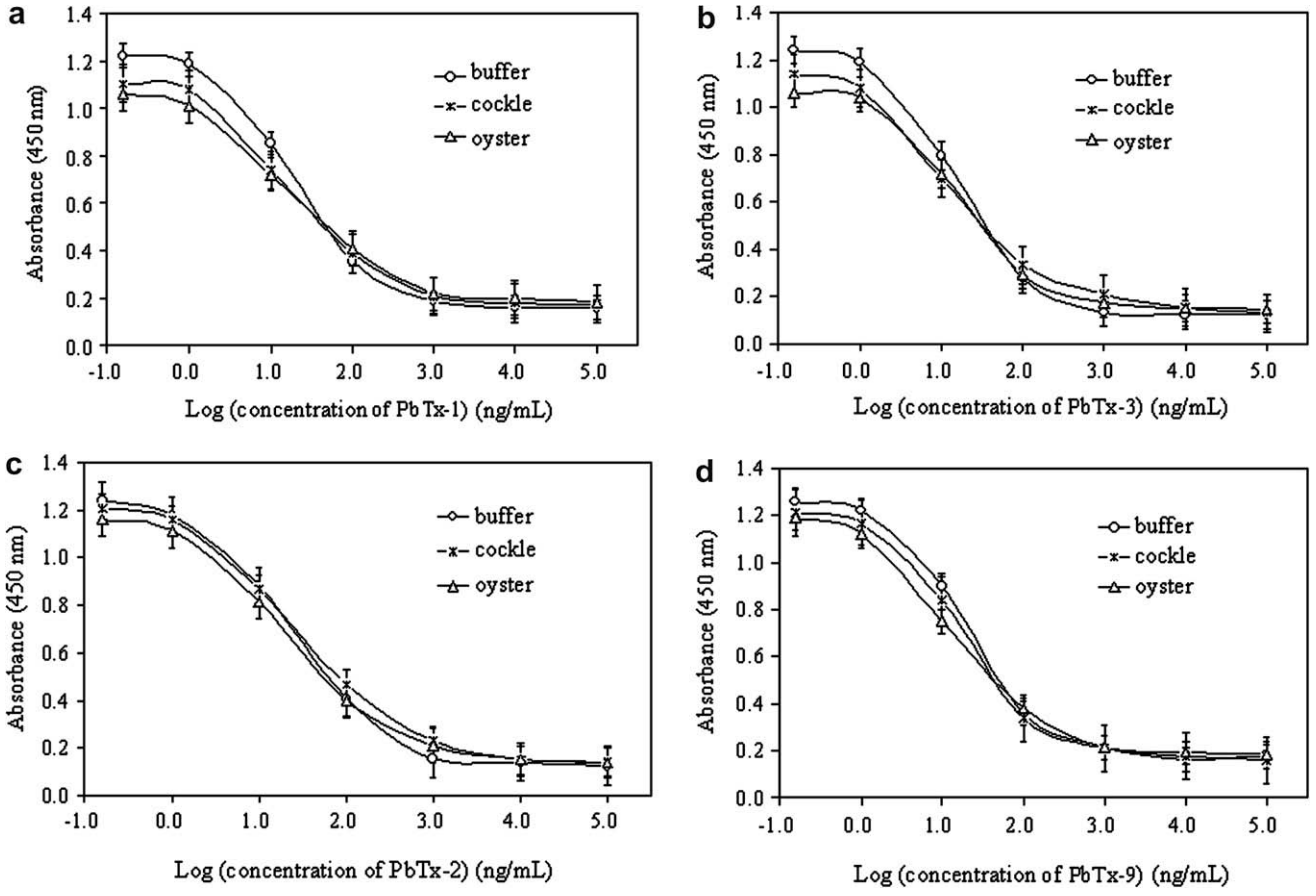

Fig. 2. Direct competition ELISA curves for PbTxs in matrix extract of cockle and oyster. Standard curve (a) PbTx-2 in extract by direct competition ELISA, (b) PbTx-1 in extract by direct competition ELISA, (c) PbTx-3 in extract by direct competition ELISA, (d) PbTx-9 in extract by direct competition ELISA. The details of assay protocol were described in text.

Table 3
Rcoveries of toxins from spiked homogenates of whole meat of shellfish[a].

Toxin	Concentration (ng/g)	Recovery (%) of toxins from	
		Cockle	Oyster
PbTx-2	4	102.1 ± 1.3	98.7 ± 2.4
	40	99.7 ± 0.8	104.3 ± 0.3
	400	101.3 ± 0.6	102.2 ± 2.7
PbTx-1	4	98.4 ± 1.3	92.9 ± 3.2
	40	101.2 ± 2.1	99.5 ± 2.2
	400	97.8 ± 0.7	95.4 ± 3.4
PbTx-3	4	95.4 ± 1.6	103.2 ± 3.1
	40	99.3 ± 2.5	101.8 ± 2.3
	400	102.3 ± 0.9	98.5 ± 4.1
PbTx-9	4	88.4 ± 3.1	92.3 ± 3.3
	40	98.6 ± 0.4	89.4 ± 2.9
	400	99.3 ± 1.2	96.2 ± 0.8

Results are mean ± SD (n = 5).
[a] Assay conditions were described in the text.

0.6 ng well^{-1}, close to the sensitivity of immunochromatographic assay (Zhou et al., 2009), higher than electrochemi-luminescence-based competitive displacement immunoassay (Poli et al., 2007) and lower than ELISA (Naar et al., 2001). The assay could be accomplished within 1.5 h, less than that of other immunoassays (Naar et al., 2001; Twiner et al., 2007).

4. Conclusions

We produced a monoclonal antibody which shows high-affinity against PbTxs, and developed monoclonal antibody-based competitive ELISA for detection of PbTxs. The IC50 value of the optimised direct competitive ELISA was 5.3 ng mL^{-1} with a detection limit of 0.6 ng well^{-1}. The antibody showed high CR with PbTx-1, PbTx-3 and PbTx-9, negligible CR with ciguatoxin-1 and okadaic acid, and no signigcant CR with microcystin LR and dinophysistoxin. Recoveries of PbTxs from spiked cockle and oyster ranged 88.4%–102.3% and 89.4%–104.3%, respectively. The newly developed competitive ELISA seems to be a useful method for monitoring PbTxs in mollusk.

Acknowledgement

This work was supported by the National Natural Science Foundation of China (No. 30771657).

References

Dechraoui, M. Y., Naar, J., Pauillac, S. A., & Legrand, M. (1999). Ciguatoxins and brevetoxins, neurotoxic polyether compounds active on sodium channels. *Toxicon, 37*, 125–143.
Dong, Z. W., & Wang, Y. (2002). *Antibody engineering*. Beijing: Beijing Medical University Press. p. 281.
Fairey, E. R., Bottein Dechraoui, M. Y., Sheets, M. F., & Ramsdell, J. S. (2001). Modification of the cell based assay for brevetoxins using human cardiac voltage dependent sodium channels expressed in HEK-293 cells. *Biosensors & Bioelectronics, 16*, 579–586.
Kamps, C., Carlin, R. G., & Shefield, L. (1993). Analysis of hapten-carrier protein conjugates by nondenaturing gel electrophoresis. *Journal of Immunological Methods, 164*, 245–253.
Kentaro, K., Yonekazu, H., & Tamao, N. (1999). Production and characterization of a monoclonal antibody against domoic acid and its application to enzyme immunoassay. *Toxicon, 37*, 1579–1589.
Levine, L., & Shimizu, Y. (1992). Antibodies to brevetoxin B: Serologic differentiation of brevetoxin B and brevetoxin A. *Toxicon, 30*, 411–418.
Lewis, R. J. (1995). Detection of ciguatoxins and related benthic dinoagellate toxins: In vivo and in vitro methods. *Manual on Harmful Marine Microalgae, 923*, 135–161.
Liu, X. B., Cai, M. Y., Wang, X., & Li, X. R. (1999). One simple and efficient method for purification of IgG McAb from mice ascites: Caprylic acid/ammonium sulfate precipitation. *Journal of Sichuan University (Medical Science Edition), 30*, 455–456.
Melinek, R., Rein, K. S., Schultz, D. R., & Baden, D. G. (1994). Brevetoxin PbTx-2 immunology: differential epitope recognition by antibodies from two goats. *Toxicon, 32*, 883–890.
Naar, J., Branaaa, P., Bottein-Dechraoui, M. Y., Chinain, M., & Pauillac, S. (2001). Polyclonal and monoclonal antibodies to PbTx-2-type brevetoxins using minute amount of hapten-protein conjugates obtained in a reversed micellar medium. *Toxicon, 39*, 869–878.
Plakas, S. M., Jester, E. L. E., El Said, K. R., Granade, H. R., Abraham, A., Dickey, R. W., et al. (2008). Monitoring of brevetoxins in the *Karenia brevis* bloom-exposed Eastern oyster (*Crassostrea virginica*). *Toxicon, 52*, 32–38.
Poli, M. A., Rein, K. S., & Baden, D. G. (1995). Radioimmunoassay for PbTx-2-type brevetoxins: Epitope specificity of two anti-PbTx sera. *Journal of AOAC International, 78*, 538–542.
Poli, M. A., Rivera, V. R., Neal, D. D., Baden, D. G., Messer, S. A., Plakas, S. M., et al. (2007). An electrochemi-luminescence-based competitive displacement immunoassay for the type-2 brevetoxins in oyster extracts. *Journal of AOAC International, 90*, 173–178.
Trainer, V. L., & Baden, G. D. (1990). An enzyme immunoassay for the detection of Florida red tide brevetoxins. *Toxicon, 29*, 1387–1394.
Trainer, V. L., & Baden, D. G. (1991). An enzyme immunoassay for the detection of Florida red tide brevetoxins. *Toxicon, 29*, 1387–1394.
Twiner, M. J., Bottein Dechraoui, M. Y., Wang, Z. H., Mikulski, C. M., Henry, M. S., Pierce, R. H., et al. (2007). Extraction and analysis of lipophilic brevetoxins from the red tide dinoflagellate *Karenia brevis*. *Analytical Biochemistry, 369*, 128–135.
Zhou, Y., Li, Y. S., Pan, F. G., Tan, J. H., Liu, Z. S., & Wang, Z. (2006). The study of purified methods of mice ascites IgG McAb. *Heilongjiang Animal Science and Veterinary Medicine, 10*, 14–17.
Zhou, Y., Pan, F. G., Li, Y. S., Zhang, Y. Y., Zhang, J. H., Lu, S. Y., et al. (2009). Colloidal gold probe-based immunochromatographic assay for the rapid detection of brevetoxins in fishery product samples. *Biosensors and Bioelectronics, 24*, 2744–2747.

Food Chemistry 118 (2010) 472–481

Contents lists available at ScienceDirect

Food Chemistry

journal homepage: www.elsevier.com/locate/foodchem

Analytical Methods

Development and validation of two new sensitive ELISAs for Hesperetin and Naringenin in biological fluids

Svitlana Shinkaruk [a,b], Valérie Lamothe [a,b], Jean-Marie Schmitter [c,d], Claudine Manach [e], Christine Morand [e], Annie Berard [f], Bernard Bennetau [g,h], Catherine Bennetau-Pelissero [a,b,*]

[a] Université de Bordeaux, EA 2975 UBX1-UBX2-ENITA de Bordeaux, F-33405, France
[b] ENITA de Bordeaux, UMRS, F-33175, France
[c] Université de Bordeaux, IECB, F-33607, France
[d] CNRS, UMR 5248 UBX1-ENITA de Bordeaux, F-33607, France
[e] INRA Clermont-Ferrand Theix, UNH, UMR 1019, Saint Genes Champanelle, F-63122, France
[f] CHU de Bordeaux – Université Victor Ségalen Bordeaux 2, ERI "Facteurs de risques vasculaires, nutriments, prévention de l'athérome", case 49, 146 rue Léo-Saignat, F-33076, France
[g] Université de Bordeaux, UMR 5255 ISM, F-33405, France
[h] CNRS, UMR 5255 ISM, F-33405, France

ARTICLE INFO

Article history:
Received 24 July 2008
Received in revised form 13 March 2009
Accepted 2 May 2009

Keywords:
Flavanone
Hesperetin
Naringenin
Haptens
Polyclonal antibodies
ELISA
Plasma
Urine

ABSTRACT

Carboxylic acid haptens were synthesised, for Hesperetin (**Hesp**) and Naringenin (**Nar**). They had a spacer arm (4 or 6 carbons long) on the C7 position. Haptens were coupled to bovine serum albumin. Polyclonal antibodies were generated. Enzyme-linked immunosorbent assays (ELISAs) were developed. Owing to sensitivity, one antibody for each flavanone was retained, namely anti-**h4-Hesp** and anti-**h4-Nar**. For **Hesp** and Nar, IC_{50} of the standard curves were 1.29 pmol/well and 0.72 pmol/well, respectively. Intra-assay and inter-assay variations were 10.24% and 10.53%, respectively for **Hesp** and 10.03% and 10.79%, respectively for **Nar**. Anti-**h4-Hesp** was highly specific when **anti-h4-Nar** showed cross-reactions with liquiritigenin and eriodictyol, which were significantly reduced in heterologous assay conditions. Assays were validated by comparisons with HPLC Coularray. Measurements were done on diet, plasma and urine samples from mice fed on diets enriched with **Hesp** or **Nar** and on a range of diluted mice urine samples.

1. Introduction

Hesperetin (**Hesp**) and Naringenin (**Nar**) belong to the flavanone family, which is one category of flavonoids. All flavonoids have a C6–C3–C6 backbone. There has been considerable interest in the flavonoid content of foods since the early 1980s when a link was established between a diet rich in fruits and vegetables and a reduced risk of chronic diseases (Steinmetz & Potter, 1991a, 1991b). Among other compounds, a high intake of **Hesp** and/or **Nar** was shown to be associated with a reduced risk of several chronic diseases (Knekt et al., 2002). This includes vascular risk in humans for which various mechanisms have been proposed like increased nitric oxide production (Liu, Xu, & Cheng, 2008), significant decrease of triacylglycerol, total cholesterol and phospholipid levels in serum (Huong, Takahashi, & Ide, 2006), and significant increase in high density lipoprotein (HDL) in plasma (Jeon et al., 2007). **Hesp** and **Nar** also display anti-atherogenic effects (Lee et al., 2003). **Nar** has been shown to present oestrogenic effects (Bovee, Schoonen, Hamers, Bento, & Peijnenburg, 2008) although essentially via non genomic pathways (Koohi, Walther, & Ivell, 2007). **Hesp** and **Nar** were also shown to exhibit anti-oestrogenic effects in MCF-7 and fibroblasts co-culture through anti-aromatase effects (van Meeuwen, Korthagen, de Jong, Piersma, & van den Berg, 2007). Several studies are in accordance and show a preventive effect of **Nar** against lung cancer (Hsiao et al., 2007; Malaveille et al., 1996).

Hesp and **Nar** are commonly conjugated in plants with a variety of groups like glycoside, malonyl or acetyl. Their concentrations in citrus fruits are exceptionally high, reaching 180–320 mg/L for

Abbreviations: Bi, OD of sample or standard wells; Bo, OD of positive control; BSA, bovine serum albumin; DMF, *N,N*-dimethylformamide; DMSO, dimethyl sulfoxide; ELISA, enzyme linked immunosorbent assay; IC_{50}, concentration for 50% inhibition; IR, infrared spectroscopy; MALDI, matrix assisted laser desorption ionisation; NBS, *N*-bromosuccinimide; NMR, nuclear magnetic resonance; OD, optical density; PBS, phosphate buffer saline; ppm, part per million; PS, pork serum; TLC, thin layer chromatography; Thyr, thyroglobulin.

* Corresponding author. Address: ENITA de Bordeaux, 1, Cours du Général de Gaulle, 33175 Gradignan, France. Tel.: +33 557 350 754; fax: +33 557 350 749.
E-mail address: c-bennetau@enitab.fr (C. Bennetau-Pelissero).

0308-8146/$ - see front matter © 2009 Elsevier Ltd. All rights reserved.
doi:10.1016/j.foodchem.2009.05.002

hesperidin (**Hesp**-glycoside) in orange juice (Gil-Izquierdo, Riquelme, Porras, & Ferreres, 2004) and 26 mg **Nar** (equivalent aglycones)/100 g fresh grapefruit (Harnly et al., 2006) while in strawberries or tomatoes, **Nar** concentrations (equivalent aglycones) are about 1.8 or 2 mg/100 g fresh fruit.

Numerous methods have been reported for the determination of flavonoids. They rely essentially on chromatographic separation associated with various detection methods allowing the concomitant determination of several compounds in one run (Sakakibara, Honda, Nakagawa, Ashida, & Kanazawa, 2003). Generally, quantification in vegetal foodstuffs is achieved after the hydrolysis of the glycosylated flavonoids to allow comparison with commercially available aglycone standards and to reduce the number of compounds to analyse. The hydrolysis procedure included refluxing the samples in an acidified methanolic solution but this hydrolysis procedure may also lead to the degradation of the aglycones (Merken, Merken, & Beecher, 2001). In biological fluids, flavonoids are not present as native forms or aglycones but as conjugated derivatives resulting from the intestinal and hepatic conjugation process (namely glucuronidation, sulfatation, methylation). Thus quantification of flavonoids in plasma and urine is achieved after enzymatic hydrolysis of conjugates (Morand, Manach, Donovan, & Remesy, 2001) followed by a chromatographic analysis coupled to diode array detection (Radtke, Linseisen, & Wolfram, 2002), coulometric detection (Manach, 2003), photo-diode array electrospray mass spectrometry (Franke et al., 2002), UV detection (Kanaze, Kokkalou, Georgarakis, & Niopas, 2004) or MS–MS detection (Grace, Mistry, Carter, Leathem, & Teale, 2007). All these techniques induce rather high costs and require high physicochemical skills. Detection in biological fluids enables the determination of the flavonoid bioavailability and the correlation of the ingested amounts with the registered effects. They may prove that when the plasma concentrations increase, the effect is higher. Such an approach can also exhibit the high inter-individual variation of plasma concentrations, thus explaining the large variety of effects registered in consumers. Naringin, namely the **Nar**-glycoside from food, is first deglycosylated into **Nar** by the β-glycosidases of enterocytes. Then colonic bacteria are able to metabolize **Nar** into various compounds including **Nar** aglycone phloroglucinol, 3-(4-hydroxyphenyl)-propionic acid, and 3-phenylpropionic acid depending on the human subject and on the quality of gut microflora (Rechner et al., 2004). Then, in rat and human plasmas, flavanones are present as glucuronide and sulphate conjugates (Felgines et al., 2000; Manach, Morand, Gil-Izquierdo, Bouteloup-Demange, & Remesy, 2003). In addition, **Hesp** and probably **Nar** as well, can bind with human serum albumin to form a polyphenol–protein complex in molecular association ranging from 0.3 to 7 (Xie, Xu, & Wang, 2005). This can influence **Hesp** availability at the cellular level. Rat liver microsomes are also able to convert flavanones into flavones and hydroxy-quinones having different activities compared to their parent compounds (Nikolic & van Breemen, 2004). Therefore, plasma bioavailability of **Nar** and **Hesp** results from complex processes.

In this context and to further explore the biological effects of these compounds it appeared relevant to develop easy-to-use methods and limited cost methodologies for biological fluid analysis. This can help to correlate an ingested quantity of glycosylated compounds with circulating forms and biological effects, and demonstrate a dose dependant effect based on circulating concentrations rather than on ingested amount. Therefore this paper relates the chemical synthesis of new haptens of **Nar** and **Hesp**, and the production of specific antibodies and their use in quantitative ELISA for measuring **Nar** and **Hesp** concentrations in diets and in animal fluids.

2. Materials and methods

2.1. Chemicals

Hesp (4′-methoxy-3′,5,7-trihydroxyflavanone) and **Nar** (4′,5,7-trihydroxyflavanone) were purchased from Sigma–Aldrich Chemical Co. (Saint Quentin Fallavier, France). Ethyl 4-bromobutyrate, ethyl 6-bromohexanoate, and potassium *tert*-butoxide were obtained from Alfa Aesar (Bischheim, France). Dimethylformamide (DMF) was dried by distillation over CaO and stored over 4 Å molecular sieves. All moisture-sensitive reactions were performed under argon atmosphere in oven-dried or flame-dried glassware. Biological reagents were purchased from Sigma–Aldrich (Saint Quentin Fallavier, France) except for the secondary antibody, i.e. goat anti-rabbit IgG-horseradish peroxidase purchased from DAKO (Trappes, France) and the enzyme used to hydrolyse the samples, i.e. β-D-glucuronoside glucuronosohydrolase-arylsulfate sulfohydrolase from *Helix pomatia* which was purchased from Roche Diagnostic (Mannheim, Germany).

2.2. Instruments

Melting points were determined with a Stuart Scientific melting point SMP3 apparatus and were uncorrected. ^{1}H and ^{13}C NMR spectra were recorded with a Bruker AC-300 FT (^{1}H: 300 MHz, ^{13}C: 75 MHz) or with a Bruker AC 250 (^{1}H: 250 MHz, ^{13}C: 63 MHz). The spectra were calibrated using the frequency of the deuterated solvent (the lock frequency). The chemical shifts (δ) and coupling constants (J) are, respectively expressed in ppm and Hz. IR spectra were recorded with a Perkin–Elmer paragon 1000 FT-IR spectrophotometer. Thin-layer chromatography (TLC) was performed using Merck TLC plates, (0.25 mm, particle size 15 μm, pore size 60 Å). Merck silica gel 60 (70–230 mesh, 0.063–0.200 mm) was used for flash chromatography. The spots were visualised with a UV lamp. Mass spectra of **Hesp** and **Nar** haptens were acquired on a QStar Elite mass spectrometer (Applied Biosystems). The instrument was equipped with an ESI source and the spectra were recorded in the positive mode. The electrospray needle was maintained at 4500 V and operated at room temperature. Samples were introduced by injection through a 10 μL sample loop into a 200 μL/min flow of methanol from the LC pump.

Optical densities (OD) of microtitration plates were read on a Dynex MRX II microtitration plate reader at 490 nm. The plates were NUNC Maxisorp® 96 wells microtitration plates.

2.3. Chemical synthesis

2.3.1. Ethyl 4-{[5-hydroxy-2-(4-hydroxyphenyl)-4-oxo-3,4-dihydro-2H-chromen-7-yl]oxy} butanoate (**5**)

Typical procedure. **Nar** (4′,5,7-trihydroxyflavanone, 2.72 g, 10 mmol) was dissolved in acetone (30 mL), K_2CO_3 (2.76 g, 20 mmol) and ethyl 4-bromobutyrate (2.93 g, 15 mmol) were then added. The mixture was refluxed for 5 h and then allowed to cool to room temperature. The reaction mixture was filtered, and the filtrate was evaporated to dryness to give a yellow oil (5.8 g). Flash chromatography using dichloromethane: methanol (97:3) as an eluent gave the desired compound (**6**) as a pale yellow oil (R_f = 0.15, 3.0 g, 78%).

^{1}H NMR ($CDCl_3$, 300 MHz): δ1.24 (t, J = 7.1 Hz, 3H, CH_3), 2.08 (quintuplet, J = 6.8 Hz, 2H, CH_2), 2.48 (t, J = 6.8 Hz, 2H, CH_2), 2.69 (dd, J = 17, 3 Hz, 1H, H-3b), 3.06 (dd, J = 17, 13 Hz, 1H, H-3a), 3.98 (t, J = 6.8 Hz, 2H, CH_2), 4.12 (q, J = 7.1 Hz, 2H, CH_2), 5.27 (dd, J = 13, 3 Hz, 1H, H-2), 5.97 (d, J = 2.3 Hz, 1H, H_{ar}, 6), 6.01 (d, J = 2.3 Hz, 1H, H_{ar}, 8), 6.86 (d, J = 8.7 Hz, 2H, H_{ar}, 3′,5′), 7.27 (d, J = 8.7 Hz, 2H, H_{ar}, 2′,8′).

Table 1
Experimental conditions for synthesis of haptens 1–4.

Hapten	Step 1		Step 2	
	Conditions	Yield (%)	Conditions	Yield (%)
For Nar				
1	K_2CO_3 (3 eq), acetone, reflux	78	1 M LiOH, MeOH	45
3	K_2CO_3 (3 eq), DMF, 70 °C[a]	76	1 M LiOH, MeOH	34
For Hesp				
2	*t*-BuOK (2 eq), DMF, 70 °C[b]	80	1 M LiOH, MeOH	29
4	*t*-BuOK (2 eq), DMF, 70 °C[b]	65	1 M LiOH, acetonitrile	30

[a] Low yield of reaction in acetone and in *i*-propanol (ambient temperature, reflux).
[b] No reaction in conditions used for Naringenin haptens.

^{13}C NMR ($CDCl_3$, 75 MHz): δ196.3 (C=O), 173.4 (COOEt), 167.2 (CQ), 164.0 (CQ), 163.0 (CQ), 156.8 (CQ), 129.9 (CQ), 127.9 (CH_{ar}, 2′,6′), 115.7 (CH_{ar}, 3′,5′), 103.1 (CQ), 95.5 (CH_{ar}, 6), 94.6 (CH_{ar}, 8), 79.0 (CH-2), 67.3 (CH_2O), 60.8 (CH_2CH_3), 43.0 (CH_2-3), 30.7 (CH_2C=O), 24.3 (CH_2), 14.2 (CH_3).

The compounds (**6**), (**7**), and (**8**) were prepared as described for (**5**). The conditions used for each reaction are summarised in Table 1.

*2.3.2. Ethyl 4-{[5-hydroxy-2-(4-hydroxyphenyl)-4-oxo-3,4-dihydro-2H-chromen-7-yl]oxy} hexanoate (**7**)*

Nar (4′,5,7-trihydroxyflavanone, 2.72 g, 10 mmol) was reacted with ethyl 6-bromohexanoate (3.35 g, 15 mmol) as described for (**6**) except for the solvent used (see Table 1). The purification by flash chromatography using dichloromethane:methanol (95:5) as an eluent gave the target compound (**8**) as a yellow oil (R_f = 0.3, 3.16 g, 78%).

^{1}H NMR ($CDCl_3$, 300 MHz): δ1.24 (t, J = 7.1 Hz, 3H, CH_3), 1.47 (quintuplet, J = 7 Hz, 2H, CH_2), 1.66 (quintuplet, J = 7.0 Hz, 2H, CH_2), 1.87 (quintuplet, J = 7.0 Hz, 2H, CH_2), 2.32 (t, J = 7.0 Hz, 2H, CH_2), 2.76 (dd, J = 17, 3 Hz, 1H, H-3b), 3.08 (dd, J = 17, 12.8 Hz, 1H, H-3a), 3.95 (t, J = 7.0 Hz, 2H, CH_2), 4.12 (q, J = 7.1 Hz, 2H, CH_2), 5.33 (dd, J = 12.8, 3 Hz, 1H, H-2), 6.01 (m, 2H, H_{ar}, 6, 8), 6.89 (d, J = 8.7 Hz, 2H, H_{ar}, 3′, 5′), 7.30 (d, J = 8.7 Hz, 2H, H_{ar}, 2′,8′).

^{13}C NMR ($CDCl_3$, 75 MHz): δ196.1 (C=O), 173.7 (COOEt), 167.4 (CQ), 164.0 (CQ), 162.9 (CQ), 156.8 (CQ), 129.9 (CQ), 127.9 (CH_{ar}, 2′,6′), 115.7 (CH_{ar}, 3′,5′), 103.0 (CQ), 95.5 (CH_{ar}, 6), 94.5 (CH_{ar}, 8), 79.0 (CH-2), 68.1 (CH_2O), 60.3 (CH_2CH_3), 43.1 (CH_2-3), 34.1 (CH_2C=O), 32.4 (CH_2), 27.6 (CH_2), 24.1 (CH_2), 14.2 (CH_3).

*2.3.3. Ethyl 4-{[5-hydroxy-2-(3-hydroxy-4-methoxyphenyl)-4-oxo-3,4-dihydro-2H-chromen-7-yl] oxy}butanoate (**6**)*

Hesp (4′-methoxy-3′,5,7-trihydroxyflavanone, 2 g, 6.6 mmol) was reacted with ethyl 4-bromobutyrate (1.95 g, 10 mmol) under the conditions described in Table 1. The cooled reaction mixture was poured onto ice and the pH was adjusted to 2 with 10% HCl. The EtOAc/H_2O work-up gave the target compound (**5**) as an oil (2.1 g, 80%) which was used without further purification.

^{1}H NMR ($CDCl_3$, 250 MHz): δ1.23 (t, J = 7.1 Hz, 3H, CH_3), 2.01 (quintuplet, J = 6.8 Hz, 2H, CH_2), 2.46 (t, J = 7.3, 2H, CH_2COOEt), 2.74 (dd, J = 17, 3 Hz, 1H, H-3b), 3.09 (dd, J = 17, 12.8 Hz, 1H, H-3a), 3.88 (s, 1H, OCH_3), 4.04 (t, J = 6.3 Hz, 2H, CH_2O), 4.12 (q, J = 7.1 Hz, 2H, CH_2), 5.30 (dd, J = 12.8, 3 Hz, 1H, H-2), 6.04 (m, 2H, H_{ar}, 6, 8), 6.90 (m, 2H, H_{ar}, 5′, 6′), 7.02 (d, J = 1.9 Hz, 1H, H_{ar}, 2′).

^{13}C NMR ($CDCl_3$, 63 MHz): δ196.5 (C=O), 174.8 (COO), 167.1 (CQ), 163.7(CQ), 163.0 (CQ), 147.9 (CQ), 146.4 (CQ), 131.5 (CQ), 117.6 (CH_{ar}, 6′), 113.2 (CH_{ar}, 2′), 111.1 (CH_{ar}, 5′), 102.7 (CQ), 94.8 (CH_{ar}, 6), 93.0 (CH_{ar}, 8), 79.0 (CH-2), 67.1 (CH_2O), 60.3 (CH_2CH_3), 55.0 (OCH_3), 42.6 (CH_2-3), 29.8 (CH_2C=O), 24.1 (CH_2), 14.2 (CH_3).

*2.3.4. Ethyl 4-{[5-hydroxy-2-(3-hydroxy-4-methoxyphenyl)-4-oxo-3,4-dihydro-2H-chromen-7-yl]oxy}hexanoate (**8**)*

Hesp (4′-methoxy-3′,5,7-trihydroxyflavanone, 3.02 g, 10 mmol) was reacted with ethyl 6-bromohexanoate (3.35 g, 15 mmol) as described above. The purification by flash chromatography using diethyl ether:pentane (8:2) gave the target compound (**7**) as a yellow solid (2.8 g, 65%).

^{1}H NMR ($CDCl_3$, 300 MHz): δ1.27 (t, J = 7.2 Hz, 3H, CH_3), 1.48 (quintuplet, J = 7.2 Hz, 2H, CH_2), 1.75 (m, 4H, CH_2CH_2), 2.34 (t, J = 7.3, 2H, CH_2COOH), 2.79 (dd, J = 17, 3 Hz, 1H, H-3b), 3.08 (dd, J = 17, 12.8 Hz, 1H, H-3a), 3.93 (s, 1H, OCH_3), 3.98 (t, J = 6.4 Hz, 2H, CH_2O), 4.16 (q, J = 7.2 Hz, 2H, CH_2), 5.34 (dd, J = 12.8, 3 Hz, 1H, H-2), 6.04 (d, J = 2.3 Hz, 1H H_{ar}, 6), 6.06 (d, J = 2.3 Hz, 1H H_{ar}, 8), 6.90 (d, 1H, J = 8.3 Hz, H_{ar}, 5′), 6.94 (dd, J = 8.3, 1.9 Hz, 1H, H_{ar}, 6′), 7.06 (d, J = 1.9 Hz, 1H, H_{ar}, 2′), 12.02 (s, OH).

^{13}C NMR ($CDCl_3$, 63 MHz): δ196.3 (C=O), 174.0 (COO), 167.8 (CQ), 164.4 (CQ), 163.2 (CQ), 147.4 (CQ), 146.3 (CQ), 131.9 (CQ), 118.5 (CH_{ar}, 6′), 113.1 (CH_{ar}, 2′), 111.0 (CH_{ar}, 5′), 103.4 (CQ), 95.8 (CH_{ar}, 6), 94.9 (CH_{ar}, 8), 79.3 (CH-2), 68.6 (CH_2O), 60.7 (CH_2CH_3), 56.4 (OCH_3), 43.5 (CH_2-3), 34.5 (CH_2C=O), 28.9 (CH_2), 25.9 (CH_2), 24.9 (CH_2), 14.6 (CH_3).

*2.3.5. 4-{[5-Hydroxy-2-(4-hydroxyphenyl)-4-oxo-3,4-dihydro-2H-chromen-7-yl]oxy}butanoic acid (**1**) or **h4-Nar***

An ice-cooled 1 M LiOH solution (10 mL) was added dropwise to a solution of (**6**) (1.22 g, 3.15 mmol) in methanol (10 mL) at 0 °C and the mixture was allowed to reach room temperature. After stirring for 2 h the pH was adjusted to pH 2–3 with 10% HCl. The aqueous phase was extracted with ethyl acetate (3 × 40 mL). The combined organic extracts were washed with water (50 mL) and brine (50 mL), dried ($MgSO_4$) and concentrated under reduced pressure. Flash chromatography using diethyl ether:pentane (8:2) as an eluent gave the desired compound (**2**) as white crystals (R_f = 0.24, 0.4 g, 45%, m.p. 172 °C).

^{1}H NMR (CD_3OD, 300 MHz): δ2.06 (quintuplet, J = 6.8 Hz, 2H, CH_2),2.48 (t, J = 8.0 Hz, 2H, CH_2), 2.73 (dd, J = 17, 3 Hz, 1H, H-3b), 3.17 (dd, J = 17, 13 Hz, 1H, H-3a), 4.06 (t, J = 7.4 Hz, 2H, CH_2), 5.38 (dd, J = 13, 3 Hz, 1H, H-2), 6.06 (m, 2H, H_{ar}, 6, 8), 6.82 (d, J = 8.6 Hz, 2H, H_{ar}, 3′,5′), 7.33 (d, J = 8.6 Hz, 2H, H_{ar}, 2′,8′).

^{13}C NMR (CD_3OD, 63 MHz): δ197.9 (C=O), 174.4 (COOH), 168.3 (CQ), 165.2 (CQ), 165.0 (CQ), 164.5 (CQ), 130.9 (CQ), 129.3 (CH_{ar}, 2′,6′), 116.4 (CH_{ar}, 3′,5′), 116.3 (CQ), 96.1 (CH_{ar}, 6), 95.2 (CH_{ar}, 8), 80.3 (CH-2), 68.6 (CH_2O), 43.8 and 43.7 (CH_2-3), 30.6 (CH_2C=O), 25.4 (CH_2).

IR (cm^{-1}, KBr): 3443, 3138, 1699, 1640, 1611, 1570, 1519, 1308, 1197, 1168, 1090.

MS (ESI+) m/z 739 $[2M+Na]^+$, 381 $[M+Na]^+$, 359 $[M+H]^+$.

HR-MS (ESI+) m/z calculated for $C_{19}H_{18}O_7$: 359.1125 $[M+H]^+$; found: 359.1124.

*2.3.6. 6-{[5-Hydroxy-2-(4-hydroxyphenyl)-4-oxo-3,4-dihydro-2H-chromen-7-yl]oxy}hexanoic acid (**3**) or **h6-Nar***

According to the procedure described above for compound (**2**), the intermediate (**8**) (2.2 g, 5.3 mmol) was treated with an ice-cooled 1 M LiOH solution (16 mL). Flash chromatography using diethyl ether: pentane (85:15) as an eluent gave a beige solid (R_f = 0.23) which was purified again by recrystallization from methanol to afford the desired compound (**3**) as white crystals (0.7 g, 34%, m.p. 144 °C).

^{1}H NMR ($(CD_3)_2CO$, 250 MHz): δ1.51 (quintuplet, J = 7.0 Hz, 2H, CH_2), 1.67 (quintuplet, J = 7.0 Hz, 2H, CH_2), 1.80 (quintuplet, J = 7.0 Hz, 2H, CH_2), 2.32 (t, J = 7.3, 2H, CH_2COOH), 2.75 (dd, J = 17, 3 Hz, 1H, H-3b), 3.20 (dd, J = 17, 13 Hz, 1H, H-3a), 4.07 (t, J = 6.4 Hz, 2H, CH_2), 4.97 (dd, J = 13, 3 Hz, 1H, H-2), 6.04 (m, 2H, H_{ar}, 6, 8), 6.90 (d, J = 8.5 Hz, 2H, H_{ar}, 3′,5′), 7.39 (d, J = 8.5 Hz, 2H, H_{ar}, 2′,8′), 12.13 (br s, OH).

^{13}C NMR ($(CD_3)_2CO$, 75 MHz): δ197.6 (C=O), 174.6 (COOH), 168.3 (CQ), 165.0 (CQ), 164.7 (CQ), 158.7 (CQ), 130.7 (CQ), 129.0 (CH_{ar}, 2′,6′), 116.1 (CH_{ar}, 3′,5′), 103.7 (CQ), 95.9 (CH_{ar}, 6), 95.0 (CH_{ar}, 8), 80.0 (CH-2), 69.1 (CH_2O), 43.5 (CH_2-3), 34.1 (CH_2C=O), 29.3 (CH_2), 26.2 (CH_2), 25.3 (CH_2).

IR (cm^{-1}, KBr): 3308, 2946, 1718, 1708, 1638, 1615, 1519, 1379, 1302, 1167, 1090.

MS (ESI+) *m*/*z* 795 [2 M+Na]$^+$, 409 [M+Na]$^+$, 387 [M+H]$^+$.

HR-MS (ESI+) *m*/*z* calculated for $C_{21}H_{22}O_7$: 387.1444 [M+H]$^+$; found: 387.1438.

2.3.7. 4-{[5-Hydroxy-2-(3-hydroxy-4-methoxyphenyl)-4-oxo-3,4-dihydro-2H-chromen-7-yl]oxy} butanoic acid (**2**) or ***h4-Hesp***

According to the procedure applied for compound (**2**), the intermediate (**6**) (416 mg, 1 mmol) was treated with an ice-cooled 1 M LiOH solution (10 mL). Flash chromatography using diethyl ether: pentane (8:2) as an eluent gave a beige solid (R_f = 0.15) which was purified again by recrystallization from methanol to afford (**1**) as beige crystals (110 mg, 29%, m.p. 175 °C).

^{1}H NMR (CD_3OD, 300 MHz): δ2.05 (quintuplet, *J* = 6.8 Hz, 2H, CH_2), 2.49 (t, *J* = 7.3, 2H, CH_2COOH), 2.74 (dd, *J* = 17, 3 Hz, 1H, H-3b), 3.09 (dd, *J* = 17, 12.8 Hz, 1H, H-3a), 3.87 (s, 1H, OCH_3), 4.04 (t, *J* = 6.3 Hz, 2H, CH_2), 5.33 (dd, *J* = 12.8, 3 Hz, 1H, H-2), 6.04 (m, 2H, H_{ar}, 6, 8), 6.94 (m, 3H, H_{ar}, 2′, 5′, 6′).

^{13}C NMR (CD_3OD, 75 MHz): δ196.6 (C=O), 175.4 (COOH), 167.3 (CQ), 163.8 (CQ), 163.1 (CQ), 148.0 (CQ), 146.4 (CQ), 131.6 (CQ), 117.6 (CH_{ar}, 6′), 113.1 (CH_{ar}, 2′), 111.1 (CH_{ar}, 5′), 102.7 (CQ), 94.8 (CH_{ar}, 6), 94.0 (CH_{ar}, 8), 79.0 (CH-2), 67.2 (CH_2O), 55.0 (OCH_3), 42.6 (CH_2-3), 29.8 (CH_2C=O), 24.1 (CH_2).

IR (cm^{-1}, KBr): 3537, 3085, 2968, 1715, 1642, 1599, 1519, 1442, 1306, 1277, 1213, 1167, 1091, 1029.

MS (ESI+) *m*/*z* 799 [2M+Na]$^+$, 411 [M+Na]$^+$, 389 [M+H]$^+$.

HR-MS (ESI+) *m*/*z* calculated for $C_{20}H_{20}O_8$: 411.1050 [M+Na]$^+$; found: 411.1032.

2.3.8. 4-{[5-Hydroxy-2-(3-hydroxy-4-methoxyphenyl)-4-oxo-3,4-dihydro-2H-chromen-7-yl]oxy} hexanoic acid (**4**) or ***h6-Hesp***

As for compound (**2**), the intermediate (**8**) (710 mg, 1.6 mmol) (dissolved in acetonitrile (25 mL)) was treated with an ice-cooled 1 M LiOH solution (10 mL). Flash chromatography using diethyl ether:pentane (9:1) as an eluent gave (**4**) as a beige solid (R_f = 0.15, 200 mg, 30%, m.p. 163 °C).

^{1}H NMR (CD_3OD, 300 MHz): δ1.51 (quintuplet, *J* = 7.2 Hz, 2H, CH_2), 1.66 (quintuplet, *J* = 7.2 Hz, 2H, CH_2), 1.80 (quintuplet, *J* = 7.2 Hz, 2H, CH_2), 2.33 (t, *J* = 7.3, 2H, CH_2COOH), 2.75 (dd, *J* = 17, 3 Hz, 1H, H-3b), 3.11 (dd, *J* = 17, 12.8 Hz, 1H, H-3a), 3.88 (s, 1H, OCH_3), 4.02 (t, *J* = 6.4 Hz, 2H, CH_2), 5.36 (dd, *J* = 12.8, 3 Hz, 1H, H-2), 6.04 (m, 2H, H_{ar}, 6, 8), 6.94 (m, 3H, H_{ar}, 2′, 5′, 6′).

^{13}C NMR (CD_3OD, 75 MHz): δ197.1 (C=O), 174.9 (COOH), 167.3 (CQ), 163.6 (CQ), 163.2 (CQ), 148.4 (CQ), 146.9 (CQ), 131.4 (CQ), 118.2 (CH_{ar}, 6′), 114.5 (CH_{ar}, 2′), 112.4 (CH_{ar}, 5′), 103.0 (CQ), 95.4 (CH_{ar}, 6), 94.6 (CH_{ar}, 8), 78.8 (CH-2), 68.6 (CH_2O), 56.1 (OCH_3), 42.6 (CH_2-3), 34.0 (CH_2C=O), 28.6 (CH_2), 25.4(CH_2), 24.6 (CH_2).

IR (cm^{-1}, KBr): 3309, 2949, 1742, 1633, 1572, 1517, 1468, 1438, 1366, 1300, 1274, 1196, 1165, 1099, 1018.

MS (ESI+) *m*/*z* 855 [2M+Na]$^+$, 439 [M+Na]$^+$, 417 [M+H]$^+$.

HR-MS (ESI+) *m*/*z* calculated for $C_{22}H_{24}O_8$: 417.1543 [M+H]$^+$; found: 417.1528.

2.4. Preparation of the conjugates

The haptens (**h4-Hesp**, **h6-Hesp**, **h4-Nar** and **h6-Nar**) were coupled to bovine serum albumin (BSA) for injection into rabbits and to swine Thyr for coating. The conjugation procedure was derived from that described in Riggle (1991) and Szurdoki, Szekacs, Le, and Hammock (2002). Briefly, tributylamine (17.3 μl, 0.072 mmol), isobutyl chloroformate (4.7 μl, 0.036 mmol) and hapten (0.036 mmol) were added to 1 mL of DMF at 4 °C and stirred in an ice bath for 30 min. The resulting activated hapten solution in DMF was added dropwise to the protein solution (BSA: 6.1 mg, 0.069 μmol or Thyr: 48.24 mg, 0.087 μmol) in 5 mL of a borate buffer (borate-boric buffer 0.2 M, pH 8.7). The mixture was stirred for 6 h at room temperature, dialysed against phosphate buffer saline (PBS: 0.01 M, pH 7.4, 0.9% NaCl) and then against distilled water. The hapten–protein conjugates were lyophilised and stored at −20 °C.

2.5. Matrix assisted laser desorption–ionisation mass spectrometry (MALDI-MS)

The mass spectra of the hapten-BSA conjugates were recorded in the linear mode with a Bruker Reflex III mass spectrometer equipped with a UV laser (337 nm). Samples (10 μM aqueous solutions) were mixed (1/1 v/v) with matrix solutions (sinapinic acid or α-cyano-4-hydroxy-cinnamic acid, 10 mM in water/acetonitrile containing 0.1% trifluoroacetic acid) and 1 μl of the mixture was applied on a stainless steel target and left to dry at room temperature. Spectra were acquired in the external calibration mode using BSA as a reference. The hapten/carrier protein ratio of each conjugate was estimated by measuring the change in molecular weight due to covalent hapten attachment through the lysine ε-amino groups of BSA: hapten number = $(MW_{conjugate} - MW_{BSA})/MW_{hapten}$. For **h4-Nar** MW was considered as 340, for **h6-Nar** MW = 368, for **h4-Hesp** MW = 370, and for **h6-Hesp** MW = 398.

2.6. Immunisation of the rabbits

Immunisation was performed on germ- and pathogen-free New Zealand rabbits from Millegen (Labège, France). Rabbits were ear-sampled before immunization to collect pre-immunserum. During the immunization procedure performed subcutaneously at multiple points, 500 μg of hapten–BSA conjugates were injected at each injection. The first three injections were performed at one-week intervals. Two additional injections then followed after a three-week interval. Fifty millilitre were collected one week after the last injection. After blood clotting at 4 °C for 24 h, serum was centrifuged at 3000*g* for 10 min at 4 °C. Sera were stored at −20 °C in small aliquots. For each hapten–BSA conjugate, two rabbits were injected and only one serum was retained based on a cross-test (direct binding of the antibody onto the coated conjugate) checking for antibody titre. Titres of all antisera obtained against h4- or h6-**Hesp** and Nar were compared using the homologous coupled molecule (Thyr-**h-Hesp** was used with anti-**h-Hesp** and Thyr-**h-Nar** was used with the anti-**h-Nar**, the immobilized antigens exhibiting an homologous length of the spacer arm). OD were compared for a 1/10,000 2nd antibody dilution at 490 nm.

2.7. Validation of the assays

2.7.1. Origin of the samples

Mice blood samples were collected between 02:30 pm and 03:00 pm on animals starved from 08:00 pm the day before and fed a single meal the following morning at 08:30 am. The diet was a semi-synthetic diet enriched with 0.02%, 0.05% and 0.1% hesperidin or 0.02% naringin. 24 h-urine samples were collected from mice fed for 18 weeks on a diet enriched either with 0.02% hesperidin or 0.02% naringin.

2.7.2. Hydrolysis of flavanone glucuronides

Hesp and **Nar**-glucuro and sulfo-conjugates contained in the food matrix and in the plasma, respectively, were hydrolysed using β-glucuronidase aryl-sulfatase from *Helix pomatia* (Roche

Table 2
Optimal conditions for each assay procedure.

Antisera		Anti-**h4-Hesp**	Anti-**h4-Nar**
Coating flavanone-Thyr (μg mL^{-1})		0.8	0.8
Specific antibody dilution		1/20,000	1/20,000
2nd antibody dilution		1/10,000	1/10,000
Standard curve limit (ng mL^{-1})		125–0.06	125–0.06
IC_{50} ng mL^{-1}		*1.95*	*0.98*
Detection limit (ng mL^{-1})		0.24	0.12
Slope		0.0805 ± 0.009	0.0778 ± 0.08
Intra-assay variation (%) n = 22	High (1000 ng mL^{-1})	9.06	10.01
	Low (5 ng mL^{-1})	11.42	10.03
Inter-assay variation (%) n = 10	High (1000 ng mL^{-1})	10.87	9.24
	Low (5 ng mL^{-1})	10.18	12.33

IC_{50}: Concentration of the analyte required for 50% inhibition of the antibody binding to the coating antigen.

Diagnostic). The hydrolysis recovery ratio was monitored as described in Bennetau-Pelissero et al. (2003).

2.7.3. Flavanone extraction from plasma

Free flavanone aglycones were extracted using a liquid–liquid extraction with acidified ethyl acetate (1% HCl). After evaporation to dryness, the extracts were stored at −20 °C until assay. In addition, three external standards of extraction, i.e. control plasma containing either **Hesp** or **Nar** in known quantities were run in parallel to the sample extraction to check the extraction recovery.

2.7.4. Extraction procedure for mice diets

The extraction procedure for diet samples was as described by Bennetau-Pelissero et al. (2003) and implied a re-suspension of 1 g of finely grounded diet into 100 mL of distilled water with vigorous shaking and sonications. The procedure then included

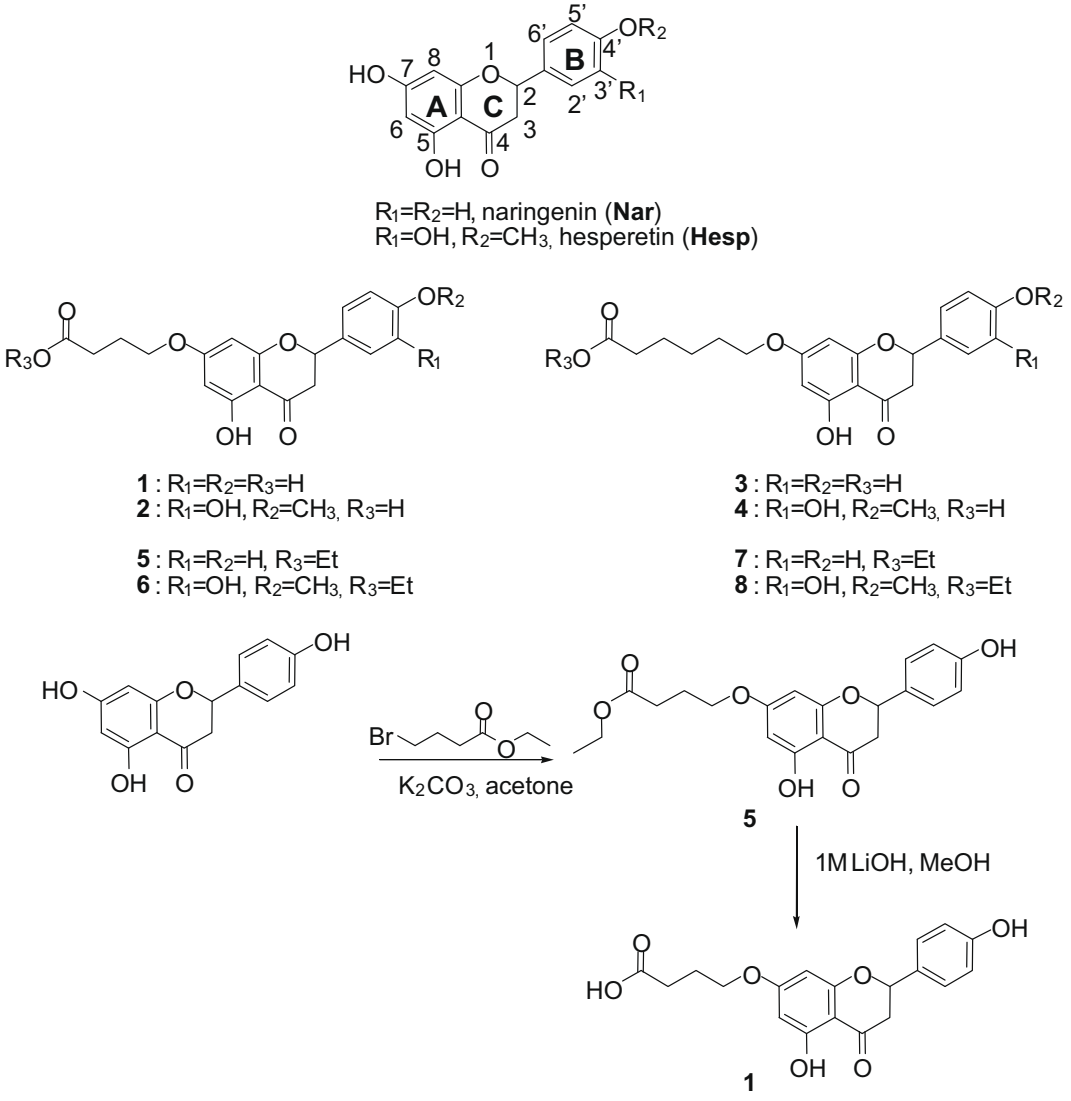

Fig. 1. Structure and synthesis of Naringenin and Hesperetin haptens.

an enzymatic hydrolysis with β-glucuronidase-aryl sulfatase (from Roche) before ethyl acetate extraction. This enzyme was demonstrated to hydrolyse glycosides. The recovery was monitored as previously described.

2.7.5. Assay procedure

Coating of the wells was performed overnight at 4 °C with the homologous hapten (with the corresponding spacer arm) coupled to Thyr (i.e. Thyr-**h**-**Hesp** and Thyr-**h**-**Nar** for **Hesp** and **Nar**, respectively) (200 μL/well). The conjugates were dissolved in a carbonate buffer (0.05 M, pH 9.6). Wells were then saturated at 37 °C for 30 min with PBS–Tween–PS–DMSO (PBS containing 1 mg mL^{-1} BSA, 0.05% Tween 20 and 1% DMSO) in order to avoid further unspecific binding. Then, plates were washed three times with PBS–Tween–DMSO (PBS, 0.05% Tween 20, 1% DMSO). Twelve serial dilutions (1 in 2) from 125 to 0.06 ng mL^{-1} of the appropriate analyte in PBS–Tween–PS–DMSO were prepared for the standard curves (100 μL/well). Specific antibodies in PBS–Tween–PS–DMSO were then added (100 μL/well). The competition incubation lasted for 2 h at 37 °C. The plates were washed three times with PBS–Tween–DMSO. The secondary antibody (goat anti-rabbit IgG coupled to horseradish peroxidase from Dako) was added as 200 μL/well in PBS–Tween–PS–DMSO. The incubation was performed at 37 °C for 30 min. Peroxidase activity was revealed by adding 200 μL/well of substrate solution (0.005 M *o*-phenylenediamine, 0.00025% H_2O_2 in citrate-phosphate buffer (0.15 M, pH 5.0)). The enzymatic reaction lasted for 30 min at room temperature and was stopped with 4 M H_2SO_4 (50 μL/well). ODs were read at 490 nm. The standard curves were expressed as log[flavanone] = f((Bi − Blank)/(Bo − Blank))* 100, where Bi is the OD of the sample or of the standard wells, Bo is the positive control, i.e. the ODmax obtained by making the antibody to react on the coating without any competitor added. Blanks are the negative controls obtained in wells regularly coated but without adding the primary antibody. The assays demonstrated that anti-h4-haptens gave the best results in homologous conditions. For these haptens and antibodies, the best assay conditions allowing the best sensitivity, are presented in Table 2. This is also shown in Fig. 2A.

2.7.6. Cross-reactivity tests

The cross-reactivity of an antibody is defined as its ability to react with a molecule distinct from the one it was initially raised against. The cross-reactivities of the antibodies were tested using a competitive procedure. Following the previously optimised

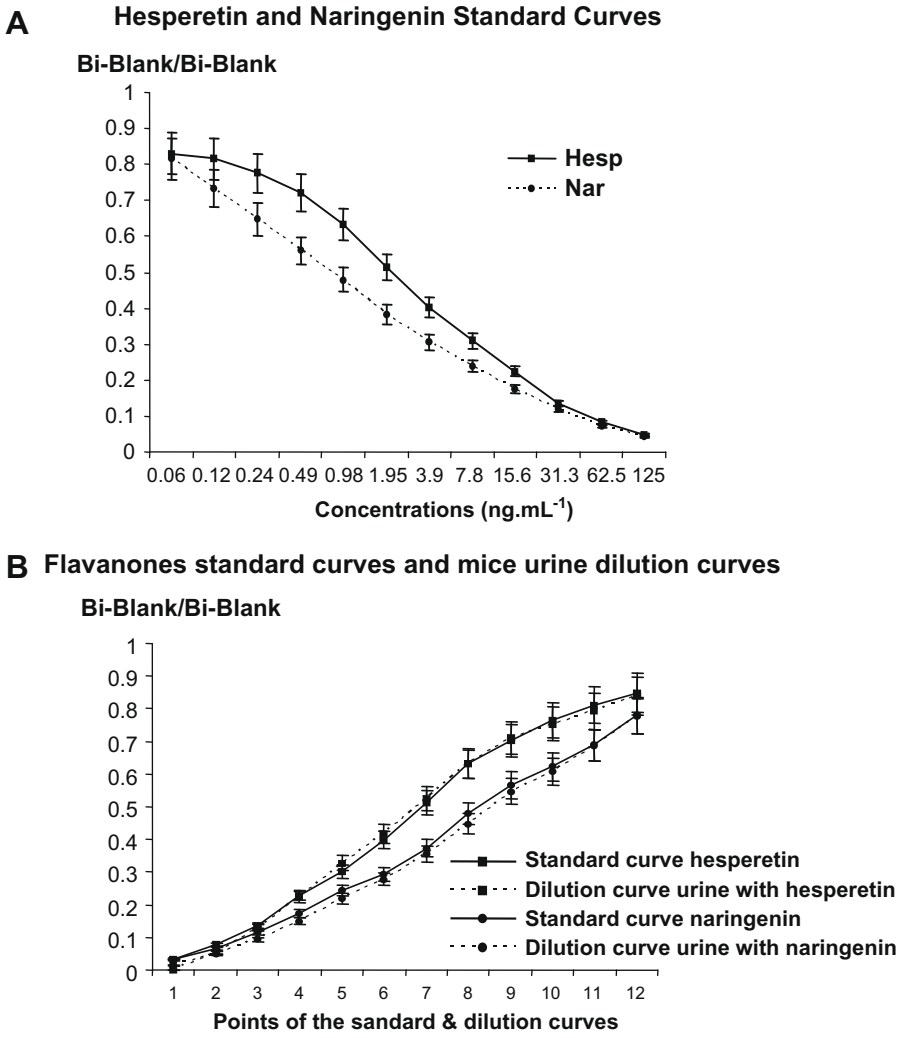

Fig. 2. In both figures points are the mean of duplicates. The equation of the competitive assay is Log [**Nar** or **Hesp** concentrations] = f(Bi − NC)/(Bo − NC) * 100, where Bi is the optical density of the sample or the standard, NC is the negative control obtained without the antibody, Bo is the total binding without any competitor. Analyte-antibody combinations are listed in Table 2. (A) Standard curves obtained with the two antibodies. (B) Standard curves obtained with each of the two antibodies and urine dilution curves. One urine sample contained 6979.35 ng mL^{-1} Hesperetin, after enzymatic hydrolysis and the other contained 10364.00 ng mL^{-1} Naringenin, after the same hydrolysis.

Table 3
Specificity tests.[a]

Compounds tested	Anti-**h4-Hesp**	Anti-**h4-Nar**	
	on h4-**Hesp-Thyr**	on **h4-Nar–Thyr**	on **h6-Nar–Thyr**
Genistein	0.007	0.375	
Daidzein	0.004	0.062	
Naringenin	0.5	100	
Hesperetin	100	1.5	
Naringin	<0.001	<0.001	
Hesperidin	<0.001	<0.001	
8-Prenyl Naringenin	0.031	8	
Isosakuranetin	4	0.025	
Eriodictyol	1	26.7	15
Liquiritigenin	0.03	50	31
Chrysin	0.0156	0.0019	
(−)-Homoeriodictyol	1.5	3	
Flavanone	0.12	0.25	
Luteolin	0.0156	0.1	

[a] Expressed as percentages of cross reaction in comparison to the homologous standard curves.

conditions (Table 2), the antibodies were challenged with **h4-Hesp** or **h4-Nar** coupled to Thyr as the coating and to serial dilutions of other compounds diluted in PBS–Tween–PS–DMSO as competitors. Eight concentrations of the various competitors were tested (from 50 μg mL^{-1} to 0.003 μg mL^{-1}) with a 4-fold decrease between each concentration. Other cross-reactivity tests were performed with the anti-**h4-Nar** in attempt to obtain lower cross-reactivity. These tests reside in heterologous competition between the free competitors and Thyr-**h6-Nar** as the immobilized coating. For these tests the antibody was at a concentration of 1/400,000 with a coating at 0.5 μg mL^{-1}, a secondary antibody dilution of 1/10,000 and a peroxidase revelation of 10 min at 37 °C.

2.8. Validation tests

The assays for **Hesp** and **Nar** were undertaken on plasma samples from mice fed on semi-synthetic diets based on 73% wheat starch, 15% casein, 6% mineral mixture (AIN 93 M), 1% vitamin mixture (93VX), and 5% corn oil. These semi-synthetic diets were enriched or not with hesperidin (**Hesp**-glycoside, 0.02%) or naringin (**Nar**-glycoside, 0.02%). To check for the absence of cross-reactions with **Hesp** and **Nar** metabolites, serial dilutions of urine samples collected on mice fed with the corresponding semi-synthetic diet were compared to the **Hesp** and **Nar** standard curves (Fig. 2B). Data obtained using the new ELISA techniques on plasmas were compared to values obtained on the same samples by the HPLC method coupled to coularray detector (Table 4).

2.9. HPLC analysis

HPLC analysis was performed using a system consisting of two pumps (Model 580, ESA, Chelmsford, USA) for high pressure gradients, a temperature-controlled autosampler (Gilson, Villiers-le-Bel, France), a 150 × 4.6 mm Hypersil BDS C18–5μ column (Touzard et Matignon, Les Ulis, France), a thermostatic chamber and an eight-channel Coularray detector (model 5600, Eurosep, Cergy, France). Mobile phases consisted of a 30 mmol/L NaH_3PO_4 buffer (pH 3) containing 20% acetonitrile (A) or 40% acetonitrile (B). Separation was achieved using a gradient elution (35 °C, 0.8 mL/min): 0–3 min: 100% A, 3–30 min: linear gradient from 100%A to 100%B, 30–35 min: 100%B, 35.01–45 min: 100%A. Potentials were set at 25–350–480–550–650–750–850 mV (with Pd as the reference). **Hesp** and **Nar** were quantified using the sums of the areas obtained on the electrodes 2, 3 and 4, 5, 6, respectively.

3. Results and discussion

3.1. Immunogen design

Specificity and selectivity of an antibody is crucial for immunologic assays since the comparison to a standard curve is only relevant if the compound detected in the sample is the same. Otherwise the assay is only semi-quantitative. **Hesp** and **Nar** are small molecules and, thus, are not immunogenic. Design and preparation of the corresponding haptens and the hapten-protein conjugates are necessary for efficient antibody generation. Previous studies, demonstrated that the hapten chemical structure has a relevant influence on the process of antigen–antibody recognition and thus on the specificity and the sensitivity of an immunoassay (Bennetau-Pelissero et al., 2000; Le Houerou et al., 2000). **Hesp** and **Nar** have a common chemical structure and differ by functional groups present on the B ring (Fig. 1). The high hydroxylation degree of the flavanone skeleton offers the opportunity for easy introduction of an *O*-carboxyalkyl spacer arm. So, the linkers bearing a carboxylic function required for covalent coupling to carrier proteins were introduced at the C7-OH position (ring A) in order to exhibit the flavanone skeleton and the specific recognising sites to allow the best discrimination between **Hesp** and **Nar**. The linker length variation (4 carbon atoms for haptens **1** and **2**, and 6 carbon atoms for haptens **3** and **4**, Fig. 1) for both compounds was expected to improve the specificity of the immunoassay in heterologous combination of the coating and the immunizing haptens. Our previous experience led to us developing polyclonal antibodies, as they previously demonstrated to be more specific than monoclonal when used against small molecules. Indeed, within the flavonoid

Table 4
Validation of the Hesperetin ELISA on mice plasma samples. Comparison with the HPLC method.

% of hesperidin supplementation in diets (%)	Dilution factor for plasmas	Concentrations in each plasma (ng mL^{-1})[a]	Mean ± SD (ng/mL^{-1})	Concentrations (μM) ELISA	Concentrations (μM) HPLC[b]	Mean ± SD (μM) HPLC[b]
0	80–160	80	81.53 ± 12.6	NS	NS	NS
	80–160	69.8				
	80–160	94.8				
0.02	160–320	1197.8	1037 ± 146.6	3.43 ± 0.48	2.84	2.7 ± 0.10
	160–320	1003.2			2.69	
	160–320	910.4			2.59	
0.05	200–400	1494.4	2014 ± 907.6	6.66 ± 3.00	5.38	7.11 ± 1.33
	200–400	1484.8			5.07	
	200–400	3061.6			8.62	
0.1	1000–2000	4764	4157 ± 1733	13.75 ± 5.73	17.58	16.03 ± 2.54
	1000–2000	2202			12.44	
	1000–2000	5506			18.08	

NS is non significant.
[a] For each plasma, values are duplicates of two dilutions.
[b] HPLC was performed with a coulometric detection (Coularray).

family all molecules are strongly structurally related. Therefore specific recognition of this kind of molecule needs the recognition of different combined epitopes on the molecule by different IgG. This can be achieved using polyclonal antibodies. In this case, the specificity results from the combination of different IgG towards different portions of the antigen used at a concentration avoiding cross-reactivities with one particular epitope rather than another. Each combination is unique and is characteristic of each individual rabbit.

3.2. Synthetic work

The C7-hydroxyl group of **Hesp** and **Nar**, which was selected as the site for linker attachment, is the most reactive hydroxyl functions available. For this reason, it can be easily region selectively alkylated without using any protective group. Thus, all haptens were prepared in the same two steps. The synthesis of hapten **1** is outlined in Fig. 1 and the experimental conditions for all haptens **1–4** are summarised in Table 1. In the first step, the corresponding ethyl esters **5–8** were obtained in good yields with a classic Williamson ether synthesis. A stronger base was needed in the case of **Hesp** derivatives. In the saponification step the yields were lower. Ester hydrolysis was not completed. For **Hesp** derivatives, the formation of transesterification products was observed and for hapten **4**, the yield of the reaction was improved by using acetonitrile.

3.3. Analysis of the BSA conjugates

Haptens (**1**), (**2**), (**3**) and (**4**) were then reacted with a carrier protein, i.e. BSA, to produce immunogenic constructions in order to obtain anti-**Hesp** and anti-**Nar** antibodies. The molecular ratios of haptens to protein were estimated by MALDI-MS. The hapten-protein ratios in all cases were nearly the same: approximately 10 haptens per carrier protein. This density was considered to be sufficient to obtain a good antibody quality (Malaitsev & Azhipa, 1993).

3.4. Immunization tests

In Table 2 it appears that the titres of the antibodies were rather similar since they were both used at the same dilution (1/20,000). This means that the immunization protocol was suitable for the generation of antibodies to flavonoids, to be used in ELISA tests.

3.5. ELISA tests

The optimal conditions of the two ELISAs are shown in Table 2. Before ELISAs, the recovery ratios registered in parallel to all tested samples, showed recovery between 98% and 100%. For each conjugate of **Hesp** and **Nar**, two antibodies were generated, selected for their relative sensitivity and the best were used thereafter. The standard sigmoid curves obtained for the best antibodies (anti-**h4-Hesp** and anti-**h4-Nar**) and the conditions are presented in Fig. 2A. Anti-**h4-Nar** allows the best sensitivity (IC_{50} at 0.98 ng mL^{-1}), and anti-h4-Hesp exhibits an IC_{50} at 1.96 ng mL^{-1}. For **Hesp** and **Nar**, the best detection limits were 0.24 and 0.12 ng mL^{-1}, respectively. This is correlated to a weaker specificity for anti-**h4-Nar**. This is in accordance with literature (Avrameas, 1992). It must be noted that the sensitivity reached here was obtained with a Thyr-h-flavanone complex characterised by a ratio of 20 molecules of h-flavanone for 1 molecule of Thyr. In previous works (Bennetau-Pelissero et al., 2000, 2003; Le Houerou et al., 2000), it was shown that the sensitivity of an assay can be improved by reducing this coupling ratio. The present ELISAs present a good sensitivity and compare favourably with other analytical techniques. Indeed, Felgines et al. (2000) had a detection limit of 820 ng mL^{-1}, using HPLC coupled to UV detection (320 nm). In parallel, Harnly et al. (2006) had detection limits of 6 g mL^{-1} and 5 g mL^{-1} of **Hesp** and **Nar**, respectively using HPLC coupled to UV diode array detection. Kanaze, Kokkalou, Georgarakis, and Niopas (2004) obtained detection limits of 10 ng mL^{-1} for both **Hesp** and **Nar** using HPLC coupled to UV detection (288 nm). Only Franke, et al. (2002) reported better sensitivity using LC–MS with detection limits of 1.75 ng mL^{-1} and 0.05 ng mL^{-1} in urine and 0.2 ng mL^{-1} and 0.05 ng mL^{-1} in plasma for **Hesp** and **Nar**, respectively.

Intra and inter-assay variation coefficients were determined for both antibodies using either high (1000 ng mL^{-1}) or low concentrated solutions (5 ng mL^{-1}). Inter-plate variations were calculated as variation coefficients of measurements carried out on 11 microtitration plates. Intra-assay variations were calculated as the variation coefficients obtained on 22 values of the same sample. These variations were always below 11% (Table 2). Therefore these assays appeared to be as reliable as other physicochemical techniques (Felgines et al., 2000; Franke et al., 2002; Kanaze et al., 2004).

3.6. Cross-reactivity of the antibodies

The two antisera, anti-**h4-Hesp** and anti-**h4-Nar**, were tested against various other flavonoids for cross-reactivities (Table 3). For anti-**h4-Hesp**, only isosakuranetin presents a cross-reaction of 4%. There were no other significant cross-reactions. Isosakuranetin differs from **Hesp** because it lacks a hydroxyl group at the C3′ position. These structures are therefore rather similar and this could explain the low cross-reaction registered here. On the other hand, for anti-**h4-Nar** some significant cross-reactions were registered for liquiritigenin and eriodictyol (50% and 26.4% respectively). Cross-reactions with liquiritigenin may find their origin in the bounding between BSA and **h4-Nar**. Most likely, BSA produces steric hindrance towards the C5 position that lies in the vicinity of the C—O-linker. Since liquiritigenin differs from **Nar** by the occurrence of a hydroxyl group at the C5 position, it is likely that the antibodies cannot discriminate very well between the two molecules for this reason. One solution would be to harvest the polyclonal antibody using liquiritigenin but this would affect its titre and therefore its sensitivity. Fortunately, liquiritigenin occurs only in licorice and in specific medicinal herbs used in Chinese traditional medicine and it will be easy to avoid it on a regular basis. Eriodictyol, a major flavanone from lemon, presents an additional hydroxyl group at the C3′ position when compared to **Nar**. The observed cross-reaction seems hard to explain since previous works showed that polyclonal antibodies were quite powerful at discriminating molecules in such configuration. Again, the antibody can be harvested with eriodictyol at the expense of a loss of sensitivity. Another way to reduce cross-reactions is to perform heterologous competition using a coating molecule having another affinity with the antibody. Tests were performed with anti-**h4-Nar** on an immobilized Thyr-**h6-Nar**. Cross-tests previously showed that the affinity of the anti-**h4-Nar** was higher for Thyr-**h6-Nar** than for Thyr-**h4-Nar**. In these conditions cross-reactivities were reduced from 50% to 31% and from 26.4% to 15% for liquiritigenin and eriodictyol, respectively (Table 3). These cross-reactions can give fairly good assay results, considering that eriodictyol concentration in grapefruit is much lower than that of **Nar**. Therefore, the dilution needed to assay these types of samples or biological fluids will reduce the risk of miss-quantification.

3.7. Validation of the assays

Validation was undertaken on mouse and Human plasmas enriched with known quantities of **Hesp** and **Nar** (data not shown) as well as on specifically enriched semi-synthetic diets. A semi-

synthetic diet was enriched with 200 μg/g of Hesperidin, i.e. after hydrolysis, enriched with 96.7 μg/g equivalent Hesperetin. When treated in triplicates as previously described, our assay detected 96.22 ± 15.29 μg/g where 15.29 was the standard deviation. Another semi-synthetic diet was enriched with 200 μg/g of Naringin, i.e. after hydrolysis, enriched with 93.9 μg/g equivalent Naringenin. When treated in triplicates as mentioned in the technical section, our assay measured 102.90 ± 16.34 μg/g where 16.34 was the standard deviation. The results obtained were therefore in accordance with the expected data, and the lower specificity of the Naringenin assay could be seen when comparing the accuracy of the results obtained with the two assays.

Then several mouse plasmas were tested to check for the ability of the assay to detect **Hesp** and **Nar** in natural biological fluid samples. Data obtained on plasma from mice fed with a diet enriched with 0.02%, 0.05% or 0.1% hesperidin are presented in Table 4. There were three plasmas for each treatment and each determination was done in duplicate. As shown in Table 4, the flavanone concentrations in the plasma were strictly correlated with their concentration in the diet. Some interindividual variations were observed, as in the case of previously published results (Felgines et al., 2000; Franke et al., 2002). However there was a twofold increase between each group of Hesp plasma concentrations in agreement with the hesperidin proportions in the diets. Moreover, ELISA values were in close agreement with HPLC-Coularray values. It was possible to get highly concentrated urine samples from mice fed either with a 0.02% hesperidin or a 0.02% naringin-enriched diet. Urine sample were enzymatically hydrolysed and dilution curves were compared to draw a parallel between the corresponding standard curve and the biological fluid. The agreement was found to be excellent as shown in Fig. 2B. This demonstrated that the cross-reactions of the antibody with other urine constituents including **Hesp** and **Nar** metabolites were negligible and that the antibodies could be used for assays in biological fluids.

In conclusion, although **Hesp** and **Nar** are closely related molecules, it appeared here that the specificity obtained in similar conditions was not identical. **Hesp** is well-discriminated, and as demonstrated by the good concordance between the urine dilution curve and the **Hesp** standard curve, the cross-reactions with the parent compounds likely to be present in biological samples are very low. Fortunately, because eriodictyol and liquiritigenin are likely not to be present in large amounts in grapefruits and in biological fluids from subjects having had this food matrix, the cross-reactions observed with anti-**h-Nar** do not reduce the interest of the assay. Once again the good agreement between the urine dilution curve and the **Nar** standard curve shows the interest of the assay for biological samples. Using heterologous competition, it was demonstrated that the specificity of the Nar assay could be improved.

Acknowledgements

This work was funded by the PNRA (ANR program on food) through the AGRUVASC project and by the Aquitaine Region. We gratefully thank Russell Wallace and Zoé Tebby for careful reading of the manuscript.

References

Avrameas, S. (1992). Amplification systems in immunoenzymatic techniques. *Journal of Immunological Methods, 150*(1–2), 23–32.

Bennetau-Pelissero, C., Arnal-Schnebelen, B., Lamothe, V., Sauvant, P., Sagne, J. L., Verbruggen, M. A., et al. (2003). ELISA as a new method to measure genistein and daidzein in food and human fluids. *Food Chemistry, 82*, 645–658.

Bennetau-Pelissero, C., Le Houerou, C., Lamothe, V., Le Menn, F., Babin, P., & Bennetau, B. (2000). Synthesis of haptens and conjugates for ELISAs of phytoestrogens. Development of the immunological tests. *Journal of Agricultural Food Chemistry, 48*(2), 305–311.

Bovee, T. F., Schoonen, W. G., Hamers, A. R., Bento, M. J., & Peijnenburg, A. A. (2008). Screening of synthetic and plant-derived compounds for (anti)estrogenic and (anti)androgenic activities. *Analytical; Bioanalytical Chemistry, 390*(4), 1111–1119.

Felgines, C., Texier, O., Morand, C., Manach, C., Scalbert, A., Regerat, F., et al. (2000). Bioavailability of the flavanone naringenin and its glycosides in rats. *American Journal of Physiology-Gastrointestinal and Liver Physiology, 279*(6), G1148–G1154.

Franke, A. A., Custer, L. J., Wilkens, L. R., Le Marchand, L. L., Nomura, A. M., Goodman, M. T., et al. (2002). Liquid chromatographic-photodiode array mass spectrometric analysis of dietary phytoestrogens from human urine and blood. *Journal of Chromatography B Analytical Technology Biomedical Life Science, 777*(1–2), 45–59.

Gil-Izquierdo, A., Riquelme, M. T., Porras, I., & Ferreres, F. (2004). Effect of the rootstock and interstock grafted in lemon tree (Citrus limon (L.) Burm.) on the flavonoid content of lemon juice. *Journal of Agricultural Food Chemistry, 52*(2), 324–331.

Grace, P. B., Mistry, N. S., Carter, M. H., Leathem, A. J., & Teale, P. (2007). High throughput quantification of phytoestrogens in human urine and serum using liquid chromatography/tandem mass spectrometry (LC-MS/MS). *Journal of Chromatography B Analytical Technology Biomedical Life Science, 853*(1–2), 138–146.

Harnly, J. M., Doherty, R. F., Beecher, G. R., Holden, J. M., Haytowitz, D. B., Bhagwat, S., et al. (2006). Flavonoid content of US Fruits, vegetables, and nuts. *Journal of Agricultural Food Chemistry, 54*(26), 9966–9977.

Hsiao, Y. C., Kuo, W. H., Chen, P. N., Chang, H. R., Lin, T. H., Yang, W. E., et al. (2007). Flavanone and 2′-OH flavanone inhibit metastasis of lung cancer cells via down-regulation of proteinases activities and MAPK pathway. *Chemistry and Biology Interaction, 167*(3), 193–206.

Huong, D. T., Takahashi, Y., & Ide, T. (2006). Activity and mRNA levels of enzymes involved in hepatic fatty acid oxidation in mice fed citrus flavonoids. *Nutrition, 22*(5), 546–552.

Jeon, S. M., Kim, H. K., Kim, H. J., Do, G. M., Jeong, T. S., Park, Y. B., et al. (2007). Hypocholesterolemic and antioxidative effects of naringenin and its two metabolites in high-cholesterol fed rats. *Translation Research, 149*(1), 15–21.

Kanaze, F. I., Kokkalou, E., Georgarakis, M., & Niopas, I. (2004). A validated solid-phase extraction HPLC method for the simultaneous determination of the citrus flavanone aglycones hesperetin and naringenin in urine. *Journal of Pharmaceutical and Biomedical Analysis, 36*(1), 175–181.

Knekt, P., Kumpulainen, J., Jarvinen, R., Rissanen, H., Heliovaara, M., Reunanen, A., et al. (2002). Flavonoid intake and risk of chronic diseases. *American Journal of Clininical Nutrition, 76*(3), 560–568.

Koohi, M. K., Walther, N., & Ivell, R. (2007). A novel molecular assay to discriminate transcriptional effects caused by xenoestrogens. *Molecular and Cellular Endocrinology, 276*(1–2), 45–54.

Le Houerou, C., Bennetau-Pelissero, C., Lamothe, V., Le Menn, F., Babin, P., & Bennetau, B. (2000). Syntheses of Novel Hapten-Protein Conjugates for production of Highly Specific Antibodies to Formononetin, Daidzein and Genistein. *Tetrahedron, 56*, 295–301.

Lee, S., Lee, C. H., Moon, S. S., Kim, E., Kim, C. T., Kim, B. H., et al. (2003). Naringenin derivatives as anti-atherogenic agents. *Bioorganic and Medicinal Chemistry Letters, 13*(22), 3901–3903.

Liu, L., Xu, D. M., & Cheng, Y. Y. (2008). Distinct effects of naringenin and hesperetin on nitric oxide production from endothelial cells. *Journal of Agricultural Food Chemistry, 56*(3), 824–829.

Malaitsev, V. V., & Azhipa, O. (1993). The effect of epitope density on the immunogenic properties of hapten-protein conjugates. *Biulleten Eksperimentalnol Biologii I Meditsiny, 115*(6), 645–646.

Malaveille, C., Hautefeuille, A., Pignatelli, B., Talaska, G., Vineis, P., & Bartsch, H. (1996). Dietary phenolics as anti-mutagens and inhibitors of tobacco-related DNA adduction in the urothelium of smokers. *Carcinogenesis, 17*(10), 2193–2200.

Manach, C. (2003). *The use of HPLC with coulometric array detection in the analysis of flavonoids in complex matrices. Santos-Buelga C., W. G., In Methods in polyphenol analysis, (pp. 63–91)*. Cambridge: Royal Society of Chemistry.

Manach, C., Morand, C., Gil-Izquierdo, A., Bouteloup-Demange, C., & Remesy, C. (2003). Bioavailability in humans of the flavanones hesperidin and narirutin after the ingestion of two doses of orange juice. *European Journal of Clinical Nutrition, 57*(2), 235–242.

Merken, H. M., Merken, C. D., & Beecher, G. R. (2001). Kinetics method for the quantitation of anthocyanidins, flavonols, and flavones in foods. *Journal of Agricultural Food Chemistry, 49*(6), 2727–2732.

Morand, C., Manach, C., Donovan, J., & Remesy, C. (2001). Preparation and characterization of flavonoid metabolites present in biological samples. *Methods in Enzymology, 335*, 115–121.

Nikolic, D., & van Breemen, R. B. (2004). New metabolic pathways for flavanones catalyzed by rat liver microsomes. *Drug Metabolism and Disposition, 32*(4), 387–397.

Radtke, J., Linseisen, J., & Wolfram, G. (2002). Fasting plasma concentrations of selected flavonoids as markers of their ordinary dietary intake. *European Journal of Nutrition, 41*(5), 203–209.

Rechner, A. R., Smith, M. A., Kuhnle, G., Gibson, G. R., Debnam, E. S., Srai, S. K., et al. (2004). Colonic metabolism of dietary polyphenols: influence of structure on microbial fermentation products. *Free Radical Biology and Medicine, 36*(2), 212–225.

Riggle, B. (1991). Development of a preliminary enzyme-linked immunosorbent assay for the herbicide trifluralin. *Bulletin of Environmental Contamination and Toxicology, 46*(3), 404–409.

Sakakibara, H., Honda, Y., Nakagawa, S., Ashida, H., & Kanazawa, K. (2003). Simultaneous determination of all polyphenols in vegetables, fruits, and teas. *Journal of Agricultural Food Chemistry, 51*(3), 571–581.

Steinmetz, K. A., & Potter, J. D. (1991a). Vegetables, fruit, and cancer I. Epidemiology. *Cancer Causes and Control, 2*(5), 325–357.

Steinmetz, K. A., & Potter, J. D. (1991b). Vegetables, fruit, and cancer II. Mechanisms. *Cancer Causes and Control, 2*(6), 427–442.

Szurdoki, F., Szekacs, A., Le, H. M., & Hammock, B. D. (2002). Synthesis of haptens and protein conjugates for the development of immunoassays for the insect growth regulator fenoxycarb. *Journal of Agricultural Food Chemistry, 50*(1), 29–40.

van Meeuwen, J. A., Korthagen, N., de Jong, P. C., Piersma, A. H., & van den Berg, M. (2007). (Anti)estrogenic effects of phytochemicals on human primary mammary fibroblasts, MCF-7 cells and their co-culture. *Toxicology and Applied Pharmacology, 221*(3), 372–383.

Xie, M. X., Xu, X. Y., & Wang, Y. D. (2005). Interaction between hesperetin and human serum albumin revealed by spectroscopic methods. *Biochimica Et Biophysica Acta, 1724*(1–2), 215–224.

Food Chemistry 118 (2010) 482–487

Contents lists available at ScienceDirect

Food Chemistry

journal homepage: www.elsevier.com/locate/foodchem

Analytical Methods

Application of real-time PCR on the development of molecular markers and to evaluate critical aspects for olive oil authentication

Maria J. Giménez [a,*], Fernando Pistón [b], Antonio Martín [a], Sergio G. Atienza [a]

[a] I.A.S. – C.S.I.C., Dpto. de Mejora Genética Vegetal, Apdo. 4084, E-14080 Córdoba, Spain
[b] Dpto. de Genética, Universidad de Córdoba, Campus Rabanales Edif. C-5, 14071 Córdoba, Spain

ARTICLE INFO

Article history:
Received 3 March 2009
Received in revised form 31 March 2009
Accepted 6 May 2009

Keywords:
Olive oil authentication
DNA-based markers
qRT-PCR

ABSTRACT

Olive oil authentication using DNA-based markers is becoming very important. qRT-PCR was an efficient tool in investigating the utility of PCR primers for olive oil authentication allowing to discard primers with low PCR efficiency. It also allows investigating of the relative effectiveness among four DNA isolation methods and therefore qRT-PCR would be useful for further optimisation of the DNA extraction protocols. The number of target molecules for the amplification of 80 bp amplicons was higher than that of 200 bp. Therefore the amplicon size should be optimised for olive oil authentication since the higher the number of templates the greater the probability of successful amplification. On conclusion, qRT-PCR is a useful tool in the development of molecular markers for olive oil authentication and it should be used for the optimisation of critical parameters such as the amplicon size and the DNA extraction method.

1. Introduction

Olive (*Olea europaea* L. subsp. *europaea* var. *europaea*) is one of the most ancient crops of the Mediterranean basin. The main use of this crop is the production of olive oil but its drupes can also be consumed as table olives. Olive oil has been traditionally very important in all the Mediterranean area but its consumption is increasing throughout the world due to its importance in the diet and its beneficial effect on health.

Food authenticity and traceability have become very important in the last years to allow consumers to perform informed choices about the foods they buy and eat. There are several ways in which food can be misdescribed including the substitution of one ingredient by a similar but cheaper one and over-declaring a quantitative ingredient. Accordingly, olive oil authentication has become very important.

Several Protected Denomination of Origin (PDO) olive oil regions have been established by legislation to ensure both producer's profits and consumer's rights. In this context, it is mainly the identification of the olive cultivar used for the oil production which is of importance for authentication (Luykx & van Ruth, 2008) since the contribution of cultivars is known for each designation.

The authenticity of olive oil has been addressed using different techniques such as proton transfer reaction mass spectrometry (PTR-MS), nuclear magnetic resonance spectroscopy (NMR) or high performance liquid chromatography (HPLC) among others (Luykx & van Ruth, 2008). However, the chemical composition of olive oil may differ among seasons and growing areas. Besides, investigations concerning the origin and authenticity of olive oil through the chemical analysis of different oil's components have shown that no single known parameter could detect the presence of hazelnut and almond oils in olive oil, in percentages lower than or equal to 5% (Christopoulou, Lazaraki, Komaitis, & Kaselimis, 2004). Consequently chemical analyses *per se* are not sufficient to assure olive oil authenticity.

This has promoted a growing interest towards the application of DNA-based markers since it is independent from environmental conditions. Thus, specific protocols for DNA isolation from olive oil have been developed (Breton, Claux, Metton, Skorski, & Berville, 2004; Busconi et al., 2003; Consolandi et al., 2008; De la Torre, Bautista, Cánovas, & Claros, 2004). Besides, different types of DNA markers including RAPDs (Belaj, Trujillo, de la Rosa, Rallo, & Gimenez, 2001; Doveri, O'Sullivan, & Lee, 2006), AFLPs (Belaj, Rallo, Trujillo, & Baldoni, 2004), SCARs (Busconi et al., 2003; De la Torre et al., 2004; Doveri, O'Sullivan, & Lee, 2006), SNPs (Doveri, O'Sullivan, & Lee, 2006) and microsatellites (Breton et al., 2004; Diaz, De la Rosa, Martin, & Rallo, 2006) have been applied to cultivar identification or olive oil traceability. A summary of PCR-based methods applied in the authentication of olive plant origin has been recently reviewed (Mafra, Ferreira, & Oliveira, 2008).

Whatever the DNA isolation method, tiny amounts of degraded DNA are obtained when isolating DNA from oil samples. Because of their low detection limits, PCR and the adapted kinetic qRT-PCR (real-time quantitative PCR) have been used extensively for the

* Corresponding author. Tel.: +34 957 499241; fax: +34 957 499252.
E-mail address: ge1gialm@uco.es (M.J. Giménez).

0308-8146/$ - see front matter © 2009 Elsevier Ltd. All rights reserved.
doi:10.1016/j.foodchem.2009.05.012

detection and quantification of nucleic acids (Freeman, Walker, & Vrana, 1999). However, the usefulness of the PCR technique for traceability purposes depends on the quality and quantity of the isolated DNA. At the detection limits of an assay, mathematical models (Taberlet et al., 1996) and experimental evidence (Morrison, Weis, & Wittwer, 1998) have shown that nucleic acids are detected inconsistently and quantified imprecisely. Considering the tiny amounts of DNA isolate from olive oil, the DNA isolation method needs optimisation in order to obtain enough DNA quantity (Breton et al., 2004). Consequently, comparison between different DNA isolation methods is crucial in order to be successful in olive oil authentication.

Besides, there are other factors that may affect the application of the DNA technology for olive oil authentication. DNA technology should rely on amplification products smaller than 200 bp in food products where a high degradation of DNA may occur (Hupfer, Hotzel, Sachse, & Engel, 1998; Unseld, Beyermann, Brandt, & Hiesel, 1995), but the size of the amplifiable DNA has not been considered for olive oil authentication.

Finally, olive is an allogamous wind-pollinated species and therefore DNA isolated from olive oil represents a composite profile of the maternal alleles juxtaposed with alleles contributed by the pollen donors (Doveri, O'Sullivan, & Lee, 2006). Cytoplasmic DNA is maternally inherited and thus it is not affected by the pollen donors. Therefore, the isolation of this DNA type from olive oil should be addressed as a first step towards its use in olive oil traceability.

The aim of this present work was to use qRT-PCR as a tool in the development of molecular markers for olive oil authentication and to identify critical aspects which should be optimised for this purpose.

2. Material and methods

2.1. DNA isolation

DNA from the olive cultivar 'Picual' was isolated from young leaves following the method described by Belaj et al., 2001. Isolation of DNA from one commercial 'Picual' monovarietal oil was carried out by using four different protocols.

2.1.1. CTAB based method (Doyle, 1991)

To 1 ml of a homogenised oil sample, 500 μl of pre-warmed (60 °C) CTAB extraction buffer (2% CTAB, 1.4 M NaCl, 50 μM DTT, 20 mM EDTA, 100 mM Tris–HCl, pH 8.0) were added, mixed and incubated for 30 min at 60 °C. After addition and mixing of 500 μl of cold chloroform (C):isoamyl alcohol (I) (24:1) the mixture was centrifuged at 20,000*g* for 30 min, 4 °C, and the upper phase was transferred to a new tube. This step was performed once again to obtain a clearer supernatant. For DNA precipitation, 1 volume of cold isopropanol was added, mixed smoothly by inverting the tube and kept at −20 °C overnight. The supernatant was discarded after centrifugation (30 min, 4 °C, 20,000*g*). The pellet was then washed with 500 μl of 70% v/v ethanol/water, centrifuged (30 min, 4 °C, 20,000*g*) and dried.

2.1.2. Hexane method (Consolandi et al., 2008)

One millilitre of oil sample and 500 μl of hexane were pipetted into a 2 ml microcentrifuge tube, vortexed vigorously for 5 min and centrifuged (15 min, 4 °C, 20,000*g*). The oily supernatant was transferred to a fresh 2 ml tube and mixed with 400 μl lysis buffer (50 mM Tris pH 8.5, 1 mM EDTA, 0.5% v/v Tween 20) and 2 μl of 10 mg/ml Proteinase K. The same reagents were also added to the centrifugation pellet. Both samples were incubated at 48 °C for 2 h and centrifuged (30 min, 4 °C, 20,000*g*). The oily upper phase and the two aqueous phases were each transferred to a new microtube, avoiding contact with the oil–water interphase and sediment, and then heated to 95 °C to inactivate Proteinase K. The DNA was precipitated by mixing samples with 500 μl of cold absolute isopropanol, incubating them at −20 °C overnight, followed by centrifugation (30 min, 4 °C, 20,000*g*) and discarding of liquid phases. The residue of each tube was washed with 500 μl of 70% ethanol, centrifuged (30 min, 4 °C, 20,000*g*) and dried at 36 °C for 15 min.

2.1.3. CTAB–hexane method

The extraction was carried out in a 2 ml microtube by adding 500 μl of pre-warmed CTAB extraction buffer to a mixture of 500 μl of hexane and 1 ml of olive oil. The sample was shaken vigorously, incubated at 60 °C for 30 min and centrifuged (30 min, 4 °C, 20,000*g*) and aqueous phase was then transferred to a new tube. Precipitation and washing of DNA was completed as described in the CTAB based method.

2.1.4. CTAB–hexane–chloroform method

This method is a modification of the previous one, but, in this case, half the volumes of oil (500 μl), CTAB lysis buffer (250 μl) and hexane (250 μl) were mixed in a 2 ml microtube and incubated at 60 °C for 30 min. Cold C:I (24:1) was then added (500 μl), the mixture centrifuged (30 min, 4 °C, 20,000*g*) and 1 ml of the upper part of the solution was transferred to new tube and mixed with a volume of chloroform:isoamyl alcohol (24:1). After centrifugation (30 min, 4 °C, 20,000*g*), the aqueous phase was transferred to a microtube. Prior to precipitation and washing of DNA performed as in the CTAB base method, 10–20 μg/ml linear acrylamide (Ambion) were added to the sample to improve DNA recovery.

Dried DNA pellets obtained by each method were resuspended in 25 μl of 0.1 × TE buffer/ml of oil. Four independent extractions of 1 ml of oil, or eight extractions of 500 μl of oil (CTAB–hexane–chloroform method), were carried out for each oil sample. DNA of the replicates was pooled in a single tube for PCR reactions.

2.2. Oligonucleotide primers

In order to asses the quantity and length of the different types of DNA extracted from all the samples, primers pairs for amplification of specific cytoplasmic and nuclear DNA fragments of (approximately) 80 and 200 bp were designed from *O. europaea* sequences available in GenBank (Table 1). The PCR primers were designed using the Primer Express software (Applied Biosystems, Foster City, CA, USA), in accordance with the criteria required for qRT-PCR primer design. The primers were synthesised by TAGN (Gateshead, United Kingdom).

2.3. Quantitative real-time PCR (qRT-PCR) amplification

For qRT-PCR amplification 2.5 μl of DNA was added to 7.5 μl of milliQ water, 12.5 μl of 2X SYBR Green™ Master Mix (Applied Biosystems), 2.5 μl of a mixture of 2 μM of each (forward and reverse) primer, for each primer pair. Three duplicate reactions were used for each sample, and each set included template controls containing water to check for contamination in the reaction components. The qRT-PCR amplifications were conducted using an ABI PRISM® 7000 Sequence Detection System (Applied Biosystems, Foster City, CA, USA), with thermocycling initiated by 10 min of initial denaturation at 94 °C followed by 40 cycles (94 °C for 15 s; 60 °C for 60 s) with a single fluorescent reading (SYBR Green I chemistry) at the end of each cycle. After the amplification, a dissociation protocol was performed to estimate the melting point (T_m) curves. The threshold cycle (Ct) was calculated by the ABI PRISM 7000 software after removing the effect of background (β_0).

Table 1
Sequences of primers pairs for specific amplification of chloroplastic and nuclear DNA fragments, size of amplicons, and source sequence used for designing them.

Primer	Forward 5′–3′	Reverse 5′–3′	Size (bp)[a]	SCF	GenBank accesion
C4-80	GGTGTTATTCCCGTGGCTTCAG	ACGGAATCATCCCCAAAGATCTC	80	0.96	AJ001766
C4-200	AAAGGGCGATGCTACCATATTGA	GGGATTCGCAGATCTTCCAGAC	182	2.19	AJ001766
N3-80	GTTCGCCAAAAGGACCGACAT	GCCAGACATGGTGCAGCAGTT	83	1	AJ416321
N3-200	TACACCACGGTCATGCAAGTCC	TGGCGAACAGAAGACCGATAATG	193	2.33	AJ416321

[a] SCF: size calibration factor = A_{si}/A_{sref}, where A_{si} is the number of base pairs of the amplicon *i*, and A_{sref} is the number of base pairs of amplicon N3-80.

2.4. Estimation of the PCR efficiencies

Concentration gradients of genomic leaf DNA obtained as described above, were used for generating the calibration curves. Each dilution reaction was set up in triplicate. The Ct values were plotted *vs* the concentrations (logarithmic value) of the input DNA, and parameters of the linear regression curves were used for calculating the efficiencies of each primer according to the equation $E = 10^{-1/b}$, where b is the slope of the curve.

2.5. Initial fluorescence (F_0) calculation

Initial fluorescence (F_0) was calculated according to the equation: $F_t = \beta_0 + F_0 \times E^{Ct}$ since F_0 is a good estimator of the input number of molecules for each amplicon type (Rutledge, 2004), where F_t is threshold fluorescence value, β_0 is the background, E is the efficiency of the primer, and Ct is the threshold cycle. As the amount of SYBR Green I dye bound to double stranded DNA is dependent on amplicon size, in order to compare fluorescence of amplicons differing in the number of base pairs, F_0 was corrected by a size calibration factor (SCF), $F_0^* = F_0/\text{SCF}$ being SCF = A_{si}/A_{sref}, where A_{si} is the number of base pairs of the amplicon *i*, and A_{sref} is the number of base pairs of amplicon N3-80 (Table 1), set as reference.

3. Results and discussion

3.1. Utility of qRT-PCR in the development of molecular markers for olive oil authentication

A great effort has been conducted during the last decade towards the identification of olive cultivars using molecular markers. At present SSR are the markers of choice for cultivar identification (De la Rosa, James, & Tobutt, 2002; Diaz et al., 2006; Diaz et al., 2007). Previous works on olive oil authentication have suggested the use of microsatellite markers for DNA tracking due to their small size (200–300 bp) (Pasqualone, Montemurro, Caponio, & Blanco, 2004). At first sight, SSRs developed for cultivar identification would seem to be the obvious choice when their amplicon size is adequate. Despite their utility for cultivar identification, primer pairs showing a good performance when tested on DNA isolated from leafs might not be suitable if the PCR efficiency is too low for producing detectable amounts of amplicons from very small input DNA.

To demonstrate this we used the primers developed to amplify the locus EMO3 used for cultivar identification (De la Rosa et al., 2002). The performance of EMO3 primers was assessed using qRT-PCR and DNA extracted from 'Picual' young leaves and 'Picual' monovarietal oil (Fig. 1). The amplification using leaf-extracted DNA was allowed to reach the exponential phase of the PCR reaction. However, the amplification conducted with oil-extracted DNA did not yield a detectable amplification since it could not reach the exponential phase (Fig. 1). Thus, EMO3 primers are not suitable for olive oil authentication due to their low PCR efficiency when using DNA extracted from oil. Furthermore small changes in the PCR efficiency might eventually allow the exponential phase to be reached and thus to obtain a detectable signal which would lead to haphazard detection and thus to false negatives when using conventional PCR.

To further demonstrate the effect of the PCR efficiency on the applicability of primers for olive oil traceability we designed a new set of primers using as a template the same sequence used to design EMO3 primers (AJ416321). These primers were named N3-200 (Table 1) and they amplify a PCR product of equivalent size to that of EMO3 (around 200 bp).

The results obtained with this primer pair are also shown in Fig. 1. The assay efficiency using this new set of primers is much higher as seen from the greater slope of the logarithmic transformation of the increase in the fluorescent signal (ΔRn). As a consequence, the amplification derived from leaf-extracted DNA is detected much earlier (around eight cycles before than when using EMO3). Furthermore, this difference in amplification efficiency can explain differences in detection of amplification of this locus for samples of oil-DNA. A detectable amplification was produced when using N3-200 primers whereas this was not the case when using EMO3 primers (Fig. 1).

Since qRT-PCR allows inspection into the PCR efficiency, it is a very useful tool in determining the utility for olive oil authentication of primers developed for other purposes. The higher the assay efficiency, the greater the slope of the logarithmic transformation of the increase in the fluorescent signal (ΔRn). Thus it is possible to overcome low PCR efficiencies by designing new primers for the same locus.

3.2. Utility of qRT-PCR to optimise the amplicon size

When degradation of DNA is expected, amplification products smaller than 200 bp have been proposed for food authentication (Hupfer et al., 1998; Unseld et al., 1995).

DNA isolated with the CTAB and the hexane methods (set as reference protocols within the framework of the European Project Oliv-Track) was used to investigate whether the size of amplicons might be optimised for olive oil authentication.

The relative quantity of target molecules for the amplification of either 200 or 80 bp amplicons was determined using qRT-PCR. To do this, primer pairs yielding an amplicon size of around 200 or 80 bp were designed for amplifying each specific locus (AJ001766 or AJ416321, Table 1). Thus, N3-80 and N3-200 were used for nuclear DNA while C4-80 and C4-200 were used for chloroplastidial DNA (Table 1). As explained in the materials and methods section, a corrected $F_0^* = F_0/\text{SCF}$ was calculated to perform direct comparisons among amplicons differing in size (Table 2).

Fig. 2 shows the quantity of input molecules as estimated from F_0^* for each DNA type and isolation method considered (CTAB and hexane). It clearly indicates that independently of the isolation method used or the DNA type considered, the quantity of templates for the amplification of PCR products around 80 bp is much higher than that of 200 bp.

Indeed, the ratio F_0^*N3-80/F_0^*N3-200 = 9.96 (see Table 2 for F_0^* values), which means that the number of input molecules for the amplification of PCR products around 80 bp is tenfold higher than that of 200 bp for nuclear DNA when using the Hexane method. This ratio is 5.40 when considering chloroplastic DNA. For the CTAB

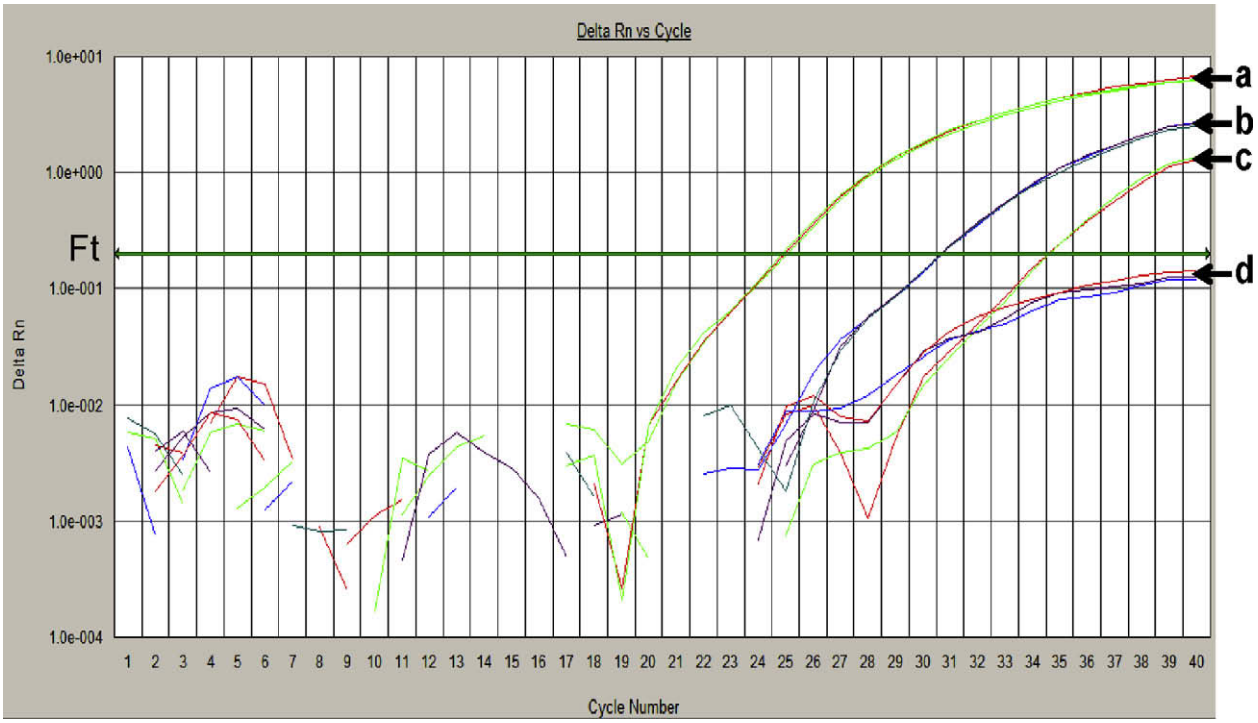

Fig. 1. Real-time PCR with DNA samples from cultivar 'Picual' using two set of primers designed on the basis of the sequence AJ416321. (a) Amplification with primers N3-200 using leaf-extracted DNA; (b) EMO3 amplification using leaf-extracted DNA; (c) N3-200 amplification using oil-extracted DNA; (d) EMO3 amplification using oil-extracted DNA. Values of fluorescence (delta Rn = ΔRn) are logarithmic. Note that for the same amount of input DNA, the EMO3 primers were allowed to reach the threshold fluorescence (Ft) when using leaf-extracted DNA but not in the case of oil-extracted DNA due to low assay efficiency. On the contrary, in the case of N3-200 primers the threshold limit is reached in both cases.

method, these ratios were 3.23 and 4.84 for nuclear and chloroplastic DNA, respectively.

Although it is known that DNA degradation takes place during olive oil extraction its influence on olive oil authentication has been neglected so far. Previous works on olive oil authentication using DNA-based markers have suggested that microsatellites may constitute a good possibility for DNA tracking due to their small size (200–300 bp) (Pasqualone et al., 2004). However, our results show that the quantity of templates for the amplification of PCR products around 80 bp is much higher than that of 200 bp whatever the extraction protocol, suggesting that the determination of optimal amplicon size should be considered for olive oil authentication.

Table 2
Quantity of template molecules in DNA extracted from 'Picual' commercial oil as estimated from corrected fluorescence (F_0^*) for each isolation method and primer pair.

DNA isolation method[a]	Primer pair	F_0^*[b]	±SE
CTAB	N3-80	3.36E−11	5.33E−12
CTAB	C4-80	1.37E−10	1.95E−12
CTAB	N3-200	1.04E−11	2.14E−12
CTAB	C4-200	2.83E−11	9.83E−12
Hexane	N3-80	2.47E−10	5.68E−11
Hexane	C4-80	2.58E−10	1.53E−11
Hexane	N3-200	2.48E−11	4.06E−12
Hexane	C4-200	4.78E−11	1.17E−11
CTAB + hexane	N3-80	5.19E−12	1.59E−12
CTAB + hexane	C4-80	1.22E−11	2.73E−12
CTAB + hexane + chloroform	N3-80	3.20E−10	2.69E−11
CTAB + hexane + chloroform	C4-80	2.62E−09	5.29E−11

[a] The methods are abbreviated as follows in the text: CTAB = CTAB; hexane = Hex; CTAB + hexane = CHex; CTAB + hexane + chloroform = CHex–Chl.

[b] F_0^*: corrected fluorescence. $F_0^* = F_0/SCF$ (SCF = size calibration factor, see Table 1).

3.3. Utility of qRT-PCR to compare between DNA isolation methods

The third task of this work was to compare the relative performance of four different protocols for DNA isolation from olive oil. The methods used are abbreviated as follows: CTAB + hexane = CHex; CTAB = CTAB; hexane = Hex; CTAB + hexane + chloroform = CHex–Chl.

The comparison among the methods used in this work is shown in Fig. 3 for both chloroplastic and nuclear DNA. It is clear that the

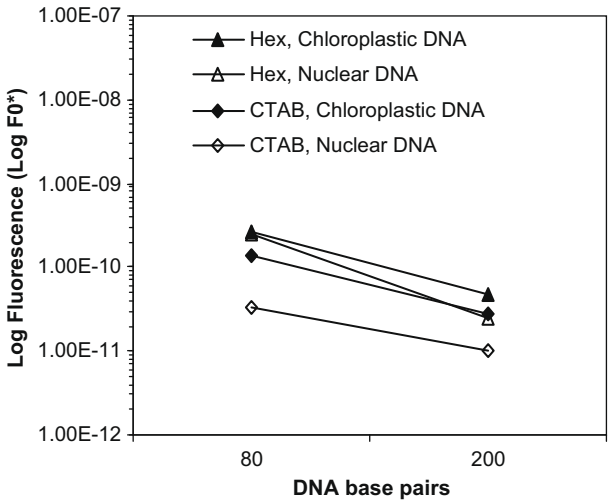

Fig. 2. Comparison between amplifiable DNA of sizes of 80 and 200 bp using qRT-PCR. Quantity of input molecules as estimated from F_0^* (shown in logarithmic scale) for each DNA type and isolation method (only hexane = Hex and CTAB methods were used).

worse method is CHex independently of the DNA type used. Besides, this figure allows a ranking to be established considering the quantity of DNA isolated as follows: CHex–Chl > Hex > CTAB > - CHex independently of the DNA type with but one exception since both CHex–Chl and Hex were almost equally efficient in isolating nuclear DNA (F_0^*N3-80$_{CHex-Chl}$/F_0^*N3-80$_{Hex}$ = 1.3, data from Table 2).

The CHex method had the poorest performance but the modifications proposed for the CHex–Chl allowed increasing the DNA obtained up to 61.7 and 214.7 times for nuclear and chloroplastic DNA, respectively (ratios of F_0^* values shown in Table 2).

The CHex–Chl method is based upon the CHex method with two modifications, the use of chloroform and the addition of nuclear acrylamide in order to improve DNA recovery. Therefore, either one or both modifications allowed to substantially improve the results obtained using the CHex method. The former method was the best for the isolation of both DNA types with one exception since the Hex protocol was almost equally efficient for nuclear DNA isolation. The Hex method was recently reported as the best protocol for nuclear DNA isolation (Martins-Lopes, Gomes, Santos, & Guedes-Pinto, 2008) but the differences found in our work indicate that further work is needed to optimise the isolation protocols and that qRT-PCR will be a useful tool for this purpose.

Regarding the DNA type, the quantity of chloroplastic DNA was higher than that of nuclear DNA for all the methods but Hex, where the ratio F_0^*C4-80$_{Hex}$/F_0^*N3-80$_{Hex}$ was 1.04 (F_0^* values from Table 2). For the other methods the ratio of chloroplastidial *vs* nuclear DNA was higher than 2 and as high as 8.19 in CHex-CHl (considering amplicon sizes of 80 bp).

Although not included in this work, it would be expected that similar results would be obtained when using mitochondrial DNA. Therefore, we think that more attention should be paid to cytoplasmic DNA (either mitochondrial or chloroplastic) for olive oil authentication since it is maternally inherited which offers several advantages over nuclear DNA. The use of this type of DNA would circumvent one of the limitations for olive oil authentication, the contribution of pollinators. Olive is a diploid species and most cultivars are considered self-incompatible, being that the flowers are wind pollinated. As a consequence the embryo of the seeds contains genetic information not only from the maternal parent but also from the pollen donor. Since olive oil is produced by crushing whole fruits, paternal DNA may hamper the traceability when using markers based on nuclear DNA (Doveri, O'Sullivan, & Lee, 2006).

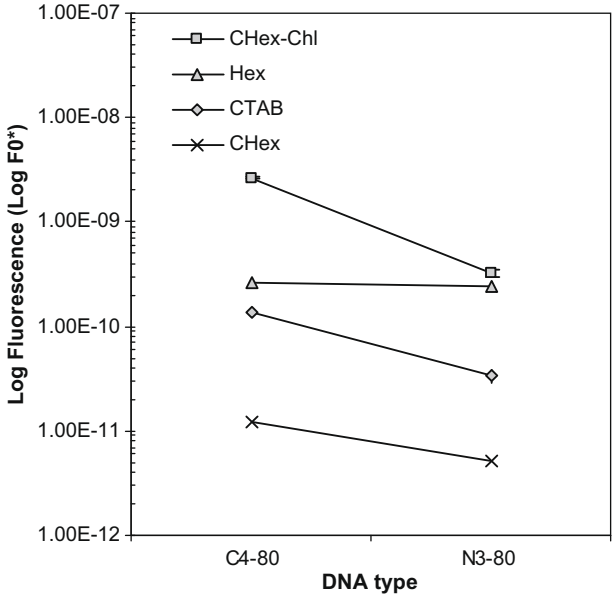

Fig. 3. Comparison among DNA isolation methods and DNA types (C = chloroplastic; N = nuclear) using qRT-PCR. Quantity of input molecules as estimated from F_0^* (shown in logarithmic scale) for each DNA type and isolation method (the methods used are abbreviated as follows: CTAB + hexane = CHex; CTAB = CTAB; hexane = Hex; CTAB + hexane + chloroform = CHex–Chl).

The higher quantity of cpDNA isolated from olive oil and the avoidance of the effect of the pollen donor on traceability cytoplasmic DNA (either mitochondrial or chloroplastic) should not be discarded for olive oil authentication, despite its use for the protection of PDOs (Luykx & van Ruth, 2008) would be more difficult at present.

Chloroplast polymorphism using microsatellites and PCR–RFLP has been reported (Besnard & Berville, 2002). The possibilities of developing new molecular markers to identify olive cultivars using cpDNA has been stated (Intrieri, Muleo, & Buiatti, 2007) but at present it is not known whether cpDNA is polymorphic enough to be used for unique cultivar identification.

The level of cpDNA variation differs among species. For instance, in tomato no variation in the plastome between an European and a Latin American tomato cultivar (Kahlau, Aspinall, Gray, & Bock, 2006) was found. In cucumber, the comparison of the cpDNA sequence between a frost-tolerant and a frost-sensitive genotype indicated that both sequences were identical with the exception of three polymorphic sites (Chung, Gordon, & Staub, 2007). On the contrary, the perennial species *Trifolium pratense* exhibits extremely high degrees of chloroplast DNA variation (Milligan, 1991).

Mitochondrial variation has been reported in olive (Besnard, Khadari, Baradat, & Berville, 2002). A higher degree of variation is usually reported for mitochondria than for chloroplast. For instance, 454 SNPs (single nucleotide polymorphisms) where detected for mitochondria between two genotypes of sugar beet, mostly in the non-coding regions (Satoh et al., 2004). Therefore, the applicability of citoplasmic DNA to olive oil authentication will depend on the degree of variation between olive cultivars which cannot be hypothesised *a priori*.

Recent advances in the sequencing technologies may allow the rapid sequencing of the chloroplast from different cultivars in the near future. This would allow the potential of cpDNA for cultivar determination to be evaluated.

4. Conclusions

The detection of frauds, either due to the mixtures with oils of other species such as hazelnut, or to the certification of PDOs would need quantitative tools. At its best, conventional PCR remains a semi-quantitative technique, and therefore, it is not optimal for authentication purposes when quantification is needed. The use of real-time chemistries allows for the detection of PCR amplification during the early phases of the reaction, providing a distinct advantage over detection of amplification at the final phase or end-point of the PCR reaction. qRT-PCR is a useful tool in the development of molecular markers for olive oil authentication since it allows inspecting the PCR efficiency. Besides qRT-PCR should be used for the optimisation of the amplicon size and the DNA isolation procedure which are critical aspects in olive oil authentication. The potential of cpDNA for olive oil authentication should be addressed in the future.

Acknowledgements

This research was financed by the Project Olive-Track, contract number QLK1-CT-2002-02386. Fernando Piston acknowledges financial support from Juan de la Cierva program from Ministry of Science and Innovation and European Social Fund (ESF).

References

Belaj, A., Rallo, L., Trujillo, I., & Baldoni, L. (2004). Using RAPD and AFLP markers to distinguish individuals obtained by clonal selection of 'Arbequina' and 'Manzamila de Sevilla' olive. *Hortiscience, 39*(7), 1566–1570.

Belaj, A., Trujillo, I., de la Rosa, R., Rallo, L., & Gimenez, M. J. (2001). Polymorphism and discrimination capacity of randomly amplified polymorphic markers in an olive germplasm bank. *Journal of the American Society for Horticultural Science, 126*(1), 64–71.

Besnard, G., & Berville, A. (2002). On chloroplast DNA variations in the olive (*Olea europaea* L.) complex: Comparison of RFLP and PCR polymorphisms. *Theoretical and Applied Genetics, 104*(6–7), 1157–1163.

Besnard, G., Khadari, B., Baradat, P., & Berville, A. (2002). Combination of chloroplast and mitochondrial DNA polymorphisms to study cytoplasm genetic differentiation in the olive complex (*Olea europaea* L.). *Theoretical and Applied Genetics, 105*(1), 139–144.

Breton, C., Claux, D., Metton, I., Skorski, G., & Berville, A. (2004). Comparative study of methods for DNA preparation from olive oil samples to identify cultivar SSR alleles in commercial oil samples: Possible forensic applications. *Journal of Agricultural and Food Chemistry, 52*(3), 531–537.

Busconi, M., Foroni, C., Corradi, M., Bongiorni, C., Cattapan, F., & Fogher, C. (2003). DNA extraction from olive oil and its use in the identification of the production cultivar. *Food Chemistry, 83*(1), 127–134.

Christopoulou, E., Lazaraki, M., Komaitis, M., & Kaselimis, K. (2004). Effectiveness of determinations of fatty acids and triglycerides for the detection of adulteration of olive oils with vegetable oils. *Food Chemistry, 84*(3), 463–474.

Chung, S.-M., Gordon, V. S., & Staub, J. E. (2007). Sequencing cucumber (*Cucumis sativus* L.) chloroplast genomes identifies differences between chilling-tolerant and -susceptible cucumber lines. *Genome, 50*(21), 5–225.

Consolandi, C., Palmieri, L., Severgnini, M., Maestri, E., Marmiroli, N., Agrimonti, C., et al. (2008). A procedure for olive oil traceability and authenticity: DNA extraction, multiplex PCR and LDR – universal array analysis. *European Food Research and Technology, 227*, 1429–1438.

De la Rosa, R., James, C. M., & Tobutt, K. R. (2002). Isolation and characterization of polymorphic microsatellites in olive (*Olea europaea* L.) and their transferability to other genera in the Oleaceae. *Molecular Ecology Notes, 2*(26), 5–267.

De la Torre, F., Bautista, R., Cánovas, F. M., & Claros, G. (2004). Isolation of DNA from olive oil and oil sediments: Application in oil fingerprinting. *Food and Agricultural Environment, 2*, 84–89.

Diaz, A., De la Rosa, R., Martin, A., & Rallo, P. (2006). Development, characterization and inheritance of new microsatellites in olive (*Olea europaea* L.) and evaluation of their usefulness in cultivar identification and genetic relationship studies. *Tree Genetics and Genomes, 2*(3), 165–175.

Diaz, A., De la Rosa, R., Rallo, P., Munoz-Diez, C., Trujillo, I., Barranco, D., et al. (2007). Selections of an olive breeding program identified by microsatellite markers. *Crop Science, 47*(6), 2317–2322.

Doveri, S., O'Sullivan, D. M., & Lee, D. (2006). Non-concordance between genetic profiles of olive oil and fruit: A cautionary note to the use of DNA markers for provenance testing. *Journal of Agricultural and Food Chemistry, 54*(24), 9221–9226.

Doyle, J. J. (1991). DNA protocols for plants. In G. Hewitt, A. W. B. Johnson, & J. P. W. Young (Eds.). *Molecular techniques in taxonomy. NATO ASI series H, cell biology* (Vol. 57, pp. 283–293). Berlin, Heidelberg, New York: Springer.

Freeman, W. M., Walker, S. J., & Vrana, K. E. (1999). Quantitative RT-PCR: Pitfalls and potential. *Biotechniques, 26*(1), 112.

Hupfer, C., Hotzel, H., Sachse, K., & Engel, K. H. (1998). Detection of the genetic modification in heat-treated products of Bt maize by polymerase chain reaction. *Zeitschrift Fur Lebensmittel-Untersuchung Und-Forschung a-Food Research and Technology, 206*(3), 203–207.

Intrieri, M. C., Muleo, R., & Buiatti, M. (2007). Chloroplast DNA polymorphisms as molecular markers to identify cultivars of *Olea europaea* L. *Journal of Horticultural Science and Biotechnology, 82*(1), 109–113.

Kahlau, S., Aspinall, S., Gray, J., & Bock, R. (2006). Sequence of the tomato chloroplast DNA and evolutionary comparison of solanaceous plastid genomes. *Journal of Molecular Evolution, 63*(2), 194–207.

Luykx, D. M. A. M., & van Ruth, S. M. (2008). An overview of analytical methods for determining the geographical origin of food products. *Food Chemistry, 107*(2), 897–911.

Mafra, I., Ferreira, I., & Oliveira, M. (2008). Food authentication by PCR-based methods. *European Food Research and Technology, 227*(3), 649–665.

Martins-Lopes, P., Gomes, S., Santos, E., & Guedes-Pinto, H. (2008). DNA markers for Portuguese olive oil fingerprinting. *Journal of Agricultural and Food Chemistry, 56*, 11786–11791.

Milligan, B. G. (1991). Chloroplast DNA diversity within and among populations of *Trifolium pratense*. *Current Genetics, 19*(5), 411–416.

Morrison, T. B., Weis, J. J., & Wittwer, C. T. (1998). Quantification of low-copy transcripts by continuous SYBR (R) green I monitoring during amplification. *Biotechniques, 24*(6), 954.

Pasqualone, A., Montemurro, C., Caponio, F., & Blanco, A. (2004). Identification of virgin olive oil from different cultivars by analysis of DNA microsatellites. *Journal of Agricultural and Food Chemistry, 52*(5), 1068–1071.

Rutledge, R. G. (2004). Sigmoidal curve-fitting redefines quantitative real-time PCR with the prospective of developing automated high-throughput applications. *Nucleic Acids Research, 32*(22), e178.

Satoh, M., Kubo, T., Nishizawa, S., Estiati, A., Itchoda, N., & Mikami, T. (2004). The cytoplasmic male-sterile type and normal type mitochondrial genomes of sugar beet share the same complement of genes of known function but differ in the content of expressed ORFs. *Molecular Genetics and Genomics, 272*(3), 247–256.

Taberlet, P., Griffin, S., Goossens, B., Questiau, S., Manceau, V., Escaravage, N., et al. (1996). Reliable genotyping of samples with very low DNA quantities using PCR. *Nucleic Acids Research, 24*(16), 3189–3194.

Unseld, M., Beyermann, B., Brandt, P., & Hiesel, R. (1995). Identification of the species origin of highly processed meat-products by mitochondrial-DNA sequences. *PCR-Methods and Applications, 4*(4), 241–243.

Food Chemistry 118 (2010) 489–496

Contents lists available at ScienceDirect

Food Chemistry

journal homepage: www.elsevier.com/locate/foodchem

A new antioxidant from wild nutmeg

C.A. Calliste [a], D. Kozlowski [a], J.L. Duroux [a], Y. Champavier [b], A.J. Chulia [c], P. Trouillas [a,*]

[a] Université de Limoges, EA 4021, Laboratoire de Biophysique, Faculté de Pharmacie, 2 rue du Docteur Marcland, 87025 Limoges, France
[b] Université de Limoges, Service commun de RMN, Faculté de Pharmacie, 2 rue du Docteur Marcland, 87025 Limoges, France
[c] Université de Limoges, EA 4021, Laboratoire de Pharmacognosie, Faculté de Pharmacie, 2 rue du Docteur Marcland, 87025 Limoges, France

ARTICLE INFO

Article history:
Received 12 February 2009
Received in revised form 26 March 2009
Accepted 6 May 2009

Keywords:
Antioxidant
Natural lignan
Nutmeg (*Myristica argentea*)
Lipid peroxidation
DFT calculation

ABSTRACT

Nutmeg (*Myristica fragans* and *Myristica argentea*) is a spice widely used in food. Argenteane is a dilignan which has been isolated from nutmeg mace (the lace-like seed membrane of nutmeg). On the basis of the experimental measurements of the lipid peroxidation inhibition, argenteane appeared to be an antioxidant as powerful as vitamin E. The present joint experimental and theoretical study helped to understand the mechanism of action of this compound. The density functional theory (DFT) calculations of the O–H bond dissociation enthalpies (BDEs) correlated with the capacity to scavenge free radicals. We demonstrated that the central moiety is able to release one or two H atom(s) to the free radicals. This mechanism was confirmed by (i) the BDE calculations and (ii) the free radical-scavenging capacity measurements of two lignans and 3,3′-dimethoxy-1,1′-biphenyl-4,4′-diol (i.e., the argenteane central moiety). In addition to this active part, two lipophilic chains participate in the molecule's capacity to react with the oxidative species generated in the membrane vicinity.

1. Introduction

The present paper reports on the biological properties of a natural lignan derivative (argenteane), which was isolated for the first time by our group (Filleur, Pouget, Allais, Kaouadji, & Chulia, 2002). Argenteane ((*bis*-*erythro*-5,5′-*bis*[1-(4-hydroxy-3-methoxyphenyl)-4-(3,4-methylenedioxyphenyl)-2,3-dimethylbutane])) is actually a dilignan (Fig. 1), the first of this type described in the plant kingdom. It has been isolated from nutmeg, together with other lignans (Filleur et al., 2002).

Nutmeg is the seed of the fruit of *Myristica*. The most common species is *Myristica fragans* but other species are used including *Myristica argentea* and *Myristica malabarica*, which are known to be less tasty but are still used in Indonesian diets. It is wrapped in a red or orange lace-like membrane, i.e., the mace. Both nutmeg and mace are spices with similar tastes. The former is sweeter while the latter is known to release more delicate flavors. Mace is also preferred in some dishes for the orange colour that is released (saffron-like colour). Nutmeg is a tropical fruit; it is native to Banda, a Mollucca island of Indonesia. Over the ages it has been cultivated in other regions (e.g., Malaysia and Grenada) but preferentially on volcanic soil. Nutmeg is used as thin slices or more generally as a powder. It is used in numerous recipes, including a lot of desserts (e.g. fruit cakes, muffins, pies) but in main courses as well (e.g., potato dishes, sauces). Nutmeg is also added to beverages (e.g., tea, mulled wine) and it is an ingredient of some curry powders.

Lignans constitute a group of polyphenolic compounds (Harworth, 1942) whose skeleton results from the establishment of a connection between β carbons of the lateral chains of two 1-phenyl propane moieties (Fig. 1). Six different groups of lignans are described: dibenzylbutanes which are just formed from the 8–8′ connexion, and the other five groups containing cyclised compounds (i.e., monofuranic lignans 9-*O*-9′, 7-*O*-9′ and 7-*O*-7′, butyrolactones, arylnaphthalenes, dibenzocycloctanes, furanofuranic lignans). Lignan derivatives obtained from nutmeg essentially belong to the dibenzylbutane group, with either a guaiacyl or piperonyl moieties on the aromatic rings.

Numerous studies have reported on the beneficial effects of diets rich in lignan derivatives. As isoflavonoids, they are phytooestrogens and thereby may prevent breast cancer (Le Bail, Champavier, Chulia, & Habrioux, 2000). As a lot of phenolic compounds, lignans also exhibit antioxidant properties (Filleur, Pouget, Duroux, Simon, & Chulia, 2001).

The present study is a joint theoretical and experimental study of the antioxidant property of argenteane (**1**) and two other derivatives derived from nutmeg (*meso*-dihydroguaiaretic acid (**2**) and *erythro*-austrobailignan-6 (**3**)) (Fig. 1). The antioxidant capacity is measured by the capacity, (i), to scavenge the stable free radical DPPH (2,2-diphenyl-1-picrylhydrazyl), and (ii), to inhibit lipid peroxidation. In order to gain a better understanding of these activities and to draw up a structure-activity relationship, the experimental results are then supported by theoretical calculations

* Corresponding author. Tel.: +33 (0) 555 435 927; fax: +33 (0) 555 435 844.
E-mail address: trouillas@unilim.fr (P. Trouillas).

0308-8146/$ - see front matter © 2009 Elsevier Ltd. All rights reserved.
doi:10.1016/j.foodchem.2009.05.010

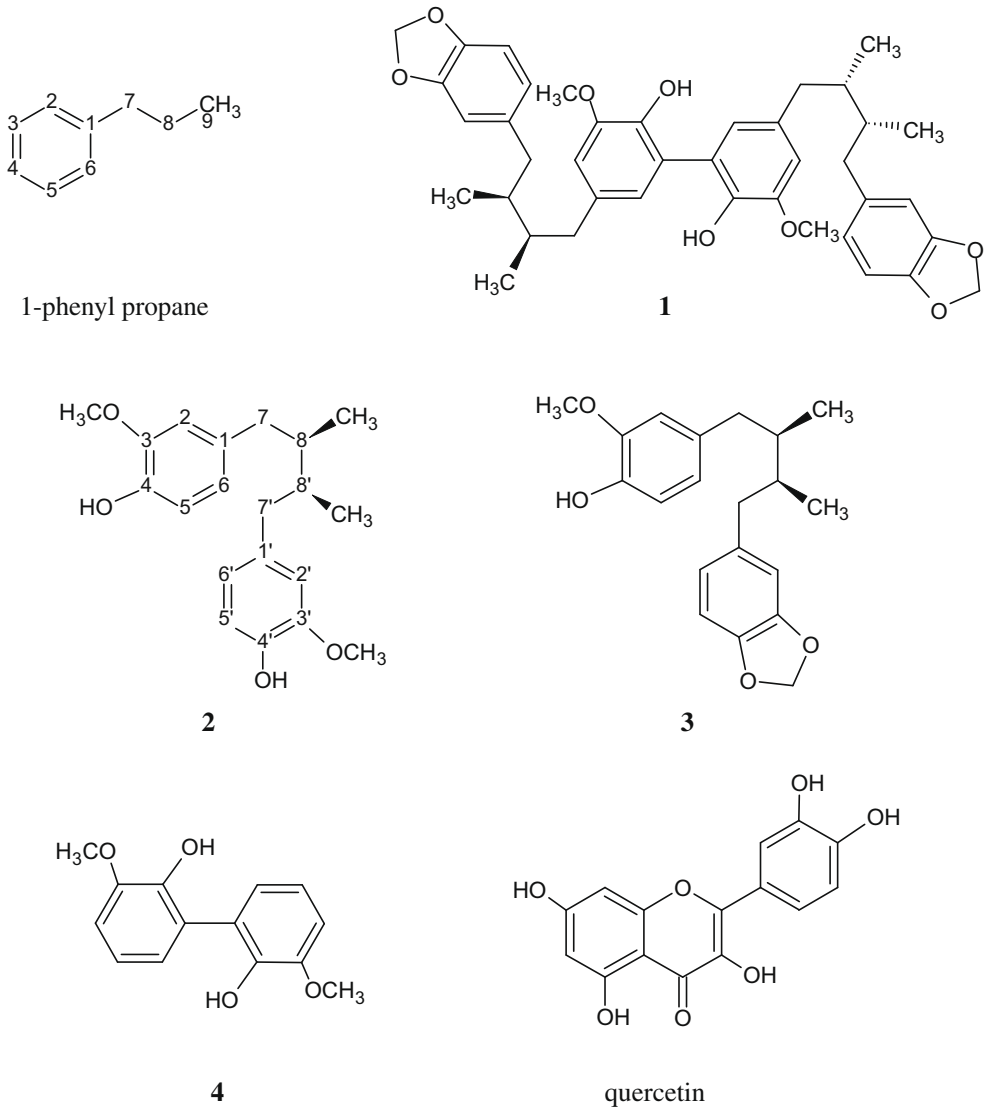

Fig. 1. Molecular structures of **1** (the dilignan, argenteane), **2** (*meso*-dihydroguaiaretic acid) and **3** (*erythro*-austrobailignan-6), **4** (3,3′-dimethoxy-1,1′-biphenyl-4,4′-diol) and quercetin.

at the DFT (density functional theory) level. We first detail the conformational features of **1**–**3**, which are described for the first time. Then we focus on the redox properties of those compounds and especially on their capacity to lose and to transfer a hydrogen to the free radicals involved in oxidative stress. Compounds **1**–**3** are compared to each other, to reference antioxidants (i.e., vitamin E and quercetin) and finally to the central moiety of **1** (i.e., compound **4**). Compound **4** was synthesised for the present study and its antioxidant capacity was evaluated. Again the quantum calculations help to establish the structure-activity relationship and finally to propose the mechanism of action of this new and effective lipid peroxidation inhibitor (as compared to quercetin and vitamin E).

2. Material and methods

2.1. Extraction and purification of argenteane

In order to reduce the number of steps for the isolation and purification of **1**, as compared to the previous reports (Filleur et al., 2002), a new processing method was developed here. Powdered mace of *M. argentea* Warb. (1 kg) was extracted with petroleum ether (10 l), thus yielding 675 g of extract. This extract was defatted by freezing and by partition against *n*-hexane and methanol (1:1). The defatted extract became a red viscous oil (340 g) that was afterwards dried under vacuum. In order to concentrate **1**, a Sephadex LH-20 column (45 × 800 mm) was used with methanol as the eluant. The subsequent extract (60 g) enriched in **1** was obtained. Compound **1** was isolated and purified by three successive MPLC (medium-pressure liquid chromatography) procedures: (i), silica gel column (Polygoprep (Ø 20–60 μm, 26 × 460 mm) eluted with *n*-hexane/$CHCl_3$ (100:0–50:50, 8 ml/min, 1200 ml), (ii), C-18 column (LiChroprep RP-18, Ø 18–25 μm, 15 × 230 mm) using methanol/water (90:10–100:0, 3 ml/min, 500 ml) as the eluant, and (iii), the same C-18 column using methanol/water (90:10–93:7, 3 ml/min, 400 ml) as the eluant. The different chromatographic steps were monitored by UV-detection at 254 nm. Pure compound **1** (60 mg) was thus obtained from 1 kg of *M. argentea* Warb. mace. The structure was confirmed by NMR, in agreement with the literature (Filleur et al., 2002).

Compounds **2** and **3** were obtained and identified following the procedure described by Filleur et al. (2002).

2.2. Enzymatic synthesis of compound **4**

Compound **4** (3,3′-dimethoxy-1,1′-biphenyl-4,4′-diol) was synthesised by a method derived from that previously described by Simmons, Minard, and Bollag (1988). Guaiacol (4 mM) was enzymatically oxidised by horseradish peroxidase (2 U/ml) in a citrate–phosphate buffer (pH 5.5) containing hydrogen peroxide (2 mM). The reaction was achieved at room temperature in 30 min. Enzyme activity was stopped by acidification of the reaction mixture with acetic acid. Separation of **4** was performed by MPLC, using three successive different systems: (i), C-18 column (LiChroprep RP-18, Ø 18–25 μm, 15 × 230 mm) using methanol/water (60:40–90:10, 3 ml/min, 600 ml) as the eluant, (ii), a silica gel column (Polygoprep Ø 20–60 μm, 15 × 230 mm) using *n*-hexane/ethyl acetate as the mobile phase (70:30–0:100, 3 ml/min, 500 ml), and (iii), a C-18 column using methanol/water (50:50–90:10, 3 ml/min, 550 ml) as the eluant. Purification was achieved on a Sephadex LH-20 column (15 × 600 mm) with methanol as the eluant.

^{1}H NMR and ^{13}C NMR spectra were measured in $(CD_3)_2CO$ on a Bruker DPX 400 MHz Avance spectrometer, using tetramethylsilane as an internal standard. Complete proton and carbon assignments were based on 1D and 2D (COSY, HMQC, HMBC) NMR experiments.

^{1}H NMR (400 MHz, acetone-d6) 6.94 (2H, dd, J = 7.5, 2.0 Hz, H-4, H-4′), 6.87 (2H, dd, J = 7.8, 2.0 Hz, H-6, H-6′), 6.83 (2H, br t, J = 7.6 Hz, H-5, H-5′), 3,87 (6H, s, H-7, H-7′). ^{13}C NMR (100 MHz, acetone-d6) 148.8 (C-3, C-3′), 144.9 (C-2, C-2′), 126.6 (C-1, C-1′), 124.4 (C-6, C-6′), 119.8 (C-5, C-5′), 111.3 (C-4, C-4′), 56.4 (OCH_3, C-7, C-7′) confirmed the molecular structure of **4** (Fig. 1).

2.3. DPPH free radical-scavenging capacity

Because of its paramagnetic properties, DPPH exhibits a characteristic ESR (electron spin resonance) signal. The ESR spectra were obtained with a Bruker model ESP300E spectrometer, using microsampling pipettes at room temperature under the following conditions: modulation frequency of 100 kHz, microwave frequency of 9.78 GHz, microwave power of 2 mW, modulation amplitude of 1.97 G, and time constant of 10.24 ms. The ESR spectra were recorded 3 min after sample preparation.

Mixtures that contained 50 μl of compound, dissolved in methanol at different concentrations, and 50 μl of DPPH ethanol solution (5×10^{-4}M) were tested. *Inhibition* was calculated as follows:

$$\text{Inhibition} = [ref - compound]/[ref - bg],$$

where *ref* and *compound* are the values of the double integrals for the ESR spectrum of the reference (DPPH + solvent) and the tested solution (DPPH + solvent + compound), respectively; *bg* represents the background signal (solvent). Each data point is the result of the average of three independent measurements. The IC_{50} value was calculated from the plot of inhibition against concentration.

2.4. Preparation of large unilamellar vesicles (LUV)

PLPC prepared from Sigma–Aldrich (St. Louis, MO) in chloroform was evaporated under vacuum in a round-bottomed flask to produce thin PLPC film. Multilamellar vesicles (MLV) were produced by vortexing the thin film after hydration with distillated water. MLVs were passed through 0.1 micron double-layer polycarbonate membrane using a Lipex™ extruder (Northern Lipids Inc., Burnaby, Canada) to produce LUV. The preparation resulted in a 250 mM PLPC LUV in water solution. Particle size ranged from 90 to 110 nm, determined using an N4 Plus submicron particle size analyser (Beckman-Coulter Inc., Fullerton, CA).

The tested compounds of various concentrations (10 μl in methanol) were added to 1 ml of LUVs mixture prior to the lipid peroxidation initiation. Oxidative stress was generated by γ-irradiation (400 Gy, Oris experimental irradiator; Oris Industries, Gif-sur-Yvette, France) of the liposomal mixture, which produces $OH^{\cdot}$ from the solvent. The oxidative stress effect was determined following the formation of conjugated dienes at 233 nm (Shimadzu UV-2401PC; Shimadzu, Kyoto, Japan).

2.5. Theoretical methodology

Over the past decade, the theoretical description of phenolic compounds has been achieved by using semi-empirical and DFT methods (Fiorucci, Golebiowski, Cabrol-Bass, & Antonczak, 2007; Lemaska et al., 2001; Leopoldini, Marino, Russo, & Toscano, 2004a; Leopoldini, Pitarch, Russo, & Toscano, 2004b; Lucarini, Pedulli, & Guerra, 2004; Priyadarsini et al., 2003; Russo, Toscano, & Uccella, 2000; Trouillas et al., 2004; Wright, Jonhson, & DiLabio, 2001; Zhang, Sun, & Chen, 2001; Zhang, Sun, & Wang, 2003). While the former method only gives good trends, the latter has given very good agreement with experimentation. In particular the description of redox properties may be reproduced by using hybrid functionals. The B3P86 functional has given very good BDE values for phenolic compounds. Indeed the theoretical O–H BDE of phenol obtained with this very functional is around 87 kcal/mol (Trouillas, Marsal, Siri, Lazzaroni, & Duroux, 2006), while the experimental value is 87 ± 1 kcal/mol (Wayner et al., 1995). A similar accuracy was obtained for catechol (Trouillas et al., 2006). Afterwards the use of B3P86 was successfully extrapolated to larger phenolic compounds to establish structure-activity relationships (Kozlowski et al., 2007a, 2007b; Trouillas et al., 2008). The use of other functionals, e.g., B3LYP has also given a reliable comparative description of polyphenols but the phenol BDE is shifted by about 4 kcal/mol, compared to the experimental value. The use of the 6-31+G(d,p) basis set is sufficient to reach a perfect agreement between the experimental and theoretical BDE of phenol (Trouillas et al., 2006), in order to describe the energies of molecules and corresponding radicals.

In the case of antioxidant polyphenols and due to the importance of electron delocalisation effects, calculations have to be performed over the entire molecules at the same level. In order to find the best conformation, we explored the potential energy surfaces at the B3P86/6-31G(d) level. Afterwards most stable geometries and energies were re-calculated at the B3P86/6-31+G(d,p) level. Both B3P86/6-31+G(d,p)//B3P86/6-31G(d) and B3P86/6-31+G(d,p) schemes gave very similar results (difference lower than 0.5 kcal/mol), indicating that the description of geometries can be carried out by using the 6-31G(d) basis set. This approximation was used for all the different structures since it is very accurate and since a PCM-B3P86/6-31+G(d,p) optimisation for compound **1** and the corresponding radical is not feasible. Indeed, the use of diffuse functions makes the convergence procedure a tricky problem for such a system.

The geometries and energies of the phenoxyl radicals ($ArO^{\cdot}$), obtained after the H abstraction from an OH group, were achieved starting from the optimised structure of the parent molecule. Following Pople, Gill, and Handy (1995), we decided to use an unrestricted approach for these open-shell systems. Compared to a restricted open-shell scheme, an unrestricted calculation allows more flexibility, e.g., this helps to describe the spin polarisation. Unrestricted DFT calculations may induce spin contamination since the unrestricted determinants are not eigenfunctions of $\langle S^2 \rangle$ operator. Nonetheless in our case spin contamination appeared to be weak.

For the four compounds (**1**–**4**) and the corresponding radicals, the most stable conformer exhibits a stabilising H-bonding interac-

tion between the OH group and the *ortho*-OCH_3 group. The vibrational frequencies have been evaluated and all conformations have been checked to have no imaginary frequency.

BDEs were calculated at 298 K using the sum of electronic and thermal enthalpies, which is the total electronic energy + ZPE + $E_{vibration}$ + $E_{rotation}$ + $E_{translation}$ + RT. Frequencies were calculated at the B3P86/6-31G(d) level (in which geometries have been optimised), using a scale factor of 0.9557 (Merrick, Moran, & Radom, 2007).

The solvent effects were implicitly taken into account by using a PCM (polarisable continuum model) method, since using a box of explicit solvent molecules is not feasible with such compounds. The effects of explicit water molecules in the surrounding of the OH group of phenol were investigated (Guerra, Amorati, & Pedulli, 2004), and confirmed that the use of PCM gives a relatively good description of BDEs. We also tested the use of a hybrid model (i.e., one or two molecules surrounding the OH groups + PCM) for quercetin (Kozlowski et al., 2007a), a bigger system than phenol. We observed only a slight difference in BDE as compared to a pure PCM calculation, while computational time was dramatically increased. Thus, in the present paper, calculations were performed with IEFPCM (Integral Equation Formalism PCM) and UA0 radii, well-adapted for phenol BDE description (data not shown).

All calculations were achieved in Gaussian 03 and implemented methods (Frisch, Trucks, Schlegel, et al., 2004).

The antioxidant (e.g., free radical-scavenging) capacity of phenolic compounds (ArOH) is strongly related to their redox properties, either H atom or electron transfer. The reactivity of those antioxidants usually follows one of those two reactions:

$$\text{HAT (H atom transfer)}: \text{ArOH} + R^{\cdot} \rightarrow \text{ArO}^{\cdot} + \text{RH} \quad (1)$$

$$\text{ET (electron transfer)}: \text{ArOH} + R^{\cdot} \rightarrow \text{ArOH}^{+\cdot} + R^{-} \rightarrow \text{ArO}^{\cdot} + RH \quad (2)$$

where R· is any radical implicated in oxidative stress, including DPPH·, ·OH, $O_2^{\cdot -}$, ROO· or NO·.

Reaction (1) is the homolytic dissociation of the O–H bond, and this is in relation to the BDE of the OH groups. Reaction (2) is a heterolytic dissociation in relation to the ionisation potential (IP) of ArOH and by the enthalpy of the $ArOH^{+\cdot}$ cation formation. Actually there exists a third mechanism, so-called sequential proton-loss-electron-transfer (SPLET), in which the proton is first lost, thereby allowing electron transfer (Zhang & Ji, 2006).

Different studies have demonstrated a very good agreement between BDEs and the free radical-scavenging capacity of phenolic compounds, thus indicating that reaction (1) is predominant for polyphenols (Fiorucci et al., 2007; Lemaska et al., 2001; Leopoldini et al., 2004a, 2004b; Lucarini et al., 2004; Priyadarsini et al., 2003; Russo et al., 2000; Trouillas et al., 2004; Wright et al., 2001; Zhang et al., 2001, 2003). We calculated the BDE (i.e., $H^{298K}(\text{ArOH}) - H^{298K}(\text{ArO}^{\cdot}) - H^{298K}(H)$) of each group for compounds **1**–**4**, in order to evaluate the capacity of each group to release one or two H atoms. BDE is a chemical descriptor related to the first mechanism. We also calculated ΔH and ΔG of reactions between **1**–**4** and free radicals (i.e., from reactants ArOH and $R^{\cdot}$ to final products $ArO^{\cdot}$ and RH). Let us insist on the fact that ΔH and ΔG are the same for the three mechanisms, as they are taken in their entirety (from initial to final products), i.e., $\Delta H = H^{298K}(\text{ArO}^{\cdot}) + H^{298K}(\text{RH}) - H^{298K}(\text{ArOH}) + H^{298K}(R)$. Those values give a global description of the free radical-scavenging action, whatever the mechanism involved, that is ΔH and ΔG take into account the different contributions, even if competition exists between the three mechanisms. Here we focus on two radicals $R^{\cdot}$ = DPPH and ROO·; the former is used to estimate the capacity of compounds to be oxidised, while the latter is involved in the lipid peroxidation process.

3. Results and discussion

3.1. Argenteane: a dimer issued from oxidation of lignan

Argenteane (**1**) is a dilignan formed in nutmeg. This is a natural dimer of the lignan compound **3**. Dimers, trimers and other oligomers of polyphenols are known to be formed in plants and they are called procyanidins or condensed tannins in the case of flavonoids. Numerous oligomers of catechin exist and they are classified in different sub-groups, depending on the carbon atoms involved in the covalent C–C bond formation. The presence of other types of dimers including quercetin and phenolic acid dimers, is reported as well (Ngoc Ly et al., 2005; Ralph, Quideau, Grabber, & Hatfield, 1994; Sang et al., 2002).

The natural dimerisation of **3** to form **1** can be explained by the capacity of the guaiacyl moiety (in **3**) to undergo enzymatically catalysed oxidation. The guaiacyl as well as the catechol moieties are known to bind to the active site of such oxidative enzymes (e.g., laccases) thus losing an H atom. Following the loss of one electron and one proton in the active site, a radical is formed from **3** and exhibits a strong spin density on carbon atom C5 (Fig. 2); this makes C–C bond formation easier.

3.2. Conformational analysis

The potential energy surface was first studied for compound **2**, following in particular the two torsion angles τ_1 = C1–C7–C8–C8′ and τ_2 = C8–C8′–C7′–C1′. Two conformers (**2a** and **2b**) were obtained, corresponding to ($\tau_1 = -168°$; $\tau_2 = 169°$) and ($\tau_1 = -170°$; $\tau_2 = 55°$), respectively. The guaiacyl moiety was computed so that a H-bonding existed between the H atom of the OH group and the O atom of the OCH_3 group. Conformations of **3** (**3a** and **3b**) were directly deduced from those of **2**, except that one of the guaiacyl moieties was turned to a piperonyl moiety (Fig. 1). We demonstrated that conformer **2a** (**3a**) is more stable than **2b** (**3b**) by

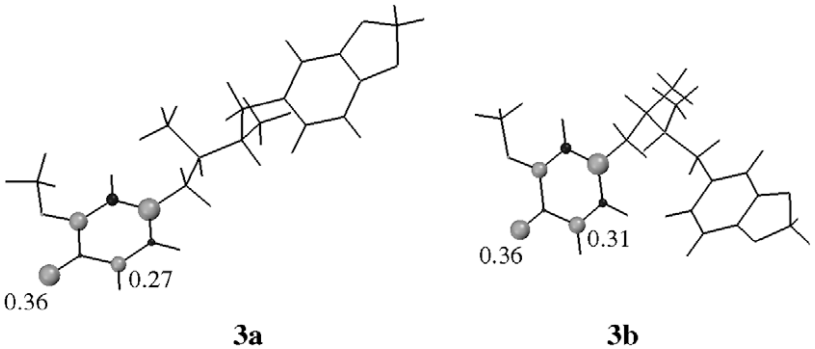

Fig. 2. Spin density distribution of the radicals obtained after H abstraction from **3**.

about 1 kcal/mol. Nevertheless this difference is too small to definitely exclude the latter.

As quoted above in text, the B3P86 functional has appeared to be relevant to evaluate phenol-BDE. Concerning the conformational analysis, no significant differences have been observed when changing the functional (data not shown). In this paper the energy difference between both conformers of **2** (**2a** and **2b**) was thoroughly evaluated. The effect of the Hartree–Fock (HF) weight included in the exchange part was especially investigated. In addition to the hybrid functional B3P86 (using 20% of HF), the two functionals BP86 (i.e., pure DFT functional with 0% HF) and BHandHP86 (i.e., 50% HF) were used to compute energies of **2**. The difference in energy between both conformers (**2a** and **2b**) was very similar with the three functionals and was lower than 1 kcal/mol. This result helped to state that, (i), B3P86 is relevant to estimate the properties of compounds **1**–**4**, and (ii), both conformers probably co-exist in solutions.

In a second step, two conformations of **4** were obtained after analysis of the potential energy curve corresponding to the variation of the torsion angle τ = C2–C1–C1′–C2′. The two conformations **4a** and **4b** correspond to $\tau = 135°$ and $-59°$. The H bond between the OH and OCH_3 groups was also favoured. In addition, for the latter conformer (**4b**), H bonding exists between the two hydroxyl groups. Both conformers possess exactly the same energy.

The conformations of **1** were then found by calculating the energies and conformations of all the different combinations of τ, τ_1 and τ_2. Some of the combinations led to dramatic steric interactions, and we finally obtained three different conformations **1a**–**1c**.

Conformers **1b** and **1c** exhibit H-bonding between the two OH groups of the central 3,3′-dimethoxy-1,1′-biphenyl-4,4′-diol moiety (as for **4b**). On the contrary, conformer **1a** does not possess this H bond, and exhibits a relatively planar shape. The three different conformers have very similar relative stability, since they possess energies lower than 0.5 kcal/mol, thus having the same Boltzmann's population and thus co-existing in solution. This conclusion may be a little bit different if the biosynthesis is oriented and favours one conformer rather than another, but to the best of our knowledge the active site of enzymes involved in dimer biosynthesis is only specific to the moiety where the oxidative process will occur, and not to rest of the molecule. Indeed such dimerisation occurs in different phenolic compounds regardless of the system size (e.g., phenolic acid (Ralph et al., 1994), catechin (Sang et al., 2002), quercetin (Ngoc Ly et al., 2005; Zhou, Kikandi, & Sadik, 2007), silybin (Gazak, Sedmera, Marzorati, Riva, & Kren, 2008)). Thus the dimer biosynthesis probably cannot influence one of the three conformers.

We studied the three conformers and the antioxidant activity is *a priori* an average of them, which is especially true for a redox action that does not require any stereospecific interaction, as for free radical-scavenging activity in solution.

3.3. Antioxidant properties of compounds *1*–*3*

In order to estimate the capacity of **1** and other two lignan derivatives from nutmeg to act as antioxidants we studied their capacity to scavenge the DPPH free radical and to inhibit the liposomal lipid peroxidation process. The former test directly gives the capacity to scavenge a free radical, usually by the HAT mechanism (Goupy, Dufour, Loonis, & Dangles, 2003). This test has been widely used over the past decades to give a quick and reliable estimation of the free radical-scavenging capacity. The latter directly gives the capacity of the molecule to react in the vicinity of the membrane in which an oxidative stress is generated. This test gives a better estimation of the actual antioxidant capacity that may occur in a stressed organism. Nonetheless both tests often correlate (Trouillas et al., 2008).

Table 1
Antioxidant capacity of **1**–**4** and two reference antioxidants, vitamin E and quercetin.

Compound	DPPH scavenging IC_{50} (μM)	Lipid peroxidation inhibition IC_{50} (μM)
1	70 ± 2	0.68 ± 0.04
2	46 ± 2	0.41 ± 0.01
3	103 ± 4	0.82 ± 0.04
4	70 ± 4	2.70 ± 0.05
Vitamin E	58 ± 1	0.60 ± 0.05
Quercetin	24 ± 2	0.24 ± 0.01

As we can see in Table 1, compound **2** is twice as effective a free radical scavenger (i.e. lower IC_{50} of about 46 μM) as compared to **3** ($IC_{50} \sim 103$ μM). Compound **1** exhibits an intermediate activity with an IC_{50} of 70 μM. The DPPH free radical-scavenging capacity of these three compounds is in the same range as that of vitamin E, but less active than quercetin. Quercetin is known to have a strong redox capacity (strong capacity to release an electron or an H atom) (Fiorucci et al., 2007; Leopoldini et al., 2004a, 2004b; Trouillas et al., 2006). Let us also note that guaiacol is much less active than **3** (IC_{50}(Guaiacol) = 300 μM, data from Kozlowski et al. (2007b) obtained under the same conditions as in the present paper). The same conclusions can be made for lipid peroxidation inhibition: (i), compound **2** is twice as active as **3** (IC_{50} = 0.41 and 0.82 μM, respectively), (ii), compound **1** is an intermediate inhibitor (IC_{50} = 0.68 μM), (iii), vitamin E is in the same range (IC_{50} = 0.60 μM) and (iv), quercetin is more active (IC_{50} = 0.24 μM).

3.4. Bond dissociation enthalpy

The BDEs of **1** and other derivatives are reported in Table 2. Two different values were obtained depending on the initial conformation. Concerning conformation without H bonding between the two OH groups (i.e., **1a**) the BDE was about 83.5 kcal/mol. In the absence of this H bond (i.e., **1b** and **1c**) the value is ~3 kcal/mol lower. This difference comes from the better stabilising effects that exist in the radical obtained after H abstraction from **1b** and **1c**. First the spin density is more delocalised for the radical derived from those two conformers, thus allowing a lower spin density on the oxygen atom (from which the H atom has been removed) (Fig. 3). Second the H bonding between the OH group of one ring and the O atom of the other ring is stronger in the radical (1.55 Å) than in the parent molecule (1.74 Å) (Figs. 3 and 4). Both stabilising effects are closely inter-linked since we obtained a non-zero spin density on the H atom involved in the H bond. As the three conformers may co-exist in a solution in which nothing favours one conformer over another, the BDE value can be seen as the mean value of the three values (i.e., 81.8 kcal/mol).

The OH BDE values obtained for compounds **2** and **3** are very similar to each other, whatever the conformer. That is, the intrinsic redox property of those two compounds does not explain their difference in activity. No differences in conformation and in electron delocalisation were noticed either. Thus the difference in the DPPH free radical-scavenging capacity was only due to the presence of two OH groups in **2**, rather than one in **3**. In conclusion, **2** scavenges twice as many radicals as **3**, by HAT mechanism. This helps and confirms the importance of the BDE parameter in order to explain the free radical-scavenging capacity of phenolic compounds.

Compound **3** is the monomer of **1**, nonetheless the chemical surrounding of the OH group is very different in both cases, and actually the BDE of **1** is lower than that of **3** by about 4 kcal/mol (gas phase calculation) and such a difference is sufficient to change the free radical-scavenging capacity and to make **1** a better antioxidant than its monomer (i.e., DPPH scavenging IC_{50} = 70 and

Table 2
BDEs (kcal/mol) of compounds **1**–**4** and of corresponding ArO· radicals (to form bi-radicals isomerised to quinones). The BDEs of quercetin at the same level, i.e., B3P86/6-31+G(d,p) are 80.0, 92.1, 90.3, 82.4 and 79.7 kcal/mol for the 3OH, 5OH, 7OH, 3′OH and 4′OH groups, respectively.

	Gas		Solvent	
	BDE	Bi-radical BDE	BDE	Bi-radical BDE
1a	83.5	83.8		
1b	81.0	92.8		
1c	80.9	91.7		
2a	85.5	107.7	81.9	
2b	85.9	106.0	82.3	
3a	85.5		81.9	
3b	85.9		81.8	
4a	85.0	84.6	82.9	85.6
	84.9[a]			
4b	82.3	93.3	82.0	89.4
	82.0[a]			

[a] B3P86/6-31+G(d,p) calculations (in this case the scale factor is 0.9588 (Merrick et al., 2007)).

103 μM, for **1** and **3**, respectively; lipid peroxidation inhibition IC_{50} = 0.68 and 0.82 μM, for **1** and **3**, respectively).

Moreover, in the case of **1**, a second HAT mechanism can occur on the second OH group to form a quinone. For conformer **1a** (without H bonding) the BDE of the second HAT is exactly the same as for the first, while for the other two conformers **1b** and **1c** (with H bond) the second BDE is much higher (by more than 10 kcal/mol). The higher BDE obtained in the latter case comes from the loss of the stabilising H bonding in the phenoxy radical. As a consequence of this high BDE, contrary to **2**, compound **1** cannot be twice as active as **3** as a free radical scavenger. This theoretical observation is accurately confirmed by experimental data from which we observed that IC_{50} values of **1** are between those of **2** and **3** (i.e., compound **1** with two OH groups is more active than **3** but less active than **2**).

From the calculation of ΔH and ΔG (Table 3), the conclusions are relatively similar to those drawn from BDE analysis, in terms of the comparative study between **1**, **2** and **3**. From the general point of view it must be noted that the entropic effects are negligible in the gas phase calculations but are a little bit more significant when taking the solvent effect into account.

The DPPH free radical-scavenging reaction with the different compounds is neither spontaneous (ΔG positive) nor exothermic (ΔH positive). Nevertheless the ΔH and ΔG values are relatively small indicating that the reaction is relatively neutral. The equilibrium may be shifted by secondary reactions (e.g., dimerisation) as suggested by different authors (Sang et al., 2002).

Concerning peroxy radical inhibition, the reaction is more favourable, i.e., spontaneous as well as exothermic.

3.5. Comparison between *1* and *4*

In the present study we synthesised compound **4**, which is the central moiety of compound **1**, which is the part of the molecule from which the HAT mechanism can occur. Compound **4** was evaluated for its DPPH free radical-scavenging capacity as well as for its capacity to inhibit lipid peroxidation. Like compound **1**, compound

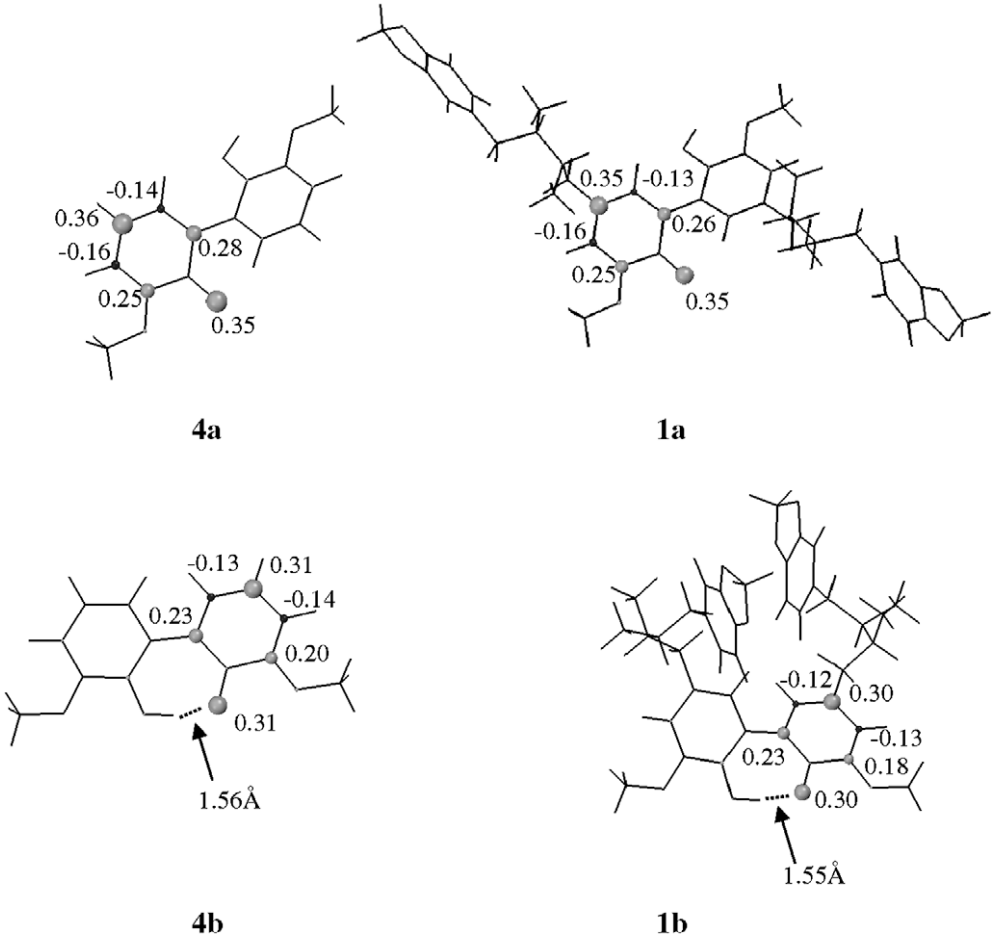

Fig. 3. Spin density distribution of the radicals obtained after H abstraction from (top) **4a** and **1a**, and (bottom) **4b** and **1b**.

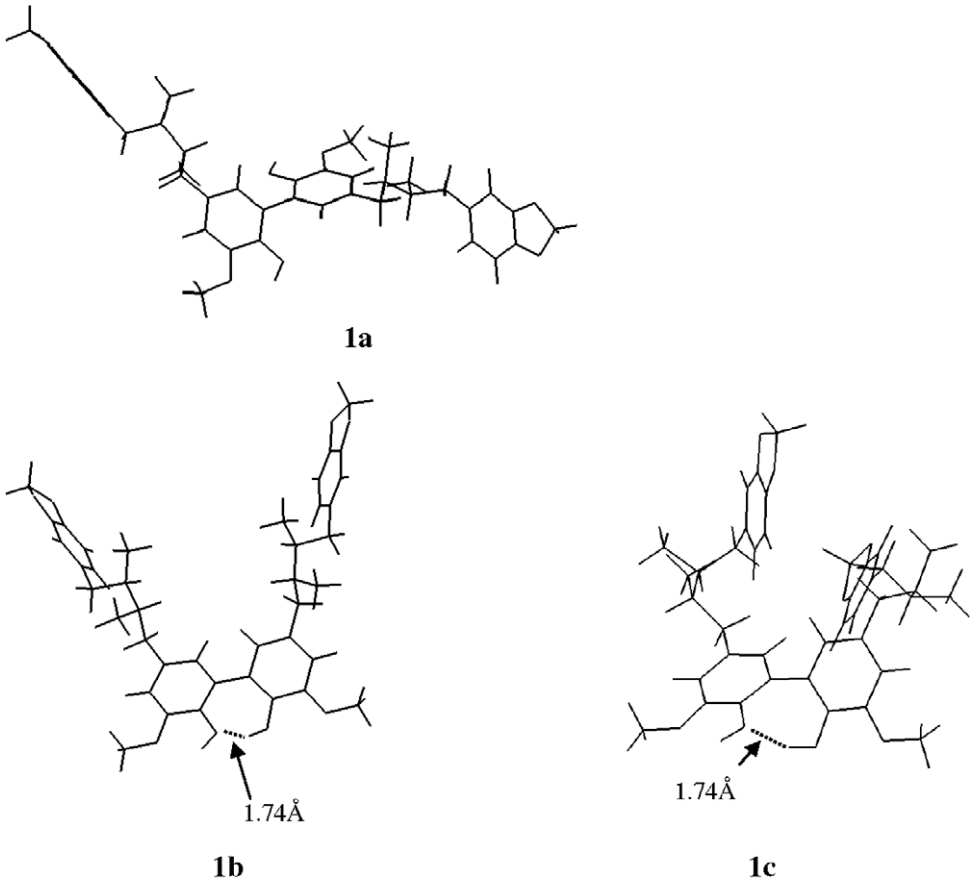

Fig. 4. Geometries of the three most stable conformers of **1**.

4 exists as different rotamers without or with H bonding interaction (i.e., **4a** and **4b**, respectively). As for **1b** and **1c**, the conformer with the H bond (**4b**) exhibits a BDE lower than its counterpart (i.e., conformer **4a** without H bond), by about 3 kcal/mol. Nonetheless, the calculations show that **4** has BDEs higher than **1**, by about 1–1.5 kcal/mol. This significant difference remains very small and should be attributed to a small but better capacity to delocalise spin density and to stabilise the ArO· radical by H-bonding (see the case of the conformers with H bonds).

In both cases (compounds **1** and **4**), as the different conformers (three and two conformers, respectively) may co-exist in a solution in which nothing favours one conformer over another, the BDE value is the mean value of the three or two values, respectively (i.e., 81.8 and 83.6 kcal/mol in the gas phase for **1** and **4**, respectively).

Table 3
ΔH and ΔG (kcal/mol) for the oxidative reaction between the different compounds and the DPPH and $CH_3OO^{\cdot}$ radicals. Calculations of conformations, enthalpies and Gibbs free energies of both radicals are performed at the B3P86/6-31+G(d,p) as for the different compounds and corresponding radicals.

	Gas				Solvent			
	DPPH		ROO·		DPPH		ROO·	
	ΔH	ΔG	ΔH	ΔG	ΔH	ΔG	ΔH	ΔG
1a	4.2	2.3	−0.6	−1.8				
1b	1.7	0.7	−3.0	−3.4				
1c	1.5	1.6	−3.2	−2.4				
2a	6.2	6.1	1.4	2.1	2.3	6.1	−6.6	−6.0
2b	6.5	6.2	1.8	2.1	2.8	6.9	−6.1	−5.2
3a	6.2	5.8	1.5	1.8	2.4	6.3	−6.5	−5.8
3b	6.5	6.1	1.8	2.1	2.2	8.3	−6.7	−3.9
4a	5.7	5.4	0.9	1.4	3.4	7.2	−5.5	−4.9
4b	2.9	2.7	−1.8	−1.3	2.5	6.3	−6.4	−5.8

The DPPH free radical-scavenging capacities of **1** and **4** are very similar (Table 1), so the difference in BDE is not enough to induce a difference in this activity. Let us confirm that this is also the case when we look at the ΔG and ΔH values. The reaction is neither spontaneous nor exothermic, as for **1**. Thus one can definitely conclude that the sheer free radical-scavenging capacities of **1** and **4** are equivalent; in other words, the free radical-scavenging capacity of **1** comes from the capacity of the central moiety (**4**) to release one or two H atoms. The influence of the rest of the molecule is very weak in this case.

Concerning the capacity of lipid peroxidation inhibition, the activity of **4** is dramatically decreased compared to **1**. This result cannot be explained by the sheer redox capacity, otherwise the behaviour would have been similar to the DPPH scavenging. The only parameter that may explain this difference in activity comes from the lower lipophilicity of **4** compared to **1** (log P = 3.0 and 10.6, respectively).

Argenteane (**1**) appears to be a powerful antioxidant, especially as a lipid peroxidation inhibitor since it is as effective as vitamin E. This activity comes from (i), a reliable HAT capacity of the two central OH groups, and (ii), an adapted lipophilicity.

It is well-known that vitamin E acts as an antioxidant directly from the membrane in which it is incorporated (Bisby & Parker, 1995). It is difficult to confirm that **1** is also inserted in the membrane; nonetheless here we confirmed the important role of its lipophilicity, thus concluding that **1** is at least relatively close to the membrane, closer than a more polar compound with the same redox capacity like compound **4**. So **1** acts either as a component of the membrane or accumulated in the very vicinity of the mem-

brane. In both cases, **1** has the capacity to accumulate in a relatively thin region, which increases its potential activity. Indeed as far as it could be accumulated in a relatively narrow region, its concentration is virtually (or artificially) increased. Thus, even if **1** is present in a relatively low concentration in the diet, its role as a protective agent against oxidative stress may be considered as powerful.

It must be stressed that the redox property of this compound could be improved by replacing the two piperonyl moieties with two guaiacyl moieties, or better still with two catechol moieties. Such a change is feasible with a conventional synthesis procedure (Nakai et al., 2003), nevertheless the lipophilic property would consequently be decreased for those two hypothetical compounds, thus reducing the capacity to act in the vicinity of the membrane. Argenteane seems to exhibit the perfect compromise between good redox capacity (for an effective free radical-scavenging capacity) and good lipophily (for a good interaction with membranes).

Acknowledgments

The authors thank the "Conseil Régional du Limousin" for financial support, IDRIS (Institut du Développement et des Ressources Informatiques Scientifiques, Orsay, Paris) and CALI (CAlcul en LImousin) for computing facilities. The authors are grateful to Daovy Allais and Sylvie Gautier for fruitful discussions that help to improve the quality of this work. The authors also thank Fabrice Collin and Monique Gardès-Albert for help and discussion concerning the lipid peroxidation experiments.

Appendix A. Supplementary data

Supplementary data associated with this article can be found, in the online version, at doi:10.1016/j.foodchem.2009.05.010.

References

Bisby, R. H., & Parker, A. W. (1995). Reaction of ascorbate with the alpha-tocopheroxyl radical in micellar and bilayer membrane systems. *Archives of Biochemistry and Biophysics, 317*(1), 170–178.

Filleur, F., Pouget, C., Allais, D. P., Kaouadji, M., & Chulia, A. J. (2002). Lignans and neolignans from *Myristica argentea* Warb.. *Natural Product Letters, 16*(1), 1–7.

Filleur, F., Pouget, C., Duroux, J. L., Simon, A., & Chulia, A. J. (2001). Antiproliferative, anti-aromatase, anti-17β-HSD and antioxidant activities of lignans isolated from *Myristica argentea* Warb.. *Planta Medica, 67*(8), 700–704.

Fiorucci, S., Golebiowski, J., Cabrol-Bass, D., & Antonczak, S. (2007). DFT study of quercetin activated forms involved in antiradical, antioxidant, and prooxidant biological processes. *Journal of Agricultural and Food Chemistry, 55*(3), 903–911.

Frisch, M. J., Trucks, G. W., Schlegel, H. B., et al. (2004). *Gaussian 03, revision C.02*. Wallingford, CT: Gaussian, Inc..

Gazak, R., Sedmera, P., Marzorati, M., Riva, S., & Kren, V. (2008). Laccase-mediated dimerization of the flavonolignan silybin. *Journal of Molecular Catalysis B: Enzymatic, 50*, 87–92.

Goupy, P., Dufour, C., Loonis, M., & Dangles, O. (2003). Quantitative kinetic analysis of hydrogen transfer reactions from dietary polyphenols to the DPPH radical. *Journal of Agricultural and Food Chemistry, 51*(3), 615–622.

Guerra, M., Amorati, R., & Pedulli, G. F. (2004). Water effect on the O–H dissociation enthalpy of para-substituted phenols: A DFT study. *Journal of Organic Chemistry, 69*, 5460–5467.

Harworth, R. D. (1942). The chemistry of the lignan group of natural products. *Journal of the Chemical Society*, 448–456.

Kozlowski, D., Marsal, P., Steel, M., Mokrini, R., Duroux, J. L., Lazzaroni, R., et al. (2007a). Theoretical investigation of the formation of a new series of antioxidant depsides from the radiolysis of flavonoid compounds. *Radiation Research, 168*(2), 243–252.

Kozlowski, D., Trouillas, P., Calliste, C., Marsal, P., Lazzaroni, R., & Duroux, J. L. (2007b). Density functional theory study of the conformational, electronic, and antioxidant properties of natural chalcones. *The Journal of Physical Chemistry A, 111*(6), 1138–1145.

Le Bail, J. C., Champavier, Y., Chulia, A. J., & Habrioux, G. (2000). Effects of phytoestrogens on aromatase, 3beta and 17beta-hydroxysteroid dehydrogenase activities and human breast cancer cells. *Life Sciences, 66*(14), 1281–1291.

Lemaska, K., Szymusiak, H., Tyrakowska, B., Zieliski, R., Soffers, A. E. M. F., & Rietjens, I. M. C. M. (2001). The influence of pH on antioxidant properties and the mechanism of antioxidant action of hydroflavones. *Free Radical Biology and Medicine, 31*, 869–881.

Leopoldini, M., Marino, T., Russo, N., & Toscano, M. (2004a). Density functional computations of the energetic and spectroscopic parameters of quercetin and its radicals in the gas phase and in solvent. *Theoretical Chemistry Accounts, 111*, 210–216.

Leopoldini, M., Pitarch, I. P., Russo, N., & Toscano, M. (2004b). Structure, conformation, and electronic properties of apigenin, luteolin, and taxifolin antioxidants. A first principle theoretical study. *The Journal of Physical Chemistry A, 108*, 92–96.

Lucarini, M., Pedulli, G. F., & Guerra, M. (2004). A critical evaluation of the factors determining the effect of intermolecular hydrogen bonding on the O–H bond dissociation enthalpy of catechol and of flavonoid antioxidants. *Chemistry European Journal, 10*, 933–939.

Merrick, J. P., Moran, D., & Radom, L. (2007). An evaluation of harmonic vibrational frequency scale factors. *The Journal of Physical Chemistry A, 111*, 11683–11700.

Nakai, M., Harada, M., Nakahara, K., Akimoto, K., Shibata, H., Miki, W., et al. (2003). Novel antioxidative metabolites in rat liver with ingested sesamin. *Journal of Agricultural and Food Chemistry, 51*(6), 1666–1670.

Ngoc Ly, T., Hazama, C., Shimoyamada, M., Ando, H., Kato, K., & Yamauchi, R. (2005). Antioxidative compounds from the outer scales of onion. *Journal of Agricultural and Food Chemistry, 53*(21), 8183–8189.

Pople, J. A., Gill, P. M. W., & Handy, N. C. (1995). Spin-unrestricted character of Kohn–Sham orbitals for open-shell systems. *International Journal of Quantum Chemistry, 56*, 303–305.

Priyadarsini, K. I., Maity, D. K., Naik, G. H., Kumar, M. S., Unnikrishnan, M. K., Satav, J. G., et al. (2003). Role of phenolic O–H and methylene hydrogen on the free radical reactions and antioxidant activity of curcumin. *Free Radical Biology and Medicine, 35*, 475–484.

Ralph, J., Quideau, S., Grabber, J. H., & Hatfield, R. D. (1994). Identification and synthesis of new ferulic acid dehydrodimers present in grass cell. *Journal of the Chemical Society – Perkin Transactions, 1*(23), 3485–3498.

Russo, N., Toscano, M., & Uccella, N. (2000). Semiempirical molecular modeling into quercetin reactive site: structural, conformational, and electronic features. *Journal of Agricultural Food Chemistry, 48*, 3232–3237.

Sang, S., Cheng, X., Stark, R. E., Rosen, R. T., Yang, C. S., & Ho, C. T. (2002). Chemical studies on antioxidant mechanism of tea catechins: Analysis of radical reaction products of catechin and epicatechin with 2,2-diphenyl-1-picrylhydrazyl. *Bioorganic and Medicinal Chemistry, 10*(7), 2233–2237.

Simmons, K. E., Minard, R. D., & Bollag, J. M. (1988). Oxidative coupling and polymerization of guaiacol, a lignin derivative. *Soil Science Society of America Journal, 52*(5), 1356–1360.

Trouillas, P., Fagnère, C., Lazzaroni, R., Calliste, C. A., Marfak, A., & Duroux, J. L. (2004). A theoretical study of the conformational behavior and electronic structure of taxifolin correlated with the free radical-scavenging activity. *Food Chemistry, 88*, 571–582.

Trouillas, P., Marsal, P., Siri, D., Lazzaroni, R., & Duroux, J. L. (2006). A DFT study of the reactivity of OH groups in quercetin and taxifolin antioxidants: The specificity of the 3-OH site. *Food Chemistry, 97*, 679–688.

Trouillas, P., Marsal, P., Svobodová, A., Vostálová, J., Gažák, R., Hrbáč, J., et al. (2008). Mechanism of the antioxidant action of silybin and 2,3-dehydrosilybin flavonolignans: A joint experimental and theoretical study. *The Journal of Physical Chemistry A, 112*(5), 1054–1063.

Wayner, D. D. M., Lusztyk, E., Page, D., Ingold, K. U., Mulder, P., Laarhoven, L. J. J., et al. (1995). Effects of solvation on the enthalpies of reaction of tert-butoxyl radicals with phenol and on the calculated O–H bond strength in phenol. *Journal of American Chemical Society, 117*, 8737–8744.

Wright, J. S., Jonhson, E. R., & DiLabio, G. A. (2001). Predicting the activity of phenolic antioxidants: Theoretical method, analysis of substituent effects, and application to major families of antioxidants. *Journal of the American Chemical Society, 123*, 1173–1183.

Zhang, H.-Y., & Ji, H.-F. (2006). How vitamin E scavenges DPPH radicals in polar protic media. *New Journal of Chemistry, 30*(4), 503–504.

Zhang, H. Y., Sun, Y. M., & Chen, D. Z. (2001). O–H bond dissociation energies of phenolic compounds are determined by field/inductive effect or resonance effect? A DFT study and its implication. *QSAR, 20*, 148–152.

Zhang, H. Y., Sun, Y. M., & Wang, X. L. (2003). Substituent effects on O–H bond dissociation enthalpies and ionization potentials of catechols: A DFT study and its implications in the rational design of phenolic antioxidants and elucidation of structure–activity relationships for flavonoid antioxidants. *Chemistry: A European Journal, 9*, 502–508.

Zhou, A., Kikandi, S., & Sadik, O. A. (2007). Electrochemical degradation of quercetin: Isolation and structural elucidation of the degradation products. *Electrochemistry Communications, 9*, 2246–2255.

Food Chemistry 118 (2010) 497–503

Contents lists available at ScienceDirect

Food Chemistry

journal homepage: www.elsevier.com/locate/foodchem

Antioxidant and nutritive constituents during sweet pepper development and ripening are enhanced by nitrophenolate treatments

María Serrano [b], Pedro J. Zapata [a], Salvador Castillo [a], Fabián Guillén [a], Domingo Martínez-Romero [a], Daniel Valero [a,*]

[a] Dept. Food Technology, EPSO, University Miguel Hernández, Ctra. Beniel km. 3.2, 03312 Orihuela, Alicante, Spain
[b] Dept. Applied Biology, EPSO, University Miguel Hernández, Ctra. Beniel km. 3.2, 03312 Orihuela, Alicante, Spain

ARTICLE INFO

Article history:
Received 13 February 2009
Received in revised form 16 April 2009
Accepted 7 May 2009

Keywords:
Capsicum annum L.
Sweet pepper
Total antioxidant activity
Polyphenols
Sugars
Organic acids
Nitrophenolates

ABSTRACT

A mix of nitrophenolates was applied to pepper plants in the irrigation system along the growth cycle. Fruits were labelled at fruit set to study the evolution of fruit growth and ripening based on fruit size and colour. In addition, at 3-day intervals, samples were taken in which the evolution of fruit weight, colour, nutritive (sugars and organic acids) and bioactive compounds (total phenolics, carotenoids, and ascorbic acid) was evaluated. Pepper fruit growth followed a simple sigmoid curve reaching its maximum size at 49 days after fruit set, although nitrophenolate treatments led to significant increases in fruit weight due to higher length, diameter, and pericarp thickness, without affecting the normal ripening process, since colour and carotenoid evolution was similar for both control and treated fruits. Glucose, fructose, ascorbic acid, citric acid, total antioxidant activity (TAA) and total phenolics increased during pepper development, and their levels were significantly enhanced by nitrophenolate applications. Thus, this treatment induced beneficial effects in terms of the improvement of fruit quality, and especially its nutritive and antioxidant constituents. Finally, it is advisable to consume peppers at the full red stage in order to achieve the maximum health-beneficial effects by consumers.

1. Introduction

Nowadays, agricultural practices are focused on the optimisation of nutrient management through a better control of plant water and nutrient requirements to improve plant health and crop yield. In this sense, the use of organic agriculture in peppers has demonstrated that quality was similar with respect to conventional or intensive practices, and thus avoiding the use of chemical fertilisers, lowering production costs and reducing grown water pollution (del Amor, 2006). Accordingly, natural compounds such as nitrophenolates (NPLs), have been shown to increase yield in sugar beet (Cerny & Ondrisik, 2003), cotton (Djanaguiraman, Sheeba, Devi, & Bangarusamy, 2005) and tomato (Djanaguiraman, Pandiyan, & Devi, 2005; Serrano et al., 2005), in which their effect were due to an increase in auxin concentration.

Peppers are fruits with a high importance in human diet due to their versatility to be consumed as fresh vegetable in salads, cooked meals or dehydrated for spices. Traditionally, commercial growers have harvested peppers at the mature green stage when pericarp becomes thick and the fruit has reached its maximum size. However, in recent years, there has been an increasing interest in picking peppers at the red colour with improved flavour, nutritional aspects and high acceptation by consumers (Frank, Nelson, Simonne, Behe, & Simonne, 2005). In fact, mature red peppers are considered one of the richest sources of natural pigments (carotenoids), and is thus used as a food colourant in the form of ground powder (Hornero-Méndez, Costa-García, & Mínguez-Mosquera, 2002). Apart from carotenoids, pepper fruit at the red stage is rich in vitamin C and phenolic compounds such as phenolics acids, flavonoids, hydroxycinnamates and flavones (Marín, Ferreres, Tomás-Barberán, & Gil, 2004). Moreover, fresh pepper is considered to be one of the vegetables with the highest content of vitamin C within the plant kingdom. Additionally, it is well known that phenolic compounds contribute to fruit sensory and nutritive quality in terms of modifying colour, taste, aroma and flavour, and also providing health-beneficial effects (Tomás-Barberán & Espín, 2001).

Literature exists on the evolution of physicochemical parameters during pepper fruit growth and development, such as weight, colour, firmness, total soluble solids, and acidity (Martínez, Curros, Bermúdez, Carballo, & Franco, 2007; Tadesse, Hewett, Nichols, & Fischer, 2002). In addition, differences in bioactive compounds, such as ascorbic acid, total phenolics, carotenoids and antioxidant activity, between mature green and red stages at harvest have been reported, although contradictory results were obtained probably due to varietal differences (Fox, Del Pozo, Lee, Sargent, & Talcott,

* Corresponding author. Tel.: +34 96 6749743; fax: +34 96 6749677.
E-mail address: daniel.valero@umh.es (D. Valero).

0308-8146/$ - see front matter © 2009 Elsevier Ltd. All rights reserved.
doi:10.1016/j.foodchem.2009.05.006

2005; Howard, Talcott, Brenes, & Villalon, 2000; Matterska & Perucka, 2005; Navarro, Flores, Garrido, & Martínez, 2006). However, as far as we are aware, no detailed information is available about the evolution of nutritive and antioxidant constituents along the whole growth and ripening process of peppers on plant, and there are no scientific reports about the effect of nitrophenolates on these issues. Therefore, the aim of this paper was to investigate the changes in nutritive compounds (glucose, fructose, sucrose and organic acids) and antioxidant constituents (total phenolics, total carotenoids, and ascorbic acid) during pepper development and ripening on plants and how this can be affected by the application of nitrophenolates. Moreover, total antioxidant activity (TAA) is analysed in two separate fractions (hydrophilic and lipophillic, H-TAA and L-TAA) and their relation with the antioxidant compounds is provided.

2. Material and methods

2.1. Plant material and experimental design

The experiment was carried out in a commercial plastic glasshouse located at Pilar de la Horadada (Alicante, Spain) in two consecutive growing cycles (2005 and 2006). Pepper plants (*Capsicum annum* L. cv. Herminio) were sowed in December and the production cycles finished on September next year under conventional cultural practices and fertilisation. The experiment was designed at totally random choosing 6 rows (six replicates) of 90 plants in each (540 plants/treatment) for the following treatments: Nitrophenolates (NPLs) were added to the irrigation system (1 l/ha), and control (no treatment). Treatments consisted of a mixture of Na-*p*-nitrophenolate (0.3%), Na-*o*-nitrophenolate (0.3%) and Na-nitroguaiacol (0.1%) and were applied at 2 week intervals from the development of first floral bunch (1st week March) to end of July.

After the fruit set (beginning June), for each row 10 fruits were marked at random to evaluate the fruit growth (diameter and length, mm) and maturation on plant (external colour). Taking into account these data, 6 samples of 5 similar fruits to those labelled on plant (one sample per row) were taken at 3-day intervals and transferred to the laboratory for further analytical determinations.

2.2. Growth parameters

For each sampling date, length (mm), diameter (mm), pericarp thickness (mm), weight (g) and colour (L*, a* and b* parameters using the Hunter Lab System in a Minolta colourimeter CR200, Minolta Camera Co., Japan) were individually measured in each fruit. Data are the mean ± SE of two consecutive years.

2.3. Samples preparation

For chemical determinations 6 sub-samples of 5 peppers were made by homogenising with liquid N_2 either the entire fruit pericarp (for smaller fruits) or taking a ring of the equatorial zone without placentary tissue, and the following parameters were quantified in duplicate in each of these sub-samples (data are the mean ± SE of the two years on a fresh weight basis).

2.4. Total acidity, total antioxidant activity, total phenolic compounds, sugars and organic acids

Total acidity was determined using 1 ml of the juice obtained from pepper samples diluted in 25 ml of distilled H_2O. The pH of the juice was recorded and then titratable acidity was calculated by potentiometric titration with 0.1 N NaOH up to pH 8.1. Results were the mean ± SE expressed as g of citric acid equivalent per 100 g^{-1}.

TAA was quantified according to Arnao, Cano, and Acosta (2001), which enables the determination of TAA due to both hydrophilic and lipophilic compounds in the same extraction. Briefly, for each sub-sample, five grams of tissue were homogenised in 5 ml of 50 mM phosphate buffer pH 7.8 and 3 ml of ethyl acetate, and then centrifuged at 10,000*g* for 15 min at 4 °C. The upper fraction was used for total antioxidant activity due to lipophilic compounds (L-TAA) and the lower for total antioxidant activity due to hydrophilic compounds (H-TAA). In both cases, TAA was determined using the enzymatic system composed of the chromophore 2,2′-azino-bis-(3-ethylbenzothiazoline-6-sulphonic acid) diammonium salt (ABTS), the horse radish peroxidase enzyme (HRP) and its oxidant substrate (hydrogen peroxide), in which $ABTS^{\bullet+}$ radicals are generated and monitored at 730 nm. The decrease in absorbance after adding the pepper extract was proportional to the TAA of the sample. A calibration curve was performed with Trolox ((R)-(+)-6-hydroxy-2,5,7,8-tetramethyl-croman-2-carboxylic acid) (0–20 nmol) from Sigma (Madrid, Spain), and results are expressed as mg of Trolox equivalent 100 g^{-1}.

Phenolic extraction for each sub-sample was performed using water:methanol (2:8) containing 2 mM NaF (to inactivate polyphenol oxidase activity and prevent phenolic degradation) as described by Tomás-Barberán et al. (2001) and quantified using the Folin–Ciocalteu reagent and results were expressed as mg gallic acid equivalent 100 g^{-1}. Sugars and organic acids were extracted with 50 mM phosphate buffer pH 7, according to a previous report (Serrano, Guillén, Martínez-Romero, Castillo, & Valero, 2005), and quantified by HPLC, using 0.1% phosphoric acid running isocratically with a flow rate of 0.5 ml min^{-1} through a Supelco column (Supelcogel C-610H, 30 cm × 7.8 mm, Supelco Park, Bellefonte, USA). Organic acids were detected by absorbance at 210 nm and expressed as g 100 g^{-1} for citric acid, and mg 100 g^{-1} for the remaining organic acids using a standard curve of pure L-ascorbic, citric, malic, oxalic and succinic acids (Sigma, Poole, Dorset, UK). The detection of sugars was obtained by a refractive index detector and results were expressed as g 100^{-1} using a standard curve of pure sugars (glucose, fructose and sucrose) purchased from Sigma.

2.5. Total carotenoids

Total carotenoids were extracted according to Mínguez-Mosquera and Hornero-Méndez (1993). Briefly, 5 g of flesh tissue were extracted with acetone and shaken with diethyl ether and 10% NaCl to separate out the two phases. The lipophilic phase was washed with Na_2SO_4 (2%), saponified with 10% KOH in methanol, and the pigments were subsequently extracted with diethyl ether, evaporated and then made up to 25 ml with acetone. Total carotenoids were estimated by taking the absorbance at 450 nm according to Deepa, Kaur, George, Singh, and Kapoor (2007) in a UNICAM Helios-α spectrophotometer (Cambridge, UK), and expressed as mg of β-carotene equivalent 100 g^{-1}, taking into account the $\varepsilon^{1\%}_{cm} = 2560$.

2.6. Statistical analysis

Data for the analytical determinations were subjected to analysis of variance (ANOVA). Sources of variation were sampling dates and treatment. Mean comparisons were performed using HSD the Tukey's test to examine if differences were significant at $p < 0.05$ (Table 1). To know which compounds contribute to TAA, linear regressions were performed amongst the functional compounds taking into account data from all sampling dates (from both control to treated fruits). All analyses were performed with SPSS software package v. 12.0 for Windows (2001).

Table 1
ANOVA for dependent variables for treatment applied, storage time and their interactions for peppers[a].

	Time	Treatment	Time × treatment
Fruit weight	***	**	**
Colour a*	***	NS	NS
Total carotenoids	***	NS	NS
Glucose	***	**	**
Fructose	***	**	**
Total acidity	***	**	**
Citric acid	***	**	**
Ascorbic acid	***	**	**
H-TAA	***	**	**
L-TAA	***	NS	NS
Phenolics	***	***	***

[a] ***, **, and * represent significance at the 0.01, 0.01, and 0.05 levels, respectively, and NS represents non-significance at $P < 0.05$.

3. Results

3.1. Pepper fruit growth and maturation

The growth of pepper fruit exhibited a single-sigmoid pattern, with the maximum growth rate being found between 25 and 40 days after fruit set (DAFS). However, differences were obtained depending on treatment (Fig. 1), since those plants treated with NPLs yielded fruits with significantly higher fruit weight than controls. The maximum fruit weight was reached after 46 and 49 DAFS, with final values of ≈343 and ≈317 g, for treated and control peppers, respectively. These differences were attributed to the higher length, diameter and pericarp thickness found in the treated (134.68 ± 1.86, 93.66 ± 1.06 and 7.86 ± 0.01 mm, respectively) than in control fruits (128.22 ± 0.92, 88.39 ± 1.03 and 6.75 ± 0.13 mm, respectively), taken into account data from the last 6 sampling dates. With respect to colour (Fig. 1), its evolution was similar in both control and treated fruits. The colour a* parameter varied very little from fruit set to day 36 and increased sharply from 39 to 57 DAFS, due to colour changes from green to red, which occurred in the last phase of fruit growth, when the fruit was near its maximum weight. The carotenoid pigments were analysed from 28 DAFS when peppers were still at the green stage to a weight of ca. 100 g, and their behaviour was similar to colour evolution. Thus, a significant increase was obtained at the later growth phase and maturation without differences irrespective of treatment, with a final concentration of ≈50 mg 100 g^{-1} (Fig. 1).

3.2. Sugars, acidity and organic acids

Glucose and fructose were found to be the major sugars by HPLC, the concentrations being higher for fructose than glucose. The concentrations of both sugars increased along the fast growth phase and especially during the maturation process. Moreover, those peppers from treated plants reached significantly higher levels of both glucose and fructose than control fruits (Fig. 2). Thus, final levels of glucose and fructose were 3.25 ± 0.13 and 3.59 ± 0.12 g 100 g^{-1}, respectively, in treated fruits and 2.42 ± 0.07 and 2.79 ± 0.14 g 100 g^{-1}, respectively, in control peppers. Sucrose occurred at low levels (<0.5%) and was not affected by treatment or the growth period (data not shown). On the other hand, total acidity increased continuously as did the growth cycle, and treated peppers also showed higher levels of acidity than controls, with final values of 0.33 ± 0.01 and 0.40 ± 0.02 g 100 g^{-1}, respectively (Fig. 3). The main organic acid contributing to pepper acidity was citric acid, which evolved in a similar way to total acidity (Fig. 3), and was also at higher concentrations in pepper from NPLs-treated plants, than in those from control ones. It is interesting to point out the ascorbic acid results due to its role as vitamin C. Thus, ascorbic acid significantly increased along the growth cycle reaching final concentrations of 132 ± 4 mg 100 g^{-1} in control fruits, although the contents were significantly higher (155 ± 3 mg 100 g^{-1}, over a 18% greater) in pepper from NPLs-treated plants (Fig. 3). Other organic acids such as succinic, malic, oxalic and fumaric acids were also detected in pepper fruits although at much lower concentrations, ranging from 20 to 120 mg 100 g^{-1}, with slight but not significant increases along the growth cycle and were not affected by treatment either (data not shown).

3.3. Total antioxidant activity and phenolics

Total antioxidant activity was evaluated in both hydrophilic (H-TAA) and lipophilic (L-TAA) fractions. As can been seen in Fig. 4, H-TAA was significantly higher (ca. 10-fold) than L-TAA along the fruit growth and maturation. H-TAA increased sharply from 18 to 31 DAFS (from ≈40 to 200 mg 100 g^{-1}) coinciding with the fast growth phase, the enhancement being found at a much lower rate from this time. The NPLs treatment affected H-TAA, since it was

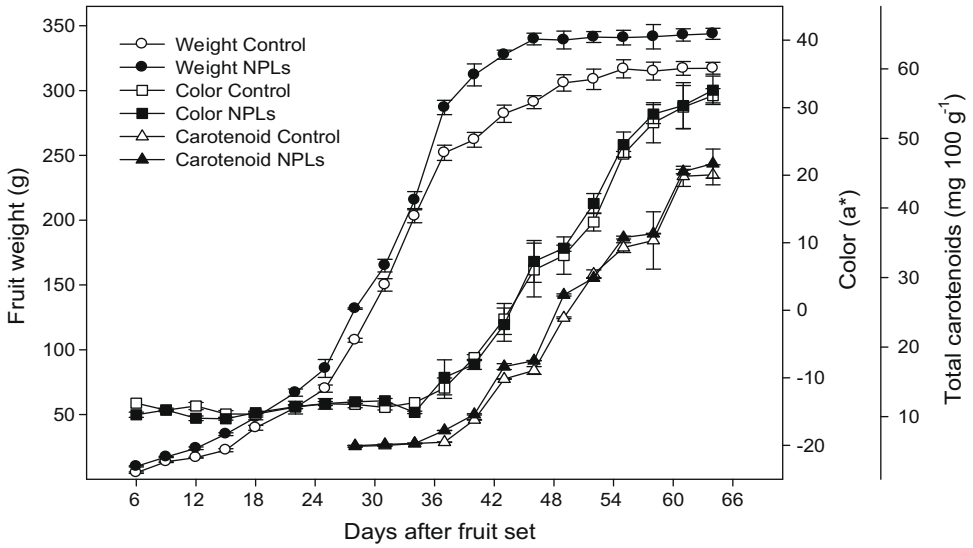

Fig. 1. Changes in fruit weight, colour a* and total carotenoids along the growth and ripening of pepper from control and nitrophenolates (NPLs)-treated plants.

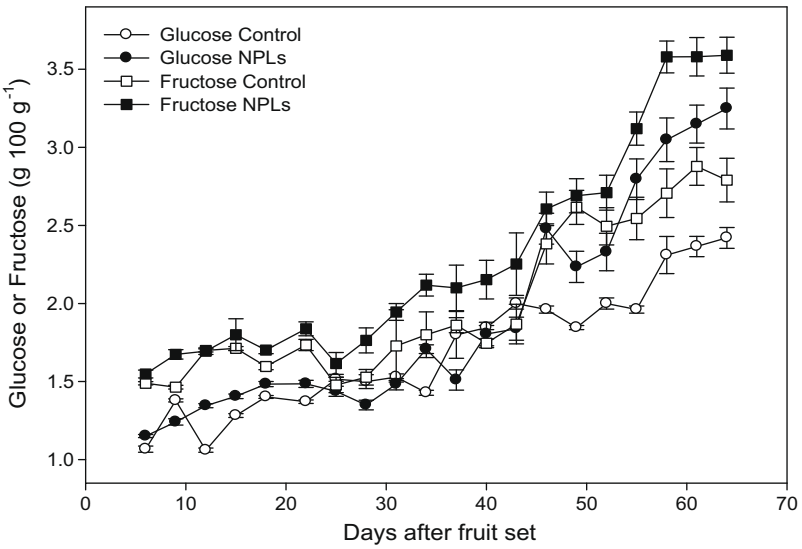

Fig. 2. Evolution of glucose and fructose along the growth and ripening of pepper from control and nitrophenolates (NPLs)-treated plants.

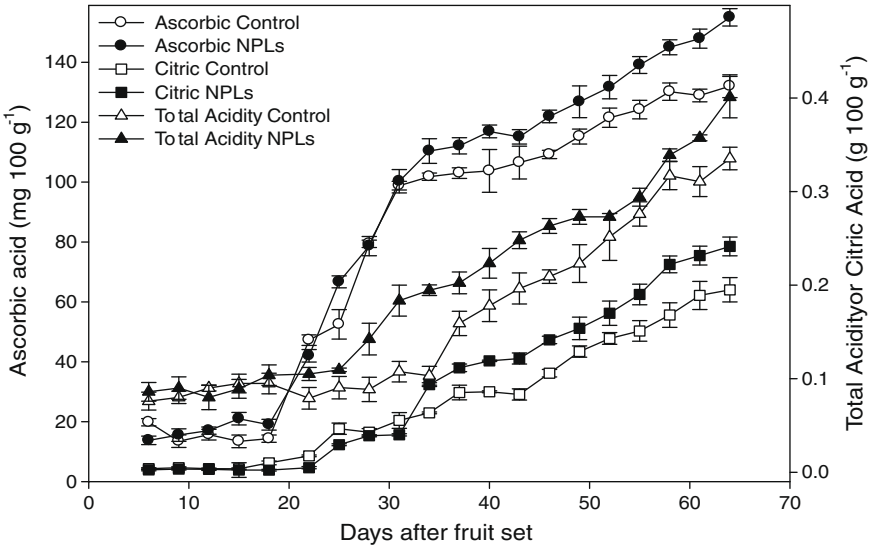

Fig. 3. Evolution of total acidity, and citric and ascorbic acids along the growth and ripening of pepper from control and nitrophenolates (NPLs)-treated plants.

significantly higher in treated peppers than in controls, with final values of 303 ± 12 and 246 ± 5 mg 100 g^{-1}, respectively. Contrarily, L-TAA was not affected by NPLs treatment, although it increased also along pepper growth and maturation, from levels of ≈7 mg 100 g^{-1} at early phases of development to final values of ≈28 mg 100 g^{-1} at full ripe stage. The phenolic content evolved in a similar way to H-TAA and was increased also by NPLs treatment. The final levels were 173 ± 3 and 142 ± 3 mg 100 g^{-1} for treated and control fruits, respectively (Fig. 4).

3.4. Correlations

To know which bioactive compounds are contributing to TAA in pepper, linear regressions were performed with data from either control or treated peppers (Table 2). Results revealed that the total phenolics and ascorbic acid were highly correlated (r^2 = 0.92–0.99) to H-TAA, whilst total carotenoids were highly correlated (r^2 = 0.81–0.97) to L-TAA and colour a* (r^2 = 0.81–0.97). In addition, colour a* parameter was also correlated to L-TAA in both control (r^2 = 0.78) and treated peppers (r^2 = 0.84).

4. Discussion

The current intensive agriculture is focused on obtaining vegetable crops with elevated yield and high quality fruits. However, there is a goal for producers to increase crop inputs for those commodities that have an elevated efficacy under intensive cultural practices, using greenhouses with an optimum control in irrigation, fertilisation, temperature, illumination, weed control, etc. However, there are few studies on the changes in nutritive and bioactive compounds with functional properties along the fruit development on plant and any report on the effect of NPLs on the behaviour of the above compounds. In this paper, we have demonstrated that glucose, fructose, ascorbic acid, citric acid, both H- and L-TAA, total phenolics and total carotenoids increased during pepper development, although their levels were significantly en-

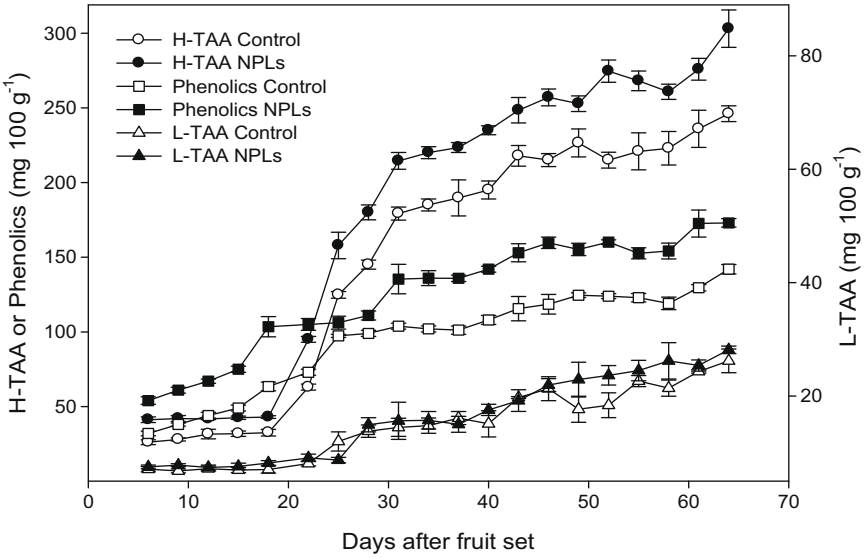

Fig. 4. Evolution of total phenolics and total antioxidant activity in the hydrophilic (H-TAA) or lipophilic (L-TAA) fraction along the growth and ripening of pepper from control and nitrophenolates (NPLs)-treated plants.

Table 2
Linear regressions between bioactive compounds and H-TAA (hydrophilic total antioxidant activity), L-TAA (lipophilic total antioxidant activity) or colour a^* in peppers from control and nitrophenolates (NPLs) treated plants.

	Control	Treated
H-TAA vs. phenolics	$y = 2.36x - 74.67$ $r^2 = 0.942$	$y = 2.41x - 119.97$ $r^2 = 0.921$
H-TAA vs. ascorbic acid	$y = 1.85x + 1.66$ $r^2 = 0.976$	$y = 1.87x + 16.01$ $r^2 = 0.985$
L-TAA vs. carotenoids	$y = 0.24x + 13.68$ $r^2 = 0.813$	$y = 0.30x + 14.08$ $r^2 = 0.937$
Colour a^* vs. carotenoids	$y = 1.17x - 19.20$ $r^2 = 0.973$	$y = 1.18x - 20.02$ $r^2 = 0.971$
L-TAA vs. colour a^*	$y = 0.32x + 15.29$ $r^2 = 0.777$	$y = 0.37x + 16.86$ $r^2 = 0.840$

hanced by NPLs application in the irrigation system, with the exception of L-TAA and total carotenoids.

Pepper fruit (*Capsicum annum* L. cv. Herminio) growth followed a simple sigmoid curve reaching its maximum size around 49 DAFS under our experimental conditions (summer time), although NPLs led to significant increases in fruit weight due to higher length, diameter, and pericarp thickness. Then, NPLs treatment improved fruit quality, since pepper fruit with high sizes are more appreciated by consumers and reach higher prices than smaller fruits at markets. The colour changes from green to red started when fruit had almost reached their final size, at 39 DAFS, and reached the full colour red (end of ripening) at day 55 of development. It is noticeable that NPLs did not modify the normal colour evolution of pepper fruit on plant. This pattern of fruit development (growth and colour changes) has been found in other pepper cultivars, although the time necessary to reach final size and full colour depended on cultivar and growth conditions. Thus, in cultivar 'New ace' final growth and colour changes occurred after 50 days of fruit set (Yahia, Contreras-Padilla, & González-Aguilar, 2001), whilst in 'Domino' cultivar, 56 days were needed (Hornero-Méndez et al., 2002), both cultivars being grown in greenhouse under controlled hydroponic conditions and receiving standard cultural practices. The colour change from green to red has been associated to ripening in sweet pepper, and it is well known that the red colour is due to carotenoid pigments (Mínguez-Mosquera & Hornero-Méndez, 1993; Pretel, Serrano, Amorós, Riquelme, & Romojaro, 1995), which is in agreement with the correlation found between colour a^* evolution and total carotenoid concentration reported herein. The main carotenoid compounds in pepper fruit have been found to be capsanthin followed by *cis*-capsanthin, β-carotene and zeaxanthin (Marín et al., 2004; Mínguez-Mosquera & Hornero-Méndez, 1993). The total carotenoid concentration in 'Herminio' pepper was within the range reported for other cultivars such as 'Vergasa' (Marín et al., 2004) and 'Robusta' (Fox et al., 2005), although higher carotenoid contents have been reported in 'Agridulce' and 'Bola' varieties (Mínguez-Mosquera & Hornero-Méndez, 1993).

The content of glucose and fructose started to accumulate at higher rates when fruit was approaching its final size (from 49 DAFS), although those peppers treated with NPLs exhibited a higher increase in these sugars. In addition, sucrose occurred at a very low concentration and did not change throughout the development process. This behaviour in sugar profile, evolution and final concentration has been reported for other pepper cultivars, since increases in both glucose and fructose were shown from green to red ripe stages in 'Mazurka' and 'Evident' cultivars (Lunning et al., 1994). However, in those peppers that are generally consumed at green stage, such as 'Padrón' the concentrations of sugars are 3–4-fold lower (López-Hernández, Oruña-Concha, Simal-Lozano, Vázquez-Blanco, & González-Castro, 1996). With respect to acidity, this parameter increased along the growth and maturation periods, although peppers from NPLs-treated plants showed higher acidity than controls. This acidity behaviour was further confirmed by the evolution of individual organic acids by HPLC. The main organic acid was citric acid followed by succinic, malic, oxalic and fumaric acids. These increases in soluble sugars and acidity have also been found during physiological ripening in many cultivars of both hot and sweet pepper, being correlated to colour changes (Behera, Pal, Sen, & Singh, 2004; Orowski, Grzeszczuk, & Jadczak, 2004; Tadesse et al., 2002). Moreover, NPLs application led to higher sugar and organic acid concentration in pepper pericarp as compared to pepper from control plants, which could be attributed to a higher net photosynthesis in NPLs-treated plants, and in turn, to higher levels of photo-assimilates to partitioning between plant sinks. In fact, NPLs increased photosynthesis in the cotton plant (Gou & Oosterhuis, 1995) and tomato plant growth by increasing the activity of antioxidant enzymes such as superoxidedismutase, catalase and peroxidase and the auxin contents (Djanaguiraman, Pandiyan,

et al., 2005). Accordingly, some bio-fertilizers applied to pepper plants to increase fruit weight and total yield also increased total soluble solids and acidity (Ghoname & Shafeek, 2005). In addition, the foliar application of Biozyme®, which contains phytohormones and micronutrients, induced also significantly higher levels of non-structural carbohydrates such as glucose and fructose (Belakbir et al., 1996). In a comparative study combining instrumental and sensory evaluation of flavour in fresh peppers, a close relationship between sweetness and concentration of glucose and fructose in pepper for red ripe stage has been reported, whilst the perceived sourness increased from the green to red maturation stages mainly due to an increased concentration of citric acid (Lunning et al., 1994). In this sense, the application of NPLs would induce an extra benefit related to consumer's acceptability, since red peppers with high contents of both sugars and acidity are more appreciated (Frank et al., 2005).

Fresh sweet peppers have exceptionally high ascorbic acid content, since a 100 g serving supply twice the current RDA (recommended daily administration) of 60 mg day^{-1}. In fact, concentrations ranging from 15 to 250 mg 100 g^{-1} of ascorbic acid have been found depending on cultivar, fruit ripening stage and growing conditions (Deepa, Kaur, Singh, & Kapoor, 2006; Fox et al., 2005; Howard et al., 2000; Jiménez, Romojaro, Gómez, Llanos, & Sevilla, 2003; Marín et al., 2004; Özden & Bayindirli, 2002). In the 'Herminio' cultivar, ascorbic acid concentration increased as did the developmental process, the enhancement being higher in NPLs-treated fruits, with final concentrations being considered as relatively high when compared to other pepper cultivars. According to our results, increases in ascorbic acid content have been reported to occur along the ripening process of both, hot and sweet pepper fruit and then, red fruit have higher vitamin C content than green ones (Behera et al., 2004; Jiménez et al., 2003; Marín et al., 2004; Navarro et al., 2006; Orowski et al., 2004; Pérez-López, del Amor, Serrano-Martínez, Fortea, & Núñez-Delicado, 2007). However, in bell pepper cultivars either maintenance or even a 2-fold decrease in ascorbic acid concentration from mature green to full red stages have been reported (Fox et al., 2005; Yahia et al., 2001).

In recent years phenolic compounds have attracted the interest of researchers because they show antioxidant activity and can protect the human body from free radicals, and have a certain role in the prevention of some diseases, including cancer, cardiovascular disease and neurodegenerative disorders (Ferrari & Torres, 2003; Kaur & Kapoor, 2001). Phenolic concentration was accumulated along the developmental stages of pepper fruit, and NPLs application led to higher total phenolic concentration. This evolution in phenolics does not seem to be a general behaviour during pepper fruit maturation, since decreases or increases in total phenolics have been associated with changes from green to red stage depending on cultivar (Conforti, Statti, & Menichini, 2007; Marín et al., 2004). Sweet pepper contains a very rich polyphenols pattern, since it has been identified to contain 5 hydroxycinamic acids and 23 flavonoids as the major phenolics compounds (Marín et al., 2004). Accordingly, in hot peppers flavonoids have been also identified as the main phenolics compounds, although capsaicinoids, such as capsaicin and dihydrocapsaicin, were also important (Hornero-Méndez et al., 2002).

Total antioxidant activity (TAA) is an important parameter in establishing the health functionality of a vegetable product and there are many methods for its measurement (Kaur & Kapoor, 2001). With the used method, we were able to measure TAA in two fractions, and the results showed that TAA was 10-fold higher in the hydrophilic fraction (H-TAA) than in the lipophilic one (L-TAA), according to previous reports in cv. 'Orlando', a California type pepper (Navarro et al., 2006) and in bell pepper 'Robusta' cultivar (Fox et al., 2005), indicating that the main compounds responsible for antioxidant properties of pepper fruits are water soluble compounds. In fact, the behaviour of total phenolics and ascorbic acid along the growth and maturation stages showed a similar pattern than that obtained for H-TAA, these compounds being highly correlated to H-TAA, which could be the responsible for this H-TAA. However, discrepancies exist in understanding the relationship between TTA and total phenols, since weak correlations between both parameters were found in several pepper cultivars at red stage (Belakbir et al., 1996; Deepa et al., 2006). Finally, L-TAA was correlated with colour a^* evolution and total carotenoids, which would be the main lipophilic compounds with antioxidant activity.

In conclusion, NPLs treatment induced beneficial effects during the growth cycle and maturation of sweet pepper in two ways. Firstly, NPLs yielded bigger fruits with higher contents of sugars (glucose and fructose) and organic acids, without affecting the normal ripening process on plant as showed by colour and carotenoid evolution. Secondly, this pre-harvest treatment also increased the bioactive compounds with functional properties, such as total phenolics and ascorbic acid, which were the main compounds contributing to TAA. In addition, since sugars, organic acids, total phenolics, carotenoids, and vitamin C increased along with the fruit ripening on plant, it should be advisable to harvest the peppers at the full red stage, in order to achieve the maximum benefit of their consumption in terms of nutritive and functional properties.

References

Arnao, M. B., Cano, A., & Acosta, M. (2001). The hydrophilic and lipophilic contribution to total antioxidant activity. *Food Chemistry, 73*, 239–244.

Behera, T. K., Pal, R. K., Sen, N., & Singh, M. (2004). Effect of maturity at harvest on physicochemical attributes of sweet pepper (*Capsicum annuum* Var Grossum) varieties. *Indian Journal of Agricultural Science, 74*, 251–253.

Belakbir, A., Lamrani, Z., Ruiz, J. M., López-Cantarero, I., Valenzuela, J. L., Romero, L., et al. (1996). Influence of year and Atonik application on variability on sugar beet yield and digestion. *Journal of Central European Agriculture, 4*, 411–418.

Cerny, I., & Ondrisik, I. (2003). Influence of year and Atonik application on variability on sugar beet yield and digestion. *Journal of Central European Agriculture, 4*, 411–418.

Conforti, F., Statti, G. A., & Menichini, F. (2007). Chemical and biological variability of hot pepper fruits (*Capsicum annuum* var *acuminatum* L.). *Food Chemistry, 102*, 1096–1104.

Deepa, N., Kaur, C., George, B., Singh, B., & Kapoor, H. C. (2007). Antioxidant constituents in some red sweet pepper (*Capsicum annuum* L.) genotypes during maturity. *Lebensmittel Wissenchaft Und Technologie, 40*, 121–129.

Deepa, N., Kaur, C., Singh, B., & Kapoor, H. C. (2006). Antioxidant activity in some red sweet pepper cultivars. *Journal of Food Composition and Analysis, 19*, 572–578.

del Amor, F. M. (2006). Growth, photosynthesis and chlorophyll fluorescence of sweet pepper plants as affected by the cultivation method. *Annals of Applied Biology, 148*, 133–139.

Djanaguiraman, M., Pandiyan, M., & Devi, D. D. (2005). Abscission of tomato fruit follows oxidative damage and its manipulation by Atonik spray. *International Journal of Agricultural Biology, 7*, 39–44.

Djanaguiraman, M., Sheeba, J. A., Devi, D. D., & Bangarusamy, U. (2005). Response of cotton to Atonik and TIBA for growth, enzymes and yield. *Journal of Biological Science, 5*, 158–162.

Ferrari, C. K. B., & Torres, E. A. F. S. (2003). Biochemical pharmacology of functional foods and prevention of chronic diseases of aging. *Biomedical Pharmacotherapy, 57*, 251–260.

Fox, A. J., Del Pozo, D., Lee, J. H., Sargent, S. A., & Talcott, S. T. (2005). Ripening-induced chemical and antioxidant changes in bell peppers as affected by harvest maturity and postharvest ethylene exposure. *HortScience, 40*, 732–736.

Frank, C. A., Nelson, R. G., Simonne, E. H., Behe, B. K., & Simonne, A. H. (2005). Consumer preferences for color, price and vitamin C content of bell peppers. *HortScience, 36*, 795–800.

Ghoname, A., & Shafeek, M. R. (2005). Growth and productivity of sweet pepper (*Capsicum annum* L.) growth in plastic house as affected by organic, mineral and bio-N-fertilisers. *Journal of Agronomy, 4*, 369–372.

Hornero-Méndez, D., Costa-García, J., & Mínguez-Mosquera, M. I. (2002). Characterization of carotenoid high-producing *Capsicum annuum* cultivars for paprika production. *Journal of Agricultural and Food Chemistry, 50*, 5711–5716.

Howard, L. R., Talcott, S. T., Brenes, C. H., & Villalon, B. (2000). Changes in phytochemical and antioxidant activity pepper cultivars (*Capsicum* species) as influenced by maturity. *Journal of Agricultural and Food Chemistry, 48*, 1713–1720.

Jiménez, A., Romojaro, F., Gómez, J. M., Llanos, M. R., & Sevilla, F. (2003). Antioxidant system and their relationship with the response of pepper fruits to storage at 20 °C. *Journal of Agricultural and Food Chemistry, 51*, 6293–6299.

Kaur, C., & Kapoor, H. C. (2001). Antioxidants in fruits and vegetables – the millennium's health. *International Journal of Food Science and Technology, 36*, 703–725.

López-Hernández, J., Oruña-Concha, M. J., Simal-Lozano, J., Vázquez-Blanco, M. E., & González-Castro, M. J. (1996). Chemical composition of Padrón peppers (*Capsicum annuum* L.) grown in Galicia (N.W. Spain). *Food Chemistry, 57*, 557–559.

Lunning, P. A., de Vries, R. V. D. W., Yuksel, D., Ebbenhorst-Seller, T., Wichers, H. J., & Roozen, J. P. (1994). Combined instrumental and sensory evaluation of flavor of fresh bell peppers (*Capsicum annuum*) harvested at three maturation stages. *Journal of Agricultural and Food Chemistry, 42*, 2855–2861.

Marín, A., Ferreres, F., Tomás-Barberán, F. A., & Gil, M. I. (2004). Characterization and quantitation of antioxidant constituents of sweet pepper (*Capsicum annuum* L.). *Journal of Agricultural and Food Chemistry, 52*, 3861–3869.

Martínez, S., Curros, A., Bermúdez, J., Carballo, J., & Franco, I. (2007). The composition of Arnoia peppers (*Capsicum annuum* L.) at different stages of maturity. *International Journal of Food Science and Nutrition, 58*, 150–161.

Matterska, M., & Perucka, I. (2005). Antioxidant activity of the main phenolics compounds isolated from hot pepper fruit (*Capsicum annuum* L.). *Journal of Agricultural and Food Chemistry, 53*, 1750–1756.

Mínguez-Mosquera, M. I., & Hornero-Méndez, D. (1993). Separation and quantification of the carotenoid pigments in red peppers (*Capsicum annuum* L.), paprika, and oleoresin by reversed-phase HPLC. *Journal of Agricultural and Food Chemistry, 41*, 1616–1620.

Navarro, J. M., Flores, P., Garrido, C., & Martínez, V. (2006). Changes in the contents of antioxidant compounds in pepper fruits at different ripening stages, as affected by salinity. *Food Chemistry, 96*, 66–73.

Orowski, M., Grzeszczuk, M., & Jadczak, D. (2004). The estimation of the yield and content of some chemical compounds in the fruits of chosen hot pepper (*Capsicum annuum* L.) cultivars. *Folia Horticulturae, 16*, 11–16.

Özden, Ç., & Bayindirli, L. (2002). Effects of combinational use of controlled atmosphere, cold storage and edible coating applications on shelf life and quality attributes of green peppers. *European Food Research and Technology, 214*, 320–326.

Pérez-López, A. J., del Amor, F. M., Serrano-Martínez, A., Fortea, M. A., & Núñez-Delicado, E. (2007). Influence of agricultural practices on the quality of sweet pepper fruits as affected by the maturity stage. *Journal of the Science of Food and Agriculture, 87*, 2075–2080.

Pretel, M. T., Serrano, M., Amorós, A., Riquelme, F., & Romojaro, F. (1995). Non-involvement of ACC and ACC oxidase activity in pepper fruit ripening. *Postharvest Biology and Technology, 5*, 295–302.

Serrano, M., Guillén, F., Martínez-Romero, D., Castillo, S., & Valero, D. (2005). Chemical constituents and antioxidant activity of sweet cherry at different ripening stages. *Journal of Agricultural and Food Chemistry, 53*, 2741–2745.

Serrano, M., Martínez-Romero, D., Castillo, S., Etchepare, O., Dupille, E., & Valero, D. . *Efecto del Atonik® en la productividad y calidad de los tomates. V congresso ibérico de ciências hortícolas* (Vol. 1). Porto, Portugal: Associação Portuguesa de Horticultura.

SPSS, VERSION 12.0 for Windows; SPSS Inc.: Chicago, IL; 2001.

Tadesse, T., Hewett, E. W., Nichols, M. A., & Fischer, K. J. (2002). Changes in physicochemical attributes of sweet pepper cv. Domingo during fruit growth and development. *Scientia Horticulturae, 93*, 91–103.

Tomás-Barberán, F. A., & Espín, J. C. (2001). Phenolic compounds and related enzymes as determinants of quality in fruits and vegetables. *Journal of the Science of Food and Agriculture, 81*, 853–876.

Tomás-Barberán, F. A., Gil, M. I., Cremin, P., Waterhouse, A. L., Hess-Pierce, B., & Kader, A. A. (2001). HPLC-DAD-ESIMS analysis of phenolic compounds in nectarines, peaches, and plums. *Journal of Agricultural and Food Chemistry, 49*, 4748–4760.

Yahia, E. M., Contreras-Padilla, M., & González-Aguilar, G. (2001). Ascorbic acid content in relation to ascorbic acid oxidase activity and polyamine content in tomato and bell pepper fruits during development, maturation and senescence. *Lebensmittel Wissenchaft Und Technologie, 34*, 452–457.

Food Chemistry 118 (2010) 504–507

Contents lists available at ScienceDirect

Food Chemistry

journal homepage: www.elsevier.com/locate/foodchem

Oil, micronutrient and heavy metal contents of tomatoes

Ayhan Demirbas *

Sila Science, Universite Mah., Mekan Sok., No: 24, 61040 Trabzon, Turkey

ARTICLE INFO

Article history:
Received 19 February 2009
Received in revised form 1 April 2009
Accepted 7 May 2009

Keywords:
Tomato fruit
Tomato seed oil
Fatty acids
Heavy metal
Micronutrient

ABSTRACT

In this study, oils, micronutrients and heavy metal contents of tomato seeds and tomato (*Lycopersicon esculentum*) fruits from different Turkish resources were determined. The tomato seed oil contains more than 84% unsaturated fatty acids, such as oleic acid, linoleic acid and linolenic acid. The fatty acid composition of tomato seed oil was similar to that of soybean oil. Under supercritical conditions, partial thermal degradation occurs on the double bonds of unsaturated aliphatic carbons chains in fatty acids. Linoleic acid was the major unsaturated fatty acid in tomato seed oil. The concentrations of metals (Pb, Cd, Fe, Cu, Zn, Na, K, Ca and Mg) were determined in tomato samples.

1. Introduction

Tomato (*Lycopersicon esculentum*) is one of the world's major vegetables with a worldwide production of 126 million tons in 2005 (FAOSTAT, 2007). It is an excellent source of many nutrients and secondary metabolites that are important for human health: mineral matter, vitamins C and E, β-carotene, lycopene, flavonoids, organic acids, phenolics and chlorophyll (Giovanelli & Paradiso, 2002).

Tomato fruits contain several anti-oxidants such as vitamin C, provitaminic A carotenes, phenolic compounds, flavonoids and phenolic acids. Consumption of its components, β-carotene and lycopene, has been related epidemiologically to a lower incidence of cardiovascular disease and of prostate, gastrointestinal and epithelial cell cancer (Rao & Rao, 2007).

Heavy metal and nutritive contents of tomatoes depend on growing conditions (Miteva, Maneva, Hristova, & Bojinova, 2001). Heavy metal and nutritive contents of tomatoes grown using conventional and organic methods were determined (Rossi et al., 2008). Compared to crops grown using conventional and organic methods, organic tomatoes contained more salicylic acid but less vitamin C and lycopene. Organic tomatoes had higher Cd and Pb levels but a lower Cu content. Organic fruits had slightly higher protein content than conventionally cultivated fruits, but the difference was minimal and consequently the nutritive significance was poor (Rossi et al., 2008).

Several unit operations such as drying, grinding, squeezing and filtrating were used to obtain tomato seed oil from tomato seeds. Tomato seed oil was extracted with supercritical carbon dioxide in a semibatch-flow extraction apparatus. The effect of milling of seeds and solvent flow rate on the extraction behaviour was studied. The extraction rate increased as solvent flow rate increased (Roy, Goto, & Hirose, 2003; Roy, Goto, Hirose, Navaro, & Hortacsu, 1994). Supercritical fluid extraction is generally carried out by mechanically stirring or in a rocking batch reactor at the critical temperature and pressure of the solvent. The yield of soluble material increases with increasing pressure (Paul & Wise, 1971).

2. Materials and methods

2.1. Sampling

The samples of tomato (*L. esculentum*) seeds, tomato peels and industrial tomato wastes were supplied from different Turkish resources. Only tomato seeds were used for oil analyses. Whole tomato fruits were used for determination of mineral matter and phenolic compounds. The tomatoes were washed in distilled water before each experiment.

2.2. Supercritical acetone extraction of tomato seeds

Tomato seed oil was extracted with supercritical acetone in a batch pressure vessel (autoclave) within the temperature range 513–518 K and the pressure range 6.0–6.5 MPa. In addition, tomato seed oil was extracted with simple Soxhelet acetone solid–liquid extraction.

* Tel.: +90 462 230 7831; fax: +90 462 248 8508.
E-mail address: ayhan.demirbas@hotmail.com

0308-8146/$ - see front matter © 2009 Elsevier Ltd. All rights reserved.
doi:10.1016/j.foodchem.2009.05.007

2.2.1. Fractionation of supercritical acetone extract

The deionised water was added into the acetone extract (1/1, v/v); and extracted with equal portions of petroleum ether (b.p. 413–433 K). Petroleum ether solubles were saponified for 3.5 h at 338 K using 0.5 N of methanolic potassium hydroxide to liberate the fatty acids present as their esters or acylglycerols. The unsaponifiables present in the mixture were then extracted 3–4 times with equal portions of petroleum ether. Upon removal of petroleum ether the unsaponifiables were obtained. The solution of saponifiables was diluted with an equal volume of water, then acidified to pH 3–4 by addition of 1.5 N hydrochloric acid. The fatty acids present in the solution were extracted using diethyl ether. After evaporation of ether, the acids were weighed. The fatty acids were methylated with diazomethane according to the method of Schelenk and Gellerman (1960).

2.3. Fatty acid analysis

The methyl esters of the fatty acids were analysed by gas chromatography (Hewlett–Packard 5790) on a 12 m 0.2 mm capillary column coated with Carbowax PEG 20 (Demirbas, 2009). The physico-chemical properties such as saponification value, acid value, iodine value and peroxide value of the tomato seed oils were determined.

2.3.1. Physico-chemical properties

The physico-chemical properties such as saponification value, acid value, iodine value and peroxide value of the tomato seed oils were determined by AOCS Tentative Methods (AOAC, 1990). All tests were performed in triplicate.

2.4. Mineral matter analysis

Mineral matter contents were determined according to earlier methods (Demirbas, 2000, 2001, 2002; Tuzen, Ozdemir, & Demirbas, 1998). Digestion of tomato seed samples was performed using an oxi-acidic mixture of HNO_3:H_2SO_4:H_2O_2 (4:1:1) (12 ml 97 for 2–4 g sample) and heating at 348 K for 3 h. After cooling, 20 ml-demineralised water was added, then the digest was again heated up to 423 K for 4 h and brought to a volume of 25 ml with demineralised water (Tuzen et al., 1998).

Cd levels in the samples were determined using a GBC 3000 graphite furnace for AAS. Determination of metal ion (Cu^{+2}, Fe^{+2}, Zn^{+2}) content was carried out with a GBC 905 model AAS using flame atomisation. For the determination of Pb and Cd contents, euterium and Smith-Hieftje background correction have been used (Demirbas, 2002). The wavelength and slit values, in nm, used for the determination of Pb, Cd, Fe, Cu and Zn were: 283.3 and 0.5, 228.8 and 0.5, 248.3 and 0.2, 324.7 and 0.5 and 213.9 and 0.5, 108 respectively. A flame photometer (Biotechnical Instruments, Model 8T 624D) was used for determinations of Na and K (Demirbas, 2005). For determination of Ca and Mg, the resulting digest solution was titrated with 0.01 M EDTA solution. The standard-addition procedure was used in all determinations.

2.5. Determination of phenolic substances

To obtain total phenolic substances from the supercritical acetone extract, 10 g of the extract obtained from tomato fruits were extracted four times with 250 ml of a 5% heated solution of NaOH at 343 K. 200-ml of the caustic solution was extracted twice with 25-ml of pentane to remove hydrocarbons. After addition of a 15% HCl solution to adjust the pH of the solution to 6, a 5% solution of $NaHCO_3$ was added to the solution until PH8.3 was obtained. As a result of this the precipitate dissolved (Morrison and Boyd, 1983). The clear solution was extracted four times with equal volumes of diethyl ether and then the ethereal layer, containing the phenols, was washed with distilled water and dried overnight with $MgSO_4$. The pH was measured using a glass electrode (Jenway 3010 model pH metre).

2.5.1. Antioxidative activity of phenolic substances

The antioxidative activity of total phenolic substances was determined using the nitric oxide method. The antioxidative activity of the isolated phenolics was determined by the ferric thiocyanate method (Nagatsu et al., 2004).

2.6. Statistical analysis

All analytical determinations were performed in triplicate and the mean values were reported. Results presented are means ± standard deviations of triplicate values. The percentages of fatty acid were compared by analysis of variance (ANOVA) taking $p < 0.05$ as the minimum criterion for statistical significance. Comparisons between means were performed with Tukey's test.

3. Results and discussion

3.1. Fatty acid analysis results

The percentage yields of supercritical acetone extractions are present in Table 1. The extract yield slightly increased with increasing temperature.

The chemical compositions of fatty acids of tomato seed oil and methyl esters from Soxhelet acetone extraction and supercritical acetone extraction are presented in Table 2. Mrystic (14:0), palmitic (16:0), stearic (18:0), arachidic (20:0), myristoleic (14:1), palmitoleic (16:1), oleic (9c-18:1), linoleic (9c, 12c-18:2) and gadoleic (20:1) fatty acids were observed in the oil samples. Unsaturated fatty acid as myristoleic acid, palmitoleic acid, oleic acid, linoleic acid, linolenic (9c, 12c, 15c-18:3) acid and gadoleic (9c-20:1) reach as high as 75.8%. In both extractions, palmitic acid was the major saturated fatty acid, followed by stearic acid. Linoleic acid was the major unsaturated fatty acid followed by oleic acid. The fatty acid composition of tomato seed oil was similar to that of soybean oil (Demirbas, 1998).

Table 1
Yields of supercritical acetone extraction (wt.% of dry tomato seed).

Runs	Temperature (K)	Total extract	Oil fraction	Unsaponifiables
1	513	39.1	35.3	3.8
2	515	40.7	36.4	4.3
3	518	41.8	36.9	4.9

Table 2
Chemical compositions of fatty acids in tomato seed oil and methyl esters by Soxhelet extraction (SAE) and supercritical acetone extraction (SCAE).

Fatty acid	Tomato seed oil (%)	Methyl esters from SAE and SCAE	
		SAE (%)	SCAE (%)
Myristic (14:0)	1.1	0.6	2.0
Palmitic (16:0)	18.1	16.4	22.6
Stearic (18:0)	4.0	3.5	5.2
Arachidic (20:0)	1.0	0.8	1.6
Myristoleic (14:1)	0.2	0.3	0.1
Palmitoleic (16:1)	3.2	3.5	3.0
Oleic (9c-18:1)	24.6	26.3	21.8
Linoleic (9c, 12c-18:2)	46.8	47.2	42.4
Linolenic (9c, 12c, 15c-18:3)	0.4	0.6	0.2
Gadoleic (9c-20:1)	0.6	0.8	1.1

Compared to Soxhelet extraction, the unsaturated fatty acid levels decreased significantly during supercritical acetone extraction from 78.7% to 68.6%. Partial thermal degradation of the unsaturated fatty acids may occur in the supercritical acetone extraction due to high temperature (<513 K). The high temperature had a much greater effect on the polyunsaturated fatty acids than saturated and monounsaturated fatty acids. Under supercritical conditions partial thermal degradation occurs on the double bonds of unsaturated aliphatic carbons chains in fatty acids (Balat, 2009; Hashem, Hussein, Senousi, Saad, & Khoda, 2009). Oxidation of methyl esters might be causing the formation of hydroperoxides. Many of the vegetable oils contain polyunsaturated fatty acid chains and their double bonds are very reactive (Browne & Armstrong, 2000). Oxidation to CO_2 of the methyl ester results in the formation of hydroperoxides. The formation of the hydroperoxide follows a well known peroxidation chain mechanism. Oxidative lipid modifications occur through lipid peroxidation mechanisms in which free radicals and reactive oxygen species abstract a methylene hydrogen atom from polyunsaturated fatty acids, producing a carbon-centred lipid radical. Spontaneous rearrangement of the 1,4-pentadiene yields a conjugated diene, which reacts with molecular oxygen to form a lipid peroxyl radical (Porter, Wolfe, & Weenan, 1979). Abstraction of a proton from neighbouring polyunsaturated fatty acids produces a lipid hydroperoxide (LOOH) and regeneration of a carbon-centred lipid radical, thereby propagating the radical reaction (Browne & Armstrong, 2000). After a hydrogen is removed, oxygen attacks rapidly and a LOOH is ultimately formed where the polyunsaturation has been isomerised to include a conjugated diene. This reaction is a chain mechanism that can proceed rapidly once an initial induction period has occurred. The greater the level of unsaturation in a fatty oil or ester, the more susceptible it will be to oxidation. Once the LOOHs have formed, they decompose and inter-react to form numerous secondary oxidation products including higher molecular weight oligomers often called polymers.

The oxidative and thermal degradation occurs on the double bonds of unsaturated aliphatic carbons chains in fatty acids. Oxidation of the methyl esters result in the formation of hydroperoxides. The formation of the hydroperoxide follows a well known peroxidation chain mechanism. The olefinic unsaturated fatty acid oxidation is a multi-step reaction process where primary products (conjugated diene hydroperoxides) decompose and chemically interact with each other to form numerous secondary oxidation products. The oxidative and thermal instability are determined by the amount and configuration of the olefinic unsaturation on the fatty acid chains (Demirbas, 2008).

3.2. Physico-chemical properties

The physico-chemical properties of the tomato seed oils are given in Table 3. Acid value is a measure of the free fatty acid content in fats and oils. The acid value is the number of mg of potassium hydroxide necessary to neutralise the free fatty acids present in 1 g of oil or fat sample (Beare-Rogers, Dieffenbacher, & Holm, 2001). The saponification value (SV) is the milligrams of KOH necessary to saponify 1 g of oil sample. The iodine value (IV) is the amount of iodine (in grams) necessary to saturate 100 g of oil sample (Demirbas, 1998). The IV is a measure of the amount of unsaturation in fats and oils. The peroxide value (PV) is a measure of the extent of oxidation of a fat or oil. The value indicates the quantity of oxidised substances, normally hydroperoxides that liberate iodine from potassium iodide under specified conditions. The PV is expressed in milliequivalents of active oxygen per kg fat (Bala, 2005).

Table 3
Physico-chemical properties of the tomato seed oils.

Property	Soxhelet acetone extraction	Supercritical acetone extraction
Acid value (mg KOH/g oil)	0.241	0.006
Saponification value (mg KOH/g oil)	190.2	183.6
Iodine value (g I/l00 g oil)	126.8	109.7
Peroxide value (mmol peroxide/kg oil)	15.0	36.2
Moisture and volatility (%)	0.052	4.18
Specific gravity (g/mL)	0.9177	0.9185
Refractive index	1.4733	1.4714
Color	Yellow	Reddish yellow

3.3. Mineral matter analysis results

The average heavy metal levels (mg/kg, dry-weight basis) of the tomato samples are given in Table 4. Table 5 shows the average levels (mg/kg, dry-weight basis) of Na, K, Ca, and Mg in tomato samples.

From Table 4, the highest and the lowest Pb content was 0.48 ± 0.11 (0.48 is average value and 0.11 is s.d.) and 0.38 ± 0.07 mg/kg in the tomatoes, respectively. The highest 210 Cd content was determined as 0.71 ± 0.15 mg/kg. The highest Cu content was 18.7 ± 3.2 mg/kg. The highest Fe and Zn contents were 2.41 ± 0.34 and 78.4 ± 6.8 mg/kg, respectively. The heavy metal levels in the plants are hardly affected by pH and organic matter content of the soil (Gast, Jansen, Bierling, & Haanstra, 1988). From Table 5, the highest and the lowest Na content were 7.18 ± 0.69 mg/kg and 5.57 ± 0.53 mg/kg in the tomatoes, respectively. The highest and the lowest K contents are 20.81 ± 3.5 mg/kg and 16.59 ± 2.3 mg/kg in the tomatoes, respectively. The highest Ca and Mg contents were 3.54 ± 0.32 and 6.32 ± 0.55 mg/kg, respectively.

The mineral matter composition of vegetables characterises their nutrition conditions and indicates the yield potentials. Excessive amounts of K and Mg in tomato inhibits the Ca uptake and blossom-end rot, which is a result of Ca deficiency (Adams & Ho, 1993). In the case of Ca deficiency in growth substrate, the Ca and P levels in tomato plants have decreased (Morard, Pujos, Bernadac, & Bertony, 1996).

Heavy metals may have significant toxic and hazardous effects on human health, especially cadmium and lead, as non-essential elements (Bakirdere & Yaman, 2008). Chronic cadmium exposures result in kidney damage, bone deformities and cardiovascular

Table 4
Average levels (average ± s.d.) of heavy metals (Pb, Cd, Fe, Cu and Zn) in tomato samples (mg/kg, dry-weight basis).

Run	Pb	Cd	Fe	Cu	Zn
1	0.43 ± 0.08	0.65 ± 0.12	2.13 ± 0.30	14.1 ± 2.4	73.1 ± 6.2
2	0.38 ± 0.07	0.61 ± 0.11	1.98 ± 0.26	12.9 ± 1.8	64.8 ± 5.3
3	0.48 ± 0.11	0.71 ± 0.15	2.41 ± 0.34	18.7 ± 3.2	78.4 ± 6.8
4	0.42 ± 0.09	0.67 ± 0.13	2.32 ± 0.29	17.3 ± 3.0	67.5 ± 6.2
5	0.40 ± 0.10	0.69 ± 0.14	2.18 ± 0.27	16.9 ± 3.1	75.7 ± 6.6

Table 5
Average levels (average ± s.d.) of Na, K, Ca and Mg in tomato samples (mg/kg, dry-weight basis).

Run	Na	K	Ca	Mg
1	6.43 ± 0.62	18.26 ± 2.8	3.08 ± 0.28	5.26 ± 0.46
2	5.57 ± 0.53	16.59 ± 2.3	2.88 ± 0.23	4.22 ± 0.41
3	7.18 ± 0.69	20.81 ± 3.5	3.54 ± 0.32	6.32 ± 0.55
4	6.28 ± 0.61	17.86 ± 3.1	3.17 ± 0.30	6.02 ± 0.52
5	6.88 ± 0.65	19.09 ± 3.3	2.98 ± 0.24	5.89 ± 0.50

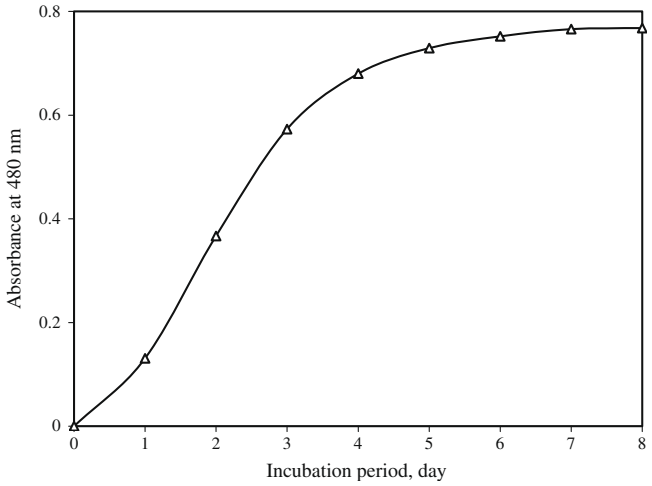

Fig. 1. Plot for antioxidative activity of phenolics determined by ferric thiocyanate method.

problems (Fritioff & Greger, 2007). It is known that copper is an essential element, but it may be toxic to both human and animals when its concentration exceeds the safe limits (Bakirdere & Yaman, 2008; Yaman, Akdeniz, Bakidere, & Atici, 2005).

3.4. Phenolic substances and antioxidative activity of phenolic substances

The highest and the lowest phenolic substance levels are 4.27 ± 0.36% and 2.48 ± 0.28% in the tomatoes, respectively. The average phenolic substance level was 3.50 ± 0.31%.

Fig. 1 shows the plot for the antioxidative activity of phenolics determined by ferric thiocyanate method. From Fig. 1, the antioxidative activity of phenolics increases sharply with time from 1 to 4 days when it reaches a plateau value.

4. Conclusion

The present work indicates that tomato seed wastes were a potential source of edible oil. The oil yield of tomato seeds was about 36% on a dry weight basis. Palmitic acid (18.1%) was the major saturated fatty acid, followed by stearic acid (4.0%) in tomato seed samples. Linoleic acid (46.8%) was the major unsaturated fatty acid followed by oleic acid (24.6%). This vegetable oil has low volatility, low sulphur, low ash content, and high viscosity.

There were considerable differences in the mineral matter composition among the tomato samples. The phenolic component yield of the tomato samples was about 3.5% on a dry weight basis. The antioxidative activities of phenolic compounds sharply increased with time from 1 to 4 days.

References

Adams, P. L., & Ho, L. C. (1993). Effects of environment on the uptake and distribution of calcium in tomato and on the incidence of blossom-end rot. *Plant and Soil, 154*, 127–132.

AOAC. (1990). *Official methods of analysis* (15th ed., pp. 951–986). Arlington, VA.

Bakirdere, S., & Yaman, M. (2008). Determination of lead, cadmium and copper in roadside soil and plants in Elazig, Turkey. *Environmental Monitoring and Assessment, 136*, 401–410.

Bala, B. K. (2005). Studies on biodiesels from transformation of vegetable oils for diesel engines. *Energy Education Science and Technology, 15*, 1–45.

Balat, M. (2009). New biofuel production technologies. *Energy Education Science and Technology Part A, 22*, 147–161.

Beare-Rogers, J., Dieffenbacher, A., & Holm, J. V. (2001). Lexicon of lipid nutrition (IUPAC Technical Report). *Pure Applied Chemistry, 73*, 685–744.

Browne, R. W., & Armstrong, D. (2000). HPLC analysis of lipid-derived polyunsaturated fatty acid peroxidation products in oxidatively modified human plasma. *Clinical Chemistry, 46*, 829–836.

Demirbas, A. (1998). Fuel properties and calculation of higher heating values of vegetable oils. *Fuel, 77*, 1117–1120.

Demirbas, A. (2000). Accumulation of heavy metals in some edible mushrooms from Turkey. *Food Chemistry, 68*, 415–419.

Demirbas, A. (2001). Levels of trace elements in the fruiting bodies of mushrooms growing in the East Black Sea region. *Energy Education Science and Technology, 7*, 67–81.

Demirbas, A. (2002). Metal ion uptake by mushrooms from natural and artificially enriched soils. *Food Chemistry, 78*, 89–93.

Demirbas, A. (2005). Beta-glucan and mineral nutrient contents of cereals grown in Turkey. *Food Chemistry, 90*, 773–777.

Demirbas, A. (2008). *Biodiesel: A realistic fuel alternative for diesel engines*. London: Springer-Verlag.

Demirbas, A. (2009). Oil from tea seed by supercritical fluid extraction. *Energy Sources Part A, 31*, 217–222.

FAOSTAT. (2007). FAOSTAT agricultural production database. <http://faostat.fao.org/site/336/default.aspx> Accessed 11. 07.

Fritioff, A., & Greger, M. (2007). Fate of cadmium in *Elodea canadensis*. *Chemosphere, 6*, 365–375.

Gast, C. H., Jansen, E., Bierling, J., & Haanstra, L. (1988). Heavy metals in mushrooms and their relationship with soil characteristics. *Chemosphere, 17*, 789–799.

Giovanelli, G., & Paradiso, A. (2002). Stability of dried and intermediate moisture tomato pulp during storage. *Journal of Agricultural and Food Chemistry, 50*, 7277–7281.

Hashem, A., Hussein, H. A., Senousi, M. A., Saad, E. E., & Khoda, M. (2009). Preparation and application of algenic acid for the removal of Pb (II) from aqueous solution. *Energy Education Science and Technology Part A, 22*, 107–115.

Miteva, E., Maneva, S., Hristova, D., & Bojinova, P. (2001). Heavy metal accumulation in virus-infected tomatoes. *Journal of Phytopathology, 149*, 179–184.

Morrison, R. T., & Boyd, R. N. (1983). *Organic Chemistry* (4th ed.). Singapore: Allyn and Bacon, Inc.

Morard, P., Pujos, A., Bernadac, A., & Bertony, G. (1996). Effect of temporary calcium deficiency on tomato growth and mineral nutrition. *Journal of Plant Nutrition, 19*, 115–127.

Nagatsu, A., Sugitani, T., Mori, Y., Okuyama, H., Sakakibara, J., & Mizuka, H. (2004). Antioxidants from rape (*Brassica campestris* Vir. *Japonica hara*) oil cake. *Natural Product Research, 18*, 231–239.

Paul, P. F. M., & Wise, W. S. (1971). *The principle of gas extraction*. London: Mills and Boon.

Porter, N., Wolfe, R., & Weenan, H. (1979). The free radical oxidation of polyunsaturated lecithins. *Lipids, 15*, 163–167.

Rao, A. V., & Rao, L. G. (2007). Carotenoids and human health. *Pharmacological Research, 55*, 207–216.

Rossi, F., Godani, F., Bertuzzi, T., Trevisan, M., Ferrari, F., & Gatti, S. (2008). Health promoting substances and heavy metal content in tomatoes grown with different farming techniques. *European Journal of Nutrition, 47*, 266–272.

Roy, B. C., Goto, M., & Hirose, T. (2003). Temperature and pressure effects on supercritical CO_2 extraction of tomato seed oil. *International Journal of Food Science and Technology, 31*, 137–141.

Roy, B. C., Goto, M., Hirose, T., Navaro, O., & Hortacsu, O. (1994). Extraction rates of oil from tomato seeds with supercritical carbon dioxide. *Journal of Chemical Engineering of Japan, 27*, 768–772.

Schelenk, H., & Gellerman, J. J. (1960). Esterification of fatty acids with diazomethane on a small scale. *Analytical Chemistry, 32*, 1412–1414.

Tuzen, M., Ozdemir, M., & Demirbas, A. (1998). Study of heavy metals in some cultivated and uncultivated mushrooms of Turkish origin. *Food Chemistry, 63*, 247–251.

Yaman, M., Akdeniz, I., Bakidere, S., & Atici, D. (2005). Comparison of trace metal concentrations in malign and benign human prostate. *Journal of Medicinal Chemistry, 48*, 630–634.

Food Chemistry 118 (2010) 508–511

Contents lists available at ScienceDirect

Food Chemistry

journal homepage: www.elsevier.com/locate/foodchem

Oxidation of (−)-epicatechin is a precursor of litchi pericarp enzymatic browning

Liang Liu [a], Shaoqian Cao [c], Yujuan Xu [a], Mingwei Zhang [a], Gengsheng Xiao [a], Qianchun Deng [d], Bijun Xie [b,*]

[a] Sericulture and Farm Produce Processing Research Institute, Guangdong Academy of Agricultural Sciences, Guangzhou 510610, PR China
[b] College of Food Science and Technology, Huazhong Agricultural University, Wuhan 430070, PR China
[c] College of Biological and Environmental Sciences, Zhejiang Wanli University, Ningbo 315100, PR China
[d] Oil Crops Research Institute, Chinese Academy of Agricultural Sciences, Wuhan 430062, PR China

ARTICLE INFO

Article history:
Received 9 March 2009
Received in revised form 31 March 2009
Accepted 7 May 2009

Keywords:
Flavanols
Epicatechin
Polyphenol oxidase
Browning
Oxidation

ABSTRACT

The degradation of flavanols had been studied both in the litchi pericarp during the storage and in the model system containing PPO and flavanols of litchi pericarp. The results showed that (−)-epicatechin was the optimal endogenous substrate of litchi pericarp PPO, and the procyanidins of litchi pericarp were oxidised very slowly when incubated alone with PPO. However, (−)-epicatechin could accelerate the oxidation of the other flavanols in litchi pericarp through a coupled oxidation pathway. The results obtained allowed us to draw a conclusion that the oxidation of (−)-epicatechin was a precursor of litchi pericarp browning. A pathway of enzymatic browning of litchi pericarp was proposed as follows: with the loss of cellular compartmentation, the litchi pericarp PPO and flavanols mixed and, then, (−)-epicatechin was oxidised by the PPO and *o*-quinones formed. The *o*-quinones reacted with other flavanols and anthocyanins, accelerating the oxidation of other polyphenols. Finally, the oxidation of (−)-epicatechin and other polyphenols led to the formation of the brown-coloured compounds, resulting in the enzymatic browning of litchi pericarp.

1. Introduction

Litchi (*Litchi chinensis Sonn.*) is a subtropical fruit of high commercial value for its white, translucent aril and attractive red colour. However, the fruit rapidly loses its bright red colour and turns brown once harvested. Postharvest browning of litchi was thought to be caused by the rapid degradation of the red pigment and oxidation of phenolic compounds by polyphenol oxidase (PPO), producing brown-coloured products (Akamine, 1960; Huang, Hart, Lee, & Wicker, 1990; Jiang, Zauberman, & Fuchs, 1997; Tan & Li, 1984).

Enzymatic browning is caused by the oxidation of phenolic substrates by PPO to produce reactive quinones. These quinones are highly reactive species involved in different reaction pathways. They are powerful electrophiles which may suffer nucleophilic attack by other polyphenols, amino acids, proteins to produce dark-brown or black pigment in senescent and postharvested fruits and vegetables (Cabanes, García-Cánovas, & García-Cármona, 1987; Fulcrand, Cheminat, Brouillard, & Cheynier, 1994; García-Carmona, Cabanes, & García-Cármona, 1987; Hurrel & Finot, 1984; Matheis & Whitaker, 1984).

In our previous studies, we found that (−)-epicatechin was the main endogenous substrate of PPO in litchi pericarp (Liu et al., 2007a, 2007b), and the enzymically generated (−)-epicatechin *o*-quinone could induce anthocyanins degradation (Liu, Cao, Xie, Sun, & Wu, 2007c). However, those results were obtained in the model systems, and whether those proposed reactions occurred in the litchi pericarp was ambiguous. Thus, the purpose of the present work was to investigate the relationship between the polyphenols oxidation by PPO and the litchi pericarp browning during the storage, so as to confirm our previous conclusions and give a further understanding for the mechanism of litchi pericarp browning.

2. Materials and methods

2.1. Plant material

The fruit of litchi (*Litchi chinensis Sonn. cv.* Feizixiao) at commercial maturation were obtained from Guangdong. The fruit arrived in the laboratory within 24 h after harvest. Fresh fruits were distributed randomly into groups of 10 fruits, packed in 0.03 mm thick PPE bags (20 × 30 cm) and airproofed with rubber bands, and stored at 3 °C.

2.2. Chemicals

(−)-Epicatechin, (+)-catechin, catechol, 4-methylcatechol and chlorogenic acid were purchased from Sigma (St. Louis, MO),

* Corresponding author. Tel./fax: +86 27 87282966.
E-mail address: bijunfood@yahoo.com.cn (B. Xie).

0308-8146/$ - see front matter © 2009 Elsevier Ltd. All rights reserved.
doi:10.1016/j.foodchem.2009.05.019

procyanidin B2 was purchased from Nakahara Science Co. (Ltd). Procyanidin A2 and epicatechin-(4β→8, 2β→O→7)–epicatechin-(4β→8)–epicatechin were obtained and characterised in our previous study (Liu et al., 2007a).

2.3. Colour measurements of litchi pericarp

The Hunter L^*, a^* and b^* values were measured using an UltraScan XE colourimeter (Hunterlab). Hunter L^* values show a gradual lightness of the pericarp. The Hunter a^* values indicate a measure of redness (or $-a^*$ of greenness) and b^* indicate a measure of yellowness (or $-b^*$ of blueness) on the hue-circle. Chroma C^* gives further information on the saturation or intensity of colour. Chroma C^* was calculated as follow equation:

$$C^* = (a^{*2} + b^{*2})^{1/2}$$

2.4. Membrane permeability measurement of litchi pericarp

Membrane permeability, expressed by relative leakage rate, was determined according to the method of Jiang and Chen (1995a) with some modifications. Discs were obtained by using a cork borer (10 mm in diameter) from 10 fruit pericarps. Twenty discs were rinsed twice and then incubated in 25 ml of distilled water at 25 °C, and shaken for 30 min. Electrolyte leakage was determined with a conductivity meter, and then the discs and incubated solution were boiled for 15 min and then cooled to 25 °C to assess total electrolytes. The relative leakage was expressed as a percentage of the total electrolytes.

2.5. Extraction of flavanols from litchi pericarp

Fresh litchi pericarp (5 g) from 5 fruits was extracted using acidified methanol (methanol:1.5 N HCl (85:15)) in a domestic ultrasonic bath (Kunshan), at room temperature for 0.5 h. The extract was filtered and the filter residue re-extracted using the same method until a colourless solution was obtained. Filtrates were combined and the final volume was adjusted to 100 ml in a volumetric flask. The sample was filtered through a 0.45 μm filter before RP-HPLC analysis.

2.6. Reversed-phase HPLC analysis

The analysis of flavanols of litchi pericarp by reversed-phase HPLC was performed on a Varian liquid chromatograph, and the detection was carried out using a photodiode array detector. The column was a VP-ODS column (150 mm × 4.6 mm ID, 5 μm particle size, SHIMADZU). The method utilised a binary gradient with a mobile phase of 2.5% v/v aqueous formic acid (mobile phase A) and acetonitrile/water/formic acid (57.5:40:2.5, v/v/v) (mobile phase B). A 10-μl sample solution was injected and the elution conditions were as follow: a linear gradient from 5% to 35% B in 40 min, from 35% to 50% B in 5 min, and from 50% to 80% B in 5 min, followed by washing and reconditioning of the column. Flow rate was 1 ml/min. Calibrations were performed for each compound by injection of known dilutions. Quantifications were based on peak areas at 280 nm for flavanols, at 510 nm for anthocyanins.

2.7. PPO activity analysis

Fresh litchi pericarp (5 g) from 5 fruits were triturated with liquid nitrogen, and then homogenised with 50 ml of 0.1 M phosphate buffer (pH 7.5) and 1 g of PVPP for 10 min. After centrifugation at 8000*g* for 5 min, the supernatant was collected and the final volume was adjusted to 100 ml in a volumetric flask. PPO activity was assayed spectrophotometrically at 25 °C using (−)-epicatechin as a substrate by monitoring at 440 nm (Liu et al., 2007b). The reaction medium (3 ml) contained 1 ml of 3 mM (−)-epicatechin, 1.98 ml of 50 mM of phosphate buffer (pH 7.5), and 0.02 ml of the enzyme solution. One unit of enzyme was defined as the amount of enzyme that caused an increase in absorbance of 0.001/min at 25 °C.

2.8. Statistical analysis

The Hunter L^*, a^* and b^* values were measured 10 times on each of the 10 fruits, and the average Hunter values were calculated. For enzyme activity measurement and quantification of flavanols, each sample was assayed in triplicate. Means were compared using Tukey Test with a significance level $P < 0.05$.

3. Results and discussion

3.1. Change in PPO activity of litchi pericarp during the storage

To evaluate the role of PPO activity played in the browning of litchi pericarp, we investigated the change in the PPO activity during the storage. However, there was no significant change ($P > 0.05$) in the PPO activity of litchi pericarp during the whole storage (Fig. 1). This suggested that the change in the PPO activity had no correlation with the browning of litchi pericarp, and the browning might be more dependent on whether the PPO mixed with its phenolic substrates.

3.2. Changes in polyphenols and membrane permeability of litchi pericarp during the storage

According to the previous structural identifications (Liu et al., 2007a, 2007c), we found that cyanidin 3-rutinoside was the major anthocyanins and (−)-epicatechin, procyanidin A2, procyanidin B2 and epicatechin-(4β→8, 2β→O→7)–epicatechin-(4β→8)–epicatechin were the four major flavanols in the litchi pericarp (Fig. 2). These results were in agreement with the previous descriptions (Le Roux, DoCo, Sarni-manchado, Lozano, & Cheynier, 1998; Sarni-manchado, Le Roux, Le Guerneve, Lozano, & Cheynier, 2000).

To investigate the relationship between the change of polyphenols and litchi pericarp browning, the contents of cyanidin 3-rutinoside and each major flavanol, the membrane permeability and browning of litchi pericarp were measured at intervals of 7 days during the storage. Browning of litchi pericarp during the storage

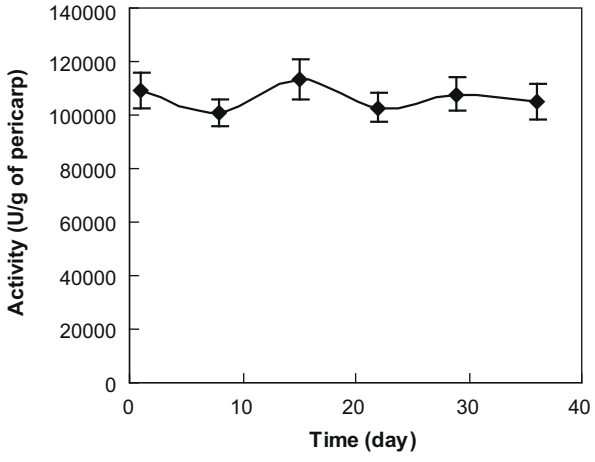

Fig. 1. Change in the PPO activity during storage at 3 °C. Vertical bars indicate SD.

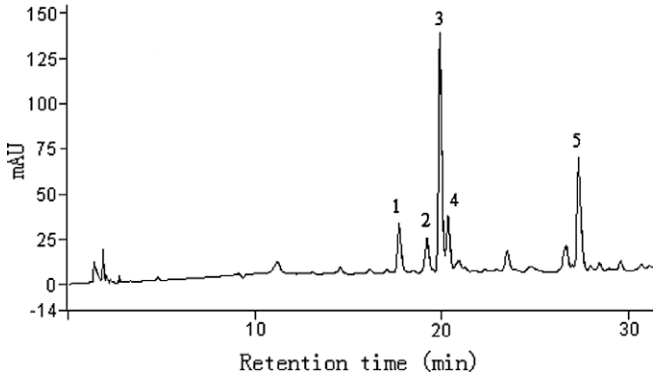

Fig. 2. RP-HPLC chromatographic profile of polyphenols of litchi pericarp, detected at 280 nm. 1: procyanidin B2; 2: cyanidin 3-rutinoside; 3: (−)-epicatechin; 4: epicatechin-(4β→8, 2β→O→7)–epicatechin-(4β→8)–epicatechin; 5: procyanidin A2.

was assessed by the changes of pericarp colour, expressed as the Hunter L^*, a^*, b^* and C^* values. The contents of each major flavanol had no significant change ($P > 0.05$) in the first 22 days with storage at 3 °C (Table 1). Simultaneously, the membrane permeability did not increase significantly ($P > 0.05$) and litchi pericarp browning did not occur (Table 2).

However, the membrane permeability began to increase and browning occurred after 22 days storage (Table 2). This result agreed with the previous description that the loss of cellular compartmentation, associated with the enhanced lipid peroxidation, reduced membrane fluidity and increased membrane permeability would occur during the storage of litchi (Jiang & Chen, 1995a, 1995b; Lin et al., 1988). Our results also showed that the contents of major flavanols and anthocyanins began to decline after the membrane permeability increased (Table 1). For example, the content of (−)-epicatechin declined to 71.12% over 29 days, and then only 21.39% of the content remained at day 36. This could easily be explained by the fact that the deterioration in membrane function allows PPO and polyphenols to mix, causing the oxidation of flavanols and the degradation of anthocyanins in the litchi pericarp.

3.3. Oxidation of endogenous polyphenols of litchi pericarp by PPO

In our previous study, we found that (−)-epicatechin was the main endogenous substrate of PPO in litchi pericarp (Liu et al., 2007b), while cyanidin 3-rutinoside was not a direct substrate for PPO (Liu et al., 2007c). However, the oxidation of the other endogenous polyphenols, especially flavanols in litchi pericarp by PPO is unknown. In an attempt to determine the optimal endogenous substrate of litchi pericarp PPO, the reaction of litchi pericarp PPO with endogenous flavanols of litchi pericarp had been investigated.

Table 2
Changes in colour and membrane permeability of litchi pericarp during storage at 3 °C.

Day	Hunter colour parameters				Membrane permeability (%)[a]
	L^*	a^*	b^*	C	
1	35.61a	15.61a	22.72a	27.57a	17.54 ± 2.87c
8	35.7a	15.51a	21.97a	26.89a	17.24 ± 4.38c
15	34.64a	15.64a	21.84a	26.86a	18.74 ± 2.79c
22	34.22a	13.54a	21.98a	25.82a	18.42 ± 3.96c
29	34.97a	12.60ab	22.44a	25.74a	26.14 ± 6.52b
36	29.09b	11.00b	16.38b	19.73b	52.22 ± 14.85a

In each column, values with the same letter are not significantly different; $P < 0.05$, Tukey comparison.
[a] Mean ± SD.

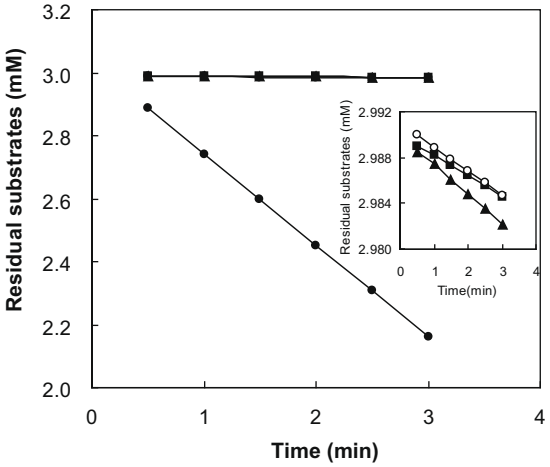

Fig. 3. Oxidation rate of (−)-epicatechin (●), procyanidin A2 (▲), procyanidin B2 (○) and epicatechin-(4β→8, 2β→O→7)–epicatechin-(4β→8)–epicatechin (■) by PPO of litchi pericarp. Inset: amplified plot for the oxidation rate of procyanidin A2 (▲), procyanidin B2 (○) and epicatechin-(4β→8, 2β→O→7)–epicatechin-(4β→8)–epicatechin (■) by PPO of litchi pericarp.

From Fig. 3, we found that the oxidation rate of (−)-epicatechin by litchi pericarp PPO was much faster than the other flavanols of litchi pericarp. The low oxidation rates of procyanidin A2, procyanidin B2 and epicatechin-(4β→8, 2β→O→7)–epicatechin-(4β→8)–epicatechin indicated that procyanidins in litchi pericarp were poor substrates for PPO (Fig. 3). This result was in agreement with the previous studies on apple and grape (Cheynier, Owe, & Rigaud, 1988; Cheynier & Silva, 1991; Le Bourvellec, Le Quere, Sanoner, Drilleau, & Guyot, 2004).

However, those three procyanidins of litchi pericarp disappeared much faster than expected in the litchi pericarp during the storage (Table 1). This was probably due to the fact that those

Table 1
Changes in the major polyphenols in litchi pericarp during storage at 3 °C.

Polyphenols (mg/g of pericarp)[b]	Day of storage					
	1	8	15	22	29	36
Procyanidin B2	1.08 ± 0.05a	1.04 ± 0.03a	1.03 ± 0.04a	1.01 ± 0.03a	0.53 ± 0.02b	0.15 ± 0.01c
(−)-Epicatechin	3.74 ± 0.10a	3.68 ± 0.08a	3.58 ± 0.06a	3.54 ± 0.07a	2.66 ± 0.03b	0.80 ± 0.02c
Procyanidin A2	1.87 ± 0.08a	1.84 ± 0.06a	1.77 ± 0.04a	1.74 ± 0.05a	1.38 ± 0.03b	0.32 ± 0.02c
Trimer[a]	0.82 ± 0.06a	0.80 ± 0.03a	0.80 ± 0.05a	0.73 ± 0.04a	0.58 ± 0.04b	0.28 ± 0.02c
Cyanidin 3-rutinoside	0.34 ± 0.02a	0.33 ± 0.02a	0.33 ± 0.03a	0.30 ± 0.02a	0.24 ± 0.02b	0.11 ± 0.01c

In each row, values with the same letter are not significantly different; $P < 0.05$, Tukey comparison.
[a] Trimer was epicatechin-(4β→8, 2β→O→7)–epicatechin-(4β→8)–epicatechin.
[b] Mean ± SD.

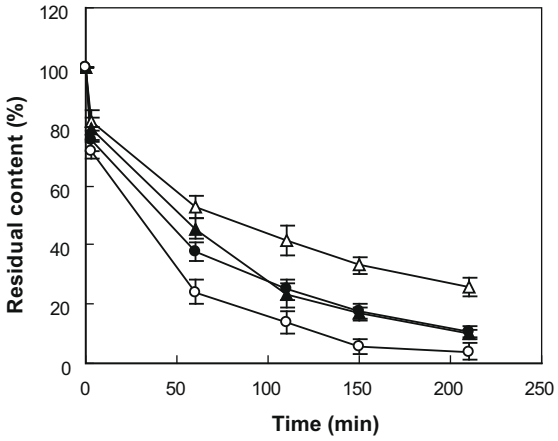

Fig. 4. Changes of (−)-epicatechin (●), procyanidin A2 (▲), procyanidin B2 (○) and epicatechin-(4β→8, 2β→O→7)–epicatechin-(4β→8)–epicatechin (Δ) during the reaction between PPO and flavanols extract of litchi pericarp. The reaction medium (3 ml) contained 1 ml of 0.5 mg/ml litchi pericarp flavanols, 1.98 ml of 50 mM of phosphate buffer (pH 7.5), and 0.02 ml of the enzyme solution. Vertical bars indicate SD.

procyanidins were oxidised by the enzymatically generated *o*-quinone of (−)-epicatechin. Interestingly, procyanidin B2 disappeared even faster than (−)-epicatechin in litchi pericarp during the storage (Table 1). This was probably attributed to the high antioxidant activity of procyanidin B2, which could more easily react with the *o*-quinone of (−)-epicatechin, resulting in the reduction of the *o*-quinone of (−)-epicatechin back to (−)-epicatechin and the oxidation of itself.

In order to confirm the above conclusion that the *o*-quinone of (−)-epicatechin could accelerate the oxidation of flavanols, this oxidation had been investigated in the model system which contained both flavanols and PPO of litchi pericarp. The rate of this reaction was very fast and the solution turned dark yellow-brown rapidly. The HPLC analysis showed that the degradation rates of procyanidin B2, procyanidin A2 and epicatechin-(4β→8, 2β→O→7)–epicatechin-(4β→8)–epicatechin were similar to the degradation rate of (−)-epicatechin in this model system (Fig. 4), confirming the above conclusion. A similar result had been obtained by Cheynier et al. (1988) who suggested that caftaric acid could induce coupled oxidation of other polyphenols in grape must-like model solutions containing grape PPO.

The degradation of flavanols could be observed both in the litchi pericarp during the browning of litchi pericarp and in the model system containing PPO and flavanols of litchi pericarp. This indicated that oxidation of flavanols by PPO played an important role in litchi pericarp browning. The results presented in this paper further indicated that the oxidation of flavanols in litchi pericarp was mainly caused by the couple oxidation of (−)-epicatechin *o*-quinone. Moreover, it has been described previously that (−)-epicatechin *o*-quinone could induce the degradation of anthocyanins in litchi pericarp through the couple oxidation pathway (Liu et al., 2007c). Thus, we proposed that the oxidation of (−)-epicatechin was a precursor of litchi pericarp browning.

In accordance with these results, the pathway of enzymatic browning of litchi pericarp was probably as follows: with the loss of cellular compartmentation, the litchi pericarp PPO and flavanols mixed. Then, (−)-epicatechin was oxidised by PPO and *o*-quinones formed. The *o*-quinones reacted with other flavanols and anthocyanins, accelerating the oxidation of the other polyphenols. Finally, the oxidation of (−)-epicatechin and other polyphenols led to the formation of the brown-coloured compounds, resulting in the enzymatic browning of litchi pericarp.

Acknowledgement

The financial support provided by the Key Program of United Funds of National Natural Science Foundation of China – Natural Science Foundation of People's Government of Guangdong (u0731005) and the Key Program of Natural Science Foundation of Guangdong (07117971) is greatly appreciated.

References

Akamine, E. K. (1960). *Preventing the darkening of fresh lychees prepared for transport*. Technical Programme Report. Hawaii Agricultural Experimental Station, University of Hawaii, 127, 3–17.

Cabanes, J., García-Cánovas, F., & García-Cármona, F. (1987). Chemical and enzymatic oxidation of 4-methylcatechol in the presence and absence of L-serine. Spectrophotometric determination of intermediates. *Biochimica and Biophysica Acta, 914*, 190–197.

Cheynier, V., Owe, C., & Rigaud, J. (1988). Oxidation of grape juice phenolic compounds in model solutions. *Journal of Food Science, 55*, 1729–1732.

Cheynier, V., & Silva, J. M. R. (1991). Oxidation of grape procyanidins in model solutions containing trans-caffeoyltartatic acid and polyphenol oxidase. *Journal of Agriculture and Food Chemistry, 39*, 1047–1049.

Fulcrand, H., Cheminat, A., Brouillard, R., & Cheynier, V. (1994). Characterization of compounds obtained by chemical oxidation of caffeic acid in acidic conditions. *Phytochemistry, 35*, 499–505.

García-Carmona, F., Cabanes, J., & García-Cármona, F. (1987). Enzymatic oxidation by frog epidermis tyrosinase of 4-methylcatechol and *p*-cresol. Influence of L-serine. *Biochimica and Biophysica Acta, 914*, 198–204.

Huang, S., Hart, H., Lee, H. S., & Wicker, L. (1990). Enzymic and colour changes during postharvest storage of lychee fruit. *Journal of Food Science, 55*, 1762–1763.

Hurrel, R. F., & Finot, P. A. (1984). Nutritional consequences of the reactions between proteins and oxidized polyphenolic acids. *Advances in Experimental Medicine and Biology, 177*, 423–435.

Jiang, Y. M., & Chen, F. (1995a). A study on polyamine change and browning of fruit during cold storage of litchi fruit. *Postharvest Biology and Technology, 5*, 245–250.

Jiang, Y. M., & Chen, F. (1995b). Effect of spermidine on regulation of senescence of litchi fruit and its relation to ethylene. *Chinese Journal of Botany, 2*, 22–25.

Jiang, Y. M., Zauberman, G., & Fuchs, Y. (1997). Partial purification and some properties of polyphenol oxidase extracted from litchi fruit pericarp. *Postharvest Biology and Technology, 10*, 221–228.

Le Bourvellec, C., Le Quere, J. M., Sanoner, P., Drilleau, J. F., & Guyot, S. (2004). Inhibition of apple polyphenol oxidase activity by procyanidins and polyphenol oxidation products. *Journal of Agriculture and Food Chemistry, 52*, 122–130.

Le Roux, E., DoCo, T., Sarni-manchado, P., Lozano, Y., & Cheynier, V. (1998). A-type proanthocyanidins from pericarp of *Litchi chinensis*. *Phytochemistry, 48*, 1251–1258.

Lin, Z. F., Li, S. S., Zhang, D. L., Liu, S. X., Li, Y. B., Lin, G. Z., et al. (1988). The changes of oxidation and peroxidation in postharvest litchi fruit. *Acta Botanica Sinica, 30*, 383–387.

Liu, L., Cao, S., Xie, B., Sun, Z., Li, X., & Miao, W. (2007b). Characterization of polyphenol oxidase from litchi pericarp using (−)-epicatechin as substrate. *Journal of Agriculture and Food Chemistry, 55*, 7140–7143.

Liu, L., Cao, S., Xie, B., Sun, Z., & Wu, J. (2007c). Degradation of cyanidin-3-rutinoside in the presence of (−)-epicatechin and litchi pericarp polyphenol oxidase. *Journal of Agriculture and Food Chemistry, 55*, 9074–9078.

Liu, L., Xie, B., Cao, S., Yang, E., Xu, X., & Guo, S. (2007a). A-type procyanidins from *Litchi chinensis* pericarp with antioxidant activity. *Food Chemistry, 105*, 1446–1451.

Matheis, G., & Whitaker, J. R. (1984). Modification of proteins by polyphenol oxidase and peroxidase and their products. *Journal of Food Biochemistry, 8*, 137–162.

Sarni-manchado, P., Le Roux, E., Le Guerneve, C., Lozano, Y., & Cheynier, V. (2000). Phenolic composition of litchi fruit pericarp. *Journal of Agriculture and Food Chemistry, 48*, 5995–6002.

Tan, X. J., & Li, Y. B. (1984). Partial purification and properties of polyphenol oxidase in litchi fruit peel. *Acta Phytophysiologica Sinica, 10*, 339–346.

Food Chemistry 118 (2010) 512–518

Contents lists available at ScienceDirect

Food Chemistry

journal homepage: www.elsevier.com/locate/foodchem

Effect of fermentation temperature on the microbial and physicochemical properties of silver carp sausages inoculated with *Pediococcus pentosaceus*

Yanshun Xu [a], Wenshui Xia [a,*], Fang Yang [a], Jin Moon Kim [a,*], Xiaohua Nie [b]

[a] State Key Laboratory of Food Science and Technology, School of Food Science and Technology, Jiangnan University, Wuxi, Jiangsu 214122, China
[b] College of Biological and Environmental Engineering, Zhejiang University of Technology, Hangzhou, Zhejiang 310014, China

ARTICLE INFO

Article history:
Received 27 January 2009
Received in revised form 25 March 2009
Accepted 7 May 2009

Keywords:
Fermentation temperature
Silver carp
Fermented sausages
Pediococcus pentosaceus

ABSTRACT

The effect of fermentation with *Pediococcus pentosaceus* at different temperatures ranging from 15 to 37 °C on the quality characteristics of silver carp sausages was investigated. Higher temperature stimulated the rapid growth of lactic acid bacteria, resulting in a rapid decline in pH, and consequently suppressed the growth of *Pseudomonas*, *Micrococcaceae* and *Enterobacteriaceae*. However, increasing fermentation temperature gave a progressive increase in total volatile basic nitrogen and biogenic amines in fermented silver carp sausages. Histamine was the main biogenic amine, exceeding 100 mg/kg after 48 h of fermentation at temperatures above 30 °C. Higher content of non-protein nitrogen and α-amino nitrogen correlated with the electrophoretic studies, which showed that proteolysis of high molecular weight myofibrillar and sarcoplasmic proteins was more prominent at higher fermentation temperatures. Products fermented at 23–30 °C showed greatest consumer preference and most favourable textural properties.

1. Introduction

In China, freshwater fishes account for about 45% of total aquacultural production, reaching 18 million tons in 2004. Silver carp (*Hypophthalmichthys molitrix*) is one of the main freshwater fish species, due to its fast growth rate, easy cultivation, high feed efficiency ratio as well as high nutritional value (Luo, Shen, Pan, & Bu, 2008). However, freshwater fish including silver carp often have strong earthy/musty taste and odour, due to significant concentrations of geosmin or 2-methyl-isobomeol (MIB) in fish flesh (Howgate, 2004). Furthermore, silver carp contains many intramuscular small bones. Therefore, the consumption of silver carp has been limited and the price of the fish is low.

Lactic acid fermentation is an important method of preserving perishable fish and marine products in developing countries (Adams, Cooke, & Twiddy, 1987). Lactic acid bacteria (LAB) could cause rapid acidification of the raw material, through the production of organic acids, mainly lactic acid and acetic acid, and also produce a variety of antimicrobial substances, which can consequently prevent the growth of most hazardous food microorganisms (Hu, Xia, & Ge, 2008).

Fermented minced fish, which is an excellent source of protein, is widely consumed throughout Southeast Asia. It is typically composed of freshwater fish species, salt (2–7%), a carbohydrate source and spices (Paludan-Müller, Huss, & Gram, 1999). Nevertheless, most fish fermentation is still conducted as spontaneous processes at household or small-scale levels in developing countries. Initiation of a spontaneous fermentation process takes a relatively long time, and the quality of the products varies considerably, limiting their acceptability and commercial importance (Twiddy, Cross, & Cooke, 1987).

The use of starter cultures in food fermentation has been studied widely and introduced into commercial practice to increase processing rates and product consistency in recent years. Using starter cultures to develop novel fish products, which would be free of fishy odour and taste, is attracting increasing interest (Hu et al., 2008). A minced fish-salt-glucose system with *Lactobacillus plantarum* and *Pediococcus pentosaceus* was investigated for its ability to promote rapid fermentation at 30 °C (Twiddy et al., 1987). *P. pentosaceus*, *L. plantarum* and *Leuconostoc mesenteroides* were inoculated into the minced frozen fillet of yellowfin tuna and fermented at 8 °C to develop novel fish food products with desired meat properties (Glatman, Drabkin, & Gelman, 2000). *L. plantarum*, *Pediococcus acidilactici*, and *P. pentosaceus* BT520 have been used for the production of Som-fug, a Thai fermented fish at 30 °C (Riebroy, Benjakula, & Visessanguan, 2008). Yin, Pan, and Jiang (2002) used several LAB, including *L. plantarum* CCRC10069, *Lactococcus lactis* subsp. *lactis* CCRC 12315 and *Lactobacillus helveticus* CCRC 14092, as starter cultures to ferment mackerel mince at 37 °C, which could substantially inhibit the development of volatile basic nitrogen, suppress the growth of spoilage microflora and improve the organoleptic qualities and digestibility of the product. Mixed starter cultures were

* Corresponding authors. Tel.: +86 510 85919121; fax: +86 510 85329057.
E-mail addresses: xiaws@jiangnan.edu.cn (W. Xia), jin.moon.kim@hotmail.com (J.M. Kim).

0308-8146/$ - see front matter © 2009 Published by Elsevier Ltd.
doi:10.1016/j.foodchem.2009.05.008

also reported to substantially suppress the accumulation of biogenic amines, and improve the flavour and nutritional value of fish muscle at 30 °C (Hu, Xia, & Liu, 2007b; Hu et al., 2008). A fermented cold-smoked fish with lactic acid bacteria was prepared at 20–22 °C (Petäjä, Eerola, & Petäjä, 2000).

Although these widely varying temperatures are used on different types and batches of fermented fish, there are only a few publications concerning the effect of fermentation temperature on the characteristics of fermented fish products (Adams et al., 1987). Temperature is one of the key environmental parameters that affect the microbial growth and the rate of fermentation. Better understanding of the temperature effects on the fermentation process will facilitate improvement of product quality and safety.

The objectives of this study were to develop a value-added product, a sausage using silver carp meat, and to investigate the effect of temperature on the characteristics of the sausages inoculated with *P. pentosaceus*, in terms of microbial and physicochemical changes during fermentation.

2. Materials and methods

2.1. Preparation of starter culture

P. pentosaceus was obtained from the Technology Center of the Shuanghui Group (Luohe, Henan, China). *P. pentosaceus* was subcultured twice in de Man Rogosa Sharpe (MRS) broth at 30 °C for 24 h. Cells were harvested by centrifugation at 10,000*g* for 15 min at 4 °C, and washed twice with saline water (0.85% NaCl); then the cell pellets were resuspended in the same saline water. After adjusting the level of cells to 7–8 log CFU/ml by using a UV-2100 spectrophotometer (Unico, Shanghai, China), the resulting cell suspension was stored at 4 °C for the inoculation of fish mince on the same day.

2.2. Preparation of silver carp sausages

Frozen silver carp (2–3 kg/fish), purchased from a local market (Wuxi, Jiangsu, China), was thawed in running tap water and then beheaded, gutted, and scaled. Prepared fish was then manually filleted. The fillets were passed through a deboner (Model 694, Baader North America, New Bedford, MA) with a drum having 5 mm-diameter perforations, to remove many intramuscular small bones and to obtain the mince. The fish mince was then mixed uniformly with 2% NaCl, 1% glucose, 4% sucrose, 0.05% sodium ascorbate, and 0.5% seasoning mix. Finally, an appropriate amount of *P. pentosaceus* suspension was inoculated to a final level of 6–7 log CFU/g fish mince, and well mixed using a sterile glass rod. The resulting mince was then stuffed into collagen casings (38 mm diameter) and incubated at 15, 23, 30 and 37 °C, RH 90–93% for 2 days. Sausage samples were taken every 12 h for analysis.

2.3. Microbiological analysis

Ten grams of sausage sample were aseptically transferred into a sterile plastic bag and stomached for 2 min in a stomacher (Lab-Blender 400; Seward Medical, London, UK) with 90 ml sterile peptone saline diluent (containing 0.1% peptone and 0.85% NaCl). Appropriate decimal dilutions of the samples were prepared with the same diluent and 0.1 ml aliquots of appropriate dilution were spread on the different agar plates and incubated as follows: total aerobic bacteria on plate count agar (PCA, Oxoid, CM325), incubated at 37 °C for 48 h; lactic acid bacteria on de Man Rogosa Sharpe agar (MRS, Oxoid, CM0361), incubated anaerobically at 30 °C for 48 h; *Enterobacteriaceae* on violet red bile dextrose agar (VRBD, Oxoid, CM485) with double layer, incubated at 37 °C for 24 h; *Micrococcaceae* on mannitol salt agar (MSA, BD Difco), incubated at 30 °C for 48 h; *Pseudomonas* on *Pseudomonas aeromonas* selective agar base (GSP Agar, Merck, Nr 10230), incubated at 26 °C for 72 h. Bacteria counts were expressed as log CFU/g sample.

2.4. Determination of pH and water content

Each of five-gram sausage samples was homogenised (Ultra Turrax homogeniser, IKA Labortechnik, Selangor, Malaysia) with 45 ml of boiled distilled water at 11,000 rpm for 1 min, and the pH was measured (Mettler Toledo 320-s, Shanghai, China). Water content was determined by drying 3–5 g of sausage sample at 100–102 °C to a constant weight (AOAC, 1998).

2.5. Determination of non-protein nitrogen (NPN), α-amino nitrogen (AAN) and total volatile basic nitrogen (TVB-N)

NPN was extracted from 5–10 g of sausage sample with 5% (w/v) trichloroacetic acid (TCA) for Kjeldahl procedure. The α-amino nitrogen (AAN) was analysed according to the Sorensen method by titration with formaldehyde (AOAC, 1998). TVB-N content was determined by the Conway micro-diffusion technique (Cobb, Alaniz, & Thompson, 1973).

2.6. Sodium dodecyl sulphate–polyacrylamide gel electrophoresis (SDS–PAGE)

Sarcoplasmic proteins and myofibrillar proteins were extracted according to the method of Joo, Kauffman, Kim, and Park (1999) with slight modification. Using a homogeniser (Ultra Turrax), 2 g of sausage sample were homogenised (12,000 rpm, 1 min) with 20 ml of chilled 0.025 M potassium phosphate buffer (pH 7.2) and centrifuged at 5000*g* for 20 min. The supernatant was used as sarcoplasmic proteins. The resulting precipitate was homogenised (Ultra Turrax homogeniser) with 20 ml of chilled 1.1 M potassium iodide in 0.1 M phosphate buffer (pH 7.2) at 12,000 rpm for 1 min. The supernatant was collected by centrifugation at 5000*g* for 20 min and used as myofibrillar proteins.

SDS–PAGE was carried out in a vertical gel electrophoresis unit (Mini-Protean-3 Cell, Bio-Rad, Richmond, CA) according to the method of Laemmli (1970), using 10% separating gel and 4% stacking gel. Aliquots of 10 μl were injected in each well including standard protein marker. Electrophoresis was done at 90–120 V. After electrophoresis was completed, gels were stained with 0.125% Coomassie Brilliant Blue R-250 in 25% methanol and 10% acetic acid. Destaining was performed using 40% methanol and 10% acetic acid.

2.7. Determination of biogenic amines

Finely ground sausage sample (5 g) was transferred to 50-ml centrifuge tubes and homogenised (Ultra Turrax homogeniser) with 20 ml of 5% TCA solution for about 2 min. The supernatant was collected by centrifugation (10,000*g*, 4 °C, 10 min) and the residue was extracted again with an equal volume of TCA solution. Both supernatants were combined and filtered through a filter paper (Whatman No. 4). The filtrate was made up to 50 ml with 5% TCA solution and stored at 0–4 °C for high-performance liquid chromatography (Agilent 1100 Series; Agilent, Santa Clara, CA) analysis within a week.

The derivatisation reagent was prepared by transferring 100 mg *o*-phthalaldehyde (OPA), 1 ml acetonitrile and 130 μl 2-mercaptoethanol to a 10-ml volumetric flask, and then diluting with 0.4 M borate buffer (pH 10.2) to 10 ml. The resulting solution was mixed well, and stored refrigerated and used within 24 h. Pre-column derivatisation with OPA was performed automatically.

A reverse-phase Hypersil ODS C_{18} (125 × 4.60 mm, particle size 5 μm) column was used for separation. The column temperature

and flow rate were set at 40 °C and 1.0 ml/min, respectively. The mobile phase consisted of solvent A (pH 7.2), 7.35 mM sodium acetate solution:triethylamine:tetrahydrofuran (500:0.12:2.5 v/v), and solvent B (pH 7.2), 7.35 mM sodium acetate solution:methanol:acetonitrile (1:2:2 v/v). Fluorescence was monitored at an emission wavelength of 450 nm using an excitation wavelength of 340 nm.

Biogenic amine standards, tyramine, tryptamine, putrescine dihydrochloride, cadaverine dihydrochloride were purchased from Sigma (St. Louis, MO) and histamine dihydrochloride from Fluka Biochemica (Buchs, Switzerland). Double-distilled and deionised water was used for dilution and chromatographic separation.

2.8. Texture profile analysis (TPA)

Texture profile analysis was carried out as described by Bourne (1978), using a Universal TA-XT2i texture analyser (Stable Micro Systems, Godalming, UK) equipped with a cylindrical P/25 probe. Three slices of sausage sample (1.5 cm thick and 2.0 cm diameter) were allowed to equilibrate to room temperature and then compressed twice to 50% of their original height. A time of 5 s was allowed to elapse between the two compression cycles. Force–time deformation curves were obtained with a 25 kg load cell applied at a cross-head speed of 1 mm/s. Hardness, springiness, cohesiveness, adhesiveness and chewiness were calculated using Texture Expert software version 1.22 (Stable Micro Systems).

2.9. Sensory evaluation

The sensory qualities of taste, flavour, texture, and overall acceptability of fermented silver carp sausages were evaluated by 15 untrained panellists, who were graduate students and teachers in the School of Food Science and Technology. The nine-point hedonic scale was used for evaluation, with 9 being extreme liking, 5 being neither like or dislike and 1 being extreme dislike.

2.10. Statistical analysis

For data analysis, analysis of variance (ANOVA) was used. Significant differences were defined at $p < 0.05$. Comparisons of group means were obtained using Duncan's multiple range test. All statistical analysis was performed using SPSS 11.0 for windows software (SPSS Inc., Chicago, IL).

3. Results and discussion

3.1. pH and water content

As shown in Fig. 1, with the progress of fermentation, the decrease in pH was directly proportional to the increase in fermentation temperature from 15 to 37 °C. The pH of fish mince decreased rapidly during fermentation, from initial values of around 6.7–4.5 within 48 h at the higher temperature, whilst fermentation at 15 °C caused the pH to remain above 6.0 after 48 h. The rapid decrease in pH was also related to the higher growth rate of LAB noted in Fig. 2. According to Adams et al. (1987), rapid growth of LAB causing pH to decrease to below 4.5 within 2 days is essential to prevent spoilage and to ensure safety of the product.

Water content decreased continuously during fermentation (Fig. 1). The rate of decrease increased as the fermentation temperature increased. The results indicated that higher fermentation temperature caused faster dehydration. This was probably related to rapid decline of pH to a value close to the isoelectric point of fish proteins, caused by the rapid growth of LAB at higher temperatures, resulting in lower water-holding capacity of the fish muscle proteins in the sausages (Huff-Lonergan & Lonergan, 2005).

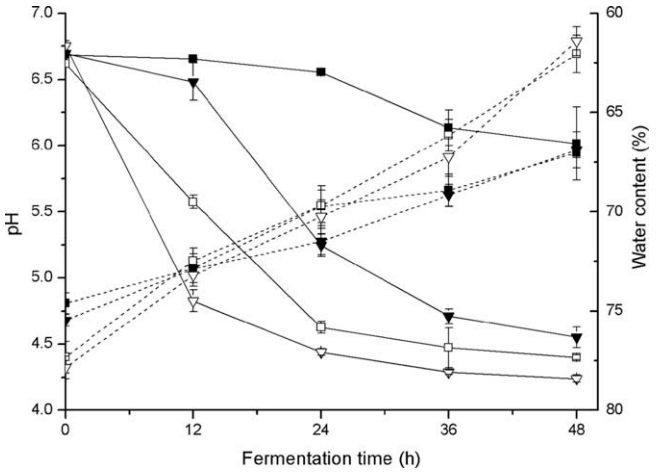

Fig. 1. Changes in pH and water content in silver carp sausages during fermentation at different temperatures (■) 15 °C; (▼) 23 °C; (□) 30 °C; (▽) 37 °C.

3.2. Microbiological analysis

Microbial changes during fermentation at different temperatures are shown in Fig. 2. The initial counts of LAB in inoculated fish mince ranged from 6.5 to 7.0 log CFU/g. During fermentation, LAB showed a faster growth at higher temperatures, reaching up to 8 log CFU/g within 24 h. In contrast, the growth of LAB at 15 °C was clearly slowed and it took longer for the population to reach 8 log CFU/g. It took 36 h at 15 °C, 24 h at 23 °C, and 12 h at both 30 °C and 37 °C to reach 8 log CFU/g for the total bacteria. LAB count showed a similar trend. This indicates that LAB was considered the dominant species during fermentation at the given temperatures.

Micrococcaceae numbers showed an increase at first to 5–6 log CFU/g and a subsequent decrease during fermentation at temperatures above 23 °C, whilst for fermentation at 15 °C, the counts increased continually up to 6.3 log CFU/g after 48 h of fermentation. Hugas and Monfort (1997) have reported that acidification and anaerobic conditions inhibited the growth of *Micrococcaceae* during ripening of fermented sausages. The growth of *Enterobacteriaceae* and *Pseudomonas* exhibited a similar pattern with *Micrococcaceae*. The results indicated that temperature had a pronounced influence on the growth of these microorganisms during lactic fermentation. At higher temperature, LAB grew more rapidly. This quickly lowered the pH, thereby inhibited the growth of undesirable microorganisms. Several authors have also reported that growth of the majority of spoilage bacteria and pathogens present in minced fish was inhibited more effectively by rapid attainment of low pH (Adams et al., 1987; Hu, Xia, & Ge, 2007a; Yin et al., 2002). The inhibition of spoilage and pathogenic bacteria was probably due to the accumulation of lactic acid produced by the starter culture, which could cause acidification of the cytoplasm (Lambert & Stratford, 1999). Although the rate of pH reduction was slower at lower temperature, little variation was encountered in the LAB counts after 48 h of fermentation at different temperatures, and this is in accordance with the findings by Adams et al. (1987). Temperature is a major factor in food deteriorative reactions, especially for microbial spoilage, since specific growth rate and lag phase are highly temperature-dependent (Cayre, Vignolo, & Garro, 2003).

3.3. TVB-N

The levels of TVB-N increased progressively with the increase in temperature and time during fermentation (Table 1). Increasing temperature clearly enhanced the development of TVB-N. After

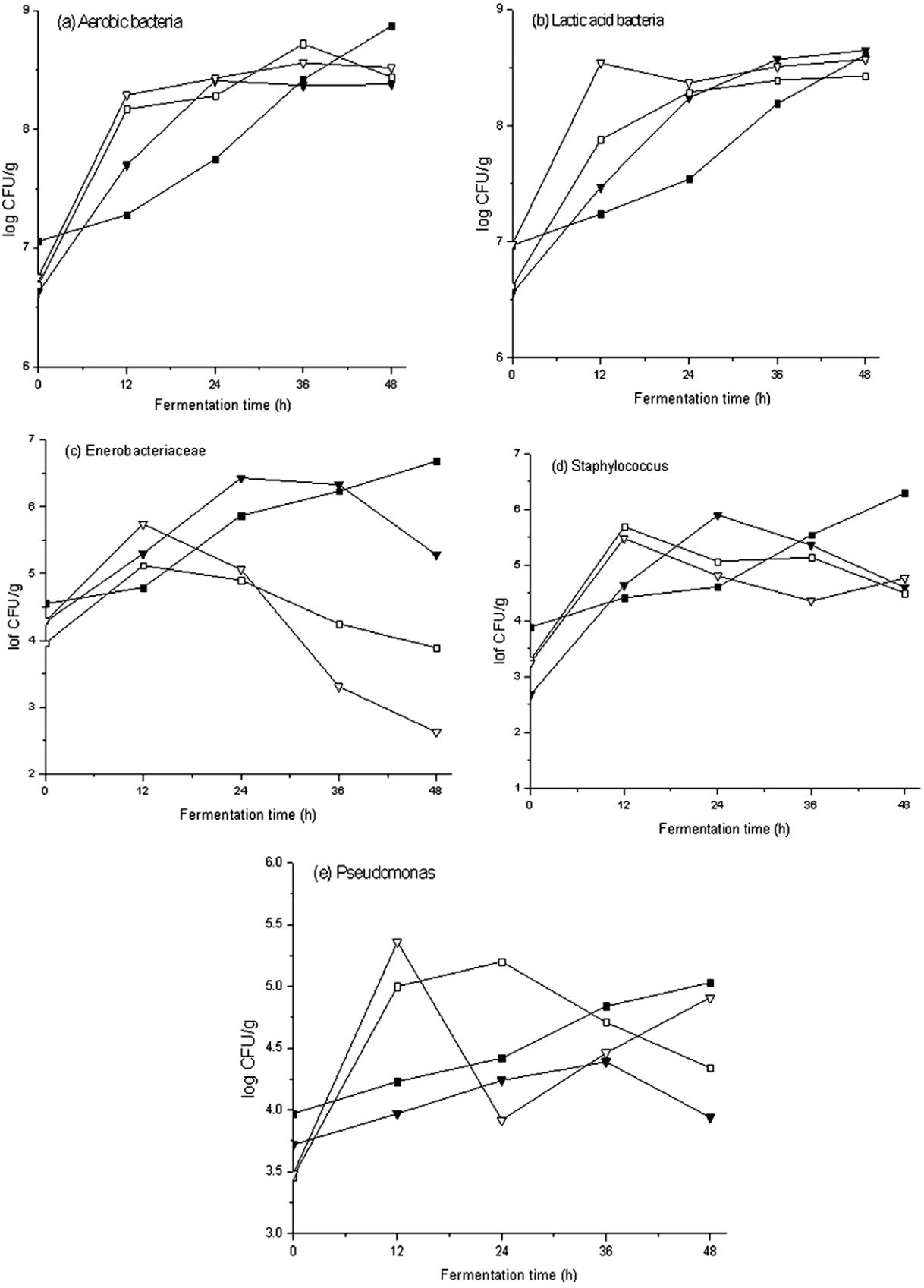

Fig. 2. Microbiological changes in silver carp sausages during fermentation at different temperatures (■) 15 °C; (▼) 23 °C; (□) 30 °C; (▽) 37 °C.

48 h of fermentation, the TVB-N content was less than 30 mg/100 g fish meat at all tested temperatures except for 37 °C. TVB-N content of 30 mg/100 g is generally regarded as the acceptable limit for fish (Riebroy, Benjakul, Visessanguan, & Tanaka, 2007). The results

Table 1
Changes in TVB-N in silver carp sausages during fermentation at different temperatures (mg/100 g)[1].

Fermentation temperatures (°C)	Fermentation time (h)				
	0	12	24	36	48
15	8.35 ± 0.86^{aA}	9.21 ± 0.91^{aA}	11.8 ± 0.72^{aB}	12.6 ± 0.95^{aB}	14.3 ± 1.11^{aC}
23	8.93 ± 0.79^{aA}	9.83 ± 0.61^{aA}	12.9 ± 1.18^{aB}	14.6 ± 0.89^{bC}	16.7 ± 1.24^{aD}
30	7.97 ± 0.58^{aA}	11.7 ± 0.63^{bB}	15.1 ± 0.83^{bC}	18.7 ± 0.94^{cD}	20.9 ± 1.31^{bE}
37	8.80 ± 0.78^{aA}	15.9 ± 0.88^{cB}	19.8 ± 1.24^{cC}	26.3 ± 1.15^{dD}	31.2 ± 2.33^{cE}

[a–d]Means with different superscript letters in the same column indicate significant differences ($p < 0.05$).
[A–E]Means with different superscript letters in the same row indicate significant differences ($p < 0.05$).
[1] Data are expressed as means ± standard deviation ($n = 3$).

indicated that although the growth of undesirable bacteria (Fig. 2) could be effectively suppressed by LAB at higher temperature, the metabolic activity for the production of TVB-N still continued. Several authors have reported that fermentation with LAB in fish could substantially inhibit the accumulation of TVB-N (Glatman et al., 2000; Hu et al., 2008; Yin et al., 2002).

3.4. Proteolysis

Proteolysis-related parameters (AAN and NPN) showed a different behaviour during fermentation of fish sausages (Table 2). Values of NPN did not change significantly ($p < 0.05$) at lower temperature (15, 23 and 30 °C) after 12 h of fermentation, whilst AAN contents showed a continuous increase across the same temperature range and fermentation period. However, higher contents of AAN and NPN were obtained at 37 °C. This suggested that a relatively intense proteolysis occurred at higher temperature. This was probably attributed to the enhanced activity of both endogenous and microbial proteolytic enzymes at the higher temperature, especially at low pH, which could stimulate acidic proteinase activity. Similar results in dry sausage have been reported by Bover-Cid, Izquierdo-Pulido, and Vidal-Carou (2001). Several investigators have reported that acidic pH could improve activity of proteolytic enzymes, especially cathepsins (Molly et al., 1997; Riebroy et al., 2008).

SDS–PAGE electrophoretograms of the sarcoplasmic and myofibrillar proteins in fish sausages after 48 h of fermentation are shown in Fig. 3. Sarcoplasmic and myofibrillar proteins with molecular weights of 40–200 kDa and lower than 30 kDa disappeared or decreased in intensity to different degrees after 48 h of fermentation, depending on the temperature applied. Furthermore, the intensity of a polypeptide with a molecular weight of ~35 kDa progressively increased with increasing temperature. This is partially due to the intense degradation of sarcoplasmic and myofibrillar proteins at higher temperature (23, 30 and 37 °C). In contrast, there was no marked degradation of proteins after 48 h of fermentation at 15 °C. Martin, Cordoba, Antequera, Timon, and Ventanas (1998) also found that intense proteolysis took place in Iberian ham when higher temperature was applied. Both endogenous and microbial proteases contributing to the degradation of muscle proteins have been reported by other studies (Fadda et al., 1999). The initial hydrolysis of muscle proteins is attributed mainly to endogenous cathepsins, followed by the action of microbial peptidases, which further degrade the protein fragments to small peptides and free amino acids, and consequently have an important influence on meat flavour development (Fadda et al., 1999; Molly et al., 1997).

It should be noted that the bands with high molecular weight disappeared completely after 48 h of fermentation at temperatures above 23 °C, whilst no proportional increase in intensity of the bands with lower molecular weight was observed. It is possible that proteins denatured and formed large aggregates with higher molecular weights, through covalent bonds and non-disulphide covalent bonds as pH decreased during fermentation, which prevented proteins being extracted under the experimental conditions.

3.5. Biogenic amines

As shown in Table 3, the higher fermentation temperature resulted in higher amounts of biogenic amines, coinciding with higher free amino acid contents (AAN, Table 2). Histamine was quantitatively the most important biogenic amine formed during fermentation in fish sausages, reaching up to 100 mg/kg after 48 h of fermentation at 30–37 °C, which exceeded the limit of 50 mg/kg established by the FDA for Scombridae (FDA, 1996). It is remarkable that histamine content in sausage samples fermented at 23 °C was even lower than that before fermentation. This can be explained that histamine might have been consumed by the fermenting microflora as a nitrogen source (Bover-Cid et al., 2001). Histamine is potentially hazardous and the causative agent of amine intoxication associated with the consumption of seafood (Flick, Oria, & Douglas, 2001).

A minor production of less than 8 mg/kg of tyramine was observed at tested temperatures, which was much less than that in dry sausages (Bover-Cid et al., 2001). The allowable level of tyramine in foods is 100–800 mg/kg whilst 1080 mg/kg is toxic (Shalaby, 1996).

Table 2
Changes in AAN[2] and NPN[3] in silver carp sausages during fermentation at different temperatures[1].

Fermentation time (h)	AAN (mg/100 g dry matter)				NPN (mg/g dry matter)			
	15 °C	23 °C	30 °C	37 °C	15 °C	23 °C	30 °C	37 °C
0	237 ± 7.98^{aA}	236 ± 14.3^{aA}	249 ± 12.7^{aA}	249 ± 12.1^{aA}	9.54 ± 0.20^{bA}	9.66 ± 0.27^{cAB}	10.2 ± 0.11^{bB}	10.2 ± 0.29^{abB}
12	242 ± 9.15^{aA}	234 ± 12.2^{aA}	247 ± 9.42^{aA}	296 ± 12.6^{abB}	8.30 ± 0.10^{aA}	8.73 ± 0.11^{aB}	8.77 ± 0.16^{aB}	9.49 ± 0.18^{aC}
24	241 ± 11.47^{aA}	238 ± 9.90^{aA}	260 ± 8.62^{aA}	295 ± 11.8^{abB}	8.44 ± 0.03^{aA}	9.14 ± 0.06^{bB}	10.3 ± 0.22^{bC}	10.7 ± 0.27^{bC}
36	252 ± 4.88^{aA}	247 ± 8.81^{aA}	275 ± 11.8^{aA}	363 ± 23.8^{bcB}	7.99 ± 0.33^{aA}	9.26 ± 0.07^{bB}	10.2 ± 0.08^{bC}	13.0 ± 0.54^{cD}
48	254 ± 8.36^{aA}	272 ± 5.62^{bA}	311 ± 19.5^{bB}	380 ± 17.0^{cC}	8.09 ± 0.12^{aA}	9.09 ± 0.12^{bB}	10.5 ± 0.13^{bC}	12.4 ± 0.36^{cD}

[a–c]Means with different superscript letters in the same column indicate significant differences ($p < 0.05$).
[A–D]Means with different superscript letters in the same row indicate significant differences ($p < 0.05$).
[1] Data are expressed as means ± standard deviation ($n = 3$).
[2] AAN, α-amino nitrogen.
[3] NPN, non-protein nitrogen.

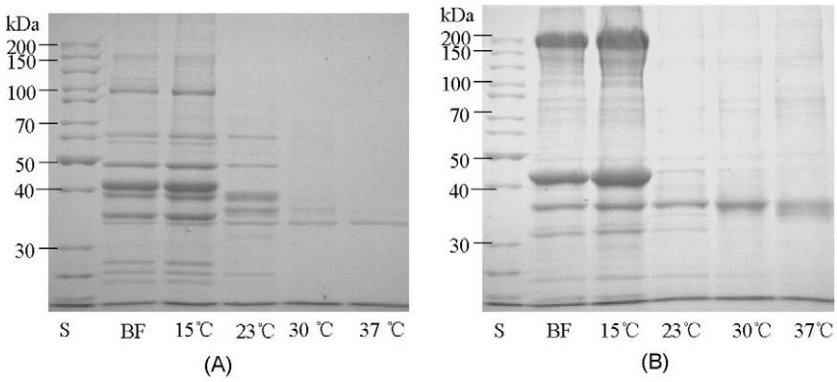

Fig. 3. SDS–PAGE profile of sarcoplasmic proteins (A) and myofibrillar proteins (B) in silver carp sausages after 48 h of fermentation at different temperatures. BF, before fermentation.

Lower levels of putrescine, cadaverine and tryptamine were also observed at tested temperatures in this study. Putrescine is produced by decarboxylation of either ornithine or agmatine, and cadaverine is produced by decarboxylation of lysine (Özogul, Ahmad, Hole, Özogul, & Deguara, 2006). Although putrescine and cadaverine have no direct adverse effect on human health, they play an important role in food poisoning, as they can potentiate the toxicity of histamine by inhibiting histamine-metabolising enzymes, such as diamine oxidase and histamine methyl transferase; they can also react with nitrites to form nitrosamines, which are carcinogenic compounds (Shakila, Vasundhara, & Kumudavally, 2001).

From the results it may be concluded that the increase in biogenic amines in fish sausages was due to the enhanced residual activity of microbial decarboxylase and the higher amounts of precursor amino acids resulting from proteolysis at elevated temperatures. Besides the use of good quality raw material, fermentation at low temperature is necessary to prevent the formation of increased amounts of biogenic amines during the manufacture of fermented fish sausages. It has been reported that biogenic amines production was attributed to both surviving microorganisms and residual activity of decarboxylase produced by microorganisms (Komprda, Neznalova, Standara, & Bover-Cid, 2001). In fermented foods, besides the active growth of microflora, the acidification and the proteolytic processes occurring during fermentation make the environment particularly favourable for biogenic amine production (Bover-Cid et al., 2001).

Table 3
Biogenic amines content in silver carp sausages after 48 h of fermentation at different temperatures.

Samples	Biogenic amines (mg/kg)				
	Histamine	Tyramine	Putrescine	Cadaverine	Tryptamine
BF[a]	21.4	2.61	0.95	0.22	0.19
15 °C	44.9	5.13	1.22	1.01	0.79
23 °C	18.6	4.09	1.10	1.91	1.37
30 °C	102	5.66	2.69	60.4	36.3
37 °C	129	6.72	4.68	31.5	19.5

[a] BF, before fermentation.

3.6. Sensory evaluation and TPA analysis

Sensory evaluation and the texture profile for fish sausages fermented at different temperatures are shown in Table 4. No significant differences in appearance, taste, flavour, and acceptability were observed amongst batches fermented at 23–37 °C. Lower acceptance in all attributes was observed in sausages fermented at 15 °C, and this was due to less sourness, too fishy a smell, and a grey colour. The better taste of the sausages fermented at higher temperature could be linked to higher concentration of free amino acids (Hu et al., 2007a). In addition, the lactic acid produced not only gives the product a unique lactic acid flavour, masking or suppressing fishy smell, but also increases the firmness and mouthfeel resulting from the acid denaturation of muscle proteins (Yin & Jiang, 2001).

As shown in Table 4, fermentation temperature had a great influence on the textural properties of silver carp sausages. At the end of fermentation, sausage samples showed a marked increase in all TPA

Table 4
Sensory evaluation[1] and texture profile analysis[2] of silver carp sausage after 48 h of fermentation at different temperatures.

Parameter	Sample				
	BF[3]	15 °C	23 °C	30 °C	37 °C
Appearance	ND[4]	1.81 ± 0.46^{a}	7.06 ± 1.37^{b}	6.43 ± 1.27^{b}	6.38 ± 148^{b}
Flavour	ND	2.89 ± 0.78^{a}	5.90 ± 1.10^{b}	6.00 ± 1.06^{b}	5.25 ± 1.28^{b}
Taste	ND	ND	5.88 ± 1.25^{a}	6.25 ± 1.58^{a}	5.50 ± 1.69^{a}
Overall acceptability	ND	1.87 ± 0.99^{a}	6.63 ± 1.12^{bc}	6.50 ± 1.30^{bc}	5.00 ± 1.51^{b}
Hardness (g)	112 ± 13.2^{a}	592 ± 127^{b}	2280 ± 89.4^{c}	2890 ± 143^{d}	3770 ± 88.3^{e}
Springiness	0.53 ± 0.03^{a}	0.80 ± 0.04^{c}	0.81 ± 0.03^{c}	0.76 ± 0.03^{c}	0.66 ± 0.04^{b}
Cohesiveness	0.57 ± 0.03^{ab}	0.64 ± 0.04^{bc}	0.69 ± 0.02^{c}	0.63 ± 0.01^{bc}	0.55 ± 0.02^{a}
Adhesiveness (g × s)	-54.5 ± 3.08^{a}	-45.3 ± 11.9^{a}	-7.19 ± 0.41^{b}	-5.18 ± 0.61^{b}	-0.58 ± 3.86^{b}
Chewiness (g)	46.3 ± 12.9^{a}	314 ± 80.2^{b}	1260 ± 39.0^{c}	1340 ± 42.7^{c}	1360 ± 16.9^{c}

[a–c] Means with different superscript letters in the same row indicate significant differences ($p < 0.05$).
[1] Data are expressed as means ± standard deviation ($n = 15$).
[2] Data are expressed as means ± standard deviation ($n = 3$).
[3] BF, before fermentation.
[4] ND, not detected.

texture attributes, compared to the samples before fermentation. Products at higher temperature (23–37 °C) seemed to possess greater hardness, whilst no significant differences in other TPA parameters, like springiness, cohesiveness, adhesiveness and chewiness, were observed across the same temperature range. The development of firmness is related to pH reduction and moisture removal (Baumgartner, 1980). Riebroy et al. (2008) also reported that texture formation of fermented fish mince was closely associated to the rapid decline in pH, which induced conformational changes of muscle proteins and caused the formation of acid-induced gelation. Higher acidity in the sausages resulted in superior organoleptic properties.

4. Conclusions

Temperature is a technologically important parameter to control fish sausage fermentation. Higher fermentation temperature would be advisable for faster and shorter fermentation. However, the production of fermented silver carp sausages at higher temperature could cause some quality defects, such as higher content of biogenic amines and TVB-N. Further research should be conducted to improve the overall quality of the product.

Acknowledgements

This research was financially supported by PCSIRT0627, 111 Project-B07029, 863 Project (No. 2006AA09Z444), 863 Project (No. 2007AA09Z442), the earmarked fund for Modern Agro-industry Technology Research System and Guangdong Production-Education-Research Cooperation Project of the Ministry of Education (No. 2007A090302059).

References

Adams, M. R., Cooke, R. D., & Twiddy, D. R. (1987). Fermentation parameters involved in the production of lactic acid preserved fish-glucose substrates. *International Journal of Food Science and Technology, 22*, 105–114.

AOAC (1998). *Official methods of analysis* (16th ed.). Gaithersburg, MD: Association of Official Analytical Chemists.

Baumgartner, P. A. (1980). The influence of temperature on some parameters for dry sausage during ripening. *Meat Science, 4*, 191–201.

Bourne, M. C. (1978). Texture profile analysis. *Food Technology, 32*(7), 62–66.

Bover-Cid, S., Izquierdo-Pulido, M., & Vidal-Carou, M. C. (2001). Effect of the interaction between a low tyramine-producing *Lactobacillus* and proteolytic staphylococci on biogenic amine production during ripening and storage of dry sausages. *International Journal of Food Microbiology, 65*(1–2), 113–123.

Cayre, M. E., Vignolo, G., & Garro, O. (2003). Modeling lactic acid bacteria growth in vacuum-packaged cooked meat emulsions stored at three temperatures. *Food Microbiology, 20*(5), 561–566.

Cobb, B. F., Alaniz, I., & Thompson, C. A. (1973). Biochemical and microbial studies on shrimp: Volatile nitrogen and amino acid analysis. *Journal of Food Science, 38*(3), 431–436.

Fadda, S., Sanz, Y., Vignolo, G., Aristoy, M., Oliver, G., & Toldra, F. (1999). Characterization of muscle sarcoplasmic and myofibrillar protein hydrolysis caused by *Lactobacillus plantarum*. *Applied and Environment Microbiology, 65*(8), 3540–3546.

FDA (1996). Decomposition and histamine in raw, frozen tuna and mahi-mahi; canned tuna; and related species. *Compliance Policy Guides 7108*. 240, sec. 540, 525.

Flick, G. J., Oria, M. P., & Douglas, L. (2001). Potential hazards in cold-smoked fish: Biogenic amines. *Journal of Food Science, 66*, s1088–s1099.

Glatman, L., Drabkin, V., & Gelman, A. (2000). Using lactic acid bacteria for developing novel fish food products. *Journal of the Science of Food and Agriculture, 80*, 375–380.

Howgate, P. (2004). Tainting of farmed fish by geosmin and 2-methyl-iso-bomeol: A review of sensory aspects and of uptake/depuration. *Aquaculture, 234*(1–4), 155–181.

Hu, Y. J., Xia, W. S., & Ge, C. R. (2007a). Effect of mixed starter cultures fermentation on the characteristics of silver carp sausages. *World Journal of Microbiology & Biotechnology, 23*(7), 1021–1031.

Hu, Y. J., Xia, W. S., & Ge, C. R. (2008). Characterization of fermented silver carp sausages inoculated with mixed starter culture. *Lwt-Food Science and Technology, 41*(4), 730–738.

Hu, Y. J., Xia, W. S., & Liu, X. Y. (2007b). Changes in biogenic amines in fermented silver carp sausages inoculated with mixed starter cultures. *Food Chemistry, 104*(1), 188–195.

Huff-Lonergan, E., & Lonergan, S. M. (2005). Mechanisms of water-holding capacity of meat: The role of postmortem biochemical and structural changes. *Meat Science, 71*(1), 194–204.

Hugas, M., & Monfort, J. M. (1997). Bacterial starter cultures for meat fermentation. *Food Chemistry, 59*(4), 547–554.

Joo, S. T., Kauffman, R. G., Kim, B. C., & Park, G. B. (1999). The relationship of sarcoplasmic and myofibrillar protein solubility to colour and water-holding capacity in porcine longissimus muscle. *Meat Science, 52*(3), 291–297.

Komprda, T., Neznalova, J., Standara, S., & Bover-Cid, S. (2001). Effect of starter culture and storage temperature on the content of biogenic amines in dry fermented sausage polican. *Meat Science, 59*(3), 267–276.

Laemmli, U. K. (1970). Cleavage of structural proteins during the assembly of the head of bacteriophage T4. *Nature, 227*(5259), 680–685.

Lambert, R. J., & Stratford, M. (1999). Weak-acid preservatives: Modelling microbial inhibition and response. *Journal of Applied Microbiology, 86*(1), 157–164.

Luo, Y. K., Shen, H. X., Pan, D. D., & Bu, G. H. (2008). Gel properties of surimi from silver carp (*Hypophthalmichthys molitrix*) as affected by heat treatment and soy protein isolate. *Food Hydrocolloids, 22*(8), 1513–1519.

Martin, L., Cordoba, J. J., Antequera, T., Timon, M. L., & Ventanas, J. (1998). Effects of salt and temperature on proteolysis during ripening of Iberian Ham. *Meat Science, 49*(2), 145–153.

Molly, K., Demeyer, D., Johansson, G., Raemaekersm, M., Ghistelinck, M., & Geenen, I. (1997). The importance of meat enzymes in ripening and flavour generation in dry fermented sausages: First results of a European project. *Food Chemistry, 59*(4), 539–545.

Özogul, Y., Ahmad, J. I., Hole, M., Özogul, F., & Deguara, S. (2006). The effects of partial replacement of fish meal by vegetable protein sources in the diet of rainbow trout (*Onchorynchus mykiss*) on postmortem spoilage of fillets. *Food Chemistry, 96*(4), 549–561.

Paludan-Müller, C., Huss, H. H., & Gram, L. (1999). Characterization of lactic acid bacteria isolated from a Thai low-salt fermented fish product and the role of garlic as substrate for fermentation. *International Journal of Food Microbiology, 46*(3), 219–229.

Petäjä, E., Eerola, S., & Petäjä, P. (2000). Biogenic amines in cold-smoked fish fermented with lactic acid bacteria. *European Food Research and Technology, 210*(4), 280–285.

Riebroy, S., Benjakul, S., Visessanguan, W., & Tanaka, M. (2007). Effect of iced storage of bigeye snapper (*Priacanthus tayenus*) on the chemical composition, properties and acceptability of Som-fug, a fermented Thai fish mince. *Food Chemistry, 102*(1), 270–280.

Riebroy, S., Benjakula, S., & Visessanguan, W. (2008). Properties and acceptability of Som-fug, a Thai fermented fish mince, inoculated with lactic acid bacteria starters. *Lwt-Food Science and Technology, 41*(4), 569–580.

Shakila, R. J., Vasundhara, T. S., & Kumudavally, K. V. (2001). A comparison of the TLC-densitometry and HPLC method for the determination of biogenic amines in fish and fishery products. *Food Chemistry, 75*(2), 255–259.

Shalaby, A. R. (1996). Significance of biogenic amines to food safety and human health. *Food Research International, 29*(7), 675–690.

Twiddy, D. R., Cross, S. J., & Cooke, R. D. (1987). Parameters involved in the production of lactic acid preserved fish-starchy substrate combinations. *International Journal of Food Science and Technology, 22*, 115–121.

Yin, L. J., & Jiang, S. T. (2001). *Pediococcus pentosaceus* L and S utilization in fermentation and storage of mackerel sausage. *Journal of Food Science, 66*(5), 742–746.

Yin, L. J., Pan, C. L., & Jiang, S. T. (2002). Effect of lactic acid bacterial fermentation on the characteristics of minced mackerel. *Journal of Food Science, 67*(2), 786–792.

Food Chemistry 118 (2010) 519–524

Contents lists available at ScienceDirect

Food Chemistry

journal homepage: www.elsevier.com/locate/foodchem

Glucosinolates, volatile constituents and biological activities of *Erysimum corinthium* Boiss. (Brassicaceae)

A.A. Al-Gendy [a,*], O.D. El-gindi [b], Al.S. Hafez [b], A.M. Ateya [a]

[a] Department of Pharmacognosy, Faculty of Pharmacy, Zagazig University, Zagazig 44519, Egypt
[b] Department of Pharmacognosy, Al-Azhar University, Egypt

ARTICLE INFO

Article history:
Received 3 November 2008
Received in revised form 18 March 2009
Accepted 7 May 2009

Keywords:
Erysimum corinthium
Brassicaceae
Glucosinolates
Isothiocyanates
Volatile constituents
Antimicrobial and cytotoxicity

ABSTRACT

Fresh leaves, roots and ripe seeds of *Erysimum corinthium* Boiss. (Brassicaceae) were investigated to uncover their glucosinolate contents through natural autolysis and exogenous myrosinase hydrolysis. The hydrolysis products were submitted to GC–MS analysis. Six glucosinolates were identified for the first time in this plant; namely, sinigrin, progoitrin, glucoiberin, 3-(methylcarbonyl)propyl glucosinolate, glucocheirolin and glucoerysolin. Glucocheirolin was the major compound accumulated in the seeds and progoitrin was the major compound in the roots, while 3-(methylcarbonyl)propyl glucosinolate was the major compound in the leaves. Other volatile constituents, e.g., terpenes and fatty acids esters were also identified. Seeds and leaves showed higher antimicrobial activity than roots. Seeds showed a marked cytotoxicity *in vitro* against colorectal, hepatic and Hela cell lines.

1. Introduction

Glucosinolates are an important group of phytochemicals present exclusively in 15 botanical families of the order Capparales and very abundant in Brassicaceae (Barbieri, Pernice, Maggio, De Pascalr, & Fogliano, 2008). The crucifer family Brassicaceae is an economically important family for its many food and oilseed crops, as well as containing many important ornamental plants and noxious weeds (Vaughn & Borhow, 2005).

Chemically, glucosinolates are glucose and sulfur-containing organic compounds whose decomposition products are produced when plant cells are ruptured, and the glucosinolates present in vacuoles are hydrolysed by the enzyme myrosinase (β-thioglucosidase glucohydrolase (EC 3.2.3.1). These hydrolysis products include substituted isothiocyanates, nitriles, thiocyanates, epithionitriles and oxazolidinethiones (Fig. 1), which vary depending on the plant species studied, side-chain substitution, cell pH and cell iron concentration (Fenwick, Heaney, & Mullin, 1983; Gil & MacLeod, 1980).

Many glucosinolate degradation products are of interest because of their biological activities. Several of these hydrolysis products have biocidal activity against a wide variety of organisms, such as insects, plants, fungi and bacteria (Vaughn, 1999), while others have cancer chemoprotective attributes (Fahey, Zalcmann, & Talalay, 2001). Moreover, the consumption of cruciferous vegetables has been associated with a reduced risk of cancer of the lung, stomach, breast, prostate, pancreas, colon and rectum, which has been attributed to its isothiocyanate contents (Heber, 2004; Higdon, Delage, Williams, & Dashwood, 2007).

Taxonomically, *Erysimum* is one of the most complex genera of the Cruciferae (Al-Shehbaz & Al-Shammary, 1987). Erysimum plants are characterised by the presence of methylthioalkyl, methylsulfinylalkyl and methylsulfonylalkyl glucosinolates (Daxenbichler et al., 1991). To our knowledge, there is no pervious report or publication on the chemistry and biological activities of *Erysimum corinthium*. Thus, this encouraged us to investigate glucosinolate contents and the possible biological activity of this plant.

2. Materials and methods

2.1. Plant materials

E. corinthium (Boiss.) Wettst. (*Cheiranthus corinthius* Boiss.) seeds were collected from Al-Sharkya district, Egypt and cultivated in the botanical garden, Faculty of Pharmacy, Zagazig University. The plant material was collected in April to May 2005. It was identified by Dr. Sean Edwards, Botanical Herbarium, Manchester University. Voucher samples are kept in the Pharmacognosy Department Herbarium, Faculty of Pharmacy, Zagazig University. Other samples are kept in Manchester University Herbarium.

* Corresponding author. Tel./fax: +20 2 383 71549.
E-mail address: Amalalgendy@hotmail.com (A.A. Al-Gendy).

0308-8146/$ - see front matter © 2009 Elsevier Ltd. All rights reserved.
doi:10.1016/j.foodchem.2009.05.009

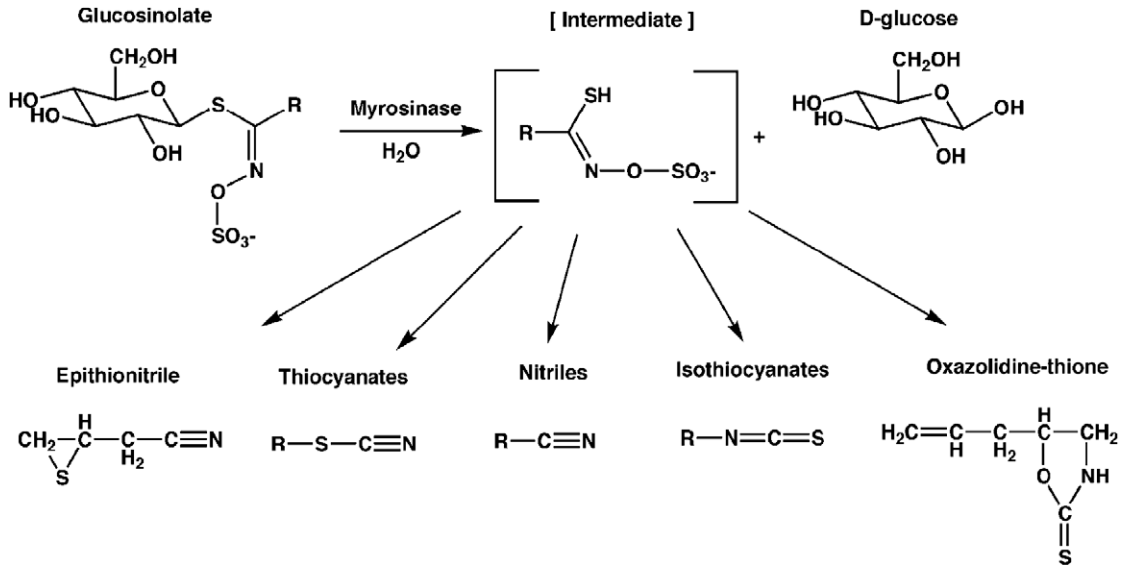

Fig. 1. The general structure of glucosinolates and their enzymatic degradation products (adapted from Rask et al. (2000)).

2.2. Preparation of hydrolysis products

2.2.1. Exogenous myrosinase hydrolysis (method ***A***)

Crushed undefatted seeds (500 mg), fresh leaves (10 g) and fresh roots (10 g) were homogenised separately with distilled water (200 ml), myrosinase enzyme (1–2 units, Sigma) and 2–5 mg L-ascorbic acid and allowed to hydrolyse for 2 h. Dichloromethane (50 ml) was added, the mixtures were shaken for 30 min and separated by centrifugation for 5 min at 3500 rpm. The separated organic layer was dried over anhydrous sodium sulfate, and concentrated under nitrogen to about 0.5 ml. The concentrated hydrolysate was kept (in a tightly closed vial) in a freezer until analysis (Al-Gendy & Lockwood, 2003).

2.2.2. Natural autolysis (method ***B***)

Each plant organ was homogenised separately with distilled water (200 ml) and left for natural autolysis overnight (17 h) at room temperature, followed by extraction as described above (Al-Gendy, 2008; Al-Gendy & Lockwood, 2003).

2.3. Identification and quantitative determination of breakdown products using gas chromatography–mass spectrometry (GC–MS)

One microlitre aliquots of the concentrated extract prepared by methods **A** and **B** were subjected to GC–MS analysis using a Trace GC 2000 gas chromatograph attached to a Finnigan MAT SSQ 7000 mass spectrometer operated at 70 eV. The column used was a DB-5MS fused silica capillary column (30 m × 0.25 mm × 0.25 μm; Agilent, Santa Clara, CA). The carrier gas was helium and the flow rate was 1 ml/min. The injector temperature was 250 °C and the temperature program was 50 °C initially for 2 min, followed by an increase of 5 °C/min to 280 °C.

2.4. Antimicrobial activity

Plant extracts prepared by natural autolysis and exogenous myrosinase hydrolysis were concentrated under a stream of nitrogen to dryness, weighed and dissolved in DMSO at concentration of 1 mg/ml.

For screening of antimicrobial activities, the Gram-positive bacteria used were *Bacillus subtilis, Staphylococcus aureus* and *Streptococcus faecalis,* while *Escherichia coli*, *Neisseria gonorrhea* and *Pseudomonas aeroginosa* were the used Gram-negative bacteria. *Candida albicans* and *Aspergillus flavus* were the used fungi. The standard antibiotic was tetracycline while the standard antifungal was amphotericin B.

A sterilised filter paper disc saturated with 1 mg of each sample was placed on a plate containing solid bacterial medium (nutrient agar broth) or fungal medium (Dox's medium), the latter of which had been heavily seeded with a spore suspension of the tested organism. After incubation, the diameter of the clear zone of inhibition surrounding the sample was taken as a measure of the inhibitory power of the sample against the particular test organism (Irobi, Moo-Young, & Anderson, 1996; Muanza, Kim, Euler, & Williams, 1994).

2.5. Cytotoxic activity

Crushed seeds (500 mg) were boiled with 200 ml water for 5 min to inactivate the natural enzyme. Light petroleum ether (50 ml) was added to extract fatty materials and the pH of the separated aqueous layer was adjusted to 6.5. Then, 1–2 units of myrosinase enzyme and 2–5 mg L-ascorbic acid were added and allowed to hydrolyse for 2 h, followed by extraction as described above.

Potential cytotoxicity of the seeds' crude extract (containing glucosinolate hydrolysis products) was tested using the method reported by Skehan et al. (1990). The tested cell lines were colorectal (HCT116), hepatic (HEPG2-1) and Hela. Cells were plated in 96-multiwell plate (10^4 cells/well) for 24 h before treatment with the extracts, to allow attachment of cell to the wall of the plate. Different concentrations of hydrolysate (1, 2.5, 5 and 10 μg/ml) were added to the cell monolayer and triplicate wells were prepared for each individual dose. Monolayer cells were incubated with the hydrolysates for 48 h at 37 °C and in an atmosphere of 5% CO_2. Cells were then fixed, washed and stained with Sulfo-Rhodamine-B stain. Excess stain was washed with acetic acid and attached stain was recovered with Tris–EDTA buffer. Colour intensity was measured in an ELISA reader and the relation between surviving fraction against the extract concentration was plotted to get the survival curve of each tumour cell line.

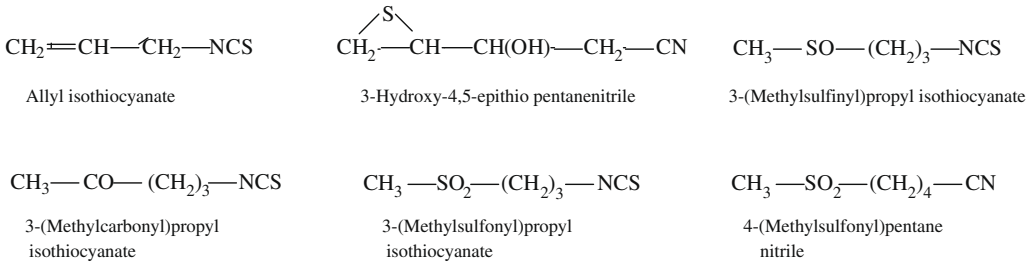

Fig. 2. Structure of glucosinolate hydrolysis products identified in *E. corinthium*.

3. Results and discussion

3.1. Identification of glucosinolate hydrolysis products and other volatile components

GC–MS analysis of extracts obtained by exogenous myrosinase hydrolysis and natural autolysis of seeds, leaves and roots of *E. corinthium* revealed the presence of glucosinolate hydrolysis products and other volatile components, e.g., terpenes and fatty acid methyl esters. Structure and mass spectra data of isothiocyanates, nitriles and epithioalkane nitriles formed by glucosinolate break down are given in Fig. 2 and Table 1 while other volatile components are given in Table 2.

Individual peaks were identified by comparing their retention time and mass spectrum with spectra in our home-made library, as well as with the literature data (Adams, 1995; Al-Gendy,

Table 1
GC–MS analysis of glucosinolate hydrolysis products of *E. corinthium*.

Parent GLS / Identified compound (molecular formulae)	t_R (min)	$[M]^+$	MS spectral data *m/z* (% relative abundance)	Relative %					
				Seeds		Leaves		Roots	
				A	**B**	**A**	**B**	**A**	**B**
Sinigrin									
Allyl isothiocyanate (C_4H_5NS)	4.8	99 (100)	72 (24), 41 (48)	–	4.4	–	–	–	–
Progoitrin									
3-Hydroxy 4,5-epithio pentanenitrile (C_5H_7NOS)	24.3	129 (100)	111 (38), 101 (15), 83 (10), 55 (90), 41 (77)	0.13 T	0.6	1.2	0.8	9.6	0.9
Glucoiberin									
3-(Methylsulfinyl)propyl isothiocyanate (Iberin) ($C_5H_9NOS_2$)	24.4	163 (7)	130 (12), 116 (44), 100 (27), 72 (100), 63 (17), 41 (65)	0.7	1.1	–	–	–	–
3-Methylcarbonylpropyl GLS									
3-Methylcarbonylpropyl isothiocyanate (C_6H_9NOS)	26.5	143 (35)	125 (10), 85 (13), 59 (27), 43 (100)	–	–	3.2	–	–	–
Glucocheirolin									
3-(Methylsulfonyl)propyl isothiocyanate (cheirolin) ($C_5H_9NO_2S_2$)	27.6	179 (100)	146 (1), 121 (18), 99 (63), 81 (12), 72 (70), 41 (52)	94.3	43.7	–	0.4	–	–
Glucoerysolin									
4-(Methylsulfonyl)pentane nitrile (erysoline nitrile) ($C_6H_{11}NO_2S$)	29.03	161 (<1)	129 (20), 100 (17), 82 (24), 55 (98), 41 (100)	–	–	0.8T	0.6	3.5	1.1

A: exogenous hydrolysis, **B**: natural autolysis; GLS: glucosinolate, T: tentatively identified.

Table 2
GC–MS analysis of miscellaneous volatile compounds of *E. corinthium*.

Identified compounds (molecular formula)	t_R (min)	Relative %					
		Seeds		Leaves		Roots	
		A	**B**	**A**	**B**	**A**	**B**
1,8-Cineole ($C_{10}H_{18}O$)	8.5	–	3.02	–	0.5	–	–
γ-Terpinene ($C_{10}H_{16}$)	9.2	–	0.2	–	–	–	–
2,5-Dimethylcyclohexanol ($C_8H_{16}O$)	10.6	–	–	–	0.3	–	–
Verbanol (*cis*) ($C_{10}H_{16}O$)	11.8	–	–	–	0.7	–	–
Pentyl Benzene ($C_{11}H_{16}$)	11.98	–	0.2	–	–	–	–
Verbenone ($C_{10}H_{14}O$)	13.47	–	–	–	0.4	–	–
2,4-Decadienal ($C_{10}H_{16}O$)	15.9	–	0.2	–	–	–	–
Urea, tetrabutyl ($C_{17}H_{36}N_2O$)	17.3	–	0.2	–	–	–	–
Benzene 1-methyl-4-methylthio ($C_8H_{10}S$)	17.7	0.1	–	–	–	–	–
Neophytadiene ($C_{20}H_{38}$)	28.6	–	–	–	1.2	–	–
Methyl palmitate ($C_{17}H_{34}O_2$)	32.5	–	–	0.8	–	–	–
Methyl linolenate ($C_{19}H_{32}O_2$)	33.72	–	–	–	0.7	–	–
Methyl oleate ($C_{19}H_{36}O_2$)	33.78	–	0.4	–	–	–	–
Phytol ($C_{20}H_{40}O$)	34.07	–	–	–	1.5	–	–
Sicol ($C_{19}H_{20}O_4$)	40.2	–	–	–	–	1.6	–
Dioctyl adipate ($C_{22}H_{42}O_4$)	40.8	–	–	1.7	–	–	–
Stigmast-4-en-3-one ($C_{29}H_{48}O$)	56.2	–	–	–	0.6	–	–

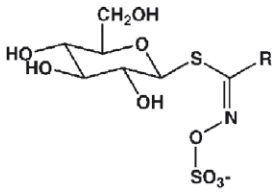

R	Glucosinolate
$CH_2{=}CH{-}CH_2{-}$	Sinigrin
$CH_3{-}SO{-}(CH_2)_3{-}$	Glucoiberin
$CH_3{-}SO_2{-}(CH_2)_3{-}$	Glucocheirolin
$CH_3{-}SO{-}(CH_2)_4{-}$	Glucoerysolin
$CH_3{-}CO{-}(CH_2)_3{-}$	3-Methyl carbonylpropyl glucosinolate
$CH_2{=}CH{-}CH(OH){-}CH_2{-}$	Progoitrin

Fig. 3. Glucosinolates identified in *Erysimum corinthium*.

2008; Al-Gendy & Lockwood, 2003; Odham & Stenhagen, 1972, chap. 8; Spencer & Daxenbichler, 1980; Vaughn & Borhow, 2005) and computer matching against the Wiley database.

3.1.1. Seeds

Four glucosinolates were identified: sinigrin, progoitrin, glucoiberin and glucocheirolin (Fig. 3). The major hydrolysis product of the seeds was cheirolin, liberated from glucocheirolin, which represents a major glucosinolate for many *Erysimum* species (Bennett, Mellon, & Kroon, 2004; Daxenbichler et al., 1991). Allyl isothiocyanate liberated from sinigrin was detected only by natural autolysis, while iberin liberated from glucoiberin could be detected by the two applied methods.

Bennett et al. (2004) had investigated the seeds of eight *Erysimum* species; glucoiberin was identified in all of them, while glucocheirolin was detected in six of them. Also, glucoerysolin and sinigrin were detected in two species. According to their results, they recommend *Erysimum pumillum* as the best seed source for glucoiberverin. Our results recommend *E. corinthium* as a good source for isolation and commercial production of glucocheirolin. Moreover, Daxenbichler et al. (1991) had investigated 12 *Erysimum* species, where glucoiberin and glucocheirolin were the most common glucosinolates identified.

3-Hydroxy-4,5-epithio pentanenitrile liberated from progoitrin was detected by natural autolysis only. To our knowledge, there is no previous report for the identification of progoitrin hydrolysis products in *Erysimum* species. Glucosinolate concentration in the reproductive tissues (florets, flowers and seeds) are often as much as 10–40 times higher than in the vegetative tissues. Thus, seed material can be a very good source of glucosinolates (Bennett et al., 2004). Our results are in agreement with this concept, due to the high concentration of glucocheirolin in the seed materials, compared to leaves, and its absence in the root.

The seeds contained volatile compounds including terpenes, e.g., 1,8-cineole and γ-terpinene, fatty acid esters, such as methyl oleate, and other miscellaneous volatile compounds formed mainly by natural autolysis. On the other hand, only 1-methyl-4-(methylthio)benzene is detected by exogenous myrosinase hydrolysis.

3.1.2. Leaves

The glucosinolate contents of the leaf are much smaller than those of the seeds. Only four glucosinolates were identified: progoitrin, 3-(methylcarbonyl)propyl glucosinolate, glucocheirolin and glucoerysolin (Fig. 3). On the other hand, many volatile components were detected by natural autolysis, while only two compounds, dioctyl adipate and methyl palmitate, were detected after exogenous hydrolysis (Table 2).

3.1.3. Roots

Our results showed that the root has the highest concentration of progoitrin and glucoerysolin, compared to leaves and seeds (Table 1). On the other hand, no glucoiberin and glucocheirolin were detected. It is clear that the amount of glucosinolate hydrolysis products obtained by exogenous hydrolysis is higher than that of natural autolysis.

Regarding the other volatile compounds, the root seems to be a poor source for these compounds as only sicol (1.6%) was detected by exogenous hydrolysis.

3.2. Antimicrobial activity

The antimicrobial activities of the applied plant extracts obtained by methods **A** and **B** of seeds, leaves and roots are given in Table 3. All tested extracts showed inhibition of growth for the tested organisms, except *A. flavus*, which means that *E. corinthium* has the ability to inhibit the growth of Gram-positive and

Table 3
Antimicrobial activity of *E. Corinthium* seeds, leaves and roots.

Microorganism	Inhibition zone diameter (mm/mg sample)								
	Seeds		Leaves		Roots		Standard		C
	A	**B**	**A**	**B**	**A**	**B**	T	Am	
Bacillus subtilis	17	22	15	15	12	9	30	0	0
Staphylococcus aureus	16	19	14	14	11	9	32	0	0
Streptococcus faecalis	15	20	15	15	10	9	31	0	0
Escherichia coli	15	17	14	14	14	10	34	0	0
Neisseria gonorrhea	17	19	14	13	10	10	31	0	0
Pseudomonas aeroginosa	14	16	14	14	11	10	34	0	0
Aspergillus flavus	0	0	0	0	0	0	0	0	0
Candida albicans	16	18	14	15	10	10	37	21	0

A: exogenous myrosinase hydrolysis, **B**: natural autolysis, T: tetracycline, Am: amphotericin B, C: control.

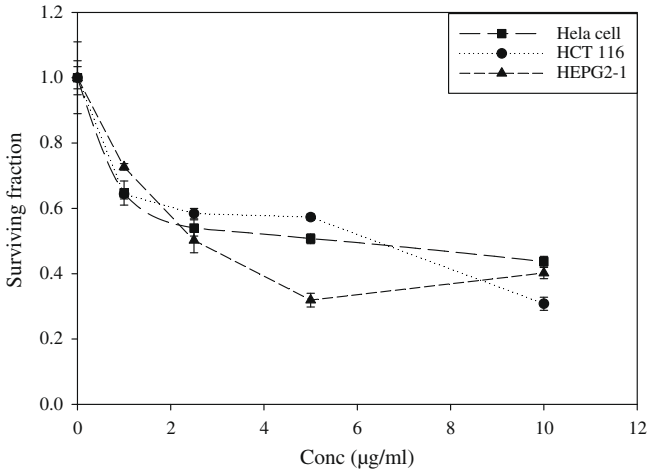

Fig. 4. Cytotoxic activity of *Erysimum corinthium* seeds.

Gram-negative bacteria, as well as fungi. The obtained results showed that the hydrolysis products of seeds have the highest activity while the hydrolysis products of roots have the lowest activity.

Although the concentration of cheirolin liberated by method **A** in seeds is nearly double that liberated by method **B**, the antimicrobial activity of seed extract prepared by method **B** is higher than that prepared by method **A**, especially against Gram-positive bacteria. This is mostly due to the presence of allyl isothiocyanate, which could not be detected by method **A** and also due to 3-hydroxy-4,5-epithio pentanenitrile liberated from progoitrin, and the higher concentration of iberin. Sinigrin, glucoiberin and progoitrin previously showed a marked similar activity that was attributed to their hydrolysis products (Brabban & Edwards, 1995; Manici, Lazzeri, & Palmieri, 1997; Tolonen et al., 2004).

In an earlier report, allyl isothiocyanate and crude plant extracts containing allyl isothiocyanate exhibited similar antimicrobial properties (Kanemaru & Miyamoto, 1990). Moreover, allyl isothiocyanate was reported to reduce *E. coli* in fresh ground beef during refrigerated or frozen storage (Nadarajah, Han, & Holley, 2005).

The toxic activity of glucosinolate hydrolysis products has been demonstrated towards a range of fungi *in vitro*, including both pathogens and non-pathogens (Fenwick et al., 1983; Osbourn, 1996). Also, allyl isothiocyanate was found to be one of the most fungitoxic glucosinolate hydrolysis products (Mithen, Lewis, Fenwick, & Heaney, 1986). Previously, allyl isothiocyanate showed nematocide effect for *Globodera rostochiensis,* which suggests the use of autolysis products of plant materials containing sinigrin to control the potato cyst nematode in soil (Buskov, Serra, Rosa, Sørensen, & Sørensen, 2002).

The antimicrobial activity of leaf extracts prepared by the two described methods is nearly equal. On the other hand, root extract prepared by method **A** showed higher activity than that prepared by method **B**.

3.3. Measurements of cytotoxic activity

The purified crude extract of seeds of *E. corinthium* could inhibit the growth of colorectal HCT 116, hepatic HEPG2-1 and Hela cells *in vitro*. The IC_{50} values were 6.7, 2.5 and 6.5 μg/ml, respectively, which means that hepatic HEPG2-1 cells are the most sensitive towards the tested plant extract (Fig. 4).

The hydrolysis products of sinigrin, progoitrin and glucocheirolin had previously showed a marked *in vitro* cytotoxicity against human erythroleukaemic K562 cells. Although it has been proposed that some isothiocyanates inhibit protein synthesis and affect carbohydrate metabolism, the activity of these compounds seems to be mainly ascribed to the chemical reactivity of the isothiocyanate group, which can bind easily to protein. Moreover, some hydrolysis products could be considered as antimitotic substances, given their strong antiproliferative activity (Nastruzzi et al., 1996).

A previous report showed that allyl isothiocyanate could inhibit cell cycle progression of Hela cells at G_2/M phase in a dose-dependent manner and the IC_{50} was about 15 μM (Hasegawa, Nishino, & Iwashima, 1993).

Rats fed a broccoli diet, which has a high concentration of sulforaphane, showed a significant increase in colon and hepatic quinone reductase (Keck, Qiao, & Jeffery, 2003). In adult male rats, oral administration of a mixture of glucosinolate derivatives, including iberin, caused a modification of both phase I and phase II detoxification enzymes, which was greater than the sum of the effects of individual components (Staack, Kingston, Wallig, & Jeffery, 1998).

4. Conclusion

There is a variation of glucosinolate levels in seeds, leaves and roots of *E. corinthium*. The highest percentage of glucosinolates is detected in seeds. A significant difference was observed between glucosinolate hydrolysis products identified by exogenous myrosinase hydrolysis and natural autolysis. The leaves showed the highest percentage of non-glucosinolate volatile components, while the roots showed the lowest. The seeds extract showed the highest antimicrobial activity, compared to the leaves and roots. Moreover, the seeds extract could participate in inhibiting the proliferation of colorectal HCT 116, hepatic HEPG2-1 and Hela cells *in vitro*.

Acknowledgement

The authors are very grateful to the staff of Micro-Analytical Center, Faculty of Science, Cairo University and Cancer Biology Unit, National Cancer Institute, Cairo University, for their great help in carrying out antimicrobial and cytotoxic activities, respectively.

References

Adams, R. P. (1995). *Identification of essential oil components by gas chromatography/mass spectroscopy*. Carol Stream, Illinois USA: Allured Publishing Corporation.

Al-Gendy, A. A. (2008). Phytochemical and biological screening of glucosinolates and volatile constituents of different Brassicaceae plants growing in Egypt. *Bulletin of Faculty of Pharmacy, Cairo University, 46*, 235–244.

Al-Gendy, A. A., & Lockwood, G. B. (2003). GC–MS analysis of volatile hydrolysis products from glucosinolates in *Farsetia aegyptia* var. *Ovalis*. *Flavour and Fragrance Journal, 18*, 148–152.

Al-Shehbaz, I. A., & Al-Shammary, K. I. (1987). Distribution and chemotaxonomic significance of glucosinolates in certain middle-eastern Cruciferae. *Biochemical Systematics and Ecology, 15*, 559–569.

Barbieri, G., Pernice, R., Maggio, A., De Pascalr, S., & Fogliano, V. (2008). Glucosinolates profile of *Brassica rapa* L. Subsp. *Sylvestris* L. Janch. Var. *Esculenta* Hort. *Food Chemistry, 107*, 1687–1691.

Bennett, R. N., Mellon, F. A., & Kroon, P. A. (2004). Screening crucifer seeds as sources of specific intact glucosinolates using ion-pair high-performance liquid chromatography negative ion electrospray mass spectrometry. *Journal of Agricultural and Food Chemistry, 52*, 428–438.

Brabban, A., & Edwards, C. (1995). The effects of glucosinolates and their hydrolysis products on microbial growth. *Journal of Applied Bacteriology, 79*, 171–177.

Buskov, S., Serra, B., Rosa, E., Sørensen, H., & Sørensen, J. C. (2002). Effects of intact glucosinolates and products produced from glucosinolates in myrosinase-catalyzed hydrolysis on the potato cyst nematode (*Globodera rostochiensis* Cv. Woll). *Journal of Agricultural and Food Chemistry, 50*, 690–695.

Daxenbichler, M. E., Spencer, G. F., Carlson, D. G., Rose, G. B., Brinker, A. M., & Powell, R. G. (1991). Glucosinolate composition of seeds from 297 species of wild plants. *Phytochemistry, 30*, 2623–2638.

Fahey, J. W., Zalcmann, A. T., & Talalay, P. (2001). The chemical diversity and distribution of glucosinolates and isothiocyanates among plants. *Phytochemistry, 56*, 5–51.

Fenwick, G. R., Heaney, R. K., & Mullin, W. J. (1983). Glucosinolates and their breakdown products in food and food plants. *Critical Reviews in Food Science and Nutrition, 18*, 123–301.

Gil, V., & MacLeod, A. (1980). Benzylglucosinolate degradation in *Lepidium sativum*: Effect of plant age and time of autolysis. *Phytochemistry, 19*, 1365–1368.

Hasegawa, T., Nishino, H., & Iwashima, A. (1993). Isothiocyanates inhibit cell cycle progression of hela cells at G_2/M phase. *Anti-Cancer Drugs, 4*, 273–279.

Heber, D. (2004). Vegetables, fruits and phytoestrogens in the prevention of diseases. *Journal of Postgraduate Medicine, 50*, 145–149.

Higdon, J. V., Delage, B., Williams, D. E., & Dashwood, R. H. (2007). Cruciferous vegetables and human cancer risk: Epidemiologic evidence and mechanistic basis. *Pharmacological Research, 55*, 224–236.

Irobi, O. N., Moo-Young, M., & Anderson, W. A. (1996). Antimicrobial activity of Annato (*Bixa orellana*) extract. *Pharmaceutical Biology, 34*, 87–90.

Kanemaru, K., & Miyamoto, T. (1990). Inhibitory effects on the growth of several bacteria by brown mustard and allyl isothiocyanate. *Nippon Shokuhin Kogyo, 37*, 823–829.

Keck, A.-S., Qiao, Q., & Jeffery, E. (2003). Food matrix effects on bioactivity of Broccoli-derived sulforaphane in liver and colon of F344 rats. *Journal of Agricultural and Food Chemistry, 51*, 3320–3327.

Manici, L., Lazzeri, L., & Palmieri, S. (1997). *In vitro* fungitoxic activity of some glucosinolates and their enzyme-derived products toward plant pathogenic fungi. *Journal of Agricultural and Food Chemistry, 45*, 2768–2773.

Mithen, R., Lewis, B. G., Fenwick, G. R., & Heaney, R. K. (1986). *In vitro* activity of glucosinolates and their products against *Leptosphaeria maculans*. *Transactions of the British Mycological Society, 87*, 433–440.

Muanza, D. N., Kim, B. W., Euler, K. L., & Williams, L. (1994). Antibacterial and antifungal activity of nine medical plants from Zaire. *Pharmaceutical Biology, 32*, 337–345.

Nadarajah, D., Han, J. H., & Holley, R. A. (2005). Inactivation of *Escherichia coli* O 157:H7 in packaged ground beef by allyl isothiocyanate. *International Journal of Food Microbiology, 99*, 269–279.

Nastruzzi, C., Cortesi, R., Esposito, E., Menegatti, E., Leoni, O., Iori, R., et al. (1996). *In vitro* cytotoxic activity of some glucosinolate-derived products generated by myrosinase hydrolysis. *Journal of Agricultural and Food Chemistry, 44*, 1014–1021.

Odham, G., & Stenhagen, E. (1972). Fatty acids. In G. Waller (Ed.), *Biochemical applications of mass spectrometry* (pp. 211–228). New York, London, Sydney, Toronto: John Wiley and Sons (Chapter 8).

Osbourn, A. E. (1996). Preformed antimicrobial compounds and plant defense against fungal attack. *The Plant Cell, 8*, 1821–1831.

Rask, L., Andreasson, E., Ekbom, B., Eriksson, S., Pontoppidan, B., & Meijer, J. (2000). Myrosinase: Gene family evolution and herbivore defense in Brassicaceae. *Plant Molecular Biology, 42*, 93–113.

Skehan, P., Storeng, R., Scudiero, D., Monks, A., McMahon, J., Vistica, D., et al. (1990). New colorimetric cytotoxicity assay for anticancer-drug screening. *Journal of the National Cancer Institute, 82*, 1107–1112.

Spencer, G. F., & Daxenbichler, M. E. (1980). Gas chromatography–mass spectrometry of nitriles, isothiocyanates and oxazolidinethiones derived from cruciferous glucosinolates. *Journal of the Science of Food and Agriculture, 31*, 359–367.

Staack, R., Kingston, S., Wallig, M. A., & Jeffery, E. H. (1998). A comparison of the individual and collective effects of four glucosinolate breakdown products from Brussels Sprouts on induction of detoxification enzymes. *Toxicology and Applied Pharmacology, 149*, 17–23.

Tolonen, M., Rajaniemi, S., Pihlava, J.-M., Johansson, T., Saris, P. E., & Ryhanen, E.-L. (2004). Formation of nisin, plant-derived biomolecules and antimicrobial activity in starter culture fermentations of sauerkraut. *Food Microbiology, 21*, 167–179.

Vaughn, S. F. (1999). Glucosinolates as natural pesticides. In H. G. Cutler & S. J. Cutler (Eds.), *Principles and practices in plant allelochemical interactions* (pp. 81–91). Boca Raton, FL: CRC Press.

Vaughn, S. F., & Borhow, M. A. (2005). Glucosinolates hydrolysis products from various plant sources: pH effects, isolation, and purification. *Industrial Crops and Products, 21*, 193–202.

Food Chemistry 118 (2010) 525–528

Contents lists available at ScienceDirect

Food Chemistry

journal homepage: www.elsevier.com/locate/foodchem

Effect of canned tuna fish processing steps on lead and cadmium contents of Iranian tuna fish

Maryam Ganjavi [a], Hamid Ezzatpanah [a,*], Mohammad Hadi Givianrad [b], Akbar Shams [a]

[a] Department of Food Science and Technology, Islamic Azad University, Science and Research Branch, P.O. Box 14515.775, Tehran, Iran
[b] Department of Chemistry, Islamic Azad University, Science and Research Branch, P.O. Box 14515.775, Tehran, Iran

ARTICLE INFO

Article history:
Received 23 February 2009
Received in revised form 8 April 2009
Accepted 8 May 2009

Keywords:
Lead
Cadmium
Iranian tuna fish
Processing
Yellowfin
Skipjack
Electrothermal atomic absorption spectrometry

ABSTRACT

The contents of Pb and Cd in two species of Iranian tuna fish (*yellowfin* and *skipjack*), which were caught from the Persian Gulf and Oman Sea, and the effects of canning processing steps on their contents were assessed by electrothermal atomic absorption spectrometry. The results revealed that the levels of lead and cadmium throughout the processing steps in *yellowfin* were in range of 0.154 ± 0.019–0.441 ± 0.025 μg/g and 0.029 ± 0.002–0.084 ± 0.0005 μg/g, respectively. Pb and Cd concentrations from received fish to final product in *skipjack* were found to be in range of 0.072 ± 0.031–0.218 ± 0.031 μg/g and 0.016 ± 0.001–0.062 ± 0.002 μg/g, respectively. The limit of detection for lead and cadmium were 0.058 μg/g (11.6022 μg/l) and 0.0007 μg/g (0.1485 μg/l), respectively. Results from paired sample *t*-test analysis showed that defrosting, cooking, and sterilisation by autoclave would reduce the contents of lead and cadmium, considerably.

1. Introduction

A great number of major pollutants have entered aquatic systems such as rivers, lakes, and oceans (Rashed, 2001). Several pollutants such as heavy metals (e.g., lead and cadmium) are very toxic, stable and not easily biodegradable (Ikem & Egibor, 2005). The ingestion of food is known as an important way of exposure to heavy metals. Heavy metals such as lead and cadmium can be very harmful even at low concentrations when ingested over a long time (Celik & Oehlenschlager, 2004; Tuzen & Soylak, 2007; Voegborlo, El-Methnani, & Abedin, 1999). Amongst food, fish are constantly exposed to heavy metals present in polluted water. These heavy metals can accumulate in their tissues in different amounts depending on the size and age of fish (Burger et al., 2002; Demirezen & Uruc, 2006; Emami khansari, Ghazi – khansari, & Abdolahi, 2005; Kagi & Schaffer, 1998; Marijic & Raspor, 2007; Tuzen & Soylak, 2007). Thus, fish have been found to be good bioindicators or biosensor of heavy metal contamination in aquatic systems (Burger et al., 2002; Keskin et al., 2007; Kuroshima, 1987).

Consumption of fish is very popular amongst people all around the world because it has high protein content, low saturated fatty acids, and high omega fatty acids content (Ikem & Egibor, 2005; Tuzen & Soylak, 2007). In Iran, like many other countries the consumption of canned fish especially canned tuna fish is privilege because of its convenient and affordable use. The main source of providing fish for Iranian canned tuna fish factories are the Persian Gulf and Oman Sea where the possibility of heavy metal contamination is high because of heavy trafficking of oil.

Processing steps may change the concentration of heavy metals in fish before consumption. In this study the influence of processing steps on the concentration of lead and cadmium in two species of tuna fish (*yellowfin* and *skipjack*) has been investigated since such effects has not been previously investigated.

2. Materials and methods

2.1. Apparatus

A Varian Spectra AA-220 (Melbourne, Australia) atomic absorption spectrometer equipped with a GTA-100 graphite furnace atomiser, deuterium lamp as a background corrector, a Varian programmable sample dispenser, wavelengths 217 nm and 326.1 nm, spectral bandwidth 1 nm and 0.5 nm monochromator were used for determination of lead and cadmium, respectively.

All glassware used in analytical work were soaked in commercial detergent for 24 h, rinsed with water, soaked in sulfochromic solution, rinsed with deionised water then kept in an oven at 110 °C until needed.

* Corresponding author. Tel.: +98 21 44865023; fax: +98 21 44865025.
E-mail addresses: hamidezzatpanah@yahoo.com, hamidezzatpanah@srbiau.ac.ir (H. Ezzatpanah).

0308-8146/$ - see front matter © 2009 Elsevier Ltd. All rights reserved.
doi:10.1016/j.foodchem.2009.05.018

2.2. Reagents and standards

All reagents used were of analytical reagent grade. Standard stock solutions of lead and cadmium were prepared by diluting concentrated solutions to obtain a solution of 1000 mg/l with deionised water, Nanopure water system with specific resistivity of 18.3 MΩ cm^{-1} (Millipore), was used for all working and standard solutions.

2.3. Sample preparation and digestion

Samples of two species of tuna fish were collected before and after four processing steps (defrosting, butchery, cooking, and sterilisation by autoclave) from canned tuna fish factories in Tehran-Iran, which provide their fish from the Persian Gulf and Oman Sea. First, the oil content of samples (before and after sterilisation) was drained off, and all samples were homogenised in a food blender with stainless steel cutters, followed by digestion.

For the determination of lead and cadmium 5 ± 0.01 g of each samples was weighed into a 150 ml beaker and 50 ml of freshly 1:1 (v/v) H_2O_2 (30%):HNO_3 (65%) was added slowly in portion. Each beaker was covered with a watch glass and stored at room temperature for 48 h. The samples were heated on hot plate until the solutions were clear. The solutions were then allowed to cool and sonicated for five minutes. The clear solutions were transferred into 25 ml flasks and diluted to the mark with deionised water and transferred into lidded tubes in a water-bath of 60 °C for 30 min. Finally, 170 μl of phosphoric acid as a modifier was added to each tube and shaken using a tube-shaker. The concentrations of cadmium and lead were determined using a Graphite Furnace Atomic Absorption Spectrophotometer (GFAAS) in different samples. The GFAAS determinations were carried out in triplicate.

3. Results and discussion

3.1. The influence of different species on concentrations of lead and cadmium

The concentrations of Pb and Cd in *yellowfin* and *skipjack* species which were caught from the Persian Gulf and Oman Sea are shown in Table 1. Literature values for lead were reported as 0.58–4.03 μg/g dry weight (Sharif, Mustafa, Hossain, Amin, & Safiullah, 1993), 0.5–9 μg/g (Aucoin et al., 1999), 4.9–5.30 μg/g (Chale, 2002), 0.22–0.85 μg/g dry weight (Tuzen, 2003), 0.7–2.4 μg/g (Mendil et al., 2005), 0.09–6.95 μg/g dry weight (Turkmen, Turkmen, Tepe, & Akyurt, 2005), 0.068–0.874 μg/g (Yilmaz, Ozdemir, Demirak, & Tuna, 2007) & 0.33–0.93 μg/g (Uluozlu, Tuzen, Meendil, & Soylak, 2007).

Cadmium concentrations in literature have been reported in the range of 0.04–0.13 μg/g dry weight (Sharif et al., 1993), 0.25–0.39 μg/g (Chale, 2002), 0.09–0.48 dry weight (Tuzen, 2003), 0.01–4.16 μg/g dry weight (Turkmen et al., 2005), 0.1–1.2 μg/g (Mendil et al., 2005), 0.010–0.084 μg/g (Yilmaz et al., 2007), and 0.45–0.90 μg/g (Uluozlu et al., 2007).

The concentration of lead in *yellowfin* was slightly higher than the permissible level for tuna fish according to European communities (EC) (0.4 Pb μg/g). Also, the concentrations of cadmium in both species were lower than the permissible levels for tuna fishes established by (EC) (0.1 Cd μg/g) (Commission of the European Communities (2001)).

The concentrations of lead and cadmium were significantly higher in *yellowfin* than those in *skipjack* (Table 1). Statistical analysis based on student paired sample *t*-test showed significant differences ($p < 0.05$) between the two species for the amount of lead and cadmium, which could be related to the bigger size of *yellowfin* and the differences between these species were attributed to their behaviours and habitats.

3.2. Processing effects on lead and cadmium contents

Statistical analysis using paired sample *t*-test showed that the concentrations of lead (Table 2) and cadmium (Table 3) in *skipjack* were significantly different ($p < 0.05$) before and after cooking and sterilisation by autoclave. Significant differences ($p < 0.05$) were also found in the lead (Table 2) and cadmium (Table 3) concentrations of *yellowfin* before and after defrosting, cooking, and sterilisation.

Thus defrosting might significantly reduce the concentration of lead and cadmium in canned tuna fish due to possible separation of serum. Furthermore, it could be concluded that cooking and sterilisation might decline the concentration of lead and cadmium in tuna fish during processing. The reduction in metal contents of fish during the heating process may be related to the decrease of protein content and release of these metals with the loss of water as free salts, possibly associated with soluble amino acids and uncoagulated proteins (Atta, El-sebaie, Noaman, & Kassab, 1997; Howarth & Sprague, 1978 Bryan & Hummerstone, 1971).

Table 4 shows the concentrations of Pb and Cd in final canned products of *yellowfin* and *skipjack* species. Lead concentrations in literature have been reported as 0.18–0.40 μg/g (Voegborlo et al., 1999), 0.0126–0.0726 μg/g (Emami khansari et al., 2005), 0.0–0.03 μg/g (Ikem & Egibor, 2005), and 0.09–0.40 μg/g (Tuzen & Soylak, 2007). Literature values for cadmium were reported in the range of 0.09–0.32 μg/g (Voegborlo et al., 1999), 0.0046–0.0720 μg/g (Emami khansari et al., 2005), 0.0–0.05 μg/g (Ikem & Egibor, 2005), and 0.06–0.25 μg/g (Tuzen & Soylak, 2007).

The concentrations of lead and cadmium in all canned tuna fish samples were found to be lower than the limits established by the Institute of Standards and Industrial Research of Iran (ISIRI), and European communities (Commission of the European Communities, 2001; Institute of Standards and Industrial Research of Iran, 2003).

3.3. Analytical Figures of merit

Sensitivity was studied by means of the limit of detection (LOD), defined as follows:

$$\mathrm{LOD} = \frac{3\delta_b}{m}$$

where δ_b is standard deviation of eight successive measurements of blank; m means the slope of the standard calibration curve.

Table 1
Assessment of heavy metal concentrations (μg/g wet weight) in tuna fish species of the Persian Gulf and Oman Sea (expressed as mean concentration ± SD, $N = 10$).

Fish species	Pb (X ± SD)	Permissible[a] level of Pb μg/g	Mean differences of Pb	Significance level of Pb	Cd (X ± SD)	Permissible[a] level of Cd μg/g	Mean differences of Cd	Significance level of Cd
Yellowfin	0.441 ± 0.025	0.4	0.223	0.018	0.084 ± 0.0005	0.1	0.022	0.026
Skipjack	0.218 ± 0.031	0.4			0.062 ± 0.002	0.1		

[a] European communities.

Table 2
The effect of four steps of processing on concentration of lead in *skipjack and yellowfin*.

Fish species	Steps	Significance level	Standard deviation	Differences
Skipjack	Before and after defrosting	0.064	0.012	0.084
	Before and after butchery	0.318	0.008	−0.011
	Before and after cooking	0.041	0.002	0.021
	Before and after sterilisation by autoclave	0.042	0.006	0.061
Yellowfin	Before and after defrosting	0.012	0.004	−0.029
	Before and after butchery	0.230	0.015	0.091
	Before and after cooking	0.003	0.0006	0.072
	Before and after sterilisation by autoclave	0.042	0.007	0.148

Table 3
The effect of four steps of processing on the concentration of cadmium in *skipjack and yellowfin*.

Fish species	Steps	Significance level	Standard deviation	Differences
Skipjack	Before and after defrosting	0.025	0.002	0.037
	Before and after butchery	0.145	0.003	0.005
	Before and after cooking	0.044	0.0003	0.003
	Before and after sterilisation by autoclave	0.029	0.0003	0.005
Yellowfin	Before and after defrosting	0.007	0.0007	0.042
	Before and after butchery	0.214	0.0006	-0.001
	Before and after cooking	0.007	0.0001	0.008
	Before and after sterilisation by autoclave	0.032	0.0005	0.007

Table 4
Heavy metal concentrations (μg/g wet weight) in Final canned tuna fish species of the Persian Gulf and Oman Sea (expressed as mean concentration ± SD, $N = 10$).

Fish species	Pb (X ± SD)	Permissible level[a] of Pb μg/g	National permissible level[b] of Pb μg/g	Cd (X ± SD)	Permissible[a] level of Cd μg/g	National permissible level[b] of Cd μg/g
Yellowfin	0.154 ± 0.019	0.2	0.5	0.029 ± 0.002	0.05	0.1
Skipjack	0.072 ± 0.031	0.2	0.5	0.016 ± 0.001	0.05	0.1

[a] European communities.
[b] Institute of Standards and Industrial Research of Iran.

According to this equation, the LOD of lead and cadmium were 0.058 μg/g (11.6022 μg/l) and 0.0007 μg/g (0.1485 μg/l), respectively.

Precision, which is a measure of reproducibility, expressed as percent relative standard deviation (RSD) within the liner range, was obtained by using the following equation (Saber-Tehrani, Givianrad, & Hashemi-Moghadam, 2006a; Saber-Tehrani, Hashemi-Moghadam, Givianrad, & Aberoomand-Azar, 2006b):

$$\mathrm{RSD} = \frac{100\delta}{\bar{x}}$$

The repeatability of measurements, as the means of RSD was 1.7% for lead and 0.9% for cadmium for 8 successive individual measurements of the same sample. In addition, RSD of the whole procedure, expressed as the RSD of the concentration measured for three replicated analyses of the same sample, were 2.2% for lead and 0.2% for cadmium.

The accuracy of method has been investigated by means of spiking different amounts of lead and cadmium into samples (Saber-Tehrani et al., 2006a; Saber-Tehrani et al., 2006b). The recoveries were found within the range of 86%–90% for lead and 85%–92% for cadmium, which are tabulated in Table 5.

3.4. Pearson

Correlation analysis based on Pearson coefficient was performed. Significant positive correlation is the relationship between two sets of data in which the values of two variables increase or decrease together significantly (Saber-Tehrani, Givianrad, & Kahkashan, 2007; Saber-Tehrani et al., 2006a).

In this study, positive correlations in the non-thermal process were found between the lead concentration of *skipjack* and *yellowfin* and also, between the cadmium concentration of *yellowfin* and lead concentration of *skipjack* at a confidence level of 95% (Table 6). Moreover positive correlations in the thermal process were found amongst cadmium concentrations of *yellowfin* and *skipjack*, and also, between the cadmium concentration of *skipjack* and lead concentration of yellowfin at a confidence level of 95% (Table 6). Furthermore, in whole process cadmium concentration in *skipjack*

Table 5
Recoveries corresponding to lead and cadmium by means of spiking different contents of lead and cadmium to the samples.

Lead content (μg l^{-1})	Lead spiked (μg l^{-1})	Recovery (%)	Cadmium content (μg l^{-1})	Cadmium spiked (μg l^{-1})	Recovery (%)
	25	85.8		25	84.8
26.86	50	90.1	1.2	50	89.1
	100	87.3		100	92.1

Table 6
Pearson correlation matrix for lead and cadmium contents of tuna fish species in thermal, non-thermal, and whole process.

	Lead content of *yellowfin*	Lead content of *skipjack*	Cadmium content of *yellowfin*	Cadmium content of *skipjack*
Lead content of *yellowfin*	1	0.635	0.539	0.569
		0.598	0.572	0.592
		0.571	**0.558**	0.531
Lead content of *skipjack*		1	0.661	0.573
			0.673	0.521
			0.584	0.496
Cadmium content of *yellowfin*			1	0.541
				0.683
				0.563
Cadmium content of *skipjack*				1

Note: Bold numbers indicate a significant correlation (99% confidence) and underline numbers show a significant correlation (95% confidence). The numbers in the first row correspond to non-thermal process, those in the second row correspond to thermal process, and those in the third row correspond to whole process of canned tuna fish.

and lead concentration in *yellowfin* had positive correlations at a confidence level of 95%. In addition, positive correlations were recognised at a confidence level of 99%, amongst lead and cadmium concentrations in both species and amongst cadmium concentration in *yellowfin* and lead concentration in *skipjack* (Table 6). Thus, whole process (defrosting, butchery, cooking, and sterilisation by autoclave) can reduce lead and cadmium concentrations in both species.

4. Conclusion

A suitable and sensitive method was developed for determination of lead and cadmium in biological samples by ETAAS. Moreover, by considering the concentrations of lead and cadmium in unprocessed tuna fish species, it can be commented that nowadays the pollution of the Persian Gulf and Oman Sea is in the permissible range.

It was also found that the concentration of lead and cadmium in *yellowfin* was significantly higher than those of *skipjack*.

More importantly, defrosting, cooking, and sterilisation could result in a significant reduction of lead and cadmium in the final product. Therefore, the consumption of Iranian canned tuna fish of the Persian Gulf and Oman Sea can be safe for human health in spite of possible contamination with heavy metals.

Acknowledgments

The authors are grateful to the Canned Tuna Fish Factories of Tehran-Iran for providing the samples, Laboratory Complex of Islamic Azad University for valuable technical assistance and also, Prof. H. Lelieveld and Dr. K. Shamsi for their cooperative guidance.

References

Atta, M. B., El-sebaie Noaman, M. A., & Kassab, H. E. (1997). The effect of cooking on the content of heavy metals in fish (*Tilapia nilotica*). *Food Chemistry, 58*, 1–4.

Aucoin, J., Blanchard, R., Billiot, C., Partridge, C., Schultz, D., Mandhare, K., et al. (1999). Trace metals in fish and sediments from Lake Boeuf, Southeastern Louisiana. *Microchemical Journal, 62*, 299–307.

Bryan, G. W., & Hummerstone, L. G. (1971). Adaptation of the polychaete, *Nereis diverscolor* to sediments containing high concentration of heavy metals. *Journal of the Marine Biological Association of the United Kingdom, 51*, 857–863.

Burger, J., Gaines, K. F., Shane Boring, C., Stephens, W. L., Snodgrass, J., Dixon, C., et al. (2002). Metal levels in fish from the Savannah River: Potential hazards to fish and other receptors. *Environmental Research, 89*, 85–97.

Celik, U., & Oehlenschlager, J. (2004). Determination of zinc and copper in fish samples collected from Northeast Atlantic by DPSAV. *Food Chemistry, 87*, 343–347.

Chale, F. M. M. (2002). Trace metal concentrations in water, sediments and fish tissue from Lake Tanganyika. *The Science of the Total Environment, 299*, 115–121.

Commission of the European Communities (2001). *Commission Regulation (EC) No. 221/2002 of 6 February 2002 amending regulation (EC) No. 466/2002 setting maximum levels for certain contaminants in foodstuffs*. Official Journal of the European Communities, Brussels, 6 February 2002.

Demirezen, D., & Uruc, K. (2006). Comparative study trace elements in certain fish meat and meat products. *Meat Science, 74*, 255–260.

Emami khansari, F., Ghazi – khansari, M., & Abdolahi, M. (2005). Heavy metals contents of canned tuna fish. *Food Chemistry, 93*, 293–296.

Howarth, R. S., & Sprague, J. B. (1978). Copper lethality to rainbow Trout in waters of various hardness and pH. *Water Research, 12*, 455–462.

Ikem, A., & Egibor, N. O. (2005). Assessment of trace elements in canned fishes (mackerel, tuna, salmon, sardines and herrings) in Georgia and Alabama (United state of America). *Journal of Food Composition and Analysis, 18*, 771–787.

ISIRI number 6952 (2003). Institute of Standards and Industrial Research of Iran. *Fish and fish products – Canned tuna fish in brine-specifications and test methods*. Tehran, Iran.

Kagi, J. H., & Schaffer, A. (1998). Biochemistry of metallothionein. *Biochemistry, 27*, 8509–8515.

Keskin, Y., Baskaya, R., Ozyaral, O., Yurdun, T., Luleci, N. E., & Hayran, O. (2007). Cadmium, lead, mercury and copper in fish from the Marmara Sea, Turkey. *Bulletin of Environmental Contamination and Toxicology, 78*, 258–261.

Kuroshima, R. (1987). Cadmium accumulation and its effect on calcium metabolism in the *Girella punctata* during a long term exposure. *Nippon Suisan Gakkaishi, 53*(3), 445–450.

Marijic, V. F., & Raspor, B. (2007). Metal exposure assessment in native fish, *Mullus barbatus* L., from the Eastern Adriatic Sea. *Toxicology Letters, 168*(3), 292–301.

Mendil, D., Uluozlu, O. D., Hasdemir, E., Tuzen, M., Sari, H., & Suicmez, M. (2005). Determination of trace metal levels in seven fish species in Lakes in Tokat, Turkey. *Food chemistry, 90*, 175–179.

Rashed, M. N. (2001). Cadmium and lead levels in fish (*Tilapia nilotica*) tissues as biological indicator for lake water pollution. *Environmental Monitoring and Assessment, 68*(1), 75–89.

Saber-Tehrani, M., Givianrad, M. H., & Hashemi-Moghadam, H. (2006a). Determination of total methyl mercury in human permanent healthy teeth by electrothermal atomic absorption spectrometry after extraction in organic phase. *Talenta, 71*, 1319–1325.

Saber-Tehrani, M., Givianrad, M. H., & Kahkashan, P. (2007). Assessment of some elements in human permanent healthy teeth, their dependence on number of amalgam filling and interelements relationships. *Biological Trace Element Research, 116*, 155–169.

Saber-Tehrani, M., Hashemi-Moghadam, H., Givianrad, M. H., & Aberoomand-Azar, P. (2006b). Methylmercury determination in biological samples using electrothermal atomic absorption spectrometry after acid leaching extraction. *Analytical and Bioanalytical Chemistry, 386*, 1407–1412.

Sharif, A. K. M., Mustafa, A. I., Hossain, M. A., Amin, M. N., & Safiullah, S. (1993). Lead and cadmium contents in ten species of tropical marine fish from the Bay of Bengal. *The Science of the Total Environment, 133*, 193–199.

Turkmen, A., Turkmen, M., Tepe, Y., & Akyurt, I. (2005). Heavy metals in three commercially valuable fish species from Iskenderun Bay, Northern East Mediterranean Sea, Turkey. *Food Chemistry, 91*, 167–172.

Tuzen, M. (2003). Determination of heavy metals in fish samples of the middle Black Sea (Turkey) by graphite furnace atomic absorption spectrometry. *Food Chemistry, 80*, 119–123.

Tuzen, M., & Soylak, M. (2007). Determination of trace metals in canned fish marketed in Turkey. *Food Chemistry, 10*, 1378–1382.

Uluozlu, O. D., Tuzen, M., Meendil, D., & Soylak, M. (2007). Trace metal content in nine species of fish from the Black and Aegean Seas. *Food chemistry, 104*, 835–840.

Voegborlo, R. B., El-Methnani, A. M., & Abedin, M. Z. (1999). Mercury, cadmium and lead content of canned tuna fish. *Food Chemistry, 67*, 341–345.

Yilmaz, F., Ozdemir, N., Demirak, A., & Tuna, A. L. (2007). Heavy metal levels in two fish species *Leuciscus cephalus* and *Lepomis gibbosus*. *Food Chemistry, 100*, 830–835.

Food Chemistry 118 (2010) 529–533

Contents lists available at ScienceDirect

Food Chemistry

journal homepage: www.elsevier.com/locate/foodchem

Changes on the levels of serotonin precursors – tryptophan and 5-hydroxytryptophan – during roasting of Arabica and Robusta coffee

Ana Carolina C.L. Martins, M. Beatriz A. Gloria *

LBqA – Laboratório de Bioquímica de Alimentos, FAFAR, Universidade Federal de Minas Gerais, Av. Antonio Carlos 6627, Belo Horizonte, MG 31270 901, Brazil

ARTICLE INFO

Article history:
Received 20 February 2009
Received in revised form 5 April 2009
Accepted 8 May 2009

Keywords:
Coffee
Arabica
Robusta
Tryptophan
5-Hydroxytryptophan
Roasting

ABSTRACT

The levels of free and total tryptophan and of 5-hydroxytryptophan (5-HTP) were investigated in green and roasted grains and beverages of *Coffea arabica* L. (Arabica) and *Coffea canephora* Pierre var. *robusta* (Robusta). Grains were light, medium and dark roasted. Free and protein tryptophan were extracted before and after hydrolysis. The levels of tryptophan and 5-HTP were quantified simultaneously by ion-pair HPLC and fluorimetric detection after derivatisation with *o*-phthalaldehyde. Robusta green coffee had higher total and protein tryptophan, whereas Arabica had higher free tryptophan levels. 5-HTP was not detected in the samples before and after roasting. Free tryptophan was completely degraded during roasting. Roasting significantly affected protein tryptophan. The rate of loss was smaller in Arabica compared to Robusta at every roasting degree. A beverage prepared the Brazilian way with a medium-roasted coffee provided 1.4–2.5 mg tryptophan/50 ml cup.

1. Introduction

Coffee plays a major social and economical role. It is one of the most widely consumed beverages throughout the world due to its pleasant taste and aroma and stimulant effect. It is the second major commodity commercialised worldwide, losing only to petroleum. It represents an important financial source for developing countries, involving a large number of workers in the production chain (Embrapa Café, 2007). Brazil is the largest green coffee producer and exporter, accounting for approximately 30% of the world market. Among the most economically relevant Brazilian coffee species are *Coffea arabica* and *Coffea canephora* (Perrone, Farah, Donangelo, de Paulis, & Martin, 2008).

Recent studies have attributed beneficial health effects to coffee. Coffee is frequently recommended as a stimulant and to prevent hypertension; furthermore, it is a bronchodilator and a good source of potassium in the diet. Studies have also described the association of the daily moderate consumption of coffee with lower prevalence of cirrhosis, lower risk of diabetes type 2, decreased prevalence of some types of cancer, inhibition of fat absorption and activation of lipid metabolism in the liver (Higdon & Frei, 2006).

Several epidemiological studies have associated coffee intake with beneficial effects in the central nervous system (CNS). Coffee consumption has been positively associated with alertness, humour, lower risk of suicides, lower incidence of Parkinson disease, prevention of depression, and decrease of alcohol consumption and cigarette smoking (Dórea & Da Costa, 2005; Higdon & Frei, 2006). The majority of the studies blame caffeine for these effects. However, coffee has many other compounds, and, therefore, the possible functional role of other substances present in coffee must be investigated.

Serotonin – 5-hydroxytryptamine or 5-HT (3-(2-aminoethyl)-1H-indol-5-ol) – is a neurotransmitter in the CNS. It is synthesised from the amino acid L-tryptophan by a short metabolic pathway consisting of two enzymes: tryptophan hydroxylase (EC 1.14.16.4) and amino acid decarboxylase (EC 4.1.1.28) with 5-hydroxytryptophan (5-HTP) as an intermediate (Fig. 1). Serotonin has broad activities in the brain, playing an important role in the modulation of anger, aggression, body temperature, mood, sleep, human sexuality, appetite, and metabolism, as well as stimulating vomiting (Ruddick et al., 2006; Shaw, Turner, & Del Mar, 2009; Turner, Loftis, & Blackwell, 2005). Cirilo et al. (2003) detected the presence of serotonin in green and roasted coffee. According to their study, an increase in the degree of roasting resulted in a significant increase in serotonin levels. The authors suggested that serotonin could have been formed by the thermal degradation of their precursors – tryptophan and 5-hydroxytryptophan (5-HTP) – during roasting. However information is scarce on the levels of serotonin and its precursors in coffee and also, how they are affected during production and processing.

* Corresponding author. Tel.: +55 31 34982419; fax: +55 31 34096911.
E-mail address: mbeatriz@ufmg.br (M.B.A. Gloria).

0308-8146/$ - see front matter © 2009 Elsevier Ltd. All rights reserved.
doi:10.1016/j.foodchem.2009.05.016

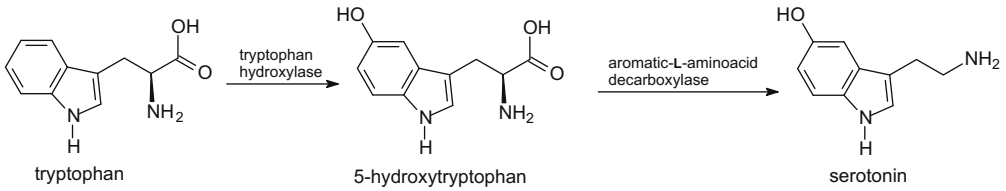

Fig. 1. Metabolic pathway from tryptophan to serotonin.

According to Lyons and Truswell (1988) and Goihl (2006), serotonin taken orally does not pass into the serotonergic pathways of the CNS because it does not cross the blood–brain (hematoencephalic) barrier. However, tryptophan and 5-hydroxytryptophan, from which serotonin is synthesised, cross the blood–brain barrier. Synthesis and turnover of brain serotonin depend directly on the uptake of its precursors – tryptophan and 5-hydroxytryptophan – across the blood–brain barrier.

Tryptophan (2-amino-3-(1H-indol-3-yl)-propionic acid) is an essential amino acid in the human diet. Besides acting as building blocks in protein biosynthesis, tryptophan functions as a biochemical precursor for serotonin, melatonin and niacin. Serotonin is synthesised *via* tryptophan hydroxylase. However, it can be converted to melatonin. Niacin is synthesised from tryptophan *via* kynurenine and quinolinic acids as key biosynthetic intermediates (Delgado-Andrade, Rufian-Henares, Jimenez-Perez, & Morales, 2006; Goihl, 2006; Ruddick et al., 2006).

5-Hydroxytryptophan or 5-HTP (2-amino-3-(5-hydroxy-1H-indol-3-yl) propanoic acid) is a naturally occurring amino acid. It is decarboxylated to serotonin by the aromatic-L-amino-acid decarboxylase in the presence of vitamin B6. This reaction occurs both in nervous tissue and in the liver (Birdsall, 1998; Shaw et al., 2009).

Both serotonin precursors – tryptophan and 5-HTP – in the diet can affect brain serotonin levels. High levels of non-protein (free) tryptophan, which is easily absorbed, could increase its availability in the brain. 5-HTP has advantages over tryptophan, as its intestinal absorption does not require the presence of a transporter and it is not affected by the presence of other amino acids and carbohydrates in the diet (Birdsall, 1998; Comai et al., 2007; Higdon & Frei, 2006; Turner et al., 2005).

Very little information is available regarding the levels of serotonin precursors in coffee. Therefore, the objective of this study was to determine the levels of free and total tryptophan and of 5-HTP in green coffee beans and to investigate the influence of roasting on their levels.

2. Material and methods

2.1. Standards and chemicals

Tryptophan and 5-hydroxytryptophan were purchased from Sigma Chemical Co. (St. Louis, MO, USA). All reagents were of analytical grade, except HPLC solvents which were chromatographic grade. LC water was used throughout the experiments (Milli-Q System, Millipore Corp., Bedford, MA, USA).

2.2. Coffee samples, roasting and beverage preparation

Samples of green economically relevant Brazilian coffee – *C. arabica* L. cv Catuaí Amarelo (Arabica) and *C. canephora* Pierre var. *robusta* (Robusta) – were kindly provided by Incofex Armazéns Gerais LTDA, Viçosa, MG, Brazil. These samples included two good cup quality green samples of Arabica (Catuaí amarelo, hard beverage, 2007/2008) from Viçosa, MG, and Robusta (soft beverage, 2006/2007) from Lajinha, MG. Samples from three different lots of each species were used.

The green coffee grains (100 g) were roasted in a commercial fluidised bed (hot air stream) roaster (i-Roast® Model No. 40009, Hearthware Home Products, USA) at three different conditions: 171 °C/8 min, 171 °C/15 min, and 210 °C/15 min to obtain light, medium and dark roasts, respectively. A 1 min cooling period was included in the roasting procedure. Roasting degrees of the coffee were determined by means of percent weight loss during roasting and colour characteristics (CIE $L^*a^*b^*$ colour system) of the roasted coffee (Almeida, Farah, Silva, Nunan, & Gloria, 2006; Perrone et al., 2008).

Before and after roasting, the coffee grains were ground and analysed for free and protein-bound tryptophan, 5-hydroxytryptophan, moisture content and total nitrogen levels.

The beverages were prepared the Brazilian way with medium-roasted samples of Arabica and Robusta coffee (Almeida et al., 2006). 20 g of ground coffee (20 mesh) were added to 150 ml of water at 90 °C. The mixture was kept under agitation for 3 min and was filtered through filter paper (No. 102, Melita, São Paulo, SP, Brazil). The beverages were also analysed for total solids, extraction yield and concentration.

The samples were analysed immediately. When necessary, samples were stored under nitrogen, refrigeration (−23 °C) and protected from light in order to minimise tryptophan loss due to oxidation.

2.3. Weight loss during roasting

The percent weight loss (%WL) of the coffee beans after roasting was calculated by using the following equation (Perrone et al., 2008)

$$\%\,\mathrm{WL} = 100(\mathrm{WBR} - \mathrm{WAR})/\mathrm{WBR}$$

where WBR is the weight before roasting and WAR is the weight after roasting.

2.4. CIE $L^*a^*b^*$ colour characteristics

The CIE $L^*a^*b^*$ colour characteristics were determined using a ColorTec colourimeter PCM (Accuracy Microsensor, Pittsford, NY, USA) with standard illumination D_{65} and colourimetric normal observer angle of 10°. The L^* (luminosity), a^* (intensity of red (+) and green (−)) and b^* (intensity of yellow (+) and blue (−)) values were taken straight from the equipment. The chroma $[c = (a^2 + b^2)^{1/2}]$ and the hue angle [h = arctg a/b] were calculated. The L^*, chroma and hue values were used to infer the degree of roasting of the coffee (Almeida et al., 2006).

2.5. Determination of moisture content

The moisture content of ground green and roasted coffee was determined by dehydration in an oven with forced air ventilation (Tecnal, Piracicaba, SP, Brazil) at 105 ± 2 °C until constant weight (Reh, Gerber, Prodolliet, & Vuataz, 2006). This information was used to express the amounts of the analytes on a dry weight basis.

2.6. Determination of total nitrogen levels

The total levels of nitrogen were determined by the Micro-Kjeldahl method, and the levels of protein were estimated using 6.25 (AOAC, 2000).

2.7. Simultaneous HPLC determination of tryptophan and 5-hydroxytryptophan

Free and protein-bound tryptophan were extracted from the samples with 50% methanol before and after hydrolysis with 4.2 N NaOH, respectively (AOAC, 2000). The levels of tryptophan and 5-HTP were quantified simultaneously by ion-pair HPLC, post-column derivatisation with *o*-phthalaldehyde and fluorimetric detection at 340 and 445 nm of excitation and emission, respectively (Martins, 2008).

2.8. Extraction rate and concentration of the beverage

The beverages were analysed for solid content (dehydration in air-oven at 105 ± 2 °C). Extraction rate and concentration were calculated as the percentage of total solids per amount of coffee used and beverage volume, respectively (López-Galilea, De Peña, & Cid, 2007).

2.9. Statistical analysis

The analyses were performed in duplicate. Data are presented as means ± standard deviations. The data were submitted to ANOVA (one way and two-way) followed by Tukey test at 5% probability using SIGMA STAT 2.0 (Systat Software Inc, Richmond, CA, USA). Pearson correlation was used to correlate the levels of serotonin precursors with the degree of roasting.

3. Results and discussion

3.1. Physico-chemical characteristics and serotonin precursors in green coffee

The levels of moisture, protein, 5-HTP and tryptophan in green Arabica and Robusta coffee are indicated on Table 1. Robusta coffee had significantly higher moisture content compared to Arabica. The moisture levels found and the difference between green Arabica and Robusta coffee is reported in the literature with values ranging from 8 to 12 g/100 g (Casal, Mendes, Oliveira, & Ferreira, 2005; Mazzafera, 1999; Montavon, Mauron, & Duruz, 2003).

In order to eliminate interference of the moisture content between samples, the levels of the other analytes were expressed on a dry weight basis (dw). Protein levels were of approximately 13 g/100 g dry weight basis (dw), with no significant difference between the two species. The levels found are similar to literature values ranging from 8.7 to 13.6 g/100 g (Casal et al., 2005; Mazzafera, 1999). However, these results are probably over-estimated as part of the levels of nitrogen detected by the Kjeldahl method in green coffee is not only available as amino acids or proteins, but other sources of nitrogen such as caffeine, and trigonelline (Bekedan, Schols, Van Boekel, & Smit, 2006; Mazzafera, 1999). According to these investigators, non-protein nitrogen corresponds to approximately 17–30% of the total levels.

Table 1
Levels of moisture, protein, 5-hydroxytryptophan (5-HTP) and free and protein-bound tryptophan in Arabica and Robusta green coffee.

Parameters	Green coffee[a]	
	Arabica	Robusta
Moisture (g/100 g)	8.65 ± 0.21^{B}	10.24 ± 0.16 ^{A}
Protein (g/100 g, dw[c])	13.92 ± 0.98	13.73 ± 0.74
5-HTP (mg/100 g, dw)	nd[b]	nd
Tryptophan		
Free (mg/100 g, dw)	22.08 ± 1.53^{A}	3.09 ± 0.10^{B}
Protein-bound (mg/100 g, dw)	120.8 ± 3.3^{B}	154.0 ± 4.5^{A}
Total (mg/100 g, dw)	142.9 ± 2.9^{B}	157.0 ± 4.5^{A}

[a] Mean values (±standard deviation) with different capital letters in the same line are significantly different (ANOVA, $p \leqslant 0.05$).
[b] Not detected (<0.3 mg/100 g).
[c] dw = dry weight.

The presence of serotonin precursors in green coffee was investigated for the first time. 5-HTP was not detected in any of the green coffee samples analysed; whereas tryptophan was present at high levels (Table 1). Free tryptophan was present at higher concentrations in Arabica (22.08 mg/100 g dw) compared to Robusta (3.09 mg/100 g dw). It corresponded to 15% and 2% of the total tryptophan levels in Arabica and Robusta coffees, respectively.

Significantly higher protein-bound tryptophan (154.0 mg/100 g dw) was found in Robusta green coffee compared to Arabica (120.8 mg/100 g dw). These values represent 1.12 and 0.87 g tryptophan/100 g of protein, respectively. Therefore, Robusta green coffee had significantly higher protein-bound tryptophan compared to Arabica.

The levels of tryptophan found are similar to reported values (Arnold & Ludwig, 1996; Casal, Alves, Mendes, Oliveira, & Ferreira, 2003; Casal et al., 2005). Differences in the profile and levels of amino acids in coffee can result from several factors, among them, species, varieties, degree of ripening, post-harvest conditions, and method of analysis (Arnold & Ludwig, 1996; Casal et al., 2003; Mazzafera, 1999).

According to Comai et al. (2007), tryptophan is a minor amino acid in the human diet. However, it is one of the most abundant free amino acids in green coffee, along with alanine, proline, asparagine, glutamic acid and phenylalanine (Casal et al., 2003; Mazzafera, 1999). Therefore, green coffee is a good source of free and protein-bound tryptophan.

3.2. Roasting effects on weight loss, CIE colour characteristics, moisture and protein levels

The weight loss during roasting, the CIE colour characteristics and the levels of moisture and protein in the roasted coffee samples are indicated on Table 2. There was a significant loss of weight of samples after roasting. The weight loss increased with an increase in the intensity of the roasting process for both coffee species. A significant difference was also observed between species, with higher weight loss in Robusta compared to Arabica in every degree of roasting. Similar results were reported by Perrone et al. (2008).

A significant difference was observed on the CIE $L^*a^*b^*$ colour characteristics among roasted samples. According to the literature, the degree of roasting can be inferred by coffee's colour: the stronger the roasting degree, the lower the L^* values will be (Almeida et al., 2006; Cirilo et al., 2003; Summa, De La Calle, Brohee, Stadler, & Anklam, 2007). Significant differences were also observed for the chroma, which refers to the perceived colourfulness. It decreased significantly throughout the roasting process. Such differences during roasting of distinct varieties under the same conditions have also been observed in previous studies. According to Murkovic and Derler (2006), the higher sucrose content of Arabica compared to Robusta coffee, can favour colour development during roasting. The significant difference in the weight loss during roasting and in colour characteristics (L^* and chroma values) confirmed that the samples were submitted to three different degrees of roasting – light, medium and dark (Perrone et al., 2008).

Table 2
Colour characteristics, levels of moisture and protein in Arabica and Robusta coffee submitted to different roasting conditions.

Parameter	Coffee roasting[a]		
	Light (171 °C/8 min)	Medium (171 °C/15 min)	Dark (210 °C/15 min)
Weight loss (%)			
Arabica	13.90 ± 0.20^{BZ}	17.91 ± 0.85^{BY}	29.55 ± 0.99^{BX}
Robusta	16.40 ± 0.10^{AZ}	21.22 ± 0.56^{AY}	33.07 ± 0.94^{AX}
CIE colour			
L^* (luminosity)			
Arabica	27.97 ± 2.00^{AX}	18.97 ± 0.78^{AY}	12.74 ± 0.83^{BZ}
Robusta	28.84 ± 1.61^{AX}	18.67 ± 1.32^{AY}	14.53 ± 2.06^{AZ}
Chroma			
Arabica	27.90 ± 3.43^{AX}	12.20 ± 1.46^{AY}	2.64 ± 1.24^{BZ}
Robusta	29.10 ± 2.90^{AX}	11.67 ± 1.12^{AY}	$5.65 + 1.57^{AZ}$
Hue			
Arabica	66.97 ± 5.28^{BY}	57.59 ± 8.32^{AY}	220 ± 52.2^{BX}
Robusta	70.88 ± 4.03^{AZ}	56.53 ± 10.22^{AY}	164 ± 25.3^{AX}
Moisture content (g/100 g)			
Arabica	1.31 ± 0.38	1.40 ± 0.38	1.53 ± 0.49
Robusta	1.63 ± 0.33	1.45 ± 0.30	1.57 ± 0.38
Protein (g/100 g)			
Arabica	13.37 ± 1.58	14.26 ± 1.64	14.67 ± 2.70
Robusta	14.10 ± 0.66	14.39 ± 1.27	14.78 ± 1.72

[a] Mean values (±standard deviation) with different letters (AB) for the same parameter in the same column and with different letters (XYZ) in the same line are significantly different (Tukey tests, $p \leqslant 0.05$).

There was a significant loss of moisture content after roasting – 85% loss – for both Arabica and Robusta coffee, reaching values which did not differ significantly between species and among the different roasting degrees. During coffee roasting there are two major phases: dehydration and pyrolysis. Most of the water is lost during dehydration, at the beginning of the roasting process, reaching very low levels. During pyrolysis, there is still water loss, along with CO_2 and CO, however at a very slow rate (Casal et al., 2005; Montavon et al., 2003). The gravimetric method used in the determination of moisture is not sensitive enough to detect such a small loss.

The levels of protein in the roasted coffee varied from 13.37 to 14.78 g/100 g. Similar results are described in the literature (Casal et al., 2005). However, these results are also over-estimated because of other sources of nitrogen in the roasted coffee such as caffeine, trigonelline and the Maillard reaction derived melanoidins (Bekedan et al., 2006; Mazzafera, 1999). There was no significant difference on total nitrogen levels between species or roasting degrees.

3.3. Influence of roasting on the levels of serotonin precursors in Arabica and Robusta coffee

5-HTP was not detected (<0.3 mg/100 g) in any of the roasted coffee samples, similar to what was found in green coffee. Free tryptophan, which was present in green coffee, was not detected (<0.3 g/ml) in roasted coffee either. Its total loss during roasting indicates the sensitivity of free tryptophan, irrespective of the degree of roasting.

Protein-bound tryptophan was detected in the roasted samples at levels which decreased as the intensity of the roasting process increased (Fig. 2). No significant difference was observed on tryptophan levels between species at each degree of roasting. During the initial minutes of roasting there was a significant decrease on the levels of tryptophan in Robusta coffee compared to Arabica. The loss of tryptophan correlated significantly (Pearson correlations, $R^2 \geqslant 0.979$) with the roasting degree, with higher rates for Robusta (−39.504) compared to Arabica (−29.925). This result suggests that there might be factors in Arabica coffee which decreased tryptophan loss. The higher lipid content of Arabica coffee could afford this protective effect (Casal et al., 2003).

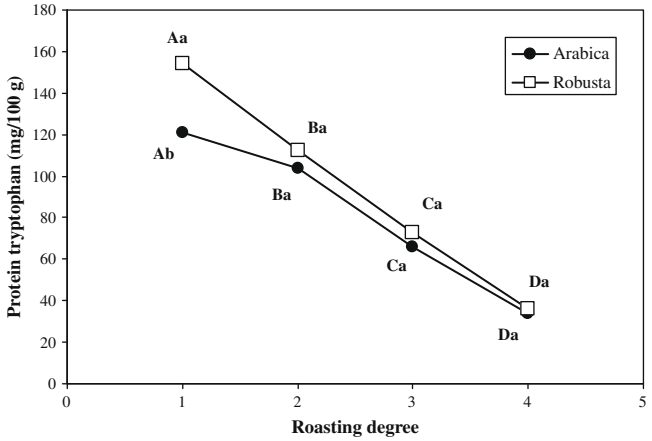

Fig. 2. Levels of protein-bound tryptophan in Arabica and Robusta green (1) and roasted coffee to different degrees: (2) light roast – 171 °C/8 min, (3) medium roast – 171 °C/15 min and (4) dark roast – 210 °C/15 min. Mean levels with different letters ab for species and ABCD for roasting degree are significantly different (Tukey test, $p \leqslant 0.05$).

According to Turner et al. (2005) and Ruddick et al. (2006), 5-HTP can be formed through oxidation of free or protein-bound tryptophan, however, it is much more susceptible to oxidation than tryptophan itself. Furthermore, 5-HTP can be decarboxylated during roasting forming serotonin (Cirilo et al., 2003). Therefore, it is possible that 5-HTP could have been produced and degraded during roasting.

3.4. Serotonin precursors in Arabica and Robusta coffee beverages

The coffee beverages prepared with the medium-roasted coffee (171 °C/15 min) had ~24% extraction rate (Table 3), which is typical of a homemade beverage with good body (López-Galilea et al., 2007). The levels of nitrogen detected by the Kjeldahl method overestimates protein levels as indicated previously.

5-HTP and free tryptophan were not detected. However, protein-bound tryptophan was found in the beverages from both species. Significantly higher tryptophan levels were detected in Robusta compared to Arabica beverage. The levels of tryptophan in the beverages varied from 28.1 to 49.5 μg/ml, which represents 1.4 to 2.5 mg of tryptophan/50 ml cup. Based on these results, three cups of coffee a day would provide the recommended daily intake (DRI, 2005).

Table 3
Total solids, extraction rate, protein, 5-hydroxytryptophan (5-HTP), free and protein-bound tryptophan in coffee beverage from medium-roasted Arabica and Robusta.

Parameters	Levels[a]	
	Arabica	Robusta
Total solids (mg/ml)	32.74 ± 0.39^{B}	$33.87 \pm 0.18^{*}$
Extraction rate (g/100 ml)	24.56 ± 0.29^{a}	24.40 ± 0.14^{A}
Protein (g/100 ml)	0.11 ± 0.01^{B}	0.12 ± 0.01^{A}
5-HTP (mg/100 ml)	Nd[b]	nd
Tryptophan	nd	nd
Free (mg/100 ml)	nd	nd
Protein-bound (μg/ml)	28.1 ± 4.1^{B}	49.5 ± 4.6^{A}

[a] Mean values ± standard deviation with the different capital letters in the same line are significantly different ($p \leqslant 0.05$).
[b] nd – not detected (<0.3 μg/ml).

The presence of tryptophan in coffee beverages suggests that it might contribute to the diet tryptophan pool. However its uptake as a precursor of the neurotransmitter serotonin must be further investigated, as it will also depend on protein digestibility, presence of anti-nutritional factors, ratio of tryptophan/neutral amino acids and presence of added carbohydrates to the beverage (Comai et al., 2007; Lyons & Truswell, 1988).

4. Conclusions

Based on these results, green coffee did not have 5-HTP, however it was observed to be a good source of free and protein-bound tryptophan. During roasting, there was a complete degradation of free tryptophan and the levels of protein bound-tryptophan decreased with the intensity of the roasting process. A beverage prepared with medium-roasted Arabica and Robusta coffee provides a good dietary source of protein-bound tryptophan.

Acknowledgements

The authors thank CNPq (Conselho Nacional de Desenvolvimento Científico e Tecnológico) and Fapemig (Fundação de Amparo a Pesquisa do Estado de Minas Gerais) for the financial support.

References

Almeida, A. A. P., Farah, A., Silva, D. A. M., Nunan, E. A., & Gloria, M. B. A. (2006). Antibacterial activity of coffee extracts and selected coffee chemical compounds against enterobacteria. *Journal of Agricultural and Food Chemistry, 54*, 8738–8743.

AOAC (2000). *Official methods of analysis* (17th ed.). Gaithersburg, MD, USA: AOAC.

Arnold, U., & Ludwig, E. (1996). Analysis of free amino acid in green coffee beans. II. Changes of the amino acid content in arabica coffees in connection with post-harvest model treatment. *Zeitschrift für Lebensmittel-Untersuchung und-Forschung, 203*, 379–384.

Bekedan, E. K., Schols, H. A., Van Boekel, M. A. J. S., & Smit, G. (2006). High molecular weight melanoidins from coffee brew. *Journal of Agricultural and Food Chemistry, 54*, 7658–7666.

Birdsall, T. C. (1998). 5-Hydroxytryptophan: A clinically-effective serotonin precursor. *Alternative Medicine Review: A Journal of Clinical Therapeutic, 3*, 271–280.

Casal, S., Alves, M. R., Mendes, E., Oliveira, M. B. P. P., & Ferreira, M. A. (2003). Discrimination between arabica and robusta coffee species on the basis on their amino acid enantiomers. *Journal of Agricultural and Food Chemistry, 51*, 6495–6501.

Casal, S., Mendes, E., Oliveira, M. B. P. P., & Ferreira, M. A. (2005). Roast effects on coffee amino acid enantiomers. *Food Chemistry, 89*, 333–340.

Cirilo, M. P. G., Coelho, A. F. S., Araújo, C. M., Gonçalves, F. R. B., Nogueira, F. D., & Gloria, M. B. A. (2003). Profile and levels of bioactive amines in green and roasted coffee. *Food Chemistry, 82*, 397–402.

Comai, S., Bertazzo, A., Bailoni, L., Zancato, M., Costa, C., & Allegri, G. A. (2007). Content of proteic and nonproteic tryptophan in quinoa and cereal flours. *Food Chemistry, 100*, 1350–1355.

Delgado-Andrade, C., Rufian-Henares, J. A., Jimenez-Perez, S., & Morales, F. J. (2006). Tryptophan determination in milk-based ingredients and dried sport supplements by liquid chromatography with fluorescence detection. *Food Chemistry, 98*, 580–585.

Dórea, J. G., & Da Costa, T. H. M. (2005). Is coffee a functional food? *British Journal of Nutrition, 93*, 773–782.

DRI. (2005). Dietary reference intake. Food and Nutrition Information Center, USDA. <http://fnic.nal.usda.gov/nal_display/index.php?info_center>.

Embrapa Café (2007). Histórico. 01nov2007. <http://www22.sede.embrapa.br/cafe/unidade>.

Goihl, J. (2006). Tryptophan can lower aggressive behavior. *Feedstuffs, 78*, 12–22.

Higdon, J. V., & Frei, B. (2006). Coffee and health: A review of recent human research. *Critical Reviews in Food Science and Nutrition, 46*, 101–123.

López-Galilea, I., De Peña, M. P., & Cid, C. (2007). Correlation of selected constituents with the total antioxidant capacity of coffee beverages: Influence of the brewing procedure. *Journal of Agriculture and Food Chemistry, 55*, 6110–6117.

Lyons, P. M., & Truswell, A. S. (1988). Serotonin precursors influenced by type of carbohydrate meal in healthy adults. *American Journal of Clinical Nutrition, 47*, 433–439.

Martins, A. C. C. (2008). *Determination of serotonin precursors – tryptophan and 5-hydroxytryptophan – in coffee by ion-pair HPLC*. MSc Dissertation in Food Science. Universidade Federal de Minas Gerais, 99p.

Mazzafera, P. (1999). Chemical composition of defective coffee beans. *Food Chemistry, 64*, 547–554.

Montavon, P., Mauron, A. F., & Duruz, E. (2003). Changes in green coffee profiles during roasting. *Journal of Agriculture and Food Chemistry, 51*, 2335–2343.

Murkovic, M., & Derler, K. (2006). Analysis of amino acids and carbohydrates in green coffee. *Journal of Biochemical and Biophysical Methods, 69*, 25–32.

Perrone, D., Farah, A., Donangelo, C. M., de Paulis, T., & Martin, P. R. (2008). Comprehensive analysis of major and minor chlorogenic acids and lactones in economically relevant Brazilian coffee cultivars. *Food Chemistry, 106*, 859–867.

Reh, C. T., Gerber, A., Prodolliet, J., & Vuataz, G. (2006). Water content determination in green coffee – method comparison to study specificity and accuracy. *Food Chemistry, 96*, 423–430.

Ruddick, J. P., Evans, A. K., Nutt, D. J., Lightman, S. L., Rook, G. A. W., & Lowry, C. A. (2006). Tryptophan metabolism in the central nervous system: Medical implications. *Expert Reviews in Molecular Medicine, 8*, 1–27.

Shaw, K., Turner, J., & Del Mar, C. (2009). Tryptophan and 5-hydroxytryptophan for depression. *Cochrane Database of Systematic Reviews, 3*, 1–8.

Summa, C. A., De La Calle, B., Brohee, M., Stadler, R. H., & Anklam, E. (2007). Impact of the roasting degree of coffee on the in vitro radical scavenging capacity and content of acrylamide. *LWT-Food Science and Technology, 40*, 1849–1854.

Turner, E. H., Loftis, J. M., & Blackwell, A. D. (2005). Serotonin a la carte: Supplementation with the serotonin precursors 5-hydroxytryptophan. *Pharmacological Therapy, 109*, 325–338.

Food Chemistry 118 (2010) 534–539

Contents lists available at ScienceDirect

Food Chemistry

journal homepage: www.elsevier.com/locate/foodchem

Antioxidant mechanisms of Trolox and ascorbic acid on the oxidation of riboflavin in milk under light

Naeemah K. Hall, Timothy M. Chapman, Hyun Jung Kim *, David B. Min

Department of Food Science and Technology, The Ohio State University, 2015 Fyffe Road, Columbus, OH 43210, USA

ARTICLE INFO

Article history:
Received 23 February 2009
Received in revised form 3 April 2009
Accepted 8 May 2009

Keywords:
Riboflavin
Milk
Trolox
Ascorbic acid
Singlet oxygen

ABSTRACT

Antioxidant activities and the mechanism of water-soluble Trolox and ascorbic acid on the oxidation of riboflavin in milk were studied. Trolox or ascorbic acid at 0, 100, 250, 500, or 1000 ppm was added to milk with or without added 50 ppm riboflavin and stored under light at 27 °C. Headspace oxygen was analysed by GC and Trolox, ascorbic acid, and riboflavin were determined by HPLC. The headspace oxygen of milk with added 50 ppm riboflavin depleted faster than that of milk without added riboflavin ($p < 0.05$). Trolox and ascorbic acid decreased during storage under light and riboflavin was completely destroyed within 24 h. As the concentration of Trolox or ascorbic acid increased, the riboflavin loss decreased. Riboflavin, Trolox, and ascorbic acid competed to react with singlet oxygen which was formed in the presence of riboflavin under light. Trolox and ascorbic acid protected riboflavin in milk under light by reacting with singlet oxygen.

1. Introduction

Riboflavin (Vitamin B2) is required for the metabolism of fats, carbohydrates and proteins and for red blood cell formation and respiration. Riboflavin is also essential in healthy hair and nail growth and thyroid activity (Choe, Huang, & Min, 2005; Siassi & Ghadirian, 2005). Riboflavin must be obtained from foods because the body does not synthesise or store the vitamin.

Milk is the most important source of riboflavin. Children between the ages 3–5 get approximately one-fifth of their total riboflavin intake from milk (Wells, 2000). Children ages 8–11 who drank no school milk, as compared to children who drank milk everyday at school, were more likely to have riboflavin intakes below the recommended levels (Cook, Altman, Jacoby, & Holland, 1975). The Recommended Daily Allowances for men is 1.3 mg/day, 1.1 mg/day for women and up to 0.9 mg/day for children up to age 14 (Institute of Medicine, 1998). Milk is stored in refrigerated dairy cases and exposed to fluorescent light to enhance consumer attraction prior to purchase at the supermarket (Bradley, Kim, & Min, 2006; Cladman, Scheffer, Goodrich, & Griffiths, 1998; Shiota, Ikeda, Konishi, & Yoshioka, 2002; Van Aardt et al., 2005). The light exposure lowers the nutritional quality of milk by destroying riboflavin rapidly. The vitamin content claimed on the label may not be the actual vitamin content upon purchase (Whited, Hammond, Chapman, & Boor, 2002). Riboflavin loss is dependant on light intensity and wavelength, exposure time, and packaging materials (Min & Boff, 2002). Researchers are continually studying effective ways to protect riboflavin in foods.

Oxidation of milk during light storage causes a significant loss of vitamins and produces off-flavours. The type, concentration, and solubility of oxygen can increase the oxidation of milk. Triplet oxygen oxidation is temperature dependant requiring higher activation energies, whilst singlet oxygen oxidation occurs at very low temperatures (Huang, Choe, & Min, 2004a; Min & Boff, 2002). Milk fat can affect the formation of off-flavours, where pentanal, heptanal and hexanal levels increased as the fat content increased from 0.5% to 3.4% (Lee, 2002). High concentrations of riboflavin in milk produce high amounts of volatile compounds (Huang et al., 2004a; Jung, Yoon, Lee, & Min, 1998; Lee, 2002).

In addition to protecting milk from light through the use of modified packaging materials, food additives can be used to prevent oxidation of milk. Tocopherols are the most powerful hydrophobic natural antioxidants. Trolox is an α-tocopherol derivative. The hydrophobic phytyl group of tocopherol has been replaced with a hydrophilic carboxylic group to produce Trolox, which is soluble in water (Priyadarsini, Kapoor, & Naik, 2001). Trolox is a synthetic compound that has been used as a food additive and as an active ingredient in cosmetic products (Carlotti, Sapino, Vione, Pelizzetti, & Trotta, 2004; Delicado, Ferrer, & Carmona, 1997). Studies show that the phytyl group of tocopherol has little effect on its antioxidant activity (Niki et al., 1985). α-Tocopherol and Trolox donate hydrogen from the hydroxyl group of a chroman ring to food radicals. Since the active antioxidant site for α-tocopherol and

* Corresponding author. Tel.: +1 614 292 7801; fax: +1 614 292 0218.
E-mail address: hyunjkim@iastate.edu (H.J. Kim).

0308-8146/$ - see front matter © 2009 Elsevier Ltd. All rights reserved.
doi:10.1016/j.foodchem.2009.05.017

Trolox are the same, the hydrogen-donating ability of Trolox will be similar to that of α-tocopherol.

Trolox reduced lipid oxidation and oxymyoglobin oxidation in bovine muscle (O'Grady, Monahan & Brunton, 2001) and protein oxidation in chicken breast meat (Lin & Liang, 2002). Cardiac recovery was significantly enhanced with Trolox after ischaemia and reperfusion (Sagach et al., 2002). Trolox inhibited the formation of thiobartituric acid reactive substances, which are indirect makers of lipid oxidation (Sagach et al., 2002). Trolox reduced the oxidation of blood plasma (Barclay, Basque, Stephenson, & Vinqvist, 2003). Many studies have reported the antioxidant effects of Trolox in food and biological systems but none have reported the antioxidant effect of Trolox in milk during light storage. The objective of this research was to study the antioxidant activities and mechanisms of Trolox and ascorbic acid to protect riboflavin in milk during storage under light.

2. Materials and methods

2.1. Materials

Commercial whole milk was purchased from a local grocery store (Krogers, Columbus, OH, USA). Teflon-coated rubber septa, aluminium caps and glass serum vials were purchased from Supelco, Inc. (Bellefonte, PA, USA). Riboflavin, ascorbic acid, and Trolox™ ((±)-6-Hydroxy-2,5,7,8-tetramethylchromane-2-carboxylic acid) were purchased from Sigma Chemical Co. (St. Louis, MO, USA). A Milli-Q purification system was obtained from Millipore Co. (Bedford, MA, USA).

2.2. Sample preparation and storage

Two gallons of milk were sterilised before experimentation to reduce microbial growth during storage. Milk was commercially sterilised by Abbott Nutrition Supply Chain (Columbus, OH, USA.) and aseptically packaged in a can (200 ml). Trolox or ascorbic acid at 0, 100, 250, 500, or 1000 ppm was added to sterilised milk with or without the addition of 50 ppm riboflavin. Ten millilitres of milk sample was transferred to a 20-ml serum vial (22.6 × 150 mm, Supelco Inc., Bellefonte, PA, USA). Sample vials were sealed airtight with a Teflon-coated rubber septa and aluminium caps and stored under light at 27 °C. The light source was four Sylvania fluorescent lamps (General Electrics, Cleveland, OH, USA) with 1500 Lux light intensity. Samples were prepared in duplicate at each sample analysis. Headspace oxygen of samples was measured daily for 3 days. Riboflavin, Trolox, and ascorbic acid in milk were analysed every 3 h for 12 h.

2.3. Determination of headspace oxygen by GC

Headspace oxygen in the milk bottle was measured by injecting 100 μl of headspace gas into a Hewlett–Packard 5890 gas chromatograph (GC) equipped with a thermal conductivity detector. A stainless steel column (1.8 m × 0.32 cm) packed with 80/100 molecular sieve 13× (Alltech Asso Inc., IL, USA) was used. High purity (99.995%) helium was used as the carrier gas at 20 ml/min. The temperature of injection port, oven, and detector were 120, 40, and 150 °C, respectively. The gas chromatographic peak was measured by electronic count using a HP 3396A integrator. The percent of headspace oxygen of the sample bottle was determined by comparing the gas chromatographic peak of that of air which was considered to have 20.9% oxygen (Huang, Choe, & Min, 2004b; King & Min, 1998).

2.4. Determination of Trolox, ascorbic acid, and riboflavin by HPLC

To analyse Trolox and ascorbic acid in milk, 5 ml of 3% metaphosphoric acid in 50% methanol solution was added to 5 ml milk. Milk samples were filtered with a 0.45 μm membrane filter (25 mm i.d., Whatman, NY, USA) and collected into a 2-ml vial. Trolox and ascorbic acid were also determined by HPLC (Agilent 1100, Agilent Technologies, Inc., Santa Clara, CA, USA) equipped with a multiple wavelength detector and a Discovery C18 column (5 μm 4.6 mm × 15 cm, Supelco Inc., Bellefonte, PA, USA). The injection volume was 100 μl. The flow rate of mobile phase was 1 ml/min. The mobile phase for Trolox analysis was 60% methanol in 50 mM potassium phosphate. The mobile phase for ascorbic acid analysis was 50 mM potassium phosphate. Trolox and ascorbic acid was detected at 290 nm and 254 nm, respectively.

To analyse riboflavin in milk, 20 ml of 3% metaphosphoric acid in water was added to 10 ml milk to precipitate proteins. Milk samples were diluted with 50 ml deionised water and 1 ml was filtered with a 0.45 μm membrane filter into a vial. The riboflavin of milk was measured by reverse phase liquid chromatography using a High Pressure Liquid Chromatography system (HPLC, Agilent 1100, Agilent Technologies, Inc., Santa Clara, CA, USA) equipped with an Ultrasphere IP column (C-18, 5 μm 4.6 mm × 15 cm, Fullerton, CA, USA). The injection volume was 50 μl. The flow rate of the mobile phase, 10% acetonitrile in 4.0 mM aqueous octane sulphonate with 0.74% triethylamine at pH 4.09 (adjusted with 1% formic acid), was 0.8 ml/min. Riboflavin was measured by a fluorescence detector at an emission wavelength of 518 nm with an excitation at 366 nm.

2.5. Statistical analysis

All experiments were done in duplicate. Two-way analysis of variance and Tukey's test were used to analyse the effects of Trolox and ascorbic acid on the headspace oxygen content and riboflavin content using XLSTAT at $\alpha = 0.05$ (Microsoft 2007).

3. Results and discussion

3.1. Milk sample preparation

A preliminary work showed that microorganisms in milk depleted headspace oxygen in the sample bottle during storage under light. In the current study, the oxidation of milk during storage under light was studied by headspace oxygen determination in the sample bottle. To eliminate the depletion of headspace oxygen by microorganisms in milk, milk was sterilised. Riboflavin contents of milk with and without sterilisation were analysed and essentially the same.

3.2. Reproducibility of GC and HPLC analyses

The coefficients of variation for measuring headspace oxygen by GC and Trolox, ascorbic acid, and riboflavin content by HPLC for 5 replicates were 2.1, 1.7, 1.4, and 1.4%, respectively (data not shown). The low coefficients of variations were considered good to determine headspace oxygen by GC and Trolox, ascorbic acid, and riboflavin content in milk by HPLC.

3.3. Effect of riboflavin concentration on headspace oxygen of milk

The riboflavin content of milk measured by HPLC was 1.3 ppm. Milk added with 50 ppm riboflavin contained a total amount of 51.3 ppm riboflavin. Milk with 0 ppm riboflavin was prepared by passing milk through a Florisil column according to Jung et al.

Table 1
Effect of riboflavin on the headspace oxygen of milk during 3 days of storage under light and in dark at 27 °C.

Storage	Riboflavin (ppm)	Headspace oxygen (%)[a]			
		0 day	1 day	2 day	3 day
Light	0	20.9 ± 0.02	20.7 ± 0.03	20.6 ± 0.02	20.7 ± 0.04
	1.3	20.9 ± 0.02	18.2 ± 0.25	17.3 ± 0.26	15.9 ± 0.22
	51.3	20.9 ± 0.02	15.1 ± 0.24	13.0 ± 0.32	11.2 ± 0.35
Dark	0	20.9 ± 0.02	20.8 ± 0.04	20.7 ± 0.07	20.6 ± 0.04
	1.3	20.9 ± 0.02	20.9 ± 0.03	20.8 ± 0.09	20.7 ± 0.06
	51.3	20.9 ± 0.02	20.8 ± 0.03	20.8 ± 0.06	20.7 ± 0.03

[a] Values are the average of three measurements ± standard deviation.

(1998). The effects of 0, 1.3, and 51.3 ppm riboflavin on the headspace oxygen of milk under light and in dark for 3 days at 27 °C are shown in Table 1. Riboflavin had a significant effect on the depletion of headspace oxygen in milk under light ($p < 0.05$). The headspace oxygen of milk with 0, 1.3, and 51.3 ppm riboflavin under light for 1 day decreased from 20.9% to 20.7, 18.2, and 15.1%, respectively. The depletion of headspace oxygen in the airtight bottle was assumed to be a result of the reaction between oxygen and milk components. The headspace oxygen of milk with 0, 1.3, and 51.3 ppm riboflavin stored in dark were essentially the same, remaining at approximately 20.9% throughout storage. Riboflavin accelerated the depletion of headspace oxygen in milk under light but not in dark. Riboflavin in milk or soymilk increased the formation of volatiles and the depletion of headspace oxygen under light (Bradley et al., 2006; Huang et al., 2004a, 2004b; King & Min, 1998; Lee, 2002). Riboflavin-free milk did not produce volatiles during 8 h of storage under light (Jung et al., 1998).

Riboflavin increased the depletion of headspace oxygen in milk under light but not in dark (Table 1). It suggested that the type of oxygen in milk under light may not be the same type of the oxygen in milk in the dark. The chemical reaction of riboflavin under light is shown in Fig. 1. Ground state riboflavin having conjugated double bonds easily absorbs light and becomes excited singlet riboflavin (^{1}Riboflavin$*$). The excited singlet state riboflavin becomes excited triplet riboflavin (^{3}Riboflavin$*$) through intersystem crossing mechanism. The diradical excited triplet riboflavin reacts with diradical triplet oxygen to produce singlet oxygen by triplet–triplet annihilation (Huang et al., 2004b; Min & Boff, 2002). Singlet oxygen

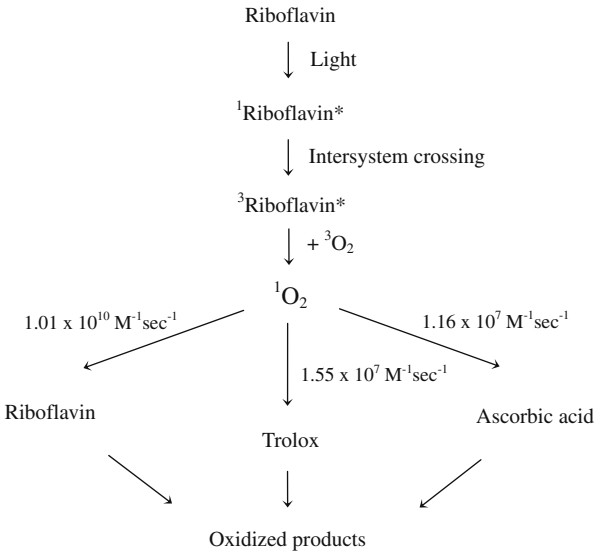

Fig. 1. Formation of singlet oxygen by riboflavin under light and the reaction rates of riboflavin, Trolox, and ascorbic acid with singlet oxygen in milk system.

is an electrophilic, very reactive, and high-energy molecule. Singlet oxygen quickly reacts with food components containing double bonds such as riboflavin, polyunsaturated lipids, aromatic amino acids, and vitamins. Singlet oxygen was detected in skim milk by electron spin resonance spectroscopy (Bradley et al., 2006), which showed singlet oxygen was formed in the presence of riboflavin and triplet oxygen under light. The headspace oxygen in milk did not deplete during storage in dark but rapidly depleted under light (Table 1). Singlet oxygen can not be formed in dark, even in the presence of riboflavin. Therefore, the headspace oxygen in milk under light decreased due to singlet oxygen which reacted with food components such as riboflavin, unsaturated lipids, aromatic or sulphur containing proteins, or vitamins in milk to form oxidised products (Jung et al., 1998; King & Min, 1998; Lee, 2002).

3.4. Effect of Trolox or ascorbic acid on headspace oxygen of milk without or with added 50 ppm riboflavin

The effects of 0, 100, 250, 500 and 1000 ppm Trolox on the headspace oxygen of milk without or with added 50 ppm riboflavin are shown in Fig. 2. As the concentration of Trolox increased from 0 to 100, 250, 500, and 1000 ppm, the depletion of headspace oxygen increased ($p < 0.05$). After 3 days of storage under light, the headspace oxygen of milk without added riboflavin with 0 ppm Trolox and 1000 ppm Trolox decreased from 20.9% to 15.9% and 11.1%, respectively (Fig. 2A). The addition of 1000 ppm Trolox nearly doubled headspace oxygen depletion in milk without added riboflavin. In the milk with added 50 ppm riboflavin, the addition of Trolox increased the rate of headspace oxygen depletion (Fig. 2B). The headspace oxygen of milk with added 50 ppm riboflavin containing 250, 500, and 1000 ppm Trolox were significantly lower than that of 0 ppm or 100 ppm Trolox ($p < 0.05$).

The effects of 0, 100, 250, 500 and 1000 ppm ascorbic acid on the headspace oxygen of milk without or with added 50 ppm riboflavin are shown in Fig. 3. As the concentration of ascorbic acid increased, the depletion of headspace oxygen increased. The headspace oxygen of milk without added 50 ppm riboflavin containing ascorbic acid were significantly lower than milk with 0 ppm ascorbic acid ($p < 0.05$). The headspace oxygen of milk with added 50 ppm riboflavin decreased more than those of milk without added riboflavin. The headspace oxygen content of milk with added 50 ppm riboflavin containing 500 and 1000 ppm ascorbic acid were significantly lower than those containing 100 and 250 ppm ascorbic acid ($p < 0.05$).

As the concentration of Trolox and ascorbic acid in milk increased, the headspace oxygen depletion increased. The higher depletion of headspace oxygen in milk containing Trolox and ascorbic acid might be due to the reaction between Trolox or ascorbic acid and oxygen in the sample vial during storage.

3.5. Effect of Trolox or ascorbic acid on riboflavin destruction of milk without or with added 50 ppm riboflavin

The effects of 0, 100, 250, 500 and 1000 ppm Trolox or ascorbic acid on the riboflavin content of milk without added 50 ppm riboflavin under light for 12 h are shown in Fig. 4. Milk initially contained 1.3 ppm riboflavin. Milk with 0 ppm Trolox lost 100% riboflavin for 9 h under light. Riboflavin in milk with 100, 250, 500 and 1000 ppm Trolox after 12 h of storage under light were 0, 0.07, 0.07, and 0.10 ppm, respectively (Fig. 4A). As the concentration of Trolox increased from 0 to 100, 250, 500, and 1000 ppm, the riboflavin destruction decreased ($p < 0.05$). Riboflavin in milk with 100, 250, 500 and 1000 ppm ascorbic acid after 12 h of storage under light were 0.06, 0.05, 0.09, and 0.27 ppm, respectively (Fig. 4B). Ascorbic acid protected more riboflavin than Trolox at the corresponding concentration.

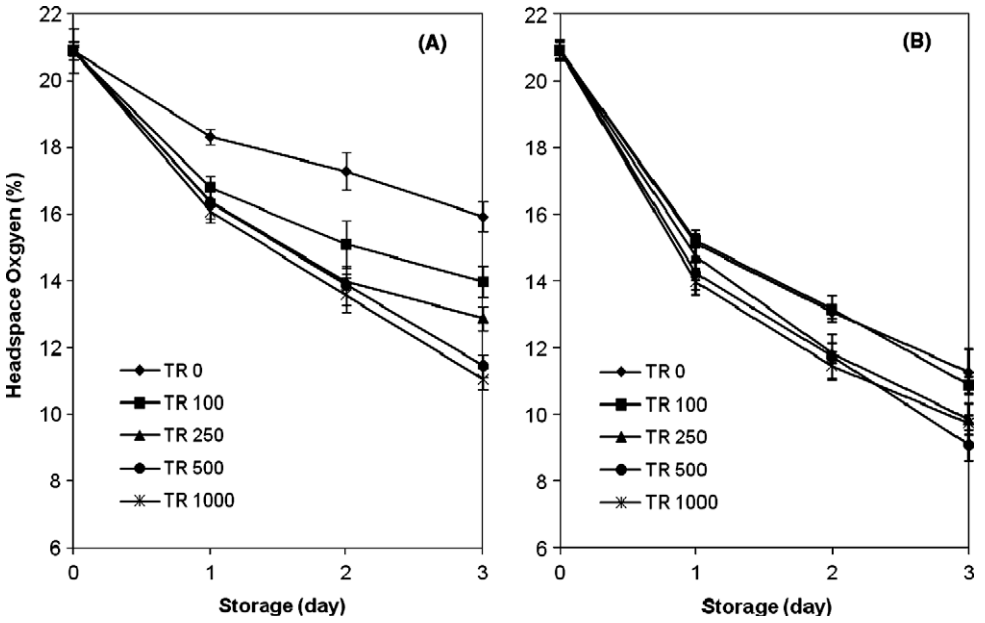

Fig. 2. Effects of 0, 100, 250, 500, and 1000 ppm Trolox on the headspace oxygen of milk without (A) and with (B) added 50 ppm riboflavin during the storage of 3 days under light at 27 °C (TR: Trolox).

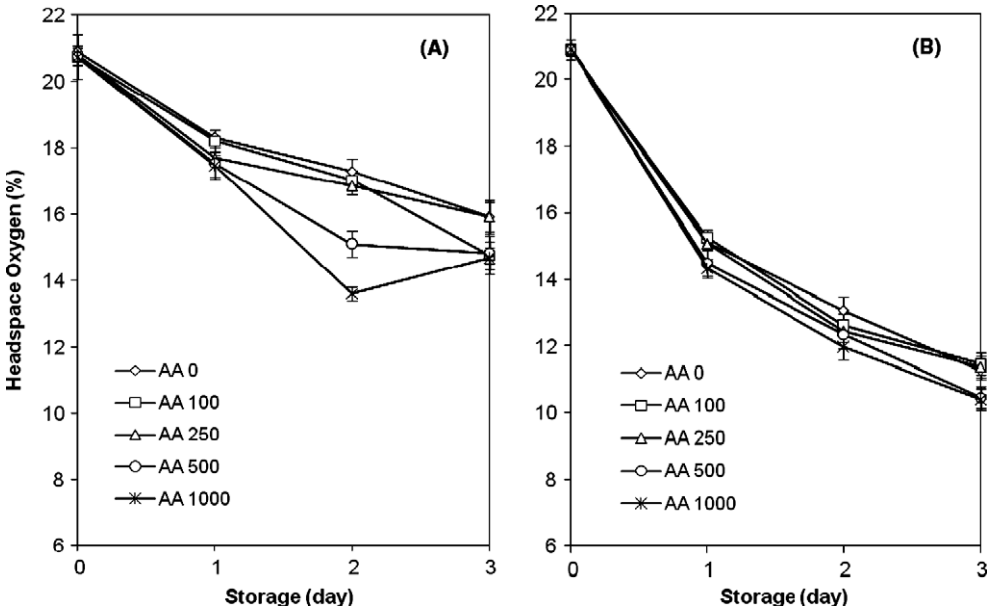

Fig. 3. Effects of 0, 100, 250, 500, and 1000 ppm ascorbic acid on the headspace oxygen of milk without (A) and with (B) added 50 ppm riboflavin during the storage of 3 days under light at 27 °C (AA: ascorbic acid).

The effects of 0, 100, 250, 500 and 1000 ppm Trolox or ascorbic acid on the riboflavin content of milk with added 50 ppm riboflavin under light for 12 h are shown in Fig. 5. Milk without Trolox or ascorbic acid lost 92% riboflavin after 12 h and 100% riboflavin after 24 h of storage under light. As the concentration of Trolox increased from 0 or 100 ppm to 250, 500, and 1000 ppm, the riboflavin destruction significantly decreased ($p < 0.05$) (Fig. 5A). After 24 h under light, milk with 1000 ppm Trolox contained 3.7 ppm riboflavin whilst riboflavin in milk without Trolox was completely lost. As the concentration of Trolox increased from 0 or 100 ppm to 250, 500, and 1000 ppm, the riboflavin destruction significantly decreased ($p < 0.05$) (Fig. 5B). Riboflavin in milk containing 1000 ppm ascorbic acid was 4.3 ppm after 24 h of storage under light. Ascorbic acid was effective at minimising riboflavin destruction in milk. The destruction of riboflavin in milk with 500 or 1000 ppm ascorbic acid was significantly slower than milk with 0, 100, or 250 ppm ascorbic acid ($p < 0.05$).

The concentrations of 1000 ppm Trolox or 1000 ppm ascorbic acid in milk with added 50 ppm riboflavin during storage under light are shown in Table 2. As the storage time increased from 0 to 24 h, Trolox and ascorbic acid in milk decreased from 1000 ppm to 333 and 285 ppm, respectively. Ascorbic acid decreased faster than Trolox during storage under light. The decrease of Trolox and ascorbic acid required both riboflavin and light during storage. The effects of singlet oxygen on the stability of ascorbic acid and tocopherol (Trolox is α-tocopherol derivative) have al-

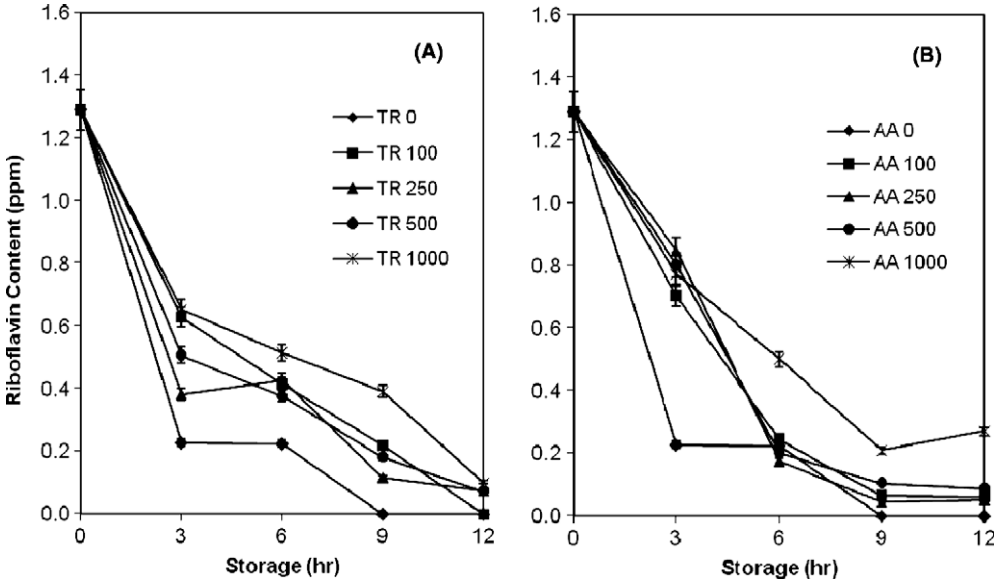

Fig. 4. Effects of 0, 100, 250, 500, and 1000 ppm Trolox (A) and ascorbic acid (B) on the riboflavin content of milk without added 50 ppm riboflavin during the storage of 12 h under light at 27 °C (TR: Trolox, AA: ascorbic acid).

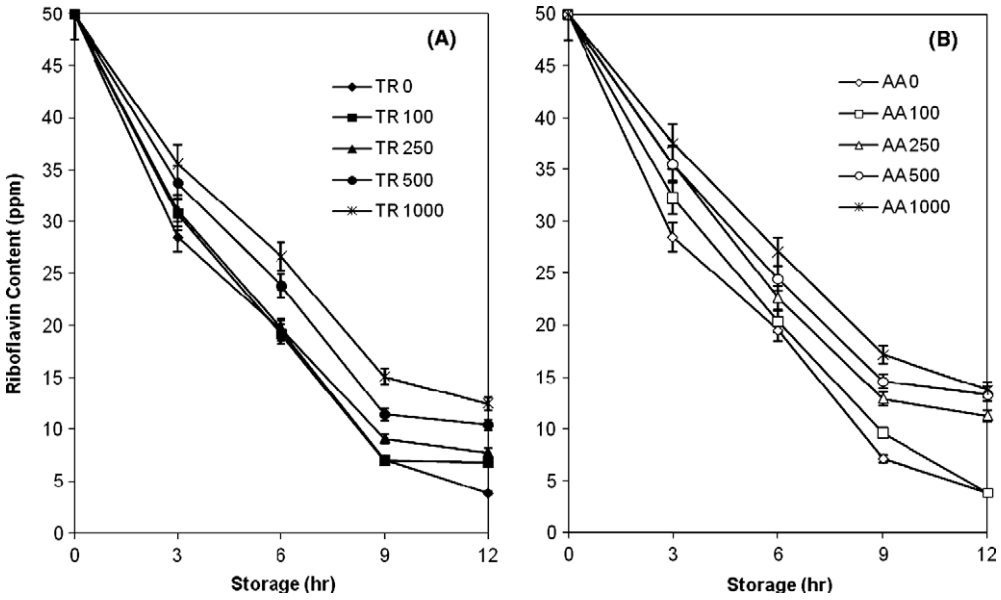

Fig. 5. Effects of 0, 100, 250, 500, and 1000 ppm Trolox (A) and ascorbic acid (B) on the riboflavin content of milk with added 50 ppm riboflavin during the storage of 12 h under light at 27 °C (TR: Trolox, AA: ascorbic acid).

ready been studied (Jung, Kim, & Kim, 1995; Jung et al., 1998; Kim, Lee, & Min, 2006). Ascorbic acid was completely destroyed after 12 min light exposure with 6 ppm riboflavin added, whereas only 2% was destroyed in the sample to which no riboflavin was added or stored in the dark (Jung et al., 1995). Kim et al. (2006) reported that the loss of tocopherols in the absence of a photosensitiser under light or in the presence of a photosensitiser in the dark was not detectable. Singlet oxygen formed in the presence of riboflavin under light reacted with Trolox and ascorbic acid in milk.

3.6. Reaction of riboflavin, Trolox, and ascorbic acid with singlet oxygen

Trolox is a polar antioxidant and locates itself in the water phase of milk (Huang, Hopia, Schwarz, Frankel, & German, 1996).

Table 2
Trolox and ascorbic acid concentration in milk with added 50 ppm riboflavin during storage under light.

Storage (h)	Trolox (ppm)	Ascorbic acid (ppm)
0	1000	1000
3	867 ± 13.56	792 ± 19.55
6	713 ± 15.43	635 ± 10.24
9	586 ± 9.56	514 ± 8.23
12	440 ± 6.87	376 ± 9.45
24	333 ± 5.14	285 ± 7.27

Trolox was reported to prevent protein oxidation effectively but lipid oxidation less effectively in chicken dispersions because it partitioned more into the water phase (Lin & Liang, 2002). The

effectiveness of an antioxidant is dependant on its location within a multiphase system, such as milk. The affinity of Trolox or ascorbic acid to the water phase and lipid phases of milk may determine its effectiveness as an antioxidant. Riboflavin is water-soluble and will locate itself in the water-phase of milk. The protection of riboflavin by Trolox may not be as efficient as the protection by ascorbic acid which could be more soluble in the water phase than Trolox. Partitioning studies on Trolox and ascorbic acid may explain why milk with Trolox lost more headspace oxygen and more riboflavin than milk with ascorbic acid.

Electrophilic singlet oxygen reacts with the double bond containing riboflavin, Trolox, and ascorbic acid (Fig. 1). Huang et al. (2004b) reported that the reaction rate between riboflavin and singlet oxygen in purified water was $1.01 \times 10^{10}\,M^{-1}\,s^{-1}$, which is a diffusion-controlled rate and explained the extremely fast degradation of riboflavin in foods under light. The reaction rates of Trolox and ascorbic acid with singlet oxygen in water were $1.55 \times 10^{7}\,M^{-1}\,s^{-1}$ and $1.16 \times 10^{7}\,M^{-1}\,s^{-1}$, respectively (Yettella & Min, 2008). Trolox and ascorbic acid could rapidly react with singlet oxygen. Riboflavin, Trolox, and ascorbic acid in milk will compete to react with singlet oxygen at different reaction rates.

Singlet oxygen in milk was formed in the presence of riboflavin and triplet oxygen under light. Trolox, ascorbic acid, and riboflavin in milk competed to react with singlet oxygen. As the concentration of Trolox and ascorbic acid in milk increased, the amount of singlet oxygen to react with riboflavin decreased. The more Trolox or ascorbic acid added to milk, the less singlet oxygen reacted with riboflavin. Trolox and ascorbic acid protected riboflavin in milk under light by reacting with singlet oxygen.

In conclusion, the concentration of riboflavin and the addition of Trolox or ascorbic acid affected the headspace oxygen depletion and riboflavin destruction of milk during storage under light. The depletion of headspace oxygen in milk could be attributed to the formation of singlet oxygen and the subsequent oxidation of food components in milk, including riboflavin, Trolox, and ascorbic acid. Trolox and ascorbic acid protected riboflavin in milk under light by reacting with singlet oxygen but did not completely protect it.

References

Barclay, L. R. C., Basque, M. C., Stephenson, V. C., & Vinqvist, M. R. (2003). Photooxidations initiated or sensitized by biological molecules: Singlet oxygen versus radical peroxidation in micelles and human blood plasma. *Photochemistry and Photobiology, 78*(3), 248–255.

Bradley, D. G., Kim, H. J., & Min, D. B. (2006). Effect, quenching mechanism, and kinetics of water soluble compounds in riboflavin photosensitized oxidation of milk. *Journal of Agricultural and Food Chemistry, 54*, 6016–6020.

Carlotti, M. E., Sapino, S., Vione, D., Pelizzetti, E., & Trotta, M. (2004). Photostability of Trolox in water/ethanol, water, and oramix CG 110 in the absence and in the presence of TiO_2. *Journal of Dispersion Science and Technology, 25*(2), 193–207.

Choe, E., Huang, H., & Min, D. B. (2005). Chemical reactions and stability of riboflavin in foods. *Journal of Food Science, 70*(1), 28–36.

Cladman, W., Scheffer, S., Goodrich, N., & Griffiths, M. W. (1998). Shelf life of milk packaged in plastic containers with and without treatment to reduce light transmission. *International Dairy Journal, 8*, 629–636.

Cook, J., Altman, D. G., Jacoby, A., & Holland, W. W. (1975). The contribution made by school milk to the nutrition. *British Journal of Nutrition, 34*, 91–103.

Delicado, E. N., Ferrer, A. S., & Carmona, F. G. (1997). A kinetic study of the one-electron oxidation of Trolox C by the hydoperoxidase activity of lipoxygenase. *Biochemica et Biophysica Acta, 1335*, 127–134.

Huang, R., Choe, E., & Min, D. B. (2004a). Effects of riboflavin photosensitized oxidation on the volatile compounds of soymilk. *Journal of Food Science, 69*(9), 733–738.

Huang, R., Choe, E., & Min, D. B. (2004b). Kinetics for singlet oxygen formation by riboflavin photosensitization and the reaction between riboflavin and singlet oxygen. *Journal of Food Science, 69*(9), 726–732.

Huang, S., Hopia, A., Schwarz, K., Frankel, E., & German, J. (1996). Antioxidant activity of α-tocopherol and Trolox in different lipid substrates: bulk oils vs. oil-in-water emulsions. *Journal of Agricultural and Food Chemistry, 44*, 2496–2502.

Institute of Medicine (1998). Report – *Dietary reference intakes for thiamin, riboflavin, niacin, vitamin B6, folate, vitamin B12, pantothenic acid, biotin, and choline* (pp. 87–121). National Academy of Sciences: Institute of Medicine, Food and Nutrition Board.

Jung, M. Y., Kim, S. K., & Kim, S. Y. (1995). Riboflavin sensitized photooxidation of ascorbic acid kinetics and amino acid effects. *Food Chemistry, 53*, 397–403.

Jung, M. Y., Yoon, S. H., Lee, H. O., & Min, D. B. (1998). Singlet oxygen and ascorbic acid effects on dimethyl disulfide and off-flavor in skim milk exposed to light. *Journal of Food Science, 63*(3), 408–412.

Kim, H. J., Lee, M. Y., & Min, D. B. (2006). Singlet oxygen oxidation rates of α-, γ-, and δ-tocopherols. *Journal of Food Science, 71*(8), 465–468.

King, J. M., & Min, D. B. (1998). Riboflavin photosensitized singlet oxygen oxidation of Vitamin D. *Journal of Food Science, 63*(1), 31–34.

Lee, J. (2002). *Photooxidation and photosensitized oxidation of linoleic acid, milk, and lard*. PhD dissertation, Columbus, Ohio: The Ohio State University.

Lin, C. C., & Liang, J. H. (2002). Effect of antioxidants on the oxidative stability of chicken breast meat in a dispersion system. *Journal of Food Science, 67*(2), 530–533.

Min, D. B., & Boff, J. M. (2002). Chemistry and reaction of singlet oxygen in foods. *Comprehensive Reviews in Food Science and Food Safety, 1*(2), 58–72.

Niki, E., Kawakami, A., Saito, M., Yamamoto, Y., Tsuchiya, J., & Kamiya, Y. (1985). Effect of phytyl side chain of vitamin E on its antioxidant activity. *Journal of Biological Chemistry, 260*(4), 2191–2196.

O'Grady, M. N., Monahan, F. J., & Brunton, N. P. (2001). Oxymyoglobin oxidation and lipid oxidation in bovine muscle—Mechanistic studies. *Journal of Food Science, 66*(3), 386–392.

Priyadarsini, K. I., Kapoor, S., & Naik, D. B. (2001). One- and two-electron oxidation reactions of Trolox by peroxynitrite. *Chemical Research in Toxicology, 14*, 567–571.

Sagach, V. F., Scrosati, M., Fielding, J., Rossoni, G., Galli, C., & Visioli, F. (2002). The water-soluble vitamin E analogue Trolox protects against ischaemia/reperfusion damage in vitro and ex vivo: A comparison with vitamin E. *Pharmaceutical Research, 45*(6), 435–439.

Shiota, M., Ikeda, N., Konishi, H., & Yoshioka, T. (2002). Photooxidative stability of ice cream prepared from milk fat. *Journal of Food Science, 67*(3), 1200–1207.

Siassi, F., & Ghadirian, P. (2005). Riboflavin deficiency and esophageal cancer: A case control-household study in the Caspian Littoral of Iran. *Cancer Detection and Prevention, 29*, 464–469.

Van Aardt, M., Duncan, S. E., Marcy, J. E., Long, T. E., O'Keefe, S. F., & Nielsen-Sims, S. R. (2005). Aroma analysis of light-exposed milk stored with and without natural and synthetic antioxidants. *Journal of Dairy Science, 88*, 881–890.

Wells, A. (2000). Drinks for young children: The dental and nutritional benefits of milk. *Nutrition and Food Science, 30*(2), 76–79.

Whited, L. J., Hammond, B. H., Chapman, K. W., & Boor, K. J. (2002). Vitamin A degradation and light-oxidized flavor defects in milk. *Journal of Dairy Science, 85*, 351–354.

Yettella, R. R., & Min, D. B. (2008). Quenching mechanisms and kinetics of Trolox and ascorbic acid on the riboflavin-photosensitized oxidation of tryptophan and tyrosine. *Journal of Agricultural and Food Chemistry, 56*, 10887–10892.

Food Chemistry 118 (2010) 540–547

Contents lists available at ScienceDirect

Food Chemistry

journal homepage: www.elsevier.com/locate/foodchem

Comparison of bioactive compounds, antioxidant and antiproliferative activities of Mon Thong durian during ripening

Ratiporn Haruenkit [a], Sumitra Poovarodom [b], Suchada Vearasilp [c], Jacek Namiesnik [d], Magda Sliwka-Kaszynska [e], Yong-Seo Park [f], Buk-Gu Heo [g], Ja-Yong Cho [h], Hong Gi Jang [g], Shela Gorinstein [i,*]

[a] Faculty of Agricultural Industry, King Mondkut's Institute of Technology Ladkrabang, Ladkrabang, Bangkok 10520, Thailand
[b] Department of Soil Science, King Mondkut's Institute of Technology Ladkrabang, Ladkrabang, Bangkok 10520, Thailand
[c] Post Harvest Technology Research Institute, Chiang Mai University, Chiangmai 50200, Thailand
[d] Department of Analytical Chemistry, Chemical Faculty, Gdansk University of Technology, 80 952 Gdansk, Poland
[e] Department of Organic Chemistry, Chemical Faculty, Gdansk University of Technology, 80 952 Gdansk, Poland
[f] Department of Horticultural Science, Mokpo National University, Muan, Jeonnam, South Korea
[g] Naju Foundation of Natural Dyeing Culture, Naju 520-931, South Korea
[h] Department of Medicated Diet and Food Technology, Jeonnam Provincial College, Damyang 517-802, South Korea
[i] Department of Medicinal Chemistry and Natural Products, School of Pharmacy, The Hebrew University, Hadassah Medical School, Jerusalem 91120, Israel

ARTICLE INFO

Article history:
Received 12 March 2009
Received in revised form 7 May 2009
Accepted 11 May 2009

Keywords:
Mon Thong durian
Ripening
Bioactive compounds
Fatty acids
Antioxidant
Antiproliferative activities

ABSTRACT

The aim of this investigation was to compare the bioactive and nutrient compounds, fatty acids, and antioxidant and antiproliferative activities of Mon Thong durian at different stages of ripening. It was found that the total polyphenols, flavonoids, flavanols, ascorbic acid, tannins and the antioxidant activity determined by four assays (CUPRAC, DPPH, ABTS and FRAP) differed in immature, mature, ripe and overripe samples. The content of polyphenols and antioxidant activity were the highest in overripe durian, flavonoids were the highest in ripe durian, and flavanols and antiproliferative activity were the highest in mature durian ($p < 0.05$). FTIR spectra of polyphenols, HPLC profiles of fatty acids, the antioxidant and antiproliferative activities can be used as indicators to characterise different stages of durian ripening.

1. Introduction

Durian (*Durio zibethinus Murray*) is one of the most important seasonal fruits in tropical Asia. Durian cultivars are derived from *D. zibethinus Murray*, originating in the Malay Peninsula (Voon, Hamid, Rusul, Osman, & Quek, 2007). The importance of this fruit is mostly connected with its composition and antioxidant properties (Arancibia-Avila et al., 2008; Leontowicz et al., 2008; Toledo et al., 2008). It has been reported that durian has additional valuable health properties: polysaccharide gel, extracted from the fruit hulls, reacts on immune responses and is responsible for cholesterol reduction (Chansiripornchai, Chansiripornchai, & Pongsamart, 2008). The glycaemic index of durian was the lowest in comparison with papaya and pineapple (Daniel, Aziz, Than, & Thomas, 2008). The heath properties of durian are based not only on the antioxidant properties, but also on its fatty acid composition. Cholesterol hypothesis implied that reducing the intake of saturated fats and cholesterol while increasing that of polyunsaturated oils is effective in lowering serum cholesterol, and thereby in reducing coronary heart disease. The protective activity is linked with a high supply of $n-3$ fatty acids coming from fish and seafood, and high consumption of wholegrain products, as well as fruits and vegetables (Siondalski & Lysiak-Szydlowska, 2007). Durian is rich in $n-3$ fatty acids, compared to some other fruits (Phutdhawong, Kaewkong, & Buddhasukh, 2005).

Recently, it has been shown that individuals who eat daily five servings or more of fruits and vegetables have approximately half the risk of developing a wide variety of cancer types, particularly those of the gastrointestinal tract (Gescher, Pastorino, Plummer, & Manson, 1998). Therefore the antiproliferative activities of methanol extracts of Mon Thong durian at different stages of ripening on human cancer cell lines (Calu-6 for human pulmonary carcinoma and SNU-601 for human gastric carcinoma) were determined using MTT (3-(4,5-dimethylthiazol-2-yl)-2,5-diphenyltetrazolium bromide) assay. As far as we know there are no published results of such investigations.

* Corresponding author. Address: David R. Bloom Center for Pharmacy at the Hebrew University of Jerusalem, Jerusalem, Israel. Tel.: +972 2 6758690; fax: +972 2 6757076.
E-mail address: gorin@cc.huji.ac.il (S. Gorinstein).

0308-8146/$ - see front matter © 2009 Elsevier Ltd. All rights reserved.
doi:10.1016/j.foodchem.2009.05.029

2. Materials and methods

2.1. Chemicals

6-Hydroxy-2,5,7,8-tetramethylchroman-2-carboxylic acid (Trolox), 2,2-azino-bis(3-ethylbenzthiazoline-6-sulphonic acid) (ABTS), 1,1-diphenyl-2-picrylhydrazyl (DPPH), Folin–Ciocalteu reagent (FCR), lanthanum (III) chloride heptahydrate, $FeCl_3{\cdot}6H_2O$, $CuCl_2{\cdot}2H_2O$, 2,9-dimethyl-1,10-phenanthroline (neocuproine), ascorbic acid and butylated hydroxyanisole (BHA) were purchased from Sigma Chemical Co., St. Louis, MO. 2,4,6-Tripyridyl-*s*-triazine (TPTZ) was purchased from Fluka Chemie, Buchs, Switzerland. Individual fatty acids were purchased from Sigma–Aldrich (Steinheim, Germany). All solvents used as reaction media were of analytical grade and were obtained from POCh (Gliwice, Poland). Acetonitrile (ACN) and tetrahydrofuran (THF) used as mobile phases were of HPLC grade and were purchased from Merck (Darmstadt, Germany).

2.2. Samples and preparation

All durian samples were harvested in May, 2008, from a 25-year old Mon Thong commercial durian orchard, in Chantaburi province, eastern Thailand.

The maturity of the durian fruits was determined by combined techniques: day count, character of fruit spines, tapping the fruit, colour and shape of the fruit (Yaacob & Subhadrabandhu, 1995). The Mon Thong durian samples at various stages of ripening (1, immature; 2, mature; 3, ripe; 4, overripe) were chosen according to the following criteria:

1. Immature durian (80% maturity) was taken 5 days before the harvest.
2. Mature durian (100% maturity): harvested around 120–125 days after fruit set, using several methods and was prepared 1 day after harvest. Harvesting and determination of durian maturity was carried out by skilled workers. The mature samples were cut with peduncle intact and brought down carefully. The samples were left for 1 day and cut open to get mature durian flesh with firm texture and no smell.
3. Ripe durian: mature samples were left to soften (the stage that can be consumed), which normally takes 3–5 days till the flesh is losing contact with the thick shell.
4. Overripe durian: ripe durian after 3–5 days of ripening.

2.3. Fourier-transform infrared (FTIR) spectra of polyphenols

The presence of polyphenols (flavonoids and phenolic acids) in the investigated durian samples was studied by Fourier-transform infrared (FTIR) spectroscopy. A Bruker Optic GMBH Vector FTIR spectrometer (Bruker Optic GMBH, Attingen, Germany) was used to record IR spectra. A potassium bromide microdisk was prepared from finely ground lyophilised powder of 2 mg of durian sample with 100 mg of KBr (Edelmann & Lendl, 2002).

2.4. Determination of nutrients, polyphenols, flavonoids, flavanols, tannins and ascorbic acid

Elemental analysis, minerals and trace elements were determined as previously described (Poovarodom & Phanchindawan, 2006). The following solvents were used for extraction of bioactive compounds: sample/methanol, sample/water and sample/acetone as 25, 25 and 40 mg/ml, respectively, at room temperature for 2 h twice as previously described (Leontowicz et al., 2008, 2007). To determine the total amount of polyphenols in the studied extracts, Folin–Ciocalteu reagent (FCR) was used, and the measurement was performed at 765 nm with gallic acid as the standard. Results were expressed as mg of gallic acid equivalents (GAE). Flavonoids, extracted with 5% $NaNO_2$, 10% $AlCl_3{\cdot}6H_2O$ and 1 M NaOH, were measured at 510 nm. The total flavanols were estimated using the *p*-dimethylaminocinnamaldehyde (DMACA) method, and then the absorbance at 640 nm was read. The extracts of condensed tannins (procyanidins) with 4% methanol vanillin solution were measured at 500 nm. (+)-Catechin served as a standard for flavonoids, flavanols, and tannins, and the results were expressed as catechin equivalents (CE).

Total ascorbic acid was determined by CUPRAC assay (Ozyurek, Guclu, Bektasoglu, & Apak, 2007). The water extract was prepared from 100 mg of lyophilised sample and 5 ml of freshly prepared nitrogen-bubbled water, and stirred for 30 min at 4 °C and centrifuged. This extract (1 ml) was mixed with 2 ml of 3.0 mM lanthanum (III) chloride heptahydrate, also prepared with nitrogen-bubbled water. Ethyl acetate (EtAc) was used for extraction of flavonoids, in order to avoid interference. The remaining tannin in aqueous solution of fruit extracts after ethyl acetate treatment was checked.

Ascorbic acid was quantified in the aqueous phase. One millilitre of Cu (II)–neocuproine (Nc), in ammonium acetate-containing medium at pH 7, was added to 1 ml of the obtained extract. The absorbance of the formed bis-(Nc)–copper (I) chelate was measured at 450 nm (Ozyurek et al., 2007).

2.5. Determination of the antioxidant activity

The following four tests were applied:

1. Cupric reducing antioxidant capacity (CUPRAC) is based on utilising the copper (II)–neocuproine [Cu (II)–Nc] reagent as the chromogenic oxidising agent. To the mixture of 1 ml of Cu (II), Nc, and NH_4Ac buffer solution, extract of durian sample (or standard) solution (x ml) and H_2O [$(1.1 - x)$ ml] was added to make a final volume of 4.1 ml. The absorbance at 450 nm was recorded against a reagent blank (Apak, Guclu, Ozyurek, & Karademir, 2004).
2. 1,1-Diphenyl-2-picrylhydrazyl (DPPH) solution (3.9 ml, 25 mg/l) in methanol was mixed with the samples extracts (0.1 ml). The reaction progress was monitored at 515 nm until the absorbance was stable (Ozgen, Reese, Tulio, Scheerens, & Miller, 2006).
3. 2,2-Azino-bis(3-ethyl-benzothiazoline-6-sulphonic acid) diammonium salt ($ABTS^{\cdot+}$) was generated by the interaction of ABTS (7 mM) and $K_2S_2O_8$ (2.45 mM). This solution was diluted with methanol until the absorbance reached 0.7 at 734 nm (Ozgen et al., 2006).
4. Ferric-reducing/antioxidant power (FRAP) assay measures the ability of the antioxidants contained in the samples to reduce ferric-tripyridyltriazine (Fe^{3+}-TPTZ) to a ferrous form (Fe^{2+}), which absorbs light at 593 nm (Ozgen et al., 2006; Szeto, Tomlinson, & Benzie, 2002).

2.6. Fatty acids

2.6.1. Chromatographic procedure

2.6.1.1. Sample preparation. Lyophilised durian samples (~150 mg) were hydrolysed with 1 ml of 2 M KOH in MeOH:H_2O (1:1; v/v) at 80–85 °C for 1.5 h in PTFE linked screw-capped amber coloured tubes. After cooling, the hydrolysates were acidified with 4 M HCl (~0.5 ml) to pH ~2, and the free fatty acids were extracted twice with 1 ml of *n*-heptane. The upper organic layer was separated, dried with Na_2SO_4, and then heptane was removed under

a gentle stream of nitrogen at 40 °C. The residue was used for derivatisation (Czauderna & Kowalczyk, 2001).

2.6.1.2. Derivatisation procedure. Fatty acid standards (0.5–100 μg/ml) and fatty acids released by saponification from durian lipid extract were converted to fatty acid *p*-bromophenacyl ester, according to the modified method of Wood and Lee (1983) (Fig. 1). To the residue in a PTFE linked screw-capped amber coloured tube 200 μl of α-bromoacetophenone solution (10 mg/ml in acetone) and 200 μl of triethylamine solution (10 mg/ml in acetone) were added. The contents were ultrasonicated and heated for 30 min at 50 °C in an ultrasonic bath. The resulting solution was evaporated to dryness under a gentle stream of nitrogen at 40 °C. A 250 μl volume of acetonitrile:acetone (1:1; v/v) was added to the tube. The resulting solution was filtered and injected into the column. Analytes were dissolved in a mixture of acetonitrile:acetone (1:1; v/v) and 5 μl of the solution were injected onto the chromatographic column. A mixture of **A**, water and **B**, ACN + THF (99:1; v/v), was used as a mobile phase in gradient mode at flow rate of 2.0 ml min^{-1}. Gradient at 5 min was 80% **B**; at 8 min – 85% **B**; at 20 min – 98% **B**. The UV detector was operated at 258 nm (diode-array detector in single wavelength mode). All analyses were thermostatted at 40 °C. The concentrations of fatty acids in biological samples were calculated using fatty acid standards and an internal standard (hexadecanoic acid) as a measure of extraction yield. The limit of detection (LOD) was calculated as a signal-to-noise ratio of three, while the limit of quantification (LOQ) was defined as 10 times the noise level (Czauderna & Kowalczyk, 2001; Meyer, 1999; Wood & Lee, 1983).

2.6.1.3. Apparatus. Chromatographic analyses were performed using liquid chromatograph Series 1200 (Agilent Technology Inc., Santa Clara, CA) equipped with quaternary pump, autosampler, thermostatted column compartment and diode-array detector. Supelcosil LC-18 HPLC column (150 × 4.6 mm; particle size 3 μm) was obtained from Supelco (Bellefonte, PA).

2.7. Determination of the antiproliferative activity

The antiproliferative activities of 100% methanol extracts of four stages of durian ripening on human cancer cell lines (Calu-6 for human pulmonary carcinoma and SNU-601 for human gastric carcinoma) were measured using MTT (3-(4,5-dimethylthiazol-2-yl)-2,5-diphenyltetrazolium bromide) assay. The cell lines were purchased from Korean Cell Line Bank (KCLB: Seoul, Korea). Cells were grown in RPMI-1640 medium at 37 °C under 5% CO_2 in a humidified incubator. Cells were harvested, counted (3×10^4 cells/ml), and transferred into a 96-well plate, and incubated for 24 h prior to the addition of methanol extracts of durian. Serial dilutions of the extracts were prepared by dissolving compounds in dimethyl sulfoxide (DMSO), followed by dilution with RPMI-1640 medium to give final concentrations at 125, 250, 500, 1000 and 2000 μg/ml. Stock solutions of samples were prepared for cell lines at 90 μl and samples at 10 μl, and incubated for 72 h. MTT solution at 5 mg/ml was dissolved in 1 ml of phosphate buffer solution (PBS), and 10 μl of it were added to each of the 96 wells. The wells were wrapped with aluminium foil and incubated at 37 °C for 4 h. The solution in each well containing media, unbound MTT and dead cells were removed by suction and 150 μl of DMSO were added to each well. The plates were then shaken and optical density was recorded using a microplate reader at 540 nm. Distilled water was used as positive control and DMSO as solvent control (Chon, Heo, Park, Kim, & Gorinstein, 2009). The effect of the durian extract on the proliferation of cancer and normal cells was expressed as relative cell survival rate:

$$\text{percent survival rate} = 100 \times (OD \text{ of durian extract treated sample}/OD \text{ of non-treated sample}),$$

where *OD* is optical density (Kim et al., 2006).

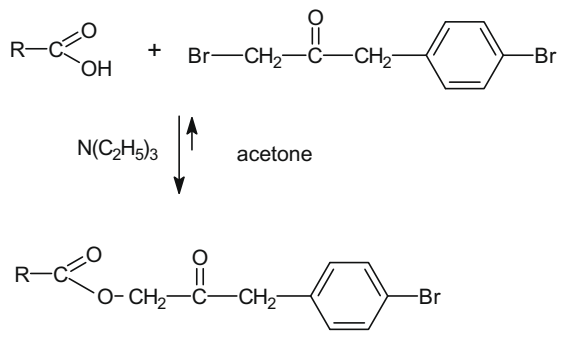

Fig. 1. Free fatty acids derivatisation reaction.

2.8. Statistical analyses

The results of this investigation *in vitro* are means ± SD of five measurements. Differences between groups were tested by two-way ANOVA. In the assessment of the antioxidant potential, Spearman correlation coefficient (*r*) was used. Linear regressions were also calculated; *p* values of <0.05 were considered significant.

3. Results

3.1. Bioactive compounds

The soil of the durian orchard was a sandy loam with pH 4.2, EC 224 μS/cm, organic matter 2.8%, available P (BrayII) 200 mg/kg, exchangeable (NH_4OAc) K, Ca and Mg, 156, 347 and 51 mg/kg, respectively; extractable (DTPA) Fe, Mn, and Zn, 17.7, 2.0 and 2.4 mg/kg, respectively. It was suggested that KCl could be used as an effective replacement for K_2SO_4 in this soil. These results were similar with our previous data (Poovarodom & Phanchindawan, 2006). According to the results summarised in Table 1, the contents of most nutrients were significantly higher ($p < 0.05$) in the immature samples (P, Ca, Mg, Fe, Cu, Zn and B). Durian samples at different stages of ripening are relatively rich in all nutrients.

The wavenumbers of FTIR spectra for catechin at 827, 1039, 1115, 1143, 1286, 1478, 1511 and 1610 cm^{-1} were assigned to

Table 1
Nutrient concentration in durian flesh at four different maturities (mg/kg DW).[A,B]

Indices	Immature	Mature	Ripe	Overripe
N	9868 ± 412^b	8826 ± 4^a	11084 ± 419^c	11322 ± 421^c
P	1382 ± 64^b	946 ± 48^a	1094 ± 51^a	1103 ± 52^a
K	15907 ± 611^a	13811 ± 502^a	14493 ± 511^a	14167 ± 507^a
Ca	406 ± 19^b	172 ± 9^a	181 ± 9^a	181 ± 9^a
Mg	1100 ± 52^b	701 ± 32^a	628 ± 29^a	612 ± 28^a
Na	233 ± 12^b	212 ± 11^b	200 ± 10^a	187 ± 9^a
Fe	9.4 ± 0.5^b	5.7 ± 0.2^a	6.1 ± 0.3^a	6.2 ± 0.3^a
Mn	9.6 ± 0.5^b	8.3 ± 0.4^a	7.5 ± 0.4^a	9.2 ± 0.5^b
Cu	7.8 ± 0.4^b	4.8 ± 0.2^a	4.5 ± 0.2^a	4.3 ± 0.2^a
Zn	8.1 ± 0.4^b	6.5 ± 0.3^a	5.8 ± 0.3^a	6.3 ± 0.3^a
B	6.2 ± 0.3^b	7.0 ± 0.4^b	4.1 ± 0.2^a	3.9 ± 0.2^a

[A] Values are means ± SD of five measurements.
[B] Values in rows with different superscript letters are significantly different ($p < 0.05$).

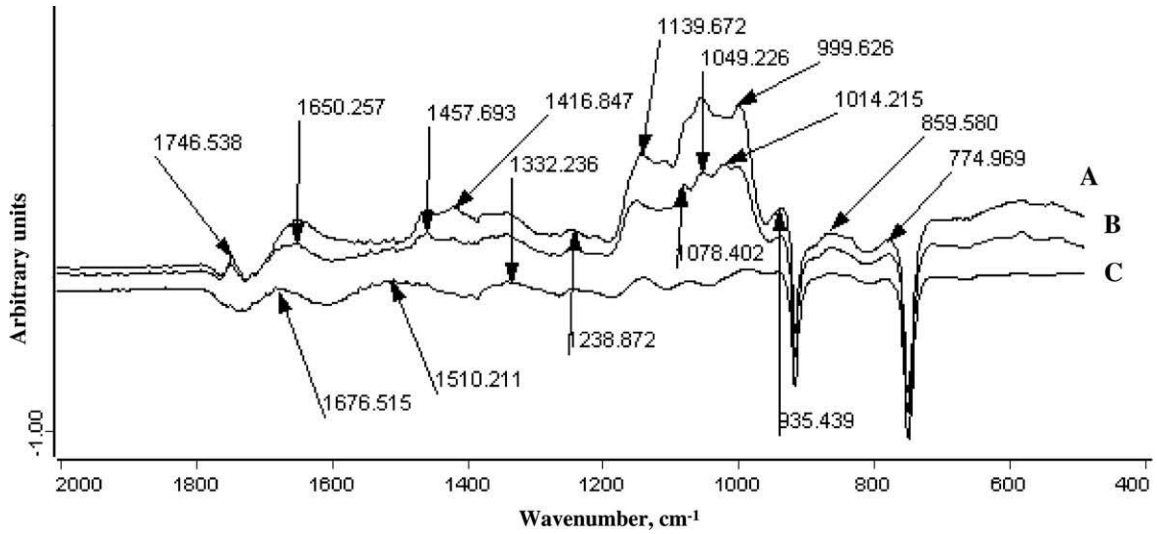

Fig. 2. FTIR spectra of ripe (C), mature (B) and overripe (A) durian samples.

C–H alkenes, –C–O alcohols, C–OH alcohols, –OH aromatic, C–O alcohols, C–H alkanes, C=C aromatic ring and C=C alkenes. Gallic acid showed the following wavenumbers (cm^{-1}) of 866, 1026, 1238, 1450, 1542 and 1618. Immature, mature, ripe and overripe durian samples in the region of polyphenols showed slightly different bands than the standards, but the wavenumbers of the bands were similar in this group (Fig. 2). The absorption bands at 1650, 1458, 1417 and 1014 cm^{-1} were absent in ripe durian, in comparison with the immature, mature and overripe samples. Oppositely, bands at 1677 and 1510 cm^{-1} were observed in ripe durian. Other bands in the durian samples were slightly shifted in comparison with the standards (Fig. 2).

3.2. Polyphenols, flavonoids, flavanols, tannins and ascorbic acid

Different solvents (water, acetone and methanol) showed variation in the amounts of the bioactive compounds. Methanol was the most effective solvent based on extraction yield. The amount of polyphenols (mg GAE/g) extracted from four durian samples with methanol, water and acetone was 12.3, 10.3 and 7.2, respectively (Tables 2 and 3). The contents (Table 2) of polyphenols in overripe durian, flavonoids in ripe durian, flavanols in mature durian, and tannins in mature and ripe durian were the highest in methanol extracts ($p < 0.05$). Polyphenols in acetone extracts were the highest in overripe samples (Table 2, $p < 0.05$). The contents of flavanols and ascorbic acid were the highest in overripe samples extracted with water (Table 3).

3.3. Antioxidant activity

The antioxidant activity of the methanol extract of overripe sample was the highest ($p < 0.05$), according to CUPRAC, DPPH, ABTS and FRAP tests. Acetone extract of immature sample by CUPRAC and ABTS (Table 4) showed the lowest value. The antioxidant activity of the water extracts (Table 5) was the highest in mature and ripe durian using ABTS test and in overripe durian using FRAP test samples ($p < 0.05$).

3.4. Fatty acids

The contents (Table 6) of capric acid was the highest in overripe durian, myristic and palmitic acids in overripe and ripe durian, oleic acid in ripe and linoleic acid in immature and mature samples ($p < 0.05$). The HPLC profiles (Fig. 3) revealed that the major unsaturated fatty acids were oleic and linoleic, while the main saturated was palmitic. Capric, myristic, stearic and arachidic acids were determined in the samples. Palmitic (16:0), oleic (18:1) and linoleic (18:2) acids were among the major fatty acids throughout the maturation and ripening of the fruits. The levels of these fatty acids were found to be significantly different ($p < 0.05$) between the four maturity stages. These results show that durian has moderate levels of fatty acids that significantly changed during maturation and ripening.

Table 2
The contents of the studied biocompounds extracted with methanol and acetone at different stages of durian ripening.[A,B,C]

Samples	Methanol				Acetone
	Polyphenols (mg GAE/g)	Flavonoids (mg CE/g)	Flavanols (μg CE/g)	Tannins (mg CE/g)	Polyphenols (mg GAE/g)
Immature	1.3 ± 0.2^{a}	1.0 ± 0.1^{a}	116.3 ± 8.6^{a}	0.7 ± 0.07^{a}	1.2 ± 0.1^{a}
Mature	3.4 ± 0.3^{b}	1.2 ± 0.1^{a}	135.5 ± 8.9^{c}	0.8 ± 0.07^{b}	2.0 ± 0.2^{b}
Ripe	3.3 ± 0.3^{b}	2.2 ± 0.1^{c}	101.0 ± 8.2^{a}	0.8 ± 0.07^{b}	1.7 ± 0.1^{a}
Overripe	4.3 ± 0.4^{c}	1.7 ± 0.1^{b}	121.6 ± 8.7^{b}	0.7 ± 0.07^{a}	2.3 ± 0.2^{b}

[A] Values are means ± SD of five measurements.
[B] Values in columns with different superscript letters are significantly different ($p < 0.05$).
[C] Per g DW (dry weight).

Table 3
The contents of the studied biocompounds extracted with water at different stages of durian ripening.[A,B,C]

Samples	Polyphenols (mg GAE/g)	Flavonoids (mg CE/g)	Flavanols (μg CE/g)	Vit. C (mg Asc/g)	Tannins (mg CE/g)
Immature	2.0 ± 0.2^{a}	0.5 ± 0.03^{a}	34.9 ± 2.6^{a}	4.3 ± 0.3^{a}	0.2 ± 0.02^{a}
Mature	2.8 ± 0.2^{b}	1.5 ± 0.1^{b}	62.0 ± 5.6^{b}	9.4 ± 0.7^{c}	0.6 ± 0.05^{c}
Ripe	2.6 ± 0.3^{b}	1.5 ± 0.1^{b}	67.1 ± 5.2^{b}	8.0 ± 0.6^{b}	0.5 ± 0.04^{c}
Overripe	2.9 ± 0.3^{b}	1.6 ± 0.1^{b}	73.9 ± 6.4^{c}	11.3 ± 1.1^{d}	0.4 ± 0.03^{b}

[A] Values are means ± SD of five measurements.
[B] Values in columns with different superscript letters are significantly different ($p < 0.05$).
[C] Per g DW (dry weight).

Table 4
The antioxidant activity (μmol Trolox equiv./g) of the studied biocompounds extracted with methanol and acetone at different stages of durian ripening.[A,B,C]

Sample	CUPRAC[D]	CUPRAC[E]	DPPH[D]	ABTS[D]	ABTS[E]	FRAP[D]
Immature	17.3 ± 1.1[a]	5.0 ± 0.4[a]	4.6 ± 0.3[a]	12.4 ± 1.6[a]	3.8 ± 0.3[a]	10.3 ± 1.1[a]
Mature	22.5 ± 1.4[b]	7.1 ± 0.6[b]	8.0 ± 0.6[c]	20.6 ± 1.8[b]	4.9 ± 0.4[b]	12.0 ± 1.2[a]
Ripe	26.1 ± 2.1[b]	6.8 ± 0.5[b]	6.1 ± 0.5[b]	31.3 ± 2.6[c]	4.1 ± 0.4[b]	14.9 ± 1.3[b]
Overripe	29.3 ± 2.5[c]	7.1 ± 0.6[b]	10.0 ± 0.8[d]	44.1 ± 3.3[d]	4.4 ± 0.4[b]	17.0 ± 1.4[c]

[A] Values are means ± SD of five measurements.
[B] Values in columns with different superscript letters are significantly different ($p < 0.05$).
[C] Per g DW (dry weight).
[D] Extraction at room temperature in concentration of 25 mg lyophilised sample in 1 ml methanol.
[E] Extraction at room temperature in concentration of 40 mg lyophilised sample in 1 ml acetone.

Table 5
The antioxidant activity (μmol Trolox equiv./g) of the studied biocompounds extracted with water at different stages of durian ripening.[A,B,C]

Sample	CUPRAC	DPPH	ABTS	FRAP
Immature	17.0 ± 1.5[a]	4.8 ± 0.3[a]	32.1 ± 2.6[a]	14.1 ± 1.3[a]
Mature	22.9 ± 1.9[b]	5.7 ± 0.4[b]	40.0 ± 4.1[c]	25.8 ± 2.2[b]
Ripe	22.1 ± 1.9[b]	5.2 ± 0.4[b]	39.4 ± 3.9[c]	17.1 ± 1.3[a]
Overripe	22.9 ± 1.9[b]	5.8 ± 0.5[b]	36.8 ± 3.1[b]	40.0 ± 3.5[c]

[A] Values are means ± SD of five measurements.
[B] Values in columns with different superscript letters are significantly different ($p < 0.05$).
[C] Per g DW (dry weight).

Table 6
Fatty acids composition (μg/g DW) of the durian samples.[A]

Durian samples	Capric C 10:0	Myristic C 14:0	Palmitic C 16:0	Stearic C 18:0	Arachidic C 20:0	Oleic C 18:1	Linoleic C 18:2
Immature	2.9 ± 0.1[a]	26.2 ± 5.4[a]	2214.5 ± 30.2[a]	98.9 ± 6.2[a]	18.0 ± 2.7[a]	1789.7 ± 37.8[a]	711.3 ± 12.5[b]
Mature	3.5 ± 0.1[a]	48.9 ± 10.9[a]	2754.6 ± 52.8[a]	113.4 ± 20.9[a]	18.9 ± 3.0[a]	2113.8 ± 41.6[a]	513.0 ± 10.6[b]
Ripe	6.1 ± 2.2[b]	94.2 ± 8.9 [b]	3421.3 ± 26.6[b]	125.5 ± 10.1[a]	18.8 ± 1.8[a]	2608.3 ± 28.3[c]	351.2 ± 39. 9[a]
Overripe	8.8 ± 0.5[c]	102.9 ± 11.5[b]	3268.2 ± 41.2[b]	121.0 ± 15.7[a]	20.3 ± 1.9[a]	2314.6 ± 30.1[b]	354.6 ± 48.5[a]

[A] Values are mean ± SD of triplicate extractions.

3.5. Antiproliferative activity

It was observed that the antiproliferative activities of the methanol extracts of immature, mature, ripe and overripe durian samples on two cell lines (Calu-6 for human pulmonary carcinoma and SNU-601 for human gastric carcinoma) were different (Fig. 4). The cell survival rate (%) for concentrations of 2000 μg/ml for mature durian on Calu-6 was 86.8 ± 1.5, and on SNU-601 was 88.5 ± 2.5%, showing the highest antiproliferative activity in comparison with other samples. Our investigation shows that antioxidant activity of the studied samples was not always correlated with their antiproliferative activity.

4. Discussion

Fruits and vegetables contain a variety of phytochemicals, including flavonoids, which have antioxidant and anticancer properties. The purpose of this study was to evaluate the bioactive and nutrient compounds, fatty acids, antioxidant activity and the antiproliferative effects of durian at different stages of ripening on human cell lines.

Our results in observation of FTIR polyphenol spectra were in accordance with others (Edelmann & Lendl, 2002; Sinelli, Spinardi, Di Egidio, Mignani, & Casiraghi, 2008). FTIR spectroscopy can be used as an additional tool to screen fruits for the content of phenolic compounds during their ripening.

Our results correspond with Harris and Brannan (2009), who reported that total phenolics were affected by ripeness, so the concentration of total phenolics in pawpaw pulp were in the order: underripe = ripe > overripe, while the concentration of flavonoids was in the order: ripe < underripe < overripe. Total phenolics were positive correlated with reducing and radical-scavenging potentials. These results indicate that pawpaw pulp of varying ripeness levels is a potential source of natural phenolic and flavonoid antioxidants that could lead to the development of value-added products from pawpaw. Durian, like pawpaw, can be used as a nutritional supplement to the everyday diet.

Our results were compared with Chaisuksant, Boonyuen, and Sunthornwat (2008), where immature green, mature green and orange ripe fruits of bullet wood (*Mimusops elengi*) were investigated. The methanol–acetone extracts were further separated into three different fractions designated as free phenolic acid (F1), soluble phenolic ester (F2) and insoluble phenolic acid ester (F3). The relative antioxidant capacities of extracts of immature and mature fruits, expressed as gallic acid equivalents, were F2 > F3 > F1 and of ripe fruit F2 = F3 > F1. The antioxidant capacity of crude methanol–acetone extract from immature fruit was higher than that of either the mature or the ripe fruit. Our results differ and showed that the antioxidant activity of overripe fruit was higher than the other samples.

The antioxidant activity of some fruits at different stages of ripening depends on the scavenging methods used for their determination (Lin, Wu, Tsai, Yang, & Chen, 2007). For example the oxygen-scavenging capacity of mature meifruit (*Prunus mume Seibu. et Zucc*) in water fraction was lower than that of Trolox. However, both oxygen- and hydroxyl-scavenging capacities of

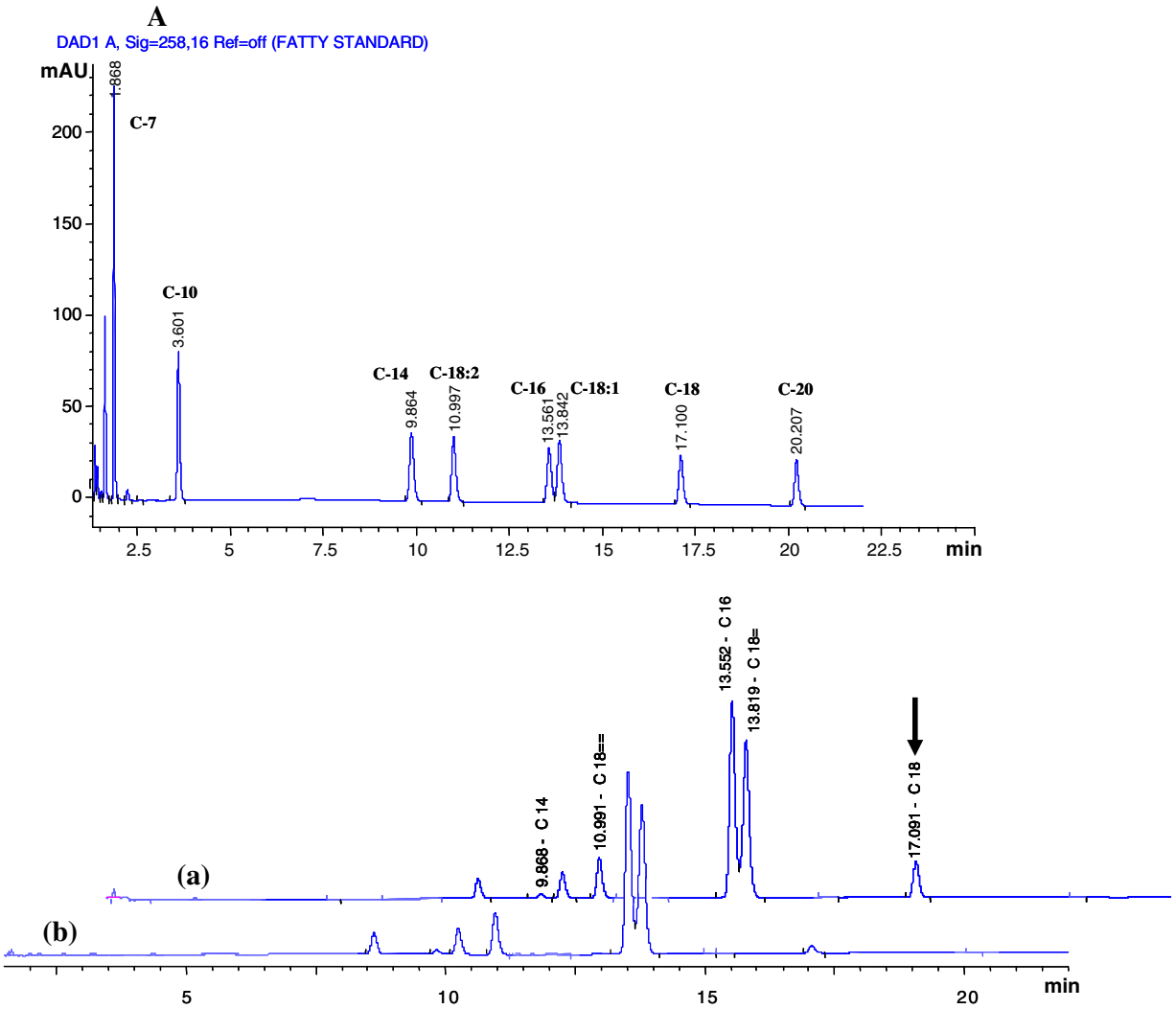

Fig. 3. (A) The typical chromatogram of fatty acids standard solution. Analytes: C-7, enanthic acid; C-10, capric acid; C-14, myristic acid; C-18:2, linoleic acid; C-16, palmitic acid; C-18:1, oleic acid; C-18, stearic acid; C-20, arachidic acid. (a) Chromatograms of derivatised mature durian hydrolysates spiked with C_{18} fatty acid; (b) not spiked.

immature fruit and hydroxyl-scavenging capacities of mature fruit showed no significant difference from Trolox. Similar results were obtained with the ABTS-scavenging method in durian samples of water extracts. The amount of polyphenols in this fruit was about 5 times higher than in overripe durian water extract (Table 3).

The change in the amount of polyphenols during ripening was reported also in three apricot cultivars (Dragovic-Uzelac, Levaj, Mrkic, Bursac, & Boras, 2007). The content of individual polyphenols during ripening was quite similar, whereas their amounts differed significantly. Immature fruits showed the highest level of polyphenols, which decreased at semi-mature fruits and did not change remarkably in mature fruits. The quantity of polyphenols during fruits ripening depends on cultivars, therefore this comparison would not give results similar to those for durian fruit.

The fatty acid composition in durian samples similar to other reports with some slight differences (Phutdhawong et al., 2005): the most prominent component was stearic acid Me ester (35.9%), then palmitic acid Me ester (32.9%), oleic acid Me ester (4.67%), myristic acid Me ester (2.5%) and linoleic acid Me ester (2.2%). Other authors found that during ripening the content of fatty acids increases significantly. Wissem, Baya, and Brahim (2008), reported that total fatty acid contents of *Myrtus communis* var. italica fruit varied from 0.8% to 3.1% during fruit maturation and the predominant fatty acids were linoleic (12.2–71.3%), palmitic (13.6–37.1%) and oleic (6.5–21.9%) acids. The linoleic acid proportions correlated inversely with palmitic and oleic acids during all the stages of ripening.

The content of fatty acids in durian was similar to the banana fruit. The most abundant fatty acids in the banana pulp (29–90% of the total amount of lipophilic extract), were linoleic, linolenic and oleic acids (Oliveira, Freire, Silvestre, & Cordeiro, 2008).

This information can be used by nutritionists and food technologists to improve the nutrition of local people and develop food products that would be beneficial to human health.

Epidemiological studies have consistently linked abundant consumption of fruits and vegetables to a reduction of the risk of developing several types of cancer. The methanolic fractions of different durian samples showed the highest antioxidant activity in comparison with the acetone and water extracts. The methanol fractions were selected for testing of their effect on cells. In most cases, however, the identification of specific fruits and vegetables that are responsible for these effects is still lacking, retarding the implementation of effective dietary-based chemopreventive approaches. Our previous investigations showed that the results of the antiproliferative effect of different plants of Korean salads were not consistent with the findings of DPPH radical-scavenging activ-

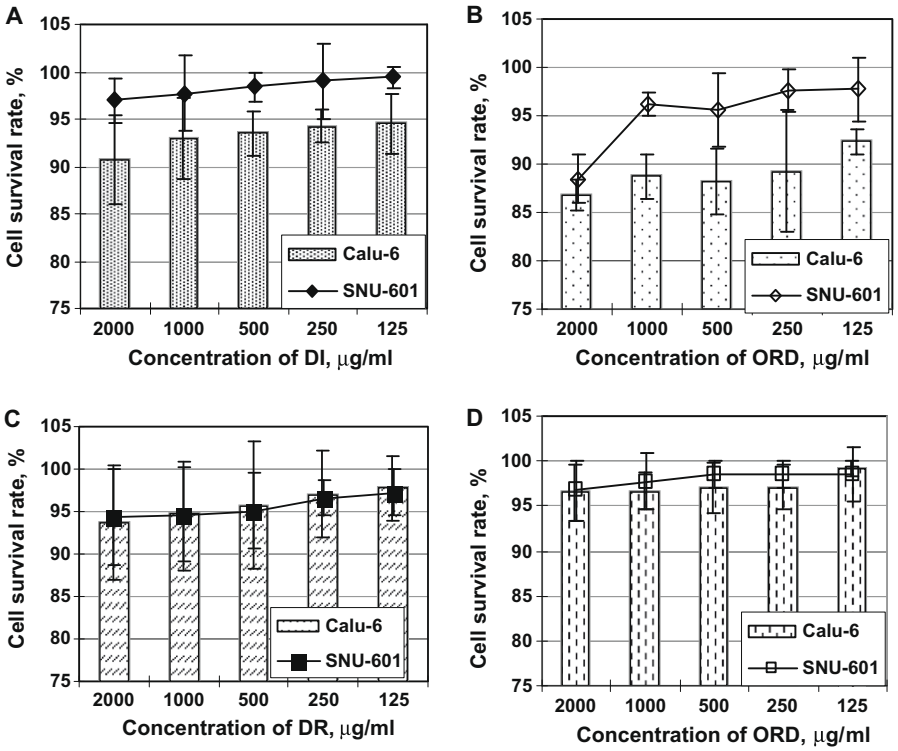

Fig. 4. Cytotoxic effect of methanol extracts from durian samples on human cancer cell lines Calu-6 (for human pulmonary carcinoma) and SNU-601 (for human gastric carcinoma): (A) DI, durian immature; (B) DM, durian mature; (C) DR, durian ripe; (D) ORD, overripe durian.

ity or total phenolic content (Chon et al., 2009). Mature durian sample showed the highest antiproliferative activity. This can be explained not only by relatively high antioxidant activity, but by the amount of flavonoids and other bioactive compounds. The results on cell proliferation can be explained as a synergistic effect of flavonoids, flavanols and ascorbic acid in mature durian. Our data correspond with others (Campbell, King, Harmston, Lila, & Erdman, 2006), that combinations of flavonoids, which are naturally present in whole fruits and vegetables, are more effective in cancer cell growth inhibition than the individual flavonoids. Durian can be used as a potential source of high-value phytochemicals with nutraceutical and functional food additive applications.

5. Conclusions

It was found that the contents of polyphenols, flavonoids, flavanols, ascorbic acid and tannins in Mon Thong durian cultivar in its different stages of ripening (immature, mature, ripe and overripe) and the antioxidant activity as determined by four complementary assays (CUPRAC, DPPH, ABTS and FRAP) was different. The content of flavonoids was the highest in ripe durian and flavanols in mature samples ($p < 0.05$). The antiproliferative activity of mature durian was the highest ($p < 0.05$).

Acknowledgements

Authors thank to Dr. Prof. Resat Apak (Analytical Chemistry Division, Faculty of Engineering, Istanbul University, Turkey) for sending us his data in spectrophotometric determination of ascorbic acid by the modified CUPRAC method with extractive separation of flavonoids–La (III) complexes as well as for making useful suggestions in this matter; to Dr. Elena Katrich (Hebrew University of Jerusalem, School of Pharmacy) for her technical assistance in determination of antioxidant activity. We also wish to thank the reviewer who made useful suggestions that hopefully improved the arguments and presentation of this paper.

References

Apak, R., Guclu, K., Ozyurek, M., & Karademir, S. E. (2004). Novel total antioxidant capacity index for dietary polyphenols and vitamins C and E, using their cupric ion reducing capability in the presence of neocuproine: CUPRAC method. *Journal of Agricultural and Food Chemistry, 52*, 7970–7981.

Arancibia-Avila, P., Toledo, F., Park, Y.-S., Jung, S.-T., Kang, S.-G., Heo, B. G., et al. (2008). Antioxidant properties of durian fruit as influenced by ripening. *LWT-Food Science and Technology, 41*, 2118–2125.

Campbell, J. K., King, J. L., Harmston, M., Lila, M. A., & Erdman, J. W. Jr., (2006). Synergistic effects of flavonoids on cell proliferation in Hepa-1c1c7 and LNCaP cancer cell lines. *Journal of Food Science, 71*, S358–S363.

Chaisuksant, R., Boonyuen, C., & Sunthornwat, O. (2008). Radical scavenging tests of phenolic fractions from *Mimusops elengi* fruits. *Acta Horticulturae, 787*, 313–317.

Chansiripornchai, N., Chansiripornchai, P., & Pongsamart, S. (2008). A preliminary study of polysaccharide gel extracted from the fruit hulls of durian (*Durio zibethinus*) on immune responses and cholesterol reduction in chicken. *Acta Horticulturae, 786*, 57–60.

Chon, S.-U., Heo, B.-G., Park, Y.-S., Kim, D.-K., & Gorinstein, S. (2009). Total phenolics level, antioxidant activities and cytotoxicity of young sprouts of some traditional Korean salad plants. *Plant Foods for Human Nutrition, 64*, 25–31.

Czauderna, M., & Kowalczyk, J. (2001). Separation of some mono-, di- and tri-unsaturated fatty acids containing 18 carbon atoms by high-performance liquid chromatography and photodiode array detection. *Journal of Chromatography B, 760*, 165–178.

Daniel, R. S., Aziz, Al-s. I., Than, W., & Thomas, W. M. S. (2008). Glycemic index of common Malaysian fruits. *Asia Pacific Journal of Clinical Nutrition, 17*, 35–39.

Dragovic-Uzelac, V., Levaj, B., Mrkic, V., Bursac, D., & Boras, M. (2007). The content of polyphenols and carotenoids in three apricot cultivars depending on stage of maturity and geographical region. *Food Chemistry, 102*, 966–975.

Edelmann, A., & Lendl, B. (2002). Toward the optical tongue: Flow-through sensing of tannin–protein interactions based on FTIR spectroscopy. *Journal of the American Chemical Society, 124*, 14741–14747.

Gescher, A., Pastorino, U., Plummer, S. M., & Manson, M. M. (1998). Suppression of tumour development by substances derived from the diet – Mechanisms and clinical implications. *British Journal of Clinical Pharmacology, 45*, 1–12.

Harris, G. G., & Brannan, R. G. (2009). A preliminary evaluation of antioxidant compounds, reducing potential, and radical scavenging of pawpaw (*Asimina triloba*) fruit pulp from different stages of ripeness. *LWT-Food Science and Technology, 42*, 275–279.

Kim, M. J., Kim, Y. J., Park, H. J., Chung, J. H., Leem, K. H., & Kim, H. K. (2006). Apoptotic effect of red wine polyphenols on human colon cancer SNU-C4 cells. *Food Chemistry and Toxicology, 44*, 898–902.

Leontowicz, H., Leontowicz, M., Haruenkit, R., Poovarodom, S., Jastrzebski, Z., Drzewiecki, J., et al. (2008). Durian (*Durio zibethinus Murr.*) cultivars as nutritional supplementation to rat's diets. *Food and Chemical Toxicology, 46*, 581–589.

Leontowicz, M., Leontowicz, H., Jastrzebski, Z., Jesion, I., Haruenkit, R., Poovarodom, S., et al. (2007). The nutritional and metabolic indices in rats fed cholesterol-containing diets supplemented with durian at different stages of ripening. *Biofactors, 29*, 123–136.

Lin, S.-B., Wu, Ch.-A., Tsai, M.-J., Yang, H.-T., & Chen, R.-Y. (2007). Antioxidative activity and amygdalin content of water extract of meifruit (*Prunus mume Seibu. Et Zucc*) and its processed products. *Taiwan Nongye Huaxue Yu Shipin Kexue, 45*, 46–53.

Meyer, V. R. (1999). *Practical high-performance liquid chromatography* (p. 78). Chichester, UK: Wiley.

Oliveira, L., Freire, C. S. R., Silvestre, A. J. D., & Cordeiro, N. (2008). Lipophilic extracts from banana fruit residues: A source of valuable phytosterols. *Journal of Agricultural and Food Chemistry, 56*, 9520–9524.

Ozgen, M., Reese, R. N., Tulio, A. Z., Jr., Scheerens, J. C., & Miller, A. R. (2006). Modified 2,2-azino-bis-3-ethylbenzothiazoline-6-sulfonic acid (ABTS) method to measure antioxidant capacity of selected small fruits and comparison to ferric reducing antioxidant power (FRAP) and 2,20-diphenyl-1-picrylhydrazyl (DPPH) methods. *Journal of Agricultural and Food Chemistry, 54*, 1151–1157.

Ozyurek, M., Guclu, K., Bektasoglu, B., & Apak, R. (2007). Spectrophotometric determination of ascorbic acid by the modified CUPRAC method with extractive separation of flavonoids–La(III) complexes. *Analytica Chimica Acta, 588*, 88–95.

Phutdhawong, W., Kaewkong, S., & Buddhasukh, D. (2005). GC–MS analysis of fatty acids in Thai durian aril. *Chiang Mai Journal of Science, 32*, 169–172.

Poovarodom, S., & Phanchindawan, N. (2006). Effects of chloride and sulfate in various N and K fertilizers on soil chemical properties and nutrient concentrations in durian leaf and fruit. In J. B. Retamales (Ed.), *Proceedings of the Vth international symposium on mineral nutrition of fruit plants*. *Acta Horticulturae, 721*, 191–197.

Sinelli, N., Spinardi, A., Di Egidio, V., Mignani, I., & Casiraghi, E. (2008). Evaluation of quality and nutraceutical content of blueberries (*Vaccinium corymbosum* L.) by near and mid-infrared spectroscopy. *Postharvest Biology and Technology, 50*(3), 1–36.

Siondalski, P., & Lysiak-Szydlowska, W. (2007). Food components in the protection of the cardiovascular system. In Z. E. Sikorski (Ed.), *Chemical and functional properties of food components* (3rd ed., pp. 439–450). Boca Raton, FL: CRC Press LLC.

Szeto, Y. T., Tomlinson, B., & Benzie, I. F. F. (2002). Total antioxidant and ascorbic acid content of fresh fruits and vegetables: Implications for dietary planning and food preservation. *British Journal of Nutrition, 87*, 55–59.

Toledo, F., Arancibia-Avila, P., Park, Y.-S., Jung, S.-T., Kang, S.-G., Heo, B. G., et al. (2008). Screening of the antioxidant and nutritional properties, phenolic contents and proteins of five durian cultivars. *International Journal of Food Sciences and Nutrition, 59*, 415–427.

Voon, Y. Y., Hamid, N. S. A., Rusul, G., Osman, A., & Quek, S. Y. (2007). Characterisation of Malaysian durian (*Durio zibethinus Murr.*) cultivars: Relationship of physicochemical and flavour properties with sensory properties. *Food Chemistry, 103*, 1217–1227.

Wissem, A. W., Baya, M., & Brahim, M. (2008). Variations in essential oil and fatty acid composition during *Myrtus communis* var. Italica fruit maturation. *Food Chemistry, 112*, 621–626.

Wood, R., & Lee, T. (1983). High-performance liquid chromatography of fatty acids: Quantitative analysis of saturated, monoenoic, polyenoic and geometrical isomers. *Journal of Chromatography, 254*, 237–246.

Yaacob, O., & Subhadrabandhu, S. (1995). *The production of economic fruits in South-East Asia* (pp. 90–108). Kuala Lumpur: Oxford University Press.

Food Chemistry 118 (2010) 548–553

Contents lists available at ScienceDirect

Food Chemistry

journal homepage: www.elsevier.com/locate/foodchem

Protective activity of components of an edible plant, *Mallotus japonicus*, against oxidative modification of proteins and lipids

Hiromasa Tabata [a,b,*], Takuya Katsube [a], Koko Moriya [b], Toshihiko Utsumi [b], Yukikazu Yamasaki [a]

[a] Shimane Institute for Industrial Technology, 1 Hokuryo-cho, Matsue, Shimane 690-0816, Japan
[b] Department of Biological Chemistry, Faculty of Agriculture, and Applied Molecular Bioscience, Graduate School of Medicine, Yamaguchi University, Yamaguchi 753-8515, Japan

ARTICLE INFO

Article history:
Received 13 February 2009
Received in revised form 9 April 2009
Accepted 11 May 2009

Keywords:
Mallotus japonicus
Mallotusinic acid
Protein protection
Lipid peroxidation
LDL oxidation

ABSTRACT

Protective activities of components of *Mallotus japonicus* leaves, namely mallotinic acid, mallotusinic acid, corilagin, and geraniin, against oxidation of both intracellular and extracellular proteins including lipoproteins and lipids were evaluated. These four components dose-dependently protected bovine serum albumin (BSA) against protein degradation by ClO·, one of the reactive oxygen species (ROS) generated in the human body, in a manner similar to epigallocatechin gallate (EGCG), a strong antioxidant in green tea. Lipid peroxidation assay indicates they also inhibit lipid peroxidation suggesting they may protect elements of the human body against oxidation induced diseases. As a model element, low-density lipoprotein (LDL) was chosen and the anti-LDL oxidation activity of the four tannin components were evaluated. All four showed strong protective activity against LDL oxidation at levels greater than EGCG. These observations suggest that the leaves of the edible plant, *M. japonicus*, containing mallotinic acid, mallotusinic acid, corilagin, and geraniin, may be useful in controlling oxidative stress in the human body.

1. Introduction

ROS cause damage to intracellular and extracellular proteins, lipids, and nucleic acids (DNA and RNA), and play important roles in the development of tissue damage, various diseases, and the acceleration of the aging process (Ramarathnam, Osawa, Ochi, & Kawakishi, 1995). The potential of antioxidants for preventing oxidation in human tissue has therefore attracted much attention. It has been suggested that certain plant extracts or products such as green tea (Cabrera, Gimenez, & Lopez, 2003), and wine (Kanner, Frankel, Granit, German, & Kinsella, 1994), which contain phenolic components serve to control oxidation activity (Katsube et al., 2006; Kim & Lee, 2004) and reduce the risk of illness such as cardiovascular disease including atherogenesis (Katsube et al., 2004; Sanches-Moreno, Jimenez-Escrig, & Saura-Calixto, 2000). Notably, green tea exhibits strong antioxidative activity, and catechins such as EGCG, a principal component, have been isolated as the active components (Cabrera et al., 2003). Polyphenols such as catechins, are present in many edible plants and vegetables (Chen et al., 1998). Furthermore, EGCG was found to have strong antioxidative activity (Kim & Lee, 2004). As a result, EGCG is often used as a standard for assessing antioxidative activity.

We have previously reported the screening for antioxidants in edible plants, using low-density lipoprotein (LDL) oxidation, DPPH radical-scavenging, and Folin–Ciocalteu assays (Katsube et al., 2004). It was suggested that the combination of LDL oxidation assay and DPPH radical-scavenging assay is useful for assessing antioxidative potential in plants. A 70% ethanol extract of *Mallotus japonicus* leaf, a plant used in drugs and folk medicine, showed the strongest antioxidative activity among 52 edible plant extracts including extract of green tea. We have previously isolated and evaluated the radical-scavenging activity of antioxidants in *M. japonicus* leaves (Tabata et al., 2008). Certain phenolic components, including four tannins, namely mallotinic acid, mallotusinic acid, corilagin, and geraniin, were isolated and identified as the chemical components responsible for such activity in the *M. japonicus* leaves. We clarified that these four tannins have activity to scavenge radicals such as the DPPH, superoxide, and hydroxyl radicals. These radical-scavenging activities were much greater than those of gallic acid, rutin, quercetin, and chlorogenic acid, and were as strong as EGCG.

Since oxidative modification of protein and lipid peroxidation are important models, there are numerous reports describing the protective activity for proteins and lipids against oxidation stress (Nagasawa, Yonekura, Nishizawa, & Kitts, 2001; Srinivasan, Sabitha, & Shyamaladevi, 2007; Terashima, Nakatani, Harima, Nakamura, & Shiba, 2007). It has also been reported that tea extract and its components such as EGCG protect proteins and lipids (Aldini, Yeum, Carini, Krinsky, & Russell, 2003; Hodgson et al., 1999). We therefore

* Corresponding author. Address: Shimane Institute for Industrial Technology, 1 Hokuryo-cho, Matsue, Shimane 690-0816, Japan. Tel.: +81 852 60 5126; fax: +81 852 60 5136.
E-mail address: tabata-hiromasa@shimane-iit.jp (H. Tabata).

0308-8146/$ - see front matter © 2009 Elsevier Ltd. All rights reserved.
doi:10.1016/j.foodchem.2009.05.033

compared the protective activities of the four tannin components with those of EGCG. It is believed that oxidative modification of a component of human plasma, LDL, plays a key role in the pathogenesis of early artherosclerosis (Aviram, 1993; Steinberg, Parthasarathy, Carew, Khoo, & Witztum, 1989). Further studies suggest that antioxidants from plants protect LDL from oxidative modification *in vitro* (Hodgson et al., 1999) and decrease morbidity in heart disease (Enstrom, Kanim, & Klein, 1992; Rimm et al., 1993).

In the present study, we evaluated the protective activity of the *M. japonicus* leaf components, namely mallotinic acid, mallotusinic acid, corilagin, and geraniin, for proteins, lipids, and LDL against oxidative damage.

2. Materials and methods

2.1. Chemicals, reagents, and solvents

BSA was purchased from Wako Pure Chemical Industries, Ltd. (Osaka, Japan). EGCG was obtained from SIGMA–ARDRICH CO. (St. Louis, USA). All other chemicals and solvents used were of analytical grade.

2.2. Extraction and isolation

The lyophilised samples of *M. japonicus* leaves in distilled water was boiled in a hot water bath. The supernatant was concentrated to dryness under reduced pressure, and the residue was used as the dried hot water extract (HWE). Mallotinic acid, mallotusinic acid, corilagin, and geraniin were isolated from *M. japonicus* leaves (Tabata et al., 2008). Each structural formula is shown in Fig. 1. The supernatant from the hot water extract was applied to an ODS-80Ts column (21.5 × 300 mm i.d.) (TOSOH Co.) using an AKTA purifier (Amersham Biosciences Co.), and eluted with a stepwise gradient of 0–50% acetonitrile containing 0.1% formic acid (0%: 218 ml, 15%: 218 ml, 30%: 648 ml, and 50%: 218 ml) at a flow rate of 5 ml/min and fractionated. Mallotinic acid, mallotusinic acid, corilagin, and geraniin were repeatedly applied to the same column, and eluted with 15% acetonitrile containing 0.1% formic acid until purified.

2.3. Analysis of protein protective activity

After the extracts were adequately diluted with distilled water, protein protective activity was determined. One hundred-fifty microliters of 3 mg/ml BSA in PBS, 5 μl of PBS, and 80 μl of each sample were pipetted into a microtube. Fifteen microliters of 83 mM sodium hypochlorite were added and incubated for 30 min at 37 °C. After denaturing with mercaptethanol, 8 μl of the solution were applied to 12.5% SDS–PAGE. Coomassie staining detection was carried out by Quick-CBB (Wako Pure Chemical Industries, Ltd., Osaka, Japan). The protein protective activities were calculated by densitometric analysis.

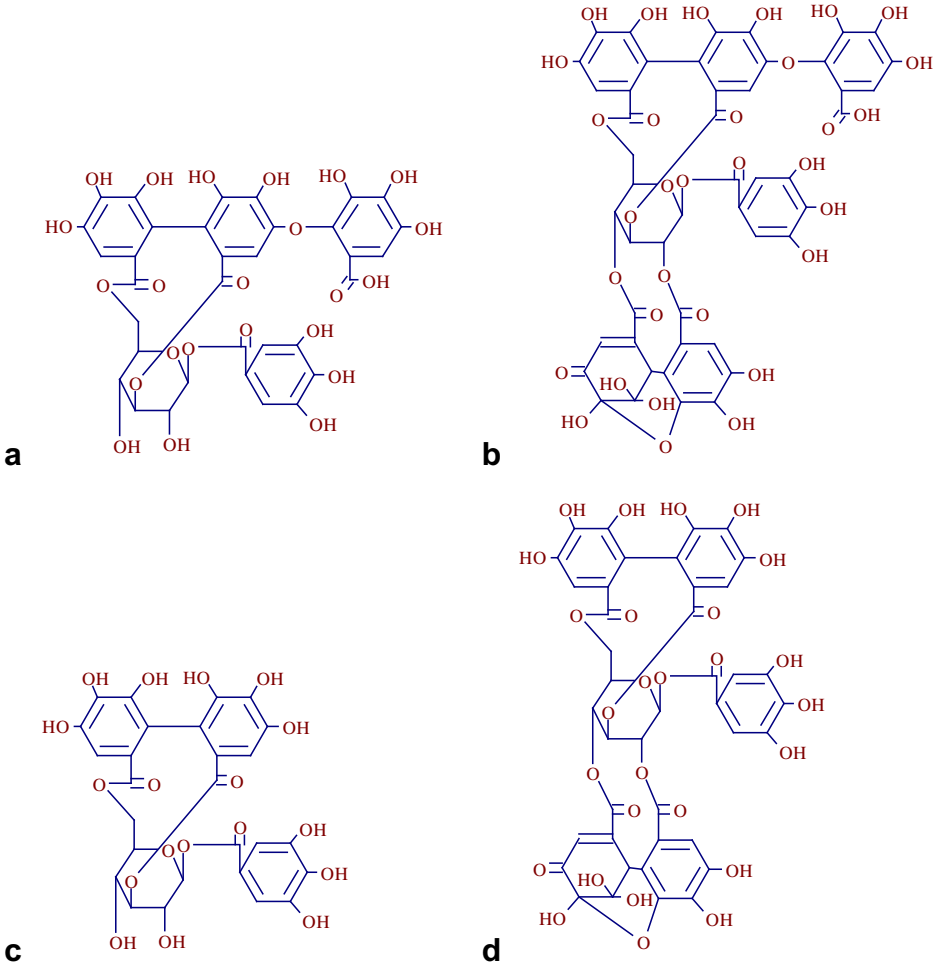

Fig. 1. Structural formulas of (a) mallotinic acid ($C_{34}H_{26}O_{23}$), (b) mallotusinic acid ($C_{48}H_{32}O_{32}$), (c) corilagin ($C_{27}H_{22}O_{18}$), and (d) geraniin ($C_{41}H_{28}O_{27}$).

2.4. Densitometric analysis

A densitometric assay was performed using a MultiImage Light Cabinet (Alpha Innotech Co., San Leandro, CA) controlled by Alpha-Imager software.

2.5. Lipid peroxidation assay

A modified thiobarbituric acid-reactive species (TBARS) assay (Banerjee, Dasgupta, & De, 2005) was used to measure the lipid peroxide formed, using egg yolk as lipid-rich media.

One hundred microliters of egg yolk homogenate (10% v/v) and sample were added to a test tube and filled up to 190 μl with distilled water. Ten microliters of $FeSO_4$ (0.01 M) were added to induce lipid peroxidation and incubated at 37 °C for 30 min. Then 300 μl of 20% acetic acid (pH adjusted to 3.5 with NaOH), 300 μl of 0.8% (w/v) TBA in 1.1% sodium dodecyl sulfate, and 10 μl of 20% TCA were added and the mixture was vortexed and heated in a boiling water bath for 60 min. After cooling, 1 ml of butan-1-ol was added to each tube and centrifuged at 3000 rpm for 10 min. As the blank, 10 μl of $FeSO_4$ were added after incubation. The absorbance of the upper layer was measured at 540 nm using a Multilabel Counter (PerkinElmer, Inc., Wellesley, MA). Inhibition of lipid peroxidation (%) by the sample was calculated according to $(1\text{-}(E - E_b)/(C - C_b)) \times 100$ where E is A_{540} of the sample, E_b is A_{540} of the sample blank, C is A_{540} of the fully oxidised control (distilled water), and C_b is A_{540} of the control blank.

2.6. Lipoprotein separation

Venous blood was obtained from fasting, healthy adult human volunteers into a tube containing ethylenediamine-N,N,N′,N′-tetra-acetic acid (EDTA). LDL was isolated from freshly separated plasma, to which butylhydroxytoluene had been previously added as an antioxidant, by preparative ultracentrifugation according to described technique (Rodriguez-Sureda, Julve, Llobera, & Peinado-Onsurbe, 2002). Isolated LDL was subdivided and stored at −80 °C and used within a 2-month period. LDL was concentrated and desalted using a Centricon-3 (Amicon, Inc., Beverly, MA). Protein concentration in LDL was determined using a Protein Assay Rapid kit (Wako Pure Chemical Industries, Ltd., Osaka, Japan).

2.7. LDL oxidation assay

LDL oxidation assay was carried out (Katsube et al., 2004). After preincubation with water-diluted sample solution for 5 min, reaction was initiated by adding 5 μM $CuSO_4$ to a 20 μg/ml LDL mixture in phosphate-buffered saline (pH 7.4) at 37 °C. Formation of conjugated dienes was monitored continuously at 234 nm for 7 h using a spectrophotometer (Shimadzu UV-1700, Tokyo, Japan) equipped with a 16-position automated sample changer.

Oxidation kinetics were analysed on the basis of oxidation lag time, defined as the interval between initiation of oxidation and the intercept of the tangent for the slope of the absorbance curve during the propagation phase. Antioxidant activity was calculated as EGCG equivalent.

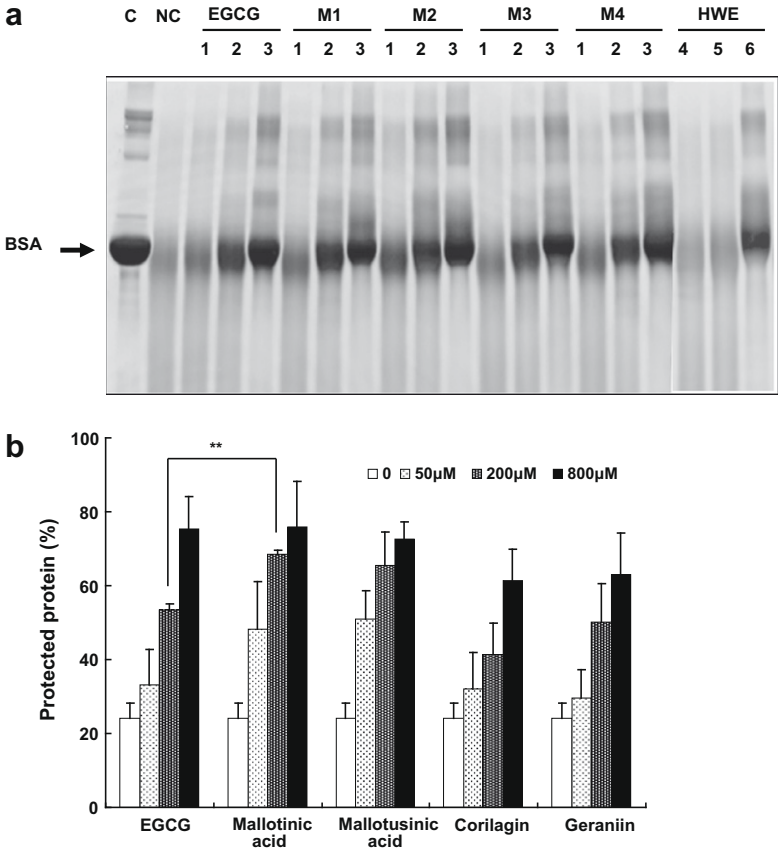

Fig. 2. Protective activity of HWE and four components of *M. japonicus* leaf against degradation of BSA by $ClO^{\cdot}$. (a) Coomassie staining after SDS–PAGE of: C; non-treated with $ClO^{\cdot}$ (control), NC; without antioxidant (negative control), M1; Mallotinic acid, M2; Mallotusinic acid, M3; Corilagin, M4; Geraniin, 1; 50 μM, 2; 200 μM, 3; 800 μM, 4; 40 μg/ml, 5; 160 μg/ml, 6; 640 μg/ml. (b) The result of densitometric analysis. $^{**}p < 0.01$ vs. EGCG.

2.8. Statistical analysis

Data was subjected to analysis of variance using *T*-test to evaluate the significance difference among samples and standards.

3. Results

3.1. Protective activity against degradation of BSA by ClO·

The protective activity against degradation of BSA by ClO·, of HWE and components, mallotinic acid, mallotusinic acid, corilagin, and geraniin is shown in Fig. 2. Coomassie staining after SDS–PAGE clearly shows the protective activity against protein degradation (Fig. 2a). The BSA band was detected in the non ClO·-treated sample (control). While the BSA band almost disappeared in the sample treated with ClO· in the absence of antioxidative material (negative control), the BSA band was retained in the antioxidative material-added samples (EGCG, HWE, and four components). As a result of the densitometric scanning of the SDS–PAGE gel (Fig. 2b), it was shown that all tannin components as well as EGCG dose-dependently protected BSA from degradation. The relative intensity of the negative control sample was 24% (vs. control), and the intensity increased as the concentration of the added antioxidant increased. At 200 μM, the order in terms of protein protective activity was as follows: mallotinic acid > mallotusinic acid > EGCG > geraniin > corilagin; however, statistic analysis suggests that there was no significant difference between each component and EGCG except for mallotinic acid. There were no significant differences at 50 and 800 μM.

3.2. Protective activity against lipid peroxidation

When the lipids in the egg yolk were peroxidated by Fe^{2+}, the absorbance of the reaction mixture containing TBARS at 595 nm increased. The protective activity against lipid peroxidation was evaluated by calculating the ratio of blank mixture and materials-treated mixture. HWE dose-dependently inhibited lipid peroxidation, and the inhibitory effect was evident even at a concentration of 0.03 mg/ml (Fig. 3a). All tannin components, and EGCG, also dose-dependently inhibited lipid peroxidation (Fig. 3b). The levels of inhibitory activity were almost the same at concentrations from 30 to 300 μM, and there were no significant differences between each component and EGCG. Only at the concentrations of 10 μM, corilagin and mallotusinic acid showed significantly weaker activity than that of EGCG. All materials inhibited lipid peroxidation more than 60% at 100 μM and more than 80% at 300 μM.

3.3. Protective activity against LDL oxidation

Protective activity of components, mallotinic acid, mallotusinic acid, corilagin, and geraniin were assessed using Cu^{2+}-induced LDL oxidation. When LDL oxidation was induced by Cu^{2+}, the absorbance at 234 nm increased. Changes in lag time of LDL oxidative modification were observed following the addition of various concentrations of EGCG, HWE, and the four components. As shown in Fig. 4, lag time without EGCG was about 38 min and increased dose-dependently with the addition of EGCG. Similar results were observed when each of HWE and the four components were added (data not shown). The lag time plots of EGCG and four components were straight lines from 0 to 0.4 μM and that of HWE were from 0 to 0.75 μg/ml, and each correlation coefficient was greater than 0.99 (Fig. 5). LDL protective activity was calculated using the ratio of the slope, and the results are summarised in Table 1. HWE showed LDL protective activity and the value was 0.32 mg EGCG equivalent/mg. All the four components showed higher anti-LDL oxidation activity than that of EGCG, and Mallotusinic acid showed the highest activity. As compared with EGCG, the relative protective activity ranged from 128% (corilagin) to 192% (mallotusinic acid).

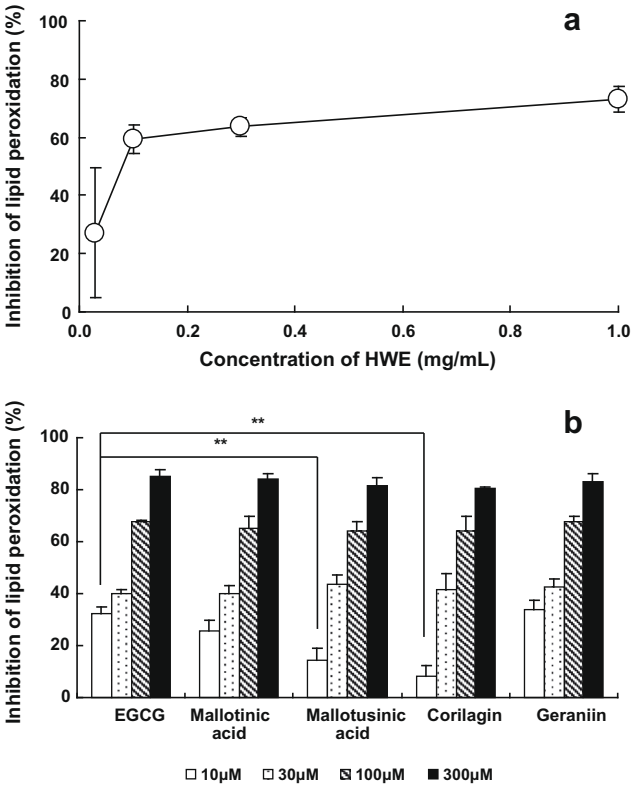

Fig. 3. Protective activity of HWE and four components of *M. japonicus* leaf against lipid peroxidation. (a) The result of protective activity of HWE of *M. japonicus* leaves against lipid peroxidation. (b) The result of protective activity of components against lipid peroxidation. $^{**}p < 0.01$ vs. EGCG.

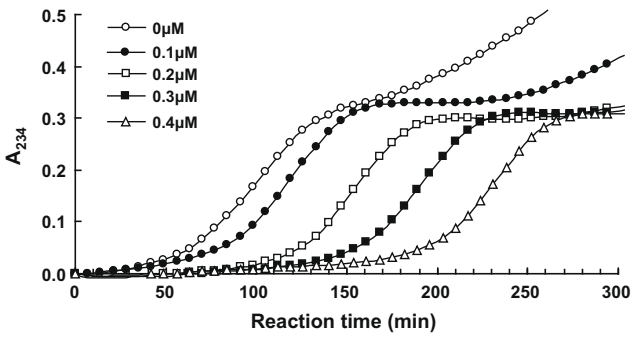

Fig. 4. Lag time increase by EGCG addition against LDL oxidation. (○) no addition, (●) 0.1 μM, (□) 0.2 μM, (■) 0.3 μM, (△) 0.4 μM.

4. Discussion

Our previous systematic screening for antioxidative activity in edible plants using LDL oxidation assays, DPPH radical-scavenging assays, and Folin–Ciocalteu assays revealed that the *M. japonicus* leaf extract exhibited the strongest activity among 52 edible plant extracts (Katsube et al., 2004). In a more recent study, we reported that the active compounds in *M. japonicus* leaf had been isolated

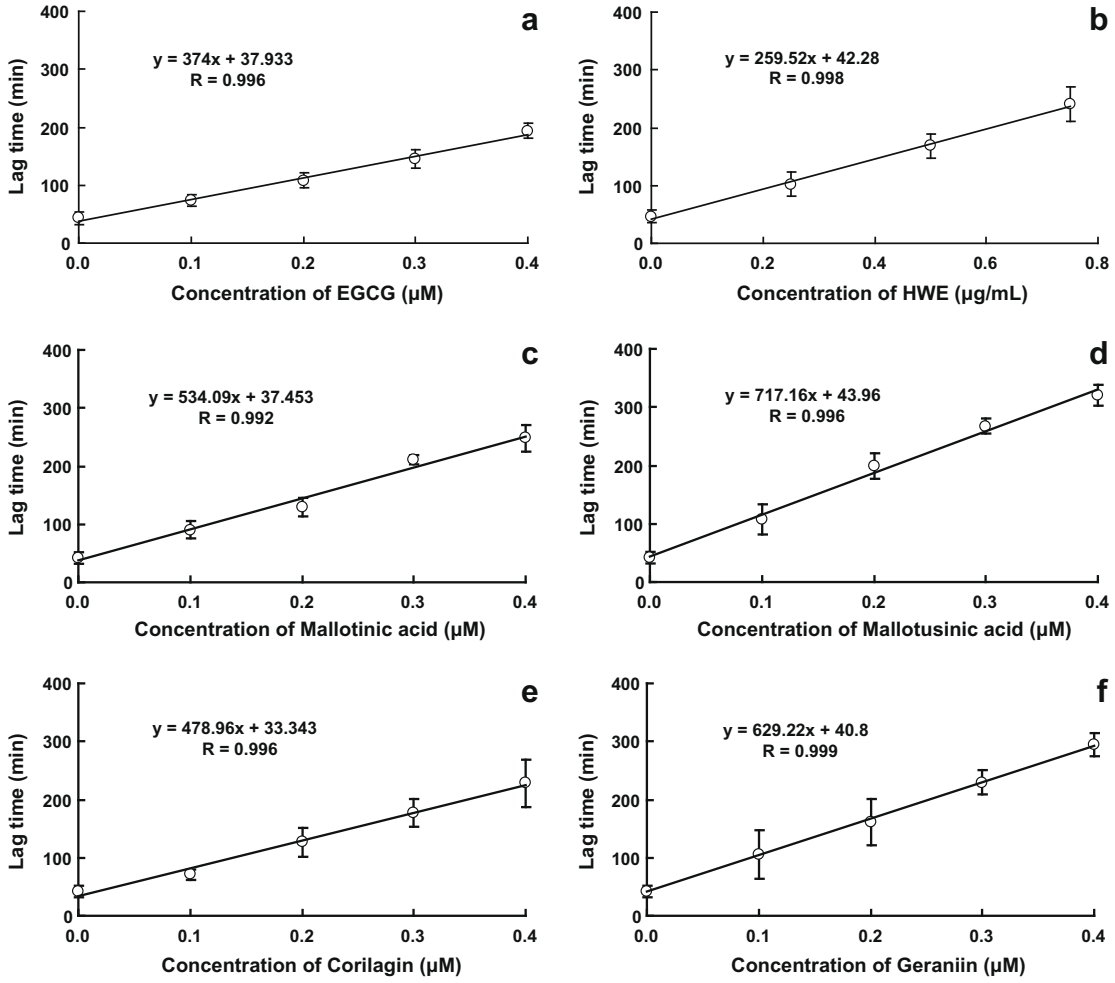

Fig. 5. Protective activity of four components of *M. japonicus* leaf against LDL oxidation. (a) EGCG, (b) HWE, (c) Mallotinic acid, (d) Mallotusinic acid, (e) Corilagin, and (f) Geraniin.

Table 1
Summary of protective activity against LDL oxidation.

	Slop	Relative activity (%)	Relative activity (mg EGCG eq./mg)
EGCG	374	100	
Mallotinic acid	534	143	
Mallotusinic acid	717	192	
Corilagin	479	128	
Geraniin	629	168	
HWE	260		0.32

and identified, and four of them, mallotinic acid, mallotusinic acid, corilagin and geraniin, exhibited strong radical-scavenging activity (Tabata et al., 2008). In the present study, we attempted to evaluate the protective activity of these four *M. japonicus* leaf components against oxidation of intracellular and extracellular protein and lipid, and plasma LDL.

We first evaluated the protective activity against degradation of protein, BSA by $ClO^{\cdot}$.

$ClO^{\cdot}$ is generated from H_2O_2 by myeloperoxidase (MPO) produced by activated neutrophils. The MPO system of activated phagocytes is central to the normal host defense mechanism, and dysregulated MPO contributes to the pathogenesis of inflammatory disease states ranging from atherosclerosis to cancer. It has been suggested that materials exhibiting protective activity for proteins against oxidative stress-induced modification may be useful in controlling diseases and aging generally (Hipkiss, Worthington, Himsworth, & Herwig, 1998). HWE and the four antioxidative components in *M. japonicus* leaf all protected BSA from oxidative modification. The components, as well as EGCG, exhibited significant protective activity at 200 μM, and 60–75% of BSA was protected at 800 μM (Fig. 2a). The fact that HWE, the four tannin components, and EGCG showed similar activity to protect against oxidative modification of proteins indicated that the four tannin components are active compounds in HWE for protecting protein against ROS.

Lipid peroxidation is a free-radical mediated process and damages cells (Upasani, Khera, & Balaraman, 2001). It has been shown that EGCG exhibits protective activity against lipid peroxidation (Chen & Ho, 1995). Therefore, we next evaluated the ability of HWE and four *M. japonicus* leaf components to protect against lipid peroxidation. Although the protective activity of EGCG against lipid peroxidation was stronger than that of mallotusinic acid and corilagin at 10 μM, the activity of all the four tannin components were comparable to EGCG (Fig. 2). We suggest that they have the potential to protect lipids in the body.

LDL oxidation is one aspect of the process of atherogenesis. Since the *M. japonicus* leaf antioxidative components showed potential for protective activity for proteins and lipids, we evaluated protective activity for LDL against oxidative modification by Cu^{2+}. All of EGCG, HWE, and the *M. japonicus* leaf antioxidative components showed dose-dependent activity (Fig. 5). The activity of four

components was greater than that of EGCG; particularly, that of mallotusinic acid was 1.92 fold stronger than EGCG (Table 1). As shown in Fig. 1, the number of the hydroxyl substitutions of the four components are larger than 10 and larger than that of EGCG. Since the hydroxyl substitutions play an important role in antioxidative activity, the level of antioxidative activity appeared related to the number of them, and we previously reported a similar trait on radical-scavenging activity (Tabata et al., 2008). It has also been noted that methylated derivatives of catechines have a lower protective activity against lipid oxidation than their corresponding precursors (Su et al., 2004). Since the physiological concentration of phenolic compounds is less than a few μM, our results suggest that the *M. japonicus* leaf antioxidative component of mallotinic acid, mallotusinic acid, corilagin, and geraniin can protect intracellular and extracellular components against oxidative stress under the physiological conditions.

In the present study, we suggest that four components of the *M. japonicus* leaf provide protective activity in the human body against oxidative stress and various related diseases. As the major phenolic components of the *M. japonicus* leaf are mallotusinic acid (2.3% of flesh leaf weight) and geraniin (1.2% of flesh leaf weight), their relative content (% of total) being 50.9% and 28.2%, respectively (Tabata et al., 2008), they show the greatest potential for such purposes. As the *M. japonicus* leaf is edible and contains potent antioxidative components, it may prove to be a natural functional food.

References

Aldini, G., Yeum, K.-J., Carini, M., Krinsky, I. N., & Russell, M. R. (2003). (−)-Epigallocatechin-(3)-gallate prevents oxidative damage in both the aqueous and lipid compartments of human plasma. *Biochemical and Biophysical Research Communications, 302*, 409–414.

Aviram, M. (1993). Modified forms of low-density lipoprotein and atherosclerosis. *Atherosclerosis, 98*, 1–9.

Banerjee, A., Dasgupta, N., & De, B. (2005). *In vitro* study of antioxidant activity of *Syzygium cumini* fruit. *Food Chemistry, 90*, 727–733.

Cabrera, C., Gimenez, R., & Lopez, C. M. (2003). Determination of tea components with antioxidant activity. *Journal of Agricultural and Food Chemistry, 51*, 4427–4435.

Chen, C.-W., & Ho, C.-T. (1995). Antioxidant properties of polyphenols extracted from green and black teas. *Journal of Food Lipids, 2*, 35–46.

Chen, Z.-Y., Wang, L.-Y., Chan, T. P., Zhang, Z., Chung, Y. H., & Liang, C. (1998). Antioxidative activity of green tea catechin extract compared with that of rosemary extract. *Journal of the American Oil Chemists' Society, 75*, 1141–1145.

Enstrom, J. E., Kanim, L. E., & Klein, M. A. (1992). Vitamin C intake and mortality among a sample of the United States population. *Epidemiology, 3*, 194–202.

Hipkiss, R. A., Worthington, C. V., Himsworth, J. T. D., & Herwig, W. (1998). Protective effects of carnosine against protein modification mediated by malondialdehyde and hypochlorite. *Biochimica et Biophysica Acta, 1380*, 46–54.

Hodgson, M. J., Proudfoot, M. J., Croft, D. K., Puddey, B. I., Mori, A. T., & Beilin, J. L. (1999). Comparison of the effects of black and green tea on *in vitro* lipoprotein oxidation in human serum. *Journal of the Science of Food and Agriculture, 79*, 561–566.

Kanner, J., Frankel, E., Granit, R., German, B., & Kinsella, E. J. (1994). Natural antioxidants in grapes and wines. *Journal of Agricultural and Food Chemistry, 42*, 64–69.

Katsube, T., Imawaka, N., Kawano, Y., Yamazaki, Y., Shiwaku, K., & Yamane, Y. (2006). Antioxidant flavonol glycosides in mulberry (*Morus alba* L.) leaves isolated based on LDL antioxidant activity. *Food Chemistry, 97*(2), 5–31.

Katsube, T., Tabata, H., Ohta, Y., Yamasaki, Y., Anuurad, E., Shiwaku, K., et al. (2004). Screening for antioxidant activity in edible plant products: Comparison of low-density lipoprotein oxidation assay, DPPH radical-scavenging assay, and Folin–Ciocalteu assay. *Journal of Agricultural and Food Chemistry, 52*, 2391–2396.

Kim, D.-O., & Lee, Y. C. (2004). Comprehensive study on vitamin C equivalent antioxidant capacity (VCEAC) of various polyphenolics in scavenging a free radical and its structural relationship. *Critical Reviews in Food Science and Nutrition, 44*, 253–273.

Nagasawa, T., Yonekura, T., Nishizawa, N., & Kitts, D. D. (2001). *In vitro* and *in vivo* inhibition of muscle lipid and protein oxidation by carnosine. *Molecular and Cellular Biochemistry, 225*, 29–34.

Ramarathnam, N., Osawa, T., Ochi, H., & Kawakishi, S. (1995). The contribution of plant food antioxidants to human health. *Trends in Food Science and Technology, 6*, 75–82.

Rimm, E. B., Stampfer, M. J., Ascherio, A., Giovanniucci, E., Colditz, G. A., & Willett, W. C. (1993). Vitamin E consumption and the risk of coronary heart disease in men. *New England Journal of Medicine, 328*, 1450–1456.

Rodriguez-Sureda, V., Julve, J., Llobera, M., & Peinado-Onsurbe, J. (2002). Ultracentrifugation micromethod for preparation of small experimental animal lipoproteins. *Analytical Biochemistry, 303*, 73–77.

Sanches-Moreno, C., Jimenez-Escrig, A., & Saura-Calixto, F. (2000). Study of low-density lipoprotein oxidizability indexes to measure the antioxidant activity of dietary polyphenols. *Nutrition Research, 20*, 941–953.

Srinivasan, P., Sabitha, E. K., & Shyamaladevi, S. C. (2007). Attenuation of 4-Nitroquinoline 1-oxide induced *in vitro* lipid peroxidation by green tea polyphenols. *Life Science, 80*, 1080–1086.

Steinberg, D., Parthasarathy, S., Carew, T. R., Khoo, J. C., & Witztum, J. L. (1989). Beyond cholesterol: Modifications of low-density lipoproteins that increase its atherogenicity. *New England Journal of Medicine, 320*, 915–924.

Su, Y.-L., Xu, J.-Z., Ng, H. C., Leung, K. L., Huang, Y., & Chen, Z.-Y. (2004). Antioxidant activity of tea theaflavins and methylated catechins in canol oil. *Journal of the American Oil Chemists' Society, 81*, 269–274.

Tabata, H., Katsube, T., Tsuma, T., Ohta, Y., Imawaka, N., & Utsumi, T. (2008). Isolation and evaluation of the radical-scavenging activity of the antioxidants in the leaves of an edible plant, *Mallotus japonicus*. *Food Chemistry, 109*, 64–71.

Terashima, M., Nakatani, I., Harima, A., Nakamura, S., & Shiba, M. (2007). New method to evaluate water-soluble antioxidant activity based on protein structural change. *Journal of Agricultural and Food Chemistry, 55*, 165–169.

Upasani, C. D., Khera, A., & Balaraman, R. (2001). Effect of lead and vitamin E, C or spiruline on malondialdehyde, conjugated dienes and hydro peroxides in rat. *Indian Journal of Experimental Biology, 39*, 70–74.

Food Chemistry 118 (2010) 554–558

Contents lists available at ScienceDirect

Food Chemistry

journal homepage: www.elsevier.com/locate/foodchem

Antioxidant potentials of buntan pumelo (*Citrus grandis* Osbeck) and its ethanolic and acetified fermentation products

Hung-Der Jang [a,*], Ku-Shang Chang [a], Tsan-Chang Chang [b], Chuan-Liang Hsu [c,*]

[a] Department of Food Science, Yuanpei University, Hsin-chu 300, Taiwan, ROC
[b] Department of Nursing, St. Mary's Medicine, Nursing and Management College, Yi-lan 266, Taiwan, ROC
[c] Department of Food Science, Tunghai University, Taichung 407, Taiwan, ROC

ARTICLE INFO

Article history:
Received 26 February 2009
Received in revised form 31 March 2009
Accepted 11 May 2009

Keywords:
Buntan pumelo
Citrus grandis Osbeck
Antioxidant potential
Total phenolic contents
Total flavonoid contents

ABSTRACT

The antioxidant potentials of buntan pumelo (*Citrus grandis* Osbeck) and its fermented products were determined. The essential oil from peel had higher total phenolic (214 mM) and flavonoid (134 mg QE/g of dried material) contents than those of different solvent extracts from fruit pulp. In addition, DPPH free radical-scavenging activity and ferric-reducing antioxidant power values determined for the essential oil were 26.1 ± 1.2% and 2.3 ± 0.3 mM, respectively, which were significantly higher than those of various fruit pulp extracts. The ethanol-fermented products of pumelo juice had higher total phenolic and flavonoid contents than those of fresh juice. For maintenance of the substantial antioxidant properties of pumelo products, ethanol-fermented juice rather than fresh or acetate-fermented juice is recommended. Through correlation analysis, the phenolic compounds in the fermented pumelo products were found to be the major contributors to the free radical-scavenging activity and ferric-reducing power.

1. Introduction

Many researchers have reported that high consumption of fruits and vegetables is associated with a lowered incidence of degenerative diseases, including cancer, heart disease, inflammation, arthritis, immune system decline, brain dysfunction and cataracts (Di Matteo & Esposito, 2003; Gerber et al., 2002; Kris-Etherton et al., 2002). In the past decade, the essential oils and various extracts of fruits have been screened for their potential uses as alternative remedies for the treatment of many infectious diseases and the preservation of foods from the toxic effects of oxidants (Lis-Balchin & Deans, 1997).

The protective action of citrus fruits has been attributed to the presence of antioxidants, especially polyphenolic compounds, such as tannins and anthocyanins, and antioxidant vitamins, including ascorbic acid, tocopherol and β-carotene (Saskia et al., 1996; Soong & Barlow, 2004; Wang, Cao, & Prior, 1997). Citrus plants are also rich in naturally-occurring flavonoids, which are primarily found in peel. Flavonoids have a wide range of biological activities, such as cell-proliferation-inhibiting, apoptosis-inducing, enzyme-inhibiting, antibacterial, and antioxidant effects (Cao, Sofic, & Prior, 1997; Havsteen, 2002). Moreover, flavonoids possess various clinical properties, such as anti-atherosclerotic, anti-inflammatory, anti-tumour, anti-thrombogenic, anti-osteoporotic, and antiviral effects (Havsteen, 2002; Hertog, Feskens, Hollman, Katan, & Kromhout, 1993).

The Chinese fruit, *Citrus grandis* Osbeck is also known as buntan pumelo. Buntan pumelo is a fruit indigenous to tropical regions of Asia, which contains an array of biologically active phytochemicals. Buntan pumelo is also a traditionally popular fruit consumed at the Mid-Autumn Festival in Taiwan. Fruits of pumelo are rich in vitamin C and dietary fibre, which can reduce the risk of cardiovascular disease, similar to the effect of other citrus fruits. Although some researchers have investigated the antioxidant capacity of the buntan pumelo, few studies have focused on the stability of its antioxidant compounds. The results of Mokbel and Suganuma (2006) revealed that 100% and 80% methanol extracts of buntan fruits albedo contained groups of compounds including sitosterol, limonoids, fatty acids, coumarins, furanocoumarins, etc. Mokbel and Hashinaga (2006) evaluated the antioxidant activity of buntan using various solvents. Their work indicated that ethyl acetate extracts of flavedo and albedo from buntan fruits showed a high DPPH free radical-scavenging effect. However, they did not reveal the principal compounds related to these antioxidant activities.

Research has indicated that the antioxidant activities of fruits or vegetables could be affected by fermentation (Su & Chien, 2007; Yang, Paulino, Janke-Stedronsky, & Abawi, 2007). For maintenance of the substantial antioxidant properties of fermented products, determination of the principal antioxidant components is vital.

The antioxidant properties of various solvent extracts from buntan pumelo have been reported (Mokbel & Hashinaga, 2006). However, the principal components contributing to antioxidant

* Corresponding authors. Tel.: +886 3 5381183x8482; fax: +886 3 6102342 (H.-D. Jang); tel.: +886 3 5381183x8487; fax: +886 3 6102342 (C.-L. Hsu).
E-mail addresses: hungder@mail.ypu.edu.tw (H.-D. Jang), clhsu@mail.ypu.edu.tw (C.-L. Hsu).

0308-8146/$ - see front matter © 2009 Elsevier Ltd. All rights reserved.
doi:10.1016/j.foodchem.2009.05.020

capacity need to be determined. In order to evaluate its potential use as an antioxidant in food, the antioxidant capacity of buntan pumelo cultivated in Taiwan was determined. The objectives of this study were: (1), to compare the antioxidant (phenolic and flavonoid) content and antioxidant activity of different extracts of the peel and pulp of buntan pumelo, (2), to compare the same for pumelo juice and its ethanol and acetate-fermented products, and (3), to correlate the antioxidant load with the antioxidant activity of the extracts.

2. Materials and methods

2.1. Sample preparation and chemicals

Buntan pumelo (*C. grandis* Osbeck) fruit was purchased in Yunlin County, Taiwan. The pumelo fruits were peeled and dried at 45 °C for 7 days. The fruit pulps were cut into small pieces (about 1 cm^3), freeze-dried at –20 °C, and then pulverised into fine powder. The peels of pumelo were cleaned, and also cut into small pieces. All of the samples, including dried fruit pulp powder and peels, were then stored in pill vials at room temperature until further use. Ethanol, methanol, acetone, and ethyl acetate were purchased from Fisher Scientific, Loughborough, UK.

2.2. Extraction of fruit material

The dried pumelo pulp powder was treated using distilled water, acetone, ethyl acetate, ethanol and methanol, respectively. Two grams of the dried fruit pulp powder were extracted 3 times using 20 ml of each solvent at 37 °C; 24 h for each extraction. The extracts were dried using a rotary evaporator at 40 °C for further analysis. The extracts were then diluted with each solvent. The peel part was squeezed with a juice squeezer to obtain the essential oil.

2.3. Preparation of fermented products from buntan fruit

Saccharomyces sp. SH 26 was inoculated in a sugar solution (13 °Brix). *Acetobacter* sp. was cultivated in a nutrient broth at 37 °C. One hundred grams of pumelo fruit pulp, obtained as described above, were homogenised with 400 ml distilled water in a juicer. The pumelo juice was obtained after filtration through gauze. The sugar content of the juice filtrate was adjusted with sucrose to 13 °Brix using a digital refractometer. The diluted citrus solution was inoculated with a 5% (v/v), 48-h-old yeast solution and fermented at 25 °C until the concentration of ethanol reached 10%. A portion of the ethanol solution was inoculated with a 5% (v/v), 48-h-old *Acetobacter* solution and statically incubated at 37 °C for 14 days until reaching 2.7% acidity. Total phenolic content and total flavonoid content of the ethanol-fermented products (EFP) and the acetate-fermented products (AFP) were determined as described in the following sections. Antioxidant activities of the ethanol or acetate-fermented products were then determined using DPPH radical-scavenging and ferric-reducing antioxidant power (FRAP) assays.

2.4. Determination total phenolics content

The Folin–Ciocalteu reagent assay was used to determine the total phenolics content (Su & Silva, 2006). The fruit pulp extracts or essential oil (0.5 ml) was mixed with 0.5 ml Folin–Ciocalteu reagent previously diluted with 7 ml deionised water. The solution was allowed to stand for 3 min at 25 °C before adding 0.2 ml of saturated sodium carbonate solution. The mixed solution was diluted to 10 ml with deionised water and allowed to stand for another 120 min before the absorbance at 725 nm was measured. Gallic acid was used as standard for the calibration curve. The total phenolic content was expressed as mmol gallic acid equivalents (GAE) per litre of sample (mM).

2.5. Determination total flavonoid content

The total flavonoid contents were determined according to the aluminium chloride colorimetric method described by Chang, Yang, Wen, and Chern (2002). Briefly, aliquots of 0.1 ml of fruit pulp extracts or essential oil were dissolved and mixed with 0.9 ml of 95% alcohol, 0.1 ml of 10% aluminium chloride hexahydrate, 0.1 ml of 1 M potassium acetate, 4.3 ml of 80% ethanol and 2.8 ml of deionised water. After incubation at room temperature for 40 min, the absorbance of the reaction mixture was measured at 415 nm against a deionised water blank using a spectrophotometer (Hitachi Model 100-20; Hitachi, Tokyo, Japan). Quercetin was chosen as a standard. Using a seven point standard curve (0–50 mg/l), the total flavonoid contents were determined in triplicate, respectively. The data were expressed as milligram quercetin equivalents (QE)/g lyophilised powder. The data were then converted into milligram quercetin equivalents (QE) per gram of fresh matter from fruit, based on the moisture contents of lyophilised powder and fresh fruit materials.

2.6. DPPH free radical-scavenging assay

The DPPH free radical-scavenging assay was carried out according to the modified method of Su and Chien (2007). Five millilitres of 0.03 g/l DPPH (2,2-diphenyl-1-picrylhydrazyl) methanol solution were reacted with 0.1 ml fruit pulp extracts or essential oil at room temperature. The extraction solvent was used as control. The absorbance was measured at 517 nm after 30 min of reaction in the dark. The DPPH radical-scavenging activity was calculated as follows:

DPPH radical-scavenging activity (%) = $100 \times (1 - A_s/A_c)$, where A_c is the absorbance reading of DPPH without sample (control) at 517 nm, A_s is the absorbance reading of DPPH added to sample at 517 nm.

2.7. Ferric-reducing antioxidant power (FRAP) assay

The FRAP assay was carried out, using a modified version of the method of Benzie and Szeto (1999). A 20-μl aliquot of the fruit pulp extract or essential oil was mixed with 1.8 ml of FRAP reagent and 1.8 ml deionised water. Deionised water was used as control. The absorbance reading at 593 nm was taken after standing at 37 °C for 30 min. Aqueous solutions of 0–5 mM ferrous sulphate heptahydrate were used for calibration and reducing power was expressed as mM.

2.8. Statistical analysis

The triplicate data were subjected to an analysis of variance for a completely random design, using Statistical Analysis System (SAS Institute Inc., Cary, NC) program. Comparison of means was analysed by Duncan's multiple range test and differences were considered significant when $p < 0.05$.

3. Results and discussion

3.1. Total phenolic contents and total flavonoid contents of buntan pumelo fruit pulp extracts and peel essential oil

The total phenolic content of fruit pulp and peel extracts of buntan pumelo is shown in Table 1. Total phenolic contents from different fruit pulp extracts ranged from 4.8 ± 0.3 to 1.5 ± 0.2 mM GAE. This study showed that total phenolic contents in the various

Table 1
Total phenolic contents, total flavonoid contents and antioxidant properties of buntan pumelo fruit pulp extracts and essential oil of peel.

Buntan pumelo sample	DPPH free radical-scavenging activity (%)	FRAP (mM)	Total phenolic contents (mM GAE)	Total flavonoid contents (mg QE/g)
Ethyl acetate extracts	10.3 ± 1.5B[a]	0.4 ± 0.1A	3.5 ± 0.3B	0.2 ± 0.0A
Methanol extracts	15.5 ± 0.5D	1.0 ± 0.2C	4.6 ± 0.4C	0.3 ± 0.0A
50% ethanol extracts	4.8 ± 0.3A	0.7 ± 0.1B	1.5 ± 0.2A	0.2 ± 0.0A
Acetone extracts	12.9 ± 0.5C	1.1 ± 0.1C	4.0 ± 0.2B,C	0.2 ± 0.0A
Water extracts	16.3 ± 0.6D	1.2 ± 0.2C	4.8 ± 0.3C	0.3 ± 0.0A
Essential oil	26.1 ± 1.2E	2.3 ± 0.3D	214 ± 10.3D	134 ± 0.2B

[a] Data are expressed as the average of three determinations ± SD. Data with different capital case letters in the individual plant extracts are significantly different at 5% level according to Duncan's multiple range test.

extracts of fruit pulp as: water (4.8 ± 0.3 mM GAE) > methanol (4.6 ± 0.4 mM GAE) > acetone (4.0 ± 0.2 mM GAE) > ethyl acetate (3.5 ± 0.3 mM GAE) > 50% ethanol (1.5 ± 0.2 mM GAE). The essential oil from peels had higher total phenolics content than the extracts of fruit pulp. Total phenolic concentrations of essential oil from peel were 214 ± 10.3 mM GAE. The total flavonoid contents in the fruit pulp and essential oil varied considerably. The essential oil from peels had higher total flavonoid contents than the extracts of fruit pulp. Total flavonoid contents of essential oil from peel were 134 ± 0.2 mg QE/g. However, total flavonoid contents in the extracts of fruit pulp ranged from 0.2 ± 0.0 to 0.3 ± 0.0 mg QE/g. The results showed that pumelo peel possesses high concentrations of phenolic compounds and flavonoids; results were similar to previous reports about citrus peel (Bocco, Cuvelier, Richard, & Berset, 1998; Zia-ur-Rehman, 2006).

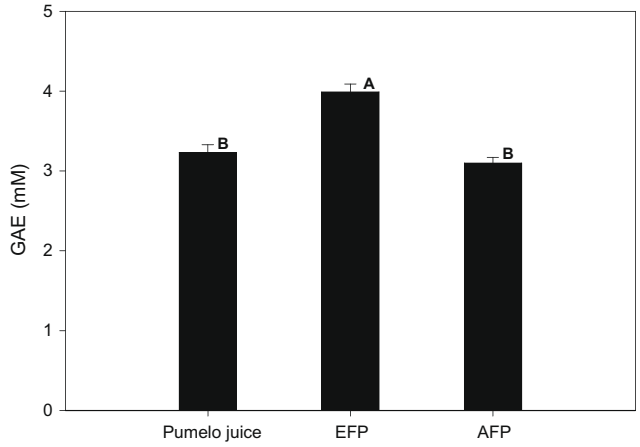

Fig. 1. Total phenolics content of buntan pumelo juice and its fermented products. Data are expressed as the average of three determinations ± SD. Data that do not share the same capital case letter on the top of vertical bar are significantly different at 5% level according to Duncan's multiple range test. EFP, ethanol-fermented products; AFP, acetate-fermented products.

3.2. Antioxidant properties of buntan pumelo fruit pulp extracts and peel essential oil

The DPPH free radical-scavenging activity of pumelo fruit pulp extracts and peel essential oil are also presented in Table 1. The results were shown as relative activities against the control. The relative activities of essential oil were 26%, which were higher than those of freshly-prepared fruit pulp extracts. The DPPH free radical-scavenging activity of various fruit pulp extracts were between 5% and 16%. In addition, relative activities of water or methanol extracts were significantly higher than acetone, ethyl acetate, or 50% ethanol extracts. Due to different antioxidant potentials of different compounds, the antioxidant activity of citrus extracts is strongly dependent on the extraction solvent.

The reducing power of fruit pulp extracts and essential oil using FRAP assay are also shown in Table 1. Among all citrus preparations investigated, essential oil from peel had higher FRAP value (2.3 mM) than those of fruit pulp extracts. The essential oil of pumelo peel also showed stronger antioxidant activities than the fruit pulp extracts. There was more than 3-fold difference between FRAP values in various fruit pulp extracts. The FRAP values of water, acetone or methanol extracts were over 1 mM, which were significantly higher than those of ethyl acetate or 50% ethanol extracts. Comparing all of the fruit pulp extracts, the water extracts had the highest FRAP value (1.2 mM) followed by the acetone extracts, methanol extracts, 50% ethanol extracts and ethyl acetate extracts.

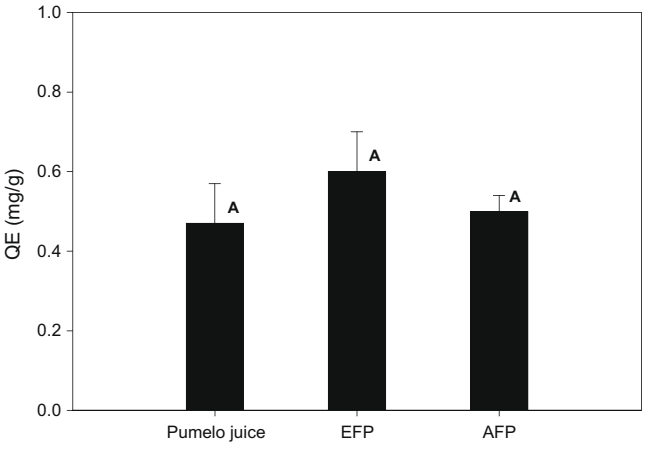

Fig. 2. Total flavonoid contents of buntan pumelo juice and its fermented products. Data are expressed as the average of three determinations ± SD. Data that do not share the same capital case letter on the top of vertical bar are significantly different at 5% level according to Duncan's multiple range test. EFP, ethanol-fermented products; AFP, acetate-fermented products.

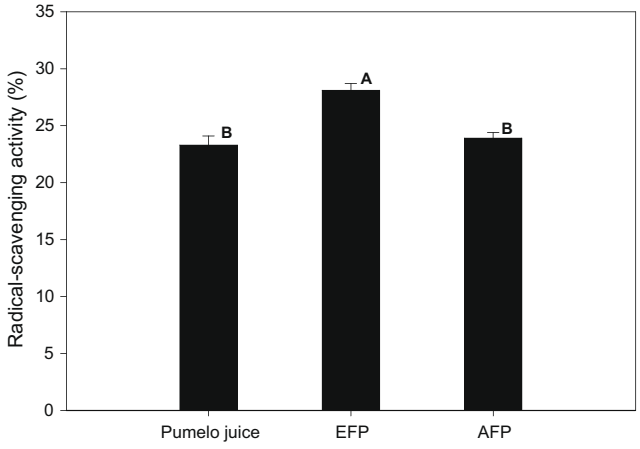

Fig. 3. DPPH radical-scavenging assay of buntan pumelo juice and its fermented products. Data are expressed as the average of three determinations ± SD. Data that do not share the same capital case letter on the top of vertical bar are significantly different at 5% level according to Duncan's multiple range test. EFP, ethanol-fermented products; AFP, acetate-fermented products.

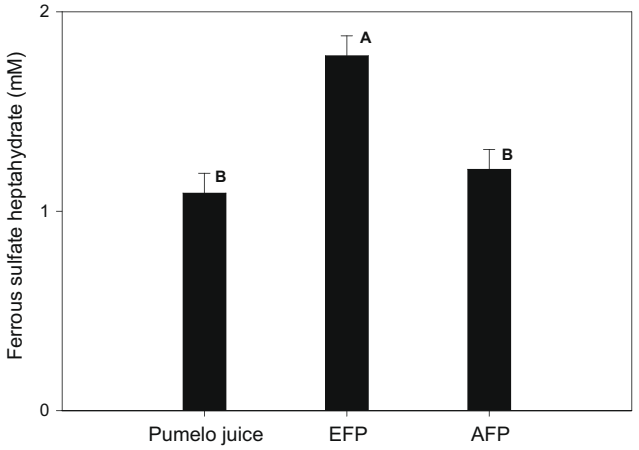

Fig. 4. Antioxidant activity of buntan pumelo juice and its fermented products using FRAP assay. Data are expressed as the average of three determinations ± SD. Data that do not share the same capital case letter on the top of vertical bar are significantly different at 5% level according to Duncan's multiple range test. EFP, ethanol-fermented products; AFP, acetate-fermented products.

3.3. Total phenolic contents and total flavonoid contents of fruit pulp extracts and fermented products

As shown in Fig. 1, total phenolics content of the EFP (4.0 mM GAE) of buntan pumelo juice was higher than that of pumelo juice. During the alcoholic fermentation, the polyphenols in the product increased. The reason is that less oxidation of polyphenols occurred during the fermentation process. Phenolic compounds can act as antioxidants and also can easily be oxidised. In order to retain or increase antioxidant activity of products, oxidation of the phenolic composition should be taken into account. Salmon (2006) proposed that the yeast *Saccharomyces cerevisiae* used in the alcoholic fermentation required oxygen for lipid synthesis, and can consume much oxygen with no detrimental effect on the fermentation process. As yeasts have much higher affinities for oxygen than polyphenols, viable yeast and yeast lees compete with phenolic compounds. However, total phenolics content in the AFP was not significantly different from that of pumelo juice. According to the studies of Su and Chien (2007), oxidation may still affect phenolic content during the acetification process. The results of their study are in agreement with Andlauer, Stumpf, and Furst (2000), who reported alterations in total phenolic content of vinegars due to the acetification process.

Total flavonoid contents of the buntan pumelo fermented products are shown in Fig. 2. In general, total flavonoid contents did not show a significant difference between the pumelo juice and the fermented products. Total flavonoid content did not vary between the EFP and the AFP; total flavonoid contents in the EFP and the AFP were 0.6 ± 0.1 and 0.5 ± 0.0 mg QE/g, respectively. The results showed that contents of flavonoid were low in the buntan pumelo and its fermented products.

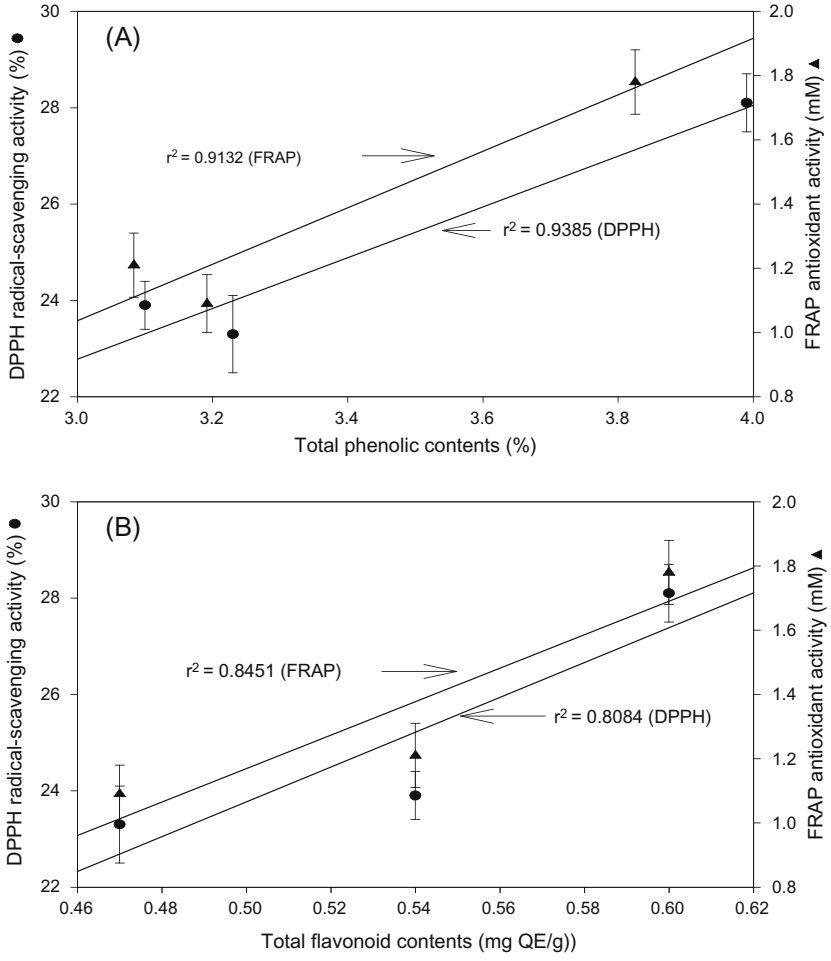

Fig. 5. Correlation of total phenolic contents (A) or total flavonoid contents (B) with antioxidant properties. Data are expressed as the average of three determinations ± SD.

3.4. The DPPH free radical-scavenging activity of fruit pulp extracts and its fermented products

As shown in Fig. 3, the DPPH free radical-scavenging activities of fermented products ranged from 24% to 28%, which were higher than those of fresh pumelo juice (23%). Furthermore, the EFP had higher DPPH free radical-scavenging activity than AFP. We postulated that the higher free radical-scavenging activity in AFP and EFP might be due to the higher total phenolic and total flavonoid contents in the fermented products. The DPPH free radical-scavenging activity of essential oil was similar to the results reported by Mokbel and Hashinaga (2006). Furthermore, The DPPH free radical-scavenging activity of pumelo fruit pulp extract was about 13% higher than the result described by Su, Shyu, and Chien (2008).

3.5. FRAP assay of fruit pulp extracts and its fermented products

The FRAP values of the various fermented products ranged from 1.2 to 1.8 mM; the EFP had higher reducing power using FRAP assay than that of AFP. The FRAP values of EFP were significantly higher than those of pumelo juice; however, those of AFP and pumelo juice were not significantly different (Fig. 4). The results suggested that the EFP had higher reducing power than the pumelo juice without fermentation. The higher total phenolic and total flavonoid contents might account for the higher reducing power in the EFP using FRAP assay.

3.6. Correlation of total phenolic contents or total flavonoid contents with antioxidant properties

Correlation analysis was used to elucidate if phenolic compounds or flavonoids conferred stronger antioxidant activity in the pumelo juice or its fermented products. Statistical analysis revealed that the total phenolic contents in the pumelo juice or its fermented products and the DPPH free radical-scavenging activity or reducing power using FRAP assay were positively correlated (Fig. 5A). Correlation between free radical-scavenging ability ($r^2 = 0.939$) or reducing power ($r^2 = 0.913$) and total phenolic contents in pumelo juice and its fermented products in this study was high and significant. According to some studies, free radical-scavenging activity depends on the structural conformation of phenolic compounds (Bors, Michel, & Stettmaier, 1997; Larrauri, Ruperez, & Calixto, 1996). Thus, free radical-scavenging activity is greatly influenced by the phenolic composition of the sample. However, the correlation between the total flavonoid contents in the pumelo juice or its fermented products and both free radical-scavenging activity ($r^2 = 0.808$) and reducing power ($r^2 = 0.845$) were lower, compared to the effect of total phenolic contents, and not significant (Fig. 5B). This indicates that the flavonoid components might not have good free radical-scavenging ability and reducing power. In addition, we might conclude that the total phenolic contents could be used as an index for free radical-scavenging and reducing power in the buntan pumelo fruit pulp juice or its fermented products.

4. Conclusions

The contents of phenolic and flavonoid compounds obtained from the essential oil of pumelo peel were approximately 45-fold higher than those of fruit pulp extracts. The free radical-scavenging and antioxidant activities of water or methanol extracts were highest among the various extracts of pumelo fruit pulp. The total phenolic contents and antioxidant capacity varied considerably from pumelo juice to its fermented products in this study. For maintenance of the antioxidant properties of pumelo products, ethanol-fermented juice is recommended. Furthermore, the correlation analysis revealed that the total phenolic contents could be used to evaluate the antioxidant capacity of the pumelo extracts.

References

Andlauer, W., Stumpf, C., & Furst, P. (2000). Influence of the acetification process on phenolic compounds. *Journal of Agricultural and Food Chemistry, 48*, 3533–3536.

Benzie, I. F. F., & Szeto, Y. T. (1999). Total antioxidant capacity of teas by the ferric reducing/antioxidant power assay. *Journal of Agricultural and Food Chemistry, 47*, 633–636.

Bocco, A., Cuvelier, M.-E., Richard, H., & Berset, C. (1998). Antioxidant activity and phenolic composition of citrus peel and seed extract. *Journal of Agricultural and Food Chemistry, 46*, 2123–2129.

Bors, W., Michel, C., & Stettmaier, K. (1997). Antioxidant effects of flavonoids. *Biofactors, 6*, 399–402.

Cao, G., Sofic, E., & Prior, R. L. (1997). Antioxidant and pro-oxidant behavior of flavonoids: Structure-activity relationships. *Free Radical Biology and Medicine, 22*, 749–760.

Chang, C. C., Yang, M. H., Wen, H. M., & Chern, J. C. (2002). Estimation of total flavonoid content in propolis by two complementary colorimetric methods. *Journal of Food and Drug Analysis, 10*, 178–182.

Di Matteo, V., & Esposito, E. (2003). Biochemical and therapeutic effects of antioxidants in the treatment of Alzheimer's disease, Parkinson's disease, and amyotrophic lateral sclerosis. *Current Drug Targets-CNS and Neurological Disorder, 2*, 95–107.

Gerber, M., Boutron-Ruault, M. C., Hercberg, S., Riboli, E., Scalbert, A., & Siess, M. H. (2002). Food and cancer: State of the art about the protective effect of fruits and vegetables. *Bulletin du Cancer, 89*, 293–312.

Havsteen, B. H. (2002). The biochemistry and medical significance of the flavonoids. *Pharmacology and Therapeutics, 96*, 67–202.

Hertog, M. G. L., Feskens, E. J. M., Hollman, P. C. H., Katan, M. B., & Kromhout, D. (1993). Dietary antioxidant flavonoids and risk of coronary heart disease: The Zutphen elderly study. *Lancet, 342*, 1007–1011.

Kris-Etherton, P. M., Hecker, K. D., Bonanome, A., Coval, S. M., Binkoski, A. E., Hilpert, K. F., et al. (2002). Bioactive compounds in foods: Their role in the prevention of cardiovascular disease and cancer. *American Journal of Medicine, 113*(Suppl. 9B), 71S–88S.

Larrauri, J. A., Ruperez, P., & Calixto, F. S. (1996). Antioxidant activity of wine pomace. *American Journal of Enology and Viticulture, 47*, 369–372.

Lis-Balchin, M., & Deans, S. G. (1997). Bioactivity of selected plant essential oils against *Listeria monocytogenes*. *Journal of Applied Bacteriology, 82*, 759–762.

Mokbel, M. S., & Hashinaga, F. (2006). Evaluation of the antioxidant activity of extracts from buntan (*Citrus grandis* Osbeck) fruit tissues. *Food Chemistry, 94*, 529–534.

Mokbel, M. S., & Suganuma, T. (2006). Antioxidant and antimicrobial activities of the methanol extracts from pummelo (*Citrus grandis* Osbeck) fruit albedo tissues. *European Food Research and Technology, 224*, 39–47.

Salmon, J. M. (2006). Interactions between yeast, oxygen and polyphenols during alcoholic fermentations: Practical implications. *LWT, 39*, 959–965.

Saskia, A. B. E., Van Acker, S., Van de Berg, D., Tromp, M., Griffoen, D., Van Bennekom, W., et al. (1996). Structural aspect of antioxidant activity of flavonoids. *Free Radical Biology and Medicine, 3*, 331–342.

Soong, Y. Y., & Barlow, P. J. (2004). Antioxidant activity and phenolic content of selected fruit seeds. *Food Chemistry, 88*, 411–417.

Su, M. S., & Chien, P. J. (2007). Antioxidant activity, anthocyanins, and phenolics of rabbiteye blueberry (*Vaccinium ashei*) fluid products as affected by fermentation. *Food Chemistry, 104*, 182–187.

Su, M. S., Shyu, Y. T., & Chien, P. J. (2008). Antioxidant activities of citrus herbal product extracts. *Food Chemistry, 111*, 892–896.

Su, M. S., & Silva, J. L. (2006). Antioxidant activity, anthocyanins, and phenolics of rabbiteye blueberry (Vaccinium ashei) by-products as affected by fermentation. *Food Chemistry, 97*, 447–451.

Wang, H., Cao, G., & Prior, R. L. (1997). Oxygen radical absorbing capacity of anthocyanins. *Journal of Agricultural and Food Chemistry, 45*, 304–309.

Yang, J., Paulino, R., Janke-Stedronsky, S., & Abawi, F. (2007). Free-radical-scavenging activity and total phenols of noni (*Morinda citrifolia* L.) juice and powder in processing and storage. *Food Chemistry, 102*(30), 2–308.

Zia-ur-Rehman, (2006). Citrus peel extract – A natural source of antioxidant. *Food Chemistry, 99*, 450–454.

Food Chemistry 118 (2010) 559–565

Contents lists available at ScienceDirect

Food Chemistry

journal homepage: www.elsevier.com/locate/foodchem

Purification and identification of novel antioxidant peptides from enzymatic hydrolysates of sardinelle (*Sardinella aurita*) by-products proteins

Ali Bougatef [a], Naima Nedjar-Arroume [b], Laïla Manni [a], Rozenn Ravallec [b], Ahmed Barkia [a], Didier Guillochon [b], Moncef Nasri [a,*]

[a] Laboratoire de Génie Enzymatique et de Microbiologie, Ecole Nationale d'Ingénieurs de Sfax, B.P. "W" 3038 Sfax, Tunisia
[b] Laboratoire de Procédés Biologiques, Génie Enzymatique et Microbien, IUT A Lille I, BP 179, 59653 Villeneuve d'Ascq Cedex, France

ARTICLE INFO

Article history:
Received 24 January 2009
Received in revised form 14 April 2009
Accepted 11 May 2009

Keywords:
Heads and viscera
Antioxidant activity
Radical-scavenging activity
Peptide
Mass spectrometry
Sardinella aurita

ABSTRACT

In order to utilise sardinelle (*Sardinella aurita*) protein by-products, which is normally discarded as industrial waste in the process of fish manufacturing, heads and viscera proteins were hydrolysed by different proteases to obtain antioxidative peptides. All hydrolysates showed different degrees of hydrolysis and varying degrees of antioxidant activities. Hydrolysate generated with crude enzyme extract from sardine (*Sardina pilchardus*) displayed high antioxidant activity, and the higher DPPH radical-scavenging activity (87 ± 2.1% at 2 mg/ml) was obtained with a degree of hydrolysis of 6%. This hydrolysate was fractionated by size exclusion chromatography on a Sephadex G-25 into eight major fractions (P_1–P_8). Fraction P_4, which exhibited the highest DPPH scavenging activity, was then fractionated by reversed-phase high performance liquid chromatography (RP-HPLC). Seven antioxidant peptides were isolated. The molecular masses and amino acids sequences of the purified peptides were determined using ESI-MS and ESI-MS/MS, respectively. Their structures were identified as Leu-His-Tyr, Leu-Ala-Arg-Leu, Gly-Gly-Glu, Gly-Ala-His, Gly-Ala-Trp-Ala, Pro-His-Tyr-Leu and Gly-Ala-Leu-Ala-Ala-His. The first peptide displayed the highest DPPH radical-scavenging activity (63 ± 1.57%; at 150 μg/ml) among these peptides.

The results of this study suggest that sardinelle by-products protein hydrolysates are good source of natural antioxidants.

1. Introduction

Lipid oxidation is of great concern to the food industry and consumers because it leads to the development of undesirable off-flavours, odours and potentially toxic reaction products (Lin & Liang, 2002). Furthermore, cancer, coronary heart disease and Alzheimer's diseases are also reported to be caused in part by oxidation or free radical reactions in the body (Diaz, Frei, Vita, & Keaney, 1997). To prevent foods from undergoing such deterioration and to provide protection against serious diseases, it is very important to inhibit lipid peroxidation occurring in foodstuffs and the living body. Antioxidants are used to preserve food products by retarding discolouration and deterioration as a result of oxidation (Decker, Warner, Richards, & Shahidi, 2005).

Many synthetic antioxidants, such as butylated hydroxyanisole (BHA) and butylated hydroxytoluene (BHT), are used as food additives to prevent deterioration. Although these synthetic antioxidants show stronger antioxidant activities than those of natural antioxidants, such as α-tocopherol and ascorbic acid, the use of these chemical compounds has begun to be restricted because of their induction of DNA damage and their toxicity (Ito et al., 1986). In recent years, there has been great interest in finding new antioxidants from natural sources for use in food and medicinal materials to replace synthetic antioxidants. Vitamin C, α-tocopherol and phenolic compounds, which are present naturally in vegetables, fruits and seeds, possess the ability to reduce oxidative damage associated with many diseases, including cancer, cardiovascular diseases, atherosclerosis, etc. Recently, the ability of phenolic substances, including flavonoids and phenolic acids to act as antioxidants has been extensively investigated (Katalinic, Milos, Kulisic, & Jukic, 2006; Madhujith & Shahidi, 2006; Miraliakbari & Shahidi, 2008; Rice-Evans, Miller, & Paganda, 1996; Shahidi, 2008; Shahidi, Alasalvar, & Liyana-Pathirana, 2007; Wong, Li, Cheng, & Chen, 2006; Zhong, Khan, & Shahidi, 2007).

In recent years, hydrolysed proteins from many animal and plant sources have been found to possess antioxidant activity, such as milk casein (Blanca, Ana, Lourdes, & Isidra, 2007), soybean (Gibbs, Zougman, Masse, & Mulligan, 2004), rice bran (Parrado et al., 2006), quinoa seed protein (Aluko & Monu, 2003), canola (Cumby, Zhong, Naczk, & Shahidi, 2008), egg-yolk protein (Sakanaka, Tachibana, Ishihara, & Juneja, 2004) and porcine myofibrillar

* Corresponding author. Tel.: +216 74 274 088; fax: +216 74 275 595.
E-mail addresses: mon_nasri@yahoo.fr, moncef.nasri@enis.rnu.tn (M. Nasri).

0308-8146/$ - see front matter © 2009 Elsevier Ltd. All rights reserved.
doi:10.1016/j.foodchem.2009.05.021

proteins (Saiga, Tanabe, & Nishimura, 2003). In addition, aquatic products and by-products have also proven to be good sources of antioxidant peptides, such as smooth hound (*Mustelus mustelus*) protein (Bougatef et al., 2009), capelin protein (Amarowicz & Shahidi, 1997), mackerel protein (Wu, Chen, & Shiau, 2003), jumbo squid skin (Mendis, Rajapakse, Byun, & Kim, 2005), hoki frame protein (Kim, Je, & Kim, 2007), yellowfin sole frame protein (Jun, Park, Jung, & Kim, 2004), yellow stripe trevally (*Selaroides leptolepis*) (Klompong, Benjakul, Kantachote, & Shahidi, 2007), yellowfin sole skin gelatine hydrolysate (Kim, Lee, Byun, & Jeon, 1996), Alaska pollack skin gelatine hydrolysate (Kim et al., 2001), and Alaska pollack frame protein hydrolysate (Je, Park, & Kim, 2005).

In Tunisia, sardinelle (*Sardinella aurita*) catches were about 13,300 tonnes in 2002 (F.A.O., 2004). During processing, solid wastes including heads and viscera are generated and constitute as much as 30% of the original material. These wastes, which represent an environmental problem to the fishing industry, constitute an important source of proteins. Traditionally, this material is transformed into powdered fish flour for animal feed (Ström & Eggum, 1981). Nevertheless, novel processing methods are required to convert sardinelle by-products into more profitable and marketable products. An interesting alternative would be to transform fish proteins by-products into biologically active peptides by protease treatments.

In this study, we investigated the antioxidative activity of sardinelle heads and viscera protein hydrolysates obtained by various enzymatic treatments. Furthermore, seven new antioxidative peptides were isolated from the hydrolysate obtained by treatment with crude enzyme extract from sardine viscera and their amino acids sequences were determined.

2. Materials and methods

2.1. Reagents

Chemicals required for the assays including 1,1-diphenyl-2-picrylhydrazyl (DPPH), BHA, α-tocopherol and linoleic acid were purchased from Sigma Chemical Co. (St. Louis, MO, USA). Sephadex G-25 was from Pharmacia (Uppsala, Sweden). Other chemicals and reagents used were of analytical grade.

2.2. Materials

Sardinelle (*S. aurita*) was purchased from the fish market of Sfax city, Tunisia. It was washed twice with water; heads and viscera were separated, rinsed with cold distilled water, and then stored in sealed plastic bags at −20 °C until used.

2.3. Enzymes

The enzyme preparations used were: Alcalase® 2.4L serine-protease from *Bacillus licheniformis* supplied by Novozymes® (Bagsvered, Denmark), crude enzyme preparation from *Aspergillus clavatus* ES1 (Hajji, Kanoun, Nasri, & Gharsallah, 2007), alkaline proteases from *B. licheniformis* NH1 (El Hadj-Ali et al., 2007), and crude enzyme extract from viscera of sardine (*Sardina pilchardus*) (Bougatef, Souissi, Fakhfakh, Triki-Ellouz, & Nasri, 2007).

2.4. Preparation of endogenous enzyme extract from sardine viscera

Viscera from sardine (150 g) were homogenised for 60 s with 300 ml of extraction buffer (10 mM Tris–HCl, pH 8.0). The homogenate was centrifuged at 8500*g* for 30 min at 4 °C and the supernatant was collected. The supernatant referred to as the crude enzyme extract was stored at 4 °C prior to analysis. All enzymatic assays were conducted within a week after extraction. For a long conservation, supernatant was lyophilised.

Crude enzymes from *B. licheniformis* NH1 and *A. clavatus* ES1 were prepared in our laboratory as described by El Hadj-Ali et al. (2007) and Hajji et al. (2007).

The protease activity in the crude enzyme extract was determined by the method of Kembhavi, Kulkarni, and Pant (1993) using casein as a substrate. One unit of protease activity was defined as the amount of enzyme required to liberate 1 μg of tyrosine per minute under the experimental conditions used.

2.5. Preparation of sardinelle protein hydrolysates using various proteases

Heads and viscera (500 g), in 500 ml distilled water, were first minced, using a grinder (Moulinex Charlotte HV3, France) then cooked at 90 °C for 20 min to inactivate endogenous enzymes. The cooked heads and viscera sample was then homogenised in a Moulinex® blender for about 2 min. The samples were adjusted to optimal pH and temperature for each enzyme; crude enzyme from NH1 (pH 10.0; 50 °C), Alcalase and crude enzyme extract from sardine viscera (pH 8.0; 50 °C) and crude enzyme from ES1 (pH 8.0; 40 °C). Then, the substrate proteins were digested with enzymes at a 0.27:1 (U/mg) enzyme/protein ratio for 3 h. Enzymes were used at the same activity levels to compare hydrolytic efficiencies. During the reaction, the pH of the mixture was maintained at the desired value by continuous addition of 4 N NaOH solution. The enzymatic hydrolysis was stopped by heating the solutions at 80 °C during 20 min. The protein hydrolysates were then centrifuged at 5000*g* for 20 min to separate soluble and insoluble fractions. Finally, the soluble fraction was freeze-dried using freeze-dryer (Bioblock Scientific Christ ALPHA 1-2) and stored at −18 °C for further use. The powders were used as sardinelle protein hydrolysates.

2.6. Determination of the degree of hydrolysis

The degree of hydrolysis (DH), defined as the percent ratio of the number of peptide bonds broken (h) to the total number of peptide bonds per unit weight (h_{tot}), in each case, was calculated from the amount of base (NaOH) added to keep the pH constant during the hydrolysis (Adler-Nissen, 1986) as given below:

$$\mathrm{DH}\,(\%) = \frac{h}{h_{tot}} \times 100 = \frac{B \times Nb}{MP} \times \frac{1}{\alpha} \times \frac{1}{h_{tot}} \times 100$$

where B is the amount of NaOH consumed (ml) to keep the pH constant during the reaction, Nb is the normality of the base, MP is the mass (g) of protein (N × 6.25), and α is the average degree of dissociation of the α-NH_2 groups released during hydrolysis expressed as:

$$\alpha = \frac{10^{\mathrm{pH}-\mathrm{pK}}}{1 + 10^{\mathrm{pH}-\mathrm{pK}}}$$

where pH and pK are the values at which the proteolysis was conducted. The total number of peptide bonds (h_{tot}) in a fish protein concentrate was assumed to be 8.6 meq/g (Adler-Nissen, 1986).

2.7. Antioxidant activity

2.7.1. DPPH radical-scavenging assay

The DPPH radical-scavenging activity of the hydrolysates was determined as described by Bersuder, Hole, and Smith (1998). Samples dissolved in 500 μl of distilled water (2 mg/ml for hydrolysates H1–H4; 1 mg/ml for G-25 fractions and 150 μg/ml for RP-HPLC fractions) were mixed with 500 μl of 99.5% ethanol and

125 μl of a DPPH solution (0.02% in 99.5% ethanol). The mixtures were incubated for 60 min in the dark at room temperature, and the reduction of DPPH radicals was measured at 517 nm. In its radical form, DPPH has an absorption band at 517 nm which disappears upon reduction by an antiradical compound. Lower absorbance of the reaction mixture indicated higher free radical-scavenging activity. DPPH radical-scavenging activity was calculated as:

$$\text{DPPH radical} - \text{scavenging activity } (\%) = \frac{\text{Absorbance of control} - \text{Absorbance of sample}}{\text{Absorbance of control}} \times 100$$

The control was conducted in the same manner, except that distilled water was used instead of sample. BHA was used as positive standard. The test was carried out in triplicate.

2.7.2. Inhibition of linoleic acid autoxidation

The lipid peroxidation inhibition activity of hydrolysates was measured in a linoleic acid emulsion system according to the method of Osawa and Namiki (1985). A 20 mg of hydrolysates, dissolved in 10 ml of 50 mM phosphate buffer (pH 7.0), was added to a solution of 0.13 ml of linoleic acid and 10 ml of 99.5% ethanol. The total volume was then adjusted to 25 ml with distilled water. The mixture was incubated in a 50 ml assay tube with a screw cap at 40 ± 1 °C for 5 days in a dark room. The degree of oxidation of linoleic acid was measured using the ferric thiocyanate method of Mitsuda, Yasumoto, and Iwami (1996). To 0.1 ml of the reaction mixture were added 4.7 ml of 75% ethanol, 0.1 ml of 30% ammonium thiocyanate, and 0.1 ml of 20 mM ferrous chloride solution in 3.5% HCl. After 3 min incubation, the colour development, which represents the linoleic acid oxidation, was measured at 500 nm. α-Tocopherol, a natural antioxidative agent, was used as reference and 50 mM phosphate buffer (pH 7.0) as control. The antioxidative capacity of inhibiting the peroxide formation in linoleic acid system was expressed as follows:

$$\text{Inhibition } (\%) = \left[1 - \frac{\text{Absorbance of sample}}{\text{Absorbance of control}}\right] \times 100$$

2.7.3. Reducing power assay

The ability of the protein hydrolysates or purified peptides to reduce iron(III) was determined by the method of Yildirim, Mavi, and Kara (2001). An aliquot of 1 ml sample (2 mg of hydrolysate/ml) was mixed with 2.5 ml of 0.2 M phosphate buffer (pH 6.6) and 2.5 ml of 1% (w/v) potassium ferricyanide. The mixtures were incubated at 50 °C for 30 min. After incubation, 2.5 ml of 10% (w/v) trichloroacetic acid was added and the reaction mixtures were centrifuged for 10 min at 1650*g*. Finally, 2.5 ml of the supernatant solution were mixed with 2.5 ml of distilled water and 0.5 ml of 0.1% (w/v) ferric chloride solution. After a 10 min reaction time, the absorbances of the resultant solutions were measured at 700 nm. Higher absorbance of the reaction mixture indicated higher reducing power. The test was carried out in triplicate.

2.8. Purification and characterisation of antioxidant peptides

2.8.1. Fractionation of protein hydrolysates with Sephadex G-25 gel filtration

The freeze-dried hydrolysate (1 g), with a DH of 6% obtained by treatment with crude alkaline protease extract from sardine was suspended in 20 ml of distilled water, then loaded onto a Sephadex G-25 gel filtration column (2.5 cm × 54 cm), pre-equilibrated and eluted with distilled water. Fractions (5 ml each) were collected at a flow rate of 60 ml/h, and absorbance was measured at 226 nm to determine the elution profile of the sample. Fractions associated with each peak showing antioxidant activity were pooled and freeze-dried.

2.8.2. Reversed-phase high pressure liquid chromatography (RP-HPLC)

The peptide mixture in fraction P_4 from Sephadex G-25, which exhibited the highest DPPH scavenging activity, was dissolved in distilled water, filtered through 0.22 μm filters, and then separated by RP-HPLC on a Vydac C_{18} column (10 mm × 250 mm). Peptides were eluted with eluent A (water containing 0.1% trifluoric acetic acid (TFA) for 10 min), then with a linear gradient of acetonitrile (0–100% in 25 min) containing 0.1% TFA at a flow rate of 1 ml/min. On-line UV absorbance scans were performed between 200 and 300 nm at a rate of one spectrum per second with a resolution of 1.2 nm. Chromatographic analyses were completed with Millennium software. The antioxidative activities of the eluted peaks were determined.

The liquid chromatographic system consisted of a Waters 600E automated gradient controller pump module, a Waters Wisp 717 automatic sampling device and a Waters 996 photodiode array detector. Spectral and chromatographic data were stored on a NEC image 466 computer. Millennium software was used to plot, acquire and analyse chromatographic data.

2.8.3. Determination of the amino acid sequence of the purified peptides

The molecular mass and peptide sequencing were done on positive ion mode using Electrospray ionisation-mass spectrometry (ESI-MS) and the tandem mass spectrometry (MS/MS). ESI mass spectrometry was performed using a triple quadrupole instrument Applied Biosystems API 3000 (PE Sciex, Toronto, Canada) equipped with an electrospray ion source. The system is controlled by the Analyst Software 1.4, allowing the control of the spectrometer, the analysis and the processing data. Interpretations of spectra MS–MS were made with the Bioanalyst software. The freeze-dried samples from RP-HPLC were dissolved in acetonitrile/water (20/80; v/v) containing 0.1% formic acid for the positive mode. The solution was injected with a flow rate of 5 μl/min. The potential of ionisation was of 5000 V in positive mode. At the time of the recording of the spectrum, 30 scans on average were added (MCA mode) for each spectrum. The gases used (nitrogen and air) were pure (up to 99%) and produced by a compressor Jun-Air 4000-40M and a nitrogen generator Whatman model 75–72 (Whatman Inc, Haverhill, MA the USA). The polypropylene glycol was used for the calibration and the optimisation of the machine. The peptide sequence was determined from the CID spectrum of the protonated analyse $[M+H]^+$ by MS/MS experiments. Peptide sequences were done using the bioanalyst software (Applied Biosystems, USA).

2.9. Statistical analysis

Statistical analyses were performed with Statgraphics ver. 5.1, professional edition (Manugistics Corp., USA) using ANOVA analysis. Differences were considered significant at $p < 0.05$.

3. Results and discussion

3.1. Preparation of protein hydrolysates using various proteases

It has been demonstrated that the antioxidant activities of proteins can be increased through hydrolysis with certain enzymes, and some peptides or fractions possess stronger antioxidant potential than others (Chen, Muramoto, & Yamauchi, 1995). Further, the antioxidant activity of protein hydrolysates depends on the protein substrate, the specificity of the enzyme, the conditions used during proteolysis and the degree of hydrolysis. Since enzymes have

specific cleavage positions on polypeptides chain, protein hydrolysates were prepared from sardinelle by-products by treatment with different enzymes to obtain peptides with different amino acids sequences and peptides length. Alcalase®, crude enzyme preparations from *B. licheniformis* NH1 and *A. clavatus* ES1, and crude enzyme extract from sardine viscera were used in the present study. The hydrolysis curves of sardinelle by-products proteins after 3 h of incubation are shown in Fig. 1. Enzymes were used at the same activity levels to compare hydrolytic efficiencies.

The hydrolysis of the sardinelle by-products proteins was characterised by a high rate of hydrolysis for the first 1 h. The rate of enzymatic hydrolysis was subsequently decreased, and then the enzymatic reaction reached the steady-state phase when no apparent hydrolysis took place. Crude enzyme preparation from *B. licheniformis* NH1 was the most efficient while crude enzyme preparation from *A. clavatus* ES1 was the lowest efficient. After 3 h of hydrolysis, the DH reached about 11% with crude enzyme preparation from NH1 strain, 8% with Alcalase® and crude extract from sardine viscera, and 5% with crude enzyme preparation from *A. clavatus* ES1. The shape of the hydrolysis curves is similar to those previously reported for sardine (Quaglia & Orban, 1987), Atlantic salmon (Kristinsson & Rasco, 2000), yellowfin tuna (Guérard, Dufossé, De La Broise, & Binet, 2001), and sardinelle (Bougatef et al., 2008).

3.2. Antioxidant activity of sardinelle by-products hydrolysates

The resulting hydrolysates were freeze-dried and assayed for antioxidative activity using various antioxidant assays, including 1,1-diphenyl-2-picrylhydrazyl (DPPH) radical-scavenging activity, reducing power and lipid peroxidation inhibition assay.

3.2.1. DPPH free radical-scavenging activity

DPPH is a stable free radical that shows maximum absorbance at 517 nm. When DPPH radicals encounter a proton-donating substrate such as an antioxidant, the radicals would be scavenged and the absorbance is reduced (Shimada, Fujikawa, Yahara, & Nakamura, 1992). The decrease in absorbance is taken as a measure for radical-scavenging activity.

Fig. 2 shows the DPPH radical-scavenging activity of sardinelle by-products hydrolysates at 2 mg/ml and BHA. The results clearly indicated that hydrolysate obtained by treatment with crude enzyme from sardine viscera exhibited the highest radical-scavenging activity (53.76 ± 1.2%), while the lowest DPPH radical-scavenging activity was obtained with crude enzyme from *A. clavatus* ES1 (10.55 ± 1.55%). However, all hydrolysates showed lower radical-scavenging activity than BHA (2 mM; 92.5 ± 1.7%). The results obtained suggested that some peptides within sardinelle protein hydrolysates were significantly strong radical scavengers.

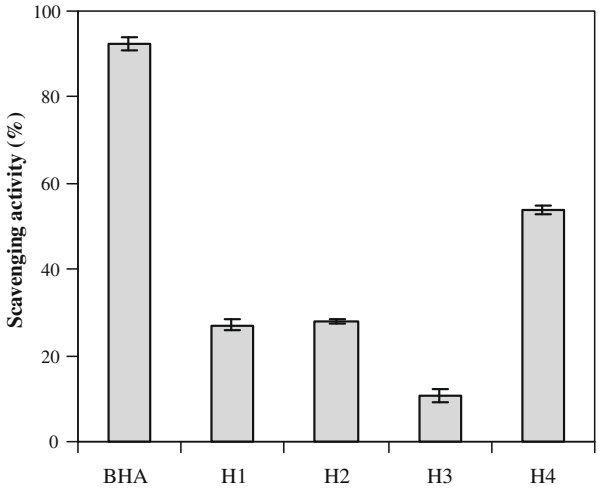

Fig. 2. DPPH scavenging activity of sardinelle by-products protein hydrolysates. H1, H2, H3 and H4 are hydrolysates obtained by treatment with Alcalase® (DH = 8%), crude enzymes from *B. licheniformis* NH1 (DH = 11%) and *A. clavatus* ES1 (DH = 5%), and crude enzyme extract from sardine viscera (DH = 8%), respectively. Values presented are the mean of triplicate analyses.

3.2.2. Reducing power

The reducing power assay is often used to evaluate the ability of an antioxidant to donate an electron or hydrogen (Yildirim et al., 2000). Many reports have revealed that there is a direct correlation between antioxidant activities and reducing power of certain bioactive compounds. In this assay, the ability of hydrolysates to reduce Fe^{3+} to Fe^{2+} was determined. The presence of antioxidants in the protein hydrolysate results in reduction of the Fe^{3+}/ferric cyanide complex to the ferrous form. Therefore, the Fe^{2+} complex can be monitored by measuring the formation of Perl's Prussian blue at 700 nm. Fig. 3 shows the reducing power activities (as indicated by the absorbance at 700 nm) of the different protein hydrol-

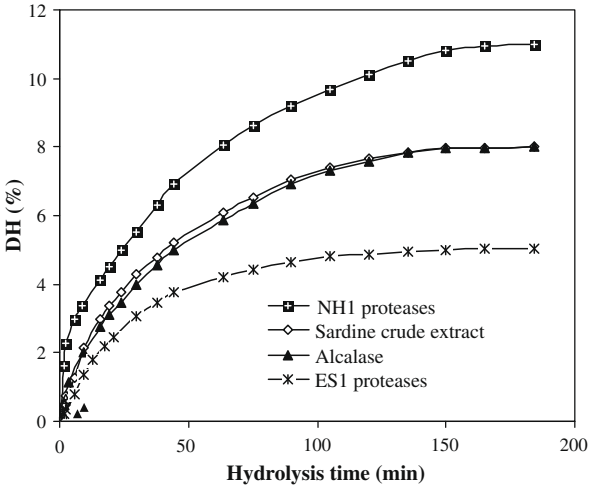

Fig. 1. Hydrolysis curves for sardinelle by-products treated with different enzymes.

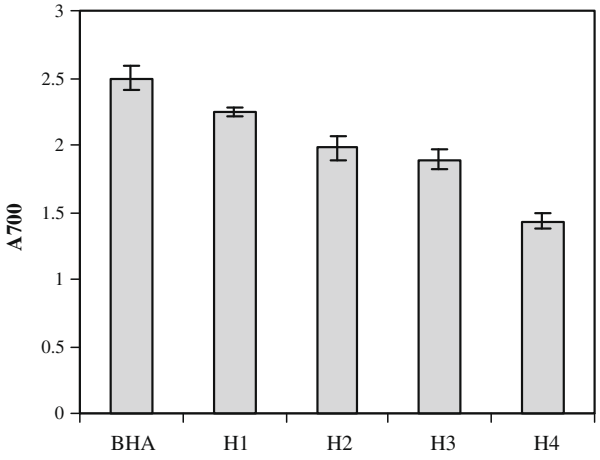

Fig. 3. Reducing power activity of the different hydrolysates. H1, H2, H3 and H4 are hydrolysates obtained by treatment with Alcalase® (DH = 8%), crude enzymes from *B. licheniformis* NH1 (DH = 11%) and *A. clavatus* ES1 (DH = 5%), and crude enzyme extract from sardine viscera (DH = 8%), respectively. Values presented are the mean of triplicate analyses.

ysates compared with BHA as standard. All hydrolysates showed some degree of electron donation capacity. The hydrolysate obtained by treatment with Alcalase® was the most potent reducing power (2.24 ± 0.48) followed by that obtained by treatment with crude enzyme preparation from *B. licheniformis* NH1 (1.98). The hydrolysate treated with sardine crude enzyme extract showed the weakest activity. However, all hydrolysates showed lower reducing power than BHA.

3.2.3. Lipid peroxidation inhibition assay

Peroxidation of lipids is a complex process that involves formation and propagation of lipid radicals and lipid hydroperoxides are formed as primary oxidation products in the presence of oxygen. The antioxidative activity of the four hydrolysates at 2 mg/ml, against the peroxidation of linoleic acid, was investigated and compared to α-tocopherol which has been widely used as a natural antioxidative agent. As shown in Table 1, the control (without antioxidant) had the highest absorbance value, indicating the highest degree of oxidation among samples, while the sample with α-tocopherol, used as a reference, had the lowest absorbance. All hydrolysates prevented linoleic acid peroxidation, which was smaller than α-tocopherol providing about 77% inhibition of linoleic acid peroxidation. Hydrolysate obtained by treatment with crude enzyme from sardine viscera, exhibited the highest inhibition of lipid peroxidation in the linoleic acid emulsion system (53.76 ± 0.42%), and followed by Alcalase and NH1 crude enzyme hydrolysates.

3.3. Antioxidant activity at different degrees of hydrolysis

The above results demonstrated that hydrolysate obtained by treatment with crude enzyme extract from sardine viscera exhibited high antioxidant activity. Therefore, this crude extract was chosen for the isolation and identification of antioxidant peptides.

The degree of hydrolysis is a measure of the extent of hydrolysis degradation of a protein, and it is the most widely used indicator for comparison among different protein hydrolysates. During hydrolysis, a wide variety of larger, medium and smaller peptides are generated, depending on enzyme specificity. In order to study the effect of the DH on the evolution of antioxidative properties, protein hydrolysates having DH values of 2%, 4%, 6% and 8% were generated from heads and viscera of sardinelle by treatment with sardine crude enzyme extract. As shown in Table 2, hydrolysate with 6% DH exhibited the highest DPPH radical-scavenging activity (87 ± 2.1%). In addition, according to the results reported in Table 2, the reducing power was correlated with the degree of hydrolysis, and higher activity (1.43 ± 0.77) was obtained with DH of 8%. From this result, it appears that protein hydrolysate from sardinelle by-products could function by donating electrons to the free radicals.

3.4. Isolation and purification of antioxidant peptides

To purify antioxidant peptides, hydrolysate with 6% DH, which exhibited the highest DPPH scavenging activity, was initially separated into eight fractions (P_1–P_8) by size exclusion chromatography on Sephadex G-25 column (Fig. 4). Each fraction was pooled, lyophilised and its antioxidant activity was assayed. As shown in Fig. 4, all fractions (at 1 mg/ml) displayed antioxidant activities. Fraction P_4 possessed the highest radical-scavenging activity (48%) among all fractions. This fraction was further separated by reversed-phase HPLC and fractionated into six major sub-fractions ($P_{4\text{-}1}$, $P_{4\text{-}2}$, $P_{4\text{-}3}$, $P_{4\text{-}4}$, $P_{4\text{-}5}$ and $P_{4\text{-}6}$). The elution profile of peptides is shown in Fig. 5. Fractions were collected separately through repeated chromatography using reversed-phase HPLC column and concentrated in vacuo prior to testing the radical-scavenging activities. As shown in Fig. 5, all fractions showed varying degrees of DPPH radical-scavenging activity, and sub-fraction $P_{4\text{-}3}$ possessed the strongest activity (63 ± 1.57%; at 150 μg/ml).

Table 2
DPPH radical-scavenging activity and reducing power of sardinelle by-product hydrolysates, with different DHs, produced by treatment with crude extract from sardine viscera.

DH (%)	DPPH (%)	Reducing power (A700)
2	47.5 ± 0.22	0.3 ± 0.06
4	47.77 ± 0.18	0.36 ± 0.04
6	87 ± 1.5	0.8 ± 0.23
8	53.76 ± 1.2	1.43 ± 0.77
BHA	92.5 ± 1.7	2.5 ± 0.12

The concentration of protein hydrolysates was 2.0 mg/ml. BHA (2.0 mM; 0.36 mg/ml) was used as standard.

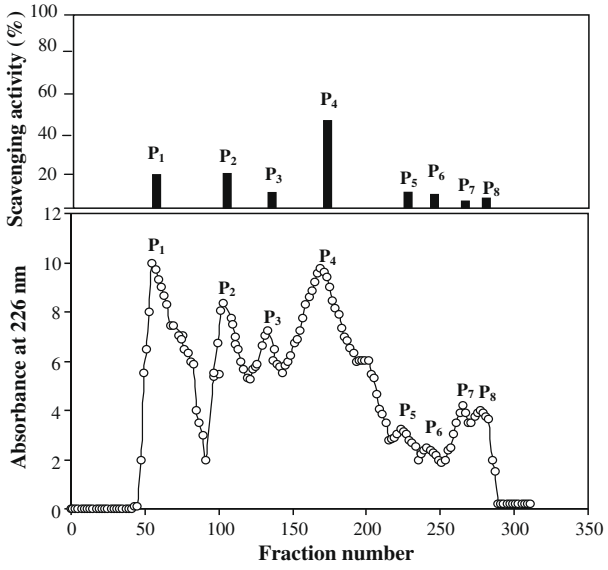

Fig. 4. Elution profile of sardinelle by-product protein hydrolysates separated by size exclusion chromatography on Sephadex G-25 (lower panel) and the DPPH radical-scavenging activities of the separated fractions (upper panel). The column (2.5 cm × 54 cm) was equilibrated and eluted with distilled water at a flow rate of 60 ml/h. Values presented are the mean of triplicate analyses.

Table 1
Antioxidant activity of sardinelle by-products hydrolysates in linoleic acid autoxidation system measured by the ferric thiocyanate method.

	Absorbance at 500 nm	Inhibition (%)	DH (%)
Control	2.65 ± 0.02	0	–
Alcalase®	1.75 ± 0.01	33.96 ± 0.6	8
Proteases from *B. licheniformis* NH1	1.85 ± 0.01	28.14 ± 0.52	11
Proteases from *A. clavatus* ES1	2.25 ± 0.015	15 ± 0.3	5
Crude extract from sardine viscera	1.28 ± 0.012	53.76 ± 0.42	8
α-Tocopherol	0.6 ± 0.01	77.35 ± 0.11	–

The concentration of protein hydrolysates was 2.0 mg/ml. α-Tocopherol (2.0 mM; 0.86 mg/ml) was used as standard.

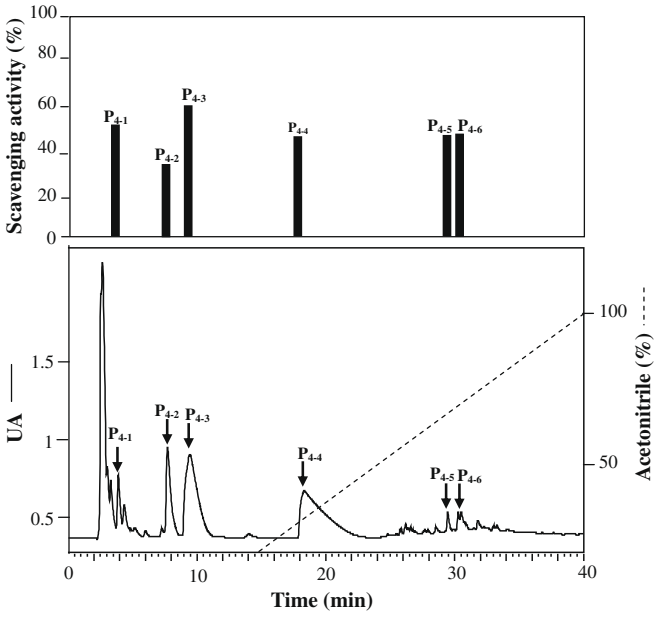

Fig. 5. Reversed-phase HPLC pattern on a Vydac C_{18} column of the P_4 fraction obtained from Sephadex G-25 gel filtration (lower panel). The antioxidant activity of the eluted peaks was measured by DPPH radical-scavenging effect (upper panel). Flow rate, 1 ml/min; monitoring absorbance, 215 nm. Values presented are the mean of triplicate analyses.

3.5. Identification of antioxidative peptides

Peptides in sub-fractions (P_{4-1}–P_{4-5}) were analysed by ESI-MS for molecular mass determination and ESI-MS/MS for the characterisation of peptides. Four purified peptides were identified in sub-fractions P_{4-1} (Leu-Ala-Arg-Leu), P_{4-2} (Gly-Gly-Glu), P_{4-3} (Leu-His-Tyr) and P_{4-5} (Gly-Ala-Leu-Ala-Ala-His) (Table 3). Leu-His-Tyr displayed the highest DPPH radical-scavenging activity (63 ± 1.57% at 150 μg/ml). In addition, sub-fraction P_{4-4} contains three peptides and the antioxidant activity if this sub-fraction may result from the three peptides, which contained His, Trp or Tyr residues. In fact, Da'valos, Miguel, Bartolome, and Lo'pez-Fandino (2004) reported that among the amino acids, Trp, Tyr and Met showed the highest antioxidant activity, followed by Cys, His and Phe. The antioxidant activity of histidine-containing peptides has been reported and attributed to the chelating and lipid radical-trapping ability of the imidazole ring (Murase, Nagao, & Terao, 1993; Park, Jung, Nam, Shahidi, & Kim, 2001; Uchida & Kawakishi, 1992).

In this study, four of the seven antioxidant peptides identified had His residue. Further, Leu-His-Tyr peptide, which displayed high activity, may be due to the presence in this sequence of both His and Tyr residues. All identified peptides are novel peptides with antioxidant activity that had never been reported.

Table 3
Peptides identified by MS/MS in fractions P_{4-1}, P_{4-2}, P_{4-3}, P_{4-4} and P_{4-5} separated by RP-HPLC.

Fractions	MW (Da)	Sequence	DPPH scavenging activity (%)
P_{4-1}	471.3	Leu-Ala-Arg-Leu	51 ± 1.31
P_{4-2}	263.08	Gly-Gly-Glu	38 ± 1.27
P_{4-3}	431.2	Leu-His-Tyr	63 ± 1.5
P_{4-4}	283.1	Gly-Ala-His	
	403.1	Gly-Ala-Trp-Ala	52 ± 1.44
	528.2	Pro-His-Tyr-Leu	
P_{4-5}	538.2	Gly-Ala-Leu-Ala-Ala-His	54 ± 1.38

4. Conclusions

In the present study, sardinelle by-products protein hydrolysates obtained by various proteases were found to possess antioxidant activity. Among four proteolytic preparations, the hydrolysis with crude extract from sardine viscera resulted in the production of the hydrolysate with the highest antioxidant activity.

By gel permeation chromatography on Sephadex G-25, and reversed-phase HPLC, seven antioxidant peptides were purified from the combined heads and viscera of sardinelle hydrolysates (DH 6%) and their sequences were identified by ESI/MS/MS and molecular weight analysis. The peptide Leu-His-Tyr displayed the highest radical-scavenging activity.

These results suggest that hydrolysate from sardinelle by-products could be used as natural antioxidant in enhancing antioxidants properties of functional foods and in preventing oxidation reactions in food processing.

Further research should be done in order to purify and identify antioxidative peptides in the other fractions collected by gel filtration.

Acknowledgment

This work was funded by "Ministry of Higher Education, Scientific Research and Technology, Tunisia".

References

Adler-Nissen, J. (1986). A review of food hydrolysis specific areas. In J. Adler-Nissen (Ed.), *Enzymic hydrolysis of food proteins* (pp. 57–109). Copenhagen, Denmark: Elsevier Applied Science Publishers.

Aluko, R. E., & Monu, E. (2003). Functional and bioactive properties of quinoa seed protein hydrolysates. *Journal of Food Science, 68*, 1254–1258.

Amarowicz, R., & Shahidi, F. (1997). Antioxidant activity of peptide fractions of capelin protein hydrolysates. *Food Chemistry, 58*, 355–359.

Bersuder, P., Hole, M., & Smith, G. (1998). Antioxidants from a heated histidine–glucose model system. I. Investigation of the antioxidant role of histidine and isolation of antioxidants by high performance liquid chromatography. *Journal of the American Oil Chemist's Society, 75*, 181–187.

Blanca, H. L., Ana, Q., Lourdes, A., & Isidra, R. (2007). Identification of bioactive peptides after digestion of human milk and infant formula with pepsin and pancreatin. *International Dairy Journal, 17*, 42–49.

Bougatef, A., Hajji, M., Balti, R., Lassoued, I., Triki-Ellouz, Y., & Nasri, M. (2009). Antioxidant and free radical-scavenging activities of smooth hound (*Mustelus mustelus*) muscle protein hydrolysates obtained by gastrointestinal proteases. *Food Chemistry, 114*, 1198–1205.

Bougatef, A., Nedjar-Arroume, N., Ravallec-Plé, R., Leroy, Y., Guillochon, D., Barkia, A., et al. (2008). Angiotensin I-converting enzyme (ACE) inhibitory activities of sardinelle (*Sardinella aurita*) by-products protein hydrolysates obtained by treatment with microbial and visceral fish serine-proteases. *Food Chemistry, 111*, 350–356.

Bougatef, A., Souissi, N., Fakhfakh, N., Triki-Ellouz, Y., & Nasri, M. (2007). Purification and characterization of trypsin from the viscera of sardine (*Sardina pilchardus*). *Food Chemistry, 102*, 343–350.

Chen, H. M., Muramoto, K., & Yamauchi, F. (1995). Structural analysis of antioxidative peptides from soybean β-conglycinin. *Journal of Agricultural and Food Chemistry, 43*, 574–578.

Cumby, N., Zhong, Y., Naczk, M., & Shahidi, F. (2008). Antioxidant activity and water-holding capacity of canola protein hydrolysates. *Food Chemistry, 109*, 144–148.

Da'valos, A., Miguel, M., Bartolome, B., & Lo'pez-Fandino, R. (2004). Antioxidant activity of peptides derived from egg white proteins by enzymatic hydrolysis. *Journal of Food Protection, 67*, 1939–1944.

Decker, E. A., Warner, K., Richards, M. P., & Shahidi, F. (2005). Measuring antioxidant effectiveness in food. *Journal of Agricultural and Food Chemistry, 53*, 4303–4310.

Diaz, M. N., Frei, B., Vita, J. A., & Keaney, J. F. (1997). Antioxidants and atherosclerotic heart disease. *The New England Journal of Medicine, 337*, 408–416.

El Hadj-Ali, N., Agrebi, R., Ghorbel-Frikha, B., Sellami-Kamoun, A., Kanoun, S., & Nasri, M. (2007). Biochemical and molecular characterization of a detergent stable alkaline serine-protease from a newly isolated *Bacillus licheniformis* NH1. *Enzyme and Microbial Technology, 40*, 513–523.

F.A.O. (2004). *Food and agriculture organisation*. Rome, Italy: Fishery Statistics.

Gibbs, B. F., Zougman, A., Masse, R., & Mulligan, C. (2004). Production and characterization of bioactive peptides from soy hydrolysate and soy fermented food. *Foods Research International, 37*, 123–131.

Guérard, F., Dufossé, L., De La Broise, D., & Binet, A. (2001). Enzymatic hydrolysis of proteins from yellowfin tuna (*Thunnus albacares*) wastes using Alcalase. *Journal of Molecular Catalysis, 11*, 1051–1059.

Hajji, M., Kanoun, S., Nasri, M., & Gharsallah, N. (2007). Purification and characterization of an alkaline serine-protease produced by a new isolated *Aspergillus clavatus* ES1. *Process Biochemistry, 42*, 791–797.

Ito, N., Hirose, M., Fukushima, S., Tsuda, H., Shirai, T., & Tatematsu, M. (1986). Studies on antioxidants: Their carcinogenic and modifying effects on chemical carcinogenic. *Food and Chemical Toxicology, 24*, 1099–1102.

Je, J. Y., Park, P. J., & Kim, S. K. (2005). Antioxidant activity of a peptide isolated from Alaska pollack (*Theragra chalcogramma*) frame protein hydrolysate. *Food Research International, 38*, 45–50.

Jun, S. Y., Park, P. J., Jung, W. K., & Kim, S. K. (2004). Purification and characterization of an antioxidative peptide from enzymatic hydrolysate of yellowfin sole (*Limanda aspera*) frame protein. *European Food Research and Technology, 219*, 20–26.

Katalinic, V., Milos, M., Kulisic, T., & Jukic, M. (2006). Screening of 70 medicinal plant extracts for antioxidant capacity and total phenols. *Food Chemistry, 94*, 550–557.

Kembhavi, A. A., Kulkarni, A., & Pant, A. (1993). Salt-tolerant and thermostable alkaline protease from *Bacillus subtilis* NCIM No. 64. *Applied Biochemistry and Biotechnology, 38*(8), 3–92.

Kim, S. Y., Je, J. Y., & Kim, S. K. (2007). Purification and characterization of antioxidant peptide from hoki (*Johnius belengerii*) frame protein by gastrointestinal digestion. *Journal of Nutritional Biochemistry, 18*, 31–38.

Kim, S. K., Kim, Y. T., Byun, H. G., Nam, K. S., Joo, D. S., & Shahidi, F. (2001). Isolation and characterization of antioxidative peptides from gelatine hydrolysate of Alaska Pollak skin. *Journal of Agricultural and Food Chemistry, 49*, 1984–1989.

Kim, S. K., Lee, H. C., Byun, H. G., & Jeon, Y. T. (1996). Isolation and characterization of antioxidative peptides from enzymatic hydrolysates of yellowfin sole skin gelatine. *Journal of the Korean Fisheries Society, 29*, 246–255.

Klompong, V., Benjakul, S., Kantachote, D., & Shahidi, F. (2007). Antioxidative activity and functional properties of protein hydrolysate of yellow stripe trevally (*Selaroides leptolepis*) as influenced by the degree of hydrolysis and enzyme type. *Food Chemistry, 102*, 1317–1327.

Kristinsson, H. G., & Rasco, B. A. (2000). Fish protein hydrolysates: Production, biochemical, and functional properties. *Critical Reviews in Food Science and Nutrition, 40*, 43–81.

Lin, C. C., & Liang, J. H. (2002). Effect of antioxidants on the oxidative stability of chicken breast meat in a dispersion system. *Journal of Food Science, 67*, 530–533.

Madhujith, T., & Shahidi, F. (2006). Optimization of the extraction of antioxidative constituents of six barley cultivars and their antioxidant properties. *Journal of Agricultural and Food Chemistry, 54*, 8048–8057.

Mendis, E., Rajapakse, N., Byun, H. G., & Kim, S. K. (2005). Investigation of jumbo squid (*Disidicus gigas*) skin gelatin peptides for their antioxidant effects. *Life Sciences, 77*, 2166–2178.

Miraliakbari, H., & Shahidi, F. (2008). Antioxidant activity of minor components of tree nut oils. *Food Chemistry, 111*, 421–427.

Mitsuda, H., Yasumoto, K., & Iwami, K. (1996). Antioxidative action of indole compounds during the autoxidation of linoleic acid. *Eiyo to Shokuryo, 19*, 210–214.

Murase, H., Nagao, A., & Terao, J. (1993). Antioxidant and emulsifying activity of *N*-(long-chain-acyl) histidine and *N*-(long-chain-acyl) carnosine. *Journal of Agricultural and Food Chemistry, 41*, 1601–1604.

Osawa, T., & Namiki, M. (1985). Natural antioxidant isolated from eucalyptus leaf waxes. *Journal of Agriculture and Food Chemistry, 33*, 777–780.

Park, P. J., Jung, W. K., Nam, K. S., Shahidi, F., & Kim, S. K. (2001). Purification and characterization of antioxidative peptides from protein hydrolysate of lecithin-free egg yolk. *Journal of the American Oil Chemist's Society, 78*, 651–656.

Parrado, J., Miramontes, E., Jover, M., Gutierrez, J. F., de Teran, L. C., & Bautista, J. (2006). Preparation of a rice bran enzymatic extract with potential use as functional food. *Food Chemistry, 4*, 742–748.

Quaglia, G. B., & Orban, E. (1987). Enzymic solubilisation of proteins of sardine (*Sardina pilchardus*) by commercial proteases. *Journal of Science of Food and Agriculture, 38*, 263–269.

Rice-Evans, C. A., Miller, N. J., & Paganda, G. (1996). Structure–antioxidant activity relationships of flavonoids and phenolic acids. *Free Radical Biology and Medicine, 20*, 933–956.

Saiga, A., Tanabe, S., & Nishimura, T. (2003). Antioxidant activity of peptides obtained from porcine myofibrillar proteins by protease treatment. *Journal of Agricultural and Food Chemistry, 51*, 3661–3667.

Sakanaka, S., Tachibana, Y., Ishihara, N., & Juneja, L. R. (2004). Antioxidant activity of egg-yolk protein hydrolysates in a linoleic acid oxidation system. *Food Chemistry, 86*, 99–103.

Shahidi, F. (2008). Nutraceuticals and functional foods: Whole versus processed foods. *Trends in Food Science and Technology*. doi:10.1016/j.tifs.2008.08.004.

Shahidi, F., Alasalvar, C., & Liyana-Pathirana, C. M. (2007). Antioxidant phytochemicals in hazelnut kernel (*Corylus avellana* L.) and hazelnut byproducts. *Journal of Agricultural and Food Chemistry, 55*(121), 2–1220.

Shimada, K., Fujikawa, K., Yahara, K., & Nakamura, T. (1992). Antioxidative properties of xanthan on the antioxidation of soybean oil in cyclodextrin emulsion. *Journal of Agricultural and Food Chemistry, 40*, 945–948.

Ström, T., & Eggum, B. O. (1981). Nutritional value of fish viscera silage. *Journal of Science of Food and Agriculture, 32*, 115–120.

Uchida, K., & Kawakishi, S. (1992). Sequence-dependant reactivity of histidine-containing peptides with copper(II)/ascorbate. *Journal of Agricultural and Food Chemistry, 40*, 13–16.

Wong, C., Li, H., Cheng, K., & Chen, F. (2006). A systematic survey of antioxidant activity of 30 Chinese medicinal plants using the ferric reducing antioxidant power assay. *Food Chemistry, 97*, 705–711.

Wu, H. C., Chen, H. M., & Shiau, C. Y. (2003). Free amino acids and peptides as related to antioxidant properties in protein hydrolysates of mackerel (*Scomber austriasicus*). *Food Research International, 36*, 949–957.

Yildirim, A., Mavi, A., & Kara, A. A. (2001). Determination of antioxidant and antimicrobial activities of *Rumex crispus* L. extracts. *Journal of Agricultural and Food Chemistry, 49*, 4083–4089.

Yildirim, A., Mavi, A., Oktay, M., Kara, A. A., Algur, Ö. F., & Bilaloglu, V. (2000). Comparison of antioxidant and antimicrobial activities of tilia (*Tilia argentea Desf Ex DC*) sage (*Salvia triloba* L.) and black tea (*Camellia sinensis*) extracts. *Journal of Agricultural and Food Chemistry, 48*, 5030–5034.

Zhong, Y., Khan, M. A., & Shahidi, F. (2007). Compositional, characteristics and antioxidant properties of fresh and processed sea cucumber (*Cucumaria frondosa*). *Journal of Agricultural and Food Chemistry, 54*, 1188–1192.

Food Chemistry 118 (2010) 566–574

Contents lists available at ScienceDirect

Food Chemistry

journal homepage: www.elsevier.com/locate/foodchem

Construction of a novel beer proteome map and its use in beer quality control

Takashi Iimure [a,*], Nami Nankaku [b], Naohiko Hirota [a], Zhou Tiansu [a], Takehiro Hoki [a], Makoto Kihara [a], Katsuhiro Hayashi [a], Kazutoshi Ito [c], Kazuhiro Sato [b]

[a] Bioresources Research and Development Department, Sapporo Breweries Ltd., 37-1, Nittakizaki, Ota, Gunma 370-0393, Japan
[b] Barley Germplasm Center, Research Institute for Bioresources, Okayama University, 2-20-1, Chuo, Kurashiki, Okayama 710-0046, Japan
[c] Frontier Laboratories of Value Creation, Sapporo Breweries Ltd., 10 Okatohme, Yaizu, Shizuoka 425-0013, Japan

ARTICLE INFO

Article history:
Received 30 January 2009
Received in revised form 19 March 2009
Accepted 12 May 2009

Keywords:
Beer protein
Hordeum vulgare
Saccharomyces cerevisiae
Two-dimensional gel electrophoresis
Proteome

ABSTRACT

Beer proteins were analysed by two-dimensional gel electrophoresis (2DE). The protein species associated with major spots on 2DE gels were identified by mass spectrometry followed by a database search to construct a comprehensive beer proteome map. As a result, 85 out of 199 protein spots examined were positively identified and categorised into 12 protein species. A total of 11 beer samples were brewed from the malt of eight cultivars having different levels of protein modification. This experiment was designed to demonstrate the influences of barley cultivar and malt modification on beer protein composition and beer quality characters. The beers produced from these brewing trails were subsequently analysed by 2DE and their proteomes were compared. Cultivars and malt modification affected the concentration of several proteins in beer. Beer protein concentration was associated with differences in the desirable beer quality trait, foam stability. In addition, expression of yeast derived proteins were observed that may also influence beer quality. Overall, the application of a comprehensive beer proteome map provides a strong platform for detection and potential manipulation of beer quality related proteins.

1. Introduction

Beer foam quality is one of the important characteristics that a consumer uses to determine beer quality. Foam quality is defined by its stability, lacing, whiteness, intensity, strength, and creaminess (Bamforth, 1985). In clear beer, colloidal haze formation is also a serious quality problem. Consumers judge a beer as stale or not fit to drink if it displays colloidal haze. Foam stability (Bamforth, 1985; Evans & Sheehan, 2002) and haze formation (Asano, Shinagawa, & Hashimoto, 1982; Iimure et al., 2009; Siebert, 1999) have been assumed to be major quality traits controlled by proteins. In beer foam stability, several beer proteins have been identified as either foam-positive or negative. Previous reports suggested that protein Z (Evans, Sheehan, & Stewart, 1999; Evans et al., 2003; Kaersgaard & Hejgaard, 1979; Maeda, Yokoi, Kamada, & Kamimura, 1991) and lipid transfer protein 1 (LTP1) (Jégou, Douliez, Mollé, Boivin, & Marion, 2000; Sorensen, Bech, Muldbjerg, Beenfeldt, & Breddam, 1993) play important roles in beer foam stability. In addition, recent studies have suggested that barley dimeric α-amylase inhibitor-1 (BDAI-1) and yeast thioredoxin are foam-positive and foam-negative proteins, respectively (Iimure et al., 2008; Okada et al., 2008). In beer colloidal haze, CMe component tetrameric α-amylase inhibitor (CMe), BDAI-1 and hordein were suggested as haze active (Asano et al., 1982; Evans et al., 2003; Iimure et al., 2009; Robinson et al., 2007; Siebert, 1999). However, conclusive identification of protein factors causing beer foam stability and haze formation still requires validation. One of the reasons for the poor understanding of protein factors may come from the lack of knowledge of the spectrum of proteins in beer. Thus, comprehensive analysis of beer protein identity is necessary to reveal the relationship between beer proteins with respect to quality characters including foam stability and haze formation.

Barley cultivar and the level of protein modification during malting are also known as important malting related factors that can modify beer quality (Evans, Nischwitz, Stewart, Cole, & MacLeod, 1998; Iimure et al., 2008). Protein modification is judged by malt modification which is conventionally measured in the brewing industry as the Kolbach index (soluble nitrogen/total nitrogen × 100). Therefore, the understanding of beer protein also requires an understanding of the effect of different barley cultivar and malt modification combinations in important quality proteins (i.e., hordeins, protein Z).

Proteome analysis, which separates a sample of proteins by two-dimensional gel electrophoresis (2DE) which is followed by mass spectrometry analysis and database searches, is a powerful tool to comprehensively detect the spectrum of proteins present in a beer sample. In several reports, proteins from barley grain and malt were analysed by 2DE and major protein spots were

* Corresponding author. Tel.: +81 276 56 1454; fax: +81 276 56 1605.
E-mail address: takashi.iimure@sapporobeer.co.jp (T. Iimure).

0308-8146/$ - see front matter © 2009 Elsevier Ltd. All rights reserved.
doi:10.1016/j.foodchem.2009.05.022

identified (Bak-Jensen, Laugesen, Roepstorff, & Svensson, 2004; Østergaard, Finnie, Laugesen, Roepstorff, & Svensson, 2004). Also major beer proteins were identified by mass spectrometry (Hao et al., 2006; Perrocheau, Rogniaux, Boivin, & Marion, 2005). Similarly, Iimure et al. (2008) and Iimure et al. (2009) identified foam proteins and haze active proteins using a proteome analysis.

To expand these pioneering analyses, this study develops a comprehensive proteome map of beer for Japanese style lager beer. Recent advancements in protein analysis enable the development of a proteome map with greater resolution by identifying relatively minor spots. The use of the proteome map is applied practically, to assess eleven beer samples that were prepared with different barley cultivars and levels of malt modification. The efficient application of protein spot intensities on 2DE images is discussed to control foam stability and haze formation.

2. Materials and methods

2.1. Barley sample, malting and malt quality analysis

The barley-malt materials used in this study are described in Table 1. Each 75 kg barley grain sample from a single cultivar (>2.5 mm screen) was processed according to Okada et al. (2008). For cultivars F, G and H, two different ex-steep moisture levels, i.e., low (36–37%) and high (43–44%), were used to influence malt modification, thus assess its influence on beer protein composition. Malt quality characters were analysed according to the standard methods of the European Brewery Convention (European Brewery Convention & Analytica, 1987).

2.2. Pilot-scale brewing

Wort was prepared and fermented at a 400 l pilot-scale plant according to Okada et al. (2008), except for mashing in temperature which was either 50 or 60 °C (Table 1). Beer quality characteristics were analysed according to the standard methods of European Brewery Convention (European Brewery Convention, Analytica, 1987). Beer foam stability (NIBEM value) was scored by foam stability tester type NIBEM-T (Haffmans B. V., Venlo, Holland) according to the manufacturer's instructions. Colloidal stability was scored by a forcing test (FT-3). For the FT-3 haze test, the bottled beer samples were stored at 60 °C for 3 days and then 0 °C for 1 day. Subsequently, the beer clarity, FT-3, was measured in terms of haze formation (Iimure et al., 2009).

2.3. Two-dimensional gel electrophoresis (2DE)

Completely degassed beer samples were desalted using a PD-10 column (GE Healthcare Biosciences, Japan). After the protein concentration was determined by the Bradford method using bovine serum albumin as a standard, desalted protein was lyophilised. The lyophilised protein was dissolved in 8 M urea (Wako, Japan) + 2% 3-[(3-cholamidopropyl) dimethylammonio] propanesulfonic acid (CHAPS) (Dojindo Laboratories, Japan) solution containing 0.28% dithiothreitol (Wako, Japan). Subsequently, the protein solution was applied to IPG dry strips pI 3–10 or 4–7 or 6–9 (GE Healthcare Bioscience, Japan). 2DE and silver staining were carried out according to Okada et al. (2008).

2.4. Mass spectrometry analysis

The protein spots were excised from the gels and decolorised by a solution containing 15 mM potassium ferricyanide and 50 mM sodium thiosulphate. Sample gels were treated for in gel reduction using dithiothreitol and S-alkylation using monoiodoacetic acid. After adding ammonium hydrogencarbonate buffer containing trypsin, sample gels were incubated for 4 h at 37 °C. The resultant sample solution was desalted using Zip-Tip (Nihon Millipore Ltd., Japan), and eluted with 80% acetonitrile. The sample was analysed using matrix-assisted laser desorption ionisation time-of-flight mass spectrometry (MALDI-TOF-MS) using Voyager-DE STR (Applied Biosystems, USA). Internal mass was calibrated using trypsin autolysis products. Protein species were identified by peptide mass fingerprinting (PMF) on the non-redundant amino acid database of the National Center for Biotechnology Information (NCBI-nr) using the MASCOT search engine (Perkins, Pappin, Creasy, & Cottrell, 1999). The following parameters were used for searches in MASCOT. Database: NCBInr; Taxonomy: all entries, enzyme: trypsin, number of missed cleavages: up to 1 missed cleavage, fixed modification: carbamidometyl cysteine, variable modification: oxidation of methionine, peptide tolerance: below 50 ppm, mass values: MH+. The protein was considered as a positive candidate when it satisfied all of the following three criteria, (1) significant MASCOT score ($P < 0.05$), (2) more than four peptides matched and (3) sequence coverage of more than 15%. When candidate was not identified in NCBI-nr, barley gene index (http://compbio.dfci.harvard.edu/tgi/), HarvEST #31 (http://harvest.ucr.edu/) and mass spectrometry protein sequence database (MSDB) (http://proteomics.leeds.ac.uk/bioinf/msdb.html) were searched under the same conditions to attempt protein identification. When a protein was not identified by PMF analysis using trypsin as proteinase, the sample was double digested by trypsin and lysil endopeptidase. The decolorised sample gel was treated with a Tris–HCl buffer (pH 8.0) containing lysil endopeptidase and incubated for 3 h at 35 °C. After adding trypsin, the sample was incubated for 20 h at 35 °C. Subsequently, the samples were analysed by liquid chromatography mass spectrometry/mass spectrometry (LC-MS/MS) by following conditions. The sample solution was ap-

Table 1
Characteristics and materials of beer samples used for protein analysis.

Beer sample name	Barley cultivar	Area of production	Year	Mashing in temperature (°C)	Malt Kolbach index[a]	Beer bitterness unit	NIBEM (s)	FT-3[b]
Beer A	Cultivar A	Japan	2007	60	42.5	21.7	258	4.19
Beer B	Cultivar B	Japan	2004	60	42.2	20.8	226	4.10
Beer C	Cultivar C	Japan	2007	60	43.3	19.5	232	5.49
Beer D	Cultivar D	Japan	2003	60	46.6	16.3	229	5.95
Beer E	Cultivar E	Canada	2004	60	42.5	19.1	247	1.77
Beer F(L)	Cultivar F	Japan	2002	50	43.7	23.4	281	1.39
Beer F(H)	Cultivar F	Japan	2002	50	49.1	22.4	234	1.41
Beer G(L)	Cultivar G	Japan	2000	50	47.3	23.0	251	1.18
Beer G(H)	Cultivar G	Japan	2000	50	54.0	21.3	223	1.63
Beer H(L)	Cultivar H	Canada	2000	50	39.4	23.6	269	1.51
Beer H(H)	Cultivar H	Canada	2000	50	50.0	22.9	269	1.02

[a] Soluble nitrogen/total nitrogen × 100.
[b] Beer clarity after the forcing test (see Section 2).

plied to LC-MS/MS as follows. Equipment: MAGIC 2002 (Michrom BioResources Inc., USA), column: MAGIC C18 (0.1 × 150 mm, Michrom BioResources Inc.), mobile phase: 2% acetonitrile + 0.1% formic acid, and 90% acetonitrile + 0.1% formic acid, flow rate: 250–300 nL/min, mass spectrometer: Q-Tof2 (Micromass, UK), ionisation method: Nanoflow-LC ESI, ionisation mode: positive mode, electric potential of capillary: 1.8 kV, collision energy: 20–56 eV. In order to identify protein species, NCBI-nr was searched by resultant values of product ion from all precursor ions using MASCOT search engine.

3. Results

3.1. Identification of major beer proteins on the 2DE gels

Proteins in standard beer samples (i.e., Beer F(L)), were separated by 2DE (pI 4–7 and 6–9) (Fig. 1) and individual protein spots were analysed by MALDI-TOF-MS or LC-MS/MS followed by database searches to determine spot identity. The search engines identified 85 out of 199 protein spots which were categorised into 12 protein species (Table 2). According to the source of sequences

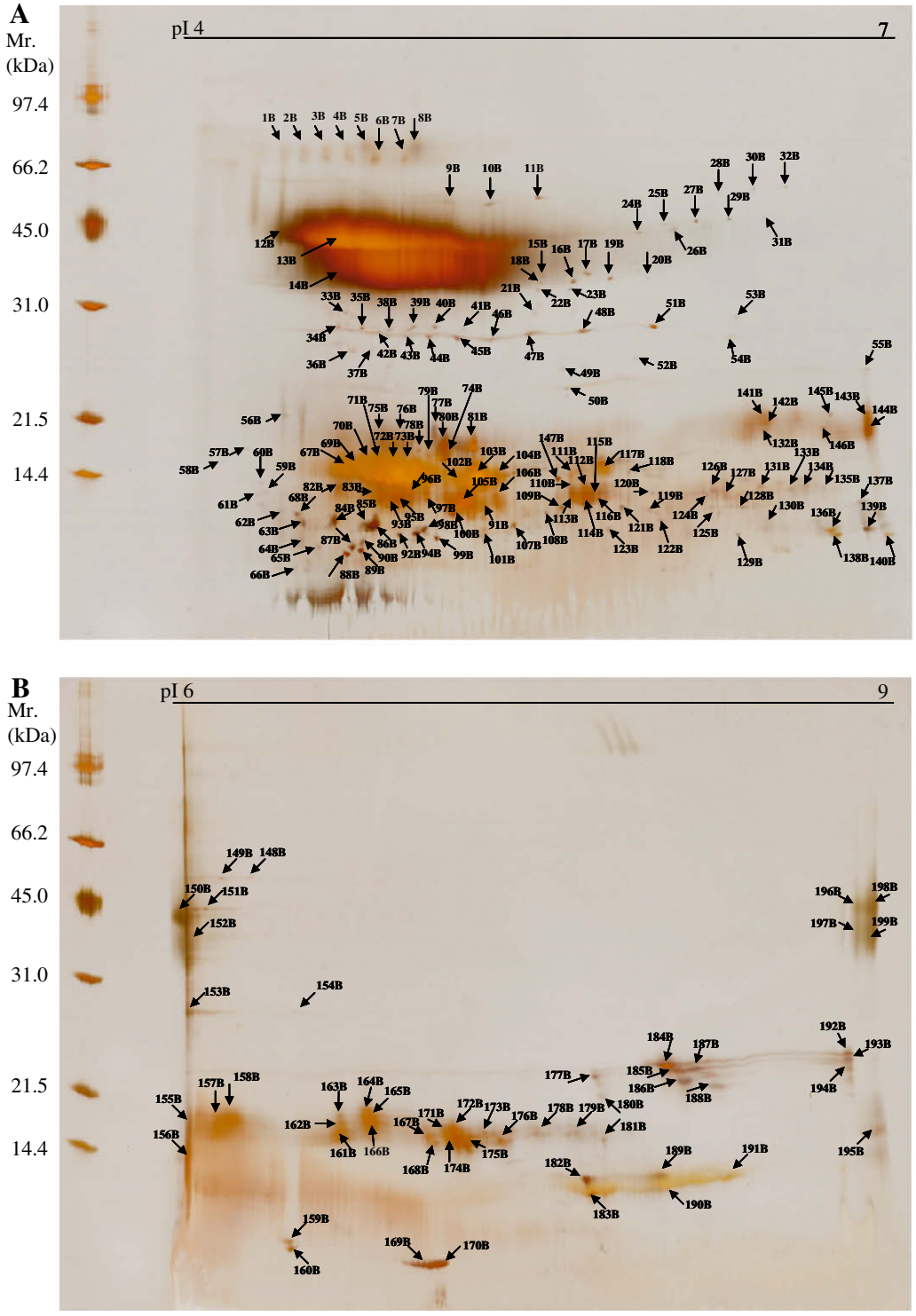

Fig. 1. Two-dimensional gel electrophoresis (2DE) images of proteins of Beer F(L). (A) 2DE image of pI 4–7, (B) 2DE image of pI 6–9. Arrows indicate spot numbers in Table 2.

Table 2
Beer protein species identified by MALDI-TOF-MS or LC-MS/MS analysis followed by MASCOT database search on NCBI-nr or HarvEST #31.

Spot no.	Protein name	Accession no.	Organisms	Theoretical Mr (Da)	Observed Mr (Da)	Theoretical pI	Observed pI
004B	Protein z-type serpin	gi|1310677	H[h]	43,307	69,245	5.61	4.64
005B	Protein z-type serpin	gi|1310677	H	43,307	71,496	5.61	4.73
007B	Protein z-type serpin	gi|1310677	H	43,307	68,147	5.61	4.86
008B	Protein z-type serpin	gi|1310677	H	43,307	70,361	5.61	4.93
009B	Protein z-type serpin	gi|1310677	H	43,307	54,478	5.61	5.08
010B	Protein z-type serpin	gi|1310677	H	43,307	54,045	5.61	5.25
012B	Serpin-Z7 (HorvuZ7) (BSZ7)	gi|75282567	H	42,851	47,176	5.45	4.37
013B	Serpin-Z7 (HorvuZ7) (BSZ7)	gi|75282567	H	42,851	45,692	5.45	4.61
014B	Protein z-type serpin	gi|1310677	H	43,307	41,181	5.61	4.55
015B	Protein z-type serpin	gi|1310677	H	43,307	38,630	5.61	5.46
018B	Protein z-type serpin	gi|1310677	H	43,307	37,116	5.61	5.46
019B	Protein z-type serpin	gi|1310677	H	43,307	37,714	5.61	5.75
023B	Protein z-type serpin	gi|1310677	H	43,307	35,948	5.61	5.58
024B	Protein z-type serpin	gi|1310677	H	43,307	47,176	5.61	5.86
029B	Enolase[c]	gi|20151217	S[i]	46,683	50,292	6.17	6.25
032B	Enolase[c]	gi|20151217	S	46,683	58,077	6.17	6.48
039B	Protein z-type serpin	gi|1310677	H	43,307	29,910	5.61	4.92
044B	Chain B, triosephosphate isomerase[d]	gi|230406	S	26,762	28,509	5.75	4.99
045B	Chain B, triosephosphate isomerase[d]	gi|230406	S	26,762	28,509	5.75	5.11
046B	Chain A, triosephosphate isomerase[e]	gi|230405	S	26,762	28,282	5.75	5.25
047B	Chain A, triosephosphate isomerase[e]	gi|230405	S	26,762	28,738	5.75	5.41
048B	Chain A, triosephosphate isomerase[e]	gi|230405	S	26,762	29,201	5.75	5.63
051B	Chain A, triosephosphate isomerase[e]	gi|230405	S	26,762	30,150	5.75	5.92
053B	Chain A, triosephosphate isomerase[e]	gi|230405	S	26,762	31,379	5.75	6.27
054B	Chain B, crystal structure of the yeast Phosphorelay protein Ypd1	gi|6435746	S	18,996	28,282	4.58	6.24
062B	Lipid transfer protein 1[f]	gi|47168353	H	10,145	12,413	8.19	4.36
063B	Lipid transfer protein 1[f]	gi|47168353	H	10,145	11,644	8.19	4.46
067B	Trypsin/amylase inhibitor pUP13	gi|225102	H	15,307	15,404	5.35	4.63
068B	Lipid transfer protein 1[f]	gi|47168353	H	10,145	12,022	8.19	4.44
069B	Trypsin/amylase inhibitor pUP13	gi|225102	H	15,307	15,404	5.35	4.69
071B	Trypsin/amylase inhibitor pUP13	gi|225102	H	15,307	15,652	5.35	4.77
072B	Trypsin/amylase inhibitor pUP13	gi|225102	H	15,307	15,404	5.35	4.84
073B	Trypsin/amylase inhibitor pUP13	gi|225102	H	15,307	15,652	5.35	4.90
074B	Chloroform/methanol-soluble protein CMb[g]	gi|585290	H	17,199	16,686	5.77	5.06
075B	Lipid transfer protein 1[f]	gi|47168353	H	10,145	18,074	8.19	4.78
076B	Lipid transfer protein 1[f]	gi|47168353	H	10,145	17,505	8.19	4.87
079B	Chloroform/methanol-soluble protein CMb[g]	gi|585290	H	17,199	16,160	5.77	4.98
080B	Chloroform/methanol-soluble protein CMb[g]	gi|585290	H	17,199	18,074	5.77	5.03
081B	Chloroform/methanol-soluble protein CMb[g]	gi|585290	H	17,199	16,955	5.77	5.18
082B	trypsin/amylase inhibitor pUP13	gi|225102	H	15,307	13,883	5.35	4.61
086B[a]	Thioredoxin; Trx2p	gi|6321648	S	11,197	11,644	4.79	4.77
091B	Lipid transfer protein 1[f]	gi|47168353	H	10,145	12,714	8.19	5.15
093B	Alpha-amylase inhibitor BDAI-1 precursor	gi|123970	H	17,045	12,816	5.36	4.82
095B	Trypsin/amylase inhibitor pUP13	gi|225102	H	15,307	13,023	5.35	4.87
096B	Trypsin/amylase inhibitor pUP13	gi|225102	H	15,307	13,023	5.35	4.93
102B	Trypsin/amylase inhibitor pUP13	gi|225102	H	15,307	14,449	5.35	5.10
103B	Chloroform/methanol-soluble protein CMb[g]	gi|585290	H	17,199	14,800	5.77	5.18
104B	trypsin/amylase inhibitor pUP13	gi|225102	H	15,307	14,682	5.35	5.27
105B	Lipid transfer protein 1[f]	gi|47168353	H	10,145	13,023	8.19	5.13
106B	Lipid transfer protein 1[f]	gi|47168353	H	10,145	13,127	8.19	5.27
108B	Lipid transfer protein 1[f]	gi|47168353	H	10,145	12,216	8.19	5.49
109B	Lipid transfer protein 1[f]	gi|47168353	H	10,145	12,512	8.19	5.54
110B	Alpha-amylase inhibitor BDAI-1 precursor	gi|123970	H	17,045	13,883	5.36	5.59
111B	Trypsin/amylase inhibitor pUP13	gi|225102	H	15,307	14,682	5.35	5.58
112B	Lipid transfer protein 1[f]	gi|47168353	H	10,145	13,772	8.19	5.65
113B	Alpha-amylase inhibitor BDAI-1 precursor	gi|123970	H	17,045	13,023	5.36	5.59
114B	Alpha-amylase inhibitor BDAI-1 precursor	gi|123970	H	17,045	13,023	5.36	5.65
115B	Lipid transfer protein 1[f]	gi|47168353	H	10,145	13,554	8.19	5.71
116B	Lipid transfer protein 1[f]	gi|47168353	H	10,145	13,023	8.19	5.68
117B	Chloroform/methanol-soluble protein CMb[g]	gi|585290	H	17,199	15,159	5.77	5.73
118B	Lipid transfer protein 1[f]	gi|47168353	H	10145	15,038	8.19	5.82
120B	Lipid transfer protein 1[f]	gi|47168353	H	10,145	13,554	8.19	5.91
126B	Lipid transfer protein 1[f]	gi|47168353	H	10,145	13,663	8.19	6.18
127B	Lipid transfer protein 1[f]	gi|47168353	H	10,145	13,446	8.19	6.22
128B	Lipid transfer protein 1[f]	gi|47168353	H	10,145	12,613	8.19	6.28
131B	Lipid transfer protein 1[f]	gi|47168353	H	10,145	13,883	8.19	6.37
133B	Lipid transfer protein 1[f]	gi|47168353	H	10,145	13,772	8.19	6.49
134B	Lipid transfer protein 1[f]	gi|47168353	H	10,145	13,772	8.19	6.56
135B	Lipid transfer protein 1[f]	gi|47168353	H	10,145	13,772	8.19	6.63
137B	Lipid transfer protein 1[f]	gi|47168353	H	10,145	12,919	8.19	6.79
140B[b]	Subtilisin-chymotrypsin inhibitor CI-1B	CONTIG3945	H	17,480	10,922	9.63	6.89
144B[b]	BTI-CMe3.1 protein	CONTIG218	H	24,106	18,219	8.90	6.80
147B	Lipid transfer protein 1[f]	gi|47168353	H	10,145	14,449	8.19	5.52
150B	Protein z-type serpin	gi|1310677	H	43,307	45,692	5.61	6.04
152B	Protein z-type serpin	gi|1310677	H	43,307	39,885	5.61	6.09

Table 2 (*continued*)

Spot no.	Protein name	Accession no.	Organisms	Theoretical Mr (Da)	Observed Mr (Da)	Theoretical pI	Observed pI
153B	Chain A, triosephosphate isomerase[e]	gi|230405	S	26,762	28,056	5.75	6.08
155B	Lipid transfer protein 1[f]	gi|47168353	H	10,145	16,686	8.19	6.08
156B	Lipid transfer protein 1[f]	gi|47168353	H	10,145	13,994	8.19	6.08
182B	Lipid transfer protein 1[f]	gi|47168353	H	10,145	12,714	8.19	7.75
183B	Lipid transfer protein 1[f]	gi|47168353	H	10,145	11,737	8.19	7.78
189B	Lipid transfer protein 1[f]	gi|47168353	H	10,145	12,919	8.19	8.06
190B	Lipid transfer protein 1[f]	gi|47168353	H	10,145	11,926	8.19	8.06
191B	Lipid transfer protein 1[f]	gi|47168353	H	10,145	12,919	8.19	8.37
195B	Trypsin/amylase inhibitor pUP13	gi|225102	H	15,307	15,904	5.35	8.98
199B	Protein z-type serpin	gi|1310677	H	43,307	36,820	5.61	8.95

[a] Analysed using LC-MS/MS, the other spots were analysed by MALDI-TOF-MS.
[b] Protein identified on HarvEST #31 (http://harvest.ucr.edu/).
[c] Chain A, Mg-phosphonoacetohydroxamate complex of S39a yeast enolase 1.
[d] Chain B, structure of yeast triosephosphate isomerase at 1.9-Å resolution.
[e] Chain A, structure of yeast triosephosphate isomerase at 1.9-Å resolution.
[f] Chain A, non-specific lipid transfer protein 1 from barley in complex with L-alfa-lysophosphatidylcholine, laudoyl.
[g] Alpha-amylase/trypsin inhibitor CMb precursor (chloroform/methanol-soluble protein CMb).
[h] *Hordeum vulgare* subsp. vulgare.
[i] *Saccharomyces cerevisiae*.

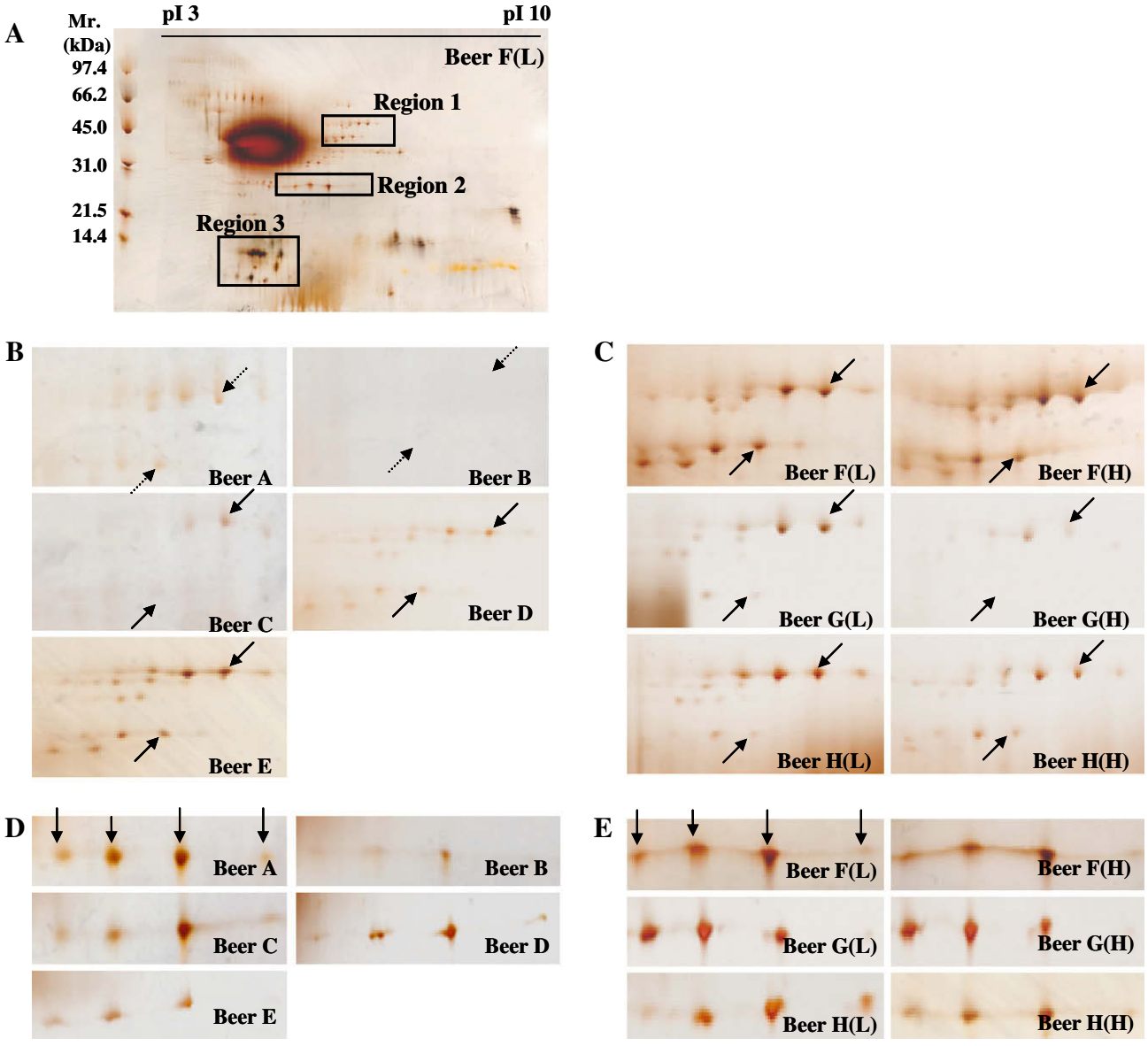

Fig. 2. The differences of two-dimensional gel electrophoresis (2DE) images on Regions 1 and 2 containing the spots of enolase and triose phosphate isomerase (TPI), respectively. (A) Whole image (pI 3–10) of 2DE, (B) 2DE images on Region 1 of the beer from each five cultivars, (C) 2DE images on Region 1 of the beer from each three cultivars with low(L) or high(H) malt modifications. (D) 2DE images on Region 2 of the beer from each five cultivars, (E) 2DE images on Region 2 of the beer from each three cultivars with low(L) or high(H) malt modifications. In B and C, arrows indicate the protein spots of enolase, and in D and E arrows indicate the protein spots of TPI.

on the databases, 8 out of the 12 protein species were derived from *Hordeum vulgare* subsp. *vulgare* and the remaining four proteins were derived from *Saccharomyces cerevisiae*.

3.2. The contribution of barley cultivars on beer proteins

To estimate differences of the beer protein composition among barley cultivars, we processed five beer samples from cultivars A–E (Table 1). The beer proteins were separated by 2DE and their images were compared (Figs. 2 and 3). Major differences were observed in gel Regions 1–3 (Fig. 2A).

The spot intensities of these three Regions in the five beer samples are summarised in Table 3. As shown in Fig. 1 and Table 2, Regions 1 and 2 contained the *S. cerevisiae* protein spots of enolase and triose phosphate isomerase (TPI), respectively. Among five beer samples, the spots of yeast enolase (at Region 1) in Beer E were intense compared to the other four samples (Fig. 2B and Table 3). On the other hand, these spots were not observed in Beer B. Spots of TPI (at Region 2) in Beers B and E were less intense than the others (Fig. 2D and Table 3).

In Region 3, five protein species were identified (Fig. 3A). The protein spots were not detectable in Beer F(L) but were detectable in Beer H(L), to allow identification by mass spectrometry analysis (Fig. 3B). The spot of yeast thioredoxin (y-TRX2p) in Beer D was less intense than the others (Fig. 3C and Table 3). In Beer A, the spot intensities of alpha amylase/trypsin inhibitor CMb precursor (CMb) were more intense than the others. Comparatively, the spot of lipid transfer protein 1 (LTP1) in Beer A was relatively low. The spot of LTP1 on Beer E was the most intense among the five beer samples.

3.3. The influence of malt modification levels on beer proteins

Malt modification can be influenced by increasing the ex-steep moisture during malting. Beers were brewed from cultivars F, G and H with low (36–37%) or high (43–44%) levels of ex-steep moisture. Low ex-steep moisture resulted in relatively low KI/modification while high ex-steep moistures provided malt with relatively high KI/modification. The 2DE images of the beer proteins made from these malts were compared to detect interactions between cultivar and malt modification levels on beer protein composition. As expected the spot intensities of proteins derived from yeast were almost constant in all three cultivars despite the level of malt modification being changed, although some changes in the level of enolase in Beer G and y-TRX2p in Beer H was observed (Figs. 2 and 3). In Beers F(L) and F(H), spot intensities of barley proteins TAI, CMb and LTP1 were lower at the higher malt modification level. However, these spot intensities were unchanged in Beers H(L) and H(H) at both malt modification levels. In addition, in Beers H(L) and H(H), the spot intensities of barley dimeric α-amylase inhibitor-1 (BDAI-1) were almost constant at both malt modification levels. On the other hand, they were lower in beers made from the more modified malts for Beers G(L) and G(H) and faint in both Beers F(L) and F(H).

4. Discussion

A total of 85 protein spots on 2DE gels (Fig. 1 and Table 2) together with data set for the 2DE images were identified in the current proteome analysis. Perrocheau et al. (2005) also analysed beer proteins by 2DE and mass spectrometry but resulted in identification of only 31 protein spots. Hao et al. (2006) identified major proteins in beer foam by mass spectrometry following sodium dodecyl sulphate polyacrylamide gel electrophoresis (SDS–PAGE), which made protein composition comparison difficult between samples. Thus, we assume the data set in current protein analysis as one of the most comprehensive beer proteome maps yet to be made.

Multiple proteomic locations for beer proteins were observed for protein Z4, LTP1, BDAI-1, and triose phosphate isomerase from

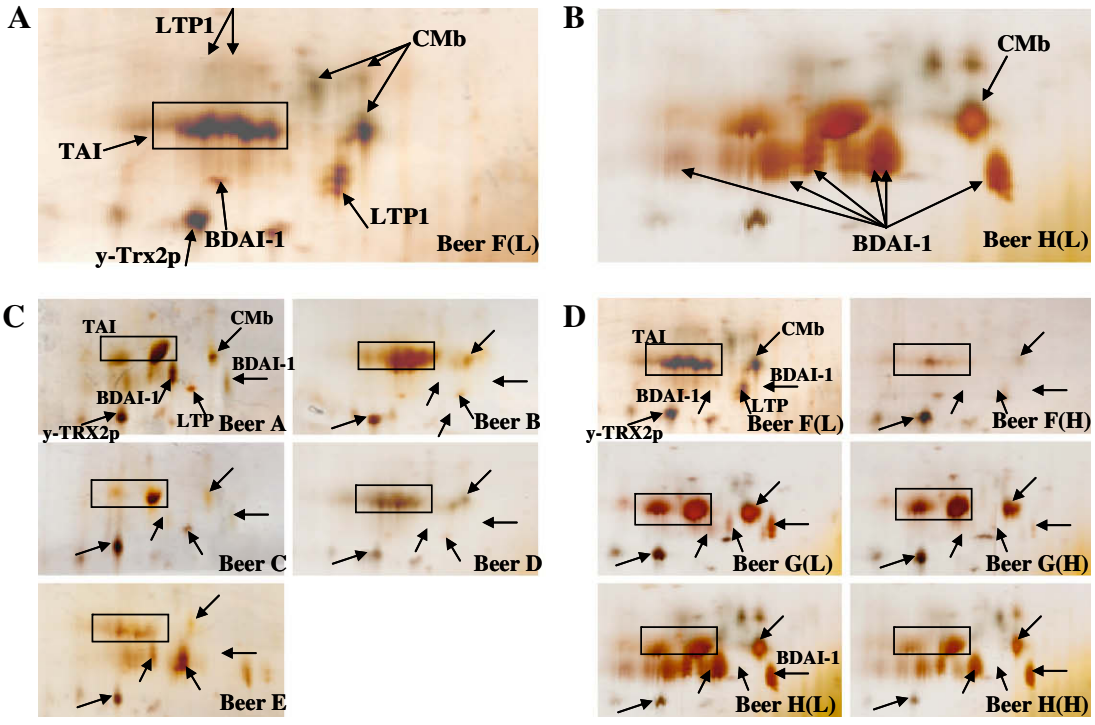

Fig. 3. The differences of two-dimensional gel electrophoresis (2DE) images on Region 3 (see Fig. 2A). (A) The 2DE image of proteins in Beer F(L). (B) The 2DE image of proteins in Beer H(L). (C) 2DE images of the beers brewed from each five cultivars. (D) 2DE images of the beers from each three cultivars with low(L) or high(H) malt modifications. The squares indicate the spot region of TAI.

Table 3
Summary of protein spot intensities on two-dimensional gels from beers of each five cultivars, and the beers from three cultivars with different malt modification.

	Enolase[a]	TPI[b]	y-TRX2p[c]	TAI[d]	CMb[e]	BDAI-1[f]	LTP[g]	Malt Kolbach index[h]	NIBEM (s)	FT-3[i]
Beer A	△[j]	○	○	○	○	△	△	42.5	258	4.19
Beer B	×	△	○	○	△	×	×	42.2	226	4.10
Beer C	△	○	○	○	×	×	△	43.3	232	5.49
Beer D	△	○	△	△	△	×	×	46.6	229	5.95
Beer E	○	△	○	△	×	△	○	42.5	247	1.77
Beer F(L)	○	○	○	○	○	×	○	43.7	281	1.39
Beer F(H)	○	○	○	△	×	×	×	49.1	234	1.41
Beer G(L)	○	○	○	○	○	△	△	47.3	251	1.18
Beer G(H)	△	○	○	○	○	×	×	54.0	223	1.63
Beer H(L)	○	○	○	○	○	○	×	39.4	269	1.51
Beer H(H)	○	○	△	○	○	○	×	50.0	269	1.02

[a] Chain A, Mg-phosphonoacetohydroxamate complex of S39a yeast enolase 1.
[b] Chains A and B, structure of yeast triosephosphate isomerase at 1.9-Å resolution.
[c] Thioredoxin; Trx2p.
[d] Trypsin/amylase inhibitor pUP13.
[e] Alpha-amylase/trypsin inhibitor CMb precursor (chloroform/methanol-soluble protein CMb).
[f] Alpha-amylase inhibitor BDAI-1 precursor.
[g] Chain A, non-specific lipid transfer protein 1 from barley in complex with L-alfa-lysophosphatidylcholine, laudoyl.
[h] Soluble nitrogen/total nitrogen × 100.
[i] Beer clarity after the forcing test (see Section 2).
[j] '○' indicates that the protein spot intensity was relatively intense, 'Δ' indicates that the protein spot intensity was relatively low, and '×' indicates that the spot intensity was relatively faint or invisible.

yeast (Fig. 1 and Table 2). For the barley proteins it is known that for each protein there is only one or a small number of barley genes from which these proteins are transcribed. Therefore, electrophoretic mobility of these beer proteins is assumed to be the result of various relatively minor protein modifications such as reduction of disulphide bonds, partial proteolytic cleavage, glycosylation and phosphorylation. These protein modifications have important implications for the properties of these proteins with respect to the beer quality properties that they influence. LTP1, in particular has been well studied with respect to these modifications (Perrocheau, Bakan, Boivin, & Marion, 2006; van Nierop, Evans, Axcell, Cantrell, & Rautenbach, 2004). In future work, beer quality related proteins such as protein Z4 and BDAI-1 will be more intensively studied to better understand the implications for modifications that occur during the malting and brewing processes.

The present beer proteome map shows eight species of barley proteins, which includes protein Z-type serpin (protein Z4), serpin-Z7 (protein Z7), BDAI-1, CMb, LTP1, TAI, BTI-CMe and subtilisin-chymotrypsin inhibitor CI-1B. These beer proteins mostly have inhibitory properties such as protease or amylase inhibitors except LPT1 which may also have antimicrobial properties (Kader, 1996). These beer proteins survive the malting and brewing process relatively intact, retaining their apparent molecular weight as well as their immunochemical identity (Hejgaard, 1977; Kaersgaard & Hejgaard, 1979; Sorensen et al., 1993). As shown in Fig. 3 and Table 3, it has been suggested that the beer protein composition and level is substantially dependent on barley cultivar and level of malt modification.

Recent studies have shown that BDAI-1 may be a foam-promoting protein (Iimure et al., 2008; Okada et al., 2008). Among five beer samples from the five cultivars, the spot intensities of beer BDAI-1 were invisible in Beers B–D that had lower foam stability (NIBEM = 226–232 s), compared to Beers A and E which had higher levels of BDAI-1 and higher foam stability (NIBEM = 247–258 s) (Table 3). Significantly in cultivar H (higher foam stability at both lower and higher malt modification), the spot intensities of BDAI-1 were not changed by malt modification conditions. In comparison the spot intensities of BDAI-1 were invisible in Beer F(L) in spite of the highest foam stability. This is perhaps not surprising as beer foam stability cannot be explained by a single protein in isolation but combination of proteins and by several processing factors (Evans & Bamforth, 2008; Iimure et al., 2008). Although beer foam stability was not completely explained by only BDAI-1, these data support the hypothesis that BDAI-1 is a foam-promoting protein (Iimure et al., 2008).

The spot intensity of LTP1, long identified as foam-promoting protein (Sorensen et al., 1993), was more intense in Beer E that had higher foam stability (NIBEM = 247 s) (Table 3). However, the spot for LTP1 in Beer A (higher foam stability: NIBEM = 258 s) was relatively low. The contribution of LTP1 to foam stability depends on its modification and conformation (Perrocheau et al., 2006; van Nierop et al., 2004). During the kettle boil, LTP1 is irreversibly denatured, which substantially reduces its immuno-reactivity to the barley LTP1 antibodies (Bech, Vaag, Heinemann, & Breddam, 1995; Lusk, Goldstein, & Ryder, 1995), but improves its foam-promoting properties (Bech et al., 1995; Lusk et al., 1995; Sorensen et al., 1993). Conversely, van Nierop et al. (2004) observed that increased denaturation of LTP1 by boiling could in fact be detrimental to foam stability due to the reduced ability of denatured LTP1 to bind foam destabilizing lipids. Where the level of lipids in beer was low or the level of LTP1 was high there was little impact on beer foam stability; however, where the level in beer of LTP1 was low, and the level of lipids high, substantial reductions in foam stability were observed. The observations of this study imply that LTP1 with acidic pI has relatively low foam stabilizing properties. In addition, there were 30 LTP1 spots identified at both acidic and basic pI (Fig. 1 and Table 2). The protein spots of LTP1 on the basic side were not comparable between samples due to their relatively poor resolution. Because of difficulties to compare beer LTP1 concentrations by only one LTP1 spot in Region 3, our results could not confirm that LTP1 is foam-positive. Thus, a more reliable detection system, e.g., LTP1 specific antibody, is required to further investigate the relationship between LTP1 and foam stability.

Recently it was observed that CMb, CMe and BDAI-1 were not major haze active proteins but were factors promoting haze formation (Iimure et al., 2009). As shown in Table 1, FT-3 in Beer D was the highest (most hazy) among the beers produced in this study. However, in Beer D, CMb was relatively low and BDAI-1 was invisible (Fig. 3C and Table 3). Similarly, spot intensities of CMb and BDAI-1 were relatively low or invisible in beer samples with higher FT-3 (Beers B and C). These results confirmed that CMb and BDAI-1 are not predominant haze active proteins. However, in our previ-

ous paper, CMb, CMe and BDAI-1 were contained in all four haze samples examined; therefore CMb, CMe and BDAI-1 may be factors promoting haze formation, actually being concentrated in the haze particles being formed (Iimure et al., 2009). In this study, a protein spot directly corresponding to haze stability was not observed in the beer samples. Accordingly, no haze active or predominant protein was detected by the 2DE analysis. It is suggested that beer protein contents may depend not only on the barley cultivar of origin, but also proteolytic activity during malting and mashing (Kihara et al., 2002). Therefore, to improve the levels of foam-positive proteins, i.e., BDAI-1, and to decrease the proteins promoting haze formation, i.e., CMb and CMe, it is important that relationship between protein and malt protease activity is better understood.

Four species of yeast proteins, enolase, TPI, y-TRX2p and yeast phosphorelay protein Ypd1 were identified in Beer F(L) (Fig. 1 and Table 2). The contributions of yeast enolase, TPI and yeast phosphorelay protein Ypd1 to beer quality is not unknown at present. y-TRX2p is reported as an intracellular protein (Gan, 1991; Pedrajas et al., 1999). Generally, glycolytic enzymes including enolase and TPI are cytoplasmic, but it was reported that several glycolytic enzymes locate at cell surfaces (López-Villar et al., 2006). In this study, these three yeast proteins were identified in beer. Perrocheau et al. (2005) also identified enolase and TPI in beer. These results suggest that yeast cells were damaged during brewing, resulting in release of these yeast proteins to beer. On the other hand, there were no obvious accordance for spot intensity levels in enolase, TPI and y-TRX2p (Table 3). For example enolase was not detected but y-TRX2p was distinct in Beer B. On the other hand, enolase and TPI were distinct, although y-TRX2p was relatively low in Beer H(H). If these three yeast proteins in beer are dependent on only cell damage, the spot intensities of these proteins should be correlated with each other. Therefore, these protein concentrations in beer might depend not only on the yeast cell damage but also the expression level of the proteins. Since y-TRX2p is upregulated under oxidative stress (Kuge & Jones, 1994), levels of these proteins might relate to the stresses exposure in yeast cells during brewing processes. It has been suggested that the physiological condition of yeast cells influences several quality traits including foam stability (Dreyer, Biedermann, & Ottesen, 1983) and flavour stability (Guido, Rodrigues, Rodrigues, Gonçalves, & Barros, 2004). However, evaluation methods for physiological conditions of yeast cells are not well established even there are several methods such as the acidification power test (Fernandez, Gonzalez, & Sierra, 1991) and flow cytometry analysis (Hutter, 2002). If the relationships between each yeast protein such as enolase, TPI and y-TRX2p and the level of stress conditions on yeast cells are confirmed, these proteins may become excellent markers to monitor the brewing process.

Among four yeast proteins, y-TRX2p was suggested as a foam-negative protein (or indicator) (Iimure et al., 2008). In Beer H(H) (higher foam stability), the spot intensity of y-TRX2p was lower than the other beer samples (Fig. 3D and Table 3). However, y-TRX2p in Beer D (lower foam stability) was also low. As described by Iimure et al. (2008), foam stability may not be controlled by a single protein, but by a combination of a number of factors such as protein Z, BDAI-1 and y-TRX2p. In addition, it has been shown that the extent of LTP1 denaturation has important consequences for foam stability if the levels of foam destabilizing lipids are relatively high (van Nierop et al., 2004). Hop iso-α-acids isomerised from α-acids during wort boiling play important roles for beer bitter taste. Beer bitterness unit derived from hop iso-α-acids is also an important factor for beer foam stability (Evans, Surrel, Sheehy, Stewart, & Robinson, 2008; Kunimune & Shellhammer, 2008). Accordingly, the lower foam stability in Beer D could result from the lower beer BDAI-1 and beer bitterness unit (Tables 1 and 3) or higher levels of lipid in the beer which was beyond the scope of this study. Therefore, if the beer bitterness unit and/or BDAI-1 were higher, the beer foam stability could be improved by a synergetic effect with lower y-TRX2p.

Overall, the current comprehensive beer proteome map provides a strong detection platform for the behaviours of beer quality related proteins. For instance, foam stability is a useful beer quality target whose level could be manipulated using the procedures applied in this report. The nucleotide and amino acid sequences defined by the protein identification in the beer proteome map may have advantages for barley breeding and process control for beer brewing. The nucleotide sequences also give us access to DNA markers in barley breeding by detecting sequence polymorphisms. As such, DNA markers of such target proteins could be applied to selection of barley lines to optimise the level of these proteins in future barley malting cultivars with higher brewing quality. Additionally, the amino acid sequences from both barley and yeast can supply control methods during the brewing processes to potentially enable monitoring of protein expression levels. Further development of efficient and rapid (real time) techniques for protein detection in the commercial brewing industry are expected to maximise the use of the beer proteome map developed in this investigation.

Acknowledgements

We are grateful to T. Yazawa, K. Ito and N. Yatabe, the Bioresources Research and Development Department, Sapporo Breweries Ltd. for their technical assistance. We are also grateful to K. Takoi for the beer sample preparation. This study was supported by the Program for Promotion of Basic Research Activities for Innovative Biosciences, Japan (PROBRAIN).

References

Asano, K., Shinagawa, K., & Hashimoto, N. (1982). Characterization of haze-forming proteins of beer and their roles in chill haze formation. *Journal of the American Society of Brewing Chemists, 40*, 147–154.

Bak-Jensen, K. S., Laugesen, S., Roepstorff, P., & Svensson, B. (2004). Two-dimensional gel electrophoresis pattern (pH 6–11) and identification of water-soluble barley seed and malt proteins by mass spectrometry. *Proteomics, 4*, 728–742.

Bamforth, C. W. (1985). The foaming properties of beer. *Journal of the Institute of Brewing, 91*, 370–383.

Bech, L. M., Vaag, P., Heinemann, B., & Breddam, K. (1995). Throughout the brewing process barley lipid transfer protein1 (LTP1) is transformed into a more foam-promoting form. In *Proceedings of the 25th European brewery convention congress* (pp. 561–568). Oxford: IRL Press.

Dreyer, T., Biedermann, K., & Ottesen, M. (1983). Yeast proteinase in beer. *Carlsberg Research Communications, 48*, 249–253.

European Brewery Convention, Analytica (1987). *European brewery convention* (fourth ed.). Zurich: Brauerei und Getraenke Rundschau.

Evans, D. E., Nischwitz, R., Stewart, D. C., Cole, N., & MacLeod, L. C. (1998). The influence of malt foam positive proteins and non-starch polysaccharides on beer foam quality. *European Brewery Convention Monograph, 27*, 114–128.

Evans, D. E., Sheehan, M. C., & Stewart, D. C. (1999). The impact of malt derived proteins on beer foam quality. Part II. The influence of malt foam-positive proteins and non-starch polysaccharides on beer foam quality. *Journal of the Institute of Brewing, 105*, 171–177.

Evans, D. E., & Sheehan, M. C. (2002). Don't be fobbed off: The substance of beer foam, a review. *Journal of the American Society of Brewing Chemists, 60*, 47–57.

Evans, D. E., Robinson, L. H., Sheehan, M. C., Tolhurst, R. L., Hill, A., Skerritt, J. S., et al. (2003). Application of immunological methods to differentiate between foam-positive and haze-active proteins originating from malt. *Journal of the American Society of Brewing Chemists, 61*, 55–62.

Evans, D. E., Surrel, A., Sheehy, M., Stewart, D., & Robinson, L. H. (2008). Comparison of foam quality and the influence of hop α-acids and proteins using five foam analysis methods. *Journal of the American Society of Brewing Chemists, 66*, 1–10.

Evans, D. E., & Bamforth, C. W. (2008). Beer foam: Achieving a suitable head. In C. W. Bamforth, I. Russell, & G. G. Stewart (Eds.), *Handbook of alcoholic beverages: Beer, a quality perspective* (pp. 1–60). Burlington, MA: Elsevier.

Fernandez, S., Gonzalez, G., & Sierra, A. (1991). The acidification power test and the behavior of yeast in brewery fermentations. *Technical Quarterly-Master Brewers Association of the Americas, 28*, 89–95.

Gan, Z. R. (1991). Yeast thioredoxin genes. *The Journal of Biological Chemistry, 266*, 1692–1696.

Guido, L. F., Rodrigues, P. G., Rodrigues, J. A., Gonçalves, C. R., & Barros, A. A. (2004). The impact of the physiological condition of the pitching yeast on beer flavor stability: An industrial approach. *Food Chemistry, 87*, 187–193.

Hao, J., Li, Q., Dong, J., Yu, J., Gu, G., Fan, W., & Chen, J. (2006). Identification of the major proteins in beer foam by mass spectrometry following sodium dodecyl sulfate–polyacrylamide gel electrophoresis. *Journal of the American Society of Brewing Chemists, 64*, 166–174.

Hejgaard, J. (1977). Origin of a dominant beer protein. Immunochemical identity with a β-amylase associated protein from barley. *Journal of the Institute of Brewing, 83*, 94–96.

Hutter, K. J. (2002). Flow cytometry. A new tool for direct control of fermentation processes. *Journal of the Institute of Brewing, 108*, 48–51.

Iimure, T., Takoi, K., Kaneko, T., Kihara, M., Hayashi, K., Ito, K., et al. (2008). Novel prediction method of beer foam stability using protein Z, barley dimeric α-amylase inhibitor-1 (BDAI-1) and yeast thioredoxin. *Journal of Agricultural and Food Chemistry, 56*, 8664–8671.

Iimure, T., Nankaku, N., Watanabe-Sugimoto, M., Hirota, N., Tiansu, Z., Kihara, M., et al. (2009). Identification of novel haze-active beer proteins by proteome analysis. *Journal of Cereal Science, 49*, 141–147.

Jégou, S., Douliez, J. P., Mollé, D., Boivin, P., & Marion, D. (2000). Purification and structural characterization of LTP1 polypeptides from beer. *Journal of Agricultural and Food Chemistry, 48*, 5023–5029.

Kader, J. C. (1996). Lipid transfer proteins in plants. *Annual Review of Plant Physiology and Plant Molecular Biology, 47*, 627–654.

Kaersgaard, P., & Hejgaard, J. (1979). Antigenic beer macromolecules. An experimental survey of purification methods. *Journal of the Institute of Brewing, 85*, 103–111.

Kihara, M., Saito, W., Okada, Y., Kaneko, T., Asakura, T., & Ito, K. (2002). Relationship between proteinase activity during malting and malt quality. *Journal of the Institute of Brewing, 108*, 371–376.

Kuge, S., & Jones, N. (1994). YAP1 dependent activation of TRX2 is essential for the response of *Saccharomyces cerevisiae* to oxidative stress by hydroperoxides. *The EMBO Journal, 13*, 655–664.

Kunimune, T., & Shellhammer, T. H. (2008). Foam-stabilizing effects and cling formation patterns of iso-α-acids and reduced iso-α-acids in lager beer. *Journal of Agricultural and Food Chemistry, 56*, 8629–8634.

López-Villar, E., Monteoliva, L., Larsen, M. R., Sachon, E., Shabaz, M., Pardo, M., et al. (2006). Genetic and proteomic evidences support the localization of yeast enolase in the cell surface. *Proteomics, 6*, 107–118.

Lusk, L. T., Goldstein, H., & Ryder, D. (1995). Independent role of beer proteins, melanoidins and polysaccharides in foam formation. *Journal of the American Society of Brewing Chemists, 53*, 93–103.

Maeda, K., Yokoi, S., Kamada, K., & Kamimura, M. (1991). Foam stability and physicochemical properties of beer. *Journal of the American Society of Brewing Chemists, 49*, 14–18.

Okada, Y., Iimure, T., Takoi, K., Kaneko, T., Kihara, M., Hayashi, K., et al. (2008). The influence of barley malt protein modification on beer foam stability and their relationship to the barley dimeric α-amylase inhibitor-I (BDAI-I) as a possible foam-promoting protein. *Journal of Agricultural and Food Chemistry, 56*, 1458–1464.

Østergaard, O., Finnie, C., Laugesen, S., Roepstorff, P., & Svensson, B. (2004). Proteome analysis of barley seeds: Identification of major proteins from two-dimensional gels (pI 4–7). *Proteomics, 4*, 2437–2447.

Pedrajas, J. R., Kosmidou, E., Miranda-Vizuete, A., Gustafsson, J., Wright, A. P. H., & Spyrou, G. (1999). Identification and functional characterization of a novel mitochondrial thioredoxin system in *Saccharomyces cerevisiae*. *The Journal of Biological Chemistry, 274*, 6366–6373.

Perkins, D. N., Pappin, D. J. C., Creasy, D. M., & Cottrell, J. S. (1999). Probability-based protein identification by searching sequence databases using mass spectrometry data. *Electrophoresis, 20*, 3551–3567.

Perrocheau, L., Rogniaux, H., Boivin, P., & Marion, D. (2005). Probing heat-stable water-soluble proteins from barley to malt and beer. *Proteomics, 5*, 2849–2858.

Perrocheau, L., Bakan, B., Boivin, P., & Marion, D. (2006). Stability of barley and malt lipid transfer protein 1 (LTP1) toward heating and reducing agents: Relationships with the brewing process. *Journal of Agricultural and Food Chemistry, 54*, 3108–3113.

Robinson, L. H., Juttner, J., Milligan, A., Lahnstein, J., Eglinton, J. K., & Evans, D. E. (2007). The identification of a barley haze active protein that influences beer haze stability: Cloning and characterization of the barley SE protein as a barley trypsin inhibitor of the chloroform/methanol type. *Journal of Cereal Science, 45*, 343–352.

Siebert, K. J. (1999). Effects of protein-polyphenol interactions on beverage haze, stabilization, and analysis. *Journal of Agricultural and Food Chemistry, 47*, 353–362.

Sorensen, S. B., Bech, L. M., Muldbjerg, M., Beenfeldt, T., & Breddam, K. (1993). Barley lipid transfer protein 1 is involved in beer foam formation. *Technical Quarterly-Master Brewers Association of the Americas, 30*, 136–145.

van Nierop, S. N. E., Evans, D. E., Axcell, B. C., Cantrell, I. C., & Rautenbach, M. (2004). Impact of different wort boiling temperatures on the beer foam stabilizing properties of lipid transfer protein 1. *Journal of Agricultural and Food Chemistry, 52*, 3120–3129.

Food Chemistry 118 (2010) 575–581

Contents lists available at ScienceDirect

Food Chemistry

journal homepage: www.elsevier.com/locate/foodchem

Estimating the quantity of egg white and whey protein concentrate in prepared crabstick using ELISA

Zachary H. Reed, Jae W. Park *

Oregon State University, Seafood Laboratory, 2001 Marine Drive Rm 253, Astoria, OR 97103, United States

ARTICLE INFO

Article history:
Received 15 January 2009
Received in revised form 28 March 2009
Accepted 11 May 2009

Keywords:
ELISA
Dried egg white
Whey protein concentrate
Antibody
Quantification

ABSTRACT

Indirect enzyme-linked immunosorbent assays (ELISA) technique was used to identify and quantify the use of dried egg white (DEW) and whey protein concentrate (WPC) in crabsticks. The use of SDS–PAGE for the quantification of protein additives has had limited success due to the high shear and high temperature processes of surimi crabstick. Monoclonal (anti-heat-denatured ovalbumin) and polyclonal (anti-β-lactoglobulin) antibodies were used. Antibodies showed no significant cross-reactivity with non-target crabstick proteins. An optimised extraction solution of 10% SDS and 2.5% 2-ME yielded high extractability with improved consistency. Quantification of DEW and WPC was achieved using the optimised extraction solution and indirect ELISA. Estimated DEW values were within 7% of actual values, WPC samples were within 17%. Inter-assay coefficients of variance for DEW ranged from 0.9% to 3.1% and those of the WPC were 1.0–8.0%.

1. Introduction

The crabstick industry does not have a standard of identity established for protein additives such as dried egg white (DEW) and whey protein concentrate (WPC). A lack of standard of identities can lead to increased use and/or abuse of protein additives in the crabstick formulation, which decreases surimi quantity and correlates to lower quality product if the usage is not properly optimised. Surimi refers to refined fish myofibrillar proteins used as an intermediate product in many seafood flavoured products. Surimi is produced through heading, gutting, mincing, washing, dewatering and concentrating the fish myofibrillar proteins (Lee, 1984; Park & Lin, 2005). The concentrated myofibrillar protein is mixed with cryoprotectants such as sugar, sorbitol, and polyphosphates which serve to stabilize the fish myofibrillar protein during frozen storage (Park & Lanier, 1987; Park, Lanier, & Green, 1988). Surimi is comminuted with other ingredients such as starch, DEW, WPC, and other flavours in the production of crab-flavoured seafood (crabsticks). DEW has been used extensively as a functional food ingredient because of its gelling and foaming properties (Mine, 1995). β-Lactoglobulin (β-LG) is largely responsible for the physicochemical properties as well as the functional behaviour of food products that contain whey protein (Foegeding, Davis, Doucet, & McGuffey, 2002). Burgarella, Lanier, Hamann, and Wu (1985) showed that DEW and WPC can be used in low concentrations to provide an additive effect of increased gel strength and deformability.

One method used to quantify protein additives in crabstick is SDS–PAGE coupled with gel densitometry (Reed & Park, 2008). We found that SDS–PAGE was useful for detection of DEW but was not appropriate for the quantification of DEW. Enzyme-linked immunosorbent assays (ELISA) take advantage of the interaction between proteins and antibodies and can be used to qualify and quantify protein additives in food. Commercial ELISA kits are available for the detection of egg, milk, wheat, buckwheat, and peanut proteins. It is mandatory for these five allergens to be labelled in Japan (Matsuda et al., 2006) and in most countries including United States. Due to the severity of some food allergies the use of ELISA has become widespread for detection of allergenic proteins (Faeste, Egaas, Lindvik, & Lovberg, 2007; Fuller, Goodwin, & Morris, 2006). ELISA has also been shown to be effective in quantifying egg white in processed pork products (Leduc et al., 1999). Dupont et al. (2006) have developed an ELISA for bovine lactoferrin to determine lactoferrin concentrations in milk, whey, and cheese. Ovalbumin (OA) is the most abundant of egg white proteins, comprising 54% of the total proteins (Stevens, 1991). Of the whey proteins in bovine milk, β-lactoglobulin (β-LG) is the most abundant (Farrell et al., 2004).

Extraction of protein from the cooked gel sample is one of the most critical steps in obtaining a clean and reproducible ELISA assay. Commonly, Tris-buffered saline (TBS) and phosphate buffered saline (PBS) have been used to extract protein from the sample matrix. Asensio et al. (2003) used 0.85% saline solution to extract proteins from grouper, wreck fish and Nile perch fillets. Hefle, Jeanniton, and Taylor (2001) used PBS to extract proteins from pasta for the detection of egg residues in food, while Holden, Fæste,

* Corresponding author. Tel.: +1 503 325 4531; fax: +1 503 325 2753.
E-mail address: jae.park@orst.edu (J.W. Park).

0308-8146/$ - see front matter © 2009 Elsevier Ltd. All rights reserved.
doi:10.1016/j.foodchem.2009.05.023

and Egaas (2005) used 0.1 M Tris, 0.5 M glycine at pH 8.7 for the extraction of lupine from several baked goods. Preliminary studies revealed that, when crabstick samples were extracted with PBS alone either overnight at room temperature or at 90 °C for an hour, results were not reproducible. Due to the strong gel matrix of high protein content, different extraction methods were investigated.

Watanabe et al. (2005) investigated the use of an extraction solution containing sodium dodecyl sulphate (SDS) and 2-mercaptoethanol (2-ME) for the detection of raw and processed egg. In their study they found the total protein extracted using TBS could be increased 10–100-fold with the addition of 1% SDS and 7% 2-ME to the TBS extraction solution. Ochiai and Watabe (2003) found that using an extraction solution of urea, SDS, and 2-ME, allowed for species identification of processed fish products.

The overall goal of this study was to develop an indirect ELISA assay for the qualification and quantification of dried egg white and whey protein concentrate when used as an additive to a cooked and pasteurised crabstick product. In addition, we attempted to develop an optimised extraction method for fish protein gels with strong texture.

2. Materials and methods

2.1. Food products and chemicals

Alaska pollock (*Theragra chalcogramma*) surimi (FA grade, 10 kg blocks), were obtained from Western Alaska Fisheries (Seattle, Wash., USA) and stored frozen at −18 °C. The 10 kg blocks were cut into approximately twenty 1 kg blocks, individually vacuum packed, and stored at −18 °C until used for surimi crabstick paste preparation. Ingredients used for surimi crabstick paste preparation were NaCl (Morton Iodised Salt, Morton International, Inc., Chicago, Ill., USA), corn starch (Corn Products International, Westchester, Ill., USA), wheat starch (Midsol 50, MGP Ingredients, Inc., Atchison, Kans., USA), modified waxy maize starch (Polartex 06727, Cargill, Inc., Cedar Rapids, Iowa, USA), sugar (used to represent all flavour components) (Pure Cane Sugar, C&H Sugar Company, Inc., Crockett, Calif., USA), and culinary tap water. The protein additives were dried egg white (DEW) (K-200, Henningsen Foods, Omaha, Nebr., USA) and whey protein concentrate (WPC 8600, Hilmar Ingredients, Hilmar, Calif., USA). All other chemicals were reagent grade.

2.2. Antibodies

Affinity purified rabbit polyclonal antibodies produced against bovine β-lactoglobulin (pAb anti-β-LG) and goat anti-mouse IgG coupled with horse radish peroxidase (HRP-anti-mIgG) were obtained from Bethyl Laboratories (Montgomery, Tex., USA). Mouse monoclonal antibodies against heat denatured hen ovalbumin (Ab anti-H-OA) were purchased from Abcam, Inc. (Cambridge, Mass., USA). Goat anti-rabbit IgG coupled with HRP (HRP-anti-rIgG) was purchased from Sigma–Aldrich, Inc. (St. Louis, Mo., USA). All antibodies were delivered at a concentration of 1 mg/mL. Antibodies were tested against a serial dilution of purified ovalbumin (OA) or β-lactoglobulin (β-LG) which produced a linear response. The antibodies were also tested against crabsticks. When tested against crabsticks, antibodies showed no reactivity with proteins other than the target protein.

2.3. Sample preparation

2.3.1. Basic surimi paste batches

Crabsticks were made with base ingredients including: surimi (40%), water (45%), salt (2%), starches (8%), and sugar (5%). Three formulations for crabstick were made containing base ingredients and protein additives such as DEW only, WPC only, and 50/50 mixture of DEW/WPC. For each of the three formulations a total of nine batches per formulation were made. Six standard batches containing various protein additives were made (0.00%, 0.25%, 0.50%, 1.00%, 1.50%, and 2.00% protein additives). Three additional verification batches were also made (0.375%, 0.750%, and 1.750% protein additives). For batches with protein additives, starch was replaced in a 1:1 ratio (w/w) by protein additive resulting in an equal moisture concentration of approximately 75%. Final batch sizes were approximately 1300 g. Frozen surimi was allowed to thaw at room temperature (≈23 °C) for approximately 1 h and then cut into small pieces. All chopping was performed using a Stephan vertical vacuum cutter (model UM 5 universal, Stephan Machinery Co., Columbus, Ohio, USA). Surimi pieces were added to the chopping bowl and chopped at 1800 rpm for 1 min. Salt (26 g) was then added to the chopped surimi and chopping continued at 1800 rpm for 1 min. Following the integration of the salt, 65 g of sugar was added in addition to starch (50:40:10 corn:wheat:modified waxy maize), protein additive when required, and water followed by chopping at 1800 rpm for 1 min. A vacuum of 40–60 kPa was applied to the surimi paste and chopping continued for 3 min at 3000 rpm. Surimi paste was then placed in a plastic bag and refrigerated until samples were cooked.

Approximately 20–25 g of labelled surimi paste was placed into a sheet mould (stainless steel 25 cm × 7.5 cm × 1.4 mm) formed on top of a piece of aluminium foil, which had been sprayed with no-stick cooking spray (Pam® Original, ConAgra Foods, Inc., Omaha, Nebr., USA). Excess raw surimi paste was vacuum packed and frozen at −80 °C. Food grade plastic film was laid over the top of the paste and a stainless steel tube roller (11.5 cm × 4 cm dia.) was used to evenly spread out the paste to form a crabstick sheet. After the film was removed the aluminium foil containing the crabstick sheet was cooked in a steam bath (93 °C) for 90 s. After initial cooking, crabstick sheets were cut in half, wrapped in plastic film and then placed back in the 93 °C steam bath for 30 min to simulate commercial pasteurisation. Pasteurised samples were submerged in ice water to cool for 15 min. If samples were not to be used within 48 h they were frozen at −80 °C until needed.

For the verification process, three batches per formulation were made (0.375%, 0.75%, and 1.75% protein additive) and the protein concentrations were estimated using the linear equation produced from the five standard batches (0.25%, 0.50%, 1.00%, 1.50%, and 2.00% protein additives). Using Microsoft Excel software the standard curves were obtained by plotting the absorbance at 450 nm vs the protein additive concentrations of 0.25%, 0.50%, 1.00%, 1.50%, and 2.00%. The standard curve was fitted to a linear equation ($y = mx + b$), where y = absorbance at 450 nm, m = slope of the line, x = protein additive %, and b = intercept of the line. Calculation of the verification samples were given by the following equation: $x = (y - b)/m$.

2.4. Optimised sample extraction

During our preliminary experiments, we realised the optimisation of the extraction solution was extremely important to obtain consistent data. In a preliminary optimisation step 25 extraction solutions were tested. Extraction solutions contained various levels of SDS (2.5%, 5%, and 7.5% w/v), Tween 20 (0.05%, 0.075%, and 0.1% v/v) and 2-ME (5%, 7.5%, and 10% v/v). All extraction solutions were incubated for 1, 2, or 3 h at 90 °C (results not shown). A final optimised extraction protocol was achieved using 10% SDS w/v and 2.5% 2-ME v/v. Tween 20 was determined to have no significant effect on the extraction of the protein from the crabstick samples. This may be due to the much more substantial amount of SDS used as both are detergents. Samples used for the standard curve pro-

duced a linear response which then allowed for the estimation of the DEW and WPC content of the verification batches.

Approximately 2 g of sample was accurately weighed into a 50 mL centrifuge tube and 20 mL of solution containing 10% SDS and 2.5% 2-ME was added. Samples were homogenised for 1 min at speed 4 (Powergen 700, Fisher Scientific, Pittsburgh, Pa., USA) followed by extraction for 1 h at 90 °C. Extracted samples were centrifuged at 7796*g* (Sorvall RC-5B, DuPont Co., Newton, Conn., USA) for 20 min. The supernatant was filtered (70 mm dia. # 541, Whatman International Ltd., Maidstone, UK) into a 25 mL volumetric flask and brought to volume using additional 10% SDS and 2.5% 2-ME solution.

2.5. Indirect ELISA

Ovalbumin (OA) from chicken egg white, grade VI (Sigma–Aldrich, Inc., St. Louis, Mo., USA) and β-lactoglobulin (β-LG) from bovine milk (Sigma–Aldrich, Inc., St. Louis, Mo., USA) were serially diluted using PBS, containing 137 mM NaCl, 2.7 mM KCl, 10 mM phosphate buffer (Omnipur 10× PBS Concentrate, EMD Chemicals, Inc., Gibbstown, NJ, USA) and assayed in both the OA and β-LG ELISA checking for linearity and cross-reactivity. OA and β-LG were solubilised in 5% SDS (w/v) and heated at 90 °C for 1 h. Total protein content was determined using the Lowry method (Lowry, Rosebrough, Farr, & Randall, 1951). Samples were serially diluted with PBS to 25 ng/mL and tested in triplicate. Indirect ELISA results were given as the average of the three serial dilutions.

Crabstick samples were serially diluted in PBS to a final dilution of 1:10,000. Polystyrene 96 well microtiter plates (Nalge Nunc International, Rochester, NY, USA) were coated with 100 μL of serially diluted samples (6 wells/sample) and were incubated overnight at 4 °C. The plates were washed three times with PBS containing 0.5% (v/v) Tween 20 (PBS-T) and blocked with 100 μL of Superblock® blocking buffer in PBS with 0.05% Tween 20 (Thermo Scientific, Rockford, Ill., USA) at 37 °C for 30 min. After the plates were washed three times with PBS-T, 100 μL of diluted (1:5000, 1 mg/mL) Ab anti-H-OA or pAb anti-β-LG antibodies were added to the wells and incubated at 37 °C for 1 h. After three PBS-T wash cycles, 100 μL of diluted (1:5000, 1 mg/mL) HRP-anti-mIgG when detecting Ab anti-H-OA and HRP-anti-rIgG when detecting pAb anti-β-LG were added to each well and incubated at 37 °C for 30 min. Plates were washed three times using PBS-T after which 100 μL of 3,3′,5,5′-tetramethylbenzidine, 1-Step Ultra TMB ELISA (Thermo Scientific, Rockford, Ill., USA) was added and allowed to develop for 8 or 12 min at room temperature, for the DEW and WPC samples, respectively. Colour development was stopped by the addition of 100 μL of 2 N sulphuric acid per well. The plate was read at 450 nm using a Biolog Microlog (Biolog, Hayward, Calif., USA).

2.6. Immunoblotting

SDS–PAGE was performed as outlined by Laemmli (1970) using a 12.5% (% T) separating gel and a 4% (% T) stacking gel. The crabstick samples used for SDS–PAGE and immunoblotting contained both DEW and WPC. A 0.5 mL aliquot of extracted sample, that was used for the indirect ELISA, was mixed with 0.5 mL of Laemmli sample buffer (0.6 mL 1 M Tris–HCl (pH 6.8), 5.0 mL glycerol, 2.0 mL 10% (w/v) SDS, 0.5 mL 2-ME, 1.0 mL 1% (w/v) bromophenol blue, 0.9 mL H_2O). Sample and buffer were vortexed and then heated for 3 min at 90 °C to disrupt any disulphide bonds. Samples were separated using a Mini-Protean III Cell (Bio-Rad, Hercules, Calif., USA) according to the operating manual.

After electrophoresis the gels were removed and equilibrated in Towbin solution (25 mM Tris, 192 mM glycine, 20% methanol (v/v) at pH 8.3) for 20 min and transferred to a nitrocellulose membrane (Bio-Rad, Hercules, Calif., USA) using a Mini Trans-Blot® Electrophoretic Transfer Cell (Bio-Rad, Hercules, Calif., USA) using a slight modification of an earlier published method (Towbin, Staehelin, & Gordon, 1979). The membrane was blocked using Superblock® blocking buffer in PBS with 0.05% Tween 20 (Thermo Scientific, Rockford, Ill., USA) for 30 min at 25 °C. The blocked membrane was washed three times for 5 min using PBS-T. The membrane was incubated with either Ab anti-H-OA or pAb anti-β-LG (1:15,000) for 60 min at 25 °C after which the membrane was washed three times. The membrane was incubated with HRP-anti-mIgG when detecting Ab anti-H-OA and was incubated with HRP-anti-rIgG when detecting pAb anti-β-LG antibodies (1:15,000) at 25 °C for 60 min followed by three additional wash cycles. Bands were visualised using 1-Step™ TMB-Blotting (Thermo Scientific, Rockford, Ill., USA). Development was stopped by the addition of dd water. Molecular weight was determined by comparison to the Kaleidoscope™ protein standard (Bio-Rad, Hercules, Calif., USA) also run in each SDS–PAGE.

2.7. Statistical methods

For determination of the inter-assay precision, the mean coefficients of variation (CV) were based on three extractions performed on separate days. Each day an extraction was performed and the extract was assayed in triplicate on the same day. All calculations were done using Microsoft Excel (Microsoft Corporation, Redmond, Wash., USA). Each assay contained six replicates of each sample. The lower limit of detection (LLD) for the indirect assay was given as three times the standard deviation plus the background of blank wells. The lower limit of quantification (LLQ) was taken to be the lowest point (0.25% protein additive) of the standard curve.

3. Results and discussion

3.1. Optimised sample extraction

Extracting the proteins with 10% SDS and 2.5% 2-ME for 1 h at 90 °C was found to be the optimum condition yielding reproducible and reliable data for the ELISA assay. Fig. 1 shows the increased accuracy and decreased variation obtained when the optimised extraction solution was used. The calculated protein was determined using the standard curve created from the standard crabstick batches. In Fig. 1A, it is shown that the calculated % protein for DEW (calculated protein divided by protein added) ranges from 91.5% to 120.1% for the pre-optimised extraction solution (1% SDS (w/v) and 5% 2-ME (w/v)). It is our opinion that the addition of SDS and 2-ME was successful in disrupting the bonds formed during gelation. The gel matrix formed during the cooking of the crabsticks is believed to have caused steric hindrance during adsorption onto the ELISA plate. Due to the steric hindrance, some of the antibody epitopes were not available for interaction with the antibody. For the optimised extraction solution the range narrows to 100.0–101.7%. The standard deviation for the pre-optimised solution ranged from 4.6% to 24.0% and that of the optimised solution was 4.0–6.3%. The WPC extraction optimisation showed a similar trend. The pre-optimised calculated % protein ranged from 85.9% to 134.4% with a standard deviation range of 5.7–40.0%. The calculated % protein for WPC using the optimised extraction solution ranged from 95.6% to 116.7% with a standard deviation ranging from 1.7% to 11.4%.

3.2. Reactivity testing and immunoblotting

Purified OA and β-LG proteins were examined for reactivity and cross-reactivity with the Ab anti-H-OA and pAb anti-β-LG. In

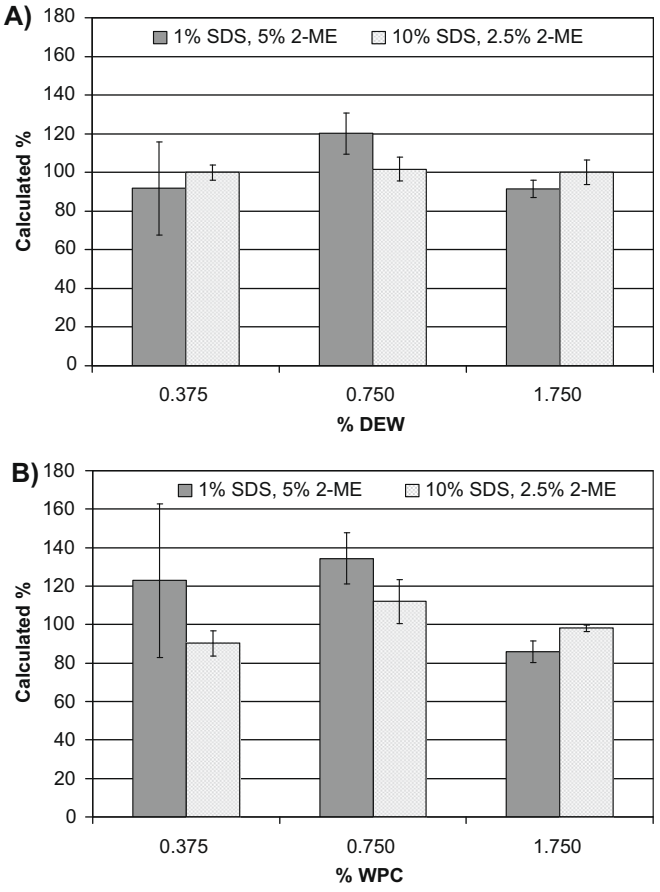

Fig. 1. Protein extraction using pre-optimised solution (1% SDS and 5% 2-ME) and optimised solution (10% SDS and 2.5% 2-ME) (A) crabstick containing DEW (B) crabstick containing WPC. The calculated protein was determined using the standard curve created from the standard crabstick batches.

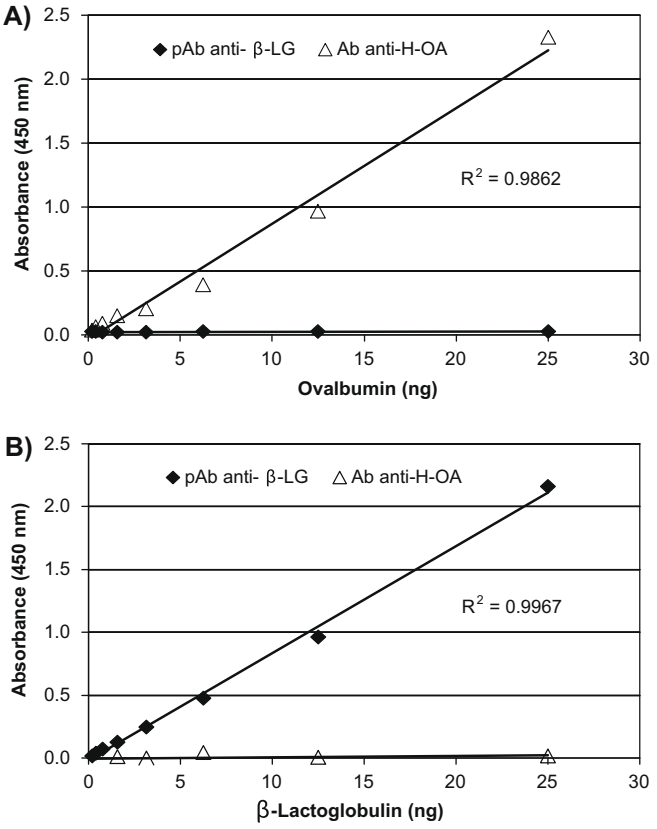

Fig. 2. Linear response of Ab anti-H-OA (A) and pAb anti-β-LG (B) tested against ovalbumin and β-lactoglobulin.

Fig. 2A, there is a linear response for OA passively absorbed to the microtiter plate and incubated with Ab anti-H-OA, while virtually no binding was observed with β-LG when incubated with the same Ab anti-H-OA. In Fig. 2B, a linear response was observed for β-LG when incubated with pAb anti-β-LG. Again virtually no response was made for the OA incubated with pAb anti-β-LG. Immunoblotting of crabstick samples for DEW detection using Ab anti-H-OA showed similar patterns to those produced from purified ovalbumin and DEW only samples (Fig. 3A). Fig. 3B shows similar results for samples tested for the presence of β-LG using pAb anti-β-LG.

3.3. Lower limit of detection vs lower limit of quantification (LLD vs LLQ)

Blank wells (36 total) were tested using Ab anti-H-OA with an average absorbance of 0.044 ± 0.006 and a LLD of 0.062 absorbance. The LLQ for the ELISA assay was calculated as the lowest point on the standard curve using 0.25% protein additives (16.5 and 12.4 ng/mL for DEW and WPC, respectively). The average absorbance value for the 0.25% DEW sample was 0.361 ± 0.034. The control sample (0% DEW) had an average absorbance of 0.101 ± 0.021 which was 3.6 times lower than that of the 0.25% DEW sample. The absorbance of the control sample was higher than the LLD but still below the LLQ. The average absorbance for the blanks were calculated using the standard curve the resulting values were negative showing that the blank values lie outside of the linear range of the standard curve. A similar trend was found using the blank values and standard curve for the WPC. The blank wells for WPC had an average absorbance of 0.057 ± 0.007 and a LLD of 0.078. The absorbance of the LLQ for WPC was 0.476 ± 0.037. The control sample (0% WPC) had an average absorbance of 0.085 ± 0.008. Again the control sample was slightly higher than the LLD but still much lower than the LLQ. The range for the standard curve was chosen so as to cover the most commonly added amounts of protein additive.

3.4. Indirect ELISA of DEW and WPC in crabstick

Using the most abundant proteins found in the respective protein additives helped in creating an accurate assay. Finding antibodies that will bind well with the heat-denatured form of OA and β-LG was a key for the success of the assay development. An indirect ELISA was used to qualify and quantify the use of DEW and WPC in prepared crabstick. Due to the highly processed nature of the crabstick, the proteins found in the sample have been completely denatured. Chemical (addition of salt) and physical (chopping and cooking) processing made it even more difficult to find the antibodies that could detect the denatured protein. The Ab anti-H-OA was produced to bind strongly with OA in denatured and modified forms such as heat-denatured and reduced. The antibody used to detect β-LG was created using native β-LG. Table 1 shows the results of the verification batches for DEW, WPC, and their mixture (DEW/WPC). The calculated % protein was determined by dividing the determined protein % from the standard curve by the actual protein % added. Samples containing DEW had a calculated % protein that ranged from 98.8% to 106.6% and a standard deviation range of 2.5–6.3%. All calculated % protein values for the samples that contained DEW were within 7% of the actual added protein value. The WPC had a calculated % protein that ranged from 90.3% to 116.7% and a standard deviation range of

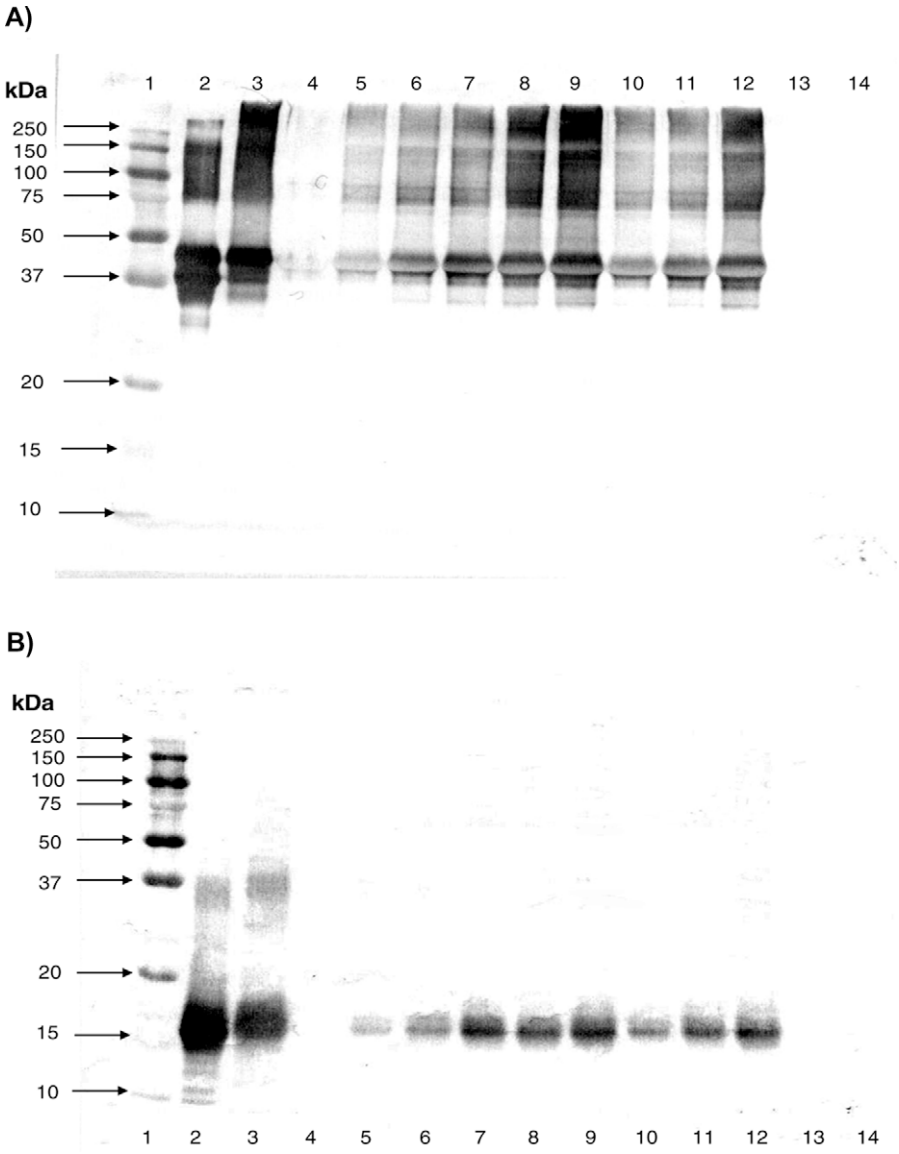

Fig. 3. Immunoblotting of DEW/WPC mixture tested using Ab anti-H-OA (A) and pAb anti-β-LG (B). (A) Lane (L) (1) Kaleidoscope marker, (2) ovalbumin, (3) DEW, lanes 4–12 crabstick batches (% DEW/WPC) (4) 0%, (5) 0.25%, (6) 0.5%, (7) 1.0%, (8) 1.5%, (9) 2.0%, (10) 0.375%, (11) 0.75%, (12) 1.75%, (13) β-LG, (14) WPC. (B) Lane (L) (1) Kaleidoscope marker, (2) β-LG, (3) WPC, lanes 4–12 crabstick batches (% DEW/WPC) (4) 0%, (5) 0.25%, (6) 0.5%, (7) 1.0%, (8) 1.5%, (9) 2.0%, (10) 0.375%, (11) 0.75%, (12) 1.75%, (13) ovalbumin, (14) DEW.

1.3–11.4%. All calculated % protein values for WPC samples were within 17%.

To understand the precision of the assay, the CV were analysed and reported in Table 2. Overall assay CV for DEW samples ranged from 0.9% to 3.1% while those for the WPC samples ranged from 1.0% to 8.0%. The difference in CV range for the two assays may be due, in part, to the nature of the antibodies used. The Ab anti-H-OA was developed against heat denatured OA. However the pAb anti-β-LG was created using the native form of β-LG. The difference in the CV may be because of increased avidity of the Ab anti-H-OA with denaturation. An antibody produced using heat denatured β-LG may possibly lead to an antibody with a stronger avidity for heat denatured β-LG.

Breton, Phan Thanh, and Paraf (1988) found that affinity purified antibodies raised against native ovalbumin had higher avidity against heat-denatured ovalbumin than against the native ovalbumin molecule. Rumbo, Chirdo, Fossati, and Anon (1996) found that avidity peaked and then began to decrease as heating time increased. This trend held true for samples tested between 70 and 100 °C. They attributed the decrease in avidity to an increase in OA unfolding. Luis, Perez, Sanchez, Lavilla, and Calvo (2007) showed that the use of native β-LG as an antigen, still allowed for the detection of highly denatured β-LG in food products including meat, bakery products, sauces, and snacks. Chicón, Belloque, Alonso, and López-Fandiño (2008) found that high pressure treatment of β-LG at 200 and 400 MPa actually increased the binding of β-LG-specific rabbit IgG antibodies when tested in an indirect ELISA format. According to Svenning, Brynhildsvold, Molland, Langsrud, and Vegarud (2000), β-LG antibody antigenicity was reduced due to the WPC processing. However, they stated that the reduction may be due to lower protein solubility. For WPC that was heated without any hydrolysis they showed 61% protein solubility and a 500-fold decrease in antigenicity. With pre-heated and hydrolysed WPC, they showed 100% protein solubility and a

Table 1
Protein additive estimation of verification batches using indirect ELISA.

	Added protein (%)	Determined protein (%)	Sample recovery	
			%[a]	CV (%)[a]
DEW	0.375	0.375	100.0	3.1
	0.750	0.763	101.7	2.9
	1.750	1.749	100.2	1.0
WPC	0.375	0.339	90.3	7.6
	0.750	0.840	112.0	5.3
	1.750	1.717	98.1	1.0
DEW/WPC[b] (mixture)	0.375	0.371	98.8	2.8
	0.750	0.799	106.6	0.9
	1.750	1.755	100.3	1.8
DEW/WPC[c] (mixture)	0.375	0.383	102.2	8.0
	0.750	0.875	116.7	3.4
	1.750	1.674	95.6	4.0

[a] Sample recovery (%) and coefficient of variance (CV) as determined from three extractions done on three separate days in triplicate plates.
[b] Sample were tested with Mab H-OA detection antibodies.
[c] Sample were tested with Pab β-LG detection antibodies.

Table 2
Inter-assay coefficient of variance[a] (%) by indirect ELISA.

	Added protein (%)	Inter-assay (% CV)
DEW	0.375	3.1
	0.750	2.9
	1.750	1.0
WPC	0.375	7.6
	0.750	5.3
	1.750	1.0
DEW/WPC[b] (mixture)	0.375	2.8
	0.750	0.9
	1.750	1.8
DEW/WPC[c] (mixture)	0.375	8.0
	0.750	3.4
	1.750	4.0

[a] Inter-assay CVs are given as the mean of three extractions done on three separate days. Each extract from each extraction was assayed in triplicate on the same day.
[b] Samples were tested with Mab H-OA detection antibodies.
[c] Samples were tested with Pab β-LG detection antibodies.

10-fold decrease in antigenicity. Their study pointed out that β-LG antibody antigenicity was affected not only by processing conditions, but also by protein solubility.

4. Conclusions

Obtaining antibodies that would bind the target protein in the highly processed crabstick proved to be a key for the success of the assay development. Ab anti-H-OA and pAb anti-β-LG were shown to be highly specific for the target protein and showed no cross-reactivity with non-target proteins found in the prepared crabstick. An optimised solution for extraction was made with 10% SDS and 2.5% 2-ME. This optimised extraction solution demonstrated high reproducibility for the prepared crabsticks. An indirect ELISA assay was tested and proved as an effective method for the qualification and quantification DEW and WPC in a cooked and pasteurised crabstick. All three levels of DEW protein additive were estimated to less than 7% of the actual value and those of the WPC were estimated to less than 17%. Accuracy of the WPC assay may be improved by producing an antibody from the heat denatured form of β-LG.

Acknowledgement

Special thanks go to James Thompson for his valuable insight and technical support.

References

Asensio, L., Gonzalez, I., Rodriguez, M. A., Mayoral, B., Lopez-Calleja, I., Hernandez, P. E., et al. (2003). Identification of grouper (*Epinephelus guaza*), wreck fish (*Polyprion americanus*), and Nile perch (*Lates niloticus*) fillets by polyclonal antibody-based enzyme-linked immunosorbent assay. *Journal of Agricultural and Food Chemistry, 51*(5), 1169–1172.
Breton, C., Phan Thanh, L., & Paraf, A. (1988). Immunochemical properties of native and heat denatured ovalbumin. *Journal of Food Science, 53*(1), 222–225.
Burgarella, J. C., Lanier, T. C., Hamann, D. D., & Wu, M. C. (1985). Gel strength development during heating of surimi in combination with egg white or whey protein concentrate. *Journal of Food Science, 50*(6), 1595–1597.
Chicón, R., Belloque, J., Alonso, E., & López-Fandiño, R. (2008). Immunoreactivity and digestibility of high-pressure-treated whey proteins. *International Dairy Journal, 18*(4), 367–376.
Dupont, D., Faurie, F., Martin, B., Beuvier, E., Arnould, C., Rolet-Repecaud, O., et al. (2006). Determination of bovine lactoferrin concentrations in cheese with specific monoclonal antibodies. *International Dairy Journal, 16*(9), 1081–1087.
Faeste, C. K., Egaas, E., Lindvik, H., & Lovberg, K. E. (2007). Extractability, stability, and allergenicity of egg white proteins in differently heat-processed foods. *Journal of AOAC International, 90*(2), 427–436.
Farrell, H. M., Jimenez-Flores, R., Bleck, G. T., Brown, E. M., Butler, J. E., Creamer, L. K., et al. (2004). Nomenclature of the proteins of cows' milk – Sixth revision. *Journal of Dairy Science, 87*(6), 1641–1674.
Foegeding, E. A., Davis, J. P., Doucet, D., & McGuffey, M. K. (2002). Advances in modifying and understanding whey protein functionality. *Trends in Food Science and Technology, 13*(5), 151–159.
Fuller, H. R., Goodwin, P. R., & Morris, G. E. (2006). An enzyme-linked immunosorbent assay (ELISA) for the major crustacean allergen, tropomyosin, in food. *Food and Agricultural Immunology, 17*(1), 43–52.
Hefle, S. L., Jeanniton, E., & Taylor, S. L. (2001). Development of a sandwich enzyme-linked immunosorbent assay for the detection of egg residues in processed foods. *Journal of Food Protection, 64*(11), 1812–1816.
Holden, L., Fæste, C. K., & Egaas, E. (2005). Quantitative sandwich ELISA for the determination of lupine (*Lupinus* spp.) in foods. *Journal of Agricultural and Food Chemistry, 53*, 5866–5871.
Laemmli, U. (1970). Cleavage of structural proteins during assembly of the head of bacteriophage T4. *Nature, 227*, 680–685.
Leduc, V., Demeulemester, C., Guizard, C., Le Guern, L., Polack, B., & Peltre, G. (1999). Immunochemical detection of egg white antigens and allergens in meat products. *Allergy, 54*(5), 464–472.
Lee, C. M. (1984). Surimi process technology. *Food Technology*(November), 69–80.
Lowry, O., Rosebrough, N., Farr, A., & Randall, R. (1951). Protein measurement with the folin phenol reagent. *Journal of Biological Chemistry, 193*(2), 265–275.
Luis, R. D., Perez, M. D., Sanchez, L., Lavilla, M., & Calvo, M. (2007). Development of two immunoassay formats to detect β-lactoglobulin: Influence of heat treatment on β-lactoglobulin immunoreactivity and assay applicability in processed food. *Journal of Food Protection, 70*(7), 1691–1697.
Matsuda, R., Sato, H., Morishita, N., Gamo, R., Mishima, T., Matsumoto, T., et al. (2006). Interlaboratory evaluation of two enzyme-linked immunosorbent assay kits for the detection of egg, milk, wheat, buckwheat, and peanut in foods. *Journal of AOAC International, 89*(6), 1600–1608.
Mine, Y. (1995). Recent advances in the understanding of egg white protein functionality. *Trends in Food Science and Technology, 6*(7), 225–232.
Ochiai, Y., & Watabe, S. (2003). Identification of fish species in dried fish products by immunostaining using anti-myosin light chain antiserum. *Food Research International, 36*, 1029–1035.
Park, J. W., & Lanier, T. C. (1987). Combined effects of phosphates and sugar or polyol on protein stabilization of fish myofibrils. *Journal of Food Science, 52*(6), 1509–1513.
Park, J. W., Lanier, T. C., & Green, D. P. (1988). Cryoprotective effects of sugar, polyols, and/or phosphates on Alaska pollock surimi. *Journal of Food Science, 53*(1), 1–3.
Park, J. W., & Lin, T. M. (2005). Manufacturing and evaluation. In J. W. Park (Ed.), *Surimi and surimi seafood* (pp. 33–106). Boca Raton: CRC Press Taylor & Francis Group.
Reed, Z. H., & Park, J. W. (2008). Qualification and quantification of fish protein in prepared surimi crabstick. *Journal of Food Science, 73*(5), C329–C334.
Rumbo, M., Chirdo, F. G., Fossati, C. A., & Anon, M. C. (1996). Analysis of structural properties and immunochemical reactivity of heat-treated ovalbumin. *Journal of Agricultural and Food Chemistry, 44*(12), 3793–3798.
Stevens, L. (1991). Egg white proteins. *Comparative Biochemistry and Physiology: B: Comparative Biochemistry, 100*(1), 1–9.

Svenning, C., Brynhildsvold, J., Molland, T., Langsrud, T., & Vegarud, G. E. (2000). Antigenic response of whey proteins and genetic variants of beta-lactoglobulin – The effect of proteolysis and processing. *International Dairy Journal, 10*(10), 699–711.

Towbin, H., Staehelin, T., & Gordon, J. (1979). Electrophoretic transfer of proteins from polyacrylamide gels to nitrocellulose sheet: Procedure and some applications. *Proceedings of the National Academy of Sciences, 76*, 4350–4354.

Watanabe, Y., Aburatani, K., Mizumura, T., Sakai, M., Muraoka, S., Mamegosi, S., et al. (2005). Novel ELISA for the detection of raw and processed egg using extraction buffer containing a surfactant and a reducing agent. *Journal of Immunological Methods, 300*(1/2), 115–123.

Food Chemistry 118 (2010) 582–588

Contents lists available at ScienceDirect

Food Chemistry

journal homepage: www.elsevier.com/locate/foodchem

Fractionation and evaluation of radical scavenging peptides from *in vitro* digests of buckwheat protein ☆

Yuanyuan Ma [a], Youling L. Xiong [a,*], Jianjun Zhai [b], Haining Zhu [b], Thomas Dziubla [c]

[a] Department of Animal and Food Sciences, University of Kentucky, 206 Garrigus Building, Lexington, KY 40546, USA
[b] Department of Molecular and Cellular Biochemistry, University of Kentucky, Lexington, KY 40506, USA
[c] Department of Chemical and Materials Engineering, University of Kentucky, Lexington, KY 40506, USA

ARTICLE INFO

Article history:
Received 8 January 2009
Received in revised form 15 April 2009
Accepted 11 May 2009

Keywords:
Buckwheat protein
In vitro digestion
Free radical scavenging
Gel filtration
Tandem mass spectrometry

ABSTRACT

Buckwheat protein (BWP) isolate was subjected to a two-stage *in vitro* digestion (1 h pepsin followed by 2-h pancreatin at 37 °C). The antioxidant potential of the BWP digests was compared by assessing their capacity to scavenge 2,2′-azinobis (3-ethylbenzothiszoline-6-sulphonic acid) ($ABTS^{+\cdot}$) and hydroxyl (·OH) radicals. The 2-h pancreatin digest, which demonstrated the strongest activity against both radicals, was subjected to Sephadex G-25 gel filtration. Of the six fractions collected, fractions IV (456 Da) and VI (362 Da) showed the highest $ABTS^{+\cdot}$ scavenging activity and were 23–27% superior to mixed BWP digest ($P < 0.05$). Fraction VI was most effective in neutralising ·OH and was 86% and 24% more efficient ($P < 0.05$) than mixed BWP digest and fraction IV, respectively. LC–MS/MS identified Trp-Pro-Leu, Val-Pro-Trp, and Val-Phe-Pro-Trp (IV), Pro-Trp (V) and tryptophan (VI) to be the prominent peptides/amino acid in these fractions.

1. Introduction

The gastrointestinal (GI) tract is one of the most vulnerable tissues inside the human body to oxidative attack by reactive oxygen species (ROS). Oxidative stress is believed to be one important cause of GI inflammation, ulcer, and colitis (Blau, Rubinstein, Bass, Singaram, & Kohen, 1999). The upper GI mucosa, itself a natural defence layer, is constantly exposed to ROS derived from endogenous as well as exogenous sources, i.e., foods, which can contain high amounts of unsaturated lipids, prooxidant transition metal ions and even directly, free radicals. For example, a diet containing iron and ascorbic acid in the presence of unsaturated fatty acids predisposed the GI lining to hydroxyl radical (·OH) mediated injury, which can lead to colitis (Carrier, Aghdassi, Platt, Cullen, & Allard, 2001). Moreover, it has been demonstrated that ·OH can form in the gastric juice, and the radical generation is implicated in GI mucosa damage and ensuing ulcer (Nalini, Ramakrishna, Mohanty, & Balasubramanian, 1992). Hence, identifying potential antioxidants that may help neutralise radicals, particularly ·OH, thereby protecting the GI system, is of great importance.

There has been growing interest in recent years to produce bioactive peptides that can exert radical scavenging activity. Carnosine, a naturally occurring dipeptide rich in muscle foods, is a classical example of peptides that can act as a strong radical scavenger and inhibit ROS-initiated lipid oxidation (Boldyrev & Johnson, 2002). Most reported antioxidants are derived from common food protein sources using commercial enzymes. For example, canola protein hydrolysate prepared using flavourzyme was shown to be antioxidative and can enhance water-holding capacity in cooked pork meat (Cumby, Zhong, Naczk, & Shahidi, 2008). Hydrolysed animal proteins, e.g., gelatin hydrolysate from Alaska polluck skin (Kim et al., 2001), also show antioxidant activity in food model systems.

Proteins in raw and processed foods can possess antioxidant peptide sequences and structural domains; the active fragments are released during the GI digestion process. Reported high-efficiency radical scavenging peptides released through *in vitro* pepsin and pancreatin digestion include those from casein (Hernandez-Ledesma, Amigo, Ramos, & Recio, 2004), maize zein (Zhu, Chen, Tang, & Xiong, 2008), oyster protein (*Crassostrea gigas*) (Qian, Jung, Byun, & Kim, 2008), and mussel protein (*Mytilus coruscus*) (Jung et al., 2007).

Buckwheat, a traditional grain widely considered as a functional food source, has gained its fame due to published studies that linked its proteins to various health benefits, e.g., cholesterol reduction (Kayashita, Shimaoka, Nakajoh, Yamazaki, & Norihisa, 1997), tumour inhibition (Liu et al., 2001), and hypotension regulation (Ma, Bae, Lee, & Yang, 2006). Because many of the health promoting functions are inherently related to the radical scavenging activity of peptides from the protein digests, it is hypothesised that hydrolysis of buckwheat protein can release the peptide fragments capable of

☆ Approved for publication as journal article number 09-07-004 by the Director of Kentucky Agricultural Experiment Station.

* Corresponding author. Tel.: +1 859 257 3822; fax: +1 859 257 5318.
E-mail address: ylxiong@uky.edu (Y.L. Xiong).

0308-8146/$ - see front matter © 2009 Elsevier Ltd. All rights reserved.
doi:10.1016/j.foodchem.2009.05.024

stabilising ROS and inhibiting lipid oxidation. A preliminary study supported this hypothesis (Ma & Xiong, 2009). However, the specific peptides or peptide fractions responsible for the antioxidant functions have not been elucidated.

In the present study, the ability of mixed as well as individual fractions of *in vitro* pepsin–pancreatin sequential digests of buckwheat protein to stabilise ·OH and $ABTS^{+\cdot}$ radicals was investigated. The objective was to identify the most effective antioxidant peptide fraction(s) from buckwheat *in vitro* digests. Initially, the digest with the highest radical scavenging capacity was fractionated by means of gel filtration. The ability to stabilise hydroxyl radical by each post-column fraction was subsequently examined, and the prominent peptides in active fractions were sequenced by liquid chromatography–tandem mass spectrometry (LC–MS/MS).

2. Materials and methods

2.1. Extraction of buckwheat protein (BWP)

Low-fat buckwheat flour was purchased from Bulkfoods.com (Toledo, OH, USA). The product specification sheet from the supplier indicated 3.6% fat, 71.4% total carbohydrate and 25% protein. Before protein extraction, the flour was stirred with hexane (1:1 w/v, four changes) for 48 h to remove residual fat. After vacuum evaporation of residual hexane, the dried defatted flour powder was subjected to the process of protein extraction according to the method of Tomotake, Shimaoka, Kayashita, Nakajoh, and Kato (2002) with some modifications. Defatted buckwheat flour (1 kg) was manually dispersed into 10 L of deionized water, and the pH was adjusted to 8.0 using 1 M NaOH. After stirring with a propeller (~50 rpm) at 4 °C for 2 h, the suspension was centrifuged at 5000*g* for 20 min. The supernatant (protein extract) was decanted and adjusted to pH 4.5 using 1 M HCl to isoelectrically precipitate protein. The protein precipitate was washed with deionized water two times and then neutralised with 0.1 M NaOH before lyophilisation. Freeze dried BWP powder was stored at −20 °C before use.

2.2. Preparation of protein digests

BWP *in vitro* digests were prepared according to the method of Lo and Li-Chan (2005). The suspension of BWP (5%, w/v) in nanopure deionized water was adjusted pH 2.0 with 1 M HCl, followed by the addition of pepsin (4%, w/w, protein basis). The mixture was incubated 1 h in a shaking water bath set at 37 °C to allow pepsin digestion. Subsequently, the pH was adjusted to 5.3 using 0.9 M $NaHCO_3$. After the addition of pancreatin (4% w/w, protein basis), the pH was adjusted to 7.5 with 1 M NaOH. The digestion was restarted and continued in the 37 °C shaking water bath for another 2 h. Aliquots of hydrolysates were removed at 0, 30, 60, 90, 120, and 180 min during the pepsin → pancreatin sequential digestion, adjusted to neutrality (pH 7.0) with 1 M NaOH/HCl, and heated at 96 °C for 5 min to inactivate the enzymes. Each aliquot was freeze dried and kept at –20 °C before use.

2.3. Gel filtration

Preliminary results showed that the two-stage *in vitro* digestion yielded a high radical scavenging activity in the final BWP digest (i.e., 180 min total digestion time). Therefore, this digest, referred to as "$D_{180\ min}$", was subjected to peptide fractionation using a low-pressure size exclusion chromatography with a 2.6 cm (dia.) × 70 cm (length) Sephadex G-25 fine column (Pharmacia XK 26/70, Piscataway, NJ, USA).

A 2 mg/mL of $D_{180\ min}$ solution, prepared from lyophilised powder by dissolving in the elution buffer (0.02 M phosphate, pH 7.4), was clarified and sterilized through a 25-mm syringe filter with a 0.22 μM membrane (Fisher Scientific, Pittsburgh, PA). The purified solution (10 mL) was loaded to the Sephadex column and eluted in a 4 °C cold room with the elution buffer at a 0.9 mL/min flow rate. Peptide fractions were collected using an automated fraction collector, and the absorbance (215 nm) of the eluents was measured. In order to collect enough peptides for antioxidant assays, a total of 23 chromatographic runs were conducted. The corresponding peptide fractions from the 23 replicates were pooled and lyophilised. Freeze dried fractions were stored at –20 °C for further analysis.

Molecular weight (MW) distribution of the individual peptide fractions was estimated from a MW calibration curve generated from the elution volume of the following standards (Sigma Chemical Co., St. Louis, MO) that were chromatographed separately in the Sephadex G-25 column under the same condition as described above: cytochrome C (12327 Da), aprotinin (6512 Da), bacitracin (1423 Da), and tetrapeptide GGYR (452 Da). The evolution volume (mL) of blue dextran was used to establish the void volume of the column. Data were fitted in the exponential decay model (modified single with three parameters) of the SigmaPlot Ver. 9 software (Systat Software Inc., Chicago, IL, USA), which yielded the following equation:

$$LogMW = 2.3429e^{\left(\frac{34.8528}{Vol-79.1592}\right)}$$

2.4. Radical scavenging activity (RSA)

The RSA of BWP *in vitro* digests and the peptide fractions of the final digest ($D_{180\ min}$) was evaluated using ·OH and $ABTS^{+\cdot}$ systems. The ·OH assay involved the inhibition of radical formation rather than scavenging radicals that are already produced (i.e., pre-existed), while the $ABTS^{+\cdot}$ scavenging assay was carried out by using pre-generated cationic radicals. Furthermore, $ABTS^{+\cdot}$, a synthetic radical species, is much larger in size than ·OH, which is known to be most reactive of all the reactive oxygen species in food systems. Therefore, the analysis of RSA of BWP digests in the two different radical generation systems may lead to a better understanding of RSA of BWB peptides than would the individual assay systems.

2.4.1. ·OH scavenging

The ·OH scavenging activity measurement was carried out according to the method of Moore, Yin, and Yu (2006). Briefly, 30 μL samples were each mixed with 170 μL of 9.28×10^{-8} M fluorescein in a 96-well polystyrene plate (Fisher Scientific, Pittsburgh, PA, USA), followed by the addition of 40 μL of 0.1999 M H_2O_2 and 60 μL $FeCl_3$. The mixed solution was immediately transferred to a Cary Eclipse fluorescence spectrophotometer equipped with a microplate reader (Varian, Victoria, Australia). The measurement with 0.1 s reading time per well and 1 min per plate was conducted with a 485 nm excitation wavelength and a 535 nm emission wavelength for 3 h to obtain the fluorescein decay curve. The ·OH scavenging capacity was expressed as trolox equivalent (μM), which was determined from the regression equation built on a series of trolox standards (20, 40, 80, and 100 μM). The concentration of the standards was set as the *x*-axis and the net area under the decay curve was set as the *y*-axis. The calculation of the area under curve (AUC) is shown below, where *f* represents the fluorescence value at a particular time during the decay:

$$AUC = 0.5 + f_1/f_0 + f_2/f_0 + f_3/f_0 + \cdots + f_{i-1}/f_0 + 0.5(f_i/f_0)$$

2.4.2. $ABTS^{+\cdot}$ scavenging

The $ABTS^{+\cdot}$ scavenging ability was determined by the decolorization assay (Re et al., 1999). Briefly, $ABTS^{+\cdot}$ was generated by a mixed solution of 7 mM ABTS and 2.45 mM potassium persulphate. After

12–16 h reaction, a dense green–blue coloured solution with excessive accumulation of $ABTS^{+\cdot}$ radical was diluted with 0.2 M phosphate buffer (pH 7.4) to the absorbance level of 0.7 ± 0.02 at 734 nm. The RSA was then determined by mixing 10 μL samples (2 mg/mL protein) and 990 μL diluted $ABTS^{+\cdot}$ solution for digestion aliquots (0, 30, 60, 90, 120 and 180 min) assay, and 100 μL samples (0.189 mg/mL protein) into 900 μL of diluted $ABTS^{+\cdot}$ solution for post-column fractions and final digest mixture ($D_{180\ min}$) for comparison. The absorbance was recorded at 1, 2, 5 and 10 min during the reaction. The extent of decolorization represented the magnitude of scavenging ability and was calculated from a standard curve generated with 50, 100, 250, 500, and 1000 μM of trolox. Trolox equivalent antioxidant capacity (TEAC) was used to express RSA.

2.4.3. LC–MS/MS

Gel filtration fractions (5 μL each) that exhibited strong radical scavenging activity were subjected to LC–MS/MS analysis using a QSTAR XL quadruple time-of-flight mass spectrometer (Applied Biosystems, Foster City, CA, USA) coupled with a nano-flow HPLC system (Eksigent Technologies, Dublin, CA, USA) through a nano-electrospray ionisation source (Protana, Toronto, Canada) (Lu & Zhu, 2005). The samples were injected by an autosampler, desalted on a trap column (300 μm i.d. × 5 mm length, LC Packings, Sunnyvale, CA, USA), and subsequently separated by reverse phase C18 column (75 μm i.d. × 150 mm length, Vydac, Columbia, MD, USA) at a flow rate of 200 nL/min. The HPLC gradient was linear from 5% to 80% mobile phase B in 55 min using mobile phase A (H_2O, 0.1% formic acid) and mobile phase B (80% acetonitrile, 0.1% formic acid).

Peptides eluted out of the reverse phase column were analyzed online by mass spectrometry (MS) and selected peptides were subjected to tandem mass spectrometry (MS/MS) sequencing. The automated data acquisition using information-dependent mode was performed on QSTAR XL under control by Analyst QS software (Applied Biosystems, Foster City, CA, USA). Each cycle typically consisted of one 1-s MS survey scan from 150 to 1200 (m/z) and two 2-s MS/MS scans of singly, doubly and triply charged species with mass range of 100–1200 (m/z). The spectra were interpreted using the *de novo* peptide sequencing module of the Analyst QS software.

2.5. Statistical analysis

The study employed a randomized complete block design with replication as the block. There were a minimum of three replications. Each analysis was done in duplicate. Data were subjected to analysis of variance using the general linear model's procedure of the Statistix software 9.0 (Analytical Software, Tallahassee, FL). When a treatment effect was found significant, Tukey HSD all-pair-wise multiple comparisons were performed to identify significant differences between individual means.

3. Results and discussion

3.1. RSA of BWP in vitro digests

In the ·OH scavenging test, the potential of an antioxidant to inhibit ·OH formation or to stabilise the radical was indicated by the rate of fluorescence decay of fluorescein (Moore et al., 2006). All BWP *in vitro* digest samples showed a slower fluorescence decay than non-hydrolysed BWP (data not shown), indicating that hydrolysis improved ·OH scavenging activity of BWP. Despite some variations, there was an overall trend that the ·OH scavenging activity increased with digestion (Fig. 1). In the Fenton reaction ($Fe^{2+} + H_2O_2 \rightarrow Fe^{3+} + {\cdot}OH + OH^-$), the impact of ·OH on susceptible compounds could be restrained by either Fe^{2+} chelation or ·OH stabilisation or both. Hence, the strong ·OH elimination activity of BWP digests, notably that of $D_{180\ min}$, can be attributed to the removal of free Fe^{2+} prooxidant and stabilisation of radicals through hydrogen or electron donation. The first mechanism was a postulation on the basis of the ·OH assay, which can be supported by the strong iron chelation ability of 2 h pancreatin digests (i.e., $D_{180\ min}$) (Ma & Xiong, 2009).

The $ABTS^{+\cdot}$ radical scavenging activity assay also demonstrated a positive and more consistent rise in the scavenging capacity with digestion time, culminating at 2 h of pancreatin treatment (i.e., end of the total 180 min *in vitro* digestion) (Fig. 2). In the $ABTS^{+\cdot}$ method, the antioxidant activity was measured exclusively by the ability of an antioxidant to act as a hydrogen or electron donor to neutralise preformed $ABTS^{+\cdot}$ radicals (Re et al., 1999). However, in the ·OH method, a test antioxidant is placed in a radical generation system where the antioxidant capacity was expressed both as inhibition of the radical initiation and elimination of formed radi-

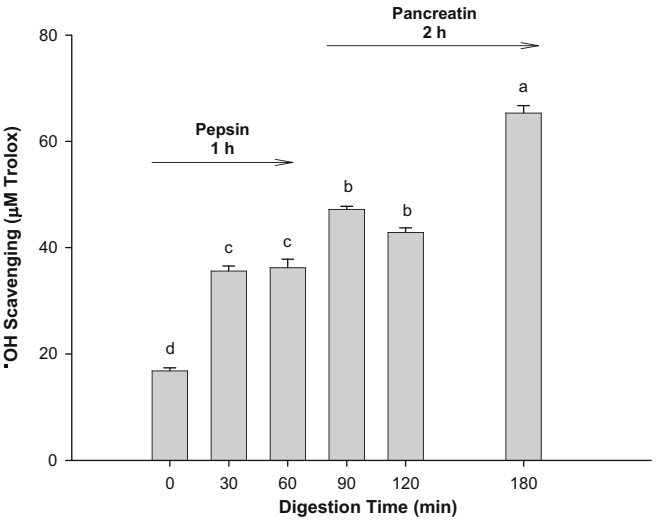

Fig. 1. Hydroxyl radical scavenging capacity of *in vitro* sequential digests of buckwheat protein. Means ($n = 3$) without a common letter differ significantly ($P < 0.05$). Sample solutions: 0.10 mg/mL protein.

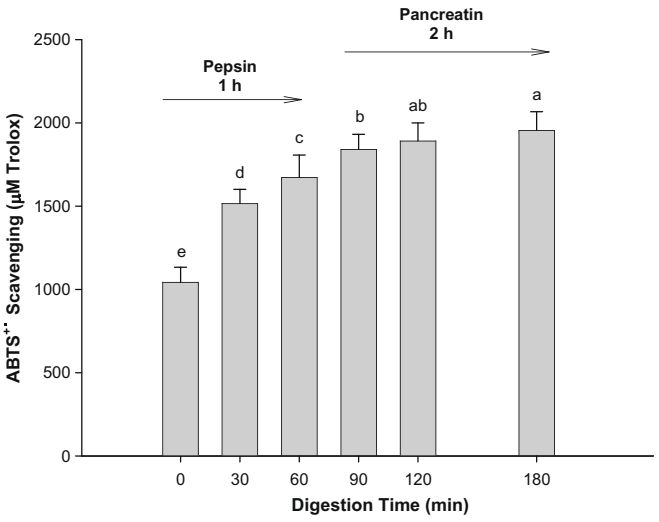

Fig. 2. $ABTS^{+\cdot}$ scavenging capacity of *in vitro* sequential digests of buckwheat protein. Means ($n = 3$) without a common letter differ significantly ($P < 0.05$). Sample solutions: 0.159 mg/mL protein.

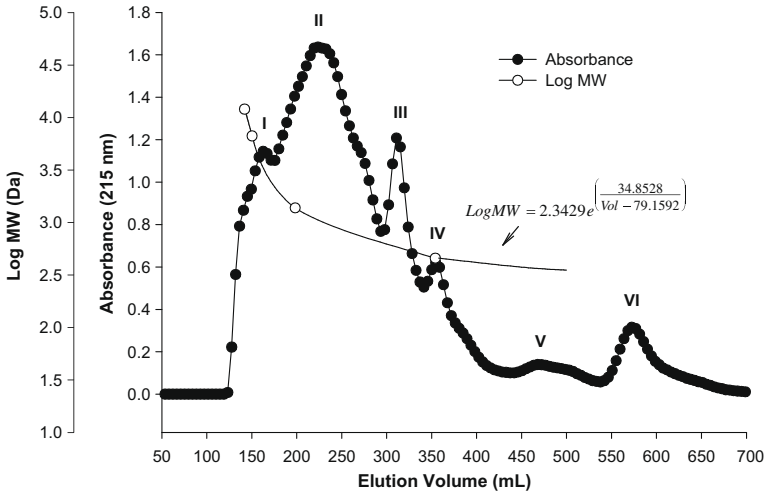

Fig. 3. Sephadex G-25 gel filtration of the final *in vitro* digest (180 min total digestion time) of buckwheat protein ($n = 23$), and regression plot of log MW vs. elution volume ($n = 3$).

cals (Moore et al., 2006). The remarkable similarity in the results of ·OH and $ABTS^{+\cdot}$ assays on different digests suggested that inhibition of radical initiation was probably not a critical factor determining the efficacy of BWP digests as antioxidants.

3.2. Peptide fractionation

Six peptide fractions were obtained by the Sephadex G-25 size exclusion gel filtration (Fig. 3). Based on the regression equation between elution volume and MW of each standard, the estimated mean MWs of these fractions were 3611 (I), 960 (II), 529 (III), 456 (IV), 365 (V), and 362 Da (IV). Assuming an average MW of 135 Da for amino acids, fraction I would be a peptide mixture consisting predominantly of those with 26 amino acid residues, and fractions II, III, IV and V or VI would have a preponderance of heptamerci, tetrameric, trimeric, or dimeric peptides, respectively. Fraction VI would also contain free amino acids. Based on the nitrogen analysis of the freeze dried eluent powders, these fractions accounted for 23.7% (I), 60.2% (II), 10.5% (III), 3.2% (IV), 1.4% (V), and 1.0% (VI) of the total eluent protein.

The incomplete separation of fractions I–IV suggested that they each contained peptides with various sizes, some of which were overlapping in neighbouring fractions. A relatively broad distribution of molecular weight masses in hydrolysed proteins is commonly associated with gel filtration (Adler-Nissen, 1986). The tailing parts of the eluents (fractions V and VI) would consist of mixed short peptides and free amino acids (Zhu et al., 2008). Thus, a more robust separation system (e.g., a high performance liquid chromatography) that enables a precise MW distribution measurement is desirable for better elucidating the relationship of peptide MW distribution with antioxidant activity.

3.3. RSA of peptide fractions

The ·OH and $ABTS^{+\cdot}$ scavenging activities of various gel filtration fractions of the final BWP *in vitro* digest ($D_{180\ min}$) are shown in Fig. 4 (·OH scavenging capacity vs. fractions) and Fig. 5 ($ABTS^{+\cdot}$ scavenging capacity vs. fractions). Fraction VI exhibited the strongest ·OH scavenging activity, which was 86% greater ($P < 0.05$) than the

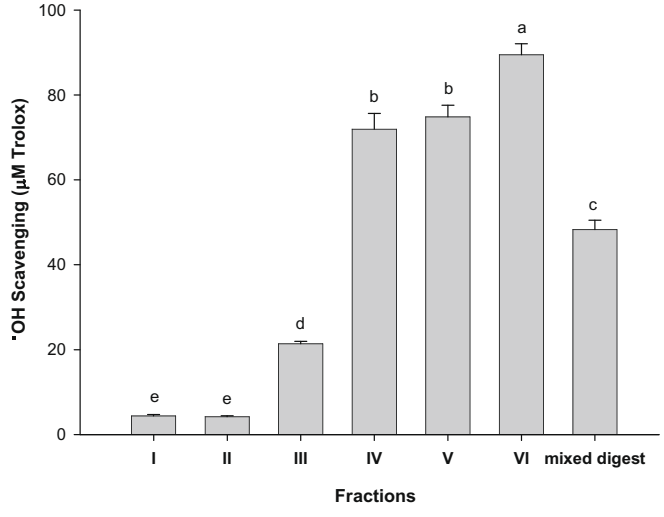

Fig. 4. Hydroxyl radical scavenging capacity of gel filtration fractions of final *in vitro* digest (180 min total digestion time) of buckwheat protein. Means ($n = 3$) without a common letter differ significantly ($P < 0.05$). Sample solutions: 0.10 mg/mL protein.

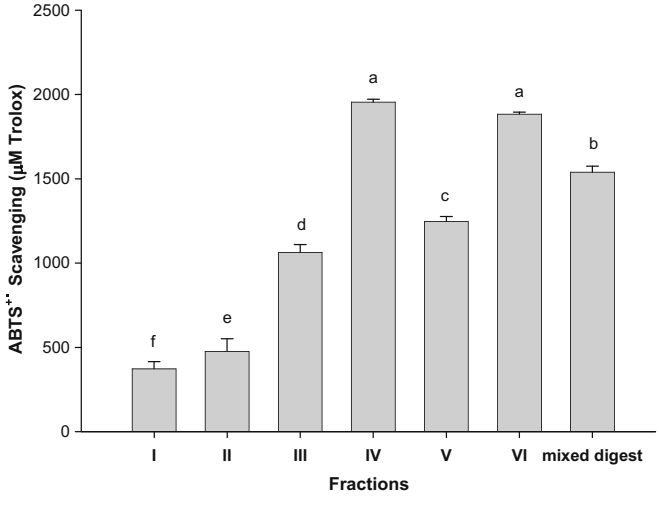

Fig. 5. $ABTS^{+\cdot}$ scavenging capacity of gel filtration fractions of the final *in vitro* digest (180 min total digestion time) of buckwheat protein. Means ($n = 3$) without a common letter differ significantly ($P < 0.05$). Sample solutions: 0.159 mg/mL protein.

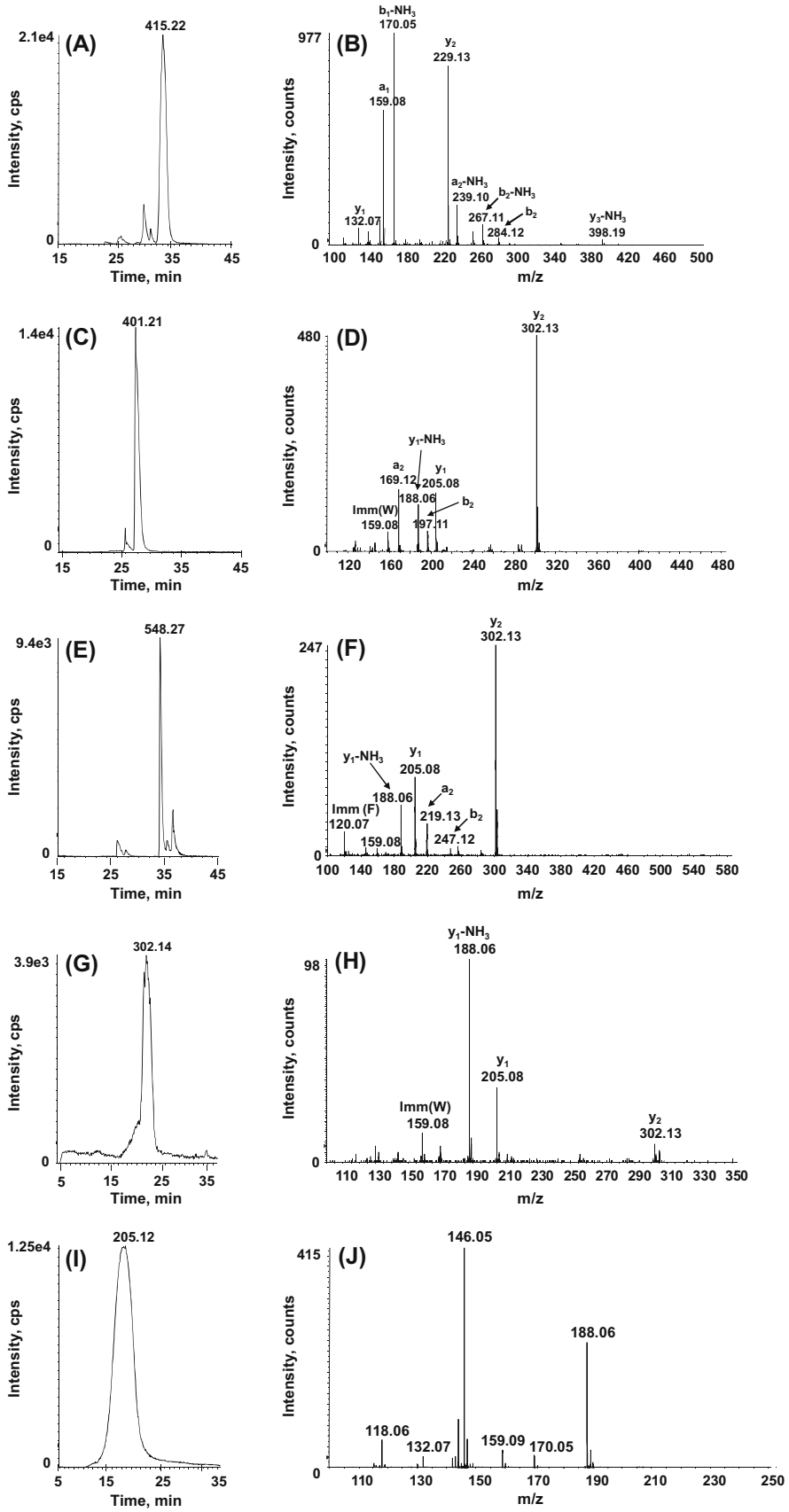

Fig. 6. Extracted ion chromatograms (A, C, E, G, I) and tandem MS/MS spectra (B, D, F, H, J) of the prominent peptides present in gel filtration fractions IV (A–F), V (G; H), and VI (I; J). The peptides/amino acid were identified as Trp-Pro-Leu (B), Val-Pro-Trp (D), Val-Phe-Pro-Trp (F), Pro-Trp (H) and Trp (J).

mixed BWP final digest ($D_{180\ min}$). Fractions IV and VI showed the highest potential in scavenging $ABTS^{+\cdot}$, and the activity was enhanced by an average of 24.5% ($P < 0.05$) compared to mixed final digest.

Although the $ABTS^{+\cdot}$ scavenging activity of fractions IV and VI indicated no significant differences, fraction VI showed a particularly strong ·OH elimination activity and was 24% more effective than fraction IV. These results suggested that fractions IV and VI were primary contributors to the radical scavenging capacity of the final BWP *in vitro* digest. The weaker antioxidant activity of the final mixed digest compared to the individual fractions IV and V can be explained by the dilution effect of relatively ineffective larger peptides. Fractions I (3611 Da), II (960 Da) and III (529 Da), which were present in the mixed final digest ($D_{180\ min}$), all displayed extremely low activity against $ABTS^{+\cdot}$ and ·OH. Yet, they made up the bulk of the total proteins/peptides in the mixed final digest.

3.4. Peptide sequence

Gel filtration fractions IV, V and VI, which exhibited relatively strong radical scavenging activity as indicated above, were subjected to individual peptide separation and sequence identification. The extracted ion chromatograms (XIC) and the tandem MS/MS spectra of the prominent peptides in these fractions are shown in Fig. 6. There were three prominent peptides in fraction IV, their XICs with the m/z values of 415.22, 401.21 and 548.27 are displayed in panels (A), (C) and (E), respectively. Their MS/MS spectra are shown in panels (B), (D) and (F). *De novo* sequencing determined the sequences of the peptides as Trp-Pro-Leu (B), Val-Pro-Trp (D) and Val-Phe-Pro-Trp (F), respectively. Fraction V produced relatively lower total signals in the LC–MS/MS analysis. A peptide with the m/z value of 302.14 was evident (panel G) and the MS/MS spectrum (panel H) supported the sequence of dipeptide Pro-Trp. Fraction VI showed a dominant XIC peak with elution time from 10 to 25 min (m/z at 205.12, panel I). The MS/MS spectrum displayed a characteristic pattern of fragments (m/z values of 118, 146 and 188) of the amino acid tryptophan as previously reported (Yamada, Miyazaki, Shibata, Hara, & Tsuchiya, 2008). Tryptophan was also detected in fractions V and IV with lower abundance (data not shown). The decreasing sizes of the prominent peptides in fractions IV, V and VI were consistent with the estimated molecular weights based on the gel filtration fractionation (Fig. 3).

These results were in concert with the general finding that short peptides with 2–10 amino acids exert greater antioxidant potential and other bioactive properties than their parent native proteins or large polypeptides (Kitts & Weiler, 2003). Through peptide bond cleavage, hydrolysis allows the release of active peptides capable of sequestering oxygen radicals, chelating prooxidant metal ions, and inhibiting lipid peroxidation in food systems (Elias, Kellerby, & Decker, 2008). For example, an oligopeptide with the sequence of His-Gly-Pro-Leu-Gly-Pro-Leu (797 Da), which was purified from fish skin hydrolysate, showed strong activity against ROS as well as linoleic acid peroxidation (Mendis, Rajapakse, & Kim, 2005). Two antioxidant short peptides, with the sequences of His-Val-Thr-Glu-Glu and Pro-Val-Pro-Ala-Glu-Gly-Val, were identified from chicken essence (Wu, Pan, Chang, & Shiau, 2005). Proline, as well as leucine, were found to play an important role in the antioxidant activity of peptides derived from soy protein, e.g., Leu-Leu-Pro-His-His (Chen, Muramoto, Yamauchi, & Nokihara, 1996). In our study, proline was present in all four prominent peptides identified in BWP digest fractions that showed strong antioxidant activity. In addition, valine was also present in two of four peptides. Zhu et al. (2008) reported that the peptide fractions rich in di-, tri-, and tetrapeptides from the zein *in vitro* digest (1–8 mg/mL protein) had comparable or stronger antioxidant activity than that of 0.1 mg/mL ascorbic acid or BHA. These peptides were superior to non-hydrolysed zein.

The dominant existence of tryptophan in fraction VI suggested that tryptophan was a potent antioxidant in BWP digests, consistent with previous findings (Christen, Peterhans, & Stocker, 1990; Elias, McClements, & Decker, 2005). It is noteworthy that tryptophan was also present in all four peptides with significant abundances in the three strong radical scavenging fractions (IV, V, VI), further supporting its antioxidant property. Furthermore, because short peptides are smaller molecules than intact proteins, at an equal weight concentration basis, the peptides' molar concentration would be significantly greater than that of intact proteins. This difference would also contribute to the higher antioxidant activity of BWP peptides.

In conclusion, free radical scavenging activity of BWP was accentuated by *in vitro* digestion, especially after 2 h pancreatin digestion following the 1 h pepsin treatment. On an equal weight concentration basis, fractions enriched with di-, tri- and tetrameric peptides containing tryptophan and proline exhibited the strongest radical scavenging activity. These short peptides are implicated in the protection of the upper digestive tract of humans from oxidative stresses and may partially explain why dietary BWP promotes the health of the GI system.

Acknowledgments

This research was supported by a CSREES/USDA NRI grant to Y.L.X. (2008-35503-18790). The Proteomics Core directed by H.Z. is in part supported by the NIH/NCRR Center of Biomedical Research Excellence in the Molecular Basis of Human Disease (P20-RR020171) and NIH/NIEHS Superfund Basic Research Program (P42-ES007380). The NIH Shared Instrumentation Grant S10RR023684 (to H.Z.) is acknowledged.

References

Adler-Nissen, J. (1986). *Enzymic hydrolysis of food proteins* (p. 427). New York, NY: Elsevier Applied Science.

Blau, S., Rubinstein, A., Bass, P., Singaram, C., & Kohen, R. (1999). Differences in the reducing power along the rat GI tract: Lower antioxidant capacity of the colon. *Molecular and Cellular Biochemistry, 194*, 185–191.

Boldyrev, A., & Johnson, P. (2002). Carnosine and related compounds: Antioxidant dipeptides. In P. Johnson & A. Boldyrev (Eds.), *Oxidative stress at molecular, cellular and organ levels* (pp. 101–114). Kerala, India: Research Signpost.

Carrier, J., Aghdassi, E., Platt, I., Cullen, J., & Allard, J. P. (2001). Effect of oral iron supplementation on oxidative stress and colonic inflammation in rats with induced coilitis. *Alimentary Pharmacology and Therapeutics, 15*, 1989–1999.

Chen, H. M., Muramoto, K., Yamauchi, F., & Nokihara, K. (1996). Antioxidant activity of designed peptides based on the antioxidative peptide isolated from digests of a soybean protein. *Journal of Agricultural and Food Chemistry, 44*, 2619–2623.

Christen, S., Peterhans, E., & Stocker, R. (1990). Antioxidant activities of some tryptophan metabolites: Possible implication for inflammatory diseases. *Proceedings of the National Academy of Sciences of the United States of America, 87*, 2506–2510.

Cumby, N., Zhong, Y., Naczk, M., & Shahidi, F. (2008). Antioxidant activity and water-holding capacity of canola protein hydrolysates. *Food Chemistry, 109*, 144–148.

Elias, R. J., Kellerby, S. S., & Decker, E. A. (2008). Antioxidant activity of proteins and peptides. *Critical Review in Food Science and Nutrition, 48*, 430–441.

Elias, R. J., McClements, D. J., & Decker, E. A. (2005). Antioxidant activity of cysteine, tryptophan, and methionine residues in continuous phase β-lactoglobulin in oil-in-water emulsions. *Journal of Agricultural and Food Chemistry, 53*, 10248–10253.

Hernandez-Ledesma, B., Amigo, L., Ramos, M., & Recio, I. (2004). Application of high-performance liquid chromatography–tandem mass spectrometry to the identification of biologically active peptides produced by milk fermentation and simulated gastrointestinal digestion. *Journal of Chromatography – A, 1049*, 107–114.

Jung, W. K., Qian, Z. J., Lee, S. H., Choi, S. Y., Sung, N. J., Byun, H. G., et al. (2007). Free radical scavenging activity of a novel antioxidative peptide isolated from *in vitro* gastrointestinal digests of *Mytilus coruscus*. *Journal of Medicinal Food, 10*, 197–202.

Kayashita, J., Shimaoka, I., Nakajoh, M., Yamazaki, M., & Norihisa, K. (1997). Consumption of buckwheat protein lowers plasma cholesterol and raises fecal

neutral sterols in cholesterol-fed rats because of its low digestibility. *The Journal of Nutrition, 127*, 1395–1400.

Kim, S. K., Kim, Y. T., Byun, H. G., Nam, K. S., Joo, D. S., & Shahidi, F. (2001). Isolation and characterization of antioxidative peptides from gelatin hydrolysate of Alaska pollack skin. *Journal of Agricultural and Food Chemistry, 49*, 1984–1989.

Kitts, D. D., & Weiler, K. (2003). Bioactive proteins and peptides from food sources. Applications of bioprocesses used in isolation and recovery. *Current Pharmaceutical Design, 9*, 1309–1323.

Liu, Z., Ishikawa, W., Huang, X., Tomotake, H., Kayashita, J., Watanabe, H., et al. (2001). A buckwheat protein product suppresses 1,2-dimethylhydrazine-induced colon carcinogenesis in rats by reducing cell proliferation. *The Journal of Nutrition, 131*, 1850–1853.

Lo, W. M. Y., & Li-Chan, E. C. Y. (2005). Angiotensin I converting enzyme inhibitory peptides from *in vitro* pepsin–pancreatin digestion of soy protein. *Journal of Agriculture and Food Chemistry, 53*, 3369–3376.

Lu, X., & Zhu, H. (2005). Tube-gel digestion: A novel proteomic approach for high throughput analysis of membrane proteins. *Molecular and Cellular Proteomics, 4*, 1948–1958.

Ma, Y., & Xiong, Y. L. (2009). Antioxidant and bile acid binding activity of buckwheat protein in vitro digests. *Journal of Agricultural and Food Chemistry, 57*, 4372–4380.

Ma, M. S., Bae, I. Y., Lee, H. G., & Yang, C. B. (2006). Purification and identification of angiotensin I-converting enzyme inhibitory peptide from buckwheat (Fagopyrum esculentum Moench). *Food Chemistry, 96*, 36–42.

Mendis, E., Rajapakse, N., & Kim, S. K. (2005). Antioxidant properties of a radical-scavenging peptide purified from enzymatically prepared fish skin gelatin hydrolysate. *Journal Agriculture and Food Chemistry, 53*, 581–587.

Moore, J., Yin, J. J., & Yu, L. (2006). Novel fluorometric assay for hydroxyl scavenging capacity (HOSC) estimation. *Journal of Agriculture and Food Chemistry, 54*, 617–626.

Nalini, S., Ramakrishna, B. S., Mohanty, A., & Balasubramanian, K. A. (1992). Hydroxyl radical formation in human gastric juice. *Journal of Gastroenterology and Hepatology, 7*, 497–501.

Qian, Z. J., Jung, W. K., Byun, H. G., & Kim, S. K. (2008). Protective effect of an antioxidative peptide purified from gastrointestinal digests of oyster, *Crassostrea gigas* against free radical induced DNA damage. *Bioresource Technology, 99*, 3365–3371.

Re, R., Pellegrini, A., Proteggente, A., Pannala, M., Yang, C., & Rice-Evans, C. (1999). Antioxidant activity applying an improved ABTS radical cation decolorization assay. *Free Radical Biology and Medicine, 26*, 1231–1237.

Tomotake, H., Shimaoka, I., Kayashita, J., Nakajoh, M., & Kato, N. (2002). Physicochemical and functional properties of buckwheat protein product. *Journal of Agriculture and Food Chemistry, 50*, 2125–2129.

Wu, H. C., Pan, B. S., Chang, C. L., & Shiau, C. Y. (2005). Low-molecular-weight peptides as related to antioxidant properties of chicken essence. *Journal of Food and Drug Analysis, 13*, 176–183.

Yamada, K., Miyazaki, T., Shibata, T., Hara, N., & Tsuchiya, M. (2008). Simultaneous measurement of tryptophan and related compounds by liquid chromatography/electrospray ionization tandem mass spectrometry. *Journal of Chromatography B, 867*, 57–61.

Zhu, L. J., Chen, J., Tang, X., & Xiong, Y. L. (2008). Reducing, radical scavenging and chelation properties of *in vitro* digests of Alcalase-treated zein hydrolysate. *Journal of Agriculture and Food Chemistry, 56*, 2714–2721.

Food Chemistry 118 (2010) 589–593

Contents lists available at ScienceDirect

Food Chemistry

journal homepage: www.elsevier.com/locate/foodchem

Biologically important thiols in aqueous extracts of spices and evaluation of their *in vitro* antioxidant properties

Kalyan Reddy Manda [a], Craig Adams [b], Nuran Ercal [a,*]

[a] Department of Chemistry, Missouri University of Science and Technology, Rolla, MO 65409, USA
[b] Department of Civil Engineering, Architectural and Environmental Engineering, 220 Butler Carlton Hall, Missouri University of Science and Technology, Rolla, MO 65409, USA

ARTICLE INFO

Article history:
Received 19 February 2009
Received in revised form 7 May 2009
Accepted 11 May 2009

Keywords:
Spices
Aqueous extracts
Thiols
Oxidative stress
Antioxidant activity

ABSTRACT

The levels of the biologically important thiols in aqueous extracts of different spices were determined using a sensitive high performance liquid chromatography (HPLC) technique. The spices analysed: turmeric, ginger, cardamom, mustard, fenugreek, and coriander showed different levels of thiols. Biologically important thiols or biothiols measured in these spices included glutathione (GSH), cysteine (CYS), N-acetylcysteine (NAC), homocysteine (HCYS), and γ-glutamyl cysteine (GGC). Our results showed that thiol levels varied from 4 to 1089 nM/g weight (dry or wet). Furthermore, none of the biothiols analysed were found in cumin, nutmeg, clove or star anise. We also studied the antioxidant abilities of these aqueous extracts using various *in vitro* antioxidant methods to correlate between the levels of these thiols and their antioxidant effects. Our results suggested that antioxidant activities may be independent of thiol content and may be, in part the combination of all the phytochemicals present. These results may be useful in explaining the effect of spices on thiol levels in *in vitro* and *in vivo* studies.

1. Introduction

Free radical mediated cell damage has been implicated in the pathology of various human chronic diseases such as Alzheimer's, Parkinson's, Crohn's, and certain cancers (Sies, 1985; Halliwell & Gutterbridge, 1989). These radicals may be generated as byproducts of various metabolic pathways, due to the metabolism of xenobiotics or by originating from the environment. These highly reactive radicals can react with biological molecules such as cell membrane lipids and DNA, which ultimately results in cell death (Kappus, 1986). However, they are also formed endogenously to perform biological functions. Radical induced damage is prevented in the body by various enzymatic antioxidant defence systems including superoxide dismutase, catalase, glutathione S-transferase, and also by biologically important thiols (biothiols) such as glutathione (GSH), cysteine (CYS), homocysteine (HCYS), and γ-glutamylcysteine (GGC) (Ross, 1989; Stoecker & Frei, 1991).

Biothiols are important antioxidants which protect the cells from oxidative damage (Meister & Anderson, 1983; Sen & Packer, 2000; Wlodek, 2002). Excessive oxidative damage can result in reduced levels of these biothiols. Over the past few decades, research has been dedicated to find natural sources of antioxidants, including biothiols. We previously reported several biothiols (mentioned above) in fruits and vegetables, including rare thiols like N-acetylcysteine (NAC) (Demirkol, Adams, & Ercal, 2004). NAC has long been used as a mucolytic agent for treating chronic bronchitis, as well as an effective antidote for acetaminophen poisoning (Bowman, Backer, Larsson, Melander, & Whalander, 1983; Prescott & Critchley, 1983).

Dietary sources like vegetables, fruits, contain a wide variety of phytochemicals like phenols and flavanoids that possess bioactive properties which may protect cellular systems against oxidative damage. Along with the phytochemicals, a significant level of thiols, known to enhance the antioxidant properties of fruits and vegetables have been reported in these dietary sources (Jones et al., 1992).

Spices, like turmeric, fenugreek, mustard, ginger, etc. may offer many health benefits and have been proven to counteract oxidative stress in *in vitro* and *in vivo* systems (Ahmed, Seth, & Banerjee, 2000; Modak et al., 2007). Most of these spices have been intensely studied only for their active components like phenolic acids, flavanoids (Kikuzaki & Nakatani, 1993). To the best of our knowledge, no known data or study is available regarding the presence of biothiols in spices. Therefore, the objective of this paper was to investigate the content of various biologically important thiols in spices. Furthermore, we wanted to determine whether the spices possessing higher thiols had higher antioxidant properties than their counterparts.

* Corresponding author. Address: Department of Chemistry, Missouri University of Science and Technology, 142 Schrenk Hall, 400 West 11th Street, Rolla, MO 65409, USA. Tel.: +1 573 341 6950; fax: +1 573 341 6033.
E-mail address: nercal@mst.edu (N. Ercal).

0308-8146/$ - see front matter © 2009 Elsevier Ltd. All rights reserved.
doi:10.1016/j.foodchem.2009.05.025

2. Materials and methods

2.1. Reagents and chemicals

All chemicals were purchased from Sigma (St. Louis, MO) unless otherwise stated. Acetonitrile, acetic acid, water, and phosphoric acid [all high performance liquid chromatography (HPLC) grade] were purchased from Fisher (St. Louis, MO). N-(1-Pyrenyl) maleimide (NPM) was purchased from Aldrich (Milwaukee, WI). Spice powders and ginger were purchased from major chain markets in Rolla and St. Louis MO.

2.2. Preparation of aqueous spice extracts

All Spices (0.1 g each), were suspended in 1 mL of serine borate buffer (100 mM Tris–HCl, 10 mM borate, 5 mM serine, and 1 mM diethylenetriaminepentacetic acid, pH 7.0). For ginger, (0.1 g) slices were homogenised in 1 mL of serine borate buffer using a tissue tearor (Model 985-370, type 2, Biospec Products Inc.) on ice for 2 min, with 5-s intervals of homogenisation. The slurry was centrifuged at 5000*g* for 1 min at 4 °C and the supernatants were filtered through 0.2 μm acrodisc. About 100 μL of the supernatant was used for the *in vitro* antioxidant assays. All samples were placed on ice during the experiments.

2.3. Determination of NAC, GSH, CYS, HCYS, and GGC by the HPLC method

An HPLC method for determining thiols was developed in this laboratory by analysing γ-glutamyl cycle intermediates (Winters, Zukowski, Ercal, Matthews & Spitz; 1995). All spices (0.1 g each) were placed in a 1 mL of serine borate buffer and homogenised on ice for 2 min. Ginger samples were prepared as described above. The slurry was centrifuged at 5000*g* for 1 min at 4 °C and supernatant (250 μL) was derivatized with 750 μL of NPM (1 mM in acetonitrile). This compound reacts with the free sulfhydryl groups to form fluorescent derivatives. The resulting solution was mixed and incubated at room temperature for 5 min. Ten micro litres of 2 N HCl were added to stop the reaction. After filtration through a 0.2 μm acrodisc, the derivatized samples were injected onto a 5 μm C_{18} column in a reverse phase HPLC system. NAC, GGC, CYS, and HCYS were determined concurrently with GSH since they also form fluorescent derivatives with NPM.

2.4. HPLC system

The HPLC system (Thermo Electron Corporation) consisted of a Finnigan™ SpectraSYSTEM SCM1000 Vacuum Membrane Degasser, a Finnigan™ SpectraSYSTEM P2000 Gradient Pump, a Finnigan™ SpectraSYSTEM AS3000 autosampler, and a Finnigan™ SpectraSYSTEM FL3000 fluorescence detector (λ_{ex} = 330 nm and λ_{em} = 376 nm). The injection volume was 5 μL for all of the samples. The HPLC column was a Reliasil ODS-1 C_{18} column (5 μm packing material) with 250 × 4.6 mm i.d. (Column Engineering, Ontario, CA, USA). The mobile phase was 30 percent water and 70% acetonitrile, containing 1 mL/L acetic acid and 1 mL/L *o*-phosphoric acid. The NPM derivatives were eluted from the column isocratically at a flow rate of 1 mL/min. Quantitation of the peaks from the HPLC system was performed with a Chromatopac, model C-R601 (Shimadzu).

2.5. Calibration curves

Calibration curves were constructed by using integrated peak areas as the *y*-axis vs concentrations as the x-axis. Linearity was achieved for NAC, GSH, GGC, CYS, and HCYS over a concentration range of 25–2500 nM ($r^2 > 0.995$).

2.6. Radical scavenging power

Radical scavenging power (RSP) of aqueous extracts of spices and ascorbic acid were assessed by the method of Hsu et al. with slight modifications (Hsu, Coupar, & Ng, 2006). The reaction mixture was a total volume of 3 mL, which included 2.9 mL of 2,2-diphenyl-1-picrylhydrazyl (DPPH, 1×10^{-4} M) and 100 μL of aqueous extracts of the corresponding spice. The solutions were left in the dark at room temperature for 30 min, and the resulting colour was measured spectrophotometrically at 520 nm against blanks. A decreasing intensity of purple colour was related to a higher RSP percentage, which was calculated using the following equation;

$$\mathrm{RSP} = [1 - (A_{s\cdot30}/B_{S\cdot30})] \times 100$$

where $A_{s.30}$ is absorbance of sample and $B_{S.30}$ is absorbance of blank at 30 min reaction time.

2.7. ·OH–scavenging activity assay

Hydroxyl radical (·OH) scavenging ability was measured according to the literature procedure with a few modifications (Smirnoff & Cumbes, 1989). The reaction mixture (2.1 mL) contained 1 mL $FeSO_4$ (1.5 mM), 0.7 mL H_2O_2 (6 mM), 0.3 mL sodium salicylate (20 mM) and 100μL of aqueous extracts of spices. This mixture was incubated at 37 °C for 1 h, after which the absorbance of the hydroxylated salicylate complex was measured at 562 nm. The percentage scavenging effect was calculated as:

$$\text{Scavenging effect} = [1 - (A_1 - A_2)/A_0] \times 100\%$$

where A_0 was the absorbance of the control (without extract) and A_1 was the absorbance in the presence of the extract, A_2 was the absorbance without sodium salicylate.

2.8. Fe^{2+}-chelating activity assay

Fe^{2+}-chelating activity was measured according to a literature procedure with a few modifications (Cheng, Kuo, Chan, Ko, & Teng, 1998). The reaction mixture (2.00 ml) contained 100μL of spice extract, 100μL $FeCl_2$ (0.6 mM), and 1.7 mL deionised water. The mixture was shaken vigorously and left at room temperature for 5 min; 100 μL of ferrozine (5 mM in methanol) were then added, mixed, and left for another 5 min to complex the residual Fe^{2+}. The absorbance of the Fe^{2+} - ferrozine complex was measured at 562 nm against a blank. Disodium Ethylenediaminetetracetic acid (EDTA-Na_2) was used as the control. The chelating activity of the extract for Fe^{2+} was calculated as:

$$\text{Chelating effect} = [1 - (A_1 - A_2)/A_0] \times 100\%$$

where A_0 was the absorbance of the control (without extract) and A_1 was the absorbance in the presence of the extract, A_2 was the absorbance without ferrozine.

2.9. Determination of total polyphenolic compounds

Total phenolic content was determined by the Folin–Ciocalteau method (Ordonez, Gomez, Vattuone, & Isla, 2006). Spice extracts (100μL) was mixed with 2.5 ml of 0.2 M Folin–Ciocalteau reagent for 5 min and 2.0 ml of 75 g/L Na_2CO_3 were then added. The absorbance was measured at 760 nm after 2 h of incubation at room temperature. Results were expressed as μg/mL of gallic acid equivalents (GAE).

2.10. Statistical analysis

All results presented in this study are the average of at least three measurements. Means ± standard deviations are shown in figures. One way Analysis of Variance (ANOVA) was performed followed by Bonferroni's multiple comparison tests.

3. Results and discussion

Due to the increased interest and commercialisation of botanicals because of their health-related benefits, many spices have been evaluated to determine their potential benefits. Several spices have exhibited antioxidant properties and, as a result, additional studies are being conducted to determine their specific health benefits. Natural antioxidants are known to protect cells from damage induced by oxidative stress, which is generally considered to be a cause of ageing, degenerative disease, and cancer (Ringman, Frautschy, Cole, Masterman, & Cummings, 2005).

Turmeric and its components, which have been widely studied over the last 25 years, have been reported to induce GSH synthesis in *in vitro* models (Dickinson, Iles, Zhang, Blank, & Forman, 2003). Thiol levels in oxidative stress conditions were increased in studies with ginger extracts (Ajith, Nivitha, & Usha, 2007; Amin & Hamza, 2006). Fenugreek extracts have been shown to produce beneficial effects, such as neutralising of free radicals and enhancing of antioxidant status (Anuradha & Ravikumar, 1998). Initiation, as well as propagation phases, of $FeCl_3$ induced lipid peroxidation was inhibited by cardamom extracts (Yadav & Bhatnagar, 2007). Although most of the antioxidant activities in these studies are attributed to polyphenolic compounds present in these spice extracts, the idea that these extracts may be sources of biothiols like GSH is ignored in most of the studies. In addition antioxidant activity does not always correlate with the presence of large quantities of these polyphenolic compounds. Hence, the presence of other antioxidants (like biothiols) in the aqueous spice extracts was determined and the correlation between antioxidant activity and thiol levels were investigated using various antioxidant assays.

In situ derivatization of the spice extracts with NPM produced the NPM-NAC, NPM-GSH, NPM-GGC, NPM-CYS, and NPM-HCYS adducts, which were rapidly separated by the HPLC system employed for this study (Demirkol et al., 2004). Fig. 1a shows a chromatogram of the mix standards using the NPM method. The chromatogram prepared from fenugreek illustrates the well-defined separation of the NPM-GSH, NPM-GGC, NPM-CYS, and NPM-HCYS adduct peaks achieved by this method.

The NAC, GSH, GGC CYS, and HCYS concentrations in the aqueous extracts of the spices are reported in Table 1. Amongst the biological thiols the highest levels of GSH and CYS were found in ginger extracts (1076 nM/g and 387 nM/g wet weight, respectively). Coriander extracts showed very low levels of thiols amongst all the spices analysed with only 35 nM/g dry weight of GSH present. Fenugreek showed the highest levels of HCYS, (62 nM/g dry weight), followed by turmeric. GGC was detected only in mustard and fenugreek as seen in Figs. 1b and 1c, respectively. Mustard contained the highest level of GGC. NAC was not detected in any of spice samples studied. Coriander had the lowest level of biological thiols amongst the spices analysed, with only GSH present in its aqueous extracts.

Our study showed that the spices analysed contained different levels of biothiols. It was therefore, necessary to determine whether the spices containing higher levels of thiols were more potent antioxidants than their counterparts with lower thiol levels. Accordingly, the antioxidant abilities of the aqueous extracts of the spices were evaluated using different *in vitro* methods. As most of the thiols were susceptible to oxidation, all of the spice samples were extracted in SBB and placed on ice during the experimental process. Ascorbic acid and EDTA-Na_2were used as standards to compare the *in vitro* antioxidant properties.

2,2-Diphenyl-1-picrylhydrazyl (DPPH) is widely used to test the ability of compounds to act as free radical scavengers or hydrogen

Table 1
Thiols concentration in spices (nM/g dry or wet weight).[a]

Spices	Botanical name	NAC	GSH	CYS	HCYS	GGC
Mustard	Brassica hirta	ND	820 ± 24	53 ± 3	ND	46 ± 6
Fenugreek	*Trigonella foenum-graecum* L.	ND	519 ± 52	57 ± 4	62 ± 1	42 ± 10
Ginger[b]	*Zingiber officinalis*	ND	1076 ± 18	387 ± 6	ND	ND
Turmeric	Curcuma longa	ND	41 ± 4	112 ± 1	51 ± 4	ND
Coriander	*Coriander sativum*	ND	35 ± 3	ND	ND	ND
Cardamom	Elettaria caradamomum	ND	112 ± 2	44 ± 2	ND	ND

[a] ND, not detectable. The results are given as Means ± S.D. ($n = 3$) of at least three samples of each spice.
[b] Thiols expressed as nM/g wet weight.

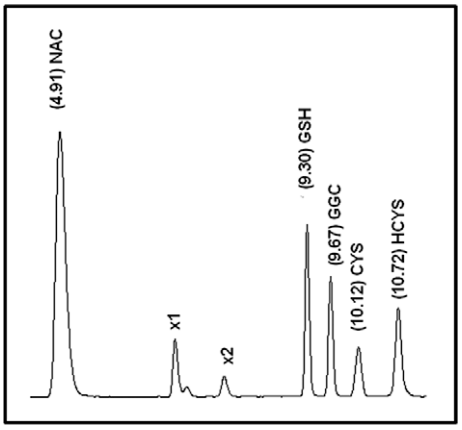

Fig. 1a. Chromatogram of a mixture of NAC (N-acetylcysteine), GSH (glutathione), GGC (γ-glutamyl cysteine), CYS (cysteine), and HCYS (homocysteine). Peaks from ×1 to ×2 represent NPM hydrolysis peaks. Retention times are given in minutes in parentheses next to the corresponding peaks.

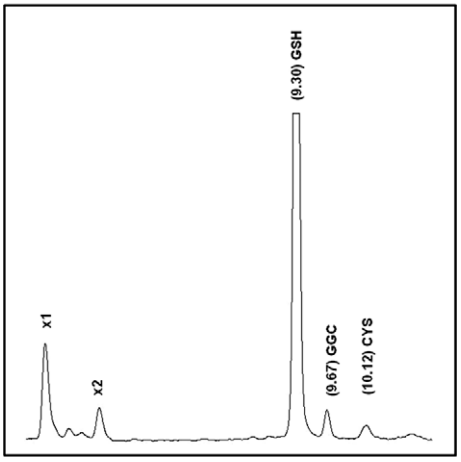

Fig. 1b. Chromatogram of NPM derivatized mustard sample showing GSH (glutathione), GGC (γ-glutamyl cysteine), and CYS (cysteine). Peaks from ×1 to ×2 represent NPM hydrolysis peaks. Retention times are given in minutes in parentheses next to the corresponding peaks.

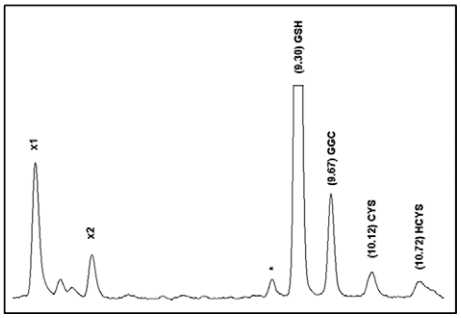

Fig. 1c. Chromatogram of NPM derivatized fenugreek sample showing GSH (glutathione), GGC (γ-glutamyl cysteine), and CYS (cysteine), and HCYS (homocysteine). Peaks from ×1 to ×2 represent NPM hydrolysis peaks. Retention times are given in minutes in parentheses next to the corresponding peaks. An unidentified peak is denoted as "*".

donors, and to evaluate antioxidant activity of foods. It has also been used in recent years to quantify antioxidants in complex biological systems. Mustard extract showed the highest DPPH activity with cardamom being the lowest of all, as seen in Fig. 2a. Ascorbic acid showed a 50% DPPH scavenging activity at 125 μg. Although mustard did not have the highest levels of thiols, the radical scavenging power of mustard extract was highest, in comparison with the other spice extracts.

The highly reactive radical (·OH) reacts with biomolecules resulting in damage to cells. Hydroxyl radicals are produced through various biological reactions; one of the common reactions is the Iron (II) - based Fenton reaction. Hydroxyl radical scavenging activity of aqueous extracts of spices was evaluated to determine their hydroxyl radical scavenging activity. Hydroxylation of salicylate is widely used as an index of hydroxyl radical formation *in vitro*. The present study showed that coriander extract, of all the spices extracts, was the strongest scavenger of hydroxyl radical, as seen in Fig. 2b. It is also noteworthy that cardamom, ginger, and turmeric extracts also showed a scavenging ability similar to that of the coriander extract.

Iron can initiate lipid peroxidation by Fenton reaction and also accelerate peroxidation by decomposing lipid hydroperoxides into peroxyl and alkoxyl radicals that can abstract hydrogen and perpetuate the chain reaction (Gülçin, Büyükokuroglu, & Küfrevioglu, 2003; Halliwell, 1991). Chelating ferrous ions illustrates one of the significant antioxidant properties. EDTA-Na_2, a standard chelator was used to compare the chelating effects of the extracts. The chelating effects of the spice extracts are as follows: cardamom › fenugreek › mustard › coriander › turmeric › ginger. Even at a minimal concentration of 20 μg, the standard chelator EDTA-Na_2, showed a 50% chelating as seen in Fig. 2c.

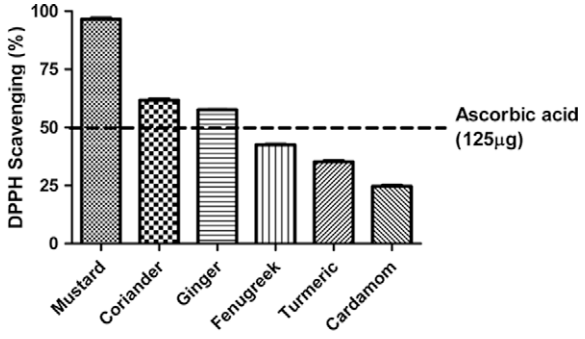

Fig. 2a. The DPPH radical-scavenging activity of spices extracts. The absorbance values were converted to the scavenging effect (%) and data plotted as the means of the replicate scavenging effect (%) values ± S.D. (n = 3).

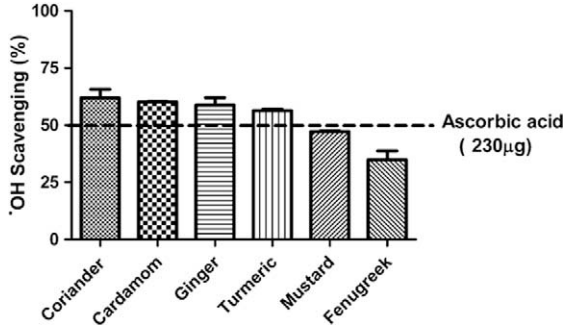

Fig. 2b. The ·OH radical-scavenging activity of spices extracts. The absorbance values were converted to the scavenging effect (%) and data plotted as the means of the replicate scavenging effect (%) values ± S.D. (n = 3).

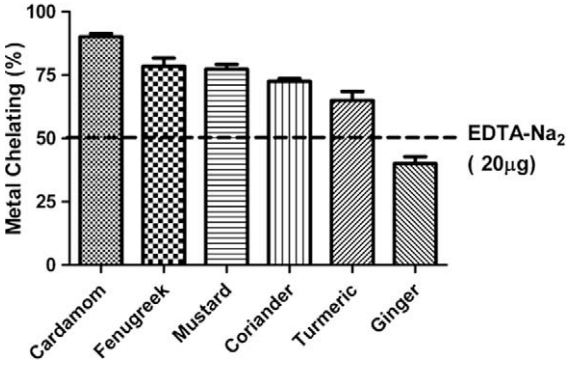

Fig. 2c. Fe^{2+}-chelating activity of spices extracts. The absorbance values were converted to the scavenging effect (%) and data plotted as the means of the replicate chelating effect (%) values ± S.D. (n = 3).

In vitro antioxidant assays performed to establish a relation between thiol levels and the antioxidant abilities did not show a thiol dependent effect. As most of the antioxidant abilities are attributed to the phenolic content of the samples, an experiment was performed to see if the antioxidant abilities measured were directly related to the levels of the phenols present in the extracts. It was observed that the antioxidant properties were independent of the phenolic content. Recent studies have also shown that many flavanoids and polyphenols contribute significantly to the total antioxidant activity in fruits and vegetables (Luo, Basile, & Kennelly, 2002). Although mustard extract showed the highest phenolic content as seen in Fig. 2d, none of the antioxidant studies showed a

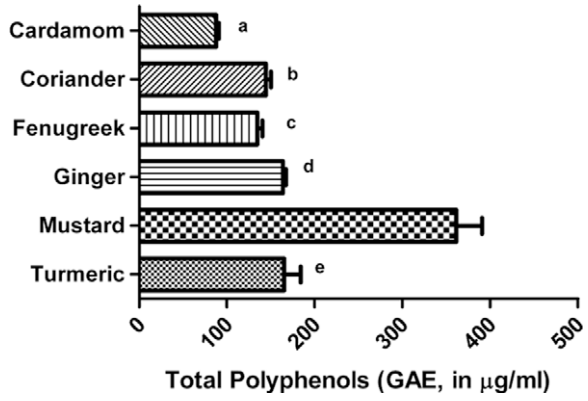

Fig. 2d. Polyphenol content of water extracts from spices. Total polyphenol content is expressed in gallic acid equivalents (GAE). Mean values ± S.D. followed by different letters are significantly different (p < 0.05).

predominant effect of mustard due to its phenolic content. It can be concluded from these studies that the antioxidant abilities of spices observed in this present study may not only be a result of the phenolic content of the spices, but may also be attributed to the presence of other potent antioxidants like thiols and flavanoids.

The findings of the present study suggest that spices can be a significant source of thiols and, along with the phenols present, can enhance the antioxidant status of the biological system. The high levels of thiols observed in some spices may reinforce the idea that incorporation of spices into everyday meals may be very beneficial, and could promote good health by protecting against oxidative stress related problems.

Acknowledgements

Dr. Ercal was supported by R15DA023409-01A2 from the NIH and the contents of this paper are solely the responsibility of the authors and do not necessarily represent official views of NIH. The authors would like to thank Barbara Harris for carefully editing this manuscript.

References

Ahmed, R. S., Seth, V., & Banerjee, B. D. (2000). Influence of dietary ginger (*Zingiber officinales* Rosc) on oxidative stress induced by malathion in rats. *Food and Chemical Toxicology, 38*, 443–450.

Ajith, T. A., Nivitha, V., & Usha, S. (2007). *Zingiber officinale* roscoe alone and in combination with alpha-tocopherol protect the kidney against cisplatin-induced acute renal failure. *Food and Chemical Toxicology, 45*, 921–927.

Amin, A., & Hamza, A. A. (2006). Effects of roselle and ginger on cisplatin-induced reproductive toxicity in rats. *Asian Journal of Andrology, 8*, 607–612.

Anuradha, C. V., & Ravikumar, P. (1998). Anti-lipid peroxidative activity of seeds of fenugreek (*Trigonella foenum graecum*). *Medical Science Research, 26*, 317–321.

Bowman, G., Backer, U., Larsson, S., Melander, B., & Whalander, L. (1983). Oral acetylcysteine reduces exacerbation rate in chronic bronchitis; report of a trial organized by the Swedish Society for Pulmonary Diseases. *European Journal of Respiratory Diseases, 63*, 405–415.

Cheng, Z. J., Kuo, S. C., Chan, S. C., Ko, F. N., & Teng, C. M. (1998). Antioxidant properties of butein isolated from *Dalbergia odorifera*. *Biochimica et Biophysica Acta, 1392*, 291–299.

Demirkol, O., Adams, C., & Ercal, N. (2004). Biologically important thiols in various vegetables and fruits. *Journal of Agricultural Food Chemistry, 52*, 8151–8154.

Dickinson, D. A., Iles, K. E., Zhang, H., Blank, V., & Forman, H. J. (2003). Curcumin alters EpRE and AP-1 binding complexes and elevates glutamate-cysteine ligase gene expression. *FASEB Journal, 17*, 473–475.

Gülçin, I., Büyükokuroglu, M. E., & Küfrevioglu, Ö. I. (2003). Metal chelating and hydrogen peroxide scavenging effects of melatonin. *Journal of Pineal Research, 34*, 278–281.

Halliwell, B. (1991). Reactive oxygen species in living systems: Source, biochemistry, and role in human disease. *American Journal of Medicine, 91*, 14–22.

Halliwell, B., & Gutterbridge, J. M. C. (1989). *Free radicals in biology and Medicine* (3rd ed.) (pp. 18–28). Clarendron Press: Oxford.

Hsu, B., Coupar, I. M., & Ng, K. (2006). Antioxidant activity of hot water extract from the fruit of the Doum palm, *Hyphaene thebaica*. *Food Chemistry, 98*, 317–328.

Jones, D. P., Coates, R. J., Flagg, E. W., Eley, J. W., Block, G., Greenberg, R. S., et al. (1992). Glutathione in foods listed in the National Cancer Institute's Health Habits and History Food Frequency Questionnaire. *Nutrition and Cancer, 17*, 57–75.

Kappus, H. (1986). Overview of enzyme systems involved in bio-reduction of drugs and redox cycling. *Biochemical Pharmacology, 35*, 1–6.

Kikuzaki, H., & Nakatani, N. (1993). Antioxidant effects of some ginger constituents. *Journal of Food Science, 55*, 2337–2340.

Luo, X. D., Basile, M. J., & Kennelly, E. J. (2002). Polyphenolic antioxidants from the fruits of *Chrysophyllum crinito* L. (star apple). *Journal of Agricultural and Food Chemistry, 50*, 1379–1382.

Meister, A., & Anderson, M. E. (1983). Glutathione. *Annual Review of Biochemistry, 52*, 711–760.

Modak, M., Dixit, P., Londhe, J., Ghaskadbi, S., Paul, A., & Devasagayam, T. (2007). Indian herbs and herbal drugs used for the treatment of diabetes. *Journal of Clinical Biochemistry and Nutrition, 40*, 163–173.

Ordonez, A. A. L., Gomez, J. D., Vattuone, M. A., & Isla, M. I. (2006). Antioxidant activities of *Sechium edule* (Jacq) Swartz extracts. *Food Chemistry, 97*, 452–458.

Prescott, L. F., & Critchley, J. A. (1983). The treatment of acetaminophen poisoning. *Annual Reviews of Pharmacology and Toxicology, 23*, 87–191.

Ringman, John M., Frautschy, Sally A., Cole, Gregory M., Masterman, Donna L., & Cummings, Jeffrey L. (2005). Potential role of the curry spice curcumin in Alzheimer's disease. *Current Alzheimer's Research, 2*, 131–136.

Ross, D. (1989). Mechanistic toxicology: A radical perspective. *Journal of Pharmacy and Pharmacology, 41*, 505–511.

Sen, C. K., & Packer, L. (2000). Thiol homeostasis and supplements in physical exercise. *American Journal of Clinical Nutrition, 72*, 653S–695S.

Sies, H. (1985). Oxidative stress. Introductory remarks. In H. Sies (Ed.), *Oxidative stress* (pp. 1–8). London: Academic press.

Smirnoff, N., & Cumbes, Q. J. (1989). Hydroxyl radical scavenging activity of compatible solutes. *Phytochemistry, 28*, 1057–1060.

Stoecker, R., & Frei, B. (1991). Endogenous antioxidant defences in human plasma. In H. Siehs (Ed.), *Oxidative stress: Oxidants and antioxidants* (pp. 213–243). London: Academic Press.

Winters, R., Zukowski, J., Ercal, N., Matthews, R. H., & Spitz, D. R. (1995). Analysis of glutathione, glutathione disulfide, cysteine, homocysteine, and other biological thiols by high-performance liquid chromatography following derivatization by N-(1-pyrenyl) maleimide. *Analytical Biochemistry, 227*, 14–21.

Wlodek, L. (2002). Beneficial and harmful effects of thiols. *Polish Journal of Pharmacology, 54*, 215–223.

Yadav, A. S., & Bhatnagar, D. (2007). Modulatory effect of spice extracts on iron-induced lipid peroxidation in rat liver. *Biofactors, 29*, 147–157.

Food Chemistry 118 (2010) 594–601

Contents lists available at ScienceDirect

Food Chemistry

journal homepage: www.elsevier.com/locate/foodchem

Effects of drying methods and conditions on release characteristics of edible chitosan films enriched with Indian gooseberry extract

Pornpimon Mayachiew, Sakamon Devahastin *

Department of Food Engineering, Faculty of Engineering, King Mongkut's University of Technology Thonburi, 126 Pracha u-tid Road, Tungkru, Bangkok 10140, Thailand

ARTICLE INFO

Article history:
Received 13 January 2009
Received in revised form 31 March 2009
Accepted 13 May 2009

Keywords:
Active packaging
Fourier-transform infrared spectroscopy
Functional group interaction
Hot air drying
Low-pressure superheated steam drying
Natural antioxidant
Swelling
Total phenolic content
Vacuum drying

ABSTRACT

The present work was aimed at studying the effects of drying methods and conditions (i.e., ambient drying, hot air drying at 40 °C, vacuum drying and low-pressure superheated steam drying within the temperature range of 70–90 °C at an absolute pressure of 10 kPa), as well as the concentration of Indian gooseberry extract, (added to edible chitosan film-forming solution as a natural antioxidant, at concentrations of 1, 2 and 3/100 g), on the residual total phenolic content (TPC) of the films. The swelling and release behaviour of TPC from the films were also studied. Drying methods and conditions were found to have significant effects on the percentage of residual TPC. The release characteristics, swelling and functional group interaction of the antioxidant films, as assessed by Fourier-transform infrared (FTIR) spectroscopy, were found to be affected by the drying methods and conditions, as well as the concentration of the Indian gooseberry extract.

1. Introduction

Edible films have recently received increased attention due to their various advantages including biodegradability and edibility. Among many materials that can be used to form edible films, chitosan (β-(1,4)-2-amino-2-deoxy-D-glucose) is one of the most promising as it has a good film-forming ability, which makes it suitable for use as a food packaging. Many investigators have evaluated chitosan films for many food-related applications (Han, Zhao, Leonard, & Traber, 2004; Sebti, Martial-Gros, Carnet-Pantiez, Grelier, & Coma, 2005). To make edible films even more useful, functional edible films that contain active agents have been developed, to enhance food quality and product shelf-life (Suppakul, Miltz, Sonneveld, & Bigger, 2003).

Chitosan can be easily formed into films by a casting/solvent evaporation technique. Different drying methods and conditions have been used to prepare chitosan films. Numerous researchers prepared chitosan films by drying them at ambient temperature (Caner, Vergano, & Wiles, 1998; Hwang, Kim, Jung, Cho, & Park, 2003; Wiles, Vergano, Barron, Bunn, & Testin, 2000); other researchers prepared chitosan films by oven drying (Butler, Vergano, Testin, Bunn, & Wiles, 1996) or infrared drying (Srinivasa, Ramesh, Kumar, & Tharanathan, 2004). Recently, Mayachiew and Devahastin (2008a) investigated the influences of different drying methods and conditions on the drying kinetics and various properties of chitosan films. Drying at control conditions (ambient air drying and hot air drying at 40 °C) were compared with vacuum drying and low-pressure superheated steam drying (LPSSD) at an absolute pressure of 10 kPa and different drying temperatures (70, 80, and 90 °C). The properties of chitosan films, in terms of colour, tensile strength, percent elongation, water vapour permeability (WVP), glass transition temperature (T_g) and degree of crystallinity were determined. In terms of the drying kinetics, the drying methods were found to have a significant effect on the rates of moisture reduction of the samples. Vacuum drying and LPSSD required much shorter drying time than did ambient and hot air drying at 40 °C. In terms of properties it was found that LPSSD at 70 °C led to films with higher tensile strength and percent elongation than the films prepared by other drying methods and under other drying conditions. Ambient dried and LPSSD films had more crystallinity than the films dried by vacuum drying.

In terms of active agents that can be incorporated into films, plant extracts have recently received much attention and have a tendency of replacing synthetic agents. Generally, plant extracts which contain high concentrations of phenolic compounds possess strong antioxidant properties. Indian gooseberry (*Phyllanthus emblica* Linn.), or "Ma-khaam Pom" in Thai, is one of the most

* Corresponding author. Tel.: +66 2 470 9244; fax: +66 2 470 9240.
E-mail address: sakamon.dev@kmutt.ac.th (S. Devahastin).

0308-8146/$ - see front matter © 2009 Elsevier Ltd. All rights reserved.
doi:10.1016/j.foodchem.2009.05.027

often-used herbs and is widely available in most tropical and subtropical countries. Indian gooseberry has been shown to possess high antioxidant activity *in vitro* (Mayachiew & Devahastin, 2008b).

Recently, many antioxidant edible films have been developed to reduce oxidation in packed foods (Gómez-Estaca, Bravo, Gómez-Guillén, Alemán, & Montero, 2009; Han & Krochta, 2007; Oussalah, Caillet, Salmiéri, Saucier, & Lacroix, 2004). For example, Oussalah et al. (2004) studied the use of milk protein-based films containing essential oils for the preservation of whole beef muscle. Films incorporated with oregano stabilised lipid oxidation in beef muscle samples, while films incorporated with pimento possessed the highest antioxidant activity. Gómez-Estaca et al. (2009) investigated the antioxidant properties of gelatin-based edible films containing oregano or rosemary aqueous extracts. It was found that the films supplemented with antioxidant extracts exhibited higher reducing ability and free radical-scavenging capacity than the control films; the degree of antioxidant power was generally proportional to the amount of the added extract.

For functional edible films, controlled release of active agents from the films to food is important, since there is a need to maintain the concentration of active compounds in packed food (Buonocore, Del Nobile, Panizza, Corbo, & Nicolais, 2003). Although many studies have been made on the effects of many parameters on the release of active agents from many types of films (Jeon, Park, Kwak, Lee, & Park, 2007; Tovar, Salafranca, Sánchez, & Nerín, 2005), the effects of drying methods and conditions used to prepare functional edible films, in particular chitosan films, on the retention and release characteristics of added antioxidant compounds have not been well established. The objectives of this study were therefore to investigate the effects of drying methods (i.e., ambient-temperature drying, hot air drying, vacuum drying, low-pressure superheated steam drying) and conditions on the total phenolic content (TPC) of chitosan films incorporated with Indian gooseberry extract. A study of the release behaviour of the antioxidant compound from the films was also conducted. Fourier-transform infrared (FTIR) spectroscopy was performed to investigate functional group interaction between chitosan and added active agent. Swelling of the films was also measured, to help explain the release behaviour of the films.

2. Materials and methods

2.1. Materials

Chitosan (molecular weight of 900,000 Da and degree of deacetylation of 90.2%) was obtained from S.K. Profishery Co., Ltd. (Bangkok, Thailand). Glycerol was purchased from Carlo Erba (Val de Reuil, Italy) while acetic acid was obtained from Merck (Darmstadt, Germany). Folin–Ciocalteu reagent, sodium carbonate and absolute ethyl alcohol were purchased from Carlo Erba (Vigevano, Italy).

2.2. Preparation of chitosan solution

Chitosan solution (1.5% w/v) was prepared by dissolving chitosan in 1% (v/v) acetic acid under constant stirring at 300 rpm using a magnetic stirrer (Framo®-Gerätechnik, model M21/1, Eisenbach, Germany) at room temperature for 24 h. Glycerol 25% (w/w chitosan) was then added into the chitosan solution; stirring was continued at room temperature for 1 h. After mixing the solution was centrifuged for 15 min at 12,400 rpm using a refrigerated centrifuge (Hitachi, model Himac CR21, Ibaragi, Japan) to remove undissolved impurities and bubbles in the solution.

2.3. Preparation of Indian gooseberry extract

To prepare Indian gooseberry extract, Indian gooseberry powder (10 g dry basis), dried by a tray dryer at 40 °C with particle size between 125–425 μm, was extracted with 50 ml of 95% (v/v) ethanol (Ahmad, Mehmood, & Mohammad, 1998). The extract was filtered through a filter paper (Ø110 mm, Cat. no. 1001 110, Schleicher and Schuell GmbH, Dassel, Germany); the filtrate was collected and concentrated using a rotary evaporator (Resona Technics, Labo Rota 300, Gossau, Switzerland) at 40 °C for 10 min and kept at 4 °C in a dark bottle until use. For a detailed preparation method the reader is referred to Mayachiew and Devahastin (2008b).

2.4. Preparation of antioxidant chitosan films

Indian gooseberry extract was added to the chitosan solution at concentrations of 1, 2 and 3/100 g. The concentration of the extract was varied since it was hypothesised that different concentrations of the extract might lead to different polymer structure modification, which would in turn affect the release behaviour of the active compound. All mixtures were homogenised by a bench top homogeniser (Ika® Works (Asia), Model T 25 basic, Selangor, Malaysia) at 9500 rpm for 2 min. The film solution (21 g) was poured onto an acrylic plate with dimensions of 13 × 10 cm to cast an antioxidant film. Drying of the film was performed by four methods, which were ambient air drying, hot air drying at 40 °C, and vacuum drying and low-pressure superheated steam drying (LPSSD) at 10 kPa, both at 70, 80 and 90 °C following the procedures of Mayachiew and Devahastin (2008a). After drying the film was conditioned for at least 48 h in a desiccator containing saturated salt solution of magnesium nitrate (Ajax Finechem, Seven Hills, Australia), which produced a relative humidity (RH) of 53%.

2.5. Determination of total phenolic content of films

The total phenolic content (TPC) of the antioxidant film was evaluated by an elution technique described by Zhang and Kosaraju (2007) with some modification. A portion of the film (0.5 g; 2 × 2 cm) was placed in 50 ml of 0.1 M NaOH and shaken with an environmental incubator shaker (New Brunswick Scientific, Model G-24, Edison, NJ) at room temperature for 48 h. The sample was then taken to determine the TPC, using Folin–Ciocalteu reagent (Zhou & Yu, 2006). The reaction mixture contained 50 μl of the eluted sample, 250 μl of the Folin–Ciocalteu reagent, 0.75 ml of 20 g/100 ml sodium carbonate and 3 ml of pure water. After 2 h of reaction at ambient temperature the absorbance at 765 nm was measured using a Shimadzu UV-2101 spectrophotometer (Shimadzu Scientific Instruments, Kyoto, Japan); the absorbance was used to calculate the TPC, using gallic acid as a standard. The results were presented in terms of the percentage of residual TPC. The percentage of residual TPC was calculated according to the following equation:

$$\%\ \text{Residual TPC} = 100 \times \left(\frac{\text{Mass of dried sample} \times (\text{conc. of TPC in dried sample})}{\text{Mass of film solution} \times (\text{conc. of TPC in film solution})}\right) \quad (1)$$

where the mass of dried sample is the mass of the sample after a drying procedure has been applied.

2.6. Release of antioxidant agent from films

A release test was conducted in an environmental incubator shaker at room temperature. A film (2 × 2 cm) was placed in a bea-

ker containing 100 ml of distilled water. The solution sample was taken out at 15 min intervals until 1 h and every 1 h afterward, to determine the TPC of the solution in order to follow the release kinetics of the antioxidant from the film. The release result was reported in terms of the percentage of release of TPC:

$$\%\ \text{Released TPC}_t = 100 \times \frac{\text{TPC}_t}{\text{TPC}_0}. \quad (2)$$

where TPC_0 is the amount of TPC after drying, TPC_t is the amount of release of TPC at any time.

2.7. FTIR analysis

Attenuated total reflection/Fourier-transform infrared spectroscopic (ATR/FTIR) spectra were collected at 25 °C by coupling the ATR accessory to an FTIR spectrometer (Perkin–Elmer Inc., Model 1760X, Norfolk, CT) available at Chulalongkorn University, Bangkok. Time-resolved experiments were collected by averaging, depending on the experiment, 10 or 2 scans at 4 cm^{-1} spectral resolution at various time intervals.

2.8. Swelling of antioxidant films

A film was cut into sizes of 2 × 2 cm and dried in a vacuum oven (Sanyo, Model Gallenkamp/OM-09980, Loughborough, UK) at 70 °C at an absolute pressure of 100 mbar for 24 h. The film was weighed and left at ambient temperature in 30 ml of distilled water for 24 h. The film was then blotted with a tissue paper and the mass of the film was measured periodically with a microbalance (Sartorius, Model RC 250S, Göttingen, Germany) until equilibrium was reached. The degree of swelling was evaluated using Eq. (3):

$$\text{Degree of swelling} = 100 \times \left(\frac{\text{Mass of film (g)} - \text{Mass of dried film (g)}}{\text{Mass of dried film (g)}}\right) \quad (3)$$

2.9. Statistical analysis

All data were subjected to analysis of variance (ANOVA) using SPSS® software (Chicago, IL) and were presented as mean values with standard deviations. Differences between mean values were established using Duncan's multiple range tests at a confidence level of 95%. All experiments were performed in duplicate except where stated otherwise.

3. Results and discussion

3.1. Total phenolic content of antioxidant films

Phenolic compounds in plants have high antioxidant activities, mainly due to redox properties, which include free radical-scavenging, hydrogen-donating and singlet oxygen-quenching. Mayachiew and Devahastin (2008b) reported that Indian gooseberry extract had high antioxidant activity *in vitro* and that phenolics were the main compounds of the extract.

Table 1 shows the percentage of residual TPC of chitosan films incorporated with various concentrations of Indian gooseberry extract and prepared by different drying methods and conditions; the drying time to reach the desired final film moisture content of 14% (d.b.) is listed in Table 2. Indian gooseberry extract concentration did not seem to have any significant effect on the percentage of residual TPC. However, antioxidant films incorporated with higher concentrations of the extract showed higher intensity of absorption peaks at 1250, 1620 and 1720 cm^{-1} and lower intensity of absorption peak at 1566 cm^{-1} (Fig. 4), indicating more intermolecular interaction between chitosan film and Indian gooseberry extract when the concentration of the added extract increased.

Table 1
Percentage of residual total phenolic content of antioxidant films prepared by different drying methods and conditions.

Drying method	Indian gooseberry extract concentration		
	1%	2%	3%
Ambient drying	97.90 ± 1.88[a]	98.18 ± 1.32[a]	98.67 ± 0.49[a]
Hot air drying	96.54 ± 2.20[a]	96.50 ± 1.08[a]	96.68 ± 1.07[a]
Vacuum drying			
70 °C	84.78 ± 1.59[c]	85.65 ± 0.60[bc]	85.36 ± 0.49[c]
80 °C	81.65 ± 1.13[d]	81.83 ± 1.20[de]	82.69 ± 1.07[d]
90 °C	76.58 ± 1.24[e]	77.18 ± 1.08[f]	77.47 ± 0.66[f]
LPSSD			
70 °C	87.82 ± 1.81[b]	86.42 ± 0.72[b]	87.76 ± 0.33[b]
80 °C	83.81 ± 1.59[c]	84.72 ± 0.48[cd]	84.44 ± 1.40[c]
90 °C	79.65 ± 1.59[de]	80.15 ± 0.96[e]	80.39 ± 0.74[e]

Values in the same column with different superscripts mean that the values are significantly different ($p < 0.05$).

Table 2
Drying time to reach final moisture content of 14% (d.b.).

Drying method	Indian gooseberry extract concentration		
	1%	2%	3%
Ambient drying	52 h	50 h	47 h
Hot air drying	17 h	16 h	15 h
Vacuum drying			
70 °C	85 min	84 min	84 min
80 °C	65 min	64 min	64 min
90 °C	60 min	59 min	59 min
LPSSD			
70 °C	130 min	129 min	129 min
80 °C	95 min	94 min	94 min
90 °C	90 min	89 min	89 min

Regarding the effects of drying methods and conditions, it was noted that drying methods and conditions had significant effects on the percentage of residual TPC of the films. It was found that ambient dried films had the highest residual TPC. The higher losses of TPC were observed for films dried by vacuum drying and LPSSD; LPSSD films had slightly higher residual TPC than the vacuum-dried films, however. This may be due to the fact that the film temperature increased more rapidly and stayed at higher levels in the case of vacuum drying, thus inducing more thermal degradation of TPC compared with the LPSSD films (Mayachiew & Devahastin, 2008a). The temperature of the vacuum-dried films increased more rapidly than that of the LPSSD films, due to the fact that the electric heater was used more often during vacuum drying, since it was the only source of energy for drying. This might increase the amount of radiation absorbed by the film surfaces. The constant rate drying periods of vacuum-dried films were also shorter than those of LPSSD films. These are typical comparative characteristics of vacuum drying and LPSSD (Devahastin, Suvarnakuta, Soponronnarit, & Mujumdar, 2004).

Higher drying temperatures led to a lower percentage of residual TPC in both vacuum-dried films and LPSSD films. The antioxidant films prepared by LPSSD at 70 °C had the highest percentage of residual TPC, compared with films prepared at other conditions of LPSSD and vacuum drying. It is indeed well recognised that thermal treatment induces degradation of phenolic compounds (Chan et al., 2009; Guan, Cenkowski, & Hydamaka, 2005; Larrauri, Rupérez, & Saura-Calixto, 1997). The minimum percentage of residual TPC was found in the case of chitosan film incorporated with 1% Indian gooseberry extract and prepared by vacuum

drying at 90 °C. The presence of oxygen in the case of ambient and low-temperature hot air drying did not seem to have any significant effect on the percentage of residual TPC.

3.2. Release of antioxidant agent from films

Figs. 1–3 show the evolution of the percentage of release of TPC from antioxidant films prepared by different drying methods and conditions. At the same concentration of Indian gooseberry extract antioxidant chitosan films prepared by ambient drying, hot air drying and LPSSD at 70 °C showed the highest percentage of release of TPC; the release was lowest in the case of the films prepared by vacuum drying at 90 °C. This might be due to the different intermolecular interactions between the extract and chitosan films (as shown by the results of FTIR spectra in Section 3.3), the microstructure of the films, as well as different degrees of film swelling. The results on film swelling will be discussed in further detail in Section 3.4.

It can be seen in Fig. 1 that the percentage of TPC released from chitosan films incorporated with 1% (w/w) Indian gooseberry extract prepared by ambient drying, hot air drying and LPSSD at 70, 80 and 90 °C reached 92%, 90%, 87%, 84% and 79% within 24 h, respectively. The percentage of TPC released from vacuum-dried films at 70, 80 and 90 °C at 24 h was approximately 86%, 81% and 75%, respectively. TPC was released from LPSSD films faster than from vacuum-dried films prepared at the same temperature. The same trends were found in the cases of chitosan films incorporated with 2% and 3% (w/w) Indian gooseberry extract (see Figs. 2 and 3).

Regarding the effect of Indian gooseberry extract concentration, the percentage of antioxidant released decreased when the Indian gooseberry extract concentration increased. Chitosan films incorporated with 3% (w/w) Indian gooseberry extract had lower percentage of antioxidant release than the films incorporated with 1% and 2% extract. This might also be due to the effect of higher intermolecular interaction.

The release profiles of the antioxidant films could be separated into two parts. During an initial period (0–8 h), the release profiles were generally non-linear; the release of TPC was rapid at first and then slowed down with an increase in time. However, the release profiles of the films incorporated with 1% Indian gooseberry extract were linear within 2 h, which might be due to the fact that the films required a shorter time to become fully hydrated, as shown later by a higher degree of swelling; the rapid release of TPC from the films was thus attributed to the rapid swelling of the films in distilled water.

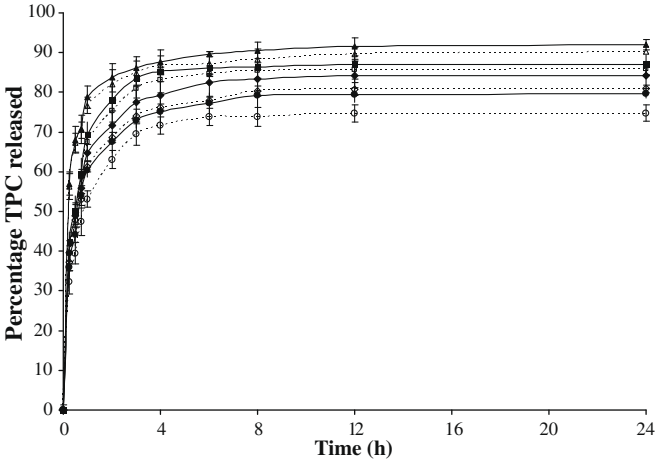

Fig. 1. Percentage of release of TPC from chitosan films enriched with 1% (w/w) Indian gooseberry extract and prepared by ambient drying (—▲—); hot air drying at 40 °C (---△---); LPSSD at 70 °C (—■—), 80 °C (—◆—), 90 °C (—●—); vacuum drying at 70 °C (---□---), 80 °C (---◇---), 90 °C (---○---).

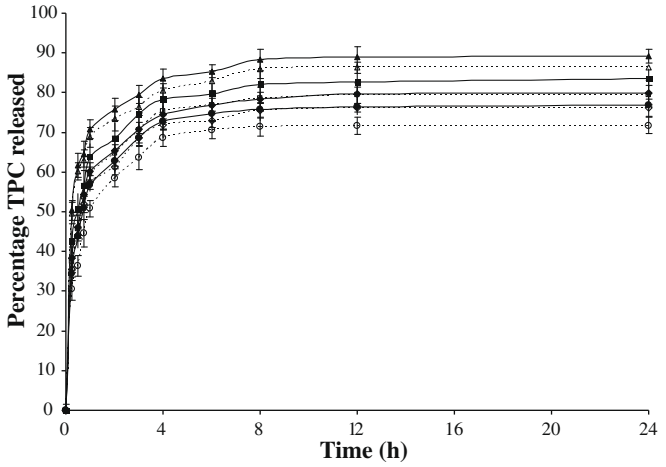

Fig. 2. Percentage of release of TPC from chitosan films enriched with 2% (w/w) Indian gooseberry extract and prepared by ambient drying (—▲—); hot air drying at 40 °C (---△---); LPSSD at 70 °C (—■—), 80 °C (—◆—), 90 °C (—●—); vacuum drying at 70 °C (---□---), 80 °C (---◇---), 90 °C (---○---).

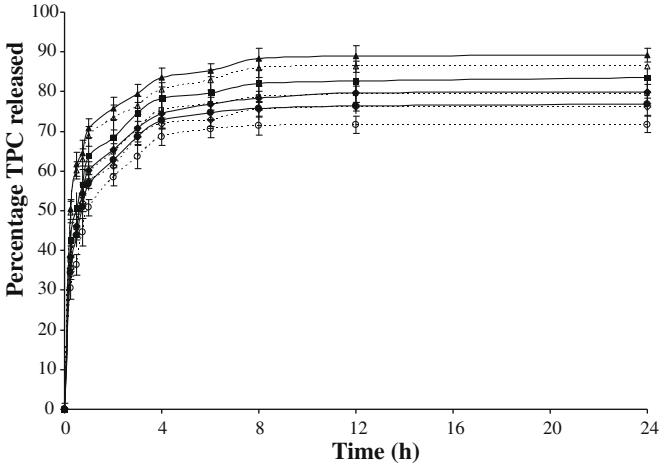

Fig. 3. Percentage of release of TPC from chitosan films enriched with 3% (w/w) Indian gooseberry extract and prepared by ambient drying (—▲—); hot air drying at 40 °C (---△---); LPSSD at 70 °C (—■—), 80 °C (—◆—), 90 °C (—●—); vacuum drying at 70 °C (---□---), 80 °C (---◇---), 90 °C (---○---).

In the second period (8–24 h) the release was rather constant. The constant rate of release might be due to the interaction of the extract with the chitosan matrix. Popa, Aelenei, Popa, and Andrei (2000) studied the interaction between chitosan and polyphenols extracted from spruce wood bark and found that chitosan and polyphenols formed a complex and that the release of polyphenols followed a two-step process as well.

Chitosan might interact with phenolic compounds of Indian gooseberry extract, mainly by weak interactions such as hydrogen bonding. Hydroxyl groups of phenolics could form H-bonds with NH_3^+ of chitosan (Kanatt, Chander, & Sharma, 2008). Moreover, the amine groups probably also contributed to ionic interactions with carboxylic groups of acid phenols (Spagna et al., 1996). These bound fractions could affect the release of phenolic compounds. On the other hand, phenolics retention might be achieved through strong covalent bonds (Popa et al. 2000).

3.3. FTIR analysis of antioxidant films

3.3.1. Effect of antioxidant agent

The interaction between chitosan and the extract was characterised by FTIR analysis. Fig. 4 shows the transmission infrared spectra of the chitosan films enriched with different concentrations of Indian gooseberry extract and prepared by ambient drying. Pure chitosan film had characteristic bands at 1631 cm^{-1} (amide I band) and 1566 cm^{-1} (amide II vibration). The present FTIR spectra are similar to the results described by many studies (Pranoto, Rakshit, & Salokhe, 2005; Ritthidej, Phaechamud, & Koizumi, 2002). Chitosan films showed a symmetric carboxylate anion stretching at 1413 cm^{-1}, indicating free chitosan films (Puttipipatkhachorn, Nunthanid, Yamamoto, & Peck, 2001).

When chitosan films were incorporated with Indian gooseberry extract, changes in FTIR spectra were noted. The spectra of antioxidant films exhibited small modifications of the positions of some bands within the range 1500–1700 cm^{-1}, which are related to amine and carbonyl groups. The new absorption peak at 1620 cm^{-1} (amide I band) was shifted from 1631 cm^{-1}. In addition, the peak was sharper with an increase in the extract concentration, indicating more interaction between chitosan and the extract. Pasanphan and Chirachanchai (2008) reported that chitosan could form a linkage with phenolic compounds, such as gallic acid, *via* an amide linkage, which is shown as the absorption peak at 1620 cm^{-1}.

Another important change was found as new peaks at 1720 cm^{-1}, indicating an ester linkage, which could be attributed to the more intensive interaction between chitosan and Indian gooseberry extract. However, the peak intensity at 1566 cm^{-1}, which is attributed to the amine group ($-NH_2$) of chitosan, decreased. The loss of this peak might be due to the interaction of the amine group with a functional group of the extract. In addition, the peak at 1250 cm^{-1}, which corresponds to C–O stretching of the phenol compounds, was stronger with an increase in the concentration of the extract.

Structurally, phenolics are compounds consisting of aromatic rings bonded to one or more hydroxyl substituents and range from simple phenolic molecules to highly polymerised compounds. Phenolic compounds are naturally present as conjugates with polysaccharides, linked to one or more of the phenolic groups and may also occur as functional derivatives such as esters (Balasundram, Sundram, & Samman, 2006). Therefore, chitosan could bind with phenolics when Indian gooseberry extract was incorporated into films.

3.3.2. Effects of drying methods and conditions

The effects of drying methods and conditions on functional group interaction were also investigated. The IR spectra of chitosan films enriched with 2% (w/w) Indian gooseberry extract and prepared by vacuum drying and LPSSD at 70 and 90 °C were compared with those of the film prepared at ambient conditions. It is seen in Fig. 5 that drying methods and conditions had some effects on the IR spectra. Antioxidant films prepared by LPSSD and vacuum drying showed stronger peak intensity of the amide linkage at 1620 cm^{-1} than did ambient dried film. However, LPSSD led to films of lower intermolecular interaction, which was shown by the lower peak intensity of the amide linkage at 1620 cm^{-1}, relative to that from vacuum drying. Drying led to intermolecular interaction in the films, which was shown by the alteration of the peak intensity at 1620 cm^{-1}.

The percentage of release of TPC decreased, due probably to an increase in the intermolecular interaction. The antioxidant film

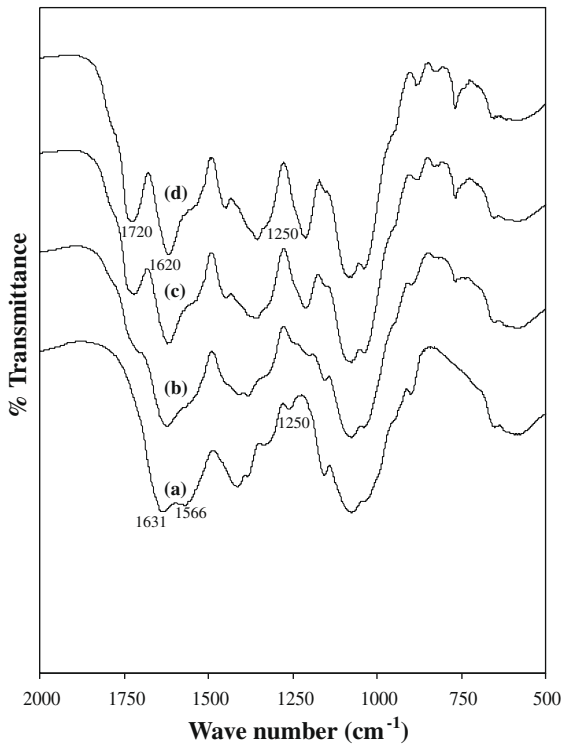

Fig. 4. FTIR spectra of ambient dried films with different concentrations of Indian gooseberry extract: (a) with no extract, (b) with 1% (w/w) Indian gooseberry extract, (c) with 2% (w/w) Indian gooseberry extract, (d) with 3% (w/w) Indian gooseberry extract.

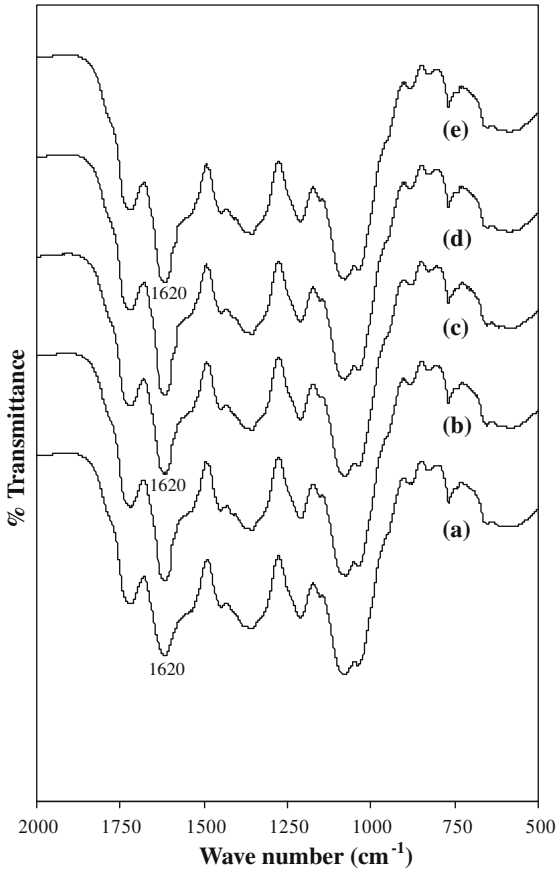

Fig. 5. FTIR spectra of chitosan films enriched with 2% (w/w) of Indian gooseberry extract prepared using different drying methods and conditions: (a) ambient drying, (b) vacuum drying at 70 °C, (c) LPSSD at 70 °C, (d) vacuum drying at 90 °C and (e) LPSSD at 90 °C.

dried by vacuum drying at 90 °C exhibited the lowest percentage of release of TPC and showed a different release profile compared with the film prepared by ambient drying. This may be due to the high intermolecular interaction between chitosan and phenolic compounds, such as gallic acid, in Indian gooseberry extract via amide linkage, which was shown by an absorption peak at 1620 cm^{-1} (Pasanphan & Chirachanchai, 2008). Muzzarelli and Muzzarelli (2005) reported that amidation, which was shown by the absorption peak at 1620 cm^{-1}, might lead to a decrease in swelling of the heat-treated films, resulting in the lower percentage of antioxidant release.

Regarding the effect of the drying temperature on intermolecular interaction, it was found that the peaks at 1620 cm^{-1} of the films dried at 90 °C were slightly sharper than those of the films dried at 70 °C. This might be due to the fact that the higher temperature induced more interchain crosslinkage, which involves NH_2 group with amide formation (Lim, Khor, & Ling, 1999). Ritthidej et al. (2002) reported that longer time of heat treatment led to a stronger peak intensity of amide I band. Higher intermolecular interaction due to the use of higher drying temperature might thus lead to the lower percentage of release of TPC mentioned earlier in Section 3.2. Lower percentage of release of TPC was observed for both LPSSD and vacuum-dried films.

Suppakul et al. (2003) indeed stated that different interactions between an active agent and chitosan had an effect on the release of the active agent from the film. Drying methods and conditions may thus be used to engineer chitosan films for controlled release applications.

3.3.3. FTIR of films after release study

FTIR spectroscopy was performed to determine the characteristics of the film matrix as well as the changes of the intermolecular interaction both before and after the release study. By considering the IR spectra of chitosan film enriched with 2% (w/w) Indian gooseberry extract prepared by ambient drying both before and after release study (Fig. 6) it was found that the polymer signal diminished when the film was in contact with water because of the sorption of moisture and subsequent film swelling (Lagaron, Fernandez-Saiz, & Ocio, 2007).

It was also found that the film after the release study exhibited a drop of the relative peak intensities at 1250, 1620 and 1720 cm^{-1}, indicating a decrease in the interaction of active agent with the film. The changes of the peak intensity could be due to the loss of active agent linkage with the chitosan matrix after being released into the liquid phase. It was indeed shown by the release profiles in Figs. 1–3 that the percentage of release of TPC from the films increased with time.

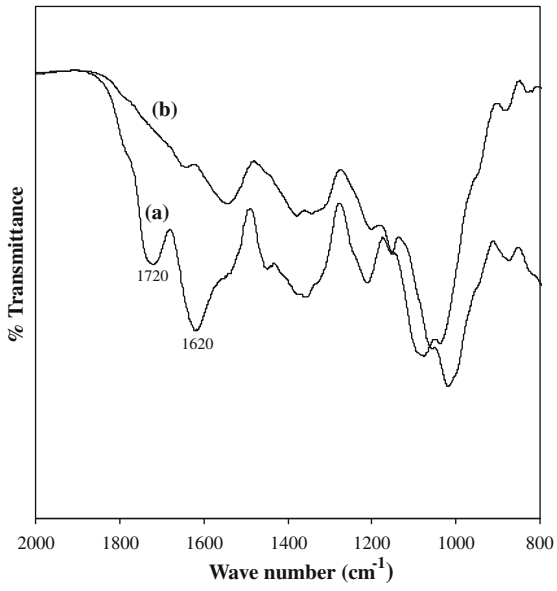

Fig. 6. FTIR spectra of chitosan films enriched with 2% (w/w) Indian gooseberry extract: (a) before release and (b) after release.

The peak remaining after release might be due to the interaction of the extract with the chitosan matrix, which was shown by the constant rate of release in the second period (8–24 h) of release study in Section 3.2. After the release study the film still retained some of the polymer signals, which indicated that part of the film still remained intact, as also observed visually.

3.4. Swelling of antioxidant films

The water resistance of films was measured in terms of swelling as shown in Table 3. It was observed that the swelling ability of antioxidant films was affected by the extract concentration. Swelling of pure chitosan film prepared at ambient conditions was around 173%, a value which is similar to that of Yao et al. (1996). The high value of swelling is due to the hydrophilic characteristic of chitosan. Nevertheless, from our observation, the films did not break apart even after the swelling study.

Swelling of the films was reduced when the films were incorporated with the extract. Although chitosan has hydrophilic groups, such as carboxylic groups, in its structure and these groups could easily interact with water, resulting in swelling of the films, upon being enriched with the extract intermolecular interaction between chitosan and the extract developed and this resulted in a decrease in the film swelling. In addition, a lower level of swelling could be attributed to the hydrophobic properties of the extract. Di Pierro et al. (2006) also reported that the degree of swelling of a polymeric material strongly depends on the amount and nature of intermolecular chain interactions.

It was noted that drying methods significantly affected the degree of swelling. It is seen in Table 3 that swelling of LPSSD and vacuum-dried films was less than that of films prepared at ambient conditions and at 40 °C. Swelling of the films could be reduced through an increase in the degree of cross-linkage. The lesser extents of swelling of LPSSD and vacuum-dried films were because of the higher extents of thermal cross-linkage, thus inducing less swelling of the films due to more rigid chains (Lim et al. 1999; Mayachiew & Devahastin, 2008a). In addition, thermal treatment of chitosan led to amide formation, which reduced the number of hydrophilic groups, thus decreasing swelling of the films (Muzzarelli & Muzzarelli, 2005; Ritthidej et al. 2002).

In addition, it was found that the degree of swelling slightly decreased with an increase in the drying temperature. This is again

Table 3
Percentage of swelling of antioxidant films.

Drying method	Indian gooseberry extract concentration		
	1%	2%	3%
Ambient drying	124.8 ± 2.8^{a}	84.0 ± 1.9^{a}	56.2 ± 0.9^{a}
Hot air drying	123.5 ± 2.6^{a}	83.0 ± 2.2^{a}	55.8 ± 1.6^{a}
Vacuum drying			
70 °C	103.9 ± 2.2^{bc}	68.3 ± 3.0^{bc}	44.0 ± 2.3^{bc}
80 °C	97.7 ± 1.9^{de}	64.3 ± 3.1^{cd}	39.9 ± 1.2^{cde}
90 °C	91.6 ± 2.8^{f}	60.7 ± 3.9^{d}	36.2 ± 2.9^{e}
LPSSD			
70 °C	109.4 ± 2.6^{bc}	73.4 ± 1.2^{b}	46.0 ± 2.6^{b}
80 °C	100.0 ± 2.7^{de}	66.6 ± 1.7^{cd}	42.6 ± 1.7^{bcd}
90 °C	95.6 ± 3.0^{ef}	62.4 ± 2.5^{cd}	38.4 ± 2.1^{de}

Values in the same column with different superscripts mean that the values are significantly different ($p < 0.05$).

because of thermal cross-linkage, which is accelerated by temperature (Lim & Wan, 1995). From release results in Figs. 1–3 it was found that higher drying temperatures of both LPSSD and vacuum drying led to lower percentage of release of TPC.

The results indicated that vacuum-dried films, which had lower degrees of swelling compared with the films prepared by LPSSD and drying at control conditions, showed the lowest percentage of release of TPC. The increased release that occurred with an increase in the degree of film swelling could be related to a change in the integrity of the film matrix (Sujja-areevath, Munday, Cox, & Khan, 1998). This is because the films might undergo relaxation during the release process, making the films become more flexible. This allowed the extract to diffuse out of the matrix more easily (Wu, Wang, Tan, Moochhala, & Yang, 2005). It was found from the release study that the films with lower degrees of swelling had lower percentage of release of TPC. Risbud, Hardikar, Bhat, and Bhonde (2000) also reported a direct correlation between the degree of swelling and release of antibiotics from chitosan films; the release of active agent from chitosan films normally increased with the degree of swelling.

In addition, release of the extract from the films might also be related to the film microstructure (Berger et al., 2004; Risbud et al., 2000). High-porosity film enhanced swelling, which was responsible for the release. It was found that at the same drying temperature LPSSD films had higher percentage of release of TPC than vacuum-dried films. This might be due to the higher porosity of the LPSSD films. It has been shown earlier that biomaterials undergoing LPSSD had higher porosity than products undergoing vacuum drying (Léonard, Blacher, Nimmol, & Devahastin, 2008).

4. Conclusion

The effects of drying methods and conditions on the percentage of residual TPC, release characteristics, intermolecular interaction and degree of swelling of chitosan films incorporated with different concentrations of Indian gooseberry extract were investigated. An increase in the extract concentration led to stronger functional group interaction, while the degree of swelling and percentage of release of TPC from antioxidant films decreased. The percentage of residual TPC, percentage of release of TPC, degree of swelling and functional group interaction were affected by drying methods and conditions. Ambient drying, low-temperature hot air drying and LPSSD at 70 °C led to antioxidant chitosan films with less intermolecular interaction, higher degree of swelling and percentage of release of TPC than did the other drying methods and conditions. Drying methods and conditions may be used to engineer chitosan films for controlled release in food packaging applications. Work is underway to develop a mathematical model that can be used to explain the release characteristics of TPC from chitosan films.

Acknowledgements

The authors express their sincere appreciation to the Thailand Research Fund (TRF), the Commission on Higher Education, Thailand and the International Foundation for Science (IFS) in Sweden for supporting the study financially.

References

Ahmad, I., Mehmood, Z., & Mohammad, F. (1998). Screening of some Indian medical plants for their antimicrobial properties. *Journal of Ethnopharmacology, 62*, 183–193.

Balasundram, N., Sundram, K., & Samman, S. (2006). Phenolic compounds in plants and agri-industrial by-products: Antioxidant activity, occurrence, and potential uses. *Food Chemistry, 99*, 191–203.

Berger, J., Reist, M., Mayer, J. M., Felt, O., Peppas, N. R., & Gurny, R. (2004). Structure and interactions in covalently and ionically crosslinked chitosan hydrogels for biomedical applications: Review. *European Journal of Pharmaceutics and Biopharmaceutics, 57*, 19–34.

Buonocore, G. G., Del Nobile, M. A., Panizza, A., Corbo, M. R., & Nicolais, L. (2003). A general approach to describe the antimicrobial agent release from highly swellable films intended for food packaging applications. *Journal of Controlled Release, 90*, 97–107.

Butler, B. L., Vergano, P. J., Testin, J. M., Bunn, J. M., & Wiles, J. L. (1996). Mechanical and barrier properties of edible chitosan films as affected by composition and storage. *Journal of Food Science, 61*, 953–955, 961.

Caner et al., 1998 C.CanerP.J.Vergano & Wiles, J. L.. Chitosan film mechanical and permeation properties as affected by acid, plasticizer, and storage. *Journal of Food Science, 63*. 1049–1053.

Chan, E. W. C., Lim, Y. Y., Wong, S. K., Lim, K. K., Tan, S. P., Lianto, F. S., et al. (2009). Effects of different drying methods on the antioxidant properties of leaves and tea of ginger species. *Food Chemistry, 113*, 166–172.

Devahastin, S., Suvarnakuta, P., Soponronnarit, S., & Mujumdar, A. S. (2004). A comparative study of low-pressure superheated steam and vacuum drying of a heat-sensitive material. *Drying Technology, 22*, 1845–1867.

Di Pierro, P., Chico, B., Villalonga, R., Mariniello, L., Damiao, A. E., Masi, P., et al. (2006). Chitosan-whey protein edible films produced in the absence or presence of transglutaminase: Analysis of their mechanical and barrier properties. *Biomacromolecules, 7*, 744–749.

Gómez-Estaca, J., Bravo, L., Gómez-Guillén, M. C., Alemán, A., & Montero, P. (2009). Antioxidant properties of tuna-skin and bovine-hide gelatin films induced by the addition of oregano and rosemary extracts. *Food Chemistry, 112*, 18–25.

Guan, T. T. Y., Cenkowski, S., & Hydamaka, A. (2005). Effect of drying on the nutraceutical quality of sea buckthorn (*Hippophae rhamnoides* L. ssp. sinensis) leaves. *Journal of Food Science, 70*, E514–E518.

Han, J. H., & Krochta, J. M. (2007). Physical properties of whey protein coating solutions and films containing antioxidants. *Journal of Food Science, 72*, E308–E314.

Han, C., Zhao, Y., Leonard, S. W., & Traber, M. G. (2004). Edible coatings to improve storability and enhance nutritional value of fresh and frozen strawberries (*Fragaria* × *ananassa*) and raspberries (*Rubus ideaus*). *Postharvest Biology and Technology, 33*, 67–78.

Hwang, K. T., Kim, J. T., Jung, S. T., Cho, G. S., & Park, H. J. (2003). Properties of chitosan-based biopolymer films with various degrees of deacetylation and molecular weights. *Journal of Applied Polymer Science, 89*, 3476–3484.

Jeon, D. H., Park, G. Y., Kwak, I. S., Lee, K. H., & Park, H. J. (2007). Antioxidants and their migration into food simulants on irradiated LLDPE film. *LWT – Food Science and Technology, 40*, 151–156.

Kanatt, S. R., Chander, R., & Sharma, A. (2008). Chitosan and mint mixture: A new preservative for meat and meat products. *Food Chemistry, 107*, 845–852.

Lagaron, J. M., Fernandez-Saiz, P., & Ocio, M. J. (2007). Using ATR–FTIR spectroscopy to design active antimicrobial food packaging structures based on high molecular weight chitosan polysaccharide. *Journal of Agricultural and Food Chemistry, 55*, 2554–2562.

Larrauri, J. A., Rupérez, P., & Saura-Calixto, F. (1997). Effect of drying temperature on the stability of polyphenols and antioxidant activity of red grape pomace peels. *Journal of Agricultural and Food Chemistry, 45*, 1390–1393.

Léonard, A., Blacher, S., Nimmol, C., & Devahastin, S. (2008). Effect of far-infrared radiation assisted drying on microstructure of banana slices: An illustrative use of X-ray microtomography in microstructural evaluation of a food product. *Journal of Food Engineering, 85*, 154–162.

Lim, L. Y., Khor, E., & Ling, C. E. (1999). Effects of dry heat and saturated steam on the physical properties of chitosan. *Journal of Biomedical Materials Research Part B: Applied Biomaterials, 48*, 111–116.

Lim, L. Y., & Wan, L. S. C. (1995). Heat treatment of chitosan films. *Drug Development and Industrial Pharmacy, 21*, 839–846.

Mayachiew, P., & Devahastin, S. (2008a). Comparative evaluation of physical properties of edible chitosan films prepared by different drying methods. *Drying Technology, 26*, 176–185.

Mayachiew, P., & Devahastin, S. (2008b). Antimicrobial and antioxidant activities of Indian gooseberry and galangal extracts. *LWT – Food Science and Technology, 41*, 1153–1159.

Muzzarelli, R. A. A., & Muzzarelli, C. (2005). Chitosan chemistry: Relevance to the biomedical sciences. *Advances in Polymer Science, 186*, 151–209.

Oussalah, M., Caillet, S., Salmiéri, S., Saucier, L., & Lacroix, M. (2004). Antimicrobial and antioxidant effects of milk protein-based film containing essential oils for the preservation of whole beef muscle. *Journal of Agricultural and Food Chemistry, 52*, 5598–5605.

Pasanphan, W., & Chirachanchai, S. (2008). Conjugation of gallic acid onto chitosan: An approach for green and water-based antioxidant. *Carbohydrate Polymers, 72*, 169–177.

Popa, M. I., Aelenei, N., Popa, V. I., & Andrei, D. (2000). Study of the interactions between polyphenolic compounds and chitosan. *Reactive and Functional Polymers, 45*, 35–43.

Pranoto, Y., Rakshit, S. K., & Salokhe, V. M. (2005). Enhancing antimicrobial activity of chitosan films by incorporating garlic oil, potassium sorbate and nisin. *LWT – Food Science and Technology, 38*, 859–865.

Puttipipatkhachorn, S., Nunthanid, J., Yamamoto, K., & Peck, G. E. (2001). Drug physical state and drug-polymer interaction on drug release from chitosan matrix films. *Journal of Controlled Release, 75*, 143–153.

Risbud, M. V., Hardikar, A. A., Bhat, S. V., & Bhonde, R. R. (2000). pH-sensitive freeze–dried chitosan–polyvinyl pyrrolidone hydrogels as controlled release system for antibiotic delivery. *Journal of Controlled Release, 68*, 23–30.

Ritthidej, G. C., Phaechamud, T., & Koizumi, T. (2002). Moist heat treatment on physicochemical change of chitosan salt films. *International Journal of Pharmaceutics, 232*, 11–22.

Sebti, I., Martial-Gros, A., Carnet-Pantiez, A., Grelier, S., & Coma, V. (2005). Chitosan polymer as bioactive coating and film against *Aspergillus niger* contamination. *Journal of Food Science, 70*, M100–M104.

Spagna, G., Pifferi, P. G., Rangoni, C., Mattivi, F., Nicolini, G., & Palmonari, R. (1996). The stabilization of white wines by adsorption of phenolic compounds on chitin and chitosan. *Food Research International, 29*, 241–248.

Srinivasa, P. C., Ramesh, M. N., Kumar, K. R., & Tharanathan, R. N. (2004). Properties of chitosan films prepared under different drying conditions. *Journal of Food Engineering, 63*, 79–85.

Sujja-areevath, J., Munday, D. L., Cox, P. J., & Khan, K. A. (1998). Relationship between swelling, erosion and drug release in hydrophilic natural gum mini-matrix formulations. *European Journal of Pharmaceutical Sciences, 6*, 207–217.

Suppakul, P., Miltz, J., Sonneveld, K., & Bigger, S. W. (2003). Active packaging technologies with an emphasis on antimicrobial packaging and its applications. *Journal of Food Science, 68*, 408–420.

Tovar, L., Salafranca, J., Sánchez, C., & Nerín, C. (2005). Migration studies to assess the safety in use of a new antioxidant active packaging. *Journal of Agricultural and Food Chemistry, 53*, 5270–5275.

Wiles, J. L., Vergano, P. J., Barron, F. H., Bunn, J. M., & Testin, R. F. (2000). Water vapor transmission rates and sorption behavior of chitosan films. *Journal of Food Science, 65*, 1175–1179.

Wu, N., Wang, L. S., Tan, D. C. W., Moochhala, S. M., & Yang, Y. Y. (2005). Mathematical modeling and in vitro study of controlled drug release via a highly swellable and dissoluble polymer matrix: Polyethylene oxide with high molecular weights. *Journal of Controlled Release, 102*, 569–581.

Yao, K. D., Liu, J., Cheng, G. X., Lu, X. D., Tu, H. L., & Da Silva, J. A. L. (1996). Swelling behavior of pectin/chitosan complex films. *Journal of Applied Polymer Science, 60*, 279–283.

Zhang, L., & Kosaraju, S. L. (2007). Biopolymeric delivery system for controlled release of polyphenolic antioxidants. *European Polymer Journal, 43*, 2956–2966.

Zhou, K., & Yu, L. (2006). Total phenolic contents and antioxidant properties of commonly consumed vegetables grown in Colorado. *LWT – Food Science and Technology, 39*, 1155–1162.

Food Chemistry 118 (2010) 602–615

Contents lists available at ScienceDirect

Food Chemistry

journal homepage: www.elsevier.com/locate/foodchem

Muscle structure responses and lysosomal cathepsins B and L in farmed Atlantic salmon (*Salmo salar* L.) *pre-* and *post-rigor* fillets exposed to short and long-term crowding stress

D. Bahuaud [a,*], T. Mørkøre [a,b], T.-K. Østbye [b], E. Veiseth-Kent [c], M.S. Thomassen [a], R. Ofstad [c]

[a] Norwegian University of Life Sciences (UMB), Department of Animal and Aquacultural Sciences (IHA), Postbox 5003, 1432 Ås, Norway
[b] Nofima Marin AS, Postbox 5010, 1432 Ås, Norway
[c] Nofima Mat AS, Osloveien 1, 1430 Ås, Norway

ARTICLE INFO

Article history:
Received 19 January 2009
Received in revised form 19 March 2009
Accepted 13 May 2009

Keywords:
Fish quality
Stress
pH
Texture
Protease
Muscle degradation
Myofibre
Myocommata
Breakages

ABSTRACT

Atlantic salmon (average body weight 2.9 ± 0.1 kg) were subjected to either minimal pre-slaughter crowding stress (NS group), 20 min (short-term stress, SS group) or about 24 h pre-slaughter crowding stress (long-term stress, LS group). Significant negative effects were mostly seen due to long-term stress (LS) at early stages *post-mortem*, but also short-term stress (SS) had significant negative impacts on muscle quality of *pre-* and *post-rigor* fillets. Pre-slaughter long-term stress (LS) significantly lowered muscle pH, softened the fillets and increased muscle *cathepsin L* gene expression, immediately *post-mortem.* A tendency of increased *cathepsin B* gene expression and cathepsin B total activity was also seen. Stress further accelerated the incidence of myofibre–myofibre detachments, increased the percentage of myofibre–myocommata detachments over the storage period and increased the percentage of myofibre breakages and contracted myofibres 96 h *post-mortem*. Significant correlations were observed between muscle pH and cathepsin B + L activity, muscle texture and muscle degradation parameters. Cathepsin B activity was correlated to muscle degradation and *cathepsin L* gene expression to muscle degradation and texture. Pre-slaughter stress, especially long-term stress (LS), thus seems to accelerate cathepsin activity, resulting in faster muscle degradation, directly or indirectly connected to the low initial muscle pH. No significant variation was observed between *pre-rigor* and *post-rigor* filleting, except that *pre-rigor* filleting significantly increased the percentage of myofibre breakages.

1. Introduction

Pre-slaughter handling stress is an important issue for salmon industry because of its effect on welfare and fillet quality. Several studies have shown that pre-slaughter stress accelerates fish fillet softening, increases gaping, affects skin and fillet colour and increases drip loss (Erikson & Misimi, 2008; Kiessling, Espe, Ruohonen, & Mørkøre, 2004; Morzel, Sohier, & Van de Vis, 2003; Mørkøre, Mazo, Tahirovic, & Einen, 2008; Roth, Slinde, & Arildsen, 2006; Skjervold, Fjæra, Østby, & Einen, 2001; Stien et al., 2005). Pre-slaughter stress accelerates the breakdown of ATP, resulting in earlier *rigor* onset and making it difficult to obtain and process *pre-rigor* fillets (Kiessling et al., 2004; Mørkøre et al., 2008; Sigholt et al., 1997; Skjervold, Fjæra, & Østby, 1999).

During stress and exhausting exercise, fish use anaerobic energy, leading to the production of lactic acid and resulting in low initial *post-mortem* pH in the muscle (Bagni et al., 2007; Erikson, Sigholt, & Seland, 1997; Lowe, Ryder, Carragher, & Wells, 1993; Poli, Parisi, Scappini, & Zampacavallo, 2005; Stien et al., 2005; Thomas, Pankhurst, & Bremner, 1999). Some authors suggested that this low initial pH could be responsible for the deteriorated final muscle quality (Lavety, Afolabi, & Love, 1988; Nakayama, Goto, & Ooi, 1996). Direct mechanical stress of the muscle fibrils or connective tissue, causing the release of proteases, could also contribute to the acceleration of muscle structure degradation (Roth et al., 2006).

Cathepsins are lysosomal proteases that are involved in mammalian and fish *post-mortem* muscle softening (Bahuaud et al., 2008; Chéret, Delbarre-Ladrat, de Lamballerie-Anton, & Verrez-Bagnis, 2007; Godiksen, Morzel, Hyldig, & Jessen, 2009; Taylor, Geesink, Thompson, Koohmaraie, & Goll, 1995; Yamashita & Konagaya, 1990, 1991). We have already underlined the importance, but complexity, of the mechanisms involving cathepsins in fish muscle degradation (Bahuaud et al., 2009). A potential role of these enzymes in the acceleration of *post-mortem* degradation of fish or mammalian muscle when subjected to pre-slaughter stress have

* Corresponding author. Tel.: +47 64 96 60 67; fax: +47 64 96 51 01.
E-mail addresses: diane.bahuaud@umb.no, bahuaud_diane@yahoo.fr (D. Bahuaud).

0308-8146/$ - see front matter © 2009 Elsevier Ltd. All rights reserved.
doi:10.1016/j.foodchem.2009.05.028

also been suggested (Bahuaud et al., 2009; Gil, Guerrero, & Sarraga, 1999; Vihko & Salminen, 1983). Calpains are calcium-dependent cytosolic proteases existing in two main ubiquitous forms according to the concentration of Ca^{2+} required for their activation: μ-calpain and m-calpain. It is well known that calpains are actively involved in *post-mortem* tenderisation of mammal muscle (Koohmaraie, 1992, 1996), but their participation in fish fillet softening, even if suggested, has drawn less attention (Chéret et al., 2007; Salem, Kenney, Killefer, & Nath, 2004). In fish, calpain activity seems to be difficult to characterise, probably due to the presence of its strong inhibitor, calpastatin (Chéret et al., 2007; Hultmann & Rustad, 2007; Salem, Nath, Rexroad, Killefer, & Yao, 2005), but the role of calpains in *post-mortem* softening is not to be excluded.

Today, most of the farmed salmon are filleted *post-rigor*, after 3–5 days of storage on ice; this period of storage being needed for an easier removal of pin bones and to avoid processing while the fish is still in *rigor*. Reducing pre-slaughter stress will increase the potential of *pre-rigor* filleting, thus providing higher freshness and quality products on the market, as *pre-rigor* fillets of Atlantic salmon have been shown to present less gaping, be thicker, firmer and offer a more intense colouration (Einen, Guerin, Fjæra, and Skjervold, 2002; Skjervold, 2002; Skjervold, Fjæra, Østby, Isaksson, Einen, et al., 2001; Skjervold et al., 2001).

Most of the studies on pre-slaughter stress in Atlantic salmon have so far focused on parameters like ATP, lactate and cortisol levels as primary stress responses, onset of *rigor mortis*, texture, colour and drip loss. The impact of pre-slaughter stress on muscle structure and the factors responsible for the quality degradation process have been less explored. The present study underlines the potential role of lysosomal cathepsins in muscle degradation, in relation to both short- and long-term pre-slaughter crowding stress.

2. Materials and methods

2.1. Fish and experimental setting

Atlantic salmon (*Salmo salar* L.) were raised in sea-water at Nofima Marin (previously Akvaforsk) Research Station, Averøy, on the west coast of Norway, where they were fed a standard commercial extruded dry feed (“Optiline S 800”, 9 mm, Skretting, Stavanger, Norway). Three weeks before slaughter, 600 salmon were randomly distributed into 4 net-pens (125 m^3) in the sea, each of them containing 150 fish. The salmon (average body weight of 2.9 ± 0.1 kg) were starved for 4 days before slaughter (sea temperature 12.7 °C, salinity 33‰) and were subjected to three different pre-slaughter handling procedures: Minimal crowding Stress (NS) (2 net-pens), Short-term crowding Stress (SS) (1 net-pen), or Long-term crowding Stress (LS) (1 net-pen). Salmon from the LS group were kept crowded in their net-pen by reducing the size of the net-pen in order to obtain a fish density of 300 kg/m^3, for about 24 h from the day before slaughter. At the day of slaughter, salmon from each group were transferred from their net-pen to a tank with refrigerated sea-water (RSW 2.0 °C ± 0.1 °C), where they were live-chilled and kept at either a low density of 65 kg/m^3 (NS group) or high density of 300 kg/m^3 (SS and LS groups) for 20 min. Salmon were then killed by percussive stunning, gill cut and bled in a tank with running RSW for 20 min. All the salmon used for analyses were collected in two harvests per group. To avoid any additional disturbance, 2 net-pens were attributed to the NS group only, so that each net-pen in this group had to be harvested only once.

Seventy-two salmon were taken from each net-pen without any specific criteria and killed for the present study; the rest of the salmon in the different net-pens being used for other studies not mentioned here. For the present study, the killed salmon (n = 72) were distributed in four batches (n = 18 in each batch, 6 salmon in each group NS, SS and LS). The first three batches were hand-filleted immediately *post-mortem* by experienced workers to obtain “*pre-rigor* fillets” that were placed on solid plastic trays in closed Styrofoam boxes with ice, and stored in a cold room (5 °C) for further analyses. Salmon from the last batch were packed as gutted fish on ice in Styrofoam boxes and stored in a cold room (5 °C) until they were filleted *post-rigor*, 96 h after slaughter, and analysed as “*post-rigor* fillets”. Only the left fillets were used for sampling and analyses in the present study. Each left fillet from each batch of salmon was used for sampling and analyses on maximum three locations at three different time-points *post-mortem*.

2.2. Instumental texture measurement (fillet firmness)

Fillet firmness was measured at 0 h, 12 h, 24 h, 48 h, 96 h and 192 h *post-mortem* on 6 *pre-rigor* fillets/time-point/group and at 96 h and 192 h *post-mortem* on 6 *post-rigor* fillets/time-point/group. Measurements were done on the front part of the fillets, in the dorsal section, above the mid-line.

A texture Analyser TA-XT2 (Stable Micro Systems Ltd., Godalming, UK) equipped with a 5 kg load cell was used for the measurements. A flat-ended cylindrical probe (12.5 mm diameter; type P/0.5) was used with a test speed of 1 mm s^{-1} and penetration depth 90% of the fillet height. The force required to puncture the fillet surface, i.e. the breaking force (F_{break}, N) was recorded from the time–force graphs. This response variable has been previously found to correlate well with sensory assessment of firmness (Mørkøre & Einen, 2003).

2.3. Measurement of muscle pH

Muscle pH was measured at 0 h, 12 h, 24 h, 48 h, 96 h and 192 h *post-mortem* on 6 *pre-rigor* fillets/time-point/group, and 96 h and 192 h *post-mortem* on 6 *post-rigor* fillets/time-point/group. The instrument used was a pH meter 330i SET (Wissenschaftlich-Technische-Werkstätten GmbH & Co. KG WTW, Weilheim, Germany) connected to a muscle electrode (Scott pH electrode, Blueline 21 pH 2.13/−5 °C/gel, WTW, Weilheim, Germany). The measurements were performed by inserting the electrode into the epaxial white muscle next to the point of instrumental texture measurement.

2.4. Microscopy of the muscle

Sampling for microscopic observations was performed at 0 h, 12 h, 24 h, 48 h and 96 h *post-mortem* on 6 *pre-rigor* fillets/time-point/group and 96 h and 192 h *post-mortem* on 6 *post-rigor* fillets/time-point/group. White muscle samples (2 x 2 × 3 mm) were taken directly after texture measurements, at the place of compression of the texture instrument’s probe, and fixed in 2.5% glutaraldehyde in cacodylate buffer, pH 7.3. Mechanical deformation of the muscle samples before sampling was made to ensure that all the samples had the same mechanical treatment and to enhance the detachments between muscle fibres and between muscle fibres and myocommata (Ando, Toyohara, Shimizu, & Sakaguchi, 1991; Nakayama et al., 1996). The fixed samples were kept at low temperature (4 °C) until they were embedded for histological analyses.

Briefly, after rinsing with cacodylate buffer (2 × 15 min) and dehydration in different gradients of ethanol (70 and 96% for 2 × 20 min and 100% for 20 min), the samples were embedded in a cold plastic resin based on hydroxyethylmethacrylate (Technovit 7100, Heraeus Kulzer). The direction of the myofibres in the embedded samples was oriented so as to obtain both cross – (for all time-points, *pre-* and *post-rigor* fillets) and longitudinal – (only for the 96 h samples, *pre-rigor* and *post-rigor* fillets) sections. Light microscopy observations at 10 and 20 time magnification were made on

thin sections (3 μm) stained in 0.05 g/100 ml toluidine blue dissolved in 0.1 M aqueous sodium acetate buffer using the method of Ofstad, Olsen, Taylor, and Hannesson (2006), with slight modifications.

In the cross-section samples, muscle degradation was evaluated according to the method of Taylor, Fjæra and Skjervold (2002) with slight modifications. Percentages of detachments between myofibres (myofibre–myofibre detachments) as well as detachments between myofibres and connective tissue (myofibre–myocommata detachments) were determined. Two plastic blocks embedding 1–2 muscle samples/fillet/time-point were analysed. For each sample, detachments were counted on minimum 250 junctions between myofibres, and 50 junctions between myofibres and connective tissue.

In the longitudinal-oriented samples, the percentage of myofibre breakages and contracted myofibres was evaluated. Two plastic blocks embedding 1–2 muscle samples/fillet were analysed. For each sample, the percentage of myofibre breakages or contracted myofibres was evaluated on a minimum of 100 myofibres/sample.

2.5. Cathepsin activity

White muscle samples were taken next to the place used for instrumental texture, pH and histology sampling and analyses, on the same 6 salmon fillets/group, 0 h *post-mortem*. The samples were immediately frozen in liquid nitrogen before being stored at −80 °C until further analyses. Cathepsin B + L, cathepsin B and cathepsin L total activities were determined by homogenising 300 mg of muscle in 1 ml extraction buffer (100 mM Na-acetate in 0.2% Triton X-100, pH 5.5) in Precellys tubes, with a Precellys 24 homogenizer (Bertin Technologies, France) (2 cycles of 20 s at 5500 rpm, separated by a 10 s break). The obtained homogenates were centrifuged at 16,000 *g* for 30 min and the supernatants were used to determine enzyme activities.

Cathepsin B + L and cathepsin B activities were measured fluorimetrically according to the method of Kirschke, Wood, Roisen, and Bird (1983). The release of the fluorogenic reagent 7-amido-4-methylcoumarin was determined by fluorescence measurement at excitation 360 nm and emission wavelengths 460 nm. N-CBZ-L-phenylalanyl-L-arginine-7-amido-4-methylcoumarin (Z-Phe-Arg-Nmec) for cathepsin B + L activity and N-CBZ-L-arginyl-L-arginine-7-amido-4-methylcoumarin (Z-Arg-Arg-Nmec) for cathepsin B activity were used as substrates. To get an idea of the level of cathepsin L activity, cathepsin B activity was subtracted from cathepsin B + L activity (Bahuaud et al., 2009; Chéret, Delbarre-Ladrat, de Lamballerie-Anton, and Verrez-Bagnis, 2007; De Ceuninck et al., 1995; Zhao et al., 2005). The assays were run twice in triplicates.

2.6. Cathepsin relative gene expression

Epaxial white muscle of Atlantic salmon was dissected immediately *post-mortem* (0 h samples) from 6 fillets/group, next to the place used for instrumental texture, pH, and histology sampling and analyses. The tissue samples were kept at −80 °C until analysis. Total RNA was isolated using TRIzol Reagent (Invitrogen, USA) according to the manufacturer instructions. Total RNA was DNase I treated with Turbo DNA-free kit (Ambion, USA). Purification of RNA was made by precipitation using 0.1 volume of 3 M Sodium Acetate and three volumes of 99% ethanol. After 30 min incubation at room temperature, centrifugation for 10 min at 4 °C and 10,000 *g*, the pellet was dried and then resuspended in 40 μl RNase free water.

Concentration and quality of RNA was measured with NanoDrop ND-1000 Spectrophotometer (NanoDrop Technologies, USA). cDNA was synthesised using oligod(T) primers from 0.5 μg RNA in a total volume of 50 μl using Taqman reverse transcriptase reagents (Applied Biosystems, USA) and according to the manufacturer protocol. BLAST search and Vector NTI Advance 10 (Invitrogen, USA) was used to identify and analyse salmon cathepsin B and cathepsin L sequences. Vector NTI Advance 10 was used to design real time PCR primers which were purchased from Invitrogen (Invitrogen, USA).

Real time PCR was performed in a LightCycler 480 Instrument (Roche Applied Science, Germany) with gene-specific primers for *cathepsin B* and *cathepsin L*. Both *RNA polymerase 2* (*rpol2*), *eukaryotic translation initiation factor 3* and *NADH-ubiquinone oxidoreductase* (*nour*) were evaluated as reference genes using Genorm (Vandesompele et al., 2002). *Rpol2* and *nour* were the most stably expressed reference genes, and the geometric mean of these was therefore used when calculating the relative gene expressions. Table 1 gives the real time PCR primer sequences for relative expression of *cathepsin B*, *cathepsin L*, *rpol2* and *nour*. PCR master mix consisted of 1 μl forward and reverse primer (final concentration of 0.5 μM), 4 μl 1:10 dilution of cDNA and 5 μl LightCycler 480 SYBR Green I Master (Roche Applied Science, Germany). All samples were analysed in triplicates with non-template control for each gene. The reaction condition was 95 °C for 5 min, 45 cycles of 95 °C/15 s and 60 °C for 1 min. A melting curve analysis (95 °C for 5 s and 65 °C for 1 min, 97 °C) was run to confirm the presence of a single PCR product. Primer efficiency was calculated for each primer pair.

The relative gene expression level was calculated according to the ΔΔCt method and adjusted for differences in primer efficiency (Plaffl, 2001).

2.7. Statistical analyses

Mean results per group (NS, SS and LS) were analysed by General Linear Model (GLM). We used SAS (Statistical Analysis System) release 8.02 (SAS Institute Inc., Cary, NC, USA) as statistical software, with "stress period length (NS, SS and LS)", "time *post-mortem*" and "time of filleting (*pre-/post-rigor)*" as explanatory variables. Significant differences among means were ranked by Least Squares Means at $p < 0.05$. Correlations between the different measured quality traits and muscle degradation parameters were obtained using the Pearson correlation coefficients, at the same level of significance.

Table 1
Real time PCR primer sequences for relative gene expression of *cathepsin B* and *cathepsin L* in the muscle.

Primer	Genbank no.		5′–3′
Cathepsin B	DR696159	Ssa cathepsin B F1	AGGGGGGAACTCCTTACTGGCT
		Ssa cathepsin B R1	CGATGCCACAGTGGTCCTTACCT
Cathepsin L	CB502996	Ssa cathepsin L F1	GTATAGTGAAATGTGTGACC
		Ssa cathepsin L R2	AACCAGAGCAATAATTCAAG
NADH-ubiquinone oxidoreductase (nour)	DW532752	Ssa nour L F1	CAACATAGGGATTGGAGAGCTGTACG
		Ssa nour L R2	TTCAGAGCCTCATCTTGCCTGCT
RNA polymerase 2 (rpol2)	CA049789	Ssa rpol2 F1	TAACGCCTGCCTCTTCACGTTGA
		Ssa rpol2 R1	ATGAGGGACCTTGTAGCCAGCAA

Multivariate analysis was performed on *pre-rigor* fillets only, using individual fish results from salmon batch number 1, at 0 h, 12 h and 48 h *post-mortem*, in order to map the overall correlations between muscle quality and stress. The data were analysed with Partial Least Squares Regression (PLSR) (Martens & Næs, 1989), using the measured muscle quality traits and muscle degradation parameters as explanatory variables and "stress period length (NS, SS and LS)" as binary response variable.

Table 2 gives a summary of the different analyses and sampling made at the different time-points on the *pre-rigor* and *post-rigor* fillets.

3. Results

3.1. Fillet firmness of pre-rigor and post-rigor fillets

Fillet firmness significantly changed with time of storage ($p < 0.0001$) in the *pre-rigor* fillets (Fig. 1). Over the whole storage period of the *pre-rigor* fillets, there was a tendency that pre-slaughter crowding stress had an effect on fillet texture (F_{break}) ($p = 0.087$) (Fig. 1) and long-term stress (LS) had a significantly different impact than short-term stress (SS) ($p = 0.029$). Immediately *post-mortem*, fillets from the LS group presented the softest fillets ($p_{(NS/LS)} = 0.0005$ and $p_{(SS/LS)} = 0.0002$). At 12 h *post-mortem*, fillets from the NS and LS groups did not present any significantly different fillet texture any longer, but the SS group showed the firmest fillets ($p_{(NS/SS)} = 0.041$ and $p_{(LS/SS)} = 0.001$). From 24 h *post-mortem*, no significant effect of crowding stress on fillet texture could be seen in the *pre-rigor* fillets.

In the *post-rigor* fillets, fillet firmness significantly decreased between 96 h and 192 h *post-mortem* ($p = 0.051$). There was a significant effect of pre-slaughter stress on fillet texture during this storage period in the *post-rigor* fillets ($p = 0.041$), with the SS group presenting the softest fillets significantly different from the NS group ($p = 0.046$). At 192 h *post-mortem*, the SS fillets were also softer than the LS fillets ($p = 0.028$) (Fig. 1).

At 96 h and 192 h *post-mortem*, time of filleting did not have any significant influence on fillet texture in general, but 96 h *post-mortem*, *pre-rigor* fillets from the NS group were significantly softer ($p = 0.054$) than *post-rigor* fillets from the same group. The same tendency could be observed in the SS group ($p = 0.080$), but these differences had disappeared by 192 h *post-mortem*.

3.2. pH of pre-rigor and post-rigor fillets

pH significantly decreased with time of storage ($p < 0.0001$) in the *pre-rigor* fillets (Fig. 2). Over the whole storage period of the *pre-rigor* fillets, a significant effect of pre-slaughter stress on muscle pH was seen in general ($p = 0.0003$), where the LS group presented the lowest pH values ($p_{(NS/LS)} = 0.002$; $p_{(SS/LS)} = 0.0001$). Fillets from the LS group also showed the lowest pH at 0 h ($p_{(NS/LS)} < 0.0001$; $p_{(SS/LS)} = 0.0001$) and 12 h *post-mortem* ($p_{(NS/LS)} = 0.004$; $p_{(SS/LS)} = 0.007$). From 24 h *post-mortem* to the end of the storage period, no significant differences in fillet pH were observed between the groups in the *pre-rigor* fillets.

Table 2
Summary: Different analyses and sampling made at the different time-points.

	Time *post-mortem* (h)	Batch	Texture	pH	Myofibre–myofibre detachments	Myofibre–myocommata detachments	Myofibre breakages	Contracted myofibres	Cathepsin B + L activity	Cathepsin B activity	Cathepsin L activity	*Cathepsin B* gene expression	*Cathepsin L* gene expression
Pre-rigor fillets	0	1	X	X	X	X			X	X	X	X	X
	12	1	X	X	X	X							
	24	2	X	X	X	X							
	48	1	X	X	X	X							
	96	3	X	X	X	X	X	X					
	192	3	X	X									
Post-rigor fillets	96	4	X	X	X	X	X	X					
	192	4	X	X	X	X							

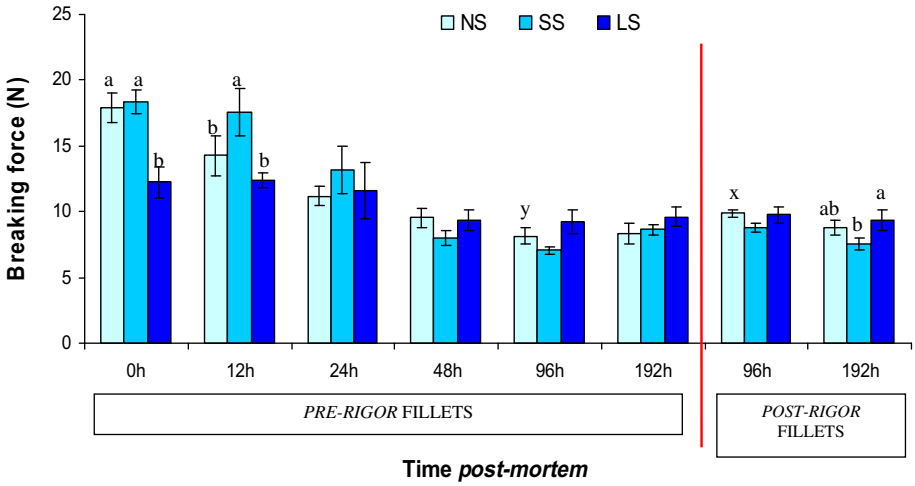

Fig. 1. Changes during the storage period (0–192 h *post-mortem*) of firmness (F_{break}) of *pre-rigor* and *post-rigor* fillets of Atlantic salmon subjected to minimal (NS), short-(SS) or long-term (LS) pre-slaughter crowding stress. Each histobar represents the mean value ± SE of one group at one time-point ($n = 6$). Different letters denote significant differences ($p < 0.05$) between the groups at the same time point (a, b) or between *pre-rigor* and *post-rigor* fillets at the same time-point within the same group (x, y).

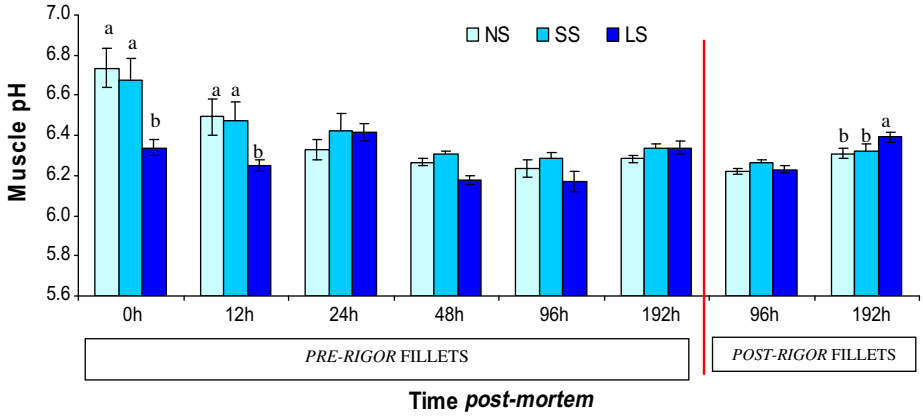

Fig. 2. Changes during the storage period (0 h to 192 h *post-mortem*) of pH of *pre-rigor* and *post-rigor* fillets of Atlantic salmon subjected to minimal (NS), short-(SS) or long-term (LS) pre-slaughter crowding stress. Each histobar represents the mean value ± SE of one group at one time-point ($n = 6$). Different letters denote significant differences ($p < 0.05$) with the other groups, at the same time-point.

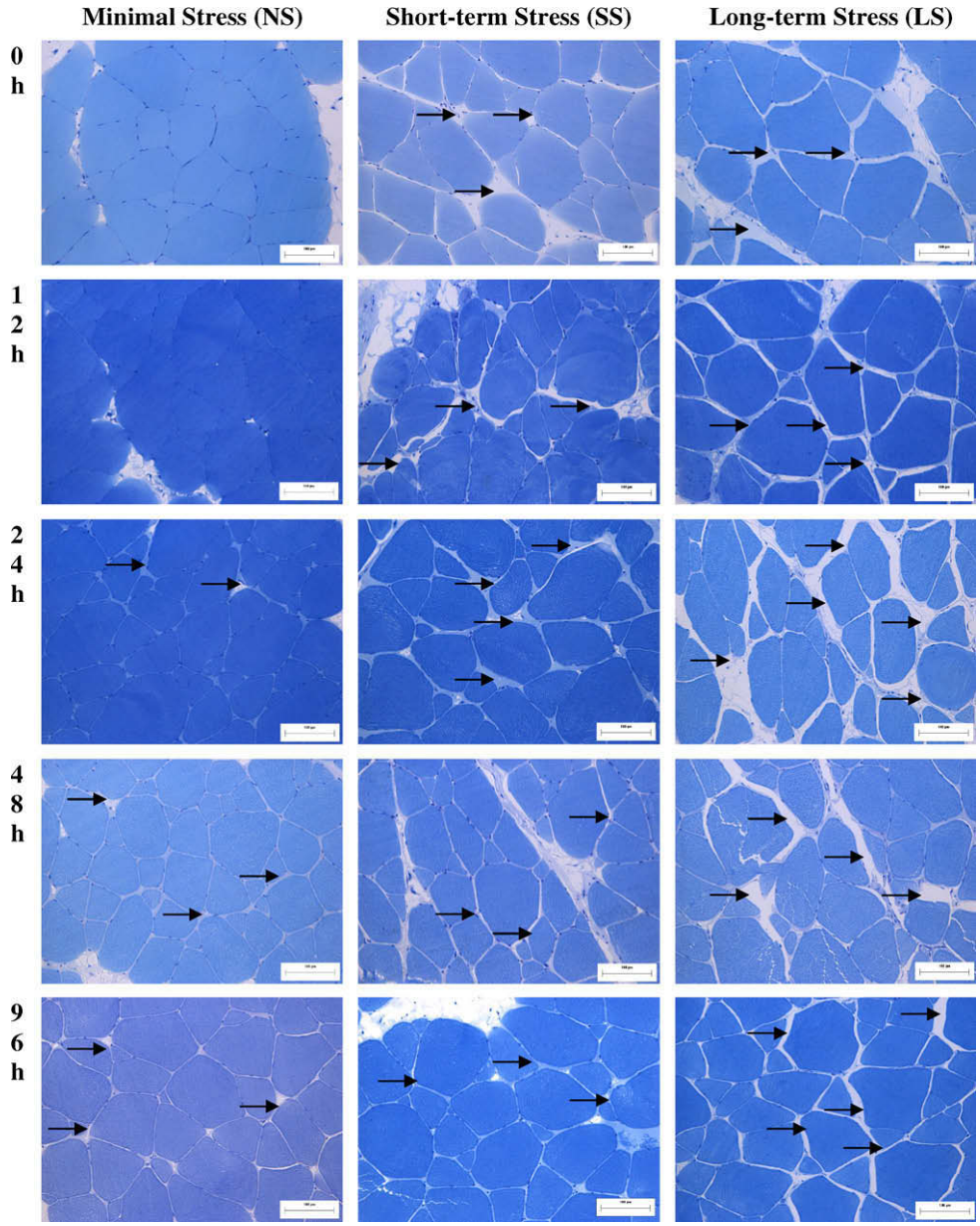

Fig. 3. Light microscopy observations (cross-sections) 0 h, 12 h, 24 h, 48 h and 96 h *post-mortem*, of *pre-rigor* fillets of Atlantic salmon subjected to minimal (NS), short-(SS) or long-term (LS) pre-slaughter crowding stress; magnification ×20. Arrows: myofibre–myofibre detachments.

In the *post-rigor* fillets, pH significantly changed between 96 h and 192 h *post-mortem* ($p < 0.0001$) but no significant effect of pre-slaughter stress was found in general during this period. At 192 h *post-mortem*, fillets from the LS group however presented the highest pH ($p_{(NS/LS)} = 0.019$ and $p_{(SS/LS)} = 0.043$) (Fig. 2).

Muscle pH values showed no significant difference between *pre-* and *post-rigor* fillets at 96 h and 192 h *post-mortem*.

3.3. Myofibre–myofibre detachments in pre-rigor and post-rigor fillets

In the *pre-rigor* fillets, the percentage of myofibre–myofibre detachments significantly increased with time of storage ($p < 0.0001$) and because of pre-slaughter crowding stress ($p < 0.0001$) (Fig. 3 and Fig. 4). Over the whole storage period, the LS group showed the highest percentage of myofibre–myofibre detachments ($p_{(NS/LS)} < 0.0001$ and $p_{(SS/LS)} < 0.0001$) in the *pre-rigor* fillets. Significant differences between groups at each time-point were mainly noticed before 24 h *post-mortem*. At 0 h *post-mortem*, salmon from the LS group showed significantly more myofibre–myofibre detachments than the NS group ($p = 0.003$), while the percentage of detachments was not significantly different between the SS and the NS groups; 12 h *post-mortem*, both the SS and LS groups presented more myofibre–myofibre detachments than the NS group ($p_{(NS/SS)} = 0.011$; $p_{(NS/LS)} < 0.0001$), the LS group showing an even more pronounced effect ($p_{(SS/LS)} < 0.0001$). At 24 h and 48 h *post-mortem*, there were no longer any significant differences in percentage of myofibre–myofibre detachments between the three groups, although the long-term stress (LS) numerically seemed to still result in more detachments. This trend was noticed until the end of the storage period, 96 h *post-mortem* in the *pre-rigor* fillets. At 96 h *post-mortem*, *pre-rigor* fillets from the SS group showed less detachments than the other groups, significantly when compared to the LS group ($p = 0.019$).

In general, no difference in percentage of myofibre–myofibre detachments was noticed between 96 h and 192 h *post-mortem* in the *post-rigor* fillets or between groups (Figs. 5 and 6). But 96 h *post-mortem*, as in the *pre-rigor* fillets, short-term stress (SS) resulted in less myofibre–myofibre detachments, significantly when compared to the NS group ($p = 0.040$). This difference had disappeared by 192 h *post-mortem*.

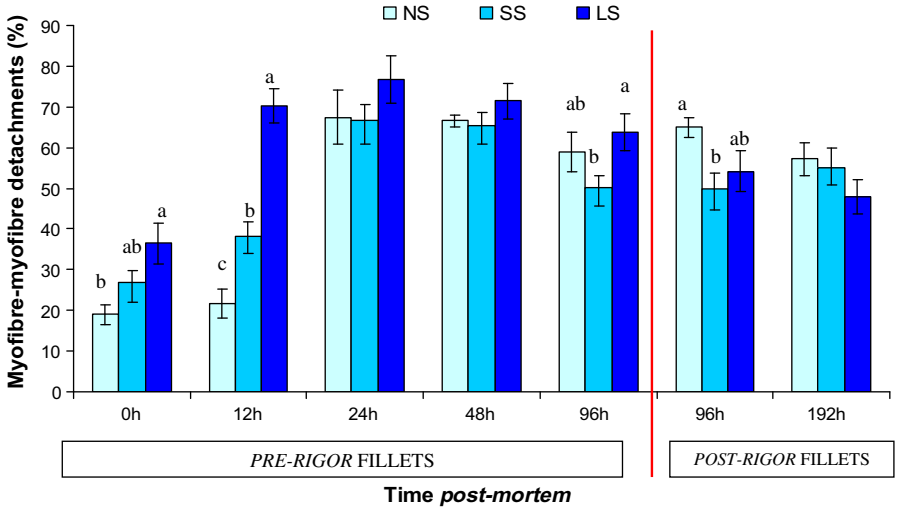

Fig. 4. Changes during the storage period (0 h to 192 h *post-mortem*) of myofibre–myofibre detachments (%) in *pre-rigor* and *post-rigor* fillets of Atlantic salmon subjected to minimal (NS), short-(SS) or long-term (LS) pre-slaughter crowding stress. Each histobar represents the mean value ± SE of one group at one time-point ($n = 6$). Different letters denote significant differences ($p < 0.05$) with the other groups, at the same time-point.

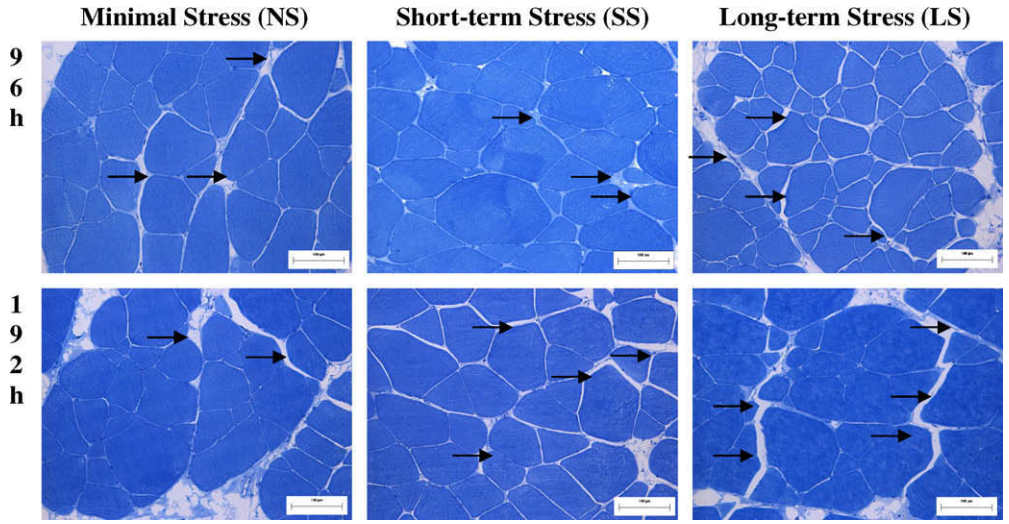

Fig. 5. Light microscopy observations (cross-sections) 96 h and 192 h *post-mortem*, of *post-rigor* fillets of Atlantic salmon subjected to minimal (NS), short-(SS) or long-term (LS) pre-slaughter crowding stress; magnification ×20. Arrows: myofibre–myofibre detachments.

At 96 h *post-mortem*, no significant differences in percentage of myofibre–myofibre detachments were found between the *pre-rigor* and the *post-rigor* fillets.

3.4. Myofibre–myocommata detachments in pre-rigor and post-rigor fillets

Due to the large variation in percentage of myofibre–myocommata detachments, no general effect of storage time was observed between 0 h and 96 h *post-mortem* in the *pre-rigor* fillets (Fig. 6). The percentage of myofibre–myocommata detachments was however significantly higher at 24 h ($p = 0.030$) and 96 h ($p = 0.033$) than at 0 h *post-mortem*. Pre-slaughter stress further increased significantly the level of myofibre–myocommata detachments in general ($p = 0.047$) over the whole storage period in the *pre-rigor* fillets, and significantly more myofibre–myocommata detachments were found in the SS ($p = 0.028$) and in the LS groups ($p = 0.037$) than in the NS group. When compared at individual time-points in the *pre-rigor* fillets, however, only the SS group 96 h *post-mortem* presented significantly more myofibre–myocommata detachments than the NS ($p = 0.042$) and LS groups ($p = 0.042$).

The level of myofibre–myocommata detachments significantly increased between 96 h and 192 h *post-mortem* ($p = 0.002$) in the *post-rigor* fillets (Fig. 6). Like in the *pre-rigor* fillets, the SS group showed significantly more myofibre–myocommata detachments than the NS group ($p = 0.035$) but this time only after 192 h of storage.

At 96 h *post-mortem*, *pre-rigor* filleting resulted in significantly more myofibre–myocommata detachments than *post-rigor* filleting, but only when salmon were subjected to short-term (SS) stress ($p = 0.034$).

3.5. Myofibre breakages and contracted myofibres in pre-rigor and post-rigor fillets

In the *pre-rigor* fillets, significantly more myofibre breakages were found in the LS than in the NS group ($p = 0.050$) (Figs. 7 and 8A). In the SS group, the percentage of myofibre breakages was numerically higher than the NS group, but the difference was not statistically significant. In the *post-rigor* fillets, no significant differences in percentage of myofibre breakages were noticed between the three groups (Fig. 8A). *Pre-rigor* filleting resulted in significantly more myofibre breakages than *post-rigor* filleting in general ($p = 0.003$), and especially when salmon were subjected to long-term stress (LS) ($p_{(LS\ pre\text{-}rigor/LS\ post\text{-}rigor)} = 0.009$).

In the *pre-rigor* fillets, pre-slaughter stress did not influence the percentage of contracted myofibres, whereas in the *post-rigor* fillets, short-term (SS) ($p = 0.058$) and long-term pre-slaughter stress (LS) ($p = 0.072$) tended to result in more contracted myofibres than minimal stress (Fig. 7 and Fig. 8A). There was also a tendency that *pre-rigor* filleting resulted in less contracted myofibres than *post-rigor* filleting ($p = 0.063$), and this difference was significant for salmon subjected to long-term stress (LS) ($p_{(LS\ pre\text{-}rigor/LS\ post\text{-}rigor)} = 0.040$).

3.6. Cathepsin activity in pre-rigor fillets

Pre-slaughter crowding stress (SS and LS) seemed to result in more cathepsin B + L activity in the muscle than minimal crowding stress (NS), even though these differences were not significant (Fig. 9A) ($p_{(NS/LS)} = 0.141$). Exactly the same pattern was observed when measuring cathepsin B activity alone (Fig. 9B) ($p_{(NS/LS)} = 0.084$), whereas cathepsin L activity did not seem to be affected by pre-slaughter crowding stress (average cathepsin L activity for NS: 1.281 ± 0.025 mU/g muscle; SS: 1.280 ± 0.029 mU/g muscle; LS: 1.281 ± 0.011 mU/g muscle).

3.7. Cathepsin relative gene expression in pre-rigor fillets

The relative gene expression of *cathepsin L* was significantly influenced by pre-slaughter stress ($p = 0.001$). When compared to the NS group, a significantly higher gene expression of *cathepsin L* was found in the LS group ($p = 0.011$), whereas no significant differences were seen with the SS group (Fig. 10). There was also a tendency that the gene expression of *cathepsin B* followed the same

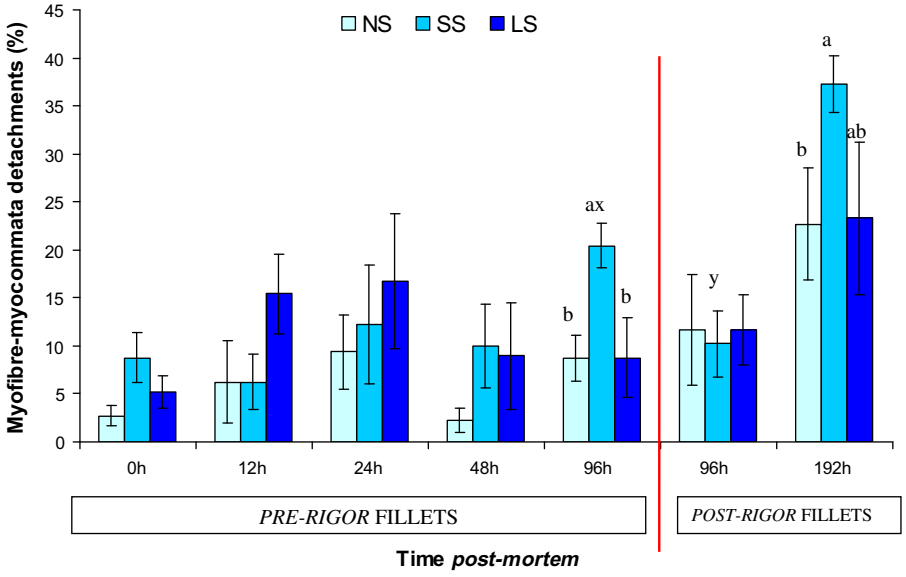

Fig. 6. Changes during the storage period (0 h to 192 h *post-mortem*) of myofibre–myocommata detachments (%) in *pre-rigor* and *post-rigor* fillets of Atlantic salmon subjected to minimal (NS), short-(SS) or long-term (LS) pre-slaughter crowding stress. Each histobar represents the mean value ± SE of one group at one time-point ($n = 6$). Different letters denote significant differences ($p < 0.05$) between the groups at the same time-point (a, b) or between *pre-rigor* and *post-rigor* fillets at the same time-point within the same group (*x*, *y*).

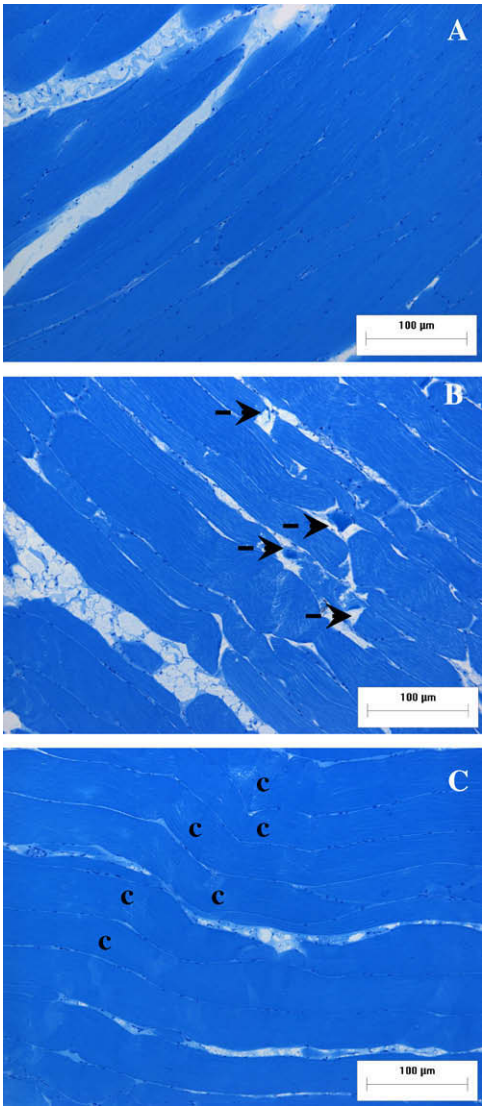

Fig. 7. Light microscopy observations (longitudinal-sections), 96 h *post-mortem*, of *pre-rigor* and *post-rigor* fillets of Atlantic salmon subjected to minimal (NS), short- (SS) or long-term (LS) pre-slaughter crowding stress; magnification ×20. A: intact myofibres; B: myofibre breakages (arrows); C: contracted myofibres (c).

pattern: a numerically higher expression was found in the LS group ($p_{(NS/LS)} = 0.186$), when compared to the NS and SS groups, even if these results were not significantly different.

3.8. Correlations between the quality traits and muscle degradation parameters in pre-rigor and post-rigor fillets

Table 3 summarises the significant effects of pre-slaughter stress and time of filleting (*pre-rigor*/*post-rigor*) on the quality traits and muscle degradation parameters measured in the present study and Table 4 gives the correlation coefficients between the results obtained.

The correlations between the different quality traits and muscle degradation parameters are also represented with a PLSR plot in Fig. 11. A correlation loading plot from PLSR summarises the data's overall covariance structure. It holds information about how the variables are related to each other, and how well each variable is explained by the model. In essence, variables located close to each other are positively correlated, while variables located on opposite side of an axis are negatively correlated. The distance from origo to each variable represents how well it is explained by the model; the inner ellipse represents 50% explained variance and the outer ellipse represents 100% explained variance. In the present study, the multivariate analysis of the data at 0 h, 12 h and 48 h *post-mortem* allowed explaining 73% of the total variation in stress-length period (NS, SS and LS). The first component (PC1) separates between long-term stress (LS) to the right and short-term (SS) or minimal crowding stress (NS) to the left. Quality traits and muscle degradation parameters that correlated with the first component were pH at 0 h, 12 h and 48 h and firmness at 0 h and 12 h to the left, and to the right we find myofibre–myofibre (MF–MF) detachments at 0 h and 12 h, myofibre–myocommata (MF–MC) detachments at 12 h, *cathepsin L* relative gene expression, cathepsin B + L activity and cathepsin B activity. This means that pH and firmness (F_{break}) were positively correlated in the present study, and salmon in the NS and SS groups had higher pH and firmness than salmon in the LS group. Myofibre–myofibre detachments were positively correlated to *cathepsin L* expression and cathepsin B activity, and negatively correlated to pH and firmness. Salmon from the LS group presented more myofibre–myofibre detachments, and higher cathepsin B activity and *cathepsin L* gene expression. The second component mainly separated between the SS and NS groups, but it only accounted for 10% of the muscle quality variation. The only variable showing some correlations with the second component is myofibre–myocommata detachments at 0 h, which had a tendency to be higher for short-term stressed (SS) salmon.

4. Discussion

Pre-slaughter stress accelerates anaerobic energy metabolism, and therefore produces a rapid increase in muscle lactic acid production (Poli et al., 2005). In the present study, salmon subjected to pre-slaughter long-term stress (LS) presented the lowest muscle pH immediately *post-mortem* and over the whole storage period. Our results agree with several other studies, which also showed a lower muscle pH immediately *post-mortem* or a higher lactate level in stressed fish than in unstressed ones (Bagni et al., 2007; Erikson, Beyer, & Sigholt, 1997; Erikson & Misimi, 2008; Lowe et al., 1993; Stien et al., 2005; Tejada & Huidobro, 2002; Thomas et al., 1999). The strong pH reduction in long-term stressed salmon immediately after slaughter may suggest an *in vivo* accumulation of lactic acid in the muscle, because long-term stress induced strong swimming activity and presumably a very slow release of lactic acid from the cells.

Ofstad et al. (2006) showed that both myofibre–myofibre and myofibre–myocommata detachments in cod and wolffish were mainly caused by fractures in the extracellular matrix, maybe due to degradation of proteoglycans and glycoproteins. In the present study, the percentage of myofibre–myofibre detachments increased with time until 24 h *post-mortem*, which has already been observed in previous studies (Bahuaud et al., 2008; Bahuaud et al., 2009) and translates the normal muscle degradation process during storage. Pre-slaughter stress significantly affected the integrity of the *pre-rigor* fillets by accelerating this degradation; the longer the pre-slaughter stress period, the faster the incidence of myofibre–myofibre detachments and this agrees with Ando et al. (2001) and Nakayama et al. (1996), who also showed that pre-slaughter stress increased the incidence of myofibre–myofibre detachments in chub mackerel and red sea-bream. Increase of plasma cortisol is a well-known primary stress response in fish, and in accordance with our results, Macdonald and Cidlowski (1982) showed that glucocorticoids in rat stimulate protein degradation. The acceleration of detachments between myofibres due to pre-slaughter stress and observed particularly in the LS group in the

present study, could also be directly or indirectly related to the significantly lower muscle pH immediately *post-mortem*, since a significant negative correlation was found between muscle pH and percentage of myofibre–myofibre detachments.

In the present study, pre-slaughter stress also increased significantly myofibre–myocommata detachments. Accordingly, Gomez-Guillen, Montero, Hurtado, and Borderias (2000) found that shear strength of the connective tissue fraction in stressed Atlantic salmon was lower, and this was associated with lower muscle pH. In earlier studies, such increase in myofibre–myocommata detachments was not noticed until 192 h *post-mortem* in Atlantic salmon and wolffish (Bahuaud et al., 2008; Bahuaud et al., 2009; Ofstad et al., 2006; Taylor, Fjæra, & Skjervold, 2002) and it was suggested that myofibre–myocommata detachments were associated with loss of *rigor* stiffness (Taylor et al., 2002). In the present study, the very low muscle pH found particularly in the LS group could be directly responsible for these detachments, as we also found a significant negative correlation between muscle pH and percentage of myofibre–myocommata detachments. Similarly, Lavety et al. (1988) showed a strong negative relationship between muscle pH and degree of gaping in salmon and rainbow trout, and also noticed that the lower the muscle pH, the easier it was to break the myocommata.

Our results on enzyme activities indicated that pre-slaughter stress increases cathepsin B total activity in the muscle, even if these results were not significant. Long-term pre-slaughter stress also enhanced significantly *cathepsin L* gene expression in the muscle, and a similar trend was seen for *cathepsin B*. These results agree with studies on rats and mice where, under stress conditions, cathepsin total activity (Pote & Altekar, 1980; Vihko & Salminen, 1983) or *cathepsin* gene expression in Atlantic salmon (Bahuaud et al., 2009) increased in the muscle. Measuring cathepsin total activity and *cathepsin* gene expression in fish muscle has been used to highlight the level of potential proteolysis (Bahuaud et al., 2009; Chéret, Hernandez-Andres, Delbarre-Ladrat, de Lamballerie, & Verrez-Bagnis, 2006; Chéret et al., 2007; Mommsen, 2004; Salem, Levesque, Moon, Rexroad, & Yao, 2006). An increase of cathepsin total activity and/or relative gene expression in fish muscle thus indicates a higher potential muscle degradation *pre-* and/or *post-mortem*. In the present study, cathepsin B activity was measured with its specific substrate. The substrate used to measure cathepsin B + L activity can be degraded by both cathepsin B and cathepsin L. To obtain cathepsin L activity, we subtracted our results of cathepsin B activity from our results of cathepsin B + L activity; this method may not truly represent the exact cathepsin L activity but was, however, previously used by several authors (Chéret,

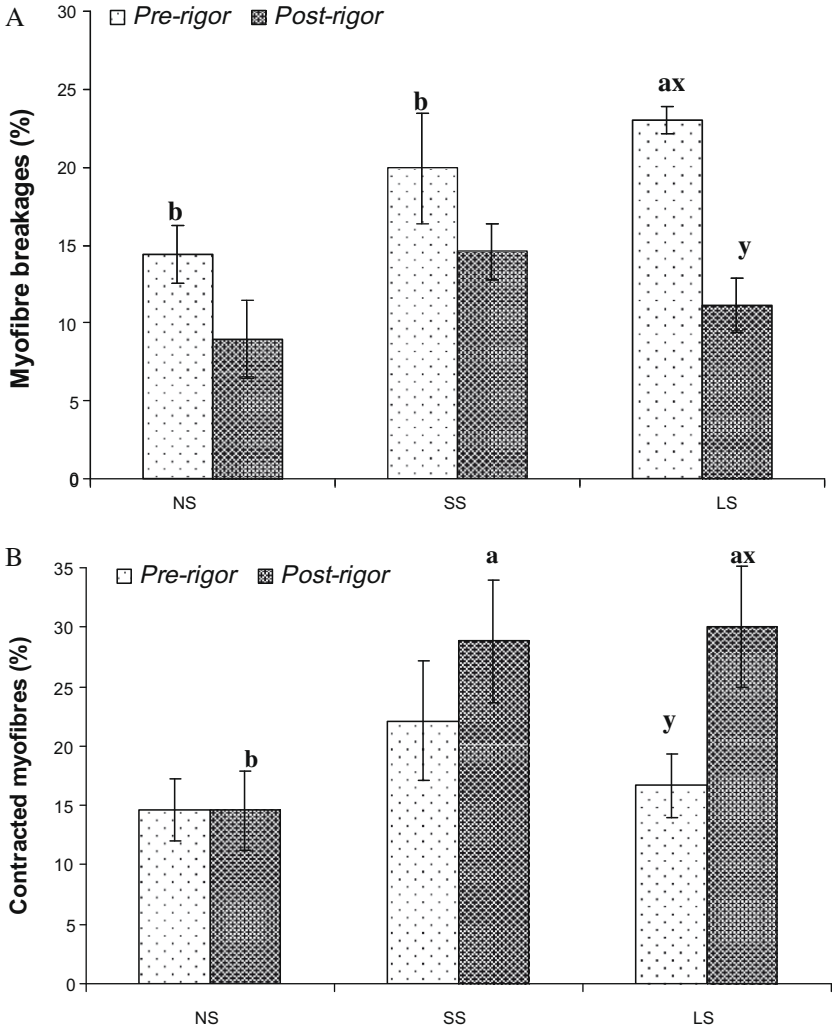

Fig. 8. A: Myofibre breakages (%); B: Contracted myofibres (%), 96 h *post-mortem,* in *pre-rigor* and *post-rigor* fillets of Atlantic salmon subjected to minimal (NS), short-(SS) or long-term (LS) pre-slaughter crowding stress. Each histobar represents the mean value ± SE of one group for a time of filleting (*pre/post-rigor* filleting) ($n = 6$). Different letters denote significant differences ($p < 0.05$) between the groups for the same time of filleting (*pre/post-rigor*) (a, b) or between *pre-* and *post-rigor* filleting within a group (*x*, *y*).

Delbarre-Ladrat, de Lamballerie-Anton, & Verrez-Bagnis, 2007; De Ceuninck et al., 1995; Zhao et al., 2005) and can at least give an idea of the level of cathepsin L activity.

In salmonids, cathepsin B and cathepsin L have been particularly associated with muscle softening, with an optimum pH for activity of 6.0–5.5 and 5.6 respectively (Aoki & Ueno, 1997; Aoki, Yamashita, & Ueno, 1995; Godiksen et al., 2009; Yamashita & Konagaya, 1990; Yamashita & Konagaya, 1991). In the present study, we found a significant negative correlation between muscle pH and level of cathepsin B + L activity. Pre-slaughter stress resulted in lower muscle pH immediately *post-mortem* than minimal-stress (NS), significantly for long-term stress (LS), and this

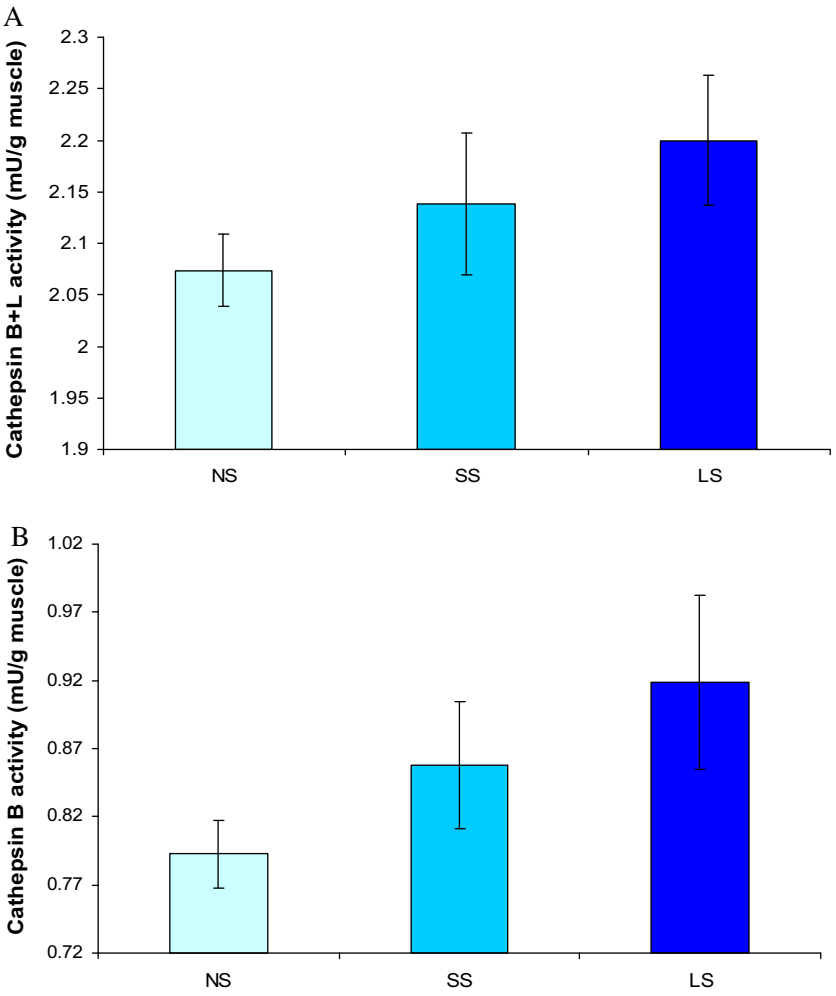

Fig. 9. A: Cathepsin B + L total activity; B: Cathepsin B total activity, 0 h *post-mortem*, in frozen *pre-rigor* fillet homogenates of Atlantic salmon subjected to minimal (NS), short- (SS) or long-term (LS) pre-slaughter crowding stress. Each histobar represents the mean value ± SE of one group ($n = 6$).

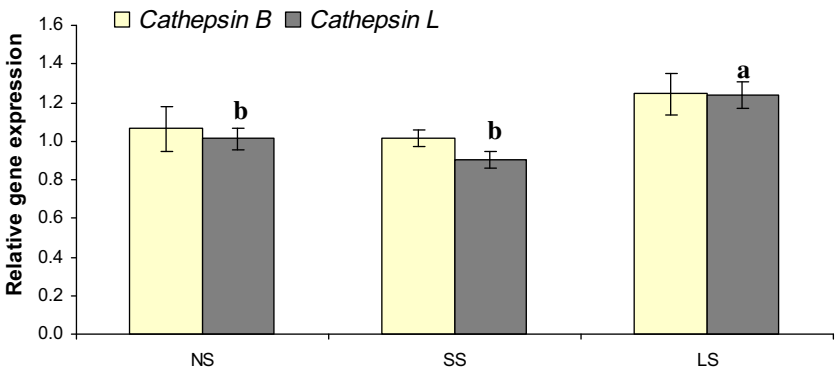

Fig. 10. Cathepsin B and cathepsin L relative gene expressions, 0 h *post-mortem*, in *pre-rigor* fillets of Atlantic salmon subjected to minimal (NS), short-(SS) or long-term (LS) pre-slaughter crowding stress. Each histobar represents the mean value ± SE of one group ($n = 6$). Different letters denote significant differences with the other groups for either cathepsin B or cathepsin L.

Table 3
Summary: effects (p values relative to NS group) of stress and time of filleting on quality of Atlantic salmon *pre-rigor* and *post-rigor* fillets.

	Effect of stress						Effect of time of filleting (*pre-rigor*/*post-rigor*)
	Pre-rigor fillets			*Post-rigor fillets*			
	General	SS	LS	General	SS	LS	
pH	0.0003	–	0.002	–	–	-	–
Myof–Myof detach	<0.0001	–	<0.0001	–	–	–	–
Myof–Myoc detach	0.047	0.028	0.037	–	–	–	–
Myof breakages	–	–	0.050	–	–	–	0.003
Contract myofibres	–	–	–	–	*0.058*	*0.072*	*0.063*
Texture	*0.087*	–	–	0.041	0.046	–	–
Cath B activity	–	–	*0.084*	nd	nd	nd	nd
Cath L activity	–	–	–	nd	nd	nd	nd
Cath B expression	–	–	–	nd	nd	nd	nd
Cath L expression	0.001	–	0.011	nd	nd	nd	nd

Negative signs denote no significant effect; nd = not determined.

Table 4
Correlation coefficients between results of the different quality traits.

	pH	Myof–myof detach	Myof–myoc detach	Firmness	Cath B + L act	Cath B act	Cath L act	*Cath B* exp	*Cath L* exp
pH		−0.548***	−0.222**	0.292***	−0.460**	–	–	–	–
Myof–myof detach	−0.548***		–	−0.516***	–	0.477**	–	–	0.513**
Myof–myoc detach	−0.222**	–		−0.204**	*−0.435**	0.455**	–	–	–
Firmness	0.292***	−0.516***	−0.204**		–	*−0.437**	–	–	*−0.469**
Cath B + L activity	−0.460**	–	*0.435**	–		nd	nd	nd	nd
Cath B activity	–	0.477**	0.455**	*−0.437**	nd		nd	–	nd
Cath L activity	–	–	–	–	nd	nd		nd	–
Cath B expression	–	–	–	–	nd	–	nd		nd
Cath L expression	–	0.513**	–	*−0.469**	nd	nd	–	nd	

nd = correlation not-determined.
* Correlation trend $p < 0.07$.
** Correlation is significant at $p < 0.05$.
*** Correlation is significant at $p < 0.001$; negative signs denote no significant correlation.

low pH could be directly responsible for the earlier higher activity of cathepsin B in the muscle of the stressed salmon, especially the LS group. Gil et al. (1999) also measured a higher activity of cathepsin B and cathepsin B + L in PSE ham with low pH, when compared with normal quality ham. Accordingly, in mammals, Taylor et al. (1995) suggested that cathepsins participated in mammalian muscle proteolysis *post-mortem* as soon as muscle pH became low.

Significant positive correlations between percentage of myofibre–myofibre detachments and cathepsin B activity on one hand, and *cathepsin L* gene expression on the other hand, were observed, as well as between percentage of myofibre–myocommata detachments and cathepsin B activity. These results agree with Vihko and Salminen (1983), who found an increase in cathepsin D activity in exhausted rat muscle, and this activity increase was associated with muscle fibre injuries, necrosis and protein degradation. Gomez-Guillen et al. (2000) also noticed that pre-slaughter stress in Atlantic salmon resulted in myofibrillar protein denaturation and greater myosin proteolysis, knowing that cathepsins are able to degrade myosin easily (Aoki & Ueno, 1997; Ladrat, Verrez-Bagnis, Noel, & Fleurence, 2003; Taylor et al., 1995). In the present study, the significantly higher percentage of myofibre–myofibre detachments until 24 h *post-mortem* and significantly higher percentage of myofibre–myocommata detachments over the whole storage period found in the stressed groups could thus be a direct consequence of the action of cathepsin B activity in the muscle, the lower initial muscle pH *post-mortem* in these groups, especially in the LS group, allowing the action of this enzyme at earlier stages than in the NS group.

On the other hand, the higher percentage of myofibre–myofibre and myofibre–myocommata detachments observed in the present study could also be due to a mechanical stress directly applied to the muscle by pre-slaughter crowding stress. Muscle structure degradation of Atlantic salmon due to mechanical stress has already been suggested in our previous study (Bahuaud et al., 2009) and Roth et al. (2006) indicated that pre-slaughter stress in Atlantic salmon could affect myofibrils or connective tissue physically, thus releasing proteases and accelerating muscle degradation. Gomez-Guillen et al. (2000), Sigholt et al. (1997) and Yamashita and Konagaya (1991) also suggested that protein denaturation resulting from exposure of *post-mortem* muscle to low pHs, may facilitate the access of substrates by proteolytic enzymes and thus enhancing muscle proteolysis. The low muscle pH observed especially in the long stressed (LS) salmon could also have caused a direct damage of the muscle structure by shrinking myofibres, thus increasing the tensions on the endomysium or at the connective tissue level, resulting in a higher number of myofibre–myofibre and myofibre–myocommata detachments.

Pre-slaughter stress tended to increase the percentage of contracted myofibres in *post-rigor* fillets 96 h *post-mortem,* and the longer the pre-slaughter stress period, the higher the percentage of contracted myofibres. This is in accordance with several authors (Erikson & Misimi, 2008; Erikson, Sigholt, Rustad, Einarsdottir, & Jørgensen, 1999; Nakayama, Toyoda, & Ooi, 1994; Skjervold et al., 1999; Skjervold, Fjæra, Østby, Einen, 2001; Stien et al., 2005; Thomas et al., 1999; Veiseth, Fjæra, Bjerkeng, & Skjervold, 2006) who pointed out that pre-slaughter stress enhances *rigor* contraction in fish.

We also observed an increase in percentage of myofibre breakages in *pre-rigor* fillets with pre-slaughter stress, and the longer the pre-slaughter stress period, the higher the percentage of myofibre breakages. In the present study, salmon subjected to long-term stress (LS) presented the highest fillet contraction (Martinsen, 2006). The higher percentage of myofibre breakages observed in

the stressed salmon could thus result from the higher tension exerted on the fillet during *rigor* contraction (Erikson & Misimi, 2008; Erikson et al., 1999; Nakayama et al., 1994; Skjervold et al., 1999; Skjervold, Fjæra, Østby, Einen, 2001; Stien et al., 2005; Thomas et al., 1999; Veiseth et al., 2006). Taylor and Koohmaraie (1998) found more breakages in the I-band region of myofibrils in normal sheep muscle than in callipyge, where callipyge muscle was associated with less proteolytic activity. In the present study, the higher cathepsin B activity in the stressed salmon 0 h *post-mortem*, even not significant, could thus also be responsible for the higher percentage of myofibre breakages observed in these fish (significantly in the LS group), when compared to the NS group.

The effect of pre-slaughter stress on fillet firmness evaluated as breaking force could be seen until at least 12 h *post-mortem*, but after this point, no significant differences in fillet texture between the groups could be noticed, except at 192 h *post-mortem* in the *post-rigor* fillets where the SS group presented the softest texture. This agrees with Erikson, Beyer, et al., 1997, Skjervold, Fjæra, Østby, Einen (2001) and Stien et al. (2005), who noticed that pre-slaughter stress had the strongest impact at early stages *post-mortem* in Atlantic salmon and cod, but gradually became less pronounced. The soft texture observed only in the SS *post-rigor* fillets 192 h *post-mortem* was not easily understood, but agrees with Kiessling et al. (2004) who found that short-term stressed Atlantic salmon presented a softer muscle texture after around 1 week of storage. Immediately *post-mortem*, fillets from the LS group were significantly the softest of all, but short-stress (SS) did not have any impact on fillet texture at that time. Ando et al. (2001) also found that the breaking strength of stressed chub mackerel was lower than in non-stressed ones at early stages *post-mortem*. Like in the present study, this softer texture was associated with a higher incidence of myofibre–myofibre detachments and Taylor et al. (2002) also suggested that myofibre–myofibre detachments highly influenced Atlantic salmon fillet texture. Godiksen et al. (2009) also showed that cathepsin B, D and L were correlated to fillet texture in rainbow trout, and these results would agree with the ones obtained here on cathepsin B activity and *cathepsin L* gene expression.

In the present study, a strong significant correlation between muscle pH and fillet softness (F_{break}) was also observed, similar to the one suggested by Stien et al. (2005) on cod. This could indicate that the lower initial muscle pH as revealed in the LS group was responsible for muscle structure degradation, influencing fillet texture, as suggested by Morzel et al. (2003) in turbot. There were also significant correlations between muscle texture and percentage of myofibre–myofibre detachments, myofibre–myocommata detachments, and *cathepsin L* gene expression. Fillet texture thus resulted from a combination of different factors as already suggested by Skjervold, Fjæra, Østby, Isaksson, et al. (2001) and Taylor et al. (2002); pre-slaughter stress causing a lower initial muscle pH, activating cathepsins earlier, and these cathepsins acting directly on muscle integrity and influencing fillet texture. In the present study, the attention has been given to the lysosomal proteases cathepsins, as these enzymes have previously been involved in *post-mortem* degradation of fish, and we established a possible link between low pH due to pre-slaughter stress and cathepsin activity. In addition, the eventual participation of other proteases like calpains cannot be excluded and investigations on these cytosolic enzymes are currently being processed in our laboratory.

The influence of time of filleting (*pre-rigor* or *post-rigor*) was compared at 96 h and 192 h *post-mortem* and little impact on the observed quality traits and muscle degradation parameters was found. Our results are in accordance with Skjervold, Fjæra, Østby, Isaksson, et al. (2001), who noticed that quality differences between *pre-rigor* and *post-rigor* fillets are reduced with time. We found, however, that *pre-rigor* filleting increased the percentage of myofibre breakages 96 h *post-mortem*. *Pre-rigor* fillets are known to contract more than *post-rigor* fillets, as in *pre-rigor* fillets, *rigor*

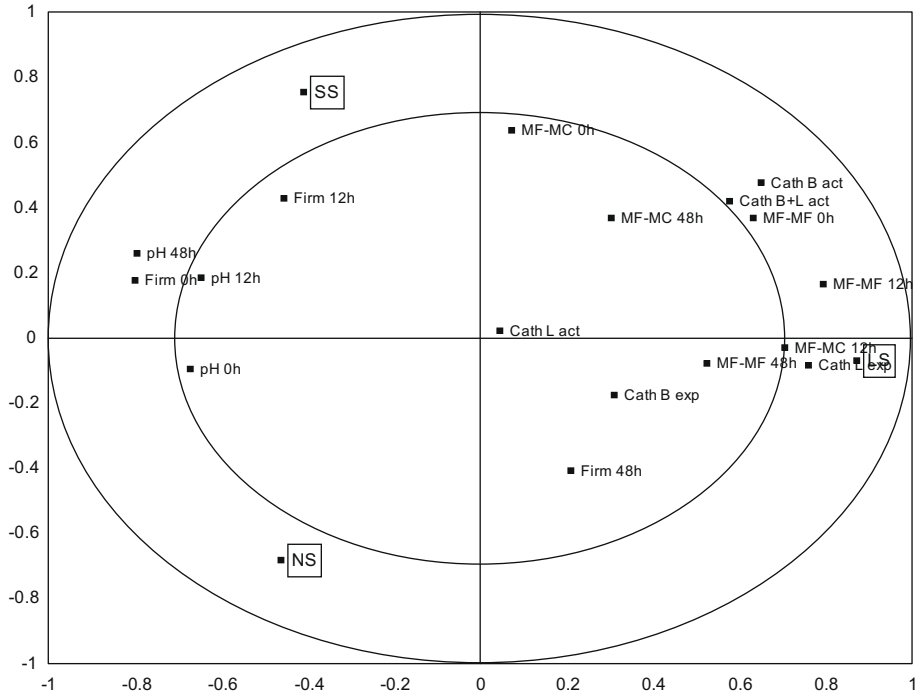

Fig. 11. Correlation loading plot from PLS regression. The first component (horizontal) (PC1) uses 34% of muscle quality variation to explain 38% of the variation in stress–length period, while the second component (vertical) (PC2) uses 10% of muscle quality variations to explain an additional 35% of variations in stress–length period. The inner and outer ellipse represent 50% and 100% explained variance respectively. MF–MF: Myofibre–myofibre detachments; MF–MC: Myofibre–myocommata detachments; Cath act: Cathepsin activity; Cath exp: *Cathepsin* relative gene expression; Firm: Fillet firmness.

contraction can progress without resistance from the fish backbone (Mørkøre et al., 2008; Skjervold, Fjæra, Østby, Isaksson, et al. 2001; Skjervold et al., 2001). This higher *rigor* contraction would then increase tensions in the myofibres, resulting in a higher number of breakages. Misimi, Erikson, Digre, Skavhaug, and Mathiassen (2008) and Mørkøre et al. (2008) also suggested that the effects of *ante-mortem* treatments (here pre-slaughter stress) are more pronounced in *pre-rigor* than *post-rigor* fillets, as significant effects of pre-slaughter stress usually occur before a noticeable onset of *rigor mortis*. *Post-rigor* filleting tending to increase the percentage of contracted myofibres 96 h *post-mortem* was, however, difficult to explain and therefore further investigations are necessary to understand this phenomenon.

5. Conclusion

Our results all converged to the fact that pre-slaughter crowding stress affects Atlantic salmon muscle quality, most significantly long-term stress (LS), especially at early stages *post-mortem*, and the longer the pre-slaughter stress period, the stronger the effects. It seemed that the low muscle pH immediately *post-mortem* resulting from the formation of lactic acid during stress, particularly in long-term stress (LS), accelerated cathepsin activity which consequently acted earlier on muscle proteolysis, leading to the acceleration of muscle degradation, when compared to minimal pre-slaughter crowding stress (NS). It can also be suggested that this low muscle pH or direct physical stress provoked shrinkage of the myofibrils; this mechanical stress increasing the tensions at the connective tissue level, and resulting in an acceleration of the muscle structure degradation. It is not excluded that other proteases like calpains could also be activated by pre-slaughter stress and may also participate in the degradation process, but this statement needs further investigations.

To conclude, pre-slaughter crowding stress in Atlantic salmon can decrease both *pre-rigor* and *post-rigor* fillet quality and has to be avoided in order to obtain high quality products. The degree of degradation seems to be related to the length of the pre-slaughter stress period; a long-term stress may produce more lactic acid and result in a lower muscle pH. *Pre-rigor* filleting still remains an interesting technique to provide fresher products on the market.

Acknowledgments

The authors would like to thank the Norwegian Research Council (NFR) for the financial support of this study, part of the Strategic University Project (SUP) 155015/110, "Atlantic salmon, our most important raw material for food production". Grethe Enersen and Målfrid T. Bjerke are warmly thanked for their help with sampling of the experimental material, as well as Ingrid Måge with the multivariate analysis of the data.

References

Ando, M., Joka, M., Mochizuki, S., Satoh, K. I., Tsukamasa, Y., & Makinodan, Y. (2001). Influence of death struggle on the structural changes in chub mackerel muscle during chilled storage. *Fisheries Science, 67*, 744–751.

Ando, M., Toyohara, H., Shimizu, Y., & Sakaguchi, M. (1991). Postmortem tenderization of rainbow-trout (Oncorhynchus-Mykiss) muscle caused by gradual disintegration of the extracellular-matrix structure. *Journal of Science and Food Agriculture, 55*, 589–597.

Aoki, T., & Ueno, R. (1997). Involvement of cathepsins B and L in the post-mortem autolysis of mackerel muscle. *Food Research International, 30*, 585–591.

Aoki, T., Yamashita, T., & Ueno, R. (1995). Purification and characterization of a cathepsin B-like enzyme from Mackerel White Muscle. *Fisheries Science, 61*, 121–126.

Bagni, M., Civitareale, C., Priori, A., Ballerini, A., Finola, M., Brambilla, G., et al. (2007). Pre-slaughter crowding stress and killing procedures affecting quality and welfare in sea bass (*Dicentrarchus labrax*) and sea bream (*Sparus aurata*). *Aquaculture, 263*, 52–60.

Bahuaud, D., Mørkøre, T., Langsrud, Ø., Sinnes, K., Veiseth, E., Ofstad, R., et al. (2008). Effects of -1.5 C Super-chilling on quality of Atlantic salmon (*Salmo salar*) pre-rigor Fillets: Cathepsin activity, muscle histology, texture and liquid leakage. *Food Chemistry, 111*, 329–339.

Bahuaud, D., Østbye, T. K., Torstensen, B. E., Rørå, M. B., Ofstad, R., Veiseth, E., et al. (2009). Atlantic salmon (*Salmo salar*) muscle structure integrity and lysosomal cathepsins B and L influenced by dietary $n-6$ and $n-3$ fatty acids. *Food Chemistry, 114*, 1421–1432.

Chéret, R., Delbarre-Ladrat, C., de Lamballerie-Anton, M., & Verrez-Bagnis, V. (2007). Calpain and cathepsin activities in post mortem fish and meat muscles. *Food Chemistry, 101*, 1474–1479.

Chéret, R., Hernandez-Andres, A., Delbarre-Ladrat, C., de Lamballerie, M., & Verrez-Bagnis, V. (2006). Proteins and proteolytic activity changes during refrigerated storage in sea bass (*Dicentrarchus labrax* L.) muscle after high-pressure treatment. *European Food Research and Technology, 222*, 527–535.

De Ceuninck, F., Poiraudeau, S., Pagano, M., Tsagris, L., Blanchard, O., Willeput, J., et al. (1995). Inhibition of chondrocyte cathepsin B and L activities by insulin-like growth factor-II (IGF-II) and its Ser29 variant in vitro: possible role of the mannose 6-phosphate/IGF-II receptor. *Molecular and Cellular Endocrinology, 113*, 205–213.

Einen, O., Guerin, T., Fjæra, S. O., & Skjervold, P. O. (2002). Freezing of pre-rigor fillets of Atlantic salmon. *Aquaculture, 212*, 129–140.

Erikson, U., Beyer, A. R., & Sigholt, T. (1997). Muscle high-energy phosphates and stress affect K-values during ice storage of Atlantic salmon (*Salmo salar*). *Journal of Food Science, 62*, 43–47.

Erikson, U., & Misimi, E. (2008). Atlantic salmon skin and fillet color changes effected by perimortem handling stress, rigor mortis, and ice storage. *Journal of Food Science, 73*, C50–C59.

Erikson, U., Sigholt, T., Rustad, T., Einarsdottir, I. E., & Jørgensen, L. (1999). Contribution of bleeding to total handling stress during slaughter of Atlantic salmon. *Aquaculture International, 7*, 101–115.

Erikson, U., Sigholt, T., & Seland, A. (1997). Handling stress and water quality during live transportation and slaughter of Atlantic salmon (*Salmo salar*). *Aquaculture, 149*, 243–252.

Gil, M., Guerrero, L., & Sarraga, C. (1999). The effect of meat quality, salt and ageing time on biochemical parameters of dry-cured Longissimus dorsi muscle. *Meat Science, 51*, 329–337.

Godiksen, H., Morzel, M., Hyldig, G., & Jessen, F. (2009). Contribution of cathepsins B, L and D to muscle protein profiles correlated with texture in rainbow trout (*Oncorhynchus mykiss*). *Food Chemistry, 113*, 889–896.

Gomez-Guillen, M. C., Montero, P., Hurtado, O., & Borderias, A. J. (2000). Biological characteristics affect the quality of farmed Atlantic salmon and smoked muscle. *Journal of Food Science, 65*, 53–60.

Hultmann, L., & Rustad, T. (2007). Effects of temperature abuse on textural properties and proteolytic activities during post mortem iced storage of farmed Atlantic cod (Gadus morhua). *Food Chemistry, 104*, 1687–1697.

Kiessling, A., Espe, M., Ruohonen, K., & Mørkøre, T. (2004). Texture, gaping and colour of fresh and frozen Atlantic salmon flesh as affected by pre-slaughter iso-eugenol or CO_2 anaesthesia. *Aquaculture, 236*, 645–657.

Kirschke, H., Wood, L., Roisen, F. J., & Bird, J. W. C. (1983). Activity of lysosomal cysteine proteinase during differentiation of rat skeletal–muscle. *Biochemical Journal, 214*, 871–877.

Koohmaraie, M. (1992). The role of Ca2+-dependent proteases (calpains) in post mortem proteolysis and meat tenderness. *Biochimie, 74*, 239–245.

Koohmaraie, M. (1996). Biochemical factors regulating the toughening and tenderization processes of meat. *Meat Science, 43*, 193–201.

Ladrat, C., Verrez-Bagnis, V., Noel, J., & Fleurence, J. (2003). In vitro proteolysis of myofibrillar and sarcoplasmic proteins of white muscle of sea bass (*Dicentrarchus labrax* L.): effects of cathepsins B, D and L. *Food Chemistry, 81*, 517–525.

Lavety, J., Afolabi, O. A., & Love, R. M. (1988). The connective tissues of fish IX. Gaping in farmed species. *International Journal of Food Science and Technology, 23*, 23–30.

Lowe, T. E., Ryder, J. M., Carragher, J. F., & Wells, R. M. G. (1993). Flesh quality in snapper, *Pagrus-Auratus*, affected by capture stress. *Journal of Food Science, 58*, 770.

Macdonald, R. G., & Cidlowski, J. A. (1982). Glucocorticoids inhibit presursor incorporation into protein in splenic lymphocytes by stimulating protein-degradation and expanding intracellular amino-acid pools. *Biochimica Et Biophysica Acta, 717*, 236–247.

Martens, H., & Næs, T., 1989. *Multivariate calibration* (1st ed., pp 419 + xvii). Chichester, New York: John Wiley and Sons.

Martinsen, T. S. (2006). *Impact of handling stress on contraction and post-mortem metabolism of pre-rigor filleted Atlantic salmon (Salmo salar L.)*. Master Thesis, Department of Animal and Aquacultural Sciences, Norwegian University of Life Sciences, Ås, p. 49.

Misimi, E., Erikson, U., Digre, H., Skavhaug, A., & Mathiassen, J. R. (2008). Computer vision-based evaluation of pre- and postrigor changes in size and shape of atlantic cod (*Gadus morhua*) and atlantic salmon (*Salmo salar*) fillets during rigor mortis and ice storage: Effects of perimortem handling stress. *Journal of Food Science, 73*, E57–E68.

Mommsen, T. P. (2004). Salmon spawning migration and muscle protein metabolism: the August Krogh principle at work. *Comparative Biochemistry and Physiology B-Biochemistry and Molecular Biology, 139*, 383–400.

Mørkøre, T., & Einen, O. (2003). Relating sensory and instrumental texture analyses of Atlantic salmon. *Journal of Food Science, 68*, 1492–1497.

Mørkøre, T., Mazo, T. P. I., Tahirovic, V., & Einen, O. (2008). Impact of starvation and handling stress on rigor development and quality of Atlantic salmon (*Salmon salar* L.). *Aquaculture, 277*, 231–238.

Morzel, M., Sohier, D., & Van de Vis, H. (2003). Evaluation of slaughtering methods for turbot with respect to animal welfare and flesh quality. *Journal of Science and Food Agriculture, 83*, 19–28.

Nakayama, T., Goto, E., & Ooi, A. (1996). Observation of characteristic muscle structure related to delay in red sea-bream rigor mortis by spinal cord destruction. *Fisheries Science, 62*, 977–984.

Nakayama, T., Toyoda, T., & Ooi, A. (1994). Physical property of carp muscle during rigor tension generation. *Fisheries Science, 60*, 717–721.

Ofstad, R., Olsen, R. L., Taylor, R., & Hannesson, K. O. (2006). Breakdown of intramuscular connective tissue in cod (*Gadus morhua* L.) and spotted wolffish (*Anarhichas minor* O.) related to gaping. *Lwt-Food Science and Technology, 39*, 1143–1154.

Plaffl, M. W. (2001). A new mathematical model for relative quantification in real-time RT-PCR. *Nucleic Acids Research, 29*, 2002–2007.

Poli, B. M., Parisi, G., Scappini, F., & Zampacavallo, G. (2005). Fish welfare and quality as affected by pre-slaughter and slaughter management. *Aquaculture International, 13*, 29–49.

Pote, M. S., & Altekar, W. (1980). Increase in rat serum aldolase levels induced by x-irradiation. *Indian Journal of Biochemistry and Biophysics, 17*, 263–266.

Roth, B., Slinde, E., & Arildsen, J. (2006). Pre or post mortem muscle activity in Atlantic salmon (*Salmo salar*). The effect on rigor mortis and the physical properties of flesh. *Aquaculture, 257*, 504–510.

Salem, M., Kenney, P. B., Killefer, J., & Nath, J. (2004). Isolation and characterization of calpains from rainbow trout muscle and their role in texture development. *Journal of Muscle Foods, 15*, 245–255.

Salem, M., Levesque, H., Moon, T. W., Rexroad, C. E., & Yao, J. B. (2006). Anabolic effects of feeding beta(2)-adrenergic agonists on rainbow trout muscle proteases and proteins. *Comparative Biochemistry and Physiology A – Molecular and Integrative Physiology, 144*, 145–154.

Salem, M., Nath, J., Rexroad, C. E., Killefer, J., & Yao, J. (2005). Identification and molecular characterization of the rainbow trout calpains (Capn1 and Capn2): Their expression in muscle wasting during starvation. *Comparative Biochemistry and Physiology Part B: Biochemistry and Molecular Biology, 140*, 63–71.

Sigholt, T., Erikson, U., Rustad, T., Johansen, S., Nordtvedt, T. S., & Seland, A. (1997). Handling stress and storage temperature affect meat quality of farmed-raised Atlantic salmon (*Salmo salar*). *Journal of Food Science, 62*, 898–905.

Skjervold, P. O. (2002). *Live-chilling and pre-rigor filleting of salmonids-technology affecting physiology and product quality*. Dr. Agric. Thesis, Agricultural University of Norway (NLH), Ås, p. 45.

Skjervold, P. O., Fjæra, S. O., & Østby, P. B. (1999). Rigor in Atlantic salmon as affected by crowding stress prior to chilling before slaughter. *Aquaculture, 175*, 93–101.

Skjervold, P. O., Fjæra, S. O., Østby, P. B., & Einen, O. (2001). Live-chilling and crowding stress before slaughter of Atlantic salmon (*Salmo salar*). *Aquaculture, 192*, 265–280.

Skjervold, P. O., Fjæra, S. O., Østby, P. B., Isaksson, T., Einen, O., & Taylor, R. (2001). Properties of salmon flesh from different locations on pre- and post-rigor fillets. *Aquaculture, 201*, 91–106.

Skjervold, P. O., Rørå, A. M. B., Fjæra, S. O., Vegusdal, A., Vorre, A., & Einen, O. (2001). Effects of pre-, in-, or post-rigor filleting of live chilled Atlantic salmon. *Aquaculture, 194*, 315–326.

Stien, L. H., Hirmas, E., Bjornevik, M., Karlsen, O., Nortvedt, R., Rørå, A. M. B., et al. (2005). The effects of stress and storage temperature on the colour and texture of pre-rigor filleted farmed cod (*Gadus morhua* L.). *Aquaculture Research, 36*, 1197–1206.

Taylor, R. G., Fjæra, S. O., & Skjervold, P. O. (2002). Salmon fillet texture is determined by myofiber–myofiber and myofiber–myocommata attachment. *Journal of Food Science, 67*, 2067–2071.

Taylor, R. G., Geesink, G. H., Thompson, V. F., Koohmaraie, M., & Goll, D. E. (1995). Is Z-disk degradation responsible for postmortem tenderization? *Journal of Animal Science, 73*, 1351–1367.

Taylor, R. G., & Koohmaraie, M. (1998). Effects of postmortem storage on the ultrastructure of the endomysium and myofibrils in normal and Callipyge Longissimus. *Journal of Animal Science, 76*, 2811–2817.

Tejada, M., & Huidobro, A. (2002). Quality of farmed gilthead seabream (*Sparus aurata*) during ice storage related to the slaughter method and gutting. *European Food Research and Technology, 215*, 1–7.

Thomas, P. M., Pankhurst, N. W., & Bremner, H. A. (1999). The effect of stress and exercise on post-mortem biochemistry of Atlantic salmon and rainbow trout. *Journal of Fish Biology, 54*, 1177–1196.

Vandesompele, E., Preter, K.D., Pattyn, F., Poppe, B., Roy, N.V., Paepe, A.D., et al. (2002). Accurate normalization of real-time quantitative RT-PCR data by geometric averaging of multiple internal control genes. *Genome Biology 3*, research0034.0031-0034.0011.

Veiseth, E., Fjæra, S. O., Bjerkeng, B., & Skjervold, P. O. (2006). Accelerated recovery of Atlantic salmon (*Salmo salar*) from effects of crowding by swimming. *Comparative Biochemistry and Physiology Part B: Biochemistry and Molecular Biology, 144*, 351–358.

Vihko, V., & Salminen, A. (1983). Acid hydrolase activity in tissues of mice after physical stress. *Comparative Biochemistry and Physiology Part B: Biochemistry and Molecular Biology, 76*, 341–344.

Yamashita, M., & Konagaya, S. (1990). Participation of cathepsin L into extensive softening of the muscle of chum salmon caught during spawning migration. *Nippon Suisan Gakkaishi, 56*, 1271–1277.

Yamashita, M., & Konagaya, S. (1991). Hydrolytic action of Salmon cathepsin-B and cathepsin-L to muscle structural proteins in respect of muscle softening. *Nippon Suisan Gakkaishi, 57*, 1917–1922.

Zhao, G. M., Zhou, G. H., Wang, Y. L., Xu, X. L., Huan, Y. J., & Wu, J. Q. (2005). Time-related changes in cathepsin B and L activities during processing of Jinhua ham as a function of pH, salt and temperature. *Meat Science, 70*, 381–388.

Food Chemistry 118 (2010) 616–619

Contents lists available at ScienceDirect

Food Chemistry

journal homepage: www.elsevier.com/locate/foodchem

Isolation and identification of the main carotenoid pigment from the rare orange muscle of the Yesso scallop

Ning Li [a], Jingjie Hu [a], Shan Wang [a], Jie Cheng [a], Xiaoli Hu [a], Zhenyu Lu [b], Zhenjian Lin [b], Weiming Zhu [b], Zhenmin Bao [a,*]

[a] Key Laboratory of Marine Genetics and Breeding, Chinese Ministry of Education, College of Marine Life Sciences, Ocean University of China, Qingdao 266003, PR China
[b] Key Laboratory of Marine Drugs, Chinese Ministry of Education, School of Medicine and Pharmacy, Ocean University of China, Qingdao 266003, PR China

ARTICLE INFO

Article history:
Received 17 December 2008
Received in revised form 25 March 2009
Accepted 14 May 2009

Keywords:
Patinopecten yessoensis
Muscle
Carotenoid
Pectenolone

ABSTRACT

The Yesso scallop (*Patinopecten yessoensis*) is one of the most important aquacultural scallops in the north of China. We identified a rare colour variant that occurs in about 0.2% of the natural population. Orange variants have not been reported before in shellfish, including scallops. Identification of the molecular basis of this colour variation will provide guidance when developing a breeding plan for these scallops. The main pigment was isolated from the muscle tissues of the variant Yesso scallop by silica gel column chromatography, and was characterised by mass spectrometry and ^{1}H and ^{13}C nuclear magnetic resonance methods. Its structure was identified as that of pectenolone (3,3′-dihydroxy-β,β-caroten-4–one). This is the first report of pectenolone, a type of carotenoid, in the muscle of the Yesso scallop.

1. Introduction

The Yesso scallop (*Patinopecten yessoensis*) is one of the most important commercial aquacultural shellfish in the north of China and has been cultured mainly in Liaoning and Shandong provinces since it was introduced from Japan in 1982 (Wang, 1984). Annual production is about 200,000 tons and the Yesso scallop industry generated about 3 billion yuan in 2007–2008.

During the course of a research project aimed at optimising a breeding strategy for this scallop, we identified a rare colour variant that occurred in about 0.2% of the natural population. The muscle tissue of this variant was orange, as opposed to the usual white.

Colours appearing in the tissues of many aquatic animals are known to be due to the presence of carotenoids (Fox, 1979; Goodwin, 1984; Haard, 1992; Latscha 1990; Simpson, 1982; Ytrestøyl, Coral-Hinostroza, Hatlen, Robb & Bjerkeng, 2004). The principal carotenoids in shellfish are β-carotene, lutein A, zeaxanthin, diatoxanthin, and pectenolone. Most of these compounds were isolated and identified during the 1980s (Goodwin, 1984; Matsuno & Hirao, 1989; Matsuno, 1989). Interestingly, these compounds cannot be synthesised *de novo* by the animals; instead, they are the result of the accumulation of carotenoids from the diet or from specific chemical modifications by metabolic reactions (Buchecker, 1982).

The ovaries of almost all Yesso scallops will turn reddish-orange during their reproductive season and then return to white after ovulation. In 1981, Matsuno, Hiraoka and Maoka isolated and identified five carotenoids from the gonad of the Yesso scallop. However, the orange-coloured muscle tissue that we encountered has not been reported before. Therefore, we aimed to determine the type of pigment responsible for the orange colour and whether the pigment was molecularly identical to the pigments previously isolated from gonads.

To identify the pigment, we used thin-layer chromatography (TLC), column chromatography, and high-performance liquid chromatography (HPLC). In addition, mass spectrometry (MS) using electrospray ionisation (ESI) and ^{1}H and ^{13}C nuclear magnetic resonance (NMR) spectrometry were applied to determine the structure of the main pigment.

2. Materials and methods

2.1. Chemicals and samples

Ultrapure water was used during all analyses. Most of the solvents and chemicals used were of analytical grade. Methanol (MeOH) for HPLC was purchased from Tianjin Shield Company, Tianjin, China. Silica gel GF254 for TLC was obtained from Qingdao Haiyang Chemical Company, Quingdao, China.

* Corresponding author. Tel./fax: +86 532 82031960.
E-mail address: zmbao@ouc.edu.cn (Z. Bao).

0308-8146/$ - see front matter © 2009 Elsevier Ltd. All rights reserved.
doi:10.1016/j.foodchem.2009.05.043

2.2. Animals

The Yesso scallops with orange muscles (Fig. 1) were obtained from the Dalian Zhangzidao Fishery in February and March of 2007. The orange muscles were removed and stored at −80 °C until analysis.

2.3. Sample extraction

Approximately 2 kg of Yesso scallop muscle were homogenised in acetone and extracted at room temperature until the colour was no longer visible. A little was retained for carotenoid content analysis. To avoid degradation and isomerisation of carotenoids, amber glassware was used and the extractions were performed in an aphotic environment. The crude acetone extract was filtered under reduced pressure to remove particles, followed by evaporation under vacuum (temperature <30 °C) to a concentrated liquid and then flushed with nitrogen. The extraction was then frozen at −80 °C until isolation.

2.4. Isolation of the main pigment

The concentrated acetone extract was applied to a silica gel column under reduced pressure and eluted using increasing percentages of acetone in petroleum ether. Twenty-one fractions were collected according to colour. Silica gel column chromatography was repeated for fractions 16–18, which were red in colour; this time the eluant was chloroform ($CHCl_3$) and MeOH. Thirty-four subfractions were obtained, of which fractions 7–12 were deep red in colour. These fractions were believed to contain the main carotenoid and were analysed further.

2.5. Purity check of the main carotenoid

The purity of the main carotenoid isolated by column chromatography was evaluated by TLC and reverse-phase HPLC. TLC analysis used a mixture of $CHCl_3$:MeOH (20:1 v/v) as the developing agent. The conditions of reverse-phase HPLC analysis were an analytical-scale (250 × 4.6 mm inner diameter) C18 ODS column; 10-μl injection volume; 30 °C column temperature; water:methanol mobile phase (90:10, v/v); 1.0 ml per minute flow rate; 200–500-nm UV–vis detection. After confirming the purity of the compound, the main pigment was further evaluated by MS and NMR.

2.6. Electrospray ionisation-mass spectrometry

To obtain the mass spectrum of the carotenoid, a small amount of the compound was dissolved in 100% methanol and applied to the probe. ESI-MS was performed on a Q-TOF Ultima Global GAA076 LC–MS (Applied Biosystems, Foster City, CA) in the positive ion mode.

Fig. 1. Muscle tissue of *Patinopecten yessoensis*. The orange colour variant is shown on the right.

2.7. ^1H and ^{13}C nuclear magnetic resonance

The main carotenoid pigment was dissolved in 500 μl d_6-acetone. ^1H and ^{13}C NMR spectra were recorded on a JEOL ECP-600 spectrometer (600 MHz), using the acetone solvent peak as a reference; chemical shifts were recorded as δ values.

2.8. Quantitative evaluation of total carotenoids from the orange muscle of Yesso scallop

The total carotenoids content from Yesso scallop was determined by spectrophotometry (λ = 450 nm) and calculated by following formula:

$$\text{Total carotenoid content from Yesso scallop (mg)} = \text{optical density value} \times \text{volume (ml)} \times \text{dilution times} \times 10 \div 2500 \ (\text{mean value } A^{1\%}_{1cm}\ 2500 \text{ of coloured carotenoids}).$$

Table 1
The ^1H and ^{13}C NMR data of the main pigment isolated from the muscle of the *Patinopecten yessoensis* orange colour variant.

No.	^1H NMR (J = Hz)	^{13}C NMR
1◆		37.0s
2	2.09m, 1,74m	46.7t
3	4.29ddd (13.2, 2.8, 1.9)	69.8d
3-OH	3.96d (2.3)	
4		200.8s
5		127.6s
6		162.0s
7●	6.75–6.83	125.8d
8◤	6.34–6.56	140.3s
9◣		137.5s
10◣	6.34–6.56	135.8d
11●	6.34–6.56	124.6d
12◤	6.34–6.56	135.9d
13◤		137.4s
14★	6.34–6.56	134.7d
15	6.75–6.83	131.7d
16	1.13s	29.0q
17	1.17s	30.9q
18	1.89s	14.1q
19▼	2.50m	12.7q
20▼	2.50m	12.8q
1′◆		37.4s
2′	1.81m, 1.38m	42.3t
3′	3.90m	64.3d
3′-OH	3.75d (4.6)	
4′	2.38m, 2.07m	47.6t
5′		138.9s
6′		124.8s
7′		90.2s
8′		99.1s
9′		120.0s
10′◤	6.34–6.56	142.8d
11′	6.66 dd(15.1, 11.5)	125.3d
12′◤	6.34–6.56	139.0d
13′		135.8s
14′★	6.34–6.56	134.5d
15′	6.75–6.83	131.5d
16′	1.35s	26.3q
17′	1.22s	31.0q
18′	1.89s	22.6q
19′▲	2.02s	18.2q
20′▲	2.02s	12.6q

▲, ▼, ◆, ●, ★, ◢, ◣, ◤, correlating assignments may be interchanged with one another; *s*, singlet; *d*, doublet; *t*, triplet; *m*, multiplet; *q*, quartet.

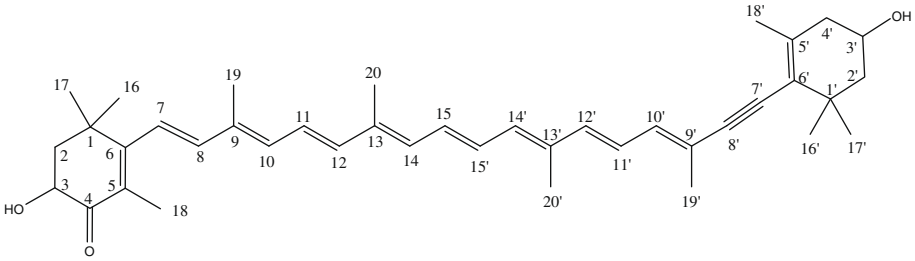

Fig. 2. Structure of the main pigment isolated from the muscle of the *Patinopecten yessoensis* orange colour variant.

3. Results and discussion

3.1. Purity of the main carotenoid from the muscle of the Yesso scallop

The carotenoids present in the orange muscles of Yesso scallops were isolated and purified by acetone extraction and silica gel chromatography. In order to determine whether a single carotenoid was responsible for producing the deep red colour that we identified as the main pigment, we performed TLC and HPLC. TLC of the main carotenoid produced a single red dot with an R_f value of 0.455. HPLC analysis of the main carotenoid showed a single peak and the absorption maximum was at about 454.6 nm (MeOH). Photodiode array measurements of the spectral properties of the peak were determined at the upslope, apex, and downslope. The degree of agreement between the three spectra indicated the degree of purity; the results indicated that a single pure substance was responsible for producing the red colour of the main pigment.

3.2. Electrospray ionisation–mass spectrometry of the main carotenoid

The positive ESI-MS exhibited a quasimolecular peak at *m/z* 581.6 $[M + H]^+$ in full scan mode. Therefore, we assumed that the relative molecular weight of the carotenoid was about 580. The ion at *m/z* 665.6 was assumed to be the corresponding quasimolecular ion of the carotenoid.

3.3. Nuclear magnetic resonance spectra of the main carotenoid

The ^1H and ^{13}C NMR spectra data of the main carotenoid from the orange Yesso scallop are shown in Table 1.

The compound showed a quasimolecular ion peak in positive ESI-MS at *m/z* 581.6 $[M + H]^+$. The molecular formula of this compound was assigned to $C_{40}H_{52}O_3$ by ESI-MS, ^1H and ^{13}C NMR data. The ^1H NMR spectrum included multiple overlapped conjugated olefinic protons (δ 6.35–6.81) and two broad signals (δ 3.96 d, J = 2.3 Hz, 1H; δ 3.75 d, J = 4.6 Hz, 1H) attributed to substitution by two secondary hydroxyl groups. Ten singlet methyl signals were also observed on ^1H NMR (δ 1.12, 3H; δ 1.17, 3H; δ 1.89, 3H; δ 2.50, 6H; δ 1.35, 3H; δ 1.22, 3H; δ 1.89, 3H; δ 2.02, 6H).

The presence of 40 distinct signals in the ^{13}C NMR spectrum concurred with a unique signal for each carbon in the formula $C_{40}H_{52}O_3$ and an unsaturation index of 14. The ^{13}C NMR spectrum showed unique signals at δ 200.8 (s), corresponding to a keto group, and δ 99.1 (s), and δ 90.2 (s), corresponding to an acetylenic group, respectively. Eighteen olefinic carbons (δ 125.8d, δ 140.3s, δ 137.5s, δ 135.8d, δ 124.6d, δ 135.9d, δ 137.4s, δ 134.7d, δ 131.7d, δ 120.0s, δ 142.8d, δ 125.3d, δ 139.0d, δ 135.8s, δ 134.5d and δ 131.5d) indicated a conjugated chain system. Another four olefinic carbons (δ 127.6s, δ 162.0s, δ 138.9s and δ 124.8s) were assigned to the double bonds in the two six-membered ring systems. The data obtained for the main carotenoid agree with previous reports for pectenolone (Matsuno & Maoka, 1981; Hiraoka et al., 1982). No effort was made to determine the stereochemistry of the compound.

The structure of the purified carotenoid is presented in Fig. 2 and it corresponds to that of pectenolone (Campbell et al., 1967). Carotenoids have been reported to possess highly nutritional and therapeutic properties, such as increasing the cytotoxic activity of killer T cells, decreasing the rate of tumour growth (Nishino, 1998; Nishino et al., 2002), and promoting wound healing. The free form of this compound was previously isolated from the gonad of the Yesso scallop and it accounted for 73% of the carotenoids present (Matsuno, Hiraoka, & Maoka, 1981).

3.4. The total content of carotenoids from the orange muscle

The total content of carotenoids from the orange muscle of Yesso scallop was about 18.6 μg/g measured by spectroscopy.

4. Conclusions

In this study, the carotenoid pectenolone was proved to be the main molecular component responsible for the orange colour of the Yesso scallop muscle. Pectenolone was isolated by column chromatography and characterised by ESI-MS, ^1H NMR, and ^{13}C NMR, and is identical to the compound previously isolated from the gonad of the Yesso scallop. The muscle is the edible part of the scallop, making it the most important feature considered during breeding and farming. Increasing the frequency of the colour variant could have a positive impact on the economic value of Yesso scallops. Our breeding experiments determined that this colour variation is heritable; therefore, future research efforts will focus on developing breeding strategies to maximise production of this orange colour variant.

Acknowledgements

We wish to acknowledge the Zhangzidao Group for collecting the scallops. Financial support for this work was provided by The National High Technology Research and Development Program of China (“863” program, 2006AA10A408), the Specialized Research Fund for the Doctoral Program of Higher Education (20060423015), the National Key Technology Research and Development Program of China (2006BAD09A09, 2006BAD09A10), and E-Institute of Shanghai Municipal Education Commission (E03009).

References

Buchecker, R. (1982). A chemist’s view of animal carotenoids. In G. Britton & T. W. Goodwin (Eds.), *Carotenoid chemistry and biochemistry* (p. 175). Oxford: Pergamon Press.

Campbell, S. A., Mallams, A. K., Waight, E. S., Weedon, B. C. L., Barbier, M., Lederer, E., et al. (1967). Pectenoxanthin, cynthiaxanthin, and a new acetylenic carotenoid, pectenolone. *Chemical Communications, 18*, 941–942.

Fox, D. L. (1979). *Biochromy: Natural colouration of living things*. Berkeley: University of California Press.

Goodwin, T. W. (1984). *The biochemistry of carotenoids. Animals* (Vol. 2). London: Chapman and Hall.

Haard, N. F. (1992). Biochemistry and chemistry of colour and colour change in seafood. In G. J. Flick & R. E. Martin (Eds.), *Advances in seafood biochemistry: Composition and quality* (pp. 305). Lancaster and Basel: Technomic Publishing Co. Inc.

Hiraoka, K., Matsuno, T., Ito, M., Tsukida, M., Schichida, Y., & Yoshizawa, T. (1982). Absolute configuration of pectenolone. *Bulletin of the Japanese Society of Scientific Fisheries, 48*, 215–217.

Latscha, T. (1990). *Carotenoids: Their nature and significance in animal feeds*. Basel: Department of Animal Nutrition and Health, Hoffmann-La Roche Ltd.

Matsuno, T. (1989). Animal carotenoids. In N. I. Krinsky, M. M. Mathews-Roth, & R. F. Taylor (Eds.), *Carotenoids chemistry and biology* (pp. 59–74). New York: Plenum Press.

Matsuno, T., Hiraoka, K., & Maoka, T. (1981). Carotenoids of shellfishes. II. Carotenoids in the gonad of scallops. *Nippon Suisan Gakkaishi, 47*(3), 385–390.

Matsuno, T., & Hirao, S. (1989). Marine carotenoids. In R. G. Ackman (Ed.). *Marine Biogenic Lipids, Fats, and Oils* (Vol. 1, pp. 251–388). Boca Raton: CRC Press.

Matsuno, T., & Maoka, T. (1981). Isolation of diatoxanthin, pectenoxanthin, pectenolone and a new carotenoid, 3,4,3′-trihydroxy-7′,8′-didehydo-β-carotene from arkshell and related three species of Bivalves. *Bulletin of the Japanese Society of Scientific Fisheries, 47*, 495–499.

Nishino, H. (1998). Cancer prevention by carotenoids. *Mutation Research, 402*, 159–163.

Nishino, H., Murakoshi, M., Ii, T., Takemura, M., Kuchide, M., Kanazawa, M., et al. (2002). Carotenoids in cancer chemoprevention. *Cancer and Metastasis Reviews, 21*, 257–264.

Simpson, K. L. (1982). Carotenoid pigments in seafood. In R. E. Martin, G. J. Flick, C. E. Hebard, & D. R. Ward (Eds.), *Chemistry and biochemistry of marine food products* (pp. 115). Westport: AVI Publishing Co Inc.

Wang, Q. C. (1984). Introduction of Japanese scallop and prospect of culture it in northern China. *Fisheries Science, 3*(4), 24–27.

Ytrestøyl, T., Coral-Hinostroza, G., Hatlen, B., Robb, D. H. F., & Bjerkeng, B. (2004). Carotenoid and lipid content in muscle of Atlantic salmon, Salmo salar, transferred to seawater as 0+ or 1+ smolts. *Comparative Biochemistry and Physiology Part B: Biochemistry and Molecular Biology, 138*(1), 29–40. Available from http://www.sciencedirect.com/science/journal/10964959.

Food Chemistry 118 (2010) 620–626

Contents lists available at ScienceDirect

Food Chemistry

journal homepage: www.elsevier.com/locate/foodchem

Yeast leavened banana-bread: Formulation, processing, colour and texture analysis ☆

Abdellatif Mohamed *, Jingyuan Xu, Mukti Singh

Cereal Products and Food Science Unit, NCAUR, Agriculture Research Service, USDA, 1815 N. University St., Peoria IL 61604, USA

ARTICLE INFO

Article history:
Received 18 December 2008
Received in revised form 6 May 2009
Accepted 13 May 2009

Keywords:
Dehydrated banana
Soluble fibre
Suspension rheology
Bread texture
Freezable water
DMA
DSC
Potassium
Dietary fibre

ABSTRACT

Banana powder (BP) was added to hard-red spring wheat (HRSW) flour intended for yeast-leavened bread formulation. Five different formulations containing 10%, 15%, 20%, 25%, and 30% BP were prepared with varying amounts of base flour, while vital gluten was maintained at 25% in all blends. Based on the added BP amounts only, the prepared bread could deliver 42.87–128.6 mg potassium/30 g of bread (one regular slice) and 0.33–1.00 g of fibre. Although the dough water absorption was increased, due to BP addition, the dough mixing tolerance (MTI) decreased. The bread loaf volume was significantly higher than the control except for the 30% blend, where the loaf volume was similar to the control. Bread staling increased with BP levels due to the high sugar content but, this effect was limited to the first two days of storage. Blends exhibited darker colour due to the high sugar and protein, while the 25% and 30% blends had the lowest percent of freezable water. The amounts of acetic acid extractable proteins from the dry blends and the dough decreased with increase in BP. The linear rheological properties of the control, 10%, and 30% blends exhibited similar viscoelastic solid behaviour, where both G' and G'' had plateaus ($G' > G''$) and they were parallel to each other over three decades of the frequency. Blends showed higher moduli values than the control.

Published by Elsevier Ltd.

1. Introduction

The addition of pre-hydrated plant fibre has been reported to improve dough water absorption and also to increase the loaf volume of high-fibre bread as well (Sosulski & Wu, 1988). Pomeranz, Shogren, Finney, and Bechtel (1977) reported that, the addition of various dry fibres to bread formulations increased dough water absorption, the mixing time, and decreased bread loaf volume. Addition of brewer's spent grain, a solid material remaining after malt brewing, to standard bread formulation resulted in low loaf volume (Prentice & D'Appolonia, 1977). The effect of oats-bran meal on dough stability and water absorption was shown to be minor as compared with bran from oat-groat (D'Appolonia and Youngs, 1978). In general, the presence of components with high water-binding capacity negatively affect flour water absorption, dough mixing, rheological properties and bread quality, such as loaf volume, crumb texture and colour (Holas & Tipples, 1978; Jelaca & Hylnka, 1971; Kim & D'Appolonia, 1977; McCleary, 1986; Michmiewicz, Biliadires, & Bushuk, 1990; Shelton & D'Appolonia, 1985). Baked products with high soluble fibre were formulated to target consumers interested in lowering their blood cholesterol (Mohamed, Rayas-Duarte, & Xu, 2008; Mohamed, Rayas-Duarte, Xu, Palmquist, & Inglett, 2004).

Barley flour and its fractions contain substantial amounts of soluble fibre, namely β-glucan in the form of (1–3)(1–4)-β-glucans (Berglund, Fastnaught, & Holm, 1992; Marlett, 1991).

The change in formulation was demonstrated to influence bread thermal properties. This was clearly established by differential scanning calorimetry (DSC), where the addition of soluble fibre was found to increase the melting temperature of ice in frozen bread (Mohamed et al., 2008; Vodovotz, Hallberg, & Chinachoti, 1996). A significant increase in loaf volume and specific loaf volume was observed upon the addition of water soluble non-starch polysaccharides (Rao, Manohar, & Muralikrishna, 2007). The dynamic mechanical analysis (DMA) testing of bread at very low temperatures (−70 °C) revealed various changes in viscoelastic properties (Hallberg & Chinachoti, 1992; Vittadini & Vodovotz, 2003).

Freeze-dried banana pulp showed a marked cholesterol-lowering effect when incorporated into a diet at the level of 300 or 500 g/kg. The soluble and insoluble components of dietary fibre participate in the hypocholesterolaemic effect of banana pulp (Horigome, Sakaguchi, & Kishimoto 1992). Potassium is the third most abundant mineral in the body and is critical in regulating blood pressure, water retention, and muscle activity. Banana is among the

☆ Names are necessary to report factually on available data; however, the USDA neither guarantees nor warrants the standard of the product, and the use of the name by the USDA implies no approval of the product to the exclusion of others that may also be suitable.

* Corresponding author. Tel.: +1 309 681 6331; fax: +1 309 681 6685.
E-mail address: a.mohamed@ars.usda.gov (A. Mohamed).

0308-8146/$ - see front matter Published by Elsevier Ltd.
doi:10.1016/j.foodchem.2009.05.044

potassium-rich fruits along with raisins, orange juice, and potato skin (Young, Lin, & McCabe 1995). In 2004, the Food and Nutrition Board of the Institute of Medicine established an adequate intake level for potassium based on intake levels that have been found to lower blood pressure, reduce salt sensitivity, and minimize the risk of kidney stones. These levels were 3800 (mg/day) for children, 4700 for adults and pregnant women, and 5100 for breast-feeding (Food & Institute of Medicine. Potassium., 2004).

The objectives of this research were to develop yeast-fermented bread formulations with high banana powder content without compromising bread quality characteristics such as loaf volume, taste, and length of storage time. The possible interactions between the components of the formulation will be addressed. This product will assist consumers in meeting their daily recommended potassium intake by consuming bread.

2. Materials and methods

2.1. Materials

Freeze-dried banana (in ¼″ diced pieces) obtained from Van Drunen Farms (Momence, IL) was ground in a food processor for 5 min and sieved through 80 mesh before use. Hard-red spring wheat (HRSW) flour (Miller's Choice) was obtained from North Dakota State Mill (Grand Forks, ND). Vital wheat gluten was obtained from Midwest Grain (Pekin, IL). Ascorbic acid was obtained from Spectrum Chemical Mfg. Corp. (Gardena, CA), α-amylase (Doh-tone) was obtained from American Ingredients (St. Louis, MO), and instant dry yeast was obtained from Fleischmann's Yeast (Chesterfield, MO). Other bread ingredients (non-fat dry milk and Crisco shortening) were obtained from a local supermarket. The banana powder proximate analysis as described in the certificate of analysis provided by the supplier were; 4% moisture; 4.09% protein; 87.19 carbohydrates (68.9% sugars, 7.5 other carbohydrates, and 10.9% dietary fibre); 1.33 g potassium; 0.089 g magnesium. Five blends with the same amount of vital gluten were used in this research: Control (100% HRS wheat flour); 10% (10% banana, 65% flour, 25% gluten); 15% (15% banana, 60% flour, 25% gluten); 20% (20% banana, 55% flour, 25% gluten); 25% (25% banana, 50% flour, 25% gluten); and 30% (30% banana, 45% flour, 25% gluten).

2.2. Methods

2.2.1. Farinograph testing

The HRSW flour and the five blends (0%, 10%, 15%, 20%, 25%, and 30% banana powder) were tested using the Farinograph according to AACCI (2000) method No. 54–21, while moisture was determined as stated by AACCI (2000) method No. 39–06. The 10 g mixing bowl was used under standard conditions (60% absorption, 14% moisture, 500 FU consistency, and 20 min run time). The dough water absorption, mixing tolerance index (MTI), and stability profiles were calculated.

2.2.2. Baking procedure

The baking procedure was based on the modified AACCI (2000) method (10-09). The ingredients for the 35 g loaf used here were a mix of solutions and dry blends. Two solutions were prepared; 350 mg ascorbic acid in 100 ml water and α-amylase solution (105 mg α-amylase (Doh-tone) in 100 ml water). The dry ingredients were prepared by combining the following; 35 g flour (or flour/banana blend); 0.875 g (2.5%) instant dry yeast; 2.1 g (6%) shortening; 1.4 g (4%) non-fat dry milk. To the dry ingredients; 5 ml ascorbic acid solution (500 ppm) and 1 ml α-amylase solution were added. The blend was mixed in a Micro mixer (National Manufacturing, Lincoln, NE).

The water absorption, as determined by mixing and feeling the dough, was as follows: Control (100% HRSW flour) = 17.5 ml; 30% = 20 ml; 25% = 21 ml; 20% = 21 ml; 15% = 22 ml; 10% = 22 ml. These amounts were added plus the 5 ml ascorbic acid and 1 ml amylase solutions added to all samples equally. Mixing times were 6 min for the control and the 10% banana, 7 min for the 15%, 20%, and the 25% banana, while the 30% banana required 8 min mixing. During initial testing, it was found that addition of the sugar/salt solution (as specified in the AACC method) to the blends containing banana caused little or no dough development (gluten-network development) due to the elevated amount of sugar in the powdered banana (68% w/w) used in the blend. Therefore, sugar and salt were eliminated in the final formulations. The method was further modified to maximize loaf volume as follows: After dough-mixing, the different formulations were proofed for 1.5 h in baking pan without punching, rather than proofing in bowls first and punched and finally in baking pans. Formulations were baked in pre-heated oven at 425 °F for 18 min. Baking performance was done in triplicate and loaf volume was recorded according to AACCI (2000) method number 10-05.

2.2.3. Bread firmness

Bread samples were tested using TA-XT2i Texture Analyzer (Texture Technologies Corp., Scarsdale, NY). Although the Texture Analyzer was used, this method was based on the AACCI (2000) method number 74-09 with a 35 mm aluminum plunger and 20 mm bread-slices. Firmness testing was performed on bread loaves that were stored at 25, 4, and −20 °C for 2, 5, and 7 days using 5 kg load cell and a 6 mm cylinder probe as described by the texture analyzer manufacturer. The bread macro available in the applications software of the texture analyzer was used without modifications. The testing was performed in triplicate, and the force recorded in grams.

2.2.4. Colour analysis

After baking, bread samples were cooled and stored at room temperature in Double Zipper, Ziploc® Brand (SC Johnson, Racine, WI), for colour measurement at the same day. The L* (Lightness), a* (Redness), and b* (Yellowness) values of the crust and the crumb were measured utilizing a HunterLab LabScan XE Spectrophotometer with a D65 light source (Hunter Associates Laboratory, Inc., Reston, VA) in triplicate.

2.2.5. Differential scanning calorimetry (DSC) and freezable water

Bread samples were analyzed using a Q2000 DSC (TA Instruments, New Castle, DE). Samples (12–16 mg) were placed in hermetically-sealed aluminum pans and cooled to −80 °C using the refrigeration system connected to the DSC. The samples were then heated from −80 to 110 °C at a rate of 5 °C/min. The onset and peak temperatures were determined by the tangent method utilized by the instrument software, which minimizes error committed by the operator in determining the onset temperature. The amount of freezable water was determined from the DSC data according to the method of Vittadini and Vodovotz (2003).

2.2.6. Acetic acid protein extraction and HPLC

Doughs were ground using a coffee grinder (Coffee Grinder GX4100-11, Oceanside, NY). The grinding was done gradually with occasional stops so that to prevent temperature rise due to friction. Dry control and blends, and their ground dough samples (4 g) were dispersed in 40 ml 0.1 M acetic acid. In order to extract the acetic acid-soluble proteins from dry blends, samples were shaken for 1 h, while dough samples were shaken overnight (~14 h) using a 32-WBS-40 shaker (John-Sam, Boocheon, NJ). After extraction (shaking), samples were centrifuged at 6000×g for 30 min at 10 °C. The supernatant and the precipitate were freeze-dried sepa-

rately. The protein content of the dried precipitate and the liquid supernatant was determined using FP-528 Nitrogen Protein Analyzer (LECO, St. Joseph, MI) (Mohamed et al., 2008). The protein content was determined by multiplying the total nitrogen by a factor of 6.25.

Supernatant of acetic-acid extracted samples were filtered through a 0.45 μm syringe filter and analyzed using size exclusion HPLC (SE-HPLC HP) 1100 system (Hewlett Packard, Ramsey, MN) with automatic injection. Samples were injected (20 μl) on a Bio-Sep-SEC-S4000 column and detected at 214 nm. The eluting solvent was acetonitrile and water (1:1, v/v) containing 0.1% trifluoroacetic acid (TFA) at a flow rate of 0.5 ml/min for 60 min (Batey, Gupta, & MacRitchie, 1991).

2.2.7. Rheological measurements

Although all formulations were baked, only three out of the six blends were used for rheological testing, the control (100% HRS wheat flour); 10% (10% banana, 65% flour, 25% gluten); and 30% (30% banana, 45% flour, 25% gluten), where testing was done on 20% (wt.%) suspensions. Samples were dispersed in a 0.05 M sodium phosphate buffer, pH 7.0 (25 °C) (Xu, Bietz, Felker, Carriere, & Wirtz, 2001) using Polytron PT10-35 homogenizer with a "low-foam" mixing head PTA 20TS (Kinematica AG, Switzerland). A duplicate of each sample were well dispersed and stored at 4 °C and used within 2 days. Rheological properties of the suspensions were measured using Rheometrics ARES strain-controlled fluids rheometer (TA Instruments Inc., New Castle, DE) equipped with 50 mm diameter cone-plate geometry (Xu et al., 2001). The angle of the cone was 0.04 radians. The sample chamber was placed in a humidity-controlled chamber to prevent moisture loss during runs, while the temperature was set at 25 ± 0.1 °C and controlled via a water circulation system. Prior to dynamic rheological parameter measurements, a strain-sweep experiment was conducted to confirm the linear viscoelastic range throughout the experiment. Linear viscoelasticity indicates that the measured parameters are independent of shear strains. Below 0.3% of strain, all measured materials in this study were in the linear range. Small-amplitude oscillatory shear experiments (shear strain = 0.1%) were conducted over a frequency (ω) range of 0.1–500 rad/sec, yielding the shear storage G' and the loss G'' moduli. The storage modulus represents the non-dissipative component of mechanical properties. The viscoelastic solid or "rubber-like" behavior is suggested if the G' spectrum is independent of frequency and greater than the loss modulus over a certain range of frequency. The loss modulus represents the dissipative component of the mechanical properties and is characteristic of viscous flow. The phase shift (δ) is defined by $\delta = \tan^{-1}(G''/G')$, and indicates whether a material is solid ($\delta = 0$), or liquid ($\delta = 90°$), or somewhere in between. Non-linear rheological measurements were conducted as steady shear in the range of shear rate of 0.01–400s^{-1}. Each measurement was repeated at least two times with different samples, where the relative errors were all within the range of ±12%.

2.2.8. Dynamic mechanical analysis (DMA)

Samples were weighed in 25.4 × 50.8 × 3 mm stainless steel windows and put in carver press at room temperature for 10 min and 2000 lbs force (8896.5 N). The samples were removed and cut into strips and placed in torsion rectangular fixture for the TA ARES LS2 controlled strain rheometer. Each sample had different dimensions, which were recorded before testing. The samples were clamped in the fixtures using a torque wrench set at 20 cN.m. The bread samples were cooled to −60 °C and measured to as high as possible temperature before samples slipped out of grips due to change in dimensions. The temperature ramps were 2 °C/min, 0.1% strain and 1 rad/s. Storage, loss modulus, and tan δ were characterized, and the storage modulus was fitted into the Fermi Equation.

2.2.9. Statistics

The statistical analysis of the bread samples data was carried out using PROC GLM in SAS Version 8.2 for PC Windows. A completely random design (CRD) was used to compare the texture data of the control and the blends stored for 2, 5 and 7 days at 25, 4, and −20 °C. From the ANOVA, F-test value was obtained and a multiple comparison test was performed on the means, using Duncan's Multiple Range Test at 0.05 levels.

3. Results and discussion

3.1. Farinograph testing

The presence of banana fibre dictated the addition of supplemental vital gluten intended for maintaining dough viscoelasticity. In general, fibre dilutes wheat gluten functionality for two reasons; due to its high water holding capacity as well as lack of viscoelasticity. Mixing flour and water for dough development is the most critical step of dough formation that requires exact mixing time and enough available water. The importance of dough mixing is evident in the disulphide bond formation between gluten (wheat proteins) fractions, where gluten film is formed, which is required for holding dough components together, thus forming a viscoelastic mass. Farinograph was used to determine the effect of powdered banana on the water absorption of the control flour and the mechanical properties of the formed dough. The water required for dough maximum consistency in the Farinograph was different from that needed for the dough used for baking. That is due to the presence of other ingredients beside the water and the different type of mixing used relative to the Farinograph mixing. Despite the difference in the amount of water required for dough formation, the Farinograph is an appropriate tool to test the effect of dried banana on the mechanical rheology of wheat flour. The presence of banana powder increased the Farinograph water absorption of the control by 5.2, 7.5, 10.3, 12.5, and 15.2% for the 10, 15, 20, 25, and 30% banana added, respectively. The dough mixing tolerance index (MTI) is the difference in Brabender Units (BU) between the top of the Farinograph-profile peak and 5 min later, where larger differences indicate increasing banana powder influence on the control. MTI of wheat flour had decreased in the presence of the banana powder, where MIT of the 15% banana was 37% lower than the control (46 versus 29 BU). Further increase in banana content resulted in additional decrease in MIT of the control but, there was little difference between 10 and 15% blends, in addition to insignificant differences between the 20 and 25% blends. Dough stability was reduced by 22.3% (control 21.1 min and blends 16.4 min) in the presence of banana powder. Dough stability is the difference in min between the time when the top of the curve reaches 500 BU and the time where it leaves the 500 BU. The increase in the banana content in the blends didn't have further influence on the dough stability. The effect of the banana on the Farinograph profile of the control could be attributed to the presence of fibre and the sugars as well as the electrolytes such as potassium. The influence of these components on MIT and dough stability is due to their ability to compete with gluten for water as well as weakening the gluten network needed for dough formation. The purpose of adding vital gluten to the blends was to manage the negative influence of the banana on the dough rheology. This way, the quality of the final product, such as loaf volume and crumb quality, will be maintained. The arrival time is also one of the dough quality parameters obtained from the Farinograph testing. It is the time needed for the curve to reach the

500 BU mark, where longer arrival time indicates slower gluten development during mixing. Consequently, this will increase dough mixing time and delay bread production. The arrival time for the control flour was 1 min while the 15% blend needed 6 min to arrive.

One of the good measures of wheat flour quality as well as the effect of added ingredients on the final bread quality characteristics is the bread loaf volume. Although, the addition of vital gluten to banana blends will increase cost, it was necessary to maintain bread quality. Among other components, banana powder contained around 11% fibre, 69% sugars, 4% proteins, and 1.5% fat. Due to their structure, sugars and the fibre absorb a large amount of water, consequently interfering with gluten development during dough mixing. Lack of fully developed gluten has a direct effect on dough formation, mixing time, and bread quality. The 10%, 15%, 20%, and 25% blends exhibited significantly ($p \leqslant 0.05$) higher loaf volume compared to the control, whereas the 30% blend loaf volume was similar to the control (Fig. 1a). Keep in mind that all blends had the same amount of vital gluten added to the control (25%). Therefore, blends with less banana powder showed higher loaf volume indicating positive effect of vital gluten. The 30% blend appeared to be the most comparable to the control. It is worth mentioning here, because of the high sugar content of the banana powder, sugar was eliminated from the baking formulation of the blend while it was added to the control. The presence of higher sugar content, instigated competition with vital gluten for available water, which delayed gluten development. Another reason for eliminating sugars was their effect on the colour (high sugar darker colour), texture, and taste of the final product.

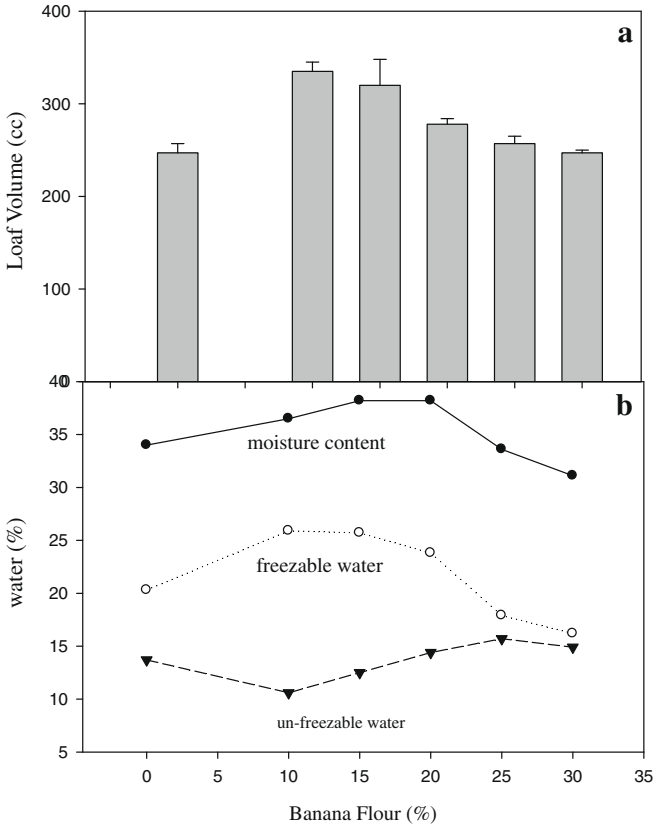

Fig. 1. (a) Loaf volume of the control and the blends. Samples with the same letter are not significantly different at 95% confidence interval. (b) Moisture content, freezable water, and un-freezable water of the control and the blends.

3.2. Bread staling

Bread staling is one of the important characteristic of stored bread, where bread aroma becomes less desired by consumers. Staling can be quantified by determining bread texture. Amylose and amylopectin retrogradation are believed to be the main cause of staling. Monoacylglycerols complexation with amylose was found to be effective in reducing staling (Willhoft, 1971). In order to determine the effect of storage time and temperature on bread, firmness testing was done at 25, 4.0, and −20 °C for 2, 5, and 7 days. The time and temperature were selected to imitate supermarket's storage conditions. The control (0% banana) exhibited higher firmness compared to the blends at all temperatures and storage time (Table 1). In addition to the increase in firmness with time, the lower temperature reduced the firmness at all storage time. The data in Table 1 also showed that higher banana powder content increased bread firmness due to the high sugar content. Elevated amounts of sugar had direct effect on water migration from other bread components, such as protein and gelatinized starch, thus causing bread stiffness. This moisture distribution and trapping by the sugars are the cause of higher firmness. Bread enriched with soluble fiber is one of the popular products in the baking industry. High soluble fibre and protein content, were found to have reduced bread firmness (Mohamed et al., 2008). The amount of banana powder added had a significant effect on bread firmness after storage, where most blends were significantly different from each other, within each temperature, except 25% and 30% blends (Table 1). Samples stored for two days at room temperature showed significantly lower firmness compared to the control, where samples with lower banana powder content exhibited lower firmness. After 5 and 7 days storage at room temperature, no significant difference in firmness was observed between blends, except the 10%, regardless of the amount of banana powder added (Table 1). At 4 °C storage, banana powder content seemed to have significant effect specially, after 5 and 7 days storage. Storage at −20 °C showed a pattern, where the 10% and 15% blends had similar firmness values, while the 20%, 25%, and 30% blends exhibited similar firmness (Table 1). The 10% blend stored at −20 °C showed the least firmness, while the greatest firmness recorded was the control stored at room temperature for 5 or 7 days.

Table 1
Bread firmness, after storage for 2, 5, and 7 days at 25, 4, and −20 °C.

Banana (%)/days	2	5	7
25 °C			
0	1563.0 ± 52.0 a	2614.0 ± 87.0 a	2871.0 ± 86.0 a
10	375.1 ± 35.1 d	954.9 ± 24.7 b	1085.0 ± 21.3 a
15	502.4 ± 22.3 cd	1016.0 ± 20.1 b	1266.0 ± 30.7 b
20	742.2 ± 28.5 bc	1392.0 ± 31.0 b	1617.0 ± 48.7 b
25	871.5 ± 24.6 b	1413.4 ± 16.3 b	1724.6 ± 19.5 b
30	887.8 ± 19.4 b	1530.3 ± 20.8 b	1754.8 ± 20.2 b
4 °C			
0	1002.6 ± 89.0 a	1143.8 ± 23.4 a	1202.9 ± 18.9 a
10	305.1 ± 51.0 c	450.7 ± 9.7 d	484.0 ± 51.1 d
15	421.1 ± 61.8 c	580.4 ± 13.8 cd	629.8 ± 82.6 cd
20	652.3 ± 15.6 b	814.5 ± 26.8 bc	855.2 ± 26.1 bc
25	763.6 ± 20.4 b	869.3 ± 12.1	1007 ± 29.8 ab
30	821.3 ± 18.8 ab	996.7 ± 29.5 ab	1032.1 ± 30.6 ab
−20 °C			
0	275.7 ± 94.4 a	269.8 ± 78 a	300.0 ± 80.0 a
10	70.7 ± 19.8 b	79.7 ± 16.4 b	84.7 ± 14.4 b
15	101.6 ± 36.8 b	106.8 ± 25.9 b	120.3 ± 39.7 b
20	211.9 ± 56.7 a	228.5 ± 36.4 a	263.1 ± 65.8 a
25	253.8 ± 83.0 a	283.9 ± 63.6 a	320.8 ± 86.0 a
30	276.1 ± 65.7 a	295.6 ± 62.6 a	332.0 ± 63.0 a

Predicted mean values followed by the same letter within temperature and column are not significantly different based on overlap of the 95% confidence intervals.

3.3. Colour analysis

Considering the high protein content of the blends, due to the additional vital gluten, it was expected they will be darker than the control (lower L^* value). Similarly, samples with more banana powder will be darker, due to the excess sugar in the banana powder. The bread crust data in Table 2 showed just that, where the L^* value decreased significantly and in accordance to the banana powder content, where the 30% blend was the darkest and the 10% was the least. The crumb showed similar pattern with less significant differences between blends. The darkness of both, the crust and crumb, is a product of the Maillard Reaction between reducing sugars and proteins. The redness (a^*) and yellowness (b^*) of the crust was also significantly different between all samples. The redness values of the crumb significantly increased relative to the banana content, while the yellowness was not significantly different, where the 10% and 15% blends were significantly lower than the remaining blends including the control (Table 2). Unlike in the crust, this indicated the difficulty in locating regions on the crumb with major colour contrast compared to the control.

3.4. Freezable water

The percent freezable water (FW) was calculated according to Vittadini and Vodovotz (2003). The method is based on DSC analysis of bread by dividing the peak enthalpy of the water in the bread sample by the latent heat of fusion of ice. The initial moisture content of the tested bread samples was directly associated with the FW (Fig. 1b). As expected, the amount of banana powder in blends influenced the moisture content and consequently altered the %FW. The %FW value of the control was in the middle of those of the blends, despite the lower amounts of water added to the control initially during dough mixing. The 25% and the 30% blends showed the lowest %FW, while the 10% and 15%, and 20% blends were the highest (Fig. 1b). It is interesting to see the differences between samples with the same amounts of water during dough mixing display different %FW values as in blends 10% and 15% as well as 25% and 30%. The effect of the banana powder on the %FW was obvious in Fig. 1b. Although, the initial excess amounts of water added to the blends compared to the control managed to increase %FW as in the 10, 15, and 20, the increase in the amounts of banana powder brought it down as shown in the 25% and 30% blends (Fig. 1b). The high sugar content of the added banana powder have interacted with the water and lowered the quantity of free water hence reducing the overall %FW of the bread. The peak temperature data of ice melting gathered from DSC profile reflected similarities between the samples, where the 10% blend as well as the control melted at −2 °C and the 30% blend at −7 °C. This trend was not apparent, neither on the moisture content and the %FW nor in the bread firmness.

3.5. Acetic acid protein extraction and HPLC

Protein extractability can be used as a measure of interaction, where low extractability indicates protein interaction with other ingredients used in the formulation. A representative sample of wheat proteins can be extracted using 0.1 M acetic acid (Mohamed et al., 2008) because wheat gluten is partially soluble in acetic acid. Additionally, it is important to determine the effect of mixing on protein extractability by extracting proteins from both, dry mixes as well as dough. The amounts of proteins extracted from both, dry mixes or dough, decreased as the banana powder increased in the formulation, even though the ratio of protein:non-protein in the dry mix was kept the same by adding extra gluten. The amount of protein in the supernatant was determined and plotted against the amount of banana powder in the blends. A linear regression of the plotted data was used to show the linearity of the amount of proteins extracted from the dry mix and the dough as a function of banana powder content. The decrease in the extractable protein from the dry mixes followed a strait line with a good fit $Y = 36.9\ X - 0.68$ ($R^2 = 0.97$), whereas the dough had a poor fit with $R^2 = 0.40$ and $Y = 39.7\ X - 0.83$. This difference could be attributed to the formation of water-insoluble aggregates as part of the gluten-network formed during mixing while gluten transformed into a viscoelastic material. Considering the extra protein added to the blends one might expect the amount of extractable protein from control to be lower than the blends, but the data presented here showed otherwise. Except for the 10 and the 15% blends, the extractable protein from the remaining blends was lower than the control.

In an attempt to show changes in protein-fractions size, the extracted proteins were analyzed using a SE-HPLC. The dough profile showed a typical wheat protein profile with different peak intensity according to the amount of protein in each sample. The first peak around 11.5 min represents the high MW glutenins followed by the low MW glutenins and finally the gliadins (Fig. 2). The SE-HPLC profile of the blends showed similar trends regarding the type of protein extracted. Although, there is similarity in the type of the extracted protein, some fractions showed more glutenins

Table 2
Bread colour analysis of the control and the blends.

Banana (%)	L^* [A]	a^* [B]	b^* [C]
Crust			
0	56.51 ± 3.7[D] a	14.83 ± 1.2 c	36.36 ± 1.2 a
10	37.85 ± 2.6 b	16.42 ± 0.37 a	27.77 ± 1.4 b
15	32.39 ± 2.9 c	15.55 ± 0.8 b	22.10 ± 1.9 c
20	28.51 ± 1.4 cd	13.45 ± 0.4 c	16.87 ± 0.6 d
25	25.79 ± 0.8 de	11.66 ± 0.3 d	13.20 ± 0.2 e
30	22.86 ± 0.3 e	9.27 ± 0.6 e	9.66 ± 0.9 f
Crumb			
0	66.21 ± 2.3 a	1.30 ± 0.7 d	19.88 ± 1.3 a
10	60.39 ± 0.5 b	1.28 ± 0.2 d	16.46 ± 0.1 b
15	57.91 ± 2.9 bc	2.14 ± 0.3 c	17.72 ± 0.3 b
20	54.40 ± 4.1 c	3.10 ± 0.6 b	19.48 ± 1.2 a
25	53.52 ± 3.7 c	3.71 ± 0.2 ab	19.78 ± 0.7 a
30	56.83 ± 1.6 bc	3.94 ± 0.3 a	20.55 ± 0.8 a

[A] L^* = lightness, higher values indicate lighter colour.
[B] a^* = redness.
[C] b^* = yellowness; higher colour intensity is indicated by higher values.
[D] Predicted mean values followed by the same letter within a column are not significantly different based on overlap of the 95% confidence intervals.

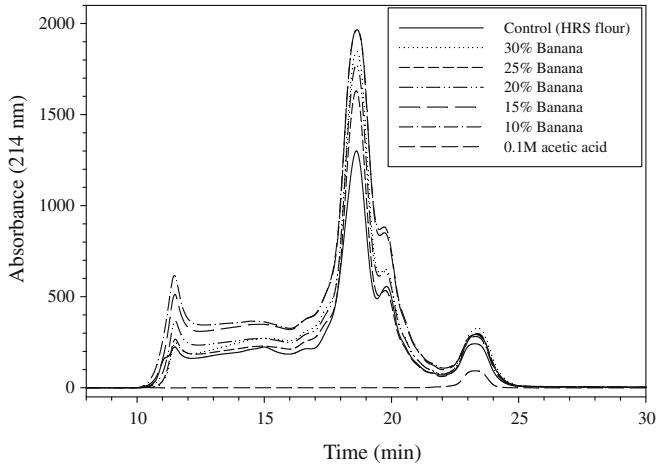

Fig. 2. SE-HPLC of acetic acid extractable proteins from doughs of control and blends.

than low MW glutenins (Fig. 2). The dry mixes extraction profile did not show sharp glutenins peak, instead, a broad peak appeared (data in not shown) between 12 and 16 min and another peak with higher intensity, compared to the dough profile. The presence of the broad peak could be due to the fact that, glutenins interacted with the banana powder while in the dough, glutenins formed aggregates, which allowed easy extraction, and thus the sharp peak was present.

3.6. Rheological measurements

The profile of the strain-sweep measurements at 1 rad/s frequency for the control (0% banana), 10%, and the 30% banana, where the linear range of control was less than 1% and the linear range of the 10% and 30% suspensions was less than 0.3% as well as the remaining blends. The elastic or storage modulus (G') for the 30% blend was the highest among the three blends. Although all samples had the amount of added vital gluten (25%), the high banana content of the 30% blend and the higher amount of gluten in the 10% blends are possibly the cause of the high G' relative to the control. The 30% blend contains higher fibre content, while the 10% blend was higher in gluten content due to the higher wheat flour in the blend. Therefore, the high fibre content facilitated the formation of a more solid like suspension, while gluten is known to have high elasticity than the other components in the flour causing higher G' of the two blends than the control. The linear rheological properties of the control, 10%, and 30% blends exhibited similar viscoelastic solid behavior (Ferry, 1980), where both G' and G'' had plateaus ($G' > G''$) and there were parallel to each other over three decades of the experimental frequency. Blends showed higher moduli values than the control. The storage or elastic moduli (G') and the phase shifts (δ) for the control were in a range of 20 to 90 Pa and 15 to 32°, respectively. The elastic moduli (G') and the phase shifts (δ) for the 10% blend were in a range of 99 to 437 Pa and 15 to 31°, respectively, while the 30% blend exhibited a 212–851 Pa elastic moduli (G') and the (δ) between 11 and 23° (Fig. 3b). The G' and the δ values of the remaining blends (10%, 15%, and 25%) were in between the 20% and 30% blend (data not shown). These results indicated that blends exhibited stronger viscoelastic solid properties than the control, suggesting that blends should have better baking quality than the control. However, the stronger viscoelastic solid-behaviour of the blends, partially caused by the fibre in the banana, may not have the same effect on the dough system and the baking process. Therefore, blends and the control flour might have similar baking quality despite their differences in the dynamic rheology testing. This is due to the difference between the suspension system tested here and the dough system used for baking, where the solid content of the dough system is much higher than the suspension used for dynamic rheology analysis.

The non-linear shear behavior of the control and the 10% as well as 30% blends showed shear-thinning behavior (Fig. 3a). The viscosity of the blends was higher than the control, whereas the viscosity of the 30% blend was highest (Fig. 3a). The remaining blends exhibited the same shear-thinning with values between the 10% and the 30% blends (data not shown), indicating that all blends has similar viscosities but, slightly higher than the control. Because the actual industrial processing shear rates are in the range of 1 to 100 s^{-1} (Bloksma, 1988), we could predict that, processing the control flour will require less mixing-energy than the blends due to the lower viscosities and should be easily processed. Although there were differences between the control and the blends in their rheological properties, it is reasonable to consider these differences being not substantial enough to cause changes in the final bread quality. Especially, if we consider the nutritional benefits due to the high potassium and fibre of the blends.

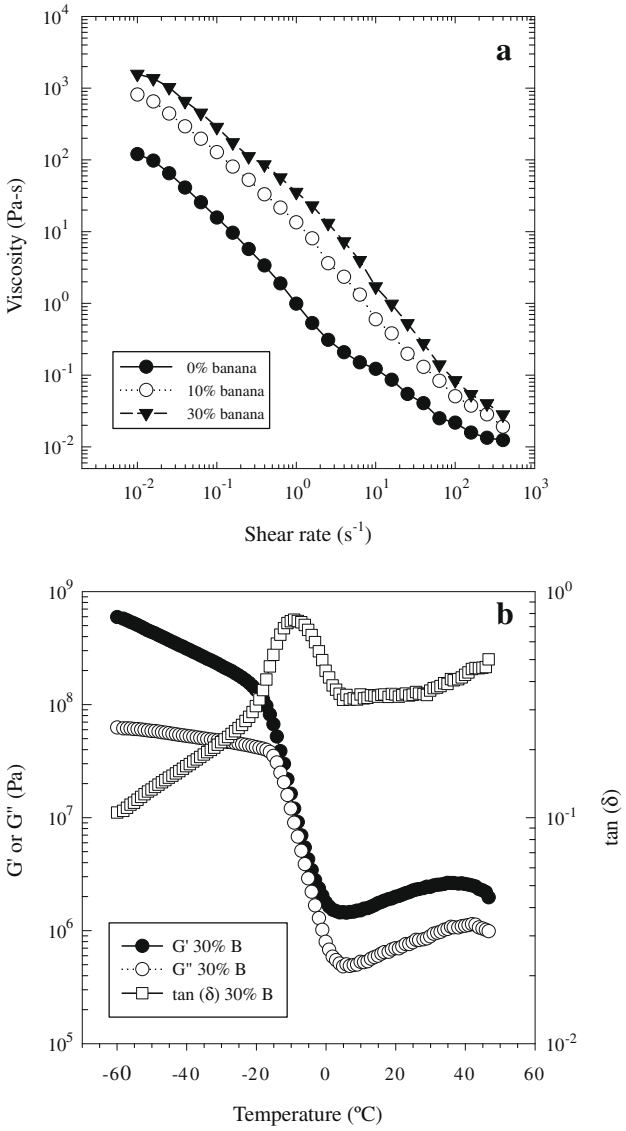

Fig. 3. (a) Non-linear steady shear viscosities for 20% suspensions of: control flour (●), 10% banana (○), and 30% banana (▼). (b) Dynamic mechanical analysis (DMA) profile of bread made from 30% banana blend G' (●), G'' (○), tan(δ) (□).

3.7. Dynamic mechanical analysis (DMA)

The storage moduli (G') obtained from DMA measurements of the bread made from the control flour and its various blends were fitted in the glass transitions model proposed by Peleg (1993, 1994). The model equation can be written as:

$$R(T) = 1/\{1 + \exp[(T - Tc)/a]\}$$

where $R(T)$ is stiffness ratio, T is temperature, Tc is temperature level which characterizes the transition region and is the inflection point of the stiffness, and a is indicator of the steepness of the curve of $R(T)$ vs. T (Fig. 3b). In our cases, $R(T)$ can be expressed as $R(T) = G'/G'$ (−30 °C). The fitting results are shown in Table 3, where all r^2 of the fitting results were above 0.71. The lower Tc value of the control bread relative to the blends signify slight shift of transition region to lower temperatures. The gradual drop in G' of the control might imply grater heterogeneity of the control compared to the blends. Overall, the variations in stiffness between the control and the blends were minimal according to the model fit, which indicated that the properties for these breads were similar around the glass transitions region.

Table 3
Storage moduli (G') obtained from DMA testing of control bread and blends.

Banana in bread (%)	*Tc* (°C)[A]	a (°C)[B]	r[B]
0	−13.1 ± 0.1	5.0 ± 0.1	0.85
30	−15.0 ± 0.2	4.4 ± 0.2	0.80
25	−15.9 ± 0.3	4.1 ± 0.3	0.71
20	−16.3 ± 0.3	4.0 ± 0.2	0.72
15	−17.3 ± 0.2	3.8 ± 0.1	0.80
10	−18.4 ± 0.1	3.3 ± 0.1	0.81

[A] *Tc* is the temperature level which characterizes the transition region and is the inflection point of the stiffness.
[B] a is indicator of the steepness of the curve of $R(T)$ vs. T; $R(T)$ is stiffness ratio; T is temperature.

4. Conclusions

Although it is considered specialty bread, by replacing up to 30% of the wheat flour, the final bread loaf volume was as good as or better than the control. The presence of BP increased the un-freezable water, which was reflected on the 50% reduction on bread staling as indicated by bread hardness. The rheological properties of the blends represented by Farinograph and the dynamic rheology showed that mechanical properties (Farinograph) are better predictor of the blends baking performance than dynamic rheology. This bread is a readily obtainable source for the daily recommended potassium intake per bread serving. This bread is also low in carbohydrates and higher in fibre relative to conventional bread.

Acknowledgements

The authors would like to thank Jason Adkins for his technical support and A. J. Thomas for conducting the DMA measurements.

References

AACCI – American Association of Cereal Chemists International (2000). *Approved methods of the AACCI. Methods 10-05, 10-09, 39-06, 54-21, and 74-09* (10th ed.). St. Paul, MN: AACCI.
Batey, I. L., Gupta, R. B., & MacRitchie, F. (1991). Use of size-exclusion high-performance liquid chromatography in the study of wheat flour proteins: An improved chromatographic procedure. *Cereal Chemistry, 68*, 207–209.
Berglund, P. T., Fastnaught, C. E., & Holm, E. T. (1992). Food use of waxy hull-less barley. *Cereal Foods World, 37*, 707–715.
Bloksma, A. H. (1988). Rheology of the breadmaking process. In *Paper presented at 8th international cereal and bread Congress, Lausanne, Switzerland*.
D'Appolonia, B. L., & Youngs, V. L. (1978). Effect of bran and high-protein concentrate from oats on dough properties and bread quality. *Cereal Chemistry, 55*, 36–743.
Ferry, J. D. (1980). *Viscoelastic Properties of Polymers* (3rd ed.). New York: John Wiley & Sons Inc.
Food and Nutrition Board, Institute of Medicine. (2004). Potassium. In *Dietary reference intakes for water, potassium, sodium, chloride, and sulfate* (pp. 173–246). Washington, D.C.: National Academies Press.
Hallberg, L. M., & Chinachoti, P. (1992). Dynamic mechanical analysis for glass transition in long shelf-life bread. *Journal of Food Science, 57*, 1201–1205.
Holas, J., & Tipples, K. H. (1978). Factors affecting farinograph and baking absorption. 1. Quality characteristics of flour stream. *Cereal Chemistry, 55*, 637–652.
Horigome, T., Sakaguchi, E., & Kishimoto, C. (1992). Hypocholesterolaemic effect of banana (Musa sapientun L. Var Cavendishii) pulp in the rat fed on a cholesterol-containing diet. *British Journal of Nutrition, 68*, 231–244.
Jelaca, S. L., & Hylnka, I. (1971). Water binding capacity of wheat flour crude pentosans and their relation to mixing characteristics of dough. *Cereal Chemistry, 48*, 211–222.
Kim, S. K., & D'Appolonia, B. L. (1977). Bread staling studies. III. Effects of pentosans on dough, bread, and bread staling rate. *Cereal Chemistry, 54*, 150–160.
Marlett, J. A. (1991). Dietary fibre content and effect of processing on two barley varieties. *Cereal Foods World, 36*, 576–580.
McCleary, B. V. (1986). Enzymatic modification of plant polysaccharides. *International Journal of Biological Macromolecules, 8*, 349–354.
Michmiewicz, J., Biliadires, C. G., & Bushuk, W. (1990). Water soluble pentosans of wheat: Composition and some physical properties. *Cereal Chemistry, 67*, 434–439.
Mohamed, A., Rayas-Duarte, P., & Xu, J. (2008). Hard-red spring wheat/C-TRIM 20 bread: Formulation, processing and texture analysis. *Food Chemistry, 107*, 516–524.
Mohamed, A., Rayas-Duarte, P., Xu, J., Palmquist, D. E., & Inglett, G. E. (2004). Hard red winter wheat/nutrim alkaline noodles: Processing and sensory analysis. *Journal of Food Science, 70*, 1–7.
Peleg, M. (1993). Mapping the stiffness-temperature-moisture relationship of solid biomaterials at and around their glass transition. *Rheology Acta, 32*, 575–580.
Peleg, M. (1994). Mathematical characterization and graphical presentation of the stiffness-temperature-moisture relationship of gliadin. *Biotechnology Progress, 10*, 652–654.
Pomeranz, Y., Shogren, M. D., Finney, K. F., & Bechtel, B. (1977). Fibre breadmaking: Effect on functional properties. *Cereal Chemistry, 54*, 25–41.
Prentice, N., & D'Appolonia, B. L. (1977). High-fibre bread containing brewer's spent grain. *Cereal Chemistry, 54*, 1084–1095.
Rao, R. S. P., Manohar, R. S., & Muralikrishna, G. (2007). Functional properties on water-soluble non-starch polysaccharides from rice and ragi: Effect on dough characteristics and baking quality. *LWT-Food Science and Technology, 40*, 1678–1686.
Shelton, D. R., & D'Appolonia, B. L. (1985). Carbohydrates functionality in the baking process. *Cereal Foods World, 30*, 437–442.
Sosulski, F. W., & Wu, K. K. (1988). High bread containing field pea hulls, wheat, corn, and wild oats bran. *Cereal Chemistry, 65*, 186–191.
Vittadini, E., & Vodovotz, Y. (2003). Changes in the physicochemical properties of wheat and soy-containing breads during storage as studied by thermal analysis. *Journal of Food Science, 68*, 2022–2027.
Vodovotz, Y., Hallberg, L., & Chinachoti, P. (1996). Effect of aging and drying on thermo-mechanical properties of white bread as characterized by dynamic mechanical analysis (DMA) and differential scanning calorimetry (DSC). *Cereal Chemistry, 73*, 264–270.
Willhoft, E. M. A. (1971). Bread staling I and II. *Journal Science Food Agriculture, 22*, 176–180.
Xu, J., Bietz, J. A., Felker, F. C., Carriere, C. J., & Wirtz, D. (2001). Rheological properties of vital wheat gluten suspensions. *Cereal Chemistry, 78*, 181–185.
Young, DB., Lin, H., & McCabe, RD. (1995). Potassium's cardiovascular protective mechanisms. *American Journal Physiology, 268*, 825–837.

Food Chemistry 118 (2010) 627–633

Contents lists available at ScienceDirect

Food Chemistry

journal homepage: www.elsevier.com/locate/foodchem

Dry milling of field pea (*Pisum sativum* L.) groats prior to wet fractionation influences the starch yield and purity

Sabaratnam Naguleswaran, Thava Vasanthan *

Department of Agricultural, Food and Nutritional Science, University of Alberta, Edmonton, AB, Canada T6G 2P5

ARTICLE INFO

Article history:
Received 16 October 2008
Received in revised form 8 May 2009
Accepted 13 May 2009

Keywords:
Field pea
Groats
Starch
Dry milling
Wet fractionation
Sonication

ABSTRACT

Field peas from two cultivars were dehulled and groats were processed by two protocols: (1) groats directly ground with water into a slurry and fractionated into fibre, protein and starch concentrates (groat wet fractionation, GWF), and (2) groats dry milled into flour and then wet fractionated using steps identical to that of protocol-1 (flour wet fractionation, FWF). The yield (%, w/w) and composition (%, w/w) of starch, protein and fibre concentrates from both protocols were determined. The data indicated that the FWF had significantly higher starch yield when compared to GWF. Scanning electron micrographs clearly suggested that better tissue fragmentation caused by dry milling may be responsible for better starch yield in FWF. The purity of starch isolate from FWF was lower than that of GWF. Brabender visco-amylographs showed differences in pasting properties of starches between protocols. Furthermore, the effect of sonication on starch yield and purity was studied between two wet fractionations. A combination of FWF with the sonication at 75% amplitude for 10 min showed better starch yield.

1. Introduction

Components of wet fractionated field pea grain offer advantages in food and non-food applications and livestock feed industries (De Graaf, Harmsen, Vereijken, & Monikes, 2001; Guillon & Champ, 2002; Hoover & Ratnayake, 2002; Otto, Baik, & Czuchajowska, 1997a; Ratnayake, Hoover, Shahidi, Perera, & Jane, 2001). Novel functional properties of purified starch, high nutritional value of protein and brighter color of dietary fibre from field pea are some of the positive attributes. Dry methods of fractionation tend to result in high starch damage and low purity starch concentrates (Czuchajowska & Pomeranz, 1994; Otto, Baik, & Czuchajowska, 1997b; Otto et al., 1997a). On the other hand, wet methods of starch fractionation are lengthy, laborious and costly. In addition, the wet fractionation process for legume starches has been problematic due to the presence of a highly hydrated fine fibre fraction and large amounts of insoluble flocculent protein (Reichert & Youngs, 1978; Schoch & Maywald, 1968).

During wet fractionation, fibre and protein components in the slurry decrease the starch sedimentation and co-settle with starch to produce undesirable brownish sediment. Low starch yield and purity may be due to inadequate breakage of cell wall and protein matrix structures, which prevents the separation of starch granules from fibre and protein. In the current commercial process for field pea fractionation, the grains are dehulled and then taken for wet milling prior to further fractionation. It is hypothesized that a front-end processing step that dry mills the groat into flour prior to wet milling would improve starch yield and purity.

Most wet fractionation studies on field peas have been carried out based on the original process developed by Schoch and Maywald (1968) for legumes. The initial slurry is typically prepared in alkaline solution. The use of alkaline chemicals (e.g. NaOH) is not well accepted by the food industry, since the necessary subsequent steps of alkali neutralization and salt removal are costly and time-consuming (Otto et al., 1997b; Sosulski, 1989). Whether the slurry is prepared from wet-milled groats or from flour affects the starch yield, recovery, purity and properties. A comparison of field pea groat wet fractionation (GWF) and flour/meal wet fractionation (FWF) in this regard has not been reported.

A simple quick fractionation technology was sought to maximize the yield and purity of starch isolated from field pea by optimising the type of wet fractionation method and sonication conditions. The objectives of this study were (1) to compare yield and chemical composition of the fractions obtained by GWF and FWF from selected field pea cultivars, (2) to compare the morphological and pasting characteristics of purified starch fractions isolated through GWF and FWF, and (3) to compare the effect of sonication on the starch yield and purity of field peas between GWF and FWF protocols.

* Corresponding author. Tel.: +1 780 492 2898; fax: +1 780 492 8914.
E-mail address: tv3@ualberta.ca (T. Vasanthan).

0308-8146/$ - see front matter © 2009 Elsevier Ltd. All rights reserved.
doi:10.1016/j.foodchem.2009.05.045

2. Materials and methods

2.1. Materials

Field pea cultivars, CDC Mozart and Eclipse, were obtained from Crop Development Centre, University of Saskatchewan (Saskatoon, Canada). The fungal protease enzyme (Flavourzyme® 1000 L) was obtained from Novozymes North America, Inc. (Franklinton, NC, USA). Commercial field pea starch was provided by the Parrheim foods (Portage La Prairie, MB, Canada). Blending of groats was performed using a Waring blender −60 Hz (Dynamics Corp. of America, New Hartford, CT, USA), and stirring of flour was performed using a magnetic stir plate. The stainless steel sieve (75 μm openings) was from W.S. Tyler, St. Catharines, ON, Canada. The centrifugations were done using Beckman J2-21 high speed centrifuge (Beckman Instruments Inc., Palo Alto, CA, USA). Drying of samples were taken place in conventional oven (Fisher Isotemp® Oven, Model: 204, Pittsburgh, PA, USA) and freeze-drier (VirTis freeze dryer, Model: 50 SRC, Gardiner, NY, USA). Megazyme assay kits for the determination of total starch and starch damage were purchased from Megazyme International Ireland Ltd. (Wicklow, Ireland). All other chemicals and solvents were of ACS certified grade.

2.2. Sample preparation

Field pea seeds in 5 kg batches were dehulled in a "tangential abrasive dehuller" (manufactured by Engineering Services Branch, Alberta Agriculture and Food, Canada), that was equipped with

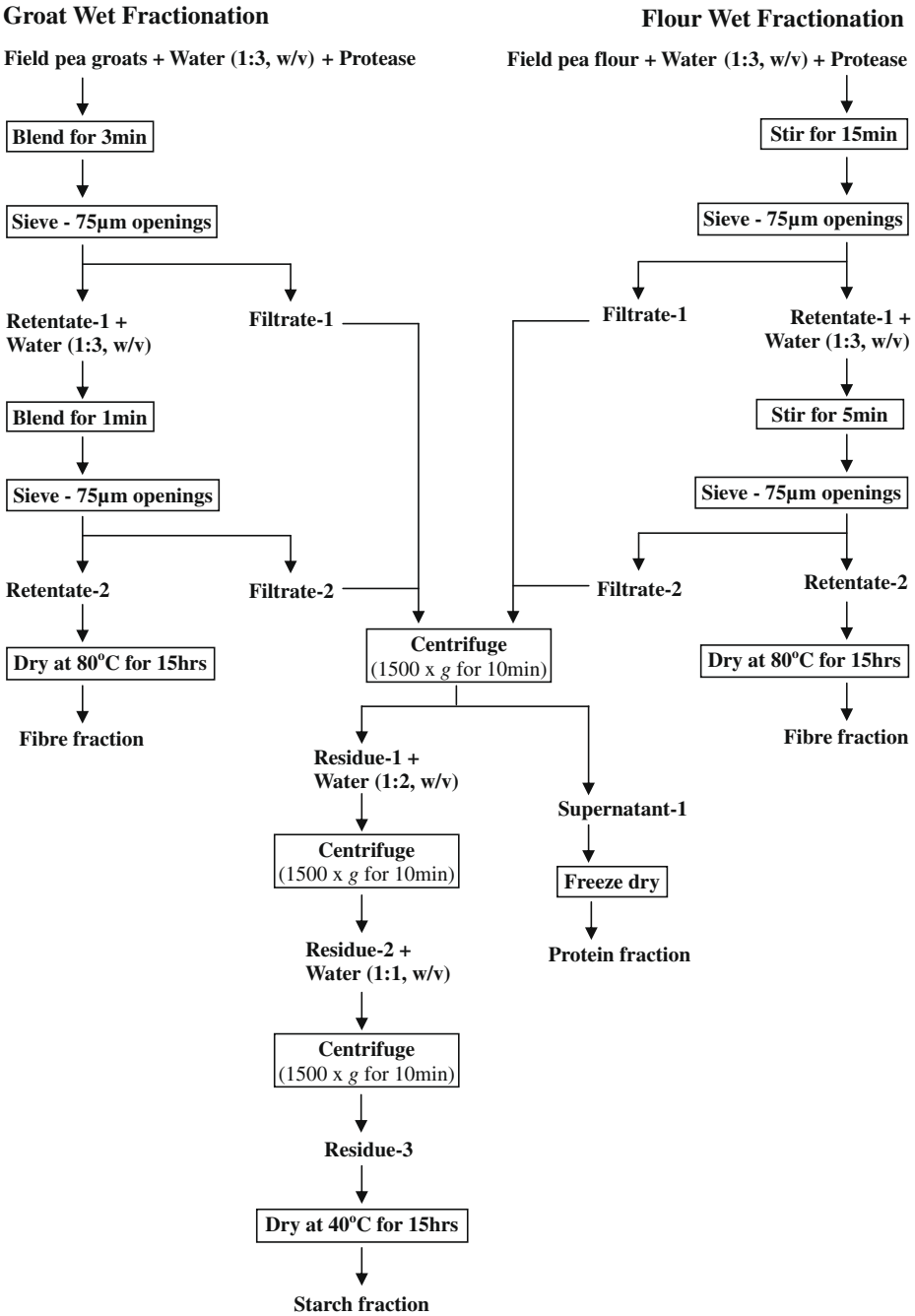

Fig. 1. Flow chart for the wet fractionations of field pea.

eight vertically oriented abrasive discs of 25 cm diameter operating at a speed of 60 Hz for 3 min. Then the dehulled grains were sifted through the Carter Day Aspirator Tester (Serial No: CD011721, Style No: COS3, Carter Day International, Inc., Minneapolis, MN, USA) at the airflow speed of 30% in order to separate the hulls from the cotyledons and the groats were collected separately for each cultivar. Field pea groats were dry milled using a lab scale cyclone sample mill (Udy Corp., Fort Collins, CO, USA) fitted with a sieve with 0.25 mm round openings. Both groats and flour from two cultivars of field pea were used in this study.

2.3. Addition of protease enzyme in wet fractionation

It is hypothesized that the addition of protease enzyme can effectively reduce the frothing during the wet fractionation process caused by its hydrolysing effect on protein. A simple experiment was conducted as wet grinding of field pea groats (100 g groats + 300 mL water) for 3 min with (1 mL) or without protease enzyme (Flavourzyme® 1000 L). Flavourzyme® 1000 L is a protease complex of both endo- and exo-protease, and it contains a concentration of aminopeptidase 15–20%. Its activity is 1.0 leucine aminopeptidase units (LAPU)/g. One LAPU is the amount of enzyme that hydrolyzes one micromole of leucine-p-nitroanilide per minute. After wet grinding of groats, with or without (control) protease enzyme, the slurry was quantitatively emptied into measuring cylinder and the volume of froth was measured in mL.

2.4. Wet fractionations

The procedure for wet fractionation of field pea groats (groat wet fractionation – GWF) and field pea flour (flour wet fractionation – FWF) is described in Fig. 1. Three replicate fractionations were done for each type of wet fractionation.

2.5. Application of sonication

Sonication treatment using a Sonic 300-Dismembrator (ARTEK Systems Corp., Farmingdale, NY, USA) was applied to the slurry of retentate-1 in both GWF and FWF (Fig. 1). The sonication amplitude was set at 60%, 75% or 90%, and the sonication duration was maintained for 10, 20 or 30 min. The temperature of the slurry during the sonication treatment was recorded. A standard wet fractionation process without sonication treatment as described in Section 2.4 (Fig. 1) was applied as a control for this experiment. Two replicated fractionations were done for each sonication treatment.

2.6. Granule morphology

Granule morphology of flour and starches was studied by scanning electron microscopy (SEM) following the procedure of Li, Vasanthan, Rossnagel, and Hoover (2001a).

2.7. Chemical composition

Moisture content was determined by the standard AACC (2004) procedure (method 44-15A). Protein content was measured by Leco® Carbon/Nitrogen determinator (TruSpec® CN, Leco Corporation St. Joseph, MI, USA). Ash content was quantified according to the AOAC (2000) procedure (method 923.03). Lipid was measured by the Goldfisch extraction method where petroleum ether was used to extract the lipid (AACC method 30.25, 2004). Total starch and damaged starch contents were estimated by the Megazyme assay procedures of AA/AMG 9/97 and SDA 11/01, respectively (Megazyme International Ireland Ltd., Wicklow, Ireland). Amylose content was determined according to the Standard Analytical Methods of the Member Companies of the Corn Refiners Association Inc., Washington, DC, USA.

2.8. Pasting properties of starch

Pasting characteristics (8% w/v, pH 5.5) of field pea starches were measured by Brabender viscometer (C.W. Brabender Instruments Inc., South Hackensack, NJ, USA) following the method of Li, Vasanthan, Rossnagel, and Hoover (2001b).

2.9. Statistical analysis

All experiments were carried out in a simple complete randomized design (CRD) at least with two replicates. One way Analysis of Variance (ANOVA) of the results was performed using General Linear Model (GLM) procedure of SAS® Statistical software, Version 9.1.2 (SAS® institute Inc., Cary, NC, 2004). The multiple comparison of the means was accomplished by Tukey (HSD) test at $\alpha = 0.05$ level. The means and standard deviations are reported.

3. Results and discussion

3.1. Composition of field pea

The chemical composition of flour from groats of two field pea cultivars, CDC Mozart and Eclipse, is summarized in Table 1. The

Table 1
Chemical composition (%) of flour[a] from two field pea varieties and their fractions[b] after fractionation by two different wet methods.

Components	Composition of field pea flour			
	CDC Mozart		Eclipse	
Moisture	9.1 ± 0.1		8.6 ± 0.1	
Starch	52.9 ± 0.6		49.3 ± 0.7	
Protein[c]	25.9 ± 0.2		22.5 ± 0.6	
Lipid	0.99 ± 0.01		0.80 ± 0.02	
Ash	2.7 ± 0.1		2.8 ± 0.0	
Amylose[d]	20.3 ± 0.3		22.5 ± 0.5	
	Yield and composition of fibre, protein concentrates and starch isolates			
	CDC Mozart		Eclipse	
	GWF[e]	FWF[f]	GWF[e]	FWF[f]
Fibre concentrate[b]				
Yield (% initial material)	28.1 ± 0.6*p*	13.9 ± 0.4*q*	30.5 ± 1.8*p*	11.6 ± 0.5*q*
Moisture	2.7 ± 0.4*p*	2.9 ± 0.3*p*	1.1 ± 0.1*q*	0.6 ± 0.2*q*
Protein[c]	3.5 ± 0.1*r*	7.9 ± 0.6*p*	2.8 ± 0.1*r*	6.3 ± 0.2*q*
Starch	66.6 ± 0.3*p*	60.1 ± 0.9*q*	67.2 ± 2.1*p*	57.8 ± 1.8*q*
Starch isolate[b]				
Yield (% initial material)	39.2 ± 1.1*q*	54.9 ± 0.7*p*	32.7 ± 1.7*r*	54.6 ± 1.2*p*
Moisture	8.4 ± 0.2*p*	7.6 ± 0.3*pq*	6.8 ± 0.6*qr*	6.3 ± 0.1*r*
Protein[c]	8.8 ± 0.1*q*	7.7 ± 0.1*r*	11.7 ± 0.2*p*	7.9 ± 0.4*r*
Starch	83.6 ± 0.2*p*	80.4 ± 0.9*qr*	81.0 ± 0.3*q*	79.0 ± 0.6*r*
Lipid	0.1 ± 0.0*q*	0.3 ± 0.0*p*	0.4 ± 0.0*p*	0.4 ± 0.0*p*
Ash	0.3 ± 0.1*pq*	0.3 ± 0.0*pq*	0.2 ± 0.0*q*	0.4 ± 0.1*p*
Damaged starch	1.3 ± 0.0*p*	1.3 ± 0.1*p*	1.2 ± 0.0*q*	1.1 ± 0.0*r*
Protein concentrate[b]				
Yield (% initial material)	26.5 ± 0.2*q*	25.8 ± 0.1*r*	28.7 ± 0.1*p*	24.7 ± 0.2*s*
Moisture	5.6 ± 0.0*p*	5.5 ± 0.1*p*	5.4 ± 0.2*p*	5.6 ± 0.1*p*
Protein[c]	61.4 ± 0.2*p*	55.9 ± 0.1*q*	53.3 ± 0.3*r*	50.6 ± 0.2*s*
Starch	4.9 ± 0.5*r*	7.3 ± 0.1*q*	5.8 ± 0.5*r*	8.5 ± 0.2*p*

[a] Mean of three replicate measurements ± standard deviation. All data reported on dry basis.
[b] Data (mean of three replicates) followed by the same letter in the same row are not significantly different ($p < 0.05$) by Tukey test. All data reported on dry basis.
[c] N × 6.25.
[d] Apparent amylose.
[e] GWF = groat wet fractionation.
[f] FWF = flour wet fractionation.

Table 2
Total dry matter recovery (TDMR), starch separation efficiency (SSE) and protein separation efficiency (PSE) of field peas fractionated by two different wet methods.[a]

(%)	CDC Mozart		Eclipse	
	GWF[b]	FWF[c]	GWF[b]	FWF[c]
TDMR	93.8 ± 0.3*p*	94.6 ± 0.5*p*	92.0 ± 0.5*q*	90.9 ± 0.9*q*
SSE[d]	61.9 ± 1.8*q*	83.5 ± 1.6*p*	53.8 ± 2.9*r*	87.5 ± 1.5*p*
PSE[e]	62.9 ± 0.2*q*	55.7 ± 0.2*r*	68.0 ± 0.3*p*	55.5 ± 0.3*r*

[a] Data (mean of three replicates) followed by the same letter in the same row are not significantly different ($p < 0.05$) by Tukey test. All data reported on dry basis.
[b] GWF = groat wet fractionation.
[c] FWF = flour wet fractionation.
[d] $\text{SSE} = \frac{(\%\text{starch in the starch fraction}) \times (\%\text{yield of the fraction})}{(\%\text{starch in the flour})}$.
[e] $\text{PSE} = \frac{(\%\text{protein in the protein fraction}) \times (\%\text{yield of the fraction})}{(\%\text{protein in the flour})}$.

moisture, starch, protein, and ash contents of the pea flours were similar to values reported in the literature (Colonna, Gallant, & Mercier, 1980; Davydova, Leontev, Genin, Sasov, & Bogracheva, 1995; Otto et al., 1997b; Sosulski, Garratt, & Slinkard, 1976; Vose, Basterrechea, Gorin, Finlayson, & Youngs, 1976). Previous studies have shown a wide variation in field pea lipid and fibre contents; 0.7–4.7%, w/w (Gujska, Reinhard, & Khan, 1994; Otto et al., 1997b) and 1.1–27.6%, w/w (Otto et al., 1997b; Tian, Kyle, & Small, 1999), respectively. In the present study, the lipid content of field pea (0.80–0.99%, w/w) was on the lower side of the literature values.

3.2. Wet fractionation of field pea

Yield and composition of field pea flour and fractions are presented in Table 1. The fractionation method significantly affected the yields of starch, fibre and protein. FWF resulted in higher starch yield but lower fibre and protein yields than GWF. The yields of starch for GWF and FWF were in the range reported in the literature (30.0–44.0% (Hoover & Ratnayake, 2002; Schoch & Maywald, 1968) and 33.6–63.1% (Colonna et al., 1980; Otto et al., 1997b), respectively). The high starch yield from FWF might be attributed to the contamination of fine fibre (Chavan, Shahidi, Hoover, & Perera, 1999; Hoover & Ratnayake, 2002; Schoch & Maywald, 1968), however, the ash content was very low, which indicated minimal contamination by the high-ash containing fine fibre. Despite lower yield, the GWF process resulted in a starch fraction of slightly higher purity than the FWF protocol. Protein was the main contaminant in all starch fractions and constituted almost 1/3 of the original protein quantity present in the initial material. The lipid content of field pea starch isolate was within the range reported by other authors (Davydova et al., 1995; Hoover & Sosulski, 1991).

The composition of fibre and protein concentrates of FWF and GWF were significantly different. Compared to GWF, the fibre fraction of FWF had a lower starch and a higher protein content. Conversely, the protein concentrates of FWF had a higher starch and a lower protein content compared to GWF. Since both by-products of starch isolation are nutritionally good sources of fibre and protein, and have useful functional properties (Dalgetty & Baik, 2003; Guillon & Champ, 2002; Nunes, Raymundo, & Sousa, 2006; Sosulski & Sosulski, 1986; Vose, 1980; Wang, Bhirud, & Tyler, 1999), they could be formulated in human food and livestock feed preparation.

The total dry matter recovery (TDMR), starch separation efficiency (SSE) and protein separation efficiency (PSE) of field peas are presented in Table 2. TDMR is the total weight of the dry fractions (fibre, starch and protein) obtained through fractionation divided by the initial dry weight of the sample. The cultivar, but not the fractionation method, had a significant effect on TDMR. All TDMR values for wet fractionations were less than 100%, likely due to loss of dry matter in between processing steps. The starch

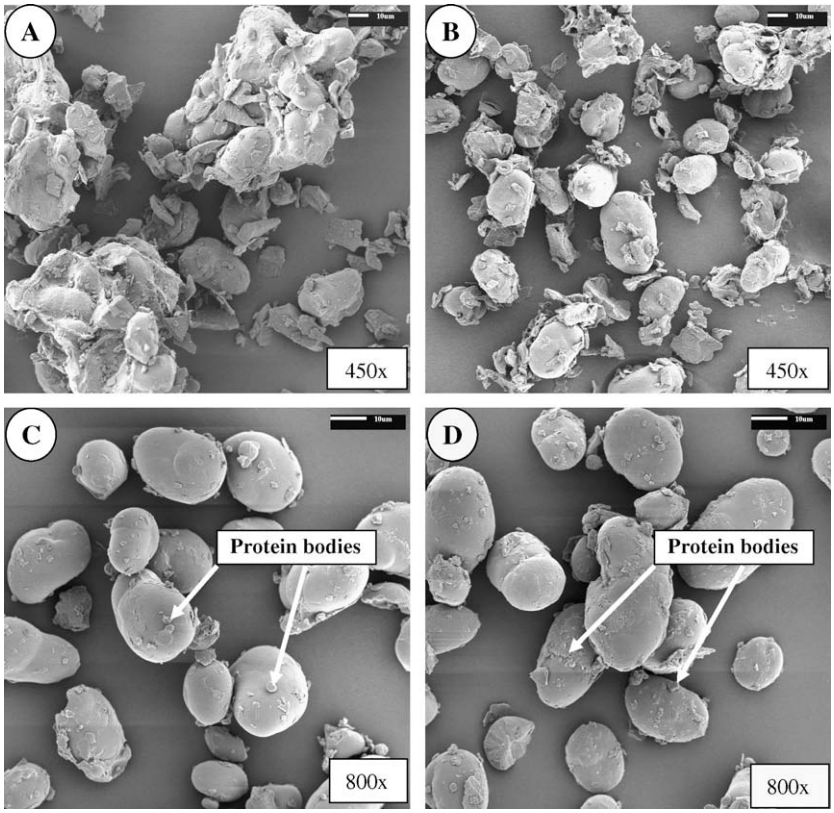

Fig. 2. Scanning electron micrographs (SEM) of flours and starches of field pea: (A) wet-milled flour, (B) dry milled flour, (C) starch isolated per groat wet fractionation (GWF), and (D) starch isolated per flour wet fractionation (FWF).

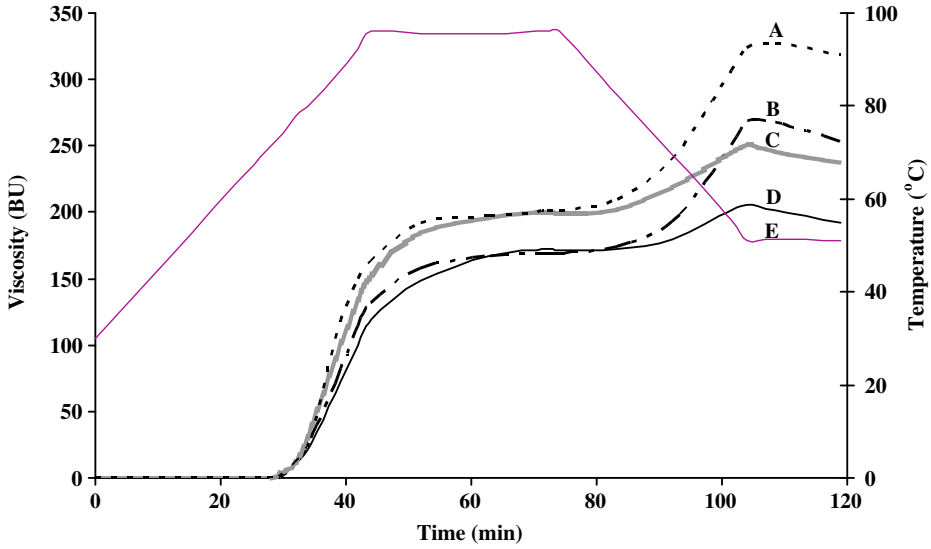

Fig. 3. Brabender viscoamylographs of field pea starches isolated by two different wet fractionation protocols: (A) Eclipse-FWF, (B) CDC Mozart-FWF, (C) Eclipse-GWF, (D) CDC Mozart-GWF, and (E) temperature (°C).

separation efficiency was higher for the FWF protocol, whereas the protein separation efficiency was higher for the GWF protocol. Sosulski (1989) previously reported separation efficiencies of starch and protein of 79.2% and 72.7%, respectively for filed pea.

To ensure efficient separation and purification, particle size distribution is crucial in a fractionation method. It was expected that dry milling prior to wet fractionation may cause the cell walls of cotyledon to disintegrate better and thereby free the embedded starch granules from the protein matrix more efficiently. Scanning electron micrographs (SEM) of flours clearly demonstrated the higher proportion of fragmented cotyledon cells with dry milling (Fig. 2B) as compared to that observed with wet milling (Fig. 2A). These observations present a reasonable explanation for higher starch yields obtained with FWF compared to GWF.

The major difficulties in purifying starch from legumes are the presence of a highly hydratable fine fibre fraction (cotyledon cell wall material) and a strong adherence of insoluble proteins to the starch granules (Schoch & Maywald, 1968). In addition, the protein causes significant frothing during grinding and screening operations that further complicates the wet fractionation process. It was observed in the present study that hydrolysing the protein with a fungal protease enzyme reduced frothing by 50–60%.

The main starch impurity was protein, which was present at levels higher than commercial field pea starch (0.55%) and literature values (0.25–0.44%, w/w) for both GWF and FWF (Otto et al., 1997b; Ratnayake et al., 2001). The scanning electron micrographs of starch isolate from GWF (Fig. 2C) and FWF (Fig. 2D), plainly show the adhered residual protein bodies on surfaces of starch granules. High residual protein content in starch fractions of the present study could be due to the following: (1) the absence of alkali use in the starch isolation, (2) brownish deposit from top of the starch layer after centrifugation was not removed, and (3) the conventional greater number of water washings was not used. However, the simple and gentle fractionation protocol used in the present study led to greatly reduced starch damage compared to other literature protocols (48%, w/w; Vose, 1977).

Due to high starch yield, dry milling of field pea groats followed by wet fractionation (FWF) used in this study was found to be more effective and efficient compared to wet grinding of groats only (GWF). In addition, the number of washings required to obtain a significant starch yield was reduced as compared to a flour wet fractionation method reported for field pea (Otto et al., 1997b).

3.3. Pasting characteristics of starches

The pasting characteristics of field pea starches are shown in Fig. 3. The four starches demonstrated a C-type amylograph pattern (low swelling and high hot paste stability) typical of most legume starches (Schoch & Maywald, 1968). The viscoamylographs showed restricted swelling and absence of peak viscosity, which is in agreement with previous studies on field pea starch (Gujska et al., 1994; Ratnayake et al., 2001; Schoch & Maywald, 1968). FWF starches had higher pasting temperatures and viscosities (notably high setback, and constant cold paste viscosity during agitation at 50 °C) compared to GWF. This effect may be due to shear effects of dry milling in the FWF procedure (Vose, 1977). In addition, the starch from cultivar Eclipse had higher viscosity than the starch from CDC Mozart in terms of corresponding wet processes. A number of intrinsic factors such as granule swelling, friction between swollen granules, amylose leaching, starch crystallinity, and amylopectin chain length may also play a role in increased viscosities observed in the present study (Ratnayake, Hoover, & Warkentin, 2002). A direct comparison between the present data and previous data is difficult, since different concentrations of starch were used in viscosity measurements.

3.4. Effect of sonication on starch yield and properties

Table 3 compares the yield, starch and protein contents of pea starch fractions for GWF and FWF methods under different sonication treatments. Sonication in GWF significantly increased starch yield by 5–8% (w/w) compared to the control, however, in FWF the starch yield was only improved by 2–3% (w/w). Higher starch yield in sonication-assisted GWF may be due to the disintegration of unfragmented cotyledon cells by ultrasound shear causing the release of more starch granules. In FWF, the cotyledon cells were already opened up by dry milling, thus no significant improvement on starch yield was expected or observed. The effect of sonication on starch yield is further supported by the SEM pictures of flour used for GWF and FWF methods (Fig. 2). It is evident in the SEM that the groat wet fractionation without sonication (control-GWF; Fig. 2A) showed presence of unfragmented cotyledon whereas control-FWF (Fig. 2B) showed highly disintegrated cotyledon structure with free starch granules.

Table 3
Chemical composition (%)[p] and yield (%, initial material) of field pea starch fractionated by two wet methods in combined with different sonication treatments.

Fractionation methods	Sonication treatments (min)	Yield (%)		Starch (%)		Protein (%)	
		CDC Mozart	Eclipse	CDC Mozart	Eclipse	CDC Mozart	Eclipse
GWF[r]	Control	32.8 ± 1.2*d*	31.8 ± 0.9*f*	83.7 ± 0.1*b–d*	81.0 ± 0.5*b–g*	8.9 ± 0.1*a*	11.8 ± 0.1*a*
	60% amp.[q] 10	34.2 ± 0.2*cd*	36.4 ± 0.7*c–e*	86.2 ± 0.6*a–c*	83.7 ± 0.9*a–c*	4.8 ± 0.7*c*	10.0 ± 0.4*ab*
	60% amp. 20	33.2 ± 0.6*d*	36.7 ± 1.8*c–e*	89.3 ± 1.1*a*	84.4 ± 1.4*ab*	4.6 ± 0.5*c*	8.9 ± 0.4*b–f*
	60% amp. 30	33.7 ± 1.2*cd*	34.2 ± 0.2*ef*	88.3 ± 0.6*ab*	83.7 ± 0.2*a–c*	4.3 ± 0.3*c*	9.7 ± 0.7*bc*
	75% amp. 10	34.9 ± 1.6*cd*	37.5 ± 0.7*c–e*	88.9 ± 0.5*a*	83.2 ± 0.9*a–d*	3.5 ± 0.2*c*	9.7 ± 0.6*bc*
	75% amp. 20	32.8 ± 0.6*d*	35.4 ± 0.4*d–f*	88.3 ± 1.9*ab*	83.5 ± 0.8*a–c*	3.7 ± 0.3*c*	8.4 ± 0.5*b–g*
	75% amp. 30	32.7 ± 1.7*d*	38.9 ± 0.5*cd*	87.4 ± 0.8*ab*	82.2 ± 0.7*a–f*	3.8 ± 0.3*c*	9.1 ± 0.8*b–d*
	90% amp. 10	35.0 ± 0.2*cd*	37.3 ± 0.4*c–e*	87.5 ± 2.8*ab*	82.9 ± 0.1*a–e*	3.8 ± 0.6*c*	9.1 ± 0.6*b–f*
	90% amp. 20	33.0 ± 0.5*d*	37.8 ± 1.3*c–e*	88.7 ± 0.5*a*	85.2 ± 0.3*a*	3.8 ± 0.7*c*	8.6 ± 0.8*b–g*
	90% amp. 30	37.6 ± 2.6*c*	39.4 ± 0.5*c*	88.0 ± 0.5*ab*	83.7 ± 0.6*a–c*	4.9 ± 0.4*c*	9.1 ± 0.9*b–e*
FWF[s]	Control	55.3 ± 0.2*ab*	53.9 ± 0.2*ab*	80.8 ± 0.7*d*	78.7 ± 0.4*g*	7.7 ± 0.2*ab*	8.1 ± 0.0*b–g*
	60% amp. 10	56.2 ± 0.1*ab*	54.7 ± 1.2*ab*	80.6 ± 0.5*d*	79.0 ± 0.0*fg*	7.6 ± 0.0*ab*	7.8 ± 0.7*c–g*
	60% amp. 20	52.6 ± 1.2*b*	54.1 ± 0.8*ab*	80.5 ± 0.4*d*	80.6 ± 2.1*c–g*	7.1 ± 0.3*b*	7.1 ± 0.2*e–g*
	60% amp. 30	53.1 ± 0.3*b*	54.6 ± 0.3*ab*	81.2 ± 1.9*d*	79.4 ± 0.8*fg*	7.0 ± 0.4*b*	7.2 ± 0.3*d–g*
	75% amp. 10	58.2 ± 0.7*a*	56.0 ± 0.7*a*	82.1 ± 0.2*cd*	79.7 ± 0.6*e–g*	7.6 ± 0.3*ab*	7.6 ± 0.0*d–g*
	75% amp. 20	53.1 ± 0.7*b*	53.3 ± 0.1*ab*	81.2 ± 1.9*d*	79.8 ± 1.3*d–g*	6.7 ± 0.4*b*	6.9 ± 0.1*g*
	75% amp. 30	53.0 ± 0.8*b*	54.7 ± 1.3*ab*	81.7 ± 1.1*cd*	79.0 ± 0.1*fg*	6.8 ± 0.3*b*	7.4 ± 0.1*d–g*
	90% amp. 10	56.7 ± 0.9*ab*	55.2 ± 0.0*ab*	81.5 ± 0.7*d*	78.6 ± 0.6*g*	7.0 ± 0.3*b*	7.8 ± 0.2*c–g*
	90% amp. 20	53.8 ± 1.6*b*	52.8 ± 1.9*ab*	81.8 ± 1.3*cd*	80.0 ± 0.7*d–g*	7.2 ± 0.2*b*	7.3 ± 0.3*d–g*
	90% amp. 30	55.3 ± 0.1*ab*	51.9 ± 1.1*b*	79.9 ± 0.4*d*	78.8 ± 0.8*fg*	7.3 ± 0.1*b*	7.1 ± 0.1*fg*

[p] Data (mean of two replicates) followed by the same letters in the same column are not significantly different ($p < 0.05$) by Tukey test. All data reported on dry basis.
[q] Amplitude.
[r] GWF = groat wet fractionation.
[s] FWF = flour wet fractionation.

The sonication treatment in GWF significantly improved the purity of starch (Table 3). Sonication treatment of GWF caused a decrease in the protein content by 3.5–5.5% (w/w of original protein weight) and an increase in the starch content by 4–5% (w/w of original starch weight) compared to control-GWF (Table 3).

High-intensity ultrasound shear in the flour slurry creates uniform distribution of the flour particles (Wang & Wang, 2004) and disrupts the cell membranes causing the cotyledon cell wall to disintegrate and release more starch granules (Zhang, Niu, Eckhoff, & Feng, 2005). During sonication, the temperature of the slurry increased as the amplitude and time of sonication increased. At amplitude of 90% for 30 min during sonication, the temperature of the slurry was 54 °C. At this temperature, significantly higher starch yield was obtained in GWF, however higher temperatures negatively affect the physicochemical properties of starch. In order to avoid the pre-gelatinization of field pea starches, a temperature below 40 °C is considered safe. To optimize the effectiveness of the sonication but control temperature rise, the condition of 75% amplitude for 10 min was found to be best. At these conditions, and in combination with the FWF protocol, a maximum starch yield of 56.0–58.2% was obtained.

4. Conclusions

This study represents a new opportunity for future researchers to investigate and refine conditions that improve field pea starch purity. A simple wet fractionation method incorporating sonication and protease treatment was used to maximize yield and purity of field pea starch. Dry milling of field peas prior to wet fractionation, in combination with 10 min sonication treatment at 75% amplitude, was found to produce the highest starch yield of the studied conditions. However, initial direct wet milling of the groats resulted in starch of higher purity.

Acknowledgements

Financial support from the Natural Sciences and Engineering Research Council (NSERC) of Canada through a research grant to Dr. T. Vasanthan is gratefully acknowledged. The authors also thank Dr. T. Warkentin of the Crop Development Center, University of Saskatchewan, Saskatoon, Canada for providing field pea grains.

References

AACC – American Association of Cereal Chemists (2004). *Approved methods of the AACC* (10th ed.). St. Paul, Minnesota, MN, USA: AACC.
AOAC International – Association of Analytical Communities (2000). *Official methods of analysis of AOAC international* (17th ed.). Gaithersburg, MD, USA: AOAC International.
Chavan, U. D., Shahidi, F., Hoover, R., & Perera, C. (1999). Characterization of beach pea (*Lathyrus maritimus* L.) starch. *Food Chemistry, 65*(6), 1–70.
Colonna, P., Gallant, D., & Mercier, C. (1980). *Pisum sativum* and *Vicia faba* carbohydrates: Studies of fractions obtained after dry and wet protein extraction processes. *Journal of Food Science, 45*, 1629–1636.
Czuchajowska, Z., & Pomeranz, Y. (1994). Process for fractionating legumes to obtain pure starch and a protein concentrate. U.S. Patent 5364,471.
Dalgetty, D. D., & Baik, B. (2003). Isolation and characterization of cotyledon fibers from peas, lentils, and chickpeas. *Cereal Chemistry, 80*(3), 310–315.
Davydova, N. I., Leontev, S. P., Genin, Y. V., Sasov, A. Y., & Bogracheva, T. Y. (1995). Some physico-chemical properties of smooth pea starches. *Carbohydrate Polymers, 27*, 109–115.
De Graaf, L. A., Harmsen, P. F. H., Vereijken, J. M., & Monikes, M. (2001). Requirements for non-food applications of pea proteins – A review. *Nahrung/Food, 45*(6), 408–411.
Guillon, F., & Champ, M. M. J. (2002). Carbohydrate fractions of legumes: Uses in human nutrition and potential for health. *British Journal of Nutrition, 88*(3), S293–S306.
Gujska, E., Reinhard, W. D., & Khan, K. (1994). Physicochemical properties of field pea, pinto and navy bean starches. *Journal of Food Science, 59*(3), 634–636.
Hoover, R., & Ratnayake, W. S. (2002). Starch characteristics of black bean, chick pea, lentil, navy bean and pinto bean cultivars grown in Canada. *Food Chemistry, 78*, 489–498.
Hoover, R., & Sosulski, F. W. (1991). Composition, structure, functionality, and chemical modification of legume starches: A review. *Canadian Journal of Physiology and Pharmacology, 69*, 79–92.
Li, J. H., Vasanthan, T., Rossnagel, B., & Hoover, R. (2001a). Starch from hull-less barley: I. Granule morphology, composition and amylopectin structure. *Food Chemistry, 74*, 395–405.
Li, J. H., Vasanthan, T., Rossnagel, B., & Hoover, R. (2001b). Starch from hull-less barley: II. Thermal, rheological and acid hydrolysis characteristics. *Food Chemistry, 74*, 407–415.
Nunes, M. C., Raymundo, A., & Sousa, I. (2006). Rheological behaviour and microstructure of pea protein/κ-carrageenan/starch gels with different setting conditions. *Food Hydrocolloids, 20*, 106–113.
Otto, T., Baik, B., & Czuchajowska, Z. (1997a). Microstructure of seeds, flours, and starches of legumes. *Cereal Chemistry, 74*(4), 445–451.
Otto, T., Baik, B., & Czuchajowska, Z. (1997b). Wet fractionation of garbanzo bean and pea flours. *Cereal Chemistry, 74*(2), 141–146.

Ratnayake, W. S., Hoover, R., Shahidi, F., Perera, C., & Jane, J. (2001). Composition, molecular structure, and physicochemical properties of starches from four field pea (*Pisum sativum* L.) cultivars. *Food Chemistry, 74*, 189–202.

Ratnayake, W. S., Hoover, R., & Warkentin, T. (2002). Pea starch: Composition, structure and properties – A review. *Starch/Starke, 54*, 217–234.

Reichert, R. D., & Youngs, C. G. (1978). Nature of the residual protein associated with starch fractions from air-classified field peas. *Cereal Chemistry, 55*(4), 469–480.

Schoch, T. J., & Maywald, E. C. (1968). Preparation and properties of various legume starches. *Cereal Chemistry, 45*(1–6), 564–573.

Sosulski, F. W. (1989). Preparation and uses of vegetable food proteins made by dry processes. In *Proceedings of the world congress on vegetable protein utilization in human foods and animal feedstuffs* (pp. 553–558). Champaign, Illinois, USA: American Oil Chemists' Society.

Sosulski, F., Garratt, M. D., & Slinkard, A. E. (1976). Functional properties of ten legume flours. *Canadian Institute of Food Science and Technology Journal, 9*(2), 66–69.

Sosulski, F. W., & Sosulski, K. (1986). Composition and functionality of protein, starch, and fiber from wet and dry processing of grain legumes. In R. L. Ory (Ed.), *Plant proteins: Applications, biological effects, and chemistry* (pp. 176–189). Washington, DC, USA: The American Chemical Society.

Tian, S., Kyle, W. S. A., & Small, D. M. (1999). Pilot scale isolation of proteins from field peas (*Pisum sativum* L.) for use as food ingredients. *International Journal of Food Science and Technology, 34*(3), 3–39.

Vose, J. R. (1977). Functional characteristics of an intermediate amylose starch from smooth-seeded field peas compared with corn and wheat starch. *Cereal Chemistry, 54*(5), 1141–1151.

Vose, J. R. (1980). Production and functionality of starches and protein isolates from legume seeds (field peas and horsebeans). *Cereal Chemistry, 57*(6), 406–410.

Vose, J. R., Basterrechea, M. J., Gorin, P. A. J., Finlayson, A. J., & Youngs, C. G. (1976). Air classification of field peas and horsebean flours: Chemical studies of starch and protein fractions. *Cereal Chemistry, 53*(6), 928–936.

Wang, N., Bhirud, P. R., & Tyler, R. T. (1999). Extrusion texturization of air-classified pea protein. *Journal of Food Science, 64*(3), 509–513.

Wang, L., & Wang, Y. (2004). Application of high-intensity ultrasound and surfactants in rice starch isolation. *Cereal Chemistry, 81*(1), 140–144.

Zhang, Z., Niu, Y., Eckhoff, S. R., & Feng, H. (2005). Sonication enhanced cornstarch separation. *Starch/Starke, 57*, 240–245.

Food Chemistry 118 (2010) 634–640

Contents lists available at ScienceDirect

Food Chemistry

journal homepage: www.elsevier.com/locate/foodchem

Structure and physicochemical properties of palmyrah (*Borassus flabellifer* L.) seed-shoot starch grown in Sri Lanka

S. Naguleswaran [a], T. Vasanthan [a,*], R. Hoover [b], Q. Liu [c]

[a] Department of Agricultural, Food and Nutritional Science, University of Alberta, Edmonton, AB, Canada T6G 2P5
[b] Department of Biochemistry, Memorial University of Newfoundland, St. John's, NL, Canada A1B 3X9
[c] Food Research Program, Agriculture and Agri-Food Canada, Guelph, ON, Canada N1G 5C9

ARTICLE INFO

Article history:
Received 18 September 2008
Received in revised form 8 May 2009
Accepted 13 May 2009

Keywords:
Palmyrah
Seed-shoot
Starch
Physicochemical properties
Resistant starch

ABSTRACT

Starch from palmyrah (*Borassus flabellifer* L.) seed-shoot flour was isolated and its composition, morphology, structure and physicochemical properties were determined. The yield of starch was 38.4% on a whole flour basis. The shape of the granule ranged from round to elliptical. Bound lipid, total lipid, apparent amylose, total amylose and resistant starch contents were 0.03%, 0.04%, 30.9%, 32.7% and 32.2%, respectively. The X-ray pattern was of the A-type and relative crystallinity was 34.1%. Palmyrah starch exhibited a high proportion (31.8%) of short amylopectin chains (DP 6–12) and a low proportion (1.2%) of long amylopectin chains (DP > 36). Gelatinization temperatures were 73.1–82.0 °C and enthalpy of gelatinization was 13.6 J/g. Pasting temperature, viscosity breakdown and set-back were 76.5 °C, 147 and 74 BU, respectively. Palmyrah starch exhibited high granular swelling, and restricted amylose leaching. Susceptibility towards *in vitro* α-amylolysis and retrogradation was low. The results showed that physicochemical properties of palmyrah starch were largely influenced by strong interactions between amylose–amylose and/or amylose–amylopectin chains within the granule interior.

1. Introduction

Palmyrah (*Borassus flabellifer* L.) is a palm tree belonging to the family *Palmae* and the sub-family *Boracidae* (Jeyaratnam, 1986). The three most economically important species of *Borassus* are *Borassus aethiopum* Mart, *B. flabellifer* Linn, and *Borassus sundaicus* Becc. (Mohanadas, 2002). The species *B. flabellifer* L. is abundant in the arid tropics of South America, West Africa, India, Sri Lanka and Southeast Asia (Mohanadas, 2002; Morton, 1988). There are about 140 million palmyrah palms distributed worldwide with over 11 million in Sri Lanka (Mohanadas, 2002). Palmyrah provides a variety of edible and non-edible products. Foremost edibles of the palmyrah include the inflorescence sap, the sweet fruit pulp, the peeled seed-shoots (seedlings), and the kernel from both the very young and mature nuts (Barminas et al., 2008; Morton, 1988).

During germination of palmyrah seeds, the excess carbohydrate is stored in the form of starch in the scale leaf of the seedling (Fig. 1). The scale leaf becomes the edible part of the seedling (shoot) and is colloquially known as "palmyrah tuber" (Jeyaratnam, 1986). The palmyrah seed-shoot is high in starch and it is widely utilised in the preparation of starch based products such as porridge and soups (Sumudunie, Janz, Jayasekara, & Wickramasinghe, 2004).

Commercial production of palmyrah seed-shoot products in South America, West Africa, Southeast Asia, India and Sri Lanka is substantial and primarily for food purposes. The objective of this study was to fractionate the starch from palmyrah seed-shoot flour (*B. flabellifer*) and to compare its molecular structure, morphology, composition, and physicochemical properties with those of other palm (giginya [*B. aethiopum*], sago [*Metroxylon* spp.], oil palm [*Elaeis guineensis* Jacq.]) and wheat starches reported in the literature. An understanding of the structure–property relationships of palmyrah starch is important to form the basis for further investigations into physical and chemical modification to improve the use of palmyrah starch for food and industrial applications.

2. Materials and methods

2.1. Preparation of raw materials

Raw palmyrah seed-shoot flour was obtained from the local market of Northern Sri Lanka where the species *B. flabellifer* L. is grown abundantly. Representative samples were ground in a cyclone sample mill (Udy Corp., Fort Collins, CO, USA) fitted with a sieve with 0.25 mm round openings. Native wheat starch (MIDSOL 50) was obtained from Midwest Grain Products Inc., 1300 Main, Atchison, KS, USA.

* Corresponding author. Tel.: +1 780 492 2898; fax: +1 780 492 8914.
E-mail address: tv3@ualberta.ca (T. Vasanthan).

0308-8146/$ - see front matter © 2009 Elsevier Ltd. All rights reserved.
doi:10.1016/j.foodchem.2009.05.046

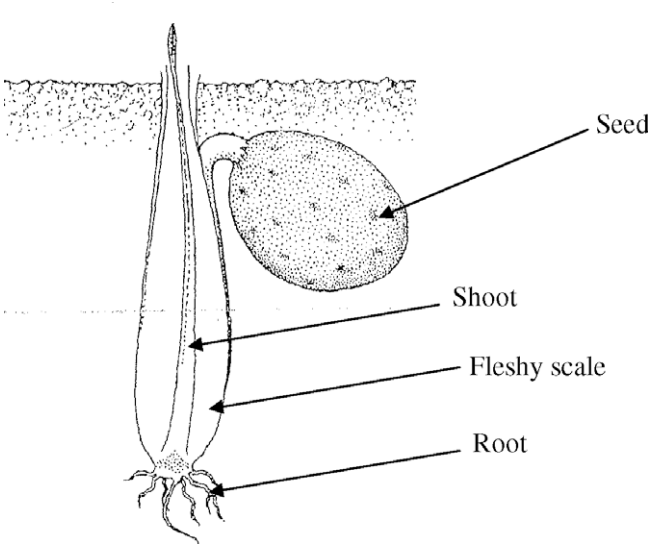

Fig. 1. Germinating palmyrah seed (adapted and modified from Arseculeratne, Panabokke, Tennekoon, & Bandunatha, 1971; Mason & Hendry, 1994).

2.2. Starch fractionation

Starch was fractionated from palmyrah seed-shoot flour according to the procedure outlined in Fig. 2. The palmyrah flour was stirred with water by means of a magnetic stirrer at medium speed. The resultant slurry was then screened using a stainless steel sieve (W.S. Tyler, St. Catharines, ON, Canada) and the filtrate-1 and retentate-1 were collected separately. The retentate-1 was mixed again with water and stirred. The filtrate (filtrate-2) was collected and retentate (retentate-2) was discarded after screening. The filtrate-1 and filterate-2 were combined together and centrifuged (Model J2-21 centrifuge, Beckman Instruments Inc., Palo Alto, CA, USA) with the conditions shown in Fig. 2. The supernatant-1 was discarded and the residual cake (residue-1) was mixed with water followed by stirred for 10 min at medium speed in a magnetic stirrer. The stirred slurry was then centrifuged with same centrifugal conditions. The supernatant-2 was decanted and residue-2 was mixed well with water and centrifuged as per previous conditions. Finally, the supernatant-3 was decanted and the residue-3 (starch cake) was quantitatively recovered and dried in a conventional oven (Fisher Isotemp® Oven, Model: 204, Pittsburgh, PA, USA) to obtain the starch fraction. Three replicated fractionations were done.

2.3. Chemical composition

Moisture content was determined by the standard AACC (2004) procedure (method 44-15A). Nitrogen was measured by Leco® Carbon/Nitrogen determinator (TruSpec® CN, Leco Corporation, St. Joseph, MI, USA). Ash content was measured according to the AOAC (2000) procedure (method 923.03). Starch lipids (free and bound) were determined by the procedures outlined in an earlier publication (Vasanthan & Hoover, 1992). Total starch, resistant starch and starch damage contents were estimated by the Megazyme assay procedures of AA/AMG 9/97, K-RSTAR 05/2008 and SDA 11/01, respectively (Megazyme International Ireland Ltd., Wicklow, Ireland). Apparent and total amylose concentrations were determined according to the Standard Analytical Methods of the Member Companies of the Corn Refiners Association Inc., Washington, DC, USA. Phosphorus content was determined by the method of Smith and Caruso (1964).

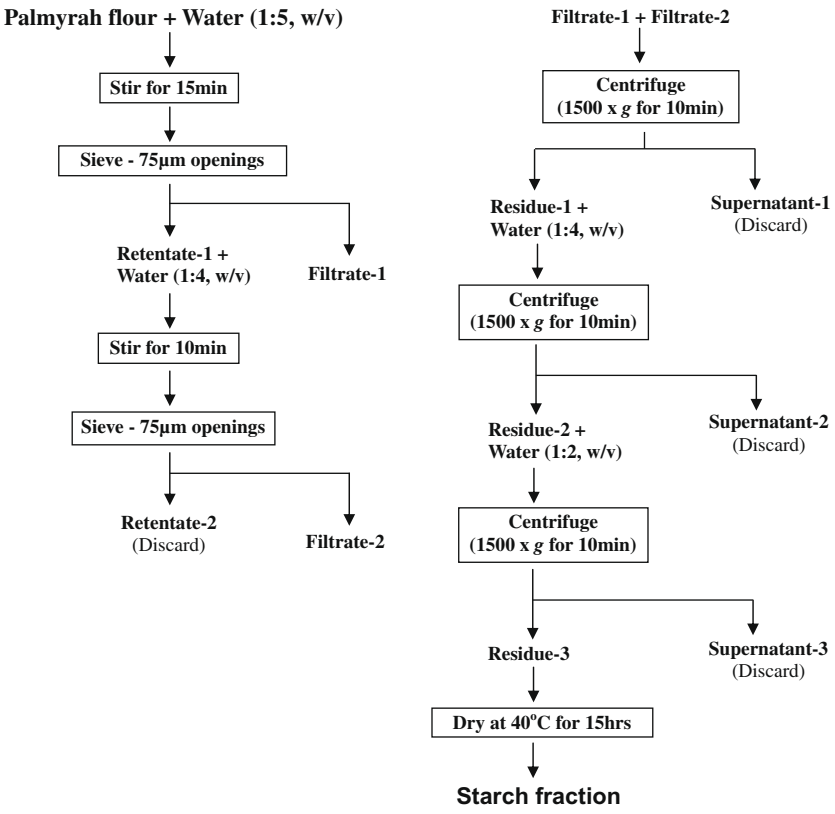

Fig. 2. Flow chart for wet fractionation of palmyrah flour.

2.4. Granule morphology and size estimation

Granule morphology of palmyrah starch was studied by scanning electron microscopy following the procedure of Li, Vasanthan, Rossnagel, and Hoover (2001a). The procedure outlined by Jayakody, Hoover, Liu, and Weber (2005) was used to measure the size and shape of starch granules using a Micromaster™ -Model CK (Japan) light microscope.

2.5. Molecular characterisation of amylopectin

The branch chain length distribution of isoamylase debranched amylopectin from debranched palmyrah starch was determined by high pressure anion exchange chromatography with pulsed amperometric detection (HPAEC-PAD) following the procedure of Jayakody et al. (2005).

2.6. X-ray diffraction

Powder X-ray diffraction was carried out by the method outlined by Jayakody et al. (2007).

2.7. Swelling factor (SF) and amylose leaching (AML)

Swelling factor of palmyrah starch when heated in the temperature range from 40 to 90 °C in excess water was measured according to the method of Tester and Morrison (1990). The percent amylose leaching of native palmyrah starch when heated in the temperature range from 40 to 90 °C was determined following the procedure of Jayakody et al. (2005). The amylose content for AML was determined as the method referred in Section 2.3.

2.8. Differential scanning calorimetry (DSC)

Gelatinization parameters of palmyrah starch were examined by a Perkin–Elmer DSC-2 differential scanning calorimeter (Perkin–Elmer Ltd., Beaconsfield, UK) following the procedure outlined by Li, Vasanthan, Rossnagel, and Hoover (2001b). The thermograms were recorded with an empty aluminium pan as a reference.

2.9. Pasting properties of starch

Pasting characteristics (8% w/v, pH 5.5) of palmyrah starch was measured by Brabender viscometer (C.W. Brabender Instruments Inc., South Hackensack, NJ, USA) following the method of Li et al. (2001b).

2.10. Enzyme digestibility

Enzymatic digestibility studies on palmyrah and wheat starches were conducted following the procedure outlined by Jayakody et al. (2007) with some modifications. The following modifications were done in the later part of the procedure. Aliquots (5 mL) of reaction mixture were collected at 24-h intervals and immediately boiled in a water bath (95–98 °C) for 5 min to terminate the enzymatic reaction, and then immediately stored frozen at −18 °C until further analysis. The degree of hydrolysis or percent reducing value of all samples was determined using the method of Bruner (1964).

2.11. Retrogradation

The retrogradation characteristics of palmyrah starch were determined by turbidity measurements. Turbidity development during storage of palmyrah starch was measured according to the method of Craig, Maningat, Seib, and Hoseney (1989). Starch (50 mg) was suspended in water (5 mL) in screwcap tubes and placed in a boiling water bath for 30 min. The tubes were thoroughly shaken every 5 min. After cooling to room temperature (5 min), the percent transmittance (T%) at 650 nm was determined against a water blank in a Jenway 6300 spectrophotometer (Jenway Ltd., Essex, UK). The tubes containing the starch pastes were kept at 4 °C for a day and then at 40 °C for 12 days. T (%) was determined at 24-h intervals.

3. Results and discussion

3.1. Chemical composition of starch

Starch yield, composition, and granule morphology are presented in Table 1. The yield and purity of starch from palmyrah flour were 38.4% and 95.8%, respectively. Thus, the recovery of starch based on the flour (73.9% starch) is 49.8%. Starch yield from other palms and wheat have been shown to be in the range of 7.1–24.7% (Noor, Mohd, Islam, & Mehat, 1999; Barminas et al., 2008; Sun & Tomkinson, 2003) and 29.0% (Vansteelandt & Delcour, 1999), respectively. The protein content of palmyrah starch (2.5%) was higher than that reported for giginya (0.18%; Barminas et al., 2008), sago (0.1%; Swinkels, 1985), oil palm (0.9%; Noor et al., 1999) and wheat (0.25%; Vansteelandt & Delcour, 1999) starches. The higher protein content of palmyrah starch may be due to differences in starch isolation protocol or genetic differences. The phosphorus content (198 ppm) of palmyrah starch was higher than those reported for giginya (86 ppm; Barminas et al., 2008) and sago (110 ppm; Srichuwong, Sunarti, Mishima, Isono, & Hismatsu, 2005) starches. The total lipid content (0.04%) was slightly lower than those reported for giginya (0.09%; Barminas et al., 2008), sago (0.13%; Ahmad, Williams, Doublier, Durand, & Buleon, 1999), oil palm (0.30%; Noor et al., 1999) and wheat (0.70%; Hoover, Vasanthan, Senanayake, & Martin, 1994) starches. The total amylose content (32.7%) was higher than those reported for giginya (26.2%; Barminas et al., 2008), oil palm (19.5%; Noor

Table 1
Yield, chemical composition, and granule morphology of palmyrah starch isolate.

Characteristics	Composition (%)[a]
Yield (% initial material)	38.4 ± 1.3
Starch	95.8 ± 1.7
Moisture	9.1 ± 0.5
Protein[b]	2.5 ± 0.7
Ash	ND[c]
Lipid	
Unbound[d]	0.01 ± 0.00
Bound[e]	0.03 ± 0.01
Amylose	
Apparent[f]	30.9 ± 0.0
Total[g]	32.7 ± 0.2
Amylose complexed with native lipid[h]	5.6 ± 0.6
Starch damage	2.6 ± 0.4
Resistant starch	32.2 ± 0.4
Granule size (μm)	
Round	5–16
Elliptical	
Shorter diameter	8
Longer diameter	32

[a] All data reported on dry basis. Values are mean ± standard deviation.
[b] $N * 6.25$.
[c] Not detected.
[d] Lipid obtained from native starch by chloroform–methanol 2:1 (v/v) at 25 °C (mainly unbound lipids).
[e] Lipid extracted by hot n-propanol–water 3:1 (v/v) from the residue left after chloroform–methanol extraction (mainly bound lipids).
[f] Apparent amylose determined by iodine binding without removal of free and bound lipids.
[g] Total amylose determined by iodine binding after removal of free and bounds lipids.
[h] [(Total amylose − apparent amylose)/total amylose] * 100.

et al., 1999), sago (24–31%; Ahmad et al., 1999) and wheat (27.3%; Hoover et al., 1994) starches.

The resistant starch (RS) content of palmyrah starch (32.2%) was much higher than the RS content (0.5–11.4%) of cereal and legume starches of nearly similar amylose content (Ranhotra, Gelroth, & Eisenbraun, 1991; Themeier, Hollmann, Neese, & Lindhauer, 2005). This suggests that the high RS content of palmyrah may be the result of strong interactions between amylose–amylose (AM–AM) and/or amylose–amylopectin (AM–AMP) chains within native starch granules. Crystallites resulting from the above interactions (especially those from AM–AM) could hinder the accessibility of glycosidic oxygens to hydrolytic enzymes. Thus, the RS of palmyrah starch could be categorised as RS2 according to the classification proposed by Englyst and Cummings (1987). There are no reports on the RS2 content of other palm starches. The RS2 content of palmyrah starch was higher than that of Hylon VII maize starch (23.0%), but lower than that in commercially available RS2 starches such as Hi-Maize 240 and Hi-Maize 260 in which the RS2 content is reported to be 42% and 60%, respectively (Champ, 2004). Starch damage during isolation of palmyrah starch was minimal (2.6%).

3.2. Morphological characteristics of starch granules

Microscopic examination showed that the starch granules of palmyrah had irregular shapes, which varied from round (5–16 μm; Fig. 3A) to oval and elliptical (shorter diameter, 8 μm; longer diameter, 32 μm; Fig. 3B). The granules were slightly smaller than oval granules of sago starch (20–40 μm; Ahmad et al., 1999), but slightly larger than granules of oil palm starch (3–25 μm; Noor et al., 1999). The granule surface of palmyrah starch appeared to be rough with indentations (Fig. 3B).

3.3. Amylopectin unit chain length distribution

The amylopectin glucan chains were classified into A (DP 6–12), B1 (DP 13–24), B2 (DP 25–36) and B3 (DP 37–50) on the basis of the number of glucose units per chain. The data are presented in Table 2A. The above distribution was similar to that reported for wheat starch (Sasaki & Matsuki, 1998) with respect to DP 13–24 and DP 25–36. However, the proportion of DP 6–12 (31.8%) and DP 37–50 (1.2%) of palmyrah starch amylopectin was different from that of wheat starch [DP 6–12 (24–25%), DP > 36 (15.9–18.1%); Sasaki & Matsuki, 1998]. There are no reports on the amylopectin chain length distribution of other palm starches.

3.4. X-ray diffraction and relative crystallinity

The X-ray diffraction pattern of palmyrah starch at 14% moisture is presented in Fig. 4A. The relative crystallinity (RC) was 34.1%. Sago palm starch, which has amylose content in the range

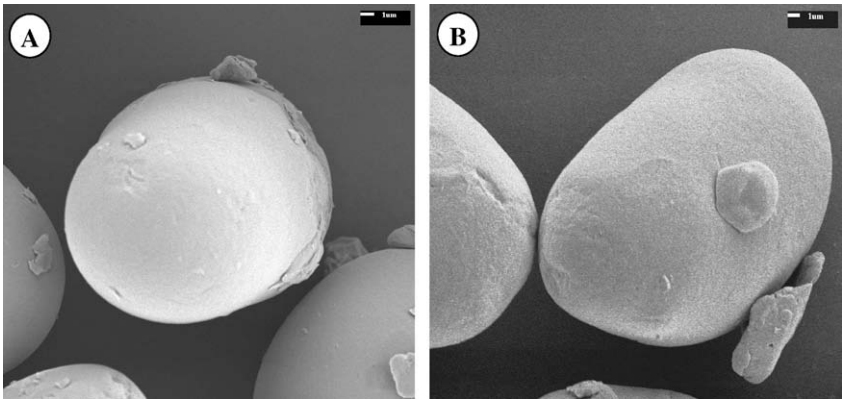

Fig. 3. Scanning electron micrographs (SEM) of palmyrah starch: (A) 3000×, (B) 5000×.

Table 2
Some physicochemical properties of palmyrah starch[a].

(A) Amylopectin chain length distribution[b]						
A (DP 6–12)[c]	B1 (DP 13–24)[c]	B2 (DP 25–36)[c]	B3 (DP 37–50)[c]	$\overline{CL}$[d]		
31.8 ± 1.8	56.5 ± 1.1	10.5 ± 0.7	1.2 ± 0.2	16.5 ± 0.3		
(B) Gelatinization parameters[e]						
T_o (C)[f]	T_p (°C)[f]	T_c (°C)[f]	$T_c - T_o$ (°C)[g]	ΔH (J/g)[h]		
73.1 ± 0.1	77.6 ± 0.3	82.0 ± 0.3	9.0 ± 0.2	13.6 ± 0.2		
(C) Pasting properties[i]						
Pasting temperature (°C)	Peak viscosity (BU)[j]	Viscosity at 95 °C (BU)	Viscosity after 30 min at 95 °C (BU)	Viscosity breakdown (BU)	Viscosity at 50 °C (BU)	Set-back (BU)
76.5	275	192	128	147[k]	202	74[l]

[a] All data reported on dry basis and represents the mean ± standard deviation.
[b] Total relative area was used to calculate percent distribution.
[c] DP indicates degree of polymerisation.
[d] $\overline{CL}$(average chain length) calculated by $\sum(DP_n \times \text{peak area}_n) \sum(\text{peak area}_n)$.
[e] Starch:water ratio 1:3 (w/w) dry basis and scanning speed 10 °C/min.
[f] T_o, T_p, T_c represent the onset, peak and conclusion temperature of gelatinization.
[g] $T_c - T_o$ represents the gelatinization temperature range.
[h] ΔH represents the gelatinization enthalpy.
[i] A 8% (w/w) aqueous starch suspension at pH 5.5.
[j] Brabender unit.
[k] Peak viscosity − viscosity after 30 min at 95 °C.
[l] Viscosity at 50 °C − viscosity after 30 min at 95 °C.

of 24–31%, exhibits a C-type X-ray pattern that is characteristic of starches with relatively high amylose content (Ahmad et al., 1999; Takeda, Takeda, Suzuki, & Hizukuri, 1989). Palmyrah starch, in spite of its higher amylose content (32.7%), exhibited the A-type X-ray pattern characteristic of cereal starches (Hizukuri, Kaneko, & Takeda, 1983; Zobel, 1988) and oil palm trunk starch (Noor et al., 1999). The difference in the X-ray spectra of palmyrah and sago is likely due to differences in their average amylopectin chain length ($\overline{CL}$ in DP), which was 16.5 for palmyrah, and 22.1 for sago (Takeda et al., 1989). Shorter chain lengths (DP < 19.7) are associated with A-type starches, whereas starches with chain lengths in the range 20.3–21.3 have been shown to exhibit A, B or C-type polymorphism (Hizukuri et al., 1983).

A low intensity peak characteristic of an amylose–lipid complex was evident in the X-ray spectrum (peak at $2\theta = 20^{\circ}$) of palmyrah starch (Hoover & Hadziyev, 1981). This was rather surprising, since the amount of lipid-complexed amylose chains in palmyrah starch was fairly low (5.6%). This finding suggests that the amylose–lipid complex in palmyrah starch is highly organised into a three dimensional crystalline structure.

3.5. Swelling factor (SF) and amylose leaching (AML)

The SF and AML of palmyrah starch heated in the temperature range 40–90 °C are presented in Fig. 4B. SF measures the amount of intragranular water, and has been shown to be influenced by: (1) amylopectin structure (Shi & Seib, 1992; Sasaki & Matsuki, 1998; Han & Hamaker, 2001; Patindol, Flowers, Kuo, Wang, & Gealy, 2006; Vandeputte, Vermeylen, Geeroms, & Delcour, 2003), (2) V-amylose–lipid complexes (Tester & Morrison, 1990), (3) amylose content (Morrison, Tester, Snape, Law, & Gidley, 1993), and (4) extent of interaction between amylose–amylose (AM–AM) and/or AM and amylopectin (AM–AMP) chains within the native granule (Hoover & Manuel, 1996). The SF increased gradually from 40 to 70 °C, increased sharply between 70 and 80 °C, and then tapered off again. At all temperatures, the SF of palmyrah starch was higher than that reported for wheat starch, although the trends were similar (Hoover & Vasanthan, 1994). A higher ratio of shorter (DP 6–12) to longer (DP > 36) amylopectin chains mean that the crystalline region would be more easily hydrated in palmyrah starch than in wheat starch. This finding together with the relatively low proportion of lipid-complexed amylose chains (5.6%, compared to 22.7% for wheat [Hoover & Vasanthan, 1994]) could explain the higher SF of palmyrah starch.

AML has been shown to be influenced by: (1) total amylose concentration, (2) extent of interaction between AM–AM and/or AM–AMP chains within the native granule, and (3) amount of lipid-complexed amylose chains (Hoover & Vasanthan, 1994). As shown in Fig. 4B, amylose leaching was detectable in palmyrah starch only at temperatures exceeding 60 °C. A rapid increase in AML occurred in the temperature range 70–85 °C, and then tapered off. A similar trend has been reported for giginya (Barminas et al., 2008) and wheat (Hoover & Vasanthan, 1994) starches. However, in giginya and wheat, AML begins at a lower temperature (~50 °C), and is more extensive than in palmyrah starch at the same temperature (Barminas et al., 2008; Hoover & Vasanthan, 1994). The small extent of leached amylose in palmyrah starch supports our earlier hypothesis that interactions between AM–AM and/or AM–AMP within the amorphous domains are much stronger than in wheat and other palm starches, and may contribute to the presence of resistant starch.

3.6. Gelatinization characteristics

Gelatinization characteristics of palmyrah starch are presented in Table 2B. At the same starch/water ratio and scanning speed,

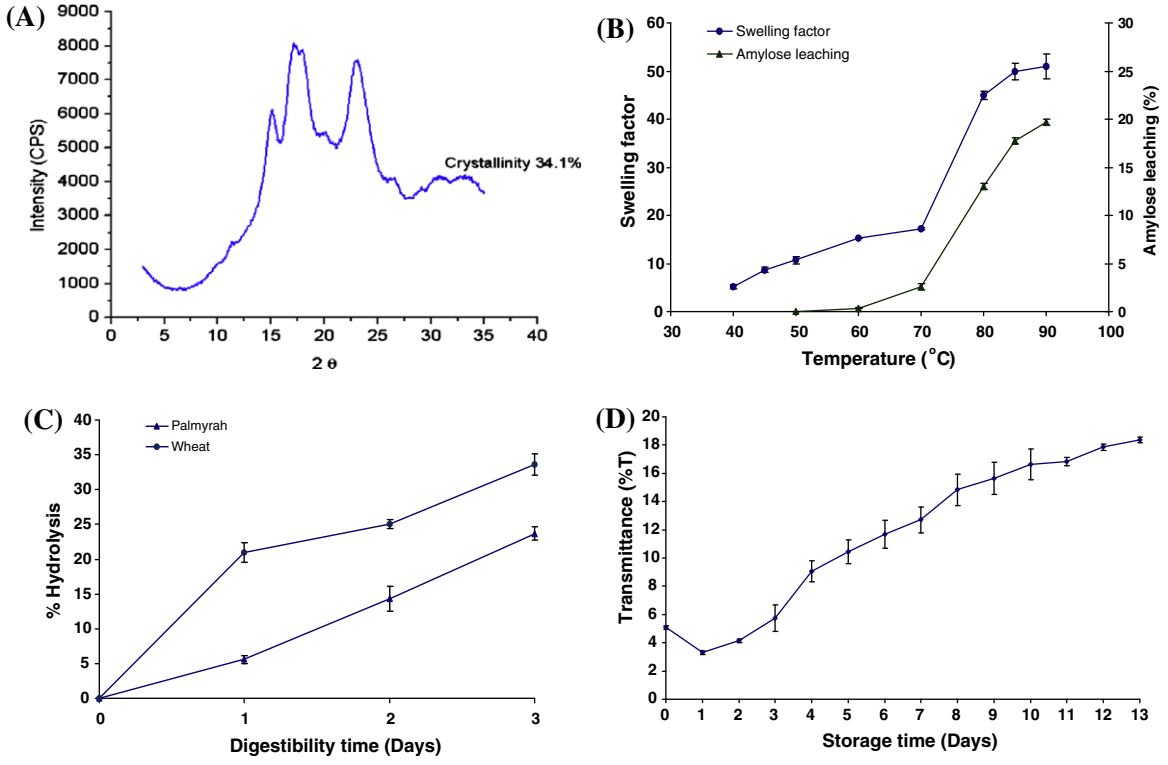

Fig. 4. Some physicochemical properties of palmyrah starch. (A) X-ray diffraction pattern of native palmyrah starch at 14% moisture; (B) swelling factor and amylose leaching of palmyrah starch at various temperatures; (C) time course of hydrolysis (%) of native palmyrah and wheat starches by porcine pancreatic α-amylase, (D) Retrogradation of palmyrah starch pastes monitored by determination of % transmission immediately after gelatinization (day 0), after storage at 4 °C (day 1) and during storage at 40 °C (days 2–13). Error bars represent standard deviations.

the gelatinization onset, peak, conclusion, range, and enthalpy of giginya starch are 61.1, 66.2, 74.2, 13.1 °C and 8.1 J/g, respectively (Barminas et al., 2008). The corresponding values for wheat starch are 57.0, 62.0, 67.0, 10 °C and 9.5 J/g, respectively (Hoover et al., 1994). The higher gelatinization temperatures and enthalpy, and the narrower gelatinization range of palmyrah starch reflect the melting of a crystalline structure of a higher stability and a lower degree of heterogeneity. The molecular architecture of the crystalline regions, which corresponds to the distribution of amylopectin short chains has been shown to have the greatest influence on gelatinization characteristics (Noda et al., 1998; Shi & Seib, 1992). The difference in the ratio of short chains (DP 6–12) to long chains (DP > 36) between palmyrah (27, Table 2A) and wheat (1.4, Sasaki & Matsuki, 1998) suggests that palmyrah starch should have exhibited lower gelatinization temperatures and enthalpy than wheat starch. The fact that palmyrah starch exhibits higher gelatinization temperatures and enthalpy (Table 2B) suggests strong interactions between AM–AM and/or AM–AMP chains (within the native granule) rather than amylopectin structure is the major factor influencing gelatinization transition parameters in palmyrah starch.

3.7. Pasting properties

Pasting properties of palmyrah starch are presented in Table 2C. Strong interactions between AM–AM and/or AM–AMP chains within the granule interior of palmyrah starch also influenced the pasting properties, as evidenced by the high pasting temperature (76.5 °C), low peak viscosity (275 BU), and low extent of viscosity breakdown (147 BU) during the holding cycle at 95 °C. The low set-back (74 BU) can be attributed to reduced amylose leaching, presence of granule fragments (due to a low breakdown viscosity) and a low proportion of long amylopectin chains (DP > 36).

3.8. α-Amylase hydrolysis

The susceptibility of palmyrah and wheat starches towards hydrolysis by α-amylase is presented in Fig. 4C. The hydrolysis data (wheat > palmyrah) suggests that stronger interactions between AM–AM and/or AM–AMP chains in palmyrah starch suggests negates the influence of bound lipid content (wheat > palmyrah), amylose content (palmyrah > wheat) and proportion of long (DP > 36) amylopectin chains (wheat > palmyrah) to α-amylase hydrolysis.

3.9. Retrogradation

Retrogradation occurs when the starch components in gelatinized starch reassociate in an ordered structure. In this study, retrogradation of palmyrah starch paste was determined by monitoring changes in light transmission during storage at 4 °C (day 1) and at 40 °C (days 2–13), as shown in Fig. 4D. The initial decrease in % T by 1.8% reflects an association between leached amylose chains. The extent of this decrease is more pronounced in wheat starch (2.7%), since AML during gelatinization is more extensive in wheat (Hoover & Vasanthan, 1994) than in palmyrah starch. Interactions involving leached starch chains have no significant impact on retrogradation in palmyrah starch because of the low degree of AML and weak interaction between amylopectin chains (due to a low proportion of long chains). The increase in % T after 24-h in palmyrah starch is likely a reflection of the disintegration of granule remnants.

4. Conclusions

This study revealed that the physicochemical properties of palmyrah starch are influenced to a large extent by strong interactions between starch chains within the amorphous domains of the granule. The high gelatinization temperature and thermal stability of palmyrah starch would make it potentially useful in products that are subjected to high temperature processing (canned foods, baby foods, sauces), whereas the low extent of retrogradation makes it suitable for use as a thickener in frozen foods. The high RS2 content may have important techno-functional benefits and physiological and/or health benefits.

Acknowledgement

The funding support from NSERC Canada through a research grant to Dr. T. Vasanthan is gratefully acknowledged.

References

AACC – American Association of Cereal Chemists. (2004). *Approved methods of the AACC* (10th ed.). St. Paul, MN, USA: AACC.

Ahmad, F. B., Williams, P. A., Doublier, J. L., Durand, S., & Buleon, A. (1999). Physico-chemical characterization of sago starch. *Carbohydrate Polymers, 38*, 361–370.

AOAC International – Association of Analytical Communities (2000). *Official methods of analysis of AOAC international* (17th ed.). Gaithersburg, MD, USA: AOAC International.

Arseculeratne, S. N., Panabokke, R. G., Tennekoon, G. E., & Bandunatha, C. H. S. R. (1971). Toxic effects of *Borassus flaberlifer* L. (Palmyrah palm) in rats. *British Journal of Experimental Pathology, 52*, 524–537.

Barminas, J. T., Onen, A. I., Williams, E. T., Zaruwa, M. Z., Mamuru, S. A., & Haggai, D. (2008). Studies on functional properties of borassus starch from fresh germinating nuts of giginya (*Borassus aethiopum*) palm. *Food Hydrocolloids, 22*, 298–304.

Bruner, R. L. (1964). Determination of reducing value: 3, 5-Dinitrosalicylic acid method. In R. L. Whistler (Ed.), *Methods in carbohydrate chemistry, (Vol. IV-Starch)* (pp. 67–71). New York, NY, USA: Academic Press.

Champ, M. (2004). Resistant starch. In A. C. Eliasson (Ed.), *Starch in food: Structure, function and application* (pp. 560–574). Cambridge, England: Woodhead Publishing Limited.

Craig, S. A. S., Maningat, C. C., Seib, P. A., & Hoseney, R. C. (1989). Starch paste clarity. *Cereal Chemistry, 66*(3), 173–182.

Englyst, H. N., & Cummings, J. H. (1987). Resistant starch, a new food component: A classification of starch for nutritional purpose. In I. D. Morton (Ed.), *Cereals in European context* (pp. 221–233). Chichester, England/Germany: Ellis Horwood Ltd./VCH.

Han, X. Z., & Hamaker, B. R. (2001). Amylopectin fine structure and rice starch paste breakdown. *Journal of Cereal Science, 34*(3), 279–284.

Hizukuri, S., Kaneko, T., & Takeda, Y. (1983). Measurement of the chain length of amylopectin and its relevance to the origin of crystalline polymorphism of starch granules. *Biochimica et Biophysica Acta, 760*(1), 188–191.

Hoover, R., & Hadziyev, D. (1981). Characterization of potato starch and its monoglyceride complexes. *Starch/Stärke, 33*(9), 290–300.

Hoover, R., & Manuel, H. (1996). The effect of heat-moisture treatment on the structure and physicochemical properties of normal maize, waxy maize, dull waxy maize and amylomaize V starches. *Journal of Cereal Science, 23*(2), 153–162.

Hoover, R., & Vasanthan, T. (1994). The effect of annealing on the physicochemical properties of wheat, oat, potato and lentil starches. *Journal of Food Biochemistry, 17*, 303–325.

Hoover, R., Vasanthan, T., Senanayake, N. J., & Martin, A. M. (1994). The effects of defatting and heat-moisture treatment on the retrogradation of starch gels from wheat, oat, potato and lentil. *Carbohydrate Research, 261*, 13–24.

Jayakody, L., Hoover, R., Liu, Q., & Weber, E. (2005). Studies on tuber and root starches. I. Structure and physicochemical properties of innala (*Solenostemon rotundifolius*) starches grown in Sri Lanka. *Food Research International, 38*, 615–629.

Jayakody, L., Lan, H., Hoover, R., Chang, P., Liu, Q., & Donner, E. (2007). Composition, molecular structure, and physicochemical properties of starches from two grass pea (*Lathyrus sativus* L.) cultivars grown in Canada. *Food Chemistry, 105*, 116–125.

Jeyaratnam, M. (1986). Studies on the chemistry and biochemistry of palmyrah products. M.Phil thesis. Sri Lanka: University of Jaffna.

Li, J. H., Vasanthan, T., Rossnagel, B., & Hoover, R. (2001a). Starch from hull-less barley. I. Granule morphology, composition and amylopectin structure. *Food Chemistry, 74*, 395–405.

Li, J. H., Vasanthan, T., Rossnagel, B., & Hoover, R. (2001b). Starch from hull-less barley. II. Thermal, rheological and acid hydrolysis characteristics. *Food Chemistry, 74*, 407–415.

Mason, D., & Hendry, C. J. K. (1994). Chemical composition of palmyrah (*Borassus flabellifer*) seed shoots – odiyal. *International Journal of Food Sciences and Nutrition, 45*, 287–290.

Mohanadas, S. (2002). The palmyrah palm and the composition of palmyrah fruit pulp. In *Hand book of Prof. S. Mageswaran memorial lecture*. Sri Lanka: University of Jaffna.

Morrison, W. R., Tester, R. F., Snape, C. E., Law, R., & Gidley, M. J. (1993). Swelling and gelatinization of cereal starches. IV. Some effects of lipid complexed amylose and lipid-force amylose in lintnerized waxy and non-waxy barley starches. *Carbohydrate Research, 245*, 289–302.

Morton, J. F. (1988). Notes on distribution, propagation, and products of *Borassus* palms (Arecaceae). *Economic Botany, 42*(3), 420–441.

Noda, T., Takahata, Y., Sato, T., Suda, I., Morishita, T., Ishiguro, K., et al. (1998). Relationships between chain length distribution of amylopectin and gelatinization properties within the same botanical origin for sweet potato and buckwheat. *Carbohydrate Polymers, 37*, 153–158.

Noor, M. A. M., Mohd, A. M. D., Islam, M. N., & Mehat, N. A. (1999). Physico-chemical properties of oil palm trunk starch. *Starch/Stärke, 51*(8–9), 293–301.

Patindol, J., Flowers, A., Kuo, M. I., Wang, Y. J., & Gealy, D. (2006). Comparison of physicochemical properties of starch structure of red rice and cultivated rice. *Journal of Agricultural and Food Chemistry, 54*(7), 2712–2718.

Ranhotra, G. S., Gelroth, J. A., & Eisenbraun, G. J. (1991). High-fiber white flour and its use in cookie products. *Cereal Chemistry, 68*(4), 432–434.

Sasaki, T., & Matsuki, J. (1998). Effect of wheat starch structure on swelling power. *Cereal Chemistry, 75*(4), 525–529.

Shi, Y.-C., & Seib, P. A. (1992). The structure of four waxy starches related to gelatinization and retrogradation. *Carbohydrate Research, 227*, 131–145.

Smith, R. J., & Caruso, J. (1964). Determination of phosphorus. In R. L. Whistler (Ed.), *Methods in carbohydrate chemistry, (Vol. IV-Starch)* (pp. 42–46). New York, NY, USA: Academic Press.

Srichuwong, S., Sunarti, T. C., Mishima, T., Isono, N., & Hismatsu, M. (2005). Starches from different botanical sources. II. Contribution of starch structure to swelling and pasting properties. *Carbohydrate Polymers, 62*(1), 25–34.

Sumudunie, K. A. V., Janz, E. R., Jayasekara, S., & Wickramasinghe, S. M. D. N. (2004). The neurotoxic effect of palmyrah (*Borassus flabellifer* L.) flour re-visited. *International Journal of Food Sciences and Nutrition, 55*(8), 607–614.

Sun, R., & Tomkinson, J. (2003). Fractional isolation and spectroscopic characterization of sago starch. *International Journal of Polymer Analysis and Characterization, 8*(1), 29–46.

Swinkels, J. J. M. (1985). Sources of starch: Its chemistry and physics. In G. M. A. VanBeynum & J. A. Roels (Eds.), *Starch conversion technology* (pp. 15–45). New York, USA: Marcel Dekker Inc..

Takeda, Y., Takeda, C., Suzuki, A., & Hizukuri, S. (1989). Structures and properties of sago starches with low and high viscosities on amylography. *Journal of Food Science, 54*(1), 177–182.

Tester, R. F., & Morrison, W. R. (1990). Swelling and gelatinization of cereal starches. I. Effects of amylopectin, amylose, and lipids. *Cereal Chemistry, 67*(6), 551–557.

Themeier, H., Hollmann, J., Neese, U., & Lindhauer, M. (2005). Structural and morphological factors influencing the quantification of resistant starch II in starches of different botanical origin. *Carbohydrate Polymers, 61*(1), 72–79.

Vandeputte, G. E., Vermeylen, R., Geeroms, J., & Delcour, J. A. (2003). Rice starches. I. Structural aspects provide insight into crystallinity characteristics and gelatinization behavior of granular starch. *Journal of Cereal Science, 38*(1), 43–52.

Vansteelandt, J., & Delcour, J. A. (1999). Characterization of starch from durum wheat (*Triticum durum*). *Starch/Stärke, 51*(2–3), 73–80.

Vasanthan, T., & Hoover, R. (1992). Effect of defatting on starch structure and physicochemical properties. *Food Chemistry, 45*, 337–347.

Zobel, H. F. (1988). Molecules to granules: A comprehensive starch review. *Starch/Stärke, 40*(2), 44–50.

Food Chemistry 118 (2010) 641–647

Contents lists available at ScienceDirect

Food Chemistry

journal homepage: www.elsevier.com/locate/foodchem

Effect of methyl jasmonate on cell wall modification of loquat fruit in relation to chilling injury after harvest

Shifeng Cao, Yonghua Zheng *, Kaituo Wang, Huaijin Rui, Shuangshuang Tang

College of Food Science and Technology, Nanjing Agricultural University, Weigang 1, Nanjing 210095, PR China

ARTICLE INFO

Article history:
Received 18 March 2009
Received in revised form 31 March 2009
Accepted 14 May 2009

Keywords:
Loquat fruit
Chilling injury
Methyl jasmonate
Lignin
Cell wall polysaccharides

ABSTRACT

Loquat fruit were pretreated with 10 μM methyl jasmonate (MeJA) for 24 h at 20 °C, and then stored at 1 °C for 35 days to investigate the effect of MeJA treatment on cell wall modification in relation to chilling injury. Loquat fruit developed chilling injury, manifested as increased fruit firmness and internal browning, decreased extractable juice during storage. These chilling injury symptoms were significantly reduced by MeJA treatment. MeJA also markedly delayed the increases in lignin, alcohol insoluble residues, hemicellulose and cellulose. Meanwhile, the MeJA-treated fruit exhibited significantly lower activities of phenylalanine ammonia lyase, peroxidase, polyphenol oxidase and higher polygalacturonase activity than the control during storage. The levels of water- and CDTA-soluble pectins in MeJA-treated fruit were also significantly higher than that in the control. These results suggest that the reduction in chilling injury by MeJA may be due to inhibited lignin accumulation and enhanced cell wall polysaccharides solubilisation.

1. Introduction

Loquat (*Eriobotrya japonica* Lindl.) fruit is very perishable due to microbial decay and mechanical damage after harvest. Low temperature storage is an effective method to control pathogenic decay and preserve quality. However, chilling injury limits the storage period and shelf-life of red-fleshed loquat cultivars (Zheng, Li, & Xi, 2000). The major symptoms of chilling injury in loquat fruit are stuck peel, firm and juiceless texture (flesh leatheriness) and internal browning. These physiological disorders are the main problems when loquats are stored at low temperature. Thus, postharvest treatments that can alleviate chilling injury and extend shelf-life of loquat fruit are urgently needed.

Previous work has shown that the development of chilling injury in cold-stored loquat fruit is attributed to the abnormal changes in cell wall metabolism (Zheng et al., 2000). Cell walls are essentially composed of three complex interpenetrated macromolecular networks: cellulose–hemicellulose, pectin and lignin (Boudet, Kajita, Grima-Pettenati, & Goffner, 2003; Carpita & Gibeaut, 1993). Pectin-rich cell wall interfaces (middle lamella and cellular junctions) are thought to play a key role in cell–cell adhesion and tissue cohesion whilst the cellulose–hemicellulose network is thought to largely contribute to rigidity (Jarvis, Briggs, & Knox, 2003; Whitney, Gothard, Mitchell, & Gidley, 1999). From a functional point of view, lignin supports and strengthens the cell wall, prevents degradation of cell wall polysaccharides and facilitates water transport (Lewis & Yamamoto, 1990). Though a lot of work has been done on process and regulation of cell wall metabolism during fruit softening (Vicente, Saladie, Rose, & Labavitch, 2007), the mechanism of cell wall changes induced by chilling in loquat fruit has not been clarified, except for the association with lignin synthesis (Shan et al., 2008).

Evidence suggests that methyl jasmonate (MeJA), as a natural plant regulator, plays an important role in plant growth and development, fruit ripening and responses to environmental stresses (Creelman & Mullet, 1997). When exogenously applied, MeJA has been shown to result in an improved chilling tolerance and reduced incidence of chilling injury in several horticultural crops (González-Aguilar, Tizuado-Hernándoz, & Wang, 2006). Since MeJA treatment is easy to set up and inexpensive, it could be a useful technique to maintain quality in postharvest storage. In our previous studies, we found that MeJA treatment at 10 μM was effective in alleviating chilling injury of cold-stored loquat fruit (Cao et al., 2007) and the reduction in chilling injury by MeJA might be due to enhanced antioxidant enzyme activity and a higher unsaturated/saturated fatty acid ratio (Cao, Zheng, Wang, Jin, & Rui, 2009). However, little information is known about the effect of MeJA treatment as a factor that affects cell wall modification in loquat fruit during cold storage. The objective of the study was to investigate whether the MeJA-induced modification in cell wall metabolism is linked to the reduced chilling injury in cold-stored loquat fruit.

* Corresponding author. Tel.: +86 25 84399080; fax: +86 25 84395618.
E-mail address: zhengyh@njau.edu.cn (Y. Zheng).

0308-8146/$ - see front matter © 2009 Elsevier Ltd. All rights reserved.
doi:10.1016/j.foodchem.2009.05.047

2. Materials and methods

2.1. Plant material and treatments

The plant material and treatments were the same as described in our previous study (Cao et al., 2009). Fruit samples were taken after MeJA treatment (time 0) and at 7-day intervals during storage for measurements of fruit firmness, extractable juice, internal browning, lignin content, cell wall polysaccharide composition and the activities of phenylalanine ammonia lyase (PAL, EC 4.3.1.5), peroxidase (POD, EC 1.11.1.7), polyphenol oxidase (PPO, EC 1.14.18.1), polygalacturonase (PG, EC 3.2.1.15) and pectin methyl esterase (PME, EC 3.1.1.11).

2.2. Determinations of fruit firmness, extractable juice and internal browning index

Fruit firmness was measured on two paired sides of 10 fruit from each replicate (skin removed) with a TA-XT2i texture analyser (Stable Micro System Ltd., UK) with a 5 mm diameter probe at a speed of 1 mm s^{-1}.

Extractable juice was estimated from the weight loss from placental tissue plugs in response to low-speed centrifugation. Four plugs (7 mm wide and 10 mm thick) were placed over sterile cotton in a 50 ml centrifuge tube and centrifuged for 10 min at 1700*g* at room temperature. The results are expressed as% fresh weight loss of the tissue plugs after centrifugation.

The internal browning (IB) index, manifested as browning discoloration near the core was evaluated visually using 10 fruit from each replicate after cutting the fruit longitudinally in half. For each fruit, IB was scored according to a 5-grade scale, where 0 = none; 1 = slight; 2 = moderate; 3 = moderately severe; 4 = severe. Results were expressed as an IB index calculated using the following formula: IB index (between 0 and 4) = [$\sum$(IB level) $\times$ (number of fruit at the IB level)]/(Total number of fruit in the treatment).

2.3. Enzyme assays

To measure the enzymes activity, ten fruit from each treatment replicate were peeled, cut into small pieces and the bulked fruit samples (from the ten fruit) were frozen in liquid nitrogen and stored at −20 °C until analysis. All extract procedures were conducted at 4 °C. PAL was extracted with 0.2 M sodium borate buffer at pH 8.7 containing 20 mM of β-mercaptoethanol. For PPO, 1 g of flesh tissue was ground with 5 ml of 0.2 M sodium phosphate buffer (pH 6.5) containing 1% polyvinylpyrrolidone (PVP), or with 50 mM sodium borate buffer at pH 8.7 for POD. For PME and PG, 1 g of flesh tissue was ground with 5 ml of 0.15 M NaCl, containing 1% PVP. The extracts were then homogenised and centrifuged at 10,000*g* for 20 min at 4 °C. The supernatants were used for the enzyme assays.

PAL was assayed by the method described by Zucker (1968). One unit of PAL activity was defined as the amount of enzyme that causes the increase in absorbance of 0.01 at 290 nm in one hour under the specified conditions.

PPO activity was assayed following the method of Murr and Morris (1974). One unit of PPO activity was defined as the amount of enzyme that causes the increase in absorbance of 0.01 at 410 nm in one minute under the specified conditions.

POD activity was assayed using guaiacol as a donor and H_2O_2 as a substrate according to the method of Kochba, Lavee, and Spiege (1977). One unit of POD activity was defined as an increase of 0.01 in absorbance per minute at 460 nm under the assay conditions.

PG activity was determined according to Zhou, Dong, Ben-Arie, and Lurie (2000a) and one unit of activity was defined as 1 μmol galacturonic acid released per mg of protein per hour.

PME activity was determined according to Zhou et al., 2000b and one unit of activity was calculated as 1 mM NaOH consumed per mg of protein per hour.

Protein content in the enzyme extracts was estimated using the Bradford method, using bovine serum albumin as a standard (1976). Specific activity of the enzymes was expressed as units per mg of protein.

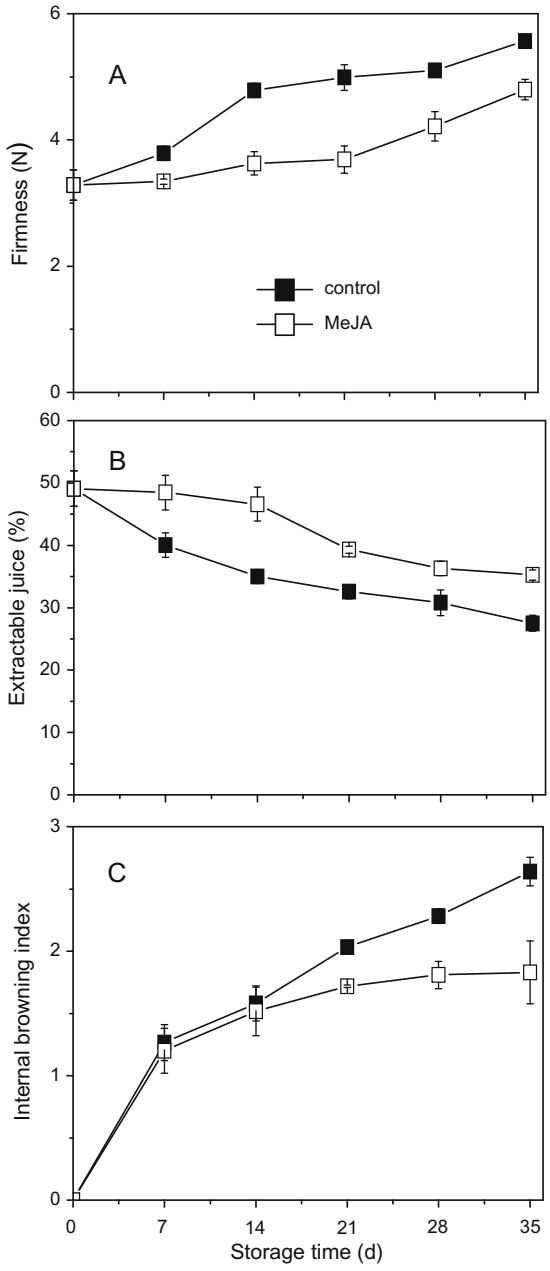

Fig. 1. Effects of MeJA on fruit firmness (A), extractable juice (B) and internal browning index (C) of loquat fruit during storage at 1 °C. Values for firmness and internal browning are the means ± SE of triplicate samples of ten fruit each. Values for extractable juice are the means ± SE of triplicate assays. Vertical bars represent the standard errors of the means.

2.4. Measurements of lignin content

The same frozen samples as used for the enzyme assays were used for lignin analysis. Lignin was gravimetrically determined according the method described previously (Cao et al., 2008). The result was expressed as a percentage.

2.5. Extraction and analysis for cell wall polysaccharides

The same frozen samples as used for the enzyme analysis were used for the extraction of alcohol insoluble residues (AIR). The AIR was prepared by homogenising 20 g of frozen tissues in 80 ml of cold 95% alcohol over ice for 3 min, which was then boiled for 25 min. The AIR was filtered under vacuum through glass fibre filters (GF/C, Whatman) and washed with 100 ml of 95% ethanol. The AIR was transferred to 100 ml of chloroform–methanol (1:1, v/v) and stirred for 30 min at room temperature. The AIR was filtered under vacuum through glass fibre filters (GF/C, Whatman) and washed with 100 ml of 100% acetone. The AIR samples were dried in an oven at 40 °C for 5 h and weighed. Results were expressed as 100 mg g^{-1} fresh weight (FW).

Then, the AIR (50 mg) was fractionated using the methods described previously (Deng, Wu, & Li, 2005). The uronic acid content in the water, CDTA and Na_2CO_3 fractions were determined by the m-hydroxydiphenyl method (Blumenkrantz & Asboe-Hansen, 1973). Galacturonic acid (Fluka) was used as the standard. Results were expressed as mg of galacturonic acid per 100 mg of AIR. The cellulose and hemicelluloses contents were quantified using a phenol–sulphuric acid method (Dubois, Gilles, Hamilton, Rebers, & Smith, 1956). Glucose was used as the standard for these assays. Results were expressed as mg of glucose per 100 mg of AIR.

2.6. Data analysis

Experiments were performed using a completely randomised design. All statistical analyses were performed with SPSS (SPSS Inc., Chicago, IL, USA). The data were analysed by one-way analysis of variance (ANOVA). Mean separations were performed by Duncan's multiple range tests. Differences at $p < 0.05$ were considered as significant.

3. Results

3.1. Effect of MeJA treatment on chilling injury

The major symptoms of chilling injury in loquat fruit are stuck peel, firm and juiceless texture and internal browning. Therefore, fruit firmness, internal browning and extractable juice were used to evaluate the development of chilling injury of loquat fruit in this work. Fruit firmness increased with increased storage time (Fig. 1A). The increase in firmness was significantly inhibited by MeJA treatment. Firmness of MeJA treated fruit was 14.1% lower than that of the control after 35 days of storage. There was also a positive effect of MeJA on extractable juice where the loss of juice was significantly ($p < 0.05$) inhibited by MeJA treatment (Fig. 1B). The internal browning index of loquat fruit increased gradually

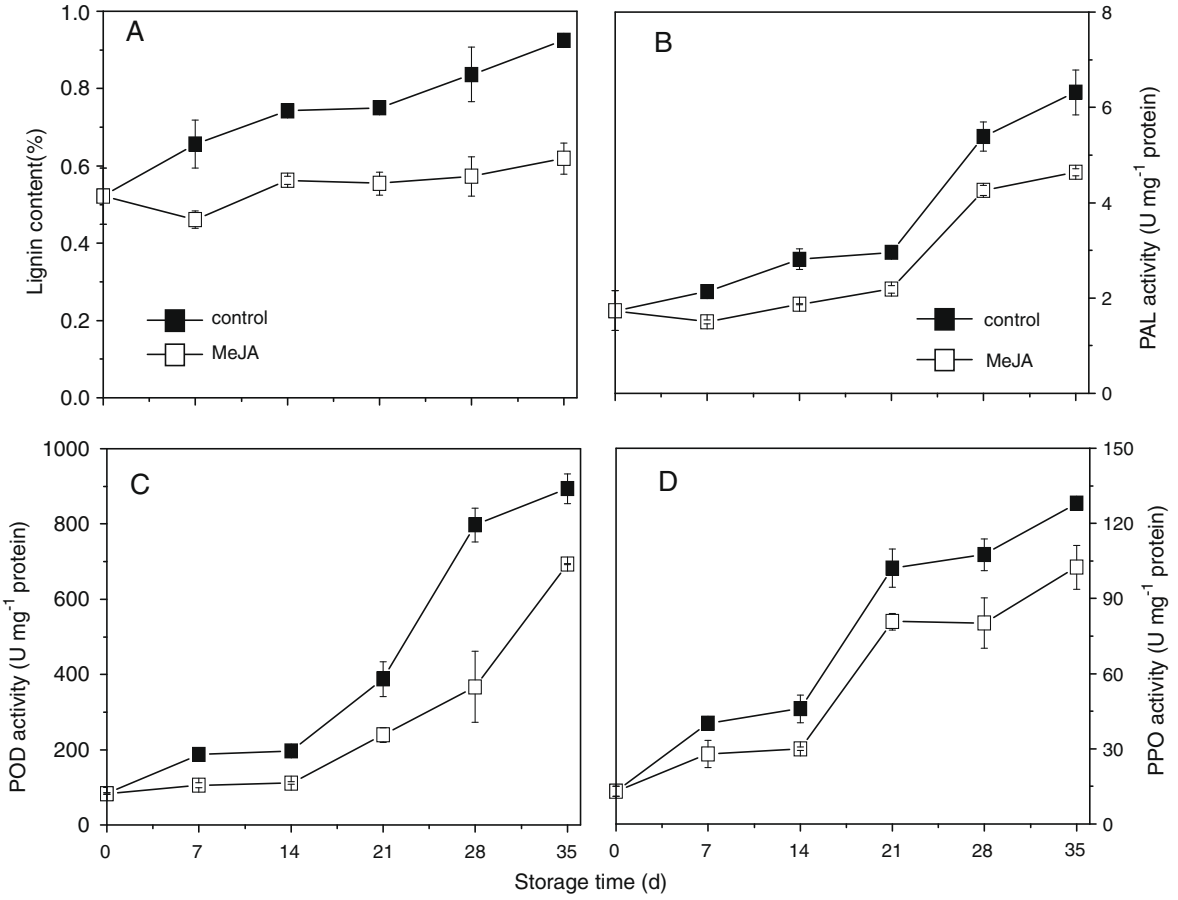

Fig. 2. Effect of MeJA on lignin content (A) and activities of PAL (B), POD (C) and PPO (D) in loquat fruit during storage at 1 °C. Values are the means ± SE of triplicate assays. Vertical bars represent the standard errors of the means.

with storage time but treatment with MeJA significantly ($p < 0.05$) inhibited the increase after 14 days of cold storage (Fig. 1C). The internal browning index increased to 264% and 183% of the initial values, respectively, in the control and the MeJA-treated fruit after 35 days of storage. The control fruit showed severe flesh leatheriness and a higher internal browning index after 21 days of storage at 1 °C. Treatment with MeJA delayed the increase in fruit firmness, internal browning index, and maintained higher levels of extractable juice, thereby delaying the development of flesh leatheriness and maintaining fruit quality.

3.2. Effect of MeJA treatment on lignin content and PAL, POD and PPO activities

The level of lignin increased steadily during the whole storage time. The lignin content in the control fruit was 76.9% higher than

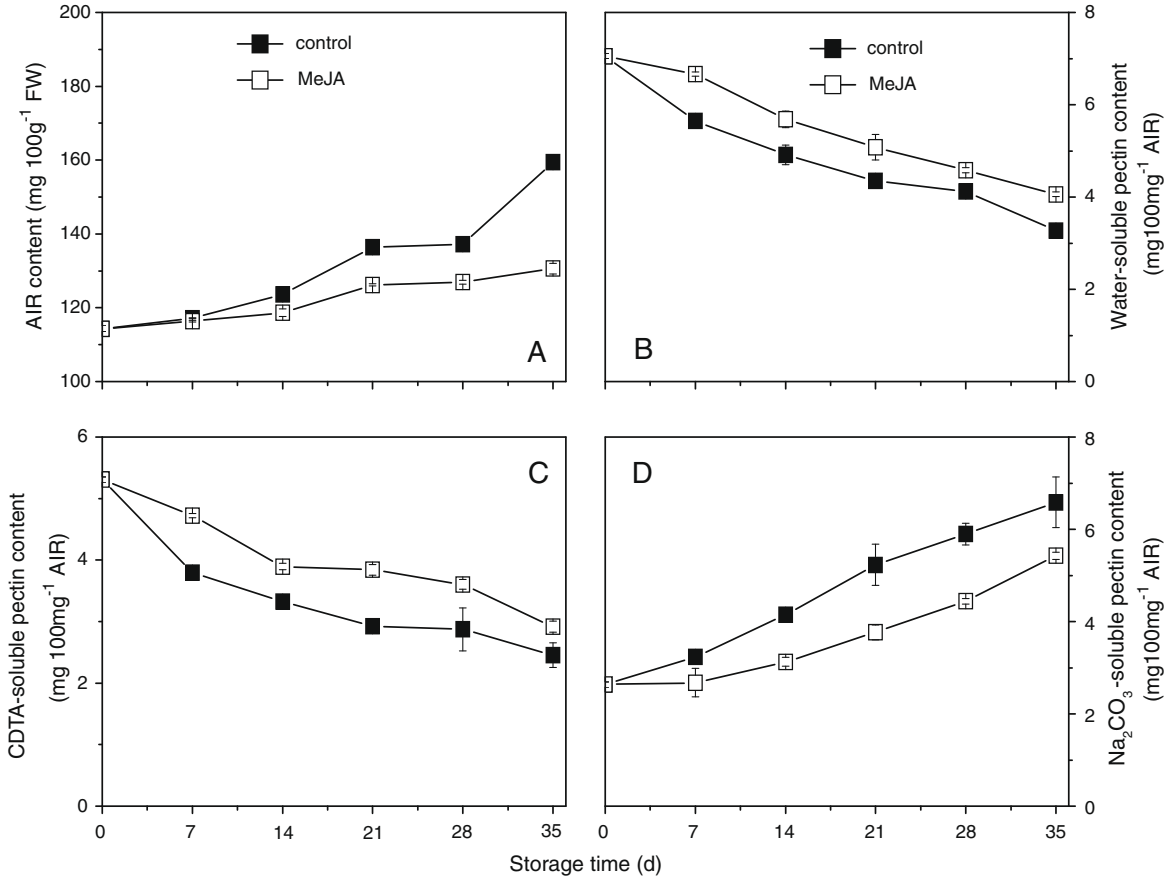

Fig. 3. Effect of MeJA on the contents of AIR (A), Water-(B), CDTA-(C) and Na_2CO_3-soluble pectins (D) in loquat fruit during cold storage at 1 °C. Values are the means ± SE of triplicate assays. Vertical bars represent the standard errors of the means.

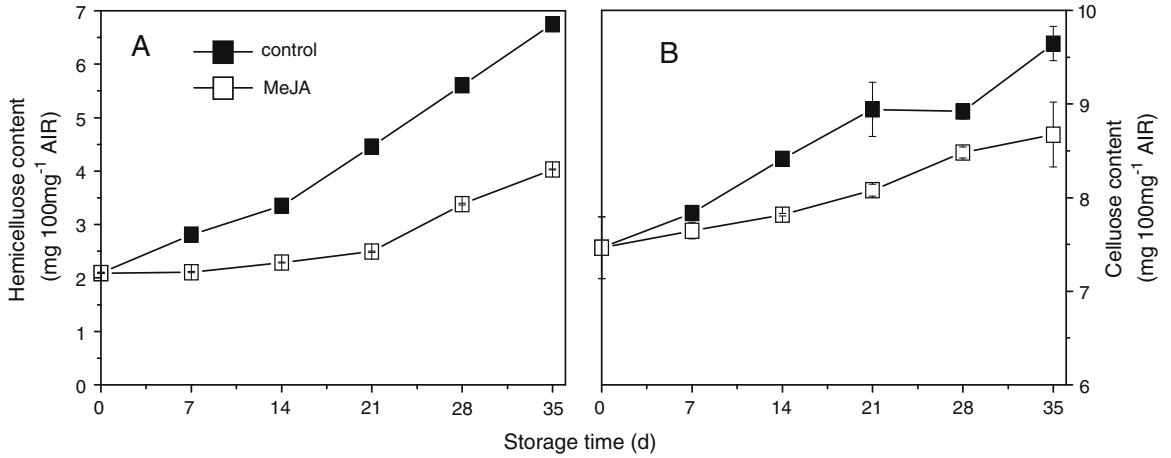

Fig. 4. Effect of MeJA on the contents of hemicelluose (A) and cellulose (B) in loquat fruit during cold storage at 1 °C. Values are the means ± SE of triplicate assays. Vertical bars represent the standard errors of the means.

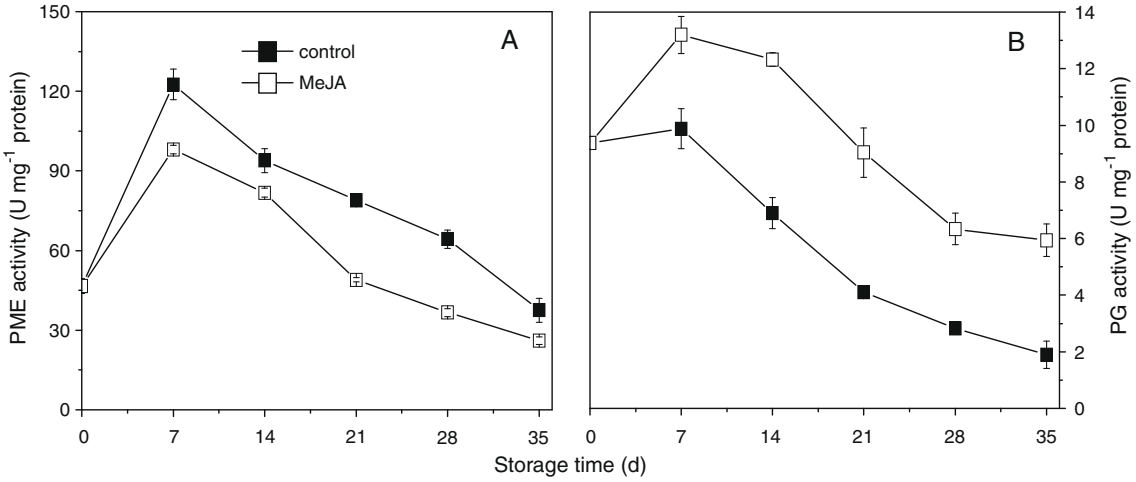

Fig. 5. Effect of MeJA on PME (A) and PG (B) activity in loquat fruit during storage at 1 °C. Values are the means ± SE of triplicate assays. Vertical bars represent the standard errors of the means.

the level at harvest. MeJA significantly ($p < 0.05$) inhibited the accumulation of lignin and after 35 days of storage the content was only 17.3% higher than the level at harvest (Fig. 2A). Activities of PAL, POD and PPO in loquat fruit increased with storage time (Fig. 2B–D). MeJA treatment significantly ($p < 0.05$) inhibited the increase in activities of these three enzymes. At the end of storage, the activities of PAL, POD and PPO in MeJA treated fruit were 26.7%, 22.3% and 20.3%, respectively, lower than that in control after storage for 35 days.

3.3. Effect of MeJA treatment on the AIR, and the water-, CDTA-, and Na_2CO_3-soluble pectins in loquat fruit

There was an increase in the AIR level over 35 days of storage (Fig. 3A). MeJA treatment significantly ($p < 0.05$) inhibited the increase of the AIR content. The AIR content in the control fruit was 39.5% higher than the level at harvest, whilst in the treated fruit it was only 14.0% higher than the amount of AIR at harvest. The levels of H_2O- and CDTA-soluble pectins decreased, whilst the Na_2CO_3 -soluble pectin level increased during storage (Fig. 3B–D) but, treatment with MeJA resulted in a significantly ($p < 0.05$) higher retention of H_2O- and CDTA-soluble pectins and a lower level of Na_2CO_3 -soluble pectin.

3.4. Effect of MeJA on contents of hemicelluose and cellulose in loquat fruit

The cell wall constituent hemicellulose and cellulose, in both the treated and the control fruit, increased progressively with storage time, however, their levels were significantly ($p < 0.05$) lower in MeJA-treated fruit. As shown in Fig. 4, the contents of hemicellulose and cellulose were, respectively, 40.2% and 10.4% lower than that in the control fruit on the 35th day.

3.5. Effect of MeJA treatment on PME and PG activities

The activity of PME increased sharply whilst that of PG increased slightly during the initial 7 days of storage, thereafter the activities of both enzymes decreased during storage. PG activity was significantly ($p < 0.05$) higher in MeJA-treated fruit than in the control fruit, whilst treatment with MeJA enhanced the decline of PME activity (Fig. 5), thus resulting in a significantly ($p < 0.05$) higher PG/PME ratio.

4. Discussion

It has been reported that lignin contributes to the development of chilling injury in cold-stored loquat fruit and its accumulation confers high rigidity and compression resistance to the cell wall (Zheng et al., 2000). Lignin synthesis is the result of coordinated action of many related enzymes including PAL, POD and PPO. PAL is a key enzyme that catalyses the conversion of phenylalanine to *trans*-cinnamic acid in the phenylpropanoid pathway, which is the first step in the biosynthesis of lignin in plants. POD catalyses the polymerisation of monolignol to form lignin. In addition, PPO can use as substrates those phenolic compounds which are precursors of lignin synthesis (Boudet et al., 2003). Therefore, the involvement of lignin synthesis in chilling injury and its related enzymes were analysed in this study. We observed an accumulation of lignin in response to low temperature after relatively long storage periods. It was also observed that MeJA treatment modified the time course of this response and reduced the magnitude of this particular response. Additionally, in all cases of lignin accumulation, increased activities of PAL, POD and PPO were detected. The activation of these three enzymes in loquat fruit has been reported in response to chilling stress (Shan et al., 2008). Treatments such as acetylsalicylic acid and 1-methylcyclopropene that reduced chilling injury have been shown to decrease the activities of PAL, POD and PPO (Cai, Li, & Chen, 2005; Cai et al., 2006). In the present study, treatment with MeJA significantly ($p < 0.05$) reduced chilling injury (Fig. 1) and decreased the activities of PAL, POD and PPO under low temperature stress (Fig. 2). These results suggest that the effect of MeJA in reducing the development of chilling injury was correlated to inhibited activities of enzymes involved in lignin synthesis. Moreover, PPO has been shown to be responsible for browning reactions during postharvest handling, storage and processing of fruits and vegetables. POD may participate in the oxidation and accumulation of phenolic materials and result in browning. The PAL activity can reflect the amount of the phenolic substrate. Hence, all of the three enzymes can also be involved in tissue browning (Peiser, Lopez-Galvez, Cantwell, & Saltveit, 1998), one of the symptoms of chilling injury in many fruits. In this study, loquat fruit had increasing PAL, POD and PPO activities, corresponding with an increase in the internal browning index during cold storage. MeJA treatment significantly inhibited the activities of the three enzymes, thus resulting in inhibition of the browning reaction and a lower internal browning index in loquat fruit.

Softening-associated changes in cell wall polysaccharides have been extensively documented in apple, carambola, mango and many tropical fruits (Vicente et al., 2007). Less attention has been paid to the changes in pectin, hemicellulose and cellulose content of loquat fruit during the development of chilling injury. In this study, we examined the possible role that cell wall polysaccharides might play in response to MeJA treatment under chilling stress. The AIR content accumulated during cold storage (Fig. 3A), and this increase was possibly related to higher firmness in cold-stored fruit as compared with freshly harvested fruit (Fig. 1A). As compared to untreated fruit, the significantly ($p < 0.05$) lower content of AIR in MeJA-treated fruit was an indicator of a higher degree of pectic polymers solubilisation. However, a previous study has shown that concomitant with the cell wall degradation in peach fruit, synthesis of cell walls also happened simultaneously during chilling injury development (Mao & Zhang, 2001). Therefore, cell wall synthesis might also be used to explain the accumulation of AIR in loquat fruit during cold storage and the chilling injury alleviation by MeJA might be partly attributed to inhibition of the synthesis.

In order to reveal the relationship between the cell wall polysaccharides and chilling injury in loquat fruit clearly, the AIRs obtained were further fractionated by sequential extraction with three pectic fractions, hemicellulose and cellulose. Typically, during fruit sofening, depolymerisation of cell wall polysaccharides was accompanied by increases in the levels of water- and chelator-soluble pectins, whilst the levels of Na_2CO_3-soluble pectin, hemicellulose and cellulose decreased (Chin, Ali, & Lazan, 1999; Redgwell, Melton, & Brasch, 1992). However, in loquat, we observed that the development of irreversible chilling injury symptoms, e.g., flesh leatheriness, was accompanied by decreased levels of water- and CDTA-soluble pectins and increased contents of Na_2CO_3-soluble pectin, hemicellulose and cellulose in the control fruit, whilst MeJA treatment maintained significantly ($p < 0.05$) higher contents of the first two pectins and lower contents of the latter three substances (Fig. 3B–D, Fig. 4). Our data presented here indicate that the chilling injury of loquat fruit might result from an increase in the cell wall stability by reducing the ability of enzymes to break down the bonds that hold the cell wall structure together, or by interacting with pectic polymers, hemicellulose and cellulose components. Loquat fruit treated with MeJA remained less firm, coinciding with higher retention of water- and CDTA-pectins and lower levels of hemicelluloses and cellulose.

The occurrence of chilling injury in loquat fruit during cold storage has been found to be associated with the imbalance of PG and PME activities (Zheng et al., 2000), which could lead to an excess of the de-esterified pectin matrix without subsequent depolymerisation (Zhou et al., 2000a). Our results indicated that the low PG activity, and the low PG/PME ratio in the control loquat fruit could induce the loss of juiciness and development of chilling injury. However, PG activity and the PG/PME ratio in MeJA-treated fruit was significantly ($p < 0.05$) higher than those in control, which was correlated with the higher levels of water- and CDTA-soluble pectins and lower incidence of chilling injury. Our results were consistent with the previous study in peach fruit (Feng et al., 2003), in which flesh leatheriness, one of the major symptoms of chilling injury in peach, was found to be a result of inhibited PME and PG activities during low temperature storage, whilst treatment with MeJA maintained significantly higher PME and PG activities, thereby preventing the development of chilling injury.

In conclusion, our data suggest that the role of MeJA treatment in reducing the incidence of chilling injury of loquat fruit appears to be mainly related to its ability to inhibit lignin accumulation and enhance the solubilisation of cell wall polysaccharides.

Acknowledgements

This study was supported by the National Natural Science Foundation of China (30671462), Qin Lan Project and National Scientific and Technical Supporting Program (2006BAD30B03, 2006BAD22B05).

References

Blumenkrantz, N., & Asboe-Hansen, G. (1973). New method for quantitative determination of uronic acids. *Analytical Biochemistry, 54*, 484–489.

Boudet, A. M., Kajita, S., Grima-Pettenati, J., & Goffner, D. (2003). Lignins and lignocellulosics: A better control of synthesis for new and improved uses. *Trends in Plant Science, 8*, 576–581.

Bradford, M. M. (1976). A rapid and sensitive method for the quantitation of microgram quantities of protein utilizing the principle-dye binding. *Analytical Biochemistry, 72*, 248–254.

Cai, C., Chen, K. S., Xu, W. P., Zhang, W. S., Li, X., & Ferguson, I. (2006). Effect of 1-MCP on postharvest quality of loquat fruit. *Postharvest Biology and Technology, 40*, 155–162.

Cai, C., Li, X., & Chen, K. S. (2005). Acetylsalicylic acid alleviates chilling injury of postharvest loquat (*Eriobotrya japonica* Lindl.) fruit. *European Food Research Technology, 223*, 533–539.

Cao, S. F., Zheng, Y. H., Wang, K. T., Jin, P., & Rui, H. J. (2009). Methyl jasmonate reduces chilling injury and enhances antioxidant enzyme activity in postharvest loquat fruit. *Food Chemistry, 115*, 1458–1463.

Cao, S. F., Zheng, Y. H., Yang, Z. F., Ma, S. J., Li, N., Tang, S. S., et al. (2007). Effects of methyl jasmonate treatment on quality and decay in cold-stored loquat fruit. *Acta Horticulture, 750*, 425–430.

Cao, S. F., Zheng, Y. H., Yang, Z. F., Tang, S. S., Jin, P., Wang, K. T., et al. (2008). Effect of methyl jasmonate on inhibition of *Colletotrichum acutatum* infection in loquat fruit and the possible mechanism. *Posthavest Biology and Technology, 47*, 151–158.

Carpita, N. C., & Gibeaut, D. M. (1993). Structural models of primary cell walls in flowering plants: Consistency of molecular structure with the physical properties of the walls during growth. *Plant Journal, 3*, 1–30.

Chin, L. H., Ali, Z. M., & Lazan, H. (1999). Cell wall modifications, degrading enzymes and softening of carambola fruit during ripening. *Journal of Experimental Botany, 50*, 767–775.

Creelman, R. A., & Mullet, J. E. (1997). Biosynthesis and action of jasmonate in plants. *Annual Review of Plant Physiology and Plant Molecular Biology, 48*, 355–381.

Deng, Y., Wu, Y., & Li, Y. F. (2005). Changes in firmness, cell wall composition and cell wall hydrolases of grapes stored in high oxygen atmospheres. *Food Research International, 38*, 769–776.

Dubois, M., Gilles, K. A., Hamilton, J. K., Rebers, P. A., & Smith, F. (1956). Colorimetric method for determination of sugars and related substances. *Analytical Chemistry, 28*, 350–356.

Feng, L., Zheng, Y. H., Zhang, Y. F., Wang, F., Zhang, L., & Lu, Z. X. (2003). Methyl jasmonate reduces chilling injury and maintains postharvest quality in peaches. *Agricultural Sciences in China, 11*, 1246–1252.

González-Aguilar, G. A., Tizuado-Hernández, M. E., & Wang, C. Y. (2006). Physiological and biochemical responses of horticultural products to methyl jasmonate. *Stewart Postharvest Review, 2*, 1–9.

Jarvis, M. C., Briggs, S. P. H., & Knox, J. P. (2003). Intercellular adhesion and cell separation in plants. *Plant, Cell and Environment, 26*, 977–989.

Kochba, J., Lavee, S., & Spiege, R. P. (1977). Difference in peroxidase activity and isoenzymes in embryogenic and non-embryogenic 'Shamouti' orange ovular callus lines. *Plant and Cell Physiology, 18*, 463–467.

Lewis, N. G., & Yamamoto, E. (1990). Lignin: Occurrence, biogenesis and biodegradation. *Annual Review of Plant Physiology and Plant Molecular Biology, 41*, 455–496.

Mao, L. C., & Zhang, S. L. (2001). Influence of intermittent low temperature stress on cell wall metabolism in peaches. *Acta Phytophysiologica Sinica, 27*, 151–155.

Murr, D. P., & Morris, L. L. (1974). Influence of O_2 and CO_2 on o-diphenol oxidase activity in mushrooms. *Journal of the American Society for Horticultural Science, 99*, 155–158.

Peiser, G., Lopez-Galvez, G., Cantwell, M., & Saltveit, M. E. (1998). Phenylalanine ammonia lyase inhibitors control browning of cut lettuce. *Postharvest Biology and Technology, 14*, 171–177.

Redgwell, R. J., Melton, L. D., & Brasch, D. J. (1992). Cell wall dissolution in ripening kiwifruit (*Actinidia deliciosa*). Solubilization of the pectic polymers. *Plant Physiology, 98*, 71–81.

Shan, L. L., Li, X., Wang, P., Cai, C., Zhang, B., Sun, C. D., et al. (2008). Characterization of cDNAs associated with lignification and their expression profiles in loquat fruit with different lignin accumulation. *Planta, 227*, 1243–1254.

Vicente, A. R., Saladie, M., Rose, J. K. C., & Labavitch, J. M. (2007). The linkage between cell wall metabolism and fruit softening: Looking to the future. *Journal of the Science of Food and Agriculture, 87*, 1435–1448.

Whitney, S. E. C., Gothard, M. G. E., Mitchell, J. T., & Gidley, M. J. (1999). Roles of cellulose and xyloglucan in determining the mechanical properties of primary plant cell walls. *Plant Physiology, 121*, 657–663.

Zheng, Y. H., Li, S. Y., & Xi, Y. F. (2000). Changes of cell wall substances in relation to flesh leatheriness in cold-stored loquat fruits. *Acta Phytophysiologica Sinica, 26*, 306–310.

Zhou, H. W., Dong, L., Ben-Arie, R., & Lurie, S. (2000a). Pectin esterase polygalacturonase and gel formation in peach pectin fractions. *Phytochemistry, 55*, 191–195.

Zhou, H. W., Lurie, S., Lers, A., Khatchitski, A., Sonego, L., & Ben-Arie, R. (2000b). Delayed storage and controlled atmosphere storage of nectarines: Two strategies to prevent woolliness. *Postharvest Biology and Technology, 18*, 133–141.

Zucker, M. (1968). Sequential induction of phenylalanineammonia lyase and a lyase-inactivating system in potato tuber disks. *Plant Physiology, 43*, 365–374.

Food Chemistry 118 (2010) 648–655

Contents lists available at ScienceDirect

Food Chemistry

journal homepage: www.elsevier.com/locate/foodchem

Effect of hydroxypropyl-β-cyclodextrin on the aggregation of (*E*)-resveratrol in different protonation states of the guest molecule

José Manuel López-Nicolás *, Francisco García-Carmona

Department of Biochemistry and Molecular Biology-A, Faculty of Biology, University of Murcia, Campus de Espinardo, 30071 Murcia, Spain

ARTICLE INFO

Article history:
Received 30 July 2008
Received in revised form 7 April 2009
Accepted 14 May 2009

Keywords:
Resveratrol
Cyclodextrin
Aggregation
Fluorescence
Absorbance

ABSTRACT

The aggregation state of (*E*)-resveratrol was studied in the presence and absence of hydroxypropyl-β-cyclodextrin (HP-β-CD) using absorption and steady-state fluorescence at different pH values. The results revealed that this potent antioxidant shows a monomer/aggregate equilibrium which is dependent on the protonation state of (*E*)-resveratrol. This equilibrium can be modified by the presence of HP-β-CD, which reduces the aggregation of the (*E*)-resveratrol molecules, producing individual molecules of the solute and preventing side effects due to aggregation phenomena. At pH values higher than the pK_{a1} of (*E*)-resveratrol, the coexistence of different protonated/deprotonated forms of this antioxidant does not permit the fluorimetric determination of the complexation constant (K_F) of (*E*)-resveratrol with HP-β-CD. However, when the Hildebrand–Benesi equation was used to calculate this constant at physiological pH, this problem was resolved, with a K_F value of 14490 ± 723 M^{-1} and the stoichiometry of the complexation process 1:1 for all the cases tested. The results obtained in this paper resolve the contradictory data published about the complexation process of (*E*)-resveratrol by cyclodextrins.

1. Introduction

Interest in the potential health benefits associated with the dietary consumption of (*E*)-resveratrol (3,5,4′-trihydrostilbene) has increased significantly in the past decade. Resveratrol is a member of the stilbene family, a group of compounds consisting of two aromatic rings joined by a methylene bridge, and can be found in several foods (Counet, Callemien, & Collin, 2006; Ragab, Van Fleet, Jankowski, Park, & Bobzin, 2006; Wang, Catana, Yang, Roderick, & van Breemen, 2002). The increased consumption of monomeric (*E*)-resveratrol and/or (*E*)-resveratrol-containing foods may be associated with improved health. These health benefits are related to a diverse range of biological activities such as anticancer, cardioprotection, antioxidant, antiviral, cytogenetic, oestrogenic and anti-inflamatory activities and the inhibition of platelet aggregation (Fang et al., 2002; Latruffe et al., 2002; Matsuoka et al., 2002; Stivala et al., 2001; Xu, Wang, Liu, Jiang Wang, & Fang Wang, 2007).

However, the problems concerning the physicochemical properties of (*E*)-resveratrol have meant that no novel food has been fortified with this antioxidant (López-Nicolás, & García-Carmona, 2008a). Despite the fact that (*E*)-resveratrol is one of the most potent antioxidants discovered in the recent years, few studies have focused on the structural determinants of this stilbene which influence its health-associated properties, such as the aggregation state, the protonation state or its solubility in aqueous solutions (López-Nicolás & García-Carmona, 2008b; Ovesná & Horváthová-Kozics, 2005), and it is these which are objectives of this work.

The aggregation state of many compounds may modify their biological activities (López-Nicolás, Bru, & García-Carmona, 1997). In solution, some molecules exhibit an aggregation behaviour that, depending on the pH, may lead to the formation of true micelles or merely to a dispersed oil phase (Bru, López-Nicolás, & García-Carmona, 1995). Thus, the knowledge of the possible equilibrium between the monomeric forms and the aggregates of this antioxidant may be essential for understanding the influence of (*E*)-resveratrol concentration on the properties attributed to it. For this reason, a study of the aggregation state of (*E*)-resveratrol in both the absence and presence of a type of compound which reduces the formation of aggregates at physiological pH is desirable.

Moreover, the aggregation of some molecules is strongly dependent on the protonation state of the molecule (López-Nicolás et al., 1997). Indeed, in the case of (*E*)-resveratrol the healthy properties of this stilbene can only be demonstrated when the three hydroxyl groups are present, i.e., when (*E*)-resveratrol is in its protonated form (Matsuoka et al., 2002). For this reason, the possible aggregation of (*E*)-resveratrol in different protonation states in the presence of modifiers of the aggregation state of this antioxidant is also worth studying.

Finally, the use of (*E*)-resveratrol as fortifier and nutraceutical is limited by its poor solubility in water and bioavailability (Trela & Waterhouse, 1996; Walle, Hsieh, Delegge, Oatis, & Walle, 2004; Wenzel & Somoza, 2005). For these reasons, the complexation of

* Corresponding author. Tel.: +34 968 364765; fax: +34 968 364147.
E-mail address: josemln@um.es (J.M. López-Nicolás).

0308-8146/$ - see front matter © 2009 Elsevier Ltd. All rights reserved.
doi:10.1016/j.foodchem.2009.05.039

(*E*)-resveratrol with the type of molecules which increase its bioavailability and solubility in aqueous solutions is strongly desirable.

To study these objectives we have used cyclodextrins (CDs), which are torus-shaped oligosaccharides made up of 6–8 glucopyranose units that originate from the enzymatic degradation of starch through the action of CD-glucano-transferase (Saenger, 1980; Szejtli, 1988; Szente & Szejtli, 2004). Poorly water-soluble compounds and hydrophobic moieties of amphiphilic molecules interact non-covalently with the CD cavity to form the so-called inclusion complexes, which are also highly water-soluble (López-Nicolás, Bru, Sánchez-Ferrer, & García-Carmona, 1995). Hydroxypropyl-β-cyclodextrin (HP-β-CD), a hydroxyalkyl derivative, is an alternative to α-, β- and γ-CD, with improved water solubility and may be slightly more toxicologically benign). As the first approved CD derivatives by FDA, HP-β-CDs have widely applications in food, agriculture and the pharmaceutical field (Yuan, Jin, & Li, 2008).

As opposed to other solubility-enhancing detergents, water-miscible solvents, etc., CDs produce individual molecules of the solute, thus preventing side effects, due to aggregation phenomena (Bru et al., 1995; Bru et al., 1996; López-Nicolás et al., 1997).

The effect of CDs on (*E*)-resveratrol has been reported in very few publications. Moreover, most works published have limited their investigation to the determination of complexation constants (K_F) using techniques such as solubility (Bertacche, Lorenzi, Nava, Pini, & Sinico, 2006), enzymology (Lucas-Abellán, Fortea, López-Nicolás, & Núñez-Delicado, 2007) or liquid chromatography, (López-Nicolás & García-Carmona, 2008a; López-Nicolás, Núñez-Delicado, Pérez-López, Carbonell, & Cuadra-Crespo, 2006). However, results concerning the K_F values of (*E*)-resveratrol complexed by CDs under different reaction conditions are contradictory. While some papers have claimed that natural CDs are the most suitable for the inclusion process (Bertacche et al., 2006), others have reported that modified CDs are the most appropriate to complex (*E*)-resveratrol (Lucas-Abellán et al., 2007). Moreover, papers have reported very different complexation constant values for the same type of complexes. Our study may help to resolve this problem because other publications have not take into account several important aspects of the complexation mechanism, such as the aggregation state of (*E*)-resveratrol, the pH values of the reaction medium, the pK_a values of the guest molecule and the UV–vis or fluorospectrometric properties of (*E*)-resveratrol in the presence of CDs.

Bearing in mind the above, this work has three principal objectives: (i) to study the aggregation state of (*E*)-resveratrol in the presence and absence of anti-aggregant agents such as CDs; (ii) to analyse the complexation of (*E*)-resveratrol with CDs in an aqueous medium under various experimental conditions and (iii) to obtain as wide a range of information as possible to clarify the contradictory data published in the literature about CD/(*E*)-resveratrol complexes.

To perform the study, several different methodologies are applied, which make use of changes in absorbance and fluorescence spectroscopic properties of (*E*)-resveratrol in the presence of CDs.

2. Material and methods

2.1. Reagents

The biochemicals were purchased from Fluka (Madrid, Spain). HP-β-CD was purchased from Sigma–Aldrich (Madrid, Spain) and used as received. (*E*)-resveratrol was from Sigma–Aldrich (Steinheim, Germany) and was used without further purification.

2.2. Stock standard solution of (*E*)-resveratrol

An accurately weighed 0.1 g standard sample of (*E*)-resveratrol was dissolved in ethanol, transferred into a 100-ml standard flask and diluted to the mark with ethanol and mixed well. The solution was stored at 4 °C. (*E*)-Resveratrol is sensitive to light and irradiation of solutions of the analyte induces the formation of (*Z*)-resveratrol and, if very intense, leads to the formation of a highly fluorescent compound. Because of this, the samples were stored in darkness. The stock standard solution was diluted to 30 μg/ml with sodium phosphate (0.1 M) before being used.

2.3. Fluorescence and absorbance spectroscopy

A PiStar-180 Spectrometer (Applied Photophysics Ltd., Leatherhead, United Kingdom) equipped with a xenon lamp source and quartz cell was used to perform all absorbance and fluorescence measurements. Excitation and emission bandwidths were both set at 2 nm. For both absorbance and fluorescence spectroscopy, excitation and emission spectra were recorded at 25 °C. To avoid inner filter effects, 2-mm quartz cells were used.

2.4. Influence of HP-β-CD concentration

The effect of HP-β-CD concentration on the absorbance and fluorescence intensity of (*E*)-resveratrol was studied. The (*E*)-resveratrol concentration was held constant at the values shown in Figs. 3–5, while the HP-β-CD concentration was varied. The HP-β-CD/(*E*)-resveratrol complexes were prepared according to the following procedure: a 1.0-ml aliquot of (*E*)-resveratrol solution at the concentrations shown in the figure legends (prepared by dilution of stock solution with water just before use) was transferred into a 5-ml volumetric flask and then an appropriate amount of HP-β-CD solution was added and the flask was filled to the mark with water. The resulting solutions were shaken and allowed to equilibrate and their fluorescence intensities were read within 1 h. All measurements were made at least in triplicate.

3. Results and discussion

3.1. Selection of the investigation conditions

Since (*E*)-resveratrol is a trihydroxyl molecule, it is important to evaluate its behaviour with changes in pH. Bearing in mind the published data for the acidic dissociation constants (López-Nicolás & García-Carmona, 2008b), and to study the aggregation state of (*E*)-resveratrol and its complexation processes by HP-β-CD under various experimental conditions of pH and concentrations, the present investigation was planned by defining the following possible situations. In all these situations, changes in the spectra of UV–vis absorption of fluorescence excitation and emission were used to study the complexation process.

3.1.1. Physiological region ($pH < pK_{a1}$)

This region can be considered as the physiological zone where (*E*)-resveratrol maintains its biological activities. The guest is the totally protonated structure of (*E*)-resveratrol (Structure A, Scheme 1) and the host is a neutral molecule (HP-β-CD). A pH value of 6.5 was selected to study the complexation of (*E*)-resveratrol by HP-β-CD in the physiological region.

3.1.2. Enzymatic oxidation region: mild basic medium ($pK_{a1} < pH < pK_{a2}$)

The oxidation of (*E*)-resveratrol by several enzymes has been described in this region. The major guest is that corresponding to

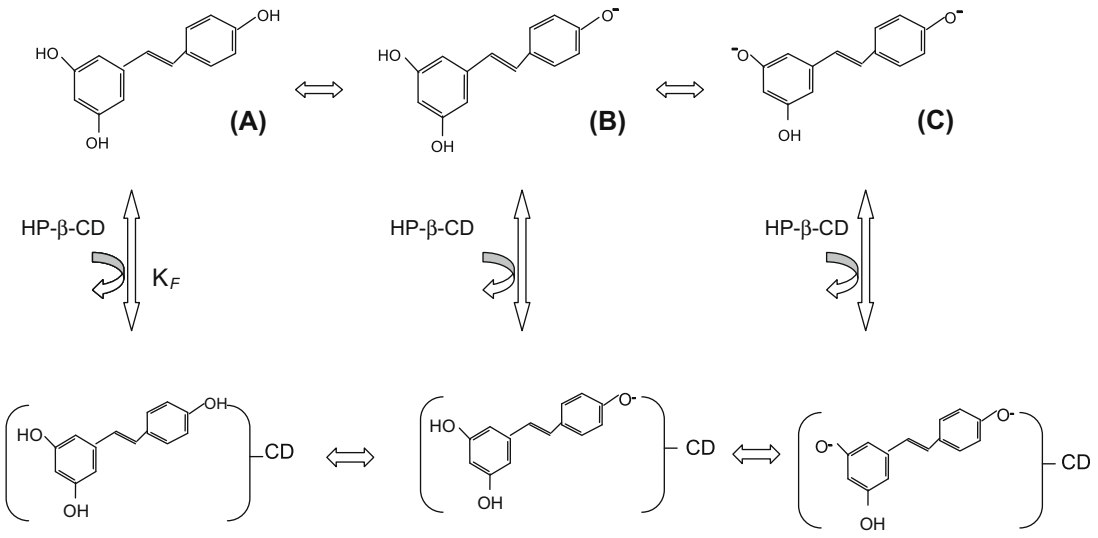

Scheme 1. Complexation of protonated and deprotonated forms of (*E*)-resveratrol with HP-β-CD.

only one deprotonated hydroxyl group in the structure of (*E*)-resveratrol (Structure B, Scheme 1) but, as the pK_a values of (*E*)-resveratrol do not greatly differ, the coexistence of minority species, such as the totally protonated (Structure A, Scheme 1) and two deprotonated (Structure C, Scheme 1) hydroxyl groups in the structure of (*E*)-resveratrol is perfectly possible. On the other hand, in the pH value selected in this zone (pH 9.2) the host is a neutral molecule (HP-β-CD), and so this pH value was selected to study the complexation of (*E*)-resveratrol by HP-β-CD.

3.1.3. Strong basic medium (pK_{a2} < pH)

In this region, the majority species is the (*E*)-resveratrol containing two deprotonated hydroxyl groups in its structure (Structure C, Scheme 1). In this paper, the complexation of this stilbene by CDs is not studied for three reasons: (i) the basic hydrolysis of this antioxidant takes place very close to this zone; (ii) no physiological activities of (*E*)-resveratrol have been described in this pH region and (iii) the enzymatic oxidation of (*E*)-resveratrol is inhibited at these pH values.

3.2. UV–vis study of the aggregation of (E)-resveratrol in the presence of cyclodextrins

3.2.1. Physiological region

As indicated in introduction section, when the pH value of the reaction medium is situated below the first acidic dissociation constant (pK_{a1}), (*E*)-resveratrol shows its biological activities (Fang et al., 2002; Matsuoka et al., 2002; Stivala et al., 2001; Xu et al., 2007). For this reason, it is very important to study the aggregation of this molecule below the pK_{a1} value. Although several papers have reported substantial differences for the pK_a values of (*E*)-resveratrol (Cao, Chen, Du, Hou, & Tian, 2006; Galeano Díaz, Durán Merás, & Airado Rodríguez, 2007; López-Nicolás & García-Carmona, 2008a, 2008b; Takagai et al., 2005), at the selected pH value of 6.5, (*E*)-resveratrol is in its protonated form.

Fig. 1A shows the spectra of the pure (*E*)-resveratrol solutions in increasing concentrations at pH 6.5. The stilbene shows two absorption bands at around 215 and 300 nm in this pH region. Moreover, the results obtained show that the band around 300 nm presents a bandwidth of 20 nm and two small maxima centred at 305 and 316 nm. As can be seen in Fig. 2A (filled circles), although the absorbance at both 215 and 305 nm increases with the (*E*)-resveratrol concentration, the absorbance ratio of the stilbene at 215 and 305 nm was not constant as was to be expected according to the Lambert–Beer law, but increased. As suggested for other compounds (Guomei, Shaomin, Chuan, & Jinghao, 2003; Zhang, Jiang, Guo, & Li, 2008), variations in the absorbance ratio between different wavelengths would have been caused by the aggregation of (*E*)-resveratrol due to the monomer (M)/aggregate (A) equilibrium of (*E*)-resveratrol:

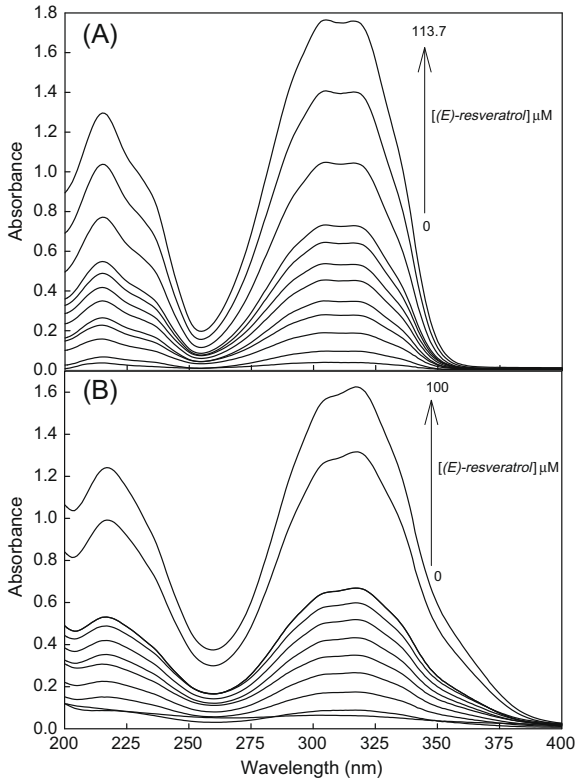

Fig. 1. The absorption spectra of (*E*)-resveratrol solutions (A) 1.26, 3.79, 7.59, 15.18, 18.93, 22.75, 26.57, 30.32, 45.56, 60.60, 76.90 and 113.7 μM at pH 6.5; and (B) 2.5, 5, 10, 15, 20, 25, 30, 35, 40, 80 and 100 μM at pH 9.2.

$$nM \rightleftharpoons A$$

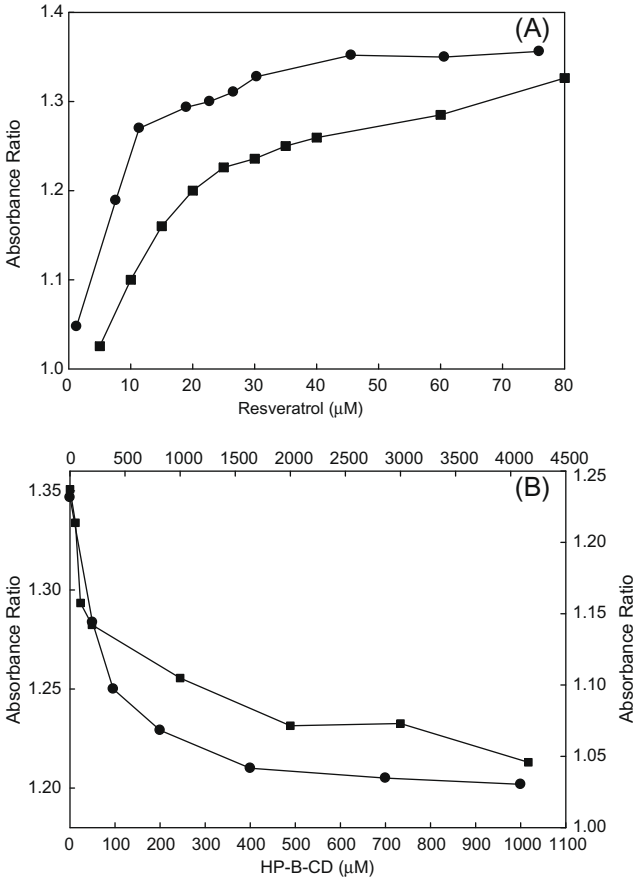

Fig. 2. (A) A plot of absorbance ratio of (*E*)-resveratrol at 305 and 215 nm versus the concentration of (*E*)-resveratrol at pH 6.5 (filled circles) and at 317 and 215 nm at pH 9.2 (filled squares); (B) the absorbance ratio of (*E*)-resveratrol in the presence of different concentrations of HP-β-CD at pH 6.5 (filled circles) and pH 9.2 (filled squares). (*E*)-Resveratrol concentration was maintained at 60.6 μM (pH 6.5) and 80 μM (pH 9.2).

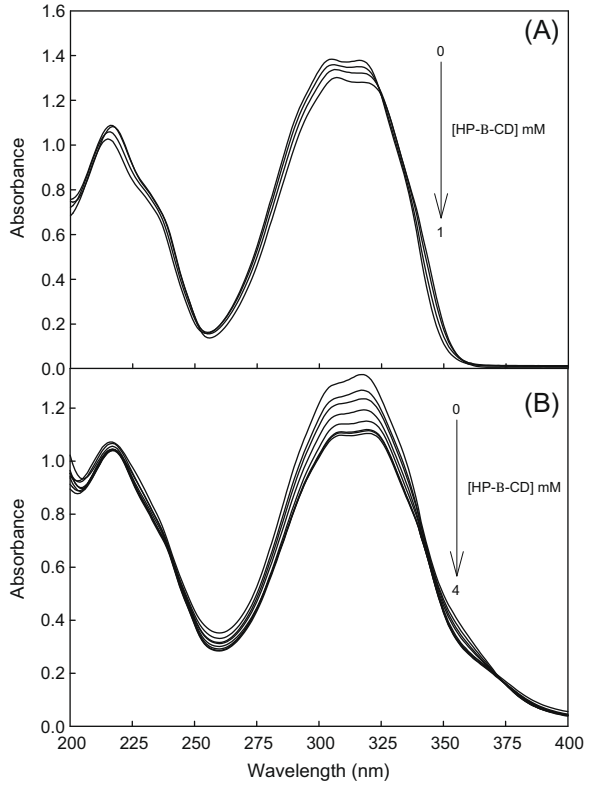

Fig. 3. (A) The absorption spectra of 60.6 μM (*E*)-resveratrol in the presence of increasing concentrations of HP-β-CD (0, 0.25, 0.5, 1 mM) at pH 6.5; and (B) absorption spectra of 80.0 μM (*E*)-resveratrol in the presence of increasing concentrations of HP-β-CD (0, 0.25, 0.5, 0.75, 1, 1.5, 2, 3, 4 mM) at pH 9.2.

As indicated in the introduction section, the aggregation state of a molecule is strongly related with its biological activity. For this reason, the use of antiaggregate compounds such as CDs, which maintains the monomer form of (*E*)-resveratrol, is advisable. Therefore, the next step was to study the effect of adding HP-β-CD on the aggregation state of (*E*)-resveratrol.

As can be seen from Fig. 2B (filled circles), the absorbance ratio of (*E*)-resveratrol at 215 and 305 nm decreased with increasing HP-β-CD concentration at pH 6.5, leading to an opposite effect to that observed in Fig. 2A (filled circles) in the absence of HP-β-CD. This may be explained by the capacity of HP-β-CD to modify the aggregation equilibrium existing in different molecules, producing individual molecules of the solute and preventing side effects due to aggregation phenomena, as has been seen to occur in polyunsaturated fatty acids (Bru et al., 1995; López-Nicolás et al., 1995). In this case, the presence of HP-β-CD modifies the equilibrium between free and aggregate (*E*)-resveratrol, leading to increase in the concentration of monomer (*E*)-resveratrol with respect to the aggregate forms as has been demonstrated by our group for other molecules (López-Nicolás et al., 1995).

To corroborate the formation of an inclusion complex between (*E*)-resveratrol and HP-β-CD, the UV–vis spectra of 60.6 μM (*E*)-resveratrol at pH 6.5 in the absence and presence of increasing concentrations of HP-β-CD are shown in Fig. 3A. With the addition of HP-β-CD the absorbance decreased gradually at around 300 nm, which suggests the formation of HP-β-CD/(*E*)-resveratrol complexes. Moreover, several works have reported that the presence (or not) of an isobestic point may determine the formation of a CD/guest complex (Guomei et al., 2003; Zhang et al., 2008). As shown in Fig. 3A, the isobestic points appears at 253 and 326 nm, which again suggests the formation of HP-β-CD/(*E*)-resveratrol complexes.

3.2.2. Enzymatic oxidation region

Although (*E*)-resveratrol shows its biological activities below the pK_{a1} value, it is still necessary to study the possible aggregation of this stilbene when (*E*)-resveratrol is deprotonated, to understand the oxidative process of this antioxidant by several enzymes, as in the case of lipoxygenase. Indeed, several authors have studied the oxidation of (*E*)-resveratrol by lipoxygenase at basic pH values (Fan & Mattheis, 2001; Lucas-Abellán et al., 2007; Pinto, García-Barrado, & Macías, 2003). However, these researchers did not take into account the aggregation and protonation state of (*E*)-resveratrol and, for this reason, this enzymatic oxidative pH region was the next region studied.

As shown in Fig. 1B, the band around 300 nm was reduced at higher pH values than those in the physiological zone, and the 340 nm band increased. However, as in the physiological region, the absorbance ratio of (*E*)-resveratrol at 215 and 317 nm increased with the (*E*)-resveratrol concentration (Fig. 2A filled squares), indicating the presence of aggregation phenomena at pH 9.2. As was also seen in the physiological zone, the absorbance ratio of (*E*)-resveratrol at 215 and 340 nm decreased with increasing HP-β-CD concentration at pH 9.2, modifying the aggregation equilibrium existing between monomeric and aggregate forms of (*E*)-resveratrol (Fig. 2B filled squares).

Demonstrating the formation of HP-β-CD/(*E*)-resveratrol inclusion complex at pH 9.2, Fig. 3B shows that the absorbance at

340 nm was significantly reduced when increasing concentrations of HP-β-CD were added to the reaction medium and that two new isobestic points appeared at 242 and 345 nm at this pH value.

The phenomenon of aggregation for (*E*)-resveratrol at different pHs described above may explain the different values reported by different researchers (Bertacche et al., 2006; Lucas-Abellán, Fortea, Gabaldón, & Núñez-Delicado, 2008), using linear regression of the phase solubility diagram to determine the K_F values at neutral pH for the (*E*)-resveratrol/CD complexes. Indeed, a technique based on the solubility of the guest molecule is not precise when aggregation phenomena of a guest molecule, such as (*E*)-resveratrol, occur in the region studied.

3.3. Effect of HP-β-CD on fluorescence of (E)-resveratrol at basic pH values

To obtain as wide a range of information as possible about the molecular interactions that drive the complexation process of (*E*)-resveratrol by HP-β-CD, a detailed fluorospectrometric study of the interaction between these compounds was carried out at different pH values.

Up to the date, in the literature there is only one paper that reports the fluorescence behaviour of (*E*)-resveratrol in the presence of CDs. Recently, Lucas-Abellán, Fortea, Gabaldón, and Núñez-Delicado (2008) studied the complexation of (*E*)-resveratrol with several types of CDs at different pHs using three different methods: enzymatic, solubility and fluorimetric. The comparison of the results obtained by the three methods by these researchers revealed that the fluorimetric method undervalued the K_F between (*E*)-resveratrol and all the CDs, while the enzymatic and solubility methods were more precise for calculating the K_F. For this reason, those researchers affirm that the fluorimetrically determined K_F is not correct.

However, the reasons for this behaviour were not explained and this fact must be clarified, taking into account different factors, such as the pK_a of the guest molecule, the medium pH, the fluorospectrometric properties of (*E*)-resveratrol and the aggregation state of this potent antioxidant.

In the paper published by Lucas-Abellán et al. (2008) only fluorescence intensity values at a single wavelength (380 nm) were presented but no excitation or emission spectra were shown. This fact led to several anomalous results, which are clarified in this paper, where an exhaustive study of the fluorospectrometric properties of (*E*)-resveratrol in the presence of CDs is carried out.

(*E*)-Resveratrol presents three relative emission bands (385 nm, 445 nm and 475 nm) depending on the pH of the reaction medium. When the pH value is lower than the pK_{a1}, (*E*)-resveratrol shows a characteristic emission spectrum with a principal emission band at λ = 385 nm, corresponding to the non-charged form of (*E*)-resveratrol (Structure A, Scheme 1). Moreover, when the pH of the medium is increased, a new emission band is showed at 445 nm which belongs to (*E*)-resveratrol with one hydroxyl group deprotonated (Structure B, Scheme 1) and, finally, when the pH value is increased to the region near to the third pK_a, the emission spectrum of (*E*)-resveratrol contains a new additional band at 475 nm (Structure C, Scheme 1), due to the deprotonation of two hydroxyl groups.

As shown in Fig. 4A, at the pH value studied in this section (9.2), (*E*)-resveratrol showed an equilibrium between its protonated/deprotonated structures (Scheme 1). Indeed, the principal emission band, in the absence of CDs, was 475 nm ((*E*)-resveratrol with two hydroxyl group deprotonated: Structure C, Scheme 1), followed by 445 nm ((*E*)-resveratrol with one hydroxyl group deprotonated: Structure B, Scheme 1) and finally 385 nm ((*E*)-resveratrol protonated: Structure A, Scheme 1).

As shown in Fig. 4A, the addition of increasing concentrations of HP-β-CD enhances the triple fluorescence emission of (*E*)-resveratrol when the protonated form is in equilibrium with deprotonated forms (Scheme 1). However, these three emission bands were surprisingly not enhanced with the same intensity. As is shown in Fig. 4A, the fluorescence intensity of the band near 385 nm increased more strongly in the presence of HP-β-CD, followed by the 445 nm band, and, finally, the 475 nm band. These results are due to the different capacity of HP-β-CD to complex the three protonated/deprotonated forms of (*E*)-resveratrol present at this pH value. However, this triple increase of the emission of (*E*)-resveratrol at different wavelengths in the presence of HP-β-CD could interfere in the determination of the complexation constants and thus explain the anomalous results showed by Lucas-Abellán et al. (2008). For this reason, the next step in our investigations was to determine the K_F values for the complexation of (*E*)-resveratrol with HP-β-CD at pH 9.2.

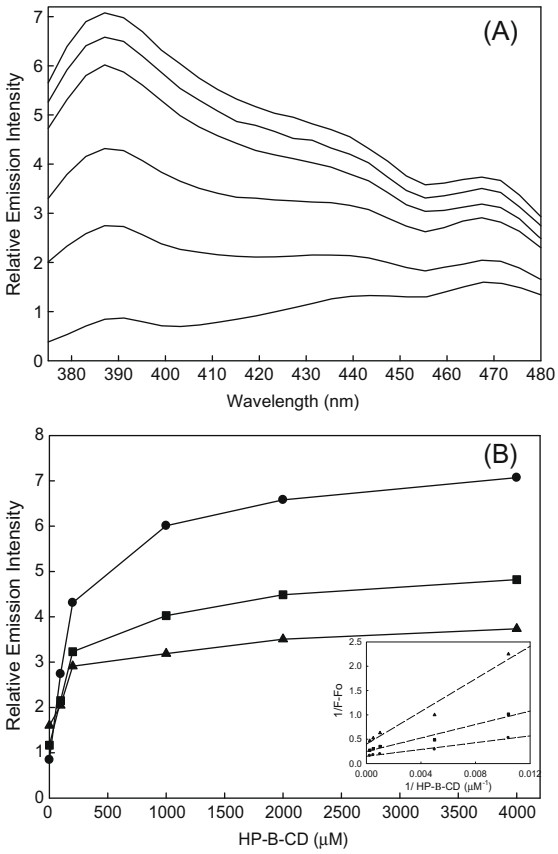

Fig. 4. (A) Emission fluorescence spectra of (*E*)-resveratrol (26.6 μM) at increasing concentrations of HP-β-CD (0, 96, 200, 1000, 2000, 4000 μM) at pH 9.2. Excitation wavelength: 344 nm. (B): Dependence of fluorescence intensities of (*E*)-resveratrol (26.6 μM) on HP-β-CD concentrations (0, 96, 200, 1000, 2000, 4000 μM) at three wavelengths: 385 nm (filled circles); 445 nm (filled squares) and 475 nm (filled triangles). *Inset:* Double reciprocal plot of (*E*)-resveratrol complexed to HP-β-CD for determination of the stoichiometry of HP-β-CD/(*E*)-resveratrol complexes: $1/(F - F_0)$ versus 1/[HP-β-CD] (assumption of 1:1 complex) at three wavelengths: 385 nm (filled circles); 445 nm (filled squares) and 475 nm (filled triangles).

3.4. Stoichiometry and complexation constant of the HP-β-CD/(E)-resveratrol complexes at basic pH values

The determination of the complexation constants for CD/(*E*)-resveratrol complexes is the subject of great controversy. Using linear regression of the phase solubility diagram, several papers have reported very different K_F values at neutral pH for the complexes between (*E*)-resveratrol and β-CD or HP-β-CD (Bertacche et al., 2006; Lucas-Abellán et al., 2008). Bertacche et al.

(2006) showed a higher K_F value using β-CD than HP-β-CD, while Lucas-Abellán et al. (2008) obtained opposite results. Moreover, the K_F values determined by Lucas-Abellán et al. (2008) were 4.5 times higher than those reported by Bertacche et al. (2006) for the same type of complex. Finally, as shown previously, Lucas-Abellán et al. (2008) reported different K_F values for the HP-β-CD /(*E*)-resveratrol, according to the method used to determine these constants.

In order to resolve these conflicting results, we have calculated the stoichiometry and K_F values for the HP-β-CD/(*E*)-resveratrol complexes at pH 9.2 using another analysis technique – steady-state fluorescence – which takes into account the changes in the physicochemical state of this antioxidant with concentration and following the Benesi–Hildebrand method.

Assuming that the composition of the complex was 1:1, the following expression can be written:

$$(E)\text{-resveratrol} + \text{HP-β-CD} \rightleftarrows \text{HP-β-CD-}(E)\text{-resveratrol} \quad (1)$$

The complexation constant, K_F is given by:

$$K_F = \frac{[\text{HP-β-CD}/(E)\text{-resveratrol}]}{[(E)\text{-resveratrol}][\text{HP-β-CD}]} \quad (2)$$

where [HP-β-CD], [(*E*)-resveratrol] and [HP-β-CD/(*E*)-resveratrol] are equilibrium concentrations.

From the experimental data of Fig. 4A, when three wavelengths corresponding to the three forms of (*E*)-resveratrol are considered, the difference in the intensity of the (*E*)-resveratrol emission fluorescence in the absence and presence of different amounts of HP-β-CD was plotted versus the HP-β-CD concentration (Fig. 4B). Representative plots of the variation in fluorescence intensity at the three wavelength bands analysed (385, 445 and 475 nm) as a function of HP-β-CD concentration were analysed by the Benesi–Hildebrand method.

The K_F value for the inclusion complex can be determined by the typical double reciprocal (or Benesi–Hildebrand) plots:

$$\frac{1}{F - F_o} = \frac{1}{(F_\infty - F_o)K_F[\text{HP-β-CD}]} + \frac{1}{F_\infty - F_o} \quad (3)$$

where [HP-β-CD] denotes the HP-β-CD concentration; F_0 the fluorescence intensity of (*E*)-resveratrol in the absence of HP-β-CD; F_∞ the fluorescence intensity when all of the (*E*)-resveratrol molecules are essentially complexed with HP-β-CD; and *F* the observed fluorescence intensity at each HP-β-CD concentration tested.

In our study, when a plot of $1/(F - F_0)$ versus 1/[HP-β-CD] is constructed (Fig. 4B inset) a straight line is obtained, which is indicative of a 1:1 stoichiometry for HP-β-CD/(*E*)-resveratrol at pH 9.2. On the other hand, assuming the stoichiometry of the inclusion complex to be 1:2, the following expression is obtained:

$$\frac{1}{F - F_o} = \frac{1}{(F_\infty - F_o)K'([\text{HP-β-CD}])} + \frac{1}{F_\infty - F_o} \quad (4)$$

When making a plot of $1/(F - F_0)$ against $1/[\text{HP-β-CD}]^2$, a non-linear relationship is obtained (data not shown), which indicates that the stoichiometry of the inclusion complex is not 1:2.

However, anomalous results were found when the complexation constants values were determined at the three wavelengths selected (385, 445 and 475 nm). Table 1 reports that the complexation constants obtained using fluorescence measurements for the three wavelengths selected were very different. The highest complexation constant value was determined at the wavelength where the totally protonated form of (*E*)-resveratrol (Structure A, Scheme 1) presents the emission maximum (385 nm) and the lowest complexation constant value was calculated at 475 nm, which is the wavelength where the structure of (*E*)-resveratrol with two deprotonated hydroxyl groups (Structure C, Scheme 1) presents its emission maximum. The fact that the complexation constant value was dependent on the wavelength selected to observe the increase of fluorescence in the presence of HP-β-CD proves that these constants are apparent complexation constants (K_{app}) and not true complexation constants (K_F).

Table 1
Apparent complexation constants (K_{app}) at pH 9.2 for the complexes between HP-β-CD and the three forms of (*E*)-resveratrol: protonated (385 nm) (Structure A, Scheme 1); one hydroxyl deprotonated (445 nm) (Structure B, Scheme 1) and two deprotonated (475 nm) (Structure C, Scheme 1). Complexation constant (K_F) at pH 6.5 for the complexes between HP-β-CD and (*E*)-resveratrol.

λ (nm)	pH 9.2		
	K_{app} (M^{-1})	K_{app} (M^{-1})	K_{app} (M^{-1})
385	4285 ± 105	–	–
445	–	3579 ± 89	–
475	–	–	2263 ± 78
	pH 6.5		
	K_F (M^{-1})		
385	14490 ± 723		

These results help explain the anomalous results obtained by Lucas-Abellán et al. (2008) mentioned above. A comparison of the results obtained by the three methods (enzymatic, solubility, and fluorimetric) by these researchers revealed that the fluorimetric method undervalued the K_F between (*E*)-resveratrol and several types of CDs. However, in the paper reported by Lucas-Abellán et al. (2008), fluorescence emission was only measured at 380 nm, i.e., the emission band of the protonated form of (*E*)-resveratrol, but the authors did not take into account the fact that, in the presence of HP-β-CD, the apparent complexation constants are dependent on the wavelength selected to analyse the interaction between the protonated form of (*E*)-resveratrol and HP-β-CD.

Moreover, although the results obtained in this work partially confirm the statement by Lucas-Abellán et al. (2008) that the steady-state fluorescence is not a suitable technique to determine the K_F between (*E*)-resveratrol and HP-β-CD because the K_F is undervalued, with respect to the values obtained using another techniques, it is very possible that this affirmation could be only correct at basic pH values, where different protonated/deprotonated forms of this antioxidant coexist complexed and not complexed by HP-β-CD (Scheme 1). However, the conclusion of Lucas-Abellán et al. (2008) may be not correct when only one structure of (*E*)-resveratrol is present in the medium. For this reason, the next step of our investigation was to study the complexation between (*E*)-resveratrol and HP-β-CD at pH values below the pK_{a1} of the stilbene. At the pH value selected (6.5) (*E*)-resveratrol shows a high biological activity and only its protonated form is present.

3.5. Effect of HP-β-CD on fluorescence of (E)-resveratrol at physiological pH values

As shown in Fig. 5A, the emission spectra of (*E*)-resveratrol at pH 6.5 in the absence and presence of HP-β-CD are very different from that observed at basic pH because, at physiological pH, only one emission band (385 nm) is presented, unlike the three emission bands observed at pH 9.2 (Fig. 4A). This result is due to the presence of only one form of (*E*)-resveratrol at pH 6.5 (protonated form, Structure A of Scheme 1).

Fig. 5A shows the fluorescence emission spectra of (*E*)-resveratrol in an aqueous solution at pH 6.5 containing different concentrations of HP-β-CD. As is shown, (*E*)-resveratrol emits relatively weak fluorescence in the absence of CDs. However, with the addition of HP-β-CD, the maximum emission wavelength slightly shifted to a shorter wavelength (from 392 to 384 nm); (Fig. 5A

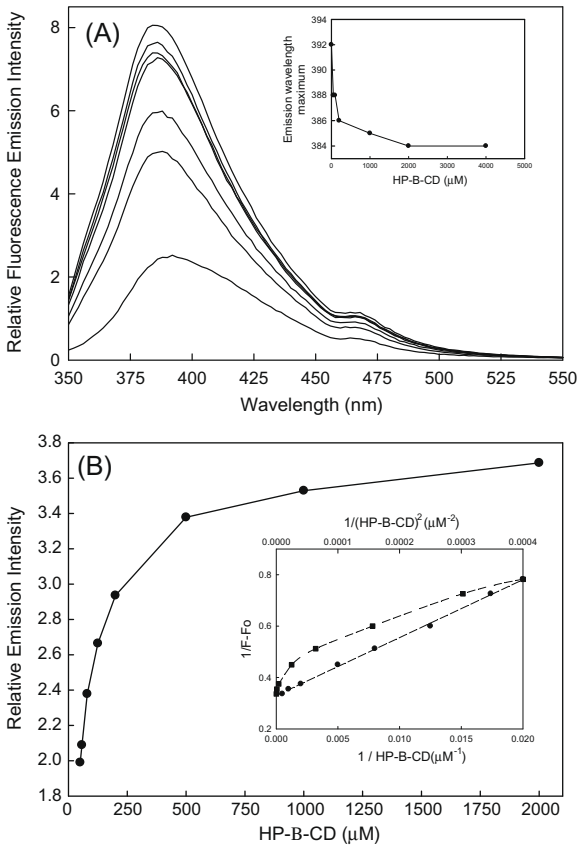

Fig. 5. (A) Emission fluorescence spectra of (*E*)-resveratrol (10 μM) at various concentrations (0, 50, 96, 200, 1000, 2000, 4000 μM) of HP-β-CD at pH 6.5. Inset: Dependence of emission wavelength maximum of (*E*)-resveratrol on HP-β-CD concentrations (0, 50, 96, 200, 1000, 2000, 4000 μM). Excitation wavelength: 334 nm. (B) Dependence of emission fluorescence intensities of (*E*)-resveratrol (10 μM) on HP-β-CD concentrations (50, 57, 125, 200, 500, 1000, 2000 μM). Excitation wavelength: 334 nm. Inset: Double reciprocal plot of (*E*)-resveratrol complexed to HP-β-CD for determination the stoichiometry of HP-β-CD/(*E*)-resveratrol complexes: $1/(F - F_0)$ versus 1/[HP-β-CD] (assumption of 1:1 complex) (filled circles); (b) $1/(F - F_0)$ versus $1/[\text{HP-β-CD}]^2$ (hypothesis of 1:2 complex) (filled squares).

inset) and the emission fluorescence intensity was markedly enhanced at pH 6.5. These changes were due to the interaction between HP-β-CDs and (*E*)-resveratrol, which again implied the formation of HP-β-CD/(*E*)-resveratrol complexes as has been reported for other guest/host interactions (Guomei et al., 2003; Zhang et al., 2008). When (*E*)-resveratrol is entrapped in the HP-β-CD cavity, this microenvironment with a smaller polarity and stronger rigidity would restrict the freedom of the guest molecules and increase the fluorescence quantum yield. Furthermore, the steric hindrance of the HP-β-CD torus would protect the excited states from non-radiative and quenching processes that normally occur in bulk aqueous solutions and enhance the fluorescence efficiencies of the guest molecule.

3.6. Stoichiometry and complexation constant of the HP-β-CD/(E)-resveratrol complexes at physiological pH values

In order to quantify the interaction between (*E*)-resveratrol and HP-β-CD in this region of pH, K_F was determined by a fluorimetric method at pH 6.5.

Following the same methodology that the applied to determine the K_F values for the complexation of (*E*)-resveratrol by HP-β-CD at basic pH, the relative emission intensity of this antioxidant was calculated at increasing HP-β-CD concentrations (Fig. 5A). The linear correlations obtained for all the fits were higher than 0.99, indicating that the presumed stoichiometry of the complexes formed was also 1:1 (Fig. 5B inset, filled circles). The plot of $1/(F - F_0)$ as a function of $1/[\text{HP-β-CD}]^2$ was also analysed because it was thought it would provide information about the presence of higher order complexes, especially at high HP-β-CD concentrations (Fig. 5B inset, filled squares). However, none of the experimental data provided a good linear fit in these plots, ruling out this possibility. Applying the data obtained to Eq. (3), the K_F value for this physiological pH was calculated ($K_F = 14490 \pm 723\ M^{-1}$).

The results obtained in this work may help to understand the interaction between (*E*)-resveratrol and HP-β-CD. If we compare the K_F obtained for the totally protonated structure of this stilbene with the K_{app} determined at basic pH (Table 1), we can observe that the K_F value determined at pH value below that of the pK_{a1} of (*E*)-resveratrol was always higher than the K_{app} calculated when (*E*)-resveratrol is partially deprotonated. This fact was expected since, in basic solutions, the complexation constant value is low, due to the presence of negative charges in its molecule, which induces better (*E*)-resveratrol solubilisation in the bulk solution rather than in the hydrophobic part of the CD. Moreover, these results are in accordance with other work published by our group (López-Nicolás et al., 2008a, 2008b), where CDs complex the protonated form of (*E*)-resveratrol (Structure A, Scheme 1) with higher efficiency than the deprotonated forms.

These results confirm that the use of fluorescence measurements to calculate the K_F value for the HP-β-CD/(*E*)-resveratrol complexes is not adequate when the pH of the medium is higher than the pK_{a1} of (*E*)-resveratrol because of the presence of different protonated/deprotonated forms (complexed or not complexed by HP-β-CD) of this stilbene. However, when (*E*)-resveratrol is presented in its totally protonated form (i.e., at pH values lower than its pK_{a1}) steady-state fluorescence is an adequate technique to study the interaction between (*E*)-resveratrol and HP-β-CD.

4. Conclusions

Although the biological activities of (*E*)-resveratrol have been studied in many papers, little information exists about the physicochemical structure of this potent antioxidant under different conditions. For this reason, its use as functional ingredient in novel foods (as a fortifier and nutraceutical compound) has been restricted to date. In this paper, we clarify diverse contradictory data existing in the literature about different properties of (*E*)-resveratrol, such as the aggregation and protonation state, which may have importance for its putative health-giving properties. Moreover, the lipophilic nature of this stilbene means that it needs a carrier which permits its "solubilisation" in aqueous media. The complete study of the complexation of (*E*)-resveratrol by cyclodextrins using absorbance and fluorescence techniques resolves the conflicting data existing in the literature about this type of complexation. Moreover, knowledge of the effect of HP-β-CD on the aggregation state of (*E*)-resveratrol and determination of the complexation constants of the different protonated and deprotonated forms of this potent antioxidant open up new possibilities for the use of (*E*)-resveratrol in the food and pharmaceutical industry.

Acknowledgments

This work was supported by AGL2007-65907 (MEC, FEDER, Spain) and by Programa de ayudas a Grupos de Excelencia de Región de Murcia, de la Fundación Séneca, Agencia de Ciencia y Tecnología de la Región de Murcia (Plan Regional de Ciencia y Tecnología 2007/2010).

References

Bertacche, V., Lorenzi, N., Nava, D., Pini, E., & Sinico, C. (2006). Host–guest interaction study of resveratrol with natural and modified cyclodextrins. *Journal of Inclusion Phenomena and Macrocyclic Chemistry, 55*, 279–287.

Bru, R., López-Nicolas, J. M., Nuñez-Delicado, E., Nortes-Ruipérez, D., Sánchez-Ferrer, A., & García-Carmona, F. (1996). Cyclodextrins as hosts for poorly water-soluble compounds in enzyme catalysis. *Applied Biochemistry and Biotechnology, 61*, 189–198.

Bru, R., López-Nicolás, J. M., & García-Carmona, F. (1995). Aggregation of polyunsaturated fatty acids in the presence of cyclodextrins. *Colloids and Surfaces, 97*, 263–269.

Cao, J., Chen, G. H., Du, Y. S., Hou, F. F., & Tian, Y. L. (2006). Determination of dissociation constants of resveratrol and polydatin by capillary zone electrophoresis. *Journal of Liquid Chromatography Research and Related Technologies, 29*, 1457–1463.

Counet, C., Callemien, D., & Collin, S. (2006). Chocolate and cocoa: New sources of trans-reveratrol and trans-piceid. *Food Chemistry, 98*, 649–657.

Fan, X., & Mattheis, J. P. (2001). Inhibition of oxidative and antioxidative enzymes by trans-resveratrol. *Food and Chemical Toxicology, 66*, 200–203.

Fang, J., Lu, M., Chen, Z., Zhu, H., Li Yang, Y., Wu, L. M., et al. (2002). Antioxidant effects of resveratrol and its analogues against the free-radical-induced peroxidation of linoleic acid in micelles. *Chemistry European Journal, 8*, 4191–4198.

Galeano Díaz, T., Durán Merás, I., & Airado Rodríguez, D. (2007). Determination of resveratrol in wine by photochemically induced second-derivative fluorescence coupled with liquid–liquid extraction. *Analytical and Bioanalytical Chemistry, 385*, 1999–2007.

Guomei, Z., Shaomin, S., Chuan, D., & Jinghao, P. (2003). Study on the interaction of methylene blue with cyclodextrin derivatives by absorption and fluorescence spectroscopy. *Spectrochimica Acta Part A, 59*, 2935–2941.

Latruffe, N., Delmas, D., Jannin, B., Cherkaoui, M., Passilly-Degrace, P., & Berlot, J. P. (2002). Molecular analysis on the chemopreventive properties of resveratrol, a plant polyphenol microcomponent. *International Journal of Molecular Medicine, 10*, 755–760.

López-Nicolás, J. M., & García-Carmona, F. (2008a). Rapid, simple and sensitive determination of the apparent formation constants of *trans-resveratrol* complexes with natural cyclodextrins in aqueous medium using HPLC. *Food Chemistry, 109*, 868–875.

López-Nicolás, J. M., & García-Carmona, F. (2008b). Aggregation state and pka values of (E)-resveratrol as determined by fluorescence spectroscopy and UV–visible absorption. *Journal Agricultural and Food Chemistry, 56*, 7600–7605.

López-Nicolás, J. M., Bru, R., Sánchez-Ferrer, A., & García-Carmona, F. (1995). Use of "soluble lipids" for biochemical processes: Linoleic acid: Cyclodextrin inclusion complexes in aqueous solutions. *Biochemical Journal, 308*, 151–154.

López-Nicolás, J. M., Núñez-Delicado, E., Pérez-López, A. J., Carbonell, A., & Cuadra-Crespo, P. (2006). Determination of stoichiometric coefficients and apparent formation constants for β-cyclodextrin complexes of trans-resveratrol using reversed-phase liquid chromatography. *Journal of Chromatography A, 1135*, 158–165.

López-Nicolás, J. M., Bru, R., & García-Carmona, F. (1997). Kinetic characteristics of the enzymatic conversion in presence of cyclodextrins: Study of the oxidation of polyunsaturated fatty acids by lipoxygenase. *Biochimica et Biophysica Acta, 1347*, 140–150.

Lucas-Abellán, C., Fortea, I., López-Nicolás, J. M., & Núñez-Delicado, E. (2007). Cyclodextrins as resveratrol carrier system. *Food Chemistry, 104*, 39–44.

Lucas-Abellán, C., Fortea, M. I., Gabaldón, J. A., & Núñez-Delicado, E. (2008). Complexation of resveratrol by native and modified cyclodextrins: Determination of complexation constant by enzymatic, solubility and fluorimetric assays. *Food Chemistry, 111*, 262–267.

Matsuoka, A., Takeshita, K., Furuta, A., Ozaki, M., Fukuhara, K., & Miyata, N. (2002). The 4′-hydroxy group is responsible for the in vitro cytogenetic activity of resveratrol. *Mutation Research-Genetic Toxicology and Environmental Mutagenesis, 521*, 29–35.

Ovesná, Z., & Horváthová-Kozics, K. (2005). Structure-activity relationship of *trans*-resveratrol and its analogues. *Neoplasma, 52*, 450–455.

Pinto, M. C., García-Barrado, J. A., & Macías, P. (2003). Oxidation of resveratrol catalyzed by soybean lipoxygenase. *Journal Agricultural and Food Chemistry, 51*, 1653–1657.

Ragab, A. S., Van Fleet, J., Jankowski, B., Park, J. H., & Bobzin, S. C. (2006). Detection and quantitation of resveratrol in tomato fruit (*Lycopersicon esculentum* Mill.). *Journal Agricultural and Food Chemistry, 54*, 7175–7179.

Saenger, W. (1980). Cyclodextrin inclusion compounds in research and industry. *Angewandte Chemie International Edition in English, 19*, 344–362.

Stivala, L. A., Savio, M., Carafoli, F., Perucca, P., Bianchi, L., Maga, G., et al. (2001). Specific structural determinants are responsible for the antioxidant activity and the cell cycle effects of resveratrol. *Journal of Biological Chemistry, 276*, 22586–22594.

Szejtli, J. (1988). *Cyclodextrin technology*. Dordrecht: Kluwer Academic Publisher.

Szente, L., & Szejtli, J. (2004). Cyclodextrins as food ingredients. *Trends in Food Science and Technology, 15*, 137–142.

Takagai, Y., Kubota, T., Kobayashi, H., Tashiro, T., Takahashi, A., & Igarashi, S. (2005). Adsorption and desorption properties of trans-resveratrol on cellulose cotton. *Analytical Sciences, 21*, 183–186.

Trela, B. C., & Waterhouse, A. L. (1996). Resveratrol: Isomeric molar absorptivities and stability. *Journal Agricultural and Food Chemistry, 44*, 1253–1257.

Walle, T., Hsieh, F., Delegge, M. H., Oatis, J. E. Jr., & Walle, U. K. (2004). High absorption but very low bioavailability of oral resveratrol in humans. *Drug Metabolism and Disposition, 32*, 1377–1382.

Wang, Y., Catana, F., Yang, Y., Roderick, R., & van Breemen, R. B. (2002). An LC-MS method for analyzing total resveratrol in grape juice, cranberry juice, and in wine. *Journal Agricultural and Food Chemistry, 50*, 435–445.

Wenzel, E., & Somoza, V. (2005). Metabolism and bioavailability of trans-resveratrol. *Molecular Nutrition and Food Research, 49*, 472–481.

Xu, S., Wang, G., Liu, H., Jiang Wang, L., & Fang Wang, H. A. (2007). DMol3 study on the reaction between trans-resveratrol and hydroperoxyl radical: Dissimilarity of antioxidant activity among O–H groups of trans-resveratrol. *Journal of Molecular Structure THEOCHEM, 809*, 79–85.

Yuan, C., Jin, Z., & Li, X. (2008). Evaluation of complex forming ability of hydroxypropyl-β-cyclodextrins. *Food Chemistry, 106*, 50–55.

Zhang, Q. F., Jiang, Z. T., Guo, Y. X., & Li, R. (2008). Complexation study of brilliant cresyl blue with beta-cyclodextrin and its derivatives by UV–vis and fluorospectrometry. *Spectrochimica Acta Part A: Molecular and Biomolecular Spectroscopy, 69*, 65–70.

Food Chemistry 118 (2010) 656–662

Contents lists available at ScienceDirect

Food Chemistry

journal homepage: www.elsevier.com/locate/foodchem

Oxidative stability of sunflower oil supplemented with carnosic acid compared with synthetic antioxidants during accelerated storage

Ying Zhang, Lei Yang, Yuangang Zu *, Xiaoqiang Chen, Fuji Wang, Fang Liu

Key Laboratory of Forest Plant Ecology, Northeast Forestry University, 150040 Harbin, PR China

ARTICLE INFO

Article history:
Received 16 July 2008
Received in revised form 9 April 2009
Accepted 14 May 2009

Keywords:
Carnosic acid
Rosmarinus officinalis L.
Antioxidant activity
Oxidative stability
Sunflower oil

ABSTRACT

In vitro antioxidant activities and protective effects in stabilising sunflower oil of three rosemary extracts high in carnosic acid (CA) were tested. The CA contents (w/w) of the extracts were 24.9% (CA25), 60.5% (CA60) and 98.3% (CA98). Total phenolic contents of CA25 and CA60 were (3.58 ± 0.026 g/100 g) and (8.20 ± 0.027 g/100 g), (3.91 ± 0.029 g/100 g) and (8.10 ± 0.056 g/100 g) expressed in gallic acid and catechin equivalents, respectively. Reducing power of CA and other antioxidants at 0.5 mg/ml followed the order of L-ascorbic acid > CA98 > TBHQ > BHA > CA60 > BHT > CA25. The IC_{50} values in the DPPH assay obtained for CA25, CA60, CA98, BHA, BHT and TBHQ were 0.30 ± 0.002, 0.20 ± 0.003, 0.12 ± 0.002, 0.19 ± 0.002, 0.42 ± 0.010, and 0.09 ± 0.001 mg/ml, respectively.

Protective effects of CA in stabilising sunflower oil were tested, compared to synthetic antioxidants, by measuring their peroxide values, thiobarbituric acid-reactive substances, free fatty acid contents and *p*-anisidine value during accelerated storage. Results indicated that CA exhibited stronger antioxidant activity in sunflower oil than BHT and BHA. However, its antioxidant activity was less than that of TBHQ.

1. Introduction

Edible oils with higher contents of unsaturated fatty acids, especially polyunsaturated fatty acids, are more susceptible to oxidation. Lipid oxidation of oils can not only produce rancid odours, unpleasant flavours and discoloration, but can also decrease the nutritional quality and safety due to degradation products, resulting in harmful effects on human health (Esterbauer, Schaur, & Zollner, 1991; Lercker & Rodriguez-Estrada, 2002). To retard or prevent oxidative deterioration, synthetic antioxidants, such as butylated hydroxyanisole (BHA), butylated hydroxytoluene (BHT) and *tert*-butyl hydroquinone (TBHQ) have widespread use as food additives in many countries. Recent reports reveal that these compounds may be implicated in many health risks, including cancer and carcinogenesis (Hou, 2003; Prior, 2004). Hence, there is a tendency towards the use of natural antioxidants of plant origin to replace these synthetic antioxidants. The application of plant extracts to prevent edible oil rancidity had been studied (Mallet, Cerrati, Ucciani, Gamisons, & Gruber, 1994; Xiong, Yang, Zhang, & Xiao, 2001). Among them, rosemary (*Rosmarinus officinalis* L.) extracts with their powerful antioxidant activities are often the first choice for processed foods and widely used in the food industry (Nissen, Mansson, Bertelsen, Huynh-Ba, & Skibsted, 2000). The antioxidant activities of rosemary extracts are related to the presence of phenolic diterpene compounds, such as carnosic acid, carnosol and rosmanol, rosmariquinone and rosmaridiphenol, which break free radical chain reactions by hydrogen atom donation (Basaga, Tekkaya, & Acikel, 1997; Frankel, Huang, Aeschbach, & Prior, 1996; Thorsen & Hildebrandt, 2003).

Carnosic acid is the primary phenolic diterpene compound found in the leaves of rosemary (Richheimer, Bemart, King, Kent, & Bailey, 1996). Carnosic acid (Fig. 1) is a lipophilic antioxidant that scavenges singlet oxygen, hydroxyl radicals, and lipid peroxyl radicals, thus preventing lipid peroxidation and disruption of biological membranes (Aruoma, Halliwell, Aeschbach, & Loliger, 1992; Haraguchi, Saito, Okamura, & Yagi, 1995). Its radical-scavenging activity is caused by the presence of two *O*-phenolic hydroxyl groups found at C11 and C12 of the molecule (Richheimer et al., 1999).

Antioxidant potential of carnosic acid *in vitro* has been proved by Erkan, Ayranci, and Ayranci (2008). In addition to its antioxidant activity, it has been reported to possess anti-inflammatory, antiproliferative, antitumorigenic and neuroprotective effects (Aruoma et al., 1992; Chang et al., 2008; Danilenko et al., 2003; Erkan et al., 2008; Rau et al., 2006; Satoh et al., 2008).

In this paper, we describe the isolation of extracts with three different contents of carnosic acid from dried rosemary leaves. Furthermore, we studied *in vitro* their antioxidant effects and stabilisation of sunflower oil under accelerated conditions, compared with synthetic antioxidants, including BHA, BHT and TBHQ.

* Corresponding author. Tel.: +86 451 82191517; fax: +86 451 82102082.
E-mail address: zygorl@vip.hl.cn (Y. Zu).

0308-8146/$ - see front matter © 2009 Elsevier Ltd. All rights reserved.
doi:10.1016/j.foodchem.2009.05.038

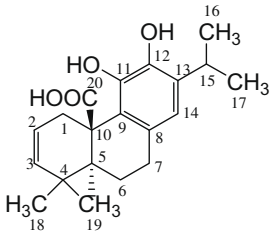

Fig. 1. Molecular structure of carnosic acid.

2. Materials and methods

2.1. Materials

Refined, bleached, and deodorised (RBD) sunflower oil was obtained from Standard Food Industries Ltd., Guangdong, China. It contained very low α-tocopherol (<4.3 mg/kg) and no synthetic antioxidants. Fresh leaves of *Rosmarinus officinalis* L. were harvested from the FuYang base of Zhe Jiang Hi Sun Pharmaceutical Co., China in September, 2007. All reagents and solvents were either of HPLC or analytical grade. Carnosic acid standard (⩾91%), L-ascorbic acid, BHA, BHT, TBHQ, Folin–Ciocalteu reagent, gallic acid standard, catechin standard, and DPPH (2,2-diphenyl-1-picrylhydrazyl) free radicals were purchased from Sigma–Aldrich Co. (St. Louis, MO).

2.2. Preparation and analysis of CA

Dried rosemary (*Rosmarinus officinalis* L.) leaves (1 kg); (carnosic acid content 2.09 g/100 g DW) were chopped into small parts with a blender and placed in a round-bottomed flask with 1 l of deionised water. The solution was steam-distilled for 60 min in a Clevenger-type apparatus for oil isolation. The residue was extracted using aqueous 80% ethanol solution by an ultrasound-assisted extraction (KQ-250DB, Kunshan Ultrasound Co. Ltd., Kunshan, China) at 40 °C for 30 min. This procedure was repeated twice, and the combined filtrate was evaporated in a rotary evaporator (Shanghai Qingpu Huxi Instrument Factory, Shanghai, China) at 50 °C, to give CA25 (70.3 g).

CA25 was dissolved in ethyl acetate (1:40, w/v), insoluble substances were removed by filtration, then 100 ml 0.8% sodium carbonate solution was added to the filtrate. The two phases were separated and the ethyl acetate layer was collected and combined with 200 ml 5% sodium chloride solution; the solution was concentrated under vacuum to a volume of about 50 ml, then filtered and the filtrate pH was adjusted to 4.5–5.0 with 10% HCl, and extracted by normal hexane. The hexane fractions were concentrated in a rotary evaporator at 50 °C (Shanghai Qingpu Huxi Instrument Factory, Shangai, China), to give crystals of CA60 (22.6 g).

CA60 was dissolved in ethyl acetate, insoluble materials were removed by filtration, then the filtrate was concentrated and purified through silica column chromatography eluted with ethyl acetate, and to give 9.0 g high purity carnosic acid (CA98).

The carnosic acid content of CA25, CA60 and CA98 were analysed by high-performance liquid chromatography (HPLC) on a Jasco HPLC system equipped with a UV detector (Jasco International Co. Ltd., Tokyo, Japan). Analyses were performed on a Curosil-PFP (4.6 mm × 250 mm, 5 μm) reversed-phase column (Phenomenex Inc., Torrance, CA). The UV detector was set at a wavelength of 230 nm. The mobile phase was acetonitrile:0.5% phosphorous acid (60:40, v/v) at a flow rate of 1 ml/min and the injection volume was 10 μl.

The carnosic acid recoveries were calculated relative to the amount of carnosic acid in dried rosemary leaves.

2.3. Determination of total phenolic content

The total phenolic contents of CA25 and CA60 were determined using the Folin–Denis method (Swain & Hills, 1959) with a little modification. This method is based on the reducing power of the phenolic hydroxyl groups (Hahn, Rooney, & Earp, 1984); 0.1 ml of CA25 or CA60 (10 mg/ml in ethanol) and 1.0 ml Folin–Ciocalteu reagent (1:1 with water) were mixed. After 5 min, 1 ml of 10% Na_2CO_3 was added and the volume was accurately adjusted to 25 ml. Then the mixture was left at room temperature for 60 min. The absorbance was measured with a spectrophotometer (Shimadzu UV-2550; Shimadzu, Kyoto, Japan) at 765 nm against a blank. The determination was performed three times. Total phenolic contents were calculated from standard curves of gallic acid ($y = 0.27x - 0.022$, $r = 0.993$) and catechin ($y = 0.29x - 0.023$, $r = 0.995$), respectively, and then expressed as g/100 g sample.

2.4. Measurement of reducing power

The reducing power of CA25, CA60, CA98 and positive standards L-ascorbic acid, BHA, BHT, TBHQ was determined according to the method of Ardestani and Yazdanparast (2007). The reducing power was measured using chemical reduction of Fe(III) to Fe(II). Various concentrations of sample (62.5–1000 μg/ml in ethanol) were mixed with sodium phosphate buffer (2.5 ml, 0.2 M, pH 6.6) and 2.5 ml of 1% potassium ferricyanide ($K_3Fe(CN)_6$). The mixture was incubated at 50 °C for 20 min, 2.5 ml of 10% trichloroacetic acid (TCA) was added to the mixture, which was then centrifuged for 10 min at 3000*g*. The upper layer of solution (2.5 ml) was mixed with distilled water (2.5 ml) and $FeCl_3$ (0.5 ml, 0.1%), and the absorbance was measured with multiplate spectrophotometer at 700 nm (UV-2550, Shimadzu, Kyoto, Japan). A higher absorbance indicates a higher reducing power.

2.5. DPPH radical-scavenging assay

DPPH (2,2-diphenyl-1-picrylhydrazyl) radical-scavenging activity of CA25, CA60 and CA98 compared with commonly-employed synthetic antioxidants BHA, BHT and TBHQ was measured according to the method of Blois (1958) and modified slightly. Briefly, 0.1 ml of sample at variable concentrations (62.5–1000 μg/ml in ethanol) was added to 3.9 ml of a DPPH solution (25 mg/l in ethanol) as the free radical source and kept for 30 min at room temperature. The decrease in the solution absorbance, due to proton-donating activity, was measured at 517 nm (UV-2550, Shimadzu, Kyoto, Japan). The DPPH radical-scavenging activity was calculated using the following formula:

$$\text{DPPH radical} - \text{scavenging activity } (\%) = [(1 - A_1/A_0) \times 100],$$

where A_0 is the absorbance of the control, and A_1 is the absorbance of CA25, CA60 and CA98 or the commercial synthetic antioxidants.

2.6. Oxidative stability determination

2.6.1. Sample preparation

CA25, CA60 and CA98 were added to sunflower oil at a concentration of 200 mg/kg. Synthetic antioxidants (BHA, BHT and TBHQ) were employed at their legal limit of 200 mg/kg (Duh & Yen, 1997) as reference. All the samples (250 ml) were placed in dark brown coloured reagent bottles with narrow necks and mixed for 30 min in an ultrasonic water bath of 60 °C (KQ-250DB, Kunshan Ultrasound Co. Ltd.). Then all the samples (250 ml) were stored in an incubator at a fixed temperature of 60 °C. Control samples without antioxidants were also maintained under the same storage conditions. Analyses were conducted at 4-day intervals for thiobarbituric

acid-reactive substances assay (TBARS) and 3-day intervals for all other assays.

2.6.2. Analysis of peroxide value

The peroxide value (*PV*) of all samples was measured according to GB/T 5009.37-2003 with a slight modification. Sunflower oil samples (2 g) were dissolved in 30 ml of chloroform:glacial acetic acid (3:2, v/v). Then 1 ml saturated solution of KI was added. The mixture was shaken by hand for 1 min and was then kept in the dark for 5 min. After the addition of 75 ml distilled water, the mixture was titrated against sodium thiosulfate (0.002 M) until the yellow colour almost disappeared. Then about 0.5 ml of starch indicator (1%) solution was added. Titration was continued until the blue colour just disappeared. The blank was also analysed under similar conditions. Peroxide value (meq/kg) was calculated according to the equation:

$$PV = C \times (V - V_k) \times 12.69 \times 78.8/m$$

where C is the concentration of sodium thiosulfate (M); V and V_k are the volume of sodium thiosulfate exhausted by sample and blank, respectively (ml); m is the mass of sunflower oil (g).

2.6.3. Thiobarbituric acid-reactive substances assay (TBARS)

Lipid oxidation of all samples was assessed by the 2-thiobarbituric acid (TBA) method according to GB/T 5009.181-2003 with a slight modification. In brief, 10 g of samples were homogenised in 10 ml of TCA (7.5%)–EDTA (0.1%) solution. This sample was shaken continuously for 0.5 h with a mechanical shaker, then filtered. Exactly 5 ml of filtrate was added to 5 ml of TBA (2.88 g/l) solution in a 25 ml colorimetrical tube, and heated in a water bath (90 °C) for 40 min for pink colour development. The tube was first cooled for 1 h, and was then centrifuged for 5 min at 3000*g*. The supernatant fluid was added to 5 ml of chloroform in another tube, and then shaken. This mixed solution was allowed to stand for at least 1 h. The absorbance was measured at 532 nm using a spectrophotometer (UV-2550, Shimadzu, Kyoto, Japan). TBARS were calculated from a standard curve of malondialdehyde (MDA), freshly prepared by acidification of TEP (1,1,3,3-tetraethoxypropane) in the range from 0.02 to 0.3 μg/ml ($y = 0.8885x + 0.0372$, $r = 0.9997$) and expressed as mg of malondialdehyde per kg sample.

2.6.4. Measurement of free fatty acids (FFA)

Free fatty acids, as oleic acid percentages in oil samples, were determined using an alkali titration method according to GB/T 5009.37-2003 with a slight modification. Samples (2 g) were dissolved in a 50 ml mixture of neutral ether:ethanol (2:1, v/v). Then the mixture was shaken by hand. After cooling to room temperature, the mixture was titrated against potassium hydroxide (0.05 M) using phenolphthalein solution (10 g/l) as an indicator. FFA value (mg/g) was calculated according to the equation:

$$[\mathrm{FFA}] = (V \times C \times 56.11)/m$$

where V is the volume of potassium hydroxide exhausted by samples (ml); C is the concentration of potassium hydroxide (M); m is the mass of sunflower oil (g).

2.6.5. Measurement of p-anisidine value

The *p*-anisidine value (*AnV*) was determined according to IUPAC method 2.504 (IUPAC, 1987). Sunflower oil samples (2 g) were dissolved in 25 ml isooctane and absorbance of this fat solution was measured at 350 nm using a spectrophotometer (UV-2550, Shimadzu, Kyoto, Japan). Five millilitres of the above mixture was mixed with 1 ml 0.25% *p*-anisidine in acetic acid (w/v) and after 10 min standing, absorbance was read at 350 nm using a spectrophotometer (UV-2550, Shimadzu, Kyoto, Japan). *AnV* was calculated according to the equation:

$$AnV = 25 \times (1.2A_s - A_b)/m$$

where A_s is the absorbance of the fat solution after reaction with the *p*-anisidine reagent; A_b is the absorbance of the fat solution; m is the mass of sunflower oil (g) sample.

2.7. Statistical analysis

Experiments were replicated twice on different occasions. All analyses were carried out in triplicate ($n = 3$) for each replicate which were reported as mean ± SD; an ANOVA test (using SPSS 11.5 statistical software; SPSS Inc., Chicago, IL) was used to compare the mean values of each treatment. Significant differences between the means of parameters were determined by using the Duncan test ($p < 0.05$).

3. Results and discussion

3.1. Analysis of carnosic acid

A calibration curve was prepared by plotting the peak areas of the carnosic acid standard samples. The standard curve gave a linear response for the carnosic acid concentrations and the peak areas in the range from 0.08 to 0.4 mg/ml ($y = 2 \times 10^7 x + 148{,}456$, $r = 0.9999$). The carnosic acid contents were calculated from a standard curve, and the contents were 24.9%, 60.5% and 98.3%, respectively. Recoveries of CA25, CA60 and CA98 were 83.9%, 65.5% and 42.4%, respectively. The structure of CA98 was identified by comparison of its spectral properties (^{1}H NMR) (Model: FD-PNMR-2; China Motion Network Technology Co. Ltd., Zhengzhou City, China) with those reported in the literature (Schwarz & Ternes, 1992). CA25, CA60 and CA98 were then kept in the dark at −20 °C until tested.

3.2. Total phenolic contents

Phenols are very important plant constituents because of their scavenging ability on free radicals due to their hydroxyl groups (Hatano et al., 1989). Therefore, phenolic contents of plants may contribute directly to their antioxidant action. The main phenolic compounds identified in rosemary are rosmarinic acid, carnosic acid, carnosol, methyl carnosate, rosmanol, epirosmanol and rosmadial (Ivanova, Gerova, Chervenkov, & Yankova, 2005). Total phenolic contents in CA25 and CA60 are presented in Table 1. The higher CA contents may account for the higher total phenolic content. Generally, total phenolic content of CA60 was 2–3 times higher than that of CA25. The results expressed as gallic acid equivalents or catechin equivalents were similar.

3.3. Reducing power assay

The reducing capacity of a compound may serve as a significant indicator of its potential antioxidant activity (Hsu, Coupar, & Ng, 2006). In the present study, the reducing power was assessed based on measurement of Fe^{3+} to Fe^{2+} transformation. Fig. 2 shows the reductive capability (absorbance at 700 nm) of CA25, CA60 and CA98, relative to L-ascorbic acid, BHA, BHT, and TBHQ. In this assay,

Table 1
Total phenolic contents of CA25 and CA60.

Sample	g Gallic acid equivalents/100 g sample	g Catechin equivalents/100 g sample
CA25	3.58 ± 0.026[a]	3.91 ± 0.029[a]
CA60	8.20 ± 0.027[a]	8.10 ± 0.056[a]

[a] Data are given as means ± SD, $n = 3$.

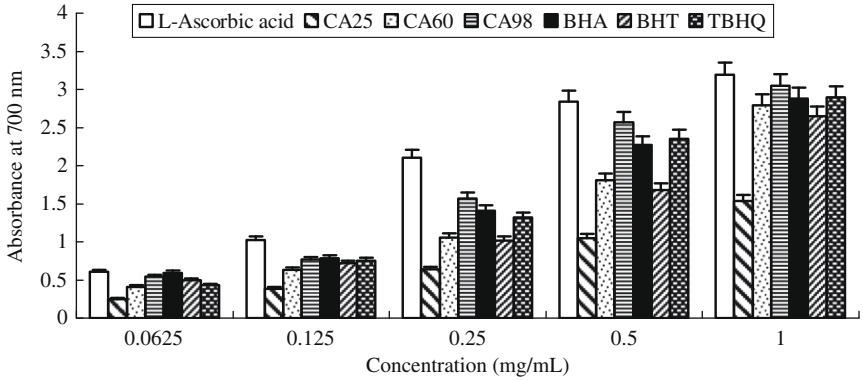

Fig. 2. Reducing capability of CA25, CA60, CA98 compared with commercial natural or synthetic antioxidants.

increased absorbance indicated increased reducing power. The reducing power of all these test compounds increased in a concentration-dependent manner. The reducing power of all these test compounds at 0.5 mg/ml was markedly lower than that of L-ascorbic acid. At the same concentration, reducing power of CA98 showed better activities than synthetic antioxidants. The reducing power of antioxidants at 0.5 mg/ml followed the order of L-ascorbic acid > CA98 > TBHQ > BHA > CA60 > BHT > CA25. These results suggest that carnosic acid has a remarkable potency to donate electrons to reactive free radicals, converting them into more stable non-reactive species and terminating the free radical chain reaction.

3.4. Scavenging effect on DPPH radicals

The DPPH assay, which measures the ability of compounds to transfer labile H-atoms to radicals, is the commonest method of antioxidant activity evaluation (Brand-Williams, Cuvelier, & Berset, 1995). The abstraction of hydrogen by this stable free radical is known to lead to bleaching with a maximum absorption band around 515–528 nm and can easily be monitored spectrophotometrically.

DPPH radical-scavenging abilities of CA25, CA60 and CA98 along with the reference standards BHA, BHT and TBHQ are shown in Table 2. A lower value of IC_{50} (defined as the concentration of compound that was able to inhibit 50% of the total DPPH radicals) indicates a higher antioxidant activity. All tested compounds demonstrated a concentration-dependent scavenging activity by quenching DPPH radicals; DPPH radical-scavenging activities of carnosic acids increased with increased content. Scavenging activities of CA25, CA60 and CA98 were significantly higher ($p < 0.05$) than that of BHT but less than that of TBHQ. As shown in Table 2, the scavenging activity of DPPH radicals decreased in the following order: TBHQ > CA98 > BHA > CA60 > CA25 > BHT, all values significantly different at $p < 0.01$.

These results indicated that CA has a noticeable effect on scavenging free radicals. This could be attributed to its molecular structure. It has been documented that antiradical scavenging activity is related to substitution of hydroxyl groups in the aromatic rings of phenolics, thus contributing to their hydrogen-donating ability (Brand-Williams et al., 1995; Yen, Chang, & Duh, 2005).

Table 2
Scavenging activity of antioxidants for DPPH radical; data are shown as IC_{50} (mg/ml) and % inhibition at 0.5 mg/ml of antioxidants.

Sample	IC_{50}[a,b]	Inhibition (%)[c]
CA25	0.30 ± 0.002	64.18 ± 0.12
CA60	0.20 ± 0.003	75.94 ± 0.10
CA98	0.12 ± 0.002	82.23 ± 0.08
BHA	0.19 ± 0.002	71.28 ± 0.11
BHT	0.42 ± 0.010	53.29 ± 0.13
TBHQ	0.09 ± 0.001	88.74 ± 0.07

[a] Defined as the concentration of the compounds that was able to inhibit 50% of the total DPPH radicals.
[b] Data are given as means ± SD, $n = 3$.
[c] % inhibition at 0.5 mg/ml.

3.5. Effect on peroxide value

Peroxide value (*PV*) is a measure of the concentration of peroxides and hydroperoxides formed in the initial stages of lipid oxidation. Peroxide value is one of the most widely-used tests for the measurement of oxidative rancidity in oils and fats. In this paper, oxidation degree on sunflower oil samples was determined by measuring *PV* in the absence and presence of antioxidants at 60 °C for 21 days. The influence of antioxidants during storage on *PV* in the sunflower oil samples is shown in Fig. 3. Results showed that peroxide value increased linearly with storage time and increased in acceleration after the ninth day. Sunflower oil samples without the antioxidant (control) reached a maximum *PV* of 272 ± 0.65 meq/kg after 21 days of storage. A significant difference ($p < 0.01$) in *PV* was observed between the control and sunflower oil samples containing CA and synthetic antioxidants, all of which slowed the rate of peroxide formation. The *PV* of sunflower oil samples with CA25, CA60, CA98, BHA, BHT and TBHQ were 75.7 ± 0.47, 61.5 ± 0.54, 39.4 ± 0.48, 205 ± 0.68, 160 ± 0.55 and 20.0 ± 0.49 meq/kg, respectively. The corresponding inhibition rates were 72.2%, 77.4%, 85.5%, 24.8%, 41.2% and 92.6%, respectively, after 21 days under accelerated storage conditions compared with the control. Furthermore, the antioxidant effects of CA25, CA60 and CA98 were better than BHT and BHA, and with the increase of content of CA, the antioxidant effect was better. However, among these treatments, TBHQ remained the most effective and gave the lowest *PV*.

3.6. Effect on thiobarbituric acid-reactive substances (TBARS)

TBA is defined as the quantity of malondialdehyde (in mg) present in 1 kg of sample. The TBA value is an index of lipid oxidation measuring malondialdehyde (MDA) content. Hydroperoxides, the initial reaction product of PUFA, reacted with oxygen to form MDA, which may contribute to off-flavour of oxidised oils. The method is based on the spectrophotometric quantification of the pink complex formed at an absorbance of 532 nm after reaction of one molecule of MDA with two molecules of 2-thiobarbituric acid (TBA). The effects of CA25, CA60, CA98 and synthetic antioxidants on TBARS values of sunflower oil at 60 °C for 24 days are shown in Fig. 4. TBARS values gradually increased in experimental

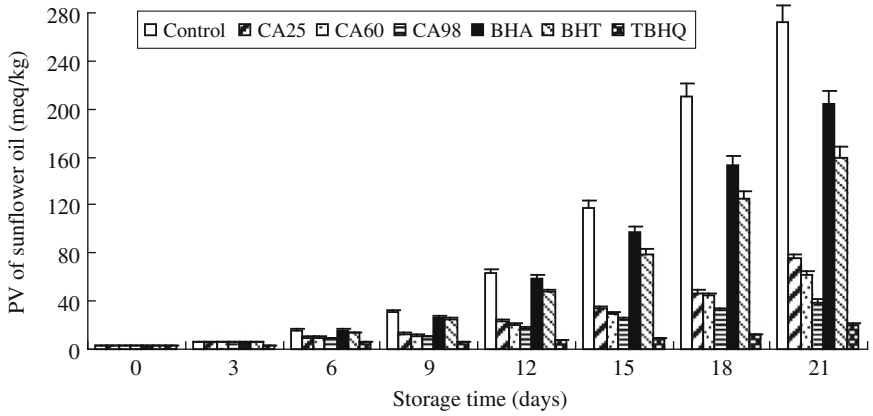

Fig. 3. Effect of adding antioxidants on *PV* of sunflower oil under accelerated storage at 60 °C for 21 days.

sunflower oil during the storage period, with increased acceleration after the fourth day. After 24 days of storage, TBARS value of the control sample reached a maximum of 0.3 ± 0.004 mg/kg, which was 1.86-fold higher than that of the sample treated with CA25, 1.99-fold higher than that of the sample treated with CA60, 2.86-fold higher than that of the sample treated with CA98. Additionally, TBARS value of the control was 1.75-fold, 1.63-fold and 4.35-fold higher than that of the sample treated with BHT, BHA and TBHQ, respectively. A significant difference ($p < 0.05$) was observed. We can see from Fig. 4 that CA inhibited the formation of TBARS at all concentrations: inhibitory effects on TBARS were stronger than BHA and BHT, but lower than TBHQ.

3.7. Effect on free fatty acids content (FFA)

Formation of free fatty acids might be an important measure of rancidity of foods. FFA are formed due to hydrolysis of triglycerides and may get promoted by reaction of oil with moisture (Frega, Mozzon, & Lercker, 1999).

Addition of antioxidants caused significant reductions in FFA of sunflower oil during 21 days' storage at 60 °C, as shown in Fig. 5. It is evident from these results that, as the content of CA increased, inhibitory effects on FFA also increased considerably, which increased acceleration after the ninth day. After 21 days' storage at 60 °C, FFA value of the control sample reached a maximum of 0.71 ± 0.05 mg/g. FFA values of sunflower oil treated with CA25, CA60 and CA98 were 0.45 ± 0.04, 0.42 ± 0.02, and 0.38 ± 0.02 mg/g, whereas values for oil treated with synthetic antioxidants BHA, BHT and TBHQ were 0.46 ± 0.03, 0.34 ± 0.03 and 0.20 ± 0.01 mg/g, respectively (Fig. 5). Significant differences ($p < 0.05$) in free fatty acids were observed between the control and the sunflower oil treated with CA25, CA60, CA98 and synthetic antioxidants. However, inhibitory effects of CA25, CA60 and CA98 on FFA were better than those of BHT, but lower than BHA and TBHQ.

3.8. Effect on p-anisidine value

p-Anisidine value (*AnV*) plays an important role in the oxidation process of edible oil and edible fats. Calculating *AnV* is one of the oldest methods for evaluating secondary lipid oxidation. It is based on the reactiveness of the aldehyde carbonyl bond on the *p*-anisidine amine group, leading to the formation of a Schiff base that absorbs at 350 nm (Laguerre, Lecomte, & Villeneuve, 2007):

$$\mathrm{R{=}CH{=}O + H_2N{-}\Phi{-}OMe \rightarrow R{-}CH{=}N{-}\Phi{-}OMe\ (Schiff\ base) + H_2O} \quad (1)$$

Results of *AnV* measurements are very similar to the results of TBARS values measurements, as shown in Fig. 6. We can see *AnV* increased significantly throughout the storage time, which increased in acceleration after the sixth day. Addition of CA25, CA60 and CA98 caused significant reduction in *AnV* of sunflower oil during 21 days' storage at 60 °C. It is evident from these results that, the same order of CA efficiency was observed as the content of CA increased, inhibitory effects on *AnV* also increased considerably, better than BHA and BHT but lower than TBHQ.

This difference in antioxidant activity may be accounted for on the basis of chemical structures. The stability of phenoxy radicals reduces the rate of propagation and further reactions and thus increases the oxidative stability of lipids (Gordon, 1990), with

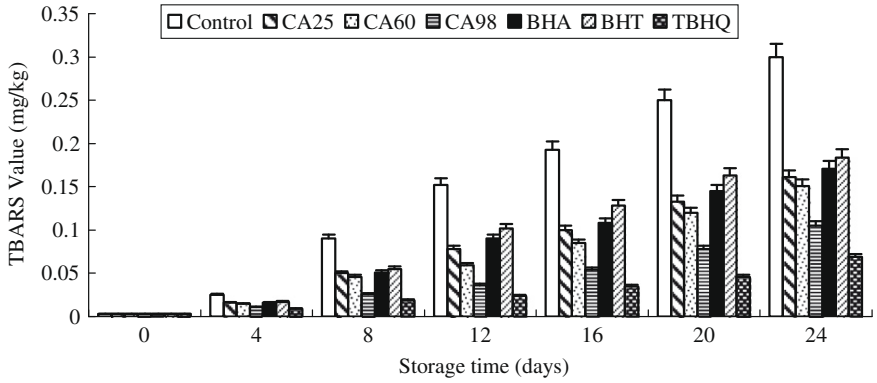

Fig. 4. Effect of adding antioxidants on TBARS of sunflower oil under accelerated storage at 60 °C for 24 days.

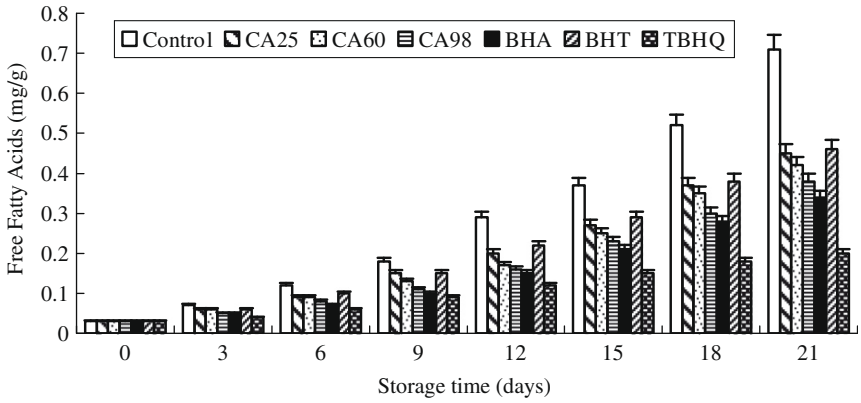

Fig. 5. Effect of adding antioxidants on free fatty acid content (FFA) of sunflower oil under accelerated storage at 60 °C for 21 days.

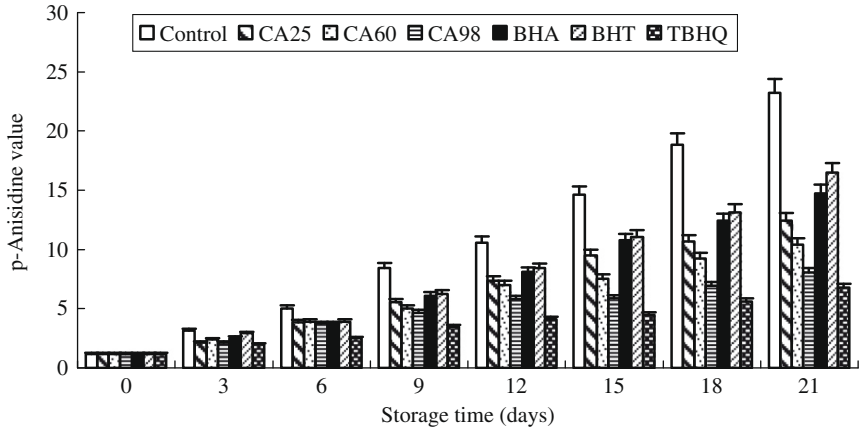

Fig. 6. Effect of adding antioxidants on *p*-anisidine value (*AnV*) of sunflower oil under accelerated storage at 60 °C for 21 days.

two phenolic hydroxyl groups (Fig. 1) being responsible for the higher antioxidant activity of CA. In addition, in most cases, of all the test compounds, the synthetic antioxidant TBHQ which has two *para*-hydroxyl groups can make the phenols more easily donate hydrogen atoms to active free radicals to interrupt the chain reaction of antioxidation (Jiang & Wang, 2006) and this is responsible for superior antioxidant activity in various edible oils (Madhavi, Singhal, & Kulkarni, 1995). In this study, in comparison with synthetic antioxidants, in addition to existing structural differences, effects of CA content may also play an important role in the observed trends.

4. Conclusions

Generally, results of the present study apparently indicated that CA25, CA60 and CA98, separated from rosemary dried leaves, executed very good antioxidant activity.

Though sunflower oil is difficult to stabilise because of high linoleic acid content, CA25, CA60 and CA98 were proved to show strong protective effects against lipid oxidation of sunflower oil during accelerated storage. They showed content-dependent inhibitory effects on retarding lipid oxidation of sunflower oil. This is in accordance with results of Braida, Mattea, and Cardarelli (2008) and Trojakova, Reblova, Nguyen, and Pokorny (2001), who have reported that there was high correlation between the carnosic acid content and the protection factor in high linoleic acid content oil. Also, CA98 was to a greater extent more effective than commonly-employed synthetic antioxidants BHT and BHA, but less effective than the synthetic antioxidant TBHQ. This is in accordance with results of Aruoma et al. (1992) who reported that in soybean oil carnosic acid was more active than BHT and BHA, but less active than TBHQ. Results observed in our experiments showed that CA25, CA60 and CA98 could be considered as satisfactory for large scale applications.

Acknowledgement

This work was financially supported by National Key Technology Research and Development Program, China (No. 2006BAD18B04).

References

Ardestani, A., & Yazdanparast, R. (2007). Antioxidant and free radical-scavenging potential of *Achillea santolina* extracts. *Food Chemistry, 104*, 21–29.

Aruoma, O. I., Halliwell, B., Aeschbach, R., & Loliger, J. (1992). Antioxidant and pro-oxidant properties of active rosemary constituents: Carnosol and carnosic acid. *Xenobiotica, 22*, 257–268.

Basaga, H., Tekkaya, C., & Acikel, F. (1997). Antioxidative and free radical scavenging properties of rosemary extract. *Lebensmittel-Wissenschaft und -Technologie, 30*, 105–108.

Blois, M. S. (1958). Antioxidant determination by the use of a stable free radical. *Nature, 181*, 1199–1200.

Braida, I., Mattea, M., & Cardarelli, D. (2008). Extraction–adsorption–desorption process under supercritical condition as a method to concentrate antioxidants from natural sources. *The Journal of Supercritical Fluids, 45*(2), 195–199.

Brand-Williams, B., Cuvelier, M. E., & Berset, C. (1995). Use of a free radical method to evaluate antioxidant activity. *LWT-Food Science and Technology, 28*, 25–30.

Chang, C. H., Chyau, C. C., Hsieh, C. L., Wu, Y. Y., Ker, Y. B., Tsen, H. Y., et al. (2008). Relevance of phenolic diterpene constituents to antioxidant activity of supercritical CO(2) extract from the leaves of rosemary. *Natural Products Research, 22*, 76–90.

Danilenko, M., Wang, Q., Wang, X., Levy, J., Sharoni, Y., & Studzinski, G. P. (2003). Carnosic acid potentiates the antioxidant and prodifferentiation effects of 1alpha 25-dihydroxyvitamin D(3) in leukemia cells but does not promote elevation of basal levels of intracellular calcium. *Cancer Research, 63*, 1325–1332.

Determination of the p-Anisidine Value, Method 2.504 (1987). *IUPAC standard methods for the analysis of oils, fats and derivatives* (7th ed., pp. 210–211). Oxford: Alden Press.

Duh, P. D., & Yen, G. C. (1997). Antioxidant efficacy of methanolic extracts of peanut hulls in soybean and peanut oils. *Journal of American Oil Chemists Society, 74*, 745–748.

Erkan, N., Ayranci, G., & Ayranci, E. (2008). Antioxidant activities of rosemary (*Rosmarinus officinalis* L.) extract, blackseed (*Nigella sativa* L.) essential oil, carnosic acid, rosmarinic acid and sesamol. *Food Chemistry, 110*(7), 6–82.

Esterbauer, H., Schaur, R. F., & Zollner, H. (1991). Chemistry and biochemistry of 4-hydroxynonenal, malonaldehyde and related aldehydes. *Free Radical Biology and Medicine, 11*, 81–128.

Frankel, E. N., Huang, S., Aeschbach, W. R., & Prior, E. (1996). Antioxidant activity of a rosemary extract ant its constituents, carnosicacid, carnosol, and rosemaric acid, in bulk oil and oil-in-water emulsion. *Journal of Agricultural and Food Chemistry, 44*, 131–135.

Frega, N., Mozzon, M., & Lercker, G. (1999). Effects of free fatty acids on oxidative stability of vegetable oil. *Journal of the American Oil Chemists Society, 76*(3), 325–329.

Gordon, M. H. (1990). The mechanisms of antioxidant action in vitro. In B. J. F. Hudson (Ed.), *Food antioxidants* (pp. 1–18). London: Elsevier Applied Science.

Hahn, D. H., Rooney, L. W., & Earp, C. F. (1984). Tannins and phenols of sorghum. *Cereal Foods World, 29*, 776–779.

Haraguchi, H., Saito, T., Okamura, N., & Yagi, A. (1995). Inhibition of lipid peroxidation and superoxide generation by diterpenoids from *Rosmarinus officinalis*. *Planta Medica, 61*, 333–336.

Hatano, T., Edamatsu, R., Mori, A., Fujita, Y., Yasuhara, T., Yoshida, T., et al. (1989). Effects of the interaction of tannins with co-existing substances. VI. Effects of tannins and related polyphenols on superoxide anion radical and on DPPH radical. *Chemical and Pharmaceutical Bulletin, 37*, 2016–2021.

Hou, D. X. (2003). Potential mechanism of cancer chemoprevention by anthocyanin. *Current Advancements in Molecular Medicines, 3*, 149–159.

Hsu, B., Coupar, I. M., & Ng, K. (2006). Antioxidant activity of hot water extract from the fruit of the *Doum palm*, *Hyphaene thebaica*. *Food Chemistry, 98*, 317–328.

Ivanova, D., Gerova, D., Chervenkov, T., & Yankova, T. (2005). Polyphenols and antioxidant capacity of Bulgarian medicinal plants. *Journal of Ethnopharmacology, 96*, 145–150.

Jiang, A. L., & Wang, C. H. (2006). Antioxidant properties of natural components from *Salvia plebeia* on oxidative stability of ascidian oil. *Process Biochemistry, 41*, 1111–1116.

Laguerre, M., Lecomte, J., & Villeneuve, P. (2007). Evaluation of the ability of antioxidants to counteract lipid oxidation: Existing methods, new trends and challenges. *Progress in Lipid Research, 46*, 244–282.

Lercker, G., & Rodriguez-Estrada, M. T. (2002). Cholesterol oxidation mechanism. In F. Guardiola, P. C. Dutta, R. Codony, & G. P. Savage (Eds.), *Cholesterol and phytosterol oxidation products: Analysis, occurrence and biological effects* (pp. 1–26). Champaign, IL: AOCS Press.

Madhavi, D. L., Singhal, R. S., & Kulkarni, P. R. (1995). Technological aspects of food antioxidants. In D. L. Madhavi, S. S. Deshpande, & D. K. Salunkhe (Eds.), *Food antioxidants: Technological, toxicological and health perspectives* (pp. 159–265). New York: Marcel Dekker.

Mallet, J. F., Cerrati, C., Ucciani, E., Gamisons, J., & Gruber, M. (1994). Antioxidant activity of plant leaves in relation to their alpha-tocopherol content. *Food Chemistry, 49*, 61–65.

Nissen, L. R., Mansson, L., Bertelsen, G., Huynh-Ba, T., & Skibsted, L. H. (2000). Protection of dehydrated chicken meat by natural antioxidants as evaluated by electron spin resonance spectrometry. *Journal of Agricultural and Food Chemistry, 48*, 5548–5556.

Prior, R. L. (2004). Absorption and metabolism of anthocyanins: Potential health effects. In M. Meskin, W. R. Bidlack, A. J. Davies, D. S. Lewis, & R. K. Randolph (Eds.), *Phytochemicals: Mechanisms of action* (pp. 1–19). Boca Raton, FL: CRC Press.

Rau, O., Wurglics, M., Paulke, A., Zitzkowski, J., Meindl, N., Bock, A., et al. (2006). Carnosic acid and carnosol, phenolic diterpene compounds of the labiate herbs rosemary and sage, are activators of the human peroxisome proliferator-activated receptor gamma. *Planta Medica, 72*, 881–887.

Richheimer, S. L., Bailey, D. T., Bernart, M. W., Kent, M., Vininski, J. V., & Anderson, L. D. (1999). Antioxidant activity and oxidative degradation of phenolic compounds isolated from rosemary. *Recent Research Development in Oil Chemistry, 3*, 45–58.

Richheimer, S. L., Bemart, M. W., King, G. A., Kent, M. C., & Bailey, D. T. (1996). Antioxidant activity of lipid-soluble phenolic diterpenes from rosemary. *Journal of the American Oil Chemists' Society, 73*, 507–514.

Satoh, T., Kosaka, K., Itoh, K., Kobayashi, A., Yamamoto, M., Shimojo, Y., et al. (2008). Carnosic acid, a catechol-type electrophilic compound, protects neurons both in vitro and in vivo through activation of the Keap1/Nrf2 pathway via Salkylation of targeted cysteines on Keap1. *Journal of Neurochemistry, 104*, 1116–1131.

Schwarz, K., & Ternes, W. (1992). Antioxidative constituents of *Rosmarinus officinalis* and *Salvia officinalis*. *Z Lebensm-Unters – Forsch, 195*, 95–98.

Swain, T., & Hills, W. E. (1959). The phenolic constituents of *Prunus domestica*. *Journal of the Science of Food and Agriculture, 10*, 63–68.

Thorsen, M. A., & Hildebrandt, K. S. (2003). Quantitative determination of phenolic diterpenes in rosemary extracts: Aspects of accurate quantification. *Journal of Chromatography A, 995*, 119–125.

Trojakova, L., Reblova, Z., Nguyen, H., & Pokorny, J. (2001). Antioxidant activity of rosemary and sage extracts in rapeseed oil. *Journal of Food Lipids, 8*(1), 1–13.

Xiong, H. P., Yang, W. L., Zhang, Y. S., & Xiao, W. J. (2001). Recent advances in natural plant antioxidants. *Natural Product Research and Development, 13*(5), 75–79.

Yen, W. J., Chang, L. W., & Duh, P. D. (2005). Antioxidant activity of peanut seed testa and its antioxidative component, ethyl protocatechuate. *Lebensmittel-Wissenschaft und -Technologie, 38*, 193–200.

Food Chemistry 118 (2010) 663–669

Contents lists available at ScienceDirect

Food Chemistry

journal homepage: www.elsevier.com/locate/foodchem

Evaluation of Asian salted noodles in the presence of *Amaranthus* betacyanin pigments

Fan Zhu, Yi-Zhong Cai, Harold Corke *

School of Biological Sciences, The University of Hong Kong, Pokfulam Road, Hong Kong, China

ARTICLE INFO

Article history:
Received 18 February 2009
Received in revised form 27 March 2009
Accepted 13 May 2009

Keywords:
Amaranthus betacyanin pigments
Asian salted noodles
Colour
Texture
Pasting

ABSTRACT

The effect of betacyanin pigments from *Amaranthus tricolor* on the functional properties and colour of wheat flour in relation to the quality of Asian salted noodles was studied. Addition of *Amaranthus* pigments significantly decreased the viscosity of wheat flour pastes as well as hardness and adhesiveness of the gels. Low levels of *Amaranthus* pigments (0.1% and 0.5%) imparted a more pink shade to flour gels, dried raw noodles, and cooked noodles, whereas higher levels (1.0% and 2.0%) gave a more red shade with decreased brightness. Pigment addition at low levels had no significant effect on the cooking and textural properties of noodles, whereas high level (2.0%) did have a significant influence. Several RVA and textural parameters of wheat flour pastes and gels were highly correlated to quality of cooked noodles and may be used in predicting actual noodle quality in the presence of *Amaranthus* pigments.

1. Introduction

The perception of flavour is intrinsically linked to multisensory interactions including colour when tasting food (Auvray & Spence, 2008). Colour interferes with our judgments on flavour perception. For example, colour has been shown to be able to quantitatively replace sugar and still maintain sweetness perception in flavoured foods. Colour has also been indicated to considerably affect the acceptability of foods and is strongly related to different social segments (Clydesdale, 1993). It plays a critical role in the attractive appearance of beverages and foods. Favourable colour tone stimulates our appetite and contributes significantly to our enjoyment of foods (Auvray & Spence, 2008). For example, colour of tomato concentrates, whose colorant is mainly beta-carotene, has been shown to play an essential part in consumers' preference (Hayes, Smith, & Morris, 1998).

Many colorants are more than just for appearance. Natural pigments, such as carotenoids, anthocyanins, and betalains, can not only enhance the sensory properties of food products, but also functionally improve their nutritional quality due to their potential role in human health as natural antioxidants (Cai, Sun, & Corke, 2003; Stintzing & Carle, 2004). It has been shown that anthocyanins from various plants can be beneficial due to their potential bioactivities such as anti-carcinogenicity, anti-mutagenicity, anti-inflammation, protection against age-related declines of neuronal signal transduction, and cholesterol reduction (Galvano et al., 2004). It has also been clinically proved that consumption of cactus pear fruit, which is rich in betalain pigments with good antioxidant capacity, can positively influence the redox balance in human body, decrease oxidation to lipids, and improve antioxidant status in healthy humans (Tesoriere, Butera, Pintaudi, Allegra, & Livrea, 2004). Betanin, a major class of betalain, can inhibit the myeloperoxidase/nitrite-induced oxidation of human low-density lipoproteins by scavenging the initiator radical nitrogen dioxide and lipoperoxyl radical (Allegra, Tesoriere, & Livrea, 2007). Extracts from *Amaranthus spinosus* could inhibit spontaneous and dexamethasone-induced apoptosis in murine primary splenocytes (Lin, Li, & Lin, 2008).

Betalains, as a promising novel colorant with great potential for human health, has been recently gained increased research focus (Stintzing & Carle, 2004). Many new betalains, including the yellow betaxanthins and red or violet betacyanins, have been identified and characterised from various plant or fungal sources (Kumar & Sinha, 2004). Among them, *Amaranthus* betacyanin pigments from various species in the family Amaranthaceae have also been systematically researched (Cai, Sun, & Corke, 2005). It has been shown that betacyanins from plants in the Amaranthaceae could be good natural antioxidants against free radicals (DPPH·) *in vitro* (Cai et al., 2003). However, *Amaranthus* betacyanin pigments are not as developed or commonly used globally as betalains colorants from red beet, though some *Amaranthus* species have higher biomass yield potential than red beet. Cai and Corke (1999) applied betacyanin pigments from *Amaranthus cruentus* in model food systems, i.e. jelly, ice cream, and beverage for colouring and concluded that betacyanins may be a feasible natural colorant for jelly, higher

* Corresponding author. Tel.: +852 22990314; fax: +852 28583477.
E-mail address: hcorke@yahoo.com (H. Corke).

0308-8146/$ - see front matter © 2009 Elsevier Ltd. All rights reserved.
doi:10.1016/j.foodchem.2009.05.041

pH beverages, and ice cream under selected conditions. Another preliminary study showed that *Amaranthus* betacyanin pigments might be used as an efficient colorant in wheat-based system (Zhu, Cai, Sun, & Corke, 2008). However, no scientific report has been found on the application of *Amaranthus* betacyanins in staple foods.

Asian noodles are one of the most popular cereal foods. Noodles in various formulations and shapes have been staple foods for many Oriental countries since ancient times. Major types of Asian noodles are white salted noodles and yellow alkaline noodles. These two noodle types differ greatly in various aspects such as formulation, production procedures, and sensory attributes (Corke & Bhattacharya, 1999). Noodle quality has various aspects: appearance, eating quality, taste, cooking properties, etc., and is influenced by various factors such as the composition of protein subunits and starch properties (Corke & Bhattacharya, 1999). Though coloured pasta and bread products can be seen in the marketplace, no scientific report has been found on the development of novel coloured noodles incorporated with *Amaranthus* betacyanins.

Amaranthus tricolor was selected for this study because of its good colouring efficacy for foods and high biomass for betacyanin production, compared with other *Amaranthus* species (Cai et al., 2005; Zhu et al., 2008). Furthermore, pigment extract from *A. tricolor* (code: GB08.130) has been legally approved as a natural colorant according to Hygienic Standards for Food Additives in China (GB 2760-1996).

The objective of this study was to evaluate the effect of *Amaranthus* betacyanin pigments from mature leaves of *A. tricolor* in Asian salted noodles. This study may stimulate further utilisation of betalains as natural food colorants in novel food product development.

2. Materials and methods

2.1. Wheat flour

'Red Bicycle' brand, commercial wheat flour made from U.S. hard red winter wheat, was purchased from Hong Kong Flour Mills (Kowloon, Hong Kong). Proximate analysis (crude protein, ash, crude fat) of wheat flour (wet basis) was performed according to AACC methods in triplicate and the results were expressed as average. Moisture content was obtained using LJ16 Moisture Analyser (Mettler-Toledo, Switzerland). The contents of crude protein, ash, crude fat, and moisture were 11.6%, 0.43%, 1.35%, and 13.2% (w/w), respectively.

2.2. Amaranthus betacyanin pigments

The mature leaves of *A. tricolor* (Tr35) grown in Wuhan, Hubei Province, China were collected. Pigment extraction followed previous methods (Cai, Sun, & Corke, 2001) with minor modification. Briefly, the fresh leaves were washed, cut into small pieces, and extracted, followed by centrifugation, concentration, and freeze drying. The dried pigment extracts were tightly sealed in plastic bags and stored at 4 °C in the dark until use. The betacyanins in these two pigment extracts were identified as amaranthin and its isomer (Cai et al., 2001). On the basis of spectrophotometeric analysis, total betacyanin concentration of *A. tricolor* pigment extract was 86.5% (w/w, dry basis) (Zhu et al., 2008).

2.3. Pasting analysis

Pasting properties of various wheat flour systems were determined using a Rapid Visco Analyser (RVA, Model 3D, Newport Scientific, Warriewood, Australia) with Thermocline for Windows software (Version 2.0). Suspensions of pure double deionized water (24.6 g) with pure wheat flour (3 g, dry basis) as control, or flours (3 g, dry basis) with addition of pigment powder (28 mg, 140 mg, 280 mg, and 560 mg, respectively), were prepared to give a series of concentration of 0.0%, 0.1%, 0.5%, 1.0%, and 2.0% (w/w) *Amaranthus* betacyanins in the canisters, respectively. The suspension was then manually homogenised using the plastic paddle to avoid lump formation. Then, the pH of the wheat flour–water–pigments slurry was recorded by a pH meter (Orion model 720A, Boston, MA, USA) right before the RVA test. A programmed heating and cooling cycle (22 min) was used (Zhu et al., 2008). The samples were held at 50 °C for 1 min, heated to 95 °C in 7.5 min, held at 95 °C for 5 min before cooling to 50 °C in 7.5 min and holding at 50 °C for 2 min. The peak time (PT), peak viscosity (PV), hot paste viscosity (HPV), cool paste viscosity (CPV) and their derivative parameters: breakdown, BD = PV–HPV, setback, SB = CPV–PV were recorded. The viscosities were expressed in Rapid Visco Units (RVU). All tests were performed in triplicate.

2.4. Salted noodle preparation

Noodle making followed the previous methods (Sui, Lucas, & Corke, 2006; Wu & Corke, 2005) with some modifications. Wheat flour (30.0 g, moisture basis) was mixed with 10.0 g of 6% (w/w) NaCl solution to make salted noodles as control. For pigmented noodle production, *Amaranthus* betacyanins pigment powder (40 mg, 200 mg, 400 mg, and 800 mg) was completely dissolved in 10.0 g of 6% (w/w) NaCl solution before 30.0 g of wheat flour was added for mixture. The mixture was manually kneaded for 5 min in a plastic bowl to obtain a crumbly dough ball. After resting for 5 min in the bowl, the crumbly dough was then sheeted through the first roll gap 15 times and folded in half each time on a domestic-type electric pasta machine (Atlas Electric model 150, Marcato Co., Campodarsego, Italy). Then the dough sheet was further passed through the next six successively reduced gaps 8 times each without intermediate resting. Finally, the resultant thin dough sheet was cut through a slitter to produce noodles of around 2 mm width. The raw noodles were placed on tissue to dry at 25 °C for around 8 h in an oven with the ventilation setting for fresh air at six (maximum) (Model 600, Memmert Co., Schwabach, Germany). The dried raw noodles were stored in transparent plastic bags at room temperature (23–26 °C) until use within a week. For each group, final *Amaranthus* betacyanins pigment content of the noodles were 0%, 0.1%, 0.5%, 1.0%, and 2.0% (w/w), respectively.

2.5. Cooking properties

Noodle cooking followed the previous methods (Sui et al., 2006; Wu & Corke, 2005) with some modifications. After storage for one day and seven days, dried raw noodles (5 g) were cooked in boiling water (300 mL) in a beaker with lid for 5 min until the white core disappeared. They were cooled in cool water (~20 °C) for 10 s before dried on a paper towel for 15 min until further texture and colour testing.

For cooking yield and loss analysis, cooked noodle strands on the paper towel were softly blotted for about 1 min to remove the excess surface moisture on the noodles surface. Cooking yield (CY) was calculated as:

$$CY = Mco/Md$$

where Mco = weight of cooked noodles (g); Md = weight of dried raw noodles (g).

After cooking, the remaining water (~300 mL) in the beaker was further boiled for evaporation until around 20 mL was left. Then the beaker with left water was further dried in an oven at

95 °C until constant weight (Mc, g). Cooking loss % (CL) was calculated as:

$$CL\,\% = (Mc - Mb) \times 100/(Md - Mm)$$

where Mb = weight of beaker (g); Mm = weight of moisture in dried raw noodles. All analysis was conducted at least in triplicate.

2.6. Colour analysis

The Hunter colour parameters *L*, *a*, and *b* (CIE 1976) were measured by a colorimeter (Chroma Meter CR-301, Minolta Co., Osaka, Japan) through round plastic optical cells (21 mm in diameter and 5 mm in depth), standardised with calibration plate sets CR-A47 and a white plate. Colour results were expressed as tristimulus parameters (*L*, *a*, *b*, *C*, and *H*). *H* (hue angle = arctan *b*/*a*) indicates sample colour (0° or 360° = red; 90° = yellow; 180° = green; 270° = blue), and *C* [Chroma = $(a^2 + b^2)^{1/2}$] indicates colour purity or saturation (higher values are more vivid). All measurements were performed at least in triplicate.

Colour characteristics of flour gels during storage for one week were determined on the wheat flour gels from the RVA analysis. Gels were transferred into screw-capped and transparent cylinder plastic cups (5.5 cm in diameter and 5.5 cm in height for the cups, and around 1.1 cm in thickness for the gels in cup) right after RVA testing. The cups were sterilized beforehand by wiping with ethanol and subjecting to violet ray to prevent microbial growth. Colour characteristics of dried raw noodles were determined on their surface. Colour characteristics of cooked noodles were measured on their surface at around 20 min after cooking.

2.7. Textural analysis of flour gels and cooked noodles

All texture properties were analysed with an SMS Model TA-XT2*i* texture analyser (Stable Micro Systems Ltd., Godalming, Surry, England) equipped with Texture Expert software (version 1.2). The methods followed the previous studies (Collado & Corke, 1997; Wu & Corke, 2005; Zhu et al., 2008) with some modifications.

For the texture of flour gels, after RVA testing, the paddle was removed immediately and the paste in the canister was sealed tightly by parafilm and stored at room temperature for 24 h before testing. The testing mode was Texture Profile Analysis (TPA). The probe was a flat-ended stainless steel cylinder probe with a diameter of 5 mm (P/5). The pre-test, test, and post-test speeds were 1 mm/s. The distance in strain was 30%. The trigger type was auto with a trigger force of 2.0 g. The data acquisition rate was 25 pps.

For the tensile and compression tests of cooked noodles, noodles were cooked in separated batches and got tested separately between 15 and 20 min after cooking to avoid rapid textural changes of cooked noodles right after cooking (Corke & Bhattacharya, 1999). For tensile strength analysis, the instrument was equipped with spaghetti/noodle tensile grips (A/SPR). The noodle strand was winded two, three or four times around parallel friction roller of the grip to anchor the samples and avoid slippage. The distance between the parallel rollers was 4 cm. The mode was measure force in tension. Pre-test and test speeds were 3.0 mm/s, post-test speed was 3.0 mm/s. Distance was 100 mm. The trigger type was auto with a trigger force of 5.0 g. The data acquisition rate was 200 pps. The maximum force required to break down the strand was termed tensile force (g). At least 10 individual strands were tested for each group. The five minimum values were discarded. For compression analysis, the probe was a cylinder probe with a diameter of 36 mm (P/36). The mode was measure force in compression with single cycle. The pre-test, test, and post-test speeds were 2 mm/s. The strain was 30%. The trigger type was auto with a trigger force of 5.0 g. The data acquisition rate was 200 pps. Two noodle strands were put parallel on the platform and tested close together at a time. The maximum force (g) was noted firmness. For at least 6 times was tested each group.

2.8. Scanning electron microscopy (SEM)

Dried noodles stored at room temperature for a week were manually broken to expose the cross-sectional surface. The surfaces of both noodles and its cross-section were mounted on a silver specimen holder and coated with gold–palladium alloy under vacuum for 60 s. Morphology was randomly investigated by a Scanning Electron Microscope Hitachi S-4800 FEG (Tokyo, Japan). The images were obtained at an accelerating voltage of 5.0 kV at various magnifications.

2.9. Statistical analysis

Data analysis and statistical computations for analysis of variance (ANOVA), Pearson correlation analysis and Duncan's test were performed with the Statistical Analysis System (SAS Institute Inc., Cary, N.C., USA) and Microsoft Office Excel (Microsoft Corporation, Redmond).

3. Results and discussion

3.1. Effect of Amaranthus betacyanin pigments on the pasting properties of wheat flour

Addition of *Amaranthus* betacyanin pigments at various levels (0.1–2.0%) generally decreased the pasting viscosities of wheat flour (Table 1). *Amaranthus* betacyanin pigments at a concentration of 2.0% achieved the greatest reduction in both paste viscosity and peak time (PT), whereas that of 0.1% least changed them. Peak viscosity (PV) with addition of *Amaranthus* betacyanin pigments at 0.1% (229 RVU) was not significantly different to control (234 RVU). Addition of betacyanin pigments at higher levels significantly reduced PV (PV at 1.0% and 2.0% of 210 and 209 RVU, respectively). For hot paste viscosity (HPV), addition of *Amaranthus* betacyanin pigments at all levels decreased HPV considerably in a dose-dependent manner (the lowest value 52 RVU at 2.0%),

Table 1
Influence of *Amaranthus* betacyanin pigments on the pasting and gelling properties of wheat flours[a].

Pigment concentrations (%) (w/w)	pH	PV (RVU)	HPV (RVU)	BD (RVU)	CPV (RVU)	SB (RVU)	PT (min)	HD (g)	ADH (g s)	COH
0.0	5.92a	234a	126a	108a	251a	125a	9.00ab	11.9a	13.9a	0.436a
0.1	5.93a	229a	113b	116b	218b	106b	9.04a	10.1b	12.2a	0.518ab
0.5	5.87b	218b	81c	137c	162c	81c	8.97ab	7.5c	9.4b	0.524ab
1.0	5.79c	210c	67d	143d	137d	69d	9.02ab	5.6d	6.9c	0.580b
2.0	5.65d	209c	52e	157e	102e	50e	8.93b	3.7e	4.2d	0.776c

[a] Values in the same column with the same letters do not differ significantly ($p < 0.05$); PV = peak viscosity; HPV = hot paste viscosity; BD = breakdown; CPV = cold paste viscosity; SB = setback; PT = peak time; HD = hardness; ADH = adhesiveness; COH = cohesiveness.

compared with control (126 RVU). Breakdown (BD) is the derivative of PV and HPV and showed similar but negative trend with HPV. Pigment addition did not alter peak time (PT) except for a small effect at 2.0%. Cold paste viscosity (CPV) was considerably reduced in a dose-dependent manner (lowest value at 102 RVU at 2.0%), compared with control (251 RVU) by addition of the pigment. Setback (SB) is a derivative of CPV and PV and showed similar trend with CPV.

Pasting properties of flour are primarily related to the swelling and rupture of starch granules in a system (Rojas, Rosell, & de Barber, 1999). Different food additives in the system can alter the pasting behaviour to various extents. Several previous studies showed that sugars and sugar alcohols could increase the viscosity of various starch–water systems, depending on the type used (Gunaratne, Ranaweera, & Corke, 2007). For example, addition of various polyhydroxy compounds, i.e. sucrose, glucose, glycerol, and hydroxypropyl beta-cyclodextrin, increase all the pasting parameters of potato and wheat starches (Gunaratne et al., 2007). However, no such trend was observed here. On the other hand, acid treatments of various starches could decrease all the pasting parameters and increase the gelatinization parameters and cause early development of peak viscosity and delay the onset of gelatinization (Gunaratne & Corke, 2007). For example, hydrochloric acid treatments reduced peak viscosity (PV) in wheat, potato, and maize starches, both modified and unmodified (Gunaratne & Corke, 2007). This trend was also observed in this study. pH of the system has also been reported to be critical for the pasting and gelatinization behaviour of various starch and flour (Bao & Corke, 2002; Rodriguezsosa, Parsiros, & Gonzalez, 1981). For example, lower pH could result in viscosity reduction of pasting for rice flours (Bao & Corke, 2002). In this study, addition of betacyanin pigment reduced the pH of the suspension in the first place with the level at 2.0% achieved the greatest reduction by 0.27 with the exception of 0.1% which showed little effect (Table 1). The major constituents of *Amaranthus* betacyanin pigment are amaranthin and its isomer (Cai et al., 2001; Herbach, Stintzing, & Carle, 2006; Zhu et al., 2008). When subjected to heating, amaranthin and its isomer would degrade into a series of related chemicals with acid moieties (Herbach et al., 2006). Structurally, these compounds possess the sugar (glucose) and acid moieties (glucuronic acid and betalamic acid), and effect of the latter might surpassed the former as the data shown (Table 1). They may subject the wheat flour to acid presence during pasting and also altered the pH of the system as shown in Table 1.

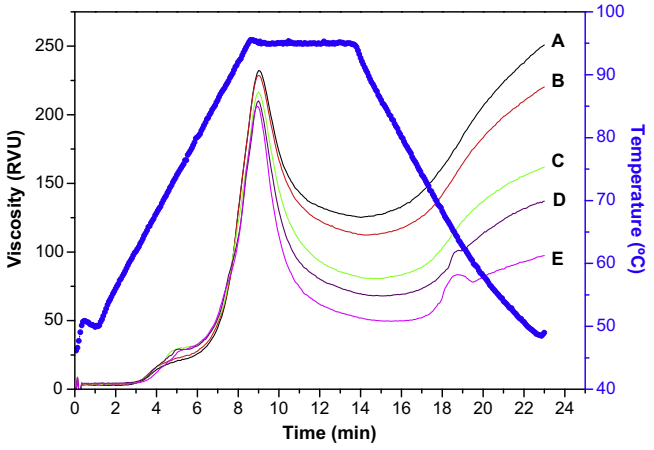

Fig. 1. Pasting characteristics of Red Bicycle flour as affected by *Amaranthus* betacyanin pigments at various concentration. (A) control; (B): 0.1%; (C): 0.5%; (D): 1.0%; (E): 2.0%.

Bump area appeared in the pasting profile during the cooling stage for pigment addition at concentrations of both 1.0% and 2.0% (Fig. 1). No observable bump area was noted for lower pigment concentrations (0.1% and 0.5%) or control. The bump area has been positively related with the extent of the formation and content of amylose–lipid complex during the cooling phase (Rojas et al., 1999). The amylose–lipid complex can retard the retrogradation of various gelatinized starch systems (Eliasson, 1994). Higher pigment concentration (2.0%) increased the size of the bump area compared with that at 1.0%, indicating that addition of betacyanin pigments could facilitate the formation of complex between amylose and free lipids present in wheat flour (1.35%).

3.2. Effect of Amaranthus betacyanin pigments on the textural properties of flour gels

Addition of *Amaranthus* betacyanin pigments at various levels generally decreased gel hardness (HD) and adhesiveness (ADH) and increased cohesiveness (COH) generally in a dose-dependent manner (Table 1). For example, addition of betacyanin pigments at 2.0% caused the greatest reduction in both HD and ADH by 8.2 g and 9.7 g s, respectively, and increased COH by 0.340. Statistically, pigments concentration at 0.1% showed no effect on both ADH and COH, whereas 0.5% had no effect on COH. Flour gel formed after gelatinization is a result of starch retrogradation, in 24 h mainly being attributed to amylose re-association and aggregation (Wang & Wang, 2001). As discussed in Section 3.1, amaranthin and its isomer isoamaranthin in the *Amaranthus* pigments may adversely affect molecular environment for amylose re-association, interacting with starch amylose chains, hinder amylose aggregation via hydrogen bonding in the paste, thus resulting softer gels (Gunaratne & Corke, 2007).

Pearson correlation analysis showed that several gel textural parameters correlated well with pasting parameters. For example, CPV was highly positively correlated with HD ($r = 0.997$), and BD with ADH ($r = 0.997$); whereas COH was highly negatively correlated with SB ($r = -0.898$). This is in accordance with previous studies (Wu & Corke, 1999).

3.3. Effect of Amaranthus betacyanin pigments on the colour of flour gels, dried, and cooked noodles

Addition of *Amaranthus* betacyanin pigments at various levels significantly ($p < 0.05$) changed the colour characteristics of wheat flour gels, and both dried and cooked noodles, imparting to all products shades of pink-redness to various extents (Table 2). The shades of gels, dried noodles, and cooked noodles for the control were generally in light grey with the low colour purity (C) compared with pigment-treated samples.

Addition of pigments significantly decreased lightness (L) of all products after cooking at day 1 and day 7 in a dose-dependent manner with the greatest reduction at 2.0% pigment addition. For example, at day 1, 2.0% level reduced lightness (L) by 32.8, 40.9, and 32.0 for gels, dried, and cooked noodles, respectively. High negative correlation existed between *Amaranthus* pigment concentration and lightness (L) of flour gels, dried, and cooked noodles ($p < 0.05$). For example, correlation coefficients (r) between pigment concentration and L of cooked noodles at day 1 and day 7 were −0.914 and −0.919, respectively. Addition of pigments considerably increased Chroma (C) of gels, dried, and cooked noodles, but not in a dose-dependent manner. For example, at day 1, 0.5% level most increased C of flour gels by 18.3, whereas 2.0% level most increased C of cooked noodles by 21.2, compared with control (1.8). Addition of pigments considerably imparted pink-redness to gels, dried, and cooked noodles as reflected in hue angle (H). For example, at day 1, addition of pigment at 2.0% decreased H of

Table 2
Influence of *Amaranthus* betacyanin pigments on the colour of flour gels, dried noodles and cooked noodles at day 1 and day 7[a].

Samples	Pigment concentrations (%) (w/w)	Day 1			Day 7		
		L	*C*	*H*	*L*	*C*	*H*
Flour gels	0.0	64.3a	1.8a	142.9a	64.7a	1.5a	144.5a
	0.1	51.9b	11.6b	34.8b	55.0b	11.3b	73.6b
	0.5	38.0c	20.1c	10.2c	40.4c	20.8c	21.0c
	1.0	33.6d	19.0d	8.2d	35.6d	20.9c	11.4d
	2.0	31.5e	13.9e	9.4e	32.8e	12.5d	11.7d
Dried noodles	0.0	79.6a	12.6a	84.1a	78.9a	13.1a	83.8a
	0.1	65.7b	27.2b	354.9b	65.8b	28.5b	355.5b
	0.5	55.9c	31.2c	351.3c	55.5c	32.9c	351.8c
	1.0	44.9d	36.6d	354.8b	46.8d	36.6d	354.4b
	2.0	38.7e	33.6e	357.4d	35.7e	32.2c	357.4d
Cooked noodles	0.0	73.9a	6.3a	99.1a	72.8a	6.2a	99.4a
	0.1	65.2b	10.3b	22.2b	65.7b	11.8b	23.7b
	0.5	54.0c	20.8c	8.5c	53.5c	20.2c	11.6c
	1.0	49.4d	23.5d	11.5d	50.2d	27.5d	11.6c
	2.0	41.9e	27.5e	9.5e	42.1e	30.0e	11.3c

[a] Values in the same column with the same letters do not differ significantly ($p < 0.05$); *L* = lightness; *C* = Chroma; *H* = hue angle.

cooked noodles from 99.1 (control) to 9.5 which is very "red". Generally, pigment addition levels at 0.5%, 1.0%, and 2.0% achieved more or less similar *H*. This indicated that efficient adjustment in pigment addition level could be done without compromising the colour shade or colour purity.

Cooking either increased or decreased lightness (*L*), depending on the pigment concentrations. Storage treatment didn't alter this trend. Take lightness changes at day 1 for example, cooking decreased *L* of control by 5.7. As for the noodles treated at lower pigment concentration (0.1% and 0.5%), cooking decreased their lightness, however, noodles with higher pigment concentration (1.0% and 2.0%) had the opposite trend. Cooking treatment generally decreased *C* and altered *H* with the greatest reduction at 0.1% pigment addition (16.9 for *C*, and 27.3 for *H*), whereas *C* and *H* were altered the least at 2.0% pigment addition (6.1 for *C*, and 12.1 for *H*). This indicated that increasing pigment concentration to certain degree may be used as an effective way to protect colour loss during noodle cooking.

Colour stability during storage could be reflected from the changes in colour parameters between day 1 and day 7. Dried noodles treated with *Amaranthus* betacyanin pigments at lower concentration showed much better colour stability compared with the flour gels which had much higher moisture content. The former had average moisture of 8.31% and the latter 90%. For example, with 0.5% betacyanin pigments, the change in *H* for flour gel from day 1 to day 7 was 10.8 whereas that for dried noodles was only 0.5. Higher pigment concentration increased colour stability for the flour gels. For example, the change in *H* for flour gel at 0.1% pigment concentration was 38.8, whereas that of 2.0% was only 2.3. This is generally consistent with previous studies (Zhu et al., 2008). *Amaranthus* betacyanin pigment used in wheat flour gels at 4 °C showed great stability (Zhu et al., 2008). In this study, the storage temperature was much higher (23–26 °C) and the colour stability was lower compared that at 4 °C reported in that study (Zhu et al., 2008), indicating that lower temperature could favour the colour retention in wheat gel system during storage.

3.4. Effect of Amaranthus betacyanin pigments on the microstructure of dried noodles

The surface and cross-section of dried raw noodles were examined using Scanning Electron Microscopy at magnifications of 1000 and 1500 (Fig. 2). Cross-sectional surfaces of dried noodles were heavily covered by non-uniform amorphous gluten protein. The starch granules (both the large size type A and small size type B) were imbedded deeply in the gluten network (Fig. 2A). Morphology of dried noodle surface (Fig. 2B) differed greatly from their cross-section. The starch granules were more clearly visible compared with their cross-sectional counterpart. The cracks between starch granule (type A) and gluten network were obvious, which might be attributed to the drying processing. No apparent distinction

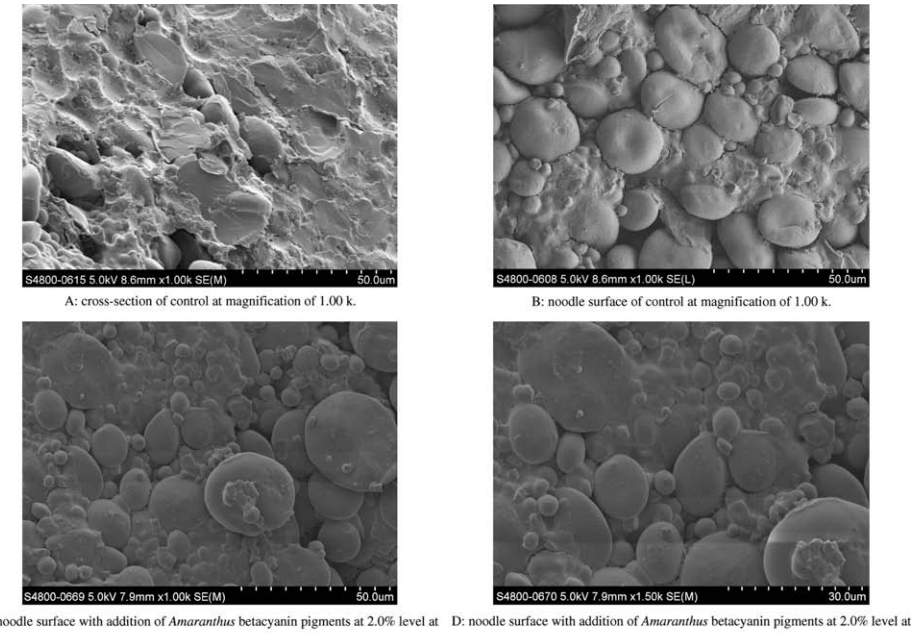

Fig. 2. Scanning electron micrographs of surface and cross-section of dried raw noodles at day 7. (A) cross-section of control (×1.0 k); (B) noodle surface of control (×1.0 k); (C) noodle surface with addition of *Amaranthus* betacyanin pigments at 2.0% level (×1.0 k); (D) noodle surface with addition of *Amaranthus* betacyanin pigments at 2.0% level (×1.5 k).

Table 3
Influence of *Amaranthus* betacyanin pigments on the textural and cooking properties of cooked noodles at day 1 and day 7[a].

Pigment concentrations (%) (w/w)	Day 1				Day 7			
	Tensile (g)	Firmness (g)	Cooking yield	Cooking loss (%)	Tensile (g)	Firmness (g)	Cooking yield	Cooking loss (%)
0.0	11.4ab	3061.5a	2.98a	0.39a	12.3a	2848.0a	2.95ab	0.38ab
0.1	12.3a	2984.3ab	2.91a	0.42a	11.0ab	2835.8a	2.92bc	0.31a
0.5	11.9a	2946.6ab	2.96a	0.33a	11.8ab	2803.3a	2.89bc	0.46bc
1.0	10.4b	2835.4bc	2.84a	0.46a	11.2ab	2784.2a	3.01a	0.50c
2.0	10.3b	2740.2c	2.71b	0.63b	10.1b	2547.1b	2.79c	0.54c

[a] Values in the same column with the same letters do not differ significantly ($p < 0.05$).

was observed on the micro-morphology of cross-section between control and samples treated with pigments. However, the surface of noodle with betacyanin pigment addition at 2.0% (Fig. 2C and D) was more coherent and smoother between gluten network and starch granules than the control (Fig. 2B), indicating that betacyanin pigment presence could improve the surface connectivity between starch granules and gluten for dried raw noodles, which may further influence the surface properties of cooked noodles (Ross, 2006).

3.5. Effect of Amaranthus betacyanin pigments on the textural and cooking properties of cooked noodles

Addition of *Amaranthus* betacyanin pigments influenced the textural and cooking properties of cooked noodles to various extents (Table 3). Addition of betacyanin pigments at low concentration had no significant effect on the tensile force ($p < 0.05$). For example, at day 7, addition levels at 0.1%, 0.5%, and 1.0% did not significantly change the tensile force compared with control. However, addition of 2.0% considerably decreased the tensile force by 2.2 g, compared with control (12.3 g). Similar trend was also found on day 1 test.

Compression tests were employed to assess the deformation properties of cooked noodles. The data in Table 3 indicated that only at higher concentrations did the addition of betacyanin pigments decrease the firmness of the cooked noodles. Similar trends were observed both at day 1 and day 7. For day 1, addition at 1.0% and 2.0% significantly reduced the firmness by 226.1 and 321.3 g, respectively, compared with control (3061.5 g), whereas lower addition levels had no effect ($p < 0.05$). For day 7, only addition level at 2.0% significantly reduced the firmness (by 300.9 g), in comparison with control (2848.0 g), whereas lower addition levels had little effect. It was reported that pH reduction in wheat flour dough could result in dough with less shear thinning and subsequently tensile strength and cutting force of extruded noodles, as well as increased gelatinization degree and cooking loss, whereas pH increase could increase both the tensile strength and cutting force (Shiau & Yeh, 2001). In this study, the decreases in both firmness and tensile strength in the presence of *Amaranthus* pigments may be attributed to the pH reduction effect caused by *Amaranthus* betacyanin pigments as discussed in pasting session. The trends in the changes of both firmness and tensile strength as affected by the betacyanin pigments were similar. This was generally in agreement with previous studies that some instrumental descriptors for noodle texture as well as wheat flour properties could be positively correlated (Shiau & Yeh, 2001; Lee et al., 2008).

After storage at room temperature for a week, the tensile force of noodles with or without pigment addition did not significantly vary, whereas the firmness of the noodles of both control and those with pigments was reduced to various extents. For example, during a week of storage the firmness of the control decreased by 213.5 g, whereas that of cooked noodles at 2.0% pigments addition level decreased by 203.1 g. This may be due to the endogenous amylase enzyme in the wheat flour which could soften the texture of noodles during storage (Cato, Halmos, & Small, 2006).

Noodles with high quality should require a minimum loss of solids into the water to maintain their integrity during cooking. And water absorption capacity of noodles could be reflected in their cooking yield. At day 1, addition of *Amaranthus* betacyanin pigments at lower levels (0.1% and 0.5%) did not affect both cooking yield and cooking loss significantly ($p < 0.05$). However, pigment addition at 2.0% increased cooking loss and decreased cooking yield significantly ($p < 0.05$), compared with control (0.39%). This indicated that addition level of pigment could be adjusted without compromising cooking properties of the noodles (e.g. cooking loss). At day 7, similar trends were observed on both the cooking loss and yield that pigment addition at 2.0% significantly increased the former and decreased the latter, indicating that noodle cooking quality was stable during one week storage at room temperature.

Pasting and textural properties of wheat flour correlated well with some parameters of noodle textural and cooking properties. The concentration of *Amaranthus* betacyanin pigments significantly and negatively correlated with noodle's firmness at both day 1 ($r = -0.970$) and day 7 ($r = -0.954$), whereas it highly and positively correlated with cooking loss at both day 1 ($r = 0.869$) and day 7 ($r = 0.871$). CPV and SB of wheat flour positively correlated with firmness of cooked noodle at day 1 ($r = 0.963$ and 0.968), and also at day 7 to some extent ($r > 0.8$). This was partially in agreement with previous studies on sweetpotato starch noodles (Collado & Corke, 1997). The flour gel textural properties also showed some high correlation with noodle quality. For example, hardness (HD) of the gels positively and highly correlated with cooked noodles' firmness at day 1 and day 7 ($r = 0.980$ and 0.819), whereas cohesiveness (COH) negatively and significantly correlated with cooked noodles firmness at day 1 and day 7 ($r = -0.951$ and -0.968). This was partially consistent with previous studies on rice noodles which suggested that some physicochemical properties of rice flour could be high correlated with quality of cooked rice noodles (Bhattacharya, Zee, & Corke, 1999). In this study, correlation analysis indicated that gels from RVA test or parameters from pasting analysis, which could be easily and accurately obtained, could be employed as alternative methods to predict the quality of wheat noodles in the presence of *Amaranthus* betacyanin pigments.

4. Conclusions

Addition of *Amaranthus* betacyanin pigments significantly decreased the pasting viscosities of wheat flour in a dose-dependent manner. Addition of pigment at 2.0% decreased the peak time. Addition of *Amaranthus* pigments decreased the hardness and adhesiveness of the gels from the RVA test and increased their cohesiveness. *Amaranthus* pigments imparted to Asian salted noodles and flour gels a colour shade of pink or red, with great colour stability during one week storage at room temperature. Addition of

Amaranthus pigments had no observable influence on the microstructure of cross-section of dried raw noodles, whereas the high addition level (2.0%) made the noodle surface smoother. Addition of *Amaranthus* pigments at low levels (0.1% and 0.5%) generally had little effect on the cooking and textural properties of cooked noodles. But high addition level (2.0%) significantly decreased the tensile strength and firmness, as well as the cooking yield, and increased the cooking loss of cooked noodles.

Amaranth grains have been under intensive development in China during the last two decades. This is the first report about *Amaranthus* betacyanin pigments applied in Asian noodles. This laboratory study may provide a basis for food technologists to develop novel coloured foods incorporating with functional natural colorants with good antioxidant capacity.

Acknowledgement

This work was supported by The University of Hong Kong Seed Funding for Basic Research (200811159062) and Hong Kong RGC-GRF Grant (760308).

References

Allegra, M., Tesoriere, L., & Livrea, M. A. (2007). Betanin inhibits the myeloperoxidase/nitrite-induced oxidation of human low-density lipoproteins. *Free Radical Research, 41*, 335–341.

Auvray, M., & Spence, C. (2008). The multisensory perception of flavor. *Consciousness and Cognition, 17*, 1016–1031.

Bao, J., & Corke, H. (2002). Pasting properties of γ-irradiated rice starches as affected by pH. *Journal of Agricultural and Food Chemistry, 50*, 336–341.

Bhattacharya, M., Zee, S. Y., & Corke, H. (1999). Physicochemical properties related to quality of rice noodles. *Cereal Chemistry, 76*, 861–867.

Cai, Y., & Corke, H. (1999). *Amaranthus* betacyanin pigments applied in model food systems. *Journal of Food Science, 64*, 869–873.

Cai, Y. Z., Sun, M., & Corke, H. (2001). Identification and distribution of simple and acylated betacyanin pigments in the Amaranthaceae. *Journal of Agricultural and Food Chemistry, 49*, 1971–1978.

Cai, Y. Z., Sun, M., & Corke, H. (2003). Antioxidant activity of betalains from plants in the Amaranthaceae. *Journal of Agricultural and Food Chemistry, 51*, 2288–2294.

Cai, Y. Z., Sun, M., & Corke, H. (2005). Characterization and application of betalain pigments from plants of the Amaranthaceae. *Trends in Food Science and Technology, 16*, 370–376.

Cato, L., Halmos, A. L., & Small, D. M. (2006). Impact of alpha-amylases on quality characteristics of Asian white salted noodles made from Australian white wheat flour. *Cereal Chemistry, 83*, 491–497.

Clydesdale, F. M. (1993). Color as a factor in food choice. *Critical Reviews in Food Science and Nutrition, 33*, 83–101.

Collado, L. S., & Corke, H. (1997). Properties of starch noodles as affected by sweetpotato genotype. *Cereal Chemistry, 74*, 182–187.

Corke, H., & Bhattacharya, M. (1999). Wheat products: 1. Noodles. In C. Y. W. Ang, K. Liu, & Y. W. Huang (Eds.), *Asian Foods: Science and Technology* (pp. 43–65). Boca Raton: CRC.

Eliasson, A. C. (1994). Interactions between starch and lipids studied by DSC. *Thermochimica Acta, 246*, 343–356.

Galvano, F., La Fauci, L., Lazzarino, G., Fogliano, V., Ritieni, A., Ciappellano, S., et al. (2004). Cyanidins: Metabolism and biological properties. *Journal of Nutritional Biochemistry, 15*, 2–11.

Gunaratne, A., & Corke, H. (2007). Influence of prior acid treatment on acetylation of wheat, potato and maize starches. *Food Chemistry, 105*, 917–925.

Gunaratne, A., Ranaweera, S., & Corke, H. (2007). Thermal, pasting, and gelling properties of wheat and potato starches in the presence of sucrose, glucose, glycerol, and hydroxypropyl beta-cyclodextrin. *Carbohydrate Polymers, 70*, 112–122.

Hayes, W. A., Smith, F. G., & Morris, A. E. J. (1998). The production and quality of tomato concentrates. *Critical Reviews in Food Science and Nutrition, 38*, 537–564.

Herbach, K. M., Stintzing, F. C., & Carle, R. (2006). Betalain stability and degradation – structural and chromatic aspects. *Journal of Food Science, 71*, 41–50.

Kumar, J. K., & Sinha, A. K. (2004). Resurgence of natural colorants: A holistic view. *Natural Product Research, 18*, 59–84.

Lee, S., Bae, I. Y., Jung, J. H., Jang, K. I., Kim, Y. W., & Lee, H. G. (2008). Physicochemical, textural and noodle-making properties of wheat dough containing alginate. *Journal of Texture Studies, 39*, 393–404.

Lin, J. Y., Li, C. Y., & Lin, B. F. (2008). *Amaranthus spinosus* L. inhibits spontaneous and dexamethasone-induced apoptosis in murine primary splenocytes. *Journal of Food and Drug Analysis, 16*, 52–61.

Rodriguezsosa, E. J., Parsiros, O., & Gonzalez, M. Z. (1981). Effect of pH on pasting properties of Habanero (*Dioscorea rotundata*) yam starch. *Journal of Agriculture of the University of Puerto Rico, 65*, 154–159.

Rojas, J. A., Rosell, C. M., & de Barber, C. B. (1999). Pasting properties of different wheat flour–hydrocolloid systems. *Food Hydrocolloids, 13*, 27–33.

Ross, A. (2006). Instrumental measurement of physical properties of cooked Asian wheat flour noodles. *Cereal Chemistry, 83*, 42–51.

Shiau, S. Y., & Yeh, A. I. (2001). Effects of alkali and acid on dough rheological properties and characteristics of extruded noodles. *Journal of Cereal Science, 33*, 27–37.

Stintzing, F. C., & Carle, R. (2004). Functional properties of anthocyanins and betalains in plants, food, and in human nutrition. *Trends in Food Science and Technology, 15*, 19–38.

Sui, Z. Q., Lucas, P. W., & Corke, H. (2006). Optimal cooking time of noodles related to their notch sensitivity. *Journal of Texture Studies, 37*, 428–441.

Tesoriere, L., Butera, D., Pintaudi, A. M., Allegra, M., & Livrea, M. A. (2004). Supplementation with cactus pear (*Opuntia ficus–indica*) fruit decreases oxidative stress in healthy humans: A comparative study with vitamin C. *American Journal of Clinical Nutrition, 80*, 391–395.

Wang, L. F., & Wang, Y. J. (2001). Structures and physicochemical properties of acid-thinned corn, potato and rice starches. *Starch-Stärke, 53*, 570–576.

Wu, H. X., & Corke, H. (1999). Genetic diversity in physical properties of starch from a world collection of *Amaranthus*. *Cereal Chemistry, 76*, 877–883.

Wu, J. P., & Corke, H. (2005). Quality of dried white salted noodles affected by microbial transglutaminase. *Journal of the Science of Food and Agriculture, 85*, 2587–2594.

Zhu, F., Cai, Y. Z., Sun, M., & Corke, H. (2008). Influence of *Amaranthus* betacyanin pigments on the physical properties and color of wheat flours. *Journal of Agricultural and Food Chemistry, 56*, 8212–8217.

Food Chemistry 118 (2010) 670–674

Contents lists available at ScienceDirect

Food Chemistry

journal homepage: www.elsevier.com/locate/foodchem

Triterpenic acids in table olives

Concepción Romero, Aranzazu García, Eduardo Medina, Mª Victoria Ruíz-Méndez, Antonio de Castro, Manuel Brenes *

Instituto de la Grasa (CSIC), Avda. Padre García Tejero 4, 41012-Seville, Spain

ARTICLE INFO

Article history:
Received 12 March 2009
Received in revised form 6 May 2009
Accepted 13 May 2009

Keywords:
Table olives
Maslinic acid
Oleanolic acid
Triterpenic acid, variety

ABSTRACT

An experimental investigation was carried out for the first time on the triterpenic acids in table olives. Maslinic acid was found in a higher concentration than oleanolic acid in the flesh of 17, unprocessed olive varieties, with the Picual and the Manzanilla varieties showing the highest and almost the lowest contents, respectively. The level of triterpenic acids in several types of commercial black and green olives ranged from 460 to 1470 mg/kg fruit, which represents a much higher value than reported for virgin olive oils. In fact, the NaOH treatment employed to debitter black and green olives reduced the concentrations of these substances in the flesh because of their solubilisation into alkaline solutions. Thus, natural black olives, which are not treated with NaOH, showed a higher concentration than 2000 mg/kg in the olive flesh. These results will contribute to the reevaluation of table olives from a nutritional and functional point of view because of the promising bioactivity properties attributed to olive triterpenic acids.

Published by Elsevier Ltd.

1. Introduction

Triterpenic acids are widespread in plants in the form of free acids or aglycones for triterpenoid saponins. Their extracts have been used for centuries in folk medicine as anti-inflammatory, anti-diabetes and hepatoprotective agents (Liu, 1995) and they have recently attracted interest in the scientific community because of their anti-carcinogenic activity (He & Liu, 2007; Struch, Jaeger, Schempp, Scheffler, & Martin, 2008) which makes them very attractive for use in cosmetics and healthcare products as functional compounds.

Among the free triterpenic acids, oleanolic, betulinic, ursolic and maslinic are some of the most abundant in the plant kingdom. Olive fruits and leaves are especially rich in oleanolic and maslinic acids (Vázquez & Janer, 1969), and small amounts of ursolic and betulinic have also been occasionally described in olive products (Bianchi & Vlahov, 1994). Both oleanolic and maslinic acids are concentrated on the surface of olive leaves to form a physical barrier that prevents microbes from penetrating into the leaf (Kubo, Matsumoto, & Takase, 1985). They are also present in high concentrations in the epicarp of the fruit forming part of the waxes that cover them; and oleanolic acid has even been found in the endocarp, wood shell and seeds of olives (Bianchi & Vlahov, 1994).

The presence of triterpenic acids in olive oil is gaining interest because of their anti-tumour activities (Rodríguez-Rodríguez, Herrera, Álvarez de Sotomayor, & Ruíz-Gutiérrez, 2007). However, the concentration of these compounds in oils depends on the oil quality (Pérez-Camino & Cert, 1999): extra virgin olive oils with low acidity did not reach 200 mg/kg, virgin olive oils with acidity higher than 1% exceeded 300 mg/kg, and crude pomace olive oils had up to 10,000 mg/kg, although the latter oils have to be refined before consumption. In fact, an enrichment in triterpenic acids occurs in the crude pomace oil during the storage of the pomace paste (alpeorujo, García, Brenes, Dobarganes, Romero, & Ruíz-Méndez, 2008) but a significant loss in these substances is produced during the refining process of the oil, particularly when a neutralisation step is used (chemical refining, Pérez-Camino & Cert, 1999).

In the case of table olives, very few data on these substances are available. Earlier, Gaviña and Viguera (1964) detected oleanolic and maslinic acids in the sodium hydroxide solutions (lye) generated during the processing of Spanish-style green olives and this was confirmed later by other researchers (Bianchi, 2003; Vázquez & Janer, 1969), but, to our knowledge, no more data have been published until now. Because of the recent interest surrounding the triterpenic acids of olives, a deeper understanding of their contents in commercial table olives, their changes during olive processing and their contents in table olive varieties is required. At the same time, the olive triterpenic acids, oleanolic and maslinic, have been attributed with anti-oxidant (Tsai & Yin, 2008), anti-hyperglycemic (Liu, Hongbin, Weigang, Dongyan, & Luyong, 2007; Sato et al., 2007), anti-microbial (Horiuchi et al., 2007) and anti-cancer activity (Juan, Planas, Ruíz-Gutiérrez, Daniel, & Wenzel, 2008; Reyes-Zurita, Rufino-Palomares, Lupiáñez, & Cascante, 2009) They have also been proposed to feed rainbow trout (Fernández-Navarro, de la Higuera, Lupiáñez, Peragón, & Amores, 2008) and to enrich

* Corresponding author. Tel.: +34 954690850; fax: +34 954691262.
E-mail address: brenes@cica.es (M. Brenes).

0308-8146/$ - see front matter Published by Elsevier Ltd.
doi:10.1016/j.foodchem.2009.05.037

vegetable oils as new functional compounds (Guinda, Albi, Pérez-Camino, & Lanzón, 2004).

Therefore, the aim of this research was to study the triterpenic acid contents of table olives as well as the wastewaters generated during their processing as a potential source of these high-value substances.

2. Materials and methods

2.1. Samples

Olive fruits of Ascolana, Domat, Aloreña, Arbequina, Morona, Conservolea, Gordal, Picual, Hojiblanca, Leccino, Koroneiki, Verdial, Picholine, Cacereña, Kalamata, Galega and Manzanilla varieties were hand-harvested with a green–yellow colour on the surface from two different orchards located in the provinces of Seville and Cordoba (Spain) during September–October.

Commercial table olives were purchased in Spanish and Greek markets. Three samples of three different commercial brands were obtained for each table olive preparation.

2.2. Processing Spanish-style green olives

Olive fruits of Manzanilla, Hojiblanca and Gordal varieties with a green–yellow colour on the surface were put into PVC vessels. Five kilograms of fruits were covered with 4 l of 2% NaOH and maintained in the alkaline solution until the alkali penetrated 2/3 the way to the pit of the olives. Subsequently, olives were washed with tap water for 16 h and covered with brine (11% NaCl). All experiments were run in duplicate.

2.3. Processing natural black olives

Olive fruits of the Manzanilla variety with a black colour on the surface were put into PVC vessels. Five kilograms of fruits were covered with an acidified brine (8% NaCl, 0.8% acetic acid) and maintained under anaerobic conditions by covering the surface of the brine with a floating cap. Experiments were run in duplicate.

2.4. Processing black olives

Olive fruits of Manzanilla and Hojiblanca varieties with a green–yellow colour on the surface were preserved as commented above for natural black olives for 6 months. Subsequently, fruits were treated in cylindrical containers over two consecutive days with NaOH solutions (lye) of 1.5% and 1.2%, which were permitted to penetrate 1–2 mm into the flesh and to the pit, respectively. After each lye treatment, tap water was added every day to complete a 24 h cycle. On the third day a new washing cycle of 24 h was used. Subsequently, fruits were suspended in a ferrous gluconate solution (0.1%) for another 24 h. Air was continuously bubbled through the mixture of fruits and liquid. Experiments were run in duplicate.

2.5. Extraction of triterpenic acids from liquids

An amount of 0.8 ml of sample (lyes, washing solutions and brines) was mixed with 2 ml of ethyl acetate in a 10 ml centrifuge tube. The mixture was vortexed for 1 min, centrifuged at 9500 rpm for 5 min at 20 °C, and the organic solvent was separated from the water phase. This step was repeated six times. Subsequently, the pooled organic ethyl acetate extract was vacuum evaporated and the residue dissolved in 0.8 ml of methanol, which was filtered through 0.2 μm pore size and an aliquot (20 μl) was injected into the liquid chromatograph. In order to check the exhaustiveness of the method, the pH of lyes and washing solutions was dropped below 3. Subsequently, triterpenic acids were extracted from the supernatant with ethyl acetate and they were not detected in these solutions. By contrast, the precipitate formed during pH correction was dissolved in methanol and it was analysed by HPLC. The amount of triterpenic acids in the precipitate was the same as found when lyes and washing solutions without any pH modification were analysed by using ethyl acetate as extracting solvent.

2.6. Extraction of triterpenic acids from olive flesh

Twenty grams of destoned and cut olive fruits were triturated, and desiccated at 105 °C until weight stabilisation. Subsequently, 1 g of dry olives were mixed in a 10 ml centrifuge tube with 4 ml of methanol/ethanol (1:1, v/v) and vortexed for 1 min, centrifuged at 9500 rpm for 5 min at 20 °C, and the solvent was separated from the solid phase. This step was repeated six times, and the pooled solvent extract was vacuum evaporated. The residue was dissolved in 2 ml of methanol, which was filtered through 0.2 μm pore size and an aliquot (20 μl) was injected into the liquid chromatograph.

2.7. HPLC analysis of triterpenic acids: UV and MS detection

The chromatography system consisted of a Waters 717 plus auto sampler, a Waters 600E pump, and a Waters 996 diode array detector (Waters Inc., Mildford, MA, USA). A Spherisorb ODS-2 (5 μm, 25 × 46 mm i.d.; Waters Inc.) column was used. The temperature of the column was kept constant at 35 °C by using a Waters column heater. The mobile phase (methanol/acidified water with phosphoric acid at pH 3.0, 92:8, v/v) was delivered to the column at a flow rate of 0.8 ml/min and the eluate was monitored at 210 nm. Triterpenic acids (oleanolic and maslinic acids) were quantified using oleanolic acid (Sigma, St. Louis, MO, USA) as external standard. A similar response factor was assumed for both triterpenic acids on the basis of their similar UV spectra. The calibration equation, concentration (mg/l) = 0.0001 × peak area, was calculated in a range of 0–3000 mg/l, and the determination coefficient was 0.996.

An Alliance Waters chromatography system connected to UV and MS detectors was used to identify the compounds. The chromatography method was similar to that explained above and the mass spectra were acquired using a quadrupole mass analyser (ZMD4; Waters Inc.), equipped with a electrospray ionisation (ESI) probe and working in the negative mode. Cone voltage fragmentation was at 10 V, capillary voltage was 3 kV, desolvation temperature was 200 °C, source temperature was 120 °C, and extractor voltage was 12 V. Standards linolenic, linoleic and oleanolic acids were used to identify peaks 2–4, respectively.

2.8. Statistical analysis

Statistica software version 6.0 was used for data processing (Statistica for Windows, Tulsa, OK, USA). Comparison between mean variables was made by the Duncan's multiple range tests and the differences considered significant when $p < 0.05$.

3. Results and discussion

Despite the recent relevance of olive triterpenic acids, there is no information on the amount of these substances in whole olive fruits. Some reports have indicated that they are concentrated in the epicarp of the fruits and contribute to more than 60% of the total waxes (Bianchi, 2003), with oleanolic and maslinic found in similar concentrations. In contrast, the amount of these substances in the mesocarp of olives is low and maslinic acid is the main com-

ponent. Nevertheless, the triterpenic acid contents in whole olive fruits have never been quantified, particularly in those intended for table olives.

In this study, oleanolic and maslinic acids were extracted from the olive fruits, which were previously dried to avoid water interference during the analysis, with a mixture of methanol/ethanol (1:1), a similar method to that employed for "alpeorujo" olive oil (García et al., 2008). The chromatographic system used was also the same developed to analyse triterpenic acids in "alpeorujo olive oil" and a similar chromatographic profile was obtained. A good separation of maslinic and oleanolic acid was achieved (Fig. 1), and the presence of peaks corresponding to linoleic and linolenic acids along with the absence of other triterpenic acids were confirmed by HPLC-MS. Compounds corresponding to these four peaks had molecular masses of 472, 278, 280 and 456 uma. Peak 1 had a molecular mass similar to that of maslinic acid and its fragmentation pattern was the same as that of oleanolic acid (peak 4). Besides, UV spectra of peaks 1 and 4 were similar. Based on all these results and literature data, peak 1 was assigned to maslinic acid.

The raw fruits of the varieties studied showed important differences in their triterpenic acid contents (Fig. 2). The sum of maslinic and oleanolic acids ranged from 1500 to 3000 mg/kg olive flesh, with the concentration of maslinic being higher than that of oleanolic acid for all the studied varieties. Surprisingly, olives of the Manzanilla variety, which is the main variety processed for table olives, practically had the lowest content in triterpenic acids, lower than other important table olive varieties such as Hojiblanca, Kalamata, Gordal or Conservolea. Indeed, the Manzanilla olive variety is rich in phenolic compounds (Romero et al., 2004) and triterpenic alcohols (López-López, Montaño, Ruíz-Méndez, & Garrido-Fernández, 2008) but this is not the case for maslinic and oleanolic acids. In contrast, the Picual variety, which is seldom used for table olives but it is the most important variety for olive oil worldwide, showed the highest content in maslinic and oleanolic acids.

Concerning the evolution of triterpenic acids during olive processing, Figs. 3 and 4 reflect the concentration of these substances in the different solutions generated during the two main table olive preparation methods: Spanish-style green olives and black olives. Triterpenic acids were extracted from the olive solutions (lyes, washing waters and brines) with ethyl acetate without any pH correction because it is well-known that the solubility of triterpenic acids is very low in aqueous media at pH below neutrality, and it increases at alkaline pH (Jäger, Winkler, Pfüller, & Scheffler, 2007), which is in accordance with results obtained in this study.

Results revealed that the alkaline treatment gave rise to the solubilisation of maslinic and oleanolic acids into the lyes and the washing solutions. It must be said that the pH of the lyes and washing water was in most cases higher than 8. Thus, maslinic acid was found in a range of 800–1000 mg/l in the lyes of the

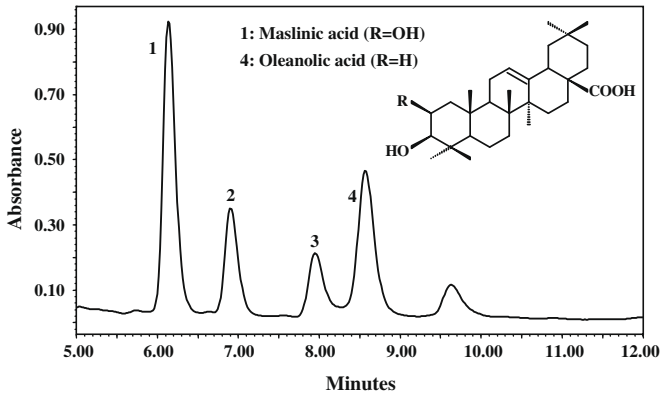

Fig. 1. HPLC chromatogram at 210 nm of the triterpenic acid extract of a Spanish-style green olives sample. Peaks: (1) maslinic acid; (2) linolenic acid; (3) linoleic acid; and (4) oleanolic acid.

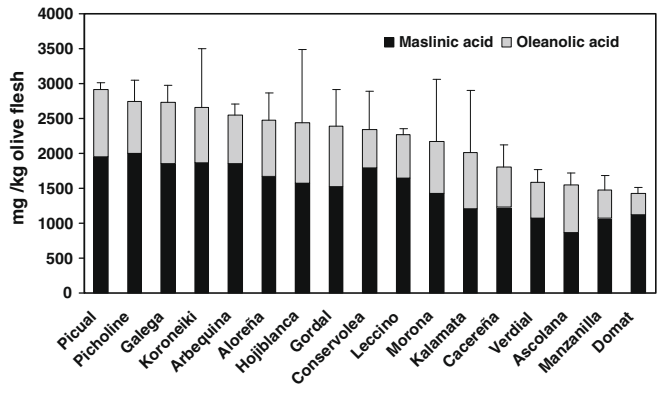

Fig. 2. Concentration in triterpenic acids of several raw olive varieties intended for table olives. Bars indicate the standard deviation of two samples obtained from different orchards.

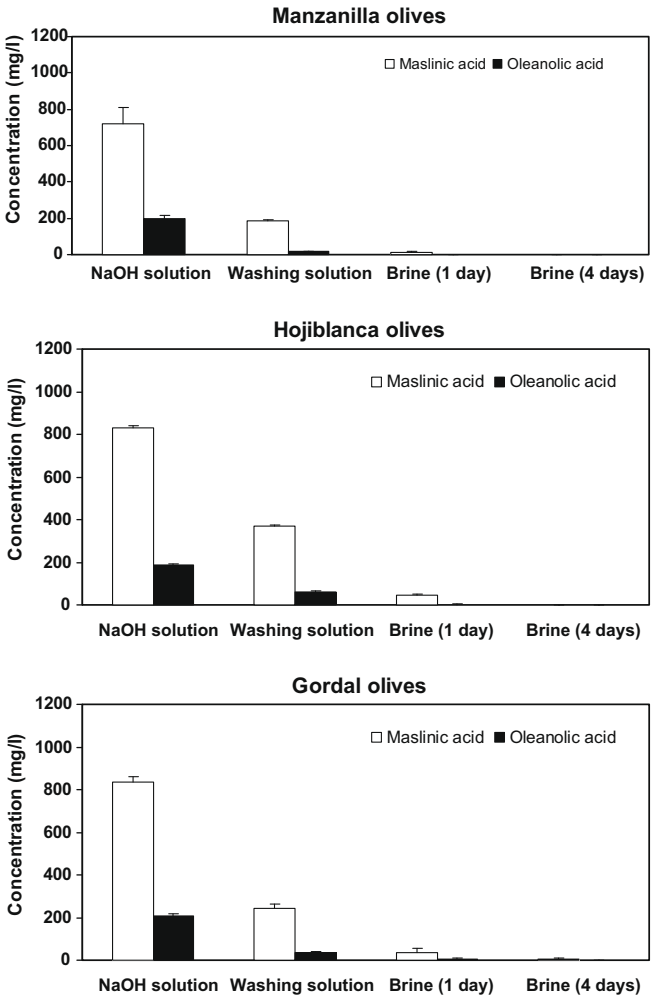

Fig. 3. Concentration in triterpenic acids of the different solutions generated during the processing of Spanish-style green olives of the Manzanilla, Hojiblanca and Gordal varieties. Bars mean the standard deviation.

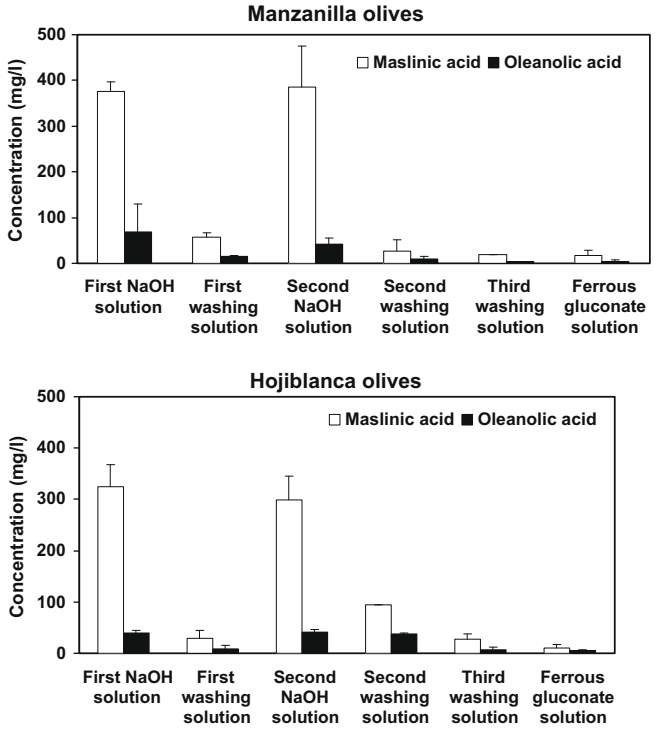

Fig. 4. Concentration in triterpenic acids of the different solutions generated during the processing of black olives of the Manzanilla and Hojiblanca varieties. Bars mean the standard deviation.

Manzanilla, Gordal and Hojiblanca varieties processed according to the Spanish-style green method. The values are comparable to those reported by Bianchi (2003) for the lyes of Italian varieties, and maslinic was always detected in a higher concentration than oleanolic. Although the concentration of triterpenic acids was lower in the washing solutions than in the lyes, the ratio maslinic/oleanolic was similar for both types of olive solutions. A low concentration of triterpenic acids was found in brines during the first days of fermentation when the pH varied from 9 to 7 and they were not detected thereafter as fermentation progressed and pH dropped below neutrality. Hence, it seems that these substances precipitated at low pH. In fact, an inhibitory activity against the lactic acid bacteria growth by a precipitate formed during the acidification of brines and washing waters has been reported (De Castro, Romero, & Brenes, 2005). Because triterpenic acids possess anti-microbial activity (Horiuchi et al., 2007) and are insoluble in aqueous media at acid pH, it can be supposed that these substances are components of this precipitate and could contribute to the anti-lactic acid bacteria activity of it. Moreover, it must be taken into account that Jäger et al. (2007) have reported that the solubility of triterpenic acids in plant extracts was higher than expected due to their interaction with large molecules or aggregates.

On the other hand, the most concentrated solutions in triterpenic acids of all the wastewaters generated during the processing of black olives were again the lyes, followed by the washing waters and the ferrous gluconate solutions, all of them having alkaline pH (Fig. 4). These streams, as well as those generated during the processing of green olives, represent a big environmental problem for the olive factories, and our results disclosed them as a good source of these new potential functional compounds, especially the lyes and the washing waters.

Likewise, maslinic and oleanolic acids were never found in the brines of natural black olives (data not shown) since they were not treated with NaOH, and were initially acidified with acetic acid up to pH 4. Therefore, this acidic medium did not allow the solubilisation of the triterpenic acids into the brines.

Olives and olive oil are recognised as healthy foods from a nutritional point of view because of their content in monounsaturated fatty acids, anti-oxidant phenolic compounds and others. Triterpenic acids could contribute to the good perception that consumer have of these products, although it is necessary to know their amounts in these foods. There are few data on the concentration of triterpenic acids in edible fruits (He & Liu, 2007; Cui et al., 2006; Frighetto, Welendorf, Nigro, Frighetto, & Siani, 2008), some on olive oil (Pérez-Camino & Cert, 1999) and none on table olives.

The data presented in Table 1 reflect the amount of maslinic and oleanolic acids in the main trade olive preparations. As could be expected from the data in Fig. 2–4, maslinic acid was always found in a higher concentration than oleanolic acid and olives non-treated with alkali (turning colour olives, natural black olives) were richer in these substances than those elaborated as green and black olives. Additionally, the pitting and stuffing steps did not significantly affect the concentration of triterpenic acids in olives as opposite to the decrease in hydrophilic phenolic compounds (Romero et al., 2004).

Regarding olive varieties, differences were also found, with the Hojiblanca variety having a higher amount of triterpenic acids than the Manzanilla. However, the concentration of triterpenic acids in commercial table olives was more affected by the alkaline treatment and further washing cycles than other variables. Thus, turning colour olives and natural black olives had an amount of triterpenic acids as high as 1000–2000 mg/kg olive flesh, much higher than reported for virgin olive oils (Pérez-Camino & Cert, 1999). Indeed, green and black olives also had a higher concentration in these substances than olive oils.

Table 1
Content in triterpenic acids (mg/kg olive flesh) of commercial table olives.

Cultivar	Presentation	Maslinic acid	Oleanolic acid
Manzanilla	Plain green olives	384.1 ± 50.0 a	202.6 ± 57.3 a
Manzanilla	Pitted green olives	497.3 ± 87.8 ac	330.0 ± 185.7 a
Manzanilla	Green olives stuffed with pimento	355.5 ± 88.4 a	191.2 ± 89.7 a
Hojiblanca	Plain green olives	904.7 ± 259.6 b	565.2 ± 107.1 bc
Gordal	Plain green olives	414.2 ± 89.3 a	294.3 ± 4.5 a
Manzanilla	Plain black olives	287.1 ± 66.6 a	178.8 ± 43.7 a
Manzanilla	Pitted black olives	290.7 ± 129.1 a	169.7 ± 121.0 a
Hojiblanca	Plain black olives	506.8 ± 232.5 ab	364.5 ± 242.3 ac
Cacereña	Plain black olives	295.1 ± 203.9 a	185.1 ± 121.1 a
Manzanilla	Plain turning colour olives	824.9 ± 179.5 bc	274.2 ± 61.4 a
Kalamata	Plain natural black olives	1318.4 ± 401.0 d	841.4 ± 162.9 b

Each value is the mean ± standard deviation of three samples. Letters within columns designate statistically significant differences ($p < 0.05$) according to the Duncańs New Multiple Range Test. Triterpenic acids were extracted from olives as described in Section 2.6.

4. Conclusions

On the basis of our results, it can be stated that table olives are a food product rich in triterpenic acids, in particular maslinic acid. However, the NaOH treatment used to debitter the fruits leads to the solubilisation of these substances into the alkaline solutions and, therefore, to significant losses in the final product. Likewise, the alkaline wastewaters have been revealed as a good source of these valuable triterpenic acids.

These results may contribute to the revaluation of table olives in view of the promising bioactivity properties attributed to olive triterpenic acids (Juan et al., 2008; Reyes-Zurita et al., 2009).

Acknowledgements

This study was supported by a grant from the Spanish-Government and the European Union FEDER Funds (Projects AGL-2006-01552 and AGL-2007-63-647). The authors thank Virginia Martín for technical assistance.

References

Bianchi, G., & Vlahov, G. (1994). Composition of lipid classes in the morphologically parts of the olive fruit, cv. Coratina (*Olea europaea* Linn.). *Fat Science Technology, 96*, 72–77.

Bianchi, G. (2003). Lipids and phenols in table olives. *European Journal of Lipids Science and Technology, 105*, 229–242.

Cui, T., Li, J., Kayahara, H., Ma, L., Wu, L., & Nakamura, K. (2006). Quantification of the polyphenols and triterpene acids in Chinese hawthorn fruit by high-performance liquid chromatography. *Journal of Agricultural and Food Chemistry, 54*, 4574–4581.

De Castro, A., Romero, C., & Brenes, M. (2005). A new polymer inhibitor of lactobacillus growth in table olives. *European Food Research and Technology, 221*, 192–196.

Fernández-Navarro, M., de la Higuera, V., Lupiáñez, M., Peragón, J. A., & Amores, J. (2008). Maslinic acid added to the diet increases growth and protein-turnover rates in the white muscle of rainbow trout (*Oncorhynchus mykiss*). *Comparative Biochemistry and Physiology Part C: Toxicology and Pharmacology, 147*, 158–167.

Frighetto, R. T. S., Welendorf, R. M., Nigro, E. N., Frighetto, N., & Siani, A. C. (2008). Isolation of ursolic acid from apple peels by high speed counter-current chromatography. *Food Chemistry, 106*, 767–771.

García, A., Brenes, M., Dobarganes, M. C., Romero, C., & Ruíz-Méndez, Mª. V. (2008). Enrichment of pomace olive oil in triterpenic acids during storage of Alpeorujo olive paste. *European Journal of Lipid Science and Technology, 110*, 1136–1141.

Gaviña, F., & Viguera, J. Mª. (1964). Transformaciones químicas de la aceituna durante el aderezo. VII. Identificación de un dihidroxitriterpénico asilado de la lejía residual. *Grasas y Aceites, 15*, 143–146.

Guinda, A., Albi, T., Pérez-Camino, M. C., & Lanzón, A. (2004). Suplementation of oils with oleanolic acid from the olive leaf (Olea europaea). *European Journal of Lipid Science and Technology, 106*, 22–26.

He, X. J., & Liu, R. H. (2007). Triterpenoids isolated from apple peels have potent antiproliferative activity and may be partially responsible for applés anticancer activity. *Journal of Agricultural and Food Chemistry, 55*, 4366–4370.

Horiuchi, K., Shiota, S., Hatano, T., Yoshida, T., Kuroda, T., & Tsuchiya, T. (2007). Antimicrobial activity of oleanolic acid from *Salvia officinalis* and related compounds on vancomycin-resistant Enterococci (VRE). *Biological and Pharmaceutical Bulletin, 30*, 1147–1149.

Jäger, S., Winkler, K., Pfüller, U., & Scheffler, A. (2007). Solubility studies of oleanolic acid and betulinic acid in aqueous solutions and plant extracts of *Viscum album* L.. *Planta Medica, 73*, 157–162.

Juan, M. E., Planas, J. M., Ruíz-Gutiérrez, V., Daniel, H., & Wenzel, U. (2008). Antiproliferative and apoptosis-inducing effects of maslinic and oleanolic acids, two pentacyclic triterpenes from olives, on HT-29 colon cancer cells. *British Journal of Nutrition, 100*, 36–43.

Kubo, I., Matsumoto, A., & Takase, I. (1985). A multichemical defense mechanism of bitter olive *Olea europaea* (Oleaceae). Is oleuropein a phytoalexin precursor? *Journal of Chemical Ecology, 11*, 251–263.

Liu, J. (1995). Pharmacology of oleanolic acid and ursolic acid. *Journal of Ethnopharmacology, 49*, 57–68.

Liu, J., Hongbin, S., Weigang, D., Dongyan, M., & Luyong, Z. (2007). Maslinic acid reduces blood glucose in KK-Ay mice. *Biological and Pharmaceutical Bulletin, 30*, 2075–2078.

López-López, A., Montaño, A., Ruíz-Méndez, M. V., & Garrido-Fernández, A. (2008). Sterols, fatty alcohols, and triterpenic alcohols in commercial table olives. *Journal of the American Oil Chemistś Society, 85*, 253–262.

Pérez-Camino, M. C., & Cert, A. (1999). Quantitative determination of hydroxy pentacyclic triterpene acids in vegetable oils. *Journal of Agricultural and Food Chemistry, 47*, 1558–1562.

Reyes-Zurita, F. J., Rufino-Palomares, E. E., Lupiáñez, J. A., & Cascante, M. (2009). Maslinic acid, a natural triterpene from *Olea europaea* L. induces apoptosis in HT29 human colon-cancer cells via the mitochondrial apoptotic pathway. *Cancer Letters, 273*, 44–54.

Rodríguez-Rodríguez, R., Herrera, Mª. D., Álvarez de Sotomayor, M., & Ruíz-Gutiérrez, V. (2007). Pomace olive oil improves endothelial function in spontaneously hypertensive rats by increasing endothelial nitric oxide synthase expressión. *American Journal of Hypertension, 20*, 728–734.

Romero, C., Brenes, M., Yousfi, K., García, P., García, A., & Garrido, A. (2004). Effect of cultivar and processing method on the contents of polyphenols in table olives. *Journal of Agricultural and Food Chemistry, 52*, 479–484.

Sato, H., Genet, C., Strehle, A., Thomas, C., Lobstein, A., Wagner, A., Mioskowski, C., Auwerx, J., & Saladin, R. (2007). Anti-hyperglycemic activity of a TGR5 agonist isolated from *Olea europaea*. *Biochemical and Biophysical Research Communications, 362*, 793–798.

Struch, C. M., Jaeger, S., Schempp, C. M., Scheffler, A., & Martin, S. F. (2008). Solubilized triterpenes from mistletoe show anti-tumor effects on skin-derived cell lines. *Planta Medica, 74*, 1130.

Tsai, S. J., & Yin, M. C. (2008). Antioxidative and anti-inflammatory protection of oleanolic acid and ursolic acid in PC12 cells. *Journal of Food Science, 73*, H174–H178.

Vázquez, A., & Janer, Mª. L. (1969). Triterpenic acids from olive tree. *Grasas y Aceites, 20*, 133–138.

Food Chemistry 118 (2010) 675–680

Contents lists available at ScienceDirect

Food Chemistry

journal homepage: www.elsevier.com/locate/foodchem

Structural characterisation and antioxidant properties of polysaccharides from the fruiting bodies of *Russula virescens*

Zhong-wei Sun [1], Li-xiang Zhang [1], Bin Zhang, Tian-gui Niu *

College of Food Science and Nutritional Engineering, China Agricultural University, Beijing 100083, PR China

ARTICLE INFO

Article history:
Received 16 January 2009
Received in revised form 17 March 2009
Accepted 14 May 2009

Keywords:
Antioxidant property
Polysaccharide
Russula virescens
Scavenging ability

ABSTRACT

Water-soluble crude polysaccharide named as RVP was obtained from the fresh fruiting bodies of *Russula virescens* by boiling-water extraction. DEAE-Sepharose CL-6B column chromatography was used for the fractionation of polysaccharide RVP. Two fractions were obtained, namely RVP-1 and RVP-2. RVP-1 and RVP-2 were composed mainly of glucose, with the estimated equivalent dextran molecular weights of 3.1×10^5 and 4.2×10^5 Da, respectively. Analysis by Periodate oxidation–Smith degradation indicated that RVP-1 was composed of 68.3% (1 →)- or ((1 → 6)-glycosidic linkages and 31.7% (1 → 3)-glycosidic linkages, and RVP-2 7.9% (1 →)- or (1 → 6)-glycosidic linkages, 9.6% (1 → 2)-glycosidic linkages, 35.7% (1 → 4)-glycosidic linkages, and 46.8% (1 → 3)-glycosidic linkages. RVP-1 exhibited equivalent inhibiting power for self-oxidation of 1,2,3-phentriol to vitamin C (Vc), a little higher scavenging activity of superoxide radical and hydroxyl radical than Vc. The reducing power of RVP-1 at 20.0 mg/ml was 0.77, and RVP-1 was a good chelating agent for ferrous ions. Overall, RVP-1 possessed good antioxidant properties and should be developed as a novel potential antioxidant.

1. Introduction

Oxidation is essential to many organisms for the production of energy fuel biological processes. However, the uncontrolled production of oxygen-derived free radicals is involved in the onset of many diseases such as cancer, rheumatoid arthritis, and atherosclerosis, as well as in degenerative processes associated with aging (Mau, Lin, & Song, 2002). Almost all organisms have natural antioxidant properties and can repair oxidative damage in their systems, but these systems are unable to prevent the damage completely. Antioxidants are substances that can delay or prevent oxidative cellular oxidisable substrates. They work in two ways: by scavenging reactive oxygen species (ROS) and by inhibiting the generation of ROS. At present, synthetic antioxidants are used for industrial processing to preserve food quality. However, the most commonly used ones have been suspected of being responsible for liver damage and carcinogenesis (Grice, 1988; Qi et al., 2005). Thus, there has been increasing interest in finding natural, effective, and safe antioxidants, since they can protect the human body from free radicals and retard the progress of many chronic diseases (Kinsella, Frankel, German, & Kanner, 1993; Nandita & Rajini, 2004). Published data indicate that some plant polysaccharides have strong antioxidant activities and can be explored as novel potential antioxidants (Hu, Xu, & Hu, 2003; Jiang, Jiang, Wang, & Hu, 2005; Ramarahnam, Osawa, Ochi, & Kawaishi, 1995). In addition, polysaccharides extracted from mushrooms, such as *Grifola frondosa* and *Auricularia auricular*, have also shown antioxidant properties as shown by their free radical scavenging abilities (Fan, Zhang, Yu, & Ma, 2007; Lee et al., 2003; Liu, Ooi, & Chang, 1997).

Russula virescens is a wild mushroom that grows on the roots of pine trees, and has long been used as a folk remedy in traditional Chinese medicine. To date, no investigation has been carried out on polysaccharides that may account for the antioxidant activities of *R. virescens*. In this study, we reported on the extraction and purification of two novel water-soluble polysaccharides of *R. virescens* using DEAE-Sepharose CL-6B column chromatography. In addition, we attempted to investigate the molecular weights, chemical compositions, structure, and antioxidant activities, of the polysaccharides isolated from the fresh fruiting bodies of *R. virescens*.

2. Materials and methods

2.1. Materials

Fresh fruiting bodies of *R. virescens* were purchased from Chengdu, Sichuan Province, China. T-series dextrans of different molecular weights were purchased from Sigma Chemical Co. (St.

* Corresponding author. Address: College of Food Science and Nutritional Engineering, China Agricultural University, P.O. Box 111, No. 17 Qinghua East Road, Beijing 100083, PR China. Tel./fax: +86 10 62737045.
E-mail address: niu2009niu@hotmail.com (T.-g. Niu).
[1] These authors contributed equally to this work.

0308-8146/$ - see front matter © 2009 Elsevier Ltd. All rights reserved.
doi:10.1016/j.foodchem.2009.05.036

Louis, MO, USA). Nitro blue tetrazolium (NBT), phenazine methosulphate (PMS), dihydronicotineamidadenine dinucleotide (NADH), thiobarbituric acid (TBA), butylated hydroxyanisol (BHA), hydrogen peroxide (H_2O_2), ferrozine, 1,2,3-phentriol, α-tocopherol, deoxyribose, L-rhamnose, D-glucose, D-arabinose, D-xylose, D-fructose, D-galactose, and D-mannose were purchased from Sigma Chemical Co. (St. Louis, MO, USA), whilst DEAE-Sepharose CL-6B was from the Pharmacia Co. (Sweden). All other reagents used were of analytical grade.

2.2. Isolation and purification of the polysaccharide

A standard procedure was followed for the isolation of the polysaccharide. The fresh fruiting bodies of *R. virescens* were dried and powdered. The powder (100 g) was defatted with 95% ethanol at room temperature for 48 h under stirring, then autoclaved in 2 l of double-distilled water at 120 °C for 3 h and later filtered. The residue was further extracted with 750 ml of water for 1 h. The combined aqueous extracts were concentrated in a rotary evaporator under reduced pressure at 50 °C and filtered. The filtrate was then precipitated by adding ethanol (four times the volume of aqueous extract) at 4 °C, followed by centrifugation at 4800 rpm for 20 min. The precipitate was dissolved in 300 ml of water and deproteinised 20 times as described by Sevag (Staub, 1965). The resulting aqueous fraction was extensively dialysed against double-distilled water for three days and precipitated again by adding fourfold volume of ethanol. After centrifugation, the precipitate was washed with anhydrous EtOH and then dissolved in water and lyophilised to yield the crude polysaccharide (RVP). Further fractionation was performed in anion-exchange chromatography. RVP (1000 mg) was dissolved in 10 ml distilled water, centrifuged, and the supernatant was then injected to a column (4.6 × 30 cm) of DEAE-Sepharose CL-6B equilibrated with distilled water. After being loaded with the sample, the column was eluted with distilled water for 1000 ml at 4 ml/6 min, followed stepwise by NaCl aqueous solution (0 and 1 M) for 400 ml, respectively, at 40 ml/h. The elution was detected by the phenol–sulphuric acid method, using glucose as standard (Dubois, Gilles, Hamilton, Rebers, & Smith, 1956). The major polysaccharide fractions were collected with a fraction collector, dialysed against tap water and distilled water for 48 h, concentrated in a rotary evaporator, and finally lyophilised in a freeze dryer (Tokyo Rikakikai Co., Ltd., Japan).

2.3. Components analysis and properties

The protein content was measured according to Bradford's method (Bradford, 1976). The chemical composition of these polysaccharides was analysed following the procedure in Zhang's investigation (Zhang et al., 2007). The acetate derivatives were analysed by gas chromatography (GC) with a HP-5 capillary column (HP6820, Hewlett–Packard). The temperature programme was increased from 120 to 300 °C at an increment of 5 °C/min using N_2 as carrier gas. The standard monosaccharides were then measured following the same procedure.

The infrared spectra of the polysaccharides were recorded with a Nicolet NEXUS-470 FT-IR (Spectrum One, Perkin Elmer Co., USA) spectrometer in the range of 4000–500 cm^{-1} using the KBr disk method.

2.4. Determination of molecular weights

The molecular weights of RVP-1 and RVP-2 were evaluated and determined by high performance liquid chromatography (HPLC) on two Water Ultrahydrogel TM Linear 7.8 × 300 mm columns and were eluted with 0.1 M of sodium nitrate solution at a flow rate of 0.9 ml/min at 45 °C. Elution was monitored by a refractive index detector. The column was calibrated with glucose (molecular weight: 180 Da) and T-series Dextran standards (molecular weight: 4600, 10,000, 21,400, 41,100, 1,33,800, 4,82,000, and 20,00,000 Da). Individual molecular weight standard solutions were freshly prepared daily by dissolving 25 mg each of the eight standards from 180 to 20,00,000 Da in 50 ml DMSO. RVP-1 and RVP-2 solutions were prepared in a similar fashion. The standard solutions were then injected in duplicate in the order of decreasing molecular weight, with the GPC software (Thermo Labsystems, Shrewsbury, MA, USA) used to perform a narrow band linear regression standard calibration curve of log molecular weight versus HPLC retention time. The sample preparations were later injected in duplicate.

2.5. Periodate oxidation–Smith degradation

Sample (50 mg) was dissolved in 25 ml of distilled water and 25 ml of 30 mM $NaIO_4$ were added. The solution was kept in the dark at 4 °C, 0.1 ml aliquots were withdrawn at 6 h intervals, diluted to 25 ml with distilled water and read in a spectrophotometer at 223 nm. The reaction was complete when absorbency did not descend, and the excess of $NaIO_4$ was decomposed with glycol (2 ml). The solution of periodate product (2 ml) was sampled to calculate the yield of formic acid by 0.005 M sodium hydroxide, and the rest was extensively dialysed against tap water and distilled water for 24 h, respectively. The content inside was concentrated and reduced with sodium borohydride (160 mg), and the mixture was left for 24 h at 25 °C, neutralised to pH 6.0 with 50% acetic acid, dialysed as described above, and concentrated to a volume (10 ml). One-third of solution described above was freeze-dried and analysed with GC. Others were added to the same volume of 1 M sulphuric acid, kept for 40 h at 25 °C, neutralised to pH 6.0 with barium carbonate, and filtered. The filtrate was dialysed as foresaid, and the content out of sack was desiccated for GC analysis; the content inside was diluted with ethanol, and after centrifugation, the supernatant and precipitate were also dried out for the GC analysis.

2.6. Assay for antioxidant activity

2.6.1. Hydroxyl radical assay

The hydroxyl radical assay was measured by the method of Ghiselli, Nardini, Baldi, and Scaccini (1998) with a minor modification. Samples were dissolved in distilled water at 0 (control), 0.1, 0.2, 0.4, 0.8, 1.6, 3.2, 6.3, 12.5, 25, or 50 mg/ml. The sample solution (0.1 ml) was mixed with 0.6 ml of reaction buffer [0.2 M phosphate buffer (pH 7.4), 2.67 mM deoxyribose, and 0.13 mM ethylenediaminetetraacetic acid (EDTA)], 0.2 ml of 0.4 mM ferrous ammonium sulphate, 0.05 ml of 2.0 mM ascorbic acid, and 0.05 ml of 20 mM H_2O_2 was then added to the reaction solution. The reaction solution was incubated for 15 min at 37 °C, and then 1 ml of 1% thiobarbituric acid and 1 ml of 2.0% trichloroacetic acid were added to the mixture. The mixture was boiled for 15 min and cooled on ice. The absorbance of the mixture was measured at 532 nm. The inhibition percentage of hydroxyl radical was calculated as: (1 − absorbance of sample/absorbance of control) × 100%.

2.6.2. Superoxide radical assay

The superoxide radical assay was measured by the method of Robak and Gryglewski (1988) with a minor modification. Samples were dissolved in distilled water at 0 (control), 0.78, 1.56, 3.125, 6.25, 10, 20, 40, 50, 80, or 100 mg/ml. A 0.1-ml aliquot of each sample solution was mixed with 1 ml of 16 mM Tris–HCl (pH 8.0) containing 557 μm NADH, 1 ml of 16 mM Tris–HCl (pH 8.0) containing 45 μm PMS, and 1 ml of 16 mM Tris–HCl (pH 8.0) containing 108 μm NBT. After 5 min of incubation at 25 °C, the absorbance was measured at 560 nm. The superoxide radical effect was calcu-

lated as: scavenging activity (%) = (1 − absorbance of sample/absorbance of control) × 100%.

2.6.3. Self-oxidation of 1,2,3-phentriol assay

The scavenging ability for self-oxidation of 1,2,3-phentriol of all different contents were investigated according to the method of Marklund and Marklund (1974) with a minor modification. Briefly, samples were dissolved in distilled water at 0 (control), 5, 10, 40, or 80 mg/ml. The sample solution (0.1 ml) was mixed with 2.8 ml of 0.05 M Tris–HCl buffer (pH 8.0) containing 1 mM EDTA and 1,2,3-phentriol (0.2 ml, 6 mM), and was shaken rapidly at room temperature. The absorbance of the mixture was measured at 325 nm per 30 s for 4 min against a blank, and a slope was calculated as the absorbance per min. The ability of different scavenging abilities for self-oxidation of 1,2,3-phentriol of all fractions was calculated as: (1 − slope of sample/slope of control) × 100%.

2.6.4. Reducing power assay

The reducing power was determined according to the method of Oyaizu (1986). The different concentrations of samples (0.1–20 mg/ml, 2.5 ml) were mixed with phosphate buffer (2.5 ml, 0.2 M, pH 6.6) and 2.5 ml of potassium ferricyanide [$K_3Fe(CN)_6$] (1%, w/v). The mixture was incubated at 50 °C for 20 min. After 2.5 ml of trichloroacetic acid (10%, w/v) were added to terminate the reaction, the mixture was centrifuged at 2000 *g* for 10 min. The upper layer of solution (5 ml) was mixed with water (5 ml) and $FeCl_3$ (1 ml, 0.1%), and the absorbance was measured at 700 nm against a blank. Ascorbic acid, BHA, and α-tocopherol were used for comparison.

2.6.5. Metal chelating assay

Chelating ability was determined according to the method of Dinis, Madeira, and Almeida (1994). The different concentrations of samples (0.1–20 mg/ml, 1 ml) were mixed with 3.7 ml of methanol and 0.1 ml of 2 mM ferrous chloride. The reaction was initiated by the addition of ferrozine (0.2 ml, 5 mM). After 10 min at room temperature, the absorbance of the mixture was determined at 562 nm against a blank. Citric acid and EDTA were used for comparison. The ferrous ion-chelating activity was given by the following equation:

$$\text{Chelating ability}\ (\%) = (1 - \text{absorbance of sample/absorbance of control}) \times 100\%.$$

3. Results and discussion

3.1. Isolation, purification and composition of fractions

The crude polysaccharide was isolated from the hot water extract of *R. virescens* by a yield of 1.94%. After being fractioned on DEAE-Sepharose CL-6B column, RVP-1 (0.46%) and RVP-2 (0.17%) were obtained from the distilled water eluent and NaCl eluent, respectively. The protein content in RVP-1 and RVP-2 were 1.77% and 1.25%, respectively.

According to GC analysis, both RVP-2 and RVP-1 were composed of xylose, mannose, glucose, galactose and fructose, with molar ratios of 6.8:13.2:136.7:7.8:1.0 and 1.2:3.2:195.6:11.6:1.0, respectively. These data revealed great differences in the polysaccharides' distribution of xylose, mannose, glucose, galactose, and fructose, strongly indicating that the polysaccharides were heterogeneous. It is worth mentioning that the polysaccharides consisted mainly of glucose.

The infrared spectroscopy (IR) spectra of samples RVP-1 and RVP-2 displayed the characteristic IR absorption of polysaccharides at 1650 and 1250 cm^{-1}. The broadly stretched intense peak at 3400 cm^{-1} was due to the hydroxyl stretching vibration. A weak C–H group stretching band at 2930 cm^{-1} could also be observed. On the other hand, the absorptions at 1424 and 1371 cm^{-1} were possibly due to non-symmetrical and symmetrical CH_3 bending, respectively. A band at 1250 cm^{-1} caused by non-symmetrical C–O–C stretching vibration could likewise be observed.

3.2. Molecular weight

HPLC was applied to elucidate the molecular weights of RVP-1 and RVP-2. The equivalent dextran molecular weights of RVP-1 and RVP-2 were around 3.1×10^5 and 4.2×10^5 Da, respectively.

3.3. Structure characterisation of RVP-1 and RVP-2

Both RVP-1 and RVP-2 showed abundance HIO_4 uptake, whilst they were oxidised. The consumption of HIO_4 (1.369 mmol) in RVP-1 was about two times than the amount of formic acid (0.683 mmol) that was produced per mol sugar residue after 72 h of periodate treatment, indicating the existence of large amounts of monosaccharide which were 1 → linked or 1 → 6 linked or more branched. In addition, it was concluded that sugar residues oxidised or linkages of (1 →)-glycosidic linkages accounted for 68.3%. The periodate-oxidised products were hydrolysed and examined by gas chromatography. The presence of glucose revealed that there were (1 → 3)-glycosidic linkages, namely linkages that cannot be oxidised. Erythritol was absent, indicating there was no (1 → 4)-glycosidic linkage in RVP-1. According to the results above, the main chain linkages could be alternately arrayed by (1 → 3)-glycosidic linkages and (1 → 6)-glycosidic linkages, or the main chain linkages could be (1 → 6)-glycosidic linkages with branch (1 → 3)-glycosidic linkages.

Results from 96 h of Periodate oxidation of RVP-2 showed that the ratio of the consumption of HIO_4 (0.611 mol/mol sugar residue)

Table 1
GC results from fractions of Smith degradation of RVP-1 and RVP-2.

Fractions	RVP-1			RVP-2			
	Glu[a]	Gly[b]	Ery[c]	Glu	Gly	Ery	Man[d]
Full acid hydrolysis	+[e]	+[f]	–	+	+	+	+
Smith degradation							
Out of sack	+	+	–	+	+	+	–
Precipitation in the sack	+	–	–	+	–	–	+
Supernatant in the sack	–	–	–	–	–	–	+

[a] Glucose.
[b] Glycerol.
[c] Erythritol.
[d] Mannose.
[e] Detectable.
[f] Undetectable.

to the production of formic acid (0.079 mol/mol sugar residue) was more than 2, indicating the existence of little amounts of monosaccharide which were 1 → linked or 1 → 6 linked and little branching. In addition, it was inferred that sugar residues oxidised and linkages of (1 →)-glycosidic linkages accounted for 53.2% and 7.9%, respectively. The periodate-oxidised products were hydrolysed and examined by gas chromatography (Table 1). The presence of glucose indicated (1 → 3)-glycosidic linkages, namely linkages that cannot be oxidised by HIO_4. The presence of mannose revealed some residues of mannose were (1 → 3)-linked, (1 → 2,3)-linked, (1 → 2,4)-linked, (1 → 3,4)-linked, (1 → 3,6)-linked, or (1 → 2,3,4)-linked, which cannot be oxidised by HIO_4. Results of Smith degradation analysis of fractions were summarised in Table 1. The glycerol and erythritol were found with a molar ratio of 1.00:1.32 by GC after conversion to the corresponding alditol acetates. It was thus deduced that (1 → 2)-glycosidic linkages accounted for 9.6%, and (1 → 4)-glycosidic linkages 35.7%. At the same time, the branching of RVP-2 was little, so the linkages of the main chain could be alternately arrayed by (1 → 3)-glycosidic linkages and (1 → 2)-glycosidic linkages or (1 → 4)-glycosidic linkages, according to the presence of glycerin and erythritol, or the linkages of main chain could be the (1 → 2)-glycosidic linkages or (1 → 4)-glycosidic linkages and the linkages of branches (1 → 3)-glycosidic linkages.

3.4. Scavenging activity of hydroxyl radical

Hydroxyl radicals can easily cross cell membranes, can readily react with most biomolecules including carbohydrates, proteins, lipids, and DNA in cells, and cause tissue damage or cell death. Thus, removing hydroxyl radicals is important for the protection of living systems.

Hydroxyl radicals, generated by the reaction of iron–EDTA complex with H_2O_2 in the presence of ascorbic acid, attack deoxyribose to form products which, upon heating with 2-thiobarbituric acid under acid conditions, yield a pink tint. Added hydroxyl radical scavengers compete with deoxyribose for the resulting hydroxyl radicals and diminish tint formation (Cheng, Ren, Li, Chang, & Chen, 2002). The above-mentioned model was used to measure inhibitory activities of all fractions on hydroxyl radicals.

Both RVP-1 and RVP-2 had higher scavenging effect than Vitamin (Vc) (Fig. 1). Their scavenging effects increased with increasing concentration. The scavenging effects of RVP-1 and RVP-2 were 0–67.3% and 3.3–98.1%, respectively, at the amount of 0.01–5.0 mg, and that of Vc was about 0–60.7%. This result proved that polysaccharides from the fresh fruiting bodies of *R. virescens* had a significant effect on scavenging hydroxyl radicals, and RVP-1 and RVP-2 were more pronounced than Vc.

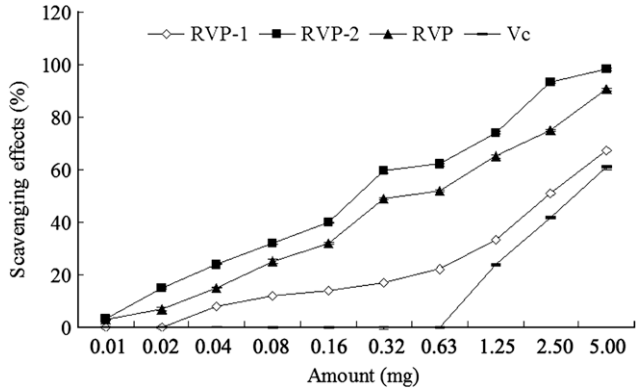

Fig. 1. Scavenging activities of hydroxyl radical by RVP-1, RVP-2, RVP and Vc. Each value is expressed as mean ± standard deviation ($n = 3$).

3.5. Scavenging activity of superoxide radical

Although superoxide was a weak oxidant, in most organisms, it could degrade continuously and form other active ROS, triggering peroxidation of lipids, and then induce pathological incidents such as arthritis and Alzheimer's disease. Thus, it is important to remove superoxide radicals.

Superoxide radicals were generated in a PMS/NADH system for assay in the reduction of nitro blue tetrazolium (NBT). The scavenging activities of RVP-1 on superoxide radicals were shown to be significant in a concentration-dependent fashion (Fig. 2). As shown in Fig. 2, RVP-1 was found to have more scavenging activities of superoxide radicals than RVP and Vc. The purification fraction RVP-2 showed no scavenging activities. At the amount of between 0.156 mg and 5.0 mg, the effects on scavenging superoxide of RVP-1 were 2.4–88.1%. However, the scavenging activity of Vc for superoxide radical was 0–83.1%. On the basis of these results, RVP-1 had stronger scavenging activity for superoxide radicals compared to vitamin C.

3.6. Scavenging activity of self-oxidation of 1,2,3-phentriol

Fig. 3 illustrates the scavenging power for self-oxidation of 1,2,3-phentriol of RVP-1 and RVP-2. Their scavenging powers correlated well with increasing concentrations. Moreover, the scavenging power of RVP-1 was stronger than those of RVP and RVP-2, and corresponded to that of Vc. These results indicate that RVP-1 has strong scavenging power for self-oxidation of 1,2,3-phentriol and should be explored as novel potential antioxidants.

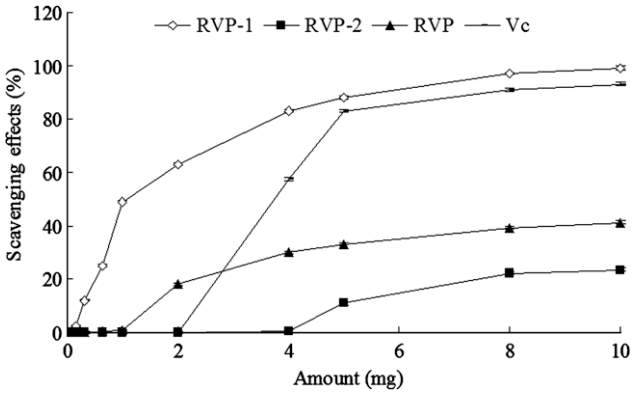

Fig. 2. Scavenging effects of RVP-1, RVP-2, RVP and Vc on super oxide radicals. Each value is expressed as mean ± standard deviation ($n = 3$).

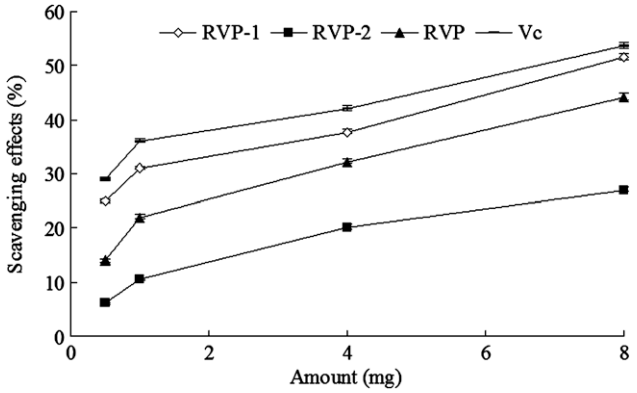

Fig. 3. Inhibitory effects of RVP-1, RVP-2, RVP and Vc on self-oxidation of 1,2,3-phentriol. Each value is expressed as mean ± standard deviation ($n = 3$).

3.7. Reducing power

Fig. 4 depicts the reducing power of tested samples. Higher absorbance value means stronger reducing power of samples. In this assay, the reducing power of the tested polysaccharides steadily increased with increasing sample concentration. The reducing abilities of RVP-1, RVP-2, and RVP at 20.0 mg/ml were 0.77, 0.96, and 0.46, respectively, which were weaker than those of butylated hydroxyanisol (BHA) and ascorbic acid. BHA showed a reducing power of 0.93 at 0.1 mg/ml and the reducing powers of ascorbic acid and α-tocopherol were 0.87 and 0.96 at 1 mg/ml, respectively. The reducing properties were generally associated with the presence of reductones, which have been shown to exert antioxidant action by breaking the free-radical chain which is done by donating a hydrogen atom. Zhu, Hackman, Ensunsa, Holt, and Keen (2002) reported that in most cases, irrespective of the stage in the oxidative chain in which the antioxidant action is assessed, most nonenzymatic antioxidative activities, such as scavenging of free radicals or inhibition of peroxidation, are mediated by redox reaction. Our data showed that the reducing power of these fractions probably play a role in the antioxidation of *R. virescens*.

3.8. Chelating effect on ferrous ions

At 5 mg/ml, RVP-1 chelated ferrous ions by 75.6% whereas the chelating abilities of RVP-2 and RVP were 30.1% and 50.8%, respectively (Fig. 5). At 10 mg/ml, the chelating abilities of RVP-1, RVP-2, and RVP were 93.3%, 51.2%, and 80.1%, respectively. However, EDTA showed an excellent chelating ability of 90.6% at 0.1 mg/ml. Citric acid was not a good chelating agent for ferrous ions in this assay and its chelating ability was 16.7% at 20 mg/ml.

Obviously, RVP-1 and RVP were good chelating agents for ferrous ions. Since ferrous ions are the most effective pro-oxidants in the food system (Yamaguchi, Tatsumi, Karo, & Yoshimitsu, 1988), the high ferrous-ion chelating abilities of polysaccharides from *R. virescens* would be somewhat beneficial.

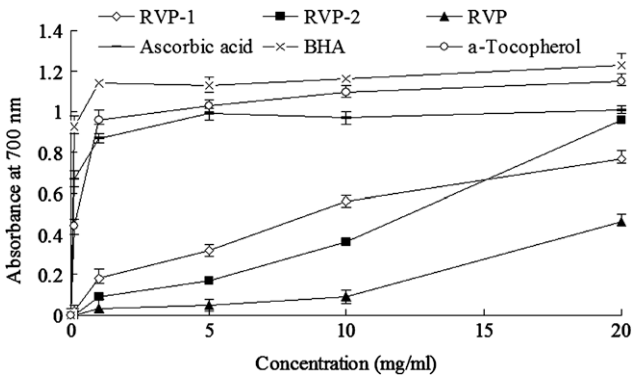

Fig. 4. Reducing power of RVP-1, RVP-2 and RVP. Each value is expressed as mean ± standard deviation ($n = 3$).

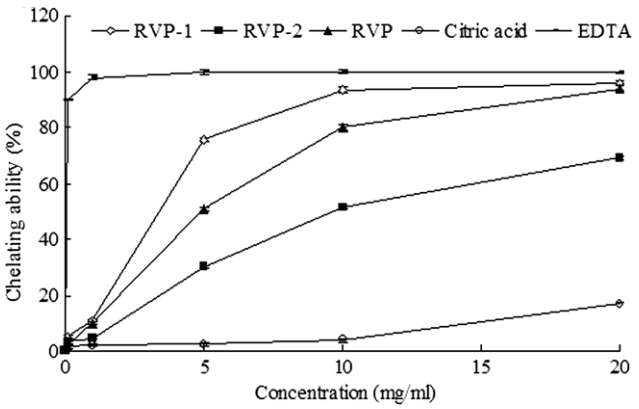

Fig. 5. Chelating effects of RVP-1, RVP-2 and RVP on ferrous ions. Each value is expressed as mean ± standard deviation ($n = 3$).

4. Conclusions

On the basis of the previously mentioned results, it was concluded that the water extracting crude polysaccharide of *R. virescens* contained predominantly two fractions (RVP-1 and RVP-2) purified by DEAE-Sepharose CL-6B column chromatography. RVP-1 and RVP-2 were heteropolysaccharides in which glucose was the major component. The estimated equivalent dextran molecular weights of RVP-1 and RVP-2 were around 3.1×10^5 and 4.2×10^5 Da, respectively. Analysis by Periodate oxidation–Smith degradation indicated that RVP-1 was composed of 68.3% (1 →)- or ((1 → 6)-glycosidic linkages and 31.7% (1 → 3)-glycosidic linkages, and RVP-2 7.9% (1 →)- or (1 → 6)-glycosidic linkages, 9.6% (1 → 2)-glycosidic linkages, 35.7% (1 → 4)-glycosidic linkages, and 46.8% (1 → 3)-glycosidic linkages.

RVP-1 and RVP-2 had a little higher scavenging activity of hydroxyl radical than that of Vc, and RVP-1 had a higher activity at scavenging superoxide radical compared to Vc and equivalent inhibiting ability to Vc on self-oxidation of 1,2,3-phentriol.

Overall, RVP-1 possessed good antioxidant properties and can be developed as a novel potential antioxidant for the treatment and prevention of some diseases relating to ROS. We can rationally assume that *R. virescens* has curative effect in traditional medicine partly because of antioxidation of polysaccharides in it. Thus, RVP-1 should be explored and investigated further in view of its potential as a therapeutic agent.

References

Bradford, M. M. (1976). A rapid and sensitive method for the quantitation of microgram quantities of protein utilizing the principle of protein binding. *Analytical Biochemistry, 72*, 248–254.

Cheng, Z. Y., Ren, J., Li, Y. Z., Chang, W. B., & Chen, Z. D. (2002). Study on the multiple mechanisms underlying the reaction between hydroxyl radical and phenolic compounds by qualitative structure and activity relationship. *Bioorganic and Medicinal Chemistry, 10*, 4067–4073.

Dinis, T. C. P., Madeira, V. M. C., & Almeida, L. M. (1994). Action of phenolic derivatives (acetaminophen, salicylate, and 5-amino salicylate) as inhibitors of membrane lipid peroxidation and as peroxyl radical scavengers. *Archives of Biochemistry and Biophysics, 315*, 161–169.

Dubois, M., Gilles, K. A., Hamilton, J. K., Rebers, P. A., & Smith, F. (1956). Colorimetric method for determination of sugars and related substances. *Analytical Chemistry, 28*, 350–356.

Fan, L., Zhang, S., Yu, L., & Ma, L. (2007). Evaluation of antioxidant property and quality of breads containing *Auricularia auricula* polysaccharide flour. *Food Chemistry, 101*, 1158–1163.

Ghiselli, A., Nardini, M., Baldi, A., & Scaccini, C. (1998). Antioxidant activity of different phenolic fractions separated from an Italian red wine. *Journal of Agricultural Food and Chemistry, 46*, 361–367.

Grice, H. C. (1988). Safety evaluation of butylated hydroxyanisole from the perspective of effects on forestomach and oesophageal squamous epithelium. *Food and Chemical Toxicology, 26*, 717–723.

Hu, Y., Xu, J., & Hu, Q. H. (2003). Evaluation of antioxidant potential of aloe vera (*Aloe barbadensis* Miller) extracts. *Journal of Agricultural and Food Chemistry, 51*, 7788–7791.

Jiang, Y. H., Jiang, X. L., Wang, P., & Hu, X. K. (2005). In vitro antioxidant activities of water-soluble polysaccharides extracted from *Isaria farinosa* B05. *Journal of Food Biochemistry, 29*, 323–335.

Kinsella, J. E., Frankel, E. N., German, J. B., & Kanner, J. (1993). Possible mechanisms for the protective role of antioxidants in wine and plant foods. *Food Technology, 47*, 85–89.

Lee, B. C., Bae, J. T., Pyo, H. B., Choe, T. B., Kim, S. W., Hwang, H. J., et al. (2003). Biological activities of the polysaccharides produced from submerged culture of the edible *Basidiomycete Grifola frondosa*. *Enzyme and Microbial Technology, 32*, 574–581.

Liu, F., Ooi, E. C., & Chang, S. T. (1997). Free radical scavenging activities of mushroom polysaccharide extracts. *Life Science, 60*, 763–771.

Marklund, S., & Marklund, G. (1974). Involvement of superoxide anion radicals in the autoxidation of pyrogallol and a convenient assay for superoxide dismutase. *European Journal of Biochemistry, 47*, 469–471.

Mau, J. L., Lin, H. C., & Song, S. F. (2002). Antioxidant properties of several specialty mushroom. *Food Research International, 5*, 519–526.

Nandita, S., & Rajini, P. S. (2004). Free radical scavenging activity of an aqueous extract of potato peel. *Food Chemistry, 85*, 611–616.

Oyaizu, M. (1986). Studies on products of browning reactions: Antioxidative activities of products of browning reaction prepared from glucosamine. *Japanese Journal of Nutrition, 44*, 307–315.

Qi, H. M., Zhang, Q. B., Zhao, T. T., Chenc, R., Zhang, H., Niu, X. Z., et al. (2005). Antioxidant activity of different sulfate content derivatives of polysaccharide extracted from *Ulva pertusa* (Chlorophyta) in vitro. *International Journal of Biological Macromolecules, 37*, 195–199.

Ramarahnam, N., Osawa, T., Ochi, H., & Kawaishi, S. (1995). The contribution of plant food antioxidants to human health. *Trends in Food Science and Technology, 6*, 75–82.

Robak, J., & Gryglewski, R. (1988). Flavonoids are scavengers of superoxide anions. *Journal of Biochemical Pharmacology, 37*, 837–841.

Staub, A. M. (1965). Removal of protein – Sevag method. *Methods in Carbohydrate Chemistry, 5*, 5–6.

Yamaguchi, R., Tatsumi, M. A., Karo, K., & Yoshimitsu, U. (1988). Effect of metal salts and fructose on the autoxidation of methyl linoleate in emulsions. *Agricultural and Biological Chemistry, 52*, 849–850.

Zhang, J., Wu, J., Liang, J. Y., Hu, Z. A., Wang, Y. P., & Zhang, S. T. (2007). Chemical characterization of *Artemisia* seed polysaccharide. *Carbohydrate Polymers, 67*, 213–218.

Zhu, Q. Y., Hackman, R. M., Ensunsa, J. L., Holt, R. R., & Keen, C. L. (2002). Antioxidative activities of oolong tea. *Journal of Agricultural and Food Chemistry, 50*, 6929–6934.

mechanisms for the high oxidative stability of SO during thermal oxidation have not been fully understood. Initial concentration of antioxidants including sesamol or tocopherol in SO may play a crucial role or other new antioxidant compounds may be formed during heating treatment.

Recently, our research group has developed a new method, which can predict the oxidative stability of edible oils by measuring absorbance of a mixture of DPPH and oil sample. Using this method, profile changes of antioxidants or radicals in thermally oxidised oils including olive oil, soybean oil, lard, and corn oil could be explained (Lee, Chung, Chang, & Lee, 2007). DPPH method may explain the exceptionally high oxidative stability of SO from roasted sesame seeds through monitoring the changes of hydrogen donating compounds and/or radicals with the combinations of sesamol and sesamolin analysis and other conventional methods such as conjugated dienoic acid (CDA) and headspace oxygen contents.

The objectives of this study were to determine the oxidative stability of SO pressed from sesame seeds roasted different time and temperature and to monitor major contributing factors for the extended oxidative stability of SO through a combination of DPPH, CDA, headspace oxygen analysis, and profile changes of sesamol and sesamolin.

2. Materials and methods

2.1. Materials

White sesame seeds in package were purchased from a local grocery market (Seoul, Korea). DPPH and sesamol were purchased from Sigma–Aldrich (St. Louis, MO, USA). Isooctane was bought from Junsei Chemical Co. (Tokyo, Japan). Other chemicals including sodium chloride, *n*-hexane, acetonitrile, and methanol were purchased from Daejung Chemical Co. (Seoul, Korea).

2.2. Sample preparation

2.2.1. Sesame oil preparation

Sesame seeds were put in a drum of a coffee roaster (Model CBR-101, Genesis Co., Ltd. Gyeonggi, Korea) and roasted at the temperature of 213, 230, or 247 °C with the duration of 14, 21, or 28 min. Therefore nine roasting condition (3 roasting temperature × 3 roasting time) was used in this study. Oil from roasted sesame seeds was extracted using an oil maker with a pressing unit (Model DO-9990, Dong-A Oscar Co., Ltd. Seoul, Korea). Crude SO was centrifuged (Model Mega 17R, Hanil Science Ltd. Gyeonggi, Korea) at 2208*g* for 20 min and supernatant was separated. Control was SO prepared from sesame seeds without roasting treatment. SO from sesame seed roasted at 247 °C for 28 min was designated as SO247/28. All samples were prepared triplicates.

2.2.2. Thermal treatment for oxidative stability of SO

One gram of SO was put in a 10-mL vial without caps. Samples were placed in a convection oven (Model LDO-250F, Win Science, Seoul, Korea) at 180 °C for 90 min and then analysed by CDA and DPPH methods at every 15 min.

Samples for the headspace oxygen analysis were prepared in 10-mL vials sealing air-tightly with Teflon-coated rubber septa and aluminum caps. Samples were thermally oxidised at 93 °C for 32 h and headspace oxygen contents was analysed at 0, 2.5, 4.5, 12, 16, and 32 h.

For the analysis of sesamol and sesamolin, SO from 213, 230, and 247 °C for 21 min were selected and thermally oxidised at 180 °C for 90 min in the convection oven (Win Science, Seoul, Korea). All samples were prepared triplicate.

2.3. CDA analysis

CDA of samples was measured according to AOCS (1980) method Ti la-64. The absorbance of oil sample in isooctane was determined at 233 nm using a UV–vis spectrophotometer (Model UV-1650PC, Shimadzu, Kyoto, Japan). CDA (%) was calculated using equation of $(0.84 \times A)/(bc - K_0)$, where A is the absorbance of samples at 233 nm, b is the cell length (cm), c is the gram per litre, and K_0 is the absorptivity by acid group, 0.03.

2.4. Analysis for headspace oxygen

Headspace oxygen in samples was analysed according to previous reports (Min, Li, & Lee, 1998; Yang, Lee, & Min, 2002; Lee & Min, 2009). The oxygen contents of headspace gas in sample bottles was determined by a gas chromatograph (GC) equipped with a thermal conductivity detector (TCD) (Agilent Technology, Palo Alto, CA, USA) and a stainless steel column (3.0 m × 0.2 cm) packed with 60/80 Molecular Sieve 5A (Restek, Bellefonte, PA, USA). Injection volume was 25 μL using an air-tight syringe and the flow rate of helium gas was 20 mL/min. Temperatures of oven, injector, and detector were 60, 180, and 180 °C, respectively.

2.5. DPPH measurement

DPPH method was adapted from a previous report of our research groups with minor modification (Lee et al., 2007). Briefly, 5 mL of 0.10 mM DPPH in isooctane was mixed with 56 μL oil samples and the absorbance of the sample mixture was measured at 509 nm after 30 min in the dark using the UV/VIS-spectrometer (Shimadzu, Kyoto, Japan).

2.6. Sesamol and sesamolin analysis

Sesamol and sesamolin in SO were separated and isolated using a high performance liquid chromatograph (HPLC) equipped with an ultraviolet detector (Model L-2400, Hitachi, Tokyo, Japan). A 4 μm Waters Novapak C_{18} reversed-phase HPLC column (150 mm × 3.9 mm I.D.) was used as stationary phase. Mobile phase was a mixture of deionized water and acetonitrile (70:30, v/v) at flow rate 1.0 mL/min. Sesame oil was diluted in *n*-hexane (0.1 g/mL) and 10 μL was injected. Sesamol and sesamolin in eluent were detected at 290 nm and identified based on the retention times of standard compound of sesamol and results of previous reports (Lee & Choe, 2006). Standard curves of sesamol were prepared to quantify the peak of sesamol in HPLC.

2.7. Statistical analysis

The data of CDA results, headspace oxygen of thermally oxidised SO at 32 h, and sesamol contents in SO before thermal oxidation were analysed statistically by ANOVA and Duncan's multiple range test using commercially available software package SPSS software program (SPSS Inc., Chicago, IL, USA). Also, contents of sesamol and sesamolin in thermally oxidised SO213/21, SO230/21, and SO247/21 were statistically analysed. A p value <0.05 was considered significant.

3. Results and discussion

3.1. CDA analysis

CDA values of SO during thermal oxidation at 180 °C for 90 min are shown in Table 1. CDA determines the formation of conjugated dienes or primary oxidation products of polyunsaturated fatty

Table 1
CDA values of SO prepared from roasted sesame seeds during thermal oxidation at 180 °C for 90 min.

	0 min	15 min	30 min	45 min	60 min	75 min	90 min
Control (0/0)	0.349 ± 0.020Aa[a]	0.420 ± 0.016Abc	0.528 ± 0.019Bbc	0.654 ± 0.145Cb	1.034 ± 0.017Df	1.157 ± 0.029Ee	1.362 ± 0.006Ff
SO213/14[b]	0.333 ± 0.004Aa	0.355 ± 0.011Aa	0.450 ± 0.035Bab	0.534 ± 0.024Cab	0.689 ± 0.009Dcd	0.937 ± 0.016Ed	1.097 ± 0.020Fe
SO213/21	0.335 ± 0.008Aa	0.380 ± 0.050Aab	0.459 ± 0.039Bab	0.560 ± 0.006Cab	0.723 ± 0.028Dde	0.959 ± 0.026Ed	1.155 ± 0.027Fe
SO213/28	0.337 ± 0.006Aa	0.398 ± 0.019ABabc	0.416 ± 0.058Ba	0.540 ± 0.005Cab	0.756 ± 0.010De	0.939 ± 0.035Ed	1.118 ± 0.078Fe
SO230/14	0.354 ± 0.023Aa	0.417 ± 0.049Bbc	0.483 ± 0.011Cab	0.546 ± 0.008Dab	0.747 ± 0.022Ee	0.953 ± 0.048Fd	0.951 ± 0.044Fd
SO230/21	0.394 ± 0.002Ab	0.445 ± 0.042Ac	0.466 ± 0.017Aab	0.602 ± 0.154Bab	0.596 ± 0.024Bb	0.640 ± 0.031Bda	0.685 ± 0.056Bab
SO230/28	0.422 ± 0.012Ab	0.392 ± 0.027Aabc	0.528 ± 0.021Bbc	0.517 ± 0.007Ba	0.571 ± 0.028Cb	0.640 ± 0.044 Da	0.695 ± 0.008Eab
SO247/14	0.542 ± 0.044Ac	0.506 ± 0.026Ad	0.676 ± 0.135ABd	0.571 ± 0.002ABCab	0.536 ± 0.016BCa	0.656 ± 0.053Ca	0.647 ± 0.015Ca
SO247/21	0.582 ± 0.010Ad	0.591 ± 0.018Ae	0.594 ± 0.055Acd	0.608 ± 0.044ABab	0.656 ± 0.023Bc	0.757 ± 0.039Cc	0.723 ± 0.002Db
SO247/28	0.687 ± 0.022Ae	0.633 ± 0.004ABe	0.676 ± 0.015ABd	0.653 ± 0.038BCab	0.726 ± 0.019CDe	0.745 ± 0.035Db	0.820 ± 0.016Ec

[a] Different capital letters are significant among the same low and small letters are significant among the same column at 0.05.
[b] SO213/14 indicates SO prepared at 213 °C roasting temperature and 14 min roasting time.

acids. CDA values have been used to determine the oxidative stability of edible oils under thermal oxidation and to evaluate the antioxidant ability (Lee & Choe, 2006; Lee et al., 2007). CDA values of SO from roasted sesame seeds at 213 °C and SO 230/14 were not significant at 0 min ($p > 0.05$) while those of SO230/21, SO230/28, and SO from 247 °C roasted sesame seeds were significant compared to those of control ($p < 0.05$), which implies that SO were more oxidised when sesame seeds roasted at higher temperature and longer time (Table 1). Yoshida and Takagi (1997) analysed characteristics of sesame oils from different roasting conditions (160–250 °C) and observed minor increases in the lipid oxidation products including peroxide value, carbonyl value, anisidine value, and thiobarbituric acid reactive substances in more roasted samples.

Generally, SO from 230 to 247 °C roasted sesame seeds had significantly lower CDA values than SO from 213 °C roasted sesame seeds and control samples during thermal oxidation for 90 min ($p < 0.05$) (Table 1). For example, CDA values of control, SO213/14, SO230/14, and SO247/14 for 90 min oxidation at 180 °C were 1.362, 1.155, 0.685, and 0.723, respectively (Table 1), which shows that SO from sesame seeds received higher roasting temperature and longer duration possessed higher oxidative stability at 180 °C oxidation.

3.2. Analysis for headspace oxygen

Headspace oxygen of SO during thermal oxidation are shown in Fig. 1. Headspace oxygen contents in control samples decreased from 20.94% to 11.82% for 32 h at 93 °C while those from SO213/21, SO230/21, and SO247/21 changed by 5.69%, 3.00%, and 2.55%, respectively. Headspace oxygen of SO from 213 °C roasted sesame seeds was significantly higher than those from 230 to 247 °C ($p < 0.05$). As the degree of oxidation in oil increases, headspace oxygen in air-tight sample bottles decreases due to the reaction of oxygen with unsaturated fatty acids. Therefore, control samples had the lowest oxidative stability and SO247/28 had the highest oxidative stability. Measuring headspace oxygen is one of reliable methods to determine the oxidative stability of lipid samples (Min et al., 1998; Vittadini, Lee, Frega, Min, & Vodovotz, 2003; Yang et al., 2002). Generally, it is accepted that SO from roasting condition have relatively high oxidative stability (Miles & Doucette, 2001). In this study, SO from higher temperature and longer roasting time had higher oxidative stability than SO from lower temperature and shorter roasting time based on the results of CDA and headspace oxygen analysis, which agrees with previous reports (Miles & Doucette, 2001). However, major contributing factors for the high oxidative stability of SO during thermal oxidation are not understood yet.

3.3. DPPH analysis

Absorbance changes of DPPH in SO roasted at 213 (a), 230 (b), and 247 °C (c) are shown in Fig. 2. Absorbance of a mixture of DPPH

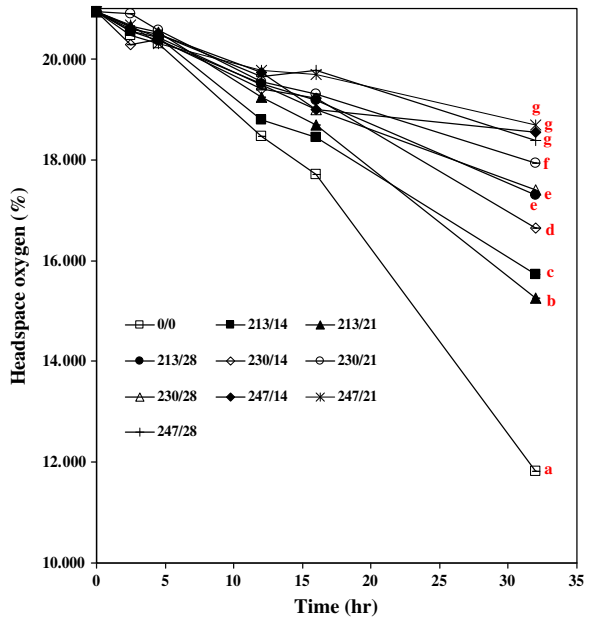

Fig. 1. Headspace oxygen of SO from roasted sesame seeds during thermal oxidation at 93 °C for 32 h. Statistical analysis was conducted on the headspace oxygen in SO oxidised at 32 h and different letters are significant at 0.05.

and control, SO213/21, SO230/21, or SO247/21 at 0 min were 0.589, 0.583, 0.451, and 0.220, respectively. SO from higher roasting temperature and longer roasting time had lower absorbance of DPPH at 0 min than control (Fig. 2). The low absorbance of DPPH implies that DPPH abstracted more hydrogen atom or electrons from SO and escaped from radical state. SO247/21 may have relatively higher concentration of free radical scavenging compounds or oxidised lipid radicals than control. Absorbance of control (symbol of 0/0 in Fig. 2) increased up to 45 min oxidation and started to decrease. This pattern of DPPH absorbance of control samples agrees with the previous reports on the oxidation of edible oils such as olive oil, soybean oil, lard, and corn oil (Lee et al., 2007).

As oxidation time increased, the absorbance of DPPH in SO from sesame seeds roasted at 213 °C with 14, 21, and 28 min increased gradually (Fig. 2a). The increase of absorbance implies that hydrogen donating free radical scavengers in SO was continuously depleted to retard the formation of lipid radicals. SO from sesame seeds roasted at 230 °C showed different pattern of DPPH absorbance depending on the roasting time (Fig. 2b). Absorbance of DPPH from SO230/14 increased up to 45 min and stared to decrease like control samples. However, the decreasing patterns of absorbance between control and SO230/14 were different. The thermal oxidation time for pattern changes of DPPH absorbance

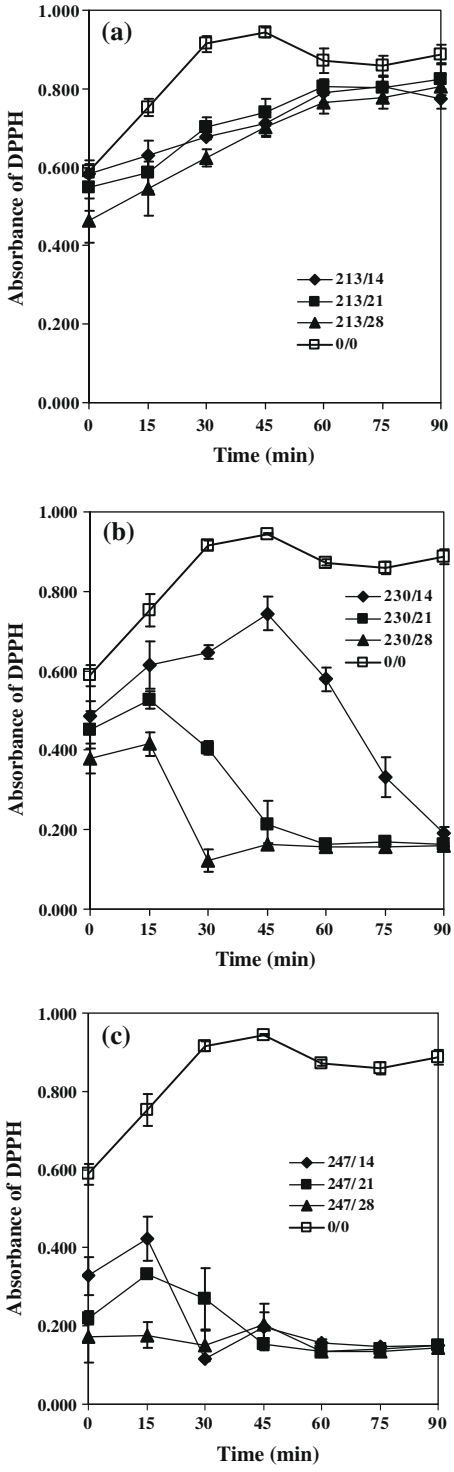

Fig. 2. Changes of absorbance of DPPH in SO from roasted sesame seeds at 213 °C (a), 230 °C (b), and 247 °C (c) during thermal oxidation at 180 °C.

in both SO230/21 and SO230/28 was 15 min rather than 45 min of SO230/14 (Fig. 2b). It is interesting that SO from sesame seeds roasted at longer roasting time showed shorter time for pattern changes. This trend can be observed in SO from sesame seeds roasted at 247 °C. SO247/28 did not show great changes of absorbance while SO247/14 and SO247/21 showed increases of DPPH absorbance up to 15 min and started to decrease like SO230/21 and SO230/28 (Fig. 2c). This observation of DPPH results implies that new free radical scavenging compounds may be generated continuously in SO from 230 to 247 °C roasted sesame seeds during thermal oxidation. Therefore, SO from sesame seeds roasted at higher temperature may have enough free radical scavenging compounds and absorbance of DPPH did not change during heat treatment. This observation was confirmed by the results of sesamol and sesamolin analysis.

3.4. Sesamol and sesamolin analysis

Effects of roasting condition on the sesamol contents in SO before heat treatment are shown in Fig. 3. As roasting time and temperature increased, contents of sesamol in SO significantly increased ($p < 0.05$). Sesamol contents in SO247/28 were significantly higher than those in SO213/14 by 6.42 times while control samples did not contain sesamol. Wu (2007) analysed lignan contents of 14 brands of sesame oils, and found their mean of total lignans as 11.5 mg/g; 82% and 15% of the lignans were sesamin and sesamolin, respectively. The author reported that sesamol contents were relatively higher in darker coloured SO. Previous studies showed that extended oxidative stability of SO from roasting conditions was closely related with the sesamol contents and γ-tocopherol (Frank, 2005).

Changes of sesamol and sesamolin contents in SO prepared from sesame seeds roasted at 213, 230, and 247 °C for 21 min at 180 °C oxidation are shown in Fig. 4. As heat treatment increased from 0 to 90 min, concentration of sesamol in SO230/21 and SO247/21 increased significantly and peak areas of sesamolin decreased significantly ($p < 0.05$). DPPH absorbance did not change in SO247/21 during thermal oxidation (Fig. 2c), which may be due to the sufficient amount of sesamol generated from sesamolin (Fig. 4). In case of SO230/21, relative peak areas of sesamolin changed from 100% to 6.61% for 90 min, while concentration of sesamol in SO230/21 increased from 0.16 to 0.42 mM. DPPH absorbance in SO230/21 started to decrease from 15 min oxidation, which was the time for the increases of sesamol contents. Therefore, increase of sesamol in SO230/21 seemed to be closely related with the decrease of DPPH absorbance like SO247/21. Suja et al. (2004) showed that second order rate constants of sesamol and DPPH were 11.1 and 30.7 times higher than those of sesamin and sesamolin, respectively. Therefore, formation of sesamol from sesamolin played important roles on the decreases of DPPH absorbance and exceptional thermal stability of SO during heat treatment. The results of this study agree with the previous reports of Fukuda et al. (1986) and Shahidi & Naczk (2004).

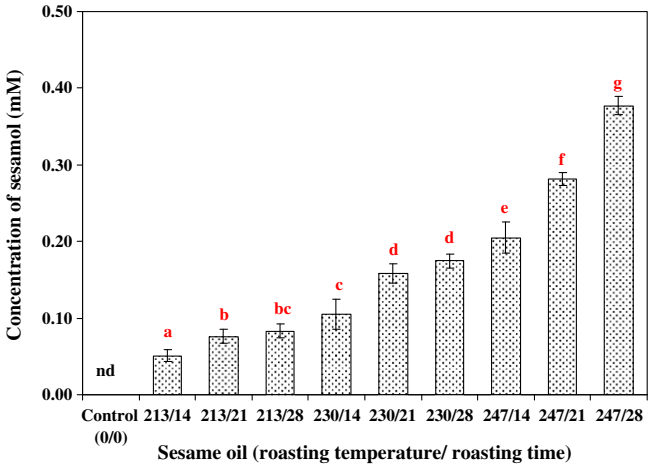

Fig. 3. Effects of roasting condition on the sesamol contents in SO before thermal oxidation at 180 °C. nd: not detected. Different letters are significant at 0.05.

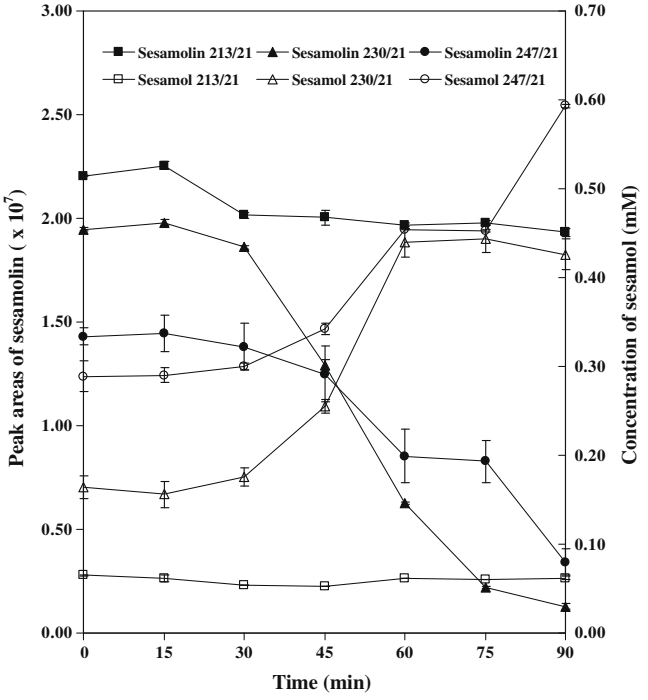

Fig. 4. Changes of sesamol and sesamolin in SO from roasted sesame seeds at 213, 230, or 247 °C for 21 min at 180 °C thermal oxidation. Right and left *Y*-axes are for the peak areas of sesamolin and concentration of sesamol, respectively.

Interestingly, changes of sesamol and sesamolin in SO from 213 °C were relatively smaller than those in SO from 230 to 247 °C during thermal oxidation, which matched the patterns of DPPH absorbance in Fig. 2. The pattern changes of SO from 230 to 247 °C strongly indicates that new free radical scavenging compounds were continuously formed and this antioxidant compound was tentatively confirmed as sesamol from the decomposition of sesamolin (Figs. 2 and 4).

The decreases in the absorbance of DPPH showed that SO from roasted sesame seeds already contained substantial amounts of hydrogen donating antioxidants and oxidised lipid radicals before thermal treatment. CDA values and sesamol contents in SO confirmed the presence of oxidised lipids and hydrogen donating free radical scavengers, respectively. If conventional methods like CDA and headspace oxygen analysis methods were used only, sesamol and antioxidants such as γ-tocopherol in SO would be concluded as a crucial ingredient for the extraordinary high oxidative stability of SO during heat treatment. DPPH method has revealed that hydrogen donating compounds were continuously generated in SO from 230 to 247 °C roasted sesame seeds. This speculation was confirmed by sesamol and sesamolin analysis showing the formation of sesamol from sesamolin during 180 °C treatment.

It is well-known that the concentration of γ-tocopherol decreases as thermal oxidation prolonged. Therefore, γ-tocopherol could be one factor for the decreases of absorbance of DPPH in SO before thermal oxidation. However, γ-tocopherol may not be a major compound for the decreases of DPPH during thermal oxidation at 180 °C. Rather than this, formation of sesamol is more important factor for the low absorbance of DPPH in SO. Interestingly, SO213/21 produced low concentration of sesamol compared to samples at SO230/21 and SO247/21 during thermal oxidation (Fig. 4). The formation rate of sesamol from sesamolin should be similar in SO at 180 °C oxidation irrespective of roasting temperature for sesame seeds. Therefore, other factors in SO from 230 to 247 °C roasted sesame seeds may influence the stability of sesamolin and the formation of sesamol, which needs further researches.

References

Abou-Gharbia, H. A., Shahidi, F., Shehata, A. A. Y., & Youssef, M. M. (1997). Effect of processing on oxidative stability of sesame oil extracted from intact and dehulled seed. *Journal of American Oil Chemists' Society, 74*, 215–221.

Abou-Gharbia, H. A., Shehata, A. A. Y., & Shahidi, F. (2000). Effect of processing on oxidative stability and lipid classes of sesame oil. *Food Research International, 33*, 331–340.

AOCS (1980). *AOCS official and tentative methods of the American oil chemists' society* (3rd ed.). Champaign, IL: AOCS Press.

Chung, J., & Choe, E. O. (2001). Effects of sesame oil on thermooxidative stability of soybean oil. *Food Science and Biotechnology, 10*, 446–450.

Frank, J. (2005). Beyond vitamin E supplementation: An alternative strategy to improve vitamin E status. *Journal of Plant Physiology, 162*, 834–843.

Fukuda, Y., Nagata, M., Osawa, T., & Namiki, M. (1986). Chemical aspects of the antioxidative activity of roasted sesame seed oil, and the effect of using the oil for frying. *Agricultural and Biological Chemistry, 50*(4), 857–862.

Kamal-Eldin, A., & Appelqvist, L. A. (1994). Variation in fatty acid composition of the different acyl lipids in seed oils from four sesamum species. *Journal of the American Oil Chemists' Society, 71*, 135–139.

Kaur, I. P., & Saini, A. (2000). Sesamol exhibits antimutagenic activity against oxygen species mediated mutagenicity. *Mutation Research, 470*, 71–76.

Lee, J. M., Chung, H., Chang, P. S., & Lee, J. H. (2007). Development of a method predicting the oxidative stability of edible oils using 2,2-diphenyl-1-picrylhydrazyl (DPPH). *Food Chemistry, 103*, 662–669.

Lee, J. Y., & Choe, E. O. (2006). Extraction of lignan compounds from roasted sesame oil and their effects on the autoxidation of methyl linoleate. *Journal of Food Science, 71*, 430–436.

Lee, J. Y., Kim, M. J., & Choe, E. O. (2007). Antioxidant activity of lignan compounds extracted from roasted sesame oil on the oxidation of sunflower oil. *Food Science and Biotechnology, 16*, 981–987.

Lee, J. Y., Lee, Y. S., & Choe, E. O. (2008). Effects of sesamol, sesamin, and sesamolin extracted from roasted sesame oil on the thermal oxidation of methyl linoleate. *Food Science and Technology, LWT, 42*, 1871–1875.

Lee, J. H., & Min, D. B. (2009). Effects of photooxidation and chlorophyll photosensitization on the formation of volatile compounds in lard model systems. *Food Science and Biotechnology, 18*, 413–418.

Miles, R. A., & Doucette, W. J. (2001). Assessing the aerobic biodegradability of 14 hydrocarbons in two soils using a simple microcosm/respiration method. *Chemosphere, 45*, 1085–1090.

Min, D. B., Li, T. L., & Lee, H. O. (1998). Effects of processing steps on the contents of minor compounds and oxidation of soybean oil. *Advances in Experimental Medicine and Biology, 434*, 161–180.

Namiki, M. (1990). Antioxidants/antimutagens in food. *Critical Reviews of Food Science and Nutrition, 29*, 273–300.

Sankar, D., Sambandam, G., Ramakrishna, R. M., & Pugalendi, K. V. (2005). Modulation of blood pressure, lipid profiles and redox status in hypertensive patients taking different edible oils. *Clinica Chimica Acta, 355*, 97–104.

Shahidi, F., & Naczk, M. (2004). *Phenolics in food and nutraceuticals*. Florida: CRC press (pp. 108–109).

Suja, K. P., Jayalekshmy, A., & Arumughan, C. (2004). Free radical scavenging behavior of antioxidant compounds of sesame (*Sesamum indicum* L.) in DPPH system. *Journal of Agricultural and Food Chemistry, 52*(4), 912–915.

Utsunomiya, T., Chavali, S. R., Zhong, W. W., & Forse, R. M. (2000). Effects of sesamin-supplemented dietary fat emulsions on the ex vivo production of lipopolysaccharide-induced prostanoids and tumor necrosis factor a in rats. *American Journal of Clinical Nutrition, 72*, 804–808.

Vittadini, E., Lee, J. H., Frega, N. G., Min, D. B., & Vodovotz, Y. (2003). DSC determination of thermally oxidized olive oil. *Journal of the American Oil Chemists' Society, 80*, 533–537.

Wu, W. H. (2007). The contents of lignans in commercial sesame oils of Taiwan and their changes during heating. *Food Chemistry, 104*, 341–344.

Yang, W. T., Lee, J. H., & Min, D. B. (2002). Quenching mechanisms and kinetics of α-tocopherol and β-carotene on the photosensitizing effect of synthetic food colorant FD & C Red No. 3. *Journal of Food Science, 67*(2), 507–510.

Yoshida, H., & Takagi, S. (1997). Effects of seed roasting temperature and time on the quality characteristics of sesame (*Sesamum indicum*) oil. *Journal of the Science of Food and Agriculture, 75*(1), 19–26.

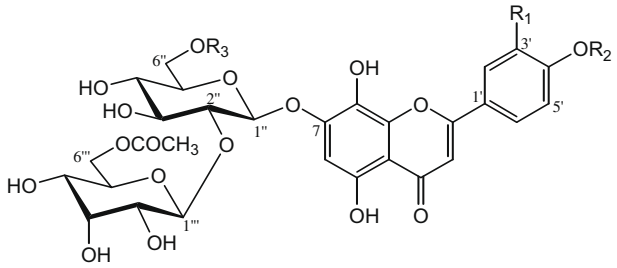

	R_1	R_2	R_3
1	OH	H	H
4	OH	H	Ac
2	H	H	H
5	H	H	Ac
3	OH	Me	H
6	OH	Me	Ac

Fig. 1. Structures of compounds **1**–**6** isolated from the butanol fraction of a methanol extract from *Sideritis brevibracteata*.

teins; and oxidants have been considered in eye disorders such as cataract and retrolental fibroplasia. Aldose reductase, the key enzyme of the polyol pathway, has been demonstrated to play an important role in the etiology of the complications of diabetes (Enomoto et al., 2004).

2. Material and methods

2.1. Plant material

The aerial parts of *S. brevibracteata* P.H. Davis were collected from C3 Antalya: Alanya, Alanya-Türbelinaz road, around Bektaş, calcareous rocks, in macchie, 200 m, N 36° 33.560′, E 32° 00 484′, by *Hayri Duman* 875, 27.05.2001. Voucher specimens (coll. *Hayri Duman* 875) are deposited in the Botany Department Herbarium at Gazi University (GAZI) Turkey.

2.2. General experimental procedures

CC: silica gel 60 (70–230 mesh, Merck, Darmstadt, Germany); thin layer chromatography (TLC): silica gel 60 F_{254} precoated aluminium plates (0.2 mm, Merck, Germany). Detection: UV fluorescence and spraying 1% vanillin/H_2SO_4, followed by heating at 105 °C for 1–2 min. IR spectra were recorded on Jasco FT/IR 420 spectrometer (Japan) as KBr pellets. UV spectra: Shimadzu UV-1601 (Japan), UV–visible spectrophotometer. ^{1}H- and ^{13}C-NMR spectra were measured with Varian Mercury 400 FT-NMR spectrometer (Varian Inc., Palo Alto, CA, USA). The spectra were measured in CD_3OD and referenced against residual non-deuterated solvent. Electrospray ionization mass spectrometer (ESI-MS) (Manchester, UK) was recorded using Waters Micromass Spectrometer ZQ.

2.3. Extraction and isolation

The air-dried and powdered aerial parts of *S. brevibracteata* (350 g) were extracted with 3500 ml MeOH in a Soxhlet apparatus for 12 h. The MeOH extract was then evaporated in vacuum (40 °C). The residue (82.80 g) was dissolved in 500 ml H_2O–MeOH mixture (9:1, v/v), then partitioned three times with chloroform (3 × 250 ml), AcOEt (3 × 250 ml) and *n*-BuOH saturated with water (3 × 250 ml). These three phases were evaporated under reduced pressure and total extracts of chloroform (10.50 g), AcOEt (9.38 g) and *n*-BuOH (25.11 g) were obtained. An aliquot of *n*-BuOH extract (2.72 g) was subjected to medium-pressure liquid chromatography (MPLC), using water (200 ml) and H_2O–MeOH mixtures (5 → 45% MeOH in steps of 5% of MeOH (each 200 ml)). Flavonoids were eluted in the following order: **1** (88 mg) (fractions 61–62), **2** (142 mg) (fractions 65–69), **3** (87 mg as crude) (fractions 71–74), **4** (292 mg) (fractions 79–81), **5** (118 mg) (fractions 82–83) and **6** (44 mg) (fractions 86–87). Fractions 71–74 (87 mg) containing crude compound **3** were subjected to a silica gel using $CHCl_3$–MeOH–H_2O mixtures (90:10:1 → 61:27:7, v/v/v) as solvent system yielding pure **3** (13 mg). Rechromatography of fractions 59–60 (64 mg) on a silica gel column using $CHCl_3$–MeOH–H_2O solvent mixtures (80:20:1 → 80:20:2, v/v/v) afforded compound **7** (27.2 mg). Compounds **1**–**7** were also obtained from the AcOEt extract.

2.4. Medium-pressure chromatography

MPLC separations were carried out using a Buchi glass column (C-690: 04437; 460 × 26 mm i.d.) packed with Lichroprep C_{18} (Merck, Germany) using Buchi 681 chromatography pump combined with a Buchi 684 fraction collector.

2.4.1. Hypolaetin 7-O-[6‴-O-acetyl-β-D-allopyranosyl-(1 → 2)]-β-D-glucopyranoside (*1*)

Amorphous yellow powder. UV λ_{max} nm (MeOH): 276, 302, 342; IR ν_{max} cm^{-1} (KBr): 3408 (OH), 2924 (C–H), 1717 (ester C=O), 1655 (γ-pyrone C=O), 1614, 1585, 1505 (aromatic ring); ESI-MS: m/z 691.14 $[M + Na]^+$, calculated for $C_{29}H_{32}O_{18}$; ^{1}H NMR (CD_3OD, 400 MHz); ^{13}C-NMR (CD_3OD, 100 MHz). All data were similar to those previously reported (Lenherr & Mabry, 1987; Rodriguez-Lyon et al., 2000) and assignments confirmed by COSY, HMQC and HMBC.

2.4.2. Isoscutellarein 7-O-[6‴-O-acetyl-β-D-allopyranosyl-(1 → 2)]-β-D-glucopyranoside (*2*)

Amorphous yellow powder. UV λ_{max} nm (MeOH): 276, 307, 325(sh); IR ν_{max} cm^{-1} (KBr): 3400 (OH), 2923 (C–H), 1725 (ester C=O), 1658 (γ-pyrone C=O), 1608, 1585, 1503 (aromatic ring); ESI-MS: m/z 675.15 $[M + Na]^+$, calculated for $C_{29}H_{32}O_{17}$; ^{1}H NMR (CD_3OD, 400 MHz); ^{13}C-NMR (CD_3OD, 100 MHz). All data were in good accordance with those previously reported (Albach et al., 2003; Lenherr & Mabry, 1987; Rios et al., 1992).

2.4.3. 3′-hydroxy-4′-O-methylisoscutellarein 7-O-[6‴-O-acetyl-β-D-allopyranosyl-(1 → 2)]-β-D-glucopyranoside (*3*)

Amorphous yellow powder. UV λ_{max} nm (MeOH): 279, 299(sh), 339; IR ν_{max} cm^{-1} (KBr): 3410 (OH), 2921 (C–H), 1732 (ester C=O), 1659 (γ-pyrone C=O), 1614, 1585, 1506 (aromatic ring); ESI-MS: m/z 705.19 $[M + Na]^+$, calculated for $C_{30}H_{34}O_{18}$; ^{1}H NMR (CD_3OD, 400 MHz); ^{13}C-NMR (CD_3OD, 100 MHz). All data were in accordance with reported data (Lenherr & Mabry, 1987; Rios et al., 1992).

2.4.4. Hypolaetin 7-O-[6‴-O-acetyl-β-D-allopyranosyl-(1 → 2)]-6″-O-acetyl-β-D-glucopyranoside (*4*)

Amorphous yellow powder. UV λ_{max} nm (MeOH): 276, 301, 343; IR ν_{max} cm^{-1} (KBr): 3410 (OH), 2920 (C–H), 1723 (ester C=O), 1659 (γ-pyrone C=O), 1610, 1585, 1503 (aromatic ring); ESI-MS: m/z 733.19 $[M + Na]^+$, calculated for $C_{31}H_{34}O_{19}$; ^{1}H NMR (CD_3OD, 400 MHz); ^{13}C-NMR (CD_3OD, 100 MHz) and assignments confirmed by COSY, HMQC and HMBC. All data were similar to those previously reported (Lenherr & Mabry, 1987; Rodriguez-Lyon et al., 2000).

*2.4.5. Isoscutellarein 7-O-[6‴-O-acetyl-β-D-allopyranosyl-(1 → 2)]-6″-O-acetyl-β-D-glucopyranoside (**5**)*

Amorphous yellow powder. UV λ_{max} nm (MeOH): 277, 307, 325(sh); IR ν_{max} cm^{-1} (KBr): 3410 (OH), 2920 (C–H), 1725 (ester C=O), 1659 (γ-pyrone C=O), 1608, 1585, 1504 (aromatic ring); ESI-MS: m/z 717.20 $[M + Na]^+$, calculated for $C_{31}H_{34}O_{18}$; ^1H NMR (CD_3OD, 400 MHz); ^{13}C-NMR (CD_3OD, 100 MHz). All data were in accordance with reported data (Lenherr & Mabry, 1987; Skaltsa et al., 2000).

*2.4.6. 3′-hydroxy-4′-O-methylisoscutellarein 7-O-[6‴-O-acetyl-β-D-allopyranosyl-(1 → 2)]-6″-O-acetyl-β-D-glucopyranoside (**6**)*

Amorphous yellow powder. UV λ_{max} nm (MeOH): 279, 298(sh), 338; IR ν_{max} cm^{-1} (KBr): 3420 (OH), 2922 (C–H), 1726 (ester C=O), 1659 (γ-pyrone C=O), 1613, 1585, 1503 (aromatic ring); ESI-MS: m/z 747.20 $[M + Na]^+$, calculated for $C_{32}H_{36}O_{19}$; ^1H NMR (CD_3OD, 400 MHz); ^{13}C-NMR (CD_3OD, 100 MHz). All data were similar to those previously reported (Lenherr & Mabry, 1987).

*2.4.7. Verbascoside (**7**)*

Amorphous colourless powder; UV λ_{max} nm (MeOH) = 220, 234 (sh), 290, 329; IR ν_{max} (KBr) cm^{-1} = 3390 (OH), 1700 (conjugated ester C=O), 1630 (conjugated C=O), 1604, 1523 (aromatic ring), $C_{29}H_{36}O_{15}$; ^1H- and ^{13}C-NMR (CD_3OD). All data were in accordance with reported data (Sticher & Lahloub, 1982).

2.5. Pharmacological procedures

2.5.1. Animals

Male Swiss Albino mice (20–25 g) were purchased from the animal breeding laboratories of Refik Saydam Central Institute of Health (Ankara, Turkey). The animals, left for two days for acclimatization to animal room conditions, were maintained on standard pellet diet and water *ad libitum*. The food was withdrawn on the day before the experiment, but animals were allowed free access to water. A minimum of six animals was used in each group. Throughout the experiments, animals were processed according to the suggested ethical guidelines for the care of laboratory animals.

2.5.2. Preparation of test samples for bioassay

All extracts were administered in 100 mg/kg dose after suspending in 0.5% sodium carboxymethyl cellulose (CMC) suspension in distilled water. The control group animals received the same experimental handling as those of the test groups except that the drug treatment was replaced with appropriate volumes of the dosing vehicle. Either indomethacin (10 mg/kg and 0.5 mg/ear) or acetyl salicylic acid (ASA) (100 mg/kg) in 0.5% CMC was used as reference drug.

2.5.3. Antinociceptive activity

p-Benzoquinone (PBQ)-induced abdominal constriction test (Okun, Liddon, & Lasagnal, 1963) was performed on mice for determination of antinociceptive activity. According to the method, 60 min after the oral administration of test samples, the mice were intraperitoneally injected with 0.1 ml/10 g body weight of 2.5% (w/v) PBQ (Merck) solution in distilled H_2O. Control animals received an appropriate volume of dosing vehicle. The mice were then kept individually for observation and the total number of abdominal contractions (writhing movements) was counted for the next 15 min, starting at the 5th min after the PBQ injection. The data represent the average of the total number of writhes observed. The antinociceptive activity was expressed as percentage change from writhing controls. Aspirin (ASA) at 100 mg/kg dose was used as the reference drug in this test.

2.5.4. Anti-inflammatory activity

2.5.4.1. Carrageenan-induced hind paw edema model. Carrageenan-induced hind paw edema model was used for determination of anti-inflammatory activity (Yeşilada & Küpeli, 2002). The difference in footpad thickness between the right and left foot was measured with a pair of dial thickness gauge calipers (Ozaki Co., Tokyo, Japan). Mean values of treated groups were compared with mean values of a control group and analyzed using statistical methods. One hour after the oral administration of the test sample or dosing vehicle, each mouse was injected with freshly prepared (0.5 mg/25 μl) suspension of carrageenan (Sigma, St. Louis, Missouri, USA) in physiological saline (154 nM NaCl) into the subplantar tissue of the right hind paw. As the control, 25 μl saline solutions were injected into that of the left hind paw. Paw edema was measured every 90 min for 6 h from induction of inflammation. The difference in footpad thickness was measured by gauge calipers (Ozaki Co., Tokyo, Japan). Mean values of the treated groups were compared with mean values of a control group and analyzed using statistical methods. Indomethacin (10 mg/kg) was used as the reference drug.

2.5.4.2. TPA-induced mouse ear edema. Each mouse received 2.5 μg of TPA (12-*O*-tetradecanoylphorbol 13-acetate) dissolved in 20 μl of EtOH 70% (De Young, Kheifets, Ballaron, & Young, 1989). This was applied by an automatic pipette in 20 μl volumes to both anterior and posterior surfaces of the right ear. The left ear (control) received the same volume of solvent (EtOH 70%) simultaneously with TPA. Indomethacin (0.5 mg/ear) was used as a standard drug. For evaluation of the activity, two methods were used as presented below.

1. The thickness of each ear was measured 4 h after induction of inflammation using gauge calipers (Ozaki Co., Tokyo, Japan). The edema was expressed as the difference between right and left ears due to TPA application and consequently, inhibition percentage was expressed as a reduction in thickness with respect to the control group.
2. After 4 h, the animals were sacrificed under deep ether anesthesia. Disks 6 mm in diameter were removed from each ear and weighed on a balance. The swelling was estimated as the difference in weight between the punches from right and left ears, and expressed as an increase in ear thickness.

2.5.4.3. Prostaglandin (PGE_2)-induced hind paw edema model. PGE_2-induced hind paw edema model was used for determination of anti-inflammatory activity (Kasahara, Hikino, Tsurufiji, Watanabe, & Ohuchi, 1985). The difference in footpad thickness between the right and left foot was measured with a pair of dial thickness gauge calipers (Ozaki Co., Tokyo, Japan). Mean values of treated groups were compared with mean values of a control group and analyzed using statistical methods. One hour after the oral administration of the test sample or dosing vehicle, each mouse was injected with freshly prepared (5 μg/5 μl) suspension of PGE_2 (Fluka Chemie AG, Art. 82475) in Tyrode's solution into the subplantar tissue of the right hind paw. As the control, 5 μl Tyrode's solution was injected into that of the left hind paw. Paw edema was measured every 15 min for 75 min from induction of inflammation. The difference in footpad thickness was measured by gauge calipers (Ozaki Co., Tokyo, Japan). Mean values of the treated group were compared with mean values of a control group and analyzed using statistical methods. Indomethacin (10 mg/kg) was used as the reference drug.

2.5.4.4. Acute toxicity. Animals employed in the carrageenan-induced paw edema experiment were observed over 48 h and mor-

bidity or mortality was recorded, if present, for each group at the end of the observation period.

2.5.4.5. Gastric-ulcerogenic effect. After the antinociceptive activity experiment, mice were sacrificed under deep ether anesthesia and stomachs were removed. The abdomen of each mouse was then opened through the greater curvature and examined under dissecting microscope for lesions or bleedings.

2.5.4.6. Statistical analysis of data. Data obtained from animal experiments were expressed as mean standard error (±SEM). Statistical differences between the treatment and control groups were evaluated by ANOVA and Students–Newman–Keuls post hoc tests. $p < 0.05$ was considered to be significant ($^{*}p < 0.05$; $^{**}p < 0.01$; $^{***}p < 0.001$).

2.5.5. Antioxidant activity

2.5.5.1. Reduction of DPPH radical. Methanolic solutions (0.1%) of compounds **1**–**7** were chromatographed on a silica gel plate using $CHCl_3$–MeOH–H_2O (70:30:3, v/v/v). After drying, TLC plates were sprayed with 0.2% 2,2-diphenyl-1-picrylhydrazyl (DPPH) radical (Fluka, Switzerland) solution in MeOH. Compounds showing a yellow-on-purple spot were regarded as antioxidant (Takao, Kitatani, Watanebe, Yagi, & Sakata, 1994).

2.5.5.2. The lipid peroxidation of liposomes assay. The principal components of the assay, apart from the standardized liposomes source (Brain extract, Sigma, Germany), are ascorbic acid (Aldrich, Germany) and an iron source ($FeCl_3$, Sigma, Germany). Brain extract suspension was made in PBS (phosphate buffered saline, Sigma, Germany) and sonicated in an ice-water bath until all lipids had been suspended. For the test reaction of the pure compounds, a mixture of liposomes, $FeCl_3$, ascorbic acid and PBS was used. All of the tubes were incubated at 37 °C for 20 min. The TBA test was performed thereafter by adding butylated hydroxytoluene (Sigma, Germany) in ethanol followed by thiobarbituric acid (TBA, Sigma, Germany) in NaOH (Merck, Germany) and HCl (Merck, Germany). The tubes were heated to 90 °C for 30 min and then allowed to cool completely. The chromogens were extracted by *n*-butanol (Merck, Germany). The mixture was vortexed to ensure complete extraction of the chromogen and then centrifuged at 3500 rpm for 15 min at room temperature in order to separate the two layers. The absorbance of the upper layers, which contain the chromogen, was determined by a Shimadzu UV-1601(Japan) UV–vis spectrophotometer at 532 nm. The incorporation of any antioxidant compound in the mixture will lead to a reduction in the extent of peroxidation (Güvenç et al., 2005). The calculation of percentage inhibitions of lipid peroxidation was assessed by comparing the absorbance of the full reaction mixture with that of the extract test reaction mixtures where the substance to be assessed was included. The half-maximal inhibitory concentrations (IC_{50}) of compounds **1**–**7** were calculated by linear regression analysis.

Compounds were prepared in MeOH and seven different concentrations (1; 0.20; 0.04; 0.008; 0.0016; 0.00032; 0.000064 mg/ml). Propyl gallate was used as a reference compound in the same concentrations.

2.5.6. Effect on aldose reductase (AR)

2.5.6.1. Preparation of sample solution. All compounds were dissolved in dimethyl sulphoxide (DMSO). Usually a 3 μg/mL solution was prepared and diluted to the desired concentrations with DMSO.

2.5.6.2. Assay of AR activity. Assays were performed at 25 °C in 0.2 M sodium phosphate buffer (pH 6.2) containing 10 mM DL-glyceraldehyde, 0.5 mM NADPH and enzyme (3×10^{-3} unit) in a total volume of 1.0 mL. The effect of enzyme inhibition was determined by adding 3 μL of an inhibitor solution to the reaction mixture; the appropriate blank was prepared. The reaction was initiated by adding substrate, and the rate of NADPH oxidation was indicated by the decrease of absorbance at 340 nm on a Shimadzu UV 160A spectrophotometer (Enomoto et al., 2004). Quercetin was used as positive control.

2.5.6.3. Determination of IC_{50}. The concentration of inhibitors (μg/0.1 mL reaction mixture) giving 50% inhibition of enzyme activity was estimated from the least-squares regression line of the logarithmic concentrations plot against the remaining activities.

3. Results and discussion

For the scientific evaluation of the aerial parts of *S. brevibracteata*, used as an herbal tea in Turkish folk medicine, various extracts and pure compounds (**1**–**7**) were investigated. These extracts and pure compounds were then investigated for their *in vivo* anti-inflammatory activity using carrageenan-induced hind paw edema model (Table 1), PGE_2-induced hind paw edema model (Table 2) and TPA-induced mouse ear edema model (Table 3) and for their

Table 1
Effects of the extracts and the pure compounds of *S. brevibracteata* against carrageenan-induced paw edema in mice.

Extract/cpd.	Dose mg/kg	Swelling thickness ($\times 10^{-2}$mm) ± SEM (% inhibition)			
		90 min	180 min	270 min	360 min
Control		47.9 ± 3.4	53.2 ± 2.9	58.8 ± 3.5	63.7 ± 3.8
MeOH extract	100	51.2 ± 3.8	58.8 ± 3.7	61.2 ± 2.9	66.4 ± 3.1
$CHCl_3$ extract	100	46.5 ± 3.2 (2.9)	51.1 ± 3.0 (3.9)	56.2 ± 3.4 (4.4)	61.7 ± 3.2 (3.1)
BuOH extract	100	36.8 ± 2.4 (23.2)	38.9 ± 2.6 **(26.9)***	40.1 ± 3.0 **(31.8)****	41.2 ± 3.3 **(35.3)****
Remaining H_2O extract	100	48.8 ± 3.9	54.5 ± 3.1	58.9 ± 3.9	64.5 ± 3.5
Hypolaetin (**1**)	100	39.7 ± 2.0 (17.1)	41.2 ± 3.2 (22.6)	43.2 ± 3.0 **(26.5)***	44.8 ± 2.8 **(29.7)****
(**4**)	100	42.3 ± 3.0 (11.7)	45.6 ± 2.8 (14.3)	47.8 ± 3.1 (18.7)	48.9 ± 2.9 **(23.2)***
Isoscutellarein (**2**)	100	46.3 ± 2.7 (3.3)	47.8 ± 2.9 (10.2)	50.6 ± 3.4 (13.9)	52.2 ± 3.0 (18.1)
(**5**)	100	47.5 ± 2.9	48.8 ± 3.2 (8.3)	50.1 ± 3.0 (14.8)	57.8 ± 3.2 (9.3)
3′-Hydroxy-4′-*O*-methylisoscutellarein (**3**)	100	48.3 ± 4.2	53.4 ± 3.9	60.7 ± 4.4	64.8 ± 4.1
(**6**)	100	38.7 ± 1.9 (19.2)	42.2 ± 2.4 (20.7)	41.3 ± 2.6 **(29.8)****	42.5 ± 3.0 **(33.3)****
Verbascoside = acteoside (**7**)	100	43.6 ± 3.3 (8.9)	45.6 ± 2.9 (14.3)	41.5 ± 3.1 **(29.4)***	45.1 ± 3.3 **(29.2)****
Indomethacin	10	33.5 ± 2.7 **(30.1)****	34.8 ± 2.5 **(34.6)****	35.7 ± 2.5 **(39.3)*****	38.1 ± 2.9 **(40.2)*****

MeOH: methanol extract; $CHCl_3$: chloroform extract; BuOH: *n*-butanol extract; SEM: standard error mean.
* $p < 0.05$.
** $p < 0.01$.
*** $p < 0.001$.

Table 2
Effects of the extracts and the pure compounds of *S. brevibracteata* against PGE_2-induced paw edema in mice.

Extract/cpd.	Dose (mg/kg)	Swelling thickness ($\times 10^{-2}$mm) ± SEM (% inhibition)					
		0 min	15 min	30 min	45 min	60 min	75 min
Control		1.9 ± 0.9	15.4 ± 1.7	21.3 ± 1.9	23.3 ± 2.1	19.7 ± 2.5	11.9 ± 1.9
MeOH extract	100	2.1 ± 1.1	16.3 ± 1.5	22.4 ± 1.8	25.7 ± 2.3	21.1 ± 2.0	13.4 ± 1.8
$CHCl_3$ extract	100	1.8 ± 0.8 (5.3)	14.8 ± 1.2 (3.9)	19.7 ± 1.1 (7.5)	21.7 ± 1.6 (6.9)	17.5 ± 1.4 (11.2)	10.5 ± 1.3 (11.8)
BuOH extract	100	1.7 ± 0.7 (10.5)	11.5 ± 1.1 **(25.3)***	14.8 ± 1.5 **(30.5)****	16.9 ± 1.2 **(27.5)***	15.1 ± 1.4 (23.4)	9.9 ± 1.7 (16.8)
Remaining H_2O extract	100	1.9 ± 1.0	16.7 ± 1.9	23.4 ± 1.7	26.9 ± 1.9	22.4 ± 2.7	15.6 ± 2.3
Hypolaetin (**1**)	100	1.8 ± 1.3 (5.3)	11.9 ± 1.8 (22.7)	16.0 ± 1.3 **(24.9)***	17.1 ± 1.5 **(26.6)***	16.9 ± 1.5 (14.2)	10.8 ± 1.7 (9.2)
(**4**)	100	1.8 ± 1.1 (5.3)	12.8 ± 1.5 (16.9)	16.8 ± 1.4 (21.1)	17.9 ± 1.2 (23.2)	18.1 ± 1.9 (8.1)	10.9 ± 2.0 (8.4)
Isoscutellarein (**2**)	100	2.0 ± 0.7	11.8 ± 1.7 (23.4)	17.6 ± 1.9 (17.4)	19.9 ± 2.3 (14.6)	17.1 ± 2.6 (13.2)	10.1 ± 2.1 (15.1)
(**5**)	100	2.1 ± 1.1	13.9 ± 1.4 (9.7)	18.7 ± 1.7 (12.2)	19.5 ± 1.5 (16.3)	17.0 ± 1.3 (13.7)	10.4 ± 1.6 (12.6)
3′-Hydroxy-4′-*O*-methylisoscutellarein (**3**)	100	2.5 ± 1.1	14.3 ± 1.1 (7.1)	22.5 ± 2.3	25.7 ± 1.9	17.8 ± 1.5 (9.6)	11.3 ± 1.1 (5.0)
(**6**)	100	1.9 ± 1.0	11.4 ± 1.1 **(25.9)***	15.8 ± 1.4 **(25.8)***	17.5 ± 1.3 **(24.9)***	17.9 ± 1.7 (9.1)	9.8 ± 1.4 (17.6)
Verbascoside = acteoside (**7**)	100	1.8 ± 1.1 (5.3)	12.7 ± 1.3 (17.5)	15.8 ± 1.6 **(25.8)***	18.5 ± 1.4 **(20.6)***	18.1 ± 1.9 (8.1)	10.3 ± 1.8 (13.4)
Indomethacin	10	1.7 ± 0.5 (10.5)	11.2 ± 1.2 **(27.3)***	13.9 ± 1.4 **(34.7)****	14.9 ± 1.1 **(36.1)*****	13.9 ± 1.4 **(29.4)****	9.2 ± 1.3 (22.7)

PGE2: prostaglandin; MeOH: methanol extract; $CHCl_3$: chloroform extract; BuOH: *n*-butanol extract; SEM: standard error mean.
* $p < 0.05$.
** $p < 0.01$.
*** $p < 0.001$.

Table 3
Effects of the extracts and the pure compounds of *S. brevibracteata* against TPA-induced ear edema in mice as measurement of swelling thickness and weight measurement of edema.

Extract/cpd.	Dose (mg/ear)	Swelling thickness (μm) ± SEM	Inhibition %	Weight edema (mg) ± SEM	Inhibition %
Control		248.2 ± 35.6		23.5 ± 3.9	
MeOH extract	0.5	234.5 ± 42.6	5.5	20.4 ± 3.7	13.2
$CHCl_3$ extract	0.5	221.7 ± 33.5	10.7	18.8 ± 3.5	20.0
BuOH extract	0.5	156.7 ± 29.6	**36.9****	15.6 ± 3.1	**33.6****
Remaining H_2O extract	0.5	254.2 ± 27.8	–	22.8 ± 4.1	2.9
Hypolaetin (**1**)	0.5	166.9 ± 23.9	**32.8****	16.9 ± 2.9	**28.1***
(**4**)	0.5	170.5 ± 30.5	**31.3***	17.1 ± 2.7	**27.2***
Isoscutellarein (**2**)	0.5	215.4 ± 31.8	13.2	19.9 ± 4.8	15.3
(**5**)	0.5	202.1 ± 21.7	18.6	20.2 ± 3.4	14.0
3′-Hydroxy-4′-*O*-methylisoscutellarein (**3**)	0.5	223.5 ± 25.2	9.9	24.1 ± 5.9	–
(**6**)	0.5	163.2 ± 20.8	**34.2****	16.1 ± 2.9	**31.4****
Verbascoside = acteoside (**7**)	0.5	226.5 ± 31.2	8.7	21.4 ± 3.7	8.9
Indomethacin	0.5	53.3 ± 17.8	**78.5*****	12.1 ± 1.1	**48.5*****

TPA: 12-*O*-tetradecanoylphorbol 13-acetate; MeOH: methanol extract; $CHCl_3$: chloroform extract; BuOH: *n*-butanol extract; SEM: standard error mean.
* $p < 0.05$.
** $p < 0.01$.
*** $p < 0.001$.

antinociceptive activity using PBQ-induced writhing model in mice (Table 4); pure phenolic compounds of this plant were also studied *in vitro* for antioxidant and AR inhibitory activities (Table 5).

Compounds **1**–**7** were isolated with MPLC using reversed phase material (RP C-18) and increasing amount of MeOH in water as eluent from *n*-butanol extract of the MeOH extract of aerial parts of *S. brevibracteata*. Compounds **1**–**6** were obtained as yellow solids. Their IR spectra showed absorption bands for hydroxyl, ester carbonyl, conjugated carbonyl and aromatic ring. The UV spectra and NMR data resulted in grouping the compounds in three pairs (**1**/**4**, **2**/**5** and **3**/**6**). The UV, IR, ^{1}H- and ^{13}C-NMR data of compounds **1**/**4**, **2**/**5** and **3**/**6** were identical with those of hypolaetin 7-*O*-[6‴-*O*-acetyl-β-D-allopyranosyl-(1 → 2)]-β-D-glucopyranoside (**1**) (Lenherr & Mabry, 1987; Rodriguez-Lyon et al., 2000), isoscutellarein 7-*O*-[6‴-*O*-acetyl-β-D-allopyranosyl-(1 → 2)]-β-D-glucopyranoside (**2**) (Albach et al., 2003; Lenherr & Mabry, 1987; Rios et al., 1992), 3′-hydroxy-4′-*O*-methylisoscutellarein 7-*O*-[6‴-*O*-acetyl-β-D-allopyranosyl-(1 → 2)]-β-D-glucopyranoside (**3**) (Lenherr & Mabry, 1987; Rios et al., 1992), hypolaetin 7-*O*-[6‴-*O*-acetyl-β-D-allopyranosyl-(1 → 2)]-6″-*O*-acetyl-β-D-glucopyranoside (**4**) (Lenherr & Mabry, 1987; Rodriguez-Lyon et al., 2000), isoscutellarein 7-*O*-[6‴-*O*-acetyl-β-D-allopyranosyl-(1 → 2)]-6″-*O*-acetyl-β-D-glucopyranoside (**5**) (Lenherr & Mabry, 1987; Skaltsa et al., 2000), and 3′-hydroxy-4′-*O*-methylisoscutellarein 7-*O*-[6‴-*O*-acetyl-β-D-allopyranosyl-(1 → 2)]-6″-*O*-acetyl-β-D-glucopyranoside (**6**) (Lenherr & Mabry, 1987), respectively (Fig. 1). Compound **7** was identified as verbascoside (=acteoside). The UV, IR, ESI-MS and NMR data were in good accordance with those previously reported (Sticher & Lahloub, 1982).

Anti-inflammatory activity has been reported in different kinds of extracts of several *Sideritis* species (Alcaraz et al., 1989; Barberán, Manez, & Villar, 1987; Hernandez-Perez, Sanches-Mateo, Montalbetti-Moreno, & Rabanal, 2004). However, studies performed on the pure compounds are rare (Küpeli, Şahin, Çalış, Yeşilada, & Ezer, 2007; Villar, Gasco, & Alcaraz, 1984). In the present study, the results in Tables 1–4 indicated that the *n*-butanol extract of *S. brevibracteata* exhibited the highest anti-inflammatory and antinociceptive activity. These results are in good accordance with the uses of this genus. The dried flowering spikes of *Sideritis* species are used as herbal tea in the western and southern coastal regions of Turkey due to their pleasant smell and aroma. Tea is the hot water extract of a plant and it contains all water soluble extractives such as sugars, glycosides, phenolics, etc. (Başer, 1995). It was considered that the active compounds for both anti-inflammatory and antinociceptive activities could be flavonoids, which are the major components of the *n*-butanol fraction.

Table 4
Effects of the extracts and the pure compounds of *S. brevibracteata* against *p*-benzoquinone-induced writhings in mice.

Extract/cpd.	Dose (mg/kg)	Number of writhings ± SEM	Inhibitory ratio (%)	Ratio of ulceration
Control		53.2 ± 3.7		0/6
MeOH extract	100	49.8 ± 3.5	6.4	0/6
$CHCl_3$ extract	100	44.5 ± 2.9	16.4	0/6
BuOH extract	100	29.9 ± 2.0	**43.8*****	0/6
Remaining H_2O extract	100	59.6 ± 3.1	–	2/6
Hypolaetin (**1**)	100	33.2 ± 2.3	**37.6****	0/6
(**4**)	100	37.9 ± 3.1	**28.8***	0/6
Isoscutellarein (**2**)	100	39.8 ± 3.9	25.2	0/6
(**5**)	100	43.2 ± 2.4	18.8	0/6
3′-hydroxy-4′-*O*-methylisoscutellarein (**3**)	100	50.1 ± 5.6	5.8	0/6
(**6**)	100	32.6 ± 2.3	**38.7****	0/6
Verbascoside = acteoside (**7**)	100	39.9 ± 3.2	**25.0***	0/6
ASA	100	25.2 ± 2.1	**52.6*****	4/6

MeOH: methanol extract; $CHCl_3$: chloroform extract; BuOH: *n*-butanol extract; SEM: standard error mean; ASA: acetyl salicylic acid.
* $p < 0.05$.
** $p < 0.01$.
*** $p < 0.001$.

Table 5
Antioxidant and aldose reductase inhibitory activities of pure compounds obtained from *S. brevibracteata*.

Compounds	Antioxidant activity in the TBA test IC_{50} value (μg/mL) ± SD	Aldose reductase inhibitory activity IC_{50} value (μg/mL)
Hypolaetin (**1**)	0.78 ± 0.07	0.61
(**4**)	0.57 ± 0.03	0.47
Isoscutellarein (**2**)	3.48 ± 1.75	1.16
(**5**)	3.14 ± 2.18	1.02
3′-Hydroxy-4′-*O*-methylisoscutellarein (**3**)	1.33 ± 0.02	1.25
(**6**)	1.96 ± 0.41	>1000
Verbascoside = acteoside (**7**)	0.99 ± 0.01	2.11
Propyl gallate	0.21 ± 0.01	
Quercetin		1.16

All the above arguments are in agreement with experiments undertaken by other research groups reporting similar chemical compounds from other *Sideritis* species (Alcaraz et al., 1989; Küpeli et al., 2007; Villar et al., 1984). As shown in Table 1, *n*-butanol extract was significantly active against carrageenan-induced edema. Hence, the phenolic compounds isolated from the *n*-butanol extract were also assayed in the same *in vivo* system. All extracts and the pure compounds were given in standard dose of 100 mg/kg, in order to make a direct comparison of their activities. Hypolaetin derivatives (**1**,**4**) and 3′-hydroxy-4′-*O*-methylisoscutellarein7-*O*-[6‴-*O*-acetyl-β-D-allopyranosyl-(1 → 2)-6″-*O*-acetyl-β-D-glucopyranoside] (**6**) showed activity in carrageenan-induced paw edema, ear edema and PBQ-induced writhings in mice. Compounds **1** and **6** were found to be active against PGE_2-induced paw edema in mice. Compound **7** showed activity in all the test systems. On the other hand, the anti-inflammatory properties of verbascosides (**7**) as a major constituent of *Stachytarpheta cayennesis* (L.C. Rich) Vahl were shown in a previous study (Penido et al., 2006).

Our results are supported by the previous studies showing the anti-inflammatory and antinociceptive activities of certain *Sideritis* species due to their flavonoid and phenylethanoid contents (Hernandez-Perez et al., 2004; Küpeli et al., 2007; Penido et al., 2006). Compounds **1** (hypolaetin 7-*O*-[6‴-*O*-acetyl-β-D-allopyranosyl-(1 → 2)-β-D-glucopyranoside]) and **7** (verbascoside) were found to be the most active compounds. Isoscutellarein derivatives (**2**, **5**) were found to have lower anti-inflammatory and antinociceptive activities.

The water soluble part of the MeOH extract was partitioned between chloroform and *n*-BuOH. According to the TLC autographic assay with DPPH**.**, seven compounds (**1**–**7**) were found to be responsible for the scavenging properties of *S. brevibracteata* (Takao et al., 1994). These compounds were rich in *n*-BuOH extract of the aerial parts of this species. The antioxidant activity of the compounds was investigated using TBA method, in which the highest activity was observed for compounds **1**, **4** and **7**. Among the flavone glycosides, hypolaetin derivatives (**1**, **4**) were found to have stronger activity than isoscutellarein. It was shown that compounds **3** and **6** have higher antioxidant activity than compounds **2** and **5**. Compounds **3** and **6,** which carry hydroxyl group at C-3′ position and methoxyl group at C-4′ position on ring B, are more active than compounds **2** and **5,** having one hydroxyl group at C-4′ position on ring B. These results are in good accordance with those reported by Rios et al. (Rios et al., 1992). *O*-glycosylation at C-7 has been reported as weakly negative on activity by Mora et al. (Mora, Paya, Rios, & Alcaraz, 1990). However, Rios et al. observed that compounds having the 6‴-acetylallopyranosyl-(1 → 2)-glucopyranoside group were also active (Rios et al., 1992). In the present study, it was observed that the acetyl group on the allose unit was ineffective on antioxidant activity. Furthermore, the antioxidant activity of compound **7** has been reported in previous studies (Aldini et al., 2006; Siciliano et al., 2005). Thus, the presence of *ortho*-hydroxyl groups on phenolic moieties is responsible for the remarkable antioxidant activity, as previously reported for flavonoids (Rios et al., 1992) and for phenylethanoid glycosides (Heilmann et al., 2000). Moreover, we examined six flavonoid compounds along with verbascoside for their inhibitory activities on human AR. A structure activity relationship among the seven compounds was not found in the AR inhibitory assay. However, among the flavone glycosides, hypolaetin derivatives (**1**, **4**) gave similar activity. Isoscutellarein derivatives (**2**, **5**) also showed the same activity.

The distribution of the flavone glycosides in the genus *Sideritis* is of interest from a taxonomic viewpoint. In particular, 8-OH-flavone glycosides are characteristic for some sections of *Sideritis*. The 7-allosylglycosides of hypolaetin, isoscutellarein and 3′-hydroxy-4′-*O*-methylisoscutellarein were also reported from different *Sideritis* species, as *S. hypsophila* (Rodriguez-Lyon et al., 2000), *S. javalambrensis* (Rios et al., 1992), and *S. mugronensis* (Alcaraz et al., 1989; Villar et al., 1984). In 1993, in contrast to the sections of *Empedocleopsis* and *Creticae*, the section *Marrubiastrum* was reported as one of the richest *Sideritis* species containing 8-OH-flavone glycosides (Gil, Ferreres, Marrero, Tomás-Lorente, & Tomás-Barberán, 1993). Among the Ibero-North African *Sideritis* species, species of the section *Sideritis* (*Eusideritis* Bentham) were also characterized by the accumulation of the 7-glycosides of 8-OH-flavones

(isoscutellarein, hypolaetin and their methyl ethers), as in this study (Barberán, Rejdali, Harborne, & Heywood, 1988). Moreover, the presence of 6-OH-flavone and 8-OH-flavone 7-glycosides is also a characteristic feature for the Lamiaceae, Scrophulariaceae and chemically related families (Barberán, Grayer-Barkmeijer, Gil, & Harborne, 1988).

Consequently, it was observed that *S. brevibracteata* became a good anti-inflammatory, antinociceptive, antioxidant and AR inhibitory herbal tea, since among the 17 species (18 taxa) of *Sideritis* investigated (Güvenç et al., 2005), this species was found to be richest in 8-OH-flavone glycoside content.

Acknowledgement

The authors thank Prof. Dr. Hakan Göker (Ankara University, Faculty of Pharmacy) for the measurements of the NMR spectra and Prof. Dr. Erhan Palaska (Hacettepe University, Faculty of Pharmacy) for the ESI-MS spectra of the compounds reported in this study.

References

Albach, D. C., Grayer, R. J., Jensen, S. R., Özgökçe, F., & Veitch, N. C. (2003). Acylated flavone glycosides from Veronica. *Phytochemistry, 64*, 1295–1301.

Alcaraz, M. J., Jimenez, M. J., Valverde, S., Sanz, J., Rabanal, R. M., & Villar, A. (1989). Anti-inflammatory compounds from *Sideritis javalambrensis* *n*-hexan extract. *Journal of Natural Products, 52*, 1088–1091.

Aldini, G., Piccoli, A., Beretta, G., Morazzoni, P., Riva, A., Marinello, C., et al. (2006). Antioxidant activity of polyphenols from solid olive residues of c.v. Coratina. *Fitoterapia, 77*(12), 1–128.

Aytaç, Z., & Aksoy, A. (2000). A new *Sideritis* species (Labiatae) from Turkey. *Flora Mediterranea, 10*, 181–184.

Barberán, F. A. T., Grayer-Barkmeijer, R. J. G., Gil, M. I., & Harborne, J. B. (1988). Distribution of 6-hydroxy-, 6-methoxy- and 8-hydroxyflavone glycosides in the Labiatae, the Scrophulariacea and related families. *Phytochemistry, 27*, 2631–2645.

Barberán, F. A. T., Manez, S., & Villar, A. (1987). Identification of antiinflammatory agents from *Sideritis* species growing in Spain. *Journal of Natural Products, 50*, 313–314.

Barberán, F. A. T., Rejdali, M., Harborne, J. B., & Heywood, V. H. (1988). External and vacuolar flavonoids from Ibero-North African *Sideritis* species. A chemosystematic approach. *Phytochemistry, 27*, 165–170.

Başer, K. H. C. (1995). Flavours, fragrances and essential oils. In *Proceedings of the thirteenth international congress of flavours, fragrances and essential oils*, Istanbul, 15–19 October.

Baytop, T. (1999). *Türkiye'de Bitkiler ile Tedavi. Geçmişte ve Bugün* (2nd ed.). İstanbul: Nobel Tıp Kitabevleri.

De Young, L. M., Kheifets, J. B., Ballaron, S. J., & Young, J. M. (1989). Edema and cell infiltration in the phorbol ester treated mouse ear are temporally separate and can be differently modulated by pharmacologic agents. *Agents Activity, 26*, 335–341.

Enomoto, S., Okada, Y., Güvenç, A., Erdurak, C. S., Coşkun, M., & Okuyama, T. (2004). Inhibitory effect of traditional Turkish folk medicines on aldose reductase (AR) and hematological activity, and on AR inhibitory activity of quercetin-3-*O*-methyl ether isolated from *Cistus laurifolius* L. *Biological and Pharmaceutical Bulletin, 27*, 1140–1143.

Gil, M. I., Ferreres, F., Marrero, A., Tomás-Lorente, F., & Tomás-Barberán, F. A. (1993). Distribution of flavonoid aglycones and glycosides in *Sideritis* species from the Canary Islands and Madeira. *Phytochemistry, 34*, 227–232.

Güvenç, A., Houghton, P. J., Duman, H., Coşkun, M., & Şahin, P. (2005). Antioxidant activity studies on some *Sideritis* species native to Turkey. *Pharmaceutical Biology, 43*, 173–177.

Heilmann, J., Calıs, I., Kırmızıbekmez, H., Schühly, W., Harput, S., & Sticher, O. (2000). Radical scavenger activity of phenylethanoid glycosides in FMLP stimulated human polymorphonuclear leucocytes: Structure-activity relationships. *Planta Medica, 66*, 746–748.

Hernandez-Perez, H., Sanches-Mateo, C. C., Montalbetti-Moreno, Y., & Rabanal, R. M. (2004). Studies on the analgesic and anti-inflammatory effects of *Sideritis candicans* Ait Var. *eriocephala* Webb aerial part. *Journal of Ethnopharmacology, 93*, 284–297.

Huber-Morath, A. (1982). *Sideritis* L. In P. H. Davis (Ed.), *Flora of Turkey and the Aegean Islands* (Vol. 7, pp. 178–199). Edinburgh, UK: University Press

Kasahara, Y., Hikino, H., Tsurufiji, S., Watanabe, M., & Ohuchi, K. (1985). Antiinflammatory actions of ephedrines in acute inflammations. *Planta Medica, 51*, 325–331.

Küpeli, E., Şahin, F. P., Çalış, I., Yeşilada, E., & Ezer, N. (2007). Phenolic compounds of *Sideritis ozturkii* and their in vivo anti-inflammatory and antinociceptive activities. *Journal of Ethnopharmacology, 112*, 356–360.

Lenherr, A., & Mabry, T. J. (1987). Acetylated allose-containing flavonoid glucosides from *Stachys anisochila*. *Phytochemistry, 26*, 1185–1188.

Mora, A., Paya, M., Rios, J. L., & Alcaraz, M. J. (1990). Structure-activity relationships of polymethoxyflavones and other flavonoids as inhibitors of non-enzymic lipid peroxidation. *Biochemical Pharmacology, 40*, 793–797.

Okun, R., Liddon, S. C., & Lasagnal, L. (1963). The effect of aggregation, electric shock and adrenergic blocking drugs on inhibition of the "writhing syndrome". *Journal of Pharmacology and Experimental Therapeutics, 139*, 107–109.

Penido, C., Costa, K. A., Futuro, D. O., Paiva, S. R., Kaplan, M. A. C., Figueiredo, M. R., et al. (2006). Anti-inflammatory and anti-ulcerogenic properties of *Stachytarpheta cayennensis* (L.C. Rich) Vahl. *Journal of Ethnopharmacology, 104*, 225–233.

Rios, J. L., Mañez, S., Paya, M., & Alcaraz, M. J. (1992). Antioxidant activity of flavonoids from *Sideritis javalambrensis*. *Phytochemistry, 31*, 1947–1950.

Rodriguez-Lyon, M. L., Diaz-Lanza, A. M., Bernabe, M., & Villaescusa-Castillo, L. (2000). Flavone glycosides containing acetylated sugars from *Sideritis hyssopifolia*. *Magnetic Resonance Chemistry, 38*, 684–687.

Siciliano, T., Bader, A., Vassallo, A., Braca, A., Morelli, I., Pizza, C., et al. (2005). Secondary metabolites from *Ballota undulata* (Lamiaceae). *Biochemical Systematics and Ecology, 33*, 341–351.

Skaltsa, H., Bermejo, P., Lazari, D., & Silvan, A. M. (2000). Inhibition of prostaglandin E2 and leukotriene C4 in mouse peritoneal macrophase and thromboxane B2 production in human platelets by flavonoids from *Stachys chrysantha* and *Stachys candida*. *Biological and Pharmaceutical Bulletin, 23*, 47–53.

Sticher, O., & Lahloub, M. F. (1982). Phenolic glycosides of *Paulownia tomentosa* bark. *Planta Medica, 46*, 145–148.

Takao, T., Kitatani, F., Watanebe, N., Yagi, A., & Sakata, K. (1994). A simple screening method for antioxidants and isolation of several antioxidants produced by marine-bacteria from fish and shellfish. *Bioscience Biotechnology and Biochemistry, 58*, 1780–1783.

Villar, A., Gasco, M. A., & Alcaraz, M. J. (1984). Anti-inflammatory and anti-ulcer properties of hypolaetin-8-glucoside, a novel plant flavonoid. *Journal of Pharmacy and Pharmacology, 36*, 820–823.

Yeşilada, E., & Küpeli, E. (2002). *Berberis crataegina* DC. root exhibits potent anti-inflammatory, analgesic and febrifuge effects in mice and rats. *Journal of Ethnopharmacology, 79*, 237–248.

2005). Similarly, chlorogenic acids were reported to accumulate with an increase in altitude in one study (Avelino et al., 2005) but to remain stable in another (Guyot et al., 1996). These discrepancies may be due to the fact that previous surveys were not performed using experimental sites that were strictly designed to study the effect of altitude: i.e. the soil–climatic conditions may also have varied at the sites (soil type and solar exposure, for example) as well as agricultural management. In addition, the studies covered a low altitude range ($\leqslant$400 m). However, a recent study investigated the effect of altitude on coffee bean composition using eight experimental plots located at regular intervals within an altitude range of 550 m on the same slope of the Poas volcano in Costa Rica (Bertrand et al., 2006). Positive statistical relationships were found between altitude and caffeine, CGA (on the basis of the main CGA component, 5-CQA), and total lipids of green beans, estimated by NIRS. Unfortunately, mesoclimate parameters were not recorded locally and it was therefore not possible to conclude whether the effects of altitude were mainly related to a temperature gradient or to other soil–climatic variables. Consequently, a rigorous study is still required to comprehensively analyse the relationships between main climatic variables (temperature, rainfall, irradiance and evapotranspiration potential) and the composition of the coffee seed.

Concerning post-harvest treatments, green coffee is traditionally produced by either wet or dry processing. Both methods aim to remove the pericarp of the coffee cherry and to dry the raw coffee seed to a moisture content of 10–12% fresh weight. In the dry process, whole coffee fruits are dried in the sun and then hulled mechanically. In the wet process, ripe coffee cherries are mechanically depulped and the mucilaginous residues are degraded during a 'fermentation' step and then washed off. The resulting beans are still covered by the endocarp, termed parchment. The parchment coffee is then dried and subsequently hulled. The chemical composition of wet- and dry-processed seeds may differ significantly, as observed for free amino acids, organic acids, and non-structural carbohydrates (Bytof, Knopp, Schieberle, Teutsch, & Selmar, 2005; Knopp, Bytof, & Selmar, 2006). Dry-processed coffees are generally characterised by more body, whereas in most *terroirs,* wet-processed coffees have a better aroma, generally resulting in higher acceptance (Selmar, Bytof, & Knopp, 2002). In both treatments, the freshly processed coffee beans remain viable and exhibit active metabolic processes (Bytof et al., 2007). This observation established a novel and stimulating bridge between two distant disciplines in the coffee community: seed physiology and the chemistry of green bean technology.

It is now widely accepted that the metabolic reactions that occur during wet-processing help generate pleasant cup quality attributes (Selmar et al., 2002). Based on the observation of the early induction of the isocitrate lyase gene involved in the glyoxylate cycle, it was recently suggested that the germination process was initiated during the course of wet processing (Selmar et al., 2006). The concomitant increase in the abundance of β-tubulin, a marker for cell division or elongation, corroborates this hypothesis (Bytof et al., 2007). While chemical differences between wet and dry-processed seeds are well documented, data on the changes induced by the treatment itself (metabolic shift between fresh and processed seeds) are very scarce. Moreover, in contrast to the knowledge acquired on the metabolic processes that occur in the course of coffee seed development (Joët et al., 2009), no data is available on how environmental factors and post-harvest processes interplay.

Considering the importance of *terroirs* and post-harvest treatments in the generation of flavour, a better understanding of the chemical transformations occurring during wet processing, and their relationships with the metabolic status of the seed at harvest, seems highly warranted. The present study was carried out using samples from 16 Arabica coffee plots located throughout Reunion Island. Its rich homogeneous volcanic soil and various microclimates within short distances, combined with a dense network of meteorological stations, make Reunion Island a valuable experimental site to document the effects of environmental factors on the final composition of the bean. In order to estimate these effects precisely, all plots were planted the same year with exactly the same cultivar and underwent identical agricultural management. We quantified changes in lipid, chlorogenic acid, sugar and caffeine contents caused by wet processing and analysed how these changes were affected by the chemical variations induced by the environment.

2. Materials and methods

2.1. Biological material

Experiments were performed in Reunion Island on seeds of *C. arabica* cv. 'Laurina' (a natural dwarf mutant of cv. 'Bourbon') presenting two specific traits identified so far: rather low caffeine content and a typical oblong shape. The experimental plots were planted in 2003 without shade and were in their second (2006) production year (about 2 m high). Plant spacing was 2 m between rows and 1 m within rows. Fertilisers were applied and pests and diseases were controlled according to locally recommended practices. Among 107 experimental plots available throughout the island, sixteen plots that maximise variations in altitude (150–1032 m asl.) and climatic conditions (Table 1) were selected. The survey unit was a compact plot of about 240 coffee trees.

2.2. Meteorological observations and date of harvests

Reunion Island hosts a dense meteorological network of more than 50 automated stations dedicated to sugarcane agronomy (this service is under the supervision of Meteo France and Cirad). Climatic conditions (temperatures, rainfall, total irradiance, and potential evapotranspiration) were estimated for each plot from records at the nearest meteorological stations (data from Meteo France and Cirad) and corrected taking into account the difference in altitude. Temperatures were also recorded locally (under the coffee canopy) using portable temperature recorders. Dates of harvest differed depending on the location (Table 1).

2.3. Berry harvest and processing

Coffee berries were collected at the harvest peak for each plot (from April to December 2006), when the coffee was of best quality. Only just-ripe cherries (when pericarp turns purple) were harvested. For each experimental plot studied, fruits were collected on 20 trees randomly selected in the experimental plot. After cross-section, fresh seeds were separated from the pericarp and locules and immediately frozen in liquid nitrogen in the field and then stored at −80 °C. Seeds that were subjected to wet processing were harvested in the morning (2 kg of coffee cherries), transported to the CIRAD processing factory (Ligne Paradis, Saint Pierre), and directly processed in the afternoon by the wet method (de-pulping, fermentation and drying) to obtain approximately 500 g of green coffee beans (11% moisture). The temperature was recorded during the fermentation process which was divided into three successive steps: 'dry' fermentation with only mucilage (24 h), maceration by adding water to cover the seeds (15 h) and, finally, washing by changing the water three times during this step (11 h) (Table 1). The green coffee samples were screened through a size 15 sieve and the defective beans were discarded. For chemical analysis, seed tissues were freeze-dried and ground to a fine powder using an analytical grinder (IKA A10, Staufen, Germany). Powdered seed

Table 1
Geographic and climatic data for the last 5 months preceding harvest. Altitude (m); latitude and longitude (degrees); mean of minimum, average, and maximum daily temperatures (°C) (T_{min}, T_{aver} and T_{max}, respectively); TR, temperature range (calculated as T_{max}–T_{min}); RAIN, rainfall (mm d^{-1}); IR, irradiance (J cm^{-2} d^{-1}); ETP, evapotranspiration potential (mm d^{-1}); T_{ferm}, mean temperature during wet processing (°C). Cv = coefficient of variation.

Sites	Harvest	Alt	Long	Lat	T_{min}	T_{aver}	T_{max}	TR	RAIN	IR	ETP	T_{ferm}
1	04-2006	150	55 23 38	21 16 00	21.8	25.3	28.6	6.8	3.8	1728	4.6	24.0
2	04-2006	270	55 40 39	21 03 16	22.5	23.9	26.4	3.9	9.0	1783	2.1	25.3
3	07-2006	315	55 38 39	21 20 08	16.3	19.3	24.3	8.0	4.7	1284	2.5	19.6
4	08-2006	463	55 21 08	20 57 36	18.4	21.2	25.2	6.8	1.5	1488	2.5	20.3
5	05-2006	500	55 21 08	20 57 36	18.0	22.0	26.6	8.6	2.7	1150	2.9	21.6
6	08-2006	549	55 31 32	21 17 38	15.8	19.5	24.1	8.2	3.8	1374	3.4	19.7
7	07-2006	585	55 16 48	21 05 18	14.6	18.9	23.8	9.2	3.0	1043	2.2	18.7
8	09-2006	661	55 36 23	21 19 36	12.6	16.2	20.9	8.4	5.1	1199	2.4	21.3
9	09-2006	757	55 32 52	21 17 29	13.7	17.0	21.1	7.4	4.2	1148	2.6	20.3
10	10-2006	790	55 24 02	21 13 17	10.8	14.4	19.2	8.4	2.7	1164	2.7	23.0
11	08-2006	805	55 18 12	21 07 20	14.0	17.5	22.0	7.9	3.0	1031	2.2	19.5
12	09-2006	880	55 30 24	21 03 16	12.3	16.4	21.6	9.3	1.4	1270	1.9	18.9
13	09-2006	980	55 21 03	21 00 31	9.6	13.4	17.3	7.7	2.6	1023	1.9	20.8
14	10-2006	985	55 18 41	21 07 09	10.3	14.3	19.1	8.8	2.9	973	2.2	22.1
15	09-2006	1014	55 33 39	21 16 59	10.7	14.9	20.0	9.3	4.2	1133	2.6	19.7
16	12-2006	1032	55 25 02	21 12 35	9.9	14.0	17.7	7.8	2.0	1349	3.3	26.4
Cv (%)					28.2	20.2	15.0	16.7	51.1	19.0	26.0	10.8

tissue from fresh and wet-processed seeds was stored over silica-gel in a hermetic plastic box at −20 °C until analysis.

2.4. Lipid, sugar, caffeine and chlorogenic acid determination

Lipids, sugars, caffeine and chlorogenic acids were determined as described in Joët et al. (2009). Roughly, fatty acid methyl esters (FAMEs) were prepared according to the ISO-5509 standard and measured by GC. Sugars were determined by High-Performance Anion Exchange Chromatography coupled with Pulsed Amperometric Detection (Dionex Chromatography Co., Sunnyvale, USA). The seed CWP content was estimated by measuring the defated alcohol insoluble residue (DAIR). Chlorogenic acids and caffeine were analysed by HPLC at 325 and 276 nm, respectively. All metabolites were analysed in triplicate (from 3 different extractions) using a completely random experimental design.

2.5. Statistical analysis

Statistical significance of variations in metabolite content due to wet processing was verified by analysis of variance (one-way ANOVA with fixed effect). Correlations between climatic variables and metabolites levels as well as correlations among metabolites levels were analysed by linear regression using Pearson's correlation coefficient. For both, ANNOVA and linear regression, a significance threshold of $P = 0.01$ was retained.

3. Results

3.1. Air temperature during seed development influences routing within sugar, chlorogenic acid and fatty acid metabolic pathways

CGA, caffeine, CWP, lipid and free sugar contents, as well as fatty acid composition, were measured in fresh mature seeds sampled in 16 experimental coffee plots. These plots showed very high climatic variations, especially a very broad temperature gradient, which was highly correlated ($R = 0.93$, $P = 0.0000$ for T_{min} and T_{aver}, $R = 0.92$, $P = 0.0000$ for T_{max}) with altitude, which ranged from 150 to 1032 m (Table 1).

Relationships between metabolite contents and environmental factors were analysed by linear regression (Table 2). With the exception of caffeine, the overall lipid, sugar, and CGA composition of fresh seeds (Table 3) did not differ from that previously observed in other varieties. No environmental factor significantly influenced the accumulation of the four main classes of storage compounds studied. Indeed, total CWP, total lipids, total free sugars and total CGA, did not show any significant correlation with any climatic variable. Caffeine was not influenced by any of the environmental factors we measured. However, within a given chemical family (CGA, lipids or free sugars), some components were significantly influenced by the environment. Out of the 28 metabolites analysed, half showed significant correlations with the mean average air temperature during the last five months of seed development – i.e. the period when storage compounds accumulate in the seed (Joët et al., 2009). Significant correlations were also found with altitude and with mean minimum and maximum daily temperatures (data not shown), but the highest correlation coefficients were with the daily average temperature. In contrast, no significant correlation was found between rainfall or potential evapotranspiration and any of the compounds studied and only weak correlations were found with solar irradiance.

Within a given chemical family, when significant ($P < 0.01$), the slope of regression equations could differ among the compounds of the family concerned. For instance, 3-caffeoyl quinate (3-CQA) and 4-CQA content were positively correlated with temperature while the reverse trend was observed for 5-CQA (Fig. 1A). Interestingly, the same phenomenon was found for di-CQA: i.e. di3.4-CQA and di-4.5-CQA were positively influenced by temperature while a negative correlation was observed for di3.5-CQA. These results suggest that temperature may act directly on routing towards the different isomers within the CGA metabolic pathway without affecting the final CGA content. A similar routing regulation was observed within the FA biosynthetic pathway. Indeed, the relative contents of the two major FA, namely linoleic and palmitic acids (35–45% each), were negatively correlated with environmental temperature, while stearic acid (about 7%) accumulated more in warmer conditions (Fig. 1B). Similarly, oleic acid (about 7% of FA) was positively correlated with temperature, but the correlation coefficient was weaker ($R = 0.57$; $P = 2.10^{-2}$, data not shown).

3.2. Wet processing affects storage compounds differently

Nine of the 28 metabolite variables analysed showed significant differences in fresh and wet-processed seeds, as tested by one-way ANOVA ($P < 0.01$; Table 3). At the level of the biochemical class, post-harvest treatment did not influence total free sugar, total CGA or caffeine contents. In contrast, wet processing caused a significant increase in total CWP and lipid contents, suggesting

Table 2
Correlation matrix between metabolite contents in fresh and wet-processed seeds and mean environmental factors calculated during the last 5 months of fruit development. Numbers in brackets are correlations with wet-processed seeds. R = Pearson's linear-correlation coefficients. R values in bold indicate P values < 0.01. T_{aver}, average daily temperatures; RAIN, rainfall; IR, irradiance; ETP, evapotranspiration potential; T_{ferm}, mean temperature during wet processing. CGA, chlorogenic acid; CQA, caffeoyl quinic acid; FQA, feruloyl quinic acid.

	T_{aver}	RAIN	IR	ETP	T_{ferm}
Total CWP	−0.01 (−0.03)	0.18 (0.25)	−0.01 (0.01)	−0.11 (−0.51)	(−0.19)
Total soluble sugars	0.14 (−0.29)	0.31 (0.21)	0.14 (−0.20)	−0.26 (−0.33)	(0.41)
Myo-inositol	−0.49 (0.15)	0.00 (0.55)	−0.20 (0.55)	−0.01 (−0.05)	**(0.77)**
Glucose	**−0.71** (0.03)	−0.41 (−0.14)	−0.28 (0.03)	−0.15 (−0.32)	(−0.33)
Fructose	0.18 (−0.03)	−0.41 (−0.19)	0.12 (−0.05)	0.42 (−0.34)	(−0.41)
Sucrose	0.19 (−0.23)	0.36 (0.22)	0.15 (−0.16)	−0.29 (−0.27)	(0.43)
Raffinose	0.02 (0.45)	−0.08 (0.20)	0.11 (0.15)	0.16 (0.35)	(0.13)
Stachyose	**0.59** (0.16)	0.48 (0.27)	**0.63** (−0.05)	0.54 (−0.01)	(−0.16)
Sorbitol	−0.19 **(−0.89)**	0.14 (−0.26)	−0.09 (−0.58)	−0.37 (−0.30)	(0.05)
Caffeine	−0.06 (0.01)	0.07 (0.44)	−0.28 (−0.21)	−0.56 (−0.31)	(0.05)
Total CGA	−0.31 (−0.24)	0.02 (0.10)	−0.31 (−0.35)	−0.53 (−0.27)	(−0.13)
3-CQA	**0.80 (0.87)**	0.53 (0.53)	0.60 **(0.78)**	−0.03 (0.36)	(0.41)
4-CQA	**0.71 (0.80)**	0.53 (0.53)	0.53 **(0.70)**	−0.14 (0.32)	(0.38)
5-CQA	**−0.64** (−0.59)	−0.12 (−0.09)	−0.49 (−0.61)	−0.51 (−0.39)	(−0.28)
4-FQA	0.23 (0.61)	0.19 (0.61)	0.28 (0.42)	−0.40 (−0.06)	(0.15)
5-FQA	0.10 (0.30)	−0.26 (0.01)	−0.17 (0.01)	0.07 (0.26)	(0.27)
di3.4-CQA	**0.82 (0.85)**	0.42 (0.42)	0.57 **(0.67)**	0.03 (0.35)	(0.39)
di3.5-CQA	**−0.72 (−0.73)**	−0.48 (−0.36)	**−0.73 (−0.73)**	−0.24 (−0.46)	(−0.47)
di4.5-CQA	**0.76 (0.89)**	0.38 (0.42)	0.60 **(0.69)**	−0.03 (0.40)	(0.41)
Total lipids	−0.29 (−0.34)	−0.51 (−0.52)	−0.24 (−0.27)	0.32 (0.42)	(−0.03)
Palmitic (16:0)	**−0.71 (−0.70)**	−0.44 (−0.28)	−0.59 (−0.54)	−0.50 (−0.54)	(−0.26)
Stearic (18:0)	**0.89 (0.90)**	0.35 (0.28)	**0.64 (0.72)**	0.39 **(0.63)**	(0.25)
Oleic (18:1)	0.57 **(0.82)**	−0.13 (0.12)	0.11 (0.50)	0.21 (0.45)	(−0.25)
cis-Vaccenic (18:1-n7)	**−0.81 (−0.86)**	−0.18 (−0.31)	−0.48 (−0.59)	−0.44 (−0.54)	(0.06)
Linoleic (18:2)	**−0.70 (−0.85)**	−0.05 (−0.16)	−0.28 (−0.56)	−0.09 (−0.42)	(0.07)
Linolenic (18:3)	0.39 (0.49)	0.18 (−0.04)	0.14 (0.22)	0.02 (0.37)	(−0.06)
Arachidic (20:0)	**0.90 (0.96)**	0.54 (0.36)	**0.72 (0.66)**	0.27 (0.43)	(0.19)
Gondoic (20:1)	−0.05 (−0.01)	0.37 (0.16)	0.02 (0.01)	0.17 (0.08)	(0.16)
Behenic (22:0)	**0.81 (0.87)**	0.49 (0.28)	**0.65** (0.59)	0.22 (0.37)	(0.30)
Lignoceric (24:0)	0.09 (0.49)	0.40 (0.44)	−0.03 (0.53)	0.13 (−0.04)	(0.38)

Table 3
Cell wall polysaccharide (CWP), soluble sugar, chlorogenic acid (CGA), caffeine and lipid composition of mature seeds before (fresh seeds) and after wet processing. Values are expressed as percentages of dry mass (% DM) except for fatty acids which are expressed as relative contents (% of total fatty acids). CQA, caffeoyl quinic acid; FQA, feruloyl quinic acid. Effect of wet processing on chemical composition was tested using one-way ANOVA.

	Fresh seeds	Wet-processed seeds	Effect	$F_{1,30}$	P value
Total CWP	62.479 ± 1.284	64.478 ± 1.145	**	21.60	0.000063
Total soluble sugars	8.653 ± 0.798	8.276 ± 0.536		2.464	0.126960
Myo-inositol	0.142 ± 0.038	0.078 ± 0.020	**	34.86	0.000002
Glucose	0.261 ± 0.056	0.031 ± 0.033	***	201.21	$<10^{-6}$
Fructose	0.122 ± 0.051	0.031 ± 0.033	**	35.85	0.000001
Sucrose	8.081 ± 0.785	7.956 ± 0.532		0.28	0.602957
Raffinose	0.013 ± 0.008	0.021 ± 0.016		3.43	0.073792
Stachyose	0.015 ± 0.016	0.084 ± 0.023	***	94.25	$<10^{-6}$
Sorbitol	0.020 ± 0.015	0.074 ± 0.053	**	15.52	0.000451
Caffeine	0.736 ± 0.099	0.725 ± 0.066		0.13	0.721017
Total CGA	7.359 ± 0.499	7.646 ± 0.655		1.95	0.173191
3-CQA	0.310 ± 0.100	0.370 ± 0.116		2.45	0.128056
4-CQA	0.527 ± 0.093	0.579 ± 0.110		2.08	0.159210
5-CQA	4.962 ± 0.420	5.159 ± 0.609		1.13	0.295579
4-FQA	0.056 ± 0.007	0.056 ± 0.008		0.00	0.983787
5-FQA	0.414 ± 0.028	0.417 ± 0.048		0.03	0.861936
di3.4-CQA	0.157 ± 0.049	0.189 ± 0.055		2.96	0.095590
di3.5-CQA	0.816 ± 0.144	0.645 ± 0.144	**	11.19	0.002219
di4.5-CQA	0.117 ± 0.040	0.232 ± 0.058	***	42.84	$<10^{-6}$
Ratio CQA/diCQA	5.348 ± 0.415	5.747 ± 0.469	**	6.46	0.016430
Total lipids	16.022 ± 0.941	16.912 ± 0.707	**	9.15	0.005063
Palmitic (16:0)	35.637 ± 0.878	35.419 ± 1.027		0.42	0.523271
Stearic (18:0)	7.022 ± 0.717	7.086 ± 0.980		0.04	0.834560
Oleic (18:1)	7.438 ± 0.828	7.209 ± 1.027		0.48	0.493860
cis-Vaccenic (18:1-n7)	0.442 ± 0.038	0.437 ± 0.043		0.15	0.703753
Linoleic (18:2)	43.581 ± 1.359	44.024 ± 1.859		0.59	0.447809
Linolenic (18:3)	1.898 ± 0.169	1.882 ± 0.136		0.09	0.762305
Arachidic (20:0)	2.361 ± 0.353	2.372 ± 0.452		0.01	0.941386
Gondoic (20:1)	0.284 ± 0.010	0.288 ± 0.011		1.25	0.273248
Behenic (22:0)	0.522 ± 0.114	0.491 ± 0.111		0.60	0.443342
Lignoceric (24:0)	0.209 ± 0.032	0.198 ± 0.026		1.10	0.302051

** $P < 0.01$.
*** $P < 10^{-6}$.

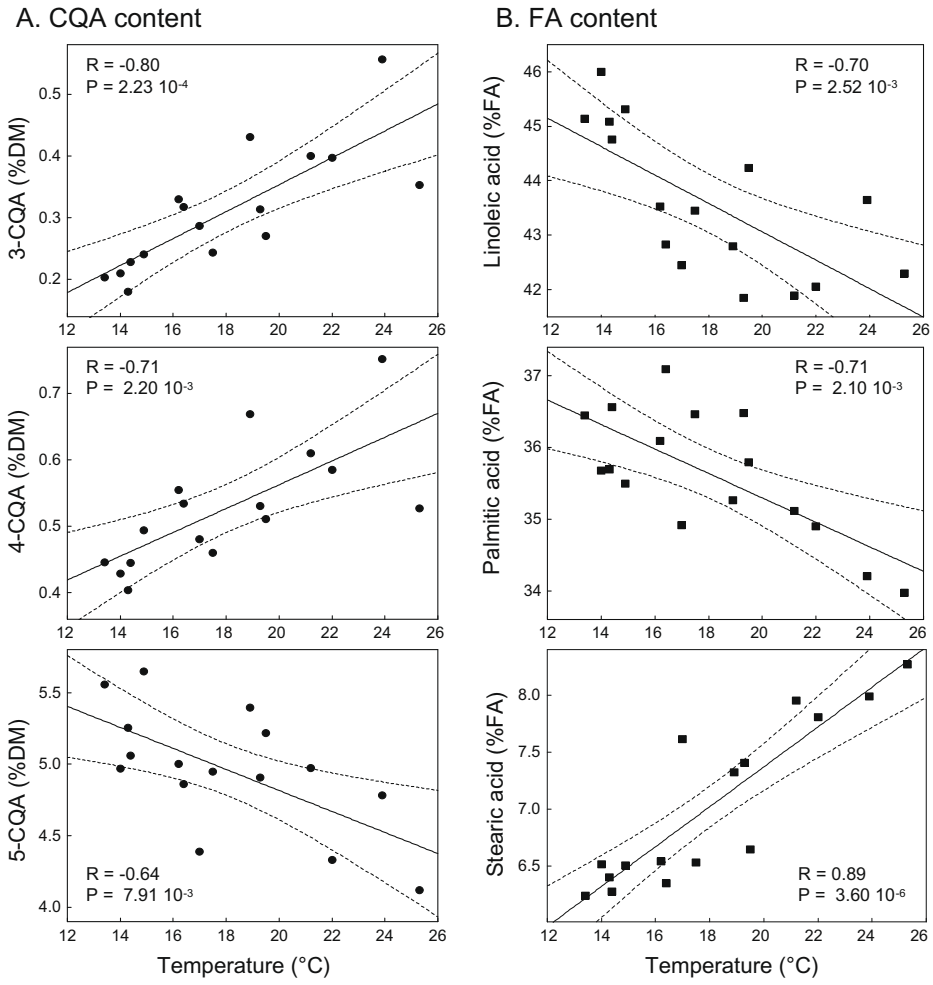

Fig. 1. Effect of the mean average temperature during the last 5 months of fruit development on the CGA composition (A) and FA composition (B) of fresh seeds. *R* and *P* = Pearson's linear correlation coefficient and probability of significance. Dotted lines represent the 95% confidence interval.

intense metabolic reconversion during this treatment. At the compound level within each class, free sugars (including sugar alcohols and oligosaccharides) were the most affected by wet processing since five out of the seven soluble sugars studied showed significant variations (Table 3). Moreover, while glucose, fructose and myo-inositol contents decreased during the post-harvest treatment, stachyose and sorbitol contents increased. In contrast, although lipid content increased, FA composition of total lipids was stable. Finally, CGA were relatively unaffected, as only two minor isomers underwent significant changes (a slight drop in di-3,5CQA and an increase in di-4,5CQA). However, the ratio between CQA and di-CQA increased significantly during wet processing.

3.3. Correlations between compound balances are possible indicators of metabolic inter-conversion

To better understand the reactions that occur during wet processing, the net gain or loss of each compound (difference between contents in wet-processed and fresh seeds) was calculated and correlations between the variations in the compounds were analysed by linear regression. Among the 45 relationships studied, only four were highly significant ($P < 0.01$). The increase in CWP induced by wet processing was highly correlated with loss of sucrose (Fig. 2) suggesting a link between sucrose mobilisation during wet processing and CWP metabolism. Similarly, the extent of sorbitol accumulation during wet processing was highly correlated with glucose and myo-inositol losses, suggesting that their variations were tightly inter-connected in the reactions that took place during wet processing. Indeed, the only one positive correlation was found between glucose and myo-inositol losses, most probably linked to the process of sorbitol accumulation (Fig. 2).

Relationships between metabolite contents and mean temperature during the fermentation process were also analysed by linear regression (Table 2). Myo-inositol was the only compound whose content showed a significant correlation with T_{ferm}. Similarly, when considering variations in compounds (data not shown), only net gains of stachyose ($R = -0.55$, $P = 0.027$), 3-CQA ($R = 0.55$, $P = 0.028$) and di3.4-CQA ($R = 0.57$, $P = 0.021$) showed significant correlations with T_{ferm}, underlining the modest role played by fermentation temperature on the metabolic interconversions that occur during post-harvest processing.

3.4. The metabolic status of the seed at harvest plays a primordial role in variations in soluble sugars during wet processing

Since CGA and fatty acids were almost unaffected by wet processing (Table 3), compounds of these two families which were significantly influenced by temperature in fresh seeds were, as expected, also significantly correlated with temperature in wet-processed seeds (Table 2). In contrast, among the soluble sugars, three compounds – glucose, stachyose and sorbitol – showed a

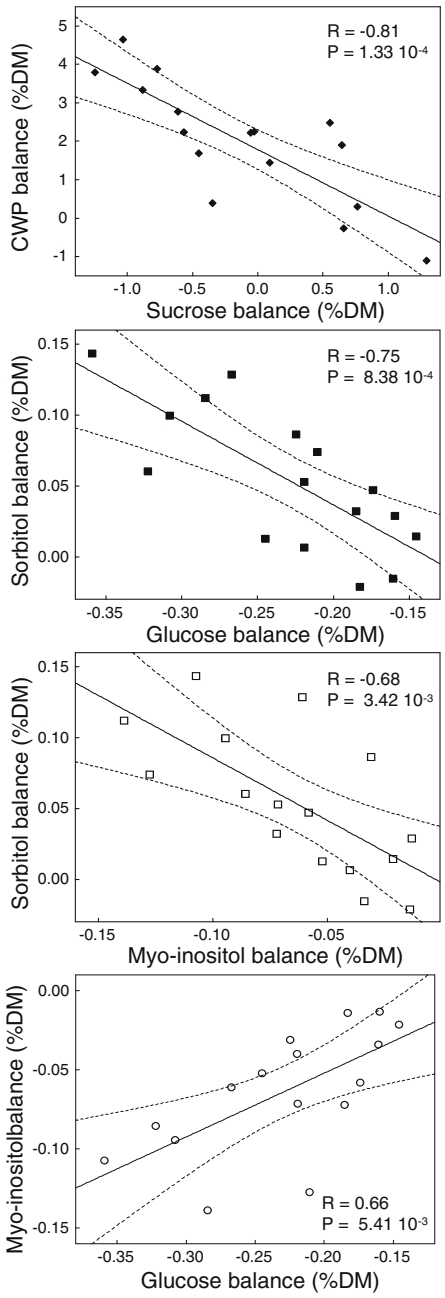

Fig. 2. Correlations between increases and decrease in free sugars caused by wet-processing. *R* and *P* = Pearson's linear correlation coefficient and probability of significance. Dotted lines represent the 95% confidence interval.

significant correlation with temperature in fresh seeds but not in processed seeds (or the reverse). For instance, the glucose content of fresh seeds was highly influenced by field temperature during development (Fig. 3A), but since glucose was almost completely degraded during post-harvest treatment (Table 3), the correlation between the two variables was lost in processed seeds (Fig. 3B). Interestingly, the reverse situation occurred for sorbitol (Fig. 3A and B). Since the glucose and sorbitol contents of the bean did not depend on the fermentation temperature (Table 2), one could logically hypothesise that during post-harvest treatment, sorbitol synthesis was directly influenced by glucose content (its precursor) in unprocessed seeds. This is a valuable example of the influence of the seed metabolic status at harvest on the interconversions that occur during wet processing.

4. Discussion

Through comprehensive metabolite profiling of samples from 16 experimental coffee plots, we showed for the first time that neither altitude, temperature, rainfall, irradiance nor evapotranspiration had a significant direct influence on final total CWP, CGA, lipid and caffeine contents of fresh (Laurina) coffee seeds. The only study which provides comparable data is that performed in Central America by Bertrand et al. (2006). These authors found that total lipid content of the seed was highly significantly correlated with altitude in the traditional variety Caturra but not in recent F1 hybrids. These authors hypothesised that trees of the variety Caturra suffered from a decreased leaf lifespan at low altitudes resulting in an impaired leaf-to-fruit ratio and therefore in a lower carbon supply to developing seeds (Vaast, Angrand, Franck, Dauzat, & Genard, 2005). By contrast, F1 hybrids exhibited high vigour in the whole range of altitudes tested, and thus no excessive fruit charge. We did not observe any noticeable differences in the leaf-to-fruit ratio with varying altitude in our Laurina field trials during the experiment. The relationships between altitude/temperature and final total CWP, CGA, lipid and caffeine contents thus appear to be highly dependent on the variety, even if a common trend towards 5-CQA accumulation with altitude was observed in both studies. However, it is not possible to ascertain whether the positive effect of altitude on seed lipid content observed by Bertrand et al. (2006) in Caturra was directly linked to temperature or to another climatic parameter. Clearly, the effects of climate on allocations to the main pools of storage compounds in the developing coffee seed require further investigations using a broad panel of *C. arabica* varieties.

However, our results evidenced for the first time in coffee that during seed development, environmental temperature had a direct impact on routing within several major metabolic pathways. Without affecting total CGA, lipid and soluble sugar contents, temperature directly influenced the composition of each of these three pools. For instance, the percentage of linoleic acid increased with decreasing temperatures, while the percentage of its precursor, oleic acid, decreased. Temperature has previously been shown to have a dramatic effect on the FA composition of the seed in many cold-tolerant crops such as soybean or rapeseed (Byfield, & Upchurch, 2007; Deng, & Scarth, 1998), and in the model plant *Arabidopsis thaliana* (Blodner, Goebel, Feussner, Gatz, & Polle, 2007). By contrast, to our knowledge, the influence of climatic conditions on seed FA has only very rarely been studied in cold-sensitive species such as coffee. Moreover, the response of each individual FA to temperature variations in coffee did not differ from that observed in the cold-tolerant species cited above. For instance, an increase in polyunsaturated FA (PUFA) and a decrease in oleic acid with decreasing temperature are mechanisms shared by all these species. It is therefore plausible that the effects of temperature on the FA composition of the bean are governed by mechanisms shared by this wide diversity of species. Temperature-mediated modulation of PUFA membrane content is believed to enable cell survival across a broad range of growth temperatures through the control of membrane fluidity (Kodama, Hamada, Horiguchi, Nishimura, & Iba, 1994). The modulation of FA composition in storage lipids may be controlled at both transcriptional and post-transcriptional levels (Byfield, & Upchurch, 2007; Tang, Novitzky, Griffin, Huber, & Dewey, 2005), but also through the O_2 concentration of the seed and the stability of the FA biosynthetic enzyme, which both depend directly on environmental temperature (Rolletschek et al., 2007). Interestingly, a recent study demonstrated that in cotton, another cold-sensitive subtropical crop, the leaf linoleic acid content also increased at low temperatures, together with a higher transcription of the gene encoding the enzyme that converts

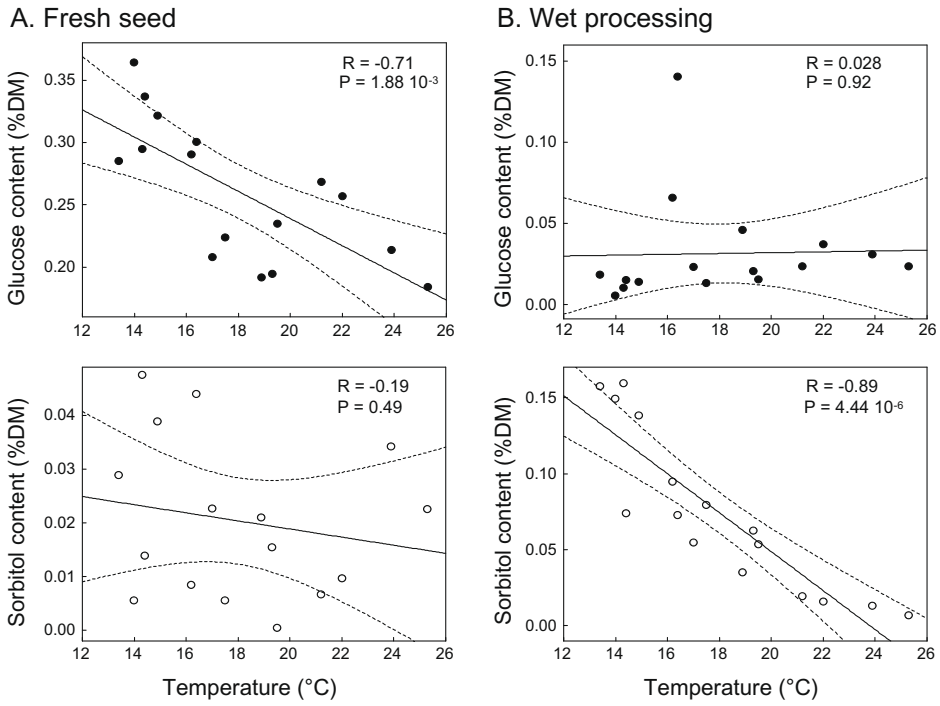

Fig. 3. Relationships between the mean average environmental temperature during the last 5 months of fruit development and seed glucose and sorbitol contents before (A) and after (B) wet-processing. *R* and *P* = Pearson's linear correlation coefficient and probability of significance. Dotted lines represent the 95% confidence interval.

oleic acid into linoleic acid, Δ12 desaturase (Kargiotidou, Deli, Galanopoulou, Tsaftaris, & Farmaki, 2008). Similarly, changes in phenolic compounds in the seed with variations in temperature could be a cold acclimation mechanism. For example, accumulation of anthocyanins and flavonoids was observed in *A. thaliana* under cold conditions (Leyva, Jarillo, Salinas, & Martinezzapater, 1995). Since changes in CGA isomer composition as a function of temperature is reported here for the first time, additional work is necessary to better understand its physiological role.

The chemical analysis of fresh and wet-processed seeds clearly confirmed the significant influence of post-harvest treatments on the final composition of green beans. The measurement of net gains and losses during wet processing illustrated the occurrence of an important catabolism, such as that of glucose and fructose, but also revealed the neo-synthesis of other non-structural carbohydrates, such as sorbitol, raffinose and stachyose. More importantly, we showed for the first time, that non-negligible amounts of CWP and lipids accumulated during this short period of time. Our results therefore reinforce the assumption that significant metabolism occurs within coffee seeds during wet processing. This was previously shown for free amino-acids and γ-aminobutyric acid on the one hand, and for reducing sugars on the other hand, whose contents respectively significantly increased (Bytof et al., 2005) and massively decreased (Knopp et al., 2006) during post-harvest treatment. In the latter study, variations in glucose and fructose contents were in the same range as those described in the present study. Moreover, as previously reported (Menezes, 1994), we showed that the CQA/diCQA ratio, reported as a marker of bean maturity and quality, was positively affected by wet processing. Our data are therefore in agreement with most previous reports and suggest that these metabolic processes are independent of the variety. Metabolic reactions that occur during wet processing are targeted towards particular metabolites, mainly non-structural carbohydrates and CWP, while most of the other compounds we studied, i.e. caffeine, most CGA isomers, and FA were unaffected by post-harvest treatment.

The major decrease in glucose and fructose contents that occurred during wet processing has previously been interpreted as a consequence of the glucose turnover due to anaerobic fermentation, which enables ATP biosynthesis in the coffee seed under the hypoxia conditions conferred by flooding (Knopp et al., 2006). However, the overexpression of the glyoxylate cycle-specific isocitrate lyase (ICL) gene during wet processing was also recently interpreted as an early mobilisation of reserves: in other words, the early induction of germination processes (Selmar et al., 2006). This assumption was reinforced by the observation using flow cytometry of a peak in cell division (4-C nuclei), concomitant with an increase in the abundance of β-tubulin, a marker for cell division or elongation (Bytof et al., 2007). One of the main features of germination metabolism is the mobilisation of reserves. Since free amino acids are typical products of storage protein hydrolysis, their increase during wet processing was interpreted as reflecting the mobilization of reserves (Bytof et al., 2005). Similarly, during seed germination, soluble carbohydrates are among the first components which are affected by the resumption of active metabolism. However, taken together, our results do not support the hypothesis of the mobilisation of reserves during wet processing. Conversely, we detected a significant accumulation of the two major storage compounds in coffee, namely CWP and lipids. Moreover, we observed the concomitant biosynthesis of oligosaccharides such as raffinose and stachyose. Finally, the decrease in glucose content was highly correlated to sorbitol biosynthesis, suggesting the conversion of glucose to sorbitol in addition to its catabolism through the ethanol fermentative pathway. Instead, our results argue for the induction of a stress metabolism linked to the hypoxia and the osmotic shock caused by flooding during wet processing. In this respect, the recent report of early induction of ICL gene expression under hypoxic conditions in submerged rice seedlings is worth mentioning (Lu, Wu, & Han, 2005). In flooded rice seedlings, the glyoxylate cycle appeared to be unrelated to the mobilisation of storage lipids but rather served to replenish carbons for the Krebs cycle (Fan, Lane, & Higashi, 2003). Similarly,

accumulation of the β-tubulin transcript has been linked to osmotic priming in tomato seeds (De Castro, Zheng, Bergervoet, De Vos, & Bino, 1995) and could be triggered in coffee seeds by the hypo-osmotic conditions that occur during wet processing.

The biosynthesis of sorbitol during wet processing, which was directly correlated with the decrease in the glucose and myo-inositol pools, is reported here for the first time. Sorbitol could be synthesised either from glucose-6P by sorbitol-6-phosphate dehydrogenase (S6PDH), as it is the case in fruit trees of the Rosaceae family, or directly from glucose *via* aldose reductase activity, as already evidenced in germinating soybean seeds (Kuo, Doehlert, & Crawford, 1990). Interestingly, an increase in the sorbitol pool was associated with myo-inositol depletion in transgenic tobacco overexpressing S6PDH (Sheveleva et al., 1998), suggesting that myo-inositol and sorbitol were both synthesised from the same glucose-6P pool in processed coffee seeds. The myo-inositol depletion observed in processed seeds could be due to the decrease of its turnover from glucose-6P in favour of sorbitol biosynthesis. However, the sorbitol biosynthetic pathway in coffee seed remains to be characterised at the molecular level as no candidate gene has been found for S6PDH and aldose reductase in coffee EST databases. From this point of view, it is worth mentioning that sorbitol was also shown to transiently accumulate during coffee seed development (Joët et al., 2009). This transient rise in polyol content was concomitant with the peak of expression of a gene encoding a sorbitol dehydrogenase (SDH), an enzyme that catalyses the reversible oxidation of sorbitol to fructose. This enzyme could be also involved in sorbitol biosynthesis (Ohta, Moriguchi, Kanahama, Yamaki, & Kanayama, 2005). We thus suggest that the accumulation of sorbitol during wet processing could be related to the induction of stress-related metabolism induced under the hypoxic and highly reductive conditions caused by flooding. Sorbitol and other polyols play important roles as osmoprotectants. Many previous reports indicated that marginal accumulation of polyols increases stress tolerance, likely through the stabilisation of macromolecular structures (Tarczynski, Jensen, & Bohnert, 1993). Alternatively, the reduction of glucose to sorbitol could act as a safety redox valve, consuming NAD(P)H and supporting the storage of reducing power under the highly reductive conditions encountered during flooding.

Our results also revealed a clear negative relationship between variations in sucrose content during wet processing and variations in CWP. This trade-off can be easily interpreted by considering the roles played by sucrose synthase (SUSY), a key enzyme controlling carbon partitioning in sink tissues. SUSY catalyses the reversible interconversion of sucrose to UDP-glucose and fructose. A membrane-bound isoform of SUSY is directly involved in CWP synthesis by channelling UDP-glucose to cellulose synthase (Amor, Haigler, Johnson, Wainscott, & Delmer, 1995). Interestingly, SUSY was shown to be regulated at both the transcriptional and post-transcriptional levels by oxygen depletion caused by flooding (Dejardin, Sokolov, & Kleczkowski, 1999).

5. Conclusions

Using samples from 16 plots with considerable variations in their climatic characteristics, the present work established for the first time the effects of temperature on the final composition of the coffee seed. Similarly, we demonstrated the influence of wet processing on the chemical composition of beans and its interactions with the metabolic status of seeds at harvest. This study also highlighted the fact that most changes can be interpreted by physiological processes decrypted in other plants with regard to the effects of temperature during seed development and of hypoxic conditions during wet processing. One of the most important outcomes of this study is therefore to support the development of approaches coupling genomics and metabolomics to improve our understanding of the influence of the environment on coffee bean 'quality'.

However, despite the very wide range of metabolites covered, it seems unlikely that any of them explains to a large extent the better flavour and aroma of high-altitude coffees. Indeed, among compounds exhibiting a significant correlation with temperature, none showed an absolute variation high enough to be involved in the considerable quality differences reported elsewhere between low- and high-altitude Arabica coffees. Similarly, none of the variations revealed during wet processing are likely to play a major role in the generation of aroma and flavour. Obviously, future chemical targets of metabolomics approaches cannot be the compounds that are classically reported in the coffee literature (chlorogenic acids, caffeine, soluble sugars, fatty acids, etc.). Instead, we suggest focusing such studies on other compounds whose content is non-negligible (diterpenes, amino acids, organic acids) and on volatile molecules that could be more directly involved in beverage quality attributes.

Acknowledgments

This work was supported by the European Union, *Région Réunion* and IRD (*DOCUP Réunion* 2000-2006).

References

Amor, Y., Haigler, C. H., Johnson, S., Wainscott, M., & Delmer, D. P. (1995). A membrane-associated form of sucrose synthase and its potential role in synthesis of cellulose and callose in plants. *Proceedings of the National Academy of Science U S A, 92*(20), 9353–9357.

Avelino, J., Barboza, B., Araya, J. C., Fonseca, C., Davrieux, F., Guyot, B., et al. (2005). Effects of slope exposure, altitude and yield on coffee quality in two altitude terroirs of Costa Rica, Orosi and Santa Maria de Dota. *Journal of the Science of Food and Agriculture, 85*(11), 1869–1876.

Bertrand, B., Vaast, P., Alpizar, E., Etienne, H., Davrieux, F., & Charmetant, P. (2006). Comparison of bean biochemical composition and beverage quality of Arabica hybrids involving Sudanese-Ethiopian origins with traditional varieties at various elevations in Central America. *Tree Physiology, 26*(9), 1239–1248.

Blodner, C., Goebel, C., Feussner, I., Gatz, C., & Polle, A. (2007). Warm and cold parental reproductive environments affect seed properties, fitness, and cold responsiveness in *Arabidopsis thaliana* progenies. *Plant Cell and Environment, 30*(2), 165–175.

Byfield, G. E., & Upchurch, R. G. (2007). Effect of temperature on delta-9 stearoyl-ACP and microsomal omega-6 desaturase gene expression and fatty acid content in developing soybean seeds. *Crop Science, 47*(4), 1698–1704.

Bytof, G., Knopp, S. E., Kramer, D., Breitenstein, B., Bergervoet, J. H. W., Groot, S. P. C., et al. (2007). Transient occurrence of seed germination processes during coffee post-harvest treatment. *Annals of Botany, 100*(1), 61–66.

Bytof, G., Knopp, S. E., Schieberle, P., Teutsch, I., & Selmar, D. (2005). Influence of processing on the generation of gamma-aminobutyric acid in green coffee beans. *European Food Research and Technology, 220*(3–4), 245–250.

De Castro, R. D., & Marraccini, P. (2006). Cytology, biochemistry and molecular changes during coffee fruit development. *Brazilian Journal of Plant Physiology, 18*(1), 175–199.

De Castro, R. D., Zheng, X., Bergervoet, J., De Vos, C., & Bino, R. J. (1995). [beta]-Tubulin accumulation and DNA replication in imbibing tomato seeds. *Plant Physiology, 109*(2), 499–504.

Decazy, F., Avelino, J., Guyot, B., Perriot, J. J., Pineda, C., & Cilas, C. (2003). Quality of different Honduran coffees in relation to several environments. *Journal of Food Science, 68*, 2356–2361.

Dejardin, A., Sokolov, L. N., & Kleczkowski, L. A. (1999). Sugar/osmoticum levels modulate differential abscisic acid-independent expression of two stress-responsive sucrose synthase genes in *Arabidopsis*. *Biochemical Journal, 344*(2), 503–509.

Deng, X., & Scarth, R. (1998). Temperature effects on fatty acid composition development of low-linolenic oilseed rape (*Brassica napus* L.). *Journal of the American Oil Chemists Society, 75*(7), 759–766.

Fan, T. W. M., Lane, A. N., & Higashi, R. A. (2003). In vivo and in vitro metabolomic analysis of anaerobic rice coleoptiles revealed unexpected pathways. *Russian Journal of Plant Physiology, 50*(6), 787–793.

Flament, I. (2002). *Coffee flavour chemistry*. Chichester, UK: John Wiley and Sons.

Guyot, B., Gueule, D., Manez, J. C., Perriot, J. J., Giron, J., & Villain, L. (1996). Influence de l'altitude et de l'ombrage sur la qualité des cafés Arabica. *Plantations, Recherche, Développement, 3*, 272–280.

Joët, T., Laffargue, A., Salmona, J., Doulbeau, S., Descroix, F., Bertrand, B., et al. (2009). Metabolic pathways in tropical dicotyledonous albuminous seeds: *Coffea arabica* as a case study. *New Phytologist, 182*(1), 146–162.

Kargiotidou, A., Deli, D., Galanopoulou, D., Tsaftaris, A., & Farmaki, T. (2008). Low temperature and light regulate delta 12 fatty acid desaturases (FAD2) at a transcriptional level in cotton (*Gossypium hirsutum*). *Journal of Experimental Botany, 59*(8), 2043–2056.

Knopp, S., Bytof, G., & Selmar, D. (2006). Influence of processing on the content of sugars in green Arabica coffee beans. *European Food Research and Technology, 223*(2), 195–201.

Kodama, H., Hamada, T., Horiguchi, G., Nishimura, M., & Iba, K. (1994). Genetic enhancement of cold tolerance by expression of a gene for chloroplast omega-3-fatty-acid desaturase in transgenic tobacco. *Plant Physiology, 105*(2), 601–605.

Kuo, T. M., Doehlert, D. C., & Crawford, C. G. (1990). Sugar metabolism in germinating soybean seeds: Evidence for the sorbitol pathway in soybean axes. *Plant Physiology, 93*(4), 1514–1520.

Leroy, T., Ribeyre, F., Bertrand, B., Charmetant, P., Dufour, M., Montagnon, C., et al. (2006). Genetics of coffee quality. *Brazilian Journal of Plant Physiology, 18*(1), 229–242.

Leyva, A., Jarillo, J. A., Salinas, J., & Martinezzapater, J. M. (1995). Low-temperature induces the accumulation of phenylalanine ammonia-lyase and chalcone synthase messenger-RNAs of *Arabidopsis thaliana* in a light-dependent manner. *Plant Physiology, 108*(1), 39–46.

Lu, Y., Wu, Y. R., & Han, B. (2005). Anaerobic induction of isocitrate lyase and malate synthase in submerged rice seedlings indicates the important metabolic role of the glyoxylate cycle. *Acta Biochimica et Biophysica Sinica, 37*(6), 406–414.

Menezes, H. C. (1994). The relationship between the state of maturity of raw coffee beans and the isomers of caffeoylquinic acid. *Food Chemistry, 50*(3), 293–296.

Ohta, K., Moriguchi, R., Kanahama, K., Yamaki, S., & Kanayama, Y. (2005). Molecular evidence of sorbitol dehydrogenase in tomato, a non-Rosaceae plant. *Phytochemistry, 66*(24), 2822–2828.

Rolletschek, H., Borisjuk, L., Sanchez-Garcia, A., Gotor, C., Romero, L. C., Martinez-Rivas, J. M., et al. (2007). Temperature-dependent endogenous oxygen concentration regulates microsomal oleate desaturase in developing sunflower seeds. *Journal of Experimental Botany, 58*(12), 3171–3181.

Selmar, D., Bytof, G., Knopp, S. E., & Breitenstein, B. (2006). Germination of coffee seeds and its significance for coffee quality. *Plant Biology (Stuttg), 8*(2), 260–264.

Selmar, D., Bytof, G., & Knopp, S. (2002). New aspects of coffee processing: The relation between seed germination and coffee quality. In *Proceedings of the international congress of ASIC*, (p. 19).

Sheveleva, E. V., Marquez, S., Chmara, W., Zegeer, A., Jensen, R. G., & Bohnert, H. J. (1998). Sorbitol-6-phosphate dehydrogenase expression in transgenic tobacco. High amounts of sorbitol lead to necrotic lesions. *Plant Physiology, 117*(3), 831–839.

Tang, G. Q., Novitzky, W. P., Griffin, H. C., Huber, S. C., & Dewey, R. E. (2005). Oleate desaturase enzymes of soybean: Evidence of regulation through differential stability and phosphorylation. *Plant Journal, 44*(3), 433–446.

Tarczynski, M. C., Jensen, R. G., & Bohnert, H. J. (1993). Stress protection of transgenic tobacco by production of the Osmolyte Mannitol. *Science, 259*(5094), 508–510.

Vaast, P., Angrand, J., Franck, N., Dauzat, J., & Genard, M. (2005). Fruit load and branch ring-barking affect carbon allocation and photosynthesis of leaf and fruit of *Coffea arabica* in the field. *Tree Physiology, 25*(6), 753–760.

Vaast, P., Bertrand, B., Perriot, J. J., Guyot, B., & Genard, M. (2006). Fruit thinning and shade improve bean characteristics and beverage quality of coffee (*Coffea arabica* L.) under optimal conditions. *Journal of the Science of Food and Agriculture, 86*(2), 197–204.

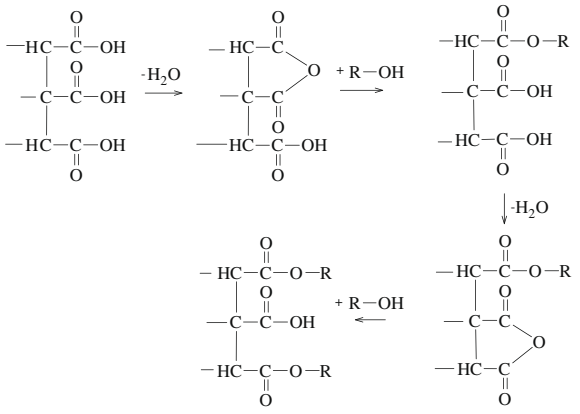

Scheme 1. Mechanism of the conventional dry cross-linking of cellulose using carboxylic acids in the presence of acid catalysts. R represents cellulose (Yang & Wang, 1996; Yang et al., 1997).

antibacterial and acidulant effects of citric acid. It was reported that adding citric acid decreased the strength of the starch–PVA film but provided better strength than glycerol-added starch–PVA films. The better strength of the citric acid-added starch–PVA film compared to glycerol-added starch–PVA films was attributed to the better hydrogen bonding between citric acid and starch–PVA molecules compared to glycerol and starch–PVA molecules (Yoon, Chough, & Park, 2006, 2007).

In this research, we show that citric acid can cross-link starch and improve the mechanical properties and decrease dissolution of starch in water and formic acid. The effect of various amounts of citric acid and glycerol used on the mechanical properties of the films and changes in the morphology and physical structure, thermal stability, water vapour permeability, and colour and stability of the films in water and formic acid has been studied.

2. Materials and methods

2.1. General

Commercially-available corn starch was purchased from American Maize Products Co., Hammond, IN). Glycerol, citric acid, sodium hypophosphite, sodium hydroxide and acetic acid were reagent-grade chemicals purchased from VWR International, Bristol, CT.

2.2. Preparing starch films

Starch films were prepared by dispersing 3% (w/w) starch in water. The starch dispersion was heated on a hot plate to 90 °C and held at that temperature for 20 min. The heated starch solution was cooled to about 65 °C and the required amount of glycerol was added to the starch solution. The starch solution was then poured onto Teflon-coated glass plates. The cast starch films were allowed to air dry for about 48 h before peeling them from the plates.

2.3. Cross-linking starch films

A specified amount of citric acid and the catalyst sodium hypophosphite (50% w/w, on weight of citric acid used) was dissolved in the starch solution. The starch solution containing the cross-linking agent and catalyst was heated to 90 °C, held at that temperature for 20 min, then cooled to 65 °C and poured onto Teflon-coated glass plates. The cast films were allowed to air dry for about 48 h and later peeled from the plates. The starch films were then treated in a hot air oven at 165 °C for various periods of time for the cross-linking reaction to occur. After heating, the films were immediately transferred to a conditioning chamber maintained at 23 °C and 50% relative humidity.

2.4. Tensile properties

The tensile properties of the starch films were determined on an MTS tensile tester (QTest 10; MTS, Eden Prairie, MN) according to ASTM standard D 882-02. Testing was done on five samples each measuring 10 cm × 1 cm randomly cut from the cast films. Two replications were done for a total of 10 tests for each condition. Before testing, all samples were conditioned for at least 40 h in a conditioning chamber maintained at 23 ± 0.5 °C and 50 ± 1% relative humidity.

2.5. Fourier-transform infrared

FTIR spectra were collected from the non-cross-linked and cross-linked starch films on an attenuated total reflectance ATR spectrophotometer (Nicolet 380; Thermo-Fisher, Waltham, MA). The samples were thoroughly washed in water to remove unattached citric acid and catalysts. The washed samples were placed on a germanium plate and 128 scans were collected for each sample.

2.6. Thermal analysis

A differential scanning calorimeter (DSC 822; Mettler-Toledo Inc., Columbus, OH) and a thermogravimetric analyzer (Leco TGA 701; Leco, St Joseph, MI) were used to study the thermal behaviour of the starch films before and after cross-linking. DSC curves were obtained by heating the samples at a rate of 20 °C per minute and holding at 50 °C for 3 min to remove moisture and then to 250 °C at 20 °C per minute. The samples were then cooled to 25 °C and a second heating cycle was performed by heating the samples again to 250 °C at 20 °C per minute. Thermogravimetric analysis was performed by heating the sample at a rate of 15 °C per minute.

2.7. Morphological structure

The surface features of the non-cross-linked and cross-linked films were observed using a scanning electron microscope (Hitachi Model S3000N Variable Pressure SEM; Hitachi Ltd., Tokyo, Japan). The samples were sputter coated with gold palladium and observed under the SEM at a voltage of 15 kV.

2.8. Water vapour permeability

The water vapour permeability of the control and cross-linked starch films was determined according to ASTM standard E96/E96M-05. Three replications were done for the control and cross-linked films and the average water vapour permeability is reported along with ± one standard deviation.

2.9. X-ray diffraction

A Rigaku D-max/BΘ2Θ X-ray diffractometer (Rigaku Americas, Woodlands, TX) with Bragg–Brentano parafocusing geometry, a diffracted beam monochromator, and a copper target X-ray tube set to 40 kV and 30 mA was used to observe the diffraction pattern of the control and cross-linked starch films. The diffraction patterns were recorded for 2θ values ranging from 5° to 40° on samples measuring 2 cm × 2 cm.

2.10. Changes in colour

The changes in the colour of the starch films due to cross-linking were measured in terms of the yellowness index (*YI*) using a spectrophotometer (Hunter Lab, Model: Ultra scan XE; Hunter Associates Laboratory Inc., Reston, VA) with a 1-inch opening and D65/10° observer. The film samples conditioned in the standard testing atmosphere were folded in the middle and the two layers were used for measurement. Three readings were taken from three different places in each film and the measurements were repeated on three films that were cast separately. The average and standard deviations of the *YI* are reported.

2.11. Weight loss in water under various pH conditions

The control and cross-linked starch films were treated in phosphate-buffered saline water (pH 7.2) at 50 °C for 3–35 days. About 0.5 g of the films were put in water (1:5 film to water ratio) and taken out after a specified time. The samples taken out were rinsed in distilled water and allowed to dry in a standard conditioning chamber maintained at 23 ± 0.5 °C and 50 ± 1% relative humidity. The weight of the conditioned specimen after treating in water was used to determine the % weight loss of the films in water.

2.12. Weight loss in formic acid

The weight loss of the non-cross-linked and cross-linked starch films in formic acid was studied at two temperatures (20 and 50 °C). Precisely 0.2 g of the films were put in 5 g of formic acid in glass vials and sealed. The vials were kept at 20 °C for 24 h and at 50 °C for 5 h. After the treatment, the formic acid was removed and the remaining starch was thoroughly washed in distilled water. The dry weight of the samples after formic acid treatment was recorded to calculate the % weight loss. Two replications were repeated for each condition and the average and standard deviation are reported.

3. Results and discussion

3.1. Effect of adding glycerol

The effect of adding glycerol on the tensile strength and elongation of the cross-linked starch films is shown in Fig. 1. Both the control and cross-linked films with less than 10% glycerol became brittle after curing and were not considered for further studies. Increasing the concentration of glycerol to 15% from 10% increases the tensile strength and elongation and provides flexible films. Further increase in glycerol concentration above 15% increased the elongation but considerably decreased the tensile strength of the films. A glycerol concentration of 15% provided the highest tensile strength to the films and was used for all further studies. At low concentrations of glycerol (<10%), there is not enough plasticising effect and the starch molecules become brittle. At concentrations above 15% the plasticising effect is too pronounced and makes the starch molecules move easily, leading to high elongation but decrease in tensile strength. The amount of glycerol to be added should be decided based on the tensile strength and elongation required for a particular application.

3.2. Effect of curing time

The effect of curing time on the tensile strength of the citric acid cross-linked films is shown in Fig. 2. As seen from the figure, there is a narrow range of curing time (3–5 min) that provides the optimum tensile strength to the films. Further increase in curing time substantially decreases the tensile strength of the films at this curing temperature. Curing time is one of the most important factors determining the efficiency of carboxylic acid cross-linking and hence the properties of the cross-linked materials. Sufficient curing time is necessary for the cross-linking reaction to occur but excess curing will damage the starch molecules, leading to decrease in tensile strength and unwanted changes in the colour of the films. An optimum curing time of about 5 min at about 165–170 °C was also reported for citric acid cross-linking of cotton fabrics. Although longer curing times may be suitable, if lower curing temperatures are used, it is more preferable to have shorter curing times for large-scale processing of films, due to economic and technical reasons. Since the citric acid cross-linking of starch occurs at high temperatures, a one-step cross-linking process may be possible, in order to develop cross-linked starch products by extrusion.

3.3. Effect of citric acid concentration

Cross-linking starch films with citric acid improved the tensile strength of the films by more than 150%, as seen from Fig. 3. However, there is an optimum amount of citric acid that is necessary to obtain good increase in the tensile strength of the films. Concentrations of citric acid less than 5% provided relatively low

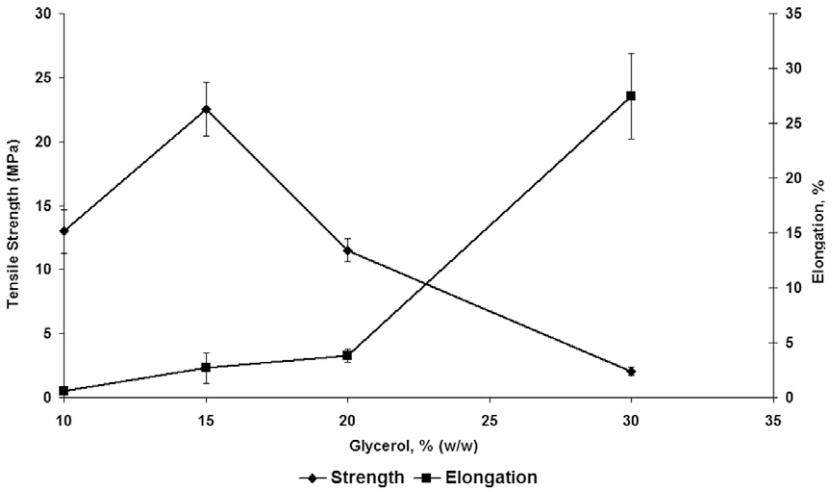

Fig. 1. Effect of adding glycerol on the strength and elongation of cross-linked starch films. Films were cast from 3% starch and cross-linked using 5% (w/w) citric acid and cured at 165 °C for 5 min.

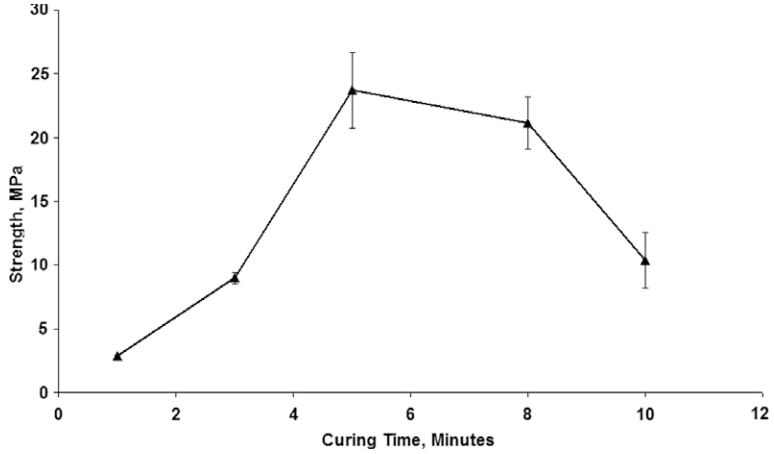

Fig. 2. Effect of curing time on the strength of cross-linked starch films. Films were cast from 3% starch and cross-linked using 5% (w/w) citric acid.

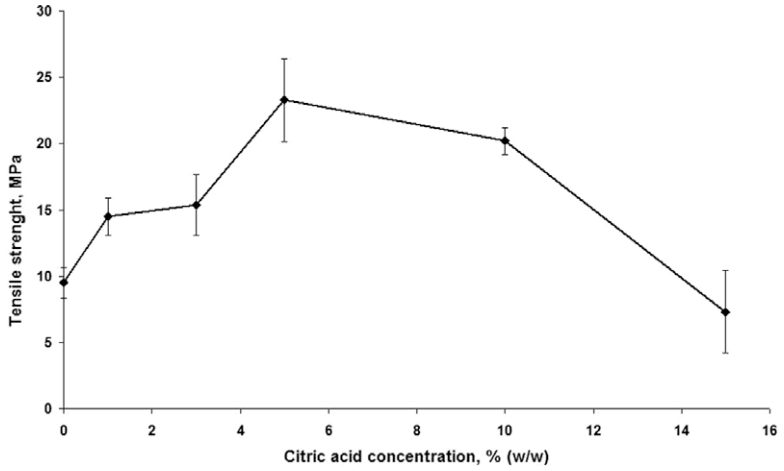

Fig. 3. Effect of increasing citric acid concentration on the strength of cross-linked starch films. Films were cast from 3% starch with 15% glycerol and cured at 165 °C for 5 min.

improvement in tensile strength and concentrations above 5% decreased the tensile strength of the films. Cross-linking interconnects the starch molecules in the film, which could increase the molecular weight of the starch and also provides better intermolecular interactions between molecules, leading to better tensile strength, compared to the non-cross-linked starch films. At low concentrations of citric acid, there is not enough cross-linking between the starch molecules to improve the tensile strength of the films. At high concentrations, however, there is excess cross-linking that limits the mobility of the starch molecules, leading to lower tensile strength (Yang et al., 1996, 1997).

Previously, high amylose starch films cross-linked with epichlorohydrin (6%) had tensile strength of about 38 MPa, higher than the strength of the films obtained in this research but normal starch was used to produce the films in this research (Rioux, Ispas-Szabo, Ait-Kadi, Mateescu, & Juhasz, 2002). Apart from the report on cross-linking high amylose starch films, to the best of our knowledge, there is no literature available on cross-linking pure starch films. Most of the cross-linked starch films reported in the literature are blends of cross-linked starch with synthetic polymers. Films made using epichlorohydrin-cross-linked starch and polyethylene (1:1 ratio) had strength ranging from 12 to 15 MPa with varying amounts of epichlorohydrin (0.1–2%), compared to 24 MPa for the 5% citric acid cross-linked films (Kim & Lee, 2002). Similarly, starch–polyethylene films cross-linked with boric acid (0.5–2.5%) had tensile strength ranging from 8.9 to 10.1 MPa and the breaking elongation decreased from 60% to 8% after cross-linking (Yin, Li, Liu, & Li, 2005). However, starch–polyvinyl alcohol films cross-linked with hexamethoxymethylmelamine had tensile strength ranging from 50 to 65 MPa, and the non-cross-linked films also had high strengths, ranging from 45 to 55 MPa (Chen, Imam, Gordon, & Greene, 1997). In another report, starch–LDPE films made using epichlorohydrin cross-linked and/or glycerol modified starch had strength ranging from 5 to 14 MPa (Garg & Jana, 2007). Using high amylose starch or other poly(carboxylic acids) may be two approaches to further increase the strength of the starch films developed in this research.

3.4. FTIR

The FTIR spectra of the non-cross-linked films and films cross-linked with 5% citric acid are shown in Fig. 4. Both the films have similar peaks, except for the additional peak in the cross-linked film at 1724 cm^{-1}. The band at 1724 cm^{-1} (indicated by an arrow in Fig. 4) is ascribed to the carboxyl and ester carbonyl bands (Yang et al., 1991). Since the films were thoroughly washed to remove the unbound citric acid and catalyst, the presence of the carbonyl peak confirms the chemical linkages between citric acid and starch.

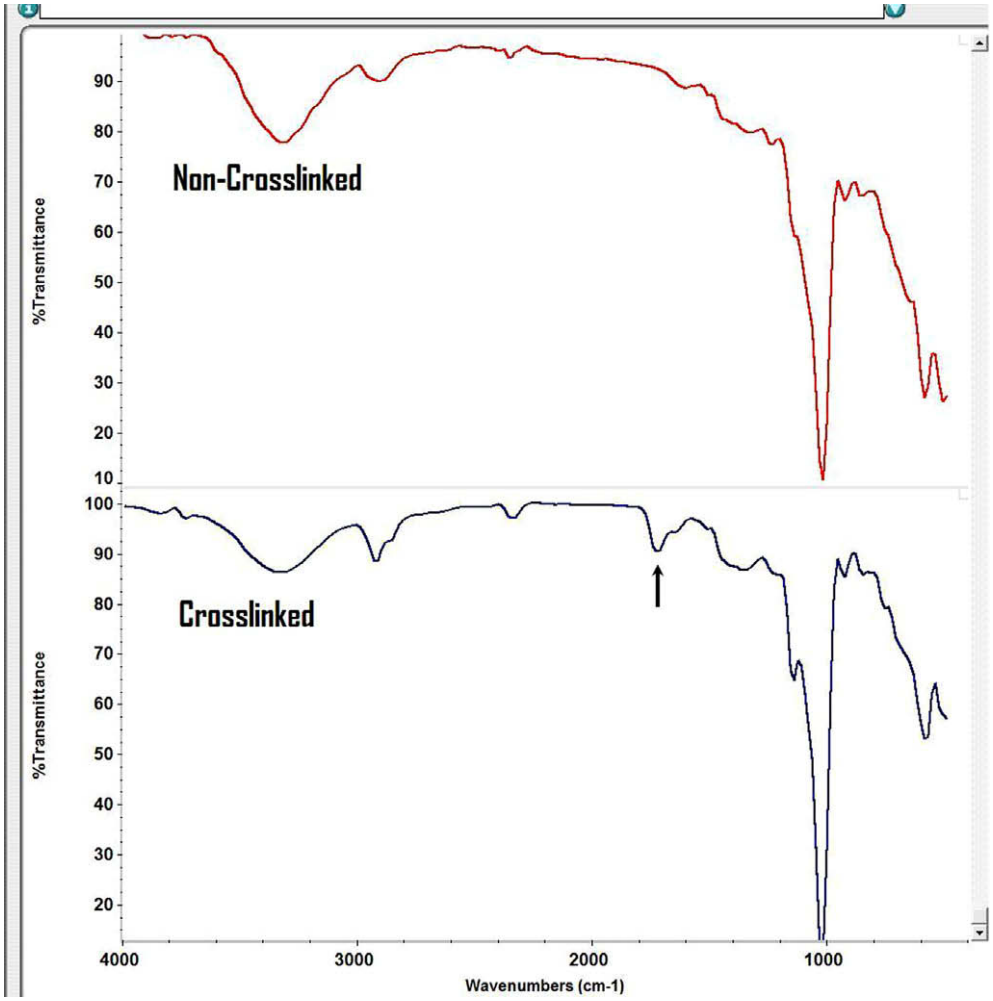

Fig. 4. FTIR spectra of the non-cross-linked starch films and starch films cross-linked with 5% citric acid.

3.5. Thermal analysis

The DSC thermograms of the non-cross-linked films and films cross-linked with 5% citric acid are shown in Fig. 5a and b. Fig. 5a is the DSC thermogram of the films collected during the first heating cycle. The thermogram of the non-cross-linked film (5a) show a endothermic curve that peaks at about 100 °C, whereas the thermogram of the cross-linked film has an endothermic curve that peaks at about 150 °C. The peak in both the non-cross-linked and cross-linked films disappears after the second heating cycle of the same sample, as shown in Fig. 5b. The disappearance of the peaks seen during the first heating cycle indicates that the peaks are most likely due to the presence of moisture in the films. The shift of the water evaporation peak to the higher temperature for the cross-linked films indicated the cross-linkages made water evaporation more difficult than from non-cross-linked film.

The thermal degradation of the starch films can be observed in Fig. 6. Overall, the cross-linked starch films have about 20% lower weight loss than the non-cross-linked films after heating the films to 600 °C, indicating much improved resistance to thermal degradation, due to cross-linkages. The non-cross-linked films begin to show weight loss at about 70 °C, whereas the weight loss of the cross-linked films starts at about 100 °C. The first main increase in weight loss of both the films initiated at about 120 °C, with the non-cross-linked films showing slightly more weight loss than the cross-linked films. The lower weight loss of the cross-linked films between 120 and 220 °C should be due to the higher thermal stability of the starch molecules after cross-linking. However, the cross-linked films showed a higher weight loss than the non-cross-linked films between 220 and 320 °C. This is probably due to the degradation of some of the starch molecules in the cross-linked films when they were cured at high temperatures for the cross-linking reaction to occur. The cross-linked films have much higher thermal stability than the non-cross-linked films above 320 °C, due to the cross-linking of the starch molecules.

3.6. Morphological structure

Scanning electron microscope pictures of the control and cross-linked films do not show any appreciable change in surface morphology due to cross-linking, as seen from Fig. 7a and b, respectively. The films are homogenous without pores or cracks and the starch molecules have been well dispersed without the many granules that were observed in films made from epichlorohydrin cross-linked starch mixed with low-density polyethylene (Garg & Jana, 2007).

3.7. Physical structure

X-ray diffraction patterns of the cross-linked and non-cross-linked starch are similar, with two prominent peaks at about 17° and 22°, as seen from Fig. 8. However, typical starch peaks seen at about 5° and 14° were not seen in either cross-linked or non-cross-linked film, indicating changes in crystallinity and/or the crystal structure. The control and cross-linked starch films had

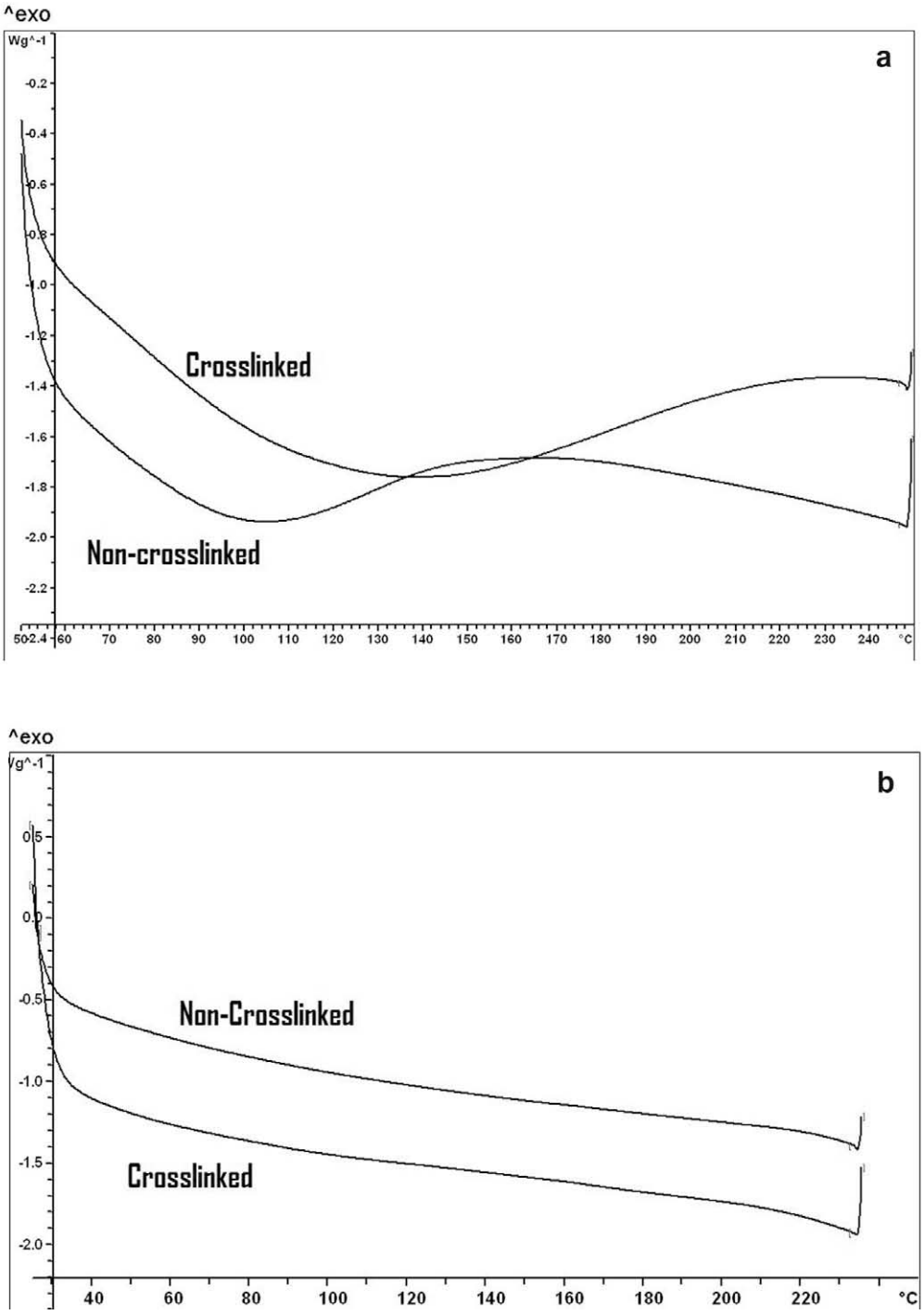

Fig. 5. DSC thermograms of the non-cross-linked starch films and starch films cross-linked with 5% citric acid during the first (a) and second (b) heating cycles.

similar % crystallinity of about 17% and 14%, respectively. Epichlorohydrin cross-linked starch films also did not show any change in % crystallinity or peak positions, compared to native starch (Garg & Jana, 2007; Kim & Lee, 2002). The increase in the diffraction intensity of the cross-linked starch films but decrease in the % crystallinity suggests that some of the amorphous regions may be better oriented after cross-linking.

3.8. Water vapour permeability

Citric acid cross-linked films have slightly lower water vapour permeability, compared to the non-cross-linked films. The control and cross-linked films had a water vapour permeability of 33 ± 0.5 and 31 ± 0.8 g h^{-1} m^{-2}, respectively. The formation of a more tight structure after cross-linking prevents the swelling of starch and also restricts the movement of molecules, leading to a decrease in the water vapour permeability.

3.9. Colour change

Citric acid cross-linking is reported to cause yellowing, especially in proteins when cured at high temperatures and/or long periods of time (Schramm, Vukusic, & Katovic, 2002; Yang et al., 1996). The changes in the *YI* of the starch films before and after

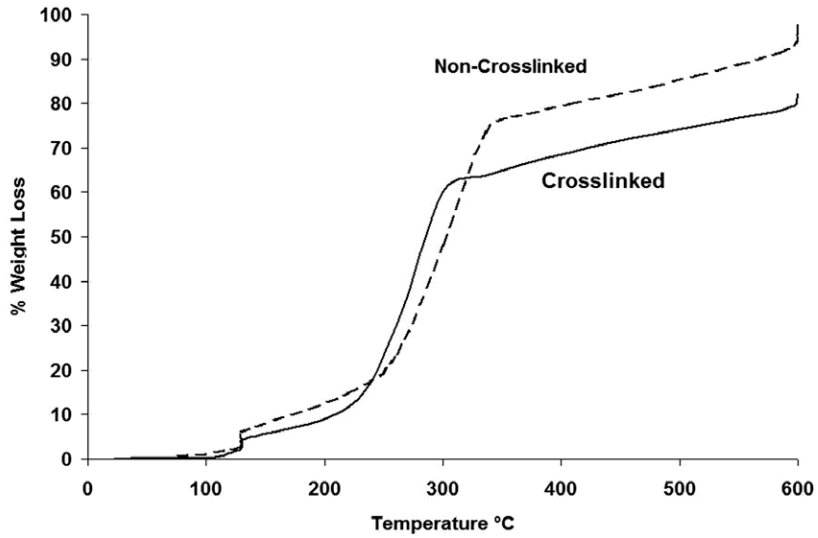

Fig. 6. Weight-loss (%) of the non-cross-linked starch films and starch films cross-linked with 5% citric acid in a thermogravimetric analyser.

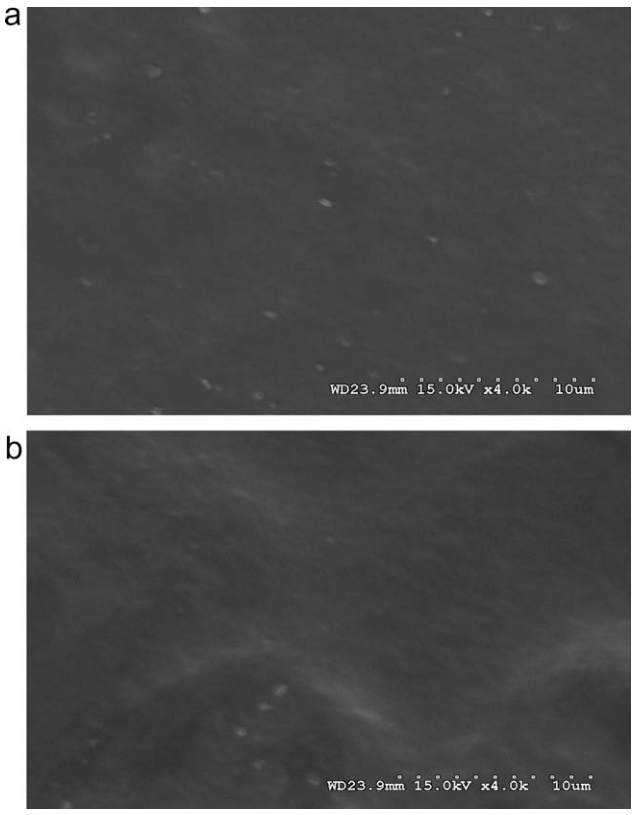

Fig. 7. SEM pictures of cross-linked (a) and control films (b) magnified 4000×. The films are homogenous without any pores or cracks.

curing are shown in Fig. 9. There is no change in the *YI* of the starch films with various amounts of citric acid before curing. After curing at 165 °C for 5 min, the films turn slightly yellow, with the *YI* increasing with increasing amount of citric acid in the films. The non-cross-linked films also show a slight increase in *YI* after curing. Films cross-linked with 1%, 3% and 5% citric acid have similar *YI*, about 10% higher than their corresponding *YI* before curing. The *YI* of the films treated with 10% citric acid increases substantially after curing and those treated with 20% citric acid have nearly 13 times higher *YI* than that of the non-cross-linked films after curing. The discoloration of the films after curing at high temperatures is mainly due to the dehydration of citric acid that leads to the formation of an unsaturated acid that imparts colour to the films (Andrews & Welch, 1989). The higher the amount of citric acid in the films is, the higher the quantities of unsaturated acids formed, leading to more yellowness. In addition to the formation of the unsaturated acids, starch will also degrade to a certain extent at high temperatures, leading to discoloration, as seen from the higher *YI* of the non-cross-linked films after curing, compared to the *YI* of the non-cross-linked films before curing.

3.10. Weight loss in water

The cross-linked starch films had only about 25% weight loss, even after being in pH 7.2 water at 50 °C for 35 days, whereas the non-cross-linked fibres lost about 75% of their weight, as seen from Fig. 10. After 3 days in water, both the cross-linked and non-cross-linked fibres lose about 25% of their weight. On further treatment in water, the cross-linked fibres do not show any considerable loss in weight but the weight loss of the non-cross-linked films increases to about 70% after 10 days in water. The non-cross-linked fibres do not experience much weight loss on further treatment in water for up to 35 days. Cross-linking not only increases the strength of the films but also creates a more dense structure. This prevents the swelling of starch and decreases the accessible regions, leading to an improvement in the resistance to dissolution, compared to the non-cross-linked films.

3.11. Weight loss in formic acid

The weight loss of starch films in formic acid decreases considerably after cross-linking, as seen from Fig. 11. The non-cross-linked starch films lose about 50% of their weight after being in formic acid for 24 h at 20 °C. Films cross-linked with 1% and 3% formic acid have weight loss of about 25% and those cross-linked with 5% and 10% citric acid have weight loss of 17% and 15%, respectively, when treated in formic acid for 24 h at 20 °C. The non-cross-linked and films cross-linked with 1% citric acid completely dissolved in formic acid when treated with formic acid at 50 °C for 5 h. Films cross-linked with higher amounts of citric acid showed substantial decrease in weight loss in formic acid at 50 °C. Starch films cross-linked with 3% and 5% citric acid had weight loss of 53% and 36%,

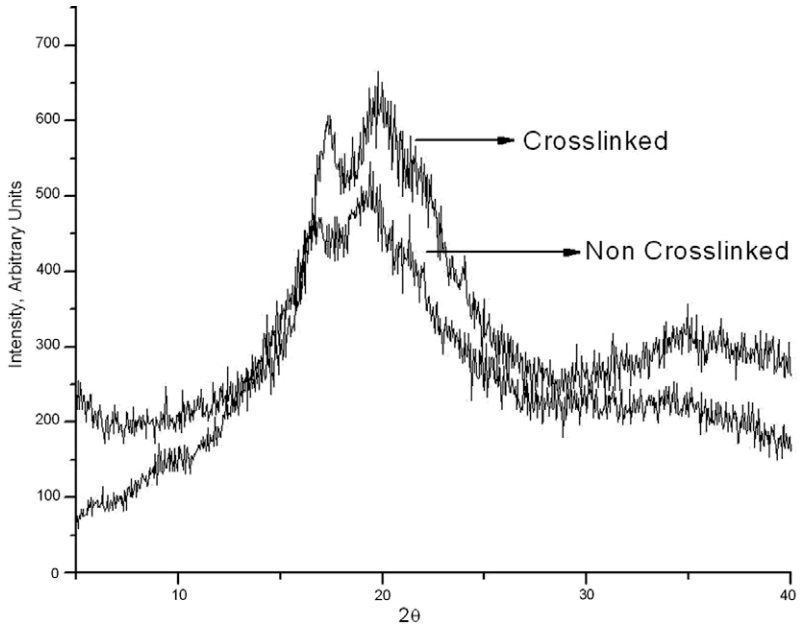

Fig. 8. Diffraction patterns of cross-linked and non-cross-linked starch films show similar diffraction peaks and intensities without any considerable change in the starch crystals due to cross-linking.

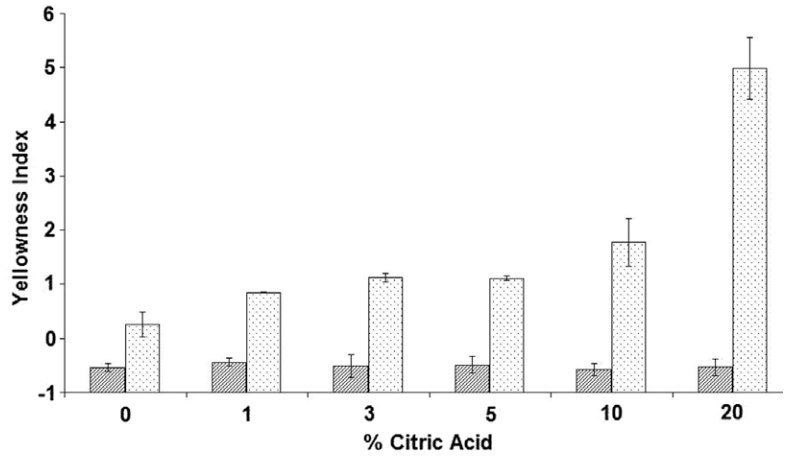

Fig. 9. Changes in the yellowness index of the starch films before and after curing at 165 °C for 5 min with various amounts of citric acid.

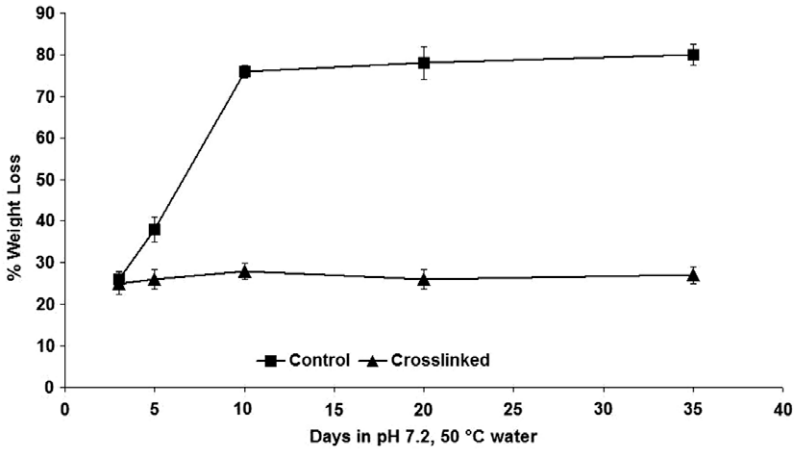

Fig. 10. Weight-loss (%) of the non-cross-linked and cross-linked starch films after treating in pH 7.2 water at 50 °C for various periods of time.

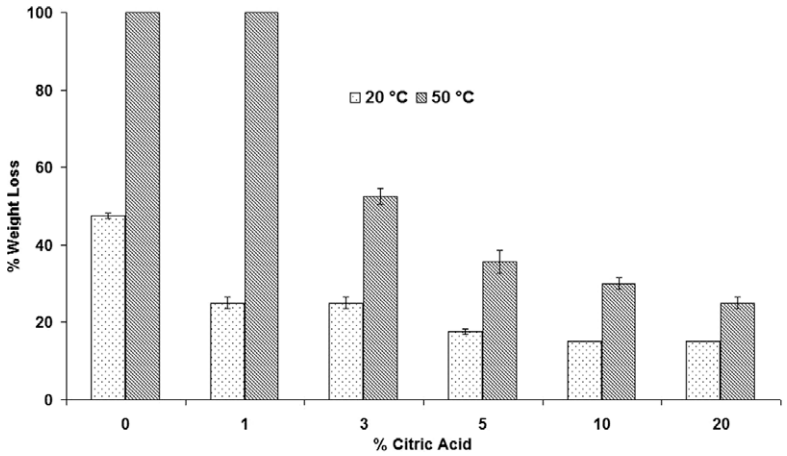

Fig. 11. Weight-loss (%) of the starch films after treating in formic acid at 20 °C for 24 h and 50 °C for 5 h.

respectively whereas 10% and 20% citric acid cross-linked films lost only 30% and 25% of their weight after being in formic acid for 5 h at 50 °C. The higher strength of the starch films and less swelling of the starch molecules after cross-linking should be the major reasons for the better stability of the cross-linked films in formic acid, compared to the non-cross-linked films. Although the 10% and 20% cross-linked starch films have lower strength than the 5% citric acid cross-linked films, the higher amounts of citric acid would prevent the dissolution of the starch in the 10% and 20% films, leading to better resistance to dissolution. The extent of citric acid to be used for cross-linking should therefore be selected based on the end use requirements for the films.

3.12. Advantages of citric acid cross-linking

Citric acid is preferable for starch cross-linking since low levels (5% or less) are required for cross-linking; it can be derived from fermentation and could therefore be considered as a green chemical. Citric acid also has price advantages over a few other compounds commonly used to cross-link starch. Based on reagent-grade chemicals for laboratory purchase, citric acid costs about $0.05 per gram, compared to $0.09, $0.04, $0.08 and $0.07 for glutaraldehyde, epichlorohydrin, boric acid and sodium trimetaphosphate, respectively. From MSDS ratings, citric acid, boric acid and sodium trimetaphosphate have health hazard rating of 1, whereas glutaraldehyde is rated 2 and epichlorohydrin is rated 3. Sodium hypophosphite is reported to be hazardous to the environment. In addition to citric acid, other poly(carboxylic acids) may also be suitable for cross-linking starch films.

4. Conclusions

Citric acid effectively cross-links starch and improves the strength and considerably decreases the weight loss of the films in water and formic acid. Cross-linked starch films have about 150% higher strength than non-cross-linked films and also better strength than most cross-linked and/or synthetic polymer blended starch films previously developed. Cross-linked starch films show a broad melting peak and have considerably higher thermal stability (lower weight loss) compared to the non-cross-linked samples at temperatures between 320 and 600 °C. Citric acid cross-linking slightly decreases the water vapour permeability and colour (*YI*) of the films but the morphology and % crystallinity of the films are not adversely affected. Starch films cross-linked with 3–20% of citric acid have only about 15–25% weight loss, whereas the non-cross-linked films immediately dissolved in formic acid.

Acknowledgements

The authors wish to thank the Agricultural Research Division at the University of Nebraska-Lincoln, USDA Hatch Act and Multi-State Research Project S-1026 for their financial support.

References

Andrews, B. A. K., & Welch, C. M. (1989). Efficient ester cross-link finishing for formaldehyde-free durable press cotton fabrics. *American Dyestuff Reporter, 78*(6), 15–23.

Chen, L., Imam, S. H., Gordon, S. H., & Greene, R. V. (1997). Starch-polyvinyl alcohol cross-linked film-performance and biodegradation. *Journal of Polymers and the Environment, 5*(2), 111–117.

Garg, S., & Jana, A. K. (2007). Studies on the properties and characteristics of starch–LDPE blend films using cross-linked, glycerol modified, cross-linked and glycerol modified starch. *European Polymer Journal, 43*, 3976–3987.

Hirsch, J. B., & Kokini, J. L. (2002). Understanding the mechanism of cross-linking agents ($POCl_3$, STMP and EPI) through swelling behaviour and pasting properties of cross-linked waxy maize starches. *Cereal Chemistry, 79*(1), 102–107.

Kim, M., & Lee, S. (2002). Characteristics of cross-linked potato starch and starch-filled linear low-density polyethylene. *Carbohydrate Polymers, 50*, 331–337.

Kunaik, L., & Marchessault, R. H. (1972). Study of cross-linking reaction between epichlorohydrin and starch. *Starch, 24*(4), 110–116.

Raj, B., Udaya Sankar, K., & Siddaramaiah (2004). Low density polyethylene/starch blend films for food packaging applications. *Advanced Polymer Technology, 23*(1), 32–45.

Ramaraj, B. (2007). Cross-linked poly(vinyl alcohol) and starch composite films: Study of their physiochemical, thermal and swelling properties. *Journal of Applied Polymer Science, 103*, 1127–1132.

Rioux, B., Ispas-Szabo, P., Ait-Kadi, A., Mateescu, M., & Juhasz, J. (2002). Structure–properties relationship in cross-linked high amylose starch cast films. *Carbohydrate Polymers, 50*, 371–378.

Schramm, C., Vukusic, S. B., & Katovic, L. (2002). Non-formaldehyde durable press finishing of dyed fabrics: Evaluation of cotton-bound polycarboxylic acids. *Coloration Technology, 118*, 244–249.

Seker, M., & Hanna, M. A. (2006). Sodium hydroxide and trimetaphosphate levels affect properties of starch extrudates. *Industrial Crops and Products, 23*, 249–255.

Simkovic, I., Hricovini, M., Mendichi, R., & Soest, J. J. G. (2004). Cross-linking of starch with 1,2,3,4-diepoxybutane or 1,2,7,8-diepoxyoctane. *Carbohydrate Polymers, 55*, 299–305.

Wattanachant, S., Muhammad, K., Hashim, D. M., & Rahman, R. A. (2003). Effect of cross-linking reagents and hydroxypropylation levels on dual-modified sago starch properties. *Food Chemistry, 80*, 463–471.

Yang, C. Q., & Andrews, B. A. K. (1991). Infrared spectroscopic studies of the non-formaldehyde durable press finishing of cotton fabrics by use of polycarboxylic acids. *Journal of Applied Polymer Science, 43*, 1609–1616.

Yang, C. Q., & Wang, X. (1996). Formation of cyclic anhydride intermediates and esterification of cotton cellulose by multifunctional carboxylic acids: An infrared spectroscopy study. *Textile Research Journal, 66*(9), 595–603.

Yang, C. Q., Wang, X., & Kang, I. (1997). Ester cross-linking of cotton fabric by polymeric carboxylic acids and citric acid. *Textile Research Journal, 67*(5), 334–342.

Yang, Y., Wang, L., & Li, S. J. (1996). Formaldehyde-free zein fiber-preparation and investigation. *Journal of Applied Polymer Science, 59*, 433–441.

Yin, Y., Li, J., Liu, Y., & Li, Z. (2005). Starch cross-linked with poly(vinyl alcohol) by boric acid. *Journal of Applied Polymer Science, 96*, 1394–1397.

Yoon, S., Chough, S., & Park, H. (2006). Properties of starch-based blend films using citric acid as additive II. *Journal of Applied Polymer Science, 100*, 2554–2560.

Yoon, S., Chough, S., & Park, H. (2007). Preparation of resistant starch/poly(vinyl alcohol) blend films with added plasticizer and cross-linking agents. *Journal of Applied Polymer Science, 106*, 2485–2493.

Yu, J., Wang, N., & Ma, X. (2005). The effects of citric acid on the properties of thermoplastic starch plasticized by glycerol. *Starch/Starke, 57*, 494–504.

more than 50% protein, whilst the depleted starch phase showed less than 2% protein. These values were obtained at constant process conditions (rotational speed, temperature and moisture content); no attempts were made yet to investigate the influence of these parameters on separation behaviour. The gluten obtained from shear induced separation showed higher R_{max} (maximum resistance to extension) and area under curve (energy for extension) in large-strain uniaxial extension tests as compared to commercial gluten. In this paper, we elaborate on separation principles based on differences in rheology between the starch and gluten phase using simple shear flow.

The main mechanism that contributes to the separation of gluten is shear-induced segregation or demixing of gluten and starch. Gluten with its visco-elastic characteristic and starch with dilatant characteristics undergoes segregation (Kieffer & Stein, 1999). This phenomenon is in accordance with the reported segregation behaviour of polymeric systems under shear flow, which is a known effect for synthetic (non-food) polymer blends or polymeric suspensions (Hobbie, Lin-Gibson, Wang, Pathak, & Kim, 2004; Olmsted, 1999; Vermant, 2001).

However, for using this separation principle more information is needed about the driving forces in the system and how the driving forces are influenced by process conditions. Therefore, the objective of the study reported here was to investigate the influence of the process conditions (rotational speed, temperature and shearing time) on the separation behaviour of gluten and starch.

2. Experimental

2.1. Materials

Flour of Soissons (single French wheat cultivar) was kindly obtained from Top Institute Food and Nutrition (TIFN), Wageningen, The Netherlands. Protein, GMP wet weight, moisture and ash contents for flour used were 10.65 (%db), 188 (g/100 g dry matter of the flour), 12.7% and 0.48 (%db), respectively. The Farinograph characteristics of this flour are: water absorption 54% (based on 14% flour moisture), arrival time 10.5 min, time to peak 15 min, stability 21 min and time to breakdown 31.5 min.

2.2. Preparation of starting material for shear experiments

Non-developed or "Zero developed" (ZD) dough was prepared according to the method of Campos, Steffe, and Ng (1996) with modifications described by Peighambardoust, van der Goot, van Vliet, Hamer, and Boom (2006). ZD dough is a "zero mechanical energy input" developed dough which is completely hydrated prior to processing. NaCl at a concentration of 2% (w/w flour basis), and moisture content of 49% (5% lower than Farinograph water absorption) was used in preparation of the ZD doughs. A comparison between characteristics of ZD dough and flour–water mixture has been reported earlier (Peighambardoust, van der Goot, Boom, & Hamer, 2006).

Based on previous experiences, for running a successful shear experiment one has to reduce dough moisture content to a level 5% lower than flour's Farinograph water requirement (Peighambardoust, van Brenk, van der Goot, Hamer, & Boom, 2007; Peighambardoust, van der Goot, van Vliet, et al., 2006; Peressini, Peighambardoust, Hamer, Sensidoni, & van der Goot, 2008). Doughs prepared at a high moisture content become sticky upon long processing leading to difficulties in handling and sampling of the processed dough. Previous results showed that shearing of the dough (at Farinograph moisture content) at 120 min led to re-distribution of the separated gluten phase throughout the product (Peighambardoust et al., 2008). Therefore, in the present study a moisture content of 5% lower than Farinograph water absorption was used in the preparation of the ZD doughs.

2.3. Shearing process

We used the same apparatus and methods for the shearing trials as described previously (Peighambardoust et al., 2008). Increasing rotational speeds of 2–6 rpm, 10–20 rpm, 20–30 rpm, 30–40 rpm and 40–50 rpm for different trials were used to ensure a good (non-slippage) shearing conditions. Process temperature set of 5, 15, 20, 30 and 40 °C and processing time of 50, 80, 90, 120 and 180 min were used.

A schematic drawing of the shear cell geometry was shown previously (Peighambardoust et al., 2008). The shear rate in the device can be calculated using the following equation:

$$\dot{\gamma} = \frac{\frac{2\pi N}{60} R\cos(\alpha)}{\delta + R\tan(\theta)\cos(\alpha)} \quad (1)$$

In this equation, $\dot{\gamma}$ is the shear rate (s^{-1}), N is the rotational speed (rpm), R is the distance (in m) from the centre of the cone, δ is the distance between the two cones in the centre (in m), α and θ are the angles of the external and internal cones (in degree), respectively (see also Fig. 1), when δ is zero, the shear rate has the same value throughout the system; however when it is larger, the shear rate will be larger away from the centre of the cones.

2.4. Sampling of dough for subsequent analysis

After stopping the process and disassembling the cell, four or five regions (rings) of dough from top to bottom were sampled using a razor blade. The reason for selecting five samples in some experiments was to see whether or not there is any difference in the composition of the gluten phase (in terms of glutenin macropolymer) separated exactly at the tip part of the cone, where the gluten concentration reaches to its maximum. The sampling time before the dough is frozen in the liquid nitrogen was about 5 min and this was kept constant for all trials. The samples from top to bottom were encoded as 1–4 or 1–5 depending on the conditions for some experiments. The samples were immediately frozen in liquid nitrogen and freeze-dried overnight to an average moisture content of 4% and kept in sealed plastic containers at ambient temperature until further analysis.

2.5. Measurement of protein

The protein contents ($N \times 5.7$) of freeze-dried dough samples were determined by the Dumas method (Sebecic & Balenovic, 2001) using an NA2100 Nitrogen and Protein Analyzer (Thermo-Quest-CE Instruments, Rodeno, Italy). Methionine was used as a standard.

2.6. Measurement of GMP wet weight

Freeze-dried dough sample was weighed (1.55 g) in an ultra-centrifuge tube of approximately 33 ml. The tube was then placed on a Vortex mixer. Whilst rigorous vortexing, 9.125 ml demi-water was added with a calibrated dispensor. Vortexing was continued for about 10–15 s till a homogenous and lump-free suspension was obtained. Immediately after suspending, 3.875 ml 12% (w/v) SDS solution was added, followed by the addition of two portions of 9 ml demi water with a dispensor to reach a final concentration of 1.5% (w/v) SDS. The tubes were then ultra-centrifuged (Graveland, Bosveld, Lichtendonk, Moonen, & Scheepstra, 1982) (80,000g, 30 min at 20 °C) in a Kontron Ultracentrifuge. The supernatant (SUP) was decanted and the gel-like layer found on top of the starch sediment (called GMP) was weighed immediately as GMP wet

weight. This amount was expressed as grams of gel per 100 g of sample (db). The measurements of GMP wet weight were performed at least in triplicate.

3. Results

3.1. Effect of rotational speed

3.1.1. Visual inspection of dough after processing

The sheared doughs showed accumulation of the gluten phase at the apex of the cones for all rotational speed regimes used. Nevertheless, doughs sheared at higher rotational speeds (>30 rpm) appeared to be softer, whilst still giving reasonable gluten accumulation in the apex of the cone. Low rotational speed treatments led to the appearance of gluten domains in the form of strands in the middle regions of the cone (samples 2 and 3). This effect disappeared at higher shear rates.

3.1.2. Changes in protein concentration

Table 1 shows the protein content in the sheared dough as a function of the rotational speed at different locations in the shearing device. The amount of protein at the apex of the cone was at least 32.6% at low rotational speeds of 2–6 rpm. Increasing the rotational speed to 30–40 rpm led to a significant increase in the protein content of the gluten at the apex (sample 5). An additional increase to 40–50 rpm did not increase the protein content of sample 5.

At rotational speeds of more than 30 rpm, there was a significant increase in the protein content of samples in region 3. This was in parallel with protein accumulation at the apex of those trials. In total, increasing rotational speed (>30 rpm) led to an increase in the protein content of the bottom half of the cone (samples 3–5, which comprises 31.8% of total dough weight, see Table 1). In contrast with this, the upper half of the cone (samples 1–2, which comprise 68.2% of total dough weight) stays protein-depleted (<4% protein).

At all rotational speeds, the upper regions of the cone (layers 1 and 2, which comprise 68% of the total dough weight) became protein-depleted (and therefore starch-enriched). In general, it seems that the rotational speed did not have a large influence on the extent of protein separation.

3.1.3. Changes in GMP wet weight

Table 1 also shows the influence of the rotational speed on the GMP wet weight (in non-rested dough or gluten). Increasing the rotational speed from 2–6 to 10–20 rpm led to a decrease in the GMP wet weight of samples 4 and 5. Upper samples (1 and 2) showed increased GMP wet weights at rotational speed of 10–20 rpm. When the rotational speed increased from 10–20 to 20–30 rpm, GMP wet weight decreased in all zones in the cell. This decrease might be related to the breakdown of glutenin particles at higher shear rates. Especially at 20 rpm, a large peak in the torque was observed, which could account for the gluten breakdown. However, a further increase in speed (>30 rpm) did not result in a further decrease in the GMP wet weight of the separated gluten.

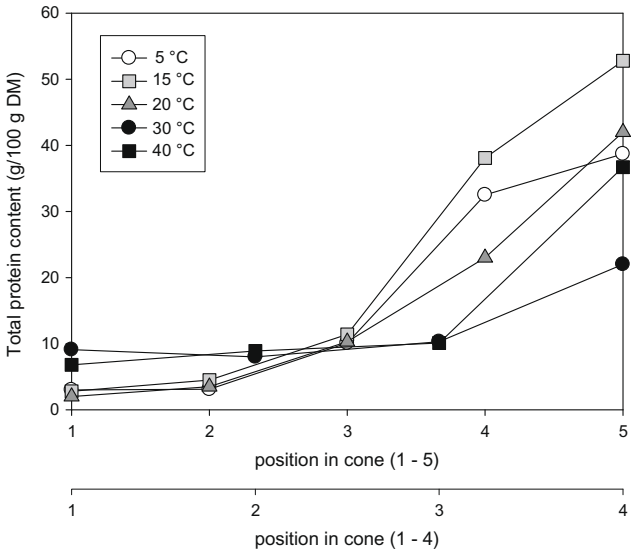

Fig. 1. Effect of temperature on total protein content of dough as function of sampling locations (1–5). Rotational speed regimes for 5, 15, 20, 30 and 40 °C experiments were 10–20, 5–15, 5–10, 5–15 and 5–30 rpm, respectively. Processing times for all experiments were 60 min, except for 40 °C for which a processing time of 40 min was used. Error bars are not shown as they were of a similar size to the symbols used.

3.2. Effect of temperature

3.2.1. Visual inspection of dough

The sheared doughs yielded gluten separation at a temperature of 15 °C. Upon increasing the shearing temperature, accumulation of the gluten phase at the apex of the cone became less. Large gluten domains in the form of long fibres in the middle part of the cone (regions 2 and 3) were observed at a temperature of 20 °C. Shearing at 30 °C showed only minor gluten separation, and shearing at 40 °C resulted in only small gluten domains at the apex of the cone. At this temperature, the rest of dough was soft and sticky.

3.2.2. Changes in protein concentration

The total protein content as a function of sampling position and temperature is shown in Fig. 1. A cold shearing regime (5 °C) gave a protein enrichment of up to 39% at the apex of the cone. Increasing the temperature to 15 °C resulted in a considerable increase in the separation of total protein content. A further increase in temperature did not further increase the separation. At higher temperatures, especially at 30 °C, the enrichment of protein became lower. Shearing at 40 °C, however, led to a slight increase in the to-

Table 1
Effect of rotational speed on total protein content and GMP wet weight of the dough at different sampling locations (1–5). Processing temperature and time were 5–7 °C and 60 min, respectively. Please note that for 2–6 rpm, the four-segmented sampling scheme was used, whilst for the other runs the five-segmented sampling scheme was used.

	Samples	2–6 rpm	10–20 rpm	20–30 rpm	30–40 rpm	40–50 rpm
Protein content (g/100 g DM)	1	2.4 ± 0.2[a]	3.0 ± 0.4	4.0 ± 0.4	2.4 ± 0.2	3.4 ± 0.3
	2	3.8 ± 0.4	3.1 ± 0.3	3.6 ± 0.3	3.9 ± 0.3	3.9 ± 0.4
	3	14.6 ± 0.5	10.1 ± 0.4	10.8 ± 0.4	14.8 ± 0.4	15.6 ± 0.2
	4	32.6 ± 0.4	32.5 ± 0.7	26.7 ± 0.1	27.1 ± 0.3	28.6 ± 0.1
	5		38.7 ± 0.5	38.5 ± 0.3	40.6 ± 0.5	40.4 ± 0.5
GMP wet weight (g/100 g DM)	1	40 ± 5	98 ± 11	54 ± 4	66 ± 15	76 ± 3
	2	59 ± 5	171 ± 16	69 ± 11	85 ± 12	100 ± 4
	3	202 ± 6	153 ± 26	69 ± 16	86 ± 6	84 ± 2
	4	337 ± 11	107 ± 17	75 ± 11	88 ± 11	75 ± 8
	5		269 ± 21	126 ± 17	105 ± 10	111 ± 17

[a] Standard deviation of triplicate measurements.

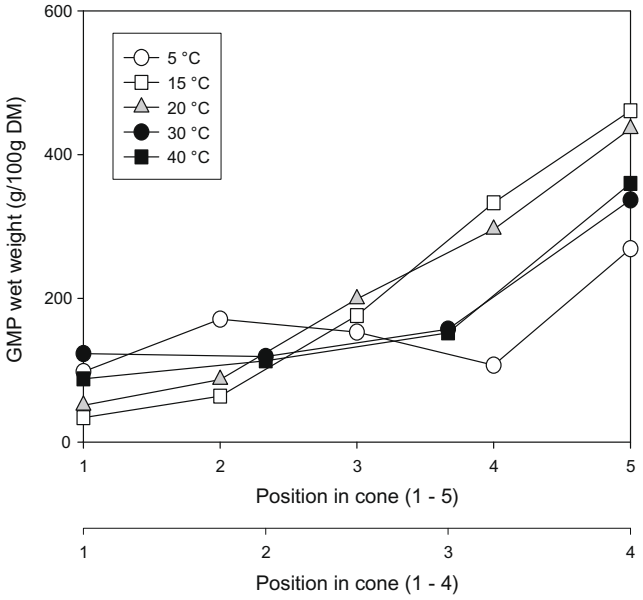

Fig. 2. Effect of shearing temperature on the GMP wet weight (in non-rested dough) at different sampling locations (1–5). Rotational speed and processing time were mentioned in Fig. 1. Error bars are not shown as they were of a similar size to the symbols used.

tal protein content of the material at the apex of the cone, probably due to increased interactions in the gluten phase. It is remarkable that the protein depletion in the starch-rich regions is severely reduced at higher temperatures.

3.2.3. Changes in the GMP wet weight

The effect of the shearing temperature on the GMP wet weight (in non-rested dough) was investigated. Fig. 2 demonstrates GMP wet weight variations as function of shearing temperature. At all temperatures, GMP data showed significantly higher values at the apex of the cone (sample 4) compared to other sampling locations, indicating separation in terms of glutenin macro-polymer. In terms of the effect of shearing temperature, the GMP wet weights followed the trend in the total protein content (in Fig. 1), except for the 5 °C experiment, which showed lower GMP values in samples 4 and 5. There is an optimum in the enrichment of the glutenin macro-polymer at shearing temperatures of 15 and 20 °C. No clear difference was seen between GMP wet weight values of sheared doughs at 15 or 20 °C. Increasing the temperature from 20 to 30 °C led to a decrease in the GMP wet weight.

3.3. Influence of shearing time

3.3.1. Visual inspection of sheared dough

Regardless of small differences in terms of rotational speed and processing temperatures, separation of gluten and starch was observed for all shearing runs. Shearing for 50 min already gave a reasonable separation. At the moisture content used in this study, a shearing time of 120 min gave the most complete separation, as judged visually. Prolonged shearing (for 180 min) exhausted the dough, leading to a smaller volume of the gluten phase in the apex of the cone. This dough was sticky and appeared over-processed.

3.3.2. Changes in protein concentration

Fig. 3 shows that the apex of the cone is enriched in protein for all shearing times, whilst the top of the cone was depleted of protein (<4%), thus rich in starch. Especially after 120 min, a low protein content was found in the starch phase. There was no clear difference in protein content of samples in the same locations and sheared for 50–80 min. The highest level of protein enrichment (43–49%) was found for shearing times of 90–120 min. Further shearing for 180 decreased the protein content in zones 4 and 5.

3.3.3. Changes in the GMP wet weight

Fig. 4 shows the GMP wet weights as a function of the shearing time. Shearing for 50 min already led to an increase in the GMP wet weight at the apex of the cone. Changes in GMP wet weight paralleled changes in the total protein content of the dough upon differ-

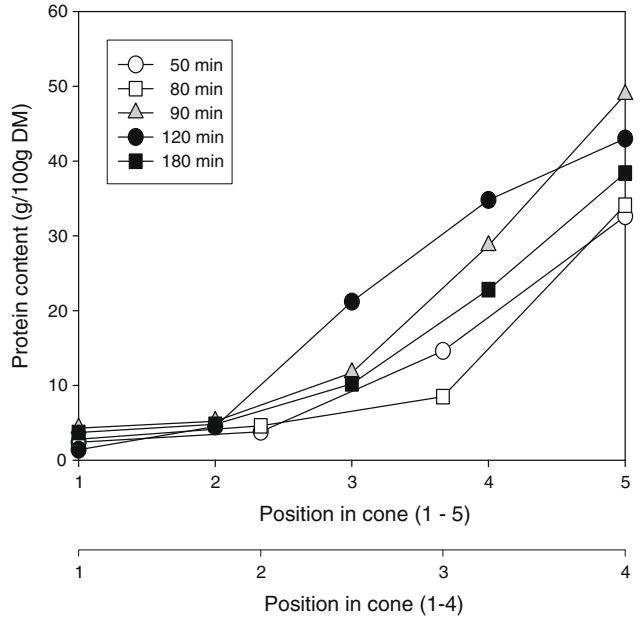

Fig. 3. Effect of shearing time on total protein content of dough as function of sampling locations (1–5). The shearing runs of 50 min and 180 min were carried out at a temperature of 5 °C. Temperature for shear runs of 90 and 120 min was 15 and 10 °C, respectively. Rotational speed regimes for shearing times of 50, 90, 120 and 180 min were 2–6, 5–20, 5–15 and 4–15 rpm, respectively. Error bars are not shown as they were of a similar size to the symbols used.

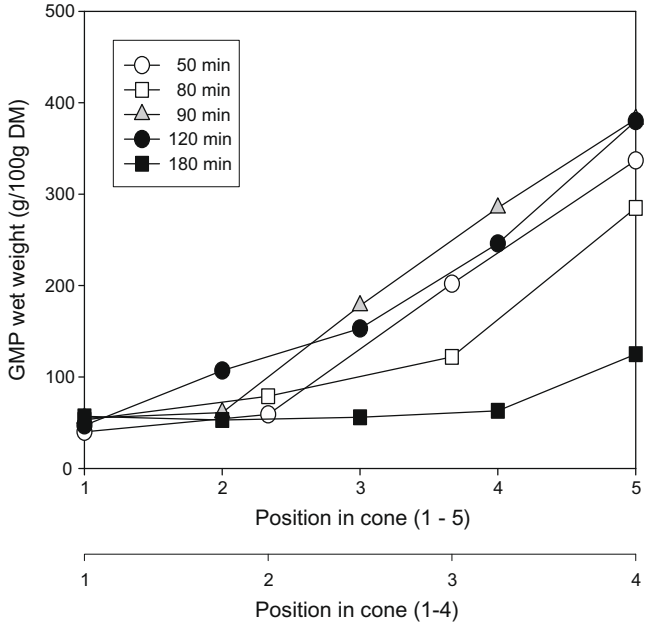

Fig. 4. Effect of shearing time on GMP wet weight (in non-rested dough) at different sampling locations (1–5). Processing temperature and rotational speed was mentioned in Fig. 3. Error bars are not shown as they were of a similar size to the symbols used.

ent shearing times (Fig. 3), except that upon prolonged shearing (180 min) GMP wet weight of gluten samples (at the apex) were considerably lower (125 g) than its amount in other shearing times. Similarly with the total protein content, an optimum for separation was observed in terms of GMP wet weight for shearing times of 90–120 min.

4. Discussion

We previously reported that the separation of wheat dough into gluten-rich and gluten-poor fractions occurs through a two-stage mechanism (Peighambardoust et al., 2008). The first stage leads to the formation of gluten domains. The size of these local gluten domains decreases with increasing shear rate (Peressini et al., 2008) that was explained by a rupture of those domains due to the shear forces. The second stage comprises of the migration of local gluten domains to the centre part of the shear cell. As this is an exchange (binary transfer) process, the gluten migration is accompanied by migration of starch particles to the outer part of the cell.

There are numerous publications on the effect of simple shear on the migration of polymers (MacDonald & Muller, 1996; Shelby & Caflisch, 2004) and macromolecules (Agarwal, Dutta, & Mashelkar, 1994; Ponche & Dupuis, 2005). Shelby and Caflisch (2004) mentioned that a gradient in shear rate causes a gradient in the elastic strain energy for HMW molecules. As a result, they diffuse away from the wall and towards the centreline in order to reduce their potential energy. Consequently, the smaller particles would migrate toward the wall surface. Carrying this thought further and considering that dough comprises of a visco-elastic gluten phase and inert starch particles (Kieffer & Stein, 1999), we think that the migration in the cell is due to the visco-elastic nature of the gluten. Because starch particles are unlikely to deform upon the shear field applied due to their rigid nature, they will not store elastic strain energy. Therefore, starch particle will not experience a driving force for migration towards the apex of the cone. This leads us to the conclusion that inward migration is induced by the gluten phase. Nevertheless, a number of studies report on migration phenomena in particle containing, viscous and visco-elastic media (Highgate, 1966; Ponche & Dupuis, 2005). Shear-induced normal stresses in cone-and-plate systems can lead to outward migration of particles (Feng & Joseph, 1996; Morris & Boulay, 1999). If this effect is also present when shearing dough, there will be an active driving force for starch particles to migrate away from the apex of the cone. Unfortunately, we are not able to indicate which of the two migration effects is dominant in the experiments reported at this stage.

Dill (1979) and Agarwal et al. (1994) derived an equation describing the migration of a DNA macromolecule in a cone and plate shear field. They assumed that the DNA molecule is a random coil that behaves as a Hookean spring when stretched. This gives rise to a migration velocity towards the centre of the cell:

$$v_m \cong -\frac{\eta_c \dot{\gamma}^2(R)}{R k_B T} r_0^5 \tag{2}$$

where η_c is the viscosity of the continuous phase, R is the radial position, $\dot{\gamma}$ is the shear rate, k_B the Boltzman constant, T the temperature and r_0 the undisturbed radius of the macromolecule. Here we interpret that r_0 is the size of the gluten domain at rest. Combining equations 1 and 2 leads to:

$$v_m \cong \frac{\eta_c R}{k_B T}\left(\frac{2\pi N \cos(\alpha)}{\delta + R\tan(\theta)\cos(\alpha)}\right)^2 r_0^5 \tag{3}$$

It is clear that a single DNA molecule in water behaves differently than a gluten domain in dough. Nevertheless, we think that the driving force for migration is similar, namely elongation of an elastic particle. Since, the elongation is elastic, it leads to an inward migration. In qualitative terms, the equation seems therefore useful for the first and initial explanations in our observation in the dough systems.

Eq. (3) indicates that the size of the gluten domains strongly determines the radial migration velocity of the gluten. Thus, the gluten domains need to have a minimum size before migration can become significant. Furthermore, the visco-elastic nature of the gluten seems to be important in the second step.

4.1. Influence of moisture content

We previously (Peighambardoust et al., 2008) reported on the separation of gluten and starch under shear field at a moisture content of 54% (according to Farinograph moisture absorption of the flour). In the present study, a lower moisture content (49%) was used. The results shown for shearing time (Section 3.3) indicated that at a low moisture content, it takes longer (>60 min) to reach an optimum time for separation. In the previous study we showed that a shearing time of 40 min already gave enhanced separation followed by the disappearance of a separated phase at a longer time (120 min). The higher dough viscosity might play a role here, because a positive correlation has been reported between the radial migration velocity and the viscosity of the medium (Agarwal et al., 1994). This is all in agreement with Eq. (3). The increased viscosity induces the stretching of the gluten domains, enhancing the radial force on these gluten domains. Nevertheless, local aggregation of gluten is probably less at low moisture contents, most likely due to a smaller volume of the gluten phase at lower moisture contents. Thus, a longer shearing time is necessary to obtain local gluten domains that are large enough to induce radial migration. Therefore, the total effect of the moisture content on the separation rate is difficult to predict, though the experiments showed that a lower moisture content leads to a slower separation. Compared to our previous study, it seems that a lower moisture content had a positive effect on gluten stability, as it was possible to shear the dough for 120 min without re-dispersion of the gluten throughout the dough.

4.2. Effect of rotational speed

The migration velocity is proportional to the square of the rotational speed (via the shear rate – see Eq. (2)) (Agarwal et al., 1994; Dill, 1979). This faster migration is however counteracted by the fact that gluten domains become more susceptible to breaking at higher shear rates (Peressini et al., 2008). Thus, their radius will be smaller on average. Furthermore, an increased rotational speed also reduces the dough viscosity (Data not shown). Though the migration of gluten domains is positively effected by an increased shear rate, the lower viscosity reduces this positive effect.

Visual inspection of the processed dough revealed the presence of strongly elongated gluten domains at low speeds. Higher speeds led to softer dough, but still gluten migration could be obtained. However, this gluten contained less GMP (see Table 1), suggesting a reduced gluten vitality. Therefore, a low rotational speed in the range of 10 to 20 rpm seems to work best in the shearing device used here.

4.3. Effect of temperature

The process temperature has a significant effect on the dough viscosity. At higher temperatures the hydrophobic interactions become more important (Fasina, Walter, Fleming, & Simunovic, 2003) as a result of the fact that formation of gluten domains are favoured. Thus, an increased temperature would have a positive ef-

fect on step 1. However, the increased hydrophobic interaction will exhaust the dough more quickly, as a result of which over-processing can occur. The lower average GMP-values at 40 °C hints in this direction. Step 2 is negatively influence by the temperature as shown by Eq. (3). In addition, the dough viscosity will be lowered, which reduces the driving force for migration even further.

4.4. Outlook towards industrial application

Wheat flour can be separated into a gluten-rich and gluten-poor phase using a broad range of process conditions. The separation is not influenced strongly by the process conditions, which can be explained by the multitude of the effects that play a role. Overall, a low rotational speed in combination with a moderate temperature seems to work best because those conditions minimise gluten damage. The shear separation process could also benefit starch quality, since the process does not apply multiple washing steps for separation or purification of the starch, and therefore the loss of suspending small starch granules in the water is restricted.

Since the experiments reported here were not optimised to yield the highest possible protein content, it is relevant to consider whether one could further increase the protein content (e.g. by changing device geometry and dough formulation). In our previous study, we showed that the remaining gluten is present in small domains in the starch-enriched phase (in other words it is not dispersed throughout the starch phase as it is in an over-mixed dough). Also the starch particles are clustered in the gluten-rich phase. The formation of those gluten domains and starch clusters indicate that further purification should be possible. Eq. (3) suggests that a modification of the shear rate profile might lead to enhanced purification. The distance between the cones and possibly the shape of the cones could be modified. Furthermore, since the separation mechanism has two distinct stages, it might be beneficial to separate both stages into isolated process steps, which can then both be optimised. Many changes in conditions yield opposing effects results in stages 1 and 2, which may be avoided in a two stage process. Nevertheless, we think that the use of differences in rheological behaviour of dough constituents is a challenging new principle, which merits further exploration.

It is clear that for industrial application, dedicated and new equipment has to be developed, in which the shear rate and absolute velocities are key design parameters. The development of new separation equipment faces many challenges. We still need a better understanding of the driving forces present in this system in order to optimise the process conditions. It is not clear yet, how the separation principle presented here can be translated to a continuous set-up. Finally, it can be mentioned that the long shearing times lead to large energy inputs, which should be reduced to make this process industrially feasible.

5. Conclusions

The influence of process conditions on the separation of starch and gluten in a cone-cone shearing device was reported. Separation of the dough into a starch-rich and a gluten-rich region was clearly observed under all experimental conditions tested. The migration of gluten was not strongly influenced through variations in the process conditions. A possible explanation is that the two stages in the mechanism (formation of local small gluten domains followed by macroscopic radial migration) respond oppositely to most changes in process conditions. Nevertheless, the experiments described in this paper showed that a low rotational speed combined with a moderate temperature seem most favourable. A higher shear rate at lower temperature, prolonged shearing, and a higher process temperature all lead to certain extent of gluten damage, thereby softening the dough and reducing the driving force for separation.

Acknowledgements

Financial support of Cargill (Bergen op Zoom, The Netherlands) in performing this study is gratefully acknowledged. The helpful discussions given by Rob Hamer (Top Institute Food and Nutrition, TIFN, Wageningen, The Netherlands) and Remko Boom (Food Process Engineering Group, Wageningen University, The Netherlands) during this study is highly appreciated. We thank the mechanical and electronic workshops of Wageningen University (Wageningen, the Netherlands) for constructing the shear cell.

References

Agarwal, U. S., Dutta, A., & Mashelkar, R. A. (1994). Migration of macromolecules under flow: The physical origin and engineering implications. *Chemical Engineering Science, 49*, 1693–1717.

Campos, D. T., Steffe, J. F., & Ng, P. K. W. (1996). Mixing wheat flour and ice to form undeveloped dough. *Cereal Chemistry, 73*, 105–107.

Christophersen, C., Andersen, E., Jakobsen, T. S., & Wagner, P. (1997). Xylanases in wheat separation. *Starch–Starke, 49*, 5–12.

Day, L., Augustin, M. A., Batey, I. L., & Wrigley, C. W. (2006). Wheat-gluten uses and industry needs. *Trends in Food Science and Technology, 17*, 82–90.

Del Castillo, L. F., Criado-Sancho, M., & Jou, D. (2000). Nonequilibrium chemical potential and shear-induced migration of polymers in dilute solutions. *Polymer, 41*, 2633–2638.

Dik, T., Yöndem-Makascioglu, F., Aytac, C. H., & Kincal, N. S. (2002). Wet separation of wheat flours into starch and gluten fractions: The combined effects of water to flour ratio-dough maturation time and the effects of flour aging and ascorbic acid addition. *Journal of the Science of Food and Agriculture, 82*, 405–413.

Dill, K. A. (1979). Theory for the separation of very large DNA-molecules by radial migration. *Biophysical Chemistry, 10*, 327–334.

Don, C., Lichtendonk, W. J., Plijter, J. J., Van Vliet, T., & Hamer, R. J. (2005). The effect of mixing on Glutenin-particle properties: Aggregation factors that affect gluten function in dough. *Journal of Cereal Science, 41*, 69–83.

Fasina, O. O., Walter, W. M., Jr., Fleming, H. P., & Simunovic, N. (2003). Viscoelastic properties of restructured sweet potato puree. *International Journal of Food Science and Technology, 38*, 421–425.

Feng, D., & Joseph, D. (1996). The motion of solid particles suspended in viscoelastic liquids under torsional shear. *Journal of Fluid Mechanics, 324*, 199–222.

Frederix, S. A., Courtin, C. M., & Delcour, J. A. (2004). Influence of process parameters on yield and composition of gluten fractions obtained in a laboratory scale dough batter procedure. *Journal of Cereal Science, 39*, 29–36.

Graveland, A., Bosveld, P., Lichtendonk, W. J., Moonen, J. H. E., & Scheepstra, A. (1982). Extraction and fractionating of wheat flour protiens. *Journal of the Science of Food and Agriculture, 33*, 1117–1128.

Hamer, R. J., Weegels, P. L., Marseille, J. P., & Kelfkens, M. (1989). A study of the factors affecting the separation of wheat flour into starch and gluten. In: Y. Pomeranz (Ed.), Wheat is unique: Structure, composition, processing, end-use properties, and products. St. Paul, MN: American Association of Cereal Chemists, pp. 467–477.

Highgate, D. (1966). Particle migration in cone–plane viscometry of suspension. *Nature, 211*, 1390–1391.

Hobbie, E. K., Lin-Gibson, S., Wang, H., Pathak, J. A., & Kim, H. (2004). Ubiquity of domain patterns in sheared viscoelastic fluids. *Physical Review E, 061503*, 1.

Kelfkens, M., & Hamer, R. J. (1991). Agronomic factors related to the quality of wheat for the starch industry. 2. Nitrogen-fertilization and overall conclusions. *Starch–Starke, 43*(34), 4–347.

Kieffer, R., & Stein, N. (1999). Demixing in wheat doughs – Its influence on dough and gluten rheology. *Cereal Chemistry, 76*, 688–693.

Ma, H., & Graham, M. D. (2005). Theory of shear-induced migration in dilute polymer solutions near solid boundaries. *Physics of Fluids, 17*, 1–13.

MacDonald, M. J., & Muller, S. J. (1996). Experimental study of shear-induced migration of polymers in dilute solutions. *Journal of Rheology, 40*, 259–283.

Morris, J. F., & Boulay, F. (1999). Curvilinear flows of non-colloidal suspensions: The role of normal stresses. *Journal of Rheology, 43*, 1213–1217.

Olmsted, P. D. (1999). Dynamics and flow-induced phase separation in polymeric fluids. *Current Opinion in Colloid and Interface Science, 4*, 95–100.

Peighambardoust, S. H., Hamer, R. J., Boom, R. M., & van der Goot, A. J. (2008). Migration of gluten under shear flow as a novel mechanism for separating wheat flour into gluten and starch. *Journal of Cereal Science, 48*, 327–338.

Peighambardoust, S. H., van Brenk, S., van der Goot, A. J., Hamer, R. J., & Boom, R. M. (2007). Dough processing in a Couette-type device with varying eccentricity: Effect on glutenin macro-polymer properties and dough micro-structure. *Journal of Cereal Science, 45*, 34–48.

Peighambardoust, S. H., van der Goot, A. J., Boom, R. M., & Hamer, R. J. (2006). Mixing behaviour of a zero-developed dough compared to a flour–water mixture. *Journal of Cereal Science, 44*, 12–20.

Peighambardoust, S. H., van der Goot, A. J., van Vliet, T., Hamer, R. J., & Boom, R. M. (2006). Microstructure formation and rheological behaviour of dough under simple shear flow. *Journal of Cereal Science, 43*, 183–197.

Peressini, D., Peighambardoust, S. H., Hamer, R. J., Sensidoni, A., & van der Goot, A. J. (2008). Effect of shear rate on microstructure and rheological properties of sheared wheat doughs. *Journal of Cereal Science, 48*, 426–438.

Ponche, A., & Dupuis, D. (2005). On instabilities and migration phenomena in cone and plate geometry. *Journal of Non-Newtonian Fluid Mechanics, 127*, 123–129.

Sebecic, B., & Balenovic, J. (2001). Rapid ecologically acceptable method for wheat protein content determination – Comparison of methods. *Deutsche Lebensmittel Rundschau, 97*, 221–225.

Shelby, M. D., & Caflisch, G. B. (2004). Shear field induced diffusion and molecular weight fractionation during polymer processing. *Polymer Engineering and Science, 44*, 1283–1294.

Usta, O. B., Butler, J. E., & Ladd, A. J. C. (2006). Flow-induced migration of polymers in dilute solution. *Physics of Fluids, 18*, 031703-1–031703-4.

Van der Borght, A., Goesaert, H., Veraverbeke, W. S., & Delcour, J. A. (2005). Fractionation of wheat and wheat flour into starch and gluten: Overview of the main processes and the factors involved. *Journal of Cereal Science, 41*, 221–237.

Vermant, J. (2001). Large-scale structures in sheared colloidal dispersions. *Current Opinion in Colloid and Interface Science, 6*, 489–495.

Weegels, P. L., Hamer, R. J., & Schofield, J. D. (1996). Functional properties of wheat glutenin. *Journal of Cereal Science, 23*, 1–18.

Weegels, P. L., Marseille, J. P., & Hamer, R. J. (1988). Small-scale separation of wheat-flour in starch and gluten. *Starch–Starke, 40*, 342–346.

Weegels, P. L., Marseille, J. P., & Hamer, R. J. (1992). Enzymes as a processing aid in the separation of wheat-flour into starch and gluten. *Starch-Starke, 44*, 44–48.

Zheng, J. J., & Yeung, E. S. (2003). Mechanism for the separation of large molecules based on radial migration in capillary electrophoresis. *Analytical Chemistry, 75*, 3675–3680.

were taken. The fruits were washed, cut into four equal pieces (rinds) parallel to the major axis, then ground after the removal of seeds. HPLC-grade methanol, acetonitrile, glacial acetic acid, and hydrochloric acid were procured from Merck India Ltd., Mumbai. C18 Sep-Pak cartridges and Sephadex LH-20 were procured from Waters India Private Ltd., Bangalore and from Sigma Chemicals, Bangalore, respectively. All the other chemicals used were of analytical grade. A consolidated experimental plan has been presented in Fig. 1.

2.2. Extraction of anthocyanins

The pulp, thus obtained as described in Section 2.1, was mixed in a 1:2 ratio with acidified water (0.1% hydrochloric acid). The mixture was subjected to hydraulic press (M/s B. Sen & Berry, New Delhi, India). The extract was filtered using muslin cloth and stored in a cold room at 4–5 °C and used for experiments as and when required.

2.3. Monomeric anthocyanin content

Monomeric anthocyanin content in the whole extract was determined using pH differential method (Wrolstad et al., 2005). All the experiments were carried out in triplicate and average values were reported.

2.4. Purification of anthocyanins

The aqueous extract of *kokum* was passed through a 500 mg sorbent C-18 Sep-Pak cartridge (Waters Associates, Milford, MA) which was previously activated with methanol followed by 0.01% aqueous HCl. Anthocyanins were adsorbed onto the cartridge, whereas sugars, organic acids and other water soluble compounds were washed off the cartridge with 0.01% aqueous hydrochloric acid. Anthocyanins were eluted using acidified methanol (0.01%, v/v HCl). Methanol was evaporated using a rotary evaporator at 35 °C and pigments were dissolved in double distilled water containing 0.01% HCl. These partially purified concentrated anthocyanins were loaded (0.8 ml) onto a Sephadex LH20 column (1.0 × 60 cm) and eluted with a mixture of methanol/water/trifluoroacetic acid at a ratio of 20:79.5:0.5 (Wrolstad et al., 2005). Separated fractions from the Sephadex LH20 column were pooled and were concentrated using a lyophiliser (ThermoLab, UK) separately and subjected to NMR spectroscopy.

2.5. Thin-layer chromatography

Partially purified anthocyanins were streaked on cellulose-based thin-layer chromatography plates. Mobile phase was acetic acid:HCl:water in the ratio of 15:3:82 (Krishnamurthy, 1984). The solvent was allowed a run time of 6 h. Subsequently, the thin layer chromatography plate was dried and retention factors of separated components were determined.

2.6. High-performance liquid chromatography

The anthocyanins sample was diluted accordingly with methanol, filtered through a 0.45-μm membrane filter type HA (Millipore, Billerica, MA) and analysed by high-performance liquid chromatography (HPLC), with a photodiode array detector. The detection was carried out at 520 nm. The flow rate was maintained at 1.0 ml/min. A C-18 ODS column (250 mm × 4.6 mm; SGE, Ringwood, Australia) having a particle size of 5.0 μm was used for HPLC analysis of anthocyanins. A gradient mobile phase was used for elution: eluant **A** was acetonitrile and **B** was 3.0% acetic acid/5.0% acetonitrile/1.0% phosphoric acid in water. The elution profile has been described by Wrolstad et al. (2005).

2.7. Alkaline hydrolysis of anthocyanins

Purified pigments (1.0 ml) were hydrolysed (saponified) in a screw-cap test tube with 10 ml of 10% aqueous KOH for 8 to 10 min at room temperature in the dark as described by Wrolstad et al. (2005). The solution was neutralised using 2 N HCl, and

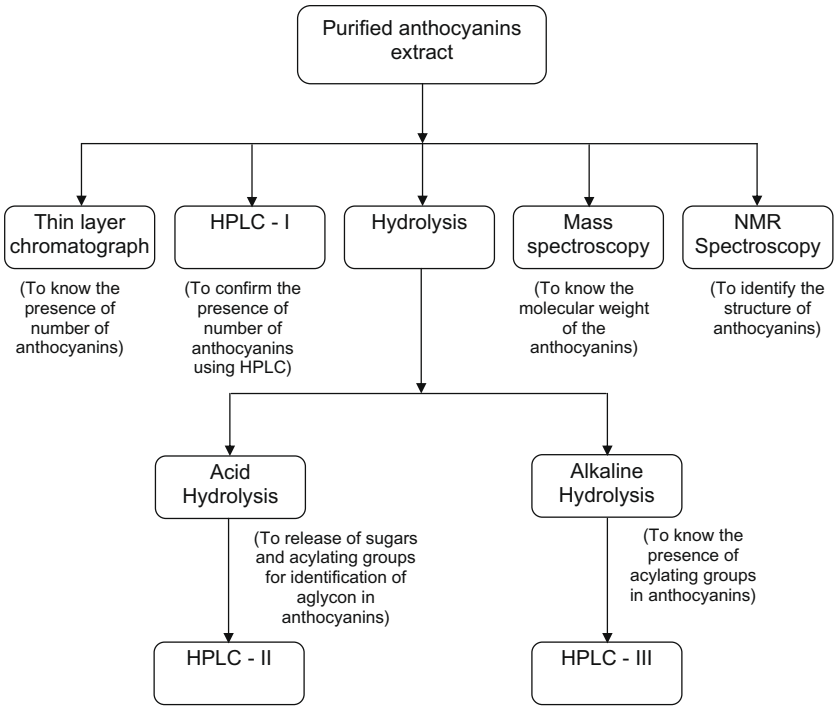

Fig. 1. Experimental plan of work for the characterisation of anthocyanins from *Garcinia indica* Choisy.

Table 1
Anthocyanin content (mg/100 g) in selected plants.

Source	Scientific name	Pigment content (mg/100 g)	References
Banana bracts	*Musa X paradisica*	32–250	Pazmino-Duran, Giusti, Wrolstad, & Gloria (2001)
Red radish	*Raphanus sativus L.*	154	Giusti & Wrolstad (1996)
Strawberry	*Fragaria ananassa* D	13–315	Silva, Bailon, Alonso, Gonzalo, & Buelga (2007)
Capulin	*Prunus serotina* Ehrh	31.7	Ordaz-Galindo et al. (1999)
Black raspberries	*Rubus occidentalis L.*	145–607	Tian et al. (2006)
Roselle	*Hibiscus Sabdariffia*	230	Tsai, McIntosh, Pearce, Camden, & Jordan (2002)
Corncobs	*Zea mays* L.	290–1323	Jing and Giusti (2005)
Berries	*Similax aspera L.*	23.7	Longo and Vasapollo (2006)
Kokum	*Garcinia indica* Choisy	1000–2400	Present work

saponified anthocyanins were purified by subjecting to C18 Sep-Pak cartridge as previously described in Section 2.4, and concentrated using a rotary evaporator.

2.8. Acid hydrolysis of anthocyanins

Ten millilitres of 2 N HCl was added to the pigment (1.0 ml) in a screw-cap test tube, which was flushed with nitrogen gas and capped. The pigment was hydrolysed for 1 h at 100 °C, and then cooled in an ice bath. Anthocyanins after hydrolysis were purified using a C18 Sep-Pak cartridge, as described in Section 2.4.

2.9. Electrospray ionisation mass spectroscopy of anthocyanins

Partially purified as well as purified sample collected from Sephadex LH-20 was diluted with methanol and analysed by ESI-MS. Q-TOF Ultima ™ mass spectrometer, with electrospray ionisation (ESI-MS) interface (Waters Corporation, Milford, MA) and loop injection. A 5.0-μl sample of purified anthocyanin extracts was injected into the system. Samples were analysed in duplicate. Posi-

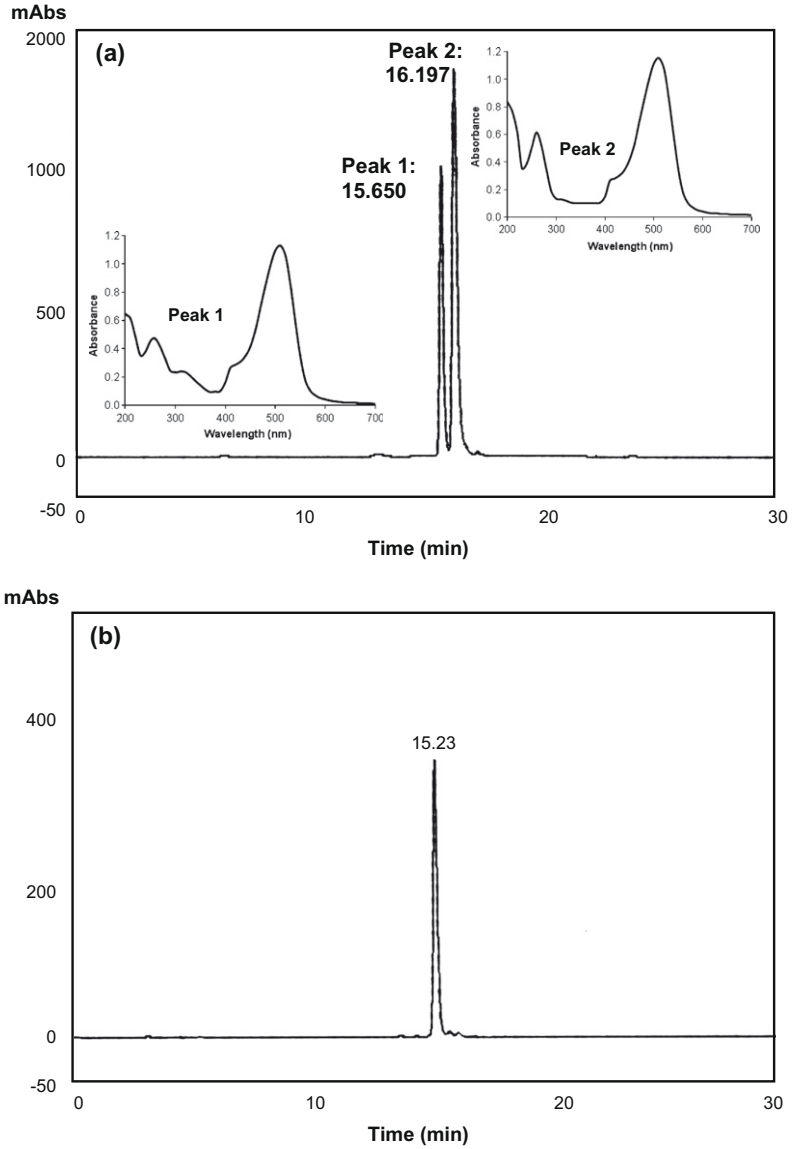

Fig. 2. HPLC chromatogram at 520 nm corresponding to (a) purified anthocyanins of *kokum*, (b) purified extract of acid-hydrolysed anthocyanins of *kokum*.

tive ion spectra of the column eluate were recorded in the range of *m/z* 250–1000 at a scan rate of 2.0 s/cycle under the following conditions: collision energy 10.0; capillary voltage 35 V; cone voltage 100 kV; source temperature 30 °C; desolvation temperature 300 °C; cone gas flow 0.8 l/min; desolvation gas flow (8.3 l/min). Argon was used as a collision gas. Data acquisition and processing were performed using MassLynxTM 4.0 SP4 software (Veigas, Narayan, Laxman, & Bhagyalakshmi, 2007).

2.10. NMR spectroscopy

Purified anthocyanin compounds were analysed by ^{1}H and ^{13}C NMR on a Bruker Avance 500 instrument. Sample (10.0 mg) was dissolved in 0.5 ml deuterated methanol for recording ^{1}H and ^{13}C spectra. Chemical shifts and coupling constants were expressed in δ and Hz, respectively (Kucharska & Oszmianski, 2002).

3. Results and discussion

The extraction of anthocyanins from *kokum* rinds yielded 2400 mg of monomeric anthocyanins/100 g of fresh fruit on a dry weight basis. This anthocyanins content was higher than the one reported for banana bracts, red radish, strawberry, capulin cherry, black raspberries, roselle hibiscus, berries and corn cobs (Table 1).

3.1. Thin-layer chromatography of anthocyanins

Thin-layer chromatography of the extract indicated two distinct red bands with retention factors of 0.26 and 0.52, which showed presence of two anthocyanins in the *kokum* extract. Krishnamurthy (1984) reported similar results.

3.2. High-performance liquid chromatography separation of kokum anthocyanins

HPLC chromatograms of *kokum* showed the presence of two major peaks with a concentration of 36% and 64% of the total peak area at 520 nm with retention times of 15.65 and 16.20 min, respectively (Fig. 2a). Individual anthocyanins (anthocyanindins) from *kokum* were isolated by HPLC. Absorbance spectra of the individual peaks (Fig. 2a) showed that the maxima of both the peaks were at 512 nm, which indicated the presence of the same anthocyanindin (Giusti & Jing, 2008, chap. 6.3). Further, absorbance spectra of anthocyanins provide information with respect to position of

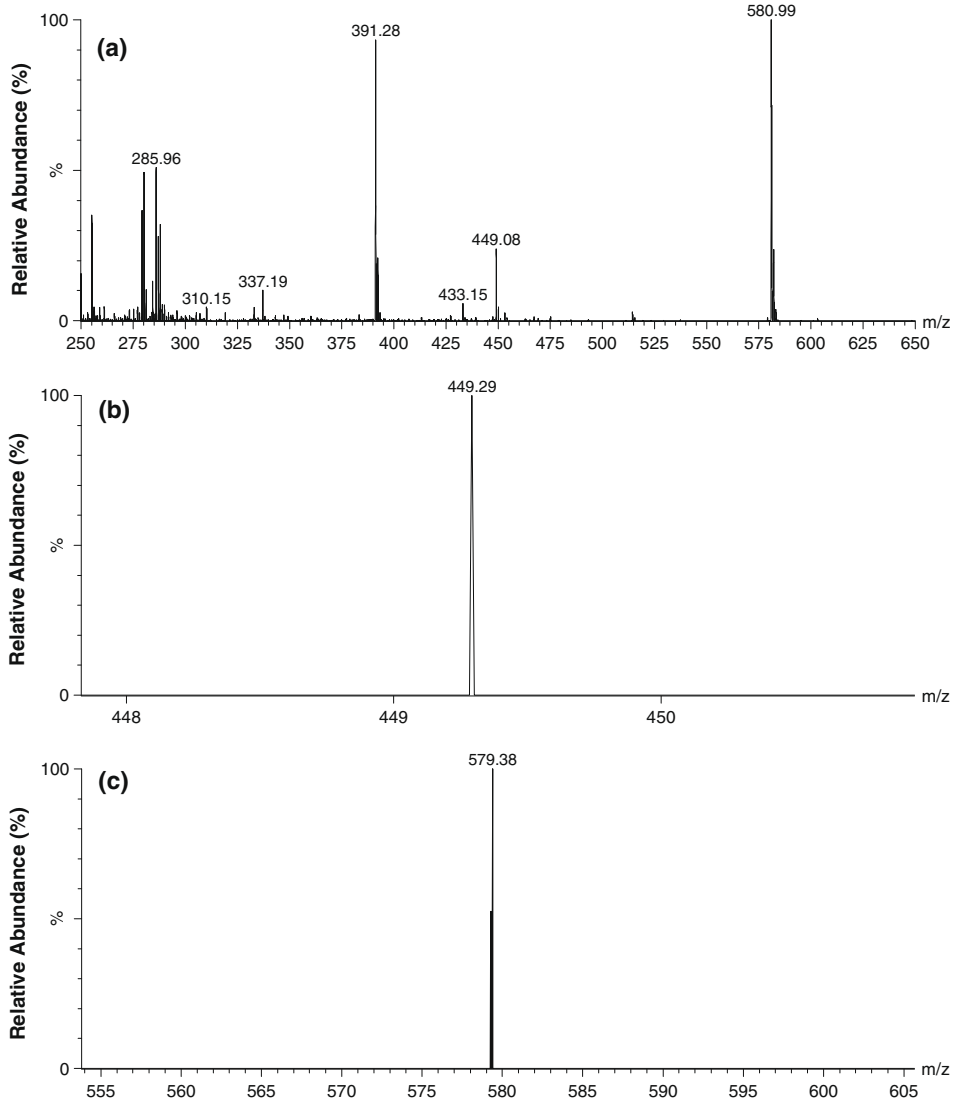

Fig. 3. Electrospray mass spectrum of (a) crude *kokum* (b) peak 1 of the HPLC (c) peak 2 of the HPLC.

glycosylation as well as the presence of acylating groups. The ratio of absorbance at 440 nm to the absorbance at visible maximum wave length ($A_{440nm}/A_{\lambda max}$ ratio) for peaks 1 and 2 were found to be 0.29 and 0.31, respectively, which indicated the possibility of glycosylation at the C-3 position of anthocyanin for both the compounds (Giusti & Jing, 2008, chap. 6.3; Longo & Vasapollo, 2006). The absence of peaks in the absorption spectra (Fig. 2a) in the region from 300 to 350 nm indicated that the pigment was not acylated (Giusti & Jing, 2008, chap. 6.3).

Acid hydrolysis of anthocyanins results in the release of sugars and acylating groups to form the aglycone, without affecting its structure. The *kokum* anthocyanins after acid hydrolysis yielded a single peak with a retention time of 15.23 min (Fig. 2b), which corresponded to cyanidin aglycone, as confirmed by comparing the results with grape anthocyanins. Wrolstad et al. (2005) demonstrated that grape anthocyanins can be used a standard for the purpose of comparison and identification. Similarly, Chiang and Wrolstad (2005) compared their results with blackberries for identification of anthocyanins.

Alkaline hydrolysis does not affect the glycosidic bond, but it will break ester linkages of acylating groups, if any are present (Giusti & Jing, 2008, chap. 6.3; Hong & Wrolstad, 1990). The chromatographic profile of alkaline-hydrolysed *kokum* anthocyanins was found to be same as that of unsaponified extract, as shown in Fig. 2a, which indicated that the anthocyanins of *kokum* were not acylated. Ordaz-Galindo, Wesche-Ebeling, Wrolstad, Rodriguez-Saona, and Argaiz-Jamet (1999) and Veigas et al. (2007) reported that there was no difference in chromatographic profiles of saponified and unsaponified fractions in the case of anthocyanins obtained from *Syzygium cumini* and capulin fruits. These results conclusively showed that anthocyanins in both cases were not acylated.

3.3. Mass spectroscopy

The mass spectrum for partially purified anthocyanin pigments shows strong ion peaks at *m/z* 286, 391, 449 and 581 (Fig. 3a). The precursor ion scan demonstrated that an ion peak at *m/z* 286 corresponding with cyanidin molecule, as the aglycone moiety (Tian, Giusti, Stoner, & Schwartz, 2006). The component corresponding to an ion peak at *m/z* 391 could not be identified in the present work. Bhaskaran and Mehta (2006) have also obtained ion peak at *m/z* 391 and regarded it as an error in the mass spectroscopy. The ion peaks at *m/z* 581 and 449 indicated the presence of anthocyanins.

Mass spectra of the peaks collected from HPLC are shown in Fig. 3b and c. The component corresponding to the ion peak at *m/z* 449 (Fig. 3b) coincided with cyanidin 3-glucoside ($C_{21}H_{21}O_{11}$) (Ordaz-Galindo et al., 1999; Zhang, Xuequn, Yang, Ji, & Jiang, 2004). The ion peak at *m/z* 581 (Fig. 3c) showed that the molecular weight of the major anthocyanin in *kokum* coincided with cyanidin 3-sambubioside ($C_{26}H_{28}O_{15}$) (Tian et al., 2006).

3.4. ^{1}H and ^{13}C NMR spectroscopy

^{1}H spectra data of compounds, corresponding to peaks 1 and 2 (Fig. 2a) isolated by chromatography exhibited signals characteristic of cyanidin aglycone moiety (Table 2a, Fig. 4). Compound corresponding to peak 1 showed a singlet at 9.03, with doublets at 6.68 and 6.93 corresponding to protons 4, 6 and 8, respectively, in the flavone group. Two doublets at 8.07 and 7.05 are observed with coupling constants of 2 and 8.5 Hz corresponding to 2′ and 5′ aromatic protons respectively. The 6′ aromatic proton appears in the spectrum at 8.27 as a double doublet with *J* values of 2 and 8.5 Hz. The doublet at 5.32 corresponds to the anomeric proton of the sugar portion with a β-configuration. Other protons corresponding to the sugar moiety appear at 3.93 (dd, 1H), 3.69–3.75 (m, 2H), 3.56–3.60 (m, 2H) and 3.47 (d). Corresponding ^{13}C spectra show fifteen carbons for the cyanidin moiety and six carbons for the glycoside portion and the spectral assignments are presented in Table 2b. These data along with the molecular mass of [449 (M^+)] indicate the compound to be cyanidin β-3-glucoside (I). This anthocyanidin was reported in black raspberries, hibiscus flowers and elderberry (Chiang & Wrolstad 2005; Nakamura, Hidaka,

Table 2a
^{1}H spectral assignments for cyanidin 3-glucoside and cyanidin 3-sambubioside.

Protons	Cyanidin β-3-glucoside	Cyanidin β-3-sambubioside
Cyanidn (Aglycone)		
4	9.03 (1H, s)	8.96 (1H, s)
6	6.68 (1H, d, J = 1.5 Hz)	6.67 (1H, d, J = 1.5 Hz)
8	6.93 (1H, d, J = 1.5 Hz)	6.92 (1H, d, J = 1.5 Hz)
2'	8.07 (1H, d, J = 2 Hz)	8.05 (1H, d, J = 2 Hz)
5'	7.05 (1H, d, J = 8. 5 Hz)	7.04 (1H, d, J = 9 Hz)
6'	8.27 (1H, dd, J = 8. 5 & 2 Hz)	8.28 (1H, dd, J = 9 & 2.5 Hz)
Anomeric sugar protons		
1″	5.32 (1H, d, *J* = 8 Hz)	5.46 (1H, d, *J* = 8 Hz)
1‴	–	4.77 (1H, d, *J* = 8 Hz)
Glycosidic protons		
	3.93 (1H, dd, *J* = 2.5 and 12.5 Hz)	3.80(1H, t, *J* = 9 Hz)
	3.69–3.75 (2H, m)	3.74 (1H, d, *J* = 6 Hz)
	3.56–3.60 (2H, m)	3.71 (1H, dd, *J* = 5.5 and 6 Hz)
	3.47 (1H, d, *J* = 9 Hz)	3.67 (1H, d, *J* = 5.5 Hz)
		3.60 (1H, m)
		3.52 (1H, t, *J* = 9.5 Hz)
		3.42 (1H, m)
		3.18 (2 H, t, *J* = 8.5 Hz)
		3.06 (2 H, t, *J* = 11 Hz)

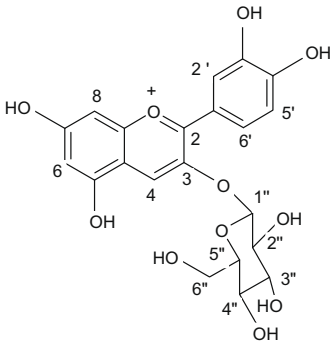

Cyanidin 3-O-ß-glucopyranoside (I)

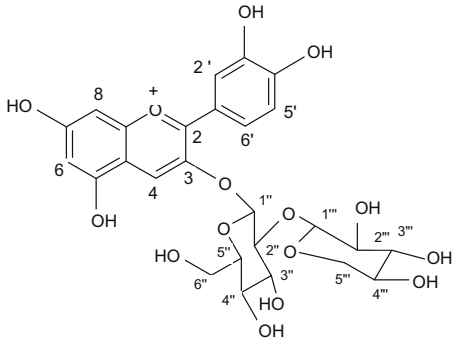

Cyanidin 3-O-(2"-ß-xylopyranosyl-ß-glucopyranoside (II)
(Cyanidin 3-O-ß-sambubioside)

Fig. 4. Structures of anthocyanins.

Table 2b
^{13}C spectral assignments for cyanidin β-3-glucoside and cyanidin β-3-sambubioside.

Carbons	Cyanidin β-3-glucoside	Cyanidin β-3-sambubioside
Aglycone		
2	168.24	168.72
3	135.29	143.52
4	128.44	134.56
5	163.52	162.52
6	111.75	111.56
7	169.82	170.25
8	93.47	93.40
9	157.53	157.51
10	113.18	116.89
1′	126.51	126.85
2′	115.76	115.69
3′	143.88	145.70
4′	151.35	154.02
5′	116.83	115.44
6′	119.58	119.55
Sugar moiety		
1-O-β-glucoside		
1″	101.99	101.76
2″	70.37	76.95
3″	76.36	76.07
4″	68.17	73.95
5″	77.04	69.06
6″	60.64	60.52
2-O- β-xylanoyl		
1‴	–	103.95
2‴	–	79.99
3‴	–	76.41
4‴	–	69.23
5‴	–	65.40

Masaki, Seto, & Uozumi, 1990; Watanabe, Yamamoto, Nagai, & Terabe, 1998).

Similarly, compound corresponding to peak 2 showed singlet at 8.96 and doublets at 6.67 and 6.92 for the flavone aromatic protons 4, 6 and 8, respectively. The aromatic protons 2′, 5′ and 6′ are seen as two doublets and a double doublet at 8.05, 7.04 and 8.28, respectively, with *J* values of 2.5 and 9 Hz. The anomeric sugar protons at 5.46 and 4.77 appear as doublets with $J = 8$ Hz, indicating it to be a diglycoside with β-configuration at the anomeric positions. Other protons corresponding to the glycoside group appeared as four triplets at 3.80, 3.52, 3.18 and 3.06, corresponding to one, one, two and two protons respectively. The spectrum also contained two doublets at 3.74 and 3.67, along with a double doublet at 3.71. Two multiplets were seen in the spectrum at 3.60 and 3.42. A total of thirteen protons were seen for the glycoside moiety showing it to consist of a disaccharide comprising an aldohexose and an aldopentose. ^{13}C spectral data (Table 2b) clearly show fifteen carbons for the cyanidin aglycone portion and thirteen carbons for the sugar moiety. The molecular mass of [580 (M^+)] along with NMR spectral data agreed well with literature values (Watanabe et al., 1998) of cyanidin β-3-sambubioside (II).

4. Conclusion

Monomeric anthocyanin content of *kokum* was 2400 mg/100 g of fresh fruits, which was quite high as compared to other fruits and vegetables. Acid and alkaline hydrolysis of *kokum* pigment indicated that the *kokum* anthocyanin consisted of single aglycone and did not contain any acylation. Pure anthocyanin compounds were isolated in high purity and analysed by mass spectrophotometry, ^{1}H and ^{13}C NMR Spectroscopy. The pigments were characterised as cyanidin 3-glucoside and cyanidin 3-sambubioside.

Acknowledgements

The authors thank Dr. V Prakash, Director CFTRI, Mysore for constant encouragement. Thanks are also due to Dr. KSMS Raghavarao, Head, Department of Food Engineering, CFTRI for his support. The authors acknowledge Mr. Manjunath and Dr. H.B. Sowbhagaya for their help in conducting the NMR studies and pigment isolation experiments. One of the authors, Chetan A Nayak, expresses gratitude and sincere thanks to the Council of Scientific and Industrial Research, New Delhi for providing senior research fellowship.

References

Bhaskaran, S., & Mehta, S. (2006). *Stabilized anthocyanin extract from Garcina indica*. US Patent No: 2006/0230983A1.
Bhat, D. J., Kamat, N., & Shirodkar, A. (2005). *Compendium and proceedings of 2nd National seminar on kokum (Garcinia indica Choisy)*, March 4–5, Goa University.
Chandran, M. D. S. (1996). Nature watch: The *kokum* tree. *Resonance, 1*, 86–89.
Chiang, H. J. F., & Wrolstad, R. E. (2005). Anthocyanin pigment composition of blackberries. *Journal of Food Science, 70*(3), C198–C202.
Du, C. T., & Francis, F. J. (1977). Anthocyanins from mangosteen, *Garcinia mangostana*. *Journal of Food Science, 42*(6), 1667–1668.
Giusti, M. M., & Wrolstad, R. E. (1996). Characterization of red radish anthocyanins. *Journal of Food Science, 61*(2), 322–326.
Giusti, M. M., & Jing, P. (2008). Analysis of anthocyanins. In S. Carmen (Ed.), *Food colorants chemical and functional properties* (pp. 479–506). New York, USA: CRC Press.
Hong, V., & Wrolstad, R. E. (1990). Use of HPLC separation/photodiode array detection for characterization of anthocyanins. *Journal of Agricultural and Food Chemistry, 38*, 708–715.
Jing, P., & Giusti, M. M. (2005). Characterization of anthocyanin rich waste from purple corncobs (*Zea mays* L.) and its applications to color milk. *Journal of Agricultural and Food Chemistry, 53*, 8775–8781.
Krishnamurthy, N. (1984). *Chemical and technological studies on coloring matters from natural sources for use in foods*. PhD Thesis, Mysore University.
Krishnamurthy, N., Lewis, Y. S., & Ravindranath, B. (1982). Chemical constituents of *kokum* fruit rind. *Journal of Food Science and Technology, 19*, 97–100.
Kucharska, A. Z., & Oszmianski, J. (2002). Anthocyanins in fruits of *Prunus padus* (bird cherry). *Journal of the Science of Food and Agriculture, 82*, 1483–1486.
Longo, L., & Vasapollo, G. (2006). Extraction and identification of anthocyanin from *Smilax aspera* L. berries. *Food Chemistry, 94*, 226–231.
Nakamura, Y., Hidaka, M., Masaki, H., Seto, H., & Uozumi, T. (1990). Major anthocyanin of the flowers of Hibiscus (*Hibiscus rosa-sinensis* L.). *Agricultural Biological Chemistry, 54*(12), 3345–3346.
Nayak, C. A., Rastogi, N. K., & Raghavarao, K. S. M. S. (2009). Bioactive constituents present in *Garcinia indica* Choisy and its potential food applications. International Journal of Food Properties, in press.
Nayak, C. A., Chethana, S., Rastogi, N. K., & Raghavarao, K. S. M. S. (2006). Enhanced mass transfer during solid-liquid extraction of gamma irradiated red beetroot. *Radiation Physics and Chemistry, 75*, 173–178.
Ordaz-Galindo, A., Wesche-Ebeling, P., Wrolstad, R. E., Rodriguez-Saona, L., & Argaiz-Jamet, A. (1999). Purification and identification of Capulin (*Prunus serotina* Ehrh) anthocyanins. *Food Chemistry, 65*, 201–206.
Pazmino-Duran, E. A., Giusti, M. M., Wrolstad, R. E., & Gloria, M. B. A. (2001). Anthocyanins form banana bracts (*Musa X paradisiaca*) as potential food colorants. *Food Chemistry, 73*, 327–332.
Silva, F. M., Bailon, M. T. E., Alonso, J. J. P., Gonzalo, J. C. R., & Buelga, C. S. (2007). Anthocyanin pigment in strawberry. *Lebensmittel Wissenschaft und Technologie, 40*, 374–382.
Tian, Q., Giusti, M. M., Stoner, G. D., & Schwartz, S. J. (2006). Characterization of a new anthocyanin in black raspberries (*Rubus occidentalis*) by liquid chromatography electrospray ionization tandem mass spectrometry. *Food Chemistry, 94*, 465–468.
Tsai, P. J., McIntosh, J., Pearce, P., Camden, B., & Jordan, B. R. (2002). Anthocyanin and antioxidant capacity in Roselle (*Hibiscus Sabdariffia* L.) extract. *Food Research International, 35*, 351–356.
Veigas, J. M., Narayan, M. S., Laxman, P. M., & Bhagyalakshmi, N. (2007). Chemical nature, stability and bioefficacies of anthocyanins from fruit peel of *syzygium cumini* Skeels. *Food Chemistry, 105*, 619–627.
Watanabe, T., Yamamoto, A., Nagai, S., & Terabe, S. (1998). Analysis of elderberry pigments in commercial food samples by micellar electrokinetic chromatography. *Analytical Sciences, 14*, 839–844.
Wrolstad, R. E., Acree, T. E., Decker, E. A., Reid, D. S., Schawartz, S. J., Shoemaker, C. F., Smith, D., & Sporns, P. (2005). *Hand book of food analytical chemistry – Pigments, colorants, flavor, texture, and bioactive components*. New Jersey: Wiley.
Zhang, Z., Xuequn, P., Yang, C., Ji, Z., & Jiang, Y. (2004). Purification and structural analysis of anthocyanins from litchi pericarp. *Food Chemistry, 84*, 601–604.

different families, A, B, X, and Y (Friedberg, Feaver, & Gerlach, 2000). Family A includes mitochondrial pol γ, and pol θ, family B includes three replicative pols (α, δ, and ε) and pol ζ, family X includes pols β, λ, μ, and TdT, and family Y includes pols η, ι, κ, and REV1. Pols are not only essential for DNA replication, repair and recombination, but are also involved in cell division. Selective inhibitors of pol are considered to be a group of potentially useful anticancer and antiparasitic agents, because some inhibitors suppress human cancer cell proliferation and have cytotoxicity (Sakaguchi, Sugawara, & Mizushina, 2002).

This paper described the structural elucidation of chemical constituents in the chloroform-soluble phase of the root of *M. citrifolia*, which inhibited the activities of mammalian pols. Furthermore, we focused on the anticancer effect of the isolated anthraquinones (i.e., compounds **1**–**10**, Fig. 1) from the chloroform extract, and investigated the chemical constituents which inhibited the activities of mammalian pol families and colon cancer cell line, HCT116, proliferation.

2. Materials and methods

2.1. Materials

Roots of the tropical plant "Noni" (*M. citrifolia*) were collected in Okinawa in August 2004. Nucleotides and chemically synthesised template-primers, such as poly(dA), oligo(dT)$_{12-18}$, and [^{3}H]-dTTP (2′-deoxythymidine 5′-triphosphate) (43 Ci/mmol), were purchased from GE Healthcare Bio-Sciences (Little Chalfont, UK). All other reagents were of analytical grade and purchased from Nacalai Tesque Inc. (Kyoto, Japan).

2.2. Enzymes

Pol α was purified from calf thymus by immuno-affinity column chromatography, as described by Tamai et al. (1988). Recombinant rat pol β was purified from *Escherichia coli* JMpβ5, as described by Date et al. (1988). The human pol γ catalytic gene was cloned into pFastBac. The histidine-tagged enzyme was expressed using the BAC-TO-BAC HT Baculovirus Expression System according to the supplier's manual (Life Technologies, MD, USA) and purified using ProBoundresin (Invitrogen Japan, Tokyo, Japan) (Umeda et al., 2000). Human pols δ and ε were purified by the nuclear fractionation of human peripheral blood cancer cells (Molt-4) using the second subunit of pols δ and ε-conjugated affinity column chromatography, respectively (Oshige, Takeuchi, Ruike, Kuroda, & Sakaguchi, 2004). A truncated form of human pol η (residues 1–511) tagged with His6 at its C-terminal was expressed in *E. coli* cells and purified as described previously (Kusumoto, Masutani, Shimmyo, Iwai, & Hanaoka, 2004). A recombinant mouse pol ι tagged with His$_6$ at its C-terminal was expressed and purified by Ni-NTA column chromatography. A truncated form of pol κ (residues 1–560) with 6 × His-tags attached at the C-terminus was overproduced in *E. coli* and purified as described previously (Ohashi et al., 2004). Recombinant human His-pol λ was overexpressed and purified according to a method described previously (Shimazaki et al., 2002). Fish pol δ was purified from the testis of cherry salmon (*Oncorhynchus masou*) (Yamaguchi et al., 2006). Fruit fly pols α, δ and ε were purified from early embryos of *Drosophila melanogaster*, as described previously (Aoyagi, Matsuoka, Furunobu, Matsukage, & Sakaguchi, 1994; Aoyagi et al., 1997). Pol α from a higher plant, cauliflower inflorescence, was purified according to the methods outlined by Sakaguchi, Hotta, and Stern (1980). Calf thymus TdT and bovine pancreas deoxyribonuclease I (DNase I) were obtained from Stratagene Cloning Systems (La Jolla, CA, USA). Human immunodeficiency virus type-1 (HIV-1) reverse transcriptase (recombinant) and the Klenow fragment of pol I from *E. coli* were purchased from Worthington Biochemical Corp. (Freehold, NJ, USA). T4 pol, *Taq* pol, T7 RNA polymerase and T4 polynucleotide kinase were purchased from Takara Bio (Tokyo, Japan). Recombinant mouse inosine 5′-monophosphate (IMP) dehydrogenase (type II) was overexpressed using *E. coli* and purified according to the method described previously (Mizushina et al., 2007).

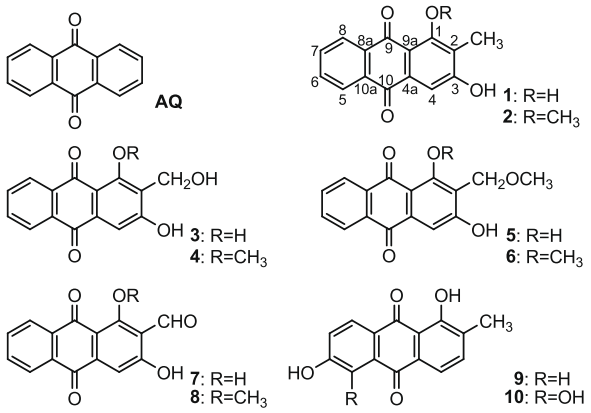

Fig. 1. Isolated anthraquinones (compounds **1**–**10**) from the chloroform-soluble phase of *M. citrifolia* root. Anthraquinone (AQ), rubiadin (**1**), rubiadin 1-methyl ether (**2**), lucidin (**3**), damnacanthol (**4**), 1,3-dihydroxy-2-methoxymethylanthraquinone (**5**), 3-hydroxy-1-methoxy-2-methoxymethylanthraquinone (**6**), nordamnacanthal (**7**), damnacanthal (**8**), sorandidiol (**9**) and morindone (**10**).

2.3. DNA polymerase assays

The reaction mixtures for pol α, pol β, plant pol α and prokaryotic pols were described previously (Mizushina et al., 1996; Mizushina, Yoshida, Matsukage, & Sakaguchi, 1997), and those for pol γ, and pols δ and ε were as described by Ogawa, Murate, Suzuki, Nimura, and Yoshida (1998) and Umeda et al. (2000), respectively. The reaction mixtures for pols η, ι and κ were the same as for pol α, and the reaction mixture for pol λ was the same as for pol β. For pols, poly(dA)/oligo(dT)$_{12-18}$ (A/T = 2/1) and dTTP were used as the DNA template-primer and nucleotide (i.e., dNTP) substrate, respectively. For HIV-1 reverse transcriptase, poly(rA)/oligo(dT)$_{12-18}$ (A/T = 2/1) and dTTP were used as the template-primer and nucleotide substrate, respectively. For TdT, oligo(dT)$_{12-18}$ (3′-OH) and dTTP were used as the DNA primer and nucleotide substrate, respectively.

The compounds were dissolved in distilled dimethyl sulfoxide (DMSO) at various concentrations and sonicated for 30 s. Aliquots of 4 μl sonicated samples were mixed with 16 μl of each enzyme (final amount 0.05 units) in 50 mM Tris–HCl (pH 7.5) containing 1 mM dithiothreitol, 50% glycerol and 0.1 mM EDTA, and kept at 0 °C for 10 min. These inhibitor-enzyme mixtures (8 μl) were added to 16 μl of each enzyme standard reaction mixture, and incubation was carried out at 37 °C for 60 min, except for *Taq* pol, which was incubated at 74 °C for 60 min. Activity without the inhibitor was considered 100%, and the remaining activity at each concentration of the inhibitor was determined relative to this value. One unit of pol activity was defined as the amount of enzyme that catalysed the incorporation of 1 nmol dNTP (i.e., dTTP) into synthetic DNA template-primers in 60 min at 37 °C under the normal reaction conditions for each enzyme (Mizushina et al., 1996, 1997).

2.4. Other DNA metabolic enzymes assays

The activities of calf primase of pol α, T7 RNA polymerase, mouse IMP dehydrogenase, T4 polynucleotide kinase and bovine DNase I were measured in standard assays according to the manu-

facturer's specifications, as described by Lu and Sakaguchi (1991), Mizushina et al. (2007), Nakayama and Saneyoshi (1985), Soltis and Uhlenbeck (1982), and Tamiya-Koizumi et al. (1997), respectively.

2.5. Cell growth assay of cultured human cancer cell line

Human colon carcinoma cell line, HCT116, was a kind gift from Dr. Bert Vogelstein (Johns Hopkins University, Baltimore, MO, USA). HCT116 cells were trypsinised and resuspended in McCoy's 5A medium with 10% FBS, and 5×10^3 cells were seeded in 96-well tissue culture plates for 24 h. The cells were then stimulated with the isolated compounds **1**–**10** for 24 h. After treatment, the survival rate was determined by MTT (3-(4,5-dimethylthiazol-2-yl)-2,5-diphenyl tetrazolium bromide) assay (Mosmann, 1983).

3. Results and discussion

3.1. Isolation and structure determination of anthraquinones from M. citrifolia root

Since the chloroform-soluble phase of the root of tropical plant "Noni" (*M. citrifolia*) had inhibitory activity of mammalian pols, the chloroform extract (122 g) was chromatographed on Sephadex LH-20 using $CHCl_3$–MeOH (1:1) to give an anthraquinone-containing fraction. This fraction was subjected to repeated SiO_2 column chromatography using a *n*-hexane–$CHCl_3$ solvent system and was finally purified by preparative TLC using a $CHCl_3$–MeOH solvent system to afford compounds **1**–**10**.

HPLC was performed with a Diol column (Inertsil Diol 5 mm, 4.6 × 250 mm, GL Sciences). The detection wavelength was 254 nm. Elution was carried out with *n*-hexane:$CHCl_3$ (A, 25:75), (B, 50:50) and (C, 75:25) at a flow rate of 1 ml/min. The injection volume was 10 μl (1.0 mg/ml, chloroform-soluble phase in $CHCl_3$). Compounds **1**–**10** contained in the chloroform-soluble phase could be separated by HPLC using three solvent systems (Fig. 2). The yields of 10 compounds from the dried root were (**1**: 0.009%), (**2**: 0.094%), (**3**: 0.011%), (**4**: 0.186%), (**5**: 0.051%), (**6**: 0.012%), (**7**: 0.086%), (**8**: 0.434%), (**9**: 0.015%) and (**10**: 0.105%). The purified compounds **1**–**10** were analysed by IR, UV, ^1H and ^{13}C NMR spectra, and the chemical structures of the isolated anthraquinones (**1**–**10**) are shown in Fig. 1.

*Rubiadin (**1**):* Yellow amorphous powder; IR ν_{max}^{KBr} cm^{-1}: 3396, 1660, 1623, 1588, 1484, 1430, 1339, 1313, 1294, 1121; UV λ_{max} (MeOH) nm (log ε): 410 (3.75), 278 (4.40), 245 (4.33), 206 (4.38); ^1H NMR (400 MHz, DMSO-d_6) δ: 13.05 (1H, s, 1-OH), 7.19 (1H, s, H-4), 8.08 (1H, dd, J = 7.0, 2.1 Hz, H-5), 7.84 (1H, td, J = 7.0, 1.7 Hz, H-6), 7.87 (1H, td, J = 7.2, 2.1 Hz, H-7), 8.14 (1H, dd, J = 7.2, 1.7 Hz, H-8), 2.03 (3H, s, H-11); ^{13}C NMR (100 MHz, DMSO-d_6) δ: 162.39 (C-1), 117.26 (C-2), 162.87 (C-3), 107.35 (C-4), 131.64 (C-4a), 126.64 (C-5), 134.34 (C-6), 134.35 (C-7), 126.31 (C-8), 132.94 (C-8a), 186.10 (C-9), 108.85 (C-9a), 181.72 (C-10), 132.82 (C-10a), 8.06 (C-11).

*Rubiadin 1-methyl ether (**2**):* Yellow needles; IR ν_{max}^{KBr} cm^{-1}: 3300, 2945, 1672, 1651, 1580, 1566, 1448, 1410, 1337, 1300, 1281, 1121; UV λ_{max} (MeOH) nm (log ε): 279 (4.57), 238 (4.22), 203 (4.46); ^1H NMR (400 MHz, DMSO-d_6) δ: 7.51 (1H, s, H-4), 8.10 (1H, dd, J = 7.4, 1.4 Hz, H-5), 7.83 (1H, td, J = 7.4, 1.4 Hz, H-6), 7.89 (1H, td, J = 7.5, 1.4 Hz, H-7), 8.15 (1H, dd, J = 7.5, 1.4 Hz, H-8), 2.16 (3H, s, H-11), 3.79 (3H, s, 1-OCH_3); ^{13}C NMR (100 MHz, DMSO-d_6) δ: 161.09 (C-1), 126.63 (C-2), 162.26 (C-3), 109.51 (C-4), 135.00 (C-4a), 126.51 (C-5), 133.82 (C-6), 134.21 (C-7), 127.11 (C-8), 134.98 (C-8a), 180.64 (C-9), 118.35 (C-9a), 183.09 (C-10), 132.54 (C-10a), 9.50 (C-11), 61.07 (1-OCH_3).

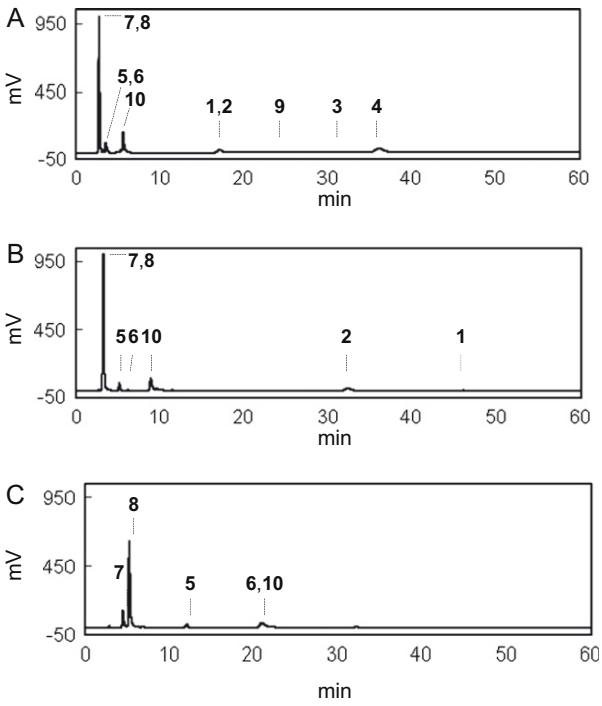

Fig. 2. HPLC profiles of chloroform-soluble phase of *M. citrifolia* root. Elution was carried out with *n*-hexane:chloroform = 25:75 (A), 50:50 (B) and 75:25 (C).

*Lucidin (**3**):* Yellow amorphous powder; IR ν_{max}^{KBr} cm^{-1}: 3413, 2945, 1660, 1615, 1590, 1439, 1413, 1333, 1307, 1284, 1008, 985; UV λ_{max} (MeOH) nm (log ε): 411 (3.69), 279 (4.23), 245 (4.24), 204 (4.27); ^1H NMR (400 MHz, DMSO-d_6) δ: 13.20 (1H, s, 1-OH), 7.26 (1H, s, H-4), 8.15 (1H, dd, J = 7.4, 1.8 Hz, H-5), 7.89 (1H, td, J = 7.4, 1.7 Hz, H-6), 7.93 (1H, td, J = 7.4, 1.8 Hz, H-7), 8.22 (1H, dd, J = 7.4, 1.7 Hz, H-8), 4.54 (2H, s, H-11); ^{13}C NMR (100 MHz, DMSO-d_6) δ: 161.09 (C-1), 126.63 (C-2), 162.26 (C-3), 109.51 (C-4), 135.00 (C-4a), 126.51 (C-5), 133.82 (C-6), 134.21 (C-7), 127.11 (C-8), 134.98 (C-8a), 180.64 (C-9), 118.35 (C-9a), 183.09 (C-10), 132.54 (C-10a), 51.18 (C-11).

*Damnacanthol (**4**):* Yellow needles; IR ν_{max}^{KBr} cm^{-1}: 3300, 2851, 1672, 1651, 1566, 1450, 1423, 1331, 1281, 1119, 968; UV λ_{max} (MeOH) nm (log ε): 277 (4.54), 239 (4.30), 203 (4.49); ^1H NMR (400 MHz, DMSO-d_6) δ: 7.52 (1H, s, H-4), 8.11 (1H, dd, J = 7.5, 1.5 Hz, H-5), 7.83 (1H, td, J = 7.5, 1.4 Hz, H-6), 7.89 (1H, td, J = 7.5, 1.5 Hz, H-7), 8.16 (1H, dd, J = 7.5, 1.4 Hz, H-8), 4.57 (2H, s, H-11), 3.87 (3H, s, 1-OCH_3); ^{13}C NMR (100 MHz, DMSO-d_6) δ: 161.66 (C-1), 128.80 (C-2), 162.17 (C-3), 109.80 (C-4), 135.37 (C-4a), 126.10 (C-5), 133.36 (C-6), 134.56 (C-7), 126.57 (C-8), 134.60 (C-8a), 179.98 (C-9), 117.85 (C-9a), 182.56 (C-10), 132.03 (C-10a), 52.15 (C-11), 62.40 (1-OCH_3).

*1,3-Dihydroxy-2-methoxymethylanthraquinone (**5**):* Yellow amorphous powder; IR ν_{max}^{KBr} cm^{-1}: 3300, 2922, 2850, 1674, 1626, 1580, 1556, 1368, 1277, 1159, 1097, 935; UV λ_{max} (MeOH) nm (log ε): 411 (3.66), 281 (4.27), 245 (4.31), 205 (4.31); ^1H NMR (400 MHz, DMSO-d_6) δ: 13.22 (1H, s, 1-OH), 7.21 (1H, s, H-4), 8.08 (1H, dd, J = 7.1, 1.4 Hz, H-5), 7.85 (1H, td, J = 7.1, 1.4 Hz, H-6), 7.88 (1H, td, J = 7.1, 1.4 Hz, H-7), 8.15 (1H, dd, J = 7.1, 1.4 Hz, H-8), 4.40 (2H, s, H-11), 3.25 (3H, s, 11-OCH_3); ^{13}C NMR (100 MHz, DMSO-d_6) δ: 163.78 (C-1), 116.60 (C-2), 164.71 (C-3), 107.92 (C-4), 133.82 (C-4a), 126.70 (C-5), 134.36 (C-6), 134.59 (C-7), 126.31 (C-8), 133.02 (C-8a), 185.88 (C-9), 106.69 (C-9a), 181.77 (C-10), 132.76 (C-10a), 57.58 (C-11), 61.07 (11-OCH_3).

*3-Hydroxy-1-methoxy-2-methoxymethylanthraquinone (**6**):* Yellow amorphous powder; IR ν_{max}^{KBr} cm^{-1}: 3287, 2967, 1672, 1653, 1568, 1423, 1335, 1302, 1284, 1106, 1065, 977; UV λ_{max} (MeOH)

nm (log ε): 277 (4.52), 240 (4.29), 204 (4.42); ^{1}H NMR (400 MHz, DMSO-d_6) δ: 7.51 (1H, s, H-4), 8.05 (1H, dd, *J* = 7.5, 1.1 Hz, H-5), 7.78 (1H, td, *J* = 7.5, 1.1 Hz, H-6), 7.84 (1H, td, *J* = 7.5, 1.1 Hz, H-7), 8.10 (1H, dd, *J* = 7.5, 1.1 Hz, H-8), 4.43 (2H, s, H-11), 3.81 (3H, s, 1-OCH_3), 3.29 (3H, s, 11-OCH_3); ^{13}C NMR (100 MHz, DMSO-d_6) δ: 162.33 (C-1), 125.23 (C-2), 162.89 (C-3), 109.90 (C-4), 135.86 (C-4a), 126.04 (C-5), 133.25 (C-6), 134.52 (C-7), 126.60 (C-8), 134.52 (C-8a), 179.77 (C-9), 117.46 (C-9a), 182.49 (C-10), 131.97 (C-10a), 62.41 (1-OCH_3), 62.23 (11-OCH_3).

*Nordamnacanthal (**7**):* Yellowish-orange needles; IR ν_{max}^{KBr} cm^{-1}: 3075, 1651, 1628, 1600, 1574, 1381, 1331, 1283, 1196, 984; UV λ_{max} (MeOH) nm (log ε): 291 (4.33), 258 (4.40), 207 (4.25); ^{1}H NMR (400 MHz, pyridine-d_5) δ: 7.42 (1H, s, H-4), 8.24 (1H, dd, *J* = 7.1, 1.8 Hz, H-5), 7.68 (1H, td, *J* = 7.1, 1.8 Hz, H-6), 7.71 (1H, td, *J* = 7.1, 1.8 Hz, H-7), 8.28 (1H, dd, *J* = 7.1, 1.8 Hz, H-8), 10.57 (1H, s, H-11); ^{13}C NMR (100 MHz, pyridine-d_5) δ: 168.33 (C-1), 113.14 (C-2), 169.27 (C-3), 109.53 (C-4), 139.45 (C-4a), 127.56 (C-5), 134.78 (C-6), 134.86 (C-7), 127.02 (C-8), 133.58 (C-8a), 186.71 (C-9), 109.36 (C-9a), 181.59 (C-10), 133.63 (C-10a), 192.99 (C-11).

*Damnacanthal (**8**):* Yellow amorphous powder; IR ν_{max}^{KBr} cm^{-1}: 3070, 1668, 1647, 1565, 1344, 1329, 1261, 1132, 980; UV λ_{max} (MeOH) nm (log ε): 283 (4.23), 247 (4.26), 203 (4.12); ^{1}H NMR (400 MHz, pyridine-d_5) δ: 7.77 (1H, s, H-4), 8.24 (1H, dd, *J* = 7.5, 1.3 Hz, H-5), 7.64 (1H, td, *J* = 7.5, 1.2 Hz, H-6), 7.70 (1H, td, *J* = 7.5, 1.3 Hz, H-7), 8.33 (1H, dd, *J* = 7.5, 1.2 Hz, H-8), 10.57 (1H, s, H-11), 4.14 (3H, s, 1-OCH_3); ^{13}C NMR (100 MHz, pyridine-d_5) δ: 166.58 (C-1), 119.51 (C-2), 166.41 (C-3), 112.67 (C-4), 141.58 (C-4a), 126.96 (C-5), 133.67 (C-6), 134.89 (C-7), 127.39 (C-8), 135.41 (C-8a), 180.07 (C-9), 118.21 (C-9a), 182.22 (C-10), 132.92 (C-10a), 194.98 (C-11), 64.31 (1-OCH_3).

*Sorandidiol (**9**):* Yellowish-orange powder; IR ν_{max}^{KBr} cm^{-1}: 3394, 1666, 1634, 1594, 1577, 1474, 1431, 1362, 1300, 1277, 1257, 1032; UV λ_{max} (MeOH) nm (log ε): 411 (3.95), 292 (4.26), 269 (4.53), 220 (4.51); ^{1}H NMR (400 MHz, DMSO-d_6) δ: 13.01 (1H, s, 1-OH), 7.54 (1H, d, *J* = 7.7 Hz, H-3), 7.48 (1H, d, *J* = 7.7 Hz, H-4), 7.39 (1H, d, *J* = 2.3 Hz, H-5), 7.17 (1H, dd, *J* = 8.6, 2.3 Hz, H-7), 8.02 (1H, d, *J* = 8.6 Hz, H-8), 2.22 (3H, s, H-11); ^{13}C NMR (100 MHz, DMSO-d_6) δ: 159.89 (C-1), 134.09 (C-2), 136.69 (C-3), 118.48 (C-4), 130.99 (C-4a), 112.44 (C-5), 163.75 (C-6), 121.32 (C-7), 129.62 (C-8), 124.39 (C-8a), 187.46 (C-9), 114.54 (C-9a), 181.59 (C-10), 135.46 (C-10a), 15.70 (C-11).

*Morindone (**10**):* Orange needles; IR ν_{max}^{KBr} cm^{-1}: 3460, 1628, 1606, 1454, 1359, 1320, 1286, 1259, 1229, 1155, 1080, 1018; UV λ_{max} (MeOH) nm (log ε): 447 (3.90), 299 (4.00), 259 (4.37), 230 (4.35), 201 (4.15); NMR (400 MHz, pyridine-d_5) δ: 13.65 (1H, s, 1-OH), 7.38 (1H, d, *J* = 7.7 Hz, H-3), 7.76 (1H, d, *J* = 7.7 Hz, H-4), 7.35 (1H, d, *J* = 8.3 Hz, H-7), 7.92 (1H, d, *J* = 8.3 Hz, H-8), 2.27 (3H, s, H-11); ^{13}C NMR (100 MHz, pyridine-d_5) δ: 161.35 (C-1), 135.62 (C-2), 136.72 (C-3), 118.94 (C-4), 131.66 (C-4a), 152.23 (C-5), 155.50 (C-6), 121.63 (C-7), 122.22 (C-8), 123.78 (C-8a), 187.57 (C-9), 115.80 (C-9a), 188.91 (C-10), 116.91 (C-10a), 16.07 (C-11).

As shown in Fig. 1, eight (**1**–**8**) of 10 anthraquinone compounds were 1,2,3-trisubstituted anthraquinones and were classified into four types according to the kind of functional group bonded to the C-2 position of the anthraquinone skeleton. These four types were a methyl group for compounds **1** and **2**, a hydroxymethyl group for compounds **3** and **4**, a methoxymethyl group for compounds **5** and **6**, and an aldehyde group for compounds **7** and **8**. The remaining two compounds (**9** and **10**) contained common 1-hydroxy and 2-methyl groups on the anthraquinone skeleton.

3.2. Effects of isolated anthraquinones (compounds **1**–**10**) on mammalian pols α, β and κ

First, 10 anthraquinones (i.e., compounds **1**–**10**) obtained from the chloroform-soluble phase together with three anthraquinone glycosides and two iridoid glycosides (Fig. 3) previously isolated from the *n*-butanol-soluble phase were tested for their inhibitory activities on pols. In mammalian pols, calf pol α, rat pol β, and human pol κ were used as representative replicative pol (i.e., B-family), repair/recombination-related pol (i.e., X-family), and repair of translation synthesis (TLS) pol (i.e., Y-family), respectively (Bebenek and Kunkel, 2004; Friedberg et al., 2000). Three anthraquinone glycosides and two iridoid glycosides did not influence the activities of these pols (data not shown), but several compounds obtained from the chloroform-soluble phase exhibited inhibitory activities (Fig. 4). These results suggest that the glycoside moiety of the compounds might prevent pol inhibitory activity.

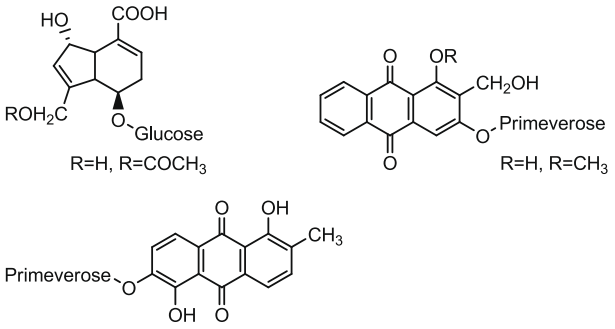

Fig. 3. Iridoid and anthraquinone glycosides isolated from the *n*-butanol-soluble phase of *M. citrifolia* root (Kamiya et al., 2008).

As shown in Fig. 4, anthraquinone (AQ) and the 1,2,3-trisubstituted anthraquinones which possessed 2-methyl or 2-hydroxymethyl groups (i.e., compounds **1**–**4**) did not show prominent inhibitory activities against these pols. 2-Methoxymethyl or 2-aldehyde groups attached to 1,2,3-trisubstituted anthraquinones (i.e., compounds **5**–**8**) exhibited remarkable inhibition against the activities of pols α and κ, but did not affect pol β activity. In anthraquinones that possessed 1-hydroxy and 2-methyl groups on one aromatic ring, compound **9**, which possessed a hydroxyl group at the C-6 position of the other aromatic ring, did not show the same pol inhibitory activity as compound **1**, whereas compound **10**, which had the hydroxyl group at the C-5 position of compound **9**, showed remarkably strong inhibitory activity against pols α and κ.

3.3. Effects of compound **10** on various pols and other DNA metabolic enzymes

Since compound **10** was the strongest inhibitor of mammalian pols α and κ in the anthraquinones (compounds **1**–**10**) investigated (Fig. 4), we focused on compound **10** in this section. As

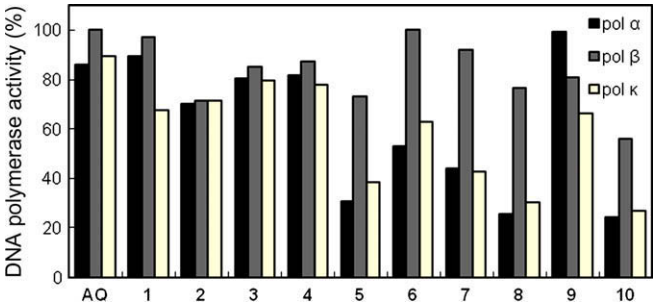

Fig. 4. Effect of anthraquinones (compounds **1**–**10**) on the activities of mammalian pols. Ten micromolar of each compound isolated from *M. citrifolia* root was incubated with calf pol α, rat pol β and human pol κ (0.05 units each). Pol activity in the absence of the compound was taken as 100%. AQ is anthraquinone.

Table 1
IC_{50} values of morindone (compound **10**) on the activities of various DNA polymerases and other DNA metabolic enzymes.

Enzyme	IC_{50} value (μM)
Mammalian DNA polymerases	
[A-family]	
Human DNA polymerase γ	35.9
[B-family]	
Calf DNA polymerase α	28.1
Human DNA polymerase δ	30.7
Human DNA polymerase ε	29.8
[X-family]	
Rat DNA polymerase β	>100
Human DNA polymerase λ	>100
Calf terminal deoxynucleotidyl transferase	>100
[Y-family]	
Human DNA polymerase η	33.3
Mouse DNA polymerase ι	32.5
Human DNA polymerase κ	29.7
Fish DNA polymerases	
Cherry salmon DNA polymerase δ	34.0
Insect DNA polymerases	
Fruit fly DNA polymerase α	28.5
Fruit fly DNA polymerase δ	29.2
Fruit fly DNA polymerase ε	29.6
Plant DNA polymerases	
Cauliflower DNA polymerase α	>100
Prokaryotic DNA polymerases	
E. coli DNA polymerase I (Klenow fragment)	>100
T4 DNA polymerase	>100
Taq DNA polymerase	>100
Other DNA metabolic enzymes	
Calf primase of DNA polymerase α	>100
HIV-1 Reverse transcriptase	>100
T7 RNA polymerase	>100
Mouse IMP dehydrogenase (type II)	>100
T4 polynucleotide kinase	>100
Bovine deoxyribonuclease I	>100

Compound **10** was incubated with each enzyme. Enzymatic activity in the absence of the compound was taken as 100%.

shown in Table 1, this compound inhibited the activities of some mammalian pols, such as A-family of pol γ, B-family of pols α, δ and ε, and Y-family of pols η, ι and κ, and these pols were suppressed to the same extent, with IC_{50} values of 28.1–35.9 μM; however, compound **10** did not inhibit the activities of X-family pols (i.e., pols β, λ and TdT). Furthermore, this compound also inhibited animal pols from fish (cherry salmon) pol δ, and insect (fruit fly) pols α, δ and ε at almost the same concentration as the inhibition of mammalian pols. On the other hand, compound **10** had no significant influence on the activities of pol α from plants (cauliflower) and prokaryotes, such as the Klenow fragment of *E. coli* pol I, *Taq* pol and T4 pol. This compound did not inhibit the activities of the other DNA metabolic enzymes tested, including calf primase of pol α, HIV-1 reverse transcriptase, T7 RNA polymerase, mouse IMP dehydrogenase (type II), T4 polynucleotide kinase and bovine DNase I.

To determine whether the inhibitor resulted in binding to DNA or the enzyme, the interaction of compound **10** with double-stranded DNA (dsDNA) was investigated based on the thermal transition of dsDNA with or without the compound. The Tm of dsDNA with an excess amount of compound **10** (100 μM) was measured using a spectrophotometer equipped with a thermoelectric cell holder. In the concentration range used, thermal transition of Tm was not observed, whereas ethidium bromide used as a positive control, a typical intercalating compound, produced a clear thermal transition. We then investigated whether an excessive amount of nucleic acid (i.e., poly(rC)) or protein (i.e., bovine serum albumin (BSA)) could prevent the inhibitory effect of compound **10** to determine whether the effect resulted from their non-specific adhesion to mammalian pols α and κ, or selective binding to specific sites. Poly(rC) and BSA had little or no influence on the effect of compound **10**, suggesting that the binding to the pols occurs selectively. These observations indicated that compound **10** did not intercalate to DNA as a template-primer, and the compound could directly bind to the enzyme and inhibit its activity.

These results suggested that compound **10** might be a potent and selective inhibitor of animal A-, B- and Y-families of pols.

3.4. Effects of anthraquinones on cultured human cancer cells

Furthermore, the inhibitory effect of the isolated anthraquinones (compounds **1**–**10**) on human colon cancer cells (HCT116 cells) was investigated. As shown in Fig. 5, 100 μM of compounds **5**, **7**, **8** and **10** suppressed cell growth by less than 100 μM of LD_{50} values. The effect of anthraquinone (AQ) and the 10 derivatives on cancer cell growth showed almost the same tendency as the inhibitory effect on pols α and κ (Fig. 4). The cell growth suppression of compound **10** was strongest in the anthraquinones (compounds **1**–**10**) tested, and the LD_{50} value was 32.2 μM. Since the LD_{50} value of compound **10** for cancer cell growth was almost the same as the IC_{50} values for animal pols, such as pol α (Table 1), this compound might be able to penetrate cancer cells and reach the nucleus, inhibiting the activities of A-, B- and Y-families of pols, and inhibition of pol activities by compound **10** might lead to cell growth suppression.

In summary, the presence of a methoxymethyl or aldehyde group at the C-2 position on the anthraquinone skeleton could be important for inhibitory activities against pols and the cell growth suppression of a human colon cancer cell line, HCT116. Furthermore, from the comparison of these bio-activities between compound **1** and compound **10**, a substituent at 3-position was unnecessary, but the hydroxyl group at 5-position was very important.

In animal pol families, the B-family of pols α, δ and ε is a replicative form and is essential for DNA replication during cell proliferation. Biologically active anthraquinones isolated from the root of the healthy tropical plant "Noni" (*M. citrifolia*) are assumed to suppress the proliferation of colon cancer cells by inhibiting DNA replication from the positive correlation between the suppression of HCT116 cell growth and the inhibition of B-family pol activities. The Noni root containing anthraquinones may be used as an anti-cancer functional food based on the inhibitory activities of pols A-, B- and Y-families. The anthraquinones, especially morindone (compound **10**), may be useful in providing valuable information to develop a drug design strategy for anti-cancer chemotherapy agents.

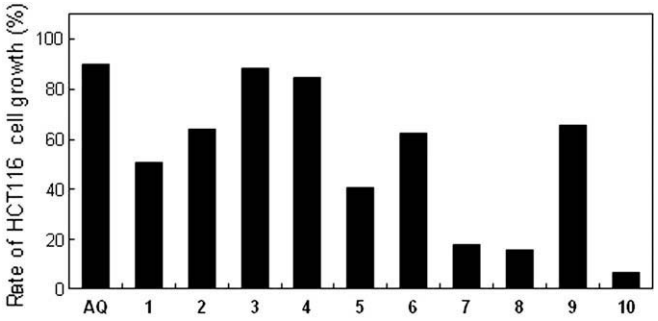

Fig. 5. Effect of anthraquinones (compounds **1**–**10**) on the proliferation of a human colon cancer cell line, HCT116. Each compound (100 μM) was added to the culture of HCT116 cells, and incubated for 24 h. The cell growth rate was determined by MTT assay (Mosmann, 1983). The proliferation of cancer cells in the absence of the compound was taken as 100%. AQ is anthraquinone.

Acknowledgements

This work was supported in part by a Grant-in-Aid for Kobe-Gakuin University Joint Research (A) (W.H., S.T., H.Y. and Y.M.), the "Academic Frontier" Project for Private Universities: matching fund subsidy from the Ministry of Education, Science, Sports, and Culture of Japan (MEXT), 2006–2010 (K.K., W.H., S.T., H.Y. and Y.M.), and a Grant from the Industrial Technology Research Program from NEDO (Japan) (K.H. and Y.M.). Y.M. acknowledges a Grant-in-Aid for Young Scientists (A) (No. 19680031) from MEXT, and The Salt Science Research Foundation, No. 09S3 (Japan).

References

Aoyagi, N., Matsuoka, S., Furunobu, A., Matsukage, A., & Sakaguchi, K. (1994). *Drosophila* DNA polymerase δ: Purification and characterization. *Journal of Biological Chemistry, 269*(8), 6045–6050.

Aoyagi, N., Oshige, M., Hirose, F., Kuroda, K., Matsukage, A., & Sakaguchi, K. (1997). DNA polymerase ε from *Drosophila melanogaster*. *Biochemical and Biophysical Research Communications, 230*(2), 297–301.

Bebenek, K., & Kunkel, T. A. (2004). In W. Yang (Ed.), *DNA repair and replication*. *Advances in protein chemistry* (Vol. 69, pp. 137–165). San Diego: Elsevier.

Date, T., Yamaguchi, M., Hirose, F., Nishimoto, Y., Tanihara, K., & Matsukage, A. (1988). Expression of active rat DNA polymerase β in *Escherichia coli*. *Biochemistry, 27*(8), 2983–2990.

Friedberg, E. C., Feaver, W. J., & Gerlach, V. L. (2000). The many faces of DNA polymerases: Strategies for mutagenesis and for mutational avoidance. *Proceedings of the National Academy of Sciences USA, 97*(11), 5681–5683.

Hirazumi, A., Furusawa, E., Chou, S. C., & Hokama, Y. (1994). Anticancer activity of *Morinda citrifolia* (Noni) on intraperitoneally implanted Lewis lung carcinoma in syngeneic mice. *Proceedings of the Western Pharmacology Society, 37*, 145–146.

Hubscher, U., Maga, G., & Spadari, S. (2002). Eukaryotic DNA polymerases. *Annual Review of Biochemistry, 71*, 133–163.

Kamiya, K., Tanaka, Y., Endang, H., Umar, M., & Satake, T. (2004). Chemical constituents of *Morinda citrifolia* fruits inhibit copper-induced low-density lipoprotein oxidation. *Journal of Agricultural and Food Chemistry, 52*(19), 5843–5848.

Kamiya, K., Hamabe, W., Harada, S., Murakami, R., Tokuyama, S., & Satake, T. (2008). Chemical constituents of *Morinda citrifolia* fruits inhibit copper-induced low-density lipoprotein oxidation. *Biological & Pharmaceutical Bulletin, 31*(5), 935–938.

Kornberg, K., & Baker, T. A. (1992) (pp. 197–225). *Eukaryotic DNA polymerase* (2nd ed.). *DNA replication*. New York: Freeman W.D. and Co..

Krishna, M. N., & Shama, R. G. (1970). *The Antiseptic, 67*, 167.

Kusumoto, R., Masutani, C., Shimmyo, S., Iwai, S., & Hanaoka, F. (2004). DNA binding properties of human DNA polymerase η: Implications for fidelity and polymerase switching of translesion synthesis. *Genes to Cells, 9*(12), 1139–1150.

Lu, B. C., & Sakaguchi, K. (1991). An endo-exonuclease from meiotic tissues of the basidiomycete *Coprinus cinereus*: Its purification and characterization. *Journal of Biological Chemistry, 266*(31), 21060–21066.

Mizushina, Y., Tanaka, N., Yagi, H., Kurosawa, T., Onoue, M., Seto, H., et al. (1996). Fatty acids selectively inhibit eukaryotic DNA polymerase activities in vitro. *Biochimica et Biophysica Acta, 1308*(3), 256–262.

Mizushina, Y., Yoshida, S., Matsukage, A., & Sakaguchi, K. (1997). The inhibitory action of fatty acids on DNA polymerase β. *Biochimica et Biophysica Acta, 1336*(3), 509–521.

Mizushina, Y., Dairaku, I., Yanaka, N., Takeuchi, T., Ishimaru, C., Sugawara, F., et al. (2007). Inhibitory action of polyunsaturated fatty acids on IMP dehydrogenase. *Biochimie, 89*(5), 581–590.

Mosmann, T. (1983). Rapid colorimetric assay for cellular growth and survival: Application to proliferation and cytotoxicity assays. *Journal of Immunology Methods, 65*(1–2), 55–63.

Nakayama, C., & Saneyoshi, M. (1985). Inhibitory effects of 9-β-D-xylofuranosyladenine 5′-triphosphate on DNA-dependent RNA polymerase I and II from cherry salmon (*Oncorhynchus masou*). *Journal of Biochemistry (Tokyo), 97*(5), 1385–1389.

Ogawa, A., Murate, T., Suzuki, M., Nimura, Y., & Yoshida, S. (1998). Lithocholic acid, a putative tumor promoter, inhibits mammalian DNA polymerase β. *Japanese Journal of Cancer Research, 89*(11), 1154–1159.

Ohashi, E., Murakumo, Y., Kanjo, N., Akagi, J-i, Masutani, C., Hanaoka, F., et al. (2004). Interaction of hREV1 with three human Y-family DNA polymerases. *Genes to Cells, 9*(6), 523–531.

Oshige, M., Takeuchi, R., Ruike, R., Kuroda, K., & Sakaguchi, K. (2004). Subunit protein-affinity isolation of *Drosophila* DNA polymerase catalytic subunit. *Protein Expression and Purification, 35*(2), 248–256.

Sakaguchi, K., Hotta, Y., & Stern, H. (1980). Chromatin-associated DNA polymerase activity in meiotic cells of lily and mouse. *Cell Structure and Function, 5*(4), 323–334.

Sakaguchi, K., Sugawara, F., & Mizushina, Y. (2002). Inhibitors of eukaryotic DNA polymerases. *Seikagaku, 73*(3), 244–251.

Sang, S., He, K., Liu, G., Zhu, N., Wang, M., Jhoo, J. W., et al. (2001). Citrifolinin, a new unusual iridoid with inhibition of Activator Protein-1 (AP-1) from the leaves of Noni (*Morinda citrifolia* L.). *Tetrahedron Letters, 42*(10), 1823–1825.

Shimazaki, N., Yoshida, K., Kobayashi, T., Toji, S., Tamai, T., & Koiwai, O. (2002). Over-expression of human DNA polymerase λ in *E. coli* and characterization of the recombinant enzyme. *Genes to Cells, 7*(7), 639–651.

Soltis, D. A., & Uhlenbeck, O. C. (1982). Isolation and characterization of two mutant forms of T4 polynucleotide kinase. *Journal of Biological Chemistry, 257*(19), 11332–11339.

Takata, K., Shimizu, T., Iwai, S., & Wood, R. D. (2006). Human DNA polymerase N (POLN) is a low fidelity enzyme capable of error-free bypass of 5S-thymine glycol. *Journal of Biological Chemistry, 281*(33), 23445–23455.

Tamai, K., Kojima, K., Hanaichi, T., Masaki, S., Suzuki, M., Umekawa, S., et al. (1988). Structural study of immunoaffinity-purified DNA polymerase α-DNA primase complex from calf thymus. *Biochimica et Biophysica Acta, 950*(3), 263–273.

Tamiya-Koizumi, K., Murate, T., Suzuki, M., Simbulan, C. G., Nakagawa, M., Takemura, M., et al. (1997). Inhibition of DNA primase by sphingosine and its analogues parallels with their growth suppression of cultured human leukemic cells. *Biochemistry & Molecular Biology International, 41*(6), 1179–1189.

Umeda, S., Muta, T., Ohsato, T., Takamatsu, C., Hamasaki, N., & Kang, D. (2000). The D-loop structure of human mtDNA is destabilized directly by 1-methyl-4-phenylpyridinium ion (MPP+), a parkinsonism-causing toxin. *European Journal of Biochemistry, 267*(1), 200–208.

Wang, M. Y., West, B. J., Jansen, C. J., Nowicki, D., Su, C., Palu, A. K., et al. (2002). *Morinda citrifolia* (Noni): A literature review and recent advances in Noni research. *Acta Pharmacologica Sinica, 23*(12), 1127–1141.

Yamaguchi, T., Saneyoshi, M., Takahashi, H., Hirokawa, S., Amano, R., Liu, X., et al. (2006). Synthetic nucleoside and nucleotides. 43. Inhibition of vertebrate telomerases by carbocyclic oxetanocin G (C.OXT-G) triphosphate analogues and influence of C.OXT-G treatment on telomere length in human HL60 cells. *Nucleosides Nucleotides Nucleic Acids, 25*(4–6), 539–551.

Youngken, H. W., Jenkis, H. J., & Butler, C. L. (1960). *Journal of the American Pharmacists Association, 40*, 271–273.

is a collection of statistical and mathematical techniques that have been successfully used in developing, improving and optimising bio-processes (Bandeira, Tininis, Bolzani, & Cavalheiro, 2006; Juntachote, Berghofer, Bauer, & Siebenhandl, 2006; Liyana-Pathirana & Shahidi, 2005; Paz, Vázquez, Riobó, & Franco, 2006; Vázquez, González, & Murado, 2006).

In this study, the optimal conditions for antioxidant extraction from soybeans fermented with *Aspergillus oryzae* were investigated using two complementary and sequential approaches. A factorial design was initially proposed. Kinetic analyses were then performed at the temperature–ethanol concentration points of the design. The parameters obtained from the fits of the kinetic data to a modified first-order model were the dependent variables to formulate the empirical equations of the second-order design. Finally, optimal conditions for a maximum antioxidant extraction were obtained from the response surfaces.

2. Materials and methods

2.1. Microorganism

A. oryzae was originally obtained from soy sauce industry (Wang, Law, & Webb, 2005). A distilled water suspension of the fungi spores was kept at −30 °C until used. The volume of inoculum was 1.5 ml with a cell concentration of 1.2×10^8 cells/ml.

2.2. Soybeans fermentation

Split soybeans (150 g) and 73.5 ml of distilled water were separately placed in 500 ml capped Duran bottles and autoclaved at 121 °C for 20 min. After the soybeans and the distilled water cooled down (at room temperature) they were both mixed with the spore suspension and manually shaken (vertically and horizontally) for 10 min to homogenise the inoculum. The inoculated soybeans were poured into Petri dishes and incubated at 30 °C for 5 days. Soybean samples were crushed with a mortar and pestle before being sealed in plastic bags and store at −30 °C until used.

2.3. Crude phenolic extraction

Detailed extraction conditions of temperature and concentration of ethanol are shown in Table 1. Ground samples (2 g) were extracted with 20 ml of the corresponding aqueous ethanol concentration at the temperature pre-established in the factorial design using a Soxtec System HT (1043 – Tecator). Subsequently, the extract was dehydrated to obtain a dry extract and diluted with ethanol up to 20 mg/ml of extract concentration. After that, the extract was centrifugated at 16,249×*g* for 5 min, and the supernatant was used for the antioxidant determination.

Table 1
Experimental domain and codification of independent variables in the factorial rotatable design.

Coded values	Natural values of temperature (T) and ethanol concentration (E)	
	T (°C)	E (%)
−1.41	40	21
−1	45	32
0	57	60
+1	69	88
+1.41	74	100

Codification: $V_c = (V_n - V_0)/\Delta V_n$; Decodification: $V_n = V_0 + (\Delta V_n \times V_c)$.
V_n = natural value in the centre of the domain.
ΔV_n = increment of V_n per unit of V_c.
Shaded area: values corresponding to the first-order design.

2.4. Determination of total phenolic content

The total phenolic content was determined based on the method of Singleton, Orthofer, and Lamuela-Raventós (1999), using the Folin–Ciocalteu Reagent (FCR) with gallic acid as a standard. Fifty microlitre of sample or blank were added to 3 ml of distilled water in 12 ml test tubes. A volume of FCR (250 μl) was placed into the tube and mixed before adding 750 μl of saturated Na_2CO_3. The final volume of the reaction mixture was adjusted to 5 ml with distilled water. The absorbance at 765 nm was read in 1 cm cuvettes after incubation for 2 h at room temperature, and readings were compared with a standard curve of gallic acid. The total phenolic content was expressed as mg of gallic acid equivalent per gram dry basis of fermented soybeans (mg GAE /g db).

2.5. Determination of DPPH radical scavenging activity

The effect of the extract on the 2,2-diphenyl-1-picrylhydrazyl (DPPH) radical was estimated according to the procedure described by Brand-Williams, Cuvelier, and Berset (1995). The extract (0.1 ml) was added to 3.9 ml of DPPH radical 6×10^{-5} M in methanol which was prepared daily. The decrease in absorbance was determined at 515 nm after incubation for 30 min. A DPPH radical solution without sample was used as a control and the DPPH percentage inhibition was calculated according to the following equation:

$$\text{DPPH radical scavenging effect } (\%) = \left(1 - \frac{\text{absorbance}_{\text{sample}}}{\text{absorbance}_{\text{control}}}\right) \times 100 \quad (1)$$

2.6. Experimental design and statistical analysis

The antioxidant activities (total phenolic content and DPPH radical scavenging capacity) as a function of the extraction time was studied using a rotatable second-order design with quintuple replication in the centre of the experimental domain (Akhnazarova & Kafarov, 1982; Box et al., 2005). The range of independent variables studied, temperature (T) and ethanol concentration (E), is shown in Table 1.

The experiments were planned using two different approaches. The variation of the antioxidant extraction (measured as total phenolic concentration and DPPH radical scavenging activity) with time were fitted to appropriate mathematical models to obtain a group of kinetic parameters that could describe these trends. A rotatable second-order design was then implemented using the kinetic parameters as response.

In the first case, the calculation was carried out using a non linear least-squares (quasi-Newton) method *via* the macro 'Solver' in the Microsoft Excel XP spreadsheet. Later, the Statistica 6.0 program (StatSoft, Inc. 2001) was used to calculate the significance of the estimated parameters (Student t-test, $\alpha = 0.05$) and the robustness of the model (Fisher F-test, $\alpha = 0.05$). Results of the factorial designs were employed to obtain empirical equations that describe the significant parameters as a function of temperature and ethanol concentration. The statistical significance of the coefficients was verified by means of the Student t-test ($\alpha = 0.05$), and the model consistency by the Fisher F-test ($\alpha = 0.05$) using the following mean squares ratios:

	The model is acceptable if
F_1 = model/total error	$F_1 \geqslant F_{\text{den}}^{\text{num}}$
F_2 = (model + lack of fitting)/model	$F_2 \leqslant F_{\text{den}}^{\text{num}}$
F_3 = total error/experimental error	$F_3 \leqslant F_{\text{den}}^{\text{num}}$
F_4 = lack of fitting/experimental error	$F_4 \leqslant F_{\text{den}}^{\text{num}}$

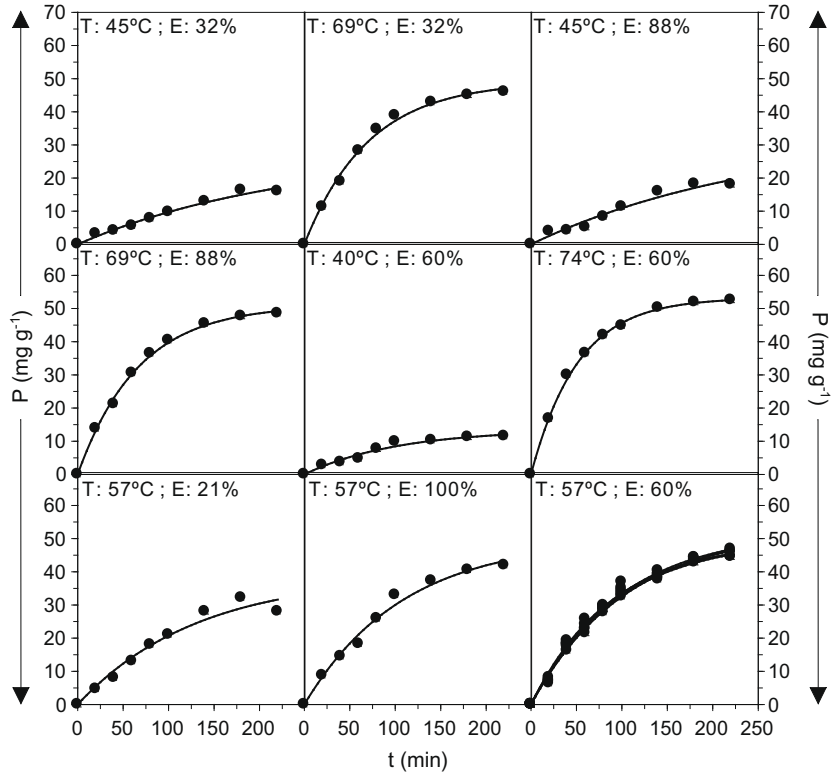

Fig. 1. Kinetics of total phenolic content extracted from soybeans fermented with *Aspergillus oryzae* in each one of the experimental conditions (in natural values) defined in Table 1. The experimental data (symbols) were fitted to the model (2) (continuous line).

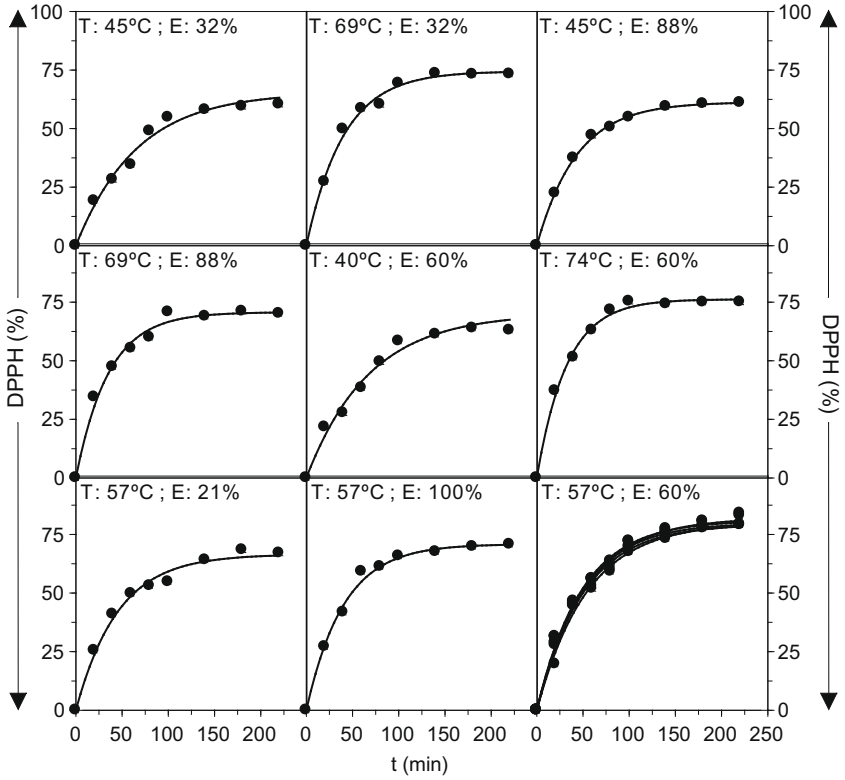

Fig. 2. Kinetics of DPPH radical scavenging activity extracted from soybeans fermented with *Aspergillus oryzae* in each one of the experimental conditions (in natural values) defined in Table 1. The experimental data (symbols) were fitted to the model (3) (continuous line).

3. Results and discussion

Previous experiments using different solvents (acetone, methanol, ethanol, hexane and ethyl acetate) at various concentrations demonstrated that methanol and ethanol were the most efficient compounds in the extraction of antioxidant compounds from fermented soybeans (data not shown). Among these, ethanol was selected since it has less restriction in food applications. The aim of this study was to evaluate the combined effects of extraction temperature and ethanol concentration for the recovery of antioxidant compounds from fermented soybeans.

3.1. Kinetics of antioxidants activities

Kinetics of the antioxidant extraction were firstly performed at the points selected in the factorial design. The results for total phenolic content and DPPH scavenging activity are shown in Figs. 1 and 2. In both cases the experimental data follow hyperbolic curves, and for this reason a modified first-order kinetic model with a final asymptote was chosen to describe the extraction of antioxidants with time

$$P = P_m \cdot (1 - e^{-k_p \cdot t}) \quad (2)$$

where P is the phenolic concentration at time t (mg GAE/g db), P_m is the maximum concentration when time approaches infinite, and k_p is the specific rate of the total phenolic concentration (min^{-1}). Similarly, for the DPPH scavenging capacity

$$D = D_m \cdot (1 - e^{-k_d \cdot t}) \quad (3)$$

where D is the DPPH radical scavenging activity (%), D_m the maximum DPPH radical scavenging activity when time approaches infinite, and k_d is the specific rate of DPPH radical scavenging activity (min^{-1}). The continuous curves in Figs. 1 and 2 represent the models obtained by fitting the experimental data to these equations. The statistical analyses of the kinetic models are summarised in Tables 2 and 3.

In general, the proposed models were statistically robust (Fisher's F-test and p-values < 0.001), and the parametric estimations were significant (Student's t-test $\alpha = 0.05$). The coefficients of linear correlation (r) between predicted and observed values were in all cases higher than 0.964. This indicates that the proposed kinetic models can be used to describe and predict the extraction of antioxidants from fermented soybeans in the range of temperature and ethanol concentration assayed.

Table 2
Parametric estimations corresponding to the modified first-order kinetic model (2) applied to the extraction of total phenolic compounds from fermented soybeans by *Aspergillus oryzae* at the experimental conditions studied. Independent variables are expressed in natural values in brackets.

Design conditions	[a]$P_m \pm$ [b]CI	[c]$k_p \pm$ CI	[d]F ($df_1 = 2$, $df_2 = 7$; $\alpha = 0.05$)	p-Value	[e]r (O:P)
T: −1 (45 °C); E: −1 (32%)	27.61 ± 12.82	0.0043 ± 0.0029	702.72	<0.0001	0.983
T: 1 (69 °C); E: −1 (32%)	49.15 ± 3.20	0.0142 ± 0.0023	2931.01	<0.0001	0.995
T: −1 (45 °C); E: 1 (88%)	33.59 ± 26.58	0.0039 ± 0.0038	305.02	<0.0001	0.964
T: 1 (69 °C); E: 1 (88%)	51.08 ± 2.07	0.0151 ± 0.0016	6904.27	<0.0001	0.998
T: −1.41 (40 °C); E: 0 (60%)	13.54 ± 3.29	0.0098 ± 0.0048	416.68	<0.0001	0.967
T: 1.41 (74 °C); E: 0 (60%)	53.26 ± 1.07	0.0195 ± 0.0012	20067.38	<0.0001	0.999
T: 0 (57 °C); E: −1.41 (21%)	38.86 ± 13.56	0.0076 ± 0.0048	345.59	<0.0001	0.966
T: 0 (57 °C); E: 1.41 (100%)	49.87 ± 7.75	0.0092 ± 0.0028	1160.07	<0.0001	0.988
T: 0 (57 °C); E: 0 (60%)	52.85 ± 5.74	0.0096 ± 0.0021	2210.10	<0.0001	0.994
T: 0 (57 °C); E: 0 (60%)	49.80 ± 3.32	0.0108 ± 0.0015	4580.68	<0.0001	0.997
T: 0 (57 °C); E: 0 (60%)	52.55 ± 5.11	0.0097 ± 0.0019	2668.48	<0.0001	0.995
T: 0 (57 °C); E: 0 (60%)	52.41 ± 7.53	0.0101 ± 0.0030	1118.99	<0.0001	0.988
T: 0 (57 °C); E: 0 (60%)	49.37 ± 5.21	0.0114 ± 0.0026	1688.54	<0.0001	0.992

[a] Maximum total phenolic concentration.
[b] Confidence intervals ($\alpha = 0.05$; $df = 7$).
[c] Specific rates of total phenolic production.
[d] F-Fisher test (df_1 = degrees of freedom of the model; df_2 = degrees of freedom of the error).
[e] Correlation coefficient between observed and predicted data.

Table 3
Parametric estimations corresponding to the modified first-order kinetic model (3) applied to the extraction of DPPH radical scavenging activity from fermented soybeans by *Aspergillus oryzae* at the experimental conditions studied. Independent variables are expressed in natural values in brackets.

Design conditions	[a]$D_m \pm$ [b]CI	[c]$k_d \pm$ CI	[d]F ($df_1 = 2$, $df_2 = 7$; $\alpha = 0.05$)	p-Value	[e]r (O:P)
T: −1 (45 °C); E: −1 (32%)	65.51 ± 6.11	0.0152 ± 0.0041	1124.24	<0.0001	0.992
T: 1 (69 °C); E: −1 (32%)	74.48 ± 3.17	0.0248 ± 0.0037	3386.46	<0.0001	0.997
T: −1 (45 °C); E: 1 (88%)	61.32 ± 1.03	0.0232 ± 0.0013	23578.91	<0.0001	0.999
T: 1 (69 °C); E: 1 (88%)	70.71 ± 3.75	0.0284 ± 0.0057	1978.03	<0.0001	0.994
T: −1.41 (40 °C); E: 0 (60%)	70.32 ± 6.65	0.0147 ± 0.0042	1071.03	<0.0001	0.991
T: 1.41 (74 °C); E: 0 (60%)	76.23 ± 2.49	0.0308 ± 0.0041	4860.86	<0.0001	0.998
T: 0 (57 °C); E: −1.41 (21%)	66.53 ± 4.03	0.0221 ± 0.0042	1961.18	<0.0001	0.995
T: 0 (57 °C); E: 1.41 (100%)	70.99 ± 3.02	0.0249 ± 0.0037	3453.07	<0.0001	0.997
T: 0 (57 °C); E: 0 (60%)	79.34 ± 2.76	0.0199 ± 0.0021	6576.57	<0.0001	0.999
T: 0 (57 °C); E: 0 (60%)	79.91 ± 2.14	0.0206 ± 0.0017	10498.72	<0.0001	0.999
T: 0 (57 °C); E: 0 (60%)	82.02 ± 6.11	0.0192 ± 0.0039	1569.18	<0.0001	0.994
T: 0 (57 °C); E: 0 (60%)	79.96 ± 5.15	0.0185 ± 0.0034	2103.97	<0.0001	0.996
T: 0 (57 °C); E: 0 (60%)	80.98 ± 3.70	0.0206 ± 0.0026	4099.41	<0.0001	0.997

[a] Maximum DPPH radical scavenging activity.
[b] Confidence intervals ($\alpha = 0.05$; $df = 7$).
[c] Specific rates of DPPH radical scavenging activity.
[d] F-Fisher test (df_1 = degrees of freedom of the model; df_2 = degrees of freedom of the error).
[e] Correlation coefficient between observed and predicted data.

From the values of the parameters in the fitted models, it can be concluded that the highest phenolic concentration (P_m) and specific rate of total phenolic content (k_p) are found at the highest temperature studied (74 °C). The highest DPPH scavenging activity (D_m) was achieved at the centre of the experimental domain ($T = 0$, $E = 0$), but the maximum specific rate of DPPH scavenging activity (k_d) is obtained at the point $T = 1.41$ and $E = 0$ (see Table 1).

3.2. Factorial design

As stated before, the second approach was to study the correlation between the kinetic parameters and the combined effects of temperature (T) and ethanol concentration (E). The parameters obtained from the fitted kinetic models were adjusted to the polynomic function

$$R = b_0 + b_1T + b_2E + b_{12}TE + b_{11}T^2 + b_{22}E^2 \quad (4)$$

where R is any of the response variables (D_m, P_m, k_p or k_d).

The best-fit model and the statistical analysis of the rotatable second-order design when R was the maximum total phenolic content (P_m) are shown in Table 4. The statistical analysis indicates that the combined term TE in Eq. (4) was not significant.

The response surfaces obtained from fitting the total phenolic parameters P_m and k_p to Eq. (4) are plotted in Fig. 3. The maximum phenolic content (P_m, left) shows a well defined maximum within the experimental domain. The maximum can be calculated by

Table 4
Results of the factorial design and tests of significance for the model of maximum total phenolic concentration (P_m).

T	E	[a]P_m	[b]$\hat{P}_m$	Coefficients from the least-squares regression	t	[c]Adjusted model	
−1	−1	27.61	24.74	51.39	68.84	**51.39**	*i.t.*
1	−1	49.15	48.57	11.92	20.16	**11.92**	***T***
−1	1	33.59	30.61	2.94	4.97	**2.94**	***E***
1	1	51.08	54.44	−1.01	1.21	NS	*TE*
−1.41	0	13.54	17.38	−8.66	13.62	**−8.66**	$\boldsymbol{T^2}$
1.41	0	53.26	50.98	−3.15	4.95	**−3.15**	$\boldsymbol{E^2}$
0	−1.41	38.86	40.99				
0	1.41	49.87	49.28				
0	0	52.85	51.39	Average value = 44.149			
0	0	49.80	51.39	Expected average value = 51.396			
0	0	52.55	51.39	Var(Ee) = 2.7867			
0	0	52.41	51.39	$t(\alpha < 0.05;\ v = 4) = 2.776$			
0	0	49.37	51.39				
	[d]SS	[e]v	[f]MS	[g]Mean square ratios			
Model	1747.66	4	436.92	MSM/MSE = 53.99	$F_8^4\ (\alpha = 0.05) = 3.838$		
Error	64.74	8	8.092	MSMLF/MSM = 0.515	$F_4^8\ (\alpha = 0.05) = 6.041$		
Exp. error	11.15	4	2.787	MSE/MSEe = 2.904	$F_4^8\ (\alpha = 0.05) = 6.041$		
Lack of fitting	53.59	4	13.398	MSLF/MSEe = 4.808	$F_4^4\ (\alpha = 0.05) = 6.388$		
Total	1812.40	12					
				$r^2 = 0.964$			
				r^2 adjusted = 0.946			

[a] Experimental values of maximum total phenolic concentration.
[b] Estimated values of maximum total phenolic concentration from the adjusted model.
[c] Coefficients for the terms of the adjusted model: *i.t.*, independent term; *E*, ethanol concentration (%); *T*, temperature (°C); NS, not significant coefficient.
[d] SS: sum of squares.
[e] v: degrees of freedom.
[f] MS: mean squares.
[g] Mean square ratios: MSM, mean squares of the model; MSE, mean squares for error; MSMLF, mean squares for model lack of fit; MSEe, mean squares for experimental error.

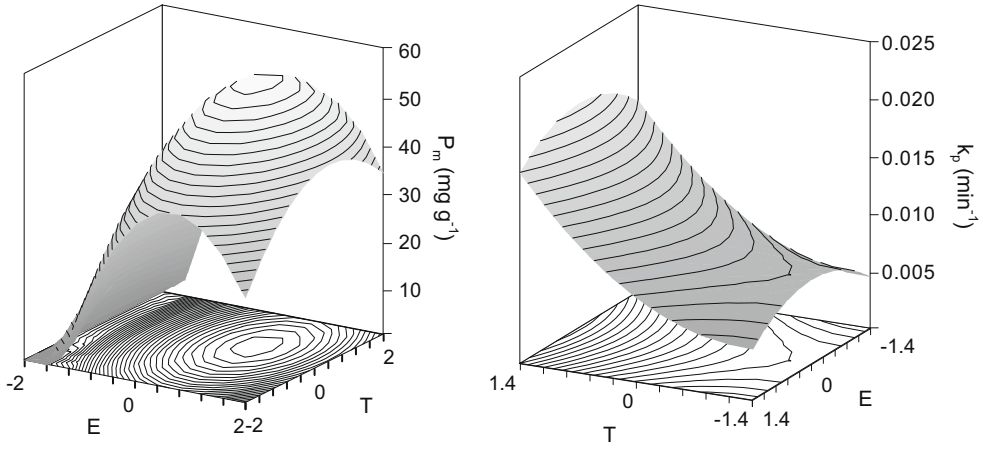

Fig. 3. Response surface corresponding to the joint effect of ethanol (E) and temperature (T) on the maximum total phenolic production (P_m, left) and in the specific rates of total phenolic production (k_p, right) according to the equations described in Tables 4 and 5. Independent variables are expressed in codified values.

deriving the response equation with respect to the independent variables T and E

$$\left.\frac{\partial P_m}{\partial T}\right|_{T=T_m} = 11.915 - 17.32T \quad \text{and} \quad \left.\frac{\partial P_m}{\partial E}\right|_{E=E_m} = 2.937 - 6.29E$$

Since at the maximum both derivatives must be zero, it is possible to calculate the optimum temperature and ethanol concentration for a maximum antioxidant extraction; $T_m = 0.690$ and $E_m = 0.467$ in codified values, equivalent to 65.3 °C and 73.1% ethanol in real values (see Table 1 for codification/decodification). At this point the predicted maximum total phenolic concentration was 56.2 mg GAE/g db.

The best-fit model and the statistical analysis of the rotatable second-order design for the specific rate of the total phenolic concentration (k_p) are shown in Table 5. In this case the statistical analysis indicates that neither the combined term TE nor the E term in Eq. (4) are significant. The response for k_p (Fig. 3, right) is a convex surface with a line of maxima at $E = 0$. An absolute maximum response cannot be obtained within the experimental domain. However, in all cases the specific rate of total phenolic concentration increases with temperature.

The results for maximum DPPH radical scavenging activity (D_m) were similar to those for the total phenolic. Fig. 4 (left) shows the parabolic response surface obtained from the equation in Table 6. Both the E and TE terms in Eq. (4) were not significant. The maximum can be equally calculated deriving the response equation with respect to the independent variables T and E

$$\left.\frac{\partial D_m}{\partial T}\right|_{T=T_m} = 3.35 - 8.70T \quad \text{and} \quad \left.\frac{\partial D_m}{\partial E}\right|_{E=E_m} = -13.24E$$

Table 5
Results of the factorial design and tests of significance for the model of the specific rate of total phenolic production (k_p).

T	E	[a]k_p	[b]$\hat{k}_p$	Coefficients from the least-squares regression	t	[c]Adjusted model	
−1	−1	0.0043	0.0061	0.0103	30.29	**0.0103**	*i.t.*
1	−1	0.0142	0.0148	0.0043	16.07	**0.0043**	***T***
−1	1	0.0039	0.0061	0.0003	1.24	NS	*E*
1	1	0.0151	0.0148	0.0003	0.83	NS	*TE*
−1.41	0	0.0098	0.0074	0.0016	5.60	**0.0016**	$\boldsymbol{T^2}$
1.41	0	0.0195	0.0197	−0.0015	5.15	**−0.0015**	$\boldsymbol{E^2}$
0	−1.41	0.0076	0.0074				
0	1.41	0.0092	0.0074				
0	0	0.0096	0.0103	Average value = 0.0104			
0	0	0.0108	0.0103	Expected average value = 0.0103			
0	0	0.0097	0.0103	Var(Ee) < 0.00001			
0	0	0.0101	0.0103	$t(\alpha < 0.05;\ \nu = 4) = 2.776$			
0	0	0.0114	0.0103				
	[d]SS	[e]ν	[f]MS	[g]Mean square ratios			
Model	0.00019	3	0.000063	MSM/MSE = 28.34	F_9^3 ($\alpha = 0.05$) = 3.863		
Error	0.00002	9	0.000002	MSMLF/MSM = 0.410	F_3^9 ($\alpha = 0.05$) = 8.845		
Exp. Error	0.000002	4	0.000001	MSE/MSEe = 3.818	F_4^9 ($\alpha = 0.05$) = 5.999		
Lack of fitting	0.00002	5	0.000004	MSLF/MSEe = 6.073	F_4^5 ($\alpha = 0.05$) = 6.256		
Total	0.00021	12					
				$r^2 = 0.904$			
				r^2 adjusted = 0.872			

[a] Experimental values of the specific rates of total phenolic production.
[b] Estimated values of the specific rates of total phenolic production from the adjusted model.
[c] Coefficients for the terms of the adjusted model: *i.t.*, independent term; *E*, ethanol concentration (%); *T*, temperature (°C); NS, not significant coefficient.
[d] SS: sum of squares.
[e] ν: degrees of freedom.
[f] MS: mean squares.
[g] Mean square ratios: MSM, mean squares of the model; MSE, mean squares for error; MSMLF, mean squares for model lack of fit; MSEe, mean squares for experimental error.

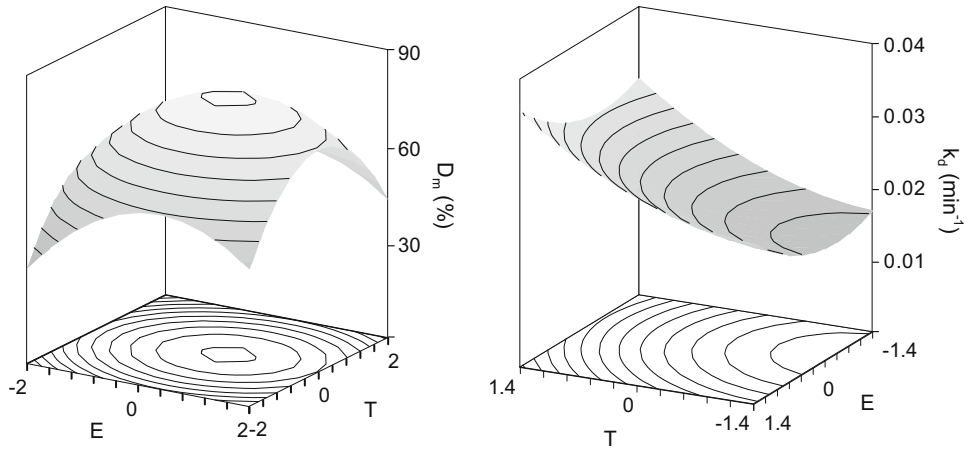

Fig. 4. Response surface corresponding to the joint effect of ethanol (E) and temperature (T) on the maximum DPPH radical scavenging activity (D_m, left) and in the specific rates of DPPH radical scavenging activity (k_d, right) according to the equations described in Tables 6 and 7. Independent variables are expressed in codified values.

The maximum D_m was found at $T_m = 0.385$ (61.6 °C) and $E_m = 0$ (60%). At this point the predicted maximum DPPH scavenging activity was 81.6%.

Table 7 summarises the results of the factorial design for the specific rate of DPPH scavenging activity (k_d) plotted in Fig. 4 (right). Only the combined term *TE* was not significant, and the model defines a concave response surface with a line of maximum slope in the proximity of $E = 0$. As for the k_p model, a maximum response cannot be calculated within the experimental domain, but k_d increases with the temperature.

Table 6
Results of the factorial design and tests of significance for the model of maximum DPPH scavenging activity (D_m).

T	*E*	[a]D_m	[b]$\hat{D}_m$	Coefficients from the least-squares regression	*t*	[c]Adjusted model	
−1	−1	65.51	66.13	80.45	169.31	**80.45**	*i.t.*
1	−1	74.48	72.82	3.35	8.90	**3.35**	***T***
−1	1	61.32	66.13	−0.21	0.55	NS	*E*
1	1	70.71	72.82	0.10	0.20	NS	*TE*
−1.41	0	70.32	67.03	−4.35	10.76	**−4.35**	$\boldsymbol{T^2}$
1.41	0	76.23	76.52	−6.62	16.37	**−6.62**	$\boldsymbol{E^2}$
0	−1.41	66.53	67.28				
0	1.41	70.99	67.28				
0	0	79.34	80.45	Average value = 73.716			
0	0	79.91	80.45	Expected average value = 80.443			
0	0	82.02	80.45	Var(Ee) = 1.1290			
0	0	79.96	80.45	$t(\alpha < 0.05;\ v = 4) = 2.776$			
0	0	80.98	80.45				
	[d]SS	[e]*v*	[f]MS	[g]Mean square ratios			
Model	478.29	3	159.430	MSM/MSE = 23.88	F_9^3 ($\alpha = 0.05$) = 3.863		
Error	60.09	9	6.677	MSMLF/MSM = 0.419	F_3^8 ($\alpha = 0.05$) = 8.845		
Exp. error	4.52	4	1.129	MSE/MSEe = 5.914	F_4^9 ($\alpha = 0.05$) = 5.999		
Lack of fitting	55.58	5	11.115	–	–		
Total	538.38	12					
				$r^2 = 0.881$			
				r^2 adjusted = 0.851			

[a] Experimental values of maximum DPPH radical scavenging activity.
[b] Estimated values of maximum DPPH radical scavenging activity from the adjusted model.
[c] Coefficients for the terms of the adjusted model: *i.t.*, independent term; *E*, ethanol concentration (%); *T*, temperature (°C); NS, not significant coefficient.
[d] SS: sum of squares.
[e] *v*: degrees of freedom.
[f] MS: mean squares.
[g] Mean square ratios: MSM, mean squares of the model; MSE, mean squares for error; MSMLF, mean squares for model lack of fit; MSEe, mean squares for experimental error.

Table 7
Results of the factorial design and tests of significance for the model of the specific rate of DPPH radical scavenging activity (k_d).

T	*E*	[a]k_d	[b]k_d	Coefficients from the least-squares regression	*t*	[c]Adjusted model	
−1	−1	0.0152	0.0164	0.0198	47.28	**0.0198**	*i.t.*
1	−1	0.0248	0.0258	0.0047	14.22	**0.0047**	***T***
−1	1	0.0232	0.0203	0.0019	5.86	**0.0019**	***E***
1	1	0.0284	0.0297	−0.0011	2.32	NS	*TE*
−1.41	0	0.0147	0.0160	0.0015	4.09	**0.0015**	$\boldsymbol{T^2}$
1.41	0	0.0308	0.0293	0.0018	5.12	**0.0018**	$\boldsymbol{E^2}$
0	−1.41	0.0221	0.0206				
0	1.41	0.0249	0.0261				
0	0	0.0199	0.0198	Average value = 0.0218			
0	0	0.0206	0.0198	Expected average value = 0.0198			
0	0	0.0192	0.0198	Var(Ee) < 0.00001			
0	0	0.0185	0.0198	$t(\alpha < 0.05;\ v = 4) = 2.776$			
0	0	0.0206	0.0198				
	[d]SS	[e]*v*	[f]MS	[g]Mean square ratios			
Model	0.00024	4	0.000060	MSM/MSE = 20.52	F_8^4 ($\alpha = 0.05$) = 3.838		
Error	0.00002	8	0.000003	MSMLF/MSM = 0.541	F_4^8 ($\alpha = 0.05$) = 6.041		
Exp. error	0.000003	4	0.000001	MSE/MSEe = 3.349	F_4^8 ($\alpha = 0.05$) = 6.041		
Lack of fitting	0.00002	4	0.000005	MSLF/MSEe = 5.698	F_4^4 ($\alpha = 0.05$) = 6.388		
Total	0.00026	12					
				$r^2 = 0.911$			
				r^2 adjusted = 0.867			

[a] Experimental values of the specific rates of DPPH radical scavenging activity.
[b] Estimated values of the specific rates of DPPH radical scavenging activity from the adjusted model.
[c] Coefficients for the terms of the adjusted model: *i.t.*, independent term; *E*, ethanol concentration (%); *T*, temperature (°C); NS, not significant coefficient.
[d] SS: sum of squares.
[e] *v*: degrees of freedom.
[f] MS: mean squares.
[g] Mean square ratios: MSM, mean squares of the model; MSE, mean squares for error; MSMLF, mean squares for model lack of fit; MSEe, mean squares for experimental error.

The empirical models obtained show a good fitting and consistency. The correlation with the observed values ($r^2_{adjusted}$) was higher that 0.85 and the experimental variability of the replica in the centre of the experimental domain was considerably low, allowing for construction of highly predictive models.

The improvement of the antioxidant extraction with temperature was probably due to the increasing diffusivity of the solvent in the solid matrix and the solubility of the phenolic compounds in the solvent, which favour the extraction (Cacace & Mazza, 2003; Herrero, Martin-Alvarez, Señoráns, Cifuentes, & Ibáñez, 2005; Juntachote et al., 2006). However, it should be noted that increasing temperature beyond a certain value can lead to decomposition of some phenolic compounds. Rostagno, Palma, and Barroso (2007) reported decomposition of isoflavones in soybean during heat treatments. Malonyl isoflavones also degrade when the extraction is performed between 75 and 100 °C. Extraction between 100 and 125 °C affects acetyl isoflavones and higher temperatures sharply reduced the glucosides concentrations.

It is not surprising to find out that the DPPH results showed a similar trend to the total phenolic concentration. However, the optimum extraction conditions were slightly different for the two assays. This could be due to the fact that each assay measures different kinds of phenolics, and each phenolic compound shows different antioxidant properties, which depends on the chemical structure and substitution position (Pokorny, 2003).

The fit of models to second-order polynomial equations was in agreement with other authors who used temperature, solvent concentration and time as variables in a similar approach using other food matrices. Wettasinghe and Shahidi (1999) studied the antioxidant properties of an ethanol extract of defatted borage seeds, and Herrero et al. (2005) investigated antioxidants from *Spirulina platensis* microalga. Liyana-Pathirana and Shahidi (2005) studied phenolic compounds from wheat, and Juntachote et al. (2006) tested phenolic extracts of lemon grass, galangal, holy basil and rosemary. However, only Herrero et al. (2005) reported that temperature had the strongest influence amongst all variables. In the other studies, the solvent concentration was the main factor affecting antioxidant extraction. These discrepancies highlight the need for appropriate extraction protocols, with suitable solvent polarity, time and temperature for each food matrix, and using multivariable experimental design techniques.

4. Conclusions

A factorial design combined with a kinetic approach was successfully applied to maximise the extraction of antioxidant compounds from soybeans fermented with *A. oryzae*. The highest values of P_m and D_m were obtained close to the centre of the experimental domain studied. Both k_p and k_d showed a marked increase with temperature, but absolute maxima for this parameters were not predicted within the experimental domain. In general, higher temperatures lead to higher yields of total phenolics and DPPH scavenging activity. However, over a certain temperature value decomposition of some phenolic compounds may occur. In this case, the optimal conditions for antioxidant extraction were 65.3 °C and 73.1% ethanol for maximum total phenolic concentration, and 61.6 °C and 60% ethanol for maximum DPPH radical scavenging activity.

Acknowledgements

The authors wish to acknowledge the SPMU-TPSD Diponegoro University (Indonesia) for the Grant awarded to Dyah Hesti Wardhani to do this research (ADB Loan No. 1792-INO). Dr. José Antonio Vázquez has been awarded a postdoctoral Grant (Programa de bolsas para estadías fóra de Galicia, 2008) by the Dirección Xeral de Investigación, Desenvolvemento e Innovación, Xunta de Galicia, Spain.

References

Akhnazarova, S., & Kafarov, V. (1982). *Experiment optimization in chemistry and chemical engineering*. Moscow: MIR Publishers.

Bandeira, K. F., Tininis, A. G., Bolzani, V. D. S., & Cavalheiro, A. J. (2006). Optimisation of conditions for the extraction of casearins from *Caesaria sylvestris* using response surface methodology. *Phytochemical Analysis, 17*, 168–175.

Box, G. E., Hunter, J. S., & Hunter, W. G. (2005). *Statistics for experimenters: Design, innovation, and discovery*. Hoboken, NJ: John Wiley and Sons, Inc.

Brand-Williams, W., Cuvelier, M. E., & Berset, C. (1995). Use of a free radical method to evaluate antioxidant activity. *Lebensmittel Wissenschaft und Technologie, 28*, 25–30.

Cacace, J. E., & Mazza, G. (2003). Mass transfer process during extraction of phenolic compounds from milled berries. *Journal of Food Engineering, 59*, 379–389.

Calliste, C. A., Trouillas, P., Allais, D. P., Simon, A., & Duroux, J. L. (2001). Free radical scavenging activities measured by electron spin resonance spectroscopy and B16 cell antiproliferative behaviors of seven plants. *Journal of Agricultural and Food Chemistry, 49*, 3321–3327.

Cuppett, S., Schnepf, M., & Hall, C. (1997). Natural antioxidants – Are they a reality? In F. Shahidi (Ed.), *Natural antioxidants: Chemistry, health effects, and applications* (pp. 12–24). Illinois: AOCS Press.

Da Silva Pinto, M., Lajolo, F. M., & Genovese, M. I. (2005). Effect of storage temperature and water activity on the content and profile of isoflavones, antioxidant activity, and in vitro protein digestibility of soy protein isolates and defatted soy flours. *Journal of Agricultural and Food Chemistry, 53*, 6340–6346.

Esaki, H., Onozaki, H., Kawakishi, S., & Osawa, T. (1997). Antioxidant activity and isolation from soybeans fermented with *Aspergillus* spp. *Journal of Agricultural and Food Chemistry, 45*, 2020–2024.

Halliwell, B., & Gutteridge, J. M. C. (1999). *Free radicals in biology and medicine* (3rd ed.). Oxford: Oxford University Press.

Hayes, R. E., Bookwalter, G. N., & Bagley, E. B. (1977). Antioxidant activity of soybean flour and derivatives – A review. *Journal of Food Science, 42*, 1527–1532.

Herrero, M., Martin-Alvarez, P. J., Señoráns, F. J., Cifuentes, A., & Ibáñez, E. (2005). Optimization of accelerated solvent extraction of antioxidants from *Spirulina plantesis* microalga. *Food Chemistry, 93*, 417–423.

Hinneburg, I., & Neubert, R. H. H. (2005). Influence of extraction parameters of the phytochemical characteristics of extracts from buckwheat (*Fagopyrum esculentum*) herb. *Journal of Agricultural and Food Chemistry, 53*, 3–7.

Hubert, J., Berger, M., Nepveu, F., Paul, F., & Daydé, J. (2008). Effects of fermentation on the phytochemical composition and antioxidant properties of soy germ. *Food Chemistry, 109*, 709–721.

Isanga, J., & Zhang, G.-N. (2008). Soybean bioactive components and their implications to health – A review. *Food Reviews International, 24*, 252–276.

Juntachote, T., Berghofer, E., Bauer, F., & Siebenhandl, S. (2006). The application of response surface methodology to the production of phenolic extracts of lemon grass, galangal, holy basil and rosemary. *International Journal of Food Science and Technology, 41*, 121–133.

Lin, C. H., Wei, Y. T., & Chou, C. C. (2006). Enhanced antioxidative activity of soybean koji prepared with various filamentous fungi. *Food Microbiology, 23*, 628–633.

Liu, F. F., Ang, C. Y. W., & Springer, D. (2000). Optimization of extraction conditions for active components in *Hypericum perforatum* using response surface methodology. *Journal of Agricultural and Food Chemistry, 48*, 3364–3371.

Liyana-Pathirana, C., & Shahidi, F. (2005). Optimization of extraction of phenolic compounds from wheat using response surface methodology. *Food Chemistry, 93*, 47–56.

McCue, P., & Shetty, K. (2003). Role of carbohydrate-claving enzyme in phenolic antioxidant mobilization from whole soybean fermented with *Rhizopus oligosporus*. *Food Biotechnology, 17*, 27–37.

Naczk, M., & Shahidi, F. (2006). Phenolics in cereal, fruits and vegetables: Occurrence, extraction and analysis. *Journal of Pharmaceutical and Biomedical Analysis, 41*, 1523–1542.

Paz, B., Vázquez, J. A., Riobó, P., & Franco, J. M. (2006). Study of the effect of temperature, irradiance and salinity on growth and yessotoxin production by the dinoflagellate *Protoceratium reticulatum* in culture by using a kinetic and factorial approach. *Marine Environmental Research, 62*, 286–300.

Pokorny, J. (2003). Natural antioxidants. In P. Zeuthen & L. S. Sorensen (Eds.), *Food preservation techniques* (pp. 31–48). Cambridge: Woodhead Publishing Ltd.

Pratt, D. E., & Birac, P. M. (1979). Source of antioxidant activity of soybeans and soy products. *Journal of Food Science, 44*, 170–1722.

Pratt, D. E., & Hudson, B. J. F. (1990). Natural antioxidants not exploited commercially. In B. J. F. Hudson (Ed.), *Food antoxidants* (pp. 171–191). London: Elsevier Science Publishers Ltd.

Romero, A. M., Doval, M. M., Sturla, M. A., & Judis, M. A. (2004). Antioxidant properties of polyphenol-containing extract from soybean fermented with *Saccharomyces cerevisiae*. *European Journal of Lipid Science and Technology, 106*, 424–431.

Rostagno, M. A., Palma, M., & Barroso, C. G. (2007). Microwave assisted extraction of soy isoflavones. *Analytica Chimica Acta, 588*, 274–282.

Shahidi, F., & Wanasundara, U. N. (1997). Measurement of lipid oxidation and evaluation of antioxidant activity. In F. Shahidi (Ed.), *Natural antioxidants: Chemistry, health effects, and applications* (pp. 379–396). Illinois: AOCS Press.

Singleton, V. L., Orthofer, R., & Lamuela-Raventós, R. M. (1999). Analysis of total phenols and other oxidation substrates and antioxidants by means of Folin-Ciocalteu reagent. In L. Packer (Ed.). *Methods in enzymology, oxidants and antioxidants* (Vol. 299, pp. 152–178). San Diego, CA: Academic Press.

Tsao, R., & Deng, Z. (2004). Separation procedures for naturally occurring antioxidant phytochemicals. *Journal of Chromatography B, 812*, 85–99.

Vázquez, J. A., González, M. P., & Murado, M. A. (2006). Preliminary assays on the nisin and pediocin production using waste protein sources. Factorial and kinetic studies. *Bioresource Technology, 97*, 605–613.

Wang, R., Law, R., & Webb, C. (2005). Protease production and conidiation by *Aspergillus oryzae* in flour fermentation. *Process Biochemistry, 40*, 217–227.

Wardhani, D. H., Vázquez, J. A., & Pandiella, S. S. (2008). Kinetics of daidzin and genistin transformations and water absorption during soybean soaking at different temperatures. *Food Chemistry, 111*, 13–19.

Wardhani, D. H., Vázquez, J. A., & Pandiella, S. S. (2009). Mathematical modeling of the development of antioxidant activity in soybeans fermented with *Aspergillus oryzae* and *Aspergillus awamori* in the solid state. *Journal of Agricultural and Food Chemistry, 57*, 540–544.

Wettasinghe, M., & Shahidi, F. (1999). Antioxidant and free radical-scavenging properties of ethanolic extracts of defatted borage (*Borago officinalis* L.) seeds. *Food Chemistry, 67*, 399–414.

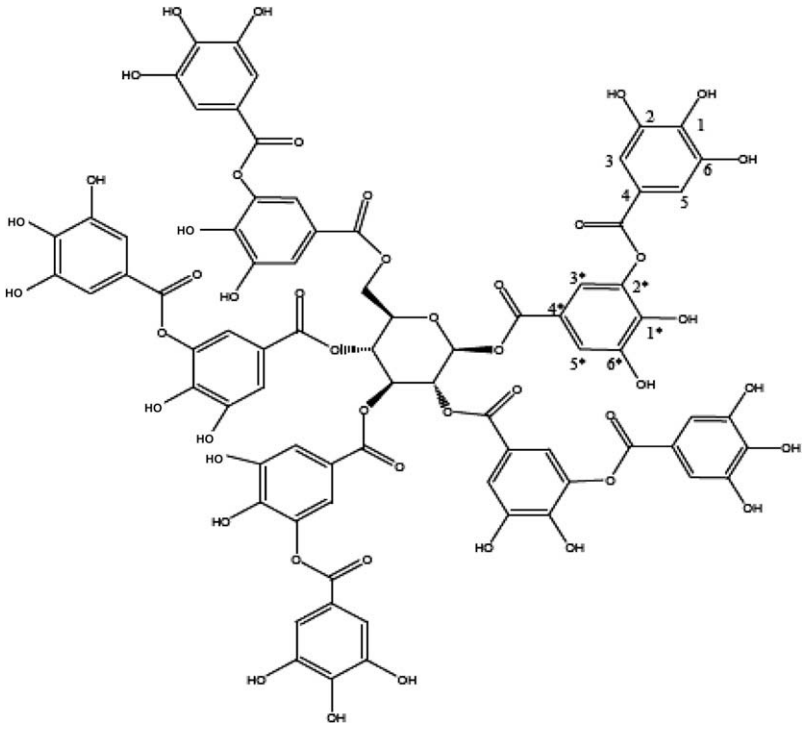

Fig. 1. Structure of tannic acid.

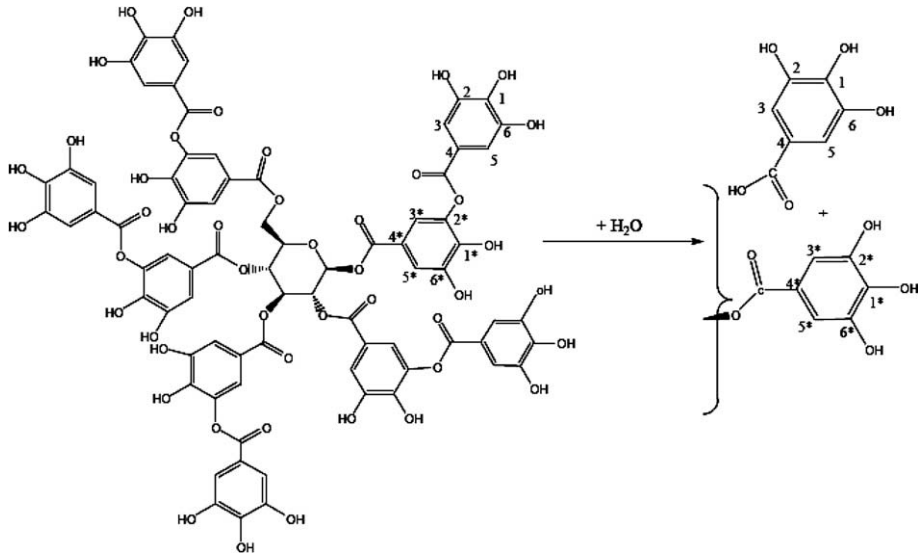

Fig. 2. The hydrolysis of tannic acid at an ester linkage between two gallic groups.

2. Materials and methods

2.1. Thermal processing of tannic acid

To prepare processed tannic acid (PTA, 30% w/v), fresh tannic acid (FTA, 30% w/v) (Sigma–Aldrich, Saint Louis, MO) was diluted in deionised water (pH 6.5). The FTA (5 ml) solution was placed in a glass bottle and hermetically sealed with a cap, and then autoclaved (121 °C, 103.4 kPa) in an autoclave (Market Forge Industries, Inc., Everett, MA) up to 60 min.

2.2. Measurement of lipid oxidation in soybean oil

The induction period (IP) measured volatile products such as aldehydes, acids, and alcohols that occur during the secondary phase of soybean oil treated with FTA and PTA at various concentrations (250, 500, 1000, 2000 and 3000 ppm). A Metrohm Rancimat® apparatus (743 Rancimat®, Brinkmann Instruments, Inc., Westbury, NY) was used to determine IP. Air flow was circulated at 10 ± 0.2 l/h through three gram samples at 110 ± 0.2 °C. Air was then passed through deionised water and the conductivity of

the water was measured. The IP was measured as the intersection of the tangent lines (first derivative) using the software provided with the instrument.

2.3. HPLC analysis of gallic acid in fresh and processed tannic acid

HPLC was used to separate and quantify gallic acid in tannic acid, as described by Kim et al. (2008), with the following modifications. The tannic acid sample was centrifuged at 16,000 *g* for 5 min and the supernatant was filtered through a 0.45 μm syringe filter and 10 μl was injected into a Gemini C18, 250 × 4.6 mm, C18 column at 25 °C. The mobile phases were 0.01 N H_2SO_4/acetonitrile (90:10, v/v) with the flow rate of 1.0 ml/min. Peaks were detected at 215 nm. The peak corresponding to gallic acid was identified, based on retention time of standard gallic acid and quantified using a calibration curve.

2.4. Effects of tannic acids processed for different processing time on lipid oxidation

Tannic acid (30%) was autoclaved at different processing times (0, 1, 5, 10, 15, 30 and 60 min). Autoclave condition was the same as described above. The processed tannic acids (300 ppm) with different processing times were added in soybean oil to measure the induction points. Fresh tannic acid (FTA) at 300 ppm was used as an unprocessed control. The concentration of gallic acid was also measured in processed tannic aid (PTA) by HPLC as described above. To determine the gallic acid effect in soybean oil, the same amount of gallic acid formed in processed tannic acid was added to soybean oil with FTA (300 ppm).

2.5. Bacterial strains

E. coli O157:H7 (ATCC 43890, 43895 and 35150), *Salmonella enterica* serovar Typhimurium (ATCC 19585 and 14028), *Salmonella typhi* (ATCC 6539), *L. monocytogenes* (ATCC 7694 and Δ*inl*AB) and *Enterobacter sakazakii* were used for this study. *E. sakazakii* Fec39 and *E. sakazakii* MSDH were kindly provided by Dr. Yoshen Chen (Department of Food Science and Technology, Mississippi State University). *E. sakazakii* Fec39 were clinically isolated by Dr. Römling (Microbiology and Tumorbiology Center, Sweden) (Zogaj, Bokranz, Nimtz, & Römling, 2003) and *E. sakazakii* MSDH by Mississippi State Department of Health, USA. An internalin A and B negative mutant (Δ*inl*AB) of *L. monocytogenes* was kindly provided with Dr. Pascale Cossart (*Département de Biologie Cellulaire et Infection*, France). All stock cultures were kept at −65 °C in tryptic soy broth (TSB, Becton Dickinson, Sparks, MD) containing 10% glycerol. The cultures were thawed and reactivated by subculture in TSB. Reactivated cells were maintained on tryptic soy agar (TSA, Becton Dickinson, Sparks, MD) slant.

2.6. Antimicrobial test

The antimicrobial test was carried out according to a disc diffusion test (Ali-Shtayeh, Yaghmour, Faidi, Salem, & Al-Nuri, 1998; Mau, Chen, & Hsieh, 2001). Each microbial culture was activated by transferring a loopful of the TSA slant culture into an Erlenmeyer flask with a cotton cap containing TSB (20 ml/flask), incubating at 37 °C for 18 h, and adjusting the cell numbers to 5 log CFU/ml with peptone (Becton Dickinson, Sparks, MD) water prior to use in tests. Each bacterial culture was uniformly streaked on Mueller–Hinton agar (Becton Dickinson, Sparks, MD), as described by O'Bryan, Crandall, Chalova, and Ricke (2008). Two sterile filter papers (Whatman GF/D, diameter = 7.5 mm) were aseptically placed on the agar. Fresh (FTA) and processed (PTA) tannic acid solutions (30%, w/v) were aseptically pipetted onto the discs (50 μl/disc). After 20 min, the agar plate was inverted and incubated at 37 °C for 24 and 48 h. Diameters of zones of inhibition were measured in mm and recorded. Analyses were performed a total of three times per strain.

2.7. ^{13}C NMR spectra of tannic acid samples

^{13}C NMR spectra of FTA and PTA solutions (30% w/v) were obtained on a Techmag 100 MHz NMR spectrometer (Spectral Data Services, Inc., Champaign, IL) at ambient temperature using a 12-μs pulse-width and 10-s delay for maximum quantification results with a 340 scan accumulation. Peaks were integrated and the integral values of the two spectra were compared to estimate the characteristics of the FTA and PTA samples.

2.8. Statistical analysis

A completely randomised design with three replications was used for antimicrobial and antioxidant studies. Analysis of variance and means were computed using the Statistical Analysis System (SAS, 2001). Fisher's least significant difference test ($p \leqslant 0.05$) was used to determine differences between treatment means. A value $p \leqslant 0.05$ was considered statistically significant.

3. Results

3.1. Antioxidant effect of fresh and processed tannic acid in soybean oil

The oxidative stability of soybean oil increased by 5–43% (from 5.93 to 6.23–8.48 h) for FTA and by 35–147% (to 7.98–14.68 h) for PTA (Fig. 3A and B). The induction time (IP) increased ($p < 0.05$) with increasing concentration of FTA or PTA. While there was no difference ($p \geqslant 0.05$) in IP between the control and soybean oil treated with FTA (500 ppm), the addition of PTA (250 ppm) to soybean oil increased ($p < 0.05$) induction time up to 7.98 h, comparable to the value of FTA at 3000 ppm (Fig. 3B). In all concentrations tested, PTA showed much stronger ($p < 0.05$) antioxidant capacity in soybean oil than FTA (Fig. 3B).

3.2. Effects of processing time of tannic acid and the combination of gallic acid and fresh tannic acid on soybean oil oxidation

Gallic acid was investigated as a possible hydrolysed product of tannic acid by thermal processing (Fig. 2). HPLC was used to quantify gallic acid for both FTA (control) and PTA at 300 ppm. As the processing time of PTA was increased from 1 to 15 min, the induction point and gallic acid were also increased ($p < 0.05$) up to 1.24 h and 1.26 μg/100 ml (Fig. 4). However, there were no changes ($p \geqslant 0.05$) beyond 15 min processing. Adding gallic acid at the same concentration found in PTA to fresh tannic acid increased the induction point of soybean oil oxidation, implying that the enhanced antioxidant capacity of processed tannic acid could be due to the galloyl group newly formed by thermal processing (Fig. 4).

3.3. Antimicrobial effect of fresh and processed tannic acid

Ten species of foodborne pathogens were used to evaluate the antimicrobial effect of fresh and processed tannic acid. An inhibition zone of 12 mm was considered as an effective indicator for good inhibitory effect (Mau et al., 2001). Processed tannic acid (PTA) possessed ($p < 0.05$) a broad antimicrobial activity on all tested microorganisms at days 1 and 2 whereas fresh tannic acid (FTA) showed good antimicrobial activity on only two strains, *S. enterica* serovar Typhimurium (ATCC 14028) and *E. sakazakii* MSDH (Table 1). At day 2, cell growth of the tested organisms was ob-

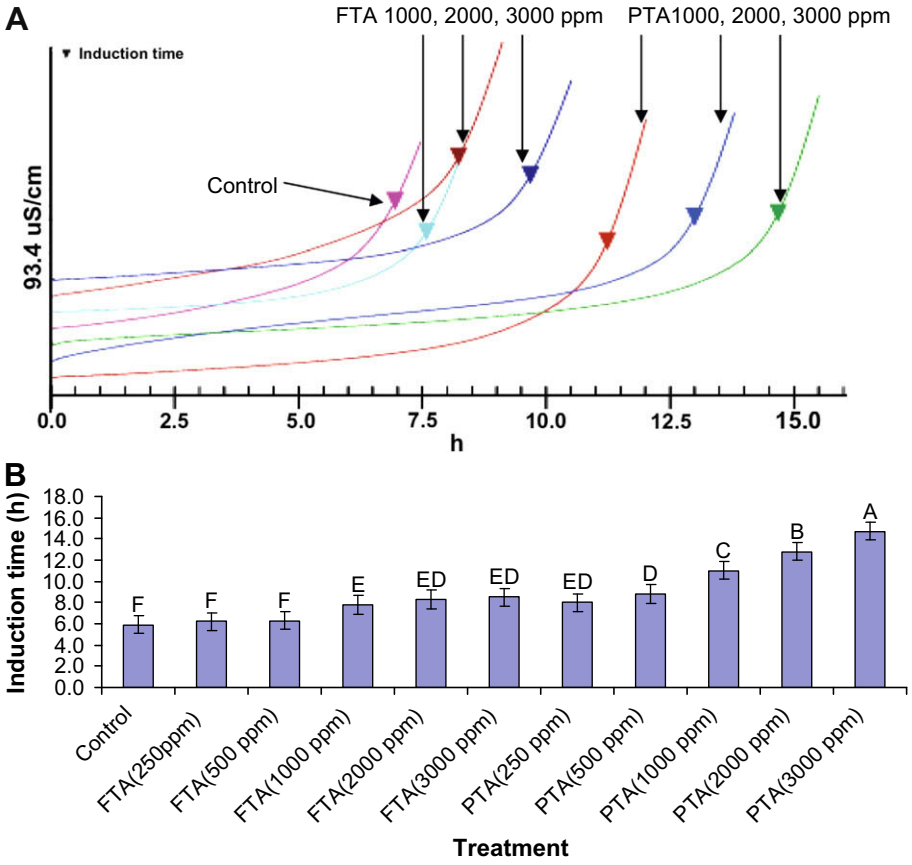

Fig. 3. (A) Induction curve of soybean oil treated with different concentrations of fresh (FTA) and processed tannic acid (PTA). (B) Induction time of soybean oil treated with different concentrations of fresh (FTA) and processed tannic acid (PTA).

served on FTA, which showed a slight decreased inhibition zone, while the cells on PTA did not show growth in the same time period.

3.4. ^{13}C NMR spectra of fresh and processed tannic acids

^{13}C NMR spectroscopy was used to see whether thermal processing causes a structural rearrangement of tannic acid. ^{13}C NMR spectral integration was carried out with different chemical shift scales for 200–100 and 100–0 ppm ranges. For the data interpretation, the chemical structure of tannic acid used in this study is shown in Fig. 3. The ^{13}C NMR spectra (Fig. 5) indicated the presence of unknown impurity peaks at 176, 36, and 20 ppm and also the presence of hydrolysed forms of tannic acid was apparent at 169–170 ppm for the aromatic carboxylic acid groups (Table 2). Thus, about 17% of ester groups of processed tannic acid were in the hydrolysed form in the PTA which showed more hydrolysation than FTA. By comparing with ^{13}C NMR spectra of pyrogallol, gallic acid, *n*-propyl gallate, and D-glucose (Stothers, 1972), other peaks were assigned as follows: aromatic acid ester carbons at 164–

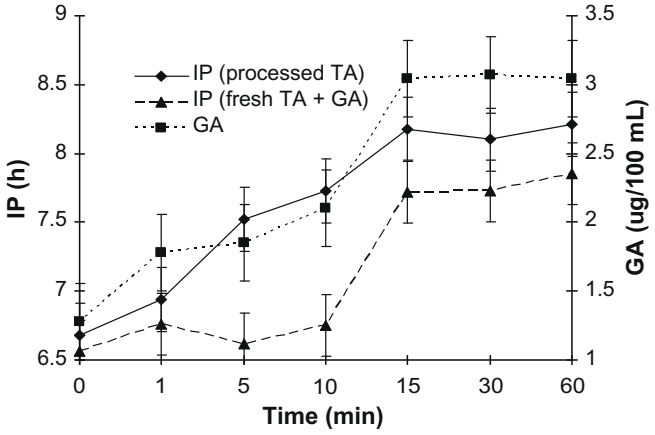

Fig. 4. Effects of processing time of tannic acid (TA) on induction point (IP, time) of soybean oil (solid diamond), their production of gallic acid (GA) (solid square), and the combination of GA and fresh TA on IP (solid triangle).

Table 1
Antimicrobial activity of fresh (FTA) and processed (PTA) tannic acid (30% w/v) on selected foodborne pathogens.

Strain	Inhibition zone diameter (mm)			
	Day 1		Day 2	
	FTA	PTA	FTA	PTA
LM 7694	10.7a*	14.5b	10.2a	14.5b
LM (ΔA, ΔB)	10.7a	14.2b	10.0a	14.5b
Salmonella Typhi 6539	10.3a	13.7b	10.0a	13.8b
Salmonella Typhimurium 19585	11.3a	14.2a	10.7a	14.2b
Salmonella Typhimurium 14028	12.8a	14.2b	12.2a	14.7b
E. sakazakii MSDH	13.2a	17.0b	12.2a	16.5b
E. sakazakii Fec39	11.0a	13.7a	9.0a	13.7b
E. coli 35150	11.0a	14.7b	10.7a	14.8b
E. coli 43890	11.5a	15.7b	10.6a	14.7b
E. coli 43895	10.8a	14.8b	10.5a	15.0b

* Means within day for each strain followed by a different letter are different ($p < 0.05$).

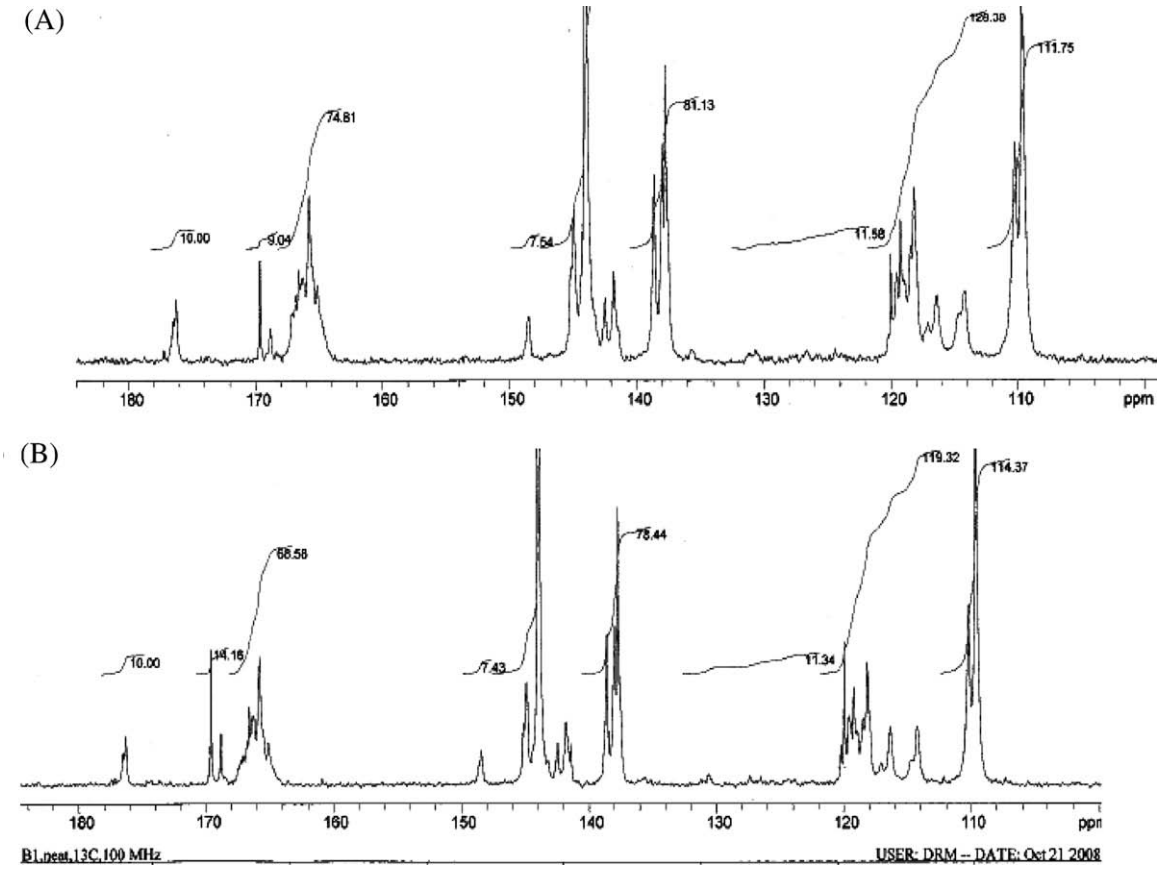

Fig. 5. ^{13}C NMR spectra of fresh (A) and processed tannic acids (B).

Table 2
^{13}C NMR spectral integration of fresh (FTA, 30%) and processed (PTA, 30%) tannic acids.

	Peak (ppm)	169–170	164–168	CO total	146–140	139–137	121–117.5	117.5–108	Ar C total	96–90	77–60	Aliph total
FTA	Integral (%)	9.04	68.6	82.7	157.5	78.4	73.0	160.7	469.6	8.6	80.9	89.5
		10.7	83.0	100.0	33.5	16.7	15.6	34.2	100.0	9.6	90.4	100
PTA	Integral (%)	14.2	74.8	83.9	162.4	81.1	81.2	158.2	482.9	11.2	90.3	101.5
		17.0	89.3	100.0	33.6	16.8	16.8	32.8	100.0	11.0	89.0	100.0
% Change		6.3	−6.3	0	−0.1	−0.1	−1.2	1.4	0.0	−1.4	1.4	0
Group ratio (theory)		1.1	9.3	10.4	20.2	10.1	10.1	19.7	60.0	0.7	5.3	6.0
		0	10.0	10.0	20.0	10.0	10.0	20.0	60.0	1.0	5.0	6.0

168 ppm; 2, 6 and 2′, 6′ aromatic carbons at 139–137 ppm; 1 and 1′ aromatic carbons at 146–140 ppm; 4 and 4′ aromatic carbons at 121–117.5 ppm; 3, 5 and 3′, 5′ aromatic carbons at 117.5–108 ppm; anomeric carbons of glucose at 96–90 ppm; and remaining glucose carbons at 77–60 ppm. The overall quantification of the integration values appears to be reasonable in that the carboxylic acid carbons (10.4 groups) are only slightly higher than the theoretical value of 10 based on the aromatic carbon value of 60 for untreated tannic acid. The aromatic carbons also showed small differences from theoretical values. These levels of variation are common in ^{13}C NMR quantitation analyses (Levy & Nelson, 1972). For glucose carbons, the ratio of the anomeric vs. other carbons is 0.7:5.3, in somewhat poor agreement with the theoretical ratio of 1:5. These differences could arise from the inherent nature of the ^{13}C NMR technique, but it is also possible that they might arise from the chemical structural changes, such as from oxidation or reduction reactions, involving the carbon groups.

4. Discussion

Tannic acid is present in many different plant species and foods including tea, cocoa beans, grapes, strawberry and persimmon and is considered as a 'generally recognised as safe' (GRAS) food substance and also as an officinal in Europe and North America (Akiyama et al., 2001; Shi, 1983). Since tannic acid showed strong antioxidant capacity to quench lipid peroxidation, prevent DNA oxidative damage, and scavenge hydroxyl radicals (·OH) (Andrade et al., 2005; Khan et al., 2000), the Rancimat® method was used to evaluate the antioxidant effects of fresh and processed tannic acid on soybean oil. While Reynhout (1991) previously reported no increased induction time (~6.5 h) of soybean oil fortified with butylated hydroxyanisole (BHA, 200 ppm), butylated hydroxytoluene (BHT, 200 ppm), tocopherol (400 ppm) or rosemary extract (400 ppm), our results showed that both soybean oils treated with PTA (8.0 h at 250 ppm) and FTA (7.8 h at 1000 ppm) had much

higher induction times than the control (5.9 h) (Fig. 3A and B). These findings are in agreement with the findings of Sanchez-Moreno, Larrauri, and Saura-Calixto (1999). They reported that tannic acid showed much stronger activity in the inhibition of lipid oxidation than BHA, quercetin, DL-α-tocopherol, and caffeic acid. As compared to FTA, PTA at the same concentration dramatically increased the induction time of soybean oil oxidation. Our results also showed that increasing thermal processing time of PTA up to 15 min increased oxidation stability of soybean oil. Heat treatment of plant materials such as *Hibiscus syriacus* had better antioxidant activity than the non-treated control. The increased antioxidant activity could be due to hydroxyl groups such as phenolic acids, flavonoids, and tocopherol formed by heat treatment (Kwon, Hong, Kim, & Ahn, 2003). Our results also showed that the addition of gallic acid and fresh tannic acid to soybean oil increased the induction point on oil oxidation, though they are not as effective as processed tannic acid, which implies that enhanced antioxidant capacity of processed tannic acid could be explained by hydrolysed gallic acid and the hydroxyl groups newly formed on the galloyl group as a result of thermal hydrolysis. Khan et al. (2000) reported that the antioxidant property appears to be related to the number of hydroxyls on the tannic acid while gallic acid and its structural analogues were found to be non-inhibitory or partially inhibitory on hydroxyl radical and singlet oxygen mediated cleavage of plasmid DNA. They also showed that the highest antioxidant efficiency is exhibited by flavonoids such as myricetin having there hydroxyl groups in the B ring.

Numerous studies have shown a broad antimicrobial activity of tannic acid on *H. pylori* (Funatogawa et al., 2004), *S. aureus* (Akiyama et al., 2001), enterotoxigenic *E. coli* (Taguri et al., 2004), *L. monocytogenes* Scott A and *Salmonella enteritidis* (Chung et al., 1993). The antimicrobial mechanism of tannic acid could be iron deprivation which may work like a siderophore to chelate essential iron from the medium and make its iron unavailable to the microorganisms (Chung et al., 1998). This activity appears to depend on the structure of the plant polyphenols, i.e., the presence of a galloyl group (3,4,5-trihydroxybenzoyl group) (Taguri et al., 2004). Puupponen-Pimiä et al. (2005) have reported that polyphenol compounds that contain three hydroxyl groups in the B ring such as flavonol myricetin have more active antimicrobial activity than other flavonols which have less hydroxyl groups in the B ring. When tannic acid, a mixture of polygalloyl glucopyranose is hydrolysed, the hydrolysis ends up forming one more gallic acid and other galloyl groups on gallotanins which could enhance tannic acid's antimicrobial activity. Since tannic acid is highly water-soluble and relatively rigid and spherical (Taguri et al., 2004), thermal processing could breakdown the ester bonds of a polygalloyls and enhance hydrolysis of tannic acid. Even though gallic acid is known to be a less effective antimicrobial than tannic acid, it is well known that both tannic and gallic acids also bind to and precipitate proteins and enzymes. This mechanism could be explained by hydrogen binding of polygalloyl glucopyranose and hydrophobic interactions by gallic acid with surface proteins on bacteria cells. Yang, Wei, Zhang, Chen, and Chen (2006) have shown that, in certain cancer tissues, tannic acid was bound to the ATP binding pockets of tyrosine kinases through unique hydrogen and hydrophobic interactions between the amino acids of tyrosine kinases and groups of tannic acid. Labieniec and Gabryelak (2006) proved that there is a direct interaction between tannic and gallic acids and DNA or bovine serum albumin (BSA) and this interaction causes the conformational changes in DNA and BSA. Kawamato, Mizutani, and Nakatsubo (1997) also showed that a sufficient number of galloyl groups are needed to form a strong binding between ligand and BSA in a polyphenol molecule. Even though gallic acid is not as effective as tannic acid (Akiyama et al., 2001; Labieniec & Gabryelak, 2006), an increased number of hydrolysed gallic acid and galloyl groups on PTA could enhance the antimicrobial activity by increasing their protein binding capacity (Kawamato et al., 1997). Sterilisation of utensils and equipment is usually conducted at 121 °C for 15 min. This process is sufficient to even kill any spores in these materials. This process is also sufficient to induce hydrolysis, including tannic acid. Thus, additional heating (time) does not provide any effect.

5. Conclusions

Thermal processed tannic acid showed stronger antioxidant capacity and antibacterial activity than fresh tannic acid. Addition of thermally processed tannic acid (up to 15 min) also increased oxidation stability of soybean oil. The thermal process enhanced the hydrolysis of tannic acid, producing one free gallic acid and a galloyl group on the remaining gallotanins, which are responsible for biological activity.

Acknowledgements

Approved for publication as Journal Article No. J-11602 of the Mississippi Agricultural and Forestry Experiment Station, Mississippi State University. This work was supported in part by the Mississippi Agricultural and Forestry Experiment Station Project Number MIS-371272 and by USDA-ARS Grant No. 58-0790-5-137.

References

Akiyama, H., Fujii, K., Yamasaki, O., Oono, T., & Iwatsuki, K. (2001). Antibacterial action of several tannins against *Staphylococcus aureus*. *Journal of Antimicrobial Chemotheraphy, 48*, 487–491.

Ali-Shtayeh, M. S., Yaghmour, R. M. R., Faidi, Y. R., Salem, K., & Al-Nuri, M. A. (1998). Antimicrobial activity of 20 plants used in folkloric medicine in the Palestinian area. *Journal of Ethnopharmacology, 60*, 265–271.

Andrade, R. G., Jr., Dalvi, L. T., Silva, J. M. C., Jr., Lopes, G. K. B., Alonso, A., & Hermes-Lima, M. (2005). The antioxidant effect of tannic acid on the in vitro copper-mediated formation of free radicals. *Archives of Biochemistry and Biophysics, 437*, 1–9.

Carson, R. S., & Frisch, A. W. (1953). The inactivation of influenzae viruses by tannic acid and related compounds. *Journal of Bacteriology, 66*, 572–575.

Chung, K. T., Stevens, S. E., Jr., Lin, W. F., & Wei, C. I. (1993). Growth inhibition of selected food-borne bacteria by tannic acid, propyl gallate and related compounds. *Letters in Applied Microbiology, 17*, 29–32.

Chung, K. T., Wong, T. Y., Wei, C. I., Huang, Y. W., & Lin, Y. (1998). Tannins and human health: A review. *Critical Reviews in Food Science and Nutrition, 38*, 421–464.

Chung, K. T., Zhao, G., Stevens, S. E., Jr., Simco, B. A., & Wei, C. I. (1995). Growth inhibition of selected aquatic bacteria by tannic acid and related compounds. *Journal of Aquatic Animal Health, 7*, 46–49.

Funatogawa, K., Hayashi, S., Shimomura, H., Yoshida, T., Hatano, T., Ito, H., et al. (2004). Antibacterial activity of hydrolyzable tannins derived form medicinal plants against *Helicobacter pylori*. *Microbiology and Immunology, 48*, 251–261.

Green, R. H. (1948). Inhibition of multiplication of influenza virus by tannic acid. *Proceedings of the Society for Experimental Biology and Medicine, 67*, 483–488.

Kaur, S., Grover, I. S., Singh, M., & Kaur, S. (1998). Antimutagenicity of hydrolyzable tannins from *Terminalia chebula* in *Salmonella* typhimurium. *Mutation Research: Genetic Toxicology and Environmental Mutagenesis, 419*, 169–179.

Kawamato, H., Mizutani, K., & Nakatsubo, F. (1997). Binding nature and denaturation of protein during interaction with galloylglucose. *Phytochemistry, 46*, 473–478.

Khan, N. S., Ahmad, A., & Hadi, S. M. (2000). Anti-oxidant, pro-oxidant properties of tannic acid and its binding to DNA. *Chemico-Biological Interaction, 125*, 177–189.

Kim, T. J., Silva, J. L., & Jung, Y. S. (2009). Antibacterial activity of fresh and processed red muscadine juice and the role of their polar compounds on *Escherichia coli* O157:H7. *Journal of Applied Microbiology*, doi:10.1111/j.1365-2672.2009.04239.x.

Kim, T. J., Silva, J. L., Weng, W. L., Chen, W. W., Corbitt, M., Jung, Y. S., et al. (2009). Inactivation of *Enterobacter sakazakii* by water-soluble muscadine seed extracts. *International Journal Food Microbiology, 129*, 295–299.

Kim, T. J., Weng, W. L., Stojanovic, J., Lu, Y., Jung, Y. S., & Silva, J. L. (2008). Antimicrobial effect of water-soluble muscadine seed extracts on *Escherichia coli* O157:H7. *Journal of Food Protection, 71*, 1465–1468.

Kwon, S. W., Hong, S. S., Kim, J. I., & Ahn, I. H. (2003). Antioxidant properties of heat-treated *Hibiscus syriacus*. *Biology Bulletin, 30*, 20–21.

Labieniec, M., & Gabryelak, T. (2006). Interactions of tannic acid and its derivatives (ellagic and gallic acid) with calf thymus DNA and bovine serum albumin using

spectroscopic method. *The Journal of Photochemistry and Photobiology B: Biology, 82*, 72–78.
Levy, G. C., & Nelson, G. L. (1972). *Carbon-13 NMR for organic chemist*. New York: Wiley-Interscience Publishing.
Mau, J. L., Chen, C. P., & Hsieh, P. C. (2001). Antimicrobial effect of extracts from Chinese chive, cinnamon, and corini fructus. *Journal of Agriculture and Food Chemistry, 49*, 183–188.
Mizumo, T., Uchino, K., Toukairin, T., Tanabe, A., Nakashima, H., Yamamoto, N., et al. (1992). Inhibitory effect of tannic acid sulfate and related sulfates on infectivity, cytopathic effect, and giant cell formation of human immunodeficiency virus. *Planta Medica, 58*, 535–539.
O'Bryan, C. A., Crandall, P. G., Chalova, V. I., & Ricke, S. C. (2008). Orange essential oils antimicrobial activities against *Salmonella* spp. *Journal of Food Science, 73*, M267–267.
Okuda, T. Y., & Hatano, T. (1995). Hydrolyzable tannins and related polyphenols. *Fortschritte der Chemie Organischer Naturstoffe, 66*, 1–117.
Puupponen-Pimiä, R., Nohynek, L., Alakomi, H. L., & Oksman-Caldentey, K. M. (2005). Bioactive berry compounds-novel tools against human pathogens. *Applied Microbiology and Biotechnology, 67*, 8–18.
Reynhout, G. (1991). The effect of temperature on the induction time of a stabilized oil. *Journal of the American Oil Chemists' Society, 68*, 983–984.
Rodríguez, H., Rivas, B., Gómez-Cordovés, C., & Muñoz, R. (2008). Degradation of tannic acid by cell-free extracts of *Lactobacillus plantarum*. *Food Chemistry, 107*, 664–670.
Sanchez-Moreno, C., Larrauri, A. J., & Saura-Calixto, F. (1999). Free radical scavenging capacity and inhibition of lipid oxidation of wines, grape juices and related polyphenolic constituents – History, production and role in disease prevention. *Food Research International, 32*, 407–412.
SAS Institute (2001). *SAS companion of the Microsoft windows environment (version 8.1)*. Cary, NC: SAS Institute, Inc..
Shi, T. S. (1983). Use of combined traditional Chinese and western medicine in the management of burns. *Panminerva Medica, 25*, 197–202.
Stothers, J. B. (1972). *Carbon-13 NMR spectroscopy*. New York: Academic Press Publishing.
Taguri, T., Tanaka, T., & Kouno, I. (2004). Antimicrobial activity of 10 different plant polyphenols against bacteria causing food-borne disease. *Biological and Pharmaceutical Bulletin, 27*, 1965–1969.
Yang, E. B., Wei, L., Zhang, K., Chen, Y. Z., & Chen, W. N. (2006). Tannic acid, a potent inhibitor of epidermal growth factor receptor tyrosine kinase. *Journal of Biochemistry, 139*, 495–502.
Zhao, G., Chung, K. T., Milow, K., Wang, W., & Stevens, S. E. Jr., (1997). Antibacterial properties of tannic acid and related compounds against the fish pathogen *Cytophaga columnaris*. *Journal of Aquatic Animal Health, 9*, 309–313.
Zogaj, X., Bokranz, W., Nimtz, M., & Römling, U. (2003). Production of cellulose and curli fimbriae by members of the family *Enterobacteriaceae* isolated form the human gastrointestinal tract. *Infection and Immunology, 71*, 4151–4158.

treated with 0.1% polyethyleneimine to precipitate nucleotides. The resulting pellet was discarded and supernatant brought to 65% saturation with ammonium sulphate. The pellet was dissolved in 20 mM Tris buffer, pH 7.4 (NH_4SO_4 extract). The NH_4SO_4 extract (21 mg) was loaded onto a Sephadex G-75 column (14 × 73 cm), pre-equilibrated and eluted with 20 mM Tris buffer, pH 7.4, at a flow rate of 1.5 ml/5 min. Protein elution was monitored at 280 nm using a spectrophotometer. The antibacterial activities of eluted samples were tested by agar diffusion method on nutrient agar. Active peak II (8 mg), pooled and lyophilised was further fractionated on a Sephadex G-75 column by eluting with 20 mM Tris buffer, pH 7.4, to give a homogenous preparation, APC, which showed antibacterial activity.

2.2. Antibacterial activity of APC

Antibacterial activity was evaluated by the well diffusion method on nutrient agar medium (Forbes, Sahm, Weissfeld, & Trevino, 1990). This was confirmed by the inhibitory effect on bacterial growth as reflected by the inhibition zone, compared to that of known antibiotics. The sterile nutrient agar medium (20 ml) in Petri dishes was uniformly smeared using sterile cotton swabs with test pure cultures of human pathogenic bacteria *S. aureus, B. subtilis, E. coli, S. typhi, V. cholerae, K. pneumoniae* and *S. paratyphi.* The nutrient agar media was prepared by dissolving 0.3% beef extract, 0.3% yeast extract, 0.5% peptone, 0.5% NaCl and 1.5% agar in 1 l of distilled water. The wells of 5 mm diameter were made using a sterile cork borer in each petri dish and the buffer extract (0–100 μg), NH_4SO_4 extract (0–74 μg), G-75 eluted samples (0–50 μg) and isolated APC (0–24 μg) were added; a blank well loaded without test compound was regarded as control. For each treatment 10 replicates were prepared. The plates were incubated at 37 °C for 24 h and the resulting zone of inhibition was measured by comparing control and the standard antibiotic.

2.3. Determination of minimum inhibitory concentration (MIC)

The minimum inhibitory concentration of isolated APC were determined by serial dilution in the nutrient agar, with concentrations ranging from 5, 10, 20, 25, 50, 75 and 100 μg/ml. The inoculum was prepared from fresh overnight broth culture in nutrient broth. Plates were incubated for 24 h at 37 °C. *MIC* was recorded as the lowest extract concentration demonstrating no visible growth in the broth (Prescot, Harley, & Klein, 1996).

2.4. Estimation of protein

The protein estimation was determined by Bradford's method (Bradford, 1976) using bovine serum albumin as standard.

2.5. Assay for ribonuclease activity

The ribonuclease activity of APC was estimated according to the method of Lam and Ng (2001), by measuring the production of acid-soluble, UV-absorbing species. Briefly, yeast tRNA (200 μg) was incubated with the APC (0–100 μg) in 150 μl 100 mM MES buffer (pH 6.0) at 37 °C for 15 min. The reaction was terminated by adding 350 μl of ice-cold 3.4% (v/v) perchloric acid. After standing on ice for 15 min, the mixture was centrifuged at 15,000*g* for 15 min at 4 °C. The absorbance of the supernatant, after suitable dilution, was measured at 260 nm. One unit of ribonuclease activity is defined as the amount of ribonuclease that produces an absorbance increase at 260 nm of 1 min^{-1} in the acid-soluble fraction per ml of reaction mixture under the specified conditions.

2.6. Assay for deoxyribonuclease activity

The deoxyribonuclease activity of APC was estimated according to the method of Wang and Ng (2001). Briefly, sperm DNA (1 mg) in 0.2 ml of ammonium acetate buffer (0.1 M), pH 5.5, and 100 μl of APC (0–100 μg) were incubated at 25 °C for 15 min. The reaction was terminated by adding 0.3 ml of ice-cold 20 mM lanthanum nitrate in 1.2% (v/v) perchloric acid, and incubated for 20 min at room temperature. Then, samples were centrifuged at 3000*g* for 5 min at 0 °C. The supernatant was diluted three-fold with water and the optical density was read at 260 nm against a blank without APC. One unit of enzymatic activity is defined as the amount of enzyme required to increase the absorbance at 260 nm of 0.001 min^{-1} ml^{-1} at pH 5.5 and 37 °C using sperm DNA.

2.7. Assay of protease activity

Proteolytic activity was assayed according to the method of Murata, Satake, and Suzuki (1963), using 2% fat-free casein in Tris–HCl buffer pH 8.5 as substrate. APC sample (0–100 μg) was incubated with casein substrate (0.5 ml) for 120 min at 37 °C. Adding 1 ml of 0.44 M trichloroacetic acid terminated the reaction. After standing for 30 min the mixture was then centrifuged. Sodium carbonate (5 ml, 0.4 M) and Folin–Ciocalteu's reagent (0.5 ml diluted to 1/3 of its original strength) were added to 1 ml of supernatant and the absorbance read at 660 nm. One unit of enzyme activity is defined as the amount of enzyme required to cause an increase per min in OD of 0.01 at 660 nm. Enzyme activity is expressed in terms of specific activity.

2.8. Haemolytic activity assay

Haemolytic (direct/indirect) activity of APC was determined according to the method of Boman and Kaletta (1957), using packed human erythrocytes (blood group A). The direct and indirect haemolytic assays were carried out using washed erythrocytes. For the direct haemolytic assay, packed erythrocytes (1 ml) were suspended in nine volumes of phosphate-buffered saline (PBS), which formed the stock. The stock (1 ml) was incubated with various concentrations of APC (0–250 μg) for 30 min at 37 °C. For the indirect haemolytic assay, stock was prepared by mixing packed erythrocytes (1 ml), egg yolk (1 ml) and phosphate-buffered saline (8 ml). One millilitre of suspension from stock was incubated with various concentrations of APC (0–250 μg) for 30 min at 37 °C. The reaction was terminated by adding 10 ml of ice-cold PBS and then centrifuged at 4 °C and 800*g*. The amount of haemoglobin released in the supernatant was measured at 540 nm. One millilitre of stock erythrocytes with 10 ml ice-cold PBS alone was considered as 0% lysis.

Table 1
Total protein yield and antibacterial activities of fractions from different chromatographic steps of isolation procedure.

Chromatographic fraction	Yield (%)	Antibacterial activity
1. Buffer extract	100	+
2. 65% $(NH_4)_2SO_4$ Precipitation	53 ± 4	+
3. Gel filtration on Sephadex G-75		
Peak I	25 ± 3	–
Peak II	22 ± 2	+
Peak III	14 ± 2	–
4. Rechromatography on Sephadex G-75		
APC	17 ± 2	+

The symbols + and – denote the presence and absence of antibacterial activity, respectively.

2.9. Cytotoxicity assay

Cytotoxicity was determined according to the method of Chwetzoff, Tsunasawa, Sakiyama, and Ménez (1989). EAT cells were suspended in Tyrode's solution (5×10^6 cells/2 ml) and incubated with APC (0–250 μg) for 30 min. Trypan blue saline (1%, 100 μl) solution was then added, and unstained (viable) cells were counted using a haemocytometer. The percentage of viable cells was determined by comparing with the number of viable cells in the control (designated as 100%).

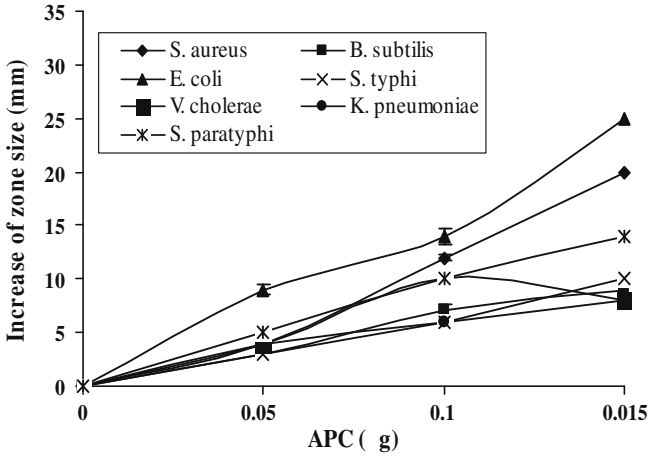

Fig. 1. Dose-dependent antibacterial activity of APC against different human pathogenic strains in agar diffusion assays. The diameter of the clear zone was measured and plotted after subtracting the diameter of the well (5 mm). Results are mean ± SD for three independent assays each performed in triplicate.

Table 2
Antibacterial activity of APC from curry leaves and antibiotics[a,b].

Microorganisms	Diameter of inhibition zone (mm)			
	APC	G	Cp	Sm
Staphylococcus aureus	25 ± 3	18 ± 1	21 ± 2	26 ± 3
Bacillus subtilis	14 ± 1	18 ± 2	17 ± 3	30 ± 2
Escherichia coli	30 ± 3	18 ± 1	17 ± 1	26 ± 3
Salmonella typhi	15 ± 1	16 ± 1	18 ± 1	24 ± 1
Vibrio cholerae	13 ± 1	16 ± 2	18 ± 1	23 ± 3
Klebsiella pneumoniae	13 ± 2	16 ± 2	18 ± 2	21 ± 1
Salmonella paratyphi	19 ± 3	18 ± 2	18 ± 2	20 ± 2

[a] The results are mean ± SD ($n = 6$).
[b] G, gentamycin; Cp, chloramphenicol; Sm, streptomycin.

Table 3
Minimum inhibitory concentrations (*MIC*) of APC and antibiotics[a,b] in serial dilution method.

Microorganisms	*MIC* (μg/ml)			
	APC	G	Cp	Sm
Staphylococcus aureus	24.5 ± 3	20.8 ± 0.7	14.4 ± 0.3	13.6 ± 0.4
Bacillus subtilis	25.2 ± 3	20.8 ± 0.4	14.4 ± 0.5	16.8 ± 0.3
Escherichia coli	14.7 ± 1	24.2v0.1	14.4 ± 0.3	16.3 ± 0.7
Salmonella typhi	15.2 ± 1	19.2 ± 0.4	12.8 ± 0.7	14.4 ± 0.5
Vibrio cholerae	13.6 ± 1	18.4 ± 0.3	12.8 ± 0.5	14.4 ± 0.3
Klebsiella pneumoniae	13.3 ± 2	16.8 ± 0.1	12.8 ± 0.6	14.4 ± 0.4
Salmonella paratyphi	19.2 ± 3	16.2 ± 0.2	12.4 ± 0.4	11.2 ± 0.4

[a] Values are expressed as mean ± SD ($n = 10$).
[b] G, gentamycin; Cp, chloramphenicol; Sm, streptomycin.

2.10. Statistical analysis

Statistical analysis was done using SPSS (Windows version 10.0.1; SPSS Inc., Chicago, IL) using a one-way student's *t*-test; $p < 0.05$ was considered as statistically significant, when comparing with relevant controls. All results refer to mean ± SD.

3. Results and discussion

Murraya koenigii is a common plant with medicinal properties. In our study, when the aqueous extract of *M. koenigii* was tested for antibacterial activity against human pathogenic bacteria, it showed inhibition of bacterial growth. This initial observation prompted us to systematically evaluate the active principle.

The Tris buffer extract (39 mg) of curry leaves upon 65% ammonium sulphate saturation yielded 21 mg of protein with antibacterial activity. The ammonium sulphate extract was fractionated with Sephadex G-75 column chromatography, into three peaks (Peaks I, II and III), amongst which peak II showed antibacterial activity. Peak II upon rechromatography on Sephadex G-75 column resulted in homogenous preparation with antibacterial activity referred to as antioxidant protein from curry leaves (APC) (Table 1). The preparation was homogeneous with a single peak with molecular mass of ~35 kDa according to mass spectrometry (Ningappa & Srinivas, 2008). Antimicrobial protein WSG isolated from *W. sominifera* has a molecular mass of ~28 kDa (Girish et al., 2006). An antimicrobial protein of about 10 kDa, called Ace-AMP1, was isolated from onion (*A. cepa* L.) seeds (Cammue et al., 1995). Recently, hevein, a small (4.7 kDa) cysteine-rich protein with antibacterial activity was isolated from latex of *H. brasiliensis* (Kanokwiroon et al., 2008). The observed molecular mass of ~35 kDa is well within the range of antibacterial proteins reported.

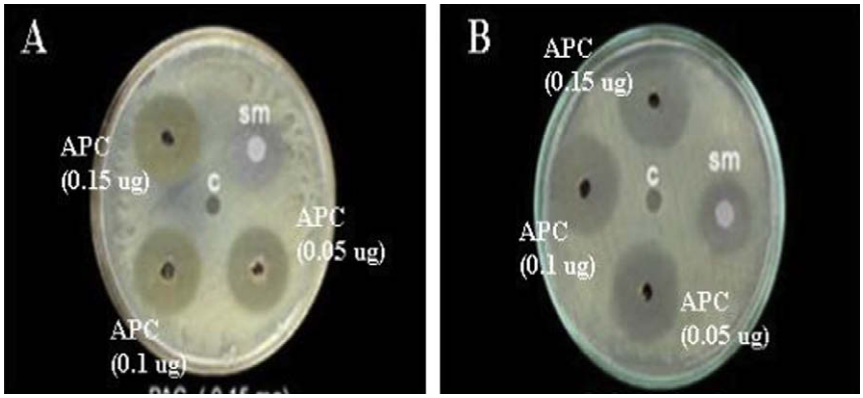

Fig. 2. Agar diffusion assay. Effect of APC on growth of (A) *Escherichia coli* and (B) *Staphylococcus aureus*. Sm, 20 μg streptomycin (positive control); C, 10 mM Tris–HCl buffer (negative control).

The dose-dependent antibacterial activity of APC against human pathogenic bacteria is shown in Fig. 1. APC showed a broad spectrum of very significant antibacterial activity by producing a clear zone of inhibition (20–25 mm) against *E. coli* and *S. aureus* (Table 2). *V. cholerae*, *K. pneumoniae, S. typhi and B. subtilis* were found to be moderately sensitive to APC, which showed an inhibition zone of 12–16 mm of (Table 2). It was interesting to observe that inhibition was comparable to that of the standards; chloramphenicol, streptomycin and gentamycin. Fig. 2 shows inhibition of *E. coli* and *S. aureus* growth by APC at 0.15 μg as studied by agar diffusion method. These results are well comparable with the antibacterial proteins listed earlier.

When APC was tested, using the agar dilution assay for determining minimum inhibitory concentration (*MIC*), it was observed that it inhibited bacterial growth, with *MIC* values ranging from 13 to 24 μg/ml APC. APC showed comparable *MIC* values with standard antibiotics, which ranged from 11.2 to 20 μg/ml (Table 3). Thus APC is as potent as standard antibiotics in inhibiting the growth of bacterial strains.

It is known that some ribonucleases/deoxyribonucleases/proteases exhibit antibacterial activity (Girish et al., 2006; Lam & Ng, 2001; Ng, 2004a; Wang & Ng, 2001). In order to know which class APC belongs to, it was screened for different enzyme activities. The results indicated that APC was devoid of ribonuclease, deoxyribonuclease and protease activity when tested at 50 and 100 μg amounts. This observation ruled out the possibility that APC is a ribonuclease, deoxyribonuclease or protease.

In our study we also investigated the toxicity of APC using EAT cells. It was interesting to observe that there was no decrease in the number of viable cells when APC was added. Further, no haemolysis occurred, either directly or indirectly, when APC was added to human erythrocytes up to 0.25 mg. These results clearly indicate that APC is a non-toxic protein having antibacterial activity. Similarly, antimicrobial protein WSG isolated from *W. sominifera,* is also reported to be non-toxic (Girish et al., 2006). Further studies on the mechanism of action by which APC exhibits antibacterial activity are in progress.

In conclusion, the ~35 kDa APC isolated from *M. koenigii* exhibited a broad spectrum of antibacterial activity against human pathogenic bacteria, comparable to commercial antibiotics. As it is non-toxic, it appears to be a promising candidate for development of an effective antioxidant antibiotic.

Acknowledgements

The authors acknowledge the Adichunchanagiri Mahasamstana Mutt and Shikshana Trust for providing facilities in the Adichunchanagiri Biotechnology and Cancer Research Institute (ABCRI) and Adichunchanagiri Institute of Technology (AIT) for providing continuous Internet facilities for carrying out this work. We acknowledge microbiology department, Adichunchanagiri Institute of Medical Sciences (AIMS), B.G. Nagara, Karnataka, India for providing bacterial strains.

References

Boman, H. G., & Kaletta, U. (1957). Chromatography of rattlesnake: A separation of three phosphodiesterases. *Biochimica et Biophysica Acta, 24*, 619–623.

Bradford, M. M. (1976). A rapid and sensitive method for the quantification of microgram quantities of protein utilizing the principle of protein dye binding. *Analytical Biochemistry, 7*, 248–254.

Broekaert, W. F., Terras, F. R., Cammue, B. P., & Osborn, R. W. (1995). Plant defensins: Novel antimicrobial peptides as components of the host defense system. *Plant Physiology, 108*, 1353–1358.

Cammue, B. P., Thevissen, K., Hendriks, M., Eggermont, K., Goderis, I. J., Proost, P., et al. (1995). A potent antimicrobial protein from onion seeds showing sequence homology to plant lipid transfer proteins. *Plant and Cell Physiology, 109*, 445–455.

Chwetzoff, S., Tsunasawa, S., Sakiyama, F., & Ménez, A. (1989). Nigexine, a phospholipase A_2 from cobra venom with cytotoxic properties not related to esterase activity. Purification, amino acid sequence and biological properties. *The Journal of Biological Chemistry, 264*, 13289–13297.

Forbes, B. A., Sahm, D. F., Weissfeld, A. S., & Trevino, E. A. (1990). Methods for testing antimicrobial effectiveness. In E. J. Baron, L. R. Petrson, & S. M. Finegold (Eds.), *Bailey and Scott's diagnostics microbiology* (pp. 171–194). St. Louis, Missouri: Mosby Co.

Girish, K. S., Machiah, K. D., Ushanandini, S., Harish Kumar, K., Nagaraju, S., Govindappa, M., et al. (2006). Antimicrobial properties of a non-toxic glycoprotein (WSG) from *Withania somnifera* (Ashwagandha). *Journal of Basic Microbiology, 46*, 365–374.

Kanokwiroon, K., Teanpaisan, R., Wititsuwannakul, D., Hooper, A. B., & Wititsuwannakul, R. (2008). Antimicrobial activity of a protein purified from the latex of *Hevea brasiliensis* on oral microorganisms. *Mycoses, 51*, 301–307.

Khanum, F., Anilakumar, K. R., Sudarshana Krishna, K. R., Viswanathan, K. R., & Santhanam, K. (2000). Anticarcinogenic effects of curry leaves in dimethylhydrazine-treated rats. *Plant Foods for Human Nutrition, 55*, 347–355.

Kiba, A., Saitoh, H., Nishihara, M., Omiya, K., & Yamamura, S. (2003). C-terminal domain of a hevein-like protein from *Wasabia japonica* has potent antimicrobial activity. *Plant and Cell Physiology, 44*, 296–303.

Lam, S. K., & Ng, T. B. (2001). Isolation of a novel thermolabile heterodimeric ribonuclease with antifungal and antiproliferative activities from roots of the sanchi ginseng *Panax notoginseng*. *Biochemical and Biophysical Research Communications, 285*, 419–423.

Murata, J., Satake, M., & Suzuki, T. (1963). Studies on snake venom. XII. Distribution of proteinase activities among Japanese and Formosan snake venoms. *Journal of Biochemistry, 53*, 431–443.

Ng, T. B. (2004a). Proteins and peptides from fungi. *Peptides, 25*, 1055–1073.

Ng, T. B. (2004b). Antifungal proteins and peptides of leguminous and non-leguminous origins. *Peptides, 25*, 1215–1222.

Ningappa, M. B., Dinesha, R., & Srinivas, L. (2008). Antioxidant and free radical scavenging activities of polyphenol-enriched curry leaf (*Murraya koenigii* L.) extracts. *Food Chemistry, 106*, 720–728.

Ningappa, M. B., & Srinivas, L. (2008). Purification and characterization of approximately 35 kDa antioxidant protein from curry leaves (*Murraya koenigii* L.). *Toxicology in Vitro, 22*, 699–709.

Prescot, L. M., Harley, J. P., & Klein, D. A. (1996). *Introduction to microbiology* (5th ed.). The Benjamin Cummins Publishing Co. Inc (pp. 681–684).

Ramsewak, R. S., Nair, M. G., Strasburg, G. M., De Witt, D. L., & Nitiss, J. L. (1999). Biologically active carbazole alkaloids from *Murraya koenigii*. *Journal of Agricultural and Food Chemistry, 47*, 444–447.

Selitrennikoff, C. L. (2001). Antifungal proteins. *Applied and Environmental Microbiology, 67*, 2883–2894.

Terras, F. R., Schoofs, H. M., De Bolle, M. F., Van Leuven, F., Rees, S. B., Vanderleyden, J., et al. (1992). Analysis of two novel classes of plant antifungal proteins from radish (*Raphanus sativus*) seeds. *Journal of Biological Chemistry, 267*, 15301–15309.

Wang, H. X., & Ng, T. B. (2001). Isolation of a novel deoxyribonuclease with antifungal activity from *Asparagus officinalis* seeds. *Biochemical and Biophysical Research Communications, 289*, 120–124.

Yadav, S., Vats, V., Dhunnoo, Y., & Grover, J. K. (2002). Hypoglycemic and antihyperglycemic activity of *Murraya koenigii* leaves in diabetic rats. *Journal of Ethnopharmacology, 82*, 111–116.

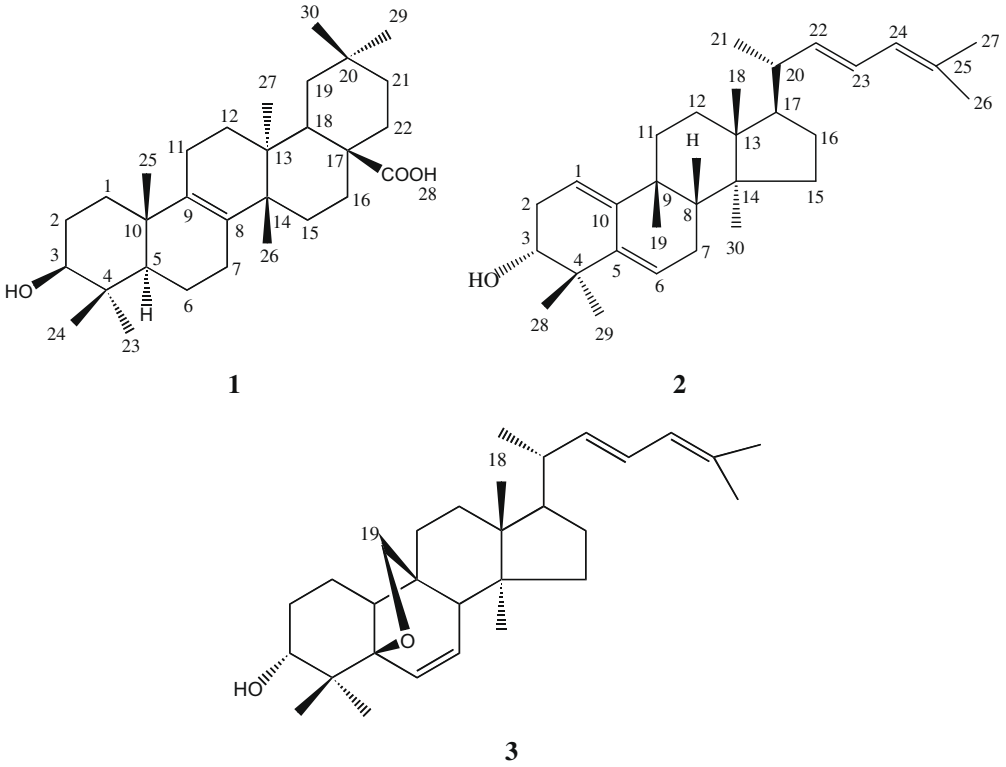

Fig. 1. Structures of triterpenoids.

2. Materials and methods

Instruments: Optical rotations were recorded with a JASCO-370 polarimeter, UV spectra on a Jasco UV–vis spectrophotometer, IR spectra on a Hitachi 260–30 spectrometer, ^{1}H (400 MHz) and ^{13}C NMR (100 MHz) spectra and ^{1}H–^{1}H COSY, NOESY, HMQC and HMBC experiments on a Varian Unity-400 NMR spectrometer and MS on a JMS-HX-100 mass spectrometer. Silica gel (Merck), particle size 15–40 μm, was used for column chromatography. Silica gel 60 F254 precoated aluminium sheets (0.2 mm, Merck) were employed for TLC. All solvents were HPLC grade. Xanthine, xanthine oxidase, and allopurinol were purchased from Sigma Chemicals.

2.1. Plant material

The stems of *M. charantia* (460 g) were collected at Hualien Hsien, Taiwan, March, 2006 and a voucher specimen (2006-1) has been deposited in the Department of Medicinal Chemistry, Kaohsiung Medical University.

2.2. Extraction and Isolation

The air-dried stems of *M. charantia* (460 g) were extracted with MeOH (Akihisa et al., 2007). The MeOH extract was concentrated under reduced pressure to give a dark brown residue (140 g), which was suspended in H_2O and then partitioned between H_2O and $CHCl_3$, H_2O and EtOAc and H_2O and *n*-BuOH, respectively. The $CHCl_3$ extract (40 g) was chromatographied on silica gel (1000 g), eluted successively with solvents of increasing polarity (*n*-hexane–EtOAc, 4:1 (3.0 l), 3:2 (2.5 l), 2:3 (2.0 l), 1:4 (2.0 l); EtOAc–MeOH, 9:1 (3.0 l), 6:1 (2.5 l), 3:1 (2.0 l), 2:1 (5.0 l), afforded 28 fractions. Fraction 12 was subjected to repeated chromatography on silica gel and eluated with CH_2Cl_2–EtOAc (1:2) to give **1** (25 mg). Fraction 6 was subjected to repeated chromatography on silica gel and eluted with *n*-hexane–CH_2Cl_2 (1:1) to give **2** (16 mg) and **3** (14 mg), respectively.

2.3. Spectral measurements

3β-Hydroxymultiflora-8-en-17-oic acid (**1**): white powder; $[\alpha]_D^{25}$ 70 (*c* 0.05, MeOH); IR ν_{max} (KBr): 3446, 1680 cm^{-1}; ^{1}H NMR and ^{13}C NMR see Table 1; ESIMS: 479 ([M+Na]$^+$), 381; HRESIMS: 479.3504 [M+Na]$^+$, $C_{30}H_{48}O_3Na$; calc. 479.3501.

Cucurbita-1(10),5,22,24-tetraen-3α-ol (**2**): yellow oil; $[\alpha]_D^{25}$ 82 (*c* 0.1, $CHCl_3$); UV (MeOH) λ_{max} (log ε): 240 (4.01) nm; IR ν_{max} (KBr): 3433, 1684 cm^{-1}; ^{1}H NMR and ^{13}C NMR see Table 1; ESIMS: 445 [M+Na]$^+$; HRESIMS: 445.3449 [M+Na]$^+$, $C_{30}H_{46}ONa$; calc. 445.3446.

5β,19β-Epoxycucurbita-6,22,24-trien-3α-ol (**3**): yellow oil; $[\alpha]_D^{25}$ −3 (*c* 0.1, $CHCl_3$); UV (MeOH) λ_{max} (log ε): 240 (4.02) nm; IR ν_{max} (KBr): 3469, 1685 cm^{-1}; ^{1}H NMR and ^{13}C NMR see Table 1; EIMS: (probe) 70 eV, *m/z* (rel. int.): 438 [M]$^+$ (19), 390 [M–H_2O–CH_2O]$^+$ (4), 281 (390-side chain) (100), 109 (81); HREIMS: 438.3498 [M]$^+$, $C_{30}H_{46}O_2$; calc. 438.3497.

2.4. Free radical scavenging activity

Radical scavenging activity of **1**–**3** and tocopherol (TOC) was determined using 1,1-diphenyl-2-picrylhydrazyl (DPPH) as a reagent (Kabouche, Kabouche, Öztürk, Kolak, & Topcu, 2007) with modification by using 96-well plates. A 0.1 mM solution of DPPH radical in MeOH was prepared and then 150 μl of this solution was mixed with 50 μl of sample solution. The mixture were incubated for 30 min in a dark room at room temperature. Scavenging capacity was read spectrophotometrically by monitoring the decrease in absorbance at 490 nm using a MRX Microplate Reader (Dynex MRX II, Dynex Technologies, 14340 Sullyfield Circle, Chantility VA 20151-1683, USA). TOC was used as standard. The percentage DPPH scavenging effect was calculated using the following equation:

Table 1
^{1}H and ^{13}C NMR spectroscopic data (δ in ppm, J in Hz) of **1** and **2** (in $CDCl_3$) and **3** (in pyridine-d_5).

	1		**2**		**3**	
	δ_H	δ_C	δ_H	δ_C	δ_H	δ_C
1	1.02 (bs), 2.49 (td, J = 13.6, 4.0)	35.1	5.49 (bs)	133.3	1.43 (m)	17.6
2	1.84 (m), 2.11 (dd, J = 17.6, 5.6)	28.0	2.06 (m), 2.48 (m)	32.1	1.76 (m)	27.3
3	3.39 (t, J = 7.6)	78.0	3.46 (dd, J = 8.4, 5.6)	73.8	3.40 (bd, J = 8.8)	76.1
4		39.4		39.5		45.5
5	1.11 (d, J = 9.6)	50.9		140.3		87.5
6	1.42 (m), 1.73 (m)	19.6	5.60 (bs)	120.8	6.03 (dd, J = 10.0, 2.0)	131.7
7	1.60 (m)	35.5	1.96 (m), 2.42 (m)	24.9	5.62 (dd, J = 10.0, 4.0)	131.5
8		134.1	1.52 (m)	50.5	2.29 (dd, J = 11.2, 6.8)	38.8
9		134.6		37.1		48.6
10		40.6		139.8	2.34 (t, J = 2.8)	52.0
11	1.92 (m)	21.1	1.64 (m), 1.94 (m)	31.1	1.43 (m), 1.73 (m)	23.6
12	1.88 (m)	28.7	1.10 (m), 1.15 (m)	34.0	1.58 (m), 1.65 (m)	30.8
13		37.7		47.1		37.2
14		42.1		49.9		45.3
15	1.38 (m), 1.60 (m)	25.4	1.42 (m)	30.4	1.26 (m)	33.2
16	1.36 (m), 1.45 (td, J = 14.0, 4.4)	30.5	1.22 (m), 1.68 (m)	28.2	1.34 (m), 1.76 (m)	28.3
17		37.8	1.84 (m)	42.6	1.50 (m)	50.2
18	1.60 (m)	45.1	0.72 (s)	16.6	0.89 (s)	15.1
19	1.38 (m), 1.74 (m)	37.5	0.97 (s)	32.2	3.51 (d, J = 8.4), 3.66 (d, J = 8.4)	79.8
20		31.3	2.12 (m)	40.5	2.14 (m)	40.3
21	1.88 (m), 2.60 (d, J = 13.6)	30.7	0.74 (s)	16.6	1.01 (d, J = 6.4)	20.5
22	1.74 (m), 2.76 (d, J = 15.6)	31.1	5.37 (dd, J = 14.8, 8.8)	138.9	5.40 (dd, J = 15.2, 8.8)	138.4
23	1.22 (s)	28.6	6.12 (dd, J = 14.8, 10.4)	123.9	6.15 (dd, J = 15.2, 10.4)	124.2
24	1.06 (s)	22.4	5.73 (d, J = 10.4)	125.2	5.74 (d, 10.4)	125.1
25	1.00 (s)	20.1		132.2		132.9
26	1.09 (s)	31.4	1.73 (s)	18.2	1.73 (s)	18.2
27	1.05 (s)	16.5	1.74 (s)	25.9	1.74 (s)	26.0
28		181.3	1.90 (s)	23.9	0.86 (s)	20.0
29	1.29 (s)	18.0	0.90 (s)	20.3	1.19 (s)	20.5
30	1.43 (s)	33.3	0.89 (s)	15.8	0.89 (s)	24.5

$$\text{DPPH scavenging effect } (\%) = [1 - (S - SB)/(C - CB)] \times 100\%$$

where S, SB, C and CB are the absorbencies of the sample, the blank sample, the control and the blank control, respectively (Kabouche et al., 2007).

2.5. Determination of ABTS radical cation scavenging capacity

The radical scavenging activity of the isolated compounds was carried out using an improved ABTS decolourisation assay with some modification (Han, Weng, & Bi, 2008). The ABTS radical cation ($ABTS^{\cdot+}$) was produced by reacting 7 mM stock solution of ABTS with 2.45 mM potassium persulfate (final concentration) and allowing the mixture to stand in the dark at room temperature for 12–16 h before use. The $ABTS^{\cdot+}$ solution was diluted with ethanol, to an absorbance of 0.7 ± 0.02 at 630 nm. An ethanolic solution (30 μl) of the samples at various concentrations was mixed with 170 μl diluted $ABTS^{\cdot+}$ solution. After reaction at room temperature for 20 min, the absorbance at 630 nm was measured. A lower absorbance of the reaction mixture indicates higher $ABTS^{\cdot+}$ scavenging activity. The capability to scavenge the $ABTS^{\cdot+}$ was calculated using the formula given below:

$$ABTS^{\cdot+}\text{scavenging activity } (\%) = [1 - (S - SB)/(C - CB)] \times 100\%$$

where S, SB, C and CB are the absorbencies of the sample, the blank sample, the control, and the blank control, respectively.

2.6. Assay of xanthine oxidase

The xanthine oxidase activity with xanthine as the substrate was measured at 25 °C, according to the protocol of Kong and others (Kong, Zhang, Pan, Tan, & Cheng, 2000) with modification. The assay mixture consisting of 50 μl of test solution, 60 μl of 70 mM phosphate buffer (pH 7.5) and 30 μl of enzyme solution [0.1 units/ml in 70 mM phosphate buffer (pH 7.5)] was prepared immediately before use. After preincubation at 25 °C for 15 min, the reaction was initiated by the addition of 60 μl of substrate solution (150 μM xanthine in the same buffer). The reaction was monitored for 5 min at 295 nm. The xanthine oxidase activity was expressed as micromoles of uric acid per minute.

2.7. Statistical analysis

Data were expressed as the mean ± SD. Statistical analysis were performed using the Bonferroni t-test method after ANOVA for multigroup comparison and the student's t-test method for two group comparison. $p < 0.05$ was considered to be statistically significant. Analysis of linear regression (at least three data within 20–80% inhibition) was used to calculated IC_{50} values.

3. Results and discussion

Compound **1** was obtained as a white powder, $[\alpha]_D^{25}$ 70 (c = 0.05, MeOH). Its IR spectrum showed absorption bands for hydroxyl (3446 cm^{-1}) and carboxylic acid (1680 cm^{-1}). The molecular formula of **1** was determined to be $C_{30}H_{48}O_3$ on the basis of its HRESIMS ($[M+Na]^+$, 479.3504, Δ−0.0003 mmu), which was consistent with its ^{1}H and ^{13}C NMR data. The ^{1}H and ^{13}C NMR spectra of **1** (Table 1) revealed the presence of 7 methyls, 11 methylenes, 3 methines including one oxymethine and 9 quaternary carbons including a carboxylic quaternary carbon. Analysis of ^{1}H–^{1}H COSY and HMQC experiments for **1** established the connectivities of eight ^{1}H–^{1}H and ^{1}H–^{13}C spin systems presented as bold lines (Fig. 2). The HMBC and NOESY correlations (Fig. 2) indicated that the Me-23 and Me-24, Me-29 and Me-30 and C-28–COOH located at C-4, C-20 and C-17, respectively, and the connectivities between C-4/C-3 and C-5, C-10/C-1, C-10/C-5 and C-9, C-9/C-11, C-8/C-7, C-9 and C-14, C-13/C-12, C-18 and C-14, C-14/C-15, C-17/C-18

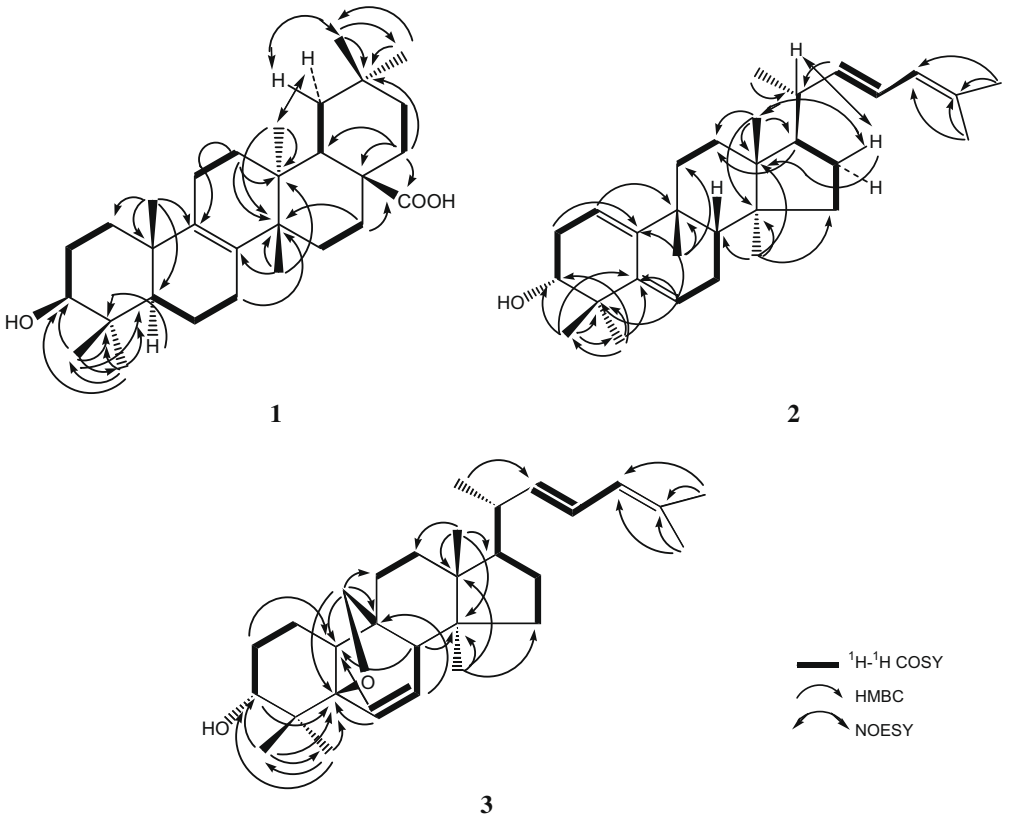

Fig. 2. Key ^{1}H–^{1}H COSY, HMBC and NOESY correlations of compounds **1**–**3**.

and C-28 and C-20/C-19 and C-21. The above result indicated that the structure of **1** was elucidated as shown **1**. The NOESY correlations of H_α-2/H-3 and Me-23, Me-23/H-5, Me-27/H_α-19 and Hβ-19/Me-30 suggested H-3, Me-23, H-5, Me-27 and Me-29 are α-oriented and that Me-24 and Me-30 are β-oriented. The NOESY correlations of Hβ-1/Me-25 and H_β-15/Me-26 suggested Me-25 and Me-26 are β-oriented. In addition, the comparison of carbon signals at C-16, C-17, C-18 and C-20 of **1** with those of reported data (Biemann, 1989a; Biemann, 1989b; Shan, Hu, & Chen, 2001; Wu et al., 2005) supported the C-28–COOH is β-oriented. Thus the structure of **1** was characterised as 3β-hydroxymultiflora-8-en-17-oic acid (**1**).

Compound **2** was assigned a molecular formula of $C_{30}H_{46}O$, as determined from its HRESIMS ([M+Na]$^+$, 445.3449, Δ−0.0003 mmu). The UV spectrum showed the presence of a heteroannular or an acyclic diene moiety (Scott, 1964). The IR absorption of **2** implied the presence of OH (3433 cm^{-1}) and *trans*-form of C=C (1684 cm^{-1}) (Biemann, 1989a; Biemann, 1989b) functionalities. The ^{1}H and ^{13}C NMR spectra of **2** (Table 1) showed the presence of eight methyls, six methylenes, nine methines including an oxymethine and seven quaternary carbons. Analysis of ^{1}H–^{1}H COSY and HMQC experiments for **2** established the connectivities of nine ^{1}H–^{1}H and ^{1}H–^{13}C spin systems presented as bold lines (Fig. 2). The HMBC correlations (Fig. 2) suggested that **2** possesses a cucurbitane skeleton. The HMBC correlations of Me-28 and Me-29/C-3 and C-4, H-1/C-9, H-2/C-10, H-6/C-5, C-4 and C-10, Me-26 and Me-27/C-24 and C-25 and H-22/C-20 suggested that **2** is a cucurbita-1(10),5,22,24-tetraen-3-ol. The NOESY correlations of H_β-2/H-3 and H-3/Me-28, H_β-16/Me-18, Me-18/H-8, H-8/Me-19 suggested that H-3, Me-28, H-8, Me-19 and Me-18 are β-oriented. The NOESY correlations of Me-30/H_α-15 and H-20/H_β-16 and H-23 suggested that Me-21 and Me-30 are α-oriented. Thus, compound **2** is characterised as cucurbita-1(10),5,22, 24-tetraen-3α-ol (**2**).

Compound **3** exhibited a [M]$^+$ at *m/z* 438.3498, Δ−0.0001 mmu, in the HREIMS, compatible with the formula, $C_{30}H_{46}$ O_2. The UV spectrum was similar to that of **2**. The IR absorption of **3** exhibited absorption bands for hydroxy (3469 cm^{-1}) and *trans*-form of C=C (1684 cm^{-1}) (Biemann, 1989a; Biemann, 1989b) moieties. The structure of **3** was identified by a combination of one- and two-dimensional NMR methods. Its ^{1}H and ^{13}C NMR spectra of **3** (Table 1) showed the presence of seven methyls, seven methylenes including an oxygenated methylene, 10 methines including an oxymethine and six quaternary carbons including an oxygenated quaternary carbon. ^{1}H–^{1}H COSY and HMQC spectra established the connectivities of ten ^{1}H–^{1}H and ^{1}H–^{13}C spin systems represented as bold lines (Fig. 2). The HMBC as shown in Fig. 2 supported that **3** was a cucurbitane triterpenoid. The HMBC correlations of H-6/C-5 and C-10, H-19/C-5, C-10, C-9 and C-11 established an epoxy moiety linked between C-5 and C-19. The ^{1}H–^{1}H COSY correlations between C-6/C-7 and C-22/C-23 and HMBC correlations between Me-26 and Me-27/C-25 and C-24 established three double bonds located between C-6/C-7, C-22/C-23 and C-24/C-25. The NOESY correlations between H_α-19/H-10, H-10/Me-28 and H_α-11/Me-30, and Me-29/H-3, Me-18/H_β-11 and H_β-19/H_β-11 suggested that H-10, Me-28, Me-30 and H-3, Me-18, Me-29 and the linkage between C-19/C-9 are on α and β-side of **3**, respectively. The relative configurations at C-5 and C-19 was established by the fact that the bridge C-5 and C-19 can only exist in the cis form (Winkelmann, Heilmann, Zerbe, Rali, & Sticher, 2000). The above result suggested that the structure of **3** was elucidated as 5β,19β -epoxycucurbita-6,22,24-trien-3α-ol (**3**).

The presence of significant peaks at *m/z* 390 [M–H_2O–CH_2O]$^+$ and 281 [390-side chain]$^+$ (base peak) also supported the characterization of **3**. The above result indicated that constituents isolated from the stems of *M. charantia* collected at Hualien Hsien,

Taiwan were different from that of collected at Pingtung County Taiwan (Chang et al., 2008).

A recent study demonstrated that the water extracts of *M. charantia* have a significant antioxidant effect (Kubola & Siriamornpun, 2008). For evaluating the antioxidant effects of isolated constituents, we used several methods, namely, 1,1-diphenyl-2-picrylhydrazl (DPPH) radical-scavenging activity, 2,2′-azinobis (3-ethylbenzothiazoline-6-sulphonic acid) (ABTS) radical cation scavenging activity and inhibition of XO activity.

The effect of antioxidant on DPPH· is thought to be due to their hydrogen donating activity (Mathew & Abraham, 2006). Compounds **2** and **3** with inhibitory effect of XO showed weak DPPH·-scavenging activity with 10.1 ± 10.9% and 13.6 ± 4.2% inhibition at 200 μM while **1** also a XO inhibitor did not show DPPH·-scavenging activity. The positive control TOC showed DPPH·-scavenging activity with 81.9 ± 1.2% inhibition at 200 μM. The relative antioxidant ability to scavenge the radical $ABTS^{\cdot+}$ has been compared to positive control TOC and is an excellent method for determining the antioxidant activity of hydrogen donating antioxidants and of chain breaking antioxidants. As shown in Fig. 3, compounds **1**, **2**, **3** and positive control TOC indicated ABTS radical cation scavenging activity in a concentration-dependent manner with IC_{50} values of 268.5 ± 7.9, 352.1 ± 11.5, 458.9 ± 13.0 and 79.9 ± 2.9 μM, respectively. It clearly showed that 1 with a hydroxyl and a carboxylic acid group displayed stronger ABTS radical cation scavenging activity.

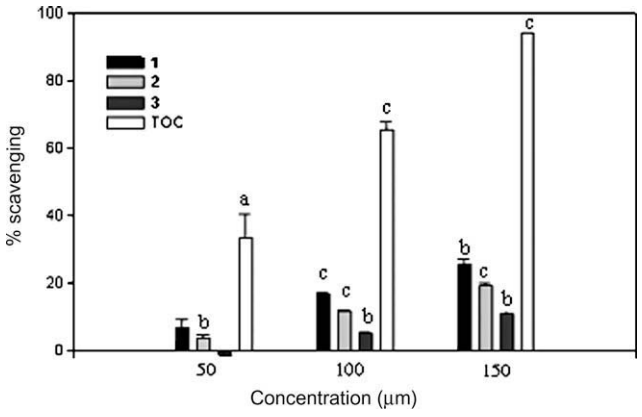

Fig. 3. ABTS radical scavenging activity of various concentrations of **1**–**3** and TOC. Values are means ± S.D., $n = 3$. $^{a}P < 0.05$, $^{b}P < 0.01$, $^{c}P < 0.001$ compared to the control value, respectively.

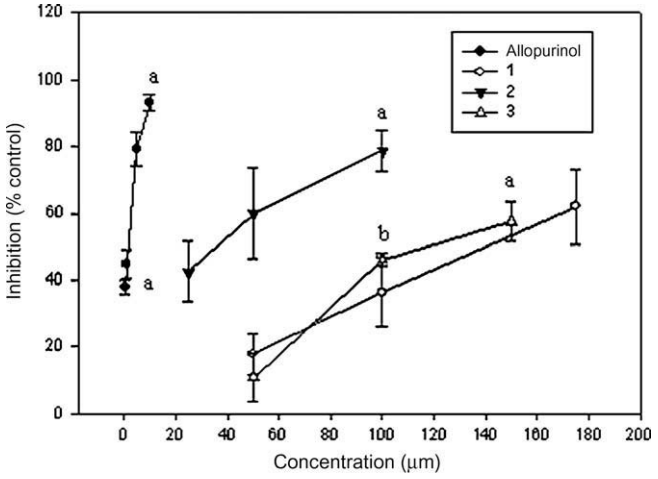

Fig. 4. Dose-dependent inhibition of XO by **1**–**3** and allopurinol. Data as means ± SD $n = 3$. $^{a}P < 0.05$, $^{b}P < 0.01$ compared to the control value, respectively.

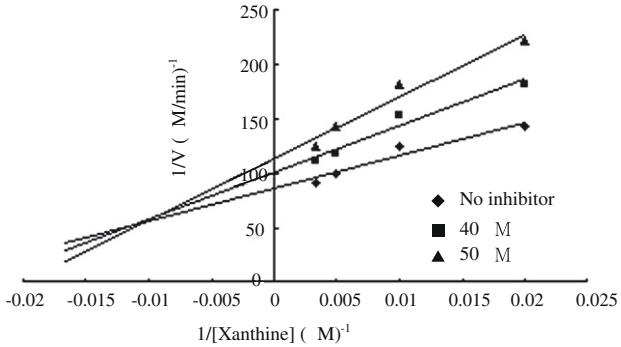

Fig. 5. Lineweaver–Burk plot of XO inhibition of **2** with various concentrations of xanthine. Lineweaver–Burk transformed data were plotted and followed by line regression of the points. Data represent the average of triplicated experiments.

As shown in Fig. 4, compound **2** was identified as a stronger XO inhibitor than those of the same chemical skeleton such as **3**. It indicated that an epoxy moiety linked between C-5 and C-19 such as **3** attenuated the inhibitory effect on XO activity.The multiflorane triterpenoid such as **1** did not show a stronger inhibitory effect on XO activity than those of cucurbitane triterpenoids. As shown in Fig. 5. selective compound **2** was established to be a competitive-noncompetitive inhibitor. It revealed that **2** could be bound to the free enzyme and the enzyme–substrate complex. Biochemically, the enzyme inhibition is associated with hydrogen binding of phenolic hydroxyls and/or carbonyls of substrate with the amide carbonyls and/or amino groups in the peptide chain of enzyme (Jiao, Ge, Shi, & Tan, 2006). Therefore, in addition to chemical skeleton and conformation of compound, the alcoholic hydroxyl in **1**–**3** may interfere with the interaction between enzyme and enzyme–substrate complex.

4. Conclusion

Two new cucurbitane triterpenoids and a new multiflorane triterpenoid were isolated from the stems of *M. charantia*. Compounds **2** and **3**, and **1**–**3** showed weak DPPH·-scavenging and ABTS radical cation scavenging activities, respectively. Compound **2** also showed a significant inhibitory effect on XO activity. Multiflorane triterpenoids have been isolated and reported from *M. cochinchinensis*, *Trichosanthes kiriloroii*, *Polypodium niponicum* and *P. formosanum* (Ageta & Arai, 1983; Shan et al., 2001; Wu et al., 2005). This is the first report of a multiflorane triterpenoid being isolated from this plant and the first report of cucurbitane triterpenoid and multiflorane triterpenoid as antioxidants. These compounds may serve as antioxidant agents for the treatment of reactive oxygen species (ROS) induced diseases.

Acknowledgments

This work was partially supported by a grant from the National Science Council (NSC 95-2320-B-037-036), Council of Agriculture (95AS-6.2.1-ST-a1 & 96AS-1.2.1-ST-a1) of Republic of China and a fund of KMU-EM-97-2.1.b.

References

Ageta, H., & Arai, Y. (1983). Fern constituents: Pentacyclic triterpenoids isolated from *Polypodium niponicum* and *P. formosanum*. *Phytochemistry, 22*, 1801–1808.

Akihisa, T., Higo, N., Tokuda, H., Ukiya, M., Akazawa, H., Tochigi, Y., et al. (2007). Cucurbitane-type triterpenoids from the fruits of *Momordica charantia* and their cancer chemopreventive effects. *Journal of Natural Products, 70*, 1233–1239.

Biemann, K. (1989). Tables of spectral data for structure determination of organic compounds. Cambridge, MA, C 70.

Biemann, K. (1989). Tables of spectral data for structure determination of organic compounds. Cambridge, MA, I 30.

Chang, C.-H., Chen, C.-R., Liao, Y.-W., Cheng, H.-L., Chen, Y.-C., & Chou, C.-H. (2008). Cucurbitane-type triterpenoids from the stems of *Momordica charantia*. *Journal of Natural Products, 71*, 1327–1330.

Cheng, H.-L., Huang, H.-K., Chang, C.-I., Tsai, C.-P., & Chou, C.-H. (2008). A cell-based screening identifies compounds from the stems of *Momordica charantia* that overcome insulin resistance and active AMP-activated protein kinase. *Journal of Agricultural and Food Chemistry, 56*, 6835–6843.

Cheng, J.-H., Hung, C.-F., Yang, S.-C., Wang, J.-P., Won, S.-J., & Lin, C.-N. (2008). Synthesis and cytotoxic, anti-inflammatory, and anti-oxidant activities of 2′,5′-dialkoxylchalcones as cancer chemopreventive agents. *Bioorganic and Medicinal Chemistry, 16*, 7270–7276.

Han, J., Weng, X., & Bi, K. (2008). Antioxidants from a Chinese medicinal herb-*Lithospermum erythrorhizon*. *Food Chemistry, 106*, 2–10.

Jiao, R. H., Ge, H. M., Shi, D. H., & Tan, R. X. (2006). An apigenin-derived xanthine oxidase inhibitor from *Palhinhaea cernua*. *Journal of Natural Products, 69*, 1089–1091.

Kabouche, A., Kabouche, Z., Öztürk, M., Kolak, U., & Topcu, G. (2007). Antioxidant abietane diterpenoids form *Salvia barrelieri*. *Food Chemistry, 102*, 1281–1287.

Kong, L. D., Zhang, Y., Pan, X., Tan, R. X., & Cheng, C. H. K. (2000). Inhibition of xanthine oxidase by liquiritigenin and isoliquiritigenin isolated from *Sinofranchetia chinensis*. *CMLS Cellular and Molecular Life Sciences, 57*, 500–505.

Kubola, J., & Siriamornpun, S. (2008). Phenolic contents and antioxidant activities of bitter gourd (*Momordica charantia* L.) leaf, stem and fruit fraction extracts in vivo. *Food Chemistry, 110*, 881–890.

Mathew, S., & Abraham, T. E. (2006). *In vitro* antioxidant activity and scavenging effects of *Cinnamom verum* leaf extract assayed by different methodologies. *Food and Chemical Toxicology, 44*, 198–206.

Scott, A. I. (1964). *Interpretation of the ultraviolet spectra of natural products* pp. 45–48. London: Pergamon Press.

Shan, M. D., Hu, L. H., & Chen, Z. L. (2001). A new multiflorane triterpenoid ester from *Momordica cochinchinensis* Spreng. *Natural Product Letters, 15*, 139–145.

Tan, M. J., Ye, J. M., Tumer, N., Hohnen-Behrens, C., Ke, C.-Q., Tang, C.-T., et al. (2008). Antidiabetic activities of triterpenoids isolated from bitter melon associated with activation of the AMPK pathway. *Chemistry and Biology, 15*, 263–273.

Thi Nguyen, M. T., Awale, S., Tezuka, Y., Ueda, J.-Y., Tran, Q. L., & Kadota, S. (2006). Xanthine oxidase inhibitors from the flowers of *Chrysanthemum sinense*. *Planta Medica, 72*, 46–51.

Winkelmann, K., Heilmann, J., Zerbe, O., Rali, T., & Sticher, O. (2000). New phloroglucinol derivatives from *Hypericum papuanum*. *Journal of Natural Products, 63*, 104–108.

Wu, T., Cheng, X.-M., Annie Bligh, S. W., Chou, G.-X., Wang, Z.-T., Bashall, A., et al. (2005). Multiflorane triterpene esters from the seeds of *Trichosanthes kirilowii*. *Helvetica Chimica Acta, 88*, 2617–2623.

2. Materials and methods

2.1. Plant materials

The ripe fruits of Chinese quince (*Pseudocydonia sinensis* Schneider var. Toukarin) were obtained from a local orchard in Nagano Prefecture, Japan.

2.2. Chemicals and reagents

(−)-Epicatechin, vanillic acid, 4-hydroxybenzoic acid, β-glucuronidase type H-2 (including sulfatase), and 2,4,6-tri(2-pyridyl)-s-triazine (TPTZ) were purchased from Sigma–Aldrich, Ltd. (St. Louis, MO, USA). Cyanidin chloride was purchased from Funakoshi Co. (Tokyo, Japan). Salicylic acid, protocatechuic acid, hippuric acid, citric acid were purchased from Nacalai Tesque, Inc. (Kyoto, Japan). 3-Hydroxyphenylacetic acid was purchased from Alfa Aesar (Karlsruhe, Germany). Solvents were purchased from Nacalai Tesque. Folin–Ciocalteu reagent was purchased from Wako Pure Chemical Industries, Ltd. (Osaka, Japan). Procyanidin B2 was purchased from Funakoshi Co., Ltd. (Tokyo, Japan). The other dimers (B1, B3 and B4) were chemically synthesised from catechin and epicatechin (Mohri et al., 2007).

2.3. Extraction of crude polyphenols (CP) from Chinese quince fruit

The semi-purified Chinese quince polyphenols were prepared using the procedure described in a previous report (Hamauzu et al., 2007). The freeze–dried powder of the flesh (30 g) was washed with 300 ml of petroleum ether to remove lipids and then the polyphenols were extracted with 60% aqueous acetone (300 ml, three times), rotary evaporated, and semi-purified using a Sep-Pak Vac 20 cm^3 (5 g) C18 cartridge (Waters Co., Milford, MA). The end result was approx. 3.0 g of freeze–dried crude polyphenols (CP) in powder form.

2.4. Breakdown of CP by heating with citric acid (preparation of CPT)

An aqueous solution of CP (final conc. of 0.1%, w/v, as epicatechin equivalent) was heated in the presence of citric acid (final conc. of 2.0%, w/v) in a screw-capped test tube for 0, 2, 4, 8, or 12 h using a dry bath incubator (GENIUS two block, Nippon Genetics Co., Ltd., Tokyo, Japan) at 95 °C. For the *in vivo* experiment, CP subjected to the same heat treatment for 0 h (CPT-0 = CP plus citric acid), 2 h (CPT-2) and 8 h (CPT-8) were prepared for administration to the rats.

2.5. Total phenolic assay

The experimental procedure was adapted from that of Hamauzu et al. (2007). About 2 ml of sample solution were mixed with 2 ml of diluted Folin–Ciocalteu reagent (1 N) in a test tube. After 3 min, 2 ml of Na_2CO_3 (10 g/100 ml) were added and the mixture was incubated for 60 min at room temperature. The absorbance was measured at 700 nm with a Shimadzu UV-1200 spectrophotometer (Tokyo, Japan) against a blank (2 ml of deionized water, plus reagents) in the reference cell. (−)-Epicatechin was used as the standard (r = 0.99975).

2.6. Reversed phase HPLC

Chromatographic separation was carried out on a Luna 5μ C18 column (150 × 4.6 mm, Phenomenex, Inc., Torrance, CA., USA) with a security guard cartridge (3.0 × 4.6 mm) at 40 °C. Solvents were 0.1% trifluoroacetic acid (A) and 0.1% trifluoroacetic acid in acetonitrile (B). The gradient program began with 5% B and was changed to obtain 15% B at 30 min, 32% B at 35 min, 40% B at 45 min, and 75% B at 50 min. The 75% B was maintained until 65 min. The flow rate was 1.0 ml/min and the injection volume was 20 μl. Detection was performed at 280 nm for flavan-3-ols and 325 nm for hydroxycinnamic derivatives on a Shimadzu SPD-M10Avp photodiode array detector. For the detection of reddish coloured substances, 458 nm and 525 nm were also used. Peaks were identified by comparing retention times and UV–visible spectra with those of standards. Polymeric and oligomeric procyanidins were identified by comparing the absorption spectra with that of (−)-epicatechin, and the denaturation of them was confirmed by thioacidolysis (Hamauzu et al., 2007) as well as the spectral changes. The presence of protocatechuic and vanillic acids in the Chinese quince polyphenols subjected to heat treatment was also checked by retention time and absorption spectra of peaks on the HPLC chromatogram.

2.7. Animals

Male Wistar rats weighing 230–270 g were conditioned in standard boxes for 3 days before the experiments. They were fed a standard laboratory diet (CE-2, CLEA Japan, Inc.), provided with water ad libitum and kept on a 12/12 h light–dark cycle. The animals were fasted 24 h before the experiment but allowed free access to water. Use of animals for the experiment was approved by the Ethics Committee of Shinshu University.

2.8. Oral administration of polyphenols and blood sampling

Each rat received (oral administration) approx. 40 mg of CP or CPT (containing 20 mg of polyphenols as (−)-epicatechin equivalent estimated by the Folin–Ciocalteu method) suspended in 2 ml of water. Each sample destined for heat treatment (CPT-2 and CPT-8) had its (−)-epicatechin equivalent (20 mg) confirmed before heat treatment because the estimation of phenolic content by the Folin–Ciocalteu method is affected by heating. Control rats were given 2 ml of water. Two hours after administration, rats were anaesthetized with diethylether, the abdominal wall was opened, and blood was collected from the abdominal aorta into heparinised tubes. The plasma was separated from the blood solids by centrifugation (800×g for 5 min at 4 °C).

2.9. The FRAP assay in rats

The experimental procedure for the FRAP (ferric reducing ability of plasma) method basically followed that of Benzie and Strain (1996) with minor modifications. The FRAP method reagent was prepared as a mixture of 10 ml of 300 mM acetate buffer (pH 3.6), 1 ml of 10 mM TPTZ–40 mM hydrochloric solution, and 1 ml of 20 mM $FeCl_3$ solution. The FRAP reagent, once prepared, was immediately incubated for 10 min at 37 °C, then 1.5 ml of the reagent was added to 50 μl of the plasma sample. The reaction mixture was incubated for 4 min at room temperature and the absorbance at 593 nm was measured using a UV-1200 spectrophotometer.

2.10. Analysis of aromatic acid metabolites

Plasma (2 ml) was added to 1.05 ml of 0.58 mM acetic acid to obtain a pH of 4.9, and 1000 U of β-glucuronidase Type H-2 containing 50 U of sulfatase was added and then incubated at 37 °C for 45 min. After acidification to pH 2 with 6 M HCl (46 μl), the solution was then extracted twice with ethyl acetate (4 ml) and centrifuged at 2400×g, 4 °C for 10 min. The resulting supernatant was evaporated under an N_2 gas stream and then re-dissolved in

500 μl of 25% (v/v) methanol. A 200 μl sample of the solution was added to 1800 μl of 10 μM salicylic acid as an internal standard and analysed by Waters LC-electrospray ionisation (ESI)-MS/MS system (Quattro Micro API, Micromass, UK). For the quantitative analysis of aromatic acid metabolites, a single ion monitoring (SIR) mode was used. The MS/MS mode was also used for qualitative analysis by monitoring the product ions.

2.11. LC-ESI-MS conditions

The column was a Luna 5μ C18 column (150 × 4.6 mm) with a security guard cartridge (3.0 × 4.6 mm) and the mobile phases consisted of 5% acetonitrile in 0.1% aqueous formic acid (solvent A) and 50% acetonitrile in 0.1% aqueous formic acid (solvent B). The flow rate was 0.3 ml/min. The following gradient was applied: 0–40 min, linear gradient from 25% B to 50% B; 40–60 min, from 50% B to 100% B; 60–65 min, 100% B. Detection was carried out using ESI conducted in negative mode with a capillary voltage of −3 kV. A cone voltage of −20 V was applied for the detection of aromatic acids and −40 V for catechin metabolites. A source temperature of 120 °C and a desolvation temperature of 350 °C were applied. The cone gas and desolvation gas flow were 50 and 600 L/h, respectively. MS data collected were processed using MassLynx v.4.0.

2.12. LC-ESI-MS/MS conditions

The peaks in the total ion chromatogram (TIC) obtained by MS scan or SIR mode were further confirmed using the same LC-ESI-MS/MS system described above. Argon gas was used as a collision gas, and the potential change defining the collision energy was optimised in the range of 10–20 V as appropriate for both parent and product ions. Aromatic acid metabolites and salicylic acid (internal standard) were detected according to the respective *m/z* values of their parent and product ions: 4-hydroxybenzoic acid (137/93), protocatechuic acid (153/109), vanillic acid (167/123), 3-hydroxyphenylacetic acid (151/107), hippuric acid (178/134) and salicylic acid (137/93).

2.13. Statistics

Data are expressed as means ± SE. Means were compared by one-way ANOVAs followed by Tukey–Kramer tests using Excel 2004 with the add-in software Statcel 2 (OMS, Tokyo, Japan). Differences with $P < 0.05$ were considered significant.

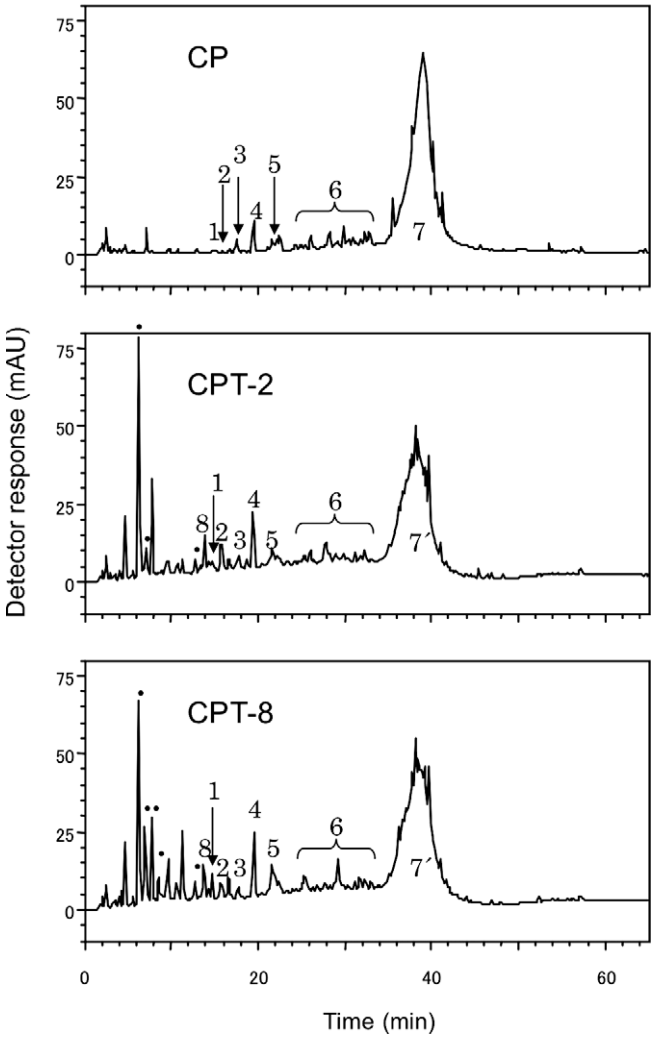

Fig. 1. RP-HPLC profiles of Chinese quince phenolics (CP) and CP subjected to heating for 2 h (CPT-2) and 8 h (CPT-8) in the presence of citric acid. 1, procyanidin B3; 2, (+)-catechin; 3, procyanidin B4; 4, procyanidin B2; 5, (−)-epicatechin; 6, oligomeric procyanidins; 7, clump of polymeric procyanidins; 7′, clump of polymeric components including procyanidin polymers and denatured polyphenols. Peaks indicated with '•' are new peaks with absorption spectra were similar to that of catechin.

3. Results and discussion

3.1. Changes in polyphenolic profile during heat treatment

During 12 h of the heat treatment, the CP solution turned reddish, and the colour intensity (measured at 458 nm) increased linearly as described previously (Hamauzu et al., 2007). During the treatment, increases in (+)-catechin, (−)-epicatechin, procyanidin dimers (B1–B4) and other oligomeric procyanidins were observed (Figs. 1 and 2). The increase in monomeric catechins (catechin plus epicatechin) and in dimers was considerable in the first 2 h. Monomers increased such that their concentrations were approx. 4 times the initial concentration after 2 h of heating, and they reached 5.4 times the initial value at 12 h after the treatment. The (+)-Catechin that was not detected in the initial solution rapidly increased during 2 h of heating and slightly decreased thereafter. Meanwhile, (−)-epicatechin increased continuously over 12 h of heating and reached 3.8 times its initial concentration. The pattern of change in total dimers was similar to that of monomers; it increased to be 3 times the initial concentration after the first 2 h and slightly increased thereafter to be 4 times the initial concentration.

In addition, some compounds having an absorption maximum at 280 nm (with a spectrum shape similar to that of catechin) appeared as peaks on the RP-HPLC chromatogram at early retention times. Small amounts of protocatechuic acid were detected in Chinese quince polyphenols before heating and the amount seemed to increase with long-term heating because a clear absorption spectra peculiar to protocatechuic acid was observed in a peak of CPT-12. However, this was unclear in the same peak of CPT-2 and CPT-8 because the peak was not separated from another peak that appeared with heat treatment. Meanwhile, vanillic acid was not detected in any polyphenolic samples with or without heat treatment. In the chromatogram, a peak of cyanidin and two peaks having an absorption maximum at 458 nm were observed as well as those from the previous report (Hamauzu et al., 2007) (data not shown). The unseparated clump of polymeric procyanidins decreased (approx. 30%) after 2 h of heating, and increased thereafter (Fig. 2). However, the increase was accompanied by the increase of visible absorbency (around 400–550 nm) indicating that polymeric

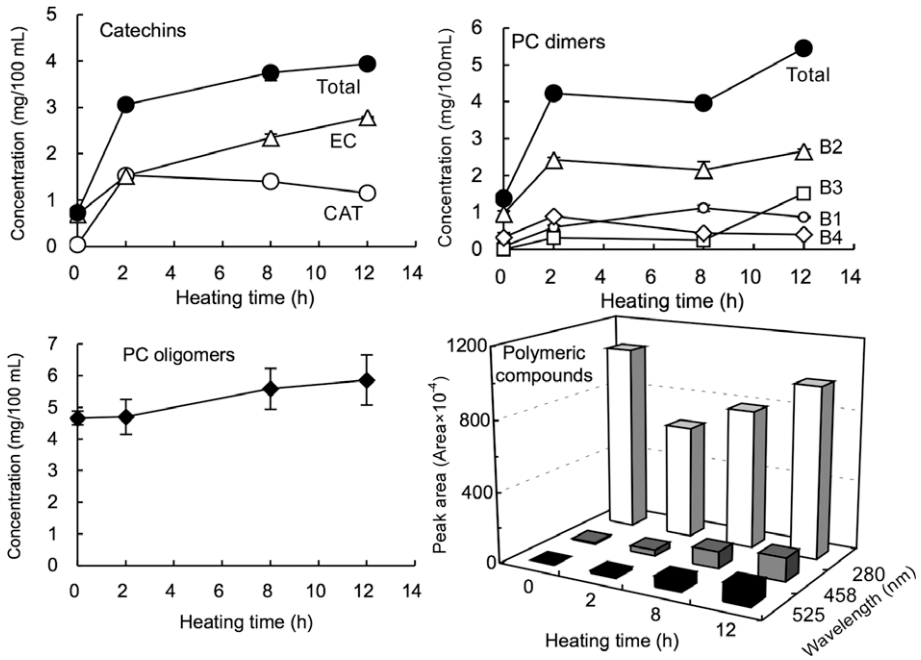

Fig. 2. Change in catechin and procyanidin concentrations and the area of polymeric compounds detected at 280, 458 and 525 nm during the heating of the Chinese quince phenolic solution in the presence of citric acid. Bars indicate SE (n = 3). EC, (−)-epicatechin; CAT, (+)-catechin; PC, procyanidin; B1–B4, procyanidin B1–B4.

procyanidins had been denatured and then re-polymerised to novel polyphenols during heat treatment.

The changes in the *in vitro* antioxidant properties and metal reducing ability were confirmed and the same trend was observed as that described previously (Hamauzu et al., 2007); they markedly increased during the first 2 h of heat treatment and the high levels were maintained until the end of the treatment (data not shown).

From the results, Chinese quince polyphenols heated with 2% citric acid seem to change from having features characteristic of more highly polymerised molecules to those characteristic of relatively less polymerised molecules as a result of the breakdown of polymerised procyanidins during the treatment. These phenomena have already been documented in our previous report (Hamauzu et al., 2007), but that experiment was conducted with 5% of citric acid. It is well known that procyanidins are transformed to cyanidin when broken down by heating with mineral acids (Porter, Hrstich, & Chan, 1986; Santos-Buelga & Scalbert, 2000). However, it has also been shown that, even with HCl, epicatechin monomers and dimers can be produced from oligomers if experimental conditions are pH 2.0 and 37 °C (Spencer et al., 2000). In the current experiment with citric acid, the conditions seemed to be moderate, so that the procyanidins were partially transformed to cyanidin and their breakdown to (−)-epicatechin and dimer B2 occurred. According to Spencer et al. (2000), the procyanidin dimer seems to be more stable than other oligomers and this is supported by our observation that the (−)-epicatechin and procyanidin B2 levels increased during heat treatment.

Protocatechuic acid was detected clearly in the samples subjected to long heating (CPT-12) times, indicating that the heat treatment decomposed polyphenols not only to the levels of monomers but also to smaller molecules such as phenolic acids. It has been known that protocatechuic acid results from the thermal processing of flavonols (Buchner, Krumbein, Rohn, & Kroh, 2006) or from cyanidin (Sadilova, Stintzing, & Carle, 2006). Sadilova et al. (2006) reported that protocatechuic acid concentration was found to increase in purified anthocyanin isolates from some plant materials after heat exposure at 95 °C and pH 1. In the current experiment, protocatechuic acid observed especially in a long-heated sample may be a result of cleavage of cyanidin that derived from 'extention units' of procyanidins.

The clump of polymeric procyanidins partially decreased during 2 h of heat treatment but it increased as denatured forms thereafter with increasing heating time. Because the absorbance increased in the visible light range, elongation of the conjugated diene seems to have occurred. In addition, new components appeared with an absorption maximum of 458 nm after heat treatment. From the shape of their absorption spectra, it is likely that those components have a xanthylium structure. It has been reported that procyanidins or catechins produce xanthylium pigments by polymerisation in the presence of an organic acid (Jurd & Somers, 1970; Labrouche, Clark, Prenzler, & Scollary, 2005).

The increase in the antioxidant properties of Chinese quince polyphenols during heat treatment seemed to be due to changes in their composition and proportions, such as would occur through the lowering of the degree of polymerisation and re-polymerisation to form new components. The antioxidant properties of oligomeric procyanidins have been reported to be superior to those of polymers (Lu & Foo, 2000).

3.2. In Vivo antioxidant activity and aromatic acids in rat plasma

The antioxidant activity of rat plasma as assessed by the FRAP method tended to increase after oral administration of CP, and the tendency was stronger in rats given CP with citric acid (CPT-0) (Fig. 3). The FRAP was also higher in rats given CPT-2 or CPT-8 than in the plasma of the controls, and in rats given CPT-2, the increase was significant ($P < 0.05$).

Aromatic acids detected in rat plasma 2 h after the administration of Chinese quince polyphenols were 3-hydroxyphenylacetic acid, protocatechuic acid, 4-hydroxybenzoic acid, vanillic acid, and hippuric acid (Fig. 4). An additional peak (m/z 209, peak 7) was also detected, indicating a possible metabolite that may have been 3,4-dihydroxyvaleric acid. However, we could not confirm this using its product ions. Although these aromatic acids were also detected in the controls' plasma, protocatechuic acid increased in the plasma of all rats after the administration of polyphenols

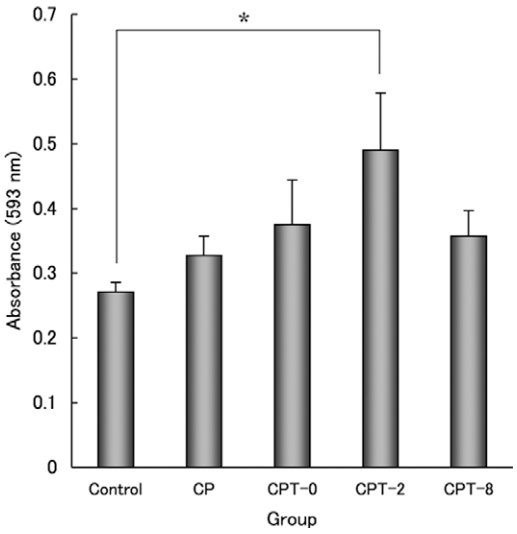

Fig. 3. Ferric reducing ability of the plasma (FRAP) of control rats and rats administered Chinese quince phenolics, some of which were subjected to heat treatment (see text for explanation of group codes). Bars indicate SE ($n = 10$ for control and CP group; $n = 4–5$ for CPT group). $^{*}P < 0.05$ (by Tukey–Kramer test).

(Fig. 5). Moreover, vanillic acid levels increased significantly in the plasma of rats administered CPT-2 and CPT-8, being 4.7 μM and 3.1 μM, respectively (4.7 and 3.1 times, respectively, that of the control or CP group (1.0 μM)). Because it has been reported that vanillic acid is transformed from protocatechuic acid by catechol-*O*-methyl transferase (COMT) in the liver (Gonthier et al., 2003b), the total amount of those two compounds (PCA + VA) was also compared in Fig. 5. The concentration of PCA + VA in the CPT-2 group (5.8 μM) was significantly higher ($P < 0.05$) than that of other groups and it was approx. 4 , 2.5 and 2 times that of the control, CP and CPT-0 groups, respectively. Levels of hippuric acid tended to be higher in rats administered CPT than those of the control or CP group. However, they did not seem to reflect the administration of polyphenols; rather they seemed to be related to the citric acid administered with polyphenols. The plasma levels of two other aromatic acids, 3-hydroxyphenylacetic acid and 4-hydroxybenzoic acid, did not show any particular trends, with a concentration of 7.0–12 μM in the former and 60–82 μM in the latter.

These results suggested that polyphenols from Chinese quince fruit might raise the antioxidant activity of plasma after intake, and that heating the polyphenols in the presence of an organic acid could improve the effect by increasing the plasma concentrations of vanillic acid. Administration of CPT-2 resulted in the most effective increase in the FRAP, which might be explained by the fact that CPT-2 had the lowest proportion of polymeric components and the highest proportion of monomers, dimers and oligomers. It has been thought that procyanidins that are larger than trimers are unlikely to be absorbed in the small intestine in their native forms (Manach, Scalbert, Morand, Rémésy, and Jiménez, 2004) and that, therefore, polymeric procyanidins may not contribute to an increase in the antioxidant activity of plasma in their intact forms. However, they can be absorbed once they reach the colon and are subjected to metabolism by the microflora there into various aromatic acids (Santos-Buelga & Scalbert, 2000; Déprez et al., 2000; Gonthier et al., 2003a), and act as functional compounds. The yields of aromatic acids of microbial origin have been reported to decrease with an increase in the degree of polymerisation of procyanidins (Gonthier et al., 2003b). Therefore, breakdown of procyanidins into smaller polymers by 2 h of heating in the presence of 2% citric acid seemed to be an effective method of bringing about a high yield of aromatic acids by the acceleration of microbial metabolism. The highest concentration of vanillic acid was detected in the plasma of rats that had received CPT-2, indicating that metabolism of the polyphenols into aromatic acids and the intestinal absorption of those metabolites were most active in rats given CPT-2.

Because protocatechuic acid was detected in Chinese quince polyphenols especially in samples heated for a long time, this compound detected in rat plasma seems to be partly the result of direct absorption from the samples administered. However, the plasma concentration of protocatechuic acid (and vanillic acid, the metabolite of protocatechuic acid) did not reflect the tendency of the efficacy of heating time. Therefore, the action of the intestinal flora of rats might also be important in increasing the plasma concentration of these phenolic acids. 3-Hydroxyphenylacetic acid, protocatechuic acid and 4-hydroxybenzoic acid have been reported to be produced from the metabolism of (+)-catechin, (−)-epicatechin or procyanidins by the intestinal microflora, whereas vanillic acid might have been transformed from protocatechuic acid by COMT in the liver (Gonthier et al., 2003b). Among these aromatic metabolites, only protocatechuic and vanillic acids reflected the effect of administration of CP or heat-treated CP; the other aromatic acids might have been derived from other ingested items such as pre-fasting food components or the citric acid administered with the polyphenols. Protocatechuic acid increased in the plasma of all rats given Chinese quince polyphenols and vanillic acid increased in the plasma of rats given CPT-2 and CPT-8, reflecting a positive effect of heat treatment. Since vanillic acid exists as protocatechuic acid before transformation by COMT in the liver, the total concentration of protocatechuic acid and vanillic acid seemed to reflect the total amount of the incorporated protocatechuic acid. This incorporation may have occurred in two ways: (1) direct incorporation from breakdown products of Chinese quince polyphenols; (2) indirect incorporation after the heated polyphenols were subjected to decomposition by intestinal microflora. Since heat treatment must have advantages for both type of incorporation, these two compounds in the plasma could be useful as indicators for the intake of Chinese quince polyphenols and especially for the effect of the heat treatment on them.

It has been reported that protocatechuic acid and vanillic acid have antioxidant activity (Mansouri, Makris, & Kefalas, 2005; Guan, Bao, Jiang, & An, 2006; Shyamala, Naidu, Sulochanamma, & Srinivas, 2007). Therefore, these compounds might contribute to an increase in the FRAP of rats given Chinese quince polyphenols. In fact, the difference of the FRAP between the groups seemed to reflect the plasma PCA + VA level of them, although the actual FRAP value cannot be explained just from the concentration of aromatic acids detected.

Not only increased antioxidant activity but also other beneficial properties have been reported for those two aromatic acids. Protocatechuic acid has been reported to have an inhibitory effect on histamine release from rat mast cells (Osawa et al., 1999), anti-inflammatory activity (Fernández, Sáenz, & García, 1998) and an anti-cancer effect on TPA-induced tumour promotion (Tseng et al., 1998). In addition, recent reports have shown that protocatechuic acid could inhibit the formation of H_2O_2-induced reactive oxygen species at the cytosolic level and also could inhibit H_2O_2-induced apoptotic events, such as the loss of mitochondrial functioning and DNA fragmentation (Tarozzi et al., 2007). Vanillic acid has been reported to have antimicrobial activity (De Moura, Pereira, Januário, França, and Dias, 2004), inhibitory effects on platelet aggregation (Yasuda, Takasawa, Nakazawa, Ueda, & Ohsawa, 2003) and a stimulatory effect on the expression of human endothelial NO synthase (Wallerath, Li, Gödtel-Ambrust, Schwarz, & Förstermann, 2005). Therefore, a heat treatment-induced increase in the plasma concentration of these aromatic acids may confer health benefits through their effects on the circulatory system.

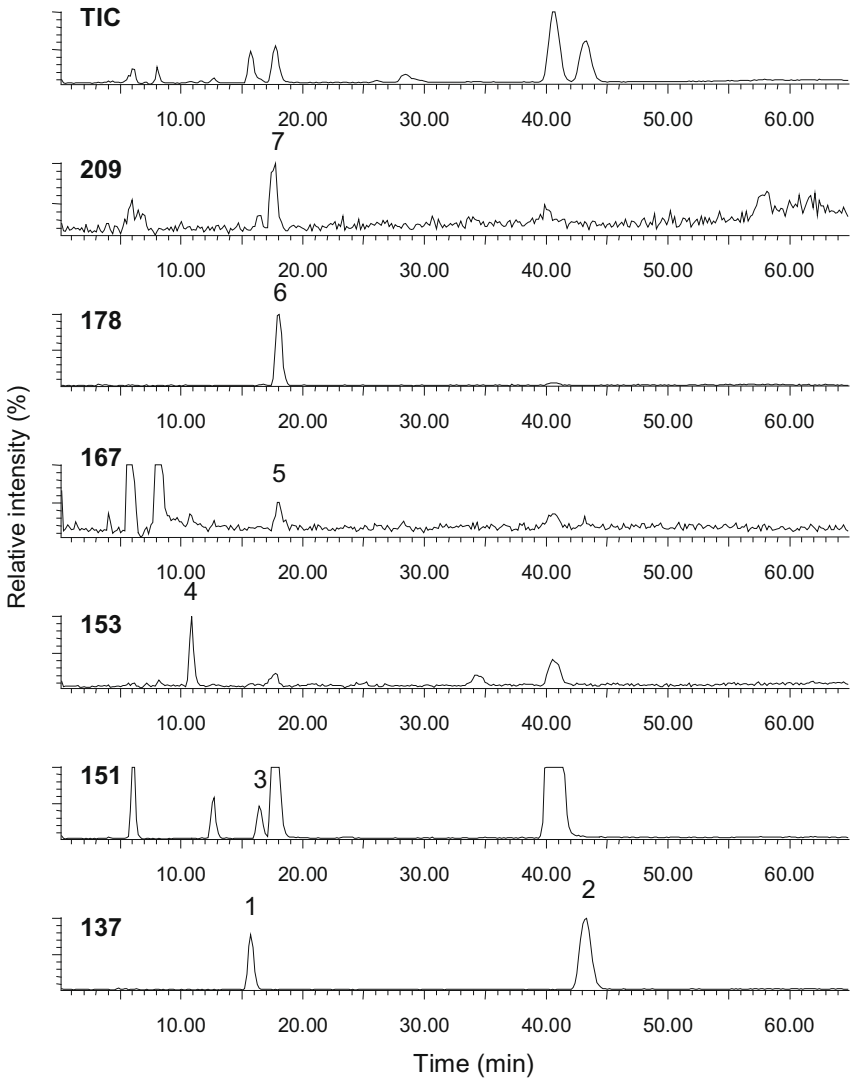

Fig. 4. LC/MS single ion recording (SIR) mass chromatogram profile of representative rat plasma after the administration of Chinese quince phenolics. Peaks: 1 = 4-hydroxybenzoic acid; 2 = salicylic acid (IS); 3 = 3-hydroxyphenylacetic acid; 4 = protocatechuic acid; 5 = vanillic acid; 6 = hippuric acid; 7 = 3,4-dihydroxyphenylvaleric acid (?).

There are some additional advantages to the breakdown of Chinese quince polyphenols by heat treatment in the presence of citric acids. The treatment can increase their bioavailability, as indicated by the observed increase in monomers such as (−)-epicatechin (which can be absorbed in their intact forms) (Manach et al., 2004). In the current experiment, however, this compound could not be detected in any of the rat plasma samples. The proportion of monomers in the polyphenolic samples given to rats was too small for monomers to be detected in the plasma after administration, even CPT-2 (it contained only 3% of total polyphenols). Moreover, using citric acid might have an additional effect on the intestinal absorption of polyphenols. The FRAP and PCA + VA concentration were both higher in the plasma of rats given CPT-0 than in the rats given CP, although the difference was not significant, suggesting that the presence of citric acid might affect the absorption of polyphenols. Yamashita et al. (2002) reported that tartaric acid enhanced the absorption of catechin in rats. Another beneficial aspect of the breakdown of Chinese quince polyphenols by heat treatment is a decreased amount of highly polymerised procyanidins. Highly polymerised procyanidins are the main component of Chinese quince polyphenols, and by having strong tannic activity, they are associated with some food problems such as astringency and may be related to some types of iron deficiency (Santos-Buelga & Scalbert, 2000). Thus, the heat-induced breakdown of polymeric procyanidins is beneficial because of the decrease in astringency and increase in functionality although polymeric procyanidins themselves may also have some beneficial functions such as antioxidant activity, anti-ulcerative activity, anti-influenza viral activity (Hamauzu et al., 2005; Hamauzu et al., 2006) and anti-proliferative activity (Miura et al., 2008). Polymeric procyanidins may have important functions in the digestive tract rather than in the circulatory system.

In conclusion, the breakdown of Chinese quince polyphenols by heating in the presence of citric acid seems to be an effective method to improve their biological activity through the increasing of lower molecular compounds and the *in vivo* production of aromatic acids such as protocatechuic and vanillic acids. The treatment could lower the proportion of polymeric procyanidins and increase the proportion of smaller molecules, such as dimers, monomers and protocatechuic acid. Thus, their ability to be absorbed in the small intestine and susceptibility to metabolism by microflora increases and the plasma concentration of aromatic acids of microbial origin will also increase. However, the results also suggest that heating for too long a period may decrease the efficiency of

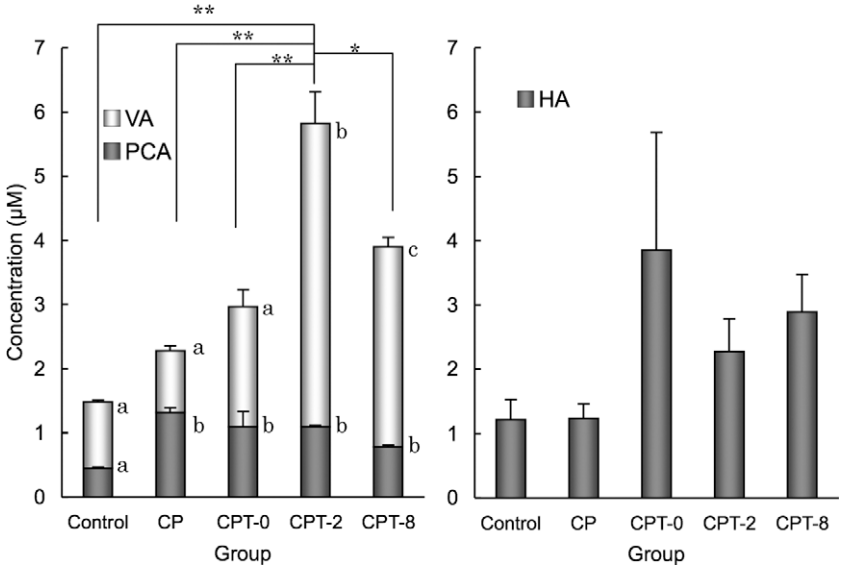

Fig. 5. Aromatic acid concentrations in the plasma of control and trial rats 2 h after the administration of Chinese quince phenolics, some of which were subjected to heat treatment (see text for explanation of group codes). PCA, protocatechuic acid; VA, vanillic acid; HA, hippuric acid. Bars indicate SE ($n = 4–5$). $^{*}P < 0.05$, $^{**}P < 0.01$ (by one-way ANOVA and Tukey–Kramer test for total amount of PCA and VA) For each administration, different letters in PCA or VA were significantly different ($P < 0.05$).

the treatment. The appropriate conditions to improve the health-promoting properties of Chinese quince polyphenols are under investigation.

References

Benzie, I. F., & Strain, J. J. (1996). The ferric reducing ability of plasma (FRAP) as a measure of "antioxidant power": The FRAP assay. *Analytical Biochemistry, 239*, 70–76.

Buchner, N., Krumbein, A., Rohn, S., & Kroh, L. W. (2006). Effect of thermal processing on the flavonols rutin and quercetin. *Rapid Communications in Mass Spectrometry, 20*, 3229–3235.

De Moura, R. M. X., Pereira, P. S., Januário, A. H., França, S. C., & Dias, D. A. (2004). Antimicrobial screening and quantitative determination of benzoic acid derivative of *Gomphrena celosioides* by TLC-densitometry. *Chemical and Pharmaceutical Bulletin, 52*, 1342–1344.

Déprez, S., Brezillon, C., Rabot, S., Philippe, C., Mila, I., Lapierre, C., et al. (2000). Polymeric proanthocyanidins are catabolized by human colonic microflora into low-molecular-weight phenolic acids. *Journal of Nutrition, 130*, 2733–2738.

Fernández, M. A., Sáenz, M. T., & García, M. D. (1998). Anti-inflammatory activity in rats and mice of phenolic acids isolated from *Scrophularia frutescens*. *Journal of Pharmacy and Pharmacology, 50*, 1183–1186.

Gonthier, M.-P., Cheynier, V., Donovan, J., Manach, C., Morand, C., Mila, I., et al. (2003a). Microbial aromatic acid metabolites formed in the gut account for a major fraction of the polyphenols excreted in urine of rats fed wine polyphenols. *Journal of Nutrition, 133*, 461–467.

Gonthier, M.-P., Donovan, J. L., Texier, O., Felgines, C., Rémésy, C., & Scalbert, A. (2003b). Metabolism of dietary procyanidins in rats. *Free Radical Biology and Medicine, 837*, 844.

Guan, S., Bao, Y.-M., Jiang, B., & An, L.-J. (2006). Protective effect of protocatechuic acid from *Alpinia oxyphylla* on hydrogen peroxide-induced oxidative PC12 cell death. *European Journal of Pharmacology, 538*, 73–79.

Hamauzu, Y., Yasui, H., Inno, T., Kume, C., & Omanyuda, M. (2005). Phenolic profile, antioxidant property, and anti-influenza viral activity of Chinese quince (*Pseudocydonia sinensis* Schneid.), quince (*Cydonia oblonga* Mill.), and apple (*Malus domestica* Mill.) fruits. *Journal of Agricultural and Food Chemistry, 53*, 928–934.

Hamauzu, Y., Inno, T., Kume, C., Irie, M., & Hiramatsu, K. (2006). Antioxidant and antiulcerative properties of phenolics from Chinese quince, quince, and apple fruits. *Journal of Agricultural and Food Chemistry, 54*, 765–772.

Hamauzu, Y., Kume, C., Yasui, H., & Fujita, T. (2007). Reddish coloration of Chinese quince (*Pseudocydonia sinensis*) procyanidins during heat treatment and effect on antioxidant and antiinfluenza viral activities. *Journal of Agricultural and Food Chemistry, 55*, 1221–1226.

Jurd, L., & Somers, T. C. (1970). The formation of xanthylium salts from proanthocyanidins. *Phytochemistry, 9*, 419–427.

Labrouche, F., Clark, A. C., Prenzler, P. D., & Scollary, G. R. (2005). Isomeric influence on the oxidative coloration of phenolic compounds in a model white wine: comparison of (+)-catechin and (−)-epicatechin. *Journal of Agricultural and Food Chemistry, 53*, 9993–9998.

Lu, Y., & Foo, L. Y. (2000). Antioxidant and radical scavenging activities of polyphenols from apple pomace. *Food Chemistry, 68*, 81–85.

Manach, C., Scalbert, A., Morand, C., Rémésy, C., & Jiménez, L. (2004). Polyphenols: food sources and bioavailability. *American Journal of Clinical Nutrition, 79*, 727–747.

Mansouri, A., Makris, D. P., & Kefalas, P. (2005). Determination of hydrogen peroxide scavenging activity of cinnamic and benzoic acids employing a highly sensitive peroxyoxalate chemiluminescence-based assay: Structure–activity relationships. *Journal of Pharmaceutical and Biomedical Analysis, 39*, 22–26.

Miura, T., Chiba, M., Kasai, K., Nozaka, H., Nakamura, T., Shoji, T., et al. (2008). Apple procyanidins induce tumor cell apoptosis through mitochondrial pathway activation of caspase-3. *Carcinogenesis, 29*, 585–593.

Mohri, Y., Sagehashi, M., Yamada, T., Hattori, Y., Morimura, K., Kamo, T., et al. (2007). An efficient synthesis of procyanidins. Rare earth metal Lewis acid catalyzed equimolar condensation of catechin and epicatechin. *Tetrahedron Letters, 48*, 5891–5894.

Oku, H., Ueda, Y., & Ishiguro, K. (2003). Antipruritic effects of the fruits of *Chaenomeles sinensis*. *Biological and Pharmaceutical Bulletin, 26*, 1031–1034.

Osawa, K., Miyazaki, K., Imai, H., Arakawa, T., Yasuda, H., & Takeya, K. (1999). Inhibitory effects of Chinese quince (*Chaenomeles sinensis*) on hyaluronidase and histamine release from rat mast cells (in Japanese with English summary). *Natural Medicines, 53*, 188–193.

Porter, L. J., Hrstich, L. N., & Chan, B. G. (1986). The conversion of procyanidins and prodelphinidins to cyanidin and delphinidin. *Phytochemistry, 25*, 223–230.

Sadilova, E., Stintzing, F. C., & Carle, R. (2006). Thermal degradation of acylated and nonacylated anthocyanins. *Journal of Food Science, 71*, 504–512.

Santos-Buelga, C., & Scalbert, A. (2000). Proanthocyanidins and tannin-like compounds–nature, occurrence, dietary intake and effects on nutrition and health. *Journal of the Science of Food and Agriculture, 80*, 1094–1117.

Shyamala, B. N., Naidu, M. M., Sulochanamma, G., & Srinivas, P. (2007). Studies on the antioxidant activities of natural vanilla extract and its constituent compounds through *in vitro* models. *Journal of Agricultural and Food Chemistry, 55*, 7738–7743.

Spencer, J. P. E., Chaudry, F., Pannala, A. S., Srai, S. K., Debnam, E., & Rice-Evans, C. (2000). Decomposition of cocoa procyanidins in the gastric milieu. *Biochemical and Biophysical Research Communications, 272*, 236–241.

Tarozzi, A., Morroni, F., Hrelia, S., Angeloni, C., Marchesi, A., Cantelli-Forti, G., et al. (2007). Neuroprotective effects of anthocyanins and their in vivo metabolites in SH-SY5Y cells. *Neuroscience Letters, 424*, 36–40.

Tseng, T., Hsu, J., Lo, M., Chu, C., Chou, F., Huang, C., et al. (1998). Inhibitory effect of *Hibiscus* protocatechuic acid on tumor promotion in mouse skin. *Cancer Letters, 126*, 199–207.

Wallerath, T., Li, H., Gödtel-Ambrust, U., Schwarz, P. M., & Förstermann, U. (2005). A blend of polyphenolic compounds explains the stimulatory effect of red wine on human endothelial NO synthase. *Nitric Oxide, 12*, 97–104.

Yamashita, S., Sakane, T., Harada, M., Sugiura, N., Koda, H., Kiso, Y., et al. (2002). Absorption and metabolism of antioxidative polyphenolic compounds in red wine. *Annals of the New York Academy of Sciences, 957*, 325–328.

Yasuda, T., Takasawa, A., Nakazawa, T., Ueda, J., & Ohsawa, K. (2003). Inhibitory effects of urinary metabolites on platelet aggregation after orally administering Shimotsu-To, a traditional Chinese medicine, to rats. *Journal of Pharmaceutical and Pharmacology, 55*, 239–244.

Information depicting a comparative analysis of the fatty acid profiles of wild and reared perch, that so far originate from one source, demonstrate the impact of geographic source, rearing system and the domestication process on the fatty acid composition of muscle lipids (Mairesse, Thomas, Gardeur, & Brun-Bellut, 2006; Mairesse, Thomas, Gardeur, & Brun-Bellut, 2007). The presented work describes a study undertaken in order to determine fatty acid composition of various body parts of European perch originating from natural aquifers and reared in the intensive system in a closed circuit and fed an artificial feed mixture.

2. Materials and methods

2.1. Experimental material

The experimental material was perch from intensive fattening with an artificial feed mixture and wild fish of that species. The reared fish originated from the "Dgał" Experimental Stocking Station belonging to the Institute of Inland Fisheries in Olsztyn, Poland. Larval fish obtained as a result of artificial reproduction were pre-reared in tanks with a volume of 1 m^3, in a recirculating cycle. Afterwards, the material was transferred into tanks with a volume of 2 m^3. The fish were fed with excess Nutra Classic trout pellets by Trouvit; Trouw, Fontaine-les-vervins, France. In the final 6 months of fattening, the feed mixture was changed into T-2P Classic (Nutreco; Amersfoort, The Netherlands) with the following composition: protein 45%, fat 16%, carbohydrates 20.8%, ash 8.5%, fibre 1.7%, total phosphorus 1.2%; vitamin A 10,000 u/kg, vitamin D3 1500 u/kg and vitamin E 150 u/kg. Digestible energy accounted for 18.8 MJ/kg, and the size of pellets was 4.0 mm. The feed mixture (a daily dose of 0.3–0.5% of stock biomass) was administered by means of automatic feeders 24 h a day. In the last 2 months, the stock density reached 30–60 kg m^{-3}. In the fattening period, the temperature of water ranged from 17.9 to 22.8 °C. The content of oxygen at the outlet did not drop below 5.1 mg O_2/l. The water reaction accounted for 7.79–8.43, whereas the concentration of total ammonia nitrogen (TAN = NH_4 + NH_3) accounted for 0.08–0.52 mg TAN/l, and that of nitrites for 0.019–0.236 mg NO_2–N/l.

In mid-November, 18 fish from the tank rearing (age 1+) and 18 wild fish (age 3+) were caught. The latter were obtained as a result of a net catch at Dgał Wielki Lake (Mazurian Lake District, Northern Poland). The fish were selected so as to provide the same number of males and females in each group and so that the mean body mass of reared (119.3 g) and wild (116.0 g) perches was alike. Immediately after the catch, the fish were killed and kept in ice for 24 h. Fillets, liver and mesenteric fat obtained after fish dissections served as an analytical material for assays of the fatty acid profile. In each group, analyses were conducted on 18 fish.

2.2. Fatty acid profile

The quantitative and qualitative analysis of fatty acid composition was conducted after the cold extraction of lipids (Folch, Less, & Stanley, 1957). Fatty acids were methylated with the use of a chloroform:methanol:sulphuric acid mixture (100:100:1) (Peisker, 1964). Chromatographic separation was conducted on a gas chromatograph (Agilent Technologies 6890N), with flame ionisation detector, and a capillary column (30 m × 0.32 mm i.d.). The liquid phase used was Supelcowax 10, and film thickness was 0.25 μm. The carrier gas was helium at a flow rate of 1 ml/min. The detector temperature was 250 °C, that of the injector was 225 °C, and that of the column was 180 °C. The detector signal was recorded by means of a Philips recorder with a 1 mV scale at a tape feed of 10 mm/min. Individual acids were identified by comparing their retention times with those of standards by Supelco (Bellefonte, PA).

2.3. Atherogenic and thrombogenicity indices

Lipid quality indices, i.e., atherogenic index (AI) and thrombogenicity index (TI), were calculated according to Ulbricht and Southgate (1991). AI = [12:0 + (4 × 14:0) + 16:0]/[(PUFA $n-6$ + $n-3$) + 18:1 + other MUFA]; TI = [14:0 + 16:0 + 18:0]/[0.5 × 18:1 + 0.5 × other MUFA + 0.5 × $n-6$ PUFA + 3 × $n-3$ PUFA + ($n-3$ PUFA/$n-6$ PUFA)].

2.4. Statistical analysis

Differences between mean values were computed using a one-way analysis of variance (ANOVA). Use was also made of Duncan's test, statistically significant differences were demonstrated at $p \leqslant 0.01$. All calculations were performed by means of Statistica 6.0 PL software (StatSoft Inc., Tulsa, OK).

3. Results

Data referring to the fatty acid composition of the artificial feed mixture and natural feed show that the content of unsaturated fatty acids (UFA) was lower by 6.11% in the natural feed. It was due to a lower (by 9.92%) content of monoenoic fatty acids (MUFA), whilst the content of polyenoic fatty acids (PUFA) was higher by 3.81% as compared to the artificial feed mixture. The greatest differences in contents of individual fatty acids were observed for 16:1 (palmitoleic) and 20:4 $n-6$ (AA, arachidonic), the concentrations of which were higher in the natural feed, and for *cis*18:1 $n-9$ (oleic), 18:2 $n-6$ (LA, linoleic), and 20:1 $n-9$ (erucic) occurring in higher amounts in the artificial feed mixture (Table 1).

Table 1
Fatty acid composition (% of total fatty acids) in an artificial feed mixture and natural feed.

Fatty acid	Artificial feed mixture	Natural feed
C14:0	4.62	6.58
C14:1	0.33	–
C15:0	0.46	0.96
C16:0	15.92	18.38
C16:1	6.64	11.08
C16:4	1.02	–
C17:1	1.10	1.29
C18:0	3.20	4.51
C18:1 $n-9$	27.02	16.14
C18:1 $n-11$	2.00	2.20
C18:2 $n-6$	11.21	7.69
C18:3 $n-3$	3.32	4.61
C8:4 $n-3$	1.26	2.18
C20:0	0.41	0.29
C20:1 $n-7$	0.23	–
C20:1 $n-9$	2.13	0.46
C20:2 $n-6$	0.13	0.41
C20:3 $n-6$	0.11	–
C20:4 $n-6$	0.55	6.86
C20:4 $n-3$	0.38	1.52
C20:5 $n-3$	7.68	7.09
C21:5	0.38	–
C22:1 $n-11$	1.31	0.12
C22:1 $n-9$	0.45	–
C22:5 $n-6$	0.20	0.94
C22:5 $n-3$	0.97	1.60
C22:6 $n-3$	6.97	5.09
∑SFA	24.61	30.72
∑UFA	75.39	69.28
∑MUFA	41.21	31.29
∑PUFA	34.18	37.99
∑$n-3$ PUFA	20.58	22.09
∑$n-6$ PUFA	12.20	15.90

The fatty acid compositions of the total lipids of the analysed body parts of perch are presented in Tables 2 and 3. Out of 48 fatty acids detected, 28 were identified as fitting in a range from C14:0 to C22:6 $n-3$.

The qualitative composition of muscle fatty acids of perch from both groups was identical, except for 16:4 acid, occurring exclusively in muscles, liver and mesenteric fat of the reared fish. Out of the three acids predominating in the muscles in terms of relative content, two, namely 16:0 (palmitic) and DHA, occurred at similar concentrations. The content of the third acid, i.e., oleic, was higher in perch fed the artificial feed mixture. Analyses demonstrated higher concentrations of such fatty acids as: 14:0, 18:4, 20:1 $n-9$ and 22:1 $n-11$ and a lower concentration of 18:0, *cis*18:1 $n-11$, 18:3 $n-3$, 20:4 $n-6$ and 22:5 $n-6$ in the reared fish. In addition, the study showed no differences in the contents of SFA and UFA as well as a relatively higher content of MUFA and a lower content of PUFA in the reared perch. The meat of the latter was additionally found to contain less $n-6$ PUFA. However, $n-3$ PUFA occurred in similar quantities in both groups of perch.

Liver lipids of the reared perch were characterised by a higher content of oleic, a lower content of DHA and a similar concentration of 16:0. Differences were also observed in the concentrations of 14:0, 16:1, 18:2 $n-6$, 18:4 and 20:1 $n-9$ acids (higher in the reared fished) as well as in those of 18:0, *cis*18:1 $n-11$, 20:4 $n-6$ and 22:5 $n-6$ acids (lower in the reared fish). In turn, no differences were found in the total contents of SFA and UFA, however, a higher content of MUFA and a lower content of PUFA, including both $n-6$ PUFA and $n-3$ PUFA, were demonstrated in the fish from intensive rearing.

In the mesenteric fat of the reared perch, analyses demonstrated a higher content of oleic, a lower content of DHA and a similar content of 16:0, as compared to the wild fish. Differences

Table 2
Fatty acid profile of muscles, liver and mesenteric fat of reared and wild perch (% of total fatty acids) (mean ± S.E.M).

Fatty acid	Muscles		Liver		Mesenteric fat	
	Reared fish ($n=18$)	Wild fish ($n=18$)	Reared fish ($n=18$)	Wild fish ($n=18$)	Reared fish ($n=18$)	Wild fish ($n=18$)
C14:0	4.48 ± 0.18[a]	1.71 ± 0.15[b]	5.87 ± 0.60[a]	2.28 ± 0.06[b]	7.18 ± 0.20[a]	3.34 ± 0.15[b]
C14:1	0.76 ± 0.07[a]	0.38 ± 0.04[a]	0.32 ± 0.12[a]	0.49 ± 0.05[a]	0.86 ± 0.03[a]	0.63 ± 0.10[a]
C15:0	0.46 ± 0.03[a]	0.55 ± 0.02[a]	0.73 ± 0.12[a]	0.75 ± 0.02[a]	0.55 ± 0.01[a]	0.64 ± 0.02[a]
C16:0	19.80 ± 0.59[a]	20.13 ± 0.16[a]	21.96 ± 2.03[a]	21.34 ± 0.42[a]	19.16 ± 0.41[a]	18.95 ± 0.27[a]
C16:1	12.01 ± 0.39[a]	8.86 ± 0.89[a]	17.40 ± 1.70[a]	9.51 ± 0.62[b]	14.74 ± 0.32[a]	10.50 ± 0.27[b]
C16:4	0.47 ± 0.02	–	1.01 ± 0.07	–	0.82 ± 0.02	–
C17:1	0.97 ± 0.01[a]	0.86 ± 0.06[a]	0.18 ± 0.12[a]	0.84 ± 0.07[a]	1.26 ± 0.02[a]	1.29 ± 0.10[a]
C18:0	2.20 ± 0.10[a]	5.18 ± 0.27[b]	2.04 ± 0.26[a]	6.83 ± 0.17[b]	1.29 ± 0.03[a]	3.27 ± 0.11[b]
C18:1 $n-9$	17.14 ± 0.36[a]	13.74 ± 1.27[b]	14.10 ± 0.67[a]	10.59 ± 0.32[b]	19.26 ± 0.19[a]	13.77 ± 0.39[b]
C18:1 $n-11$	2.60 ± 0.03[a]	4.56 ± 0.24[b]	3.10 ± 0.06[a]	5.40 ± 0.17[b]	2.79 ± 0.02[a]	7.37 ± 0.24[b]
C18:2 $n-6$	4.90 ± 0.09[a]	3.75 ± 0.26[b]	6.32 ± 0.38[a]	2.79 ± 0.16[b]	6.23 ± 0.07[a]	6.14 ± 0.15[a]
C18:3 $n-3$	0.89 ± 0.03[a]	2.11 ± 0.17[b]	1.16 ± 0.10[a]	1.27 ± 0.06[a]	1.13 ± 0.02[a]	3.94 ± 0.05[b]
C18:4	1.15 ± 0.04[a]	0.44 ± 0.03[b]	0.86 ± 0.15[a]	0.34 ± 0.07[b]	1.63 ± 0.01[a]	0.68 ± 0.05[b]
C20:1 $n-9$	2.86 ± 0.13[a]	0.62 ± 0.11[b]	2.37 ± 0.53[a]	1.01 ± 0.07[b]	3.23 ± 0.14[a]	0.47 ± 0.01[b]
C20:4 $n-3$	0.42 ± 0.08[a]	0.60 ± 0.11[a]	0.47 ± 0.14[a]	0.43 ± 0.09[a]	0.56 ± 0.01[a]	0.29 ± 0.01[a]
C20:4 $n-6$	0.78 ± 0.16[a]	7.27 ± 0.36[b]	0.31 ± 0.15[a]	7.11 ± 0.24[b]	0.52 ± 0.06[a]	8.40 ± 0.15[b]
C20:5 $n-3$	7.24 ± 0.20[a]	7.29 ± 0.31[a]	3.50 ± 0.59[a]	3.95 ± 0.18[a]	6.14 ± 0.13[a]	7.45 ± 0.25[b]
C22:1 $n-11$	1.34 ± 0.38[a]	0.11 ± 0.09[b]	0.41 ± 0.36[a]	0.03 ± 0.00[a]	1.45 ± 0.08[a]	0.01 ± 0.00[b]
C22:5 $n-3$	1.74 ± 0.06[a]	2.19 ± 0.16[a]	1.07 ± 0.29[a]	1.32 ± 0.11[a]	1.47 ± 0.05[a]	0.64 ± 0.03[b]
C22:5 $n-6$	0.17 ± 0.06[a]	1.67 ± 0.11[b]	0.04 ± 0.03[a]	1.52 ± 0.07[b]	0.06 ± 0.04[a]	0.36 ± 0.04[b]
C22:6 $n-3$	16.82 ± 0.76[a]	16.71 ± 1.42[a]	16.40 ± 1.37[a]	21.28 ± 0.44[b]	8.53 ± 0.35[a]	10.55 ± 0.05[b]

The table does not provide values for: 20:0, 20:1 $n-7$, 20:2, 20:3 $n-3$, 20:3 $n-6$, 21:5 and 22:1 $n-9$ acids whose contents in all samples did not exceed 0.5%.
Mean values denoted with various letters in the same row for a given body part are statistically significantly different ($p \leqslant 0.01$).

Table 3
Groups of fatty acids (% of total fatty acids), $n-3/n-6$, atherogenic index (AI) and thrombogenicity index (TI) in muscles, liver and mesenteric fat of reared and wild perch (mean ± S.E.M).

Specification	Muscles		Liver		Mesenteric fat	
	Reared fish ($n=18$)	Wild fish ($n=18$)	Reared fish ($n=18$)	Wild fish ($n=18$)	Reared fish ($n=18$)	Wild fish ($n=18$)
∑SFA	27.08 ± 0.80[a]	27.78 ± 0.20[a]	30.63 ± 2.91[a]	31.37 ± 0.50[a]	28.20 ± 0.47[a]	26.50 ± 0.29[a]
∑UFA	72.92 ± 0.80[a]	72.22 ± 0.20[a]	69.37 ± 2.91[a]	68.63 ± 0.50[a]	71.80 ± 0.47[a]	73.50 ± 0.29[a]
∑MUFA	37.94 ± 0.73[a]	29.20 ± 1.79[b]	38.12 ± 1.31[a]	27.89 ± 0.92[b]	44.07 ± 0.29[a]	34.19 ± 0.36[b]
∑PUFA	34.98 ± 1.09[a]	43.02 ± 1.93[b]	31.25 ± 2.49[a]	40.74 ± 0.81[b]	27.73 ± 0.66[a]	39.31 ± 0.42[b]
∑$n-3$ PUFA	27.13 ± 0.90[a]	29.18 ± 1.68[a]	22.64 ± 2.67[a]	28.49 ± 0.72[b]	17.83 ± 0.54[a]	23.11 ± 0.24[b]
∑$n-6$ PUFA	5.95 ± 0.16[a]	13.13 ± 0.37[b]	6.69 ± 0.25[a]	11.85 ± 0.19[b]	6.92 ± 0.13[a]	15.15 ± 0.35[b]
$n-3/n-6$	4.56 ± 0.09[a]	2.22 ± 0.09[b]	3.38 ± 0.15[a]	2.40 ± 0.06[b]	2.58 ± 0.06[a]	1.53 ± 0.06[b]
IA	0.53 ± 0.02[a]	0.38 ± 0.01[a]	0.67 ± 0.08[a]	0.45 ± 0.01[b]	0.70 ± 0.02[a]	0.45 ± 0.01[b]
IT	0.25 ± 0.01[a]	0.24 ± 0.01[a]	0.32 ± 0.09[a]	0.28 ± 0.02[a]	0.34 ± 0.01[a]	0.27 ± 0.01[a]

SFA contain 14:0, 15:0, 16:0, 18:0 and 20:0.
UFA contain 14:1, 16:1, 16:4, 17:1, 18:1cis9, 18:1cis11, 18:2 $n-6$, 18:3 $n-3$, 18:4, 20:1 $n-7$, 20:1 $n-9$, 20:2, 20:3 $n-3$, 20:3 $n-6$, 20:4 $n-3$, 20:4 $n-6$, 20:5 $n-3$, 21:5, 22:1 $n-9$, 22:1 $n-11$, 22:5 $n-3$, 22:5 $n-6$ and 22:6 $n-3$.
MUFA contain 14:1, 16:1, 17:1, 18:1cis9, 18:1cis11, 20:1 $n-7$, 20:1 $n-9$, 22:1 $n-9$ and 22:1 $n-11$.
PUFA contain 16:4, 18:2 $n-6$, 18:3 $n-3$, 18:4, 20:2, 20:3 $n-3$, 20:3 $n-6$, 20:4 $n-3$, 20:4 $n-6$, 20:5 $n-3$, 21:5, 22:5 $n-3$, 22:5 $n-6$ and 22:6 $n-3$.
$n-3$ PUFA contain 18:3 $n-3$, 20:3 $n-3$, 20:4 $n-3$, 20:5 $n-3$, 22:5 $n-3$ and 22:6 $n-3$.
$n-6$ PUFA contain 18:2 $n-6$, 20:3 $n-6$, 20:4 $n-6$ and 22:5 $n-6$.
Mean values denoted with various letters in the same row for a given body part are statistically significantly different ($p \leqslant 0.01$).

between the groups examined were also observed for such fatty acids as: 14:0, 16:1, 18:4, 20:1 $n-9$, 22:1 $n-11$ and 22:5 $n-3$ occurring in a higher relative quantity in the reared fish, as well as for 18:0, *cis*18:1 $n-11$, 18:3 $n-3$, 20:4 $n-6$ and EPA whose concentrations in that group of fish appeared to be lower. The total content of SFA and UFA was alike in both groups of fish, whereas the total content of MUFA was higher and that of PUFA was lower in the fish from intensive rearing. Additional differences were observed in the total $n-6$ PUFA and $n-3$ PUFA whose content was higher in the mesenteric fat of wild perch.

4. Discussion

The above-presented results pointed to an identical dependency referring to the total content of SFA and UFA in muscles, liver and mesenteric fat of wild and reared perch. Quantities of those groups of fatty acids were similar. Lipids of the examined body parts of perch from both groups were also characterised by the same tendency in respect of contents of MUFA and PUFA, i.e., the wild fish contained less MUFA and more PUFA. The total content of $n-3$ PUFA was similar only in muscles, whereas the total content of $n-6$ PUFA turned out to be different in muscles, liver and mesenteric fat; its higher values were determined in the wild perch.

Thus, the differences observed between both groups of perch, resulting from different ratio of MUFA and PUFA, corresponded to a relationship determined between the artificial feed mixture and natural feed. The higher content of MUFA in the artificial feed mixture was manifested in their higher content in the reared perch. Analogously, the higher content of PUFA in natural feed corresponded to their higher concentration in the wild fish. An identical dependency referring to MUFA and PUFA was demonstrated in a study by Mairesse et al. (2007) conducted on wild and reared perch as well as in other predatory fish (Alasavar, Taylor, Zubcov, Shahidi, & Alexis, 2002; Jankowska, Zakęś, Żmijewski, & Szczepkowski, 2008; Periago et al., 2005; Yildiz & Şener, 2004).

The higher content of MUFA in muscles, liver and mesenteric fat of the reared perch was due to higher concentrations of *cis*18:1 $n-9$ and 20:1 $n-9$, as well as 22:1 $n-11$ in muscles and omental fat. However, the content of *cis*18:1 $n-9$ in all body parts of both wild and reared perch was lower than that determined in feed; hence it may be speculated that this acid was utilised as a source of metabolic energy. Differences in the contents of the other two MUFA resulted from the type of diet. High concentrations of 20:1 $n-9$ and 22:1 $n-11$ are typical of fish meal in which Atlantic herring or that originating from the North Sea as well as other sea fish are constituents (Aidos, van der Padt, Luten, & Boom, 2002; Ratnayake & Ackman, 1979). In freshwater wild fish, the content of both of those fatty acids is low (Ahlgren, Blomqvist, Boberg, & Gustafsson, 1994; Linko, Rajasilta, & Hiltunen, 1992a, 1992b). Likewise, in the wild perch, the content of both those fatty acids was lower as compared to the reared perch fed an artificial feed mixture containing fish meals.

The total content of $n-3$ PUFA in the artificial feed mixture and natural feed was similar. The same observations were made for those acids in muscles, yet their concentrations in live mesenteric fat were different and in both organs were higher in the wild perch. This was mostly due to DHA, the content of which was similar in muscles but different in the two other tissues. The same relationship between muscles and liver as well as internal fat was demonstrated by Rueda et al. (2001) for wild and reared sharpsnout sea brea (*Diplodus puntazzo*). It should also be noted that the mesenteric fat of both groups of perch contained about half the DHA as compared to muscles and liver. Likewise, according to Jezierska, Hazel, and Gerking (1982) in rainbow trout (*Oncorhynchus mykiss* Walb.*i*) the mesenteric fat accumulates less DHA than the fat of muscles or liver. Such a dependency may be linked with the fact that this fatty acid is the major component of phosphoglycerols of cellular biomembranes in fish (Henderson & Tocher, 1987).

In addition, it should be added that the content of DHA, and the resultant total content of $n-3$ PUFA, in the wild and reared perch was usually higher than that determined in the natural feed and artificial feed mixture. This could have been due to the selective retention of that fatty acid or transformation of fatty acids of the $n-3$ family, with a shorter carbon chain and a lower number of double bonds in their long-chain derivatives with a higher degree of unsaturation. The process of bioconversion of $n-3$ fatty acids in that species of fish has been confirmed by Xu and Kestemont (2002), as well as by Xu, Fontaine, Mélard, and Kestemont (2001) using reared perch fed a diet with the addition of various vegetable oils and a diet with various contents of fat. These authors point to the high activity of desaturases $\Delta5$ and $\Delta6$ in fish of that species and to 18:3 $n-3$ as a preferred reaction substrate.

A reference to the findings of the above-cited authors may also be found in the case of $n-6$ PUFA. The study demonstrated that the differences in the content of predominating AA between the wild and reared perch were very similar to those determined between the artificial feed mixture and natural feed. In addition, it is common knowledge that fatty acids of the $n-3$ and $n-6$ families compete for desaturating enzymes and that desaturases $\Delta6$ and $\Delta4$ more readily utilise PUFA $n-3$ than PUFA $n-6$ (Henderson, 1996). It may be speculated, thus, that the content of AA was determined, most of all, by the type of feed and not by bioconversion of its precursor, i.e., LA. Hence, as a result of substantially higher content of AA in the natural feed, the content of that acid in the wild perch was repeatedly higher as compared to the reared fish.

Owing to their predominating quantity, two fatty acids, namely DHA and AA, were responsible to the greatest extent for changes in the essential fatty acid ratio ($n-3/n-6$), a reliable indicator that enables a comparison of the relative nutritive value of lipids. According to Valfré, Caprino, and Turchini (2003), in freshwater fish the $n-3/n-6$ ratio fluctuates between 1 and 4. Values determined for muscles, liver and mesenteric fat were also within that range, however in the case of the wild perch they were lower as compared to the same tissues and organs of the reared perch. This was mostly due to the higher concentration of AA and, consequently, of $n-6$ PUFA in the wild perch. The higher value of the $n-3/n-6$ ratio increases the nutritive value of the reared perch. The $n-3/n-6$ ratio shown in the study is consistent with that determined between wild and reared gilthead sea bream (*Sparus aurata*) and pike (*Esox lucius*) (Jankowska et al., 2008; Orban, Nevigato, Di Lena, Casini, & Marzetti, 2003), but differs from that determined for Atlantic salmon (*Salmo salar*), rainbow trout and European eel (*Anguilla anguilla* L.) as well as sea bass (*Dicentrarchus labrax* L.), indicating the lower $n-3/n-6$ value in reared fish (Krajnovic-Ozretic, Najdek, & Ozretic, 1994; van Vliet & Katan, 1990).

Human health is additionally affected by saturated, monoenoic and polyenoic fatty acids, other than $n-3$ PUFA. Lipid quality indicators that depend on the relative contents of particular groups of fatty acids are the atherogenic index (AI) and thrombogenicity index (TI), which indicate the global dietetic quality of lipids and their potential effect on the development of coronary disease (Ulbricht et al., 1991). In the current study, the wild and reared perch were found not to differ in the values of those indices except for IA of liver and omental fat lipids. Thus, it may be stated that relationships between pro-atherogenic and anti-atherogenic fatty acids of perch muscles were not determined by its origin. No differences between the groups were either observed in comparing dependencies between pro- and anti-thrombogenic fatty acids of all body parts of both wild and reared perch.

In summarising the results obtained, it may be concluded that the intensive rearing of perch in recirculating cycles produces fish whose muscle lipids do not diverge from those of wild fish in terms of contents of EPA and DHA acids, the most valuable to a consumer, or in the values of such indicators of the nutritional quality of lipids as AI and TI. Hence, in this respect the reared perch is not inferior to the wild one. Nevertheless, the contents of fatty acids in liver (DHA) and mesenteric fat (EPA, DHA) of both groups of perch are still different. Fish of this species display a high bioconversion efficiency of $n-3$ fatty acids, which results in a higher concentration of DHA in muscles, liver and mesenteric fat of the fish compared to their diet.

References

Ahlgren, G., Blomqvist, P., Boberg, M., & Gustafsson, I.-B. (1994). Fatty acid content of the dorsal muscle – an indicator of fat quality in freshwater fish. *Journal of Fish Biology, 45*, 131–157.

Aidos, I., van der Padt, A., Luten, J. B., & Boom, R. M. (2002). Seasonal changes in crude and lipid composition of herring fillets, byproducts and respective products oils. *Journal of Agricultural and Food Chemistry, 50*, 4589–4599.

Alasavar, C., Taylor, K. D. A., Zubcov, E., Shahidi, F., & Alexis, M. (2002). Differentation of cultured and wild sea bass (*Dicentrarchus labrax*): Total lipid content, fatty acid and trace mineral composition. *Food Chemistry, 79*, 145–150.

Cahu, C., Salen, P., & de Lorgeril, M. (2004). Farmed and wild fish in the prevention of cardiovascular diseases: Assessing possible differences in lipid nutritional values. *Nutrition Metabolism and Cardiovascular Diseases, 14*, 34–41.

Cejas, J. R., Almansa, E., Jérez, S., Bolaños, A., Samper, M., & Lorenzo, A. (2004). Lipid and fatty acid composition of muscle and liver from wild and captive mature female broodstocks of white seabream, *Diplodus sargus*. *Comparative Biochemistry and Physiology B – Biochemistry and Molecular Biology, 138*, 91–102.

Folch, H., Less, M., & Stanley, H. A. (1957). A simple method for isolation and purification of total lipids from animal tissues. *Journal Biological Chemistry, 226*, 497–499.

Fontaine, P., & Kestemont, P. (2008). Perface. In P. Fontaine, P. Kestemont, F. Teletchea, & N. Wang (Eds.), *Percid fish culture. From research to production* (pp. 8–10). Namur, Belgium: Presses Universitaires de Namour.

Grigoriakis, K., Alexis, M. N., Taylor, K. D. A., & Hole, M. (2002). Comparison of wild and cultured gilthead sea bream (*Sparus aurata*); composition, appearance and seasonal variations. *International Journal of Food Sciences and Technology, 37*, 477–484.

Henderson, R. J. (1996). Fatty acid metabolism in freshwater fish with particular reference to polyunsaturated fatty acids. *Archives of Animal Nutrition, 49*, 5–22.

Henderson, R. J., & Tocher, D. R. (1987). The lipid composition and biochemistry of freshwater fish. *Progress in Lipid Research, 26*, 281–347.

Jankowska, B., Zakęś, Z., Żmijewski, T., & Szczepkowski, M. (2008). Fatty acids composition of wild and cultured northern pike (*Esox Lucius*). *Journal of Applied Ichthyology, 24*, 196–201.

Jezierska, B., Hazel, J., & Gerking, S. (1982). Lipid mobilization during starvation in the rainbow trout, *Salmo gairdneri* Richardson, with attention to fatty acids. *Journal of Fish Biology, 21*, 681–692.

Kolanowski, W., & Laufenberg, G. (2005). Enrichment of food products with polyunsaturated fatty acids by fish oil addition. *European Food Research and Technology, 222*, 472–477.

Krajnovic-Ozretic, M., Najdek, M., & Ozretic, B. (1994). Fatty acids in liver and muscle of farmed and wild sea bass (*Dicentrarchus labrax* L.). *Comparative Biochemistry and Physiology A – Physiology, 109*, 611–617.

Linko, M., Rajasilta, M., & Hiltunen, R. (1992a). Comparison of lipid and fatty acid composition in vendace (*Coregonus albula* L.) and available plankton feed. *Comparative Biochemistry and Physiology A – Physiology, 103*, 205–212.

Linko, R. R., Rajasilta, M., & Hiltunen, R. (1992b). Comparison of lipid and fatty acid composition in vendance (*Coregonus albula* L.) and available plankton feed. *Comparative Biochemistry and Physiology A – Physiology, 103*, 205–212.

Mairesse, G., Thomas, M., Gardeur, J.-N., & Brun-Bellut, J. (2006). Effects of geographic source, rearing system, and season on the nutritional quality of wild and farmed *Perca fluviatilis*. *Lipids, 41*, 221–229.

Mairesse, G., Thomas, M., Gardeur, J.-N., & Brun-Bellut, J. (2007). Effects of dietary factors, stocking biomass and domestication on the nutritional and technological quality of the Eurasian perch *Perca fluviatilis*. *Aquaculture, 262*, 86–94.

Orban, E., Nevigato, T., Di Lena, G., Casini, I., & Marzetti, A. (2003). Differentiation in the lipid quality of wild and farmed seabass (*Dicentrarchus labrax*) and gilthead sea bream (*Sparus aurata*). *Journal of Food Science, 68*, 128–132.

Peisker, K. (1964). Rapid semi-micro method for methyl esters from triglycerides using chloroform, methanol, sulphuric acid. *Journal of the American Oil Chemists Society, 11*, 87–90.

Periago, M. J., Ayala, M. D., López-Albors, O., Abdel, I., Martínez, C., Garcia-Alcázar, A., et al. (2005). Muscle cellularity and flesh quality of wild and farmed sea bass, *Dicentrarchus labrax* L.. *Aquaculture, 249*, 175–188.

Ratnayake, W. N., & Ackman, R. G. (1979). Fatty alcohols in capelin, herring and mackerel oils and muscle lipids: II. A comparison of fatty acids from wax esters with those of triglycerides. *Lipids, 14*, 804–810.

Rueda, F. M., Hernández, M. D., Eges, M. A., Aguado, F., Garcia, B., & Martínez, F. J. (2001). Differences in tissue fatty acid composition between reared and wild sharpsnout seabream, diplodus puntazzo (Cetti, 1777). *British Journal of Nutrition, 86*, 617–622.

Rueda, F. M., López, J. A., Martinem, F. J., Zamora, S., Divanach, P., & Kentouri, M. (1997). Fatty acids in muscle of wild and farmed red porgy, *Pagrus pagrus*. *Aquaculture Nutrition, 3*, 161–165.

Sağlik, S., Alpasian, M., Gezgin, T., Çetintürk, K., Tekinay, A., & Güven, K. C. (2003). Fatty acid composition of wild and cultivated gilthead seabream (*Sparus aurata*) and sea bass (*Dicentrarchus labrax*). *European Journal of Lipid Science and Technology, 105*, 104–107.

Sèrot, T., Gandemer, G., & Demaimay, M. (1998). Lipid and fatty acid compositions of muscle from farmed and wild adult turbot. *Aquaculture International, 6*, 331–343.

Sheik-Eldin, M., De Silva, S., Anderson, T. A., & Gooley, G. (1996). Comparsion of fatty acid composition of muscle, liver, mature oocytes, and diets of wild and captive Macquarie perch, *Macquaria australasica*, broodfish. *Aquaculture, 144*, 201–216.

Steffens, W. (1997). Effects of variation in essential fatty acids in fish feeds on nutritive value of freshwater fish for humans. *Aquaculture, 151*, 97–119.

Suzuki, H., Okazaki, K., Hayakawa, S., Wada, S., & Tamura, S. (1986). Influence of commercial dietary fatty acids on polyunsaturated fatty acids of cultured freshwater fish and comparison with those of wild fish of the same species. *Journal of Agricultural and Food Chemistry, 34*, 58–60.

Ulbricht, T. L. V., & Southgate, D. A. T. (1991). Coronary disease seven dietary factors. *Lancet, 338*, 985–992.

Valfré, F., Caprino, F., & Turchini, G. M. (2003). The health benefit of seafood. *Veterinary Research Communications, 27*, 507–512.

van Vliet, T., & Katan, M. B. (1990). Lower ratio of $n-3$ to $n-6$ fatty acids in cultured than in wild fish. *American Journal of Clinical Nutrition, 51*, 1–2.

Watson, L. (2008). The European market for perch (*Perca fluviatilis*). In P. Fontaine, P. Kestemont, F. Teletchea, & N. Wang (Eds.), *Percid fish culture. From research to production* (pp. 10–15). Namur, Belgium: Presses Universitaires de Namour.

Xu, X. L., Fontaine, P., Mélard, C., & Kestemont, P. (2001). Effects of dietary fat levels on growth, feed efficiency and biochemical composition of Eurasian perch *Perca fluviatilis*. *Aquaculture International, 9*, 437–449.

Xu, X., & Kestemont, P. (2002). Lipid metabolism and FA composition in tissues of Eurasian perch *Perca fluviatilis* as influenced by dietary fats. *Lipids, 37*, 297–304.

Yildiz, M., & Şener, E. (2004). The effect of dietary oils of vegetable origin on the performance, body composition, fatty acid profiles of sea bass (*Dicentrarchus labrax* L. 1785) juveniles. *Turkish Journal of Veterinary and Animal Sciences, 28*, 553–562.

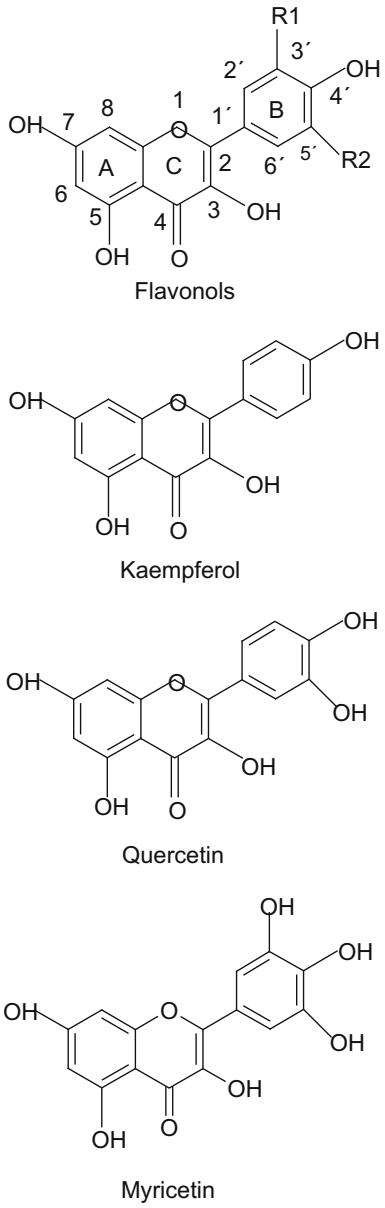

Fig. 1. Flavonols structures.

as drugs, vitamins and food colourants, increasing the solubility, stability and bioavailability of the guest molecule (Buschmann & Schollmayer, 2002; Loftsson & Brewster, 1996).

The ability of CDs to form inclusion complexes with guest molecules depends on the relative size of the internal cavity of CD to the size of the guest molecule or certain key functional groups within the guest. While the height of the CD cavity is the same for all types (7.9 Å), the number of glucose units determines the internal diameter of the cavity and its volume. Based on these dimensions β-CDs (cavity diameter 6–6.5 Å) will complex mainly aromatics and heterocycles (Martín Del Valle, 2004).

As recently described by our group, CDs can be used as flavonoids complexation agents, not only to increase the total flavonoid concentration in aqueous solutions, while the free flavonoids concentration remains constant, but also to decrease the free flavonoid concentration in aqueous solution, while the total concentration remains constant (Lucas-Abellán, Fortea, López-Nicolás, & Núñez-Delicado, 2007). In all cases, CDs acts as substrate reservoir in a dosage-controlled manner. In the case of resveratrol, its complexation with hydroxypropyl-β-cyclodextrins (HP-β-CDs) led to an increase not only in its aqueous solubility but also in its antioxidant activity due to its protection towards free radical attack (Lucas-Abellán et al., 2008).

The complexation of myricetin and quercetin in CDs has been described by our group and their complexation constants (K_c) were calculated by using both solubility and enzymatic methods (Lucas-Abellán, Fortea, Gabaldón, & Núñez-Delicado, 2008). However, it is still unknown whether entrapment in the internal cavity of CDs affects the antioxidant capacity of those flavonols.

Based on the statement described above and tacking into account radial distances, flavonols could be entrapped by β-CDs via phenoxyl group of ring A (C6–C8 = 2.68 Å) or ring B having one (C3′–C5′ = 2.68 Å), two (–OHC4′–OH–C5′ = 3.09 Å) or three OH groups (OH–C3′–OH–C5′ = 5.27 Å) (Fig. 1).

As continuing research examines the effect of antioxidants on health, the testing for antioxidant protection has become focus of attention in the dietary and natural products industry. Researchers associated with the natural product industry have pushed for a standardised method for measuring antioxidant capacity in natural products (Honzel et al., 2008). A large number of methods have been developed to evaluate the antioxidant capacity in foods, one of the most popular and best standardised chemical antioxidant methods being the oxygen radical absorbance capacity (ORAC) test (Ou, Huang, Hampsch-Woodill, & Prior, 2001). The ORAC method is based on the inhibition of the peroxyl-radical-induced oxidation initiated by thermal decomposition of azo-compounds, like 2,2′-azobis(2-amidino-propane) dihydrochloride (AAPH), and it is the only method that combines inhibition time and inhibition degree into a single quantity. This test is widely used for the evaluation and comparison of the antioxidant capacity of natural food products and plasma (Prior et al., 2007).

In the present paper, the effect of the complexation of three flavonols kaempferol, quercetin and myricetin, with HP-β-CDs on their antioxidant capacity against reactive oxygen species (ROS) has been studied by means of ORAC-fluorescein (ORAC-FL) assay (Ou et al., 2001). The antioxidant capacity of myricetin, quercetin and kaempferol in aqueous solution in the absence and presence of CDs is studied for the first time, using the ORAC-FL assay adapted to manual handling, and a conventional fluorescence plate reader.

2. Material and methods

2.1. Chemicals

FL, AAPH, 6-hydroxy-2,5,7,8-tetramethylchroman-2-carboxylic acid (Trolox C), myricetin, quercetin and kaempferol were purchased from Sigma (Madrid, Spain). HP-β-CDs were from TCI (Europe). All other chemicals used were of analytical grade.

A FL stock solution (4 μM) was made in 75 mM sodium phosphate buffer (pH 7.4) and was stored at −20 °C for 4 weeks. The FL solution was prepared daily in 75 mM sodium phosphate buffer (pH 7.4) by diluting the FL stock to a final concentration of 6 nM. Solutions of 0.25 mM Trolox C and 15 μM myricetin, quercetin and kaempferol in 75 mM sodium phosphate buffer (pH 7.4) were prepared and aliquoted into small vials for storage at −80 °C until use. A 127 mM AAPH solution in 75 mM sodium phosphate buffer (pH 7.4) was prepared daily.

2.2. ORAC-FL assay

The ORAC analyses were carried out on a Synergy HT multi-detection microplate reader, from Bio-Tek Instruments, Inc. (Winooski, USA), using 96-well polystyrene microplates with black

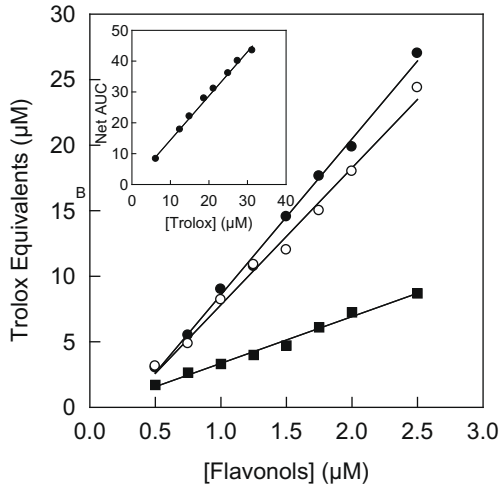

Fig. 2. Regression of μM Trolox equivalents of kaempferol (●), quercetin (○) and myricetin (■) at different concentrations. *Inset:* regression of net AUC of Trolox C on different concentrations of Trolox C. The net AUC = $AUC_{sample} - AUC_{blank}$.

sides and clear bottom, purchased from Nalge Nunc International. Fluorescence was read through the clear bottom, with an excitation wavelength of 485/20 nm and an emission filter of 528/20 nm. The plate reader was controlled by KC4, version 3.4, software. The oxygen radical absorbance capacity was determined as described by Dávalos, Gómez-Cordovés, and Bartolomé (2004), with slight modifications. The reaction was carried out in 75 mM sodium phosphate buffer (pH 7.4), and the final reaction mixture was 200 μL. FL (100 μL; 3 nM, final concentration) and myricetin, quercetin, or kaempferol in the absence or presence of β-CDs or HP-β-CDs (70 μL) solutions, were placed in the wells of the microplate. The mixture was preincubated for 30 min at 37 °C, before rapidly adding the AAPH solution (30 μL; 19 mM, final concentration) using a multichannel pipette. The microplate was immediately placed in the reader and the fluorescence recorded every 1.14 min for 120 min. The microplate was automatically shaken prior to each reading. A blank with FL and AAPH using sodium phosphate buffer instead of the antioxidant solution and eight calibration solutions using Trolox C (6.25, 12.5, 15.0, 18.75, 21.25, 25, 27.5 and 31.25 μM) as antioxidant were also used in each assay. The inhibition capacity was expressed as Trolox equivalents (mM), and is quantified by integrating of the area under the curve (AUC). All reaction mixtures were prepared in triplicate and at least three independent assays were performed for each sample. In order to avoid a temperature effect, only the inner 60 wells were used for experimental purposes, while the outer wells were filled with 200 μL of distilled water.

The results were expressed as μM Trolox equivalents by using the calibration curve of Trolox C ($y = 0.12 + 1.43x$) (Fig. 2, insert). The area under the fluorescence decay curve (AUC) was calculated by the following equation:

$$AUC = 1 + \sum_{i=1.14}^{i=120} f_i/f_0 \quad (1)$$

where f_0 is the initial fluorescence read at 0 min and f_i is the fluorescence read at time i. The net AUC corresponding to the sample was calculated by subtracting the AUC corresponding to the blank. Data processing was performed using Sigmaplot software package 9.0 (Jandel Scientific, Germany).

3. Results and discussion

Synthetic antioxidants such as butylated hydroxyanisole (BHA), butylated hydroxytoluene (BHT) and tertbutylhydroquinone (TBHQ) have been widely used as antioxidants in foods, but concerns over their safety have led to increased interest in natural antioxidants (Wanasundara & Shahidi, 1998). Synthetic antioxidants have in many cases been substituted by phenolic compounds and much research effect has been directed at these natural antioxidants, in particular flavonoids (Martínez-Valverde, Periago, Provan, & Chesson, 2002).

In the present paper, the effect of including of myricetin, quercetin and kaempferol in CDs on their antioxidant activity is studied by using the ORAC-FL method in the presence of increasing concentrations of CDs. These three flavonols were selected for study become of their on chemical structure characteristics, availability and prevalence in plants foods.

Fig. 2 presents the concentration-dependent data of antioxidant activity obtained for each flavonol tested: myricetin (filled square), quercetin (open circle) and kaempferol (filled circle). Least squares regression lines were computed between flavonols concentration and antioxidant activity (expressed as μM Trolox equivalents). As can be seen in Fig. 2, the regression analysis showed linear relation between each flavonol concentration and μM Trolox equivalents, yielding the equations: $y = -3.3 + 11.9x$; $y = -2.6 + 10.45x$ and $y = -0.2 + 3.56x$ for kaempferol, quercetin and myricetin, respectively. Considering that a slope of 1.0 in the lines of Fig. 2 would mean that the ORAC activity of 1 μM of the tested flavonol is equivalent to 1 μM Trolox, kaempferol (slope 11.9), quercetin (slope 10.45) and myricetin (slope 3.56) had ORAC activities from 3–12-fold greater than Trolox. These results agree with those presented by Tabart, Kevers, Pincemail, Defraigne, and Dommes (2009), in which the antioxidant activity of the same three flavonols was determined by several methods, including ORAC assay.

In general, the antioxidant activity of flavonoids depends on the structure and substitution pattern of their hydroxyl groups. As stated in other papers the presence of 3-OH group, which provides a catechol-like structure in ring C, is beneficial for the antioxidant activity of flavonoids. Additional hydroxyl groups at positions C5 and C7 of the A ring appear to be less important. The presence of the C2–C3 double bond with a 4-keto arrangement is known to be responsible for electron delocalisation from ring B, which it increases the radical-scavenging activity. The flavonols tested in this work have a different number of OH in ring B. We observed (Fig. 2) the antioxidant activity to be as follows: kaempferol > quercetin > myricetin, which is inversely proportional to the number of hydroxyl groups in the B ring. Kaempferol, which had only one OH group in position C4′ of ring B, showed a slightly higher antioxidant activity than quercetin (with a catechol moiety). Both flavonols appeared to be much better antioxidants than myricetin, which has a galloyl structure in ring B.

Once the antioxidant activity of each flavonol had been established, our purpose was to demonstrate the effect of the inclusion of kaempferol, quercetin and myricetin in HP-β-CDs on the antioxidant activity of the flavonols using the ORAC-FL assay.

The respective areas, under the curve, when the FL decay curves obtained in the presence of kaempferol (Fig. 3, insert), quercetin or myricetin (0.5 or 0.75 μM) (*data not shown*) in the absence of HP-β-CDs were smaller than those obtained in the presence of 1.75 mM HP-β-CDs. Because ORAC assay data combines inhibition time and inhibition degree in a single datum, it is important to note that any increase in the inhibition time and decrease in the inhibition degree of the FL decay curve was greater in the presence of flavonols–CD complexes in all cases than in the presence of flavonols alone (Fig. 3, insert).

When increasing concentrations of HP-β-CDs were added to the reaction medium at too flavonoid concentrations (0.5 or 0.75 μM), a clear increase in the antioxidant activity was observed in all cases (Figs. 3–5). It was not possible to measure the net AUC of kaempferol, quercetin and myricetin at concentrations higher than

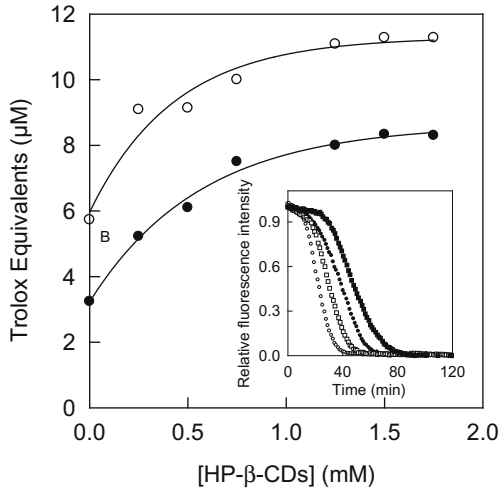

Fig. 3. Effect of HP-β-CDs concentration on the μM Trolox equivalents of kaempferol 0.5 μM (●) and 0.75 μM (○). *Inset:* FL fluorescence decay curves induced by AAPH in the presence of kaempferol alone (0.5 μM (○) and 0.75 μM (□)) and with HP-β-CDs 1.75 mM (kaempferol 0.5 μM (●) and 0.75 μM (■)).

0.75 μM in the presence of CDs, because the measuring times exceeded 2 h, which was established as optimum for the ORAC assay (Lucas-Abellán et al., 2008).

When the concentration of HP-β-CDs increased, the μM Trolox equivalents of flavonols also increased reaching saturation level at approximately 1 mM of HP-β-CDs in all cases. At the saturation level, flavonols showed approximately double the antioxidant activity in the presence than in the absence of CDs in all the cases studied (Figs. 3–5). This effect on antioxidant activity may have been due to the formation of inclusion complexes between these flavonoids and HP-β-CDs.

In order to corroborate that those three flavonols were complexed by HP-β-CDs in 75 mM sodium phosphate buffer (pH 7.4), their complexation constants, K_c were calculated by constructing phase solubility diagrams (*data not shown*). The K_c values obtained for kaempferol, quercetin and myricetin were 1411, 900 and 850 M^{-1}, respectively (Table 1). Kaempferol showed the highest K_c, whereas quercetin and myricetin had lower (and very similar) values.

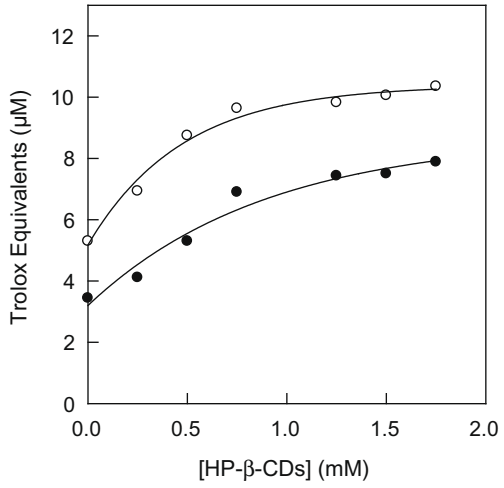

Fig. 4. Effect of HP-β-CDs concentration on the μM Trolox equivalents of quercetin 0.5 μM (●) and 0.75 μM (○).

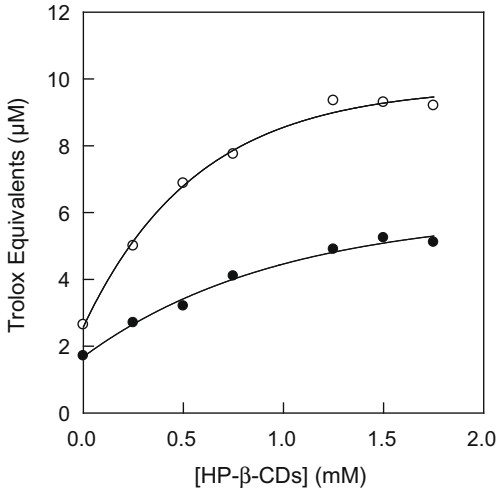

Fig. 5. Effect of HP-β-CDs concentration on the μM Trolox equivalents of myricetin 0.5 μM (●) and 0.75 μM (○).

As can be seen in Fig. 6, at an HP-β-CDs concentration of 1.75 mM, the concentration at which almost all flavonols were complexed, kaempferol presented the highest antioxidant activity (Fig. 6, black bars) and myricetin the lowest, as in the absence of HP-β-CDs. It is important to note that there was little difference between the antioxidant activities observed for the tree flavonols when all of them were totally complexed in HP-β-CDs. However,

Table 1
Complexation constant (K_c), aqueous solubility (S_0), free flavonol ([flavonol]$_f$) and antioxidant activity (AA) normalised with respect to the Trolox measurement.

Flavonol	K_c (M^{-1})	S_0 (μM)	[Flavonol]$_f$ (μM)			AA normalised respect to Trolox (μM TE/μM flavonol)	
			0 mM HP-β-CDs	0.25 mM HP-β-CDs	1.75 mM HP-β-CDs	0 mM HP-β-CDs	1.75 mM HP-β-CDs
Kaempferol	1411	4	0.75	0.556	0.217	11.9	15.1
Quecetin	900	26	0.75	0.612	0.291	10.4	13.5
Myricetin	850	62	0.75	0.619	0.3	3.6	11.2

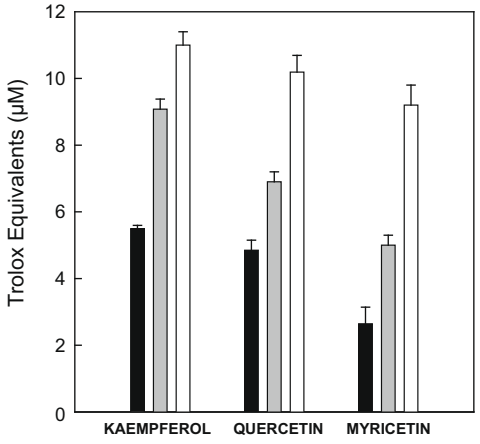

Fig. 6. Effect of HP-β-CDs concentration in the μM Trolox equivalents of kaempferol, quercetin and myricetin alone, 0.75 μM (black bars) and in the presence of HP-β-CDs 0.25 mM (grey bar) or HP-β-CDs 1.75 mM (white bars).

at 0.25 mM HP-β-CDs, a concentration at which not all the flavonol is complexed, the differences between the antioxidant activities of three flavonols were greater (Fig. 6, grey bars). As can be seen in Fig. 6, the increase in antioxidant activity at 0.25 mM HP-β-CDs was close to the increase observed at 1.75 mM in the case of kaempferol, while in the case of quercetin and myricetin, the antioxidant activity at 0.25 mM HP-β-CDs was much lower than at 1.75 mM. This can be explained taking by the higher K_c of kaempferol is compared with quercetin or myricetin.

At flavonol concentrations studied in this paper (up to 0.75 μM), kampferol, quercetin and myricetin were soluble in the reaction medium (Table 1). Therefore, the increase in μM Trolox equivalent observed in Figs. 3–5 when increasing CDs concentration were added to the reaction medium, cannot be attributed to the solubilisation of flavonols, as has been previously described for lycopen (Bangalore, McGlynn, & Scott, 2005) and α-tocopherol (Huang, Ou, Hampsch-Woodill, Flanagan, & Deemer, 2002). In all cases, when the flavonols were complexed, HP-β-CDs acted as a reservoir of controlled substrate dosage protecting flavonols against their rapid oxidation by AAPH radical. So, their antioxidant activity was prolonged and only reached a maximum when all the flavonols had been complexed (a minimum quantity of free flavonols was always present because the complexation phenomenon is a dynamic equilibrium).

To complete the study, an experiment was carried out in which increasing concentrations of each flavonol were added to the reaction medium at a fixed HP-β-CDs concentration (1.75 mM). In this case, the values of antioxidant activity normalised with respect to Trolox increased in all cases (Table 1).

In order to clarify whether the increase in antioxidant activity of flavonols was due to the protection afforded by HP-β-CDs, the free flavonol concentrations ($[\text{flavonols}]_f$) at each bar of Fig. 6, were calculated using the K_c value previously obtained for each flavonol (Table 1) and the following Eq. (2) (Lucas-Abellán et al., 2008):

$$[\text{flavonols}]_f = (-([\text{CD}]_t K_c - [\text{flavonols}]_t K_c + 1) + \sqrt{([\text{CD}]_t K_c - [\text{flavonols}]_t K_c + 1)^2 + 4K_c[\text{flavonols}]_t})/2K_c \quad (2)$$

where $[\text{flavonols}]_t$ is total flavonol and $[\text{CD}]_t$ is total CD.

As can be seen in Table 1, in the absence of HP-β-CDs, the concentration of free flavonol was the same in all cases. However, as shown in Fig. 6, kaempferol presented the highest antioxidant activity, due to its chemical structure. Moreover, as HP-β-CDs concentration increased, free flavonol concentration decreased in all cases, kaempferol being the most complexed flavonol, due to its higher K_c (Table 1). Due to the similar K_c value for quercetin and myricetin, both flavonols presented similar free concentrations at a fixed HP-β-CDs concentration, (Table 1). However, as can be seen in Fig. 6, quercetin presented greater antioxidant activity, as in the absence of HP-β-CDs, due to its chemical structure.

In summary, the antioxidant activity of kaempferol, quercetin and myricetin increased when as they are complexed in HP-β-CDs. Kaempferol presented the highest antioxidant activity both in the absence and presence of HP-β-CDs, while myricetin showed the lowest antioxidant activity.

Acknowledgements

This work was partially supported by Ministerio de Educación y Ciencia (AGL2006-08702/ALI). C.L.A. is a holder of a Research Grant from the Programa Nacional de Formación de Personal Investigador (FPI), Ministerio de Educación y Ciencia (Spain).

References

Bangalore, D. V., McGlynn, W., & Scott, D. D. (2005). Effect of b-cyclodextrin in improving the correlation between lycopene concentration and ORAC values. *Journal of Agricultura and Food Chemistry, 53*, 1878–1883.

Benavente-García, O., Castillo, J., Marín, F. R., Ortuno, A., & Del Río, J. A. (1997). Uses and properties of citrus flavonoids. *Journal of Agricultural and Food Chemistry, 45*, 4505–4515.

Buschmann, H. J., & Schollmayer, E. (2002). Application of cyclodextrins in cosmetic products: A review. *Journal of Cosmetic Science, 53*, 185–191.

Cao, G., Sofic, E., & Prior, R. (1997). Antioxidant and prooxidant behaviour of flavonoids: Structure–activity relationships. *Free Radical Biology and Medicine, 22*, 749–760.

Dávalos, A., Gómez-Cordovés, C., & Bartolomé, B. (2004). Extending applicability of the oxygen radical absorbance capacity (ORAC-fluorescein) assay. *Journal of Agricultural and Food Chemistry, 52*, 48–54.

Espín, J. C., García-Conesa, M. T., & Tomás-Barberán, F. A. (2007). Nutraceuticals: Facts and fiction. *Phytochemistry, 68*, 2986–3008.

Heim, K. E., Tagliaferro, A. R., & Bobilya, D. J. (2002). Flavonoid antioxidants: Chemistry, metabolism and structure–activity relationships. *The Journal of Nutritional Biochemistry, 13*, 572–584.

Honzel, D., Carter, S. G., Redman, K. A., Schauss, A. G., Endres, J. R., & Jensen, G. S. (2008). Comparison of chemical and cell-based antioxidant methods for evaluation of food and natural products: Generating multifaceted data by parallel testing using erythrocytes and polymorphonuclear cells. *Journal of Agricultural and Food Chemistry, 56*, 8319–8325.

Huang, D., Ou, B., Hampsch-Woodill, M., Flanagan, J. A., & Deemer, E. K. (2002). Development and validation of oxygen radical absorbance capacity assay for lipophilic antioxidants using randomly methylated β-cyclodextrin as the solubility enhancer. *Journal of Agricultural and Food Chemistry, 50*, 1815–1821.

Huber, G. M., Rupasinghe, V., & Shahidi, F. (2009). Inhibition of oxidation of omega-3 polyunsaturated fatty acids and fish oil by quercetin glycosides. *Food Chemistry*. doi:10.1016/j.foodchem.2009.04.007.

Loftsson, T., & Brewster, M. E. (1996). Pharmaceutical application of cyclodextrins. Drug solubilisation and stabilization. *Journal of Pharmaceutical Science, 85*, 1017–1025.

Lucas-Abellán, C., Fortea, M. I., Gabaldón, J. A., & Núñez-Delicado, E. (2008). Encapsulation of quercetin and myricetin in cyclodextrins at acidic pH. *Journal of Agricultural and Food Chemistry, 56*, 255–259.

Lucas-Abellán, C., Fortea, M. I., López-Nicolás, J. M., & Núñez-Delicado, E. (2007). Cyclodextrins as resveratrol carrier system. *Food Chemistry, 104*, 39–44.

Lucas-Abellán, C., Mercader-Ros, M. T., Zafrilla, M. P., Fortea, M. I., Gabaldón, J. A., & Núñez-Delicado, E. (2008). ORAC-fluorescein assay to determine the oxygen radical absorbance capacity of resveratrol complexed in cyclodextrins. *Journal of Agricultural and Food Chemistry, 56*, 2254–2259.

Manach, C., Mazur, A., & Scalbert, A. (2005). Polyphenols and prevention of cardiovascular diseases. *Current Opinions in Lipidology, 16*, 77–84.

Martín del Valle, E. M. (2004). Cyclodextrins and their uses: A review. *Process Biochemistry, 39*, 1033–1046.

Martínez-Valverde, I., Periago, M. J., Provan, G., & Chesson, A. (2002). Phenolic compounds, lycopene and antioxidant activity in commercial varieties of tomato (*Lycopersicum esculentum*). *Journal of the Science of Food and Agriculture, 82*, 323–330.

Middleton, E., Kandaswami, C., & Theoharides, T. C. (2000). The effects of plant flavonoids on mammalian cells: Implications for inflammation, heart disease and cancer. *Pharmacological Reviews, 52*, 673–751.

Ou, B., Huang, D., Hampsch-Woodill, M., & Prior, R. L. (2001). Development and validation of an improved oxygen radical absorbance capacity assay using fluorescein as the fluorescent probe. *Journal of Agricultural and Food Chemistry, 49*, 4619–4626.

Parr, A. J., & Bolwell, G. P. (2000). Phenols in the plant and in man. The potential for possible nutritional enhancement of the diet by modifying the phenols content or profile. *Journal of the Science of Food and Agriculture, 80*, 985–1012.

Prior, R. L., Gu, L., Wu, X., Jacob, R. A., Sotoudeh, G., Kader, A. A., et al. (2007). Plasma antioxidant capacity changes following a meal as a measure of the ability of a food to alter in vivo antioxidant status. *Journal of American College Nutrition, 26*, 170–181.

Puupponen-Pimiä, R., Nohynek, L., Meier, C., Kähkönen, M., Heinonen, M., Hopia, A. J., et al. (2001). Antimicrobial properties of phenolic compounds from berries. *Journal of Applied Microbiology, 90*, 494–507.

Samman, S., Lyons Wall, P. M., & Cook, N. C. (1998). Flavonoids and coronary heart disease: Dietary perspectives. *Baillieres Clinic Endocrinology Metabolic, 12*, 589–604.

Soobrattee, M. A., Neergheen, V. S., Luximon-Ramma, A., Aruoma, O. I., & Bahorum, T. (2005). Phenolics as potential antioxidant therapeutic agents: Mechanism and actions. *Mutation Research, 579*, 200–213.

Szejtli, J. (2004). Past, present, and future of cyclodextrin research. *Pure and Applied Chemistry, 76*, 1825–1845.

Tabart, J., Kevers, C., Pincemail, J., Defraigne, J. O., & Dommes, J. (2009). Comparative antioxidant capacities of phenolic compounds measured by various tests. *Food Chemistry, 113*, 1226–1233.

Wanasundara, U. N., & Shahidi, F. (1998). Antioxidant and prooxidant activity of green tea extracts in marine oils. *Food Chemistry, 63*, 335–342.

Wojdylo, A., Oszmianski, J., & Czemerys, R. (2007). Antioxidant activity and phenolic compounds in 32 selected herbs. *Food Chemistry, 105*, 940–949.

information is available on the effect of 1-MCP treatment on physiological and biochemical responses, towards, for example, antioxidant enzymes and lipid peroxidation, as well as the alteration of nutritional quality in broccoli florets. To date, there are no reports on the effect of 1-MCP treatment on glucosinolates of products including broccoli florets. The objective of the present study was to investigate the effect of treatment of broccoli florets with 2.5 μl/l 1-MCP on shelf life, visual quality, physiological and biochemical responses and health-promoting compounds during storage at 20 °C.

2. Materials and methods

2.1. Plant material

Broccoli heads (*Br. oleracea* var. *italica* cv. Lvxiong) of prime quality were harvested in the early morning from the greenhouse of Zhejiang University (Hangzhou, China), top-iced and then transported to the Postharvest Laboratory of Vegetable Institute, Zhejiang University within 10 min. Broccoli heads with a diameter ranging from 15 to 20 cm were chosen, and the inner branches (with florets having stalks of approximately 2 cm) were then cut from these heads for experimentation. The florets were surface-sterilised by washing with a solution of 50 mg/kg NaOCl for 1 min and dried using a household model spin drier for 2 min. The florets were then randomly distributed into the required number of treatment units.

2.2. 1-MCP and storage treatments

Broccoli florets were treated with air (control), 0.1, 1, 2.5, 5 and 10 μl/l 1-MCP for 6 h at 20 °C. The broccoli florets were placed in plastic bags and 1-MCP was injected, then the injection pore of the bags was immediately sealed and the samples were stored for 6 h at 20 °C. After treatment, all experimental units were stored according to randomised complete block design in incubation chamber with 95% RH at 20 °C. The shelf life was then determined. The concentration of 2.5 μl/l 1-MCP was selected for further study.

There were three replicates per treatment with 200 g of broccoli florets per replicate. Shelf life, visual quality and visual colour scale rating were made in replicates of 10 florets taken daily. The treated broccoli florets were used for determination of chlorophyll, antioxidant enzymes, polyphenol oxidase (PPO, EC 1.14.18.1), lipoxygenase (LOX, EC 1.13.11.12), malondialdehyde (MDA), ascorbic acid, total carotenoids and glucosinolates.

2.3. Determination of shelf life

Shelf life was determined according to previous reports (Ku & Wills, 1999; Xu, Guo, Yuan, Yuan, & Wang, 2006). The time for quality to decline to 30% yellowing in florets was assigned as their shelf life.

2.4. Determination of visual colour rating scale and visual quality

Visual quality was determined as previously described (Jia et al., 2009). Visual quality of florets was scored on a 1–9 scale, where 9 refers to excellent and fresh appearance, 7 to good, 5 to fair (limit of marketability), 3 to fair (useable but not saleable), and 1 to unusable. Intermediate numbers were assigned where appropriate. Colour of broccoli florets was visually rated using colour rating scales 1–5, as described by Rangkadilok et al. (2002), where 1 refers to dark green, 2 to trace yellow (10% yellow), 3 to slightly yellow (25% yellow), 4 to medium yellow (50% yellow), and 5 to completely yellow (100%).

2.5. Determination of chlorophyll content

Florets (0.5 g) were ground and extracted in 10 ml of 80% acetone, centrifuged at 3000 rpm for 10 min at room temperature, and then residue was removed. Total chlorophyll content was determined by reading the absorbance at 652 nm with a spectrophotometer. Total chlorophyll content was estimated as mg/g fresh weight (FW).

2.6. Enzyme assay

Broccoli florets (0.5 g) were homogenised with 5 ml, 50 mM phosphate buffer (pH 7.8) in an ice-water bath, and then centrifuged at 8000 rpm for 20 min at 4 °C. The supernatant was collected and used for enzyme assay.

Total superoxide dismutase (SOD, EC 1.15.1.1), catalase (CAT, EC 1.11.1.6) and peroxidase (POD, EC 1.11.1.7) activities were assayed according to the method of Toivonen and Sweeney (1998). SOD activity was determined based on the ability of SOD to inhibit the reduction of nitroblue tetrazolium. The absorbance was monitored at 560 nm. One unit of SOD is the amount of extract that gives 50% inhibition of the reduction rate of NBT. CAT activity was determined by monitoring the enzyme-catalysed decomposition of H_2O_2 by potassium permanganate. One unit of CAT activity was defined as the amount of H_2O_2 (μmol) depleted per min at 240 nm. POD activity was measured based on the determination of guaiacol oxidation at 470 nm by H_2O_2. The change in absorbance at 470 nm was followed every 30 s by spectrophotometer. PPO activity was assayed by measuring the increase in absorbance at 420 nm with 100 mM catechol solution as substrate, according to Kumar, Mohan, and Murugan (2008). One unit of enzyme activity was defined as the amount of enzyme that caused an increase in absorbance of 0.001 min^{-1}. LOX activity was determined according to the method of Anese and Sovrano (2006) with minor changes. The substrate solution was prepared by mixing 20 μl of linoleic acid, 48 ml of H_2O, 2 ml of 0.1 N NaOH and 10 μl of Tween 20. Each test contained 0.1 ml enzymatic extracts, 0.15 ml substrate solution and 1.25 ml phosphate buffer (pH 5.7). One unit of LOX is defined as the amount of enzyme which caused an increase in absorption at 234 nm of 0.1 min^{-1} (3 min period).

The SOD, CAT, POD, PPO and LOX activities were estimated by units/mg protein. Protein content of samples was determined by using Folin phenol reagent (Lowry, Rosebrough, Farr, & Randall, 1951).

2.7. Malondialdehyde (MDA) determination

MDA was measured by 2-thiobarbituric acid reaction. One gram fresh weight of broccoli florets sample was homogenised in 5 ml of 0.1% (w/v) TCA. The homogenate was centrifuged at 12,500 rpm for 20 min. One millilitre of supernatant was precipitated with 4 ml 20% TCA containing 0.5% (w/v) 2-thiobarbituric acid. The mixture was heated in a water-bath shaker at 95 °C for 30 min and quickly cooled in an ice-bath. The absorbance was read at 532 nm after centrifugation at 3000 rpm for 10 min and the value for non-specific absorption at 600 nm was subtracted. The MDA content was calculated using its extinction coefficient of 155 mM^{-1} cm^{-1}. The amount of MDA was estimated as μmol/g FW.

2.8. Total carotenoids determination

Five grams of florets were ground and extracted with a mixture of acetone and petroleum ether (1:1, v/v) repeatedly using the mortar and pestle until a colourless residue was obtained. After washing several times with water, the upper phase was collected and combined as crude extract. The extracts were made up to a

known volume with petroleum ether. Total carotenoids content was determined by reading the absorbance at 451 nm with a spectrophotometer. Total carotenoids content was estimated as mg/100 g FW.

2.9. Ascorbic acid determination

Twenty grams of frozen broccoli florets were ground to a fine powder at liquid nitrogen temperature, extracted twice with 20 ml of 1.0% (w/v) oxalic acid and centrifuged for 20 min at 3000 rpm. The combined aqueous extract was filtered under vacuum in a volumetric flask. Each sample was filtered through a 0.45 μm cellulose acetate filter prior to injection. HPLC analysis of ascorbic acid was carried out using a Shimadzu (Tokyo, Japan) mode VP liquid chromatograph with a dual-wavelength spectrophotometer. Samples (5 μl) were separated at room temperature on a Waters Spherisorb C18 column (150 × 4.6 mm id; 5 μm particle size) (Milford, MA) using a solution of 0.05 M KH_2PO_4 at a flow rate of 1.0 ml/min. The amount of ascorbic acid was calculated from absorbance at 254 nm, using ascorbic acid as a standard. Results were expressed as mg/100 g FW.

2.10. Glucosinolate assay

Freshly harvested and stored broccoli florets were frozen in liquid N_2 and kept in polyethylene bags at −70 °C until freeze-drying. Freeze-dried broccoli samples were stored in sealed polyethylene bags at 4 °C until analysis. Glucosinolates were extracted and analysed as previously described with minor modifications (Wang, Grubb, & Abel, 2002; Xu et al., 2006). Freeze-dried samples (25 mg) were boiled in 1 ml water for 10 min. After recovery of the liquid, the residues were washed with water (1 ml), and the combined aqueous extract was applied to a DEAE-Sephadex A-25 (40 mg) column (pyridine acetate form) (GE Healthcare, Piscataway, NJ). The column was washed three times with 20 mM pyridine acetate and twice with water. The glucosinolates were converted into their desulfo analogues by overnight treatment with 100 μl of 0.1% (1.4 units) aryl sulfatase, and the desulfoglucosinolates were eluted with 2 × 0.5 ml water. HPLC analysis of desulfoglucosinolates was carried out using a Shimadzu mode VP liquid chromatograph with a dual-wavelength spectrophotometer. Samples (100 μl) were separated at 30 °C on a Waters Spherisorb C18 column (150 × 4.6 mm id; 5 μm particle size) using acetonitrile and water at a flow rate of 1.0 ml/min. The procedure employed isocratic elution with 1.5% acetonitrile for the first 5 min; a linear gradient to 20% acetonitrile over the next 15 min, followed by isocratic elution with 20% acetonitrile for the final 10 min. Absorbance was measured at 226 nm and 280 nm. *ortho*-Nitrophenyl-β-D-galactopyranoside (Sigma) was used as an internal standard for HPLC analysis. Concentrations of individual glucosinolates were determined according to published response factors. The integrated area of the desulfo-4-methylsulfinylbutyl glucosinolate peak was converted to a molar amount under the assumption that this compound has a molar extinction coefficient at 226 nm equal to that of sinigrin.

2.11. Statistical analyses

Statistical analysis was performed using the SPSS package program version 11.5 (SPSS Inc., Chicago, IL). Data was analysed by analysis of variance (ANOVA model one-way). Sources of variation were storage duration and treatments. The means were compared by the least significant differences (LSD) test at a significance level of 0.05. The values are reported as means with their standard deviations for all results.

3. Results

3.1. Effect of 1-MCP treatment on shelf life

All 1-MCP treatments greatly extended the shelf life of broccoli florets, the most significant being broccoli florets treated with 2.5 μl/l 1-MCP (Fig. 1). The shelf life of broccoli florets treated with 2.5 μl/l 1-MCP was extended to two times that of control florets (2.5 days at 20 °C). Based on the results of shelf life studies, 1-MCP at a dose of 2.5 μl/l was selected, to analyse the effect of 1-MCP treatment on visual and nutritional quality of broccoli florets.

3.2. Effect of 1-MCP treatment on colour, visual quality and chlorophyll degradation

There was yellowing and rapid loss in visual quality occurred in control florets during storage at 20 °C. 1-MCP treatment effectively inhibited this yellowing and visual quality deterioration of broccoli florets. A significant difference in colour and visual quality between 1-MCP treatment and control was observed after 1 days storage at 20 °C (Fig. 2). Chlorophyll content decreased in both control and 1-MCP-treated broccoli florets during storage. However, chlorophyll degradation rate was significantly lower in treated broccoli florets than in control florets (Fig. 2). After storage at 20 °C for 5 days, 1-MCP-treated broccoli florets contained 67% of the initial chlorophyll content, while control florets contained only 24% of initial value.

3.3. Effect of 1-MCP treatment on SOD, CAT, POD and PPO activities

SOD activity in both the control and treatment declined during the first 3 days of storage, significantly increased during the following day and then fell again at the 5th day. CAT activity in both the control and treatment showed the same trend as SOD during the first 3 days of storage, and then increased steadily to the 5th day. 1-MCP treatment significantly improved the SOD and CAT activities, which made the SOD and CAT activities always higher in the treatment than in control across the whole storage period (Fig. 3). POD activity increased in both control and 1-MCP treatment during the first day, decreased over the next 3 days and then

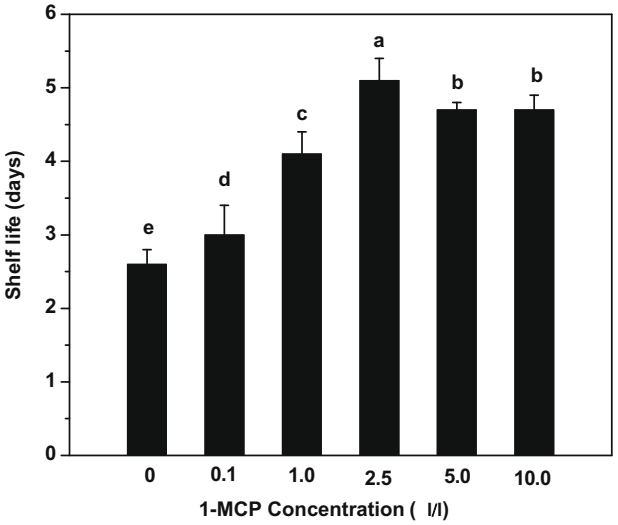

Fig. 1. Shelf life of broccoli florets treated with different concentrations of 1-MCP during storage at 20 °C. Each data is the mean of three replicate samples. Values not sharing a common letter are significantly different at $p < 0.05$.

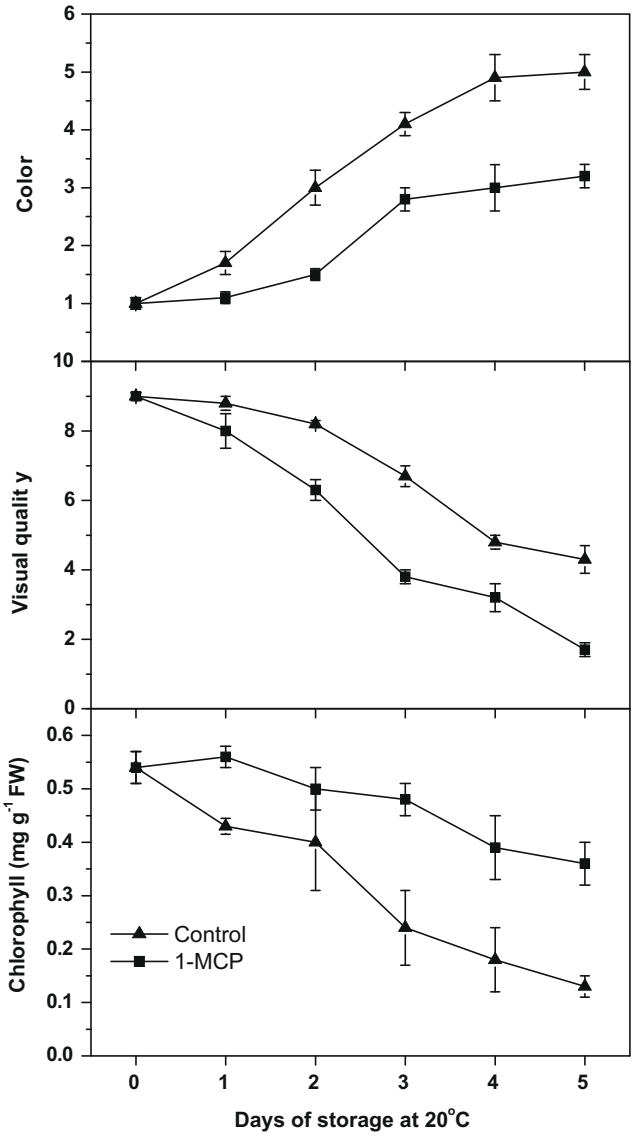

Fig. 2. Changes of colour, visual quality and chlorophyll content in broccoli florets. Florets were treated with air (control) and 2.5 μl/l 1-MCP for 6 h at 20 °C. Florets were stored at 20 °C for 5 days. Each data point is the mean of three replicate samples. Vertical bars represent standard deviation of the mean.

increased again. The activity of POD in treated broccoli florets was significantly higher than in the control florets during 5 days storage at 20 °C (Fig. 3). PPO activity in both control and treatment markedly increased during the initial 4 days of storage and then decreased at day 5. However, the florets treated with 1-MCP possessed relatively lower PPO activity in comparison with the control florets during storage (Fig. 3).

3.4. Effect of 1-MCP treatment on MDA content and LOX activity

The initial content of MDA was 1.54 μmol/g FW, and no significant difference in MDA content was observed between control and 1-MCP treatment during the first day of storage; subsequently a larger rise in MDA content was found in control florets than in florets treated with 2.5 μl/l 1-MCP from the second day at 20 °C (Fig. 4). The results indicated that 1-MCP treatment could inhibit the rise of MDA content. Similarly, the rise of LOX activity during storage was inhibited by the 1-MCP treatment (Fig. 4).

3.5. Effect of 1-MCP treatment on the contents of ascorbic acid and total carotenoids

The contents of ascorbic acid and total carotenoids in both control and 1-MCP treated broccoli florets declined progressively, with a higher level of both in 1-MCP treated florets than in the control after 5 days of storage at 20 °C. The loss of ascorbic acid and total carotenoids were 19.4% and 30.0%, respectively, in 1-MCP-treated florets, while losses of as much as 57.8% and 50.0% occurred, respectively, in control florets over 5 days of storage at 20 °C. The contents of ascorbic acid and total carotenoids were 2-fold and 1.3-fold higher, respectively, in 1-MCP treatment florets than in control florets on the 5th day (see Fig. 5).

3.6. Effect of 1-MCP treatment on total and individual glucosinolates

The total glucosinolate content as well as the individual aliphatic (methylsulfinylalkyl: glucoiberin, glucoraphanin and progoitrin) and indole (glucobrassicin, neoglucobrassicin and 4-methoxyglucobrassicin) glucosinolate contents were quantitatively determined in broccoli florets over 5 days of storage (Fig. 6). The predominant aliphatic glucosinolates in broccoli florets were 4-methylsulfinylbutyl glucosinolate (glucoraphanin), followed by 3-methylsulfinylpropyl glucosinolate (glucoiberin), while the predominant indole glucosinolates were 3-indolylmethyl glucosinolate (glucobrassicin) and 1-methoxy-3-indolymethyl glucosinolate (neoglucobrassicin).

The change of the total aliphatic glucosinolates content was not significant in both control and 1-MCP treatment over the first two days storage, then a rapid decrease of total aliphatic glucosinolates content was observed in florets of control and 1-MCP treatment. However, the decrease rate in treated florets was significantly lower than in control florets. The total aliphatic glucosinolates was reduced by 71.2% after 5 days of storage at 20 °C in control florets, but only reduced by 51.3% in florets treated with 2.5 μl/l 1-MCP (Fig. 6). Amongst the individual aliphatic glucosinolates, glucoraphanin, progoitrin and glucoiberin showed similar trends to total aliphatic glucosinolates in both control and treatment during 5 days of storage at 20 °C. The loss rates of glucoraphanin, progoitrin and glucoiberin in broccoli florets treated with 1-MCP (56.4%, 23.6% and 32.4%, respectively) were much lower than those in control florets (77.7%, 48.6% and 42.7%, respectively) at the end of the 5 days storage period (Fig. 6).

The total indole glucosinolates content decreased during 5 days storage at 20 °C, although lower losses of indole glucosinolates than aliphatic glucosinolates in both control and treatment were detected. The total indole glucosinolates decreased by 37.0% in the control, but only 23.7% in the treatment (Fig. 6). The decrease in total indole glucosinolates was predominantly due to the progressive degradation of glucobrassicin and neoglucobrassicin in both control and treatment. However, the decrease rate of glucobrassicin and neoglucobrassicin in the treatment (26.7% and 20.6%, respectively) was lower than in the control (41.5% and 33.2%, respectively) (Fig. 6).

4. Discussion

The effect of 1-MCP treatment on shelf life, visual quality, antioxidant enzymes and health-promoting compounds in broccoli florets was investigated in the present study. The results showed that the shelf life of broccoli florets treated with various concentrations of 1-MCP was significantly improved. This is consistent with the findings of Ku and Wills (1999), Fan and Mattheis (2000), Able, Wong, Prasad and O'Hare (2002), and Forney, Song, Fan, Hildebrand, and Jordan (2003). However, Ku and Wills (1999) found that

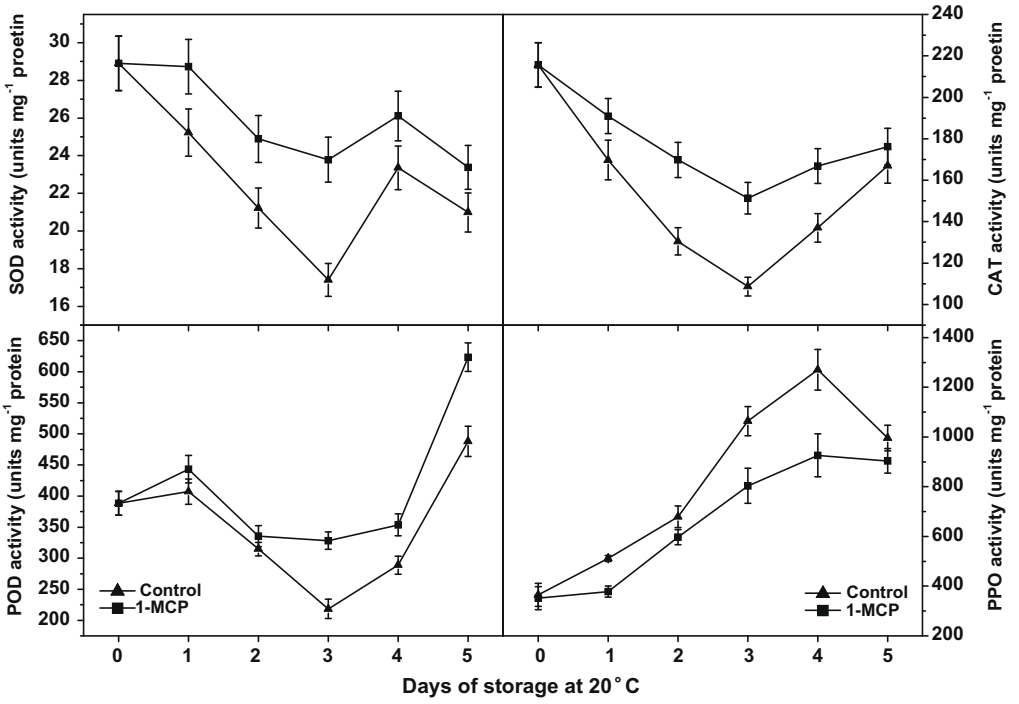

Fig. 3. Changes of superoxide dismutase (SOD), peroxidase (POD), catalase (CAT) and polyphenol oxidase (PPO) activities in broccoli florets. Florets were treated with air (control) and 2.5 μl/l 1-MCP for 6 h at 20 °C. Florets were stored at 20 °C for 5 days. Each data point is the mean of three replicate samples. Vertical bars represent standard deviation of the mean.

the higher the concentration of 1-MCP was (ranging from 0.02 to 50 μl/l), the greater was the storage life of broccoli florets, but also suggested that a lower concentration range (1–10 μl/l) needs to be used to avoid toxicity. Able et al. (2002) showed that a concentration of 12 μl/l 1-MCP was considered optimal for extension of the shelf life of broccoli florets. Our study showed that the extension of shelf life was most significant in broccoli florets treated with 2.5 μl/l 1-MCP. This discrepancy could be due to different cultivars and temperatures used.

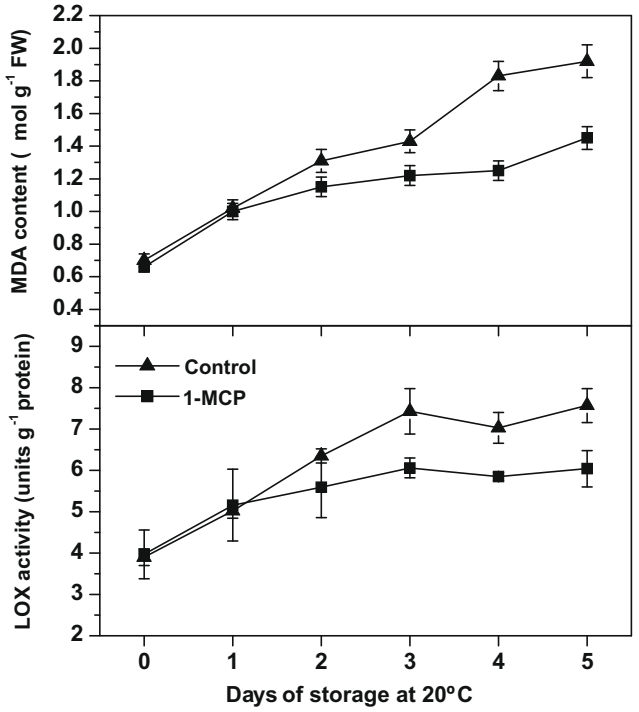

Fig. 4. Change of malondialdehyde (MDA) content and lipoxygenase (LOX) activity in broccoli florets. Florets were treated with air (control) and 2.5 μl/l 1-MCP for 6 h at 20 °C. Florets were stored at 20 °C for 5 days. Each data point is the mean of three replicate samples. Vertical bars represent standard deviation of the mean.

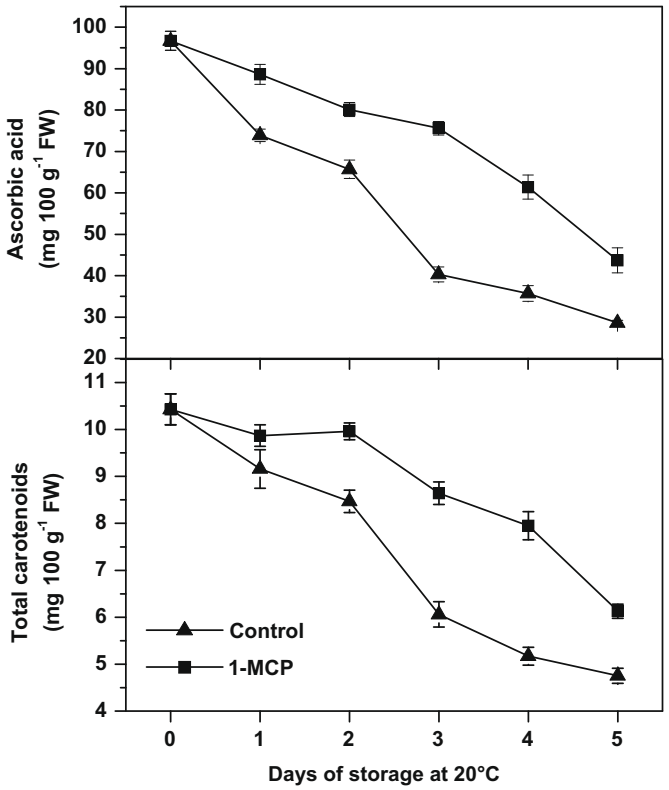

Fig. 5. Changes of ascorbic acid and total carotenoids in broccoli florets. Florets were treated with air (control) and 2.5 μl/l 1-MCP for 6 h at 20 °C. Florets were stored at 20 °C for 5 days. Each data point is the mean of three replicate samples. Vertical bars represent standard deviation of the mean.

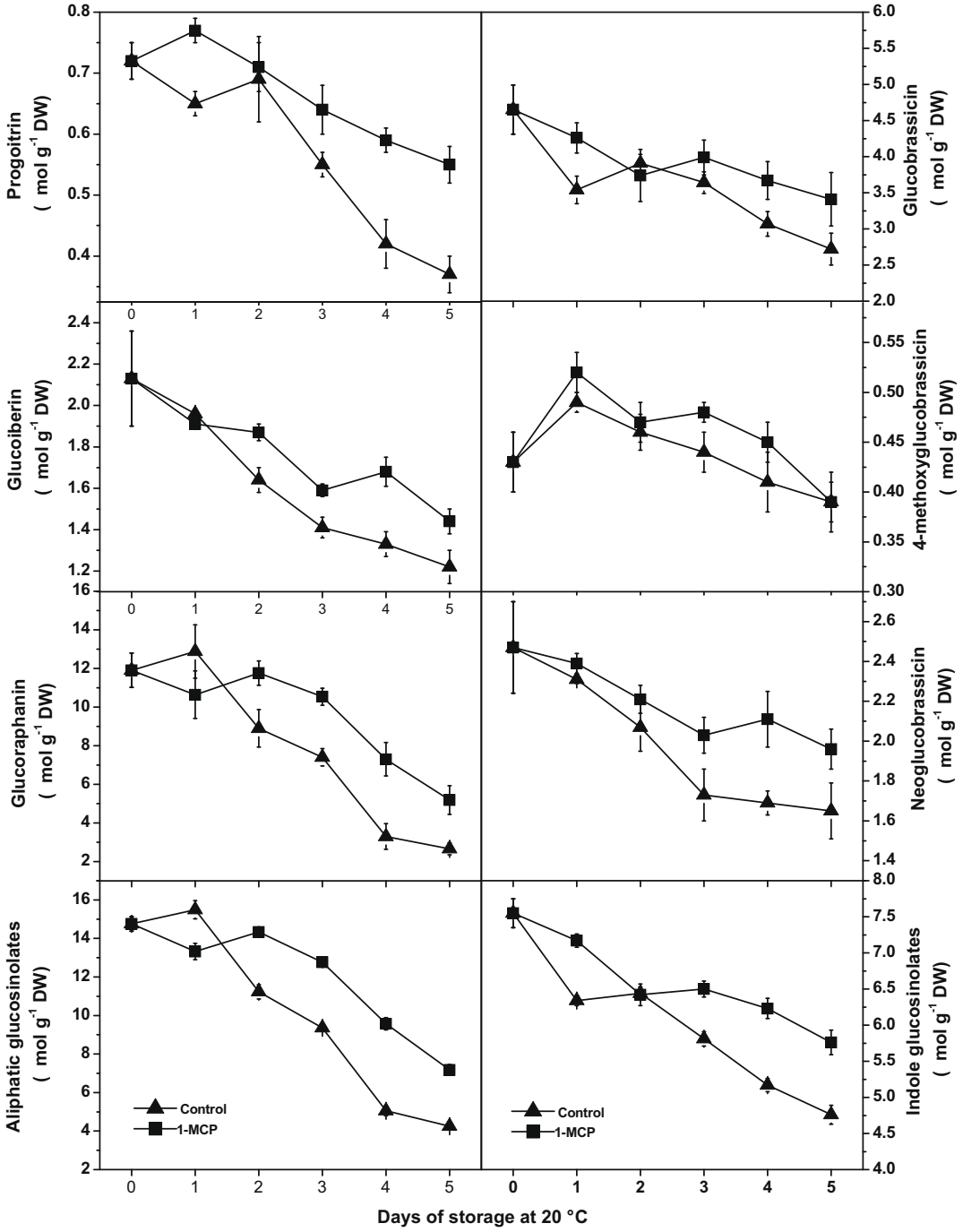

Fig. 6. Changes of total aliphatic, total indole and individual glucosinolates in broccoli florets. Florets were treated with air (control) and 2.5 μl/l 1-MCP for 6 h at 20 °C. Florets were stored at 20 °C for 5 days. Each data point is the mean of three replicate samples. Vertical bars represent standard deviation of the mean.

The green colour of broccoli is an important commercial quality index. Degreening of broccoli after harvest occurs rapidly during storage at 20 °C (Wang, 1977). Treatment of broccoli with 1-MCP resulted in delayed loss of green colour and delayed onset of yellowing (Fan & Mattheis, 2000; Gong & Mattheis, 2003; Ku & Wills, 1999). Our study supported the evidence that treatment of broccoli florets with 2.5 μl/l 1-MCP inhibited chlorophyll degradation, yellowing and quality deterioration.

Senescence is considered to be associated with the defence system, including antioxidant enzymes and antioxidants. Antioxidant enzymes (SOD, CAT and POD) are considered to be important in the oxy-radical detoxification process in plant tissues (Han et al., 2006; Mittler, 2002). Toivonen and Sweeney (1998) reported that antioxidant protection offered by SOD and POD is important for the retention of green colour in broccoli flower buds, and the increases in SOD, POD and CAT were likely responses to the increases in oxygen radical production in broccoli, which could subsequently lead to yellowing. Postharvest treatment could change the activity of antioxidant enzymes in vegetables and fruits. Ethanol vapour treatment leads to higher activities of SOD, POD and CAT in broccoli florets during storage, as compared with the control (Han et al., 2006). 1-MCP treatment has also been shown to increase the activities of antioxidant enzymes in mango (Singh & Dwivedi, 2008) and *Yali* pear (Fu, Cao, Li, Lin, & Jiang, 2007). In our study,

it was found that SOD, CAT and POD activities were consistently higher in the 1-MCP treatment than in the control during 5 days storage at 20 °C. It was suggested that the increases in the activities of SOD, CAT and POD were generally a consequence of the system ability to delay senescence (Toivonen & Sweeney, 1998). From the results of our study, it can be hypothesised that 1-MCP might delay the senescence of broccoli florets by means of regulating the antioxidant enzymes system. The specific mechanism of 1-MCP in delaying the senescence of broccoli florets and its relationship with the antioxidant enzymes still remain to be further investigated. PPO represents a marker compound for the extent of oxidation and is responsible for browning in fresh-cut fruits and vegetables. 1-MCP treatment has been shown to reduce browning, which was associated with reduced PPO activity in avocados (Watkins, 2006). It is suggested in the present study that 1-MCP treatment could reduced the browning of broccoli florets by reduction of PPO activity.

The thiobarbituric acid-reactive substance MDA is the product of membrane peroxidation and has been used as a direct indicator of membrane injury. According to Zhuang, Hildebrand, and Barth (1995, 1997), postharvest senescence of broccoli is correlated with lipid peroxidation (MDA content), leading to cell-membrane disintegration. LOX are regarded to be responsible for membrane degradation because they catalyse the peroxidation of polyunsaturated fatty acids, producing hydroperoxy fatty acids (Macri, Braidot, Petrusa, & Vianello, 1994). It was found in our study that 1-MCP treatment could inhibit the increase of lipid peroxidation (MDA content) and LOX activity in broccoli florets, compared with control florets, during postharvest storage.

Vitamin C is one of the most important nutritional components in broccoli, as well as in many other horticultural crops, and has many biological activities in the human body. The concentration of vitamin C/ascorbic acid (the predominant form of vitamin C) in broccoli generally decreased during storage and the loss rate during storage could be lowered by postharvest handling (Serrano et al., 2006; Vallejo et al., 2003). In our study, the control florets lost more than half of their initial ascorbic acid after 5 days of storage, while these losses were minimised in those florets treated with 1-MCP. The present study showed that 1-MCP treatment resulted in significantly better retention of ascorbic acid during postharvest storage. Carotenoids have been extensively studied for their potential protection against numerous cancers. However, limited information is available on the effect of postharvest handling on carotenoids in broccoli. In the present work, total carotenoids in both control and treated florets decreased during 5 days of storage. However, treatment of broccoli florets with 2.5 μl/l 1-MCP significantly lowered the magnitude of total carotenoids loss during postharvest storage.

Glucosinolates are among the most important health-promoting natural products in broccoli florets. They are known to contribute to the anticarcinogenic activity of broccoli. Several hydrolysis products of methylsulfinyl aliphatic glucosinolates, such as glucoraphanin, in broccoli are considered to reduce the risk of cancers. Sulforaphane (derived from glucoraphanin) is the most potent, naturally-occurring inducer of Phase 2 enzymes that detoxify carcinogens (Brown et al., 2002). The same is true for breakdown products of indole glucosinolates, notably glucobrassicin (Weng, Tsai, Kulp, & Chen, 2008). However, higher losses of glucoraphanin (or sulforaphane) and other glucosinolates have been reported after harvesting (Cieslik, Leszczynska, Filipiak-Florkiewicz, Sikora, & Pisulewski, 2007; Jia et al., 2009; Rangkadilok et al., 2002; Vallejo et al., 2003). In fact, control florets lost over half of their initial glucosinolates after 5 days storage at 20 °C (Fig. 6). Broccoli florets suffer a series of stresses after harvest (washing/pre-cutting) and during storage, which might trigger complex metabolism of glucosinolates. Cutting of broccoli heads to broccoli florets brings myrosinase in contact with glucosinolates, which might lead to a high degree of glucosinolate hydrolysis. On the other hand, it might also induce the biosynthesis of glucosinolates during 1-MCP treatment and storage. The glucosinolate level of stored broccoli florets is a reflection of two opposing mechanisms, hydrolysis of glucosinolates by myrosinase and induction of glucosinolate biosynthesis by an unknown mechanism. The elevated level of some individual glucosinolates (progoitrin, glucoraphanin, and 4-methoxyglucobrassicin) in broccoli florets during the first day of storage under control or 1-MCP treatment was observed in our study (Fig. 6). The predominance of the induction of biosynthesis of these glucosinolates might be the cause of the increase of the content under these cases during storage, though the specific mechanism involved remains to be further elucidated.

Postharvest handing is required to maintain glucosinolate content in broccoli florets and low temperature and high relative humidity are effective conditions (Jia et al., 2009; Jones et al., 2006; Rodrigues & Rosa, 1999). The present study showed that 1-MCP treatment leads to better retention of glucosinolates, in comparison with the control, during storage at 20 °C, which suggested that 1-MCP treatment is also an effective method to maintain glucosinolate content. To the best of our knowledge, this is the first report on the effect of 1-MCP treatment on the glucosinolate content of foods. The mechanism by which broccoli florets treated with 2.5 μl/l 1-MCP inhibited the decrease rate of glucosinolate content compared with the control is not clear. However, previous studies and the data from the current study could provide possible explanations. Firstly, as mentioned above, 1-MCP treatment inhibited the increase of MDA as compared with the control. MDA is the product of membrane peroxidation, and could damage the structure and integrity of membrane during the senescence of broccoli florets. Thus, it can be hypothesised that 1-MCP could inhibit probable loss of membrane integrity and mixing of glucosinolates with myrosinase, leading to less glucosinolates hydrolysis. Furthermore, the biosynthesis of secondary metabolites, such as glucosinolates, is thought to be part of the plant defensive mechanism, and ethylene seems to play a role in this process (Mikkelsen et al., 2003). On the other hand, 1-MCP is well-known as an ethylene inhibitor and ethylene production was decreased by 1-MCP treatment. It is possible that the blockage of ethylene action by 1-MCP treatment favoured the biosynthesis of glucosinolates or inhibited some ethylene-related degradative pathways. Further studies are warranted to provide a clearer understanding of the effect of 1-MCP treatment on glucosinolate content.

It was reported that aliphatic glucosinolates were generally more stable than indole glucosinolates during storage and processing of Brassica vegetables (Jia et al., 2009; Rungapamestry, Duncan, Fuller, & Ratcliffe, 2007). Boiling of these vegetables leads to inactivation of myrosinase and partial decomposition of thermolabile glucosinolates, especially indole glucosinolates (Cieslik et al., 2007). The observation that indole glucosinolates were preserved better than aliphatic glucosinolates under 1-MCP treatment in the current study suggests that 1-MCP treatment might have different effects on the stability of myrosinase and individual glucosinolates metabolites, though the mechanism involved remains to be further investigated.

Previous studies have found that glucoraphanin, the predominant glucosinolate in broccoli, dramatically decreased at room temperature (Rodrigues & Rosa, 1999). Our current study showed similar results. On the other hand, 1-MCP treatment significantly inhibited the loss rate of glucoraphanin and glucobrassicin. In this regard, it is likely that broccoli florets treated with 1-MCP will be preferable for human consumption than control broccoli florets.

As high temperatures are often encountered during the handling, transportation and retail marketing of broccoli, they have become the main cause of postharvest loss of broccoli, especially in developing countries. The use of 1-MCP can reduce the require-

ment for low temperature while still extending the shelf life, and reducing the loss of visual and nutritional quality. It has tremendous potential for maintaining broccoli florets quality during storage at relatively higher temperature.

In conclusion, 2.5 μl/l 1-MCP treatment significantly extended the shelf life, reduced the postharvest deterioration, retarded the chlorophyll degradation and inhibited the increase of MDA content and the activities of PPO and LOX of broccoli florets. The activities of SDO, POD and CAT in florets treated with 1-MCP were higher than those in control florets. 1-MCP treatment reduced the losses of total carotenoids, ascorbic acid and total aliphatic, total indole and individual glucosinolates in broccoli florets when compared to those in the control. These results indicated that 1-MCP treatment could be a good candidate for extending shelf life, maintaining the visual quality and reducing the loss of health-promoting compounds, particularly chemopreventive glucosinolates in broccoli florets stored at 20 °C.

Acknowledgements

The authors thank Dr. Duo Li for critical reading of the manuscript. This work was supported by National High-tech R&D Program of China (863 program 2008AA10Z111), China Postdoctoral Science Foundation Funded Project (20080441259), National Natural Science Foundation of China (30320974) and Fok Ying Tong Education Foundation (104034).

References

Able, A. J., Wong, L. S., Prasad, A., & O'Hare, T. J. (2002). 1-MCP is more effective on a floral brassica (*Brassica oleracea* var. *italica* L.) than a leafy brassica (*Brassica rapa* var. *chinensis*). *Postharvest Biology and Technology, 26*(2), 147–155.

Anese, M., & Sovrano, M. (2006). Kinetics of thermal inactivation of tomato lipoxygenase. *Food Chemistry, 95*, 131–137.

Brown, A. F., Yousef, G. G., Jeffrey, E. H., Klein, B. P., Wallig, M. A., Kushad, M. M., et al. (2002). Glucosinolate profiles in broccoli: Variation in levels and implications in breeding for cancer chemoprotection. *Journal of the American Society for Horticultural Science, 127*(5), 807–813.

Cartea, M. E., & Velasco, P. (2008). Glucosinolates in Brassica foods: Bioavailability in food and significance for human health. *Phytochemistry Reviews, 7*, 213–229.

Cieslik, E., Leszczynska, T., Filipiak-Florkiewicz, A., Sikora, E., & Pisulewski, P. M. (2007). Effects of some technological processes on glucosinolate contents in cruciferous vegetables. *Food Chemistry, 105*(3), 976–981.

Fan, X. T., & Mattheis, J. P. (2000). Yellowing of broccoli in storage is reduced by 1-methylcyclopropene. *Hortscience, 35*(5), 885–887.

Forney, C. F., Song, J., Fan, L. H., Hildebrand, P. D., & Jordan, M. A. (2003). Ozone and 1-methylcyclopropene alter the postharvest quality of broccoli. *Journal of the American Society for Horticultural Science, 128*(3), 403–408.

Fu, L., Cao, J., Li, Q., Lin, L., & Jiang, W. (2007). Effect of 1-methylcyclopropene on fruit quality and physiological disorders in *Yali* pear (*Pyrus bretschneideri Rehd.*) during storage. *Food Science and Technology International, 13*(1), 49–54.

Gong, Y. P., & Mattheis, J. P. (2003). Effect of ethylene and 1-methylcyclopropene on chlorophyll catabolism of broccoli florets. *Plant Growth Regulation, 40*(1), 33–38.

Han, J. H., Tao, W. Y., Hao, H. K., Zhang, B. L., Jiang, W. B., Niu, T. G., et al. (2006). Physiology and quality responses of fresh-cut broccoli florets pretreated with ethanol vapor. *Journal of Food Science, 71*(5), S385–S389.

Izumi, H., Watada, A. E., & Douglas, W. (1996). Optimum O_2 or CO_2 atmospheres for storing broccoli florets at various temperatures. *Journal of the American Society for Horticultural Science, 121*, 127–131.

Jia, C. G., Xu, C. J., Wei, J., Yuan, J., Yuan, G. F., Wang, B. L., et al. (2009). Effect of modified atmosphere packaging on visual quality and glucosinolates of broccoli florets. *Food Chemistry, 114*, 28–37.

Jones, R. B., Faragher, J. D., & Winkler, S. (2006). A review of the influence of postharvest treatments on quality and glucosinolate content in broccoli (*Brassica oleracea* var. *italica*) heads. *Postharvest Biology and Technology, 41*(1), 1–8.

Ku, V. V. V., & Wills, R. B. H. (1999). Effect of 1-methylcyclopropene on the storage life of broccoli. *Postharvest Biology and Technology, 17*(2), 127–132.

Kumar, V. B. A., Mohan, T. K. C., & Murugan, K. (2008). Purification and kinetic characterization of polyphenol oxidase from Barbados cherry (*Malpighia glabra* L.). *Food Chemistry, 110*(32), 8–333.

Lowry, O. H., Rosebrough, N. J., Farr, A. L., & Randall, R. J. (1951). Protein measurement with the Folin phenol reagent. *Journal of Biological Chemistry, 193*, 265–275.

Luo, Z. S., Xu, X. L., Cai, Z. Z., & Yan, M. (2007). Effects of ethylene and 1-methylcyclopropene (1-MCP) on lignification of postharvest bamboo shoot. *Food Chemistry, 105*(2), 521–527.

Macri, F., Braidot, E., Petrusa, E., & Vianello, A. (1994). Lipoxygenase activity associated to isolated soybean plasmamembranes. *Biochimica et Biophysica Acta, 1215*, 109–114.

Mikkelsen, M. D., Petersen, B. L., Glawischnig, E., Jensen, A. B., Andreasson, E., & Halkier, B. A. (2003). Modulation of CYP79 genes and glucosinolate profiles in Arabidopsis by defense signaling pathways. *Plant Physiology, 131*(1), 298–308.

Mittler, R. (2002). Oxidative stress, antioxidants and stress tolerance. *Trends in Plant Science, 7*(9), 405–410.

Rangkadilok, N., Tomkins, B., Nicolas, M. E., Premier, R. R., Bennett, R. N., Eagling, D. R., et al. (2002). The effect of post-harvest and packaging treatments on glucoraphanin concentration in broccoli (*Brassica oleracea* var. *italica*). *Journal of Agricultural and Food Chemistry, 50*(25), 7386–7391.

Rodrigues, A. S., & Rosa, E. A. S. (1999). Effect of post-harvest treatments on the level of glucosinolates in broccoli. *Journal of the Science of Food and Agriculture, 79*(7), 1028–1032.

Rungapamestry, V., Duncan, A. J., Fuller, Z., & Ratcliffe, B. (2007). Effect of cooking Brassica vegetables on the subsequent hydrolysis and metabolic fate of glucosinolates. *Proceedings of the Nutrition Society, 66*(1), 69–81.

Serrano, M., Martinez-Romero, D., Guillen, F., Castillo, S., & Valero, D. (2006). Maintenance of broccoli quality and functional properties during cold storage as affected by modified atmosphere packaging. *Postharvest Biology and Technology, 39*(1), 61–68.

Singh, R., & Dwivedi, U. N. (2008). Effect of Ethrel and 1-methylcyclopropene (1-MCP) on antioxidants in mango (*Mangifera indica* var. *Dashehari*) during fruit ripening. *Food Chemistry, 111*(4), 951–956.

Toivonen, P. M. A., & Sweeney, M. (1998). Differences in chlorophyll loss at 13 degrees C for two broccoli (*Brassica oleracea* L.) cultivars associated with antioxidant enzyme activities. *Journal of Agricultural and Food Chemistry, 46*(1), 20–24.

Vallejo, F., Tomas-Barberan, F., & Garcia-Viguera, C. (2003). Health-promoting compounds in broccoli as influenced by refrigerated transport and retail sale period. *Journal of Agricultural and Food Chemistry, 51*(10), 3029–3034.

Wang, C. Y. (1977). Effect of amimoethyoxy analog of rhizobitoxine and sodium benzoate on senescence of broccoli. *Hortscience, 12*, 54–56.

Wang, Q., Grubb, C. D., & Abel, S. (2002). Direct analysis of single leaf disks for chemopreventive glucosinolates. *Phytochemical Analysis, 13*(3), 152–157.

Watkins, C. B. (2006). The use of 1-methylcyclopropene (1-MCP) on fruits and vegetables. *Biotechnology Advances, 24*(4), 389–409.

Weng, J. R., Tsai, C. H., Kulp, S. K., & Chen, C. S. (2008). Indole-3-carbinol as a chemopreventive and anti-cancer agent. *Cancer Letters, 262*(2), 153–163.

Xu, C. H., Guo, D. P., Yuan, J., Yuan, G. F., & Wang, Q. M. (2006). Changes in glucoraphanin content and quinone reductase activity in broccoli (*Brassica oleracea* var. *italica*) florets during cooling and controlled atmosphere storage. *Postharvest Biology and Technology, 42*(2), 176–184.

Zhuang, H., Hildebrand, D. F., & Barth, M. M. (1995). Senescence of broccoli buds as related to changes in lipid peroxidation. *Journal of Agricultural and Food Chemistry, 43*(10), 2589–2591.

Zhuang, H., Hildebrand, D. F., & Barth, M. M. (1997). Temperature influenced lipid peroxidation and deterioration in broccoli buds during postharvest storage. *Postharvest Biology and Technology, 10*(1), 49–58.

extracts (~6–10% of coffee composition) but not in roasted (~0.01% of coffee composition) (Farah, Monteiro, Calado, Franca, & Trugo, 2006) was not considered. Furthermore, a few natural active substances in coffee of low molecular weight such as trigonelline, caffeic acid and 5-caffeoylquinic acid (139, 180 and 354 Da, respectively) have shown activity against the growth of *Legionella pneumophila* (Furuhata, Dogasaki, Hara, & Fukuyama, 2002), Enterobacteria (Almeida et al., 2006) and *S. mutans* (Almeida et al., 2004).

In view of existing contradictory results and of the persistent need for new strategies for caries control, the aim of the present study was to verify if natural coffee compounds contribute to the antibacterial activity against *S. mutans*, correlating results of minimum inhibitory concentration (MIC), minimum bactericidal concentration (MBC), biofilm inhibition concentration and biofilm reduction concentration assays with the concentration of major bioactive compounds in various coffee extracts with different chemical composition. Additionally, this study aimed at investigating the effect of species, decaffeination and roasting on such antibacterial effect.

2. Materials and methods

2.1. Coffee chemical compounds

5-Caffeoylquinic acid (chlorogenic acid, 5-CQA), caffeic acid, ferulic acid, trigonelline, nicotinic acid and caffeine (Sigma–Aldrich, St. Louis, MO, USA) solutions at 1 mg/mL were prepared using Milli-Q purified water (Millipore Corporation, Billerica, MA, USA). All standard solutions were filtered through sterile filter paper discs (TPP, 0.22 μm membrane, Zurich, Switzerland) prior to microbiological tests.

2.2. Coffee samples and aqueous extracts

Regular *C. arabica* cv. Yellow Bourbon and *C. canephora* cv. Conillon beans were harvested, respectively, in Minas Gerais and Espírito Santo, Brazil (Group 1). One blend of *C. arabica* harvested in São Paulo and a second sample of *C. canephora* cv. Conillon harvested in Espírito Santo were used in both regular and decaffeinated forms (Group 2). Decaffeination was performed using water and dichloromethane (Cocam, Brazil). Samples from Group 2 were of inferior quality comparing to those of Group 1.

Samples were roasted in a commercial spouted bed roaster (I-Roast, Gumee, IL, USA), operating at a maximum temperature of 220 °C, for 6, 7, 8, 13 and 15 min. The Roast Colour Classification system (Agtron-SCAA, Reno, NV; 1995), the percent weight loss values on a wet basis (Farah et al., 2005, 2006) and the instrumental colour (Colourgap 1A, Leogap-Probat, Brazil) were used as tools for roasting degree determination. Green and roasted coffee beans were ground in a laboratory-scale mill to pass through a 0.46 mm sieve.

Coffee extracts at 10% were obtained by a coffee brewing procedure commonly used in Brazil, percolating 100 mL of pre-boiling (95 °C) Milli-Q purified water through 10 g of green or roasted coffee samples. The extracts were filtered through Whatman #1 qualitative filter paper (Whatman, Maidstone, UK). Prior to microbiological tests, all coffee extracts were re-filtered through sterile filter papers (TPP, 0.22 μm membrane) and aliquots of the filtered extracts were reserved for chromatographic analyses.

2.3. Chemical characterisation of coffee extracts

The pH of the extracts was obtained by means of a pH metre (DM20 Digimed, Santo Amaro, SP, Brazil). The contents of caffeic, ferulic and chlorogenic acids (3-, 4- and 5-caffeoylquinic acids – 3-, 4- and 5-CQA; 3-, 4- and 5-feruloylquinic acids – 3-, 4- and 5-FQA; 3-, 4- and 5-coumaroylquinic acids – 3-, 4- and 5-CoQA; 3,4-, 3,5- and 4,5-dicaffeoylquinic acids – 3,4-, 3,5- and 4,5-diCQA; caffeoylferuloylquinic acids – CFQA), their respective 1,5-quinolactones (3- and 4-caffeoylquinide – 3- and 4-CQL; 3- and 4-feruloylquinide – 3- and 4-FQL; 3,4-dicaffeoylquinide – 3,4-diCQL) were determined by gradient LC-DAD-ESI-MS according to Farah et al. (2006), using a Magic C30 column (150 × 2.0 mm, 5 μm, 100 Å, Michrom Bioresources, Inc., Auburn, CA). The contents of caffeine, trigonelline, nicotinic acid and sucrose were determined by LC-ESI-MS according to Perrone, Donangelo, and Farah (2008), using a Spherisorb® S5 ODS2 Microbore column (150 × 2.0 mm, 5 μm, Waters, Milford, MA, USA). The LC equipment (Shimadzu, Kyoto, Japan) comprised a LC-10AD*vp* quaternary pump, a CTO-10AS*vp* column oven, an 8125 manual injector (Rheodyne) with a 5 μL loop and a SPD-M10A*vp* diode array detector. This LC system was interfaced with a LC–MS 2010 mass spectrometer (Shimadzu, Kyoto, Japan).

For sample clarification prior to the chromatographic analyses of phenolic compounds, 500 μL of each coffee extract were mixed with 500 μL of each Carrez solution and the volume was made up to 50 mL with Milli-Q water. For the determination of trigonelline, nicotinic acid, caffeine and sucrose Carrez solutions were replaced by 1 mL of saturated basic lead acetate solution (Farah et al., 2006). The mixtures were shaken, let rest for 10 min and filtered through a Whatman #1 qualitative filter paper and a 0.22 μm membrane (Millipore). The filtrates were used directly for chromatography. Chemical analyses were performed in triplicate.

2.4. Bacterial strains and culture

The bacterial strain used was from the American Type Culture Collection (ATCC): *S. mutans* ATCC 25175. Bacteria were kept at −20 °C in Tryptic Soy Broth [TSB] (Oxoid, Hampshire, England) with 20% glycerol and activated by transfer into blood agar, and incubation at 36.5 ± 1.0 °C, in anaerobic conditions, for 48 h in a candle jar. Bacterial cells were suspended, according to the McFarland protocol (1907), in saline solution to produce a suspension of about 1.5×10^8 CFU/mL. Three-hundred microlitres of this suspension were mixed with 9.7 mL of Mueller–Hinton bacterial broth medium (Difco, Sparks, USA), resulting in an inoculum with $4–5 \times 10^6$ CFU/mL.

2.5. Minimum inhibitory concentration (MIC) and minimum bactericidal concentration (MBC) determination

MIC was evaluated by the dilution method in Mueller–Hinton broth medium (Difco) according to Clinical and Laboratory Standards Institute (CSLI, formerly NCCLS) guidelines (NCCLS, 2003), with concentrations ranging from 1 to 10 mg/mL of the 10% coffee extracts. The concentrations varied from 1 to 1000 μg/mL for the standard solutions. The inoculum was added to each tube and the MIC value was evaluated after 24 h of incubation at 36.5 ± 1.0 °C, as the lowest concentration that completely inhibited the formation of visible growth. The MBC determination was used to assess if the inhibitory effect observed in MIC determinations was through a lethal (bactericidal) action. Samples from tubes where the MIC results showed no bacterial growth were removed with a loop, inoculated onto a blood agar plate, and incubated at 36.5 ± 1.0 °C, for 48 h in a candle jar. MBC was considered to be the concentration at which microorganisms were totally unable to grow. In the cases where the referred samples showed no bactericidal activity, the number of colonies formed (colony-forming units – CFU) on that plate was calculated at the inhibitory concentrations (no presence of turbidity). The controls included an inocu-

lated Mueller–Hinton broth medium (Difco) without the test compounds. Experiments were performed three times in duplicate.

2.6. Ethanol test

Based on the fact that ethanol has been used as a vehicle for chemical compounds or as an extraction solvent for plant extracts in various antibacterial studies (Almeida et al., 2004; Dall'Agnol et al., 2003; Xiao et al., 2007), and in order to choose a solution vehicle eliminating the possibility of false-positive results, ethanol alone was tested – in replacement of standard solution or coffee extracts – for *S. mutans* growth inhibition. HPLC grade ethanol (0.4 mL) (Tedia, Brazil) at 5%, 10% and 20% was added to test tubes containing 3.6 mL inoculated Mueller–Hinton broth medium. Experiment was performed in duplicate.

2.7. Sucrose supplemented medium test

The *S. mutans* inoculum was made as described above in Section 2.4. Three-hundred microlitres of the inoculum were transferred to two test tubes, one containing only 9.7 mL of Mueller–Hinton broth medium (control) and one containing the same amount of medium supplemented with 5.06 mg of sucrose. After incubation at 36.5 ± 1 °C for 6 h, diluted samples from the tubes were inoculated onto a blood agar plate and incubated at the same temperature for 48 h in a candle jar. The number of CFU was calculated. The experiment was performed in duplicate.

2.8. Biofilm susceptibility assay

The standard solutions and extracts showing better performance in relation to the cell-growth inhibition (MIC and MBC results) were selected for this assay. All 6 min roasted coffee extracts were tested. The effect of 5-CQA, trigonelline and selected extracts on *S. mutans* biofilm formation was examined by microdilution method. Twofold serial dilutions of extracts were prepared in 96-well polystyrene tissue culture plates (TPP, Zellkultur Testplatte 96 F) containing brain–heart infusion growth supplemented with 2% sucrose (BHIS, Difco, 200 μL/well) with final concentrations of 1.25, 2.5, 5.0, 50 and 90 mg/mL of the 10% selected coffee extracts. The selected standard solutions were tested at the concentration of 0.8 mg/mL. Chlorhexidine (0.05%, w/v) was used as the positive control; the medium without the tested agents was used as the non-treated control and the medium alone as the blank control. Aliquots (20 μL) of *S. mutans* ATCC 25175 cell suspension (final concentration of cells 5×10^7 CFU/mL) were inoculated in the wells of the polystyrene tissue culture plate except in the wells with the cell culture media alone as the blank control. After incubation in an anaerobic incubator (10% CO_2, 80% N_2, 10% H_2, 37 °C, 24 h), absorbance at 570 nm was recorded to assess the culture growth. Culture supernatants from each well were then decanted and planktonic cells were removed by washing with PBS, pH 7.2. The biofilm was air-dried (room temperature), stained (1 h) with 0.1% (w/v) Crystal Violet (Sigma) and rinsed thoroughly with water until control wells appeared colourless. Biofilm formation was quantified by the addition of 200 μL of 80% ethanol and 20% acetone to each Crystal Violet-stained well. The absorbance at 570 nm (A_{570}) was determined using a microplate reader (model 550 – Bio Rade Microplate Reader, Marnes – La-Coquete, France). The percentage of inhibition was calculated using the equation $(1 - A_{570}$ of the test$/A_{570}$ of non-treated control$) \times 100$ (Wei, Campagna, & Bobek, 2006).

To examine the effects of the selected chemical compounds and coffee extracts, *S. mutans* ATCC 25175 cells (20 μL aliquots of 5×10^7 CFU/mL) were inoculated into the wells of a polystyrene microtitre plate containing BHIS at a volume of 200 μL/well. Following incubation in an anaerobic incubator (10% CO_2, 80% N_2, 10% H_2, 37 °C, 24 h), the culture supernatant from each well was decanted and planktonic cells were removed by washing with PBS. BHIS containing the test samples, prepared in another microtitre plate, was then transferred to the one-day biofilm plate, and the plates were further incubated at 37 °C for 24 h under anaerobic conditions. Following, the cell growth was assessed by measurement of the absorbance at 570 nm, and the biofilm was fixed, stained and quantified as described above. The biofilm assays were performed in quadruplicate.

2.9. Statistical analysis

The association between chemical composition and number of colonies formed on the plate surface results was investigated using Pearson correlation analysis. CFU and biofilm results were analysed using Student's *t* test. SSPS software, version 11.0 was used for all statistical analysis. A 5% significance level was considered.

3. Results and discussion

In the present study, six bioactive compounds and 36 coffee extracts with distinct chemical composition were tested for *S. mutans* growth inhibition. For those compounds and coffee extracts showing growth inhibition in any of the tested concentrations, MIC was determined. Additionally, the coffee extracts showing the best performances in these assays were tested for biofilm inhibition and reduction.

3.1. Ethanol test

All tubes containing ethanol inhibited the growth of *S. mutans*, compared to the control with Milli-Q purified water. Therefore, for the evaluation of antibacterial activity Milli-Q water was chosen as the vehicle for selected chemical compounds and for coffee extracts preparation.

3.2. Selected coffee compounds

5-CQA, caffeic acid and trigonelline were able to inhibit the growth of *S. mutans*, with MIC of 0.8 mg/mL (bacteriostatic activity). No bactericidal activity was observed at this concentration. Nicotinic acid, caffeine and ferulic acid did not show bacteriostatic activity against *S. mutans* at tested concentrations. Although it is possible that at higher concentrations nicotinic acid, caffeine and ferulic acid would show bacteriostatic activity and 5-CQA, caffeic acid and trigonelline would show bactericidal activity, this test was not performed because we opted for testing concentrations that would mimic those found in coffee or other food sources.

The number of CFU from the tube containing trigonelline (0.1×10^2) was significantly lower than those containing 5-CQA and caffeic acid (0.3×10^2 and 0.5×10^2, respectively) ($p < 0.01$), evidencing a stronger antibacterial activity of trigonelline against *S. mutans* compared with those of the tested phenolic compounds. Among the phenolic compounds, 5-CQA showed the highest inhibitory performance. These results are in accordance with previous studies investigating the antibacterial activity of coffee compounds against *S. mutans* and other bacteria (Almeida et al., 2004; Almeida et al., 2006; Furuhata et al., 2002). Furuhata et al. (2002) reported antibacterial activity of caffeic and 5-CQA against a strain of *L. pneumophila*, while Almeida et al. (2006), Almeida et al. (2004) described antibacterial effects of trigonelline, 5-CQA and caffeic acid on the growth of Enterobacteria and *S. mutans*, respectively, using the agar diffusion method. To our knowledge, the antibacterial activity of ferulic and nicotinic acids against *S. mutans* had not been

tested until the present study. Despite the inhibitory effect of 5-CQA and trigonelline on *S. mutans* cell-growth, these compounds did not exert inhibition or reduction of the bacteria biofilm formation at the tested concentration (correspondent to MIC result). This is not surprising, given that biofilm is less susceptible to antimicrobial agents compared with planktonic cells (Wei et al., 2006).

The colour characterisation, percent weight loss on a wet basis during roasting and pH of the tested coffee extracts from Groups 1 and 2 are presented in Table 1. Sucrose, caffeine, trigonelline and nicotinic acid concentrations in the coffee extracts are presented in Table 2. Phenolic compounds concentrations are presented in Table 3.

3.3. Coffee extracts from Group 1

In Group 1 regular coffee samples of different species (*C. arabica* cv. Yellow Bourbon and *C. canephora* cv. Conillon) were tested before and after 6, 7, 8, 13 and 15 min of roasting. Both species inhibited *S. mutans* growth when roasted for 6, 7 and 8 min, with MIC of 5.0 mg/mL. The extracts obtained from green beans and at 13 and 15 min of roasting did not show inhibitory activity at tested concentrations. Inoculation of positive tubes onto a blood agar plate showed that at tested concentrations (5 and 10 mg/mL), the lighter the roasting degree the higher was the inhibitory activity (Table 4). Daglia et al. (1998) observed higher antibacterial activity in acidic fractions of coffee extracts. In our study, samples showing higher inhibitory activity (lighter samples) also showed lower pH compared to darker samples (Table 1).

Our MIC results are also in agreement with those obtained in the tests with isolated compounds. Trigonelline and 5-CQA are thermo-labile compounds and therefore the darker the roasting degree the lower their concentration (Tables 2 and 3). Trigonelline is a *N*-metyl-betaine (Farah et al., 2006) and 5-CQA is an ester of caffeic acid with quinic acid (Farah et al., 2006). During roasting, trigonelline is demethylated to form nicotinic acid or degraded into low molecular weight compounds (Farah et al., 2006), while chlorogenic acids may be isomerised, epimerised, lactonised and also degraded to low molecular weight compounds (Farah et al., 2006).

Table 1
Roasting time and degree, instrumental colour, percent weight loss on a wet basis during roasting and pH of coffee samples from Groups 1 and 2.

Roasting time (min)	Roasting degree	Colour[a]	Weight loss (%)	pH[b]
C. canephora (Group 1)				
–	Green	>200	0.0	5.3
6	Very light	172	13.5	4.9
7	Very light	150	14.8	5.1
8	Moderately light	100	16.4	5.1
13	Moderately dark	72	21.9	5.2
15	Dark	59	25.2	5.2
C. arabica (Group 1)				
–	Green	>200	0.0	6.0
6	Moderately light	104	15.1	5.0
7	Moderately dark	68	17.8	5.2
8	Dark	60	20.1	5.3
13	Very dark	40	24.8	5.5
15	Very dark	40	26.2	5.6
C. canephora (Group 2)				
–	Green	>200	0.0	5.1
6	Very light	196	12.6	5.3
7	Very light	140	14.0	5.5
8	Medium	88	16.9	5.7
13	Moderately dark	62	23.4	5.9
15	Dark	47	23.7	6.0
C. arabica (Group 2)				
–	Green	>200	0.0	5.6
6	Very light	172	12.3	5.3
7	Light	134	14.1	5.6
8	Moderately Light	111	15.2	5.7
13	Moderately dark	65	20.9	5.8
15	Dark	58	21.4	5.9
Decaffeinated C. canephora (Group 2)				
–	Green	>200	0.0	5.0
6	Very light	187	10.3	5.3
7	Very light	144	12.1	5.5
8	Light	134	12.3	5.5
13	Moderately light	107	14.0	5.7
15	Light medium	93	15.5	5.8
Decaffeinated C. arabica (Group 2)				
–	Green	>200	0.0	5.0
6	Very light	198	9.2	5.1
7	Very light	164	10.2	5.3
8	Very light	162	10.8	5.5
13	Light medium	96	14.9	5.7
15	Medium	81	16.2	5.8

[a] Measured by luminosity degree. Results are means of determinations in triplicate.
[b] Means of determinations in duplicate.

Table 2
Sucrose, caffeine, trigonelline and nicotinic acid contents in green and roasted coffee extracts from Groups 1 and 2.[a]

Roasting time (min)	Sucrose	Caffeine	Trigonelline	Nicotinic acid
C. canephora (Group 1)				
–	4770.1	1031.2	698.7	ND[b]
6	74.7	1111.1	536.3	8.8
7	35.3	1100.2	430.0	13.1
8	20.5	997.2	317.0	18.9
13	11.1	971.1	72.0	24.2
15	12.4	955.8	24.3	23.6
C. arabica (Group 1)				
–	10213.7	513.6	850.5	ND[b]
6	112.3	540.2	641.3	6.5
7	41.8	519.2	320.6	18.3
8	31.2	496.7	169.1	20.2
13	21.2	413.6	25.9	19.2
15	20.2	387.2	10.3	16.8
C. canephora (Group 2)				
–	4086.7	666.7	557.9	ND[b]
6	424.2	759.6	508.2	2.9
7	122.2	730.1	456.1	6.3
8	37.3	750.6	226.1	14.0
13	24.4	719.7	23.4	21.0
15	21.0	599.4	23.5	18.5
C. arabica (Group 2)				
–	4603.8	357.1	958.8	ND[b]
6	725.7	485.9	652.9	5.0
7	228.9	476.2	523.3	11.7
8	61.7	505.4	335.4	39.8
13	27.6	524.6	28.3	32.6
15	20.6	536.9	21.1	33.4
Decaffeinated C. canephora (Group 2)				
–	2451.1	18.4	712.3	ND[b]
6	273.0	20.9	687.6	3.7
7	98.5	18.2	578.8	8.6
8	82.2	17.9	520.0	8.4
13	38.2	17.1	386.0	13.2
15	39.1	13.9	237.7	21.7
Decaffeinated C. arabica (Group 2)				
–	4002.5	16.0	1001.2	ND[b]
6	1116.6	14.6	852.3	2.2
7	475.4	14.5	803.5	4.0
8	331.1	16.4	774.2	5.4
13	52.8	13.1	404.1	15.6
15	47.2	13.2	198.2	30.1

[a] Results are shown as mean of triplicate of analysis, expressed in μg/mL. Analyses' coefficient of variation was <5%.
[b] ND = not detected.

Table 3
Contents of cinnamic acid derivatives in green and roasted coffee extracts from Groups 1 and 2.[a,b,c]

Roasting time	CA	5-CQA	Total CQA	Total FQA	Total *p*-CoQA	Total diCQA	CFQA	Total CGA	Total CQL	Total FQL	3,4-diCQL	Total CGL
C. canephora (Group 1)												
–	3.8	3588.9	5804	423.2	40.9	642.6	116.1	7026.8	ND	ND	ND	ND
6	ND	946.3	2048.5	254.7	42.1	84.4	21.7	2451.6	242.3	44.9	1.9	289.1
7	ND	514.1	1161.5	185.5	28	30.8	11.6	1417.5	160	36.9	1.0	199.4
8	ND	218.1	499.5	101.2	17.3	10.3	5.4	633.8	81	24.1	0.3	106.8
13	ND	18.2	40.2	18.7	10.8	0.5	ND	59.4	9.2	6.6	ND	15.4
15	ND	7.2	16	6.8	ND	0.4	ND	23.2	6	2.7	ND	5.4
C. arabica (Group 1)												
–	2.7	2132.5	2770.1	254.8	71.7	93.1	13.2	3202.9	ND	ND	ND	ND
6	ND	727.0	1674.9	159.5	56	31.2	3.6	1925.2	66.2	8.7	ND	74.9
7	ND	224.2	557	52.8	23.7	7.1	ND	640.5	40.8	5.3	ND	46.1
8	ND	92.7	235.7	30.3	13.8	3.4	ND	283.2	19.8	1.4	ND	21.2
13	ND	8.9	22	5.2	1.5	ND	ND	28.7	3.3	ND	ND	3.3
15	ND	5.9	15.1	3.3	0.6	ND	ND	19.1	2.9	ND	ND	2.9
C. canephora (Group 2)												
–	4.0	1527.5	2489.6	476.7	44	96.7	37.2	3143.9	ND	ND	5.4	5.4
6	ND	1118.6	2340	315.1	25.1	143.1	63.0	2886.3	151.2	31.9	1.4	184.5
7	ND	853.4	1894	299.1	29.5	63.4	31.9	2317.9	207.9	44.9	41.0	293.8
8	ND	220.1	521.2	135.6	18.7	11.9	4.9	692.3	91	30	ND	130.5
13	ND	6.8	17.4	7.2	ND	1.1	2.1	27.8	10.0	2.1	ND	12.1
15	ND	11.0	24.6	15.9	ND	ND	ND	40.6	2.2	2.9	ND	5.1
C. arabica (Group 2)												
–	2.9	1499.9	2527.2	252.4	67.5	114.4	25.6	2987.1	ND	ND	ND	ND
6	ND	1098.4	2402.1	168.8	63.7	86.1	17.4	2738.2	152.1	15.5	1.9	169.5
7	ND	709.7	1605.1	122.4	48	43	8.3	1826.9	132.0	18.4	0.4	150.8
8	ND	429.1	1003.4	78.8	40.2	21.2	4.6	1148.1	110.1	14.1	0.2	124.4
13	ND	10.6	27.9	4.3	1	2.1	3.1	38.4	11.5	ND	ND	11.5
15	ND	15.0	33.7	6.3	0.9	3	8.0	51.9	6.6	3.0	ND	9.6
Decaffeinated C. canephora (Group 2)												
–	5.5	1678.1	4283.6	672.1	40	275.3	123.6	5394.8	10.6	5.1	6.7	22.4
6	ND	1470.3	3192.9	556.1	50	110.6	64.2	3973.7	290.2	67.5	3.4	361.1
7	ND	692.8	1542.5	309.9	35	44.1	24.2	1955.8	178.9	50.1	2.3	231.3
8	ND	608.4	1363.3	284.2	32.8	37.6	22.2	1740.2	155.3	38.5	1.0	194.8
13	ND	185.6	445.3	104.2	10.4	18.5	5.4	583.8	64.0	21.2	ND	85.2
15	ND	75.2	175.2	52.6	4.9	3.8	3.6	240.2	18.6	9	ND	27.6
Decaffeinated C. arabica (Group 2)												
–	3.3	2359.2	6075.3	839.1	78.8	410.5	131.7	7535.2	5.4	7.3	8.4	21.2
6	ND	2188.6	4956.3	650.3	64.8	200.7	72.2	5944.2	242.9	42.7	6.2	291.8
7	ND	2010.4	4356.6	565.2	68.3	180.6	66.6	5237.3	370.4	81.1	3.8	455.3
8	ND	1479.8	3222.5	440.6	64.4	118.8	48.1	3894.4	275.9	52.3	4.5	332.7
13	ND	148.6	365	58.3	28.8	13.9	31.5	497.5	94.0	28.4	ND	122.4
15	ND	76.4	180.4	47.1	11.1	3.6	2.1	244.3	21.9	7.6	ND	29.5

[a] Results are shown as mean of triplicate of analysis, expressed in μg/mL. Analyses' coefficient of variation was <5%.
[b] No ferulic acid was observed in any of the analysed samples from both groups.
[c] CA, caffeic acid; CQA, cafeoylquinic acids; FQA, feruloylquinic acids; *p*-CoQA, *p*-coumaruloylquinic acids; diCQA, dicaffeoylquinic acids; CFQA, cafeoylferuloylquinic acids; CGA, chlorogenic acids; CQL, caffeoylquinide; FQL, feruloylquinide; diCQL, dicaffeoylquinide; CGL, chlorogenic acids lactones.

Like 5-CQA, other CQA and diCQA isomers are also formed from caffeic and quinic acid, and it is very possible that all these compounds, which together are responsible for more than 90% of the chlorogenic acids content in the coffee extracts, exert antibacterial activity. On the other hand, since ferulic acid did not show activity against *S. mutans*, it is possible that feruloylquinic acids and their lactones do not exert such activity. The mechanisms of growth inhibition of chlorogenic acids and trigonelline are not clear, but according to Cowan (1999) the causes for phenolic toxicity to microorganisms may include enzymatic inhibition by oxidised compounds, possibly through reaction with sulfidryl groups or also through more nonspecific interactions with proteins.

Although the contents of 5-CQA and trigonelline in the coffee extracts were similar to those of the standard solutions with bacteriostatic activity (Tables 2 and 3), other non-bacteriostatic compounds such as polysaccharides and aminoacids that are also part of coffee composition may have contributed to increase the MIC of coffee extract compared to those of the isolated compounds.

Despite caffeic acid inhibitory activity, the amount of this phenolic acid in its non-esterified form in coffee is generally very low, especially in the roasted beans (Farah et al., 2005). In the present study, we only identified caffeic acid in the green coffee extracts (Table 3). Although the high concentrations of chlorogenic acids, trigonelline and caffeic acid were found in the green coffee extracts (4.0 and 7.0 mg/mL altogether in *C. arabica* and *C canephora*, respectively) (Tables 2 and 3), sucrose concentration in these extracts was quite high (10.2 and 4.8 mg/mL, respectively), being equivalent to 2.6 and 0.7 times those of the sum of the tested antibacterial compounds in *C. arabica* and *C. canephora*, respectively (Table 2). The majority of the oral microbiota depends on sugar as energy source (McNeill & Hamilton, 2004). Although glucose is the preferred sugar for bacterial growth, bacteria may use a large variety of sugars such as sucrose, maltose and lactose as alternative sources of energy (Wen, Browngardt, & Burne, 2001). Therefore, it is most likely that sucrose has promoted the growth of the referred bacteria, counteracting the inhibitory effect of trigonelline and chlorogenic acids in the green coffee extracts.

The present results are in accordance with Daglia et al. (1998, 2007) who did not observe inhibitory activity in green coffee extracts. However, one of these studies (Daglia et al., 2007) reported

Table 4
Number of colony-forming units (CFU) for coffee extracts from Group 1(G1) and Group 2 (G2) with inhibitory activity against *Streptococcus mutans*.

Roasting time (min)	Concentration (mg/mL)	CFU[a]
C. canephora (G1)		
6	10	1.85
	5	2.48
7	10	2.28
	5	2.90
8	10	3.04
	5	2.31
C. arabica(G1)		
6	10	1.70
	5	2.36
7	10	2.20
	5	2.85
8	10	2.95
	5	3.26
Regular C. canephora (G2)		
6	10	2.26
	5	2.81
7	10	2.65
	5	3.18
8	10	3.00
	5	3.48
Regular C. arabica (G2)		
6	10	2.08
	5	2.78
7	10	2.60
	5	2.99
8	10	3.11
	5	3.30
Decaffeinated C. canephora (G2)		
6	10	2.38
	5	2.89
7	10	3.04
	5	3.97
Decaffeinated C. arabica (G2)		
6	10	2.36
	5	2.85
7	10	2.78
	5	3.96

[a] Results are shown in $\log_{10}$ scale for better comparison.

that due to the lack of antibacterial activity of green coffee, along with a positive activity of dark roasted coffee, the compounds with inhibitory activity could not be naturally present in coffee, being formed by Maillard reaction during roasting process. The study went further identifying α-dycarbonil compounds as the main coffee agents with inhibitory activity (Daglia et al., 2007). Nevertheless, such compounds are present in very low concentrations in commonly consumed aqueous coffee extracts (Daglia et al., 2007). Furthermore, even though the medium roasted coffee extract evaluated by Daglia et al. (2007) was about six times more concentrated than the light roasted extracts (6 and 7 min of roasting) used in the present study, all extracts exhibited similar MIC results. This indicates that the antibacterial effect of the referred α-dycarbonil compounds may be lower than those of natural coffee compounds such as 5-CQA, trigonelline, caffeic acid and possibly other compounds that are more abundant in lighter roasted coffees, although results from the present study and from Daglia et al. (2007) cannot be directly compared. This matter should be investigated in future studies.

In order to confirm our hypotheses that the high concentration of sucrose present in green coffee beans was counteracting the antibacterial effect of natural coffee compounds, we performed an additional experiment incubating the *S. mutans* inoculum in test tubes containing plain medium (control) or the same medium supplemented with sucrose. The concentration of sucrose used in this test was similar to that found in the *C. canephora* sample from Group 1. The number of CFU from the control tube was 1.2×10^6, while the number of CFU of the supplemented medium tube was 5.3×10^6, 4.4 times higher than in non-supplemented media. This result increases evidence that sucrose may counteract the antibacterial effect of natural occurring compounds in green coffee beans.

Regarding differences between both investigated species, *C. arabica* cv. Yellow Bourbon extracts showed similar inhibitory activity on the growth of *S. mutans* when compared to *C. canephora* cv. Conillon. No significant difference was observed between the numbers of CFU of both species (Table 4). In the biofilm formation assays, however, while *C. arabica* cv. Yellow Bourbon extract did not inhibit the biofilm formation at tested concentrations, *C. canephora* cv. Conillon showed an inhibition of 39.6% (compared to 91.7% of the positive control chlorhexidine) at 90 mg/mL, a concentration similar to that commonly used in Brazil and other countries for coffee preparation (100 mg/mL). As far as we know, this is the first study evaluating the inhibitory activity of coffee on biofilm formation, but it is possible that the anti-adhesive property reported for coffee (Daglia et al., 2002) is related to this activity. Considering that the contribution of caffeine for the anti-adhesive property of coffee has previously been discarded (Daglia et al., 2002), the possible involvement of chlorogenic acids and their lactones in such activity should be investigated, since the amount of both classes of compounds in the active *C. canephora* extract (6 min roasted) was about 27% and 73% higher than in *C. arabica*, respectively.

Regarding the biofilm reduction assay, *C. canephora* extract of Group 1 showed a low biofilm viability reduction (6.6%) at 90 mg/mL (against 20.6% by chlorhexidine), while *C. arabica* did not show reduction at tested concentrations. The low reduction of mature biofilm when compared to the inhibition of biofilm formation was expected, since in a biofilm, bacteria are invariably less susceptible to antimicrobial agents than their planktonic counterparts (Wilson, 1996). Nonetheless, the inhibition of early biofilm formation is more important than the reduction of mature biofilm because once the formation of biofilm is inhibited, mature biofilm existence may be prevented.

3.4. Coffee extracts from Group 2

With the intention to confirm the results from Group 1 and because decaffeination process may considerably change coffee chemical composition (Farah et al., 2006; Toci, Farah, & Trugo, 2006), a group of green and roasted regular and decaffeinated *C. arabica* and *C. canephora* samples from the same lot was tested. As in Group 1, all regular coffee extracts roasted for 6, 7 and 8 min inhibited the growth of *S. mutans*, with a MIC of 5 mg/mL. No activity was observed in extracts roasted for 13 and 15 min. No significant difference was observed between the numbers of CFU of both species (Table 4). Also, as in Group 1, regular *C. canephora* showed biofilm formation inhibition (18.3% inhibition at 90 mg/mL), while regular *C. arabica* did not exhibit inhibitory activity at tested concentrations.

Only *C. arabica* and *C. canephora* extracts prepared from beans roasted for 6 and 7 min inhibited the bacterial growth (MIC of 5 mg/mL). Differently from the regular samples, extracts from decaffeinated beans roasted for 8 min did not show inhibitory activity. Additionally, none of the decaffeinated extracts inhibited the biofilm formation. Although in the present study caffeine alone did not exert inhibitory activity on the growth of *S. mutans*, studies performed by Daglia et al. (2007) and Almeida et al. (2004) observed that at concentrations of 5.0 and 2.0 mg/mL, respectively, caffeine provided antimicrobial activity against *S. mutans*. These authors also showed that caffeine was able to enhance the inhibi-

tory effect of coffee compounds. This could explain why decaffeinated coffee roasted for 8 min did not show inhibitory effect. Furthermore, other possibly inhibitory compounds may have been washed out by water and dichloromethane during decaffeination process. As in regular samples, a significant inverse correlation was found between roasting degree and inhibitory activity among decaffeinated samples (Table 4). Group 2 samples did not show biofilm reduction at tested concentrations.

Regular samples from Group 1 showed a tendency ($p = 0.08$) to exhibit better antibacterial performance than those from Group 2. Additionally, regular *C. canephora* samples from Group 1 showed better inhibitory performance of biofilm formation than those from Group 2. This could probably be explained by the inferior quality of samples from Group 2, which contained a higher number of fermented defective beans such as black and sour (Farah et al., 2006; Toci & Farah, 2008) possibly presenting unknown substances that could counteract the antibacterial effects of natural coffee components.

In conclusion, this study showed that 5-CQA, trigonelline, and caffeic acid from coffee exert inhibitory activity against the growth of *S. mutans*; that such activity is enhanced by the presence of caffeine and/or other compounds extracted by decaffeination; that *C. canephora* extracts seems to exert better performance in relation to inhibition of biofilm formation than those of *C. arabica* and that roasting degree is inversely associated with antibacterial activity against *S. mutans*.

Coffee is a natural ingredient that may be obtained in large quantities at low cost. Furthermore, the advantage of coffee as an antibacterial beverage is that it is consumed in a concentrated form (6–10%) as opposed to various medicinal infusions that have shown such effect *in vitro* and are usually consumed at 1–2% (Bravo, Goya, & Lecumberri, 2007). So, the fact that the coffee derived extract used in this study exhibited antibacterial activity against *S. mutans* cell-growth and against *S. mutans* biofilm formation supports the hypothesis that it may be highly beneficial as an anticariogenic ingredient, when consumed without sucrose addition. However, in the *in vivo* situation, *S. mutans* does not occur in monoculture, but rather in a complex ecosystem biofilm. As the *in vitro* tests employed in this study are essentially preliminary screenings, further investigation – especially *in vivo* – should be performed to verify the effect of regular light roasted *C. canephora* and *C. arabica* extracts and their components in the prevention of dental caries.

Acknowledgments

The authors would like to thank Professor José Mauro Costa Monteiro (Minas Gerais, Brazil) and Mr. Robert Machtans Junior from Cocam Cia. de Café Solúvel e Derivados (São Paulo, Brazil) for generously providing the coffee samples. The financial support of the National Council for Technological Development (CNPq), Consórcio Brasileiro de Pesquisa e Desenvolvimento do Café (CBP&D)/EMBRAPA (Brazil) and Fundação Carlos Chagas Filho de Amparo à Pesquisa do Estado do Rio de Janeiro (FAPERJ) is acknowledged.

References

Almeida, A. A. P., Farah, A., Silva, D. A. M., Nunan, E. A., & Glória, M. B. (2006). Antibacterial activity of coffee extracts and selected coffee chemical compounds against Enterobacteria. *Journal of Agricultural and Food Chemistry, 54*, 8738–8743.

Almeida, A. A. P., Naghetini, C. C., Santos, V. R., & Glória, M. B. (2004). *In vitro* antibacterial activity of coffee extracts on *Streptococcus mutans*. In *Proceedings of the 20th international conference on coffee science* (pp. 242–248). Bangalore, India: ASIC.

Bravo, L., Goya, L., & Lecumberri, E. (2007). LC/MS characterization of phenolic constituents of mate (ilex paraguariensis, St. Hil.) and its antioxidant activity compared to commonly consumed beverages. *Food Research International, 40*, 393–405.

Cowan, M. M. (1999). Plant products as antimicrobial agents. *Clinical Microbiology Reviews, 12*, 564–582.

Daglia, M., Cuzzoni, M. T., & Dacarro, C. (1994). Antibacterial activity of coffee: Relationship between biological activity and chemical markers. *Journal of Agricultural and Food Chemistry, 42*, 2273–2277.

Daglia, M., Papetti, A., Dacarro, C., & Gazzani, G. (1998). Isolation of an antibacterial component from roasted coffee. *Journal of Pharmaceutical and Biomedical Analysis, 18*, 219–225.

Daglia, M., Papetti, A., Grisoli, P., Aceti, C., Spini, V., Dacarro, C., et al. (2007). Isolation, identification, and quantification of roasted coffee antibacterial compounds. *Journal of Agricultural and Food Chemistry, 55*, 10208–10213.

Daglia, M., Tarsi, R., Papetti, A., Grisoli, P., Dacarro, C., Pruzzo, C., et al. (2002). Antiadhesive effect of green and roasted coffee on *Streptococcus mutans*' adhesive properties on saliva-coated hydroxyapatite beads. *Journal of Agricultural and Food Chemistry, 50*, 1225–1229.

Dall'Agnol, R., Ferraz, A., Bernardi, A. P., Albring, D., Nör, C., Sarmento, L., et al. (2003). Antimicrobial activity of some Hypericum species. *Phytomedicine, 10*, 511–516.

Farah, A., de Paulis, T., Moreira, D. P., Trugo, L. C., & Martin, P. R. (2006). Chlorogenic acids and lactones in regular and water-decaffeinated arabica coffees. *Journal of Agricultural and Food Chemistry, 54*, 374–381.

Farah, A., de Paulis, T., Trugo, L. C., & Martin, P. R. (2005). Effect of roasting on the formation of chlorogenic acid lactones in coffee. *Journal of Agricultural and Food Chemistry, 53*, 1505–1513.

Farah, A., Monteiro, M. C., Calado, V., Franca, A. S., & Trugo, L. C. (2006). Correlation between cup quality and chemical attributes of Brazilian coffee. *Food Chemistry, 98*, 373–380.

Furuhata, K., Dogasaki, C., Hara, M., & Fukuyama, M. (2002). Inactivation of *Legionella pneumophila* by phenol compounds contained in coffee. *Journal of Antibacterial and Antifungical Agents, 30*, 291–297.

Johnston, K. L., Clifford, M. N., & Morgan, L. M. (2003). Coffee acutely modifies gastrointestinal hormone secretion and glucose tolerance in humans: Glycemic effects of chlorogenic acid and caffeine. *American Journal of Clinical Nutrition, 78*, 728–733.

Kendrick, S. F. W., & Day, C. P. (2007). A coffee with your brandy, Sir? *Journal of Hepatology, 46*, 980–982.

McFarland, J. (1907). Nephelometer: An instrument for estimating the number of bacteria in suspensions used for calculating the opsonic index and for vaccines. *Journal of the American Medical Association, 14*, 1176–1178.

McNeill, K., & Hamilton, I. R. (2004). Effect of acid stress on the physiology of biofilm cells of *Streptococcus mutans*. *Microbiology, 150*, 735–742.

NCCLS (2003). Methods for dilution antimicrobial susceptibility tests for bactéria that grow aerobically. In *Approved standard M7–A6* (6th ed.). Wayne, PA: NCCLS.

Ohshima, T., Miyakawa, Y., Watanabe, T., & Ohyama, K. (2003). Effect of amphotericin B dilution with various beverages on the survival of *Candida albicans* cells. *Kansenshogaku Zasshi, 77*, 29–33.

Osawa, K., Miyazaki, K., Shimura, S., Okuda, J., Matsumoto, M., & Ooshima, T. (2001). Identification of cariostatic substances in the cacao bean husk: Their anti-glucosyltransferase and antibacterial activities. *Journal of Dental Research, 80*, 2000–2004.

Perrone, D., Donangelo, C. M., & Farah, A. (2008). Fast simultaneous analysis of caffeine, trigonelline, nicotinic acid and sucrose in green and roasted coffee by liquid chromatography–mass spectrometry. *Food Chemistry, 110*, 1030–1035.

Rosengren, A., Dotevall, A., Wilhelmsen, L., Thelle, D., & Johansson, S. (2004). Coffee and incidence of diabetes in Swedish women: A prospective 18-year follow-up study. *Journal of Internal Medicine, 255*, 89–95.

Smith, D. J. (2002). Dental caries vaccines: Prospects and concerns. *Critical Reviews in Oral Biology and Medicine, 13*, 335–349.

Thimothe, J., Bonsi, I. A., Padilla-Zakour, O. I., & Koo, H. (2007). Chemical characterization of red wine grape (*Vitis vinifera* and *Vitis* interspecific hybrids) and pomace phenolic extracts and their biological activity against *Streptococcus mutans*. *Journal of Agricultural and Food Chemistry, 55*, 10200–10207.

Toci, A., & Farah, A. (2008). Volatile compounds as potential defective coffee beans markers. *Food Chemistry, 108*, 1133–1141.

Toci, A., Farah, A., & Trugo, L. C. (2006). Efeito do processo de descafeinação com diclorometano sobre a composição química dos cafés arábica e robusta antes e após a torração. *Química Nova, 29*, 965–971.

Wei, G.-X., Campagna, A. N., & Bobek, L. A. (2006). Effect of MUC7 peptides on the growth of bacteria and on *Streptococcus mutans* biofilm. *Journal of Antimicrobial Chemotherapy, 57*, 1100–1109.

Wen, Z. T., Browngardt, C., & Burne, R. A. (2001). Characterization of two operons that encode components of fructose-especific enzyme II of the sugar: Phosphotransferase system of *Streptococcus mutans*. *FEMS Microbiology Letters, 205*, 337–342.

Wilson, M. (1996). Susceptibility of oral bacterial biofilms to antimicrobial agents. *Journal of Medical Microbiology, 44*, 79–87.

Xiao, J., Zhou, X. D., Feng, J., Hao, Y. Q., & Li, J. Y. (2007). Activity of Nidus Vespae extract and chemical fractions against *Streptococcus mutans* biofilms. *Letters in Applied Microbiology, 45*, 547–552.

Blacnchard, 1994). There are several ways available to study the properties of a gel and the mechanism of their formation e.g. employing the two main rheological studies available, namely small strain and large strain testing. The combination of these measurements can give valuable information on gel properties and qualities. Small strain testing is a study where a sample is deformed without breaking the structure. Heating and cooling of a gel, using low frequency and small strain oscillatory experiments, is one of the best suited methods to follow changes in physical properties relating molecular properties of a gel (Hamman, 1991; Hamman & MacDonald, 1992). Large strain testing is when a sample is deformed until the structure is permanently broken. Large strain testing, such as torsion estimates fundamental properties of a gel and has shown to correlate with sensory. The torsion test is a typical method to test the hardness (shear stress) and elasticity (shear strain) of surimi gels.

The overall objective of this study was to evaluate the quality of gels prepared using muscle proteins isolated from tilapia white muscle using the acid and alkali-aided processes and compare to gels prepared using washed tilapia muscle which simulates surimi without added cryoprotectants.

2. Materials and methods

2.1. Raw material

Tilapia fillets (170–200 g) were obtained fresh from a local supplier (Rain Forest Aquaculture, Sunrise, FL). The fillets were processed immediately after fish were killed and transported in Styrofoam boxes on ice to the laboratory and stored in a cold room at 4 °C until processed (within 24 h from the time of filleting). Red muscle was manually excised from the white muscle and discarded. The remaining white muscle was ground using a Scoville grinder (Hamilton Beach, Washington, NC) with 6 mm holes. All sample preparation was performed in a cold room at 4 °C or on ice when applicable to maintain temperature below 5 °C.

2.2. Preparation of washed muscle

Ground muscle was mixed with cold DI water (1:3, w/w) and allowed to sit for 15 min, stirring every few minutes with a plastic spatula. The slurry was poured into a strainer covered with double layer of cheesecloth and the water manually squeezed out. This was repeated 2×, with the last wash water containing 0.2% NaCl to aid in the dewatering of the tilapia white muscle proteins. The washed muscle was placed in a zip-lock bag and stored overnight on ice in a cold room at 4 °C before gel preparation.

2.3. Preparation of protein isolates

Ground muscle was mixed with cold DI water (1:9, w/w), homogenised for 60 s (2 × 30s) using a Waring blender (Waring Products Division, New Hartford, CT) at 40% electrical output and carefully poured (to avoid foaming) into a plastic beaker on ice. The homogenates were adjusted to pH 2.5, 2.9, 11.0 or 11.2 to solubilise the proteins, using 2 M HCl or 2 M NaOH. The adjusted homogenate was poured into centrifuge bottles and centrifuged at 10,000*g* for 20 min in a Sorvall RC-5B using a GS-3 rotor. Centrifugation resulted in the formation of three layers. The supernatant was separated from the top layer and the sediment by pouring the contents of the centrifuge bottles through a strainer covered with two layers of cheesecloth. The collected supernatant was subjected to isoelectric precipitation by adjusting the pH to 5.5, following centrifugation at 10,000*g* for 20 min. The sediment (protein isolate) was placed in a zip-lock bag and stored on ice in a cold room at 4 °C over night.

2.4. Moisture content

To determine moisture content of the protein isolates and washed muscle a ~5 g sample was placed in a Cenco moisture balance (CSC Scientific Company, Inc., Fairfax, VA). Prior to sample preparation for rheological measurements moisture content of protein isolate and washed muscle was adjusted to 90% by adding cold DI water based on the following formula:

$$g\ H_2O = \frac{X\ g_{\text{sample}}\left(X_{\text{moisture of sample}} - X_{\text{desired moisture}}\right)}{X_{\text{desired moisture}} - 1}. \quad (1)$$

For gel quality analysis the protein isolates were adjusted to 83% moisture content by squeezing the water out manually. The washed muscle required centrifugation at 10,000*g* for 20 min in a RC-5B centrifuge using a GS-3 rotor to reach the desired moisture content.

2.5. Rheology

Samples for rheology measurements were prepared by placing ~25 or 30 g of the protein isolate/washed muscle (90% moisture) in a 100 mL plastic beaker. The isolate/washed muscle was homogenised with a hand held Tissue Tearor (Biospec Products, Inc., Bartlesville, OK) for 1 min on speed six, then 25 mM of sodium phosphate dibasic (pulverised with a mortar and pestle to reduce particle size) was added and the paste homogenised again for 2 min on same speed for thorough mixing. Finally 2% NaCl was added (when applicable) and mixed well with a stainless steel spatula. The pH of the paste was adjusted to pH 7.1–7.2 with 2 M NaOH followed by mixing with a stainless steel spatula. After the pH adjustment the beaker was covered with parafilm and the paste was kept on ice for 30 min before rheological measurements. Sample preparation time including the 30 min setting time was ~50–60 min.

Viscoelastic changes on heating and cooling were determined using single gap geometry in an AR2000 Advanced Rheometer (TA Instruments, New Castle, DE). Approximately 20 g of sample (prepared as previously described) was placed in the sample chamber at 5 °C and the head set to a specified gap (4950 μm). After reaching the gap, excess sample was removed with a stainless steel spatula and a layer of mineral oil was placed on top of the sample to prevent evaporation on heating. The opening was covered with a metal moisture trap to prevent evaporation. The samples were heated from 5 to 80 °C at a rate of 2 °C/min and cooled from 80 to 5 °C at the same rate and measurement conducted using a oscillatory mode with constant frequency set at 0.1 Hz and maximum strain at 0.01 (Kristinsson & Hultin, 2003b).

2.6. Gel quality

Approximately 130 g of isolate/washed muscle were accurately weighed and placed in a Mini Chopper (Sunbeam Products Inc., Boca Raton, FL) with 25 mM sodium phosphate dibasic buffer added after blending for 20 s, and after ~1 min 2% NaCl was added when applicable. The pH was adjusted to 7.1–7.2 by adding 2 M NaOH drop wise. The paste was mixed for a total of 4 min with all steps performed in a cold room at 4 °C. The paste was then manually stuffed into steel tubes (diameter 19 mm) and the ends sealed with a rubber cap and fastened with a hose clamp. The paste was cooked for 30 min at 80 °C in a Precision water bath (Precision Scientific, Winchester, VA) and cooled in ice water for 15 min. Gels were removed from stainless steel tubes and placed in zip-lock bags and stored in a cold room at 4 °C for 48 h prior to testing.

After storing the gels at 4 °C for 48 h they were cut into 28.7 mm long samples using a cutting motive. After reaching room temperature (~40 min) the gels were milled into dumbbell shape with a minimum centre diameter of 1.0 cm. Gels were tested using

a modified Brookfield DV-II viscometer (Gel Consultants, Raleigh, NC) and the gels twisted at 2.5 rpm until structure failed. Shear stress (resistance to breakage) and shear strain (distance until breakage) of the gels were obtained using computer software linked to the viscometer.

2.7. Folding

Folding test was performed within 60 h of storage at 4 °C, according to the method of Kudo, Okada, and Miyauchi (1973). Approximately 3 mm slices were cut and folded by hand at room temperature. The ability of the gels to fold was graded using a five point system.

2.8. Water-holding capacity

Water-holding capacity of the gels on pressing was determined using the method of Feng and Hultin (2001) where pressing loss is defined as the water loss of a 3 mm thick slice under 3000 g pressure (using a 3 L beaker full of water) for 1 min. The sample was sandwiched between 5 layers of Whatman filter paper (Whatman Inc., Clifton, NJ) which absorbed the expressible water. Weight before and after pressing was recorded and moisture content was determined by drying the samples overnight at 106 °C in a moisture oven.

2.9. Sulphydryl content

Total sulphydryl (SH) content was determined on the protein paste before cooking and on the gels after cooking by using the method of Choi and Park (2002) with slight modifications. The pastes and gels were diluted 100× to give a protein concentration between 1 and 2 mg/mL. A 0.25 mL sample of the protein solution was added to 2.5 mL of 8 M urea, 2% sodium dodecylsulphate (SDS) and 10 mM EDTA in 0.2 M Tris–HCl buffer at pH 7.1. To this solution 50 uL of 10 mM Ellman's reagent (10 mM 5,5′-dithiobis(2-nitrobenzoic acid) was added, mixed and heated in a water bath at 40 °C for 15 min. After the reaction the absorbance of the solution was measured at 420 nm using an Agilent 8453 UV–VIS spectrophotometer (Agilent Technologies, Palo Alto, CA) and total SH content was calculated using a molar extinction coefficient of 13,600 mol/cm.

2.10. Statistics

Analysis of variance (ANOVA) was used to determine significant differences between treatments. All results were analysed by using the Statistical Analysis System (SAS). Results are expressed as means ± SD.

3. Results and discussions

Gel forming ability of tilapia white muscle protein isolates prepared with the acid and alkali-aided processes were determined and compared to gel forming ability of washed tilapia white muscle (analogue to conventional lab scale surimi without added cryoprotectants). Gel characteristics were evaluated by using small strain (viscoelastic changes) and large strain (torsion) testing, folding and water-holding capacity. Gels were prepared with or without addition of 2% NaCl (w/w) and the paste was adjusted to pH 7.1–7.2 which are common conditions for gelation of fish muscle.

3.1. Torsion

Shear stress (i.e. resistance to breakage) of gels prepared using 2% NaCl (w/w) was significantly higher ($p < 0.01$) than that seen for gels without added NaCl, except for gels prepared from washed muscle (Fig. 1a). For gels with 2% added salt, the lowest shear stress, thus least resistance to breakage, was obtained for gels prepared from washed muscle, 32.1 ± 4.3 kPa. Gels from protein isolates prepared by solubilising the proteins at pH 2.5, 11.0 and 11.2 gave the highest shear stress values, ranging from 80 to 84 kPa. There was however no significant difference between these gels ($p > 0.05$). For gels without added salt, the highest stress value, 69.1 ± 12.0 kPa, was obtained for the isolates prepared using pH 11.0 while the lowest stress value was obtained for the isolates prepared using pH 2.9 and the washing procedure, 30.4 ± 7.0 and 26.0 ± 2.0 kPa, respectively.

Resistance of gels to deformation or shear strain (Fig. 1b) showed that the addition of 2% NaCl (w/w) resulted in significantly higher ($p < 0.01$) strain values for all treatments compared to gels without added NaCl. For samples without added salt, isolates prepared using pH 11.0 and 11.2 gave significantly ($p < 0.05$) higher strain values (1.6 ± 0.1 and 1.5 ± 0.2, respectively) compared to acid treated proteins and washed muscle. On the other hand, the isolate prepared using pH 2.9 and the washed muscle had the lowest shear strain values (1.1 ± 0.1 and 1.2 ± 0.1, respectively), which is in line with the results seen for shear stress. If isolates prepared using low pH treatment are compared it is clear that pH 2.5 treatment with and without 2% NaCl (w/w) gave significantly ($p < 0.01$) higher strain values than the pH 2.9 treatment, thus being significantly more elastic.

The strain values obtained for the treatments were lower or borderline for the ideal shear strain values for surimi from fish muscle, which are expected to be between 2 and 3. The reason for lower values could be explained by the absence of cryoprotectants and setting which are used in surimi production. Bakir, Hultin, and Kelleher (1994) had similar findings for gels prepared from Atlantic mackerel and Bluefish.

Shear stress and strain values were significantly higher for samples with 2% added NaCl (w/w). Salt is believed to improve gelation ability and water retention by solubilising myofibrillar proteins (Xiong, 1997). Addition of salt above 300 mM (~1%) solubilises the myofibrillar proteins by breaking up the interactions between myosin in the thick filament and actin in the thin filaments, along with other cytoskeletal proteins (Lanier, 2000). In a concentrated gel paste (prior to gelation), the osmotic pressure is probably too high to obtain complete solubilisation of the myofibrillar proteins. Uniform dispersion of partially solubilised or unravelled proteins is likely to be more important in a gel paste. Addition of salt is also believed to contribute to a more elastic gel by dispersing the proteins more evenly, which is a consequence of partial or full solubilisation.

It was interesting to note the difference between the two low pH treatments. A difference in gel performance between different low pH treatments has been seen with other species. A study performed by Kim, Park, and Choi (2003) on Pacific whiting showed by using a puncture test that deformation of gels containing 1.5% beef plasma protein was higher for proteins treated at pH 2.0 compared to pH 3.0 which was in part explained by increased hydrophobicity of the proteins at low pH. Davenport, Theodore, and Kristinsson (2004) also found a significant difference in gel forming ability between three different low pH treatments which could on the other hand not be explained by hydrophobicity changes or changes in protein conformation using tryptophan as a structural probe.

The pH 2.9 treatment in particular resulted in the formation of weak gels. During isoelectric precipitation of proteins solubilised at pH 2.9 it was observed that the proteins seemed to form larger aggregates compared to proteins at pH 2.5 and 11.0. Larger aggregates do not form as ordered three dimensional structures and thus form a weaker gel. Hermansson (1978) reported that denaturation of proteins prior to aggregation results in a finer gel structure,

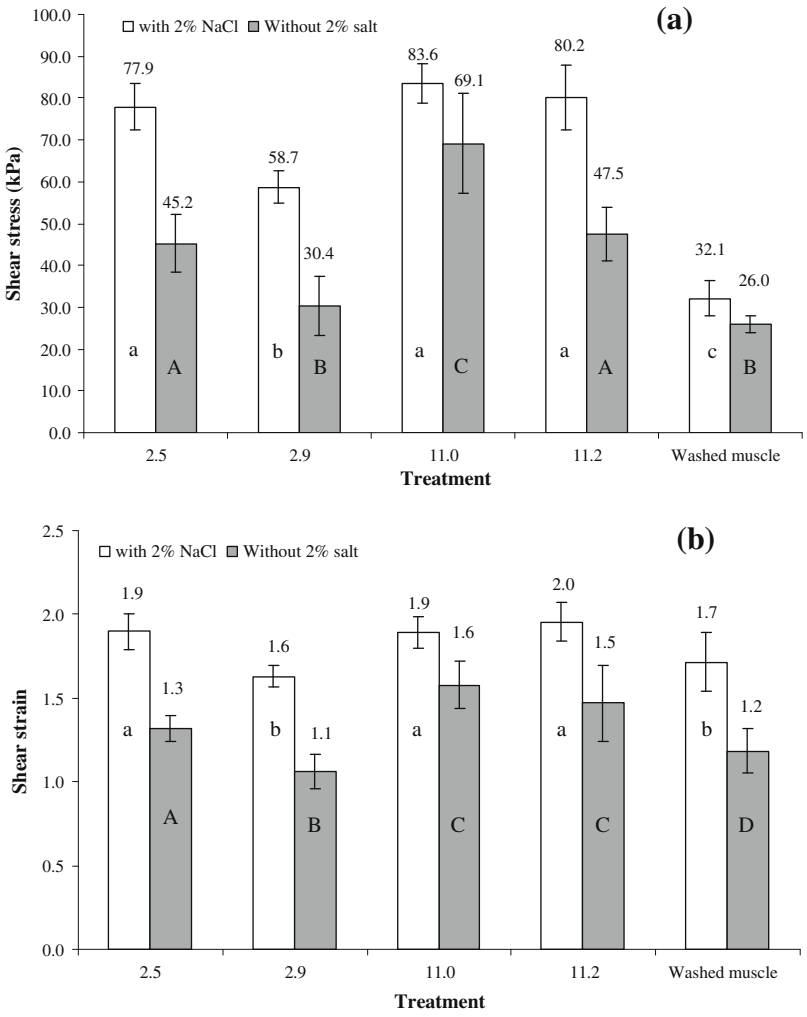

Fig. 1. Shear stress (kPa) (a) and shear strain (b) of gels produced from proteins extracted from tilapia white muscle. Low and high solubilisation pH treatment was compared to a three cycle washing treatment (control). Different capital letters indicate significant difference ($p < 0.01$) for treatments without 2% NaCl. Different small letters indicate a significant difference for treatments with 2% NaCl.

exhibiting greater elasticity than if random aggregation occurs prior to denaturation. Too many protein–protein interactions might result in a hard and inelastic gel whereas too many protein–water interactions might result in a soft and fragile gel (Cortes-Ruiz, Pacheco-Aguilar, Garcia-Sanches, & Lugo-Sanches, 2001). Hydrolysis of the myosin heavy chain was observed for isolates produced with the acid process (Kristinsson & Ingadottir, 2006), which could in part explain their reduced gel forming abilities. This is in agreement with results by Undeland et al. (2002) who suggested that reduced amount of myosin heavy chain (possibly due to proteolysis) contributed to lower stress values at acidic conditions. It is interesting to note however that the pH 2.5 treatment with tilapia proteins was better than the pH 2.9 treatment. It is possible the proteases in question were more active at pH 2.9 than pH 2.5. Differences in protein conformation between the two treatments may also be causing the difference, as discussed above.

Kristinsson and Ingadottir (2006) reported that washed muscle, acid isolates and alkali isolates have different protein compositions, which may contribute to the different gel forming ability of these treatments. Interestingly the alkali process and the washing process removed similar proteins but had significantly different gel forming abilities. The very low stress values obtained for the washed muscle compared to the acid and alkali treated proteins indicate that conformational differences of proteins contribute to variations in gelation properties.

3.2. Folding

The fold test is a common test used in the surimi industry for a quick evaluation of gel quality. All treatments with 2% added NaCl exhibited excellent folding ability and received the highest score available, or 5 (Table 1). Gels prepared using alkali treated proteins without 2% NaCl (w/w) exhibited excellent folding ability and were double folded without breaking. The salt free gels prepared using acid treated proteins and washed muscle performed very poorly. The lowest folding score was obtained for gels prepared from isolates made with pH 2.9 treatment which split in two during the first fold (score 1). Gels prepared from washed muscle and pH 2.5 cracked without splitting during the first fold and received a score of 2.

3.3. Rheology

Small strain oscillatory rheological testing was used to follow changes in viscoelastic properties of gels during heating and cooling. Initial and final storage modulus (G') during gelation was determined for all treatments (Fig. 2a). All treatments exhibited

Table 1
Quality of protein gels as assessed by the fold test. Gel quality was estimated by folding ~3 mm thick gel slices by hand at room temperature and graded by using a five point system (Kudo et al., 1973).

Added NaCl (%)	Treatment				
	pH 2.5	pH 2.9	pH 11	pH 11.2	Washed muscle
2	$5.0 \pm 0.0^{a,1}$	$5.0 \pm 0.0^{a,1}$	$5.0 \pm 0.0^{a,1}$	$5.0 \pm 0.0^{a,1}$	$5.0 \pm 0.0^{a,1}$
0	$2.0 \pm 1.5^{b,1}$	$1.0 \pm 0.0^{b,2}$	$5.0 \pm 0.0^{a,3}$	$5.0 \pm 0.0^{a,3}$	$2.0 \pm 1.2^{b,1}$

Different letters within each column indicate significant difference ($p < 0.05$). Different numbers within each row indicate significant difference ($p < 0.05$).

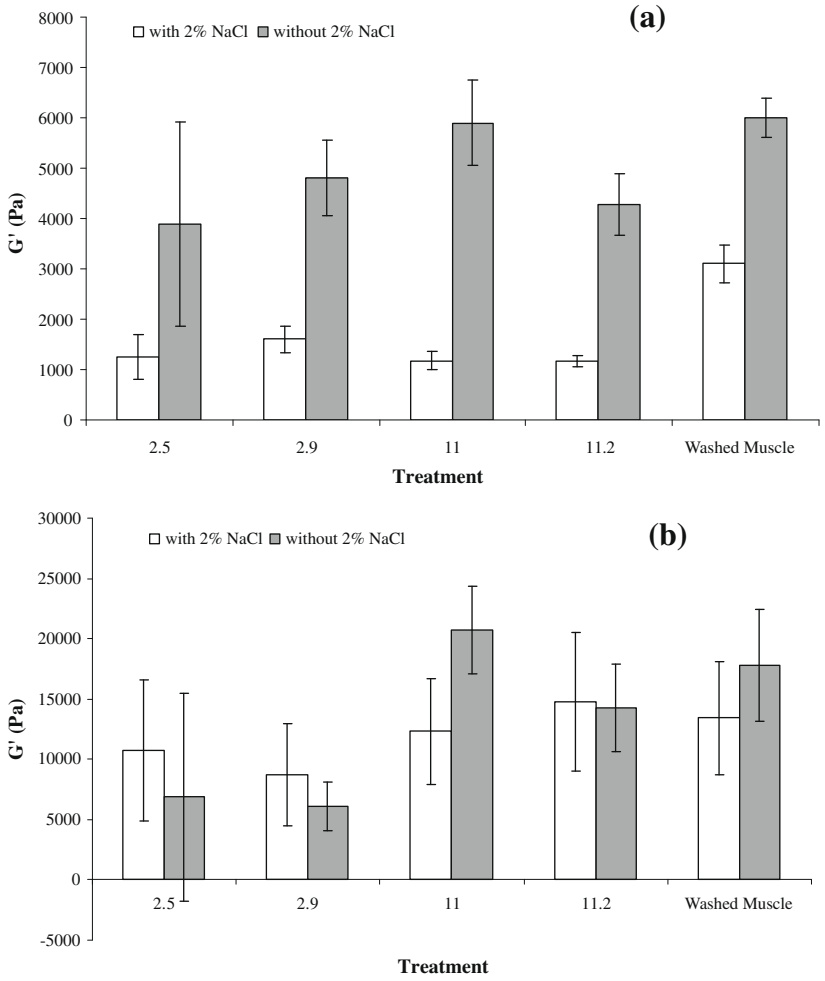

Fig. 2. Storage modulus (G') of protein pastes at 5 °C before thermal gelation (a) and at 5 °C after thermal gelation (b). Samples (~10% protein (w/w)) were adjusted to pH 7.1–7.2. Samples measured at 5 °C before gelation were allowed to sit for 30 min on ice prior to recording G'.

higher initial G' (Pa) in the absence of NaCl (Fig. 2a) compared to samples with 2% NaCl (w/w). A higher G' translates to a more rigid system. The protein paste was adjusted to pH 7.1–7.2 which would give the muscle proteins a substantial negative charge (Feng & Hultin, 1997). This negative charge creates strong repulsive forces between the proteins, creating more space for water to enter giving a more expanded and rigid system. When 2% NaCl (w/w) is added the ions screen some of the repulsive forces bringing the proteins closer together and thus decreasing the space available for water to enter (Kristinsson & Hultin, 2003c) and therefore decrease hydration and leads to less expansion of the system. Differences in initial G' between treatments were observed. Washed muscle showed the highest value among the samples that contained salt. This is likely due to more structure in the washed muscle, since some of the myofibrils would still be intact for that system and many of the myofibrillar proteins would still be part of their native structural elements.

The final G' represents samples that have undergone thermally induced gelation along with setting on cooling (Fig. 2b). The results for final G' showed significant variations for the acid treated samples which could be attributed to the procedures used, the isolate or the raw material. There is evidence that the acid process may lead to larger variations in gelation when using small strain oscillatory testing compared to the alkali process (Theodore, Kristinsson, & Crynen, 2003). The reason for this is unknown, but is hypothesised to be due to unstable structural protein conformations that can form at low pH, thus leading to many different refolded structures at pH 5.5, where the proteins are precipitated. Although variations were large, the results indicate that the proteins from the alkali process have the ability to form stronger gels

compared to the proteins from the acid process, which partly agrees with the torsion results.

In contrast to the torsion results where samples containing 2% NaCl (w/w) exhibited better gelling ability, samples without salt seemed to form better gels, except for the isolates made at pH 2.9. The small strain oscillatory testing and the torsion testing are not necessarily expected to go hand in hand, since they are different tests done at different protein concentrations. The small strain oscillatory testing gives more insight into the gel forming mechanism and protein–protein interaction potential of the muscle proteins at lower concentrations, while the torsion test measures the final gel strength and quality at high protein concentration. It is interesting to note the higher G' for the isolates from the alkaline process, suggesting they have substantially more protein–protein interactions and higher gel forming potential at lower protein concentrations than higher concentrations compared to the isolates from acid process which performed poorer at lower concentrations compared to higher concentrations. The rheology results also indicated that the washed muscle performs better relative to the alkali isolates, at low compared to high protein concentrations.

Fig. 3a–d shows the changes in G' during heating and cooling for the acid and alkali treated proteins, respectively, compared to the washed tilapia white muscle. These graphs allow us to gain an insight into possible differences in gel forming mechanisms between the samples. Washed tilapia muscle with 2% (w/w) added NaCl (Fig. 3a) had a stable G', from 5 to 38 °C, where it started to increase until peaking at ~44 °C and then declining down to a minimum of 53 °C. The G' then rose steadily until 80 °C was reached. A similar curve for heating was observed by Klesk, Yongsawatdigul, Park, Viratchakul, and Virulhakul (2000b) which studied the effect of state of rigor on the gel forming ability of washed tilapia muscle. The increase up to 44 °C has been attributed to cross-linking of myosin and the drop in G' after that to denaturation of light meromyosin, leading to increased fluidity. The second increase in G' has been attributed to the formation of permanent cross-linked myosin filaments (Xiong, 1997). A rapid increase in G' was observed during cooling of the gel indicating formation of a firm gel structure.

Myofibrillar proteins, especially myosin and actin are believed to be largely responsible for gelation. Therefore, gelation of myosin, actin and their complex actomyosin has been the subject of many studies. For myosin, the heavy chain is believed to be the main subunit involved in gelation. The role of the light chain seems to depend on ionic strength where at high ionic strength they may be less important than at low ionic strength. At low ionic strength, removal of the light chains substantially lowered the rigidity of myosin gels (Xiong, 1997). Results from studies on key isolated muscle proteins have been used to try to elucidate gelation mechanism of complex mixture of myofibrillar proteins (Xiong, 1997). The increase in G' that was observed for the washed muscle on heating may be attributed to dissociation of light chains from the heavy chains resulting in conformational changes to the molecule. Cross-linking of myosin is also believed to be responsible for the

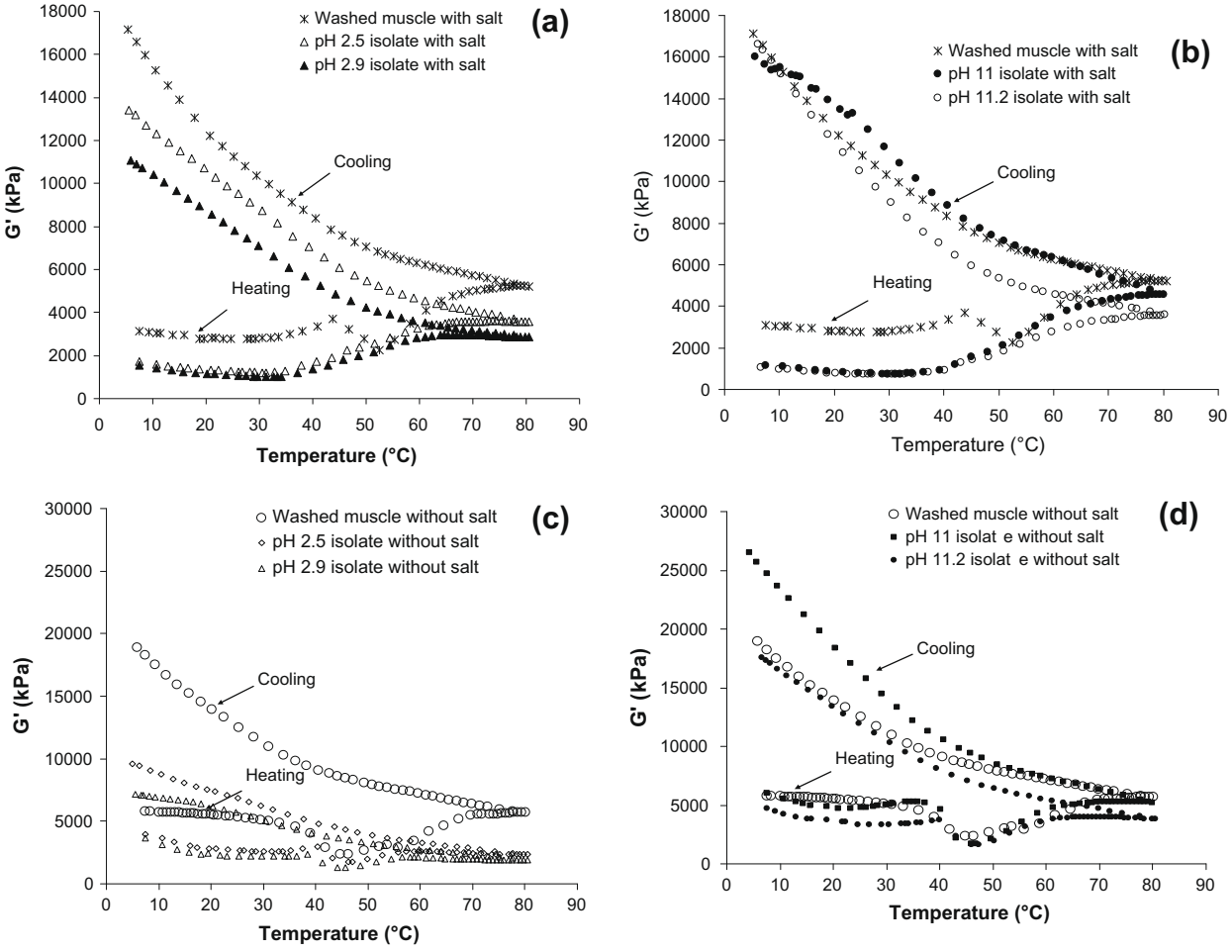

Fig. 3. Rheograms of washed tilapia muscle and protein isolates with 2% NaCl (w/w) added (a) and (b), and with no NaCl added (c) and (d). The rheograms show storage modulus (G') development during heating at 5–80 °C followed by cooling from 80 to 5 °C at 2 °C/min. Samples (~10% protein (w/w)) were adjusted to pH 7.1–7.2 were allowed to sit for 30 min on ice prior to thermal gelation.

increase in G' since it forms a strong elastic network. The subsequent drop is postulated to relate to dissociation of the actin–myosin complex and unfolding of the alpha-helix portion of the myosin rod (Xiong & Blacnchard, 1994). This transformation leads to a large increase in fluidity and might disrupt some protein networks that have already formed (Xiong & Blacnchard, 1994). All these structural changes lead to rapid aggregation and formation of gel networks resulting in a steady increase in G' (Xiong, 1997).

Acid treated proteins with 2% NaCl (w/w) behaved quite differently from the washed muscle. The pH 2.5 treated proteins showed a continuous increase in G' which started around 36 °C and leveled off at ~65 °C (Fig. 3a). A similar pattern was observed for the heating phase of the pH 2.9 treatment (Fig. 3a). The onset of gelation was thus at a significantly lower temperature that that seen for washed tilapia muscle. This could be due to a more unfolded structure of the acid treated proteins, thus requiring a lower temperature to further unfold and interact on heating. The same was seen for cod muscle proteins by Kristinsson and Hultin (2003b). The large difference observed between replicates of the acid treated proteins has been discussed in the previous section and may be attributed to unstable protein structures at low pH leading to different refolded structures which can affect the gelation properties.

The alkali treated proteins showed a similar viscoelastic curve on heating in the presence of 2% NaCl (w/w) as the acid treated proteins (Fig. 3b). The G' started to gradually increase around 40 °C but as presented previously had a larger final G' indicating the formation of a firmer gel compared to the acid treated proteins (Fig. 3a). The slightly higher onset temperature of gelation for the alkali treated proteins compared to acid treated proteins may suggest that they are more refolded than the acid treated proteins. The protein composition differences between the two isolates (Kristinsson & Ingadottir, 2006), might also partly account for the differences in temperature sensitivity.

The acid and alkali treated proteins with added 2% NaCl (w/w) did not show the same transitions as were observed for washed muscle likely due to denaturation and dissociation of the muscle proteins during processing. It has been found that major changes occur with myosin on acid and alkali treatment (Kristinsson & Hultin, 2003b). It was for example found that acid treatment led to complete dissociation of cod myosin while alkaline treatment only led to the dissociation of the light chains from the myosin head. As a result the proteins had different viscoelastic behaviour on heating and cooling compared to a washed cod muscle (Kristinsson & Hultin, 2003b). It was believed that the absence of light chains led to protein aggregation and cross-linking at lower temperatures due to a more exposed myosin head group. Yongsawatdigul and Park (2004) also observed that acid and alkali treated proteins from rockfish were denatured during treatment while still retaining ability to form gels. The lower gelation ability of the acid treated proteins compared to the alkali treated could be due to different conformational changes in part due to loss of myosin heavy chain during processing or the presence of unfavourable conformation of the proteins during acidic treatments, e.g. too many hydrophobic groups leading to bigger aggregates and a less ordered gel. Another explanation for the poor gelling ability of the acid treated proteins could be the presence of denatured sarcoplasmic proteins, many which were retained in the acid process but not in the alkali and washed process (Kristinsson, Theodore, Demir, & Ingadottir, 2005). Crynen and Kristinsson (2003) demonstrated with catfish proteins that the acid process not only negatively affects the myofibrillar proteins but also leads to changes in the sarcoplasmic proteins that, when mixed with the myofibrillar proteins, have a very detrimental effect on gelation. These authors however found that when sarcoplasmic proteins were subjected to alkaline pH treatment they in many cases increased the gel forming ability of the myofibrillar proteins.

Washed muscle without 2% added NaCl (Fig. 3c) exhibited different viscoelastic behaviour on heating compared to the washed muscle containing salt. Initial G' was higher and decreased with increasing temperature until it reached a minimum at 46 °C, which was 7 °C lower than the minimum observed for washed muscle with 2% NaCl (w/w). This decrease suggests that protein complexes may have dissociated instead of forming cross-links as in the system with salt. A steady increase, similar to the one seen for the proteins in salt, was then observed with increasing heating excluding a small bump at ~56 °C. The increase in G' on cooling was similar for both washed muscle in the presence and absence of salt, so differences between the two systems were only seen during the heating/denaturation part of the rheology experiments.

When the viscoelastic curves for isolates without added NaCl were compared to isolates with 2% NaCl (w/w) they were quite different and resembled the curves for washed tilapia muscle. The acid treated proteins (pH 2.5) showed a slight decrease in G' on heating until they reached approximately 40 °C, where the G' dropped down to a minimum at 47 °C (Fig. 3c). The G' then increased again and leveled off at higher temperatures. Protein isolates made with the pH 2.9 treatment showed a very similar trend, however with a lower final G' (Fig. 3c). The alkali treated proteins without added salt showed the same trend as the acid treated proteins except for a higher final G' (Fig. 3d).

Not many gelation studies have been performed with fish proteins in the absence of salt, in part due to the long held believe that salt was necessary for gelation. The results here show that gels can form in the absence of salt, and higher final G' values were in most cases seen in the absence of salt. The absence of salt leads to more electrostatic repulsion between the proteins at pH 7.1–7.2 compared to samples with salt, which may explain the higher G'. The onset of thermal gelation was also different for samples in the absence of salt. For example the rheological curve of washed muscle without salt exhibited a similar pattern reaching a minimum 7 °C lower than compared with salt. Another observation was that the rheology curves for acid and alkali treated proteins without salt exhibited all similar drop in G' around 40 °C. This drop could be explained by a breakup of protein aggregates with higher temperatures, and the subsequent increase in G' due to proteins denaturing and forming permanent cross-links at higher temperatures. Washed muscle consists mainly of myofibrillar proteins because much of the sarcoplasmic proteins are removed during the washing step (Park & Lanier, 2000). The acid produced protein isolate contains on the other hand sizable amount of sarcoplasmic proteins while the alkali isolate had significantly less of the sarcoplasmic proteins. The types of proteins recovered therefore do not seem to explain this similar behaviour of the acid and alkali isolates on heating. The above emphasises that the differences between the two systems are far from trivial and more investigation is needed to understand the underlying mechanisms for gelation in salt and no salt.

3.4. Water-holding capacity

Good water-holding capacity is an important factor in muscle protein gels as it not only affects the economics of their production but also their quality. Same gels as were tested with the Torsion Gelometer were analysed for water loss on pressing (Fig. 4). Gels with no added salt lost from about 5% to 14% water on pressing. Addition of 2% NaCl (w/w) significantly reduced ($p < 0.05$) water loss for protein isolates, while the difference was not significant ($p > 0.05$) for the washed muscle. The range of water loss, ~4.5–6%, for gels with salt was also smaller than that of gels with no salt. Most water loss, or ~14%, was observed for gels with no added NaCl from isolated made from pH 2.9 treated proteins, while the gels with added salt from the isolate made from pH 11 treated proteins had least water loss, or ~4.5%.

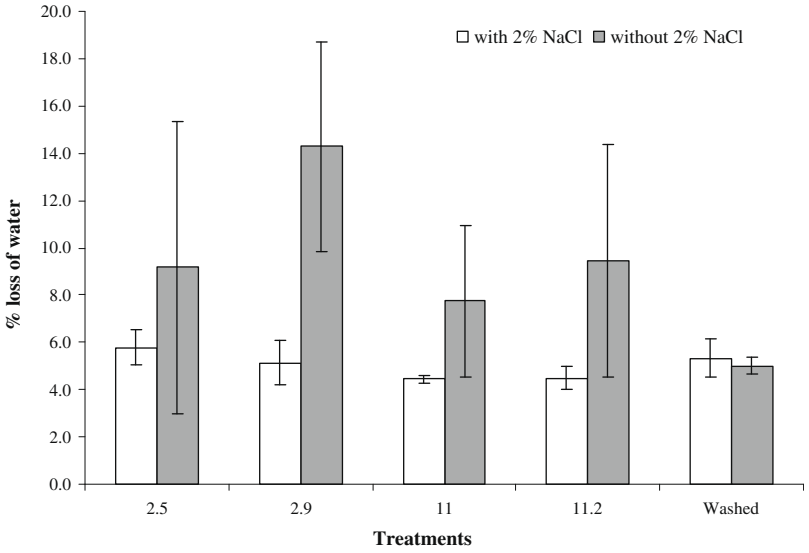

Fig. 4. Water loss of heat-induced tilapia protein isolates and washed muscle gel slices (3 mm) under pressure (3 kg). Samples contained either 2% added NaCl and no added NaCl.

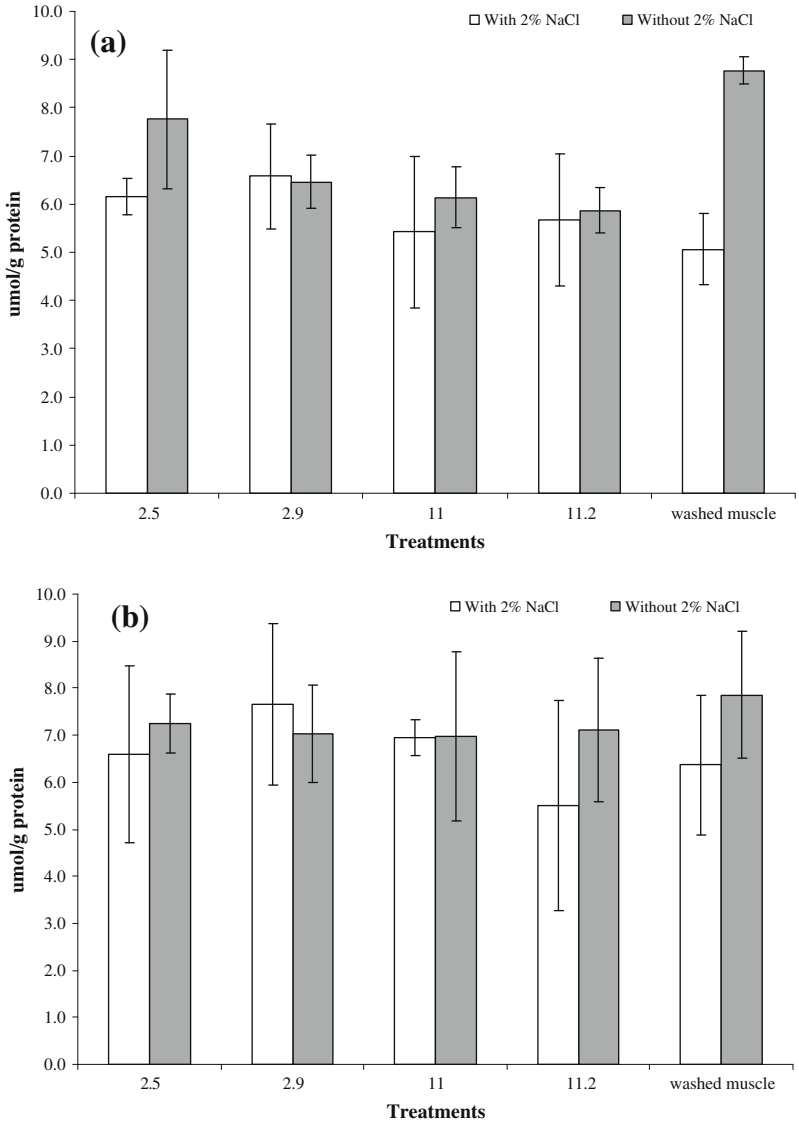

Fig. 5. Level of total sulphydryl groups (μmol/g protein) in tilapia protein isolates and washed muscle before (a) and after (b) thermal gelation (20 min at 80 °C).

Gel structure is believed to greatly influence the ability of a gel to hold water. In a well ordered gel, movement of water might be restricted compared to a less ordered structure (Hamman & MacDonald, 1992). This is partly due to strong capillary forces within the ordered structure and also high gel pressure if water is being held due to strong repulsive forces between negative charges in the protein matrix (Kristinsson & Hultin, 2003c). Between pH 7.1 and 7.2 there are strong repulsive forces between muscle proteins and these repulsive forces strengthen even more in the absence of salt (Kristinsson & Hultin, 2003c). The water-holding results agree with the gelation results, in that the weaker and more brittle gels had lower water-holding capacity. Feng and Hultin (2001) reported that gels with an evenly distributed gel structure showed improved WHC whereas a poor gel matrix can lead to syneresis, i.e. a discharge of water from the gel. Formation of localised aggregates is believed to contribute to lower gel forming ability (Feng & Hultin, 2001) and a correlation between a gel elasticity and water-holding capacity has been seen for chicken-breast gels (Kristinsson & Hultin, 2003c). For example the gels from the pH 2.9 treatment had the poorest gel forming ability (especially in the absence of salt), thus having a poorer gel structure, and also had the least ability to hold water than any of the other treatments. The salt free gels in general had poorer gel forming ability than the gels with salt, and these did also have worse water-holding ability. The addition of salt to the proteins thus appears to have led to a better ordered structure than the absence of salt. The salt is able to partially "solubilise" the muscle proteins, and this could have been important for the formation of an ordered structure since proteins would have been dispersed better prior to gelation.

3.5. SH-content

Changes in free sulphydryl (SH) groups and disulphide bonds (S–S) are often associated with gelation of muscle proteins. It is also known that SH-groups become more reactive at the high pH values representative of the alkaline process (Yongsawatdigul & Park, 2004). Washed muscle exhibited the highest total SH content before cooking for samples without added NaCl, whereas washed muscle with 2% NaCl (w/w) had significantly lower ($p < 0.05$) total SH content (Fig. 5a). There were no significant differences ($p > 0.05$) between pastes with no added salt and added salt between acid or alkali isolates. There was also no significant difference ($p > 0.05$) in total SH-groups after cooking between treatments and salt concentrations (Fig. 5b). It was also interesting to see that there were no significant ($p > 0.05$) difference in total SH-groups before and after gel formation.

A reduction in total SH-groups indicates the formation of S–S bonds between proteins, and has been found on many occasions when gelation of muscle proteins is studied (Lanier, 2000). A significant difference in SH group between the low and high pH treatments was not found. Other studies with the acid and alkali processes have either reported differences or no differences in reactive and total SH-groups. Kristinsson and Hultin (2003a) showed that alkali treated myosin had more reactive SH-groups than acid treated myosin, and also had better gel forming ability. A study by Yongsawatdigul and Park (2004) performed on rockfish muscle showed that washed muscle had lower content of total SH compared to unwashed muscle. These authors observed a higher amount of total SH-groups in proteins made with the alkaline process compared to acid process, thus suggesting S–S bonds formed during the acid process. Rockfish proteins made with the alkali process had the largest decrease in SH-groups, suggesting that more S–S bonds were formed during gelation for that treatment compared to other treatments. This was not seen with the tilapia muscle proteins. Another study performed on Pacific whiting showed a significantly higher total SH content of isolates made at low pH compared to high pH, suggesting SH-groups became more reactive on alkali treatment. Even though differences were seen in SH-groups with Pacific whiting proteins there were no link between these and gel forming ability. A study performed on threadfin bream showed that total sulphydryl groups were stable up to 30 °C but decreased from 40 to 80 °C which indicates formation of disulphide linkages during heating (Yongsawatdigul & Park, 2003). Again, the data with the tilapia proteins indicate that no significant S–S bonds were formed on heating and thus differences in SH-groups could not explain the different functionality of the proteins.

4. Conclusions

Gel forming ability of the acid and alkali treated proteins was determined and compared to washed tilapia muscle. Large strain testing (torsion) showed that gels with 2% added NaCl were stronger and more elastic compared to samples without 2% NaCl. The alkali treated proteins also gave better results when compared to acid treated proteins and washed muscle. The use of small strain oscillatory testing gave interesting results. Samples without 2% NaCl performed in some cases better than samples with 2% NaCl. Variability at low pH was high possibly due to a more unstable structure of the proteins. The small and large strain testing are however not necessarily expected to go hand in hand. Levels of total sulphydryl groups before and after thermal gelation did not explain differences in gel forming ability or gel quality. More investigation is needed to understand the underlying mechanism and the molecular properties involved in gelation of tilapia muscle proteins. The overall findings from this research indicate that alkali treated tilapia muscle proteins can form strong and elastic gels upon heating.

Acknowledgements

This work was supported by the Cooperative State Research, Education and Extension Service, US Dept. of Agriculture by Grant 2002-34135-12467 of the T-STAR Grants Program and by Grant 2004-35503-14119 of the USDA NRI Competitive Grants Program.

References

Bakir, H. M., Hultin, H. O., & Kelleher, S. D. (1994). Gelation properties of fatty fish processed with or without added sodium chloride, cryoprotectants and antioxidants. *Food Research International, 27*, 443–449.

Choi, Y. J., & Park, J. W. (2002). Acid-aided protein recovery from enzyme-rich pacific whiting. *Journal of Food Science, 67*(8), 2962–2967.

Cortes-Ruiz, J. A., Pacheco-Aguilar, R., Garcia-Sanches, G., & Lugo-Sanches, M. E. (2001). Functional characterization of protein concentrates from bristly sardine under acidic conditions. *Journal of Aquatic Food Product Technology, 10*, 2–23.

Crynen, S., & Kristinsson, H. G. (2003). The effect of acid and alkali treatments on the gelation properties of sarcoplasmic and myofibrillar proteins of channel catfish. In *IFT Annual Meeting, Chicago, Ill.* Abstr. 87-3.

Davenport, M. P., & Kristinsson, H. G. (2003). Low and high pH treatments induce a molten globular structure in myosin which improves its gelation properties. In *IFT Annual Meeting, Chicago, Ill.* Abstr. 42-9.

Davenport, M. P., Theodore, A., & Kristinsson, H. G. (2004). Influence of insoluble muscle components on the gelation properties of catfish protein isolates made with acid and alkali aided processing. In *IFT Annual Meeting, Las Vegas, NV.* Abstr. 83A-21.

Feng, Y. M., & Hultin, H. O. (1997). Solubility of the proteins of mackerel light muscle at low ionic strength. *Journal of Food Biochemistry, 21*(6), 479–496.

Feng, Y. M., & Hultin, H. O. (2001). Effect of pH on the rheological and structural properties of gels of water-washed chicken-breast muscle at physiological ionic strength. *Journal of Agricultural and Food Chemistry, 49*(8), 3927–3935.

Hamman, D. D. (1991). A tool for understanding thermally induced protein gelation. In P. Nicholas & R. Barford (Eds.), *Interactions of food proteins* (pp. 212–227). Washington, DC: American Chemical Society.

Hamman, D. D., & MacDonald, G. A. (1992). Rheology and texture properties of surimi and surimi based foods. In T. C. Lanier & C. M. Lee (Eds.), *Surimi technology* (pp. 429–500). New York: Marcel Dekker.

Hermansson, A. M. (1978). Physico chemical aspects of soy proteins structure formation. *Journal of Texture Studies, 9*(1–2), 33–58.

Huang, C. H., Lai, H. T., & Weng, Y. M. (1998). Suitability of hybrid tilapia (*Oreochromis niloticus* × *Oreochromis aureus*) muscle for gel formation. *International Journal of Food Science and Technology, 33*, 339–344.

Hultin, H. O., & Kelleher, S. D. (2000). Surimi processing from dark muscle fish. In J. W. Park (Ed.), *Surimi and surimi seafood* (pp. 59–77). New York: Marcel Dekker.

Kim, Y. S., Park, J. W., & Choi, Y. J. (2003). New approaches for the effective recovery of fish proteins and their physiochemical characteristics. *Fisheries Science, 69*, 1231–1239.

Klesk, K., Yongsawatdigul, J., Park, J. W., Viratchakul, S., & Virulhakul, P. (2000a). Gel forming ability of tropical tilapia surimi as compared with Alaska pollock and pacific whiting surimi. *Journal of Aquatic Food Product Technology, 9*(3), 91–104.

Klesk, K., Yongsawatdigul, J., Park, J. W., Viratchakul, S., & Virulhakul, P. (2000b). Physical behavior of tropical tilapia surimi gels at various thermal treatments as compared with Alaska pollock and pacific whiting surimi. *Journal of Aquatic Food Product Technology, 9*(3), 91–104.

Kongpun, O. (1999). The gel forming ability of washed and unwashed fish meat (lizardfish and nile tilapia). *Natural Science, 33*, 258–269.

Kristinsson, H. G., & Demir, N. (2003). Functional fish protein ingredients from fish species of warm and temperate waters: Comparison of acid and alkali-aided processing vs. conventional surimi processing. In P. Bechtel (Ed.), *Advances in seafood byproducts* (pp. 277–298). Fairbanks, Alaska: Univ. of Alaska Press.

Kristinsson, H. G., & Hultin, H. O. (2003a). Changes in conformation and subunit assembly of cod myosin at low and high pH and after subsequent refolding. *Journal of Agricultural and Food Chemistry, 51*(24), 7187–7196.

Kristinsson, H. G., & Hultin, H. O. (2003b). Effect of low and high pH treatment on the functional properties of cod muscle proteins. *Journal of Agricultural and Food Chemistry, 51*, 5103–5110.

Kristinsson, H. G., & Hultin, H. O. (2003c). Role of pH and ionic strength on water relationships in washed minced chicken-breast muscle gels. *Journal of Food Science, 68*(3), 917–922.

Kristinsson, H. G., & Ingadottir, B. (2006). Recovery and properties of muscle proteins extracted from tilapia (*Oreochromis niloticus*) light muscle by pH shift processing. *Journal of Food Science, 71*(3), 132–141.

Kristinsson, H. G., Theodore, A., Demir, N., & Ingadottir, B. (2005). A comparative study between acid- and alkali-aided processing and surimi processing for the recovery of proteins from channel catfish muscle. *Journal of Food Science, 70*(4), 298–306.

Kudo, G., Okada, M., & Miyauchi, D. (1973). Gel-forming capacity of washed and unwashed flesh of some pacific coast species of fish. *Marine Fisheries Review, 32*, 10–15.

Lanier, T. C. (2000). Surimi gelation chemistry. In J. W. Park (Ed.), *Surimi and surimi seafood* (pp. 237–265). New York: Marcel Dekker.

Onibala, H., Takayama, T., Shindo, J., Hayashi, S, & Miki, H. (1997). Influence of freshness on occurrence of setting and disintegrating in heat-induced gels from tilapia. *Fisheries Science, 63*(2), 276–280.

Park, J. W., Korhonen, R. W., & Lanier, T. C. (1990). Effects of rigor-mortis on gel-forming properties of surimi and unwashed mince prepared from tilapia. *Journal of Food Science, 55*(2), 353–355, 366.

Park, J. W., & Lanier, T. C. (2000). Processing of surimi and surimi seafoods. In R. E. Martin (Ed.), *Marine and freshwater products handbook*. Lancaster, NH: Technomic Publishing Company.

Theodore, A., Kristinsson, H. G., & Crynen, S. (2003). The effect of pH and salt on the gelation properties of catfish surimi and catfish protein isolates from acid and alkali-aided processing. In *IFT Annual Meeting, Chicago, Ill.* Abstr. 76A-10.

Undeland, I. A., Kelleher, S. D., & Hultin, H. O. (2002). Recovery of functional proteins from herring (*Clupea harengus*) light muscle by an acid or alkaline solubilization process. *Journal of Agricultural and Food Chemistry, 50*, 7371–7379.

Xiong, Y. L. (1997). Structure–function relationship of muscle proteins. In S. Damodaran & A. Paraf (Eds.), *Food proteins and their applications* (pp. 341–392). New York: Marcel Dekker.

Xiong, Y. L. (2000). Meat processing. In S. Nakai & H. W. Modler (Eds.), *Food proteins processing applications* (pp. 89–145). New York: Wiley-VCH.

Xiong, Y. L., & Blacnchard, S. P. (1994). Dynamic gelling properties of myofibrillar protein from skeletal muscles of different chicken parts. *Journal of Agricultural and Food Chemistry, 42*, 670–674.

Yongsawatdigul, J., & Park, J. W. (2003). Thermal denaturation and aggregation of threadfin bream actomyosin. *Food Chemistry, 83*, 409–416.

Yongsawatdigul, J., & Park, J. W. (2004). Effects of alkali and acid solubilization on gelation characteristics of rockfish muscle proteins. *Journal of Food Science, 69*(7), 499–505.

2. Materials and methods

2.1. Materials

Chufa [*Eleocharis tuberosa* (Roxb.) Roem. et Schult. cv. Guilin] corms were purchased from a commercial market in Nanning of China. The healthy corms with uniform size were selected, washed, peeled and then cut into small pieces using a sharp stainless steel knife. These fresh-cut samples were stored at −20 °C until further extraction and analysis.

2.2. Chemicals and reagents

Standards (−)-gallocatechin gallate, (−)-epicatechin gallate and (+)-catechin gallate were purchased from Sigma–Aldrich (St. Louis, MO, USA). Acetonitrile was HPLC grade and obtained from Merck (Darmstadt, Germany). Other reagents were analytical grade.

2.3. Partial purification and activity determination of PPO

PPO was extracted by the modified methods of Jiang, Giora, and Yoram (1997). At 4 °C, 30 g of corm samples were homogenised in 200 ml of 0.1 M sodium phosphate buffer (pH 6.8) containing 2 g of polyvinyl pyrrolidone (PVP) and 1.0% (v/v) Triton X-100. After filtration of the homogenate through cheesecloth, the filtrate was centrifuged at 10,000 rpm for 15 min. The supernatant was collected and fractionated with solid ammonium sulfate (30–80% saturation). The precipitate was collected by centrifugation at 10,000 rpm for 15 min, which was further re-dissolved in a small volume of 10 mM sodium phosphate buffer (pH 6.8). After overnight dialysis against the same buffer, the dialysed solution was collected as the partially purified PPO to analyse its biochemical properties. PPO activity was spectrophotometrically assayed according to the modified method of Jiang (1999) with catechol as an exogenous substrate. The enzyme solution (0.2 ml) was rapidly added into 2.8 ml of 10 mM catechol solution (prepared in 10 mM sodium phosphate buffer, pH 6.8). The increase in absorbance at 400 nm at 25 °C was recorded automatically for 3 min using a UV-1700 spectrophotometer (Shimadzu, Kyoto, Japan). One unit of PPO activity was defined as the amount of the enzyme that caused a change of 0.001 in absorbance per minute. Relative activity described enzymatic activity as the percentage of the activity expressed as $(A/A_{max}) \times 100$, where A indicated the increase in optical density per minute (Montero, Ávalos, & Pérez-Mateos, 2001). Protein content was determined by the dye-binding method of Bradford (1976).

2.4. Effects of pH and temperature on PPO properties

PPO activity was assayed in a pH range of 4–6 in 50 mM citric acid–phosphate buffer and 7–9 in 50 mM Tris–HCl buffer using catechol as the substrate. To determine the optimal pH values of chufa PPO, 1 ml of 10 mM catechol and 1.9 ml of buffer solution were mixed at 25 °C prior to adding 0.1 ml of enzyme solution. On the other hand, the PPO activity was measured in a temperature range of 20–60 °C using a water bath. A total of 2.8 ml of 10 mM catechol was pre-warmed to the corresponding temperatures. Then, 0.2 ml of enzyme solution was added. To determine the effects of high temperature, the enzyme solution was incubated in water bath at 70, 80 and 90 °C for 4 min. Every one minute, 0.2 ml of enzyme solution was transferred into 2.8 ml of 10 mM catechol to assay the enzyme stability. The relative activities were compared by the method described above.

2.5. Effects of inhibitors and metal ions on PPO properties

To determine the effects of inhibitors on PPO activity, 2.9 ml of 10 mM catechol and 25 μl of 0.1 M inhibitor solutions were mixed immediately at 25 °C prior to adding 75 μl of enzyme solution. To determine the effects of metal ions, 2 ml of 10 mM catechol and 1 ml of 2 mg/ml metal compounds were mixed before adding 0.5 ml of enzyme solution. The control was the substrate–enzyme reaction system without any inhibitor or metal compounds.

2.6. Determination of kinetic parameters

The enzyme kinetic parameters (Doğan & Doğan, 2004), Michaelis–Menten constant (K_m) and maximal reaction velocity (V_{max}) for chufa PPO were determined at 25 °C when using catechol as the substrate. The assay cuvette (3 ml) contained 2.8 ml of catechol solution with gradient concentration (from 0.002 to 0.01 M) and 0.2 ml of the enzyme solution. The kinetic parameters were estimated by linear regression analysis using the following equation.

$$v = \frac{V_{max} \cdot [S]}{K_m + [S]}, \quad (1)$$

where [S] corresponds to the substrate concentration. The data were plotted as $1/v$ vs $1/[S]$. K_m and V_{max} were determined as the reciprocal absolute values of the intercepts on the x- and y-axes of the regression curve (Lineweaver & Burk, 1934).

2.7. Identification and estimation of endogenous PPO substrates

Polyphenols in plants are often considered as PPO substrates. The identification of polyphenols in chufa corms were performed by high performance liquid chromatography using a Waters 2695 HPLC system (Waters, Milford, MA, USA) with a dual wavelength absorbance detector. The separation was carried out on a 250 × 4.6 mm i.d., 5 μm Pinnacle C_{18} column (Restek, Bellafonte, PA, USA). The mobile phase consisted of acetonitrile (A) and acidified water containing 2% acetic acid (B). The linear gradient program was as follows: 0 min, 1% A; 4 min, 1% A; 38 min, 50% A; 42 min, 80% A and then held for 3 min before returning to the initial conditions. The flow rate was 1 ml/min and the injection volume was 20 μl. The monitoring wavelength was at 280 nm. The recognition of phenolic compositions was achieved by comparison with retention times (Rt) and ultraviolet spectra of standards. HPLC profile ranged from 5 to 30 min, in which the obvious peaks appeared, was obtained by Waters Empower software.

2.8. Data analysis

In the present study, all experiments were performed in triplicate ($n = 3$), and the results represented mean ± standard deviations (SD) of three replicated determinations.

3. Results and discussion

3.1. Protein content and PPO activity

During the extraction of chufa PPO, an undesirable reaction between the natural phenols and PPO was prevented by adding PVP, which could extract phenols by a well-postulated hydrogen bonding of the ionisable hydrogens of phenol to the oxygens of polyvinylpyrrolidone (Andersen & Sowers, 1968). The addition of Triton X-100 during extraction might improve the PPO activity because this surfactant could extract enzymatic proteins in plasma membranes (Broothaerts et al., 2000; Sun et al., 2008). Using the dye-

binding method, the calibration curve was linear in a protein content range of 10–100 μg, with $R^2 > 0.99$ and the calibration curve equation was $y = 0.0074x - 0.0422$. Based on this equation, the protein content of the dialysed PPO enzyme solution in the present study was around 52.7 μg protein/ml with a total activity of 45 units/ml when catechol as the substrate.

3.2. Optimal pH and temperature

In general, PPO shows maximum activity at or near neutral pH values. However, the optimum pH has been found to vary with the enzymatic source and the substrate over a relatively wide range of values, including in alkaline medium (Cestari, Vieira, Nascimento, Santos Filha, & Airoldi, 2002). The pH profile for the oxidation of catechol by chufa PPO is shown in Fig. 1A. At 25 °C, the highest peak for relative enzyme activity was observed at pH 5, which indicated that the optimal pH for chufa PPO activity was pH 5. From Fig. 1A, the enzyme activity only slightly decreased between pH 5 and 6. However, it steeply declined under pH 5 and above pH 6. At pH 3 and 9, the PPO activities were only about 52.9% and 17.6% of the maximal activity. Plant PPO is suggested to contain Cu^{2+} in its active site (Kuwabara & Katoh, 1999), and Cu^{2+} will depart from the active site in the acidic or alkaline pH range, leading to the loss in PPO activity (Huang, Zhang, & Wang, 2005). This is the possible reason for steep decrease of chufa PPO activity under pH 5 and above pH 6 in the present study.

In addition, when using catechol as the substrate, the optimal temperature for chufa PPO activity was shown in Fig. 1B. The temperature has a two-sided influence on enzymatic activity, i.e. increasing incubation temperature enhances enzymatic reaction velocity but simultaneously results in denaturalisation of the enzyme. The optimal temperature depends on the effect of the two-sided equilibrium (Sun et al., 2008). From Fig. 1B, chufa PPO activity exhibited a gradually increasing trend in a temperature range of 20–45 °C, and then rapidly decreased above 45 °C due to the denaturalisation of the enzyme. The optimal temperature for chufa PPO activity was at 45 °C. The PPO in plant tissues is relatively heat labile and high temperatures can inactivate it. Thermal inactivation of PPO usually increases with increasing temperature and follows first-order kinetics, which has been reported in many studies (Chutintrasri & Noomhorm, 2006; Lee & Smith, 1979; Rapeanu, Loey, Smout, & Hendrickx, 2006; Schweiggert, Schieber, & Carle, 2005). The effects of high temperatures on chufa PPO are shown in Fig. 1C. The PPO was relatively stable at 70 °C but unstable at 80 and 90 °C. After heating for 4 min at 70 °C, the relative PPO activity were similar to that of heating for 0 min. While heating PPO at 80 and 90 °C, its relative activities remained at 79.4% and 61.8% after 4 min. The above results indicated that chufa PPO activity would obviously decline when heating it above 70 °C, which owes to the degradation of PPO at higher temperatures.

3.3. Effects of various inhibitors and metal ions

The effects of various inhibitors and metal ions on chufa PPO activity are listed in Table 1. Compared with the control, ethylenediaminetetraacetic acid disodium salt (EDTA-2Na) and L-cysteine had no inhibiting effects on the PPO activity. Contrarily, both compounds somewhat improved the enzymatic reaction between the PPO and catechol. Adding ascorbic acid, sodium thiosulfate pentahydrate ($Na_2S_2O_3{\cdot}5H_2O$) and anhydrous sodium sulfite (Na_2SO_3) into the substrate–enzyme system reduced the PPO activity. Amongst three inhibitors, $Na_2S_2O_3{\cdot}5H_2O$ exhibited the strongest inhibiting effect, followed by ascorbic acid and Na_2SO_3. The mechanism of inhibition differs, depending on the compound used. Ascorbic acid, owing to its nontoxic nature at the levels employed, is widely used to inhibit the activity of PPO in vegetable or fruit tissues. Ascorbic acid may act more as an antioxidant than as an enzyme inhibitor because it reduces the initial quinone formed by PPO to the original diphenol before it undergoes the browning reaction (Aydemir, 2004). On the other hand, ascorbic acid can also reduce Cu^{2+} of PPO into Cu^{+} (Hsu, Shieh, Bills, & White, 1988). Na_2-

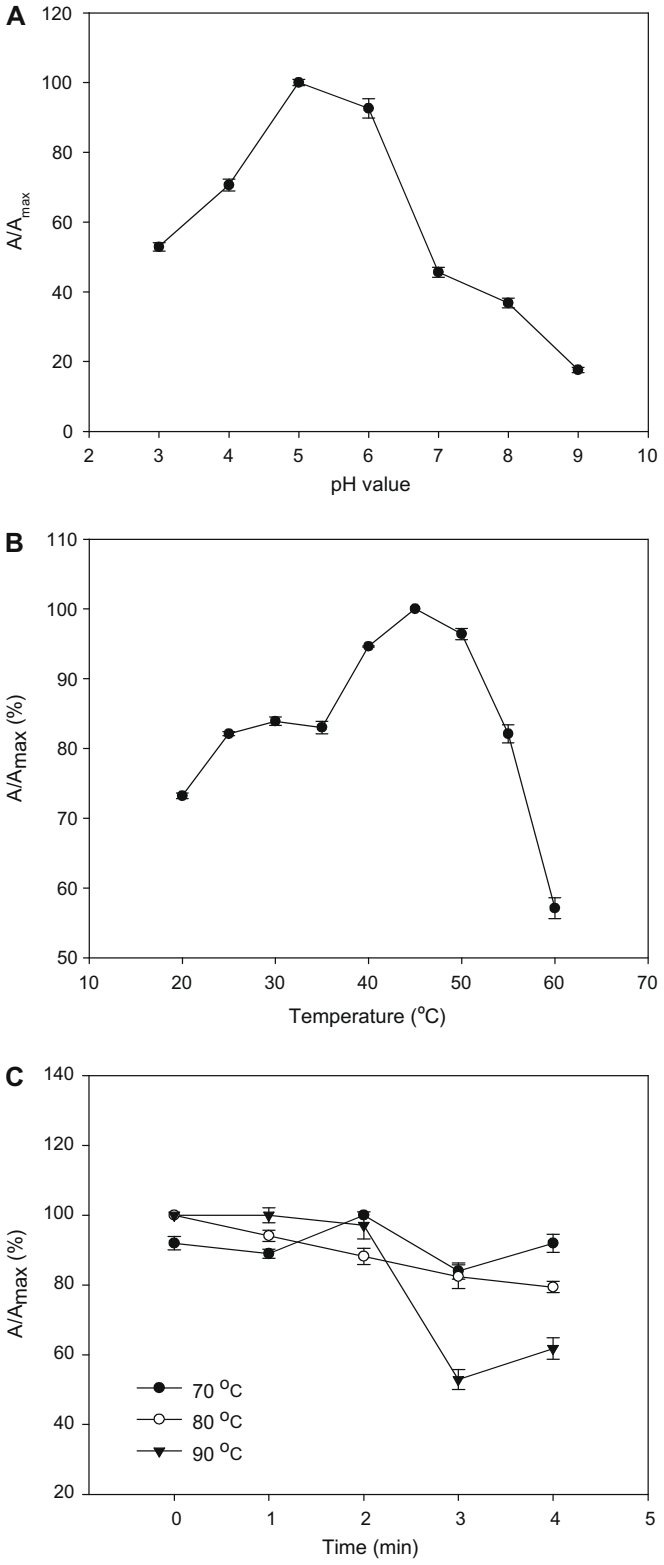

Fig. 1. Effects of pH values and temperatures on chufa PPO activity. (A) The optimal pH, (B) the optimal temperature and (C) the heat stability.

Table 1
Effects of various inhibitors and metal compounds on chufa PPO activity.

Compounds	Concentration	A/A_{max} (%)
Inhibitors[*]		
Control	0.1 M	76.5 ± 0.7
EDTA-2Na	0.1 M	80.4 ± 0.6
Ascorbic acid	0.1 M	45.1 ± 1.2
$Na_2S_2O_3{\cdot}5H_2O$	0.1 M	41.2 ± 1.1
Na_2SO_3	0.1 M	64.7 ± 0.7
L-Cysteine	0.1 M	100 ± 0.0
Metal compounds[**]		
Control	2 mg/ml	37.3 ± 0.2
NaCl	2 mg/ml	44.1 ± 0.8
KCl	2 mg/ml	36.3 ± 1.4
$ZnSO_4{\cdot}7H_2O$	2 mg/ml	100 ± 0.0
$CaCl_2$	2 mg/ml	71.6 ± 3.5
$CuSO_4{\cdot}5H_2O$	2 mg/ml	87.3 ± 1.7
$FeSO_4{\cdot}7H_2O$	2 mg/ml	50.0 ± 2.2
$FeCl_3{\cdot}6H_2O$	2 mg/ml	74.5 ± 1.0

[*] Enzyme reaction system: 2.9 ml of 10 mM catechol (prepared in 10 mM sodium phosphate buffer, pH 6.8) + 25 μl of inhibitor + 75 μl of enzyme solution.
[**] Enzyme reaction system: 2 ml of 10 mM catechol (prepared in 10 mM sodium phosphate buffer, pH 6.8) + 1 ml of metal compounds + 0.5 ml of enzyme solution.

$S_2O_3{\cdot}5H_2O$ and Na_2SO_3 are the good reducing agents of *o*-quinone. Both may react directly with sulfhydryl groups, resulting in the reduction of *o*-quinone and formation of colourless complexes with *o*-quinone (Sun et al., 2008). Sulfites are effective in inhibiting PPO activity but they are subject to regulatory restrictions due to adverse effects on human health.

Generally speaking, adding 2 mg/ml metal compounds into the substrate–enzyme system had considerable influences on the PPO activity. Except for K^+, other metal ions accelerated the enzymatic reaction between the PPO and catechol. Amongst them, Zn^{2+} exhibited the strongest accelerating effect and the PPO activity increased most after adding it. Cu^{2+}, Fe^{3+} and Ca^{2+} also improved this enzymatic reaction. Furthermore, adding Fe^{2+} and Na^+ into the substrate–enzyme system weakly increased the PPO activity. Plant PPO is suggested to have one binuclear Cu site per protein molecule for the reaction centre (Kuwabara & Katoh, 1999), and various metal ions may affect the substrate combining this reaction centre so as to alter the PPO activity. Some metal ions that increase PPO activity have already found by other researchers who suggested that the effect of metal ions on PPO activity was concentration-dependent or pH-dependent. Chu, Yeh, and Shaw (1993) reported that Cu^{2+} activated banana leaf PPO activity at concentrations lower than 0.6 mM but inhibited it at higher concentrations. Using a kinetic study on the effect of sodium chloride on latent grape PPO activity, Valero and García-Carmona (1998) observed that this metal compound showed a strongly pH-dependent inhibitory effect at pH values lower than 5 but acted as an activator at higher values. Whether the effect of metal ions on chufa PPO activity is dependent on concentration and pH value needs further study.

3.4. Kinetic study

A Lineweaver–Burk double reciprocal plot (Fig. 2) showed a correlation coefficient of $R^2 = 0.9635$, and the regression curve equation was $y = 0.1307x + 12.125$. The K_m and V_{max} values of chufa PPO for catechol were calculated from above equation. The results showed that the apparent K_m and V_{max} values of the present enzymatic reaction were about 10.77 mM and 82 units/ml min at 25 °C, respectively.

3.5. Evaluation of potential endogenous PPO substrates

By HPLC analysis, three major polyphenols isolated from chufa corms were identified as (−)-gallocatechin gallate (Rt = 18.4 min),

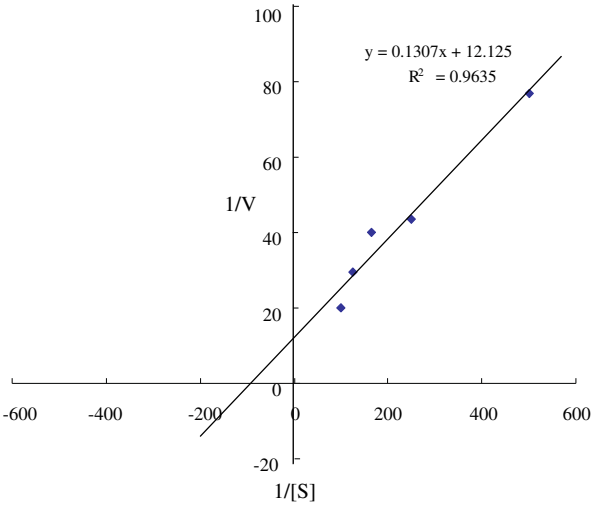

Fig. 2. Lineweaver–Burk double reciprocal plot of chufa PPO. The substrate concentrations were 0.002, 0.004, 0.006, 0.008 and 0.01 M, respectively.

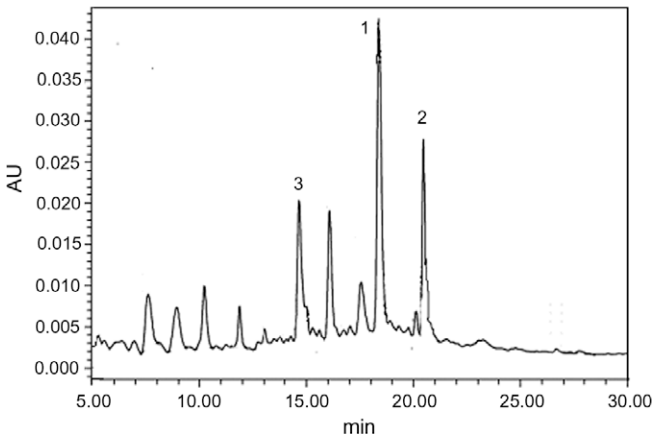

Fig. 3. HPLC–chromatogram of polyphenol components extracted from chufa corms ($\lambda = 280$ nm). Peak 1: (−)-gallocatechin gallate; peak 2: (−)-epicatechin gallate; and peak 3: (+)-catechin gallate.

(−)-epicatechin gallate (Rt = 20.5 min) and (+)-catechin gallate (Rt = 14.7 min) (Fig. 3). These three polyphenols possessed similar chemical structures to catechol, i.e. the *ortho*-diphenolic or pyrogallolic hydroxyls, which were the locations of enzymatic action of PPO (Jiang, 1999; Martinez & Whitaker, 1995; Sun et al., 2006). A wide range of compounds with *ortho*-dihydroxyphenolic or pyrogallolic structures are substrates for the PPO in higher plants because of the presence of oxidisable OH groups (i.e. those phenolic OHs that are adjacent to each other) (Martinez & Whitaker, 1995). Therefore, just like catechol which served as substrate of chufa PPO, these three polyphenols (as the potential endogenous substrates) might also be catalysed by chufa PPO in the presence of oxygen and finally polymerised into the yellow or brown coloured by-products, causing the browning of corm tissues after fresh-cut processing. In chufa corms, the phenolic compositions catalysed by PPO and the PPO properties when reacting with endogenous substrates will be investigated in further studies. These studies will be necessary for exactly elucidating enzyme-catalysed browning mechanism of fresh-cut chufa corms.

Acknowledgements

The financial support provided by Scientific Research Foundation for Doctoral Personnel (Grant No. 20090306) and Foundation

of Fundamental Research Project from Guangxi Academy of Agricultural Sciences was appreciated.

References

Andersen, R. A., & Sowers, J. A. (1968). Optimum conditions for bonding of plant phenols to insoluble polyvinylpyrrolidone. *Phytochemistry, 7*, 293–301.

Ayaz, F. A., Demir, O., Torun, H., Kolcuoglu, Y., & Colak, A. (2008). Characterization of polyphenoloxidase (PPO) and total phenolic contents in medlar (*Mespilus germanica* L.) fruit during ripening and over ripening. *Food Chemistry, 106*(29), 1–298.

Aydemir, T. (2004). Partial purification and characterization of polyphenol oxidase from artichoke (*Cynara scolymus* L.) heads. *Food Chemistry, 87*(5), 9–67.

Bradford, M. M. (1976). A rapid and sensitive method for the quantitation of microgram quantities of protein using the principle of protein–dye binding. *Analytical Biochemistry, 72*, 248–254.

Broothaerts, W., McPherson, J., Li, B., Randall, E., Lane, W. D., & Wiersma, P. A. (2000). Fast apple (*Malus domestica*) and tobacco (*Nicotiana tobacum*) leaf polyphenol oxidase activity assay for screening transgenic plants. *Journal of Agricultural and Food Chemistry, 48*, 5924–5928.

Cestari, A. R., Vieira, E. F. S., Nascimento, A. J. P., Santos Filha, M. M., & Airoldi, C. (2002). Factorial design evaluation of some experimental factors for phenols oxidation using crude extracts from jackfruit (*Artocarpus integrifolia*). *Journal Brazilian Chemical Society, 13*, 260–265.

Chu, H.-L., Yeh, D.-B., & Shaw, J.-F. (1993). The biochemical properties of polyphenol oxidase from banana leaf. *Botanical Bulletin of Academia Sinica, 34*, 169–174.

Chutintrasri, B., & Noomhorm, A. (2006). Thermal inactivation of polyphenoloxidase in pineapple puree. *LWT-Food Science and Technology, 39*, 492–495.

Dincer, B., Colak, A., Aydin, N., Kadioglu, A., & Güner, S. (2002). Characterization of polyphenoloxidase from medlar fruits (*Mespilus germanica* L., Rosaceae). *Food Chemistry, 77*, 1–7.

Doğan, S., & Doğan, M. (2004). Determination of kinetic properties of polyphenol oxidase from *Thymus* (*Thymus longicaulis* subsp. Chaubardii var. Chaubardii). *Food Chemistry, 88*, 69–77.

Duangmal, K., & Owusu Apenten, R. K. (1999). A comparative study of polyphenoloxidases from taro (*Colocasia esculenta*) and potato (*Solanum tuberosum* var. Romano). *Food Chemistry, 64*, 351–359.

Hsu, A. F., Shieh, J. J., Bills, D. D., & White, K. (1988). Inhibition of mushroom polyphenoloxidase by ascorbic acid derivatives. *Journal of Food Science, 53*, 765–767, 771.

Huang, J., Zhang, H., & Wang, Y. (2005). Characteristics of polyphenol oxidase in *Pteridium aquilinum*. *Food and Machinery, 21*, 12–13, 16 (in Chinese).

Jiang, Y. M. (1999). Purification and some properties of polyphenol oxidase of longan fruit. *Food Chemistry, 66*, 75–79.

Jiang, Y. M., Giora, Z., & Yoram, F. (1997). Partial purification and some properties of polyphenol oxidase extracted from litchi fruit pericarp. *Postharvest Biology and Technology, 10*, 221–228.

Kuwabara, T., & Katoh, Y. (1999). Involvement of the binuclear copper site in the proteolytic activity of polyphenol oxidase. *Plant and Cell Physiology, 40*, 1029–1035.

Lee, C. Y., & Smith, N. L. (1979). Blanching effect on polyphenol oxidase activity in table beets. *Journal of Food Science, 44*, 82–83.

Lineweaver, H., & Burk, D. (1934). The determination of enzyme dissociation constant. *Journal of American Chemists' Society, 56*, 658–661.

Liu, X., Zhao, L., & Zhou, A. (2006). Preliminary study on functional component and functional activities of waste slurry derived in processing water chestnut starch. *Food Science, 27*, 251–256 (in Chinese).

Martinez, M. V., & Whitaker, J. R. (1995). The biochemistry and control of enzymatic browning. *Trends in Food Science and Technology, 6*, 195–200.

Montero, P., Ávalos, A., & Pérez-Mateos, M. (2001). Characterization of polyphenoloxidase of prawns (*Penaeus japonicus*). Alternatives to inhibition: additives and high-pressure treatment. *Food Chemistry, 75*, 317–324.

Parr, A. J., Waldron, K. W., Ng, A., & Parker, M. L. (1996). The wall-bound phenolics of Chinese water chestnut (*Eleocharis dulcis*). *Journal of the Science of Food and Agriculture, 71*, 501–507.

Pen, L. T., & Jiang, Y. M. (2003). Effects of chitosan coating on shelf life and quality of fresh-cut Chinese water chestnut. *Lebensmittel-Wissenschaft und-Technologie, 36*, 359–364.

Peng, L., & Jiang, Y. (2006). Exogenous salicylic acid inhibits browning of fresh-cut Chinese water chestnut. *Food Chemistry, 94*, 535–540.

Rapeanu, G., Loey, A. V., Smout, C., & Hendrickx, M. (2006). Biochemical characterization and process stability of polyphenoloxidase extracted from Victoria grape (*Vitis vinifera* ssp. *Sativa*). *Food Chemistry, 94*, 253–261.

Schlimme, D. V. (1995). Marketing lightly processed fruits and vegetables. *HortScience, 30*, 15–17.

Schweiggert, U., Schieber, A., & Carle, R. (2005). Inactivation of peroxidase, polyphenoloxidase, and lipoxygenase in paprika and chili powder after immediate thermal treatment of the plant material. *Innovative Food Science and Emerging Technologies, 6*, 403–411.

Sun, J., Jiang, Y., Wei, X., Shi, J., You, Y., Liu, H., et al. (2006). Identification of (−)-epicatechin as the direct substrate for polyphenol oxidase isolated from litchi pericarp. *Food Research International, 39*, 864–870.

Sun, J., Shi, J., Zhao, M., Xue, S. J., Ren, J., & Jiang, Y. (2008). A comparative analysis of property of lychee polyphenoloxidase using endogenous and exogenous substrates. *Food Chemistry, 108*, 818–823.

Valero, E., & García-Carmona, F. (1998). pH-dependent effect of sodium chloride on latent grape polyphenol oxidase. *Journal of Agricultural and Food Chemistry, 46*, 2447–2451.

sensory attributes (especially focusing on the umami-taste attribute) according to their grades.

2. Materials and methods

2.1. Pine-mushroom

Pine-mushrooms of four grades cultivated in Inje-eup, Gangwon-do, Republic of Korea, in 2006 were used in this study. Fresh pine-mushrooms were wrapped in LLD-PE (low-level-density-polyethylene) film and stored at −70 °C in a deep freezer until use. Then they were thawed at 4 °C in a refrigerator for 3 h before sliced using a cutter (model SFS-102, Shinomura, Sanjo, Niigata, Japan). Then the pine-mushrooms were freeze-dried for the analysis of free amino acids and 5′-nucleotides.

2.2. Free amino acids assay

Free amino acids were extracted and analysed using EZ:faast-free amino acid analysis kit (Phenomenex, Torrance, CA) combined by gas chromatograph-flame ionisation detector (GC-FID) as described by Elmore, Koutsidis, Dodson, Mottram, and Wedzicha (2005). Freeze-dried pine-mushroom powder (1 g) was extracted with 15 ml of methanol at 75 °C for 25 min and cooled to room temperature. Then 15 ml of water and 17 ml of chloroform were added and this was centrifuged at 3000 rpm for 10 min. The supernatant was used as an extract sample for EZ:faast analysis. The preparation of a sample for GC-FID began with the addition of 20 nmol of novaline internal standard, followed by a solid phase extraction and then two derivatisation steps at room temperature. The derivatised amino acids were extracted into isooctane/chloroform (100 μl) and analysed by an HP 6890 GC-FID (Hewlett–Packard, Palo Alto, CA).

An aliquot of the derivatised amino acid solution (2 μl) was injected at 250 °C in split mode (1:15) onto a ZB AAA capillary column (60 m length × 0.25 mm i.d. × 0.25 mm film thickness, Phenomenex). The oven temperature was held at 110 °C for 1 min, then increased to 320 °C at 32 °C/min, and then held at 320 °C for 2 min. The carrier gas was helium at a constant flow rate of 1.5 ml/min. Each free amino acid was identified by matching its retention time with that of EZ:faast standard in GC chromatogram and quantified using its respective calibration curve.

2.3. 5′-Nucleotides

5′-Nucleotides were extracted and analysed as described by Taylor, Hershey, Levine, Coy, and Olivelle (1981). Freeze-dried pine-mushroom powder (500 mg) was extracted with 25 ml of deionised water. This suspension was heated to boil for 1 min, cooled, and then centrifuged at 3000 rpm for 15 min. The extraction was repeated twice. The combined supernatants were then evaporated, and filtered using a 0.45 μm PVDF filter (26 mm, Phenomenex) prior to HPLC analysis.

HPLC analysis was carried out using a HP series 1100 ultra performance liquid chromatograph (UPLC) system equipped with a G1311A quaternary pump, variable wavelength detector, and auto sampler (Hewlett–Packard). 5′-Nucleotides were separated by Sunfire C18 column (4.6 × 250 mm, 5 μl) (Waters Co., Milford, MA) using an isocratic mobile phase of 0.5 M potassium phosphate (pH 4.0 with phosphoric acid) at a flow rate of 1 ml/min and UV detection at 254 nm. Each 5′-nucleotide was identified by matching its retention time with that of an authentic standard in HPLC chromatogram and quantified using its respective calibration curve.

2.4. Equivalent umami concentration (EUC)

EUC (g MSG/100 g) is the concentration of MSG equivalent to the umami intensity given by a mixture of MSG and 5′-nucleotides and is represented by the following addition equation (Yamaguchi, Yoshikawa, Ikeda, & Ninomiya, 1971):

$$Y = \Sigma a_i b_i + 1218(\Sigma a_i b_i)(\Sigma a_j b_j)$$

where Y is the EUC of the mixture in terms of g MSG/100 g; a_i is the concentration (g/100 g) of each umami amino acid [aspartic acid (Asp) or glutamic acid (Glu)]; a_j is the concentration (g/100 g) of each 5′-nucleotide [5′-IMP, 5′-GMP, 5′-XMP, 5′-AMP]; b_i is the relative umami concentration (RUC) for each umami amino acid to MSG (Glu, 1 and Asp, 0.077); b_j is the RUC for each umami 5′-nucleotide to 5′-IMP (5′-IMP, 1; 5′-GMP, 2.3; 5′-XMP, 0.61 and 5′-AMP, 0.18); and 1218 is a synergistic constant based on the concentration (g/100 g) used.

2.5. Statistical analysis

Analysis of variance (ANOVA) was performed using the general line model (GLM) procedure to determine significant differences in the amounts of free amino acids and 5′-nucleotides of pine-mushrooms according to their grades. Duncan's multi-range test was conducted when the samples exhibited a significance difference between samples, with the level of significance set at $P < 0.05$. Both ANOVA and Duncan's multiple range test were performed with SPSS (version 10.1, Chicago, IL).

3. Results and discussion

The quality of mushrooms depends on various factors such as their aroma, taste, texture, and colour, with the aroma and taste being the most important. Pine-mushrooms have been classified according to their appearance by the Korean National Forestry Cooperatives Federation (http://www.koreanforest.com), which is affected mostly by their ripening stages and cultivating conditions. Our previous studies demonstrated that the flavour characteristics of pine-mushrooms vary distinctively with their grades, with the intensities of most sensory flavour attributes being either strongest or weakest in pine-mushrooms of the highest grade. A total of 15 sensory attributes, such as sweet, salty, sour, bitter, umami, piny, floral, alcohol-like, meaty, moldy, wet soil-like, fishy, fermented, metallic, and astringent properties, in pine-mushrooms, were described by eight trained panelists. The intensities of sweet, piny, floral, and meaty attributes were strongest in pine-mushrooms of the highest grade, whereas those of sour, bitter, alcohol-like, moldy, wet soil-like, fermented, metallic, and astringent attributes were highest in pine-mushrooms of the lowest grade, both ones being decreased or increased according to their grades. However, it was noteworthy that the umami-taste was strongest in pine-mushrooms of second grade (7.84), followed by third grade (6.56), fourth grade (5.84), and first grade (5.00), respectively (Cho et al., 2007).

As indicated in Table 1, 23 amino acids were identified in the two parts of the four grades of pine-mushrooms, with ANOVA their mean contents differed significantly with part and grade ($P < 0.05$). Free amino acids were grouped according to Komata (1969) into the following four classes of taste components: MSG-like, sweet, bitter, and tasteless. Chen (1986) found that sweet components (alanine, glycine, and threonine) and MSG-like components (aspartic and glutamic acids) were taste-active amino acids in mushrooms. In the present study, the content of glutamic acid decreased in the order of second grade > third grade > fourth grade > first grade. Also, the content of aspartic acid was highest in

Table 1
Contents of free amino acids identified in pine-mushrooms of two different parts according to their four grades.

	Content (mg/g dry weight)							
	In the pileus				In the stipe			
	1st	2nd	3rd	4th	1st	2nd	3rd	4th
Amino acids								
Alanine	3.95 ± 0.36A[a]	3.96 ± 0.11A	4.00 ± 0.48A	4.03 ± 0.26A	1.96 ± 0.15C	1.95 ± 0.24C	3.15 ± 0.37B	1.34 ± 0.09D
Glycine	0.96 ± 0.10B	1.09 ± 0.05A	0.87 ± 0.04C	0.83 ± 0.03C	0.58 ± 0.04D	0.64 ± 0.06D	0.81 ± 0.07C	0.34 ± 0.02E
Valine	1.08 ± 0.13AB	1.04 ± 0.03A	0.83 ± 0.06AB	0.57 ± 0.01B	0.53 ± 0.04B	0.55 ± 0.05B	0.70 ± 0.06AB	0.00 ± 0.00C
Leucine	1.70 ± 0.18B	1.84 ± 0.07A	1.50 ± 0.14C	0.99 ± 0.07E	0.86 ± 0.05F	0.95 ± 0.07EF	1.24 ± 0.10D	0.40 ± 0.01G
Isoleucine	0.00 ± 0.00D	0.69 ± 0.01A	0.58 ± 0.03B	0.38 ± 0.02C	0.36 ± 0.01C	0.35 ± 0.02C	0.00 ± 0.00D	0.00 ± 0.00D
Proline	1.73 ± 0.19C	1.78 ± 0.07BC	1.62 ± 0.03C	2.05 ± 0.20A	1.68 ± 0.12C	1.86 ± 0.12B	0.00 ± 0.00E	1.25 ± 0.01D
Thioproline	0.00 ± 0.00B	0.45 ± 0.06A	0.00 ± 0.00B	0.00 ± 0.00B	0.00 ± 0.00B	0.00 ± 0.00B	0.00 ± 0.00B	0.00 ± 0.00B
Aspartic acid	3.28 ± 0.26C	5.45 ± 0.36A	3.84 ± 0.44B	3.22 ± 0.36D	0.78 ± 0.08G	1.38 ± 0.08E	0.86 ± 0.14F	0.70 ± 0.04H
Methionine	0.30 ± 0.06B	0.25 ± 0.02C	0.35 ± 0.01A	0.34 ± 0.00A	0.00 ± 0.00D	0.00 ± 0.00D	0.00 ± 0.00D	0.00 ± 0.00D
Hydroxyproline	0.41 ± 0.07C	0.29 ± 0.04F	0.48 ±.20AB	0.36 ± 0.01DE	0.34 ± 0.01E	0.49 ± 0.08A	0.46 ± 0.06B	0.38 ± 0.07D
Glutamic acid	4.42 ± 0.19F	8.60 ± 1.03A	6.91 ± 1.02C	5.24 ± 0.21D	2.50 ± 0.18H	7.48 ± 0.49B	5.01 ± 0.64E	3.40 ± 0.24G
Phenylalanine	2.81 ± 0.35D	3.03 ± 0.14C	3.60 ± 0.80A	2.68 ± 0.10D	2.37 ± 0.13E	3.16 ± 0.30B	3.33 ± 0.40BC	1.93 ± 0.21F
Aminoadipic-acid	0.27 ± 0.02D	0.37 ± 0.06B	0.31 ± 0.04C	0.41 ± 0.03A	0.15 ± 0.00F	0.23 ± 0.00E	0.29 ± 0.04CD	0.00 ± 0.00G
Ornithine	9.49 ± 0.49G	12.60 ± 0.36F	21.95 ± 1.42B	15.68 ± 1.48D	15.00 ± 0.99D	26.82 ± 2.56A	20.66 ± 2.70C	13.63 ± 1.27E
Lysine	3.73 ± 0.12C	4.93 ± 0.19B	7.86 ± 2.49A	5.30 ± 0.43B	3.48 ± 0.05C	5.06 ± 0.98B	5.57 ± 0.74B	2.84 ± 0.23D
Histidine	2.98 ± 0.09E	4.18 ± 0.16C	5.78 ± 1.75A	4.83 ± 0.30B	2.09 ± 0.14G	3.35 ± 0.55D	2.63 ± 0.20F	1.67 ± 0.13H
Tyrosine	3.44 ± 0.18E	4.17 ± 0.31D	7.20 ± 2.24A	4.55 ± 0.34CD	4.12 ± 0.52D	5.68 ± 0.60B	4.72 ± 0.24C	3.03 ± 0.08E
Hydroxyproline	0.00 ± 0.00B	0.17 ± 0.03A	0.00 ± 0.00B	0.00 ± 0.00B	0.00 ± 0.00B	0.37 ± 0.06B	0.00 ± 0.00B	0.00 ± 0.00B
Tryptophane	0.79 ± 0.09G	0.93 ± 0.07F	1.17 ± 0.28D	1.49 ± 0.05B	1.21 ± 0.22D	1.62 ± 0.14A	1.03 ± 0.14E	1.40 ± 0.11C
Cystathionine	0.57 ± 0.03AB	0.63 ± 0.11A	0.50 ± 0.22CD	0.61 ± 0.06A	0.14 ± 0.00F	0.44 ± 0.04D	0.34 ± 0.05E	0.00 ± 0.00G
Umami-taste active amino acids[b]	7.70 ± 0.23E	14.05 ± 0.70A	10.75 ± 0.73B	8.46 ± 0.29D	3.28 ± 0.13H	8.86 ± 0.29C	5.88 ± 0.39F	4.10 ± 0.14G
5′-Nucleotides								
5′-AMP[c]	0.57 ± 0.04B	0.67 ± 0.03A	0.65 ± 0.01A	0.65 ± 0.01A	0.14 ± 0.01E	0.34 ± 0.01C	0.25 ± 0.02D	0.22 ± 0.01D
5′-CMP[d]	0.76 ± 0.03C	1.38 ± 0.05A	0.95 ± 0.03B	0.74 ± 0.03C	0.49 ± 0.04E	0.58 ± 0.01D	0.59 ± 0.02D	0.44 ± 0.04E
5′-GMP[e]	0.64 ± 0.03B	0.80 ± 0.01A	0.79 ± 0.05A	0.69 ± 0.05B	0.16 ± 0.01E	0.40 ± 0.01C	0.31 ± 0.05D	0.29 ± 0.05D
5′-UMP[f]	0.51 ± 0.01B	0.58 ± 0.05	0.56 ± 0.01AB	0.55 ± 0.02AB	0.17 ± 0.01F	0.33 ± 0.04 C	0.27 ± 0.03D	0.22 ± 0.02E
Flavor 5′-nucleotides[g]	0.64 ± 0.03B	0.80 ± 0.01A	0.79 ± 0.05A	0.69 ± 0.05B	0.16 ± 0.01E	0.40 ± 0.01C	0.31 ± 0.05D	0.29 ± 0.05D
Equivalent umami concentration (EUC)[h]								
EUC	90.59 ± 0.03D	204.26 ± 0.06A	164.63 ± 0.04B	109.89 ± 0.11C	13.26 ± 0.02G	85.32 ± 0.01D	44.87 ± 0.06E	28.09 ± 0.01F

[a] Each values are expressed as mean ± SD ($n = 3$) are significant differences ($P < 0.05$) among pine-mushrooms using Ducan's multiple comparison test between the samples having the different letter in a row.
[b] Umami-taste active amino acids, aspartic acid + glutamic acid.
[c] 5′-AMP, 5′-adenosine monophosphate.
[d] 5′-CMP, 5′-cytosine monophosphate.
[e] 5′-GMP, 5′-guanosine monophosphate.
[f] 5′-UMP, 5′-uridine monophosphate.
[g] Flavor 5′-nucleotides, 5′-GMP + 5′-IMP + 5′-XMP.
[h] Calculated based on the equation: $Y = \Sigma a_i b_i + 1218(\Sigma a_i b_i)(\Sigma a_j b_j)$ (Yamaguchi, Yoshikawa, Ikeda, & Ninomiya, 1971) where Y is the EUC of the mixture in terms of g MSG/100 g; a_i is the concentration (g/100 g) of each umami amino acid [aspartic acid (Asp) or glutamic acid (Glu)]; a_j is the concentration (g/100 g) of each 5′-nucleotide [5′-IMP, 5′-GMP, 5′-XMP, 5′-AMP]; b_i is the relative umami concentration (RUC) for each umami amino acid to MSG (Glu, 1 and Asp, 0.077); b_j is the RUC for each umami 5′-nucleotide to 5′-IMP (5′-IMP, 1; 5′-GMP, 2.3; 5′-XMP, 0.61 and 5′-AMP, 0.18); and 1218 is a synergistic constant based on the concentration (g/100 g) used.

pine-mushrooms of second grade, followed by those of third, first, and fourth grades. The contents of both aspartic and glutamic acids were higher in the pileus than in the stipe, irrespective of the grade. Moreover, as for the umami-taste, the total contents of aspartic and glutamic acids were highest and lowest in pine-mushrooms of second and first grades, respectively, which is consistent with the sensory results in our previous study (Cho et al., 2007).

Yamaguchi et al. (1971) reported that four of the six 5′-nucleotides (5′-AMP, 5′-IMP, 5′-GMP, and 5′-XMP) normally detected in mushrooms contribute to umami-taste. Table 1 lists the contents of the 5′-nucleotides (5′-AMP, 5′-CMP, 5′-GMP, and 5′-UMP) identified in the pileus and stipe of pine-mushrooms of the four grades. The contents of 5′-AMP and 5′-GMP exhibiting umami-taste decreased in the order of second grade > third grade > fourth grade > first grade. As for the umami-taste active free amino acids, the contents of 5′-AMP and 5′-GMP were higher in the pileus than in the stipe.

Yamaguchi et al. (1971) suggested that the combination of umami amino acids and umami 5′-nucleotides would synergistically increase the umami-taste of mushrooms. The EUC value of 100% indicates that the umami intensity of mushrooms per 1 g dry matter is equivalent to the umami intensity of 1 g of MSG; in other words, 1 g MSG/g dry matter. The EUC values of pine-mushrooms varied widely, ranging from 204.26% in the pileus of second grade mushrooms to 13.26% in the stipe of first grade mushrooms. Mau (2005) grouped the EUC values into four levels: (1) >1000 g, (2) 100–1000 g, (3) 10–100 g, and (4) <10 g per 100 g of dry matter, corresponding to >10, 1–10, 0.1–1, and <0.1 g MSG/g, respectively. Therefore, the EUC values of our tested pine-mushrooms were in the second level. On the other hand, it was noteworthy that the EUC values and umami sensory intensities exhibited the same patterns in pine-mushrooms of different grades. Also, the EUC values were higher in the pileus than in the stipe.

In conclusion, the total contents of umami-taste active free amino acids and 5′-nucleotides were highest and lowest in pine-mushrooms of second and first grades, respectively. Also, the EUC value, which could express the synergistic effect between umami-taste components, decreased in the order of second grade > third grade > four grade > first grade. All of these results are highly consistent with those of the sensory tests performed in our previous study (Cho et al., 2007), showing that amino acids (e.g., aspartic acid and glutamic acid) and 5′-nucleotides (e.g., 5′-AMP and 5′-

GMP) are key umami-taste components of pine-mushrooms. Moreover, the contents of umami-taste active free amino acids and 5′-nucleotides and the EUC values were higher in the pileus than in the stipe in all four grades of pine-mushrooms.

Acknowledgements

This study was supported by both the Korea Science and Engineering Foundation (R01-2004-000-10276-0) and the Korea Research Foundation (KRF-2005-908-C00064).

References

Altamura, M. R., Robbins, F. M., Andreotte, R. E., Long, L., & Hasselstrom, T. (1967). Mushroom ninhydrin-positive compounds. Amino acids, related compounds, and other nitrogenous substances found in cultivated mushroom, *Agaricus campestris*. *Journal of Agricultural and Food Chemistry, 15*, 1040–1043.

Bellisle, F. (1999). Glutamate and the umami taste: Sensory, metabolic, nutritional and behavioural considerations. A review of the literature published in the last 10 years. *Neuroscience and Biobehavioral Reviews, 23*, 423–438.

Chang, H.-L., Chao, G.-R., Chen, C.-C., & Mau, J.-L. (2001). Non-volatile taste components of *Agaricus blazei*, *Antrodia camphorate* and *Cordyceps militaris* mycelia. *Food Chemistry, 74*, 203–207.

Chen, H.-K. (1986). *Studies on the characteristics of taste-active components in mushroom concentrate and its powderization*. Master Thesis, National Chung-Hsing University, Taichung, Taiwan.

Chiang, P.-D., Yen, C.-T., & Mau, J.-L. (2006). Non-volatile components of canned mushrooms. *Food Chemistry, 97*, 431–437.

Cho, I. H., Choi, H.-K., & Kim, Y.-S. (2006). Difference in the volatile composition of pine-mushrooms (*Tricholoma matsutake* Sing.) according to their grades. *Journal of Agricultural and Food Chemistry, 54*, 4820–4825.

Cho, I. H., Kim, S. Y., Choi, H.-K., & Kim, Y.-S. (2006). Characterization of aroma-active compounds in raw and cooked pine-mushrooms (*Tricholoma matsutake* Sing.). *Journal of Agricultural and Food Chemistry, 54*, 6332–6335.

Cho, I. H., Lee, S. M., Kim, S. Y., Choi, H.-K., Kim, G.-O., & Kim, Y.-S. (2007). Differentiation of aroma characteristics of pine-mushrooms (*Tricholoma matsutake* Sing.) of different grades using gas chromatography–olfactometry and sensory analysis. *Journal of Agricultural and Food Chemistry, 55*, 2323–2328.

Cho, I. H., Namgung, H.-J., Choi, H.-K., & Kim, Y.-S. (2008). Volatiles and key odorants in the pileus and stipe of pine-mushroom (*Tricholoma matsutake* Sing.). *Food Chemistry, 106*, 71–76.

Craske, J. D., & Reuter, F. H. (1965). The nitrogenous constituents of the dehydrated mushroom, *Boletus edulis*, and their relation to flavour. *Journal of the Science of Food and Agriculture, 16*, 243–250.

Elmore, J. S., Koutsidis, G., Dodson, A. T., Mottram, D. S., & Wedzicha, B. L. (2005). Measurement of acrylamide and its precursors in potato, wheat, and rye model systems. *Journal of Agricultural and Food Chemistry, 53*, 1286–1293.

Hac, L. R., Long, M. L., & Blish, M. (1949). The occurrence of free L-glutamic acid in various foods. *Food Science and Technology, 3*, 351–354.

Holts, R. B. (1971). Qualitative and quantitative analyses of free neutral carbohydrates in mushroom tissues by gas–liquid chromatography and mass spectroscopy. *Journal of Agricultural and Food Chemistry, 19*, 1272–1273.

Hommond, J. B. W., & Nichols, R. (1975). Changes in respiration and soluble carbohydrates during the post-harvest storage of mushrooms *Agaricus bisporus*. *Journal of the Science of Food and Agriculture, 26*, 835–842.

Komata, Y. (1969). The taste and constituents of foods. *Nippon Shokuhin Kogyo Gakkaishi, 3*, 26.

Lee, Y.-L., Jian, S.-Y., & Mau, J.-L. (2009). Composition and non-volatile taste components of *Hypsizigus marmoreus*. *Food Science and Technology, 42*, 594–598.

Lin, S.-Y. (1988). *Studies on the characteristics of taste-active components in shiitake mushroom and the powderization of the concentrate*. Master Thesis, National Chung-Hsing University, Taichung, Taiwan.

Maga, J. A. (1981). Mushroom flavor. *Journal of Agricultural and Food Chemistry, 29*, 1–4.

Mau, J.-L. (2005). The umami taste of edible and medicinal mushrooms. *International of Journal of Medicinal Mushrooms, 7*, 119–125.

Mau, J.-L., Chyau, C.-C., Li, J.-Y., & Tseng, Y.-H. (1997). Flavor compounds in straw mushrooms *Volvariella volvacea* harvested at different stages of maturity. *Journal of Agricultural and Food Chemistry, 45*, 4726–4729.

Mau, J.-L., Lin, H.-C., Ma, J.-T., & Song, S.-F. (2001). Non-volatile components of several speciality mushrooms. *Food Chemistry, 73*, 461–466.

Mau, J.-L., Wu, K.-T., Wu, Y.-H., & Lin, Y.-P. (1998). Nonvolatile taste components of ear mushrooms. *Journal of Agricultural and Food Chemistry, 46*, 4583–4586.

Taylor, M. W., Hershey, R. A., Levine, R. A., Coy, K., & Olivelle, S. (1981). Improved method of resolving nucleotides by reverse-phase high performance liquid chromatography. *Journal of Chromatography A, 219*, 133–139.

Tsai, S.-Y., Tsai, H.-L., & Mau, J.-L. (2008). Non-volatile taste components of *Agaricus blazei*, *Agrocybe cylindracea* and *Boletus edulis*. *Food Chemistry, 107*, 977–983.

Tsai, S.-Y., Wu, T.-P., Husang, S.-J., & Mau, J.-L. (2007). Nonvolatile taste components of *Agaricus bisporus* harvested at different stages of maturity. *Food Chemistry, 103*, 1457–1464.

Tseng, Y.-H., & Mau, J.-L. (1999). Contents of sugars, amino acids and free 5′-nucleotides in mushrooms, *Agaricus bisporus*, during post-harvest storage. *Journal of the Science of Food and Agriculture, 79*, 1519–1523.

Yamaguchi, S. (1979). The umami taste. In J. C. Boudreau (Ed.), *ACS symposium series: 115. Food taste chemistry* (pp. 33–51). Washington, DC: American Chemical Society.

Yamaguchi, S., Yoshikawa, T., Ikeda, S., & Ninomiya, T. (1971). Measurement of the relative taste intensity of some α-amino acid and 5′-nucleotides. *Journal of Food Science, 36*, 846–849.

Yang, J.-H., Lin, H.-C., & Mau, J.-L. (2001). Non-volatile taste components of several commercial mushrooms. *Food Chemistry, 72*, 465–471.

pH of soy milk from 7.5 to 6.0 (Nsofor & Maduako, 1992). Pasteurised soy milks were fortified with Ca, followed by serial concentrations of potassium citrate (used as CA) and SHMP, to compare their effectiveness in the study of Yazici et al. (1997). They found that heat stability of soy milks with SHMP were lower than for potassium citrate. They discussed that this might be because the final pH attained with potassium citrate was higher than that of SHMP and also might be due to conformational changes in protein structure due to specific reactions of CA.

There has been no report on the effect of pasteurisation on the properties of Ca-fortified soy milk, which would be useful for their manufacture. The objective of the present study is to investigate [Ca^{2+}], pH, absolute viscosity, particle diameter and dry sediment content of Ca-fortified soy milk incorporating SHMP, DSHP, TSC or EDTA-Na_2, before and after pasteurisation.

2. Materials and methods

2.1. Materials

Dried soybeans, *Glycine max*, (product of Canada) were purchased from a supermarket in Reading, UK.

The following CAs was used: SHMP ($(NaPO_3)_6$, Fisher Scientific Ltd., Loughborough, UK), DSHP ($Na_2HPO_4{\cdot}2H_2O$, Fisher Scientific Ltd., Loughborough, UK), TSC ($Na_3C_6H_5O_7{\cdot}2H_2O$, Fisher Scientific Ltd., Loughborough, UK) and EDTA-Na_2 ($C_{10}H_{14}N_2Na_2O_8{\cdot}2H_2O$, BDH Laboratory Supplies, Poole, UK). Ca chloride ($CaCl_2{\cdot}2H_2O$) was obtained from VWR International Ltd., Poole, UK.

2.2. Preparation of soy milk

Soybeans (100 g) were washed in de-ionised water. The cleaned beans were soaked in 1 kg of water for 14 h at 4 °C. The swollen soybeans were drained and blended with 1 kg of boiling water in a blender (Model A707A, Kenwood MFG, Surrey, UK) at low speed for 5 min. The slurry was heated for 10 min at 80 °C. The hot mixture was filtered through four layers of cheese cloth and the filtrate (~850 g) was collected. The soy milk was cooled to room temperature and then kept at 4 °C.

2.3. Preparation of samples

Soy milk (700 g) was heated to 45 °C on a heated magnetic stirrer, and SHMP, DSHP, TSC or EDTA-Na_2 was added at concentrations of 0.5% or 1.0%. The mixtures were stirred on a heated magnetic stirrer for 10 min at 45 °C. The soy milks (600 ml) containing chelating agents were warmed to 45 °C and Ca chloride was added at a concentration of 25 mM, followed by stirring under the same conditions. Each sample of Ca-fortified soy milk was divided into two, and one was pasteurised at 72 °C for 15 s in a glass bottle (500 ml capacity) in a water bath, with the temperature controlled at 75 °C, and subsequently cooled to room temperature. The remaining portions of Ca-fortified soy milks were not pasteurised. Control samples before and after pasteurisation were prepared without addition of CAs. All samples were allowed to equilibrate at 4 °C for 2 h. Preparation of samples was carried out in triplicate.

2.4. Analysis of samples

2.4.1. Ionic Ca concentration

Ionic Ca concentration was measured using a Ca^{2+}/pH analyser (Model 634, Ciba Corning Diagnostics, Essex, UK), described by Lin, Lewis, and Grandison (2006). The mV value for standards and samples was obtained directly from the analyser. Five ionic Ca standards (0.1–11 mM) were used to produce a calibration curve (log [Ca^{2+}] versus mV) on each day of analysis.

2.4.2. pH

A pH meter (Model SA 720, Orion Research Inc., Massachusetts, USA) was used to measure pH of samples at 25 °C.

2.4.3. Absolute viscosity

Kinematic viscosity of samples at 25 °C was measured with an Ostwald U-tube as described by Lewis (1996). The density of samples at 25 °C was analysed using specific gravity bottles (Lewis, 1996). Absolute viscosity was calculated according to Eq. (1)

$$\text{Absolute viscosity} = \text{kinematic viscosity} \times \text{density} \quad (1)$$

2.4.4. Particle diameter

Particle diameters of diluted samples (100 μl samples in 3 ml de-ionised water) were measured with a Zetamaster (Model ZEM 5002, Malvern Instruments Ltd., Malvern, UK).

2.4.5. Dry sediment

An accurately weighed (A, g) sample (approximately 23 g) was added to a centrifuge tube. The tube was then centrifuged at 4200 rpm for 30 min (2760 G) in a centrifuge (Model Centaur 2, Fisons, Loughborough, UK). The supernatant was discarded. The pellet was transferred to a moisture dish and dried in a hot air oven at 105 °C to constant weight (B, g). The equation below was applied to find% dry sediment

$$\%\ \text{Dry sediment} = \left(\frac{B}{A}\right) \times 100 \quad (2)$$

2.5. Statistical analysis

Statistical analysis of data for effects of CA and pasteurisation on properties of soy milk was performed by one-way ANOVA using SPSS 15.0 for Windows. Mean differences were analysed using Duncan's multiple-range test at $p \leqslant 0.05$.

3. Results and discussion

3.1. Effect of CA and pasteurisation on [Ca^{2+}]

Table 1 shows how [Ca^{2+}] of Ca-fortified soy milks is affected by addition of four types of CA. Control samples (with no addition of CA) before and after pasteurisation had the highest [Ca^{2+}]. Adding 25 mM Ca chloride clearly precipitated soybean protein in the control samples. This Ca level was within the range (10–100 mM) reported necessary to form a good curd in soy milk (Wang & Hesseltine, 1982). Soybean curd was found at the bottom of the bottle and clear whey formed the top layer. In a previous study, it was found that [Ca^{2+}] in soy milk was very low (<0.02 mM) Pathomrungsiyounggul et al. (2007). Thus, most of the [Ca^{2+}] (0.28–8.55 mM) in Table 1 was derived from the added Ca chloride.

[Ca^{2+}] in the pasteurised control sample in the present study (8.38 mM) was slightly higher than that produced in the previous study (7.66 mM) (Pathomrungsiyounggul et al., 2007). Note that different batches of soybeans were used to make the soy milks. It was found that approximately one third of the added Ca dissociated to Ca ion in the control samples. The remainder would be either undissociated or bound to the proteins. It is known that Ca does bind to soy protein. The two main storage proteins of soybean, 7S and 11S globulin are both involved in soy curd formation (Saio, Kamiya, & Watanabe, 1969). The binding sites are on the side-chain carboxyl groups of the aspartic and glutamic acid resi-

Table 1
Calcium ion concentration (mM) of soy milks and its reduction following addition of chelating agents.

Chelating agent			$[Ca^{2+}]$ (mM)		Reduction of $[Ca^{2+}]$ (mM) per mM of CA	
Type	%	mM	Before pasteurisation	After pasteurisation	Before pasteurisation	After pasteurisation
SHMP	0 (control)	0	8.55 ± 0.17 c*	8.38 ± 0.38 c*	-	–
	0.5	8.2	0.82 ± 0.14 b	0.91 ± 0.15 b*	0.94	0.91
	1.0	16.5	0.37 ± 0.06 a	0.38 ± 0.06 a	0.50	0.49
DSHP	0 (control)	0	8.55 ± 0.17 c*	8.38 ± 0.38 c*	–	–
	0.5	28.2	1.11 ± 0.17 b	0.78 ± 0.13 b	0.26	0.27
	1.0	56.8	0.32 ± 0.05 a	0.28 ± 0.05 a	0.14	0.14
TSC	0 (control)	0	8.55 ± 0.17 c*	8.38 ± 0.38 c*	–	–
	0.5	17.1	1.53 ± 0.20 b*	1.51 ± 0.18 b*	0.41	0.40
	1.0	34.3	0.50 ± 0.06 a	0.50 ± 0.06 a	0.23	0.23
EDTA-Na_2	0 (control)	0	8.55 ± 0.17 c*	8.38 ± 0.38 c*	–	–
	0.5	13.5	3.76 ± 0.26 b*	3.75 ± 0.21 b*	0.35	0.34
	1.0	27.1	1.25 ± 0.23 a*	1.21 ± 0.20 a*	0.27	0.26

* = Sample showed coagulation.
Means ± standard deviation of samples using the same type of chelating agent followed by the same letter are not significantly different ($p > 0.05$).
No significant effect of pasteurisation on $[Ca^{2+}]$ of samples.

dues, as well as on the imidazole group of histidine (Kroll, 1984). Besides binding with protein, Ca ions also bind with phytate in soy milk (Torikata, Ishihara, & Yano, 1986).

As well as in the control samples, coagulation also occurred in the pasteurised sample containing 0.5% SHMP; and in both unheated and heated soy milks with 0.5% added TSC, and for all samples with added EDTA-Na_2.

Addition of all types of CA led to a significant ($p \leqslant 0.05$) reduction in $[Ca^{2+}]$ of both unheated and pasteurised soy milks, compared to their controls. They function by reducing the chemical activity of metal ions, forming complexes with their unshared electron pair (Lindsay, 1996; Martell & Motekaitis, 2002). Higher additions of added CA resulted in significantly lower $[Ca^{2+}]$ levels in the samples, ($p \leqslant 0.05$).

Similar results have been found in other drinks. A model nutritional beverage, (soybean oil-in-water emulsion stabilised by whey protein isolate) containing Ca chloride, had lower $[Ca^{2+}]$ when EDTA-Na_2 or TSC were added (Keowmaneechai & McClements, 2002). Tsioulpas (2005) found that increasing levels of SHMP, DSHP or TSC caused a significant drop of $[Ca^{2+}]$ in raw cows' milk. For all types of CA, the reduction of $[Ca^{2+}]$, measured in mM of added CA, was higher for 0.5% addition compared to 1% addition (Table 1).

Pasteurisation did not significantly change $[Ca^{2+}]$ (Table 1). Tessier and Rose (1958) reported a similar finding for skim milk pasteurised at 66 °C for 30 min, although heating milk at 82 °C for 30 min lowered $[Ca^{2+}]$. In the study of May and Smith (1998), a 7.3% decrease in $[Ca^{2+}]$ was found in milk after pasteurisation at 72.8 °C for 15 s and this supported the previous findings that Ca transferred from the soluble to the colloidal state.

It was noted for non-pasteurised samples that non-coagulated samples contained lower $[Ca^{2+}]$ than coagulated samples. The contents of Ca ions were generally in a range of 0.28–0.82 mM for non-coagulated and 0.91–8.55 mM for coagulated samples, respectively. However, the sample with 0.5% added DSHP showed no coagulation although its $[Ca^{2+}]$ was 1.11 mM.

3.2. Effect of CA and pasteurisation on pH

Table 2 shows the pH of Ca-fortified soy milk with various CAs before and after pasteurisation. Soy milk fortified with Ca had a pH of 5.66 and 5.65, before and after pasteurisation. It has been reported that the pH of soy milk (pH 6.7) was reduced to ~5.8 when 14 mM Ca were added (using Ca chloride) (Shun-Tang, Ono, & Mikami, 1999). It is expected that pH of soy milks with added Ca would be lower, as hydrogen ions are released. The hydrogen ions compete with Ca ions for the same binding sites on the protein molecule (Kroll, 1984) and these hydrogen ions should dissociate from protein molecules because of Ca ions binding to protein.

Adding 0.5% SHMP reduced the pH of control samples. This reduction was not significant for non-pasteurised samples but became significant ($p \leqslant 0.05$) for pasteurised samples. Adding 1% SHMP significantly increased ($p \leqslant 0.05$) the pH of control samples. The reduction of pH when adding low levels of SHMP might have arisen because hydrogen ions were released through the binding of protein with sodium ions from SHMP. Salts of Ca and magnesium have been used to bind to protein in the preparation of tofu resulting in a reduction in its pH (Prabhakaran, Perera, & Valiyaveettil, 2005). Adding 0.3% and 0.5% SHMP was previously found to decrease the pH of the 25 mM Ca-fortified soy milk but 0.7–1.2% addition raised its pH (Pathomrungsiyounggul et al., 2007). A drop in pH was observed when 0.3–1.5% SHMP were added to stabilise the Ca-fortified soy milk (Yazici et al., 1997). A slight increase of pH was reported in raw cows milk when 0.05–0.2% SHMP was added (Tsioulpas, 2005). These data indicate that using SHMP to stabilise beverages causes variable effects, sometimes decreasing and sometimes increasing the pH.

Addition of 0.5% and 1% DSHP significantly ($p \leqslant 0.05$) increased the pH of control samples; a higher concentration of added DSHP led to a higher pH. The same trend was found in raw cow milk (Tsioulpas, 2005). The pH of 1% DSHP solution was 9.14 (Table 2), forming an alkaline solution in water, leading to an increase of pH when added to soy milk.

Tri-sodium citrate caused similar, although less marked, pH changes to DSHP. A 1% TSC solution had a pH of 8.28 (Table 2), again contributing to this pH increase. At the 1% level of addition, TSC increased pH by less than DSHP. It was noted that the pH of a 1% TSC was lower than that of a 1% DSHP solution. The greater ability of DSHP to raise pH might be due to its higher molar concentration (at same % addition). The increase in pH of samples when adding a greater concentration of TSC in the present study was in agreement with its effects on cows' milk in the study of Tsioulpas (2005). Moreover, the addition of 0.3–1.5% potassium citrate as stabiliser in Ca-fortified soy milk caused an increase in pH, (Yazici et al., 1997).

All samples prepared with EDTA-Na_2 had much lower pH values (pH 4.33–4.69) compared with control samples (pH 5.65–5.66). The pH decreased significantly ($p \leqslant 0.05$) as the concentration of EDTA-Na_2 increased. Addition of EDTA-Na_2 as its disodium salt results in a reduction in pH of the system. For example, the pH of the

Table 2
pH of soy milks and changes following addition of chelating agents.

Chelating agent			Pasteurisation		pH of solution 1% CA
Type	%	mM	Before	After	
SHMP	0 (control)	0	5.66 ± 0.01 a*	5.65 ± 0.01 b*	6.00
	0.5	8.2	5.59 ± 0.14 a	5.51 ± 0.10 a*	
	1.0	16.5	5.92 ± 0.03 b(b)	5.80 ± 0.05 c(a)	
DSHP	0 (control)	0	5.66 ± 0.01 a*	5.65 ± 0.01 a*	9.14
	0.5	28.2	6.62 ± 0.01 b(b)	6.47 ± 0.03 b(a)	
	1.0	56.8	7.09 ± 0.02 c	7.06 ± 0.03 c	
TSC	0 (control)	0	5.66 ± 0.01 a*	5.65 ± 0.01 a*	8.28
	0.5	17.1	5.98 ± 0.07 b*	6.02 ± 0.05 b*	
	1.0	34.3	6.44 ± 0.02 c	6.44 ± 0.02 c	
EDTA-Na_2	0 (control)	0	5.66 ± 0.01 c*	5.65 ± 0.01 c*	4.57
	0.5	13.5	4.66 ± 0.06 b*	4.69 ± 0.08 b*	
	1.0	27.1	4.33 ± 0.06 a*	4.36 ± 0.07 a*	

* = Sample showed coagulation.
a, Means ± standard deviation in the same column, for samples used the same type of chelating agent, followed by the same letter are not significantly different ($p > 0.05$).
(a), Means ± standard deviation in the same row followed by the same letter are not significantly different ($p > 0.05$).

1% EDTA-Na_2 solution was as low as 4.57 (Table 2), because weakly acidic acetic acid is released into water. The isoelectric point (p*I*) of soy protein is about 4.2 (Liu et al., 2004). Protein molecules have a minimum solubility at their p*I* and are often seen to precipitate. Coagulation occurred in all samples treated with EDTA-Na_2, probably because their pH was lower, approaching the p*I*.

It was reported that soy protein in soy milk began to coagulate when the pH was reduced to about 6.0 regardless of the type of Ca salts, and that pH, rather than Ca ions is the most important factor for the precipitation of soy protein (Lu, Carter, & Chung, 1980). All samples showing coagulation in Table 2 had pH's near to or less than 6.0. Non-coagulated samples following the addition of DSHP and TSC had pH's higher than 6.0 but those using SHMP had pH's lower than 6.0.

Overall, most of the measured changes in pH following pasteurisation were not significant. In the case of the control and soy milk with added phosphates (SHMP and DSHP), pH decreased slightly after pasteurisation, and there were two samples (addition of 0.5% DSHP and 1% SHMP) in which the pH dropped significantly ($p \leqslant 0.05$) after pasteurisation. However, for soy milk with added TSC and EDTA-Na_2, the trend was for pasteurisation to increase the pH, although these changes were not statistically significant. Pasteurisation of skim milk at 66 °C for 30 min brought about a slight reduction of pH, from 6.79 to 6.72 in a previous study (Tessier & Rose, 1958). Sterilisation caused a small reduction in the pH of soy milks which were fortified with Ca using mixtures of Ca citrate and tri-Ca phosphate (Weingartner, Nelson, & Erdman, 1983). In contrast, a much larger reduction of pH after sterilisation was found in soy milks produced from blanched soybean (from 7.5 to 6.0), sprouted-blanched soybean (from 7.5 to 6.2) and sprouted-unblanched soybean (from 6.5 to 5.8) (Nsofor & Maduako, 1992).

3.3. Effect of CA and pasteurisation on absolute viscosity

Absolute viscosities of samples before and after pasteurisation are shown in Table 3. Viscosity will affect consumer acceptability of Ca-fortified soy milk. Some coagulated samples could not be measured because their curd blocked the capillary tube of the smaller diameter viscometer whereas flow times were too quick (<100 s) in the larger diameter viscometer. Flow times between 100 and 500 s offer accurate and reproducible results (Lewis, 1996). In the case of SHMP, DSHP and TSC, reductions of absolute viscosity were observed when their concentration was increased from 0.5% to 1%. Similar trends were reported previously in Ca-fortified soy milk. Adding 0.35–1% SHMP reduced absolute viscosity from 140 to 30 cp (Yazici et al., 1997). The viscosity dropped from 6.5 to 4.4 cp when TSC was increased from 0.2% to 0.7% TSC (Prabharaksa et al., 1989). Absolute viscosity is affected by total solids as well as the suspended matter, which usually increases the viscosity (Bourne, 2002). When Ca ions bind to the protein molecules, the

Table 3
Absolute viscosity (cp, mPa s) of soy milks.

Chelating agent			Pasteurisation	
Type	%	mM	Before	After
SHMP	0 (control)	0	NA*	NA*
	0.5	8.2	9.33 ± 2.28 b	NA*
	1.0	16.5	3.46 ± 0.30 a	6.10 ± 2.27
DSHP	0 (control)	0	NA*	NA*
	0.5	28.2	5.71 ± 1.46	8.42 ± 3.20
	1.0	56.8	3.71 ± 0.27	3.79 ± 0.30
TSC	0 (control)	0	NA*	NA*
	0.5	17.1	5.66 ± 1.69*	5.17 ± 1.62*
	1.0	34.3	3.62 ± 0.36	4.35 ± 0.59
EDTA-Na_2	0 (control)	0	NA*	NA*
	0.5	13.5	3.98 ± 0.88*	3.93 ± 1.03*
	1.0	27.1	5.61 ± 1.21*	5.30 ± 1.11*

* = Sample showed coagulation.
NA = Results not available due to time being <100 s.
a, Means ± standard deviation in the same column, for samples used the same type of chelating agent, followed by the same letter are not significantly different ($p > 0.05$).
No significant effect of pasteurisation on absolute viscosity of samples.

hydrophobic interaction of the neutralised proteins becomes more predominant and induces the aggregation (Kohyama et al., 1995). The aggregates of soy protein might influence the viscosity of samples in the same way as suspended matter. At lower concentration of CA, more Ca ions might bind with protein resulting in more aggregates in the samples, leading to higher absolute viscosities.

However, there was an increase in absolute viscosity when the concentration of EDTA-Na_2 increased from 0.5% to 1%. As mentioned, all samples with added EDTA-Na_2 coagulated. Therefore the higher solute concentration in the samples from high concentration of EDTA-Na_2 might increase the absolute viscosity of the samples. The relationship between the concentration of a solute and viscosity is a direct non-linear function (Bourne, 2002).

For samples prior to pasteurisation, the absolute viscosity of samples containing 1% SHMP, DSHP and TSC was low, in the range of 3.5–3.7 cp. Pasteurised samples which had not coagulated had absolute viscosities in a range of 3.79–8.42 cp. For more severe heat treatment of Ca lactate fortified soy milk by sterilisation containing 0.1–0.4% TSC, decreased the viscosity of samples about 3–4 times (Prabharaksa et al., 1989). They observed that viscosities of samples before and after sterilisation were 8.98–12.49 cp and 3.00–3.50 cp, respectively. Weingartner et al. (1983) reported that pasteurised soy beverages, containing 25 mM Ca using the mixtures of Ca citrate and tri-Ca phosphate, were acceptable to sensory panels and indistinguishable from the control (pasteurised soy milk no added Ca) and their viscosities were in the range 4.9–5.7 cp. Prabharaksa et al. (1989) found that Ca soy milk formulated for infants and young children by adding 0.45% Ca lactate and 0.3% TSC had a viscosity of 3.12 cp. Thus in comparison with this data, it should be possible to prepare the pasteurised-Ca-fortified soy milk with the desired viscosity by addition of 1% of either DSHP or TSC.

3.4. Effect of Ca and pasteurisation on particle diameter

The effects of different CAs and pasteurisation on the particle diameter are summarised in Table 4. In control samples, their particle sizes were bigger than 1000 nm. In the case of adding SHMP, particle size dropped following the addition of SHMP, with higher concentrations of SHMP giving a significantly smaller particle size. These results were in agreement with published data (Pathomrungsiyounggul et al., 2007). The reduction of particle diameter when Ca ions were bound by CA might be because the binding caused the repulsive force of negatively charged protein molecules to become predominant and protein molecules were less likely to aggregate. This drop of particle diameter in the present study contrasted with the results reported by Tsioulpas (2005), who added various concentrations of SHMP (from 0.8 to 3.2 mM) to unheated milks and sterilised them. His results showed that unheated milks and heated milks had larger casein micelles when increasing the concentration of SHMP.

For DSHP, it also reduced the particle diameter compared to control samples. A slightly larger particle diameter was found in non-pasteurised samples when increasing DSHP concentration from 0.5% to 1%, but a reduction in particle size was observed in pasteurised samples. Tsioulpas (2005) found that adding DSHP from 3.5 to 14 mM in milk, led to an unpredictable trend of casein micelle size in non-heated milk, whereas increase of casein micelle size was found in sterilised milk.

Samples containing 1% TSC had a smaller particle diameter than those containing 0.5% TSC. At 0.5%, TSC was less effective than other CAs in retarding aggregation but at 1% addition, it was able to reduce the size of samples to as low as ~487 and 509 nm for non-heated and heated samples, respectively. Keowmaneechai and McClements (2002) reported that sequestering of ionic Ca with TSC prevented droplets from aggregating and retarded the formation of larger flocs of the whey protein-stabilised oil-in-water emulsions. Their study showed that particle diameter of the beverage became smaller when TSC was added at 2.5 to 10 mM. In milk, addition of 2–8 mM TSC caused increase in size of casein micelles in non-sterilised and sterilised milk (Tsioulpas, 2005).

Particle diameter of samples containing 0.5% EDTA-Na_2 was smaller than control samples. Raising the EDTA-Na_2 concentration from 0.5% to 1% led to an increase in the particle diameter. Samples with 1% added EDTA-Na_2 had particle size >1000 nm which had been observed in control samples. This enlargement of particle diameter resulted possibly from the acidic function of EDTA-Na_2 (Table 2) on p*I* of protein molecules as mentioned. Keowmaneechai and McClements (2002) found the decrease and the increase of particle diameter of the whey protein-stabilised oil-in-water emulsions containing 10 mM Ca when increasing the concentration of EDTA-Na_2. Particle size of their sample was found to decrease when 2.5–10 mM EDTA-Na_2 were used and attributed to chelating free ionic Ca with EDTA. However, the particle size increased when the EDTA-Na_2 concentrations were used at 20–40 mM. They suggested that this was probably due to the ability of free sodium cation and EDTA anion to increase the ionic strength of the aqueous phase resulting in the reduction of the electrostatic repulsion between the droplets.

At a concentration of 0.5%, TSC was less effective in reducing the particle diameter than EDTA-Na_2. Even so, TSC gave a greater reduction in the particle diameter than EDTA-Na_2, at a concentra-

Table 4
Particle diameter (nm) of soy milks.

Chelating agent			Pasteurisation	
Type	%	mM	Before	After
SHMP	0 (control)	0	>1000*	>1000*
	0.5	8.2	595.9 ± 60.2 b	>1000*
	1.0	16.5	468.2 ± 43.5 a	534.2 ± 17.8
DSHP	0 (control)	0	>1000*	>1000*
	0.5	28.2	554.2 ± 67.1	>1000
	1.0	56.8	587.6 ± 55.3	597.7 ± 20.4
TSC	0 (control)	0	>1000*	>1000*
	0.5	17.1	>1000*	>1000*
	1.0	34.3	487.0 ± 38.3	508.7 ± 42.1
EDTA-Na_2	0 (control)	0	>1000*	>1000*
	0.5	13.5	675.3 ± 112.4*	768.7 ± 150.4*
	1.0	27.1	>1000*	>1000*

* = Sample showed coagulation.
a, Means ± standard deviation in the same column, for samples used the same type of chelating agent, followed by the same letter are not significantly different ($p > 0.05$). No significant effect of pasteurisation on particle diameter of samples.

Table 5
Dry sediment (%) of soy milks.

Chelating agent			Pasteurisation	
Type	%	mM	Before	After
SHMP	0 (control)	0	4.42 ± 0.07 b*	4.35 ± 0.09 b*
	0.5	8.2	4.78 ± 0.31 b	4.89 ± 0.33 b*
	1.0	16.5	0.89 ± 0.13 a(a)	2.66 ± 1.01 a(b)
DSHP	0 (control)	0	4.42 ± 0.07 c*	4.35 ± 0.09 c*
	0.5	28.2	3.36 ± 0.32 b	3.74 ± 0.40 b
	1.0	56.8	1.86 ± 0.30 a	1.86 ± 0.29 a
TSC	0 (control)	0	4.42 ± 0.07 b*	4.35 ± 0.09 b*
	0.5	17.1	4.84 ± 0.55 b*	4.83 ± 0.54 b*
	1.0	34.3	0.90 ± 0.13 a	1.26 ± 0.17 a
EDTA-Na_2	0 (control)	0	4.42 ± 0.07*	4.35 ± 0.09*
	0.5	13.5	4.81 ± 0.23*	4.83 ± 0.29*
	1.0	27.1	4.99 ± 0.17*	5.01 ± 0.07*

* = Sample showed coagulation.
a, Means ± standard deviation in the same column, for samples used the same type of chelating agent, followed by the same letter are not significantly different ($p > 0.05$).
(a), Means ± standard deviation in the same row followed by the same letter are not significantly different ($p > 0.05$).

tion of 1%. TSC was shown previously to be somewhat less effective than EDTA-Na_2 at preventing flocculation at a low concentration in the whey protein-stabilised oil-in-water emulsion (Keowmaneechai & McClements, 2002).

Overall, all CAs improved the stability of control samples as a result of lowering particle diameter. The smallest particle diameter among pasteurised samples was observed in the sample containing 1% TSC. The particle sizes of three commercial soy milks were 380–440 nm according to a report by Saeseaw et al., (2005). It should be noted that the smallest size of pasteurised sample in this study was not as small as the particle size in the previous study.

Prior to pasteurisation, non-coagulated samples had a particle diameter of 468–596 nm. Pasteurisation increased their particle diameter but this was not significant ($p > 0.05$). For milk with added SHMP, DSHP and TSC at 0.05–0.2%, high heat treatment by sterilisation increased their casein micelle size by approximately 100–200 nm (Tsioulpas, 2005).

3.5. Effect of CA and pasteurisation on dry sediment

The dry sediment content is used to indicate the solids sedimented by applying a centrifugal force (Table 5). Control samples had dry sediment levels of 4.42% and 4.35%, before and after pasteurisation. There were significant ($p < 0.05$) reductions in dry sediment of samples with added SHMP, DSHP and TSC. However, in the case of addition of EDTA-Na_2, there was a small but non significant increase in dry sediment. These high levels of sediment are unacceptable.

Within the non-pasteurised group, all samples which had coagulated had a higher dry sediment content than that of control sample. The same result was also found among the pasteurised samples. For the non-pasteurised sample with 0.5% SHMP, although it did not show coagulation after 2 h, it contained higher dry sediment than the control sample. For the other non-coagulated samples addition of SHMP, DSHP and TSC reduced the dry sediment content when compared with their control samples, both before and after pasteurisation. The higher the level of CA, the lower the content of dry sediment.

Pasteurisation influenced significantly ($p \leqslant 0.05$) the dry sediment of the sample with 1% added SHMP. Its dry sediment content increased about three times following pasteurisation. For the remaining treatments, pasteurisation did not significantly change the dry sediment content of samples. The effect of soy milk temperature (60, 70 and 80 °C) at the time of adding $CaCl_2$ on total solid mass of samples was studied (Wang & Hesseltine, 1982). They found that the total solids mass remained about the same.

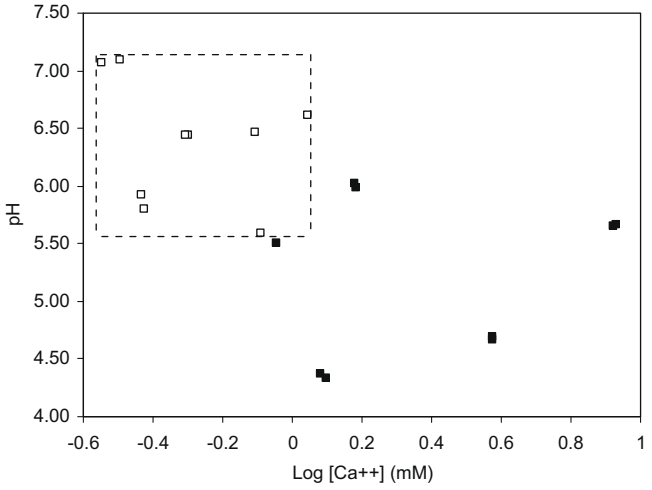

Fig. 1. Relationship between log [Ca^{2+}] and pH (□ non-coagulated and ■ coagulated sample).

It is desirable to minimise sediment formation. After pasteurisation, the sample with 1.0% added TSC contained the minimum amount of sediment content (1.26%). However, its level was higher than that of 25 mM Ca-fortified soy milk with 1.2% added SHMP, which was 0.76% (Pathomrungsiyounggul et al., 2007).

3.6. Relationship between [Ca^{2+}] and pH

It was found that increase in log [Ca^{2+}] led to a decrease in pH of samples (Fig. 1) This was similar to the observation of Pathomrungsiyounggul et al. (2007). To prepare Ca-fortified soy milk without coagulation, its Ca^{2+} and pH needs to be adjusted with values in the area indicated in Fig. 1. These were within the ranges log [Ca^{2+}] between −0.55 and 0.05 mM (i.e. 0.28–1.12 mM) and pH 5.6–7.1.

3.7. Relationship between [Ca^{2+}] and dry sediment

Fig. 2 indicates that the dry sediment of non-coagulated samples increase very quickly when [Ca^{2+}] is slightly higher whereas

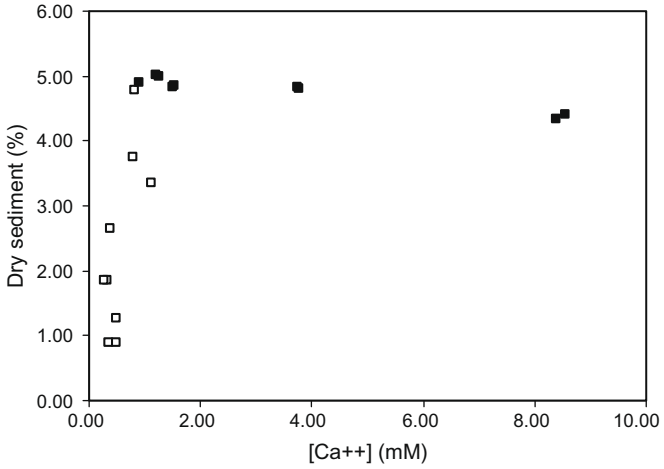

Fig. 2. Relationship between log [Ca^{2+}] and dry sediment (□ non-coagulated and ■ coagulated sample).

those of the coagulated samples were almost the same (~4.4–5.0%). The result in the present study agrees with the previous work in Ca-fortified soy milk (Pathomrungsiyounggul et al., 2007).

4. General discussion

Ca chloride is not the best salt for Ca fortification of soy milk, as the pH is reduced and ionic Ca is increased. The negative effects these factors have on heat stability are shown in Fig. 1. However, this can be corrected by the addition of stabilisers, and those which tend to work best are those which increase pH and decrease ionic Ca. Therefore, measuring pH and ionic Ca provides an effective method to monitor the effects of stabiliser addition. For soy milk, this has not been routinely reported. Since pH and ionic Ca provide good indicators of the susceptibility of sediment formation, this needs to be evaluated at higher temperatures, to evaluate heat stability during UHT processing and in-container sterilisation.

It is interesting to compare and contrast heat stability and sediment formation in milk of animal origin (e.g. cows' milk) and vegetable origin (e.g. soy milk).

On-Nom (2007) have found that when milk is heated, its pH falls and ionic Ca decreases, but that this is largely reversible on cooling. They measured pH and ionic Ca in milk at temperatures between 80 and 120 °C using dialysis. It has been argued that in order to evaluate heat stability, it is important be able to measure pH and ionic Ca at the pasteurisation and sterilisation conditions, although there is no reported data on how these properties change with temperature in soy milk.

EDTA-Na_2 is an interesting salt, as it chelates Ca in soy milk but also reduces pH and thus does not improve heat stability. An alternative chelating agent would be the tetra sodium salt, which when added to milk has been found to decrease ionic Ca and also increase pH. This is currently being investigated further.

References

Bourne, M. C. (2002). *Food texture and viscosity: Concept and measurement*. UK: Academic Press.

Gerstner, G. (2005). Feasibility of calcium fortification in dairy and soy drinks. *Food Marketing and Technology, 18*, 10–13.

Hirotsuka, M., Taniguchi, H., Narita, H., & Kito, M. (1984). Calcium fortification of soy milk with calcium–lecithin liposome system. *Journal of Food Science, 49*, 1111–1112. 1127.

Keowmaneechai, E., & McClements, D. J. (2002). Influence of EDTA and citrate on physicochemical properties of whey protein-stabilized oil-in-water emulsions containing $CaCl_2$. *Journal of Agricultural Food Chemistry, 50*, 7145–7153.

Kohyama, K., Sano, Y., & Doi, E. (1995). Rheological characteristics and gelation mechanism of Tofu (soybean curd). *Journal of Agricultural and Food Chemistry, 43*(7), 1808–1812.

Kroll, R. D. (1984). Effect of pH on the binding of calcium-ions by soybean proteins. *Cereal Chemistry, 61*(6), 490–495.

Lewis, M. J. (1996). *Physical properties of foods and food processing systems*. England: Woodhead Publishing Ltd.

Lin, M-J., Lewis, M. J., & Grandison, A. S. (2006). Measurement of ionic calcium in milk. *International Journal of Dairy Technology, 59*, 192–199.

Lindsay, R. C. (1996). Food additives. In O. R. Fennema (Ed.), *Food chemistry* (pp. 767–823). USA: Marcel Dekker, Inc.

Liu, Z., Chang, S. K. C., Li, L., & Tatsumi, E. (2004). Effect of selective thermal denaturation of soybean proteins on soymilk viscosity and tofu's physical properties. *Food Research International, 37*, 815–822.

Lu, J. Y., Carter, E., & Chung, R. A. (1980). Use of calcium salts for soybean curd preparation. *Journal of Food Science, 45*, 32–34.

Martell, A. E., & Motekaitis (2002). *Chelation*. New York, USA: The McGraw-Hill Companies, Inc.

May, R. J., & Smith, D. E. (1998). Effect of storage and various processing conditions on the amount of ionic calcium in milk. *Milchwissenschaft, 53*(11), 605–608.

Nauta, T. (1991). Chelating agents. In J. Smith (Ed.), *Food additive user's handbook* (pp. 273–279). UK: Blackie and Son Ltd.

Nsofor, L. M., & Maduako, O. (1992). Stabilized soymilk for ambient tropical storage: A preliminary report. *International Journal of Food Science and Technology, 27*, 573–576.

On-Nom, N. (2007) Measurement of calcium partitioning, ionic calcium and pH of milk at high temperature, MSc dissertation. School of Food Biosciences, University of Reading, UK.

Pathomrungsiyounggul, O., Grandison, A. S., & Lewis, M. J. (2007). Effect of calcium chloride and sodium heametaphosphate on certain chemical and physical properties of soymilk. *Journal of Food Science, 72*, 428–434.

Prabhakaran, M., Perera, C. O., & Valiyaveettil, S. (2005). Effect of different coagulants on the isoflavone levels and physical properties of prepared firm tofu. *Food Chemistry, 99*, 492–499.

Prabharaksa, C., Olek, A. C., & Steinkraus, K. H. (1989). Enrichment of soybean milk with calcium. *Acta Biotechnologica, 9*(1), 9–16.

Rasyid, F., & Hansen, P. M. T. (1991). Stabilization of soy milk fortified with calcium gluconate. *Food Hydrocolloids, 4*(5), 415–422.

Saio, K., Kamiya, M., & Watanabe, T. (1969). Food processing characteristics of soybean 11S and 7S proteins. *Agricultural and Biological Chemistry, 33*, 1301–1308.

Shun-Tang, G., Ono, T., & Mikami, M. (1999). Incorporation of soy milk lipid into protein coagulum by addition of calcium chloride. *Journal of Agricultural Food Chemistry, 47*, 901–905.

Tessier, H., & Rose, D. (1958). Calcium ion concentration in milk. *Journal of Dairy Science, 41*, 351–359.

Torikata, Y., Ishihara, J., & Yano, T. (1986). Protein coagulation through reversible and irreversible bindings of calcium. *Agricultural and Biological Chemistry, 51*, 707–714.

Tsioulpas, A. (2005). *Role of minerals on casein micelle stability of bovine milk* (p. 150), PhD Thesis, School of Food Biosciences. University of Reading: Reading.

USDA (2008). *USDA national nutrient database for standard reference* (Vol. 20). Release 2008.

Wang, H. L., & Hesseltine, C. W. (1982). Coagulation conditions in tofu processing. *Process Biochemistry, 17*, 7–12.

Weingartner, K. E., Nelson, A. I., & Erdman, J. W. J. (1983). Effect of calcium addition on stability and sensory properties of soy beverage. *Journal of Food Science, 48*, 256–257. 263.

Yazici, F., Alvarez, V. B., Mangino, M. E., & Hansen, P. M. T. (1997). Formulation and processing of a heat stable calcium-fortified soy milk. *Journal of Food Science, 62*(3), 535–538.

However, the genetic basis of the aroma formation in melon is still unknown. One strategy to gain knowledge and improve aroma volatiles is the identification of genes or quantitative trait loci (QTLs) associated with certain compounds of the melon aroma profile. This strategy would help to implement quality-oriented breeding programme in order to design fruit with new or improved aroma.

The goal of the present work is to characterize the aroma profile of a collection of NILs that, with PI 161375 introgressions, encompassed many of the twelve linkage groups (LG) of the melon genome. Secondarily, some QTLs associated with aroma volatiles are reported and non-climacteric behaviour verified.

2. Material and methods

2.1. Plant material

The set of 25 melon near-isogenic lines (NILs) developed by introgressing Korean accession 'Shongwan Charmi' PI 161375 (SC; Group Conomon) genomic regions into 'Piel de sapo' (PS) [*C. melo* var. inodorus H. Jacq. (Group Inodorus)] genome (Eduardo, Arús, & Monforte, 2005) used in this study was described by Eduardo et al. (2007). Eighteen NILs contained a single molecular marker-defined introgression from SC into the PS genetic background (Eduardo et al., 2007), and the rest had two or more. The introgressions from SC presented in this set of NILs covered at least 85% of melon genome. In the present study the NIL SC3–5 was not used because of its evident climacteric behaviour (Obando-Ulloa et al., 2008). NILs were coded with the prefix "SC" followed by *x*–*y* numbers and, in some cases, one or two *z* letters (SC*x*–*y z*, for example SC3–5*ab*): the first *x* number indicates the linkage group (LG), and the second number *y* indicates the number of the NIL within the LG. The letters indicates additional genetic facts: "*a*", there is more than one introgression; "*b*" the NIL has an introgression slightly different from the introgression of the NIL with the same number described in Eduardo et al. (2005), although it covers the same genomic region; "*h*", the introgression is heterozygous and "*d*", part of the introgression is heterozygous (Eduardo et al., 2007). Although the mapping resolution of this population is not very high, it is sufficient for focusing research effort.

2.2. Experimental design

Crop management, harvesting practices, and harvesting indices have been previously described (Obando et al., 2008). Nine samples for the parental PS and 86 more for the NILs were analyzed. Only two replicates of NILs SC8–3, SC11–2*hab*, SC12–4*hb* and SC11–4*d* were available for analysis, while three samples of the remaining 21 NILs were analyzed (Table 1).

2.3. Fruit respiration rate

To confirm climacteric or non-climacteric behaviour, the fruit respiration rate in the NILs of interest was monitored over a period of 14*d* at 18.6 ± 1.1 °C and 68 ± 9% relative humidity. Nine NILs and PS were tested according to the static method (Fernández-Trujillo et al., 2008; Obando-Ulloa et al., 2008). The NILs were chosen based on the suspicion of climacteric behaviour in the field.

2.4. Juice sampling for aroma volatile analysis

Juice samples were obtained according to Obando-Ulloa et al. (2008) and stored at –60 °C until analysis. Juice was squeezed with a Simplex Super metal juicer (Italy) using 20 mm long and 15 mm diameter flesh cylinders obtained with an apple cork borer from the middle of one of the longitudinal sections of every fruit. Samples were taken by filtering juice through a powder funnel and four-layer cheesecloth. After 3 min, 4 ml of a saturated calcium chloride solution were added to 10 ml of juice and the mixture was homogenized, according to Baldwin, Goodner, Plotto, Pritchett, and Einstein (2004). A 1.33-ml mixture aliquot was poured into 4-ml glass vials for chromatography analysis. These samples were stored in a freezer at −70 °C until transportation for eight hours by car to the laboratory in Cáceres (Spain) in a 10 mm-thick polystyrene icebox with eight dry-CO_2 tablets of 100 g, and then stored at −80 °C until analysis.

2.5. Volatile analysis: headspace formation, solid-phase microextraction (SPME), gas chromatography–mass spectrometry (GC–MS) analysis

The methodology for gas chromatography–mass spectrometry (GC–MS) analysis of the samples was based on Ruiz, Ventanas, Cava, Andrés, and García (1999) and García-Esteban, Ansorena, Astiasarán, Martín, and Ruiz (2004), taking into account the information supplied by Kourkoutas et al. (2006). The method was described in a previous publication (Obando-Ulloa et al., 2008), but was slightly modified as a result of manual operation. The 4-ml vials were heated at 37 °C in a stirred shaken water bath for 30 min until equilibrium, and then aroma volatiles were extracted from the headspace for 30 min with a SPME fibre (StableFlex Divinylbenzene/Carboxen/polydimethyl siloxane 50/30 μm or DVD/CAR/PDMS) with 1 cm long standard needle for manual operation (Supelco Ref. 57328-U, Bellefonte, PA, USA), which was previously preconditioned at 280 °C for 50 min in the gas chromatography injection port.

After extraction, the fibre was manually introduced in the split/split-less injector at 280 °C in order to desorb the aroma volatile compounds during three minutes. The injector was mounted on a HP-6890 gas chromatograph (Agilent Technol., Wilmington, DEL) coupled to a selective single quadrupole mass spectrometer (HP-5973 Network, Agilent Technol.). For the split/split-less injector, the liner used had a 0.75 mm diameter (Supelco, Bellefonte, PA). The volatiles were separated into a 30 m × 0.25 mm internal diameter with 5% phenyl–methylsiloxane as stationary phase (HP-5MS, Agilent Technol.). The injection port was in split-less mode and the temperature was isothermal for 10 min at 40 °C, rising to 200 °C at 5 °C min^{-1}, and holding for 5 min. The transfer line to the mass spectrum was maintained at 280 °C.

The mass spectra were obtained by electronic impact at 70 eV, a multiplier voltage of 1756 V and collecting data at a rate of 1 scan·s^{-1} over the *m/z* range of 30–500 AMU. Compounds were tentatively identified by comparing their mass spectra with those included in the National Institute for Standards and Technology (NIST98, search version 2.0) data bank and by comparison of Kovats indices with those reported in the literature (Kondjoyan & Berdagué, 1996). The retention times from a series of straight-chain alkanes (C8–C20) supplied by Fluka were used under identical conditions to calculate the Kovats indices for all the identified volatile compounds (Kondjoyan & Berdagué, 1996; for "DB-5 like" phases). C6 and C7 were calculated from compounds present in our chromatograms. In addition, the Chemical Abstract Service (CAS) numbers of the volatiles reported in the NIST98 database also found in the website http://webbook.nist.gov/chemistry/name-ser.html (Table 2), were used to obtain their corresponding IUPAC names by checking the website http://www.chemindustry.com/apps/chemicals (Obando-Ulloa et al., 2008). The results of the volatile analyzes were expressed as percentage of total chromatographic area of the 28 volatile compounds of the profile reported in Table 2 (Muriel, Antequera, Petrón, Andrés, & Ruiz, 2004). These compounds were recovered and positively identified within the run time (Beaulieu, 2005, 2006; Muriel et al., 2004).

Table 1
Mean relative content of the probable aromatic compounds identified in the headspace of the fruit of the collection of near-isogenic lines (NILs) of melon and the parental line 'Piel de sapo' (PS). Mean physiological activities at harvest of the fruit analyzed are also reported. NIL means within rows highlighted with * showed statistical differences from PS data, according to a Dunnett's test at $P = 0.05$.

Compound	SC1–3*d*	SC1–4*a*	SC2–2*a*	SC2–3*d*	SC3–3	SC4–1*hb*	SC4–3*b*	SC4–4	SC5–2	SC5–3	SC6–4	SC7–2	SC7–4ab	SC8–1	SC8–2	SC8–3	SC8–4	SC9–2*a*	SC9–1*a*	SC9–3	SC10–2	SC11–2*hab*	SC11–4*d*	SC12–1*ab*	SC12–4*hb*	PS
Butyl acetate	0.27	0.18	0.24	0.28	0.22	0.29	0.35	0.39	0.24	0.29	0.35	0.22	0.41	0.26	0.22	0.22	0.30	0.13	0.20	0.27	0.17	0.37	0.22	0.37	0.17	0.27
1-Methoxypropan-2-yl acetate	0.57	0.60	0.62	0.88	0.33	0.85	0.74	0.84	0.71	0.72	0.42	0.45	0.66	0.77	0.39	0.25	0.60	0.22	0.74	0.71	0.34	0.93	0.29	0.69	1.26	0.73
3-Hydroxy-2,4,4-trimethylpentyl 2-methylpropanoate	0.60	1.16	0.99	0.91	0.92	0.89	1.58*	2.45*	1.03	1.15	0.96	1.44	0.66	1.28*	1.56	0.00	1.12	2.17	0.71	1.01	0.42	0.71	1.27	1.09	1.19	0.99
Pentanal	2.69	3.58	2.14	2.26	2.14	2.79	2.23	0.86	1.88	2.09	3.32	1.10	1.52	2.71	1.35	2.43	0.94	0.50	3.43	2.96	2.67	4.96	2.62	0.33	1.97	2.57
Hexanal	29.96	39.87	25.18	25.97	27.44	33.63	31.01	8.40	22.21	22.30	30.94	15.37	22.01	30.39	16.06	28.76	12.27	10.83	42.05	33.41	32.56	48.95	28.24	4.98	21.48	29.53
Heptanal	1.88	3.07	3.05	2.21	2.12	2.19	3.09	1.32	1.96	1.78	3.51	1.41	2.00	3.54	1.61	2.00	1.31	0.59	2.16	3.00	1.71	1.94	2.18	0.66	2.11	2.74
Benzaldehyde	0.93	0.87	0.79	0.96	0.89	0.83	1.23	1.32	1.30	1.14	0.77	0.78	0.80	0.73	0.56	0.82	0.57	0.88	1.22	0.87	1.10	1.17	0.56	1.17	0.79	1.16
Octanal	1.35	1.81	1.44	1.91	1.86	1.75	2.53	2.11	1.56	1.49	1.60	1.23	1.08	1.97*	1.39	1.28	1.52	1.50	1.51	2.05	1.51	1.98	1.87	1.35	2.50	1.77
Decanal	0.60	0.86	0.84	1.07	0.78	0.88	1.41	0.91	0.91	0.83	0.73	0.75	0.62	0.63	0.61	0.59	0.69	0.92	0.67	1.04	0.65	0.68	0.66	1.14	1.82	0.69
2-Methylpentane	3.15	1.42	1.76	2.39	2.52	2.25	1.81	4.36	3.06	2.42	2.98	2.98	1.94	1.04	3.70	3.59	2.66	2.25	1.31	2.58	1.91	0.00	2.41	4.54	3.98	2.40
3-Methylpentane	1.14	1.26	1.51	2.16	1.93	2.09	1.96	3.96	2.78	2.46	2.99	3.13	1.55	1.18	3.60	3.53	2.64	3.14	1.42	1.74	1.78	0.86	2.41	2.57	4.06	2.18
Methylcyclopentane	2.47	2.60	1.21	3.49	3.61	2.97	4.31	4.74	1.78	3.01	4.79	2.97	2.76	1.95	4.64	4.83	3.28	1.59	2.94	3.00	3.29	1.02	3.60	3.72	6.63	2.50
Ethylbenzene	0.35	0.23	0.32	0.33	0.34	0.32	0.38	0.50	0.33	0.38	0.34	0.33	0.43	0.31	0.48	0.25	0.46	0.43	0.47	0.41	0.36	0.23	0.31	0.62	0.59	0.44
1,4-Dimethylbenzene	0.79	0.48	0.75	0.89	0.78	0.84	1.16	1.29	0.95	1.00	0.86	0.74	0.96	0.68	1.06	0.47	1.13	1.28	0.99	0.95	0.79	0.68	0.82	1.48	1.58	1.09
1,2-Dimethylbenzene	0.48	0.38	0.43	0.46	0.42	0.46	0.62	0.73	0.62	0.55	0.43	0.45	0.48	0.50	0.53	0.30	0.58	0.61	0.56	0.56	0.43	0.53	0.48	0.73	0.69	0.54
4,7,7-Trimethylbicyclo[3.1.1]-3-heptene	0.29	0.12	0.18	0.26	0.17	0.21	0.28	0.39	0.25	0.21	0.26	0.24	0.29	0.14	0.32	0.21	0.22	0.29	0.15	0.24	0.12	0.21	0.17	0.29	0.28	0.25
Terpene not identified (41 69 95 108 119 137 152)	1.97	1.59	1.62	1.65	2.04	1.82	1.71	1.91	1.72	1.83	1.67	2.39	2.46	2.13	2.11	2.23	2.69	2.07	1.78	1.42	1.40	2.07	2.11	2.88	0.67	2.19
6-Methyl-5-heptene-2-one	0.53	0.93	0.72	1.07	0.73	0.94	1.60	1.20	0.95	1.09	0.68	0.88	0.93	0.79	0.75	0.69	1.21	0.87	0.60	0.93	0.53	0.87	0.63	0.99	1.62	0.87
5,5,6-Trimethyl-, endo-bicyclo[2.2.1]-2-heptanone	0.31	0.46	0.43	0.54	0.38	0.24	0.87	0.49	0.48	0.45	0.30	0.30	0.30	0.49	0.42	0.43	0.35	0.47	0.29	0.37	0.23	0.31	0.36	0.60	0.90	0.46
Methanethiol	12.47	8.77	14.01	12.30	8.82	12.49	6.64	11.66	13.34	11.73	7.75	14.06	7.61	10.51	13.90	10.91	15.74	10.43	7.35	10.96	12.43	9.41	8.26	13.73	17.47	10.59
Ethanol	5.27	5.77	5.40	8.19	10.13	8.12	11.35	13.77	10.60	8.55	7.76	9.14	12.39	5.68	9.02	7.93	6.67	6.99	4.35	8.43	6.68	0.22	10.45	5.60	12.50	6.37
Ethyl ether	1.60	4.45	5.50	4.12	7.68	3.15	3.12	5.66	5.55	4.50	8.43	5.76	3.25	5.61	7.37	9.24	4.42	6.41	5.37	4.28	6.25	1.14	5.00	5.62	6.69	4.56
1-Methyl-4-prop-1-en-2-yl-cyclohexene (D-limone)	0.34	0.52	0.50	0.44	0.60	0.58	0.64	0.62	0.39	0.47	0.38	0.56	0.40	0.36	0.54	0.38	0.60	0.70	0.45	0.53	0.49	0.31	0.52	0.58	0.67	0.42
1,7,7-Trimethylnorbornan-2-one (Camphor)	17.52	17.78	15.58	16.44	19.44	19.24	19.40	23.02	19.41	20.87	17.78	23.60	21.49	25.91	21.63	18.64	26.80	21.65	19.06	15.85	12.75	20.45	19.75	28.73	8.39	21.00
Respiration rate (nmol kg^{-1} s^{-1})	71.61	63.41	64.13	79.99	66.21	54.40	85.77	71.14	66.25	63.99	61.14	77.51	77.44	66.06	76.26	71.98	68.99	72.85	72.76	56.82	48.53	56.63	59.43	63.08	76.83	65.19
Ethylene production rate (nmol kg^{-1} s^{-1})	19.20	18.10	12.00	14.70	17.21	19.71	29.02	12.93	19.59	12.76	12.98	17.60	18.71	13.42	14.90	10.72	17.29	17.49	18.70	20.28	18.31	10.29	14.81	12.83	16.40	16.20

Table 2
Description of the probable aromatic compounds identified in the headspace of fruit of the collection of near-isogenic lines of melon (NILs) and the parental 'Piel de sapo' (PS).

Compound's name	No. CAS	Mass-to-charge ratio (*m/z*)	KI	ID
Esters				
Butyl acetate	123-86-4	43 (999), 56 (442), 41 (147), 61 (144), 73 (142), 55 (74), 29 (66), 27 (50), 57 (41), 15 (36)	815	a
1-Methoxypropan-2-yl acetate	108-65-6	43 (999), 45 (497), 15 (239), 72 (203), 29 (91), 58 (120), 41 (90), 87 (87), 27 (65), 39 (58)	870	a, b
3-Hydroxy-2,4,4-trimethylpentyl 2-methylpropanoate	74367-34-3	71 (999), 56 (756), 43 (609), 89 (455), 41 (235), 55 (203), 73 (162), 57 (162), 72 (89), 85 (81)	1389	a, b
Aldehydes				
Pentanal	110-62-3	44 (999), 29 (690), 41 (522), 27 (461), 43 (311), 58 (282), 39 (268), 57 (257), 28 (192), 42 (151)	696	a, b
Hexanal	66-25-1	44 (999), 56 (816), 41 (655), 43 (531), 57 (441), 29 (382), 27 (330), 72 (197), 45 (196), 55 (147)	799	a, b
Heptanal	111-71-7	44 (999), 43 (861), 41 (844), 70 (662), 27 (611), 42 (555), 55 (512), 57 (423), 39 (287), 45 (204)	900	a,b
Benzaldehyde	100-52-7	77 (999), 106 (944), 105 (944), 51 (384), 50 (185), 78 (139), 52 (93), 107 (72), 74 (62), 39 (62)	965	a, b
Octanal	124-13-0	41 (999), 43 (883), (57) 809, 56 (785), 55 (690), 44 (684), 84 (564), 29 (478), 69 (418), 42 (418)	1000	a, c
Decanal	112-31-2	43 (999), 41 (985), 57 (785), 55 (549), 44 (542), 29 (451), 70 (380), 56 (351), 42 (342), 71 (333)	1209	a, c
Branched alkanes				
2-Methylpentane	107-83-5	43 (999), 42 (528), 41 (354), 27 (305), 71 (285), 39 (200), 29 (179), 57 (106), 15 (95), 70 (67)	558	a
3-Methylpentane	96-14-0	57 (999), 56 (756), 41 (675), 29 (604), 27 (398), 43 (292), 39 (218), 15 (89), 55 (88), 28 (82)	576	a, b
Methylcyclopentane	96-37-7	56 (999), 41 (547), 69 (438), 39 (263), 55 (261), 42 (201), 28 (160), 27 (159), 84 (106), 43 (79)	622	a, c
Aromatic hydrocarbon				
Ethylbenzene	100-41-4	91 (999), 106 (282), 51 (114), 65 (113), 77 (99), 78 (87), 92 (73), 39 (70), 50 (62), 105 (61)	866	a, c
1,4-Dimethylbenzene	106-42-3	91 (999), 106 (658), 105 (288), 77 (118), 51 (85), 39 (79), 92 (74), 79 (70), 103 (58), 78 (57)	873	a, c
1,2-Dimethylbenzene	95-47-6	91 (999), 106 (430), 105 (177), 51 (135), 39 (135), 77 (129), 65 (87), 79 (82), 78 (72), 27 (68)	896	a, c
Terpenes				
4,7,7-Trimethylbicyclo[3.1.1] -3-heptene	Not previously identified		940	a, b
Terpene not identified (41 69 95 108 119 137 152)	Not previously identified		1118	a
Ketones				
6-Methyl-5-heptene-2-one	110-93-0	43 (999), 41 (460), 69 (341), 55 (330), 108 (276), 58 (171), 111 (165), 68 (153), 39 (130), 71 (129)	985	a, c
5,5,6-Trimethyl-, endo-bicyclo[2.2.1] -2-heptanone	3767-44-0	108 (999), 95 (793), 41 (503), 55 (448), 69 (348), 39 (257), 67 (254), 109 (254), 81 (242), 110 (242)	1215	a
Other compounds				
Methanethiol	74-93-1	47 (999), 48 (758), 45 (614), 46 (147), 44 (126), 33 (121), 32 (116), 14 (67), 49 (56), 13 (43)	ND	a, c
Ethanol	64-17-5	31 (999), 45 (514), 29 (298), 27 (224), 46 (216), 43 (114), 26 (98), 30 (81), 15 (66), 42 (47)	ND	a
Ethyl ether	60-29-7	31 (999), 29 (627), 59 (396), 27 (346), 45 (326), 74 (225), 15 (174), 43 (90), 26 (88), 28 (85)	504	a, b
1-Methyl-4-prop-1-en-2-yl-cyclohexene (D-limone)	5989-27-5	68 (999), 93 (590), 67 (446), 79 (227), 94 (225), 136 (225), 121 (194), 41 (192), 92 (187), 107 (170)	1034	a, b
1,7,7-Trimethylnorbornan-2-one (Camphor)	76-22-2	95 (999), 41 (794), 81 (739), 108 (388), 69 (386), 55 (376), 27 (348), 39 (335), 83 (331), 109 (282)	1163	a

KI, Kovats index; ND, not determined; ID, identification: a, GC/MS; b, Kovats index and literature Kondjoyan and Berdagué (1996); c, Kovats index not previously published.

2.6. Statistical analysis

Data were subjected to a one-way ANOVA using general linear model procedures, with pedigree as factor in JMP® v5.1.2 for Windows (SAS Institute Inc., NC). If significant differences were found by ANOVA using pedigree, the differences between NILs and PS were evaluated by Dunnett's test at $P = 0.05$, using JMP, according to Obando et al. (2008).

Aroma data were also subjected to principal components analysis (PCA), using JMP. This analysis was used to identify the volatiles that explain the most part of the volatile differences among NILs and to group the NILs according their aroma profile. The NIL PC values of all the compounds were analyzed by ANOVA with pedigree as factor and Dunnett's test in JMP. The PCA graph was split into two graphs (score and loading plots, respectively) in order to clarify the analysis due to the high number of samples and volatiles considered in this study. Otherwise, the PCA figure with the score plot overlapping the loading plot would be a cloud of data with no sense. The score plot was performed with the mean component value (prin) obtained for each PC, while the loading plot was reached with the eigenvectors greater than 0.20 for the aroma volatile compounds that better define the orientation of each PC axis.

3. Results

3.1. Respiration rate

The PS showed a non-climacteric pattern, while four NILs showed a similar non-climacteric behaviour (Fig. 1). Compared with the respiration rate levels of PS, SC8–4 and SC9–2*a* showed slightly higher levels, while SC2–3*d* showed slightly lower levels. The NIL SC3–3 was classified as having a slightly climacteric behaviour (Fig. 1). Other NILs checked at harvest (Table 1) or in other experiments, such as SC10–2, also showed the levels of non-climacteric PS or a typical non-climacteric pattern (data not shown).

3.2. Definition of the aroma profile

About 206 aroma volatile compounds were tentatively identified in the headspace of the NILs analyzed, although only 48 compounds were preliminarily identified in most of the NILs and in PS. The definition of the aroma profile was based on the number of samples in which the compound was detected. So, in cases in which there were two NIL samples and the compound was detected in only one of them, the compound was not considered for the profile. On the other hand, if there were three samples and the compound was identified in two of the three or in all three samples, it was considered for the profile. That is why only 24 compounds defined the probable aroma profile in the whole collection and PS (Table 1). The profile was composed of six aldehydes, three esters, three branched alkanes, three aromatic branched hydrocarbons, two terpenes, two ketones and five compounds from other groups (Tables 1 and 2).

It was also found that (*Z*,*Z*)-3,6 nonadienal was only detected in NIL SC8–1, with a relative content levels of around 0.51%.

3.3. Principal component analysis of the aroma volatile data

PCA transformed a number of possibly correlated variables of single aroma volatiles into a smaller number of uncorrelated variables called principal components. Principal components were obtained as linear combinations of the original variables, so the first principal component has maximum possible variance, the second principal component is orthogonal to the first principal component and has the maximum possible variance and so on. PC components explain better the melon aroma than single compounds individually. The first three PCs contributed to 57% of the total variance (30%, 15% and 12%, respectively). Fig. 2A depicts PC1 versus PC2. The parental line PS was located close to the centre of the graph. The NIL SC12–1*ab* showed the higher PC1 levels, significantly higher than PS, according to the Dunnett's test (Table 1; data not shown). NILs SC4–3*b*, SC11–2*hab* showed higher PC2 values than PS, while SC7–2 showed lower PC2 values according to Dunnett's tests (Fig. 2A; data not shown).

PC1, representing 30% of the total variance, was mostly affected by the relative concentrations of 2-methylpentane, 3-methylpentane, ethylbenzene, 1,4-dimethylbenzene, 1,2-dimethylbenzene and 5,5,6-trimethyl-, endo-bicyclo[2.2.1]-2-heptanone in the positive direction, while pentanal, hexanal, and heptanal defined the negative orientation of the PC1 axis (Fig. 2B). PC2, representing 15% of the total variance, was affected by relative concentrations of methanethiol, ethanol, ethyl ether, methylcyclopentane, which defined its negative orientation, while its positive orientation was defined by 1-methoxypropan-2-yl acetate, 6-methyl-5-heptene-2-one, octanal and decanal. The third component PC3, representing 12% of the total variance, was mainly affected in its negative orientation by the relative concentration of butyl acetate, a non-identified terpene and 1,7,7-trimethylnorbornan-2-one (camphor) (data not shown).

3.4. Univariate analysis of the compounds identified in the aroma profile

Three compounds of the profile [hexanal, 1,7,7-trimethylnorbornan-2-one (camphor), and methanethiol] showed noticeably higher levels than the rest of the compounds but with no significant pedigree effect.

However, compounds with lower relative content were more affected by the pedigree factor. Some of them, such as the 3-hydroxy-2,4,4-trimethylpentyl 2-methylpropanoate, showed a higher relative content compared with PS (29–148% in the NILs SC4–3*b*, SC4–4 and SC11–4*d*). On the other hand, octanal showed a 11.3% lower level in the NIL SC8–1 than PS (Table 1).

3.5. QTL mapping

Only three QTLs were associated with the aroma profile of these NILs. Two of them increased the ester 3-hydroxy-2,4,4-trimethylpentyl 2-methylpropanoate (2 QTLs in LG IV and XI), while other in LG VIII reduced the relative content of octanal. Additionally, another QTL in LG VIII was responsible for the cucumber-like aroma [(*Z*,*Z*)-3,6 nonadienal], characteristic of NIL SC8–1, as mentioned above.

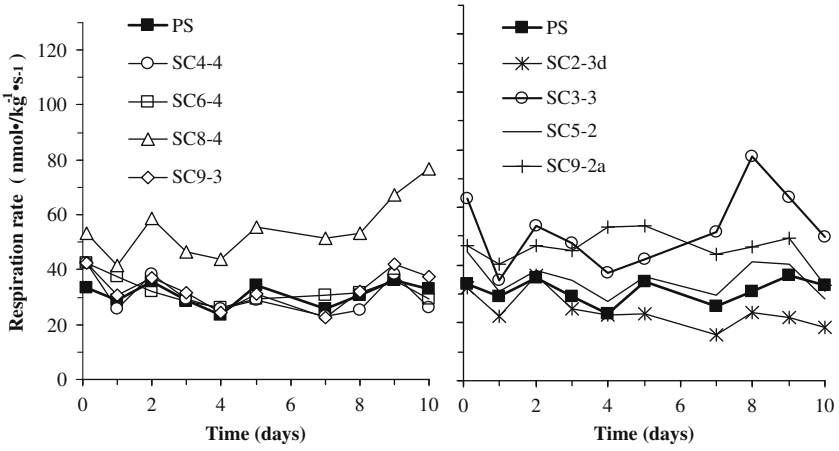

Fig. 1. Respiration rate (mean of representative fruit, $n = 3–5$) in the parental line 'Piel de Sapo' (PS) and five selected near-isogenic lines (NILs) of melon measured over 10 d at 18.6 °C.

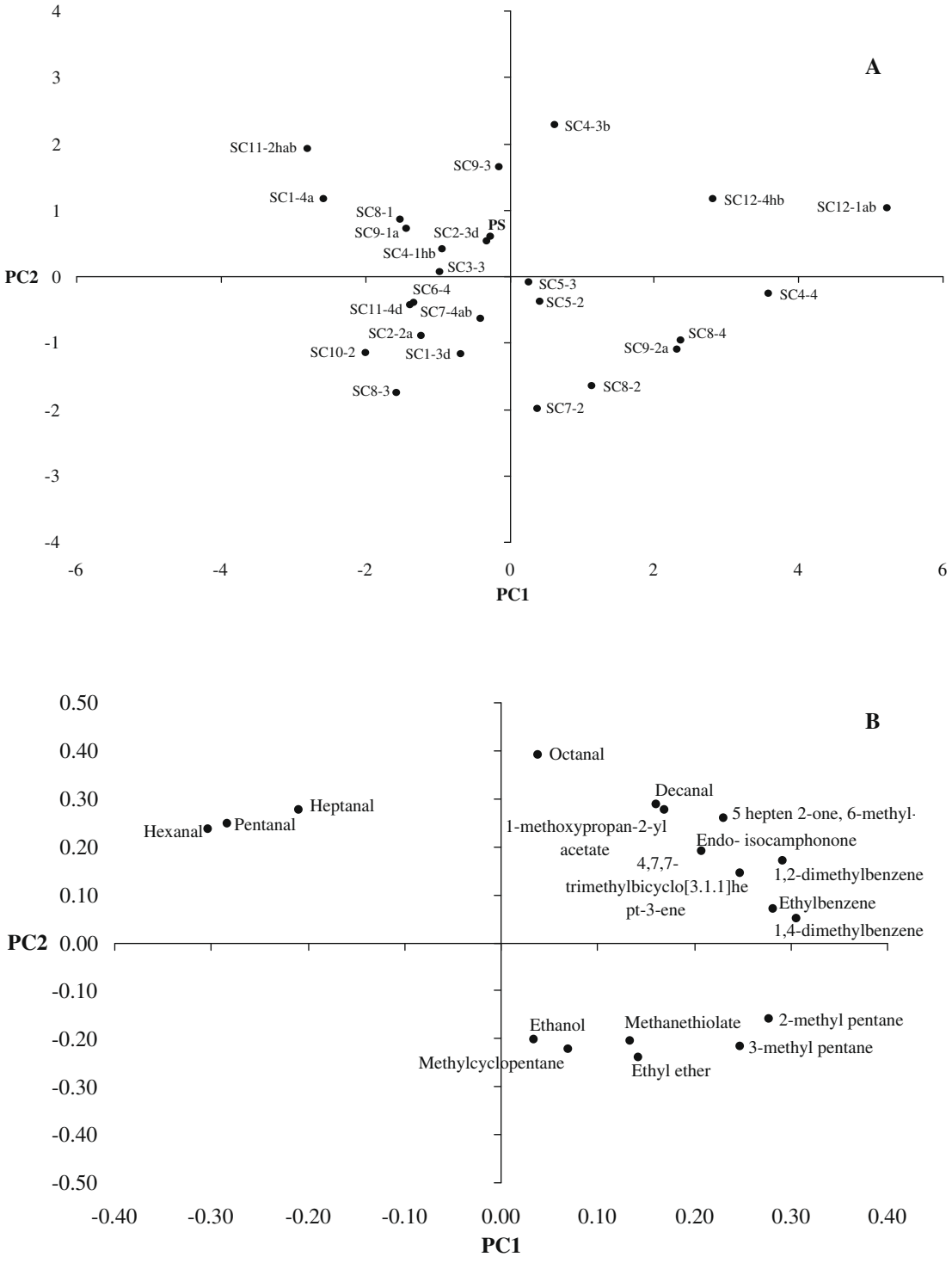

Fig. 2. Plot of the centroids of scores (A) and loading plots (B) of the the two main principal component analyzes (PCA) of the aroma volatiles identified in the collection of near-isogenic lines (NILs) of melon at harvest. The loading plots higher than 0.20% allowed the orientation of the PC axis to be defined. The first two PC's explained 30% and 15% of the total variance, respectively. The biplot was divided in two figures in order to provide a clearer graph for a better understanding of the results.

4. Discussion

Overall, PI 161375 did not really affect the physiological behaviour of the NILs studied, which showed a non-climacteric behaviour, except NIL SC8–4 with its respiration rate that seemed to be higher and showed a trend to increase (Fig. 1), and the NIL SC3–5 previously studied (Moreno et al., 2008; Obando-Ulloa et al., 2008; data not shown). The aroma profile of non-climacteric *Inodorous* melons has received little attention in the literature (Kourkoutas et al., 2006), but these melons have great interest as intact, fresh-cut or processed fruit due to their longer shelf-life than the climacteric ones (Beaulieu & Baldwin, 2002; Fernández-Trujillo et al., 2008; Oms-Oliu, Odriozola-Serrano, Soliva-Fortuny, & Martin-Belloso, 2008).

Usually, ethylene burst aroma biosynthesis is easy to detect by the human nose, while in non-climacteric fruit the external aroma is scarcely detected except when the fruit become senescent or rotten (Obando-Ulloa et al., 2009). The non-climacteric PS type, how-

ever, shows many aroma compounds, most of them aldehydes (Table 1). Even though some aldehydes are not easily detectable by the human nose, others have a low human detection threshold (Baldwin, 2002; Beaulieu & Baldwin, 2002; Canoles, Beaudry, Li, & Howe, 2006), and are important for the flavour of tomato, cucumber, peppers and other vegetables (Baldwin, 2002; Canoles et al., 2006). Aldehydes with low molecular weight are associated with immature stages in climacteric Cantaloupe melons (Beaulieu & Grimm, 2001). However, most aldehydes are present at high levels or increase markedly during early growth stages and then decrease with increasing harvest maturity (Beaulieu & Grimm, 2001). In this collection, aldehydes are present in between 15–40% relative levels of the total aroma of the profile, and hexanal shows the highest relative content with respect to other aldehydes, in agreement with previous results working with PS and other non-climacteric NILs with introgression in LG III (Obando-Ulloa et al., 2008). Hexanal is considered to contribute to green notes and, secondarily, to melon aroma, and benzaldehyde has been defined as a pleasant aroma for Cantaloupe type melons (Beaulieu, 2006; Beaulieu & Grimm, 2001), and high concentrations are usually associated with a high degree of melon ripening (Beaulieu & Grimm, 2001). Also, it is not unlikely that the unsaturated aldehyde fraction and, particularly, hexanal, may be due to lipid peroxidation during sampling and freezing (Ma et al., 2007). It has also been reported that hexanal increases with increasing harvest maturity, which could lead to development of off-flavours in stored melon and fresh-cut products (Beaulieu & Grimm, 2001) and in tomato (Canoles et al., 2006). However, hexanal slightly changes during PS senescence compared with other NILs (Obando-Ulloa et al., 2009).

The rest of the main compounds of the profile have previously been reported as aroma components in other foods. For example, methanethiolate has been associated with food heating and/or cooking, and is also an essential compound for the flavour of cured ham (Ruiz et al., 1999). However, the high concentrations in some NILs and reference cultivars seem to contribute to the *musky* notes of the aroma (Obando-Ulloa et al., 2008).

On the other hand, 1,7,7-trimethylnorbornan-2-one (camphor) have also been reported in other melon cultivars (Lamikanra & Richard, 2002), and in NILs with introgression of the melon LG III (Obando-Ulloa et al., 2008). The three QTLs mapped for three different compounds and LG's can be used as a good model for melons to study the relationship between aroma biosynthesis and aroma precursors (Baldwin, 2002). Octanal is an aldehyde previously reported as a major component (12.7% v/v) in orange flavourings (Muñoz-Aguirre, Yoshino, Nakamoto, & Morizumi, 2007), but also reported in the flesh of Queen Ann's pocket melons (Aubert & Pitrat, 2006), fresh-cut Cantaloupe melons (Beaulieu & Lancaster, 2007), in and in seedless watermelon juice (Beaulieu & Lea, 2006).

The compound 3-hydroxy-2,4,4-trimethylpentyl 2-methylpropanoate is a complex ester not previously reported in PS or the NILs studied with introgression in LG III (Obando-Ulloa et al., 2008). This compound has been found in green tea (Hattori, 2006) and as a minor compound of the extracellular secretion from living brown algae (Shibata, Hama, Miyasaki, Ito, & Nakamura, 2006).

The compound (*Z,Z*)-3,6-nonadienal is one of the precursors of the cucumber-like aroma which is produced from fatty acid oxidation (Ma et al., 2007). The pleasant odour in cucumber has been attributed to (*E,Z*)-2,6-nonadienal, while two unsaturated aldehydes (2-hexenal and 2-nonenal) and three saturated aldehydes (ethanal, propanal and hexanal) were considered to contribute secondarily to overall flavour (Beaulieu and Baldwin, 2002; Beaulieu, 2005; Beaulieu & Grimm, 2001; Palma-Harris, McFeeters, & Fleming, 2002), but (*Z,Z*)-3,6-nonadienal was not recovered in Cantaloupe melons (Beaulieu & Grimm, 2001). The NIL SC8–1 can be used as a model to avoid cucumber-like aroma in melons or to study the biosynthetic pathways of C6 and C9 unsaturated aldehydes and alcohols from linolenic precursors (Ma et al., 2007). Hydroxyperoxide lyases (HPL) cleave these C9 aldehydes (Tijet, Schneider, Muller, & Brash, 2001). HPL form very unstable hemiacetals from hydroperoxides (HPO) generated by lipoxygenases from the polyunsaturated fatty acids, leading to the generation of aldehydes and aldehyde enols by spontaneous dissociation (Pech et al., 2008, chap. 13). The compound (*E,Z*)-2,6-nonadienal is a muskmelon-like or musky aroma and and (*Z,Z*)-3,6-nonadien-1-ol is a grassy boiled leaf-like aroma (Kourkoutas et al., 2006), Due to the reasons mentioned above, the former compounds can be easily obtained from (*Z,Z*)-3,6-nonadienal by isomerisation.

This aroma profile has multiple uses for the characterization of melon cultivars of the Inodorus Group, particularly of the 'Piel de sapo' type. For example, this profile can be used for present or future European protected geographical indications (PGI). Additionally, the compounds can be used to train and establish melon test panel and sensorial protocols, or to correlate sensory and instrumental parameters, for new or traditional melon cultivars (Pardo et al., 2000). Finally, the profile is useful for standardizing or developing new natural melon flavours and fragances; for the on-line control using the right sensors of fresh or processed melon products (Muñoz-Aguirre et al., 2007), such as fresh-cut halves, slices or cubes; or cremogenates, soups, canning balls, etc. This profile is also useful for developing new melon fruit spirits and distillates (Hernández-Gomez, Ubeda, & Briones, 2003) with aroma volatiles closer to the fresh fruit aroma.

5. Conclusions

The aroma profile of this collection was composed of 24 compounds with predominance of aldehydes in non-climacteric melons, particularly hexanal and methanethiolate. The introgressions of PI 161375 studied also had higher levels of one ester and lower levels of octanal with no significant effects on the rest of the compounds of the profile. Three QTLs associated with ester and aldehyde biosynthesis were mapped, while another QTL was associated with the cucumber-like aroma [(*Z,Z*)-3,6 nonadienal].

Acknowledgements

This work was funded by Grants BIO-AGR06/02-0011 (Consejería de Educación y Cultura de la Región de Murcia), 05676/PI/07 and 00620/PI/04 (Fundación Séneca de la Región de Murcia), AGL2003-09175-C02-01 and AGL2003-09175-C02-02 from the Spanish Ministry of Education and Science and European Fund for Regional Development (FEDER, European Union). J. Obando was partly supported by a fellowship from the Spanish Ministry of Foreign Affairs (MAE-AECI). The authors are indebted to Ana Belén Pérez and Manuela Selma for sampling assistance and to Semillas Fitó S.A. (Barcelona, Spain) for providing the PS seeds.

References

Aubert, C., & Pitrat, M. (2006). Volatile compounds in the skin and pulp of Queen Anne's pocket melon. *Journal of Agricultural and Food Chemistry, 54*, 8177–8182.

Baldwin, E. (2000). Flavor trivia and tomato aroma. Biochemistry and possible mechanisms for control of important aroma components. *HortScience, 35*, l013–1022.

Baldwin, E. (2002). Fruit flavor, volatile metabolism and consumer perceptions. In M. Knee (Ed.), *Fruit quality and its biological basis* (pp. 89–106). Sheffield, UK: Sheffield Academic Press Ltd.

Baldwin, E., Goodner, K., Plotto, A., Pritchett, K., & Einstein, M. (2004). Effects of volatiles and their concentration on perception of tomato descriptors. *Journal of Food Science, 69*, S310–S318.

Beaulieu, J. (2005). Within-season volatile and quality differences in stored fresh-cut cantaloupe cultivars. *Journal of Agricultural and Food Chemistry, 53*, 8679–8687.

Beaulieu, J. (2006). Volatile changes in cantaloupe during growth, maturation, and in stored fresh-cuts prepared from fruit harvested at various maturities. *Journal of the American Society of Horticultural Science, 131*, 127–139.

Beaulieu, J. C., & Baldwin, E. (2002). Flavor and aroma of fresh cut fruits and vegetables. In O. Lamikanra (Ed.), *Fresh cut fruits and vegetables. Science, technology and market* (pp. 391–425). Boca Ratón, Fla: ORC Press LLC.

Beaulieu, J. C., & Grimm, C. C. (2001). Identification of volatile compounds in cantaloupe at various developmental stages using solid phase microextraction. *Journal of Agricultural and Food Chemistry, 49*, 1345–1352.

Beaulieu, J. C., & Lancaster, V. A. (2007). Correlating volatile compounds, sensory attributes, and quality parameters in stored fresh-cut cantaloupe. *Journal of Agricultural and Food Chemistry, 55*, 9503–9513.

Beaulieu, J. C., & Lea, J. M. (2006). Characterization and semiquantitative analysis of volatiles in seedless watermelon varieties using solid-phase microextraction. *Journal of Agricultural and Food Chemistry, 54*, 7789–7793.

Canoles, M. A., Beaudry, R. M., Li, C. Y., & Howe, G. (2006). Deficiency of linolenic acid in Lefad7 mutant tomato changes the volatile profile and sensory perception of disrupted leaf and fruit tissue. *Journal of the American Society for Horticultural Science, 131*, 284–289.

Eduardo, I., Arús, P., & Monforte, A. J. (2005). Development of a genomic library of near isogenic lines (NILs) in melon (*Cucumis melo* L.) from the exotic accession PI 161375. *Theorethical and Applied Genetics, 6*, 1–10.

Eduardo, I., Obando, J., Martínez, J. A., Alarcón, A. L., Arús, P., Álvarez, J. M., et al. (2007). Estimating the genetic architecture of fruit quality traits in melon (*Cucumis melo* L.) using a genomic library of near-isogenic lines. *Journal of the American Society of Horticultural Science, 132*, 80–89.

Fallik, E., Alkali-Tuvia, S., Horev, B., Copel, A., Rodov, V., Aharoni, Y., et al. (2001). Characterisation of 'Galia' melon aroma by GC and mass spectrometric sensor measurements after prolonged storage. *Postharvest Biology and Technology, 22*, 85–91.

Fernández-Trujillo, J. P., Obando, J., Martínez, J. A., Moreno, E., García-Mas, J., & Monforte, A. J. (2008). Climacteric or non-climacteric behavior in melon fruit 2. Linking climacteric pattern and main postharvest disorders and decay in a set of near-isogenic lines. *Postharvest Biology and Technology, 50*, 125–134.

García-Esteban, M., Ansorena, D., Astiasarán, I., Martín, D., & Ruiz, J. (2004). Comparison of simultaneous distillation extraction (SDE) and solid-phase microextraction (SPME) for the analysis of volatile compounds in dry-cured ham. *Journal of Science and Food Agriculture, 84*, 1364–1370.

Hattori, S. (2006). Study of new approach for evaluation of Japanese green tea using OASIS method. *Bulletin of the Faculty of Agriculture Hokkaido University, 28*(1), 85–120. eprints.lib.hokudai.ac.jp/dspace/bitstream/2115/8282/1/28(1)_2.pdf.

Hernández-Gomez, L. F., Ubeda, J., & Briones, A. (2003). Melon fruit distillates: Comparison of different distillation methods. *Food Chemistry, 82*, 539–543.

Kondjoyan, N., & Berdagué, J. L. (1996). A compilation of relative retention indices for the analysis of aromatic compounds. In Laboratoire de Flaveur et Diazol (Ed.), Clermont-Ferrand, France.

Kourkoutas, D., Elmore, J. S., & Mottram, D. S. (2006). Comparison of volatile compositions and flavour properties of cantaloupe, Galia and honeydew muskmelons. *Food Chemistry, 97*, 95–102.

Lamikanra, O., & Richard, O. A. (2002). Effect of storage on some volatile aroma compounds in fresh-cut Cantaloupe melon. *Journal of Agricultural and Food Chemistry, 50*, 4043–4047.

Ma, Y., Hu, X., Chen, J., Chen, F., Wu, J., Zhao, G., et al. (2007). The effect of freezing modes and frozen storage on aroma, enzyme and micro-organism in Hami Melon. *Food Science and Technology International, 13*, 259–267.

Moreno, E., Obando, J., Dos-Santos, N., Fernández-Trujillo, J. P., Monforte, A. J., & García-Mas, J. (2008). Candidate genes and QTLs for fruit ripening and softening in melon. *Theoretical and Applied Genetics, 116*, 589–602.

Muñoz-Aguirre, S., Yoshino, A., Nakamoto, T., & Morizumi, T. (2007). Odor approximation of fruit flavors using a QCM odor sensing system. *Sensors and Actuators B – Chemical, 123*, 1101–1106.

Muriel, E., Antequera, T., Petrón, M. J., Andrés, A. I., & Ruiz, J. (2004). Volatile compounds in Iberian dry-cured loin. *Meat Science, 68*, 391–400.

Obando, J., Fernández-Trujillo, J. P., Martínez, J. A., Alarcón, A. L., Eduardo, I., Arús, P., et al. (2008). Identification of melon fruit quality quantitative trait loci using near-isogenic lines. *Journal of the American Society of Horticultural Science, 133*, 139–151.

Obando-Ulloa, J. M., Moreno, E., García-Mas, J., Nicolai, B., Lammertyn, J., Monforte, J. A., et al. (2008). Climacteric or non-climacteric behavior in melon fruit 1. Aroma volatiles. *Postharvest Biology and Technology, 49*, 27–37.

Obando-Ulloa, J. M., Nicolai, B., Lammertyn, J., Bueso, M. C., Monforte, A. J., & Fernández-Trujillo, J. P. (2009). Aroma volatiles associated with the senescence of climacteric or non-climacteric melon fruit. *Postharvest Biology and Technology, 52*, 146–155.

Oms-Oliu, G., Odriozola-Serrano, I., Soliva-Fortuny, R., & Martin-Belloso, O. (2008). The role of peroxidase on the antioxidant potential of fresh-cut 'Piel de Sapo' melon packaged under different modified atmospheres. *Food Chemistry, 106*, 1085–1092.

Palma-Harris, C., McFeeters, R. F., & Fleming, H. P. (2002). Fresh Cucumber flavor in refrigerated pickles: Comparison of sensory and instrumental analysis. *Journal of Agricultural and Food Chemistry, 50*, 4875–4877.

Pardo, J. E., Alvarruiz, A., Varón, R., & Gómez, R. (2000). Quality evaluation of melon cultivars. Correlation among physical–chemical and sensory parameters. *Journal of Food Quality, 23*, 161–170.

Pech, J. C., Latché, A., & Van der Rest, B. (2008). Genes involved in the biosynthesis of aroma volatiles and biotechnological applications. In B. Bruckner & S. G. Wyllie (Eds.), *Fruit and vegetable flavour: Recent advances and future prospects* (pp. 254–271). Abington, Cambridge, UK: Woodhead Pub. Ltd.

Ruiz, J., Ventanas, J., Cava, R., Andrés, A. I., & García, C. (1999). Volatile compounds of dry-cured Iberian ham as affected by the length of the curing process. *Meat Science, 52*, 9–27.

Shibata, T., Hama, Y., Miyasaki, T., Ito, M., & Nakamura, T. (2006). Extracellular secretion of phenolic substances from living brown algae. *Journal of Applied Phycology, 18*, 787–794.

Tijet, N., Schneider, C., Muller, B. L., & Brash, A. R. (2001). Biogenesis of volatile aldehydes from fatty acids hydroperoxides: Molecular cloning of a hydroperoxide lyase (CYP74C) with specificity for both the 9- and 13-hydroperoxides of linoleic and linolenic acids. *Archives of Biochemistry and Biophysics, 386*, 281–289.

Villanueva, M. J., Tenorio, M. D., Esteban, M. A., & Mendoza, M. C. (2004). Compositional changes during ripening of two cultivars of muskmelon fruits. *Food Chemistry, 87*, 179–185.

were washed thoroughly with tap water, dried by forced air circulation and pulverised in a blender. Algal powder (270 g) was depigmented using sequential extraction with petroleum ether (24 h) and acetone (24 h) as solvent in a Soxhlet apparatus. The unextracted material was placed in a plastic beaker and air dried to yield depigmented algal powder (DAP; 173 g).

2.1.2. Extraction with acid

Extractions of DAP (3 g) with 0.1 M HCl (w/v::1:100) were conducted at 30–35 °C for 12 h under constant stirring (twice). Separation of the residue from the extract was performed by filtration through a glass filter (G-2). The residue was washed with additional 0.1 M HCl and the wash was collected to maximise polysaccharide recovery. The extracts were combined, dialysed and lyophilised to give fraction A (yield, 8.8%).

2.1.3. Extraction with alkali

The acid insoluble residue was extracted with 3% Na_2CO_3 (w/v::1:100) at 45–50 °C for 4 h under constant stirring (twice). The extract was carefully acidified with concentrated HCl to pH ~1, the precipitate formed was collected by centrifugation, washed with 0.1 M HCl, suspended in water and dissolved by careful addition of NaOH. The slightly alkaline solution was dialysed and diluted with 4.0 M $CaCl_2$ solution to make a final concentration of 2% $CaCl_2$. The precipitate formed at this stage was isolated by centrifugation, washed with water and treated with 0.1 M HCl (4 × 50 ml, stirring at room temperature for ~2 h). Then the precipitate was dissolved in dilute NaOH as above, the solution dialysed and finally lyophilised to yield sodium alginate (B, yield, 22.6%).

2.1.4. Extraction with water

The residue left after extraction with alkali was once again extracted with water at 80 °C (twice) and the combined extract (C) dialysed. Then 4.0 M $CaCl_2$ solution was added to the extract to make a final concentration of 2% $CaCl_2$, and the suspension kept at 5–9 °C overnight. After separating the precipitate (C2) by centrifugation the supernatant dialysed, concentrated and lyophilised to give fraction C1 (yield, 6.2%).

The resulting insoluble residue was dialysed against distilled water and finally lyophilised (INS).

2.1.5. Anion exchange chromatography (AEC)

A solution (20 ml) of dilute acid extracted polymer (fraction A) in 50 mM sodium acetate (pH 5.5) was applied to a column (2.6 × 25 cm) of DEAE-Sepharose FF (AcO^-). Thereafter, the column was eluted (0.6 ml min^{-1}) successively with 0.05 M (fraction AF1), 0.7 M (fraction AF2) and 2.0 M (fraction AF3) NaOAc buffer in a stepwise manner. Appropriate fractions were pooled, dialysed and lyophilised.

2.1.6. Size exclusion chromatography (SEC)

System A: Size exclusion chromatography of fraction C1 on Superdex-30 column (2.6 × 50 cm; Amersham Biosciences AB) was carried out using 0.5 M sodium acetate buffer (pH 5.0) as solvent. Fractions (5 ml) were collected and analysed for neutral sugar content by phenol–sulphuric acid method (Dubois, Gilles, Hamilton, Rebers, & Smith, 1956). Appropriate fractions (namely, C1F1 and C1F2) were pooled, dialysed and lyophilised.

System B: Apparent molecular mass of the fucoidan fraction (AF3) was determined by size exclusion chromatography on Sephacryl S-200 column (2.6 × 90 cm, Amersham Biosciences AB) using standard dextrans (M_w range 1000–5,00,000 Da), as described previously (Adhikari et al., 2006).

2.2. General methods

Chemicals used were analytical grade or best available. All experiments were conducted at least in duplicate, the mean and standard deviation was directly calculated from the functions present in excel program. Evaporations were performed under diminished pressure at ~45 °C (bath) and small volume of aqueous solutions was lyophilised. Dialysis against distilled water was performed with continuous stirring, toluene being added to inhibit microbial growth. Moisture was determined by drying ground material in an air-circulated oven at 110 °C for 3 h. Gas liquid chromatography (GLC) was carried out on a Shimadzu GC-17A (Shimadzu, Kyoto, Japan) gas chromatograph equipped with FID, and nitrogen was used as a carrier gas. Gas liquid chromatography–mass spectrometry (GLC–MS) analysis was carried out on a Shimadzu QP 5050 A, Shimadzu, and the ionisation potential was 70 eV.

2.3. Sugar analysis

Total sugars and uronic acids were determined by the phenol–sulphuric acid (Dubois et al., 1956) and *m*-hydroxydiphenyl (Ahmed & Labavitch, 1977) assay, respectively. All fractions were hydrolysed with 2 M trifluoro acetic acid (2 h, 100 °C) for measurement of individual neutral sugar. Sugars were reduced, acetylated and analysed as their alditol acetate by GLC (Blakeney, Harris, Henry, & Bruce, 1983) on columns of 3% SP-2340 on Supelcoport 100–120 mesh, and DB-225 (JW) and by GLC-MS. Myo-inositol was used as an internal standard. Sugars in the acid hydrolysate were also analysed by thin layer chromatography as described elsewhere (Adhikari et al., 2006). DAP was hydrolysed with 2 M trifluoro acetic acid (2 h at 100 °C) for soluble substances. For insoluble residues, this hydrolysis was followed by a treatment of the residue with 72% (w/w) H_2SO_4 for 1 h at room temperature and then with 1 M H_2SO_4 for 2 h at 100 °C. Alternatively, trimethylsilyl (TMS) derivatives of methyl glycosides were analysed by gas chromatography.

2.4. Sulphate estimation and desulphation

Estimation of sulphate by modified barium chloride method and FT-IR spectroscopy and solvolytic desulphation were carried out as described (Mandal et al., 2007).

2.4.1. Methylation analysis

The laminaran fraction (C1F2), the fucoidan (AF3) and its desulphated (AF3-D) derivatives (~2 mg of each) were subjected to two rounds of methylation (Blakeney & Stone, 1985). The methylated polysaccharides were hydrolysed, and the liberated glycoses converted into their partially methylated alditol acetates and analysed by GLC and GLC/MS.

2.4.2. Fourier transform infra red spectroscopy (FT-IR)

Recording of IR spectra were carried out as described previously (Adhikari et al., 2006).

2.4.3. Nuclear magnetic resonance spectroscopy (NMR)

The ^1H NMR spectra were recorded on a Bruker 500 spectrometer (Bruker Biospin AG, Fallanden, Switzerland) operating at 500 MHz, respectively, for ^1H.

The samples (~10 mg of each) was heated (at 80 °C for 30 min) with water (1 ml), centrifuged and the resulting supernatant lyophilised. The freeze-dried sample was deuterium-exchanged by lyophilisation with D_2O and then examined in 99.9% D_2O.

2.4.4. Ferric ion reducing/antioxidant power (FRAP) assay

The FRAP assay was conducted according to Benzie and Strain (1996) as modified by Pulido, Bravo, and Saura-Calixto (2000).

Briefly, the oxidant was prepared by mixing 2.5 ml of a 10 mM TPTZ [2,4,6-tri(2-pyridyl-5-triazine) Fluka Chemicals, Madrid, Spain] solution in 40 mM HCl with 25 ml of 0.3 M acetate buffer (pH 3.6) and 2.5 ml of 20 mM $FeCl_3 \cdot 6H_2O$. The final solution has Fe(III) of 1.67 mM and TPTZ of 0.83 mM. To measure FRAP value, 900 μl of freshly prepared FRAP reagent was warmed to 37 °C and a reagent blank reading was taken at 593 nm; then 30 μl of test sample and 90 μl of distilled water were added. Absorbance readings were taken after 0.5 s and every 15 s until 30 min using a Shimadzu UV-1601 (PC) Spectrophotometer. The change of absorbance ($\Delta A = A_{30\ min} - A_{0\ min}$) was calculated and related to ΔA of an Fe(II) standard solution. Aqueous solutions of known Fe(II) concentrations (100–2000 μM $FeSO_4 \cdot 7H_2O$) were used for calibration.

2.4.5. Scavenging capability for 1,1-diphenyl-2-picrylhydrazyl (DPPH) radicals

The method reported by Shimada, Fujikawa, Yahara, and Nakamura (1992) was adopted for measurement of free radical scavenging capability. To each 4 ml of sample solution, 1 ml of freshly prepared methanolic DMSO solution of DPPH (0.5 mM) was added, mixed well and then let stand for 30 min at room temperature in the dark. The absorbance of the resulting was recorded at 517 nm. Butylated hydroxyanisole (BHA) was used as reference compound. The capability to scavenge the DPPH radical was calculated using the following equation:

$$\text{Scavenging effect}\ (\%) = \left[1 - \frac{\text{absorbance of sample at 517 nm}}{\text{absorbance of control at 517 nm}}\right] \times 100$$

3. Results and discussion

3.1. General

The central goal of this study was to determine the classes of polysaccharides present in brown alga *T. conoides*. For this sugar composition of depigmented algal powder (DAP) was determined. It contained 35% 2 M TFA hydrolysable sugars of which about seventh were uronic acids. The main neutral sugar was fucose and it also contained other sugar including glucose, galactose and xylose (Table 1). The sequential extraction procedure as shown in Fig. 1 was based on the different solubility, molecular mass and charge distribution of polysaccharides from brown seaweeds. Laminarans are soluble in warm waters and therefore extracted at 80 °C. Fucans were extracted with diluted hydrochloric acid, whereas alginates were extracted with sodium carbonate. Alginates form insoluble precipitates with bivalent calcium and at acid pH, and are stable in solution between pH 6 and 9.

Table 1
Yields and chemical composition of fractions obtained from the marine brown alga *Turbinaria conoides*.

	DAP[d]	A[d]	AF3[d]	AF3D[d]	B[d]	C1[d]	C1F2[d]
Yield[a]	100	8.8	nd	nd	22.6	6.2	nd
Sulfate[b]	nd	3	4	tr	1	2	tr
TS[b]	35	36	37	56	46	41	58
Protein[b]	nd	1.3	nd	nd	2.4	2.1	nd
Fuc[c]	56	57	54	52	tr	59	6
Xyl[c]	11	15	18	19	tr	12	5
Man	7	tr	tr	–	tr	tr	tr
Gal[c]	15	23	28	29	tr	18	–
Glc[c]	12	5	–	–	–	11	89

nd, not determined; tr, trace. –, not detected; TS, total sugar.
[a] Percent weights of depigmented algal powder (DAP) dry weight.
[b] Percent weights of the fraction.
[c] Mole% of anhydro sugar.
[d] For a description of fractions obtained see Section 2.

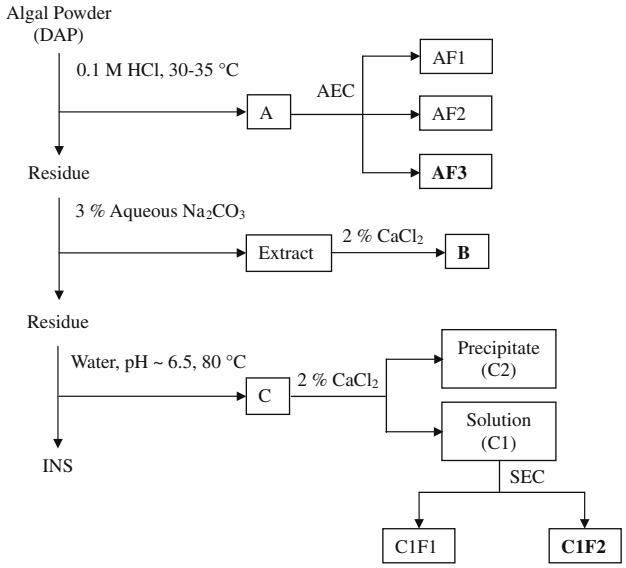

Fig. 1. Scheme for the extraction and purification of polysaccharides from the marine brown alga *Turbinaria conoides*.

3.2. Chemical characterisation of the fucoidan from Turbinaria conoides

3.2.1. General

Sugar compositional analysis revealed that fraction A consist mainly of fucose as the major neutral sugar together with smaller amount of galactose and xylose units (Table 1). The uronide content of this fraction was 6% and it also contained sulphate groups.

Anion exchange chromatography on a DEAE-Sepharose column separated fraction C into three components (AF1, AF2 and AF3). AF1, which accounted for 11% of the total polymers recovered from the anion exchanger, was the minor component of A fraction. It consisted mostly of fucose together with smaller amount of galactose, xylose and glucose residues (Table 1). The second fraction AF2, eluted at the beginning of the salt gradient, is the second largest fraction. AF3 was the major fraction, amounting to 51% of the total polymers recovered from the column. Sugar compositional analyses revealed that AF3 consists mainly of fucose together with smaller amount of galactose and xylose units (Table 1). Thin layer chromatographic analysis of the monosaccharides present in the hydrolysate indicates the presence of an uronic acid with an R_f value similar to that of glucuronic acid. GLC analysis of the TMS derivatives of the derived methyl glycosides confirmed this result. The presence of glucuronic acid has already been reported in fucoidan from brown seaweeds (Adhikari et al., 2006; Mandal et al., 2007). Therefore, AF3 is essentially a fucoidan that might contain a high number of sulphate groups, as indicated by its late elution. Indeed, the high charge density of this polysaccharide was confirmed by its sulphate content (4%, w/w). The FT-IR spectrum (Supplementary Fig. 1) of AF3 showed an absorption band at 1252 cm^{-1} related to a >S=O stretching vibration of the sulphate group. An additional sulphate absorption band at 848 cm^{-1} (C–O–S, secondary axial sulphate) indicated that the sulphate group is located at position 4 of the fucopyranosyl residue (Patankar, Oehninger, Barnett, Williams & Clark, 1993). Solvolytic desulphation of the purified (AF3) fucoidan (as pyridinium salt) produces a desulphated derivative (AF3D). Preliminary experiments (data not shown) showed a higher recovery with this method compared to methanol–HCl and

auto-desulphation methods. In the IR spectrum of desulphated derivative (AF3D) absorbances at 1252 cm^{-1} and 848 cm^{-1} become weak, demonstrating that they were associated with sulphate groups. This purified fucoidan had negative specific rotation $[\alpha]_D^{33}$ − 109° (*c* 0.2, H_2O), revealing that fucose in AF3 belongs to the L-series, like other fucoidan from brown seaweeds (Adhikari et al., 2006; Kariya et al., 2004; Mandal et al., 2007).

3.2.2. Molecular mass

AF3 was subjected to further chemical analysis. First, the apparent molecular mass was determined by size exclusion chromatography. The elution profile of this macromolecule on Sephacryl S-200 suggests that this polymer is homogeneous (Supplementary Fig. 2). Based on calibration with standard dextrans, the apparent molecular mass of AF3 would be 50 kDa.

3.2.3. Glycosidic linkages

Table 2 shows that the desulphated fucoidan yielded partially methylated alditol acetates corresponding to (1 → 2)-Xyl_p (xylopyranose), (1 → 3)-linked Fuc_p, and (1 → 3)- and (1 → 2,3)-linked Gal_p residues, consistent with the presence of fucoidan. The presence of large quantities of T-Xyl_p (terminal xylopyranose) and T-Fuc_p residues suggest that this polymer is highly branched with 29 terminals for every 71 residues in the main chain. Interestingly, 33–34% of the total fucose residues are terminal, 27–28% are (1 → 3)-linked, 21–22% are branched points (Table 2). Small amount of (1 → 4)- and (1 → 2)-linked Fuc_p residues were also present. So far, fucose residues in algal fucoidans are either (1 → 3)- or (1 → 3)- and (1 → 4)-linked (Cumashi et al., 2007; Pomin & Mourão, 2008). Linkage analysis of the native fucan sulphate AF3 yielded a variety of monomethylated, dimethylated and trimethylated products (Table 2) indicating that the structure of this polymer is highly complex. The amount of sulphate groups in the native polysaccharide as calculated from methylation was not in good agreement with the experimentally determined sulphate. But, methylation of sulphated polysaccharides does not always yield reliable proportions of methylated alditol acetates (Adhikari et al., 2006; Pereira, Mulloy, & Mourao, 1999;). 2-*O*-methyl fucitol, and unmethylated fucitol were amongst the abundant products of methylation analysis of the native polymer. The increase in the proportions of 2,4-di-*O*-methyl fucitol after desulphation, as a consequence of decreased proportions of 2-*O*-methyl fucitol residues, suggests that sulphate groups, when present, are located at position 4 of the (1 → 3)-linked fucosyl residues. This result also confirms the prediction made by IR analysis regarding the position of sulphate group.

Table 2
Partially methylated alditol acetates derived from the fucoidan (AF3) of *Turbinaria conoides* and its desulphated derivative (AF3D).

Methylation products[a]	Deduced linkage	Peak area[b]	
		AF3	AF3D
2,3,4-Xyl	Xyl_p(1 →	11	12
3,4-Xyl	→ 2)Xyl_p(1 →	7	9
2,3,4-Fuc	Fuc_p(1 →	8	17
2,4-Fuc	→ 3)Fuc_p(1 →	3	14
2,3-Fuc	→ 4)Fuc(1 →	3	3
3,4-Fuc	→ 2)Fuc_p(1 →	5	6
2-Fuc	→ 3,4)Fuc(1 →	17	5
3-Fuc	→ 2,4)Fuc_p(1 →	2	6
Fuc	→ 2,3,4)Fuc_p(1 →	16	-
3,4,6-Gal	→ 2)Gal_p(1 →	6	7
2,4,6-Gal	→ 3)Gal_p(1 →	10	10
4,6-Gal	→ 2,3)Gal_p(1 →	6	6
2-Gal	→ 3,4,6)Gal(1 →	6	5

–, not detected.
[a] 2,3,4-Xyl denotes 1,5-di-*O*-acetyl-2,3,4-tri-*O*-methylxylitol, etc.
[b] Percentage of total area of the identified peaks.

3.2.4. NMR spectroscopy

We employed ^1H NMR spectroscopy to determine the anomeric configuration and the sulphation pattern of the fucoidan AF3. The native polysaccharide has a very complex ^1H NMR spectrum (Fig. 2). A number of separate spin systems ranging from 5.02 to 5.43 ppm attributable to anomeric protons of α-fucose residues were distinguishable in the spectrum of the pure fucoidan (Kariya et al., 2004; Mandal et al., 2007; Mourao et al., 1996). The appearance of large number of anomeric signals suggest that the environment of the fucose residues are different and this may arise from varied sulphation pattern, different glycosidic linkage positions and/or diverse sequence of monosaccharide residues. This spectrum also included resonances characteristic of fucoidan, such as signals from ring protons (H-2 to H-5) between 3.34 and 4.34 ppm, and intense signals from the methyl protons H-6 at ~1.02–1.28 ppm. This later envelope of signals confirms the presence of different types of fucosyl residues. The signals between 4.45 and 4.90 ppm were attributed to anomeric protons of β-linked sugars. The high proportion of xylose and galactose residues must be responsible for these signals in the spectrum, but was not possible to assign any particular signals to these residues. Therefore, it is apparent that the NMR spectrum of this polysaccharide is complex as observed for fucoidan from other marine brown algae (Adhikari et al., 2006; Mandal et al., 2007; Mourao et al., 1996; Pereira et al., 1999).

3.3. Structural features of the laminaran and alginic acid rich fractions from Turbinaria

Laminarans are soluble, but their water solubility depends on the branching level: the higher the branching degree, the higher the solubility. The less branched laminarans are soluble only in warm water (60–80 °C). The alginic acid (C2) present in the hot water extract (C) was removed by taking advantage of the insolubility of Ca-alginate in water. The molecular mass of laminarans is small (5–

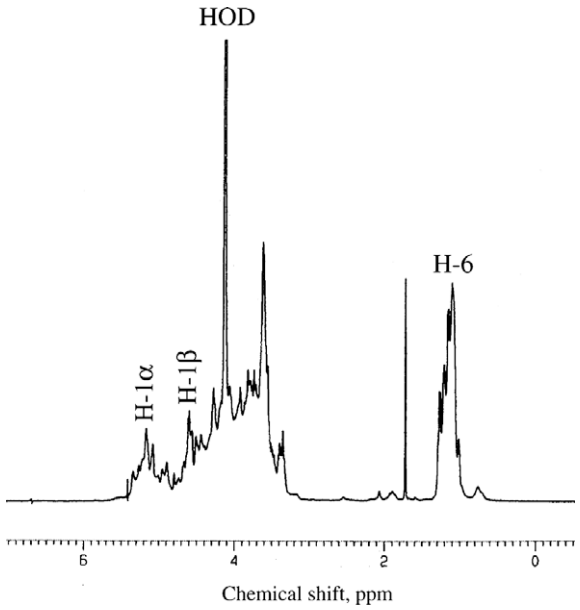

Fig. 2. ^1H NMR spectrum at 500 MHz of the fucoidan (AF3) of *Turbinaria conoides*. The spectrum was recorded at 80 °C for sample in D_2O solution. H-1α, H-1β and H-6 refer to anomeric signals of α-linked fucose, β-linked sugars and methyl protons of fucose residues, respectively. The signal for the residual water was designated as HOD.

10 kDa). Therefore, attempts have been made to separate them from fucoidan fraction by size exclusion chromatography. Indeed, SEC on Superdex-30 separates C1 into two fractions C1F1 and C1F2 (Supplementary Fig. 3). The minor fraction, C1F2, which accounted for 35% of the total sugar recovered from the column consisted of mainly glucose as neutral sugar. Based on calibration with standard dextrans, the apparent molecular weight of this glucan would be 5 kDa. This glucan containing fraction (C1F2) does not produce blue colouration with iodine. Moreover ^{1}H NMR spectrum of this polymer clearly shows the presence of only one anomeric signal at 4.827 ppm indicative of β-configuration. Finally, methylation analysis of this glucan revealed the presence of 1,3,5-tri-*O*-acetyl-2,4,6-tri-*O*-methylglucitol (98%) and 1,5-di-*O*-acetyl-2,3,4,6-tera-*O*-methylglucitol (2%) residues. On the basis of the glycosidic linkage and ^{1}H NMR analysis it may be concluded that the glucan of *T. conoides* is a linear polysaccharide and contained β-(1 → 3)-linked glucopyranosyl residues.

Sodium alginates form insoluble precipitates at acid pH and with calcium salts, but they are stable in solution between pH 6 and 9. Therefore, these macromolecules were extracted with Na_2CO_3. The fractional product (B) was analysed using FT-IR and ^{1}H NMR spectroscopy. The FT-IR spectrum of this fraction contains band at 3400 (OH stretching), 2925 (CH stretching), 1675 and 1420 (COO stretching) cm^{-1} characteristic of alginate. Moreover two bands at approximately 1100 and 1025 cm^{-1} responsible for mannuronic (M) and guluronic (G) units, respectively, were also observed (Supplementary Fig. 4).

To evaluate the content of G, M and G–G linkage, we have investigated the ^{1}H NMR spectrum (Fig. 3) of sodium alginate using procedures as described previously (Grasdalen, 1983; Matsushima et al., 2005). The relative areas of anomeric protons G-1 (H-1 of G) and M-1 (H-1 of M) correspond to the mole fractions of G and M, respectively. The peak areas of G-5 (H-5 resonances of G) give the distribution of G in G-block and GM-block, and the algebraic sum of their intensities accounts for the total G content, i.e., the relative area of G-5 is equal to that of G-1. From the measurement

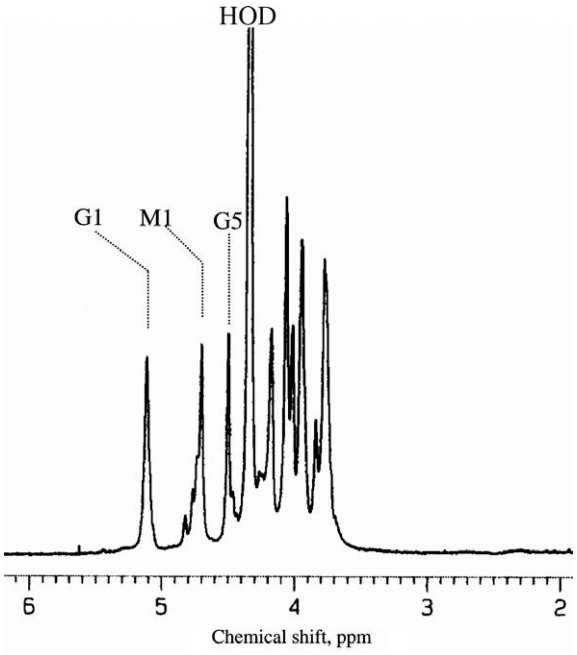

Fig. 3. ^{1}H NMR spectrum at 500 MHz of the alginic acid containing fraction (B) isolated from the brown seaweed *Tubinaria conoides*. G1 and M1 are the anomeric signals of guluronic acid and mannuronic acid, respectively, and G5 is the signals of the H-5 proton of guluronic acid residue. The spectrum was recorded at 80 °C for sample in D_2O solution. The signal for the residual water was designated as HOD.

of peak areas of A (δ_H 5.13 (G-1)), B (δ_H 4.72–4.84 (G-5 in GM-block and M-1)) and C (δ_H 4.45–4.52 (G-5 in G-block)), the guluronic acid content (G%) and G–G diad frequency (GG%) were calculated using Eqs. (1) and (2), and the calculated values are 46.19 and 42.12, respectively

$$G\%(\%) = \frac{\text{area of } A}{(\text{area of } B) + (\text{area of } C)} \times 100 \quad (1)$$

$$GG\%(\%) = \frac{\text{area of } C}{(\text{area of } B) + (\text{area of } C)} \times 100 \quad (2)$$

3.4. Antioxidant activity of polysaccharides

3.4.1. Frap assay

In recent years many different methods are being used to evaluate antioxidant capacity of foods and biological samples (Huang, Ou, & Prior, 2005). In some of these protocols, antioxidant assays were performed in alcoholic solutions, but in this condition polysaccharide would precipitate. Therefore, the antioxidant capacity of sulphated polysaccharides (AF3, B and C1F2) from *Turbanaria* was determined by the FRAP assay. This assay in which a ferric salt $Fe(III)(TPTZ)_2Cl_3$ (TPTZ = 2,4,6-tripyridyl-s-triazine) is used as oxidant (Benzie & Strain, 1996) takes advantage of electron transfer reactions (Huang et al., 2005). FRAP values increased considerably from 4 to 30 min, as it has been described for other vegetable and seaweed samples (Ruperez et al., 2002).

Regarding antioxidant capacity of the polysaccharides of present study it is clear that the fucoidan (AF3) showed the highest reducing power at 4 and 30 min (165 and 190 mol Fe(II) per g sample dry weight, respectively). This is followed by alginic acid and laminaran (Table 3). Results are expressed as mol Fe(II) per g sample dry weight. For comparison of potencies, values are also calculated as mol Trolox/g sample dry weight from regression equations as described by Pulido et al. (2000) of Trolox at 4 and 30 min of reaction with the FRAP reagent.

3.4.2. Scavenging effect on1,1-diphenyl-2-picrylhydrazyl (DPPH) radicals

For further insight into the activation mechanism, we examined whether the protective effect was associated with DPPH radicals. The proton radical scavenging action is known to be one of the various mechanisms for antioxidation. DPPH is one of the compounds that possess a proton free radical and shows a characteristic absorption at 517 nm (purple) (Matsukawa et al., 1997). When DPPH encounters proton radical scavengers, its purple colour would fade rapidly (Yamaguchi, Takamura, Matoba, & Terao, 1998). An excellent scavenging capability on DPPH radicals at a dosage of 1 mg/ml (61%) was found with the fucoidan fraction AF3 as compared with the control BHA (100%) regarding the low dosage ranges used (Fig. 4). More significant and effective radical scavenging capability (90%) was also found with the fraction AF3 at a higher dosage (5 mg/ml). Comparable results with the fraction

Table 3
Ferric ion reducing ability[a] of polysaccharide containing fractions from *Turbinaria conoides*.

	4 min		30 min	
	μmol Trolox/g	μmol Fe(II)/g	μmol Fe(II)/g	μmol Trolox/g
AF3[b]	165	79	190	96
B[b]	92	53	137	85
C1F2[b]	72	38	82	43

[a] Results are expressed as equivalent of Fe(II) or Trolox per gram dry weight of fractions in aqueous solution. Each value, which is given to its nearest whole number, was the mean of two replicates.
[b] For a description of fractions obtained see Section 2.

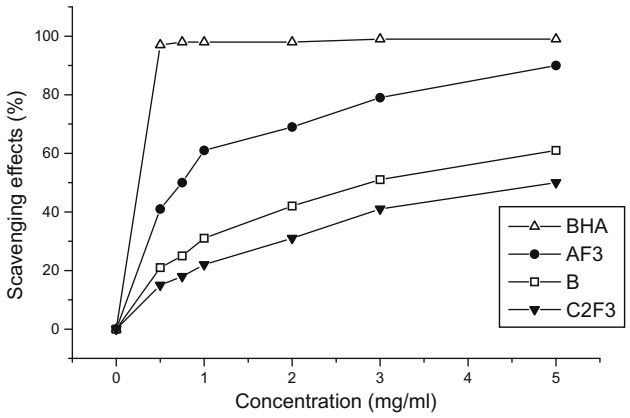

Fig. 4. Scavenging effect of polysaccharides isolated from the brown seaweed *Tubinaria conoides* on DPPH radicals. BHA: Butylated hydroxyanisole. AF3: The fucoidan rich fraction. B: The alginic acid containing fraction. C2F3: The laminaran rich fraction.

AF3 were found to be 62% at the dosages of 5.0 mg/ml for the alginate rich fraction B (Fig. 4). In contrast, the laminaran fraction C2F3 obtained from demonstrated least scavenging capability (50%) among three fractions at the concentration of 5.0 mg/ml. Moreover, the marked inhibitory effect of these polysaccharides on DPPH radicals was found to be concentration dependent (Fig. 4), though the activities were low. These results reveal that the polysaccharides of present study are potent scavenger and their antioxidative activity may be attributed to their proton-donating ability (Shimada et al., 1992). Probably, these fractions might contain a higher amount of reductone which could react with radicals to stabilise and terminate radical chain reaction. Whether the structures can be related to scavenging capacity for DPPH radicals remains to be determined in future studies. However, our preliminary results suggest that different bioactivities of these fractions apparently may be, in some respects, linked to their different molecular structures.

Most of earlier data on antioxidant of foods and biological samples were on phenolic compounds and many researchers have been reported positive correlation between free radical scavenging activity and total phenolic compound. But this correlation between structure and activity is not always valid. For example, selected enzymatic extracts of seaweeds (*Ecklonia cava* and *Sargassum coreanum*) did not possess antioxidant activity, although they contained as much phenolic compounds as the other extracts of *E. cava*. Feruloyl oligosaccharides showed a higher antioxidant capacity than free ferulic acid (Yuan, Wang, Yao, & Chen, 2005). Moreover, the former showed greater antioxidant capacity in vivo than in vitro when compared with vitamin C (Ou et al., 2007). Therefore, it is believed that other materials in seaweed extracts, such as small molecular weight polysaccharides, pigments, proteins or peptides, may influence the activity. Indeed, recent data showed that a number of polysaccharide containing fractions isolated from various sources such as medicinal mushrooms (Jiang et al., 2008; Shimada et al., 1992), higher plants (Aguirre, Isaacs, Matsuhiro, Mendoza, & Zúñiga, 2009), marine algae (Rocha de Souza et al., 2007; Ruperez et al., 2002; Wang, Zhang, Duan & Li, 2009; Wang et al., 2008) and even some enzymatic extracts (Je et al., 2009) possess antioxidant activity. Our results are in agreement with these studies. In addition, the polysaccharides used in this study were purified and, therefore, conclusively prove their antioxidant potency.

Literature data also shows that some polysaccharides have higher antioxidative potency than the others. For example, the antioxidant potential of sulphated polysaccharides from the brown seaweed *Fucus vesiculosus* was higher than that of agar-like sulphated galactans from the red seaweed Nori (Ruperez, 2001). In a more recent study this group (Ruperez et al., 2002) found that antioxidant potency of fucoidan containing fraction from the brown alga *Fucus vesiculosus* was higher than that of laminaran and alginic acid containing fractions. The laminaran (C1F2) and alginate (B) rich fractions of present study exhibited lower antioxidant potentials than the fucoidan containing fraction AF3 (Table 3). This result is in agreement with that of Ruperez et al. (2002) except that the antioxidant potency of the purified polysaccharides of present study is lower.

Although the antioxidant capacity of polysaccharide has been proven, the relationships between structure and antioxidative capacity have not yet been elucidated. This is primarily due to the interplay of two important factors. Firstly, the huge structural diversity of these polysaccharides has given a major hindrance in the structure–activity relationship establishment. However, on the basis of the accumulated data several common structural motifs emerge that are important for activity. Secondly, many of the hitherto used sulphated polysaccharides contained a number of other molecules. These later molecules may have their own activities, and or at least dilute the efficacy of the sulphated polymer itself. However, the polysaccharides described in this work are purified and therefore, conclusively proves their antioxidant activities.

4. Conclusions

In this study, we found that the soluble polysaccharides of *T. conoides* can be an excellent antioxidant. The fucoidan (40 kDa) exhibit more potency than the laminaran (5 kDa) and, therefore, this potency may be directly related with the molecular mass of these polysaccharides. These differences can as well be attributed to the differences in structure and perhaps to the actual availability of the functionality in each individual structure. The antioxidative activity of *Turbinaria* polysaccharides may be attributed to their proton-donating activity as evidenced through DPPH radical scavenging results.

Because the polysaccharides tested in this study was basically prepared without toxic chemical reagents, it can be assumed to be potentially useful as a safe antioxidant in food processing industries. Furthermore, as the isolation of these polysaccharides involves a few inexpensive and easy steps it will be of an added advantage.

Acknowledgements

This work was supported by Department of Science and Technology (SR/S1/OC-50/2007) to B.R. We thank Director, CSMCRI, Gujarat, India for his help for the collection and identification of the alga. Standard dextrans were gift from Dr. Tapani Vuorinen, Finland. T.G. thanks CSIR, New Delhi for a fellowship.

Appendix A. Supplementary data

Supplementary data associated with this article can be found, in the online version, at doi:10.1016/j.foodchem.2009.05.069.

References

Adhikari, U., Mateu, C. G., Chattopadhyay, K., Pujol, C. A., Damonte, E. B., & Ray, B. (2006). Structure and antiviral activity of sulphated fucans from *Stoechospermum marginatum*. *Phytochemistry, 67*, 2474–2482.

Aguirre, M. J., Isaacs, M., Matsuhiro, B., Mendoza, L., & Zúñiga, E. A. (2009). Characterization of a neutral polysaccharide with antioxidant capacity from red wine. *Carbohydrate Research*. doi: 10.1016/j.carres.2009.03.024.

Ahmed, A., & Labavitch, J. M. (1977). A simplified method for accurate determination of cell wall uronide content. *Journal of Food Biochemistry, 1*, 361–365.

Benzie, I. F. F., & Strain, J. J. (1996). The ferric reducing ability of plasma (FRAP) as a measure of "antioxidant power": The FRAP assay. *Analytical Biochemistry, 239*, 70–76.

Blakeney, A. B., Harris, P., Henry, R. J., & Bruce, A. B. (1983). A simple rapid preparation of alditol acetates for monosaccharide analysis. *Carbohydrate Research, 113*, 291–299.

Blakeney, A. B., & Stone, B. A. (1985). Methylation of carbohydrates with lithium methylsulphinyl carbanion. *Carbohydrate Research, 140*, 319–324.

Cumashi, A., Ushakova, N. A., Preobrazhenskaya, M. E., D'Incecco, A., Piccoli, A., Licia, T., et al. (2007). A comparative study of the anti-inflammatory, anti-coagulant, anti-angiogenic and anti-adhesive activities of nine different fucoidans from brown seaweeds. *Glycobiology, 17*, 541–552.

Dubois, M., Gilles, K. A., Hamilton, J. K., Rebers, P. A., & Smith, F. (1956). Colorimetric method for determination of sugars and related substances. *Analytical Chemistry, 28*, 350–366.

Ghosh, T., Chattopadhyay, K., Marschall, M., Karmakar, P., Mandal, P., & Ray, B. (2009). Focus on antivirally active sulphated polysaccharides: From structure-activity analysis to clinical evaluation. *Glycobiology, 19*, 2–15.

Grasdalen, H. (1983). High-field ^{1}H NMR spectroscopy of alginate: Sequential structure and linkage conformations. *Carbohydrate Research, 118*, 255–260.

Halliwell, B., & Gutteridge, J. M. C. (1984). Oxygen toxicity, oxygen radicals, transition metals and disease. *Biochemical Journal, 219*, 1–4.

Huang, D., Ou, B., & Prior, R. L. (2005). The Chemistry behind antioxidant capacity assays. *Journal of Agricultural and Food Chemistry, 53*, 1841–1856.

Je, J.-Y., Park, P.-J., Kim, E.-K., Park, J.-S., Yoon, H.-D., Kim, K.-R., et al. (2009). Antioxidant activity of enzymatic extracts from the brown seaweed *Undaria pinnatifida* by electron spin resonance spectroscopy. *LWT – Food Science and Technology, 42*, 874–878.

Jiang, Y.-H., Jiang, X.-L., Wang, P., Mou, H.-L., Hu, X.-K., & Liu, S.-Q. (2008). The antitumor and antioxidative activities of polysaccharides isolated from *Isaria farinosa* B05. *Microbiological Research, 163*, 424–430.

Kariya, Y., Mulloy, B., Imai, K., Tominaga, A., Kaneko, T., Asari, A., et al. (2004). Isolation and partial characterization of fucan sulphates from the body wall of sea cucumber *Stichopus japonicus* and their ability to inhibit osteoclastogenesis. *Carbohydrate Research, 339*, 1339–1346.

Mandal, P., Mateu, C. G., Chattopadhyay, K., Pujol, C. A., Damonte, E. B., & Ray, B. (2007). Structural features and antiviral activity of sulphated fucans from the brown seaweed *Cystoseira indica*. *Antiviral Chemistry and Chemotherapy, 18*, 153–162.

Matsukawa, R., Dubinsky, Z., Kishimoto, E., Masaki, K., Masuda, Y., & Takeuchi, T. (1997). A comparison of screening methods for antioxidant activity in seaweeds. *Journal of Applied Phycology, 9*, 29–35.

Matsushima, H., Minoshima, H., Kawanami, H., Ikushima, Y., Nishizawa, M., Kawamukai, A., et al. (2005). Decomposition reaction of alginic acid using subcritical and supercritical water. *Industrial and Engineering Chemistry Research, 44*, 9626–9630.

Mayer, A. M. S., & Lehmann, V. K. B. (2000). Marine pharmacology in 1998: Marine compounds with antibacterial, anticoagulant, antifungal, anti-inflammatory, anthelmintic, antiplatelet, antiprotozoal and antiviral activities; with actions on the cardiovascular, endocrine, immune and nervous systems: And other miscellaneous mechanisms of action. *Pharmacologist, 42*, 62–69.

Mourao, P. A. S., Pereira, M. S., Pavao, M. S. G., Mulloy, B., Tollefsen, D. M., Mowinckel, M. C., et al. (1996). Structure and anticoagulant activity of a fucosylated chondroitin sulphate from Echinoderm. *Journal of Biological Chemistry, 271*, 23973–23984.

Ou, S.-Y., Jackson, G. M., Jiao, X., Chen, J., Wu, J.-Z., & Huang, X.-S. (2007). Protection against oxidative stress in diabetic rats by wheat bran feruloyl oligosaccharides. *Journal of Agricultural and Food Chemistry, 55*, 3191–3195.

Patankar, M. S., Oehninger, S., Barnett, T., Williams, R. L., & Clark, G. F. (1993). A revised structure for sulphated fucan may explain some of its biological activities. *Journal of Biological Chemistry, 268*, 21770–21776.

Pereira, M. S., Mulloy, B., & Mourao, P. A. S. (1999). Structure and anticoagulant activity of sulphated fucans. *Journal of Biological Chemistry, 274*, 7656–7667.

Pomin, V. H., & Mourão, P. A. S. (2008). Structure, biology, evolution and medical importance of sulphated fucans and galactans. *Glycobiology, 18*, 1016–1027.

Pulido, R., Bravo, L., & Saura-Calixto, F. (2000). Antioxidant activity of dietary polyphenols as determined by a modified ferric reducing/antioxidant power assay. *Journal of Agricultural and Food Chemistry, 48*, 3396–3402.

Renn, D. W. (1997). Biotechnology and the red seaweed polysaccharide industry: Status, needs and prospects. *TIBTECH, 15*, 9–14.

Rocha de Souza, M. C., Marques, C. T., Dore, C. M. G., Ferreira da Silva, F. R., Rocha, H. A. O., & Leite, E. L. (2007). Antioxidant activities of sulphated polysaccharides from brown and red seaweeds. *Journal of Applied Phycology, 19*, 153–160.

Ruperez, P. (2001). Antioxidant activity of sulphated polysaccharides from the Spanish marine seaweed Nori. In *Proceedings of the COST 916 European conference on bioactive compounds in plant foods* (p. 114). Tenerife, Canary Islands, Spain: Health Effects and Perspectives for the Food Industry.

Ruperez, P., Ahrazem, O., & Leal, A. (2002). Potential antioxidant capacity of sulphated polysaccharides from the edible marine brown seaweed *Fucus vesiculosus*. *Journal of Agricultural and Food Chemistry, 50*, 840–845.

Shimada, K., Fujikawa, K., Yahara, K., & Nakamura, T. (1992). Antioxidative properties of xanthan on the autoxidation of soybean oil in cyclodextrin emulsion. *Journal of Agricultural and Food Chemistry, 40*, 945–948.

Wang, B.-G., Zhang, W.-W., Duan, X.-J., & Li, X.-M. (2009). In vitro antioxidative activities of extract and semi-purified fractions of the marine red alga, *Rhodomela confervoides* (Rhodomelaceae). *Food Chemistry, 113*, 1101–1105.

Wang, J., Zhang, Q., Zhang, Z., & Li, Z. (2008). Antioxidant activity of sulphated polysaccharide fractions extracted from *Laminaria japonica*. *International Journal of Biological Macromolecules, 42*, 127–132.

Yamaguchi, T., Takamura, H., Matoba, T., & Terao, J. (1998). HPLC method for evaluation of the free radical scavenging activity of foods by using 1, 1,-diphenyl-2-picrylhydrazyl. *Bioscience Biotechnology and Biochemistry, 62*, 1201–1204.

Yuan, X. P., Wang, J., Yao, H. Y., & Chen, F. (2005). Free radical scavenging capacity and inhibitory activity on rat erythrocyte hemolysis of feruloyl oligosaccharides from wheat bran insoluble dietary fiber. *LWT – Food Science and Technology, 38*, 877–883.

emulsions, their ability to inhibit lipid oxidation could increase (Heins, McPhail, Sokolowski, Stockmann, & Schwarz, 2007).

Most free radical scavenging antioxidants in food systems contain active hydroxyl groups that can donate hydrogen to lipid radicals. These hydroxyl groups are most commonly associated with phenolic compounds. Many phenolic compounds are surface active (e.g., accumulate at water–lipid interfaces) since they contain both oxygen and hydrocarbon ring structures (Chaiyasit, Elias, McClements, & Decker, 2007). Unfortunately, phenolic compounds are not strongly surface active and sometimes contain other functional groups such as carboxylic acids that can make them very water soluble. If phenolic acids could be made more surface active by esterifying them with hydrocarbon chains, this would potentially increase their concentration at water–lipid interfaces in oil-in-water emulsions where they could potentially be more effective at inhibiting lipid oxidation.

Previous work in our lab looked at the ability of free or esterified (butyl or dodecyl groups) *p*-hydroxyphenylacetic acid (HPA) to inhibit lipid oxidation in oil-in-water emulsions (Yuji et al., 2007). Unexpectedly, free HPA was a more effective antioxidant than its more surface active butyl and dodecyl conjugates in menhaden oil-in-water emulsions as determined by both lipid hydroperoxides and thiobarbituric acid reactive substances. One potential reason for this discrepancy could be that the esterification of the butyl and dodecyl groups onto HPA resulted in compounds with different free radical scavenging activity.

The objective of this work was to determine if the esterification of chlorogenic acid (CGA) to hydrocarbon chains would improve its ability to inhibit lipid oxidation in oil-in-water emulsions. Chlorogenic acid, a commonly occurring polyphenol found in plants, is widely recognised to be an active free radical scavenger (Clifford, 1999). Since esterification of hydrocarbons onto phenolic acids can alter their antioxidant activity, the free CGA and CGA esters (C_4, C_8, or C_{12}) were added to oil-in-water emulsions at equal free radical scavenging activities.

2. Materials and methods

2.1. Materials

Menhaden oil was donated by Omega Protein (Houston, TX). 2,2-Azobis (2-methylpropionamidine) dihydrochloride (AAPH), fluorescein, hexadecane, and ethylenediaminetetraacetic acid (EDTA) were obtained from Sigma–Aldrich (St. Louis, MO). Brij 35 was purchased from Acros Organics (Morris Plains, NJ). All other chemicals were reagent grade or purer and were obtained from Fisher Scientific (Pittsburgh, PA). Double distilled water was used throughout the experiments.

2.2. Methods

2.2.1. Enzymatic synthesis of chlorogenic acid conjugates

The chemo-enzymatic synthesis of chlorogenate fatty esters was carried out from methyl chlorogenate following the procedure described by Lopez Giraldo et al. (2007). Typically, methyl chlorogenate (5 mmol) was added to 375 ml of desired fatty alcohol and the mixtures were then placed in sealed flasks, and stirred on an orbital shaker (250 rpm, 55 °C) until complete dissolution of methyl chlorogenate. *Candida antarctica* B lipase 5% w/w (calculated from the total weight of both substrates) was added to start the reaction. The mixture then stirred at 55 °C for 96 h under a nitrogen flow. The final lipophilised esters were then purified using a two step liquid–liquid extraction procedure as described by Lopez Giraldo et al. (2007). All recovered esters were characterised by mass spectrometry.

2.2.2. Preparation of emulsion

Oil-in-water emulsions were prepared by mixing menhaden oil with an emulsifier solution (17 mM Brij 35 in 10 mM phosphate buffer, pH 7.0) to achieve a final lipid concentration of 20% (w/w) lipid. A coarse emulsion was produced first by homogenising at high speed for 2 min with a Bio-homogenizer (Tekmar Company, Cincinnati, OH). Emulsion droplet size was then further reduced with an ultrasonicator (Fisher Sonic Dismembrator 500, Pittsburgh, PA) at 4 °C for 3 min at 70% power and 0.5 s duty cycles. A laser light scattering instrument (Mastersizer, Malvern Instruments, Ltd., Worcestershire, UK) was used to measure the particle size distribution. The mean particle size of the emulsion was reported as the volume–surface mean diameter (d_{32}). The mean particle diameter in all emulsions ranged from 0.35 to 0.45 μm and did not change during the storage studies.

2.2.3. Removal of continuous phase surfactant

Excess Brij 35 in the continuous phase of the emulsion was removed because surfactants not absorbed to the emulsion droplets have been shown to form micelles and change the physical location of antioxidants (Richards, Chaiyasit, McClements, & Decker, 2002). To remove excess Brij 35, emulsions were divided into centrifuge tubes (Sorvall 75 ml, Asheville, NC) and centrifuged at 30,000 rpm at 4 °C for 40 min. After centrifugation, the aqueous phase (lower layer) was removed with a syringe and discarded and fresh buffer was added. The emulsion was redispersed by vortexing for 5 min. This procedure of centrifugation, removal of continuous phase and reconstitution of emulsion droplets was repeated a total of three times (Elias, McClements, & Decker, 2007). Following the final wash, the total lipid content of the creamed emulsion (1.0 g) was determined gravimetrically after extracting the lipid using a modified method of Folch, Lees, and Stanley (1957). After determination of lipid content of the creamed emulsion, the creamed layer was diluted into fresh 10 mM phosphate buffer (pH 7.0) to a final lipid concentration of 2% (w/w). Antioxidants dissolved in 10 mM phosphate buffer (pH 7.0) were then added to the emulsion at final antioxidant concentrations ranging from 47 to 120 μM.

2.2.4. Measurement of antioxidants concentration in continuous phase of the oil-in-water emulsions

To determine the concentration of antioxidants in the continuous phase, fresh menhaden oil-in-water emulsions containing 50 μM of antioxidants were put into centrifuge tubes (Sorvall 9.8 ml, Asheville, NC) and centrifuged at 30,000 rpm at 4 °C for 40 min. After centrifugation, the aqueous phase (lower layer) was withdrawn with a syringe and filtered through a 0.22 μm syringe filter (Millex-GS, Bedford, MA). The concentration of each antioxidant in the continuous phase was measured at 285 nm using a UV–VIS scanning spectrophotometer (UV-2010PC, Shimazu, Kyoto, Japan). The concentration of the antioxidants was determined using a standard curve prepared with each antioxidant over the concentration range of 1–50.0 μM. Limit of detection was 0.5 μM.

2.2.5. Interfacial tensiometry

The surface activity of antioxidants was determined by interfacial tensiometry using a drop shape analyzer (DSA 10; Kruss USA, Charlotte, NC). Antioxidants were dissolved in hexadecane at 0–500 μM. Hexadecane was used as a non-oxidisable lipid to prevent oxidation of the antioxidants during analysis. The mixture was loaded in a syringe and ejected to form a droplet at the inverted tip of a hypodermic needle that was submerged in double distilled water. The tip of the needle was positioned on an optical bench between a light source and a high speed charge couple device (CCD) camera. The CCD camera was connected to a video frame-grabber board to record the image onto the hard drive of a computer at a speed of one frame per 1 min. The shape of pendent

drops was determined through numerical analysis of the entire drop shape. The interfacial tension was calculated from the drop shape using the Young–Laplace equation of capillarity (Nicole, Kristianto, Osman, & Michael, 2005). This methodology requires accurate determination of solution densities, which were measured using a digital density metre (DMA 35 N; Anton Paar USA, Ashland, VA). All interfacial tension measurements were carried out after 1 h of equilibrium.

2.2.6. Free radical scavenging activity as determined by the oxygen radical absorbance capacity (ORAC) assay

The ability of the free and esterified CGA to scavenge peroxyl radicals was determined using the ORAC assay (Huang, Ou, Hampsch-Woodill, Flanagan, & Deemer, 2002; Ou, Hampsch-Woodill, & Prior, 2001; Prior, Wu, & Schaich, 2005). Chlorogenic acid and its conjugates were dissolved in acetone/water mixture (50:50, v/v) to a final concentration of 1 mM. A 300 mM solution of 2,2′-azobis (2-methylpropionamidine) dihydrochloride (AAPH) and 50 nM solution of fluorescein in 75 mM potassium phosphate buffer at pH 7.0 were prepared and kept on ice. Fluorescein was held at 37 °C in a water bath for 15 min and then brought to a final concentration of 45 nM in a cuvette with 0–10 μM antioxidant, 0.1 mM EDTA, and 20 mM AAPH in 75 mM phosphate buffer (pH 7.0). Analyses were performed on a Fluorolog fluorometer (Photon Technology International Inc., Birmingham, NJ) set at an excitation wavelength of 493 nm and an emission wavelength of 515 nm with the temperature being maintained at 37 °C. Fluorescence was recorded every minute for 40 min and the fluorescence relative to the fluorescence at time zero (F/F_0) was calculated from the fluorescence decay curve. The area under the curve (AUC) was obtained by subtracting the AUC of the blank from that of the sample. AUC was calculated using PeakFit v4.12 (SeaSolve Software Inc.). Data were expressed as micromoles of Trolox equivalents (TE) per gram of sample as determined from a Trolox standard curve over the range of 1.0–20 μM.

2.2.7. Lipid oxidation measurements

Emulsion samples (1 ml) were placed into 10 ml headspace vials and sealed with polytetrafluoroethylene (PTFE)/butyl rubber septa and allowed to oxidise in the absence of light at 20 °C for up to 7 days. Headspace propanol was measured using a Shimazu GC-2014 gas chromatograph equipped with a solid phase microextraction (SPME) AOC-5000 auto injector (Shimazu, Kyoto, Japan) according to the method described by Yuji et al. (2007). The SPME head space conditions were as follows: sample incubation temperature, 45 °C; sample incubation time, 15 min; extraction time, 2 min; injection time, 3 min. A 50/30 μm DVB/Carboxen/PDMS SPME fibre was used for extraction (Supelco, Bellefonte, PA). The GC operating conditions were as follows: samples were injected in split mode (5:1); oven temperature program was 40 °C for 4 min followed by an increase of 10 °C/min to 110 °C, then an increase of 20 °C/min to a final temperature of 250 °C held for 2 min; injector was 250 °C; flame ionisation detector was 250 °C. The aldehydes were separated on a Supelco (Equity™-1) fused silica capillary column (30 m, 0.32 mm i.d., 1.0 μm film thickness). Concentrations were determined from peak area using a standard curve made from authentic propanol over the range of 0.025–1.0 mM.

Following headspace analysis, vials were opened and emulsion samples were used for lipid hydroperoxide measurements. Lipid hydroperoxides were measured using a modified method from Shantha and Decker (1994). Emulsions (0.3 ml) were mixed with 1.5 ml of isooctane/isopropanol (3:1, v/v) by vortexing (10 s, three times) and centrifuged at 1000*g* for 2 min. The upper layer (0.2 ml total volume containing 0.02–0.2 ml of lipid extract) was added to 2.8 ml of methanol/butanol (2:1, v/v), followed by 15 μl of 3.94 M ammonium thiocyanate and 15 μl of ferrous iron solution (prepared by adding equal amounts of 0.132 M $BaCl_2$ and 0.144 M $FeSO_4$). After 20 min, the absorbance of the solutions was measured at a wavelength of 510 nm using a UV–visible spectrophotometer (Genesys 20; Thermo Fisher Scientific Inc., Waltham, MA). Lipid hydroperoxide concentrations were determined using a standard curve prepared with cumene hydroperoxides over the range of 0.03–50 mM.

2.2.8. Statistical analysis

All experiments were performed in triplicate. Differences between means were determined with the least-squares means procedure at $p < 0.05$ (Snedecor & Cochran, 1989).

3. Results and discussion

To determine if the esterification of hydrocarbon chains onto CGA altered its physical properties, continuous phase concentrations in the menhaden oil-in-water emulsions and surface activity of the free and esterified antioxidants was determined. As expected, hydrocarbon chain esterification was able to change the partitioning behaviour of chlorogenic acid in the oil-in-water emulsions. The concentration of antioxidants in the aqueous phase of the menhaden oil-in-water emulsions was in the order of CGA > butyl CGA > octyl CGA > dodecyl CGA (Fig. 1). The concentration of CGA in the aqueous phase was more than 80% compared to dodecyl CGA which was 16%. These results indicate that esterification of CGA to hydrocarbon chains resulted in a greater retention of antioxidant in the lipid droplets of the emulsion.

To determine if the esterification also would increase the ability of CGA to concentrate at the oil–water interface of emulsion droplets where oxidation is thought to be most prevalent (McClements & Decker, 2000), the surface activity of CGA and its esters was determined. Fig. 2 shows that CGA and butyl CGA were not able to decrease the interfacial tension in a hexadecane–water system over a concentration range of 0–500 μM. In contrast, both octyl and dodecyl CGA were surface active decreasing interfacial tension by 20% and 60% at a concentration of 500 μM, respectively, compared to the control (no added chlorogenic acid). The greater reduction of interfacial tension by dodecyl than octyl CGA indicated that increasing the hydrocarbon chain from 8 to 12 carbons

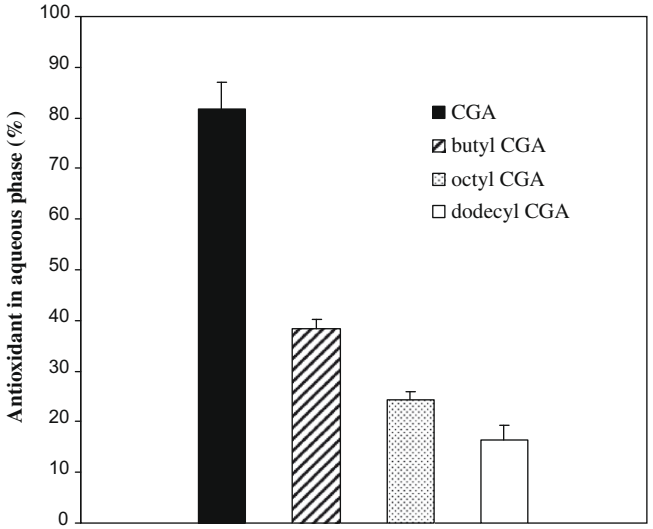

Fig. 1. Chlorogenic acid (CGA), butyl CGA, octyl CGA, and dodecyl CGA concentrations in the continuous phase of Brij 35-stabilized 2% menhaden oil-in-water emulsions. Data points represent means ($n = 3$) ± standard deviations (some error bars may lie within the data points).

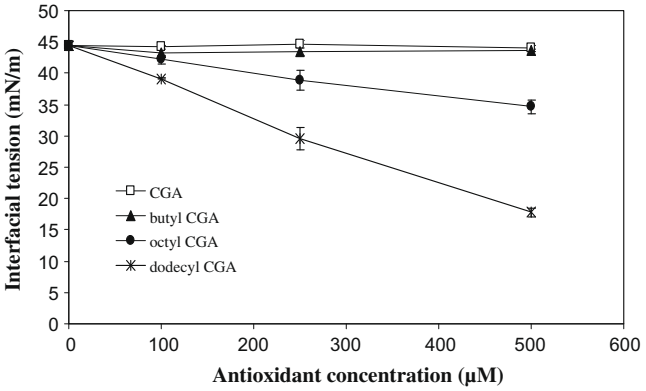

Fig. 2. Interfacial tension of chlorogenic acid (CGA), butyl CGA, octyl CGA, and dodecyl CGA in a water–hexadecane interface. Data points represent means ($n = 3$) ± standard deviations (some error bars may lie within the data points).

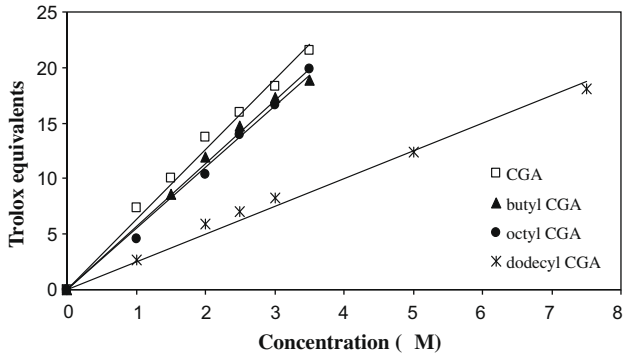

Fig. 3. The Trolox equivalents of chlorogenic acid (CGA), butyl CGA, octyl CGA, and dodecyl CGA at different concentrations as determined by the oxygen radical absorbance capacity (ORAC).

would increased the ability of dodecyl CGA to concentrate at the oil–water interface instead of partitioning into the lipid core of the emulsion droplet.

Previous research showed that the esterification of hydrocarbon chains onto *p*-hydroxyphenylacetic acid decreased its ability to scavenge peroxyl radicals (Yuji et al., 2007). Therefore, prior to conducting experiments on the ability of the CGA esters to inhibit lipid oxidation in oil-in-water emulsions, their peroxyl radical scavenging activity was determined using the ORAC assay. Fig. 3 shows the linear response between the concentration and the radical scavenging capacity, expressed as Trolox equivalents, for CGA and each of its derivatives. Peroxyl radical scavenging activity was in the order of CGA > butyl CGA = octyl CGA > dodecyl CGA. The peroxyl radical scavenging activity of the dodecyl CGA esters was about 50% less than that of the other antioxidants. As in our previous work, the free *p*-hydroxyphenylacetic acid was also the most effective free radical scavenger (Yuji et al., 2007). However, unlike CGA, the *p*-hydroxyphenylacetic acid dodecyl ester was a more effective free radical scavenger than the butyl ester.

The ability of CGA and its esters to inhibit lipid oxidation in oil-in-water emulsions would be expected to be a function of both their physical location and free radical scavenging activity. To control for the differences in free radical scavenging activity between CGA and its esters, the antioxidants were added at equal free radical scavenging activities. This was done by calculating the concentration of CGA and its esters that would give a Trolox equivalent of 7.2 as determined by the standard curves in Fig. 3. The resulting concentrations of antioxidants added to the menhaden oil-in-water emulsions are shown in Table 1.

Table 1
The concentrations of chlorogenic acid (CGA) and its esters that produced an equivalent oxygen radical absorbance capacity (ORAC) value (expressed as μmol of Trolox equivalents (TE) and concentration of antioxidants added to an the oil-in-water emulsion lipid oxidation test so that all antioxidants were added at equal free radical scavenging activity.

Sample	Conc. at ORAC = 7.2 TE	Conc. in oxidation test (μM)
CGA	2.37	47.4
Butyl CGA	2.67	53.3
Octyl CGA	2.71	54.2
Dodecyl CGA	6.00	120.0

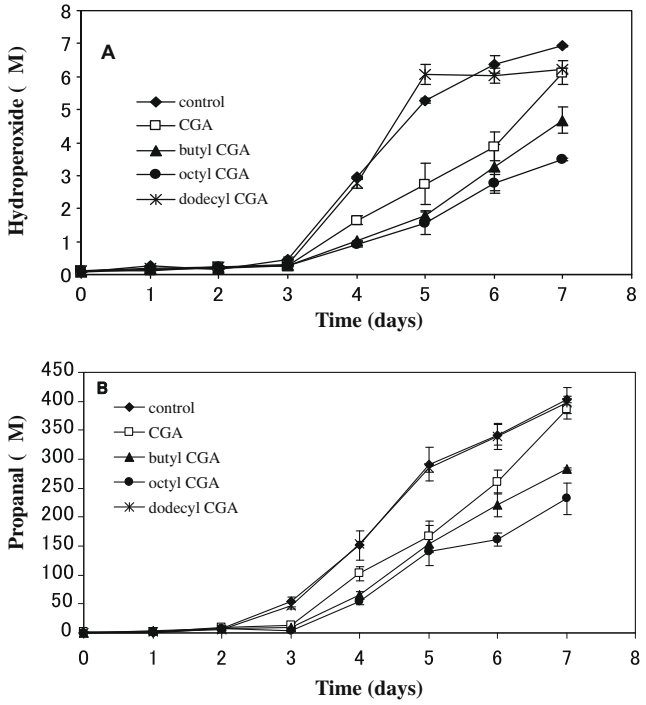

Fig. 4. Ability of chlorogenic acid (CGA), butyl CGA, octyl CGA and dodecyl CGA to inhibit formation of (A) lipid hydroperoxides and (B) propanol in a 2% menhaden oil-in-water emulsions (pH 7.0) stored at 20 °C. Data points represent means ($n = 3$) ± standard deviations (some error bars may lie within the data points).

Surfactants are normally used to stabilize oil-in-water emulsions against flocculation and coalescence by changing the physical properties of the emulsion droplet interface. However, after homogenisation there are often significant quantities of non-adsorbed surfactant molecules present in the aqueous phase of emulsions. Above a critical micelle concentration (CMC), the non-adsorbed surfactant will form micelles. Surfactant micelles are capable of incorporating molecules such as antioxidants within their hydrophobic core. In previous studies we found that excess surfactant will increase the solubilisation of antioxidants into the aqueous phase of oil-in-water emulsions (Richards et al., 2002). Therefore, in all experiments we used an emulsion to which excess surfactant was removed by a repeated washing procedure as described in the methods section.

Fig. 4 shows the results of lipid oxidation measurements. All antioxidants, except dodecyl CGA, inhibited lipid hydroperoxide formation up to 4 days of storage ($p < 0.05$) and propanol formation up to 3 days of storage ($p < 0.05$). Dodecyl CGA was not able to inhibit either lipid hydroperoxide or propanol formation compared to the control. Lipid hydroperoxide formation was inhibited 44% by CGA, 66% by butyl CGA and 70% by octyl CGA when compared to the control at 4 days storage. Propanol formation was inhibited 32% by CGA, 57% by butyl CGA, and 65% by octyl CGA

compared to the control at 4 days of storage. In general, as the chain length increased, antioxidant activity was increased compare to CGA with the exception of dodecyl CGA. However, little differences in antioxidant activity were observed between butyl CGA and octyl CGA.

Dodecyl CGA had higher lipid partitioning and surface activity than CGA, butyl CGA and octyl CGA. According to the antioxidant polar paradox hypothesis, non-polar antioxidants which are retained in the oil phase of oil-in-water emulsions should be more effective than antioxidants which tend to partition more into the aqueous phase (Frankel, 2005). Some investigators have also suggested that increasing the surface activity of an antioxidant would also increase its ability to inhibit lipid oxidation since it would concentrate at the oil–water interface where oxidation is most prevalent (Heins et al., 2007).

The results of this research suggest that neither retention in the lipid phase concentration nor surface activity were good predictors of antioxidant activity in oil-in-water emulsions. Increasing the size of the hydrocarbon chain esterified to chlorogenic acid increased both lipid partitioning in oil-in-water emulsion droplets (Fig. 1) and surface activity (Fig. 2). However, the esters with the highest lipid partitioning and surface activity were not an effective antioxidant when CGA and its esters were added at equal free radical scavenging activities. In addition, dodecyl CGA which had greater lipid partitioning and surface activity than butyl CGA (Figs. 1 and 2) did not have substantially greater ability to inhibit lipid hydroperoxide and propanol formation compared to butyl CGA (Fig. 4). Similar results were also reported by Yuji and coworkers (2007).

In this research all antioxidants were added at equal free radical scavenging activity to minimise differences in the ability of the different antioxidants to scavenge free radicals that could be caused by the esterification of a hydrocarbon chain onto the chlorogenic acid. However, in addition to free radical scavenging, chlorogenic acid can also inhibit lipid oxidation by chelating prooxidant metals (Andjelkovic et al., 2006). Since transition metals such as iron are major prooxidants in oil-in-water emulsions (Mancuso et al., 1999), it is possible that CGA and its derivates are inhibiting lipid oxidation by a combination of both free radical scavenging and metal chelation. This could mean that partitioning of the CGA esters into the lipid phase could decrease their ability to chelate aqueous phase prooxidative metals while simultaneously increasing their ability to scavenge free radicals in the lipid phase. If loss of chelating activity in the aqueous phase of the emulsions was important in the overall antioxidant activity of the tested compounds than increasing antioxidant concentration in the lipid phase my not result in an increase in antioxidant activity.

The ability of CGA and its esters to inhibit lipid oxidation in oil-in-water emulsions could also be influenced by interactions with other antioxidants. Antioxidant interactions such as the ability of ascorbic acid to regenerate oxidised α-tocopherol to reactivate α-tocopherol in biological membranes (Buettner, 1993; Porter, 1993) have been used to explain why antioxidant combination can work better than single antioxidants. Since the oil used in these experiments would contain α-tocopherol, it is possible that it or other lipid soluble antioxidants endogenous to the oil could be regenerated at the oil–water interface of the emulsion droplets by an antioxidant in the aqueous phase. Therefore, the CGA esters could also become less effective at regenerating antioxidants at the lipid–water interface as their partitioning into the lipid phase increased.

Interestingly, the dodecyl CGA had little to no antioxidant activity in the oil-in-water emulsion when added at equal free radical scavenging activity even though it had the highest lipid partitioning and surface activity. Since the dodecyl CGA had approximately one half the free radical scavenging activity as the other CGA derivatives, it was added at approximately twice the concentrations. At high concentrations, antioxidants can promote lipid oxidation through pathways such as transition metal reduction (Mei, McClements, & Decker, 1999) which could help explain why dodecyl CGA did not inhibit lipid oxidation.

4. Conclusions

The antioxidant polar paradox hypothesis states that antioxidants that are retained in lipid droplets are better antioxidants in oil-in-water emulsions. To test this hypothesis, chlorogenic acid was esterified with hydrocarbon chains to alter its physical properties. Esterification of chlorogenic acid resulted in increase lipid solubility and surface activity as the number of carbons on the hydrocarbon chains increased. Esterification of chlorogenic acid did not change its ability to scavenge free radicals with the exception of the dodecyl ester which had approximately half the free radical scavenging activity as free CGA and the other CGA esters. Since the antioxidant polar paradox hypothesis was developed for free radical scavenging antioxidants, CGA and its esters were added to oil-in-water emulsions at equal free radical scavenging activity. Even though the CGA esters had greater lipid partitioning and surface activity than free CGA, their ability to inhibit lipid oxidation did not increase. This suggests that the presence of CGA in the aqueous phase of oil-in-water emulsions could also contribute to total antioxidant activity possibly by chelating prooxidants metals or regeneration of antioxidants within the emulsion droplet.

Acknowledgements

We thank Tokyo University of Marine Science and Technology (Japan) for the financial support of Keiichi Sasaki. This research was partially funded by Grant 2004-02422 from NRI CSREES, USDA. Luis Javier López Giraldo thanks the support from Programme Alβan, the European Union Programme of High Level Scholarships for Latin America, Scholarship No. E05D055786CO.

References

Andjelkovic, M., Van Camp, J., De Meulenaer, B., Depaemelaere, G., Socaciu, C., Verloo, M., et al. (2006). Iron-chelation properties of phenolic acids bearing catechol and galloyl groups. *Food Chemistry, 98*, 23–31.

Buettner, G. R. (1993). The pecking order of free radicals and antioxidants: Lipid peroxidation, α-tocopherol, and ascorbate. *Archives of Biochemistry and Biophysics, 300*, 535–543.

Chaiyasit, W., Elias, R. J., McClements, D. J., & Decker, E. A. (2007). Role of physical structures in bulk oils on lipid oxidation. *Critical Reviews in Food Science and Nutrition, 47*, 299–317.

Clifford, M. N. (1999). Chlorogenic acids and other cinnamates nature, occurrence and dietary burden. *Journal of the Science of Food and Agriculture, 79*, 362–372.

Decker, E. A. (1998). Strategies for manipulating the prooxidative/antioxidative balance of foods to maximize oxidative stability. *Trends in Food Science and Technology, 9*, 241–248.

Decker, E. A., Warner, K., Richards, M. P., & Shahidi, F. (2005). Measuring antioxidant effectiveness in food. *Journal of Agricultural Food Chemistry, 53*, 4303–4310.

Elias, R. J., McClements, D. J., & Decker, E. A. (2007). Impact of thermal processing on the antioxidant mechanisms of continuous phase β-lactoglobulin in oil-in-emulsions. *Food Chemistry, 104*, 1402–1409.

Folch, J., Lees, M., & Stanley, G. H. S. (1957). A simple method for the isolation and purification of total lipids from animal tissues. *Journal of Biological Chemistry, 226*, 497–509.

Frankel, E. N. (1996). Antioxidants in lipid foods and their impact on food quality. *Food Chemistry, 57*, 51–55.

Frankel, E. N. (2005). *Lipid oxidation* (2nd ed.). University of California, Davis, California, USA, Bridgewater, England: The Oily Press, PJ Barnes & Associates.

Frankel, E. N., & Meyer, A. S. (2000). The problems of using one-dimensional methods to evaluate multifunctional food and biological antioxidants. *Journal of the Science of Food Agriculture, 80*, 1925–1941.

Halliwell, B. (1990). How to characterize a biological antioxidant. *Free Radical Research Communication, 9*, 1–32.

Heins, A., McPhail, D. B., Sokolowski, T., Stockmann, H., & Schwarz, K. (2007). The location of phenolic antioxidants and radicals at interfaces determines their activity. *Lipids, 42*(6), 537–582.

Huang, D., Ou, B., Hampsch-Woodill, M., Flanagan, J. A., & Deemer, E. K. (2002). Development and validation of oxygen radical absorbance capacity assay for lipophilic antioxidants using randomly methylated β-cyclodextrin as the solubility enhancer. *Journal of Agricultural Food Chemistry, 50*, 1815–1821.

Lopez Giraldo, L. J., Laguerre, M., Lecomte, J., Figueroa-Espinoza, M. C., Barouh, N., Baréa, B., et al. (2007). Lipase-catalyzed synthesis of chlorogenate fatty esters in solvent-free medium. *Enzyme and Microbial Technology, 41*, 721–726.

Mancuso, J. R., McClements, D. J., & Decker, E. A. (1999). The effects of surfactant type, pH, and chelators on the oxidation of salmon oil-in-water emulsions. *Journal of Agricultural Food Chemistry, 41*, 4112–4116.

McClements, D. J. (2005). *Food emulsions: Principles, practice, and techniques*. Boca Raton, FL: CRC Press.

McClements, D. J., & Decker, E. A. (2000). Lipid oxidation in oil-in-water emulsions: Impact of molecular environment on chemical reactions in heterogeneous food systems. *Journal of Food Science, 65*, 1270–1282.

Mei, L., McClements, D. J., & Decker, E. A. (1999). Lipid oxidation in emulsions as affected by the charge status of antioxidants and emulsion droplets. *Journal of Agricultural Food Chemistry, 47*, 2267–2273.

Nicole, M. D., Kristianto, T., Osman, A. B., & Michael, T. H. (2005). A finite element based algorithm for determining interfacial tension (γ) from pendant drop profiles. *Journal of Colloid and Interface Science, 286*, 647–660.

Nuchi, C. D., McClements, D. J., & Decker, E. A. (2001). Impact of tween 20 hydroperoxides and iron on the oxidation of methyl linoleate and salmon oil dispersions. *Journal of Agricultural Food Chemistry, 49*, 4912–4916.

Ou, B., Hampsch-Woodill, M., & Prior, R. L. (2001). Development and validation of an improve oxygen radical absorbance capacity assay using fluorescein as the fluorescent probe. *Journal of Agricultural Food Chemistry, 49*, 4619–4626.

Porter, W. L. (1993). Paradoxical behavior of antioxidants in food and biological systems. *Toxicology and Industrial Health, 9*(1–2), 93–122.

Prior, R. L., Wu, X., & Schaich, K. (2005). Standardized method for the determination of antioxidant capacity and phenolics in foods and dietary supplements. *Journal of Agricultural Food Chemistry, 53*, 4290–4302.

Richards, M. P., Chaiyasit, W., McClements, D. J., & Decker, E. A. (2002). Ability of surfactant micelles to alter the partitioning of phenolic antioxidants in oil-in-water emulsions. *Journal of Agricultural Food Chemistry, 50*, 1254–1259.

Shantha, N. C., & Decker, E. A. (1994). Rapid, sensitive, iron-based spectrophotometric methods for determination of peroxide values of food lipids. *Journal of AOAC International, 77*, 421–424.

Snedecor, G. W., & Cochran, W. G. (1989). *Statistical methods* (8th ed). Ames: Iowa State University Press.

Yuji, H., Weiss, J., Villeneuve, P., Giraldo, L. J. L., Figueroa-Espinoza, M. C., & Decker, E. A. (2007). Ability of surface-active antioxidants to inhibit lipid oxidation in oil-in-water emulsion. *Journal of Agricultural Food Chemistry, 55*, 11052–11056.

2. Materials and methods

2.1. Plant material

Seeds of *L. bipinnata* were collected from Asangihal village in Sindagi taluk of Bijapur district, India, in October 2007 and grown in the botanical garden, Department of Botany, Karnatak University, Dharwad, India. The species was identified by Dr. M. Jayaraj, and a voucher specimen was prepared and deposited in the Department of Botany, Karnatak University, Dharwad, India.

2.2. Isolation procedure

The dried leaves were extracted using a soxhlet apparatus for 8 h in petroleum ether (40–60 °C). The essential oil obtained was dried under vacuum and stored at 4–6 °C before analysis.

2.3. Gas chromatography–mass spectrometry (GC–MS)

The analysis was carried out on a Shimadzu-GCMS-QP2010S fitted with a 30 m × 0.25 mm × 0.25 μm Rtx-5ms capillary column. The oven temperature was programmed as follows: from 60 to 180 °C at 3 °C/min and isothermally held for 15 min. Helium was used as carrier gas at 1 ml/min and 1 μl of sample was injected for analysis.

2.4. Identification of constituents

The identifications of the components were based on the comparison of their mass spectra with those of reference spectra in the computer library, as well as by comparison of their retention indices with literature values and our data are in accordance with those previously reported (Alberto et al., 2006).

2.5. Antimicrobial activity

2.5.1. Microbial strains

The antimicrobial activity of the essential oils samples was tested towards 11 different microorganisms. Three gram-negative bacteria, namely *Escherichia coli* ATCC 25922, *Pseudomonas aeruginosa* ATCC 27853, *Shigella dysentery*. Five gram positive bacteria namely *Enterococcus faecalis* ATCC 29212, *Staphylococcus aureus* ATCC 29213, *Vancomycin resistant enterococcus* ATCC 51299, *Bacillus subtilis, Micrococcus. Aspergillus niger, Penicillium notatum* and *Candida albicans* were the three fungi used for the study.

2.5.2. Determination of antimicrobial activity and minimum inhibitory concentration (MIC)

Antibacterial activity of essential oils of *L. bipinnata* was tested by the paper disc diffusion method according to the slightly modified National Committee for Clinical Laboratory Standards Guidelines (National Committee for Clinical Laboratory Standard, 2001), using 100 μl of suspension of the tested microorganisms, containing 2.0×10^6 colony forming units (cfu/ml) for inoculating the plates (William, 1977). A test oil solution was prepared in dimethyl sulphoxide (DMSO) and loaded (10 μl) onto sterile filter paper discs (6 mm diameter, HiMedia Laboratories Pvt. Limited, India), which finally contained 300 μg/μl of the compound per disc. Since the essential oil was dissolved in DMSO, it was used as a control. Impregnated disks were then dried for 1 h and placed on inoculated plates. The seeded plates were incubated at 37 °C for 24 h and 25 °C for 72 h for bacteria and fungi, respectively. The diameters of the inhibition zones were measured in millimetres. Studies were performed in triplicate, and the developing inhibition zones were compared with those of reference discs. Antibiotic streptomycin was used as a reference for bacteria and nystatin for fungi. The minimal inhibitory concentration of essential oil was determined by a micro dilution assay. The essential oil was twofold serially diluted with DMSO containing 0.125–8 μg/μl of oil. The MIC of the essential oil was defined, as the lowest concentration at which there was 100% inhibition of growth compared with the growth for a drug free control. In order to ensure that the solvent had no effect on fungal growth, a control test was also performed containing broth supplemented with only DMSO at the same dilution used in the assay. Each experiment for the antibacterial assay and MIC was repeated thrice.

3. Results and discussion

The essential oil of *L. bipinnata* obtained on extraction was analysed by gas chromatography–mass spectrometry (GC–MS). Twenty-nine components, representing 72.38% of the total essential oil, were identified (see Table 1). The constituents identified by GC–MS analysis, their retention indices and area percentages (concentrations) are summarised in Table 1. The essential oil was dominated by terpenes and alcohols which accounted for 34.44% and 28.03% of the essential oil, respectively. The major terpenes were pulegone (8.45%) and camphor (7.09%) while the alcohols consisted mainly of transcarveol (18.93%) and menthol (5.89%). Other terpenes present in appreciable amounts are caryophyllene oxide (3.68%), linalyl acetate (3.37%), bicyclogermacrene (3.09%) and thymol (2.35%) as mentioned in Table 1. The chemical composition of the essential oil was, however, different from that observed from other *Lavandula* species. Carveol and pulegone are used as a fragrance in cosmetics and flavour additive in food industry, pulegone is also used in aromatherapy. Camphor and menthol are readily absorbed through skin and produces a felling of cooling and acts as a slight local anaesthetic and antimicrobial substance. There are anti-itch gel and cooling gels with camphor and menthol

Table 1
The essential oil components of leaves of *L. bipinnata* (data were obtained using GC–MS analysis).

Compound	Retention index	Area (%)
α-Pinene	939	1.01
Camphene	964	0.35
Sabinen	975	0.39
Cis-pinine	986	0.43
Myrcene	991	0.25
Δ-3-carene	1011	0.37
Fenchone	1087	1.05
Linalool	1098	0.94
Fenchol	1117	0.36
Camphor	1143	7.09
Isopulegol	1146	0.80
Pinocarvone	1162	0.38
Lavandulol	1166	0.38
Menthol	1165	5.89
Terpinen-4-ol	1177	0.73
Myrtenal	1193	0.53
Transcarveol	1217	18.93
Pulegone	1219	8.45
Pipertone	1228	4.65
Linalyl acetate	1257	3.37
Bornyl acetate	1285	0.21
Lavandulyl acetate	1289	1.79
Thymol	1290	2.35
Carvacrol	1298	0.44
Myrtenyl acetate	1327	0.63
β-Caryophyllene	1418	0.18
Germacrene-D	1480	1.66
Bicyclogermacrene	1494	3.09
Caryophyllene oxide	1581	3.68
	Total (%)	72.38

Table 2
The zone of inhibition (mm) and minimum inhibitory concentration (MIC) values (μg/μl) of the essential oil of *L. bipinnata* and standard streptomycin against bacteria.

No.	Bacteria	Zone of inhibition (mm)		MIC (μg/μl)	MIC (μg/μl)
		L. bipinnata oil	Streptomycin	*L. bipinnata* oil	Streptomycin
1.	*E. coli* ATCC 25922	10	24	⩽0.5	⩽0.005
2.	*P. aeruginosa* ATCC 27853	07	15	⩽2.0	⩽0.010
3.	*Sh. dysentery*	11	17	⩽1.0	⩽0.020
4.	*E. faecalis* ATCC 29212	10		⩽2.0	⩽0.010
5.	*S. aureus* ATCC 29213	13	29	⩽1.0	⩽0.005
6.	*VRE* ATCC 51299	11	21	⩽2.0	⩽0.010
7.	*B. subtilis*	13	23	⩽1.0	⩽0.010
8.	*Micrococcus*	12	32	⩽0.5	⩽0.005

as the active ingredients. The essential oil of *L. bipinnata* is rich in transcarveol, pulegone, camphor and menthol and hence it can be used as a source of these components.

The essential oil was evaluated for antimicrobial activity against gram positive (*E. faecalis* ATCC 29212, *S. aureus* ATCC 29213, *VRE* ATCC 51299, *B. subtilis*, *Micrococcus*), gram-negative (*E. coli* ATCC 25922, *P. aeruginosa* ATCC 27853, *Sh. dysentery*) bacteria and fungi (*A. niger*, *P. notatum* and *C. albicans*). It was found to be active against all the microbes used for the activity. The essential oil was very active against *B. subtilis*, *S. aureus*, *Micrococcus*, *A. niger*, Moderately active against *E. coli*, *Sh. dysentery*, *E. feacalis*, *VRE*, *C. albicans* and low activity against *P. aureginosa and P. notatum* (see Tables 2 and 3). The minimum inhibiting concentration (MIC) of essential oil ranged from 0.5 to 2.0 μg/μl and 2 to 4 μg/μl for bacteria and fungi respectively. The MIC values for the standard ranged from 0.005 to 0.02 μg/μl and 0.04 to 0.16 μg/μl for streptomycin and nystatin, respectively. In general, the essential oil showed better antibacterial activity than antifungal activity (see Tables 2 and 3). The gram positive bacterium is more susceptible to the antimicrobial properties of essential oils than gram-negative bacteria and it is considered to be due to its outer membrane (Cox et al., 2001). The activity of the essential oil varies with its concentration and kind of bacteria. These differences in the susceptibility of the test organisms to essential oil could be attributed to a variation in the rate of the essential oil constituent's penetration through the cell wall and cell membrane structures. The ability of essential oil to disrupt the permeability barrier of cell membrane structures and the accompanying loss of chemiosmotic control are the most likely reasons for its lethal action (Cox et al., 2001). Although the concentrations of the essential oil were generally about 100 times more than those of the standard antibiotic (streptomycin and nystatin), they showed marked antibacterial and antifungal activities, as evidenced by their zones of inhibition (see Table 2). This difference between concentrations of the essential oil and the standard antibiotic can be explained in terms of the fact that the active components in the essential oil comprise only a fraction of the oil used. Therefore, the concentration of the active components could be much lower than the standard antibiotics used. It is important to note that, if the active components were isolated and purified, they would probably show higher antimicrobial activities than those observed here.

The increasing antibiotic resistance of pathogens associated with infectious disease as well as undesirable side effects of antibiotics suggested the use of natural products such as essential oils as antibiotics or its components as alternatives to antibiotics. However further research is required to evaluate the practical values of therapeutic application.

Mass spectral data of six major compounds are as follows

Camphor (152): 152 [M^+], 135, 123, 108, 95, 81, 69. 152 is the molecular ion peak corresponding to molecular weight of the compound and 95 is the base peak.
Menthol (156): 152 [M^+], 138, 123, 109, 95, 81, 71, 55, 53. 156 is the molecular ion peak corresponding to the molecular weight of the compound and 71 is the base peak.
Transcarveol (152): 152 [M^+], 137, 119, 109, 91, 84, 77. 152 is the molecular ion peak corresponding to molecular weight of the compound and 109 is the base peak.
Pulegone (152): 152 [M^+], 137, 123, 109, 95, 81, 67, 53. 152 is the molecular ion peak corresponding to molecular weight of the compound and 81 is the base peak.
Piperitone (152): 152 [M^+], 137, 124, 111, 95, 82, 67, 54. 152 is the molecular ion peak corresponding to molecular weight of the compound and 82 is the base peak.
Caryophyllene oxide (220): 220 [M^+], 205, 187, 177, 161, 145, 131, 121, 107, 93, 79, 69, 55, 43, 41. 220 is the molecular ion peak corresponding to molecular weight of the compound and 41 is the base peak.

Table 3
The zone of inhibition (mm) and minimum inhibitory concentration (MIC) values (μg/μl) of the essential oil of *L. bipinnata* and standard nystatin against fungi.

		Zone of inhibition (mm)		MIC (μg/μl)	MIC (μg/μl)
		L. bipinnata oil	Nystatin	*L. bipinnata* oil	Nystatin
1.	*A. niger*	13	21	⩽2.0	⩽0.040
2.	*P. notatum*	09	13	⩽4.0	⩽0.160
3.	*C. albicans*	10	23	⩽4.0	⩽0.160

4. Conclusions

Our results demonstrated that transcarveol, pulegone, camphor and menthol were the main constituents of essential oil of *L. bipinnata*. Since, these constituents are used as flavouring agents in cosmetic and food industry, the essential oil of *L. bipinnata* can be used as a source of these constituents. The essential oil of *L. bipinnata* showed antimicrobial activity against both bacteria and fungi, therefore it can be used as an herbal medicine. The plant is not known to be toxic because it has been consumed by mankind for centuries without showing any signs of toxicity.

Acknowledgement

This work was partially financed by University Grants Commission under the Special Assistance programme.

References

Adam, K., Afroditi, S., Stella, K., Thomas, L., & Minas, A. (1998). Antifungal activities of *Origanum vulgare* subsp. *hirtum*, *Mentha spicata*, *Lavandula angustifolia*, and *Salvia fruticosa* essential oils against human pathogenic fungi. *Journal of Agriculture and Food Chemistry, 46*(5), 1739–1745.

Alberto, A., Andrea, B., Valentina, C., Sandro, D., & Paolo, C. (2006). Chemical composition, seasonal variability, and antifungal activity of *Lavandula stoechas L. Ssp. stoechas* essential oils from stem/leaves and flowers. *Journal of Agriculture and Food Chemistry, 54*(12), 4364–4370.

Buchbauer, G., Jirovetz, L., Jager, W., Dietrich, H., Plank, C., & Karamat, E. (1991). Aromatherapy: Evidence for the sedative effect of the essential oil of lavender after inhalation. *Zeitschrift fur Naturforschung C, 46*(11–12), 1067–1072.

Catherine, J. C., & Kathi, J. K. (2001). *The longwood herbal task force* (<http://www.mcp.edu/herbal/>) *and the center for holistic pediatric education and research* (<http://www.childrenshospital.org/holistic/>) *Lavender* (*Lavandula spp.*).

Cavanagh, H. M. A., & Wilkinson, J. M. (2005). Lavender essential oil: A review. *Australian Infection Control, 10*(1), 35–37.

Cox, S. D., Mann, C. M., Markham, J. L., Gustafson, J. E., Warmington, J. R., & Wyllie, S. G. (2001). Determination the antimicrobial action of tea tree oil. *Molecules, 6*(1), 87–91.

Delaveau, P., Guillemain, J., Narcisse, G., & Rousseau, A. (1989). Neurodepressant effects of lavender essential oil. *Comptes Rendus des Seances de la Societe de Biologie et des ses Filiales (Paris), 183*(4), 342–348.

Jagtap, S. D., Deokule, S. S., Pawar, P. K., & Harsulkar, A. M. (2009). Traditional ethnomedicinal knowledge confined to the Pawra tribe of Satpura Hills, Maharashtra, India. *Ethnobotanical Leaflets, 13*, 98–115.

Maria, L. B. (2002). *Lavender: The genus Lavandula*. United Kingdom: CRC press. p. 30.

Moon, T., Cavanagh, H. M. A., & Wilkinson, J. M. (2004). Lavender as an antibacterial essential oil – are all lavenders equal?. In *AICA national conference*, p. 46.

Muyima, N. Y. O., Zulu, G., Bhengu, T., & Popplewell, D. (2002). The potential application of some novel essential oils as natural cosmetic preservatives in an aqueous cream formulation. *Flavour and Fragrance, 17*(4), 258–266.

Nair, R. V. (2004). *Controversial drug plants*. India: Orient Blackswan. p. 201.

National Committee for Clinical Laboratory Standard (2001). In *Performance standards for anti-microbial susceptibility testing: 11th informational supplement*. Document M100-S11, Wayne, PA.

Pullaiah, T. (2006). *Biodiversity in India*. India: Daya Books. p. 350.

Roy, G. P., Shukla, B. K., & Bhaskar, D. (1992). *Flora of Madhya Pradesh: Chhatrapura and Damoh*. India: APH publishing. p. 351.

Valiollah, H., Alireza, G., & Badie, S. (2003). Anti-inflammatory and analgesic properties of the leaf extracts and essential oil of *Lavandula angustifolia* mill. *Journal of Ethnopharmacology, 89*(1), 67–71.

Welsh, C. (1995). Three essential oils for the medicine cabinet. *Alternative Health Practitioner, 3*(1), 11–15.

William, H. (1977). *Microbiological Assay. An introduction to quantitative principles and evaluation*. New York: Academic Press.

two yellow rock sugars (*gula batu*) from cane; two palm sugars (*gula anau* and *gula Melaka*); and three fancy sugars, varieties of rock honey sugar, also from cane (see Table 1). One of these fancy sugars, china rock honey sugar, listed dried chrysanthemum flowers amongst its contents.

Sugars were dissolved in phosphate buffer (50 mM, pH 6.2). The raw sugar and the soft brown sugar were both light brown, granulated, sugars coloured and flavoured by coating with caramel or molasses. The red sugars were refined, granulated, sugars whose crystals were coloured artificially. All the rock sugars were refined, lightly coloured, sugars in large lumps or crystals. The palm sugars were unrefined: the *gula Melaka* was a single piece of solid sugar, and the *gula anau* was a viscous liquid. The lump sugars were crushed in a mortar with a pestle in order to aid dissolution. Each sugar was tested over a concentration range from 0.1% to 50% (w/v). Each individual sample concentration was tested twice, and each individual sugar was tested at least three times.

2.2. Chrysanthemum flowers

Dried chrysanthemum flowers are used in traditional Chinese medicines and were obtained from a Chinese apothecary. The dried petals were infused with hot, double-distilled, water, just off the boil at room temperature (25 °C) for 15 min at a concentration of 1% (w/v). This infusion was diluted further in phosphate buffer to produce solutions of 0.1–50% v/v stock/buffer.

2.3. Cyclic voltammetry

Cyclic voltammetry was performed using an eDAQ system (www.eDAQ.com), consisting of an E190 potentiostat connected to an e-corder which inputted to eChem software (running on a PC using Microsoft Windows Vista platform). The working electrode was a 3 mm diameter glassy carbon electrode; the reference electrode was Ag/AgCl in 3 M NaCl (+207 mV *vs*. standard hydrogen electrode); the auxiliary electrode was a 0.25 mm diameter Pt wire. The working electrode was polished for at least 4 min before individual cycles of voltammetry. Unless otherwise stated, applied potentials ranged from −200 to +800 mV, and the scan rate was 200 mV s^{-1}. The volume of the voltammetric cell was approximately 15 ml.

Vitamin C (ascorbic acid) was used as a standard antioxidant for comparison of the sugars. Cyclic voltammograms were constructed for vitamin C at concentrations from 5.1 μM to 2.6 mM. Vitamin C (Krüger GmbH & Co., Germany) was dissolved freshly at the start of the experiments. All solutions were prepared using double-distilled water.

2.4. Diffusion coefficients

According to the Randles–Ševcik equation (Randles, 1948):

$$I_{pa} = kn^{3/2}AD^{1/2}C.v^{1/2}$$

where I_{pa} = peak anodic current; k = Randles–Ševcik constant (2.69×10^5 A.s.$V^{-1/2}$ mol^{-1}) at 25 °C; n = electron stoichiometry (i.e., the number of electrons transferred to the substrate molecule); A = exposed surface area of the electrode (cm^2); D = diffusion coefficient of the substrate molecule (cm^2 s^{-1}); C = concentration of the substrate molecule (mol cm^{-3}); v = scan rate (V s^{-1}).

Thus, if the concentration of the substrate is kept constant, a plot of I_{pa} *vs.* $v^{½}$ will yield a straight line whose slope can be used to determine the diffusion coefficient. Samples of sugars were scanned at rates from 50 to 3200 V s^{-1}, in steps of $\log_2$ units.

2.5. Redox potentials and peak potentials

In cases where the oxidation of compounds was, at least partially, reversible, the redox potential was calculated form $(E_{pa} + E_{pc})/2$ and the peak potential was calculated from $(E_{pc} - E_{pa})$, where E_{pa} and E_{pc} were the potentials at which the peak anodic and peak cathodic currents (I_{pa} and I_{pc}, respectively) were recorded.

3. Results

3.1. Vitamin C standards

Over a range of 5.1 μM to 2.6 mM, vitamin C produced a concentration-dependent peak anodic current (I_{pa}) (Figs. 1 and 2).

Table 1
Peak anodic currents per unit concentration.

Sugar	Current Constant[a] (concentration μA^{-1})	$C.D^{0.5}$ (mol cm^{-2} $s^{-0.5}$) × 10^{-6}
Cane sugars		
Nazri soft brown sugar peak1	8.1 ± 1.10 (0.931, 6)	1.6 ± 0.24 (0.884)
Nazri soft brown sugar peak2	3.7 ± 0.16 (0.992, 6)	4.4 ± 0.47 (0.936)
SIS raw sugar peak 1	18.2 ± 1.57 (0.978, 4)	0.7 ± 0.06 (0.956)
SIS raw sugar peak 2	8.2 ± 0.51 (0.989, 4)	1.5 ± 0.09 (0.979)
Sunflower *gula merah*	0.65 ± 0.039 (0.975, 8)	17.9 ± 0.24 (0.999)
Chek Hup white rock sugar	–	–
Granulated pure white sugar	–	–
Nabila *gula merah*	–	–
STM *gula merah*	–	–
Sunflower yellow lump sugar	–	–
Yellow *gula batu*	–	–
Fancy sugars		
China rock honey sugar	6.9 ± 0.46 (0.982, 5)	4.9 ± 0.47 (0.947)
Luo Han Guo rock honey sugar	–	–
Luo Han Guo winter melon sugar	–	–
Palm sugars		
Gula anau	0.41 ± 0.006 (0.998, 9)	29.3 ± 0.37 (0.999)
Gula Melaka	–	–

Values for $C.D^{0.5}$ (±standard error) were calculated from the slopes of the regressions of I_{pa} on (scan rate)$^{0.5}$, as shown in Fig. 10, constraining the line to pass through the origin; the correlation coefficient (r^2) is given within parentheses. The values of $C.D^{0.5}$ for vitamin C (mol.cm^{-2} $s^{-0.5}$ × 10^{-6}) were: 38.9 ± 0.58 (0.999), 21.3 ± 0.53 (0.996) and 3.3 ± 0.04 (0.999) at concentrations of 0.51, 0.26 mM and 51.1 μM, respectively. For chrysanthemum flower infusion (10% v/v buffer) the slope was 10.8 ± 0.73 × 10^{-6} mol cm^{-2} $s^{-0.5}$ (r^2 = 0.973). All data are for 7 d.f.

[a] Current constants were obtained form the slope of the regression of I_{pa}^{-1} on [analyte]$^{-1}$, constraining the regression to pass through the origin. The regressions are drawn in Fig. 8; values are slope ± s.e. slope, with the correlation coefficient (r^2) and degrees of freedom given within parentheses. The units of concentration for all the sugars is *g*% (w/v) phosphate buffer.

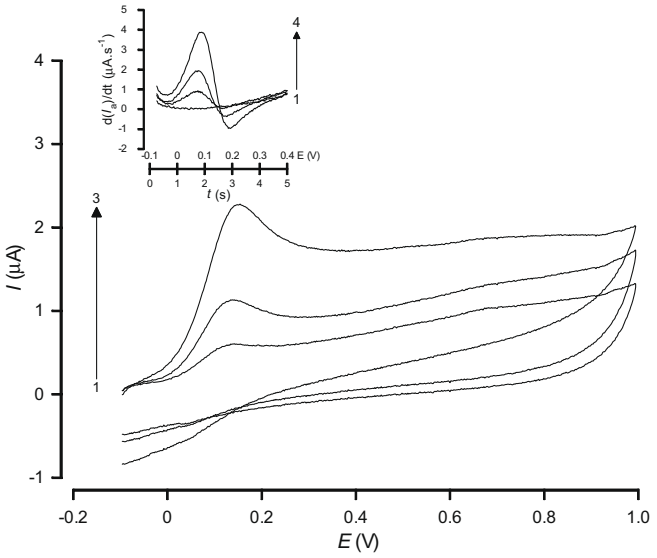

Fig. 1. Vitamin C. Cyclic voltammograms for vitamin C in 0.1 M phosphate buffer, pH 6.2. The numbers 1 → 3 correspond to concentrations of 0.010, 0.026 and 0.051 mM vitamin C in phosphate buffer. Inset are differentiated recordings, with the numbers 1 → 4 corresponding to concentrations of 0, 0.010, 0.026 and 0.051 mM vitamin C in phosphate buffer.

The potential (E_{pa}) at which I_{pa} occurred was 168–218 mV for concentrations from 5.1 μM to 2.6 mM (Fig. 2). There were no observable peak cathodic currents (I_{pc}).

The relationship between I_{pa} and concentration of vitamin C appeared to be linear over the concentration range of 5.1 μM to 2.6 mM (Fig. 2A). When both the ordinate and abscissa were plotted on reciprocal scales the regression was also linear (Fig. 2B). The slope of this transformation, 0.03 ± 0.007 mM μA^{-1}, gives the concentration of vitamin C per unit I_{pa} which was termed the "current constant".

The voltammograms were subjected to first order differentiation with respect to time (using eChem software). The resulting transformed voltammograms give $d(I_a)/dt$ with a peak corresponding to the fastest rate of increase of the I_{pa} (Fig. 1 inset). In other words, the differentiated traces give the rate of oxidation of vitamin C. There was a linear correlation between the amplitude of the signal produced by vitamin C and the rate of increase of that signal (Fig. 2C).

When the concentration of vitamin C was kept fixed at either 0.05, 0.25 or 0.51 mM, the I_{pa} was linearly dependent upon the scan rate for a range from 50 to 3200 mV s^{-1} (Fig. 2D). Using the slope of this regression and the Randles–Ševcik equation, the diffusion coefficient of vitamin C was calculated and found to be $1.89 \times 10^{-6} \pm 2.67 \times 10^{-7}$ (mean ± s.e. mean, of the three different concentrations of vitamin C, three different samples each measured in duplicate using two different recording electrodes). The negative logarithm of this, i.e. the p*D*, is 5.74 ± 0.064 ($n = 3$).

3.2. Sugars

Refined white granulated sugar, up to 50% w/v buffer, gave a signal no different from the phosphate buffer alone. No signal was found for two of the three red sugars (Nabila *gula merah* and STM *gula merah*), nor for the white or yellow rock sugars, nor for *gula Melaka* palm sugar, nor for the two Luo Han Guo mixed sugars. No peaks were observed in the anodic or cathodic directions of the cyclic voltammograms, nor were any peaks identified on the differentiated traces. Potentials were applied from −200 to +1200 mV.

In contrast, anodic current peaks were found in four refined cane sugars (SIS raw sugar, Nazri soft brown sugar, China rock honey sugar and *gula merah*) and one unrefined palm sugar (*gula anau*) (Figs. 3–7, respectively). The cyclic voltammograms for SIS raw sugar, soft brown sugar and China rock honey sugar had more than one peak, however the smaller peaks tended to be obscured by the main peak; it was often easier to discern that there was a second or third compound present from the differentiated recording (Figs. 3–5).

The relationship between the I_{pa} amplitude and the concentration was similar for all the five positive sugars, in that for low level signals the relationship looked linear but at higher level signals (higher concentrations) the relationship deviated from linearity as if to plateau. Using double-reciprocal plots, the graphs were

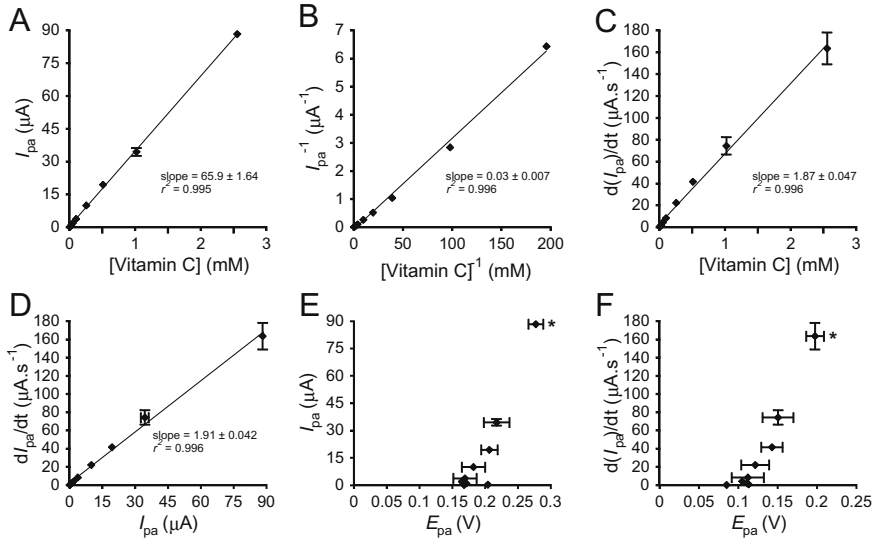

Fig. 2. Characteristics of vitamin C by voltammetry. (A) Vitamin C produces a concentration-dependent linear increase in peak anodic current (I_{pa}). (B) The double reciprocal plot of I_{pa}^{-1} on concentration^{-1} is linear. (C) The first order derivative of the I_{pa} also has a linear dependency on concentration. (D) The first order derivative has a linear relation with the I_{pa}. (E) From 5.11 μM to 1.02 mM there was no significant change in the potential (E_{pa}) at which the I_{pa} occurred, only at the highest concentration tested (∗, 2.56 mM) does the E_{pa} lie significantly more positive (two-way ANOVA and *post hoc t*-test). (F). For dI_{pa}/dt, there was no significant shift in E_{pa} over a concentration range from 5.11 μM to 1.02 mM, but at 2.56 mM (∗) the rightward shift is statistically significant ($p < 0.01$) two-way ANOVA and *post hoc t*-test).

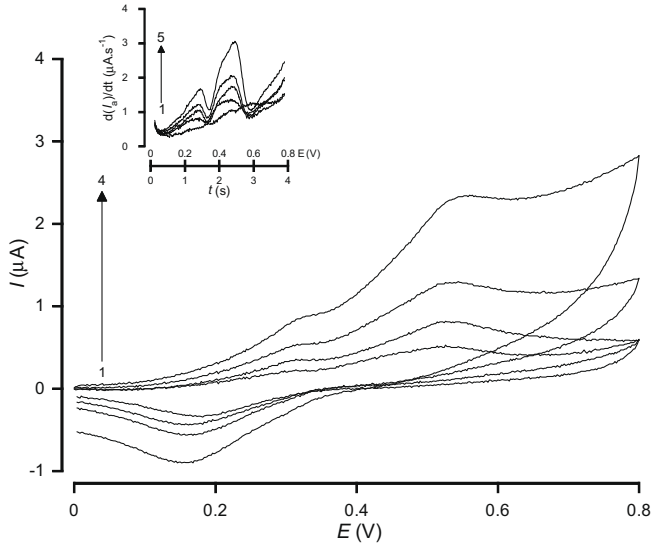

Fig. 3. SIS raw sugar. Cyclic voltammograms for SIS raw sugar in 0.1 M phosphate buffer, pH 6.2. The numbers 1 → 4 correspond to concentrations of 3%, 6%, 12% and 25% (w/v) sugar in phosphate buffer. Inset are differentiated recordings, with the numbers 1 → 5 corresponding to concentrations of 0%, 3%, 6%, 12% and 25% (w/v) sugar in phosphate buffer.

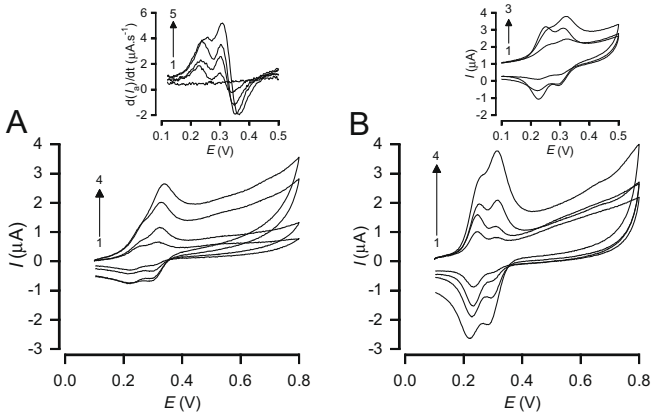

Fig. 5. China rock honey sugar and chrysanthemum flowers infusion. Cyclic voltammograms for: (A) China rock honey sugar in 0.1 M phosphate buffer, pH 6.2. The numbers 1 → 4 correspond to concentrations of 3%, 6%, 12% and 25% (w/v) sugar. Inset are differentiated recordings, with the numbers 1 → 5 corresponding to concentrations of 0%, 3%, 6%, 12% and 25% (w/v) sugar in phosphate buffer; (B) chrysanthemum flower infusion in phosphate buffer, pH 6.2. The background (phosphate buffer alone) has been subtracted. The numbers 1 → 4 correspond to concentrations of 0.5%, 1%, 2% and 5% (v/v) infusion. Inset are current recordings, with the numbers 1 → 3 corresponding to concentrations of 6.25% (w/v) China rock honey sugar in phosphate buffer, chrysanthemum flowers infusion 2% (v/v) in phosphate buffer, and an equal volume mixture of these two.

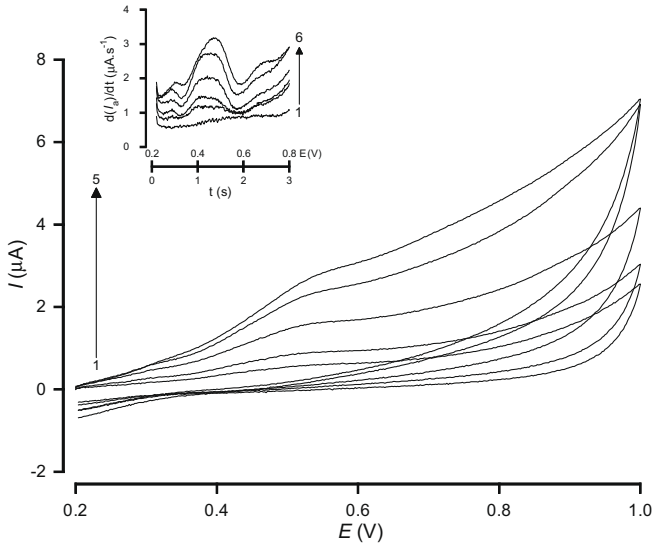

Fig. 4. Soft brown sugar. Cyclic voltammograms for soft brown sugar in 0.1 M phosphate buffer, pH 6.2. The numbers 1 → 5 correspond to concentrations of 1%, 3%, 6%, 12% and 25% (w/v) sugar in phosphate buffer. Inset are differentiated recordings, with the numbers 1 → 6 corresponding to concentrations of 0, 1, 3, 6, 12 and 25% (w/v) sugar in phosphate buffer.

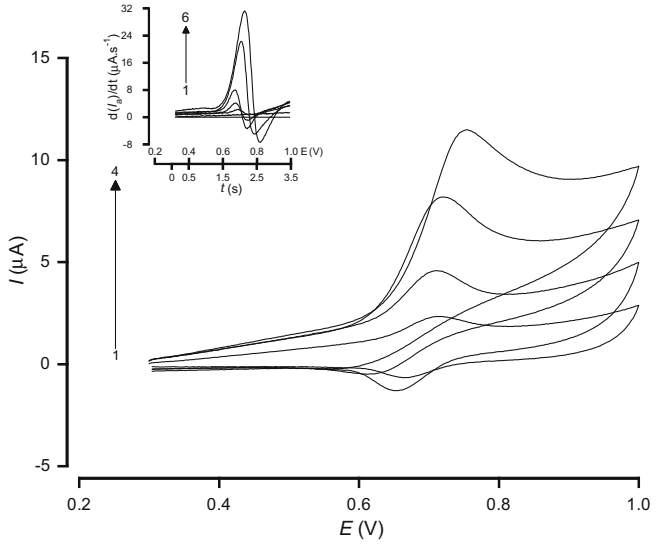

Fig. 6. *Gula merah*. Cyclic voltammograms for *gula merah* in 0.1 M phosphate buffer, pH 6.2. The numbers 1 → 4 correspond to concentrations of 1.5%, 3%, 6%, and 12% (w/v) sugar in phosphate buffer. Inset are differentiated recordings, with the numbers 1 → 6 corresponding to concentrations of 0%, 1%, 3%, 6%, 12% and 25% (w/v) sugar in phosphate buffer.

linearised (Fig. 8); as for vitamin C, the slope of this transformation gave the concentration of analyte per unit I_{pa}, or current constant (Table 1), and allows a direct comparison between the sugars and vitamin C. Assuming that the I_{pa} reflects antioxidant activity, comparing these values with vitamin C gives a rank order of antioxidant activity of the five sugars: *gula anau* > *gula merah* > China rock honey sugar > soft brown sugar > SIS raw sugar.

The red sugar, sunflower *gula merah*, was certainly red in colour. When it was being dissolved it was noticeable that the red colour came away from the sugar crystals so that in the early stages of dissolution there was a reddish coloured liquid with white crystals on the bottom of the beaker. The same was true for the two negative red sugars, Nabilah *gula merah* and STM *gula merah*.

The two refined brown sugars and the China rock honey sugar contained compounds whose oxidation appeared to be at least partially reversible, because the cathodic current traces in the cyclic voltamograms also displayed peaks (I_{pc}) (Figs. 3–5).

For the China rock honey sugar, for the first peak, which was due to a substance with a redox potential of 258 ± 8.4 mV (n = 5), the I_{pa}/I_{pc} ratio was 1.1 ± 0.18 (n = 5) and the peak potential was 44.7 ± 5.28 mV (n = 5). This peak was only measurable at a concentration of 3.13% (w/v) buffer because otherwise it merged into the peak for a second substance. This second peak was due to a substance with a redox potential of 302 ± 6.7 mV (n = 6, at five concentrations from 3.13% to 50% w/v buffer); the I_{pa}/I_{pc} ratio was 2.3 ± 0.26 and the peak potential was 54.6 ± 3.80 mV.

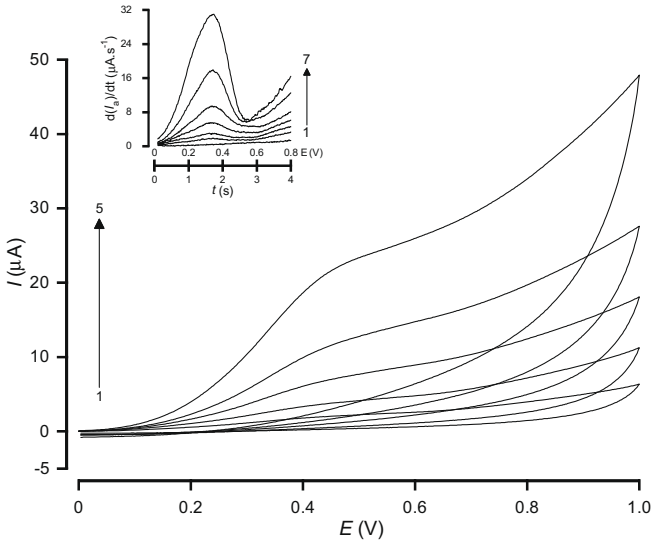

Fig. 7. *Gula anau*. Cyclic voltammograms for *gula anau* in 0.1 M phosphate buffer, pH 6.2. The numbers 1 → 5 correspond to concentrations of 1%, 2%, 5%, 10% and 20% (w/v) sugar in phosphate buffer. Inset are differentiated recordings, with the numbers 1 → 7 corresponding to concentrations of 0%, 1%, 2%, 5%, 10%, 20% and 50% (w/v) sugar in phosphate buffer.

3.3. Chrysanthemum flowers

The solutions of infused dried chrysanthemum flowers yielded multiple peaks in the cyclic voltammograms. Two prominent peaks were discernible below 400 mV and occurred close together (Fig. 5). The potentials at which these peaks occurred were similar to those observed in the China rock honey sugar, and when the China rock honey sugar (6.25%) was mixed with an equal volume of the chrysanthemum infusion (2%), there were still only two peaks in either the anodic or cathodic current traces (Fig. 5). Furthermore, on the differentiated traces, no additional peaks were seen. The first peak, was due to a substance with a redox potential of 238 ± 1.3 mV (n = 5); the I_{pa}/I_{pc} ratio was 1.0 ± 0.04 (n = 5) and the peak potential was 38.4 ± 17.7 mV (n = 5). This peak was measurable only at concentrations from 0.1% to 2% (w/v) buffer because otherwise it merged into the second peak. The second peak was due to a substance with a redox potential of 284 ± 5.3 mV (n = 7), at concentrations from 0.5% to 50% w/v buffer; the I_{pa}/I_{pc} ratio was 1.9 ± 0.37 and the peak potential was 52.9 ± 18.3 mV. The peak potentials for both the first and second peaks were not significantly different from those for the corresponding peaks in the China rock honey sugar (unpaired Student's t-tests). Likewise, the peak ratios did not significantly differ between the flower infusion and the sugar, nor did the redox potentials (unpaired t-tests, $p > 0.05$).

3.4. Peak anodic current potentials

Of all the compounds tested, vitamin C had the lowest E_{pa}, at approximately 200 mV (Fig. 9). None of the sugars had compounds with an oxidation potential in this region. The main antioxidant in the China rock honey sugar, the raw sugar (peak1), the soft brown sugar (peak1) and the chrysanthemum infusion all had values for E_{pa} in the region of 300–400 mV. The antioxidant compounds in *gula anau* and in the second peaks of the refined raw sugar and the soft brown sugar had potentials that were similar at 500–650 mV. The compound in *gula merah,* that yielded an anodic current peak, had a very high potential, greater than 700 mV. Furthermore, the peak potential of this compound became more positive, in a concentration-dependent fashion (Fig. 8), up to 900 mV at the highest concentration tested (50% w/v).

3.5. Diffusion coefficients

For the five positive sugars, vitamin C and the chrysanthemum flower infusion, the plots of I_{pa} against the square root of the scan

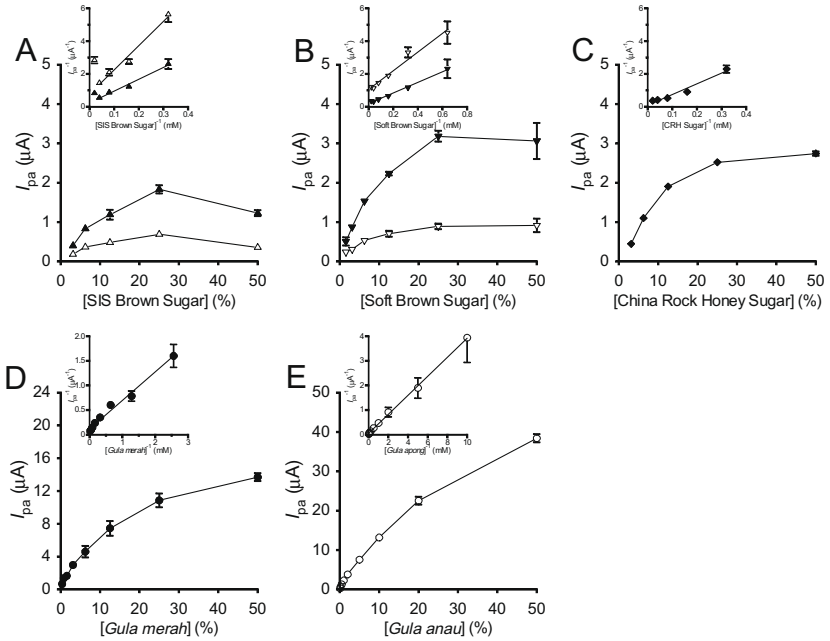

Fig. 8. Sugars displaying peak anodic currents (I_{pa}). (A) SIS raw sugar peak1 (open upward triangle); SIS raw sugar peak2 (closed upward triangle). (B) Soft brown sugar peak1 (open downward triangle); soft brown sugar peak2 (closed downward triangle). (C) China rock honey sugar (closed diamond). (D) *Gula merah* (closed circle). (E) *Gula anau* (open circle). Concentrations are given as w/v phosphate buffer. Graphs show concentration dependency of I_{pa}, insets show double-reciprocal plots of I_{pa}^{-1} *versus* concentration^{-1}. Regression slopes and correlation coefficients are given in Table 1 (N.B. For SIS brown sugar, the points at a concentration of 50% were not included in the regression). Points show mean ± s.e. mean, unless occluded by symbol.

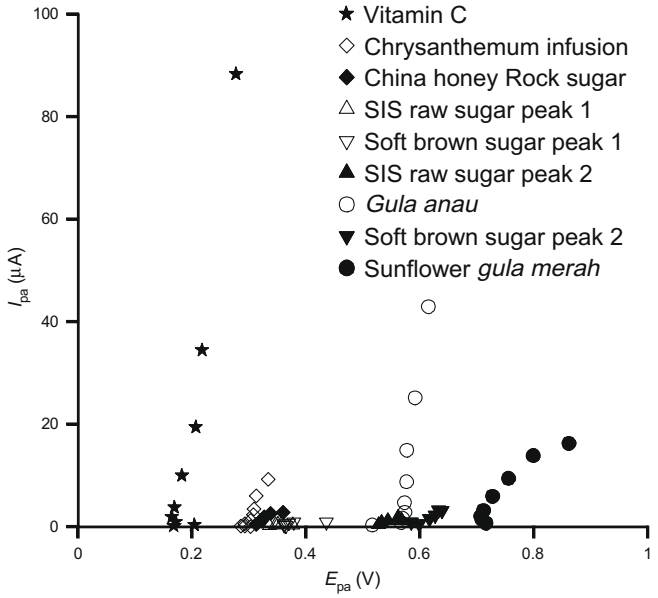

Fig. 9. Relationships between peak anodic currents (I_{pa}) and oxidation potentials (E_{pa}). Vitamin C (closed star), chrysanthemum flowers infusion (open diamond), China rock honey sugar (closed diamond), SIS raw sugar peak1 (open upward triangle), soft brown sugar peak1 (open downward triangle, occluding open upward triangles), *gula anau* (open circle), SIS raw sugar peak2 (closed upward triangle), soft brown sugar peak2 (closed downward triangle) and *gula merah* (closed circle). The highest concentrations tested, and the highest I_{pa} for each analyte, were: vitamin C, 2.6 mM; chrysanthemum flower infusion 50% v/v buffer; all sugars, 50% w/v buffer.

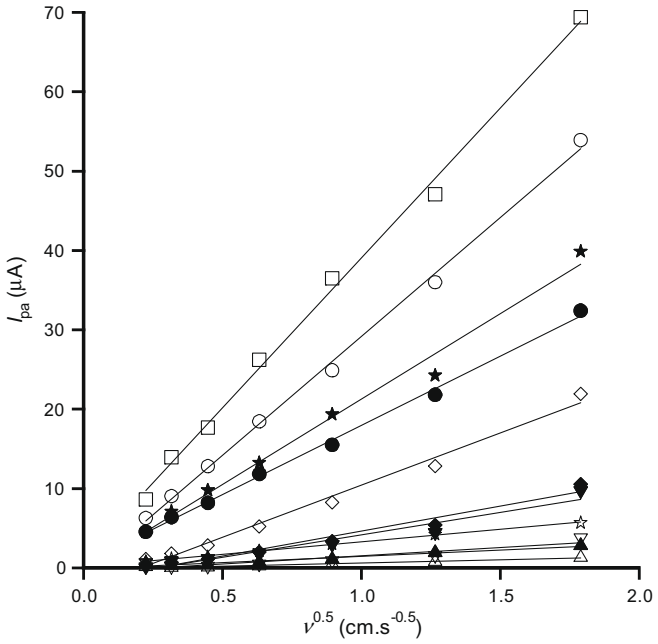

Fig. 10. Regressions of peak anodic currents (I_{pa}) on the square root of the scan rate ($v^{0.5}$). Vitamin C (10%, open square; 5% closed star; 1% open star), chrysanthemum flowers infusion (open diamond), China rock honey sugar (closed diamond), SIS raw sugar peak1 (open upward triangle), soft brown sugar peak1 (open downward triangle), *gula anau* (open circle), SIS raw sugar peak2 (closed upward triangle), soft brown sugar peak2 (closed downward triangle) and *gula merah* (closed circle). All the sugars were tested at concentrations of 10% w/v buffer; the chrysanthemum flower infusion was tested at 10% v/v buffer.

rate are shown in Fig. 10. In each case, the regression of I_{pa} on the square root of the scan rate was linear (least-squares regression); the regression lines were constrained to passing through the origin and their slopes are given in Table 1 together with their correlation coefficients. For the China honey rock sugar, and for the infusion of chrysanthemum flowers, there was not a clear enough separation of the two peaks to allow separate analysis, and data for the I_{pa} that occurred around 300 mV in both cases are shown. The slope of the regression is the value $C.D^{0.5}$ (from the Randles–Ševcik equation), but the diffusion coefficients for compounds contained in the sugars could not be calculated, because their concentration is unknown.

4. Discussion

The results show that some refined and unrefined sugars do contain antioxidants. Previous studies relating the redox potential of a compound to a lipid peroxidation assay showed that compounds with a redox potential below 450 mV were antioxidant, and that compounds with a redox potential of 490 mV or above were pro-oxidant (Simic, Manojlovic, Šegan, & Todorovic, 2007). The highest levels of antioxidant activity appeared to be found in the palm sugar *gula anau*. This sugar had an antioxidant activity equivalent to 1.7 mg of vitamin C per 1 g of *gula anau*. The nature of the antioxidant has not been described, but it is unlikely to be vitamin C itself because, even though the diffusion coefficient of this compound was close to that of authentic vitamin C, the potential at which the peak anodic currents occurred was approximately 100 mV more positive than that of authentic vitamin C.

A red sugar, *gula merah*, also contained a substance in appreciable amount that was oxidisable, however, the potential at which the peak anodic current arose were very high, around 700 mV. This means that this substance is not a powerful antioxidant (Simic et al., 2007). Because the colour readily came away from the sugar crystals during dissolution, and also because the red colour of this product did not look like that of any other sugar, there is some doubt as to the origin of this antioxidant. No further information has been supplied by the manufacturer.

The mixed sugar, China rock honey sugar, had a comparatively low level of antioxidant activity. This is almost certainly entirely due to its chrysanthemum flower content. The two peaks of anodic current, that were present in this mixed sugar, were also present in aqueous extracts of dried chrysanthemum petals alone. When samples of the sugar and flowers were mixed, there were still only the two anodic peaks. Furthermore, the I_{pa}/I_{pc} ratios, the redox potentials and the peak potentials for the two substances did not significantly differ between the two samples. Finally, the predominant peaks in these two substances also had similar diffusion coefficients. Two other mixed sugars with similar or identical contents apart from the chrysanthemum flowers had no discernible antioxidant activity. Therefore, it is probable that any antioxidant activity present in the China rock honey sugar is due to the dried chrysanthemum flowers.

The refined SIS raw sugar and the Nazri soft brown sugar both had low levels of antioxidant activity from two compounds. From the current constants, assuming that the compounds in the two sugars are the same, the concentrations of both compounds in the soft brown sugar were just over double (2.25 and 2.22 times great for peaks 1 and 2, respectively) those in the raw sugar; the oxidation potentials for the compounds were the same. When this difference in concentration is taken into account, the diffusion coefficients for the compound of peak1 become almost identical, while those for peak2 become very close. The main difference between these two products appeared to be particle size; the raw sugar was composed of larger crystals.

From the potentials at which the anodic current peaks arose, it would appear that the antioxidant in the refined raw and soft

brown sugars could be the same as that in the unrefined palm sugar. From the values of the current constants, the amount present in the *gula anau* was 20 times greater than that in the raw sugar. Correcting the value of $C.D^{0.5}$ to reflect this 20-fold difference, gives a compound with the same diffusion coefficient in the two sugars (the corrected $C.D^{0.5}$ for gula anau becomes 1.47 μmol $cm^{-2}.s^{-0.5}$ c.f. 1.5 μmol cm^{-2} $s^{-0.5}$ for the raw sugar).

The antioxidants in the chrysanthemum petals and the China rock honey sugar were the most powerful amongst the sugars, arising at potentials approximately 100 mV lower than any other. As noted above, it was not always possible to resolve the peaks for these compounds because they merged into each other. Antioxidant activity has been reported in chrysanthemum flower buds from three different species (Woo et al., 2008), and at least 17 polyphenol compounds which may have antioxidant activity can be extracted from *Chrysanthemum morifolium* flowers (Lai et al., 2007).

The calculated diffusion coefficient for vitamin C (1.89×10^{-6} cm s^{-1}) is in agreement with values in the literature obtained using modified carbon paste electrodes (5.7×10^{-6} cm s^{-1}, Marian, Sandulescu, & Bonciocat, 2000) or glassy carbon electrodes (3.2×10^{-6} cm s^{-1}, Sabzi & Pournaghi-Azar, 2005).

The cyclic voltammograms for *gula anau* show a remarkable similarity to those for vanillic acid. Simic et al. (2007) showed that vanillic acid (1 mM) has a single broad-based peak at a potential of 0.73 mV, with a linear relationship between I_{pa} and the square root of the scan rate. The voltammograms also showed no peak on the reduction curve. These authors also used a glassy carbon electrode with a Ag/AgCl reference electrode. Vanillic acid is among several antioxidant compounds found in refined or coated brown sugars from sugarcane (Payet, Sing, & Smadja, 2005).

Using a colourimetric assay which determined the total amount of antioxidants in a sample, Halvorsen et al. (2006) showed that raw cane sugar had nearly twice the antioxidant capacity of turbinado sugar, and that the level of antioxidant activity in refined granulated sugar was approximately 80 times less than that in the raw cane sugar. Using cyclic voltammetry, antioxidant activity was not detected in any of the white or yellow sugars that were tested.

In conclusion, it is evident that most types of refined sugars on the market do not contain any antioxidants. Very low levels of antioxidant activity were found in the refined raw and brown cane sugars. Higher levels were found in a rock honey sugar (also refined) which also contained chrysanthemum flowers, and the activity was due to the flowers.

An oxidisable substance was found at appreciable levels in the unrefined palm sugar, *gula anau*, however whether or not this functions as an antioxidant remains to be determined. If it is, then *gula anau*, should be promoted as the sweetener of choice because of its antioxidant content.

Acknowledgements

This work is funded by Kementarian Bangunan Negara Brunei Darussalam, under grant STIC-3 RKN9. The authors gratefully acknowledge this support. Dr. Khor Vi An, Kedai Ubat Beserah, Kuantan, Malaysia, is thanked for the gift of dried chrysanthemum flowers.

References

Halvorsen, B. L., Carlsen, M. H., Phillips, K. M., Bøhn, S. K., Holte, K., Jacobs, D. R., et al. (2006). Content of redox-active compounds (i.e. antioxidants) in foods consumed in the United States. *American Journal of Clinical Nutrition, 84*, 95–135.

Kilmartin, P. A., & Hsu, C. F. (2003). Characterisation of polyphenols in green, oolong, and black teas, and in coffee, using cyclic voltammetry. *Food Chemistry, 82*, 501–512.

Lai, J-P., Lima, Y. H., Sua, J., Shen, H-M., & Ong, C. M. (2007). Identification and characterization of major flavonoids and caffeoylquinic acids in three *Compositae* plants by LC/DAD-APCI/MS. *Journal of Chromatography B, 848*, 215–225.

Li, Y., & Schellhorn, H. E. (2007). New developments and novel therapeutic perspectives for vitamin C. *Journal of Nutrition, 137*, 2171–2184.

Marian, I. O., Sandulescu, R., & Bonciocat, N. (2000). Diffusion coefficient (or concentration) determination of ascorbic acid using carbon paste electrodes in Fredholm alternative. *Journal of Pharmaceutical and Biochemical Analysis, 23*, 227–230.

Payet, B., Sing, A. S. C., & Smadja, J. (2005). Assessment of antioxidant activity of cane brown sugars by ABTS and DPPH radical scavenging assays: determination of their polyphenolic and volatile constituents. *Journal of Agricultural Food Chemistry, 53*, 10074–10079.

Randles, J. E. B. (1948). A cathode ray polarograph. Part II. The current–voltage curves. *Transaction of the Faraday Society, 44*, 327–338.

Roginsky, V., Barsukova, T., Hsu, C. F., & Kilmartin, P. A. (2003). Chain-breaking antioxidant activity and cyclic voltammetry characterization of polyphenols in a range of green, Oolong, and black teas. *Journal of Agricultural Food Chemistry, 51*, 5798–5802.

Sabzi, R. E., & Pournaghi-Azar, M. H. (2005). Electrocatalytic determination of ascorbic acid on a glassy carbon electrode chemically modified with cobalt pentacyanonitrosylferrate. *Analytical Sciences, 21*, 689–692.

Simic, A., Manojlovic, D., Šegan, D., & Todorovic, M. (2007). Electrochemical behavior and antioxidant and prooxidant activity of natural phenolics. *Molecules, 12*, 2327–2340.

Valdés, F. (2006). Vitamina C. *Actas Dermo-sifiliográficas, 97*, 557–568.

Vita, J. A. (2005). Polyphenols and cardiovascular disease: effects on endothelial and platelet function. *American Journal of Clinical Nutrition, 81*, 292S–297S.

Woo, K. S., Yu, J. S., Hwang, I. G., Lee, Y. R., Lee, C. H., Yoon, H-S., et al. (2008). Antioxidative activity of volatile compounds in flower of *Chrysanthemum indicum*, *C. morifolium*, and *C. zawadskii*. *J. Korean Society Food Science Nutrition, 37*, 805–809.

problems of different nature as to heart and circulatory, or complications in the immunization system. Other researchers, however, when developing some experiments concerning the influence of injected caffeine on the urinary excretion of some metal ions, e.g. potassium, sodium, magnesium, calcium, zinc, copper, in rats, conclude that the urinary excretion of zinc and copper were found to be unaffected by caffeine (YeH et al., 1986).

Whilst earlier data on diffusion coefficients of copper chloride in aqueous solutions at 25 °C and 37 °C over the concentration range from 0.001 to 0.05 mol dm^{-3} have been reviewed (Ribeiro et al., 2005), no data on mutual diffusion coefficients of Cu(II) salts in the presence of caffeine at 25 °C and 37 °C – relevant data for *in vivo* pharmaceutical applications- have been published, as far as careful literature searches have shown. This paper reports experimental data for differential ternary mutual diffusion coefficients (D_{11}, D_{22}, D_{12} and D_{21}) of copper chloride in aqueous solutions at carrier concentrations from (0.000 to 0.020 mol dm^{-3}), for each solute, respectively, in the presence of caffeine at different concentrations (that is from 0.000 to 0.020 mol dm^{-3}) using the Taylor dispersion equipment for aqueous solutions of $CuCl_2$-caffeine at 25 °C and 37 °C.

2. Experimental

2.1. Reagents and solutions

Copper chloride (Sigma–Aldrich, *pro analysi* > 99.9%) and caffeine (Sigma, *pro analysi* > 98.5%) were used as supplied, without further purification. All the solutions were freshly prepared before each experiment (concentration uncertainty less than ± 0.1%). They were prepared in calibrated volumetric flasks using bi-distilled water and de-aerated during 30 min, approximately, before use.

2.2. Equipment and procedure for diffusion measurements

The theory of the Taylor dispersion technique is well described in literature (Barthel, Gores, Lohr, & Seidl, 1996; Callendar & Leaist, 2006; Vitagliano, 1991), and therefore, we only indicate some relevant points concerning this method on the experimental determination of ternary diffusion coefficients, D_{11}, D_{22}, D_{12} and D_{21}, respectively.

The above dispersion method is based on the dispersion of small amounts of solution injected into laminar carrier streams of solvent or solution of different composition, flowing through a long capillary tube. The length of the Teflon dispersion tube used in the present study was measured directly by stretching the tube in a large hall and using two high quality theodolytes and appropriate mirrors to accurately focus on the tube ends. This technique gave a tube length of 3.2799 (±0.0001) × 10^4 mm, in agreement with less-precise control measurements using a good-quality measuring tape. The radius of the tube, 0.5570 (±0.00003) mm, was calculated from the tube volume obtained by accurately weighing (resolution 0.1 mg) the tube when empty and when filled with distilled water of known density.

At the start of each run, a 6-port Teflon injection valve (Rheodyne, model 5020) was used to introduce 0.063 mL of solution into the laminar carrier stream of slightly different composition. A flow rate of 0.17 mL min^{-1} was maintained by a metering pump (Gilson model Minipuls 3) to give retention times of about 1.1 × 10^4 s. The dispersion tube and the injection valve were kept at 298.15 K and 303.15 K (±0.01 K) in an air thermostat.

Dispersion of the injected samples was monitored using a differential refractometer (Waters model 2410) at the outlet of the dispersion tube. Detector voltages, $V(t)$, were measured at accurately 5 s time intervals with a digital voltmeter (Agilent 34401A) with an IEEE interface. Binary diffusion coefficients, D, were evaluated by fitting the dispersion equation

$$V(t) = V_0 + V_1 t + V_{\max}(t_R/t)^{1/2} \exp\left[-12D(t - t_R)^2/r^2 t\right] \quad (1)$$

to the detector voltages. The additional fitting parameters were the mean sample retention time t_R, peak height $V_{\max}$, baseline voltage V_0, and baseline slope V_1.

Diffusion in a ternary solution is described by the diffusion equations

$$-(J_1) = (D_{11})_v \frac{\partial c_1}{\partial x} + (D_{12})_v \frac{\partial c_2}{\partial x} \quad (2)$$

$$-(J_2) = (D_{21})_v \frac{\partial c_1}{\partial x} + (D_{22})_v \frac{\partial c_2}{\partial x} \quad (3)$$

where J_1, J_2, $\frac{\partial c_1}{\partial x}$ and $\frac{\partial c_2}{\partial x}$ are the molar fluxes and the gradients in the concentrations of solutes 1 and 2, respectively. Main diffusion coefficients, D_{11} and D_{22}, give the flux of each solute produced by its own concentration gradient. Cross diffusion coefficients D_{12} and D_{21} give the coupled flux of each solute driven by a concentration gradient in the other solute. A positive D_{ik} cross- coefficient ($i \neq k$) indicates co-current coupled transport of solute i from regions of higher concentration of solute k to regions of lower concentration of solute k. However, a negative D_{ik} coefficient indicates counter-current coupled transport of solute i from regions of lower to higher concentration of solute k.

Extensions of the Taylor technique have been used to measure ternary mutual diffusion coefficients (D_{11}, D_{22}, D_{12} and D_{21}) for multicomponent solutions. These coefficients were evaluated by fitting the ternary dispersion equation (Eq. (4)) to two or more replicate pairs of peaks for each carrier-stream.

$$V(t) = V_0 + V_1 t + V_{\max}(t_R/t)^{1/2} \quad (4)$$

$$\left[W_1 \exp\left(-\frac{12D_1(t - t_R)^2}{r^2 t}\right) + (1 - W_1)\exp\left(-\frac{12D_2(t - t_R)^2}{r^2 t}\right)\right] \quad (5)$$

Two pairs of refractive-index profiles, D_1 and D_2, are the eigenvalues of the matrix of the ternary D_{ik} coefficients.

In these experiments, small volumes of ΔV of solution, of composition $\bar{c}_1 + \overline{\Delta c}_1$, $\bar{c}_2 + \overline{\Delta c}_2$ are injected into carrier solutions of composition, $\bar{c}_1$, $\bar{c}_2$ at time $t = 0$.

3. Results and discussion

The diffusion coefficients values for the ternary system $CuCl_2$ + caffeine + water at 25 °C and 37 °C, D_{11}, D_{12}, D_{21} and D_{22}, are summarised in Tables 1 and 2. These results are the average of 4 experiments. Good reproducibility was observed, as seen by the small standard deviations of the mean, S_{Dav}. Previous papers (Ribeiro, Leaist, et al., 2006; Ribeiro, Valente, et al., 2007; Ribeiro et al., 2008) reporting data obtained with this technique have shown that the error limits of our results should be close to the imprecision, therefore, giving an experimental uncertainty of 1–3%.

These results are compared with those obtained for binary systems at same temperature and same technique (Tables 1 and 2), that is, for $CuCl_2$ and caffeine in aqueous solutions, respectively.

From the above results, it is evident that caffeine molecules exert a significant influence on the diffusion of $CuCl_2$ in aqueous solution (that is, in general, for [caffeine]/[$CuCl_2$] ratio values $\geqslant 1$, increasing this effect with the increase of these ratios, and with increase of the concentrations but for the same ratio). Main coefficients D_{11} and D_{22} give the molar fluxes of the $CuCl_2$ (1) and caffeine (2) components driven by their own concentration

Table 1
Diffusion coefficients of the ternary system copper chloride (1) + caffeine (2) solutions, D_{11}, D_{12}, D_{21} and D_{22}, and the respective standard deviations, S_D, at 25 °C.

c_1[a]	c_2[a]	R[b]	$D_{11} \pm S_D/(10^{-9}\ m^2\ s^{-1})$	$D_{12} \pm S_D/(10^{-9}\ m^2\ s^{-1})$	$D_{21} \pm S_D/(10^{-9}\ m^2\ s^{-1})$	$D_{22} \pm S_D/(10^{-9}\ m^2\ s^{-1})$	D_{12}/D_{22}[c]	D_{21}/D_{11}[d]
0.000	0.001	—				0.760[f]		
0.000	0.005	—				0.738[f]		
0.000	0.010	—				0.703[f]		
0.000	0.020	—				0.663[f]		
0.001	0.000	—	1.284[e]					
0.005	0.000	—	1.235[e]					
0.010	0.000	—	1.199[e]					
0.020	0.000	—	1.128[e]					
0.001	0.001	1	1.260 ± 0.024	0.018 ± 0.006	−0.017 ± 0.005	0.750 ± 0.011	0.024	−0.013
0.001	0.005	5	1.180 ± 0.021	0.019 ± 0.006	−0.018 ± 0.020	0.721 ± 0.012	0.026	−0.015
0.005	0.005	1	1.174 ± 0.002	0.024 ± 0.009	−0.054 ± 0.038	0.711 ± 0.009	0.033	−0.046
0.005	0.010	2	1.148 ± 0.003	0.067 ± 0.025	−0.082 ± 0.017	0.649 ± 0.016	0.034	−0.046
0.010	0.010	1	1.146 ± 0.028	0.026 ± 0.020	−0.053 ± 0.036	0.685 ± 0.022	0.038	−0.046
0.020	0.020	1	1.116 ± 0.014	0.103 ± 0.001	−0.104 ± 0.003	0.627 ± 0.011	0.164	−0.093

[a] c_1 and c_2 in units of mol dm^{-3}.
[b] $R = c_2/c_1$ for ternary systems.
[c] D_{12}/D_{22} give the number of moles of $CuCl_2$ co-transported per mole of caffeine.
[d] D_{21}/D_{11} give the number of moles of caffeine counter-transported per mole of $CuCl_2$.
[e] Our experimental binary D values for aqueous $CuCl_2$ (Ribeiro, Esteso, et al. (2006).
[f] Taylor binary D values for aqueous *caffeine* (Leaist and Hui (1990)).

Table 2
Diffusion coefficients of the ternary system copper chloride (1) + caffeine (2) solutions, D_{11}, D_{12}, D_{21} and D_{22}, and the respective standard deviations, S_D, at 37 °C.

c_1 [a]	c_2 [a]	R[b]	$D_{11} \pm S_D/(10^{-9}\ m^2\ s^{-1})$	$D_{12} \pm S_D/(10^{-9}\ m^2\ s^{-1})$	$D_{21} \pm S_D/(10^{-9}\ m^2\ s^{-1})$	$D_{22} \pm S_D/(10^{-9}\ m^2\ s^{-1})$	D_{12}/D_{22}[c]	D_{21}/D_{11}[d]
0.000	0.001	—				1.050		
0.000	0.005	—				0.980		
0.000	0.010	—				0.944		
0.000	0.020					0.890		
0.001	0.000	—	1.683[e]					
0.005	0.000	—	1.660[e]					
0.010	0.000	—	1.630[e]					
0.020	0.000	—	1.580 [e]					
0.001	0.001	1	1.599 ± 0.024	0.009 ± 0.006	−0.008 ± 0.020	0.982 ± 0.011	0.001	−0.005
0.001	0.005	5	1.520 ± 0.035	0.001 ± 0.065	−0.010 ± 0.005	0.981 ± 0.041	0.001	−0.007
0.005	0.005	1	1.539 ± 0.024	0.041 ± 0.021	−0.056 ± 0.020	0.927 ± 0.021	0.044	−0.037
0.005	0.010	2	1.450 ± 0.010	0.019 ± 0.014	−0.030 ± 0.038	0.920 ± 0.011	0.021	0.021
0.010	0.010	1	1.455 ± 0.034	0.026 ± 0.011	−0.003 ± 0.017	0.934 ± 0.012	0.028	−0.002
0.020	0.020	1	1.302 ± 0.014	0.104 ± 0.003	0.110 ± 0.036	0.795 ± 0.019	0.131	0.084

[a] c_1 and c_2 in units of mol dm^{-3}.
[b] $R = c_2/c_1$ for ternary systems.
[c] D_{12}/D_{22} give the number of moles of $CuCl_2$ co-transported per mole of caffeine.
[d] D_{21}/D_{11} give the number of moles of caffeine counter-transported per mole of $CuCl_2$.
[e] Our experimental binary D values for aqueous $CuCl_2$ (Ribeiro et al. (2005)).

gradient. In general, these coefficients are lower than the binary diffusion coefficients of aqueous $CuCl_2$ and caffeine for both temperatures (deviations between 1% and 10%). However, in general, at the concentrations used in this study, we verify that added $CuCl_2$ produces relatively minor changes in D_{22} for caffeine, whilst added caffeine produces major chances in D_{11} for $CuCl_2$. Some copper ions can be present in solution as complexes 1:1 Cu(II):caffeine, as indicated in the literature (Franska, 2008). Consequently, they will have less mobility and, consequently, they can be responsible for relatively large decreases in D_{11}. This effect is less accentuated when we consider the effect of $CuCl_2$ on transport of caffeine, probably due to the similarity of the mobilities of caffeine free species and eventual aggregates of $CuCl_2$ and caffeine (Spiro et al., 1989).

The limiting values for infinitesimal concentration of cross-coefficients D_{12} and D_{21} should be zero within experimental error. However, at finite concentrations, the cross-coefficients D_{12} and D_{21} values different from zero may be used to understand the influence of these solutes in diffusion of solution components. In our case, the gradient in the concentration of $CuCl_2$ produces co-current coupled flows of caffeine. Considering that D_{12}/D_{22} gives the number of moles of $CuCl_2$ co-transported per mole of caffeine, we may say that, at the concentrations used, a mole of diffusing caffeine co-transports at most 0.02 mol of $CuCl_2$, increasing the co-transport with the increase of its concentration. Through D_{21}/D_{11} values, at the same concentrations, we can expect that a mole of diffusing $CuCl_2$ counter transports at most 0.01 mol of caffeine.

At 310.15 K, the of $CuCl_2$ co-transported per mole of caffeine, $D_{12}/D_{22,}$ is about 0.001 mol, whilst the number of moles of caffeine transported per mole of copper chloride, D_{21}/D_{11}, and their direction strongly depend on the concentration of the caffeine (that is, for concentrations of caffeine for the concentration range 0.001–0.020 M, the number of moles of this component can change between 0.002 and 0.084, as well as their direction).

These interactions can be explained with basis in electrostatic mechanism (Callendar & Leaist, 2006; Leaist, 1986). In binary solutions of $CuCl_2$, the condition of electroneutrality requires that Cu^{2+} and Cl^- ions diffuse at the same rate, even though the mobility of Cl^- is approximately two times larger than the mobility of Cu^{2+}. In fact, the electrical field produced by the flow of the $CuCl_2$ slows down Cl^- and speeds up Cu^{2+}, so that they travel at the same rate and thereby preventing charge separation. If caffeine is added, amounts of copper and chloride can be transported as complexes 1:1 Cu(II):caffeine and, in that situation, most the free copper is consumed by formation of these complexes. As a result, the gradi-

ent in $CuCl_2$ produces a gradient with opposite sign in the concentration of Cu^{2+} species. As these species diffuses toward the region of higher copper chloride concentration, as electric field is induced to slow Cl^- migration and maintain electroneutrality. The electric field pulls the caffeine (as a mixture of monomer caffeine molecules, and of a significant fraction of dimmers and higher caffeine multimers species, as shown as by dimerisation constant, K_D = 6.8 kg mol^{-1} at 25 °C Spiro et al., 1989) along with Cl^-, counter-current to the main flow of copper chloride, and resulting, hence, negative values of D_{21}. However, with the increase of the temperature (Table 2), we obtain, for some concentrations, values of D_{21} and D_{12} lower, indicating us that eventual interactions present in those systems are less accentuated at physiological temperature, (37 °C). The contribution of all species for the influence on this transport property may eventually be difficult to make. In fact, clarifying the nature of these interactions is not an easy task. However, we could say that what eventually can be more important for some areas of interest (e.g. pharmaceutical applications) is the thermodynamic behaviour of the involved species, not so much the complex question of the nature of their internal binding forces.

4. Conclusions

Based on these ternary diffusion measurements, we may conclude that in the concentration range studied, for each solute, caffeine plays a role on the behaviour of the diffusion copper chloride in aqueous solutions. In fact, we can see that the diffusion of $CuCl_2$ in aqueous solutions at both temperatures, 25 °C and 37 °C, may be affected by the eventual presence of new different species resulting from various equilibria (e.g. dimmers and higher caffeine multimers, different complexes as 1:1 Cu(II):caffeine, and monomers of protonated caffeine).

In conclusion, diffusion coefficients measured for aqueous solutions of $CuCl_2$ and caffeine provide transport data necessary to model diffusion in practical applications.

Acknowledgment

A.C.F.R. is grateful for the Sabbatical Leave Grant (BSAB) from "Fundação para a Ciência e Tecnologia".

References

Aldrian, P. S., Keen, C. L., Lonnerdal, B., & Dewey, K. G. (1997). Effects of coffee consumption on iron, zinc and copper status in nonpregnant Sprague-Dawely rats. *International Journal of Food Sciences and Nutrition, 48*, 177–189.

Barthel, J., Gores, H. J., Lohr, C. M., & Seidl, J. J. (1996). Taylor dispersion measurements at low electrolyte concentrations. 1. Tetraalkylammonium perchlorate aqueous solutions. *Journal Solution Chemistry, 25*(92), 1–935.

Callendar, R., & Leaist, D. G. (2006). Diffusion coefficients for binary, ternary, and polydisperse solutions from peak-width analysis of Taylor dispersion profiles. *Journal Solution Chemistry, 35*, 353–379.

Cingi, M. B., Borromei, R., & Oleari, L. (1977). Influence of copper (II) salts on the solubility of caffeine in water: Complex formation and the salting-out effect. *Journal Chemical Society-Dalton Transactions, 22*, 2276–2280.

David, L., Cozar, O., Forizs, E., Craciun, C., Ristoiu, D., & Balan, C. (1999). Local structure analysis of some Cu(II) theophylline complexes. *Spectrochimica Acta Part A, 55*, 2559–2564.

Falk, M., Chew, W., Waiter, J. A., Kwiatkowski, W., Barclay, D. K., & Klassen, G. A. (1998). Molecular modelling and NMR studies of the caffeine dimmer. *Canadian Journal of Chemistry-Revue Canadienne de Chimie, 76*, 48–56.

Franska, M. (2008). Detection of binuclears copper-caffeine complexes under electrospray ionization condition. *European Journal of Mass Spectrometry, 14*, 81–86.

Kolayli, S., Ocak, M., Küçük, M., & Abbasoğlu, R. (2004). Does caffeine bind to metal ions? *Food Chemistry, 84*, 383–388.

Leaist, D. G. (1986). Transport in aqueous zinc chloride–potassium chloride electrolytes. *Berichte Bunsenges Physikalische Chemie, 90*, 797–802.

Leaist, D. G., & Hui, L. (1990). Intradiffusion coefficients and integral mutual diffusion coefficients of dilute associating solutes are identical. Caffeine in water. *Journal Physics Chemistry, 94*, 8741–8744.

Nafisi, S., Shamloo, D. S., Mohajerani, N., & Omidi, A. (2002). A comparative study of caffeine and theophylline binding to Mg(II) and Ca(II) ions: Studied by FTIR and UV spectroscopic methods. *Journal of Molecular Structure, 608*(1), 1–7.

Nafisi, S., Monajemi, M., & Ebrahimi, S. (2004). The effects of mono-and divalent metal cations on the solution structure of caffeine and theophylline. *Journal Molecular Structure, 705*(1–3), 35–39.

Nafisi, S., Manouchehri, F., Tajmir-Riahi, H. A., & Varavipour, M. (2008). Structural features of DNA interaction with caffeine and theophylline. *Journal of Molecular Structure, 875*(1–3), 392–399.

Ribeiro, A. C. F., Esteso, M. A., Lobo, V. M. M., Valente, A. J. M., Simões, S. M. N., Sobral, A. J. F. N., et al. (2005). Diffusion coefficients of copper chloride in aqueous solutions at 298.15 K and 310.15 K. *Journal of Chemistry and Engineering Data, 50*(198), 6–1990.

Ribeiro, A. C. F., Esteso, M. A., Lobo, V. M. M., Valente, A. J. M., Simões, S. M. N., Sobral, A. J. F. N., et al. (2006). Interactions of copper (II) chloride with B-cyclodextrin in aqueous solutions at 25 °C. *Journal Carbohydrate Chemistry, 25*, 173–185.

Ribeiro, A. C. F., Leaist, D. G., Lobo, V. M. M., Esteso, M. A., Valente, A. J. M., Santos, C. I. A. V., et al. (2006). Binary mutual diffusion coefficients of aqueous solutions of β-cyclodextrin at temperatures from 298.15 to 312.15 K. *Journal of Chemical and Engineering Data, 51*(136), 8–1371.

Ribeiro, A. C. F., Esteso, M. A., Lobo, V. M. M., Valente, A. J. M., Simões, S. M. N., Sobral, A. J. F. N., et al. (2007). Interactions of copper (II) chloride with sucrose, glucose and fructose in aqueous solutions. *Journal Molecular Structure, 826*, 113–119.

Ribeiro, A. C. F., Valente, A. J. M., Santos, C. I. A. V., Prazeres, P. M. R. A., Lobo, V. M. M., Burrows, H. D., et al. (2007). Binary mutual diffusion coefficients of aqueous solutions of α-cyclodextrin, 2-hydroxypropyl-α-cyclodextrin and 2-hydroxypropyl-β-cyclodextrin at temperatures from 298.15 to 312.15 K. *Journal of Chemistry and Engineering Data, 52*(58), 6–590.

Ribeiro, A. C. F., Santos, C. I. A. V., Valente, A. J. M., Ascenso, O. S., Lobo, V. M. M., Burrows, H. D., et al. (2008). Some transport properties of γ-cyclodextrin aqueous solutions at (298.15 and 310.15 K). *Journal of Chemical and Engineering Data, 53*(75), 5–759.

Spiro, M., Grandoso, D. M., & Price, W. E. P. (1989). Protonation constant of caffeine in aqueous solution. *Journal of the Chemical Society-Faraday Transactions I, 85*(12), 4259–4267.

Vitagliano, V. (1991). Some phenomenological and thermodynamic aspects of diffusion in multicomponent systems. *Pure and Applied Chemistry, 63*, 1441–1448.

YeH, J. K., Aloia, J. F., Semla, H. M., & Chen, S. Y. (1986). Influence of injected caffeine on the metabolism of calcium and the retention and excretion of sodium, potassium, phosphorus, magnesium, zinc and copper in rats. *Journal of Nutrition, 116*, 273–280.

It is well known that post-harvest processing has pronounced effects on the chemical composition of coffee seeds, specially in water-soluble components like sugars, caffeine, trigonelline and chlorogenic acids (Smith, 1985). Despite the considerable availability of studies comparing coffees processed by dry and wet methods in the literature (Balylaya & Clifford, 1995; Clifford & Ramirez-Martinez, 1991; Guyot, Guele, Assemar, Tchana, & Pomathios, 1995; Knopp, Bytof, & Selmar, 2006; Leloup et al., 2004; Mazzafera & Padilha-Purcino, 2004), data on the chemical composition of coffees processed by semi-dry methods are still scarce.

Chlorogenic acids (CGA), a major family of phenolic compounds that represent 6–12% of coffee constituents in mass (Farah, DePaulis, Trugo, & Martin, 2005), are known to be responsible for coffee pigmentation and astringency (Farah & Donangelo, 2006). The thermal degradation of chlorogenic acids during roasting will result in formation of phenolic substances that contribute to bitterness (Clifford, 1985a) and aromatic compounds like phenols, which are undesirable to cup quality (Toci & Farah, 2008). Additionally, CGA participates in colour formation through its incorporation into the backbone of melanoidins (Farah & Donangelo, 2006). The major CGA classes in coffee are the caffeoylquinic acids (CQA), feruloylquinic acids (FQA) and dicaffeoylquinic acids (diCQA), with at least three isomers per class (Clifford, 2000). Caffeine is a xanthine derivative that gives a bitter characteristic taste to coffee (Farah, DePaulis, Moreira, Trugo, & Martin, 2006). Trigonelline is a pyridine derivative known to contribute indirectly to the formation of desirable and undesirable aroma compounds during roasting (Macrae, 1985; Moreira, Trugo, & Maria, 2000). Trigonelline content has also been correlated to good cup quality (Farah, Monteiro, Calado, Franca, & Trugo, 2006). Sugars, particularly sucrose, which is the most abundant simple carbohydrate in coffee, act as aroma precursor, originating several volatile substances during roasting such as furans, aldehydes and carboxylic acids (Farah, DePaulis et al., 2006; Farah, Monteiro et al., 2006; Teixeira et al., 1995). In the last few years, CGA, caffeine and trigonelline have also been the subject of several investigations in view of their potentially positive biological effects in humans.

The aim of this study was to compare the composition of the nine main chlorogenic acids, caffeine, trigonelline and sucrose in Brazilian green coffee seeds produced by wet and semi-dry post-harvesting methods.

2. Materials and methods

2.1. Samples

Seventeen coffee samples were used in this study, being four Arabica cultivars (Red Catuaí; Rubi; Yellow Bourbon and Topázio) and 11 hybrids, 10 from the crossing of *C. arabica* cv. Yellow Catuaí with Timor Hybrid (numbers 1–11) and two from the crossing of cv. Red Caturra with Timor Hybrid (numbers 12 and 13). The coffee fruits were produced in a farm located in Paula Cândido, Minas Gerais, Brazil. After harvesting, fruits were processed by wet and semi-dry methods.

2.1.1. Post-harvesting treatments

The ripe coffee cherries were harvested by hand picking, followed by wet or semi-dry processing. For wet processing, coffee fruits were quickly washed, manually pulped, followed by 8 h soaking for fermentation and mucilage removal. After soaking, parchment coffees were washed and de-hulled. The semi-dry processed seeds, were quickly washed and manually pulped, followed by washing and de-hulling, without mucilage removal. After wet or semi-dry processing, coffee seeds were stored in plastic bags under −20 °C until chemical analysis.

2.2. Extractions for chromatographic analyses

Prior to extraction, all seeds were milled to pass a 0.46 mm sieve. CGA were extracted with aqueous methanol (40%) and clarified with Carrez solutions according to Trugo and Macrae (1984), also described in Farah et al. (2005). Caffeine and trigonelline were extracted with 95 °C distilled water and clarified with aqueous plumb acetate (20%) (Farah, DePaulis et al., 2006; Farah, Monteiro et al., 2006; Trugo & Macrae, 1984). For sucrose evaluation, green coffee seeds were extracted with aqueous methanol (40%) and clarified with acetonitrile (Trugo, Farah, & Cabral, 1995). Extractions were performed in duplicates.

2.2.1. HPLC analyses

2.2.1.1. Chlorogenic acids. CGA were analysed, using a HPLC gradient system with a high-precision pump (Shimadzu model LC-10-AD, Kyoto, Japan), a UV detector (Shimadzu model LC-10-AD) operating at 325 nm, and a ODS-C18 column (Rexchrom: 5 μm, 250 × 4.6 nm, Regis Technologies, Morton Grove, IL) coupled with a guard column (Rexchrom: 5 μm, 10 × 3 nm, Regis Technologies). Chromatographic data was recorded and integrated in the Class VP computer software (Shimadzu). A gradient using 10 mM citric acid solution and methanol was performed (Farah et al., 2005). The identity of CGA was confirmed by LC–MS analyses as described by Farah, DePaulis et al. (2006) and Farah, Monteiro et al. (2006). In this work, the authors used IUPAC numbering system for CGA. When citing other authors, their numbering has been changed when necessary for consistency.

2.2.1.2. Caffeine and trigonelline. Caffeine and trigonelline analyses were performed according to Trugo and Macrae (1984), also described in Farah, DePaulis et al. (2006) and Farah, Monteiro et al. (2006). Analyses were performed by an isocratic system consisting of pump (Knauer, Model 64, Germany), integrator (Shimadzu, Model C-R6A) and UV detector (Shimadzu, model SPD-1-AV) operating at 272 nm for caffeine and 264 nm for trigonelline. A reversal phase column (ODS C-18 Merck, Darmstadt, Germany) was used with 40% methanol as mobile phase for caffeine and with 5% methanol for trigonelline. Flow rate was 1 mL/min.

2.2.1.3. Sucrose. Sucrose analyses were performed according to Trugo et al. (1995), adapted. A pump (Knauer, model 64) with a 20 μL Rheodyne fixed loop injector (Oak Harbor, WA, USA), Spherisorb NH_2 column (Supelco, Bellefonte, PA, USA), RI detector (Waters, Milford, MA, USA) and integrator (Hewllet Packard, model) were used. A mobile phase with acetonitrile 80%, at 1 mL/min was used.

2.3. Water content

In order to express the results in dry matter basis (dm), the water content of all samples was determined according to AOAC procedures (2000).

2.4. Statistical analysis

HPLC results were tested for differences by GraphPad Prism® software, version 4.0 (San Diego, CA, USA), using paired *t*-test method and considered significant when $p \leqslant 0.05$.

3. Results and discussion

3.1. Chlorogenic acids

The levels of CQA, FQA and diCQA in green coffee seeds processed by wet and semi-dry post-harvesting methods are

presented in Tables 1 and 2, respectively. For the first time, the distribution and content of nine CGA (3-CQA; 4-CQA; 5-CQA; 3-FQA; 4-FQA; 5-FQA; 3,4-diCQA; 3,5-diCQA; 4,5-diCQA) are compared in Brazilian coffees processed by wet and semi-dry methods. The CGA contents observed in this work are consistent with previous data for coffee in general (Farah & Donangelo, 2006). In the wet method, the average contents of CQA, di-CQA and FQA were, respectively, 4.94 ± 0.41; 0.94 ± 0.05 and 0.32 ± 0.02 g/100 g (dm), representing 81.3%, 13.3% and 5.3% of total CGA content (6.08 ± 0.44 g/100 g, dm). In this group, the sample with highest level of CGA was hybrid **1** (7.4 ± 0.21 g/100 g, dm), while the one with the lowest level was *C. arabica* cv. Topázio (5.2 ± 0.57 g/100 g, dm).

In the semi-dry method, the mean levels of CQA were 4.70 ± 0.37 g/100 g (dm), followed by diCQAs with 0.98 ± 0.02 g/100 g (dm) and FQA with 0.30 ± 0.01 g/100 g (dm). These classes accounted for 81.0%, 14.0% and 5.1% of total CGA levels (5.8 ± 0.38 g/100 g, dm), respectively. The highest content of total CGA was observed in hybrid **2** (6.7 ± 0.58 g/100 g, dm), mainly due to higher contents of 5-CQA and, to a lesser extent, 3,5-diCQA. The lowest content was observed in hybrid **3** (5.4 ± 0.25 g/100 g, dm). The highest and lowest CGA contents present in hybrids **2** and **3**, respectively, may result from different genetic inheritance of *C. arabica* and *C. canephora*, since Timor hybrid samples were produced by crossing of these two species. The higher CGA content in *C. canephora* comparing to *C. arabica* has been extensively reported (Clifford & Ramirez-Martinez, 1991; Farah & Donangelo, 2006).

Although the distribution profile of CGA classes in samples treated by the semi-dry method was similar to those treated by the wet method, on average, coffees processed by the wet method presented significantly higher total CGA content ($p = 0.02$) than those processed by the semi-dry method. This difference was observed in all CGA classes, except for the diCQA.

No data on CGA composition of semi-dry method is available in the literature. However, literature has reported a higher CGA content in wet processed Robusta seeds than in dry processed seeds. This difference in CGA contents has been attributed to losses of other water-soluble components by lixiviation and fermentation in the wet method (Wootton, 1974), in addition to slight degradation of such components in dry processed seeds exposed to sun heat. In this work, it is possible to observe that the CGA composition of semi-dry seeds are intermediate to those of dry and wet processed seeds, being more comparable to results obtained for dry processed seeds. This result is coherent, since semi-dry pro-

Table 1
Chlorogenic acids contents in coffee samples processed by semi-dry post-harvesting method.

Samples	3-CQA	4-CQA	5-CQA	3-FQA	4-FQA + 5-FQA	3,4-diCQA	3,5-diCQA	4,5-diCQA
Hybrid 1	460.0 ± 30.2	615.1 ± 10.5	4200.4 ± 100.1	28.0 ± 0.5	258.2 ± 20.1	158.3 ± 15.3	367.3 ± 10.1	181.1 ± 7.1
Hybrid 2	476.1 ± 18.1	666.3 ± 24.3	4116.4 ± 98.5	29.3 ± 2.5	264.6 ± 14.5	203.7 ± 12.8	459.4 ± 19.3	249.7 ± 14.6
Hybrid 3	391.2 ± 25.3	534.3 ± 65.8	3362.2 ± 52.7	27.5 ± 3.4	246.1 ± 17.2	151.9 ± 19.7	328.1 ± 21.2	201.6 ± 15.0
Hybrid 4	455.5 ± 15.4	590.7 ± 89.0	3210.1 ± 74.3	30.7 ± 1.2	309.2 ± 14.3	186.7 ± 9.8	353.6 ± 12.8	189.1 ± 4.5
Hybrid 5	465.5 ± 22.4	657.3 ± 58.1	4317.5 ± 101.5	28.3 ± 1.3	299.8 ± 15.7	154.1 ± 17.6	343.9 ± 16.7	190.6 ± 9.1
Hybrid 6	502.8 ± 20.0	657.4 ± 20.5	3562.2 ± 78.4	28.6 ± 2.4	316.9 ± 16.8	216.6 ± 18.2	414.4 ± 19.1	204.4 ± 16.0
Hybrid 7	438.0 ± 14.6	615.1 ± 32.0	4090.3 ± 70.5	29.4 ± 5.6	285.4 ± 35.3	149.9 ± 19.1	312.4 ± 21.1	197.4 ± 12.2
Hybrid 8	472.1 ± 26.5	647.4 ± 16.7	3907.9 ± 35.2	27.9 ± 2.3	259.9 ± 17.1	168.8 ± 11.1	313.2 ± 17.6	170.2 ± 6.8
Hybrid 9	440.7 ± 15.2	624.8 ± 37.6	3723.5 ± 40.1	26.9 ± 6.0	290.0 ± 24.3	191.3 ± 21.7	387.8 ± 11.0	240.5 ± 9.7
Hybrid 10	479.2 ± 22.6	660.3 ± 41.9	3905.2 ± 98.2	28.2 ± 2.4	270.0 ± 25.2	194.3 ± 17.3	380.2 ± 10.0	219.0 ± 12.4
Hybrid 11	480.1 ± 38.9	662.3 ± 18.8	3920.3 ± 84.1	31.3 ± 1.7	271.3 ± 36.4	196.3 ± 16.2	380.3 ± 10.0	220.3 ± 18.4
Hybrid 12	509.1 ± 19.2	676.2 ± 22.5	2967.4 ± 14.6	39.0 ± 1.9	253.9 ± 30.5	253.5 ± 28.3	431.6 ± 15.0	243.2 ± 18.2
Hybrid 13	510.5 ± 52.3	680.3 ± 20.9	3005.2 ± 65.2	41.2 ± 2.8	267.0 ± 22.7	249.3 ± 31.4	432.6 ± 10.0	250.1 ± 14.3
Yellow Bourbon	403.9 ± 41.2	582.6 ± 74.0	3305.0 ± 74.0	27.1 ± 6.5	221.4 ± 50.3	220.6 ± 14.4	462.1 ± 8.5	125.0 ± 17.0
Red Catuaí	437.9 ± 40.5	605.8 ± 30.2	3226.3 ± 41.2	32.8 ± 7.1	247.1 ± 47.8	214.5 ± 21.7	440.4 ± 13.3	229.4 ± 4.5
Rubi	445.9 ± 17.1	617.9 ± 24.6	3191.5 ± 54.2	28.0 ± 1.3	206.9 ± 12.7	238.0 ± 8.5	442.3 ± 12.5	248.5 ± 13.0
Topázio	536.0 ± 15.3	689.4 ± 28.2	3251.2 ± 35.4	28.6 ± 1.3	257.9 ± 19.9	238.3 ± 9.7	423.2 ± 12.2	225.8 ± 10.0

CQA = caffeoylquinic acids; FQA = feruloylquinic acids; diCQA = dicaffeoylquinic acids. Results are shown as mean of duplicate extraction ± standard deviation, expressed as mg/100 g of coffee in dry weight basis.

Table 2
Chlorogenic acids contents in coffee samples processed by wet post-harvesting method.

Samples	3-CQA	4-CQA	5-CQA	3-FQA	4-FQA + 5-FQA	3,4-diCQA	3,5-diCQA	4,5-diCQA
Hybrid 1	530.2 ± 20.1	675.6 ± 52.1	4845.1 ± 84.2	30.2 ± 10.3	298.2 ± 21.8	196.2 ± 10.1	410.2 ± 30.5	220.3 ± 10.2
Hybrid 2	504.0 ± 41.5	716.3 ± 21.3	4351.7 ± 13.2	31.3 ± 8.5	264.6 ± 40.1	212.1 ± 14.6	401.7 ± 2.8	292.1 ± 15.4
Hybrid 3	487.6 ± 15.6	677.3 ± 17.1	3901.7 ± 5.4	29.7 ± 7.1	263.1 ± 35.1	178.8 ± 2.8	366.0 ± 14.4	266.4 ± 17.1
Hybrid 4	416.0 ± 48.9	547.3 ± 18.4	3395.8 ± 98.3	32.4 ± 0.3	330.7 ± 1.2	160.9 ± 17.5	314.1 ± 10.4	206.9 ± 9.5
Hybrid 5	479.8 ± 16.6	701.0 ± 7.4	4396.5 ± 11.5	35.1 ± 9.5	379.2 ± 9.1	184.1 ± 24.6	401.1 ± 9.7	247.5 ± 10.4
Hybrid 6	478.9 ± 17.2	609.0 ± 10.0	3239.6 ± 76.6	30.7 ± 5.1	305.6 ± 10.1	234.3 ± 18.1	419.8 ± 10.5	273.5 ± 11.6
Hybrid 7	464.7 ± 18.1	619.4 ± 28.0	3862.2 ± 65.3	29.8 ± 4.0	366.7 ± 18.7	153.2 ± 17.1	351.0 ± 15.4	102.4 ± 10.7
Hybrid 8	467.2 ± 33.5	646.3 ± 25.2	4574.7 ± 90.3	27.7 ± 3.4	317.1 ± 52.2	207.3 ± 11.0	402.5 ± 32.5	290.9 ± 9.8
Hybrid 9	540.4 ± 74.0	727.9 ± 21.3	4017 ± 30.2	31.4 ± 8.2	327.8 ± 0.20.0	189.5 ± 18.3	342.2 ± 38.0	218.7 ± 10.4
Hybrid 10	535.6 ± 50.1	705.2 ± 17.1	4125.8 ± 21.3	32.1 ± 9.9	328.7 ± 41.8	205.7 ± 13.3	325.0 ± 7.5	215.8 ± 3.2
Hybrid 11	512.4 ± 20.6	732.3 ± 19.8	4125.8 ± 20.8	35.6 ± 10.0	315.8 ± 4.6	223.5 ± 19.0	402.5 ± 18.6	265.7 ± 17.2
Hybrid 12	506.3 ± 13.5	662.0 ± 30.8	3527.8 ± 15.2	30.9 ± 8.9	236.9 ± 31.1	203.5 ± 16.8	383.4 ± 16.1	247.6 ± 14.3
Hybrid 13	480.8 ± 10.2	627.9 ± 20.9	2852.0 ± 15.4	38.5 ± 0.9	252.6 ± 20.0	216.3 ± 17.0	387.1 ± 18.0	260.1 ± 12.0
Yellow Bourbon	501.5 ± 17.0	605.2 ± 15.6	3410.2 ± 17.5	34.1 ± 0.1	269.6 ± 15.8	275.6 ± 21.7	510.1 ± 17.0	198.4 ± 16.1
Red Catuaí	528.1 ± 23.3	685.3 ± 24.3	3256.8 ± 41.6	34.9 ± 7.1	283.4 ± 19.7	280.1 ± 22.8	270.5 ± 22.9	274.8 ± 17.0
Rubi	421.1 ± 21.7	571.8 ± 21.2	3682.6 ± 38.8	26.6 ± 7.0	228.7 ± 21.5	180.8 ± 19.0	205.2 ± 28.0	268.5 ± 18.1
Topázio	384.0 ± 14.6	503.2 ± 17.1	3162.8 ± 19.0	20.5 ± 0.5	209.4 ± 17.0	189.2 ± 9.0	363.2 ± 7.5	238.0 ± 18.1

CQA = caffeoylquinic acids; FQA = feruloylquinic acids; diCQA = dicaffeoylquinic acids. Results are shown as mean of duplicate extraction ± standard deviation, expressed as mg/100 g of coffee in dry weight basis.

cessed seeds do not undergo soaking and fermentation like wet processed seeds. Moreover, it is noteworthy to point that this difference between the chemical composition of semi-dry and wet processed seeds may be considerably amplified if soaking time is increased in the wet method. While in this work, seeds have been soaked for 8 h, soaking time may be increased to up to 48 h (Teixeira et al., 1995).

Considering the similarity of dry and semi-dry methods, the present results are in agreement with results from Balylaya and Clifford (1995), using three dry and wet-processed *C. canephora* cv. Robusta samples and Leloup et al. (2004) for six Robusta samples. On the other hand, in Balylaya and Clifford (1995), wet-processed Arabica seeds ($n = 3$) showed lower levels of total chlorogenic acids compared to dry processed seeds. In this work, when only Arabica seeds ($n = 4$) were compared statistically, no significant difference was observed between wet and semi-dry methods. Therefore, the difference observed between both methods ($p = 0.02$) is attributed to the hybrid samples ($n = 13$), which presented a similar behaviour to Robusta samples. This difference between the results obtained for Arabica and Robusta/hybrids samples may be attributed to differences in their cell-wall constitutions (Toci & Farah, 2008).

3.2. Caffeine

In the coffee seeds processed by the wet method, the contents ranged from 1.05 ± 0.02 to 1.53 ± 0.01 g/100 g (dm) while in those seeds processed by semi-dry method, caffeine contents ranged from 1.12 ± 0.02 to 1.54 ± 0.02 g/100 g (dm) of coffee (Table 3). These results are in agreement with literature reports (Farah, DePaulis et al., 2006; Farah, Monteiro et al., 2006; Macrae, 1985). No significant difference between both methods was observed regarding caffeine contents. This is in agreement with results from Balylaya and Clifford (1995) and Leloup et al. (2004) for dry and wet processed seeds, and may be possibly due to the thermo-stability and the lower contents of caffeine in coffee compared to CGA.

3.3. Trigonelline

Trigonelline contents in seeds processed by the wet method ranged from 0.80 ± 0.02 to 1.40 ± 0.01 g/100 g (dm) with average of 0.90 ± 0.01 g/100 g (dm), while in seeds processed by semi-dry method, trigonelline contents ranged from 0.64 ± 0.01 to 0.92 ± 0.01 g/100 g (dm) with average of 0.81 ± 0.02 g/100 g (dm) (Table 3). These contents are in agreement with general coffee data (Farah, DePaulis et al., 2006; Farah; Martín, Pablo, & Gonzaléz, 1998; Monteiro et al., 2006). As with CGA, the relative increase in trigonelline content of coffee seeds processed by wet method compared to semi-dry method ($p < 0.0001$) may be due to loss of other components with higher water solubility by lixiviation and thermal degradation.

3.4. Sucrose

The content of sucrose in coffee treated by the wet method ranged from 8.0 ± 0.02 to 10.8 ± 0.05 g/100 g (dm), with average of 9.0 ± 0.03 g/100 g (dm) (Table 3). Sucrose content in seeds treated by the semi-dry method ranged from 7.10 ± 0.02 g/100 g to 14.5 ± 0.05 g/100 g (dm) with average of 12.3 ± 0.07 g/100 g (dm) (Table 3). These contents are generally in agreement with reports by Farah, DePaulis et al. (2006), Farah, Monteiro et al. (2006) and Knopp et al. (2006). Sucrose content in coffee seeds processed by the semi-dry method was significantly higher than in those processed by the wet method ($p = 0.02$) when including hybrids and Arabica samples. However, when evaluating only Arabica samples, no differences were found between semi-dry and wet methods. These results are also in agreement with those by Knopp et al. (2006).

In contrast with our results, Leloup et al. (2004) did not find differences when comparing sugar contents in dry and wet Robusta samples. However, our results are comparable to results from Guyot et al. (1995) who evaluated samples of *C. canephora* cv. Robusta treated by dry and wet methods.

As stated above, differently from the wet method, in the semi-dry method the mucilage is kept on the bean. According to Avallone, Guiraud, Guyot, Olguin, and Brillouet (2001), the mucilage is composed mostly by cell well polysaccharides, pectic substances and monosaccharides. Sucrose is not present in a dominant proportion in the mucilage when compared with other sugars. The authors state that this disaccharide is present mostly inside the coffee bean. Thus, it would not be possible to easily conclude that coffees produced by semi-dry methods have more sucrose than those produced by the wet method. Therefore, sucrose losses observed in our wet processed hybrid seeds are possibly mostly due to the high water solubility of this compound during washing and soaking and due to its use as a substrate for fermentation (Wootton, 1974). As with the CGA, the difference between the results obtained for Arabica and hybrids from Robusta samples might

Table 3
Caffeine, trigonelline and sucrose contents in coffee samples processed by semi-dry and wet post-harvesting methods.

Samples	Semi-dry method			Wet method		
	Caffeine	Trigonelline	Sucrose	Caffeine	Trigonelline	Sucrose
Hybrid 1	1.54 ± 0.02	0.83 ± 0.03	11.21 ± 0.02	1.53 ± 0.01	0.87 ± 0.01	10.41 ± 0.01
Hybrid 2	1.38 ± 0.02	0.81 ± 0.03	11.6 ± 0.01	1.42 ± 0.01	0.96 ± 0.01	10.56 ± 0.01
Hybrid 3	1.40 ± 0.01	0.64 ± 0.02	7.13 ± 0.02	1.45 ± 0.01	0.88 ± 0.01	8.78 ± 0.01
Hybrid 4	1.30 ± 0.02	0.84 ± 0.02	10.39 ± 0.01	1.15 ± 0.01	0.93 ± 0.01	9.73 ± 0.01
Hybrid 5	1.34 ± 0.02	0.76 ± 0.02	10.10 ± 0.01	1.46 ± 0.01	0.93 ± 0.01	9.89 ± 0.01
Hybrid 6	1.37 ± 0.03	0.77 ± 0.02	9.82 ± 0.01	1.19 ± 0.03	0.85 ± 0.01	10.49 ± 0.05
Hybrid 7	1.32 ± 0.01	0.79 ± 0.03	9.25 ± 0.02	1.39 ± 0.01	0.86 ± 0.01	8.53 ± 0.05
Hybrid 8	1.35 ± 0.01	0.78 ± 0.03	9.50 ± 0.03	1.47 ± 0.02	0.86 ± 0.01	9.64 ± 0.05
Hybrid 9	1.25 ± 0.01	0.85 ± 0.03	10.31 ± 0.05	1.29 ± 0.01	1.03 ± 0.02	9.34 ± 0.05
Hybrid 10	1.20 ± 0.01	0.90 ± 0.03	9.01 ± 0.01	1.05 ± 0.01	0.92 ± 0.01	8.05 ± 0.04
Hybrid 11	1.11 ± 0.02	0.89 ± 0.03	8.88 ± 0.01	1.14 ± 0.01	1.12 ± 0.01	9.61 ± 0.04
Hybrid 12	1.19 ± 0.01	0.76 ± 0.03	14.54 ± 0.02	1.23 ± 0.01	0.80 ± 0.02	8.98 ± 0.01
Hybrid 13	1.12 ± 0.03	0.77 ± 0.02	13.41 ± 0.02	1.22 ± 0.01	0.83 ± 0.01	10.03 ± 0.01
Yellow Bourbon	1.13 ± 0.02	0.90 ± 0.01	10.05 ± 0.01	1.05 ± 0.02	0.89 ± 0.01	10.88 ± 0.04
Red Catuaí	1.13 ± 0.02	0.78 ± 0.04	11.68 ± 0.01	1.26 ± 0.02	0.92 ± 0.01	9.85 ± 0.03
Rubi	1.21 ± 0.01	0.74 ± 0.01	11.98 ± 0.02	1.19 ± 0.02	0.80 ± 0.01	9.16 ± 0.05
Topázio	1.43 ± 0.01	0.92 ± 0.01	12.66 ± 0.02	1.16 ± 0.01	0.85 ± 0.02	8.49 ± 0.04

Results are shown as mean of duplicate extraction ± standard deviation, expressed as mg/100 g of coffee in dry weight basis.

be attributed to differences in their cell-wall constitutions (Toci & Farah, 2008) but should be thoroughly investigated.

4. Conclusions

For the first time, the contents of nine chlorogenic acids, caffeine, trigonelline and sucrose were evaluated together in Brazilian Arabica coffee cultivars and hybrids treated by wet and semi-dry post-harvesting methods. The wet method produced an increase in chlorogenic acids and trigonelline contents and a small loss in sucrose contents comparing to semi-dry method. However, since the soaking period in the wet method is largely variable, more dramatic changes may be observed in these coffee components when seeds are soaked for longer periods of time. Sensorial analysis should be carried out in order to correlate the chemical differences observed between both post-harvesting methods with cup quality.

Acknowledgements

The authors would like to thank Henrique Theodoro Martins Peixoto, Dartanhan Augusto Fernandes Lima and José Carlos Silva Guimarães for assistance with coffee production, harvesting and processing; and to Carolina Castro Borges for technical assistance with trigonelline analysis. The financial support of CBPandD/Café-EMBRAPA; CNPq and FAPERJ is greatly acknowledged.

References

ABIC. (2008). Notícias. <http://www.abic.com.br/exportação.html> Accessed 20.04.2008.

AOAC (2000). *Official methods of analysis of the association of official analytical chemists* (17th ed.). Gaithersburg, MD, USA: Association of Official Analytical Chemists.

Avallone, S., Guiraud, J. P., Guyot, B., Olguin, E., & Brillouet, J. M. (2001). Fate of mucilage cell wall polysaccharides during coffee fermentation. *Journal of Agricultural and Food Chemistry, 49*, 5556–5559.

Balylaya, K. J., & Clifford, M. N. (1995). Chlorogenic acids and caffeine contents of monsooned Indian Arabica and robusta coffees compared with wet and dry processed coffees from the same geographic area. In *ASIC proceedings of 16th colloque coffee* (pp. 316–324). Kyoto.

Clifford, M. N. (1985a). Chlorogenic acids. In R. J. Clarke & R. Macrae (Eds.), *Coffee chemistry* (pp. 153–202). Elsevier, Applied Science: Amsterdam.

Clifford, M. N. (2000). Chlorogenic acids and others cinnamates-nature, occurrence, dietary burden, absorption and metabolism. *Journal of Science and Food Agricultural, 80*, 1033–1043.

Clifford, M. N., & Ramirez-Martinez, J. R. (1991). Phenols and caffeine in wet-processed coffee seeds and coffee pulp. *Food Chemistry, 40*, 35–42.

Farah, A., DePaulis, T., Moreira, D. P., Trugo, L. C., & Martin, P. R. (2006). Chlorogenic acids and lactones in regular and water-decaffeinated Arabica coffees. *Journal of Agricultural and Food Chemistry, 54*, 374–381.

Farah, A., DePaulis, T., Trugo, L. C., & Martin, P. R. (2005). Formation of chlorogenic acids lactones in roasted coffee. *Journal of Agricultural and Food Chemistry, 53*, 1105–1113.

Farah, A., & Donangelo, C. M. (2006). Phenolic compounds in coffee. *Brazilian Journal Plant Physiology, 18*(1), 23–36.

Farah, A., Monteiro, M. C., Calado, V., Franca, A. S., & Trugo, L. C. (2006). Correlation between cup quality and chemical attributes of Brazilian coffee. *Food Chemistry, 98*, 373–380.

Guyot, B., Guele, D., Assemar, S., Tchana, E., & Pomathios, L. (1995). Influence du mode de préparation du café vert robusta sur as composition chimique et ses qualités organoleptiques. In *ASIC proceedings of the 16th colloque scientifique international sur le Café* (pp. 267–277). Paris.

Knopp, S.-E., Bytof, G., & Selmar, D. (2006). Influenced of processing on the content of sugars in green Arabica coffee seeds. *European Food Research and Technology, 223*, 195–201.

Leloup, V., Cancel, C., Liardon, R., Rytz, A., & Pithon, A. (2004). Impact of wet and dry process on green composition and sensory characteristics. In *ASIC proceedings of 20th colloque coffee* (pp. 93–100). Bangalore, India.

Macrae, R. (1985). Nitrogenous compounds. In R. J. Clarke & R. Macrae (Eds.), *Coffee chemistry* (pp. 115–152). Elsevier, Applied Science: Amsterdam.

Martín, M. J., Pablo, F., & Gonzaléz, A. G. (1998). Discrimination between arabica and robusta green coffee varieties according to their chemical composition. *Talanta, 46*, 1259–1264.

Mazzafera, P., & Padilha-Purcino, R. (2004). Post harvest processing methods and alterations in coffee fruit. In *ASIC proceedings of 20th colloque coffee*. Bangalore, India.

Moreira, R. F. A., Trugo, L. C., & Maria, C. A. B. (2000). Compostos voláteis do café torrado. Parte II. Compostos alifáticos, alicíclicos e aromáticos. *Quimica Nova, 23*, 195–201.

Rothfos, B. (1980). *Coffee production*. Hamburg: Gordian-Max-Rieck.

Smith, A. W. (1985). Agricultural practices. In R. J. Clarke & R. Macrae (Eds.), *Coffee chemistry* (pp. 18–23). Elsevier, Applied Science: Amsterdam.

Teixeira, A. A., Brando, C. H. J., Thomaziello, R. A., & Teixiera, R. (1995). In A. Illy & R. Viani (Eds.), *Espresso coffee: The science of quality* (pp. 91–95). Italy: Elsevier Academic Press. 197, 198.

Toci, A. T., & Farah, A. (2008). Volatile compounds as potential defective coffee seeds' markers. *Food Chemistry, 108*, 1133–1141.

Trugo, L. C., Farah, A., & Cabral, L. (1995). Oligosaccharides distribution in Brazilian soybean cultivars. *Food Chemistry, 52*(4), 385–387.

Trugo, L. C., & Macrae, R. A. (1984). Chlorogenic acid composition of instant coffee. *Analyst, 109*, 263–266.

Wootton, A. E. (1974). The dry matter loss from parchment coffee during field processing. In *ASIC proceedings of the 16th Colloque Scientifique International sur la Chimie des Cafés Verts* (pp. 316–324). Paris.

The characterisation of the animal origin of raw materials used for production of gelatin is now of concern for both manufacturers and consumers. This paper describes the potential utilisation of FTIR spectroscopy as a rapid method to differentiate and authenticate the source of gelatin.

2. Materials and methods

2.1. Sample preparation

Two different gelatin samples from porcine and bovine sources were obtained from Sigma and Merck, respectively (Table 1). Gelatin jellies were prepared by dissolving gelatins in deionized water and the mixtures were placed in a sonicator at 50 °C for 10 min until a clear solution was acquired. The jellies were poured into aluminum foil moulds (68 mm × 8 mm × 5 mm) and allowed to set for 1 h at 16–20 °C. The jellies were then cut into 68 mm × 8 mm × 3 mm according to ATR surface area. In this study, a total of 19 samples of porcine and bovine jellies were prepared, the concentrations of which were between 2% w/v and 16% w/v. The concentrations were chosen to be similar to those found in typical desserts and pastilles.

2.2. FTIR measurement

A Nicolet 6700 spectrometer model (Thermo-Nicolet, USA) with a DTGS-KBR detector was used in the measurements. An ATR accessory equipped with ZnSe cell was used. All spectra were recorded within a range of 4000–650 cm^{-1} with a 4 cm^{-1} resolution and 32 scans. Two replicate spectra were obtained from two independent experiments and the average spectrum was taken for further investigation. All measurements were performed in a dry atmosphere at room temperature (25 ± 0.5 °C). A single beam spectrum was obtained for all samples. These spectrums were subtracted against a background air spectrum and the results were presented in absorbance units.

ATR is a technique whereby the sample is placed in contact with ATR element (ZnSe crystal, 45° ends) and a spectrum is recorded because of that contact. This sampling technique allows radiation through the sample without transmission and only small amount of sample is sufficient to allow transmission of the incident radiation provided the sample is sufficient to cover the entire ATR surface (Griffiths & Haseth, 2007).

2.3. Acquisition of infrared spectra and data

All data were subjected to discriminant analysis (DA) using TQ Analyst software (Thermo-Nicolet, Madison, WI, USA). DA was performed for the wavenumber ranges between 3300–3280 cm^{-1} and 1660–1217 cm^{-1}. Constant pathlength was used for calculations. There are six principal components used for calculation to reduce spectral information. The Mahalanobis distance was used to formulate a distance between clusters. It was made on the variables of the study with the aim to determine which of these variables best discriminated according to the right sources of gelatin as well as establishing a mathematical model for this purpose. The distance is measured in terms of standard deviations from the mean of the training samples.

2.4. Discriminant analysis

In the TQ Analyst Software, the validation needs to be carried out by splitting the spectrum into two groups. One group for calibration and the other one for validation. Only three to four spectra were selected as validation spectra. The rest were performed as calibration spectra. When all validation spectra lay inside their cluster, the modules is consider correct.

3. Results and discussion

3.1. Spectral for gelatins

The frequencies at which major peaks occurred are shown in Fig. 1. Gelatins derived from porcine exhibited spectra very similar to those for gelatins derived from bovine. Four regions involves are 3600–2300 cm^{-1} (Amide A), 1656–1644 cm^{-1} (Amide I), 1560–1335 cm^{-1} (Amide II) and 1240–670 cm^{-1} (Amide III). These peaks were identified to be similar with those reported by Muyonga et al. (2004).

A typical gelatin spectrum showed low intensities of Amides I and II bands, with the Amide III band almost non-existent. This is consistent with changes expected because of denaturation of collagen to gelatin. A very low intensity showed for Amide III region is associated with loss of triple helix state during high temperature gelatin extraction (Muyonga et al., 2004). The 3290–3280 cm^{-1} region is donated by N–H bond-stretching mode of hydrogen bonded amide groups. The absorption is polarised parallel to N–H bond, which is parallel to the helix axis in α-helical structures and perpendicular to the polypeptide chain in β-sheets. The band might be shifted to lower frequency when the hydrogen bonding strength increases (Krimm & Bandekar, 1986).

The carbonyl C=O double bond-stretching mode, with contributions from in-phase bending of the N–H bond and stretching of the C–N bond, occurs in frequency range 1660–1620 cm^{-1} region which is often referred to as Amide I band. The frequency range 1660–1650 cm^{-1} was known as α-helical and 1640–1620 cm^{-1} as β-sheets structures. The frequency range of 1550–1520 cm^{-1} is due to Amide II with α-helical structure between 1550–1540 cm^{-1} and β-sheets at 1525–1520 cm^{-1}. The Amide II vibration is caused by deformation of the N–H bonds. Fischer, Cao, Cox, and Francis (2005) and Lagant, Vergoten, Loucheux-Lefebvre, and Fleury (1983) attributed 1500–1200 cm^{-1} to CH_2 deformation. It is known that this region contains vibrations corresponding to groups present in fatty acids, proteins, polysaccharides and phosphate derivatives.

Table 1
General description of gelatin samples employed in this study.

Gelatin type	Company name	Batch no.	Gelatine type	Bloom value
Gelatin bovine skin	Sigma	115K0144	Type B	~225
Gelatin bovine skin	Sigma	047K0005	Type B	~225
Gelatin bovine skin	Sigma	126K0053	Type B	~225
Gelatin porcine skin	Sigma	087K0125	Cell culture tested	–[a]
Gelatin porcine skin	Sigma	084K0211	Cell culture tested	–[a]
Gelatin porcine skin	Sigma	047K00061	Cell culture tested	–[a]
Gelatin powder (bovine)	Merck	K37294478719	Type B	80–120
Gelatin sheet (porcine)	Merck	K35519572612	Type A	160–240

[a] Not stated.

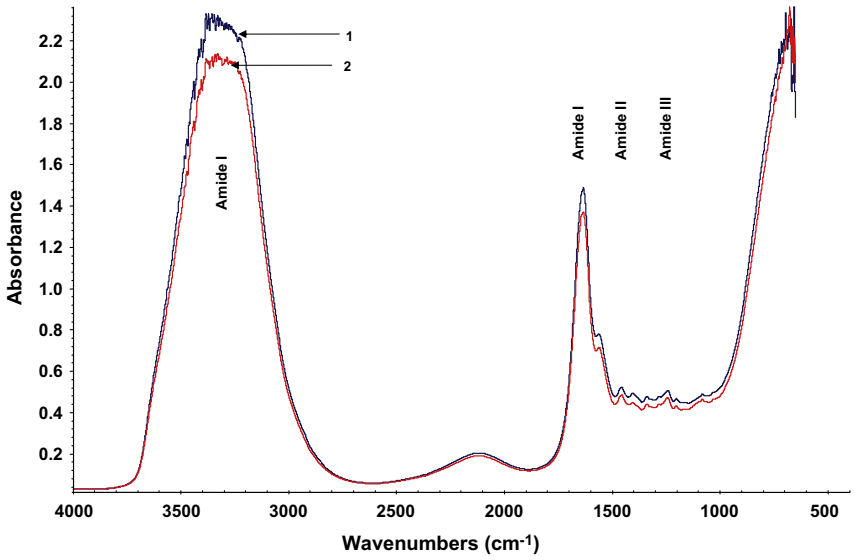

Fig. 1. FTIR spectra for bovine gelatin (1) and porcine gelatin (2).

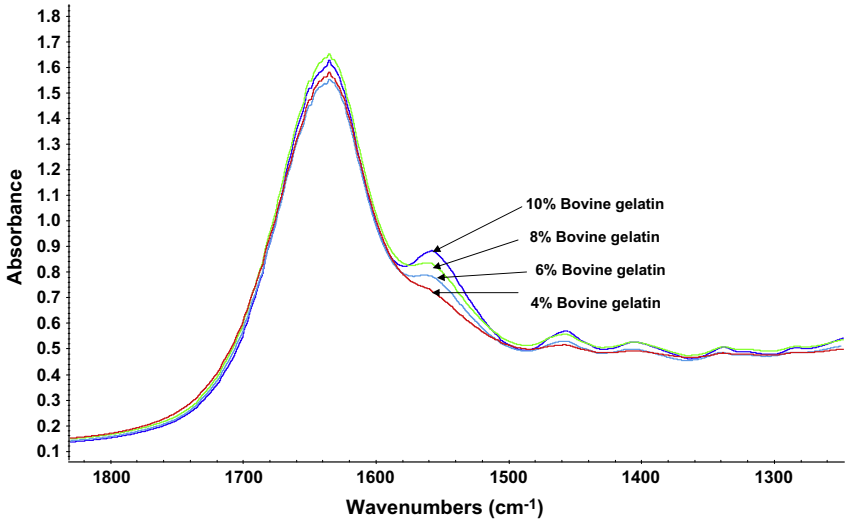

Fig. 2. Concentration-dependent FTIR spectra of bovine gelatin in the range of 1720–1060 cm^{-1}.

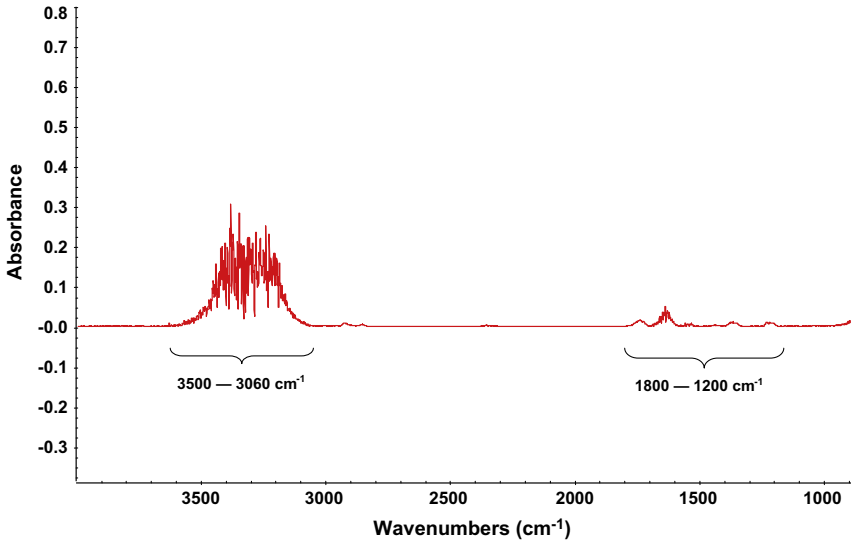

Fig. 3. Differences of variances between bovine and porcine spectrum.

Table 2
Performance index (PI) and principal component spectra diagnostic of the analysis region contribution.

Day	Performance index	PC1	PC2
1	91.6	94.81	99.56
2	91.2	90.28	99.24
3	89.9	98.93	99.33
Mean ± SD	90.9 ± 0.89		

PC1 – Principal component 1.
PC2 – Principal component 2.

The FTIR spectra obtained from porcine and bovine gelatin show wide and overlapping absorption bands since it covers multitude of functional groups that contain more information than that offered by all the chemical components considered individually. As illustrated in Fig. 2, samples with different concentration of gelatin showed different spectra and all of them follow the correct sequences according to the concentrations. The spectrum showed the sensitivity of FTIR and its capability of discriminating between sample concentrations.

3.2. Discriminant analysis and characterisation of FTIR spectrum of standard gelatin

A multivariate DA based on criterion groups formed by cluster analysis was performed to determine the extent to which the groups were separated by the cluster solution (Duckworth, 1998). It can be performed as follow-up procedure where the results can be used as the predictor to form the groups in the cluster phase.

Even though both porcine and bovine gelatins have a very similar spectrum to each other, the discrimination was made by focusing on protein and polypeptides since these are the main components which in turn determine its function in food systems. Infrared spectra of these are affected by coupling of the vibrations of neighbouring peptide groups (Brauner, Dugan, & Mendelsohn 2000; Brauner, Flach, & Mendelsohn 2005; Krimm & Bandekar 1986). The maximum differences among gelatins spectra were found in two main windows (3290–3280 cm^{-1} and 1660–1200 cm^{-1}) of the complete spectral range. These window were specified through analysis using differences of variance between spectrum of bovine gelatin and porcine gelatin (Fig. 3).

Principal component analysis (PCA) was performed using TQ Analyst software to find out spectral features that had significant influence on spectral variance. Table 2 showed performance index (PI) and principal component spectra diagnostic of the analysis region contribution. The PI signifies how well the calibrated method can classify the validation standards where the higher value of PI indicates the closer of standard to its class. For the three different days of analysis, the average of PI values is 90.9 ± 0.89, showing the ability of this method to produce good repeatability results. The

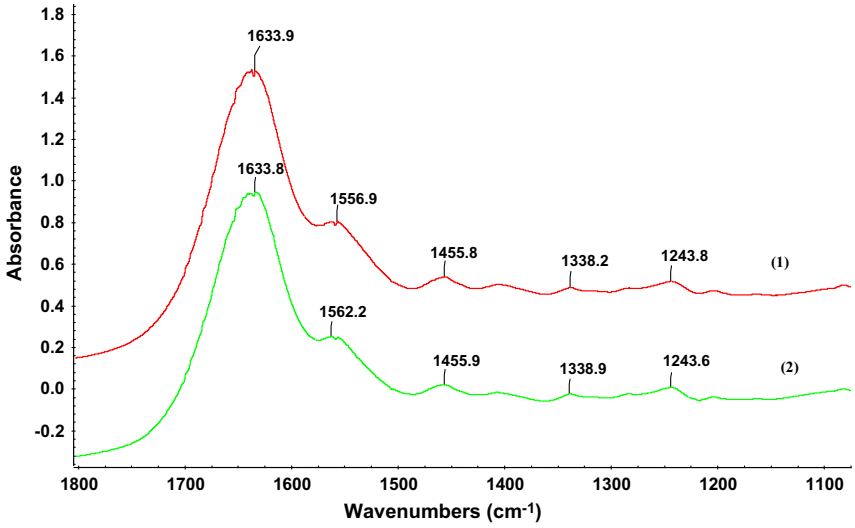

Fig. 4. Component peak location FTIR for average of three spectra of bovine gelatins (1) and average of three spectra of porcine gelatins (2).

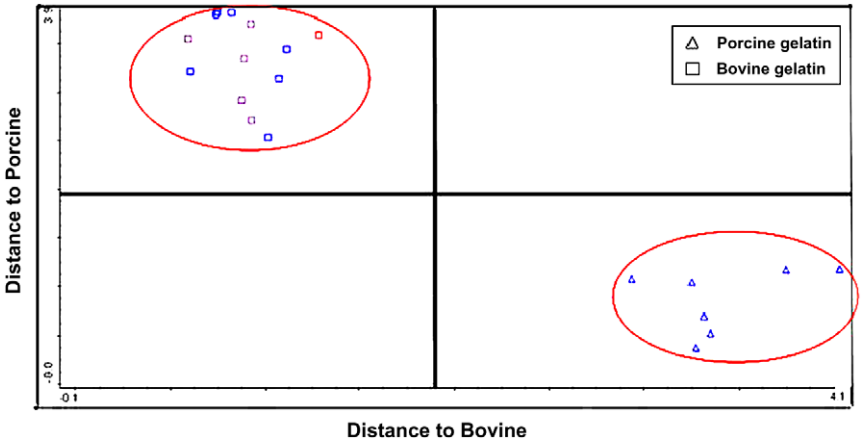

Fig. 5. Cooman's plot for two classes of gelatin: porcine gelatin and bovine gelatin.

principal component spectra diagnostic elaborate more on the spectral information in a calibration set which is determined by the principal component. It also described the amount of total spectra variation for each principal component.

Muyonga et al. (2004) have shown that the secondary structure of gelatin can be analysed at absorption band between 1600 and 1700 cm^{-1}. However, the spectra of both porcine and bovine gelatin samples were found to be indistinguishable when analysed at a resolution of 2 cm^{-1} (Fig. 4). However, when the comparison was done based on the intensity of the spectra, a slight difference was obtained to enable the results to be clustered using the discriminant analysis technique.

Infrared spectra of all sample of gelatins were used to perform the discriminant analysis using TQ Analyst software. The results obtained from discriminant analysis is best visualise using Cooman's plot that were obtained using Mahalanobis distance value of the FTIR spectrum of standard bovine and porcine gelatin (Pettersen, Svartengren, & Lundstedt, 1998). The axes are the distance to the models and the coordinates are calculated OMNIC distance (sample standard deviation). The distances to the principal component models for the porcine gelatins and bovine gelatins are plotted in Fig. 5. Both samples were successfully classified according to their respective group.

4. Conclusion

The FTIR spectroscopic techniques can be used for rapid classification of gelatin. In order to determine unknown gelatin sources, the deformation of N–H bonds found in the range 3290–3280 cm^{-1} and 1660–1200 cm^{-1} were analysed using discriminant analysis. These regions were found to give information about the origin of the gelatin. Cooman's plot proved to be useful for visualising the discriminant analysis approach for the classification. This qualitative method may provide a rapid determination of gelatin source for application in food, pharmaceutical and photographic applications. Two independent PCA models were calculated defining two separate classes of samples. A future use of such a qualitative approach may be established by the food industry as well as second derivative study of FTIR spectrum can be done to alleviate any doubts about the gelatin source as to whether it is porcine or bovine.

Acknowledgements

We would like to thank the Ministry of Science, Technology and Innovation Malaysia (MOSTI) for funding this study (Science Fund No. 05-01-04-SF0625 awarded to Prof. Dr. Yaakob B. Che Man).

References

Brauner, J. W., Dugan, C., & Mendelsohn, R. (2000). C-13 isotope labeling of hydrophobic peptides. Origin of the anomalous intensity distribution in the infrared amide I spectral region of β-sheet structures. *Journal of the American Chemical Society, 122*, 677–683.

Brauner, J. W., Flach, C. R., & Mendelsohn, R. (2005). A quantitative reconstruction of the amide I contour in the IR spectra of globular proteins: From structure to spectrum. *Journal of the American Chemical Society, 127*, 100–109.

Cao, H., & Xu, S. (2008). Purification and characterization of type II collagen from chick sterna cartilage. *Food Chemistry, 108*, 439–445.

Che Man, Y. B., Syahariza, Z. A., Mirghani, M. E. S., Selamat, J., & Bakar, J. (2005). Analysis of potential lard adulteration in chocolate and chocolate products using Fourier transform infrared spectroscopy. *Food Chemistry, 90*, 815–819.

Defernez, M., & Wilson, R. H. (1995). Mid infrared spectroscopy and chemometrics for determining the type of fruit used in jam. *Journal of the Science of Food and Agriculture, 67*, 461–467.

Duckworth, J. (1998). Spectroscopic qualitative analysis. *Applied Spectroscopy, 16*, 5–177.

Fischer, G., Cao, X., Cox, N., & Francis, M. (2005). The FTIR spectra of glycine and glycylglycine zwitterions isolated in alkali halide matrices. *Journal of Chemical Physics, 313*, 39–49.

Friess, W., & Lee, G. (1996). Basic thermoanalytical studies of insoluble collagen matrices. *Biomaterials, 17*, 2289–2294.

Griffiths, P. R., & Haseth, J. A. (2007). *Fourier transform infrared spectrometry* (pp. 171–175). New York: Wiley Interscience.

Hidaka, S., & Liu, S. Y. (2002). Effects of gelatins on calcium phosphate precipitation: A possible application for distinguishing bovine bone gelatin from porcine skin gelatin. *Journal of Food Composition and Analysis, 16*, 477–483.

Krimm, S., & Bandekar, J. (1986). Vibrational spectroscopy and conformation of peptides, polypeptides and proteins. *Advances in Protein Chemistry, 38*, 181–364.

Kumosinski, T. F., & Farrell, H. M. (1993). Determination of the global secondary structure of proteins by Fourier transform infrared (FTIR) spectroscopy. *Trends in Food Science and Technology, 4*, 169–175.

Lagant, P., Vergoten, G., Loucheux-Lefebvre, M. H., & Fleury, G. (1983). Raman spectra and normal vibrations of dipeptides I. Glycylglycine. *Biopolymers, 22*, 1267.

Lai, Y. W., Kemsley, E. K., & Wilson, R. H. (1995). Quantitative analysis of potential adulterant of extra virgin olive oil using infrared spectroscopy. *Food Chemistry, 53*, 95–98.

Muyonga, J. H., Cole, C. G. B., & Duodu, K. G. (2004a). Fourier transform infrared (FTIR) spectroscopy study of acid soluble collagen and gelatin from skins and bones of young and adult Nile perch (*Lates niloticus*). *Food Chemistry, 86*, 325–332.

Muyonga, J. H., Cole, C. G. B., & Duodu, K. G. (2004b). Extraction and physico-chemical characterization of Nile Perch (*Lates niloticus*) skin and bone gelatin. *Food Hydrocolloids, 18*, 581–592.

Nemati, M., Oveisi, M. R., Abdollahi, H., & Sabzevari, O. (2004). Differentiation of bovine and porcine gelatins using principal component analysis. *Journal of Pharmaceutical and Biomedical Analysis, 34*, 139–143.

Paradkar, M. M., & Irudayaraj, J. (2002). A Rapid FTIR spectroscopic method for estimation of caffeine in soft drinks and total methylxanthines in tea and coffee. *Journal of Food Science. Food Chemistry and Toxicology, 67*, 2507–2511.

Petibois, C., & Deleris, G. (2006). Chemical mapping tumor progression by FTIR imaging: Towards molecular histopathology. *Trends in Biotechnology, 24*(10).

Pettersen, J., Svartengren, J., & Lundstedt, T. (1998). A multivariate investigation of the effect of the hormone leptin on body weight reduction. *Chemometrics and Intelligent Laboratory Systems, 44*, 373–380.

Prystupa, D. A., & Donald, A. M. (1996). Infrared study of gelatin conformations in the gel and sol states. *Polymer Gels and Networks, 4*, 87–110.

Syahariza, Z. A., Che Man, Y. B., Jinap, S., & Bakar, J. (2005). Detection of lard adulteration in cake formulation by Fourier transform infrared (FTIR) spectroscopy. *Food Chemistry, 92*, 365–371.

Venien, A., & Levieux, D. (2005). Differentiation of bovine from porcine gelatines using polyclonal anti-peptide antibodies in indirect and competitive indirect ELISA. *Journal of Pharmaceutical and Biomedical Analysis, 39*, 418–424.

natural flavours, while maintaining inhibition of bacterial and enzymatic degradation. Mild heat treatment would be sufficient enough to destroy vegetative microorganisms, removing that requirement from the irradiation process, without strongly impacting flavour. The application of irradiation was hypothesised to offer other benefits, such as improved texture, additional protection from spore-forming organisms, and better retained nutrients.

Minimal literature reports exist on irradiation of juices. Papaya juice has been shown to quench hydroxyl free radicals formed during exposure to gamma rays (Gray & Mower, 1991). Glucose, fructose and sucrose were found to primarily absorb the rays, with malonaldehyde and other sugar derivatives being formed. Niemand, den Drijver, Pretorius, Holzapfel, and van der Linde (1983) reported that irradiation of sugar solutions resulted in mutagenic compounds; these mutagenic compounds did not form in irradiated mango juice. Organic acids and phenols contributed to 85% of the protective effect. These results would likely apply to papaya as well, since the sugar, organic acid and phenol contents are similar (Luximon-Ramma et al., 2003). A WHO Technical Report (1997) also concluded there were no safety concerns with high (>10 kGy) doses of irradiation.

In designing a process for preparing papaya pulp, pasteurisation was first explored (Brekke, Chan, & Cavaletto, 1973). However, cooked flavour development in papaya occurs to a much greater degree than in other pasteurised fruit products (Argaiz & Lopez-Malo, 1995). As a result, products have been developed that mix papaya with other components in an effort to minimise off-flavours produced from papaya heat treatment (Mostafa, Abd El Hady, & Askar, 1997; Tiwari, 2000). Producing a papaya beverage where the primary flavours come from papaya requires different processing approaches to avoid off-flavours produced by heat treatment. A combination of moderate irradiation and mild heat should decrease the need for flavour masking, and allow a higher percentage of the flavour to come from papaya.

The purpose of this research was to evaluate irradiation and mild heat treatment together as a viable alternative to heat treatment alone. Also, the aim was to minimise required processing as much as possible to maximise nutrient retention. It was hypothesised that a combination treatment using both irradiation and mild heat would result in a safe product that retained flavour and a nutritional profile more similar to fresh papaya than pasteurised pulp. This would make possible a wider acceptability of a fruit pulp with superior nutrient density.

2. Materials and methods

2.1. Materials

Carica papaya L. var.'s *Rainbow* and *SunUp* were donated by the Hawaiian Papaya Industry Association and the Hawaii Department of Agriculture. They were harvested when approximately 25% yellow and vapour-heat treated to eliminate fruit fly infestation (by heating to 47 °C over at least 4 h at 90% humidity, then cooling for 1 h) in Hawaii before shipment (second day air). Fruit were stored at 23 °C for 3–5 days until at least 80% yellow before pulping.

Escherichia coli K12 was provided by Dr. Scott Martin from the University of Illinois and cultured in Luria-Bertani (LB) broth. *Listeria innocua* (ATCC, Manassas, VA) was received freeze-dried and cultured in Brain Heart Infusion medium (Fisher Scientific, Fairlawn, NJ). *Salmonella typhimurium* (Carolina Biological Supply, Burlington, NC) was received in MicroKwik nutrient agar and cultured in LB broth. *Clostridium sporogenes* (Carolina Biological Supply) was received in thioglycollate medium in a MicroKwik vial and cultured using reinforced Clostridium medium (Fisher Scientific). AAPH (2,2′-azobis(2-amidino-propane)dihydrochloride) was obtained from Wako Chemical (Richmond, VA). Trolox, ascorbic acid, ferrous sulphate and EDTA were purchased from Fisher Scientific. Fluorescein, α-(4-pyridyl-1-oxide)-*N*-*tert*-butylnitrone (POBN), quercetin and pectin were acquired from Sigma Chemical (St. Louis, MO).

2.2. Sample preparation

Papaya was divided into sets (5 fruit per set) which were washed, dried, halved, and the seeds were removed. The pulp was transferred into a KitchenAid K5SS with a pulper attachment (Hobart Corporation, Troy, OH) and collected. Brix was measured using a Westover Scientific (Mill Creek, WA) RHB-32ATC hand held refractometer and papaya pulp was diluted with double distilled H_2O (ddH_2O) to 8 °Brix. Diluted pulp was separated into glass containers labelled for the following treatments and frozen (−20 °C): control (C), heated to 80 °C for 5 min (H), 5 kGy irradiation (5), 7.5 kGy (7.5), 5 kGy + heat (5H), 7.5 kGy + heat (7.5H). Samples were irradiated in triplicate while frozen in a Gammacell 220 Excel with a cobalt-60 source (MDS Nordion, Ottawa, ON, Canada). Combination treatments were irradiated prior to heat treatment.

2.3. Titratable acidity

Titratable acidity was performed according to a modified AOAC (2002, chapter 11) method, conducted as follows: the pH of 5 g diluted papaya was measured after addition of 125 ml ddH_2O. This solution was quickly titrated with 0.02 N NaOH to reach a final pH 8.2. The volume of NaOH consumed was used to calculate citric acid equivalents.

2.4. Viscometry

Freshly thawed papaya samples were centrifuged (to remove pulp) and transferred onto the Advanced Rheometric Expansion System Rheometric Fluid Spectrometer III (ARES RFS III) with an attached SR5 Peltier Circulator (TA Instruments, New Castle, DE). It was connected to TA Orchestrator Software Version 8.03 (TA Instruments) with the gap set at 0.5 mm and a temperature of 5 °C. Treatment samples were run in triplicate and ddH_2O was used as a standard for calibration. Values are reported as shear rate/shear stress (s^{-1} Pa^{-1}).

2.5. Colourimetry

Papaya samples were poured into a glass container, placed on the reading area of the HunterLab LabScan II 0/45 (Hunter Associates Laboratory Inc., Reston, VA), and covered. Measurements were analysed with HunterLab Universal Software™ Version 3.8. After automatic standardisation, samples were analysed in triplicate. Each treatment was compared to the control with respect to differences in L, a, b, and ΔE values.

2.6. Microbiology

Four non-pathogenic or opportunistic organisms were selected to represent a variety of potential contaminating organisms (Busta et al., 2003). Frozen *E. coli* K12 cultures were thawed and added to LB media. Cultures were incubated (24 h, 37 °C) with rotation. Thawed *Rainbow* and *SunUp* papaya pulp samples were spiked with sufficient *E. coli* K12 culture to result in 10^{10} CFU of *E. coli* added per container. Inoculated papaya pulp was frozen overnight and treated the following day, after which inoculated papaya was plated on LB plates in duplicate. The plates were then incubated (24 h, 37 °C). Observations for *S. typhimurium* were conducted in

a similar fashion. Growth and bacterial counts were verified before papaya spiking began. *L. innocua* was prepared in a similar fashion to *E. coli* with the following exceptions: it was cultured in and grown on Brain Heart Infusion broth and plates, respectively. *C. sporogenes* starter culture was added to reinforced Clostridial media in a Type A Anaerobic Chamber 7000000 (Coy Laboratory Products Inc.; Grass Lake, MI) maintained at 37 °C with a gas mixture of 5% carbon dioxide, 5% hydrogen, and nitrogen to balance and incubated (24 h). Inoculation and plating for *C. sporogenes* spiked papaya was conducted similar to *E. coli* K12, except for the use of Clostridial media plates and incubation (24 h, 37 °C) in the anaerobic chamber. After incubation of duplicate plates for all four organisms, colonies were counted. Values are reported as number of colonies per 1.0 ml diluted (8 °Brix) papaya pulp plus spike.

2.7. Pectinesterase (PE) activity

Pectinesterase activity was determined by the method of Kertesz (1955), with minor alterations. A 1% pectin solution was adjusted to pH 7.5, found to be optimal by Chang, Morita, and Yamamoto (1965) and maintained at 30 °C. Diluted papaya and 1.7 M NaCl were mixed and vortexed for 30 s. The optimum NaCl concentration of 0.2 M (Chang et al., 1965; Lourenco & Catutani, 1984) was achieved upon addition of the papaya/NaCl solution to the 1% pectin solution. The pH was readjusted with 0.02 N NaOH to 7.5 before beginning the trial. For 7 min, the pH was maintained at 7.5 with titration of 0.02 N NaOH. Trials were performed in triplicate for each treatment. The baseline for methyl de-esterification of pectin was determined in the absence of papaya, under the same conditions as above and subtracted from all trials. One unit of pectinesterase activity (PEU) is expressed as mmol NaOH consumed per min per g fresh undiluted papaya.

2.8. Consistometry

Papaya pulp samples were placed in the closed reservoir of a level Bostwick Consistometer (Fairfax, VA). Trials (30 s) began once the gate was released allowing treatments to flow. The minimum and maximum flow was recorded and averaged. Remaining puree in the weighing boats was subtracted from the initial weight to determine actual treatment weight. Pulp samples in the consistometer were returned to their containers and stored in the refrigerator. Measurements were continued daily or every other day over a 10-day period or until the sample had gelled such that it flowed 6 cm or less (*Rainbow* variety) or 4 cm or less (*SunUp* variety).

2.9. High performance liquid chromatography (HPLC)

2.9.1. Phenolics extraction

Papaya samples were weighed into 15 ml plastic tubes and centrifuged (17,000*g*, 1 min). The supernatant was collected in a round bottom flask. Pulp extractions began with the addition of 5 ml 100% warm MeOH (~40 °C), vortexing (30 s), sonication (2 min, 40 °C), and centrifugation (17,000*g*, 1 min). The supernatant was added to the round bottom flask and the extraction was repeated three times. Combined extracts were dried (37 °C) in a Brinkmann Büchi RE 111 Rotavapor (New Castle, DE). Dried extracts were reconstituted with warm MeOH and continuous mild heat to ensure complete extraction. The supernatant was placed in a test tube, followed by additional extractions until the dried extract was pale yellow. The MeOH extracts were dried continuously under N_2 at 37 °C to 1 ml. The resulting volume was centrifuged (17,000*g*, 5 min) and the supernatant was poured into a new tube. One last extraction (as above) was performed on the pulp remaining in the tube using warm MeOH. After drying to 1 ml, the extract was filtered (0.45 μm) and injected onto the HPLC. Quercetin was added to the original pulp to monitor phenolic recovery using this extraction protocol.

2.9.2. HPLC phenolic measurements

A Waters Corp. 2695 separations module and autosampler (Millford, MA) and Hewlett Packard 1050 diode array detector model G1306A (Agilent Technologies Inc., Santa Clara, CA) was used with simultaneous detection at 260, 280, 320 and 360 nm using Chemstation software (Agilent Technologies, Palo Alto, CA). Absorption spectra were recorded from 190 to 600 nm for all peaks. Peak separation was accomplished with a Waters Xterra RP18 (5 μm) 3.1 × 150 mm column preceded by a guard column containing Sepralyte C18 (10 μm, Analytichem Intl., Harbor City, CA). Solvent A consisted of 0.1% H_3PO_4 in ddH_2O and solvent B was 0.1% H_3PO_4 in 95% acetonitrile. At a flow rate of 1 ml/min, the elution program followed a linear gradient from 0% B to 50% B in 20 min, from 50% back to 40% in 0.1 min, holding at 40% for 10 min, from 40% to 95% in 15 min, from 95% to 0% in 3 min, and holding 10 min (Franke, Custer, Arakaki, & Murphy, 2004). Treatment peak areas were calculated from a quercetin standard curve. Samples were analysed in triplicate.

2.9.3. Ascorbic acid extraction

Extraction was performed according to Lee and Coates (1999). Papaya pulp samples were diluted to 1 ml with dithiothreitol (DTT) (4.2 mM in 0.1 M K_2HPO_4, pH 7.0) and vortexed. An aliquot of this mixture was added to freshly prepared 4.5% *m*-phosphoric acid (*m*-PA) in a new tube. Treatments were mixed, spin filtered (0.45 μm), and injected onto the HPLC column.

2.9.4. HPLC-ascorbic acid measurements

A Waters Xterra column and guard column were used as above. Solvent A consisted of 0.1% H_3PO_4 in ddH_2O and solvent B was 100% methanol. At a flow rate of 0.8 ml/min, the elution program followed a linear gradient from 0% to 30% B over 8 min, back to 0% B in 3 min and held for 6 min. Peak detection was at 240 nm. An external ascorbic acid standard curve with three different concentrations was used to quantify the results. The ascorbic acid standard was also treated with DTT and *m*-PA solutions. Samples were analysed in triplicate.

2.10. Electron paramagnetic resonance (EPR)

2.10.1. Extraction of papaya samples

Frozen papaya pulp samples were thawed at RT. Samples (1 g) were carefully weighed into Eppendorf tubes and centrifuged in a tabletop microfuge (max speed, 1 min). The supernatant was transferred to 2 ml vials. The papaya pellet was resuspended by addition of 500 μl 100% MeOH and vortexing; the suspension was sonicated (2 min with intermittent shaking) and centrifuged (max speed, 1 min). The resulting supernatant was added to the 2 ml vial to complete the first extraction. The above MeOH extraction was repeated with a final centrifugation of 2 min. Combined supernatants were centrifuged (max speed, 1 min) a final time to remove residual pulp. Remaining papaya pulp from the original 2 ml freezer vials was also centrifuged (max speed, 2 min) and the resulting supernatant was used as a water extract.

2.10.2. EPR

The EPR protocol and solution preparation was performed according to Falchi et al. (2006). A quartz flat cell (SP Industries Inc., Wilmad-LabGlass, Buena, NJ) was used. Scans began 3 min after the addition of H_2O_2. Spectra were recorded at X-band (~9.5 GHz) on a Varian E-122 spectrometer with a TE102 cavity (Palo Alto, CA). Other parameters: frequency, ~9.51 GHz; field centre, 3390; gain, 3200; number of scans, 5; scan range, 80; scan

time, 30 s; 2 s between each scan; modulation amplitude, 1; time constant, 0.032 s; and power, 20 mW (10 db). Fenton controls were subtracted from control and treated papaya samples and the values adjusted to a scale that placed the control papaya at a value of 100 arbitrary units. Samples were run in triplicate.

2.11. Oxygen radical absorbance capacity (ORAC)

2.11.1. Fruit extractions

Extractions followed the procedure of Wu et al. (2004), with minor adjustments: papaya samples (1 g) were added to 15 ml Corning polypropylene tubes (Corning Inc., Corning, NY). Extractions began with the addition of 10 ml 70:29.5:0.5 acetone:water:acetic acid (AWA) to papaya samples followed by the Wu et al. (2004) extraction method. The extract was then further diluted (1:5) with AWA to fit the Trolox standard curve used in the assay.

2.11.2. $ORAC_{FL}$ analysis

$ORAC_{FL}$ assays were conducted according to Davalos, Gomez-Cordoves, and Bartolome (2004) in a preheated (37 °C) BioTek FLx600 fluorometer (BioTek Instruments Inc., Winooski, VT) using 96-well black side with clear bottom plates (Corning Inc., Corning, NY). Data were collected using KC4 software (BioTek Instruments Inc.). Parameters: emission wavelength, 515 nm (530/25); excitation wavelength, 493 nm (485/15); reading every minute for 80 min with shaking for 3 s at intensity 3 before each reading. Reagent concentrations and plate organisation were as described in Davalos et al. (2004).

2.12. Statistics

Data were compiled using Microsoft Excel (Microsoft Corporation, Redmond, WA). Treatments were compared within each variety as well as among varieties using analysis of variance (Tukey's HSD, $p < 0.05$, SAS statistical software, SAS Institute Inc., Cary, NC). The Tukey adjustment was utilised to control experiment wise errors across papaya varieties. Consistometry was measured using analysis of variance repeated measures ($p < 0.05$).

3. Results and discussion

3.1. Processing conditions

It was the goal of this study to produce a shelf stable processed pulp-based papaya beverage, similar in consistency to tomato juice (a drinkable, commercially available pulp-containing nectar), while maintaining product quality, nutritional value and flavour. If irradiation alone were to be used to create a shelf-stable pulp, this would require 48 kGy to guarantee destruction of *C. botulinum* (WHO Technical Report, 1997). This high dosage would be cost prohibitive and unfeasible due to the extremely long process required. Less than 10 kGy is sufficient to destroy vegetative cells, depending on the food product being examined; this would however require refrigeration of the product to account for *C. botulinum* risk. No guidelines have yet been issued for irradiation of the pulp or juice of papaya.

In addition to microbiological concerns, papaya processing would also have to address inactivation of the enzyme pectin methylesterase (PE, further discussed below), which causes papaya pulp to gel (Chang et al., 1973). Fresh (non-processed) diluted pulp was demonstrated to undergo rapid gel formation (within 1–2 days) as indicated by consistometry (Figs. 1 and 2) and visual observation. Thus, it was necessary to modify processing to include enzymatic inactivation. Doses of irradiation up to 7.5 kGy applied

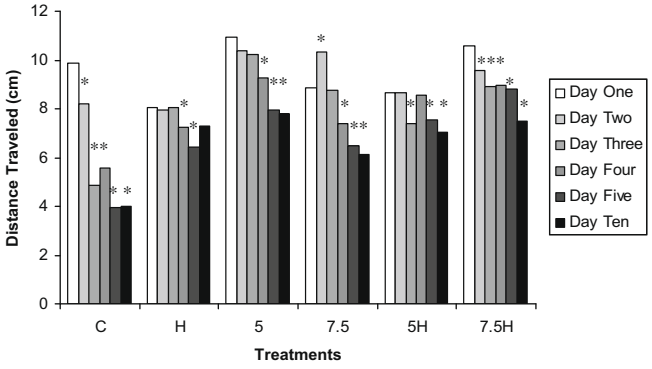

Fig. 1. Consistency of *Rainbow* papaya over 10 days. Each bar represents the distance the papaya sample travelled in the consistometer. *Significant at 0.05 level compared to day 1 for each sample using repeated measures analysis of variance. C, control; H, heat (80 °C, 5 min); 5, 5 kGy; 7.5, 7.5 kGy; 5H, 5 kGy + heat; and 7.5H, 7.5 kGy + heat ($n = 3$).

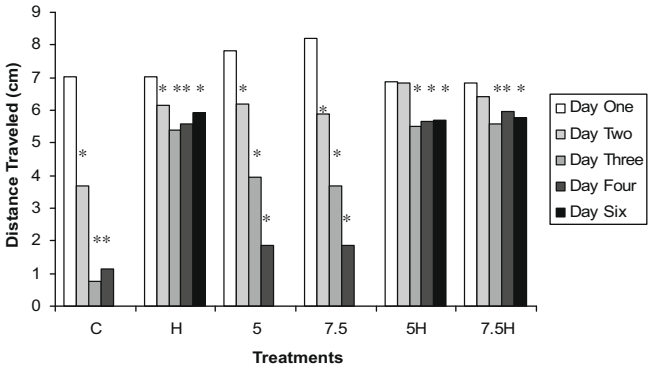

Fig. 2. Consistency of *SunUp* papaya over 6 days. Each bar represents the distance the papaya sample travelled in the consistometer. *Significant at 0.05 level compared to day 1 for each sample using repeated measures analysis of variance. C, control; H, heat (80 °C, 5 min); 5, 5 kGy; 7.5, 7.5 kGy; 5H, 5 kGy + heat; and 7.5H, 7.5 kGy + heat ($n = 3$).

in this study did not affect PE activity (Fig. 3). Though we did not test PE activity on samples irradiated at higher doses, others have demonstrated that up to 48 kGy did not have a significant impact on elimination of destructive enzyme activity (Wilkinson & Gould, 1996). This necessitated the use of mild heat treatment to reduce PE activity to acceptable levels.

Preliminary indications of aroma and flavour of the irradiated product indicated that favourable flavour and aroma could be obtained with irradiation dosages between 5 and 15 kGy. Although 10 and 15 kGy were preferred by a few tasters during informal

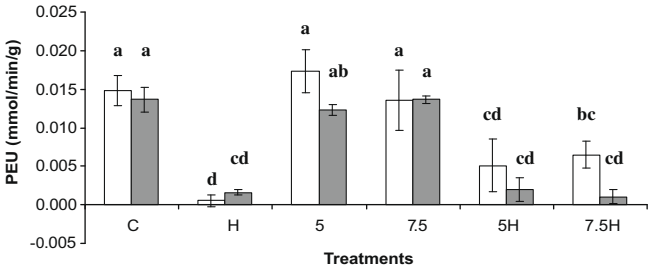

Fig. 3. Pectinesterase activity units (PEU) of *Rainbow* (white bars) and *SunUp* (grey bars) papaya. Values are reported as mean ± SD. Bars not sharing the same lowercase letter are significantly different ($p < 0.05$). C, control; H, heat (80 °C, 5 min); 5, 5 kGy; 7.5, 7.5 kGy; 5H, 5 kGy + heat; and 7.5H, 7.5 kGy + heat ($n = 3$).

testing (~8 students and faculty in the laboratory evaluated 5, 7.5, 10 and 15 kGy papaya treatments), the longer time required for irradiation and potential cost were problematic. Thus, 5 and 7.5 kGy were selected. More than one dose was included to quantify the independent effects on microbiological organisms, particularly in combination with heat, as well as any differences in impact on nutrient content.

Heat treatment temperature and time were chosen based on the work of Magalhães, Tosello, and de Massaguer (1996). Our results were within the ranges of residual pectin methylesterase activities found by Castaldo et al. (1997) in thermally processed fruit preparations. When administered before heat treatment, both selected doses resulted in a greater destruction of *C. sporogenes* (see Section 3.6 below) and improved flavour and texture compared to heat followed by irradiation. The pulp texture was smoother, with fewer clumps.

3.2. pH and °Brix

For *Rainbow* variety samples, the pH of heat treatment alone was the only value significantly higher than the control (Table 1). The pH was not significantly different than the control for any treatments applied to the *SunUp* variety samples, nor were the pH values significantly different from each other across varieties. Others have reported various varieties of papaya to have a pH between 4.9 and 5.1 (Ahmed & Ramaswamy, 2004; Brekke et al., 1973; Penteado & Leitão, 2004). Significant changes from control values were noted in °Brix for the 5H treatment for *Rainbow* papaya; Brix did not change for the *SunUp* variety (Table 1). Across varieties, only the 5H treatments were significantly different from one another. By informal testing it was noted that all irradiated samples tasted sweeter than control samples. Preliminary sugar compositional analysis of our treatments resulted in no significant change in carbohydrates (data not shown, Hawaiian Agricultural Research Center, Oahu, HI). Thus, perceived changes in sweetness were likely due to changes in other components, such as flavour compounds, which can mask sweetness levels (Bakker, 1995). These flavour components may change during food processing and thus change sweetness perception.

3.3. Titratable acidity

Titratable acidity was conducted to quantify the amount of citric acid, the most predominant organic acid, within each variety of papaya (Table 1). Within each papaya variety there were no significant differences between the control and any of the five treatments. However, there were significant differences between *Rainbow* and *SunUp* varieties between controls and 5H samples. This is likely due to varietal differences.

3.4. Viscometry

The juices of each treatment (pulp removed) were analysed for viscosity compared to the control within that variety (Table 1). For the *Rainbow* papaya samples, all treatments were significantly different from the control, but not from each other. For the *SunUp* papaya samples, there were no significant differences from the control, though 5H was significantly less viscous than 7.5. It is unclear how the latter should be interpreted. Though controls were not significantly different from one another across varieties, many of the other treatments were. It was hypothesised that differences may be due to different varietal responses to treatments. The results may also help explain why the *SunUp* papaya was thicker in general (see consistometry results below). We chose to measure the viscometry of the fluid portion of the papaya pulp to determine if our processing conditions would result in any immediate effects

Table 1
Effects of papaya variety and treatment on pH, °Brix, viscometry, and titratable acidity.[A]

	Rainbow						*SunUp*					
	C	H	5	7.5	5H	7.5H	C	H	5	7.5	5H	7.5H
pH	4.9 ± 0.0^{bcd}	5.1 ± 0.0^{a}	4.9 ± 0.0^{bcd}	4.9 ± 0.0^{bcd}	5.1 ± 0.0^{ab}	5.1 ± 0.0^{ab}	5.0 ± 0.1^{bcd}	5.0 ± 0.0^{abc}	4.9 ± 0.0^{cd}	4.8 ± 0.1^{d}	5.0 ± 0.1^{bcd}	5.0 ± 0.1^{bcd}
°Brix	8.07 ± 0.12^{b}	9.00 ± 0.00^{ab}	7.90 ± 0.79^{b}	8.30 ± 0.17^{b}	9.83 ± 1.04^{a}	9.33 ± 1.04^{ab}	8.37 ± 0.06^{b}	8.27 ± 0.06^{b}	8.10 ± 0.10^{b}	7.97 ± 0.06^{b}	8.37 ± 0.06^{b}	8.47 ± 0.06^{ab}
Viscometry[B]	7.51 ± 0.95^{ab}	4.16 ± 1.14^{d}	4.53 ± 0.22^{cd}	5.14 ± 0.50^{cd}	4.18 ± 0.43^{d}	4.62 ± 0.13^{d}	7.50 ± 0.70^{ab}	6.43 ± 0.51^{abc}	7.57 ± 0.81^{ab}	8.00 ± 0.28^{a}	5.60 ± 0.29^{bcd}	6.32 ± 0.84^{abc}
Titratable acidity[C]	0.09 ± 0.01^{ab}	0.09 ± 0.00^{abc}	0.09 ± 0.00^{ab}	0.10 ± 0.00^{a}	0.10 ± 0.00^{a}	0.09 ± 0.00^{abc}	0.07 ± 0.01^{c}	0.08 ± 0.00^{bc}	0.08 ± 0.00^{bc}	0.09 ± 0.01^{abc}	0.08 ± 0.01^{bc}	0.08 ± 0.01^{bc}

C, control; H, heat (80 °C, 5 min); 5, 5 kGy; 7.5, 7.5 kGy; 5H, 5 kGy + heat; and 7.5H, 7.5 kGy + heat (n = 3).

[A] Values not sharing the same letter within each row are significantly different ($p < 0.05$) and are reported as mean ± SD.

[B] Values are reported as shear/stress (s^{-1} Pa^{-1}).

[C] Values are reported as g/100 ml citric acid.

on the viscosity of the juice. Consistometry measurements would determine thickening of the entire pulp, thus allowing us to separate where changes, if any, were occurring. If we observed an increased viscosity, further dilution might be necessary, as consumer preference decreases for a product that is more viscous than expected (Grigelmo-Miguel & Martín-Belloso, 1999). All significant changes that occurred after our treatments resulted in a less viscous juice.

Comparison of an untreated fresh sample of *SunUp* papaya to a frozen (then thawed) untreated *SunUp* papaya sample indicated no significant viscosity differences between fresh and frozen samples (data for fresh samples found in Table 1; frozen data not shown). This supported the decision to freeze samples rather than add citric acid to avoid gelation. Tomato juice was compared to the *Rainbow* papaya control sample, as our papaya samples were diluted to the same °Brix as tomato juice (~8% dissolved solids). Papaya juice is significantly more viscous than tomato juice ($p < 0.05$, data not shown). This suggests that °Brix is not the only contributor to viscosity in papaya.

3.5. Colourimetry

In *Rainbow* papaya samples the only significant colour differences from the control were localised to '*a*' values, losing some of its redness when heated with or without irradiation (H, 5H, and 7.5H; Table 2). Significant changes in the '*a*' values resulted in a significant change in the overall ΔE values as well. For *SunUp* papaya, significant differences from the control were also found only in the '*a*' measurements. However, values were only significantly less red for H and 7.5H. Surprisingly, 7.5 was significantly more red than the control. None of the ΔE values were significantly different from the control for this variety. These results suggest that, in *SunUp* samples, heat resulted in loss of red colour while irradiation resulted in enhanced red colour. Overall, the two treatments work in opposition, resulting, for the *SunUp* variety, in combination treatments having a colour similar to that of the control. The same did not seem to occur, at least not significantly, in the *Rainbow* variety. *SunUp* papaya gets its red colour from lycopene, a carotenoid not produced in *Rainbow* papaya. This gives *SunUp* papaya an increased overall carotenoid content (Yamamoto, 1964) and its distinct red colour. Carotenoids are easily destroyed by heat (Beyers & Thomas, 1979) but have the ability to absorb high energy radicals, such as singlet oxygen (Lee, Koo, & Min, 2004). Heat resulted in a loss of red colour, and thus carotenoids, in both varieties of papaya. Irradiation may have changed the structure or ratios of the carotenoids, and thus the apparent colour, depending on their concentrations and/or ability to absorb free radicals produced during irradiation. In a side-by-side comparison of papaya pulp, the colour difference between control and heat treated *Rainbow* samples is visible, with heat treated samples having a slightly more pale yellow colour. No colour difference was visually apparent between control and treated *SunUp* papaya. The overall darker red colour likely masked the colour changes resulting from our treatments.

3.6. Microbiology

Before treatment, the final concentration of the organisms in the papaya pulp was as follows: 4.65×10^8 CFU/ml for *E. coli*; 5.58×10^8 CFU/ml for *S. typhimurium*; 5.63×10^8 CFU/ml for *L. innocua*; 4.21×10^6 CFU/ml for *C. sporogenes.* Administration of heat, whether alone or in combination with irradiation, was sufficient to eliminate all growth of *E. coli* and *S. typhimurium*. All *E. coli* was also destroyed with 7.5 kGy, while 530 CFU/ml (*Rainbow*) and 930 CFU/ml (*SunUp*) remained after 5 kGy. Neither irradiation treatment alone was sufficient to destroy *S. typhimurium* (plates were confluent or uncountable). For *L. innocua*, in *Rainbow* and

Table 2
Effects of papaya variety and treatment on colourimetry.[A]

	Rainbow						*SunUp*					
	C	H	5	7.5	5H	7.5H	C	H	5	7.5	5H	7.5H
L[B]	28.48 ± 2.05^{ab}	25.55 ± 1.31^{bc}	28.84 ± 1.98^{ab}	29.22 ± 1.89^{a}	25.51 ± 1.37^{bc}	25.91 ± 0.97^{abc}	23.83 ± 0.27^{cd}	22.56 ± 0.22^{cd}	23.65 ± 0.22^{cd}	24.51 ± 0.14^{cd}	22.00 ± 0.36^{d}	22.93 ± 0.18^{cd}
a	6.92 ± 0.04^{e}	5.16 ± 0.58^{f}	7.34 ± 0.17^{e}	7.08 ± 0.16^{e}	4.70 ± 0.40^{fg}	3.94 ± 0.45^{g}	13.19 ± 0.36^{b}	11.17 ± 0.06^{d}	13.37 ± 0.12^{b}	14.43 ± 0.10^{a}	12.89 ± 0.16^{bc}	12.23 ± 0.15^{c}
b	44.20 ± 3.69^{abc}	41.79 ± 0.73^{cd}	46.42 ± 1.28^{ab}	47.44 ± 0.67^{a}	42.68 ± 1.20^{bc}	43.60 ± 1.01^{abc}	37.78 ± 0.94^{e}	37.10 ± 0.90^{e}	38.60 ± 0.22^{de}	40.48 ± 0.18^{cde}	37.07 ± 0.63^{e}	38.73 ± 0.43^{de}
ΔE	0.00^{c}	4.89 ± 0.27^{ab}	2.39 ± 2.28^{abc}	3.40 ± 3.00^{abc}	5.68 ± 0.55^{a}	5.49 ± 1.37^{a}	0.00^{c}	2.49 ± 0.54^{abc}	0.97 ± 0.90^{c}	3.11 ± 0.52^{abc}	2.12 ± 0.68^{abc}	1.64 ± 0.84^{bc}

C, control; H, heat (80 °C, 5 min); 5, 5 kGy; 7.5, 7.5 kGy; 5H, 5 kGy + heat; and 7.5H, 7.5 kGy + heat ($n = 3$).

[A] Values not sharing the same letter within each row are significantly different ($p < 0.05$) and are reported as mean ± SD.

[B] L measures lightness on a scale of $L = 0$ (black) to $L = 100$ (white); a measures the degree of red (+a) or green (−a) present in a sample; b indicates the degree of yellow (+b) or blue (−b) present in the sample; and ΔE combines all three values.

SunUp papaya, respectively, 50 and 20 CFU/ml remained after heat alone, 60 and 3890 after 5 kGy, and no colonies survived after 7.5 kGy or either or the combination treatments. For *C. sporogenes*, heat alone left 370 and 710 CFU/ml, 5 and 7.5 kGy resulted in a distinguishable but uncountable number of colonies (for both varieties), 5H left 90 and 140 CFU/ml and 7.5H left 320 and 130 CFU/ml.

To completely eliminate *C. sporogenes* and *L. innocua* by heat treatment alone, higher temperatures would be necessary; however, this would lead to detrimental changes in flavour, odour, colour, and texture of papaya pulp (Argaiz & Lopez-Malo, 1995). The combination treatment of irradiation followed by heat produced a stronger elimination of all organisms tested, while minimising detrimental changes. The 5H and 7.5H treatments were effective at eliminating growth of all bacteria tested except *C. sporogenes* in both varieties of papaya. *C. sporogenes* is a resilient spore-forming bacterium that can survive harsh conditions to a greater degree than organisms that do not form spores; yet its viability was reduced to countable colonies by both combination treatments applied in this study. While this is an encouraging result, our combination treatments did not completely eliminate the spore-forming bacteria. Use of our processing method will require that the product be refrigerated to ensure it is safe for consumption. Almost no *Clostridium* species will grow at refrigeration temperatures (Hauschild, 1989).

3.7. Pectinesterase (PE) activity

PE is responsible for demethylation of methyl ester groups on the alpha-galacturonic acid residues of pectin polymers (Powell, Morris, Gidley, & Rees, 1982). This results in a greater number of carboxylic acid groups available to interact with divalent cations present in the pulp. Many of these cations will bind to adjacent pectin molecules, resulting in less fluidity and subsequent gel formation in the fresh papaya pulp. A significant reduction in PE activity (from the control) was achieved in both varieties of papaya with heat treatment, whether or not it was combined with irradiation (Fig. 3). Irradiation alone did not significantly reduce PE activity for either variety. Results were not significantly different between varieties for any of the treatments.

3.8. Consistometry

Initially, *Rainbow* papaya pulp had a longer flow distance, indicating lower viscosity, than *SunUp* papaya; however, it did not decrease as dramatically over time (Figs. 1 and 2). Irradiated *Rainbow* papaya did not gel as quickly as the *SunUp* variety despite similar PE activities. The *SunUp* irradiated samples gelled much more similarly to the control than irradiated *Rainbow* samples. For both varieties, all treatments decreased significantly from the control within a few days. It is unclear how much of this is due to enzyme activity. Since there was a reduction in the enzymatic activity of PE after heat treatment, it was expected that there would only be significant differences over time in control or irradiated samples. Though there were significant drops in flow distance for all samples, heat treated samples maintained the lowest flow distance over a number of days. Control and irradiated samples flowed shorter distances with time.

Because of the small but significant decrease in flow distance in all samples, the goal was to confirm that the change was not due to PE activity increasing with time. Some of the stable form of PE may have only been partially denatured and may have regained activity over time (Magalhães et al., 1996). A follow-up PE assay was performed after consistometry measurements were completed. PE values were very similar to the PE values obtained before the consistometry measurement began (data not shown). Thus, slight thickening of the pulp of both varieties after a few days of measurements must be due to some other factor yet to be determined.

3.9. HPLC-flavonoids

Extractions of both varieties were performed multiple times with various solvent mixtures. No flavonoids were detected after any of the extractions attempted. Even after preparation of a 10× concentrated papaya sample, no flavonoids were detected for either *Rainbow* or *SunUp* varieties. A quercetin spike was added to the method described above to confirm the quality of the extraction/concentration process (80% recovery). Other researchers (Franke et al., 2004) also reported undetectable levels of flavonoids in papaya.

3.10. HPLC-ascorbic acid

The ascorbic acid concentration significantly decreased after both doses of irradiation in the *Rainbow* variety compared to control (Fig. 4); however, combination treatments were not significantly different from the control. In the *SunUp* variety, 7.5 and combination treatments were significantly lower than the control. Comparing varieties, H, 5H, and 7.5H were significantly different from one another. This suggests that *SunUp* papaya ascorbic acid may be more susceptible to heat or that *Rainbow* papaya may not be as susceptible to it. Overall, irradiation was more detrimental to ascorbic acid than the mild heat treatment applied, and in the *Rainbow* variety, combination treatments significantly removed the negative effects of irradiation on ascorbic acid content. This may be due to decompartmentalisation of ascorbic acid in the pulp. Other researchers (Wilkinson & Gould, 1996) have found an 8–20% reduction of ascorbic acid content after irradiation at 3 kGy. For comparison, ascorbic acid loss in this study after 5 kGy was 18% in *Rainbow* papaya samples and 11% in *SunUp* papaya samples.

3.11. EPR analysis

EPR provided a unique method to evaluate papaya's response to hydroxyl radicals (Rødtjer, Skibsted, & Andersen, 2006). Two different extraction methods were employed to evaluate the antioxidant capacity of both *SunUp* and *Rainbow* papaya varieties and to determine if any differences were apparent due to extraction method (Figs. 5 and 6). There were no significant differences observed between any samples for either extraction method, though the trends were similar to the results of ascorbic acid analysis. Other researchers (Tzika, Papadimitriou, Sotiroudis, & Xenakis, 2008) have also recently applied this methodology to a number of fruit and vegetables juices.

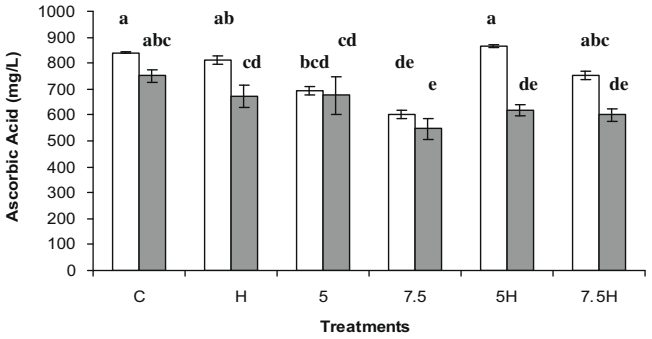

Fig. 4. Ascorbic acid content of *Rainbow* (white bars) and *SunUp* (grey bars) papaya. Values are reported as mean ± SD. Bars not sharing the same lowercase letter are significantly different ($p < 0.05$). C, control; H, heat (80 °C, 5 min); 5, 5 kGy; 7.5, 7.5 kGy; 5H, 5 kGy + heat; and 7.5H, 7.5 kGy + heat ($n = 3$).

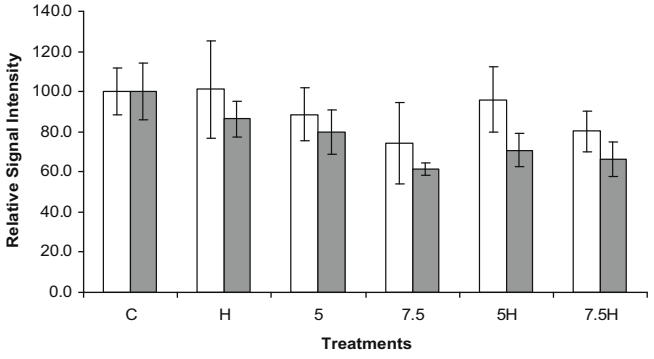

Fig. 5. EPR signal intensity of water extracts of *Rainbow* (white bars) and *SunUp* (grey bars) papaya. For ease of comparison, the average control EPR signal was adjusted to a value of 100 with other subsequent treatments shown relative to the control. Values are reported as mean ± SD. No treatments were significantly different ($p < 0.05$). C, control; H, heat (80 °C, 5 min); 5, 5 kGy; 7.5, 7.5 kGy; 5H, 5 kGy + heat; and 7.5H, 7.5 kGy + heat ($n = 3$).

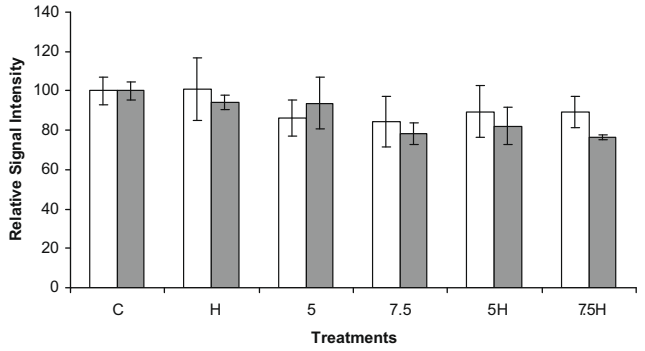

Fig. 6. EPR signal intensity of methanolic extracts of *Rainbow* (white bars) and *SunUp* (grey bars) papaya. For ease of comparison, the average control EPR signal was adjusted to a value of 100 with other subsequent treatments shown relative to the control. Values are reported as mean ± SD. No treatments were significantly different ($p < 0.05$). C, control; H, heat (80 °C, 5 min); 5, 5 kGy; 7.5, 7.5 kGy; 5H, 5 kGy + heat; and 7.5H, 7.5 kGy + heat ($n = 3$).

3.12. ORAC analysis

No significant antioxidant capacity differences were observed between controls and any treatments for either variety of papaya (Fig. 7). However, the antioxidant capacity of the 5H treatment in *Rainbow* samples was significantly higher than that of either irradiation treatment alone. There were no significant differences between the two papaya varieties for control or treated samples. Comparing these results with EPR and ascorbic acid results, it is likely that the decrease in ORAC after irradiation is primarily due to loss of ascorbic acid. Though *Rainbow* and *SunUp* papaya contain undetectable levels of flavonoids, papaya does contain phenolic compounds (total phenolics assayed by Luximon-Ramma et al. (2003); individual papaya phenolics have not been quantified). However, as no differences were seen between the water and methanol extracts in the EPR assay, either most of the phenolic compounds are water-soluble or irradiation does not have a large effect on the phenolic content. The latter is most likely, as papaya sugars have been shown to be primarily responsible for quenching gamma ray-produced radicals (Gray & Mower, 1991).

With an average ORAC value of 5 μmol TE/g (undiluted papaya), papaya has a higher ORAC value than cantaloupe or watermelon, but lower than grapes, carrots or apples (Wu et al., 2004). To our knowledge, no other researchers have explored the impact of ionising radiation on ORAC values at the doses applied in this study.

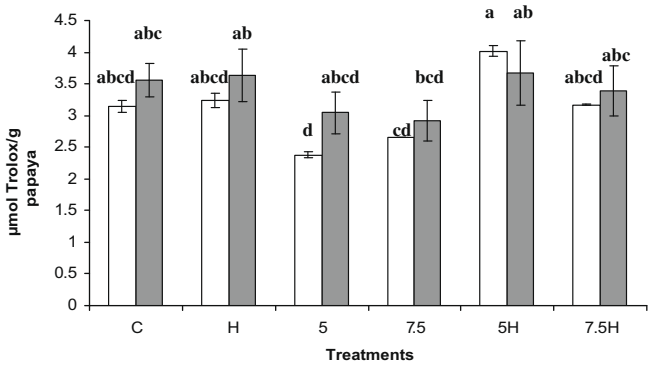

Fig. 7. ORAC values of *Rainbow* (white bars) and *SunUp* (grey bars) papaya (diluted to 8 °Brix). Values are reported as mean ± SD. Bars not sharing the same lowercase letter are significantly different ($p < 0.05$). C, control; H, heat (80 °C, 5 min); 5, 5 kGy; 7.5, 7.5 kGy; 5H, 5 kGy + heat; and 7.5H, 7.5 kGy + heat ($n = 3$).

Reyes and Cisneros-Cevallos (2007) found no change in ORAC value on whole mangoes at doses of up to 3 kGy. Due to the significant decrease in ascorbic acid after irradiation described above, it would be expected that higher doses of irradiation would result in a significant reduction of ORAC value. The trend toward a decreased ORAC value at the doses used in this study support this hypothesis. It would be of interest to explore the rate of change in ORAC value at doses of irradiation that would be expected to oxidise all of the ascorbic acid, and attempt to determine what other compounds in papaya would be subsequent targets. Niemand et al. (1983) found that phenols and organic acids accounted for most of the protection from mutagen formation in mango juice. Their contribution to ORAC value should be further explored.

A combination of moderate irradiation and mild heat resulted in a microbiologically safe (if refrigerated), enzyme inactive, and nutritionally optimised papaya pulp. Irradiation resulted in a sweeter papaya flavour, though there was no significant change in sugar profiles. Drinkable consistency is maintained for at least 10 days. Colour changed slightly in the *Rainbow* variety, though was not as important as aroma and flavour in informal tasting. Ascorbic acid was significantly reduced after irradiation in both varieties, but was similar to controls after heat treatment in the *Rainbow* variety samples. Neither EPR nor ORAC antioxidant analyses of treatments were significantly different from controls, though the results were patterned similarly to ascorbic acid results. This suggests that in diluted papaya pulp, the antioxidant primarily affected by irradiation is ascorbic acid. Challenges to the implementation of this process include the requirement for refrigeration, consumer resistance to irradiation, and potential costs of irradiation. If implemented, processed papaya pulp will retain more of its fresh flavour and nutritional qualities, increasing papaya marketability.

Support

Funding for this research was provided by a grant from the Hawaiian Farm Bureau. Papaya was provided by the Hawaiian Papaya Industry Association by arrangement through the Hawaii Department of Agriculture. Support for T. Parker and S. Esgro was provided by a Jonathan Baldwin Turner Fellowship (University of Illinois at Urbana-Champaign).

Acknowledgements

We would like to thank the following from the University of Illinois at Urbana-Champaign for use of their equipment: Dr. Stoyan Toshkov for use of the Gammacell irradiator; Dr. William Helferich

for the use of the fluorometer; Dr. Mark Nilges and the EPR centre for the use of their spectrometer; Dr. Shelly Schmidt for use of the viscometer; Dr. Keith Cadwallader and John Jerrell for use of their HPLC equipment; Dr. Susan Brewer for use of the colourimeter; and Dr. Michael Miller for use of the anaerobic chamber.

References

Ahmed, J., & Ramaswamy, H. S. (2004). Response surface methodology in rheological characterization of papaya puree. *International Journal of Food Properties, 7*, 45–58.

AOAC (2002). *Official methods of analysis of the Association of Official Analytical Chemists* (pp. 2–3) (17th ed.). Gaithersburg, MD: AOAC International.

Argaiz, A., & Lopez-Malo, A. (1995). Kinetics of first change on flavour, cooked flavour development and pectinesterase inactivation on mango and papaya nectars and purees. *Revista Espanola de Ciencia y Tecnologia de Alimentos, 35*, 92–100.

Bakker, J. (1995). Flavor interactions with the food matrix and their effects on perception. In A. G. Gaonkar (Ed.), *Ingredient interactions: Effects on food quality* (pp. 411–439). New York, NY: Marcel Dekker Inc.

Beyers, M., & Thomas, A. C. (1979). Gamma irradiation of subtropical fruits. 4. Changes in certain nutrients present in mangoes, papayas, and litchis during canning, freezing, and gamma irradiation. *Journal of Agricultural and Food Chemistry, 27*, 48–51.

Brekke, J. E., Chan, H. T., Jr., & Cavaletto, C. G. (1973). Papaya puree and nectar. *Research Bulletin, Hawaii Agricultural Experiment Station, 1*(170), 1–13.

Busta, F. F., Suslow, T. V., Parish, M. E., Beuchat, L. R., Farber, J. N., Garrett, E. H., et al. (2003). The use of indicators and surrogate microorganisms for the evaluation of pathogens in fresh and fresh-cut produce. *Comprehensive Reviews in Food Science and Food Safety, 2*, 179S–185S.

Castaldo, D., Laratta, B., Loiudice, R., Giovane, A., Quagliuolo, L., & Servillo, L. (1997). Presence of residual pectin methylesterase activity in thermally stabilized industrial fruit preparations. *Lebensmittel-Wissenschaft & Technologie, 30*, 479–484.

Chan, H. T., Jr., Flath, R. A., Forrey, R. R., Cavaletto, C. G., Nakayama, T. O. M., & Brekke, J. E. (1973). Development of off-odors and off-flavors in papaya puree. *Journal of Agricultural and Food Chemistry, 21*, 566–570.

Chang, L. W. S., Morita, L. L., & Yamamoto, H. Y. (1965). Papaya pectinesterase inhibition by sucrose. *Journal of Food Science, 30*, 218–222.

Davalos, A., Gomez-Cordoves, C., & Bartolome, B. (2004). Extending applicability of the oxygen radical absorbance capacity (ORAC-fluorescein) assay. *Journal of Agricultural and Food Chemistry, 52*, 48–54.

Falchi, M., Bertelli, A., Lo Scalzo, R., Morassut, M., Morelli, R., Das, S., et al. (2006). Comparison of cardioprotective abilities between the flesh and skin of grapes. *Journal of Agricultural and Food Chemistry, 54*, 6613–6622.

Franke, A. A., Custer, L. J., Arakaki, C., & Murphy, S. P. (2004). Vitamin C and flavonoid levels of fruits and vegetables consumed in Hawaii. *Journal of Food Composition and Analysis, 17*, 1–35.

Gray, J., & Mower, H. F. (1991). The role of simple carbohydrates in the suppression of hydroxyl free radicals in gamma-irradiated papaya juice. *Food Chemistry, 41*, 293–301.

Grigelmo-Miguel, N., & Martín-Belloso, O. (1999). Influence of fruit dietary fibre addition on physical and sensorial properties of strawberry jams. *Journal of Food Engineering, 41*, 13–21.

Hauschild, A. H. W. (1989). *Clostridium botulinum*. In M. P. Doyle (Ed.), *Foodborne bacterial pathogens* (pp. 111–189). New York, NY: Marcel Dekker Inc.

Kertesz, Z. I. (1955). Pectic enzymes (1st ed.. In S. P. Colowick & N. O. Kaplan (Eds.). *Methods of enzymology* (vol. 1, pp. 158–166). New York, NY: Academic Press.

Lee, H. S., & Coates, G. A. (1999). Measurement of total vitamin C activity in citrus products by HPLC: A review. *Journal of Liquid Chromatography & Related Technologies, 22*, 2367–2387.

Lee, J., Koo, N., & Min, D. B. (2004). Reactive oxygen species, aging, and antioxidative nutraceuticals. *Comprehensive Reviews in Food Science and Food Safety, 3*, 21–33.

Liebman, B. (1992). Fresh fruit: A papaya a day? *Nutrition Action Healthletter*, 10–11.

Lim, Y. Y., Lim, T. T., & Tee, J. J. (2007). Antioxidant properties of several tropical fruits: A comparative study. *Food Chemistry, 103*, 1003–1008.

Lourenco, E. J., & Catutani, A. T. (1984). Purification and properties of pectinesterase from papaya. *Journal of the Science of Food and Agriculture, 35*, 1120–1127.

Luximon-Ramma, A., Bahorun, T., & Crozier, A. (2003). Antioxidant actions and phenolic and vitamin C contents of common Mauritian exotic fruits. *Journal of the Science of Food and Agriculture, 83*, 496–502.

Magalhães, M. M. dos A., Tosello, R. M., & de Massaguer, P. R. (1996). Thermal inactivation of pectinesterase in papaya pulp (pH 3.8). *Journal of Food Process Engineering, 19*, 353–361.

Morton, J. (1987). Papaya. In J. F. Morton (Ed.), *Fruits of warm climates* (1st ed., pp. 336–346). Miami, FL: Florida Flair Books.

Mostafa, G. A., Abd El Hady, E. A., & Askar, A. (1997). Preparation of papaya and mango nectar blends. *Fruit Processing, 7*, 180–185.

Murcia, M. A., Jimenez, A. M., & Martinez-Tome, M. (2001). Evaluation of the antioxidant properties of Mediterranean and tropical fruits compared with common food additives. *Journal of Food Protection, 64*, 2037–2046.

Niemand, J. G., den Drijver, L., Pretorius, C. J., Holzapfel, C. W., & van der Linde, H. J. (1983). A study of the mutagenicity of irradiated sugar solutions: Implications for the radiation preservation of subtropical fruits. *Journal of Agricultural and Food Chemistry, 31*, 1016–1020.

Penteado, A. L., & Leitão, M. F. F. (2004). Growth of *Salmonella enteriditis* in melon, watermelon and papaya pulp stored at different times and temperatures. *Food Control, 15*, 369–373.

Powell, D. A., Morris, E. R., Gidley, M. J., & Rees, D. A. (1982). Conformation and interactions of pectins: II. Influence of residue sequence on chain association in calcium pectate gels. *Journal of Molecular Biology, 155*, 517–531.

Reyes, L. F., & Cisneros-Cevallos, L. (2007). Electron-beam ionizing radiation stress effects on mango fruit (*Mangifera indica* L.) antioxidant constituents before and during postharvest storage. *Journal of Agricultural and Food Chemistry, 55*, 6132–6139.

Rødtjer, A., Skibsted, L. H., & Andersen, M. L. (2006). Antioxidative and prooxidative effects of extracts made from cherry liqueur pomace. *Food Chemistry, 99*, 6–14.

Tiwari, R. B. (2000). Studies on blending of guava and papaya pulp for RTS beverage. *Indian Food Packer, 54*, 68–72.

Tzika, E. D., Papadimitriou, V., Sotiroudis, T. G., & Xenakis, A. (2008). Antioxidant properties of fruits and vegetables shots and juices: An electron paramagnetic resonance study. *Food Biophysics, 3*, 48–53.

USDA National Nutrient Database for Standard Reference. <http://www.nal.usda.gov/fnic/foodcomp/search/> Accessed April 2008.

WHO Technical Report 890 (1997). *High-dose irradiation: Wholesomeness of food irradiated with doses above 10 kGy*. Joint FAO/IAEA/WHO Study Group, Geneva, Switzerland.

Wilkinson, V. M., & Gould, G. W. (1996). *Food irradiation: A reference guide* (p. 130). CRC Press.

Wu, X., Beecher, G. R., Holden, J. M., Haytowitz, D. B., Gebhardt, S. E., & Prior, R. L. (2004). Lipophilic and hydrophilic antioxidant capacities of common foods in the Unites States. *Journal of Agricultural and Food Chemistry, 52*, 4026–4037.

Yamamoto, H. Y. (1964). Comparison of the carotenoids in yellow- and red-fleshed *Carica papaya*. *Nature, 20*, 1049–1050.

Among them synthetic peptides hippuryl-L-histidyl-L-leucine (HHL) and furanacryloyl-L-phenylalanylglycyl-glycine (FAPGG) are the most commonly used but other peptides can be used like fluorescent molecules (for example, o-aminobenzoylglycyl-p-nitrophenylalanylproline) for specific detection and quantification (Carmel & Yaron, 1978; Sentandreu & Toldra, 2006).

In most of the previous cited works, the assay used for ACE activity was based on the method developed by Cushman and Cheung (1971). The amount of hippuric acid (HA) formed from HHL by action of ACE is extracted with ethyl acetate and the concentration is determined by a spectrophotometric assay. Different modifications of this method have been reported in which the ethyl acetate extraction was replaced by a specific binding of His-Leu with 2,4,6-trinitrobenzene sulphonate (TNBS) (Matsui, Matsufuji, & Osajima, 1992) or a specific reaction of HA with benzene sulfonyl chloride (Li, Liu, Shi, & Le, 2005). Although this assay has been very useful during decades, it has some limitations such as the required extraction of the product from the reaction mixture with an organic solvent which is an additional source of error.

Another method was described by Holmquist, Bünning, and Riordan (1979) using FAPGG as substrate. This method, consisting in the measurement of the absorbance decrease due to the substrate hydrolysis by action of ACE, was adopted for testing ACE-inhibitory activity of peptides (Vermeirssen, Van Camp, & Verstraete, 2002). Different modifications were also reported with fixed time conditions (Murray, Walsh, & FitzGeralg, 2004), using 96-wells microtiter plate (Otte et al., 2007) or HPLC determination (Anzenbacherová, Anzenbacher, Macek, & Květina, 2001). Shalaby, Zakora, and Otte (2006) have compared the performance of the ACE inhibition assays using FAPGG and HHL as substrates.

Both methods showed similar performance but HHL substrate in solution seemed to be less stable than FAPGG substrate and the assay with FAPGG consumed less chemicals per sample. It was also pointed out that ACE preparation showed various activities. So, it is important to control the ACE-activity in the assays or to use the same enzyme preparation to compare the ACE-inhibitory activity of different samples.

In the present study, the objective was to determine the antihypertensive activity of a fish hydrolysate produced industrially from by-products normally discarded in the process of fish manufacture. Different methods have been tested and adapted. A HPLC method using FAPGG as substrate was finally selected and optimised. The determination of Hill coefficient allowed us to confirm the number of ACE active sites corresponding to low-molecular inhibitory peptides.

2. Materials and methods

2.1. Chemicals and reagents

Fish by-products hydrolysate was produced by ID.MER (Lorient, France). ACE (angiotensin-converting enzyme, EC 3.4.15.1) from rabbit lung, Captopril, HHL (Hippuryl-His-Leu), FAPGG (N-(3-[2-furylacryloyl)-Phe-Gly-Gly) and all other reagents were purchased from Sigma. Water and acetonitrile were HPLC grade.

2.2. Preparation of ACE working solution

Commercial angiotensin I-converting enzyme (Unit) was diluted in buffer (50 mM Tris–HCl pH 7.5 containing 0.3 M NaCl) to obtained a concentration of 100 mU/mL. Aliquots of 250 μL were then stored at −20 °C until use.

2.3. Methods

2.3.1. Determination of ACE inhibition using HHL as substrate

The method used was a HPLC method based on the assay developed by Cushman and Cheung (1971) and Wu, Aluko, & Muir (2002). The substrate HHL was dissolved (5 mM) in 0.1 M sodium-borate buffer (pH 8.3) containing 0.3 M NaCl. The assay was performed by mixing 100 μL of substrate solution with 25 μL of inhibitor solution (or borate buffer for control). After 10 min of incubation at 37 °C, 10 μL of ACE solution (100 mU/mL) were added and the sample was further incubated at 37 °C for 30 min with continuous agitation at 450 rpm. The reaction was stopped by addition of 100 μL of 1 M HCl and the solution was filtered through a 0.45-μm nylon syringe filter before being analyzed by reversed-phase HPLC.

The HPLC analysis was performed on a C18 column (150 × 3.0 mm i.d.), particle size 5 μm with a Varian chromatographic system and analytes were detected at the wavelength of λ = 228 nm. The column was eluted at a flow rate of 0.5 mL min^{-1} with a two solvents system: (A) 0.05% TFA in water and (B) 0.05% TFA in acetonitrile. The gradient consisted 5–60% B in 10 min, maintained for 2 min at 60% B, then returned to 5% B for 1 min. This was followed by isocratic elution for 4 min at 5% B.

2.3.2. Determination of ACE inhibition using FAPGG as substrate

To 125 μL of buffer (50 mM Tris–HCl pH 7.5 containing 0.3 M NaCl), 100 μL of substrate solution (2.5 μM FAPGG in the same buffer) and 50 μL of inhibitor solution were added. The reaction was started by addition of 25 μL of enzyme (100 mU/mL ACE solution) and the mixture was incubated 45 min at 37 °C in a water bath. The reaction was then stopped by addition of 200 μL of methanol and the reaction mixture was then analyzed by HPLC. ACE inhibition was determined by measuring the level of FAP with and without inhibitor, in the same conditions.

The HPLC analysis was performed on a ODS Hypersil column (250 × 4.6 mm i.d.), particle size 5 μm with a Varian chromatographic system. FAP and FAPGG were separated isocratically at room temperature with a mobile phase consisting of a mixture of 0.02 M nonylamine (adjusted to pH 2.4 with H_3PO_4) – acetonitrile (67.5:32.5 v/v). The flow rate was 1 mL min^{-1} and the injection volume was 100 μL. Analytes were detected at the wavelength of λ = 305 nm.

2.3.3. ACE inhibition measurement

The evaluation of ACE inhibition was based on the comparison between the concentration of FAP in presence or not (control sample) of an inhibitor. After injection in HPLC of the control and the assay with inhibitor, the FAP peak areas obtained in the two cases were measured (Fig. 1) and the degree of ACE inhibition (in%) was calculated according to the equation (A):

$$\text{ACE inhibition } (\%) = [1 - (A_{\text{inhibitor}}/A_{\text{control}})] \times 100 \quad \text{(A)}$$

where $A_{\text{inhibitor}}$ and A_{control} are respectively, the relative areas of the FAP peak of the assay with inhibitor and of the control sample without inhibitor.

This protocol was reproduced 15 times with the fish hydrolysate in order to be validated. The retention times were constant and the experimental error for the determination of ACE inhibition was around 3.5%.

The relation previously described supposed a linearity of UV response between the peak area and the FAPGG amount. Known rising amounts of substrate FAPGG were injected in HPLC to determine in which interval the UV response curve was linear. The results obtained showed this relationship was linear until 0.25 nmol of FAPGG but not over. Given that the amount of FAPGG injected during the ACE inhibition measurement was 0.05 nmol,

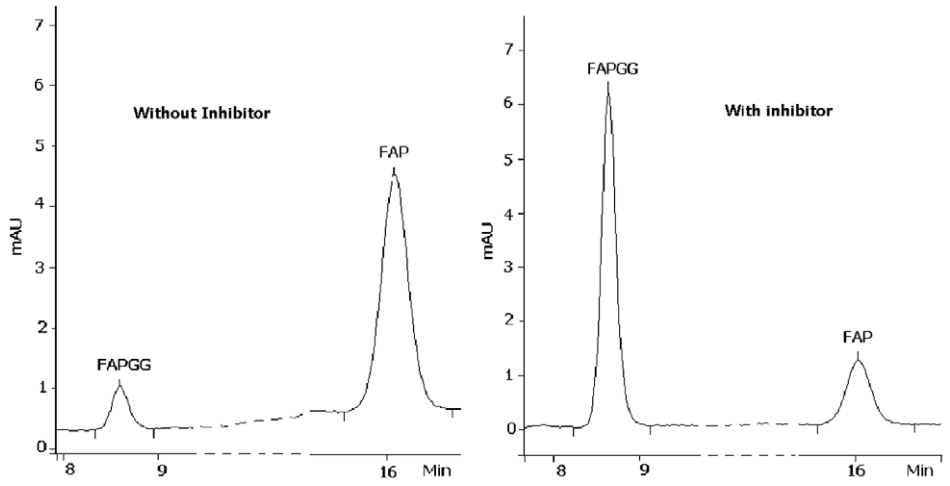

Fig. 1. HPLC profiles of the control sample without inhibitor and the assay sample with inhibitor. Retention times of the substrate FAPGG and the product formed by ACE hydrolysis (FAP) were, respectively of 8.6 and 16.1 min.

the comparison of peak areas could be used to calculate the inhibition.

2.3.4. Determination of Hill coefficient

ACE is known to possess two binding sites for low-molecular weight inhibitors. In order to know if the fish hydrolysate peptides responsible for the ACE inhibition are low-molecular peptides, the Hill coefficient corresponding to the number of binding sites was determined for the fish hydrolysate in comparison to Captopril.

The experimental data were evaluated for fitting with an equation of type Hill equation: $y = a/[1 + (b/x)^n]$, where y was the meaning of the inhibition (I), x was the inhibitor concentration (C), a was the maximum of inhibition (I_{max}), b was the inhibitor concentration corresponding to a 50% inhibition (IC_{50}) and n was the Hill coefficient corresponding to the number of the binding sites of the ACE (steepness of the curves below).

2.3.5. Optimization of the E/S ratio and the incubation time

Before measuring ACE inhibition, the best conditions for the FAPGG hydrolysis by ACE were determined. Different ratios of enzyme/substrate (E/S) were first tested with an incubation time of 30 min (0.4, 4, 8, 10 and 17.5 mU ACE/nmol substrate). Then, various incubation times were assayed using the optimum E/S ratio (15, 30, 45 and 60 min).

2.3.6. Influence of NaCl content in buffer

In the literature, the NaCl concentration in buffer currently used was 300 mM but we noticed in some cases, other concentrations (Jung et al., 2006; Matsui et al., 1992). To evaluate the influence of the NaCl content in buffer on the ACE inhibition, three different buffers were prepared with various amounts of NaCl (5 mM, 300 mM and 1 M). ACE inhibition measurement was performed as described on Section 2.3.2. using the fish hydrolysate as inhibitor. The E/S ratio was 10 mU ACE/nmol substrate and the incubation time was 45 min.

2.3.7. Determination of ACE-inhibitory activity of Captopril

Captopril, an inhibitor of ACE, was used as a reference. The degree of ACE inhibition was measured using different amounts of Captopril from 5 to 100 μL of a 5 ng/mL solution as described in the Section 2.3.1. The IC_{50} value, corresponding to the amount required to inhibit 50% of the ACE activity, was determined from the ACE inhibition curve. Five different inhibition curves were realised to evaluate the IC_{50} standard deviation.

2.3.8. Determination of ACE-inhibitory activity of a fish hydrolysate

As for Captopril, IC_{50} value and standard deviation were determined from five ACE inhibition curves obtained with different amounts of a same batch of fish hydrolysate. Other batches of the fish hydrolysate were then tested in terms of ACE inhibition to evaluate the reproducibility of the process.

2.4. Statistical analysis

The IC_{50} values were calculated from ACE inhibition curves obtained with increasing amounts of inhibitor (Captopril and the fish hydrolysate). The results for each inhibitor were expressed as the mean ± S.D. of five values obtained from five inhibition curves.

3. Results and discussion

3.1. Choice of substrate

In this work, the analyses were carried out by HPLC-UV and HHL and FAPGG were tested. The choice of the substrate was based on (i) the sensitivity (corresponding detection limits have been estimated) and (ii) the cost and more precisely the ACE amounts required for hydrolysis. The chromatographic conditions lead to a good separation of the products HHL and HA with respective retention times of 10.8 and 7.5 min. Nevertheless, the background signal is unstable and disturbs a precise quantification. The corresponding detection limit is high and insufficient for the study: 0.25 nmol of HHL are hardly detected.

FAPGG constitutes a better substrate: 0.05 nmol were easily detected. The substrate and the hydrolysed compound were separated in good conditions with a stable and low background. The retention times were 8.6 and 16.1 min for FAPGG and FAP, respectively.

Moreover, from the point of view of reactant consumption, FAPGG is excellent. With a same enzyme/substrate ratio, the degree of hydrolysis was lower with HHL (33%) while it approaches 90% with FAPGG.

3.2. E/S ratio and incubation time

The results of FAPGG hydrolysis by ACE showed it needed a great amount of enzyme to reach a hydrolysis rate of 50%. As a steady state was obtained from a E/S ratio of 10 mU/nmol, it was decided to go on with this ratio for all measurements (Fig. 2).

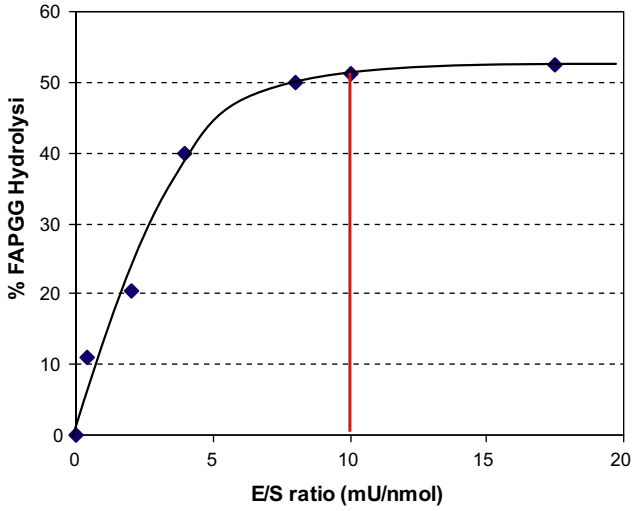

Fig. 2. FAPGG hydrolysis rate obtained with different E/S ratio after 30 min incubation at 37 °C. A steady state was reached from a E/S ratio of 10 mU/nmol.

With regard to the incubation time (Fig. 3), the different assays showed the FAPGG hydrolysis was not optimum after 30 min incubation and began to decrease after 45 min. So, the ACE inhibition measurements were carried out with an incubation time of 45 min.

3.3. Influence of NaCl content in buffer

The ACE inhibition with 5 mM NaCl was the lowest with an IC_{50} of 23.4 μg peptides. In the other hand, there were less differences between 1 M and 300 mM NaCl with IC_{50}, respectively of 15.3 μg and 12.3 μg peptides. However, the ACE inhibition was slightly higher with 300 mM NaCl and, as it was currently described in the literature, we decided to work with this concentration in buffer.

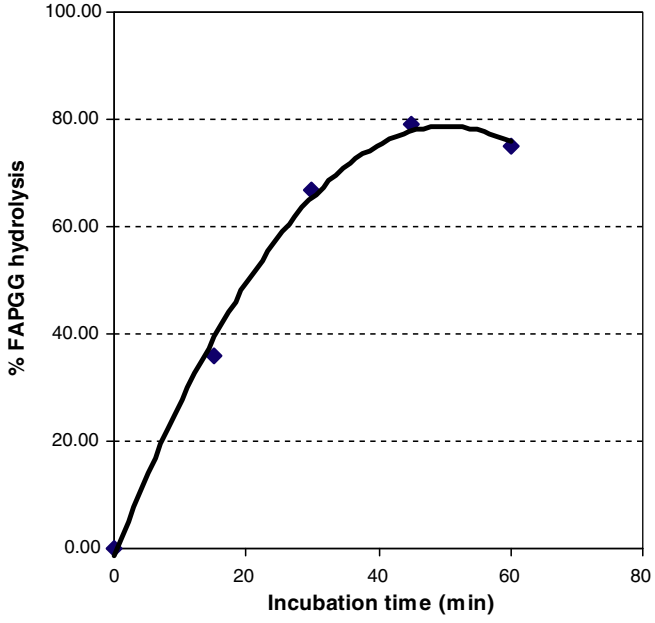

Fig. 3. FAPGG hydrolysis rate obtained with a E/S ratio of 12.5 mU/nmol after different incubation times at 37 °C. The hydrolysis reached an optimum after 45 min of incubation.

3.4. IC_{50} of Captopril

The measurement of ACE inhibition with Captopril allowed us to determine an IC_{50} value of 0.19 ng (±0.09) corresponding to a concentration of 1.75 nM. This value corresponds well with literature where a value of 1.56 nM has been reported by Vermeirssen et al. (2002).The repeated measurements showed also the high sensibility but the low stability of the Captopril solution. Indeed, we noticed a decrease of 28% of the inhibition activity after only 2 days storage at −20 °C. Captopril in aqueous solution is known to undergo oxidative degradation at its thiol function to yield Captopril-disulphide which possesses no ACE inhibiting activity. In solution in Sterile Water for Irrigation, USP, Captopril 1 mg/mL is stable only three days at 5 °C (Anaizi & Swenson, 1993). This explained the important standard deviation of the IC_{50} value (Fig. 4).

3.5. IC_{50} of fish hydrolysate

The IC_{50} value obtained with a same batch of fish hydrolysate was of 43 μg (±5) and the mean value of IC_{50} obtained with four different batches of fish hydrolysate was of 46 μg (±5) (Fig. 5).

Many studies have reported ACE inhibition activity of fish hydrolysates and the IC_{50} values were very different according to the fish species and the purity level of the hydrolysate. Crude hydrolysates showed IC_{50} values of 0.88–0.26 mg/mL (Jung et al., 2006; Matsui et al., 1993) while the value for a purified fraction by RP-HPLC was 0.013 mg/mL (Je, Park, Kwon, & Kim, 2004) and 2.4 μM or 12.2 μM for purified peptides (Fujita & Yoshikawa, 1999; Kawasaki et al., 2000).

Considering those results, our non-purified fish hydrolysate appears to be very interesting and it underlines the interest of the peptides purification and identification.

Furthermore, this fish hydrolysate shows a relatively good stability even after several months of storage at −20 °C. The results show the same standard deviation between the measurements intra- and inter-batches. So, the industrial process of the fish by-products hydrolysis showed a good repeatability and allowed to produce a standardised active product.

3.6. Determination of Hill coefficient

The values of Hill coefficient obtained for Captopril and the fish hydrolysate were about 2 (respectively 1.83 and 1.98) expressing

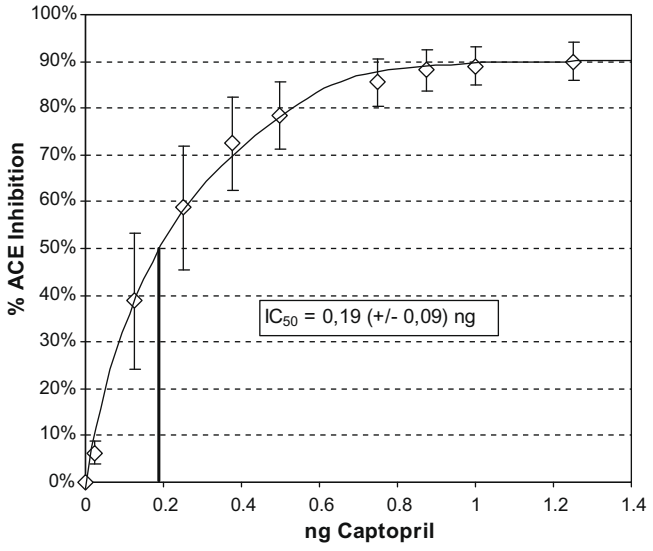

Fig. 4. ACE inhibition curve of Captopril obtained with a E/S ratio of 10 mU/nmol and an incubation time of 45 min.

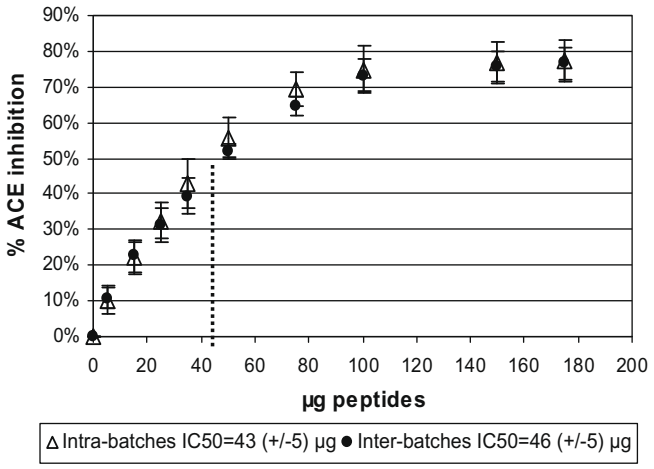

Fig. 5. ACE inhibition curve of a fish hydrolysate obtained with a E/S ratio of 10 mU/nmol and an incubation time of 45 min (intra-batches) and mean curve of ACE inhibition obtained from different fish hydrolysate batches (inter-batches).

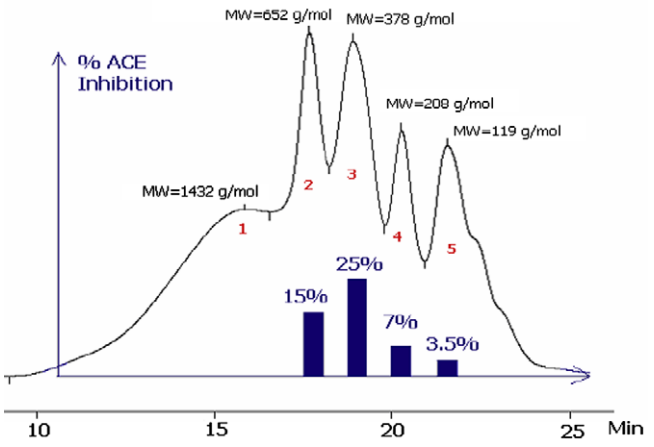

Fig. 6. Gel filtration profile of fish hydrolysate and ACE inhibition activity of the different fractions.

well the property of the ACE to possess two binding sites for low-molecular weight inhibitors. This result confirms the inhibitors present in the fish hydrolysate are low-molecular peptides. Moreover, the first results obtained on the ACE inhibition activity of the fish hydrolysate fractions isolated by gel filtration showed the most active fractions were those with molecular weights less than 600 g/mol (Fig. 6).

All those results pointed out we have to deal with peptides composed of about 2–5 amino acids.

4. Conclusion

After testing different methods for the determination of a fish hydrolysate ACE inhibition activity, we finally opted for a sensitive, extraction-free HPLC method using N-(3-[2-furylacryloyl)-Phe-Gly-Gly (FAPGG) as substrate. By varying the experimental conditions, the optimum enzyme/substrate ratio was defined as 10 mU/nmol. The incubation time was optimised at 45 min and the NaCl concentration at 300 mM.

In this way, IC_{50} values for Captopril and the fish hydrolysate were, respectively of 0.19 ng (±0.09) and 43 µg (±5). Those results allowed to underline the fish hydrolysate produced by ID. Mer had a significant ACE-inhibitory activity with a good repeatability.

The determination of the Hill coefficient and the results obtained on the gel filtration fractions tend to prove that the peptides responsible for this activity are very small molecules (2–5 amino acids). Further analyses are actually in progress to isolate and identify those peptides using different chromatographic and detection methods. The identification of those peptides constitutes the next step of this study because the knowledge of the peptides structure will allow the development of a novel functional food for preventing hypertension.

References

Anaizi, N. H., & Swenson, C. (1993). Instability of aqueous Captopril solutions. *American Journal of Hospital Pharmacy, 50*, 486–488.

Anzenbacherová, E., Anzenbacher, P., Macek, K., & Květina, J. (2001). Determination of enzyme (angiotensin convertase) inhibitors based on enzymatic reaction followed by HPLC. *Journal of Pharmaceutical and Biomedical Analysis, 24*, 1151–1156.

Beneteau-Burnat, B., & Baudin, B. (1991). Angiotensin-converting enzyme: Clinical applications and laboratory investigations on serum and other biological fluids. *Critical Reviews in Clinical Laboratory Sciences, 28*(5–6), 337–356.

Carmel, A., & Yaron, A. (1978). An intramolecularly quenched tripeptide as a fluorogenic substrate of angiotensin-I converting enzyme and bacterial dipeptidyl carboxypeptidase. *European Journal of Biochemistry, 87*(2), 265–273.

Cushman, D. W., & Cheung, H. S. (1971). Spectrophotometric assay and properties of the angiotensin-converting enzyme of rabbit lung. *Biochemical Pharmacology, 20*, 1637–1648.

Ferreira, I. M. P. L. V. O., Eça, R., Pinho, O., Tavares, P., Pereira, A., & Roque, A. C. (2007). Development and validation of an HPLC/UV method for quantification of bioactive peptides in fermented milks. *Journal of Liquid Chromatography and Related Technologies, 30*, 2139–2147.

Ferreira, I. M. P. L. V. O., Pinho, O., Mota, M. V., Tavares, P., Pereira, A., Gonçalves, M. P., et al. (2007). Preparation of ingredients containing an ACE-inhibitory peptide by tryptic hydrolysis of whey protein concentrates. *International Dairy Journal, 17*, 481–487.

Fujita, H., Yokoyama, K., & Yoshikawa, M. (2000). Classification and antihypertensive activity of angiotensin I-converting enzyme inhibitory peptides derived from food proteins. *Journal of Food Science, 65*(4), 564–569.

Fujita, H., & Yoshikawa, M. (1999). LKPNM: A prodrug-type ACE-inhibitory peptide derived from fish protein. *Immunopharmacology, 44*, 123–127.

Holmquist, B., Bünning, P., & Riordan, J. F. (1979). A continuous spectrophotometric assay for angiotensin converting enzyme. *Analytical Biochemistry, 95*, 540–548.

Je, J.-Y., Park, P.-J., Kwon, J. Y., & Kim, S.-K. (2004). A novel angiotensin I converting enzyme inhibitory peptide from Alaska Pollack (*Theragra chalcogramma*) frame protein hydrolysate. *Journal of Agricultural and Food Chemistry, 52*, 7842–7845.

Jung, W. K., Mendis, E., Je, J. Y., Park, P. J., Son, B. W., Kim, H. C., et al. (2006). Angiotensin I-converting enzyme inhibitory peptide from yellow sole (*Limanda aspera*) frame protein and its antihypertensive effect in spontaneously hypertensive rats. *Food Chemistry, 94*, 26–32.

Kawasaki, T., Seki, E., Osajima, K., Yoshida, M., Asada, K., & Matsui, T. (2000). Antihypertensive effect of Valyl-tyrosine, a short chain peptide derived from sardine muscle hydrolyzate, on mild hypertensive subjects. *Journal of Human Hypertension, 14*, 519–523.

Kohama, Y., Matsumoto, S., Oka, H., Teramoto, T., Okabe, T., & Mimura, T. (1988). Isolation of angiotensin-converting enzyme inhibitor from tuna muscle. *Biochemical and Biophysical Research Communications, 155*(1), 332–337.

Li, G.-H., Liu, H., Shi, Y.-H., & Le, G.-W. (2005). Direct spectrophotometric measurement of angiotensin I-converting enzyme inhibitory activity for screening bioactive peptides. *Journal of Pharmaceutical and Biomedical Analysis, 37*, 219–224.

Lieberman, J. (1975). Elevation of serum angiotensin-converting-enzyme (ACE) level in sarcoidis. *American Journal of Medicine, 59*(3), 365–372.

Maruyama, S., Nakagomi, K., Tomizura, N., & Suzuki, H. (1985). Angiotensin I-converting enzyme inhibitor derived from an enzymatic hydrolysate of casein. II. Isolation and bradykinin-potentiating activity on the ileum of rat. *Agricultural Biology and Chemistry, 49*, 1405–1409.

Matsui, T., Matsufuji, H., & Osajima, Y. (1992). Colorimetric measurement of angiotensin I-converting enzyme inhibitory activity with trinitrobenzene sulfonate. *Bioscience, Biotechnology and Biochemistry, 56*, 517–518.

Matsui, T., Matsufuji, H., Seki, E., Osajima, K., Nakashima, M., & Osajima, Y. (1993). Inhibition of angiotensin I-converting enzyme by *Bacillus licheniformis* alkaline protease hydrolysates derived from sardine muscle. *Bioscience, Biotechnology and Biochemistry, 57*(6), 922–925.

Miguel, M., Alvarez, Y., Lopez-Fandino, R., Alonso, M. J., & Salaices, M. (2007). Vasodilator effects of peptides derived from egg white proteins. *Regulatory Peptides, 140*, 131–135.

Murray, B. A., Walsh, D. J., & FitzGeralg, R. J. (2004). Modification of the furanacryloyl-L-phenylalanylglycylglycine assay for the determination of angiotensin-I-converting enzyme inhibitory activity. *Journal of Biochemical and Biophysical Methods, 59*, 127–137.

Otte, J., Shalaby, S. M. A., Zakora, M., & Nielsen, M. S. (2007). Fractionation and identification of ACE-inhibitory peptides from α-lactalbumin and β-casein

produced by thermolysin-catalysed hydrolysis. *International Dairy Journal, 17*, 1460–1472.

Sentandreu, M. A., & Toldra, F. (2006). A rapid, simple and fluorescence method for the assay of angiotensin-I converting enzyme. *Food chemistry, 97*, 546–554.

Shalaby, S. M., Zakora, M., & Otte, J. (2006). Performance of two commonly used angiotensin-converting enzyme inhibition assays using FA-PGG and HHL as substrates. *Journal of Dairy Research, 73*, 178–186.

Skeggs, L. T., Kahn, J. R., & Shumway, N. P. (1957). The preparation and function of the angiotensin-converting enzyme. *Journal of Experimental Medicine, 103*, 295–299.

Tauzin, J., Miclo, L., & Gaillard, J. L. (2002). Angiotensin I-converting enzyme inhibitory peptides from tryptic hydrolysate of bovine α_{S2}-casein. *FEBS Letters, 531*, 369–374.

Vermeirssen, V., Van Camp, J., & Verstraete, W. (2002). Optimisation and validation of an angiotensin-converting enzyme inhibition assay for the screening of bioactive peptides. *Journal of Biochemical and Biophysical Methods, 51*, 75–87.

Wu, J., Aluko, R. E., & Muir, A. D. (2002). Improved method for direct high-performance liquid chromatography assay of angiotensin-converting enzyme-catalysed reactions. *Journal of Chromatography A, 950*, 125–130.

Wu, J., & Ding, X. (2002). Characterization of inhibition and stability of soy-protein-derived angiotensin I-converting enzyme inhibitory peptides. *Food Research International, 35*, 367–375.

Yoshii, H., Tachi, N., Ohba, R., Sakamura, O., Takeyama, H., & Itani, T. (2001). Antihypertensive effect of ACE inhibitory oligopeptides from chicken egg yolks. *Comparative Biochemistry and Physiology, Part C, 128*, 27–33.

However, tannin and amino acid levels in tea vary during each manufacturing stage. Young two-leaf flushes are typically chosen for manufacturing the finest tea because theanine accumulates in growing shoots (Chu, Kobayashi, Juneja, & Yamamoto, 1997). During the withering and fermentation processes for Oolong tea and black tea, the composition of polyphenolic compounds changes significantly. Colorless epigallocatechin (EGC) derivates are oxidised, polymerised and transferred into theasinensins and reddish theaflavins in Oolong tea, and finally red-brown thearubigins in black tea (Haslam, 2003). Amino acids also increase during black tea fermentation, a result of protein hydrolysis. Furthermore, the tannin and amino acid contents in tea infusions are influenced by brewing (extraction) conditions, namely, temperature and time. Therefore, a rapid assay for both tannin and total amino acid in tea is essential for quality control, evaluation and classification in tea processing.

High-performance liquid chromatography (HPLC) (Reich et al., 2006; Ying, Ho, Chen, & Wang, 2005; Zhu et al., 2004) and capillary electrophoresis (CE) (Aucamp, Hara, & Apostolides, 2000; Chen et al., 2003; Horie & Kohata, 1998) techniques combined with ultraviolet detection, fluorescent detection and mass spectrometry are commonly utilised for analysing individual tea compounds. However, these separation-based techniques are labour- and time-consuming for quality control purposes. Near infrared reflectance (NIR) spectrometry was recently introduced as a rapid and non-destructive method for evaluating tea quality (Yan, 2005); however, the regression equations were established from a large database, and generating such a database is itself a tedious task.

Due to the requirements of simple sensing principle and equipment, photometric and fluorometric methods are widely used for assessing concentration of tannin and amino acids. These photometry techniques will be increased convenience and usability when flow-injection manifolds are also utilised in these analytical instrumentations. The Folin–Ciocalteau method, the AOAC method for tannin, is based on a redox reaction and prone to interference by reducing agents (Hagerman & Butler, 1989). An alternative method based on the complex-formation, the ferrous tartrate method, is the Japanese standard, and is not be affected by any coexisting reducing agent or ascorbate in Japanese green tea. Nevertheless, the ferrous tartrate method tends to form precipitate that is not compatible with the conventional FIA manifold (Iwasa, 1975). Recently, our research group developed a fluorometric FIA method for tannin based on the quenching effect on fluorescence of 3-aminophthalate (3-APA). The manifold is simple to assemble and the reagent utilised is both limited and eco-friendly (Chen et al., 2005).

For amino acids, chromogenic techniques, such as the ninhydrin method, are well known and extremely popular. However, for sample pretreatments, such as removing polyphenols with polyvinylpolypyrrolidone (PVPP), complicated reagent preparation and incubation procedures make pretreatments inconvenient practically for FIA system development. Although somewhat unstable in the reagent, the fluorogenic reaction of *o*-phthalaldehyde (OPA) is likely the most rapid and convenient amino acid assay (Roth, 1971). The problem in reagent stability can be overcome using a flow system.

In this study, an OPA reagent stream employed for amino acid determination was integrated with the tannin assay FIA manifold (Chen et al., 2005). Both reactions were sequentially monitored in a flow system with the same fluorometric detector fixed at the same excitation and emission wavelength (340/425 nm). The optimal analytical condition for the integrated system was determined, and was then utilised for classifying tea products with different processes. The effects of plucking position of tea leaves in tea plants, withering time and brewing method of infusions of partially fermented tea were investigated using the proposed system. Analytical results for commercial Oolong tea products and their market prices were compared.

2. Materials and methods

2.1. Chemicals and reagents

Tannic acid, *o*-phthalaldehyde and 2-mercaptoethanol were obtained from Wako (Osaka, Japan). Luminol (5-amino-2,3-dihydro-1,4-phthalazinedione), sodium bicarbonate, sodium borate and sodium hydroxide were obtained from Nacalai Tesque (Kyoto, Japan). Glutamic acid, aspartic acid and arginine were obtained from Sigma (St. Louis, MO, USA). Theanine was acquired from LKT Laboratories (St. Paul, MN, USA). All chemicals were analytical-reagent grade and used as received.

Carbonate buffers (pH 9.0–10.0) were prepared by adjusting the sodium bicarbonate aqueous solution with sodium hydroxide to a desired pH and stored at room temperature. Preparations of borax buffers (pH 11.0–12.0) were similar to those for carbonate buffers. Luminol stock solution (10 mM) was prepared by dissolving luminol powders in 0.1 M carbonate buffer (pH 10.0) and stored at 4 °C until use. Luminol reagent (0.4 mM) was prepared by diluting the stock solution with 0.1 M carbonate buffer. The OPA reagent was prepared by mixing 3 mL *o*-phthalaldehyde solution (10 mg mL^{-1} in ethanol) and 1.5 mL 2-mercaptoethanol solution (5 μL mL^{-1} in ethanol) in 100 mL carbonate buffer (0.1 M, pH 10.0). Standard tannic acid and theanine solutions were prepared and diluted prior to use. Deionised water with conductivity <1 μS cm^{-1} was used to prepare buffers and solutions.

2.2. Flow-injection manifold

The proposed system was assembled using conventional flow-injection silicon tubes (inner diameter, 1 mm), Teflon tubes and polypropylene connectors. The carrier (deionised water) and reagent (luminol reagent for tannin or OPA reagent for total amino acid content) were driven at 0.5 mL min^{-1} by a signal-controllable three-channel peristaltic pump (SMP23S, Tokyo Rika Co., Japan). A 100-μL aliquot of sample solution was injected into the carrier stream and merged with the reagent stream. After mixing in a 60-cm coiled tube (mixing coil), the resulting sample plug was delivered through a fluorometric detector (FP-1520, Jasco Co., Japan) for fluorescence monitoring (λ_{ex} = 340 nm; λ_{em} = 425 nm; slit = 10 nm). Fluorescence intensity was converted to a voltage signal and recorded using a chart pen recorder (Model 101, Cole–Parmer Co., USA). Relative outputs of fluorescence intensity were calculated by peak height.

2.3. Manufacture of tea samples from fresh tea leaves

Fresh tea leaves were harvested at the Wen-Shan Branch of the Tea Research and Extension Station, Council of Agriculture, Executive Yuan, Taiwan. Young three-leaf flushes of TTES No. 12 were plucked and dried slightly in hot air (30 °C for 20 min). Following the standard manufacturing process for Pouchong tea, the flushes were placed indoor and withered for 0–24 h. The withered flushes were then pan fired (250 °C for 5 min) and rolled. After rolling, tea-leaves were dried at 90 °C and further dried overnight at 75 °C. For comparison, fresh tea leaves of three species (TTES No. 12, TTES No. 14 and TTES No. 17) harvested with various plucking positions (the first two leaves and the bud, and leaves 3–5) were manufactured using the standard process for Pi-Lo-Chun green tea.

2.4. Preparation of extractions from dried tea leaves

Tea samples were prepared by infusing 3 g of dried tealeaves with 150 mL deionised water. Hot tea infusions were prepared

by brewing tealeaves with boiling water for 5 min. Tea extracts were filtered through standard filter paper (#1 Whatman™) and cooled to room temperature using an ice-water bath (3 min). Cold tea infusions were prepared by brewing tealeaves in water (room temperature) and then stored in a refrigerator at 4 °C. All tea samples were prepared and diluted before use.

3. Results and discussion

3.1. Dose-dependent FIA fluorescent responses

Fig. 1a shows typical response signals for determining tannic acid and theanine concentrations. The high baseline for tannin determination (left part in Fig. 1a) was from the background fluorescence of oxidised luminal, 3-aminophthalate, which was quenched by tannic acid in a dose-dependent manner ($r = 0.994$) (Chen et al., 2005) as predicted by the following modified Stern–Volmer relationship (IUPAC, 1996).

$$\frac{\Delta F}{F} = K_{SV}[Q] \quad (1)$$

where ΔF is the reduction in fluorescence intensity (peak height in the FIAgram); F is the unquenched fluorescence intensity (baseline fluorescence intensity); K_{SV} is the Stern–Volmer bimolecular quenching constant; [Q] is the quencher molecule concentration.

For amino acid determination, the luminol reagent was replaced with the non-fluorescent OPA reagent (the lowered baseline on the right in Fig. 1a). The linearity ($r = 0.999$) of the calibration curve reveals a pseudo first-order kinetics of the OPA-labelling reaction with theanine. The linear dynamic ranges for tannic acid and theanine were 50–250 and 0.1–1.0 μg mL^{-1} (CV < 5%, $n = 3$), respectively. Sample throughout was 20 samples h^{-1} in the proposed FIA system.

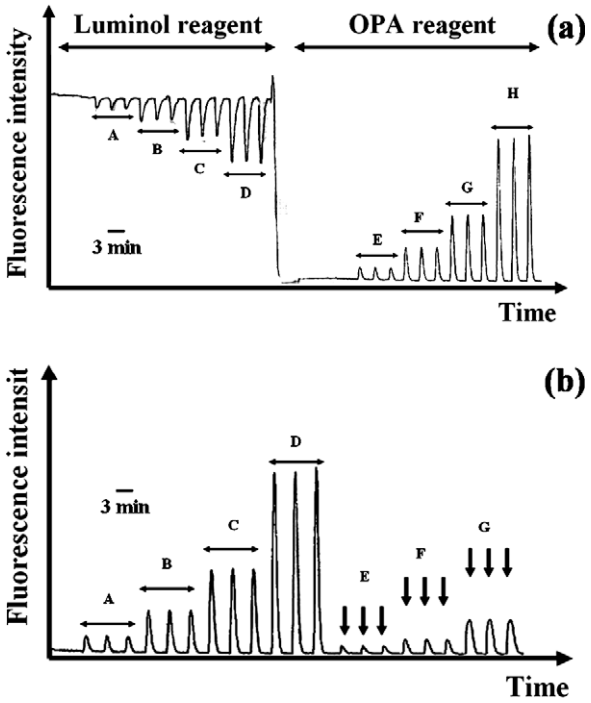

Fig. 1. (a) Dose-dependent FIAgram for calibrations of tannic acid and theanine. (A–D) Tannic acid (50, 100, 200 and 250 μg mL^{-1}). (E–H) Theanine (0.1, 0.2, 0.5 and 1 μg mL^{-1}). Luminol concentration: 0.4 mM. OPA reagent (pH 10.0): 2 mM of OPA and 1 mM of 2-mercaptoethanol. Flow rate, 0.5 mL min^{-1}. The fluorescence intensity was scaled in arbitrary unit; (b) fluorescent responses of tannic acid with OPA reagent. (A–D) Theanine (0.1, 0.2, 0.5 and 1 μg mL^{-1}). (E–G) Tannic acid (50, 100 and 500 μg mL^{-1}). OPA reagent (pH 10.0): OPA, 2 mM of OPA and 1 mM of 2-mercaptoethanol. Flow rate, 0.5 mL min^{-1}.

3.2. Cross-interference of tannin and amino acids

Concentrations of tannin and amino acids in tea infusions are generally 200–500 and 100–500 μg mL^{-1}, respectively. Significant interference occurred when tannic acid solutions of similar concentrations (50–500 μg mL^{-1}) with undiluted tea infusions were injected into the FIA system (left part in Fig. 1b). However, to determine amino acid levels in tea infusions, tea infusions diluted at minimum 100-fold should be utilised to fit the detecting range for amino acid determination. Therefore, the aforementioned interference may be negligible in practical applications.

Conversely, no fluorescence quenching effect existed even when 1000 μg mL^{-1} theanine was injected into the luminol reagent (data not shown). As this system is used in practical applications, cross-interference to both sensing subsystems will be insignificant and can be ignored.

3.3. Relative fluorescent outputs of major amino acids in tea infusions

The fluorogenic reaction of the OPA reagent with primary amines is non-specific (Roth, 1971). Other amino acids that taste sour (such as aspartic acid) or bitter (such as arginine) in tea infusions may also contribute to signal output. To evaluate the relative output from the fluorometric FIA system of major amino acids in tea leaves, treated as a percentage contribution to fluorescence by a particular amino acid in the tea leaves in the proposed OPA sensing system, the fluorescent responses of theanine, glutamic acid, aspartic acid and arginine references were initially determined using the proposed system and the OPA reagent. Fluorescent intensities of 11.8, 15.2, 16.1 and 12.7 mV were measured for 0.5 μg mL^{-1} of theanine, glutamic acid, aspartic acid and arginine, respectively (Hung, 2008). Relative output was then calculated as the product of the relative fluorescent responses and the proportions of the individual amino acids in tea leaves, taken from another study (Lee, Chen, & Matsumoto, 1996). Signal outputs of the four representative amino acids were examined; approximately 70.5% of signal response was associated with the umami-related amino acids, theanine (58.4%) and glutamate (12.1%). This experimental result for response percentage is similar to that obtained by a previous study of green tea (Lee et al., 1996) and a recent report regarding Taiwan red tea (Hsieh & Chen, 2007). Therefore, the proposed amines determination based on OPA-fluorescent was considered as an indicator of umami in tea infusions during the taste assessment.

3.4. System optimisation

The length of the mixing coil (Fig. 2a) for tannin and amino acids determinations was optimised to compromise between reaction time (especially for the OPA fluorogenic reaction) and sample dispersion. A mixing coil 60 cm long was selected based on its high peak height and short baseline reversion time.

The conditions for tannin determination were optimised in a previous study (Chen et al., 2005). For the OPA fluorogenic reaction, OPA and 2-mercaptoethanol concentrations as well as pH value were optimised (Fig. 2b and c) as 2 mM OPA, 1 mM 2-mercaptoethanol and pH 10.0 (carbonate buffer) to maximise the signal with reduced reagent consumption.

3.5. Taste quality assessment of green tea and partially fermented tea

Theanine is the predominant taste compound of umami accumulates in growing shoots (Konishi & Kasai, 1968); therefore,

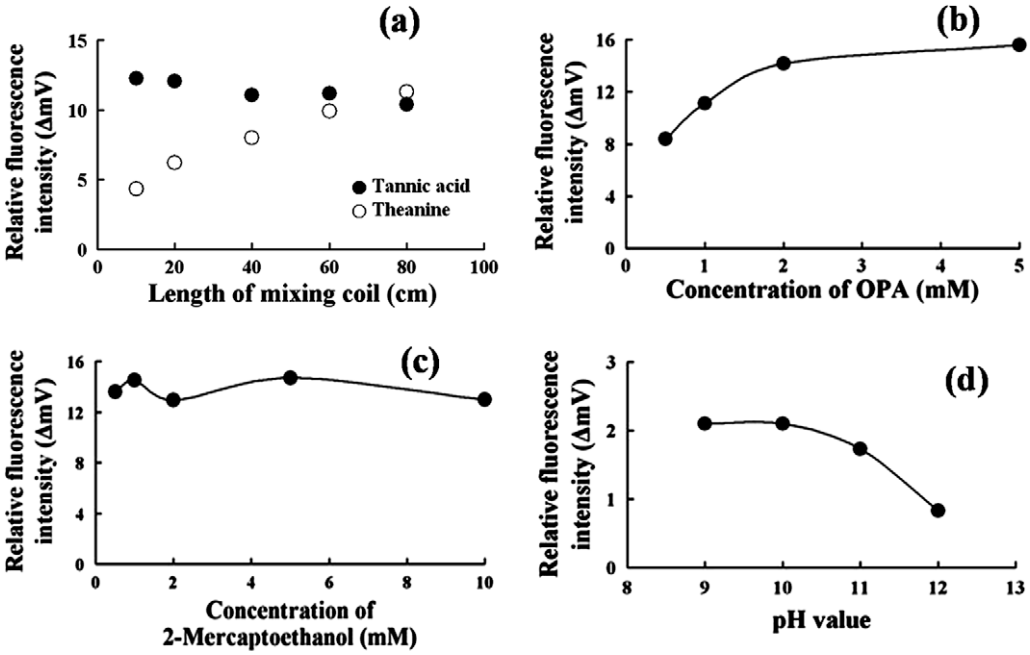

Fig. 2. Effects of the length of mixing coil for fluorescent responses of 100 μg mL^{-1} of tannic acid and 0.5 μg mL^{-1} of theanine (a). Luminol concentration: 0.4 mM. OPA reagent (pH 10.0): 2 mM of OPA and 1 mM of 2-mercaptoethanol. Flow rate, 0.5 mL min^{-1}. Effects of OPA concentration (b), 2-mercaptoethanol concentration (c) and buffer pH value (d) for fluorescent response of 0.5 μg mL^{-1} of theanine to OPA reagent. Flow rate, 0.5 mL min^{-1}. (b) 1 mM of 2-mercaptoethanol, pH value = 10.0. (b and c) 2 mM of OPA, pH value = 10.0. (d) 2 mM of OPA and 1 mM of 2-mercaptoethanol.

superior teas are typically manufactured from the youngest tea shoots. The top bud and first two leaves of tea plants produce the best teas according to tea specialists in Taiwan. The tannin and amino acids concentrations in Pi-Lo-Chun green tea infusions with young shoots and maintenance leaves were analysed using the proposed method and compared (Table 1). Typically, a significant reduction existed in both amino acids and tannin contents in tea manufactured with maintenance leaves; this experimental finding is consistent with that obtained by a free amino acid in the tea study (Nakagawa, Tokumura, Toriumi, & Nagashima, 1957). This preliminary work demonstrates that the proposed system can determine both tannin and amino acids contents in tea infusions of different teas.

According to tea experts, indoor withering time is critical for aroma development of partially fermented tea. This claim was confirmed by an experimental study (Harbowy & Balentine, 1997). Table 2 presents the effects of indoor withering time on tannin and amino acid levels. The content of tannin and amino acids in tea infusions was correlated with withering time when withering time was <24 h. A minor increase in amino acid content is consistent with free amino acids finding obtained by black and green tea study (Nagashima, Nakagawa, Tokumura, & Toriumi, 1957). However, tannin content decreased significantly after 40 h of withering. This experimental data should only be considered as a reference as 40 h of withering time is excessive for partially fermented tea. Furthermore, as diverse polyphenolic compounds are generated during withering, the relative responses of such components for quenching effect must be confirmed in further studies.

Cold water steeping is a new trend in brewing Japanese green tea and Pouchong tea because some heat-labile chemicals are preserved during low-temperature extraction. Moreover, the taste of the tea infusion may be dependant on the kinetics of extracting amino acid (umami) and tannin (astringency) at different water temperatures. As demonstrated by the FIA system, cold water steeping is effective for extracting amino acids, thus, astringency can be suppressed (Table 3). The experimental result is consistent with that obtained by a quality evaluation of green tea study (Horie et al., 1993), which showed that the major components extracted by boiling and cold water differed. This study determined that extraction efficiency for amino acids was better than that for tannin using cold water for <1 h. Therefore, tea prepared using the cold-brew method can generate a superior taste due to the reduction of astringent components (tannin) and increase in umami (amino acids), demonstrating the potential of the proposed system to optimise steeping time.

Finally, the concentrations of amino acids and tannin and local market prices of Oolong tea in Taiwan were compared (Table 4). This table indicates that the result based upon four samples from typical Oolong tea products with various grades from local market. As demonstrated by the proposed system, amino acid content is

Table 1
Effects of plucking position to tannin and amino acids in Pi-Lo-Chun green tea infusions.

Cultivar	Young shoots[a]		Maintenance leaves[b]	
	Tannin (μg mL^{-1})	Amino acids (μg mL^{-1})	Tannin (μg mL^{-1})	Amino acids (μg mL^{-1})
TTES No. 12	121 ± 5	72 ± 15	52 ± 6	55 ± 13
TTES No. 14	186 ± 17	57 ± 7	106 ± 17	34 ± 6
TTES No. 17	208 ± 15	55 ± 13	145 ± 30	17 ± 5

[a] Referred to the bud and the first two leaves in tea plants.
[b] Referred to the third, fourth and fifth leaves in tea plants.

Table 2
Effects of withering time to tannin and amino acids in Pouchong tea infusions.

Withering time (h)	Tannin (μg mL^{-1})	Amino acids (μg mL^{-1})	Ratio of amino acids to tannin
0	118 ± 21	109 ± 18	0.92
4	180 ± 28	179 ± 24	1.00
6	169 ± 22	178 ± 21	1.06
12	164 ± 16	171 ± 15	1.05
16	279 ± 27	278 ± 21	1.00
20	228 ± 29	268 ± 29	1.17
23	248 ± 23	306 ± 26	1.23
40	143 ± 19	355 ± 27	2.49

Table 3
Tannin and amino acids in Pouchong tea infusions steeped with cold water.

Extraction time (h)	Tannin (μg mL^{-1})	Amino acids (μg mL^{-1})
0.5	166 ± 21	163 ± 11
1.0	220 ± 9	270 ± 5
2.0	297 ± 37	273 ± 42
4.0	393 ± 8	329 ± 19
8.0	458 ± 8	401 ± 25
5-Min-extraction with boiling water	308 ± 37	187 ± 34

Table 4
Comparison of analytical results for Oolong teas with distinct market prices.

Tea brand	Analytical results			Detail of commercial products		
	Tannin (μg mL^{-1})[a]	Amino acids (μg mL^{-1})[a]	Ratio of amino acids to tannin	Market price (NT$/kg)	Plucking method	Elevation of tea farm (m)
B-grade Oolong	172 ± 6	58 ± 2	0.34	660	Machine	400–600
A-grade Oolong	241 ± 18	91 ± 10	0.41	1000–1300	Machine	400–600
Yu-Shan Oolong	232 ± 15	134 ± 6	0.54	2660–3000	Hand	1600
Ali-Shan Oolong	181 ± 8	158 ± 12	0.84	4000	Hand	1600–1800

[a] All values are mean ± SD obtained by triplicate analyses.

the basis for taste quality and Oolong tea prices. Similar trends were also found for Japanese green tea (Horie, Ujihara & Kohata, 2001; Lee et al., 1996). Amino acids content can only be used to differentiate between low- and high-grade Oolong teas, and is relatively less sensitive in discriminating between taste quality and price of high-grade Oolong tea (e.g., Yu-Shan Oolong and Ali-Shan Oolong). Tannin acid content in top-grade product (Ali-Shan Oolong) is significantly lower than that in high-grade (B tea) and medium-grade tea (Yu-Shan) (Table 4). Therefore, the ratio of amino acids to tannin was proposed as an advanced indicator for taste assessment of Oolong tea. This indicator has an increased ability to discriminate between high-grade Oolong teas (the discrimination percentage between Yu-Shan Oolong and Ali-Shan Oolong improved to 56% from 18%). Although, tea prices are determined by taste, labour and transportation costs, and market demand. Experimental results indicated that the proposed system with this indicator (ratio of tannin to amino acids in tea infusions) can be utilised to classify Oolong teas.

4. Conclusion

In conclusion, based on the quenching effect of tea tannin on 3-APA fluorescence and OPA fluorogenic reaction with amino acids, an on-line fluorometric system was proposed that determines the levels of astringency and umami in tea infusions using a single FIA system with the same excitation and emission wavelengths of fluorometry. Without interferences caused by reducing agents and time-consuming pretreatments, the proposed system was preliminarily applied to assess partially fermented Taiwanese teas. Analytical results show the potential of the proposed system for on-line monitoring and classification of tea. Routine analysis of a massive amount of tea samples was completed rapidly (20 samples h^{-1}), accurately (CV < 5%, $n = 3$) and conveniently using the proposed method. This method will be used to verify NIR spectrometry of tealeaves during manufacturing in future work.

Acknowledgements

The authors would like to thank the National Science Council of Taiwan for financially supporting this research under Contract Nos. NSC-95-2313-B-002-054 and NSC-96-2313-B-002-073-MY3. We also thank Director You-Zenn Tsai, Mr. Cheng-Hung Cheng and all technical assistants at Wun Shan Branch, Tea Research and Extension Station, Council of Agriculture, Taiwan for their kind help in manufacturing Pouchong tea and Pi-Lo-Chun tea.

References

Arnold, R. A., Noble, A. C., & Singleton, V. L. (1980). Bitterness and astringency of phenolic fractions in wine. *Journal of Agricultural and Food Chemistry, 28*, 675–678.

Aucamp, J. P., Hara, Y., & Apostolides, Z. (2000). Simultaneous analysis of tea catechins, caffeine, gallic acid, theanine and ascorbic acid by micellar electrokinetic capillary chromatography. *Journal of Chromatography A, 876*, 235–242.

Bakker, J. (1998). Astringency: A matter of taste. *Biologist, 45*, 104–107.

Bate-Smith, E. C. (1973). Haemanalysis of tannins: The concept of relative astringency. *Phytochemistry, 12*, 907–912.

Chen, C. N., Liang, C. M., Lai, J. R., Tsai, Y. J., Tsay, J. S., & Lin, J. K. (2003). Capillary electrophoretic determination of theanine, caffeine, and catechins in fresh tea leaves and Oolong tea and their effects on rat neurosphere adhesion and migration. *Journal of Agricultural and Food Chemistry, 51*, 7495–7503.

Chen, R. L. C., Lin, C. H., Chung, C. Y., & Cheng, T. J. (2005). Determination of tannin in green tea infusion by flow-injection analysis based on quenching the fluorescence of 3-aminophthalate. *Journal of Agricultural and Food Chemistry, 53*, 8443–8446.

Chu, D. C., Kobayashi, K., Juneja, L. R., & Yamamoto, T. (1997). Theanine – Its synthesis, isolation and physiological activity. In T. Yamamoto (Ed.), *Chemistry and applications of green tea* (pp. 129–135). Boca Raton: CRC Press.

de Freitas, V., & Mateus, N. (2002). Nephelometric study of salivary protein–tannin aggregates. *Journal of the Science of Food and Agriculture, 82*, 113–119.

Edelmann, A., & Lendl, B. (2002). Toward the optical tongue: Flow-through sensing of tannin–protein interactions based on FTIR spectroscopy. *Journal of the American Chemical Society, 124*, 14741–14747.

Glendinning, J. I. (1992). Effect of salivary proline-rich proteins on ingestive responses to tannic acid in mice. *Chemical Senses, 17*, 1–12.

Hagerman, A. E., & Butler, L. G. (1989). Choosing appropriate methods and standards for assaying tannin. *Journal of Chemical Ecology, 15*, 1795–1810.

Harbowy, M. E., & Balentine, D. A. (1997). Tea chemistry. *Critical Reviews in Plant Sciences, 16*, 415–480.

Haslam, E. (1988). Plant polyphenols (syn. vegetable tannins) and chemical defense – A reappraisal. *Journal of Chemical Ecology, 14*, 1789–1805.

Haslam, E. (2003). Thoughts in thearubigins. *Phytochemistry, 64*, 61–73.

Horie, H., Fukatsu, S., Mukai, S., Goto, T., Kawanaka, M., & Shimohara, T. (1993). Quality evaluation on green tea. *Sensors and Actuators: B. Chemical, 13*, 451–454.

Horie, H., & Kohata, K. (1998). Application of capillary electrophoresis to tea quality estimation. *Journal of Chromatography A, 802*, 219–223.

Horie, H., Ujihara, T., & Kohata, K. (2001). Elution of major tea components in tea infusion. *Tea Research Journal (Chagyo Kenkyu Hokoku), 91*, 29–33 (in Japanese).

Horne, J., Hayes, J., & Lawless, H. T. (2002). Turbidity as a measure of salivary protein reactions with astringent substances. *Chemical Senses, 27*, 653–659.

Hsieh, M.-M., & Chen, S.-M. (2007). Determination of amino acids in tea leaves and beverages using capillary electrophoresis with light-emitting diode-induced fluorescence detection. *Talanta, 73*, 326–331.

Huang, C.-Y. (2008). *Determination of polyphenols by a fluorescent flow-injection analytical system*. Bachelor report, National Taiwan University.

Hung, Y.-T. (2008). *Determination of tannin and amino acids in tea by fluorescent flow-injection analytical system*. Master thesis, National Taiwan University.

IUPAC recommendations (1996). *Compendium of chemical terminology* p. 2277 (2nd ed.). Oxford: Blackwell Scientific Publications.

Iwasa, K. (1975). Methods of chemical analysis of green tea. *Japan Agricultural Research Quarterly, 9*, 161–164.

Kallithraka, S., Bakker, J., & Clifford, M. N. (1998). Evidence that salivary proteins are involved in astringency. *Journal of Sensory Studies, 13*, 29–43.

Kaneko, S., Kumazawa, K., Masuda, H., Henze, A., & Hofmann, T. (2006). Molecular and sensory studies on the umami taste of Japanese green tea. *Journal of Agricultural and Food Chemistry, 54*, 2688–2694.

Konishi, S., & Kasai, Z. (1968). Synthesis of theanine from carbon–^{14}C dioxide in tea plants and sites of the synthesis: Metabolism and regulation of theanine and related compounds in tea plants (II). *Journal of the Science of Soil and Manure, Japan (Nippon Doji-Hiryogaku Zasshi), 39*, 439–443.

Lee, M. H., Chen, R. L. C., & Matsumoto, K. (1996). Fluorometric biosensing of the total amino acid content and the glutamate content of green tea infusions using an automated multi-channel flow system. *Bioscience, Biotechnology, and Biochemistry, 60*, 99–102.

Lesschaeve, I., & Noble, A. C. (2005). Polyphenols: Factors influencing their sensory properties and their effects on food and beverage preferences. *American Journal of Clinical Nutrition, 81*(Suppl. 1), 330S–335S.

Nagashima, Z., Nakagawa, M., Tokumura, H., & Toriumi, Y. (1957). Studies on free amino acids in the tea. Part IV. Quantitative changes in the manufacture of black and green tea. *Journal of the Agricultural Chemical Society of Japan, 31*, 169–173.

Nakagawa, M. (1975). Chemical components and taste of green tea. *Japan Agricultural Research Quarterly, 9*, 156–160.

Nakagawa, M., Tokumura, H., Toriumi, Y., & Nagashima, Z. (1957). Studies on free amino acids in the tea. Part V. Seasonal fluctuation and disturbance in the shoot. *Journal of the Agricultural Chemical Society of Japan, 31*, 771–775.

Nicola, J. B., Terence, H. L., Edwin, H., & Michael, P. W. (1997). Multiple interactions between polyphenols and a salivary proline-rich protein repeat result in complexation and precipitation. *Biochemistry, 36*, 5566–5577.

Peleg, H., Gacon, K., Schlich, P., & Noble, A. (1999). Bitterness and astringency of flavon-3-ol monomers, dimers and trimers. *Journal of the Science of Food and Agriculture, 79*, 1123–1128.

Prinz, J. F., & Lucas, P. W. (2000). Saliva tannin interactions. *Journal of Oral Rehabilitation, 27*, 991–994.

Reich, E., Schibli, A., Widmer, V., Jorns, R., Wolfram, E., & DeBatt, A. (2006). HPTLC methods for identification of green tea and green tea extract. *Journal of Liquid Chromatography and Related Technologies, 29*, 2141–2151.

Roth, M. (1971). Fluorescence reaction of amino acids. *Analytical Chemistry, 43*, 880–882.

Yan, S. H. (2005). Evaluation of the composition and sensory properties of tea using near infrared spectroscopy and principal component analysis. *Journal of Near Infrared Spectroscopy, 13*, 313–325.

Ying, Y., Ho, J. W., Chen, Z. Y., & Wang, J. (2005). Analysis of theanine in tea leaves by HPLC with fluorescence detection. *Journal of Liquid Chromatography and Related Technologies, 28*, 727–737.

Zhu, X. L., Chen, B., Ma, M., Luo, X. B., Zhang, F., Yao, S. Z., et al. (2004). Simultaneous analysis of theanine, chlorogenic acid, purine alkaloids and catechins in tea samples with the help of multi-dimension information of on-line high performance liquid chromatography/electrospray-mass spectrometry. *Journal of Pharmaceutical and Biomedical Analysis, 34*, 695–704.

ultra-performance liquid chromatography (UPLC). Remarkably shorter separation times are the hallmarks of the technique. This technique has found application in the analysis of aflatoxins (Fu et al., 2008; Ventura et al., 2006).

The incidence of aflatoxins in foods and feeds is relatively high in the tropical and sub-tropical regions due to the warm and humid weather conditions that provide ideal conditions for the growth of the aflatoxigenic moulds. Although studies on the levels of aflatoxins in food items such as corn, peanuts, spices, traditional medicines, etc. have been conducted in Malaysia (Ali, Hashim, & Yoshizawa, 1999; Ali et al., 2005), no recent data on animal feeds have been reported. A survey conducted by the Malaysian Agricultural Research and Development Institute from 1981 to 1984 indicate that 10 of the 14 feed samples were contaminated by aflatoxins (Ali, 2000). Thus, it is the aim of this study to survey the levels of aflatoxins in animal feeds that are readily available on the Malaysian market. There is considerable public concern on the adverse effects of animals consuming mycotoxin-contaminated feeds, as these aflatoxins and/or their metabolites can potentially be passed onto food products such as meat, milk or eggs.

Due to the complexity of the samples, effective sorbent materials for the cleaning-up step must be used. Immunoaffinity column enjoys widespread use due to its good specificity (Giray et al., 2007; O'Riordan & Wilkinson, 2008). However, this sorbent is expensive and commercially available as a single-use format (Calleri, Marrubini, Brusotti, Massolini, & Caccialanza, 2007; Wilson & Romer, 1991). The selective sites are more sensitive to storage conditions, thus have a somewhat shorter shelf-life compared to the more robust C18-based silica sorbent materials. Thus another objective of this work is to evaluate the suitability of multifunctional column for the cleaning-up of the extracts. The multifunctional column is furthermore attractive as it involves fewer manipulation steps, thus minimising the analysis time (Ali et al., 1999; Fu et al., 2008).

2. Experimental

2.1. Chemicals and reagents

Aflatoxin standards and trifluoroacetic acid (TFA) were purchased from Sigma–Aldrich, USA, while acetonitrile, methanol (HPLC grade) and *n*-hexane were purchased from Fisher Scientific (UK), 18 Mohm milliQ water was generated from a TKA Water Treatment System. Isolute Multimode® Columns (1 mL capacity, 100 mg), hereafter referred to as multifunctional column (MFC) were purchased from International Sorbent Technology, UK. Forty-two feed samples were obtained from various outlets in Malaysia. Most of these samples, except for copra meal and palm kernel meal, were imported from different countries.

2.2. Instrumentation and chromatographic conditions

Quantitative analyses of the aflatoxins were carried out using a HPLC unit that consisted of a pump (Jasco PU-1580) and quartenary gradient system (JASCO PU-1580-04). Fluorescence detector was used for the quantitation under the following conditions: 360 nm excitation and 440 nm emission. The analytical column was a Supelco C_{18}, 25 cm × 4.6 mm id, 5 μm particle size. All HPLC analysis were carried out under isocratic conditions using a mobile phase of acetonitrile:methanol:water (8:27:65) and the flow rate was fixed at 1.0 mL min^{-1}. The mixture was filtered using a membrane filter and degassed in an ultrasonic bath for 25 min prior to use. A 20 μL sample loop (Jasco model 7725) was used.

2.3. Preparation of standards

The aflatoxins B1, B2, G1 and G2 standards (1.0 mg of each aflatoxin in capped amber bottles) were purchased from Sigma–Aldrich. The working solutions were prepared according to the AOAC procedure (AOAC, 2000) by injecting 1 mL of acetonitrile into each vial to dissolve the aflatoxins. Working solutions (50–1000 ng g^{-1}) were diluted in acetonitrile and stored at 8 °C. They were evaporated to dryness under nitrogen before being derivatised with TFA according to the procedure describe below.

2.4. Extraction and clean-up

The method as described by Akiyama and co-workers was used with minor modifications (Akiyama, Chen, Miyahara, Toyoda, & Saito, 1996). A 20 g of sample was extracted with 80 mL acetonitrile:water (9:1) mixture for 30 min by shaking under high speed, and then filtering using a No. 4 Whatman filter paper. A 1-mL portion of the filtrate was loaded on the MFC and passed through at a flow rate of 2 mL min^{-1} (the column had previously been preconditioned with 5 mL methanol and 5 mL acetonitrile:water (9:1)). Next, 1 mL of acetonitrile:water (9:1) was applied to the column to ensure all the aflatoxins are collected. This step was repeated five times and the filtrates were combined and evaporated to dryness under nitrogen in amber bottles (5 mL capacity) and the residue was used for the derivatisation.

2.5. Pre-column derivatisation

A 100 μL of the TFA solution and 300 μL of *n*-hexane were added to the residue from the sample extract or to the aflatoxin working standards, vortexed for 30 s, and kept in the dark for 15 min at room temperature. Nine hundred microlitres of acetonitrile:water (1:9) was added to the vial, and vortexed for 30 s. The mixture was left to stand to allow the two layers to be separated. Twenty microlitres of the derivatised product (bottom layer) was injected into the HPLC column.

3. Results and discussion

3.1. Mobile phase selection

Five mobile phases consisting of acetonitrile:methanol:water (8:27:65, 17:0:83, 17:13:70, 8:20:72 and 10:20:70) were tried. Fig. 1 shows the effect of mobile phase compositions on the retention times of the aflatoxins. Aflatoxin G1 standard cannot be detected by the second and the fourth mobile phases. Shorter

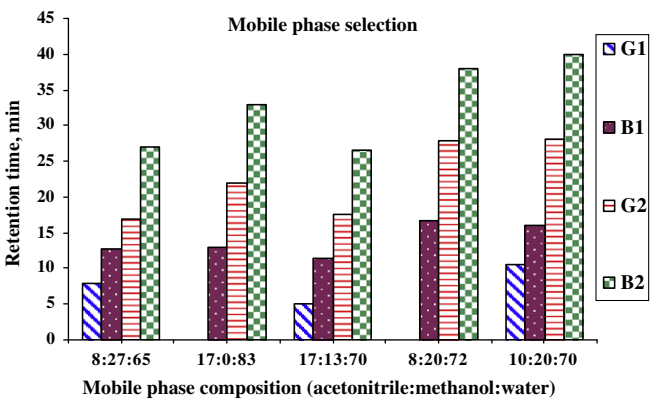

Fig. 1. Effect of mobile phase composition (acetonitrile:methanol:water) on the retention times of aflatoxins.

retention times when the third mobile phase was used, but aflatoxins B1 and B2 lower than 10 ng g^{-1} could not be detected. It appears that the sensitivity decreased when the mobile phase contained more than 70% water (mobile phases 2–4). The first mobile phase was chosen in the present study as it gave not only higher sensitivity but also with shorter retention time. This composition was also used by Akiyama et al. (2001).

3.2. Selection of extraction solvent and multifunctional column

In general, the extraction procedure depends to a great extent on the physicochemical properties of the commodities that are contaminated with aflatoxins. Commodities with high lipid and pigment content require a more selective treatment followed by extensive purification methods than those with lower content of these components. As aflatoxins are soluble in moderately polar solvents, they are normally extracted using a mixture of organic solvents such as acetonitrile, chloroform, or methanol. In earlier work, chloroform was commonly used as the extracting solvent, but has since been replaced by more environmentally-friendly solvents. It was reported that a mixture of methanol:water is more suitable compared to the use of acetonitrile:water (Gilbert & Vargas, 2003).

Different extraction mixtures involving acetonitrile:water and methanol:water was examined for the extraction efficiency of copra meal that had been spiked with 10 ng g^{-1} aflatoxin standards. Of the combinations investigated, using acetonitrile:water (9:1) and methanol:water (8:2) are more suitable than the others (Fig. 2). Using acetonitrile:water (9:1) gave more satisfactory recoveries, all the aflatoxins were at least 85% extracted. This is further supported by the recovery results when 5–30 ng g^{-1} aflatoxins were spiked and next extracted using methanol:water and acetonitrile:water (Fig. 3). Recoveries of aflatoxin G1 is significantly lower when extracted using methanol:water mixture.

Table 1
Recoveries of aflatoxins spiked to feed samples.

Sample, level spiked	% Recovery ± %RSD			
	G1	B1	G2	B2
Copra meal				
5 ng g^{-1}	98.0 ± 5.7	100.0 ± 1.0	94.0 ± 7.0	93.0 ± 1.1
15 ng g^{-1}	84.0 ± 3.9	100.6 ± 0.7	98.0 ± 4.7	95.5 ± 1.2
30 ng g^{-1}	98.0 ± 1.2	92.0 ± 0.4	98.0 ± 1.0	95.0 ± 0.6
Corn meal, 15 ng g^{-1}	95.3 ± 3.1	92.6 ± 4.6	98.6 ± 4.6	99.6 ± 1.0
Wheat bean, 15 ng g^{-1}	80.0 ± 2.7	98.0 ± 2.9	94.6 ± 5.3	86.6 ± 3.6
Mixed feed, 15 ng g^{-1}	70.0 ± 2.7	93.3 ± 6.4	104.6 ± 4.6	83.3 ± 0.4

RSD, relative standard deviation.

MFC is an interesting alternative sorbent that can be used for the cleaning-up of samples. They are designed to retain particular groups of compounds that may interfere in the analytical method but at the same time allow analytes of interest to pass through. The proprietary packing material in MFC contains both lipophilic (non-polar) and charged (polar) active sites. Lipophilic sites are largely responsible for the removal of fats and other non-polar components such as xanthophyll pigments. Charged sites consist of both dipolar and anion-exchange sites that remove proteinaceous compounds, carbohydrate and other polar interfering compounds. Contrary to solid phase extractions (SPE), the MFC procedure does not require washing or elution procedures. SPE procedures require three steps, i.e., retention of analyte on the sorbent column, washing of undesirable compounds, and elution of analyte from the sorbents. Another advantage of the MFC procedure is the elimination

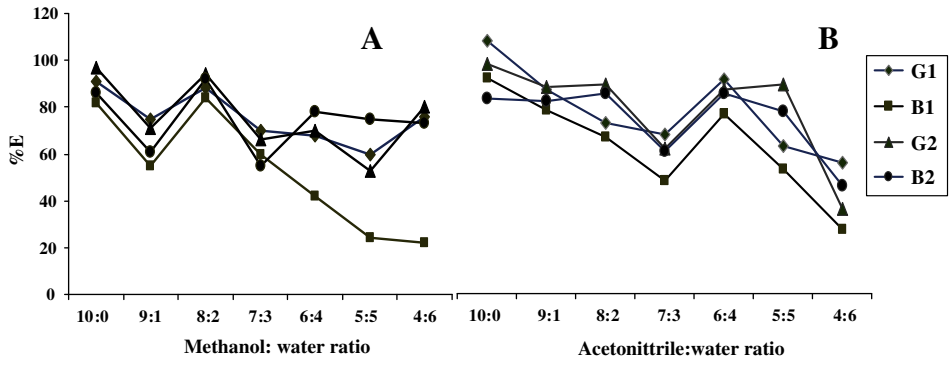

Fig. 2. Effect of extracting solvent mixtures ((A) methanol:water and (B) acetonitrile:water) on the efficiency of extraction (aflatoxins spiked, 10 ppb each).

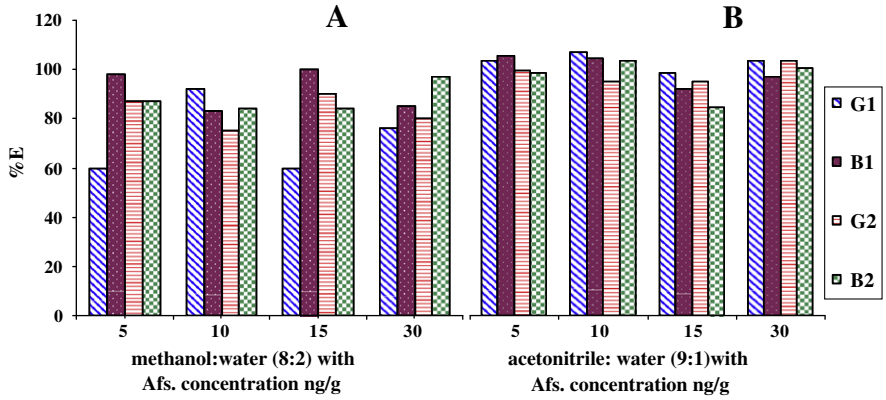

Fig. 3. Recoveries of aflatoxins that were spiked at different levels (5, 15 and 30 ng g^{-1}) when extracted with (A) methanol:water (8:2), and (B) acetonitrile:water (9:1).

of the irreversible adsorption or premature elution of analyte from the sorbent column (Krska, Welzig, Berthiller, Molinelli, & Mizaikoff, 2005; Wilson & Romer, 1991). The total analysis time is about 1 h, and this is comparable to the UPLC method (Fu et al., 2008). A direct comparison with other reports is problematic as the total analysis time is not specified by the authors.

Table 2
Levels of aflatoxins found in aflatoxin-positive feed samples.

Sample no.	Product	Aflatoxin found ng g^{-1}				
		G1	B1	G2	B2	Total
1	Maize	N.D	6.31	0.07	0.13	6.51
2	Copra meal	6.7	13.8	N.D	3.9	24.4
3	Sunflower meal	57.8	37.8	N.D	7.0	101.9
4	Wheat bean	8.6	N.D	N.D	N.D	8.6
5	Corn	6.3	2.3	N.D	N.D	8.6
6	Palm kernel expeller	9.9	N.D	N.D	N.D	9.9
7	Corn germ meal	45.6	N.D	N.D	N.D	45.6
8	Poultry feed	8.5	N.D	N.D	N.D	8.5

N.D, not detected.

3.3. Analytical characteristics

The linearity of the calibration graphs were studied by injecting in duplicate five concentrations (5–35 ng g^{-1}) of standard mixtures of the aflatoxins. Calibration plots were linear for the tested range with correlation coefficients >0.999 for all the aflatoxins. The limit of detection (LOD) was calculated to be 0.10 ng g^{-1} for both aflatoxins G1 and G2 and 0.06 ng g^{-1} for both aflatoxins B1 and B2.

The LOD was obtained by using the equation:

$$\mathrm{LOD} = ks_b/m \quad (1)$$

where m is the calibration sensitivity, s_b is the standard deviation of the blank, 3 was chosen as the factor k while the LOD was based on the signal-to-noise ratio of 3:1. LODs of 0.01 ng g^{-1} and 0.5 ng g^{-1} for each aflatoxin was reported by Ali et al. (2005) and Akiyama et al. (2001), respectively. The repeatability and reproducibility of the method was assessed by injecting five times each of the four

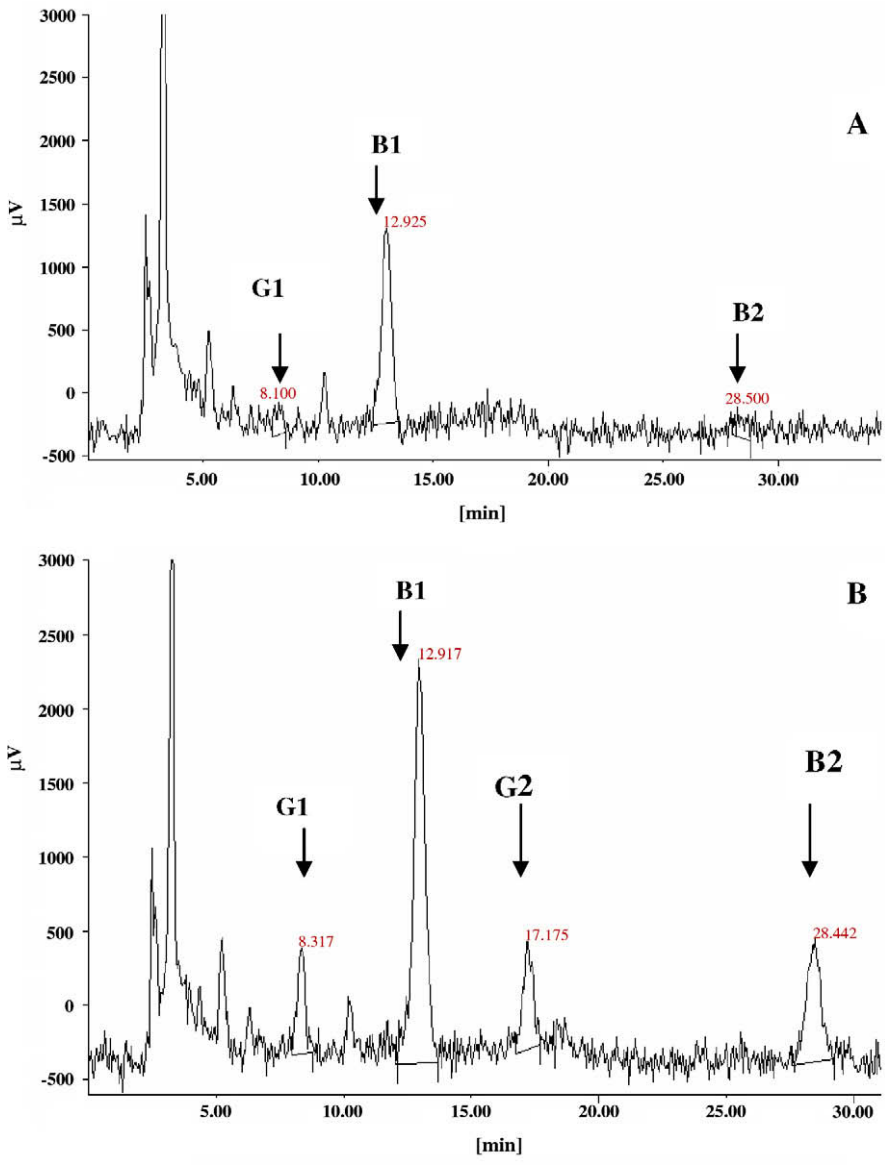

Fig. 4. Typical chromatograms of (A) extract of copra meal (sample 2), and (B) extract of copra meal that was spiked with aflatoxins B1, B2, G1 and G2 (15 ng g^{-1} each).

standard mixtures on the same day (intra-day) and over 6 days (inter-day), respectively. Good reproducibility of both the peak area (RSD $\leqslant$ 3.5%) and retention time (RSD $\leqslant$ 1.0%) were found.

3.4. Analysis of animal feeds

In the analysis of animal feed samples, peak identification was based on the comparison between the retention times of standard compounds and was confirmed by spiking standards to the samples. Quantification was based on the external standard method using calibration curves fitted by linear regression analysis. Under the stated experimental conditions, baseline separation of the aflatoxins was achieved in less than 30 min.

To further evaluate the capability of the method, aflatoxins were spiked to a few types of feed samples and analysed using the proposed method. Satisfactory recoveries, ranging from 70.0% to 104.6% were obtained (Table 1), indicating the suitability of the extracting solvents and MFC used.

Of the 42 feed samples that were tested, eight was found to be contaminated with aflatoxins (Table 2). The total aflatoxins ranged from 6.51 to 101 ng g^{-1}. Some of these samples contain aflatoxins that exceed the legal limits of 20 ng g^{-1} as imposed in many countries (e.g., USA, Austria, India, Argentina, Netherlands and Brazil) (Moss, 2002). The incidence of aflatoxins in copra (24.4 ng g^{-1}) and palm kernel (9.9 ng g^{-1}) clearly indicate that better hygienic practices must be in place in the preparation of these commodities. The traditional method of drying these items on the ground in the open air in poor hygienic conditions promotes the growth of moulds and production of mycotoxins. Surveys from other countries have reported the occurrence of aflatoxins in corn and related products from Turkey (Castells et al., 2008) and China (Li et al., 2001) and the contamination of animal feeds has been reported in Greece, Turkey (Aycicek et al., 2005). Typical chromatogram is shown in Fig. 4. It can be readily seen that all the aflatoxins are well separated from the unwanted components.

4. Conclusion

Forty-two animal feeds, comprising corn, wheat meal, sunflower meal, mixed feed, copra meal, and palm kernel expeller were analysed for the content of the aflatoxins B1, B2, G1 and G2. Three samples were found to contain total aflatoxins greater than 20 ng g^{-1}, exceeding the legal limit imposed in many countries. Cleaning-up of the extracts using the MFC is effective in removing unwanted interfering components, thus can be recommended as alternative clean-up sorbent to the more expensive immunoaffinity columns. Simpler clean-up procedure is also associated with the use of the MFC.

Acknowledgements

Wejdan Shakir Khayoon acknowledges the support of the Universiti Sains Malaysia's (USM) Research Fellowship program to support her postgraduate studies. Financial support of the work through USM Research University scheme is also acknowledged.

References

Akiyama, H., Goda, Y., Tanaka, T., & Toyoda, M. (2001). Determination of aflatoxins B1, B2, G1 and G2 in spices using a multifunctional column clean-up. *Journal of Chromatography A, 932*, 153–157.

Akiyama, H., Chen, D., Miyahara, M., Toyoda, M., & Saito, Y. (1996). Simple HPLC determination of aflatoxins B1, B2, G1 and G2 in nuts and corn. *Journal of the Food Hygienic Society of Japan, 37*, 195–201.

Ali, N. (2000). Aflatoxins in Malaysian food. *Mycotoxins, 50*, 31–35.

Ali, N., Hashim, N. H., & Yoshizawa, T. (1999). Evaluation and application of a simple and rapid method for the analysis of aflatoxins in commercial foods from Malaysia and Philippines. *Food Additives and Contaminants, 16*, 273–280.

Ali, N., Hashim, N. H., Saad, B., Safan, K., Nakajima, M., & Yoshizawa, T. (2005). Evaluation of a method to determine the natural occurrence of aflatoxins in commercial traditional herbal medicines from Malaysia and Indonesia. *Food and Chemical Toxicology, 43*, 1763–1772.

Aycicek, H., Aksoy, A., & Saygi, S. (2005). Determination of aflatoxin levels in some dairy and food products consumed in Ankara, Turkey. *Food Control, 16*, 263–266.

AOAC (2000). Natural toxins. In M. W. Trucksess (Ed.), *Official methods of analysis of AOAC international* (pp. 2–37). Gaithersburg, MD, USA: AOAC International.

Braicu, C., Puia, C., Bodoki, E., & Socaciu, C. (2008). Screening and quantification of aflatoxins and ochratoxin in different cereals cultivated in Romania using thin layer chromatography-densitometry. *Journal of Food Quality, 31*, 108–120.

Calleri, E., Marrubini, G., Brusotti, G., Massolini, G., & Caccialanza, G. (2007). Development and integration of an immunoaffinity monolithic disk for the on-line solid-phase extraction and HPLC determination with fluorescence detection of aflatoxin B1 in aqueous solutions. *Journal of Pharmaceutical and Biomedical Analysis, 44*, 396–403.

Castells, M., Marin, S., Scanchis, V., & Ramos, A. J. (2008). Distribution of fumonisins and aflatoxins in corn fractions during industrial cornflake processing. *International Journal of Food Microbiology, 123*, 81–87.

Cavaliere, C., Foglia, P., Guarino, C., Nazzari, M., Samperi, R., & Lagana, A. (2007). Determination of aflatoxins in olive oil by liquid chromatography–tandem mass spectrometry. *Analytica Chimica Acta, 596*, 141–148.

Fu, Z., Huang, X., & Min, S. (2008). Rapid determination of aflatoxins in corn and peanuts. *Journal of Chromatography A, 1209*, 271–274.

Gilbert, J., & Vargas, E. A. (2003). Advances in sampling and analysis for aflatoxins in food and animal feed. *Journal of Toxicology, 22*, 381–422.

Giray, B., Girgin, G., Engin, A. B., Aydin, S., & Sahin, G. (2007). Aflatoxin levels in wheat samples consumed in some regions of Turkey. *Food Control, 18*, 23–29.

Krska, R., Welzig, E., Berthiller, F., Molinelli, A., & Mizaikoff, B. (2005). Advances in the analysis of mycotoxins and its quality assurance. *Food Additives and Contaminants, 22*, 345–353.

Lattanzio, V. M. T., Solfrizzo, M., Powers, S., & Visconti, A. (2007). Simultaneous determination of aflatoxins, ochratoxin A and Fusarium toxins in maize by liquid romatography/tandem mass spectrometry after multitoxin immunaffinty clean up. *Rapid Communications in Mass Spectrometry, 21*, 3253–3261.

Lee, N. A., Wang, S., Allan, R. D., & Kennedy, I. R. (2004). A rapid aflatoxin B1 ELISA: Development and validation with reduced matrix effects for peanuts, corn, pistachio and soyabeans. *Journal of Agricultural and Food Chemistry, 52*, 2746–2755.

Li, F., Yoshizawa, T., Kawamura, O., Luo, X., & Li, Y. (2001). Aflatoxins and fumonisins in corn from the high-incidence area for human hepatocellular carcinoma in Guangxi, China. *Journal of Agricultural and Food Chemistry, 49*, 4122–4126.

Moss, M. O. (2002). Risk assessment for aflatoxins in foodstuffs. *International Biodeterioration and Biodegradation, 50*, 137–142.

Nawaz, S., Coker, R. D., & Haswell, S. J. (1995). HPTLC – A valuable chromatographic tool for the analysis of aflatoxins. *Journal of Planar Chromatography, 8*, 4–9.

O'Riordan, M. J., & Wilkinson, M. G. (2008). A survey of the incidence and level of aflatoxin contamination in a range of imported spice preparation on the Irish retail market. *Food Chemistry, 107*, 1429–1435.

Pena, R., Alcaraz, M. C., Arce, L., Rıos, A., & Valcarcel, M. (2002). Screening of aflatoxins in feed samples using a flow system coupled to capillary electrophoresis. *Journal of Chromatography A, 967*, 303–314.

Van Egmond, H. P., Heisterkamp, S. H., & Paulsch, W. E. (1991). EC-collaborative study on the determination of aflatoxin B1 in animal feeding stuffs. *Food Additives and Contaminants, 8*, 17–29.

Ventura, M., Guillen, D., Anaya, I., Broto-Puig, F., Llberia, J. L., Agut, M., et al. (2006). Ultra-performance liquid chromatography/tandem mass spectrometry for the simultaneous analysis of aflatoxins B1, G1, B2, G2 and ochratoxin A in beer. *Rapid Communications in Mass Spectrometry, 26*, 3199–3204.

Wilson & Romer (1991). Use of the mycosep multifunctional cleanup column for liquid chromatographic determination of aflatoxins in agricultural products. *Journal of AOAC International, 74*, 951–956.

Won-Bo, S., Yang, Z., Kim, J., Kim, J., Kang, S., Woo, G., et al. (2007). Development of immunochromatography strip-test using nanocolloidal gold-antibody probe for the rapid detection of aflatoxin B1 in grain and feed samples. *Journal of Microbiology and Biotechnology, 10*, 1629–1637.

Zinedine, A., Juan, C., Soriano, J. M., Molto, J. C., Idrissi, L., & Manes, J. (2007). Limited survey for the occurrence of aflatoxins in cereals and poultry feeds from Rabat, Morocco. *International Journal of Food Microbiology, 115*, 124–127.

Food Chemistry 118 (2010) 887

Contents lists available at ScienceDirect

Food Chemistry

journal homepage: www.elsevier.com/locate/foodchem

Preface

This Special Edition of Food Chemistry is devoted to the subject of analytical methods for authenticating food. The publication is timely as there have recently a plethora of high profile incidents where food authenticity has been compromised e.g. adulterated vodka in the UK, European frauds concerned with cheese and wine, adulteration of dairy products. The adulteration of food that takes place can sometimes be crude and can have severe implications for public safety. In this respect the recent melamine incident, although a global food safety issue, had its origins in a common food adulteration scenario, i.e. fraudsters trying to seek financial gain through mislabelling of their products, in the melamine case mislabelling the protein content of milk.

In Europe in particular, an ever more discerning consumer is prepared to pay extra for "added value" products. In many cases the products are essentially similar but with particular labelled "quality" attributes. These attributes such as local/regional/country of origin, free range, organic, species, blended or single variety, Protected Denomination of origin, to name but a few, provide food researchers with considerable challenges in terms of providing verification solutions that will satisfy consumers, food industry and control bodies alike. Our job is not helped when we are not only tasked with answering the question "is this product adulterated?" but also the more difficult question "what is the level of adulterant in the authentic product?" It is easy to see why researchers often need sophisticated solutions to authenticate food.

It is against this background that I am pleased that this special edition will present some of the latest research in this area. Approximately half of the papers are derived from research carried out within the framework of the TRACE integrated project (www.trace.eu.org). This largely European funded research programme involves over 50 participants from Europe, South America and China. TRACE has initiated research into the development of methods and systems for verifying geographical origin, species and varietal origin and methods that can verify a food using spectroscopic "fingerprinting". The analytical methods are invariably supported by chemometric interpretation in order to discriminate between the adulterated and authentic products and where possible/appropriate quantify the adulterant.

This Special edition also includes papers detailing research funded through other national and international funding bodies. In many of the manuscripts direct support has been provided by the food industry, not least in the form of highly valued provision of authentic samples and commodity expertise. This close co-operation is valued and essential for method development and validation. In addition to acknowledging the work of researchers involved in producing the manuscripts in the Special Edition we would like to acknowledge all those involved in facilitating the research and in helping through various means to develop methods to ensure the integrity of our food supply.

TRACE is delighted to help support this Special Edition and cordially invites readers to its final conference in Brussels on 2–3 December 2009 (www.trace.eu.org/admin/event/file/TRACE-Leaflet.pdf) where the final outputs from the project on methods for tracing the origin of our food will be presented.

Paul Brereton
Co-ordinator of TRACE,
Head of Food Authenticity and Traceability,
Food and Environment Research Agency,
Sand Hutton, York YO41 1LZ,
United Kingdom
Tel.: +44 1904 462625
E-mail address: paul.brereton@fera.gsi.gov.uk

0308-8146/$ - see front matter
doi:10.1016/j.foodchem.2009.05.003

Food Chemistry 118 (2010) 888–889

Contents lists available at ScienceDirect

Food Chemistry

journal homepage: www.elsevier.com/locate/foodchem

Preface

Today Port is a world-wide reputed wine known to be produced in the specific region of Douro in Portugal according to well-defined wine making-practices. The historical reasons and evolution which led to the product we drink today are probably less known to most of the consumers. At the end of the 17th century difficult political situation between France and England resulted in an increasing importation of Port wine as a replacement of the Claret Bordeaux wine for the British market. The trip on the ocean to England often spoiled the wine; the fortification or addition of distilled grape improved the shipping and preservation of the wine for its journey. This practice was further improved in the mid 19th century to stop fermentation before all the sugar is converted to alcohol, thus creating a sweeter mouth-taste typical of the Port Wines we know today. Increasing demand and high prices also gave rise to fraud and infractions. Consequently, the Portuguese government created in 1756 an institution (Companhia Geral dos Vinhos do Alto Douro) to guarantee the quality of the product. The concept of a register of vines was thus defined and Port wine became the third oldest defined and protected wine region in the world after Tokaji (1730) in Hungary and Chianti (1716) in Italy.

All world-wide reknown food products bearing traditional geographical indication of origin as distinctive signs of quality and reputation have certainly encountered a similar evolution than that of Port wine. After an initial period of commercial success, consortium of producers or government authorities establish rules for delimitation of the geographic area of origin, manufacturing practices and specifications of the finished product.

Geographic indications of products were considered in International treaties such as the Paris Convention for the Protection of Industrial Property in 1883 and the Madrid Agreements on Indications of Source and the International Registration of Marks in 1891. These international treaties and the more recent Lisbon Agreement for the Protection of Appellations of Origin and their International Registration (1958) are now administered by the World Intellectual Property Organization (WIPO), a United Nations Agency. In addition, the Agreement on Trade-Related Aspects of Intellectual Property Rights (TRIPS) deals with the international protection of geographical indications within the framework of the World Trade Organization (WTO). The European Regulation EC Reg. 2081/92 introduced the protection of Geographical Indications (PGIs) and Designations of Origin (PDOs) for agricultural products and foodstuffs in 1992. It is now replaced by the Council Regulation No. 510/2006 which also allows producers from third countries to register their names in the European Union. It should be noted that the wine-sector products (except wine vinegars) and spirits drinks are covered by their own existing Community legislation.

This frame of international agreements and regulations is important to enable the recognition of origin of a product. Food chemists are requested to provide scientific methods and perform measurements that establish the compliance of food products with the regulatory requirements. Food safety aspects are generally easily controlled with official methods determining physico-chemical or biological parameters against well-established specifications and tolerances. The analytical testing for authentication purpose such as recognition of geographic origin, or detection of adulteration is somewhat more complex. The specifications for food with geographic indication are generally based on consolidated traditional practices and often on subjective characteristics such as organoleptic properties. Although physico-chemical parameters were sometimes included in the specifications, they were generally not specific of the geographic origin and did not allow differentiation from other similar products. In this context, it is likely that imitations or adulterated products are present on the market and compete in an unfair manner with the genuine products. It is both in the interest of the consumers, the producers and also of the control bodies to dispose of analytical methods and objective parameters that enable a better control of origin of food products. The isotopic methods have shown to be an efficient tool to fight against adulteration of food products since the beginning of the 90s after the European Council has decided to establish an official European isotopic wine databank for the controls in the wine sector (EC Reg. No. 2048/89). Several European funded research projects further developed these isotopic techniques and also spectroscopic fingerprinting methods on a broader range of food products investigating applications for the control of botanical, animal and geographic origins of food products. The techniques developed in molecular biology have also led to the possibility of characterisation of species. This Special Edition of Food Chemistry illustrates the vivacity of these researches on a broad range of food products. Half of these works are based on the isotopic techniques eventually in combination with trace elements. The fingerprinting techniques are also important tools for the confirmation of origin of many food products provided that reference databank of genuine products can be established. The research works presented in this Special Edition highlight some of the analytical possibilities available today to the food chemist to provide objective physico-chemical parameters helping the recognition of origin of PDO food products and also to detect adulteration or mis-labeling. Much progress has been achieved in the past years, for instance throughout the Integrated Project TRACE.

0308-8146/$ - see front matter
doi:10.1016/j.foodchem.2009.07.034

However there is still a lot of work ahead for development of new methods, to integrate data and share databanks among official control bodies but also, when possible, with industry and producers within systems of certification at the level of quality control of the production. The strong interest in Europe for authentication and traceability of food products will continue to stimulate the research in that field. Certainly several of these works will naturally find their publication in future issues of Food Chemistry.

Claude Guillou
Joint Research Centre of the European Commission,
Institute for Health and Consumer Protection,
via E. Fermi, 21020 ISPRA (VA),
Italy,
Tel.: +39 0332 78 5678;
fax: +39 0332 78 9303.
E-mail address: claude.guillou@jrc.ec.europa.eu

to kinetic or thermodynamic isotope effects and, therefore, reflect the circumstances under which physical or (bio-) chemical processes took place. IR of the light elements provide information about climate, distance to the sea, altitude, latitude and agricultural practices.

During the last ten years IR of heavy (geo) elements (Sr, Pb) came into use in said field of application. Regional variations of respective IR are caused by radioactive decay of mother nuclides and radiogenic increase of daughter nuclides and are evolved during geologic processes. Isotopic signatures of the heavy elements in any biogenous tissue are thus inherited from the geologic environment and therefore vary spatially depending on the regional geo-, litho- and pedological situation (Horn, Schaaf, Holbach, Hölzl, & Eschnauer, 1993).

2. Juice samples

From 2002 to 2005 a Project named "Pure Juice" was funded by the European Union and coordinated by SGF International e.V., Nieder-Olm, Germany, during which especially methods using stable isotope analysis had been developed and improved to detect adulterations of fruit juices (see Results of the Pure Juice Project, 2006). One aim of the study was to establish suitable means to identify the geographic origin of fruit juices by building up a multi-element isotope data base and by developing new isotopic techniques for the elements sulphur and strontium and especially the combination of light elements' IR with those of strontium for fruit juice authenticity control. For this purpose we were supplied with numerous authentic juice samples by the SGF, amongst others, around 150 samples of orange juices from major orange cultivating regions of the world.

3. Materials and methods

For the verification of geographical origin of fruit juices the IR of hydrogen, carbon, nitrogen, sulphur and strontium proved useful in most cases.

Results of stable isotope measurement of light elements are always displayed in the delta notation, where the measured value is referred to an international standard:

$$\delta X(‰) = \left(\frac{\left(\frac{X}{Y}\right)_{Sample}}{\left(\frac{X}{Y}\right)_{Standard}} - 1 \right) \times 1000, \quad (1)$$

with X being the heavier and Y being the lighter isotope of an element.

International reference values ("Standard") are: V-SMOW (δ^2H), V-PDB ($\delta^{13}C$), AIR ($\delta^{15}N$), V-CDT ($\delta^{34}S$).

The results of Sr-isotope analyses are normally given as $^{87}Sr/^{86}Sr$ but sometimes, in analogy to those of light stable isotopes, as $\delta^{87}Sr$ with[1]

$$\delta^{87}Sr\ (‰) = \left(\frac{\left(\frac{^{87}Sr}{^{86}Sr}\right)_{Sample}}{0.7093} - 1 \right) \times 1000 \quad (2)$$

δ^2H-values of plant material are directly correlated to the water taken up from soils. Hydrogen isotopic composition of meteoric water provides information about local climatic and geographic conditions like temperature, amount of precipitation, humidity, latitude or altitude. Depending on rooting depth and water supply plants take up water either from ground water or from surface water. Although roots of orange trees can reach depths of 3 m highest root activity is found in the upper soil from 30 cm down to 60 cm; hence, water is supposed to be taken mainly from these depths (Wahid, 2001).

Although experiments have shown that – apart from ^2H-enrichment in leaf water due to evapotranspiration – no fractionation of δ^2H in the bulk plant material occurs upon water uptake (Ehleringer & Dawson, 1992), large fractionation effects caused by biochemical reactions like e.g. carbohydrate metabolism or production of lipids can be recognised within a plant (Schmidt, Werner, & Eisenreich, 2003). However, as the only source of hydrogen in oranges ultimately is meteoric water and strong correlations between δ^2H-values of the water and both plant and plant metabolites can be observed (Luo & Sternberg, 1992; Martin & Martin, 2003; Schmidt et al., 2003) it was expected to obtain useful geographic and environmental information by measuring δ^2H. Pulp turned out to be a particularly suitable material as it contains considerably less exchangeable hydrogen than carbohydrates (the latter even more than 50%).

The main source of carbon for plants is CO_2 taken up from the atmosphere for the production of carbohydrates. During photosynthetic CO_2-fixation isotope effects occur which lead to carbon isotope discrimination depending on the photosynthetic pathway a plant uses. Two pathways can be distinguished depending on the number of C-atoms built in the primary assimilation product, on the one hand the C3- or Calvin-cycle, on the other hand the C4- or the Hatch-Slack pathway (Krueger & Reesman, 1982). Regarding the carbon IR, these processes can be well discriminated as C3-plants (e.g. most species of fruit and vegetable, legumes or domestic cereals) show $\delta^{13}C$-values ranging from −24‰ to −32‰ whereas C4-plants (e.g. corn or cane sugar) display significant higher $\delta^{13}C$-values between −11‰ and −15‰. CAM (crassulacean acid metabolism) plants, like for example pineapple or vanilla can use both kinds of metabolism and consequently show intermediate values between −15‰ and −24‰ (Schmidt, Rossmann, Stöckigt, & Christoph, 2005a). Individual variation ranges are due to climatic conditions like light intensity, changes in soil water content and relative humidity (Francey & Farquhar, 1982). Hence, the distribution of carbon isotopes in plants rather acts as an indicator for different plant-physiological processes than for geographic origin. Nevertheless, in practise there are systematic differences of carbon IR between fruits e.g. coming from Mediterranean countries compared to those from South-America as a result of different growing conditions (temperature, humidity).

$\delta^{15}N$ values of plants are mainly influenced by soil nitrogen. Therefore, N-isotopes cannot directly be linked to a certain region as the main nitrogen sources for soils are fertilizers and manure – i.e. N-isotopes mainly reflect agricultural practices which, however, can be typical for certain regions (Kornexl, Werner, Rossmann, & Schmidt, 1997; Schmidt et al., 2005b).

Sulphur IR of natural compounds are influenced by several factors. On the one hand there are anthropogenic sources like industrial emissions or – though of smaller importance – fertilizers; on the other hand there are natural sources like sea spray (i.e. small drops of sea water blown to land), volcanic emissions or lithological setting of an area. Thus, the variability of $\delta^{34}S$-values is large. For example, the $\delta^{34}S$-value of seawater and that of sea spray lies around +22‰. Although $\delta^{34}S$ of volcanic emissions can vary between −20‰ and +20‰ (Thode, 1991) the average is around +5‰ (Pichlmayer, Schöner, Seibert, Stichler, & Wagenbach, 1998) and $\delta^{34}S$-values of fertilizer sulphate can vary between −6,5‰ and +24,4‰ (Vitoria, Otero, Soler, & Canals, 2004). Experiments with wheat have shown that there is no or very little isotope fractionation during sulphate uptake and transport from roots to plants (Monaghan, Scrimgeour, Stein, Zhao, & Evans, 1999). Hence, sulphur IR are very site-specific and thus can contribute significantly to the identification of geographical provenance.

[1] $^{87}Sr/^{86}Sr = 0.7093$ is an approximation for Sr-IR in (Baltic) seawater.

Like isotopes of the light elements also those of the heavy or trace elements are subject to isotope effects and mass dependent fractionation effects. But these are, according to high nuclide masses and small relative mass differences practically insignificant compared to observed variations. Applications using isotope-ratio measurements of heavy elements (Sr, Pb, Nd, etc.) are utilising variations in isotopic composition due to radioactive decay where one isotope of a given element (parent-nuclide) is transmuted into a stable isotope of another element (daughter-nuclide). The variation of the isotopic composition of strontium is due to the radioactive β-decay of ^{87}Rb with a half-life of 48 Ga resulting in an increase of the radiogenic ^{87}Sr (for further details see also Faure, 1986). For our applications it can be assumed that absolute amounts of the isotopes ^{84}Sr, ^{86}Sr and ^{88}Sr are invariant and thus remain constant in any material. Hence, $^{87}Sr/^{86}Sr$ in soils and the plants growing thereon depend – as a first approximation – on the initial Rb/Sr and the geological age of the underlying rocks. For example, plants growing on young basalts normally have low $^{87}Sr/^{86}Sr$ ratios ($^{87}Sr/^{86}Sr < 0.706$) whereas those on old crystalline rocks, like gneisses or granites display high Sr-IR ($^{87}Sr/^{86}Sr > 0.711$). According to the Sr–seawater curve (Faure, 1986) the vast majority of marine carbonatic sediments lead to intermediate $^{87}Sr/^{86}Sr$-values (0.706–0.709). In clastic sediments usually higher values between 0.709 and 0.711 can be expected as mostly material deriving from magmatic precursors is involved.

According to this, regions with different geologic histories usually show different but site-specific isotopic signatures for Sr which do not alter during (bio-) chemical and physical reactions. The biologically available, i.e. the water soluble fraction of Sr, passes from rock to soil into aerosols and water and from there enters the food chain i.e. tissues of plants, animals and humans without significant fractionation. The variability of Sr-isotopes in nature is rather wide and the concentrations of Sr in most organic materials are in the dimension of hundreds of μg/kg or mg/kg which makes sampling and sample handling easy as no large amounts of material (500 mg–5 g) are required (Horn 2005).

When interpreting Sr-IR of plant material it has to be taken into account that the isotopic composition of plants does not represent exactly that of the underlying whole rock. Several factors may influence Sr IR of organic material to different degrees. Plants take up nutrients (including Sr) from the soil by their roots and due to similar ionic radius and -charge Sr is physiologically incorporated like calcium. Formation of soil (pedogenesis) occurs through weathering of rocks. As rock forming minerals have both different Sr contents, IR and solubilities, soil and soil solution containing the bio-available Sr show either increased (mostly true for more basic rocks) or decreased (mostly true for acidic rocks) Sr IR compared to the parent rocks (Horn, 2005). Sr in soils developed on carbonates more closely resembles – due to the relatively high water solubility of $CaCO_3$ – the isotopic composition of the bulk rocks.

External factors which sometimes may significantly contribute to the Sr budget and composition of vegetation are aerosols, sea spray or fertilizers. The extend to which these sources can seriously influence the isotopic composition of plants has to be evaluated individually.

Precipitation has a mean concentration of dissolved Sr of several μg/l (Åberg, 1995). This is, although completely bio-available to plants, negligible compared to the Sr content of a typical soil which is normally several hundreds of mg/kg. Solid aerosols can strongly contribute to the Sr content of bulk soil. Whereas for example, the ubiquitous Sahara dust plays a minor role for bio-available Sr as mostly consisting of more or less insoluble minerals like mica or quartz, carbonate dust can be an important source of mobile Sr in soils. Sea spray, however, can change Sr IR in organic material significantly. Ocean water has a Sr concentration of about 8 mg/l with a $^{87}Sr/^{86}Sr$ of 0.7092 which has especially to be taken into account when interpreting Sr data of plants growing in coastal areas.

Fertilizers can play an important role for Sr IR of plants when they have both high Sr-concentrations and extreme IR like e.g. some lime or phosphate fertilizers. Nevertheless, it can be presumed that even in such special fertilizers Sr IR of plants can be altered but never falsified completely (Horn, 2005).

Thus, geographic information which can be obtained by analysing Sr IR in orange juices is mainly based on the lithologic or pedologic composition of an area. However, from case to case several different influencing factors have additionally to be taken into account.

4. Sample treatment

Three laboratories were involved in the isotope analyses: stable isotopes of C, N, S were measured at Isolab GmbH, Schweitenkirchen, δ^2H was measured at LGL, Oberschleissheim and Sr-isotope-measurements were carried out at Bavarian States Collection for Palaeontology and Geology, Munich.

Preparation steps for multi-element-isotope measurements on orange juices are schematically displayed in Fig. 1.

4.1. δ^2H, $\delta^{13}C$, $\delta^{15}N$, $\delta^{34}S$

4.1.1. Sample preparation

For the analyses of the light elements pulp, sugar, amino-acids and proteins of the juice samples were prepared. However, the stable isotope-data presented here is restricted to results of pulp as the preparation method is simple and officially accepted (see below), the material is stable and it is the only juice component which can be analysed for all isotope parameters. Pulp, which is the insoluble fraction of a juice, mainly consists of cellulose, hemicellulose, pectines and proteins and is separated from the liquid fraction by centrifugation, followed by washing several times with water and acetone (according to an officially accepted method of CEN prENV 13070, 1998). The dried samples (3–4 mg for $\delta^{13}C$, $\delta^{15}N$, $\delta^{34}S$ and 200 μg for δ^2H, respectively) are weighed into tin capsules for isotope-ratio measurements.

4.1.2. Isotope measurements

The measurements of $\delta^{13}C$, $\delta^{15}N$, $\delta^{34}S$ are carried out on an Elemental Analyser (Vario EL, Elementar, Hanau) coupled with an isotope-ratio mass spectrometer, IRMS (IsoPrime, GV Instruments). In the course of the study a system for the simultaneous determination of C, N, S has been developed and tested for routine work. Only recently a system for the simultaneous determination of H in addition to C, N and S is under development and results are compared to the conventional way of hydrogen analysis (pyrolysis at 1450° C with a Thermo Finnigan High Temperature conversion unit coupled to a Finnigan XL plus IRMS; Thermo Finnigan GmbH, Bremen, FRG) in order to get established into routine work. Detailed information about this EA-IRMS-system as well as data showing the comparability of the two systems can be found in Sieper et al. (2006).

At the beginning of each sequence of measurements six working standards are analysed, then four to six replicates of five samples alternating with six working standards – for samples discussed here this was a casein (assigned values are −23.37‰ for $\delta^{13}C$, 6.15‰ for $\delta^{15}N$, 4.4‰ for $\delta^{34}S$ and −113‰ for δ^2H) which was calibrated in a former EU-project (SMT4-CT2236-1998) by several laboratories (e.g. Camin et al., 2004). As applied since over 15 years the measured values (raw data) are referenced against this working standard. Each sequence additionally includes four to six replicates of an international reference material, e.g. NIST

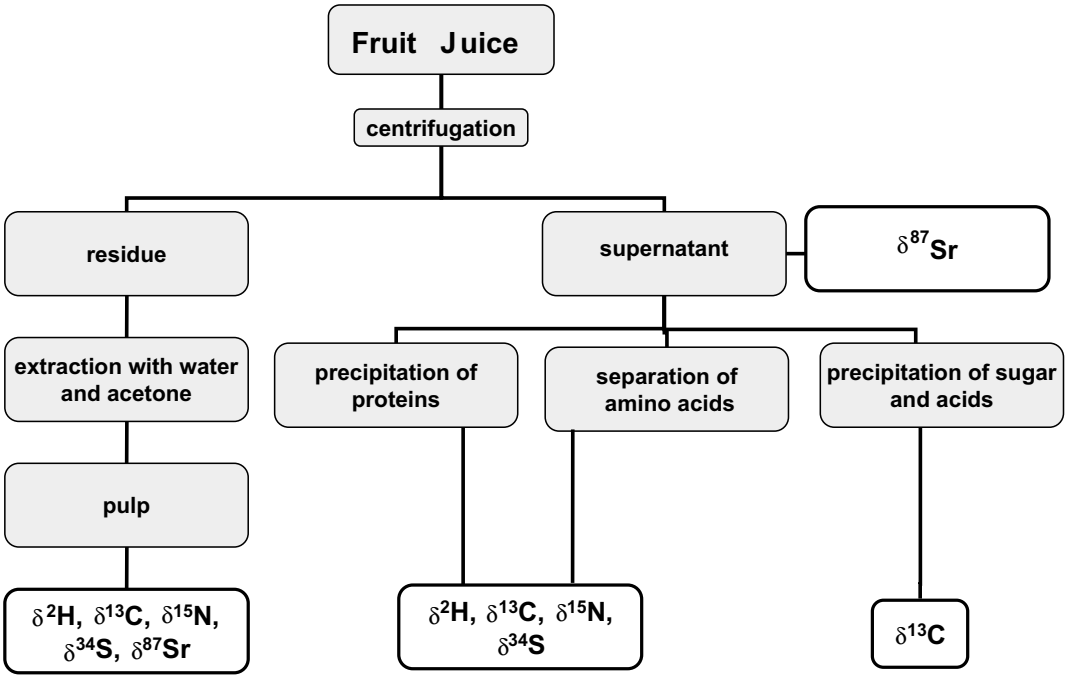

Fig. 1. Sample preparation scheme for isotope analyses in fruit juice samples.

1577b to check the accuracy of the calculation. Achieved uncertainties (1 STD) of measurements are better than ±3.0‰ (δ^{2}H), ±0.1‰ (δ^{13}C), ±0.2‰ (δ^{15}N) and ±0.3‰ (δ^{34}S). Tests for the accuracy of the measurements are regularly performed within interlaboratory round robins or by comparison with data from single-element analysis. Further details and data can be found in Rossmann, Rummel, and Kupka (2003), Camin et al. (2004), (2007) and Sieper et al. (2006).

Supposed possible exchange of hydrogen with water and/or ambient air moisture during and after preparation is corrected for by use of the "comparative equilibration technique" (Wassenaar & Hobson, 2003). The reference material was the casein standard (see above).

4.2. $^{87}Sr/^{86}Sr$

4.2.1. Sample preparation

Juice samples – 100 mg of pulp or 1 mL of bulk juice or liquid fraction – are dried for several hours and afterwards thermally ashed at 800 °C. ^{87}Rb is isobaric to ^{87}Sr and therefore cannot be distinguished by the mass spectrometer. Accordingly, it is very important to remove Rb completely. For this purpose the ashed sample is dissolved in concentrated HNO_3. Sr is then separated from other elements such as Ca, Ba and Rb by ion-chromatography on Sr-spec®, a Sr-specific crown-ether using a method modified after Pin and Bassin (1992). Due to small resin volume (50 μL) and little amounts of chemicals required (2 mL of HNO_3 in total), the usage of only extremely clean reagents (water and acid are cleaned with subboiling distillation) and multiply cleaned quartz- and teflon-beakers and the performance of separations under clean room conditions (class 100 laboratory), total blanks are below 500 pg Sr in any case. In view of a Sr content of 200 ng and more in the sample this is negligible.

4.2.2. Isotope measurement

Isotope analyses of Sr are performed on a thermal ionisation mass spectrometer (TIMS, MAT 261.8, Thermo Finnigan). Tungsten-single-filaments are used for the measurements. As Rb has a significantly – about 300 °C – lower ionisation temperature than Sr any extant Rb is evaporated from the loaded filament through controlled pre-heating before the isotopic composition of Sr is measured. For quality control and to check for proper operation of the mass spectrometer, a certified reference material ($SrCO_3$, NIST SRM 987) is analysed under the same conditions as the samples (60 single scans, $^{87}Sr/^{86}Sr$ mean value: 0.710251 ± 0.000023 (1 STD) with $n = 120$). Isotope mass fractionation during analysis is corrected for by referencing to an invariant $^{88}Sr/^{86}Sr$ value of 8.37521. The achieved precision of strontium-isotope measurements normally is <0.003% (2σm). A combined uncertainty (precision + accuracy) for $^{87}Sr/^{86}Sr$ is <0.005%.

5. Results and discussion

During the EU-project "Pure Juice" approximately 150 authentic orange juices have been analysed. The results are shown in boxplots (Fig. 2).

Samples for this project were taken from juice producing factories and not from single plantations which makes interpretation more difficult as the harvest area of the oranges can exceed several hundreds of square kilometres. Additionally, geographic details of the provenances are not available for all samples. Therefore, measured IR are supposed to reflect a mixture of values from samples grown in different environments. However, this constellation reflects "real-life" because usually laboratories do not obtain fruit juices from one single area for their market control but they will always get a final product for analysis.

Although comparisons of juices and fresh fruits of the same origin lead to corresponding results it can not be excluded that post harvest treatment could influence IR in exceptional cases. But, as detailed information is lacking and it is assumed to play a minor role, it is not considered in this study.

Seasonal variations which can play an important role for δ^{2}H- and, to a minor degree, also δ^{13}C-values, e.g. in wine authentication (Christoph, Rossmann, & Voerkelius, 2003), can be neglected in this case as normally for orange juices and, especially for concentrates fruits are taken from several harvests or even several years.

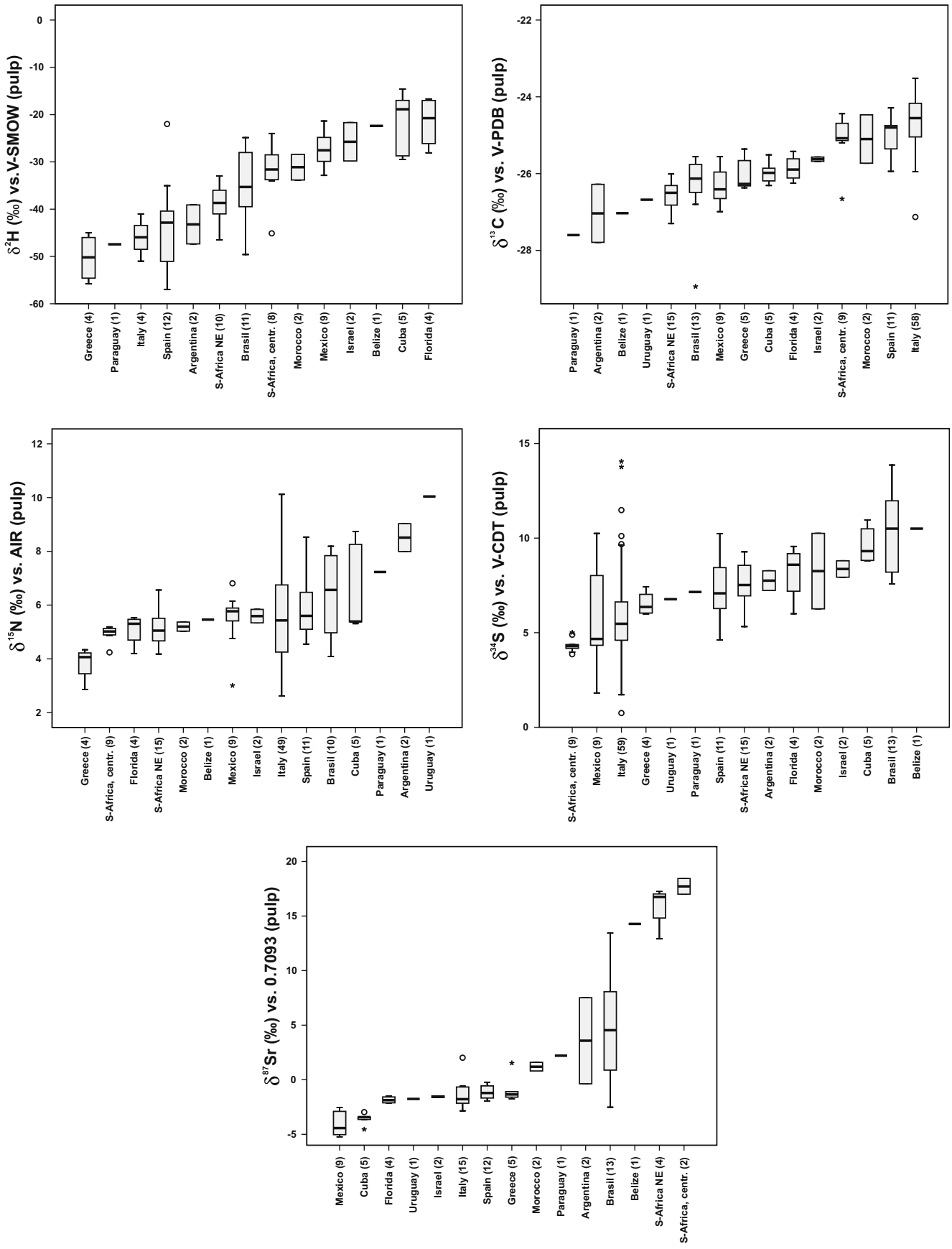

Fig. 2. All results displayed as boxplots. The boxes comprise the range between the first and the third quartile of the distribution. Box length is called interquartile range (IQR). The vertical lines (''whiskers") at the lower and upper end of the axis represent minimum and maximum values which are not considered as outliers or extreme-values. ○: outliers (data points between 1.5 and 3 times IQR lower than the first or higher than the third quartile). *: extreme-values (data points even lower or higher than outliers) The vertical line within the box is the median value of the distribution. Numbers in brackets are numbers of analysed samples.

Although all orange farms normally are located in warmer regions measured δ^2H-values of the pulps of our samples are not as similar as expected, but instead clear differences are observed. Like Heaton, Kelly, Hoogewerff, and Woolfe (2008), who analysed lipids in beef, we also find a correlation between δ^2H-values and latitude: δ^2H-values of the insoluble part of orange juices are getting more negative the further the sampling site is away from the equator. Consistently, highest values are found for samples from Cuba, Mexico and Florida, which are lying most closely to the equator. The next group are samples from Morocco showing slightly more negative values. The samples from Brazil show, expectedly, a very wide range of values as there are both samples from Northern and Southern regions included in this data set. Accordingly, samples from South-Africa show similar values as those from Brazil. Lowest δ^2H-values can be found in European samples from Italy, Spain and Greece.

In that oranges are C3-plants, δ^{13}C values of respective juices are low (−29‰ to −23‰). Nevertheless, the values show slight differences, possibly due to environmental conditions of the plants which shall not be discussed here. In any case, values can roughly be divided into three groups: the lowest values (−27.79‰ to −26.28‰) are found in the samples from Argentina, Belize and Paraguay; medium values (−28.94‰ to −25.36‰) in Brazilian-, Cuban-, Floridian-, Greek-, Mexican- and South-African (North-Eastern part) samples. Samples from South-Africa (central part) and Mediterranean countries show the highest values (−26.66‰ to −23.63‰).

Results of nitrogen isotope analysis show relatively wide overlaps between each single origin of the orange juices with values roughly between 5‰ and 8‰. While δ^{15}N values from Brazil, Cuba and Spain scatter widely and, therefore, are of limited use for origin assignments, samples from Florida, Mexico and Morocco group well within narrow ranges. Exceptions are samples from Argentina which show higher values (8–9‰) and Greek as well as Italian samples which display lower values (<4‰). The latter, after all knowledge, can be explained with application of synthetic nitrogen fertilizers. In contrast, rather high δ^{15}N values in juices from Argentina, Brazil or Cuba may be due to widespread use of organic manure.

The variation of sulphur IR in all samples of this study is covering a relatively small range (from ~0‰ to +14‰) compared to the δ^{34}S variation of vegetation worldwide (from −10‰ to +20‰) as shown by Krouse, Stewart, & Grinenko, 1991. In many cases, reasons for the observed variability can hardly be given because a combination of different sulphur sources may well lead to similar δ^{34}S values. Additionally, plants can take up sulphur from the

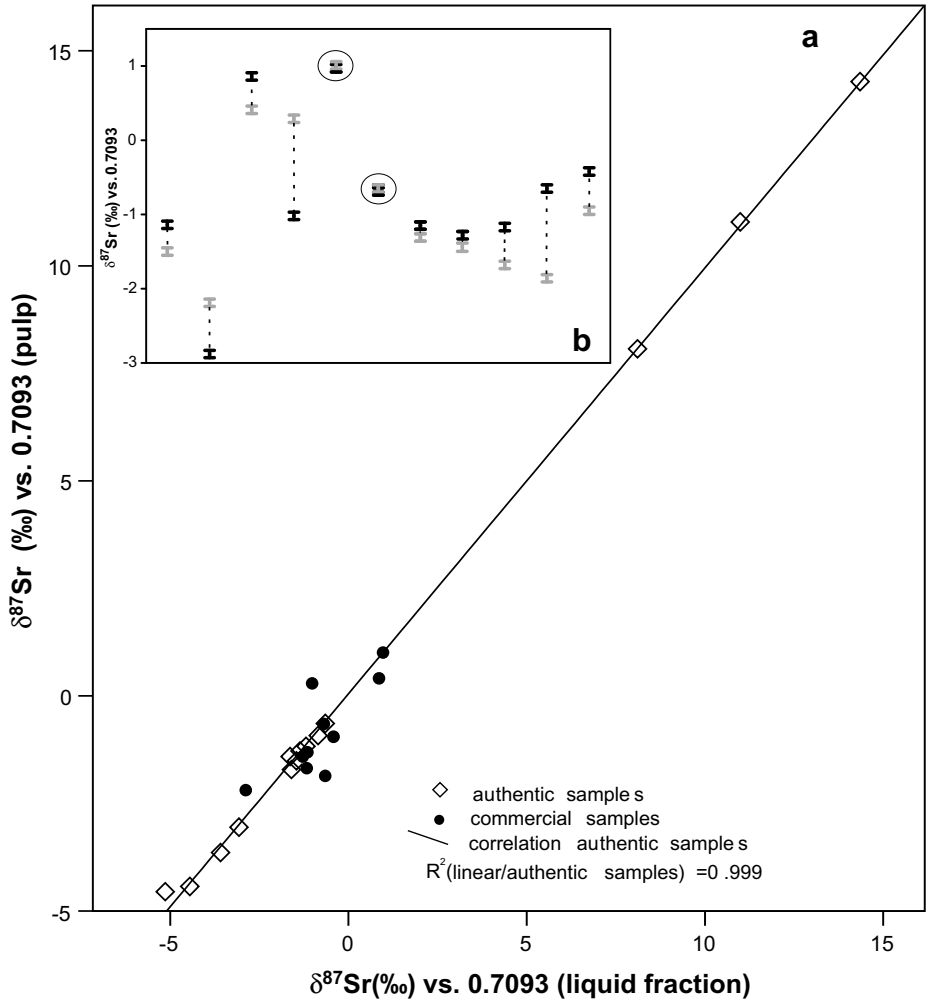

Fig. 3. (a) Comparison of δ^{87}Sr of the pulp and the liquid fraction of orange juices to detect illegal adding of foreign concentrate to single strength juices. Authentic single juice samples show identical values in both components (correlation coefficient R^2 = 0,999). Uncertainty ranges for δ^{87}Sr are much smaller than the symbol-size. (b) δ^{87}Sr values for commercial juice samples (black symbols: liquid, grey symbols: pulp) are displayed (dashed lines connect pulp-juice pairs of corresponding samples) to show the absolute differences between the fractions. The range of the symbols represents the measured value ± a combined uncertainty of 0.05‰. Samples with δ^{87}Sr-differences between pulp and liquid larger than the uncertainty are supposed to be adulterated, the two encircled samples are accepted as authentic.

atmosphere with their stomata. Hence, if there is a source of significant amounts of atmospheric sulphur, like for example, emissions of power plants, δ^{34}S-values in plants cannot be linked solely to the substrate but mixtures have to be considered.

Although results of δ^{34}S-analysis overlap to a certain degree, some sites of orange cultivation are defined very well. For example, Cuba and Mexico show overlapping values for IR of all other elements but can be discriminated by using sulphur isotopes. Obviously due to a seaspray-influence δ^{34}S-values in Cuban samples (8.8–10.96‰) are mostly higher than those from Mexico (1.81–10.25‰) where a volcanic influence is evident. Brazilian samples, mostly showing relatively higher values (7.6–13.7‰) can be well distinguished from those from Spain (4.6–10.2‰). In the case of Southern Africa it is even possible to discriminate within one country as the samples from the South-East display an average δ^{34}S-value of 7.6‰ whereas those from the central part are significantly lower with an average δ^{34}S-value of 4.3‰.

By referring to the prevailing geological conditions, Sr-isotopes often show a high potential for assigning the juice samples. The sampling sites of Cuba and Mexico show quite similar results with $^{87}Sr/^{86}Sr$ between 0.7056 and 0.7075. Sr-IR higher than 0.7065 are related to widespread Mesozoic (240–66 Ma) sediments, whereas $^{87}Sr/^{86}Sr$ below 0.7065 are due to basalts, gabbros or ultramafic rocks like serpentinites.

Both in Brazil ($^{87}Sr/^{86}Sr$: 0.7075–0.7188) and in South-Africa ($^{87}Sr/^{86}Sr$: 0.7185–0.7224) a Precambrian to Proterozoic basement (composed of 2500–600 Ma old granites and gneisses) is responsible for the mostly very high Sr-IR in the juice samples. The variation range of $^{87}Sr/^{86}Sr$ is due to heterogeneous compositions and varying grades of metamorphism of the lithology. Whereas in South-Africa large areas are exclusively dominated by Precambrian gneisses, the influence of Mesozoic sedimentary rocks and basalts is more important in Brazil – especially for the southern part in the Parana area – where also lower values (<0.7080) were found.

The $^{87}Sr/^{86}Sr$-values of the Spanish sampling sites are ranging from 0.70809 to 0.70913. This is explainable by the predominance of Mesozoic sediments in these regions.

Florida ($^{87}Sr/^{86}Sr$: 0.7078–0.7083) is completely covered with tertiary and quaternary sediments though the Sr-IR are quite similar to those we know from areas underlain by Mesozoic sediments like e.g. in Spain. An explanation for this is that the source area for the Floridian rocks, namely the youngest parts of the Appalachian Mountains is composed of Cretaceous sediments.

The Italian samples ($^{87}Sr/^{86}Sr$: 0.7073–0.7107) originate from Calabria and Sicily. In spite of this rather small area Sr-IR show – similar to the δ^{34}S values – a striking variation which is caused by very heterogeneous geological and lithological conditions in Southern Italy. There are both young basaltic rocks from the Etna volcanic complex leading to low IR, Mesozoic sediments resulting in intermediate values and crystalline rocks in Calabria with relatively high values. Large areas are covered with Cenozoic sediments consisting more or less of a mixture of these precursors. Therefore, this part of Italy is a striking example for a rather small region, where Sr IR (as well as δ^{34}S-values) can show significant variation over small distances.

A common procedure of adulteration in single strength orange juices is blending with rediluted concentrate in order to increase the production and/or to decrease the production costs. While this practice is allowed for juices made from concentrate it is illegal for single strength juices. Such kind of adulteration can be detected by analysis of both pulp and liquid fraction. Here, Sr-isotope analysis turned out to be most applicable. Authentic single strength juices do not show any significant difference in isotopic composition of Sr between soluble and insoluble components (Fig. 3a). From what is known about Sr-isotope analysis in plant material the fractions even should be identical whereas those of blended samples can show considerable differences of more than 1‰ (Fig. 3b). In routine work, samples where $^{87}Sr/^{86}Sr$ of liquid and pulp are equal within an uncertainty of ±0.05‰ are accepted as authentic but all samples with a larger inter-component-difference are judged as adulterated.

Although homogenisation between the liquids of the authentic juice and the added rediluted concentrate takes place to a certain degree, the strontium which is fixed in the pulp, (similar to cal-

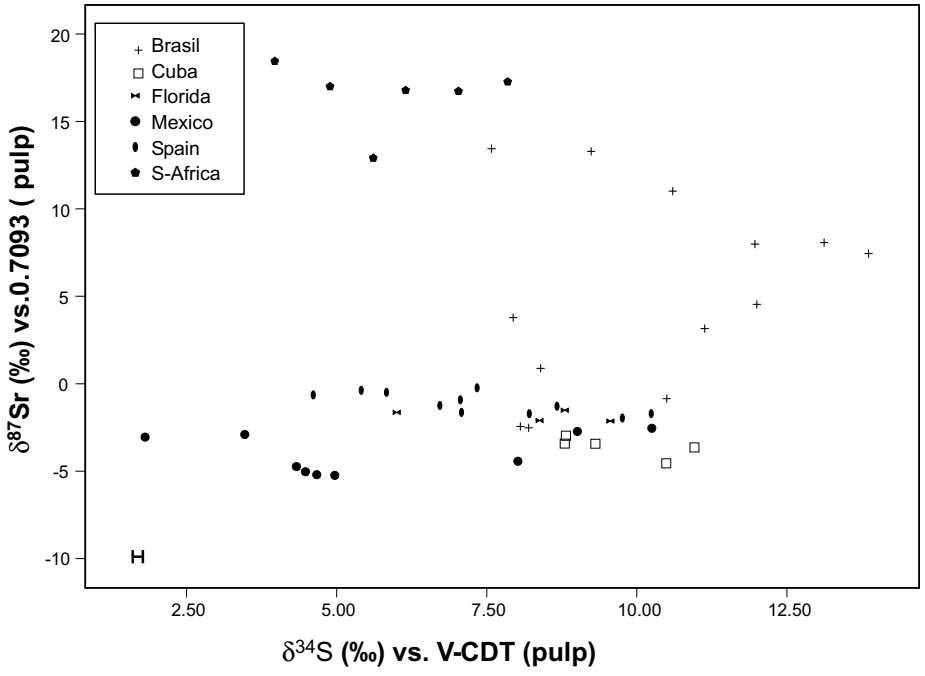

Fig. 4. δ^{87}Sr versus δ^{34}S in pulp of selected authentic orange juices. Vertical line indicates uncertainty range for δ^{34}S, uncertainty range for δ^{87}Sr is much smaller than the symbol-size.

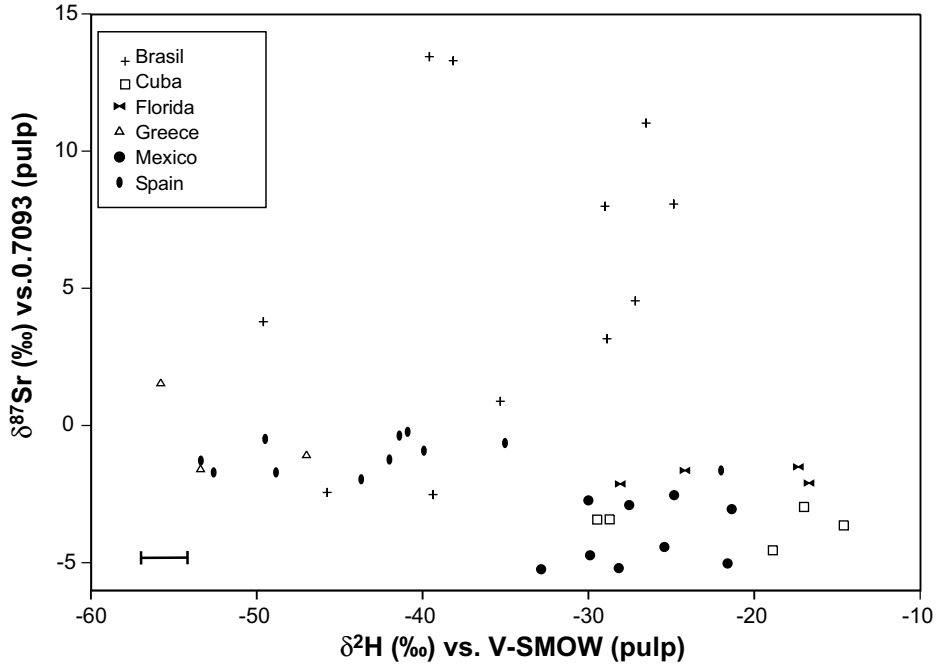

Fig. 5. $\delta^{87}Sr$ versus $\delta^{2}H$ in pulp of selected authentic orange juices. Vertical line indicates uncertainty range for $\delta^{2}H$, uncertainty range for $\delta^{87}Sr$ is much smaller than the symbol-size.

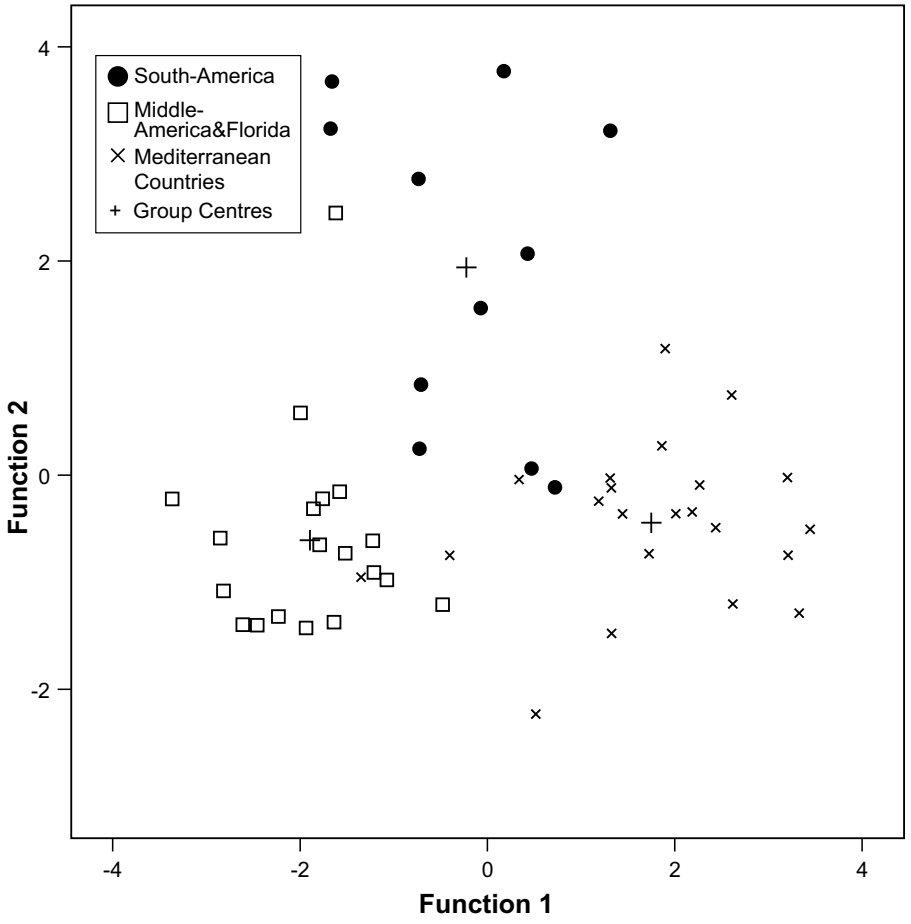

Fig. 6. Discriminant analysis for authentic orange juices samples worldwide. Employed variables are $\delta^{2}H$, $\delta^{13}C$, $\delta^{15}N$, $\delta^{34}S$, $\delta^{87}Sr$, all measured in pulp.

cium, e.g. as pectinate), remains unchanged. Therefore, it is still possible to detect such falsifications, basically using the pulp as "internal standard". However, it is only possible to quantify the amounts of added material when the concentrations of both components are known which is normally not the case. Statements about the different origins of the mixtures cannot definitely be made but sometimes be presumed if values of authentic samples are considered.

The potential of applying a multi-element approach is demonstrated in Figs. 4 and 5. Although it is sometimes possible to ascertain the geographic origin of a sample by considering only IR of one element, in most cases it is advisable or even necessary to take into account all mentioned isotopic parameters to come to an unambiguous conclusion. Additionally, it is relatively easy to falsify one parameter to pretend another origin but it is nearly impossible and – moreover – extremely costly to "adjust" several or all parameters isotopically.

For example, juices from Mexico and Cuba cannot be distinguished by means of Sr- but very well by considering S-isotopes (Fig. 4). Spanish samples can be clearly separated from Florida, Mexico and Cuba by combining $\delta^{87}Sr$ with $\delta^{2}H$ (Fig. 5) and Brazilian samples can be separated from Spanish samples – a common problem in routine – by applying a combination of $\delta^{87}Sr$, $\delta^{34}S$ and $\delta 2H$. Apart from South-African samples which can be separated from almost all others by only applying Sr-IR it can be clearly seen from the figures that an overlap between single origins exists to a certain degree. This limitation cannot be completely overcome but, however, this factor can be strongly minimised with increasing number of reference samples and by applying a multi-element-approach.

With increasing numbers of parameters evaluation and interpretation of data becomes more difficult. Therefore, we applied discriminant analysis where a classification of groups (=origins) is made which are defined by several variables (=IR). In a first step adequate parameters and discriminant functions have to be figured out which lead to a best possible separation within a data set of authentic samples. In a second step – which is not carried out here – unknown samples can be introduced in the model and are allocated to the most probable group (For further basics concerning multivariate statistics and discriminant analysis see Backhaus, Erichson, Plinke, & Weiber, 2006). Software used for statistical data evaluation here is SPSS 15.0 for windows.

A precondition for applying discriminant analysis is a homogeneous distribution of samples per group. As this is not given in our data set – on the one hand we have only one sample from Belize, on the other hand for some parameters we have over fifty samples from Italy – we split our data into three very broad groups: Mediterranean countries (Greece, Italy, Morocco, Spain), South-America (Argentina, Brazil, Paraguay, Uruguay) and Middle-America with Florida (Belize, Cuba, Mexico, Florida). Employed variables are $\delta^{2}H$, $\delta^{13}C$, $\delta^{15}N$ and $\delta^{87}Sr$, all of pulp. The result can be seen in Fig. 6. For function 1 $\delta^{2}H$ and for function 2 $\delta^{87}Sr$ proved to be the most discriminatory parameters. Function 1 accounts for 72.1%, function 2 for 27.9% of the variation. In the cross validation test, performed by the software for every sample (each sample is left out and treated as unknown), 88.5% are classified correctly.

This kind of evaluation can also be useful to distinguish between subgroups as it has been done within European regions (Fig. 7). In this case cross validation led to correct classification of 75% of the samples. Although we know that the number of sam-

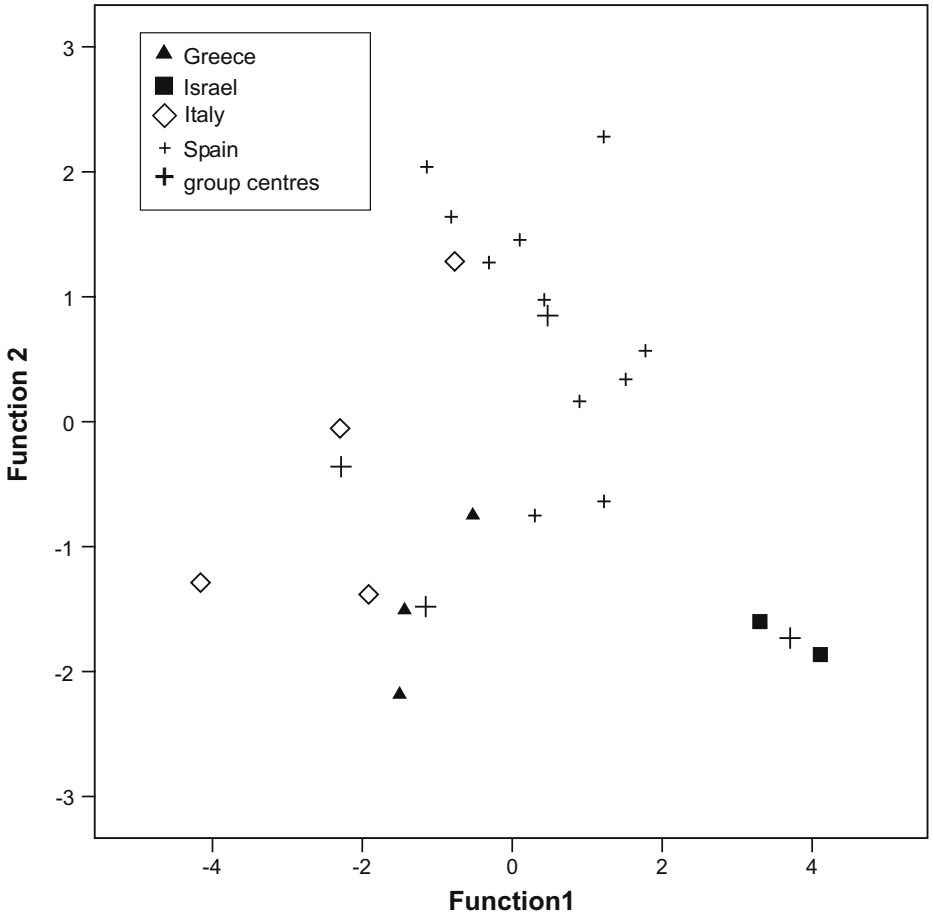

Fig. 7. Discriminant analysis for authentic Mediterranean orange juices samples. Employed variables are $\delta^{2}H$, $\delta^{13}C$, $\delta^{15}N$, $\delta^{34}S$, $\delta^{87}Sr$, all measured in pulp.

ples is much too low for an unambiguous classification, first results are looking very promising. A further improvement is expected with an increasing number of data.

However, discriminant analysis always has to be handled with care for these kind of investigations. No analytical uncertainties are taken into account and the addition of new authentic data might change the picture dramatically. Therefore, discriminant analysis provides a useful tool to get a rough idea about the provenance of a sample, but in order to avoid wrong conclusions it is essential to regard every sample individually e.g. in case of an expertise.

6. Conclusion

Within the presented project it could be clearly shown that both established and newly developed methods (i.e. sulphur- and strontium-isotope analysis as well as a combination of all investigated parameters) proved very useful for determination and verification of the geographical origin of orange juices. As in this study the regional distribution of the samples has been very patchy it is inevitable to extend the data set especially for regions which are very heterogeneous concerning climate and lithology or are relevant in practice, respectively (e.g. Brazil, Spain, Italy, etc.). Additionally, data of some important orange producers like e.g. India, China or Portugal are still missing. The collection and analysis of samples from these countries will be another future task to obtain a data set as complete as possible. It is also required to have a higher amount of authentic samples to improve further statistical evaluations.

Usually, it is not the task of the control institution to find out about the origin of the orange or the juice thereof – which would be much more difficult – but the laboratory has to confirm or to reject a declared origin. Often this problem can readily be solved by analysing the IR of the light elements. But in those cases where the results remain ambiguous strontium-isotope analysis should be performed additionally. Thus with the capability of combining several independent parameters a solid tool has been developed which allows a correct assignment of most samples.

Interpretation and evaluation of the data presented here base firstly on regional conditions influencing the isotopic parameter and secondly on results of authentic sample material. The next step would be the development of a model which allows predictions of isotope values for certain regions. This is currently done in another EU-project called TRACE. First results for different parameters have been achieved so far, e.g. for $^{87}Sr/^{86}Sr$ in mineral waters (Voerkelius et al., in preparation) or for stable IR in lamb meat (Camin et al., 2007). The planned extension to several further food commodities will be of great use also for problems concerning the origin of orange juices.

Acknowledgements

The authors would like to thank the European Union for funding and the Schutzgemeinschaft der Fruchtsaftindustrie (SGF), especially Dr. W. Rieth and Mr. K. Schulz for the coordination of the project "Pure Juice" (Projekt Nr. G6RD-CT-2002-00760). Additionally, we are grateful to two reviewers for very constructive remarks. S. Rummel would like to thank Stefan Gottschaller for careful proofreading.

References

Åberg, G. (1995). The use of natural strontium isotopes as tracers in environmental studies. *Water, Air and Soil Pollution, 79*, 309–322.

Backhaus, K., Erichson, B., Plinke, W., & Weiber, R. (2006). *Multivariate Analysemethoden. 11Auflage*. Berlin, Heidelberg: Springer.

Camin, F., Wiezterbin, K., Blanch Cortes, A., Haberhauer, G., Lees, M., & Versini, G. (2004). Application of multielement stable isotope ratio analysis to the characterization of French, Italian and Spanish cheeses. *Journal of Agricultural and Food Chemistry, 52*, 6592–6601.

Camin, F., Bontempo, L., Heinrich, K., Horacek, M., Kelly, S. D., Schlicht, C., et al. (2007). Multi-element (H, C, N, S) stable isotope characteristics of lamb from different European regions. *Analytical and Bioanalytical Chemistry, 389*, 309–320.

CEN prENV 13070, (1998). Fruit and vegetable juices – Determination of the stable carbon isotope ratio (13C/12C) in the pulp of fruit juices – Method using isotope ratio mass spectrometry. In: *CEN/TC 174 fruit and vegetable juices – methods of analysis*. European Committee for Standardization.

Christoph, N., Rossmann, A., & Voerkelius, S. (2003). Possibilities and limitations of wine authentication using stable isotope and meteorological data, data banks and statistical tests. Part 1: Wines from Franconia and Lake Constance 1992–2001. *Mitteilungen Klosterneuburg, 53*, 23–40.

Ehleringer, J. R., & Dawson, T. E. (1992). Water uptake by plants: perspectives from stable isotope composition. *Plant, Cell and Environment, 15*, 1073–1082.

Faure, G. (1986). *Principles of isotope geology* (2nd ed.). New York: John Wiley and Sons.

Fortunato, G., Mumic, K., Wunderli, S., Pillonel, L., Bosset, J. O., & Gremaud, G. (2004). Application of strontium IR measured by MC-ICP-MS for food authentication. *Journal of Analytical Atomic Spectrometry, 19*, 227–234.

Francey, R. J., & Farquhar, G. D. (1982). An explanation of $^{13}C/^{12}C$ variation in tree rings. *Nature, 297*, 28–31.

Franke, B. M., Koslitz, S., Micaux, F., Piantini, U., Maury, V., Pfammatter, E., et al. (2008). Tracing the geographic origin of poultry meat and dried beef with oxygen and strontium isotope ratios. *European Food Research and Technology, 226*, 761–769.

Heaton, K., Kelly, S. D., Hoogewerff, J., & Woolfe, M. (2008). Verifying the geographical origin of beef: The application of multi-element isotope and trace element analysis. *Food Chemistry, 107*(1), 506–515.

Horn, P. (2005). Isotopensignaturen schwerer Elemente in der ökologischen Forschung und Praxis. *Rundgespräche der Kommission für Ökologie, Bd. 30 "Auf Spurensuche in der Natur"*, 131–152.

Horn, P., Hölzl, S., Todt, W., & Matthies, D. (1998). Isotope abundance ratios of Sr in wine provenance determinations, in a tree-root activity study, and of Pb in a pollution study on tree rings. *Isotopes Environmental Health Studies, 34*, 31–42.

Horn, P., Schaaf, P., Holbach, B., Hölzl, S., & Eschnauer, H. (1993). 87Sr/86Sr from rock and soil into vine and wine. *Zeitschrift für Lebensmitteluntersuchung und-Forschung, 196*, 407–409.

Kelly, S., Heaton, K., & Hoogewerff, J. (2005). Tracing the geographical origin of food: The application of multi-element and multi-isotope analysis. *Trends in Food Science, 16*, 555–567.

Kelly, S., Baxter, M., Chapman, S., Rhodes, C., Dennis, J., & Brereton, P. (2002). The application of isotopic and elemental analysis to determine the geographical origin of premium long grain rice. *European Food Research and Technology, 214*, 72–78.

Kornexl, B. E., Werner, T., Rossmann, A., & Schmidt, H.-L. (1997). Measurement of stable isotope abundances in milk and milk ingredients — a possible tool for origin assignment and quality control. *Zeitschrift für Lebensmittel-Untersuchung und –Forschung A, 205*, 19–24.

Krouse, H. R., Stewart, J. W. B., Grinenko, V. A. (1991). Pedosphere and biosphere. In H. R. Krouse, J. W. B. Grinenko (Eds.), *SCOPE 43, Stable isotopes in the assessment of natural and anthropogenic sulphur in the environment* (pp. 267–306). John Wiley & Sons, Ltd.

Krueger, H. W., & Reesman, R. H. (1982). Carbon isotope analyses in food technology. *Mass Spectrometry Reviews, 1*, 205–236.

Larcher, R., Nicolini, G., & Pangrazzi, P. (2003). Isotope ratios of lead in Italian wines by inductively coupled plasma mass spectrometry. *Journal of Agricultural and Food Chemistry, 51*, 5956–5961.

Luo, Y.-H., & Sternberg, L. D. S. L. (1992). Hydrogen and oxygen isotopic fractionation during heterotrophic cellulose synthesis. *Journal of Experimental Botany, 43*(246), 47–50.

Martin, G. J., & Martin, M. L. (2003). Climatic significance of isotope ratios. *Phytochemistry Reviews, 2*, 179–190.

Monaghan, J. M., Scrimgeour, C. M., Stein, W. M., Zhao, W. M., & Evans, E. J. (1999). Sulphur accumulation and redistribution in wheat (*Triticum aestivum*): A study using stable sulphur isotope ratios as a tracer system. *Plant, Cell and Environment, 22*, 831–839.

Pichlmayer, F., Schöner, W., Seibert, P., Stichler, W., & Wagenbach, D. (1998). Stable isotope analysis for characterization of pollutants at high elevation alpine sites. *Atmospheric Environment, 32*(23), 4075–4085.

Pin, C., & Bassin, C. (1992). Evaluation of a strontium-specific extraction chromatographic method for isotopic analysis in geological materials. *Analytica Chimica Acta, 269*, 249–255.

Results of the Pure Juice Project, (2006). *SGF*. Nieder-Olm, Germany. www.sgf.org/de.

Rossmann, A., Haberhauer, G., Hölzl, S., Horn, P., Pichlmayer, F., & Voerkelius, S. (2000). The potential of multielement stable isotope analysis for regional assignment of butter. *European Food Research and Technology, 211*, 32–40.

Rossmann, A. (2001). Determination of stable isotope ratios in food analysis. *Food Reviews International, 17*(3), 347–381.

Rossmann, A., Rummel, S., Kupka, H.- J. (2003). L'apporto delle determinazione isotpiche innovative alla tracciabilità dei formaggi trentini (Innovative methods

of stable isotope analyses for Trentino cheese provenance determinations). In *Caratterizzazione di formaggi tipici dell'arco alpino: il contributo della ricerca. A cura di F. Gasperi e G. Versini* (pp. 143–153). San Michele all'Adige: Istituto Agrario di San Michele all'Adige, 2005.

Schmidt, H.-L., Rossmann, A., Rummel, S., Tanz, N. (in press). Stable isotope analysis for meat authenticity and origin check. In Nollet, L. M. L., Toldrá F.(Eds.), *Handbook of muscle food analysis.* Boca Raton, Florida, USA: CRC Press, Taylor and Francis Group, LLC.

Schmidt, H.-L., Rossmann, A., Stöckigt, D., & Christoph, N. (2005a). Stabilisotopenanalytik: Herkunft und Authentizität von Lebensmitteln. *Chemie in unserer Zeit, 39*, 90–99.

Schmidt, H.-L., Rossmann, A., Voerkelius, S., Schnitzler, W. H., Georgi, M., Grassmann, J., et al. (2005b). Isotope characteristics of vegetables and wheat from conventional and organic production. *Isotopes in Environmental and Health Studies, 41*(3), 223–228.

Schmidt, H.-L., Werner, R. A., & Eisenreich, W. (2003). Systematics of ^{2}H patterns in natural compounds and its importance for the elucidation of biosynthetic pathways. *Phytochemistry Reviews, 2*, 61–85.

Sieper, H.-P., Kupka, H.-J., Williams, T., Rossmann, A., Rummel, S., Tanz, N., et al. (2006). A measuring system for the fast simultaneous isotope ratio and elemental analysis of carbon, hydrogen, nitrogen and sulphide in food commodities and other biological material. *Rapid Communications in Mass Spectrometry, 20*, 2521–2527.

Thode, H. G. (1991). *Sulphur isotopes in nature and the environment: An overview. SCOPE 43. Stable isotopes in the assessment of natural and anthropogenic sulphur in the environment.* John Wiley & Sons Ltd. pp. 1–21.

Vitoria, L., Otero, N., Soler, A., & Canals, A. (2004). Fertilizer characterization: isotopic data (N, S, O, C and Sr). *Environmental Science and Technology, 38*, 3254–3262.

Voerkelius, S., Lorenz, G., Brach-Papa, C., Deters-Itzelsberger, P., Heiss, G., Hoelzl S., et al. (in preparation). Strontium isotope signatures of natural mineral waters, the reference to a simple geologic map and its potential for authentication of food. *Food Chemistry.*

Wahid, P. A. (2001). Radioisotope studies of root activity and root-level interactions in tree-based production systems: A review. *Applied Radiation and Isotopes, 54*, 715–736.

Wassenaar, L. I., & Hobson, K. A. (2003). Comparative equilibration and online techniques for determination of non-exchangeable hydrogen of keratin for use in animal migration studies. *Isotopes in Environmental and Health Studies, 39*(3), 211–217.

Angerosa et al., 1999) found that both the $^{13}C/^{12}C$ and $^{18}O/^{16}O$ of olive oils from Italy, Greece, Spain, Tunisia, Morocco and Turkey change according to the latitude, suggesting as co-factors of variability the distance from the sea and environmental conditions during the growing of plants (water stress, atmospheric moisture and temperature). Finally, Aramendia et al. (2007) observed that the $^{18}O/^{16}O$ values of bulk olive oils were influenced by the variety of the olives and by their geographical origin, but not by the altitude, ripening degree and harvesting date of olives. To our knowledge, no papers are available in the literature regarding the isotopic ratio of deuterium/hydrogen (D/H) in olive oil.

With regard to the mineral content of olive oil, interest initially focused on the presence of toxic lead or cadmium elements and of copper and nickel as catalysts for oxidative reactions affecting the flavour and stability of oils (De Souza et al., 2005). In the last few years, studies have also been carried out to verify whether the mineral profile could be a useful marker of geographical origin, cultivar, harvesting period and adulteration with cheaper vegetable oils (Benincasa, Lewis, Perri, Sindona, & Tagarelli, 2007; Cindric, Zeiner, & Steffan, 2007; Dugo, La Pera, Giuffrida, Salvo, & Lo Turco, 2004). The high organic load and viscosity and very small mineral content of olive oils were a handicap to the development of a simple and effective preparation method and subsequent analysis. Several approaches were used, such as emulsion in water with the aid of some surfactant or solvent (Anthemidis, Arvanitidis, & Stratis, 2005; Castillo, Jimenez, & Ebdon, 1999; De Souza et al., 2005; Jimenez, Velarte, & Castillo, 2003), liquid–liquid extraction (Dugo et al., 2004), wet ashing (Lo Coco et al., 2003) and total microwave digestion (Benincasa et al., 2007; Cindric et al., 2007; Zeiner, Steffan, & Cindric, 2005). Of the analytical techniques, the following were more frequently applied: electrothermal and graphite furnace atomic absorption spectrophotometry (Cindric et al., 2007; Dugo et al., 2004), derivative potentiometric stripping (Dugo et al., 2004; Lo Coco et al., 2003) and, increasingly in the last few years, inductively coupled plasma–optical emission spectrometry (Anthemidis et al., 2005; Zeiner et al., 2005; Cindric et al., 2007) and plasma–mass spectrometry (ICP–MS) (Benincasa et al., 2007; Castillo et al., 1999; Jimenez et al., 2003).

The present work focuses on the $^{13}C/^{12}C$ in bulk oil and extracted glycerol and $^{18}O/^{16}O$ in glycerol of 539 authentic PDO and PGI extra-virgin olive oils produced from 2000 to 2005 throughout Italy, sampled by the Ministry of Agricultural, Food and Forestry Policy and analysed to establish an yearly databank of isotopic reference values. This was done to evaluate the geographic authenticity of commercial samples, as has been done since 1987 for wine (EEC Reg. No. 2729/2000). Moreover, the mineral composition, the $^{18}O/^{16}O$ and, for the first time, the D/H in bulk oil of around one hundred 2005 extra-virgin olive oils are shown and discussed for their variability.

2. Materials and methods

2.1. Sampling

Authentic and well settled extra-virgin olive oils ($N = 539$) were officially collected by the Ministry of Agricultural, Food and Forestry Policy from 2000 to 2005 in the production regions of the only one PGI and the 34 out of 37 PDOs recognised at the present in Italy, according to the EC Reg. No. 510/2006. Traditionally, each PDO defines multi-varietal oils (e.g. PDO Chianti can include up to 76 varieties). The sampling tried to cover all the harvest time, the variability of the multi-varietal blends and the production area. $^{13}C/^{12}C$ in bulk olive oil and the extracted glycerol, as well as $^{18}O/^{16}O$ in the glycerol, were measured in 2000 ($N = 82$), 2001 (102), 2002 (66), 2003 (95), 2004 (58) and 2005 (136) samples. In 2005, measurement of the $^{18}O/^{16}O$ and D/H of bulk olive oil also took place. Finally, the mineral content of a selection of 99 samples of 2005 was measured.

2.2. Chemicals

2.2.1. Isotopes

All the solutions were prepared with Milli-Q water (18M Ωcm resistivity; Millipore, Bedford, MA). Sodium hydroxide 2N (RP grade; Carlo Erba Reagents, Milan, Italy), hydrochloric acid at 37% (RP; Carlo Erba Reagents), diethyl ether (Normapur; VWR International, Leuven, Belgium), ethanol at 96% (Sigma–Aldrich GmbH, Steinheim, Germany), tin and silver capsules (Säntis analytical AG, Teufen, Switzerland), P_2O_5 at 97% (Sigma–Aldrich GmbH) and nitrogen gas at 99.999% (Linde Gas, Milan, Italy) were used.

The isotopic values (expressed in $\delta‰$, as described below) were calculated against working in-house standards (commercial olive oil and glycerol), calibrated against international reference materials: fuel oil NBS-22 (IAEA-International Atomic Energy Agency, Vienna, Austria) and sugar IAEA-CH-6 (IAEA) for $^{13}C/^{12}C$ measurement; IAEA-CH-6 (IAEA) for $^{18}O/^{16}O$ and NBS-22 for D/H. Whereas in the past the data regarding $^{18}O/^{16}O$ in glycerol were usually calibrated against glycerol used in the European project SMT4-CT98-2236 (Camin et al., 2004), in this work they were calibrated against the IAEA-CH6 value ($\delta^{18}O = +36.4‰$ vs. V-SMOW) assigned since 2005 (Boschetti & Iacumin, 2005) and accepted in the European TRACE project (contract No. FP6-2003-FOOD-2-A 006942).

The isotopic values of the aforementioned international reference materials and therefore also of the samples were expressed in $\delta‰$ vs. V-PDB (Vienna - Pee Dee Belemnitella) for $\delta^{13}C$ and V-SMOW (Vienna – standard mean ocean water) for $\delta^{18}O$ and δD, according to the following formula: $[(Rs-Rstd)/Rstd] \times 1000$, where Rs is the isotope ratio measured for the sample and Rstd is the isotope ratio of the international standard.

2.2.2. Elements

Nitric acid at 69.5% (Superpure; Merck, Darmastadt, Germany), hydrochloric acid at 37% (ACS; Riedel-deHaën, Seelze, Germany), ICP Multielement Standard Solution VI (Merck), Multielement Calibration Standard 1 (Agilent Technologies, Santa Clara, CA, USA), and Cesium 1000 ug/ml (Ultra Scientific, Bologna, Italy) were used. Standard solutions were diluted and stabilized with the addition of a 1% HNO_3 and 0.2% HCl solution. SRM 2387 'Peanut butter' (National Institute of Standard and Technologies, Gaithersburg, MD, USA) was used as standard reference material to check the accuracy of the method. Sc 0.1 mg/L, Rh 0.1 mg/L and Tb 0.1 mg/L were used as internal standards. All the glassware was rinsed with nitric acid (5% v/v) and twice with milli-Q water before use.

2.3. Apparatus

2.3.1. Isotopes

The analysis was performed using an isotopic ratio mass spectrometer (IRMS) (Finnigan DELTA XP, Thermo Scientific, Bremen, Germany) coupled with an Elemental Analyser (Flash EA^{TM}1112, Thermo Scientific,) for $^{13}C/^{12}C$ measurement and with a Pyrolyser (Finnigan^{TM}TC/EA, high temperature conversion elemental analyzer, Thermo Scientific,) for D/H and $^{18}O/^{16}O$ measurement. To separate the gases, the Elemental Analyser was supplied with a Porapack QS (3 m; 6 × 4 mm, OD/ID) GC column and the Pyrolyser with a Molecular Sieve 5A (0.6 m) GC column. The devices were equipped with an autosampler (Finnigan AS 200, Thermo Scientific)

and interfaced with the IRMS through a dilutor (Conflo III, Thermo Scientific) dosing the sample and reference gases.

2.3.2. Elements

The analysis was performed using an Agilent 7500ce ICP–MS (Agilent Technologies, Tokyo, Japan) equipped with an autosampler ASX-520 (Cetac Technologies Inc., Omaha, NE, USA). After extraction, the samples were introduced into a Scott spray chamber using a MicroMist nebulizer and then into a Fassel type torch. An octopole reaction system (ORS) using He and H_2 as collision and reaction gases, respectively, was used to remove polyatomic interferences.

2.4. Sample preparation and analysis

2.4.1. Isotopes

Glycerol was obtained through hydrolysis of 20 ml of oil in NaOH, acidification of the solution, extraction of fatty acids and purification by under vacuum distillation, according to the method described for fat from cheese in Camin et al. (2004).

Aliquots of 0.3 mg of sample were weighed in tin capsules for determination of $^{13}C/^{12}C$ and silver capsules for quantification of $^{18}O/^{16}O$ and $^{2}H/^{1}H$.

For $^{13}C/^{12}C$, the precision of measurement, expressed as standard deviation when measuring an oil sample 10 times, was 0.1‰.

For $^{18}O/^{16}O$ and D/H analysis, the samples were stored in a desiccator above P_2O_5 for at least 24 h, then weighed into silver capsules and put into the auto-sampler equipped with a suitable cover. During measurement, dryness was guaranteed by flushing nitrogen continuously over the samples. The pyrolyser temperature was 1450 °C. The D/H and $^{18}O/^{16}O$ ratios of bulk olive oils were measured simultaneously in one run. The IRMS measured first D/H and then, following the magnet jump, $^{18}O/^{16}O$, taking about 10 min for each sample. Before measuring D/H, the H3 factor, which allows correction of the contribution of [H3]+ to the m/z 3 signal (Sessions, Burgoyne, & Hayes, 2001), was verified to be lower than 9. The precision of measurement, expressed as standard deviation when measuring an oil sample 10 times, was 0.3‰ for $^{18}O/^{16}O$ and 2‰ for D/H.

2.4.2. Elements

About 15 g of sample were weighed into a 50 ml conical vial of polypropylene (PP) and 15 ml of 1% HNO_3/0.2% HCl water solution was added. The mixture was thoroughly shaken for 30 s using a vortex mixer and immediately placed in an ultrasonic bath (170 W × 5 min) to extract the trace elements from the oil to the acid solution. The mixture was centrifuged (4000 rpm × 5 min) to separate the two phases. The upper oil phase was accurately removed by aspiration and the lower aqueous phase transferred into a clean PP vial and subjected to ICP–MS analysis of Li, B, Na, Mg, K, Ca, Mn, Co, Cu, Ga, Se, Rb, Sr, Mo, Cd, Cs, Ba, La, Ce, Nd, Sm, Eu, Yb, Tl, Pb, and U. Isotopes and ORS gases are shown in Table 1. Extraction and analysis was carried out in duplicate. The accuracy of the extraction method was evaluated in a natural oil sample spiked with a defined aliquot of the reference material (0.6 g of 'semi-solid' peanut butter mixed into 15 g of oil until thoroughly combined). The oil and fortified mixture were both extracted and analysed 10 times. Recoveries were calculated on the difference of the mean content of the spiked and the un-spiked samples. The detection limit (DL) of each element was calculated as three times the standard deviation of the signal of the blank sample, extracted and analysed ten times, whereas the blank sample was prepared using Milli-Q water to substitute the oil sample in the extraction step. Precision (RSD%) was evaluated by preparing and analyzing an oil sample 10 times. DL and RSD% are shown in Table 1.

Table 1
Instrumental conditions and mineral content distribution of well settled extra-virgin Italian olive oils (ORS: collision cell octopole reaction system)

Element	Isotope	ORS mode	Unit	DL	Number of Samples > DL	RSD (%)	25° Percentage	Median	75° Percentage	90° Percentage	Maximum	Range (Minimum–Maximum)	Literature
Li	7	–	μg/kg	0.005	56	18	–	0.007	0.013	0.023	0.208	–	–
Na	23	He	mg/kg	0.04	42	27	–	–	0.100	0.211	1.105	28.8–38.0	d,n
Mg	26	He	mg/kg	0.014	62	20	–	0.019	0.055	0.109	0.495	0.056–3.8	d,f,g
K	39	He	mg/kg	0.06	68	20	–	0.163	0.645	1.702	9.94	< 0.001–0.19	d,n
Ca	40	H_2	mg/kg	0.03	12	16	–	–	–	0.380	0.950	< 0.05–26.9	a, b, d,n
Mn	55	–	μg/kg	0.01	60	21	–	0.211	0.630	1.43	10.0	< 1–200	a, b, c, d, f, m, n
Co	59	–	μg/kg	0.004	20	13	–	–	–	0.012	0.033	0.023–5450	a, b, c, d, f, m, n
Cu	63	He	μg/kg	0.13	88	21	0,237	0.360	0.689	1.45	26.3	< 1–4510	a, c, d, f, g, h, l, m, n
Rb	85	–	μg/kg	0.03	83	21	0,041	0.110	0.375	1.03	13.4	–	–
Sr	88	–	μg/kg	0.04	15	17	–	–	–	0.483	3.85	1.52–48.9	b
Cs	133	–	μg/kg	0.003	67	20	–	0.004	0.005	0.012	0.819	–	–
Ba	137	–	μg/kg	0.29	22	21	–	–	–	0.543	2.49	< 0.15–700	a, c, g
La	139	–	μg/kg	0.0017	46	24	–	–	0.006	0.040	2.94	–	–
Ce	140	–	μg/kg	0.0027	50	24	–	0.003	0.008	0.046	4.72	–	–
Sm	147	–	μg/kg	0.0009	27	24	–	–	0.001	0.004	0.111	0.004–0.226	i
Eu	151	He	μg/kg	0.0002	39	20	–	–	0.001	0.002	0.023	< 0.009–0.021	b
Yb	171	–	μg/kg	0.0004	61	20	–	0.001	0.001	0.002	0.041	–	–
Pb	208	–	μg/kg	0.02	80	21	0,195	0.372	0.725	1.50	8.46	< 0.42–79.9	a, c, d, f, g, h, l, m, n
U	238	–	μg/kg	0.001	67	18	–	0.001	0.007	0.015	0.119	<0.25	c

a: Anthemidis et al. (2005); b: Benincasa et al. (2007); c: Castillo et al. (1999); d: Cindric et al. (2007); e: Dugo et al. (2004); f: Jimenez et al. (2003); g: La Pera et al. (2002); h: Lo Coco et al. (2000); i: Lo Coco et al. (2003); l: Martin-Polvillo et al. (1994); m: Solinas et al. (1987); n: Zeiner et al. (2005).

Table 2
Median, minimum and maximum values of $\delta^{13}C$ (bulk olive oil and glycerol) and of $\delta^{18}O$ values of glycerol (‰ vs. V-PDB and V-SMOW, respectively) in the Italian olive oil databank (2000–2004) and results of the non-parametric statistical test (Kruskall–Wallis' test) among crops

Region	N_{tot}	Parameter	2000				2001				2002				2003				2004			
			N	Median	Minimum	Maximum	*N*	Median	Minimum	Maximum	*N*	Median	Minimum	Maximum	*N*	Median	Minimum	Maximum	*N*	Median	Minimum	Maximum
Trentino	37	$\delta^{13}C$ bulk	5	−30.7	−31.8	−29.7	23	−30.7	−32.4	−30.1	3	−29.7	−30.4	−29.7	3	−29.5	−29.5	−29.4	3	−30.7	−30.8	−30.4
		$\delta^{13}C$ glycerol		−33.6	−34.7	−32.7		−33.5	−34.6	−32.7		−32.8	−33.3	−31.8		−32.2	−32.4	−31.9		−33.4	−33.5	−33.2
		$\delta^{18}O$ glycerol		29.2	27.8	29.2		29.1	28.0	30.5		29.3	28.5	30.2		30.9	30.8	32.4		29.3	29.2	29.3
Veneto	20	$\delta^{13}C$ bulk	3	−30.3	−30.9	−30.3	3	−30.3	−30.7	−30.3	3	−31.1	−31.2	−30.7	5	−28.8	−29.0	−27.5	6	−30.1	−31.4	−29.0
		$\delta^{13}C$ glycerol		−32.4	−33.9	−32.3		−32.5	−32.6	−32.1		−32.6	−33.3	−32.0		−31.5	−31.8	−29.2		−32.0	−33.5	−31.0
		$\delta^{18}O$ glycerol		31.3	29.1	31.7		29.8	29.5	30.8		28.9	28.0	30.3		32.7	30.2	33.1		30.6	29.7	33.1
Lombardia	16	$\delta^{13}C$ bulk	4	−30.3	−30.6	−29.9	3	−30.4	−30.6	−30.3					5	−29.1	−29.3	−28.6	4	−31.0	−31.4	−29.4
		$\delta^{13}C$ glycerol		−32.5	−33.6	−32.1		−32.2	−32.3	−31.9						−30.7	−31.3	−29.8		−32.8	−33.1	−31.7
		$\delta^{18}O$ glycerol		30.2	28.1	31.3		29.8	29.7	30.1						31.5	31.3	32.1		30.3	29.6	33.2
Emilia-	13	$\delta^{13}C$ bulk	2	−29.2			3	−29.6	−29.8	−29.4	2	−30.0			6	−29.1	−29.3	−28.7				
Romagna		$\delta^{13}C$ glycerol		−31.6				−31.6	−31.6	−31.3		−32.3				−31.2	−31.7	−30.7				
		$\delta^{18}O$ glycerol		29.7				29.8	29.1	30.1		29.7			31.1	30.9	32.4					
Liguria	18	$\delta^{13}C$ bulk	3	−30.3	−30.6	−30.1	3	−29.7	−30.0	−29.1	3	−30.3	−30.5	−29.6	6	−28.8	−29.1	−28.2	3	−30.0	−30.2	−29.6
		$\delta^{13}C$ glycerol		−33.3	−33.4	−33.1		−32.2	−32.7	−31.7		−32.7	−33.3	−32.6		−31.1	−31.7	−30.9		−33.1	−33.1	−32.6
		$\delta^{18}O$ glycerol		31.3	31.1	31.3		31.8	31.6	33.2		29.8	29.5	29.9		32.3	31.5	32.6		31.4	30.4	32.0
Tuscany	23	$\delta^{13}C$ bulk	5	−29.3	−30.0	−28.3	6	−29.3	−30.3	−29.0	9	−30.4	−30.8	−29.9	3	−28.7	−29.5	−27.9				
		$\delta^{13}C$ glycerol		−31.0	−32.3	−30.2		−31.3	−32.1	−30.9		−32.5	−33.3	−31.4		−31.4	−31.7	−30.5				
		$\delta^{18}O$ glycerol		32.9	30.9	34.2		31.0	30.2	31.8		31.2	28.4	33.1		31.9	31.6	32.8				
Umbria	30	$\delta^{13}C$ bulk	4	−29.3	−29.5	−29.2	15	−29.4	−30.0	−28.1					11	−28.9	−29.5	−28.3				
		$\delta^{13}C$ glycerol		−30.1	−31.4	−29.7		−30.9	−32.0	−29.6						−30.6	−31.7	−29.8				
		$\delta^{18}O$ glycerol		31.8	30.5	33.7		32.1	30.0	33.4						32.6	31.4	33.4				
Abruzzo	30	$\delta^{13}C$ bulk	10	−28.7	−29.7	−28.1					6	−29.4	−30.1	−29.0	8	−28.3	−28.5	−28.1	6	−29.1	−30.0	−28.4
		$\delta^{13}C$ glycerol		−30.4	−31.3	−28.8						−30.8	−31.5	−29.9		−29.8	−30.1	−29.7		−31.0	−31.8	−30.3
		$\delta^{18}O$ glycerol		32.9	31.1	34.1						31.6	30.6	32.2		33.4	33.2	33.5		32.6	31.2	33.3
Lazio	50	$\delta^{13}C$ bulk	10	−29.2	−30.3	−28.1	12	−28.8	−29.5	−28.0	12	−30.1	−31.1	−29.6	12	−28.6	−29.3	−27.8	4	−29.3	−29.9	−28.9
		$\delta^{13}C$ glycerol		−30.7	−32.1	−28.5		−30.3	−31.2	−28.9		−31.1	−32.8	−29.6		−29.8	−31.3	−28.4		−31.0	−31.7	−30.3
		$\delta^{18}O$ glycerol		33.3	31.8	33.5		32.8	30.6	33.5		31.6	29.9	33.3		33.0	32.4	33.4		32.5	32.2	32.9
Campania	35	$\delta^{13}C$ bulk	9	−29.4	−29.7	−27.5	9	−28.2	−29.3	−27.4	9	−30.0	−30.8	−28.9	6	−28.5	−29.5	−27.9	2	−28.8	−29.0	−28.6
		$\delta^{13}C$ glycerol		−31.5	−32.5	−30.0		−30.4	−31.1	−29.8		−31.7	−33.5	−29.7		−30.5	−31.5	−29.7		−30.8	−31.1	−30.5
		$\delta^{18}O$ glycerol		33.3	31.9	34.4		33.0	31.2	34.3		31.2	27.6	31.9		33.1	31.2	33.9		32.0	31.7	32.3
Apulia	55	$\delta^{13}C$ bulk	18	−29.2	−30.4	−28.2	22	−28.9	−30.0	−26.6	5	−30.6	−30.8	−30.0					10	−29.6	−30.6	−28.5
		$\delta^{13}C$ glycerol		−31.4	−32.3	−29.9		−30.8	−31.8	−29.3		−32.1	−34.4	−32.0	00					−31.8	−33.0	−30.7
		$\delta^{18}O$ glycerol		31.7	30.3	35.7		31.9	31.1	34.2		31.0	29.8	31.7						31.9	30.5	32.6
Calabria	24	$\delta^{13}C$ bulk									8	−29.8	−31.3	−28.3	9	−29.4	−30.1	−28.8	7	−29.2	−30.2	−29.0
		$\delta^{13}C$ glycerol										−31.0	−32.0	−29.9		−30.5	−31.1	−30.2		−31.0	−31.3	−30.4
		$\delta^{18}O$ glycerol										32.9	30.7	34.1		33.5	31.3	34.8		34.8	32.5	35.6
Sicily	52	$\delta^{13}C$ bulk	9	−28.4	−28.7	−28.0	3	−28.3	−28.5	−27.0	6	−28.5	−29.4	−27.7	21	−28.8	−30.0	−27.7	13	−29.1	−29.8	−28.0
		$\delta^{13}C$ glycerol		−30.4	−31.4	−29.3		−29.3	−29.4	−28.4		−29.5	−31.8	−28.8		−30.2	−31.5	−29.0		−30.6	−31.8	−29.1
		$\delta^{18}O$ glycerol		35.5	32.5	36.2		33.9	33.4	35.1		33.7	33.1	34.8		33.0	30.6	35.0		34.2	32.4	34.6
Total	403	$\delta^{13}C$ bulk	82	-29.3^{ab}	−31.8	−27.5	102	-29.2^{ab}	−32.4	−26.6	66	-30.0^{c}	−31.3	−27.7	95	-28.9^{a}	−30.1	−27.5	58	-29.4^{bc}	−31.4	−28.0
		$\delta^{13}C$ glycerol		-31.2^{b}	−34.7	−28.5		-31.2^{b}	−34.6	−28.4		-31.7^{b}	−34.4	−28.8		-30.6^{a}	−32.4	−28.4		-31.3^{b}	−33.5	−29.1
		$\delta^{18}O$ glycerol		30.0^{ab}	25.2	33.6		29.0^{b}	25.4	32.5		28.7^{b}	25.0	32.2		30.1^{a}	27.6	32.4		29.7^{ab}	26.7	33.1

Different letters correspond to significantly different median values ($p < 0.001$) *N* = number of samples.

2.5. Statistical analysis

The data were statistically evaluated according to the procedures of the software Statistica 7.1 (StatSoft Italia srl, Padua, Italy). Non parametric tests (Kruskall–Wallis and multiple bilateral comparison) were applied because of the low and unequal numbers of samples per group and the not always normal distribution (Soliani, 2003).

3. Results and discussion

3.1. Stable isotope ratios

In Table 2 the median, minimum and maximum values of bulk and glycerol $\delta^{13}C$ and of glycerol $\delta^{18}O$ were summarised for 2000–2004 production and the different Italian regions listed according to the latitude. $\delta^{18}O$ was measured in the glycerol instead of in the bulk oil because the former was assumed to be more closely related to the isotopic characteristics of ground water (Schmidt, Werner, & Rossmann, 2001).

The $\delta^{13}C$ values measured in glycerol were always lower than in bulk olive oil, with a mean difference ± standard deviation of 1.87 ± 0.67, confirming previous results (Zhang, Buddrus, Trierweiler, & Martin, 1998). Moreover, $\delta^{13}C_{glycerol}$ and $\delta^{13}C_{bulk}$ of the 403 samples were significantly correlated ($\delta^{13}C_{glycerol} = 1.1114 \times \delta^{13}C_{bulk} + 1.4057$; $p < 0.001$). If we consider 2000, 2001, 2002 and 2004 individually, the intercepts ranged from −0.3075 to +6.3585 and the slopes from 1.0435 to 1.2841. The correlation for 2003, also significant, showed particular and extreme values, both as regards intercept (−7.0134) and slope (0.8162).

Significant differences ($p < 0.001$) were found among the years of harvest (Table 2). In particular 2003, well-known as one of the hottest years in the last few decades in Italy, was different ($p < 0.001$) for at least one isotopic parameter from all the other years, showing enrichment in the heavier isotopomeres.

All the isotopic parameters showed a trend for the values to increase from Trentino to Sicily in all years (Table 2), with this being less evident in 2003. This trend, already observed in wine (Rossmann et al., 1996; Rossmann et al., 1999), is probably positively related to vicinity to the sea and dryness of the climate and negatively to latitude, as suggested by some authors (Angerosa et al., 1999; Bréas et al., 1998). Indeed, the $\delta^{13}C$ values of plant compounds are influenced by the availability of water, relative humidity and temperature, which control stomatal aperture and the internal CO_2 concentration in the leaf (O'Leary, 1995). The $\delta^{18}O$ of carbohydrates and their immediate descendants, such as glycerol, is correlated to the $\delta^{18}O$ of leaf water (Schmidt et al., 2001), which reflects the isotopic composition of groundwater and average precipitation in the region – mainly related to latitude, distance from the sea and altitude (Clark & Fritz, 1997) – and the extent of evapotranspiration, mainly influenced by humidity and temperature (Rossmann et al., 1999).

For statistical evaluation, we grouped the regions into four clusters on the basis of their latitude and the similarity of their isotopic ratios: North (Trentino, Veneto, Lombardia, Emilia Romagna), Centre (Liguria, Tuscany, Umbria, Abruzzo, Lazio), South-1 (Campania, Apulia) and South-2 (Calabria, Sicily). Applying the non parametric test of Kruskall–Wallis (Fig. 1), olive oil from Northern Italy showed isotopic values for at least one parameter significantly lower ($p < 0.01$) than for the South-2, Centre and South-1 in 5, 3 and 2 years respectively, out of the 5 years. Central Italy was never separated from South-1, whereas it was different from South-2 in two out of 5 years. The two southern macro areas could be distinguished from one another in three out of 5 years.

Comparing the few PDOs with at least five samples within each region and each year, we observed some significant differences ($p < 0.01$). In Lazio, the two 'Canino' and 'Sabina' PDOs were significantly different in 2000, 2002 and 2003 for $\delta^{13}C$ and in 2001 for $\delta^{18}O$. This could be ascribed to the inland location of the production area of 'Sabina', nearer Rieti than the 'Canino' area, closer to the sea near Tuscany, as well as to the possible effect of the prevailing olive cultivar (Aramendia et al., 2007). In Abruzzo and Apulia the comparison was only possible for one year (2000 and 2001, respectively). Significant differences in the $\delta^{13}C$ values were observed between 'Aprutino Pescarese' and 'Colline Teatine' in Abruzzo and between 'Dauno' and 'Collina di Brindisi' in Apulia.

For the 2005 samples, along with the aforementioned parameters, the $\delta^{18}O$ and δD in bulk oil were also measured (Table 3). δD was investigated as a possible additional parameter for the

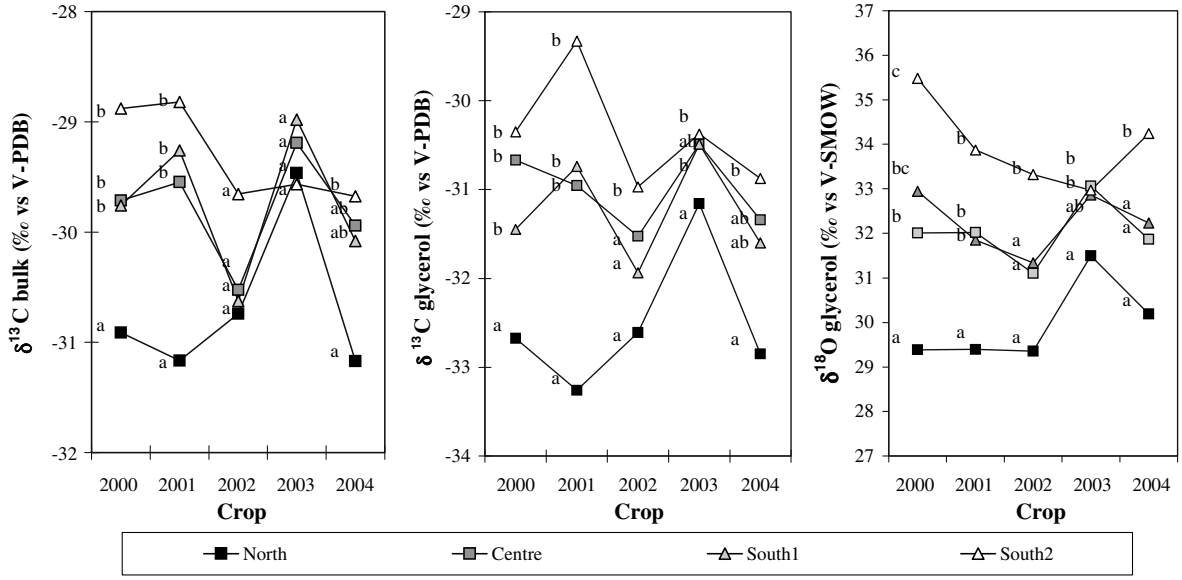

Fig. 1. Median values of the $\delta^{13}C$ (bulk olive oil and glycerol) and the $\delta^{18}O$ (glycerol) for North, Centre, South-1 and South-2 Italian olive oils (2000–2004) and results of the non-parametric statistical test (Kruskall–Wallis' test) among North, Centre, South-1 and South-2 Italian olive oils; different letters correspond to significantly different median values ($p < 0.01$).

Table 3
Median values of $\delta^{13}C$ (bulk olive oil and glycerol), $\delta^{18}O$ (bulk and glycerol) and 8D (bulk oil) for North, Centre, South-1 and South-2 Italian olive oils produced in 2005 and results of the non-parametric statistical test (KruskalWallis' test)

	N	$\delta^{13}C$ bulk (‰ vs. V-PDB)			$\delta^{13}C$ glycerol (‰ vs. V-PDB)			$\delta^{18}O$ glycerol (‰ vs. V-SMOW)			$\delta^{18}O$ bulk (‰ vs. V-SMOW)			$\delta^{2}H$ bulk (‰ vs. V-SMOW)		
		Median	Minimum	Maximum	Median	Minimum	Maximum	Median	Minimum	Maximum	Median	Minimum	Maximum	Median	Minimum	Maximum
North	45	-30.9^{a}	−31.9	−29.8	-33.9^{a}	−35.0	−32.0	28.0^{a}	26.9	31.0	20.2^{a}	19.1	22.4	-159^{a}	−165	−145
Centre	45	-30.1^{b}	−30.9	−29.0	-32.3^{b}	−33.5	−30.6	30.5^{b}	28.9	32.3	22.3^{b}	20.3	23.7	-153^{b}	−162	−142
South-1	19	-29.6^{bc}	−30.9	−29.2	-32.0^{b}	−33.3	−31.0	30.1^{b}	29.6	31.6	22.2^{b}	21.8	23.1	-149^{bc}	−156	−140
South-2	27	-29.2^{c}	−30.9	−27.9	-31.0^{c}	−32.5	−28.9	32.8^{c}	30.6	35.7	24.5^{c}	22.8	26.8	-148^{c}	−155	−137

Different letters correspond to significantly different median values $p < 0.01$.

characterisation of geographical origin, being influenced in plant products by the isotopic composition of the primary hydrogen source (source water through the leaf water) and by the geographical and climatic factors mentioned above for $\delta^{18}O$, together with their biosynthetic pathways (Schmidt, Werner, & Eisenreich, 2003).

As compared to previous years (Fig. 1), the median values of the isotopic parameters were lower, as a consequence of the rainy and cold climate characterising 2005.

The $\delta^{18}O$ values measured in bulk were significantly correlated with those in glycerol ($p < 0.001$): $\delta^{18}O_{bulk} = 0.837 * \delta^{18}O_{glycerol} - 3.2213$ ($R^2 = 0.8772$), the first always being lower, with a mean difference ± standard deviation of 8.15‰ ± 0.66.

The $\delta^{18}O$ and δD values in bulk olive oil were also correlated ($p < 0{,}001$), as happens in water (Clark & Fritz, 1997); the correlation equation is $\delta^{2}H_{bulk} = (-208{,}1 + 2{,}5091) \times \delta^{18}O_{bulk}$, but the R^2 value (0.4582) is low.

The $\delta^{18}O$ values of bulk olive oil showed the same capability as the $\delta^{18}O$ of glycerol in terms of distinguishing the four regional groups. The δD values showed similar capability to that of $\delta^{13}C$ and $\delta^{18}O$ to differentiate the four groups.

3.2. Mineral composition

The recoveries of the extraction method evaluated with the NIST sample were generally satisfactory for all the certified elements, being 82% for Zn, 84% for Mn, 90% for Ca, 92% for Mg, 95% for K, and 101 for Na. The precision of the analytical method ranged from 13% to 27% for the different elements (Table 1). Such values can be deemed satisfactory, considering the very low content of elements in olive oil.

Tables 1 and 4 show the concentration of the elements quantifiable over the DL in at least 10 samples. The content of Mo, Cd and Tl were below the respective DLs (0.18, 0.02 and 0.005 μg/kg respectively) in all the samples. Ga was found in quantifiable amounts (DL = 0.004 μg/kg) only in one Terra di Bari PDO oil (0.023 μg/kg). B was found in measurable amounts (DL = 1 μg/kg) only in five samples, with a maximum of 12.2 μg/kg for a Monte Etna PDO oil, in agreement with the results shown by Eschnauer for wines from grapes grown in volcanic areas (Eschnauer, 1982). Se was only detectable (DL = 0.014 μg/kg) in seven samples, with a maximum of 0.021 μg/kg, far below the content reported by Dugo et al. (2004), for 50 Sicilian oils analysed using cathodic stripping potentiometry and by Benincasa et al. (2007) for 36 oils from 4 Central–Southern Italian regions digested by microwave and analysed using ICP–MS. Nd was only quantifiable (DL = 0.023 μg/kg) in nine samples, with a maximum value of 0.932 μg/kg in a Terra di Bari PDO oil.

Tables 1 and 4 show the distribution of the mineral element content in the total sampling and for each PDO. As regards the content of Li, Rb, Cs, La, Ce and Yb shown in Table 1, we could not find other data for extra-virgin olive oils in the literature, while Mg, Ca, Mn, Sr, Sm, Eu and U were found in the concentration ranges reported in the literature. Na and K were measured in notably lower and higher amounts respectively, as compared to olive oils from Croatia analysed by Zeiner et al. (2005), and Cindric et al. (2007). The Co and Cu content were also in the ranges reported in literature, with the exclusion of the maximum values found for some of the aforementioned Croatian oils. The Ba content agreed with that found by Jimenez et al. (2003), and Anthemidis et al. (2005), but was far below the maximum content (700 μg/kg) measured by Castillo et al. (1999), using a semi-quantitative ICP–MS approach with direct emulsion nebulisation of the oil sample. The Pb content was low and always below the legal limits (0.1 mg/kg, EEC Reg. No. 466/2001), probably as a consequence of the increasingly widespread use of adequate equipment throughout the olive oil processing chain.

Table 4
Mineral content of well settled 2005 extra-virgin Italian olive oils displayed for region and for PDO or PGI

		Region	South Italy										Centre Italy					North Italy	
			Calabria			Apulia	Sicily						Lazio		Tuscany		Umbria	Veneto	Trentino - Veneto
		PDO/ PGI	Alto Crotonese	Bruzio	Lametia	Terra diBari	Monte Etna	Monti Iblei	Val Demone	Valdi Mazara	Valli del Belice	Valli Trapanesi	Canino	Sabina	Lucca	Toscano PGI	Umbria	Veneto	Garda
Element	Unit	No. Obs.	3	2	3	10	3	3	3	3	3	3	6	6	3	3	12	7	26
Li	μg/kg	median		0.003	0.010	0.007	0.031	0.013		0.011	0.007	0.008	0.004		0.006	0.006		0.016	0.003
		max	0.010	0.006	0.013	0.039	0.208	0.046	0.008	0.013	0.007	0.010	0.018	0.012	0.014	0.007	0.029	0.064	0.091
Na	mg/kg	median			0.049		0.280	0.189	0.066				0.069			0.060		0.154	
		max	0.124		0.100	0.170	1.11	0.492	0.161	0.129		0.052	0.326	0.124		0.133	0.340	0.609	0.312
Mg	mg/kg	median				0.042	0.082	0.087	0.015	0.047	0.016		0.031			0.034		0.050	0.046
		max	0.016		0.017	0.225	0.495	0.139	0.017	0.081	0.017	0.016	0.110	0.056		0.047	0.053	0.104	0.264
K	mg/kg	median		0.038	0.180	0.415	0.726	1.171	0.116	0.418	0.079		0.033			0.292	0.109	0.424	0.516
		max	0.32	0.08	0.22	3.79	9.94	1.70	0.17	0.90	0.10	0.12	0.56	1.13	0.12	0.43	0.64	2.06	3.13
Ca	mg/kg	median																	
		max				0.395	0.447	0.603											0.950
Mn	μg/kg	median			0.408	0.598	0.491	0.351		0.134			0.312	0.058		0.921		0.392	0.507
		max			0.566	10.0	3.42	1.21		0.522			3.61	0.655	0.173	1.17	0.623	1.49	2.87
Co	μg/kg	median				0.003	0.006												
		max				0.033	0.024	0.030		0.009				0.005	0.014		0.030	0.012	0.031
Cu	μg/kg	median	0.160	0.334	0.343	0.404	2.107	0.446	0.360	0.434	0.311	0.171	0.251	0.127	0.416	0.324	0.258	0.583	0.493
	μg/kg	max	0.237	0.363	0.952	2.37	15.8	1.47	0.689	0.472	0.885	0.430	0.663	0.824	0.778	0.355	0.810	1.72	26.3
Rb	μg/kg	median		0.040	0.108	0.394	0.199	0.628	0.040	0.178	0.060	0.036	0.237	0.173		0.214	0.058	0.336	0.183
		max	0.263	0.049	0.175	4.19	13.4	1.59	0.081	0.802	0.065	0.074	2.98	2.69	0.055	0.214	0.584	1.013	1.110
Sr	μg/kg	median																	
	μg/kg	max					1.23	3.85					1.12						1.40
Cs	μg/kg	median	0.003	0.008	0.004	0.004	0.004	0.012	0.004	0.004	0.005	0.004	0.006	0.004	0.003	0.003	0.004	0.004	
		max	0.035	0.012	0.005	0.012	0.038	0.014	0.004	0.013	0.005	0.005	0.819	0.011	0.012	0.004	0.012	0.007	0.012
Ba	μg/kg	median																	
	μg/kg	max				2.05	2.49	0.550					1.13			0.309	0.435	1.34	0.695
La	μg/kg	median			0.064	0.032	0.002						0.016			0.009	0.001	0.002	
		max			0.158	2.94	0.008	0.023		0.004			0.225	0.012		0.035	0.040	0.011	0.005
Ce	μg/kg	median		0.002	0.043	0.058							0.020			0.013		0.004	0.003
	μg/kg	max		0.004	0.111	4.72	0.018	0.045		0.008			0.161	0.024		0.056	0.056	0.013	0.009
Sm	μg/kg	median			0.005	0.003							0.001			0.001			
		max			0.010	0.111		0.002					0.015	0.001		0.004	0.003		0.002
Eu	μg/kg	median		0.0010	0.0017	0.0021	0.0004									0.0004			
	μg/kg	max	0.0020	0.0020	0.0017	0.0226	0.0008	0.0004		0.0020	0.0020	0.0021	0.0032	0.0021		0.0028	0.0025	0.0023	0.0006
Yb	μg/kg	median	0.0012	0.0007	0.0019	0.0022		0.0007		0.0006	0.0011	0.0011	0.0007	0.0012		0.0012	0.0003	0.0007	
		max	0.0017	0.0014	0.0032	0.0412	0.0015	0.0009		0.0017	0.0017	0.0015	0.0032	0.0022		0.0033	0.0030	0.0020	0.0011
Pb	μg/kg	median	0.180	0.262	0.595	0.380	211	0.439	0.815	0.292	0.300		0.329	0.234	0.790	0.345	0.516	0.691	0.260
	μg/kg	max	1.47	0.299	1.50	2.69	3.86	0.972	1.24	0.733	0.409	0.468	1.84	0.464	2.60	0.573	2.76	0.904	8.46
U	μg/kg	median			0.0021	0.0021	0.0104	0.0008	0.0009		0.0030		0.0130	0.0050		0.0067	0.0012	0.0314	0.0023
		max	0.0014		0.0176	0.0401	0.0802	0.0017	0.0016		0.0145	0.0067	0.1190	0.0939		0.0211	0.0044	0.0131	0.0390

Comparison between the mineral content of the individual PDOs was not an aim of this first work carried out on Italian extra-virgin olive oils in agreement with the Italian Ministry of Agricultural, Food and Forestry Policy. At all events – taking into account only the 3 PDOs with at least 10 samples each, namely Garda, Umbria and Terra di Bari – a trend toward higher Mg, Ca, Mn and Sr content would seem to characterise the Garda oils, especially if compared to the Umbrian oils, possibly related to the soil of the region, mainly originating from dolomitic limestone rock.

4. Conclusions

This paper, shows the results of the largest investigation ever carried out on multi-element stable isotope ratio and mineral composition using IRMS and ICP–MS in authentic PDO and PGI Italian extra-virgin olive oils. The study was done in collaboration with the Ministry of Agricultural, Food and Forestry Policy to establish a national databank for olive oils.

The stable isotope ratios of carbon, oxygen and hydrogen in olive oil were shown to increase from Trentino to Sicily, making it possible to distinguish Northern Italy from Sicily and Calabria each year and confirming the trend observed for other commodities such as wine. Significant differences were found among the years of harvest and in some cases also between PDOs from the same region. The $\delta^{13}C$ and $\delta^{18}O$ values in bulk oil were significantly correlated with those in glycerol. The $\delta^{18}O$ in glycerol showed the same capability to differentiate the geographic origin as $\delta^{18}O$ in bulk, whereas in some years the $\delta^{13}C$ of glycerol showed a better capability to discriminate as compared to bulk. Because the discriminating capability achievable using $\delta^{13}C$ in glycerol is the same as that of $\delta^{18}O$ in bulk, it would seem preferable to directly measure the isotopic ratios in bulk, making savings in terms of time and costs. The δD values, measured in 2005 for the first time in oil, showed promising geographical discrimination capability.

The content of each mineral element in well settled olive oil, measured after ultrasound acid extraction, was basically low and similar to that seen in the literature. The capability to discriminate on the basis of minerals in PDOs could only be checked for few oils produced in specific areas with different geology and requires further research in order to be confirmed.

References

Alves, R. M., Cunha, S. C., Amaral, J. S., Pereira, J. A., & Oliveira, M. B. (2005). Classification of PDO olive oils on the basis of their sterol composition by multivariate analysis. *Analytica Chimica Acta, 549*, 166–178. doi:10.1016/j.aca.2005.06.033.

Angerosa, F., Bréas, O., Contento, S., Guillou, C., Reniero, F., & Sada, E. (1999). Application of stable isotope ratio analysis to the charachterization of the geographical origin f olive oils. *Journal of Agriculture and Food Chemistry, 47*, 1013–1017. doi:10.1021/jf9809129.

Angerosa, F., Camera, L., Cumitini, S., Gleixner, G., & Reniero, F. (1997). Carbon stable isotopes and olive oil adulteration with pomace oil. *Journal of Agriculture and Food Chemistry, 45*, 3044–3048.

Anthemidis, A. N., Arvanitidis, V., & Stratis, J. A. (2005). On-line emulsion formation and multi-element analysis of edible oils by inductively coupled plasma atomic emission spectrometry. *Analytica Chimica Acta, 537*, 271–278. doi:10.1016/j.aca.2005.01.035.

Aparicio, R., & Aparicio-Ruiz, R. (2000). Authentication of vegetable oils by chromatographic techniques. *Journal of Chromatography A, 881*, 93–104.

Aramendia, M. A., Marinas, A., Marinas, J. M., Moreno, J. M., Moalem, M., Rallo, L., et al. (2007). Oxygen-18 measurement of Andalusian olive oils by continuous flow pyrolysis/isotope ratio mass spectrometry. *Rapid Communications in Mass Spectrometry, 21*, 487–496.

Benincasa, C., Lewis, J., Perri, E., Sindona, G., & Tagarelli, A. (2007). Determination of trace elements in Italian virgin olive oils and their characterization according to geographical origin by statistical analysis. *Analytica Chimica Acta, 585*, 366–370. doi:10.1016/j.aca.2006.12.040.

Bortoleto, G. G., Pataca, L. C. M., & Bueno, M. I. M. S. (2005). A new application of X-ray scattering using principal component analysis – classification of vegetable oils. *Analytica Chimica Acta, 539*, 283–287. doi:10.1016/j.aca.2005.03.025.

Boschetti, T., & Iacumin, P. (2005). Continous flow $\delta^{18}O$ measurements: New approach to standardisation, high-temperature thermodynamic and sulphate analysis. *Rapid Communications in Mass Spectrometry, 19*, 1–8.

Bréas, O., Guillou, C., Reniero, F., Sada, E., & Angerosa, F. (1998). Oxygen-18 measurement by continuous flow pyrolysis/isotope ratio mass spectrometry of vegetable oils. *Rapid Communications in Mass Spectrometry, 12*(4), 188–192.

Camin, F., Wietzerbin, K., Cortes, A. B., Haberhauer, G., Lees, M., & Versini, G. (2004). Application of multielement stable isotope ratio analysis to the characterization of French, Italian, and Spanish cheeses. *Journal of Agriculture and Food Chemistry, 52*, 6592–6601.

Castillo, J., Jimenez, M. S., & Ebdon, L. (1999). Semiquantitative simultaneous determination of metals in olive oil using direct emulsion nebulization. *Journal of Analytical Atomic Spectrometry, 14*, 1515–1518.

Cindric, I. J., Zeiner, M., & Steffan, I. (2007). Trace elemental characterization of edible oils by ICP–AES and GFAAS. *Microchemical Journal, 85*, 136–139. doi:10.1016/j.microc.2006.04.011.

Clark, I., & Fritz, P. (1997). *Environmental isotopes in hydrogeology*. New York: Lewis Publishers. pp. 35–78.

De Souza, R. M., Mathias, B. M., Da Silveira, C. L. P., & Aucelio, R. Q. (2005). Inductively coupled plasma optical emission spectrometry for trace multi-element determination in vegetable oils, margarine and butter after stabilization with propan-1-ol and water. *Spectrochimica Acta Part B, 60*, 711–715. doi:10.1016/j.sab.2005.02.025.

D'Imperio, M., Dugo, G., Alfa, M., Mannina, L., & Segre, A. L. (2007). Statistical analysis on Sicilian olive oils. *Food Chemistry, 102*, 956–965. doi:10.1016/j.foodchem.2006.03.003.

Dugo, G., La Pera, L., Giuffrida, D., Salvo, F., & Lo Turco, V. (2004). Influence of the olive variety and the zone of provenience on selenium content determined by cathodic stripping potentiometry (CSP) in virgin olive oils. *Food Chemistry, 88*, 135–140. doi:10.1016/j.foodchem.2003.12.036.

Eschnauer, H. (1982). Trace elements in must and wine: Primary and secondary contents. *American Journal of Enology and Viticulture, 33*(4), 226–230.

Jimenez, M. S., Velarte, R., & Castillo, J. R. (2003). On-line emulsion of olive oil samples and ICP–MS multi-elemental determination. *Journal of Analytical Atomic Spectrometry, 18*, 1154–1162. doi:10.1039/b303131d.

La Pera, L., Lo Curto, S., Visco, A., La Torre, L., & Dugo, G. (2002). Derivative potentiometric stripping analysis (dPSA) used for the determination of cadmium, copper, lead and zinc in Sicilian olive oils. *Journal of Agriculture and Food Chemistry, 50*, 3090–3093. doi:10.1021/jf0113124.

Lo Coco, F., Monotti, P., Rizzotti, S., & Ceccon, L. (2000). Determination of copper (II) and lead (II) in olive oils by derivative potentiometric stripping analysis. *Italian Journal of Food Science, 12*(4), 477–483.

Lo Coco, F., Ceccon, L., Circolo, L., & Novelli, V. (2003). Determination of cadmium (II) and zinc (II) in olive oils by derivative potentiometric stripping analysis. *Food Control, 14*, 55–59.

Lopez-Feria, S., Cardenas, S., Garcia-Mesa, J. A., Fernandez-Hernandez, A., & Valcarcel, M. (2007). Quantification of the intensity of virgin olive oil sensory attributes by direct coupling headspace–mass spectrometry and multivariate calibration techniques. *Journal of Chromatography A, 1147*, 144–152. doi:10.1016/j.chroma.2007.02.107.

Martin-Polvillo, M., Albi, T., & Guida, A. (1994). Determination of trace elements in edile vegetable oils by atomic absorption spectrometry. *Journal AOCS, 71*(4), 347–353.

O'Leary, M. H. (1995). Environmental effects on carbon isotope fractionation in terrestrial plants. In E. Wada, T. Yoneyama, M. Mingawa, & T. Ando (Eds.), *Stable isotope in the biosphere* (pp. 78–91). Japan: Kyoto Univeristy Press.

Rezzi, S., Axelson, D. E., Heberger, K., Reniero, F., Mariani, C., & Guillou, C. (2005). Classification of olive oils using high throughput flow ^1H-NMR fingerprinting with principal component analysis, linear discriminant analysis and probabilistic neural networks. *Analytica Chimica Acta, 552*, 13–24. doi:10.1016/j.aca.2005.07.057.

Rossmann, A., Reniero, F., Moussa, I., Schmidt, H. L., Versini, G., & Merle, M. H. (1999). Stable oxygen isotope content of water of EU databank wines from Italy, France and Germany. *Zeitschrift fuer Lebensmittel-Untersuchung und -Forschung, 208*, 400–407.

Rossmann, A., Schmidt, H. L., Reniero, F., Versini, G., Moussa, I., & Merle, M. H. (1996). Stable carbon isotope content in ethanol of EC databank wines from Italy, France and Germany. *Zeitschrift fuer Lebensmittel-Untersuchung und -Forschung, 203*, 293–301.

Royer, A., Gerard, C., Naulet, N., Lees, M., & Martin, G. J. (1999). Stable isotope charachterization of olive oils. I-compositional and carbon-13 profiles of fatty acids. *Journal of the American Oil Chemist Society, 76*(3), 357–363.

Schmidt, H.-L., Werner, R. A., & Eisenreich, W. (2003). Systematics of 2H patterns in natural compounds and ist importance fort he elucidation of biosynthetic pathways. *Phytochemistry Reviews, 2*, 61–85.

Schmidt, H.-L., Werner, R. A., & Rossmann, A. (2001). 18O pattern and biosynthesis of natural plant products. *Phytochemistry, 58*, 9–32.

Sessions, A. L., Burgoyne, T. W., & Hayes, J. M. (2001). *Analytical Chemistry, 73*, 200. doi:10.1021/ac000488m.

Soliani, L. (2003). *Statistica applicata alla ricerca biologicae ambientale*. Parma: UNINOVA.

Solinas, M., Angerosa, F., & Cichelli, A. (1987). Determinazione del contenuto di metalli negli oli vergini di oliva prodotti con diverse tecniche. Nota 2: dosaggio di cobalto, manganese, rame, piombo, stagno per spettrofotometria di assorbimento atomico con fornace di grafite. *Annali dell'Istituto Sperimentale per la Elaiotecnica 1984-1987*, X.

Spangenberg, J. E., Macko, S. A., & Hunziker, J. (1998). Characterization of olive oil by carbon isotope analysis of individual fatty acids: Implications for authentication. *Journal of Agriculture and Food Chemistry, 46*, 4179–4184. doi:10.1021/jf980183x.

Tay, A., Singh, R. K., Krishnan, S. S., & Gore, J. P. (2002). Authentication of olive oil adulterated with vegetables oils using fourier transform infrared spectroscopy. *LWT – Food Science and Technology, 35*, 99–103. doi:10.1006/fstl.2001.0864.

Vichi, S., Pizzale, L., Conte, L. S., Buxaderas, S., & Lopez-Tamames, E. (2007). The occurrence of volatile and semi-volatile aromatic hydrocarbons in virgine olive oils from north–eastern Italy. *Food Control, 18*, 1204–1210. doi:10.1016/j.foodcont.2006.07.015.

Zeiner, M., Steffan, I., & Cindric, I. J. (2005). Determination of trace elements in olive oil by ICP–AES and ETA-AAS: A pilot study on the geographical characterization (2005). *Microchemical Journal, 81*, 171–176. doi:10.1016/j.microc.2004.12.002.

Zhang, B.-L., Buddrus, S., Trierweiler, M., & Martin, G. J. (1998). Characterization of glycerol from different origins by 2H- and 13C NMR studies of site-specific natural isotope fractionation. *Journal of Agriculture and Food Chemistry, 46*, 1374–1380.

Fig. 1. Photographs of the minced meat samples and the meat chunk stored in a cold storage during the experiment. At intervals, one sample of minced meat and one slice from the chunk was taken, sealed and freeze-stored until the preparation for analysis.

stored next to the piece of meat in a cold storage (Fig. 1). At the same intervals as the chunk of pork was sub-sampled, one sample container with minced pork was removed from the tray, sealed and frozen. In this way we were able to get an estimate of maximum possible changes (as minced meat has more surfaces to evaporate water) and average changes of the isotope composition (taking slices from the chunk of meat) with storage time. The experiment started at 6.9.2005 and sampling took place approximately every hour per day over a period of almost 60 h.

Experiment 2: One big chunk of beef was taken from a fresh carcass from cattle from the Czech Republic. Half of it was minced, the second half remained intact. Sample preparations were performed in a similar manner to those described in Experiment 1 in a cold storage of the slaughterhouse. The experiment started at 27.9.2005 and lasted over an interval of approximately 26 h. This experiment was carried out in a different slaughterhouse to that used for Experiment 1 in order to test whether results varied between locations.

Experiment 3: One big chunk of pork was taken from a fresh carcass, also from a pig from Styria, and minced. The experiment started at 3.3.2006 and was carried out as described above. Once or twice a day over a period of 14 days, one sample container was removed, sealed and frozen to study the change of δ18O of meat juice over longer time periods.

Experiment 4: For the investigation of changes in δ18O of meat juice during the frying process, 1 cm of superficial meat was removed from one joint of meat from cattle from Lower Austria, after which it was cut into several slices of 1 cm thickness and similar size. The meat slices were put on a hot surface (~250 °C) and turned several times. At intervals of 1, 2, 3, 5, 7 and 9 min, one sample was removed from the hot surface, put into a sample bag and sealed.

Meat slice samples and sub-samples from the meat were cut into small pieces, put into a centrifuge container and centrifuged for 20 min at 6500 rpm.

Afterwards the extracted liquid was transferred to another sample container. If this procedure produced insufficient liquid it was repeated until the required sample amount had been extracted. The minced meat samples were put directly into centrifuge containers and centrifuged as described above. The extracted meat juice was pipetted into a glass flask for the oxygen isotope analysis and, when there was sufficient sample liquid, also for hydrogen isotope analysis.

δ^2H and $\delta^{18}O$ values of the water samples were measured using mass spectrometers Finnigan MAT 251 and Finnigan Delta + XL, each of which was coupled to an automatic equilibration device equipped with pneumatic valves (manufacturer: Finnigan and Parcom). For δ^2H, 5 ml of water was put into each vessel containing a platinum catalyst "Hokko Beads" (manufacturer: Shoko Ltd.) at a bath temperature of 20 °C. The whole system was evacuated and then filled with hydrogen up to a pressure of 300 mb. Isotope equilibrium was achieved within half an hour and the measuring process started. For $\delta^{18}O$ an aliquot of 3 ml was put into a glass vessel and attached to the equilibration device at a bath temperature of 20 °C. The system was evacuated automatically and filled with CO_2 up to a pressure of 300 mb. Each vessel was equipped with a magnetic stirrer to speed up the initial degassing of the water sample and to attain isotope equilibrium within 4 h. Evaluation of the raw data of ratios of mass 3–2 and 46–44, respectively, to δ^2H and $\delta^{18}O$ values was accomplished using two laboratory standards (Adriatic sea water and Vienna tap water), which were measured along with each batch of samples. These standards have been calibrated using the international standards VSMOW (Vienna Standard Mean Ocean Water) and SLAP (Standard Light Antarctic Precipitation) distributed by the IAEA (2001) (International Atomic Energy Agency).

All isotope results are reported using the conventional δ notation, defined as per mil (‰) deviation vs. VSMOW. Measurement uncertainty is 0.1‰ and 1‰ VSMOW for oxygen and hydrogen, respectively (1σ).

3. Results

Experiment 1: The initial $\delta^{18}O$ values in the minced pork and the chunk of pork were −4.9 and −5.6‰, respectively (Fig. 2). This difference in the initial values is explained by the minced pork and the pork chunk having been taken from different carcasses. Within the first 24 h there was a variation of ±0.4‰ of the values of the minced pork sample, without a trend but the initial value was the most depleted one. The pork chunk sample has a variation of up to 0.7‰ heavier and 0.1‰ lighter than the initial value. The following samples for the ground as well as for the chunk of pork remained within the limits found for the first 24 h, without a clear trend. The minced pork gained a daily average of about 0.1‰, a value that is within the uncertainty of measurement and less than the initial variation (first 24 h). Sub-samples from the pork chunk did not show a trend towards enriched values during the same time period.

The δ^2H values were only investigated for samples that had sufficient water extracted. The minced pork showed δ^2H values ranging from −21‰ to −18‰ (Fig. 3), with three outliers of significantly heavier isotope values up to −8‰. The isotopic trend was slightly positive, but if the outliers are disregarded, there was

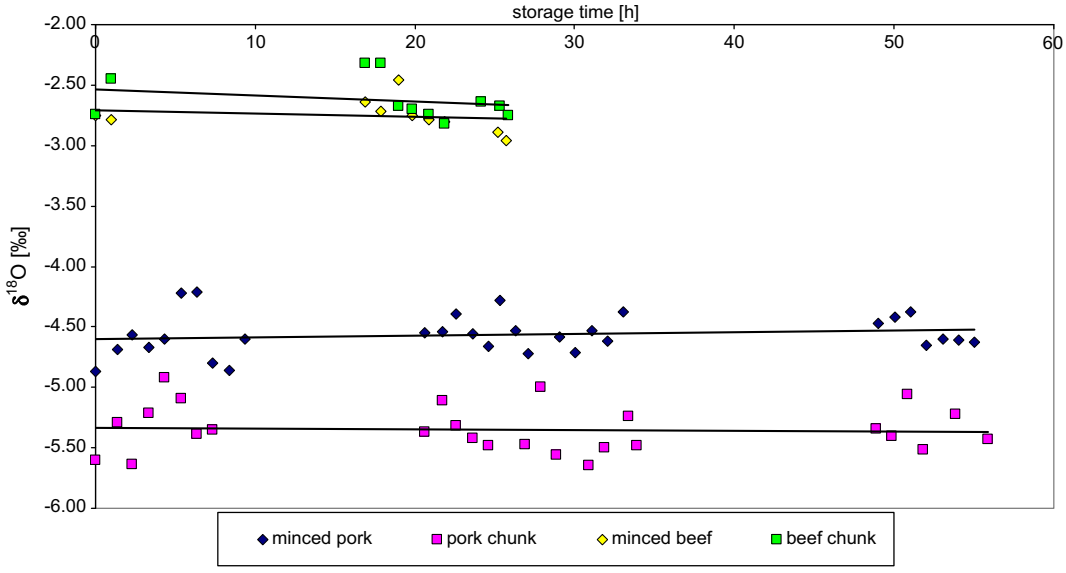

Fig. 2. Diagram with $\delta^{18}O$ V-SMOW values versus time (h) for Experiments 1 and 2 (pork and beef, respectively). Minced beef and chunk of beef come from the same carcass, minced and chunk of pork come from different animals.

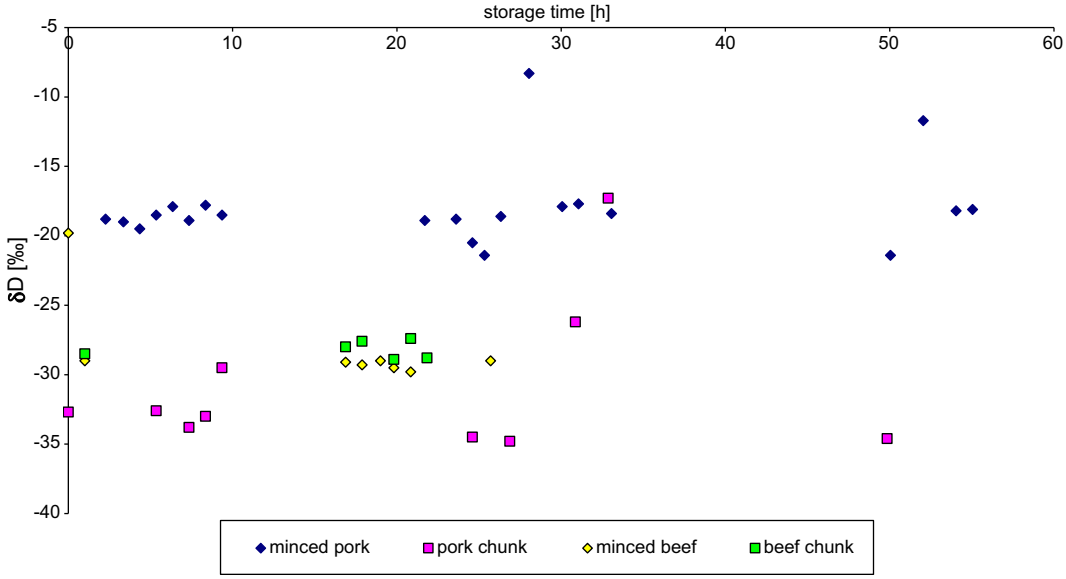

Fig. 3. Diagram with $\delta^{2}H$ V-SMOW values versus time (h) for Experiments 1 and 2 (pork and beef, respectively).

no significant change of the isotope range during the investigated period. Sub-samples from the meat chunk had $\delta^{2}H$ signatures ranging from −35‰ to −30‰, also with some outliers with heavier isotope values up to −17‰. As for the minced meat, the sub-samples taken from the meat chunk showed a small increase towards heavier values with time, but if we neglect the outliers, this trend was insignificant.

Experiment 2: The minced beef and the beef chunk were taken from the same carcass, and the initial $\delta^{18}O$ values were −2.8‰ and −2.7‰, respectively (Fig. 2). Within the experiment period the minced samples varied between −2.5‰ and −3.0‰ and the meat chunk between −2.3‰ and −2.8‰, the trends being slightly towards isotopically depleted values for both. For the $\delta^{2}H$ trends less data were available, as only the samples producing sufficient meat juice could be analysed for this parameter. However, the isotope values show almost no variations for either the minced meat or the meat chunk, ranging from −29‰ to −30‰ and −27‰ to −29‰, respectively (Fig. 3).

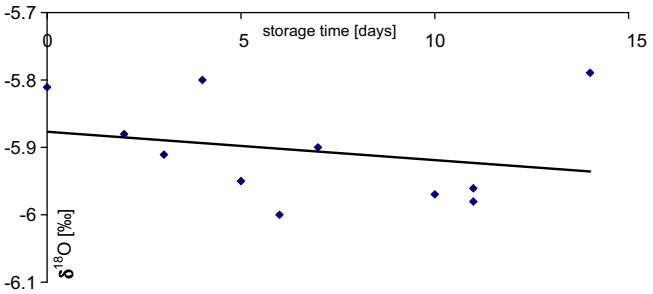

Fig. 4. Diagram showing $\delta^{18}O$ V-SMOW values versus time (14 days) for Experiment 3 (pork). No change in $\delta^{18}O$ can be detected, observed changes are within uncertainty of measurement.

Experiment 3: The pork for this experiment was not taken directly after slaughtering but from a carcass that has been slaughtered a few hours before. The initial $\delta^{18}O$ value was −5.8‰

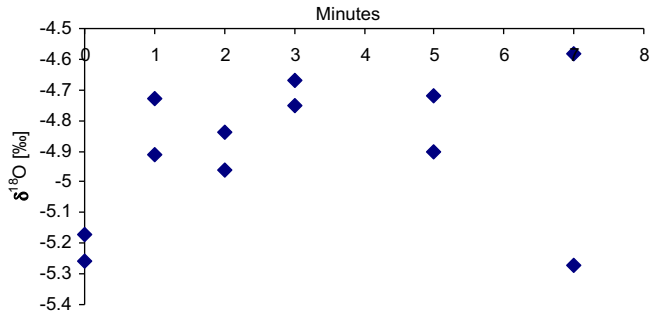

Fig. 5. Diagram showing $\delta^{18}O$ V-SMOW values versus time (min) for Experiment 4 with fried meat.

(Fig. 4). During the investigated period of 14 days, the minced samples had $\delta^{18}O$ values ranging from −5.8‰ to −6.0‰, the differences being only within experimental uncertainty and the $\delta^{18}O$ results without trend.

Experiment 4: The initial value of the raw chunk of beef was −5.2‰. The sample, that has been fried for 1 min on both sides, contained meat juice with an oxygen isotope value of −4.8‰, and there was little change with frying times up to 7 min; the 9 min sample did not contain sufficient meat juice to measure the $\delta^{18}O$ value (Fig. 5).

4. Discussion

Experiment 1, performed with pork, showed a maximum $\delta^{18}O$ variation of 0.8‰ for the chunk sub-samples and 0.7‰ of the minced samples. These variations occurred within the first 24 h and showed no significant trend. Throughout the entire experiment, the average values (per day) changed from around −4.6‰ to −4.5‰ and −5.3‰ to −5.4‰ for the minced meat and meat chunks, respectively, and thus remained within the uncertainty of measurement.

The $\delta^{2}H$ values showed a maximum variation from −21‰ to −8‰ and −35‰ to −17‰ for minced meat and the meat chunk, respectively. If we neglect the outliers the variations are reduced to −21‰ to −17‰ and −35‰ to −30‰ for minced meat and the slices from the meat chunk, respectively. If we take into account the outliers we get a slight trend towards increasing values with time, but if we disregard them there is no trend for either the minced meat or the meat chunk.

Experiment 2, performed with beef, showed a maximum $\delta^{18}O$ variation of 0.5‰ for minced beef and the slices from the meat chunk. For the investigated period of ca. 26 h, no trend towards heavier isotopes was found; on the contrary, there seemed to be a slight trend towards isotopically depleted values. The $\delta^{2}H$ ratios remain almost constant values between −28‰ and −29‰ and −27‰ and −29‰ for the minced meat and the meat chunk, respectively, almost within the uncertainty of measurement.

It is interesting to note, that the slices of meat taken from the meat chunk seem to show a slightly larger variation than the minced meat samples, although we expected to see a maximum isotope change with the minced meat samples. A possible explanation might be a slightly higher heterogeneity of the $\delta^{18}O$ in the meat chunk compared to the minced meat that would have been (at least partly) homogenised during the mincing process. The slightly negative trend for $\delta^{18}O$ in Experiment 2 raises speculation about the interaction of meat juice with air humidity. However, as no such a trend was visible in the $\delta^{2}H$ data, it can be discounted.

As previously reported by Boner and Förstel (2004), beef and pork showed different enrichments of hydrogen isotopes compared to their oxygen isotope compositions (Figs. 2 and 3). Thus the $\delta^{2}H$ values of the meat juice appear to be a potentially important tool for the control of origin and supplement the data obtained from oxygen isotope analyses. However, the presence of outliers in Experiment 1 shows that hydrogen isotopes might be less reliable at "non-ideal" storage conditions. Up to now we do not know what might have caused the outliers in $\delta^{2}H$. However, the equilibration technique with platinum catalyst used for $\delta^{2}H$ measurement sometimes experiences problems with juices, as this technique was developed for pure water samples, and it is known that contaminations of the water (e.g., sulphur) can influence the measurement. If this should be the source of error, measurement of the pure meat water can avoid this problem.

Experiment 3 was carried out to study long-time storage of meat in cold storages. The variation in $\delta^{18}O$ ranged within 0.2‰ and demonstrates that the isotope changes remained within the uncertainty of measurement.

These two experiments clearly demonstrate that the results of Thiem et al. (2004) do not apply to meat stored in industrial cold storages (Fig. 6).

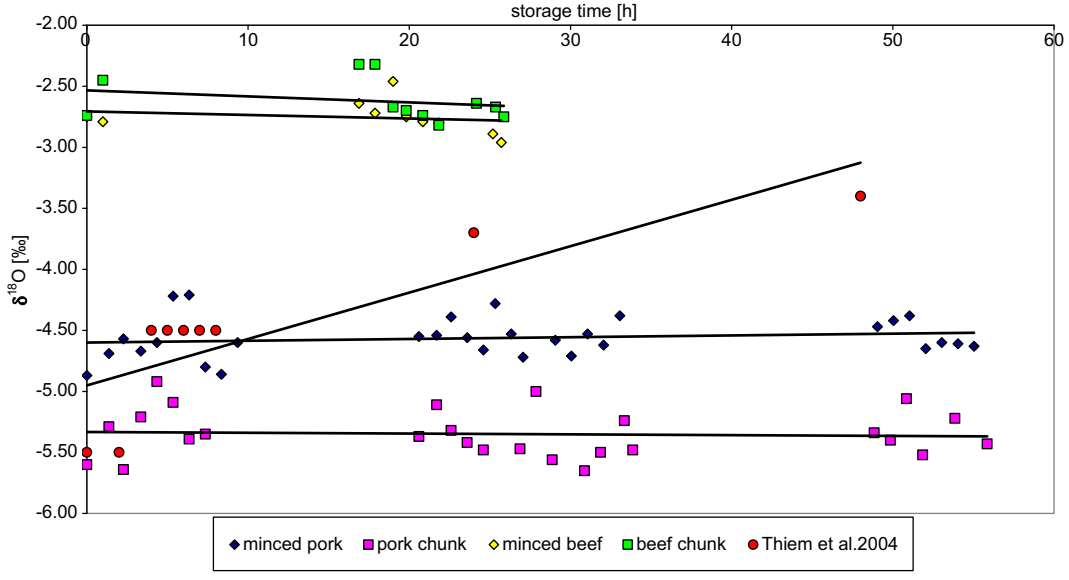

Fig. 6. Diagram with $\delta^{18}O$ V-SMOW values versus time (h) comparing the results of Experiments 1 and 2 with the results from Thiem et al. (2004) for meat stored at 0 °C.

A possible explanation for the differences in results between our findings and those of Thiem et al. (2004) is the influence of the type of cooling container used. Although not specified in their publication, we assume that Thiem et al. (2004) used a refrigerator to store the meat cube samples in their experiment. In a refrigerator there is a significant temperature gradient between the door and the cooling device, where water vapour condenses, and is permanently removed from the air in the refrigerator. Hence evaporation is increased and meat samples loose significant amounts of water. In modern industrial cold storages, air conditioning systems regulate both temperature and humidity. Almost no temperature gradients exist, keeping the air humid and preventing evaporation.

Therefore, we can conclude that meat (e.g., beef and pork) kept in industrial cold storages even for a longer period preserves its primary isotopic $\delta^{18}O$ meat juice value. However, for the processes after cool-storage of meat, such as portioning, packaging, transport to retailers and the storage of the meat at the retailer and consumer, the findings of Thiem et al. (2004) might be applicable and important.

5. Roasting

To test if it makes sense to apply $\delta^{18}O$ analyses to juice from prepared meat to authenticate its origin, we investigated changes of $\delta^{18}O$ in meat juice from fried meat. During the process of frying the meat juice experienced a maximum $\delta^{18}O$ change of 0.7‰ in our experiment. This can be explained by the small fractionation factor of water and water vapour at high temperatures (Friedman & O'Neil, 1977). As this is less than the maximum variation during storage, we regard the analysis of $\delta^{18}O$ of meat juice from roasted meat as a useful tool for estimating the $\delta^{18}O$ value of the raw meat. However, in practice "underdone" meat should be used for analysis to minimise the influence of frying, and it should be seal-packed directly after preparation, as evaporation at lower temperatures, e.g., on a plate, has a larger fractionation factor.

6. Conclusions

Our experiments clearly showed that there was no significant increase in $\delta^{18}O$ in meat juice during storage of meat in industrial cold storages. We found a maximum variation of 0.8‰ during storage, but without any trend with time. However, taking bigger samples and generously removing any meat surface in longer contact with the air should further decrease the isotopic variation. In an ideal case, as it seems to have occurred during our "long time experiment" over 14 days, the variation in meat juice $\delta^{18}O$ lies within 0.2‰. This shows that the results of Thiem et al. (2004) are not valid for meat stored in big industrial cold storages at temperatures below +5 °C. The processes after cool storing, such as portioning, packaging, transporting to supermarkets and storing in the freezers and fridges, were not investigated in the current work, and the findings of Thiem et al. (2004) suggest that such processes might have appreciable effects on the isotopic composition of meat juice.

Therefore, although it has been shown that the juice from fried meat reflects the $\delta^{18}O$ value of the raw meat, the measurement of meat juice from fried meat might not give the primary isotopic ratio, if it is not known which processes the raw meat may have undergone before it "ended in the pan".

Acknowledgments

We want to thank Schirnhofer GmbH and Marcher GmbH for allowing us to perform the experiments in their slaughterhouses and cold storages. We want to thank Mr. Höfer and especially Gerhard Rose for their support and enthusiasm and Ingrid Perz and Rudolf Tallian for reliably taking and freeze-storing the samples. Preparation of samples was done by Gerhard Spitzer and Erwin Tschank, and stable isotope measurements were carried out by Peter Kostecki. This study is part of the independent research program of the Austrian Research Centers GmbH – ARC.

References

Boner, M., & Förstel, H. (2004). *Analytical and Bioanalytical Chemistry, 378*, 301.
Camin, F., Bontempo, L., Heinrich, K., Horacek, M., Kelly, S. D., Schicht, C., et al. . *Analytical and Bioanalytical Chemistry, 389*(1), 309.
Eisinger, E., Horacek, M., & Prohaska, T. (2005). *SINA Meeting (Stable Isotope Network Austria)*. Wien.
Friedman, I., & O'Neil, J. R. (1977). In *Data of geochemistry, U.S. geological survey professional paper 440-KK* (6th ed.). Reston.
González-Martin, I., González-Pérez, C., Méndez, H. J., Marqués-Macias, E., & Sanz-Poveda, F. S. (1999). *Meat Science, 52*, 437.
Heaton, K., Kelly, S. D., Hoogewerff, J., & Woolfe, M. (2008). *Food Chemistry, 107*, 506.
Hegerding, L., Seidler, D., Danneel, H. J., Gessler, A., & Nowak, B. (2002). *Die Fleischwirtschaft, 4*, 95.
IAEA/WMO (2001). Global network of isotopes in precipitation. The GNIP Database. <http://isohis.iaea.org>.
Moser, H., & Rauert, W. (1980). Isotopenmethoden in der Hydrologie. Lehrbuch der Hydrogeologie. Bd.8. Gebrüder Borntraeger: Berlin-Stuttgart.
Piasentier, E., Valusso, R., Camin, F., & Versini, G. (2003). *Meat Science, 64*, 239.
Renou, J. P., Bielicki, G., Deponge, C., Gachon, P., Micol, D., & Ritz, P. (2004). *Food Chemistry, 86*, 251.
Thiem, I., Lüpke, M., & Seifert, H. (2004). *Isotopes Environmental Health Studies, 40*, 191.
Schmidt, O., Quilter, J. M., Bahar, B., Maloney, A. P., Scrimgeour, C. M., Begley, I. S., et al. (2005). *Food Chemistry, 91*, 545.

analysis to determine the origin of meat products has been, up to now, not very common, and the existing studies have focused on distinguishing the provenance of samples from different European countries (Boner & Förstel, 2004; Camin et al., 2007; Heaton, Kelly, Hoogewerff, & Woolfe, 2008; Nakashitaa et al., 2008). Furthermore, isotopic traceability of animal products is more complex because livestock can consume foodstuffs of various origins and also be raised on several different farms during their lifetime. Most biological and physiological factors influencing the isotopic composition of animal tissues are still poorly understood (Heaton et al., 2008; Schmidt et al., 2005).

The aim of this work was to demonstrate the potential of carbon and nitrogen stable isotope analysis to trace the geographical origin of cattle in China, and to verify if a dual-isotopic approach can be an efficient tool for cattle origin characterisation.

2. Materials and methods

2.1. Sources of samples

A total of 59 castle raised at four distinct sites which differ in their geographical locations were used for the experiment and are shown on the map in Fig. 1. Twenty-one cattle samples were collected from Yushu city, Jilin province (44.47°N, 126.08°E) in June in 2005. Yushu is located in northeast China, its mean annual temperature is 4 °C, average altitude is 407 m, and the cattle feed is mainly maize. Sixteen cattle samples were collected from Anshun city, Guizhou province (26.23°N, 105.41°E) in November in 2005, which is located in southwest China. Anshun's mean annual temperature is 14–16 °C, the average altitude is 1378 m and the cattle feed is mainly C_3 and C_4 pasture. Ten cattle samples were collected from Tongxin county, Ningxia municipality (37.33°N, 106.29°E) in October in 2005, which is located in northwest China. Tongxin's mean annual temperature is 8.6 °C and the average altitude is 1715 m, the cattle feed is mainly a mixture of wheat and maize. Twelve cattle samples were collected from Zhangbei county, Hebei province (41.08°N, 114.43°E) in November in 2005. Its mean annual temperature is 2.6 °C, the average altitude is 1325 m and the cattle feed is mainly C_3 pasture.

Fig. 1. Regions of samples.

2.2. Preparation of samples

2.2.1. Muscle samples

The samples (500 g), taken from the rump, were removed from carcasses and stored at −20 °C until processing. Muscle was dried at 70 °C for 48 h and ground in a pulverizer. Lipids were extracted from the muscle powder with petroleum ether and the residue was sieved in a 0.08 mm sieve mesh (Boner & Förstel, 2004; Schmidt et al., 2005; Yi, Li, Zhang, Zhao, & Li, 2004). Finally, the lipids were recovered using a Rotary Evaporator.

2.2.2. Tail hair samples

The samples were collected from cattle kept and raised in local regions and fed an unchanging diet for at least three months. The hair length should be 45.9 mm in three months according to a minimum hair growth rate of 0.51 mm/d (Schwertl et al., 2005). For each cattle a 40 mm section of tail hair was cut with scissors from an area 1 cm^2 close to the skin.

The hair samples were first soaked and washed with distilled water and then dried at 60 °C before soaking in a 2:1 mixture of methanol/chloroform for 2 h. After which they were washed with distilled water, soaked for another 30 min, and rinsed in the methanol/chloroform mixture again. The dried hair was cut into 1–2 mm sections (De Smet, Balcaen, Claeys, Boeckx, & Van Cleemput, 2004; Schwertl, Auerswald, & Schnyder, 2003).

2.3. Sample analysis

Dry samples were weighed into tin capsules and introduced by means of an auto sampler into the elemental analyzer (Flash EA1112). The elements of carbon and nitrogen in the samples were combusted into CO_2 and NO_x gas at 1020 °C, and then the NO_x gas was reduced over copper wires at 650 °C to N_2. The flow rate of carrier gas helium was 90 ml/min, interfaced through a Conflo III to an isotope ratio mass spectrometer (Delta plus, Thermo Finnigan). The C and N stable isotope composition of each sample was measured in the same analysis. The values of the isotopic ratios are expressed in delta (δ) notation in parts per thousands (‰) relative to the accepted international standards; $\delta^{13}C$ (‰) relative to PDB and $\delta^{15}N$ (‰) relative to atmospheric AIR. The delta values were calculated as follows:

$$\delta_x = (R_{sample}/R_{standard} - 1) \times 1000$$

where δ_x is $\delta^{13}C$ or $\delta^{15}N$, and R is the respective $^{13}C/^{12}C$ or $^{15}N/^{14}N$ ratio.

The reference working gas CO_2 was calibrated with USGS 24 ($\delta^{13}C_{PDB} = -16.049‰$), and the reference working gas N_2 was calibrated with IAEA standard N1 ($\delta^{15}N_{air} = 0.4‰$). The analytical precision was 0.2‰ for both C and N.

2.4. Statistical analysis

The analysis of data including ANOVA, Duncan's LSD test, Correlation Analysis and Discriminant Analysis (DA) were performed using the SAS software package for windows, and the box-plot figures were drawn by SAS package (version 6.12).

DA was carried out to evaluate whether cattle from different origins could be distinguished by analytical parameters. The classification rules and mathematical model was developed using Euclidean distances discriminant analysis based on the full data set of 59 samples, and then using back substitution test to evaluate the prediction capability of the mode for each parameter. The

prediction capability is expressed as a percentage of correctly classified samples relative to the entire data set, and calculated as follows:

$$x\% = (\text{number of correctly classified individual} / \text{sample population}) \times 100.$$

A box-plot provides an excellent visual summary of a set of data. It is used to show the shape of the distribution, its median value, and variability. The picture produced consists of the most extreme values in the data set (maximum and minimum values), the lower and upper quartiles, and the median.

3. Results

3.1. Difference analysis

The results of ANOVA and Duncan's LSD test showed that there were highly significant differences according to region in the mean values of carbon and nitrogen isotope ratios in the cattle tissue. The order of the geographical origin was Jinlin > Guizhou > Ningxia > Hebei according to $\delta^{13}C$ values of cattle tissues (Figs. 2a–c). For $\delta^{15}N$ values, there were highly significant differences between samples coming from pasture (Guizhou and Hebei) and cultivated land (Jilin and Ningxia) (Figs. 2d and e). This indicated that stable isotope ratios of carbon and nitrogen in cattle tissues may be used to discriminate the geographical origin in China.

3.2. Correlation analysis

A significant correlation was found in carbon and nitrogen isotope ratios between de-fatted beef, crude fat and tail hair. The correlation coefficients of $\delta^{13}C$ values between de-fatted beef, crude fat and tail hair were 0.947, 0.961 and 0.955 ($P < 0.01$) respectively, the correlation coefficient of $\delta^{15}N$ values between de-fatted beef and tail hair was 0.874 ($P < 0.01$) (Figs. 3a–d). The results implied that the three tissues respond to diet in a similar pattern and, thus,

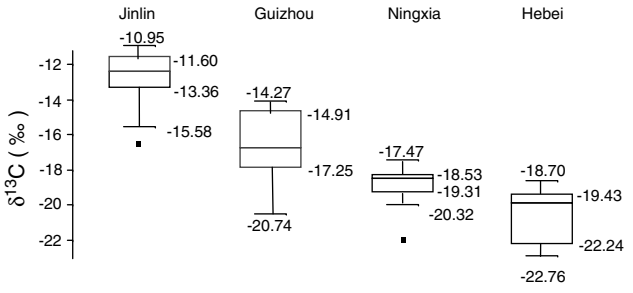

Fig. 2a. The $\delta^{13}C$ values of de-fatted beef from different regions.

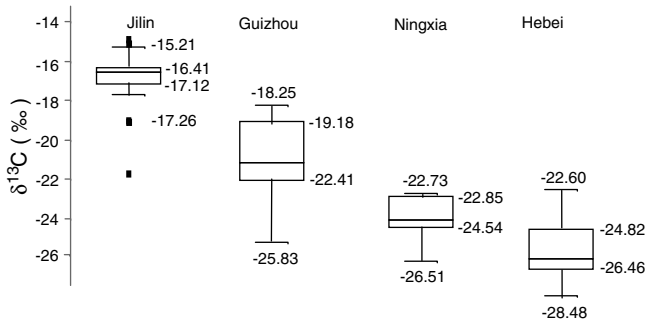

Fig. 2b. The $\delta^{13}C$ values of crude fat from different regions.

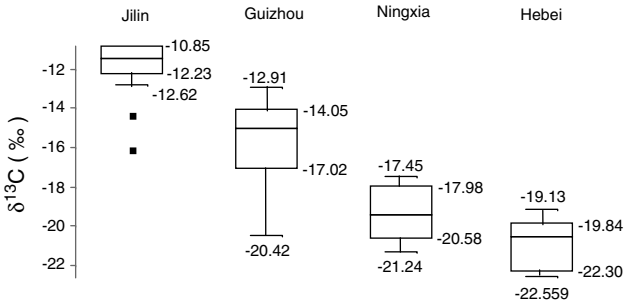

Fig. 2c. The $\delta^{13}C$ value of tail hair from different regions.

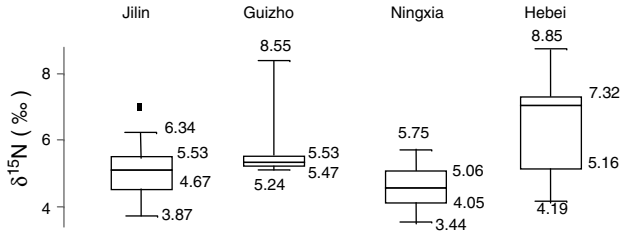

Fig. 2d. The $\delta^{15}N$ value of de-fatted beef from different regions.

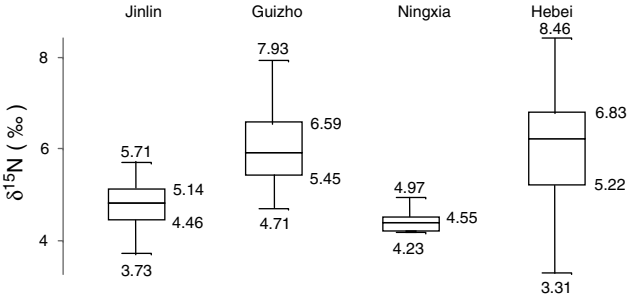

Fig. 2e. The $\delta^{15}N$ value of tail hair from different regions.

C and N isotope composition of either tissue, lipid or hair could yield useful information on dietary intake and geographical origin.

3.3. Discriminant analysis

From the comparison of discriminant analysis results based on a single indicator of $\delta^{13}C$ or $\delta^{15}N$, respectively (Table 1), it could be concluded that $\delta^{13}C$ was the better indicator to trace the origin of cattle than $\delta^{15}N$. Furthermore, correct classification could be improved by a combination of carbon and nitrogen isotope ratios, e.g., only 73% and 47% of samples were correctly classified by using the $\delta^{13}C$ and $\delta^{15}N$ in tail hair, respectively, but it could be improved to 85% by using the combination of $\delta^{13}C$ and $\delta^{15}N$ values in tail hair (Table 2).

4. Discussion

4.1. Isotopic ratios in cattle from different regions

There were significant differences based on carbon and nitrogen isotope ratios in cattle tissues from four regions in China. The $\delta^{13}C$ value of cattle was found to be highly dependent on diet composition, particularly with regard to the proportion of C_4 and C_3 plant material (De Smet et al., 2004; Schwertl et al., 2005). The main

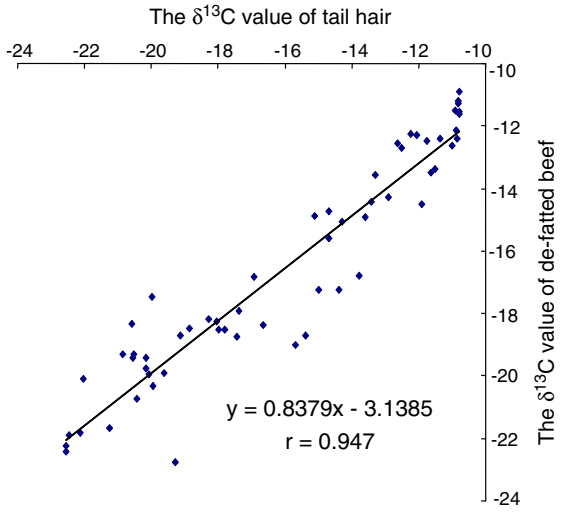

Fig. 3a. The correlation of $\delta^{13}C$ between tail hair and de-fatted beef.

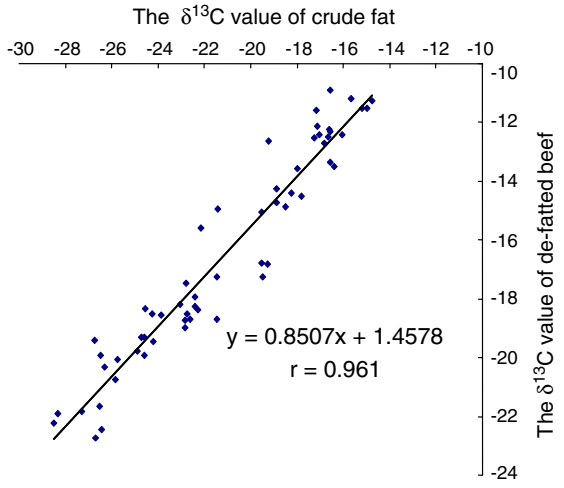

Fig. 3b. The correlation of $\delta^{13}C$ between crude fat and de-fatted beef.

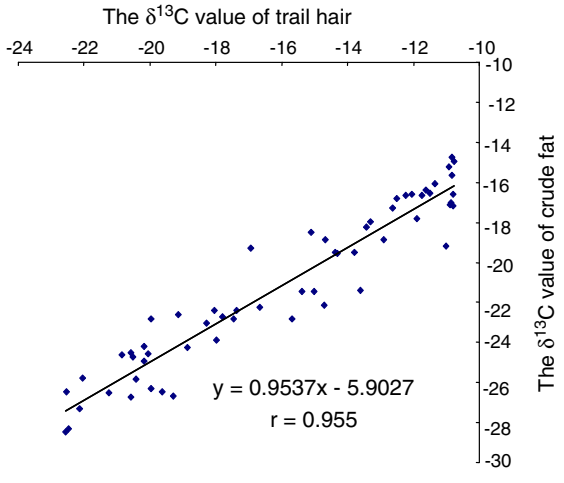

Fig. 3c. The correlation of $\delta^{13}C$ between tail hair and crude fat.

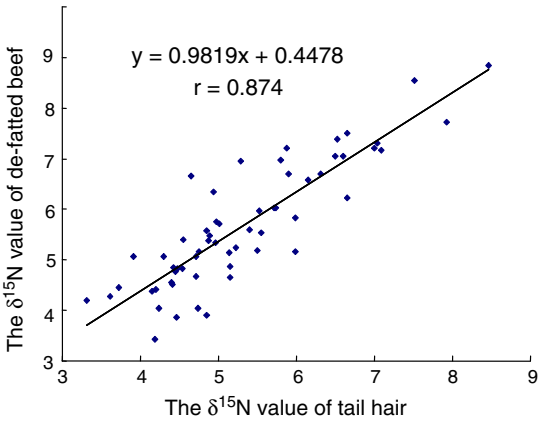

Fig. 3d. The correlation of $\delta^{15}N$ between tail hair and de-fatted beef.

feeds of cattle from four regions in China have shown significant differences, which are usually dependent upon the geographical location and climate factors. Jilin province is located in northeast China, where the mean annual temperature is relatively low (4 °C), and the maize is one of the primary crops. The cattle from Jilin were mainly fed on maize, but rice straw and soybean accounted for a small proportion of the feed. Maize is a C_4 plant; rice straw and soybean are C_3 plants, that is, cattle from Jilin were mainly fed on C_4 plants. Guizhou province is located in southwest China; cattle from here were mainly fed on C_3 and C_4 grass. Ningxia is located in northwest China, it is suitable for wheat and maize growing, and cattle from Ningxia were fed on the mixture of wheat and maize. Hebei province is adjacent to grassland; cattle reared here were mainly fed on C_3 pasture grass. These different diet compositions explain the reason why $\delta^{13}C$ values of cattle tissue from Yushu city, Jilin province were the highest among the four regions, and $\delta^{13}C$ values of samples from Zhangbei city, Hebei province were the lowest. The $\delta^{15}N$ values of animals depend on their diet and regions (Piasentier, Valusso, Camin, & Versini, 2003). Cattle from Jilin and Ningxia were mainly fed on cereal feed, while cattle from Guizhou and Hebei were mainly fed on pasture. The regions growing cereal crops usually depend on chemical fertilizer, while the regions producing pasture usually depend on organic fertilizer. Chemical fertilizer is depleted in ^{15}N relative to organic fertilizer (Cai, Zhang, & Zhang, 2002; Piasentier et al., 2003). That is the reason why the $\delta^{15}N$ value of cattle from pasture-feeding regions was significantly higher than those fed on cereal feeds. So we can draw the conclusion that $\delta^{15}N$ value may be used to differentiate the cattle from pasture-feeding regions and cereal feeding regions in the areas in China considered in this study.

4.2. Isotopic ratios in different cattle tissues

The $\delta^{13}C$ values varied significantly in different tissue. The order was tail hair > de-fatted muscle > crude fat. This result corresponds to the findings of others authors (De Smet et al., 2004; Kornexl, Werner, Roßmann, & Schmidt, 1997; Piasentier et al., 2003). De Smet et al. (2004) found that hair, muscle, blood and liver were enriched in ^{13}C compared with the $\delta^{13}C$ value of the diets, but the kidney fat was significantly depleted in ^{13}C. The $\delta^{15}N$ values in cattle tail hair were less positive than that of the de-fatted muscle, which probably may be due to the different amino acid composition between them. Though the significant differences of C and N isotopic ratios were observed between cattle tissues, high correlation coefficients were found between them. The results indicated that the three tissues respond to diet changes in a similar pattern and, thus, C and N isotope composition of either tissue could yield useful

Table 1
The percentage of observations correctly classified of cattle samples from four regions in China, on the basis of single indicator of carbon and nitrogen stable isotope ratios, respectively

Sample origin	$\delta^{13}C$ (‰)			$\delta^{15}N$ (‰)	
	De-fatted beef (%)	Crude fat (%)	Tail hair (%)	De-fatted beef (%)	Tail hair (%)
Yushu city, Jilin province	86	86	90	38	38
Anshun city, Guizhou province	50	75	69	25	6
Tongxin county, Ningxia municipality	60	50	50	70	80
Zhangbei county, Hebei province	75	67	67	75	92
% total	69	73	73	47	47

Table 2
The percentage of observations correctly classified of cattle samples from four regions in China, on the basis of combination indicators of carbon and nitrogen stable isotope ratios

Sample origin	$\delta^{13}C$ $\delta^{15}N$	$\delta^{13}C$ $\delta^{15}N$
	De-fatted beef (%)	Tail hair (%)
Yushu city, Jilin province	86	90
Anshun city, Guizhou province	69	81
Tongxin county, Ningxia municipality	80	60
Zhangbei county, Hebei province	75	100
% total	78	85

information of the dietary intake. However, the turnover rate of stable isotope showed significant difference between different tissues due to different metabolic activity (Bahar et al., 2005; De Smet et al., 2004; Harrison et al., 2007; Schwertl et al., 2003), and the correlations of isotopic ratios between different tissues depend on the sampling methods, sampling time and cattle feeding mode, which led to different results shown in previous research (Camin, Perini, Colombari, Bontempo, & Versini, 2008; De Smet et al., 2004; Piasentier et al., 2003; Renou et al., 2004). Cattle samples selected in our experiment were fed in the same regions with unchanged feeds for at least three months, and only the segment of tail hair which produced within this period was taken as samples. Therefore, most of isotopic composition in de-fatted muscle, crude fat and tail hair reached equilibrium with the feeds, and the $\delta^{13}C$ and $\delta^{15}N$ values in these three tissues could provide the regions and diets information where the cattle come from. Generally speaking, different tissues can reflect different periods of diet information, e.g., bone and bone collage provide long-term dietary information that may integrate decades of their lifetime, tissues like blood, fat, liver, muscle and brain reflect diet consumed within weeks to months (Schwertl et al., 2003). Every section of hair and hooves can be used to reconstruct an animal's dietary history (Harrison et al., 2007; Schwertl et al., 2003, 2005). Therefore, different modes should be built to predict the information of dietary change using different tissues, and the suitable tissues should be chosen according to the aims of the research undertaken.

4.3. Discriminant parameters for cattle geographical origin traceability

The $\delta^{13}C$ value was found to be a powerful parameter to determine the geographical origin of cattle followed by $\delta^{15}N$. In addition the single parameter of $\delta^{13}C$ and $\delta^{15}N$ was not sufficient to identify the cattle from different origins, due to overlap in the more extreme values, but the percentage of correctly classified observations can be significantly improved by the combination of these two parameters. That is the isotopic indicators of carbon and nitrogen could provide complementary information for tracing the geographical origin of cattle. This result is consistent with previous researchers. C-isotope ratios alone can distinguish dietary C_3/C_4 groups; N can provide additional information potentially useful for the authenticity investigation of beef (Bahar et al., 2005). In addition, the simultaneous consideration of $\delta^{13}C$, $\delta^{15}N$ and other isotope ratios such as $^{18}O/^{16}O$, $^{2}H/^{1}H$, $^{34}S/^{32}S$ and $^{87}Sr/^{86}Sr$ will improve the rate of correct classification greatly for Chinese cattle geographical origin traceability.

5. Conclusion

Carbon and nitrogen stable isotope analysis has proved a useful tool for tracing the diet and geographical origin of cattle in China. In addition, the $\delta^{13}C$ and $\delta^{15}N$ value either of de-fatted beef, crude fat and tail hair can provide similar information of the dietary intake and geographical origin.

Acknowledgements

The research is supported by Chinese National Sciences Fund (No. 30671484 and 30800862) and Eleventh Five-Year Plan for National Key Projects of Scientific and Technical Supporting Programs funded by Ministry of Science and Technology of China (No. 2006BAK02A16). We are grateful to the farmers for assistance in collecting beef samples, feeds samples and offering associated information.

References

Bahar, B., Monahan, F. J., Moloney, A. P., O'Kiely, P., Scrimgeour, C. M., & Schmidt, O. (2005). Alteration of the carbon and nitrogen stable isotope composition of beef by substitution of grass silage with maize silage. *Rapid Communication in Mass Spectrometry, 19*, 1937–1942.

Boner, M., & Förstel, H. (2004). Stable isotope variation as a tool to trace the authenticity of beef. *Analytical and Bioanalytical Chemistry, 378*, 301–310.

Branch, S., Burke, S., Evans, P., Fairman, B., & Wollff Briche, C. S. J. (2003). A preliminary study in determining the geographical origin of wheat using isotope ratio inductively coupled plasma mass spectrometry with ^{13}C, ^{15}N mass spectrometry. *Journal of Analytical Atomic Spectrometry, 18*(1), 17–22.

Cai, D. L., Zhang, S. F., & Zhang, J. (2002). Application of stable carbon and nitrogen isotope methods in ecological studies. *Journal of Ocean University of Qingdao, 32*(2), 287–295 (in Chinese).

Camin, F., Bontempo, L., Heinrich, K., Horacek, M., Kelly, S. D., Schlicht, C., et al. (2007). Multi-element (H,C,N,S) stable isotope characteristics of lamb meat from different European regions. *Analytical and Bioanalytical Chemistry*. doi:10.1007/s00216-007-1302-3.

Camin, F., Perini, M., Colombari, G., Bontempo, L., & Versini, G. (2008). Influence of dietary composition on the carbon, nitrogen, oxygen and hydrogen stable isotope ratios of milk. *Rapid Communications in Mass Spectrometry, 22*, 1690–1696.

Camin, F., Wietzerbin, K., Cortes, A. B., Haberhauer, G., Lees, M., & Versini, G. (2004). Application of multielement stable isotope ratio analysis to the characterization of French, Italian, and Spanish cheeses. *Journal of Agricultural and Food Chemistry, 52*, 6601–6952.

Coetzee, P. P., & Vanhaecke, F. (2005). Classifying wine according to geographical origin via quadrupole-based ICP-mass spectrometry measurement of boron isotope rations. *Analytical and Bioanalytical Chemistry, 383*, 977–984.

Crittenden, R. G., Andrew, A. S., LeFournour, M., Young, M. D., Middleton, H., & Stockmann, R. (2007). Determining the geographical origin of milk in Australasia using multi-element stable isotope ratio analysis. *International Dairy Journal, 17*, 421–428.

De Smet, S., Balcaen, A., Claeys, E., Boeckx, P., & Van Cleemput, O. (2004). Stable carbon isotope analysis of different tissue of beef animal in relation to their diet. *Rapid Communications in Mass Spectrometry, 18*, 1227–1232.

Gremaud, G., Quaile, S., Piantini, U., Pfammatter, E., & Corvi, C. (2004). Characterization of Swiss vineyards using isotope data in combination with trace element and classical parameters. *European Food Research and Technology, 219*, 97–104.

Hang, Z. Y., Yang, M. F., Zhuang, Z. X., Wang, X. R., & Frank, S. C. Lee (2003). Source identification of salvia miltiorrhiza BUNGE (danshen) by lead isotope ratios. *Chinese Journal of Analytical Chemistry, 31*(9), 1036–1039 (in Chinese).

Harrison, S. M., Zazzo, A., Bahar, B., Monahan, F. J., Moloney, A. P., Scrimgeour, C. M., et al. (2007). Using hooves for high-resolution isotopic reconstruction of bovine dietary history. *Rapid Communications in Mass Spectrometry, 21*, 479–486.

Heaton, K., Kelly, S. D., Hoogewerff, J., & Woolfe, M. (2008). Verifying the geographical origin of beef: The application of multi-element isotope and trace element analysis. *Food Chemistry, 107*, 506–515.

Kelly, S., Baxter, M., Chapman, S., Rhodes, C., Dennis, J., & Brereton, P. (2002). The application of isotopic and elemental analysis to determine the geographical origin of premium long grain rice. *European Food Research and Technology, 214*, 72–78.

Kornexl, B. E., Werner, T., Roβmann, A., & Schmidt, H. L. (1997). Measurement of stable isotope abundances in milk and milk ingredients – A possible tool for origin assignment and quality control. *Zeitschrift Für Lebensmitteluntersuchung Und – Forschung A, 205*, 19–24.

Manca, G., Camin, F., Coloru, G. C., Caro, A. D., Depentori, D., Franco, M. A., et al. (2001). Characterization of the geographical origin of Pecorino cheese by casein stable isotope ($^{13}C/^{12}C$ and $^{15}N/^{14}N$) ratios and free amino acid ratios. *Journal of Agricultural and Food Chemistry, 49*, 1404–1409.

Marisa, C., Almeida, R., Tiresa, M., & Vasconcelos, S. D. (2004). Does the winemaking process influence the wine $^{87}Sr/^{86}Sr$? *Food Chemistry, 85*, 7–12.

Nakashitaa, R., Suzukib, Y., Akamatsua, F., Iizumic, Y., Korenagaa, T., & Chikaraishid, Y. (2008). Stable carbon, nitrogen, and oxygen isotope analysis as a potential tool for verifying geographical origin of beef. *Analytica Chimica Acta, 617*, 148–152.

Padovan, G. J., De Jong, D., Rodrigues, L. P., & Marchini, J. S. (2003). Detection of adulteration of commercial honey sample by the $^{13}C/^{12}C$ isotope ratio. *Food Chemistry, 82*, 633–636.

Piasentier, E., Valusso, R., Camin, F., & Versini, G. (2003). Stable isotope ratio analysis for authentication of lamb meat. *Meat Science, 64*, 239–247.

Pillonel, L., Badertscher, R., Froidevaux, P., Haberhauer, G., Hölzl, S., Horn, P., et al. (2003). Stable isotope ratios, major, trace and radioactive elements in emmental cheeses of different origins. *Lebensmittel–Wissenschaft und–Technologie, 36*, 615–623.

Renou, J. P., Deponge, C., Gachon, P., Bonnefoy, J. C., Coulon, J. B., Garel, J., et al. (2004). Characterization of animal products according to geographic origin and feeding diet using nuclear magnetic resonance and isotope ratio mass spectrometry: Cow milk. *Food Chemistry, 85*, 63–66.

Rossmann, A. (2001). Determination of stable isotope ratios in food analysis. *Food Reviews International, 17*(3), 347–381.

Rossmann, A., Haberhauer, G., Hölzl, S., Horn, P., Pichlmayer, F., & Voerkelius, S. (2000). The potential of multielement stable isotope analysis for regional origin assignment of butter. *European Food Research and Technology, 211*, 32–40.

Schmidt, O., Quilter, J. M., Bahar, B., Moloney, A. P., Scrimgeour, C. M., Begley, I. S., et al. (2005). Inferring the origin and dietary history of beef from C, N and S stable isotope ratio analysis. *Food Chemistry, 91*, 545–549.

Schwertl, M., Auerswald, K., Schäufele, R., & Schnyder, H. (2005). Carbon and nitrogen stable isotope composition of cattle hair: Ecological fingerprints of production system? *Agriculture, Ecosystems and Environment, 109*, 153–165.

Schwertl, M., Auerswald, K., & Schnyder, H. (2003). Reconstruction of the isotope history of animal diets by hair segment analysis. *Rapid Communications in Mass Spectrometry, 17*, 1312–1318.

Serra, F., Guillou, C. G., Reniero, F., Ballarin, L., Cantagallo, M. I., Wieser, M., et al. (2005). Determination of the geographical origin of green coffee by principal component analysis of carbon, nitrogen and boron stable isotope ratios. *Rapid Communications in Mass Spectrometry, 19*, 2111–2115.

Simpkins, W. A., Patel, G., Harrison, M., & Goldberg, D. (2000). Stable carbon isotope ratio analysis of Australian orange juices. *Food Chemistry, 70*, 385–390.

Yi, X. F., Li, L. X., Zhang, X. A., Zhao, L., & Li, M. C. (2004). Influence of artificial food on stable carbon and nitrogen isotope composition of plateau pikas. *Zoological Research, 25*(3), 232–235 (in Chinese).

brewed from the leaves of the *Camellia sinensis* plant. Traditionally picked by hand, the harvest involves plucking the top two leaves and bud from the end of the branches. These are all collected and processed within 24 h. Tea production is dominated by Asia and Africa. 'Today over 75% of tea is produced in India, China, Sri Lanka, Kenya, Turkey and Indonesia' (Traidcraft, 2004). The price of tea is determined by the quality, flavour and the reputation of the producing area.

One of the moist prestigious areas for growing tea is Darjeeling, which is located in the West Bengal state in India. Tea has been grown commercially in Darjeeling since being planted by the British in 1852. Today tea is grown in 85 gardens covering an area of 17,400 hc to produce approximately 11.5 million kg of tea per year. Darjeeling provides a unique growing location for tea due particularly to its altitude (1800–6300 feet) and climate. These conditions, combined with strict control of production processes, result in the production of a characteristic high quality tea, which has made the name Darjeeling famous throughout the world. This quality allows the producers to command a significantly higher price for their product.

Considerable research has already been carried out to establish the origin of food and plant products with trace element analysis being used to determine the origin of a range of commodities including pistachios (Anderson & Smith, 2005), wine (Almeida & Vasconcelos, 2003; Taylor, Longerich, & Greenough, 2003), garlic (Smith, 2005), thyme, honey (Terrab, Hernanz, & Heredia, 2004) and Welsh onions (Ariyama, Horita, & Yasui, 2004). Studies into the application of isotope analysis for origin and adulteration determination have also been carried out on a range of products including wine (Majcenovic, Schneider, Lepoutre, Lempereur, & Baumes, 2002; Roßmann, Schmidt, Hermann, & Ristow, 1998; Roßmann et al., 1996), olive oil (Angerosa, Camera, Cumitini, Gleixner, & Reniero, 1997; Angerosa et al., 1999; Spangenberg & Ogrinc, 2001; Woodbury, Evershed, Rossell, Griffith, & Farnell, 1995), cheese (Manca et al., 2001) and butter (Rossmann et al., 2000).

While several studies have been conducted on tea, these generally have only small sample sets or limited classifications. Valera, Pablos and Gonzalez (1996) combined chemical analysis with discriminant analysis to broadly classify tea samples as black or green. Liu et al. (1987) analysed tea samples for their content of cellulose, hemicellulose, lignin, polyphenols, caffeine and amino acids and then used principal component analysis to classify samples as green, black or oolong. Marcos et al. (1998) determined the trace element concentrations of tea samples using inductively coupled plasma atomic emission spectroscopy (ICP-AES) and inductively coupled plasma mass spectrometry (ICP-MS). They were able to distinguish between African and Asian teas and separate Chinese samples from other Asian samples. However, this was a small study with only 15 samples from 10 different countries and cannot be considered in any way definitive. Fernandez-Caceres, Martin, Pablos, and Gonzalez (2001) applied multivariate and chemometric techniques to concentration data of the major elements in tea obtained using ICP-AES for 46 samples. Their results suggest that discrimination according to geographical origin is possible using linear discriminant analysis, however only 24 samples from five regions were used in this classification. Moreda-Pineiro, Marcos, Fisher, and Hill (2001) investigated the effects of data pre-treatment techniques on the classification of tea samples as either African or Asian. Moreda-Pineiro, Fisher, and Hill (2003) used ICP-AES and ICP-MS and were able to separate Asian and African teas and classify Chinese, Indian and Sri Lankan teas. Studies to date have typically relied on discrimination based on either light stable isotopes or trace element data rather than investigating the potential of combining both techniques to provide a more robust and universally applicable provenance determination.

The current study investigates the potential of using a combination of stable isotope (C, N & H) and trace element data for 83 tea samples to establish the growing region. The effects of differences in tea type, harvest date and tea quality on this classification have also been studied. Linear discriminant analysis has been applied to obtain separation of growing regions and to identify the provenance of samples from different tea growing regions of Asia (China, India, Sri Lanka and Taiwan). The validity of the method for the determination of origin of unknown samples was then tested through the analysis of 20 commercial samples.

2. Materials and methods

2.1. Samples

Tea samples (see Table 1) were obtained through Australian tea importers. Details were recorded as to the growing region, plantation, harvest date, type and quality. An additional 20 samples were obtained through commercial outlets. These samples were treated as 'unknowns'.

2.2. Solution analysis using inductively coupled plasma mass spectrometry (ICP-MS)

Samples of tea (1 g) were accurately weighed into conical flasks in triplicate. Nitric acid (20 mL) (Ajax Finechem, NSW, Australia, AnalR, sub-boiling quartz still redistilled) was added to each sample. The flasks were covered with watch glasses and then placed on hotplates at 140 °C for eight hours. The temperature was reduced to 90 °C and samples left overnight. After this period, the watch glasses were removed and the nitric acid evaporated to leave a yellow residue. A further volume of nitric acid (10 mL) was added and the flasks, covered by watch glasses, were placed, on hotplates at 140 °C (2 h). After this time the watch glasses were removed and the nitric acid evaporated off. When dry, 4:1 nitric/perchloric acid mixture (15 mL) (Ajax Finechem, NSW, Australia, AnalR, sub-boiling quartz still redistilled) was added to each flask. The flasks were again covered by watch glasses and placed, on hotplates at 180 °C (3 h). After this time, the temperature was reduced to 100 °C and the samples left overnight to react. In the morning, the lids were removed and the nitric/perchloric acid mixture evaporated leaving a white residue. This was cooled to room temperature and then ta-

Table 1
Summary of tea samples used in study

	Black	Green	Oolong	Total
China	6	6	0	12
India	40	2	1	43
Sri Lanka	19	4	0	23
Taiwan	1	0	4	5
Commercial	19	1	0	20
Total	85	13	5	103
Indian tea regions				
Assam	6	0	0	6
Darjeeling	10	0	1	11
Nilgiri	24	2	0	26
Total	40	2	1	43
Nilgiri tea gardens				
Chamraj	2	0	0	2
Glendale	2	0	0	2
Havukal	5	0	0	**5**
Kairbetta	8	0	0	8
Kondanaad	1	0	0	1
Korakundah	3	2	0	5
Swampy and Swampy plantations	3	0	0	3
Total	24	2	0	26

ken into solution with approx 20% nitric acid (7.5 mL) and gentle warming. The solution was transferred into pre-weighed and pre-cleaned (by soaking for 48 h in 10% nitric acid, washing with deionised water and air drying upside down) 70 mL plastic tubs. The flasks were rinsed several times with milliQ water with the washings being added to the tubs. The solutions were made up to 50 g using milliQ water.

Certified reference materials (CRMs), peach leaves and apple leaves (National Institute of Standards and Technology), were also included as samples during the digest. 0.5 g of each was weighed out in triplicate. These underwent the same acid dissolution procedure as the tea samples. Three acid blanks, which had also been taken through the entire dissolution procedure, were also included.

Prepared solution samples were analysed using solution ICP-MS (PQ3, Thermo-Elemental, Winsford, Cheshire UK) for ^{49}Ti, ^{51}V, ^{53}Cr, ^{59}Co, ^{60}Ni, ^{65}Cu, ^{66}Zn, ^{71}Ga, ^{73}Ge, ^{75}As, ^{82}Se, ^{85}Rb, ^{88}Sr, ^{89}Y, ^{90}Zr, ^{93}Nb, ^{98}Mo, ^{107}Ag, ^{111}Cd, ^{115}In, ^{120}Sn, ^{121}Sb, ^{126}Te, ^{133}Cs, ^{138}Ba, ^{139}La, ^{140}Ce, ^{141}Pr, ^{146}Nd, ^{152}Sm, ^{153}Eu, ^{158}Gd, ^{159}Tb, ^{162}Dy, ^{165}Ho, ^{166}Er, ^{169}Tm, ^{172}Yb, ^{175}Lu, ^{178}Hf, ^{181}Ta, ^{182}W, ^{203}Tl, ^{208}Pb, ^{209}Bi, ^{232}Th, and ^{238}U. A multi-element standard was run every 10 analyses to allow for drift correction. Correction and normalisation was carried out to the CRMs.

2.3. Elemental analysis isotope ratio mass spectrometry

Prior to analysing the samples for bulk isotope values, the dried tea leaves were ground to a fine powder (<500 μm) using an agate mortar and pestle. Analysis was performed using a Micromass IsoPrime isotope ratio mass spectrometer interfaced to a EuroVector EuroEA3000 elemental analyser.

2.4. $\delta^{13}C$ Analysis

Approximately 150–200 μg of the tea powder were weighed into a small tin capsule. This was then folded and compressed to contain the sample and minimise any air present. The prepared samples were introduced into the elemental analyser using an autosampler. The stable carbon isotopic composition is recorded in the delta notation relative to the Vienna Pee Dee Belemnite (VPDB) standard. CO_2 of known $\delta^{13}C$ content was introduced as a pulse of reference gas. Each sample is analysed a minimum of three times and the average and standard deviations calculated (values ranged between −29.1‰ and −23.2‰ ± 0.23 (SE)). An in-house sucrose standard and a beet sugar standard (IsoAnalytical IA-R005) of known $\delta^{13}C$ values (−10.5‰ and −26.03‰, respectively) were used for calibration purposes. Samples were analysed over a period of 18 months, with replicate samples analysed throughout the entire period to ensure reproducibility of results.

2.5. $\delta^{15}N$ Analysis

Tea powder (2–4 mg) was weighed and analysed in a similar manner to the samples used for carbon isotope analysis. Due to the increased amount of sample, the dilutor must be switched on just prior to the elution of the CO_2 peak and switched off immediately after to prevent the detector from being overloaded with CO_2. The $\delta^{15}N$ composition is reported relative to a reference gas pulse of known $\delta^{15}N$ composition. The isotopic compositions are recorded in delta notation relative to an air standard. Each sample is analysed a minimum of three times and the average and standard deviations calculated (values ranged between 0.2‰ and 7.1‰ ± 0.22 (SE)). A wheat flour standard (IsoAnalytical IA-R001) and Urea standard (EuroVector E11003) of known $\delta^{15}N$ values (2.55‰ and −0.5‰, respectively) were used for calibration purposes. Samples were analysed over a period of 18 months, with replicate samples analysed throughout the entire period to ensure reproducibility of results.

2.6. δD Analysis

The tea powder (550–650 μg) was weighed into a small silver capsule. This was folded and compressed to contain the sample and to remove any air. The prepared sample was introduced into the elemental analyser using an auto sampler. Hydrogen gas of known δD was inserted as pulses of reference gas. The gas is passed into the irMS and the isotope composition calculated using the delta notation relative to the Vienna Standard Mean Ocean Water (VSMOW) standard. Each sample is analysed a minimum of three times and the average and standard deviations calculated (values ranged between −93.4‰ and −11.5‰ ± 0.89 (SE)). Polyethylene (IAEA-CH7) and mineral oil (IA-R002) standards (δD = −100‰ and −111‰, respectively) were used for calibration purposes. Samples were analysed over a period of 18 months, with replicate samples analysed throughout the entire period to ensure reproducibility of results and that the results were not being affected by exchangeable hydrogen.

2.7. Statistical analysis

All data was transformed using a log transformation. Data analysis was performed using SPSS for Windows release 14.0.0. Discriminant analysis was undertaken to establish grouping of samples. The procedure generates a set of discriminant functions based on linear combinations of the predictor variables that provide the best discrimination between the groups. The functions are generated from a sample of cases for which group membership is known; the functions can then be applied to new cases that have measurements for the predictor variables but have unknown group membership (SPSS, 2005). Discriminant analysis was carried out using the stepwise method in which the model is built step by step. Variables are evaluated at each step; the variable that gives the best discrimination between groups is included in the analysis.

The database for discriminant analysis was formed using the data collected for the known tea samples. Samples were analysed in triplicate and each analysis was inserted into the database as an individual data point. The commercial tea samples were then inserted into the database as unlabelled cases and the discriminant analysis repeated as a test of the potential of the technique for determining the origin of unknown samples.

3. Results and discussion

3.1. Country classification

This study uses tea samples whose provenance is accurately known thereby enabling rigorous method validation and confirmation of the provenance identification potential of the methodologies used. Following the verification of the technique, test samples were analysed and subsequently classified against the database formed with the known samples. Study samples were labelled with their country of origin. In addition, Indian tea samples were subdivided into Assam, Darjeeling and Nilgiri, to allow a secondary classification following the initial country classification. These areas have distinct reputations which are carefully-protected and represent the three areas of Indian tea production which this paper is primarily concerned with uniquely identifying.

The scatter plot of the first 2 discriminant functions from the analysis of the known tea samples (Fig. 1a) confirms the capability for separation of samples into their growing region. While tea samples from Taiwan and China appear to be inseparable, inclusion of the third discriminant function (Fig. 1b) presents a clear separation of the two regions. Using these three discriminant functions 97.6% of the samples was correctly classified. The variables used to achieve this classification were δD, $\delta^{13}C$, ^{49}Ti, ^{53}Cr, ^{59}Co, ^{60}Ni,

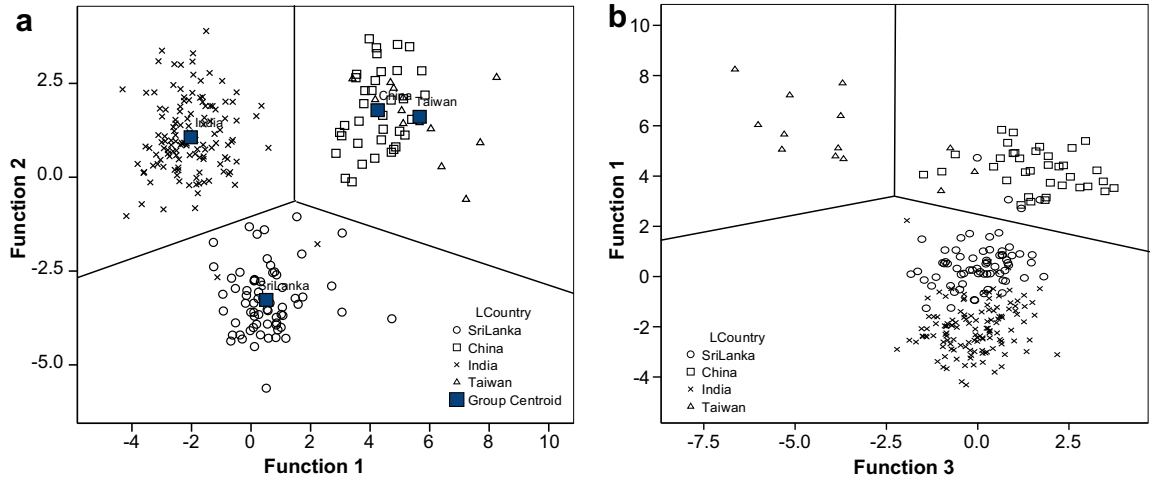

Fig. 1. (a) Scatter plot of the first 2 discriminant functions showing separation between Asian tea growing countries. (b) Scatter plot of discriminant functions 1 and 3 showing separation between China and Taiwan tea samples.

^{65}Cu, ^{71}Ga, ^{85}Rb, ^{88}Sr, ^{89}Y, ^{93}Nb, ^{111}Cd, ^{133}Cs, ^{138}Ba, ^{139}La, ^{140}Ce, ^{141}Pr, ^{153}Eu, ^{203}Tl, ^{208}Pb and ^{209}Bi.

After separation of the samples into their country region, it was investigated whether it was possible to separate the Indian tea samples into their individual growing regions. This was of particular interest due to the unique reputation of each of these regions. The discriminant analysis was repeated using a separate database consisting of the Indian samples, with classification according to region (Fig. 2).

For the method to be valid, it is important that when a sample from outside the database area is tested that it will not be incorrectly classified as coming from one of the test regions. To assess this, samples from other regions (including Africa and Australia) were inserted into the discriminant analysis as ungrouped cases. The discriminant analysis was run and the outcome assessed.

Fig. 3 presents the results from entering an African sample (labelled ungrouped cases) into the database. It can be seen that this sample forms a group completely separate from the Asian tea samples within the database, thus ensuring that misclassification would not occur.

3.2. Unknown samples

To test the validity of the method, a blind trial was conducted using 20 commercial tea samples. These samples were prepared and analysed and the data treated in the same manner as the database samples. The sample data was subsequently entered into the database as an ungrouped case and the discriminant analysis conducted to determine the likely growing region of the test samples. Following this the established origin was compared to the label. The majority of the samples could be matched with the listed growing region, while others were classified into an area different to that specified on the label.

Sample number 15, labelled Darjeeling, was inserted into the data set. Discriminant analysis grouped this sample with the Indian samples. As a further test, this sample was then inserted into the database of Indian teas to determine whether it would be possible to allocate it to a particular growing region within India. Discriminant analysis grouped this sample strongly (100%) with the Darjeeling group.

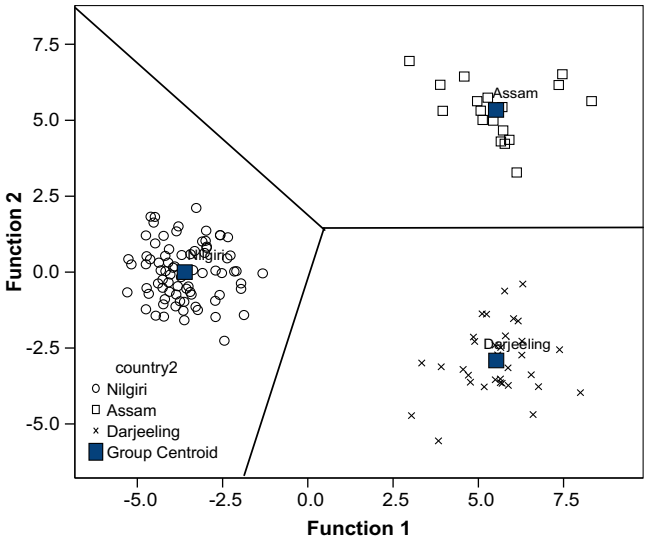

Fig. 2. Scatter plot of the first 2 discriminant functions showing separation of Indian teas according to growing region.

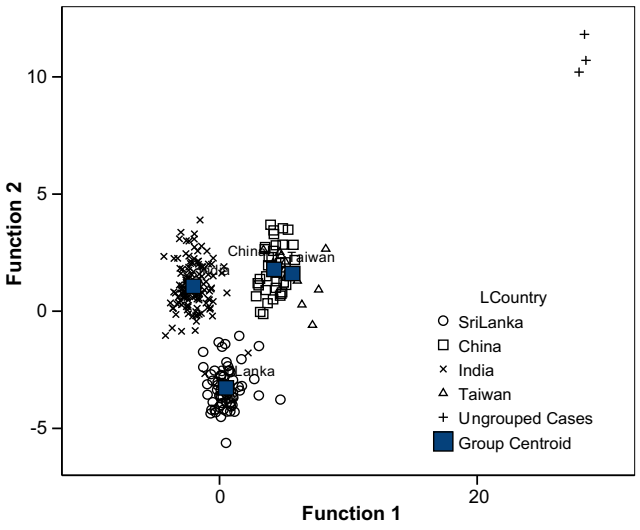

Fig. 3. Discriminant plot indicating the grouping of African tea sample (ungrouped cases) compared with the Asian tea database.

Table 2
Summary of established origin for commercial tea samples compared with the origin specified on the label

Sample #	Type	Established origin	Label
1	Jasmine	Taiwan	China
3	Black	Sri Lanka	Sri Lanka
4	Black	Sri Lanka	Sri Lanka
5	Black	2 China/1 Sri Lanka	India
6	Green	1 China/2 Sri Lanka	India
7	Black	Sri Lanka	Sri Lanka
8	Black	China	China
9	Earl Grey	China	Unlabelled
10	Black	China	China
11	Black	China	China
12	Black	India → Darjeeling	Darjeeling
15	Black	India → Darjeeling	Darjeeling
16	Black	Sri Lanka	Sri Lanka
17	Black	India → Assam	Assam
18	Black	Sri Lanka	Sri Lanka
19	Black	Sri Lanka	Sri Lanka
20	Black	Sri Lanka	Sri Lanka
21	Black	Sri Lanka	Sri Lanka
22	Black	Sri Lanka	Sri Lanka
23	Black	China	Blend

The analysis was repeated for each of the commercial tea samples. The established origin was then compared to the origin that was provided. The results are summarised in Table 2.

3.3. Intra-site variation

The tightness of the grouping of the samples gives an indication of the inter-site variation compared with the intra-site variation. The fact that the samples from one area group together, separate from the samples from other sites, indicates that the variation in chemical signatures between different sites is greater than the variation in signature between samples from the one site. This is particularly notable for the Nilgiri samples. These samples come from seven different plantations within Nilgiri. Samples also differed by grade, degree of processing, and harvest date (with a range of up to three years between harvests).

While it is obviously possible to distinguish between growing areas based on a chemical signature related to the local geology and climatology, it is also apparent from these data that the chemical signature of an individual area remains largely unchanged over a prolonged period of time. This is extremely important as it suggests that the investigator may be able to search a database of reference samples from previous harvests and determine a match. The ability to determine a match would be affected in the situation where there had been an extreme change in the climate or growing procedures of the crop, for example a change in fertilising practises. However, a benefit of the multi variable approach to the study is that it has been shown in previous studies (Gundersen, Bechmann, Behrens, & Sturup, 2000; Pilgrim, 2002) that not all minerals are significantly affected by the fertilising regime; it may therefore be possible to use the database to narrow down the regions from which further, current samples should be obtained to allow for a match. The data also suggests that there is a link between the metal content of the tea and the soil upon which it is grown. Further studies into this relationship may facilitate the development of generic databases, which will predict the chemical signature of teas on the basis of climatology, and geology, helping to identify the growing region of samples for which there is no data base entry.

Thirty-two tea samples were collected for analysis from the Nilgiri (Blue Mountains) region of Southern India. After initially establishing that the Nilgiri teas could be separated from teas the other growing regions, using discriminant analysis (Fig. 2), these samples were treated as a separate data set. The aim of this investigation was to establish whether samples could still be classified correctly despite seasonal and grade variations. In addition, the depth to which a sample could be distinguished from other samples grown in a similar area was also explored. Discriminant analysis was repeated exploring the separation that can be obtained comparing the signatures of the different plantations (Fig. 4a). 97.4% of cross-validated cases were correctly classified. The only samples that are not correctly classified are teas from the Havukal and Kairbetta gardens. The samples also appear to overlap. This is not surprising as the gardens are adjacent to each other. However, if the samples from the estates that clearly separate from each other are removed and the discriminant plot redrawn it is then possible to identify all Nilgiri teas and place samples correctly into the specific production garden (Fig. 4b). This gives an indication of the discriminatory power of the technique.

In conclusion, discriminant analysis of data obtained from trace element analysis in combination with stable isotope data, specifically δN and δD, can be used to determine the growing region of an unknown tea sample with a high degree of confidence. Results also indicate that these classifications are unaffected by the tea type (black, green or oolong), quality or harvest year. Preliminary

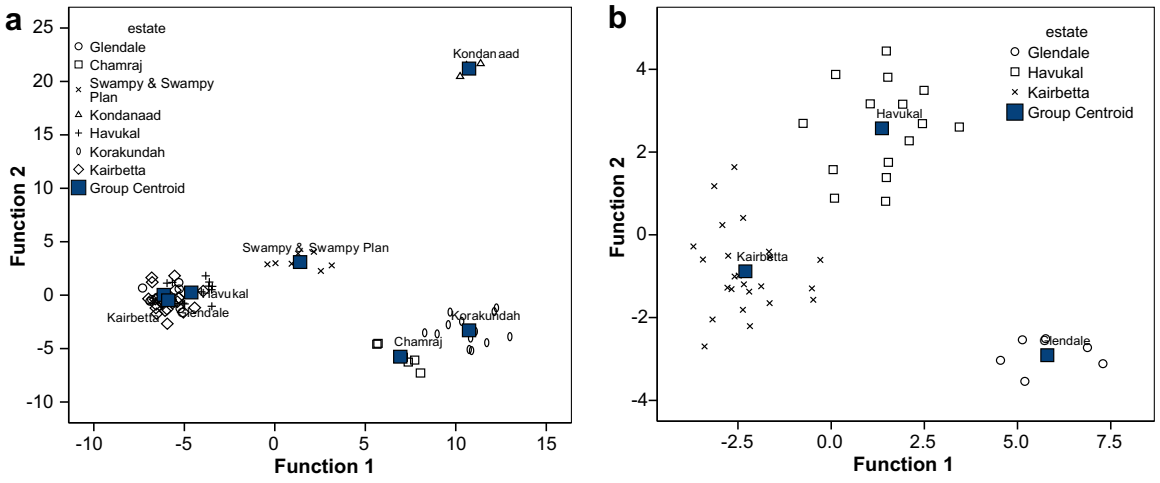

Fig. 4. (a) Scatter plot of first 2 discriminant functions showing separation between tea samples from different tea gardens within the Nilgiri region of India. (b) Scatter plot of the first 2 discriminant functions of the reduced Indian tea dataset showing separation between Havukal, Kairbetta and Glendale tea gardens.

results, based on samples from the Nilgiri region in India, indicate that once the country of origin is established, further data analysis would allow for determination of the garden on which the sample was grown.

Acknowledgements

The authors thank Sue Wang, Department of Chemistry at Curtin University of Technology, for assistance with irMS and Sven Fjastad and Allen Thomas, University of Western Australia, for assistance with ICPMS. The authors also thank Hillary and Nigel White from Elmstock Tea Company Pty. Ltd. Western Australia and David Thompson from Larsen and Thompson, Victoria for providing the tea samples and for their enthusiastic support of this research.

References

Almeida, C. M. R., & Vasconcelos, M. T. S. D. (2003). Multielement composition of wines and their precursors including provenance soil and their potentialities as fingerprints of wine origin. *Journal of Agricultural and Food Chemistry, 51*, 4788–4798.

Anderson, K. A., & Smith, B. W. (2005). Use of chemical profiling to differentiate geographic growing origin of raw pistachios. *Journal of Agricultural and Food Chemistry, 53*, 410–418.

Angerosa, F., Breas, O., Contento, S., Guillou, C., Reniero, F., & Sada, E. (1999). Application of stable isotope ratio analysis to the characterization of the geographical origin of olive oils. *Journal of Agricultural and Food Chemistry, 47*(3), 1013–1017.

Angerosa, F., Camera, L., Cumitini, S., Gleixner, G., & Reniero, F. (1997). Carbon stable isotopes and olive oil adulteration with pomace oil. *Journal of Agricultural and Food Chemistry, 45*, 3044–3048.

Ariyama, K., Horita, H., & Yasui, A. (2004). Chemometric techniques on inorganic elements composition for the determination of the geographic origin of welsh onions. *Analytical Sciences, 20*, 871–877.

Brereton, P. (2006). TRACE: Delivering integrated traceability systems that will enhance consumer confidence in the authenticity of food. Retrieved November 20, 2006, available from <http://www.trace.eu.org/menu/project/>.

Fernandez-Caceres, P. L., Martin, M. J., Pablos, F., & Gonzalez, A. G. (2001). Differentiation of tea (*Camellia sinensis*) varieties and their geographical origin according to their metal content. *Journal of Agricultural and Food Chemistry, 49*(10), 4775–4779.

Gundersen, V., Bechmann, I. E., Behrens, A., & Sturup, S. (2000). Comparative investigation of concentrations of major and trace elements in organic and conventional Danish agricultural crops. 1. Onions (*Allium cepa* Hysam) and Peas (*Pisum sativum* Ping Pong). *Journal of Agricultural and Food Chemistry, 48*, 6094–6102.

Liu, X., van Espen, P., Adams, F., Yan, S. H., & Vanbelle, M. (1987). Classification of Chinese tea samples according to origin and quality by principal component techniques. *Analytica Chimica Acta, 200*, 421–430.

Majcenovic, A. B., Schneider, R. M., Lepoutre, J.-P., Lempereur, V. R., & Baumes, R. (2002). Synthesis and stable isotope dilution assay of ethane thiol and diethyl disulfide in wine using solid phase microextraction. Effect of aging on their levels in wine. *Journal of Agricultural and Food Chemistry, 50*, 6653–6658.

Manca, G., Camin, F., Coloru, G. C., Del Caro, A., Depentori, D., Franco, M. A., et al. (2001). Characterization of the geographical origin of Pecorino Sardo cheese by casein stable isotope (13C/12C and 15N/14N) ratios and free amino acid ratios. *Journal of Agricultural and Food Chemistry, 49*, 1404–1409.

Marcos, A., Fisher, A., Rea, G., & Hill, S. J. (1998). Preliminary study using trace element concentrations and a chemometrics approach to determine the geographical origin of tea. *Journal of Analytical Atomic Spectrometry, 13*(6), 521–525.

Moreda-Pineiro, A., Fisher, A., & Hill, S. J. (2003). The classification of tea according to region of origin using pattern recognition techniques and trace metal data. *Journal of Food Composition and Analysis, 16*(2), 195–211.

Moreda-Pineiro, A., Marcos, A., Fisher, A., & Hill, S. (2001). Evaluation of the effect of data pre-treatment procedures on classical pattern recognition and principal components analysis: A case study for the geographical classification of tea. *Journal of Environmental Monitoring, 3*, 352–360.

Pilgrim, T. (2002). *Determination of the authenticity of natural and organic foodstuff from supermarket shelves*. Perth: Curtin University of Technology.

Rossmann, A., Haberhauer, G., Holzl, S., Horn, P., Pichlmayer, F., & Voerkelius, S. (2000). The potential of multielement stable isotope analysis for regional origin assignment of butter. *European Food Research and Technology, 211*(1), 32–40.

Robmann, A., Schmidt, H. L., Hermann, A., & Ristow, R. (1998). Multielement stable isotope ratio analysis of glycerol to determine its origin in wine. *European Food Research and Technology, 207*(3), 237–243.

Robmann, A., Schmidt, H. L., Reniero, F., Versini, G., Moussa, I., & Merle, M. H. (1996). Stable carbon isotope content in ethanol of EC data bank wines from Italy, France and Germany. *European Food Research and Technology, 203*(3), 293–301.

Smith, R. G. (2005). Determination of the country of origin of garlic (*Allium sativum*) using trace metal profiling. *Journal of Agricultural and Food Chemistry, 53*, 4041–4045.

Spangenberg, J. E., & Ogrinc, N. (2001). Authentication of vegetable oils by bulk and molecular carbon isotope analyses with emphasis on olive oil and pumpkin seed oil. *Journal of Agricultural and Food Chemistry, 49*(3), 1534–1540.

SPSS. (2005). Discriminant analysis. SPSS 14 for Windows Graduate Student Version-Users Guide.

Taylor, V. F., Longerich, H. P., & Greenough, J. D. (2003). Multielement analysis of Canadian wines by inductively coupled plasma mass spectrometry (ICP-MS) and multivariate statistics. *Journal of Agricultural and Food Chemistry, 51*, 856–860.

Terrab, A., Hernanz, D., & Heredia, F. J. (2004). Inductively coupled plasma optical emission spectrometric determination of minerals in thyme honeys and their contribution to geographical discrimination. *Journal of Agricultural and Food Chemistry, 52*, 3441–3445.

Traidcraft. (2004). Traidcraft and Tea. Retrieved March 27 2006, available from <http://www.traidcraft.co.uk/tem2.asp?pageID=1726&fromID=1276>.

Valera, P., Pablos, F., & Gonzalez, A. G. (1996). Classification of tea samples by their chemical composition using discriminant analysis. *Talanta, 43*, 415–419.

Woodbury, S. E., Evershed, R. P., Rossell, J. B., Griffith, R. E., & Farnell, P. (1995). Detection of vegetable oil adulteration using gas chromatography combustion/isotope ratio mass spectrometry. *Analytical Chemistry, 67*, 2685–2690.

World Intellectual Property Organization. (2006) "Geographical Indications". Retrieved May 25 2006, available from <http://www.wipo.int/about_ip/en/geographical_ind.html>.

2. Materials and methods

2.1. Feeding trials

The controlled feeding trials were conducted at Harper Adams University College. Ross and Hubbard varieties of birds were used: the birds were reared as two groups according to the strain but with the males and females together. Initially, they were all fed a proprietary wheat/soya bean meal-based broiler feed that contained no maize or maize products. At 21 and 28 days of age, respectively, the Ross and Hubbard broilers were moved to the experimental feeding house to start on the controlled feeding trials. At 42 and 56 days, respectively, the Ross and Hubbard broilers were slaughtered and 5 males and 5 female birds from each treatment pen, with body weights within 2 SD from their group/gender means, were selected for analysis.

The selected birds were plucked, eviscerated and frozen before dispatch to the laboratory for analysis.

Three feeding trials were carried out. The first two were carried out on cohorts of 10 birds of each strain and the third carried out on a cohort of 10 Ross strain birds. Trials 1, 2 and 3 had 4, 5 and 7 treatments, respectively.

In the first trial, corn was added to the feed at concentrations of 0, 25, 50 and 75% (w/w) for the duration of the finishing period (21 days for Ross and 28 days for Hubbard).

In the second trial, the feeding of the 50% (w/w) corn diet was carried out for different periods of time: (A) for the duration of the finishing period, (days 21–42 for Ross and days 28–56 for Hubbard); (B) only for the first half of the finishing period, (days 21–31 for Ross and days 28–42 for Hubbard); (C) only for the second half of the finishing period (days 32–42 for Ross and days 42–56 for Hubbard); and (D) 75% (w/w) corn diet for the final 7 days only. A control feeding trial, containing no corn, was also incorporated into the study.

The third trial investigated the effect of possible confounding dietary factors on the Ross train of birds only: (A) No corn added but 'Prairie meal' (maize gluten meal, a valuable protein source derived from corn) added throughout the finishing period (21–42 days) at 10% (w/w); (B) No corn but the natural pigment Oroglo added to the feed throughout the finishing period; (C) 40% (w/w) corn plus 10% (w/w) Prairie meal added to the feed throughout the finishing period; (D) 40% (w/w) corn plus 10% (w/w) Prairie meal plus the synthetic pigment, Carophyll Red added to the feed throughout the finishing period; and (E) 50% (w/w) corn plus Oroglo added to the feed throughout the finishing period. One control feeding trial, with no corn fed throughout the finishing period, was also included in this study.

All the diets were nutritionally complete and had similar nutrient compositions (Tables 1 and 2).

The carotenoid content of corn is, on average, 6.4–11.3 mg kg^{-1} (Cruz et al., 2004). The marigold pigment used in this experiment, Oroglo, contains 20 g kg^{-1} of xanthophylls. By adding 1.5 g kg^{-1} of Oroglo, the aim was to add 30 g more xanthophylls per tonne of feed. A similar approach was taken with the Carophyll Red, which contains canthaxanthin. This contains 450 g kg^{-1} of xanthophylls, so 66 mg kg^{-1} of this was added. The maximum amount of canthaxanthin that is allowed in the diet, by EU regulation, is currently 25 mg kg^{-1} (EC Directive 2003/7/EC).

2.2. Sample preparation

Four samples of meat were taken from the breast of each bird. The samples were freeze-dried for three days then homogenised and combined to obtain a representative sample from each bird.

Blind samples were selected from the samples prepared from the first feeding trial.

Table 1
Ingredient composition (g/kg) and calculated nutrient concentrations (g/kg) in the experimental diets in feeding trials 1 and 2

	No corn	250 g/kg corn	500 g/kg corn	750 g/kg corn
Ingredient composition				
Yellow corn		250	500	750
Wheat	750	500	250	
Soya bean meal (dehulled)	150	150	150	150
Full fat soya	20	20	20	20
Fish meal (anchovy)	20	20	20	20
Potato protein		8.3	16.7	25
Soya oil	25	16.7	8.3	
Lysine hydrochloride	4	4	4	4
Methionine	2.5	2.5	2.5	2.5
Limestone	14	14	14	14
Dicalcium Phosphate	8	8	8	8
Salt	4	4	4	4
Vitamin and trace element mix[a]	2.5	2.5	2.5	2.5
Nutrient composition				
Crude protein	181	182	183	184
Lysine	11.7	11.5	11.3	11.1
Methionine plus cystine	8.0	8.1	8.2	8.2
Calcium	9.4	9.3	9.2	9.1
Phosphorus	5.6	5.4	5.2	5.0
Sodium	2.1	2.1	2.0	1.9
Metabolisable energy (MJ/kg)	13.0	13.1	13.2	13.3

[a] Vitamin-trace mineral premix for broilers (Ian Hollows Feed Supplement, UK) added per kg of diet: 800 mg retinol, 150 mg cholecalciferol, 1.25 g tocopherol, 150 mg thiamin,500 mg riboflavin, 150 mg pyrodoxine, 750 mg cyanocobalamin, 3 g nicotinamide,0.5 g pantothenic acid, 75 mg folic acid, 6.25 g biotin, 12.5 g choline chloride, iron 1 g, 50 mg cobalt, 5 g manganese, 0.5 g copper, 4 g zinc, 50 mg iodine,10 mg selenium, and 25 mg molybdenum.

Dried meat (0.5 g) was weighed into a 4 mL vial and 2 mL of hexane was added (HPLC Grade, Sigma Aldrich) and placed in an ultrasonic bath for 20 min. The sample was then removed from the ultrasonic bath and the supernatant was removed. The liquid was filtered through a 0.45 μm PVDF (polyvinylidene fluoride) syringe filter into a 4 mL vial. The extraction procedure was repeated with a further 2 mL of hexane, and after filtering the extracts were combined. The hexane was evaporated under a stream of nitrogen to produce the lipid fraction. The remaining defatted meat (protein) fraction was air dried prior to analysis.

Chicken feed samples were analysed without prior lipid extraction.

2.4. $^{13}C/^{12}C$ Isotopic analysis

Lipid samples were diluted to a concentration of 0.2 mg mL^{-1} in hexane. Five microlitres of the resultant solutions were transferred to tin capsules (Exeter Analytical, solid, 5 × 2 mm) and the hexane was evaporated under a stream of nitrogen. One milligram aliquots of the protein fraction were weighed into tin capsules (Exeter Analytical, foil, 5 × 3.5 mm) for analysis.

The capsules containing lipid or protein fraction were placed in the autosampler of the elemental analyser (EA 1108, CE Instruments, Milan, Italy), and dropped into a vertical quartz tube maintained at a temperature of 1020 °C. The helium stream was then temporarily enriched with oxygen and the sample oxidised in a 'flash' combustion reaction. Quantitative combustion was achieved by passing the gas mixture over a catalyst layer of chromium oxide and a halogen scrubber layer of silvered cobaltous oxide. The combustion gases were then passed over elemental copper at a temperature of 650 °C, in a second quartz tube, to remove residual oxygen and convert nitrous oxides to nitrogen. Water was removed from the gas stream by a chemical trap containing anhydrous magne-

Table 2
Ingredient composition (g/kg) and calculated nutrient concentrations (g/kg) in the experimental diets in feeding trial 3

	Diet codes						
	A No corn	B 500 g/kg corn	C No corn 100 g/kg maize gluten meal	D No corn 1.5 g/kg Oroglo	E 400 g/kg corn 100 g/kg maize gluten meal	F 400 g/kg corn 100 g/kg maize gluten meal 0.067 g/kg Carophyll Red	G 500 g/kg corn 1.5 g/kg Oroglo
Ingredient composition							
Yellow corn	–	500	–	–	400	400	500
Wheat	750	250	750	750	250	250	250
Soya bean meal (dehulled)	150	150	50	150	150	150	150
Full fat soya	20	20	20	20	20	20	20
Fish meal (anchovy)	20	20	20	20	20	20	20
Potato protein	–	16.7	0	0	16.7	16.7	16.7
Maize gluten meal	–	–	100	–	100	100	–
Soya oil	25	8.3	5	25	8.3	8.3	8.3
Lysine hydrochloride	4	4	4	4	4	4	4
Methionine	2.5	2.5	2.5	2.5	2.5	2.5	2.5
Limestone	14	14	14	14	14	14	14
Dicalcium Phosphate	8	8	8	8	8	8	8
Salt	4	4	4	4	4	4	4
Vitamin and trace element mix[a]	2.5	2.5	2.5	2.5	2.5	2.5	2.5
Oroglo				1.5			1.5
Carophyll Red						0.0666	
Nutrient composition							
Crude protein	181	183	210	180	236	236	182
Lysine	11.7	11.3	9.7	11.7	12.1	12.1	11.2
Methionine plus cystine	8.0	8.2	9.5	8.0	10.7	10.7	8.1
Calcium	9.4	9.2	9.1	9.3	9.2	9.2	9.1
Phosphorus	5.6	5.2	5.3	5.5	5.3	5.3	5.2
Sodium	2.1	2.0	2.1	2.1	2.0	2.0	2.0
Metabolisable energy (MJ/kg)	13.0	13.2	13.1	12.9	13.3	13.3	13.1

[a] Vitamin-trace mineral premix for broilers (Ian Hollows Feed Supplement, UK) added per kg of diet: 800 mg retinol, 150 mg cholecalciferol, 1.25 g tocopherol, 150 mg thiamin,500 mg riboflavin, 150 mg pyrodoxine, 750 mg cyanocobalamin, 3 g nicotinamide,0.5 g pantothenic acid, 75 mg folic acid, 6.25 g biotin, 12.5 g choline chloride, iron 1 g, 50 mg cobalt, 5 g manganese, 0.5 g copper, 4 g zinc, 50 mg iodine,10 mg selenium, and 25 mg molybdenum.

sium perchlorate. Following the water trap the components of the reaction gas mixture (N_2 and CO_2) were separated on a chromatographic column (Porapak PQS, PTFE, 2 m, 6 × 5 mm). A portion of the effluent from the elemental analyser (ca. 0.5 mL min^{-1}) was transferred into the Delta S isotope ratio mass spectrometer (Thermo Finnigan, Bremen, Germany), and the signal from ions at *m/z* 44, *m/z* 45 and *m/z* 46 was monitored.

The ^{13}C content was expressed as the ratio of $^{13}C/^{12}C$. Stable isotope ratios are routinely expressed as parts per thousand (‰) difference from the isotopic ratio of an international standard VPDB (Vienna Pee Dee Belemnite). Secondary calibration of the isotope ratios was carried out by reference to in-house reference materials including gases that were traceable back to VPDB.

3. Results

The results for the Hubbard and Ross birds fed with the varying proportions of corn (treatment 1) are summarised in Figs. 1 and 2, respectively. As expected, the $\delta^{13}C‰$ value of both the lipid and protein fraction in the corn-fed chickens became more positive with increasing corn content in their feed. The natural variation in $\delta^{13}C‰$ values for both the protein fraction and lipid fraction for the chickens in the same treatment was small, (standard deviations ⩽0.67‰ for lipid and ⩽0.26‰ for protein). The trend for the $\delta^{13}C‰$ values for protein fraction, from zero to 75% (w/w) corn, was less pronounced than for the $\delta^{13}C‰$ of the lipid and this was probably due to the adipose tissue carbon being influenced by the diet more rapidly than the muscle protein. As a result of this, the apparent gap between $\delta^{13}C‰$ values of the protein and lipid fractions decreased with increasing corn in the diet, a difference of 4.86‰ for no corn in the diet decreasing to 2.86‰ for 75% (w/w) in the diet.

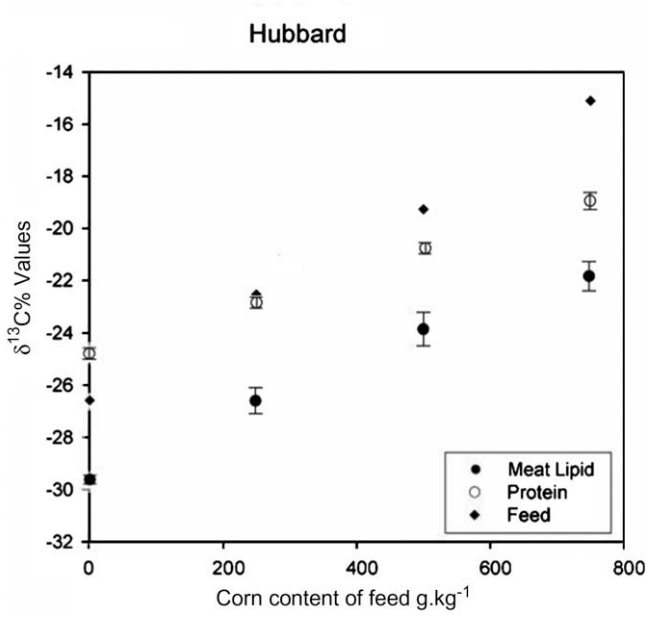

Fig. 1. The effect of corn content of diet on the $\delta^{13}C‰$ values of Hubbard birds. The error bars represent the standard deviation in the $\delta^{13}C‰$ values of 10 birds from the same treatment pen.

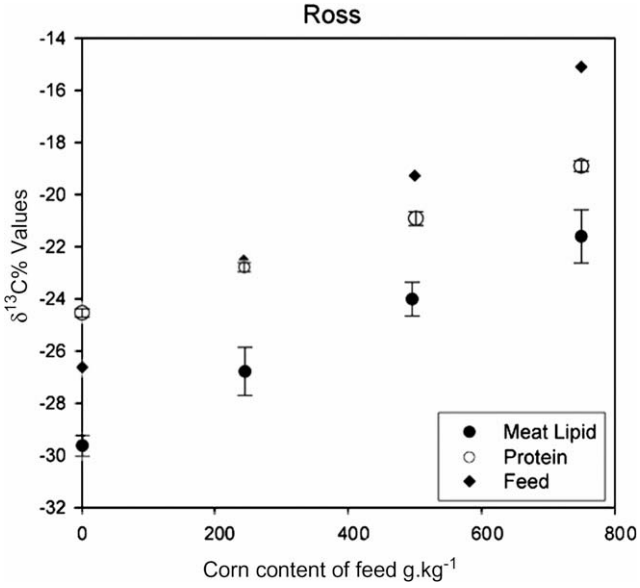

Fig. 2. The effect of corn content of diet on the $\delta^{13}C‰$ values of Ross broilers. The error bars represent the standard deviation in the $\delta^{13}C‰$ values of 10 birds from the same treatment pen.

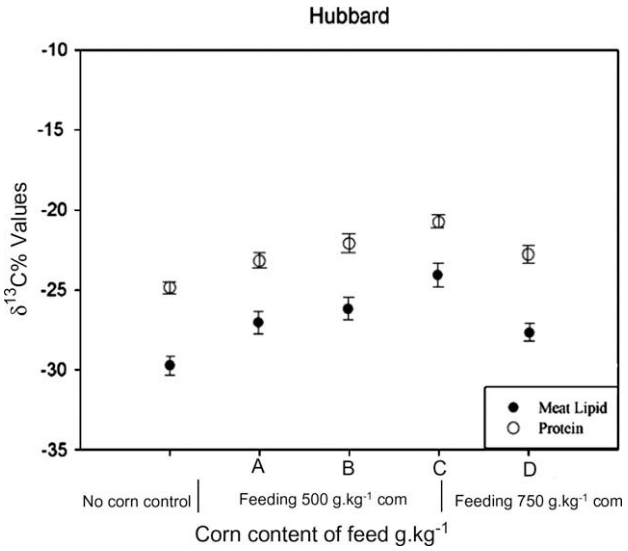

Fig. 3. $\delta^{13}C‰$ values of Hubbard birds fed with corn for varying amounts of time. A = 14 days feeding from 28 to 42 days, B = 14 days feeding from 42 to 56 days, C = 28 days feeding from 28 to 56 days and D = 7 days feeding from 49 to 56 days.

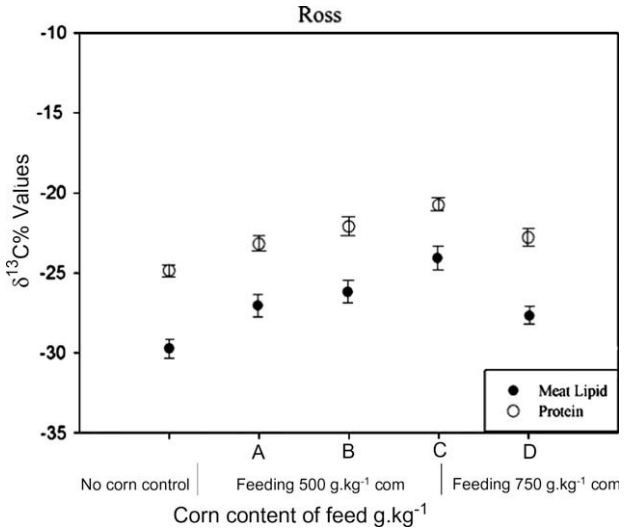

Fig. 4. $\delta^{13}C‰$ values of Ross broilers fed with corn for varying amounts of time. A = 10 days feeding from 21 to 31 days, B = 10 days feeding from 31 to 42 days, C = 21 days feeding from 21 to 42 days and D = 7 days feeding from 35 to 42 days.

Differences between the $\delta^{13}C‰$ values of both the lipid and protein fractions of the two varieties of birds were small but statistically significant ($P < 0.05$). Analysis of covariance showed that the breed had an effect on the intercept of the regression line amounting to a difference of only 0.1‰ for the protein fraction. This difference probably reflected the differences in the growth rates of the two varieties.

The carbon isotope ratio results for the chickens fed with the fixed levels of corn for varying amounts of time (treatment 2) are summarised in Figs. 3 and 4. The effect of varying the length of corn feeding was pronounced, with the 50% (w/w) corn-fed control samples, fed for all of their fattening period (half their life) having significantly more positive values than the samples where feeding was for only half the fattening period. The values for the samples from the birds fed with 50% (w/w) corn for the second half of their fattening period (42–56 days for Hubbard and 31–42 days for Ross) were more positive than the samples from the birds fed with 50% (w/w) corn in the first half of the fattening period but this was not statistically significant. The values for the samples where the feed contained 75% (w/w) corn for the last week were similar to those for 50% (w/w) corn for the second half of the fattening period for Ross broilers. However, the values for the Hubbard birds fed 75% (w/w) corn for the last week were less than those for the 50% (w/w) corn for the second half of the fattening period. Again, this probably was a reflection of the different growth rates of the two birds with the faster growing Ross strain incorporating more of the corn ^{13}C into both protein and lipid over the last quarter of the birds life.

The carbon isotope ratio results for the Ross Broilers fed with pigments and alternative feeds (treatment 3) are summarised in Fig. 5. The Prairie meal had a significant influence on the carbon values, leading to more positive $\delta^{13}C‰$ values. For the pigments, the effects on the carbon isotope ratios were less significant. There was no statistically significant difference in $\delta^{13}C‰$ values between the 50% (w/w) corn with 50% (w/w) corn plus Oroglo. This was also the case for the 40% (w/w) corn plus Prairie meal against the similar treatment with Carophyll Red added. The results also showed significant changes in the $\delta^{13}C‰$ of both the protein fraction and lipid values for the addition of Prairie meal, with the $\delta^{13}C‰$ protein fraction values increasing more than the $\delta^{13}C‰$ lipid values, contrary to what was observed with the addition of corn. (The difference between $\delta^{13}C‰$ protein and $\delta^{13}C‰$ lipid values for non corn-fed chickens was 4.97; for 50% (w/w) corn-fed chickens it was 3.05‰, and for Prairie meal-fed chicken was 5.96‰.)

Blind testing of samples from feeding trial one correctly identified all the samples that had not been fed corn and the samples that had been fed corn at 50% (w/w) in their diets for at least half of the fattening period – the generally recognised criteria for corn-fed chicken.

An evaluation of commercially grown corn-fed chickens and commercial corn chicken feed was carried out to assess whether the method was applicable to commercial conditions in the UK. Four samples of commercial chicken corn feed were analysed and had $\delta^{13}C‰$ values ranging from −19.25‰ to −21.7‰. A commercial non-corn chicken feed had a $\delta^{13}C‰$ value of −26.31‰.

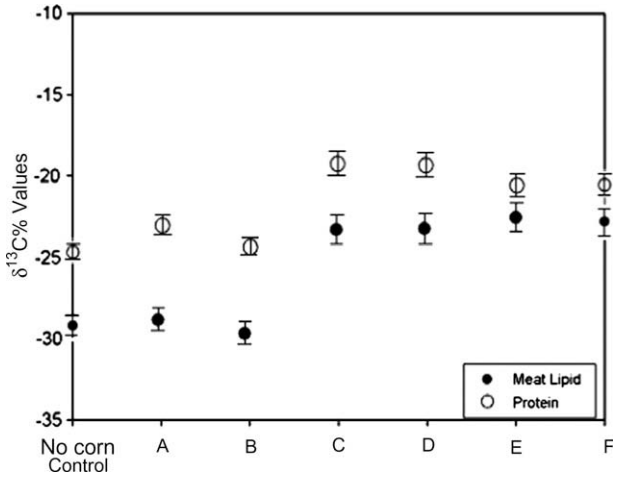

Fig. 5. The effect of feed type on the $\delta^{13}C‰$ values of Ross chickens. CR = Carophyll Red, A = Diet with Prairie meal, B = diet with Oroglo, C = 400 g kg^{-1} corn + Prairie meal, D = 400 g kg^{-1} corn + Prairie meal + Carophyll Red, E = 400 g kg^{-1} corn + Oroglo and F = 500 g kg^{-1} corn.

Analysis of the $\delta^{13}C‰$ values of protein from eight commercially grown corn-fed chickens (two producers) revealed a good correlation between $\delta^{13}C‰$ values and the corn-fed status of the birds, (mean $\delta^{13}C‰$ −20.75 st. dev. 0.37). In contrast, analysis of the chicken lipid was less conclusive, ($\delta^{13}C‰$ mean values −27.2 st. dev. 0.78) suggesting the chicken lipid was a less reliable indicator of dietary status. This reflected the observations made in the experimental samples where a larger variation was observed in the $\delta^{13}C‰$ values for lipid than for protein (standard deviations $\leqslant$0.67‰ for lipid and $\leqslant$0.26‰ for protein).

Analysis of three commercially reared chickens of different breeds to those in the experimental study (BAC 657, COB500 and Maron Gold line), grown on normal commercial diets, showed a mean $\delta^{13}C‰$ value of their protein to be −24.57 (st. dev. 0.31) and mean $\delta^{13}C‰$ value of their lipid to be −28.77 (st. dev. 0.60) indicating that the breed of chicken did not significantly influence the $\delta^{13}C‰$ value. (The Ross and Hubbard experimental samples fed on commercial diets had a mean lipid $\delta^{13}C‰$ values of 29.49 and a mean protein $\delta^{13}C‰$ value of −24.69.)

4. Discussion and conclusions

The data obtained in this study show that stable carbon isotopes can be used to differentiate between corn-fed and non corn-fed chicken. The linear trend in carbon isotope ratios with increasing amounts of corn in the diet was reflected in both the chicken lipid and protein. The amount of dietary fat that goes directly into the body fat depends on the dietary energy intake relative to the energy needs of the birds. The formulated diets were similar to commercial nutrient specifications and so were relatively energy dense, and so a high proportion of the dietary fat would have been deposited into the adipose tissue. Since all the diets contained the same amount of lipid the high corn diets would rapidly reflect the ^{13}C signature of corn lipid (Bavelaar and Beynen, 2003). This probably explains why more ^{13}C was observed in the body fat than in the protein.

The feeding time experiments indicated that it was possible to distinguish between chicken samples, where a corn diet was fed for a shorter period than recommended.

A comparison of the $\delta^{13}C‰$ data from the lipid and protein fractions from commercially produced corn-fed chicken, in order to evaluate the ability of the data to discriminate between the two rearing conditions, showed that the lipid values were less appropriate than the protein values.

The addition of Prairie meal to the diet was shown to increase the $\delta^{13}C‰$ values of both the protein and lipid in the chicken but to have a more marked effect on the protein value so that in the experimental samples it was possible to determine when Prairie meal had been used in the diet by examining the difference between the protein and lipid $\delta^{13}C‰$ values. In the light of the greater variability in the lipid $\delta^{13}C‰$ values of the commercially grown corn-fed chicken this would no longer be possible, so the addition of Prairie meal to the diet could probably not be distinguished from the addition of corn to the diet.

Analysis of the commercial feeds directly confirmed the hypothesis that the higher corn content of the feed was reflected in a more negative $\delta^{13}C‰$ value, and there were no other confounding factors in the commercial feeds.

Examining the protein $\delta^{13}C‰$ values from all of the experimental samples analysed showed that the non corn-fed chickens had a mean $\delta^{13}C‰$ value of −24.68 (st. dev. 0.17, $n = 40$), while the corn-fed chicken protein had a mean $\delta^{13}C‰$ value of −20.67 (st. dev. 0.34, $n = 50$). This compared very well with the commercial non corn-fed samples with a protein $\delta^{13}C‰$ value of −24.87; (st. dev. 0.35, $n = 14$) and the average $\delta^{13}C‰$ protein value the from commercial corn-fed samples of −20.75 (st. dev. 0.37, $n = 8$).

A calibration of $\delta^{13}C‰$ measurements against the proportion of corn in the diet produced a linear relation (Fig. 6). Four of the 140 results were judged to be outliers and were not used in the calibration. A critical value of −22.5 $\delta^{13}C‰$ was set because it was half way between the lower end of a 95% prediction interval of the calibration for 50%-corn-fed chicken and the upper end of a 95% prediction interval for 0%-corn-fed chicken. Measurement results below the critical value were used to identify chicken that had been fed less than the required 50% corn. The difference between the expected measurement results for chicken fed on 50% corn and the critical value was over eight times the standard error of prediction associated with the calibration at 50%. Hence, the false positive rate (proportion of samples from chicken fed on 50% corn identified as non corn-fed chicken) can be expected to be very low, effectively zero assuming measurement results are normally distributed (examination of the residuals showed that this assumption was reasonable). A threshold set at −22.5 $\delta^{13}C‰$ allows the method to reliably (>97.5%) assign chicken as non corn fed if the diet contains no more than 23.3% corn and by setting the threshold at −21.42 allows the method to reliably assign chicken fed on no more than 37% corn as non corn-fed.

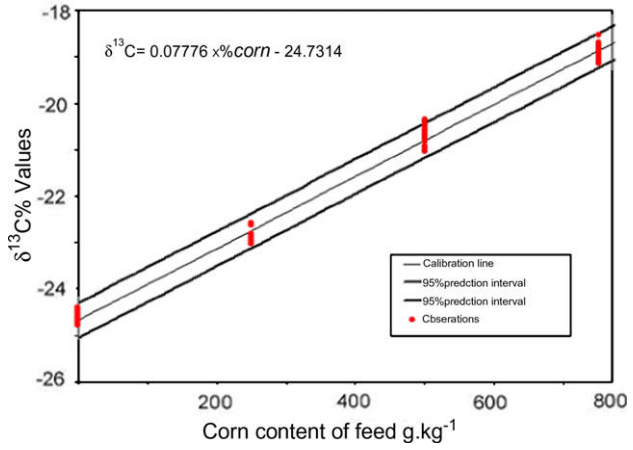

Fig. 6. Calibration curve of $\delta^{13}C‰$ values of chicken protein fraction and amount of corn in diet.

Acknowledgements

The authors would like to acknowledge the UK Food Standards Agency Food Authenticity programme for funding this work.

References

Bavelaar, F. J., & Beynen, A. C. (2003). Relationships between dietary fatty acid composition and either melting point or fatty acid profile of adipose tissue in broilers. *Meat Science, 64*, 133–140.

Council Regulation EEC 1906/90, 26th June 1990 on certain marketing standards on poultry meat.

Cruz, V. C., Pezzato, A. C., Ducatti, C., Pinheiro, D. F., Sartori, J. R., & Goncalves, J. C. (2004). Tracing metabolic routes of feed ingredients in tissues of broiler chickens using stable Isotopes. *Poultry Science, 83*, 1376–1381.

Gonzalez-Martin, I., Gonzalez-Perez, C., Mendez, J. H., Marques-Macias, E., & Poveda, F. S. (1999). Differentiation of dietary regime of Iberian Swine by means of isotopic analysis of carbon and sulphur in hepatic tissue. *Meat Science, 52*, 437–441.

Jahan, K., & Paterson, A. (2007). Lipid composition of retail organic, free-range and conventional chicken breasts. *International Journal of Food Science and Technology, 42*(3), 251–262.

O'Leary, M. H. (1981). Carbon isotope fractionation in plants. *Phytochemistry, 20*, 553–567.

Sakamoto, N., Ishida, T., Arima, T., Idenitsu, K., Inagaki, Y., & Furuya, H, et al. (2002). Concentrations of radiocarbon and isotope compositions of stable Carbon in food. *Journal of Nuclear Science and Technology, 39*(4), 323–328.

As part of the EU-funded TRACE project which aims to develop and apply analytical methods for the proof of geographical origin of food the usefulness of strontium isotope ratio investigations was evaluated.

Originally, the use of strontium isotope ratios was restricted to geosciences. However, since Chaudhuri (1978) published a study about the application of $^{87}Sr/^{86}Sr$ to investigate the origin of groundwater, the method has also been widely used in hydrology, although mostly for deep subsurface waters of higher temperature and/or salinity (Chaudhuri & Clauer, 1992; Hofmann & Baumann, 1986; Matter, Peters, & Ramseyer, 1987; Pampura, Plyusnin, & Sandimirova, 1980; Ufrecht & Hoelzl, 2006). Åberg (1995) presented the applicability of the method for several environmental studies.

More recent investigations deal with the application of strontium isotope ratios for human migration studies in archaeology (Bentley, 2006; Hodell, Quinn, Brenner, & Kamenov, 2004; Hoogewerff et al., 2001; Montgomery, Evans, & Wildman, 2006; Price, Knipper, Grupe, & Smrcka, 2004; Åberg, Fosse, & Stray, 1998), for paleodietary studies (Lee-Thorp & Sponheimer, 2003) or for forensic purposes (Beard & Johnson, 2000; Rummel, Hoelzl, & Horn, 2007). In the field of food science the first investigations of origin determination were carried out for wine (Barbaste, Robinson, Guilfoyle, Medina, & Lobinski, 2002; Horn, Hoelzl, Todt, & Matthies, 1998; Horn, Schaaf, Holbach, Hoelzl, & Eschnauer, 1993), milk (Crittenden, Andrew, LeFournour, Young, & Middleton et al., 2007), butter (Rossmann, Haberhauer, Hoelzl, Horn, & Pichlmayer et al., 2000), British mineral waters (Montgomery et al., 2006), rice (Oda, Kawasaki, & Hirata, 2002), and fruit juices (Rummel, Hoelzl, Horn, Rossmann, & Schlicht, 2008).

In order to assign origin to a food sample on the basis of its strontium isotope composition, the isotope ratio of the sample must be compared to data of authentic samples from the region in question. However, because of the usually limited possibilities to compile an adequate database of authentic samples, it cannot be assured that these samples will represent the entire strontium isotope variability of the area. This aspect is especially relevant for products from remote areas where data for authentic reference samples are lacking or unobtainable.

In order to evaluate the results, a prediction should be carried out on the basis of thorough knowledge of the geological and pedological situation of the region in question (Horn et al., 1993).

The present large scale investigation of $^{87}Sr/^{86}Sr$ in natural mineral waters is used to test if it is possible to identify geologically derived key parameters predominantly responsible for the strontium isotopic signature in the water in order to predict data ranges for samples just by the knowledge of the geographical origin and the use of a common geological map.

First results of $^{87}Sr/^{86}Sr$ analyses in "surface" water samples, ammonium nitrate extracts from soil samples, and honey as well as wheat samples from specific sample regions within the TRACE project, will be used in this study to test the applicability and transferability of predicted data ranges for strontium isotope ratios, gained by the natural mineral water investigation, to other agricultural products and food commodities.

2. Fundamentals

$^{87}Sr/^{86}Sr$ is a parameter reflecting local geochronological and lithological settings by their natural spatial variation.

Strontium isotopic signatures in rocks have evolved over geological time. ^{88}Sr, ^{86}Sr and ^{84}Sr are stable and not radiogenic whereas the abundance of 87Sr increases with radioactive decay of ^{87}Rb (half life: 48.8 x 109 years). Thus, actual $^{87}Sr/^{86}Sr$ is a function of initial $^{87}Sr/^{86}Sr$, initial Rb/Sr and time.

For example, young and rubidium-poor rocks such as Quaternary basalts have low $^{87}Sr/^{86}Sr$ (from 0.702 to around 0.706), whereas older and/or rubidium-rich rocks such as Palaeozoic granites show considerably higher ratios (Faure, 1986).

Any groundwater – in this study bottled groundwater defined as natural mineral water – obtains its characteristic strontium and isotope content from the processes of dissolution and re-precipitation of strontium from minerals. As no significant isotope fractionation occurs the groundwater obtains its isotopic signature from the minerals of the soil and rock strata through which it percolates. Precipitation processes only change the strontium content but do not alter the isotopic signature.

The strontium isotopic composition of groundwater does not reflect the $^{87}Sr/^{86}Sr$ of the bulk soil or rock it comes into contact with, but that of the soluble minerals able to exchange chemically with the water (Horn, 2005; Horn et al., 1998; Åberg, Jacks, & Hamilton, 1989).

When water circulates through the underground ongoing dissolution and precipitation is controlled by the respective recalibrated hydrochemical and hydrophysical properties of the fluid by the surrounding conditions. In the region of Hegau-Schaffhausen at the Switzerland/Germany border detailed hydrogeological investigations, which include comprehensive strontium isotope ratio analyses, appear to indicate that in earth-alkaline waters a first hydrochemical equilibrium status is reached soon after infiltration. The implication is that the specific strontium content and isotopic signature is induced by soil and surface geology within only a couple of years.

If no significant change is enforced on the quasi hydrochemical equilibrium of an earth-alkaline water, the strontium isotopic signature will remain constant for long circulation periods even in more profound and geologically different layers (InterregIIIA-Projektbericht, 2008).

The isotopic composition of groundwater from aquifers in evaporites and marine limestones resembles the isotopic composition of the rocks due to the simple geochemical composition of these rocks and the solubility of the main minerals.

As the strontium concentration and isotope ratio is closely related to the carbonate system, isotope ratios measured in groundwaters from large limestone areas follow roughly the marine curve primarily published by Burke, Denison, Hetherington, Koepnick, & Nelson et al. (1982) and Veizer and Compston (1974), continuously revised e.g. by McArthur (1994) and McArthur, Howarth, and Bailey (2001).

The isotopic composition of groundwater filtered through clastic sediments, metamorphic or magmatic rocks resemble the composition of easily weathering minerals of the corresponding rocks.

3. Sampling

Between 2005 and 2006 participants of the TRACE project collected about 650 different natural mineral water brands predominantly of western Europe. For samples from Hungary, Slovakia, Switzerland, Scandinavian countries, Slovenia, Croatia and for half the samples of Poland private contacts were used. Sampling of bottled natural mineral water was mostly done by simply buying bottles in shops. Producers have voluntarily provided only small selections of waters. The geographical origin was determined by the indicated bottling locality (city) marked on the bottle and/or by the published lists of the EU (Official Journal C59, 09-03-2005; latest update 23-10-2006).

For mapping, all geographical coordinates have been determined by the same route planning software (ADAC TourPlaner Europe 2005/2006), which turned out to be the quickest and easiest way to find even the smallest towns. It is assumed that the locality

of the source is within a distance of about 15 km, which is acceptable in this context. It is known that often more than one water source is used for the bottling of one brand, or that the sources tap multiple rock types as there are often sources in complex tectonic fault zones and/or pumped from different geological units. But for our large scale survey these details play a minor role and have therefore been neglected.

The sampling was organised to get a widespread overview of the European market and to obtain a relatively complete geologic and geographic coverage. The availability of some brands was limited or sourcing was too expensive and intricate. As several European countries have quite different drinking cultures and natural mineral water markets, not every country provides the same spatial distribution of natural mineral waters. For example, Germany offers around 800 brands, while Ireland acknowledges only four brands.

Around 700 different (ground) waters – bottled and raw ones – were sampled. Over 90% of the samples were labelled as natural mineral waters. Furthermore, for better coverage of regions with lower amount of bottling plants we included waters labelled as spring – or medical waters, which are also bottled at source. In addition, to evaluate the effect of production processes and different bottling dates on strontium isotope ratios, about 40 raw water samples were measured. These analyses showed that influences from filtering and bottling processes and seasonal variations of strontium isotope ratios can be excluded (Voerkelius & Lorenz, 2009).

The analysed parameters include the analysis of the main ion content, trace element concentration, isotope ratios of S, O, H, Sr and the tritium content (Voerkelius & Lorenz, 2009). In the context of this paper only the tritium content, the total mineral content and the strontium isotope ratio is of relevance.

4. Measurement

The strontium isotope results discussed in this paper were produced in four different laboratories. Instruments used were one Thermal Ionisation Mass Spectrometer (TIMS) and three Multi Collector Inductively Coupled Plasma Mass Spectrometers (MC-ICP-MS). As the participating laboratories already had their established methods for sample preparation, and were equipped accordingly, each followed it's own sample preparation procedures, described below. To allow for comparison of measurement results, the laboratories worked according to the same standard operating procedure (SOP). The SOP included recommendations on Rb/Sr separations, corrections for procedural blanks, the prescription of the $n(^{86}Sr)/n(^{88}Sr)$ and $n(^{87}Rb)/n(^{85}Rb)$ reference values used for discrimination and interfering element corrections (0.1194 ± 0 and 0.38565 ± 0.00030, respectively), and requiring partial internal validation of methods by regularly measuring the NIST SRM® 987 (SOP, 2006).

Depending on the Sr content, from 1 to 50 mL of natural mineral water or soil extracts were evaporated. Honey and wheat (0.3–30 g) were digested by applying microwave digestion, high pressure microwave digestion, or ashing in a muffle furnace. Residues were dissolved in HNO_3 and subsequently Sr was separated from other elements such as Ca, Ba or Rb by ion chromatography on a Sr specific crown ether resin (Sr-spec®).

The TIMS was a MAT 261/262 Thermo Finnigan and measurements were carried out on tungsten single filaments. For quality control and to check for proper operation of the mass spectrometer an international Sr-standard (NIST SRM® 987) was analysed under the same conditions as the samples. One year standard measurements ($n = 100$) yield a precision of 60 ppm for 95% probability limits (0.71025 ± 0.00004). Duplicate analyses on ten samples showed a reproducibility of <40 ppm, and total blanks are mostly below 100 pg Sr, which is negligible compared to a total Sr content between 100 and 2000 ng in the samples.

The three MC-ICP-MS involved were a Nu Plasma (Nu Instruments), an Axiom (ex-VG Instruments), and an Isoprobe (ex-Micromass). Typically, the instrumentation was equipped with a minicyclonic jacketed cinnabar spay chamber or a porous membrane based desolvation unit, a 0.2 mL min^{-1} microcentric nebuliser and Ni or Pt sampler and skimmer cones.

All four laboratories were involved in five measurement comparisons on natural mineral water test materials. These tests showed for natural mineral water samples a degree of equivalence of about 150–200 ppm between the laboratories.

The results are given as isotope ratios and as δ notation in analogy to the isotopes of the light elements commonly used in the food chemistry sector (Rossmann et al., 2000, Rummel et al., 2008). The δ value is defined as

$$\delta^{87}Sr = (^{87}Sr/^{87}Sr_{analysed}/^{87}Sr/^{86}Sr_{Standard} - 1) \times 1000$$

with $^{87}Sr/^{86}Sr$ Standard = 0.7093 (approximation for baltic sea water) according to Rossmann et al. (2000).

For groundwater dating the analysis of the tritium content of the samples was carried out by Low Level Liquid Scintillation Counting (LSC) after electrolytic 3H enrichment (e.g. Clark & Fritz, 1997). The results are expressed in Tritium Units (TU) with 1 TU = 0.119 Bq/L.

5. Development of a prediction tool

Although the strontium isotopic signature of a natural mineral water is the result of an individual and often complicated genesis, it is believed that these individual influences will be evened out by the large sample number, so that the results of this large scale investigation can be used for the development of a simplified qualitative prediction tool for the isotopic signature of unknown samples.

As described above, comprehensive investigations in the region of Hegau-Schaffhausen indicate that groundwaters with relatively low mean residence time tend to reflect the strontium isotopic signature of the surface geology (InterregIIIA-Projektbericht, 2008). As a result of these investigations and additionally by knowledge about hydrochemical equilibrium in groundwaters (Hölting, 1989), we assumed that in young natural mineral waters the strontium isotopic signature is governed by that of the soil and surface geology.

In hydrology the analysis of tritium content is used to identify young groundwater. If the tritium content is above detection limit in the natural mineral waters, the groundwater or at least part of the groundwater has a mean residence time of 50 years or less (in the current investigation before 2005 to 2006) – and is classified as young water (Clark & Fritz, 1997). In approximately 85% of all analysed brands tritium exceeds the detection limit of 0.6 TU. Therefore it is justifiable to correlate the strontium isotopic signature of the water samples with surface geology.

In order to verify a correlation between surface geology and strontium isotopic signature of the natural mineral waters, a comparison was made to a geological map. The indicated geology at the production location, as well as information of the whole catchment region including possible geological transition zones, were considered in this comparison.

The European geological map used is GIS based and provided by Pawlewicz, Steinshouer, and Gautier (2003). The map differentiates between geochronology and lithology (intrusives, volcanic rocks, metamorphic rocks and sedimentary rocks).

For improved visualisation of the correlation of the geological units and the strontium isotope values of the natural mineral waters the map was simplified with the aid of geographic information system software (GIS: ESRI ArcMap 9.2) (Fig. 1): According to the prevailing $^{87}Sr/^{86}Sr$ range of the samples located on each geological unit, the natural mineral water samples were grouped correspondingly in six groups. Geological units with similar strontium isotope data ranges to those of the samples located on these units were aggregated in the map and allocated the same colour.

In cases where a limited number of samples were available to represent a geological unit, for example the Paleozoic intrusives, assumptions were made based on fundamental geological knowledge and experience.

In the map in Fig. 1 different geological units are assigned into six distinct groups, which are indicated in the legend in six different colours. The origin locations of the natural mineral water samples are also indicated as spots in Fig. 1. The colours of the individual natural mineral water samples represent the interval into which the measured strontium isotope value was classified. All strontium isotope values were divided into six groups, which correspond to typical values associated with the geological groups indicated on the map. Visual comparison of natural mineral water strontium isotope ratios to strontium isotope ratios of underlying surface geology is now possible. As visually indicated by a difference in the colour of some spots and the underlying geological unit, it is not in all cases possible to predict the strontium isotope value

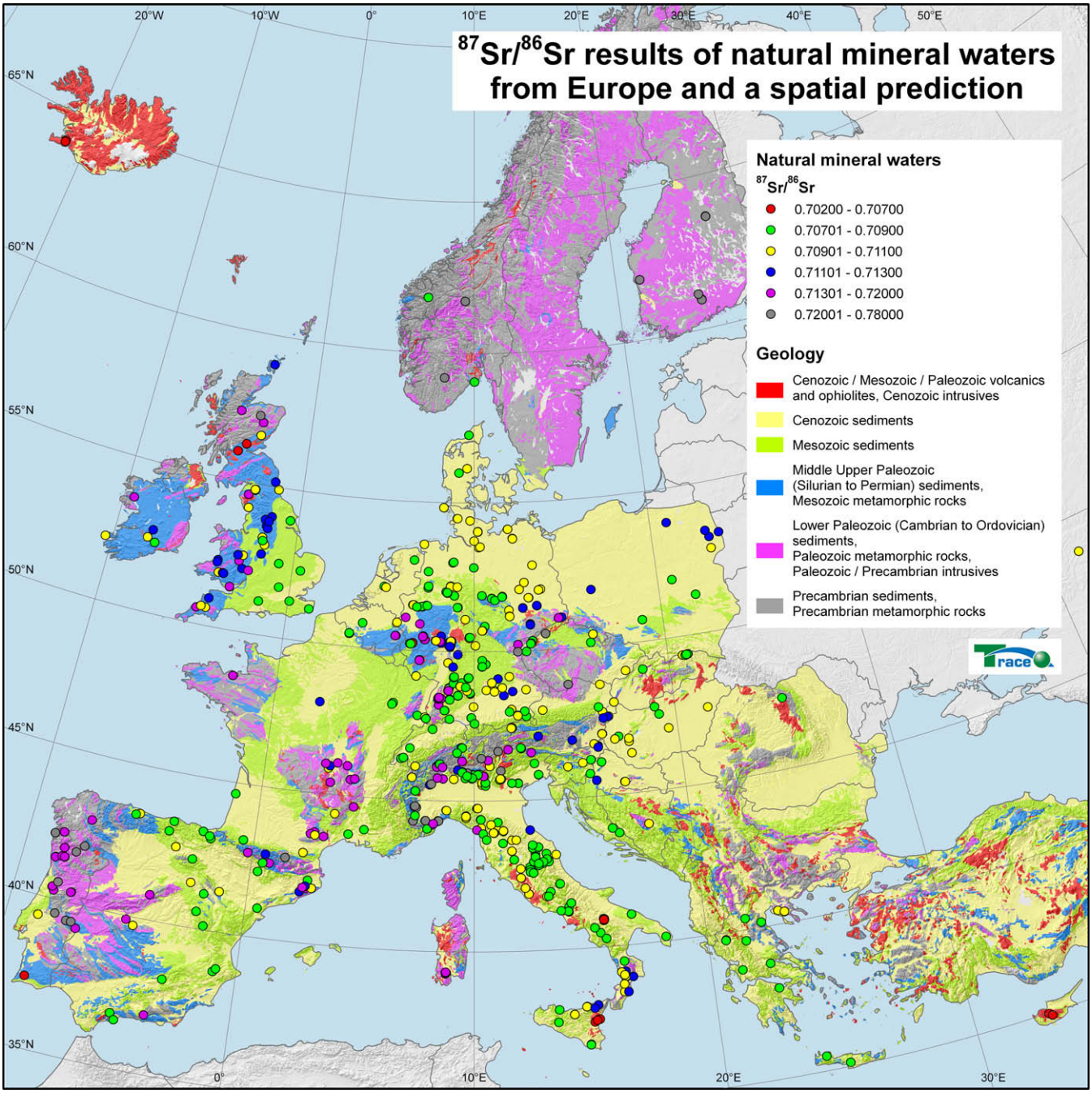

Fig. 1. Map with $^{87}Sr/^{86}Sr$ results of natural mineral waters from Europe and a spatial prediction (see Supplementary data). The map was drawn by simplifying a GIS based geological map from Pawlewicz et al. (2003).

of a sample based on the geological unit from which it was collected.

In a further iterative procedure, the data ranges were adjusted and allocated to the corresponding geological units. For this process especially natural mineral waters with their catchment area in transition zones of different geological units were checked.

6. Analytical results

656 bottled water samples were analysed and interpreted in this study. An overview of the results of the total mineral and strontium content as well as ranges for $^{87}Sr/^{86}Sr$ is given in Table 1 grouped according to the correlation ranges of surface geology of location and water samples. All results are plotted on the map of Fig. 1. The total mineral content varies from 11 to 12575 mg/L with a relatively low mean value of 797 mg/L. The strontium content ranges from <0.0002 to 22.8 mg/l (Voerkelius & Lorenz, 2009).

Results of $^{87}Sr/^{86}Sr$ of all 656 water samples show a wide range of 0.7035–0.7777 or given in δ notation from −10 ‰ to 96 ‰. This large data range of strontium isotope ratios in our water samples reflects the variation observed in young, mantle derived rocks to old continental crust.

7. Description of analytical results in correlation to the geographical origin and surface geology of production location

Low $^{87}Sr/^{86}Sr$ values of 0.7035 to 0.7070 (−8 to −3 ‰) are encountered in our natural mineral water samples from regions with basaltic volcanic rocks such as the Quaternary and Tertiary volcanic rocks of Europe (Iceland, Etna, Vulture, Alkali basalts of Latin, Eifel, Auvergne). Very low values are also observed in regions of basic Palaeozoic volcanic rocks e.g. in Scotland as also described by Montgomery et al. (2006).

The range from 0.7070 to 0.7090 (−3 to 0 ‰) is observed in water samples from regions with a surface geology of mostly Mesozoic marine sediments displayed in the map (Fig. 1) in green. Almost 40% of the analysed natural mineral waters belong to this group. It includes the natural mineral waters from large limestone areas providing natural mineral water resources of high quality compliable with modern taste.

Mudstones and more clastic sediments with lower carbonate contents but also from Mesozoic geological units, seem to produce waters with higher isotope ratios visible as blue and yellow spots on green ground. However, these rocks are underrepresented in our study and were therefore neglected for our approach.

Due to majority of clastic components in Tertiary and Quaternary sediments of the large plains and basin structures mostly derived from Palaeozoic and even Precambrian rocks, the range of analysed values of the water samples between 0.7090 and 0.7110 (0–2‰) is applied to origin regions of surface geology of these sedimentary units.

Natural mineral waters with $^{87}Sr/^{86}Sr$ values of the data range from 0.7090 to 0.7110, shown in yellow in Fig. 1, represent the second most abundant part of all analysed waters and account for about 30 %.

Surface geology of Palaeozoic low-metamorphic rock cover leads to $^{87}Sr/^{86}Sr$ from 0.7110 to 0.7130 (2–5‰) in the natural mineral waters (coloured blue in Fig. 1). The value range draws the line around Ordovician rocks. No clear differences were observed for samples of more clastic or carbonate rocks, respectively.

High ratios exceeding 0.7130 (>5‰) in natural mineral water samples are found exclusively (the only exceptions are Rhenish massif and Northern area of Black forest) in areas of Lower Palaeozoic and crystalline rocks of the old Variscian and Caledonian orogens. The clearest signal can be found in the Iberian Meseta of Portugal and Spain which also provided the highest $^{87}Sr/^{86}Sr$ of 0.7777 (96‰) analysed in one sample.

Ratios exceeding 0.7200 (>15 ‰) in water samples can even be distinguished from the lower ratios by differentiating between areas of surface geology of Palaeozoic sediments and low grade metamorphic rocks on the one hand, and areas of Precambrian and high-grade metamorphic rocks on the other hand. Although this differentiation could not be verified on every point of location, it was indicated by colouring in grey in contrast to lavender.

This study clearly shows an overall correlation between $^{87}Sr/^{86}Sr$ of the water samples with the surface geology (Fig. 1), which can easily be deduced from the compliance of the analysed values of the natural mineral waters with the postulated data ranges for the corresponding geological unit of the map. Exceptions to this correlation will now be considered:

Deviations are observed especially for samples originating in areas of Quaternary plains (coloured in yellow), which are mainly covered with glacial gravel. Samples from German plains show ratios between 0.7086 and 0.7109 (−1 and 2 ‰), whereas higher ratios even up to 0.7130 (5‰) were analysed in samples produced in Poland. The differences in value ranges can be accounted for by the detritus material which covers a wide range of rock ages and lithologies of metamorphic rocks, intrusives and volcanic rocks, and originates from Scandinavia (Henningsen & Katzung, 2006).

Other deviations were identified where Mesozoic sediments are dominated by mudstones instead of limestone as explained above.

Some of the natural mineral waters from areas with middle and upper Paleozoic surface geology in the UK and Ireland show lower ranges as indicated by the colouring of the geological unit of our map, and in contrast some samples from the Rhenish Massif in Germany show even higher ranges.

The groundwaters that are used for natural mineral waters in UK are often very young and pumped from shallow depths in comparison to other countries (Voerkelius and Lorenz; 2009). Therefore we suggest a significant unknown surface influence to account for the isotope deviation, but this point should be further addressed in future studies.

An example of deviations from the overall picture on a smaller scale is found in western Germany. The Eifel area is especially interesting because both Palaeozoic rocks and Quaternary volcanic rocks are exposed. The Volcanic area produces the CO_2 of the most traditional bottled natural mineral waters. "Natural mineral water" was originally established as a food commodity because of the popularity of natural sparkling waters (Green & Green, 1985). While sulphuric and thermal waters were used for medical applications, CO_2-rich waters of the Eifel became famous as table

Table 1
Strontium isotope ratios of 656 water samples in comparison to mineral – and strontium contents.

Number of samples	Number of samples (%)	Total mineral content (mg/L)	Sr (mg/L)	$^{87}Sr/^{86}Sr$	$\delta^{87}Sr$ (‰)
28	4	62–3523	<0.0002–3.69	<0.7070	<−3.24
245	37	29–1257	0.005–22.8	0.7070–0.7090	−3.24 to 0.42
179	27	28–8976	0.006–12.3	0.7090–0.7110	−0.42 to 2.40
66	10	36–3780	0.025–6.35	0.7110–0.7130	2.40–5.22
100	15	17–6631	<0.0005–3.45	0.7130–0.7200	5.22–15.09
38	6	11–7238	<0.0017–0.94	>0.7200	15.09–99.68

waters. Many Eifel natural sparkling waters are pumped from Devonian slate although the lower $^{87}Sr/^{86}Sr$ ratios still show the relation to the Quaternary volcanic rocks (around 0.7057– 0.7087 in contrast to >0.7136). Further detailed studies are required to determine if the observed isotope ratios refer to deep mantle fluids containing strontium or to soils and covers of the recharge, which contain easily accessible strontium from volcanic rocks and dust.

Though the highest ratios had been expected for samples coming from Scandinavia (see Fig. 1, also Henningsen & Katzung, 2006), two samples from Norway show surprisingly low values (<0.709). As carbonate sediments are rare in these regions an influence of seawater is discussed for these cases. Horn (2005) already suggested that in regions where the exposed rocks do not provide much strontium by weathering, the input of dust and precipitation will determine the strontium isotopic signature.

Although not many deviations were observed for similar geological units within the investigated Mediterranean and the northern areas of Europe, the transferability particularly for the great cratons (e.g. Africa) with thick weathering zones or arid zones remains to be proven through sampling and analysis.

8. Transferability of the prediction method to other food products

Beard and Johnson (2000) already tried to model the strontium isotope variation in the continental United States in order to use it as a general guide to expected isotopic variation in skeletal elements in a particular region. The model assumed that the $^{87}Sr/^{86}Sr$ varies only as a function of age of the surface geology. In contrast, our map (Fig. 1) is based on analysed natural mineral waters and can therefore be applied as a first estimation of strontium isotope ratios in young groundwater.

As water – and not rocks and sediments or soils – is completely bio-available to plants and animals, it is assumed that the value ranges observed and correlated with surface geology is an improvement over the use of a geological map for the prediction of strontium isotope variation in agricultural products.

The strontium isotopic signatures of water enter the food chain (i.e. plants and animals) and can be transferred to any organic material without significant fractionation (Horn et al., 1998). According to Horn (2005), in this application no significant influence by fertilizer is assumed.

Based on the map of Fig. 1 the $^{87}Sr/^{86}Sr$ value range for each of the sample regions within the TRACE project was predicted (Fig. 2). The sample regions range from 160 to 13500 sqm. The prediction considered not only the geological unit of the site but also that of the surroundings.

Comparison of the results of the mean values of the analysed "surface" water samples used for agriculture (mostly First order streams and springs) with the predicted value ranges show that around 90% of the mean values were within the predicted data range. Exceptions are the sample regions BAR and IRE: The sample region of BAR is geologically inhomogeneous with a special prediction of 0.707–0.720, sample region IRE is probably influenced by sea spray as the site is near to the Atlantic.

Comparison of first results of the samples of ammonium nitrate extracts from soil samples, as well as samples of the food commodities honey and wheat show a generally good correlation to the "surface" water samples. Noteworthy deviations from the value range of "surface" water is observed for honey and wheat samples

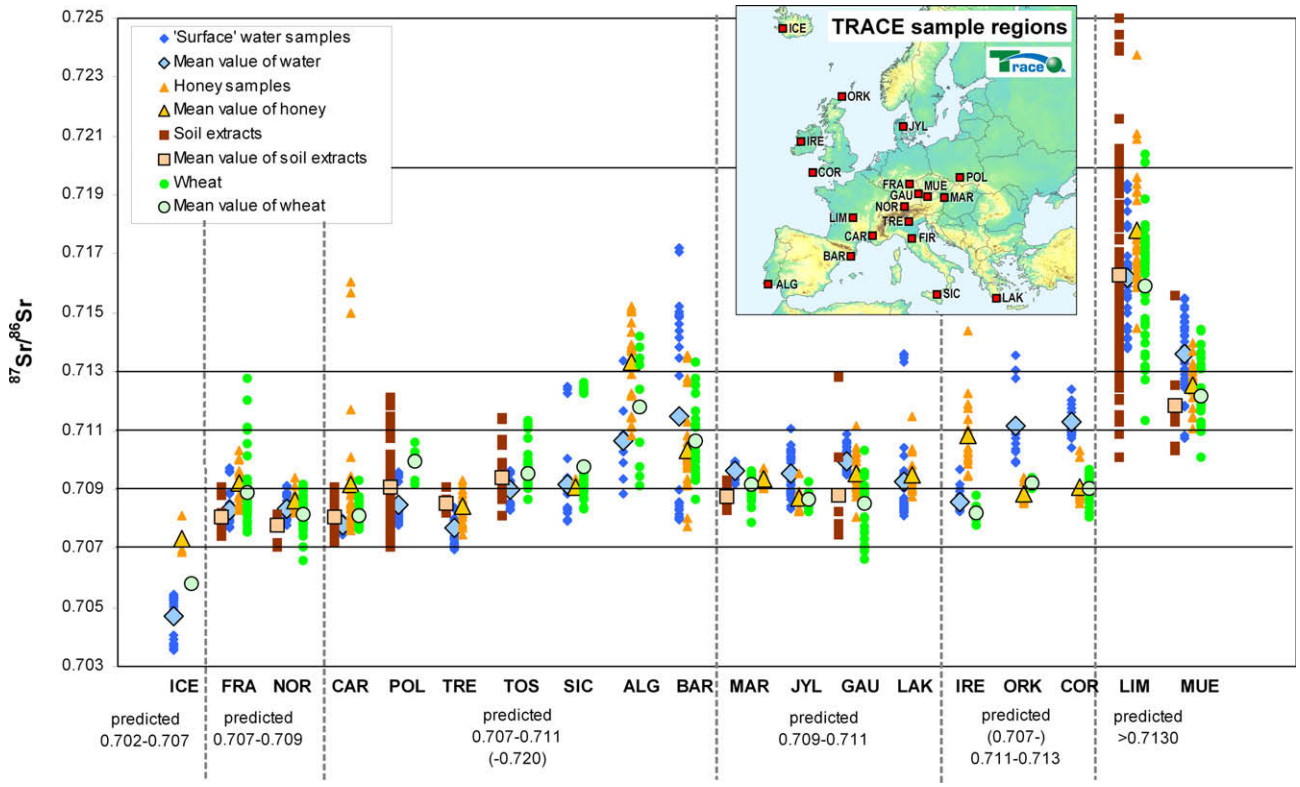

Fig. 2. $^{87}Sr/^{86}Sr$ results from water samples used for agriculture (mostly First order streams and springs), of water extracts from soil samples, of honey and wheat samples from several sample regions in Europe. The prediction of the $^{87}Sr/^{86}Sr$ value range for each of the sample region is based on the geological map of Fig. 1. The abbreviation for the sample regions are: ICE = Iceland, FRA = Germany (Franconia), NOR = Germany (Allgaeu), GAU = Germany (Gaeuboden), CAR = France (Carpentras), LIM = France (Limousin), POL = Poland, TRE = Italy (Trentino), TOS = Italy (Tuscany), SIC = Italy (Sicily), ALG = Portugal (Algarve), BAR = Spain (Barcelona), MAR = Austria (Marchfeld), MUE = Austria (Muehlviertel), JYL = Denmark (Jydland), LAK = Greece (Lakonia), IRE = Ireland, ORK = Orkney Islands and COR = England (Cornwall).

from the sample regions near the Atlantic ICE, COR, and ORK, indicating that here the influence due to sea spray is of higher significance for the $^{87}Sr/^{86}Sr$ values in the commodities than for the analysed "surface" water samples:

Honey samples from sample region ICE show higher strontium isotope values than the "surface" water samples, whereas honey and wheat samples from sample regions ORK and COR show lower values than the "surface" water samples. The food commodities from these regions seem to approach the $^{87}Sr/^{86}Sr$ value of seawater strontium of about 0.7092 (Capo & DePaolo, 1990).

Pourcelot, Stille, Aubert, Solovitch-Vella, and Gauthier-Lafaye (2008) suggest that dust and input from the atmosphere can have a significant influence on $^{87}Sr/^{86}Sr$ in the upper part of soil.

The overall correlation between the analysed and predicted value ranges (Fig. 2) confirms our assumption that our map can also be used for strontium isotope ratio prediction in other natural products.

9. Conclusion

In contrast to the numerous small scale investigations using strontium isotope ratios, this study presents results of a large scale investigation with a high amount of analysed water samples which clearly illustrate the potential of strontium isotope ratio analysis for authenticity control.

Though most of the natural mineral waters were not pumped from units of the surface geology but from deeper layers, a good or at least feasible correlation of the $^{87}Sr/^{86}Sr$ of the natural mineral water samples with the surface geology was observed.

Furthermore, the study presents an overview of the observed value ranges of this parameter. Combining the measured data with a GIS based geological map it is possible to predict qualitative spatial information of strontium isotope values. The information provided by this map can be used advantageously in authenticity control not only to estimate the isotopic signature of a natural mineral water, but also for other food products.

This is of relevance especially for the validation of the origin of products from remote areas where data for authentic reference samples are lacking or cannot be obtained. A prediction of the values from an area based on the geological map can also be used as a decisive tool to evaluate the potential of strontium isotope ratio analysis in a particular case of authenticity proof for any food product.

The applicability of the elaborated map for prediction of strontium isotope ratios for other agricultural products and food commodities was successfully tested by comparing first results of $^{87}Sr/^{86}Sr$ analyses in "surface" water samples, ammonium nitrate extracts from soil samples, as well as honey and wheat samples from specific sample regions within the TRACE project.

Based on this study it is proposed that strontium isotope ratios can contribute significantly to resolve questions of geographical origin. A prerequisite is, however, the knowledge of the spatial catchment area of an object.

An improvement of our system or provided map would be the construction of a "prediction" map with predicted value ranges for commodities produced at each geological unit. Based on complex statistical and graphical efforts the map may provide overlapping value ranges for the specific units and also consider big scale regional differences such as the observed deviations between the Quaternary plains of northern Germany and Poland (see above).

Acknowledgement

We kindly acknowledge the EU commission for funding the TRACE project. We remember gratefully ARCS, AUA, Eurofins Scientific Analyics, Fresenius, Geochem, Hydroisotop, IASMA, IFR, Insalus, NUID, UUFDG, colleagues, friends and relatives for sampling the natural mineral waters all over Europe. We thank the US Geological Survey and the United Nations for providing the georeferenced shape-file including legend of the geological map of Europe.

Appendix A. Supplementary data

Supplementary data associated with this article can be found, in the online version, at doi:10.1016/j.foodchem.2009.04.125.

References

Åberg, G. (1995). The use of natural strontium isotopes as tracers in environmental studies. *Water, Air, and Soil Pollution, 79*, 309–322.

Åberg, G., Fosse, G., & Stray, H. (1998). Man, nutrition and mobility: A comparison of teeth and bone from medieval era and the present from Pb and Sr isotopes. *The Science of Total Environment, 224*, 109–119.

Åberg, G., Jacks, G., & Hamilton, P. J. (1989). Weathering rates and $^{87}Sr/^{86}Sr$ ratios: An isotopic approach. *Journal of Hydrology, 109*, 65–78.

Barbaste, M., Robinson, K., Guilfoyle, S., Medina, B., & Lobinski, R. (2002). Precise determination of the Sr isotope ratios in wine by inductively coupled plasma sector field multicollector mass spectrometry (ICP-SF-MC-MS). *Journal of Analytical Atomic Spectrometry, 17*(2), 135–137.

Beard, B. L., & Johnson, C. M. (2000). Strontium isotope composition of skeletal material can determine the birthplace and geographic mobility of humans and animals. *Journal of Forensic Sciences, 45*(5), 1049–1061.

Bentley, R. A. (2006). Strontium isotopes from the earth to the archaeological skeleton: A review. *Journal of Archaeological Method and Theory, 13*(3), 135–187.

Burke, W. H., Denison, R. E., Hetherington, E. A., Koepnick, R. B., Nelson, H. F., & Otto, J. B. (1982). Variation of seawater $^{87}Sr/^{86}Sr$ throughout phanerozoic time. *Geology, 10*, 516–519.

Capo, R. C., & DePaolo, D. J. (1990). Seawater strontium isotopic variations from 2.5 million years ago to the present. *Science, 249*(5), 1–55.

Chaudhuri, S. (1978). Strontium isotopic composition of several oilfield brines from Kansas and Colorado. *Geochimica et Cosmochimica Acta, 42*, 329–332.

Chaudhuri, S., & Clauer, N. (1992). Signatures of radiogenic isotopes in deep subsurface waters in continents. In N. Clauer, & S. Chaudhuri (Eds.), *Lecture notes in earth sciences* (Vol. 43, pp. 497–529). Berlin: Springer.

Clark, I., & Fritz, P. (1997). *Environmental isotopes in hydrogeology*. Boca Raton, Florida: Lewis Publishers (p. 328).

Crittenden, R. G., Andrew, A. S., LeFournour, M., Young, M. D., Middleton, H., & Stockmann, R. (2007). Determining the geographic origin of milk in Australasia using multi-element stable isotope ratio analysis. *International Dairy Journal, 17*(5), 421–428.

Faure, G. (1986). *Principles of isotope geology* (2nd ed.). New York: John Wiley and Sons (p. 589).

Green, M., & Green, T. (1985). *The good water guide*. London: Rosendale Press (p. 172).

Henningsen, D., & Katzung, G. (2006). *Einführung in die Geologie Deutschlands* (Vol. 7, p. 234). Auflage, Stuttgart: Spektrum Akademischer Verlag.

Hodell, D. A., Quinn, R. L., Brenner, M., & Kamenov, G. (2004). Spatial variation of Sr isotopes ($^{87}Sr/^{86}Sr$) in the Maya region: A tool for tracking ancient human migration. *Journal of Archaeological Science, 31*(5), 585–601.

Hofmann, R., & Baumann, A. (1986). Sr isotopic composition of brines from West German thermal springs. *Neues Jahrbuch der Geologie und Paläontologie Mh, 10*, 591–598.

Hölting, B. (1989). *Hydrogeologie* (Vol. 3, p. 441). Auflage, Stuttgart: Ferdinand Enke Verlag.

Hoogewerff, J., Kralik, M., Berner, M., Vroon, P., Papesch, W., Miesbauer, H., et al. (2001). The last domicile of the iceman from Hauslabjoch: A geochemical approach using Sr, C and O isotopes and trace element signatures. *Journal of Archaeological Science, 28*(9), 983–989.

Horn, P. (2005). *Isotopensignaturen schwerer Elemente in der ökologischen Praxis. Rundgespräche der Kommission für Ökologie. Bd. 30. Auf Spurensuche in der Natur* (pp. 131–152). München: Dr. Friedrich Pfeil Verlag.

Horn, P., Hoelzl, S., Todt, W., & Matthies, D. (1998). Isotope abundance ratios of Sr in wine provenance determinations in a tree-root activity study and of Pb in a pollution study on tree-rings. *Isotopes in Environmental and Health Studies, 34*, 31–42.

Horn, P., Schaaf, P., Holbach, B., Hoelzl, S., & Eschnauer, H. (1993). $^{87}Sr/^{86}Sr$ from rock and soil into vine and wine. *Zeitschrift für Lebensmittel-Untersuchung und -Forschung, 196*, 407–409.

InterregIIIA-Projektbericht (2008). Grenzüberschreitende Bewirtschaftung des Grundwassers im Raum Hegau – Schaffhausen. Unpublished Final Report, InterregIIIA Alpenrhein Bodensee Hochrhein, (pp. 85).

Kelly, S., Baxter, M., Chapman, S., Rhodes, C., Dennis, J., & Brereton, P. (2002). The application of isotopic and elemental analysis to determine the geographical origin of premium long grain rice. *European Food Research and Technology, 214*, 72–78.

Lee-Thorp, J., & Sponheimer, M. (2003). Three case studies used to reassess the reliability of fossil bone and enamel isotope signals for paleodietary studies. *Journal of Anthropological Archaeology, 22*, 208–216.

Matter, A., Peters, T., & Ramseyer, K. (1987). $^{87}Sr/^{86}Sr$-Verhältnisse und Sr-Gehalte von Tiefengrundwässern, Mineralien sowie Gesteinen aus dem Kristallin und der Trias der Nordschweiz. *Eclogae Geologicae Helvetiae, 80*(2), 579–592.

McArthur, J. M. (1994). Recent trends in strontium isotope stratigraphy. *Terra Nova, 6*, 331–358.

McArthur, J. M., Howarth, R. J., & Bailey, T. R. (2001). Strontium isotope stratigraphy: LOWESS version 3. Best-fit line to the marine Sr-isotope curve for 0–509 Ma and accompanying look-up table for deriving numerical age. *Journal of Geology, 109*(15), 5–169.

Montgomery, J., Evans, J. A., & Wildman, G. (2006). $^{87}Sr/^{86}Sr$ isotope composition of bottled British mineral waters for environmental and forensic purposes. *Applied Geochemistry, 21*(10), 1626–1634.

Oda, H. W., Kawasaki, A., & Hirata, T. (2002). Determining the rice provenance using binary isotope signatures along with cadmium content. In *Proceedings of the seventeenth world congress of soil science* (pp. 14–20). Bangkok, Thailand, August 2002.

Pampura, V. D., Plyusnin, G. S., & Sandimirova, G. P. (1980). Geochemical and isotopic composition of strontium in mineral forming solutions of the Pauzhetka hydrothermal system (southern Kamchatka). *Geochemistry International, 17*, 57–70.

Pawlewicz, M.J., Steinshouer, D.W., & Gautier, D.L. (2003). Map Showing Geology, Oil and Gas Fields, and Geologic Provinces of Europe including Turkey. Open File Report 97–470I. Central Region Energy Resources Team, U.S. Department of the Interior U.S. Geological Survey. (http://pubs.usgs.gov/of/1997/ofr-97–470/OF97–470I/index.htm).

Pillonel, L., Buetikofer, U., Rossmann, A., Tabacchi, R., & Bosset, J. O. (2004). Analytical methods for the detection of adulteration and mislabelling of Raclette Suisse and Fontina PDO cheese. *Mitteilung Lebensmittel Hygiene, 95*, 489–502.

Pourcelot, L., Stille, P., Aubert, D., Solovitch-Vella, N., & Gauthier-Lafaye, F. (2008). Comparative behaviour of recently deposited radiostrontium and atmospheric common strontium in soils (Vosges mountains, France). *Applied Geochemistry, 23*, 2880–2887.

Price, T. D., Knipper, C., Grupe, G., & Smrcka, V. (2004). Sr isotopes and prehistoric human migration: The Bell Beaker period in central Europe. *European Journal of Archaeology, 7*(1), 9–40.

Rossmann, A., Haberhauer, G., Hoelzl, S., Horn, P., Pichlmayer, F., & Voerkelius, S. (2000). The potential of multielement stable isotope analysis for regional origin assignment of butter. *European Food Research and Technology, 211*(1), 32–40.

Rummel, S., Hoelzl, S., & Horn, P. (2007). Isotopensignaturen von Bio- und Geo-Elementen in der Forensik. In Hermann, Saternus, & Striegnitz (Eds.), *Biologische Spurenkunde, Band I: Kriminalbiologie* (pp. 381–407). Berlin, Heidelberg: Springer.

Rummel, S., Hoelzl, S., Horn, P., Rossmann, A., & Schlicht, C. (2008). The combination of stable isotope abundance ratios of H, C, N and S with $^{87}Sr/^{86}Sr$ for geographical origin assignment of orange juices. *Food Chemistry,* doi:10.1016/j.foodchem.2008.05.115.

Standard Operating Procedure SOP. (2006). Standard operating procedure for the measurement of Sr isotope ratios in various food commodities and soil samples for the TRACE project (WP1) (7 pp.). unpublished.

Ufrecht, W., & Hoelzl, S. (2006). Salinare Mineral- und Thermalwässer im Oberen Muschelkalk (Trias) im Großraum Stuttgart–Rückschlüsse auf Herkunft und Entstehung mit Hilfe der $^{87}Sr/^{86}Sr$-Strontium-Isotopie. *Zeitschrift der deutschen Gesellschaft für Geowissenschaften, 157*(2), 299–316.

Veizer, J., & Compston, W. (1974). $^{87}Sr/^{86}Sr$ composition of seawater during the phanerozoic. *Geochimica et Cosmochimica Acta, 38*, 1461–1484.

Voerkelius, S., & Lorenz, G. (2009). Final natural mineral water report. TRACE Analytical tools group WP1 and WP15. unpublished.

2. Counter-propagation artificial neural networks

To better deal with the complex statistical properties common to mineral water data, such as non-normality, strong colinearity and outlying values/populations, an advanced non-linear technique is applied known as counter-propagation artificial neural networks (CP-ANNs). Artificial neural networks belong to new evolving computer technologies in which a computer system has been designed to learn from data in a manner emulating the learning pattern in the brain. Basically, there are two main groups of artificial neural networks, which differ in architecture and in learning strategy; unsupervised and supervised self organising maps and supervised back-propagation artificial neural networks (Zupan & Gasteiger, 1999). The term "unsupervised or supervised" indicates if only input variables or descriptors plus output variables participate in the training, respectively.

Unsupervised self organising maps alias Kohonen neural networks represent a basic type of artificial neural networks. Its architecture is a two-dimensional grid of neurons (*x*–*y* in Fig. 1A), which are vectors of weights (*z* in Fig. 1A). The network is trained by taking the following steps until the weights are stabilised:

1. Prior to the learning step, the algorithm is initialised by assigning random numbers to all weights.
2. In the first learning step of learning an object from the learning set is presented to all neurons. The algorithm selects the neuron with its weights closest to the object ("winning neuron").
3. In the second step of learning the weights of the winning neuron are replaced by the object values and at the same time the neighbouring neurons are modified to become similar to them.

Counter-propagation artificial neural networks (CP-ANNs) are an extension of Kohonen neural networks. Their basic architecture is similar to the Kohonen networks, but the network and neurons now have two layers: an input layer (Kohonen layer) and an output layer (Fig. 1B). The learning in the input layer is the same as in Kohonen neural network, i.e. the similarity amongst input variables determines the arrangement of objects in the input layer map. After all object are arranged in the Kohonen layer, the positions of the objects are projected to the output where the weights are modified in a way that the weights on projected positions are equal to the values of corresponding objects. Both the weight levels and positions of the outputs can be visualised to further aid the interpretation of the results.

For this study we prepared a ANN Toolbox that performs the classification of multivariate data using the Kohonen mapping method, and predictive modelling using counter-propagation neural network (NIC_ANN_Programs). The toolbox runs under Matlab 7.

3. Experimental part

3.1. Description of the data set

For this study, 145 water samples were collected from Germany and a number of neighbouring European countries (see Fig. 2). The bulk of the samples concerns "natural mineral water" as defined in EU Directive 80/777/EEC, whereas the remaining bottled water samples are labelled as spring or table water ($N = 10$). In addition, 11 local tap water samples were included to cover areas where no mineral waters are produced.

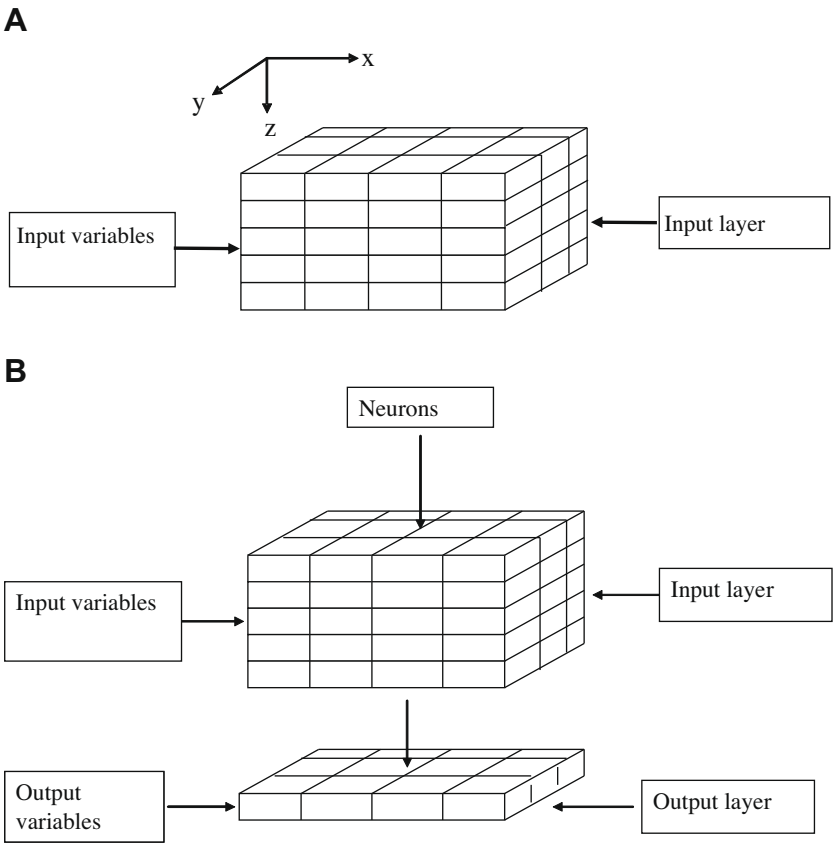

Fig. 1. Typical architecture of Kohonen neural networks (A) and counter-propagation artificial neural networks (B). Kohonen neural network architecture is two-dimensional grid of neurons, which are vectors of weights, *z* represents the number of input variables.

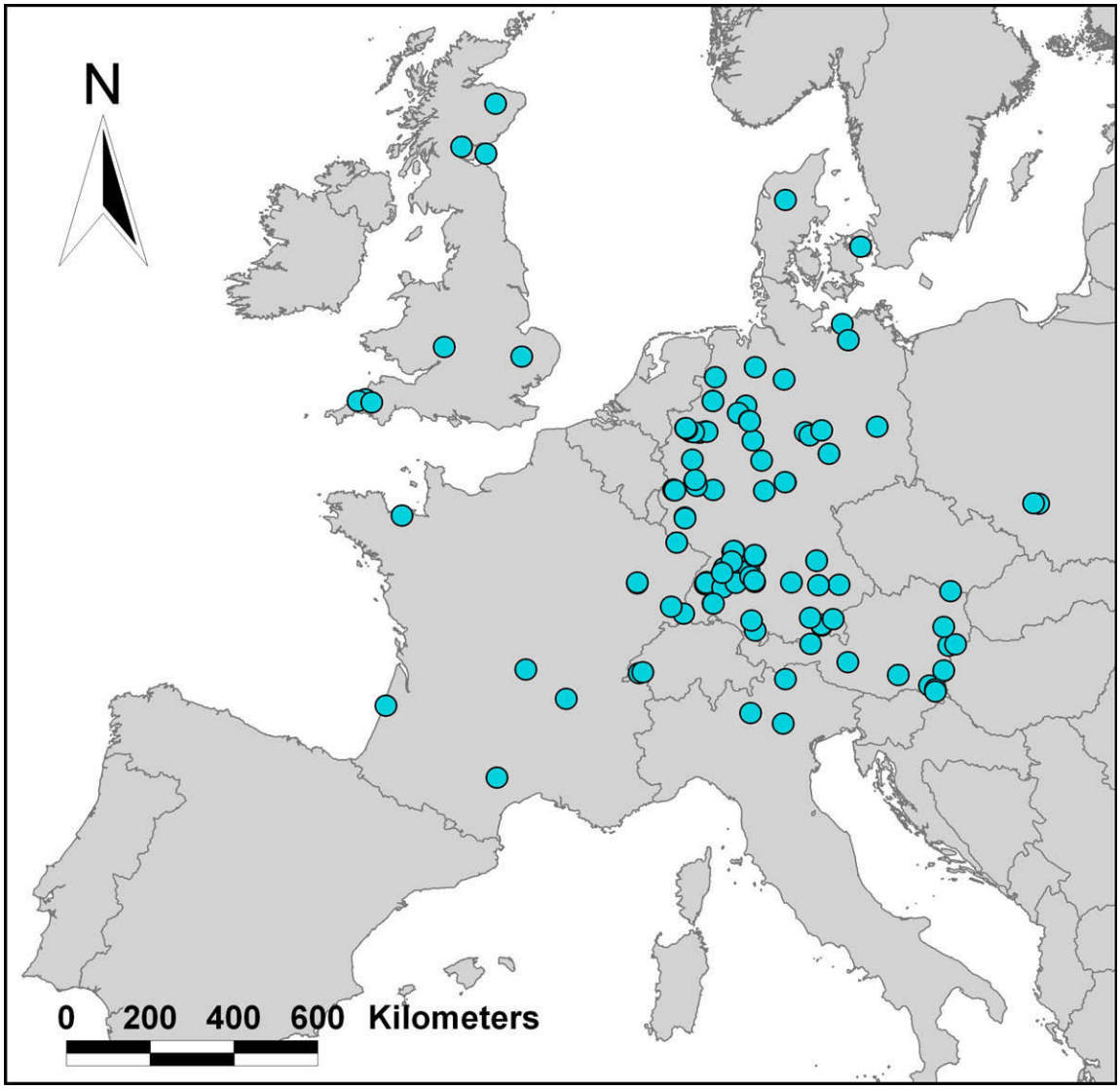

Fig. 2. Overview of mineral water sample locations (N_{tot} = 145).

For all water samples, the concentration of eight main ions (Ca^{2+}, Mg^{2+}, Na^{+}, K^{+}, HCO_3^-, SO_4^{2-}, Cl^- and F^-) and pH was determined by an independent laboratory using different analytical techniques. The consistency of the analytical data was checked by determining the ionic charge balance of the samples. The reported precision on the analysis is within ±5% relative standard deviation over the range of concentrations.

3.2. Hydrochemical modelling

From the chemical composition of the samples, the saturation indices of a number of common mineral phases (calcite, dolomite, gypsum, anhydrite, halite and fluorite) as well as CO_2 (gas) are calculated. Although, the saturation indices just represent another linear combination of the same data, they might be better related to certain mineralogical characteristics of the lithology and thus improve the prediction power. This hypothesis is further tested in this study. The saturation indices were calculated using PREEQC (Parkhurst & Appelo, 1999) using T = 10 °C and assuming charge balance (pH).

3.3. Lithological classification of the samples

For each of the water samples, the geographical position of the aquifer was determined. Next, the geology of the aquifer was determined using different information sources: (A) the mineral water brand's website, (B) local geological maps or (C) regional geological maps. It should be noted that the position as well as geology of the aquifer is therefore often known only by approximation.

The original geological description of the source lithology of the mineral water samples consists of 12 lithological groups (Table 1). As can be seen, the majority of samples is found in unconsolidated sediments and carbonate areas, which provide large and often rather permeable aquifers. Mineral waters from magmatic and metamorphic areas – where the primary flow of water goes through fractures – are much less common.

Because of the limited number of samples in some groups, two alternative classification schemes have been developed to be used for further data analysis. Whereas the first scheme (lithology 1) in Table 1 is partly based on the presence of easily dissolved minerals (carbonates and gypsum), the second scheme (lithology 2) is more

Table 1
The lithological information of the water source and the two classification schemes tested in this study (N_{tot} = 145).

Original lithology	Lithology 1 – first scheme	Class (1–5)	Lithology 2 – second scheme	Class (1–4)	No. of samples
Granite	GGMGS	1	Magmatic rocks	1	11
Gneiss, mica shist	GGMGS	1	Metamorphic rocks	2	10
Limestone, dolomite, marble	LDMMUcarb	2	Biogenic-chemical sediments (carbonates)	4	19
Limestone, dolomite, marble (gypsum bearing)	LDMMUcarbgypsum	3	Biogenic-chemical sediments (carbonates)	4	26
Marl	LDMMUcarb	2	Biogenic-chemical sediments (carbonates)	4	5
Marl (gypsum bearing)	LDMMUcarbgypsum	3	Biogenic-chemical sediments (carbonates)	4	3
Graywacke, shale	GGMGS	1	Clastic sediments	3	14
Sandstone	S	4	Clastic sediments	3	13
Sandstone (gypsum bearing)	Sgypsum	5	Clastic sediments	3	8
Unsolidated rocks	S	4	Clastic sediments	3	5
Unsolidated rocks (carbonate)	LDMMUcarb	3	Clastic sediments	3	6
Unsolidated rocks (clastic)	S	4	Clastic sediments	3	25

based a classical geological approach. Both classification schemes are evaluated in this study.

3.4. Model construction and data pre-processing

The mineral water data set consists of 145 mineral water samples and 16 variables (descriptors), i.e. nine main elements and seven saturated indices. The dataset contained missing values that were marked −9999. This key (−9999) enables our adapted Kohonen and counter-propagation neural network software (Zupan, 1994) to handle the missing data (Grošelj et al., 2004; Zupan, Novič, & Ruisanchez, 1997).

Due to the fact that multivariate data analysis depends on the normalisation of variables autoscaling has been applied to all variables x_i, $i = 1 \ldots 9 \ldots 16$, in a continuous space

$$x_{ij}^{new} = \frac{x_{ij}^{old} - \bar{x}_i}{s_i} \quad (1)$$

where s_i is the standard deviation and x_i is the mean of variable i. The variables of the samples (descriptors) were represented as inde-

Table 2
Classification matrix obtained for the different models (recall ability).

prediction / classification	GGMGS	LDMMU carb	LDMMU Carb gypsum	S	Sgypsum	uncertain
GGMGS	**22**				*2*	*11*
	18		*1*	*2*		*14*
LDMMU carb	*2*	**15**		*1*		*12*
		13	*1*	*1*		*15*
LDMMU carb gypsum	*1*		**15**	*1*		*12*
			18	*2*		*9*
S	*1*	*1*		**22**		*19*
		2		24		*17*
Sgypsum		*1*			**2**	*5*
				1	2	*5*

♦ **first model** ♦ second model

prediction / classification	magmatic rocks	metamorphic rocks	sediment A biogenic-chemical sediment	sediment B clastic sediment	uncertain
magmatic rocks	**9**				*2*
	8				*3*
metamorphic rocks		**8**			*2*
		9			*1*
sediment A biogenic-chem			**44**	*3*	*6*
			47	*1*	*5*
sediment B clastic sediment	*1*			**62**	*8*
	1		*3*	59	*8*

♦ **third model** ♦ fourth model

pendent variables (input data), whilst the classification groups as dependent variables (targets).

Four different data files were prepared. Datasets 1 and 2 were linked to the lithology classes: GGMGS, LGMMUcarb, LDMMUcarb-gypsum, S and Sgypsum (see Table 1). This is called lithology 1. Datasets 3 and 4 were linked to the lithology classes: magmatic rocks, metamorphic rocks, clastic sediments and biogenic-chemical sediments (lithology 2). Datasets 1 and 3 contain 16 descriptors, i.e. nine main elements and seven saturated indices, whereas Datasets 2 and 4 only include the nine main elements.

The four data files were trained with the artificial neural network algorithm using the ANN Toolbox (NIC_ANN_Programs; see Section 2). The network parameters were optimised by leave-one-out cross validation (Bos, Bos, & Van der Linden, 1993; Vračko, 2005) and were set as: the dimension of the network $N_x \times N_y$ = 12×12, the number of training epochs n = 1000, maximal correction factor η_{max} = 0.5 and minimal correction factor η_{min} = 0.01.

For each model, the Kohonen topmap, response surfaces and detailed position of the classes on the Kohonen topmap were obtained. The models were tested for the recall ability and validated by leave-one-out cross validation. The main difference between these two methods is that the recall ability gives the predictions of the entire training set, whereas the validation on leave-one-out classifies every object with a model built with the remaining objects.

4. Results and discussion

4.1. Recall ability

To analyse the results in more detail, the recall ability (RA) for each class was evaluated. The results are given in a classification matrix (Table 2). One can observe that the results obtained with the first and second models are more or less the same: about 50–60% of the samples are correctly classified, whereas the majority of remaining samples is classified as uncertain. Although, only few samples are incorrectly classified, the large number of uncertain answers makes the models unsuitable for prediction of the source lithology of mineral water samples on the basis of their chemical composition.

The third and fourth models in Table 2 show a much higher percentage of correctly classified samples vs. uncertain samples compared to the first and second models. For magmatic and metamorphic rocks the amount of samples classified as uncertain can still be considerable (>20%). This is most likely caused by the small number of samples contained in both classes. Nevertheless, these models appear more promising to infer the geology of the aquifer from the chemical composition of mineral water.

These results in general show that using the proper lithological classification scheme is of much more importance than including the saturation indices. The fact that the second lithological classification scheme is in general much more successful than the first scheme mostly shows that the distinction between gypsum and non-gypsum bearing aquifers (first scheme) is insufficiently reflected by the chemistry to be picked up by the CP-ANN approach. Because gypsum and anhydrite are very soluble minerals, and the saturation indices of gypsum and anhydrite were included (first model), the results are quite unexpected. The lack of a sulphate signal could be the result an SO_4^{2-} overprint from oxidising sulphides during pre-processing of mineral water derived from non-gypsum/anhydrite bearing aquifers, but such waters are expected to be rather uncommon. As we do not have any information about the uncertainty associated with the original lithological classification, it can not be excluded that the information concerning the presence or absence of gypsum is much less precise than information about other lithological properties (e.g. carbonate vs. non-carbonate).

4.2. Leave-one-out cross validation

In Table 3 the results obtained for the recall ability are compared with the leave-one-out cross validation results. The cross validation results support the previous observations showing that the best responses are obtained for the third and fourth model. The difference between the fourth and the third model is marginal, implying that inclusion of the saturation indices (not included in the fourth model) has a rather negligible effect on the predictive power of the models. This can be understood recalling the fact that the saturation indices are only a different linear (re-)combination of the concentration of the major ions. As such, they do not add additional information to the model. In case of the first model (saturation indices included), inclusion of the saturation indices even has a slightly negative effect on the predictive power of the model.

4.3. Visualisation of the model

To make the analysis of the model more evident and understandable the third model is explained by using the MATLAB visualisation tools (NIC_ANN_Programs). On the final topmap of our selected model (Fig. 3A) the classes, which predominantly occupy the individual neuron, are given. It is seen that the classes 1 and 2 (magmatic and metamorphic rocks) are grouped in the left upper corner (class 1) and in the centre of the final topmap (class 2), whilst the classes 3 and 4 (biogenic-chemical and clastic sediments) predominantly occupy right upper corner and left lower corner of the final topmap, respectively.

The same is observed for the four response surfaces (Fig. 3B), where each output level shows the grouping of the individual class. Thus, on the first, second, third and fourth output level the grouping of classes 1–4 is shown, respectively.

Comparison of the final topmap and the response surfaces in Fig. 3 shows that samples of classes 1 and 2 (magmatic and metamorphic rocks) are clearly grouped and separated from each other. The confined responses might be related to the relatively small amount of samples in each class. Contrary to classes 1 and 2, the separation of class 3 (biogenic-chemical sediment) and especially class 4 (clastic sediments) is much less evident. This is not only caused by the larger amount of samples in both classes, but also due to the fact that both classes are rather divers in terms of their mineralogical composition, which will be reflected by the hydrochemistry. Furthermore, clastic sediments commonly contain small amounts of

Table 3
Results of recall ability and leave-one-out tests.

	Recall ability test	Leave-one-out
First model		
Correct answer:	76	12
Uncertain answer:	59	17
Incorrect answer:	10	116
Second model		
Correct answer:	75	20
Uncertain answer:	60	13
Incorrect answer:	10	112
Third model		
Correct answer:	123	94
Uncertain answer:	18	9
Incorrect answer:	4	42
Fourth model		
Correct answer:	123	91
Uncertain answer:	17	11
Incorrect answer:	5	43

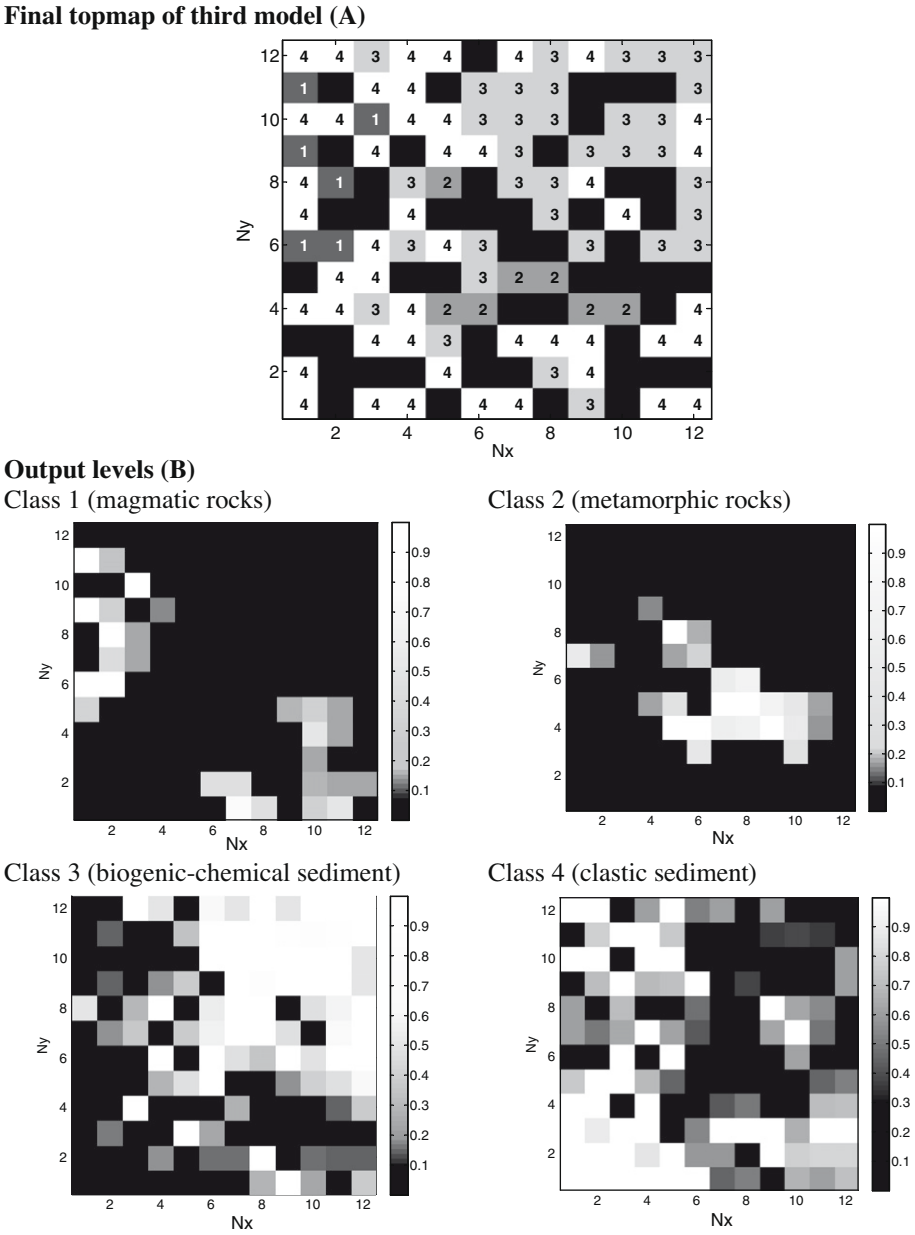

Fig. 3. Final topmap of third model. Map A shows the distribution of all four classes on the topmap. One neuron is represented on the map as a square. The colours and numbers represent the grouping and distribution of the classes: magmatic rocks (dark grey regions marked with 1), metamorphic rocks (grey region marked with 2), biogenic-chemical sediment (light grey regions marked with 3), clastic sediments (white regions marked with 4) and empty spaces (black regions). Four output levels (B) – four response surfaces (classes 1–4) – distribution of the individual class on one output level is shown.

carbonates. Because most carbonates have a high solubility, even small amounts of carbonatic material in an clastic aquifer could result in a hydrochemical signal which is more or less comparable to that from biochemic-chemical sediments such as limestones.

The observed partial overlap between classes 3 and 4 can further be explained by the fact that water from deeper aquifers could previously have been in contact with an overlying or nearby lithology of a different class, resulting in a mixed water type. This highlights the need for more detailed information about the aquifer lithology to further optimise the lithological classification scheme used for prediction.

5. Summary and conclusions

In this study we determined up to what extent the mineral water composition – in terms of the concentration of major ions (Ca^{2+}, Mg^{2+}, Na^{+}, K^{+}, HCO_3^-, SO_4^{2-}, Cl^-, F^-) and pH – can be used to verify the geological origin of mineral water. For this purpose, we analysed a dataset of 145 European mineral water samples using counter-propagation artificial neural networks.

From the mineral water dataset, four different models were built using two different geological classification schemes and a different selection of variables (with or without the calculated saturation indices). These models were tested for recall ability (RA) and validated by leave-one-out cross validation (CV-LOO).

Results show that using the CP-ANN approach, the source geology of the mineral water samples can be reasonably well predicted using a lithological classification based on four classes: magmatic rocks, metamorphic rocks, biogenic-chemical sediments and clastic sediments. Although these are preliminary results, this technique could offer opportunities to test for the geological origin of commercially sold mineral waters within Europe.

Comparison of the different models shows that the geological classification scheme used to classify the samples is of most importance for a successful prediction of the geology. Although this seems trivial, the optimal classification scheme is not always a priori evident. This implies that when using such a supervised clustering technique, multiple (re-)classification schemes should be tested and evaluated. This requires detailed knowledge of the lithological composition of the aquifer and overlying formations.

In contrast to the lithological scheme used, the effect of including the saturation indices as additional variables has negligible effect on the predictive power of the models. The fact that inclusion of the saturation indices of different mineral phases has no effect on the results shows that they do not add information in multivariate setting.

Acknowledgements

The authors like to thank the European Commission for funding this work through the Sixth Framework Program under the Food Quality and Safety Priority (TRACE Project No. 006942) and Hydroisotop GmbH for kindly providing the mineral water analysis. This publication contains results from the EU Project TRACE, No. 006942, funded under the Sixth Framework Program under the Food Quality and Safety Priority. The authors are solely responsible for the content of the publication. It does not represent the opinion of the Community, nor is the Community responsible for any use that might be made of the data herein.

References

Appelo, C. A. J., & Postma, D. (1993). *Geochemistry, groundwater and pollution*. Rotterdam: Balkema. p. 536.

Bos, M., Bos, A., & Van der Linden, W. E. (1993). Tutorial review: Data processing by neural networks in quantitative chemical analysis. *The Analyst, 118*, 323–328.

Calderone, G., Naulet, N., Guillou, C., Reniero, F., & Cortes, A. I. B. (2005). Analysis of the ^{13}C natural abundance of CO_2 gas from sparkling drinks by gas chromatography/combustion/isotope ratio mass spectrometry. *Rapid Communications in Mass Spectrometry, 19*(5), 701–705.

Caselli, M., De Giglio, A., Mangone, A., & Traini, A. (1998). Characterisation of mineral waters by pattern recognition methods. *Journal of the Science of Food and Agriculture, 76*, 533–536.

Despagne, F., & Massart, D. L. (1998). Tutorial review: Neural networks in multivariate calibration. *The Analyst, 123*, 157–178.

Grošelj, N., Zupan, J., Reich, S., Dawidowski, L., Gomez, D., & Magallanes, J. (2004). 2D mapping by Kohonen networks of the air quality data from a large city. *Journal of Chemical Information and Computer Sciences, 44*, 339–346.

Lau, O. W., & Luk, S.-F. (2002). A survey on the composition of mineral water and identification of natural mineral water. *International Journal of Food Science and Technology, 37*, 309–317.

Martin, G. J., Martin, M. L., Mabon, F., & Michon, M. J. (1983). A new method for the identification of the origin of ethanol in grain and fruit spirits: High-field quantitative deuterium nuclear magnetic resonance at the natural abundance level. *Journal of Agricultural and Food Chemistry, 31*(2), 311–315.

Müller, A., & Steinhart, H. (2007). Recent developments in instrumental analysis for food quality. *Food Chemistry, 102*, 436–444.

NIC_ANN_Programs (2007). *ANN-train program, ANN-test program, ANN-LOO program, ANN-visual program*, Laboratory of Chemometrics, National Institute of Chemistry, Ljubljana, Slovenia. <http://www.ki.si/en/research-departments/l03-laboratory-of-chemometrics/> (marjana.novic@ki.si).

Parkhurst, D. L., Appelo, C. A. J. (1999). User's guide to PHREEQC (version 2) – a computer program for speciation, batch reaction, one-dimensional transport, and inverse geochemical calculations. US Geological Survey Water-Resources Investigations, Report 99–4259.

Ravilious, K. (2004). Buyer beware. *New Scientist, 192*(2577), 40–43.

Scarmino, I. S., & Bruns, R. E. (1982). Pattern recognition classification of mineral waters based on spectrochemical analysis. *Energia Nuclear Agriculture, 4*, 99–111.

Spangenberg, J. E., & Ogrinc, N. (2001). Authentication of vegetable oils by bulk and olive oil and pumpkin seed oil. *Journal of Agricultural and Food Chemistry, 49*, 1534–1540.

Versari, A., Parpinello, G. P., & Galassi, S. (2002). Chemometric survey of Italian bottled mineral waters by means of their labeled physico-chemical and chemical composition. *Journal of Food Composition and Analysis, 15*, 251–264.

Vračko, M. (2005). Kohonen artificial neural network and counter propagation neural network in molecular structure-toxicity studies. *Current Computer-Aided Drug Design, 1*, 73–78.

Zupan, J. (1994). KCTRF-Program for Kohonen and Counter-propagation ANN. Slovenian National Institute of Chemistry. *Internal report DP-1452*.

Zupan, J., & Gasteiger, J. (1999). *Neural networks in chemistry and drug design*. Weinheim: Wiley-VCH.

Zupan, J., Novič, M., & Ruisanchez, I. (1997). Kohonen and counter-propagation ANNs in analytical chemistry. *Chemometrics and Intelligent Laborary Systems, 38*, 1–23.

from plants contain 5–10 different FAs. Simple seed oils composed of e.g. 5 different FAs may give 125 individual TAG molecules. Vegetable oils consist generally of fewer FAs than animal carcass fats, milk fats or fish oils. They seldom contain odd-numbered, branched-chain, or unsaturated FAs with fewer than 16 carbon atoms. Animal fats may be much more complex consisting of 10–40 different FAs.

In milk fat more than 400 different FAs have been identified. Most of those FAs arise from ruminal microbial metabolism and thus are unique to ruminant fats (Buchgraber et al., 2004).

Traditional analytical strategies to uncover adulteration and guarantee quality have relied on wet chemistry to determine the amount of a marker compound or compounds in a suspect material and a subsequent comparison of the value(s) obtained with those established for equivalent material (Karoui & De Baerdemaker, 2007). As the macro- and micro-components of oils are semi-volatile, both HPLC and GC techniques can be employed for their measurement. In the literature TAG and FA have received most attention. A relatively new concept is classification of oils or fats by their volatile profiles. The sensory properties of fats and oils differ considerably, which is mainly due to their volatile flavours. Therefore, volatile profiles may be useful for discrimination of fats and oils. Gas Chromatography (combined with olfactometry/flame ionization detection or mass spectrometry) (Högnadóttir & Rouseff, 2003; Luna, Morales, & Aparicio, 2006), electronic nose systems (Cosio, Ballabio, Benedetti, & Gigliotti, 2006; Hai & Wang, 2006) and proton transfer reaction-mass spectrometry (PTR-MS; Araghipour et al., 2007) are techniques for analysis of volatiles and are employed to generate classification data. As the more advanced evaluation methods used for authenticity tests of oils include a high number of variables (e.g. composition of TAGs), multivariate statistical methods are required for evaluation of the results (Cserháti et al., 2005).

In the present study the identities of seven types of fat (milk fat, cow fat, pig fat, poultry fat, coconut oil, palm oil, and palm kernel oil samples) were predicted applying partial least square discriminant analysis (PLS-DA) to (a) their multivariate FA profiles, (b) their TAG profiles, (c) their FA and TAG profiles combined, and (d) their profiles of volatile organic compounds (VOCs) measured by PTR-MS. FA and TAG profiling are rather conventional methods, but the non-targeted, non-biased chemometric approach (the PLS-DA) is an interesting new aspect, as well as the combination of multivariate datasets. PTR-MS analyses was explored because of its rapid data generation properties (full spectrum <30s). The success rates of the four approaches (FA, TAG, FA+TAG and PTR-MS) were compared.

2. Materials and methods

2.1. Materials

Eight regular and fourteen fractionated butter oil samples (8 soft and 6 hard fractions) were kindly provided by VIV Vreeland (Zelhem, the Netherlands) and Friesland Foods (Noordwijk, the Netherlands). Eight coconut oil, eight palm oil, and eight palm kernel oil samples were supplied by Unilever (Vlaardingen, The Netherlands). Samples originated from different batches. The animal fat samples from the Dutch industry consisted of eight cow fat samples, eight pig fat samples, and eight poultry fat samples. Three of them were commercial mixed samples from Smilde (Heerenveen, the Netherlands) and the others were samples from individual animals. The samples were selected taking into account as much as possible both natural and technology-induced variation. Sample material was stored at −20 °C in absence of light until analysis was carried out.

2.2. Methods

2.2.1. FA methyl ester (FAME) analysis

The fats were methylated and the fatty acid methyl esters analysed according to the international standard ISO 15885:2002. Nonanoic acid (C9:0) was added as internal standard (Sigma–Aldrich Chemie, Zwijndrecht, the Netherlands). As reference material a home-made standard FAME mixture composed of C4:0, methyl butyrate (Fluka, 19358, Sigma–Aldrich Chemie, Zwijndrecht, The Netherlands); C6:0, methyl capraote (Fluka, 21599); C8:0, methyl caprylate (Fluka, 21719); C10:0, methyl decanoate (Fluka, 21479); C12:0, methyl laurate (Fluka, 61689); C14:0, methyl myristate (Fluka, 70129); C16:0, methyl palmitate (Fluka, 76159); C18:0, methyl stearate (Fluka, 85769); C18:1, methyl oleate (Fluka, 75160); C9:0, methyl nonanoate (Sigma, 245895) was used to calculate calibration factors of the various FAMEs. Absolute concentrations (g fatty acid/100 g fat) as well as relative concentrations (the total FAME measured was normalized to 100%) were calculated. All fats and oils were analysed in triplicate.

2.2.2. TAG analysis

The TAG analysis was carried out according to the Draft International Standard ISO/DIS 17678|IDF 202 (Milk fat – Detection of foreign fats by gas chromatographic analysis of triglycerides). Tricaprion (C18) was added to each sample as internal standard. The reference material CRM 519 (IRMM, Geel, Belgium) was used for determining the calibration factor of each triglyceride. Both absolute concentrations of each TAG (g triacylglycerol/100 g fat) and relative concentrations (the total TAG measured was normalized to 100%) were measured. All fats and oils were analysed in triplicate.

2.2.3. PTR-MS analysis

For headspace analysis, 5 g of fat or oil was placed in a glass flask (100 ml) at 30 °C for 30 min to allow equilibration. Preliminary experiments showed that 30 min was sufficient for equilibration. Two replicates of each sample were analysed. The volatile organic compounds (VOCs) in the headspace of the samples were analysed at 30 °C by PTR-MS according to the method described by Lindinger, Hirber, and Paretzke (1993). A constant drift voltage of 600 V and a pressure of 2.09 ± 0.01 mbar were maintained in the reaction chamber. The headspace was drawn from the sample flask at a rate of 15 ml/min which was led through a heated transfer line into the high sensitivity PTR-MS for on-line analysis. Data were collected for the mass range m/z 20–149 using a dwell time of 0.2 s mass^{-1}. The instrument was operated at a standard E/N (ratio of electric field strength across the drift tube, E, to buffer gas density, N) of 138 Td (1Td = 10^{-17} cm^2 V molecule^{-1}). Inlet and drift chamber temperatures were 60°C. Each sample was analysed for at least 5 full mass scans. The headspace concentrations of the compounds during the cycles #2, #3 and #4 were calculated as described by Hansel et al. (1995) and background and mass discrimination corrections were applied. Headspace concentrations were subsequently averaged over the three mass scans for further statistical analysis. In preliminary experiments some of the samples were analysed for seven cycles: the results did not show consistent changes in headspace concentrations (especially no decrease) after the first cycle. Therefore, cycles #2, #3 and #4 were selected for calculations. Milk fat, coconut oil, palm oil and palm kernel oil samples were analysed in duplicate. Most animal fat samples were samples from individual animals, lack of sample material did not allow a sufficient number of PTR-MS analysis on the same samples to carry out PLS-DA analyses. Therefore, for the PTR-MS analysis, only milk fat and the vegetable oils were considered for statistical analysis.

2.2.4. Statistical analysis

PLS-DA models (Barker & Rayens, 2003) were estimated to predict the identity of the samples using either the FAME, TAG or VOC data. The analyses were carried out in Matlab using the PLS toolbox (Wise et al., 2006). PLS-DA performs a dimension reduction on the predictor variables. The dimensions (components) extracted are composed such that they exhibit maximal correlation with Y (class membership, e.g. milk fat, poultry fat, palm oil, etc.). After estimation of the classification model, its performance was evaluated by means of 10-fold cross-validation: 10% of the samples were randomly removed from the data set, and a model built with the remaining samples was used to classify these left out samples. The procedure was repeated ten times to obtain predictions for all samples. The number of components that is extracted is an important parameter in a PLS-DA model. Therefore, models with 1–8 components were investigated to select the most appropriate (optimal) number of components. Various standardization methods (on variables and on units) were investigated to improve prediction rates, i.e. mean-centering, auto-scaling, and log transformation.

After selecting the model, the 10-fold cross validation (which is a random process) was repeated 100 times to get insight into the repeatability of the classification results. The output of the 100 replications is summarized as follows. PLS-DA outputs, for each sample i, a posterior probability p_i (p_{i1}, p_{i2},. . ..p_{ik}) for membership in each of the k classes. The sample is assigned to the class with the highest posterior probability. Let p_{im} be the probability for this class, and let p_{im2} be the probability for the class with the second-largest posterior probability. Then

$$C_i = \frac{p_{it}}{p_{im} + P_{im2}}$$

(where $p_{it} = p_{im}$ when the classification is correct, and $p_{it} = p_{im2}$ when the classification is incorrect) has a value between 0 and 0.5 when sample i is incorrectly classified, and between 0.5 and 1 when it is correctly classified. The larger the difference between p_m and p_{m2}, the closer the value of C will be to either 1 or 0. If the difference between p_{im} and p_{im2} is small, C will be near 0.5. Therefore, values near 0 or 1 indicate high confidence, whereas values around 0.5 indicate lower confidence in prediction results. The box plots of C_i (one box plot for each sample) were composed as a summary of the results of the 100 repeated cross validations.

3. Results and discussion

3.1. FAME

The FAME compositions of the fats and oils characterized by 18 FAs are presented in Table 1. The FAME compositions of the cow fat (CV = 44%), pig fat (CV = 43%) and poultry fat samples (CV=34%) varied most across samples (CV based on variance between sample means, not between replicates). This is not surprising as these samples originated from different single animals.

The FAME data were subsequently subjected to PLS-DA. The best prediction rates appeared to be obtained with auto-scaling of the variables and no scaling of the units. The prediction success rates in single cross-validation runs varied from 74% (1 component) to 100% (100%: 4 and 8 components). It was therefore decided to run the 100 repeated cross-validations for 4 components to gain insight into the stability of the results. On average 1.4% of the fats were misclassified per replication. Fig. 1 shows box plots of the distribution of the 100 C_i-values obtained for each sample (for the definition of C, see the paragraph on 'Statistical Analysis'). The figure reveals that some samples are occasionally misclassified. Cow fat 8 is misclassified most often (column 38 in

Table 1
Absolute fatty acid composition of animal and vegetable fats/oils [g fatty acid/100 g fat].

	C6:0	C8:0	C10:0	C12:0	C14:0	C14:1	C15:0	C16:0	C16:1	C18:0	C18:1t1	C18:t2	C18:1	C18:1c1	C18:1c2	C18:2	C18:2conj	C18:3	CV[a] [%]
Milk fat[b]	2.4	1.4	3.1	3.9	11.5	1.0	1.0	30.4	1.9	10.6	0.4	1.6	21.0	0.6	0.6	1.4	0.6	0.5	20
Cow fat[c]	0.0	0.1	0.1	0.5	5.1	0.5	0.4	26.2	2.4	24.0	0.5	1.7	31.6	1.2	0.6	3.3	0.2	0.5	44
Pig fat[c]	0.0	0.1	0.1	0.3	1.8	0.0	0.1	27.4	1.6	17.6	0.2	0.0	35.2	2.1	0.1	12.6	0.0	1.1	43
Poultry fat[c]	0.0	0.1	0.2	3.6	2.5	0.4	0.1	23.9	4.8	5.5	0.3	0.0	36.1	1.7	0.1	18.9	0.1	1.6	34
Coconut oil[c]	0.7	8.6	6.6	49.4	18.4	0.0	0.0	10.2	0.0	3.1	0.1	0.0	7.0	0.1	0.0	1.8	0.0	0.1	14
Palm oil[c]	0.0	0.1	0.0	0.2	1.1	0.0	0.0	48.1	0.2	4.8	0.1	0.0	40.7	0.7	0.0	10.5	0.0	0.2	15
Palm kernel oil[c]	0.3	4.2	3.8	51.3	16.5	0.0	0.0	9.0	0.0	2.6	0.0	0.0	16.1	0.1	0.0	2.6	0.0	0.1	18

[a] Coefficient of variance (variance between sample means, not between replicates).
[b] Mean value of 14 fractionated and 8 unfractionated samples.
[c] Mean value of eight samples.

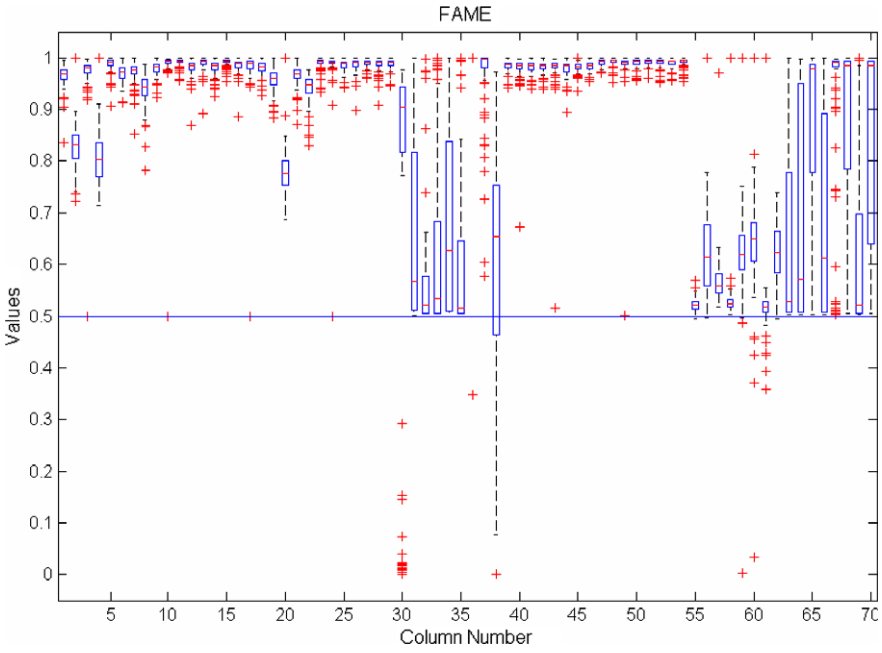

Fig. 1. Results for 100 replications of the random cross validation of the predicted classification of fat and oil samples by their absolute fatty acid compositions into identity classes (e.g. cow fat, palm oil, etc.) using PLS-DA models. For each of the samples, a box shows the location of the .25 and .75 quartiles of the quantity C (see text), the dotted lines (whiskers) are the whiskers; they have length 1.5 * the inter-quartile range (or shorter, if there are no more observations), and the crosses are outliers, lying outside the whiskers. The data have been sorted so that the 22 milk fat samples are displayed first (column 1–22), followed by 8 coconut oil (column 23–30), 8 cow fat (columns 31–38), 8 palm kernel oil (column 39–46), 8 palm oil (columns 47–54), 8 pig fat (columns 55–62), and 8 poultry fat samples (columns 63–70).

Table 2
Number and (percentages) of predicted classification of oils and fats into product classes by their absolute fatty acid composition using a four component PLS-DA model. The correctly classified samples in bold[a,b].

Sample	PLS-DA classification							Total correctly classified (%)
	Milk fat	Cow fat	Pig fat	Poultry fat	Coconut oil	Palm oil	Palm kernel oil	
Milk fat	**22 (100%)**	0 (0%)	0 (0%)	0 (0%)	0 (0%)	0 (0%)	0 (0%)	**100**
Cow fat	0 (0%)	**7 (87.5%)**	0 (0%)	1 (12.5%)	0 (0%)	0 (0%)	0 (0%)	**87.5**
Pig fat	0 (0%)	0 (0%)	**8 (100%)**	0 (0%)	0 (0%)	0 (0%)	0 (0%)	**100**
Poultry fat	0 (0%)	0 (0%)	0 (0%)	**8 (100%)**	0 (0%)	0 (0%)	0 (0%)	**100**
Coconut oil	0 (0%)	0 (0%)	0 (0%)	0 (0%)	**8 (100%)**	0 (0%)	0 (0%)	**100**
Palm oil	0 (0%)	0 (0%)	0 (0%)	0 (0%)	0 (0%)	**8 (100%)**	0 (0%)	**100**
Palm kernel oil	0 (0%)	0 (0%)	0 (0%)	0 (0%)	0 (0%)	0 (0%)	**8 (100%)**	**100**

[a] 69 out of 70 Samples were correctly classified (98.6%).
[b] Variables standardized by means of auto-scaling, no standardization on units applied.

the plot): 22 times out of 100 this sample is incorrectly classified as milk fat. However, in most cases the confidence in the incorrect classification is not very high (C_i closer to 0.5 than to 0). Four of the pig fat samples are occasionally misclassified as cow fats[1] (columns 55–62). Four more cow fat samples (columns 31–35) are sometimes incorrectly classified as pig fat. However, for these samples, the probabilities for the correct and incorrect class are almost equal, resulting in C_i -values of near 0.5. Therefore, these misclassifications are hardly visible in the box plot. Finally, one coconut fat sample (column 30) is occasionally misclassified with higher confidence, either as cow or pig fat.

More detailed results are now given for one particular cross validation run. For this run, the numbers of samples predicted into the various product groups are listed in Table 2. A scores plot of the first three dimensions of the model is shown in Fig. 2. In this run, only one cow fat sample was misclassified as poultry fat. But the posterior probability for this classification is not very high (0.13). As the second largest posterior probability is 0.05, this incorrect classification would result in a C_i-value of 0.05/0.18 = 0.28. The scores plot (Fig. 2) shows that the misclassified cow fat is positioned more or less halfway between the cow fat and the poultry fat samples.

A similar approach was adopted for the relative FAME data. With 4 components extracted, on average 1% of the classifications was incorrect.

3.2. TAG

The TAG compositions of the fats and oils were determined; they were characterized by 17 triglycerides (Table 3). The animal fats (CV = 21–40%) showed a more varied TAG composition than the vegetable oils (CV = 3–10%; CV considering variance between sample means only). TAG composition of the cow fat was generally within the ranges specified by Precht (1992), who developed a method for detection of foreign fat in milk fat. The compositions

[1] The box plot shows whether a sample is misclassified or not, it does not show into which incorrect class a misclassified sample is placed. This information is available, but due to space considerations, it is impossible to present it in a table. It was therefore decided to mention it in the text, where appropriate.

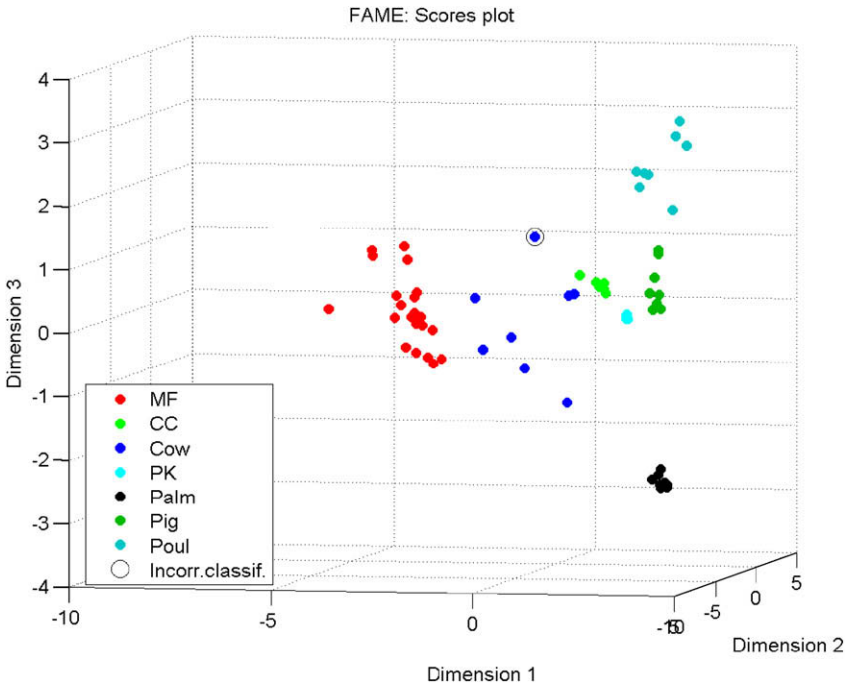

Fig. 2. Scores plot of the first three dimensions of PLS-DA on the absolute fatty acid composition data of seven oils and fats.

Table 3
Absolute triacylglycerol composition of animal and vegetable fats/oils [g triacylglycerol/100g fat].

	Chol.	C26	C28	C30	C32	C34	C36	C38	C40	C42	C44	C46	C48	C50	C52	C54	C56	CV[a] (%)
Milk fat[b]	0.4	0.3	0.6	1.3	2.7	6.3	11.0	12.7	9.8	6.9	6.5	7.3	9.0	10.8	9.6	4.6	0.3	21
Cow fat[c]	0.1	0.0	0.0	0.0	0.0	0.0	0.2	0.2	0.0	0.2	1.0	3.7	11.8	23.3	38.1	24.7	0.8	28
Pig fat[c]	0.1	0.0	0.0	0.0	0.0	0.0	0.1	0.0	0.0	0.0	0.2	0.6	2.9	15.6	62.6	20.8	1.6	25
Poultry fat[c]	0.1	0.0	0.0	0.0	0.0	0.0	0.2	0.2	0.5	1.2	2.3	5.8	9.9	20.5	36.1	26.2	1.2	40
Coconut oil[c]	0.2	0.7	1.0	3.0	11.6	15.2	17.9	16.2	10.4	7.7	4.6	2.7	2.5	2.1	1.8	1.0	0.0	9
Palm oil[c]	0.0	0.0	0.0	0.0	0.1	1.1	4.2	2.4	0.1	0.0	0.1	0.6	7.3	38.0	39.6	12.0	0.6	10
Palm kernel oil[c]	0.1	0.9	0.7	1.3	6.2	8.0	20.2	15.5	9.2	8.9	6.7	5.4	6.5	2.9	3.0	3.3	0.1	3

[a] Coefficient of variance (variance between sample means, not between replicates).
[b] Mean value of 14 fractionated and 8 unfractionated samples.
[c] Mean value of eight samples

of coconut oil and pig fat in the present study showed generally higher concentrations of the longer chain TAGs than those reported by Precht (1992).

For the TAG data too, auto-scaling of the variables and no scaling of the units appeared to give the best results. The optimal number of components was larger here than it was for the FAME data before. The cross-validation procedure was repeated 100 times for a solution with 6 components, giving a confidence box plot (Fig. 3). It appeared that all cow fat samples (columns 31–38) are occasionally classified as poultry fat samples, and all poultry fat samples (columns 63–70) sometimes as cow fat samples (see Footnote 1). Apparently, separating these two types of fat by their triglyceride compositions is a challenging task.

A similar approach was adopted for the relative TAG data. Here, with 6 components, on average 10 % of the samples was incorrectly classified. Without exception these were poultry and cow fats being confounded.

3.3. Combined FAME and TAG analysis

The FAME and TAG datasets were combined for further improvement of the identity prediction of the fats and oils. Optimal results regarding identity prediction were obtained with a six component PLS-DA model with auto-scaling of the variables and no scaling of the units. The confidence plot of this combined six component model is presented in Fig. 4. The box plot shows that all confidence levels are between 0.5 and 1.0 which indicates that the combined model classified 100% of the samples correctly. Combination of the two datasets resulted further in higher confidence in the predictions in general than for the single data sets: most values are close to 1.

A similar approach was adopted for the combined relative data. They resulted on average in a correct classification of 99 % of the samples.

3.4. VOC

Proton transfer reaction-mass spectrometry (PTR-MS) is a promising technique for analysis of volatile compounds and has been used to investigate different issues in food science. For instance the effect of technological conditions on the VOC profiles of orange juices has been studied (Biasioli et al., 2003). Pollien and co-workers used PTR-MS for on-line monitoring of acrylamide (Pollien, Lindinger, Yeretzian, & Blank, 2003). Correlation with sensory data (Biasioli et al., 2006) and real-time in-nose analysis (Fransnelli, van Ruth, Kriukova, & Hummel, 2005) are other

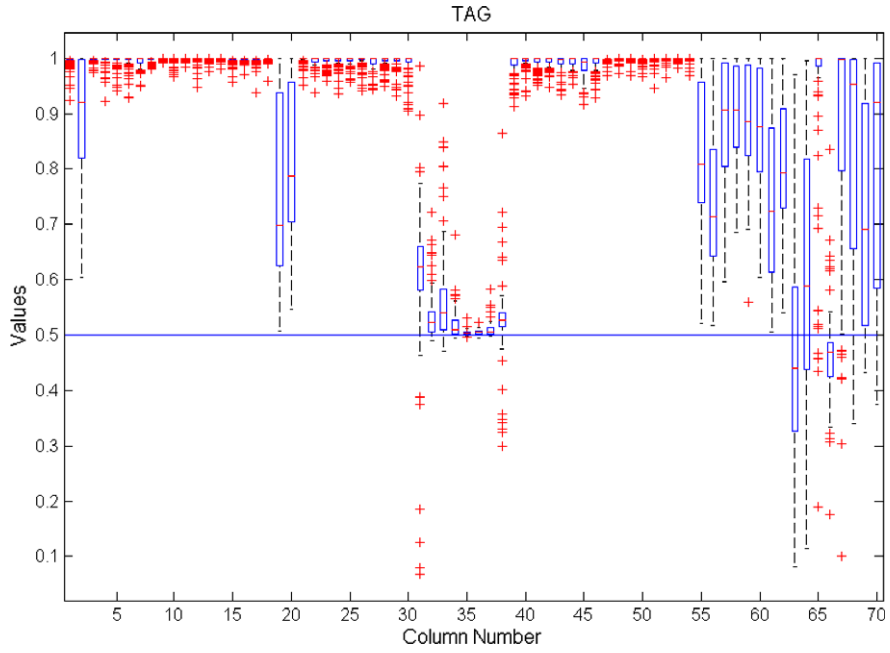

Fig. 3. Results for 100 replications of the random cross validation of the predicted classification of fat and oil samples by their absolute triacylglycerol compositions into identity classes (e.g. cow fat, palm oil, etc.) using PLS-DA models. For each of the samples, a box shows the location of the .25 and .75 quartiles of the quantity C (see text), the dotted lines (whiskers) are the whiskers; they have length 1.5 * the inter-quartile range (or shorter, if there are no more observations), and the crosses are outliers, lying outside the whiskers. The data have been sorted so that the 22 milk fat samples are displayed first (column 1–22), followed by 8 coconut oil (column 23–30), 8 cow fat (columns 31–38), 8 palm kernel oil (column 39–46), 8 palm oil (columns 47–54), 8 pig fat (columns 55–62), and 8 poultry fat samples (columns 63–70).

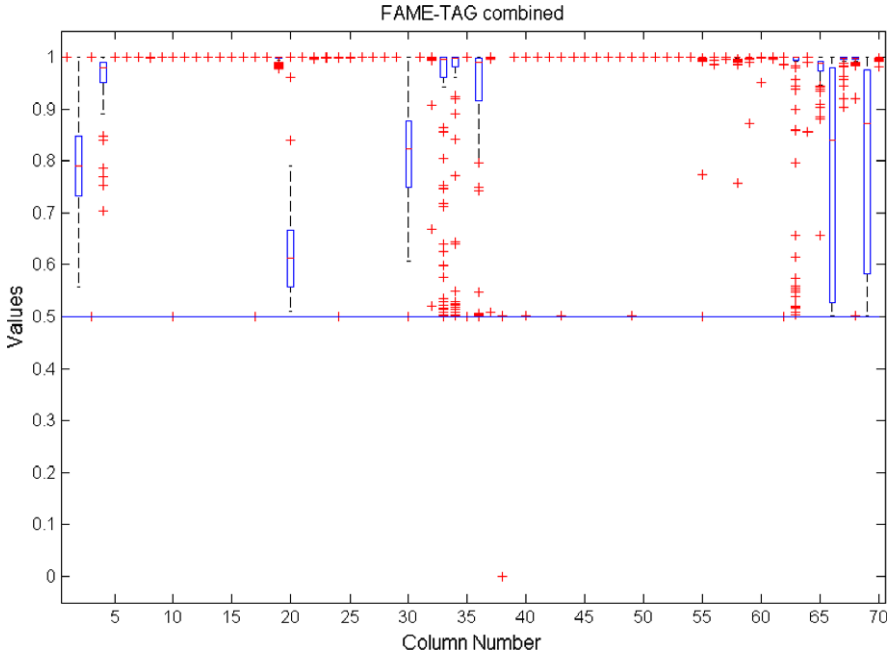

Fig. 4. Results for 100 replications of the random cross validation of the predicted classification of fat and oil samples by their combined absolute fatty acid and triacylglycerol compositions into identity classes (e.g. cow fat, palm oil, etc.) using PLS-DA models. For each of the samples, a box shows the location of the .25 and .75 quartiles of the quantity C (see text), the dotted lines (whiskers) are the whiskers; they have length 1.5 * the inter-quartile range (or shorter, if there are no more observations), and the crosses are outliers, lying outside the whiskers. The data have been sorted so that the 22 milk fat samples are displayed first (column 1–22), followed by 8 coconut oil (column 23–30), 8 cow fat (columns 31–38), 8 palm kernel oil (column 39–46), 8 palm oil (columns 47–54), 8 pig fat (columns 55–62), and 8 poultry fat samples (columns 63–70).

important applications. Proton transfer reactions are used to induce chemical ionisation of the vapours to be analysed. The sample gas is continuously introduced into a drift tube, where it is mixed with H_3O^+ ions formed in a hollow cathode ion source. Volatile compounds that have proton affinities higher than water (>166.58 kcal/mol) are ionised by proton transfer from H_3O^+, mass analysed in a quadrupole mass spectrometer and eventually detected as ion counts/s (cps) by a secondary electron multiplier. The outcome is a mass resolved fingerprint of the total volatile profile of a sample. PTR-MS is interesting for this fingerprinting

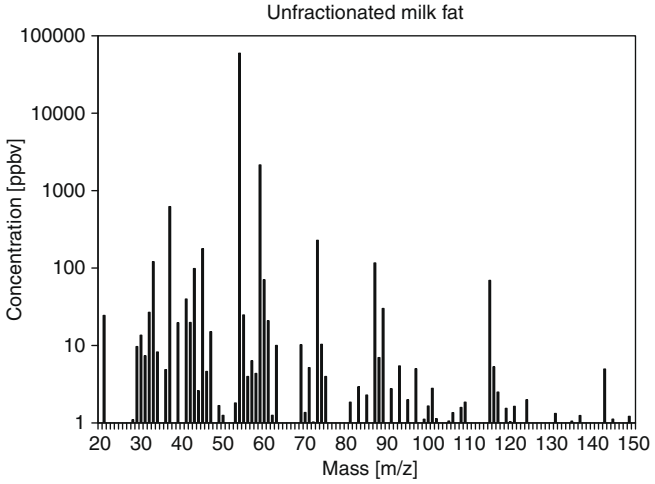

Fig. 5. Mean fingerprint mass spectrum of the volatile organic compounds in the headspace of regular milk fat obtained by proton transfer reaction mass spectrometry.

Table 4
Number and (percentages) of predicted classification of oils and fats into product classes by their volatile organic compound compositions using a three component PLS-DA model. The correctly classified samples in bold [a,b].

Sample	PLS-DA classification				Total correctly classified (%)
	Milk fat	Coconut oil	Palm oil	Palm kernel oil	
Milk fat	**22 (100%)**	0 (0%)	0 (0%)	0 (0%)	**100**
Coconut oil	0 (0%)	**7 (87.5%)**	0 (0%)	1 (12.5%)	**87.5**
Palm oil	0 (0%)	0 (0%)	**8 (100%)**	0 (0%)	**100**
Palm kernel Oil	1 (12.5%)	2 (25%)	1 (12.5%)	**4 (50%)**	**50**

[a] 41 out of 46 Samples were correctly classified (89.1%).
[b] Variables standardized by means of auto-scaling, no standardization on units applied.

approach as (i) it requires no pre-treatment of the sample, (ii) it allows rapid measurements (typically <1 min for a complete mass spectrum), and (iii) the technique is extremely sensitive (ppt level).

The PTR-MS data of the VOCs covered a range of 129 masses (data not shown). An example of the mean fingerprint mass spectrum of the regular milk fats is presented in Fig. 5. Results for one cross-validation run while applying a three component PLS-DA model with auto-scaling of the variables and no scaling of the units are presented in Table 4. The milk fats, coconut oils and palm oils were correctly classified except for one coconut oil. Palm kernel oils showed poor classification results, with only 50% of the samples being correctly classified. Misclassified palm kernel samples were placed into all product groups, therefore, it seems that the palm kernel oils were not characterized by specific VOCs, but showed great overlap with the VOCs of the other product groups. Overall, 89% of the samples were classified correctly using PTR-MS data. Therefore, classification was reasonably successful, but rates were not as high as for the FAME and TAG analysis. However, PTR-MS analysis has the advantage of being very rapid compared with the other analysis techniques, which would make it a potential technique for screening of particular fats and oils.

Table 5
Overview of correct classifications of fats and oils by their fatty acid, triacylglycerol or volatile organic compound composition using PLS-DA.

Techniques	Number of components in PLS-DA	Correct classifications (%)
Fatty acid composition, absolute data	4	99
Fatty acid composition, absolute date	6	97
Fatty acid composition, relative data	4	99
Triacylglycerol composition, absolute data	6	96
Triacylglycerol composition, relative data	6	90
Combined Fatty acid and triacylglycerol composition, absolute data	5	99
Combined fatty acid and triacylglycerol composition, relative data	6	100
Volatile organic compound composition measured by proton transfer reaction mass spectrometry	3	89

4. Conclusions

For identity prediction all techniques used were reasonably successful in classifying the various animal fats and vegetable oils (89–100%, Table 5). The identity of the samples was most successfully predicted using the combined absolute FAME and TAG data set (i.e. for the present dataset 100%). The combined FAME-TAG dataset has the additional advantage that a more robust prediction is obtained as the confidence in the predictions is generally higher than for the other datasets. Alternatively, if a certain prediction rate (e.g. 95%) is required, fewer PLS components are sufficient to obtain this success rate. PTR-MS analysis which results in a volatile fingerprint was least successful but still resulted in 89% correct classifications with the additional advantage of the speed of the technique. The technique gave promising results, but further studies are required to confirm its use as a good alternative for FA and TAG analyses.

References

Araghipour, N., Colineau, J., Koot, A., Akkermans, W., Moreno Rojas, J. M., Beauchamp, J., et al. (2007). Geographical origin classification of olive oils by PTR-MS. *Food Chemistry, 108*, 374–383.

Barker, M., & Rayens, W. (2003). Partial least squares for discrimination. *Journal of Chemometrics, 17*, 166–173.

Biasioli, F., Gasperi, F., Aprea, E., Colato, L., Boscaini, E., & Märk, T. D. (2003). Fingerprinting mass spectrometry by PTR-MS: Heat treatment vs. pressure treatment of red orange juice, a case study. *International Journal of Mass Spectrometry, 223–224*, 343–353.

Biasioli, F., Gasperi, F., Aprea, E., Endrezzi, I., Framondino, V., Marini, F., et al. (2006). Correlation of PTR-MS spectral fingerprints with sensory characterisation of flavour and odour profile of 'Trentingrana' cheese. *Food Quality and Preference, 17*, 63–75.

Buchgraber, M., Ulberth, F., Emons, H., & Anklam, E. (2004). Triacylglycerol profiling by using chromatographic techniques. *European Journal of Lipid Science and Technology, 106*, 621–648.

Cosio, M. S., Ballabio, D., Benedetti, S., & Gigliotti, C. (2006). Geographical origin and authentication of extra virgin olive oils by an electronic nose in combination with artificial neural networks. *Analytica Chimica Acta, 567*, 202–210.

Cserháti, T., Forgács, E., Deyl, Z., & Miksik, I. (2005). Chromatography in authenticity and trace ability tests of vegetable oils and dairy products: A review. *Biomedical Chromatography, 19*, 183–190.

Fransnelli, J., van Ruth, S. M., Kriukova, I., & Hummel, T. (2005). Intranasal concentrations of orally administered flavours. *Chemical Senses, 30*, 572–582.

Hai, Z., & Wang, J. (2006). Detection of adulteration in camellia seed oil and sesame oil using an electronic nose. *European Journal of Lipid Science and Technology, 108*, 116–224.

Hansel, A., Jordan, A., Holzinger, R., Prazeller, P., Vogel, W., & Lindinger, W. (1995). Proton transfer reaction mass spectrometry: On-line trace gas analysis at the ppb level. *International Journal of Mass Spectrometry and Ion Processes, 149*(150), 609–619.

Högnadóttir, A., & Rouseff, R. L. (2003). Identification of aroma active compounds in orange essential oil using gas chromatography-olfactometry and gas chromatography-mass spectrometry. *Journal of Chromatography A, 998*, 201–211.

Kamm, W., Dionisi, F., Hischenhuber, C., & Engel, K.-H. (2001). Authenticity assessment of fats and oils. *Food Reviews International, 17*(3), 249–290.

Karoui, R., & De Baerdemaker, J. (2007). A review of the analytical methods coupled with chemometric tools for the determination of the quality and identity of dairy products. *Food Chemistry, 102*, 621–640.

Lindinger, W., Hirber, J., & Paretzke, H. (1993). An ion/molecule-reaction mass spectrometer used for on-line trace gas analysis. *Journal of Mass Spectrometry and Ion Processes, 129*, 79–88.

Luna, G., Morales, M. T., & Aparicio, R. (2006). Characterisation of 39 varietal virgin olive oils by their volatile compositions. *Food Chemistry, 98*, 243–252.

Pollien, P., Lindinger, C., Yeretzian, C., & Blank, I. (2003). Proton transfer reaction mass spectrometry, a tool for on-line monitoring of acrylamide formation in the headspace of Maillard reaction systems and processed food. *Analytical Chemistry, 75*, 5488–5494.

Precht, D. (1992). Detection of foreign fat in milk fat. I. Qualitative detection by triacylglycerol formulae. II. Quantitative evaluation of foreign fat mixtures.. *Zeitschrift für Lebensmittel Untersuchung und –Forschung, 194*, 1–8.

Ulberth, F., & Buchgraber, M. (2000). Authenticity of fats and oils. *European Journal of Lipid Science and Technology, 102*, 687–694.

Wise, B. M., Shaver, J. M., Gallagher, N. B., Windig, W., Bro, R., & Koch, R. S. (2006). *PLS Toolbox Version 4.0 for use with Matlab*^{tm}, *Eigenvector Research Inc*. WA, USA: Wenatchee.

chemical and sensorial, combined with statistical analysis, has greatly facilitated the fight against fraud in this sector. Moreover, the contribution of databases and mathematical algorithms is necessary in order to provide the classification required to fully guarantee both the geographical origin and authenticity of VOO (Aparicio & Aparicio-Ruiz, 2000).

Olive oil is mainly made up of triglycerides (more than 98%), whereas the unsaponifiable fraction of virgin olive oil (VOO) represents 1–2% of the oil. This fraction is made up of minor constituents, which may vary both qualitatively and quantitatively depending on vegetal species, climatic conditions, extraction and refining procedures, and storage conditions (Cañabate-Diaz et al., 2007; Harwood & Aparicio, 2000). These also greatly influence the organoleptic quality and stability of the oil. VOO may contain up to 0.7% hydrocarbons, which is mainly constituted by squalene, a precursor of other sterols and triterpenic alcohols (Bortolomeazzi, Berno, Pizzale, & Conte, 2001; Lercker & Rodriguez-Estrada, 2000). Besides squalene, the hydrocarbon fraction of olive oil comprises of low quantities of epoxy-squalene isomers and alkanes (C16–C35) (Grob, Lanfranchi, & Mariani, 1990; Mariani & Fedeli, 1986). Plant sterols or phytosterols make up the main part of the unsaponifiable fraction of olive oil. The most abundant olive oil sterol is β-sitosterol, followed by Δ5-avenasterol. Campesterol and stigmasterol are present in lower concentrations (Harwood & Aparicio, 2000). Regarding the tracking of commercial fraud, the sterol fraction has many applications, especially where the contamination of some vegetable oils with other cheaper ones is concerned. Positional isomers of the double bond in the sterol ring have been detected and can be used as fraud tracers in VOO (Aparicio & Aparicio-Ruiz, 2000; Biedermann, Grob, Mariani, & Schmidt, 1996; Lercker & Rodriguez-Estrada, 2000; Mariani, Venturin, & Grob, 1995). Of the tocopherols, α-tocopherol comprises about 90% of the total tocopherol fraction. The stability of VOO is mainly due to their relatively low fatty acid unsaturation and to the antioxidant activity of some of the unsaponifiable components: the activity of α-tocopherol and the effect it has on the oxidative susceptibility of an olive oil was researched by Deiana et al. (2002). Moreover, α-tocopherol showed a synergistic effect in association with some phenolic compounds with significant activity. The major phenolic compounds identified and quantified in olive oil belong to three different classes: simple phenols (hydroxytyrosol, tyrosol), secoiridoids, and the lignans. The cultivar, the system of extraction, and the conditions of processing and storage are critical factors for the polyphenol content of an olive oil (Aparicio & Luna, 2002). Other constituents of the unsaponifiable matter are the pigments which impart the characteristic colour to an olive oil. They are made up of carotenoids, most importantly β-carotene, which gives a yellow colour; chlorophylls, responsible for the green shades; and pheophytins (Minguez-Mosquera, Gandul-Rojas, Garrido-Fernandez, & Gallardo-Guerrero, 1990). Other components include aliphatic alcohols made up of docosanol, tetracosanol, hexacosanol and octacosanol; and at trace levels, tricosanol, pentacosanol, and heptacosanol. In smaller quantities the following triterpenic alcohols are present: cycloartenol, 24-methylen-cycloartenol, and α- and β-amirines; diterpenic alcohols: fitol and geranilgeraniol; and triterpenic dialcohols: erythrodiol and uvaol. These numerous compounds, present in tiny percentages in olive oil, hold great biological importance and are characteristic of each type of oil (Harwood & Aparicio, 2000). In fact, the composition of the unsaponifiable fraction of VOO is affected by several factors (Harwood & Aparicio, 2000) such as olive cultivar (Aparicio, Morales, & Alonso, 1997; Esti, Cinquante, & La Notte, 1998; Pinelli et al., 2003), altitude (Mousa, Gerasopoulos, Metzidakis, & Kiritsakis, 1996), climatology (Aparicio, Ferreiro, & Alonso, 1994), agronomic factors (Gutierrez, Albi, Palma, Rios, & Olias, 1989), time of harvest (Aparicio & Morales, 1998), olive storage after harvest (Mariani, Fedeli, Grob, & Artho, 1991), and oil extraction system (Angerosa & Di Giovacchino, 1996; Ranalli & Angerosa, 1996). The diversity and interrelation amongst all these factors is reflected in the chemical composition of VOO, and it is highly unlikely that this influence would be the same in different regions. So, the geographical characterisation of VOO regards all these agronomic, pedoclimatic and botanical aspects that characterise the oil of each origin (Aparicio, Alonso, & Morales, 1994; Esti et al., 1996). Therefore, it can be expected that the unsaponifiable fraction of VOOs may contain information for the geographical characterisation of olive oils.

The more commonly used methods for minor constituent determination in olive oil usually require isolation and several procedures of separation, identification and quantification. The conventional method for quantifying sterols and triterpenic alcohols involves capillary GC–FID of the fraction isolated by TLC [Commission Regulation (EEC) No. 2568/91]. Regarding the quantification of minor components in the unsaponifiable matter of olive oil, chromatographic methods have proven to be particularly suitable (Lercker & Rodriguez-Estrada, 2000). Thus, alkanols, squalene, α-tocopherol, and sterols were determined by GC (Giacometti, 2001); sterols were quantified by GC–FID for the classification and authentication of monovarietal and PDO olive oils (Alves, Cunha, Amaral, Pereira, & Oliveira, 2005); phytosterols were analysed by GC–MS in order to compare their content with that of sunflower oil and butter (Zhang et al., 2005); SPE and GC–MS were used to characterise free and esterified sterols (Cunha, Fernandes, & Oliveira, 2006); tocopherols, and phytosterols, quantified by reversed phase HPLC, discriminate between very similar oils (Lopez Ortiz, Prats Moya, & Berenguer Navarro, 2006); and seven phytosterols analysed by LC–MS distinguished different qualities of olive oils (Cañabate-Diaz et al., 2007). FT-Raman and FT-NIR spectroscopy has also been applied to characterise olive oil. Moreover, the spectra of the unsaponifiable matter of olive oil obtained by these techniques together with univariate and multivariate statistical models enabled the detection of hazelnut oil in olive oil at a level as low as 8% (Baeten et al., 2005). FT-Raman bands due to the major unsaponifiable series of compounds, i.e. squalene, sterolic, and terpenic fractions, analysed by unsupervised multivariate techniques allow us to differentiate between olive oils and other seed oils as well as and amongst varietal VOO (Baeten, Dardenne, & Aparicio, 2001). ^{1}H, ^{13}C and/or ^{31}P NMR analysis of the bulk oil, in combination with multivariate techniques, have been used to distinguish VOOs according to their geographical origin (Rezzi et al., 2005), as well as to detect adulteration of the oil (Fragaki, Spyros, Siragakis, Salivaras, & Dais, 2005; Garcia-Gonzalez, Mannina, D'Imperio, Segre & Aparicio, 2004). IRMS methods have also been used for the authentication of olive oil by analysing the bulk oil (Angerosa, Camera, Cumitini, Gleixner, & Reniero, 1997; Bianchi, Angerosa, Camera, Reniero, & Anglani, 1993; Breas, Guillou, Reniero, Sada, & Angerosa, 1998). Isotopic measurements of alcohol and sterol fractions of olive oil also proved to be useful for its geographical characterisation (Angerosa et al., 1999). ^{1}H NMR and the more recently developed hyphenated LC–SPE–NMR technique have been applied to study phenolic compounds in the polar fraction of olive oil for authentication purposes (Christophoridou, Dais, Tseng, & Spraul, 2005; Sacco et al., 2000).

In the present work, a new approach based on ^{1}H NMR fingerprinting of the unsaponifiable fraction of VOO is presented. VOO from six countries, namely Spain, Italy, Greece, Tunisia, Turkey, and Syria, were analysed. The spectral data was subjected to pattern recognition techniques, which can be used to classify a VOO according to its geographical origin. Moreover, ^{1}H NMR spectra of the bulk oil, and its corresponding unsaponifiable fraction, as well as the subfractions of the unsaponifiable fraction (alcohol, sterol, hydrocarbon, and tocopherol fractions) were studied in the search

for the markers that multivariate techniques revealed to be related to the geographical origin of olive oils.

2. Materials and methods

2.1. Samples and chemicals

Commercial virgin olive oils (99 samples) from six countries of the Mediterranean basin, namely Italy (19 VOOs), Spain (36 VOOs), Greece (12 VOOs), Tunisia (15 VOOs), Turkey (8 VOOs), and Syria (9 VOOs), were provided by the SSOG (Stazione Sperimentale per le Industrie degli Oli e dei Grassi, Milan, Italy), which was able to assure the true type (virgin) and origin of the olive oils at least at the national level. Virgin olive oils (23 samples) from different Italian (5 VOOs), Spanish (4 VOOs), and Greek (5 VOOs) PDOs as well as samples from Tunisia (5 VOOs) and Turkey (4 VOOs) were collected directly in the country of origin by the SSOG.

Deuterated chloroform for NMR analysis (99.8 at % D), chloroform (p.a.), 1-eicosanol, α-tocopherol, β-sitosterol, stigmasterol, campesterol, and silica gel on TLC plates diethyl ether were provided by Sigma–Aldrich Chemie (Steinheim, Germany); potassium hydroxide (p.a.), anhydrous sodium sulphate (p.a.), hexane (p.a.), and 2′,7′-dichlorofluorescein (TLC grade) by Merck (Darmstadt, Germany); diethyl ether (HPLC grade) by Fluka Chemie (Buchs, Switzerland); methanol (HPLC grade) by Carlo Erba (Rodano, Italy); and erythrodiol by Extrasynthèse (Genay France). Cycloartenol standard was prepared by extracting the unsaponifiable fraction from flax oil and performing a further purification of the extract by thin layer chromatography (TLC) (see Sections 2.2 and 2.3).

2.2. Preparation of the unsaponifiable fraction of olive oil

The unsaponifiable fraction was prepared using a modification of the method described in the regulation EEC-2568/91 (annex V, Section 5.1). The sample of olive oil is dried under a nitrogen flow and filtered. Then, 50 ml of methanolic potassium hydroxide 2 N is added to an aliquot of 5 g of the dried and filtered olive oil, and heated to a gentle boil in a water bath with continuous vigorous stirring under reflux for 1 h. Then the content is transferred quantitatively into a 500 ml funnel using several rinses of distilled water (about 100 ml), and three successive extractions with ethyl ether (80 ml) are performed. The ether phase is washed with distilled water until the wash water reaches a neutral pH. Once the water is removed, the extract is dried with anhydrous sodium sulphate for 30 min, filtered and the solvent removed using a rotavapor at 40 °C to dryness. The repeatability of the method was evaluated by extracting separately four aliquots of eight different samples of VOOs of four different geographical origins.

2.3. Preparation of the alcohol, sterol, hydrocarbon, and tocopherol fractions

The unsaponifiable fraction of the oil is dissolved in chloroform (5% w/v) and fractionated by TLC using hexane-diethyl ether (50:50, v/v) as the eluent. Once the plate is developed, it is dried by leaving it for a short time under a fume hood. Then, it is sprayed with an ethanolic solution of 2,7-dichlorofluorescein (0.2%, w/v), in order to make the bands of the different fractions and components visible under ultraviolet light: the hydrocarbon fraction (HF); tocopherol fraction (TF); alcohol fraction (AF), containing cycloartenol; and the sterol fraction (SF) and erythrodiol. Then, each single band is scraped off and extracted with diethyl ether (10 ml), filtered under vacuum, washed several times with diethyl ether, and evaporated to dryness by mild heating in a gentle flow of nitrogen. An aliquot of each fraction was analysed by GC–FID (regulation EEC-2568/91, annex V, Sections 5.3 and 5.4.2.1.) in order to control the performance of the fractionation procedure.

2.4. NMR analysis

Each unsaponifiable fraction of VOO or 40 μl of the bulk oil was dissolved in 200 μl of deuterated chloroform, shaken in a vortex, and placed in a 2 mm NMR capillary. The ^{1}H NMR experiments were performed at 300 K on a Bruker (Rheinstetten, Germany) Avance 500 (nominal frequency 500.13 MHz) equipped with a 2.5 mm broadband inverse probe. The spectra were recorded using a 7.5 μs pulse (90°), an acquisition time of 3.0 s (32*k* data points) and a total recycling time of 4.0 s, a spectral width of 5500 Hz (11 ppm), 64 scans (+4 dummy scans), with no sample rotation. Prior to Fourier transformation, the free induction decays (FIDs) were zero-filled to 64*k* and a 0.3 Hz line-broadening factor was applied. The chemical shifts are expressed in δ scale (ppm), referenced to the residual signal of chloroform (7.26 ppm) (Hoffman, 2006). The interesting regions of the NMR spectra for the analysis of the unsaponifiable fraction are from 0 to 5.44 ppm, and for the bulk oil, from 0 to 7 ppm. The spectra were phase- and baseline-corrected manually, and normalised to total intensity over the region 0–5.44 ppm for the unsaponifiable fraction and over the region 4.08–4.28 ppm for the bulk oil. The region of interest of the NMR spectra was binned with 0.04 ppm-wide buckets. TopSpin 1.3 (2005) and Amix-Viewer 3.7.7 (2006) from Bruker BioSpin GMBH (Rheinstetten, Germany) were used to perform the processing of the spectra. The data table generated with the spectra of all samples was then used for pattern recognition. One bucket in the region 3.96–4.00 ppm (artifact) in the unsaponifiable fraction analysis and five buckets in the region 4.08–4.28 ppm (reference region) in the bulk oil analysis were excluded in the multivariate data analysis.

2.5. Multivariate data analysis

The data set consisted of a 99 × 135 matrix, in which rows represented the samples (99 unsaponifiable fractions of VOO analysed), and columns the 135 buckets of the ^{1}H NMR spectrum. Each VOO was represented in the 135-dimensional space by a data vector made of the 135 variables. Data vectors belonging to the same category (geographical origin: Italy, Spain, Greece, Tunisia, Turkey, or Syria) were firstly analysed by univariate procedures (ANOVA, Fisher index and Box–Whisker plots), and afterwards, by the following multivariate techniques, already described in bibliography (Berrueta, Alonso-Salces, & Héberger, 2007): unsupervised as principal component analysis (PCA); and supervised as linear discriminant analysis (LDA), partial least squares discriminant analysis (PLS-DA), classification and regression trees (CART) and soft independent modelling of class analogy (SIMCA). Statistic and chemometric data analysis were performed by means of the statistical software packages Statistica 6.1 (StatSoft Inc., Tulsa, OK, USA, 1984–2004) and The Unscrambler 9.1 (Camo Process AS, Oslo, Norway, 1986–2004). Similarly, data sets made up of the ^{1}H NMR spectral data of the bulk oil and/or the unsaponifiable fraction of 23 VOO from Italy, Spain, Greece, Tunisia, and Turkey, were analysed by PLS-DA.

In LDA, the variable selection strategy was the following. Firstly, a modified best subset selection was used, which is a variable selection procedure that performs a search for the best subsets of a small number of variables that fulfil the criterion for choosing the best one (Wilks' lambda, rate of misclassification, etc.). This can be computed relatively quickly and in several steps: first, best subset selection applied to the complete data matrix to obtain the first best (small) subset of variables; then, in a second step, using best subset selection on a data set omitting the variables selected

in the first step, a second best subset is achieved, and so on. Finally, a refined selection of the variables selected successively in the previous steps was performed using forward stepwise selection (Berrueta et al., 2007).

The supervised techniques were applied to the autoscaled (or standardised) data matrix of the profiles of the unsaponifiable fractions of VOOs (in LDA, PLS-DA, and SIMCA) or to the PCA score matrix (principal components with eigenvalue higher than 1) (in CART). The models achieved were validated by threefold cross-validation or leave-one-out cross-validation (LOO) (Berrueta et al., 2007). The reliability of the classification models achieved was studied in terms of recognition ability (percentage of the members of the training set correctly classified) and prediction ability (percentage of the members of the test set correctly classified by using the rules developed in the training step). The model achieved by SIMCA for each category was also evaluated in terms of sensitivity (percentage of objects belonging to the category which are correctly identified by the mathematical model) and specificity (the percentage of objects foreign to the category which are classified as foreign).

3. Results and discussion

3.1. ^{1}H NMR spectra of the bulk and unsaponifiable fraction and subfractions of VOOs

^{1}H NMR spectra of the 23 VOOs from five different countries (Italy, Spain, Greece, Tunisia, and Turkey) and their corresponding unsaponifiable fractions were recorded. Moreover, subfractions of the unsaponifiable fraction of two VOOs from different origins (Italy and Turkey) were also analysed by ^{1}H NMR: (i) alcohol fraction (AF), (ii) sterol fraction (SF), (iii) hydrocarbon fraction (HF), and (iv) tocopherol fraction (TF). The spectral region studied for the unsaponifiable fraction has been limited to 0–5.44 ppm, because very few signals appear at higher chemical shifts and a large hump is observable in many samples (possibly due to incomplete water removal or to the presence of microparticles). The authors are aware that in this study some information contained at fields lower than 5.44 ppm is lost, as for example characteristic ^{1}H signals of aldehydes and phenolic compounds are located at high chemical shifts in the spectral region discarded (Guillen & Ruiz, 2001; Sacchi et al., 1996). It is well known that the determination of the unsaponifiable matter is one of the most problematic methods used for oil and fat analysis (Harwood & Aparicio, 2000). However, the nature of these impurities is being studied in order to enable the use of all the information contained in the whole spectra, and further research on unsaponifiable fractions for the geographical characterisation of VOOs is being carried out.

Olive oil is mainly made up of triglycerides, differing in their substitution patterns in terms of length, degree, and kind of unsaturation of the acyl groups, and by minor components such as mono- and di-glycerides, sterols, tocopherols, aliphatic alcohols, hydrocarbons, fatty acids, pigments, and phenolic compounds (Harwood & Aparicio, 2000). The chemical shifts of the ^{1}H signals of the triglycerides are well known (Mannina & Segre, 2002; Sacco et al., 2000). Minor oil components are only observed by ^{1}H NMR when their signals do not overlap with those of the main components and their concentrations are high enough to be detected. Table 1 shows the common ^{1}H NMR signals of major and some minor compounds together with their chemical shifts and their assignments to protons of the different functional groups. Some signals of minor compounds were found in ^{1}H NMR of VOO since they were not overlapping with those of the triglyceryl protons: cycloartenol at 0.318 and 0.543 ppm, β-sitosterol at 0.669 ppm, stigmasterol at 0.687 ppm, squalene at 1.662 ppm, *sn*-1,2-diglyceryl group protons at 3.71 and 5.10 ppm, and three unknown terpenes at 4.571, 4.648, and 4.699 ppm, as already observed by other authors (Guillen & Ruiz, 2001; Sacchi et al., 1996), (D'Imperio et al., 2007; Mannina, Sobolev, & Segre, 2003).

The unsaponifiable fraction of VOOs has not been studied by NMR previously. Indeed, the ^{1}H NMR analysis of the unsaponifiable fraction provides useful data on minor compounds that are masked by the triglyceride signals in the ^{1}H NMR spectra of the bulk oil, and that can be interesting for the authentication of VOOs, as explained above. The ^{1}H NMR signals of the unsaponifiable fraction are listed in Table 2 with their chemical shifts. The ^{1}H NMR analysis of the subfractions of the unsaponifiable fraction and the standards available allow us to make assignments for the ^{1}H NMR signals by comparing their spectra, and/or using bibliographic references (D'Imperio et al., 2007; Guillen & Ruiz, 2001; Pouchert & Behnke, 1993). The signals in the spectra of the unsaponifiable fraction were slightly shifted with respect to the signals in the spectra of the bulk oil (0.013–0.015 ppm to higher chemical shifts). Some signals were due to a particular subfraction and/or could also be assigned to individual compounds: cycloartenol at 0.333, 0.558, and 0.974 ppm; β-sitosterol at 0.826, 0.834, 0.848, 0.921, and 0.934 ppm; stigmasterol at 0.702 ppm; and squalene at 1.431 ppm. The NMR spectra of the bulk oil and the unsaponifiable fraction and its subfractions provided information about the most influent NMR signals or regions for their classification of VOOs according to the geographical origin.

3.2. Repeatability of the analysis of the unsaponifiable fraction of VOOs

Four aliquots of eight VOOs of different origin were submitted to the saponification procedure and the ^{1}H NMR profiles of these unsaponifiable fractions were evaluated by PCA. Fig. 1 shows that the variability between replicates is smaller than between samples. So, the repeatability of the analytical method used for profiling unsaponifiable fractions of VOO is appropriate for the aim of this work.

3.3. Geographical characterisation of VOOs

The univariate analysis (ANOVA, Fisher test, Box and Whiskers plots) of the data set, made up of 135 variables (NMR buckets) and 99 unsaponifiable fractions of VOOs (no replicates included), revealed that none of the variables were able to discriminate between VOOs of different geographical origin by itself. Hence, it was necessary to move on to multivariate data analysis in order to achieve the desired distinction at the national level.

The presence of outliers in the dataset was analysed by PCA, and five extreme samples (three from Spain, one from Turkey and one from Tunisia) were removed after having noticed the presence of some irregularities in their NMR spectra. The tridimensional plots of the sample scores in the space defined by the three first principal components (accounting for 60% of total system variability) showed that samples were grouped according to their origin, but each cluster was partially overlapped by others. This indicates that the direction of maximum variability in the dataset did not correspond exactly to the direction of maximum discrimination amongst the classes, which suggests the presence of other sources of variability. Indeed, the influence of the saponification batch was observed in the score plots of the samples. From this observation, and taking into account the aforementioned presence of interferences due to the saponification procedure, special attention should be paid to this step of the analytical method and further research is being performed in order to reduce this effect to a minimum.

With the aim being the extraction of all the useful information contained in the dataset for the geographical classification of VOOs, several supervised pattern recognition techniques were used. The

Table 1
Chemical shift assignments of the ^{1}H NMR signals of the main components of olive oils: unsaponifiable fraction (a) and its corresponding olive oil (b)

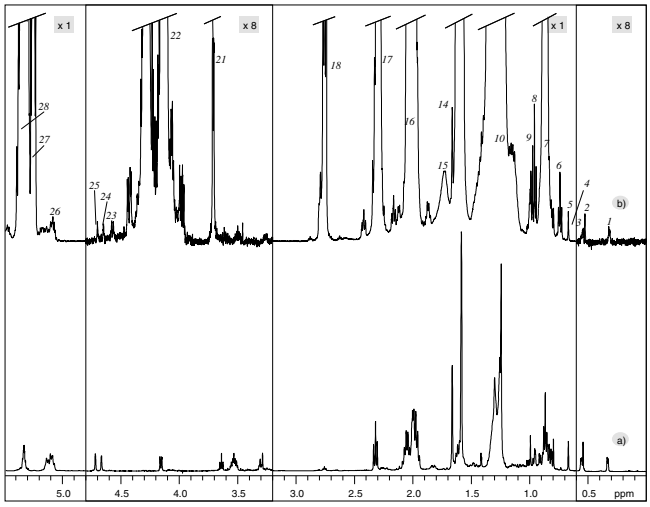

No.	Chemical shift (ppm)	Multiplicity[a]	Functional group	Attribution
1	0.318	d	–CH_2– (cyclopropanic ring)	Cycloartenol
2	0.527	s		
3	0.543	d	–CH_2– (cyclopropanic ring)	Cycloartenol
4	0.669	s	–CH_3 (C18-steroid group)	β-Sitosterol
5	0.687	s	–CH_3 (C18-steroid group)	Stigmasterol
6	0.740	t	–CH_3 (^{13}C satellite of signal at 0.87 ppm)	
7	0.866	t	–CH_3 (acyl group)	Saturated, oleic (or ω-9) and linoleic (or ω-6)
8	0.960	t	–CH_3 (acyl group)	Linolenic (or ω-3)
9	0.987	t	–CH_3 (^{13}C satellite of signal at 0.87 ppm)	
10	1.19-1.37		–$(CH_2)_n$– (acyl group)	
11	1.243		–$(CH_2)_n$– (acyl group)	Saturated (palmitic and stearic)
12	1.256		–$(CH_2)_n$– (acyl group)	Oleic
13	1.288		–$(CH_2)_n$– (acyl group)	Linoleic and linolenic
14	1.51–1.65		–OCO–CH_2–CH_2– (acyl group)	
15	1.662	s	–CH_3	Squalene
16	1.96–2.07		–CH_2–CH=CH– (acyl group)	
17	2.26–2.32	m	–OCO–CH_2– (acyl group)	
18	2.72–2.82		=CH–CH_2–CH= (acyl group)	
19	2.754	t	=CH–CH_2–CH= (acyl group)	Linoleic
20	2.789	t	=CH–CH_2–CH= (acyl group)	Linolenic
21	3.69–3.73	d	–CH_2OH (glyceryl group)	*sn*-1,2-Diglycerides
22	4.09–4.32		–CH_2OCOR (glyceryl group)	Triglycerides
23	4.571	d		Terpene
24	4.648	s		Terpene
25	4.699	s		Terpene
26	5.05–5.15	m	>CHOCOR (glyceryl group)	*sn* 1,2-diglycerides
27	5.22–5.28	m	>CHOCOR (glyceryl group)	Triglycerides
28	5.28–5.38	m	–CH=CH– (acyl group)	

[a] Signal multiplicity: s, singlet; d, doublet; t, triplet; m, multiplet.

results are shown in Table 3. The variable selection used for LDA afforded eight NMR buckets centred at the following chemical shifts: 4.86, 4.70, 3.62, 2.78, 1.46, 0.98, 0.66, and 0.54 ppm. These buckets correspond to signals of the alcoholic fraction (0.54, 0.98, 3.62, and 4.70 ppm), sterolic fraction (0.66, 1.46, and 2.78 ppm), hydrocarbon fraction (4.70 ppm), and tocopherol fraction (4.86 ppm). Hence, the four subfractions of the unsaponifiable fraction of VOOs contain information related to the geographical origin of the oils. Some of these signals could be assigned to particular compounds: cycloartenol (0.98 and 3.62 ppm), aliphatic alcohols (3.62 ppm), β-sitosterol and campesterol (0.66 and 1.46 ppm), and stigmasterol (1.46 ppm). Further studies on the identification of the individual compounds (markers) responsible of the origin differences are in progress.

The threefold cross-validated LDA model correctly classified all the Tunisian VOOs, and recognised almost all the Spanish samples (98%) and predicted 91% properly. For the Italian VOOs, the recognition and prediction abilities of the model were 87% and 84%, respectively. The model did not perform so well for the other classes, so, even though the recognition abilities were acceptable, being 93% for the Turkish VOO, 89% for the Syrian and 87% for the Greek VOOs, the prediction abilities were considerably worse, not reaching 80% of correct hits. For these three countries, the recognition and prediction abilities are substantially different, meaning that the decision rules depend too much on the actual samples in the training set, and therefore, cannot be generalised.

PLS-DA was performed on the dataset using also threefold cross-validation as in LDA, however this technique did not perform properly with this kind of validation, yielding, forepart from the Tunisian and Spanish VOOs, very low percentages of correct classification, and recognition abilities lower than the prediction abilities (data not shown). These facts indicated that these PLS models were not stable and therefore, not reliable. However, when LOO cross-validation was used to validate the PLS model, better

Table 2
Chemical shift assignments of the ^{1}H NMR signals of the unsaponifiable fraction (a) of an olive oil and its corresponding subfractions: the tocopherol fraction (b), the sterol fraction (c), the hydrocarbon fraction (d) and the alcohol fraction (e)

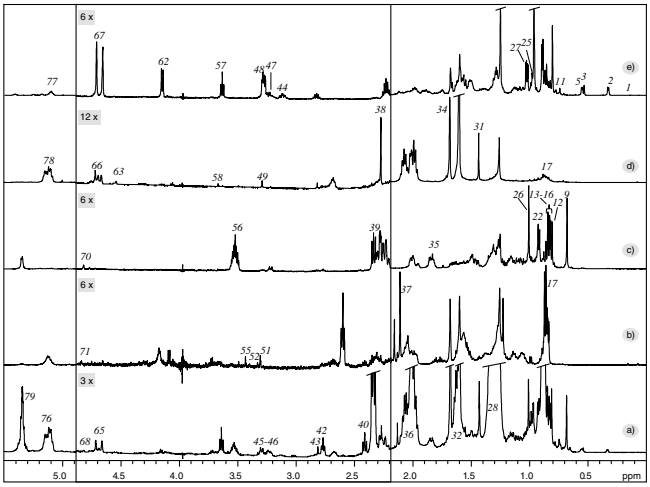

No.	Chemical shift (ppm)	Multiplicity[a]	Attribution	Subfractions[b]
1	0.141			AF
2	0.31–0.35	d		AF, SF (−)
3	0.333	d	Cycloartenol	AF
4	0.387			AF
5	0.53–0.58	d		AF, SF (−)
6	0.529			SF
7	0.539	s		AF
8	0.558	d	Cycloartenol	AF
9	0.683	s	β-Sitosterol, cycloartenol	SF
10	0.702	s	Stigmasterol	SF
11	0.747	s		AF
12	0.77–0.78			SF
13	0.813	s	β-Sitosterol, campesterol, cycloartenol	SF, AF
14	0.826		β-Sitosterol	SF
15	0.834		β-Sitosterol	SF
16	0.848	d	β-Sitosterol	SF
17	0.85–0.91		1-Eicosanol, α-tocopherol, erythrodiol	All
18	0.869		α-Tocopherol	HF, TF
19	0.881			TF
20	0.884			HF
21	0.894			TF
22	0.91–0.94			SF
23	0.921		β-Sitosterol	SF
24	0.934		β-Sitosterol	SF
25	0.974	s	Cycloartenol	AF
26	1.009		β-Sitosterol, stigmasterol, campesterol	SF
27	1.01–1.04	q		AF
28	1.22–1.40		1-Eicosanol, α-tocopherol	All
29	1.260		Cycloartenol, 1-eicosanol, α-tocopherol, erythrodiol	
30	1.316		cycloartenol, erythrodiol	
31	1.431		squalene	HF
32	1.56–1.66		1-Eicosanol, α-tocopherol	TF, HF, AF
33	1.599	s		TF, HF, AF
34	1.678	s	Squalene	HF, TF, AF
35	1.80–1.88	m	β-Sitosterol, stigmasterol, campesterol	SF
36	1.94–2.12			HF, TF, SF (−), AF (−)
37	2.131	s		TF
38	2.269	s		HF
39	2.336	t		SF
40	2.414	t		TF, HF
41	2.64–2.71			TF, HF
42	2.771	t		SF
43	2.816	s		HF, AF (−), SF (−)
44	3.10–3.17	m		AF
45	3.19–3.26			AF, SF
46	3.19–3.36		Cycloartenol, erythrodiol	All
47	3.24–3.28			AF
48	3.284			AF
49	3.287			HF
50	3.293			AF
51	3.302			TF
52	3.306			TF, AF

(*continued on next page*)

Table 2 (*continued*)

No.	Chemical shift (ppm)	Multiplicity[a]	Attribution	Subfractions[b]
53	3.315			AF
54	3.330	s		TF
55	3.416	s		TF
56	3.49–3.58	m	β-Sitosterol, stigmasterol, campesterol	SF
57	3.641	t	Cycloartenol, 1-eicosanol	AF
58	3.662	s		HF
59	3.716	s		AF
60	3.730	s		AF
61	3.744	s		AF
62	4.157	d		AF
63	4.539	d		HF
64	4.52–5.05		Cycloartenol, α-tocopherol	All
65	4.664	s		HF, AF
66	4.690	s		HF
67	4.716	s		HF, AF
68	4.749	s		TF, HF
69	4.771	s		SF
70	4.821			SF
71	4.836	s		TF
72	4.872		Cycloartenol	TF
73	4.938	s		TF
74	4.964	s		SF
75	5.001		Cycloartenol	HF, AF
76	5.05–5.21	m	Squalene	HF, TF (−), AF (−)
77	5.256	d		AF
78	5.30–5.43	m		SF
79	5.53–5.63			TF
80	5.703	s		HF
81	5.745	s		TF, HF
82	5.87–5.98			HF
83	5.988	s		TF
84	6.367	s		TF
85	6.439	t		HF
86	6.975	s		HF

[a] Signal multiplicity: s, singlet; d, doublet; t, triplet; m, multiplet.
[b] HF, hydrocarbon fraction; TF, tocopherol fraction; AF, alcohol fraction; SF, sterol fraction; (−), low intensity.

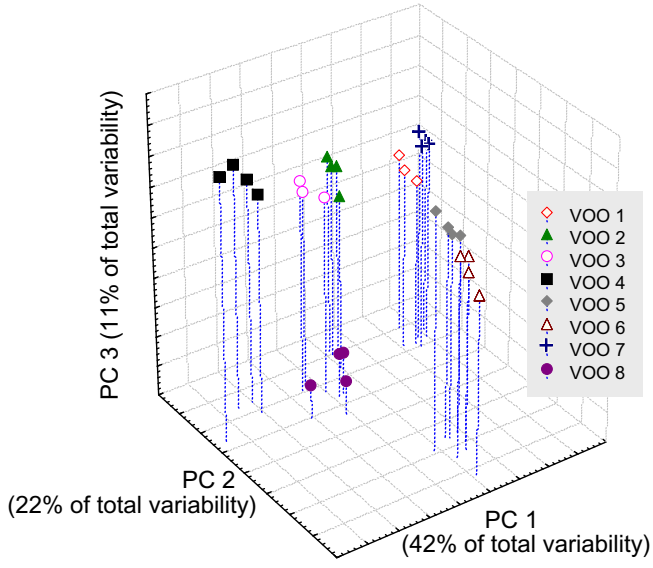

Fig. 1. Score plot of the olive oil samples used to study the repeatability of the method on the space defined two first principal components.

results were obtained. Indeed, LOO is recommended for small database sizes which present the problem of the inability to divide the data set into fairly-sized subsets for training and test sets (Basheer & Hajmeer, 2000; Berrueta et al., 2007).

In order to obtain classification models by PLS-DA using LOO, two approaches were carried out: PLS-1 and PLS-2. In the former approach, a model is computed for each class separately so that it distinguishes its samples from all the others; whereas in PLS-2, all the classes are modelled simultaneously (Esbensen, Guyot, Westad, & Houmøller, 2002). Almost the same recognition abilities were achieved by both approaches, except for the Syrian VOOs (Table 3). However, the prediction abilities of PLS-1 models were more successful. From accumulated experience in chemometrics, it can be seen that better prediction models are obtained by using a series of PLS-1 models (Esbensen et al., 2002). Indeed, all the Tunisian and Turkish VOOs were correctly classified by PLS-1 models. The Spanish and Syrian models recognised all their VOOs and satisfactorily predicted 88% and 78% of them, respectively. Regarding the Italian and Greek models, the recognition and prediction abilities were 95% and 79%, and 83% and 75%, respectively.

Table 4 shows the weighted regression coefficients (Esbensen et al., 2002) of the PLS models in the PLS-1 approach that indicate the importance of the NMR variables on the model: the larger the regression coefficient, the higher the influence of the variable on the PLS model. Thus, the most important variables for the distinction of the Italian VOO belong to the alcohol and hydrocarbon fractions, the cycloartenol content being characteristic for this class. The Spanish and Greek models are mainly influenced by signals that appear in the alcohol, hydrocarbon and sterol fractions. Some of these signals are due to β-sitosterol, campesterol, sigmasterol, and cycloartenol; particularly for the Greek class, also to aliphatic alcohols (3.62 ppm). The Tunisian VOOs present a characteristic sterol composition. What differentiated the Syrian VOOs were the signals from the tocopherol, sterol, and hydrocarbon fractions. Signals related to the four subfractions studied influence the model of the Turkish VOOs, as well as the squalene signal at 1.678 ppm. Most of LDA selected variables are also important in the PLS models, so consistent results are obtained by both pattern recognition

Table 3
Classification results obtained by supervised pattern recognition techniques for the geographical characterisation of VOO using ^{1}H NMR spectral data of the unsaponifiable fraction[a]

Origin	*N*	A priori probability		LDA[b]		PLS-DA[c]					
						PLS-2			PLS-1		
				Recognition ability (%)	Prediction ability (%)	PLS-C	Recognition ability (%)	Prediction ability (%)	PLS-C	Recognition ability (%)	Prediction ability (%)
Italy	19	20		87	84	7	89	74	5	95	79
Spain	33	35		98	91	9	100	85	7	100	88
Greece	12	13		88	67	8	83	67	4	83	75
Tunisia	14	15		100	100	4	100	100	7	100	100
Turkey	7	7		93	71	10	100	71	7	100	100
Syria	9	10		89	78	4	89	78	6	100	78

[a] *Abbreviations: N*, number of samples; PLS-C, PLS-component selected.
[b] LDA performed on Statistica using eight selected NMR buckets (0.54, 0.66, 0.98, 1.46, 2.78, 3.62, 4.70, and 4.86 ppm), threefold crossvalidation.
[c] PLS-DA performed on The Unscrambler, LOO validation.

Table 4
Weighted regression coefficients for the most important variables in the PLS-DA models (PLS-1) achieved for the geographical classification of VOO using ^{1}H NMR profiles of the unsaponifiable fraction

Model	NMR bucket	Bw	Assignment	Subfraction
Italy		5 PLS-C		
	0.58	0.0835	Cycloartenol	AF
	3.30	0.0639		TF, AF, HF
	0.34	0.0560	Cycloartenol	AF
	4.66	−0.0511		AF, HF
	4.70	−0.0468		AF, HF
Spain		7 PLS-C		
	4.66	0.0719		AF, HF
	2.78	−0.0712		SF
	0.62	−0.0695		AF, HF
	4.70	0.0692		AF, HF
	0.54	−0.0680		AF
	3.58	−0.0620	β-Sitosterol, stigmasterol, campesterol	SF
	3.14	−0.0605		AF
	2.38	0.0553		TF, SF
	0.14	0.0525		AF
	1.74	−0.0509		
	2.62	0.0498		TF
	3.34	−0.0491		TF
	1.78	−0.0431		
	0.58	−0.0416	Cycloartenol	AF
	2.46	−0.0415		SF
	3.66	−0.0400		AF, HF (−)
	0.38	0.0399		AF
	2.22	0.0373		SF, HF (−)
	4.58	−0.0365		
Greece		4 PLS-C		
	3.66	0.0721		AF, HF (−)
	3.62	0.0510	Cycloartenol, 1-eicosanol	AF
	3.58	0.0390	β-Sitosterol, stigmasterol, campesterol	SF
	4.66	−0.0389		AF, HF
	0.34	−0.0386	Cycloartenol	AF, SF (−)
Tunisia		7 PLS-C		
	2.78	0.0965		SF
	0.66	0.0614	β-Sitosterol, campesterol	SF
	5.38	0.0466		SF
	3.22	0.0444		SF (−)
	2.22	0.0387		SF, HF (−)
	3.14	−0.0362		AF
Turkey		7 PLS-C		
	2.30	0.0614		All
	4.14	0.0582		AF
	1.66	0.0494	Squalene	HF, TF, AF
	2.34	−0.0445		SF
	0.62	0.0413		
	3.42	−0.0389		TF
	1.58	0.0332		HF, AF, TF
Syria		6 PLS-C		
	2.78	0.0898		SF
	4.74	0.0800		HF, TF
	3.34	0.0623		TF
	0.70	−0.0572		SF
	3.30	−0.0455	β-Sitosterol, campesterol, stigmasterol (−)	TF, AF, HF

techniques. Moreover, these results provide information about the most important features for the characterisation of VOO according to their geographical origin, which can be useful for the identification of possible markers in further studies.

Other supervised pattern recognition techniques were also tested in the search for the best models for classification. The LOO validated models afforded by SIMCA present good sensitivities (94–100%) but in general low specificities to the other five classes (Italy: 0–57%; Spain: 0–100%; Greece: 0–14%; Tunisia: 43–89%; Turkey: 83–100%; Syria: 74–100%). These results can be explained

Table 5
Classification results obtained by supervised pattern recognition techniques for the geographical characterisation of VOO using ^{1}H NMR spectral data of the bulk oil and/or the unsaponifiable fraction

Data	Origin	*N*	a priori probability	PLS-DA					
				PLS-2			PLS-1		
				PLS-C	Recognition ability (%)	Prediction ability (%)	PLS-C	Recognition ability (%)	Prediction ability (%)
Bulk oil	Italy	5	22	5	100	60	4	100	60
	Spain	4	17	2	0	0	7	100	50
	Greece	5	22	3	100	80	5	100	100
	Tunisia	5	22	2	100	100	1	100	100
	Turkey	4	17	2	100	75	1	100	50
Unsaponifiable fraction	Italy	5	22	2	60	0	5	100	60
	Spain	4	17	3	100	25	4	100	75
	Greece	5	22	4	100	60	4	100	100
	Tunisia	5	22	2	100	100	5	100	100
	Turkey	4	17	4	100	75	8	100	50
Bulk oil + unsaponifiable fraction	Italy	5	22	1	80	60	7	100	60
	Spain	4	17	9	100	50	6	100	75
	Greece	5	22	4	100	80	3	100	100
	Tunisia	5	22	2	100	100	1	100	100
	Turkey	4	17	2	100	75	1	100	75

considering the fundamentals of SIMCA: this technique performs PCA on each class, which affords the directions of maximum variability in each class. As explained above, a source of variability due to the saponification batch was present in the data. This variability affected all classes in the same way and thus the PCA for each class. Therefore, the hyper-ellipsoids modelled by SIMCA for each class were oriented in similar directions and overlapping, which results in low specificities. Similarly, despite its great potential, CART applied on the sample scores of the principal components with eigenvalues higher than one (15 PCs), did not afford acceptable classification trees by threefold cross-validation.

Comparing the classification results obtained by the different supervised techniques used, PLS-DA (PLS-1 approach) performs better than or similar to LDA. The fact that performing LDA and CART with LOO validation was not feasible with the software available could be considered a limitation for these techniques to achieve better results, due to the relatively low number of samples available for some classes.

The results obtained by discriminant techniques (PLS-DA and LDA) are similar, so the data contains enough information to afford a model for the target classification (Berrueta et al., 2007). However, these classification results have to be considered as preliminary ones because this study has certain limitations, some of which have already been mentioned above and others are now explained. The aim of the work, i.e. the geographical characterisation of VOOs, is quite ambitious since six classes are considered, and the number of samples in each class is not balanced and for some classes relatively low. Indeed, it is known that the supervised techniques used perform worse with an increasing numbers of categories (Berrueta et al., 2007). Moreover, LDA, PLS-DA, and SIMCA are very sensitive to large imbalances in the number of samples in each class. So, if the number of objects in each class of the training set is not approximately equal, the class membership decision will be biased towards the class with the most representatives (Berrueta et al., 2007). Therefore, better results are expected in a future study for which an equal number of samples in each class is ensured by designed experiments. Furthermore, more data, i.e. a wider region of the NMR spectra will be included since the baseline distortion will be eliminated, and the source of variability due to the saponification procedure, carried out in batches, will be reduced as much as possible.

Additionally, other different analytical approaches for the geographical characterisation of VOOs were evaluated: the bulk oil and the corresponding unsaponifiable fractions of 23 different VOOs from five countries (Italy, Spain, Greece, Tunisia, and Turkey) were analysed by ^{1}H NMR. The NMR spectra of the VOOs (0–7 ppm, excluding 4.08–4.28 ppm) and the unsaponifiable fractions (0–5.44 ppm, excluding 3.96–4.00 ppm) were analysed by multivariate techniques both separately and together: (i) bulk VOO (23 samples $\times$ 170 buckets), (ii) unsaponifiable fraction of VOO (23 samples $\times$ 135 buckets), and (iii) bulk VOO and unsaponifiable fraction (23 samples $\times$ 305 buckets). In all three approaches, PCA score plots show that natural clustering occurred according to the geographical origin, but the groups were partially overlapped in the space defined by the first three principal components (accounting for 60–77% of total system variability). Since the number of variables exceeds the number of samples, LDA (without variable selection) could not be carried out, so PLS-DA was used in both versions of PLS (PLS-1 and PLS-2). Definitely, PLS-1 achieved considerably better classifications for the three analytical approaches (Table 5). These preliminary results suggest that the analysis of the bulk olive oil and its corresponding unsaponifiable fraction contain complementary information for the required classification. These approaches are being further studied with a considerably larger sample set.

4. Conclusion

Pattern recognition techniques applied to the ^{1}H NMR data of the unsaponifiable fractions of VOOs from Spain, Italy, Greece, Tunisia, Turkey, and Syria showed that these spectral data contained useful information for the geographical characterisation of VOOs. Moreover, a preliminary study of the ^{1}H NMR spectra of some oils from five different countries and their corresponding unsaponifiable fractions, suggested that they contain complementary information which would enhance the classification of VOOs according to their geographical origin. Furthermore, from the study of the subfractions of the unsaponifiable fraction (alcohol, sterol, hydrocarbon, and tocopherol fractions), some trends related to the geographical origin of the olive oils are observed. This new approach based on the NMR profile of the unsaponifiable fraction of olive oil is currently being explored and further research is being carried out. The availability of a larger data set of VOOs would further facilitate the classification at the national level and also provide a means to guarantee PDO/PGI classification CE.

Acknowledgement

The authors would like to acknowledge N. Segebarth for fruitful discussions.

References

Alves, M. R., Cunha, S. C., Amaral, J. S., Pereira, J. A., & Oliveira, M. B. (2005). Classification of PDO olive oils on the basis of their sterol composition by multivariate analysis. *Analytica Chimica Acta, 549*(1–2), 166–178.

Angerosa, F., Breas, O., Contento, S., Guillou, C., Reniero, F., & Sada, E. (1999). Application of stable isotope ratio analysis to the characterization of the geographical origin of olive oils. *Journal of Agricultural and Food Chemistry, 47*(3), 1013–1017.

Angerosa, F., Camera, L., Cumitini, S., Gleixner, G., & Reniero, F. (1997). Carbon stable isotopes and olive oil adulteration with pomace oil. *Journal of Agricultural and Food Chemistry, 45*(8), 3044–3048.

Angerosa, F., & Di Giovacchino, L. (1996). Natural antioxidants of virgin olive oil obtained by two and tri-phase centrifugal decanters. *Grasas Y Aceites, 47*(4), 247–254.

Aparicio, R., Alonso, V., & Morales, M. T. (1994). Detailed and exhaustive study of the authentication of European virgin olive oils by SEXIA expert system. *Grasas Y Aceites, 45*(4), 241–252.

Aparicio, R., & Aparicio-Ruiz, R. (2000). Authentication of vegetable oils by chromatographic techniques. *Journal of Chromatography A, 881*(1–2), 93–104.

Aparicio, R., Ferreiro, L., & Alonso, V. (1994). Effect of climate on the chemical composition of virgin olive oil. *Analytica Chimica Acta, 292*(3), 235–241.

Aparicio, R., & Luna, G. (2002). Characterisation of monovarietal virgin olive oils. *European Journal of Lipid Science and Technology, 104*(9–10), 614–627.

Aparicio, R., & Morales, M. T. (1998). Characterization of olive ripeness by green aroma compounds of virgin olive oil. *Journal of Agricultural and Food Chemistry, 46*(3), 1116–1122.

Aparicio, R., Morales, M. T., & Alonso, V. (1997). Authentication of European virgin olive oils by their chemical compounds, sensory attributes, and consumers' attitudes. *Journal of Agricultural and Food Chemistry, 45*(4), 1076–1083.

Baeten, V., Dardenne, P., & Aparicio, R. (2001). Interpretation of Fourier transform Raman spectra of the unsaponifiable matter in a selection of edible oils. *Journal of Agricultural and Food Chemistry, 49*(11), 5098–5107.

Baeten, V., Pierna, J. A. F., Dardenne, P., Meurens, M., Garcia-Gonzalez, D. L., & Aparicio-Ruiz, R. (2005). Detection of the presence of hazelnut oil in olive oil by FT-Raman and FT-MIR spectroscopy. *Journal of Agricultural and Food Chemistry, 53*(16), 6201–6206.

Basheer, I. A., & Hajmeer, M. (2000). Artificial neural networks: Fundamentals, computing, design, and application. *Journal of Microbiological Methods, 43*(1), 3–31.

Berrueta, L. A., Alonso-Salces, R. M., & Héberger, K. (2007). Supervised pattern recognition in food analysis. *Journal of Chromatography A, 1158*(1–2), 196–214.

Bianchi, G., Angerosa, F., Camera, L., Reniero, F., & Anglani, C. (1993). Stable carbon isotope ratios (13C/12C) of olive oil components. *Journal of Agricultural and Food Chemistry, 41*(11), 1936–1940.

Biedermann, M., Grob, K., Mariani, C., & Schmidt, J. P. (1996). Detection of desterolized sunflower oil in olive oil through isomerized Δ7-sterols. *Zeitschrift fur Lebensmittel-Untersuchung und -Forschung, 202*(3), 199–204.

Bortolomeazzi, R., Berno, P., Pizzale, L., & Conte, L. S. (2001). Sesquiterpene, alkene, and alkane hydrocarbons in virgin olive oils of different varieties and geographical origins. *Journal of Agricultural and Food Chemistry, 49*(7), 3278–3283.

Breas, O., Guillou, C., Reniero, F., Sada, E., & Angerosa, F. (1998). Oxygen-18 measurement by continuous flow pyrolysis/isotope ratio mass spectrometry of vegetable oils. *Rapid Communications in Mass Spectrometry, 12*(4), 188–192.

Cañabate-Diaz, B., Segura Carretero, A., Fernandez-Gutierrez, A., Belmonte Vega, A., Garrido Frenich, A., Martinez Vidal, J. L., et al. (2007). Separation and determination of sterols in olive oil by HPLC–MS. *Food Chemistry, 102*(3), 593–598.

Christophoridou, S., Dais, P., Tseng, L. I. H., & Spraul, M. (2005). Separation and identification of phenolic compounds in olive oil by coupling high-performance liquid chromatography with postcolumn solid-phase extraction to nuclear magnetic resonance spectroscopy (LC–SPE–NMR). *Journal of Agricultural and Food Chemistry, 53*(12), 4667–4679.

Commission Regulation (EEC) No. 2568/91 of 11 July 1991. European Communities 1991. *Official Journal of the European Union, L248* [Annex V].

Council Regulation (EEC) No. 2081/92 of 14 July 1992. European Communities 1992. *Official Journal of the European Union, L208*, 1–8.

Council Regulation (EEC) No. 2082/92 of 14 July 1992. European Communities 1992. *Official Journal of the European Union, L208*, 9–14.

Cunha, S. S., Fernandes, J. O., & Oliveira, M. B. P. P. (2006). Quantification of free and esterified sterols in Portuguese olive oils by solid-phase extraction and gas chromatography–mass spectrometry. *Journal of Chromatography A, 1128*(1–2), 220–227.

Deiana, M., Rosa, A., Cao, C. F., Pirisi, F. M., Bandino, G., & Dessi, M. A. (2002). Novel approach to study oxidative stability of extra virgin olive oils: Importance of α-tocopherol concentration. *Journal of Agricultural and Food Chemistry, 50*(15), 4342–4346.

D'Imperio, M., Mannina, L., Capitani, D., Bidet, O., Rossi, E., Bucarelli, F. M., et al. (2007). NMR and statistical study of olive oils from Lazio: A geographical, ecological and agronomic characterization. *Food Chemistry, 105*(3), 1256–1267.

Esbensen, K. H., Guyot, D., Westad, F., & Houmøller, L. P. (2002). *Multivariate data analysis: In practice: An introduction to multivariate data analysis and experimental design*. Oslo: Camo Process AS.

Esti, M., Cinquanta, L., Carrone, A., Trivisonno, M. C., La Notte, E., & Gambacorta, G. (1996). Composti antiossidanti e parametri qualitativi di oli vergini di oliva prodotti in Molise. *Rivista Italiana delle Sostanze Grasse, 73*(4), 147–150.

Esti, M., Cinquante, L., & La Notte, E. (1998). Phenolic compounds in different olive varieties. *Journal of Agricultural and Food Chemistry, 46*(1), 32–35.

Fragaki, G., Spyros, A., Siragakis, G., Salivaras, E., & Dais, P. (2005). Detection of extra virgin olive oil adulteration with lampante olive oil and refined olive oil using nuclear magnetic resonance spectroscopy and multivariate statistical analysis. *Journal of Agricultural and Food Chemistry, 53*(8), 2810–2816.

Garcia-Gonzalez, D. L., Mannina, L., D'Imperio, M., Segre, A. L., & Aparicio, R. (2004). Using H-1 and C-13 NMR techniques and artificial neural networks to detect the adulteration of olive oil with hazelnut oil. *European Food Research and Technology, 219*(5), 545–548.

Giacometti, J. (2001). Determination of aliphatic alcohols, squalene, α-tocopherol and sterols in olive oils: Direct method involving gas chromatography of the unsaponifiable fraction following silylation. *Analyst, 126*(4), 472–475.

Grob, K., Lanfranchi, M., & Mariani, C. (1990). Evaluation of olive oils through the fatty alcohols, the sterols and their esters by coupled LC–GC. *JAOCS, Journal of the American Oil Chemists' Society, 67*(10), 626–634.

Guillen, M. D., & Ruiz, A. (2001). High resolution H-1 nuclear magnetic resonance in the study of edible oils and fats. *Trends in Food Science and Technology, 12*(9), 328–338.

Gutierrez, F., Albi, M. A., Palma, R., Rios, J. J., & Olias, J. M. (1989). Bitter taste of virgin olive oil: Correlation of sensory evaluation and instrumental HPLC analysis. *Journal of Food Science, 54*(1), 68–70.

Harwood, J. L., & Aparicio, R. (2000). *Handbook of olive oil: Analysis and properties*. Gaithersburg, MD: Aspen.

Hoffman, R. E. (2006). Standardization of chemical shifts of TMS and solvent signals in NMR solvents. *Magnetic Resonance in Chemistry, 44*(6), 606–616.

Lercker, G., & Rodriguez-Estrada, M. T. (2000). Chromatographic analysis of unsaponifiable compounds of olive oils and fat-containing foods. *Journal of Chromatography A, 881*(1–2), 105–129.

Lopez Ortiz, C. M., Prats Moya, M. S., & Berenguer Navarro, V. (2006). A rapid chromatographic method for simultaneous determination of β-sitosterol and tocopherol homologues in vegetable oils. *Journal of Food Composition and Analysis, 19*(2–3), 141–149.

Mannina, L., & Segre, A. (2002). High resolution nuclear magnetic resonance. From chemical structure to food authenticity. *Grasas Y Aceites, 53*(1), 22–33.

Mannina, L., Sobolev, A. P., & Segre, A. (2003). Olive oil as seen by NMR and chemometrics. *Spectroscopy Europe, 15*(3).

Mariani, C., & Fedeli, E. (1986). Individuazione di oli di estrazione in quelli di pressione. *Rivista Italiana delle Sostanze Grasse, 63*(1), 3–17.

Mariani, C., Fedeli, E., Grob, K., & Artho, A. (1991). Indagine sulle variazioni dei componenti minori liberi ed esterificati di oli ottenuti da olive in funzione della maturazione e dello stoccaggio. *Riv Ital Sostanze Grasse, 68*(4), 179–186.

Mariani, C., Venturin, S., & Grob, K. (1995). Individuazione dell'olio di girasole ad alto oleico desterolato nell'olio di oliva. *Rivista Italiana Sostanze Grasse, 72*, 473–482.

Minguez-Mosquera, M. I., Gandul-Rojas, B., Garrido-Fernandez, J., & Gallardo-Guerrero, L. (1990). Pigments present in virgin olive oil. *JAOCS, Journal of the American Oil Chemists' Society, 67*(3), 192–196.

Mousa, Y. M., Gerasopoulos, D., Metzidakis, I., & Kiritsakis, A. (1996). Effect of altitude on fruit and oil quality characteristics of 'Mastoides' olives. *Journal of the Science of Food and Agriculture, 71*(3), 345–350.

Pinelli, P., Galardi, C., Mulinacci, N., Vincieri, F. F., Cimato, A., & Romani, A. (2003). Minor polar compound and fatty acid analyses in monocultivar virgin olive oils from Tuscany. *Food Chemistry, 80*(3), 331–336.

Pouchert, C. J., & Behnke, J. (1993). *The Aldrich library of ^{13}C and ^{1}H FT NMR spectra*. Milwaukee: Aldrich Chemical Co..

Ranalli, A., & Angerosa, F. (1996). Integral centrifuges for olive oil extraction the qualitative characteristics of products. *JAOCS, Journal of the American Oil Chemists' Society, 73*(4), 417–422.

Rezzi, S., Axelson, D. E., Heberger, K., Reniero, F., Mariani, C., & Guillou, C. (2005). Classification of olive oils using high throughput flow H-1 NMR fingerprinting with principal component analysis, linear discriminant analysis and probabilistic neural networks. *Analytica Chimica Acta, 552*(1–2), 13–24.

Sacchi, R., Patumi, M., Fontanazza, G., Barone, P., Fiordiponti, P., Mannina, L., et al. (1996). A high-field H-1 nuclear magnetic resonance study of the minor components in virgin olive oils. *Journal of the American Oil Chemists Society, 73*(6), 747–758.

Sacco, A., Brescia, M. A., Liuzzi, V., Reniero, F., Guillou, C., Ghelli, S., et al. (2000). Characterization of Italian olive oils based on analytical and nuclear magnetic resonance determinations. *Journal of the American Oil Chemists Society, 77*(6), 619–625.

Zhang, X., Julien-David, D., Miesch, M., Geoffroy, P., Raul, F., Roussi, S., et al. (2005). Identification and quantitative analysis of [beta]-sitosterol oxides in vegetable oils by capillary gas chromatography–mass spectrometry. *Steroids, 70*(13), 896–906.

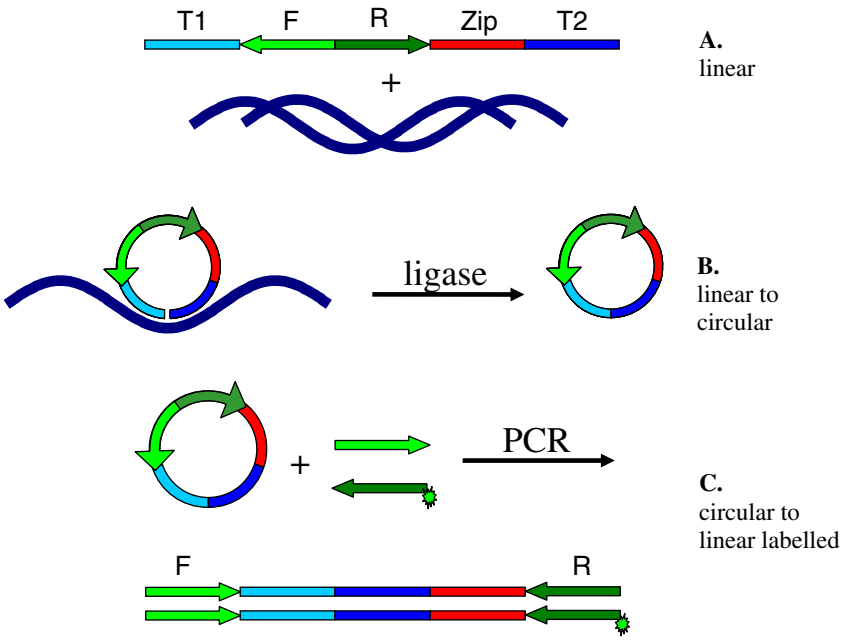

Fig. 1. Scheme of the padlock ligation procedure. A. Linear padlock with telomeric target (T) sequences can hybridise to their genomic counterpart. B. Upon hybridisation, the juxtaposed ends are ligated to form a circular molecule. C. The circular molecule are amplified by asymmetrical PCR with a forward (F) and reverse (R)-Cy3 primer to generate large amounts of linear ssDNA with a Cy3-labelled (✹) cZIP code.

a tetraploid crop with a BBA^{u}A^u genome, allowing discrimination on the absence (Golovnina et al., 2007) or presence (Bryan, Dixon, Gale, & Wiseman, 1998; Pasqualone, Montemurro, Grinn-Gofron, Sonnante, & Blanco, 2007; Terzi et al., 2005) of the D-genome. The alternative approach, positive identification of Farro della Garfagnana, is still difficult since the *Triticum* BB, A^{u}A^u and DD genome arose from a common ancestor Golovnina et al., 2007.

In this article a method for establishing the purity of Farro della Garfagnana batches is proposed that is based on the padlock ligation technology (Nilsson et al., 1994) in combination with microarrays.

Vora, Meador, Stenger, and Andreadis (2004) published the padlock probe approach to separately detect micro-organisms on a microarray. Since then, numerous related strategies were developed to fine-tune this method to tailor-made applications (Inoue, Shigemori, & Mikawa, 2006; Jarvius et al., 2006; Pang, Qureshi, Shanahan, & Harris, 2007; Szemes et al., 2005; Tian, He, & Mao, 2006). Padlock probes are based on the principle of ligation detection probes. A single stranded DNA molecule containing from left-to-right a 5′ target sequence, a reverse primer recognition site, a forward primer recognition site, a cZIP-code and a 3′ target site is hybridised with a DNA sample of interest. Upon recognition of the 5′ and 3′ target sites within the targeted DNA, the juxtaposed target sequence-ends can be ligated to form a circular molecule. Once formed, the molecule can be amplified on the basis of the primer recognition site combination on the circular probe. Since the reverse primer is Cy3-labelled, the resulting PCR products including the unique cZIP-codes also become labelled. In this way, the specific target sequence is coupled to a labelled cZIP-code. For a visual impression, the reader is referred to Fig. 1. Upon hybridisation on a microarray containing ZIP-codes, the presence of specific DNA molecules is revealed by illumination of the corresponding ZIP-code spot. Since this method is based on the amplification with two universal primers to generate unique cZIP-codes, the system is suitable for multidetection.

In this article the proof of principle is described for a robust assay to detect different cereal species and varieties in a complex cereal mixture. This assay can form the basis for effective maintenance of EU regulations with relation to EU-registered speciality products.

2. Materials and methods

2.1. Plant material and cloned sequences

Table 1 gives a listing of the plant material used in the experiments.

Cloned fragments containing the padlock probe target sequence:

The real-time PCR System for the specific detection of barley (*Hordeum vulgare*) was based on a unidentified barley sequence with accession number AY268139. The assay was developed with Primer Express 2.0 (Applied Biosystems, Foster City, USA). The forward primer: 5′ GCCAGGTCGTGAGGCAATAC 3′; reverse primer: 5′ GCCCGGGTAGAAGGATCCT 3′ and probe: 5′ FAM-CCGAGGTGCCATCCA-MGB 3′ were used in the real-time PCR, generating a fragment of 68 bp. The specificity of the system was tested with eight different cereals and proved to be specific.

The real-time PCR system for the specific detection of the D-genome was derived from the patent by Bryan and Gale (1998). Following sequences were used: forward primer: 5′ AAGGAGCTCGCCAACGG 3′; reverse primer: 5′ AACCGAGGGTCCAGAAGAGAC 3′ and probe: 5′ FAM- GCTAGATGGCTGGCTTCTATTTCATGATCCA-DQ 3′. This system proved specific for the D-genome of wheat (*T. aestivum*) and spelt wheat (*T. spelta*) generating a PCR fragment of 115 bp. In DNA of cereals lacking the D-genome no amplification was observed with this assay.

The real-time PCR was performed in a 20 μl reaction volume. It contained qPCR MasterMix (RT-QP2X-03) from Eurogentec (Seraing, Belgium); 800 nM of each primer, 400 nM of the probe and 50 ng of genomic DNA template. Amplification was performed in the ABI Prism® 7700 (Applied Biosystems, Foster City, USA) as follows: after one cycle at 50 °C for 2 min and one cycle at 95 °C for 10 min, the reaction was subjected for 50 cycles at 95 °C for 15 s and 60 °C for 60 s.

Table 1
Plant species used in the padlock experiments.

Genus and species	Name	Ploidy	1C[a] (pg)	Remarks
Avena sativa L.	Oat	2*n* = 42	13.23	
Glycine max (L.) Merr.	Soya	2*n* = 40	1.13	IRMM BF410A EKM Soya sample with a maximum of 0.03% Roundup Ready Soya (RRS)
Hordeum vulgare	Barley	2*n* = 14	5.55	
Secale cereale L.	Rye	2*n* = 14	8.28	RR
T. aestivum ssp. *Spelta*(syn. *T. spelta* L.)	Spelt	2*n* = 42		cv. Ostro, hexaploid BBAuA^{u}DD
T. aestivum ssp. *Spelta*	Spelt	2*n* = 42		cv. Oberkulmer Rotkorn, BBA^{u}A^{u}DD
T. dicoccum Schrank	Emmer	2*n* = 28	12.03	Acc. 'Züblin', EWDB 108229 from Peter Züblin (CH), BBA^{u}A^u
T. dicoccum Schrank	Emmer	2*n* = 28	12.03	Acc. 'Kleiner gelber Kahler', BBA^{u}A^u
T. monococcum	Einkorn	2*n* = 14	6.23	Diploid A^{m}A^m
T. turgidum L. ssp. *durum* (Desf.) Husn.	Durum	2*n* = 28	12.28	cv. Combo, tetraploid BBA^{u}A^u
T. turgidum ssp. *Dicoccum*(syn. *T. dicoccum*)	Farro della Garfagnana	2*n* = 28	12.28	tetraploid BBA^{u}A^u
Triticum aestivum L. ssp. *aestivum*	Wheat	2*n* = 42	17.33	Common bread wheat, hexaploid BBA^{u}A^{u}DD
Zea mays	Maize	2*n* = 20	2.73	

[a] 1C (Haploid genome weight: Bennett and Leitch (2003)).

A PCR fragment of 217 bp, specific for the chloroplast tRNA-Leu (*trnL*) gene, was amplified from genomic DNA extracted from *Avena sativa* (oat), using primers CER1F (5′-AATCCTGAGC-CAAATCCGTG-3′) and CER2R (5′-CATGTAGAATGGGACTCTCT-CTTTG-3′). Primers CER1F and CER2R have been designed by sequence homology research (alignment) of the *trnL* genes present in different plant species. These primers can amplify the *trnL* gene sequences in other species such as barley, rye and wheat, but the respective amplicon sizes differ from oat and can easily be distinguished by gel electrophoresis on a 1.6% agarose gel. On the basis of the sequence alignment, the 3′-terminal nucleotide of both primers were designed to mismatch with other species such as soybean, maize, walnut, pecan nut, almond, peanut, chestnut or rice. For this reason, those species should not be detected.

The fragments obtained by conventional PCR for oat and wheat (D-genome) and the real-time PCR fragment for barley (hordein gene) were purified using the QIAquick® PCR Purification Kit (Qiagen, Hilden, DE). The oat and wheat fragments were subsequently cloned in the pCR®2.1 vector using the Original TA Cloning® Kit (Invitrogen, Carlsbad, CA, USA). The barley sequence was cloned in the pCR®2.1-TOPO® vector using the TOPO-TA Cloning® Kit (Invitrogen, Carlsbad, CA). Subsequently, the *Eco*RI fragments containing the insert were cloned in the vector pUC18 using the Rapid DNA Ligation Kit (Roche, Mannheim, DE). Quality control was done by restriction analysis and PCR. Sequencing of the inserts was performed on a ABI Prism®3130 Genetic Analyzer using the BigDye® Terminator v3.1 Ready Reaction Cycle Sequencing kit and the universal M13 forward and reverse primers (Applied Biosystems, Foster City, CA, USA).

Based on the sequencing results for each plasmid, the clone containing the desired insert was used to make a 20 ml overnight culture. Plasmid DNA was extracted using the QIAprep® Spin Miniprep Kit (Qiagen, Hilden, DE). In the following step, two aliquots of 50 μl DNA were restricted with *Sca*I to linearise the plasmids and gel electrophoresis was performed to check if the digest was complete. The digested DNA was purified using the QIAquick® PCR Purification Kit. Elution was done in 2 steps (50 μl followed by 30 μl). The elutes were kept separately and quantified by fluorimetry (PicoGreen dsDNA assay kit, Molecular Probes Europe, Leiden, NL).

Recombinant Plasmid pIRMM-0040 contains the oat fragment, pIRMM-0044 contains the D-genome specific fragment and pIRMM-0046 contains the barley fragment.

Single stranded plant DNA-derived target sequences were derived from the combined 5′ and 3′ target sequence of the padlock probe. Target sequences were ordered (Biolegio, NL) in the reverse complement sequence to allow hybridisation and subsequent ligation of the padlock probes on the juxtaposed 5′ and 3′ target.

2.2. DNA extraction

Plant material (dry seeds and grains) was powdered under liquid nitrogen and 50 mg was used per DNA isolation. 150 μl MQ and 350 μl CTAB buffer (20 g/l CTAB; 1.4 M NaCl; 0.1 M Tris–HCl; 20 mM EDTA) was added together with 10 μl 20 mg/ml Proteinase K and incubated overnight at 42 °C. After a short centrifugation step (5 min at 14.000 rpm) the supernatant was incubated with 5 μl RNaseA (Qiagen, 100 mg/ml) and incubated at 65 °C for 15 min. Two hundred and sixty microliter of buffer AP2 (Qiagen DNeasy Plant Minikit) was added and this was incubated on ice for 5′. Further steps continued from step 10 of the Qiagen DNeasy Plant Minikit as described by the manufacturer's protocol (Qiagen: DNeasy plant handbook 07/2006) without modifications. DNA concentrations were measured with the NanoDrop spectrophotometer (NanoDrop ND-1000, software version 3.3.0).

2.3. Ligation detection probes

Padlock probes were designed by hand and checked with software available on the internet to calculate melting temperature and secondary structures. HYTHER™ (version 1.0, Nicolas Peyret and John SantaLucia, Wayne State University; Peyret, Seneviratne, Allawi, & SantaLucia, 1999; SantaLucia, 1998) was used to calculate the T_m of the 5′ and 3′ targets and of the whole linear molecule. Mfold (Zuker, 2003) was used to predict possible secondary structures. The choice of complementary ZIP-codes (Affymetrix) that were incorporated in the probes depended on cross-reactivity, availability and the likelihood of causing secondary structures. The concentration of the padlock probes (Biolegio, NL; Eurogentec Nederland bv, NL) was measured with the NanoDrop spectrophotometer and the stock contained either single probes or a mixture of probes in a concentration of 250 pM. The padlock probes all contain a 5′ phosphate group to allow ligation. See Table 2 for used sequences and cZIP-codes.

The target sequence within the plant genome and the total padlock probe sequence were checked for absence of restriction sites of endonucleases *Bam*HI, *Hin*dIII and *Eco*RI that are used to digest the genomic DNA. The padlock probes were checked with respect to the requirements to have a ~30 nt 5′ target with a T_m of 68–70 °C and a ~15 nt 3′ target with a T_m of 40 °C. The T_m calculations were performed using HYTHER™. Mfold was used to optimise the design to eliminate significant secondary structures in the

Table 2
Padlock probes: 5′ and 3′ target sequences, primer sites and coupled cZIP-codes. The sequences are in 5′-3′ direction.

Name	5′ Target	cZIP sequence	3′ Target	Target gene (GenBank)	Size (nt)
Barley	CGGTTTGCTGCTCGTATTGCCTCA CGACCTG	GTTGACCGTTAGTTATGCGA	CCTTGGATGGCACCT	CK125594	113
Maize	CTGTGGCATCATCACTGGCATCGT	GTACTACATTCGTGCGATGG	TTAGGCGTCATCAT	AF371266	124
Oat	CATCTAATAAAGTGGATTAATCGG ACGAGGACAAAGAGAGAGTCCC	TGTGATAATTTCGACGAGGC	TGAAGGAAGGGCTTTATA	DQ131557	131
Soya	GCATCATAGGTAATGAGAACCTTG GCTACTTTATTGTTGGCC	ACTCCAGTGCCAAGTACGAT	AGAGGCTGGTGGAG	K00821	142
Wheat	ATGGCTGGCTTCTATTTCATGATC CATCGTCTCTTCTG	ATTGACCAAACTGCGGTGCG	TTTTCAAATATCCAGCTAG	A92706[a]	124
	Primer sequence			Code	
Fwd primer	GCAAGAGATGGGCTACAGAGGAT				23
Rev primer	GGACAGACACGCTAAGACAGAACT				24
Positioning		GCTGAGGTCGATGCTGAGGTCGCA		cZIP-PS01	24

[a] D-genome specific (Bryan and Gale, 1998).

molecule. The length of the designed padlock probes varies slightly since the target sequences have to meet the requirements. The cZIP-codes were selected within the high intensity Bin (Affymetrix) containing the qualitatively superior oligonucleotides and compatibility of the sequence with requirements regarding T_m and secondary structures was tested.

BLAST analysis (Altschul et al., 1997: blastn for short molecules; http://www.ncbi.nlm.nih.gov/blast/Blast.cgi) was performed with the gDNA target sequence to get an estimation of the potential crops/cultivars that enable the padlock probe to circularise. It should be noted that not all genome sequences are in the database and only verification by experimentation can validate the padlock probe as crop/cultivar specific.

Prior to the initial experiments the single stranded padlock probe integrity was checked on PAGE with subsequent silver staining (GE Healthcare/Amersham, ExcelGel, PlusOne DNA Silver-staining).

2.4. Digestion and ligation

DNA (1500 ng) was digested for 1 h at 37 °C (in 1× NEB2 buffer [New England biolabs] and 0.1 μg/μl BSA with 0.33 U/μl *Bam*HI, *Eco*RI and *Hind*III resp. in a final vol. of 30 μl) and heat-inactivated at 95 °C for 10 min.

Four microliter digest (200 ng of either single DNA or mixed DNA sample) was used in a ligation assay (1× *Pfu* ligation buffer (Stratagene); 12% PEG6000; 0.1 U/μl *Pfu* ligase (Stratagene), 25 pM of each padlock probe in a final volume of 10 μl) to allow circularisation (94 °C for 5 min; 95 °C 30 s, 65 °C 5 min for 30 cycles) in the BioRad iCycler 3.021. In case of a 20% DNA sample, the amount of DNA was replenished to 200 ng with herring sperm DNA (Promega, Madison, WI, USA).

2.5. Real-time PCR

Real-Time PCR was performed using SYBR Green (1× SYBR Green Supermix containing the iTaq DNA polymerase (BioRad); 0.5 μM forward primer and 0.5 μM reverse primer; 3 μl ligation mixture) in the BioRad MyiQ single-colour Real-time Detection System (95 °C for 3 min; 95 °C 10 s, 60 °C 45 s for 40 cycles; 95 °C 1 min). The melting curve was observed from 55 to 95 °C in 80 steps of 0.5 °C per 10 s. The data were studied using the optical system software program iQ5 version 2.0 (BioRad). See Table 2 for the sequence of the forward and reverse primer.

2.6. Padlock probe specificity testing

For specificity testing 25 pM of the padlock probe was examined with 200 ng digested genomic DNA and with a mixture of the five plant DNAs. A 40 ng genomic DNA sample (made up to 200 ng DNA with 160 ng herring sperm DNA) representing 20% (w/w) of the grand total was included to allow comparison of the C_t value of the 200 ng (100%), 40 ng (20%) target DNA in herring sperm background and the 40 ng target DNA (20%) in the mixture.

DNA (200 ng) contains a limited amount of copy numbers of a certain target. With the haploid genome weight (RBG Kew Plant DNA *C*-values database: Bennett & Leitch, 2003), the *C*-value reflects the weight of a haploid genome in pg. Thus, the calculated number of targets within a haploid genome is: barley = 36,036; maize = 73,260; oat = 15,117; soya = 176,991 and wheat = 3847 (Target is D-genome-specific and therefore present only 1/3 × 11,540 = 3847 times).

2.7. Microarray visualisation

Microarrays were prepared using the MicroGrid (Apogent Discovery) and contain 50 spotted ZIP-codes (20-mer oligonucleotides from Affymetrix) with a 10-mer A-tail (and C6 to linker) in quadruplicate. The ZIP-codes are demarcated by ZIP-PS01 spots (Table 2) for positioning purposes.

The microarrays were pre-hybridised overnight at 42 °C in previously boiled and rapidly cooled pre-hybridisation mix (5× SSC; 0.1% SDS; 0.1 mg/ml herring sperm DNA). After a repeated wash with 0.1× SSC for 5′ at RT on a rotary tablet, the slides were rinsed with MQ and dried by centrifugation (2' at 1000 rpm).

For probe amplification, 3 μl ligation mixture with potentially circularised padlock probes was amplified using the forward and reverse primer (see Table 2) sites on the padlock probe (1× ThermoPol PCR buffer (New England Biolabs, containing 2 mM $MgCl_2$); 2.5 mM $MgCl_2$; 200 μM dNTPs; 2 U Vent® exo$^-$ DNA polymerase (NEB); 500 nM Cy3-labelled reverse primer; 50 nM forward primer in a total volume of 25 μl). For detection purposes, the reverse primer was labelled with Cy3. After asymmetrical PCR amplification (95 °C for 15 min; 95 °C 15 s, 51 °C 2 s, 72 °C 5 s for 80 cycles), 1 μl was applied to 64 μl hybridisation mixture (5x SSC; 0.1% SDS; 0.1 mg/ml herring sperm DNA; 192 pM 5′Cy3-labelled cZIPPS01) to hybridise to the microarray in a confined area (Gene Frame frames and cover slips 1.5 × 1.6 cm for 65 μl, ABgene, UK) for 2 h at 65 °C in a moist atmosphere.

After removing the chambers the microarrays were washed twice in 1× SSC; 0.1% SDS for 5 min, twice in 0.1× SSC; 0.1% SDS for 5′, twice in 0.1× SSC for 1 min and once with 0.01× SSC for 30 s. The slides were dried by centrifugation (2 min at 1000 rpm) and stored in the dark.

The ScanArray Express HT microarray scanner (Perkin Elmer) was used to scan the signal of the individual spots at 543 nm. Here, a PhotoMultiplier Tube (PMT) gain was used between 70 and 90 at a laser power of 90%. The individual signals were quantified using

the optical system software program ArrayVision version 8.0 (Imaging Research Inc.) and processed in Excel (Microsoft).

3. Results

3.1. Validation of padlock probes

All padlock probes were able to recognise and subsequently circularise on the target sequence. As positive controls cloned target fragments were obtained in a linearised form. In addition, for maize and oat the target sequences were ordered as single stranded oligonucleotides to perform as positive controls. Remarkably, C_t values (the threshold cycle C_t represents the PCR cycle at which the software first detects a noticeable increase in SYBR green fluorescence above a baseline signal and is a measure for significance) of reactions with 200 ng digested gDNA of oat or maize as template were lower compared to the molecular equivalent in linearised double-stranded plasmid containing the target, or the single stranded target (not shown). Plasmid and ssDNA have been complemented with herring sperm DNA to obtain a final DNA concentration of 200 ng. Although the total amount of DNA and the molar amount of target was thus comparable, more efficient ligation and subsequent amplification of padlock probe-targets was observed in genomic DNA compared to cloned and linearised plasmid or even ssDNA. The discrepancy between an artificial target and the amplification of molar equivalents in genomic DNA samples, will require further attention when quantification is required.

3.2. Specificity of padlock probes

Once padlock probes were proven to be functional on the genomic DNA for which they were designed, the padlock probes were tested with a number of cereals and other seeds for cross-reactivity. These were maize, oat, wheat, barley and soya. In Table 3, the results of the specificity of the padlock probes are depicted. The padlock probe was tested with digested genomic target DNA and with a mixture of the five plant DNAs. A genomic DNA sample representing 20% (w/w) of the grand total was included to allow comparison of the C_t value of the 100%, 20% target DNA in herring sperm background and the 20% target DNA in the mixture.

In general the padlock probes showed good performance with their target DNA (white upper area of Table 3) and hardly or not at all with the other non-target gDNA samples (grey lower area). Non-target DNAs show C_t values similar to those of the MilliQ treated water control and are therefore considered to be negative. This shows the padlock probes to be very specific for the detection of their target DNA.

As expected, the ΔC_t values (the difference between the C_t of a sample assay and the C_t of the water control: $\Delta C_t = C_{t(\text{target})} - C_{t(\text{MQ})}$ are slightly lower for the 20% sample compared to 100% target DNA. For the maize and oat padlock probe, the 20% pure DNA sample has a slightly lower C_t value than the 20% sample in the mixture. For barley and soya padlock probes the C_t value for the 20% pure sample was slightly higher while the C_t value for the wheat padlock probe was similar for the 20% pure and 20% mixture samples.

3.3. Identification of authenticity of Farro della Garfagnana

The absence of the D-genome is a criterion that molecularly distinguishes Farro della Garfagnana from spelt wheat and common bread wheat. A padlock probe for D-genome detection was developed that recognizes common bread wheat genomic DNA, but not other cereals tested (see Section 3.2.). The next step was to investigate if the padlock probe is D-genome specific, or if it does show

Table 3
ΔC_t values (ΔC_t is calculated as C_t Exp – C_t MQ) for padlock probes with target DNA (bold upper area) and presumed non-target DNA (italic lower area). 20% DNA samples and DNA mix each contain 40 ng of the target DNA compared to the 100% sample (=200 ng). ΔC_t values are calculated from at least two in duplo experiments. Outliers were omitted from the analysis. PLP = padlock probe.

Maize-specific PLP			Barley-specific PLP			Oat-specific PLP			Soya-specific PLP			Wheat-specific PLP			Wheat-specific PLP		
Target DNA	ΔC_t	SD	Target DNA	ΔC_t	SD	Target DNA	ΔC_t	SD	Target DNA	ΔC_t	SD	Target DNA	ΔC_t	SD	Target DNA	ΔC_t	SD
Maize	**8.0**	**0.1**	**Barley**	**9.6**	**0.4**	**Oat**	**14.2**	**0.4**	**Soya**	**11.2**	**0.7**	**Wheat**	**7.6**	**0.5**	**Spelt cv. Ostro**	**7.9**	**0.7**
20% Maize	**5.9**	**0.5**	**20% Barley**	**7.7**	**0.3**	**20% Oat**	**10.9**	**0.6**	**20% Soya**	**9.3**	**0.6**	**20% Wheat**	**5.6**	**0.2**	**Spelt cv. Oberkulmer Rotkorn**	**8.3**	**0.8**
DNA mix[a]	**6.1**	**0.1**	**DNA mix**	**7.0**	**0.0**	**DNA mix**	**11.7**	**0.2**	**DNA mix**	**8.7**	**0.8**	**DNA mix**	**5.5**	**0.3**	**Wheat**	**7.6**	**0.5**
Barley	*0.5*	*0.1*	*Maize*	*-0.9*	*0.0*	*Maize*	*0.5*	*0.5*	*Maize*	*0.7*	*0.9*	*Oat*	*0.4*	*0.8*	*Durum wheat cv. Combo*	*1.3*	*0.8*
Oat	*0.5*	*0.2*	*Oat*	*1.6*	*0.4*	*Barley*	*1.5*	*0.2*	*Barley*	*0.1*	*0.5*	*Barley*	*0.7*	*0.7*	*Farro della Garfagnana*	*0.7*	*0.5*
Wheat	*0.4*	*0.7*	*Wheat*	*–0.5*	*0.3*	*Wheat*	*0.2*	*0.6*	*Oat*	*1.0*	*0.8*	*Soya*	*0.2*	*0.4*	*Emmer Acc. 'Kleiner gelber Kahler'*	*1.8*	*0.4*
Soya	*0.7*	*0.0*	*Soya*	*–0.5*	*0.5*	*Soya*	*0.3*	*0.1*	*Wheat*	*0.3*	*1.1*	*Maize*	*-0.3*	*0.4*	*Emmer Acc. 'Zäblin'*	*2.4*	*0.4*
Rye[b]	*1.0*	*0.2*	*Rye*	*2.7*	*0.2*	*Rye*	*2.6*	*0.2*	*Rye*	*0.5*	*0.3*	*Rye*	*2.8*	*0.2*	*Einkorn*	*0.8*	*0.5*

[a] DNA mixture consists of barley, oat, wheat, maize and soya (20% each) in a total of 200 ng.
[b] Average of one *in duplo* experiment for all Rye samples.

some cross-reactivity with the B and A^u-genome within other members of the *Triticum* genus.

For this experiment closely related hulled cereals like einkorn (*T. monococcum*), spelt (*T. spelta* cv. Oberkulmer Rotkorn and Ostro) and two domesticated emmer lines (*T. dicoccum* line 'Züblin' and line 'Kleiner gelber Kahler') were used. In addition, durum wheat (*T. durum* cv. Combo) was included as a close relative.

As can be seen in Table 3, the wheat padlock probe strongly reacts with hexaploid *Triticum* species containing the D-genome like bread wheat, "Ostro" and "Oberkulmer Rotkorn" spelt. Of the alleged non-target species, rye and emmer lines 'Züblin' and 'Kleiner gelber Kahler' had low delta C_t values, while others do not show a reaction (maize, soya, barley, oat and einkorn). Farro della Garfagnana, which has no D-genome as such but could harbour partial D-genome copies/elements in the B or A^u-genome, showed only minor reactivity suggesting that Farro della Garfagnana is indeed not a spelt wheat but more likely an emmer.

The ΔC_t values of rye and emmer lines 'Züblin' and 'Kleiner gelber Kahler' (and Farro della Garfagnana for that matter) could be due to the fact that slight contamination with common bread wheat may be expected since no certified reference material was available. Rye and the emmer lines show the same peak in the melting curves (not shown), indicating that homoeology to the wheat target sequence might be present in their genomes. Some *Triticum* species without the D-genome show the same peak as wheat in the melting curve, but at a later C_t value. Nevertheless, the observed ΔC_t value in Farro della Garfagnana does allow discrimination between a pure sample and a mixture. Overall, the delta C_t values of non-target species (grey) are significantly lower than the target species (white).

Specificity and sensitivity of the D-genome-specific padlock probe was further tested by diluting DNA from common wheat into DNA from Farro della Garfagnana (see Figs. 2 and 3). In the previous experiment, the D-genome of common wheat was already detected in a background of 80% other genomic DNA. A dilution series was made up to 2.5% common wheat in a mixture with 97.5% Farro della Garfagnana. DNA amplification for DNA mixtures of Farro della Garfagnana and common wheat with percentages of common wheat of 20, 15, 10, 5, 2.5 and 0%, yield the standard curve in Fig. 3. At 2.5% common wheat, a ΔC_t value of 2.16 ± 0.61 was still discriminative from the background signal containing 100% Farro della Garfagnana 0.28 ± 0.02 (*t*-test: $p = 0.024$), allowing detection of contaminating D-genome sequences down to 2.5%.

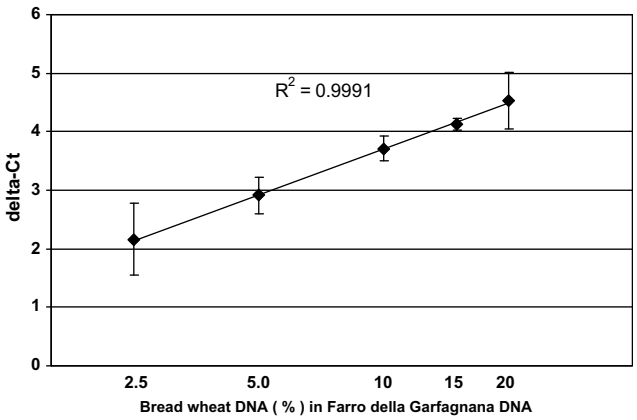

Fig. 3. ΔC_t values ($C_{t\ Exp} - C_{t\ MQ}$) of dilution series of bread wheat DNA in Farro della Garfagnana DNA using the wheat-specific padlock probe. The *x*-axis represents the log% of bread wheat DNA. Bread wheat (0%) has a delta C_t of 0.28 ± 0.02 (not shown in graph).

3.4. Microarray approach for visualisation of amplified padlock probes

A microarray approach for the detection of ligated padlock probes has the advantage that it can be rapidly extended (large numbers of) new ZIP-codes (coding for species or variety-specific padlock probes).

For this pilot experiment a microarray containing 50 spotted ZIP-codes was designed, flanked by positioning spots. This specific microarray could facilitate 50 different padlock probes to hybridise, but the microarray can easily be extended to accommodate a much larger number of target ZIP-codes. The microarray was

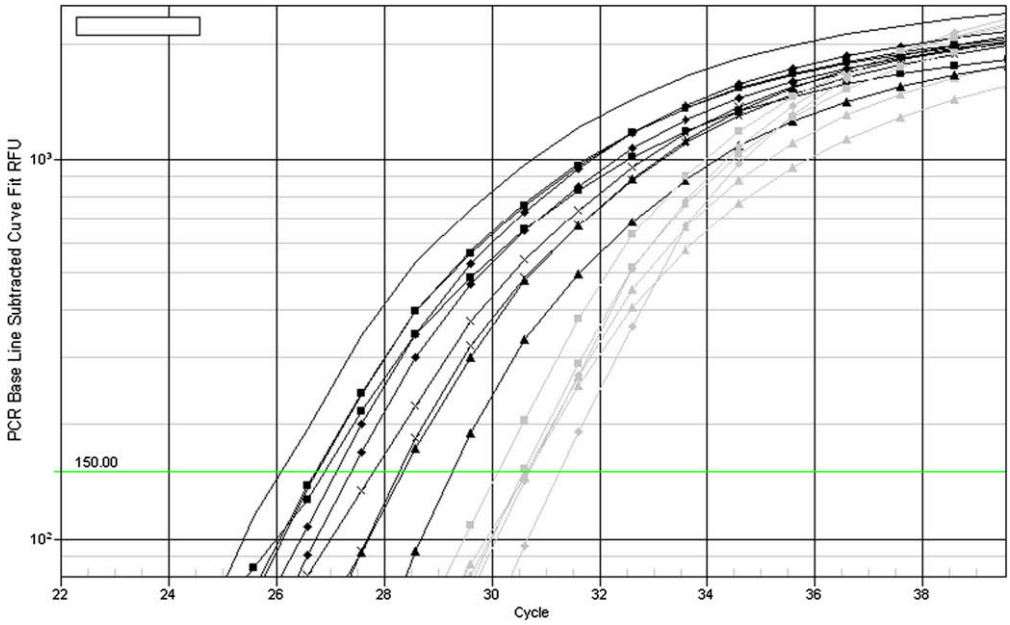

Fig. 2. Amplification plots (PCR cycles vs. relative fluorescence units) obtained from real-time PCR analysis of a dilution range (0–20% common bread wheat DNA in Farro della Garfagnana DNA) using the wheat-specific padlock probe. Black no symbol: 20% wheat; square: 15% wheat; diamond: 10% wheat; cross: 5% wheat; triangle: 2.5% wheat. Grey triangle: 0% wheat; diamond: MQ control; square: Non Target Control. The line at 150 RFU represents the threshold.

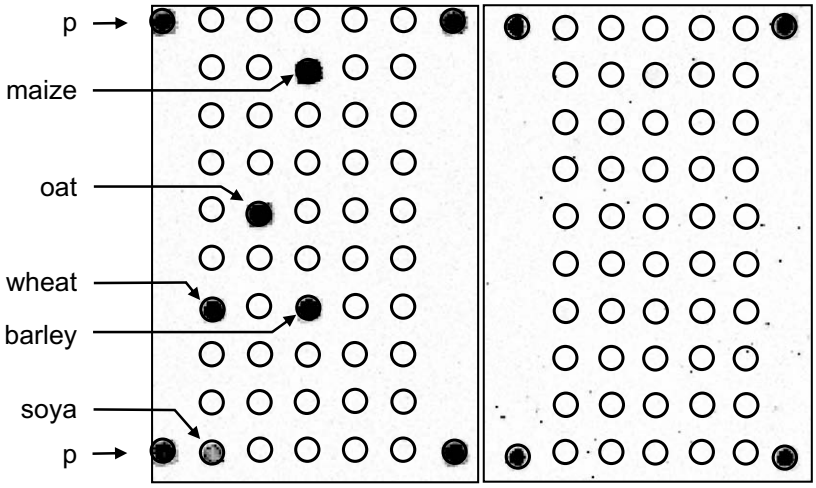

Fig. 4. Microarray hybridization shows specific and strong signals for 5-plex plant identification. Padlock probe ligation with the five corresponding probes was performed on 20% of each maize, oat, barley, wheat and soya. PCR labelling (Cy3) was followed by microarray hybridisation. Left: Microarray with the ZIP code signals corresponding to plant DNA, flanked by four positioning spots in the corners. Right: MilliQ treated water control sample.

exposed to a mixture of padlock probes (wheat, soya, maize, barley and oat), all previously allowed to circularise and amplify on a mixture of wheat:soya:maize:barley:oat at equal amounts of genomic DNA. In Fig. 4 the exposure of the five Cy3-labelled amplicons is visualised. Here, the dots representing wheat, soya, maize, barley and oat are intensely illuminated by Cy3, the resulting pattern being as anticipated. This indicates the combination of padlock probe ligation with universal PCR and microarray detection to be a truly multiplex system.

4. Discussion

For the maintenance of EU regulations related to speciality products such as PDO, PGIs and TSGs, it is necessary to develop specific and sensitive methods for the identification and establishment of authenticity of the different (agricultural) products. These methods should preferably be performed in a multiplex setting to not only allow the identification of the product itself, but also to establish the absence of any undesired admixtures in the product that will affect the quality or the economical advantage of the product.

In this paper a DNA-based method is presented that can specifically and sensitively detect a number of different cereal species in samples of speciality varieties. For the speciality product under investigation, the PGI wheat variety Farro della Garfagnana, it proved not feasible to develop product-specific markers that can be used to establish the identity of the basic product directly. But even if such markers were available, it would still be important to determine the purity of the product by eliminating the possibility that the speciality product had been mixed with other cereals with a lower economical profile. At this point only contamination by wheat varieties that do contain the D-genome as well as a limited number of other cereals can be ruled out: undesired admixture with other tetraploid emmer or durum wheat and diploid einkorn varieties will be difficult to exclude. The procedure as presented here, combining multiplex padlock ligation and microarray detection allows a rapid expansion of the approach to include more markers for individual cereal species or varieties that are either known to be speciality products or undesired admixtures. This will also further help to establish the purity of Farro della Garfagnana produce.

An additional advantage of the padlock-microarray system is that it is based on a target sequence spanning only approximately 45 nucleotides (~30 nt in the 5′ target and ~15 nt in the 3′ target of the padlock probe), compared to usually >100 nucleotides in an average PCR setting. This will improve the detection of the target in (more) processed products where some degree of DNA degradation has occurred compared to the traditional PCR approach.

For a detection system to be effective, it should be sufficiently sensitive. The padlock-microarray system described here is shown to be able to detect at least 20% of the different cereals in complex mixtures of plant genomic DNA. In a real-time PCR setting, a contamination of 2.5% common bread wheat DNA can be detected in a mixture with 97.5% Farro della Garfagnana DNA using a bread wheat specific padlock probe. This could be sufficient since Terzi, Malnati, Barbanera, Stanca, and Faccioli (2003) state that the Italian government currently prohibits the manufacture of pasta for sale in Italy containing more then 3% bread wheat. It remains to be seen what sensitivity is required to establish the authenticity of speciality products and whether this sensitivity can be achieved for all padlock probes using the system described here. The results so far are promising and make it plausible that increased sensitivity, should this be required, can indeed be achieved.

For the set-up and validation of effective detection and identification methods to underpin and maintain EU regulations on speciality products, it is of crucial importance that the basic quality of the products is well described. For the analytical characterisation of the products, reference materials for the individual products will become available. Reference materials can either confirm the purity of the authenticated product, or establish the band width of variation of the product that is still considered to be within the limits of the definition of the EU speciality product.

Acknowledgements

The authors are grateful for financial support concerning scientific activities within the Sixth Framework Programme of the European Union, project TRACE – "TRAcing food Commodities in Europe" (project no. FOOD-CT-2005-006942). The publication reflects only the authors' views and the Community is not liable for any use that may be made of the information contained therein.

We thank Angela H.A.M. van Hoek for preparing the microarrays and helpful discussions.

References

Altschul, S. F., Madden, T. L., Schaffer, A. A., Zhang, J. H., Zhang, Z., Miller, W., et al. (1997). Gapped BLAST and PSI-BLAST: A new generation of protein database search programs. *Nucleic Acids Research, 25*, 3389–3402.

Bennett, M. D., & Leitch, I. J. (2003). Plant DNA C-values database (release 2.0, January 2003). http://www.rbgkew.org.uk/cval/homepage.html.

Bryan, G. J. & Gale, M. D. (1998). Detection of D genome in wheat species. Patent number WO9804737-A/19, 05 February 1998.

Bryan, G. J., Dixon, A., Gale, M. D., & Wiseman, G. (1998). A PCR-based method for the detection of hexaploid bread wheat adulteration of Durum wheat and pasta. *Journal of Cereal Science, 28*, 135–145.

Golovnina, K. A., Glushkov, S. A., Blinov, A. G., Mayorov, V. I., Adkison, L. R., & Goncharov, N. P. (2007). Molecular phylogeny of the genus *Triticum* L. *Plant Systematics and Evolution, 264*(3–4), 195–216.

Inoue, J., Shigemori, Y., & Mikawa, T. (2006). Improvements of rolling circle amplification (RCA) efficiency and accuracy using *Thermus thermophilus* SSB mutant protein – art no. e69. *Nucleic Acids Research, 34*(9), Nil_44–Nil_52.

Jarvius, J., Melin, J., Goransson, J., Stenberg, J., Fredriksson, S., Gonzalez Rey, C., et al. (2006). Digital quantification using amplified single-molecule detection. *Nature methods, 3*(9), 725–727.

Nilsson, M., Malmgren, H., Samiotaki, M., Kwiatkowski, M., Chowdhary, B. P., & Landegren, U. (1994). Padlock probes: Circularizing oligonucleotides for localized DNA detection. *Science, 265*, 2085–2088.

Padulosi, S., Hammer, K., & Heller, J. (Eds). (1996). Hulled wheats. Promoting the conservation and use of underutilized and neglected crops. 4. In *Proceedings of the First International Workshop on Hulled Wheats, 21–22 July 1995, Castelvecchio Pascoli, Tuscany, Italy*. *International Plant Genetic Resources Institute, Rome, Italy*. 262 pp.

Pang, S., Qureshi, F., Shanahan, D., & Harris, N. (2007). Investigation of the use of rolling circle amplification for the detection of GM food. *European Food Research and Technology, 225*(1), 59–66.

Pasqualone, A., Montemurro, C., Grinn-Gofron, A., Sonnante, G., & Blanco, A. (2007). Detection of soft wheat in semolinsa and Durum wheat bread by analysis of microsatellites. *Journal of Agricultural and Food Chemistry, 55*, 3312–3318.

Pestsova, E., Ganal, M. W., & Roder, M. S. (2000). Isolation and mapping of microsatellite markers specific for the D genome of bread wheat. *Genome, 43*(4), 689–697.

Peyret, N., Seneviratne, P. A., Allawi, H. T., & SantaLucia Jr., J. (1999). Nearest-neighbor thermodynamics and NMR of DNA sequences with internal A A, C C, G G, and T T mismatches. *Biochemistry*, 38(12), 3468–3477. (http://ozone3.chem.wayne.edu/, visited on May 2008).

SantaLucia, J. Jr, (1998). A unified view of polymer, dumbbell, and oligonucleotide DNA nearest-neighbor thermodynamics. *Proceedings of the National Academy of Sciences of the United States of America, 95*(4), 1460–1465.

Szemes, M., Bonants, P., de Weerdt, M., Banér, J., Landegren, U., & Schoen, C. D. (2005). Diagnostic application of padlock probes-multiplex detection of plant pathogens using universal microarrays art. no. e70. *Nucleic Acids Research, 33*(8), Nil_1–Nil_13.

Terzi, V., Malnati, M., Barbanera, M., Stanca, A. M., & Faccioli, P. (2003). Development of analytical systems based on real-time PCR for *Triticum* species-specific detection and quantitation of bread wheat contamination in semolina and pasta. *Journal of Cereal Science, 38*, 87–94.

Terzi, V., Morcia, C., Gorrini, A., Stanca, A. M., Shewry, P. R., & Faccioli, P. (2005). DNA-based methods for identification and quantification of small grain cereal mixtures and fingerprinting of varieties. *Journal of Cereal Science, 41*, 213–220.

Tian, Y., He, Y., & Mao, C. D. (2006). Cascade signal amplification for DNA detection. *ChemBioChem, 7*(12), 1862–1864.

Vora, G. J., Meador, C. E., Stenger, D. A., & Andreadis, J. D. (2004). Nucleic acid amplification strategies for DNA microarray-based pathogen detection. *Applied and Environmental Microbiology, 70*(5), 3047–3054.

Zuker, M. (2003). Mfold web server for nucleic acid folding and hybridization prediction. *Nucleic Acids Research*, 31(13), 3406–3415. (http://www.idtdna.com/Scitools/Applications/mFold/, visited on May 2008).

In this study, the GMO content of RoundUp Ready™ soya samples, constructed by mixing two differing GMO-containing samples, in different proportions, were measured using QUIZ and commercially tested by rt-PCR. RoundUp Ready™ soya is a convenient event to test the applicability of QUIZ because: the transgene has been characterised (Windels, Taverniers, Depicker, Van Bockstaele, & De Loose, 2001), providing sequence data for event-specific primer design; CRMs are available for the event in the form of ground soya meal (Fluka Biochemika); and there is a documented single copy lectin gene in soya (Germini et al., 2004) that can be used as a reference marker.

2. Materials and methods

The overview of QUIZ is shown in Fig. 1 and the technique can be divided into a number of steps.

2.1. Preparation of DNA

Soya Roundup Ready™ GMO reference material was purchased from Fluka Biochemika. Five samples, containing different GMO content, were constructed by mixing varying proportions of 0% and 5% CRMs (Table 1). DNA was extracted from each using a DNeasy kit (QIAGEN) following the manufacturer's instructions. An aliquot of each (2 μl) was run out on an agarose gel to determine quality, and quantified by comparison with known amounts of lambda DNA (New England Biolabs) (data not shown) and estimated to be ~20 ηg μL^{-1}.

2.2. Dilution of template

The haploid genome size of soya is ~1 pg (Plant DNA *C*-values Database, Royal Botanic Gardens, Kew, UK http://www.rbgkew.org.uk/cva1/database1.html), so 20 ηg μL^{-1} equates to 20,000 genomes in 1 μL. A dilution of 10^{-3} would therefore yield 20 copies of a single copy gene per μL. For the lectin marker, 5 μL of this dilution was added to each tube containing 1 mL of reaction mix for all samples apart from the 0% GMO sample. Corresponding dilutions were made to each sample to generate an equal number of GM markers. For the 0% sample, 10^{-4} dilution was made of the template for lectin gene detection. For amplification of the GM target 25 μL of the DNA sample was added to each mL of reagents to try and equalise the numbers of each marker (Table 1).

2.3. PCR conditions and fragment analyses

Primers (Sigma–Genosys) were designed from the sequences for the transgene junction for RoundUp Ready™ soya (EMBL Accession No. AJ308515) and for the lectin gene target (EMBL Accession No. K00821) as the taxon-specific reference (Table 2A).

Reactions containing DNA were made up in amber 1.5 mL microcentrifuge tubes (Star Lab – catalogue No. I 1415 1007). These were silanised by submerging in 'Silanization Solution II' (2% dimethylchlorosilane in 1, 1, 1-trichloroethane; Fluka Biochemika) for 10 min. The tubes were rinsed 10 times with water purified by reverse osmosis using a PRO/RO unit (Labconco Corporation) and air dried before use.

The silanised tubes were used for preparing the reaction mixes, containing 1× PCR buffer (as supplied), 2.5 mM $MgCl_2$, 0.25 μM each primer, 200 μM each dNTPs, 0.05 U μL^{-1} Fastart Taq (Roche), λ DNA to 1 ηg μL^{-1} with appropriate amounts of template added prior to dispensing into 384-well microtitre plates. One millilitre of reaction mix was made for each 96-well plate. Ten microlitre of reaction mix were dispensed into each well using an epMotion 5070 workstation (Eppendorf).

Cycling parameters – 5 min 94 °C initial denaturation was followed by 50 cycles of 92 °C 30 s, 55 °C 30 s, 72 °C 30 s; with final extension of 10 min 72 °C.

After cycling, each lectin amplification reaction was mixed with a reaction for the GMO target. One microlitre of the mix was added to 10 μL of Hi-Di (Applied Biosystems) with Rox-labelled size standards (81, 106, 173, 275, 358, and 408 nucleotides) and loaded onto a 3100 Genetic Analyzer (Applied Biosystems) with an injection time of 30 s. Size standards were made by amplification of pUC19 plasmid (Yanisch-Perron, Vieira, & Messing, 1985) using a Rox-labelled primer with different non-labelled primers to give the fragment sizes required (Table 2B).

The alignment of the tracks using the size standards was performed using Genemapper 3.7 software (Applied Biosystems) though each track was manually checked to ensure correct alignment. The presence, or absence of the two markers (see Fig. 2) were recorded and their numbers used to calculate the percentage GMO

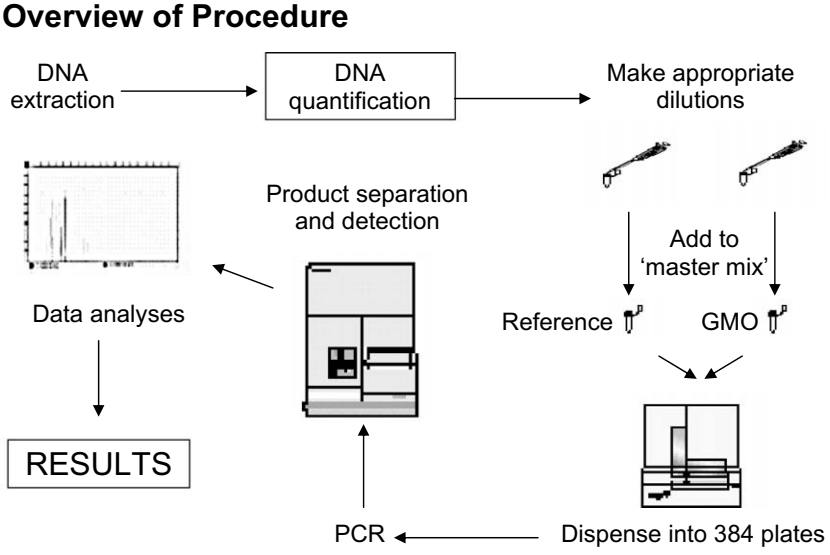

Fig. 1. Outline of the QUIZ procedure used in this study.

Table 1
Sample composition and measured GMO content

Sample	% (weight) 5% CRM	Nominal GMO content (%)	Number of lectin amplicons (total)[a]	Number of GM amplicons (total)[a]	Dilution factor	QUIZ determined GMO content (%)	% GMO content determined by rt-PCR (average)[b]
A	0	0	12	13	5×10^4	0.0022 ± 0.0009	0.009, 0.012 (0.01)
B	9.1	0.45	213 (384)	134 (368)	200	0.28 ± 0.03	0.149, 0.112 (0.130)
C	16.7	0.83	171 (384)	84 (384)	100	0.42 ± 0.06	1.253, 0.938 (1.095)
D	64.7	3.24	130 (384)	121 (368)	33.3	2.89 ± 0.37	3.078, 3.100 (3.089)
E	100	5	242 (383)	246 (382)	20	5.17 ± 0.49	4.275, 4.928 (4.601)

[a] Though 384 reactions were performed for each marker/dilution, some reactions were lost to evaporation.
[b] Samples were tested in duplicate and the results of both tests are given.

content in each sample. In cases (~20%) where the peaks were not oversized (fluorescence peak heights of >8000), peak heights greater than 500 were accepted as positives and everything else considered negatives.

2.4. Estimation of GMO content

The average number of molecules in each sample was calculated as:

$$\mu = -\log(\text{proportion of zeros}) \times \text{dilution factor}$$

The GMO content was determined as: $\mu_{gm}/\mu_{lectin} \times 100\%$.
Variance of percentage was calculated from:

$$\text{Var}_{(\text{ratio})} \approx \left(\left(\frac{p_l q_l}{N_1}\right) \cdot \left(\frac{1}{p_l}\right)^2 \cdot \left(\frac{\mu_g}{\mu_l}\right)^2 + \left(\frac{p_g q_g}{N_2}\right) \cdot \left(\frac{1}{p_g}\right)^2 \right) \cdot \left(\frac{1}{\mu_l}\right)^2$$

where p is the proportion of zeros, i.e. the proportion of negative amplifications, q is the frequency of positive $(1-p)$ amplifications for the lectin (l) and GMO (g) markers; N_1 and N_2 represent the total numbers of lectin and GMO reactions, respectively, μ_g and μ_l are the estimated numbers of molecules.

The formula for the variance of the ratio of (number of GM molecules)/(number of lectin molecules) was derived using the delta method, taking the distribution of p as binomial.

2.5. Quantification using real-time PCR

A set of samples containing 40 μL of each of the five admixtures was sent to IDna Genetics Ltd. (Norwich) to be tested for their RoundUp Ready™ content. Each sample was tested in duplicate and the results are summarised in Table 1.

3. Results and discussion

The outline of the QUIZ testing procedure is shown in Fig. 1. In this exercise we have exploited the nominal GMO contents to dilute the samples such that the expected numbers of reference and GMO targets are approximately equal. Though the number of reference targets can always be manipulated from the DNA concentrations this is not possible for samples where the GMO content is unknown. However, required dilutions can be determined empirically by testing a dilution series of the template. In fact methods of estimation can easily be extended to combine information from different dilutions and replicates of dilution series of template could be sufficient to determine whether a sample is below a given threshold without the need for further testing. Theory, verified by simulation (data not shown), demonstrates that the probabilities of no DNA template within the range 0.1–0.6 give the lowest errors in estimates of DNA concentration. This represents approximately an average of 0.5–2 target molecules per reaction giving a fourfold range of DNA concentration where the error is minimal.

The numbers of positive reactions for both lectin and GMO targets using extended numbers of PCR cycles (50 cycles) and FAM-labelled primers, for detection in automated genotypers, show successful amplification and detection from single molecules: given the DNA concentrations of the samples, it was statistically unlikely for all the reactions to contain more than one target amplicon. In fact, most peaks observed in the ABI3100 (Applied Biosystems) were oversized, even though only 0.5 μL of the reactions were used.

The amplification of near single copy template means that there are only small amounts of DNA in each reaction. Two steps were included in the procedure to reduce the loss of template DNA

Table 2A
GMO quantification: primer sequences and product length

Primer	Sequence	Amplicon length (bp)
RRS GMF	[F]-ACTGCTTCTCCCAGAATGATC	285
RRS GMR	TCGAGCTTCTTCACGAACTT	
LecF	[F]-ATGGGCTTGCCTTCTTTCT	157
LecR	CCGATGTGTGGATTTGGTG	

[F] FAM fluorophore.

Table 2B
Size standards: primer sequences and product length

Primer	Sequence	Amplicon length (bp)
Rox-labelled primer	[R]-TAGGCACCCCAGGCTTTACAC	
pUC19_83	TTTCCTGTGTGAAATTGTTATC	83
pUC19_106	TGGCGTAATCATGGTCATA	106
pUC19_173	CGACGGCCAGTGAATTCG	173
pUC19_275	TGCGGGCCTCTTCGCTATTA	275
pUC19_358	ACCGCAGATGCGTAAGGAGAA	358
pUC19_408	GCGGCATCAGAGCAGATTGTACT	408

[R] Rox fluorophore.

which would impair the measurements: the silanization of the tubes to reduce DNA binding and the addition of bacteriophage λ DNA (to 1 ηg μL^{-1}) in the reaction mixes, as competitor to DNA binding sites on the tubes and pipette tips.

In addition to the 157 bp lectin amplicon, an additional fragment of 143 bp was also detected in many of the reactions (see Fig. 2). Sequence analysis of this second product show that it is amplified from a second lectin gene (EMBL Accession No. AY342212). The spatial distance of 143 bp between the primer sequences within this gene further supports this assertion. Both primers, which have been designed to amplify the 157 bp target, contain mismatches to this copy of the lectin gene (1 for the forward and 2 for the reverse primers) yet, the amplification of the 143 bp fragment was as effective as for the larger targeted amplicon, as judged from the numbers and intensity of the two products, even when co-amplified. Where the correct amplicon was detected most of the reactions (~80%) gave oversized bands when 0.5 μL of the reactions were loaded. For the remaining samples we applied a threshold of 500. We observed that the numbers of amplicons tailed off with both GM and lectin markers and, since the experiment was designed to amplify the two markers at similar numbers, any threshold level would give similar results. This may not be true if the numbers of GM and lectin targets were considerably different.

The co-amplification of the lectin genes highlights one of the differences between rt-PCR and QUIZ for quantification. With reference to standards, rt-PCR will measure the number of genes whereas QUIZ measures the number of molecules and, if two sequences are linked, they will not behave independently. The use of genomic controls as CRMs in rt-PCR compensates for multiple genes since the assays normalises the behaviour of the reference gene(s) on a 'per genome basis'. This would not be true if plasmid standards are used (Kuribara et al., 2002; Taverniers et al., 2005).

Quantitation results obtained using QUIZ compare favourably with those of the rt-PCR assay: the correlation between the measured and nominal values are 0.9901 and 0.9878, respectively (Fig. 3). Though the number of PCR reactions performed for QUIZ greatly exceeded those for rt-PCR, the amount of DNA required is substantially less, except for the 0% sample. For determining the number of lectin genes, only 400 pg of DNA was required for each sample. Detection and quantification using small amounts of DNA make it possible to quantify from samples where DNA levels will be low, e.g. processed foods, and potential inhibitors will be diluted with the DNA.

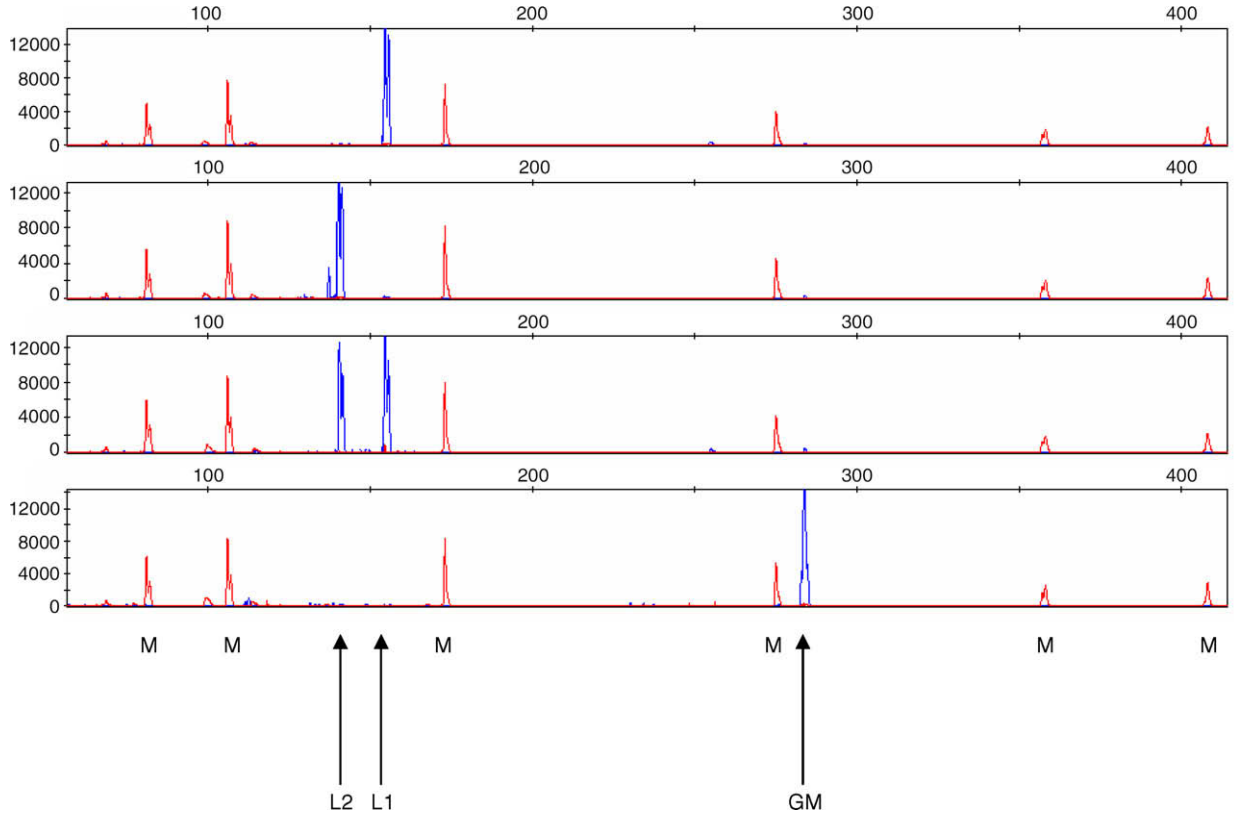

Fig. 2. Chromatograms showing the amplification of the fragments from lec 1 and lec 2 genes (L1 and L2, respectively) and event-specific amplicon (GM) in post-PCR mixes. The letter m denotes the internal Rox-labelled standards (see Table 2B) used to align tracks and numbers above the tracks represent sizes in nucleotides.

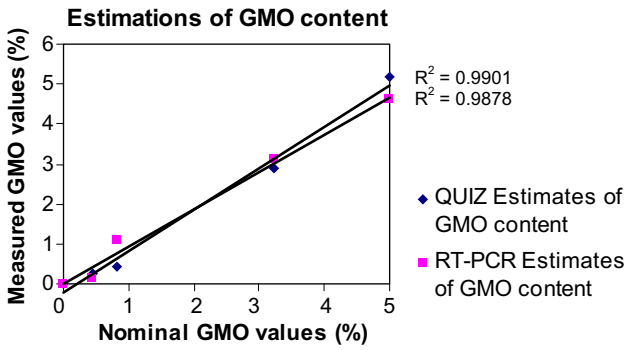

Fig. 3. The estimated GMO contents of the five samples, as determined using QUIZ and rt-PCR (iDNA Genetics Ltd.) are plotted against the nominal GMO content. The best fitting line is drawn for each method and the correlation of fit R^2 for each curve is shown.

QUIZ provides relative quantitation by comparing the abundance of each sequence which can be applicable in other systems, for example disease monitoring and gene expression. In the context of GMO testing, using GMO-specific and reference gene sequences, if the reference gene sequence is single copy, then the results from such tests can be expressed as % GMO per haploid genome, as favoured by the European Commission (EC Recommendation 2004/787). As such it does address some, but not all, of the problems of GMO labelling highlighted by Weighardt (2006). QUIZ offers a feasible alternative to quantify GMO contents of any sample, so long as suitable markers are available. The threshold for detection and quantification using QUIZ are down to single molecules: most probable number statistics are already applied to GMO detection in seed and grain (Macarthur et al., 2007; Remund, Dixon, Wright, & Holden, 2001) and the non-dependence on CRMs, which are not available for most approved events make this a potentially important GMO-testing procedure, especially for highly processed foods.

Acknowledgements

Huw Jones and Richard Horsnell are thanked for their help and patience demonstrating the ABI 3100. Jon White is thanked for helpful discussions and suggestions. This study has been carried out with financial support from the Food Standards Agency (FSA project G03025) and MLM is the recipient of a Ministero dell' Universita' e della Ricerca award from University of Naples Federico II.

References

Cankar, K., Stebih, D., Dreo, T., Zel, J., & Gruden, K. (2006). Critical points of DNA quantification by real-time PCR – effects of DNA extraction method and sample matrix on quantification of genetically modified organisms. *BMC Biotechnology, 6*, 37.

Dear, P. H., & Cook, P. R. (1989). Happy mapping: A proposal for linkage mapping the human genome. *Nucleic Acids Research, 17*, 6795–6807.

Germini, A., Zanetti, A., Salati, C., Rossi, S., Forre, C., & Schmid, S. , et al. (2004). Development of a seven-target multiplex PCR for the simultaneous detection of transgenic soybean and maize in feeds and foods. *Journal of Agricultural Food Chemistry, 52*, 3275–3280.

Hoofar, J., Malorny, B., Abdulmawjood, A., Cook, N., Wagner, M., & Fach, P. (2004). Practical considerations in design of internal amplification controls for diagnostic PCR assays. *Journal of Clinical Microbiology, 42*, 1863–1868.

Kuribara, H., Shindo, Y., Matsuoka, T., Takubo, K., Futo, S., & Aoki, N., et al. (2002). Novel reference molecules for quantitation of genetically modified maize and soybean. *Journal of AOAC International, 85*, 1077–1089.

Macarthur, R., Murray, A. W. A., Allnutt, T. R., Deppe, C., Hird, H. J., Kerins, G. M., Blackburn, J., Brown, J., Stones, R., & Hugo, S. (2007). Model for tuning GMO detection in seed and grain. *Nature Biotechnology, 25*, 169–170.

Remund, K. M., Dixon, D. A., Wright, D. L., & Holden, L. R. (2001). Statistical considerations in seed purity testing for transgenic traits. *Seed Science Research, 11*, 101–119.

Taverniers, I., Windels, P., Vaitilingom, M., Milcamps, A., Van Bockstaele, E., & Van den Eede, G., et al. (2005). Event-specific plasmid standards and real-time PCR methods for transgenic Bt11, Bt176, and GA21 maize and transgenic GT73 canola. *Journal of Agricultural Food Chemistry, 53*, 3041–3052.

Trapmann, S., Catalani, P., Conneely, P., Corbisier, P., Gancberg, D., Hannes, E., et al. (2002). The certification of reference materials of dry-mixed soya powder with different mass fractions of Roundup Ready™ soya. European Communities, Luxembourg, EUR 20273 EN, ISBN 92-894-3725-1.

Trapmann, S., & Emons, H. (2005). Reliable GMO analysis. *Analytical and Bioanalytical Chemistry, 381*, 72–74.

Weighardt, F. (2006). European GMO labeling thresholds impractical and unscientific. *Nature Biotechnology, 24*, 23–25.

Windels, P., Taverniers, A., Depicker, A., Van Bockstaele, E., & De Loose, M. (2001). Characterisation of the Roundup Ready soybean insert. *European Food Research Technology, 213*, 107–112.

Yanisch-Perron, C., Vieira, J., & Messing, J. (1985). Improved M13 phage cloning vectors and host strains: Nucleotide sequences of the M13mp18 and pUC19 vectors. *Gene, 33*, 103–119.

plants used by bees as forage during the production of "Miel de Corse". Additionally, detection systems using real-time PCR for other plant species commonly identified in honey (acacia, linden, citrus, clover, heather, olive, rape, sunflower and rosemary) were also developed and validated. These real-time PCR systems were then used to distinguish Corsican honey from samples of honey from other geographic regions.

2. Materials and methods

DNA from acacia (*Acacia decora*, *Acacia longifolia*), almond (*Prunus dulcis*), blackberry (*Rubus fruticosus*), broom (*Cytisus scoparius*), chestnut (*Aesculus hippocastanum*), citrus (*Citrus grandis*, *Citrus limon*, *Citrus sinensis*), clover (*Trifolium alpestre*, *Trifolium medium*, *Trifolium montanum*, *Trifolium rubens*), heather (*Erica carnea*), eucalyptus (*Eucalyptus erythrocorys*), hazelnut (*Corylus avellana*), lavender (*Lavandula angustifolia*, *Lavandula lanata*, *Lavandula latifolia*, *Lavandula stoechas*), linden (*Tilia platyphyllos*), maize (*Zea mays*), melissa (*Melissa officinalis*), oak (*Quercus palustris*, *Quercus pubescens*, *Quercus robur*, *Quercus rubra*, *Quercus suber*), olive (*Olea europaea*), papaya (*Carica papaya*), rape (*Brassica napus*), rockrose (*Cistus ladanifer*, *Cistus monspeliensis*), rosemary (*Rosmarinus officinalis*), sage (*Salvia fruticosa*, *Salvia lavandulifolia*), sunflower (*Helianthus annuus*), sweet chestnut (*Castanea sativa*), thyme (*Thymus vulgaris*) and wheat (*Triticum aestivum*) was extracted from plant material (leaves, flowers or pulp) purchased from the Botanical Garden in Berlin, Germany or from commercially available plants. The plant material was ground in liquid nitrogen using the A11 Basic Analytical Mill (IKA, Germany) and stored at −80 °C. The DNA was extracted using a cetyltrimethylammonium bromide (CTAB) method based on the procedure published by Tinker, Fortin, and Mather (1993). DNA extracted from cattle (*Bos taurus*) and chicken (*Gallus gallus*) were used as negative controls.

Twelve to 15 different honeys were collected from each of four regions; Corsica, Spain (Galicia), Germany and the UK (Table 1). Only four regions were considered due to the wide variety found within each. These products were obtained in the appropriate countries from commercial sources or directly from the beekeeper. It was assumed that these honeys had not be adulterated or extended with material from other sources.

The extraction of DNA from honey described below was optimised and validated in a small-scale comparison with four independent laboratories. Honey (10 g) was diluted with water to 45 ml, incubated at 65 °C in a water bath and shaken for 30 min. Following centrifugation for 30 min at 2400*g*, the pellet was resuspended in 200 μl water and ground using a 3 mm Tungsten Carbide bead in a TissueLyser (QIAGEN GmbH) for 2 min at 30 Hz. Using the DNeasy Blood and Tissue Kit (QIAGEN GmbH) the sample was digested for 30 min at 56 °C in 50 μl of buffer Al with 25 μl of proteinase K. The remainder of the DNA extraction was carried out exactly according to the manufacturer's instructions (DNeasy Blood and Tissue Kit Handbook July 2006). The DNA concentrations of samples were determined by spectrophotometry (DynaQuant 200, Hoefer, Amersham Bioscience).

Candidate genes for TaqMan™ PCR were identified and sequence data obtained from the GenBank database (Benson, Karsch-Mizrachi, Lipman, Ostell, & Wheeler, 2005) (Section 3) or where no sequence entry was available (*actin*, *tRNA-Leu* (trnL), *HMG*2 and *adh*1) by DNA sequence analysis using consensus primers. With the exception of the primer pair used to amplify the *tRNA-Leu* (trnL) gene fragment (Taberlet, Gielly, Pautou, & Bouvet, 1991), all of the primers used were developed within this project (Table 2).

Conventional PCRs were performed in a total volume of 25 μl. The reaction mixture contained 0.2 mM of each deoxynucleotide triphosphate (dNTP), 0.2 μM of each primer (listed in Table 2), 1 × PCR buffer (GeneAmp® PCR buffer, PE Applied Biosystems), 2 mM $MgCl_2$, 1.5 units Taq polymerase (AmpliTaq Gold™ DNA Polymerase, PE Applied Biosystems), and 2 μl (10–50 ng) of template DNA solution. Amplification was performed in the Thermal Cycler GeneAmp PCR System 9700 (Applied Biosystems) with the following thermal cycling protocol: 95 °C for 10 min followed by 35 cycles of 95 °C for 30 s, an annealing step for 30 s, 72 °C for 30 s and a final single step of 72 °C for 6 min. The annealing temperature used for the respective systems was determined empirically to be 60 °C, with the exception of sweet chestnut (58 °C), sunflower (56 °C), rape (57 °C), linden (58 °C), clover (58 °C) and the general actin-system for plants (57 °C).

TaqMan™ PCRs were performed in a total volume of 10 μl. The reaction mixture contained 1 × TaqMan™ Buffer A, 1.5 units AmpliTaq Gold® Polymerase, and magnesium chloride buffer (all from the Applied Biosystems TaqMan™ PCR Core Reagent Kit), 0.2 mM of each dNTP, forward and reverse primers, dual labelled fluorescent probe, and 2 μl (5–25 ng) of template DNA solution. The final concentration of the primers, probe and magnesium chloride in the respective systems was optimised empirically (Table 3). The primers and probes were purchased from TIB MOLBIOL (Germany) or Sigma (UK) and are listed in Table 2. The high magnesium chloride values determined after optimisation, might be due to the comparatively low melting temperatures of some primers and the need for probe stabilisation in TaqMan™ assays (Applied Biosystems 7700

Table 1
Honey samples ordered by country of origin

Corsica	Galicia	Germany	UK
Automne	Brezo	Blütenhonig (multi-floral)	English
Chataigneraie	Brezo	Edelkastanie (sweet chestnut)	English blossom
Maquis de Printemps	Castano	Edelkastanienhonig (sweet chestnut)	English set multi-floral
Maquis du desert des agriates	Eucalypto	Frühjahrsblüte (multi-floral, spring)	English set multi-floral
Miel de Bruyere (heather)	Galicia	Lindenhonig (linden)	English set multi-floral
Miel de Corse	Multi-floral	Lindenhonig (linden)	Exmoor heather
Miel de Corsica	Multi-floral (mainly chestnut and oak)	Raps (rape)	Heather
Miel de Printemps	Multi-floral (mixed heather + eucalyptus)	Rapshonig (rape)	Multi-floral
Miel du Maquis	Multi-flower (mainly heather)	Robinie (robinia)	North-Yorkshire multi-floral
Miel du Maquis d ete	Single-floral chestnut	Sommerblüten mit Kornblume (multi-floral, sommer)	Scottish heather
Miellats du Maquis	Single-floral eucalyptus	Sonnenblumenhonig (sunflower)	Yorkshire chunk multi-floral
Miellats du Maquis	Single-floral eucalyptus	Vielblütenhonig (multi-floral)	Yorkshire spring-blossom multi-floral
Printemps "Asphodele"	Single-floral eucalyptus	Waldhonig (forest)	
Printemps clementinier	Single-floral heather	Weißtanne (white fir)	
Printemps mille fleurs	Single-floral heather		
Printemps oranger	Single-floral (partly blackberry)		

Table 2
Specifications of primer and probe systems

Species	Gene and accession number if available	Oligonucleotide	Name	Sequence 5′–3′	Amplicon length (bp)
Acacia	*Alcohol dehydrogenase* 1 (*adh*1)	Forward primer Reverse primer Probe	Aca_adh1-f Aca_adh1-r Aca_adh1-probe	TGG GGA ATG TCC ACA TTG TAA GT TGG AGA ACC TGG TCT TGC CA FAM-AGC ATA ACA CCC CTG TCA GTG TTA ATC CTA AGA A -TAMRA	107
Broom	*Actin*	Forward primer Reverse primer Probe	Cyt_act-f Cyt_act-r Cyt_act-probe	GTT CAC CAC CTC TGC TGA GCG A TCG GCT CCA ATT GTG ATA ACT TGT FAM-CAA GAG CAG TTC TTC AGT TGA GAA AAG CTA TGA -TAMRA	160
Citrus	*Alcohol dehydrogenase* 1 (*adh*1)	Forward primer Reverse primer Probe	Cit_adh1-f Cit_adh1-r Cit_adh1-probe	TGA CAG AGG CGT CAT GCT TAA C TGA GGT TCC AAC GAA ATG ATA AAT A FAM-CTT GCC ATT GAT GGA AAA TCT CGA TTT CC -TAMRA	83
Clover	*Actin*AY372368 (*Trifolium pratense*)	Forward primer Reverse primer Probe	Tri_act-f Tri_act-r Tri_act-probe	CTG GCC GTG ATC TAA CTG AAT CTT ATC AGG AAG CTC ATA GTT TTT CTC AAT T FAM-AAG TTC TTG TTC ATA ATC CAC AGC AAC ATA GGC AA -TAMRA	191
Heather	*Alcohol dehydrogenase* 1 (*adh*1)	Forward primer Reverse primer Probe	Eri_adh1-f Eri_adh1-r Eri_adh1-probe	GGA TAG GGG AGT GAT GAT CCA T GAT GTT CCG ACG AAA TGG TAT ATG FAM-TGC CGT TTT TAG AAA ACC TTG ATT TCC CA -TAMRA	81
Eucalyptus	*Leafy*/*Floricauly* (*LFY*1)AY640313 (*Eucalyptus grandis*)	Forward primer Reverse primer Probe	Euc_LFY-f Euc_LFY-r Euc_LFY-probe	AGG AGC AAG TGG TGC AGC A TCC TCT GTT GTT GGG CGC FAM-TCA GAA AAG GAT CAG CTG GGC AGG G -TAMRA	96
Lavender	*Hydroxymethylglutaryl coenzyme A reductase* (*hmg*)	Forward primer Reverse primer Probe	Lav_HMG2-f Lav_HMG2-r Lav_HMG2-f-probe	CCA TAT CGC TCG TCT TCA ACA G TTG CCG GCG ATG GCA FAM-CAC TTG ATG CTC TGA AGC TTG GCG A -TAMRA	74
Linden	*Nitrate reductase* (*nr1*)AY138811 (*Tilia platyphyllos*)	Forward primer Reverse primer Probe	Til_nr-f Til_nr-r Til_nr-probe	GGG CAT CGA ACA TGA GCT TT TTC AAC GAG TTT GCA TGG GA FAM-AAA GAA GAT GCG CCT ACA AGA CCT GTT GC -TAMRA	101
Oak	*Phenylalanine ammonia-lyase* (*PAL*)AY443341 (*Quercus suber*)	Forward primer Reverse primer Probe	Querc_PAL-f Querc_PAL-r Querc_PAL-probe	AGT AGA GGG CGC AAG GAT AGA AA GAA TTC TCT CAC CAG TTA GTA AAC TTG TT FAM-AAA GCA GCA ATT CCT AAC CCA ATT AAG GAG T -TAMRA	136
		Forward primer	Querc_PAL2-f	AAG AAG TAG AGG GCG CAA GG	141
Olive	*Ole e 10*AY082335 (*Olea europaea*)	Forward primer Reverse primer Probe	Olea_ole10-f Olea_ole10-r2 Olea_ole10-probe	TAC CAA AGC AAG GGT CGA AAT G AGG GAT AAA ATT GTT TTA CTT ACT TGG GT FAM-TCG ATT GCG ACT TTT CGG GCA CC -TAMRA	96
Rape	*Lipase 1*AY866419 (*Brassica napus*)	Forward primer Reverse primer Probe	Bras_lip-f2 Bras_lip-r Bras_lip-probe	CAC GAC CAC GTT CTT TGT TTT CCA CTA CAA CAT TCC ATC CCC FAM-TCA CCA AAA CCG CAG CAA GCA -TAMRA	122
Rockrose	*1-Deoxy-D-xylulose 5-phosphate reductoisomerase* (*DXR*)AY297794 (*Cistus incanus*)	Forward primer Reverse primer Probe	Cis_DXR-f Cis_DXR-r Cis_DXR-probe	AAT GTT CGA TGT CCT CCT GTT CTT GCT CAC TGT TTC CAC CCA CAA FAM-CCA ATG GAT CTC TCA ATG GCG CTG TC -TAMRA	94
Rosemary	*Alcohol dehydrogenase* 1 (*adh*1)	Forward primer Reverse primer Probe	Ros_CSL-f Ros_CSL-r Ros_CSL-probe	GCG TAT GCG GCC AAC AG ACT GCC CTT GAA GAA GAA ATG G FAM-TGG CAG ATT CAT CAT TCT CCT TCA TTA GGA CC -TAMRA	74
Sunflower	*Profilin*J15210 (*Helianthus annuus*)	Forward primer Reverse primer Probe	Heli-all-nes f2 Heli-all r1 Heli-all-nes probe	CGT CAA TAC TTG TTA ATA TTA TTA AGA ATT A ATA GCT TGG CCC GTT TTC TT FAM-ATG CAT ATT CCT CCA GCT CCC TG -TAMRA	106
Sweet chestnut	*ypr10 gene for allergen Cas s* 1AJ417550 (*Castanea sativa*)	Forward primer Reverse primer Probe	Cas-all-nes f Cas-all-nes r Cas-all-nes-probe	GAG TGC TGA AAT CAT TGA AGG AAA T AAT GAT GTG TTG GAG ATG AGA ATA GAA G FAM-AGG CCC CGG AAC CAT CAA GAA GAT C -TAMRA	101
	Phenylalanine ammonia-lyase (*PAL*)	Forward primer Reverse primer Probe	Cas_PAL-f Cas_PAL-r Cas_PAL-probe	CCA AAG AAG TAG AGG GTG CAA GA GAA TTC TCT CAC CAG TTA GTA AAC TTG TT FAM-AAA GCA GCA ATT CCT AAC CCA ATT AAG GAG T -TAMRA	144
Plant	*tRNA-Leu* (*trnL*) Taberlet et al. (1991)	Forward primer Reverse primer Probe	Plant nes-2-f Plant nes-2-r Plant nes-2-probe	ATT GAG CCT TGG TAT GGA AAC CT GGA TTT GGC TCA GGA TTG CC FAM-TTA ATT CCA GGG TTT CTC TGA ATT TGA AAG TT -TAMRA	Approx. 90
	*Actin*AF111812 (*Brassica napus*), AF282624 (*Helianthus annuus*)	Forward primer Reverse primer Probe	Act-f Act-r Act-probe	CAA GCA GCA TGA AGA TCA AGG T CAC ATC TGT TGG AAA GTG CTG AG (FAM)-CCT CCA ATC CAG ACA CTG TAC TTY CTC TC -(TAMRA)	Approx. 103

(*continued on next page*)

Table 2 (*continued*)

Species	Gene and accession number if available	Oligonucleotide	Name	Sequence 5′–3′	Amplicon length (bp)
Sequencing primers	*trnL*	Forward primer	Plant 1-f	CGA AAT CGG TAG ACG CTA CG	
		Reverse primer	Plant 1-r	GGG GAT AGA GGG ACT TGA AC	
	adh1	Forward primer	Adh1-f	AGT GTT GGA GAG GGT GTG ACT GA	
		Reverse primer	Adh1-r2	CCA ACA TGC ATG ACR GTG TAC TC	
	hmg	Forward primer	HMG2-border-f-w	GGG CAG TGY TGT GAG ATG C	
		Reverse primer	HMG2-border-r-w	ATR CCG ATG ACA TCC ATG TC	
	Lipase 1	Forward primer	Bras_lip-f	CTG TTA CGC CTT TCC CAA GAA C	
		Reverse primer	Bras_lip-r	CCA CTA CAA CAT TCC ATC CCC	
	Profilin	Forward primer	Heli-all-nes f	GCG GGT GCA AAA TAT ATG GTA C	
		Reverse primer	Heli-all r1	ATA GCT TGG CCC GTT TTC TT	

R = A/G and Y = C/T (IUB code).

Table 3
Optimum concentration of primers, probes, and magnesium chloride ($MgCl_2$) for TaqMan™ PCR determined by titration

System	Forward primer (nM)	Reverse primer (nM)	Probe (nM)	$MgCl_2$ (mM)
Aca_adh1	300	300	200	8
Act	900	900	200	8
Bras_lip	900	50	200	6
Cas-all-nes	300	300	200	8
Cas_PAL	300	900	200	7
Cis_DXR	300	900	200	8
Cit_adh1	300	300	200	5
Cyt_act	500	500	200	5.5
Eri_adh1	300	300	200	8
Euc_LFY	300	900	200	5
Heli-all-nes	900	300	200	5
Lav_adh1	900	900	200	6
Lav_HMG2	300	300	200	6
Olea_ole10	300	900	200	4
Plant nes-2	300	300	200	7
Querc_PAL	300	300	200	3
Querc_PAL2	900	300	200	6
Ros_CSL	900	900	200	5.5
Til_nr	300	900	200	7
Tri_act	900	300	200	4

SDS Workshop). Amplification was performed on the Applied Biosystems 7900 HT Real-Time PCR FAST System, with the following thermal cycling protocol: 95 °C for 10 min followed by 45 cycles of 95 °C for 15 s and 60 °C for 1 min.

3. Results and discussion

The aim of this study was to develop a set of assays which, when used together on honey samples from Corsica, would provide a profile of the plant varieties visited by foraging bees, during honey production. These profiles would be indicative of the habitat on Corsica and could then be used as a reference against which honey samples could be authenticated.

The set of assays was composed of two elements: (a) a generic plant assay as proof of the presence of plants and (b) species specific assays for the detection of plants commonly found on Corsica and the EU mainland.

3.1. Development of plant specific TaqMan™ PCR systems

To develop a generic plant PCR system, which would detect a diverse range of plant pollen varieties in honey, several candidate genes were examined. It was found that the *rubisco activase*, *hydroxymethylglutaryl coenzyme A reductase*, *profilin* and *alcohol dehydrogenase* genes did not show sufficient interspecies sequence similarity to be suitable for the design of a generic plant PCR system (data not shown). However, in contrast, the *tRNA-Leu* (trnL) gene was found to be sufficiently similar between plant species and was, therefore used for the design of a generic plant PCR system (Table 2; plant nes-2), following in-house sequence analysis for a range of plant species, using primers previously shown to amplify a diverse range of plant species (Taberlet et al., 1991) (Table 2; plant 1-f, plant 1-r). This multicopy gene was particularly suitable for this application since there are very small amounts of pollen, and therefore DNA in honey and the use of a gene with more than one copy per cell increases the sensitivity of detection for TaqMan™ based assays. Fig. 1a shows the amplification plots of the generic primer and probe set using template DNA isolated from a variety of plant species.

Real-time PCR systems based on single copy gene sequences are central to the development of quantitative methods. To examine the possibility of applying a quantitative aspect to the characterisation of the plant content of honey, a PCR system (Table 2; act) based on a 103 bp region of the single copy gene *actin* was designed. When a range of plant species were tested using 5 ng DNA in a TaqMan™ PCR (Fig. 1b) the C_T values produced varied widely indicating that the assay could not be easily used to provide accurate quantitation. Factors contributing to the observed variation may include the presence of inhibitors, differing genome sizes, primer and probe sequence mismatches, and the degree of ploidy in differing species. To further complicate matters, it should be noted that the pollen profile of honeys can be season dependent, and that pollen from some plants can be strongly over or under-represented in various honeys. For example, levels of lavender pollen in honey derived from lavender plant nectar are typically very low. These factors contribute to make the characterisation of honey by the determination of the exact amount of a plant species in relation to the total plant content using real-time PCR problematical. Hence the approach in this study to characterise the origin of honeys based upon the determination of qualitative plant species markers specific for geographic regions.

3.2. Species specific detection

The design of species specific primer and probe sets used a variety of strategies, dependant upon whether sequence information was available on the NCBI database or if *de novo* sequence analysis was required. Sequence information was available for clover, eucalyptus, linden, oak, olive, rape, rockrose, sunflower and sweet chestnut. The design of most of these assays was therefore, relatively straight forward (gene, accession number and primer and probe sequences given in Table 2). There was little or no DNA sequence information available for the design of acacia, broom, citrus, heather, lavender or rosemary specific primer and probe sets. *De novo* sequence was generated for each of these species which was then used to design species specific primer and probe sets. The *alcohol dehydrogenase 1* (*adh*1) gene was amplified using consensus primers (Table 2; adh1-f, adh1-r2) designed using DNA se-

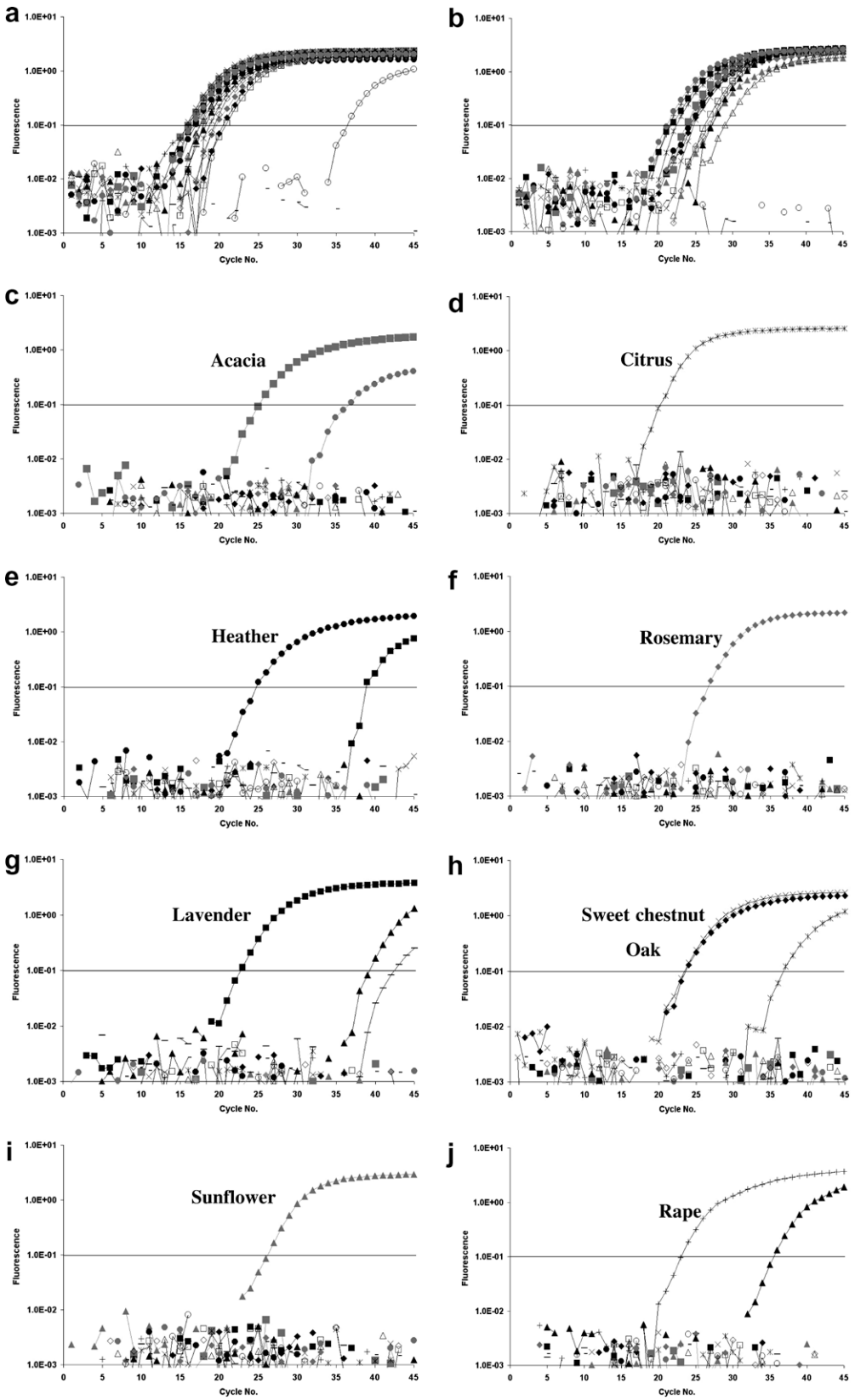

Fig. 1. *Specificity test*: fluorescence curves for samples of acacia (—■—), citrus (—✕—), heather (—●—), rosemary (—◆—), lavender (—■—), sweet chestnut (—◆—), sunflower (—▲—), rape (—┼—), linden (—⊟—), eucalyptus (—▬—), clover (—▲—), broom (—●—), rockrose (—△—), oak (—✕—), and olive (—◇—) including cattle (—⊖—) and water (—▬—) using the (a) plant nes-2, (b) act, (c) Aca_adh1, (d) Cit_adh1, (e) Eri_adh1, (f) Ros_CSL, (g) Lav_HMG2, (h) Cas-all-nes, (i) Heli-all-nes, (j) Bras_lip, (k) Til_nr, (l) Euc_LFY, (m) Tri_act, (n) Cyt_act, (o) Cis_DXR, (p) Querc_PAL and (q) olea_ole10 primer and probe system.

quence information from vine, sorghum, rice and barley. After DNA sequence analysis, specific primers and probes were successfully designed for the detection of acacia, citrus, heather and rosemary (Table 2, Fig. 1c–f, respectively). However, the primers and probe

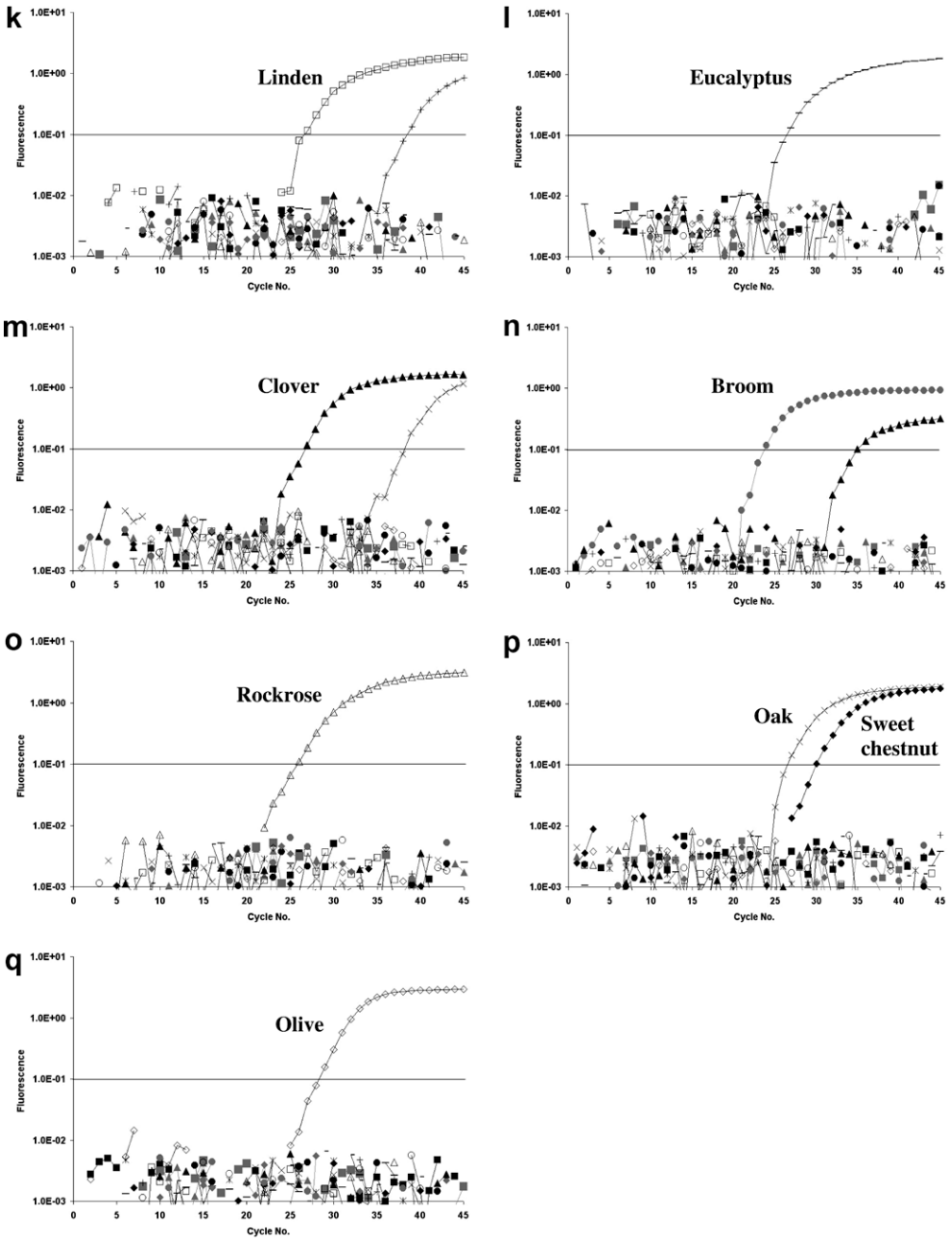

Fig. 1 *(continued)*

for the detection of *Lavandula stoechas* also amplified *Lavandula lanata* and *Lavandula latifolia*, although with significantly lower sensitivity (data not shown). An alternative PCR system was therefore developed, which would detect all lavender species with the same sensitivity. It was based on the *hydroxymethylglutaryl coenzyme A reductase* (*hmg*) gene for which sequence information for cotton, capsicum, tomato, potato and tobacco were available. After amplification and sequence analysis using consensus primers (Table 2; HMG2-border-f-w, HMG2-border-r-w) a specific primer and probe set was successfully designed which detected all lavender species with similar sensitivity (Table 2 and Fig. 1g). The detection system for sunflower was based on the *profilin* gene, however the NCBI database entry was for the mRNA and the amplicon size, for primers which had been designed to amplify a region 105 bp long, was found to be approximately 200 bp by gel electrophoresis. Sequence analysis of the amplicon (Table 2 for primers used: Heli-all-nes-f, Heli-all r1) revealed an intron/exon structure and therefore a new primer was designed which would amplify a DNA region of 106 bp. Sequence information of primers and probe is given in Table 2 and Fig. 1h shows the amplification plot for a selection of samples. The detection system for rape is based on the *lipase 1* gene. The NCBI database entry was also for the mRNA and after sequence analysis (see Table 2 for primers used: Bras_lip-f, Bras_lip-r) primers were designed to amplify a DNA region 122 bp long.

3.3. Specificity of species specific TaqMan™ PCR systems

The specificity of these primer and probe systems in TaqMan™ PCR was assessed using template DNA isolated from 25 plant species and two animal species as listed in Section 2. There was no significant cross amplification detected for the primer and probe

systems specific for acacia, broom, citrus, clover, heather, eucalyptus, lavender, linden, olive, rape, rockrose, rosemary and sunflower. Exemplary amplification curves are shown in Fig. 1. However, it was found that the sweet chestnut and oak primer and probe systems (Cas-all-nes and Querc_PAL) each cross amplified the other's DNA. Sweet chestnut (*C. sativa*) and oak (*Quercus* sp.) are closely related: in the same subfamily *Quercoideae* and on analysis of the DNA sequence it was found that there was a high degree of sequence similarity between these plant species. Therefore to distinguish sweet chestnut from oak, two alternative forward primers were designed which recognised two base differences within the PAL fragment (Cas_PAL-f and Querc_PAL2-f, Table 2). These alterations resulted in a delta C_T value of approximately 13 between oak and sweet chestnut and about six between sweet chestnut and oak using the new alternative oak and sweet chestnut primers, respectively. These differentials equate to a reduced sensitivity of approximately 100- and 10,000-fold on the alternate template DNA, for the new oak and sweet chestnut assays, respectively, and indicate a non-relevant quantity of a plant species in honey since the total DNA yield from honey is very low as described in the next section. Fig. 2 shows the fluorescence curves for a selection of samples.

3.4. Sensitivity and efficiency of the TaqMan™ PCR systems

The limit of detection (LOD), efficiency and linearity of the systems were assessed to determine the suitability and capacity of each. Tenfold dilution series of template DNA were tested in 10 replicates for each system (data not shown). It was found that for all systems the LOD was at least 25 pg, where the probability of obtaining a C_T value lower than 45 was 95%. On average a C_T value of 37 was measured. The efficiency of the systems was calculated to be between 88% and 117 % according to (Vaerman, Saussoy, & Ingargiola, 2004)

$$E = 10^{-\frac{1}{s}} - 1$$

where *E is the efficiency and s is the* slope of the regression line for the log DNA concentration plotted against C_T value. This range of efficiencies was acceptable since although logically a reaction efficiency cannot be greater than 100%, the measurement uncertainty could result in a calculated efficiency greater than 100%.

The dynamic range of the systems, where there was a linear relationship between the template concentration and the C_T values returned, were shown to be in the order of at least 3 $\log_{10}$ dilutions, confirmed by the strong linear relationship between C_T values and the $\log_{10}$ of the starting quantity up to 2.5×10^5 pg ($r^2 > 0.99$) (data not shown). The repeatability for each system was determined by measuring duplicates of three dilutions of template DNA, on three different days. The results showed a relative standard deviation of up to 33 % (data not shown).

3.5. Application of the real-time PCR systems to honey

The real-time PCR systems were used for the detection of plant species in honey. DNA was extracted and purified from honey samples from four target countries: Corsica, Spain (Galicia), Germany and England. The countries were chosen to have different flora thereby providing unique plant profiles for the honeys from each country.

Initially the DNA extracts of all the honey samples were analysed using the generic plant system and it was found that plant DNA could be unambiguously identified in all honey samples investigated. However, plant DNA was only present in low amounts, and thus at or close to the LOD of the PCR systems. In detail, using the general actin-system for plants which detects a single copy sequence an average C_T value of 34 was measured, whereas the general plant system that detects a multicopy sequence produced an average C_T value of 29. Using the plant species specific primer and probe systems an average C_T value of 36 was measured.

Analysing the DNA extracts of all the honey samples using the species specific real-time PCR systems (Table 4) it was found that there were geographical differences in the range of plant species found in honeys from Corsica, Galicia, Germany and England. In particular it was found that:

- rape was not detected in Corsican and Galician honeys, but in almost all German and English honeys analysed to date;
- sweet chestnut was detected in almost all honeys from Corsica and Galicia, but only in a few German and English honeys;
- rockrose and olive were only detected in some Corsican honeys.

These results indicated that a combination of plant species specific real-time PCR systems could be used to determine the geographical origin of honey samples from Corsica, when compared to honey samples from Galicia, Germany and England. The systems which were most informative were sweet chestnut, rockrose, rape and olive. The chi-square test was used to analyse each of the 15 detection systems to determine whether frequencies of positive results differed with geographical origin. The Fisher's exact test was used where sample sizes were too small for the chi-squared test to be accurate (expected frequency less than 5). The results are shown in Table 4 where the significance is given in terms of the *p*-value: the bigger the difference the smaller the *p*-value and where a *p*-value less than 0.05 refers to a significant difference. The results listed in Table 4 confirm that there is no statistical

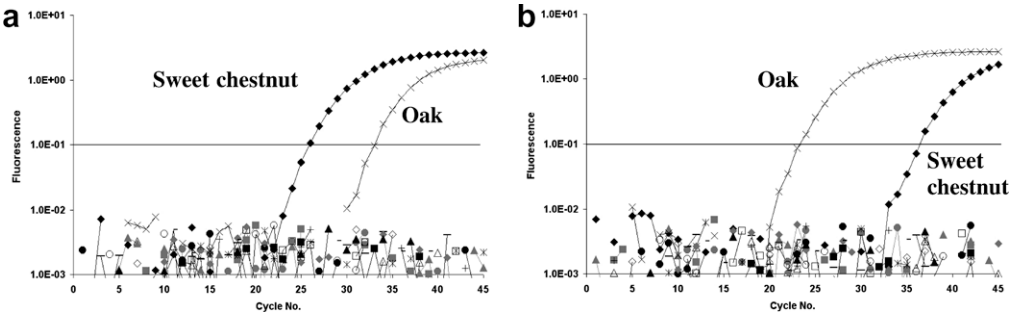

Fig. 2. Fluorescence curves for samples of acacia (—■—), citrus (—✕—), heather (—●—), rosemary (—◆—), lavender (—■—), sweet chestnut (—◆—), sunflower (—▲—), rape (—|—), linden (—□—), eucalyptus (—▬—), clover (—▲—), broom (—●—), rockrose (—△—), oak (—✕—), and olive (—◇—) including cattle (—○—) and water (—▬—) using the (a) Cas_PAL and (b) Querc_PAL2 primer and probe system.

Table 4
Statistical description for frequencies of positive results (%) using chi-square test or Fisher's exact test

Real-time PCR system specific for	Number of samples	Geographical origin of honey, percentage of positive results		*p*-Value
		Germany, UK, Galicia	Corsica	
Acacia	44	0	8	Not significant
Broom	58	5	0	Not significant
Citrus	37	0	30	0.015
Clover	47	29	0	0.019
Heather	58	17	44	0.043
Eucalyptus	58	2	0	Not significant
Lavender	53	0	13	Not significant
Linden	37	22	0	Not significant
Oak	58	7	25	Not significant
Olive	58	0	25	0.004
Rape	58	52	0	<0.001
Rockrose	58	0	63	<0.001
Rosemary	37	0	20	Not significant
Sunflower	53	5	0	Not significant
Sweet chestnut	58	57	60	Not significant

difference for Corsican honey versus German, English and Galician honeys for the frequency of the presence of DNA from acacia, broom, eucalyptus, lavender, linden, oak, rosemary, sunflower and sweet chestnut. In contrast Corsican honey samples contained DNA from citrus, heather, olive and rockrose more frequently than German, English and Galician honeys, although DNA from clover and rape could not been detected in Corsican honey. The lowest *p*-values were calculated for the olive, rape and rockrose systems. Sweet chestnut is an additional significant marker for Corsican and Galician honey compared to honey samples from Germany and England (data not shown). It was concluded therefore, that, as a proof of principle, four systems could be used to determine the geographical origin of Corsican honey. It should be noted that only 12–15 different honeys from only four countries were analysed and statistically evaluated. For more precise statements further samples, also from additional countries, should be analysed. It is very likely that honeys produced in other regions, with similar climate, would show a similar flora and therefore pollen profile. The identification of a particular plant that is only found on Corsica and the establishment of an appropriate real-time PCR detection system would have been the most promising strategy to confirm geographical origin, however, such a marker could not be identified for Corsica. Another possibility, also based on DNA methodology, would be the development of a system specific for the Corsican honey bee. Corsican honey is produced by the bee species *Apis mellifera corsica* and no other bee species have been imported onto Corsica since 1982, when a law prohibiting the importation of honeybees other than *A. mellifera corsica* came into force. Indeed, during this project, it was shown that additional DNA, other than that derived from plants, was detected in samples of honey (data not shown), where DNA from bees, aphids and bacteria were all found to be present. The identification of the Corsican honey via the identification of the species of honeybee, using genotyping, would be dependant upon the genetic drift of the Corsican honey bee since 1982, initial work on the identification of honeybee species looked promising although outside the main scope of this project.

4. Conclusions

Fifteen species specific TaqMan™ assays were developed for the detection of acacia, broom, citrus, clover, heather, eucalyptus, lavender, linden, oak, olive, rape, rockrose, rosemary, sunflower and sweet chestnut which showed no significant cross amplification when assessed on a further 10 plant species and two animal species. For the parallel detection of plants and to identify false-negative results (external amplification controls) a TaqMan™ system was developed based on a *tRNA-Leu* (trnL) sequence of approximately 90 bp. This multicopy chloroplast sequence was suitable for the detection of very low levels of plant DNA and was, therefore, applicable for the detection of plant DNA in honey. The development of a single copy *actin* sequence based system was less sensitive but may be of use for further applications, e.g. in the field of GMO or allergen analysis.

In this study, it was shown that a combination of species specific systems, selected from the pool of real-time PCR systems developed during this project, was able to produce a plant species profile unique to Corsican honey when compared to honey from Galicia, Germany and England, although the number of samples analysed was comparatively small and the locations relatively geographically remote from each other. With the detection of a particular plant in the sample that is only found in a specific location using the DNA based approach it should be possible to specifically confirm a honey's geographical origin.

Acknowledgements

The authors are grateful for financial support concerning scientific activities within the Sixth Framework Programme of the European Union, project TRACE – "Tracing Food Commodities in Europe" (Project No. FOOD-CT-2005-006942). The publication reflects the authors' views; the European Commission is not liable for any use of the information contained therein. The authors would like to thank Bettina Linke, Bundesinstitut für Risikobewertung, Germany and Theodore Allnutt, Central Science Laboratory, UK for their work in the laboratory.

References

Benson, D. A., Karsch-Mizrachi, I., Lipman, D. J., Ostell, J., & Wheeler, D. L. (2005). GenBank. *Nucleic Acids Research, 33*, D34–D38.

Holland, P. M., Abramson, R. D., Watson, R., & Gelfand, D. H. (1991). Detection of specific polymerase chain reaction product by utilization the 5′–3′ exonuclease activity of *Thermus aquaticus*. *Proceedings of the National Academy of Science of the United States of America, 88*, 7276–7280.

Louveaux, J., Maurizio, A., & Vorwohl, G. (1978). Methods of melissopalynology. *Bee World, 59*, 139–157.

Tinker, N. A., Fortin, M. G., & Mather, D. E. (1993). Random amplified polymorphic DNA and pedigree relationships in spring barley. *Theoretical and Applied Genetics, 85*, 976–984.

Taberlet, P., Gielly, L., Pautou, G., & Bouvet, J. (1991). Universal primers for amplification of three non-coding regions of chloroplast DNA. *Plant Molecular Biology, 17*, 1105–1109.

Vaerman, J. L., Saussoy, P., & Ingargiola, I. (2004). Evaluation of real-time PCR data. *Journal of Biological Regulators and Homeostatic Agents*, 212–214.

of honey including improved oral health (Molan, 2001), antimicrobial properties (Ceyhan & Ugur, 2001) and wound healing effects (Mphande, Killowe, Phalira, Jones, & Harrison, 2007). Conversely, the ingestion of grayanotoxins in 'mad honey' (Koca & Koca, 2007) can lead to mortality.

A previous study utilised NMR spectroscopy for the characterisation of Corsican honey (Donarski, Jones, & Charlton, 2008). Multivariate statistical methods were used to identify spectral regions that are characteristic of the geographical origin of Corsican honey. A wide range of European honeys were used to establish the validity of the multivariate models. The approach taken resulted in the identification of a small number of peaks in the NMR spectrum, the intensities of which were used to identify Corsican honey with an overall accuracy of 96.2%. The compounds giving rise to these peaks were only partially characterised and their source was unknown. In this manuscript we investigate the peaks identified in the NMR spectrum that are characteristic of Corsican honey and correlate these with specific honey types. Data generated from the NMR spectroscopic analysis of a second harvest of Corsican honey is included here for the first time and demonstrates the validity of the biomarkers identified.

2. Materials and methods

2.1. Materials

Honey collected during Year 1: Honey (182 samples) was collected from five countries: Austria (18), France (129), Germany (18), Ireland (2) and Italy (15).

Honey collected during Year 2: Honey (192 samples) was collected from four countries: Austria (23), France (136), Germany (18) and Italy (15).

Commercial chestnut honey: Two chestnut honeys were purchased from commercial outlets. The honeys were from the French region of Périgord and the Italian region of Piemonte.

All non-commercial honeys were received in glass jars diluted using distilled water to 70°BRIX, containing 50 g of diluted honey. A Corsican honey from the region of Châtaigneraie was used to confirm the identity of kynurenic acid. Typical °BRIX values of undiluted honey range between 75 and 85, although the original °BRIX values of the honeys analysed in this project were not provided. Therefore, where calculations were performed to determine the concentrations of biomarkers, the concentration of the biomarker in a 70°BRIX solution was calculated. It is noted that these concentrations will under represent the biomarker concentration by 6.7–17.6%. Samples were stored at room temperature in the dark. All samples were analysed within 4 months of sample receipt.

In total, 220 Corsican honeys were analysed and the distribution of the different types of Corsican honey is presented in Table 1.

Table 1
Specific types and sample numbers of Corsican honey analysed.

Corsican honey type	Number of samples analysed
Arbousier	3
Châtaigneraie	46
Autumn Maquis	31
Honeydew Maquis	34
Non-specific Maquis	6
Spring Maquis	21
Summer Maquis	11
Non-specific spring	21
Non-specific autumn	2
Non-specific	37
Spring Clémentinier	8

2.2. Chemicals

All chemicals used were of a purity of ⩾97%. Deuterium oxide (^2H_2O) was supplied by Goss Scientific Instruments Ltd. (UK). 3-Trimethylsilyl[2,2,3,3-D_4] propionic acid (TSP) and α-isophorone were supplied by Avocado Research Chemicals Ltd. (UK). Sodium azide, 2,5-dihydroxyphenylacetic acid, 4-oxoisopherone and kynurenic acid were supplied by Sigma–Aldrich Co. (UK). Di-potassium hydrogen phosphate and di-hydrogen potassium phosphate were supplied by BDH Chemicals Ltd., UK. Purine and hexakis (1H, 1H, 3H-tetrafluoropropoxy)phosphazine were supplied by Agilent Technologies (USA). Ultrapure water was obtained from an Elga Option 2 water purifier.

2.3. Sample preparation

A single 50 g jar of honey was homogenised using a Turrax mixer (11000 RPM) over five 20-s periods separated by 5 min to limit sample heating. The sample was placed onto a roller mixer at 35 RPM for 16 h until the honey was homogeneous, monitored by the distribution of a ultra-violet absorbing dye (data not shown).

2.3.1. Honey NMR spectroscopic analysis

Honey was diluted with ultrapure water to 15 ± 0.5°BRIX. All diluted samples were centrifuged to remove any remaining suspended material prior to filtration through a 0.2 μm PTFE syringe filter. The samples were prepared for NMR spectroscopic analysis by adding 480 μL of the filtered honey solution to 60 μL of sodium azide solution (10 mM dissolved in ^2H_2O, added to prevent microbial growth) and 60 μL of phosphate buffer solution (250 mM, pH 7.2 containing 10 mM TSP dissolved in ^2H_2O). The samples were thoroughly mixed using a vortex mixer prior to ^1H NMR spectroscopic analysis.

2.3.2. LC-TOF-MS analysis

A Corsican Châtaigneraie honey was diluted to 1.1 °BRIX using deionised water. The sample was centrifuged and filtered through a 0.2 μm PTFE syringe filter prior to analysis.

2.3.3. Kynurenic acid for NMR spectroscopic analysis

Kynurenic acid was prepared as a saturated solution at approximately 6 mM in ^2H_2O containing 1 mM TSP.

2.3.4. Kynurenic acid for LC-TOF-MS analysis

Kynurenic acid was prepared at a concentration of 10 μg mL^{-1} in deionised water.

2.4. NMR spectral acquisition parameters

All experiments were carried out using a Bruker Avance 500 MHz NMR spectrometer equipped with a TCI cryoprobe.

^1H NMR spectra, from all honeys, were acquired at a central frequency of 500.1323546 MHz using on-resonance pre-saturation to suppress the intensity of the water signal. A 60° observation pulse length of 5.1 μs and a delay between transients of 14 s were used. Complex data points (32768) were acquired with a spectral width of 14 ppm, giving an acquisition time of 4.6794 s. A recycle time of 18.7 s was determined experimentally to produce quantitative data with optimised sensitivity. Eight unrecorded (dummy) transients and 256 acquisition transients were used giving a total experiment time of approximately 1 h 20 min. One-dimensional (1D) ^1H NMR spectroscopic data were processed using FELIX software (Accelrys, San Diego, CA). A sine bell-shaped window function phase shifted by 90° was applied over all data points before Fourier transformation, phase and baseline correction. The chemi-

cal shift of all data was referenced to the TSP resonance at 0 ppm. The area of this resonance was set to unity for all spectra acquired.

The limit of detection of this experimental setup was determined from the signal to noise ratio of the internal standard. Representative ^{1}H NMR data from a single honey sample were used to determine a limit of detection for a resolved singlet resonance to be 6.3 μM. This is based on a minimum signal to noise ratio of 3.

^{1}H–^{1}H TOCSY NMR spectra were acquired from representative samples containing the highest concentration of each biomarker. ^{1}H–^{1}H TOCSY spectra were acquired using the standard spectrometer library pulse sequence (Bax & Davis, 1985) with 56 transients, 384 increments, a spectral width of 13.33 ppm in both dimensions and a spin-lock mixing time of 100 ms. In the F2 dimension, 4096 datapoints were collected and the F1 dimension was zero filled to give 2048 datapoints. 90° pulse lengths were calibrated for individual experiments and on-resonance pre-saturation was used to suppress the intensity of the water signal. ^{1}H–^{1}H TOCSY NMR spectra were processed using Topspin version 1.3 software (Bruker BioSpin, Germany).

2.5. Liquid chromatography and mass spectrometry parameters

Samples were analysed by LC-TOF-MS using an Agilent LC/MSD TOF (Agilent, Santa Clara, CA, USA) consisting of a 1200 Series LC and a G1620 time-of-flight mass spectrometer. Separation was facilitated using an Agilent ZORBAX Eclipse XDB-C18 100 × 2.1 mm, 3.5 μm column. The mobile phase consisted of 0.1% aqueous acetic acid (channel A) and acetonitrile (channel B). At time t minutes the percentage A was as follows t = 0 (65%), t = 5 (50%), t = 10 (50%), t = 20 (0%) and t = 25 (0%). The flow rate was 0.4 mL min^{-1} with an injection volume of 5 μL.

TOF-MS analysis was carried out in positive mode electrospray with nebuliser pressure 60 psi, capillary 4000 V, gas temperature 350 °C, drying gas flow at 12 L min^{-1}, skimmer 60 V, fragmentor 150 V and octopole RF voltage 250 V. The mass range measured was 100–1100 m/z. An additional isocratic pump was used for delivery of the reference mass solution and reference mass correction was carried out using ions at 121.05873 (purine, CAS No. 120-73-0) and 992.009798 (hexakis(1H, 1H, 3H-tetrafluoropropoxy)phosphazine, CAS No. 58943-98-9).

2.6. Statistical analyses

Statistical analysis was completed using a custom written graphical user interface (GUI) for Matlab (The Mathworks, Natick, MA; Version 7.4.0.287 [R2007a]) known as Metabolab. Statistical analyses were completed using the full NMR spectrum excluding data from the residual water resonance (4.70–4.90 ppm) and from the methyl ^{1}H atoms of ethanol (1.16–1.21 ppm).

To generate robust statistical models the data was split into a training set and a test set. All models were generated using only the training set. The data were split into training and test sets using random sequences generated using the online resource www.random.org. Each sample was randomly assigned a number in the sequence 1–374. After the samples had been assigned a number, 100 unique random numbers were generated between 1 and 374 and these samples were chosen as the test set (corresponding to 26.7% of the data). This gave a training set of 274 samples (157 Corsican samples, 117 non-Corsican samples) and an unseen test set of 100 samples (63 Corsican samples and 37 non-Corsican samples). The data were sorted by increasing value of their random number to ensure no bias was introduced into the data.

Feature selection from the NMR data was performed using two-stage GP (Davis et al., 2006) as described in Donarski et al. (2008). Briefly, each round of the GP was completed using an island population of 300, five island populations, 10 generations between island migration, an island migration rate of 10%, a maximum GP tree size of eight, and a tree mutation rate of 50%. At each generation, trees were ordered by the value of their fitness function, which in this case was the classification rate. The top 10% of GP trees were kept, and the bottom 10% were removed. The stopping conditions enforced were either classification of 100% of the data or evolution for 200 generations. The first stage of GP used all variables. The variables used in the second stage were constrained to those that were used in the generation of the final GP trees of the first stage, with a tolerance on variable position of 10 U. Venetian blind cross-validation was used omitting 10% of the data from each calculation for subsequent validation.

Classification rates are presented according to sensitivity (Corsican samples correctly classified as Corsican samples), selectivity (non-Corsican samples correctly classified as non-Corsican samples) and overall correct classification (all samples correctly classified by the model).

3. Results and discussion

It was previously reported that biomarkers of geographical origin were detected in Corsican honey analysed by ^{1}H NMR spectroscopy (Donarski et al., 2008). The results were obtained from the statistical analysis of honey samples collected during Year 1 and demonstrated the utility of GP in the determination of biomarkers within complex NMR spectroscopic data. Results obtained from the statistical analysis of honey samples collected over both years are presented herein.

3.1. Statistical results

The final classification results obtained during model generation by two-stage GP were 94.9%, 94.0% and 94.5% for the sensitivity, selectivity and overall rate, respectively. To visualise the variables that were utilised in the generation of the GP trees, a histogram showing the frequency of occurrence of the variables used in the 10 GP trees, created during cross-validation, is shown in Fig. 1A. The 10 GP trees generated were used to classify the test data and the tree that gave the highest overall classification rate was chosen and is shown in Fig. 1B. The classification results obtained from the model validation of the GP tree shown in Fig. 1B were 92.1%, 91.9% and 92.0% for the sensitivity, selectivity and overall rate, respectively.

The variables most frequently used by the two-stage GP model were converted to their corresponding 1D ^{1}H NMR chemical shifts and these resonances were examined in the acquired NMR spectra. The data showed that biomarkers were present within the Corsican honey and that these biomarkers corresponded to specific types of Corsican honey. Evaluation of the Corsican honey data determined the presence of four distinct biomarkers (referred to in this manuscript at A, B, C and D). The following section describes each of the four identified biomarkers.

3.2. Biomarker A

Biomarker A, when analysed by a combination of 1D ^{1}H and 2D ^{1}H–^{1}H TOCSY NMR spectroscopy, was shown to contain five non-exchangeable, non-equivalent ^{1}H atoms that gave rise to four resonance peaks at chemical shifts of 8.221 (1H, d, 8.3 Hz), 7.868 (2H, m and s overlapping), 7.571 (1H, m) and 6.952 (1H, s) ppm (symbols used d, doublet; m, multiplet; s, singlet). Structural elucidation using chemical shift tables and J-couplings determined that the biomarker was a fused aromatic ring system and that kynurenic acid would produce NMR resonances that matched those of the biomarker. This was confirmed by spiking kynurenic acid into a

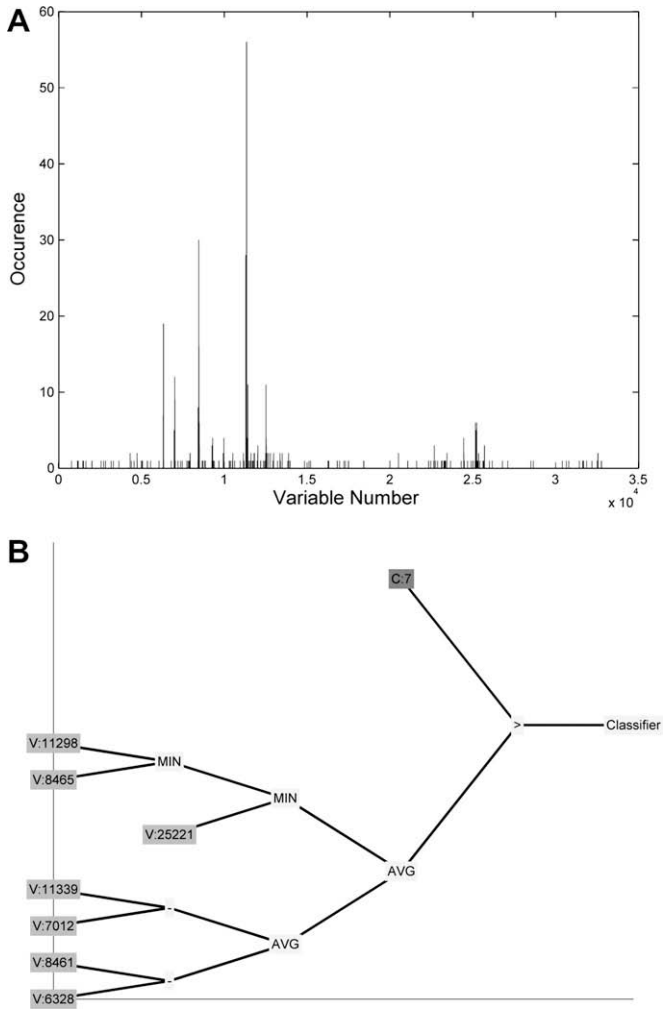

Fig. 1. (A) Variable use frequency in the final Corsican honey classification models generated by two-stage GP and (B) most successful GP tree. V, variable; C, constant; MIN, minimum; –, subtraction and AVG, average.

honey sample that contained biomarker A (Fig. 2A and B). Further confirmation of the presence of kynurenic acid was obtained using LC-TOF-MS (Fig. 2C–F). LC-TOF-MS analysis was performed using a standard solution of kynurenic acid, a Corsican honey containing biomarker A and a deionised water blank. The mass spectrum shown in Fig. 2F contains a peak not present in the kynurenic acid standard, with an accurate mass of 203.0526 Da. It was determined that this peak was from the protonated form of glucose that co-elutes with kynurenic acid using the LC conditions specified.

The relative intensity of the ^{1}H NMR spectroscopic resonance of kynurenic acid at 7.571 ppm in all of the Corsican honey analysed, is shown in Fig. 3A. Kynurenic acid was predominant in honey collected from the Châtaigneraie region of Corsica. The translation of Châtaigneraie from French to English is chestnut grove and it was hypothesised that kynurenic acid was a marker of sweet chestnut honey. It was noted that kynurenic acid was present in three non-Corsican honeys, collected from Italy, therefore this marker was not unique to Corsican honey. Two commercial non-Corsican chestnut honeys were analysed and both were shown to contain kynurenic acid, it was therefore concluded that kynurenic acid is a putative biomarker of chestnut honey.

The maximum concentration of kynurenic acid, observed by NMR spectroscopy, in the non-commercial samples was present in a Corsican honey from the region of Châtaigneraie. The concentration of kynurenic acid in this honey was determined by comparison of the peak intensities of kynurenic acid with the internal standard, TSP. The 15°BRIX solution of Châtaigneraie honey contained 0.91 mM kynurenic acid. The honeys were not supplied with their original °BRIX values so it was not possible to determine the concentration of kynurenic acid in undiluted honey. The honey was received at 70°BRIX therefore it was concluded that the concentration of kynurenic acid in the undiluted honey was $\geqslant$4.22 mM.

Kynurenic acid is a metabolite of L-tryptophan produced *via* the kynurenine pathway (Ruddick et al., 2006). It has been shown to occur naturally in human saliva (Kuc et al., 2006), urine (Furlanetto, Tognini, Carpenedo, La Porta, & Pinzauti, 1998) and cerebrospinal fluid (Stone, 1993). Kynurenic acid was previously identified by Beretta et al. in Italian honey from arboreal origin (Beretta, Caneva, & Facino, 2007) and in further work (Beretta, Caneva, Regazzoni, Bakhtyari, & Facino, 2008) they hypothesised that kynurenic acid is a biomarker of chestnut honey. Kynurenic acid was also identified in Linden, Buckwheat and multifloral honey (Kuc, Zgrajka, Parada-Turska, Urbanik-Sypniewska, & Turski, 2008) although the levels reported by Kuc et al. were approximately 150 times lower than those reported in this manuscript and that of Beretta et al. This could be due to a minor contribution from chestnut tree pollen/nectar to the composition of the honeys studied by Kuc et al. Potential neuroprotective properties of kynurenic acid have been hypothesised (Stone, 1993). Based on this hypothesis, the disruption of the kynurenine pathway is implicated in several disorders including schizophrenia (Nilsson et al., 2005), HIV related dementia (Guillemin, Kerr, & Brew, 2005) and Parkinson's disease (Németh, Toldi, & Vécsei, 2006). This has led to the development of novel drugs either based on kynurenic acid or designed to interact with the kynurenine pathway (Stone, 2000). The presence of kynurenic acid in food is not expected to affect the neurochemistry of consumers as the transport of kynurenic acid across the blood brain barrier is extremely low (Fukui, Schwarcz, Rapoport, Takada, & Smith, 1991). Kynurenic acid has also been hypothesised to contribute to the control of oral microflora (Kuc et al., 2006) and was reported to be present in human saliva at an average concentration of 3.4 nM, although patients with odontogenic abscesses showed kynurenic acid concentrations up to three times higher. It was hypothesised that this increase in kynurenic acid was produced in response to the abscesses. The consumption of kynurenic acid may therefore be beneficial to oral health.

3.3. Biomarker B

Biomarker B, when analysed by a combination of 1D ^{1}H and 2D ^{1}H–^{1}H TOCSY NMR spectroscopy, was shown to contain two non-exchangeable, non-equivalent ^{1}H chemical environments giving rise to two resonance peaks at chemical shifts of 7.350 (1H, d, 8.7 Hz) and 6.997 (1H, d, 8.7 Hz) ppm. It was concluded, based on their chemical shifts and *J*-couplings that these peaks were from a 6-membered aromatic ring system containing two non-exchangeable ^{1}H chemical environments. Analysis of the peak shapes determined that the aromatic ring system was either substituted at the 1,4 or 1,2,3,4 positions. The identity of biomarker B was not determined, aromatic compounds matching this description that have been demonstrated to be present in honey include; *p*-hydroxybenzoic acid and *p*-coumaric acid (Gheldof, Wang, & Engeseth, 2002). Acquisition of data from standard compounds determined that neither of these compounds were biomarker B. The highest concentration of biomarker B observed in a 15°BRIX solution of honey was in a spring Maquis honey and was calculated to be either 0.70 mM or 1.40 mM depending on whether biomarker B is 1,4 or 1,2,3,4 substituted, respectively. The highest concentration of biomarker B in undiluted honey was therefore calculated to be $\geqslant$ either 3.27 or 6.53 mM depending on the degree of substitution of the aromatic ring.

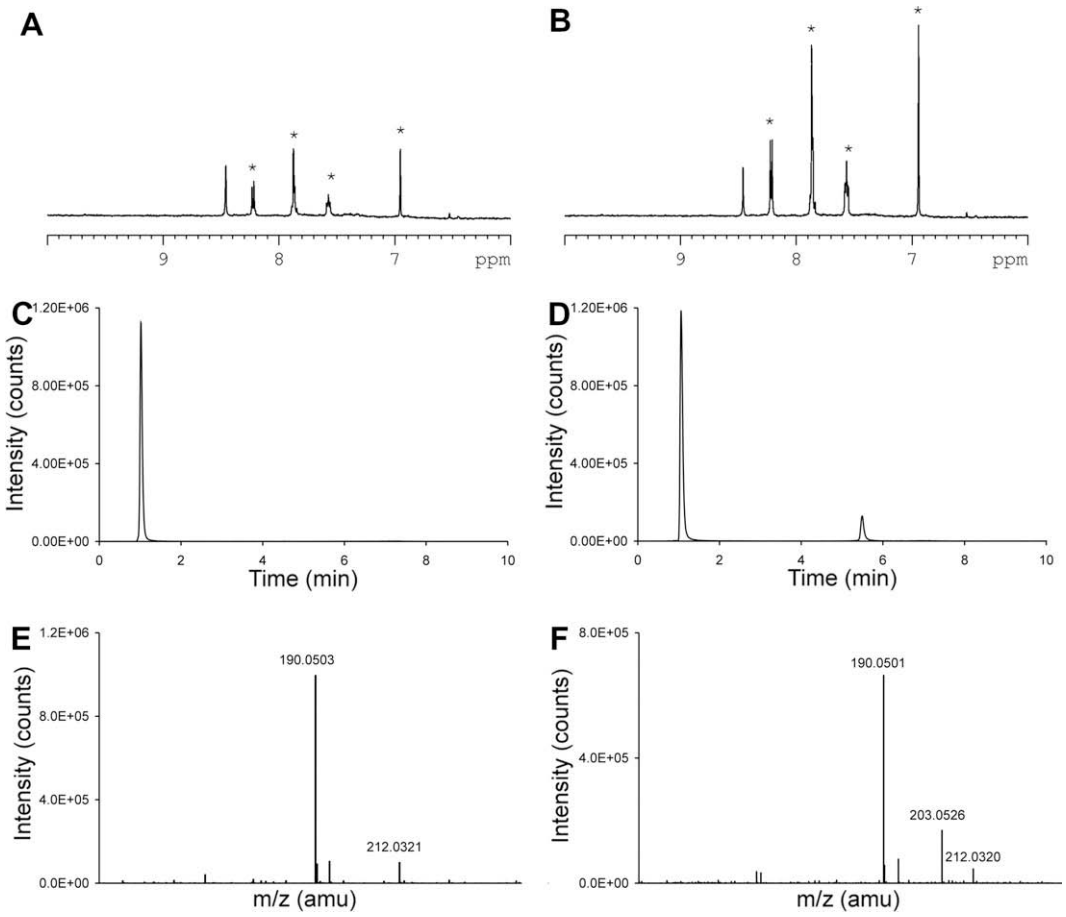

Fig. 2. Representation of the analytical data used to confirm the identity of kynurenic acid in honey. ^{1}H NMR spectrum of the region 6–10 ppm of (A) Corsican honey and (B) Corsican honey that was spiked with kynurenic acid. Peaks observed from kynurenic acid are labelled (∗). Extracted ion chromatogram of the mass range 189.8–190.3 Da corresponding to the protonated ion form of kynurenic acid in (C) kynurenic acid standard and (D) Corsican honey. Background subtracted mass spectrum observed at maximum intensity of the extracted ion chromatograms shown in (C) and (D) in the samples (E) kynurenic acid standard and (F) Corsican honey.

The relative intensity of the ^{1}H NMR spectroscopic peak of biomarker B at 6.997 ppm in all of the Corsican honey analysed is shown in Fig. 3B. Biomarker B was predominant in Corsican honey collected during the season of Spring. Spring Maquis honey contained the highest concentrations of biomarker B. Biomarker B was also detected in; Autumn Maquis, Summer Maquis and Châtaigneraie Corsican honey. Biomarker B was not detected in any non-Corsican honey. The Corsican Maquis is a shrubland consisting of different evergreen shrubs. Biomarker B was largely derived from spring flowering plants found uniquely in the Corsican Maquis, although further analysis would be required to confirm the source of this compound.

3.4. Biomarkers C and D

Biomarker C, when analysed by a combination of 1D ^{1}H and 2D ^{1}H–^{1}H TOCSY NMR spectroscopy, was shown to contain six non-exchangeable, non-equivalent ^{1}H chemical environments giving rise to six resonance peaks at chemical shifts of 6.188 (1H, bt, ~1.1 Hz), 2.752 (1H, d, 17.6 Hz), 2.503 (1H, dd, 17.6 Hz, 1.3 Hz), 1.863 (3H, d, 1.3 Hz), 1.180 (3H, bs) and 1.061 (3H, bs) ppm. (Symbols used bt, broad triplet; dd, double doublet; bs, broad singlet). All peaks associated with biomarker C were correlated by the ^{1}H–^{1}H TOCSY NMR experiment. The relative intensity and chemical shifts of each peak suggests that the biomarker contains the following chemical environments; a single alkene or aromatic environment (δ = 6.188), a methyl resonance attached to an alkene or aromatic environment (δ = 1.863), a methylene environment (δ = 2.752 and 2.503) and two methyl environments. The resonances observed for the methylene environment are at two different chemical shifts and this indicates that the molecule contains a chiral centre.

The highest concentration of biomarker C that was observed in a 15°BRIX solution of honey was in an autumn Maquis honey and was calculated to be 2.15 mM. The highest concentration of biomarker C in undiluted honey was therefore calculated to be $\geqslant$10.0 mM.

Biomarker D, when analysed by a combination of 1D ^{1}H and 2D ^{1}H–^{1}H TOCSY NMR spectroscopy, was shown to contain four non-exchangeable, non-equivalent ^{1}H chemical environments giving rise to four resonance peaks at chemical shifts of 6.811 (1H, m), 6.710 (2H, two m overlapping) and 3.482 (2H, bs) ppm. Analysis of these peaks using multidimensional NMR techniques determined that the molecule contained a six membered aromatic ring system substituted at the 1,2 and 5 positions and an alkyl chemical environment. The phenolic acid 2,5-dihydroxyphenylacetic acid, which has been reported by Cabras et al. to be a marker of Strawberry-tree honey (Cabras et al., 1999), contains these chemical environments. The ^{1}H NMR spectrum of 2,5-dihydroxyphenylacetic acid was acquired from a standard solution and confirmed biomarker D to be 2,5-dihydroxyphenylacetic acid.

The highest concentration of 2,5-dihydroxyphenylacetic acid that was observed in a 15°BRIX solution of honey was in the same autumn Maquis honey that contained the highest concentration of

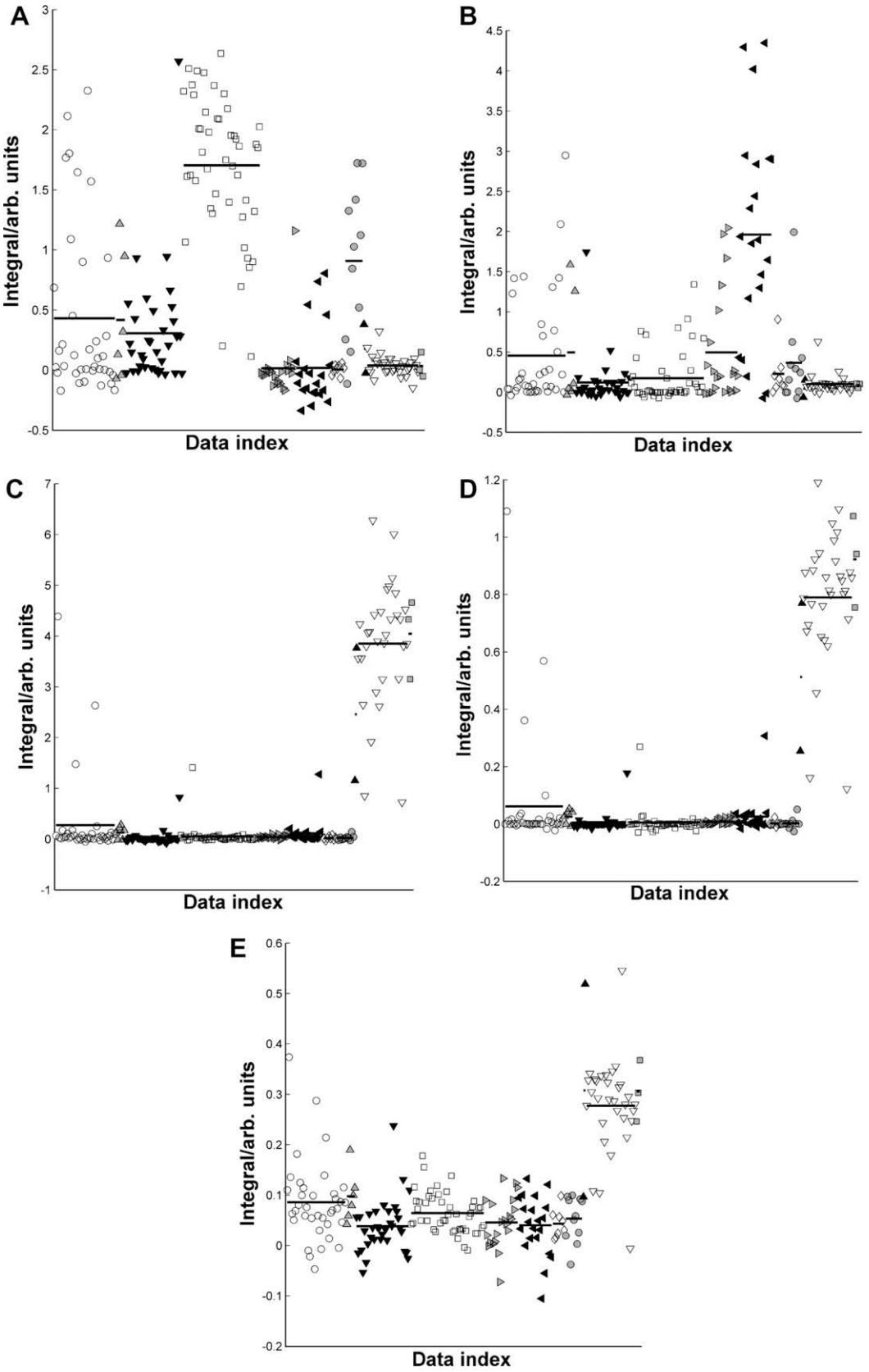

Fig. 3. Plot of the intensity of the resonances of: (A) kynurenic acid (δ = 7.571 ppm); (B) biomarker B (δ = 6.997 ppm); (C) biomarker C (δ = 6.188 ppm); (D) 2, 5-dihydroxyphenylacetic acid (δ = 6.811 ppm) and (E) α-isophorone (δ = 5.906 ppm), in all acquired Corsican ^{1}H NMR spectra. The data is labelled by Corsican honey type, ○ non-specific, ▲ non-specific Maquis, ▼ honeydew Maquis, □ Châtaigneraie, ▶ non-specific spring, ◀ spring Maquis, ◇ spring Clémentinier, ● summer Maquis, ▲ non-specific autumn, ▼ Autumn Maquis and ■ Arbousier. The mean value of each Corsican honey type is represented by a black bar passing through the range of data points from which the mean was calculated.

biomarker C and was calculated to be 0.72 mM. The highest concentration of 2,5-dihydroxyphenylacetic acid in undiluted honey was therefore calculated to be $\geqslant$3.4 mM.

The relative intensity of the ^{1}H NMR spectroscopic resonances of biomarker C and 2,5-dihydroxyphenylacetic acid at 6.188 ppm and 6.811 ppm in all of the Corsican honey analysed is shown in Fig. 3C and D, respectively. Biomarker C and 2,5-dihydroxyphenylacetic acid were predominant in Corsican honey collected during the season of Autumn. Autumn Maquis honeys contained the highest concentrations of biomarker C. Both biomarkers were also detected in; one Spring Maquis, one honeydew Maquis and in one Châtaigneraie Corsican honey. The biomarkers were also present in all three Corsican Arbousier honeys analysed. The French to English translation of Arbousier is Strawberry-tree and this is an autumn flowering tree found in the Corsican Maquis. As previously stated the phenolic acid 2,5-dihydroxyphenylacetic acid has been reported to be a biomarker of strawberry-tree honey. Other compounds reported to be markers of Strawberry-tree honey are the norisoprenoids α-isophorone, β-isophorone and 4-oxoisophorone (Bianchi et al., 2005). ^{1}H NMR spectra were therefore acquired from standards of α-isophorone and 4-oxoisophorone to determine whether these compounds were present. Data were not acquired from β-isophorone due to unavailability of the standard compound. α-Isophorone was detected in the majority of the Corsican autumn Maquis honey, but its spectral intensity was at the limit of detection of the NMR experiment. It was therefore not possible to accurately determine which non-autumn honeys, if any, contained α-isophorone or the concentration of α-isophorone present in honeys that did contain it. The relative intensity of the ^{1}H NMR spectroscopic peak of isophorone at 5.906 ppm in all of the Corsican honey is shown in Fig. 2E. 4-Oxoisophorone was not detected in any honey. It had previously been demonstrated (Bianchi et al., 2005) that the ratio of α-isophorone to β-isophorone varied between 4 and 8:1, it was therefore concluded that β-isophorone, if present, would be at a concentration too low to be observed with the ^{1}H NMR acquisition parameters used in this study.

It was noted that the ratio of biomarker C to 2,5-dihydroxyphenylacetic acid was constant in all the honey analysed. It was therefore hypothesised that biomarker C was also a biomarker of strawberry-tree honey.

4. Conclusion

^{1}H NMR spectroscopy has been shown to be a powerful analytical technique to screen for the presence of biomarkers of botanical origin in honey. The chemical properties inherent in pharmacoactive (either toxic or beneficial) organic compounds is such that when analysed by ^{1}H NMR spectroscopy they will resonate at chemical shifts usually not observed naturally in food matrices and are therefore often resolved. This is demonstrated well by the unique chemical shifts of kynurenic acid observed in honey.

Sample preparation is minimal, highly reproducible and using the acquisition parameters specified, able to detect compounds with an approximate limit of detection of 6.3 μM. Kynurenic acid is proposed as a putative biomarker of chestnut honey and the detection of 2,5-dihydroxyphenylacetic acid and α-isophorone, which corresponds with previous findings from other research groups, are also presented. Two characterised, but unidentified biomarker compounds, B and C, have been detected and it is concluded that these are marker compounds of Corsican spring Maquis and strawberry-tree honey, respectively.

Examining the prevalence of different biomarkers observed in spring, summer and autumn Maquis honey highlighted seasonal variations in honey composition. These honeys, although collected from geographically similar areas, contain different biomarkers that relate to botanical species. The determination of the geographical origin of honey using ^{1}H NMR spectroscopy is heavily dependant on variation in unrelated factors (e.g. botanical origin), which effect the product composition.

Acknowledgments

The authors thank the EU TRACE project and the UK Food Standards Agency for funding this work.

The honeys utilised in this research were collected as part of the TRACE (www.trace.eu.org) project by the Czech Bee Research Institute (Year 1) and Olivier Bidet (Year 2). The honeys were subsampled and distributed by The Irish Agriculture and Food Development Authority (Year 1) and the Institute of Chemical Technology, Prague (Year 2).

The information contained in this article reflects the authors' views; neither the European Commission nor the FSA is liable for any use of the information contained herein.

References

Andrade, P., Ferreres, F., Gil, M. I., & Tomas-Barberan, F. A. (1997). Determination of phenolic compounds in honeys with different floral origin by capillary zone electrophoresis. *Food Chemistry, 60*, 79–84.

Bax, A., & Davis, D. G. (1985). Mlev-17-based two-dimensional homonuclear magnetization transfer spectroscopy. *Journal of Magnetic Resonance, 65*, 355–360.

Beretta, G., Caneva, E., & Facino, R. M. (2007). Kynurenic acid in honey from arboreal plants: MS and NMR evidence. *Planta Medica, 73*, 1592–1595.

Beretta, G., Caneva, E., Regazzoni, L., Bakhtyari, N. G., & Facino, R. M. (2008). A solid-phase extraction procedure coupled to ^{1}H NMR, with chemometric analysis, to seek reliable markers of the botanical origin of honey. *Analytica Chimica Acta, 620*, 176–182.

Bianchi, F., Careri, M., & Musci, M. (2005). Volatile norisoprenoids as markers of botanical origin of Sardinian strawberry-tree (*Arbutus unedo* L.) honey. *Food Chemistry, 89*, 527–532.

Cabras, P., Angioni, A., Tuberoso, C., Floris, I., Reniero, F., Guillou, C., et al. (1999). Homogentisic acid: A phenolic acid as a marker of strawberry-tree (*Arbutus unedo*) honey. *Journal of Agricultural and Food Chemistry, 47*, 4064–4067.

Ceyhan, N., & Ugur, A. (2001). Investigation of in vitro antimicrobial activity of honey. *Rivista di Biologia-Biology Forum, 94*, 363–371.

Charlton, A. J., Farrington, W. H. H., & Brereton, P. (2002). Application of H-1 NMR and multivariate statistics for screening complex mixtures: Quality control and authenticity of instant coffee. *Journal of Agricultural and Food Chemistry, 50*, 3098–3103.

Davis, R. A., Charlton, A. J., Oehlschlager, S., & Wilson, J. C. (2006). Novel feature selection method for genetic programming using metabolomic H-1 NMR data. *Chemometrics and Intelligent Laboratory Systems, 81*, 50–59.

de la Fuente, E., Valencia-Barrera, R. M., Martinez-Castro, I., & Sanz, J. (2007). Occurrence of 2-hydroxy-5-methyl-3-hexanone and 3-hydroxy-5-methyl-2-hexanone as indicators of botanic origin in eucalyptus honeys. *Food Chemistry, 103*, 1176–1180.

Donarski, J. A., Jones, S. A., & Charlton, A. J. (2008). Application of cryoprobe ^{1}H nuclear magnetic resonance spectroscopy and multivariate analysis for the verification of Corsican honey. *Journal of Agriculture and Food Chemistry, 56*, 5451–5456.

Fukui, S., Schwarcz, R., Rapoport, S. I., Takada, Y., & Smith, Q. R. (1991). Blood-brain-barrier transport of kynurenines – Implications for brain synthesis and metabolism. *Journal of Neurochemistry, 56*, 2007–2017.

Furlanetto, S., Tognini, C., Carpenedo, R., La Porta, E., & Pinzauti, S. (1998). Set-up and validation of an adsorptive stripping voltammetric method for kynurenic acid determination in human urine. *Journal of Pharmaceutical and Biomedical Analysis, 18*, 67–73.

Gheldof, N., Wang, X. H., & Engeseth, N. J. (2002). Identification and quantification of antioxidant components of honeys from various floral sources. *Journal of Agricultural and Food Chemistry, 50*, 5870–5877.

Guillemin, G. J., Kerr, S. J., & Brew, B. J. (2005). Involvement of quinolinic acid in AIDS dementia complex. *Neurotoxicity Research, 7*, 103–123.

Karoui, R., Dufour, E., Bosset, J. O., & De Baerdemaeker, J. (2007). The use of front face fluorescence spectroscopy to classify the botanical origin of honey samples produced in Switzerland. *Food Chemistry, 101*, 314–323.

Kelly, S., Heaton, K., & Hoogewerff, J. (2005). Tracing the geographical origin of food: The application of multi-element and multi-isotope analysis. *Trends in Food Science & Technology, 16*, 555–567.

Koca, I., & Koca, A. F. (2007). Poisoning by mad honey: A brief review. *Food and Chemical Toxicology, 45*, 1315–1318.

Kuc, D., Rahnama, M., Tomaszewski, T., Rzeski, W., Wejksza, K., Urbanik-Sypniewska, T., et al. (2006). Kynurenic acid in human saliva – Does it influence oral microflora? *Pharmacological Reports, 58*, 393–398.

Kuc, D., Zgrajka, W., Parada-Turska, J., Urbanik-Sypniewska, T., & Turski, W. A. (2008). Presence of kynurenic acid in food and honeybee products. *Amino Acids*. doi:10.1007/s00726-008-0031-z.

Molan, P. C. (2001). The potential of honey to promote oral wellness. *General Dentistry, 49*, 584–589.

Mphande, A. N. G., Killowe, C., Phalira, S., Jones, H. W., & Harrison, W. J. (2007). Effects of honey and sugar dressings on wound healing. *Journal of Wound Care, 16*, 317–319.

Németh, H., Toldi, J., & Vécsei, L. (2006). Kynurenines, Parkinson's disease and other neurodegenerative disorders: Preclinical and clinical studies. *Journal of Neural Transmission. Supplementum*, 285–304.

Nilsson, L. K., Linderholm, K. R., Engberg, G., Paulson, L., Blennow, K., Lindström, L. H., et al. (2005). Elevated levels of kynurenic acid in the cerebrospinal fluid of male patients with schizophrenia. *Schizophrenia Research, 80*, 315–322.

Ruddick, J. P., Evans, A. K., Nutt, D. J., Lightman, S. L., Rook, G. A. W., & Lowry, C. A. (2006). Tryptophan metabolism in the central nervous system: Medical implications. *Expert Reviews in Molecular Medicine, 8*, 1–27.

Stone, T. W. (1993). Neuropharmacology of quinolinic and kynurenic acids. *Pharmacological Reviews, 45*, 309–379.

Stone, T. W. (2000). Development and therapeutic potential of kynurenic acid and kynurenine derivatives for neuroprotection. *Trends in Pharmacological Sciences, 21*, 149–154.

Weston, R. J., Brocklebank, L. K., & Lu, Y. (2000). Identification and quantitative levels of antibacterial components of some New Zealand honeys. *Food Chemistry, 70*, 427–435.

However, when specimens are small in size and once the shell is removed (as in canned products), they are generally unidentifiable. Hence, replacement with the cheaper razor clam species or mislabelling can occur, and consequently the development of a procedure for species authentication should be of the highest priority.

Genetic approaches based on DNA techniques are widely used nowadays to overcome this problem. Advantages of the use of DNA in these methodologies are: this molecule is very stable, contains more information than proteins and it is present in all tissues of all organisms. Thanks to the development of polymerase chain reaction (PCR) the molecular methods have been simplified being more easily applicable and less time-consuming. PCR amplification of species-specific fragments has been useful in fish traceability (Carrera et al., 2000; Céspedes et al., 1999) and in species identification (Asensio et al., 2001; Cross, Rebordinos, & Díaz, 2006; Rego et al., 2002).

The aim of this work was to develop an appropriate and reliable methodology for identification of five razor clams species, by means of a multiplex PCR methodology of ITS-1 region. The protocol, involving a one-step procedure, is rapid, accurate, and sensitive, enabling its use to identify razor clams in fresh and canned samples in an accurate and prompt manner.

2. Materials and methods

2.1. Materials

Samples of *E. arcuatus* and *E. siliqua* were collected by local fishermen in Rodas (Pontevedra, Spain) and Finisterre (A Coruña, Spain), respectively. Samples of *E. directus* (Denmark) were purchased from local fish suppliers and *E. macha* individuals (Chile) were supplied by Dr. Irene Lepez. All specimens were morphologically identified. A piece of foot was dissected and immediately stored in 95% ethanol until DNA extraction (less than five days). Canned and frozen products were purchased at local supermarkets.

2.2. DNA isolation and PCR amplification of ITS-1 region

Total genomic DNA was isolated from 25 mg of raw or processed foot sections using the protocol described by Fernández-Tajes and Méndez (2007).

Amplification of ITS-1 sequences were carried out using primer forward 5′-GTTTCCGTAGGTGAACCTG-3′ designed by Heath, Rawson, and Hilbish (1995) and reverse 5′-TGTGCGTTCAAGATGTCG-3′, designed in this work based on 5.8S rRNA gene sequences of several bivalve species. Amplification reactions were performed in 25 μl of reaction volume; the reaction mixture contained 15 ng of genomic DNA, 0.24 μM of each dNTP, 2 mM of $MgCl_2$, 1 μM of each primer, 0.625 U of Taq polymerase (Roche Applied Science, Barcelona, Spain) and the buffer recommended by polymerase suppliers. The thermal cycler profile consisted of an initial denaturation step of 5 min at 95 °C, 35 cycles at 94 °C for 20 s, 56 °C for 20 s and 72 °C for 1 min, and a final extension step at 72 °C for 5 min. PCR products were visualised by electrophoresis on a 2% w/v agarose gel.

2.3. Purification, cloning and sequencing of PCR products

The ITS PCR product was ligated into the plasmid pCR®2.1-TOPO®, using the TOPO-TA Cloning kit (Invitrogen), and transformed into TOP10F' cells. Plasmid DNA purification was carried out using QIAprep Miniprep Kit (Qiagen, Barcelona, Spain), which employs the modified alkaline method of Birnboim and Doly (1979). Sequencing of both strands of the insert of 4–6 clones/individual was performed with an automatic capillary DNA sequencer (CEQ™8000 Genetic Analysis System). The nucleotide sequences have been deposited in the EMBL database under accession numbers J966667-97 and AM933615-31.

2.4. Analysis of sequences and design of species-specific primers

Nucleotide sequences were aligned using ClustalX software (Thompson, Gibson, Plewniak, Jeanmougin, & Higgins, 1997), and alignments were edited with GeneDoc software (Nicholas, Nicholas, & Deerfield, 1997). Interspecific differences found at ITS-1 region of razor clams were employed for designing reverse species-specific primers using Primer3 software (Rozen & Skaletsky, 2000). Selection was done in such a way that each species-specific primer with a universal primer identical to the four species (in this case the forward described above) would produce a PCR amplification product of species-specific size. The PCR mix and thermal conditions are the previously described.

2.5. Multiplex PCR

Once all primers were tested, multiplex PCR was performed in order to simplify the species identification. Multiplex PCR was carried out using 0.24 μM of each primer, and with identical conditions as described above.

2.6. Market study

In order to evaluate the usefulness of our methodology in commercial samples 12 commercial cans were acquired in shops and stores from Galicia and Spain to check the correct labelling of the analysed products.

3. Results and discussion

The aim of this work was to develop a reliable and efficient method for genetic differentiation between European and non-European razor clam species. This identification was achieved by a multiplex PCR-based method based on ITS-1 region. The ITS spacers show more variability than their flanking coding regions, and they can be easily amplified with universal primers (Presa, Pardo, Martínez, & Bernatchez, 2002). Fresh, frozen and canned products were analysed using this methodology.

With this aim, amplification and sequencing of ITS-1 spacer of *E. arcuatus*, *E. siliqua*, *E. directus* and *E. macha* was done. Thus, PCR products of three individuals from all species were cloned and sequenced; the complete ITS-1 sequences obtained were determined to be 566 bp in *E. arcuatus* and *E. siliqua*, 535 bp in *E. directus*, and 560 bp in *E. macha*. Although there are some small differences in the length of obtained amplicons among species, they could not be detected by agarose electrophoresis.

The alignment of the sequences obtained with those from databases showed 314 variable sites, 248 nucleotide substitutions and 66 indels in a total of 585 bp, all of them in the spacer sequence. The number of species-specific sites was 11 for *E. arcuatus*, 12 for *E. siliqua*, 89 for *E. directus* and 74 for *E. macha*. The presence of this several species-specific sites allowed us to design reverse species-specific primers for razor clams characterisation. In order to make an unequivocally identification of the species, species-specific PCR can be developed because a specific sequence can be detected very sensitively in a pool of sequences of different organisms (Rodríguez et al., 2003). Table 1 shows the designed primers. No specific primers for *E. arcuatus* and *E. siliqua* were obtained, probably due to the small number of species-specific sites in both species.

Using each specific primer together with a common forward primer (ITS-F from Heath et al., 1995), a 296 bp band was obtained

Table 1
Sequence of species-specific primers designed.

Species amplified	Primer	Sequence
Forward primer	Heath et al. (1995)	5′- GTTTCCGTAGGTGAACCTG-3′
E. arcuatus/E. siliqua	ITSArSil-R	5′-CTTCGCGTCGGCAATA-3′
E. directus	ITSDir-R	5′- GACGGAGTGCATAGTGTATAAC-3′
E. macha	ITSMa-R	5′- CGTTGTTTGTGGTAATAAGGC-3′

for *E. arcuatus*/*E. siliqua*, a 223 bp PCR fragment was amplified from *E. directus* individuals, and a 386 bp band was yielded from *E. macha* samples. Amplification of 10 individuals for each razor clam species corroborated the expected product lengths.

Since our aim was to find a simple and straightforward method we carried out a multiplex PCR amplification using the three species-specific oligonucleotides (ITSArSil-R, ITSDir-R, and ITSMa-R) in the same reaction together with the ITS1N-F. The amplification of 26 individuals of *E. arcuatus/E. siliqua*, 27 individuals of *E. directus* and 20 of *E. macha* showed that no disturbance occurred among the primers during the amplification reaction and that the specific primers to each DNA species annealed on their target sequences. Fig. 1 shows the typical amplification pattern obtained with those species-specific primers. Although in this assay *E. arcuatus* and *E. siliqua* could not be identified, this problem could be solved by means of the method described by Freire, Fernández-Tajes, and Méndez (2008). Consequently, a combined protocol that implies the multiplex PCR described here and the PCR–RFLP method of ITS-1 previously developed would allow the identification of the four razor clam species.

The results shown above were obtained from raw (fresh and frozen) samples, and from processed material (canned samples). In fresh products individuals ranging in size from 10 to 15 cm, and in manufactured products 12 commercial cans were purchased at local supermarkets from Galicia and Spain. One of the main problems to apply molecular methodologies to processed products such as canned seafood is that the sterilization procedure could induce DNA fragmentation. Specifically, the sterilization process in razor clams is performed at 112.5 °C for 75 min, what produces DNA fragments about 200–700 bp. For this reason molecular methods used to identify commercial material of razor clams should employ fragments around this size. This criterion is fulfilled for the fragments generated with our specific primers. The methodology developed in this study allowed us to verify the species included in the analysed commercial products and their correct labelling.

ITS-1 and ITS-2 spacers are useful to distinguish between related species (e.g. Fernández et al., 2001; Pérez, Vieites, & Presa, 2005). In bivalves, RFLPs of this region were used for the identification of several *Mytilus* mussels (Heath et al., 1995; Toro, 1998), Veneridae clams (Fernández et al., 2001) and four scallop species (López-Piñón, Insua, & Méndez, 2002); length amplification was used to differentiate several freshwater mussels (White, McPheron, & Stauffer, 1994) and *M. edulis* from two *Modiolus* species (Dixon, Sole-Cava, Pascoe, & Holland, 1995).

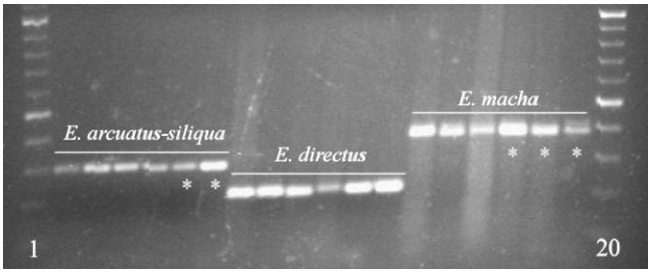

Fig. 1. ITS-1 products generated by multiplex PCR of fresh and canned (*) products with species-specific primers for *E. arcuatus/siliqua*, *E. directus* and *E. macha*. Lanes 1 and 20, 100 bp DNA ladder. Note: DNA was extracted from foot tissue sections both in canned and fresh samples.

A genetic method for the differentiation of these razor clam species, based on PCR–RFLPs of the 5S rDNA gene, was previously described (Fernández-Tajes & Méndez, 2007). Nevertheless, the organisation of ribosomal genes in multiple tandem arrays could be considered as a one of the major drawbacks in the use of these regions as genetic markers due to the intraspecific variation that could exist in the different repeats at individual level, giving rise to possible mutations and, consequently, to the loss or gain of restriction recognition sequences. However, concerted evolution tends to homogenise the repetition units present inside and among individuals of the species (Dover, Coen, & Strachan, 1982). Moreover, availability of more than one genetic marker is convenient as a technical support in the case of a legal requirement to demonstrate fraudulent substitution of species.

The results obtained in this work suggest that multiplex PCR amplification of selected ITS rDNA fragments using species-specific primers ITSArSil-R, ITSDir-R, and ITSMa-R together with ITS-F, is a powerful technique for the identification of razor clam species. Compared to alternative techniques such as direct sequencing of PCR products, PCR–RFLP or PCR–SSCP, multiplex PCR system is less consuming than these other molecular techniques, being easily performed in food inspection laboratories, especially when large numbers of samples are required to be analysed. Thus, the protocol described in this work offers an alternative tool for fraudulent species detention and for food authenticity in the market of razor clam products, as in raw as in manufactured samples.

Acknowledgements

This work was funded by a PFSHARE-90 (Sustainable HARvesing of Ensis (SHARE)) and by a TIMES (Towards a Integrated Management of Ensis stocks) grants from the European Community Initiative Programme INTERREG-IIIB "Atlantic Area" and partially funded by I3 Program 2007–08 "Programa de promoción da intensificación da actividade investigadora no sistema universitario de Galicia" financed by Xunta de Galicia. We are grateful to Mr. Jose García Gil for his technical assistance. We would also like to thank Dr. Irene Lepez for providing *E. macha* samples.

References

Asensio, L., González, I., Fernández, A., Céspedes, A., Rodríguez, M. A., Hernández, P. E., et al. (2001). Identification on nile perch (*Lates nitolicus*), grouper (*Epinephelus guaza*), and wreck fish (*Polyprion americanus*) fillets by PCR amplification of the 5S rDNA gene. *Journal of AOC International, 84*, 777–781.

Baron, P. J., Real, L. E., Ciocco, N. F., & Re, M. E. (2006). Morphometry, growth and reproduction of an Atlantic population of the razor clam *Ensis macha* (Molina, 1782). *Scientia Marina, 68*, 211–217.

Birnboim, H. C., & Dolly, J. (1979). Rapid alkaline extraction procedure for screening recombinant plasmid DNA. *Nucleic Acids Research, 7*, 1513–1523.

Carrera, E., García, T., Céspedes, A., González, I., Fernández, A., Hernández, P. E., et al. (2000). PCR-restriction fragment length polymorphism of the p53 gene as a genetic marker for identification of smoked Atlantic salmon (*Salmo salar*) and rainbow trout (*Onchorhyncus mykiss*). *Journal of AOC International, 83*, 341–346.

Céspedes, A., García, T., Carrera, E., González, I., Fernández, A., Hernández, P. E., et al. (1999). Identification of sole (*Solea solea*) and Greenland halibut (*Reinharius hippglossoides*) by PCR amplification of the 5S rDNA gene. *Journal of Agricultural and Food Chemistry, 47*, 1046–1050.

Council Regulation (EC) No 104/2000 of 17 December 1999 on the common organization of the markets in fishery and aquaculture products. (2000). *Official Journal of European Community*, *L17*, 22–52.

Cross, I., Rebordinos, L., & Díaz, E. (2006). Species identification of *Crassostrea* and *Ostrea* species by polymerase chain reaction amplification of the 5S rRNA gene. *Journal of AOC International, 89*, 145–148.

Dixon, D. R., Sole-Cava, A. M., Pascoe, P. L., & Holland, P. W. H. (1995). Periostracal adventitious hairs on spat of the mussel *Mytilus edulis*. *Journal of the Marine Biological Association of the United Kingdom, 75*, 363–372.

Dover, G., Coen, E., & Strachan, T. (1982). The dynamics of sequence turnover and concerted evolution of families of rDNA, histone genes, and non-coding DNA of *Drosophila*. *Heredity, 49*, 141.

Fernández, A., García, T., Asensio, L., Rodríguez, M. A., González, I., Hernández, P. E., et al. (2001). PCR–RFLP analysis of the internal transcribed spacer (ITS) region for identification of 3 clam species. *Food and Chemical Toxicology, 66*, 657–661.

Fernández-Tajes, J., & Méndez, J. (2007). Identification of the razor clam species *Ensis arcuatus*, *E. siliqua*, *E. directus*, *E. macha*, and *Solen marginatus* using PCR–RFLP analysis of the 5S rDNA region. *Journal of Agricultural and Food Chemistry, 55*, 7278–7282.

Freire, R., Fernández-Tajes, J., & Méndez, J. (2008). Identification of the razor clams *Ensis arcuatus* and *E. siliqua* by PCR–RFLPs analysis of ITS-1 region. *Journal of Fisheries Science*.

Gaspar, M. B., Castro, M., & Monteiro, C. C. (1999). Effect of tooth spacing and mesh size on the catch of the Portuguese clam and razor clam dredge. *ICES Journal of Marine Science, 56*, 103–110.

Hayward, P. J., & Ryland, J. S. (1998). *Handbook of the marine fauna of North–West Europe*. Oxford: Oxford University Press.

Heath, D. D., Rawson, P. D., & Hilbish, T. J. (1995). PCR-based nuclear markers identify alien blue mussel (*Mytilus* sp.) genotypes on the west coast of Canada. *Canadian Journal of Fisheries and Aquatic Sciences, 52*, 2621–2627.

López-Piñón, M. J., Insua, A., & Méndez, J. (2002). Identification of four scallop species using PCR and restriction analysis of the ribosomal DNA internal transcribed spacer region. *Marine Biotechnology, 4*, 495–502.

Luczak, C., & Dewarumez, J. M. (1992). Note on the identification of *Ensis directus* (Conrad, 1843). *Cahiers de Biologie Marine, 33*, 515–518.

Luczak, C., Dewarumez, J. M., & Essink, K. (1993). First record of the American jack knife clam *Ensis directus* on the French coast of the North Sea. *Journal of the Marine Biological Association of the United Kingdom, 73*, 233–235.

Nicholas, K. B., Nicholas, H. B., Jr., & Deerfield, D. W. (1997). Genedoc: Analysis and visualization of genetic variation. *EMBNEW News, 4*, 14.

Pérez, M., Vieites, J. M., & Presa, P. (2005). ITS-1 rDNA-based methodology to identify world-wide hake species of the genus *Merluccius*. *Journal of Agricultural and Food Chemistry, 53*, 5239–5247.

Presa, P., Pardo, B. G., Martínez, P., & Bernatchez, L. (2002). Phylogeographic congruence between mtDNA and rDNA ITS markers in Brown trout. *Molecular Biology and Evolution, 19*, 2161–2175.

Rego, I., Martínez, A., González-Tizón, A., Vieites, J., Leira, F., & Méndez, J. (2002). PCR technique for identification of mussel species. *Journal of Agricultural and Food Chemistry, 50*, 1780–1784.

Rodríguez, M. A., García, T., González, I., Asensio, L., Mayoral, B., López-Calleja, I., et al. (2003). Identification of goose, mule duck, chicken, turkey, and swine in Foie Gras by species-specific polymerase chain reaction. *Journal of Agricultural and Food Chemistry, 51*, 1524–1529.

Rozen, S., & Skaletsky, H. J. (2000). Primer3 on the WWW for general users and biologist programmers. In S. Krawetz & S. Misener (Eds.), *Bioinformatics methods and protocols: Methods in molecular biology* (pp. 365–386). Totowa, NJ: Humana Press.

Thompson, J. D., Gibson, T. J., Plewniak, F., Jeanmougin, F., & Higgins, D. G. (1997). The CLUSTAL_X windows interface. flexible strategies for multiple sequence alignment aided by quality analysis tools. *Nucleic Acids Research, 25*, 4876–4882.

Toro, J. E. (1998). Molecular identification of four species of mussels from southern Chile by PCR-based nuclear markers: The potential use in studies involving planktonic surveys. *Journal of Shellfish Research, 17*, 1203–1205.

White, L. R., McPheron, B. A., & Stauffer, J. R. (1994). Identification of freshwater mussel *Glochidia* on host fishes using restriction fragment length polymorphisms. *Molecular Ecology, 3*, 183–185.

Contents lists available at ScienceDirect

Food Chemistry

journal homepage: www.elsevier.com/locate/foodchem

Calendar

Event	Date and Venue	Details from
4th International Symposium on Sourdough	14–17 October 2009 *Munich, Germany*	Internet: http://www.sourdough.foodscience.ws
11th ASEAN Food Conference 2009	21–23 October 2009 *Bandar Seri Begawan, Brunei*	Internet: http://www.agriculture.gov.bn/DOA/BDAFST/Announcement.html
International Conference on Bio and Food Electrotechnologies	22–23 October 2009 *Compiegne, France*	Internet: http://www.utc.fr/bfe2009
International Society for Nutraceuticals and Functional Foods Annual Conference	1–4 November 2009 *San Francisco, CA*	Internet: http://isnff.org
4th International Symposium on Recent Advances in Food Analysis	4–6 November 2009 *Prague, Czech Republic*	Internet: http://www.rafa2009.eu/
2009 EFFoST Conference – New Challenges in Food Preservation: Processing – Safety – Stability	11–13 November 2009 *Budapest, Hungary*	Internet: http://www.effost-conference.elsevier.com
Pittcon 2010	28 February–5 March 2010 *Orlando, Florida*	Internet: www.pittcon.org
US/Ireland Functional Foods Conference	9–11 March 2010 *Cork, Ireland*	Internet: www.corkff2010.com
Food Colloids 2010 – On the Road from Interfaces to Consumers	21–24 March 2010 *Granada, Spain*	Internet: www.foodcolloids2010.org
IDF Symposium on the Science & Technology of Fermented Milk	7–9 June 2010 *Tromsø, Norway*	Internet: www.IDFFer2010.no
IDF Symposium on Microstructure of Dairy Products	9–11 June 2010 *Tromsø, Norway*	Internet: www.IDFMic2010.no
10th International Hydrocolloids Conference	20–24 June 2010 *Shanghai, China*	Internet: www.10ihc.org
IFT Annual Meeting and Food Expo	17–21 July 2010 *Chicago, USA*	Internet: www.ift.org
56th International Congress of Meat Science and Technology (ICoMST)	8–13 August 2010 *Jeju, South Korea*	Internet: http://icomst2010.org/
IUFoST 2010 – 15th World Congress of Food Science and Technology	22–26 August 2010 *Cape Town, South Africa*	Internet: http://www.iufost2010.org.za
Eurosense 2010 – Fourth European Conference on Sensory and Consumer Research	5–9 September 2010 *Vitoria, Spain*	Internet: TBA

This calendar of forthcoming events is based on information provided by the respective organizers and from secondary sources.
Food Chemistry welcomes information on relevant meetings. Copy deadlines are three months ahead of cover dates and information should be sent to:
Wendy Hurp, *Food Chemistry Calendar*, Elsevier Ltd, The Boulevard, Langford Lane, Kidlington, Oxford OX5 1GB, UK.
Fax: +44 (0) 1865 843960; E-mail: w.hurp@elsevier.com

doi:10.1016/S0308-8146(09)01080-2

Food Chemistry 118 (2010) I–II

Contents lists available at ScienceDirect

Food Chemistry

journal homepage: www.elsevier.com/locate/foodchem

Calendar

Event	Date and Venue	Details from
IDF World Dairy Summit	20–24 September 2009 *Berlin, Germany*	Internet:http://www.wds2009.com
Polysaccharides as a Source of Advanced Materials	21–24 September 2009 *Turku/Abo, Finland*	Internet: http://congress.utu.fi/epnoe2009/
6th NIZO Dairy Conference – Dairy ingredients: innovations in functionality	30 September–2 October 2009 *Papendal, Arnhem, The Netherlands*	Internet: www.nizodairyconf.elsevier.com
4th International Symposium on Sourdough	14–17 October 2009 *Munich, Germany*	Internet: http://www.sourdough.foodscience.ws
11th ASEAN Food Conference 2009	21–23 October 2009 *Bandar Seri Begawan, Brunei*	Internet: http://www.agriculture.gov.bn/DOA/BDAFST/Announcement.html
International Conference on Bio and Food Electrotechnologies	22–23 October 2009 *Compiegne, France*	Internet: http://www.utc.fr/bfe2009
International Society for Nutraceuticals and Functional Foods Annual Conference	1–4 November 2009 *San Francisco, CA*	Internet: http://isnff.org
4th International Symposium on Recent Advances in Food Analysis	4–6 November 2009 *Prague, Czech Republic*	Internet: http://www.rafa2009.eu/
2009 EFFoST Conference – New Challenges in Food Preservation: Processing – Safety – Stability	11–13 November 2009 *Budapest, Hungary*	Internet: http://www.effost-conference.elsevier.com
Pittcon 2010	28 February–5 March 2010 *Orlando, Florida*	Internet: www.pittcon.org
US/Ireland Functional Foods Conference	9–11 March 2010 *Cork, Ireland*	Internet: www.corkff2010.com
Food Colloids 2010 – On the Road from Interfaces to Consumers	21–24 March 2010 *Granada, Spain*	Internet: www.foodcolloids2010.org
IDF Symposium on the Science & Technology of Fermented Milk	7–9 June 2010 *Tromsø, Norway*	Internet: www.IDFFer2010.no
IDF Symposium on Microstructure of Dairy Products	9–11 June 2010 *Tromsø, Norway*	Internet: www.IDFMic2010.no
10th International Hydrocolloids Conference	20–24 June 2010 *Shanghai, China*	Internet: www.10ihc.org
IFT Annual Meeting and Food Expo	17–21 July 2010 *Chicago, USA*	Internet: www.ift.org

doi:10.1016/S0308-8146(09)00949-2

Event	Date and Venue	Details from
56th International Congress of Meat Science and Technology (ICoMST)	8–13 August 2010 *Jeju, South Korea*	Internet: http://icomst2010.org/
IUFoST 2010 – 15th World Congress of Food Science and Technology	22–26 August 2010 *Cape Town, South Africa*	Internet: http://www.iufost2010.org.za
Eurosense 2010 – Fourth European Conference on Sensory and Consumer Research	5–9 September 2010 *Vitoria, Spain*	Internet: TBA

This calendar of forthcoming events is based on information provided by the respective organizers and from secondary sources.
Food Chemistry welcomes information on relevant meetings. Copy deadlines are three months ahead of cover dates and information should be sent to:
Wendy Hurp, *Food Chemistry Calendar*, Elsevier Ltd, The Boulevard, Langford Lane, Kidlington, Oxford OX5 1GB, UK.
Fax: +44 (0) 1865 843960; E-mail: w.hurp@elsevier.com

Food Chemistry 118 (2010) I–II

Contents lists available at ScienceDirect

Food Chemistry

journal homepage: www.elsevier.com/locate/foodchem

Calendar

Event	Date and Venue	Details from
IDF World Dairy Summit	20–24 September 2009 *Berlin, Germany*	Internet:http://www.wds2009.com
Polysaccharides as a Source of Advanced Materials	21–24 September 2009 *Turku/Abo, Finland*	Internet: http://congress.utu.fi/epnoe2009/
6th NIZO Dairy Conference – Dairy ingredients: innovations in functionality	30 September–2 October 2009 *Papendal, Arnhem, The Netherlands*	Internet: www.nizodairyconf.elsevier.com
4th International Symposium on Sourdough	14–17 October 2009 *Munich, Germany*	Internet: http://www.sourdough.foodscience.ws
11th ASEAN Food Conference 2009	21–23 October 2009 *Bandar Seri Begawan, Brunei*	Internet: http://www.agriculture.gov.bn/DOA/BDAFST/Announcement.html
International Conference on Bio and Food Electrotechnologies	22–23 October 2009 *Compiegne, France*	Internet: http://www.utc.fr/bfe2009
International Society for Nutraceuticals and Functional Foods Annual Conference	1–4 November 2009 *San Francisco, CA*	Internet: http://isnff.org
4th International Symposium on Recent Advances in Food Analysis	4–6 November 2009 *Prague, Czech Republic*	Internet: http://www.rafa2009.eu/
2009 EFFoST Conference – New Challenges in Food Preservation: Processing – Safety – Stability	11–13 November 2009 *Budapest, Hungary*	Internet: http://www.effost-conference.elsevier.com
Pittcon 2010	28 February–5 March 2010 *Orlando, Florida*	Internet: www.pittcon.org
US/Ireland Functional Foods Conference	9–11 March 2010 *Cork, Ireland*	Internet: www.corkff2010.com
Food Colloids 2010 – On the Road from Interfaces to Consumers	21–24 March 2010 *Granada, Spain*	Internet: www.foodcolloids2010.org
IDF Symposium on the Science & Technology of Fermented Milk	7–9 June 2010 *Tromsø, Norway*	Internet: www.IDFFer2010.no
IDF Symposium on Microstructure of Dairy Products	9–11 June 2010 *Tromsø, Norway*	Internet: www.IDFMic2010.no
10th International Hydrocolloids Conference	20–24 June 2010 *Shanghai, China*	Internet: www.10ihc.org
IFT Annual Meeting and Food Expo	17–21 July 2010 *Chicago, USA*	Internet: www.ift.org

doi:10.1016/S0308-8146(09)001008-5

Event	Date and Venue	Details from
56th International Congress of Meat Science and Technology (ICoMST)	8–13 August 2010 *Jeju, South Korea*	Internet: http://icomst2010.org/
IUFoST 2010 – 15th World Congress of Food Science and Technology	22–26 August 2010 *Cape Town, South Africa*	Internet: http://www.iufost2010.org.za
Eurosense 2010 – Fourth European Conference on Sensory and Consumer Research	5–9 September 2010 *Vitoria, Spain*	Internet: TBA

This calendar of forthcoming events is based on information provided by the respective organizers and from secondary sources.
Food Chemistry welcomes information on relevant meetings. Copy deadlines are three months ahead of cover dates and information should be sent to:
Wendy Hurp, *Food Chemistry Calendar*, Elsevier Ltd, The Boulevard, Langford Lane, Kidlington, Oxford OX5 1GB, UK.
Fax: +44 (0) 1865 843960; E-mail: w.hurp@elsevier.com

Food Chemistry 118 (2010) I–II

Contents lists available at ScienceDirect

Food Chemistry

journal homepage: www.elsevier.com/locate/foodchem

Calendar

Event	Date and Venue	Details from
15th European Carbohydrate Symposium	19–24 July 2009 *Vienna, Austria*	Internet: www.eurocarb2009.at
8th Pangborn Sensory Science Symposium	26–30 July 2009 *Florence, Italy*	Internet: www.pangborn2009.com
ICoMST 2009 – Meat: Muscle, Manufacturing and Meals	16–21 August 2009 *Copenhagen, Denmark*	Internet: http://www.icomst2009.dk
5th CIGR International Technical Symposium on Food Processing, Monitoring Technology in Bioprocesses	31 August–2 September 2009 *Potsdam, Germany*	Internet: http://www.atb-potsdam.de/CIGRPostharvest2009/
Methods and Issues in Cheese Authenticity Studies	4–5 September 2009 *Avellino, Italy*	Internet: http://www.isa.cnr.it
CIBIA VII – Integrating Food Engineering and Wellbeing	6–9 September 2009 *Bogota, Colombia*	Internet: www.cibiacolombia.org
11th International Conference on Chitin and Chitosan	7–9 September 2009 *Taipei, Taiwan*	E-mail: iccc@tl.ntu.edu.tw Internet: http://taiwan11thiccc.ntu.edu.tw
3rd International EuroFIR Congress – European Food Composition Data for Better Diet, Nutrition and Food	8–10 September 2009 *Vienna, Austria*	Internet: www.eurofir.net
6th International Conference on Predictive Modelling in Foods	8–12 September 2009 *Washington, DC*	E-mail: vijay.juneja@ars.usda.gov; schaffner@aesop.rutgers.edu Internet: http://www.6icpmf.org/
Industrial Workshop on Microencapsulation of Flavors and Bioactives for Functional Food Applications	14–15 September 2009 *Bloomington, MN, USA*	Internet: www.bioactivesworld.com
IDF World Dairy Summit	20–24 September 2009 *Berlin, Germany*	Internet:http://www.wds2009.com
Polysaccharides as a Source of Advanced Materials	21–24 September 2009 *Turku/Abo, Finland*	Internet: http://congress.utu.fi/epnoe2009/
6th NIZO Dairy Conference – Dairy ingredients: innovations in functionality	30 September–2 October 2009 *Papendal, Arnhem, The Netherlands*	Internet: www.nizodairyconf.elsevier.com
4th International Symposium on Sourdough	14–17 October 2009 *Munich, Germany*	Internet: http://www.sourdough.foodscience.ws
11th ASEAN Food Conference 2009	21–23 October 2009 *Bandar Seri Begawan, Brunei*	Internet: http://www.agriculture.gov.bn/DOA/BDAFST/Announcement.html
International Conference on Bio and Food Electrotechnologies	22–23 October 2009 *Compiegne, France*	Internet: http://www.utc.fr/bfe2009

doi:10.1016/S0308-8146(09)00908-X

Event	Date and Venue	Details from
International Society for Nutraceuticals and Functional Foods Annual Conference	1–4 November 2009 *San Francisco, CA*	Internet: http://isnff.org
4th International Symposium on Recent Advances in Food Analysis	4–6 November 2009 *Prague, Czech Republic*	Internet: http://www.rafa2009.eu/
2009 EFFoST Conference – New Challenges in Food Preservation: Processing – Safety – Stability	11–13 November 2009 *Budapest, Hungary*	Internet: http://www.effost-conference.elsevier.com
Pittcon 2010	28 February–5 March 2010 *Orlando, Florida*	Internet: www.pittcon.org
US/Ireland Functional Foods Conference	9–11 March 2010 *Cork, Ireland*	Internet: www.corkff2010.com
Food Colloids 2010 – On the Road from Interfaces to Consumers	21–24 March 2010 *Granada, Spain*	Internet: www.foodcolloids2010.org
IDF Symposium on the Science & Technology of Fermented Milk	7–9 June 2010 *Tromsø, Norway*	Internet: www.IDFFer2010.no
IDF Symposium on Microstructure of Dairy Products	9–11 June 2010 *Tromsø, Norway*	Internet: www.IDFMic2010.no
10th International Hydrocolloids Conference	20–24 June 2010 *Shanghai, China*	Internet: www.10ihc.org
IFT Annual Meeting and Food Expo	17–21 July 2010 *Chicago, USA*	Internet: www.ift.org
56th International Congress of Meat Science and Technology (ICoMST)	8–13 August 2010 *Jeju, South Korea*	Internet: http://icomst2010.org/
IUFoST 2010 – 15th World Congress of Food Science and Technology	22–26 August 2010 *Cape Town, South Africa*	Internet: http://www.iufost2010.org.za
Eurosense 2010 – Fourth European Conference on Sensory and Consumer Research	5–9 September 2010 *Vitoria, Spain*	Internet: TBA

This calendar of forthcoming events is based on information provided by the respective organizers and from secondary sources.
Food Chemistry welcomes information on relevant meetings. Copy deadlines are three months ahead of cover dates and information should be sent to:
Wendy Hurp, *Food Chemistry Calendar*, Elsevier Ltd, The Boulevard, Langford Lane, Kidlington, Oxford OX5 1GB, UK.
Fax: +44 (0) 1865 843960; E-mail: w.hurp@elsevier.com

FOOD CHEMISTRY

Aims and Scope

Food Chemistry publishes original research papers dealing with the chemistry and biochemistry of foods and raw materials covering the entire food chain from *'farm to fork.'* Topics include:

- Chemistry relating to major and minor components of food, their nutritional, physiological, sensory, flavour and microbiological aspects;
- Bioactive constituents of foods, including antioxidants, phytochemicals, and botanicals. Data must accompany sufficient discussion to demonstrate their relevance to food and/or food chemistry;
- Chemical and biochemical composition and structure changes in molecules induced by processing, distribution and domestic conditions;
- Effects of processing on the composition, quality and safety of foods, other bio-based materials, by-products, and processing wastes;
- Chemistry of food additives, contaminants, and other agro-chemicals, together with their metabolism, toxicology and food fate.

Analytical Section

Analytical papers related to the microbiological, sensory, nutritional, physiological, authenticity and origin aspects of food. Papers should be primarily concerned with new or novel methods (especially instrumental or rapid) provided adequate validation is described including sufficient data from real samples to demonstrate robustness. Papers dealing with significant improvements to existing methods, or data from application of existing methods to new foods, or commodities produced in unreported geographical areas, will also be considered.

- Methods for the determination of both major and minor components of food especially nutrients and non-nutrient bioactive compounds (with putative health benefits) will be considered.
- Results of method inter-comparison studies and development of food reference materials for use in the assay of food components;
- Methods concerned with the chemical forms in food, nutrient bioavailability and nutritional status;
- General authentication and origin [e.g. Country of Origin Labelling (COOL), Protected Designation of Origin (PDO), Protected Geographical Indication (PGI), Certificate of Specific Character (CSC)] determination of foods (both geographical and production including commodity substitution, and verification of *organic, biological* and *ecological* labelling) providing sufficient data from authentic samples should be included to ensure that interpretations are meaningful.

FOOD CHEMISTRY

Aims and Scope

Food Chemistry publishes original research papers dealing with the chemistry and biochemistry of foods and raw materials covering the entire food chain from *'farm to fork.'* Topics include:

- Chemistry relating to major and minor components of food, their nutritional, physiological, sensory, flavour and microbiological aspects;
- Bioactive constituents of foods, including antioxidants, phytochemicals, and botanicals. Data must accompany sufficient discussion to demonstrate their relevance to food and/or food chemistry;
- Chemical and biochemical composition and structure changes in molecules induced by processing, distribution and domestic conditions;
- Effects of processing on the composition, quality and safety of foods, other bio-based materials, by-products, and processing wastes;
- Chemistry of food additives, contaminants, and other agro-chemicals, together with their metabolism, toxicology and food fate.

Analytical Section

Analytical papers related to the microbiological, sensory, nutritional, physiological, authenticity and origin aspects of food. Papers should be primarily concerned with new or novel methods (especially instrumental or rapid) provided adequate validation is described including sufficient data from real samples to demonstrate robustness. Papers dealing with significant improvements to existing methods, or data from application of existing methods to new foods, or commodities produced in unreported geographical areas, will also be considered.

- Methods for the determination of both major and minor components of food especially nutrients and non-nutrient bioactive compounds (with putative health benefits) will be considered.
- Results of method inter-comparison studies and development of food reference materials for use in the assay of food components;
- Methods concerned with the chemical forms in food, nutrient bioavailability and nutritional status;
- General authentication and origin [e.g. Country of Origin Labelling (COOL), Protected Designation of Origin (PDO), Protected Geographical Indication (PGI), Certificate of Specific Character (CSC)] determination of foods (both geographical and production including commodity substitution, and verification of *organic, biological* and *ecological* labelling) providing sufficient data from authentic samples should be included to ensure that interpretations are meaningful.

FOOD CHEMISTRY

Aims and Scope

Food Chemistry publishes original research papers dealing with the chemistry and biochemistry of foods and raw materials covering the entire food chain from *'farm to fork.'* Topics include:

- Chemistry relating to major and minor components of food, their nutritional, physiological, sensory, flavour and microbiological aspects;
- Bioactive constituents of foods, including antioxidants, phytochemicals, and botanicals. Data must accompany sufficient discussion to demonstrate their relevance to food and/or food chemistry;
- Chemical and biochemical composition and structure changes in molecules induced by processing, distribution and domestic conditions;
- Effects of processing on the composition, quality and safety of foods, other bio-based materials, by-products, and processing wastes;
- Chemistry of food additives, contaminants, and other agro-chemicals, together with their metabolism, toxicology and food fate.

Analytical Section

Analytical papers related to the microbiological, sensory, nutritional, physiological, authenticity and origin aspects of food. Papers should be primarily concerned with new or novel methods (especially instrumental or rapid) provided adequate validation is described including sufficient data from real samples to demonstrate robustness. Papers dealing with significant improvements to existing methods, or data from application of existing methods to new foods, or commodities produced in unreported geographical areas, will also be considered.

- Methods for the determination of both major and minor components of food especially nutrients and non-nutrient bioactive compounds (with putative health benefits) will be considered.
- Results of method inter-comparison studies and development of food reference materials for use in the assay of food components;
- Methods concerned with the chemical forms in food, nutrient bioavailability and nutritional status;
- General authentication and origin [e.g. Country of Origin Labelling (COOL), Protected Designation of Origin (PDO), Protected Geographical Indication (PGI), Certificate of Specific Character (CSC)] determination of foods (both geographical and production including commodity substitution, and verification of *organic, biological* and *ecological* labelling) providing sufficient data from authentic samples should be included to ensure that interpretations are meaningful.

FOOD CHEMISTRY

Aims and Scope

Food Chemistry publishes original research papers dealing with the chemistry and biochemistry of foods and raw materials covering the entire food chain from *'farm to fork.'* Topics include:

- Chemistry relating to major and minor components of food, their nutritional, physiological, sensory, flavour and microbiological aspects;
- Bioactive constituents of foods, including antioxidants, phytochemicals, and botanicals. Data must accompany sufficient discussion to demonstrate their relevance to food and/or food chemistry;
- Chemical and biochemical composition and structure changes in molecules induced by processing, distribution and domestic conditions;
- Effects of processing on the composition, quality and safety of foods, other bio-based materials, by-products, and processing wastes;
- Chemistry of food additives, contaminants, and other agro-chemicals, together with their metabolism, toxicology and food fate.

Analytical Section

Analytical papers related to the microbiological, sensory, nutritional, physiological, authenticity and origin aspects of food. Papers should be primarily concerned with new or novel methods (especially instrumental or rapid) provided adequate validation is described including sufficient data from real samples to demonstrate robustness. Papers dealing with significant improvements to existing methods, or data from application of existing methods to new foods, or commodities produced in unreported geographical areas, will also be considered.

- Methods for the determination of both major and minor components of food especially nutrients and non-nutrient bioactive compounds (with putative health benefits) will be considered.
- Results of method inter-comparison studies and development of food reference materials for use in the assay of food components;
- Methods concerned with the chemical forms in food, nutrient bioavailability and nutritional status;
- General authentication and origin [e.g. Country of Origin Labelling (COOL), Protected Designation of Origin (PDO), Protected Geographical Indication (PGI), Certificate of Specific Character (CSC)] determination of foods (both geographical and production including commodity substitution, and verification of *organic, biological* and *ecological* labelling) providing sufficient data from authentic samples should be included to ensure that interpretations are meaningful.

International Society for Nutraceuticals & Functional Foods

2009 Annual Conference

Nutraceutical, Functional Foods, and Dietary Supplements: Science, Methodologies and Applications

November 1-4, 2009
Holiday Inn-Golden Gateway Hotel
1500 Van Ness Avenue
San Francisco, CA, USA 94109

International Advisory Board
Mr. Anthony Almada (USA)
Dr. Debasis Bagchi (USA)
Dr. Colin Barrow (Australia)
Dr. Joseph Betz (USA)
Dr. Zhen-Yu Chen (Hong Kong)
Ms. Audra Davies (USA)
Dr. Colin Dennis (UK)
Dr. Xiao-Qin (Charles) Han (China)
Dr. Chi-Tang Ho (USA)
Dr. Kazuki Kanazawa (Japan)
Dr. Se-Kwon Kim (Korea)
Dr. Hannu J. Korhonen (Finland)
Dr. Hyong Joo Lee (Korea)
Dr. Kazuo Miyashita (Japan)
Dr. Bhimu Patil (USA)
Dr. Ronald B. Pegg (USA)
Dr. Peter Roupas (Australia)
Dr. Augustin Scalbert (France)
Dr. Fereidoon Shahidi (Canada)
Dr. Young-Joon Surh (Korea)
Dr. Gary Williamson (UK)
Dr. Rickey Yada (Canada)
Dr. Jerzy Zawistowski (Canada)

Conference Co-Organizers
Dr. Fereidoon Shahidi (Canada)
Dr. Chi-Tang Ho (USA)
Dr. Debasis Bagchi (USA)
Dr. C-K. Wang (Taiwan)

Conference Symposia
- Anti-aging nutraceuticals
- Nutraceuticals for arthritis and inflammatory diseases
- Nutraceuticals and brain health
- Nutraceuticals for type-2 diabetes
- Nutraceuticals for cardiovascular disease and cancer
- Nutraceuticals for obesity and weight control
- Omega-3 and other nutraceutical oils
- Marine nutraceuticals
- Nutraceutical and functional beverages
- Pre-, pro- and synbiotics
- Protein hydrolysates and biopeptides
- Phytochemicals: polyphenols, carotenoids, etc.
- Delivery systems for nutraceuticals and functional food ingredients, including nano-technology
- Absorption, metabolism and action mechanism of nutraceuticals and functional food ingredients
- Nutrigenomics, proteomics and metabolomics
- Nutraceuticals and functional food ingredients from co-products and by-products
- Global Regulations for nutraceuticals, dietary supplements and functional foods
- Analytical methodologies
- Quality assurance for nutraceuticals, dietary supplements and functional food ingredients
- Import-export issues for nutraceuticals and functional foods
- Inventor-investor and business to business
- Bioactive and minor components
- Traditional foods and health promotion
- Nuts and dried fruits: products, health and well-being
- Processing of nutraceuticals and functional food ingredients
- Voluntary papers (oral and poster)

Exhibition: 10 AM – 5 PM, November 2 & 3, 2009

Preconference:

Track A – Antioxidant Forum/Short Course-Methodologies, Assessments, Applications and Health (Oct. 31 & Nov. 1, 2009)

Track B – Omega-3 and Beyond: Fundamentals, Applications and Health (Oct. 31 & Nov. 1, 2009)

For further information, visit: ***isnff.org***

Disclaimer : Program details and speakers may change due to circumstances

International Society for Nutraceuticals and Functional Foods (ISNFF)

ANNOUNCEMENTS

The **Annual Conference and Exhibition of the International Society for Nutraceuticals and Functional Foods (ISNFF)** will be held 1-4 November 2009 in San Francisco, CA, USA. For further information and registration, please visit the website of ISNFF (www.isnff.org). For further information, please contact Peggy Ann Parsons (Tel: +1 (709) 737 8239; Fax: +1 (709) 737 4000, or E-mail: pparsons@mun.ca).

The **International Antioxidant Forum / Short Course – Methodologies, Assessments, Applications and Health** of the International Society for Nutraceuticals and Functional Foods (ISNFF) will be held in the Golden Gateway Holiday Inn in San Francisco, CA, USA on 31 October and 1 November 2009. For details visit the ISNFF website at (**www.isnff.org**). For further information, please contact Peggy Ann Parsons (Tel: +1 (709) 737 8239; Fax: +1 (709) 737 4000, or E-mail: pparsons@mun.ca).

The **Omega-3 and Beyond - Fundamentals, Applications and Health Short Course** of the International Society for Nutraceuticals and Functional Foods (ISNFF) will be held in the Golden Gateway Holiday Inn in San Francisco, CA, USA on 31 October and 1 November 2009. For details visit the ISNFF website at (**www.isnff.org**). For further information, please contact Peggy Ann Parsons (Tel: +1 (709) 737 8239; Fax: +1 (709) 737 4000, or E-mail: pparsons@mun.ca).

Fereidoon Shahidi Fellowship Award

The **International Society for Nutraceuticals and Functional Foods (ISNFF)** has announced the establishment of the above award for graduate students. The award carries a US$1500 check and a recognition plaque. For further information about nominations and applications, please visit the ISNFF website www.isnff.org or contact Peggy Ann Parsons (Tel: +1 (709) 737 8239; Fax: +1 (709) 737 4000, or E-mail: pparsons@mun.ca).

5th International Conference on Polyphenols Applications

Call for Abstracts
Network Session

Malta Polyphenols 2009

Bridging Bio-efficacy to Innovation & Applications

&

Satellite Symposium

Pomegranate Extracts: Clinical & Nutraceutical Applications

October 29 & 30, 2009

At

Radisson SAS Hotel, Bay Point Resort

St. Julian's, Malta

The aims of **Malta Polyphenols 2009** are to **provide answers** to give a **future vision** of how polyphenols can enhance human nutrition and help in the prevention and treatment of many chronic diseases. **Malta Polyphenols 2009** will target researchers and academic professors, R&D departments, clinical, pharmaceutical companies, food supplements companies, cosmetics companies, veterinary medicine companies, marketing departments, investors, start ups and all other stakeholders in the polyphenols industry.

CALL FOR ABSTRACTS

Abstracts can be sent as a word file to the following address: isanh-conferences@isanh.fr
Please indicate if you wish to submit your abstract for the Conference or Symposium and for **Oral or Poster presentation.**
All abstracts for oral or poster presentation will be submitted to the Scientific Committee.

IMPORTANT DATES

Early registration deadline: 7 September 2009
Abstract submission deadline: 1 October 2009

For further instructions on abstract submission and for details of the conference topics and sessions, visit **www.malta-polyphenols.com**